PRODUCT AND PROCESS DESIGN PRINCIPLES

Synthesis, Analysis and Evaluation

FOURTH EDITION

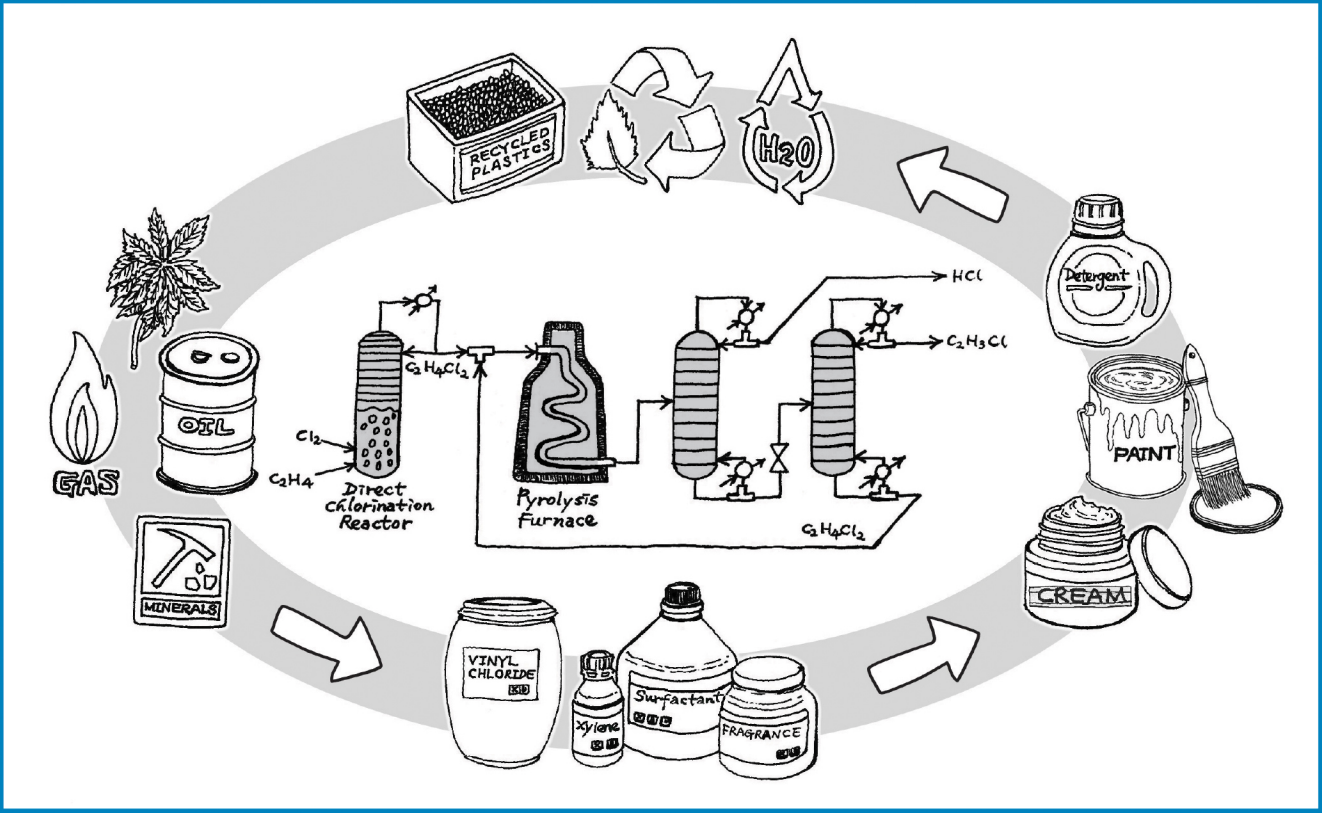

WARREN D. SEIDER • DANIEL R. LEWIN
J.D. SEADER • SOEMANTRI WIDAGDO
RAFIQUL GANI • KA MING NG

WILEY

PRODUCT AND PROCESS DESIGN PRINCIPLES

PRODUCT AND PROCESS DESIGN PRINCIPLES

Synthesis, Analysis, and Evaluation

Fourth Edition

Warren D. Seider

Department of Chemical and Biomolecular Engineering
University of Pennsylvania, Philadelphia, PA 19104-6393

Daniel R. Lewin

Department of Chemical Engineering
Technion—Israel
Institute of Technology, Haifa 32000, ISRAEL

J. D. Seader

Department of Chemical and Fuels Engineering
University of Utah, Salt Lake City, Utah 84112-9203

Soemantri Widagdo

InnoSEA International New York, USA

Rafiqul Gani

Department of Chemical and Biochemical Engineering
Technical University of Denmark, DK-2800 Lyngby, Denmark

Ka Ming Ng

Department of Chemical and Biomolecular Engineering
The Hong Kong University of Science and Technology
Clear Water Bay, Hong Kong

WILEY

VICE PRESIDENT & DIRECTOR	Laurie Rosatone
SENIOR DIRECTOR	Don Fowley
EXECUTIVE EDITOR	Linda Ratts
SPONSORING EDITOR	Mary O'Sullivan
MARKET SOLUTIONS ASSISTANT	Courtney Jordan
PROJECT MANAGER	Gladys Soto
PROJECT SPECIALIST	Nichole Urban
SENIOR MARKETING MANAGER	Daniel Sayre
ASSISTANT MARKETING MANAGER	Puja Katariwala
ASSOCIATE DIRECTOR	Kevin Holm
SENIOR CONTENT SPECIALIST	Nicole Repasky
PRODUCTION EDITOR	Sangeetha Rajan

This book was set in 10/12 Times LT Std by SPi Global and printed and bound by Lightning Source Inc.

ISBN: 978-1-119-28263-1 (PBK)
ISBN: 978-1-119-25734-9 (EVAL)

Library of Congress Cataloging in Publication Data:

Names: Seider, Warren D., author. | Lewin, Daniel R., author. | Seader, J. D., author. | Widagdo, Soemantri (Chemical engineer), author. | Gani, R. (Rafiqul), author. | Ng, Ka Ming, author.
Title: Product and process design principles : synthesis, analysis and evaluation / by Warren D. Seider, Daniel R. Lewin, J. D. Seader, Soemantri Widagdo, Rafiqul Gani, Ka Ming Ng.
Description: Fourth edition. | New York : John Wiley & Sons Inc., 2017. | Includes bibliographical references and index.
Identifiers: LCCN 2015046825 (print) | LCCN 2015047441 (ebook) | ISBN 9781119282631 (pbk.) | ISBN 9781119257332 (ePub) | ISBN 9781119261292 (Adobe PDF)
Subjects: LCSH: Chemical processes. | Synthetic products.
Classification: LCC TP155.7 .S423 2017 (print) | LCC TP155.7 (ebook) | DDC 660/.28—dc23
LC record available at http://lccn.loc.gov/2015046825

Printing identification and country of origin will either be included on this page and/or the end of the book. In addition, if the ISBN on this page and the back cover do not match, the ISBN on the back cover should be considered the correct ISBN.

Printed in the United States of America
10 9 8 7 6 5 4 3 2 1

Dedication

To the memory of my parents, to Diane, and to Deborah, Gabriel, Joe, Yishai, and Idana; Benjamin, Jaime, Ezra, and Raz

To the memory of my father, Harry Lewin, to my mother, Rebeca Lewin, to Ruti, and to Noa and Yonatan

To the memory of my parents, to Sylvia, and to my children

To the memory of my father, Theodorus Widagdo, to my mother, and to Richard

To the memory of L. E. (Skip) Scriven, H. Ted Davis, and Alkis Payatakes

To the memory of Richard R. Hughes, a pioneer in computer-aided simulation and optimization with whom two of the authors developed many concepts for carrying out and teaching process design

To all of our students: past, present, and future…

About the Authors

Warren D. Seider is Professor of Chemical and Biomolecular Engineering at the University of Pennsylvania. He received a B.S. degree from the Polytechnic Institute of Brooklyn and M.S. and Ph.D. degrees from the University of Michigan. He has contributed to the fields of process analysis, simulation, design, and control. Seider coauthored *FLOWTRAN Simulation—An Introduction* in 1974 and has coordinated the design course involving projects provided by many practicing engineers in the Philadelphia area at Penn for over 35 years. He has authored or coauthored 120 journal articles and authored or edited seven books. Seider was the recipient of the American Institute of Chemical Engineers (AIChE) Computing in Chemical Engineering Award in 1992, corecipient of the AIChE Warren K. Lewis Award in 2004 with J. D. Seader, and recipient of the AIChE F. J. and Dorothy Van Antwerpen Award in 2011. Seider served as Director of AIChE from 1984 to 1986 and as Chairman of the CAST Division and the Publication Committee. He helped to organize the Computer Aids for Chemical Engineering Education (CACHE) Committee in 1969 and served as its chairman. Seider is a member of the Editorial Advisory Board of *Computers and Chemical Engineering*. In 2008, his textbook, *Introduction to Chemical Engineering and Computer Calculations* with coauthor Alan L. Myers, was cited as one of 30 ground-breaking books in the last 100 years of chemical engineering.

Daniel R. Lewin is Churchill Family Chair Professor of Chemical Engineering and Director of the Process Systems Engineering (PSE) research group at the Technion, the Israel Institute of Technology. He received his B.Sc. from the University of Edinburgh and his D.Sc. from the Technion. Lewin's research focuses on the interaction of process design and process control and operations with emphasis on model-based methods. He has authored or coauthored over 100 technical publications in the area of process systems engineering as well as the first three editions of this textbook and the multimedia CD that accompanies it. Lewin has been awarded a number of prizes for research excellence and twice received the Jacknow Award, the Alfred and Yehuda Weissman Award, and the Yannai Prize, in recognition of teaching excellence at the Technion.

J. D. Seader is Professor Emeritus of Chemical Engineering at the University of Utah. He received B.S. and M.S. degrees from the University of California at Berkeley and a Ph.D. from the University of Wisconsin. From 1952 to 1959, he designed chemical and petroleum processes for Chevron Research, directed the development of one of the first computer-aided process design programs, and codeveloped the first widely used computerized vapor–liquid equilibrium correlation. From 1959 to 1965, he conducted rocket engine research for Rocketdyne on all of the engines that took man to the moon. Before joining the faculty at the University of Utah in 1966, Seader was a professor at the University of Idaho. He is the author or coauthor of 114 technical articles, eight books, and four patents. Seader is coauthor of the section on distillation in the sixth and seventh editions of *Perry's Chemical Engineers' Handbook.* He is coauthor of *Separation Process Principles* published in 1998 with second, third, and fourth editions in 2006, 2011, 2016, respectively. Seader was Associate Editor of *Industrial and Engineering Chemistry Research* for 12 years, starting in 1987. He was a founding member and trustee of CACHE for 33 years, serving as Executive Officer from 1980 to 1984. For 20 years, he directed the use by and distribution to 190 chemical engineering departments worldwide of Monsanto's FLOWTRAN process simulation computer program. Seader served as Chairman of the Chemical Engineering Department at the University of Utah from 1975 to 1978 and as Director of AIChE from 1983 to 1985. In 1983, he presented the 35th Annual Institute Lecture of AIChE. In 1988, he received the Computing in Chemical Engineering Award of the CAST Division of AIChE. In 2004, he received

the CACHE Award for Excellence in Computing in Chemical Engineering Education from the ASEE. In 2004, he received with Professor Warren D. Seider the Warren K. Lewis Award for Chemical Engineering Education from the AIChE. In 2008, his textbook, *Separation Process Principles* with coauthor Ernest J. Henley, was cited as one of 30 ground-breaking books in the last 100 years of chemical engineering.

Soemantri Widagdo is the founder of InnoSEA International in 2013 and formerly an R&D executive after a 15-year career at 3M Company. His last position was as the R&D Head of 3M Southeast Asia. He received his B.S. degree in chemical engineering from Bandung Institute of Technology, Indonesia, and his M.Ch.E. and Ph.D. degrees from Stevens Institute of Technology. Early in his career, Widagdo developed the first electric generator in Indonesia that used biomass gasification technology. After the completion of his graduate studies, he began his career in the United States with the Polymer Processing Institute (PPI), Hoboken, New Jersey. As the head of its computation group, he led the development of an analysis software package for twin-screw compounding. During his tenure at PPI, Widagdo was also Research Professor of Chemical Engineering at Stevens Institute of Technology. He has been involved in a variety of technology and product-development programs involving renewable energy, industrial and transportation applications, consumer office products, electrical and electronics applications, healthcare and dentistry, and display and graphics applications. He has authored and coauthored over 20 technical publications and four patents.

Rafiqul Gani is Professor of System Design at the Department of Chemical & Biochemical Engineering, The Technical University of Denmark. He is also the cofounder and former Head of the Computer Aided Product-Process Engineering Center (CAPEC). He received a B.S degree from the Bangladesh University of Engineering and Technology, and M.S., DIC, and Ph.D. degrees from Imperial College, London. Gani's current research interests include development of computer-aided methods and tools for modeling, property estimation, process-product synthesis and design, and process-tools integration. He has published more than 300 peer-reviewed journal articles and delivered over 300 lectures, seminars, and plenary/keynote lectures at international conferences, institutions, and companies all over the world. Gani was Editor-in-chief of the *Computers & Chemical Engineering* journal (until 31 December 2015), is Editor of the Elsevier CACE book series, and serves on the editorial advisory board of several other journals. He received the 2015 Computers and Chemical Engineering Award from the AIChE CAST Division. For the term 2016–2017, he has been relected as the President of the European Federation of Chemical Engineering (EFCE); he is a member of the Board of Trustees of the American Institute of Chemical Engineers (AIChE); a Fellow of the AIChE; and a Fellow of Institution of Chemical Engineers (IChemE).

Ka Ming Ng is Chair Professor of Chemical and Biomolecular Engineering at the Hong Kong University of Science and Technology. He obtained his B.S. degree from the University of Minnesota and his Ph.D. from the University of Houston. From 1980 to 2000, he served as Professor of Chemical Engineering at the University of Massachusetts, Amherst. Ng joined the Hong Kong Department of Chemical and Biomolecular Eng. in 2000 and served as Head from 2002 to 2005. He was CEO of Nano and Advanced Materials Institute Ltd., a government-funded R&D center, from 2006 to 2013 and served as Corporate Science and Technology Advisor for Mitsubishi Chemical, Japan, from 2001 to 2013. He held visiting positions at DuPont, Massachusetts Institute of Technology, and the National University of Singapore. Ng's research interests center on product conceptualization, process design, and business development involving water, natural herbs, nanomaterials, and advanced materials. He is a fellow of AIChE from which he received the Excellence in Process Development Research Award in 2002.

Preface

OBJECTIVES

The principal objective of this textbook, e-book, and accompanying materials, referred to here as *courseware,* is to present modern strategies for the systematic design of chemical products and processes. Product design deals with "What to Make," and process design deals with "How to Make."

Since the early 1960s, undergraduate education of chemical engineers has focused mainly on the engineering sciences. In recent years, however, more scientific approaches to product and process design have been developed, and the need to teach students these approaches has become widely recognized. Consequently, this courseware has been developed to help students and practitioners better use the modern approaches to product and process design. Like workers in thermodynamics; momentum, heat, and mass transfer; and chemical reaction engineering, product and process designers apply the principles of mathematics, chemistry, physics, and biology. Designers also use these principles and those established by engineering scientists to create chemical products and processes that satisfy societal needs while returning a profit. In so doing, designers emphasize the methods of synthesis and optimization in the face of uncertainties, often utilizing the results of analysis and experimentation prepared in cooperation with engineering scientists while working closely with their business colleagues.

This courseware describes the latest design strategies, most of which have been improved significantly by the advent of computers, numerical mathematical programming methods, and artificial intelligence. Because few curricula emphasize design strategies prior to design courses, this courseware is intended to provide a smooth transition for students and engineers who are called upon to design creative new products and processes.

This new edition is a result of an evolution in our approach to teaching design, starting from the first edition, which focused on commodity chemical processes; it was followed by the second edition, which expanded the scope to include the design of chemical products with emphasis on specialty chemicals involving batch rather than continuous processing. This was followed by the third edition, which presented a unified view of the design of basic, industrial, and configured consumer chemical products in the perspective of the Stage-Gate^{TM} Product-Development Process (SGPDP). In this fourth edition, we have organized the presentation of product and process design into two separate, although related, activities in a manner so that the two topics can be taught separately or together. Thus, the reader of this edition can choose to focus only on process design or on product design or can choose to study the two in parallel.

This courseware is intended for seniors and graduate students, most of whom have solved a few open-ended problems but have not received instruction in a systematic approach to product and process design. To guide this instruction, the subject matter is presented in five parts. Part I provides introductions to product design in Chapter 1 and to process design in Chapter 2. The two introductions are then followed by Chapter 3, which provides supporting materials for design activity covering literature sources, energy sources, sustainability and environmental protection, safety, and engineering ethics.

Following the introductions in Part I, Part II deals with the synthesis of products and processes. The first two chapters of this part focus on synthesis issues concerning product design, beginning with the design of molecules and mixtures to satisfy customer needs in Chapter 4. More specifically, Chapter 4 describes the use of computer-aided techniques to identify chemicals (e.g., refrigerants, solvents, polymers) and blends and solvent-based products (e.g., paints, lotions, creams) having desired properties. Chapter 5 focuses on the design of devices, functional products, and formulated products whose structure, form, shape, and/or configuration is customized.

The remainder of Part II provides a sequence of six chapters for a systematic approach to process design, starting with Chapter 6, which shows how heuristics can be harnessed to rapidly generate an initial base-case design without doing much analysis. Next, Chapter 7 presents the computational background to the use of simulation in process design, thus providing a means for verifying the heuristic decisions with quantitative analysis. In this regard, Chapter 7 also presents short-cut computation methods. It includes reliable estimation methods for thermophysical and transport properties. These two chapters are followed by chapters covering the synthesis of reactor networks (Chapter 8) and separation trains (Chapter 9), second-law analysis (Chapter 10), and heat and power integration methodology (Chapter 11). Part II also includes coverage of equipment design: Chapter 12 for heat exchangers; Chapter 13 for separation towers; Chapter 14 on pumps, compressors, and expanders; and Chapter 15 on chemical reactor design, focusing on modeling situations in which plug flow and perfect back-mixing assumptions do not hold. The last two chapters of Part II deal with equipment sizing and costing (Chapter 16) and profitability analysis (Chapter 17).

Part III discusses the analysis tools required for both product design and process design; the first two chapters cover analysis in product design. Chapter 18 provides a guide to six-sigma design strategies, which offer a means to improve product quality through the identification of the root causes of variance and their subsequent attenuation. Chapter 19 focuses on the relationship between product technical specifications and the design of the manufacturing plant and discusses issues such as product pricing and demand. Part III also consists of three chapters supporting analysis in process design, starting with Chapter 20 on plantwide controllability assessment followed by Chapter 21 on design optimization and Chapter 22 on the design and scheduling of batch processes.

Part IV describes design reporting in Chapter 23, emphasizing product and process design aspects, with a template provided for writing design reports and with recommendations for preparing oral presentations.

The last part of the book, Part V, is a collection of case studies: three featuring products and one featuring a process. Each of the three product design case studies begins with a discussion of new related technologies. Then, the most important product design steps are covered. Each case study involves some engineering design calculations and/or lab data regression to be performed by students. The process design case study involves the design process for the manufacture of ammonia and describes the development of an initial feasible, but rather unprofitable, base-case design, and then shows how the initial design is systematically refined until it is acceptable.

LIMITED TIME—PROCESS OR PRODUCT DESIGN?

When limited time is available, some faculty and students may prefer to focus on *process* design rather than *product* design by following the flow chart in Figure i-1. This can be accomplished by beginning in Part I with the introduction in Chapter 2 and coverage on design literature, innovation, energy sources, environmental sustainability, safety, and ethics in Chapter 3; then, Chapters 6–11 from Part II systematically cover heuristics, process simulation, reactor and separation system design, second-law analysis, and heat and power integration. The sequence in Chapters 12–15, detailing equipment design, may be left to students as self-study in connection with their design project work, or portions may be covered in class. Some universities teach process economics as a separate course, but those that do not will need to include Chapter 16, covering cost accounting and capital cost estimation, and Chapter 17, covering profitability analysis. Finally, all or part of the sequence of three chapters from Part III can be included: Chapter 20 on plantwide controllability assessment (probably the most important of the three to cover), Chapter 21 on design optimization (if not covered elsewhere, for example, in a course on numerical methods), and Chapter 22 on the design and scheduling of batch processes. Part IV, covering design reports, should be left to self-study. The case study in Chapter 27 could be used either by students for self-study or could be the subject for a constructive class discussion with students as preparation for their design project work.

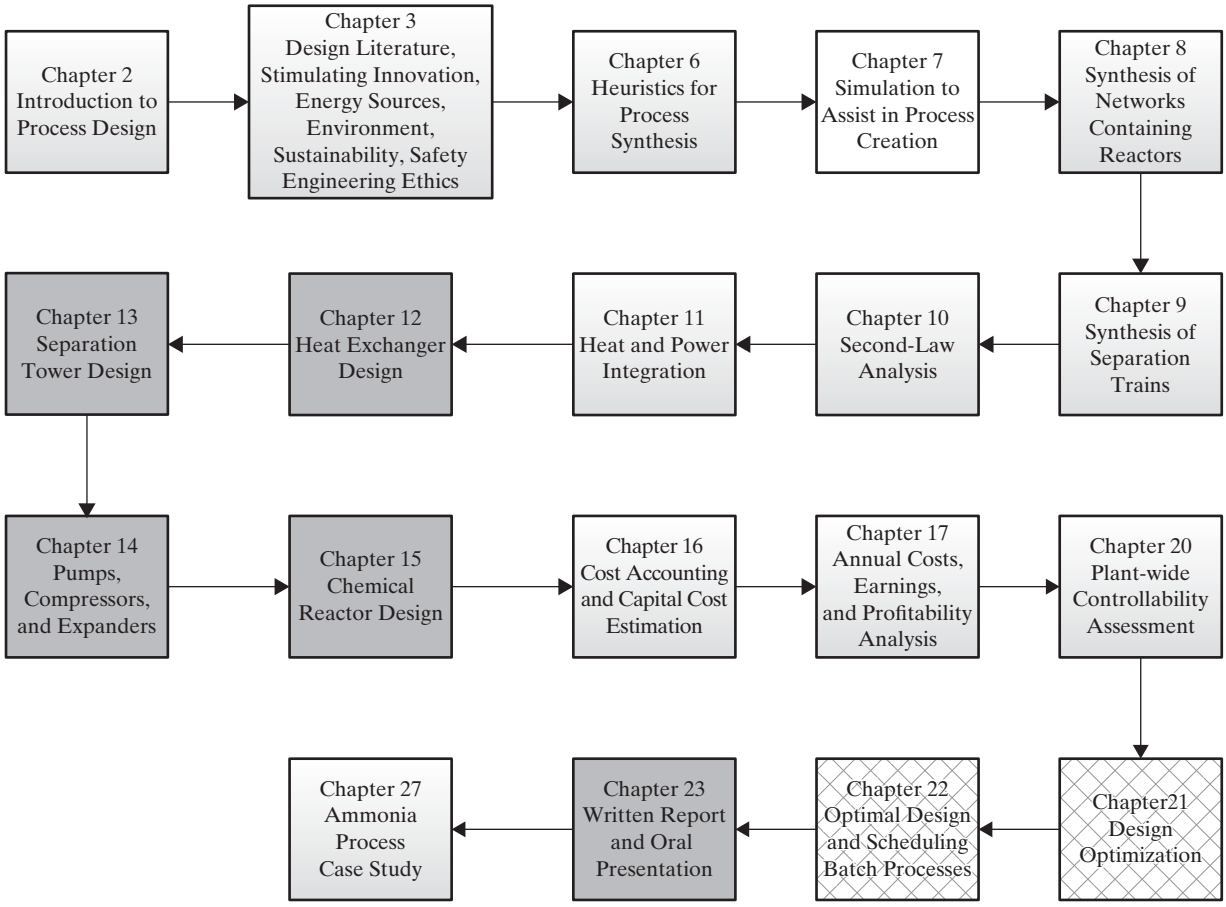

Figure i-1 Process design chapter sequence: Chapters for potential self-study are indicated in grey with optional materials indicated in cross-hatched boxes.

Courses that focus on *product* design rather than *process* design can proceed as shown in the flow chart in Figure i-2, starting with the introduction in Chapter 1 followed by materials on the design literature, innovation, energy sources, the environment, sustainability, safety, and ethics in Chapter 3. These could be followed by the two chapters on product design synthesis in Part II on the design of molecules and mixtures (Chapter 4) and on formulated products and devices (Chapter 5). Chapter 19 on decision making in product development should be covered next and then Chapters 21 on design optimization (assuming it is not covered elsewhere) and Chapter 22 on optimal design and scheduling of batch processes. It would be helpful to end the course with detailed coverage of the case studies in Chapters 24–26. As with the process design sequence, it is recommended that Part IV covering design reports be left to self-study.

FORMAT OF COURSEWARE AND SUPPORTING WEB SITE

This courseware takes the form of a conventional textbook now available for the first time as an e-book. Because the design strategies have been elucidated during the development of this courseware, fewer specifics have been provided in the chapters concerning the software packages involved. Instead, a multimedia encyclopedia has been developed to give many examples of simulator input and output with frame-by-frame instructions to discuss the nature of the models provided for the processing units, and it presents several example calculations. The encyclopedia uses voice, video, and animation to introduce new users of the steady-state simulators to the specifics of two of the most widely used process simulation programs, ASPEN PLUS and UniSim® Design, as well as instruction in MATLAB. These programs include several tutorials that provide instruction on the solution of problems for courses in mass and energy balances, thermodynamics, fluid mechanics, heat transfer, separations, and reactor design. In many cases, students will have already been introduced to the

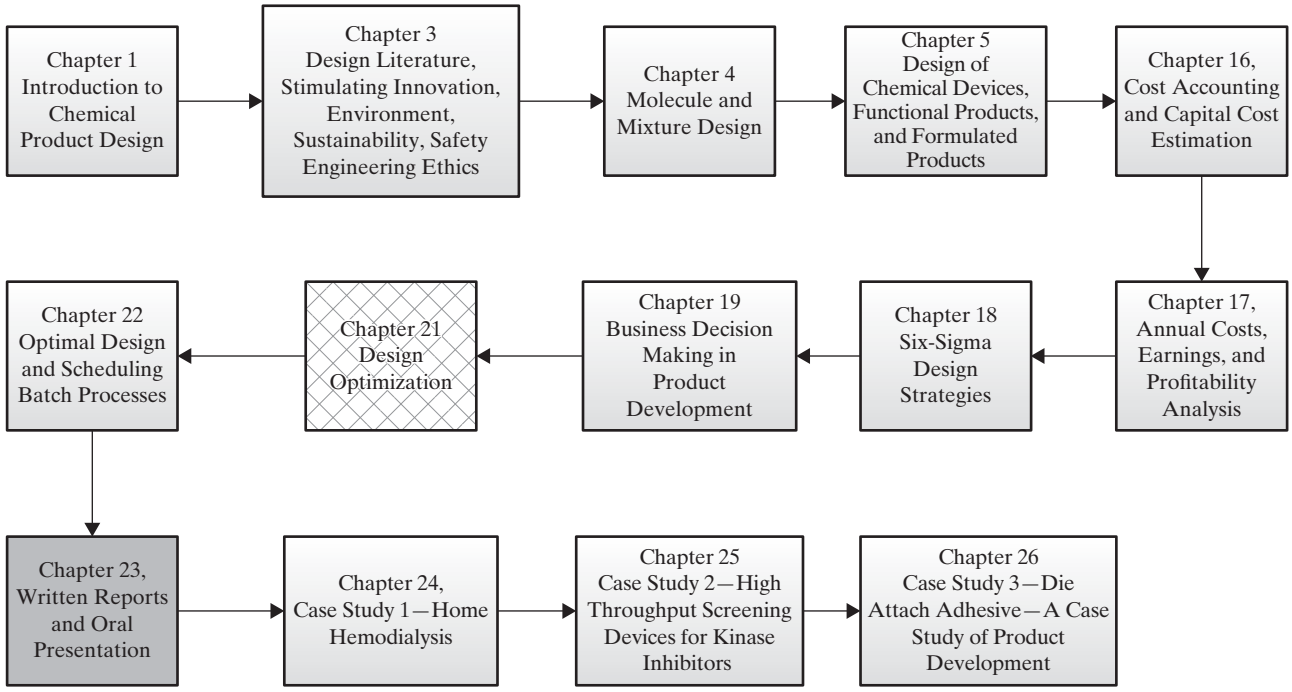

Figure i-2 Product design chapter sequence: Chapters for potential self-study are indicated in grey with optional materials indicated in cross-hatched box.

process simulators in these courses. Also, video segments show portions of a petrochemical complex in operation, including distillation towers, heat exchangers, pumps and compressors, and chemical reactors. The Wiley site[1] that supports this book also includes files that contain the solutions for many examples using either ASPEN PLUS or UniSim® Design as well as the MATLAB scripts in Chapter 20. The files are referred to in each example and can easily be used to vary parameters and to explore alternative solutions.

Supplemental sections of several chapters are provided in PDF files on the Wiley site that supports this book with only a brief summary of the material presented in the textbook. Furthermore, Appendix II lists design projects whose problem statements are provided in a PDF file on a University of Pennsylvania site.[2] These involve the design of chemical processes in several industries. Many are derived from the petrochemical industry with much emphasis on environmental and safety considerations, including the reduction of sources of pollutants and hazardous wastes and the purification before streams are released into the environment. Several projects originate in the biochemicals industry, including fermentations to produce pharmaceuticals, foods, and chemicals. Others involve the manufacture of polymers and electronic materials. Each design problem has been solved by groups of two, three, or four students at the University of Pennsylvania; copies of their design reports are available by Interlibrary Loan from the University of Pennsylvania Library. Since 2011, PDF files are also available from the University of Pennsylvania Library.

ADVICE TO STUDENTS AND INSTRUCTORS

In the use of this textbook and accompanying matter, students and instructors are advised to take advantage of the following features:

Feature 1: Well-organized Sequence of Materials to Teach Product Design

This textbook introduces the key steps in *product* design with numerous examples. These steps have been developed with the assistance and recommendations of successful practitioners of product design in industry. Students can begin with the overview in

[1] he-cda.wiley.com/WileyCDA/HigherEdTitle/productCd-0471216631.html.

[2] www.seas.upenn.edu/~dlewin/UPenn Design Problem Statements.html.

Chapter 1, which introduces the main steps involved in designing products. Computer-aided tools for design of single molecule products and of liquid mixtures and blends are covered in Chapter 4. In Chapter 5, the design of B2C chemical products for which chemical reaction and transport phenomena tend to play a dominant role is discussed in detail. The discussion of business decision making for B2C products, which is discussed in Chapter 19, is more involved than that for B2B products. Three detailed case studies for chemical products are presented in Chapters 24, 25, and 26. These examples can be expanded and/or used as the basis of design projects for student design teams. In our experience, students can frequently formulate their own product design projects based on their own experience and awareness of consumer needs.

Feature 2: Well-organized Sequence of Materials to Teach Process Design

Process synthesis is introduced primarily using heuristics in Chapters 2 and 6, whereas Chapters 8–11 provide more detailed algorithmic methods for chemical reactor network synthesis, separation train synthesis, and heat and power integration. Chapter 7, covering process simulation, provides the basis for testing process design alternatives.

This feature enables the student to begin process designs using easy-to-understand rules of thumb. Once these ideas have been mastered, students can learn algorithmic approaches that enable them to produce better designs. For example, consider how students would design a plant to produce a commodity chemical, say ammonia, from suitable raw materials—in this case, natural gas and air. Chapter 2 introduces process design focusing on the generation of a feasible base-case design, that is, one that satisfies production demands with respect to quantity and quality without necessarily being profitable. Most, if not all, of the decisions made at this point rely on heuristics, which are introduced in Chapter 2 and covered more thoroughly in Chapter 6. Because the implementation and testing of design ideas are carried out using process simulation, this is supported by the systematic coverage of the efficient use of process simulation in Chapter 7, as well as in the multimedia encyclopedia that is available on the Wiley Web site that supports this book. Attempts to improve profitability use methodologies for reactor network synthesis described in Chapter 8 (one of the examples in that chapter shows how to optimally operate a cold-shot ammonia converter) and separation network synthesis presented in Chapter 9 (although not important for ammonia synthesis). At this stage, students should be ready to learn about how heat integration can improve their design; Chapter 11 provides them a comprehensive guide, which also includes worked examples directly relevant to the problem(s) at hand. Cost accounting and profitability analysis are handled formally in Chapters 16 and 17, which provide a basis for estimating the degree to which their process is cost effective. This whole sequence can be used to support an entire design project as illustrated in Chapter 27, a case study that goes through the entire design process for a plant to produce 450 MTD of ammonia.

Feature 3: Instruction in the Use of Simulators

Throughout this courseware, various methods are used to perform extensive process-design calculations and provide graphical results that are visualized easily including the use of computer programs for simulation and design optimization. The use of these programs is an important attribute of this courseware. We believe that our approach is an improvement over an alternative approach that introduces the strategies of process synthesis *without computer methods*, emphasizing heuristics and back-of-the-envelope calculations. We favor a blend of heuristics and analysis using the computer by augmenting the heuristic approach with an introduction to the analysis of prospective flowsheets using industrial-quality simulators, such as ASPEN PLUS, HYSYS.Plant, UniSim® Design, PRO-II, CHEMCAD, FLOWTRAN, BATCH PLUS, and SUPERPRO DESIGNER. These simulators permit access to large physical property, equipment, and cost databases and the examination of aspects of numerous chemical processes. Simulators facilitate the search for optimal operating conditions to improve profitability. Emphasis is on the use of simulators to obtain data and perform tedious engineering calculations. Today, most schools use one of these simulators but often without adequate teaching materials. Consequently, the challenge for us in the preparation of this courseware was to find the proper blend of modern computational approaches with simple heuristics.

Through the use of the process simulators, which are widely used in industry, students learn how easy it is to obtain data and perform routine calculations. They learn effective approaches to building knowledge about a process through simulation. The courseware provides students the details of the methods used for property estimation and equipment modeling. They learn to use simulators intelligently and to check their results. For example, in Chapter 2, examples show how to use simulators to assemble a preliminary database and to perform routine calculations when computing heat loads, heats of reaction, and vapor–liquid equilibria. In Chapter 7, two examples show how to use the simulators to assist in the synthesis of toluene hydrodealkylation and monochlorobenzene separation processes. Most of the remaining chapters show examples of the use of simulators to obtain additional information, including equipment sizes, costs, profitability analyses, and the performance of control systems.

Because the book and the accompanying materials contain many routine self-study examples of how the simulators are useful in building a process design, the instructor has time to emphasize other aspects of process design. Through the examples and multimedia encyclopedia with emphasis on ASPEN PLUS and UniSim® Design, students obtain the details they need to use the simulators effectively, saving the instructor time in class and in answering detailed questions as students prepare their designs. Consequently, students obtain a better understanding of the design process and are exposed to a broader array of concepts in process design. In a typical situation when creating a base-case design, students use the examples in the text and the encyclopedic modules and the tutorials to learn how to obtain physical property estimates, heats of reaction, flame temperatures, and phase distributions. Then, students learn to create a reactor section using the simulators to perform routine material and energy balances. Next, students create a separation section and may eventually add recycle streams. Thanks to the coverage of the process simulators in Chapters 2 and 7 and the supporting materials, the instructor needs to review only the highlights in class.

Acknowledgments

In the preparation of this courseware, several graduate and postdoctoral students made significant contributions; they include Charles W. White III, George J. Prokopakis, Joseph W. Kovach III, Tulio R. Colmenares, Miriam L. Cygnarowicz, Alden N. Provost, David D. Brengel, Soemantri Widagdo, Amy C. Sun, Roberto Irrizary-Rivera, Leighton B. Wilson, James R. Phimister, Pramit Sarma, Thomas A. Adams II, and Cory S. Silva at the University of Pennsylvania; Oren Weitz, Boris Solovyev, Eyal Dassau, Joshua Golbert, Eytan Filiba, Eran Nahari, Uri Ash-Kurtlander, Michael Patrascu, Ronen Ben-Nun, and Elior Ben Moshe at the Technion. The successes in our product and process design courses are closely related to the many contributions of these graduate and postdoctoral students. Their help is very much appreciated.

Students at the Technion, Eyal Dassau, Joshua Golbert, Garry Zaiats, Daniel Schweitzer, and Eytan Filiba, and students at the University of Pennsylvania, Murtaza Ali, Scott Winters, Diane M. Miller, Michael DiTillio, Christopher S. Tanzi, Robert C. Chang, Daniel N. Goldberg, Matthew J. Fucci, Robyn B. Nathanson, Arthur Chan, Richard Baliban, Joshua Levin, and Larry Dooling, implemented the multimedia encyclopedia on the use of process simulators. Their efforts are also appreciated. In this regard, seed money for the initial development of the multimedia encyclopedia was provided by Dean Gregory Farrington, University of Pennsylvania, and is acknowledged gratefully. In addition, at the University of Pennsylvania, Matthew Gay, Evans Molel, and Brian Downey provided much assistance in preparing the materials on equipment sizing and profitability analysis; as did Professor Russell Dunn at Vanderbilt University. Their contributions are very much appreciated. Ideas contributed to chapters on product design and help with examples, exercises, and figures came from colleagues at the Hong Kong University of Science and Technology, Kelvin Fung, Tin Lau, Crystal Luo, Judy Zhang, and Carrie Lam; graduate students, Miki Ge, Neil Tan, Kee Tam, Faheem Mushtaq, and Lawrence Yan; former colleagues, Chris Wibowo, Tracy Liu, and Alice Cheng. Special thanks go to Tin Lau who also did the hand drawings in this book. Colleague Dr. Deenesh K Babi and Ph.D. students Mr. Anjan K Tula and Miss Sawitree Kalakul at the SPEED research group, Department of Chemical & Biochemical Engineering, Technical University of Denmark helped with the figures, the tables and to check simulation results.

Several colleagues at the University of Pennsylvania and industrial consultants from local industry in the Philadelphia area were very helpful as these materials evolved, especially Arnold Kivnick, Leonard A. Fabiano, Scott L. Diamond, John C. Crocker, Talid Sinno, Adam Brostow (Air Products and Chemicals), Robert M. Busche (Bio-en-gene-er Associates), F. Miles Julian, Robert F. Hoffman, Robert Nedwick (Penn State University, formerly ARCO Chemical Company), Robert A Knudsen (Lyondell), David Kolesar (Dow), Bruce M. Vrana (DuPont), and John A. Wismer (Arkema).

Four faculty, Michael E. Hanyak, Jr. (Bucknell University), Daniel W. Tedder (Georgia Institute of Technology), Dale E. Briggs (University of Michigan), and Colin S. Howat (Kansas University), reviewed a preliminary version of the first edition. Three additional faculty, John T. Baldwin (Texas A&M University), William L. Luyben (Lehigh University), and Daniel A. Crowl (Michigan Technology Institute), reviewed a preliminary version of the second edition. In addition, Professor Ka Ng (Hong Kong University of Science and Technology), Dr. Soemantri Widgado (3M Co.), Professor Costas Maranas (Penn State), and Professor Luke Achenie (Virginia Tech, formerly Connecticut) reviewed selected chapters for the second edition. Three additional faculty, Barry Barkel (Michigan), Miguel Bagajewicz (Oklahoma), and Dimitrios V. Papavassiliou (Oklahoma), reviewed a preliminary version of the third edition. Their suggestions and critiques were particularly helpful.

It is of special note that, during the preparation of the first edition, Professors Christodoulos A. Floudas (Texas A&M, formerly Princeton) and William L. Luyben

(Lehigh University) provided W.D. Seider an opportunity to lecture in their classes and use some of these materials as they were being developed. Their interactions and insights have been very helpful.

Throughout the development of the first and second editions and their accompanying materials, A. Wayne Anderson, the Editor for College Publishing at John Wiley, was extremely helpful. His excellent advice and guidance are very much appreciated. After our second edition appeared, Jennifer Welter, then Editor for College Publishing, provided much assistance in formulating our plans for the third edition. When preparing this fourth edition, we received much assistance from those taking her position, Dan Sayre and Vanya Gupta.

It is important to acknowledge the secretarial support provided in the most efficient and effective manner by John Linscheid, who made it possible to prepare the first edition. Also, the assistance of Meghan Godfrey and Denice Gorte in obtaining permissions to publish third-party sources was very helpful and appreciated.

Finally, W.D. Seider received two Lady Davis Visiting Professorships at the Technion during the spring of 1996 and 2002 and spent a sabbatical leave at 3M Co. in the spring of 2007. D.R. Lewin was a Visiting Professor at the University of Pennsylvania during the summer of 1997. Financial support in connection with these sabbatical leaves enabled them to work on the manuscript and is very much appreciated.

The support of 3M Co. during the preparation of the third edition is gratefully acknowledged. Soemantri Widagdo thanks Professor Saswinadi Sasmojo (Institute Technology Bandung, Indonesia) for providing his first experience in product design involving an electrical generator using biomass gasification.

February 2016
W. D. Seider,
D. R. Lewin,
J. D. Seader,
S. Widagdo,
R. Gani,
K. M. Ng.

Brief Contents

Contents

Part One

Introduction to Product and Process Design

Engineers apply science and mathematics to provide technological solutions to human and societal needs. The solutions are most often in the form of devices, machines, materials, processes, structures, and systems. The solutions are achieved by research, development, design, and operation. Chemical engineers are unique in their ability to solve technical problems using the principles of chemical kinetics, chemical and physical thermodynamic equilibrium, and mass transfer in addition to the principles of heat transfer and fluid mechanics also applied by other engineers. This textbook applies these principles to chemical **product design** and chemical **process design**.

Product design, introduced in Chapter 1, refers to product design and development steps for both business-to-business (B2B) products and business-to-consumer (B2C) products. Examples of B2B chemical products are (1) polyethylene terephthalate (PET) bottles, (2) nylon fiber, (3) Pyrex^{TM} boro-silicate glass, and (4) polyvinyl butyral. Examples of B2C chemical products are (1) sunscreen lotions, (2) insect repellent sprays, (3) light-emitting diode (LED) bulbs, (4) hemodialysis devices for home use, and (5) high throughput screening devices for kinase inhibitors.

Product design consists of a product formulation or construction and a prototype of the product suitable for testing and evaluation. The product construction shows the arrangement of product elements with specified dimensions and desired physical and chemical properties. Chemical engineers work closely with chemists, physicists, and/or material scientists to develop product formulations or construction and are responsible for combining the materials and processing technology to deliver desired product characteristics and performance.

Product development includes other nontechnical aspects of gathering customer needs, opportunity assessment, buy-or-make decision, product cost target and pricing, and sale and marketing strategy needed to launch a new product. Chemical engineers work closely with the business, legal, manufacturing, and supply-chain professionals to design a product that meets the desired cost target.

Process design, introduced in Chapter 2, refers to multiple-step chemical processes for converting raw materials into desired chemicals. The steps may include chemical reactors; equipment to separate chemical mixtures and phases; heat exchangers to set temperatures and phase conditions; and pumps, compressors, and turbines to set pressures. The process may operate continuously, batchwise, or semicontinuously. Examples of processes include the manufacture of (1) gasoline, diesel fuel, lubricants, fuel oils, and so on from crude oil; (2) vinyl chloride from ethylene and chlorine; (3) the potassium salt of penicillin V from phenoxyacetic acid, aqueous glucose, and cottonseed oil; and (4) ammonia from ambient air and natural gas.

A process design is presented in a process-design report that (PFD) showing the arrangement of the selected equipment with their connecting streams; the temperature, pressure, chemical composition, and total flow rate or amount of the material into and out of each piece of equipment; and the rate or amount of energy into or out of each piece of equipment. The PFD is accompanied by tables of stream component flow rates, stream properties, energy requirements, and equipment specifications including recommended materials of construction as well as a complete description of the process and a diagram showing process instrumentation and controllers.

Except perhaps for small projects, **plant design** is largely the province of civil, electrical, and mechanical engineers who take the information in the process-design report and do all other engineering design necessary to construct the plant, including the determination of plant location; design of the plant layout; selection and design of storage vessels for raw materials and products; detailed design of processing equipment; design of supporting structures and foundations for the equipment, design of piping and ducting

systems; selection of utilities (cooling water, compressed air, electricity, fuel oil, steam, etc.), and other service facilities. During plant design, chemical engineers may be involved in the detailed design of equipment involving chemical considerations, preparation of a piping and instrumentation diagram (P&ID), and plant layout decisions (at least where safety is a concern). Except for the most common types of processing equipment (heat exchangers, separation columns, pumps, compressors, expanders, and reactors), engineering design aspects of plant design are not treated in this textbook.

Chapter 3 of Part I discusses some supporting aspects of product and process design, including use of the design literature, stimulation of innovation, energy sources, environmental and safety considerations, sustainability with nature, and engineering ethics. The details of product and process design are presented in subsequent parts of this textbook.

Chapter 1

Introduction to Chemical Product Design

1.0 OBJECTIVES

This chapter introduces an overview of the myriad chemical products a chemical engineer designs and develops. Launching a chemical product into the market is a complex process. The tasks that need to be executed in a typical product-development project, partly in collaboration with professionals in other disciplines, are identified. The methodologies and tools for performing such tasks are discussed and illustrated with several examples.

After studying this chapter, the reader should:

1. Be cognizant of the diversity of chemical products.
2. Know the different classes of chemical products and be familiar with some representative products and their characteristics.
3. Appreciate the overall approach to product design from conceptualization to product launch.
4. Be aware of the contributions a chemical engineer can make in product design and development.
5. Be familiar with some of the tools and methodologies used in product design and development.

1.1 INTRODUCTION

The chemical industry is a vast industry with a wide variety of more than 70,000 products, including agrichemicals, ceramics, elastomers, electronic materials, explosives, foods, flavors and fragrances, fuels, industrial gases, inorganic chemicals, metals, oleochemicals, petrochemicals, pharmaceuticals, plastics, and textiles. The industry powers economic growth and raises the standard of living of modern society (Arora et al., 1998). A typical chemical engineering undergraduate curriculum initially focuses on the basics of "how to make" and primarily on organic chemicals. Thus, chemical reactors and unit operations such as distillation, crystallization, absorption, and extraction are covered in detail. Chemical kinetics, transport phenomena—heat, mass, and momentum transfer, and thermodynamics—provide the fundamental understanding of the way in which these operations function.

We consider in Chapter 1 "what to make," which is perhaps the most important decision for the management of a firm. To make a profit, all firms, public or private, large or small, have to produce products that the customer is willing to buy. With the rapid changes in technology, societal needs, consumer expectations, and competitive forces, new products have to be invented and existing products have to be improved or reduced in cost for a firm to prosper or merely to stay in business.

1.2 THE DIVERSITY OF CHEMICAL PRODUCTS

Chemical products are ubiquitous in our daily lives. We may begin the day using a soap bar and shampoo to wash up, brushing our teeth with a toothbrush and tooth paste, and moisturizing our face and hands with a lotion. The clothes we put on may be made of synthetic fibers. In our home, we may find processed foods such as ice cream and butter in the refrigerator, shortening and cooking oil in kitchen cabinets, pharmaceuticals in the medicine cabinet, nylon or polyester carpet on the floor, paint on the walls, a polymer composite countertop, and lawn fertilizer in the storage shed. In some households, there may be an air purifier with titanium dioxide, which is capable of catalytically decomposing the volatile organic compounds in the air and an air conditioner with an environmental friendly refrigerant. Going to work by automobile, we find gasoline in the gas tank, tires made of styrene-butadiene rubber, and a shatterproof glass windshield with an interlayer of transparent polyvinyl butyral.

The Chain of Chemical Products

All the products mentioned above are derived from nature—air, natural gas, petroleum (also known as crude oil), minerals, plants, and animals. Figure 1.1 is a highly simplified chemical product chain showing how the chemical products are produced successively from natural resources. For example, nitrogen can be obtained by cryogenic distillation of air whereas hydrogen is obtained from natural gas. Reaction between nitrogen and hydrogen by the Haber-Bosch process produces ammonia (see Chapter 27). Ammonia in turn reacts with carbon dioxide, also obtained from natural gas, to form urea, which is a key component in fertilizer.

A wide range of hydrocarbons such as ethylene, butadiene, benzene, toluene, xylene, and alkenes are obtained from petroleum in a refinery. In the petrochemical industry, these hydrocarbons can be used to produce a myriad of other useful chemicals. For example, ethylene, the largest chemical product

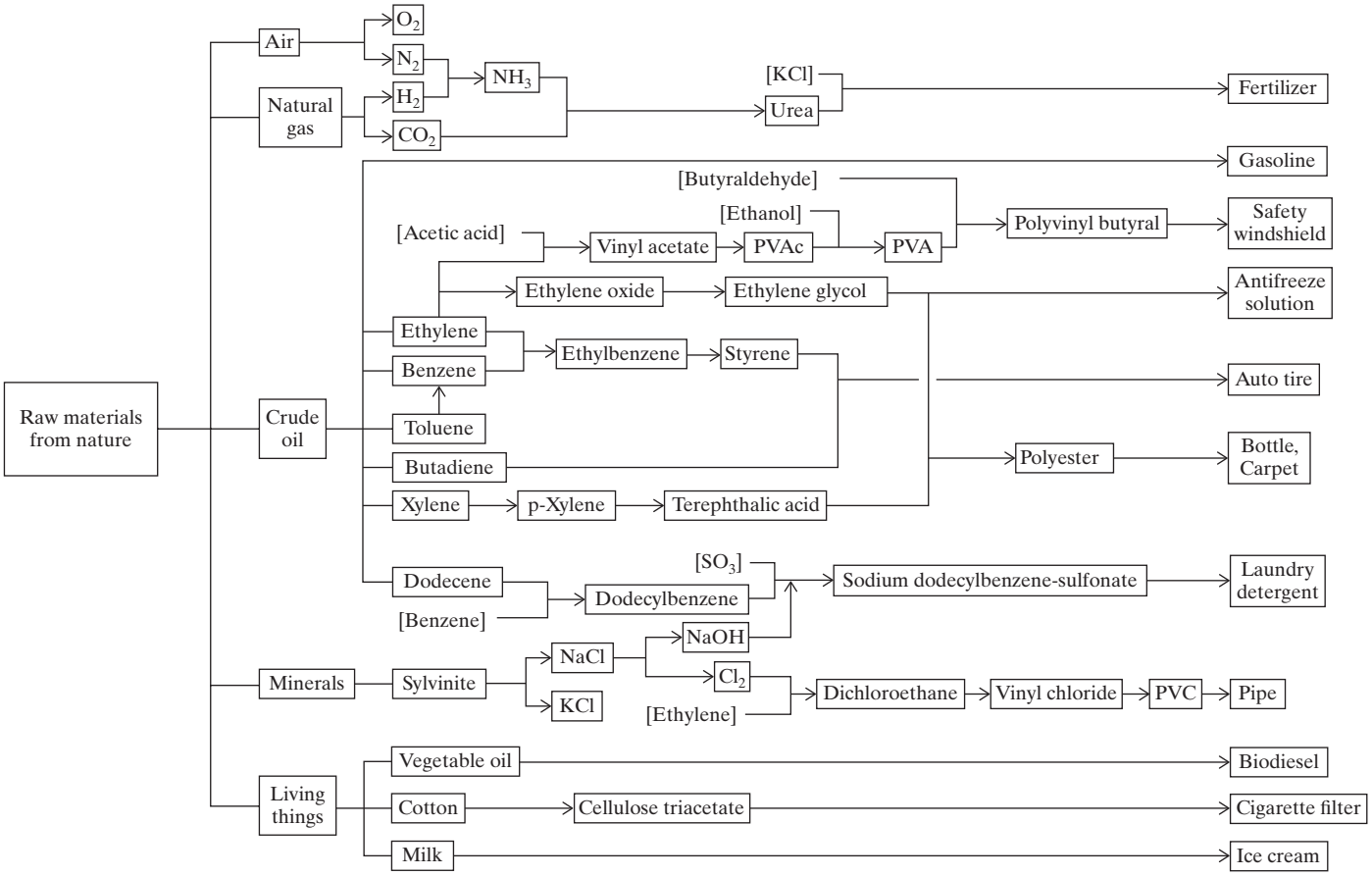

Figure 1.1 A small subset of the chain of chemical products. (The chemicals in the brackets are those not included or out of order in the product chain.)

by volume, is used in the production of rubber, plastics, solvents, and so on. It reacts with acetic acid to form vinyl acetate. Polyvinyl acetate (PVAc) reacts with ethanol to form polyvinyl alcohol (PVA). Polyvinyl butyral, the interlayer of shatterproof glass windshields, is made by reacting PVA with butyraldehyde. Ethylene can also be oxidized to ethylene oxide, which is hydrolyzed to ethylene glycol. Ethylene glycol is used in an antifreeze solution. Ethylene can also react with benzene to form ethylbenzene. Dehydrogenation of ethylbenzene forms styrene. Many automobile tires are made from various types of styrene-butadiene rubber. Sometimes, the inherent amount of benzene in the crude oil is insufficient to meet what is required in the downstream products whereas toluene is in excess. In this case, the excess toluene is converted to benzene using a process called hydrodealkylation, which is discussed in Chapter 6. Xylene contains three isomers: para-, ortho-, and meta-xylenes. Because only para-xylene is oxidized to terephthalic acid, para-xylene has to be separated from the mixture of isomers. After first removing ortho-xylene by distillation, para-xylene can be purified from para- and meta-xylene by crystallization or adsorption. A condensation reaction between terephthalic acid and ethylene glycol forms polyethylene terephthalate (PET), which is used in products such as floor carpet. PET is also used to make transparent bottles by injection molding. Dodecene, one of the alkenes in crude oil, can be converted to sodium dodecylbenzenesulfonate by reacting with benzene, sulfur trioxide, and sodium hydroxide, successively. Sodium dodecylbenzenesulfonate is a member of the linear alkylbenzenesulfonates, a major component of laundry detergent.

EXAMPLE 1.1 ***Show the main chemical reactions for producing polyester starting with ethylene and para-xylene***

SOLUTION

$2(CH_2CH_2) + O_2 \rightarrow 2(CH_2CH_2)O$	Ethylene oxide
$(CH_2CH_2)O + H_2O \rightarrow HO(CH_2)_2OH$	Ethylene glycol
$CH_3C_6H_4CH_3 + 3O_2 \rightarrow HOOCC_6H_4COOH + 2H_2O$	Terephthalic acid
$nHO(CH_2)_2OH + nHOOCC_6H_4COOH \rightarrow [(CH_2)_2OOCC_6H_4COO]_n + 2nH_2O$	Polyester

As another example, a mineral such as Sylvinite, a mixture of sodium chloride and potassium chloride, can be separated into its constituent components. Sodium chloride undergoes the chlor-alkali process to produce sodium hydroxide and chlorine. Ethylene reacts with chlorine to form dichloroethane, which is pyrolyzed to vinyl chloride, as discussed in Chapter 2. Polymerization of vinyl chloride forms polyvinylchloride (PVC), which is widely used for making pipes. Potassium chloride is used as a fertilizer.

Surfactants for soaps and detergents can also be obtained from plant oils and animal fats, which are esters of glycerol and fatty acids. Biodiesel, consisting of long-chain alkyl esters, can also be produced from plant oils. Cotton fibers are often blended with polyester fibers in a fabric for clothing. The blended fabric offers the natural feel of cotton while adding the strength and durability of polyester. Cellulose triacetate from cotton linters is used as a semipermeable membrane for water purification. A wide variety of dairy products such as cheese, ice cream, and yogurt are produced from animal milk.

Many excellent books have been written on industrial chemicals similar to those described here; see, for example, Faith et al. (1975), Austin (1984), and Chenier (2002). Books are also available on those chemical products at the end of the product chain that are used by the consumers (Cussler and Moggridge, 2011; Bröckel et al., 2007, 2013; Ng et al., 2007; Wesselingh et al., 2007).

Companies Engaging in Production of Chemical Products

The chain, or more appropriately, the network in Figure 1.1 captures only a very tiny segment of an exceedingly complex network made up of tens of thousands of products. Typically, a company focuses on a certain segment of this product chain. The separation and use of gases is dealt with by *gas companies* such as Linde, Air Products, Praxair, and Air Liquide. Petroleum exploration and refining the recovered oil into different chemicals are handled by the so-called *oil companies* such as Saudi Aramco, Exxon-Mobil, British Petroleum, and Petro China. BASF, Sinopec, Dow, SABIC, DuPont, and Mitsubishi are referred to as *chemical companies*; they convert raw materials and chemicals from oil companies into more complex compounds. Drug discovery is so challenging that it is often handled by highly specialized *pharmaceutical companies* such as Pfizer and Merck. Mineral processing tends to be handled by focused companies as well. For example, Potash Corp is the world's largest producer of potassium chloride (also known as potash). Products such as soaps, detergents, and lotions as well as some processed foods are manufactured by *consumer goods companies* such as Procter & Gamble and Unilever. In general, the companies upstream of the chemical product chain are relatively large to take advantage of economies of scale. The companies closer to actual consumers are smaller because these downstream companies have to react swiftly to meet market demands. Indeed, many small to medium-size companies produce a broad array of products such as humidity sensors, medical diagnostic kits, and fabric softeners, among others.

B2B and B2C Chemical Products

The products in the chain of chemical products can be broadly classified into two classes: *business-to-business* (*B2B*) and *business-to-consumer* (*B2C*). The former involves a transaction between two businesses, and the latter involves a sale to the consumer. Most of the oil companies' products are B2B products. For example, chemicals such as para-xylene and butadiene are supplied to the chemical companies as raw materials. These chemical products are often referred to as *commodity chemicals* because the chemical company buys such chemicals from any supplier at the lowest price possible provided that these products meet the company's raw-material specifications. Often, the primary concern for commodity chemicals is purity. The empty PET bottle that the polymer processing company sells to the bottling company is an *industrial product*; it is still a B2B chemical product but is no longer a chemical. When a consumer purchases a bottle of distilled water, the quality of terephthalic acid, a compound in the product chain leading to the PET bottle, is not the consumer's concern. However, the oxidation of para-xylene to terephthalic acid, if not done properly, produces a colored compound, 4-carboxybenzaldehyde, which makes the PET bottle yellowish. Thus, although commodity chemicals might seem remote from the consumer, their product specifications are indirectly influenced by the consumer, who is the ultimate user of the chain of products. The term *basic chemicals* is used synonymously as commodity chemicals because they are the building blocks of more complex molecules. Many novel molecules with special characteristics are derived from the basic chemicals and are produced in relatively small quantity. They belong to the class of *specialty chemicals*, which are sold based on what they can do and often offer a relatively higher profit.

The consumer has a more direct say on the specifications of B2C products, or alternatively, *consumer products*, such as shampoo, lotions, processed foods (butter, cheese, yogurt, potato chips), halogen light bulbs, masking tapes, face masks, and air purifiers. Some of the specifications are quantitative. For example, the air purifier has to be able to reduce the concentrations of certain impurities in the air of a closed room of a certain size to below specified values within a given period of time. Often, the specifications are qualitative in nature. The product has to offer consumer delight—feelings of the consumers when their expectations are fully satisfied. For example, a lotion has to feel smooth and smell good, a wine has to possess a desired bouquet, and a detergent has to impart a soft feel to the fabric. The product specifications for consumer products are often referred to as *product attributes* to reflect some of the qualitative desires. Example 1.2 shows the typical product attributes for creams and pastes (Wibowo and Ng, 2001). In addition, the product has to be safe and environmentally friendly. These seemingly obvious prerequisites can become controversial. For example, there has been a heated debate on the safety and disposal of PVC. There is no absolute safety, and it is difficult to get all parties to agree on how safe is sufficiently safe.

EXAMPLE 1.2 ***Typical product attributes for creams and pastes***

Creams and pastes such as moisturizing cream and sunscreen lotion are common consumer products. Provide a list of their typical product attributes.

SOLUTION

There are four typical product attributes:

Functional

Protects parts of the body

Cleans parts of the body

Provides a protective or decorative coating

Causes adhesion to body surface

Delivers an active ingredient to the target area

Rheological

Can be poured easily

Spreads easily when rubbed on skin

Does not flow readily under gravity but is easy to stir

Should give a uniform coating when applied to surface

Should not flow by itself but can be squeezed out of the container

Physical

Must be stable for a period of time

Melts at a certain temperature

Must release an ingredient at a controlled rate

Sensorial

Feels smooth

Does not feel oily

Appears transparent, opaque, or pearlescent

Does not cause irritation

Table 1.1 compares different aspects of B2B and B2C chemical products. B2B chemical products change hands in business-to-business transactions. Thus, an oil company sells para-xylene to a chemical company to make PET. The chemical company in turn sells the PET to a polymer processing company to make PET bottles. Most of these B2B products are in relatively pure form because they are the feedstocks for more complex molecules. An obvious exception is gasoline, which is a mixture of hydrocarbons that is sold directly to the consumer at gas stations. In contrast, most B2C chemical products such as detergent and lotion are mixtures that use chemicals from chemical companies such as surfactants and fragrances as ingredients. Some of these mixtures are randomly mixed, but some possess a specified structure. For example, CdS/ZnS quantum dots have a spherical core of CdS encapsulated by a ZnS shell. B2B product design is primarily a molecular design with considerable input from chemists whereas B2C product design often involves multicomponent systems with or without a structure. The technology involved in B2B products tends to be primarily chemistry and chemical engineering in nature. In a typical herbicide development team of 10 or so researchers, there are often nine chemists responsible for organic synthesis and only one chemical engineer in charge of product and process design. B2C products such as air purifiers or health drinks are likely to involve a more diverse team of technical personnel, including electrical and mechanical engineers and food scientists. Furthermore, for most new products, companies' marketing, financial, and legal teams are often involved to ensure that the relevant issues are properly managed.

In general, the B2B product lifetime is much longer than the B2C product lifetime. This is because the specifications for B2B products tend to be well established and remain unchanged over a long period of time whereas the B2C product attributes evolve rapidly along with the changes in consumer preferences. Figure 1.2 contrasts the product life cycle of a typical B2B product with that of a typical B2C product. It shows that the revenue of a B2B product declines because other competitors enter

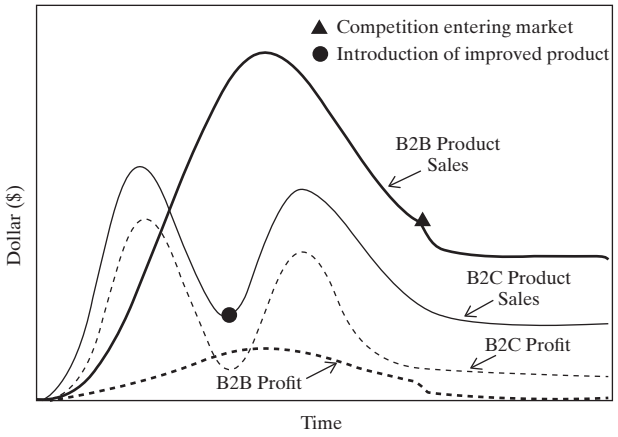

Figure 1.2 Typical life cycles of business-to-business and business-to-consumer chemical products.

Table 1.1 Comparison of Business-to-Business and Business-to-Consumer Chemical Products

	B2B Products	B2C Products
Customers	Allied chemical industries	Consumers
Nature of products	Simple or complex molecules	Devices (equipment), functional products, and formulated products
Product design	Molecular design	Selection of ingredients, product structure, and product attributes
Product life cycle	Decades	Month/year
Team	Primarily chemists and chemical engineers	A multidisciplinary team of marketing personnel, financial specialists, lawyers, electronic engineers, mechanical engineers, chemists, and chemical engineers
Financial goal	Cost reduction	New sources of revenue
Unit operations	Traditional: distillation, crystallization, extraction, absorption, adsorption, etc.	Unconventional: granulation, milling, nanomization, etching, lamination, physical vapor deposition, inkjet printing, screen printing, laser scribing, etc.
Knowledge/know-how	Well structured	Fragmented so far
Technical focus	Engineering optimization	Improved performance followed by reduced cost

the market. The B2C product lifetime is much shorter. The profit relative to sales tends to be much higher than that of the B2B products. In addition, as shown by the two peaks, this B2C product gets a second wind by introducing an improved version.

Because of the long lifetime of commodity chemicals, the research and development (R&D) for B2B products focuses on lowering the production cost of these products whereas the R&D for B2C products emphasizes the conceptualization of new and improved products to generate fresh revenue streams. Most of the manufacturing processes for B2B products are traditional processes. Reaction engineering and unit operations for the manufacturing processes of commodity chemicals including distillation, crystallization, extraction, absorption, adsorption, filtration, membrane separation, and others are well covered in a typical chemical engineering curriculum. The knowledge of commodity chemicals is well structured. The thermodynamic properties of most commodity chemicals are available in the thermodynamic database of commercial simulators. Techniques for predicting the properties of new B2B chemicals are available. If a consumer product is a mixture without a structure such as a liquid fabric softener, processing can be simply mixing operations. For consumer products with a structure, such as solar cells and lithium ion batteries, unconventional processing techniques such as granulation, sputtering, inkjet printing, screen printing, etching, calendering, and so on can be involved. The technical focus of B2B products, except for new molecules, tends to be process optimization; the technical focus of B2C products tends to be the use of advanced materials or technologies to make products with new or improved attributes for the consumer.

Market Sectors and Classes of Chemical Products

Chemical products can be classified by market sector in which a number of firms sell similar goods and services, and by three product classes which include (1) simple or complex molecules, (2) devices (or equipment) and functional products that perform a desired purpose or function, and (3) formulated products that are obtained by mixing selected ingredients that as a whole offer the desired product attributes. Table 1.2 shows examples of chemical products in each of the three product classes in nine market sectors. Remarks are made (in parentheses) to products that might be unfamiliar to the reader. The examples for devices (equipment) are italicized to distinguish them from those for functional products. Consider agricultural products. They can be new molecules that function as herbicides or pesticides. Microencapsulation of herbicide with ethylcellulose produces a controlled-release granule, a functional product, that provides prolonged action in the field. A mosquito mat is a small cardboard mat impregnated with an insecticide solution. It releases an insecticide on heating. It also contains a dye that gradually changes color during use to indicate the amount of insecticide that remains in the mat. The company also sells an accessory device, a heater that fits the mat with the rate of heating set in such a way that the evaporation of the mosquito repellent continues over the desired use period. An herbicide mixture should be properly formulated to manage the vegetation in a given locality. Obviously, chemical products represent only a small fraction of the total agricultural industry, which also includes the sale of wheat, corn, and so on. The rest of Table 1.2 covering other market sectors is left to the reader to explore. It should be emphasized that much thought goes into consumer products. The disposable baby or adult diaper has multiple layers of materials to move the urine away from the skin, yet it is made sufficiently inexpensive to be disposable.

1.3 PRODUCT DESIGN AND DEVELOPMENT

Design is a synthesis activity, meaning that different parts are combined to create a coherent whole that offers functions and characteristics that cannot be found in the individual parts. Because many B2B products are primarily molecules, *product design* is equivalent to the synthesis of new molecules. In the past, a chemist often synthesized molecules with the desired characteristics experimentally by trial and error based on intuition and experience. Nylon, discovered in 1934 by Wallace Carothers at DuPont, is a classic example (Hounshell and Smith, 1988). With recent advances in molecular design (Wei, 2007), computer tools are now available to facilitate the design of molecules as discussed in Chapter 4. Because B2C products are primarily mixtures and devices, *product design* is the activity that aggregates the constituent parts that already exist to generate the final product. Similar to the molecular design tools, computer tools have been developed to predict the properties of mixtures. Computer tools are also available to facilitate the design of the three-dimensional product structures of devices and equipment items such as heat exchangers and distillation columns.

After product design, many activities such as product prototyping and product testing are needed. These activities are referred to as *product development*. Product design and development is inseparable from process design and development to manufacture a product successfully. In addition, marketing, business, and financial specialists as well as engineers from different disciplines are needed to address all relevant aspects. An overview of the activities in a typical product design and development project is presented next.

Tasks and Phases in Product Design and Development

These activities span three phases in time—*product conceptualization* (*Phase I*)*, detail design and prototyping* (*Phase II*), and *product manufacturing and launch* (*Phase III*)—and can be classified by *job function* in terms of *management, business and marketing, research and design, manufacturing*, and *finance and economics*. The activities can also be grouped into various *tasks* (such as project management, market study, product design, prototyping), which may last over more than one development phase (Cheng et al., 2009). For example, economic analysis is performed in all three phases and is part of manufacturing as well as finance and economics. Of particular interest are those activities, italicized in Figure 1.3, that require the input of a chemical engineer. The rest of the issues, which are not-italicized, such as product launch are normally handled by personnel from other disciplines and are not discussed further here.

Table 1.2 Different Classes of Chemical Products in Various Market Sectors

Market Sector	Molecules	*Devices (Equipment)*/Functional Products	Formulated Products
Agriculture	Herbicide Pesticide	*Liquid mosquito repellent dispenser* Controlled-release herbicide Mosquito repellent mat Plant seeds	Fertilizer mixture Herbicide mixture Insect repellent
Automotive	Polyvinyl butyral Butadiene-Styrene copolymer	Auto tire Safety windshield Sun control window film Diesel exhaust fluid (an aqueous urea solution used with a catalytic system in a diesel vehicle to reduce nitrogen oxides in its exhaust)	Antifreeze Motor oil
Building & Construction	Refrigerant Binder Sealant	*Indoor catalytic air cleaner* *Humidity sensor* Smart window (applying voltage to change its light transmission properties) Weather barrier film Acrylic composite countertop Foamed concrete	Paint Adhesives for paneling Stucco
Electronics	Organic light-emitting diode materials Phosphor Fullerenes (as electron acceptor) Graphene	*Optical bonding equipment* LED light *Touch panel* Silver nanowire Quantum dot	Optically clear adhesive Die attach adhesive Encapsulant Copper nanoparticle paste
Energy	Lithium iron phosphate, nickel cobalt manganese (battery cathode materials) Biodiesel Bioethanol	*Solar panel* *Fuel cell* *Battery* Battery electrolyte	Heat transfer fluid Drilling mud
Environmental	Coagulant Antiscalant	Ion exchange resin *Reverse osmosis membrane* *Dehumidifier*	Air freshener Adsorbents for water filter
Food & Beverage	D-Xylose (commonly called wood sugar. It is a natural 5-carbon sugar obtained from plants. It adds flavors to prepared foods and can be used as animal feed.) Sugar ester (a food grade surfactant with sucrose as hydrophilic group and fatty acid as lipophilic group)	*Espresso coffee machine* *Ice cream machine* *Wine aerator* Textured vegetable protein (meat substitute)	Ice cream Health drinks
Personal Care, Health Care & Medical	Tetrafluorethane (a propellant for inhalant drug) Active pharmaceutical ingredient	*Medical diagnostic kit* Nylon toothbrush filaments Herbal extract Transdermal patch Tooth brush Disposable diaper Hand warmer *Hemodialysis device*	Tooth paste Sunscreen lotion Bar soap Hair spray Fabric softener Laundry detergent powder Pharmaceutical tablet
Packaging & Printing	Ethylene vinyl acetate copolymer (used as a peelable sealing layer)	*Flexo platemaking equipment* Food packaging film	Ink for digital textile printing Toner for photocopying Screen print paste

Project Management

The starting point of a product-development project is to formulate an *Objective-Time Chart* (Figure 1.4). This is part of the project management task in Phase I. It shows the objectives and subobjectives that have to be met within a given time horizon. Here, objectives A–E are the high-level objectives. For example, these might include the high-level tasks such as market study, product design, and feasibility study shown in Figure 1.3. In Figure 1.4, objective D is decomposed into objectives D1–D6. For example, if objective D is product design, D1 might be

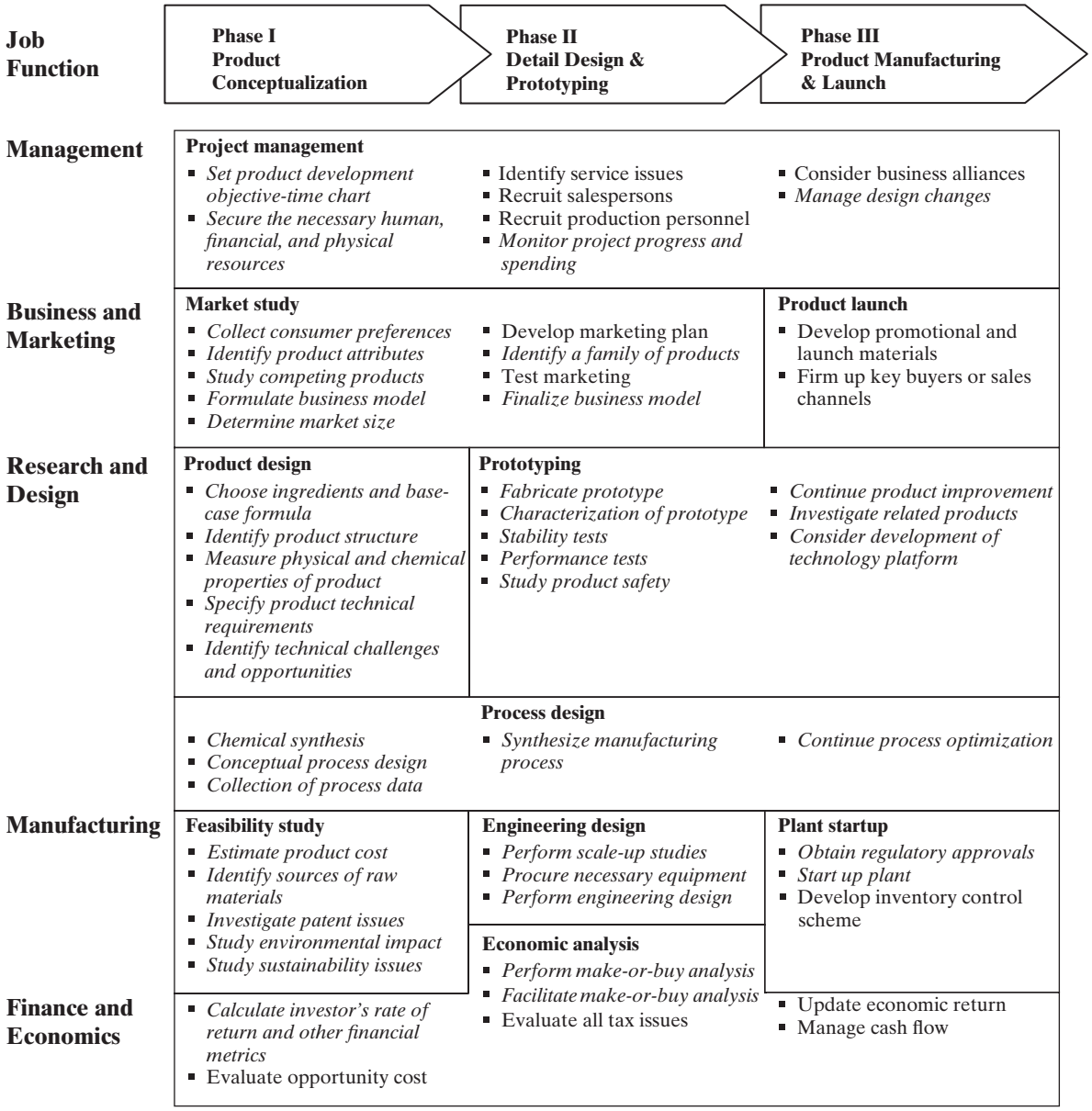

Figure 1.3 The phases and job functions in a multidisciplinary, hierarchical framework for product design and development.

selection of ingredients and D6 measurement of product's physical and chemical properties. Objective D6 is further decomposed into D61–D65. D61 could be measurement of viscosity, D62 measurement of pH, and so on. This methodology is often used by a product/process development team to show all team members the tasks that need to be performed and the time by which they should be completed. By offering a hierarchical view of the development project in its totality, that is, by viewing the whole project with successive layers of increasing details, every member knows what other members are doing to achieve the overall goal. Also, the objective-time chart highlights the tasks that can be carried out concurrently, thereby reducing the overall development time. For example, objectives D2 and D4 take place more or less concurrently and so do D3 and D5.

Different resources are needed to achieve an objective or subobjective. Figure 1.5 depicts *RAT*^{2}*IO*, a mnemonic acronym that stands for resources, activities, time and tools, input/output information, and objective. Thus, we identify in advance the *resources* (people and money) required to complete certain *activities* (experiments, modeling, and synthesis) within a specified period of *time* using proper *tools* (experimental setup or software) to generate the necessary *information* and to meet the given *objective*. The deceptively simple objective-time chart in Figure 1.4 is what distinguishes an expert from a novice. An effective project manager with the right experience can draw up a realistic timeline, ensure the availability of the necessary manpower and financial resources, and follow through to facilitate the flow of input/output information from objectives to objectives or to subobjectives. Thus, the manager should have a good appreciation of the RAT^{2}IO needed for the various tasks in a product-development project although no individual is expected to master all the details.

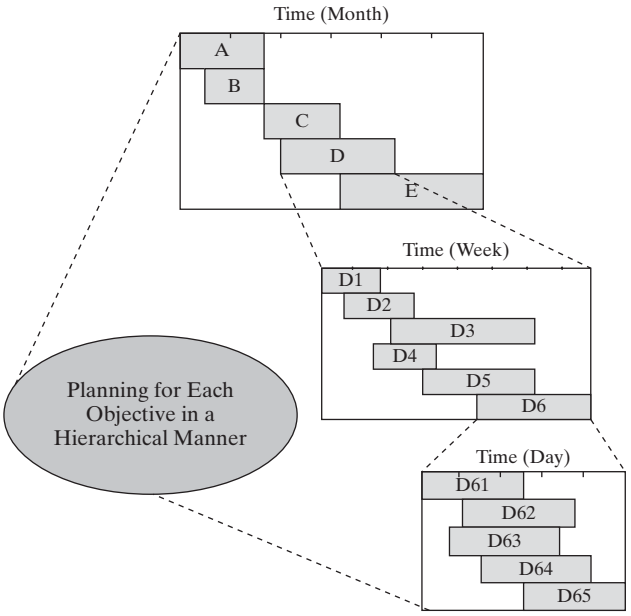

Figure 1.4 Objective-time chart details what needs to be accomplished in a hierarchical manner over the project duration.

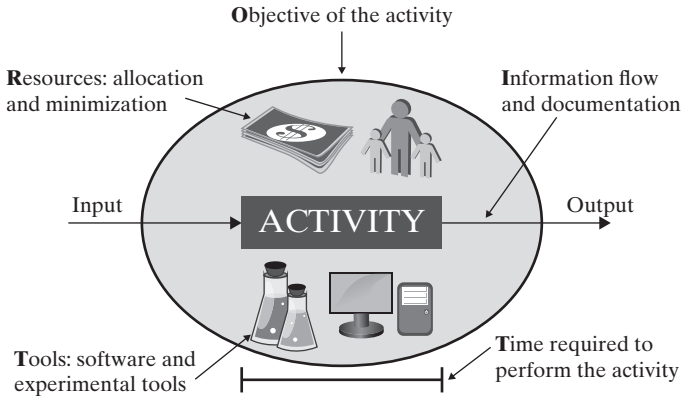

Figure 1.5 The RAT^{2}IO mnemonic acronym stands for resources, activities, time, tools, input/output information, and objective.

Complementary to the objective-time chart is the Stage-Gate™ Product-Development Process (Cooper, 2005). As shown in Figure 1.6, it consists of five stages, represented by rectangular blocks, where goals are set and five gates, represented by diamonds, and where reviews of the deliverables take place. Listed below the rectangles in the figure are the principal steps to be accomplished in each stage. Above the diamonds are brief summaries of the items to be screened or evaluated during each gate review. Each gate is intended to reduce the risk by verifying manufacturability and matching product features and performance to the consumer needs. The gate reviews are conducted by key stakeholders and decision makers from legal, business, technical, manufacturing, supply-chain, environmental, health, and safety teams. At each gate review, a decision is made to either (1) advance the design project to the next stage, (2) retain the design project at the current stage until pending critical issues are resolved, or (3) cancel the design project when a need is no longer recognized or when road blocks have been encountered that render the project infeasible.

Market Study

The decision for developing a product may be *demand-pulled* or *technology-pushed*. The former is often initiated by the business team that keeps a close watch on the market in which the company operates. An example is an antiseptic hand-cleansing gel that is now readily available after the outbreak of the SARS (severe acute respiratory syndrome) epidemic in 2003. For the latter, a product concept is stimulated by the discovery of an ingredient that gives some new or improved function or a novel processing technology that can make a new or cheaper product. The invention of nylon, as well as the subsequent marketing of nylon stockings, is a classic technology-push example. Many efforts to develop products for novel carbon materials—fullerenes, carbon nanotubes, and graphene—are currently in progress. Reactive distillation is an example of process innovation. Traditionally, chemical reactions and separations take place in their own sections of the chemical plant. For some chemical systems, reaction and separation operations can occur together in the same distillation column, thereby saving capital and operating costs.

Irrespective of the driver for product development, chemical engineers, because of their materials and processing background, are often part of the design team to form an image of the product and to define its functions to meet anticipated or existing customer needs. These needs can be collected from frontline salespersons,

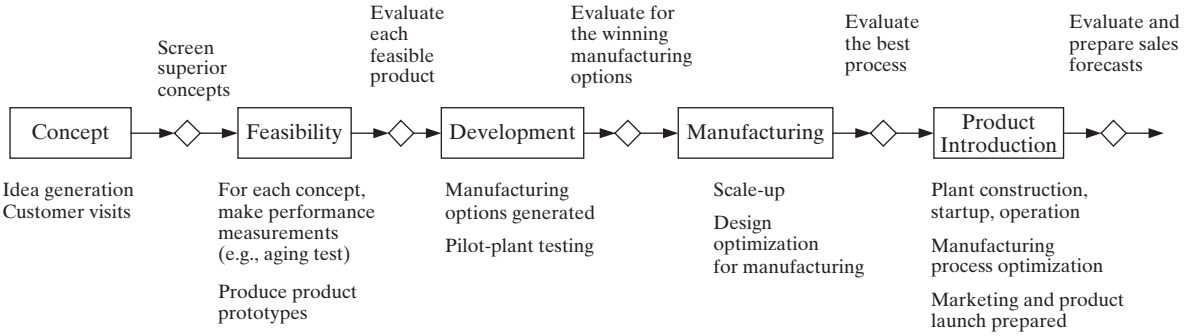

Figure 1.6 Schematic of the Stage-Gate™ Product-Development Process.

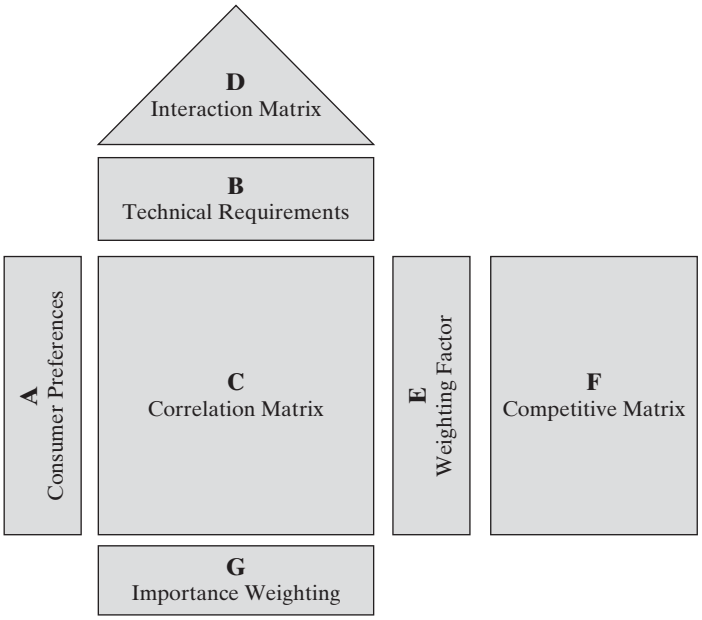

Figure 1.7 Elements of a House of Quality.

advertising agents, and potential customers. Typical considerations include:

Product Attributes

- What is the final product image?
- What are the product attributes?
- What packaging would be the most practical for the desired application?

Market Situation

- Who are the target consumers for the conceived product?
- What is the market size for the candidate product?
- Who are the competitors?
- How does the conceived product compare with the competitor's product?

Company Culture and Capability

- Does the product fit into the company's product lines?
- Can the company's technical strengths ensure product qualities?
- Are the sales channels in place to effectively market the product?

Clearly, product conceptualization requires a combination of technical know-how and marketing experience. Often, it is easy for chemical engineers to pick up marketing knowledge on the job.

A useful tool for this task is the *Quality Function Deployment (QFD)* methodology, which is particularly suitable for demand-pull products. Given a set of consumer preferences, the product-development team seeks to express them as product requirements using a more technical language involving quantitative and measurable variables. The information is captured in the *House of Quality (HOQ)*, consisting of seven blocks as shown in Figure 1.7. Block A contains the consumer preferences, and Block B contains the quantitative and measurable technical requirements that correspond to at least one of the consumer preferences. Then, the relationships between the customer and technical requirements are described by the correlation matrix in Block C where the entries represent whether a relationship exists between the given consumer preference and the technical requirement (yes or no) and, more quantitatively, the strength of this relationship (0 = none, 1 = weak, 3 = moderate, and 9 = strong). The roof of the HOQ, Block D, is the interaction matrix that shows the synergies and conflicts among the technical requirements. The synergistic requirements change in the same direction as they more or less fulfill the requirements. On the other hand, conflicting requirements change in opposite directions, signaling the need for compromises. Block E gives weighting factors for the consumer preferences, and Block F represents the capabilities of the competitors in fulfilling the consumer preferences. Block G shows the importance of each technical requirement. For each consumer preference, a score is obtained by multiplying the entry in the correlation matrix for the technical requirement under consideration with the corresponding weighting factor in Block E. Summing the scores for all the consumer preferences gives the importance weighting for the technical requirement.

EXAMPLE 1.3 ***House of quality of a hand lotion***

Figure 1.8 illustrates the creation of an HOQ for a hand lotion. There are five consumer preferences and five technical requirements. The correlation matrix pairs the consumer preferences with the technical parameters. For example, the ability of the hand lotion to protect the skin from dryness is strongly related to the emollient type and concentration. Whether the lotion spreads easily or flows under gravity depends on the viscosity of the emollient and more significantly on the thickener type and concentration. The smoothness of the hand lotion depends on the homogenizer operating conditions with a score of 9. It is also a function of the material properties of its constituents with a score of 3, 3, and 1 assigned to the parameters related to emollient, surfactant, and thickener, respectively. To render the lotion not oily, an oil-in-water emulsion is needed as stressed by a score of 9. The feel can also be affected by the emollient because it is normally oily and in relatively high concentration. At the top of the house, the interaction matrix shows the synergistic technical parameters. A blank entry indicates there is no known significant relationship between the variables. The only (–) sign indicates that when the concentration of emollient increases, the emulsion is less likely to be an oil-in-water emulsion. Thus, it signals the need for a compromise between the amount of emollient, which helps protect the skin, and the desire of having a non-oily feel.

Not all five consumer preferences are of equal importance. The column next to the correlation matrix shows that protection of the skin from dryness is the most important preference with a weighting factor of 3. An evaluation of the competitors' ability to meet the consumer preferences is given in the last block. Except for skin protection, the company's product beats the competition on all counts. The bottom row, importance weighting, shows that emollient type and concentration is the most important technical parameter to satisfy the consumer preferences.

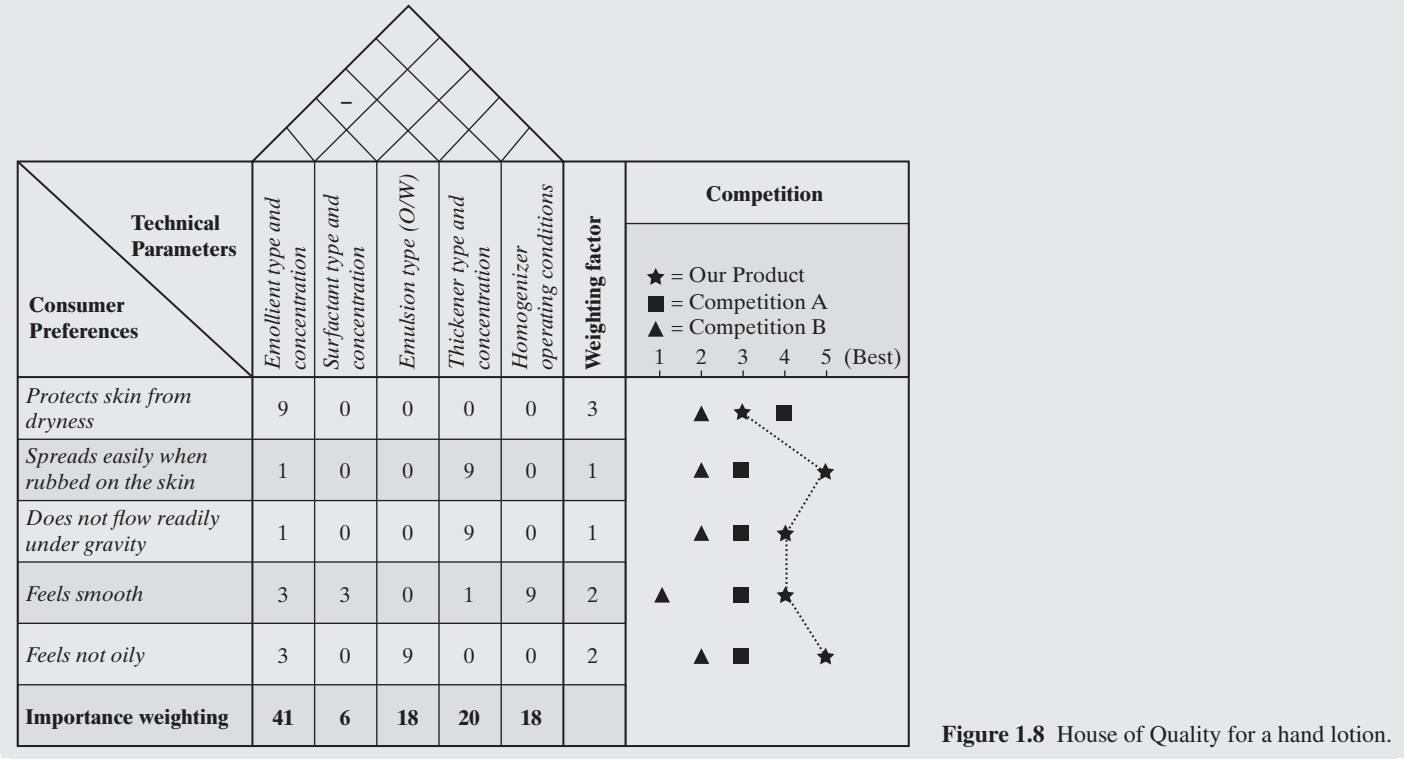

Figure 1.8 House of Quality for a hand lotion.

Products are created to meet a perceived need in the marketplace. The identification of such a product and the customers with the perceived need is an iterative process. Obviously, the greater the need is, the higher are the potential revenue and profit. However, product development is a tortuous journey replete with potholes, hurdles, and crossroads. The success stories of products, such as nylon stockings, Post-it® Notes and iPhones™ do not happen easily. A new product project more often fails than succeeds even for seasoned innovators, entrepreneurs, and investors.

To improve the odds, many approaches and methods have been proposed (Wheelwright and Clark, 1992; Blank and Dorf, 2012; Ulrich and Eppinger, 2012). The Business Model Canvas (Osterwalder and Pigneur, 2010) is one of those methods that help focus the product designer's efforts (Figure 1.9). It consists of nine building blocks arranged in a manner according to tradition:

- *Value Proposition* describes what the product offers to meet the wants and needs of a group or groups of customers.
- *Customer Segments* identify who these groups of customers are.
- *Channels* are the means by which the customers are reached and offered the product.
- *Customer Relationships* are the ways in which the product is promoted to the customers.
- *Revenue* is the income generated from the customer segments.
- *Key Resources* are the wherewithal needed to implement the business model.
- *Key Activities* are the activities undertaken to execute the business model.
- *Key Partners* are the people who play a significant role to help realize the business model, such as raw materials and manufacturing equipment suppliers.
- *Cost Structure* details the most significant costs to operate the business model.

A preliminary business model should be formulated as soon as product conceptualization begins. The answers to the questions on the canvas are expected to become more accurate and refined as information is accumulated over time. The business model is normally finalized before tackling detail design and prototyping, that is, in the early stage of Phase II of the multidisciplinary, hierarchical product-development framework (Figure 1.3).

Whereas many of the tasks in the business model are handled by the business team, chemical engineers with the relevant engineering fundamentals are indispensable in determining the value proposition, the key resources, the key activities, the key partners, and the product cost structure. It is important that the engineering team appreciates the roles of the business team and vice versa. For example, raw materials and processing costs are normally determined by the engineering team whereas the advertising and selling costs are managed by the marketing team. A collective decision by the entire project team on how much to fund these costs is essential. Only through a multidisciplinary collaborative effort can a new product be launched expeditiously and successfully.

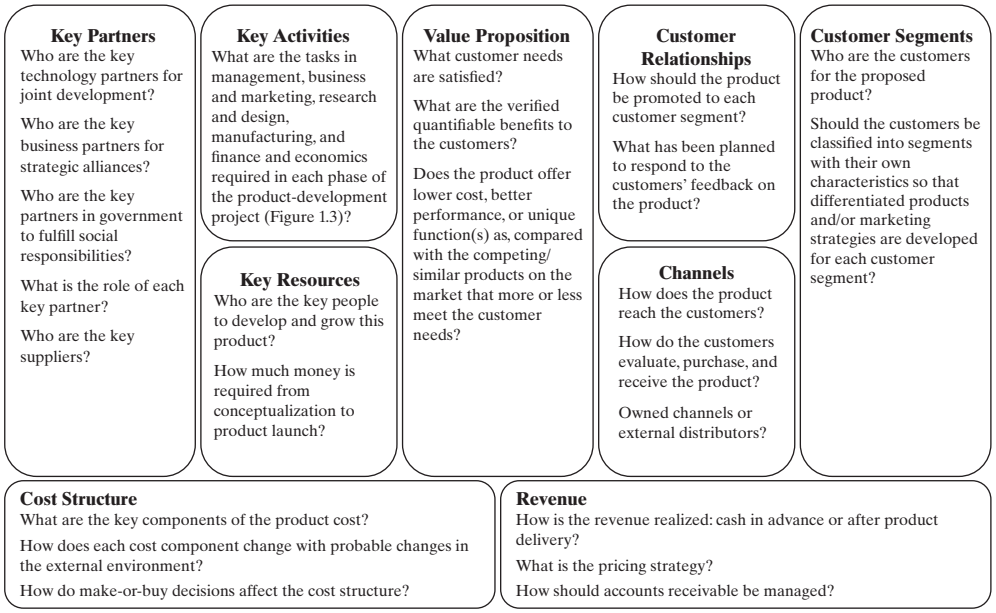

Figure 1.9 The Business Model Canvas focuses the product-development team's efforts on the essential tasks for developing a successful product.

Product Design

The objective of the research and design tasks is to translate the desirable product attributes identified by the marketing team into quantifiable *product technical specifications*, which include the type of active and supporting ingredients in the product as well as the structure of the product itself. For a multicomponent product, a base-case product recipe or formula would be developed at this time. The potential technical challenges and opportunities in making the product are identified; this information should be provided to the marketing team because product conceptualization often involves a compromise between desirability and feasibility in terms of available raw materials, manufacturing technology, and affordability.

For technology-push products driven by the discovery of a new functional ingredient, the active ingredient is already fixed. The focus is on specifying the appropriate supporting ingredients such that the product possesses additional product attributes desired by potential consumers. It is advantageous to choose supporting ingredients that are used in similar existing products. This may imply that the supply of these ingredients is not in doubt. Also, some supporting ingredients such as those for personal care products may have to be approved by the regulatory authorities.

For demand-pull products, the R&D activities begin with finding the suitable active ingredient(s). The relevant chemistry knowledge provides a good starting point to identify potential candidates. The candidates are then screened experimentally to identify a handful of lead compounds to be further investigated to verify their capability and to come up with the best choice. High throughput screening techniques, which are capable of quickly testing a large number of samples for a particular response, are valuable tools to expedite such a search.

As an alternative to the experiment-based trial and error approach, model-based search techniques such as computer-aided molecular design and computer-aided blend design can be used. Starting from the specifications for the desired product, molecular structures or mixtures that satisfy the target product attributes can be found with the help of these tools. In reality, most chemical product design problems are solved using a combination of experiments and model-based techniques. The computer tools help identify a small number of compound structures that possess the desirable properties, thereby greatly reducing the number of trial and error experiments. The experiments provide validated data, which can be used to refine the models in use.

For technology-push products, it is helpful to create an *innovation map,* which connects the new materials or processing technologies to market needs (Widagdo, 2006). It has four basic layers:

- New materials and/or processing technologies: This is the foundation layer.
- Technical-value proposition: The technical advantages/differentiations are assessed.
- Products: The potential products are identified.
- Customer-value proposition: The product advantages/differentiations, expressed from the customer point of view, are identified.

The innovation map captured in Figure 1.10 is not just the reverse of Quality Function Deployment, which begins with consumer preferences but also can be used to identify a family of products or a technology platform, expressed in the form of experience, know-how, structure, and so on that enables the creation of

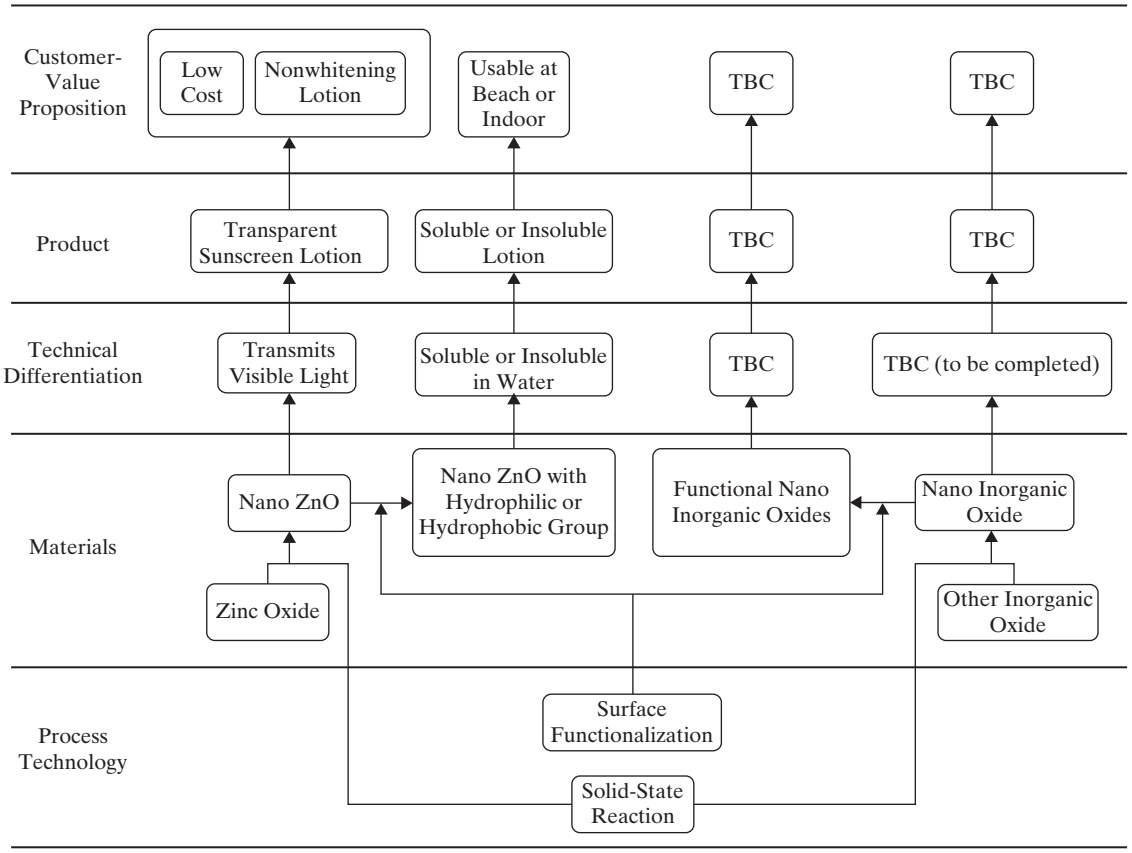

Figure 1.10 An innovation map for a sunscreen lotion with nano zinc oxide as a key ingredient.

products and processes without having to resort to a new technology. This is illustrated in Example 1.4.

EXAMPLE 1.4 ***Innovation map for zinc oxide products***

Zinc oxide is capable of absorbing UV light that can cause skin cancer while reflecting visible light. Zinc oxide nanoparticles also absorb UV light but transmit visible light. The technical team has invented a new process with which zinc oxide can be manufactured inexpensively by a solid-state reaction (Lu et al., 2008). Nano ZnO is produced by grinding zinc sulfate with potassium chloride and potassium hydroxide followed by washing to remove the soluble product (K_2SO_4 and KCl) and unreacted reactant ($ZnSO_4 \cdot 7H_2O$, KCl and KOH):

$$ZnSO_4 \cdot 7H_2O + 7.5KCl + 2KOH \rightarrow ZnO + K_2SO_4 + 7.5KCl + 8H_2O$$

Develop an innovation map for nano zinc oxide.

SOLUTION

As shown in Figure 1.10, the foundation layer of the innovation map is the solid-state reaction that does not need a solvent. Because zinc oxide absorbs UV light, it is a key component in a sunscreen lotion. The shortcoming is that such a sunscreen lotion is whitening because it reflects visible light. The use of nano zinc oxide produced by solid-state reaction leads to a low-cost transparent sunscreen lotion that is highly preferred by the consumer.

The innovation map can serve as the basis for the product-development team to create a family of products and/or a technology platform. For example, one can functionalize the zinc oxide nanoparticles by attaching hydroxyl groups to them. Such a product is water soluble and can be used as a day cream. It is not suitable for use at the beach because it readily dissolves in water. Perhaps a product that is not water soluble can be produced by using zinc nanoparticles that are functionalized with groups having long carbon chains. On the processing side, the product-development team may want to consider whether the same solid-state reaction can be used to produce nanoparticles of other materials. If affirmative, how are these nanoparticles used in other products? The innovation map is expected to evolve and become more complete with time as the product-development team moves forward.

Feasibility Study

The objective of a feasibility study is to obtain a preliminary assessment of the economic and technical feasibility of manufacturing the desired product. This will help provide an estimate of the product cost and, thus, the selling price. The selling price is decided by a balance between an acceptable return on investment and the selling price of similar products on the market. For a given production rate, material and energy balance analyses are performed to determine the raw-material consumption, waste generation, utility consumption, and required processing time. Although process details are not required, a conceptual process design (see Chapters 2 and 6) should be carried out at this stage so that the product cost can be estimated. The cost of raw materials,

especially the active ingredients, often represents a significant portion of the product cost. A trade-off exists between raw-material cost and production cost, because cheaper raw materials of lower purity may require expensive pretreatment before they can be incorporated into the product. Some impurities are totally unacceptable. For example, the presence of heavy metals in a skin-care product, even at very minute concentrations, results in disastrous product recalls. Therefore, it is crucial to identify the raw-material source. Availability and consistency of the supply of raw materials, especially natural herbs, should be assessed at this stage. In addition, transportation costs, import and export taxes, and advertising costs must be considered because they often substantially affect the overall economics.

There is no alternative to environmental compliance. Although the base-case recipe and the conceptual design of the process plant are not very exact at this point, local environmental regulations should be consulted to check whether there is any limit on the disposal of certain waste materials and whether such limits may lead to the need for expensive waste treatment facilities.

This is also the right time to consider whether to file a patent application to secure an intellectual property (IP) position for the product. A patent for an invention is a property right granted to the inventor that prevents others from practicing the invention. A patent is used to protect a product, giving the inventor an exclusivity to produce the product for a limited period of time (17 years in the United States). Patentable inventions may include (1) operating methods or processes, (2) physical structures such as the composition of matter, and (3) product features or articles. Recently, these have been expanded to include (4) algorithms and (5) business processes. Because a patent is a legal property, like a house or an automobile, it can be owned, bought, and sold. Often patents are licensed to others for fees on the order of 3–6% of gross sales.

Normally, a patent search and analysis is performed. Various search engines are available on the Internet to locate the relevant patents by user-supplied keywords, patent number, patent title, inventor name, assignee name, patent classification, issue date, and filing date. A detailed analysis of existing patents helps identify the uniqueness of the new product or process. Given the implications of the patent as a legal document, a patent attorney often rewrites the patent drafted by the chemical engineer before filing it with the patent office.

EXAMPLE 1.5 ***IP search of prior art on sunscreen lotion***

The technical team likes the idea of developing a sunscreen lotion that does not dissolve easily in water. Perform a preliminary search of the prior art using Google Advanced Patent Search. Here, prior art refers to any publicized information relevant to the originality claims in the patent to be filed.

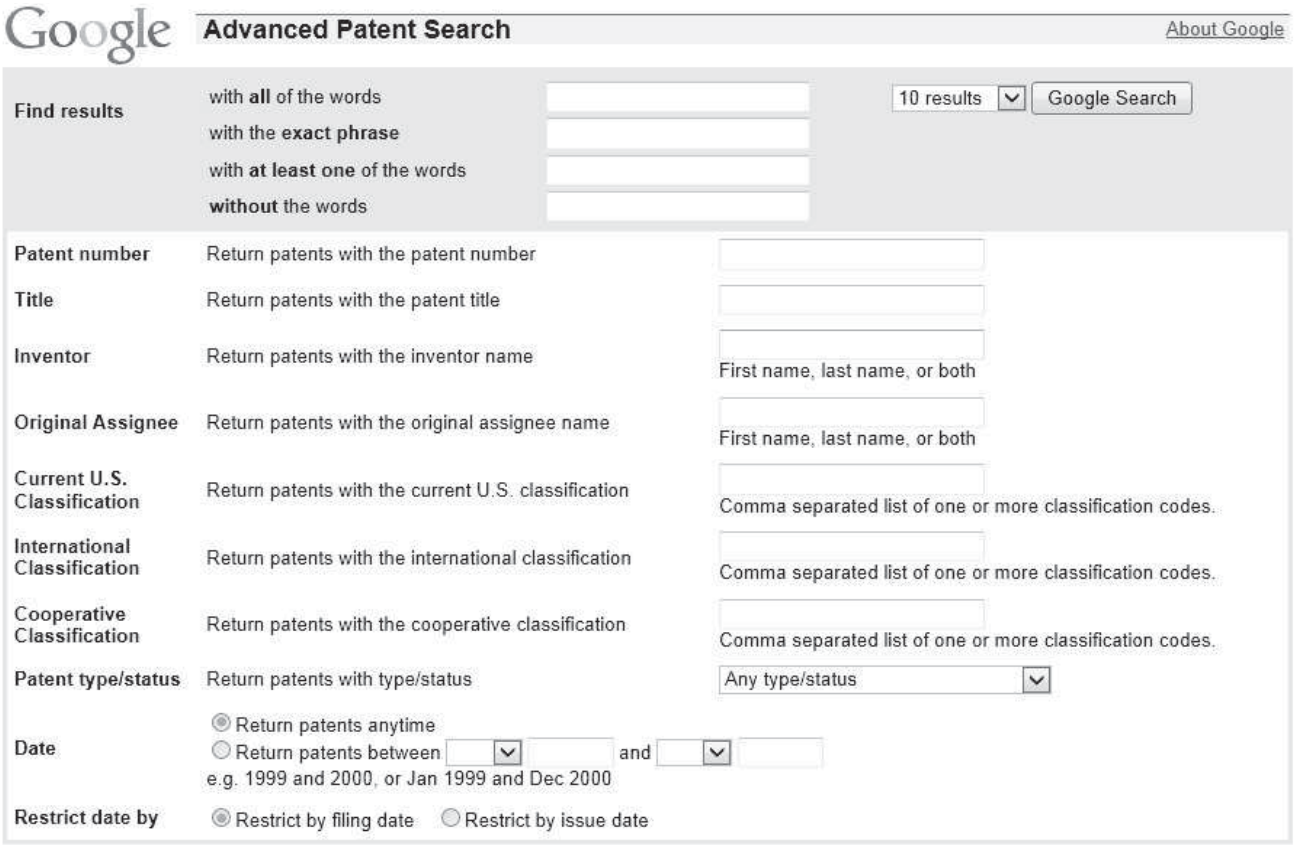

Figure 1.11 A screenshot of Google Advanced Patent Search. Google and the Google logo are registered trademarks of Google Inc. Used with permission.

SOLUTION

Figure 1.11 shows a screenshot of the home page of Google Advanced Patent Search. Normally, searches are first made using keywords. After that, searches can be limited by other attributes such as the inventor name, assignee (company) name, and filing or issue dates.

Let us perform a search by entering the following keywords: transparent sunscreen lotion nano zinc oxide in the "with **all** of the words" window and "water insoluble" in the "with the **exact phrase**" window. This yields 1610 results. We can use the search tools button "**Search tools**" on the right-hand side of the tool bar to further narrow down the search by time, patent office, filing status, and patent type. For example, if we limit ourselves to issued patents in the previous results, we can choose "**Issued patents**" with the "**Any filing status**" button. This reduces the number of results to 232. Furthermore, if only U.S. patents are considered, we can do so by choosing "**United States**" with the "**Any patent office**" button, returning 55 results. If we want to focus on patents published between Jan 1, 2012 and Dec 31, 2013, we can do so by changing "**Any time**" to "**Publication date**" and fill in the period "1/1/2012" to "12/31/2013." Now there are only 3 results.

Prototyping

Prototyping activities focus on bench-scale experiments to make a prototype of the conceived product to test the product performance. The base-case recipe or formula identified in Product Conceptualization (Phase I in Figure 1.3) is used as a starting point for the first prototype, which is then subjected to a series of standard performance tests for the product class under consideration. For example, tests for hair conditioners include assessing the condition of real human hair after applying the conditioner. All required tests and the amount of sample needed for each test should be identified so that a sufficient amount of materials required for the prototype can be prepared in advance. Prototyping is inevitably an iterative process. The product formula is revised after each round of product characterization and performance tests until the product specifications set by the marketing team are met. Physicochemical insights, previous experience, and molecular simulations are used to guide the iteration process.

1.4 SUMMARY

The chemical and allied industries, as well as their products, have been briefly reviewed. The step-by-step conversion of natural resources to basic chemicals and then to industrial and consumer products is self-organized in the marketplace (Figure 1.1). Because of the complexity, different types of firms—oil, chemical, pharmaceutical, food, consumer goods, and so on—focus on different segments of the chain of chemical products.

Although all chemical products (Table 1.2) are produced for the consumer, the consumer's preferences are closely followed only for B2C products (Table 1.1). For B2B products, consumer preference is only weakly reflected. Thus, the key demand for basic chemicals is to make these compounds as cheaply as possible and in a sustainable manner.

The general approach for product design and development is by and large the same for B2B and B2C products. The differences are in the details, particularly in product attributes and specifications. Some of the tasks in the multidisciplinary, hierarchical product design framework (Figure 1.3) are handled by professionals from other disciplines but are included here so that the reader gets a holistic view of the entire approach. It should be noted that there is a large gray area between the tasks and the approach is not meant to be strictly followed. Rather, the framework should be adapted to suit the specific product and circumstances. What is important is the proper mind-set for product design.

A number of methods are introduced to aid in the execution of the approach. The objective-time chart (Figure 1.4), the RAT^2IO mnemonic (Figure 1.5), and the stage-gate approach (Figure 1.6) are used in project management. The Quality Function Deployment and House of Quality (Figure 1.7) are used in market study. The Business Model Canvas (Figure 1.9) is used to ensure that the product-development effort is examined in a comprehensive manner. The innovation map (Figure 1.10) is used for technology-push products. Similar to the framework for product design, these design methods are not meant to be strictly followed. They remind us of the issues that need to be considered and guide us to consider them in a systematic way.

In the early stage of product development, the marketing plan and the desired product attributes may constantly change. The R&D plan has to be revised accordingly. For example, an extra active ingredient may need to be incorporated into the recipe developed in the laboratory to achieve an additional product attribute because of a newly identified market demand. Thus, it is important to keep in mind that product design is an iterative process.

Figure 1.12 is a work flow diagram that illustrates the iterative nature of product design and development. It starts with the identification of market needs and the attributes of the candidate product. The recipe for the product is first developed in the laboratory. Conceptual design of a production process allows the estimation of product cost. Then, if necessary, a product prototype is fabricated for performance testing by an evaluation panel. The manufacturing process needs to be designed and IP position has to be established. Some products may undergo a test marketing exercise in which actual samples of the product are put in a test market to assess consumer reaction. Note that the arrows returning to the previous steps are not meant to be exhaustive. For example, if the environment impact study indicates that one of the ingredients can adversely impact the environment upon product disposal, one may have to return to the laboratory to adjust the recipe to eliminate the objectionable component.

Computer-aided tools for design of single-molecule products and design of liquid mixtures and blends are covered in Chapter 4. In Chapter 5, the design of B2C chemical products for which chemical reaction and transport phenomena tend to play a dominant role is discussed. Business decision making for B2C products is more involved than that for B2B products; this is discussed in Chapter 19. Three detailed chemical product case studies are presented in Chapters 24–26. An introduction to process design is presented in Chapter 2.

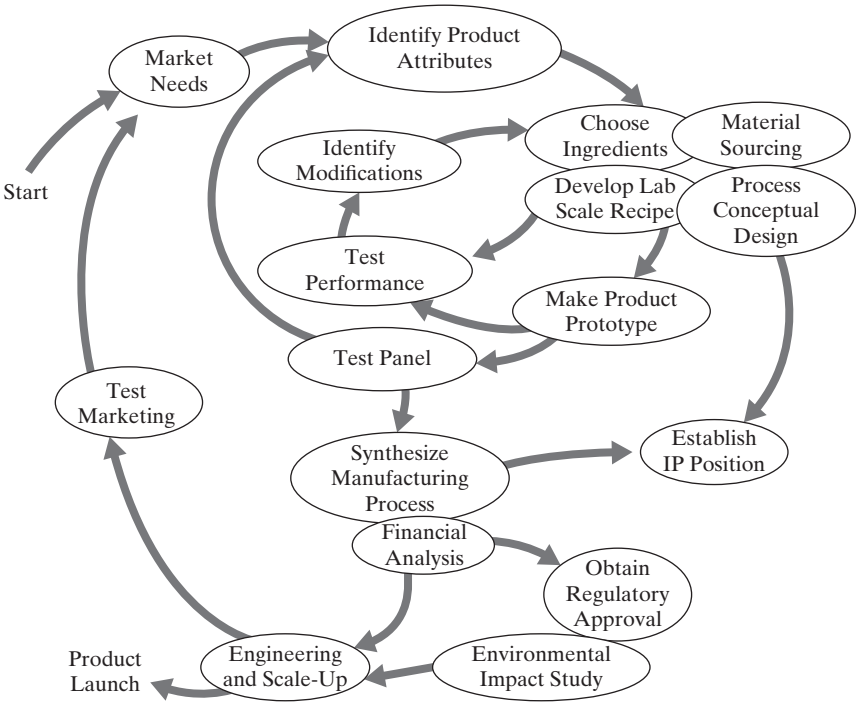

Figure 1.12 The work flow diagram illustrates the iterative nature of product design and development.

REFERENCES

1. Arora, A., R. Landau, and N. Rosenberg, *Chemicals and Long-Term Economic Growth*, Wiley, New York (1998).

2. Austin, G. T., *Shreve's Chemical Process Industries*, 5th ed., McGraw-Hill, New York (1984).

3. Blank, S., and B. Dorf, *The Startup Owner's Manual. The Step-by-Step Guide for Building a Great Company*, K&S Ranch Press, Pescadero, California (2012).

4. Bröckel, U., W. Meier, and G. Wagner (eds.), *Product Design and Engineering: Basics and Best Practices* (2 Volume Set), Wiley-VCH, Weinheim (2007).

5. Bröckel, U., W. Meier, and G. Wagner (eds.), *Product Design and Engineering: Formulation of Gels and Pastes*, Wiley, Somerset, New Jersey (2013).

6. Cheng, Y. S., K. W. Lam, K. M. Ng, K. M. Ko, and C. Wibowo, "An Integrative Approach for Product Development—A Skin-Care Cream," *Comp. Chem. Eng.*, **33**, 1097 (2009).

7. Chenier, P. J., *Survey of Industrial Chemistry*, 3rd ed., Wiley, New York (2002).

8. Cooper, R. G., *Product Leadership: Creating and Launching Superior New Products*, 2nd ed., Basic Books, Cambridge, Massachusetts (2005).

9. Cussler, E. L., and G. D. Moggridge, *Chemical Product Design*, 2nd ed., Cambridge University Press, Cambridge, United Kingdom (2011).

10. Faith, W. L., F. A. Lowenheim, and M. K. Moran, *Faith, Keyes, and Clark's Industrial Chemicals*, 4th ed., Wiley, New York (1975).

11. Hounshell, D., and J. K. Smith, *Science and Corporate Strategy: DuPont R&D, 1902-80*, Cambridge University Press, Cambridge, United Kingdom (1988).

12. Lu, J., K. M. Ng, and S. Yang, "An Efficient, One-Step Mechanochemical Process for the Synthesis of ZnO Nanoparticles," *Ind. Eng. Chem. Res.*, **47**, 1095 (2008).

13. Ng, K. M., R. Gani, and K. Dam-Johansen (eds.), *Chemical Product Design: Toward a Perspective through Case Studies*, Elsevier, Amsterdam, The Netherlands (2007).

14. Osterwalder, A., and Y. Pigneur, *Business Model Generation*, Wiley, Hoboken, New Jersey (2010).

15. Ulrich, K. T., and S. D. Eppinger, *Product Design and Development*, 5th ed., McGraw-Hill, New York (2012).

16. Wei, J., *Product Engineering: Molecular Structure and Properties*, Oxford University Press, Oxford, New York (2007).

17. Wesselingh, J. A., S. Kiil, and M. E. Vigild, *Design & Development of Biological, Chemical, Food and Pharmaceutical Products*, Wiley, Chichester, United Kingdom. (2007).

18. Wheelwright, S. C., and K. B. Clark, *Revolutionizing Product Development*, The Free Press, New York (1992).

19. Wibowo, C., and K. M. Ng, "Product-Oriented Process Synthesis and Development: Creams and Pastes," *AIChE J.*, **47**, 2746 (2001).

20. Widagdo, S, "Incandescent Light Bulb: Product Design and Innovation," *Ind. Eng. Chem. Res.*, **45**, 8231 (2006).

EXERCISES

1.1 The invention and commercialization of a new chemical is a significant undertaking. An example is the invention of nylon in the laboratory and its transformation to a nylon stocking. Please read the relevant sections in Hounshell and Smith (1988) or at the Web sites, www.dupont.com and www.acs.org, and answer the following questions:

(a) Who invented nylon?

(b) Write down the main reaction for making nylon.

(c) How was the water removed from the condensation reaction in the laboratory at that time?

(d) Which one of the two reactants for nylon was not commercially available at the time nylon was invented?

(e) How was the melt fiber spinning problem solved?

(f) Where did DuPont build the first full-scale nylon plant?

1.2 Show the main chemical reactions for producing polyvinyl butyral, assuming that ethylene, acetic acid, ethanol, and butyraldehyde are available as raw materials (see Figure 1.1).

1.3 One can follow the developments in the chemical industry in trade magazines such as the *Chemical & Engineering News*. Answer the following questions after reading the article, "Global Top 50" for the year 2013 survey by A. H. Tullo at the Web site cen.acs.org.

(a) What were the top five global chemical companies in terms of sales in 2013?

(b) Which chemical companies in China, India, South Korea, and Thailand made it into the Global Top 50 in 2013?

(c) Which were the top five companies in chemical R&D spending in 2013?

(d) What were some of the mergers, acquisitions, and divestitures in 2013?

(e) Repeat questions (a) to (d) for the most recent survey that is available at the same Web site.

1.4 The companies involved in the chemical product chain (Figure 1.1) can be categorized by product type. Gas, oil, chemical, pharmaceutical, mineral processing, and consumer goods companies have been described in the text along with the names of well-known companies in each category. Provide additional company names. In addition, identify categories not mentioned above such as specialized engineering firms and food companies and company names in these categories.

1.5 DuPont's Web site (www.dupont.com) shows 13 market sectors in which DuPont sells its products. Prepare a table similar to Table 1.2 in which the chemical products are classified by industrial sector and product form for the following eight sectors:

(a) Agriculture

(b) Automotive

(c) Building & Construction

(d) Electronics

(e) Energy

(f) Food & Beverage

(g) Health Care & Medical

(h) Packaging & Printing

Show one DuPont product for each entry in the table. If such a product is not available, enter NA (not available) in the corresponding entry of your table.

1.6 3M markets a wide variety of consumer goods. Visit its Web site (www.3M.com) and identify the attributes of the following 3M products:

(a) Ultrathon insect repellent

(b) Filtrete air purifier

(c) Water pitcher and replacement filter

(d) Sun control window film

(e) Reusable cold/hot pack

1.7 Visit the Unilever Web site (www.unilever.com) and the Procter and Gamble Web site (www.pg.com). Name some of their brands for the following consumer goods products:

(a) Soap

(b) Skin cream

(c) Shampoo

(d) Laundry detergent

1.8 A list of the typical attributes of creams and pastes is given in Example 1.2. Identify two sunscreen lotion products from two different companies. Compare them based on the four product attributes provided in the example. Make sure that quantitative product specifications such as the sun protection factor (SPF) and the protection grade of UVA (PA) are included.

1.9 The use of nano zinc oxide in sunscreen lotions is discussed in Example 1.4. The innovation map calls for an investigation of other nano inorganic oxides. Complete Figure 1.10 for the following materials:

(a) Indium tin oxide

(b) Antimony tin oxide

1.10 Use Google Advanced Patent Search to determine the number of skin care–related patents owned by the following cosmetic companies:

(a) Avon

(b) Kanebo

(c) L'Oreal

(d) Revlon

(e) Shiseido

1.11 Product quality is of paramount importance in chemical product design. Explore the following quality improvement methodologies on the Internet:

(a) Fishbone diagram

(b) Pareto analysis

(c) Process analytical technologies

(d) Quality by design

(e) Root cause analysis

(f) Taguchi method

Explain in five-six sentences how each of the methodologies works with figures if necessary.

1.12 Instead of the conventional unit operations, many B2C chemical products are manufactured using unconventional processing techniques such as etching, physical vapor deposition, and calendering. Consider the low-E double-pane insulating glass unit (IGU):

(a) Describe the structure and materials used for such an IGU.

(b) Name a company supplying each type of material used for the same.

(c) Describe the manufacturing process for the same.

(d) Name some manufacturers of these IGUs.

1.13 Repeat Exercise 1.12 for a cylindrical rechargeable battery with lithium iron phosphate as cathode, graphite as anode, and polyethylene as separator. Consult the Web site industry.siemens.com for the battery manufacturing process.

Chapter 2

Introduction to Process Design

2.0 OBJECTIVES

After studying this chapter, the reader should:

1. Understand the kinds of information gathered before designing a process to manufacture a chemical product.
2. Be able to implement the steps in creating flowsheets involving reactions, separations, and *T-P* change operations. Doing so identifies many alternatives that can be assembled into a synthesis tree containing the most promising alternatives.
3. Be aware of the major tasks in carrying out a process design with a guide to the sections and chapters of this textbook that cover methods for performing these tasks.
4. For the most promising *base-case* process flowsheets, know how to select the principal pieces of equipment and to create a detailed process flow diagram, with a material and energy balance table and a list of major equipment items.

2.1 INTRODUCTION

In process design, chemical engineers create chemical processes to convert raw materials into desired products, often identified using the product design strategies introduced in Chapter 1. In product design, the focus is on creating products that satisfy customer needs (i.e., the "voice of the customer"). Process design begins with well-defined chemical products, often available in prototype quantities from research laboratories. The process design team is challenged to design profitable processes that produce products in sufficient quantities and qualities to satisfy anticipated customer demands. Stated differently, the designers create potential processes to convert raw materials in specified states into a desired product(s) in a specified state(s).

Several key tasks/steps are involved in process design, most of which are carried out by design teams, but not necessarily in the same sequence. In this first process design chapter, these tasks are introduced, and illustrated in two principal examples, the intent being to provide introductory details while enabling readers to gain a broad appreciation of the typical approaches toward the design of manufacturing processes. For each task, references are made to subsequent chapters/sections in which more complete discussions are provided. Also, in areas where most chemical engineering students have learned techniques in earlier courses (e.g., thermodynamics, heat transfer, and separation processes), references are given and detailed methods are described later in this textbook. The first task normally involves information gathering, which is covered next.

Information Gathering

Process design problems are formulated in many ways, with many typical problem statements provided in Appendix II. Given a problem statement, usually a design group begins work to gather information that is the basis for its design. Often the project author is an excellent first source of information and data. But, in most cases, not all of the needed data are readily available, and guidance as to where to look or what assumptions are reasonable may be provided.

The data-gathering task usually involves searching the literature, especially the Internet for details about the chemical product to be manufactured. The designers need to know why the product is important. What are its uses? What are its characteristic properties? Who are the biggest producers (competitors)? For new products, much of this information is available from the product design team, which often participates on the team that designs its manufacturing process.

Gradually, the designers gain knowledge of the raw-material alternatives, and the principal chemical reactions, byproducts, and intermediates. Also, the designers begin to target a range of potential production levels and possible plant locations—usually making selections as the basis for their initial design work.

At this point, let's focus on the typical issues in designing a process to increase significantly the supply of a widely used commodity chemical, vinyl chloride. For this product, much information is readily available as provided in the problem statement that follows in Example 2.1.

EXAMPLE 2.1 ***Vinyl Chloride Manufacture—Information Gathering***

Consider the need to manufacture vinyl chloride,

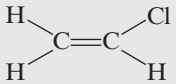

a monomer intermediate for the production of polyvinyl chloride,

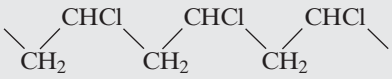

an important polymer (usually referred to just as vinyl) that is widely used for rigid plastic piping, fittings, and similar products. Over the years, large commercial plants have been built, some of which produce over 1 billion lb/yr. Hence, polyvinyl chloride and the monomer from which it is derived are referred to commonly as commodity chemicals that are produced continuously, rather than in batch, virtually everywhere. Historically, vinyl chloride was discovered in 1835 in the laboratory of the French chemist Regnault, and the first practical method for polymerizing vinyl chloride was developed in 1917 by the German chemists Klatte and Rollett (Leonard, 1971). Vinyl chloride is an extremely toxic substance and, therefore, industrial plants that manufacture it or process it must be designed carefully to satisfy government health and safety regulations.

An opportunity has arisen to satisfy a new demand, on the order of 800 million pounds per year, for vinyl-chloride monomer in a petrochemical complex on the Gulf Coast of the United States, given that an existing plant owned by the company produces 1 billion lb/yr of this commodity chemical. At this point, a design team has been formulated, and it has begun to consider four potential alternatives, including:

Alternative 1. A competitor's vinyl-chloride plant, which produces 2 MMM (billion) lb/yr of vinyl chloride and is located about 100 miles away, might be expanded to produce the required amount, which would be shipped by truck or rail in tank car quantities. In this case, the design team projects the purchase price and designs storage facilities. This might be the simplest solution to provide the monomer required to expand the local PVC plant.

Alternative 2. Chlorine from the electrolysis of NaCl solution could be processed and shipped by pipeline from a nearby plant. Then, chlorine could be reacted with in-house ethylene to produce the monomer and HCl as a byproduct.

Alternative 3. Because the existing company petrochemical complex produces HCl as a byproduct in many processes (e.g., in chloroform and carbon tetrachloride manufacture) at a depressed price because large quantities are produced, HCl is normally available at low prices. Reactions of HCl with acetylene, or ethylene and oxygen, could produce 1,2-dichloroethane, an intermediate that can be cracked to produce vinyl chloride.

Alternative 4. Design an electrolysis plant to produce chlorine. One possibility is to electrolyze the HCl, available from within the petrochemical complex, to obtain H_2 and Cl_2. Then, chlorine could be reacted according to alternative 2. Elsewhere in the petrochemical complex, hydrogen could be reacted with nitrogen to form ammonia or with CO to produce methanol.

These are typical of the alternatives that might be selected from a large number of ideas that serve as a base on which to begin the process design. For this example, it's sufficient to consider only the production of the monomer with a focus on alternatives 2 and 3.

Data from chemistry laboratories focus on several promising chemical reactions involving the chemicals in Table 2.1. Thermophysical property data (e.g., normal boiling points, vapor pressures, heat capacities, latent heats of vaporization, heats of formation, and liquid densities) for these (and many other similar chemicals) are available in extensive databases (of the process simulators; see Chapter 7) and, when not available, can be estimated fairly reliably. The availability of toxicity, safety, and purchase price data is discussed following this example.

Table 2.1 Chemicals That Participate in Reactions to Produce Vinyl Chloride

Chemical	Molecular Weight	Chemical Formula	Chemical Structure
Acetylene	26.04	C_2H_2	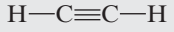
Chlorine	70.91	Cl_2	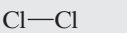
1,2-Dichloroethane	98.96	$C_2H_4Cl_2$	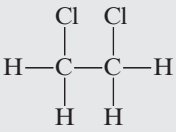
Ethylene	28.05	C_2H_4	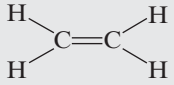
Hydrogen chloride	36.46	HCl	
Vinyl chloride	62.50	C_2H_3Cl	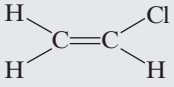

Environmental and Safety Data

As mentioned in Section 3.4, design teams need toxicity data for raw materials, products, byproducts, and intermediates incorporated in a process design. In toxicology laboratories operated by chemical companies and governmental agencies, such as the U.S. Environmental Protection Agency (EPA) and the U.S. Food and Drug Administration (FDA), tests are run to check the effects of various chemicals on laboratory animals. The chemicals are administered in varying dosages, over differing periods, and in different concentrations, stimulating effects that are measured in many ways, including effects on the respiratory system, the skin, and the onset of cancer. In most cases, the results are provided in extensive reports or journal articles. In some cases, chemicals are difficult to classify as toxic or nontoxic.

Already it is well known that a number of common chemicals are toxic to humans and need to be avoided. One source of information on these chemicals is the Toxic Chemical Release Inventory (TRI), which is maintained by the U.S. EPA, and includes over 600 chemicals. A list of these chemicals is available at the Internet site:

http://www.epa.gov/tri/chemical/index.htm

Another source is provided by the ratings of the National Fire Protection Association (NFPA), which are tabulated for many chemicals in *Data for Process Design and Engineering Practice* (Woods, 1995). The first of three categories is titled "Hazard to Health" and entries are rated from 0 to 4, with 0 meaning harmless and 4 meaning extremely hazardous.

As seen in Table 3.2 and discussed in Section 3.5, data on the flammability of organic compounds are tabulated and, for those compounds not included in the table, methods are available to estimate the data. In addition, tables of flammability data are also available for aerosols and polymers in *Perry's Chemical Engineers' Handbook* (Green and Perry, 2008). The NFPA ratings provide a less quantitative source for many chemicals under "Flammability Hazard," which is the second of the three categories (also rated from 0 to 4).

Chemical Prices

Economics data are often related to supply and demand, and consequently they fluctuate and are much more difficult to estimate. Most companies, however, carry out market studies and have a basis for projecting market size and chemical prices. In view of the uncertainties, to be safe, economic analyses are often conducted using a range of chemical prices to determine the sensitivity of the results to specific prices.

One widely used source of prices of commodity chemicals is from *ICIS Chemical Business* (formerly *Chemical Market Reporter*), a weekly publication. Their Web site, http://www.icis.com/StaticPages/Students.htm, provides information for students in their Knowledge Zone. It should be noted, however, that these prices may not reflect the market situation in a particular location; nevertheless, they provide a good starting point. In addition, commodity chemical prices may be found via ICIS pricing. This service publishes weekly pricing benchmarks to the industry and offers samples of reports that are approximately six months old via the following link: http://www.icispricing.com/il_shared/il_splash/chemicals.asp?llink%. Obviously, to obtain better estimates, at least for the immediate future, the manufacturers of the chemicals should be contacted directly. Lower prices than those listed can be negotiated. Subscribers to *ICIS Chemical Business* can also obtain more recent market trends and data derived from both their ICIS news and ICIS pricing services.

In some cases, it may be desirable to estimate the prices of utilities, such as steam, cooling water, and electricity, during process creation. Here also, appropriate prices can be obtained from local utility companies. As a start, however, values are often tabulated, as provided in Table 17.1.

Summary

To the extent possible using the literature, company files, computer data banks, and similar sources, the design team assembles a preliminary database for use in preliminary process synthesis, the subject of Section 2.3. Typically, the database contains thermophysical property data, rudimentary reaction-rate data, data concerning toxicity and flammability of the chemicals, and chemical prices. In cases where data cannot be located, estimation methods are often available. However, when the results are sensitive to the estimates, conclusions must be drawn with caution. In most cases, when a process looks promising, an experimental program is initiated, as discussed in the next section. Note that other kinds of data are normally not necessary until the detailed process flow diagram has been developed for the base-case design, and the design team is preparing to complete the detailed design of the equipment items. Note also that when molecular-structure design has been used to select the chemical product, experimental data and/or theoretical estimates are usually available in data banks, especially in drug development.

2.2 EXPERIMENTS

Many design concepts are the result of extensive experiments in the laboratory, which provide valuable data for the design team. Often, however, laboratory experiments are carried out in small vessels, using small quantities of expensive solvents, and under conditions where the conversion and selectivity to the desired product are far from optimal. For this reason, as a design concept becomes more attractive, it is common for the design team to request additional experiments at other conditions of compositions, temperatures, and pressures, and using solvents that are more representative of those suitable for large-scale production. In cases where no previous in-house experimental work has been done, laboratory programs are often initiated at the request of the design team, especially when estimates of the rates of reaction are not very reliable. When chemical reactions involve the use of catalysts, it is essential that experiments be conducted on catalyst life using feedstocks that are representative of those to be used for large-scale production, and that may contain potential catalyst poisons.

Laboratory experiments may also be necessary to aid in the selection and preliminary design of separation operations. The separation of gas mixtures requires consideration of absorption, adsorption, and gas permeation, all of which may require the search for an adequate absorbent, adsorbent, and membrane material, respectively. When nonideal liquid mixtures are to be separated, laboratory distillation experiments should be conducted early because the possibility of azeotrope formation can greatly complicate the selection of adequate separation equipment, which may involve the testing of one or more solvents or entrainers. When solids are involved, early laboratory tests of such operations as crystallization, filtration, and drying are essential.

Clearly, as data are obtained in the laboratory, they are tabulated and usually regressed, to allow addition to the preliminary database for use by the design team in preliminary process synthesis, which is the subject of the next section.

2.3 PRELIMINARY PROCESS SYNTHESIS

Having gathered information and carried out experiments, if necessary, a process design team is prepared to create an initial process flowsheet to convert the potential raw materials into chemical products. Various processing operations are used to carry out chemical reactions and to separate products and byproducts from each other and from unreacted raw materials. The assembly of these operations into a process flowsheet is known as *process synthesis*. In many respects, one of the greatest challenges in process design involves the synthesis of configurations that produce chemicals in a reliable, safe, and economical manner, at high yield and with little or no waste.

Chemical State

To initiate process synthesis, the design team must decide on raw materials, products, and byproducts specifications. These are referred to as *states*. Note that the state selections can be changed later with modifications to the flowsheets. To define the state, values of the following conditions are needed:

1. Mass (flow rate)
2. Composition (mole or mass fraction of each chemical species of a unique molecular type)
3. Phase (solid, liquid, or gas)
4. Form, if solid phase (e.g., particle size distribution and particle shape)
5. Temperature
6. Pressure

In addition, some well-defined properties, such as the intrinsic viscosity, average molecular weight, color, and odor of a polymer, may be required. These are often defined in connection with the research and marketing departments, which work to satisfy the requests and requirements of their customers. It is not uncommon for a range of conditions and properties to be desired, some of which are needed intermittently by various customers as their downstream requirements vary. When this is the case, care must be taken to design a process that is sufficiently flexible to meet changing demands.

For most chemicals, the scale (i.e., production level or flowrate) of the process is a primary consideration early in the design process. Working together with the marketing people, the scale of the process is determined on the basis of the projected demand for the product. Often the demographics of the most promising customers have an important impact on the location of the plant and the choice of its raw materials. As the scale and the location are established, the composition, phase, form, temperature, and pressure of each product and raw-material stream are considered as well. When the desired states of these streams have been identified, the problem of process synthesis becomes better defined. As shown in Figure 2.1, for the production of vinyl chloride, it remains to insert the process operations into the flowsheet.

It is noteworthy that once the state of a substance is fixed by conditions 1–6, all physical properties (except for the form of a solid), including viscosity, thermal conductivity, color, refractive index, and density, take on definite values. Furthermore, the state of a substance is independent of its position in a gravitational field and its velocity. Although there are other conditions (magnetic field strength, surface area) whose values are needed under certain conditions, the six conditions listed above are usually sufficient to fix the state of a substance.

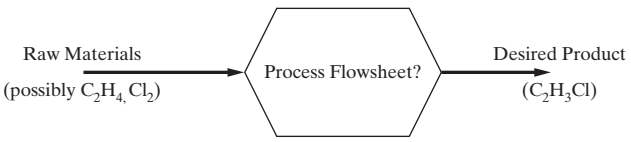

Figure 2.1 Process synthesis problem.

Process Operations

Throughout the chemical engineering literature, many kinds of equipment, so-called *unit operations*, are described, including distillation columns, absorbers, strippers, evaporators, decanters, heat exchangers, filters, and centrifuges, just to mention a few. The members of this large collection all involve one or more of these basic operations:

1. Chemical reaction
2. Separation of chemical mixtures
3. Phase separation
4. Change of temperature
5. Change of pressure
6. Change of phase
7. Mixing and splitting of streams or batches
8. Operations on solids, such as size reduction and enlargement

Since these are the building blocks of nearly all chemical processes, it is common to create flowsheets involving these basic operations as a first step in process synthesis. Then, in a *task integration* step, operations are combined where feasible. In the remainder of this section, each of the basic operations is considered in some detail before considering the steps in process synthesis.

Chemical Reaction Operations

Chemical reaction operations are at the heart of many chemical processes. They are inserted into a flowsheet to effect differences in the molecular types between raw-material and product streams. To this end, they involve the chemistry of electron transfers, free-radical exchanges, and other reaction mechanisms, to convert the molecular types of the raw materials into products of other molecular types that have the properties sought by a company's customers. Clearly, the positioning of the reaction operations in the flowsheet involves many considerations, including the degree of conversion, reaction rates, competing side reactions, and the existence of reactions in the reverse direction (which can result in constraints on the conversion at equilibrium). These, in turn, are related closely to the temperature and pressure at which the reactions are carried out, the methods for removing or supplying energy, and the catalysts that provide competitive reaction rates and selectivity to the desired products.

Separation Operations

Separation operations appear in almost every process flowsheet. They are needed whenever there is a difference between the desired composition of a product or an intermediate stream and the composition of its source, which is either a feed or an intermediate stream. Separation operations are inserted when the raw materials contain impurities that need to be removed before further processing, such as in reactors, and when products, byproducts, and unreacted raw materials coexist in a reactor effluent stream. The choice of separation operations depends first on the phase of the mixture and second on the differences in the physical properties of the chemical species involved. For liquid

mixtures, when differences in volatilities (i.e., vapor pressure) are large, it is common to use vapor–liquid separation operations (e.g., distillation), which are by far the most common. For some liquid mixtures, the melting points differ significantly and solid–liquid separations, involving crystallization, gain favor. When differences in volatilities and melting points are small, it may be possible to find a solvent that is selective for some components but not others, and to use a liquid–liquid separation operation. For other mixtures, particularly gases, differences in absorbability (in an absorbent), adsorbability (on an adsorbent; e.g., activated carbon, molecular sieves, or zeolites), or permeability through a membrane may be exploited with adsorption and membrane separation operations.

Temperature Change Operations

The need to change temperatures usually occurs throughout a chemical process. In other words, there are often differences in the temperatures of the streams that enter or leave the process or that enter or leave adjacent process operations, such as reaction and separation operations. Often a process stream needs to be heated or cooled from its *source* temperature to its *target* temperature. This is best accomplished through heat exchange with other process streams that have complementary cooling and heating demands.

Pressure Change Operations

The positioning of pressure-change operations such as gas compressors, gas turbines or expanders, liquid pumps, and pressure-reduction valves in a process flowsheet is often ignored in the early stages of process design. As will be seen, it is common to select the pressure levels for reaction and separation operations. When this is done, pressure-change operations will be needed to decrease or increase the pressure of the feed to the particular operation. In fact, for processes that have high power demands, usually for gas compression, there is often an opportunity to obtain much of the power through integration with a source of power, such as turbines or expanders, which are pressure-reduction devices. In process synthesis, however, where alternative process operations are being assembled into flowsheets, it has been common to disregard the pressure drops in pipelines when they are small relative to the pressure level of the process equipment. Liquid pumps to overcome pressure drops in lines and across control valves and to elevate liquid streams to reactor and column entries often have negligible costs. Increasingly, as designers recognize the advantages of considering the controllability of a potential process while developing the base-case design, the estimation of pressure drops gains importance because flow rates are controlled by adjusting the pressure drop across a valve.

Phase Change Operations

Often there are significant differences in the phases that exit from one process operation and enter another. For example, hot effluent gases from a reactor are condensed, or partially condensed, often before entering a separation operation, such as a vapor–liquid separator (e.g., a flash vessel or a distillation tower). In process synthesis, it is common to position a phase-change operation using temperature- and/or pressure-reduction operations, such as heat exchangers and valves.

Mixing Operations

The mixing operation is often necessary to combine two or more streams and is inserted when chemicals are recycled and when it is necessary to blend two or more streams to achieve a product specification.

Synthesis Steps

Given the states of the raw-material and product streams, process synthesis involves the selection of processing operations to convert the raw materials into products. In other words, each operation can be viewed as having a role in eliminating one or more of the property differences between the raw materials and the desired products. As each operation is inserted into a flowsheet, the effluent streams from the new operation are closer to those of the required products. For example, when a reaction operation is inserted, the stream leaving often has the desired molecular types, but not the required composition, temperature, pressure, and phase. To eliminate the remaining differences, additional operations are needed. As separation operations are inserted, followed by operations to change the temperature, pressure, and phase, fewer differences remain. In one parlance, the operations are inserted with the goal of reducing the differences until the streams leaving the last operation are identical in state to the required products. Formal, logic-based strategies, involving the proof of theorems that assert that all of the differences have been eliminated, have been referred to as *means–end analysis*. In process synthesis, these formal strategies have not been developed beyond the synthesis of simple processes. Rather, an informal approach, introduced by Rudd, Powers, and Siirola (1973) in a book entitled *Process Synthesis*, has been adopted widely. It involves positioning the process operations in the following steps to eliminate the differences:

Synthesis Step	Process Operations
1. Eliminate differences in molecular types	Chemical reactions
2. Distribute the chemicals by matching *sources* and *sinks*	Mixing
3. Eliminate differences in composition	Separation
4. Eliminate differences in temperature, pressure, and phase	Temperature, pressure, and phase change
5. Integrate tasks; that is, combine operations into *unit processes* and decide between continuous and batch processing	

Rather than discuss these steps in general, it is preferable to examine how they are applied for synthesis of a vinyl-chloride process as will be shown in Example 2.2.

Continuous or Batch Processing

When selecting processing equipment in the task-integration step, the production scale strongly impacts the operating mode. For the production of commodity chemicals, large-scale continuous processing units are selected, whereas for the production of many specialty chemicals as well as industrial and configured consumer chemical products, small-scale batch processing units are preferable. A key decision is the choice between continuous, or batch, or possibly semicontinuous operation.

Commodity Chemicals

In this subsection, an example is presented to synthesize a process for manufacture of a typical commodity chemical, vinyl chloride. See Example 2.3 for a discussion of process synthesis of a batch process to manufacture the pharmaceutical, tissue-plasminogen activator (tPA).

EXAMPLE 2.2 ***Process Synthesis of a Vinyl-Chloride Process***

Following the Process Synthesis Steps 1–5, a process flowsheet to manufacture vinyl chloride is synthesized in this example. Note that some assistance was provided by two patents (Benedict, 1960; B. F. Goodrich Co., 1963). Often, similar patents, located by design teams when gathering information, provide considerable help during process synthesis.

Step 1 Eliminate Differences in Molecular Type: For the manufacture of vinyl chloride, data from the chemistry laboratory focus on several promising chemical reactions involving the chemicals shown in Table 2.1. Note that since vinyl chloride has been a commodity chemical for many years, these chemicals and the reactions involving them are well known. For newer substances, the design team often begins to carry out process synthesis as the data are emerging from the laboratory. The challenge, in these cases, is to guide the chemists away from those reaction paths that lead to processes that are costly to build and operate, and to arrive at designs as quickly as possible, in time to capture the market before a competitive process or chemical is developed by another company.

Returning to the manufacture of vinyl chloride, the principal reaction pathways are as follows.

1. ***Direct Chlorination of Ethylene***

$$C_2H_4 + Cl_2 \rightarrow C_2H_3Cl + HCl \qquad (2.1)$$

This reaction appears to be an attractive solution to design alternative 2. It occurs spontaneously at a few hundred degrees Celsius, but unfortunately does not give a high yield of vinyl chloride without simultaneously producing large amounts of byproducts such as dichloroethylene. Another disadvantage is that one of the two atoms of expensive chlorine is consumed to produce the byproduct hydrogen chloride, which may not be sold easily.

2. ***Hydrochlorination of Acetylene***

$$C_2H_2 + HCl \rightarrow C_2H_3Cl \qquad (2.2)$$

This exothermic reaction is a potential solution for the concept denoted as alternative 3. It provides a good conversion (98%) of acetylene to vinyl chloride at 150°C in the presence of mercuric chloride ($HgCl_2$) catalyst impregnated in activated carbon at atmospheric pressure. These are fairly moderate reaction conditions, and hence, this reaction deserves further study.

3. ***Thermal Cracking of Dichloroethane from Chlorination of Ethylene***

$$C_2H_4 + Cl_2 \rightarrow C_2H_4Cl_2 \qquad (2.3)$$

$$C_2H_4Cl_2 \rightarrow C_2H_3Cl + HCl \qquad (2.4)$$

$$C_2H_4 + Cl_2 \rightarrow C_2H_3Cl + HCl \quad \text{(overall)} \qquad (2.1)$$

The sum of reactions (2.3) and (2.4) is equal to reaction (2.1). This two-step reaction path has the advantage that the conversion of ethylene to 1,2-dichloroethane in exothermic reaction (2.3) is about 98% at 90°C and 1 atm with a Friedel–Crafts catalyst such as ferric chloride ($FeCl_3$). Then, the dichloroethane intermediate is converted to vinyl chloride by thermal cracking according to the endothermic reaction (2.4), which occurs spontaneously at 500°C and has conversions as high as 65%. The overall reaction presumes that the unreacted dichloroethane is recovered entirely from the vinyl chloride and hydrogen chloride and recycled. This reaction path has the advantage that it does not produce dichloroethylene in significant quantities, but it shares the disadvantage with reaction path 1 of producing HCl. It deserves further examination as a solution to design alternative 2.

4. ***Thermal Cracking of Dichloroethane from Oxychlorination of Ethylene***

$$C_2H_4 + 2HCl + \frac{1}{2}O_2 \rightarrow C_2H_4Cl_2 + H_2O \qquad (2.5)$$

$$C_2H_4Cl_2 \rightarrow C_2H_3Cl + HCl \qquad (2.4)$$

$$C_2H_4 + HCl + \frac{1}{2}O_2 \rightarrow C_2H_3Cl + H_2O$$

$$\text{(overall)} \qquad (2.6)$$

In reaction (2.5), which *oxychlorinates* ethylene to produce 1,2-dichloroethane, HCl is the source of chlorine. This highly exothermic reaction achieves a 95% conversion of ethylene to dichloroethane at 250°C in the presence of cupric chloride ($CuCl_2$) catalyst, and is an excellent candidate when the cost of HCl is low. As in reaction path 3, the dichloroethane is cracked to vinyl chloride in a pyrolysis step. This reaction path should be considered also as a solution for design alternative 3.

5. ***Balanced Process for Chlorination of Ethylene***

$$C_2H_4 + Cl_2 \rightarrow C_2H_4Cl_2 \qquad (2.3)$$

$$C_2H_4 + 2HCl + \frac{1}{2}O_2 \rightarrow C_2H_4Cl_2 + H_2O \qquad (2.5)$$

$$2C_2H_4Cl_2 \rightarrow 2C_2H_3Cl + 2HCl \qquad (2.4)$$

$$2C_2H_4 + Cl_2 + \frac{1}{2}O_2 \rightarrow 2C_2H_3Cl + H_2O$$

$$\text{(overall)} \qquad (2.7)$$

Table 2.2 Assumed Cost of Chemicals Purchased or Sold in Bulk Quantities

Chemical	Cost (cents/lb)
Ethylene	30
Acetylene	80
Chlorine	18
Vinyl chloride	35
Hydrogen chloride	25
Water	0
Oxygen (air)	0

This reaction path combines paths 3 and 4. It has the advantage of converting both atoms of the chlorine molecule to vinyl chloride. All of the HCl produced in the pyrolysis reaction is consumed in the oxychlorination reaction. Indeed, it is a fine candidate for the solution of design alternative 2.

Given this information, it seems clear that the design team would reject reaction path 1 on the basis of its low *selectivity* with respect to the competing reactions (not shown) that produce undesirable byproducts. This leaves the other reaction paths as potentially attractive to be screened on the basis of the chemical prices. Although it is too early to estimate the cost of the equipment and its operation before the remaining process operations are in place, the design team normally computes the *economic potential*, *EP* (i.e., the sales minus the cost of raw materials, not including the cost of utilities and operating costs) for each reaction path and uses it as a vehicle for screening out those that cannot be profitable. To illustrate this process for the production of vinyl chloride, Table 2.2 provides a representative set of prices for the principal chemicals, obtained from a source such as the ICIS Business Americas (formerly the *Chemical Marketing Reporter*), as discussed earlier.

The economic potential is computed by first converting to a mass basis, as illustrated for reaction path 3:

	C_2H_4	+ Cl_2	= C_2H_3Cl	+ HCl
lbmol	1	1	1	1
Molecular weight	28.05	70.91	62.50	36.46
lb	28.05	70.91	62.50	36.46
lb/lb of vinyl chloride	0.449	1.134	1	0.583
cents/lb	30	18	35	25

Then, the economic potential is $35(1) + 25(0.583) - 30(0.449) - 18(1.134) = 15.69$ cents/lb of vinyl chloride. Similar estimates are made for the overall reaction in each of the reaction paths, it being assumed that complete conversion can be achieved without any side reactions (not shown), with the results shown in Table 2.3.

Even without the capital costs (for construction of the plant, purchase of land, etc.) and the operating costs (for labor, steam, electricity, etc.), the economic potential for reaction path 2 is negative, whereas the economic potentials for the other reaction paths are positive. This is principally because acetylene is very expensive relative to ethylene. The fairly high price of HCl also contributes to the inevitable conclusion that vinyl chloride cannot be produced profitably using this reaction path. It should be noted that the price of HCl is often very sensitive to its availability in a petrochemical complex. In some situations, it may be available in large quantities as a byproduct from another process at very low cost. At a much lower price, reaction path 2 would have a positive economic potential, but would not be worthy of further consideration when compared with the three reaction paths involving ethylene. Turning to these paths, all have sufficiently positive economic potentials, and hence are worthy of further consideration. It is noted that the price of HCl strongly influences the economic potentials of reaction paths 3 and 4, with the economic potential of reaction path 5 midway between the two. Before proceeding with the synthesis, the design team would be advised to examine how the economic potentials vary with the price of HCl.

Table 2.3 Economic Potential for Production of Vinyl Chloride (Based on Chemical Prices in Table 2.2)

Reaction Path	Overall Reaction	Economic Potential (cents/lb of vinyl chloride)
2	$C_2H_2 + HCl = C_2H_3C1$	−16.00
3	$C_2H_4 + Cl_2 = C_2H_3Cl + HCl$	15.69
4	$C_2H_4 + HCl + \frac{1}{2}O_2 = C_2H_3C1 + H_2O$	6.96
5	$2C_2H_4 + Cl_2 + \frac{1}{2}O_2 = 2C_2H_3C1 + H_2O$	11.32

Figure 2.2 shows the first step toward creating a process flowsheet for reaction path 3. Each reaction operation is positioned with arrows representing its feed and product chemicals. The *sources* and *sinks* are not shown because they depend on the *distribution of chemicals*, the next step in process synthesis. The flow rates of the external sources and sinks are computed assuming that the ethylene and chlorine sources are converted completely to the vinyl chloride and hydrogen chloride sinks. Here, a key decision is necessary to set the scale of the process, that is, the production rate at capacity. In this case, a capacity of 100,000 lb/hr (~800 million lb/yr, assuming operation 330 days annually—an operating factor of 0.904) is dictated by the opportunity presented above. Given this flow rate for the product (principal sink for the process), the flow rates of the HCl sink and the raw-material sources can be computed by assuming that the raw materials are converted to the products according to the overall reaction. Any unreacted raw materials are separated from the reaction products and recycled. By material balance, the results in Figure 2.2 are obtained, where each flow rate in lbmol/hr is 1,600.

Similar flowsheets, containing the reaction operations for reaction paths 4 and 5, would be prepared to complete Step 1 of the synthesis. These are represented in the synthesis tree in Figure 2.7, which will be discussed after all of the synthesis steps have been completed. Note that their flowsheets are not included here due to space limitations, but are requested in Exercise 2.5 at the end of the chapter. As the next steps in the synthesis are completed for reaction path 3, keep in mind that they would be carried out for the other reaction paths as well. Note, also, that only the most promising flowsheets are developed in detail, usually by an expanded design team or, in some cases, by a competitive design team.

Step 2 Distribute the Chemicals: In Step 2, where possible, the sources and sinks for each of the chemical species in Figure 2.2 are matched so that the total mass flow into a reactor equals the total mass flow out. This often entails the introduction of mixing operations to eliminate differences in flow rates when a single sink is supplied by two or more sources. In other cases, a single source is divided among several sinks. To achieve the distribution of chemicals in Figure 2.3, the ethylene and chlorine sources are matched with their sinks into the chlorination reactor. It is assumed that ethylene and chlorine enter the reactor in the stoichiometric ratio of 1:1 as in reaction (2.3). Because the raw materials are in this ratio, no differences exist between the flow rates of the sources and sinks, and hence, no mixers are needed. Flow rates of 113,400 lb/hr of chlorine and 44,900 lb/hr of ethylene produce 158,300 lb/hr of dichloroethane. When it is desired to have an excess of one chemical in relation to the other so as to completely consume the other chemical, which may be toxic or very expensive (e.g., Cl_2), the other raw material (e.g., C_2H_4) is mixed with recycle and fed to the reactor in excess. For example, if the reactor effluent contains unreacted C_2H_4, it is separated from the dichloroethane product and recycled to the reaction operation. Note that the recycle is the source of the excess chemical, and the flow rate of the external source of C_2H_4 for a given production rate of dichloroethane is unaffected. This alternative distribution of chemicals is discussed further in Section 6.3 and illustrated in Figure 6.1. Returning to the distribution of chemicals in Figure 2.3, note that, at reactor conditions of 90°C and 1.5 atm, experimental data indicate that 98% of the ethylene is converted to dichloroethane, with the remainder converted to unwanted byproducts such as trichloroethane. This loss of yield of main product and small fraction of byproduct is neglected at this stage in the synthesis.

Next, the dichloroethane source from the chlorination operation is sent to its sink in the pyrolysis operation, which operates at 500°C. Here only 60% of the dichloroethane is converted to vinyl chloride with a byproduct of HCl, according to reaction (2.4). This conversion is within the 65% conversion claimed in the patent. To satisfy the overall material balance, 158,300 lb/hr of dichloroethane must produce 100,000 lb/hr of vinyl chloride and 58,300 lb/hr of HCl. But a 60% conversion produces only 60,000 lb/hr of vinyl chloride. The additional dichloroethane needed is computed by mass balance to equal $[(1 - 0.6)/0.6] \times 158{,}300$ or 105,500 lb/hr. Its source is a recycle stream from the separation of vinyl chloride from unreacted dichloroethane, from a mixing operation inserted to combine the two sources, to give a total of 263,800 lb/hr. The effluent stream from the pyrolysis operation is the source for the vinyl-chloride product, the HCl byproduct, and the dichloroethane recycle. To enable these chemicals to be supplied to their sinks, one or more separation operations are needed and are addressed in the next synthesis step.

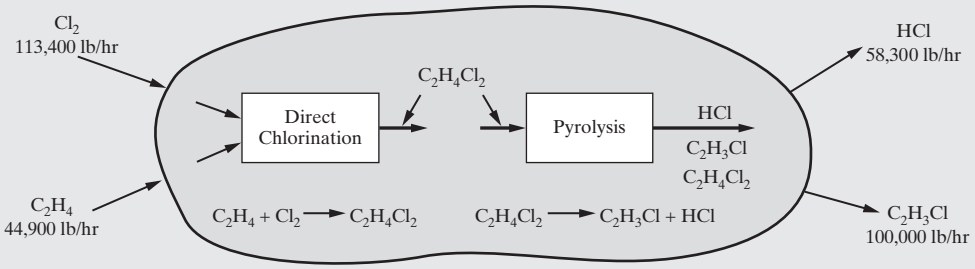

Figure 2.2 Reaction operations for the thermal cracking of dichloroethane from the chlorination of ethylene (reaction path 3)

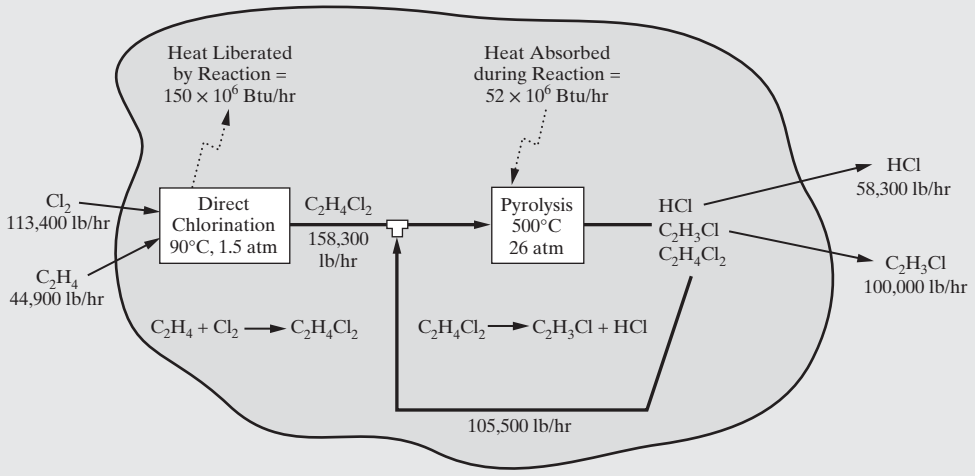

Figure 2.3 Flowsheet showing a distribution of chemicals for thermal cracking of dichloroethane from chlorination of ethylene (reaction path 3).

SUB-EXAMPLE 2.2.1 Pyrolysis Recycle Mass Balance

Assume that only 40% of the dichloroethane is converted to vinyl chloride in the pyrolysis operation. Estimate the recycle flow rate, assuming a perfect separation of dichloroethane from the pyrolysis effluent.

SOLUTION

Mass balance for dichloroethane:

$$(158{,}300 + R) \times 0.6 = R$$

Solving for R:

$$(1 - 0.6) \times R = 158{,}300 \times 0.6 = 94{,}980 \text{ lb/hr}$$

$$R = 94{,}980/0.4 = 237{,}450 \text{ lb/hr}$$

Figure 2.3 also shows the heats of reaction for the two reaction steps. These are computed at the temperatures and pressures of the reaction operations from heats of formation and heat capacities as a function of temperature. There are many sources of these data, especially the process simulators that are discussed in Chapter 7. When a simulator, such as ASPEN PLUS, is used, it is convenient to define each of the reaction operations and to perform an energy balance at reactor conditions. The simulators report the rate at which heat must be transferred to or from the reactor to achieve exit conditions from given inlet conditions or, if operated adiabatically, the exit conditions for no heat transfer, as discussed on the multimedia modules, which can be downloaded from the Wiley Web site associated with this book; follow the paths, *ASPEN → Chemical Reactors and HYSYS → Chemical Reactors*. For reaction path 3, the chlorination operation provides a large source of energy, 150 million Btu/hr, but at a low temperature, 90°C, whereas the pyrolysis operation requires much less energy, 52 million Btu/hr, at an elevated temperature, 500°C. Since this heat source cannot be used to provide the energy for pyrolysis, other uses for this energy should be sought as the synthesis proceeds. These and other sources and sinks for energy are considered during task integration in Step 5.

As for the pressure levels in the reaction operations, 1.5 atm is selected for the chlorination reaction to prevent the leakage of air into the reactor to be installed in the task-integration step. At atmospheric pressure, air might leak into the reactor and build up in sufficiently large concentrations to exceed the flammability limit. For the pyrolysis operation, 26 atm is recommended by the B.F. Goodrich patent (1963) without any justification. Since the reaction is irreversible, the elevated pressure does not adversely affect the conversion. Most likely, the patent recommends this pressure to increase the rate of reaction and, thus, reduce the size of the pyrolysis furnace, although the tube walls must be thick and many precautions are necessary for operation at elevated pressures. The pressure level is also an important consideration in selecting the separation operations, as will be discussed in the next synthesis step.

Referring to Figure 2.7, at the "Distributions of Chemicals" level, two branches have been added to the synthesis tree to represent the two distributions in connection with reaction path 3. Each of these branches represents a different partially completed flowsheet, that is, Figures 2.3 and 6.1. Other distributions arise in connection with reaction paths 4 and 5. These are represented using dashed lines in the synthesis tree.

Step 3 Eliminate Differences in Composition: As mentioned earlier, for each distribution of chemicals, the needs for separation become obvious. In Figure 2.3, for example, it is clear that the pure effluent from the chlorination reaction operation needs no separation, but the effluent from the pyrolysis operation is a mixture that needs to be separated into nearly pure species. Here, the source of the three species in the effluent is at a composition far different from the compositions of the three sinks: vinyl-chloride product, HCl byproduct, and the dichloroethane for recycle. To eliminate these composition differences, one or more separation operations are needed.

One possibility is shown in Figure 2.4, in which two distillation towers in series are inserted into the flowsheet. Distillation is possible because of the large volatility differences among the three species. This can be seen by examining

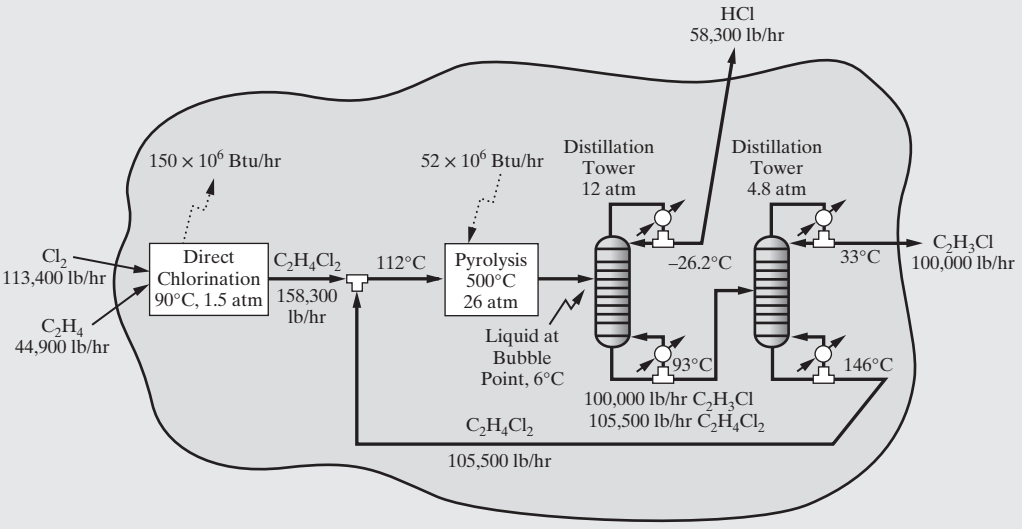

Figure 2.4 Flowsheet including the separation operations for the vinyl-chloride process.

Table 2.4 Boiling Points and Critical Constants

Chemical	Normal Boiling Point (1 atm, °C)	Boiling Point (°C) 4.8 atm	12 atm	26 atm	Critical Constants T_c(°C)	P_c(atm)
HCl	–84.8	–51.7	–26.2	0	51.4	82.1
C_2H_3Cl	−13.8	33.1	70.5	110	159	56
$C_2H_4Cl_2$	83.7	146	193	242	250	50

the boiling points in Table 2.4, which can be obtained from vapor pressure data in the preliminary database, or from a process simulator. In the first column, HCl is separated from the two organic chemicals. In the second column, vinyl chloride is separated from dichloroethane. At 1 atm, the boiling point of HCl is very low, −84.8°C, and hence if HCl were recovered at 1 atm as the distillate of the first tower, very costly refrigeration would be necessary to condense the reflux stream. At 26 atm (the pyrolysis reaction pressure), HCl boils at 0°C, and much less costly refrigeration could be used. The B.F. Goodrich patent recommends operation at 12 atm without any justification. At this pressure, HCl boils at –26.2°C and the bottoms product, comprised of vinyl chloride and dichloroethane with trace quantities of HCl, has a bubble point of 93°C, which can be calculated by a process simulator. The bottoms product at this reduced temperature and pressure is farther away from the critical points of vinyl chloride–dichloroethane mixtures at the bottom of the distillation column. It is likely, therefore, that B.F. Goodrich selected this lower pressure to avoid operation in the critical region where the vapor and liquid phases approach each other and are much more difficult to disengage (i.e., have small flooding velocities and require very large diameters and tray spacings). Furthermore, low-pressure steam is adequate for the reboiler. When this distillation tower is inserted into the flowsheet, the conditions of its feed stream, or sink, need to be identified. If the feed is a saturated liquid, the temperature is 6°C at 12 atm, with a mild refrigerant required for cooling. A preferable feed temperature would be 35°C or higher, which could be achieved by completing the cooling and partial condensation of the pyrolysis reactor effluent with cooling water, but the introduction of vapor into the column would increase the refrigeration load of the condenser at −26.2°C. Upon making this specification, key differences (temperature, pressure, and phase) appear between the effluent from the pyrolysis operation and the feed to the distillation column. These are eliminated in the next synthesis step by inserting temperature and pressure change operations, with each temperature specification leading to a somewhat different flowsheet.

After the first distillation operation is inserted into the flowsheet, the second follows naturally. The bottoms from the HCl-removal tower is separated into nearly pure species in the second tower, which is specified at 4.8 atm, as recommended by the B.F. Goodrich patent. Under these conditions, the distillate (nearly pure vinyl chloride) boils at 33°C and can be condensed with inexpensive cooling water, which is available at 25°C. The bottoms product boils at 146°C, and hence, the vapor boilup can be generated with medium-pressure steam, which is widely available in petrochemical complexes.

Note that bubble- and dew-point calculations, and phase equilibrium calculations, are discussed in Chapter 7; flooding velocities and the sizing of separation towers are discussed in Chapter 13. In summary, key decisions regarding the phases of streams (normally approximated at equilibrium) depend on the stream composition, temperature, and pressure. Iterative phase equilibrium calculations are needed to estimate bubble- and dew-point temperatures and pressures. These are normally carried out within the process simulators, even when positioning operations during process synthesis. But, in this textbook, the details of setting the stream conditions are discussed in Process Simulation Task-2 of Section 7.3 on process simulation.

Alternative separation operations can be inserted into Figure 2.3. When distillation is used, it is also possible to recover the least volatile species, dichloroethane, from the first column, and separate HCl from vinyl chloride in the second column. Yet another possibility is to use a single column with a side stream that is concentrated in the vinyl-chloride product. Absorption with water, at atmospheric pressure, can be used to remove HCl. The resulting vapor stream, containing vinyl chloride and dichloroethane, could be dried by adsorption and separated using distillation. With so many alternatives possible, the process designer needs time or help to select the most promising separation operations. As mentioned previously, this topic is considered in detail in Chapter 9.

Furthermore, as before, the synthesis tree in Figure 2.7 is augmented. In this case, the new branches represent the different flowsheets for the alternative separation operations. Clearly, as each step of the synthesis is completed, the tree represents many more possible flowsheets.

Step 4 Eliminate Differences in Temperature, Pressure, and Phase: When the reaction and separation operations are positioned, the states of their feed and product streams are selected. This is accomplished usually by adjusting the temperature and pressure levels to achieve the desired reaction conversions and separation factors. Subsequently, after the flowsheets have been created, these are often adjusted toward the economic optimum, often using the optimizers in the process simulators discussed in Chapter 21. In this synthesis step, however, the states are assumed to be fixed and operations are inserted to eliminate the temperature, pressure, and phase differences between the feed sources, the product sinks, and the reaction and separation operations.

Figure 2.5 shows one possible flowsheet. It can be seen that liquid dichloroethane from the recycle mixer at 112°C and 1.5 atm undergoes the following operations:

1. Its pressure is increased to 26 atm.
2. Its temperature is raised to the boiling point, which is 242°C at 26 atm.
3. Dichloroethane liquid is vaporized at 242°C.
4. Its temperature is raised to the pyrolysis temperature, 500°C.

Note that an alternative flowsheet would place operations 1 and 2 after operation 3. However, this is very uneconomical, as the cost of compressing a vapor is far greater than the cost of pumping a liquid because the molar volume of a vapor is so much greater than that of a liquid (typically, a factor

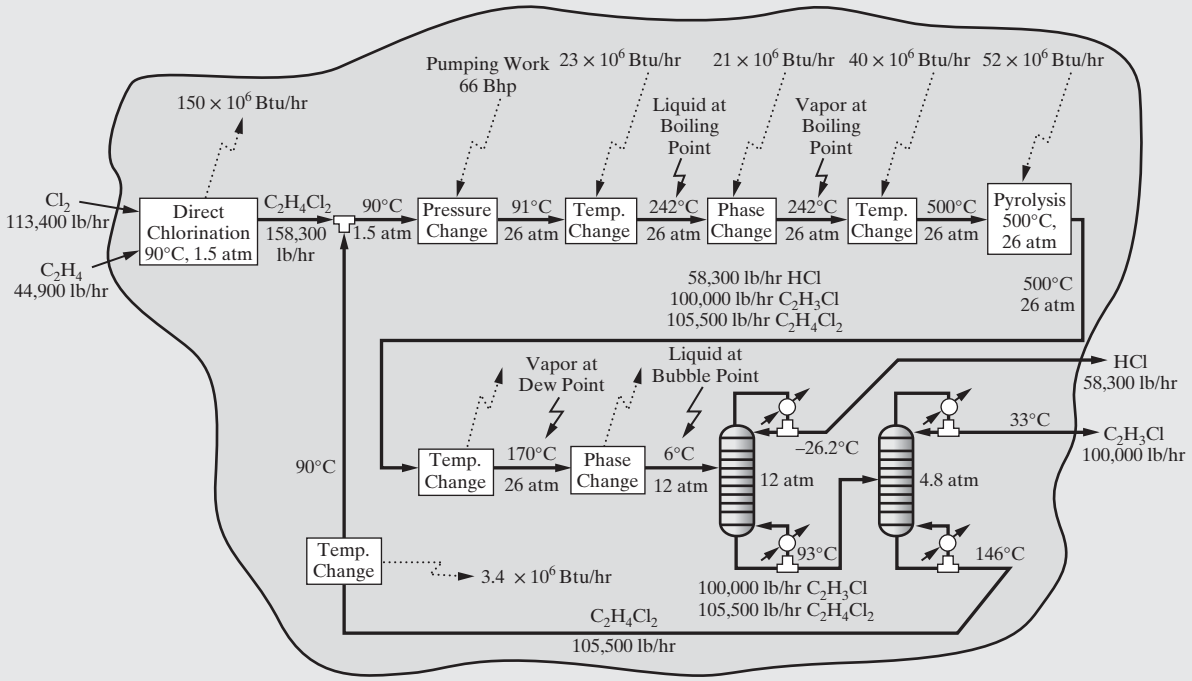

Figure 2.5 Flowsheet with temperature-, pressure-, and phase-change operations in the vinyl-chloride process.

of 100 times greater). For a more complete discussion of this observation, which is just one of many design heuristics or rules of thumb, see Section 6.7.

In addition, the hot vapor effluent from the pyrolysis operation (at 500°C and 26 atm) is operated upon as follows:

1. Its temperature is lowered to its dew point, 170°C at 26 atm.
2. The vapor mixture is condensed to a liquid at its bubble point, 6°C at 12 atm, by lowering the pressure and cooling and removing the latent heat of condensation.

Finally, the dichloroethane recycle stream is cooled to 90°C to avoid vaporization when mixed with the reactor effluent at 1.5 atm.

When positioning these operations, calculations to determine their heat duties and power loads are often carried out using process simulators. Methods for carrying out these energy balances are discussed in Process Simulation Task 3 of Section 7.3 on process simulators.

Branches to represent the two new flowsheets are added to the synthesis tree in Figure 2.7 after this synthesis step has been completed.

Step 5 Task Integration: At the completion of Step 4, each of the candidate flowsheets has a complete set of operations that eliminates the differences between the raw materials and the products. Still, with the exception of the distillation operations, specific equipment items are not shown. The selection of the processing units, often referred to as unit operations, in which one or more of the basic operations are carried out, is known as *task integration*. To assist in this selection, the reader is referred to *Chemical Process Equipment* (Walas, 1988).

Figure 2.6 shows one example of task integration for the vinyl-chloride process. At this stage in process synthesis, it is common to make the most obvious combinations of operations, leaving many possibilities to be considered when the flowsheet is sufficiently promising to undertake the preparation of a base-case design. As you examine this flowsheet, with the descriptions of the process units that follow, see if you can suggest improvements. This is one of the objectives in Exercise 2.3. Throughout the chapters that follow, techniques are introduced to obtain better integration for this and other processes that manufacture many other chemicals.

1. ***Chlorination reactor and condenser.*** The direct chlorination operation in Figure 2.5 is replaced by a cylindrical reaction vessel, containing a rectifying section, and a condenser. A pool of liquid dichloroethane, with ferric chloride catalyst dissolved, fills the bottom of the vessel at 90°C and 1.5 atm. Ethylene is obtained commonly from large cylindrical vessels, where it is stored as a gas at an elevated pressure and room temperature, typically 1,000 psia and 70°F. Chlorine, which is stored commonly in the liquid phase, typically at 150 psia and 70°F, is evaporated carefully to remove the viscous liquid (taffy) that contaminates most chlorine produced by electrolysis. Chlorine and ethylene in the vapor phase bubble through the liquid and release the heat of reaction as dichloroethane is produced. This heat causes the dichloroethane to vaporize and rise up the rectifying section into the condenser, where it is condensed with cooling water. Note that heat is needed to drive the reboiler in the first distillation column at 93°C, but the heat of reaction cannot be used for this purpose unless the temperature levels are adjusted. How can this be accomplished?

   Most of the condensate is mixed with the effluent from the recycle cooler to be processed in the pyrolysis loop. However, a portion is refluxed to the rectifying section of the column, which has several trays, to recover any of the less volatile species (e.g., trichloroethane) that may have vaporized. These *heavies* accumulate at the bottom of the liquid pool and are removed periodically as impurities.

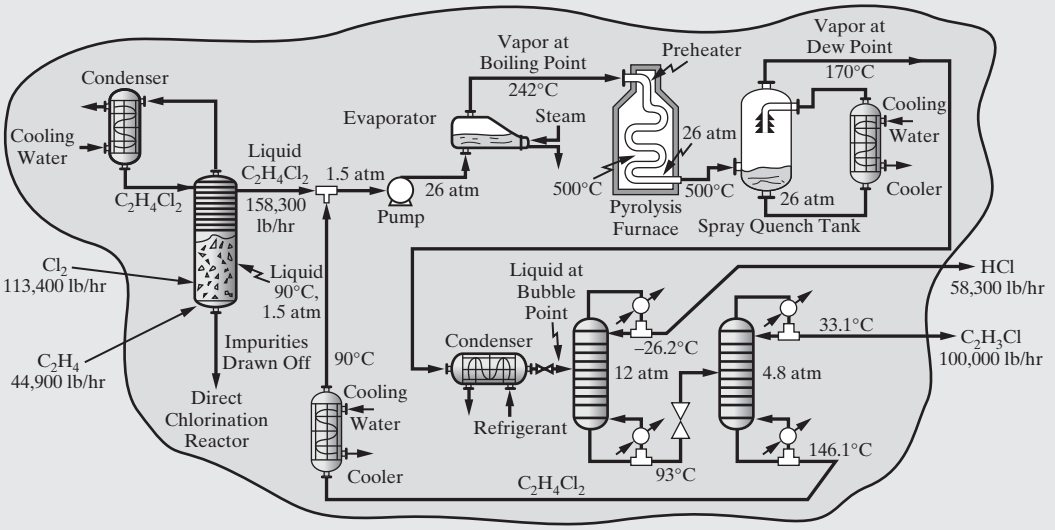

Figure 2.6 Flowsheet showing task integration for the vinyl-chloride process.

2. ***Pump.*** Since the pressure-change operation involves a liquid, it is accomplished by a pump, which requires only 66 Bhp, assuming an 80% efficiency. The enthalpy change in the pump is very small and the temperature does not change by more than 1°C.
3. ***Evaporator.*** This unit, in the form of a large kettle, with a tube bundle inserted across the bottom, performs the temperature- and phase-change operations. Saturated steam that passes through the tubes condenses as the dichloroethane liquid is heated to its boiling point and vaporized. The large vapor space is provided to enable liquid droplets, entrained in the vapor, to coalesce and drop back into the liquid pool, that is, to disengage from the vapor that proceeds to the pyrolysis furnace.
4. ***Pyrolysis furnace.*** This unit also performs two operations: It preheats the vapor to its reaction temperature, 500°C, and it carries out the pyrolysis reaction. The unit is constructed of refractory brick, with natural gas-fired heaters, and a large bundle of Nickel, Monel, or Inconel tubes, within which the reaction occurs. The tube bundle enters the coolest part of the furnace, the so-called *economizer* at the top, where the preheating occurs.
5. ***Spray quench tank and cooler.*** The quench tank is designed to rapidly quench the pyrolysis effluent to avoid carbon deposition in a heat exchanger. Cold liquid (principally dichloroethane) is showered over the hot gases, cooling them to their dew point, 170°C. As the gases cool, heat is transferred to the liquid and removed in the adjacent cooler. The warm liquid from the pool at the base of the quench vessel is circulated to the cooler, where it is contacted with cooling water. Any carbon that deposits in the quench vessel settles to the bottom and is bled off periodically. Unfortunately, this carbon deposition, as well as the corrosive HCl, is anticipated to prevent the use of the hot effluent gases in the tubes of the evaporator, which would have to be serviced often to remove carbon and replace corroded tubes. Note that coke formation in the pyrolysis products is discussed by Borsa et al. (2001). Consequently, large amounts of heat are transferred to cooling water, and the fuel requirements for the process are high. As noted later in the section on Checking the Key Assumptions in Process Synthesis, the design team is likely to measure the rate of carbon deposition and, if it is not very high, may decide to implement a design with a feed/product heat exchanger.
6. ***Condenser.*** To produce a saturated liquid at 6°C, the phase-change operation is carried out by a condenser that transfers heat to a mild refrigerant. Then the pressure is lowered to 12 atm across a valve.
7. ***Recycle cooler.*** To prevent vapor from entering the pump when the recycle stream is mixed with effluent from the direct chlorination reactor, the recycle stream is cooled to 90°C (below the boiling point of dichloroethane at 1.5 atm) using cooling water.

This completes the task integration in Figure 2.6. Can you suggest ways to reduce the need for fuel and hot utilities such as steam?

Synthesis Tree

Throughout the synthesis of the vinyl-chloride process, branches have been added to the synthesis tree in Figure 2.7 to represent the alternative flowsheets being considered. The bold branches trace the development of just one flowsheet as it evolves in Figures 2.1–2.6. Clearly, there are many alternative flowsheets, and the challenge in process synthesis is to find ways to eliminate whole sections of the tree without doing much analysis. By eliminating reaction paths 1 and 2, as much as 40% of the tree is eliminated in the first synthesis step. Similar screening techniques are applied by the design team in every step, as discussed throughout this book.

To satisfy the objective of generating the most promising flowsheets, care must be taken to include sufficient analysis in each synthesis step to check that each step does not lead to a less profitable flowsheet or exclude the most profitable flowsheet prematurely. For this reason, it is common practice in industry to mix these synthesis steps with analysis using the simulators introduced in Chapter 7.

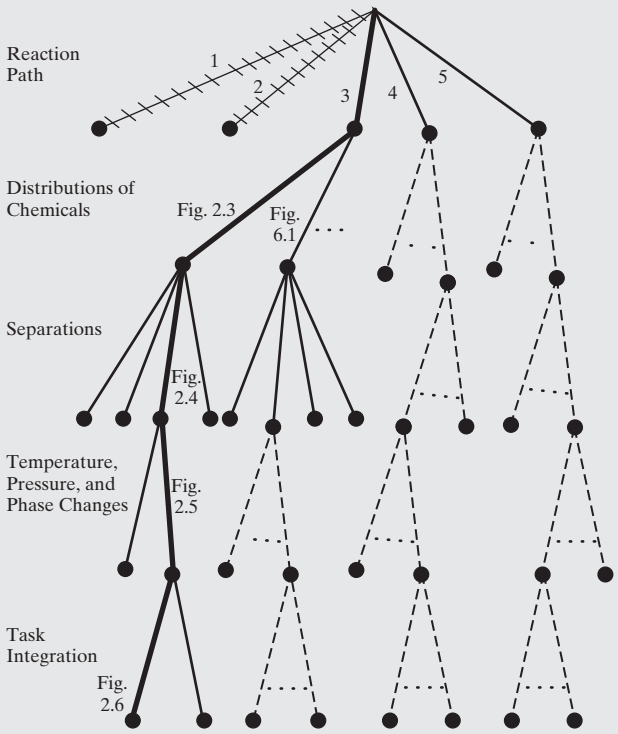

Figure 2.7 Inverted synthesis tree for the production of vinyl chloride. [Branch figure numbers must be 2.3, 2.4, 2.5, 2.6, 6.1.]

Heuristics

It is important to keep in mind that, when carrying out the steps in preliminary process synthesis, the resulting synthesis tree is closely related to any heuristics or rules of thumb used by the design team. In the vinyl-chloride example, emphasis was placed on the synthesis steps, not on the use of heuristics by the design team. An exception is the heuristic that it is cheaper to pump a liquid than compress a gas. Heuristics are covered more thoroughly in Chapter 6, where it will become clear that the synthesis tree can be improved significantly. See also *Conceptual Design of Chemical Processes* (Douglas, 1988) and Walas (1988), where many heuristics are presented.

Checking the Key Assumptions in Process Synthesis

After several promising flowsheets are synthesized, often the key assumptions are revisited before proceeding to the next steps in process design. Returning to Figure 2.6, one promising flowsheet for the vinyl-chloride process, a key limitation is that the cold $C_2H_4Cl_2$ stream is not heated by the pyrolysis products because the rate of carbon deposition in such a feed/product heat exchanger is anticipated to be high, and would cause the heat exchanger to foul with carbon. Instead, large quantities of heating utility (steam) are needed to vaporize the $C_2H_4Cl_2$ stream, and large quantities of cooling water utility are needed to cool the hot pyrolysis products. Before adopting this design, which uses excessive amounts of steam and cooling water, it becomes important to learn more about the rate of carbon deposition. Perhaps the rate is sufficiently low to allow the installation of a feed/product heat exchanger in which the carbon buildup is sufficiently low to require infrequent maintenance for carbon removal. Even at higher rates, to remove carbon deposits periodically, two heat exchangers could be installed in parallel, one of which would be operated while the other is being cleaned. This would provide substantial savings in steam and cooling-water utilities.

To check this and other assumptions, it is often desirable to construct a pilot plant that can produce quantities of product suitable for testing and evaluation by potential customers. Very few processes that include reaction steps are constructed without some form of pilot-plant testing prior to doing detailed design calculations. This is an expensive, time-consuming step that needs to be anticipated and planned for by the design team as early as possible, so as to avoid excessive delays. Also, for the vinyl-chloride process, kinetic data are needed for both the chlorination and pyrolysis reactors, as well as to determine the rate of carbon deposition. In all three cases, it is unlikely that adequate data can be located in the open literature. Consequently, unless sufficient data exist in company files or were taken in the laboratory and judged to be adequate, pilot-plant testing is needed. Generally, pilot-plant tests are conducted by a development team working closely with the design team.

Also, process simulators are often used during process synthesis, but Chapter 7 is entirely devoted to this subject.

Noncommodity Chemicals

For the manufacture of pharmaceuticals, specialty chemicals and materials, electronic materials, and foods, product throughputs are usually small leading to the design of batch, rather than continuous, processes. Example 2.3 discusses the process synthesis of such a batch process.

EXAMPLE 2.3 ***Manufacture of Tissue Plasminogen Activator (tPA)***

In the manufacture of pharmaceuticals, consider the possible production of plasminogen activators, which are powerful enzymes that trigger the proteolytic (breaking down of proteins to form simpler substances) degradation of blood clots that cause strokes and heart attacks. Since the mid-1980s, Genentech, a U.S. company, has manufactured tissue plasminogen activator (tPA), which they sold for $2,000 per 100-mg dose in the early 2000s, with annual sales of $300 MM/yr (MM in American engineering units is thousand-thousand, or 1 million). Given that their patent was set to expire in 2003, Genentech developed a next-generation, Food and Drug Administration (FDA)-approved, plasminogen activator called TNK-tPA, which is easier and safer for clinicians to use. With a rapidly growing market, the question arose as to whether an opportunity existed for another company to manufacture a generic (i.e., without a brand name) form of tPA that could compete favorably with TNK-tPA.

To examine this possibility, a design team was formulated.

It identified two potential alternatives:

Alternative 1. While a generic form of tPA may not compete well against TNK-tPA in the United States, it may be possible to market a low-cost generic tPA in foreign markets, where urokinase and streptokinase are low-cost alternatives, which sell for only $200/dose, but are associated with increased bleeding risks. Market analysis suggests that a maximum production rate of 80 kg/yr would be appropriate over the next five years.

Alternative 2. Given the possibility that lower health care reimbursements are received by hospitals in the United States, it may be reasonable to develop a similar process that competes favorably with TNK-tPA in the United States.

Other promising alternatives were likely to arise, often initiated by successes in a research laboratory.

Tissue plasminogen activator (tPA) is a recombinant therapeutic protein comprised of 562 amino acids, as shown schematically in Figure 2.8. Note that tPA is produced using a recombinant cell, which results from a recombination of genes. To eliminate blood clots, tPA activates plasminogen to plasmin, an enzyme, which dissolves fibrin formations that hold blood clots in place. In this way, blood flow is reestablished once the clot blockage dissolves, an important effect for patients suffering from a heart attack (microcardial infarction) or stroke. This example shows the steps in synthesizing a process to address the challenges posed by the opportunity suggested in alternative 1: that is, to manufacture less expensive forms of tPA that can be sold for $200 per 100-mg dose. Note that it leads to a batch process involving many small process units that must be scheduled for the manufacture of tPA, rather than a large-scale continuous process as for the manufacture of vinyl chloride.

Stated differently, based upon extensive research in the biochemistry laboratory, the tPA gene was isolated from human melanoma cells, and the process synthesis problem in Figure 2.9 created. As shown, tPA is produced using mammalian [e.g., Chinese hamster ovary (CHO)] cells that have tPA-DNA as part of their genetic contents (genome). In an aerobic bioreaction operation, the tPA-CHO cells grow in a nutrient media, HyQ PF-CHO—Hyclone media, a blend of nutrients, salts (including $NaHCO_3$), amino acids, insulin, growth factors, and transferrin, specifically for growth of CHO cells. Other ingredients include sterilized water, air, and CO_2. In addition to tPA, endotoxins may be a contaminant of the product, which must be removed because they elicit a variety of inflammatory responses in animals. Other byproducts include cell debris, wastewater, and gas emissions, especially N_2 from air, unconsumed O_2 from air, and CO_2, which regulates the pH. An important source of data, in addition to that taken in the biochemistry laboratory, is a U.S. patent, filed by Genentech (Goeddel et al., 1988), which provides considerable qualitative and quantitative information. See also the design report by Audette et al. (2000).

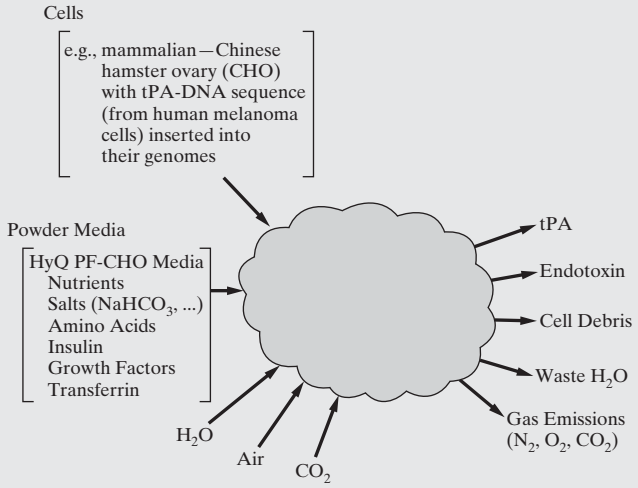

Figure 2.9 Process synthesis problem.

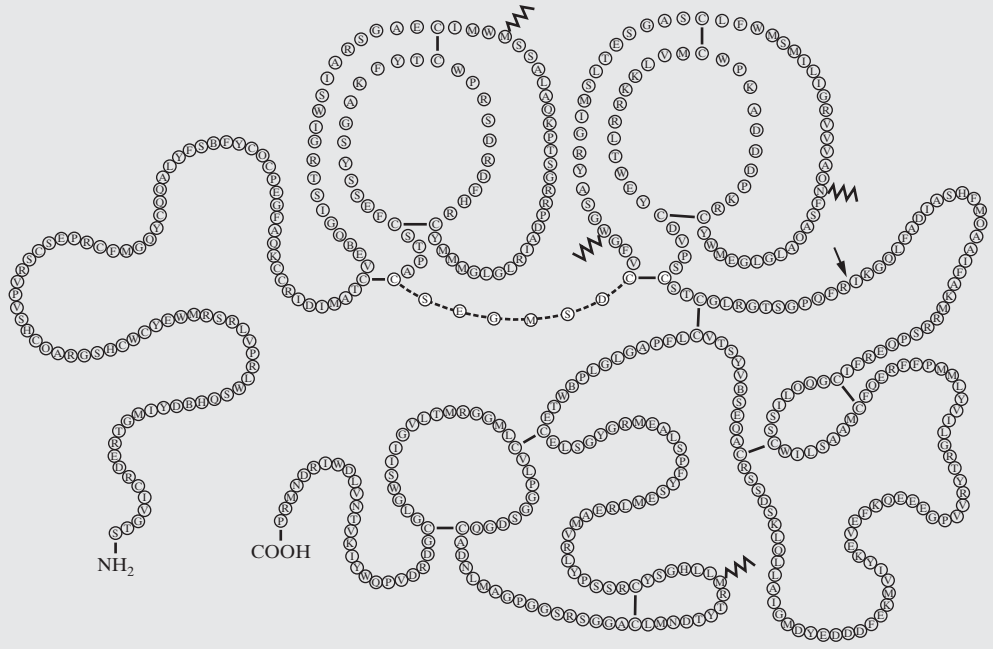

Figure 2.8 Schematic of tissue plasminogen activator (tPA).

Step 1 Eliminate Differences in Molecular Type: In the manufacture of a macromolecule like tPA through cell growth, a complex array of chemical reactions is often approximated by global reactions that are understood far less than the well-defined reactions for the manufacture of a simple monomer, like vinyl chloride. In terms of global reactions to manufacture tPA, two principal reaction paths are provided by the biochemist, as follows.

1. ***Mammalian Cells.*** Into CHO cells, the tPA-DNA sequence must be inserted and expressed. The resulting tPA-CHO cells are specially selected CHO cells with many copies of tPA-DNA inserted into their genomes, and which secrete high levels of tPA. This tPA-DNA insertion step is summarized in the reaction:

$$\begin{aligned}\text{tPA} - \text{DNA sequence} + \text{CHO cells}\\ \rightarrow \text{selected high-expressing tPA}\\ - \text{CHO cells}\end{aligned} \tag{2.8}$$

The product of this "catalyst preparation" is a master stock of tPA-CHO cells, which are prepared in the laboratory and stored in 1-mL aliquots at –70°C to be used as inoculum for the bioreaction:

$$\begin{aligned}\text{tPA} - \text{CHO cells} + \text{HyQPF} - \text{CHO media}\\ + \text{O}_2 \rightarrow \text{Increased cell numbers}\end{aligned} \tag{2.9}$$

As the cells grow in this aerobic cultivation at a rate of 0.39×10^6 cell/(ml-day), oxygen from air is consumed at the rate of 0.2×10^{-12} mol O_2/(cell-hr), and tPA is produced at the rate of 50 picogram tPA/(cell-day). The latter is secreted gradually into the liquid media solution. Note that reaction (2.8) is carried out once during the research and development phase. Initially, 1–10 mg of tPA-DNA are added to 10^6 cells to produce a few tPA-CHO cells in many unmodified CHO cells. After careful selection, one tPA-CHO cell (the "founder" cell) is selected and amplified to yield about 2×10^6 cells/mL in 10–100 L. These cells are frozen in aliquots.

2. ***Bacterial Cells.*** A promising alternative is to insert the tPA-DNA sequence into the genome of *Escherichia coli (E. coli)* cells, as summarized by the reaction:

$$\begin{aligned}\text{tPA} - \text{DNA sequence} + \textit{E.coli}\ \text{cells}\\ \rightarrow \text{selected high} - \text{expressing tPA}\\ - \textit{E. coli}\ \text{cells}\end{aligned} \tag{2.10}$$

Then, the tPA-*E. coli* bacteria cells, which are grown in the laboratory, are frozen in aliquols at –70°C to be used as inoculum for the fermentation reaction:

$$\begin{aligned}\text{tPA} - \textit{E. coli}\ \text{cells} + \text{powder media}\\ + \text{O}_2 \rightarrow \text{increased cell numbers}\end{aligned} \tag{2.11}$$

A batch fermentation of tPA–*E. coli* can produce 5–50 mg tPA/L-broth at harvest. *Escherichia coli* may require disruption to release tPA, which is then more difficult to separate. Should a process be synthesized based upon this reaction path, reaction rate data from the laboratory will be needed. Unlike CHO cells, *E. coli* cells do not add sugar groups (glycosylation) to tPA. Like CHO cells, tPA-*E. coli* cells are produced and frozen during the research and development phase.

Returning to the reaction path with CHO cells, using laboratory data, the reaction operation is inserted onto the flowsheet, as shown in Figure 2.10. At a production rate of 80 kg/yr of tPA, the lab reports that the following ingredients are consumed and waste products are produced:

Ingredients	kg/yr	Wastes	kg/yr
tPA-CHO cells	Small	Endotoxin	0.155
HyQ PF-CHO media	22,975	Cell debris	22,895
Water	178,250	Wastewater	178,250
Air	1,604	Gas emissions (N_2, O_2, CO_2)	4,036
CO_2	296		

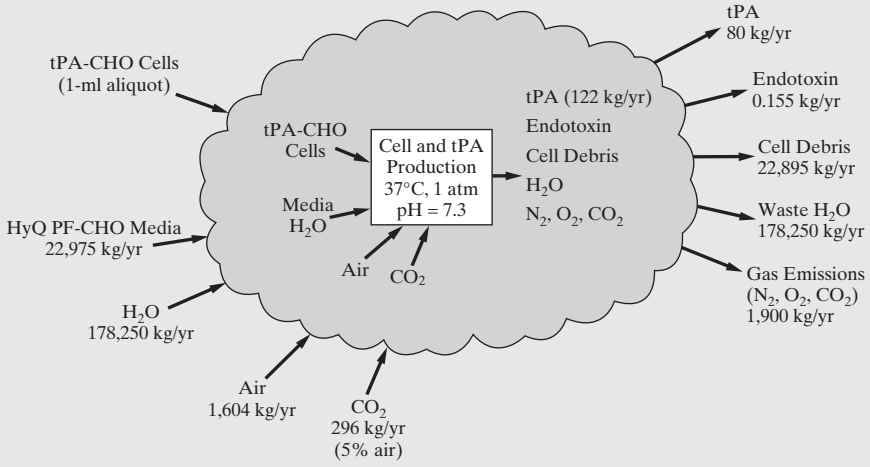

Figure 2.10 Reaction operations using mammalian CHO cells.

Table 2.5 Assumed Cost of Chemicals Produced or Sold

Chemical	kg/kg tPA	Cost ($/kg)
tPA	1	2,000,000
HyQ PF-CHO powder media	287.2	233
Water for injection (WFI)	2,228	0.12
Air	20.1	1,742
CO_2	3.7	1,447
tPA-CHO cells	—	a

[a]Not included in economic potential estimate—related to cost of research, an operating cost.

The reaction operation provides sinks for tPA-CHO cells from cold storage at –70°C, and HyQ PF-CHO media in water, air, and carbon dioxide. Its effluent is a source of tPA, at 122 kg/yr, endotoxin, cell debris, water, nitrogen, and carbon dioxide. When separated, these species are the sources for the product sinks from the flowsheet. Note that the combined cell growth and tPA production operation takes place at 37°C, 1 atm, and pH = 7.3. The latter is achieved by the $NaHCO_3$ in the powder media, with fine-tuning by manipulation of the flow rate of CO_2.

Before accepting a potential reaction path, it is important to examine the economic potential, that is, the difference between the sales revenues and the cost of ingredients. To accomplish this, the sales price of tPA is projected (e.g., $200 per 100-mg dose), and the costs of ingredients are projected, with estimates often obtained from the suppliers. A typical list of cost estimates is shown in Table 2.5. The cost of water for injection (WFI) is based upon estimates of the cost of sterilizing municipal water (12 cents/kg = 45 cents/gal = 450/1,000 gal, which is far higher than the typical cost of process water = $0.80/1,000 gal). The costs of sterilized air and carbon dioxide are for industrial cylinders of compressed gases. The cost of the tPA-CHO cells is not included, as it is associated with the cost of research, which is subsequently estimated as an operating cost.

Using these costs, the economic potential, *EP,* is estimated:

$$\begin{aligned} EP &= 2{,}000{,}000 - 287.2 \times 233 \\ &\quad - 2.228 \times 0.12 - 3.7 \times 1{,}447 \\ &\quad - 201.1 \times 1{,}742 \\ &= \$1{,}892{,}000/\text{kgtPA} \end{aligned}$$

Clearly, this is very high for tPA, a typical pharmaceutical. However, the economic potential does not account for the operating costs, which include the cost of research, the cost of utilities, and the investment cost, and are high for separations that involve expensive mass separating agents. With such a promising economic potential, the process synthesis proceeds at an accelerated pace.

Step 2 Distribute the Chemicals: In this step, the sources and sinks for each species in Figure 2.10 are matched so that the total mass flow rate into the reaction operation equals the mass flow rate out. This often entails the introduction of mixing operations, as illustrated in the previous example for vinyl chloride.

In this case, only one mixing operation is introduced, in which the HyQ PF-CHO powder media is mixed with water, as shown in Figure 2.11. Otherwise, the sources and sinks are matched directly. However, the effluent from the cell growth, tPA production reactor must be separated before its species are matched with the product sinks.

Step 3 Eliminate Differences in Composition: For most distributions of chemicals, composition differences exist between streams to be separated and the sinks to which these species are sent. Clearly, in Figure 2.11, the effluent from the cell growth, tPA production reactor must be separated.

Many separation system possibilities exist, with one provided in Figure 2.12. Here, the reactor effluent is sent to a separator for recovery of the gas emissions from the liquid mixture, with the latter sent to a centrifuge to remove wet cell debris from the harvest media or clarified broth. Note that because proteins lose their activity at temperatures above ~0°C, the centrifuge, and all other separation operations, are operated at

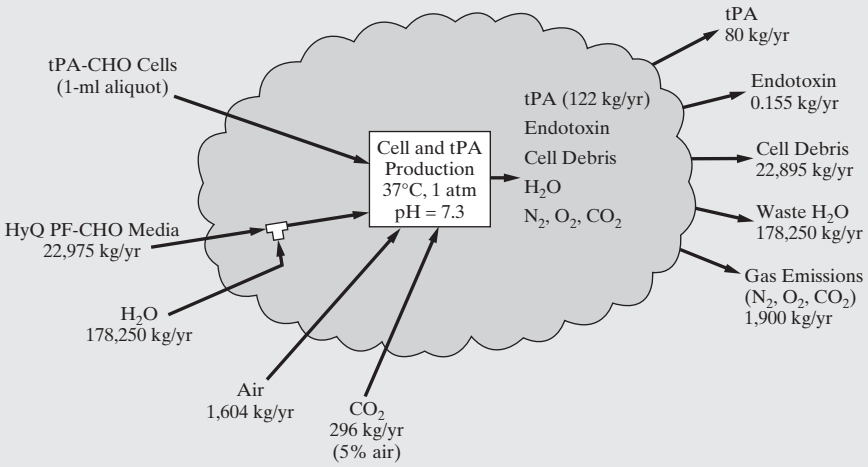

Figure 2.11 Flowsheet showing a distribution of chemicals for the tPA process.

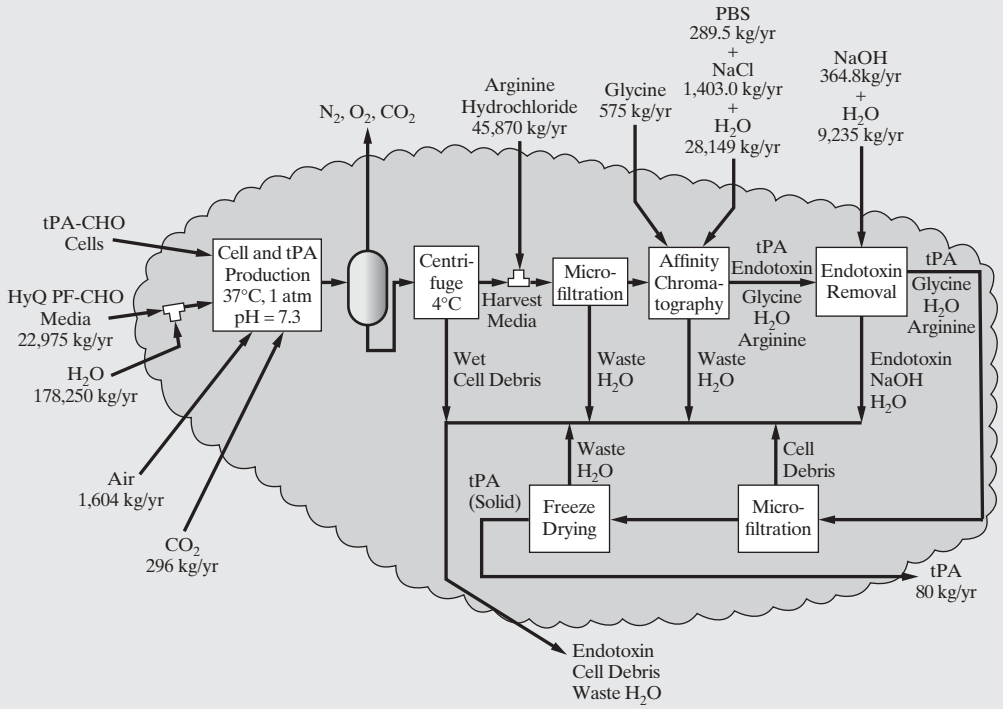

Figure 2.12 Flowsheet including the separation operations for the tPA process.

4°C, slightly above the freezing point of water. The harvest medium is mixed with arginine hydrochloride, an amino acid:

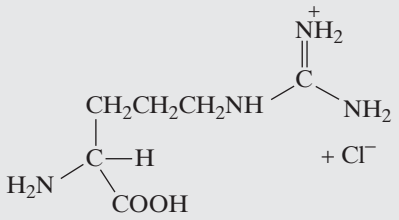

which prevents tPA from self-aggregating. Note that 45,870 kg/yr provides a concentration of 2.0 molar, which is sufficient to prevent aggregation.

The resulting mixture is sent to microfilters to remove large quantities of wastewater, which passes through the filters. For this step, alternate separators, like gel filtration and an Acticlean Etox resin (by Sterogene), should be considered. The retentate from the filter, which contains tPA, other proteins, endotoxin, arginine hydrochloride, and some water, is sent to an affinity chromatography operation. Here, tPA is selectively adsorbed on a resin (e.g., CNBr-activated Sepharose, by Amersham Biotech). The resin is then eluted with glycine, an amino acetic acid:

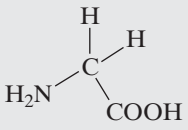

From lab measurements, 575 kg/yr of glycine are sufficient for the elution process. After the column is eluted, it is equilibrated with a mixture of 289.5 kg/yr of phosphate buffer solution (PBS) and 1,403.0 kg/yr of NaCl, with the quantities determined in the lab.

The resulting tPA solution is sent to an endotoxin removal column where the endotoxin is adsorbed selectively onto a resin (e.g., Acticlean Etox by Sterogene). This column is washed with a mixture of 364.8 kg/yr of NaOH and 9,235 kg/yr of water to remove the endotoxin. The effluent stream is microfiltered to remove cell debris that does not pass through the filter. Then, wastewater is removed in a freeze-drying operation to provide tPA in powder form.

Step 4 Eliminate Differences in Temperature, Pressure, and Phase: In the manufacture of tPA, the ingredients are assumed to be available at 20°C, water is mixed with the HyQ PF-CHO powder media at 4°C, the cultivations (cell production operations) occur at 37°C, and the separations occur at 4°C. The exothermic heat of the cultivation is removed at 37°C. Only small pressure changes occur and can be neglected at this stage of process synthesis. Similarly, no phase-change operations are added to the flowsheet. Hence, only a few temperature-change operations are added to Figure 2.12, with the resulting flowsheet shown in Figure 2.13.

Step 5 Task Integration: At this stage in the synthesis, various items of equipment are selected, often combining two or more adjacent operations into a single equipment item; that is, in task *integration*. The first key decision involves whether to operate in continuous or batch mode. For small throughputs, such as 80 kg/yr of tPA, the decision is nearly always to operate in batch mode. Choices of batch and equipment sizes, and batch time, are usually based upon the slowest operation, usually the cultivation (or fermentation) process. For tPA, it is determined using the experimental growth rate of tPA-CHO cells [0.39×10^6cell/(mL-day)], the inlet and outlet cell concentrations, and the experimental rate of tPA growth [50 pg tPA/(cell-day)], where pg ≡ picogram ≡ 10^{-12} g. One approach is shown next in Sub-Example 2.3.1.

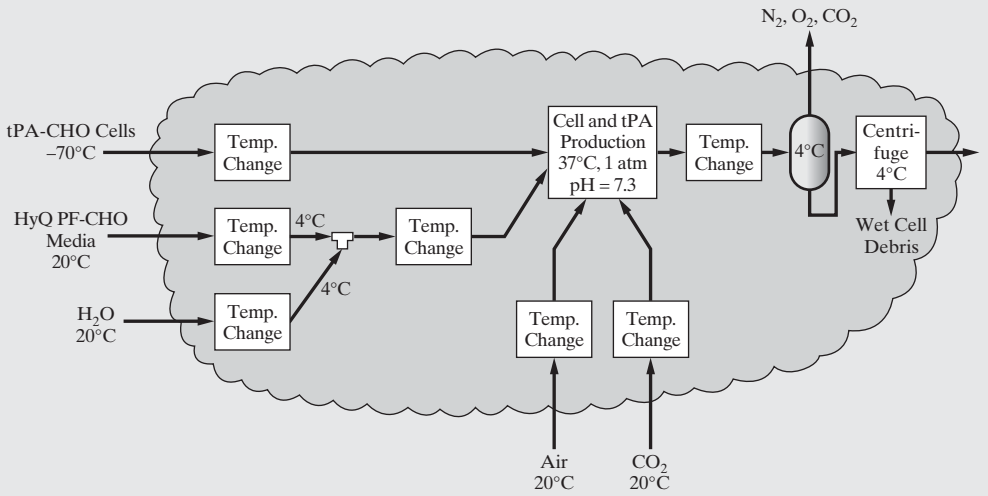

Figure 2.13 Flowsheet with the temperature-change operations in the tPA process.

SUB-EXAMPLE 2.3.1 Estimating Batch Time and Vessel Size

For nearly all cell cultivations, multiple cultivators are needed. As indicated in Step 1 of this process synthesis, 1 L of inoculum is grown in the laboratory, containing tPA-CHO cells at 2×10^6cell/mL. Next, cells are diluted and grown in progressively larger vessels. In each vessel, they are diluted to concentrations beyond which the experimental growth rate can be achieved for tPA-CHO cells, on the order of 10^5 cell/mL. Then, they are permitted to grow to concentrations limited by overcrowding, on the order of 3×10^6cell/mL for tPA-CHO cells.

As will be shown in this task integration, the last cultivator produces nearly all of the product tPA. Consequently, it is the basis for selection of batch and equipment sizes, and batch time. For typical limiting concentrations

$$c_{min} = 2 \times 10^5 \text{ cell/mL}$$
$$c_{max} = 3 \times 10^6 \text{ cell/mL}$$

the cultivation time is estimated:

$$\frac{3 \times 10^6 \frac{\text{cell}}{\text{mL}} - 2 \times 10^5 \frac{\text{cell}}{\text{mL}}}{0.39 \times 10^6 \frac{\text{cell}}{\text{mL-day}}} = 7.2 \text{ day} \cong 7 \text{ days}$$

Adding 7 days for loading, cleaning, and sterilizing the vessel, a total of 14 days are required.

Next, 50 batches annually are assumed. At two weeks per batch, two batch vessels operating in parallel are required; that is, two batch trains, each manufacturing 25 batches per year are needed. To produce 80 kg tPA/yr, the batch size is:

$$\frac{80 \text{ kg tPA}}{50 \text{ batch}} = 1.6 \frac{\text{kg tPA}}{\text{batch}}$$

One final assumption is needed. Early in the design, before the details of the separation train are considered, a 40% loss of tPA is assumed in the separations operations. Hence, $1.6 \times 1.4 = 2.24$ kg/batch must be produced in the cultivations.

Finally, at an average concentration of $(2 \times 10^5 + 3 \times 10^6)/2$ cell/mL $= 1.6 \times 10^6$cell/mL, the tPA growth per batch is

$$2{,}240 \frac{\text{g tPA}}{\text{batch}} = V \times 1.6 \times 10^6 \frac{\text{cell}}{\text{mL}} \times 50 \frac{\text{pg tPA}}{\text{cell-day}} \times \frac{1 \text{ g tPA}}{10^{12} \text{pg tPA}} \times 7 \text{ days}$$

where V is the batch volume in the third cultivator. Solving, $V = 4 \times 10^6$mL/batch $= 4{,}000$ L/batch. For this purpose, a conventional 5,000 L vessel is used.

The flowsheet in Figure 2.14a begins with a 1-L laboratory cultivator, into which a 1-mL aliquot of tPA-CHO cells, at concentration 2×10^6 cell/mL, is charged from cold storage at −70°C (after defrosting). To this, HyQ PF-CHO media, water, air, and CO_2 are added. Next, the batch time for this lab cultivator is computed in Sub-Example 2.3.2.

SUB-EXAMPLE 2.3.2 Inoculum Growth in Laboratory

After the 1-mL aliquot is defrosted and added to the 1-L cultivator, it is diluted to a concentration:

$$\frac{1 \text{ mL}}{1{,}000 \text{ mL}} \times \left(2 \times 10^6 \frac{\text{cell}}{\text{mL}}\right) = 2 \times 10^3 \frac{\text{cell}}{\text{mL}}$$

Then, the lab-cultivator batch time is:

$$\frac{2 \times 10^6 \frac{\text{cell}}{\text{mL}} - 2 \times 10^3 \frac{\text{cell}}{\text{mL}}}{0.39 \times 10^6 \frac{\text{cell}}{\text{mL-day}}} = 5.12 \text{ days} \cong 5 \text{ days}$$

and the tPA growth is:

$$0.25 \frac{\text{g tPA}}{\text{batch}} = 1{,}000 \text{ mL} \times 10^6 \frac{\text{cell}}{\text{mL}} \times 50 \frac{\text{pg tPA}}{\text{cell-day}} \times \frac{1 \text{ g tPA}}{10^{12} \text{pg tPA}} \times 5 \text{ days}$$

a small fraction of the tPA growth in the entire cultivation process. Note that to the 1-L flask, HyQ PF-CHO media is added, along with ultra-pure water, air, and CO_2, to produce 1.2 kg/batch of inoculum.

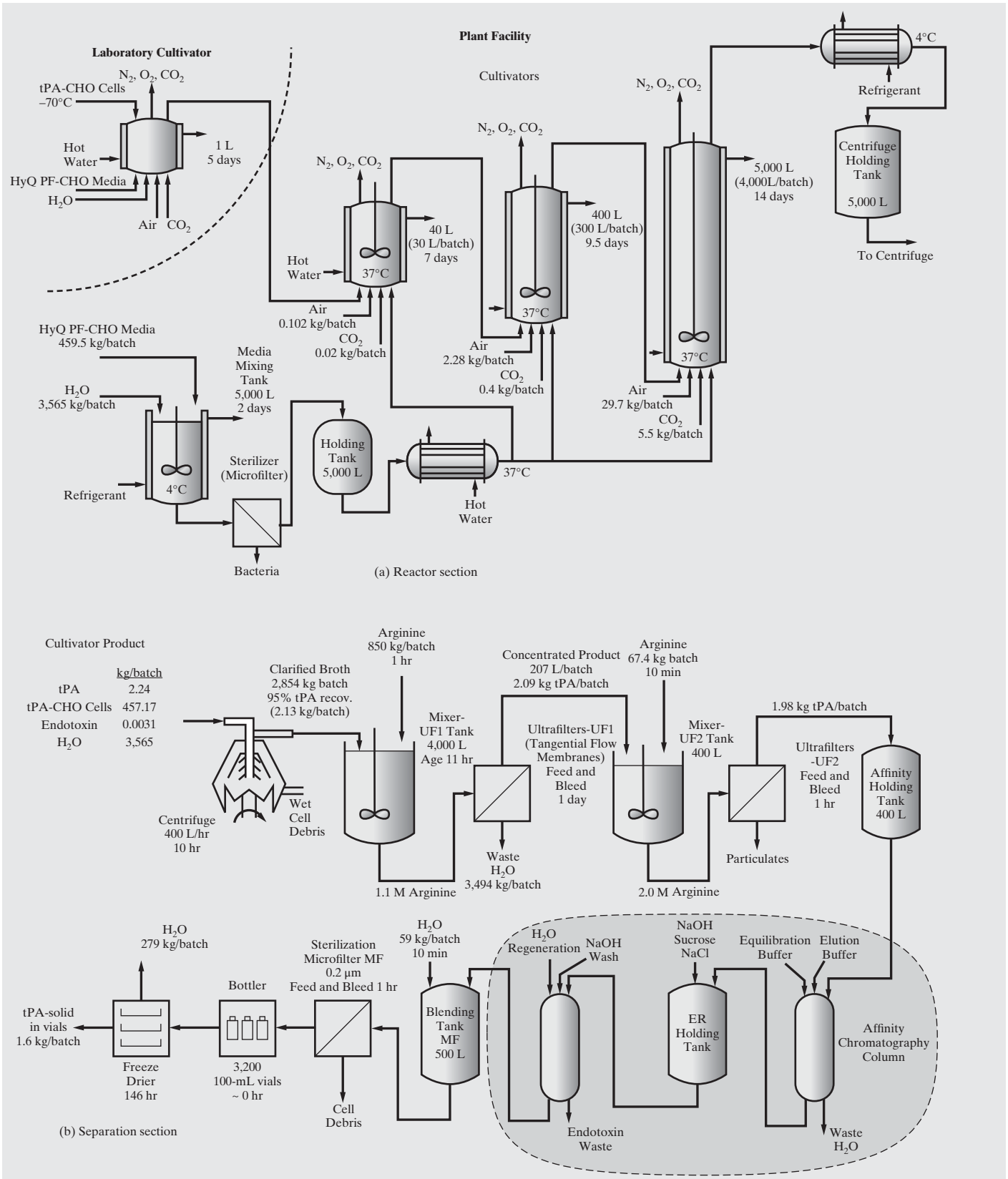

Figure 2.14 Flowsheet showing a task integration for the tPA process.

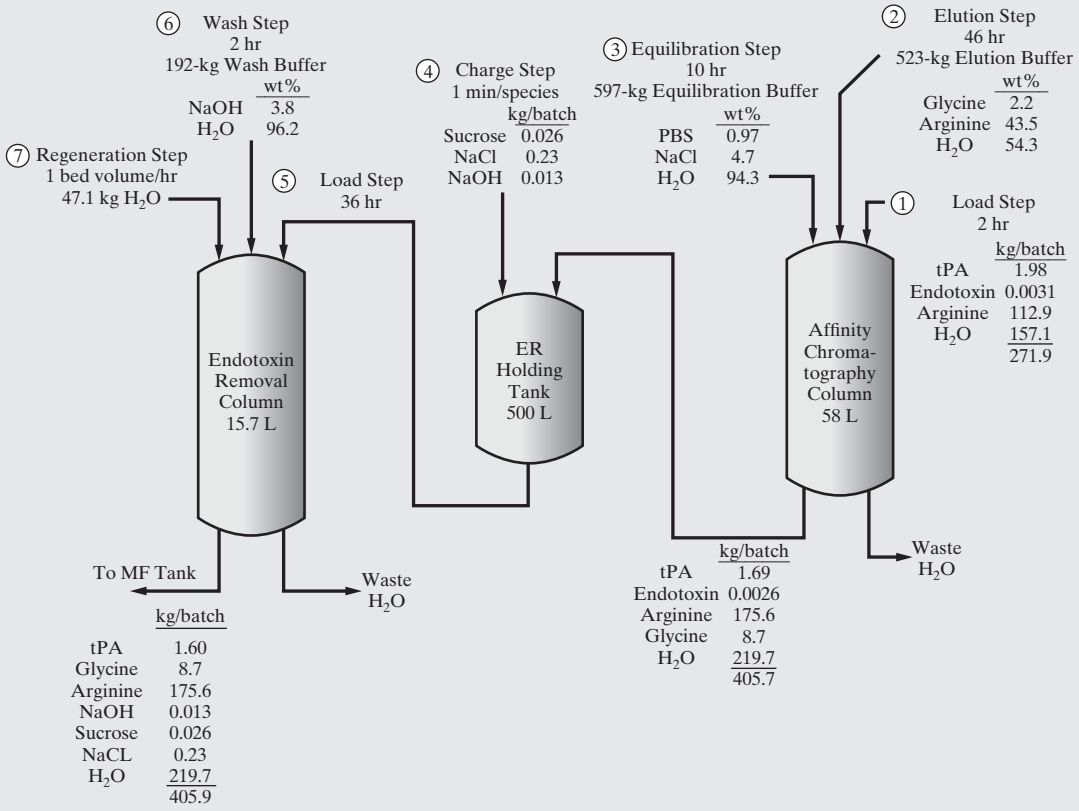

(c) Detailed separation section

Figure 2.14 (*continued*)

Next, the inoculum is taken to the plant, where it is added to the first of three cultivators, a 40-L cultivator selected to contain a 30-L batch after dilution. For this vessel, Sub-Example 2.3.3 shows how to compute the batch time, the tPA growth, and the air required.

SUB-EXAMPLE 2.3.3 Growth in Cultivator 1

After the inoculum is added to the 40-L cultivator, and diluted to 30 L, the cell concentration is:

$$\frac{1\text{ L}}{30\text{ L}} \times \left(2 \times 10^6 \frac{\text{cell}}{\text{mL}}\right) = 6.7 \times 10^4 \frac{\text{cell}}{\text{mL}}$$

Then, the growth time is:

$$\frac{2 \times 10^6 \frac{\text{cell}}{\text{mL}} - 6.7 \times 10^4 \frac{\text{cell}}{\text{mL}}}{0.39 \times 10^6 \frac{\text{cell}}{\text{mL-day}}} = 4.96 \text{ days} \cong 5 \text{ days}$$

Two days are added for loading, cleaning, and sterilization, to give a seven-day batch time.

At an average concentration of 1.03×10^6 cell/mL, the tPA growth is:

$$7.72 \frac{\text{g tPA}}{\text{batch}} = 30{,}000 \text{ mL} \times 1.03 \times 10^6 \frac{\text{cell}}{\text{mL}} \times 50 \frac{\text{pg tPA}}{\text{cell-day}} \times \frac{1 \text{ g tPA}}{10^{12} \text{ pg tPA}} \times 5 \text{ days}$$

and the O_2 consumed, at an experimental consumption rate of 0.2×10^{-12} mol O_2/cell-hr, is:

$$0.742 \frac{\text{mol O}_2}{\text{batch}} = 30{,}000 \text{ mL} \times 1.03 \times 10^6 \frac{\text{cell}}{\text{mL}} \times 0.2 \times 10^{-12} \frac{\text{mol O}_2}{\text{cell-hr}} \times \frac{24 \text{ hr}}{\text{day}} \times 5 \text{ days}$$

The weight fraction of O_2 in air is 0.233, which gives 0.102 kg air/batch.

Next, Sub-Example 2.3.4 provides similar calculations for the second and third cultivators in the plant, as shown in Figure 2.14a.

SUB-EXAMPLE 2.3.4 Growth in Cultivators 2 and 3

Cultivator 2

The second cultivator is 400 L, with contents diluted to 300 L, to give a cell concentration:

$$\frac{30\text{ L}}{300\text{ L}} \times \left(2 \times 10^6 \frac{\text{cell}}{\text{mL}}\right) = 0.2 \times 10^6 \frac{\text{cell}}{\text{mL}}$$

Its growth time is:

$$\frac{3 \times 10^6 \frac{\text{cell}}{\text{mL}} - 0.2 \times 10^6 \frac{\text{cell}}{\text{mL}}}{0.39 \times 10^6 \frac{\text{cell}}{\text{mL-day}}} = 7.2 \text{ days}$$

Here, 2.3 days are added for loading, cleaning, and sterilization, to give a 9.5-day batch time.

At an average concentration of 1.6×10^6 cell/mL, the tPA growth is:

$$173 \frac{\text{g tPA}}{\text{batch}} = 300{,}000 \text{ mL} \times 1.6 \times 10^6 \frac{\text{cell}}{\text{mL}} \times 50 \frac{\text{pg tPA}}{\text{cell-day}} \times \frac{1 \text{ g tPA}}{10^{12} \text{ pg tPA}} \times 7.2 \text{ days}$$

and the O_2 consumed, at an experimental consumption rate of 0.2×10^{-12} mol O_2/cell-hr, is:

$$16.6 \frac{\text{mol } O_2}{\text{batch}} = 300{,}000 \text{ mL} \times 1.6 \times 10^6 \frac{\text{cell}}{\text{mL}} \times 0.2 \times 10^{-12} \frac{\text{mol } O_2}{\text{cell-hr}} \times \frac{24 \text{ hr}}{\text{day}} \times 7.2 \text{ days}$$

The weight fraction of O_2 in air is 0.233, which gives 2.28 kg air/batch.

Cultivator 3

The third cultivator is 5,000 L, with contents diluted to 4,000 L, to give a cell concentration:

$$\frac{300 \text{ L}}{4{,}000 \text{ L}} \times \left(3 \times 10^6 \frac{\text{cell}}{\text{mL}}\right) = 0.225 \times 10^6 \frac{\text{cell}}{\text{mL}}$$

Its growth time is:

$$\frac{3 \times 10^6 \frac{\text{cell}}{\text{mL}} - 0.225 \times 10^6 \frac{\text{cell}}{\text{mL}}}{0.39 \times 10^6 \frac{\text{cell}}{\text{mL-day}}} \cong 7 \text{ day}$$

Here, 7 days are added for loading, cleaning, and sterilization, to give a 14-day batch time.

At an average concentration of 1.61×10^6 cell/mL, the tPA growth is:

$$2{,}254 \frac{\text{g tPA}}{\text{batch}} = 4{,}000{,}000 \text{ mL} \times 1.61 \times 10^6 \frac{\text{cell}}{\text{mL}} \times 50 \frac{\text{pg tPA}}{\text{cell-day}} \times \frac{1 \text{ g tPA}}{10^{12} \text{ pg tPA}} \times 7 \text{ days}$$

and the O_2 consumed, at an experimental consumption rate of 0.2×10^{-12}mol O_2/cell-hr, is:

$$216.4 \frac{\text{mol } O_2}{\text{batch}} = 4{,}000{,}000 \text{ mL} \times 1.61 \times 10^6 \frac{\text{cell}}{\text{mL}} \times 0.2 \times 10^{-12} \frac{\text{mol } O_2}{\text{cell-hr}} \times \frac{24 \text{ hr}}{\text{day}} \times 7 \text{ days}$$

The weight fraction of O_2 in air is 0.233, which gives 29.7 kg air/batch.

Adding the tPA growths in the laboratory and plant cultivators gives:

$$0.25 + 7.72 + 173 + 2{,}254 = 2{,}435 \text{ kg tPA/batch},$$

that is,

$$2{,}435 \text{ kg/batch} \times 50 \text{ batch/yr} = 121.7 \text{ kg tPA/yr},$$

which exceeds the throughput requirement of 80 kg tPA/yr by 52%, and should be adequate to cover anticipated separations losses. Note that, within limits, the bounding cell concentrations and batch volumes can be adjusted, affecting the batch times and tPA production rates. These parameters can be adjusted to optimize an objective function, for example, a profitability measure.

Finally, the air required for cultivation in the plant cultivators is:

$$0.102 + 2.28 + 29.7 = 32.1 \text{ kg air/batch},$$

that is,

$$32.1 \text{ kg/batch} \times 50 \text{ batch/yr} = 1{,}604 \text{ kg air/yr}$$

Returning to Figure 2.14a, note that to complete the reaction section of the process, a separate vessel for removal of gas emissions, containing N_2, O_2, and CO_2, is not needed, as these are vented continuously from the cultivators. Also, a 5,000-L mixing tank is installed to load and mix the powder media and water in two days. Note the tank jacket through which refrigerant is circulated. This vessel is followed by a microfilter, which sterilizes the mixture by removing bacteria, and a hot water heat exchanger. One last vessel, a 5,000-L holding tank, is provided to hold the contents of one cultivator batch (2.44, 457.17, 0.0031, 3,565 kg/batch of tPA, tPA-CHO cells, endotoxin, and water, respectively), in the event the centrifuge is taken off-line for servicing. The effluent from the third cultivator is cooled to 4°C in the shell-and-tube heat exchanger, which is cooled by a refrigerant on the shell side.

Turn next to the separation section in Figure 2.14b. The centrifuge is designed to handle small batches, at a rate of 400 L/hr over 10 hr. It rotates at high speed with the wet cell mass (which contains all of the tPA-CHO cells, 5 wt% of the tPA, 20 wt% of the water, and none of the endotoxin fed to the centrifuge) thrown to the outside collection volume and removed. Note that at this stage in process synthesis, recovery fractions are estimated using heuristics and experimental data when available. Also, since the endotoxin contaminant must be removed entirely, it is assumed to be entirely recovered (100%) in the effluent from the microfilters. The clarified broth (2,854 kg/batch) exits through the central tube overhead. It enters a mixing tank in which arginine hydrochloride is added to form a 1.1 molar solution, which is microfiltered to remove 3,494 kg/batch of wastewater. The concentrated product, at 207 L/batch and containing 98, 5.62, and 5.62 wt% of the tPA, arginine hydrochloride, and water fed to the microfilter, is mixed with 67.4 kg/batch of arginine in a second mixing vessel to give 2.0 molar arginine. This solution is microfiltered lo remove particulate matter before being sent to the affinity holding tank. The effluent, which contains 95, 98, 100, and 98 wt% of the tPA, arginine, endotoxin, and water fed to the microfilter, is loaded into a 58-L affinity chromatography column, which adsorbs 100, 100, 2, and 2 wt% of tPA, endotoxin, arginine, and water, as shown in Figure 2.14c. Most of the adsorbed tPA, 1.69 kg/batch, is eluted with a stream containing glycine (523 kg/batch at 2.2, 43.5, and 54.3 wt% of glycine, arginine, and water, respectively) and sent to a 500-L holding tank (405.7 kg/batch containing 1.69, 8.7, 175.6, 0.0026, and 219.7 kg/batch of tPA, glycine, arginine, endotoxin, and water, respectively). Note that the edition buffer recovers 85 wt% of the tPA and endotoxin from the resin. The affinity chromatography column is equilibrated with an equilibration buffer (597 kg/batch containing 0.97, 4.7, and 94.3 wt% PBS, NaCl, and water, respectively). After a caustic and sucrose mix is added to the holding tank (0.013, 0.026, and 0.33 kg/batch of NaOH, sucrose, and NaCl, respectively), the mixture is loaded into the endotoxin removal column (406.0 kg/batch). In this 15.7-L column, the endotoxins are adsorbed, and removed, by washing with caustic (192 kg/batch containing 3.8 and 96.2 wt% NaOH and water, respectively), which is discarded. The endotoxin removal column is regenerated with 47.1 kg/batch of water, while the endotoxin-free solution (405.9 kg/batch containing 1.6, 8.7, 175.6, 0.013, 0.026, 0.23, and 219.7 kg/batch of tPA,

glycine, arginine, NaOH, sucrose, NaCl, and water, respectively) is sent to a holding tank, where 59 kg/batch of water are added. After sterilization with a microfilter to remove cell debris, from which 99.7% of the tPA is recovered, the solution is sent to a bottler and 100-mL vials, each containing 100 mg of tPA, are conveyed to a freeze-drier, where the water is evaporated.

It is important to recognize that the batch sizes in Figure 2.14 are representative. However, as discussed subsequently in Section 7.5 and Chapter 22, the batch times and vessel sizes are key design variables in scheduling and optimizing batch processes.

Synthesis Tree

Clearly, at each step in the synthesis of the process flowsheet, alternatives are generated and the synthesis tree fills in. For the tPA process, a schematic of a synthesis tree is shown in Figure 2.15. Note that the bold branch corresponds to the flowsheets in Figures 2.10–2.14. In design synthesis, the engineer strives to identify the most promising alternatives, eliminating the least promising alternatives by inspection, wherever possible. Initially, heuristic rules help to make selections. Eventually, algorithmic methods involving optimization can be introduced to check the heuristics and identify more promising alternatives, as discussed in Chapter 22. It should be emphasized, however, that the design window, beginning during Phases 1 and 2 of the clinical trials, is small, typically on the order of 12–16 months, before Phase 3 begins. Consequently, emphasis is normally placed on the rapid development of a promising design, and less on design optimization. Stated differently, for high-priced pharmaceuticals, it is far more important to be first to market rather than to achieve relatively small savings in the capital investment or operating expenses for the plant through design optimization. For further discussion, see Pisano (1997).

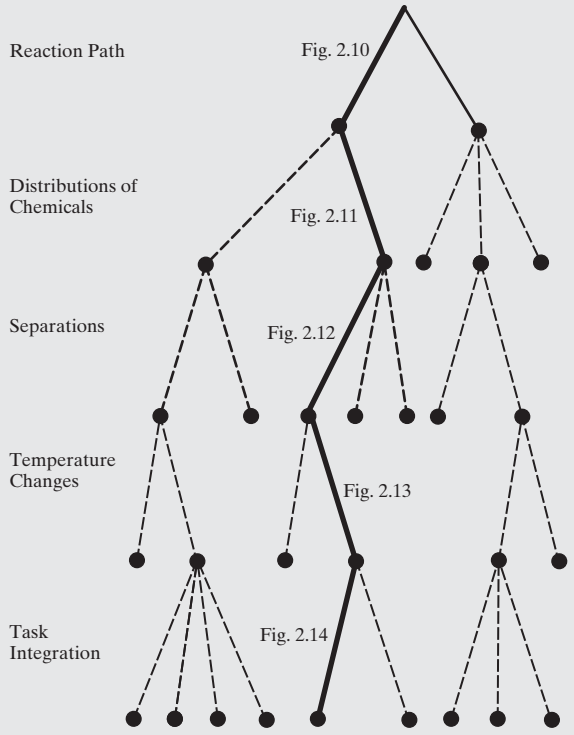

Figure 2.15 Inverted synthesis tree for the production of tPA.

2.4 NEXT PROCESS DESIGN TASKS

In the Introduction, Section 2.1, approaches for information gathering were discussed, given a process design problem statement. Then, in Section 2.2, the importance of experimentation when necessary was mentioned. These led to the key process design task, Preliminary Process Synthesis, which was discussed in Section 2.3 and illustrated to create alternative flowsheets for the manufacture of two chemical products, vinyl chloride and tissue plasminogen activator (tPA). In this section, Table 2.6 lists the remaining process design tasks, which are discussed briefly, beginning with Task-4, which involves a complete material balance for one of the promising process flowsheets—often referred to as the "base case" flowsheet. Also, for each task, the reader is referred to the chapter/section in this textbook in which approaches for carrying out the task are discussed.

Flowsheet Mass Balances

During preliminary process synthesis (Section 2.3), mass balances using approximate models are often carried out by using paper and pencil, spreadsheets, and even process simulators. For example, see Sub-Example 2.2.1. For a promising *base-case* flowsheet, block and initial process flow diagrams are often prepared, along with preliminary material balances, as shown in Section 2.5. Subsequently, mass balances are prepared using a process simulator as discussed in Chapter 7.

Process Stream Conditions

Also during preliminary process synthesis, initial stream conditions are specified, for example, temperatures and pressures, often at the bubble or dew points, or at specified vapor or liquid fractions. The latter are computed assuming phase equilibrium, often by a process simulator. In this textbook, the procedures for calculating phase equilibria and adjusting these specifications are discussed in Chapter 7 on the process simulators.

Flowsheet Material and Energy Balances

As shown earlier, simple energy balances are also carried out during preliminary process synthesis, often using a process simulator. Energy balances require estimates of the thermophysical properties (e.g., heat capacities, latent heats, internal energies, and enthalpies), which are commonly carried out by process simulators. Consequently, for base-case designs, strategies for carrying out material and energy balances for entire flowsheets are discussed in Chapter 7 on the process simulators. These are especially important for multicomponent recycle streams.

Equipment Sizing and Costing

Having completed material and energy balances for base-case designs, the next task normally involves estimating key equipment sizes and costs. Often these are estimated initially using approximate models by the process simulators as discussed in Chapter 7. Subsequently, more accurate models are inserted. For example, models to calculate the heat to be added or removed from a stream are replaced by models for shell-and-tube heat

Table 2.6 Process Design Tasks

Task	Description	Sources
1	Identify details about chemical product.	Section 2.1
2	Collect information about product's processing (e.g., raw materials, reaction paths).	Section 2.1
3	Carry out preliminary process synthesis. Select a promising base-case flowsheet.	Section 2.3, Chapters 6–11
4	Perform a mass balance on the flowsheet.	Section 2.5, Chapter 7
5	Decide on the process stream conditions.	Chapter 7
6	Perform material and energy balances on the flowsheet.	Chapter 7
7	Replace simple process unit models (e.g., heat requirement models), with more rigorous models (e.g., for a shell-and-tube heat exchanger).	Chapter 7
8	Perform equipment sizing and costing calculations for all equipment items.	Chapters 12–16, 27
9	Perform an economic evaluation for the process (e.g., a profitability analysis).	Chapter 17, 27
10	Seek opportunities for heat and mass integration.	Chapter 11, 27
11	Perform environmental impact and sustainability calculations. Check process safety.	Chapters 3
12	Check plantwide controllability.	Chapter 20
13	Seek to improve the design using process optimization.	Chapters 21, 22

exchangers. In this textbook, many of the details are provided in Chapters 12–16. Chapter 16 provides equations for estimating the sizes and costs of many equipment types.

Economic Evaluation

In some cases, just the total permanent investment is estimated, often approximately when comparing flowsheets during process synthesis. For promising base-case designs, more accurate calculations are carried out. In this textbook, Chapter 17 discusses in detail both the approximate and rigorous cost and profitability analysis methods.

Heat and Mass Integration

Often, as shown in Chapter 27 (Ammonia Process Design Case Study), heat and mass integrations are important to achieve profitable chemical processes. In this textbook, Chapter 11 thoroughly introduces the methods of heat integration, with the methods for mass integration introduced in a PDF file containing the supplement to Chapter 11.

Environment, Sustainability, and Safety

Throughout process synthesis and the subsequent tasks in process design, issues of environmental impact, sustainability, and process safety are considered carefully by most process design teams. In this textbook, Sections 3.3, 3.4, and 3.5, respectively, are devoted specifically to these issues. Also, many examples are discussed in the remaining chapters.

Controllability Assessment

It is important to check that the final flowsheet can be maintained at its desired operating conditions. There may be insufficient degrees of freedom to enable this to be carried out, and controllability assessment will uncover such deficiencies. In this textbook, Chapter 20 focuses on short-cut controllability assessment methods and introduces a conceptual plantwide control system configuration methodology, that will address these issues.

Optimization

Here, also, beginning with process synthesis, process design teams seek to select the best choices, often using optimizers within the process simulators. In this textbook, Chapter 21 focuses on optimization strategies often used in process design, with emphasis on steady-state operation of large-scale continuous processes. Chapter 22 covers the optimal design and scheduling of batch processes.

2.5 PRELIMINARY FLOWSHEET MASS BALANCES

As shown in Table 2.6, Task-4 in process design, which follows Task-3 (preliminary process synthesis), involves carrying out mass balances for the promising base-case process flowsheets. Having carried out some mass balances during process synthesis, this task is intended to complete the mass balance for the entire flowsheet, usually using approximate models and/or process simulators. Subsequently, more rigorous mass balances are carried out using process simulators (e.g., ASPEN PLUS, Aspen HYSYS, UniSim® Design, and PRO/II), as discussed in Chapter 7.

Because material balance results are normally displayed with process flow diagrams, this section discusses flow diagram conventions while presenting material balance results for the vinyl-chloride process synthesized in Example 2.2.

Flow Diagrams

Three kinds of flow diagrams are normally prepared to describe the base-case design(s). The first two, the *block flow diagram* and

the *process flow diagram*, are shown here for the vinyl-chloride process. The third, which includes the valves and process controllers, is the *piping and instrumentation diagram* (*P&ID*), which is especially important for control system design and safety (HAZOP) analysis, as discussed in Section 3.5.

Block Flow Diagram (BFD)

The block flow diagram represents the main processing sections in terms of functional blocks. As an example, Figure 2.16 shows a block flow diagram for the vinyl-chloride process, in which the three main sections in the process—namely, ethylene chlorination, pyrolysis, and separation—are shown, together with the principal flow topology. Note that the diagram also indicates the overall material balances and the conditions at each stage, where appropriate. This level of detail is helpful to summarize the principal processing sections and is appropriate in the early design stages, where alternative processes are usually under consideration.

Process Flow Diagram (PFD)

Process flow diagrams provide a more detailed view of the process. These diagrams display all of the major processing units in the process (including heat exchangers, pumps, and compressors), provide stream information, and include the main control loops that enable the process to be regulated under normal operating conditions. Often, preliminary PFDs are constructed using the process simulators. Subsequently, more detailed PFDs are prepared using software such as AUTOCAD and VISIO, the latter having been used to prepare Figure 2.17 for the vinyl-chloride process. The conventions typically used when preparing PFDs are illustrated using this figure and are described next.

Processing Units Icons that represent the units are linked by arcs (lines) that represent the process streams. The drawing conventions for the unit icons are taken from accepted standards, for example, the ASME (American Society for Mechanical Engineers) standards (ASME, 1961). A partial list of typical icons is presented in Figure 2.18. Note that each unit is labeled according to the convention U-XYY, where U is a single letter identifying the unit type (V for vessel, E for exchanger, R for reactor, T for tower, P for pump, C for compressor, etc.). X is a single digit identifying the process area where the unit is installed, and YY is a two-digit number identifying the unit itself. Thus, for example, E-100 is the identification code for the heat exchanger that condenses the overhead vapors from the chlorination reactor. Its identification code indicates that it is the 00 item installed in plant area 1.

Stream Information Directed arcs that represent the streams, with flow direction from left to right wherever possible, are numbered for reference. By convention, when streamlines cross, the

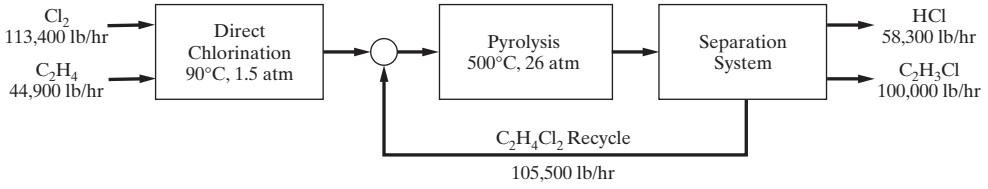

Figure 2.16 Block flow diagram for the vinyl-chloride process.

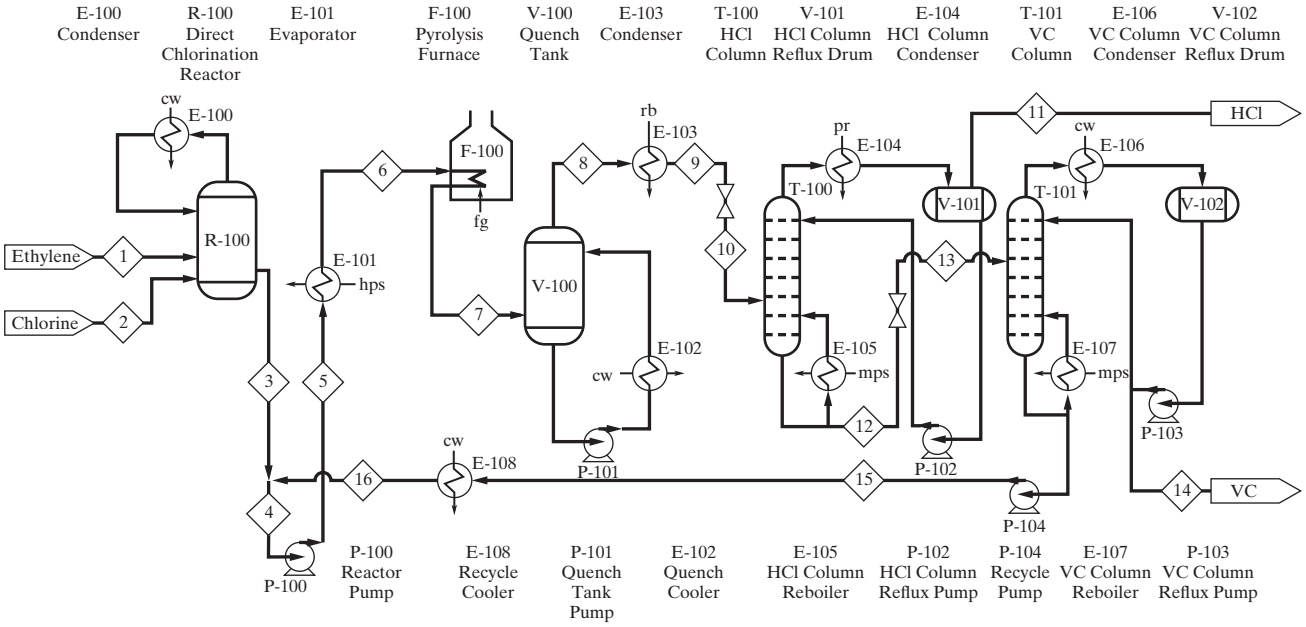

Figure 2.17 Process flow diagram for the vinyl-chloride process.

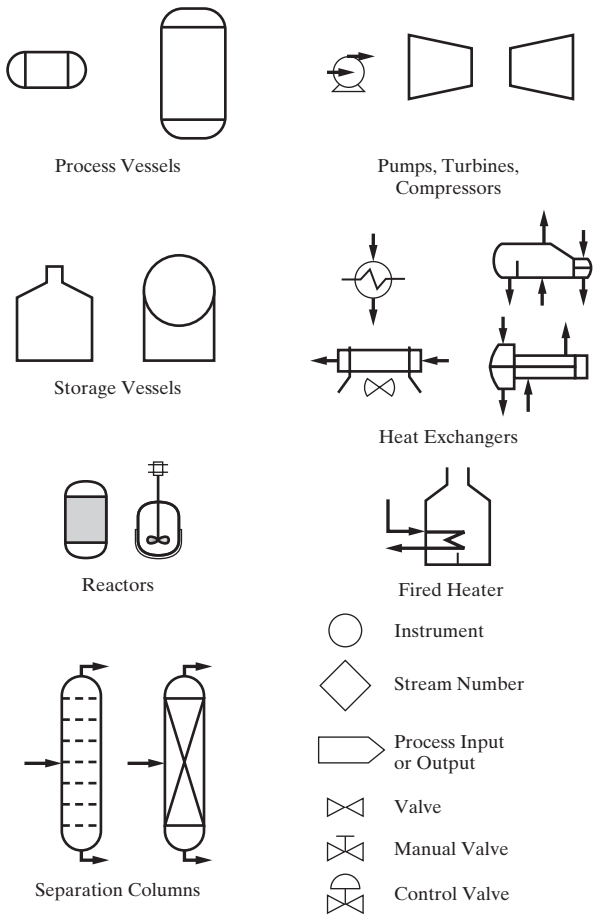

Figure 2.18 Icons in process flow diagrams.

horizontal line is shown as a continuous arc, with the vertical line broken. Each stream is labeled on the PFD by a numbered diamond. Furthermore, the feed and product streams are identified by name. Thus, streams 1 and 2 in Figure 2.17 are labeled as the ethylene and chlorine feed streams, respectively, while streams 11 and 14 are labeled as the hydrogen chloride and vinyl-chloride product streams, respectively. Mass flow rates, pressures, and temperatures may appear on the PFD directly, but more often are placed in the stream table instead, for clarity. The latter has a column for each stream and can appear at the bottom of the PFD or as a separate table. Here, because of formatting limitations in this text, the stream table for the vinyl-chloride process is presented separately in Table 2.7. At least the following entries are presented for each stream: label, temperature, pressure, vapor fraction, total and component molar flow rates, and total mass flow rate. In addition, stream properties such as the enthalpy, density, heat capacity, viscosity, and entropy may be displayed. Stream tables are often completed using a process simulator. In Table 2.7, the conversion in the direct chlorination reactor in assumed to be 100%, while that in the pyrolysis reactor in only 60%. Furthermore, both towers are assumed to carry out perfect separations, with the overhead and bottoms temperatures computed based on dew- and bubble-point temperatures, respectively.

Utilities As shown in Figure 2.17, various utility streams are utilized for heating or cooling the process streams. For example, E-100, the overhead condenser for the direct chlorination reactor, which operates at 90°C, is cooled using cooling water (*cw*). The other cooling utilities are refrigerated brine (*rb*) and propane

Table 2.7 Stream Summary Table for the Vinyl-Chloride Process in Figure 2.17

Stream Number	1	2	3	4	5	6	7	8
Temperature (°C)	25	25	90	90	91.3	242	500	170
Pressure (atm)	1.5	1.5	1.5	1.5	26	26	26	26
Vapor fraction	1.0	1.0	0.0	0.0	0.0	1.0	1.0	1.0
Mass flow (lb/hr)	44,900	113,400	158,300	263,800	263,800	263,800	263,800	263,800
Molar flow (lbmol/hr)	1,600	1,600	1,600	2,667	2,667	2,667	4,267	4,267
Component molar flow (lbmol/hr):								
Ethylene	1,600	0	0	0	0	0	0	0
Chlorine	0	1,600	0	0	0	0	0	0
1,2-dichloroethane	0	0	1,600	2,667	2,667	2,667	1,067	1,067
Vinyl chloride	0	0	0	0	0	0	1,600	1,600
Hydrogen chloride	0	0	0	0	0	0	1,600	1,600
Stream Number	9	10	11	12	13	14	15	16
Temperature (°C)	6	6.5	–26.4	94.6	57.7	32.2	145.6	90
Pressure (atm)	26	12	12	12	4.8	4.8	4.8	4.8
Vapor fraction	0.0	0.0	1.0	0.0	0.23	1.0	0.0	0.0
Mass flow (lb/hr)	263,800	263,800	58,300	205,500	205,500	100,000	105,500	105,500
Molar flow (lbmol/hr)	4,267	4,267	1,600	2,667	2,667	1,600	1,067	1,067
Component molar flow (lbmol/hr):								
Ethylene	0	0	0	0	0	0	0	0
Chlorine	0	0	0	0	0	0	0	0
1,2-dichloroethane	1,067	1,067	0	1,067	1,067	0	1,067	1,067
Vinyl chloride	1,600	1,600	0	1,600	1,600	1,600	0	0
Hydrogen chloride	1,600	1,600	1,600	0	0	0	0	0

Table 2.8 Heating and Cooling Utilities—Identifiers and Temperature Ranges

Identifier	Utility	Typical Operating Range
Hot Utilities—In increasing Cost per BTU:		
lps	Low-pressure steam, 15 to 30 psig	250 to 275°F
mps	Medium-pressure steam, 100 to 150 psig	325 to 366°F
hps	High-pressure steam, 400 to 600 psig	448 to 488°F
fo	Fuel oils	
fg	Fuel gas	Process waste stream
po	Petroleum oils	Below 600°F
dt	Dowtherms	Below 750°F
Cold Utilities—In increasing Cost per BTU:		
bfw	Boiler feed water	Used to raise process steam
ac	Air cooling	Supply at 85 to 95°F—temperature approach to process 4°F
rw	River water	Supply at 80 to 90°F (from cooling tower), return at 110°F
cw	Cooling water	Supply at 80 to 90°F (from cooling tower), return at 115 to 125°F
cw	Chilled water	45 to 90°F
rb	Refrigerated brine	0 to 50°F
pr	Propane refrigerant	–40 to 20°F

refrigerant (*pr*), each selected according to the temperature level of the required utility. Heating utilities are fuel gas (*fg*), high-pressure steam *(hps*), and medium-pressure steam (*mps*). A list of heating and cooling utilities, with temperature ranges, and the abbreviations commonly used on PFDs is presented in Table 2.8 (see also Table 17.1 and the subsection on *utilities* in Section 17.2).

Equipment Summary Table This provides information for each equipment item in the PFD, with the kind of information typically provided for each type of unit shown in Table 2.9. Note that the materials of construction (MOC), and operating temperature and pressure, are required for all units. Also note that suggestions for the materials of construction are provided in Appendix III.

In summary, the PFD is the most definitive process design document, encapsulating much of the commonly referred to design information. As such, it is used and updated throughout much of process design. However, it lacks many details required to begin the construction engineering work for the plant. Many of these details are transmitted in a *Piping and Instrumentation Diagram*.

Table 2.9 Equipment Summary Specifications

Equipment Type	Required Specification
Vessel	Height; diameter; orientation; pressure; temperature; materials of construction (MOC)
Towers	Height; diameter; orientation; pressure; temperature; number of and type of trays; height and type of packing; MOC
Pumps	Driver type; flow; suction and discharge pressures; temperature; shaft power; MOC
Compressors	Driver type; inlet flow; suction and discharge pressures; temperature; shaft power; MOC
Heat exchangers	Type; area; duty; number of shell and tube passes; for both shell and tubes: operating temperature; pressure; pressure drop; and MOC
Fired heaters	Type; tube pressure and temperature; duty; radiant; and convective heat transfer area; MOC

2.6 SUMMARY

Having studied this chapter, the reader should:

1. Be able to gather the data for use in the design of a manufacturing process, given a design problem statement.
2. Understand the five key steps in preliminary process synthesis and be able to use them to develop other flowsheets for the manufacture of vinyl chloride and tPA corresponding to the other branches of the synthesis trees in Figures 2.7 and 2.15, as well as the manufacture of other chemicals.
3. Be prepared to learn more about the 13 tasks in Table 2.6 normally carried out in preparing one or more base-case designs. Table 2.6 refers the readers to the sections and chapters that provide instructional materials.
4. After completing Task-3, Preliminary Process Synthesis, and creating promising base-case designs, be prepared to carry out Task-4 to create preliminary process flowsheets and mass balances.

REFERENCES

1. ASME, *Graphical Symbols for Process Flow Diagrams*. ASA Y32.11. Amer. Soc. Mech. Eng., New York (1961).

2. Audette, M., C. Metallo, and K. Nootrong, *Human Tissue Plasminogen Activator*, Towne Library. University of Pennsylvania, Philadelphia (2000).

3. Benedict, D.B., Process for the Preparation of Olefin Dichlorides, U.S. Patent 2, 929, 852, March 22 (1960).

4. B.F. Goodrich Co., Preparation of Vinyl Chloride, British Patent 938, 824, October 9 (1963), *Instrument Symbols and Identification*, Instrument Society of America Standard ISA-S5–1, Research Triangle Park, North Carolina (1975).

5. Borsa. A.G., A.M. Herring, J.T. McKinnon, R.L. McCormick, and G.H. Ko, "Coke and Byproduct Formation during 1.2-Dichloroethane Pyrolysis in a Laboratory Tubular Reactor." *Ind. Eng. Chem. Res.*, **40**, 2428–3436 (2001).

6. Douglas, J.M., *Conceptual Design of Chemical Processes*, McGraw-Hill, New York (1988).

7. Goeddel, D.V., W.J. Kohr, D. Pennica, and G.A. Vehar, Human Tissue Plasminogen Activator, U.S. Patent 4,.766,075, August 23 (1988).

8. Green, D.W., and R.H. Perry, (ed.), *Perry's Chemical Engineers' Handbook*, 7th (ed.), McGraw-Hill, New York (1997).

9. Leonard, E.C., (ed.), *Vinyl and Diene Monomers, Part 3*, Wiley-Interscience, New York (1971).

10. Pisano, G.P., *The Development Factory: Unlocking the Potential of Process Innovation*, Harvard Business School Press, Boston (1997).

11. Rudd, D.F., G.J. Powers, and J.J. Siirola, *Process Synthesis*, Prentice-Hall, Englewood Cliffs, New Jersey (1973).

12. Walas, S.M., *Chemical Process Equipment*, Butterworth, London (1988).

13. Woods, D.R., *Data for Process Design and Engineering Practice*, Prentice-Hall, Englewood Cliffs, New Jersey (1995).

EXERCISES

2.1 For an equimolar solution of *n*-pentane and *n*-hexane, compute:

(a) The dew-point pressure at 120°F

(b) The bubble-point temperature at 1atm

(c) The vapor fraction, at 120°F and 0.9 atm, and the mole fractions of the vapor and liquid phases

2.2 Consider a stream at 400K containing 34 mol% *n*-pentane and 66 mol% *n*-hexane.

(a) What is the bubble point pressure?

(b) What are the mole fractions in the vapor at this pressure?

2.3 For the manufacture of vinyl chloride, assemble a preliminary database. This should include thermophysical property data, MSDSs for each chemical giving toxicity and flammability data, and the current prices of the chemicals.

2.4 For the vinyl-chloride process, using heats of formation, heat capacities, and latent heats, carry-out energy balances to determine the heats liberated and absorbed in the two reaction operations. Those computed using ASPEN PLUS, as shown in Figure 2.3, are:

(a) Direct chlorination = 150 million Btu/hr; note the reactants are at 25°C and the effluent stream is at 90°C; the pressure is 1.5 atm.

(b) Pyrolysis = 52 million Btu/hr; the reactant is at 90°C and the effluent stream is at 500°C; assume the pressure is 1 atm.

2.5 Consider the flowsheet for the manufacture of vinyl chloride in Figure 2.6.

(a) If the pyrolysis furnace and distillation towers are operated at low pressure (1.5 atm), what are the principal disadvantages? What alternative means of separation could be used?

(b) For the process shown, is it possible to use some of the heat of condensation from the $C_2H_4Cl_2$ to drive the reboiler of the first distillation tower? Explain your response. If not, what process change would make this possible?

(c) Consider the first reaction step to make dichloroethane. Show the distribution of chemicals when ethylene is 20% in excess of the stoichiometric amount and the chlorine is entirely converted. Assume that 100,000 lb/hr of vinyl chloride are produced.

(d) Consider the first distillation tower. What is the advantage of cooling the feed to its bubble point at 12 atm as compared with introducing the feed at its dew point?

(e) Why isn't the feed to the pyrolysis furnace heated with the hot pyrolysis products?

(f) What is the function of the trays in the direct chlorination 3 reactor?

(g) Suggest ways to reduce the need for fuel and hot utilities such as steam.

2.6 **(a)** To generate steam at 60 atm, two processes are proposed:

(1) Vaporize water at 1 atm and compress the steam at 60 atm.

(2) Pump water to 60 atm followed by vaporization.

Which process is preferred? Why?

(b) In a distillation tower, under what circumstances is it desirable to use a partial condenser?

2.7 Synthesize a flowsheet for the manufacture of vinyl chloride that corresponds to one of the other branches in the synthesis tree in Figure 2.7. It should begin with reaction path 4 or 5.

2.8 Using the chemical engineering literature, complete the detailed database for the detailed design of the base-case process in Figure 2.17. When appropriate, indicate the kind of data needed from a pilot plant and how this data should be regressed.

2.9 Consider the tPA process reactor (cultivation) section in Figure 2.14 (a):

(a) For the third cultivator, change the reaction time to three days. To obtain a cell concentration of 3×10^6 cell/mL, estimate the liquid volume in the cultivator. What reactor volume would you recommend?

(b) For (a), estimate the kg/batch of air consumed in the third cultivator.

2.10 In 2000, when the tPA process in Example 2.3 was synthesized using Chinese hamster ovary cells, data could not be located for the second reaction path using E-coli bacterial cells. Search the literature, especially the patents, since then to locate experimental results that give the:

(a) cell growth rate [cell/(mL-day)]

(b) tPA production rate [g/cell-day)]

(c) oxygen consumption rate [mol/(cell-hr)]

To check the patent literature, see Section 1.3 (*Feasibility Study* subsection). Can you locate data for other reaction paths?

Chapter 3

Design Literature, Stimulating Innovation, Energy, Environment, Sustainability, Safety, Engineering Ethics

3.0 OBJECTIVES

Chapter 1 introduced the key issues in designing new chemical products. Similarly, Chapter 2, introduced the issues in designing processes to manufacture many of these chemical products; that is, to carry out *process design*. Next, Part II of this textbook will focus on the specifics of the synthesis steps in creating chemical products and processes; that is, carrying out *product synthesis* and *process synthesis*.

To complete Part I, this chapter introduces several subjects that underlie all aspects of chemical product and process design. First, Section 3.1 addresses the design literature and modern methods of searching for information needed to carry out design projects. Then, to create attractive new chemical products, companies take steps to stimulate invention and innovation, which are considered in Section 3.2. Following these, alternative energy sources are discussed in Section 3.3. Then, key environmental concerns are reviewed in Section 3.4, followed by sustainability issues in Section 3.5, safety issues in Section 3.6, and engineering ethics issues in Section 3.7. These considerations regularly confront chemical engineers as they develop new chemical products and processes. They arise often, especially in the example designs presented in Parts II through V.

After studying this chapter, the reader should:

1. Be knowledgeable about the design literature, especially well-edited encyclopedias, handbooks, reference books, indexes, patents, Google search engines, and Wikipedia.
2. Be prepared to consider alternative energy sources, to address the latest environmental and sustainability issues, and to apply modern safety measures in designing new products and manufacturing processes.
3. Know how to maintain high ethical principles, avoiding conflicts of interest, when designing new products and processes.

Although you will not solve any design problems in this chapter, you will obtain background information, which will be expanded upon and referred to throughout the remaining chapters of this text.

3.1 DESIGN LITERATURE

When confronted with the need to design chemical products and processes, design teams in industry have access to company employees, company files, and the open literature, including patents. These resources provide helpful leads to specific problems, as well as information about related products, thermophysical property and transport data, possible flowsheets, equipment descriptions, and process models. If the company has been manufacturing the principal products, or related chemicals, information available to the design team provides an excellent starting point, enabling the team to consider variations to current practice very early in the design cycle. In spite of this, even when designing a next-generation product or plant to expand the production of a chemical product, or retrofitting a plant to eliminate bottlenecks and expand its production, the team may find that many opportunities exist to improve the processing technologies. Several years normally separate products, plant startups, and retrofits, during which technological changes are often substantial. For example, consider the recent shift in distillation, particularly under vacuum conditions, from trays to high-performance packings. For this reason, it is important to make a thorough search of the literature to uncover the latest data, flowsheets, equipment, and models that can lead to improved products and more profitable designs.

Information Resources

Design engineers improve their performance by learning to use efficiently the vast information resources available. Engineering libraries are equipped with many books and encyclopedias created by specialists in many engineering disciplines. Many journal articles, patents, and standards provide *primary source* materials. Important information for chemical engineers concerns the chemicals, their properties, and the reactions involving them. Information on hazards, safety, and regulations can be critical to the success of product and process designs. Also, most

engineering libraries are operated by professional librarians skilled in helping chemical engineers better locate helpful information. They are an important resource in assisting designers to find the most helpful sources.

Throughout this textbook, design strategies are introduced. To be effective in carrying out product and process designs, members of design teams must appreciate their need to discover *regularly* helpful sources of information. These often improve their performance of the current design step. Ideally, designers should be finding new sources as their project work proceeds, often augmenting or redirecting aspects of their designs.

Of course, the 21st century Information Age has been stimulated by remarkable search engines, the Internet, and smart devices that increasingly give designers rapid access to information from a rapidly growing array of geographical locations. We all use Google™, Wikipedia, laptops, smartphones, and the like, to rapidly uncover information.

This is a brief section intended to recommend resources especially useful to chemical engineers in carrying out product and process designs. Clearly, one will turn to Google and Wikipedia as good *starting points*, but it's important that chemical engineers be familiar with the array of information resources created for them by chemical engineers, which can be particularly helpful in carrying out design projects. Consequently, this section first discusses these resources before offering advice on the usage of more general search engines and information resources. Many existed and were updated throughout much of the 20th century, especially the second half. Nearly all were created in classical paper format. During the past two decades, especially, many are being converted to electronic format. When available electronically, comments to this effect are provided.

Encyclopedias

Three very comprehensive, multivolume encyclopedias contain a wealth of information concerning the manufacture of many chemicals. Collectively, these encyclopedias describe uses for the chemicals, history of manufacture, typical process flowsheets and operating conditions, and related information. The three encyclopedias are the *Kirk-Othmer Encyclopedia of Chemical Technology* (1991), the *Encyclopedia of Chemical Processing and Design* (McKetta and Cunningham, 1976), and *Ullmann's Encyclopedia of Industrial Chemistry* (1988). Note that the *Kirk-Othmer Encyclopedia* and *Ullmann's Encyclopedia* can be accessed from Wiley's online Library (onlinelibrary.wiley.com). For a specific chemical or substance, it is not uncommon for one or more of these encyclopedias to have 5 to 10 pages of pertinent information together with literature references for more detail and background. Although the encyclopedias are updated too infrequently to always provide the latest technology, the information they contain is normally very helpful to a design team when beginning to assess a design problem. Other encyclopedias, which are somewhat more limited in scope, may also be helpful, including the *McGraw-Hill Encyclopedia of Science and Technology* (1987), *Van Nostrand's Scientific Encyclopedia* (Considine, 1995), the *Encyclopedia of Fluid Mechanics* (Cheremisinoff, 1986), the *International Encyclopedia of Heat and Mass Transfer* (Hewitt et al., 1997), and the *Encyclopedia of Material Science and Engineering* (Bever, 1986).

Handbooks and Reference Books

Several key handbooks and reference books are very well known to chemical engineers. These include *Perry's Chemical Engineer's Handbook* (Green and Perry, 2008), which can be accessed electronically from most engineering libraries (e.g., from the University of Pennsylvania and the *CRC Handbook of Chemistry and Physics* (the so-called *Rubber Handbook*, published annually by the CRC Press, Boca Raton, FL) (Lide, 1997), also available electronically at: www.hbcpnetbase.com. Other sources, more limited in scope, include the *JANAF Thermochemical Tables* (Chase, 1985), *Riegel's Handbook of Industrial Chemistry* (Kent, 1992), the *Chemical Processing Handbook* (McKetta, 1993a), the *Unit Operations Handbook* (McKetta, 1993b), *Process Design and Engineering Practice* (Woods, 1995b), *Data for Process Design and Engineering Practice* (Woods, 1995a), the *Handbook of Reactive Chemical Hazards* (Bretherick, 1990), and the *Standard Handbook of Hazardous Waste Treatment and Disposal* (Freeman, 1989), among many other sources. A useful Internet site for many important chemical engineering topics is www.cheresources.com.

Indexes

To search the literature, especially the research and technology journals, for information specifically helpful in designing chemical products and processes, two indexes are particularly helpful. These are *Compendex* (*Engineering Index*), which covers the journals in all areas of engineering using a controlled vocabulary that helps locate information on a topic, and *SciFinder* (*Chemical Abstracts*), which covers over 10,000 journals in all areas of the chemical sciences, as well as books and book chapters, dissertations, and so on. Other science-oriented indexes, less specific to the chemical and engineering sciences, include the *ISI Web of Science*, which covers over 8,000 journals in all areas of science, linking to bibliographies and citing references for articles; *Scopus*, which covers over 10,000 journals in all areas of science; and *PubMed Plus*, which searches the medical literature from 1947 forward.

Patents

These are important sources with which the design team must be aware to avoid the duplication of designs protected by patents. Perhaps more significantly, patent searches are often indispensable in tracing the development of new technologies when creating innovation maps. After the 17 years that protect patented products and processes in the United States are over, patents are often helpful in the design of next-generation processes to produce the principal chemicals, or improved chemical products that have preferable properties, chemical reactions, and so on. However, many patents withhold important know-how that may be vital to success. Since a patent is legal property, like a house

or a car, it, and perhaps the know-how, can be owned, bought, and sold. Often patents are licensed for fees on the order of 3–6% of gross sales. This can be important when a design team decides to incorporate a patented chemical product in its design. Patents from the United States, Great Britain, Germany, Japan, and other countries are available on the Internet, with the details of carrying out a patent search discussed in Example 1.5.

Several resources are available to search for helpful patents. *SciFinder* (*Chemical Abstracts*) is usually the most useful when designing chemical products and processes. In addition to journals and books, it can be used to search by text, chemical structure, or chemical reaction.

Searching for Chemicals by Structure and Reaction

Increasingly, searches may be carried out using a chemical structure or using a portion of the structure (called a substructure). This is possible within *SciFinder* (*Chemical Abstracts*) and *Reaxys*, which contain over 800 physical and chemical properties for more than five million organic, inorganic, and organometallic substances.

Hazards, Safety, and Regulatory Information

Here, also, many sources are provided to assist in the design of chemical products and processes. To learn about the key issues and many such sources, in this chapter, see Section 3.4 on Environmental Protection and Section 3.6 on Safety Considerations.

SRI Design Reports

SRI, a consortium of several hundred chemical companies, publishes detailed documentation for many chemical processes. Their reports provide a wealth of information, but most are written under contract for clients, and, consequently, are not available to the public. Yet some materials are available online by subscription to the public. Furthermore, most industrial consultants have access to these reports and may be able to provide helpful information to student design teams, especially those who carry out some of the design work in company libraries.

General Search Engines and Information Resources

Google™

To the lay public, so-called general search engines and information resources are easy to use, usually providing helpful responses rapidly. Thanks to advanced search algorithms and massive parallelism (a large number of processors working in parallel), millions of people regularly use the Google search engine to search the entire Internet using search terms often known only to a few individuals. Yet Google regularly returns extensive lists of pertinent information in the form of Web site addresses in the order of popularity, which is normally very helpful. The Google search engine is so effective and easy to use that its use is becoming ubiquitous. Although it is usually an excellent *starting point*, the quality of the information it retrieves, especially technical information for the design of new products and processes, must be critically assessed. Over the years, the investments of technical publishers in journals and books, edited by outstanding technical persons and subject to peer review, have produced an authoritative literature that is normally more reliable than the results of an open-ended search using a general search engine.

Google Scholar™

This less-general search engine focuses on the scholarly literature including articles, theses, and books from academic publishers, technical societies, and universities but excludes most Web sites. It permits searching for related works, citations, authors, and publications. It checks for citations of specific publications and creates an author profile. Also, it aims to rank documents weighing the full text of each document, where it was published, and who it was written by as well as how often and how recently it was cited in the scholarly literature.

Wikipedia

A far more general encyclopedia than those specifically helpful in chemical product and process design (cited above) is Wikipedia, a multilingual, Web-based, free-content encyclopedia project written collaboratively for the Internet by volunteers. The vast majority of Wikipedia articles can be edited by anyone with access to the Internet. Its primary servers are in Tampa, Florida, with additional servers in Amsterdam and Seoul. Because Wikipedia is Web based, articles can be created within minutes or hours of an announced event or development, and can be constantly updated. This makes Wikipedia the encyclopedia of choice for the latest technology with convenient access through the Google™ search engine. For example, if up-to-date information is desired on the new compact fluorescent light bulb, one need only open www.google.com on the Internet and enter the search results in the Web address for a Wikipedia article entitled "Compact Fluorescent Lamp."

Wikipedia was created in 2001, and as of mid-2014, contained more than 4.5 million articles in English (plus articles in many other languages). Because Wikipedia articles can be created and edited by anyone with Internet access, critics claim that it is susceptible to errors and unchecked information. Whereas this is true, recent studies suggest that Wikipedia is broadly as reliable as the *Encyclopedia Britannica*.

From the perspective of an information professional (e.g., librarian), Wikipedia is often a *tertiary source*, written by persons who interpret information written by others, which often begin with *primary sources*. To check for authenticity, readers should check for the availability of "sources"; that is, clear references to the primary sources. It also helps to "triangulate" information, that is, to confirm consistency from three independent sources.

General Patent Searches

In addition to Goggle patent searches, discussed in Section 1.3, several general patent search engines are available. These include the *Derwent Innovations Index*, which covers 44 patent-issuing authorities from 1963 to the present; *Esp@cenet* (European

Patent Office), which covers patents from over 80 authorities, including Europe, the World Intellectual Patent Organization, the United States, Japan, and China; *Patent Lens*, which searches patents granted from the United States, Australia, and Europe, as well as many published patent applications; *USPTO* (*United States Patent and Trademark Office*), which includes TIFF images of every patent issued by the United States (1790 forward), as well as searchable HTML full text of all patents since 1976.

3.2 STIMULATING INVENTION AND INNOVATION

Returning to the subsection Product Design in Section 1.3, the *innovation map* was introduced, showing the linkages between new technologies and customer needs in creating innovative new chemical products. The new technologies for new chemical products are normally the technical inventions by physicists, chemists, biologists, material scientists, and chemical engineers, often obtained in research laboratories. The innovations arise in applying these technologies for the design of new chemical products. This section discusses steps taken by companies to create an environment in which invention and innovation flourish. Several examples of the initiatives in practice are discussed next. Several are widely applied in industries that create and manufacture new chemical products. The first set was introduced by 3M Company.

Fifteen Percent Rule, Tech Forums, Stretch Goals, Process Innovation Tech Centers—3M Company

Fifteen Percent Rule. At 3M, managers are expected to allow employees 15% of their time to work on projects of their own choosing. This rule, which has become a fundamental part of the 3M culture, is assessed nicely by Bill Coyne, a research and development manager: "The 15% part of the Fifteen percent Rule is essentially meaningless. Some of our technical people use much more than 15% of their time on projects of their own choosing. Some use less than that; some use none at all. The number is not so important as the message, which is this: the system has some slack in it. If you have a good idea, and the commitment to squirrel away time to work on it, and the raw nerve to skirt your lab manager's expressed desires, then go for it" (Gundling, 2000).

Tech Forum. This terminology, which is used at 3M, is typical of organizational structures designed to encourage technical exchange and a cross-fertilization of ideas between persons working in many corporate divisions at widely disparate locations. At 3M, the Tech Forum is organized into chapters and committees with the chapters focused on technology, including the Physics Chapter, the Life Sciences Chapter, and the Product Design Chapter. Chapters hold seminars related to their own areas of technology, presented by outside speakers or 3M employees. Some chapters do not have a technical focus. For example, the Intellectual Property Chapter is primarily targeted at patent attorneys. Also at 3M, the Tech Forum hosts a two-day "Annual Event" at the St. Paul headquarters with each of the 3M labs invited to assemble a booth. Since the company rewards labs when other divisions use their technology, employees have an incentive to participate in this internal trade show.

Stretch Goals. Another 3M policy, intended to *stretch* the pace of innovation, is the rule that at least 30% of annual sales should come from products introduced in the past four years. The policy has recently been refined to establish an even greater sense of urgency, such that "10% of sales should come from products that have been in the market for just one year" (Gundling, 2000).

Process Innovation Technology Centers. Because 75% of manufacturing at 3M is done internally, two technology centers are provided. One is staffed with chemical engineers and material scientists to help researchers scale up a new idea for a product from the bench to production, with a focus on core technologies. The other center handles the development and scale-up for key manufacturing process technologies such as coating, drying, and inspection and measurement. The latter is staffed primarily with chemical and mechanical engineers and software development personnel. These centers work closely with researchers and engineers involved in product development and equipment design.

Open Innovation Concept—P&G

At Procter and Gamble, an open innovation concept has been embraced, with P&G having transformed its R&D process into an open innovation environment called "connect and develop," tapping collective knowledge and technologies from around the world. The executives of P&G have set targets seeking 50% of their new products from external sources. To speed up the introduction of new products, they seek to outsource some of their technology-development effort while maintaining their core technology competencies. They are leveraging the worldwide pool of inventors, scientists, and suppliers to develop new products internally.

Cross-Functional Collaboration—GE

General Electric addresses major issues by assembling teams of top performers from various disciplines for one or two weeks. Their recommendations are presented to senior executives with many implemented and involving corporate-wide changes.

Internet Surfing—Samsung

To spark their innovative spirits, Samsung mandates that its engineers allocate a portion of their time to surfing the Internet for technical and business news. Their observations of worldwide trends often lead to new foci in their product-development processes.

Learning Journeys—Starbucks and 3M

To obtain a better appreciation of local cultures, behavior patterns, and fashions, Starbucks has formulated *learning journeys*

in which groups of product developers visit several countries for a few months. This immersion into foreign cultures has led to new product ideas.

Similarly, in the current Information Age with people increasingly using personal data assistants (PDAs) and smartphones, 3M perceived this as a threat to its Post-it note™ business. Consequently, by observing how users share digital photo collections, a 3M Office Supply Business team developed Post-it Picture™ paper.

Keystone Innovation—Corning

Finally, the Corning keystone innovation strategy (Graham and Shuldiner, 2001) recognizes that many of their "top-hit" innovations combine three important ingredients for market success; they (1) address megatrend market needs, (2) address performance barriers, and (3) provide differentiated and sustainable solutions. In their major innovation (early 2000s)—ultra-thin, super-flat glass substrates for liquid crystal displays (LCDs)—Corning took advantage of the megatrend in the growing demand for high-quality displays having small footprints. As discussed in Seider et al. (2009), Sections 14.3 and 15.3, they addressed a different performance barrier, that is, the nonuniform thickness of glass substrates for high-resolution images, by inventing a novel glass formulation and the Isopipe™ manufacturing process, which are also difficult to replicate. And consequently, their *keystone* innovation strategy has created a glass substrate business poised to withstand growing competition from organic light-emitting diodes (OLEDs) display technologies.

Summary

Innovative cultures require environments with greater degrees of freedom, which collide directly with environments having few, if any, degrees of freedom, typical of the later product-development stages. Successful companies maintain this delicate balance, enabling them to launch more successful products into the market in record times.

3.3 ENERGY SOURCES

Throughout the industrial revolution and beyond, the principal energy sources have been fossil fuels: coal, oil, and natural gas. These are high-energy-density fuels that, when burned, release CO_2 (a greenhouse gas, GHG), soot and NOx (in smog), and SO_2 (which forms sulfuric acid in acid rain. Also, they are not renewable, having been formed in the Earth, often from plant matter subjected to geological processes over millions of years. And they are not sustainable beyond one to two centuries because they are being depleted largely by the developed countries (especially the United States) and at increasing rates by large developing countries, for example, China, India, and Indonesia. These countries are rapidly increasing their technology bases, including motor vehicles, electric grid infrastructures, communication devices, and product manufacturing plants.

EXAMPLE 3.1 ***Energy Density***

At 0°C and 1 atm, compare the energy densities in Kcal/Kg of H_2, CH_4, ethanol, and n-octane.

SOLUTION

The results computed using ASPEN PLUS (PRSK Property Option) are:

	CH_4	H_2	Ethanol, Liquid	*n*-Octane, Liquid
Mass heating value at 0°C, cal/g	13,295	33,961	11,530	11,547
Molar volume at 0°C, 1 atm, mol/cm^3	4.09×10^{-5}	4.08×10^{-5}	1.42×10^{-2}	5.25×10^{-3}
Density at 0°C, 1 atm, g/cm^3	6.56×10^{-4}	8.226×10^{-5}	0.6542	0.600
Volumetric heating value at 0°C, cal/cm^3	8.722	2.793	7,543	6,925

The heating value is the heat released in combustion at 0°C. On a mass basis, it is highest for hydrogen by a factor of approximately three. But on a volume basis, the liquid heating values are approximately three orders of magnitude higher than the vapor heating values.

Although this section is intended to cover each of the principal energy resources, it places emphasis on resources gaining attention in the 21st century, including shale oil, shale gas, hydrogen fuel, geothermal sources, and biofuels as well as resources being actively developed by chemical engineers. In Parts 2, 3, and 5 of this textbook, strategies and case studies are presented for design of the alternate chemical products (e.g., biodiesel, green diesel, and jet fuel and alternative pharmaceuticals) and processes to manufacture them. Note that the distribution of these resources in the United States in 2011 is shown in Figure 3.1, which is presented by the U.S. Energy Information Administration (EIA). Clearly, petroleum and coal supply more than half of the energy utilized. Natural gas is used actively and is growing rapidly due to the widespread installation of shale gas drilling rigs. Similarly, renewable energy sources are expanding rapidly, but they began at only 9% in 2011. In time, they should grow to a larger percentage, especially as environmental and sustainability issues become more widely recognized and the electrical power grid expands.

Utilization data for these principal energy sources over many years is available from the Web site of the EIA for many countries worldwide. You can access international energy statistics at www.eia.gov.

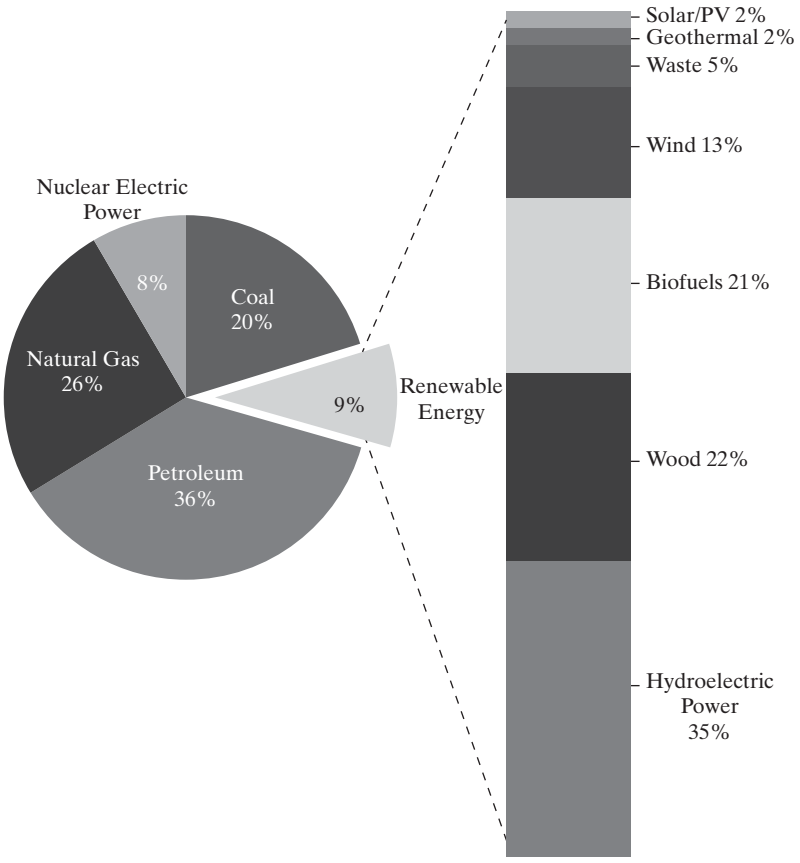

Figure 3.1 Energy distribution in the United States in 2011. (*Source:* U.S. Energy Information Administration (www.eia.gov/aer), Annual Energy Review 2011, September 2012). See the Color Figures folder on the Wiley Web site.

Coal, Oil, and Natural Gas

Until recently, probably the most dominant fuel was coal, which is mined using increasingly automated rigs that operate more safely, but still with the significant dangers of gas explosions and mine collapses. Various grades of coal (bituminous, lignite, and anthracite) have different C/H ratios, on average, about 0.9 molar. Oil is pumped using oil rigs and, on average, has C/H ratios about 0.7, producing less greenhouse gases (GHGs) (i.e., CO_2, for comparable energy yields). Natural gas (principally CH_4) has a reduced ratio of 0.25, and consequently, produces less GHGs (CO_2, but note that CH_4 is itself a significant GHG.)

Shale Oil

In 1953, a large shale deposit, mainly in North Dakota and occupying 200,000 square miles, was described by a geologist, J. W. Nordquist. The deposit, called the Bakken Formation, is estimated to hold billions of barrels of recoverable light oil. Because the cost of producing shale oil at that time by well-known thermal means was not competitive with the production of oil from conventional sources of crude oil, the Bakken shale was mostly ignored. By January 2008, the price of oil was on the order of $100 per barrel. Also, by then, horizontal drilling was developed. By combining it with a hydraulic fracking technique to free oil from the shale, shale oil could now be produced at a break-even price of about $50 per barrel. The production of oil from shale was now competitive with its production from petroleum deposits, and the production of shale oil began in earnest. By 2013, about 300 million barrels of shale oil was produced in North Dakota. In addition to the oil, about 600 million cubic feet of shale gas per day was produced. The effect of the production of shale oil on the price of a barrel of oil has been very significant. In mid-2000, the price of crude oil had risen to a high of $150 per barrel. By January 2015, the price had dropped to $50 per barrel.

Shale Gas

During the 20th century, large shale deposits were known to contain vast quantities of natural gas. Various retorting processes were developed to recover CH_4, but these were unable to compete with natural gas wells. Just over the past decade, drilling technologies have been created that insert water injection/gas removal lines vertically to great depths into the shale rock below the water table (typically 2-mile below the drilling rig), and then gradually turn them 90° before drilling horizontally long distances through shale deposits (on the order of 1-mile. In the horizontal section, a perforating device drills small holes through which water is sent to fracture the shale. Gas is released from the shale, its bubbles rising to the surface. These technologies have drastically increased the rates of shale gas production at sufficiently low prices to be competitive with natural gas wells. Large sources of competitively priced shale gas are causing

energy companies in the United States to transform rapidly from oil importers to gas exporters. And, in parallel, petrochemical companies are returning to manufacture chemicals in the United States. For several decades, these companies built plants abroad in the proximity of abundant and cheaper sources of gas and oil. Most recently, large plants have been announced to be constructed near shale gas deposits. One in southwest Pennsylvania will recover ethane (at ∼15 wt% from Marcellus shale) for conversion to ethylene and other olefin commodity chemicals (e.g., propylene), the building blocks of textiles, plastic parts, and reusable containers. In short, shale gas has been leading a boom in the U.S. chemical industry.

Hydrogen

Another source, not involving carbon, is H_2 fuel, which is the basis of the *Hydrogen Economy* proposed by Prof. John Bockris (University of Pennsylvania; Bockris, 1970). As seen in Example 3.1, H_2 has a significantly higher energy mass density than common fuels and burns cleanly with *zero* carbon emissions. On the negative side are safety concerns (H_2 explosions can be very dangerous), and the principal current source of H_2 is a fossil fuel, natural gas—to be discussed under Hydrogen Production. Currently, H_2 production is a large and growing industry with H_2 consumed principally in the Haber process to produce ammonia (NH_3; see Examples 6.4 and 8.5, and Chapter 27) for fertilizer, and for hydrocracking to convert heavy petroleum fractions into lighter fractions suitable for fuels and chemical intermediates. But although H_2 fuel is used to power fuel cells and in rocket launchers, it is not yet a major source of fuel worldwide.

Hydrogen Production

Current H_2 production is principally from fossil fuels with the majority from CH_4 in steam-methane reforming (SMR; Xu and Froment, 1989). Many other production methods are used, but in this brief discussion, just SMR and water electrolysis are discussed.

Steam-Methane Reforming (SMR)

The principal reaction is:

$$CH_4 + H_2O \rightarrow CO + 3H_2 \qquad \text{(R1)}$$

which is endothermic and normally run at temperatures between 700 and 1,100°C and pressures on the order of 30 atm over a solid catalyst. The heat of reaction normally is obtained by burning CH_4 in a furnace with reformer tubes (filled with catalyst) passing through. The front view of a typical furnace box is shown schematically in Figure 3.2.

To produce additional H_2, the effluent syngas is reacted with additional steam in the water-gas shift reaction:

$$CO + H_2O \rightarrow CO_2 + H_2 \qquad \text{(R2)}$$

an exothermic reaction performed at about 130°C. Its effluent gases (H_2, CO, CO_2, and unreacted CH_4) are normally sent to a pressure-swing adsorption (PSA) unit to produce high-purity H_2. The recovered adsorbed species are mixed with fresh CH_4 and fed to the furnace where the CH_4 and CO are completely converted to the greenhouse gas (GHG), CO_2. Overall, the conversion of CH_4 energy to H_2 energy is at a high efficiency on the order of 80%.

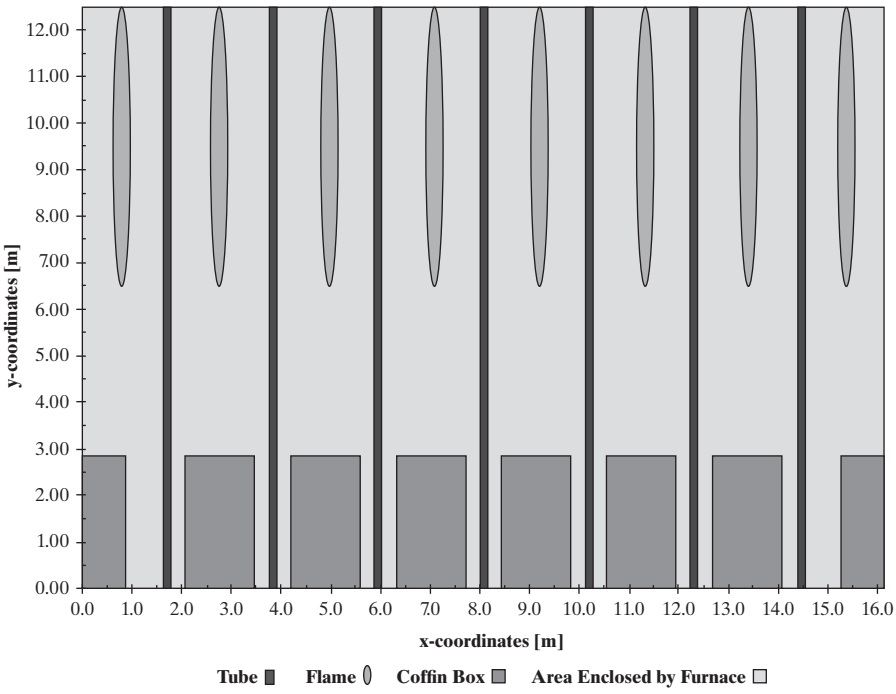

Figure 3.2 Schematic of reformer/furnace. See the Color Figures folder on the Wiley Web site.

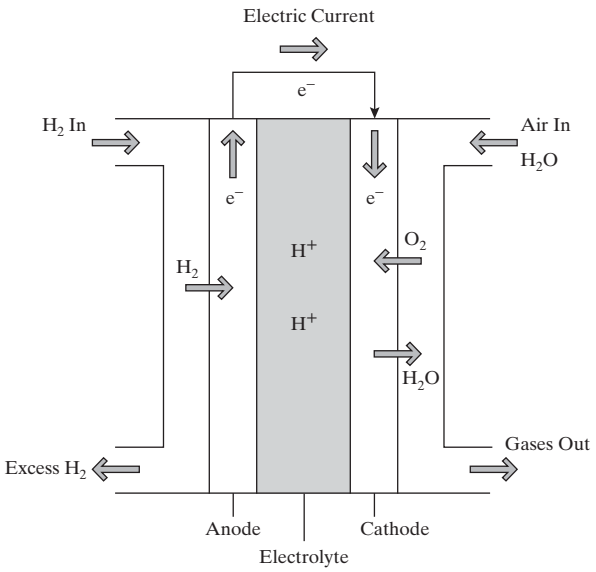

Figure 3.3 Schematic of hydrogen fuel cell.

Water Electrolysis

In this process, electrical work, often generated at low efficiency from the combustion of fossil fuels in a power plant, is used to generate H_2 and O_2. Overall, the conversion of fossil fuel energy to H_2 energy is very low and not competitive.

Fuel Cell Energy Source

An important advantage of hydrogen fuel is that it can convert more energy to electricity through fuel cells than through the use of combustion engines and turbines; that is, fuel cells are not limited by the Carnot efficiency, although they are more expensive to build than common internal combustion engines. A schematic of a hydrogen fuel cell is shown in Figure 3.3.

At the anode, H_2 releases two electrons:

$$H_2 \rightarrow 2H^+ + 2e^- \qquad \text{(R3)}$$

which travel through the external circuit producing direct current, while the two protons diffuse through the electrolyte to the cathode. At the cathode, the protons accept the two electrons and combine with O_2 from air:

$$2H^+ + 2e^- + 1/2O_2 \rightarrow 2H_2O \qquad \text{(R4)}$$

Polymer electrolyte membranes (PEMs) are used in both stationary and portable fuel cells, so-called PEMFCs. These operate at low temperatures (50–100°C) and pressures. In some designs, individual fuel cells produce electrical potentials on the order of 0.7 volt. To produce higher voltages, they are often stacked, that is placed in series (one above the other). In one application, these stacks are used to power automobiles; for example, go to www.toyota-global.com and search for "Powering the future: Hydrogen fuel cell vehicles could change mobility forever."

Hydrogen Adsorption

For H_2 as a transportation fuel, storage as a gas in cylindrical vessels creates a safety hazard. The volume required to store H_2 is also a primary concern, leading to large fuel tank costs and frequent refueling. Consequently, storage of H_2 in solids, such as in hydrates and zeolite adsorbents, is being considered to facilitate its use as a transportation fuel.

Biofuels

Of course, the consumption of increasing quantities of shale gas, although reducing the generation of GHGs compared with coal and oil sources, increases the concentrations of GHGs (principally CO_2 and CH_4) in the earth's stratosphere. To circumvent this, environmentalists are calling for alternative *carbon-neutral* energy sources, such as biofuels, which are produced through photosynthesis (Silva et al., 2015). Several alternatives have been under development over the past two decades. The first, and most mass-produced biofuel, is ethanol from cellulosic crops, including corn, switch grass, and waste plant matter. Ethanol has been fully integrated within the automotive infrastructure; however, it has a low energy density (compared with gasoline) and often competes with food production. Oilseed crops, like palm and jatropha trees, store high densities of vegetable oils (i.e., tryglycerides such as tristearin, $C_{57}H_{110}O_6$; triolein, $C_{57}H_{104}O_6$; trilinolein, $C_{57}H_{98}O_6$), which can be purified and converted to transportation-grade fuels using mature technologies. In addition, microalgae species are being explored for their ability to produce fuel-quality oils. Algae are attractive because they grow approximately 30 times faster than palm trees, yield higher oil fractions, and can be grown in either fresh or brackish water. Various processes are being developed to harvest the cells (from water), extract the oil, and convert it to fuels like biodiesel (fatty-acid methyl esters, FAMEs; e.g., methyl oleate, $C_{19}H_{36}O_2$) in three to four processing steps (Dunlop et al., 2013, Silva et al., 2014). Also, green diesel (alkanes) and jet fuel can be produced from an algae feedstock using hydrogenation methods. All these processes to produce liquid fuels are carbon neutral because plants and algae grow using CO_2 as a carbon source, which is the combustion product of the liquid fuels.

Solar Collectors

Solar energy can also be absorbed by inorganic solar collectors often mounted on the rooftops of residences and commercial buildings. Over the last two decades, the efficiencies of photovoltaic cells, which convert light into electrical current using the photovoltaic effect, have been increasing to as high as 40% (compared with plant photosynthetic efficiencies as low as 1–5%), but at high panel production costs. New products with higher photovoltaic efficiencies, such as solar shingles, are being developed by the Dow Company.

Wind Farms

In recent years, wind farms, containing an array of large windmills have been installed. Most windmills rise on the order of 30–40 ft and contain two propeller blades, each ∼30 ft long, emerging from a rotating shaft near the top. Most important, under computer control, the angle of the rotating shaft is adjusted to capture the largest draft as the wind speed and direction change. Large farms have been installed in windy valleys and off shore in the ocean. The power generated by the windmills must be transmitted to the power grid for storage during periods of low power usage. It is of special note that just 0.5% of solar energy is transformed to wind and waves (Szargut, 2005).

Hydraulic Power

Of course, over many years, dammed rivers use hydraulic power to generate shaft work that drives electric generators. Such dams also play an important role in flood control. Also, as shown in Figure 3.1, 35% renewable energy in the United States in 2011 was produced using hydraulic power. But, this represented just 3.2% of the total energy used in 2011.

Geothermal Power

Geothermal power installations provide on the order of 5% of the world's energy supply in countries well distributed around the globe. Installations vary in design from large and complex power stations to small and relatively simple pumping stations, depending on the sources of heat from the earth and the availability of competitive, low-cost energy sources. In some less-developed countries, such as the Philippines, Iceland, and El Salvador, geothermal plants produce 25% or more of their electricity. The most common current way of capturing the energy from geothermal sources is to tap into naturally occurring "hydrothermal convection" systems where cooler water seeps into the Earth's crust, is heated up, and then rises to the surface. When heated water is forced to the surface, it is a relatively simple matter to capture that steam and use it to drive electric generators. Geothermal power plants drill holes into the rock to more effectively capture the steam.

Three designs for geothermal power plants pull hot water and steam from the ground, use it, and then return it as warm water to prolong the life of the heat source. In the simplest design, the steam goes directly through a turbine and then into a condenser where the steam is condensed into water. In a second approach, very hot water is depressurized or "flashed" into steam, which can then be used to drive a turbine. In the third approach, called a binary system, the hot water is passed through a heat exchanger, where it heats a second liquid—such as isobutane—in a closed loop. The isobutane boils at a lower temperature than water, so it is more easily vaporized to run a turbine. The design choice is determined by the resource. If the water comes out of the well as steam, it can be used directly, as in the first design. If it is hot water of a high enough temperature, a flash system can be used; otherwise, it must go through a heat exchanger. Because there are more hot water resources than pure steam or high-temperature water sources, there is more growth potential in the heat exchanger design.

However, the largest geothermal system now in operation is a steam-driven plant north of San Francisco, California, known as the Geysers (but is not located at a geyser), which provides steam only. By 1990, 26 power plants had been built for a capacity of more than 2,000 MW. Of special note, in 2008, the United States had more geothermal capacity than any other country with more than 3,000 megawatts in eight states. Also, on a small scale, geothermal heat pumps have been installed underground at home sites, providing 55°F cooling in the summer and partially heating during the winter. For additional information on geothermal energy technologies, see the reference by the Union of Concerned Scientists.

Nuclear Power

Nuclear power is generated by splitting Uranium-235 (an unstable isotope) into stable isotopes of krypton and barium by nuclear fission. The energy produced is captured by converting high-pressure water to steam, which drives turbines that generate work. This energy is carbon-free but raises safety concerns, especially after the tsunami in Fukushima Daiichi, Japan, in March 2011 that disabled the water circulation system, causing a meltdown of its highly radioactive fuel rods. Widespread contamination resulted that was difficult to contain and remediate, causing over 300,000 people to be evacuated from the surroundings. Since then, there has been much resistance to planning for new nuclear power plants.

On the other hand, work continues to develop nuclear fusion (the process by which stars produce energy) on Earth as a safe, pollution-free power source. In fusion, small atomic nuclei (typically deuterium or tritium) collide and unite to produce a larger, more stable nucleus (typically helium). As with fission, mass is not conserved, and the lost mass is converted to high-energy photons. The major hurdle, thus far, has been in overcoming nuclei repulsions (Coulombic forces) in an energy-efficient manner. By confining the atoms in small geometries, energy barriers have been removed, leading to more sustained ignitions of the reactions. These can result in high temperatures, which cannot be contained in most apparati. Consequently, either high-powered magnets or lasers are employed, containing the plasma using Lorenz or inertial forces, respectively.

The use of fusion for energy production has been explored since the early 1950s, but progress has been slow. Recently, due to rising energy concerns, the National Ignition Facility (NIF) was established in California. It uses high-powered lasers to confine the atoms and drive the nuclei together. On October 7, 2013, the NIF created the first fusion reactor that produced more energy than it consumed, but the net production remains too low for fusion to become a viable energy source. On a global scale, the International Thermonuclear Experimental Reactor

(ITER) in the south of France is a collaborative effort across three continents aimed at producing a sustainable reactor by 2027. It uses high-powered magnets to contain the plasma in a Tokamak reactor. Many other fusion experiments are either in construction or in progress. A complete listing can be found on Wikipedia (search for "list of fusion experiments").

Selection of Energy Sources in Design

A key point raised by Weekman (2010) that may not be immediately obvious in this brief review of the key energy sources is the need to consider the existing chemical-conversion infrastructure when selecting energy sources, especially for commodity chemical processes. Together, its likely chemical paths toward desired products and energy sources will develop together. To quote Weekman, "Integration of solar, wind, nuclear and biomass sources with the existing chemical conversion infrastructure for fossil fuels will be key to reaching a new energy equilibrium." More specifically, it may be desirable to coprocess biomass and high-carbon fossil fuels through gasification and water-gas shift technologies. These yield CO and H_2 products (syngas) that can undergo Fischer-Tropsch reactions to yield hydrocarbons for liquid fuels or can be reacted to form the building block, methanol, for typical chemical products.

When selecting energy sources, it is important to recognize that decisions involving environmental impacts, the sustainability of natural resources, safety, and profitability are critical to successful process designs. In the next three sections, key environmental, sustainability, and safety considerations are discussed. Subsequently, throughout this textbook, examples are presented that involve all of these process design issues.

3.4 ENVIRONMENTAL PROTECTION

One of the most significant changes that has occurred since the late 1970s throughout the manufacturing and transportation sectors within the United States, and those of many other industrialized nations, is the transformation of environmental protection from a secondary to a primary issue. Through the Environmental Protection Agency (EPA), with the cooperation of the U.S. Congress, tighter environmental regulations have been legislated and enforced over this period. This has resulted in a noticeable improvement in air quality (especially in urban areas), a reduction in water pollution, and considerable progress in the remediation of many waste dumps containing toxic chemicals. In short, the United States and many other industrialized nations are rapidly increasing their emphases on maintaining a clean environment. To bring this about, in recent years large investments have been made by the chemical process industries to eliminate sources of pollution. These investments have increased the costs of manufacturing, which, in turn, have been transmitted to consumers through increased costs of end products. Because most producers are required to satisfy the same regulations, the effect has been to translate the costs to most competitors in an evenhanded manner. Problems have arisen, however, when chemicals are produced in countries that do not have strict environmental standards and are subsequently imported into the United States at considerably lower prices. Issues such as this are discussed regularly at international conferences on the environment, which convene every two or three years with the objective of increasing the environmental standards of all countries.

In this section, several of the more pressing environmental issues are reviewed, followed by a discussion of many environmental factors in process design. Then, a few primitive problem statements are reviewed, with reference to the more complete statements provided in the file, Supplement_to_Appendix_II.pdf, which can be downloaded from the website: www.seas.upenn.edu/~dlewin/UPenn Design Problem Statements.html. For more comprehensive coverage in these areas, the reader is referred to the discussions of "Environmental Protection, Process Safety, and Hazardous Waste Management" in *Frontiers in Chemical Engineering* (Amundson, 1988); *Environmental Considerations in Process Design and Simulation* (Eisenhauer and McQueen, 1993); *Pollution Prevention for Chemical Processes* (Allen and Rosselot, 1997); and *Green Engineering: Environmentally Conscious Design of Chemical Processes* (Allen and Shonnard, 2002). Early efforts to protect the environment focused on the removal of pollutants from waste gas, liquid, and solid streams. Effort has now shifted to *waste minimization* (e.g., waste reduction, pollution prevention). The need for *sustainability* in the selection of raw materials and chemical products will be considered next in Section 3.5.

Environmental Issues

At the risk of excluding many key environmental issues, the following are singled out as being closely related to the design of chemical products and processes.

Burning of Fossil Fuels for Power Generation and Transportation

Because fossil fuels are the predominant sources of power worldwide, their combustion products are a primary source of several pollutants, especially in the urban centers of industrialized nations. More specifically, effluent gases from burners and fires contain sizable concentrations of SO_2, the nitrogen oxides (NO_x), CO, CO_2, soot, ash, and unburned hydrocarbons. These, in turn, result in many environmental problems, including acid rain (principally concentrated in H_2SO_4), smog and hazes (concentrated in NO_x), the accumulation of the so-called *greenhouse gases* (CO_2 and CH_4), volatile toxic compounds (e.g., formaldehyde, phenol), and organic gases (e.g., CO), which react with NO_x, especially on hot summer days, altering the O_3 level. As the adverse impacts of pollutants on animals, plant life, and humans are being discovered by scientists and engineers, methods are sought to reduce their levels significantly. In some cases, this is accomplished by one of several methods, such as separating the sources (e.g., sulfur compounds) from fuels; adjusting the

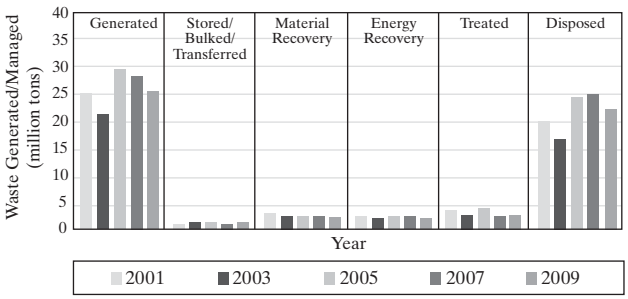

(a) Generation and management in the United States, 2001–2009

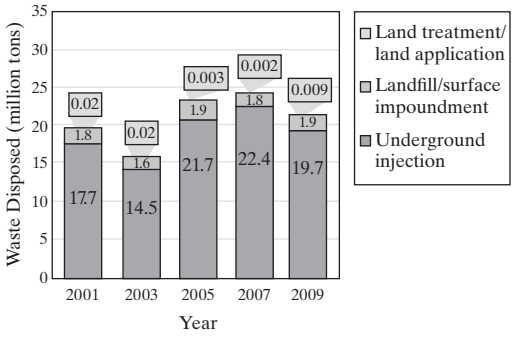

(b) Disposal to land in the United States by practice, 2001–2009

Figure 3.4 RCRA hazardous waste.
(*Source:* Eisenhauer and McQueen, 1993. See the Color Figures folder on the Wiley Web site).

combustion process (e.g., by reducing the temperature and residence time of the flame to produce less NO_x); separating soot, ash, and noxious compounds from effluent gases; reacting the effluent gases in catalytic converters; or through the use of algae to consume (through photosynthesis) large quantities of CO_2 in flue gases. As a rule of thumb, it should be noted that the cost of cleaning combustion products is approximately an order of magnitude less than the cost of removing contaminants from fuel. This is an important heuristic, especially when designing processes that are energy intensive, requiring large quantities of fuel.

Handling of Toxic Wastes

In the chemical and nuclear power industries, large quantities of toxic wastes are produced annually. The United States Congress passed the Resource Conservation and Recovery Act (RCRA) in 1976. In the first decade of the 21st century, the EPA has accumulated the data in Figure 3.4, which shows the annual quantities of hazardous wastes generated and their distribution throughout the United States. Some hazardous waste generators treat, store, and dispose of their hazardous waste onsite, and others ship their waste to treatment, storage, and disposal facilities (TSDFs). Most hazardous wastes are eventually disposed of in landfills, surface impoundments (which eventually become landfills), and land application units or by deep well injection (Figure 3.4b). Since the late 1960s, many of the burial sites (e.g., Love Canal, Times Beach) have threatened the health of nearby residents and, more broadly, have threatened to contaminate the underground water supply throughout entire states and countries. In this regard, studies by the state of California have shown that aqueous waste streams from the processing of electronic materials are posing widespread threats to the groundwater in California's Silicon Valley. In fact, this area has a leading number of sites on the U. S. National Priority List of toxic waste dumps (which comprises approximately 10,000 sites throughout the United States). In process design, it is essential that facilities be included to remove pollutants from wastewater streams. The design of mass-exchange networks (MENs) for this and other purposes is the subject of the Supplement_to_Chapter_11-2.pdf file in the Wiley Web site associated with this textbook.

Bioaccumulated Chemicals

Probably the most well-known cases of chemicals that have been discovered to *bioaccumulate* in the soil and plant life are the insecticide DDT (l,l-bis(4-chlorophenyl)-2,2,2-trichloroethane; $C_{14}H_9Cl_5$) and the solvent PCBs (polychlorinated biphenyls). DDT was sprayed in large quantities by low-flying airplanes to kill insects and pests throughout the 1950s. Unfortunately, although effective for protecting crops, forests, and plant life, toxic effects in birds, animals, and humans were strongly suspected, as discussed in Section 3.7. Consequently, DDT was banned by the U.S. EPA in 1972. Its effect, however, will remain for some time due to its having bioaccumulated in the soil and plant life.

Toxic Metals and Minerals

In this category, major changes have taken place since the late 1960s in response to the discoveries of the toxic effects of lead, mercury, cadmium, and asbestos on animals and humans. After lead poisoning (accompanied by brain damage, disfigurement, and paralysis) was related to the ingestion of lead-based paints by children (especially in older buildings that are not well maintained), the EPA banned lead from paints as well as from fuels. In fuel, tetraethyl lead had been used as an octane enhancer throughout the world. It was subsequently replaced by methyl *tertiary*-butyl ether (MTBE), which is also being replaced due to reports that it can contaminate ground water. Mercury, which has been the mainstay of manometers in chemistry laboratories, has similarly been found to be extremely toxic, with disastrous effects of accidental exposure and ingestion reported periodically. In the case of asbestos, its toxic effects have been known since the late 1940s, yet it remains a concern in all buildings built before then. Gradually, as these buildings are being renovated, sheets of asbestos insulation and asbestos ceiling tiles are being removed and replaced by nontoxic materials. Here also, the incidents of asbestos poisoning are associated most often with older buildings that have not been well maintained.

Summary

As the adverse effects of these and other chemicals become better understood, chemical engineers are being called on to

satisfy far stricter environmental regulations. In many cases, these regulations are imposed to be safe even before sufficient data are available to confirm toxic effects. For these reasons, chemical companies are carefully reexamining their existing products and processes and evaluating all proposed plants to confirm that they are environmentally sound, at least insofar as meeting the regulations imposed or anticipated to be imposed by the environmental regulation agencies.

Environmental Factors in Product and Process Design

The need to retrofit existing plants and to design new, environmentally sound plants has required chemical engineers to become far more proficient in accounting for envionmentally related factors. In this section, a few of the better-recognized factors are discussed. Additional coverage is included related to purges in Section 6.3, to fuel sources in the previous section, and to wastewater treatment in the file Supplement_to_Chapter_11-2.pdf in the PDF Files folder on the Web site associated with this textbook.

More complete coverage may be found in the comprehensive textbook *Green Engineering: Environmentally Conscious Design of Chemical Processes* (Allen and Shonnard, 2002).

Reaction Pathways to Reduce Byproduct Toxicity

The selection of reaction pathways to reduce byproduct toxicity is a key consideration during preliminary process synthesis when the reaction operations are positioned. As the reaction operations are determined by chemists and biochemists in the laboratory, the toxicity of all chemicals, especially chemicals recovered as byproducts, needs to be evaluated. For this purpose, companies have toxicity laboratories and, in many cases, large repositories of toxicity data. One useful source, especially for students at universities is the *Pocket Guide to Chemical Hazards* of the National Institute for Occupational Safety and Health (NIOSH, 1987). Clearly, when large quantities of toxic chemicals are anticipated, other reaction pathways must be sought; when these cannot be found, design concepts are rejected, except under unusual circumstances.

Reducing and Reusing Wastes

Environmental concerns have caused chemical engineers to place even greater emphasis on recycling, not only unreacted chemicals but also product and byproduct chemicals. In so doing, design teams commonly anticipate the *life cycles* of their products and byproducts, paying special attention to the waste markets, so as to select the appropriate waste quality. Stated differently, the team views the proposed plant as a producer of engineering scrap and attempts to ensure that there will be a market for the chemicals produced after their useful life is over. Clearly, this is a principal consideration in the production of composite materials and polymers. In this connection, it is important to plan on producing segregated wastes when they are desired by the waste market and, in so doing, to avoid overmixing the waste streams.

Avoiding Nonroutine Events

To reduce the possibilities for accidents and spills with their adverse environmental consequences, processes are often designed to reduce the number of transient operations, cleanup periods, and catalyst regeneration cycles. In other words, emphasis is on the design of a process that is easily controlled at or near a nominal steady state with reliable controllers and effective fault-detection sensors.

Materials Characterization

Often, waste chemicals are present in small amounts in gaseous or liquid effluents. To maintain low concentrations of such chemicals below the limits of environmental regulations, it is important to use effective and rapid methods for measuring or deducing their concentrations from other measurements. In this regard, the design team needs to understand the effect of concentration on toxicity, which can vary significantly in the dilute concentration range. Another consideration is to design the plant to use recycled chemicals—that is, someone else's waste. When this is accomplished, it is necessary to know the range of compositions within which the waste chemicals are available.

Design Objectives, Constraints, and Optimization

Environmental objectives are normally not well defined because economic objective functions normally involve profitability measures whereas the value of reduced pollution is not easily quantified by economic measures. As a consequence, design teams often formulate mixed objective functions that attempt to express environmental improvements in financial terms. In other cases, the team may settle for the optimization of an economic objective function subject to bounds on the concentrations of the solutes in the waste streams. It is important to assess whether the constraints are *hard* (not allowed to be violated) or *soft* (capable of being violated under unusual circumstances). Emphasis must be placed on the formulation of each constraint and the extent to which it must be honored.

Regulations

As mentioned previously, some environmental regulations can be treated as constraints to be satisfied during operation of the process being designed. When a mathematical model of the proposed process is created, the design team can check that these constraints are satisfied for the operating conditions being considered. When an objective function is formulated, the design variables can be adjusted to obtain the maximum or minimum while satisfying the constraints. Other regulations, however, are more difficult to quantify. These involve the expectations of the

public and the possible backlash should the plant be perceived as a source of pollution. In a similar vein, constraints may be placed on the plant location, principally because the local government may impose zoning regulations that require chemical plants to be located in commercial areas beyond a certain distance from residential neighborhoods. To keep these regulations from becoming too prohibitive, chemical companies have a great incentive to gain public confidence by satisfying environmental regulations and maintaining excellent safely records, as discussed in Section 3.6.

Intangible Costs

Like the regulations imposed by local governments, some of the economic effects of design decisions related to the environment are very difficult to quantify. These include the cost of liability when a plant is found to be delinquent in satisfying regulations, and in this connection, the cost of legal fees, public relations losses, and delays incurred when environmental groups stage protests. Normally, because these costs cannot be estimated reliably by a design team, mixed objectives are not formulated and no attempts are made to account for them in an optimization study. Rather, the design team concentrates on ensuring that the regulations will be satisfied, thereby avoiding legal fees, public relations losses, and the complications associated with public demonstrations.

Properties of Dilute Streams

Most pollutants in the effluent and purge streams from chemical plants are present in dilute concentrations. Furthermore because the regulations often require that their concentrations be kept below parts per million or parts per billion, reliable and fast analysis methods are needed to ensure that the regulations are satisfied. Beyond that, it is often important to understand the impact of the concentration on the kinetics of these species in the environment—for example, the rates of chemical reaction of organic species, such as CO with NO_x in the atmosphere to produce O_3, and the rate at which other reaction byproducts are formed. With this knowledge, a company can help regulatory agencies arrive at concentration limits more scientifically and, in some cases, at limits that are less restrictive and costly. Note that in urban smog, high concentrations of ozone often create problems for people with respiratory ailments.

Properties of Electrolytes

Many aqueous streams contain inorganic compounds that dissociate into ionic species, including acids, bases, and salts, often in dilute concentrations. These electrolytic solutions commonly occur in the manufacture of inorganic chemicals (e.g., soda ash. Na_2CO_3) in the strong solvents used in the pulp and paper industry, in the aqueous wastes associated with the manufacture of electronic materials (e.g., silicon wafers, integrated circuits, photovoltaic films), and in many other industries. Strong electrolytes dissociate into ionic species whose interactions with water and organic molecules are crucial to understanding the state of a mixture—that is, the phases present (vapor, water, organic liquid, solid precipitates, etc.) at a given temperature and pressure. Hence, when designing processes that involve electrolytes, a design team needs to include the properties of ionic species in its thermophysical properties database. Fortunately, to provide assistance for designers, databases and facilities for estimating the thermophysical properties of a broad base of ionic species over an increasing range of temperatures and pressures are available in process simulators.

Environmental Design Problems

Since the late 1970s, the number of design projects focusing on the solution of environmental problems has increased significantly. These, in turn, are closely related to environmental regulations, which have become increasingly strict. Although it is beyond the scope of this book to provide a comprehensive treatment of the many kinds of designs that have been completed, it is important that the reader gain a brief introduction to typical design problems. This is accomplished through the design projects listed in Table 3.1. As can be seen, a large fraction of the design projects are concerned with air quality; others involve water treatment; two involve soil treatment; one involves the conversion of waste fuel to chemicals; and several involve the production of fuels and chemicals from renewable resources. The problem statements for these design projects, as they were presented to student groups, are reproduced in the file Supplement_to_Appendix_II.pdf, which can be downloaded from the University of Pennsylvania website, www.seas.upenn.edu/˜dlewin/UPenn Design Problem Statements.html. Keep in mind that, as the designs proceeded, the design teams often upgraded the information provided, and in some cases created variations that were not anticipated by the originator of the problem statement.

A closer look at Table 3.1 shows that the projects address many aspects of air quality control. Two alternative approaches to sulfur removal from fuels are proposed, one involving desulfurization of the fuel and the other the recovery of sulfur from its combustion products. One is concerned with NO_x removal from combustion products, and three involve the recovery of hydrocarbons from effluent gases. Under water treatment, the projects involve the recovery of organic and inorganic chemicals from aqueous waste streams. Two alternative approaches to soil treatment are proposed, including the use of phytoremediation, that is, using plants to absorb lead and other heavy metals. Many involve the conversion of biomass to fuels and chemicals. All of the projects involve chemical reactions, and, consequently, the design teams comprise chemical engineers, chemists, and biochemists. In this respect, it seems clear that chemistry and biology are the key ingredients that qualify chemical engineers to tackle these more challenging environmental problems.

Table 3.1 Environmental Design Projects

Project	Location in Book[a]
Environmental—Air Quality	
R134a Refrigerant (2001)	App. IIS–Design Problem A-IIS.9.1
Biocatalytic Desulfurization of Diesel Oil (1994)	App. IIS–Design Problem A-IIS.9.2
Sulfur Recovery Using Oxygen-Enriched Air (1993)	App. IIS–Design Problem A-IIS.9.3
California Smog Control (1995)	App. IIS–Design Problem A-IIS.9.4
Zero Emissions (1991)	App. IIS–Design Problem A-IIS.9.5
Gas Turb. Heat Recov. for Reduced CO_2 Emission (2012)	App. IIS–Design Problem A-IIS.9.6
Recovery and Purification of HFC by Distillation (1997)	App. IIS–Design Problem A-IIS.9.7
Sunlight to Convert CO_2 into Transportation Fuels (2014)	App. IIS–Design Problem A-IIS.9.8
Bio-Butadiene from Waste Carbon Monoxide (2014)	App. IIS–Design Problem A-IIS.9.9
R125 Refrigerant Manufacture (2004)	App. IIS–Design Problem A-IIS.9.10
Zero-Emissions Solar Power Plant (2008)	App. IIS–Design Problem A-IIS.9.11
Removing CO_2 from Stack Gas and Sequestration Techs. (2008)	App. IIS–Design Problem A-IIS.9.12
Environmental—Water Treatment	
Effluent Remediation from Wafer Fabrication (1993)	App. IIS–Design Problem A-IIS.10.1
Recov. of Germanium from Optical Fiber Manufact. Effluents (1991)	App. IIS–Design Problem A-IIS.10.2
Environmental—Soil Treatment	
Phytoremediation of Lead-Contaminated Sites (1995)	App. IIS–Design Problem A-IIS.11.1
Soil Remediation and Reclamation (1993)	App. IIS–Design Problem A-IIS.11.2
Environmental—Renewable Fuels and Chemicals	
Fuel Processor for 5 KW PEM Fuel Cell Unit (2002)	App. IIS–Design Problem A-IIS.12.1
Production of Low-Sulfur Diesel Fuel (2000)	App. IIS–Design Problem A-IIS.12.2
Waste Fuel Upgrading to Acetone and Isopropanol (1997)	App. IIS–Design Problem A-IIS.12.3
Algae to Alkanes (2010)	App. IIS–Design Problem A-IIS.12.4
Algae to Biodiesel (2011)	App. IIS–Design Problem A-IIS.12.5
Furfural and Methyl-tetrahydrofuran-based Biorefinery (2008)	App. IIS–Design Problem A-IIS.12.6
Furfural and THF in China—Corn to Clothes (2008)	App. IIS–Design Problem A-IIS.12.7
Diethyl Succinate Manufacture within a Biorefinery (2008)	App. IIS–Design Problem A-IIS.12.8
1-3 Propanediol from Corn Syrup (2008)	App. IIS–Design Problem A-IIS.12.9
Butanediol as Fuel (2008)	App. IIS–Design Problem A-IIS.12.10
Green Diesel Fuel—A Biofuel Process (2008)	App. IIS–Design Problem A-IIS.12.11
ABE Fermentation of Sugar Cane (2008)	App. IIS–Design Problem A-IIS.12.12
Cellulose to Coke Bottles (2012)	App. IIS–Design Problem A-IIS.12.13
Glycerol to Renewable Propylene Glycol (2011)	App. IIS–Design Problem A-IIS.12.14
Environmental—Miscellaneous	
Combined Cycle Power Generation (2001)	App. IIS–Design Problem A-IIS.13.1
Phosgene-Free Route to Polycarbonates (2009)	App. IIS–Design Problem A-IIS.13.2
Phosgene-Free Route to Isocyanates (2010)	App. IIS–Design Problem A-IIS.13.3
Environ. Accept. Co-Solvent for Reclamation of Co-Solvents (2012)	App. IIS–Design Problem A-IIS.13.4
Drink. Water Using Concen. Solar Power with Sterling Heat Eng. (2011)	App. IIS–Design Problem A-IIS.13.5

[a] In the file, Supplement_to_Appendix_II.pdf, which can be downloaded from the University of Pennsylvania website, www.seas.upenn.edu/~dlewin/UPenn Design Problem Statements.html.

3.5 SUSTAINABILITY

Introduction—Key Issues

A sustainable product is one that meets the needs of society today while respecting the anticipated needs of future generations. Such products are also intended to avoid harming the environment. In some cases, the raw materials and products are called "green." These often help to circumvent health problems, provide environmental protection, preserve natural resources, and prevent climate change.

As mentioned in the previous Section 3.4 on Environmental Protection, the growing emphasis on sustainability is closely related to the increasing recognition of global warming due to the *greenhouse effect* as well as political problems associated with the traditional suppliers of oil and natural gas. Historically, most chemical products have been derived from methane, ethane, propane, and aromatics, normally obtained from oil and natural gas. Furthermore, a large percentage of energy for manufacturing (on the order of 80%) and wastes produced in manufacturing (also on the order of 80%) are associated with the chemical industries, including petroleum refining, chemicals production, forest products, steel, aluminum, glass, and cement. To achieve sustainability while producing high-quality products, it is desirable to use small amounts of raw materials and energy and to produce small amounts of waste.

When planning for sustainability in the 21st century, the rapid growth of the large developing nations, especially China and India, is important. Some estimates project that the world population will stabilize at 9–10 billion people with the consumption of commodities (steel, chemicals, lumber, etc) increasing by factors of 5–6 and energy by a factor of 3.5. Furthermore, the choices of resources are complicated by sustainability considerations. Decisions to take advantage of today's cheap prices and easy accessibility may result in expensive or inaccessible raw materials for future generations.

As the price of oil quadrupled in just three years, from 2005 to 2008, a move toward the usage of renewable "green" resources was initiated. Following the lead in Brazil over several decades, biomass (e.g., sugars, corn, and cellulosic wastes) was being converted to ethanol, principally as a gasoline substitute. In addition, more biomass was being used ro produced chemicals (e.g., 1,3-propanediol and tetrahydrofuran). These carbon sources, when burned as fuel or incinerated as waste, produce carbon dioxide, which is consumed as these green resources grow in photosynthesis. Also, to reduce the accumulation of GHGs, it became increasingly important to find practical ways to sequester carbon dioxide rather than release it to the atmosphere. For these reasons as mentioned in Section 3.3, alternate energy sources, such as wind, solar, geothermal, and nuclear, were gaining increased attention.

It also became common to consider the full *life cycle* when designing chemical products. A growing class of products, formed from biomass, became biodegradable. For example, biodegradable microcapsules carrying pharmaceuticals are injected into the bloodstream for delayed drug delivery over extended periods on the order of one month. In these cases, the raw materials are *renewable* and there are no waste-disposal issues.

Sustainability Indicators

In an attempt to design more sustainable industrial processes that do not compromise the ability of future generations to meet their needs, a set of sustainability indicators was introduced (Ruiz-Mercado et al., 2012a,b; 2013). These are intended to help identify aspects of potential process designs that should be revised to achieve more sustainable chemical processes. These authors at the U.S. Environmental Protection Agency have implemented the GREENSCOPE (Gauging Reaction Effectiveness for the ENvironmental Sustainability of Chemistries with a multi-Objective Process Evaluator) methodology to evaluate processes with 140 different indicators at five levels. The first four are of most concern in process design. At the lowest level 1, are facility compliance/conformance indicators (involving costs associated with environmental, health, and safety compliance). At level 2, the indicators measure material use and performance (i.e., materials use, energy use, and rates of customer complaints and returns.) Level 3 involves indicators that measure facility effects (e.g., acidification potential, percent of workers who report complete job satisfaction.) Level 4 includes supply-chain and product life cycle indicators (e.g., the percent of products designed for disassembly, reuse, or recycling). Level 5 indicators measure system effects (e.g., ecological cumulative exergy consumption; see Chapter 10, especially Section 10.4). Next, the general form of these indicators is presented, but keep in mind that other indicators/indexes have been defined (Cobb et al., 2007, 2009; Krajnc and Glavic, 2003; Sikdar, 2003).

When defining a GREENSCOPE indicator in one of four areas (environmental, efficiency, economic, and energy; that is, the 4 E's), two reference states are needed: the best-target and worst-case states. Then, all indicators are expressed on a percentage basis:

$$Percent\ Score = \frac{Actual - Worst}{Best - Worst} \times 100 \tag{3.1}$$

where the *Best* score is at 100% sustainability and the *Worst* score is at 0% sustainability. With appropriate weighting factors, w_i, $i = 1, \ldots, NI$, an overall sustainability index, SI, can be defined:

$$SI = \sum_{i=1}^{NI} w_i \times Percent\ Score_i \tag{3.2}$$

where NI is the number of sustainability indicators included.

In the environmental area, some indicators involve process input materials. For example, the *Mass of Hazardous Materials Input* indicator has a *Best* target of zero and a *Worst* target equal to the total mass of all inputs. When the *Actual mass* = 0, the *percent Score* is 100% sustainability; when the *Actual mass* = *Worst*, the *Perfect Score* is 0% sustainability. Similarly, the *Specific Hazardous Raw Materials Input* indicator can be defined:

$$m_{\text{spec haz mat}} = \frac{m_{\text{haz mat}}}{m_{\text{prod}}} \tag{3.3}$$

where $m_{\text{haz mat}}$ is the mass of the hazardous material, and m_{prod} is the total mass of the products. *Best* and *Worst* scores would be defined similarly. Another would be the *Safety Hazard, Acute Toxicity* indicator:

$$SH_{\text{acute tox}} = \frac{V_{\text{air polluted}}}{m_{\text{prod}}} \tag{3.4}$$

where $V_{\text{air polluted}}$ is the volume of air polluted at an immediate dangerous concentration. Again, *Best* = 0 and *Worst* = 10^5 m^3/kg, the latter being determined experimentally or based upon experience.

A typical efficiency indicator would be the *Reaction Yield*:

$$Rxtn\ Yield = \frac{m_{\text{prod}}}{m_{\text{theo prod}}} \tag{3.5}$$

where $m_{\text{theo prod}}$ is the theoretical mass of product to be determined for each reaction. Another would be the *Carbon Efficiency*:

$$Carbon\ Eff = \frac{m_{\text{C prod}}}{m_{\text{C reactants}}} \tag{3.6}$$

where $m_{\text{C prod}}$ and $m_{\text{C reactants}}$ are the masses of product and reactants.

Economic indicators include the *Water Cost Fraction* (fraction of production costs), the *Rate of Return on Investment*

[Eq. (17.7)], and the *Payback Period* [Eq. (17.8)]. Finally, energy indicators include the *Solvent Recovery Energy* (SRE):

$$SRE = \frac{Q_{\text{solv recov}}}{m_{\text{prod}}} \tag{3.7}$$

where $Q_{\text{solv recov}}$ is the energy required to recover the solvent and the *Specific Energy Intensity* (SEI):

$$SEI = \frac{Q_{\text{net used prim fuel equiv}}}{m_{\text{prod}}} \tag{3.8}$$

where $Q_{\text{net used prim fuel equiv}}$ is the net energy consumed as a primary fuel equivalent.

With these and similar indicators, chemical engineers can address sustainability systematically at multiple scales in a global setting with multiple objectives (Allen and Shonnard, 2012). Their role in process design is discussed by Carvalho et al. (2013), who present the SustainPro software, which implements a systematic strategy for sustainable design. Beginning with a process flowsheet, the associated material and energy balances, cost estimates, environmental impact indicators and safety indices are evaluated, and life cycle and economic analyses are carried out.

Finally, to complete this discussion of sustainability indicators, consider the study by Ruiz-Mercado et al. (2013) using GREENSCOPE to evaluate the sustainability of a process to convert vegetable oils to biodiesel using a caustic (NaOH) catalyst. To illustrate its approach, GREENSCOPE begins with the CHEMCAD simulation results for a process to transesterify the oil (assumed to be pure oleic acid) to methyl oleate, a fatty-acid methylester (FAME), which is typical of biodiesel. Space is not available herein to define the 66 environmental indicators computed by GREENSCOPE, but Figure 3.5 shows the distribution of indicator results. Clearly, most of the indicators approach

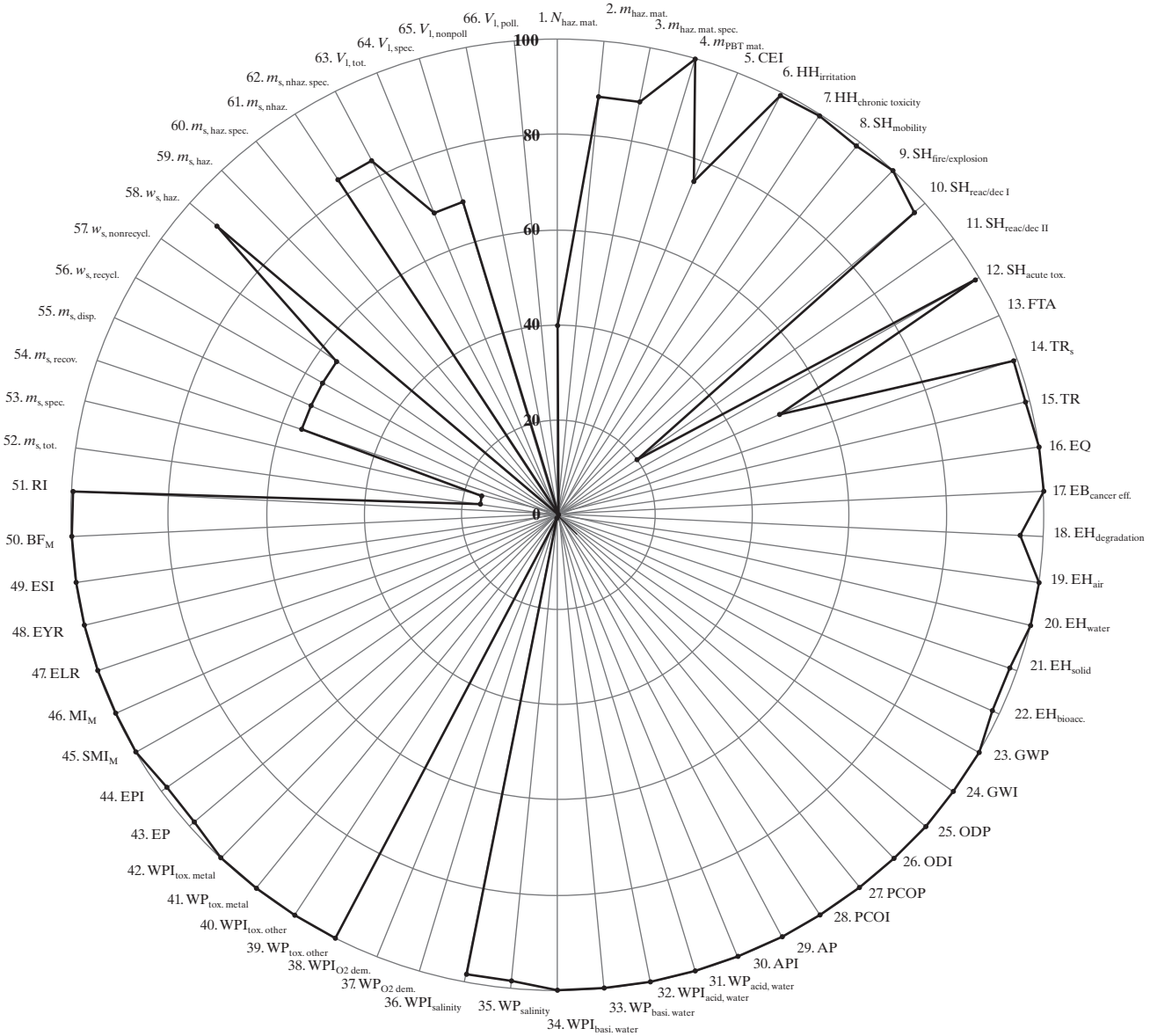

Figure 3.5 GREENSCOPE environmental indicator results for alkali-catalyzed manufacture of biodiesel.
(*Source:* Reproduced with permission from Ruiz-Mercado et al. (2013)).

unity, showing good sustainability. But the $N_{\text{haz mat}}$ indicator (1) dips to 40%, which shows a high ratio of hazardous inputs to the total number of process inputs; $m_{\text{s spec}}$ (53) dips to ∼15%, which shows a high ratio of the mass of solid waste to the mass of biodiesel product; *FTA* (13) dips to ∼50%, which shows a high probability of system failures given estimates of the component reliabilities; and a few other significant dips. These draw attention to design aspects that should be reconsidered to improve the environmental sustainability of the proposed biodiesel process. Similar charts are presented to display the efficiency, economic, and energy indicators.

Life-Cycle Analysis

A related approach to assessing the sustainability of potential product and/or process designs is to implement a life cycle analysis (LCA). For chemical products, the analysis begins with the selection of raw materials and their harvesting techniques. Then, it moves to manufacturing processes that produce the product, which is used by the customer, and then disposed of or recycled. Throughout the life cycle, energy is consumed, and wastes and emissions are generated. For each product and/or process design, various sustainability indicators for raw materials utilization, energy consumption, and the like are evaluated to assess its sustainability throughout its life cycle.

Consider, for example, the production of a biofuel product through the growth of algae. Biofuel is a renewable fuel because algae consume carbon dioxide in photosynthesis and then grow to contain triglyceride oil, which is extracted and converted to biofuel. The biofuel product is "carbon neutral" but requires large farms to cultivate algae at low concentrations in water. Much energy is required to harvest the algae, extract its oil, and convert it to biofuel. A life cycle analysis considers the needs for phosphorous nutrients, the energy requirements, the handling of byproducts, such as glycerin, and the use of residual biomass when selecting the biofuel product [e.g., biodiesel (FAME), green diesel, or jet fuel], and the alternative processes for cultivation, harvesting, extraction, and conversion to biofuel.

For a good introduction to LCA, the reader is referred to Chapter 13, "Life Cycle Concepts, Product Stewardship and Green Engineering," in *Green Engineering* (Allen and Shonnard, 2002). Also, see papers that focus on LCA for the design of biofuels produced by algae (Brentner et al., 2011; Handler et al., 2012; Stephenson et al., 2010; Frank et al., 2011).

3.6 SAFETY CONSIDERATIONS

A principal objective in the design and operation of chemical processes is to maintain safe conditions for operating personnel and inhabitants who live in the vicinity of the plants. Unfortunately, the importance of meeting this objective is driven home periodically by accidents, especially accidents in which lives are lost and extensive damage occurs. To avoid this, all companies have extensive safety policies and procedures to administer them. In recent years, these have been augmented through cooperative efforts coordinated by technical societies, for example, the Center for Chemical Plant Safety of the American Institute of Chemical Engineers, which was formed in 1985 shortly after the accident in Bhopal, India, on December 3, 1984. In this accident, which took place in a plant partially owned by Union Carbide and partially owned locally, water containing traces of rust (accumulated in pipe flow) was accidentally introduced into one of the methyl isocyanate (MIC) storage vessels (MIC was stored as an intermediate chemical in the plant) as workers carried out a routine flushing operation to clean the pipes. But the pipes were connected to the MIC storage vessels by mistake because the isolation disc, or "spectacle blind," was missing. The water reacted with the highly reactive MIC, leading to a rapid increase in temperature accompanied by boiling, which caused toxic MIC vapors to escape from the tank. The vapors passed through a pressure-relief system and into a scrubber and flare system that had been installed to consume the MIC in the event of an accidental release. Unfortunately, these systems were not operating, and approximately 25 tons of toxic MIC vapor were released, causing a dense vapor cloud that escaped and drifted over the surrounding community, killing more than 3,800 civilians and seriously injuring an estimated 30,000 more.

Like Section 3.4, on environmental issues, this section begins with a review of two safety issues that are considered by many design teams, followed by an introduction to many of the design approaches for dealing with these issues. For more comprehensive coverage of these areas, the reader is referred to *Chemical Process Safety: Fundamentals with Applications* (Crowl and Louvar, 2011); *Plant Design for Safety – A User-Friendly Approach* (Kletz, 1991); a collection of student problems, *Safety, Health, and Loss Prevention in Chemical Processes: Problems for Undergraduate Engineering Curricula—Student Problems* (American Institute of Chemical Engineers, 1990), AIChE; and *Guidelines for Engineering Design for Process Safety, CCPS,* AIChE (1993).

The U.S. Chemical Safety and Hazard Investigation Board (CSB), established by the Clean Air Act Amendments of 1990, is an independent federal agency with the mission of ensuring the safety of workers and the public by preventing or minimizing the effects of chemical incidents. CSB attempts to determine the root and contributing causes of chemical accidents. Their Web site at http://www.csb.gov is a very useful source of brief and detailed accident reports.

Safety Issues

Of the many potential safety issues, two are singled out for coverage here because they must be confronted often in the design of chemical, petroleum, and petrochemical plants and in other plants in which exothermic reactions and operations occur at elevated pressures.

Fires and Explosions

In organic chemical processes, it is not uncommon for sizable concentrations of flammable chemicals to accumulate in air or pure oxygen with the possibilities of ignition or even explosion. For this reason, laboratory studies have been carried out to determine the flammability limits for many of the common organic chemical vapors. These limits at 25°C and 1 atm are

Table 3.2 Flammability Limits of Liquids and Gases

Compound	Flash Point (°F)	LFL (%) in Air	UFL (%) in Air	Autoignition Temperature (°F)
Acetone	0.0[a]	2.5	13	1,000
Acetylene	Gas	2.5	100	
Acrolein	–14.8	2.8	31	
Acrylonitrile	32	3.0	17	
Anilin	158	1.3	11	
Benzene	12.0[b]	1.3	7.9	1,044
n-Butane	–76	1.6	8.4	761
Carbon monoxide	Gas	12.5	74	
Chlorobenzene	85[b]	1.3	9.6	1,180
Cyclohexane	–1[b]	1.3	8	473
Diborane	Gas	0.8	88	
Dioxane	53.6	2.0	22	
Ethane	–211	3.0	12.5	959
Ethyl alcohol	55	3.3	19	793
Ethylene	Gas	2.7	36.0	914
Ethylene oxide	–20[a]	3.0	100	800
Ethyl ether	–49.0[b]	1.9	36.0	180
Formaldehyde		7.0	73	
Gasoline	–45.4	1.4	7.6	
n-Heptane	24.8	1.1	6.7	
n-Hexane	–15	1.1	7.5	500
Hydrogen	Gas	4.0	75	1,075
Isopropyl alcohol	53[a]	2.0	12	850
Isopropyl ether	0	1.4	7.9	830
Methane	–306	5	15	1,000
Methyl acetate	15	3.1	16	935
Methyl alcohol	54[a]	6	36	867
Methyl chloride	32	8.1	17.4	1,170
Methyl ethyl ketone	24[a]	1.4	11.4	960
Methyl isobutyl ketone	73	1.2	8.0	860
Methyl methacrylate	50[a]	1.7	8.2	790
Methyl propyl ketone	45	1.5	8.2	941
Naphtha	–57	1.2	6.0	550
n-Octane	55.4	1.0	6.5	
n-Pentane	–40	1.51	7.8	588
Phenol	174	1.8	8.6	
Propane	Gas	2.1	9.5	
Propylene	–162	2.0	11.1	927
Propylene dichloride	61	3.4	14.5	1,035
Propylene oxide	–35	2.3	36	869
Styrene	87[b]	1.1	7.0	914
Toluene	40	1.2	7.1	997

[a]Open-cup flash point.

[b]Closed-cup flash point.

Source: Martha W. Windholtz, Ed., *The Merck Index: An Encyclopedia of Chemicals, Drugs, and Biologicals*, 10th ed. (Merck, Rahway, NJ, 1983). P. 1124; Gressner G. Hawley, Ed., *The Condensed Chemical Dictionary*, 10th ed. (Van Nostrand Reinhold, New York, 1981), pp. 860–861: Richard A. Wadden and Peter A. Scheff, *Engineering Design for the Control of Workplace Hazards* (McGraw-Hill, New York, 1987), pp. 146–156.

listed for many chemicals (Table 3.2) for which the LFL is the lower flammability limit (that is, the volume percent of the species in air below which flammability does not occur) and the UFL is the upper flammability limit (above which flammability does not occur). Within these limits, flames and explosions can occur and, consequently, design teams must be careful to keep the concentrations outside the flammability range. In addition, Table 3.2 provides autoignition temperatures above which a flammable mixture is capable of extracting enough energy from the environment to self-ignite. At lower temperatures, an ignition

source must be present. The flash point, given in the second column of Table 3.2, is the lowest temperature at which sufficient vapor exists in air to form an ignitable mixture. At the flash point, the vapor burns, but only briefly, as insufficient vapor is formed to sustain combustion.

Table 3.2 pertains to pure chemicals. For mixtures, the flammability limits are often estimated using the Le Chatelier equation that must be used with caution:

$$\mathrm{LFL_{mix}} = \frac{1}{\sum_{i=1}^{C} y_i/\mathrm{LFL}_i}, \quad \mathrm{UFL_{mix}} = \frac{1}{\sum_{i=1}^{C} y_i/\mathrm{UFL}_i} \tag{3.9}$$

where LFL_i and UFL_i are the flammability limits of species i, y_i is the mole fraction of species i in the vapor, and C is the number of chemical species in the mixture, excluding air.

To extend to elevated temperatures and pressures, the following equations have been developed:

$$\mathrm{LFL}_T = \mathrm{LFL}_{25}\left[1 - \frac{0.75\,(T-25)}{\Delta H_c}\right] \tag{3.10a}$$

$$\mathrm{UFL}_T = \mathrm{UFL}_{25}\left[1 + \frac{0.75\,(T-25)}{\Delta H_c}\right] \tag{3.10b}$$

and

$$\mathrm{UFL}_P = \mathrm{UFL} + 20.6(\log\ P + 1) \tag{3.11}$$

where T is the temperature (in °C), ΔH_c is the net heat of combustion (in kcal/mol at 25°C). P is the pressure (in MPa absolute), and UFL is the upper flammability limit at 101.3 kPa (1 atm). The lower flammability limit is not observed to vary significantly with the pressure. These equations, plus others to estimate the flammability limits for species not listed in Table 3.2, are presented by Crowl and Louvar (2011), with a more complete discussion and references to their sources. With this kind of information, the process designer makes sure that flammable mixtures do not exist in the process during startup, steady-state operation, or shutdown.

EXAMPLE 3.2 ***Flammability Limits in Air***

At 100°C, a mixture of methane (0.85 mole fraction) and ethane is exposed to air. What are its lower and upper flammability limits?

SOLUTION

From Table 3.2 and the *Handbook of Chemistry and Physics*:

	Mole Fraction	LFL_{25}	UFL_{25}	ΔH_c, Kcal/mol
CH_4	0.85	5	15	210.8
C_2H_6	0.15	3	12.5	368.4

At 100°C, for CH_4:

$$\mathrm{LFL}_{100} = 5\left[1 - \frac{0.75\,(100-25)}{210.8}\right] = 3.67 \text{ vol\% air}$$

$$\mathrm{UFL}_{100} = 15\left[1 + \frac{0.75\,(100-25)}{210.8}\right] = 19.0 \text{ vol\% } CH_4$$

and for C_2H_6:

$$\mathrm{LFL}_{100} = 3\left[1 - \frac{0.75\,(100-25)}{368.4}\right] = 2.54 \text{ vol\% air}$$

$$\mathrm{UFL}_{100} = 12.5\left[1 + \frac{0.75\,(100-25)}{368.4}\right] = 14.41 \text{ vol\% } C_2H_6$$

Then, for the mixture:

$$\mathrm{LFL_{mix}} = \frac{1}{0.85/3.67 + 0.15/2.54} = 3.44 \text{ vol\% air}$$

$$\mathrm{UFL_{mix}} = \frac{1}{0.85/19.0 + 0.15/14.41} = 18.13 \text{ vol\% mixture}$$

Toxic Releases and Dispersion Models

In chemical processing, it is desirable to avoid working with chemicals that are toxic to animals, humans, and plant life. This is an important consideration because design teams select from among the possible raw materials and consider alternate reaction paths involving intermediate chemicals and byproducts. In some cases, decisions can be made to work with nontoxic chemicals. However, toxicity problems are difficult to avoid, especially at the high concentrations of chemicals in many process streams and vessels. Consequently, the potential for a release in toxic concentrations during an accident must be considered carefully by design teams. In so doing, a team must identify the ways in which releases can occur; for example, due to the buildup of pressure in an explosion, the rupture of a pipeline due to surges at high pressure, or the collision of a tank car on a truck or train. It is also important for the team to select protective devices and processing units, to assess their potential for failure, and, in the worst case, to model the spread of a dense, toxic vapor. Given the potential for the rapid spreading of a toxic cloud, it is often necessary to find an alternative design not involving this chemical rather than take the chance of exposing the surrounding community to a serious health hazard. Although it is beyond the scope of this discussion, it should be noted that dispersion models are developed by chemical engineers to predict the movement of vapor clouds under various conditions—for example, a continuous point release at steady state with no wind; a puff with no wind; a transient, continuous point release with no wind; and all of the previously mentioned factors with wind. These and other models are described by Crowl and Louvar (2011) and de Nevers (1995) and accompanied by example calculations.

Design Approaches Toward Safe Chemical Plants

In the previous discussion of two important safety issues, design approaches to avoid accidents have been introduced. This section provides a more complete enumeration without discussing implementational details, which are covered by Crowl and Louvar (2011).

Techniques to Prevent Fires and Explosions

One method of preventing fires and explosions is *inerting*—that is, the addition of an inert gas to reduce the oxygen concentration below the minimum oxygen concentration (MOC), which can be estimated using the LFL and the stoichiometry of the combustion reaction. Another method involves avoiding the buildup of static electricity and its release in a spark that can serve as an ignition source. Clearly, the installation of grounding devices and the use of antistatic additives that increase conductivity, reducing the buildup of static charges, can help to reduce the incidence of sparking. In addition, explosion-proof equipment and instruments are often installed, for example, explosion-proof housings that do not prevent an explosion but that do absorb the shock and prevent the combustion from spreading beyond the enclosure. Another approach is to ensure that the plant is well ventilated, in most cases constructed in the open air, to reduce the possibilities of creating flammable mixtures that could ignite. Finally, sprinkler systems are often installed to provide a rapid response to fires and a means to contain them effectively.

Relief Devices

In processes where pressures can build rapidly, especially during an accident, it is crucial that the design team provide a method for relieving the pressure. This is accomplished by using a variety of relief devices, depending on whether the mixtures are vapors, liquids, solids, or combinations of these phases. In some cases, the vessels can be vented to the atmosphere; in other cases, they are vented to containment systems, such as scrubbers, flares, and condensers. The devices include relief and safety valves, knock-out drums, rupture disks, and the like. Relief system design methodologies are presented in detail in the AIChE publication *Emergency Relief System Design Using DIERS Technology* (1992).

Hazards Identification

Hazard identification is a key step in process design, normally carried out in preparation of the final design. In this step, the plant is carefully scrutinized to identify all potential causes of accidents and hazards. This requires that the design team consider the propagation of small faults into catastrophic accidents, which is complicated by the possibility of two or more faults occurring either simultaneously or in some coordinated fashion. At some point, especially after the economics are attractive, the design team normally prepares a HAZOP study, that is, a "Hazard and Operability" study in which all possible paths to an accident are identified.

HAZOP Studies. These are *qualitative* analyses that assist in the identification of possible hazards and potential catastrophes that could occur in plants under design. Most HAZOP studies lead to modifications of the Piping and Instrumentation Diagram (P&ID), reducing the likelihood of the occurrence of hazardous situations. An associated concept is a HAZAN, short for hazard analysis, which encompasses methodologies that enable *quantitative* risk analysis, and provide a means of estimating the probability and consequences of a hazard—better connecting the results of a HAZOP study to design decisions. By carrying out a HAZAN, one can provide quantitative estimates of the probabilities associated with each of the hazards identified in a HAZOP study. Given these, modifications can be made as necessary, usually incorporating appropriate backup systems to reduce each risk to acceptable levels, gauged by comparing the level of estimated risk with a prespecified target. This recognizes that every situation, even staying at home, has associated risks.

The materials that follow are drawn exclusively from the works of Trevor Kletz, and in particular from his short book, *HAZOP and HAZAN* (Kletz, 1992). This highly recommended book is less than 100 pages long with an illustration on the cover effectively summarizing many of the ideas therein, that is, a sketch of a pair of trousers held up by a belt and braces, symbolizing the need for backup systems. With his wealth of experience, backed by well-written and clear insights, Kletz is often credited as being one of the leading forces behind bringing process safety into standard engineering practice. (Kletz, 1988a, b; 1991).

EXAMPLE 3.3 ***Typical Pipe Section for HAZOP Study***

A HAZOP study is carried out on each pipe section of a P&ID, for example, the one in Figure 3.6, which shows a feed section of a process, consisting of storage tank (1) and pump (2), which supply organic feed to a distillation column through manual valve (4) as well as to an upstream plant on startup (5). Note the kickback line (6) on the pump, which ensures flow in the pump even when the upstream valve is partially or even completely closed, as well as the check-valve (3) on the pump discharge line.

The following questions are addressed in every HAZOP study:

- **What can go wrong?** The first and most important stage in any hazard study is to identify the principal things that can go wrong, leading to accidents or operating problems. A HAZOP study includes a systematic procedure in which each relevant variable associated with a pipe section (e.g., flow, temperature, pressure) is queried using one of a limited set of guide words as detailed in Table 3.3. For example, a possible concern associated with the variable "flow" in the pipe section in Figure 3.6 would be "reverse flow."
- **What will be the consequences of each incident that can occur?** One needs to know, at least qualitatively, the consequences of each incident identified to employees, members of the public, the plant, and its profits. In a HAZOP study, a qualitative assessment is made as to the severity of the hazard, using the categorization shown in Table 3.4.

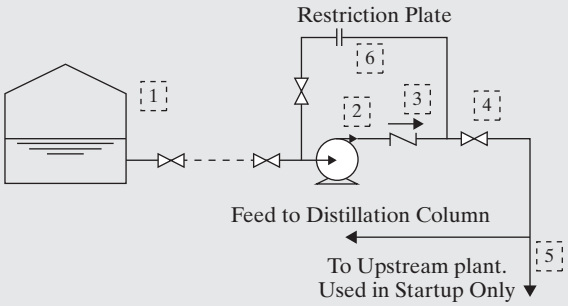

Figure 3.6 P&ID of the feed section of a process.

- **How often is each incident expected to occur?** One needs to estimate how often the hazard identified is likely to occur. In a HAZOP study, a qualitative estimate of the expected likelihood of occurrence is attempted, using the categorization shown in Table 3.5, noting that quantitative estimations are performed in HAZAN.

Table 3.3 Guide Words for a HAZOP Study

Guide Word	Deviations
NONE	No forward flow when flow is required: i.e., no flow
MORE OF	More of any relevant physical property than required: e.g., higher flow, higher temperature.
LESS OF	Less than any relevant physical property than required: e.g., lower flow, lower temperature.
REVERSE	Flow in the reverse direction than required.
PART OF	Composition of system different than required: e.g., ratio different, or species missing.
MORE THAN	More species present than required: e.g., extra phases or impurities present.
OTHER THAN	Other occurrences than normal departures from operating conditions: e.g., in startup, shutdown, failure of services.

Table 3.4 Degree of Severity of Hazard

Severity	Significance
1	High–Fatality or serious injury hazard or hazard leading to loss of greater than six months of production or $10MM.
2	Medium high–Injury hazard or hazard leading to loss of between one and six months of production or $1–10MM.
3	Medium low–Minor injury hazard or hazard leading to loss of between one and four weeks of production or $0.1–1MM.
4	Low–No injury hazard or hazard leading to loss of less than one week of production or $100,000.

Table 3.5 Degree of Likelihood of Hazard Occurrence

Likelihood	Significance
1	High–Hazard expected more than once per year
2	Medium high–Hazard expected several times in the plant life
3	Medium low–Hazard not expected more than once in the plant life
4	Low–Hazard not expected at all in the plant life

- **How can each incident be prevented?** The risk of the occurrence is assessed according to its severity and likelihood, using the chart shown in Figure 3.7. Assuming that action is called for, one needs to decide on the changes to the piping section to either prevent the identified occurrence or to reduce its probability to acceptable levels. For example, a hazard that has been classified as having the significant possibility of leading to a fatality (Severity rank 1) and being likely to occur more than once in the plant's life (Likelihood rank 3) is classified in the chart as having an undesirable risk level (C). It requires a reduction of risk to level B (undesirable risk level) at the very worst.

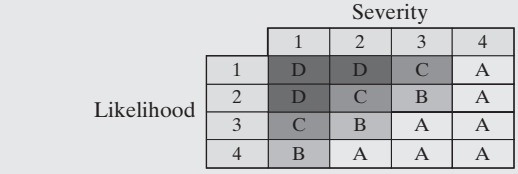

Ranking	Significance
A	Acceptable risk level.
B	**Almost acceptable risk level.** Acceptable if suitably controlled by management. Should check that suitable procedures and/or control systems are in place.
C	**Undesirable risk level.** Must be reduced to level B at the most by engineering or management control.
D	**Unacceptable risk level.** Must be reduced to level B at the most by engineering or management control.

Figure 3.7 Risk ranking in HAZOP study. See the Color Figures folder on the Wiley Web site.

In carrying out a HAZOP study, as many as possible of the incidents and their consequences (that could arise from the implementation of the raw P&ID) are identified and categorized with actions taken to modify the P&ID to reduce the likelihood and/or consequences of incidents to tolerable levels.

EXAMPLE 3.4 *Typical Improvements Due to HAZOP Procedure*

Returning to the example pipe section in Example 3.3, Figure 3.8 shows the revisions made to the P&ID in the light of hazards identified by the HAZOP procedure. A partial and far from exhaustive list of action items could include:

1. Triggered by NONE, MORE OF, and LESS OF as applied to flow, the procedure uncovers the lack of level instrumentation [level indicator (LI), and high and low level alarms (LA)] in the feed tank, leading to their addition.
2. The same key words lead to the need for a pressure gauge (PG) on the pump discharge line to provide a visual check when the pump is operating.
3. Triggered by REVERSE as applied to flow, the possibility of reverse flow over the kickback line as a consequence of a pump failure is exposed and eliminated by repositioning the check-valve downstream of the kickback line.
4. Triggered by NONE, MORE OF, and LESS OF as applied to flow, the procedure uncovers the lack of both flow measurement and flow control on the pipe section, leading to the installation of a standard flow control manifold.
5. Triggered by NONE, MORE OF, LESS OF, and REVERSE as applied to flow, the procedure uncovers the fact that nothing was previously in place to isolate the startup line during normal operating conditions. This oversight is resolved by installing both a normally closed isolation valve as well as a check valve to eliminate the possibility of reverse flow during startup.

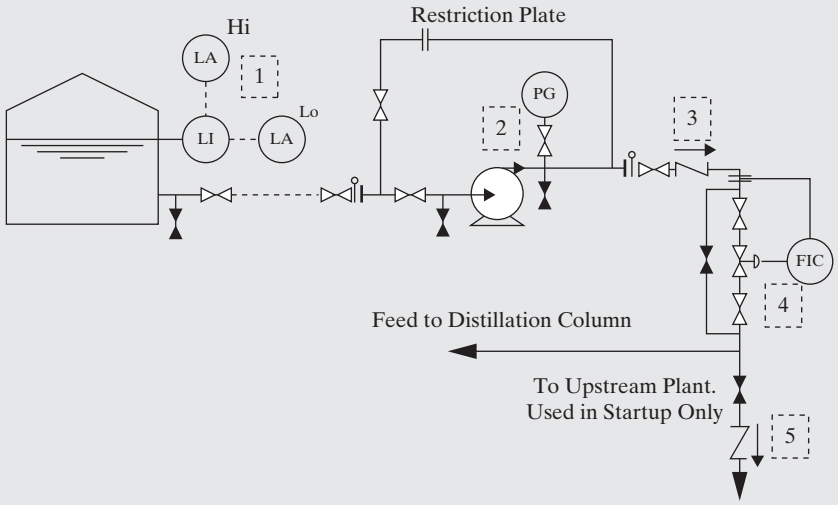

Figure 3.8 Revised P&ID of the feed section of a process.

Safety Risk Analysis When designing a chemical plant, it is important to plan strategies for alerting operators, process engineers, and plant managers as unsafe conditions develop during plant operations. This normally involves the installation of alarms and safety systems to protect the process from the consequences of abnormal events that occur when plantwide control systems (which are discussed in Chapter 20) are unable to maintain normal operating conditions. This subsection focuses on the operation of these alarm and safety systems and introduces a strategy known as dynamic risk analysis (DRA) for estimating the risks of plant shutdowns and even accidents.

Alarms, Safety Systems, and Event Trees Accidents in a chemical manufacturing process are caused by the propagation of *special-cause events*. A special-cause event, which propagates to an abnormal event (triggering an alarm), refers to any process disturbance whose consequences cannot be attenuated by the process control system. These include feedstock fluctuations that are particularly strong or sudden, a catalyst degradation or failure, a mechanical failure of a piece of equipment, sensor failures, or any other disturbances that are not fully addressed by the process control system. Once an abnormal event occurs, it is the role of the safety system(s) to return the process to normal operating conditions, and in so doing, override the process control system.

Event-tree analyses are used to estimate the failure probabilities of each safety system as it works to dampen the effects of abnormal events, which occur when alarms are triggered as variables leave their normal operating zones—that is, the green-belt zone (bounded by the high- and low-alarm thresholds) in Figure 3.9. When successful, safety systems return the variables to this zone. When unsuccessful, the variables trigger higher or lower alarms as they enter the next alarm-belt zone. When a variable remains in the red-belt zone for a prespecified length of time, an interlock trips and an emergency shutdown occurs.

Figure 3.10 shows an event tree having just three safety systems that correspond to the three zones in Figure 3.9. After an abnormal event when safety system 1 (SS_1) operates successfully, consequence C_1 (continued operation) occurs. But when it fails with failure probability x_1, SS_2 takes action and, when successful, consequence C_2 occurs (also continued operation). When unsuccessful with failure probability x_2, SS_3 takes action and, when successful, consequence C_3 (emergency shutdown) occurs. Finally, when SS_3 fails with failure probability x_3, consequence C_4 results (for example, a serious accident). In this way, event trees represent the actions of various safety systems and their end consequences after abnormal events. In DRAs, safety system actions are chronologically tracked and recorded (using the plant alarm historian) with each branch node representing the success or failure of its safety system. Using data compaction techniques and Bayesian analyses, the failure probabilities of the safety systems, and the probabilities of plant shutdowns and

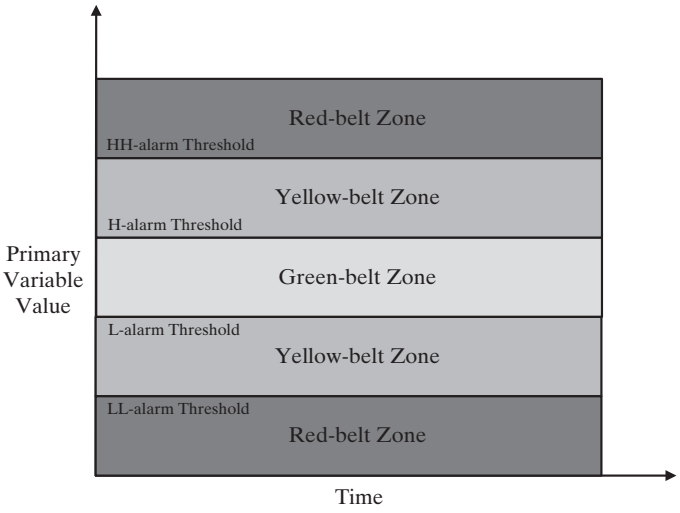

Figure 3.9 Belt-zone map for primary variables. See the Color Figures folder on the Wiley Web site.

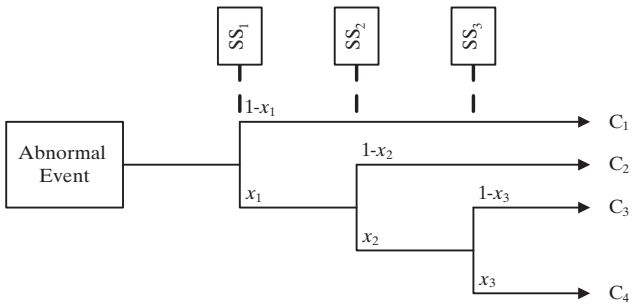

Figure 3.10 Sample event tree.

accidents have been estimated. This information becomes available to alert operators when a particular safety system is in danger of failing, or a trip or accident is likely to occur.

Dynamic Risk Analysis In the chemical manufacturing industries, much emphasis is placed on maintaining safe and reliable chemical processes. Many manufacturing processes operate at high temperatures or pressures or with chemicals that are dangerous to employees at the plant and people in the community and to the environment. Accidents at these plants can be very costly to human health, the environment, and/or, of less importance, company profits. Thus, there is clear motivation to quantify and minimize safety risk in a chemical process. Risk is defined as the expected cost of accidents:

$$Risk = (Event\ Probability) \times (Event\ Cost) \tag{3.12}$$

where the first term quantifies the probability that an unsafe event can occur (e.g., a plant shuts down or an accident occurs), and the second term is an estimated cost of the event. For plant operators, the risk associated with an event (such as switching between two operating conditions) could lead to a better choice in operating strategy (choosing an appropriate way to switch between the plant conditions). For plant managers, the quantification of risk can aid in the cost analysis of a process. It is important to note that although all chemical manufacturing plants ought to seek to minimize their risk, zero-risk processes are impossible. Rather, the chemical manufacturing industries are concerned with quantifying and minimizing risk to acceptable levels.

CSTR Example Consider a jacketed CSTR with exothermic reaction, A → B. The role of the cooling jacket is to remove heat from the exothermic reaction, allowing the vessel to operate under safe conditions, and possibly maintaining the CSTR at a temperature that maximizes product yield. A control system is typically designed to maintain a temperature at its set point in the reactor vessel by manipulating the flow rate of cooling water. When not entirely successful, moderate fluctuations in the feed flow rate of reactant to the vessel could result in temperature fluctuations that rise above safe operating conditions whereas large fluctuations in reactant feed flow rate could present serious control problems. Other events that may result in the failure of the control system include sensor failure, control-valve failure, or a leak in the cooling jacket. To maintain safe operation during such events, safety systems are installed. Suppose there is a high-temperature alarm, which activates when the reactor temperature crosses above a critical temperature, T_H, the high-alarm threshold in Figure 3.9. The high-temperature alarm would sound, and an operator would be expected to take action, possibly opening the valve on the cooling water line or closing the valve on the reactant line. If the operator failed to take action or the action the operator took was not sufficient and the temperature rises above T_{HH}, the high-high alarm threshold, triggering a second alarm, the high-high temperature alarm. When this alarm is activated, the operator has another 30 seconds, an override threshold, to take action before an automated response occurs. Here, the operator takes a more aggressive action. If the abnormal event is not arrested within 30 seconds, a quench valve is automatically opened, typically dumping cold water into the reactor and spoiling the product but avoiding a runaway reaction. When the quench tank does not function properly (the valve fails to open or the sensor to the valve fails), a runaway reaction proceeds, often resulting in the failure of the reaction vessel, or an explosion—a catastrophic event. To review, the safety systems associated with the temperature of the exothermic reactor act when:

1. An operator reacts to a high-temperature alarm.
2. An operator reacts to a high-high temperature alarm.
3. A quench valve dumps cooling water into the vessel.

As each of these three safety systems succeeds or fails, consequences C_1 through C_4 (Figure 3.10) are realized. If the failure probabilities of all three safety systems, x_1, x_2, and x_3, are known, then operators and plant managers can make informed decisions.

DRA is used to estimate failure probabilities in real time. As each safety system succeeds or fails, the failure probabilities are adjusted. Here, data in Table 3.6 for a six-month period are analyzed. The failure probabilities are estimated as sample means with the data compiled cumulatively over each month. Clearly, in each month, the probability of a plant shutdown is $x_1x_2x_3$. This is not too informative, but more complex statistical methods for estimating safety system failure probabilities (e.g., Bayesian analysis), particularly those associated with rarely used safety systems, are needed but are beyond the scope of this textbook. See instead the papers by Meel and Seider (2006) and Pariyani et al. (2012a,b).

Design Strategies During design, it is important to plan for alarm thresholds, that is, to think ahead to plant commissioning when the alarm thresholds are set. Clearly, the alarm thresholds should be set to sound under unsafe conditions and not too often to create alarm flooding. Also, during operation as failure probabilities increase, operating strategies may need to be redesigned, and when often reaching high levels, it may be necessary to renovate or replace the equipment units, their control systems, and their safety systems.

Table 3.6 Safety System Data

	January	February	March	April	May	June
Cumulative S.S. 1 activation	13	21	24	37	43	51
Cumulative S.S. 1 success	10	17	18	27	30	37
x_1 estimation	0.23	0.19	0.25	0.27	0.30	0.27
Cumulative S.S. 2 activation	3	4	6	10	13	14
Cumulative S.S. 2 success	3	4	6	9	12	13
x_2 estimation	0.00	0.00	0.00	0.10	0.08	0.07
Cumulative S.S. 3 activation	0	0	0	1	1	1
Cumulative S.S. 3 success	0	0	0	0	0	0
x_3 estimation	n/a	n/a	n/a	1.00	1.00	1.00
Overall x_1 x_2 x_3	0	0	0	0.027	0.024	0.019

Material Safety Data Sheets A process design should be accompanied by a material safety data sheet (MSDS) for every chemical appearing in the process. Developed by chemical manufacturers and kept up to date under the federal government's OSHA (Occupational Safety and Health Agency) regulations, these sheets contain safety and hazard information, physical and chemical characteristics, and precautions on safe handling and use of the chemical. The MSDSs, which usually involve several pages of information, are available on the Internet at:

http://hazard.com/msds/

http:// www. ilpi.com/msds/

http://www.msdssearch.com

3.7 ENGINEERING ETHICS

Engineers' Creed

In 1954, the National Society of Professional Engineers (NSPE) adopted the following statement, known as the Engineers' Creed:

As a Professional Engineer, I dedicate my professional knowledge and skill to the advancement and betterment of human welfare.

I pledge:

To give the utmost of performance;
To participate in none but honest enterprise;
To live and work according to the laws of man and the highest standards of professional conduct;
To place service before profit, the honor and standing of the profession before personal advantage, and the public welfare above all other considerations.
In humility and with need for Divine Guidance, I make this pledge.

ABET Ethics Statement

In 1977, a similar statement was approved by the Accreditation Board for Engineering and Technology (ABET), as follows:

Engineers uphold and advance the integrity, honor, and dignity of the engineering profession by:

I. Using their knowledge and skill for the enhancement of human welfare;
II. Being honest and impartial, and serving with fidelity the publics, their employees;
III. Striving to increase the competence and prestige of the engineering profession; and
IV. Supporting the professional and technical societies of their disciplines.

These two statements have to do with ethics, also called *moral philosophy*, which is derived from the Greek *ethika*, meaning character. Thus, ethics deals with standards of conduct or morals. Unfortunately, there are no universal standards; only the ethics of Western civilization are considered in detail here. There is a movement toward the development of global ethics, which is described briefly at the end of this section.

Engineering ethics is concerned with the personal conduct of engineers as they uphold and advance the integrity, honor, and dignity of engineering while practicing their profession. This conduct of behavior has obligations to (1) self, (2) employer and/or client, (3) colleagues and co-workers, (4) public, and (5) environment.

AIChE Code of Ethics

Specific examples of these obligations are given in individual codes of ethics adopted by the various engineering societies (e.g., AIChE, ASCE, ASME, and IEEE) and by the NSPE. The following is the Code of Ethics adopted by the American Institute of Chemical Engineers (AIChE):

Members of the American Institute of Chemical Engineers shall uphold and advance the integrity, honor, and dignity of the engineering profession by: being honest and impartial and serving with fidelity their employers, their clients, and the public; striving to increase the competence and prestige of the engineering profession; and using their knowledge and skill for the enhancement of human welfare. To achieve these goals, members shall:

1. *Hold paramount the safety, health, and welfare of the public in performance of their professional duties.*
2. *Formally advise their employers or clients (and consider further disclosure, if warranted) if they perceiv ethat a consequence of their duties will adversely affect the present or future health or safety of their colleagues or the public.*

3. *Accept responsibility for their actions and recognize the contributions of others; seek critical review of their work and offer objective criticism of the work of others.*
4. *Issue statements and present information only in an objective and truthful manner.*
5. *Act in professional matters for each employer or client as faithful agents or trustees, and avoid conflicts of interest.*
6. *Treat fairly all colleagues and co-workers, recognizing their unique contributions and capabilities.*
7. *Perform professional services only in areas of their competence.*
8. *Build their professional reputations on the merits of their services.*
9. *Continue their professional development throughout their careers, and provide opportunities for the professional development of those under their supervision.*

National Society of Professional Engineers (NSPE) Code of Ethics

A more detailed code of ethics for engineers was adopted initially by the NSPE in July 1964. Since then, it has been updated 24 times and will probably continue to receive updates. The 1997 version is reproduced in the file NSPE_CoE_1997.pdf, which can be downloaded from the PDF Folder on the Wiley Web site associated with this textbook

Online Ethics Code

It is important for an engineer or one preparing for entry into the profession to develop the ability to address in an ethical fashion significant workplace problems that may involve difficult choices. For this purpose, the Online Ethics Center (OEC) for Engineering and Science, (formerly the World Wide Web Ethics Center for Engineering and Science) was established in 1995 under a grant from the National Science Foundation (NSF). The Center, located at Case-Western Reserve University, provides very extensive educational resources, including more than 100 case studies, at the Web site: www.onlineethics.org.

Figure 3.11 provides just a sample of Center case studies dealing with public safety and welfare. The Center also sponsors conferences, addresses the ABET Readiness Committee call for a "*Guide to Ethics for Dummies,*" and provides sample student assignments from freshman to senior levels on practical ethics for use by instructors.

Example Ethical Issues

A breach of ethics or a courageous show of ethics is frequently newsworthy. An example of a breach of ethics is that of an MIT

- **Suspected Hazardous Waste**
  A supervisor instructs a student engineer to withhold information from a client about the suspected nature of waste on the client's property, to protect what the supervisor takes to be the client's interest.
- **Clean Air Standards and a Government Engineer**
  An engineer defies immediate supervisor because he believes supervisor's instruction would pose an environmental health hazard.
- **The Responsibility for Safety and the Obligation to Preserve Client Confidentiality**
  Tenants sue their building's owner, and the owner employs an engineer who finds structural detects not mentioned in the tenant's lawsuit. Issues of public safety versus client confidentiality.
- **Code Violations with Safety Implications**
  Engineer discovers deficiencies in a building's structural integrity, and it would breach client confidentiality to report them to a third party.
- **Whistleblowling City Engineer**
  An engineer privately informs other city officials of an environmental threat, a problem her supervisor has ordered her not to disclose.
- **Safety Considerations and Request for Additional Engineering Personnel**
  An engineer is concerned for worker safety during construction but yields to his client's objections at the cost of an on-site representative.
- **Engineer's Dispute with Client Over Design**
  A client believes an engineer's designs are too costly; but the engineer fears that anything less may endanger the public.
- **Do Engineers Have a Right to Protest Shoddy Work and Cost Overruns?**
  An engineer who is employed by a government contractor objects to a subcontractor's poor performance and is ignored and silenced by management.
- **Change of Statement of Qualifications for a Public Project**
  An engineering firm takes measures to remedy a deficit in a particular area of expertise needed to successfully compete for and carry out a public project.
- **Knowledge of Damaging Information**
  An engineer has a conflict between honoring an agreement to an employer and reporting a hazard to protect the public interest.

Figure 3.11 Engineering ethics cases in the Ethics Center for Engineering & Science.

student who used university hardware to distribute commercial software over the Internet. Recent examples of a more courageous show of ethics, which are presented as case studies by the WWW Ethics Center for Engineering and Science, include:

1. The attempts by Roger Boisjoly to avert the *Challenger* space disaster.
2. The emergency repair by William LeMessurier of structural supports for the Citicorp Tower in New York City.
3. The campaign of Rachel Carson for control of the use of pesticides.

The work of Rachel Carson has had a significant impact on stirring the world to action on environmental protection beginning with concerted efforts on college campuses. Carson was a U.S. Fish and Wildlife Service biologist who, in 1951, published *The Sea Around Us*, which won the National Book Award. In 1962, Carson's book *Silent Spring* was published. In that book, she criticized the widespread use of chemical pesticides, fertilizers, and weed killers, citing case histories of damage to the environment. In particular, she cited the disappearance of songbirds (thus, the title of the book) due to the use of synthetic, chlorine-containing pesticide DDT (previously discussed in Section 3.4), which kills insects by acting as a nerve poison. Synthetic pesticides were developed during a period of great economic development after World War II in an attempt to reduce insect-caused diseases in humans and to increase food production. More specifically, the use of DDT practically eliminated the anopheles mosquito that had caused malaria in many countries in Asia, Africa, and South and Central America. Carson claimed that the problems created by DDT were worse than the problems it solved. DDT disrupted reproductive processes and caused bird eggs to be infertile or deformed. Because DDT breaks down very slowly in the soil, its concentration builds up in the food chain as larger organisms eat smaller ones. Even though no adverse effects of DDT on humans have been found, its use in the United States was banned in 1972. However, it is still manufactured in the United States, and it is still used in parts of the world for malaria control.

Concern over the environment has led to much interest in the development of global ethics. Considerable information on this subject is available on the Web site (http://www.globalethics.org) of The Institute for Global Ethics, which is located at Madison, Wisconsin.

The Institute exists because many believe in their statements:

1. Because we will not survive the 21st century with the 20th century's ethics.
2. The immense power of modern technology extends globally. Many hands guide the controls and many decisions move those hands. A good decision can benefit millions, while an unethical one can cripple our future.

The Institute strongly believes that education in ethics must begin not at the middle- and high-school levels but even younger. Rush Kidder's *Good Kids, Tough Choices* includes this comment:

> *It makes excellent sense to address younger children—up through age five or six—through basic character education programs that focus on knowing what's right. (Kidder, 2010).*

Accordingly, the Institute provides instructional materials suitable for that level and stresses the concept of *moral courage*, which it is in the process of defining. In a recent white paper, the Institute makes the following statements:

> *Moral courage is different from physical courage. Physical courage is the willingness to face serious risk to life or limb instead of fleeing from it.*
>
> *Moral courage is not about facing physical challenges that could harm the body. It's about facing mental challenges that could harm one's reputation, emotional well-being, self-esteem, or other characteristics. These challenges, as the term implies, are deeply connected with our moral sense – our core moral values.*
>
> *Moral courage, … has four salient characteristics:*
>
> - *It is the courage to be moral – to act with fairness, respect, responsibility, honesty, and compassion even when the risks of doing so are substantial.*
> - *It requires a conscious awareness of those risks. The sleepwalker on the ridgepole is not courageous unless, waking up, he or she perceives the danger and goes forward anyway.*
> - *It is never formulaic or automatic, but requires constant vigilance against its opposite (moral timidity) and its counterfeit (moral foolhardiness).*
> - *It can be promoted, encouraged, and taught through precept, example, and practice.*

The teaching of engineering ethics to senior engineering students can be difficult, especially when students raise questions from their personal experiences. Years ago, a student in a senior design class, during an appointment in the instructor's office, asked the following question: "Two weeks ago, I accepted an offer of employment from a company that had set a deadline for accepting the offer. Yesterday, I received a better offer from another company for a better job opportunity at a higher starting salary. What should I do?" At that time, the instructor was inclined to tell the student to stand by the commitment to the first company. Several years later the tables were turned. A senior student told the instructor that he had accepted an offer with an excellent company and then rejected two other offers that he had received. One month later, the student informed the instructor that the company to which he had committed had reneged on the offer because of a downturn in the economy. Furthermore, job offers from the two other companies that had made offers were no longer available. From then on, when asked, the instructor recited these two episodes and told students to look out for their own best interests. If they got a better offer after accepting an earlier offer, renege on the first and take the second. Was the instructor giving ethical advice?

3.8 SUMMARY

Having studied this chapter, the reader should:

1. Be more knowledgeable about the design literature available to assist in carrying out product and process design projects. This includes well-established encyclopedias, handbooks, reference books, indexes, and patents as well as the key, recent electronic media including the Google Search Engine and Wikipedia.
2. Have been introduced to the approaches companies use to stimulate their employees to invent new technologies and innovate to create new products.
3. Be knowledgeable about the principal alternatives for generating and utilizing energy for the operation of new products and for processes to manufacturing them.
4. Be knowledgeable about the principal energy, environmental, sustainability, and safety issues that must be confronted by product and process designers. The reader should also have some familiarity with the many design methods used to protect our environment, achieve sustainability, and provide safe chemical processes.
5. Understand that it is crucial for engineers to maintain high ethical principles, especially as they relate to protecting the public against environmental and safety problems. At the minimum, the reader should be familiar with codes of ethics presented herein and recognize that engineers are often confronted with difficult choices that must be resolved using high ethical standards.

REFERENCES

1. Allen, D. T., and K. S. Rosselot, *Pollution Prevention for Chemical Processes*, John Wiley, New York (1997).

2. Allen, D. T., and D. R. Shonnard, *Green Engineering: Environmentally Conscious Design of Chemical Processes*, Prentice-Hall, Englewood Cliffs, New Jersey (2002).

3. Allen, D. T., and D. R. Shonnard, "Sustainability in Chemical Engineering Education: Identifying a Core Body of Knowledge," *AIChE J.*, **58**, 8, 2296–2302 (2012).

4. American Institute of Chemical Engineers, *Safety, Health, and Loss Prevention in Chemical Processes: Problems for Undergraduate Engineering Curricula—Student Problem,* AIChE, New York (1990).

5. American Institute of Chemical Engineers, *Emergency Relief System Design Using DIERS Technology*, AIChE, New York (1992).

6. Amundson, N. R. (ed.), *Frontiers in Chemical Engineering Research Needs and Opportunities*, National Research Council, National Academy Press, Washington, DC (1988).

7. Bever, M. B. (ed.), *Encyclopedia of Materials Science and Engineering*, Pergamon Press, Oxford, U.K. (1986).

8. Bockris, J., cited in: The History of Hydrogen, National Hydrogen Association, U. S. Dep't. of Energy. www.hydrogenassociation.org.

9. Brentner, L. B., M. J. Eckelman, and J. B. Zimmerman, "Combinatorial Life Cycle Assessment to Inform Process Design of Industrial Production of Algae Biodiesel," *Environ. Sci. Tech.*, **45**, 7060–7067 (2011).

10. Bretherick, L., *Handbook of Reactive Chemical Hazards*, Butterworth, London (1990).

11. Carvalho, A., H. A. Matos, and R. Gani, "SustainPro—A Tool for Systematic Process Analysis, Generation and Evaluation of Sustainable Design Alternatives," *Comput. Chem. Eng.*, **50**, 8–27 (2013).

12. Chase, M. W., (ed.), *JANAF Thermochemical Tables*, 3rd ed., Parts 1 and 2, in *J. Phys. Chem. Ref. Data*, 14 (Suppl. 1) (1985).

13. Cheremisinoff, N. P. (ed.), *Encyclopedia of Fluid Mechanics*, Gulf Publishing, Houston (1986).

14. Cobb, C., D. Schuster, B. R. Beloff, and D. Tanzil, "Benchmarking Sustainability," *Chem. Eng. Prog.*, **103**, 6, 38–42 (2007).

15. Cobb, C., D. Schuster, B. R. Beloff, and D. Tanzil, "The AIChE Sustainability Index: The Factors in Detail," *Chem. Eng. Prog.*, **105**, 1, 60–63 (2009).

16. Considine, D. M., (ed.), *Van Nostrand's Scientific Encyclopedia*, 8th ed., Van Nostrand, New York (1995).

17. Crowl, D. A., and J. F. Louvar, *Chemical Process Safety: Fundamentals with Applications*, 3rd ed., Prentice-Hall, Englewood Cliffs, New Jersey, 2011.

18. de Nevers, N., *Air Pollution Control Engineering*, McGraw-Hill, New York (1995).

19. Dunlop, E. H., A. K. Coaldrake, C. S. Silva, and W. D. Seider, "An Energy-limited Model of Algal Biofuel Production: Toward the Next Generation of Advanced Biofuels," *AIChE J.*, **59**, 12, 4641–4654 (2013).

20. Eisenhauer, J., and S. McQueen, *Environmental Considerations in Process Design and Simulation*, Energetics, Columbia, Maryland (1993).

21. "Energy Distribution in the U. S. in 2011," U.S. Energy Information Administration (www.eia.gov/aer), Annual Energy Review 2011 (September 2012).

22. Energy Information Administration (EIA), International Energy Statistics (2014) www.eia.gov/cfapps/ipdbproject/IEDIndex3.cfm?tid=5&pid=5&aid=2.

23. Frank, E. D., J. Han, I. Palou-Rivera, A. Elgowainy, and M. Q. Wang, *User Manual for Algae Life-Cycle Analysis with GREET: Version 0.0*, Energy Systems Division, Argonne National Laboratory (September 2011).

24. Freeman, H. M. (ed.), *Standard Handbook of Hazardous Waste Treatment and Disposal*, McGraw-Hill, New York (1989).

25. Graham, M. B. W., and A. T. Shuldiner, *Corning and the Craft of Innovation*, Oxford University Press, U.K., 2001.

26. Green, D. W., and R. H. Perry (ed.), *Perry's Chemical Engineer's Handbook*, 8th ed., McGraw-Hill, New York (2008).

27. *Guidelines for Engineering Design for Process Safety*, CCPS, AIChE (1993).

28. Gundling, E., *The 3M Way to Innovation: Balancing People and Profit*, Kodansha International, Tokyo (2000).

29. Handler, R. M., C. E. Canter, T. N. Kalnes, F. S. Lupton, O. Kholiqov, D. R. Shonnard, and P. Blowers, "Evaluation of Environmental Impacts from Microalgae Cultivation in Open-air Raceway Ponds: Analysis of the Prior Literature and Investigation of Wide Variance in Predicted Impacts," *Algal Research*, **1**, 83–92 (2012).

30. Hewitt, G. F., G. L. Shires, and Y. U. Polezhaev, (eds.), *International Encyclopedia of Heat and Mass Transfer*, CRC Press, Boca Raton (1997).

31. Hydrogen Economy, Wikipedia, en.wikipedia.org/wiki/Hydrogen_economy.

32. Institute for Global Ethics, www.globalethics.org, Madison, Wisconsin.

33. Kent, J. A., (ed.), *Riegel's Handbook of Industrial Chemistry*, 9th ed., Van Nostrand Reinhold, New York (1992).

34. Kidder, R. M., *Good Kids, Tough Choices*, Jossey-Bass (2010).

35. *Kirk-Othmer Encyclopedia of Chemical Technology*, 4th ed., Wiley-Interscience, New York (1991).

36. Kletz, T., *Learning from Accidents in Industry, Butterworths* (1988a).

37. Kletz, T., *What Went Wrong?* 2nd ed., Gulf Publishing (1988b).

38. Kletz, T., *Plant Design for Safety—A User-Friendly Approach*, Hemisphere, Washington, DC (1991).

39. Kletz, T., *HAZOP and HAZAN*, 3rd ed., IChemE (1992).

40. Krajnc, D., and P. Glavic, "Indicators of Sustainable Production," *Clean Technol. Environ. Policy*, **5**, 3, 279–288 (2003).

41. Lide, D. R., (ed.), *Handbook of Chemistry and Physics*, 78th ed., CRC Press, Boca Raton, Florida (1997).

42. *McGraw-Hill Encyclopedia of Science and Technology*, 6th ed., McGraw-Hill, New York (1987).

43. McKetta, J. J. (ed.), *Chemical Processing Handbook*, Marcel Dekker, New York (1993a).

44. McKetta, J. J. (ed.), *Unit Operations Handbook*, Marcel Dekker, New York (1993b).

45. McKetta, J. J., and W. A. Cunningham (eds.), *Encyclopedia of Chemical Processing and Design*, Marcel Dekker, New York (1976).

46. Meel, A., and W. D. Seider, "Plant-Specific Dynamic Failure Assessment using Bayesian Theory," *Chem. Eng. Sci.*, **61**, 7036–7056 (2006).

47. National Institute for Occupational Safety and Health, *Pocket Guide to Chemical Hazards*, NIOSH, Cincinnati, Ohio (1987).

48. Pariyani, A., W. D. Seider, U. G. Oktem, and M. Soroush, "Dynamic Risk Analysis Using Alarm Databases to Improve Safety and Quality: Part I—Data Compaction," *AIChE J.*, **58**(3), 812–825 (2012).

49. Pariyani, A., W. D. Seider, U. G. Oktem, and M. Soroush, "Dynamic Risk Analysis Using Alarm Databases to Improve Safety and Quality: Part II—Bayesian Analysis," *AIChE J*., **58**(3), 826–841 (2012).

50. Ruiz-Mercado, G. J., R. L. Smith, and M. A. Gonzalez, "Sustainability Indicators for Chemical Processes: I. Taxonomy," *Ind. Eng. Chem. Res.*, **51**, 2309–2328 (2012a).

51. Ruiz-Mercado, G. J., R. L. Smith, and M. A. Gonzalez, "Sustainability Indicators for Chemical Processes: II. Data Needs," *Ind. Eng. Chem. Res.*, **51**, 2399–2353 (2012b).

52. Ruiz-Mercado, G. J., M. A. Gonzalez, and R. L. Smith, "Sustainability Indicators for Chemical Processes: III. Biodiesel Case Study," *Ind. Eng. Chem. Res.*, **52**, 6747–6760 (2013).

53. Seider, W. D., J. D. Seader, D. R. Lewin, and S. Widagdo, *Product and Process Design Principles: Synthesis, Analysis, and Evaluation*, 3rd ed., Wiley, Hoboken, New Jersey (2009).

54. Sikdar, S. K., "Sustainable Development and Sustainability Metrics," *AIChE J.*, **49**, 8, 1928–1932 (2003).

55. Silva, C. S., E. Soliman, C. Wilkinson, G. Cameron, L. A. Fabiano, E. Dunlop, and W. D. Seider, "Optimal Design of an Algae Oil Transesterification Process," *Ind. Eng. Chem. Res*. **53**, 5311–5324 (2014).

56. Silva, C. S., W. D. Seider, and N. Lior, "Exergy Efficiency of Plant Photosynthesis," *Chem. Eng. Sci.*, **130**, 151–171 (2015).

57. Stephenson, A. L., E. Kazamia, J. S. Dennis, C. J. Howe, S. A. Scott, and A. G. Smith, "Life-Cycle Assessment of Potential Algal Biodiesel Production in the United Kingdom: A Comparison of Raceways and Air-Lift Tubular Bioreactors," *Energy Fuels*, **24**, 4062–4077 (2010).

58. Szargut J., *Exergy Method, Technical and Ecological Applications*, WIT Press, Billerica, Massachusetts (2005).

59. *Ullmann's Encyclopedia of Industrial Chemistry*, 5th ed., VCH, Deerfield Beach, Florida (1988).

60. Union of Concerned Scientists, How Geothermal Energy Works (Last revised December 22, 2014), www.ucsusa.org.

61. Weekman, Jr., V. W "Gazing into an Energy Crystal Ball," *Chem. Eng. Prog.*, **106**, 6, 23–27 (2010).

62. Woods, D. R., *Data for Process Design and Engineering Practice*, Prentice-Hall, Englewood Cliffs, New Jersey (1995a).

63. Woods, D. R., *Process Design and Engineering Practice*, Prentice-Hall, Englewood Cliffs, New Jersey (1995b).

64. Xu, J., and G. F. Froment, "Methane Steam Reforming, Methanation and Water-gas Shift: I. Intrinsic Kinetics," *AIChE J.*, **35**, 1, 88–96 (1989).

EXERCISES

3.1 Regarding the recent advances in drilling technologies that permit natural gas to be recovered from shale deposits cost competitively, present arguments from an environmental perspective in favor and opposed to its rapid expansion.

3.2 Two serious environmental problems have received considerable attention over the past three decades:

(a) The serious depletion of ozone in the Earth's stratosphere, especially over the North and South Poles. How has this depletion occurred, and why does it present a serious health problem?

(b) The serious buildup of ozone in the big cities due to air pollution. How has this buildup occurred and why does it present a serious health problem?

3.3 Design teams are confronted with "multiobjective" decision making. Is it possible for objectives to lead to conflicting designs? Give an example(s).

3.4 Consider the flammability limits of a mixture of methane and ethane in Example 3.2 exposed to air at 5 volume percent. Use inert nitrogen gas to prevent combustion. What volume percent of nitrogen is required?

3.5 Using Table 3.2, discuss potential safety issues associated with the usage of hydrogen as a fuel for automobiles running on fuel cells in comparison with those associated with vehicles running on gasoline.

3.6 The P&ID reproduced in the next page shows an arrangement for the cooling of a hot effluent stream using cooling water. Unfortunately, the P&ID includes a number of errors that could lead to accidents. Find as many as you can.

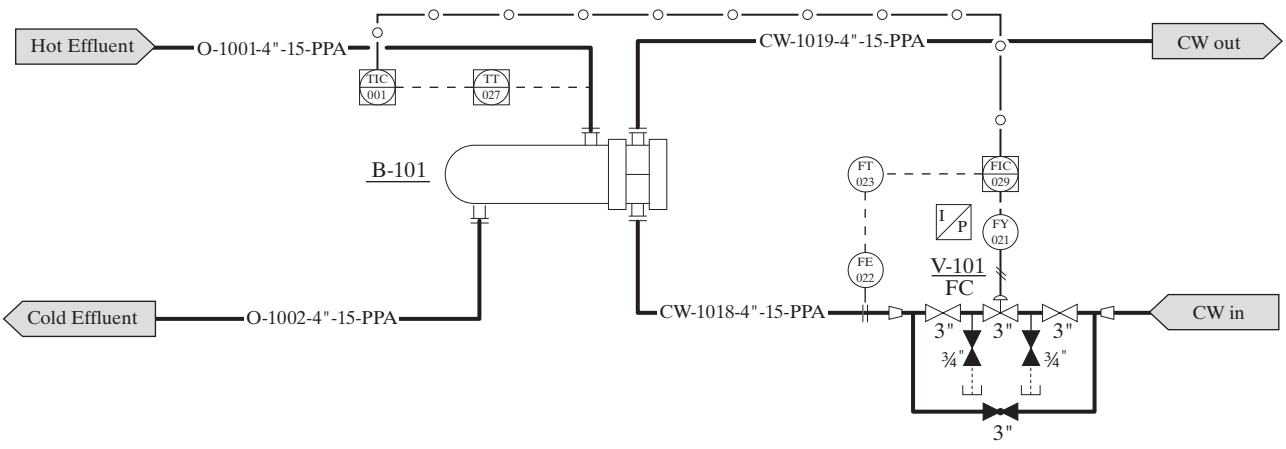

3.7 The P&ID reproduced below shows the coolant circuit for the batch reactor, R-100, in which a highly exothermic reaction occurs. The coolant circuit is intended to maintain the reactor temperature at its desired setpoint. Identify at least two serious errors in the design as indicated in the P&ID, which may lead to catastrophic failure of the reactor.

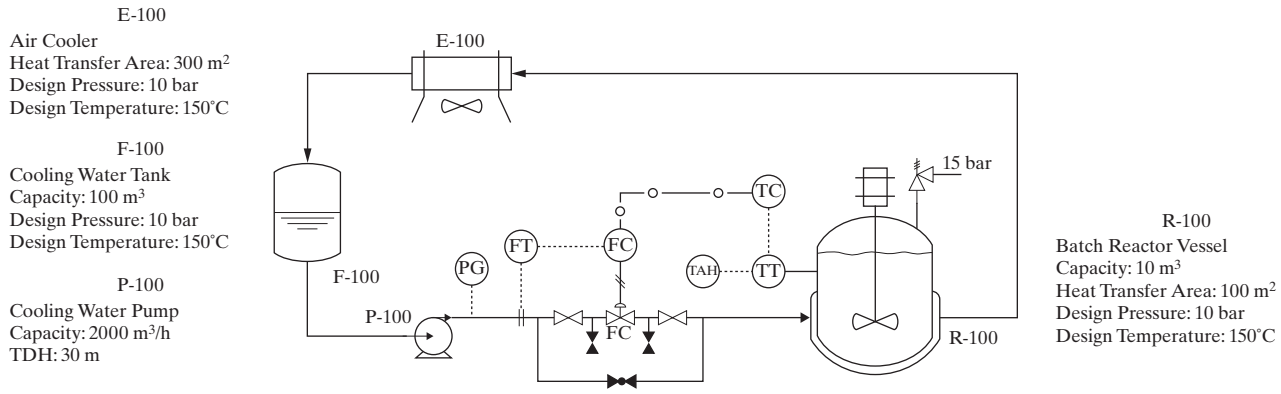

3.8 Refer to the event tree in Figure 3.10 and the data in Table 3.6. Suppose the company operating this CSTR decides to hire an expert operator in response to the runaway reaction in April. This operator claims he can perform twice as well as a regular operator (i.e., he fails half as often). Had this operator been working at the plant during April, what is the probability that the runaway reaction would not have occurred assuming that the expert operator would not have affected the malfunctioning quench valve? If there is only a 5% chance of another runaway reaction occurring in the next year using the current operators, what is the probability of a runaway reaction occurring using the expert operator. Qualitatively, if this operator is as effective as claimed, would it be in the company's best interest to hire him, even if he demanded a significantly higher salary than a regular operator?

3.9 You are an engineering manager and have been asked to work with the Public Relations Department in writing a press release about a new product that did not turn out quite as well as promised in earlier reports. How much do you reveal to the public in the press release? Consider the alternatives.

(a) I do not hint at it. It is important that the company's image is not damaged by the flawed product.

(b) I write a less-enthusiastic, but honest, release than I would if the product were perfect.

(c) I am completely honest, believing it will earn the respect of customers to be forthcoming.

3.10 You are the plant manager in charge of creating the budget report that goes to the board of directors of your company. Just before the next meeting, the president asks you to leave something negative out and just add it next time. Do you agree to do this as a favor to him? Consider the alternatives.

(a) Yes, one time will not hurt.

(b) Yes, but only after the president agrees to give you a bonus.

(c) No, one small thing can turn into many small things, which is a big deal.

3.11 You have received a job offer from a startup company headed by PhD chemists to be their chief (and only) process engineer, responsible to move their process for a novel solid adhesive from lab-scale to full production. The product is produced in the lab by cooling a "soup" of chemicals, some of which polymerize in the process. They require you

to sign a contract before they disclose any technical details. How should you respond?

(a) Disagree. You are not prepared to take on the responsibility for the process without seeing full technical details first.

(b) Agree, if the salary they are offering you is high enough.

(c) Agree, so long as you are not responsible for the process.

3.12 The Bhopal disaster was caused by a gas leak incident in India, considered one of the world's worst industrial disasters. It occurred on the night of 2–3 December 1984 at the Union Carbide India Limited (UCIL) pesticide plant in Bhopal, Madhya Pradesh, India. A leak of methyl isocyanate gas and other chemicals from the plant resulted in the exposure of hundreds of thousands of people to highly toxic chemicals. Prepare a short report or PowerPoint presentation describing:

(a) An account of the steps leading up to the reported disaster.

(b) A list of root cause(s) of the reported disaster.

(c) The ethical dilemma inherent in the reported disaster because a choice between at least two alternatives had to be made.

(d) An additional good alternative that could have either prevented the disaster or reduced the severity of its consequences.

3.13 On March 23, 2005, a hydrocarbon vapor cloud explosion occurred at the isomerization process unit at BP's Texas City Refinery in Texas City, Texas, killing 15 workers and injuring more than 170 others. Prepare a short report or PowerPoint presentation describing:

(a) The steps leading up to the reported disaster.

(b) A list of root cause(s) of the reported disaster.

(c) The ethical dilemma inherent in the reported disaster because a choice between at least two alternatives had to be made.

(d) An additional good alternative that could have either prevented the disaster or reduced the severity of its consequences.

3.14 The Chernobyl disaster was a catastrophic nuclear accident that occurred on April 26, 1986, at the Chernobyl Nuclear Power Plant in Ukraine, which was under the direct jurisdiction of the central authorities of the Soviet Union. An explosion and fire released large quantities of radioactive contamination into the atmosphere, which spread over much of Western USSR and Europe. It is widely considered to have been the worst nuclear power plant accident in history, and is one of only two classified as a level 7 event on the International Nuclear Event Scale (the other being the Fukushima Daiichi nuclear disaster in 2011). Prepare a short report or PowerPoint presentation describing:

(a) The steps leading up to the reported disaster.

(b) A list of root cause(s) of the reported disaster.

(c) The ethical dilemma inherent in the reported disaster because a choice between at least two alternatives had to be made.

(d) An additional good alternative that could have either prevented the disaster or reduced the severity of its consequences.

Part Two

Design Synthesis—Product and Processes

Part One defined product design and process design, differentiated between the two, and cited examples of each. The design of a product or a process is the subject of Part Two, which includes Chapters 4 and 5 on product design synthesis, Chapters 6–11 on process design synthesis, Chapters 12–15 on sizing of process equipment, and Chapters 16 and 17 on equipment and process cost evaluation.

Design begins with an assessment of the possible need for a new product or process. Concepts for satisfying the need are generated and examined for technical and economic feasibility, which includes consideration of safety, controllability, and environmental concerns.

The synthesis and design of new chemical products, including molecular products (consisting of a single type of molecule) and mixture-blended products (different molecules in a liquid solution or blend) are discussed in Chapter 4. In that chapter (1) preferred representations of molecular structure are presented, (2) methods are developed for selecting feasible candidate molecules and mixtures that provide the desired properties as generated from the product needs function, and (3) methods are presented for estimating the properties of molecules and mixtures when experimental values are not available. A computer-aided framework is employed and the use of software is emphasized. Many examples are given to illustrate the synthesis principles.

Chapter 5 considers devices, functional products, and formulated products whose structure, form, shape, and/or configuration are customized. Many examples are presented to illustrate how to use systematic procedures, methods, and tools to develop a conceptual design. The importance of creativity and the use of mathematical models are emphasized. These models most often employ chemical engineering principles of thermodynamics, transport phenomena, and chemical kinetics.

Heuristic methods for synthesizing the flowsheet of a chemical process are presented in Chapter 6. A total of 53 heuristics are presented that cover selection of raw materials and chemical reactions; use of excess reactants, recycle, and purges; configuration of and handling of heat of reaction in chemical reactors; selection of the type and order of separation steps for mixtures containing gases, liquids, and solids; and use and location of heat exchangers, pumps, and compressors; and handling of solids. The application of many of the heuristics is illustrated by examples.

Once a process flowsheet has been synthesized, heat and material balances and equipment design can begin. This is best carried out with computer-aided process simulation programs. This is the topic of Chapter 7 where the following steps are addressed: (1) formulation of the process simulation problem; (2) important steps in the process simulation; (3) selection of physical property and equipment-design models; and (4) systematic procedures for conducting process simulations in an efficient manner. Detailed process simulation examples apply the principles discussed to chemical and biochemical processes.

The synthesis and design of the reactor section of a chemical process should consider the use of more than one reactor to ensure that sufficient yield and selectivity of required product species are achieved in the most efficient manner. In addition, it is also necessary to consider the most efficient method for separating the components in the reactor effluent when their number is not small. The synthesis of reactor networks and separation trains are discussed and illustrated with numerous examples in Chapters 8 and 9, respectively.

Chemical processes are frequently very energy inefficient. However, without conducting an analysis based on the second law of thermodynamics, it is not possible to pinpoint and determine the extent of the inefficiency. Chapter 10 presents a method for conducting a second-law analysis where the required data for the analysis can be generated with a process simulator. Also included are heuristics and illustrative examples for improving the efficiency.

The placement and operating conditions for heat exchangers and pressure-change equipment can be crucial

in minimizing the energy requirement for a process. Chapter 11 presents systematic procedures, illustrated by many examples, for the efficient integration of heat and power in a process.

Chapters 12–15 cover the selection and sizing of process heat exchangers; trayed and packed towers for absorption, stripping, and distillation; pumps, compressors, and expanders; and chemical reactors by methods commonly employed in process simulators. Information in these chapters is essential for using process simulators effectively.

All aspects of process economics are covered in Chapters 16 and 17. Accepted methods of cost accounting are discussed in Chapter 16. This is followed by methods for estimating the capital cost of a process at different levels of accuracy, including the definitive APEA method provided by Aspen Technology, which regularly updates equipment purchase and installation costs. Methods for estimating annual costs, earnings, and profitability analysis, including discounted cash flow rate of return (DCFRR), are covered in Chapter 17.

Chapter 4

Molecular and Mixture Design

4.0 OBJECTIVES

This chapter introduces the reader to two classes of chemical products: those in which the molecules are identical in the product, to be called here a *molecular product*; and those in which different molecules are present as a liquid solution or blend, to be called here a *mixture-blended product*. The following questions, which are regarded as important for a good understanding of the issues related to molecular and mixture designs, are addressed in this chapter:

- How to represent the structure of a molecule?
- How to generate chemically feasible candidate molecules and mixtures?
- How to estimate the properties of molecules and mixtures?
- How to formulate and solve typical molecular and mixture design problems?

There are many ways to design molecular and mixture products. In this chapter, only a framework based on *computer-aided methods and software* suitable for molecular and mixture design is considered. This design approach identifies promising design alternatives through model-based computer-aided techniques that may be experimentally verified and fine-tuned at a later stage. In this way, computer-aided techniques are employed first to quickly and reliably reduce the search space within which the optimal designs are likely to be found. Then, focused experiments are performed on an identified set of promising alternatives.

After studying this chapter, the reader should:

1. Recognize the characteristics of single molecules and liquid mixtures as products.
2. Have the ability to convert the needs-functions of a product to the properties of single molecules or liquid mixtures.
3. Be familiar with computer-aided methods and software that are applicable for selection, design, and analysis of these products.
4. Be able to select, design, and analyze products composed of the same molecule throughout the product.
5. Have the ability to select, design, and analyze liquid products composed of a mixture of different molecules.

4.1 INTRODUCTION

In the classification of products in Chapter 1, the molecular and (liquid) mixture products belong to the B2B type. Typically, molecular products shown in Figures 4.1a–4.1c, and mixture-blended products shown in Figure 4.1d, find applications in the process industries as well as being incorporated in other chemicals-based products. In the former, these molecules and/or mixtures eventually help to manufacture a desired chemicals-based product; while in the latter, these molecules and/or mixtures are incorporated in the final product and have a specified function in the product.

In Figure 4.1, three types of molecular products of varying size and molecular structural complexity are highlighted. Molecules of type 4.1a usually have process-related applications or may be part of a mixture-formulated product. Molecules of types 4.1b and 4.1c are usually employed as the main active ingredient of chemicals-based products. The molecular structures of type 4.1c may be manipulated to obtain a specific product function. Figure 4.1d highlights the concept of mixture-blend design. Different chemicals are blended to obtain a liquid solution product with desired properties.

Solvents are good examples of molecular as well as mixture-blended products that may be employed in the process industries as well as in chemicals-based products. In the process industries, the feasibility of a downstream product depends on the successful performance of a solvent-based operation in a process manufacturing the product. Examples of solvent-based operations are separations, cleaning operations, and organic synthesis, to name a few. In each of these operations, the desired solvents perform different functions. The feasibility of the chemical product manufactured through the solvent-based process depends on the successful selection-design of the solvent. Unlike the solvents used in these operations, as part of a product, solvents are usually incorporated in formulated products with specific functions. For example, in cosmetic products such as lotions, their function is to deliver the active ingredient to the product application site (e.g., skin) and then leave by evaporation. The performance of the product depends on the function of the selected solvent (molecular or mixture).

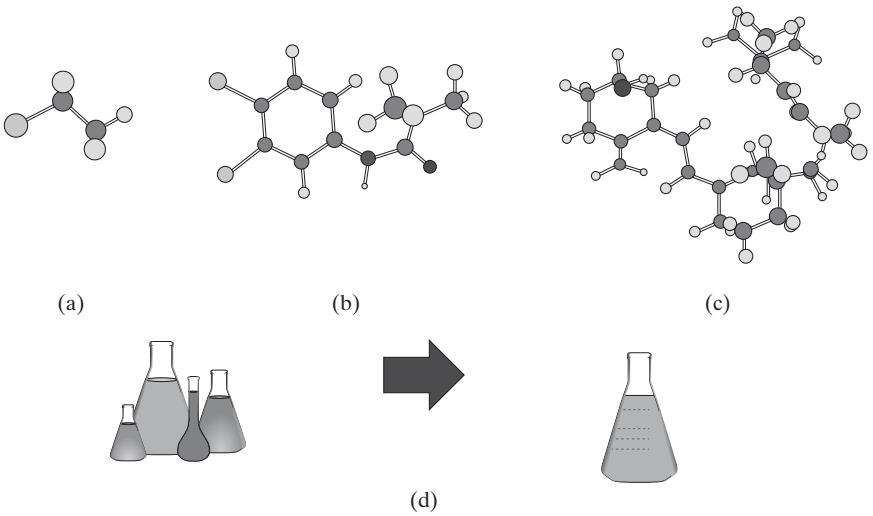

Figure 4.1 Types of molecular and mixture-blended products. See the Color Figures folder on the Wiley website.

Refrigerants and/or *heat-pump* fluids are also usually single (nearly pure) molecular products whose role is to absorb and release energy in different states defined by changes in temperature and pressure in the refrigeration or heat-pump cycle. Other examples of single molecule products are *emulsifiers* (surfactants that create an emulsion) and *active ingredients* (the chemicals performing the main function of a chemicals-based product, as in drugs and cosmetics).

An important issue with respect to all molecular products is that they need to perform specific functions related to their properties as pure chemicals and/or as species in mixtures of chemicals. These properties differ based on their *need-functions* in a processing operation or in a downstream product. A typical molecular design problem is defined as:

> *Given a set of building blocks and a specified set of target properties, determine the molecule that matches these properties.*

When the need-functions of a product cannot be matched with the properties of a single molecule, mixtures (blends) of different molecules are considered. Just like molecular products, mixtures-blends may also be employed to perform specific operations in the process industries or be employed to perform specific functions in different types of products. Examples of the former are blends of solvents, lubricants, and process fluids, while those of the latter are additives to fuels, solvent blends in paints, and aroma blends in cosmetic products. Like molecular products, applications of specific mixture products define their need-functions, which in turn define the set of properties the blend must provide to perform its functions. There are many types of mixture-blended products. In this chapter, only mixture-blends that are stable liquid solutions are covered. Other types of mixture products, such as *formulations*, are covered in Chapter 5. The typical mixture-blend design problem is defined as:

> *Given a set of chemicals and a specified set of property constraints, determine the optimal mixture and/or blend.*

Note that the chemicals in the mixture design problem could be first generated through a *molecular-product design* step.

Based on the above discussion, one of the most important issues related to molecular and/or mixture design is the set of properties of the single molecule and/or mixture that define the product's need-functions. A single-molecule solvent product must at least be a liquid at the condition of application and must dissolve an assigned solute.

EXAMPLE 4.1 ***Properties to Ensure a Solvent will be Liquid and Dissolve a Solute***

Which properties ensure that the solvent molecule will be a liquid and dissolve a solute?

SOLUTION

The boiling point and melting point of the pure compound establish whether the compound is a liquid at a specified condition. The solubility, on the other hand, can be established in many ways; for example, using the Hildebrand solubility parameter of the solvent and solute (when the solute and solvent have similar Hildebrand solubility parameters, they are mutually soluble in each other; note that the Hildebrand solubility parameter is a pure-compound property) or through calculation of the infinite-dilution activity coefficient of the solute in the solvent (solubility of the solute is inversely proportional to the infinite-dilution activity coefficient, which is a mixture property).

The needed property values may be measured or retrieved from a database of measured data, or calculated through the use of appropriate property models. Any computer-aided technique for the design of molecular products, therefore, must include a database of measured property values complemented by a library of property models to predict property values not available in the database.

Other related issues involve the structure of the molecule for molecular products, and the compositions of the molecules in mixture-blended products.

EXAMPLE 4.2 ***Molecular Stability and Stable Liquid Solutions***

How do we know: (1) from the structure of a molecule that it represents a stable chemical compound, or (2) from a mixture of stable molecules that they represent a stable liquid solution?

SOLUTION

The stability of a molecular structure must be verified through a *valence* rule. Also, the stability of a liquid mixture of stable molecules must be verified using the liquid-phase stability criterion.

Property data or estimates are, however, insufficient. To solve the molecular-product design problem, a method is needed to *generate* molecular structures by employing appropriate *building blocks* (e.g., functional groups) that can be combined to form molecules through a set of rules that ensure their molecular stability. In this way, the building blocks are assembled into molecular structures. Because some property models also require these structural data, it is advantageous to use these building blocks to predict molecular properties. Given these estimates, the generated molecules can be checked for matches with *target* property values. Then, for mixture-blended products, the specific molecules in the mixture and their compositions must be confirmed to satisfy the liquid-phase stability criterion at a specified temperature. Appropriate property models can estimate the needed property values, permitting the generated mixtures to be tested for *matches* with the *target* property values.

Based on the above, the essential ingredients for molecular design require: (1) a method to represent stable molecular structures, (2) a method to generate chemically feasible molecules, and (3) methods to estimate the required properties. Similarly, in the case of mixture-blend designs, the ingredients are: (1) a method to generate stable mixture-blend candidates, and (2) methods to estimate the needed properties. Because the number of generated, chemically feasible molecules or mixtures can be very large, a systematic framework to *generate* the molecular structures and *test* their properties, using the appropriate computer-aided methods and software, is needed.

Next, in Section 4.2, the framework for computer-aided molecular design (CAMD) and mixture-blend design (CAM^{b}D) is described, with subsections discussing molecular structure representation, the generation of molecule-mixture candidates, property prediction, CAMD/CAM^{b}D problem formulation, software for CAMD/CAM^{b}D problem solution, and CAMD/CAM^{b}D solution approaches. Then, Section 4.3 presents eight case studies highlighting solvent substitution, molecular design to find azeotropes, dichloromethane (DCM) replacement in organic synthesis, refrigerant design, active ingredient design, design of large, complex molecules, polymer design, and tailor-made gasoline-blend design.

4.2 FRAMEWORK FOR COMPUTER-AIDED MOLECULAR-MIXTURE DESIGN

The solution of all CAMD/CAM^{b}D problems can be obtained using five hierarchical steps, as shown in Figure 4.2 and listed below.

1. *Problem Formulation:* The CAMD (or CAM^{b}D) problem is defined in terms of the product needs and functions.

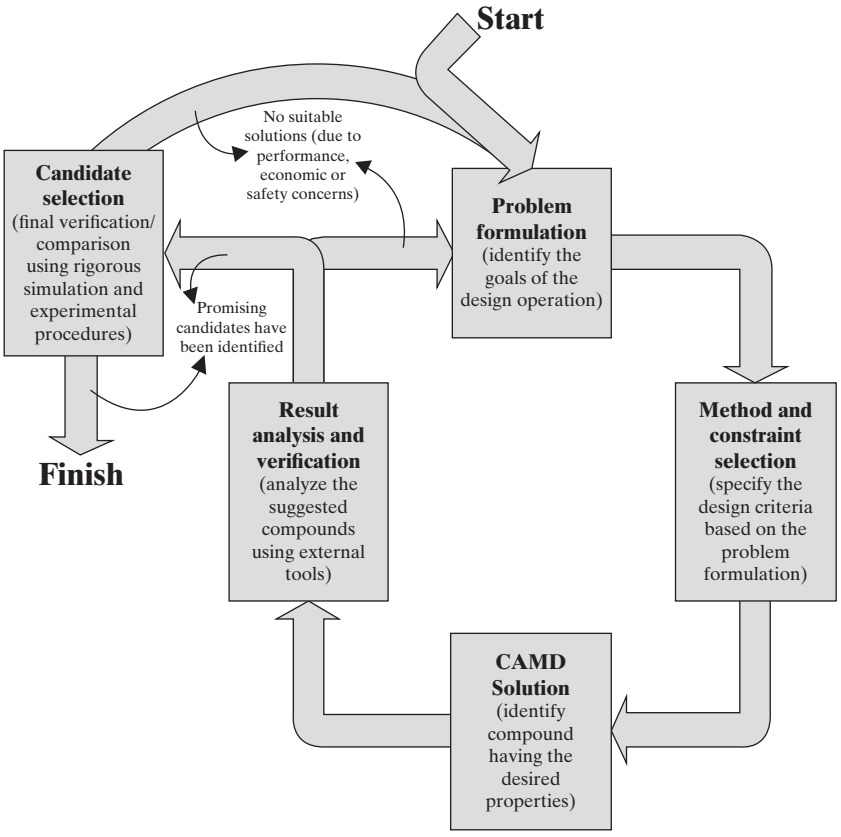

Figure 4.2 Computer-aided framework for molecular-mixture design. (*Source:* Hostrup et al., 1999. Used with permission).

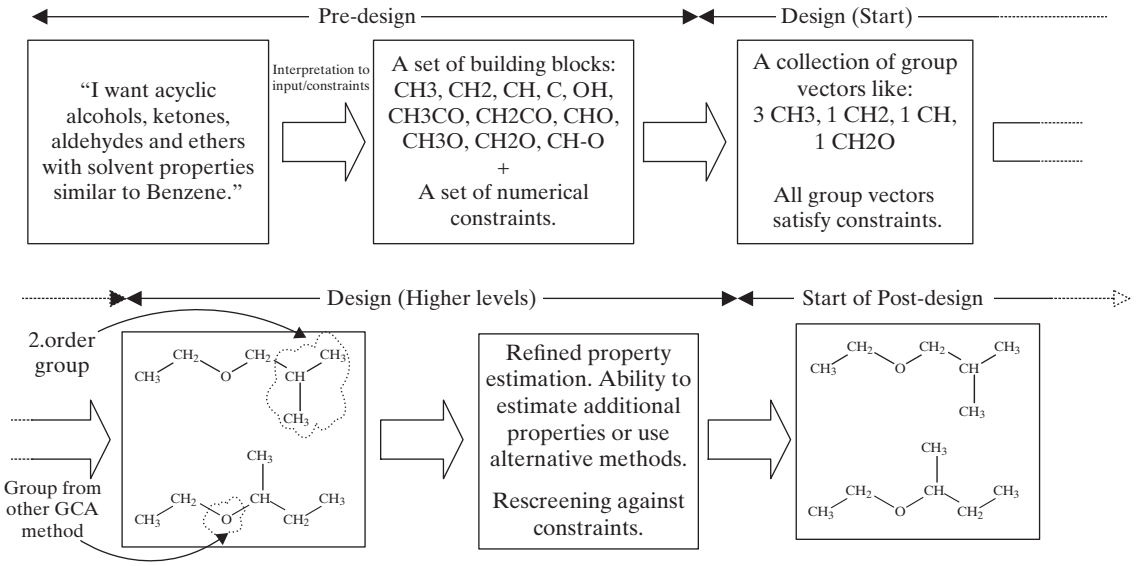

Figure 4.3 Application of the framework for CAMD (predesign: steps 1, 2; design: steps 3, 4; postdesign: step 5). (*Source:* Harper et al. 2002. Used with permission).

2. *Method and Constraint Selection:* The needs and functions of the product are converted into a specific set of properties together with their target values.
3. *CAMD/CAM^{b}D Solution:* Any CAMD (and/or CAM^{b}D) technique (for example, group-contribution-based technique) to automatically generate and test candidates is used. The selected CAMD/CAM^{b}D technique should be able to generate molecular-structure mixtures and evaluate their properties with respect to the specified target properties.
4. *Result Analysis and Verification:* The selected candidates are further analysed to confirm their desired performance. Models capable of simulating product performance during application are needed. These may be process simulation models as well as product application models (e.g., to confirm delivery of an active ingredient).
5. *Final Selection:* Through detailed verification using a combination of experiments and/or rigorous model-based tests.

A typical application of this framework is illustrated in Figure 4.3 where the objective is to find environmentally friendly substitute molecules for benzene—only the concept is highlighted here. As substitutes, environmentally friendly alternatives are likely to be acyclic molecules with C, H, and O atoms. A set of building blocks (e.g., functional groups) is used together with a set of constraints to generate candidate molecules. Because the same group vector may represent more than one molecule, all of the molecules are generated and evaluated using property models. Those that match the desired property targets are selected as candidates to replace benzene in different applications. Second-order groups are able to distinguish between some isomers, and this is highlighted also in Figure 4.3. Also, in addition to groups, groups plus connectivity may be used (Group Contribution Assembly-GCA), as highlighted in Figure 4.3.

Molecular Structure Representation

Several different representations of molecules are highlighted in Figure 4.4, but note that not all representations are shown. The simplest form of molecular representation is based on its chemical formula, where a compound is simply represented by the types of atoms it contains and the number of occurrences of each atom type (see Figure 4.4a). Although this representation applies to a large number of compounds of very different types, there is no information regarding the bonds in the compound. Another representation is as a collection of *functional groups* or *fragments*. A functional group is a molecular fragment or substructure defined by the number and types of atoms in the fragment and showing how the atoms are connected, how many free bond connections the group has available, and the atoms on which the free connections are located (see Figure 4.4b). A group vector, shown in Figure 4.4c, contains some of this connectivity information, but does not define it completely. As a result, a group vector can represent isomers, two of which are shown in Figure 4.4d, which illustrates the different compounds that can be represented using the group vector in Figure 4.4c.

Knowing the valence of the different atom types in the molecule, it is possible to generate the bond configurations. The compounds depicted in Figure 4.4d have the connectivity defined. One simple and flexible way to define the connectivity is through the adjacency matrix. An adjacency matrix is a square symmetrical matrix with rows and columns representing each atom (or fragment) in the molecule and containing nonzeroes and zeroes indicating the number of bonds or absence of bonds, respectively. Note that adjacency matrices can be expressed using fragments or atoms. Conversion from a fragment-based matrix to an atom-based matrix is achieved by replacing the entry for each fragment with the atom adjacency matrix representing the

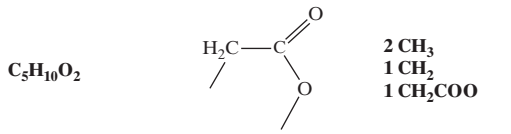

(a) (b) (c)

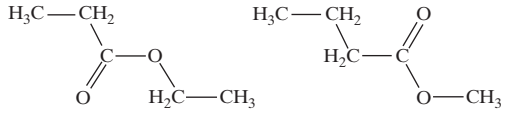

(d)

	CH_3	CH_3	CH_2	CH_2COO
CH_3	0	0	0	1
CH_3	0	0	1	0
CH_2	0	1	0	1
CH_2COO	1	0	1	0

(e)

	H	H	H	H	H	H	H	H	H	H	C	C	C	C	C	O	O
H	0										1						
H		0									1						
H			0								1						
H				0								1					
H					0							1					
H						0						1					
H							0						1				
H								0					1				
H									0					1			
H										0				1			
C	1	1	1								0		1				
C				1	1	1						0		1			
C							1	1			1		0		1		
C									1	1		1		0		1	
C													1		0	1	2
O														1	1	0	
O															2		0

(f)

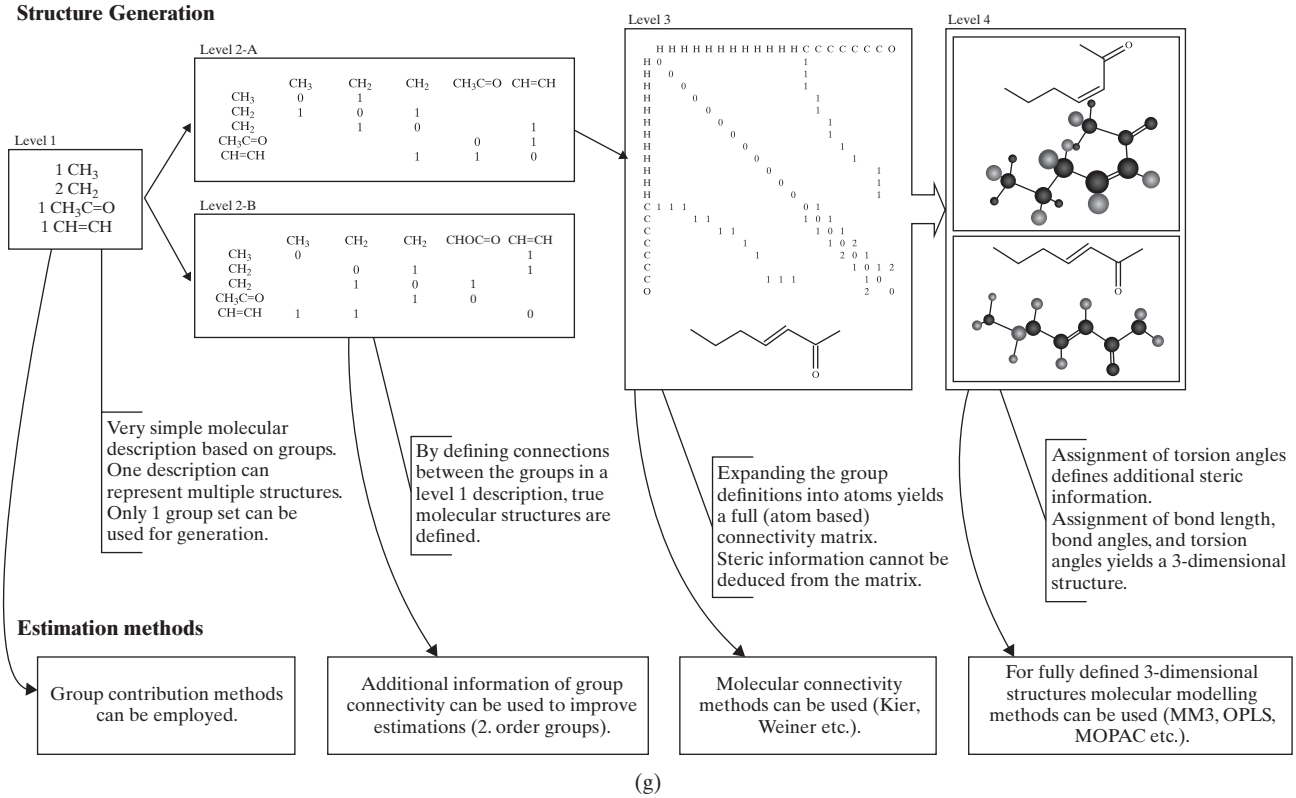

(g)

Figure 4.4 Forms of molecular structure representation and corresponding property prediction.
(*Source:* Harper et al. 2002. Used with permission).

fragment. Figures 4.4e and 4.4f show the fragment-based and atom-based adjacency matrices, respectively, for the compound in Figure 4.4d.

While the adjacency matrix defines the 2D (2-dimensional) relations between atoms in a compound, it does not contain the steric information needed to distinguish isomers. To distinguish between isomers, it is necessary to have 3D (3-dimensional) information about the atom placements. For 3D representations, adjacency matrices with a list of x, y, z Cartesian coordinates for the atoms are possible. Alternatively, the so-called *internal coordinate system*, in which atom positions are defined using bond length, bond angle, and torsion angle, is used. Choice of representation depends on the computations to be performed involving the 3D representation. Examples of 3D structures of the compounds (molecules) are developed using appropriate descriptors together with an algorithm to construct the 3D structures of the compounds and estimate their physical properties. The representation of molecular structures and estimation of properties at four levels (first- and second-order group contribution; group contribution plus connectivity index, and molecular simulation) are summarized in Figure 4.4g.

Just the representation of molecules by functional groups (fragments) is employed throughout this chapter.

Generation of Molecule-Mixture Candidates

In this subsection, first molecular structures are generated. Then, mixture-blend candidates are generated.

Generation of Molecular Structures

Having the *functional groups* as the building blocks, a *set of rules* to combine them into *chemically feasible* molecules is needed. These rules limit the combinations of groups to those in chemically feasible molecules, far fewer than the total number of unrestricted combinations.

EXAMPLE 4.3 ***Stable Molecules from Groups***

Given the groups CH_3, CH_2, and OH, how many chemically stable molecules can be generated with a minimum of two groups, a maximum of three groups, and the condition that the OH functional group appears no more than once?

SOLUTION

The following four molecules are generated:

CH_3—CH_3, CH_3—OH, CH_3—CH_2—CH_3, CH_3—CH_2—OH.

In Example 4.3, to ensure that the molecules are chemically feasible, the following rules (Odele and Macchietto, 1993) are employed:

$$\sum_{j=1}^{m}(2-u_j)n_j = 2q \tag{4.1}$$

$$\sum_{i\neq j}^{m} n_i \geq n_j(u_j-2)+2 \quad \forall j \tag{4.2}$$

$$n_j^l \leq n_j \leq n_j^u \quad \forall j \tag{4.3}$$

$$2 \leq \sum_{j=1}^{m} n_j \leq n_{\max} \tag{4.4}$$

$$n = \sum_{j=1}^{m} n_j \tag{4.5}$$

where m is the number of distinct groups in the basis set; $q = [-1, 0, 1]$ for [bicyclic, monocyclic, acyclic]; n_j and n_i are the number of groups j and i present in the molecule; u_j is the valence of group j (i.e., the number of free bond connections); n_{max} is the maximum number of groups allowed (specified) in the molecule; n is the number of groups present in a specific molecule; and n_j^{l} and n_j^{u} are the lower and upper bounds (specified) on the number of allowed groups of type j, respectively.

Equations (4.1) and (4.2) ensure that the final molecular structure satisfies the valance condition (no free attachments); Eq. (4.3) specifies the upper and lower bounds for the number of times group j appears in the molecule; Eq. (4.4) specifies the minimum and maximum of the total numbers of groups that appear in the molecule; Eq. (4.5) gives the total number of groups in the molecule.

A branch-and-bound-like approach is employed to generate the chemically feasible molecules. For example, for 2-group structures, only groups (one of each) with $u_j = 1$ can be employed. For 3-group structures, there must be at least one group with $u_j = 2$. Consequently, the two other groups must have $u_j = 1$.

Based on Eqs. (4.1)–(4.5), a general molecular generation problem can be formulated as:

Given a basis set of functional groups and the values of n_{max}, n_j^l and, n_j^u generate all the molecular structures that satisfy Eqs. (4.1)–(4.5).

EXAMPLE 4.4 ***Generating All Acyclic Molecules***

For the basis set of CH_3, CH_2, and OH functional groups, enumerate all chemically feasible acyclic molecules for $n_{\max} = 3$; $n_j^{\mathrm{l}} = 0$ (for all j); $n_j^{\mathrm{u}} = 2$ (for $j = CH_3$ and CH_2); and $n_{OH}{}^{\mathrm{u}} = 1$ that satisfy the conditions given by Eqs. (4.1)–(4.5).

SOLUTION

The valencies (u_j) of the groups in the basis set are $u_{CH_3} = 1$, $u_{CH_2} = 2$, and $u_{OH} = 1$. Now, by branch and bound, the sets of molecules that satisfy the valence rules, Eqs. (4.1)–(4.5), are generated. These molecules are listed in Table 4.1.

Obviously, the number of molecules generated for a larger set of functional groups is enormous. Even with the basis set in Table 4.2, millions of chemically feasible molecular structures are generated. One important limitation related to using first-order functional groups (as defined by Constantinou and Gani, 1994) is that isomeric structures cannot be distinguished. That is, the group set {3-CH_3; 1-CH; 2-CH_2} represents different molecules, 2-methyl pentane [CCCC(C)C; 000107-83-5], and 3-methyl pentane

[CCC(C)CC); 000096-14-0], but their calculated properties are the same—for each molecule, its SMILES notation and CAS number are given in brackets.

The full set of functional groups matching the originally proposed UNIFAC first-order functional groups can be found in Constantinou and Gani (1994); an extended set is given in Marerro and Gani (2001); and a further extended set is given in Hukkerikar et al. (2012a).

Table 4.1 Valence Test for the Generated Molecular Structures

Molecule	Conditions Satisfied	Conditions Not Satisfied
CH_3-CH_3	1, 3, 4, 5	*None [Eq. (2) not needed]*
CH_3-OH	1–5	*None*
CH_3-CH_2-CH_3	1–5	*None*
CH_3-CH_2-OH	1–5	*None*
OH-OH	1, 4, 5	3
OH-CH_2-OH	1, 2, 4, 5	3
CH_2-CH_2-CH_3	3–5	1, 2

Table 4.2 Sample Basis Set of Functional Groups

Group	Valence (u_j)	Group	Valence (u_j)
CH_3	1	COOH	1
CH_2	2	CH_3COO	1
CH	3	CH_2COO	2
C	4	CH_3O	1
ACH	2	CH_2O	2
AC	3	COO	3
OH	1	CH_3N	2
CH_3C0	1	CH_3NH	1
CH_2CO	2	$CONH_2$	1
CHO	1	$CONHCH_3$	1

In the same way chemically feasible molecules are generated, the same building blocks may be used to generate polymer repeat units. Consider the following example:

EXAMPLE 4.5 ***Generating Polymer Repeat Units***

Consider the following basis set of groups: {CH_2; CO; COO; O; CONH; CHOH; CHCl} How many polymer repeat units can be generated having a minimum of three groups and a maximum of four groups, with the condition that, except for the CH_2 group, all other groups can appear only once.

SOLUTION

All the basis set groups have a valence of 2. Note that because polymer repeat units must have two free attachments, the valence rules given by Eqs. (4.1), (4.2) need to be modified:

$$0 = \sum_{i=1}^{N} (u_i - 2) n_i \tag{4.6}$$

For 2-group structures, there are seven possible polymer repeat units (combinations of CH_2 with itself and the other six groups). Structures with three groups need at least two CH_2 and one of any other group, including itself. This gives an additional seven polymer repeat units. Structures with four groups need at least three CH_2 and one of the other groups, including itself. This gives seven more repeat units for a total of 21 polymer repeat units. Note that to obtain branched polymer repeat units, groups with valence 3 or higher must be included.

Generation of Mixture-Blend Candidates

This problem can be formulated and solved in different ways. Consider the following:

Given a basis set of n molecules, determine mixtures containing $m_{max} \geq m \geq 2$ that are stable liquid solutions at given conditions of temperature and pressure, where m_{max} is the maximum number of molecules and m is the actual number in the solution.

EXAMPLE 4.6 ***Generating Stable Liquid Solutions***

Given the molecules, methanol [OC; 000067-56-1], ethanol [OCC; 000064-17-5], benzene [C1CCCCC1; 000071-43-2], and water, find stable liquid binary and ternary mixtures at 298 K and 1 atm.

SOLUTION

The following mixtures are stable liquid solutions at the specified condition: methanol-ethanol, methanol-benzene, ethanol-benzene, methanol-water, ethanol-water, and methanol-ethanol-benzene. For each mixture, to ensure liquid-phase stability, the following criterion must be satisfied for all mixture compositions:

$$\frac{\Delta G}{RT} = \frac{G^E}{RT} + \sum_{i}^{NC} x_i \cdot ln(x_i) \qquad < 0$$

(for stable liquid solutions) (4.7)

where

$$\frac{G^E}{RT} = \sum_{i}^{NC} x_i \cdot ln(\gamma_i) \tag{4.8}$$

Here, ΔG is the Gibbs energy of mixing, G^E is the excess Gibbs energy due to mixing, x_i is the mole fraction of compound i, R is the universal gas constant, T is the absolute temperature, γ_i is the liquid-phase activity coefficient of compound i, and N_C is the number of compounds in the mixture.

Equation (4.7) is easily checked for binary mixtures to establish miscibility (stability). For multicomponent mixtures, each binary pair is checked first for miscibility. If any pair is found to be unstable, then the corresponding multicomponent mixture is likely to be unstable. Note that Eq. (4.7) is not a sufficient condition, but only a necessary condition for stability. Also, checks at equimolar binary composition are usually sufficient to identify phase instability when it arises. More details on liquid-phase stability of mixtures are presented by Conte et al. (2011).

EXAMPLE 4.7 ***Unstable Binary Pairs***

Which binary pairs in a mixture of methanol, ethanol, benzene, and water are unstable at temperature = 298 K and pressure = 1 atm?

SOLUTION

There are six binary pairs: methanol-ethanol, methanol-benzene, methanol-water, ethanol-benzene, ethanol-water, and benzene-water. For each pair, an equimolar mixture is tested for stability. The results are shown in Table 4.3.

Table 4.3 Binary Mixtures with Stability Test Results

Equimolar Mixture	$\frac{G^E}{RT} = \sum_i^{NC} x_i \cdot ln(\gamma_i)$	$\sum_i^{NC} x_i \cdot ln(x_i)$	Eq. (4.7) satisfied?
Methanol-ethanol	0.0455	−0.692	Yes
Methanol-benzene	0.5060	−0.692	Yes
Methanol-water	0.1461	−0.692	Yes
Ethanol-benzene	0.4523	−0.692	Yes
Ethanol-water	0.2940	−0.692	Yes
Benzene-water	1.3277	−0.692	No

Note: Any appropriate liquid-phase activity coefficient model (also known as G^E-model), except the Wilson model (Wilson and Deal, 1962), can be used to obtain γ_i; see the next subsection on Property Prediction.

The benzene-water pair is unstable, and consequently, multicomponent mixtures containing this pair are strong candidates to be unstable.

The size of mixture-blend design problems depends on n and m_{max}. For n molecules, the total number of binary mixtures is given by $\sum_j (n–j)$. Similarly, the number of ternary mixtures ($m_{max} = 3$), quaternary mixtures ($m_{max} = 4$), … , can be calculated. That is, for the four species in this example, there are six binary pairs, four ternary mixtures, and one quaternary mixture; a total of 11 mixtures. The binary pair of benzene-water is unstable. Therefore, only seven liquid solutions are potentially stable, with only four potentially unstable. In general, the total number of mixtures may be very large. However, when instability is detected in binary mixtures, the number of feasible multicomponent mixtures may be reduced dramatically.

Property Prediction

For CAMD/CAM^{b}D, target properties usually include pure-compound as well as mixture properties. Also, the selection of property estimation models to predict them raises additional issues and needs, including the application ranges of the selected models, the availability of model parameters, and uncertainties in their property estimations. The former limits the size of the search space for CAMD/CAM^{b}D problems. When model parameters are not available, to estimate target properties for generated molecules and/or mixtures, the latter must be removed from the list of potential candidates. This may eliminate potentially optimal products. Consequently, property estimation models with fewer parameters and having larger application ranges are needed.

The property estimation task can be arranged hierarchically based on the computational effort and cost related to calculations of the property values. Obviously, experimental measurements of properties are at the higher extremes, while simple, first-order group contribution-based methods are at the lower extremes. Normally, property prediction methods for most types of compounds are at the lower extremes, and as effort and costs increase, fewer types of compounds need to be evaluated but with more isomers included. Consequently, computationally intensive calculations (and experimental measurements) are saved only for those candidates that have satisfied all of the targets using simpler property models.

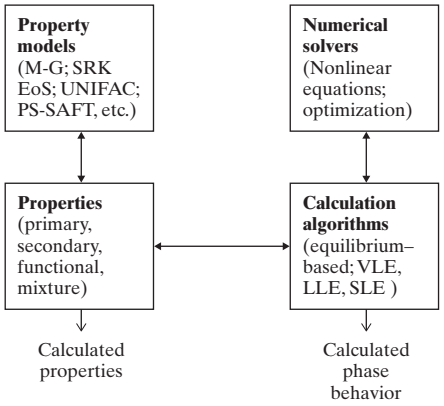

Figure 4.5 Relationships among properties, property models, solvers, and calculation algorithms.

Table 4.4 provides an example of such a hierarchy for selected sets of properties. Here, the properties are classified as primary (single-value properties, which can be calculated using structural information only); secondary (properties that, in addition to structural information, are usually a function of other properties); functional (pure-compound properties that depend on the intensive variables, temperature, and/or pressure); and mixture (properties that, in addition to structural information, depend on the intensive variables, temperature, pressure, and composition).

Similar to this classification of properties of organic chemicals, the properties of polymer repeat units can be classified as primary, secondary, functional, and mixture properties.

The relationships among the properties, property models, solvers, and calculation algorithms are illustrated in Figure 4.5. To estimate properties, first a property model is selected. For phase-equilibrium-related mixture properties, solution algorithms are employed that require estimates of other properties.

For any CAMD/CAM^{b}D problem, the required property estimates are ordered and calculated according to the classification given in Table 4.4.

EXAMPLE 4.8 ***Acyclic Molecule Design Given Properties***

Design an acyclic molecule that is a liquid at normal conditions (T = 298 K; P = 1 atm), whose heat of vaporization at 298 K is between 29 and 34 kJ/mol, and is immiscible with water.

SOLUTION

Normal boiling points (T_b) and melting points (T_m) bound the liquid state of the molecule; heat of vaporization at 298 K (ΔH_{vap}) is important when considering recovery of the molecule by distillation; the issue of miscibility with water is considered implicitly using

the octanol-water partition coefficient (when $\log K_{ow} > 1.5$, the molecule-water mixture is likely to split into two liquid phases).

According to the property classification in Table 4.4, all of the target properties (T_b, T_m, and ΔH_{vap}) are primary (that is, dependent on the molecular structure of the candidate products only). Therefore, as soon as the molecular structures of the candidate products are formulated, the target properties can be evaluated.

When, in addition to $\log K_{ow}$, the stability condition [Eq. (4.7)] is evaluated, then T_b, T_m, ΔH_{vap}, and $\log K_{ow}$ are estimated and liquid-phase activity coefficients (mixture properties) are evaluated only for candidate mixtures that satisfy the primary (target) properties ($\log K_{ow} > 1.5$). These include benzene [c(CCCC1)C1; 000071-43-2] and isopropyl acetate [O=C(OC(C)C)C; 000108-21-4].

Models for Primary Properties

Because these properties are only functions of pure-compound molecular structures, property models that employ structural variables are appropriate. The group-contribution approach based on the M-G method (Marerro and Gani, 2001) is simple, accurate, and has extensive group-parameter tables for broad arrays of properties and molecules. Recently, environmental and toxicity measures were added by Hukkerikar et al. (2012b) together with revised model parameters, providing more accurate predictions. Table 4.5 gives a partial list of the primary properties included by Hukkerikar et al. (2012a). These property prediction models have the form:

$$f(\theta) = \sum_i N_i C_i + \sum_j M_j D_j + \sum_k E_k O_k \qquad (4.9)$$

where $f(\theta)$ is a function of primary properties, θ, in Tables 4.4 and 4.5, which may contain additional adjustable model parameters (universal constants). In Eq. (4.9), C_i is the contribution of a first-order group of type i that has N_i occurrences, D_j is the contribution of a second-order group of type j that has M_j occurrences, and E_k is the contribution of a third-order group of type k that has O_k occurrences, in the molecular structures of pure compounds. To determine the contributions, C_i, D_j, and E_k, Marrero and Gani (2001) suggest a multilevel estimation approach. Eq. (4.9) is a general model for all of the primary property functions in Tables 4.4 and 4.5.

Table 4.4 Properties Arranged in Hierarchical Order

Hierarchy	Property Type	Property	Calculation Method
1	Primary	Critical temperature, T_C Critical pressure, P_C Critical volume, V_C Normal boiling point, T_b Normal melting point, T_m Heat of vaporization at 298 K, ΔH_{vap} Heat of fusion at 298 K, ΔH_{fus} Heat of formation at 298 K, ΔH_f Dipole moment, d_m Gibbs energy of formation at 298 K, ΔG_f Solubility parameter, δ_T Octanol-water partition coefficient, *Log* K_{ow} Water solubility, *Log* W_s	Additive methods (group contribution, atomic contribution, connectivity index, etc.); QSAR (Quant. Structure–Activity Relationship); molecular modeling
2	Secondary	Surface tension, σ Refractive index, n_D Acentric factor, ω Heat of vaporization at T_b, ΔH_{vap} (T_b) Entropy of formation at 298K, $\Delta S_f(298)$	$f(\delta_T)$ $f(\delta_T)$ $f(T_C, P_C, T_b)$ $f(T_C, P_C, T_b)$ $f(\Delta H_f)$
3	Functional	Vapor pressure, $P^{sat}(T)$ Density (liquid), $\rho_L(T,P)$ Diffusion coefficient, $D(T)$ Thermal conductivity, $\zeta(T)$ Solubility parameter, $\delta_T(T)$	$f(T_C, P_C, \omega, T)$ $f(T_C, P_C, T_b, \omega, T)$ $f(V_m, T_b, T)$ $f(T_C, M_w, T_b, T)$ $f(V_m, \Delta H_{vap}, T)$
4	Mixture	Activity coefficient, γ_i Fugacity coefficient, φ_i Density (liquid), ρ_L Saturation temperature, T_{sat} Saturation pressure, P_{sat} Solubility (liquid), x_L (saturated) Solubility (solid), x_S (saturated)	$f(T, \underline{x})$; $f(T, P, \underline{x})$ $f(T, P, \underline{x})$ $f(T, P, \underline{x})$ $f(P, V, T)$ $f(P, V, T)$ $f(\underline{\gamma}, \underline{x}, T, P)$ $f(\underline{\gamma}, \underline{x}, T, P)$

Table 4.5 Group Contribution Models for Selected Primary Properties

Property	Units of Measure	$f(\theta)$ [left-hand side of Eq. (4.9)]	Constant
Normal boiling point, T_b	[K]	$\exp\left(\frac{T_b}{T_{bo}}\right)$	$T_{bo} = 244.5165$
Normal melting point, T_m	[K]	$\exp\left(\frac{T_m}{T_{mo}}\right)$	$T_{mo} = 143.5706$
Critical temperature, T_C	[K]	$\exp\left(\frac{T_c}{T_{co}}\right)$	$T_{C0} = 181.6716$
Critical pressure, P_C	[bar]	$(P_c - P_{c1})^{-0.5} - P_{c2}$	$P_{C1} = 0.0519 \quad P_{C2} = 0.1347$
Enthalpy of formation, ΔH_f	[kJ/mol]	$\Delta H_f - H_{f0}$	$H_{f0} = 35.1778$
Heat of fusion, ΔH_{fus}	[kJ/mol]	$\Delta H_{fus} - H_{fus0}$	$H_{fus0} = -1.7795$
Octanol/Water partition coefficient, $Log\ K_{ow}$		$LogK_{ow} - K_{ow0}$	$K_{ow0} = 0.4876$
Heat of vaporization (298 K), ΔH_{vap}	[kJ/mol]	$\Delta H_{vap} - H_{vap0}$	$H_{vap0} = 9.6127$
Hildebrand solubility parameter, δ_T	[MPa$^{1/2}$]	$\delta_T - \delta_{T0}$	$\delta_{T0} = 21.6654$

Source: Hukkerikar et al., 2012a. Used with permission.

To use the primary property models, four steps are involved:

1. Identify the functional groups (first-, and if necessary, second-, and third-order groups).
2. Determine how many groups of each type are needed to represent the molecule.
3. Retrieve the parameters from the model parameter tables for the properties of interest.
4. Sum the contributions and use the corresponding property model functions.

EXAMPLE 4.9 ***Estimate Normal Boiling Points***

Estimate the normal boiling point of butanoic acid, di-isopropyl ester [CCCOC(=O)CCC(=O)OCCC; 000925-15-5] using the M-G method and group-contribution parameters from Hukkerikar et al. (2012a).

SOLUTION

Molecular structure

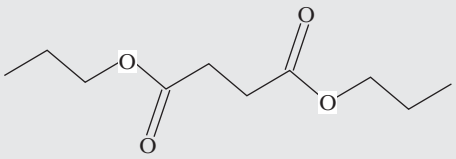

Group Representation	Group Types	Occurrences	Contribution
First-order groups	CH_3	2	0.9218
	CH_2	4	0.5780
	CH_2COO	2	2.1182
Second-order groups	OOC-CH_2-CH_2-COO	1	0.2610
Third-order groups		Not necessary	

$$T_b^{pred} = T_{bo} \ln\left(\sum_i N_i C_i + \sum_j M_j D_j + \sum_k E_k O_k\right) = 528.23\text{K}$$

Experimentally measured value = 523.95 K

For the primary properties of polymer repeat units, group-contribution-based methods are also available; for example, by van Krevelen (1990) and the M-G method adapted for polymers by Satyanarayana et al. (2009).

EXAMPLE 4.10 ***Estimate Glass-Transition Temperatures***

Estimate the glass-transition temperature for the polymer repeat unit [—(CH_2CH_2CHCl)—].

SOLUTION

The van Krevelen method for glass-transition temperature is:

$$T_g(\underline{n}) = \frac{\sum_{i=1}^{N} Y_i n_i}{\sum_{i=1}^{N} M_i n_i} = \frac{Y}{M_w} \tag{4.10}$$

The groups involved are: —CH_2— and —CHCl— Their contributions Y_i and M_i, retrieved from the CAPEC property-prediction software (Gani et al., 1997), are listed in Table 4.6.

Using Eq. (4.10), the glass–transition temperature, T_g, is:

$$T_g(\underline{n}) = \frac{2700 \times 2 + 20000 \times 1}{14 \times 2 + 48.5 \times 1} = 332\ K \tag{4.11}$$

Using the M-G method–based model for T_g in the CAPEC property prediction software (Gani et al. 1997), T_g is 315.8 K.

Table 4.6 Group Contributions for Polymer Repeat Unit Property Estimation

	Y_i	M_i	V_i	H_i
—CH_2—	2,700	14	15.85	0.000264
—CHCl—	20,000	48.5	13.4	1.98

Note: Replacing Y_i with V_i or H_i in Eq. (4.10), the molar volume and the water absorbed can be predicted for the polymer repeat unit. Also, M_i is the molecular weight of group i and M_w is the molecular weight of the repeat unit.

Models for Secondary Properties

Secondary properties are functions of other properties. Consistent with Figure 4.5 (property models → properties → calculated property values), for the secondary property of interest, three steps are needed before the specific property can be estimated:

1. Select an estimation method and property model for the specific property.
2. Identify the properties data needed to use the model and verify the application range of the estimation method for chemical species of specific types.
3. Retrieve from a database or predict the necessary properties (to be used as input).

EXAMPLE 4.11 ***Estimate Hildebrand Solubility Parameters***

Calculate the Hildebrand solubility parameter, δ_T, for acetic-acid ethyl ester [CCOC(=O)C; 000141-78-6] at 298 K.

SOLUTION

The Hildebrand solubility parameter is defined as

$$\delta_T = [(1,000\Delta H_{vap} - 8.314 \times 298)/Vm]^{1/2} \tag{4.12}$$

Just values of the heat of vaporization (ΔH_{vap}) and the molar liquid volume (Vm) at 298 K are needed. From the CAPEC database (Nielsen et al., 2001), the experimentally measured values are:

$$\Delta H_{vap}(298\ \text{K}) = 38.30\ \text{kJ/mol}$$
$$Vm\ (298\ \text{K}) = 99.66\ \text{cm}^3\text{/mol}$$

Inserting them in Eq. (4.10), gives $\delta_T = 18.23\ \text{MPa}^{1/2}$.

EXAMPLE 4.12 ***Estimate Refractive Indexes and Critical Compressibility Factors***

Calculate the refractive index and the critical compressibility factor for 1,1'-Biphenyl [C1CCC(CC1)C2CCCCC2; 000092-52-4].

SOLUTION

The model for refractive index (n_D) employs the Hildebrand solubility parameters (δ_T).

$$\begin{aligned} \text{Model:} \quad & n_D = (0.48872\delta_T + 5.55)/9.55 \\ \text{Input data:} \quad & \delta_T = 18.7\text{MPa}^{1/2} \text{ at } 298\ \text{K} \\ \text{Calculated value:} \quad & n_D = 1.35 \end{aligned} \tag{4.13}$$

The corresponding states principle is used to predict the critical compressibility factor (Z_C).

$$\begin{aligned} \text{Model:} \quad & Z_C = (P_C V_C)/(83.14 T_C) \\ \text{Input data:} \quad & P_C = 25.2\ \text{bar};\ T_C = 788.9\ \text{K}; \\ & V_C = 496.85\ \text{cm}^3\text{/mol} \\ \text{Calculated value:} \quad & Z_C = 0.295 \end{aligned} \tag{4.14}$$

EXAMPLE 4.13 ***Estimate Solubility Parameters of Polymer Repeat Units***

For the polymer repeat unit [—CH_2—CH_2—CHCl—], estimate its solubility parameter at 298 K.

SOLUTION

According to the model available in the CAPEC property prediction software (Gani et al., 1997), the solubility parameter of polymer repeat units is derived as:

$$\delta_T = (C_E/V_a)^{1/2} \tag{4.15}$$

where C_E is the cohesive energy of the polymer repeat unit and V_a is the molar volume of the amorphous polymer. According to the CAPEC property prediction software, the cohesive energy of the polymer repeat unit is 22,050.49 J/mol, and the amorphous volume is 61.30 cm^3/mol. Therefore, the solubility parameter is 18.68 J/cm^3.

Models for Functional Properties

The functional pure-compound properties are mainly functions of temperature and, in some cases, functions of pressure. For the properties of interest, the following steps are recommended:

— Check a database(s) for the availability of correlation coefficients.
- If available, use the corresponding correlation.

  Else,
- Use models based on the principle of corresponding states, if available for the necessary properties.
- Otherwise, collect experimental data and regress parameters for a preferred correlation.

EXAMPLE 4.14 ***Vapor Pressures and Liquid Density Functions of Temperature***

For the acetic-acid ethyl ester [CCOC(=O)C; 000141-78-6], predict the vapor pressure and liquid density as a function of temperature.

SOLUTION

Check the CAPEC database (Nielsen et al., 2001) for the correlations representing the needed properties. For the vapor pressure and liquid density:

Vapor pressure, P^{sat} (Antoine) [mmHg]	$P^{sat} = 10^{[A-B/(T+C)]}$, T in °C	$A = 7.261830$ $B = 1,342.109$ $C = 228.3460$
Liquid density, ρ_L [kmol/m^3]	$\rho_L = A/B^{(1+(1-T/C)D)}$	$A = 0.8996000$ $B = 0.2585600$ $C = 523.30000$ $D = 0.2780000$

Graphs of these properties are shown in Figures 4.6a and 4.6b.

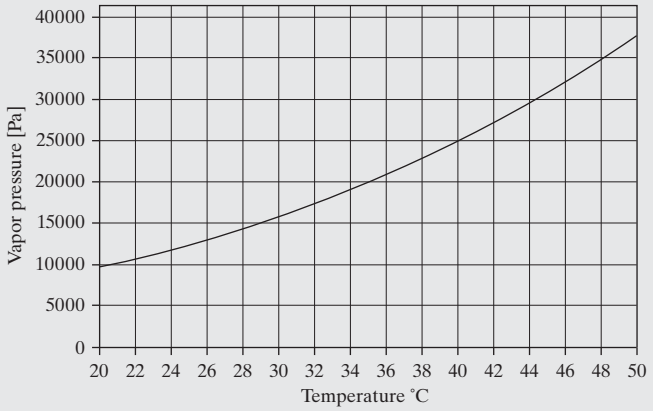

(a) Vapor pressure

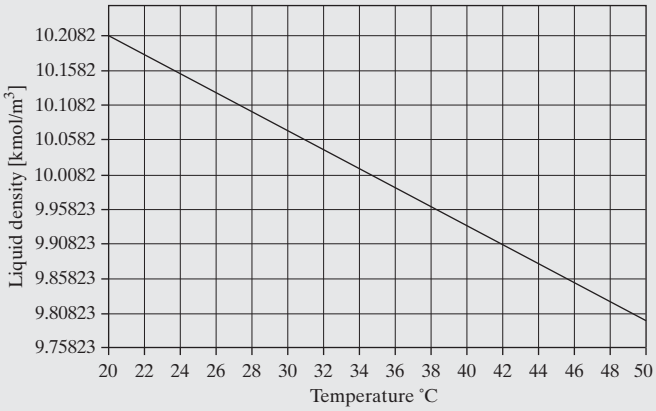

(b) Liquid density

Figure 4.6 Properties of ethyl acetate (acetic-acid ethyl ester).

Whenever correlations are employed for functional properties, the following guidelines should be followed:

- Always check the correlation limits and extrapolations beyond the limits.
- Always try to check whether sufficient accuracy is provided within these limits.
- When correlations are not available, try to check the estimates with experimental data, when available.
- Perform cross-validation, if possible.

Models for Mixture Properties

Two types of mixture properties are commonly encountered in chemicals-based product design: (1) Functional properties for a mixture in a specified phase (e.g., bulk density and enthalpy of the mixture; and (2) phase equilibrium–related properties of the compounds in the mixture (e.g., liquid-phase activity coefficients for the species in the mixture, and saturation temperatures, such as bubble- and dew-point temperatures). As illustrated in Figure 4.5, to calculate these mixture properties, pure-component properties are needed with calculation algorithms and equation solvers (when necessary). Because textbooks on thermodynamics and property prediction (Poling et al., 2001) cover this topic in detail, just a brief overview is provided next.

Functional Mixture Properties. For these properties, the compounds and their composition in the mixture are known together with the phase identity. Consequently, at the known temperature, the pure-compound property, θ_i, for each compound needs to be estimated. Using a mixing rule, the bulk property of the mixture, θ_M, is calculated:

$$\theta_{\mathrm{M}} = \theta^0 + \theta^{\mathrm{E}} \tag{4.15}$$

where θ^0 and θ^{E} are the ideal and excess mixing terms. When the excess mixing term can be neglected, the bulk mixture property is simply the molal average of the pure-compound properties:

$$\theta_{\mathrm{M}} = \Sigma_i \, (\theta_i \, x_i) \tag{4.16}$$

Models for the excess property terms vary with the property and the specific phase.

Equilibrium-Based Mixture Properties. These are estimated when two or more phases are in equilibrium. The iso-fugacity criteria for vapor-liquid equilibrium (VLE), liquid-liquid equilibrium (LLE), and solid-liquid equilibrium (SLE) are:

$$x_i \, \gamma_i \, \varphi_i^{\mathrm{sat}} \, P_i^{\mathrm{sat}} = y_i \, \varphi_i^{\mathrm{V}} P, \qquad i = 1, \ldots, N_{\mathrm{C}} \text{ (VLE)} \tag{4.17}$$

$$x_i^{\mathrm{I}} \gamma_i^{\mathrm{I}} = x_i^{\mathrm{II}} \, \gamma_i^{\mathrm{II}}, \qquad i = 1, \ldots, N_{\mathrm{C}} \text{ (LLE)} \tag{4.18}$$

$$\ln \, x_i \gamma_i = \frac{\Delta H_{\mathrm{fus}}}{R} \left(\frac{1}{T_{\mathrm{m}}} - \frac{1}{T} \right) \qquad i = 1, \ldots, N_{\mathrm{C}} \text{ (SLE)} \tag{4.19}$$

where γ_i is the liquid-phase activity coefficient of compound i; φ_i is the fugacity coefficient of compound i in the vapor phase; P_i^{sat} is the pure-compound vapor pressure at temperature, T; x_i and y_i are the liquid and vapor mole fractions of compound i; T_{m} is the melting point of the solid solute; ΔH_{fus} is the heat of fusion of the solid solute; R is the universal gas constant. Superscripts I and II indicate first and second liquid phases, superscript V indicates vapor phase, and N_{C} is the number of compounds in the mixture.

For these phase equilibrium problems, involving just two phases, the appropriate iso-fugacity equation is selected. These equations, together with mass balances (involving a feed stream and two effluent streams), along with mole fraction summations (equal unity for each stream), are solved by an appropriate solver. Solution of the VLE equations gives bubble-points, dew-points, and VLE phase diagrams. Similarly, solutions of the LLE equations give the amount and composition of each liquid phase, and solution of the SLE equations gives the saturation temperature-composition curves, as well as the solubility of the solid solute in the solvent. Examples of the needed specifications, properties, and property model parameters are shown in Table 4.7 for these two-phase equilibrium calculations.

CAMD/CAM$^{\mathrm{b}}$D—Mathematical Formulations of Molecular and/or Mixture Design Problems

The molecular and/or mixture/blend design problems can be described in the context of a generic mathematical representation:

Table 4.7 Specifications, Properties, and Model Parameters for Various Mixture Properties

Problem	Specifications Needed	Properties Needed	Model Parameters	Output
Activity coefficients using UNIFAC	T, $\underline{x}$		G^E-model parameters ($\underline{R}$, $\underline{Q}$, $\underline{\underline{a}}$)	$\underline{\gamma}$
Bubble-point temperature using Eq. (4.17)	P, $\underline{x}$	T_C, P_C, ω, P^{sat}	G^E-model parameters ($\underline{R}$, $\underline{Q}$, $\underline{\underline{a}}$)	T_{bubble}, $\underline{y}$
Liquid-phase stability using Eq. (4.18)	T, $\underline{x}$		G^E-model parameters ($\underline{R}$, $\underline{Q}$, $\underline{\underline{a}}$)	Left-hand side of Eq. (4.7)
Solid solubility using Eq. (4.19)	T	ΔH_{fus}, T_m, R	G^E-model parameters ($\underline{R}$, $\underline{Q}$, $\underline{\underline{a}}$)	x_S

Note: $\underline{R}$ and $\underline{Q}$, are vectors, and $\underline{\underline{a}}$ is a matrix of the G^E-model parameters, where $\underline{R}$ are the surface areas of the groups, $\underline{Q}$ are the volumes of the groups, and $\underline{\underline{a}}$ contains the group interaction parameters for the UNIFAC model (Fredenslund et al, 1977).

$$F_{OBJ} = \max \{C^T \underline{y} + f(\underline{x})\} \quad (4.20)$$

s.t.

$$P_r = f(\underline{x}, \underline{y}, \underline{u}, \underline{d}, \underline{\theta}) \quad (4.21)$$

$$\underline{L}_1 \le \underline{\theta}_1 (\underline{Y}, \underline{\phi}) \le \underline{U}_1 \quad (4.22)$$

$$\underline{L}_2 \le \theta_2(\underline{Y}, \underline{\phi}, \underline{\theta}) \le U_2 \quad (4.23)$$

$$L_3 \le \theta_3(\underline{Y}, \underline{\phi}, \underline{\theta}, \underline{x}) \le U_3 \quad (4.24)$$

$$L_4 \le \underline{\theta}_4(\underline{Y}, \underline{\phi}, \underline{\theta}, \underline{y}) \le U_4 \quad (4.25)$$

$$S_L \le S(\underline{Y}, \underline{\eta}) \le S_U \quad (4.26)$$

$$B\underline{x} + C^T \underline{y} \le D \quad (4.27)$$

where $\underline{x}$ represents a vector of continuous variables (such as flow rates, conditions of operation, design variables), $\underline{y}$ is a vector of measured-controlled variables (composition, temperature, pressure, etc.), $\underline{C}$ is a vector of constant coefficients, $\underline{Y}$ represents a vector of binary integer variables (such as unit operation identity, descriptor identity, compound identity), Eq. (4.21) represents the process model equations with $\underline{u}$, $\underline{d}$, and $\underline{\theta}$, vectors of input variables, manipulated-design variables, and property values, Eqs. (4.22)–(4.25) bound the four classes of property models (primary, secondary, functional, and mixture), $\underline{\phi}$ is a vector of molecular structural parameters, $\underline{\theta}$ is a vector of properties, and Eqs. (4.26) and (4.27) represent molecular and flowsheet feasibility rules, respectively, with B a matrix of constant coefficients, and D a vector of constant coefficients. The term, $f(\underline{x})$, is a linear or nonlinear portion of the objective function. For process optimization, $f(\underline{x})$ is usually a nonlinear function.

Many variations of this mathematical formulation may be derived to represent different molecular-mixture design problems. Some examples are:

1. *The Selection Problem:* Find molecules that satisfy a set of target properties; that is, satisfy only Eqs. (4.22)–(4.25). Here, molecular structure generation is not necessary. The problem is solved by simply searching within an appropriate database.
2. *The Selection-design Problem:* Here, molecular structures are generated [Eq. (4.26) ensures chemical feasibility of the generated molecule] and tested for matches with the desired properties [Eqs. (4.22)–(4.25)]. This is the most common CAMD/CAM^{b}D problem.
3. *The Optimal Design Problem:* Here, in addition to satisfying Eqs. (4.26) and (4.22)–(4.25), the molecular structure that maximizes the profit function [Eq. (4.20)] is desired.
4. *The Process-product Design Problem:* Here, the feasible molecules need to satisfy process-related specifications in Eqs. (4.21) and (4.27), in addition to satisfying Eqs. (4.22)–(4.26). This involves the simultaneous design of the product and the process that produces it (Hostrup et al., 1999; Gani, 2004).
5. *The Optimal Process-product Design Problem:* Here, all of Eqs. (4.20)–(4.27) apply.

Mixture Design Algorithm

The mixture/blend design algorithm employs a decomposition method, where the design problem is decomposed into four subproblems and solved using the workflow shown in Figure 4.7 (Yunus et al., 2014). The first level is for screening the pure-component properties, and the second level is to analyze the mixture stability. The third and fourth levels take into account the linear and nonlinear target properties, respectively.

The first compound in any mixture is the *main ingredient* (*MI*), which must be present in all mixtures. It can be a single compound or a mixture of compounds. A binary mixture is a combination of the *MI* and compound i (B_i) from the database ($MI + B_i$), whereas a ternary mixture consists of *MI* plus two compounds, i and j, from the database ($MI + B_i + B_j$). Note that subscripts i and j are compound numbers in the database. To avoid repetitions of formulations of ternary mixtures, j must always be greater than i.

Level 1: Pure-component Constraints. At this level, the pure-component properties of chemicals in the database and *MI* are compared with respect to the target values, and an initial screening is performed to remove compounds unlikely to be present in the blend. This step is applied only for linear target properties. For the remaining compounds, all feasible binary mixtures are generated.

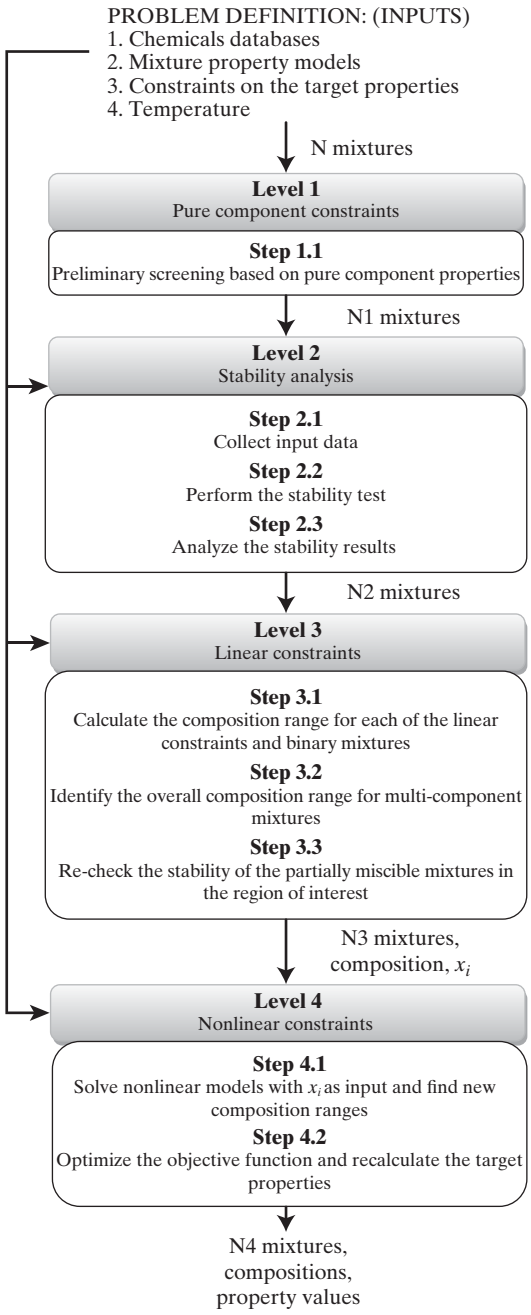

Figure 4.7 Work-flow diagram for the mixture-blend design algorithm. (*Source:* Yunus et al. 2014. Used with permission).

Level 2: Stability Analysis. The stability test [Eqs. (4.7)–(4.8)] is performed for binary mixtures. The result indicates the miscibility of the binary pairs, either totally miscible, partially miscible, or immiscible. Only total and partially miscible mixtures are retained.

Level 3: Linear Constraints. Mixture compositions are adjusted giving the desired mixture properties using ideal mixing rules [Eq. (4.16)].

EXAMPLE 4.15 ***Gasoline-Blend Problem: Linear Properties***

For a gasoline-blend problem, given the target properties and their models in Table 4.8, formulate a mixture design problem to determine the mixture (compounds and their compositions) using linear property models.

SOLUTION

Based on the property models in Table 4.8, linear, mixing-rule-based, property models are employed for η, ρ, RVP_B, RON, HHV, $-log\ LC_{50}$, and Wt_{O2}.

Therefore, the following optimization problem is solved for each candidate mixture to find the composition and the corresponding target property values:

$$\text{min or max} \quad f_{obj}(x) \tag{4.28}$$

s.t.

$$\theta_{LB} \le g_3(x,\theta) \le \theta_{UB} \tag{4.29}$$

$$g_4(x) - 1 = 0 \tag{4.30}$$

$$x \in \{x | x \in R^n, 0 \le x \le 1\}$$

where g_3 is a vector of linear constraints in Table 4.8, and g_4 is a vector of mole, weight, or volume fractions. The solution of this problem is a range of compositions for each blend within which all linear property constraints are satisfied. The stability test is performed for all feasible mixtures, with those not found to be miscible rejected. Note that because a reliable model to calculate the extent of oxidation is not available, compound selection is made without knowledge of the ability of compounds to oxidize into unwanted by-products.

Table 4.8 Target Properties for Gasoline Blend

Function	Target Property	Model Type
Ability to be burned	$45 \le RVP_B$ (kPa) ≤ 60	$\sum_{i=1}^{NC} \frac{x_i \gamma_i P_i^{sat}(T)}{RVP_B} = 1$
Flammability	T_f(K) ≤ 300	$\sum_{i=1}^{NC} \frac{x_i \gamma_i P_i^{sat}(T)}{P_i^{sat}(T_f)} = 1$
Engine efficiency	$RON \ge 92$	$\theta^k = \sum_i^{NC} x_i\, \theta_i^k$
	HHV (MJ/kg) ≥ 35	
Consistency of fuel flow	$0.30 \le \eta$(cP) ≤ 0.06	
	$0.720 \le \rho$ (g/cm^3) ≤ 0.775	
Toxicity	$-log\, LC_{50}$(mol/L) < 3.08	
Stability	$\Delta G^{mix} < 0$	
Environmental aspect	$2 \le Wt_{02}$(wt%) ≤ 20	
Low oxidation	Not available	

Note: RVP_B is the Reid vapor pressure of the blend; RON is the octane number; HHV is the heating value; $-log\ LC_{50}$ is a measure of toxicity; η is the viscosity; ρ is the density; Wt_{02} is the oxygen content.

Next, consider Level 4 in Figure 4.7 and Example 4.16.

Level 4: Nonlinear Constraints. Now, the nonlinear property models are included and an NLP problem is formulated and solved. The resulting mixtures satisfy all linear and nonlinear constraints (property models).

EXAMPLE 4.16 ***Gasoline-Blend Problem: Nonlinear Properties***

For the gasoline-blend problem in Example 4.15 and the property models in Table 4.8, formulate the mixture design problem using the nonlinear property models.

SOLUTION

Among the properties in Table 4.8, two properties require nonlinear property models: *RVP* (Reid vapor pressure) and T_f (flash temperature). Note, however, that T_f can be calculated for a potential composition by solving the following optimization problem.

$$\text{min or max} \quad f_{\text{obj}}(x) \tag{4.31}$$

s.t

$$\sum_{i=1}^{NC} \frac{x_i \gamma_i P_i^{\text{sat}}(308\text{K})}{RVP_{\text{B}}} = 1 \tag{4.32}$$

$$\sum_{i=1}^{NC} x_i - 1 = 0 \tag{4.33}$$

$$x_{\text{LB}} < x_i < x_{\text{UB}} \tag{4.34}$$

To satisfy Eq. (4.32), for a given (assumed) composition and specified temperature (308 K), γ_i and RVP_{B} are calculated. If the LHS in Eq. (4.32) equals unity, the composition has been found. A collection of compositions for the potential mixtures is obtained, and the mixture having the maximum composition of the additive *or* the minimum composition of the MI is selected because the objective is to use as little of the nonrenewable MI as possible.

A very wide range of chemical (formulation) product-design problems is solved using CAM$^{\text{b}}$D. A few examples follow:

- *Solvent Mixture:* Consider adding additional chemicals to the original solvent when the cost (of the process and/or solvent) can be reduced without having a negative effect on the solvent functional properties, or when multifunctional properties are desired (for example, when a solvent for one solute is an antisolvent for another solute). Here the important design steps involve product formulation and testing, with product manufacturing usually not an important issue.
- *Minimum Cost Additive (solvent mixture):* Paints and coatings need additives (usually solvent mixtures) where target properties include time as a variable (for example, to give a desired solvent evaporation rate). When it is not possible to satisfy product needs with a single solvent, a solvent mixture is sought. In this case, the optimal solvent mixture must satisfy the property constraints and be the lowest-cost solvent mixture. Here, also, the important design steps are product formulation and testing, with product manufacturing usually not an important issue.
- *Polymer Formulations:* The properties and performance of polymer formulations (such as blends, composites, reactive systems, lubricants, plasticizers) are critically dependent on their structure or morphology, but a specific combination of raw materials and processing is required to obtain superior performance. Here, in addition to product formulation and testing, processing is also an important issue.
- *Oil Blends:* The mixing of crude oils from different locations to obtain specified characteristics is a routine operation in refineries. Such operations often provide well-defined mixture design problems. Good property models are usually available, with the design step (defining the optimal quantities of each oil in the blend) being most important.
- *Additives in Specialty Chemicals Products:* Many complex mixtures (such as dispersions, flavors, perfumes) used in the paper, food, cosmetics, agrochemicals, textiles, and health-care industries are first manufactured as liquid (complex) products but delivered as emulsions, liposomes, or dry granules with well-defined properties. Here, multiscale models may be needed, with the formulation and testing steps being most important. Specific examples are:
  - *Pesticide Delivery and Uptake:* The problem involves formulating an additive to a pesticide product that increases its uptake into plants. Also, to control the release of the pesticide, the problem involves formulating a polymer-based membrane that achieves a desired rate of release.
  - *Drug Delivery and/or Application:* This problem involves formulating an additive to a drug, permitting it to form an emulsion that can be applied on the surface (skin) and that evaporates at a desired rate. Here, the additive compounds should be miscible with each other, should evaporate when exposed, and should form an emulsion with the drug (product), which may be a solid.

Software for CAMD/CAM$^{\text{b}}$D

Several software packages are used to solve various types of CAMD/CAM$^{\text{b}}$D problems, a few of which are briefly described here. These are not commercially available, but readers can obtain an education license for noncommercial research and education. See http://capec.kt.dtu.dk/Software/CAPEC-Software.

The CAPEC Database

This database contains a large collection of pure compound and mixture properties organized with a specially developed ontology for efficient data management. A schematic of the data representation is shown in Figure 4.8. The CAPEC database (Nielsen et al., 2001) covers 36 primary and secondary properties and nine functional properties and has access to VLE and SLE data for a large collection of binary and ternary mixtures. Properties are available for on the order of 13,000 organic chemicals.

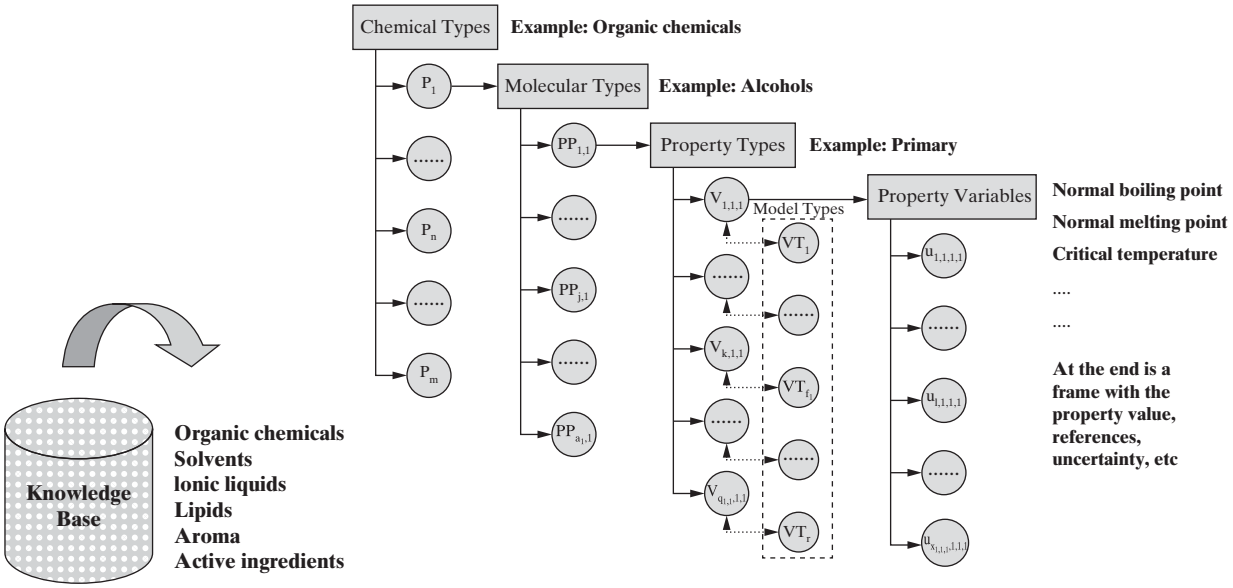

Figure 4.8 Data representation in the CAPEC database.

CAPEC Property-Prediction Software

CAPEC property-prediction software (Gani et al., 1997) integrates the CAPEC database together with a large collection of pure-compound and mixture property models. Figure 4.9 shows the architecture of the properties-prediction software.

ProCAMD Software

This software implements the work-flow shown in Figure 4.2. It has built-in solvers for CAMD, and has links to other software (for the CAPEC database and CAPEC Property Prediction).

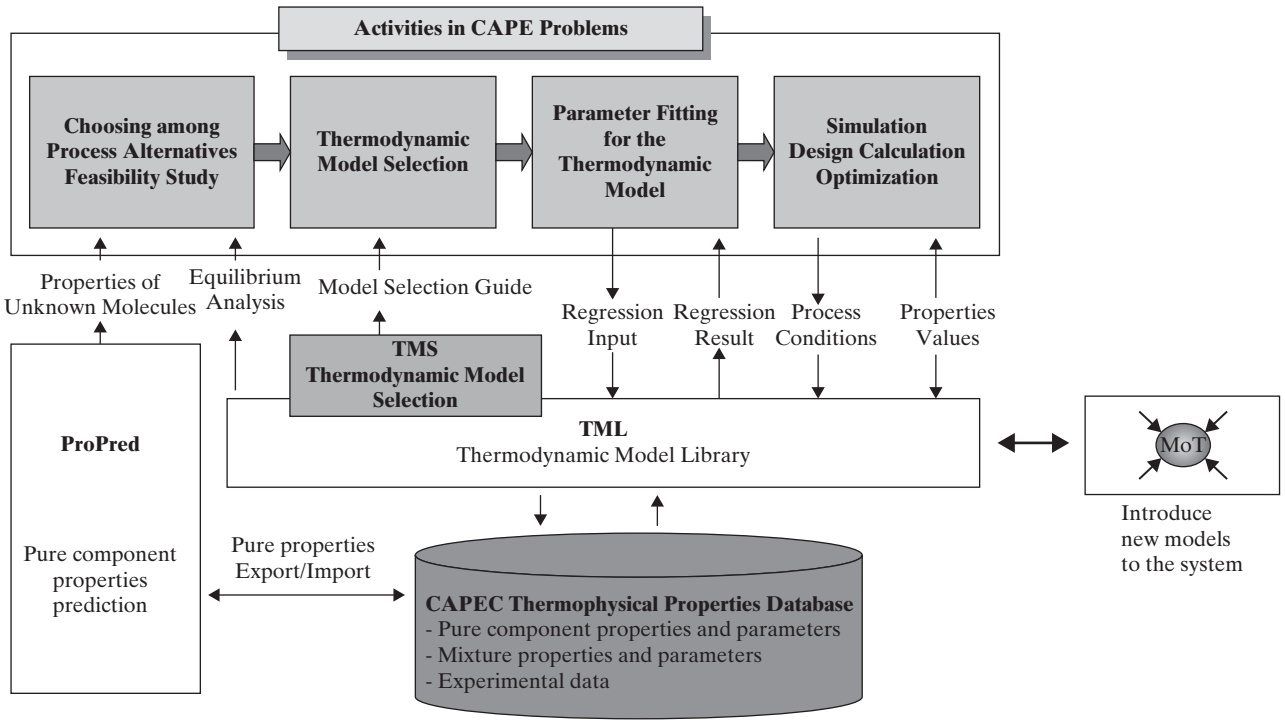

Figure 4.9 Architecture of the properties-prediction software.

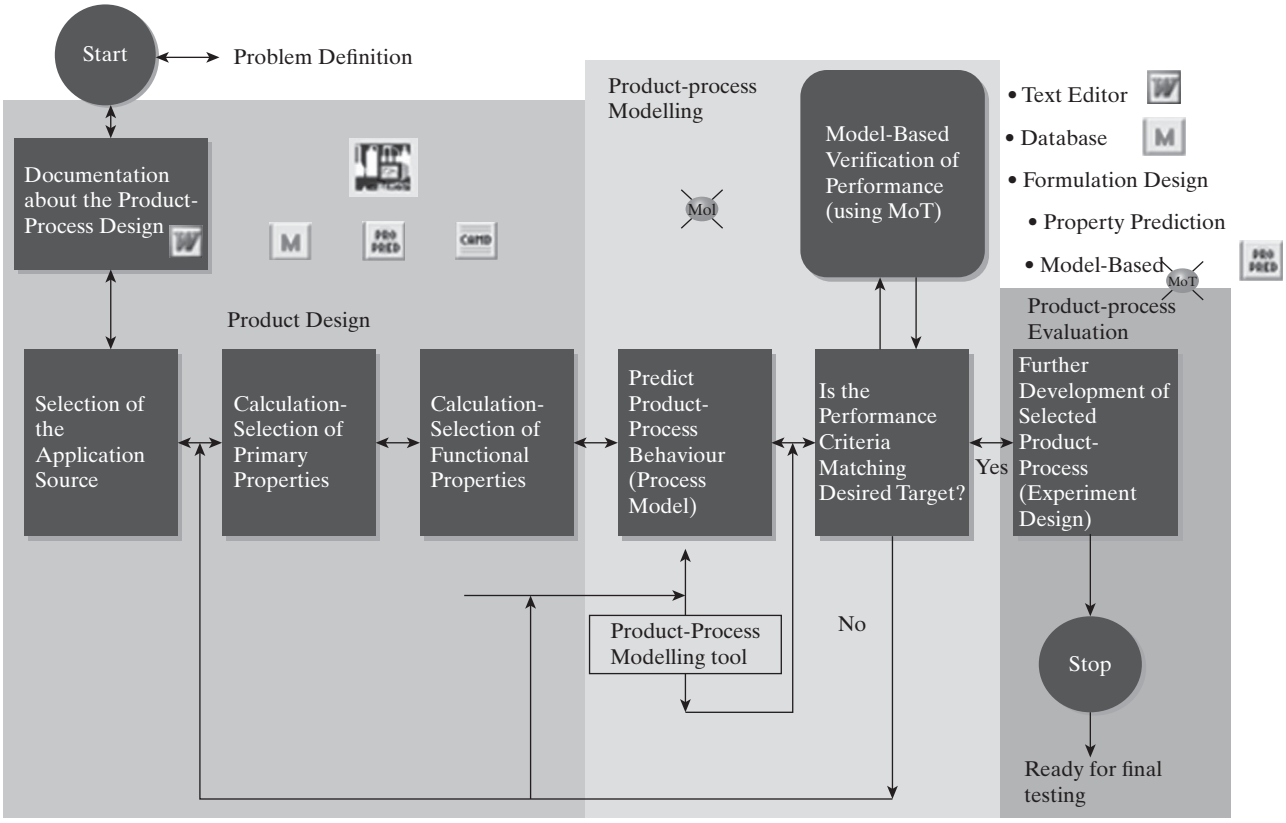

Figure 4.10 Architecture of the VPPD-Lab Software. (*Source:* Gani (2009). Used with permission).

VPPD-Lab Software

This software, which implements the so-called Virtual Product-Process Design laboratory, incorporates all software mentioned above, together with tools for formulation design (covered in Chapter 5), modeling, and simulation of product performance (that is, how the product performs when applied). For mixture design, VPPD-Lab allows the user to perform virtual experiments to rapidly identify the most promising candidates for future verification and selection using experimental measurements. The architecture of the VPPD-Lab software is highlighted in Figure 4.10. VPPD-Lab highlights a specific template (work flow) for the design of formulated products in terms of selection and evaluation of the main chemicals to be included in the formulation. The tools shown in the figure indicate the links to CAMD (tool for molecular and mixture design); ProPred (tool for product property estimation); MoT (tool for modeling of product performance); and database (tool for accessing properties of chemicals). Application of this tool for design of a formulated insect repellent is highlighted in Example 5.6 of Chapter 5.

CAMD/CAM^{b}D Solution Approaches

The examples that follow can be solved using the tool(s) highlighted in each example. These tools are accessed in the VPPD-Lab.

Database search

For efficient solution of CAMD problems using database search, a database having a large selection of properties for a very large number of compounds is needed.

EXAMPLE 4.17 ***Find Molecules that Satisfy Property Constraints***

Find molecules that satisfy the following property constraints:

$$17 < \delta_T \text{ (MPa}^{1/2}) < 21;$$

$$250 \text{ K} < T_m;\ T_b > 350 \text{ K}.$$

SOLUTION

In principle, any database of chemicals having the target properties can be used. Figures 4.11(a) and 4.11(b) highlight the search specifications and results using the CAPEC database.

Note that when an upper bound of 400 K is placed on T_b, the number of compounds matching the targets is reduced from 225 [Figure 4.11(b)] to 70.

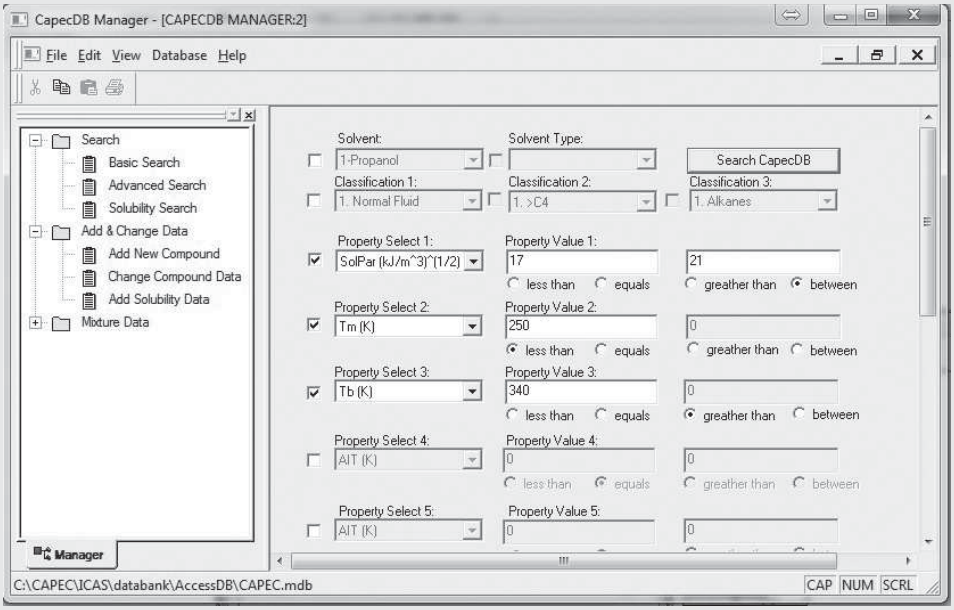

(a) Initiating the Search

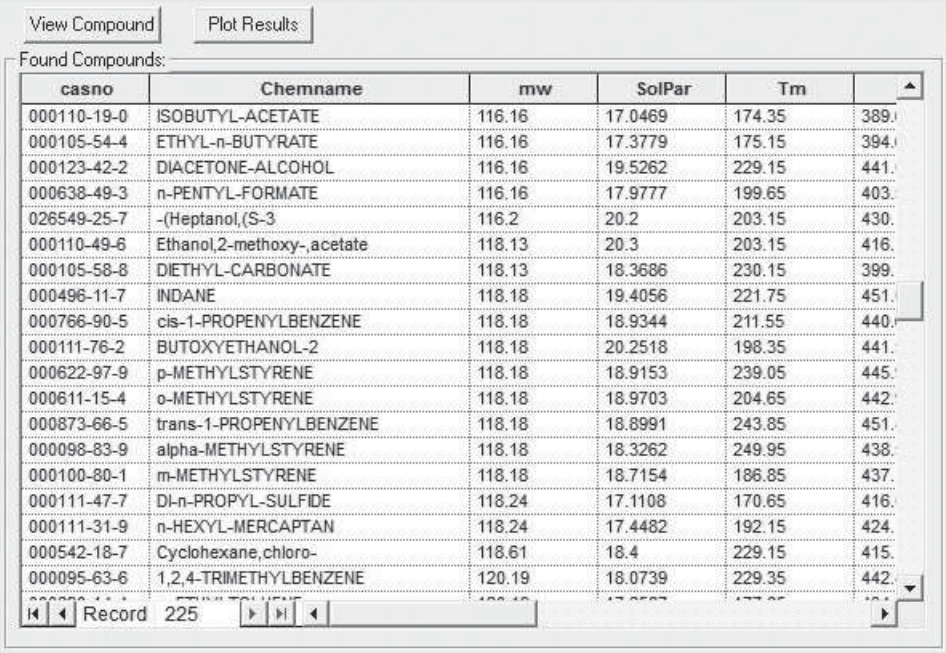

(b) Results

Figure 4.11 CAPEC database search. (*Source:* © CAPEC).

Generate and Test

Here, the building blocks, together with the combination rules [Eqs. (4.1)–(4.5) that are summarized in Eq. (4.25)], are employed to generate chemically feasible molecules, which are evaluated using a suite of property-prediction routines [Eqs. (4.21)–(4.24)]. Note that the generate-test option is easiest to implement when an objective function is not specified.

EXAMPLE 4.18 ***Find Acyclic Molecules using ProCAMD***

Solve Example 4.17 using the generate-test solution option only for acyclic compounds with C, H, and O atoms, and the additional constraints: $n_{max} = 8$; $n_j^u = 2$ (except for CH_3 and CH_2 groups).

SOLUTION

Candidate compounds to be generated are acyclic hydrocarbons, alcohols, ketones, aldehydes, acids, esters, and ethers. The molecular structures for these compounds can be generated using the following basis set of groups (building blocks): {CH_3; CH_2; CH; C; OH; CH_3CO; CH_2CO; CHO; CH_3COO; CH_2COO; HCOO; CH_3O; CH_2O; CH-O; COOH; COO}. The ProCAMD solution is shown in Figure 4.12. Based on the molecular-structure-related constraints, 3,498 chemically feasible molecules are generated. After Level-1 screening (see Figure 4.7), 754 molecules satisfy the three target property constraints. The group vector sets representing these 754 molecules generate 6,674 isomers. After Level-2 screening, 2,331 molecules satisfy the three target property constraints. Searching through the CAPEC database, 174 of these molecules are found. Note, however, that many of these compounds may not have property values in the database for all three of the target properties. Consequently, they were not found in the solution of Example 4.17 where only a database search was conducted. When, for the boiling point, an upper bound of 400 K is included, only 48 compounds are found to be feasible. Note that compared to the database search, this number is lower because the database was searched for *all* types of molecules, while in this example, only acyclic compounds are considered.

In Table 4.9, five of the molecules found in the database search are listed with their property data (found in the database) and compared with the predictions of the Constantinou and Gani (1994) and M-G methods (with parameters by Hukkerikar et al., 2012a).

Clearly, Table 4.9 shows the uncertainties in the predictions, which are an issue in model-based product design. But, the results are qualitatively correct, and consequently, promising candidates have been identified. In the end, these are verified using experimental data. In this way, the experimental data are employed for focused verification rather than sought for every candidate product.

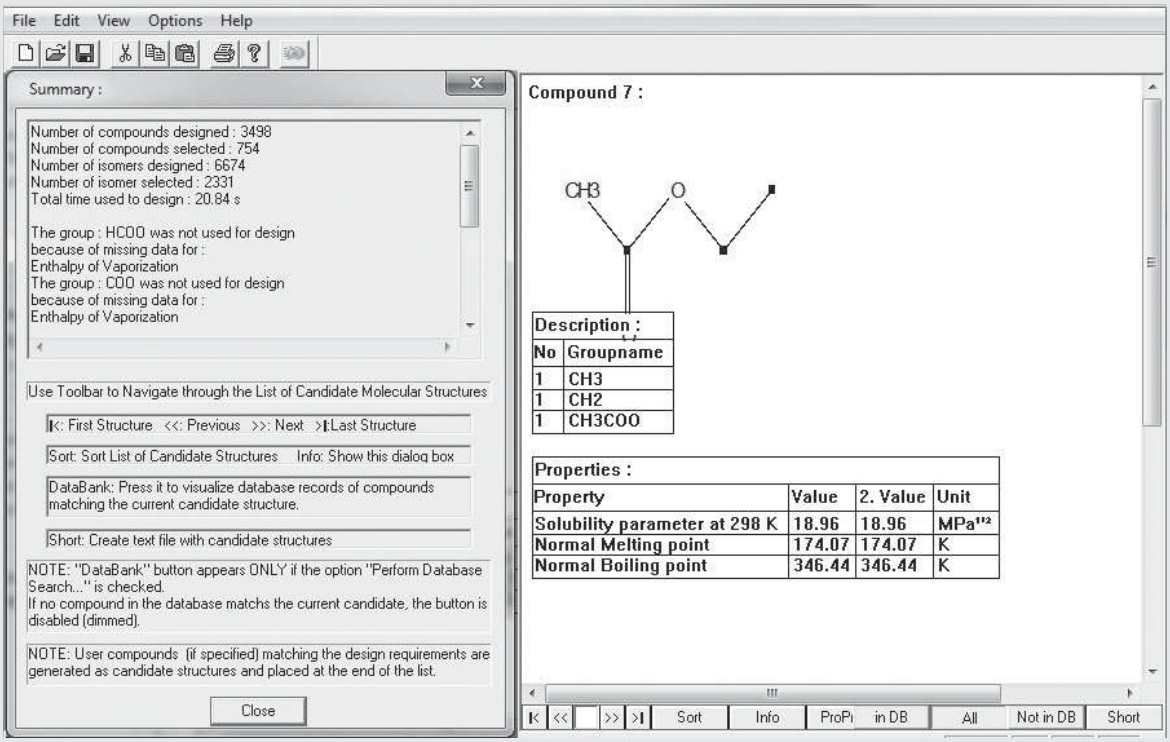

Figure 4.12 Solution of the CAMD problem. *Note:* Compound 7, shown on the RHS of the figure, is ethyl acetate; the properties shown are calculated by the Constantinou-Gani method (1994).

Table 4.9 Feasible Molecules with Experimental and Predicted Property Values

	δ_T(MPa$^{1/2}$)			T_m(K)			T_b(K)		
	Data	C-G	M-G	Data	C-G	M-G	Data	C-G	M-G
Ethyl acetate	18.9	18.3	18.7	174.0	189.6	174.5	346.4	350.2	341.7
1,2-dimethoxy-ethane	17.7	17.9	17.9	215.1	209.1	209.1	357.2	377.8	357.8
2-pentanol	21.7	20.9	20.7	200.0	186.6	191.4	392.1	394.8	391.0
Diethyl succinate	18.4	19.4	19.4	239.7	252.3	249.6	478.8	489.6	493.2
Methyl-ethyl-ketone	18.8	18.7	19.2	186.5	183.9	184.3	352.8	349.6	346.1

Mathematical Programming

This option is employed when the problem formulation includes an objective function [Eq. (4.20)] to be minimized or maximized. For selection-design problems, where molecules only need to satisfy property inequality constraints, there are no target values and, consequently, mathematical programming is not necessary. Normally, objective functions are added when the cost of manufacturing the designed molecule, or the performance of the product during application, needs to be optimized. For mixture design problems, the lowest-cost mixtures are sought. Depending on the expressions used in the objective function and the constraint functions, mixed-integer, linear programs (MILPs) or mixed-integer, nonlinear programs (MINLPs), are most often formulated. The solvers available in the GAMS-software (Brook et al., 1988) are usually sufficient. Genetic algorithm–based solutions have also been proposed (Venkatasubramanian et al., 1994). For examples of MILP and MINLP formulations, see the mixture-design case studies in Section 4.3. See also Examples 4.15 and 4.16.

EXAMPLE 4.19 ***Polymer Repeat Unit MINLP and MILP Formulations***

Derive a MINLP formulation for the polymer repeat unit design problem. Also, prepare an MILP formulation.

SOLUTION

The general MINLP for optimal polymer repeat unit design is:

$$\min_{\underline{n}} \sum_{j=1}^{P} \left(\frac{p_j(\underline{n}) - p_j^{\text{spec}}}{p_j^{\text{spec}}} \right)^2 \tag{4.35}$$

s.t.

$$0 = \sum_{i=1}^{N} (u_i - 2) n_i \tag{4.36}$$

$$p_j^{\text{L}} \le p_j(\underline{n}) \le p_j^{\text{U}}, \quad \forall j \tag{4.37}$$

$$1 \le \sum_{i=1}^{N} n_i \le n_{\max} \tag{4.38}$$

$$n_i \in \{n_i^{\text{L}}, ..., n_i^{\text{U}}\}, \quad i = 1, ..., N \tag{4.39}$$

The nonlinearity of the constraints depends on the property-model expressions in Eq. (4.37). Instead of using the van Krevelen model [Eq. (4.10)], when the property bounds for Eq. (4.37) are redefined as $p_j^{\text{L}} M_j^{\text{L}}$ and $p_j^{\text{U}} M_j^{\text{U}}$, and a linear form of property function $f(\theta)$, as in Eq. (4.9), is used, all of the property constraints are in linear forms. Here, M_j is the molecular weight of species j and the superscripts L and U are lower and upper bounds. Together with a linear objective function, an MILP is formulated (Constantinou et al., 1996). Alternatively, Eqs. (4.36), (4.38), and (4.39) can be used to generate all feasible combinations by a branch-and-bound approach, with the objective function for each combination evaluated to locate the optimal design.

4.3 CASE STUDIES

In this section, eight case studies are presented. Each is designed to solve a molecular or mixture design problem using the techniques described in Section 4.2. These include the creation of property specifications (i.e., property constraints) and structural constraints (for the generation of candidate molecules). Then, results using ProCAMD are presented, discussed, and extended as necessary.

Refrigerant Design

Problem

The main goal of this study is to combine chemical functional groups to obtain molecules having similar properties to the traditional refrigerant, chlorofluorocarbon (CFC), but with low ozone depletion and global warming potentials (*ODP* and *GWP*).

Solution

In refrigeration systems (see Example 10.3), refrigerants undergo a phase transition from liquid to gas (evaporation), in which they absorb heat at low temperature. Then, they are compressed to higher temperatures and pressures, after which they are condensed from gas to liquid while discharging absorbed heat at higher temperatures. Finally, they are partially vaporized to low temperatures before being returned for evaporation.

In the 1980s, most common commercial refrigerants were CFC-based, having superior properties, and were well-regarded as nontoxic and nonflammable. At that time, it was becoming recognized that they caused ozone depletion because of high chlorine concentrations. In response, several alternatives were introduced such as hydrofluorocarbons (HFCs). But, unfortunately, while these didn't cause ozone depletion, they were found to have high *GWP*s.

To resolve this, a refrigerant is sought that absorbs heat at low temperatures and desorbs it at high temperatures, is safe (i.e., nontoxic and nonflammable), and environmentally friendly. In this case study, the steps in finding such a refrigerant, which is also stable and inert to chemical reactions (without being converted to byproducts) compared to those used in the 1980s, are traced.

Property Constraints. Initially, these product needs are translated into a set of target properties, as illustrated in Table 4.10. Then, before selecting the goal values for these target properties, it helps to search a property database for the properties of known refrigerants. See Table 4.11, which shows the properties of the two most common refrigerants, Freon-12 and R-22, in the 1980s. Given these values, typical goal values of target properties for new refrigerants are selected, as shown in Table 4.12. Note that the *ODP* and the *GWP* are checked after the feasible set matching the five listed properties has been found.

Table 4.10 Product Needs, Target Properties, and Their Significance

Product Needs	Target Properties	Significance
Performance: Ability to transfer heat	Heat of vaporization, ΔH_{vap}	High ΔH_{vap} gives low refrigerant flow rates
	Vapor pressure, P^{sat}	Provides a measure of the pressure exerted by the vapor in thermodynamic equilibrium with the liquid at a given temperature in a closed system
	Boiling point, T_b	Corresponds to the temperature at which the vapor pressure of a liquid equals the atmospheric pressure and the liquid vaporizes
	Critical temperature, T_C	Temperature above which vaporization and condensation do not occur no matter how much pressure is applied
	Critical pressure, P_C	Pressure required to liquefy a gas at its critical temperature
Safety: Nonflammable, nontoxic	Flash point, T_f; Log LC_{50}	Nontoxic compounds having low flash points are preferred as refrigerants. LC_{50} is a measure of toxicity.
Environmental: Low ozone depletion	Ozone depletion potential (*ODP*)	*ODP* estimates the possibility of a refrigerant causing ozone depletion.
	Global warming potential (*GWP*)	Refers to the total contribution to global warming resulting from the emission of one unit of gas relative to one unit of the reference gas, CO_2, which is assigned a value of unity.

Table 4.11 Selected Target Properties for Refrigerants

Property	Dichlorodifluoro-methane (Freon-12)	Chlorodifluoro-methane (R-22)
Heat of vaporization at 20°C, ΔH_{vap} (kJ/mol)	17.17	16.32
Vapor pressure, P^{sat}, at 20°C (kPa)	565	902
Boiling point, T_b (K)	243.36	232.32
Critical temperature, T_C (K)	384.95	369.3
Critical pressure, P_C (atm)	40.711	49.06
ODP	0.82	0.034
GWP	10.600	1.700

Table 4.12 Target Property Values for the Molecular Design of Refrigerant

Target Properties	Units of Measure	Lower Bound	Upper Bound
Heat of vaporization, ΔH_{vap}	kJ/mol	16	—
Vapor pressure at 20°C, P^{sat}	kPa	550	—
Boiling point, T_b	K	—	250
Critical temperature, T_C	K	360	390
Critical pressure, P_C	atm	40	50

Structural Constraints. These constraints, Eqs. (4.1)–(4.5), are included and the basis set of groups is selected to include {CH_3; CH_2; CH; C; CF_3; CF_2; CF; CCl_2F; $HCCl_2F$; HCClF; $CClF_2$; $HCClF_2$; $CClF_3$; CCl_2F_2}. The groups containing Cl atoms with F atoms are included, but those without F atoms are excluded because of their negative impact on the *ODP* and *GWP*. Molecules with a minimum of two and a maximum of six groups are allowed, with the same group appearing a maximum of twice. Note that when the refrigerants are to be small molecules, these constraints are reasonable.

ProCAMD Results. The generated feasible compounds, together with their target properties, are displayed in Table 4.13.

Final Selection. Among the three feasible candidates, R-134a (1,1,1,2-Tetrafluoroethane) has the highest heat of vaporization, negligible ozone depletion, and negligible impact on global warming. The results show that the CAMD technique finds known molecules, having the best properties (negligible *ODP* and *GWP* and highest ΔH_{vap}) (better than Freon-12 or R-22). However, for such small molecules, the functional-group method commonly used to generate candidate molecules and test them (check whether they meet property constraints) is not very appropriate. Instead, a large database of smaller molecules is needed for the search.

Table 4.13 Promising Refrigerants from ProCAMD

Chemical	M_w (g/mol)	ΔH_{vap} (kJ/mol)	P^{sat} (kPa)	T_b (K)	T_C (K)	P_C (atm)
1,1,1,2-Tetrafluoroethane	102.03	18.78	569	247.09	374.3	40.109
Propylene	42.08	14.53	1,021	225.55	365.57	46.04
Propane	44.1	15.19	834	231.05	369.83	41.924
1,1-Difluroethane	66.05	18.59	517	248.25	386.44	44.607
Chlorofluoromethane	86.47	16.32	902	232.45	369.3	49.06

Note: Except for 1,1,1,2-tetrafluoroethane, the other compounds were added to the ProCAMD results as user-added molecules.

Large Molecule (Surfactant) Design

Problem

Design a large (surfactant) molecule having the following properties:

$$M_w > 300$$

$$T_b > 400 \text{ K}$$

$$T_m > 300 \text{ K}$$

Solution

In this problem, first a backbone is generated with ProCAMD and then it is manually extended. Its properties are calculated using the M-G method (Marerro and Gani, 2001).

Structural Constraints. Surfactant molecules have a hydrophobic part, a long tail, and a hydrophilic part. To the basis set of groups, the OH group is added for the hydrophilic part, and the ACH (aromatic ring) group is selected for the hydrophobic part. The groups CH_2, CH, and C, are included to generate a hydrocarbon tail. Also, the group CH_3 is included to terminate the molecular structures. The resulting basis set of groups is {CH_3; CH_2; CH; C; CH_2=CH; CH=CH; CH_2=C; CH=C; C=C; ACH; AC; $ACCH_3$; $ACCH_2$; ACCH; CH_2=C=CH}. Eqs. (4.1)–(4.5) are included to satisfy the molecular structural constraints (a maximum of 30 groups allowed). In this way, a relatively small backbone is generated initially, followed by manual extension with a hydrophilic group {OH} and chain-length groups {CH_2}.

ProCAMD Results. The backbone generated by ProCAMD and the final molecular structure generated manually are given in Table 4.14, together with a selected set of calculated properties. Note that the final molecule does not have the well-known nonionic surfactant (emulsifier) properties. However, by adding more O-atoms to create a chain of CH_2O groups (instead of CH_2 groups), the desired emulsifier properties are obtained. This shows how a final molecule can be generated from a backbone structure.

Active Ingredient Design/Selection

Problem

α-chloroacetamideochloroacetanilides are herbicides that have the remarkable property of stunting the growth of turf grass, without killing the grass, while enriching the green texture of the turf. These compounds are referred to as "turf retardants." Experiments have been performed to measure the biological activities measured as the decrease in vertical growth of the turf grass tall fescue. These activities are correlated to the $log\ K_{ow}$ of compounds related to α-chloroacetanilide using:

$$A = 50.374 + 5.0164(logK_{ow}) - 1.7824(logK_{ow})^2 \qquad (4.32)$$

Generate completed molecular structures from the backbone of the α-chloroacetamideo-chloroacetanilides:

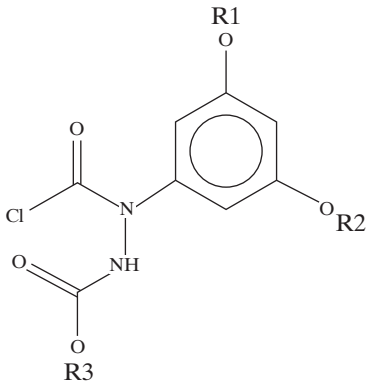

where R1 can be hydrocarbon groups (acyclic and cyclic), but R2 and R3 should only be acyclic hydrocarbon groups having 1–3 carbon atoms.

Solution

Since R1, R2, and R3 are hydrocarbons only, the basis set should comprise functional groups with C and H atoms only. For example, when generating only acyclic structures for R1, R2, and R3, the structures in Table 4.15 are generated by ProCAMD, shown with estimates for $Log\ K_{ow}$ and A.

Table 4.14 Backbone and Final Structure of Molecule Together with Calculated Properties

	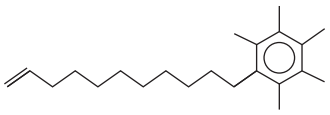	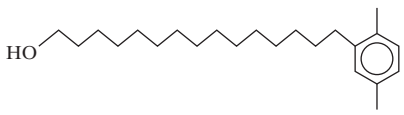
		HO
T_m	308.8	346.6
T_b	634.8	677.8
ΔH_{fus}	38.63	48.7
δ_T	14.23	20.13
$Log\ K_{ow}$	8.03	8.00
$-Log\ LC_{50}$	7.67	7.31
$-Log\ LD_{50}$	3.12	2.88

Note: LC_{50} and LD_{50} are both measures of toxicity; LC_{50} represents the concentration in water that kills 50% of fathead minnows in 96 hr. LD_{50} represents the mass of chemical per body weight of a rat that, when orally ingested, kills 50% of the rats.

Table 4.15 Molecules Generated by ProCAMD

Candidate Active Ingredient	*Log* K_{ow}	*A*	Candidate Active Ingredient	*Log* K_{ow}	*A*
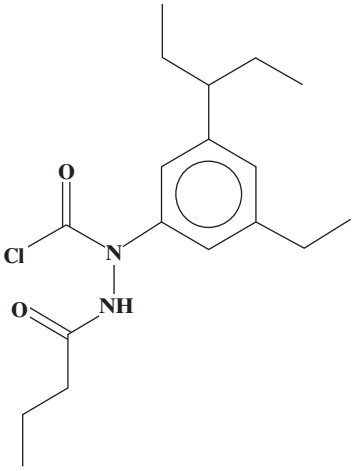	3.67	44.78	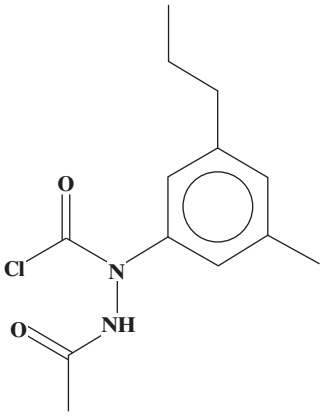	1.69	53.76
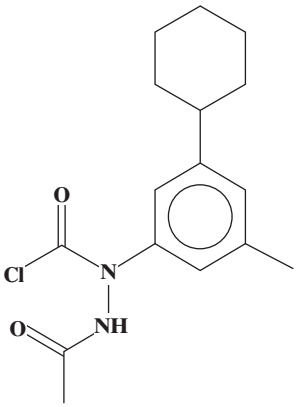	1.9	53.47	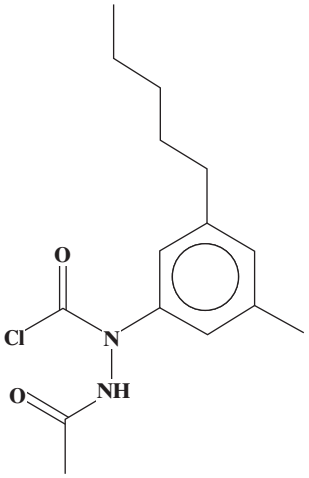	2.59	51.41
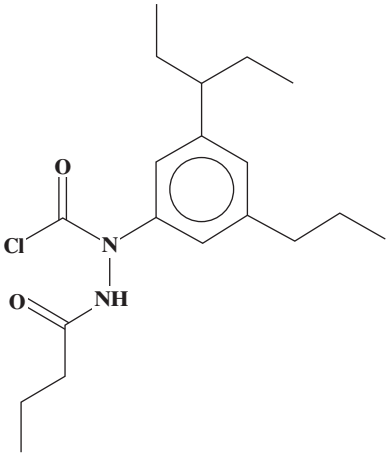	4.12	40.79			

Note: Log K_{ow} for the generated molecules were calculated with the M-G method and parameters from Hukkerikar et al. (2012a).

Polymer Design

Problem

Cookware is a class of products extensively used in everyday life, comprised commonly of aluminum, stainless steel, cast iron, copper, carbon steel, and glass materials. To increase the life span of cookware, it is advantageous to coat its surfaces with polymeric materials. Also, new cookware products are often designed with coatings of polymeric materials.

The objective of this molecular (polymeric) product-design problem is to identify polymer repeat unit structures that can coat cookware materials, like aluminum, to be resistant to heat at high temperatures, chemical reactions, and corrosion, and be easy to clean.

Solution

First, the product need-functions are converted to property specifications (constraints), which candidate products must match. In addition, a set of structural constraints, Eq. (4.6), must also be satisfied.

Property Constraints. The two most important properties that give important clues to the structure of the polymeric materials are heat-resistance functionality and Young's modulus:

- *Heat Resistance:* The required polymer should be heat resistant at cooking temperatures. For maximum cooking temperatures near 573 K, the designed polymer should have its melting temperature above 573 K. However, because it is not easy to measure and model polymer melting temperatures, the glass-transition temperature, which is approximately 50% of the melting temperature (Satyanarayana et al., 2009), can be used as a target property. Setting a 20 K safety margin, the minimum target value for T_g is 297 K.
- *Young's Modulus Measures the "Stiffness" of a Material:* Because the desired polymer is required to coat cookware, potential candidates should be sufficiently flexible while retaining optimum strength. Using graphs of Young's modulus as a function of polymeric material densities, Satyanarayana et al. (2009) confirmed that elastomers usually have Young's moduli less than 0.1 GPa while they exceed 1 GPa for crystalline polymers. Here, the goal is to set constraints on Young's modulus that are neither too flexible, as for elastomers, nor too rigid, as for highly crystalline polymers. Satyanaryana et al. (2009) suggest 0.3 and 0.6 GPa as lower and upper bounds. However, because Young's modulus is difficult to predict, the polymer amorphous density has been suggested as a target property with 1.0 and 2.4 g/cm^3 as lower and upper bounds.

Structural Constraints. The minimum number of groups in a polymer repeat unit is set at unity and the maximum number is set at three because relatively small repeat units are sought. When selecting functional groups for the basis set to generate polymer repeat unit structures, a literature search is helpful, showing that fluoropolymer resins usually have high thermal resistance, chemical inertness, and low environmental impact. Consequently, fluorinated groups like CF_2, CHF, CHF_2, CF, CF_3, and CH_2F are included together with CH_2, CH_3, CH, and C, which are used to increase or shorten the repeat-unit length and/or provide branched structures. Chlorofluoro polymers have commercial importance—and because they contain fluorine in their groups, may possibly have high thermal resistance and chemical inertness. Consequently, the groups CCl_2F, HCClF, and $CClF_2$ are included. The combined basis set is:

$$\text{Basis set} = \{CH_2,\ CH_3,\ CH,\ C,\ CF_2,\ CHF,\ CHF_2,\ CF,\ CF_3,\ CH_2F,\ CCl_2F,\ HCClF,\ CClF_2\}$$

ProCAMD Results. A total of 63 polymer repeat-unit structures satisfying the structural constraints are generated. Of these, 37 satisfy the property constraints. Excluding the isomers and ranking the remaining structures on the basis of the glass-transition temperature, the top 15 candidates are identified and listed in Table 4.16. The polymer repeat unit of Teflon®, a well-known polymer for coating cookware, is among the ranked candidates. The M-G method–based property models for polymers have been used (Satyanarayana et al., 2009).

Table 4.16 Generated Polymer Repeat Units with Target Properties

Number	Polymer Repeat Unit	T_g (K)	Density (g/cm^3)
1	–[C(CH_3)(CF_3)]n–	419.44	1.50
2	–[CF(CH_3)]n–	405.63	1.57
3	–[CH_2–CF(CF_3)]n–	390.23	1.98
4	–[CH(CF_3)]n–	389.47	1.82
5	–[CH(CF_3)–CF_2)]n–	364.23	1.89
6	–[CF_2–CF(CH_3)]n–	362.51	1.78
7	–[CH_2–CH(CF_3)]n–	357.23	1.57
8	–[CH_2–CF(CH_3)]n–	350.31	1.32
9	–[CF(CCl_2F)]n–	348.41	1.94
10	–[C(CH_3)–CCl_2F)]n–	344.77	1.41
11	–[CH_2–CF(CCl_2F)]n–	331.25	1.74
12	–[CF–HCClF]n–	325.73	1.99
13	–[CF_2–CF_2)]n–(Teflon)	322.82 (∼300)	2.02 (2.2)
14	–[C(CH_3)–HCClF]n–	319.83	1.22
15	–[CF($CClF_2$)]n–	318.68	1.97

Dichloromethane (DCM) Replacement in Organic Synthesis

Problem

The objective here is to find replacements for dichloromethane [ClCCl; 000075-09-2], which is a very well-known solvent used in organic synthesis. Note that DCM is a hazardous chemical whose release into the atmosphere needs to be strictly regulated. It is not only carcinogenic but also, when inhaled, can affect the central nervous system.

Solution

The reaction system is unknown in this organic synthesis. However, normally, the solvent is used to dissolve the reactants and/or products and is inert in the reaction mechanism.

Property Constraints. Because the reaction details are unknown, substitutes are sought that match the desirable properties only. These are solubility-related properties having the following property constraints:

$$325 < T_b < 425 \text{ K}$$

$$250 < T_m$$

$$16 < \delta_T < 19 \text{ MPa}^{1/2}$$

$$Log\ K_{ow} > 1.0$$

$$\rho_L\{298K\} > 1.0$$

Note that the liquid density is not a constraint in generating and testing candidates, but all potential molecular products are checked to satisfy typical liquid-density constraints.

Structural Constraints. Eqs. (4.1)–(4.5) are satisfied, with $n_{min} = 2$ and $n_{max} = 8$. Only acyclic molecules with C, H, and O atoms are sought. The basis set of groups is: {CH_3; CH_2; CH; C; OH; CH_3CO; CH_2CO; CHO; CH_3COO; CH_2COO; HCOO; CH_3O; CH_2O; CH-O; COO}.

ProCAMD Results. A total of 2,751 structures are generated [satisfying Eqs. (4.1)–(4.5)], but just 215 are feasible (i.e., they also satisfy the above property constraints.) A selection of these molecules, generated by ProCAMD, but also found in the database, are listed in Table 4.17. These results show the difficulty in matching the properties of DCM with those of a single molecule. However, if the first two compounds are inert in the reaction medium, they can be quite good substitutes. More examples of the design of solvents for organic synthesis are found in Gani et al. (2005).

Azeotrope Formation

Problem

Find all of the binary mixtures that form an azeotrope with ethanol at 1 atm where the other compound is an acyclic compound, having $300 < T_b < 400$ K.

Solution

Property Constraints. Besides the specified T_b constraint, the liquid miscibility with ethanol needs to be checked. For a temperature range of 300–400 K and the entire composition range, the miscibility issue is checked. Because all candidate mixtures satisfy this constraint, a check is unnecessary during the verification stage.

Structural Constraints. Acyclic compounds including hydrocarbons, aldehydes, acids, ethers, and esters are considered using the basis set of groups: {CH_3; CH_2; CH; C; CH_3CO; CH_2CO; CHO; CH_3COO; CH_2COO; HCOO; CH_3O; CH_2O; CH-O; COOH; COO}. Eqs. (4.1)–(4.5) with $n_{max} = 8$ and $n_j^u = 2$ (except for the CH_3 and CH_2 groups) are used.

ProCAMD Results. For these structural constraints, 5,614 molecules are generated, of which only 20 match the target property constraints. One of the solutions using ProCAMD is shown in Figure 4.13.

Verification. Checking the database, 1,2-dimethoxyethane [COCCOC; 000110-71-4] forms a low-boiling homogeneous azeotrope with ethanol at 350.5 K and 0.29 mole fraction. The predicted 0.34 mole fraction is in quite good agreement, considering that the vapor pressure of the generated molecule is predicted as a function of temperature. Another candidate compound from the search is methyl-ethyl-ketone [CCC(=O)C; 000078-93-3], which forms an azeotrope with ethanol at 343.8 K, having a 0.55 mole fraction (matching with measured data very well).

Solvent Substitution

Problem

Phenol has been deposited as a solid that needs to be removed from a vessel before a product can be produced. Benzene or toluene can dissolve the phenol, but a more environmentally friendly antisolvent is preferred to extract the phenol.

Solution

Property Constraints. Begin by establishing the needed properties for the replacement solvent. The CAPEC database is searched to find the properties of phenol, benzene, and toluene. In Figure 4.14, the properties of phenol are shown. Using this data, the solvent-search problem is formulated: The temperature of the operation is below 314 K (assume 300 K), at which the solvent and phenol must form a liquid solution at reasonably high phenol compositions. To achieve solubility, initially, search for solvents having melting points below 250 K and having Hildebrand solubility parameters in the range, $22 < \delta_T < 26$ $(MPa)^{1/2}$.

Generation of Candidates through CAPEC Database Search. This problem can be solved using the CAPEC database and/or ProCAMD. The search of the database gives 41 candidates, as shown in Figure 4.15. Using these results, the next step is both to generate new candidate molecules and test all candidates using ProCAMD.

Structural Constraints. The problem definition in ProCAMD is shown in Figure 4.16a and b. Note that these data can be used to

Table 4.17 Feasible DCM Substitute Molecules

	$Log\ K_{ow}$	δ_T $(MPa^{1/2})$	T_m (K)	T_b (K)	ρ_L at 298 K (g/cm^3)	Water Miscibility
Methyl n-propyl ether	1.09	16.9	169.6	328.4	0.97	No
2-methylpronal	1.31	17.6	176.0	338.3	1.06	No
Isopropyl acetate	1.29	18.1	172.1	366.7	1.16	No
Methyl isopropyl ketone	1.03	17.83	186.2	364.4	1.05	No
Butyl isobutyrate	1.61	16.7	170.9	387.7	1.16	No
Toluene	2.72	18.0	227.3	386.1	1.09	No
DCM	1.45	20.3	178.1	313.1	1.09	No

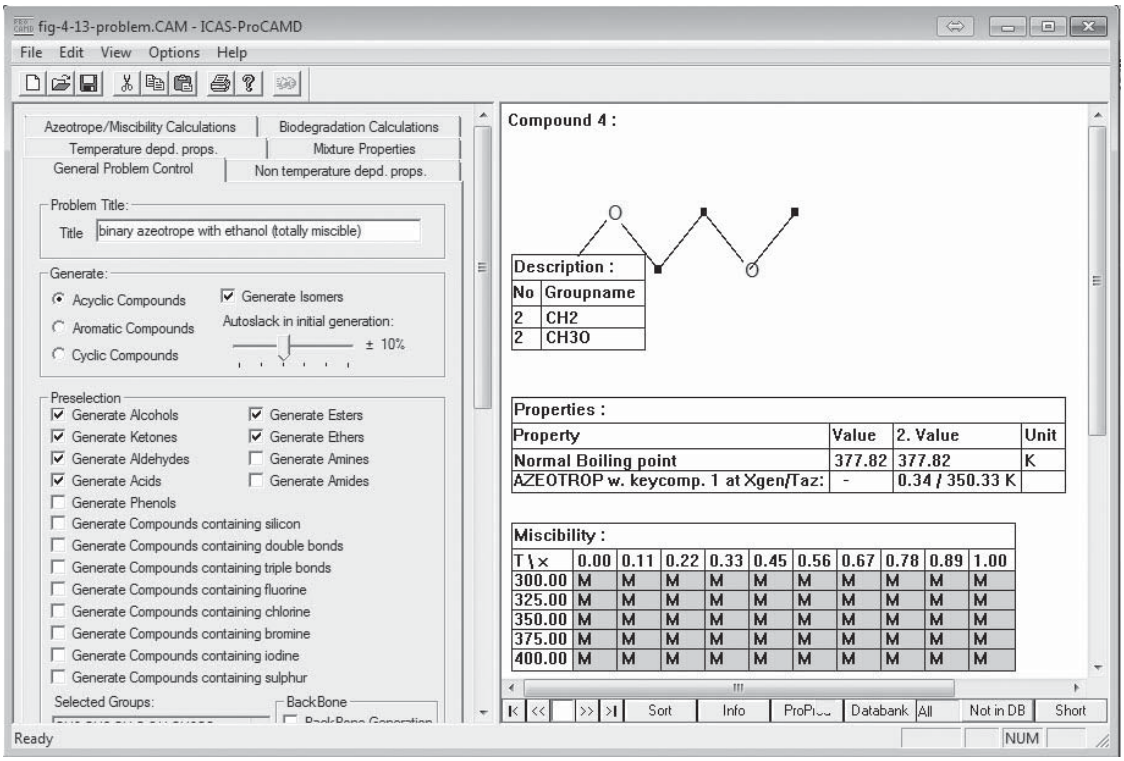

Figure 4.13 One feasible solution—Molecule forms an azeotrope and is totally miscible with ethanol. (*Source:* © ProCAMD).

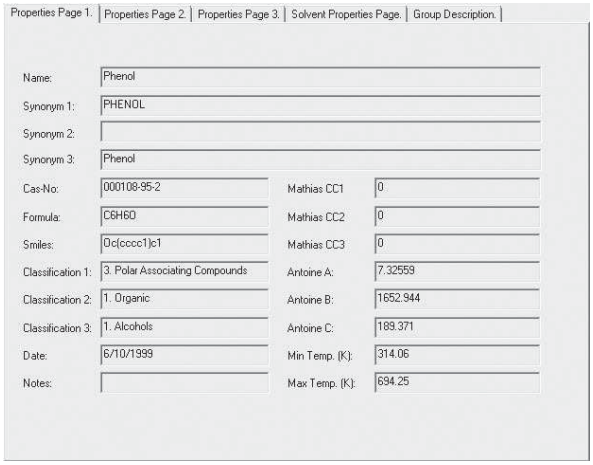

Other Properties

T_m = 314.06 K

T_b = 454.99 K

δ_T = 24.63 $(MPa)^{1/2}$

ΔH_{fus} = 11510 kJ/kmol

T_C = 694.25 K

P_C = 60.498 atm

V_C = 0.229 m^3/kmol

ν = 0.889 m^3/kmol

M_w = 94.113 g/mol

Figure 4.14 Pure-component data for phenol obtained by "basic search" in the CAPEC database. (*Source:* © CAPEC).

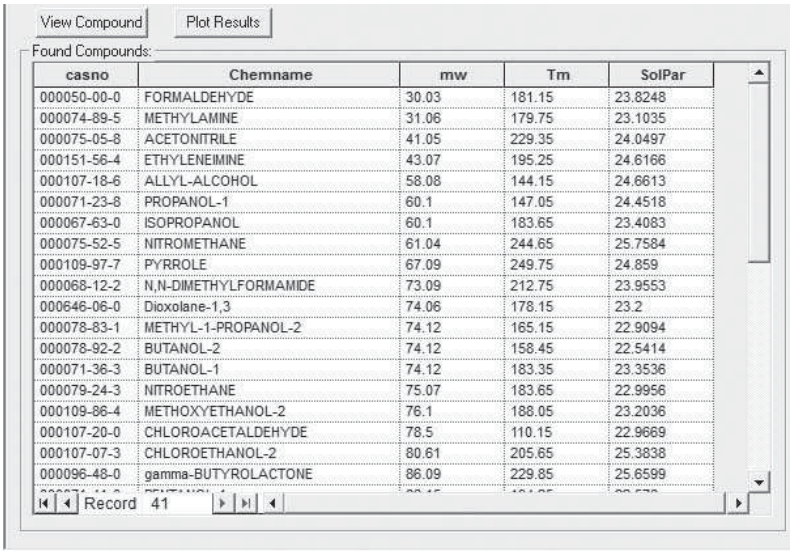

Figure 4.15 Results from solvent search. (*Source:* © ProCAMD).

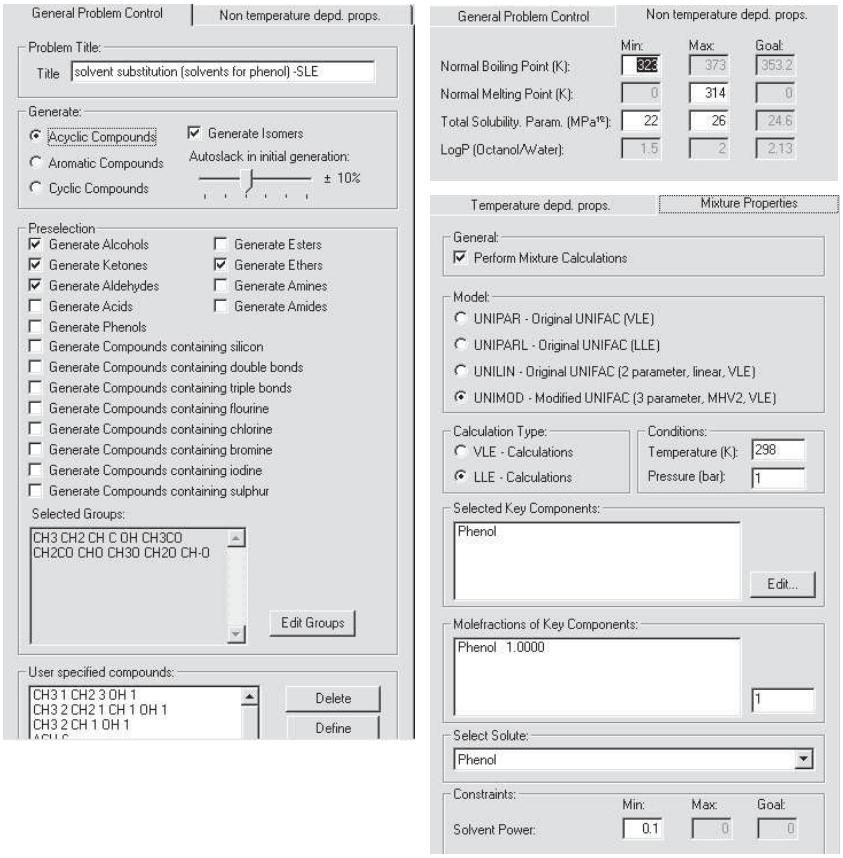

(a)

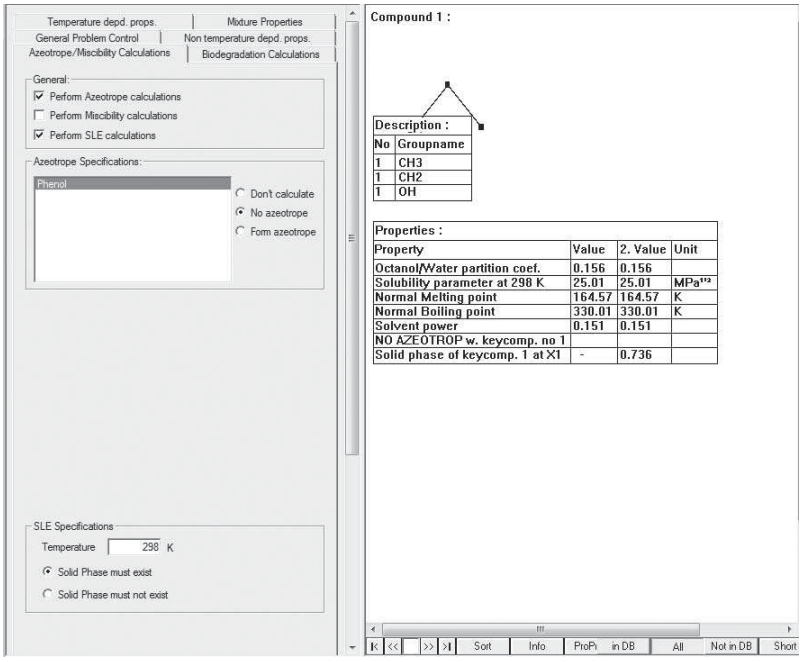

(b)

Figure 4.16 Generation of new candidate molecules and testing using ProCAMD. (a) Problem specification pages from ProCAMD. Note that four versions of the UNIFAC model for calculation of liquid-phase activity coefficients are provided. UNIMOD works well for both VLE and LLE calculations. (b) Problem specification page (left-hand side) and details of one feasible generated molecule using ProCAMD (right-hand side) Note that the properties listed for "Value" and "2. Value" are identical because in this case the second-order groups do not change the property calculations. Note also that the "octanol/water partition coefficient" is calculated, but its value is not used for checking the feasibility of the molecule. (*Source:* © ProCAMD).

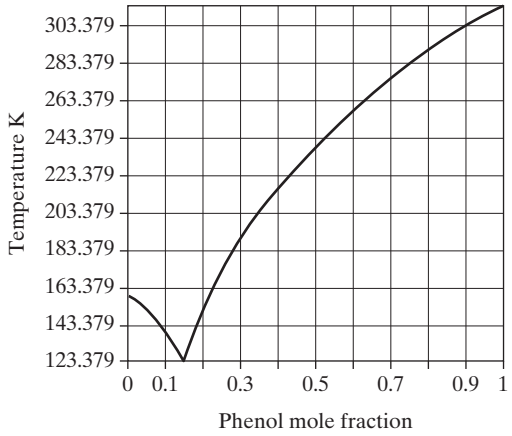

Figure 4.16 (*continued*) (c) Calculated SLE curve for phenol-ethanol system.

solve this problem through other means, including manually generating the candidate molecular structures and estimating the properties using other property prediction software.

ProCAMD Results. For this problem, ProCAMD generated 3,071 feasible molecules, of which 20 satisfied all of the property constraints. The group vectors for these 20 molecules generated 37 molecules, of which seven satisfy all of the constraints (including compound 1 in Figure 4.16b). From these figures, we can conclude that ethanol is clearly a feasible candidate solvent to be verified in the next step.

Verification of Solvent Using a Solid-liquid Equilibrium Phase Diagram. This verification can be done experimentally by measuring solid solubility data at different temperatures to display saturated solute concentrations at equilibrium as a function of temperature. Another option, used herein, is to predict the SLE phase equilibria using the calculation scheme in Table 4.7. Figure 4.16c shows the calculated SLE curve. Clearly, at 300 K, a large amount of phenol is in the liquid phase.

Alternatively, solving a slightly modified problem, as in Example 4.14, several molecules are found to be good substitutes for benzene, as shown in Table 4.18.

Table 4.18 Environmentally Friendly Substitutes for Benzene

	δ_T (MPa$^{1/2}$)	T_m (K)	T_b (K)	*Log* K_{ow}	*Log* LC_{50}
Benzene	18.7	278.1	353.0	1.82	3.44
Methyl isobutyl ketone	17.7	200.6	393.8	1.54	2.86
3-Heptanone	18.2	229.1	435.9	1.84	2.70
Methyl n-pentyl ether	17.2	200.6	392.7	2.10	2.93
Isobutyl acetate	17.9	188.4	395.9	1.79	3.28

Mixture Design

Problem

The purpose of this case study is to obtain a tailor-made gasoline blend that has a similar performance to traditional gasoline. Renewable additives to gasoline reduce the consumption of fossil fuel, extending its availability. Also, renewable additives often reduce the environmental impacts by lessening the introduction of greenhouse gases and replacing harmful chemicals (e.g., sulfur) in fossil fuels.

Solution

The gasoline blend must flow continuously from the fuel tank to the combustion chamber. It must be combustible and burned easily. Also, it should have good fuel performance and enable efficient engine operation to replace traditional gasoline. It must have a predefined flammability limit and a low toxicity level. It must be in a single liquid phase, stable, and inert to chemical reaction. Finally, oxygen content must be considered to respect environmental emissions regulations.

Problem Definition. These needs of the gasoline-blend product are converted into the target properties in Table 4.19. Also, the gasoline blend is to be used in the winter at an average ambient temperature of 5°C.

Method of Solution. The decomposition-based solution approach proposed by Yunus et al. (2014) and outlined in

Table 4.19 Target Product Needs for Gasoline Products at 5 °C Average Ambient Temperature

Product Needs	Target Properties	Symbol	Units	LB	UB
Consistency of flow in engine	Dynamic viscosity	μ	cP	0.3	0.6
	Density	ρ	g/cm^3	0.720	0.775
The ability to burn	Reid vapor pressure	*RVP*	kPa	60	90
Engine efficiency	Octane rating,	*RON*	—	92	100
	heating value	*HHV*	kJ/mol	4000	$+\infty$
Flammability	Flash point	T_f	K	$-\infty$	278
Toxicity	Lethal concentration	$-\log LC_{50}$	—	$-\infty$	3.33
Stability	Gibbs energy of mixing	ΔG_{mix}	—	$-\infty$	0
Blend regulatory issues and emissions	Oxygen content	Wt_{02}	%	2	20

Table 4.20 Binary Mixtures' Compositions and Property Values

Additive									
Gasoline	Amount	Compound No.	Chemical	*HHV* (kJ/mol)	μ (cP)	Wt_{O2} (%)	$-\text{LOG}(LC_{50})$	ρ (g/cm^3)	*RVP* (kPa)
0.6786	0.3214	71	Methyl-n-propyl-ether	4,000	0.39	6.94	3.02	0.7205	64.41
0.6762	0.3238	72	Methyl-isopropyl-ether	4,000	0.37	6.99	2.91	0.7246	78.67

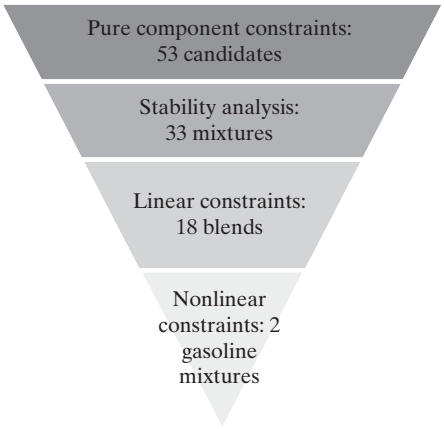

Figure 4.17 Binary gasoline-blend design using the decomposition method.

Figure 4.7 (mixture design algorithm) is employed to solve this problem. Initially, of the 1,425 compounds available in the chemical database, 89 are selected. In this case study, only binary mixtures are created. Note that the *MI* for the base gasoline is a model mixture of five compounds and, consequently, the term "binary" refers to the *MI* and the added compound. Following the steps in Levels 1–4, two binary mixtures are obtained. The reduction in the number of alternatives achieved through solution of the problems at each level is summarized in Figure 4.17. In Levels 3 and 4, the optimization problems highlighted in Examples 4.15 and 4.16 are solved, respectively. Finally, two alternatives remain after optimization to obtain the highest mole fraction of additive. The results are summarized in Table 4.20, with amounts given as molar fractions of gasoline and additive. All property values, except the lethal concentrations, are suitable for use of these two blends at 5°C. Indeed, environmentally speaking, the lethal concentrations exceed the regulations [$-log\ (LC_{50}) \leq 2.50$]. It would be preferable to avoid using the ether group in the additives to satisfy the environmental standards.

Finally, as other binary mixtures are explored to replace traditional gasoline, costs must be taken into account before experimental verifications.

4.4 SUMMARY

Using a computer-aided framework for molecular and mixture-based product design, this chapter highlights, for the reader, the important issues, methods, and software. Brief examples have been used to highlight the concepts and the work-flow in solving molecular and mixture-based design problems. Because the properties of the chemicals play a key role, successful on-line predictions within the computer-aided framework are required for CAMD/CAM^{b}D.

Specific software has been used to solve the problems herein, but sufficient information has been given for readers to use other methods and software. The parameters for the group-contribution-based property models used throughout this chapter are available publicly and can be downloaded (http://capec.kt.dtu.dk/Software/CAPEC-Software).

For further reading, edited books by Achenie et al., 2003; Kontogeorgis and Gani, 2004; and Ng et al., 2007, are recommended, as well as standard textbooks on thermodynamics and property predictions.

REFERENCES

1. Achenie, L. E. K., R. Gani, and V. Venkatasubramanian, "Computer Aided Molecular Design: Theory and Practice," *Computer-Aided Chemical Engineering*, **12**, 1–392 (2003).

2. Brook, A., D. Kendrik, and A. Meeraus, "GAMS: A User's Guide," *Scientific Press* (1988).

3. Constantinou, L., and R. Gani, "New Group-contribution Method for Estimating Properties of Pure Compounds," *AIChE J.,* **40***,* 1697–1710 (1994).

4. Constantinou, L., K. Bagherpour, R. Gani, J. A., Klein, and D. T. Wu, "Computer Aided Product Design: Problem Formulations, Methodology and Applications," *Comput. Chem. Eng.*, **20**, 685 (1996).

5. Conte, E., R. Gani, and K. M. Ng, "Design of Formulated Products: A Systematic Methodology," *AIChE J.*, **57**, 2431 (2011).

6. Fredenslund, Aa., J. Gmehling, P. Rasmussen, *Vapor-Liquid Equilibria Using UNIFAC*, Elsevier Amsterdam (1977).

7. Gani, R., "Chemical Product Design: Challenges & Opportunities," *Comput. Chem. Eng.*, **28**, 2441 (2004).

8. Gani, R., "Modeling for PSE and Product-Process Design," R. M. de Brito Alves, C.A.O. do Nascimento, and E. C. Biscaia, Jr. (eds.), 10th Int'l. Symp. Proc. Sys. Eng., Elsevier (2009).

9. Gani, R., G. Hytoft, C. Jaksland, and A. K. Jensen, "An Integrated Computer Aided System for Integrated Design of Chemical Processes," *Comput. Chem. Eng.*, **21**, 1135 (1997).

10. Gani, R., C. Jiménez-González, and D. J. C. Constable, "Method for Selection of Solvents for Promotion of Organic Reactions," *Comput. Chem. Eng.*, **29**, 1661 (2005).

11. Harper, P. M., M. Hostrup, and R. Gani, "A Hybrid CAMD Method," *Computer-Aided Chemical Engineering,* **12**, 129 (2002).

12. Hostrup, M., P. M. Harper, and R. Gani, "Design of Environmentally Benign Processes: Integration of Solvent Design and Process Synthesis," *Comput. Chem. Eng.*, **23**, 1394 (1999).

13. Hukkerikar, H. S., B. Sarup, A. Ten Kate, J. Abildskov, G. Sin, and R. Gani, "Group-Contribution+ (GC+) Based Estimation of Properties of Pure Components: Improved Property Estimation and Uncertainty Analysis," *Fluid Phase Equil.*, **321**, 25 (2012a).

14. Hukkerikar, A., S. Kalakul, B. Sarup, D. M. Young, G. Sin, and R. Gani, "Estimation of Environment-related Properties of Chemicals for Design of Sustainable Processes: Development of Group-contribution$^+$ (GC^+) Models and Uncertainty Analysis," *J. Chem. Inform. Model.*, **52**(11), 2823 (2012b).

15. Kontogeorgis, G. M., and R. Gani, "Computer-Aided Property Estimation for Process and Product Design," *Computer-Aided Chemical Engineering*, **19,** 1–425 (2004).

16. Marrero, J., and R. Gani, "Group Contribution-Based Estimation of Pure Component Properties," *Fluid Phase Equil.*, **183–184**, 183 (2001).

17. Ng, K. M., R. Gani, K. Dam-Johansen, "Chemical Product Design: Toward a Perspective through Case Studies," *Computer-Aided Chemical Engineering*, **23**, 1–501 (2007).

18. Nielsen, T. L., J. Abildskov, P. M. Harper, I. Papaeconomou, and R. Gani "The CAPEC database," *J. Chem.Eng. Data,* **46***,* 1041 (2001).

19. Odele, O., and S. Macchietto, "Computer-aided Molecular Design: A Novel Method for Solvent Selection," *Fluid Phase Equilibria*, **82**, 47 (1993).

20. Poling, B., J. Prausnitz, and J. P. O'Connell, *Properties of Gases and Liquids*, McGraw-Hill, New York (2001).

21. Satyanarayana, K. C., R. Gani, and J. Abildskov, "Computer-aided Polymer Design Using Group Contribution plus Property Models," *Comput. Chem. Eng.*, **33**, 1004 (2009).

22. Van Krevelen, D. W., *Properties of Polymers*, 3rd ed., Elsevier Science, Amsterdam, Oxford, New York (1990).

23. Venkatasubramanian, V., K. Chen, and J. M. Caruthers, "Computer-Aided Molecular Design using Genetic Algorithms," *Comput. Chem. Eng.*, **18**, 833 (1994).

24. Wilson, G. M., and C. H. Deal, "Activity Coefficients and Molecular Structure," *Ind. Eng. Chem. Fund.*, **1**, 20 (1962).

25. Yunus, N. A. B., K. V. Gernaey, J. M. Woodley, and R. Gani, "A Systematic Methodology for Design of Tailor-made Blended Products," *Comput. Chem. Eng.*, **66**, 201 (2014).

EXERCISES

4.1 Molecular Structure Generation Given the basis sets of groups Set-1{CH_3; CH_2; CH; C}; Set-2 {OH; CH_3CO; CH_3O; CH_2CO, CH_2O}, how many chemically feasible molecules can be generated [satisfying Eqs. (4.1)–(4.5)] with a minimum of two groups and a maximum of four groups and any number of groups from Set-1, but a maximum of one group from Set-2? If there were no restrictions, how many structures could be generated?

4.2 Property Prediction For 2-ethylpentanoic acid [CCCC(CC)C(=O)O; 020225-24-5], hardly any data are available in the database. To evaluate this molecule, T_b, T_m, ΔH_{fus}, and vapor pressure as a function of temperature are needed. Is this compound soluble in water? Which property models should be used to generate the missing data?

4.3 Polymer Design-1 Using the basis set in Example 4.10 and the group-contribution methods in Table 4.6, find the polymer repeat unit that has a glass-transition temperature of 383 K, density $\cong$ 1.5 g/cm^3, and water absorptivity $\cong$ 0.005 g water/g polymer.

4.4 Polymer Design-2 Fibers play an important role in the textile industries, with natural fibers usually having low tensile strength, high moisture absorption, variable quality, low durability, and so on. Synthetic fibers have gained preference over the natural fibers in certain applications. The objective of this polymer design problem is to identify polymer repeat units that can serve as synthetic fibers, avoiding some of the disadvantages of natural fibers. Find target values for the following property needs: moisture (water) absorption; tensile strength; and temperature effect (ease of ironing or pressing depends on the relative position of the glass-transition temperature) among others. Generate the polymer repeat unit structures of nylon and check whether the property needs are satisfied.

4.5 Azeotrope Formation Repeat the azeotrope formation case study for cyclic (naphthenic) and cyclic (aromatic) compounds that form azeotropes with ethanol. Also, repeat the azeotrope formation case study to identify all classes of compounds that do *not* form azeotropes with ethanol but are totally miscible with it.

4.6 API Verification-1 An identified chemical product to serve as an API (active pharmaceutical ingredient) in a drug is synthesized through a multistage reaction scheme. The key reaction step is hydrophobic, and so all of the water added to the reactor in the previous reaction stages needs to be removed. However, the product is temperature sensitive, so removing the water by evaporation at the water-boiling temperature is not an option. A suggested option is to add a solvent that forms a low-boiling azeotrope with water, has a boiling point lower than 373 K, has an octanol-water partition coefficient of less than 3, and is environmentally acceptable. The solvent when added to the system will dissolve the API, and the water will be removed together with some of the solvent by evaporating the minimum-boiling azeotrope. This is a "solvent-swap" operation typical in the development of APIs for drugs and other temperature-sensitive, high-value products. The API has a Hildebrand solubility parameter in the range 17–20 MPa$^{1/2}$.

Formulate the CAMD problem and propose at least five chemicals as desired solvents. Comment on how the solvent candidates can be verified.

4.7 API Verification-2 The drug barbiturate is well known. It has different forms—mostly different types of barbituric acid. Consider the following list of barbituric acids: {Candidate 1: 000077-02-1; Candidate 2: 061346-87-0; Candidate 3: 000076-94-8; Candidate 4: 091430-64-7; Candidate 5: 001953-33-9; Candidate 6: 007391-69-7; Candidate 7: 090197-63-0; Candidate 8: 017013-41-1; and Candidate 9: 027653-63-0}. Analyze each compound and calculate its $Log\ K_{ow}$. Use the following two models to estimate the molar concentration (C) needed to produce a 1:1 complex with protein (binding to bovine serum albumin).

$$\text{Model-1: } Log\ (1/C) = 0.58\ Log\ K_{ow} + 0.239$$

To calculate the hypnotic activity of the compound in rabbits after subcutaveous injection, use

$$\text{Model-2: } Log(1/C) = 2.09\ Log\ K_{ow} - 0.63\ (Log\ K_{ow})^2 + 1.92$$

Find which form of barbituric acid has the best (lowest) concentrations in both cases. For the best barbiturate molecule, find a solvent that is miscible with water.

4.8 Binary Liquid Mixture Design Design a binary liquid mixture that is partially miscible with water, but totally miscible with each other. The binary mixture needs to have the following properties:

Normal boiling point (K)	$370 < T_b < 390$
Hildebrand solubility parameter ($MPa^{1/2}$)	$17 < \delta_T < 19$
Liquid density (gm/cm^3)	$0.8 < \rho_L < 0.9$

Identify at least 10 chemicals from among {1-propanal; tetrahydrofuran; 2-methyl-2-butanol; methyl-ethyl-ketone; isopropyl-acetate; 2-pentanone; toluene; benzene; 1-pentanal; methyl-isopropyl-ketone; ethyl-acrylate; ethyl-acetate; methyl-n-butyrate; 1-heptanol; 2-hexanone; and n-pentyl-acetate} that are mutually soluble. Find at least one binary mixture from this list. Assume ideal mixing for each of the three properties.

4.9 Paint Formulation For a specific paint application, a mixture of solvents is needed. The mixture will be identified by its ability to mix with water (total miscibility), its normal boiling point (determines the solvent evaporation rate), its solubility parameter (determines whether paint is soluble in it), and its molecular weight (size of the candidate molecule).

For mixture properties, use the ideal mixing rule [Eq. (4.16)]. For the property ranges:

$$41 < M_{Wm}(85) < 151$$
$$350 < T_{bm}(370) < 559\ \text{K}$$
$$20 < \delta_{Tm}(25) < 34\ MPa^{1/2}$$

with target values in parentheses, find:

(a) at least one binary mixture that satisfy the target.

(b) the minimum cost binary (solvent) mixture.

The cost function is defined as

$$F = \Sigma x_i\ C\rho_i$$

where C is a cost factor (in 1,000 cost-units) and ρ_i is the density of compound i.

Note: To generate the candidate molecules, the CAPEC database (Nielsen et al., 2001) or any other database can be used. Set the specified constraints and identify all compounds found in the database to match the property constraints. Select any 10 compounds from this set. If any of the following compounds appear, place them in the short list of 10 compounds: {acetonitrile; ethyleneglycol; morpholine; 2-butoxyethanol; triethyleneglycol}.

Chapter 5

Design of Chemical Devices, Functional Products, and Formulated Products

5.0 OBJECTIVES

This chapter introduces three classes of B2C chemical products: devices, functional products, and formulated products. Each product, irrespective of its class, is made up of its own constituents in a customized structure, form, shape, or configuration. The procedures, methods, and tools for conceptual product design are discussed and are illustrated with various examples.

After studying this chapter, the reader should:

1. Be cognizant of the characteristics of devices, functional products, and formulated products.
2. Be familiar with the procedures, methods, and tools for the conceptual design of these products.
3. Be able to design chemical devices and functional products with specified product performance by modeling the dominant physicochemical phenomena and by accounting for the material properties and the product structure, form, shape, or configuration.
4. Be able to design formulated products with specified product attributes by experimental iteration guided by heuristics, correlations, and computer-aided design tools.

5.1 INTRODUCTION

B2C products such as lotions, toothpastes, antifreeze mixtures, mosquito repellent dispensers, air purifiers, and home-use water filters come in different structures, forms, shapes, and configurations. Most of these products are made up of multiple components to obtain the function(s) wanted by the consumers. Among the wide variety of products, we can identify three major classes of products: chemical devices, functional products, and formulated products. Often, a chemical product may not fall neatly into one of these classes, and the assignment of a product class to this specific product may seem arbitrary. Nonetheless, as will become clear in this chapter, this classification allows a more systematic approach to the design of B2C products.

Chemical devices are those chemical products that perform a particular purpose, especially those with mechanical and electrical parts. Often, a feed stream to a chemical device is transformed into an outlet stream with characteristics specified in the product attributes by performing reactions, fluid flow, heating/cooling, and/or separations. For example, an indoor air purifier transforms an air stream laden with volatile organic compounds (VOCs) into clean air by catalytically decomposing the VOCs with platinum-doped TiO_2 under UV irradiation (see Example 5.1). A home-use reverse osmosis (RO) module rids tap water of liquid-borne contaminants by forcing water molecules through an RO membrane. Figure 5.1 shows a spiral-wound module with multiple RO membranes. The feed flows axially between two RO membranes separated by a permeable feed spacer. The clean permeate that passes through either RO membrane encounters an impermeable permeate collecting sheet and is diverted to the permeate tube in the middle of the RO module. At the exit, the feed becomes the retentate that contains the contaminant molecules while the permeate contains the filtered water. A water filter mounted on a faucet achieves a similar objective (Figure 5.2). It removes organics using activated carbon and metal ions using ion-exchange resins. A wine aerator softens the tannins in a red wine supposedly by reaction and stripping. It takes advantage of the Venturi effect to suck air into the passing wine (Figure 5.3). Another example is a hemodialysis device that removes urea and other unwanted metabolites from the blood (see Chapter 24). A mosquito repellent dispenser lifts the solvent containing an active ingredient to the electric heater using a wick followed by vaporization of the repellent (Figure 5.4).

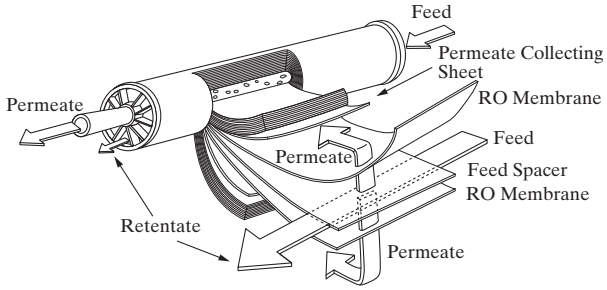

Figure 5.1 A spiral wound RO module.

In all of these examples, the physicochemical phenomena lead to the working principles of the chemical device, and the

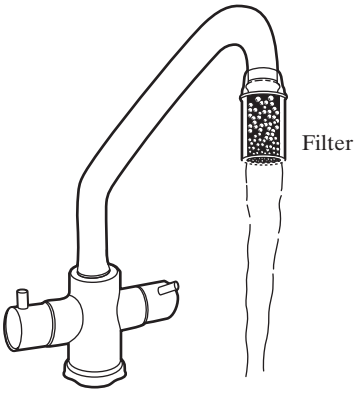

Figure 5.2 Tap water filter. A water filter consisting of activated carbon and ion-exchange resins removes organics and metal ions from the tap water.

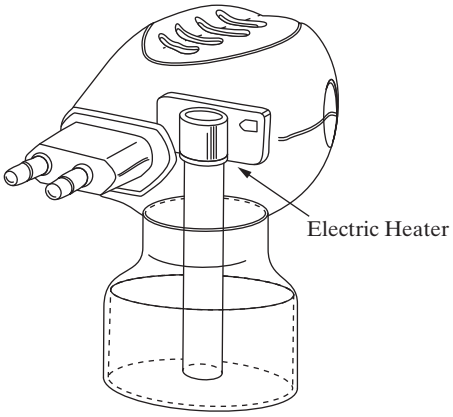

Figure 5.4 Insect repellent dispenser. The liquid insect repellent is vaporized using a heater after drawing the liquid there with a wick.

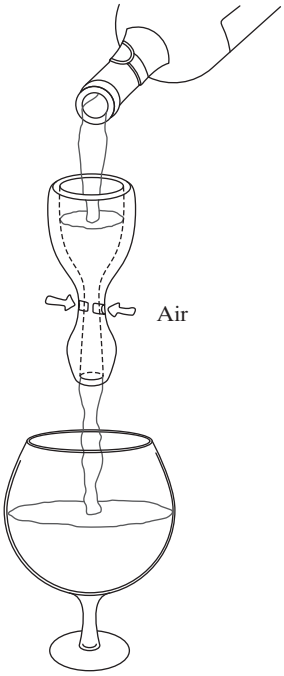

Figure 5.3 Wine aerator. Air is drawn through holes in the aerator into passing wine to soften the tannins.

materials or ingredients in a customized structure, form, shape, or configuration ensure the attainment of the desired product attributes. Thus, TiO_2 can be coated on a high efficiency particulate absorption (HEPA) filter to enhance the transport of VOCs to the catalytic sites to increase the rate of VOC decomposition in an air purifier. Similarly, an RO membrane is not in the form of a flat sheet to achieve superior performance in separations. As chemical engineers, we can view a chemical device as a single miniaturized chemical processing equipment item, a group of interconnected equipment items, or even a chemical plant. The difference is that a chemical device comprises different materials configured in a customized structure, form, shape, or configuration whereas a chemical plant is made up of reactors, distillation columns, crystallizers, evaporators, heat exchangers, filters, absorbers, extractors, and so on.

Functional products are those chemical products made up of materials that perform a desired function. Generally, these products do not have feed and outlet streams and do not involve mechanical and electrical parts. For example, a controlled-release herbicide granule can control weed growth over a prolonged period of time (see Example 5.2). A similar example is a moisture absorber using silica gel to lower the humidity in an enclosed environment such as a coat cabinet (Figure 5.5). For packaged foods, metalized polyethylene can be used to prevent the penetration of oxygen (Figure 5.6). A recent product is a high-barrier PET bottle with a thin layer of carbon on the inside of the bottle. It is several times better at limiting carbon dioxide gas permeation than the traditional PET bottle and can be used to hold carbonated drinks that require a long shelf life. Barrier functional materials can also be used to prolong the life of a tennis ball. Adhesives are an important class of functional materials. A die attach adhesive offers adhesion and a high thermal conductivity (see Chapter 26). A pharmaceutical capsule delivers a drug substance to a patient. Yet another example is a matrix type transdermal patch that delivers an active pharmaceutical

Figure 5.5 Moisture absorber. A bag of silica gel reduces the humidity in an enclosed coat cabinet.

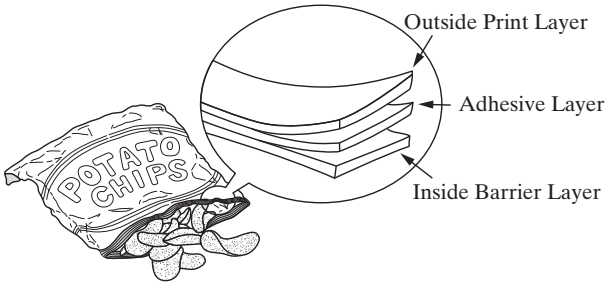

Figure 5.6 Food packaging layers. Food packaging is made up of three main layers: outside print layer, adhesive layer, and inside barrier layer. Each main layer in turn is made up of a few films of different materials. For example, a metalized plastic film is used as the inside barrier layer.

ingredient through the skin. Similarly, processed foods such as ice cream and yogurt deliver nutrients to a consumer. Thus, functional products serve as barriers (food packaging), conductors (die attach adhesive), delivery vehicles (controlled-release granule), absorbers (silica gel), and so on. Similar to devices, the performance of functional products depends on the material properties and the structure, form, shape, or configuration of the product.

Formulated products are obtained by mixing selected components together to get the desired product attributes. Thus, a sunscreen lotion may consist of zinc oxide particles and other ingredients such as emollients (see Example 5.3). An inkjet ink is a mixture of key ingredients, such as pigments or metal nanoparticles, and supporting ingredients, such as dispersants and solvents. A liquid shampoo is a mixture of surfactants, fragrances, and colorants. Paints have pigments and a solvent, normally water, which evaporates to give a solid coat of paint. Many products, such as antifreeze, do not possess a *microstructure* but some, such as a skin-care lotion, do. The lotion can be an oil-in-water or water-in-oil emulsion with different emulsion droplet sizes. The manufacture and use of formulated products generally do not involve reaction or separation. An exception is an epoxy adhesive, which might require heating to initiate the reaction between the epoxy resin and the hardener, or the blending of the two just prior to use. The formulated product is produced by mixing, but the constituent components of a formulated product are often produced by subjecting the raw materials from natural resources to multiple reaction and separation steps along the chemical product chain (Figure 1.1). Some formulated products are all solids. For example, detergent powder is carefully formulated with surfactants, bleach, enzymes, corrosion inhibitors, fluorescent whitening agents, fabric softeners, and other solid components. A formulated product can be further developed to be a device or functional product. For example, an outdoor paint with doped TiO_2 can serve both as a protective coating and as a product that decomposes VOCs.

For all of these products, the chemical engineer is responsible for determining and meeting the *product specifications*. For a chemical device, the product characteristics in product specifications should include the type and amount of the key ingredients and the structure with which these ingredients are configured. For example, before building a prototype air purifier, the amount of TiO_2 catalyst or another type of catalyst and the way in which the catalyst is placed within the air purifier need to be specified. The product specifications required for functional products are the same as those for a device except for the absence of mechanical and electrical parts, and feed/outlet streams. For formulated products, the product characteristics in product specifications include the composition of the mixture and the microstructure. The activities that we perform to obtain all of the information above are referred to as *conceptual product design*. This is analogous to conceptual process design but with a major difference. Thermodynamics, kinetics, and transport processes describe the potential mechanisms for conceptual product design, whereas process units are the building blocks for conceptual process design. This is despite the fact that process units involve the same basic chemical engineering principles.

As indicated in Figure 1.3, a chemical engineer interacts with professionals in marketing and industrial design to create a product ready for prototyping. This chapter focuses on the use of chemical engineering principles to perform conceptual product design, which takes place after a market study but before prototyping. We discuss the procedures, methods, and tools for such activities as they apply to chemical devices, functional products, and formulated products.

5.2 DESIGN OF CHEMICAL DEVICES AND FUNCTIONAL PRODUCTS

For chemical devices or functional products, the type and amount of the key ingredients, and the structure with which these ingredients are configured are identified. The same information is sought whether or not there are feed and/or outlet streams. *Key ingredients* refer to those components that are essential for achieving the desired outcome. For example, the TiO_2 catalyst for decomposing the VOCs in an air purifier is a key chemical ingredient whereas the fan for air circulation is not. The activated carbon and ion-exchange resin in a water filter are the key ingredients but the polypropylene housing is not. The amounts and configuration of the key ingredients are fixed so as to meet the required product performance. For devices, *product performance* is often quantified by the component concentrations and flow rates of the feed and outlet streams. For functional products, performance is measured by the degree to which the product achieves its designed function. The design procedure discussed here can be followed for both devices and functional products:

1. Specify the product performance.
2. Identify the key ingredients as well as the configurations that can accomplish the targeted changes to the feed stream or deliver the desired function. Keep in mind that more than one set of key ingredients and/or configuration may provide the product performance, leading to different product alternatives.
3. Identify the physicochemical phenomena ranging from reactions to separations involved in the product.
4. Use models, experiments, and available data/knowledge to identify the product specifications for meeting the desired product performance and compare product alternatives.

As with all creative work, the procedure need not be strictly followed but can be suitably adjusted under different circumstances. The fourth item is discussed next.

The Use of Models in Design of Devices and Functional Products

Modeling a transport process such as laminar flow inside a pipe using the Navier–Stokes equations or the performance of a distillation column for the separation of a binary mixture using vapor–liquid equilibrium data is a mainstay of chemical engineering. A realistic model accounts for the underlying scientific principles governing the observed behaviors and provides accurate predictions of the behaviors under different conditions without experimentation. Models can be used for product analysis and conceptual product design. As illustrated in Figure 5.7, in *product analysis*, the type and amount of the ingredients and the way in which the ingredients are configured are fixed. The results of modeling are the output information for given input information. In *product synthesis*, or conceptual product design, the input and output information are fixed. The outcome of modeling is the product itself. This seemingly small difference has huge consequences in that there is usually a large number of product alternatives that can deliver the required product performance in the output information. The art and science of product synthesis is to identify the best product alternative that the consumer is willing to buy and that leads to the desired business outcomes for the company. For example, consider the water filter in Figure 5.2. It is easy to construct a filter by mixing ion-exchange resins and activated carbon particles, send a water stream with contaminants through it, and determine the contaminant concentrations in the outlet stream. It is much harder to answer the following question: For an inlet stream with trace amounts of contaminants ranging from metal to radioactive elements, what are the types of adsorbents, their shapes, the amounts, and the way they are packed that would produce an outlet water stream with all these contaminants below specified concentrations?

Models have different degrees of complexity and accuracy (Table 5.1). The simplest is the *black-box model*. Such a model

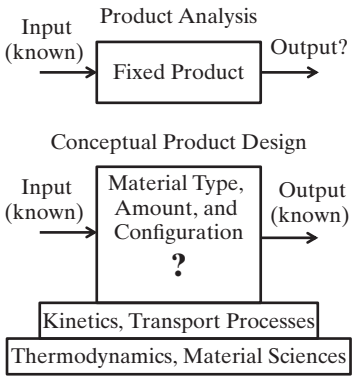

Figure 5.7 Product analysis. In product analysis, the output is calculated based on known input and a given product. In product synthesis, the product characteristics are determined based on known input and output information. Also shown is the scientific foundation for product design.

Table 5.1 Models with Different Degrees of Complexity and Accuracy

Approach	Black-box Model	Simplified Model	Rigorous Model
Technique	Data fitting	Simplified analysis of the phenomena	Detailed analysis of the phenomena
Understanding of physical phenomena	Poorly understood	Partially or completely understood	Completely understood
Range of validity	Limited to the range of collected data	Limited to the assumed conditions	Relatively wide
Predictability of model parameters	Not attempted	Case dependent	Case dependent; tends to have more unknown parameters
Experimental effort	Extensive	Minimal, directed by theory	None or for verification only

Source: Adapted from Wibowo and Ng, 2002; Ng and Wibowo, 2003.

can be obtained by relating the input and output information of the product in the form of a correlation. The parameters in the correlation are determined from experimental data through regression analysis. Obviously, the accuracy of predictions depends on the amount of data used in data regression, and the applicability of the model is limited to the range of collected data. The black-box model can be used if the physical phenomenon is poorly understood or the time for product development is very limited. A case in point is the design of an espresso machine (see Example 18.2). Product attributes such as odor intensity, flavor intensity, body, acidity, and aftertaste intensity are hard to quantify. Although it is known that these attributes depend on influencing factors, such as water temperature and pressure, the evenness of the packed ground coffee, water quality, and time of extraction, a model based on transport phenomena is unlikely to deliver accurate performance predictions. It is easier to develop a black-box model that correlates the responses of a panel of judges with the influencing factors. Many black-box models exist, and the design of experiments to obtain model parameters efficiently is a well-developed science (Dreyfus, 2005; Anderson and Whitcomb, 2007).

Simplified models may not be very accurate because some secondary physicochemical phenomena involved may be ignored. However, by accounting for the dominant mechanisms, a simplified model can be expected to capture the correct dependence of product performance on the influencing factors, thus reducing tremendously the required amount of experimental work. Consider a familiar example in simple binary distillation. The reflux ratio and number of equilibrium stages are determined using the vapor–liquid equilibrium curve in the McCabe–Thiele diagram. Although the calculated number of stages is not exact without considering mass transfer, the simple analysis provides a lower bound for the actual number of stages required for the specified separation.

When the underlying physics and chemistry are perfectly understood, rigorous modeling can account for most, if not all, of the product features and physicochemical phenomena involved. Models obtained this way are predictive, and experimental data are only needed for verification purposes. However, one has to be aware of unknown model parameters in these supposedly rigorous models. Because the secondary phenomena and effects are accounted for in such models, the number of unknown model parameters is bound to increase. Again, using binary distillation as an example, parameters such as mass-transfer coefficients and vapor–liquid interfacial area may be required in an analysis of the transport processes at each stage of a distillation column. Because these parameters often are not as exact as may be desired, the predictions of a rigorous model share the same degree of uncertainty of the model parameters.

The design procedure is illustrated next with two examples. The use of simplified models is emphasized in this chapter for pedagogical reasons. We focus on the product design procedure using only the key mechanisms. This does not imply that black-box and rigorous models, which are constructed with experimental data and advanced modeling, respectively, are not important.

EXAMPLE 5.1 *Air Purifier*

A home appliance company plans to produce an air purifier to remove indoor VOCs. As a measure of product performance, it is expected to reduce the concentration of VOCs from 150 mg/m^3 to 30 mg/m^3 in a room 200 m^3 in size within two hours.

SOLUTION

The four-step design procedure for chemical devices is as follows:

Step 1: VOCs are made up of different compounds such as acetone, benzene, toluene, and methylene chloride. As a starting point, toluene is used as the reference compound for quantifying the product performance as stated above.

Step 2: Indoor VOCs can be treated by adsorption, absorption, or photocatalytic oxidation (PCO). Because only PCO is capable of decomposing instead of just capturing VOCs, it is selected for this product. Among the various PCO catalysts, TiO_2 is the most widely used because of its reasonable price, plentiful supply, high photoactivity under UV irradiation, and capability of adsorbing the reactants. The catalyst can be deposited on any catalyst support such as carbon, alumina, and silica to obtain a high surface area.

The choice of the support and the structure, form, shape, or configuration of the product is considered next. The potential design must (1) provide intimate contact between the catalyst and the air flow with the VOCs, (2) allow sufficient and relatively uniform illumination on the catalyst, and (3) be compact, taking up as little space as possible. After careful deliberations, it is decided that a commercially available Platinum-doped TiO_2 catalyst be impregnated on a HEPA filter, which is a highly porous mat made up of randomly oriented synthetic fibers. Three of the product alternatives are shown in Figure 5.8.

In Figure 5.8a, the UV lamp is placed in front of the curved catalyst-coated HEPA filter. Air flowing through the filter allows close contact between the catalyst and the VOCs. The alternative in Figure 5.8b with a UV lamp at the center of a cylindrical HEPA filter is more compact. Air is forced to flow through the wall coated with catalyst. In Figure 5.8c, the contact area can be further increased without increasing the volume by having a folded cylindrical filter. Although the light intensity on the catalyst is less uniform in this case, particularly at the point farthest from the UV lamp, the relatively small difference in light intensity is not expected to significantly affect the catalytic reaction.

Step 3: The decomposition of VOCs on the surface of TiO_2 proceeds via several steps as illustrated in Figure 5.9. Electron-hole pairs are first generated by irradiating the TiO_2 with light having an energy level higher than the band gap energy of 3.026 eV. The electron-hole pair is separated by forming a hydroxyl radical (·OH) with adsorbed H_2O. Then, redox reactions take place between ·OH and adsorbed VOC.

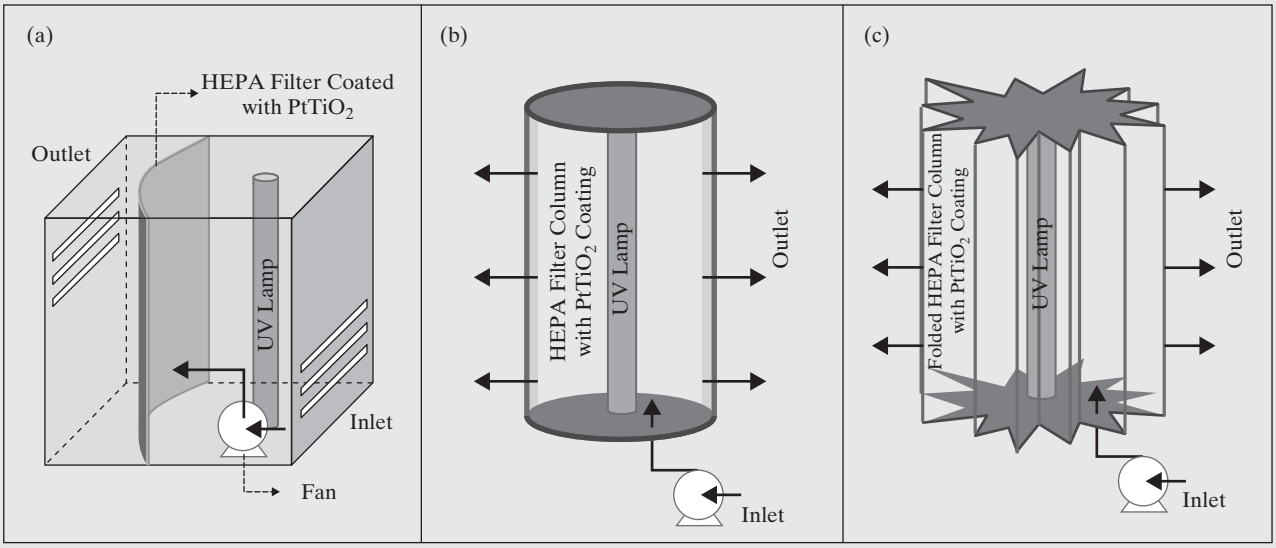

Figure 5.8 Alternative product configurations of an air purifier.

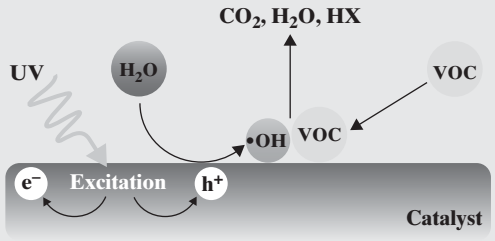

Figure 5.9 Photocatalytic oxidation of VOCs on TiO_2 surface.

The last step is desorption of reaction products, such as CO_2, water, and hydrogen halides (HX) and reconstruction of the surface.

Langmuir–Hinshelwood kinetics can be used to model the PCO reaction. The adsorption and desorption of both reactants and products are sufficiently fast as to be in equilibrium. The surface reaction of adsorbed reactants is the rate-determining step.

Step 4: No matter which product configuration is to be used, the total amount of TiO_2 coating needs to be determined to achieve the target of reducing toluene concentration from 150 mg/m^3 to 30 mg/m^3 within two hours in a 200 m^3 room. Assuming that the air in the room is perfectly mixed as a first approximation, the mass balance of toluene can be written as:

$$V_r \frac{d[C]}{dt} = r_T V_{cat} \tag{5.1}$$

where V_r and V_{cat} are the volume of the room and catalyst, respectively, $[C]$ is the toluene concentration in the air, and r_T is the rate of decomposition of toluene on the TiO_2 coating. Note that the rate of reaction depends only on $[C]$ because the catalytic coating is sufficiently thin and the temperature, pressure, reactant concentration, and light intensity across the coating are sufficiently uniform.

The bimolecular reaction of toluene and water on the catalyst surface is given by

$$r_T = -k\theta_T\theta_W \tag{5.2}$$

where k is the surface reaction rate constant, and θ_T and θ_W are the fractional coverage of the adsorption sites for toluene and H_2O, respectively. Since H_2O is in abundance and has strong interaction with the UV-excited TiO_2 surface, we can assume $\theta_W = 1$. According to the Langmuir isotherm, when the rate of adsorption equals the rate of desorption, we have

$$K_T(1 - \theta_T)[C] = \theta_T \tag{5.3}$$

where K_T, the ratio of the adsorption rate constant to the desorption rate constant, is the adsorption equilibrium constant for toluene. Solving Eq. (5.3) for θ_T and substituting it into Eq. (5.2) gives

$$r_T = \frac{-kK_T[C]}{1 + K_T[C]} \tag{5.4}$$

Substituting Eq. (5.4) into Eq. (5.1) and integrating t from $t_0 = 0$ to t_f gives

$$t_f = -\frac{\ln([C_f]/[C_0]) + K_T([C_f] - [C_0])}{kK_T(V_{cat}/V_r)} \tag{5.5}$$

where t_f is the total reaction time and $[C_0]$ and $[C_f]$ are the initial and final concentration of toluene, respectively.

According to Sanongraj et al. (2007), the surface reaction rate constant for toluene can be expressed as follows.

$$k = K_m(K_3 + K_4[C_0] + K_6[C_0]^2)(K_5 + K_2RH) \tag{5.6}$$

where K_m, K_2, K_3, K_4, K_5, and K_6 are regressed parameters and RH is the relative humidity of the air. The following table shows the values of regressed parameters for toluene degradation experiments conducted using Degussa-$PtTiO_2$-350 catalyst. The relative humidity was varied between 14 and 82%, the UVC (254 nm) light intensity was 2.2 mW/cm^2 with a $[C_0]$ value of around 150 mg/m^3 and catalyst thickness of 57.6 μm.

K_m (mg/m^3.min)	K_T (m^3/mg)	K_2	K_3	K_4 (m^3/mg)	K_5	K_6 (m^3/mg)^2
5.78	0.0189	−14.599	183873.42	−3033.00	1614.37	13.1871

If the working conditions for the air purifier are assumed to be the same as those stated above and the RH is 50%, k equals 238,103,199.5 $mg/(m^3.min)$ according to Eq. (5.6). Since 200 m^3 air needs to be cleaned within two hours (i.e., $t_f \le 2$ hr, and $V_r = 200$ m^3). Substituting k and K_T into Eq. (5.5), we get

$$t_f = -\frac{ln\frac{30}{150} + 0.0189\frac{m^3}{mg} \times (30 - 150)\frac{mg}{m^3}}{238{,}103{,}199.5\frac{mg}{m^3 \cdot min} \times 0.0189\frac{m^3}{mg}} \times \frac{200\ m^3}{V_{Cat}} \le 2\,hr \tag{5.7}$$

or $V_{cat} \ge 1.436 \times 10^{-6}$ m^3.

For any of the product configurations shown in Figure 5.8, if a HEPA filter area of 0.1 m^2 is assumed, the thickness of the catalyst coating, s, is given by

$$s \ge \frac{V_{cat}}{0.1\ m^2} = \frac{1.436 \times 10^{-6} m^3}{0.1\ m^2} = 14.4\ \mu m \tag{5.8}$$

If it is further assumed that the product configuration in Figure 5.8b is selected and that the inner diameter of the cylindrical HEPA filter is 10 cm, the length would be 32 cm.

According to Beer's law, the light intensity (I) at a certain depth (z) of the catalyst coating is

$$I = I_0 e^{-\varepsilon z \rho_b} \tag{5.9}$$

where I_0 is the light intensity at the surface, ε is the UV light absorption coefficient of the catalyst, and ρ_b is the bulk density of the catalyst. For the $PtTiO_2$ coating on the HEPA filter, $\varepsilon = 0.0386$ cm^2/g and $\rho_b = 3.56$ mg/cm^3 (Sanongraj et al., 2007). Therefore, with the surface illumination of $I_0 = 2.2$ mW/cm^2, the intensity at the back of the catalyst coating is

$$I_{14.4\,\mu m} = I_0 e^{-0.0386\ \frac{cm^2}{g} \times 0.0015\ cm \times 3.56\ \frac{mg}{cm^3}} \approx I_0 \tag{5.10}$$

which suggests negligible light attenuation for a 14.4 μm thick $PtTiO_2$ catalyst coating and the assumption of a uniform rate of toluene decomposition r_T in Eq. (5.1) is valid.

Many other design issues need to be considered. For example, air-borne particulates can clog up the coated HEPA filter. Thus, a prefilter that can be replaced periodically should be installed. Eq. (5.1) has assumed that the air in the room is perfectly mixed. Although this is not possible in reality, the fan still has to be sized to afford reasonably high air circulation rate. Obviously, toluene does not represent all possible VOC species in a household and other compounds such as ethanol, a polar compound, should be considered. Sensitivity analysis of the impact of model parameters on product performance should be performed to better understand how the product performs under different conditions. For example, the relative humidity can be in the 90s in a hot summer day and 50s in a dry winter day. The correlating parameters should not be used outside of the range of original experimental conditions. For example, the sensitivity analysis should be within the relative humidity range of 14–82%.

After performing a conceptual product design, it is highly desirable to create a prototype air purifier, which serves a number of purposes. It validates the model predictions of product performance. It ensures that the technical team begins to think in detail of the manufacturing steps, the sources of raw materials, and the product cost. Most importantly, it reassures the senior management or investors that the product design is no longer a paper exercise.

EXAMPLE 5.2 ***Controlled-release Herbicide***

Herbicides such as 2,4-dichlorophenoxyacetic acid (2,4-D) are commonly used for killing unwanted broadleaf weeds while leaving the desired crop (usually grass) to grow unmolested. However, herbicides spread on soil are easily lost due to leaching, volatilization, or biodegradation. Only a portion of the herbicide is used in killing weeds. An agrochemical company wants to develop a controlled-release granule with the active ingredient uniformly dispersed within a polymeric matrix (Figure 5.10). The controlled-release granule should release the herbicide at a fast rate at the beginning to kill weeds quickly and at a lower rate thereafter to retard the regrowth of the weeds for a long period of time.

SOLUTION

The four-step design procedure for functional products is as follows:

Step 1: Based on experimental tests, it is decided that the controlled-release granules should deliver 0.5–2 mg/m^2 day of the herbicide from days 1 to 10, followed by a lower dose of 0.1–0.5 mg/m^2 day from days 11 to 90. Thus, a total maximum amount of around 60 mg of herbicide should be applied to 1 m^2 of soil. These product attributes can be obtained by varying the granule size, the granule material, and the concentration of herbicide within the granule.

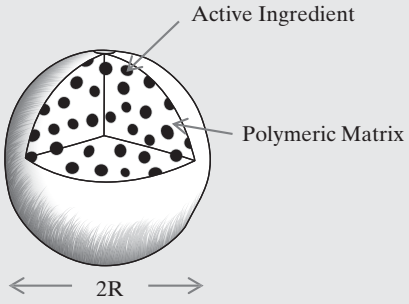

Figure 5.10 Active ingredient dispersed in a polymeric matrix in controlled-release herbicide.

Step 2: Cellulose and lignin are commonly used in the formulation of controlled-release herbicides. The polymer matrix controls the release rate of herbicide from the granules.

Step 3: The release of herbicide from the granules is controlled by two different mechanisms: the dissolution/degradation of the granule and the diffusion of herbicide within the granule. For cellulose granules, the release profile is controlled by the dissolution rate of cellulose in soil because the dissolution rate of cellulose in water is fast compared with the diffusion rate of herbicide. Although lignin is biodegradable, its degradation rate is slow, and the release profile is controlled by the diffusion rate of herbicide within the granule.

Step 4 **Dissolution of Cellulose Matrix:** The rate of herbicide release from the granule depends on the dissolution rate of cellulose, which is linearly dependent on the surface area of the granule,

$$\frac{dM_c}{dt} = 4\pi k_0 r^2 \tag{5.11}$$

where M_c is the mass of cellulose, k_0 is the dissolution rate constant, and r is the radius of the granule at time t. The amount of dissolved cellulose, M_{cd}, can be obtained by mass balance:

$$M_{cd} = \frac{4\pi\rho x_c}{3}(R^3 - r^3) \tag{5.12}$$

where ρ is particle density, x_c is the weight fraction of cellulose, and R is the initial radius of the granule. Integrating Eq. (5.11) over time after substituting M_c into it gives

$$r = R - \frac{k_0}{\rho x_c} t \tag{5.13}$$

Because the herbicide is dispersed uniformly in the matrix, the cumulative amount of herbicide released from the granule, M_h, can be obtained by replacing x_c by x_h, the weight fraction of herbicide in the granule, and substituting r from Eq. (5.13) into Eq. (5.12),

$$M_h = \frac{4\pi\rho x_h}{3}\left(R^3 - \left(R - \frac{k_0}{\rho x_c} t\right)^3\right) \tag{5.14}$$

The dissolution rate constant of cellulose is approximately 1×10^{-6} kg/m^2s (Katzhendler et al., 1997). Figure 5.11 illustrates the herbicide release profile for granules with a particle density of 2,000 kg/m^3 and an herbicide mass fraction of 0.1. It shows that all herbicide release profiles do not meet the desired product performance. The amount of herbicide released is too much during the first few days of application and the release can only be sustained for less than 25 days.

Herbicide Diffusion in Lignin Matrix: Because a lignin granule degrades very slowly, the release of herbicide occurs by diffusion from the interior of a granule into the soil followed by diffusion to the surroundings. Diffusion within a spherical granule, the rate-determining step, can be modeled using Fick's second law,

$$\frac{\partial C}{\partial t} = \frac{D}{r^2}\frac{\partial}{\partial r}\left(r^2 \frac{\partial C}{\partial r}\right) \tag{5.15}$$

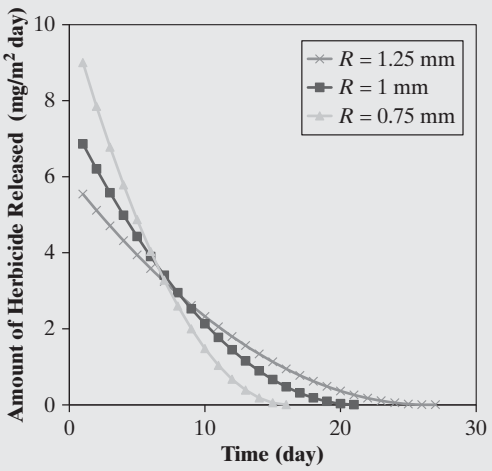

Figure 5.11 Herbicide release profile for different sizes of granules with cellulose as the polymeric matrix.

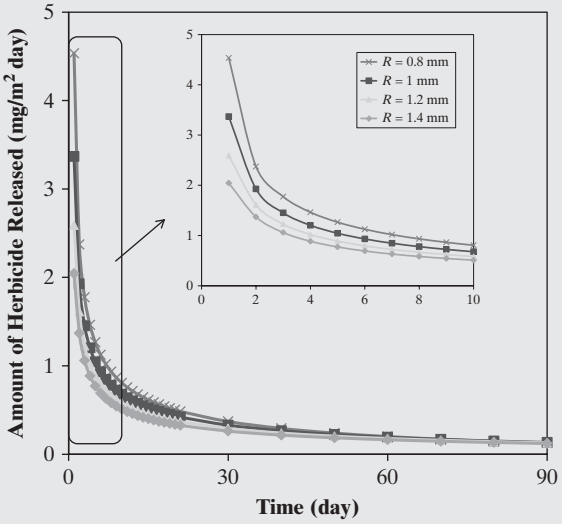

Figure 5.12 Herbicide release profile with a lignin matrix.

with the following initial and boundary conditions:

$$\begin{aligned} &0 \le r \le R;\ C = C_0 && at\ \ t = 0 \\ &r = R;\ C = C_s && for\ t > 0 \\ &r = 0;\ C = finite && for\ t > 0 \end{aligned} \tag{5.16}$$

where C is the concentration of herbicide in the granule, D is the diffusion coefficient, and C_s is the concentration of the herbicide on the surface of the granule. Solution of Eq. (5.15) gives

$$\frac{C - C_s}{C_s - C_0} = \frac{2R}{\pi r} \sum_{m=1}^{\infty} \left[\frac{(-1)^m}{m} \sin \frac{m\pi r}{R} \exp\left(-\frac{m^2 \pi^2 Dt}{R^2} \right) \right] \tag{5.17}$$

The cumulative amount of herbicide released at time t is given by

$$\begin{aligned} M_h &= -\int_0^t AD \left. \frac{\partial C}{\partial r} \right|_{r=R} dt \\ &= \frac{8R^3 (C_s - C_0)}{\pi} \sum_{m=1}^{\infty} \left[\frac{1}{m^2} \left(\exp\left(-\frac{m^2 \pi^2 Dt}{R^2} \right) - 1 \right) \right] \end{aligned} \tag{5.18}$$

where A is the surface area of the granule. The diffusion coefficient in lignin is assumed to be 1×10^{-10} cm^2/s (Pereira et al., 2002), and C_s is assumed to be the same as the herbicide concentration in the soil, which is kept at around 2 ppm to be effective (Xin et al., 2012). Figure 5.12 shows the herbicide release profile for different sizes of granules with an initial herbicide concentration of 200 kg/m^3. It clearly shows that the 1.4-mm granules with lignin matrix provide a higher dosage (0.5–2 mg/m^2 day) in the first 10 days and a lower dosage (0.1–0.5 mg/m^2 day) in the next 80 days, meeting the specified product performance. Smaller granules release too much herbicide in the first 10 days.

5.3 DESIGN OF FORMULATED PRODUCTS

Many formulated products are developed through trial-and-error experiments by specialists with extensive experience in producing the type of products under consideration. For example, an inkjet ink formulation specialist would have most of the key ingredients, typical solvents and dispersants, in the laboratory. For a new application, it is just a matter of mixing the several selected ingredients to form a mixture and adjusting its composition to obtain the desired properties such as viscosity, drying rate, and surface tension. This approach, however, is not possible for engineers with limited experience in formulating such a product. Another example is a skin-care cream that offers sunscreening, antioxidant, and moisturizing functions. Formulating such a product by iteration is challenging because it has a large number of ingredients including zinc oxide nanoparticles, emollients, emulsifiers, humectants, stabilizers, film formers, and preservatives. Another complicating factor is that some of the formulated products, such as an emulsified hand lotion, have a microstructure that affects their properties. Also, while trial-and-error might work for products that do not deviate much from existing products, the search space for novel products with new ingredients can be vast, and design by experimental iteration becomes a daunting task. The following integrated experiment-modeling procedure that helps alleviate the problems identified above can be used for the design of formulated products:

1. Collect the relevant knowledge and experiences in terms of basic scientific understanding, typical ingredients and the selection criteria, heuristics, mechanistic models, empirical correlations, computer-aided tools, and a causal table. All of this information required is self-explanatory except the *causal table,* which shows how a specific product attribute can be adjusted by changing the amount of an ingredient or the manufacturing process.

2. Convert consumer preferences into quantitative and measurable technical requirements, focusing especially on those that are perceived to be *critical to quality* (CTQ) of the product.
3. Generate a base-case formula. This can be obtained from the open literature, the database within the company, or calculations using computer-aided tools.
4. Verify the predicted physicochemical properties with experiments if necessary. Measure by experiments those properties that cannot be predicted accurately.
5. Perform experimental iteration guided by a causal table until the desired product attributes are achieved.

This procedure is illustrated with two examples. Example 5.3 shows the conventional procedure where the product is designed based on experimental trial and error.

About Formulation of Skin Creams

A skin cream is an emulsion made up of an aqueous phase and an oleic phase. Emulsions are created using emulsifiers, which are surfactant molecules with a hydrophilic (water-loving) portion and a lipophilic (oil-loving) portion. Often, one phase is dispersed in the form of emulsion droplets in the other phase with the emulsifiers at the interface of the two phases. When the aqueous phase is dispersed in the continuous oleic phase, a water-in-oil (W/O) emulsion is formed and vice versa. Oil-in-water (O/W) emulsions are common in food; examples are homogenized milk, mayonnaise, and vinaigrette. W/O emulsions are less common in food with butter, an emulsion of water in butterfat begin an example. A W/O emulsion is preferred if the product should not dissolve readily in water. An O/W emulsion with water being the continuous phase is chosen when nonstickiness on application to the skin is desired. There are many components in a skin cream distributed between the two phases. A major fraction is made up of emollients that are oleic compounds that keep the skin moist. The stability of the emulsion can be enhanced by using stabilizers (e.g., emulsifiers) to increase the repulsion between the emulsion droplets. Neutralizers are used to bring the pH of the skin cream to a desired value of around 5.5. A humectant is a hydroscopic substance that prevents the skin cream from drying out. Thickeners are substances that increase the viscosity of the cream without substantially modifying cream's other properties. The film formers promote the formation of a uniform film of the cream on the skin.

The hydrophilic-lipophilic balance (HLB) method is used to select nonionic emulsifiers (i.e., emulsifiers that do not form ions) for an oil phase consisting of several components. To select the suitable emulsifiers, we look for a mixture of emulsifiers that has an HLB value matching the HLB value of the oil phase.

The HLB of the oil phase is calculated as follows:

$$HLB_{\text{required}} = \sum w_i HLB_i \tag{5.19}$$

where w_i and HLB_i refer to the weight fraction of component i and the HLB value. The HLB values of some common emollients can be found in catalogs provided by suppliers and in the literature. The HLB value for a mixture of emulsifiers can be calculated in a similar manner by adding up the individual emulsifier's HLB values after weighting by the respective weight fractions. The HLB value of an emulsifier is also available in the literature and quantifies its relative hydrophilic and hydrophobic tendencies. A high HLB value indicates a more water soluble emulsifier, and a low HLB value indicates one that is more oil soluble. An HLB value between 12 and 16 (7 and 11) is suitable for making O/W (W/O) emulsions.

Whether a cream feels smooth or not depends on its rheological properties. A cream with shear thinning behavior (i.e., its viscosity decreases with increasing shear rate) is preferred. Theoretical and semiempirical models have been proposed to predict the rheological properties of an emulsion with different emulsion droplet sizes.

EXAMPLE 5.3 ***Sunscreen Cream (Wibowo and Ng, 2001; Cheng et al., 2009)***

A cosmetic company wants to produce a skin-care cream with three functions. The primary function is to keep the skin in a moisturized condition. Another is to block UV light, which is known to stimulate the production of reactive oxygen species (ROS) in skin cells, causing skin aging. Zinc oxide is the material of choice because, in addition to absorbing UV light, sufficiently small zinc oxide particles are transparent although large zinc oxide particles are white under visible light. The third function is to supplement the skin with an herbal antioxidant to ameliorate UV-induced skin damage. In addition, the product should be smooth, nonirritating to the skin, stable, and not feel oily or greasy. The product should not run after application. A brief introduction to skin creams is given in the box About Formulation of Skin Creams for readers unfamiliar with these products.

SOLUTION

The five-step design procedure for formulated products is as follows:

Step 1: There is an enormous amount of information on all aspects of skin-care products in the literature (Rähse, 2013). Table 5.2 shows some typical ingredients for skin-care cream with their recommended concentrations and selection criteria. Zinc oxide is not included in the table because it is only used for sunscreen lotions. It is common practice for experienced formulators to compile their own short list. The choice is also affected by other factors such as availability in the market, regulatory control, and cost of materials.

The Herschel–Bulkley model exhibits shear-thinning behavior when n < 1:

$$\mu = \frac{\tau_o}{\dot{\gamma}} + K\dot{\gamma}^{n-1} \tag{5.20}$$

Here, τ_o and K are model parameters, and $\dot{\gamma}$ is the shear rate. The Oldroyd model, which is applicable for dilute emulsions with a dispersed phase volume fraction (ϕ) less than 0.7, expresses the viscosity of the emulsion (μ_e) as a function of ϕ, the viscosity of the continuous phase (μ_c), the viscosity ratio (κ) (that is, the viscosity

Table 5.2 Ingredients for a Cream and the Corresponding Selection Criteria

Ingredients	Examples	Suggested Concentration (wt%)	Selection Criteria and Considerations
Emollient [HLB value]	*Synthetic oils:* Caprylic/Capric triglyceride [5], C_{12}-C_{15} alkyl benzoate [13] *Natural oils:* Sunflower oil [7], sweet almond oil [7], coconut oil [8] *Silicone oils:* Cyclomethicone [5], dimethicone [5]	10–40	• Natural oils are usually more acceptable to the consumers. • Silicone oils are nonsticky and highly spreadable. Their water repellent properties are good for waterproof sunblock creams.
Emulsifier [HLB value]	Steareth-2 [4.9], oleth-20 [15], glyceryl stearate [3.8], PEG-100 stearate [16], Polysorbate 20 [16.7]	1–6	• Nonionic emulsifiers are preferred in skin-care products.
Stabilizer	Sodium chloride, EDTA disodium salt dihydrate	0.01–0.2	—
Neutralizer	Triethanolamine, citric acid	0.01–0.5	—
Humectant	Glycerol, propylene glycol, butylene glycol, sorbitol	1–5	• Materials with low freezing point are preferred.
Film former	PVP/dimethylaminoethyl-methacrylate copolymer, PVP/hexadecene copolymer, aloe vera	0.1–2.5	• Film formers can increase film thickness and water resistance but also leave a sticky feel.
Thickener	Carbomers, xanthan gum, carboxymethyl cellulose	0.1–0.5	• Carbomers show thickening function in the pH range of 5–9.
Preservative	Tocopheryl, diazolidinyl urea, iodopropynyl butylcarbamate, methylparaben, propylparaben	0.01–0.5	—

of the dispersed phase to that of the continuous phase), and the capillary number N_{Ca}:

$$\mu_e = \mu_c \left[1 + \frac{(5\kappa+2)}{2(\kappa+1)}\phi + \frac{(5\kappa+2)^2}{10(\kappa+1)^2}\phi^2\right]\left[\frac{1+\lambda_1\lambda_2 N_{Ca}^2}{1+\lambda_1^2 N_{Ca}^2}\right] \tag{5.21}$$

where

$$\lambda_1 = \frac{(19\kappa+16)(2\kappa+3)}{40(\kappa+1)}\left[1 + \frac{(19\kappa+16)}{5(\kappa+1)(2\kappa+3)}\phi\right]$$

$$\lambda_2 = \frac{(19\kappa+16)(2\kappa+3)}{40(\kappa+1)}\left[1 - \frac{3\,(19\kappa+6)}{10(\kappa+1)(2\kappa+3)}\phi\right]$$

$$N_{Ca} = \frac{\mu_c d_p \dot{\gamma}}{2\sigma}$$

Here, d_p is emulsion droplet size, and σ is interfacial tension.

Heuristics are derived from experience but are often based on sound scientific rationales. Table 5.3 shows the heuristics that are useful for designing creams. Heuristics also help relate sensorial attributes described in qualitative terms such as "spreadable," to technical requirements.

In experimental iterations to determine the product formula, one or more of the product attributes often do not meet the required product attributes. Table 5.4 shows the causal table that suggests the necessary changes in ingredients or processing conditions that would nudge the product attributes toward the target attributes.

Table 5.3 Selected Heuristics for Lotions and Creams

- Use O/W emulsion if the product should not feel greasy.
- Use W/O emulsion if the product should be resistant to washing and/or perspiration.
- Prefer a product showing shear-thinning behavior if the product should be thick at rest but spread easily upon shearing.
- Aim for a viscosity of 20–100 Pa·s at rest and 0.025 Pa·s at an application shear rate of 1,000 s^{-1} to obtain the best consumer acceptance.
- A mixture of emulsifiers with high and low HLB values gives better stability results than a single emulsifier with the exact required HLB value.

Step 2: The emulsion particle size is reduced to below 5 μm to obtain a smooth cream. The pH is kept at or below around 7 so that it does not irritate the skin. To avoid an oily or greasy feel, an O/W emulsion is chosen. The viscosity should be around 0.025 Pa·s at application shear rate and around 20 Pa·s to avoid appearing runny.

Step 3: The fourth column of Table 5.5 shows the base-case formula (Prototype 1) obtained based on experience. Note that some of the ingredients go by their trade names because they are actually a mixture of compounds. For example,

Table 5.4 Causal Table for Improving Lotion and Cream Formulation Based on Test Results

Test Results	Adjustments
Emulsion cannot form instantaneously	• Adjust concentrations of emulsifiers. • Consider using different emulsifiers.
Too viscous	• Reduce thickener concentration. • Consider another thickener.
Not viscous enough	• Increase thickener concentration. • Consider another thickener or a mixture of thickeners.
Greasy	• Reduce emollient concentration. • Change emollients.
Not smooth enough	• Reduce droplet size by increasing the number of cycles and pressure of the homogenizer. • Adjust the emulsion viscosity.
Sticky	• Reduce emollient concentration. • Reduce film former concentration. • Change emollients.
pH too high	• Add acidic pH controlling compound such as citric acid.
pH too low	• Add alkaline pH controlling compound such as triethanolamine.
Emulsion not stable	• Consider other emulsifiers.

Liquid Germall® Plus is a combination of diazolidinyl urea, iodopropynyl butylcarbamate, and propylene glycol. The two key ingredients are two types of zinc oxide particles that are suspended in various organic solvents and an herbal extract. Because a market survey indicates that consumers prefer natural ingredients, sunflower oil, and sweet almond oil were selected as emollients for this product. A silicone oil, dimethicone, was chosen due to its nonsticky, highly spreadable, and water-repellent properties. Polyvinylpyrrolidone (PVP)/dimethylaminoethylmethacrylate copolymer was used to promote the formation of a uniform sunscreen film on the skin. Carbomers and xanthan gum were selected as thickeners, again on the basis of common usage. Glycerol and propylene glycol were chosen as humectants. Ethylenediaminetetraacetic acid (EDTA) disodium salt dihydrate was used as a stabilizer and Liquid Germall® Plus as a preservative. Their compositions were selected based on the suggested concentrations in Table 5.2.

The emulsifiers were selected based on the HLB method. One common practical problem was the fact that the HLB values of some ingredients such as the herbal extract were unknown. It was decided that the values could be ignored at this stage and, the required HLB was found to be around 10 using Eq. (5.19) based on the ZnO suspensions, C12-15 alkyl benzoate, sunflower oil, sweet almond oil, and dimethicone. As pointed out in Table 5.3, experience shows that a mixture of two emulsifiers with high and low HLB values that bracket the required oil HLB would give better stability than a single emulsifier having the same HLB value. Thus, 2.5% of steareth-2 and 2.5% of oleth-20 with HLB values of 4.9 and 15, respectively, were mixed to provide an HLB value of 9.95 to match the required HLB of the oil mixture. The formulator should be aware of the limitations of all design methods. Note that the HLB method provides only the relative amounts of emulsifiers; it does not indicate the amount of each emulsifier required. The emulsifier concentration was estimated again based on the suggested concentrations in Table 5.2. In addition, many other factors such as the compatibility of ingredients, the viscosity of the continuous phase, and so on might affect emulsion formation and stability.

Step 4: A panel of judges found that the emulsion produced by mixing the ingredients has acceptable softness and a nongreasy feel. The average emulsion droplet size was experimentally determined to be around 1.4 μm. Using the Oldroyd model [Eq. (5.21)], the dependence of viscosity on microstructure was estimated. It was found that the droplet size and phase volume fraction had little effect on the emulsion viscosity. Therefore, the selection of their values should rather be based on other considerations such as smoothness and stability. The viscosity at a shear rate of 1,000 s^{-1} was estimated using Eq. (5.20) to be around 0.014 Pa·s, which was close to the desired value (Table 5.3). Some characteristics of Prototype 1 were determined. It was felt that the cream was sticky after application on the skin and appeared runny on standing. Most importantly, the cream was unstable.

Step 5: The last two columns of Table 5.5 show the characteristics of Prototype 2 and Prototype 3, respectively. To remove the sticky feel, the amount of film former was reduced to zero in Prototype 2. The amount of carbomer was increased to 0.35wt% to improve the cream viscosity. To improve stability of Prototype 1, Steareth-2 and oleth-20 were replaced by Polysorbate 20 and GMS 165. A solid emollient, cocoa butter, was added to obtain a final HLB value of 11.7 for Prototype 2. To further increase the viscosity of Prototype 3, xantham gum was used along with carbomer for a total thickener concentration of 0.55wt%. This resulted in a viscosity of 15.2 Pa·s, which was within the acceptable range albeit still on the low side. The stability was also improved by adding steareth-2 back in. The pH was on the high side but could be easily adjusted using a neutralizer. The cream texture was acceptable, and it was shown to be stable for a period of more than three years. Prototypes were further optimized, but the details are omitted here.

Table 5.5 The Evolution of the Skin-care Cream Formula during Product Design

			Prototype 1	Prototype 2	Prototype 3
	HLB Value	Ingredient Type	wt%		
Oil Phase					
ZnO particles (Type 1)	5	Sunblock agent	4	4	4
ZnO particles (Type 2)	13	Sunblock agent	12	12	12
Herbal extract	—	Antioxidant	2	2	2
C12-15 alkyl benzoate	13	Emollient	1	2	2
Sunflower oil	7	Emollient	1	0.5	0.5
Sweet almond oil	7	Emollient	1	0.5	0.5
Cetyl alcohol	15.5	Coemulsifier/opacifier	1	1.5	1.5
Dimethicone	4	Emollient	2	2	2
Cocoa butter	11.5	Emollient	—	1	2
Polysorbate 20	16.7	Emulsifier	—	0.16	0.82
GMS 165 (PEG-100 stearate and Glyceryl stearate)	11	Emulsifier	—	4.84	4
Steareth-2	4.9	Emulsifier	2.5	—	0.18
Oleth-20	15	Emulsifier	2.5	—	—
Polyvinylpyrrolidone/ dimethylaminoethyl-methacrylate copolymer	—	Film former	0.2	—	—
Aqueous Phase					
Carbomer	—	Thickener	0.14	0.35	0.35
Xanthan gum	—	Thickener	—	—	0.2
Glycerol	—	Humectant	3	3	3
Propylene glycol	—	Humectant	2	2	2
EDTA disodium salt dihydrate	—	Stabilizer	0.2	0.1	0.1
Triethanolamine	—	Neutralizer	0.1	0.1	0.2
Water	—	—	Balance	Balance	Balance
Preservative Phase					
Liquid Germall® Plus	—	Preservatives	0.7	0.7	0.7
Emulsion Characteristics					
UV blocking			—	—	OK
Transparency			—	—	OK
Antioxidant activity					OK
pH			7.5–8.0	7.5–8.0	7.5–8.0
Viscosity at 0.01 s^{-1} (Pa·s)			2.14	5.09	15.2
Viscosity at 1,000 s^{-1} (Pa·s)			0.014	0.015	0.018
Average droplet size (μm)			1.4	1.4	1.4
Stickiness			Sticky	Nonsticky	Nonsticky
Stability			Phase separation	Slight phase separation	Stable

Product formulation by experimental trial and error is time-consuming. By relating the properties of pure compounds and/or blends to the molecular structures, the computer-aided design tools discussed in Chapter 4 can reduce the search space for the suitable ingredients and identify molecules that are not in the specialist's existing recipes (Mattei et al., 2014). Then, experiments are used to verify the predicted values and to determine properties such as touch and feel that cannot be predicted with models. The procedure for this integrated experiment–modeling approach is illustrated with an example next.

EXAMPLE 5.4 ***Insect Repellent Spray (Source: Conte et al., 2011, 2012. Used with permission).***

A consumer goods company wants to produce an insect repellent spray with the following characteristics: high effectiveness against mosquitoes, a water-based spray, pleasant scent, long durability, low toxicity, high stability, spray-ability, low price, and long shelf life.

SOLUTION

The five-step design procedure for formulated products is as follows:

Step 1: Effective active ingredients for repelling mosquitoes such as DEET and Picaridin are readily available. The marketing team decided on Picaridin because of its overall quality. However, the predicted solubility of Picaridin in water at 0.0086 g/cm^3 is rather low. Although water is the preferred solvent because of its safety and low cost, a water-organic solvent mixture has to be used to dissolve Picaridin. Such a solvent mixture can be designed using the computer-aided tools for mixture-blend design (CAM^{b}D) discussed in Chapter 4. The scent of the product can be improved by adding a perfume. Toxicity data are available in MSDS data sheets.

Step 2: The durability of the product is related to the evaporation time T_{90}, which is the time for evaporating 90 wt% of the solvent. The toxicity is related to the parameter LC_{50}, which is the concentration that kills 50% population of a test animal in a specified period of time. The stability of the product is related to the possibility of phase separation and can be controlled through the Hildebrand solubility parameter δ. The spray-ability depends on the kinematic viscosity ν and density ρ (or molar volume V_m) of the solvent mixture. Table 5.6 shows the desired lower and upper constraint values of the target properties described above. It was suggested that the evaporation time falls between 500 s and, 1500 s. The lethal concentration of the solvent mixtures [given in terms of $-log_{10}(LC_{50})$] is higher than 390 mol/m^3. The EPA reported no evidence for Picaridin toxicity to humans (EPA, 2005). The solubility parameter of the solvent mixture and that of the organic solvent should be close $\left(\pm 3 \text{ MPa}^{1/2}\right)$ to the solubility parameter of Picaridin, which has a value of 24.1 MPa$^{1/2}$. The viscosity and density of the solvent mixture have to be sufficiently low.

Table 5.6 Target Property Constraints for the Insect Repellent Spray

500	<	T_{90}	<	1,500 s
390	<	$-log_{10}(LC_{50})$	<	$+\infty$ mol/m^3
21.1	<	δ	<	27.1 Mpa$^{1/2}$
0	<	ν	<	75 cS
20.0	<	V_m	<	70.0 L/kmol

Step 3: The base case was identified by screening different alcohol–water mixtures that obey the constraints in Table 5.6. The properties of eight mixtures are given in Table 5.7 where the solvent mixtures are listed in terms of increasing cost. Note that mixtures 4, 6, and 7 showing a phase split were rejected.

It was suggested that the solubility parameter of the organic solvent be close $\left(\pm 3 \text{ MPa}^{1/2}\right)$ to the solubility parameter of Picaridin. Because the Hildebrand solubility parameter values for methanol and allyl alcohol (29.6 and 27.5 MPa$^{1/2}$, respectively) are higher than the upper bound value of 27.1 MPa$^{1/2}$, mixtures 1 and 3 were rejected as well.

Steps 4 and 5: Of the remaining three mixtures (mixtures 2, 5, and 8), mixture 2 was selected because it is the cheapest. The composition of the base-case formula that had a higher water content than the mixture calculated in Table 5.7 is given in Table 5.8. An aroma compound, Linalool, was added to the mixture to improve the scent.

Experiments were performed to verify the predicted results (Table 5.9). The experimental solubility of 9.3 g/L was close to the predicted value of 8.6 g/L. The base-case formulation was transparent but slightly

Table 5.7 Mixtures Matching the Target Property Constraints

	Mixtures	x_w	T_{90} (s)	LC_{50} (mol/m^3)	ν (cS)	V_m ($L/kmol$)	Cost ($/kg)	Phase Split
1	Methanol + water	0.32	819	744.7	0.83	31.0	0.65	Stable
2	2-propanol + water	0.24	661	584.8	1.31	57.1	0.92	Stable
3	Allyl alcohol + water	0.29	598	472.1	1.14	48.2	1.10	Stable
4	Tert-butyl alcohol + water	0.24	588	523.6	1.49	64.4	1.22	Unstable
5	Ethanol + water	0.27	734	413.1	1.01	43.0	1.42	Stable
6	2-methyl-1-propanol + water	0.23	597	419.8	1.66	69.9	1.72	Unstable
7	2-butanol + water	0.24	520	523.6	1.62	68.9	1.81	Unstable
8	1-propanol + water	0.25	628	452.9	1.28	55.9	2.07	Stable

Table 5.8 Formulations for the First (base-case) and Second (final) Iteration

	w_i (%)	
Chemical	First Iteration	Second Iteration
Picaridin	10.00	9.69
2-propanol	45.65	44.25
Water	43.35	42.01
Linalool	1.00	4.00
Acetic acid	—	0.05

Table 5.9 Experimental Results for the First (base-case) and Second (final) Iteration

	Experiments	First Iteration	Second Iteration
1	Solubility of Picaridin in water	9.3 g/L @ 20–23°C)	—
2	Phase stability of solvent mixture	OK	—
3	Solubility of Picaridin in the solvent mixture	OK	—
4	Solubility of linalool in the solvent mixture with Picaridin	OK	—
5	υ and ρ of pure solvents, solvent mixture, and the formulation	OK	OK
6	T_{90} of pure compounds, solvent mixture, and the formulation	OK	OK
7	Formulation sprayability	OK	OK
8	Appearance (turbidity/color), odor, stickiness, greasiness, irritation	Not satisfactory (scent of Picaridin too strong, too sticky)	Acceptable scent and stickiness
9	pH	Not satisfactory (pH = 8.5)	OK (pH = 5.5)
10	Stability at different temperatures than 300 K	—	OK at 278 K and 318 K
11	Shelf life	—	OK (over 2 months)

sticky, and the scent of Picaridin was apparent. The pH of 8.5 was too high for the skin. In the second iteration, acetic acid and additional linalool were added to the mixture. This second iteration was found to be stable between 5 and 45°C and was accepted as the final formulation after remaining unchanged in storage for two months.

A disclaimer is in order. Examples 5.3 and 5.4 are used for illustrating the product design procedure. Although the formulas for the day cream and the insect repellent spray were tested experimentally, much more work is needed to ensure that the products are indeed safe, effective, environmentally-friendly, and market ready. For example, many products are required to be certified by independent testing laboratories that the product claims are true and that relevant government regulations are satisfied.

5.4 DESIGN OF PROCESSES FOR B2C PRODUCTS

Two features distinguish B2C manufacture processes from their B2B counterparts: unconventional unit operations and manufacture for quality. Because the ingredients for B2C products are B2B products that have been manufactured upstream of the chemical product chain, processes for B2C products primarily involve operations that cast these ingredients in a customized structure, form, shape, and configuration. In general, unit operations for basic chemicals such as reaction, distillation, absorption, and so on are not involved. Instead, granulation, milling, nanomization, etching, lamination, physical vapor deposition, inkjet printing, screen printing, laser scribing, and so on are the norm for B2C product manufacturing processes (see Table 1.1). For example, selection of techniques for the impregnation of the HEPA filter with $PtTiO_2$ catalyst is the key step in manufacturing the air purifier (Example 5.1). Granulation is the main technique in the manufacture of controlled-release herbicide (Example 5.2). The inside barrier layer of the food packaging in Figure 5.6 consists of a metalized plastic film that is manufactured inexpensively by roll-to-roll coating of metal by evaporation.

Product quality is paramount for B2C products. For example, the controlled-release granules should be of approximately the same size for easy handling, and the herbicide is dispersed uniformly within them. Note that the release profile can be further refined by distributing the herbicide nonuniformly within the granule through processing. The adhesion of the $PtTiO_2$ on the HEPA filter should be sufficiently strong so that the catalyst particles would not fall off the filter throughout the lifetime of the air purifier. Preferably, the impregnated filter can be washed to remove the dust deposited on it. Also, the catalyst layer should be made sufficiently porous for the air to pass through without excessive pressure drop. Note that the demand for quality gradually increases along the chain of chemical products (Figure 1.1). Commodity chemicals are characterized primarily by purity. Specialty chemicals such as the $PtTiO_2$ catalyst for an air purifier are characterized by their composition, particle size and morphology, and effectiveness in VOC decomposition. Satisfying these requirements culminates in B2C products that deliver consumer satisfaction and pleasure.

The need for unconventional operations and the demand on quality is illustrated next. Mixing the selected ingredients together to produce the sunscreen cream in Example 5.3 might seem simple, but it is not.

EXAMPLE 5.5 ***A Cream Manufacturing Process (Source: Wibowo and Ng, 2001. Used with permission).***

One of the requirements for a cream product is that the emulsion droplets should have a diameter smaller than 5 μm to obtain a smooth cream. Develop a conceptual process design along with the key equipment characteristics and operating conditions.

SOLUTION

This is accomplished in three steps: process synthesis, selection of equipment units, and operating conditions.

Step 1 Synthesis of Flowsheet Alternatives: The flowsheet for the manufacturing of creams and pastes is usually a batch process and consists of only a few unit operations. For batch processes, the flowsheet should be interpreted as a series of sequential actions. Figure 5.13 shows a generic flowsheet for these processes. If incompatible ingredients are involved, they are mixed separately to form the continuous and dispersed phases in the premixing units. Insoluble solid ingredients may need pretreatment such as size reduction or surface modification before being dispersed into the liquid. The separate phases are then combined in the mixing unit where one phase is dispersed as droplets in the other phase to form a pre-emulsion with relatively large droplet sizes. A subsequent homogenization step is often necessary to reduce the droplet size so that the target size is met. Normally, the process up to this stage is performed at an elevated temperature (70–80°C) to facilitate mixing with a lower viscosity. The mixture is cooled down to room temperature either before or after homogenization. Heat-sensitive ingredients are added after the temperature is dropped to about 40–50°C. The last step is filling the product into appropriate containers.

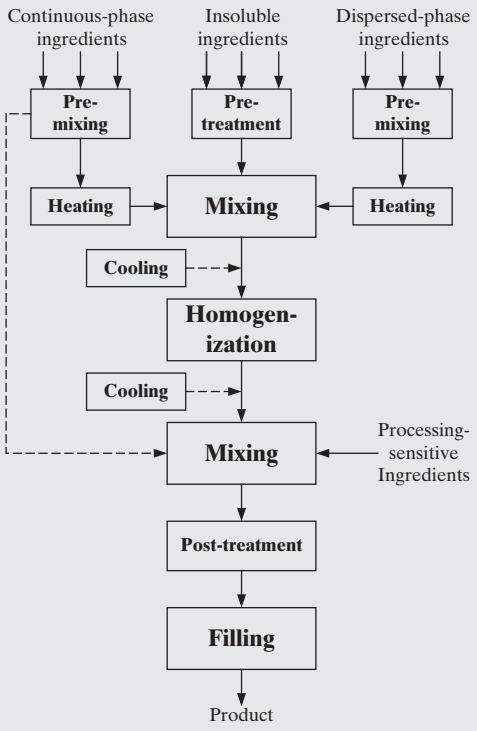

Figure 5.13 General structure of creams and pastes manufacturing process.

Step 2 Selection of Equipment: Flowsheet synthesis is followed by equipment selection. Typical capacity and energy consumption for selected emulsification units are depicted in Figure 5.14. For premixing, pre-emulsification, and dispersion of solids into liquid, an agitated vessel is normally used. Vacuuming can be used for a mixer if foaming or bubble inclusion in the product is to be avoided. Figure 5.15 depicts the schematics of three typical equipment units for homogenization. In a colloid mill (Figure 5.15a), droplet breakage is achieved by elongation and shear in laminar flow, such that the droplet bursts into several child droplets. In a pressure homogenizer (Figure 5.15b), the feed is forced to pass through a narrow valve by the application of a high pressure to induce breakage by turbulence. In an ultrasonic homogenizer (Figure 5.15c), the feed flows through an orifice and impinges on a sharp-edged knife. The impact causes the knife to rapidly vibrate and generate an intense ultrasonic field to form droplets. In practice, they are often used in combination with an agitated vessel.

Step 3 Selection of Equipment Operating Conditions: The droplet size is determined by two opposing phenomena: droplet breakup and coalescence (Walstra, 1983, 1993). In laminar flow, the shear pulls a droplet apart while the interfacial tension keeps it intact. Breakage occurs when the Weber number, which represents the ratio of viscous effect to surface tension effect, exceeds a critical value.

$$N_{We} = \frac{\dot{\gamma}\mu_c d_p}{2\sigma} \tag{5.22}$$

Here, d_p is the diameter of the droplet. When a new droplet is formed either by breakage or coalescence, it needs a layer of surfactant molecules on its surface to prevent coalescence. Therefore, whether a new drop can survive is determined by the time for surfactant migration and adsorption on the newly formed surfaces as compared to the time interval

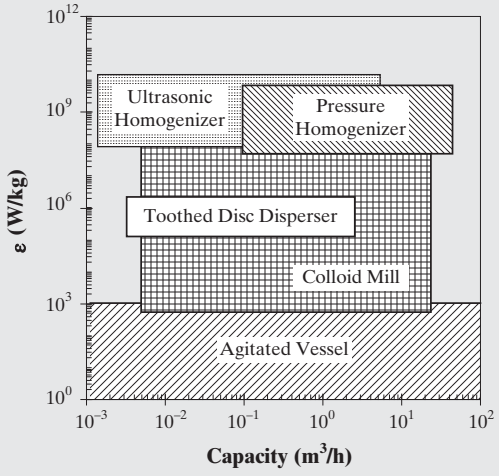

Figure 5.14 Typical capacity and energy consumption for selected emulsification units.

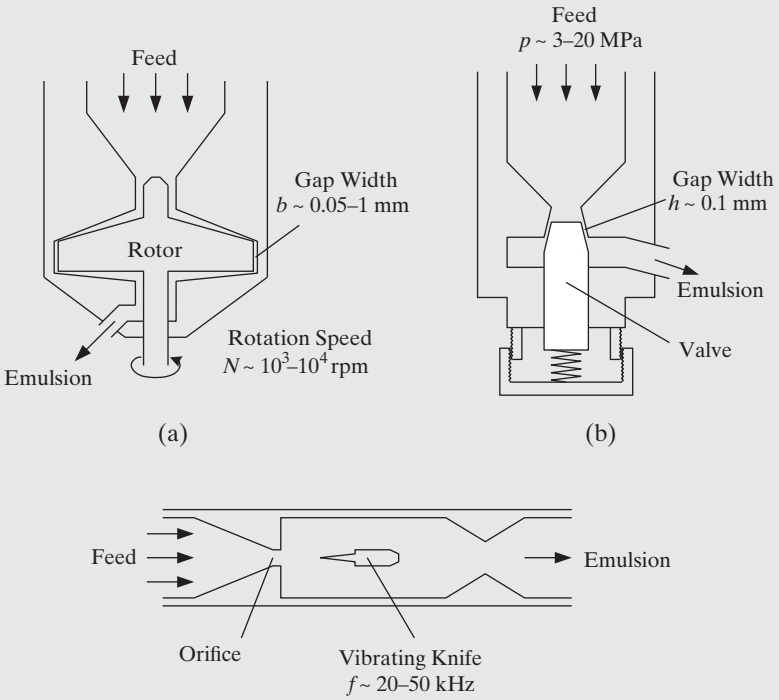

Figure 5.15 Selected equipment for homogenization in the manufacture of creams and pastes: (a) colloid mill, (b) pressure homogenizer, and (c) ultrasonic homogenizer.

between collisions. The characteristic time for adsorption of the surfactant molecules in laminar flow is given by

$$\tau_{\text{adsorption}} = \frac{20\Gamma}{d_p m_s \dot{\gamma}} \tag{5.23}$$

Here, Γ is the excess surface concentration of surfactant and m_s is the surfactant concentration. The characteristic time for collision in laminar flow is given by

$$\tau_{\text{collision}} = \frac{\pi}{8\phi\dot{\gamma}} \tag{5.24}$$

Here, ϕ is the volume fraction of the dispersed phase. Coalescence is averted when $\tau_{\text{adsorption}}/\tau_{\text{collision}} \gg 1$.

Figure 5.16 is used to estimate the required operating conditions for the colloid mill, which operates in the laminar flow regime. The solid line represents the breakup condition [Eq. (5.22)], that is, breakup is possible above the line. The dot-dash line represents the coalescence condition [Eqs. (5.23) and (5.24)], that is, breakup is possible to the right of the dot-dash line whereas re-coalescence occurs to the left of the line. It is vertical, indicating no dependence on shear rate. To obtain droplets with a size of 5 μm, the required shear rate is about 3×10^4 s^{-1}.

Figure 5.17 shows the values of the rotor rotation speed and gap width in a colloid mill with a rotor radius of 5 cm at different shear rates, calculated using the following equation (Wieringa et al.,1996),

$$\dot{\gamma} = \frac{2\pi N R_r}{b} \tag{5.25}$$

Here, N is the colloid mill rotor rotation speed, R_r is the rotor radius, and b is the gap width (Figure 5.15a). The lower boundary for the gap width (dotted line) reflects the fact that the gap is seldom narrower than 200 μm in practice. The darkened line in Figure 5.17 shows the combination of gap width and rotation speed to obtain the desired shear rate and thus the 5 μm droplets.

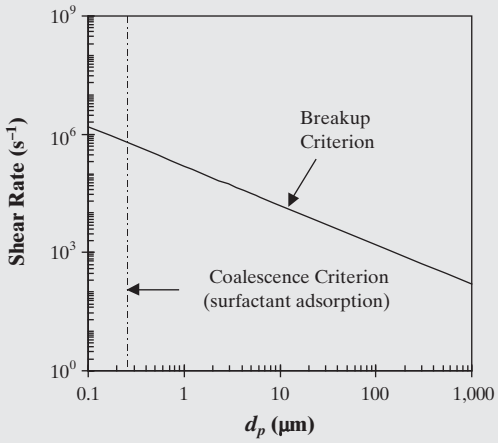

Figure 5.16 Breakup and coalescence criteria for a colloid mill.

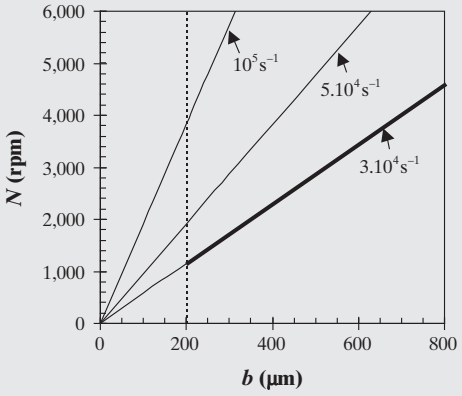

Figure 5.17 Rotation speed and gap width to obtain the desired shear rate.

5.5 SUMMARY

This chapter has focused on the design of B2C chemical products, which can be classified into devices, functional products, and formulated products. Devices are those products often with mechanical and electrical parts that change a feed stream into an outlet stream of desirable characteristics. Functional products serve as barriers, conductors, delivery vehicles, absorbers, and so on, taking advantage of the properties of the constituent materials. Formulated products often consist of a number of ingredients, most of which have to be chosen from a wide selection of similar ingredients.

To generate product designs efficiently, systematic procedures along with the related methods and tools have been developed. Figure 5.18 shows the workflow to step through a product design problem. We begin by deciding whether the intended product is a formulated product. If affirmative, product alternatives are identified by experimental iterations after several formulation steps. Then, the formulated product can be further designed as a device or functional product after selecting the ingredients. For devices and functional products, the formulation steps are often not needed although the task of identifying key ingredients uses the same methods and tools for a formulated product (see boxes enclosed with dotted lines in Figure 5.18). The seemingly simple tasks are actually very challenging because judgments and creativity are necessary. Consider the task of identifying product alternatives. There are no hard-and-fast rules to generate the four air purifier product configurations described in Example 5.1 and Exercise 5.2. They were created based on engineering experience with the desired product performance in mind. The product alternatives generated can be further optimized in terms of cost, availability of raw materials, manufacturability, and various business metrics.

Some products, such as the controlled-release herbicide in Example 5.2, are clearly chemical products. Some are less obvious because they involve elements from other engineering disciplines. For example, the air purifier (Example 5.1) can be considered a mechanical product from the viewpoint of mechanical integrity. Tradition also plays a role. The air purifier can be viewed as an electrical product simply because it is often sold in a store for appliances. Whatever the label might be, most important is how *rule-based methods* (e.g., heuristics and causal table), *model-based methods* (e.g., transport models), databases, tools (e.g., EXCEL), and experiments are used in the design activities in an integrated manner.

In conceptual product design, the key physicochemical mechanisms related to the product have to be identified. Thus, the catalytic decomposition of VOCs using platinum-doped TiO_2 is the key chemical phenomenon for the air purifier. Adsorption of moisture is the dominant mechanism for the silica gel moisture absorber (Figure 5.5). The viscosity of the sunscreen cream has to be suitably adjusted for easy application on the skin (Example 5.3).

Product specifications are obtained after conceptual product design. For formulated products, the specifications include the material type, composition, and microstructure. For chemical devices and functional products, specifications include the type and amount of the constituent materials and the way in which these materials are configured.

Product design is much more challenging than product analysis for different reasons. As illustrated in Figure 5.7, many product alternatives might satisfy the given input and output

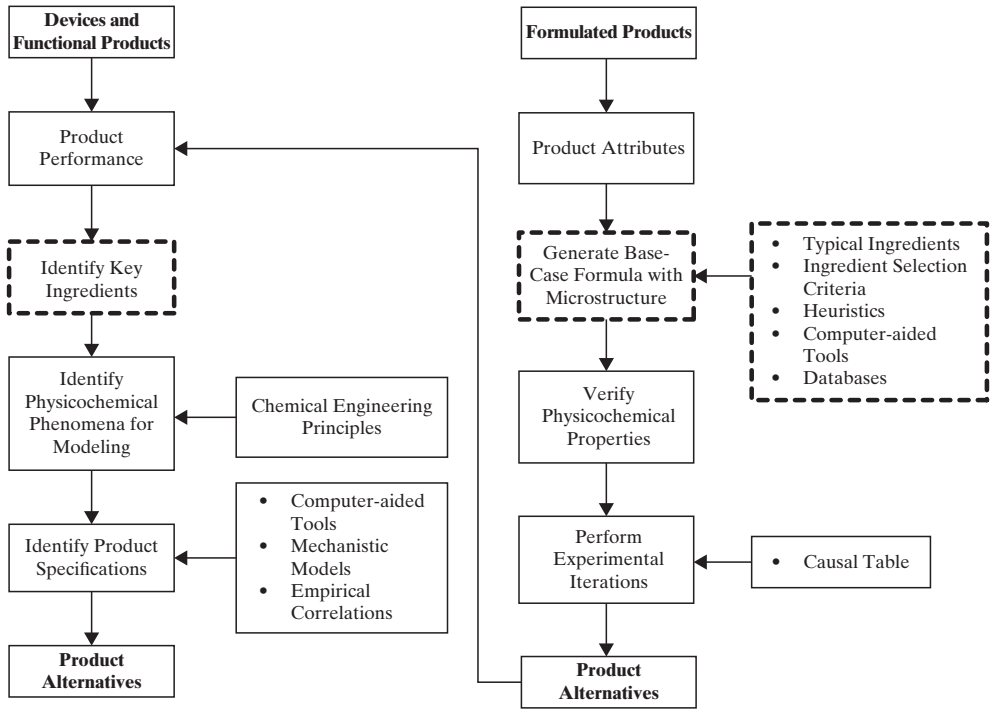

Figure 5.18 Product design workflow diagram. The key tasks and the supporting methods and tools in the design of formulated products, devices, and functional products are shown in a product design workflow diagram.

information. In addition to the large number of potential ingredients, products can be fabricated in many different structures, forms, shapes, or configurations, leading to an even wider search space. Another challenge is the fact that the output information includes hard-to-quantify product attributes such as smell, taste, touch, and feel. The demand on product quality for B2C products is a key feature distinguishing them from most B2B products that demand primarily purity.

Because the materials and physicochemical phenomena involved in the diverse chemical products can be significantly different, the chemical engineer often has to acquire some of the related domain-specific knowledge for the product under consideration to be effective in creating a design. For example, the chemical engineer must understand the basics of skin cream before designing one.

Product design requires much more effort beyond conceptual product design. Ergonomic needs, such as ease of use and aesthetic appeals including look and feel, must be considered. A detailed three-dimensional model of a product can be created using computer-aided design (CAD) software, which allows rapid screening of a large number of concepts. This is important because the packaging and appearance of a consumer product can significantly influence the consumer's perception of product quality and thus sales.

REFERENCES

1. Anderson, M. J., and P. J. Whitcom, *DOE Simplified: Practical Tools for Effective Experimentation*, 2nd ed., Productivity Press, New York (2007).

2. Cheng, Y. S., K. W. Lam, K. M. Ng, K. M. Ko, and C. Wibowo, "An Integrative Approach for Product Development—A Skin-Care Cream," *Comp. Chem. Eng.*, **33**, 1097 (2009).

3. Conte, E., R. Gani, and K. M. Ng, "Design of Formulated Products: A Systematic Methodology," *AIChE J.*, **57**, 2431 (2011).

4. Conte, E., R. Gani, Y. S. Cheng, and K. M. Ng, "Design of Formulated Products: Experimental Component," *AIChE J.*, **58**, 173 (2012).

5. Dreyfus, G., *Neural Networks: Methodology and Applications*, Springer, Berlin, Germany (2005).

6. EPA (Environmental Protection Agency, United States), New Pesticide Fact Sheet, Picaridin (2005).

7. Katzhendler, I., A. Hoffman, A. Goldberger, and M. Friedman, "Modeling of Drug Release from Erodible Tablets," *Journal of Pharmaceutical Sciences*, **86**, 110 (1997).

8. Lam, K. W., D. T. W. Lau, K. M. Ko, P. C. Leung, and K. M. Ng, "Formation of Nano-emulsion of Chinese Herbal Formula and Its Application in a Matrix-type Transdermal Patch," US Provisional Patent 61/855,966 (2013).

9. Lape, N. K., E. E. Nuxoll, and E. L. Cussler, "Polydisperse Flakes in Barrier Films," *J. Membrane Science*, **236**, 29 (2004).

10. Mattei, M., G. M. Kontogeorgis and R. Gani, "A Comprehensive Framework for Surfactant Selection and Design for Emulsion Based Chemical Product Design," *Fluid Phase Equilibrium*, **362**, 288 (2014).

11. Mullin, J. W., *Crystallization*, 4th ed., Butterworth Heinemann, Oxford, United Kingdom, (2001).

12. Ng, K. M., and Wibowo, C., "Beyond Process Design: The Emergence of a Process Development Focus," *Korean J. Chem. Eng.*, **20**, 791 (2003).

13. Paik, J. S., J. I. Shin, J. I. Kim, and P. K. Choi, "Effect of Nitrogen Flushing on Shelf-life of Packaged Potato Chips," *Packaging Technology and Science*, **7**, 81 (1994).

14. Pereira, F. M., A. R. Gonçalves, A. Ferraz, F. T. Silva, and S. C. Oliveira, "Modeling of 2,4-Dichlorophenoxyacetic Acid Controlled-release Kinetics from Lignin-based Formulations," *Applied Biochemistry and Biotechnology*, **98–100**, 101 (2002).

15. Rähse, W., "Design of Skin Care Products," *Product Design and Engineering: Formulation of Gels and Pastes*, U. Bröckel, W. Meier, and G. Wagner (eds.), Wiley, Somerset, New Jersey (2013).

16. Sanongraj, W., Y. Chen, J. C. Crittenden, H. Destaillats, D. W. Hand, D. L. Perram, and R. Taylor, "Mathematical Model for Photocatalytic Destruction of Organic Contaminants in Air," *Journal of the Air & Waste Management Association*, **57**, 1112 (2007).

17. Takahashi, S., H. A. Goldberg, C. A. Feeney, D. P. Karim, M. Farrell, K. O'Leary, and D. R. Paul, "Gas Barrier Properties of Butyl Rubber/Vermiculite Nanocomposite Coatings," *Polymer*, **47**, 3083 (2006).

18. Tock, R. W., "Permeabilities and Water Vapor Transmission Rates for Commercial Films," *Advances in Polymer Technology*, **3**, 223 (1983).

19. Walstra, P., "Formation of Emulsions," *Encyclopedia of Emulsion Technology*, Vol. 1, P. Becher (ed.), Marcel Dekker, New York (1983), p. 57.

20. Walstra, P., "Principles of Emulsion Formation," *Chem. Eng. Sci.*, **48**, 333 (1993).

21. Wankat, P. C., *Rate-Controlled Separations*, Elsevier, New York (1990).

22. Wibowo, C., and K. M. Ng, "Product-Oriented Process Synthesis and Development: Creams and Pastes," *AIChE J.*, **47**, 2746 (2001).

23. Wibowo, C., and K. M. Ng, "Product-Centered Processing: Chemical-Based Consumer Product Manufacture," *AIChE J.*, **48**, 1212 (2002).

24. Wieringa, J. A., F. van Dieren, J. J. M. Janssen, and W. G. M. Agterof, "Droplet Breakup Mechanisms during Emulsification in Colloid Mills at High Dispersed Volume Fraction," *Chem. Eng. Res. Des.*, **74**, 554 (1996).

25. Xin, Z., Z. Yu, M. Erb, T. C. J. Turlings, B. Wang, J. Qi, S. Liu, and Y. Lou, "The Broadleaf Herbicide 2,4-Dichlorophenoxyacetic Acid Turns Rice into a Living Trap for a Major Insect Pest and a Parasitic Wasp," *New Phytologist*, **194**, 498 (2012).

EXERCISES

5.1 Some of the mathematical steps in Example 5.2 are omitted. Derive Eqs. (5.14), (5.17), and (5.18).

5.2 The home appliance company decides to perform additional design work on the proposed air purifier.

(a) The $PtTiO_2$ coated HEPA filter is expected to be easily clogged by particulates in the air. It is decided that a prefilter is needed. Redesign the configuration in Figure 5.8b to include a HEPA prefilter that can be easily replaced.

(b) To avoid the use of a prefilter, a new configuration as shown in the following graphic is proposed. $PtTiO_2$ nanoparticles are coated on the inner surface of a metal cylinder. A UV lamp is placed along the central axis of the cylinder. Compare this design with that in Figure 5.8b under the same UV light intensity.

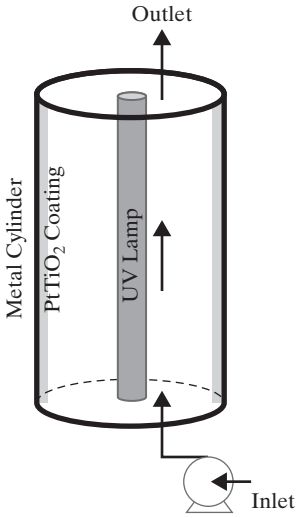

(c) VOCs are composed of different compounds. It is proposed that, in addition to toluene, ethanol be used as a reference compound for quantifying product performance. Assume that the mechanism of ethanol decomposition on UV-excited $PtTiO_2$ is the same for toluene. The following regressed parameters were obtained through experiments conducted under a light intensity of 2.2 mW/cm^2, ethanol concentration of 10–100 mg/m^3, catalyst thickness of 38.5 μm, and a relative humidity range of 17–82%. Calculate the amount of catalyst required to reduce ethanol concentration from 100 mg/m^3 to 50 mg/m^3 in the same room within two hours.

K_m (μg/L.min)	$K_{ethanol}$ (L/μg)	K_2	K_3	K_4(L/μg)	K_5	K_6($L^2/\mu g^2$)
8.4768	0.0019	0.0571	1.0525	1.0356	8.7526	8.4647

5.3 A home appliances company decides to produce an all-in-one water treatment system for treating tap water. It contains a filter to remove suspended solids, a reverse osmosis (RO) membrane unit to remove dissolved ions, an ultraviolet disinfection system, and a granular activated carbon filter for final polishing of taste and odor. We have been assigned to design the RO module (Figure 5.1). The water treatment system is attached to a faucet with a water flow rate of 7.5 L/min. The water flow rate across the membrane (i.e., permeate flow rate) is directly proportional to the pressure difference ($P_{fc} - P_p$) minus the osmotic pressure difference ($\pi_{fc} - \pi_p$),

$$Q_p = k_w A[(P_{fc} - P_p) - (\pi_{fc} - \pi_p)]$$

where k_w is the mass-transfer coefficient of water across the membrane, A is the membrane surface area, and P_{fc} and P_p (π_{fc} and π_p) are the pressure (osmotic pressure) at the feed-concentrate side and the permeate side of the membrane, respectively. The osmotic pressure π is related to the solute concentration C as follows.

$$\pi = CRT$$

where R is the universal gas constant and T is the temperature. Similarly, the solute flow rate across the membrane is proportional to the concentration difference,

$$Q_p C_p = k_s A(C_{fc} - C_p)$$

where k_s is the mass-transfer coefficient of solute across the membrane and C_{fc} and C_p are the solute concentration in the feed-concentrate side and the permeate side of the membrane, respectively.

(a) As a measure of product performance, a solute rejection ratio ($Rej = 1 - C_p/C_f$) of 99% is required for a feed stream with 100 ppm of Ca^{2+}. Determine the product specifications, particularly the membrane area and the permeate flowrate. The following parameters are available:

$$P_{fc} = 30 \text{ atm}$$
$$P_p = 1 \text{ atm}$$
$$T = 298 \text{ K}$$
$$k_w = 2.87 \times 10^{-3} \text{ m/h atm}$$
$$k_s = 6.14 \times 10^{-4} \text{ m/h}$$

(b) As water passes through the membrane, solute accumulates near the membrane surface, causing concentration polarization. C_{fc} has to be modified by multiplying with a factor β given below.

$$\beta = exp\left(\frac{Q_p}{Ak_{cp}}\right) Rej + (1 - Rej)$$

where $k_{cp} = 2.2 \times 10^{-4}$ m/s. How does it impact the design?

5.4 A household goods company decides to produce a faucet mount water filter for removing organic and metallic contaminants from tap water (Figure 5.2). The filter is made up of activated carbon and ion-exchange resin. As a measure of product performance, tap water with 346 μg/L of methyl-t-butyl ether (MTBE) and 370 μg/L of lead ions at a flow rate of 7.5 L/m at 25°C is used as a reference inlet stream. The filter must last at least two months for a four-member family. The daily drinking water consumption per person is 2 L.

(a) The equilibrium data of MTBE adsorption on activated carbon and lead on ion-exchange resin at 25°C have been obtained below. Determine from the equilibrium data the parameters for the Langmuir isotherm,

$$q = \frac{q_{max} K_A c}{1 + K_A c}$$

Here, q is the amount of solute adsorbed (mg/g of adsorbent), q_{max} is the maximum amount of solute adsorbed (mg/g), K_A is the adsorption equilibrium constant (L/mg), and c is the amount of solute in bulk liquid (mg/L).

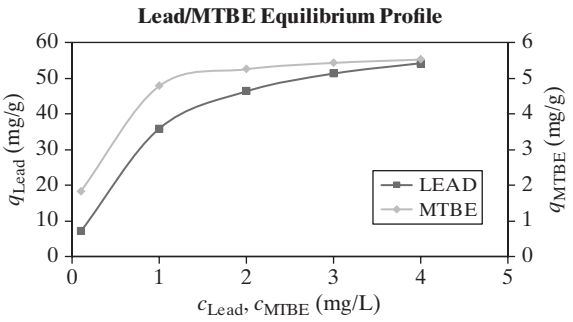

(b) Using the Langmuir parameters calculated in part (a), determine the product specifications of the faucet water filter. Specifically, what should be the dimensions of the filter? What is the ratio of activated carbon to ion-exchange resins in the filter?

To simplify the problem, local equilibrium can be assumed to take place throughout the filter. Axial dispersion and diffusion effects are negligible. MTBE is adsorbed by activated carbon and lead by activated

ion-exchange resins, separately. With these assumptions, the velocity of each solute, u, is given by (Wankat, 1990),

$$u = \frac{v_i}{1 + \frac{1 - \varepsilon}{\varepsilon}\rho_p\left(\frac{q_2 - q_1}{c_2 - c_1}\right)}$$

Here, ε is the void fraction of the filter, v_i is the interstitial velocity of fluid flow [= volumetric flow rate/(filter cross-sectional area × void fraction)], ρ_p is particle density, and 1 and 2 refer to before and after feeding the tap water to the filter, respectively. The density of the activated carbon and ion-exchange resins are 800 g/L and 1,190 g/L, respectively. The void fraction is 0.4.

(c) Discuss how to solve this design problem if local equilibrium is not valid.

5.5 A home supplies company decides to produce a reusable moisture absorber product for removing the water content in air in an enclosed space. A reduction in humidity is expected to help inhibit the growth of mold and mildew. As a measure of product performance, the moisture absorber should reduce the relative humidity of air in a closed coat cabinet with dimensions of 2m × 1m × 1m from 90% to 50% at 25°C (Figure 5.5).

(a) There are two common hygroscopic materials, silica gel and calcium chloride. Comment on their suitability as the raw materials for the intended product. What is the physicochemical behavior that governs the uptake of moisture in each material?

(b) Develop and solve the model for determining the specifications for this product. What is the minimum amount of silica gel to lower the humidity to 50%? What is the required amount of silica gel if the reduction is to be completed in two hours? Much information is available on silica gel in the literature. For example, the maximum moisture content of silica gel, defined as weight of water per unit weight of silica gel, is 0.26. The density of silica gel is 2.64 g/cm^3. The diffusion coefficient of moisture in silica gel is 0.37×10^{-8} m^2/s.

5.6 A food processing company is designing the packaging for a new product line of potato chips. The expected shelf life of the potato chips is 10 months. The bag has to hold 200 g of potato chips and 1,500 mL of nitrogen. The nitrogen gas is used as a cushion to prevent crushing the chips and to avoid lipid oxidation. The oxygen level in the bag should be less than 1% (Paik et al., 1994).

(a) The packaging generally involves three layers, each of which is made up of a few films (Figure 5.6). The outside layer is used for printing. The inside layer serves as the barrier to gas, moisture, and light and provides stiffness and heat seal. The middle layer bonds the outside and inside layers together. One of the films of the inside layer is usually aluminum coated by vaporization on a polymer film. The oxygen flux, J, through the barrier film is governed by Fick's law,

$$J = P\frac{\Delta p}{L}$$

where P is the permeability, p the pressure, and L the barrier film thickness. The accompanying table shows the permeability to oxygen of a neat polymer film as well as one with metal coating (Tock, 1983). Select with explanations the material you would use for the new packaging design. Note that the cost of materials is a major consideration in snack food packaging and the cost data can be found on the Internet.

Barrier Film Material	Film Coating	Permeability of Oxygen at 25°C (cc·mil)/(100 in^2·day.atm)	Water Vapor Transmission Rate 38°C, 50 to 100% RH (cc·mil)/(100 in^2·day)
Polyamide	None	2.6	19
	metalized	0.05	0.2
PET	None	4.5	1.2
	metalized	0.08	0.1
Polypropylene	None	250	1.75
	metalized	3	0.33

(b) What should be the dimensions of the bag? Assuming a constant permeability, calculate the minimum thickness of the selected barrier film to achieve a 10-month shelf life with respect to oxygen (i.e., retaining an oxygen concentration less than 1% inside the bag).

(c) Moisture content of the potato chips is another crucial parameter. Assume that the initial moisture content of potato chips is 1.5wt% and should not exceed 2.5wt% at the end of shelf life. Is the barrier film chosen in part (b) sufficient for the desired product performance with respect to moisture content? The data for moisture flux per unit film thickness in the table can be assumed to be constant within the stated range of RH.

5.7 A tennis ball is a rubber hollow sphere covered by a thin layer of fabric usually yellow in color. It has a diameter of 6.54–6.86 cm and weighs 56.0–59.4 g. The internal pressure of the ball filled with air is around 12 psig. The thickness of the rubber shell is around 3 mm and its composition is as follows*:

Natural Rubber	100 (per hundred rubber)
General purpose furnace black	30
Clay (mineral filler)	32
Other materials	15.5

**Source:* International Tennis Association, Balls Manufacture, www.itftennis.com, accessed Mar. 14, 2015.

Per hundred rubber (phr) is a unit used in the rubber area to indicate the relative weight of each component with respect to the weight of rubber set at 100. The purpose of clay is to reduce the air permeability of the rubber to maintain the ball pressure. Normally, tennis balls are sold as a set of three inside a pressurized plastic tube to prevent the loss of ball pressure.

(a) A manufacturer of tennis balls would like to know the impact of the gas pressure of the plastic tube on the shelf life of the balls. Plot the change of ball pressure with time at different tube pressures ranging from 0 to 12 psi above ambient pressure at room temperature. Use 6×10^{-8} cm^2/(s atm), the nitrogen permeability in natural rubber with 32 phr of clay, for your calculations. Select the appropriate tube pressure for ball storage, if the reduction in ball pressure is less than 5% in 2 years.

(b) The plastic tube is made of PET. What should be the dimensions of the tube for storing three tennis balls? Estimate the minimum wall thickness of the tube to achieve a two-year shelf life, that is, having a reduction in tube pressure of less than 5%. Use the nitrogen permeability in PET, 0.28 (cm^3 mm)/(m^2 day atm), in your calculations.

(c) Recently, a rubber coating embedded with aligned clay platelets has been developed. This nanocomposite impedes the passage of air by creating a tortuous path. The manufacturer wishes to use this material to prolong the shelf life of the tennis ball without significantly changing its size. A thin layer of butyl rubber with nitrogen permeability of 7×10^{-8} cm^2/(s atm) embedded with nanosilicate with an aspect ratio

(α) of 100 and a volume fraction (ϕ) of 0.1 is applied on the rubber core. A theory for the gas permeability of the nanocomposite ($P_{composite}$) is given by (Takahashi et al., 2006),

$$\frac{P_{composite}}{P_{matrix}} = (1-\phi)f$$

Lape et al. (2004) provides a model for the tortuosity factor, which is given by

$$f = \left(1 + \frac{(\alpha\phi)^2}{4}\right)^{-1}$$

What should be the thickness of coating to double the life span of the tennis ball, which is defined as 90% of ball pressure retention, under ambient conditions? In this case, P_{matrix} refers to the permeability of nitrogen in butyl rubber.

5.8 A healthcare company decides to produce a medicated transdermal patch to relieve the pain caused by soft tissue injuries. This product with a brand name of nanoPatch is based on a traditional herbal formula. The active ingredients are nanomized to facilitate the transdermal delivery. The transdermal patch is composed of a backing layer, a drug-in-adhesive matrix, and a liner layer (see the following figure). The protective liner is torn off prior to application and the drug-in-adhesive matrix is placed directly on the skin. There are different active ingredients in the drug-in-adhesive matrix. Of those, Ginsenoside Rg1 (Rg1), which promotes angiogenesis for injury recovery, is chosen as the reference marker for product performance.

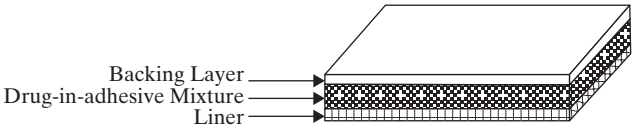

Schematic diagram of a matrix-type transdermal patch.

(a) In determining the product specifications of the nanoPatch, it is crucial to determine the diffusivity of Rg1. The research team of the company performed an *in vitro* diffusion test across a piece of porcine skin 1.2 mm thick. The concentration of Rg1 was practically constant at 10 mg/cm^3 on one side (donor side) of the skin and practically zero on the other side (acceptor side). The results are summarized in the following table. Calculate the diffusivity of Rg1 using Fick's first law.

Cumulative Amount of Rg1 Diffused Across the Porcine Skin at Different Time Intervals
Source: **Lam et al., 2013. Used with permission.**

Time (h)	Cumulative Amount ($\times 10^{-3}$ mg/cm^2)
0	0.00
4	1.47
8	5.67
12	13.55
16	22.08
20	30.05
24	37.00

(b) Clinical data show that a cumulative amount of 5 mg of Rg1 must be permeated into the skin in an eight-hour period to achieve the best results. Specifically, what should be the dimensions of the patch? What is the corresponding Rg1 concentration in the adhesive matrix? Assume steady state diffusion.

5.9 A healthcare company decides to market a hand warmer. It is basically a palm-size plastic pouch containing a supersaturated aqueous salt solution; that is, the amount of dissolved salt exceeds its solubility limit. The degree of supersaturation is the ratio of the mass of dissolved salt per unit mass of water to the mass of salt at saturation; it is expected to be in the range of 1 to 2. By flexing a small metal disk in the solution, the salt begins to crystallize, and the heat of crystallization produces a temperature rise rapidly. The amount of heat is sufficient to keep the hands holding the pouch warm over a period of up to 30 min. This hand warmer can be recharged by redissolving the salt in a microwave oven or in hot water.

From the patent literature, four potential candidates can be identified: sodium acetate, sodium thiosulfate, calcium nitrate, and lead acetate. These are all hydrated at ambient temperatures with high solubility and relatively high heats of crystallization (Mullin, 1993).

Salt	Heat of Crystallization at ~20°C (kcal/mol)	Equilibrium Solubility at 20°C (g anhyd./ 100 g Water)	Equilibrium Solubility at 40°C (g anhyd./ 100 g Water)
$NaC_2H_3O_2 \cdot 3H_2O$	−4.7	46.5	65.5
$Na_2S_2O_3 \cdot 5H_2O$	−11.4	70	103
$Ca(NO_3)_2 \cdot 4H_2O$	−8.0	129	196
$Pb(C_2H_3O_2)_2 \cdot 3H_2O$	−5.9	44.1	116

Data for the specific heat of these salts are not readily available but can be estimated using Kopp's rule, which states that the heat capacity of a solid compound or the compound in liquid form is approximately equal to the sum of the heat capacities of the individual atoms. The following table shows values for individual atoms determined from experimental data.

Values of Atomic Heat Capacity at 20°C [cal/(g atom)(°C)]

Element	Solids	Liquids
C	1.8	2.8
H	2.3	4.3
B	2.7	4.7
Si	3.8	5.8
O	4.0	6.0
F	5.0	7.0
P or S	5.4	7.4
All others	6.2	8.0

(a) The product performance calls for a temperature rise from 20°C to 40°C. If all four salts can be assumed to be able to accommodate a supersaturation of up to around 2, select one and justify its use in the hand warmer product. [Hint: Perform energy balance to determine the required amount of salt in a supersaturated solution.]

(b) Determine the product specifications. Specifically, provide the dimensions of the pouch, the amount of salt and water within the pouch, and the amount of heat available for hand warming.

5.10 One of the tasks in a product development project is to source the ingredients. Identify a supplier and the cost for the following ingredients:

(a) Zinc oxide nanoparticles under the trade name ZinClear®

(b) Sweet almond oil

(c) Demethicone

(d) GMS 165

(e) Oleth 20

(f) Xanthan gum

5.11 Example 5.5 shows how to determine the rotor rotation speed and its gap width to produce emulsion particles 5 μm in diameter. If it is decided that the emulsion particle diameter needs to be further reduced to 1 μm while keeping the gap width at its minimum size, what should be the rotor radius?

5.12 Many consumers, particularly those in developing countries, are concerned about the cleanliness of municipal water for human consumption. For this reason, distilled water is widely available at work, and water purifiers such as the water pitcher shown here are increasingly common at home. There are many brands on the market such as Brita, Aquasana, Pur, and so on. Most of the household water purifiers are based on adsorption using activated carbon and ion-exchange resins to remove organics and metal ions from tap water. Some also use UV irradiation to destroy pathogens.

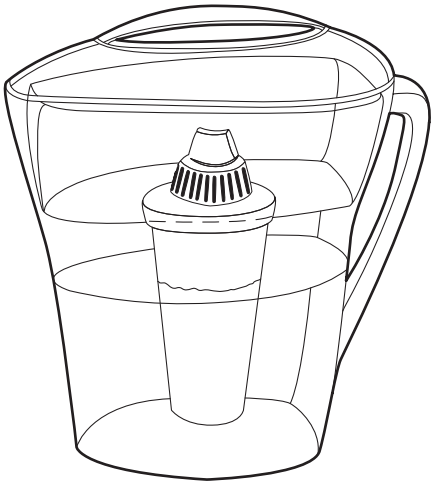

In this project, you will apply the product design concepts and methods covered in Chapters 1 and 5 to design a home-use water pitcher. Following the multidisciplinary framework, the first step is to carry out a market study to determine the market size, the desired product attributes, and the product attributes of competing products, among others. This is followed by conceptualizing the desired product and making a decision on the desired market share. Methods such as House of Quality and Business Model Canvas, and design procedure for devices are to be used. The product ingredients and structure should be identified. Product specifications are to be determined by model-based methods or experiments. Specifically, your report should cover the following:

(a) What is your product and its functions?

(b) What is the market position of your product (e.g., market size, major companies selling this and related products, comparison of your product with competing products, potentially innovative products)?

(c) What are the product specifications [e.g., product appearance, product structure, the ingredients, the amounts of the ingredients, energy consumption (if any)]?

(d) How is the product manufactured?

5.13 Many coastal cities such as Hong Kong can be very humid, particularly in spring and summer with a mean relative humidity above 80%. Dehumidifiers remove the moisture from air to provide a more pleasant living environment. In such a device, water vapor in the moist air is either condensed by cooling or adsorbed by desiccant in a refrigerant dehumidifier or desiccant dehumidifier, respectively. Common brands include Mitsubishi, Hitachi, and Whirlpool. Repeat Exercise 5.12 for such a dehumidifier.

Chapter 6

Heuristics for Process Synthesis

6.0 OBJECTIVES

This chapter returns to the steps of preliminary process synthesis in Section 2.3 in which a strategy is recommended that involves assembling the process operations to create a *base-case* process flowsheet in a specific order, as follows:

1. Chemical reactions (to eliminate differences in molecular type).
2. Mixing and recycle (to distribute the chemicals).
3. Separation (to eliminate differences in composition).
4. Temperature, pressure, and phase change.
5. Task integration (to combine operations into unit processes).

In Section 2.3, as the operations are inserted into alternative flowsheets to manufacture vinyl chloride, *rules of thumb* or *heuristics* are utilized. For example, when positioning the direct chlorination operation, it is assumed that because the reaction is nearly complete at 90°C, ethylene and chlorine can be fed in stoichiometric proportions. Furthermore, when positioning the pyrolysis operation, the temperature and pressure are set at 500°C and 26 atm to give a 60% conversion. These assumptions and specifications are based upon many factors, not the least of which is experience in the manufacture of vinyl chloride and similar chemicals. In this case, a patent by the B. F. Goodrich Co. [British Patent 938,824 (October 9, 1963)] indicates the high conversion of ethylene and chlorine over a ferric chloride catalyst at 90°C and recommends the temperature and pressure levels of the pyrolysis section. The decision not to use ethylene in excess, to be sure of consuming all of the toxic chlorine, is based upon the favorable experimental conversions reported by chemists. In the distillation operations, the choice of the key components, the quality of the feed streams and the distillation products, and the pressure levels of the towers are also based upon rules of thumb. In fact, heuristics like these and many others can be organized into an *expert system*, which can be utilized to synthesize sections of this and similar chemical processes.

Normally, design teams use heuristics when generating the alternatives that make up the synthesis tree, such as that shown in Figure 2.7. For the most part, heuristics are easy to apply; that is, they involve the setting of temperatures, pressures, excess amounts of chemicals, and so on. Often they require little analysis in that simple material balances can be completed without iterations before proceeding to the next synthesis step. Consequently, several promising flowsheets, or *base-case designs*, are generated rapidly with relatively little effort. For these flowsheets, the assumptions are checked, a process flow diagram is assembled (e.g., Figure 2.17), and a complete material balance is carried out, often using the process simulators discussed in Chapter 7.

Clearly, the heuristics used by a design team to generate the synthesis tree are crucial in the design process. Section 2.3 provides just a brief introduction to these heuristics, and hence, it is the objective of this chapter to describe the principal heuristics used in a process design more thoroughly. A total of 53 heuristics are presented in Sections 6.2 through 6.9. In many cases, the heuristics are accompanied by examples. For quick reference, the heuristics are collected together in Table 6.2 at the end of this chapter. Additional guidance in the selection of equipment is given in Chapters 16 and 17 when determining equipment purchase and operating costs, Chapter 8 when designing chemical reactors, Chapter 12 when designing heat exchangers, Chapter 13 when sizing distillation towers, and Chapter 14 when sizing pumps, compressors, and gas expanders.

After studying this chapter and the heuristics in Table 6.2, the reader should:

1. Understand the importance of selecting reaction paths that do not involve toxic or hazardous chemicals and when unavoidable, to reduce their presence by shortening residence times in the process units and avoiding their storage in large quantities.
2. Be able to distribute the chemicals, when generating a process flowsheet, to account for the presence of inert species that would otherwise build up to unacceptable concentrations, to achieve a high selectivity to the desired products, and to accomplish, when feasible, reactions and separations in the same vessels (e.g., reactive distillations).
3. Be able to apply heuristics in selecting separation processes to separate liquids, vapors, vapor–liquid mixtures and other operations involving the processing of solid particles, including the presence of liquid and/or vapor phases.

4. Be able to distribute the chemicals, by using excess reactants, inert diluents, and cold (or hot) shots, to remove the exothermic (supply the endothermic) heats of reaction. These distributions can have a major impact on the resulting process integration.
5. Understand the advantages, when applicable, of pumping a liquid rather than compressing a vapor.

Through several examples, including the synthesis of a process to hydrodealkylate toluene to benzene, and the exercises at the end of the chapter, the reader should be able to apply the heuristics in Table 6.2 when generating a synthesis tree and creating *base-case* designs.

6.1 INTRODUCTION

As introduced in Chapter 2, the first step in process design involves process synthesis, that is, the creation of alternative process flowsheets to produce a specific chemical product. For this purpose, heuristics (rules of thumb) are commonly used, at least initially. In this chapter, many more heuristics are discussed, far beyond those used in the synthesis of the vinyl-chloride and tissue plasminogen activator (tPA) processes in Chapter 2. Through usage of these heuristics, it is normally possible to create a promising "base-case flowsheet(s)," which is subsequently analyzed more carefully using process simulators, as discussed in Chapter 7. When used properly, heuristics permit the *rapid* creation of a promising base-case flowsheet(s)—one that can be refined and optimized through careful material and energy balance analysis, equipment sizing, and cost estimation using process simulators.

For each of the five synthesis steps, this chapter systematically presents a more complete set of heuristics, beginning with the first step: Select Raw Materials and Chemical Reactions in Section 6.2. Then, after sets of heuristics are presented, with examples to illustrate their use, some of the heuristics are applied for the synthesis of a base-case design, one involving the hydrodealkylation of toluene to produce benzene, which begins in Example 6.1. This chapter is intended to show how such a base-case design can be created rapidly prior to the active usage of process simulators. Note, however, that even when using heuristics, process simulators are often used for supporting calculations (e.g., to estimate physical properties) as illustrated occasionally in the examples that follow. The formal usage of process simulators for design specifications, recycle calculations, equipment sizing, cost estimation, and the like, is introduced in Chapter 7.

6.2 RAW MATERIALS AND CHEMICAL REACTIONS

Heuristic 1*: *Select raw materials and chemical reactions to avoid, or reduce, the handling and storage of hazardous and toxic chemicals.

As discussed in Section 2.3, the selection of raw materials and chemical reactions is often suggested by chemists, biologists, biochemists, or other persons knowledgeable about the chemical conversions involved. In recent years, with the tremendous increase in awareness of the need to avoid handling hazardous and toxic chemicals, in connection with environmental and safety regulations (as discussed in Sections 3.4 and 3.6), raw materials and chemical reactions are often selected to protect the environment and avoid the safety problems that are evident in Material Safety Data Sheets (MSDS). For example, recall that when the vinyl-chloride process was synthesized in Section 2.3, the reaction of acetylene with HCl was rejected because of the high cost of acetylene. Today, in addition, the reaction path would be rejected on the basis of the high reactivity of acetylene and the difficulty of ensuring safe operation in the face of unanticipated disturbances.

In connection with the handling of hazardous chemicals, the 1984 accident in Bhopal, India, in which water was accidentally mixed with the active intermediate methyl isocyanate, focused worldwide attention on the need to reduce the handling of highly reactive intermediates. As discussed in Section 3.6, within an hour of the accident, a huge vapor cloud swept across Bhopal, leading to the death of over 3,800 victims in the vicinity of the Union Carbide plant. This accident, together with the discovery of polluted groundwaters adjacent to chemical plants, especially those that process nuclear fuels, have led safety and environment experts to call for a sharp reduction in the handling of hazardous chemicals.

For these reasons, societal needs are increasingly being formulated that call for new processes to avoid or sharply reduce the handling of hazardous chemicals. As an example, consider the manufacture of ethylene glycol, the principal ingredient of antifreeze. Ethylene glycol is produced commonly by two reactions in series:

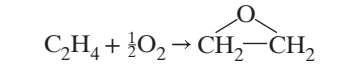

(R1)

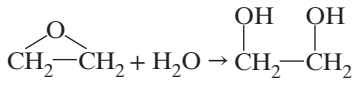

(R2)

The first reaction involves the partial oxidation of ethylene over an Ag-gauze catalyst. Because both reactions are highly exothermic, they need to be controlled carefully. More important from a safety point of view, a water spill into an ethylene oxide storage tank could lead to an accident similar to the Bhopal incident. Yet it is common in processes with two reaction steps to store the intermediates so as to permit the products to be generated continuously, even when maintenance problems shut down the first reaction operation.

Given the societal need to eliminate the storage of large quantities of reactive intermediates such as ethylene oxide, four alternative processing concepts are possible:

1. Eliminate the storage tank(s), causing intermittent interruptions in the production of ethylene glycol when the oxidation reaction shuts down.

2. Use costly chlorine and caustic (compared to oxygen from air) in a single reaction step:

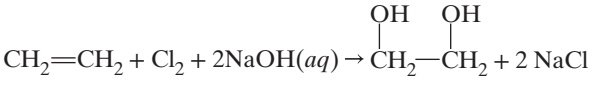

(R3)

This alternative requires more expensive raw materials, but completely avoids the intermediate.

3. As ethylene oxide is formed, react it with carbon dioxide to form ethylene carbonate, a much less active intermediate. This reaction

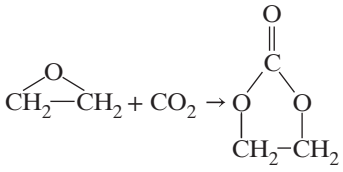

(R4)

occurs smoothly over a tetraethylammonium bromide catalyst. Ethylene carbonate can be stored safely and hydrolyzed to form the ethylene glycol product as needed.

4. Carry out reactions (R1) and (R4) consecutively over an Ag-gauze catalyst by reacting ethylene in a stream containing oxygen and carbon monoxide. To consider this as an alternative processing concept, laboratory or pilot-plant data on the rates of reaction are necessary.

In summary, there is an increasing emphasis on retrofitting processes to eliminate active intermediates and in the design of new processes to avoid these chemicals entirely. Furthermore, the designers of new processes are being asked with increasing frequency to select raw materials and reactions accordingly. These have become important considerations in the early stages of process design.

EXAMPLE 6.1 ***Synthesis of a Process to Hydrodealkylate Toluene***

This example involves the synthesis of a process to hydrodealkylate toluene, which was actively used following World War II, when it became favorable to convert large quantities of toluene, which was no longer needed to make the explosive TNT, to benzene for use in the manufacture of cyclohexane, a precursor of nylon. In this case, a product design alternative involves the conversion of toluene to benzene and, for this purpose, the principal reaction path is well defined. It involves

$$C_7H_8 + H_2 \rightarrow C_6H_6 + CH_4 \qquad \text{(R1)}$$

which is accompanied by the side reaction

$$2C_6H_6 \rightarrow C_{12}H_{10} + H_2 \qquad \text{(R2)}$$

Laboratory data indicate that the reactions proceed irreversibly without a catalyst at temperatures in the range of 1,200–1,270°F with approximately 75 mol% of the toluene converted to benzene and approximately 2 mol% of the benzene produced in the hydrodealkylation reaction converted to biphenyl. Because the reactions occur in series in a single processing unit, just a single reaction operation is positioned in the flowsheet, as shown in Figure 6.1. The plant capacity is based on the conversion of 274.2 1bmol/hr of toluene, or approximately 200 MMIb/yr, assuming operation 330 days per year.

Here, the overall mass balance is carried out assuming that *all* of the unreacted toluene is recycled and consumed in the process to be synthesized. Furthermore, 2 mol% of the entire production of benzene is converted to biphenyl.

Before inserting the reaction operation into a flowsheet, it is important to check the feasibility of the economic potential, *EP* (i.e., the sales minus the cost of raw materials, not including the cost of utilities and operating costs). Using prices for C_6H_6 and C_7H_8 from *ICIS Chemical Business* in late 2013 and 2014 estimates for H_2 and CH_4

	Cost (cent/lb)
H_2	0.59
CH_4	0.21
C_6H_6	0.54
C_7H_8	0.47
$C_{12}H_{10}$	unavailable

the economic potential per pound of benzene (assuming negligible conversion to $C_{12}H_{10}$) is only 1.4 cent/lb C_6H_6. Note, however, that after World War II with a large excess of toluene available, its unit cost was much lower—and the economic potential was much higher. Even without the cost of equipment and its operation, the *EP* was sufficiently large to proceed with the next step in process synthesis, Distribution of Chemicals.

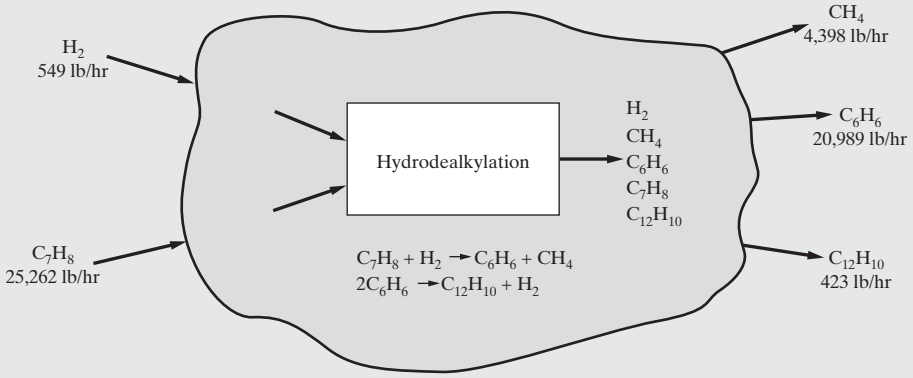

Figure 6.1 Reaction operation for the hydrodealkylation of toluene.

6.3 DISTRIBUTION OF CHEMICALS

In this subsection, several heuristics are presented beginning with the need for excess chemicals in carrying out reaction operations.

Excess Chemicals

Heuristic 2*: *Use an excess of one chemical reactant in a reaction operation to consume completely a valuable, toxic, or hazardous chemical reactant. The MSDSs will indicate which chemicals are toxic and hazardous.

After the reaction operations are positioned in a process flowsheet, the sources of chemicals (i.e., the feed streams and reactor effluents) are distributed among the sinks for chemicals (i.e., the feed streams to the reaction operations and the products from the process). In this distribution, decisions are made concerning (1) the use of one chemical reactant in excess in a reaction operation, (2) the handling of inert species that enter in the feed streams, and (3) the handling of undesired byproducts generated in side reactions. For example, as we have seen in Figure 2.3, one distribution of chemicals for the vinyl-chloride process involves stoichiometric amounts of ethylene and chlorine fed to the direct-chlorination reactor. Alternatively, an excess of ethylene can be utilized as shown in Figure 6.2. In this distribution, the reactor is designed to consume completely the hazardous and toxic chlorine, but the recovery of unreacted ethylene from the dichloroethane product is required. Clearly, an important consideration is the degree of the excess, that is, the ethylene/chlorine ratio. It governs the costs of separation and recirculation, and often plays a key role in the process economics. In many design strategies, this ratio is set using heuristics, with larger ratios used to ensure consumption of the most hazardous chemicals. Eventually, as a *base-case design* evolves, the ratio is varied systematically, often using a process simulator. In mathematical programming strategies, it is treated as a *design variable* to be varied during optimization with a lower bound. Note that for exothermic reactions, the excess chemical often serves the useful function of absorbing the heat of reaction and thereby maintaining more moderate temperatures. This is an important approach to handling large heats of reaction and is considered with several common alternatives in Section 6.5 in the subsection on heat removal from exothermic reactors. An excess of one chemical reactant is also used to increase conversion of the other (limiting) reactant when the extent of reaction is limited by equilibrium. Also, side reactions can be minimized by using an excess of one reactant.

Inert Species

Heuristic 3*: *When nearly pure products are required, eliminate inert species before the reaction operations when the separations are easily accomplished and when the catalyst is adversely affected by the inert, but not when a large exothermic heat of reaction must be removed.

Often impure feed streams contain significant concentrations of species that are inert in chemical reaction operations. When nearly pure products are required, an important decision concerns whether impurities should be removed before or after reaction operations. As an example, consider the flowsheet in Figure 6.3a in which two reaction operations have been positioned. An impure feed stream of reactant C contains the inert species D, and hence a decision is required concerning whether to remove D before or after reaction step 2, as shown in Figures 6.3b and 6.3c, respectively. Clearly, the ease and cost of the separations, that is, D from C, and D from E (plus unreacted A and C), must be assessed. This can be accomplished by examining the physical properties on which the separations are based. For example, when considering distillation, estimates of the relative volatilities are used. When the mixtures are ideal, the relative volatility, α_{ij},

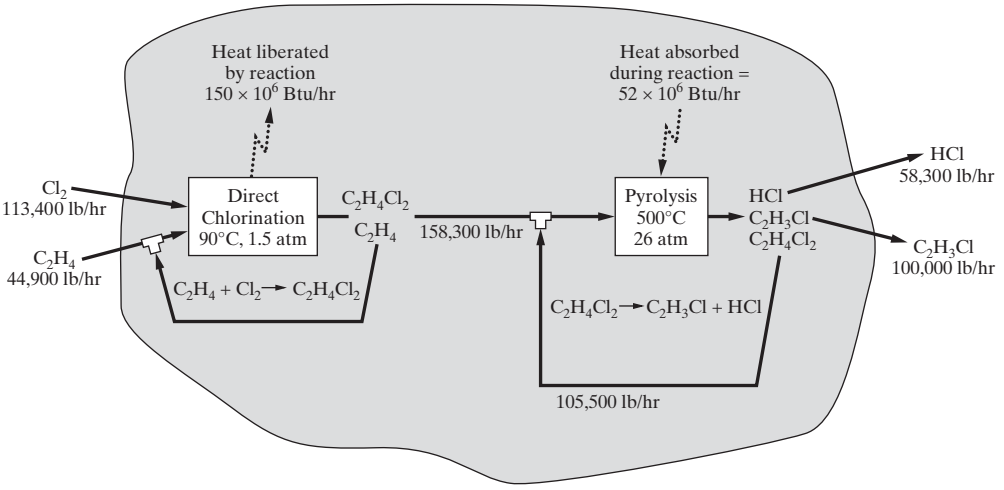

Figure 6.2 Distribution of chemicals for the production of vinyl chloride involving an excess of ethylene.

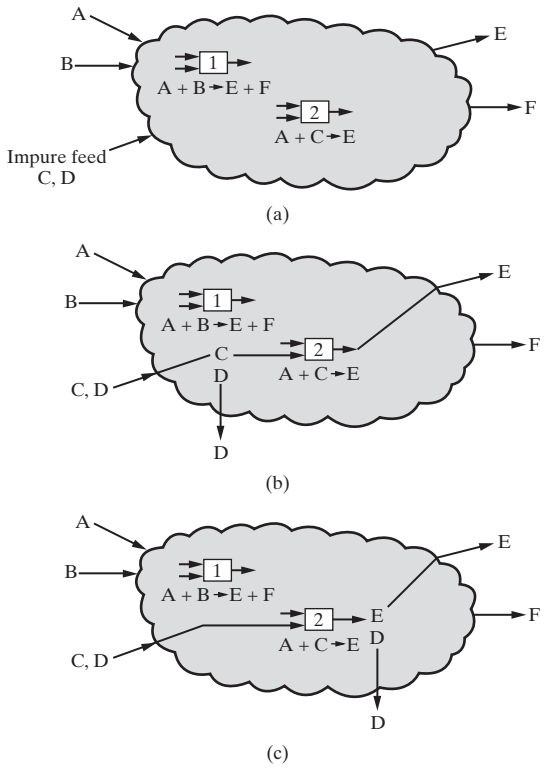

Figure 6.3 Partial distribution of chemicals showing the alternatives for removing inert species D: (a) reaction operations; (b) recovery before reaction; and (c) recovery after reaction.

is simply a ratio of the vapor pressures ($\alpha_{ij} = P_i^s/P_j^s$). Otherwise, activity coefficients are needed ($\alpha_{ij} = \gamma_i P_i^s/\gamma_j P_j^s$). When the relative volatilities differ significantly from unity, an easy and inexpensive separation is anticipated. Similarly, when considering crystallization, the differences in the freezing points are examined, and for dense membrane separations, the permeabilities of the pure species are estimated as the product of the solubility in the membrane and the molecular diffusivity. Other considerations are the sizes of the reactors and separators with larger reactors required when the separations are postponed. Also, for exothermic reactions, the inert species absorb some of the heat generated, thereby lowering the outlet temperatures of the reactors.

EXAMPLE 6.2 *Removing Inert Chemical Species*

To satisfy the Clean Air Act of 1990, gasoline must have a minimum oxygen alom content of 2.0 mol%. In the 1990s, the most common source of this oxygen was methyl *tertiary-butyl* ether (MTBE), which is manufactured by the reaction

$$CH_3OH + \textit{iso}\text{-butene} \rightleftharpoons \text{MTBE}$$

It is desired to construct an MTBE plant at your refinery, located on the Gulf Coast of Texas. Methanol will be purchased and *iso*-butene is available in a mixed-C_4 stream that contains

	Wt%
1-Butene	27
iso-Butene	26
1,3-Butadiene	47

During process synthesis, in the distribution of chemicals, a key question involves whether it is preferable to remove 1-butene and 1, 3-butadiene before or after the reaction operation. In this example, distillation is considered, although other separation methods normally are evaluated as well. It should be noted that recently MTBE was found to contaminate groundwater and, thus, in most locations is no longer the preferred source of oxygen.

SOLUTION

These hydrocarbon mixtures are only mildly nonideal, and hence it is satisfactory to examine the boiling points of the pure species or, better yet, their vapor pressures. These can be tabulated and graphed as a function of temperature using a simulator; for example, the following curves are obtained from ASPEN PLUS (and can be reproduced using the EXAM6-2.bkp file in the Program and Simulation Files folder, which can be downloaded from the Wiley Web site associated with this textbook).

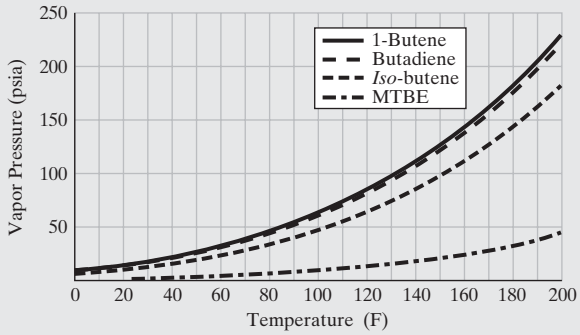

With respect to MTBE, the relative volatilities, $\alpha = P^s/P^s_{\text{MTBE}}$, at 200°F, are 5.13 (1-butene), 4.96 (1,3-butadiene), and 4.04 (*iso*-butene). Clearly, the relative volatilities of 1-butene and 1,3-butadiene are very close, but each differs significantly from the value for *iso*-butene. On this basis, the former two compounds can be separated by distillation before or after the reaction operation. Other considerations, such as their impact on the catalyst, the volumes of the reactors and distillation towers, and the temperature levels in the exothermic reactors, should be evaluated in making this decision.

EXAMPLE 6.3 *Positioning an Equilibrium Reaction Operation*

Consider the reaction and distillation operations for the isomerization of *n*-butane to *iso*-butane according to the reaction

$$n\text{-}C_4H_{10} \rightleftharpoons i\text{-}C_4H_{10}$$

The feed to the process is a refinery stream that contains 20 mol% *iso*-butane. Show the alternatives for positioning the reaction and distillation operations.

SOLUTION

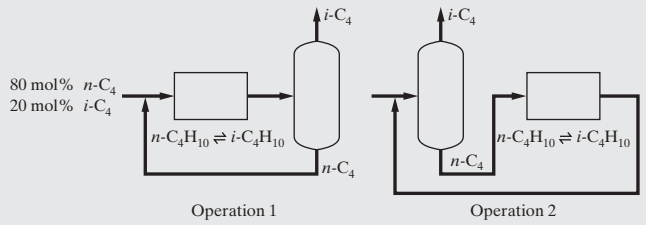

As shown in the diagram, either operation can be placed first. By positioning the distillation column first, a nearly pure feed is sent to the reaction operation, providing a higher conversion to *iso*-butane. The effectiveness of this configuration depends on the relative difficulty of achieving the distillation separation. To determine this, the two configurations should be simulated.

Purge Streams

Heuristic 4: ***Introduce purge streams to provide exits for species that enter the process as impurities in the feed or are formed in irreversible side reactions, when these species are in trace quantities and/or are difficult to separate from the other chemicals. Lighter species leave in vapor purge streams, and heavier species exit in liquid purge streams.***

Trace species, often introduced as impurities in feed streams or formed in side reactions, present special problems when the chemicals are distributed in a flowsheet. In a continuous process, these accumulate continuously unless a means is provided for their removal either by reaction, separation, or through purge streams. Because the reaction or separation of species in low concentration is usually costly, purge streams are used when the species are nontoxic and have little impact on the environment. Purge streams are also used for removing species present in larger amounts when their separation from the other chemicals in the mixture is difficult. As an example, consider the distribution of chemicals in the ammonia process ($N_2 + 3H_2 \rightleftharpoons 2NH_3$) in Figure 6.4. Trace amounts of argon accompany nitrogen, which is recovered from air, and trace amounts of methane accompany hydrogen, which is produced by steam reforming ($CH_4 + H_2O \rightleftharpoons 3H_2 + CO$). After reforming, the carbon monoxide and unreacted methane and steam are recovered, leaving trace quantities of methane. Although nitrogen and hydrogen react at high pressures, in the range of 200–400 atm depending on the process throughput, the conversion is low (usually in the range of 15–20 mol%), and large quantities of unreacted nitrogen and hydrogen are recirculated. The purge stream provides a sink for the argon and methane, which otherwise would build to unacceptable concentrations in the reactor bed, which is packed with reduced iron oxide catalyst. The light gases from the flash vessel are split into purge and recycle streams with the purge/recycle ratio being a key decision variable. As the purge/recycle ratio increases, the losses of nitrogen and hydrogen increase with an accompanying reduction in the production of ammonia. This is counterbalanced by a decrease in the recirculation rate. In the early stages of process synthesis, the purge/recycle ratio is often set using heuristics. Eventually, it can be varied with a process simulator to determine its impact on the recirculation rates and equipment sizes. Then it can be adjusted, also using a process simulator, to optimize the return on investment for the process, as discussed in Chapters 17 and 21. Note that the alternative of separating trace species from the vapor stream, thereby avoiding the purge of valuable nitrogen and hydrogen, may also be considered. These separations—for example, adsorption, absorption, cryogenic distillation, and gas permeation with a membrane—may be more expensive. Finally, it should be recognized that argon and methane are gaseous species that are purged from the vapor recycle stream. Other processes involve heavy impurities that are purged from liquid streams.

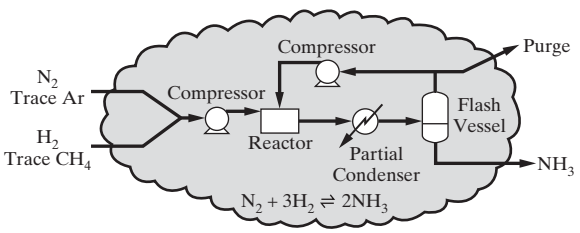

Figure 6.4 Ammonia reactor loop.

EXAMPLE 6.4 ***Ammonia Process Purge***

In this example, the ammonia reactor loop in Figure 6.4 is simulated using ASPEN PLUS to examine the effect of the purge-to-recycle ratio on the compositions and flow rates of the purge and recycle streams. For the ASPEN PLUS flowsheet below, the following specifications are made:

Simulation Unit	Subroutine	*T* (°F)	*P* (atm)
Rl	REQUIL	932	200
Fl	FLASH2	–28	136.3

and the Chao-Seader option set is selected to estimate the thermophysical properties. Note that REQUIL calculates chemical equilibria at the temperature and pressure specified, as shown on the multimedia module *ASPEN → Chemical Reactors → Equilibrium Reactors → REQUIL*, which can be downloaded from www.seas.upenn.edu/~dlewin/multimedia.html.

The combined feed stream, at 77°F and 200 atm, is composed of

	lbmol/hr	Mole Fraction
N_2	24	0.240
H_2	74.3	0.743
Ar	0.6	0.006
CH_4	1.1	0.011
	100.0	1.000

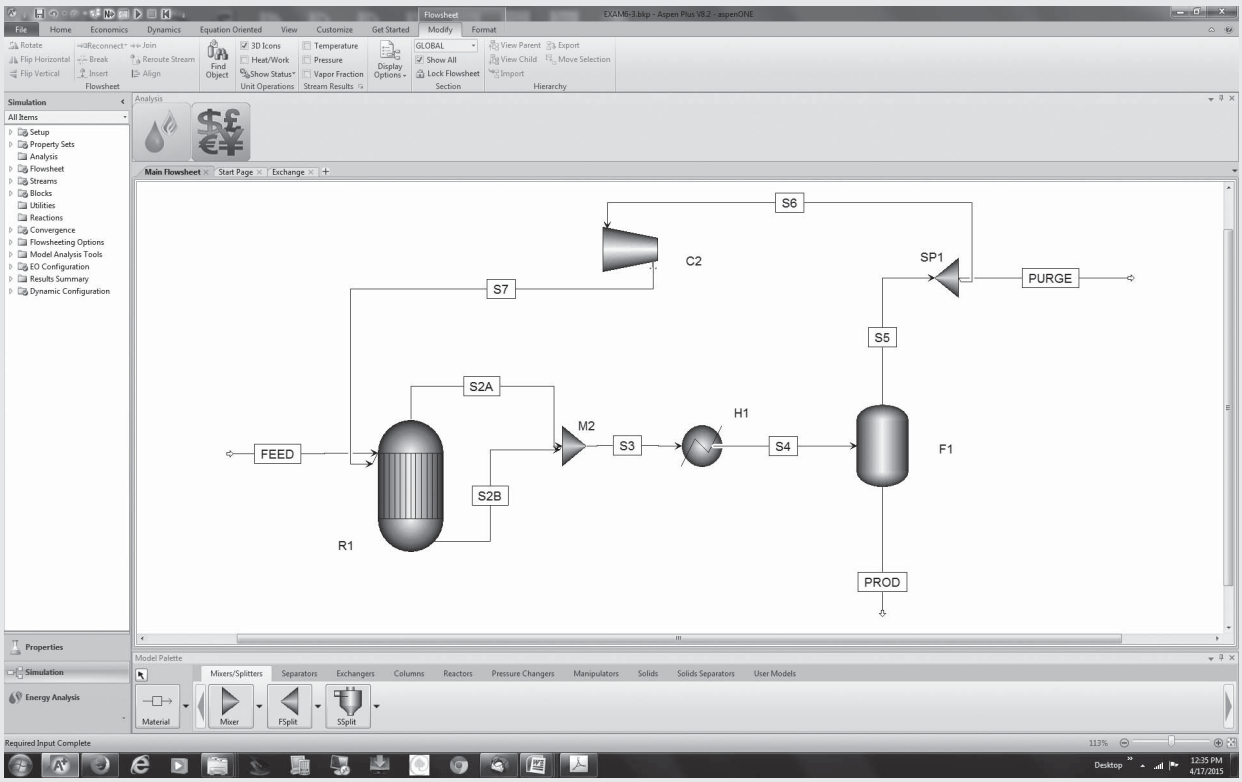

(*Source:* © AspenTech).

SOLUTION

Several variables are tabulated as a function of the purge/recycle ratio:

Purge/Recycle Ratio	PROD Flow Rate (lbmol/hr)	Recycle Flow Rate (lbmol/hr)	Purge Flow Rate (lbmol/hr)	Purge Mole Fraction Ar	Purge Mole Fraction CH_4
0.1	39.2	191.0	19.1	0.028	0.052
0.08	40.75	209.3	16.7	0.033	0.060
0.06	42.4	233.9	14.0	0.040	0.074
0.04	44.3	273.5	10.9	0.053	0.093
0.02	45.8	405.6	8.1	0.072	0.133

In all cases, the mole fractions of Ar and CH_4 in the purge are significantly greater than in the feed. As the purge/recycle ratio is decreased, the vapor effluent from the flash vessel becomes richer in the inert species and less H_2 and N_2 are lost in the purge stream. However, this is accompanied by a significant increase in the recycle rate and the cost of recirculation, as well as the reactor volume. Note that the EXAM6.4.bkp file (in the Program and Simulation Files folder, which can be downloaded from the Wiley Web site associated with this book) can be used to reproduce these results. Although not implemented in this file, the purge/recycle ratio can be adjusted parametrically by varying the fraction of stream S5 purged in a *sensitivity analysis,* which is one of the *model analysis tools* found in most simulators. The capital and operating costs can be estimated and a profitability measure optimized as a function of the purge/recycle ratio.

Heuristic 5: ***Do not purge valuable species or species that are toxic and hazardous, even in small concentrations (see the MSDSs). Add separators to recover valuable species. Add reactors to eliminate, if possible, toxic and hazardous species.***

In some situations, the recovery of trace species from waste streams is an important alternative to purging. This, of course, is the case when an aqueous stream contains trace quantities of rare metals, as can occur when catalysts are impregnated on ceramic supports. In other situations—for example, in the handling of aqueous wastes—environmental regulations are such that trace quantities of organic and inorganic chemicals must be recovered or converted into an environmentally acceptable form. One process to treat aqueous streams in the vicinity of leaking tanks is *supercritical oxidation*, using acoustic waves

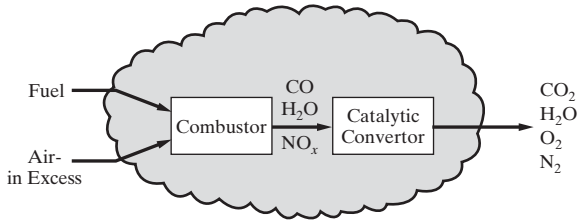

Figure 6.5 Catalytic conversion of combustion effluents.

or lasers to produce plasmas. In this process, the waste species [including chlorinated hydrocarbons, pesticides, phenols (e.g., *p*-nitrophenol), and esters] are oxidized at temperatures and pressures associated with supercritical water (Hua et al., 1995a, b). Yet another example involves the catalytic conversion of hydrocarbons and carbon monoxide in the exhaust gases from internal combustion engines. As illustrated in Figure 6.5, rather than purge the exhaust gases from a combustion engine, catalytic converters commonly convert carbon monoxide and nitrogen oxides to carbon dioxide and nitrogen, respectively. Again, the decision to insert a reaction step, rather than to separate or purge, in the early stages of process design is made often based on the availability of a catalyst and experience; that is, heuristics.

EXAMPLE 6.5 ***Hydrodealkylation of Toluene—Example 6.1 Revisited***

Turning to Step 2, the Distribution of Chemicals, in the synthesis of a process to hydrodealkylate toluene, return to the flowsheet in Figure 6.1 and determine a distribution of chemicals.

SOLUTION

One distribution of chemicals involves a large excess of hydrogen gas to prevent carbon deposition and absorb much of the heat of the exothermic hydrodealkylation reaction. Furthermore, to avoid an expensive separation of the product methane from the hydrogen gas, a purge stream is utilized in which methane leaves the process, unavoidably with a comparable amount of hydrogen. Because the performance of the separation system, to be added in the next synthesis step, is unknown, the amount of hydrogen that accompanies methane in the purge stream is uncertain at this point in the synthesis. Hence, the distribution of chemicals in Figure 6.6 is known incompletely. Note, however, that the sources and sinks of the chemicals can be connected and an estimate for the toluene recycle prepared based upon the assumption of 75 mol% conversion and complete recovery of toluene from the effluent stream. Also, at 1,268°F and 494 psia, a typical operating pressure, the heat of reaction is 5.84×10^6 Btu/hr, as computed by ASPEN PLUS using the RSTOIC subroutine and the Soave-Redlich-Kwong equation of state.

Recycle to Extinction

Heuristic 6: Byproducts that are produced in small quantities in reversible reactions are usually not recovered in separators or purged. Instead, they are usually recycled to extinction.

Often small quantities of chemicals are produced in side reactions, such as the reaction of benzene to form biphenyl in the toluene hydrodealkylation process. When the reaction proceeds *irreversibly*, small quantities of byproducts must be separated away. As shown in Figure 6.6, the biphenyl byproduct is collected in small quantities, or purged; otherwise, it will build up in the process until the process must be shut down.

When the reaction proceeds *reversibly*, in this case for the dimerization of benzene to form biphenyl, it becomes possible to achieve an equilibrium conversion at steady state by recycling product species without removing them from the process. In so doing, it is often said that undesirable byproducts are *recycled to extinction*. It is important to recognize this when distributing chemicals in a potential flowsheet so as to avoid the loss of chemicals through purge streams or the insertion of expensive separation operations. Recycle to extinction, which is considered in more detail in Section 8.8, is most effective when the equilibrium conversion of the side reaction is limited by a small chemical equilibrium constant at the temperature and pressure conditions in the reactor.

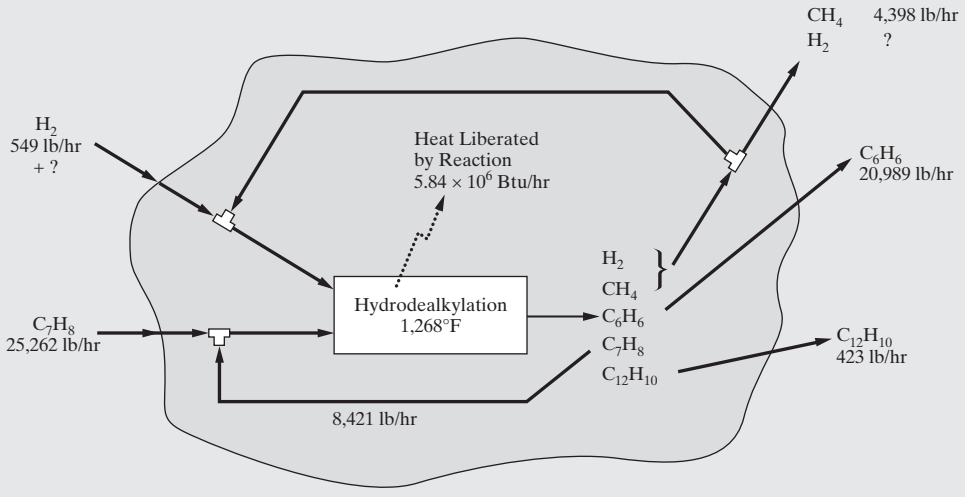

Figure 6.6 Distribution of chemicals for the hydrodealkylation of toluene.

Selectivity

Heuristic 7: ***For competing reactions, both in series and parallel, adjust the temperature, pressure, and catalyst to obtain high yields of the desired products. In the initial distribution of chemicals, assume that these conditions can be satisfied. Before developing a base-case design, obtain kinetics data and check this assumption.***

When chemical reactions compete in the formation of a desired chemical, the reaction conditions must be set carefully to obtain a desirable distribution of chemicals. Consider, for example, the series, parallel, and series-parallel reactions in Figure 6.7, where species B is the desired product. For these and similar reaction systems, it is important to consider the temperature, pressure, ratio of the feed chemicals, and the residence time when distributing the chemicals. One example of series-parallel reactions occurs in the manufacture of allyl chloride. This reaction system, which involves three competing second-order exothermic reactions, is shown in Figure 6.7d with the heats of reaction, ΔH_R, activation energies, E, and pre-exponential factors, k_0, in Table 6.1. Note that because $E_1/E_2 > 1$ and $E_1/E_3 < 1$, the conversion to allyl chloride is highest at intermediate temperatures. In the early stages of process synthesis, when distributing the chemicals, these considerations are helpful in setting the temperature, pressure, and the ratio of propylene/chlorine in the feed.

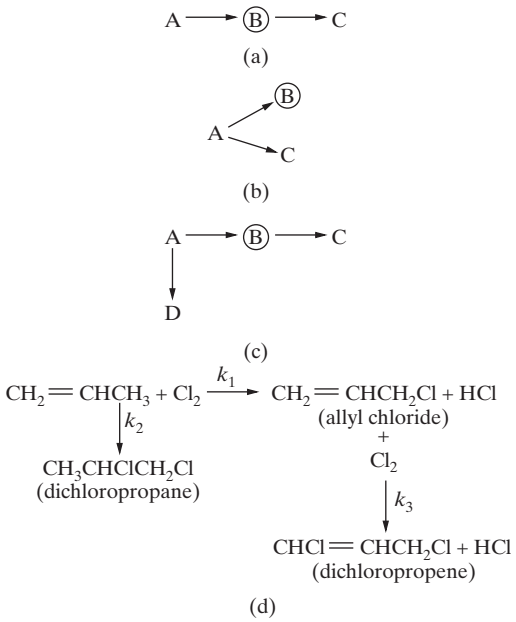

Figure 6.7 Competing reactions: (a) series reactions; (b) parallel reactions; (c) series-parallel reactions; (d) exothermic allyl-chloride reactions.

Table 6.1 Heats of Reaction and Kinetics Constants for the Allyl Chloride Process

Reaction	ΔH_R (Btu/lbmol)	k_0 [lbmol/(hrft^{3}atm^2)]	E/R (°R)
1	−4,800	206,000	13,600
2	−79,200	11.7	3,430
3	−91,800	4.6 x 10^8	21,300

When selectivity is the key to the success of a process design, it is not uncommon to carry out an extensive analysis of the reactor alone, before distributing the chemicals, and proceeding with the synthesis of the flowsheet. In other cases using simulation models, the distribution of chemicals is carried out as the process is optimized to achieve an economic objective.

EXAMPLE 6.6 ***Selectivity of the Allyl Chloride Reactions***

To demonstrate the advantages of running the reactions at intermediate temperatures, show the rate constants for the three competing reactions as a function of temperature.

SOLUTION

As shown in the following graph, the rate constant of the desirable Reaction 1 is the largest relative to the rate constants of the other two reactions at the intermediate temperatures.

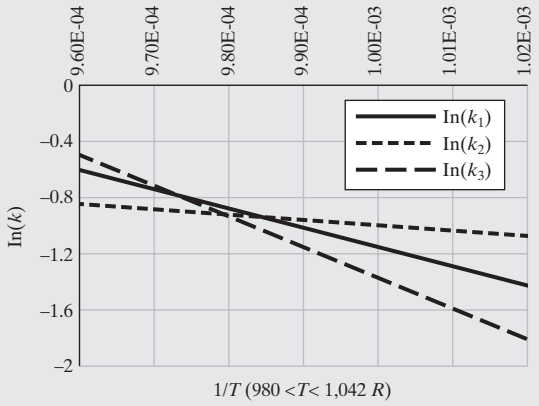

Often, adequate selectivities cannot be achieved by simply adjusting the temperature and pressure of the reactions. In these cases, the field of catalysis plays a crucial role. Chemists, biochemists, and chemical engineers work closely to design catalysts that permit the desired reactions to proceed more rapidly at lower temperatures while reducing the rates of side reactions. For this purpose, many successful reaction operations utilize crystalline zeolites, which are very effective *shape-selective catalysts.* In fact, it is possible to synthesize zeolite structures in which the cavities are just small enough to prevent the reactant molecules for the undesired side reactions from migrating to the reaction sites. Other commonly used catalysts involve the rare metals; for example, Platinum, palladium, and rhodium. Clearly, when distributing chemicals in process synthesis, it is crucial to understand the relative rates of the competing reactions. Company laboratories are a key source of this information, as are patents and articles in the scientific journals. Process designers spend considerable time searching the extensive literature to locate appropriate catalysts.

Of course, many fine books have been written on the subject of catalysis. To study how to design reactors to achieve the desired selectivity, several outstanding textbooks are available;

consider, for example, *Essentials of Chemical Reaction Engineering* (Fogler, 2011) and *The Engineering of Chemical Reactions* (Schmidt, 2004).

Reactive Separations

Heuristic 8: ***For reversible reactions especially, consider conducting them in a separation device capable of removing the products and hence driving the reactions to the right. Such reaction-separation operations lead to very different distributions of chemicals.***

The last step in process synthesis recommended in Section 2.3 is *task integration,* that is, the combination of operations into process units. In the synthesis steps recommended there, reaction operations are positioned first, chemicals are distributed (as discussed earlier in this section), and separation operations are positioned, followed by temperature-, pressure-, and phase-change operations, before task integration occurs. In some cases, however, this strategy does not lead to effective combinations of reaction and separation operations, for example, reactive distillation towers, reactive absorption towers, and reactive membranes. Alternatively, when the advantages of merging these two operations are examined by a design team, a combined reaction-separation operation is placed in the flowsheet before chemicals are distributed, with a significant improvement in the economics of the design. Although the subject of reactive separations is covered in Section 9.5, a brief introduction to reactive distillation is provided next.

Reactive distillation is used commonly when the chemical reaction is reversible, for example,

$$aA + bB \rightleftharpoons cC + dD$$

and there is a significant difference in the relative volatilities of the chemicals at the conditions of temperature and pressure suitable for the reaction. In conventional processing, when a reversible reaction operation is followed by a distillation column, it is common to use an excess of a feed chemical to drive the reaction forward. Alternatively, when the reaction takes place in the gas phase, the pressure is raised or lowered, depending on whether the summation of the stoichiometric coefficients is negative or positive. An advantage of reactive distillation, as shown for the production of methyl acetate,

$$MeOH + HOAc \rightleftharpoons MeOAc + H_2O$$

in Figure 6.8, is that the product chemicals are withdrawn from the reaction section in vapor and liquid streams, thereby driving the reaction forward without excess reactant or changes in pressure. Because methanol is more volatile than acetic acid, it is fed to the bottom of the reaction zone where it concentrates in the vapor phase and contacts acetic acid, which is fed at the top of the reaction zone and concentrates in the liquid phase. As methyl acetate is formed, it concentrates in the vapor phase and leaves the tower in the nearly pure distillate. The water product concentrates in the liquid phase and is removed from the tower in a nearly pure bottoms stream.

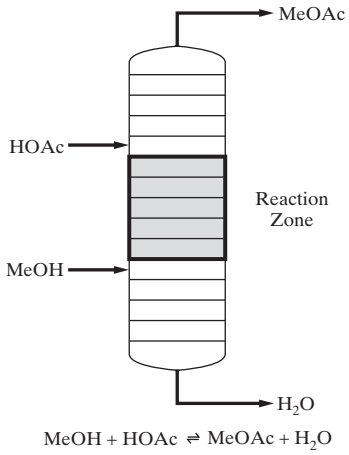

Figure 6.8 Reactive distillation to produce methyl acetate.

In summary, when the advantages of a combined operation (involving a reversible reaction and distillation, in this case) are clear to the design team, the operation can be inserted into the flowsheet *before* the chemicals are distributed in process synthesis. This is a heuristic design procedure that can simplify the synthesis steps and lead to a more profitable design.

Optimal Conversion

Consider the case of a single reaction with a large chemical equilibrium constant such that it is possible to obtain a complete conversion. However, the optimal conversion may not be complete conversion. Instead, an economic balance between a high reactor section cost at high conversion and a high separation section cost at low conversion determines the optimum. Unfortunately, a heuristic for the optimal conversion is not available because it depends on many factors. This subject is considered in more detail in Section 8.5 on reactor-separator-recycle networks.

6.4 SEPARATIONS

Separations Involving Liquid and Vapor Mixtures

Heuristic 9: ***Separate liquid mixtures using distillation, stripping, enhanced (extractive, azeotropic, reactive) distillation, liquid–liquid extraction, crystallization, and/or adsorption. The selection among these alternatives is considered in Chapter 9.***

Heuristic 10: ***Attempt to condense or partially condense vapor mixtures with cooling water or a refrigerant. Then, use Heuristic 9.***

Heuristic 11: ***Separate vapor mixtures using partial condensation, cryogenic distillation, absorption, adsorption, membrane separation, and/or desublimation. The selection among these alternatives is considered in Chapter 9.***

The selection of separation processes is dependent on the phase of the stream to be separated and the relative physical properties of its chemical species. Liquid and vapor streams are separated often using the strategy recommended by Douglas (1988) in

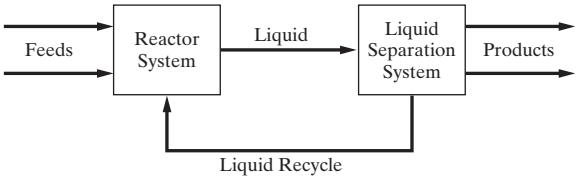

Figure 6.9 Flowsheet to separate liquid reactor effluents.
(*Source:* Modified and reprinted with permission from Douglas, 1988).

Conceptual Design of Chemical Processes. This strategy is reproduced here using the original figures, slightly modified, with the publisher's permission. It is expanded upon in Chapter 9. Note that the choice of type of separator is often influenced by the scale of the process, with distillation often favored by economies-of-scale at large throughputs, and adsorption and membrane separation gaining favor as throughputs decrease.

When the reaction products are in the liquid phase, Douglas recommends that a liquid-separation system be inserted in the flowsheet, as shown in Figure 6.9. The liquid-separation system involves one or more of the following separators: distillation and enhanced distillation, stripping. liquid–liquid extraction, and so on, with the unreacted chemicals recovered in a liquid phase and recycled to the reaction operation.

For reaction products in the vapor phase, Douglas recommends that an attempt be made to partially condense them by cooling with cooling water or a refrigerant. Cooling water can cool the reaction products typically to 35°C, as shown in Figure 6.10. However, in warm climates, a higher temperature (e.g., 45°C) is required. The usual objective is to obtain a liquid phase, which is easier to separate without using refrigeration, which involves an expensive compression step. When partial condensation occurs, a liquid-separation system is inserted with a liquid purge added when necessary to remove trace inerts that concentrate in the liquid and are not readily separated. The vapor phase is sent to a vapor recovery system, which involves one or more of the following separations: partial condensation (at elevated pressures and cryogenic temperatures), cryogenic distillation, absorption, adsorption, membrane separation, and

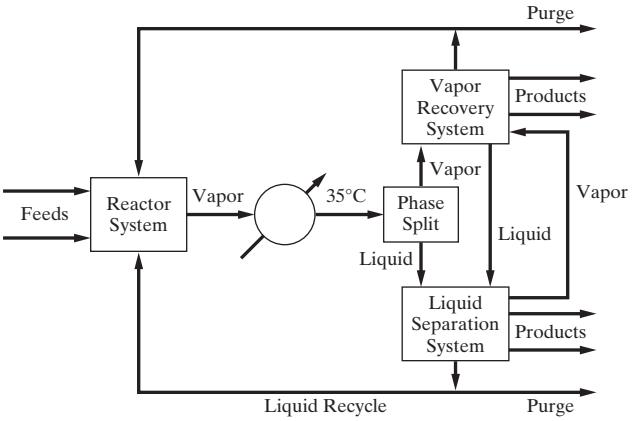

Figure 6.10 Flowsheet to separate vapor reactor effluents.
(*Source:* Modified and reprinted with permission from Douglas, 1988).

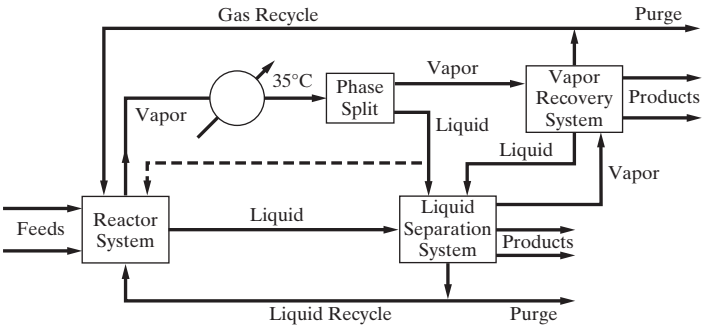

Figure 6.11 Flowsheet to separate vapor/liquid reactor effluents.
(*Source:* Modified and reprinted with permission from Douglas, 1988).

desublimation. Unreacted chemicals are recycled to the reactor section and vapor products are removed. A vapor purge is added when necessary to remove inerts that concentrate in the vapor and are not readily separated. Any liquid produced in the vapor recovery system is sent to the liquid recovery system for product recovery and the recycle of unreacted chemicals.

When the reactor effluent is already distributed between vapor and liquid phases, Douglas combines the two flowsheets, as shown in Figure 6.11. It should be recognized that the development of the separation systems for all three flowsheets involves several heuristics. First, certain separation devices, such as membrane separators, are not considered for the separation of liquids. Second, to achieve a partial condensation, cooling water is utilized initially rather than compression and refrigeration. In this regard, it is presumed that liquid separations are preferred. An attempt is made to partially condense the vapor products, but no attempt is made to partially vaporize the liquid products. Although these and other heuristics are based on considerable experience and usually lead to profitable designs, the designer needs to recognize their limitations and be watchful for situations in which they lead to suboptimal designs. Furthermore, for the separation of multicomponent streams, formal methods have been developed to synthesize separation trains involving vapors or liquids. These are covered in Chapter 9.

EXAMPLE 6.7 ***Hydrodealkylation of Toluene—Examples 6.1 and 6.5 Revisited***

Returning to the synthesis of a process to hydrodealkylate toluene, having completed the distribution of chemicals in Figure 6.6, the need to separate H_2 and CH_4 from C_6H_6, C_7H_8, and $C_{12}H_{10}$ is established. Clearly, the two vaporlike species can be easily removed in a simple vapor–liquid separator (i.e., a flash separation operation). Then, the heaviest three species can be separated in the liquid phase, as recommended by Douglas.

In the resulting flowsheet in Figure 6.12, the flash operation is adjusted to 100°F and 484 psia, slightly reduced from 494 psia in the reaction operation. The temperature is reduced using cooling water to recover the three heaviest species in the liquid phase. Then, following Douglas Heuristic 9, three distillation operations are selected to recover three products [Fuel (H_2 and CH_4), C_6H_6, and $C_{12}H_{10}$], and unreacted toluene to be recycled.

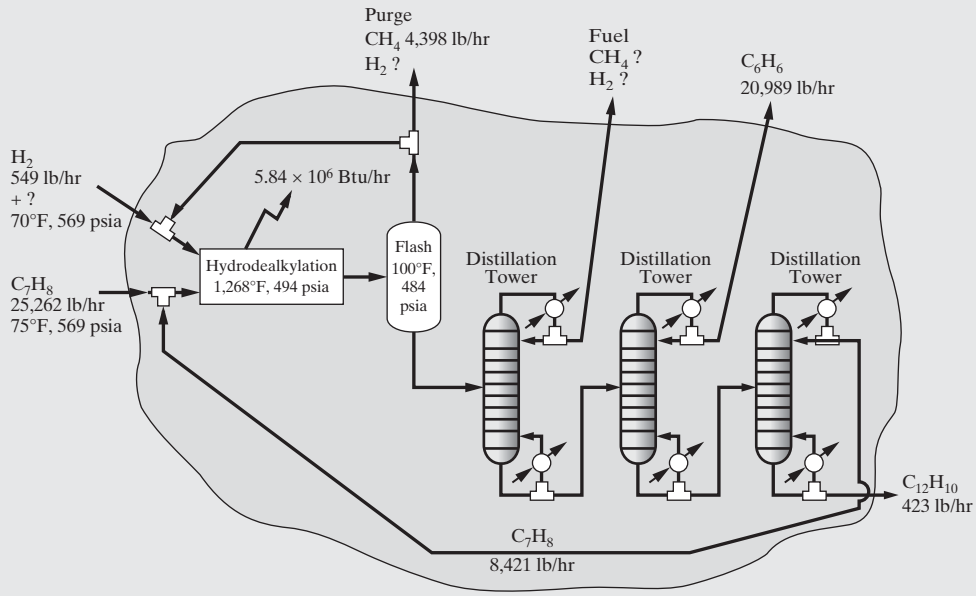

Figure 6.12 Flowsheet including the separation operations for the toluene hydrodealkylation process.

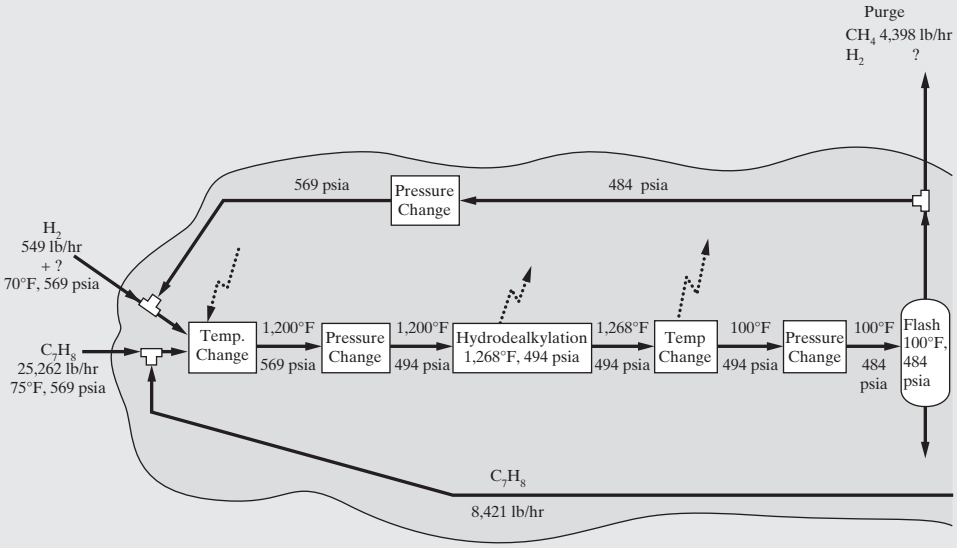

Figure 6.13 Reaction section for the toluene hydrodealkylation process with the temperature-, pressure-, and phase-change operations.

The next synthesis step involves positioning operations to change the temperatures, pressures, and phases where differences exist between the reaction and separation operations, as well as the sources of the raw materials and sinks for the product chemicals. For this process, the toluene and hydrogen feed streams are assumed to be available at elevated pressure, above that required in the hydrodealkylation reactions. When this is not the case, the appropriate operations to increase the pressure must be inserted. One arrangement of the temperature-, pressure-, and phase-change operations is shown in Figure 6.13 for the reaction section only. Clearly, large quantities of heat are needed to raise the temperature of the feed chemicals to 1,200°F, and similarly large quantities of heat must be removed to partially condense the reactor effluent. These heat loads are calculated by ASPEN PLUS as discussed shortly.

The next synthesis step involves task integration, that is, the combination of operations into process units. In one task integration, shown in Figure 6.14, reactor effluent is quenched rapidly to 1,150°F, primarily to avoid the need for a costly high-temperature heat exchanger, and is sent to a feed/product heat exchanger. There, it is cooled as it heats the mixture of feed and recycle chemicals to 1,000°F. The stream is cooled further to 100°F, the temperature of the flash separator. The liquid from the quench is the product of the reactor section, yet a portion of it is recycled to quench the reactor effluent. The vapor product is recycled after a portion is purged to keep methane from building up in the process. This recycle is compressed to the pressure of the feed chemicals, 569 psia. Returning to the feed/product heat exchanger, the hot feed mixture leaves at 1,000°F and is sent to a gas-fired furnace for further heating to 1,200°F, the temperature of the feed to the reactor. Note that the gases are heated in a tube bank that resides in the furnace, and hence a high pressure drop is estimated (70 psia). On the other hand, the hydrodealkylation reactions take place in a large-diameter vessel that has negligible pressure drop. Clearly, at a later stage in the process design, these pressure drops, along with pressure drops in the connecting pipes, can be estimated. Normally, however, small errors in the pressure drops have only a small impact on the equipment sizes and costs as well as the operating costs.

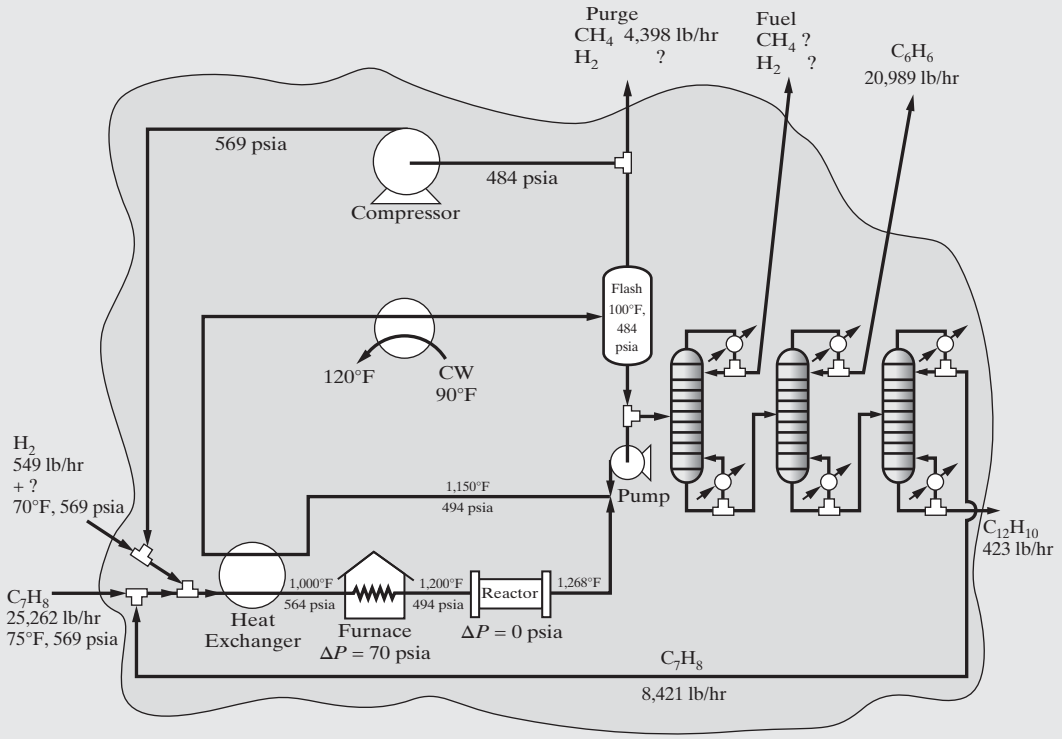

Figure 6.14 Flowsheet showing a task integration for the toluene hydrodealkylation process.

Separations Involving Solid Particles

For streams that involve solid phases or species that crystallize or precipitate, additional considerations are necessary when selecting a separation system because several steps may be necessary due to the impossibility of removing dry solids directly from a liquid. When separating inorganic chemicals, in an aqueous solution especially, the stream is often cooled or partially evaporated to recover solids by crystallization followed by filtration or centrifugation, and then drying. Often slurries are concentrated by settling, centrifugation, or filtration, before drying, as discussed in Section 9.7. Other devices for the removal of solid particles from gases and liquids are cyclones and hydroclones, respectively, as discussed in Section 6.9.

Crystallization occurs in three different modes. *Solution crystallization* applies mainly to inorganic chemicals, which are crystallized from a solvent, often water, with an operating temperature far below the melting point of the crystals. *Precipitation* is fast solution crystallization that produces large numbers of very small crystals. It usually refers to the case where one product of two reacting solutions is a solid of low solubility, for example, the precipitation of insoluble silver chloride when aqueous solutions of silver nitrate and sodium chloride are mixed together. In *melt crystallization,* two or more chemicals of comparable melting points are separated at an operating temperature in the range of the melting points. Crystallization is capable of producing very pure chemicals when conducted according to the following heuristics, noting that recovery by any mode of crystallization may be limited by a eutectic composition.

Heuristic 12: ***Crystallize inorganic chemicals from a concentrated aqueous solution by chilling when solubility decreases significantly with decreasing temperature. Keep the solution at most 1–2°F below the saturation temperature at the prevailing concentration. Use crystallization by evaporation, rather than chilling, when solubility does not change significantly with temperature.***

Heuristic 13: ***Crystal growth rates are approximately the same in all directions, but crystals are never spheres. Crystal growth rates and sizes are controlled by limiting the extent of supersaturation, $S = C/C_{saturation}$, where C is concentration, usually in the range $1.02 < S < 1.05$. Growth rates are influenced greatly by the presence of impurities and of certain specific additives that vary from case to case.***

Heuristic 14: ***Separate organic chemicals by melt crystallization with cooling, using suspension crystallization followed by removal of crystals by settling, filtration, or centrifugation. Alternatively, use layer crystallization on a cooled surface with scraping or melting to remove the crystals. If the melt forms a solid solution, instead of a eutectic, use repeated melting and freezing steps, called fractional melt crystallization, or zone melting to obtain nearly pure crystalline products.***

Prior to crystallization, it is common to employ evaporation to concentrate a solution, particularly an aqueous solution of inorganic chemicals. Because of the relatively high cost of evaporating water with its very large heat of vaporization, the following heuristics are useful for minimizing the cost.

Heuristic 15: ***Using multiple evaporators (called effects) in series, the latent heat of evaporation of water is recovered and reused. With a single evaporator, the ratio of the amount of water evaporated to the amount of external steam supplied to cause the evaporation is typically 0.8. For two effects, the ratio becomes 1.6; for three effects 2.4, and so forth. The magnitude of the boiling-point elevation caused by the dissolved inorganic compounds is a controlling factor in selecting the optimal number of effects. The elevation is often in the range of 3–10°F between solution and pure water boiling points. When the boiling-point rise is small, minimum evaporation cost is obtained with 8 to 10 effects. When the boiling point rise is appreciable, the optimal number of effects is small, 6 or less. If necessary, boost interstage steam pressures with steam-jet or mechanical compressors.***

Heuristic 16: ***When employing multiple effects, the liquid and vapor flows may be in the same or different directions. Use forward feed, where both liquid and vapor flow in the same direction, for a small number of effects, particularly when the liquid feed is hot. Use backward feed, where liquid flows in a direction opposite to vapor flows, for cold feeds and/or a large number of effects. With forward feed, intermediate liquid pumps are not necessary, whereas they are necessary for backward feed.***

Solution crystallization produces a slurry of crystals and mother liquor, which is partially separated by filtration or centrifugation into a wet cake and a mother liquor. Filtration through a filter medium of porous cloth or metal may be carried out under gravity, vacuum, or pressure. Centrifugation may utilize a solid bowl or a porous bowl with a filter medium. Important factors in the selection of equipment include (1) moisture content of the cake, (2) solids content of the mother liquor, (3) fragility of the crystals, (4) crystal particle size, (5) need for washing the crystals to replace mother liquor with pure water, and (6) filtration rate. Filtration rate is best determined by measuring the rate of cake thickness buildup using a small-scale laboratory vacuum leaf filter test with the following criteria: Rapid, 0.1–10 cm/s; Medium, 0.1–10 cm/min; Slow, 0.1–10 cm/hr.

Heuristic 17: ***When crystals are fragile, effective washing is required and clear mother liquor is desired, use gravity, top-feed horizontal pan filtration for slurries that filter at a rapid rate; vacuum rotary-drum filtration for slurries that filter at a moderate rate; and pressure filtration for slurries that filter at a slow rate.***

Heuristic 18: ***When cakes of low moisture content are required, use solid-bowl centrifugation if solids are permitted in the mother liquor; centrifugal filtration if effective washing is required.***

Wet cakes from filtration or centrifugation operations are sent to dryers for removal of remaining moisture. A large number of different types of commercial dryers have been developed to handle the many different types of feeds, which include not only wet cakes, but also pastes, slabs, films, slurries, and liquids. The heat for drying may be supplied from a hot gas in direct contact with the wet feed or it may be supplied indirectly through a wall. Depending on the thickness of the feed and the degree of agitation, drying times can range from seconds to hours. The following heuristics are useful in making a preliminary selection of drying equipment:

Heuristic 19: ***For granular material, free flowing or not, of particle sizes from 3 to 15 mm, use continuous tray and belt dryers with direct heat. For free-flowing granular solids that are not heat sensitive, use an inclined rotary cylindrical dryer, where the heat may be supplied directly from a hot gas or indirectly from tubes carrying steam that run the length of the dryer and are located in one or two rings concentric to and located just inside the dryer rotating shell. For small, free-flowing particles of 1–3 mm in diameter when rapid drying is possible, use a pneumatic conveying dryer with direct heat. For very small free-flowing particles of less than 1 mm in diameter, use a fluidized-bed dryer with direct heat.***

Heuristic 20: ***For pastes and slurries of fine solids, use a drum dryer with indirect heat. For a liquid or pumpable slurry, use a spray dryer with direct heat.***

6.5 HEAT REMOVAL FROM AND ADDITION TO REACTORS

After positioning the separation operations, the next step in process synthesis, as recommended in Section 2.3, is to insert the operations for temperature, pressure, and phase changes. To accomplish this, many excellent algorithms for heat and power integration have been developed. These are presented in Chapter 11. The objective of this section, which considers several approaches to remove the heat generated in exothermic reaction operations and to add the heat required by endothermic reaction operations, is more limited. The subject is discussed at this point because several of the approaches for heat transfer affect the distribution of chemicals in the flowsheet and are best considered after the reaction operations are positioned. These approaches are discussed next, together with other common approaches to remove or add the heat of reaction. First, the methods for removing the heat generated by exothermic reaction operations are presented. Then, some distinctions are drawn for the addition of heat to endothermic reaction operations. For the details of heat removal from or addition to complex reactor configurations, the reader is referred to Section 8.4.

Heat Removal from Exothermic Reactors

Given an exothermic reaction operation, an important first step is to compute the *adiabatic reaction temperature,* that is, the maximum temperature attainable, in the absence of heat transfer. Note that this can be accomplished readily with any of the process simulators. Furthermore, algorithms have been presented for these iterative calculations by Henley and Rosen (1969) and Myers and Seider (1976), among many sources.

EXAMPLE 6.8 *Adiabatic Reaction Temperature*

Consider the reaction of carbon monoxide and hydrogen to form methanol:

$$CO + 2H_2 \rightarrow CH_3OH$$

With the reactants fed in stoichiometric amounts at 25°C and 1 atm, calculate the standard heat of reaction and the adiabatic reaction temperature.

SOLUTION

In ASPEN PLUS, the RSTOIC subroutine is used with a feed stream containing 1 1bmol/hr CO and 2 1bmol/hr H_2 and the PSRK method (Soave-Redlich-Kwong equation of state with Holderbaum-Gmehling mixing rules). To obtain the heat of reaction, the fractional conversion of CO is set at unity with the product stream temperature at 25°C and the vapor fraction at 1.0. The latter keeps the methanol product in the vapor phase at 2.44 psia, and hence both the reactants and product species are vapor. The heat duty computed by RSTOIC is −38,881 Btu/hr, and hence the heat of reaction is $\Delta H_r = -38{,}881$ Btu/1bmol CO.

To obtain the adiabatic reaction temperature for complete conversion, the heat duty is set at zero and the pressure of the methanol product stream is returned to 1 atm. This produces an effluent temperature of 1,158°C (2,116°F), which is far too high for the Cu-based catalyst and the materials of construction in most reactor vessels. Hence, a key question in the synthesis of the methanol process, and similar processes involving highly exothermic reactions, is how to lower the product temperature. In most cases, the designer is given or sets the maximum temperature in the reactor and evaluates one of the heat-removal strategies described in this section.

Note that these results can be reproduced using the EXAM6-6.bkp file in the Program and Simulation Files folder, which can be downloaded from the Wiley Web site associated with this book. Also, RSTOIC-type subroutines are described in Section 8.1.

Heuristic 21: ***To remove a highly exothermic heat of reaction, consider the use of excess reactant, an inert diluent, or cold shots. These affect the distribution of chemicals and should be inserted early in process synthesis.***

Heuristic 22: ***For less exothermic heats of reaction, circulate reactor fluid to an external cooler or use a jacketed vessel or cooling coils. Also, consider the use of intercoolers between adiabatic reaction stages.***

To achieve lower temperatures, several alternatives are possible, beginning with those that affect the distribution of chemicals.

1. Use an excess of one reactant to absorb the heat. This alternative was discussed earlier in Section 6.3 and is illustrated in Figure 6.15a, where excess B is recovered from the separator and recirculated to the reaction operation. Heat is removed in the separator or by exchange with a cold process stream or a cold utility (e.g., cooling water).

EXAMPLE 6.9 *Excess Reactant*

Returning to Example 6.8, an excess of H_2 is specified such that the mole ratio of H_2/CO is arbitrarily 10 and the temperature of the reactor effluent stream is computed.

SOLUTION

Again, using the RSTOIC subroutine in ASPEN PLUS with a complete conversion of CO, the effluent temperature is reduced to 337°C (639°F), a result that can be reproduced using EXAM6-9.bkp file in the Program and Simulation Files folder, which can be downloaded from the Wiley Web site associated with this book. The Sensitivity command can be used to compute the effluent temperature as a function of the H_2/CO ratio, as in Exercise 6.8.

2. Use of an inert diluent, S. Figure 6.15b illustrates this alternative. One example occurs in the manufacture of methanol, where carbon monoxide and hydrogen are reacted in a fluidized bed containing catalyst. In the Marathon Oil process, a large stream of inert oil is circulated through the reactor, cooled, and recirculated to the reactor. Note that diluents like oil, with large heat capacities, are favored to maintain lower temperatures with smaller recirculation rates. The disadvantage of this approach, of course, is that a new species, S, is introduced, which, when separated from the reaction mix, cannot be removed entirely from the desired product. As in Alternative 1, heat is removed in the separator or by exchange with a cold process stream or a cold utility.

EXAMPLE 6.10 *n-Dodecane Diluent*

Returning to Example 6.8, 5 1bmol/hr of *n*-dodecane is added to the reactor feed (1 1bmol/hr CO and 2 1bmol/hr H_2) and the temperature of the reactor effluent stream is computed.

SOLUTION

In this case, the effluent temperature is reduced sharply to 77.6°C (171.7°F), a result that can be reproduced using the EXAM6-10.bkp file in the Program and Simulation Files folder, which can be downloaded from the Wiley Web site associated with this book. The *n*-dodecane flow rate is adjusted to give an adequate temperature reduction. This is accomplished in Exercise 6.9.

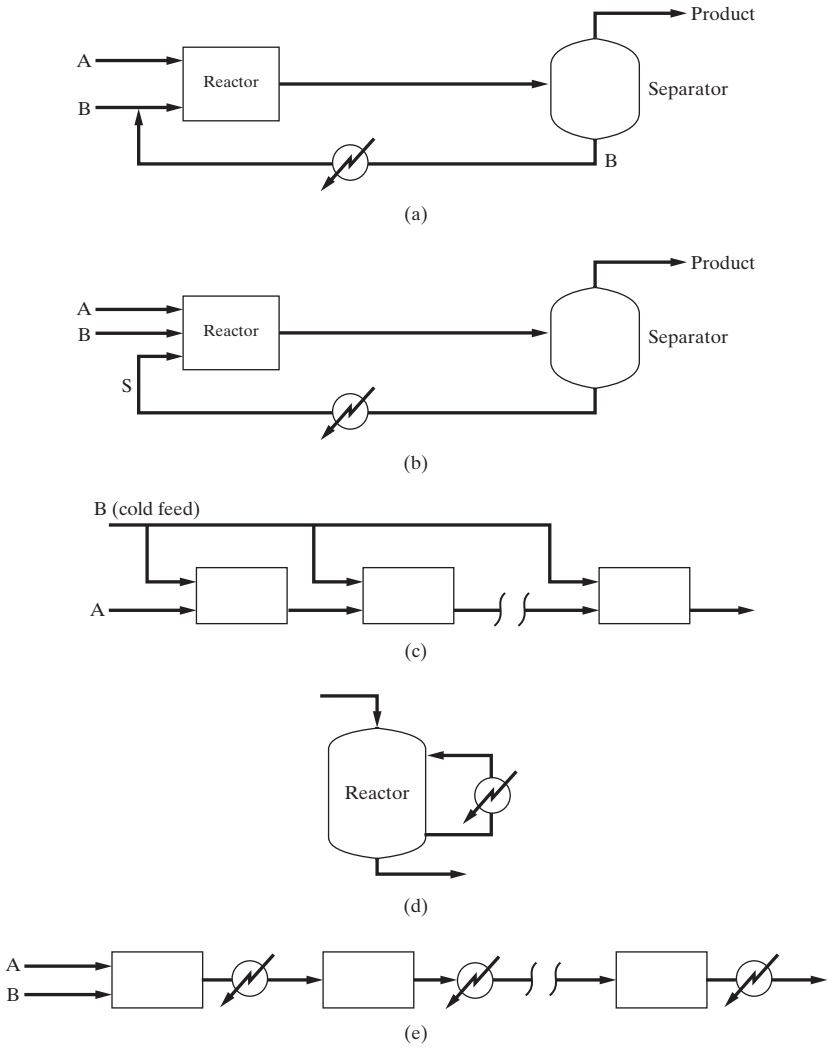

Figure 6.15 Flowsheets to remove the heat of reaction: (a) use of excess reactant; (b) use of inert diluent, S; (c) use of cold shots; (d) diabatic operation; (e) use of intercoolers.

3. Use of cold shots. In this alternative, as illustrated in Figure 6.15c, one of the reactants is cooled and distributed among several adiabatic reaction operations in series. The effluent from each stage, at an elevated temperature, is cooled with a cold shot of reactant B. In each state, additional A is reacted until it is completely consumed in the last stage. The reader is referred to Example 8.5, which shows how to adjust the cold-shot distribution in an ammonia synthesis reactor to maximize the conversion of synthesis gas to ammonia.

The next two alternatives do not affect the distribution of chemicals and are usually considered for moderately exothermic reactions, later in process synthesis—that is, during heat and power integration when opportunities are considered for heat exchange between high- and low-temperature streams.

4. Diabatic operation. In this case, heat is removed from the reaction operation in one of several ways. Either a cooling jacket is utilized or coils are installed through which a cold process stream or cold utility is circulated. In some cases, the reaction occurs in catalyst-filled tubes, surrounded by coolant, or in catalyst-packed beds interspersed with tubes that convey a coolant stream, which is often the reactor feed stream, as illustrated for the ammonia reactor (TVA design) in Figure 6.16. Here, heat transfer from the reacting species in the catalyst bed preheats the reactants, N_2 and H_2, flowing in the cooling tubes, with the tube bundle designed to give adequate heat transfer as well as reaction. The design procedure is similar to that for the design of heat exchangers in Chapter 12. It is noted that for the large-capacity, ammonia-synthesis reactors, the optimal design usually calls for a series of adiabatic beds packed with catalyst, with cooling achieved using cold shots, as shown in Figure 6.15c. Most of the commercial ammonia reactors use a combination of these two cooling arrangements. Another alternative is to circulate a portion of the reacting mixture through an external heat exchanger in which the heat of reaction is removed, as shown in Figure 6.15d.

5. Use of intercoolers. As shown in Figure 6.15e, the reaction operation is divided into several adiabatic stages with heat removed by heat exchangers placed between each stage. Here, also, heat is transferred either to cold process streams that require heating or to cold utilities.

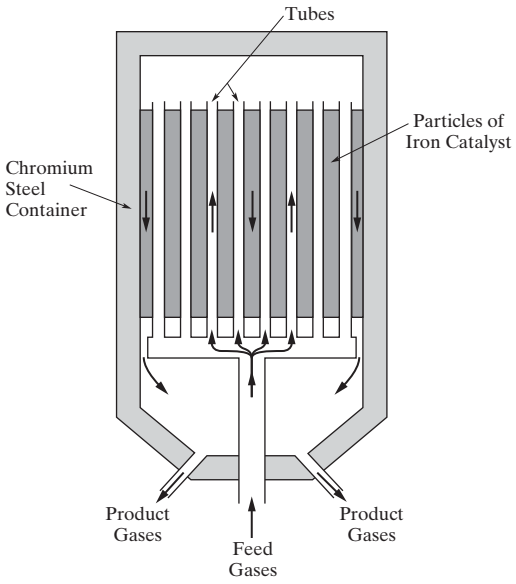

Figure 6.16 Tubular ammonia reactor. (*Source:* Based on TVA Design, from Baddour et al., 1965).

In all of these alternatives, the design team selects acceptable temperature levels and flow rates of the recirculating fluids. These are usually limited by the rates of reaction, and especially the need to avoid thermal runaway or catalyst deterioration, as well as the materials of construction and the temperature levels of the available cold process streams and utilities, such as cooling water. It is common to assign temperatures on the basis of these factors early in process synthesis. However, as optimization strategies are perfected, temperature levels are varied within bounds. See Chapters 11 and 21 for discussions of the use of optimization in process synthesis and optimization of process flowsheets, as well as Example 8.5 to see how constrained optimization is applied to design an ammonia cold-shot converter.

Heat Addition to Endothermic Reactors

Heuristic 23: ***To control temperature for a highly endothermic heat of reaction, consider the use of excess reactant, an inert diluent, or hot shots. These affect the distribution of chemicals and should be inserted early in process synthesis.***

Heuristic 24: ***For less endothermic heats of reaction, circulate reactor fluid to an external heater or use a jacketed vessel or heating coils. Also, consider the use of interheaters between adiabatic reaction stages.***

For endothermic reaction operations, sources of the heat of reaction are needed. As in the case of exothermic reaction operations, the heat of reaction and the adiabatic reaction temperature can be computed using a simulator. The latter provides a lower bound on the temperature of the reactor effluent.

When adding heat to endothermic reaction operations, three approaches for heat addition affect the distribution of chemicals in the flowsheet and are best considered immediately after the reaction operations are positioned. Given that the feed stream is preheated, these approaches closely parallel the first three approaches for heat removal from exothermic reaction operations in Figures 6.15a–6.15c. When an excess of a reactant is utilized, the decrease in effluent temperature varies inversely with the degree of excess. Similarly, when an inert diluent is added, the effluent temperature is decreased inversely with the amount of diluent. For example, when ethylbenzene is pyrolyzed to produce styrene,

$$\text{Ethylbenzene} \rightarrow \text{Styrene} + \text{H}_2$$

superheated steam is added to provide the heat of reaction and keep the reaction temperature elevated. Of course, the addition of steam significantly increases the reactor volume and both the operating and installation costs. Finally, it is possible to add hot shots of reactants to a series of reactors in a way similar to the cold shots added in Figure 6.15c.

The same two alternatives that do not affect the distribution of chemicals apply for the addition of heat to endothermic reaction operations. In this case, the diabatic operation in Figure 6.15d involves the addition of heat in ways similar to the removal of heat. Jackets, coils, and heat exchanger designs are very common. Also, interheaters between stages, as in Figure 6.15e, are used in many situations in place of intercoolers.

6.6 HEAT EXCHANGERS AND FURNACES

As discussed in the previous two sections, heat exchange is commonly used in conjunction with separation and reaction steps to change the temperature and/or phase condition of a process stream. When using a process simulator to perform heat-exchange calculations, it is necessary to select a method of heat exchange from the following six possibilities, where all but the last two involve the separation, by a solid wall, of the two streams exchanging heat.

1. Heat exchange between two process fluids using a double-pipe, shell-and-tube, or compact heat exchanger.
2. Heat exchange between a process fluid and a utility, such as cooling water or steam, using a double-pipe, shell-and-tube, air-cooled, or compact heat exchanger.
3. High-temperature heating of a process fluid using heat from the products of combustion in a furnace (also called a fired heater).
4. Heat exchange within a reactor or separator, rather than in an external heat-exchange device such as a shell-and-tube heat exchanger or furnace, as described in Section 6.5.
5. Direct heat exchange by mixing the two streams that are exchanging heat.
6. Heat exchange involving solid particles.

The following heuristics are useful in selecting an initial basis for the heat-exchange method and the operating conditions. Details of heat exchanger selection and design are presented in Chapter 12.

Heuristic 25: ***Unless required as part of the design of the separator or reactor, provide necessary heat exchange for heating or cooling process fluid streams, with or without utilities, in an external shell-and-tube heat exchanger using countercurrent flow. However, if a process stream requires heating above 750°F, use a furnace unless the process fluid is subject to chemical decomposition.***

Preliminary estimates of exit temperatures of streams flowing through a heat exchanger can be made with the following heuristics.

Heuristic 26: ***Near-optimal minimum temperature approaches in heat exchangers depend on the temperature level as follows:***

10°F or less for temperatures below ambient.

20°F for temperatures at or above ambient up to 300°F.

50°F for high temperatures.

250 to 350°F in a furnace for flue gas temperature above inlet process fluid temperature.

As an example, suppose it is desired to heat 25,000 1b/hr of toluene at 100°F and 90 psia with 25,000 1b/hr of styrene at 300°F and 50 psia. Under these conditions, assume that both streams will be liquid, but this must be verified by flash calculations after the exit temperatures and pressures have been determined. From the previous two heuristics, use a shel1-and-tube heat exchanger with countercurrent flow and a minimum approach temperature of 20°F. Let the average specific heats of the two streams be 0.43 Btu/1b-°F for toluene and 0.44 Btu/1b-°F for styrene. Initially it is not known to which end of the heat exchanger the 20°F minimum approach applies. Assume it applies at the toluene inlet end. If so, the styrene exit temperature is $100 + 20 = 120$°F. This gives a heat-exchanger duty, based on styrene, of:

$$Q = 25{,}000(0.44)(300 - 120) = 1{,}980{,}000 \text{ Btu/hr}$$

Using this duty, the exit temperature of toluene, $T_{\text{toluene out}}$, can be computed from:

$$Q = 1{,}980{,}000 = 25{,}000(0.43)(T_{\text{toluene out}} - 100)$$

Solving, $T_{\text{toluene out}} = 284.2$°F. But this gives a temperature approach of $300 - 284.2 = 15.8$°F at the styrene inlet end, which is less than the minimum approach of 20°F. Therefore. the minimum approach must be applied to the styrene inlet end. Similar calculations give $T_{\text{toluene out}} = 280$°F and $T_{\text{styrene out}} = 124.1$°F. This corresponds to an approach temperature at the toluene inlet end of 24.1°F. which is greater than the minimum approach temperature and, therefore, is acceptable.

Heuristic 27: ***When using cooling water to cool or condense a process stream, assume a water inlet temperature of 90°F (from a cooling tower) and a maximum water outlet temperature of 120°F.***

When cooling and condensing a gas, both sensible and latent heat can be removed in a single heat exchanger. However, because of the many two-phase flow regimes that can occur when boiling a fluid, it is best to provide three separate heat exchangers when changing a subcooled liquid to a superheated gas, especially when the difference between the bubble point and dew point is small. The first exchanger preheats the liquid to the bubble point; the second boils the liquid; and the third superheats the vapor.

Heuristic 28: ***Boil a pure liquid or close-boiling liquid mixture in a separate heat exchanger, using a maximum overall temperature driving force of 45° F to ensure nucleate boiling and avoid undesirable film boiling as discussed in Section 12.1.***

As discussed in detail in Section 12.1, the minimum approach temperature in a countercurrent-flow heat exchanger may occur at an intermediate location rather than at one of the two ends when one of the two streams is both cooled and condensed. If the minimum temperature approach is assumed to occur at one of the two ends of the heat exchanger, a smaller approach or a temperature crossover that violates the second law of thermodynamics may occur at an intermediate location. To avoid this situation, the following heuristic should be applied.

Heuristic 29: ***When cooling and condensing a stream in a heat exchanger, a zone analysis, described in Section 12.1, should be made to make sure that the temperature difference between the hot stream and the cold stream is equal to or greater than the minimum approach temperature at all locations in the heat exchanger. The zone analysis is performed by dividing the heat exchanger into a number of segments and applying an energy balance to each segment to determine corresponding stream inlet and outlet temperatures for the segment, taking into account any phase change. A process simulation program conveniently accomplishes the zone analysis.***

When using a furnace to heat and/or vaporize a process fluid, the following heuristic is useful for establishing inlet and outlet heating medium temperature conditions so that fuel and air requirements can be estimated.

Heuristic 30: ***Typically, a hydrocarbon gives an adiabatic flame temperature of approximately 3,500°F when using the stoichiometric amount of air. However, use excess air to achieve complete combustion and give a maximum flue gas temperature of 2,000°F. Set the stack gas temperature in the range of 650–950°F to prevent condensation of corrosive components of the flue gas.***

Pressure drops of fluids flowing through heat exchangers and furnaces may be estimated with the following heuristics.

Heuristic 31: ***Estimate heat-exchanger pressure drops as follows:***

1.5 psi for boiling and condensing.

3 psi for a gas.

5 psi for a low-viscosity liquid.

7–9 psi for a high-viscosity liquid.

20 psi for a process fluid passing through a furnace.

Unless exotic materials are used, heat exchangers should not be used for cooling and/or condensing process streams with temperatures above 1,150°F. Instead, use the following heuristic for direct heat exchange.

Heuristic 32: ***Quench a very hot process stream to at least 1,150°F before sending it to a heat exchanger for additional cooling and/or condensation. The quench fluid is best obtained from a downstream separator as in Figure 7.31 for the toluene hydrodealkylation process. Alternatively, if the process stream contains water vapor, liquid water may be an effective quench fluid.***

Streams of solid particles are commonly heated or cooled directly or indirectly. Heat transfer is much more rapid and controllable when using direct heat exchange.

Heuristic 33: ***If possible, heat or cool a stream of solid particles by direct contact with a hot gas or cold gas, respectively, using a rotary kiln, a fluidized bed, a multiple hearth, or a flash/pneumatic conveyor. Otherwise, use a jacketed spiral conveyor.***

6.7 PUMPING, COMPRESSION, PRESSURE REDUCTION, VACUUM, AND CONVEYING OF SOLIDS

As mentioned in the previous section, it is common to consider the integration of all temperature- and pressure-change operations. This is referred to as *heat and power integration* and is covered in Chapter 11 after important thermodynamic considerations are presented first in Chapter 10. At this point, however, there are several important heuristics that are useful in determining what type of operations to insert into the flowsheet to increase or decrease pressure. Details of the equipment used to perform pressure-change operations are presented in Chapter 14.

Increasing the Pressure

Gases. To increase the pressure, the most important consideration is the phase state (vapor, liquid, or solid) of the stream. If the stream is a gas, the following heuristic applies for determining whether a *fan, blower*, or *compressor* should be used.

Heuristic 34: ***Use a fan to raise the gas pressure from atmospheric pressure to as high as 40 inches water gauge (10.1 kPa gauge or 1.47 psig). Use a blower or compressor to raise the gas pressure to as high as 206 kPa gauge or 30 psig. Use a compressor or a staged compressor system to attain pressures greater than 206 kPa gauge or 30 psig***.

In Figure 6.14 for the toluene hydrodealkylation process, the pressure of the recycle gas leaving the flash drum at 100°F and 484 psia is increased with a compressor to 569 psia so that, after pressure drops 5 psia through the heat exchanger and 70 psia through the furnace, the recycle gas enters the reactor at a required pressure of 494 psia.

The following heuristic is useful for estimating the exit temperature, which can be significantly higher than the entering temperature, and the power requirement when increasing the gas pressure by a single stage of reversible, adiabatic compression.

Heuristic 35: ***Estimate the theoretical adiabatic horsepower (THp) for compressing a gas:***

$$THp = SCFM\left(\frac{T_1}{8{,}130a}\right)\left[\left(\frac{P_2}{P_1}\right)^a - 1\right] \qquad (6.1)$$

where SCFM = standard cubic feet of gas per minute at 60°F and 1 atm (379 SCF/1bmol); T_1 = gas inlet temperature in °R: inlet and outlet pressures, P_1 and P_2, are absolute pressures: and $a = (k-1)/k$ with k = the gas-specific heat ratio, C_p/C_v

Estimate the theoretical exit temperature, T_2, for a gas compressor:

$$T_2 = T_1(P_2/P_1)^a \qquad (6.2)$$

For example, if air at 100°F is compressed from 1 to 3 atm (compression ratio = 3) using $k = 1.4$, the *THp* is computed to be 128 Hp/standard million ft^3/day with an outlet temperature of 306°F.

When using a compressor, the gas theoretical exit temperature should not exceed approximately 375°F, the limit imposed by most compressor manufacturers. This corresponds to a compression ratio of 4 for $k = 1.4$ and $T_2 = 375$°F. When the exit gas temperature exceeds the limit, a single gas compression step cannot be used. Instead, a multistage compression system, with intercoolers between each stage, must be employed. Each intercooler cools the gas back down to approximately 100°F. The following heuristic is useful for estimating the number of stages, *N*, required and the interstage pressures.

Heuristic 36: ***Estimate the number of gas compression stages, N, from the following table, which assumes a specific heat ratio of 1.4 and a maximum compression ratio of 4 for each stage.***

Final Pressure/Inlet Pressure	Number of Stages
< 4	1
4–16	2
16–64	3
64–256	4

Optimal interstage pressures correspond to equal Hp for each compressor. Therefore, based on the above equation for theoretical compressor Hp, estimate

interstage pressures by using approximately the same compression ratio for each stage with an intercooler pressure drop of 2 psi or 15 kPa.

For example, in Exercise 7.8. a feed gas at 100°F and 30 psia is to be compressed to 569 psia. From the above table with an overall compression ratio of $569/30 = 19$, a three-stage system is indicated. For equal compression ratios, the compression ratio for each stage of a three-stage system $= 19^{1/3} = 2.7$. The estimated stage pressures are as follows, taking into account a 2 psi drop for each intercooler and its associated piping:

Stage	Compressor Inlet Pressure, psia	Compressor Outlet Pressure, psia
1	30	81
2	79	213
3	211	569

When compressing a gas, the entering stream must not contain liquid, and the exiting stream must be above its dew point so as not to damage the compressor. To remove any entrained liquid droplets from the entering gas, a vertical knock-out drum equipped with a demister pad is placed just upstream of the compressor. To prevent condensation in the compressor, especially when the entering gas is near its dew point, a heat exchanger should also be added at the compressor inlet to provide sufficient preheat to ensure that the exiting gas is well above its dew point.

Liquids. If the pressure of a liquid is to be increased, a pump is used. The following heuristic is useful for determining the types of pumps best suited for a given task where the head in feet is the pressure increase across the pump in psf (pounds force/ft^2) divided by the liquid density in lb/ft^3.

Heuristic 37: For heads up to 3,200 ft and flow rates in the range of 10–5,000 gpm, use a centrifugal pump. For high heads up to 20,000 ft and flow rates up to 500 gpm, use a reciprocating pump. Less common are axial pumps for heads up to 40 ft for flow rates in the range of 20–100,000 gpm and rotary pumps for heads up to 3,000 ft for flow rates in the range of 1–1,500 gpm.

For liquid water with a density of 62.4 lb/ft^3, heads of 3,000 and 20,000 ft correspond to pressure increases across the pump of 1,300 and 8,680 psi, respectively.

When pumping a liquid from an operation at one pressure, P_1, to a subsequent operation at a higher pressure, P_2, the pressure increase across the pump must be higher than $P_2 - P_1$ to overcome pipeline pressure drop, control valve pressure drop, and possible increases in elevation (potential energy). This additional pressure increase may be estimated by the following heuristic.

Heuristic 38: For liquid flow, assume a pipeline pressure drop of 2 psi/100 ft of pipe and a control valve pressure drop of at least 10 psi. For each 10-ft rise in elevation, assume a pressure drop of 4 psi.

For example, in Figure 2.6 the combined chlorination reactor effluent and dichloroethane recycle at 1.5 atm is sent to a pyrolysis reactor operating at 26 atm. Although no pressure drops are shown for the two temperature-change and one phase-change operations, they may be estimated at 10 psi total. The line pressure drop and control valve pressure drop may be estimated at 15 psi. Take the elevation change as 20 ft, giving 8 psi. Therefore, the total additional pressure increase is $10 + 15 + 8 = 33$ psi, or 2.3 atm. The required corresponding pressure increase across the pump (pressure-change operation) is, therefore $(26 - 1.5) + 2.3 = 26.8$ atm. For a liquid density of 78 lb/ft^3 or 10.4 lb/gal, the required pumping head is $26.8(14.7)(144)/78 = 730$ ft, The flow rate through the pump is $(158{,}300 + 105{,}500)/10.4/60 = 422$ gpm. Using Heuristic 37, select a centrifugal pump.

The following heuristic provides an estimate of the theoretical pump *Hp*. Unlike the case of gas compression, the temperature change across the pump is small and can be neglected.

Heuristic 39: Estimate the theoretical horsepower (THp) for pumping a liquid:

$$THp = (\text{gpm})(\text{Pressure increase, psi})/1{,}714 \qquad (6.3)$$

For example, the theoretical *Hp* for pumping the liquid in Figure 2.6, using the above data, is $(422)(26.8)(14.7)/1{,}714 = 97$ Hp.

Decreasing the Pressure

The pressure of a gas or liquid stream can be reduced to ambient pressure or higher with a single throttle valve or two or more such valves in series. The adiabatic expansion of a gas across a valve is accompanied by a decrease in the temperature of the gas. The exiting temperature is estimated from Eq. (6.2) for gas compression. For a liquid, the exit temperature is almost the same as the temperature entering the valve. In neither case is shaft work recovered from the fluid. Alternatively, it is possible to recover energy in the form of shaft work that can be used elsewhere by employing a turbinelike device. For a gas, the device is referred to as an expander, expansion turbine, or turboexpander. For a liquid, the corresponding device is a power-recovery turbine. The following heuristics are useful in determining whether a turbine should be used in place of a valve.

Heuristic 40: Consider the use of an expander for reducing the pressure of a gas or a pressure-recovery turbine for reducing the pressure of a liquid when more than 20 Hp and 150 Hp, respectively, can be recovered.

Heuristic 41: Estimate the theoretical adiabatic horsepower (THp) for expanding a gas:

$$THp = SCFM\left(\frac{T_1}{8{,}130a}\right)\left[1 - \left(\frac{P_2}{P_1}\right)^a\right] \qquad (6.4)$$

Heuristic 42: Estimate the theoretical horsepower (THp) for reducing the pressure of a liquid:

$$THp = (\text{gpm})(\text{Pressure decrease, psi})/1{,}714 \qquad (6.5)$$

In Figure 2.5, the pyrolysis effluent gas, following cooling to 170°C and condensation to 6°C at 26 atm, is reduced in pressure to 12 atm before entering the first distillation column. The flowsheet in Figure 2.5 shows the use of a valve following the condenser to accomplish the pressure reduction. Should a pressure-recovery turbine be used? Assume a flow rate of 422 gpm. The pressure decrease is $(26 - 12)\ (14.7) = 206$ psi. Using Eq. (6.5), THp = (422)(206)/1,714 = 51, which is much less than 150 Hp. Therefore, according to the above heuristic, a valve is preferred. Alternatively, the pressure reduction step could be inserted just prior to the condenser, using an expander on the gas at its dew point of 170°C. The total flow rate is (58,300 + 100,000 + 105,500)/60 = 4,397 1b/min. The average molecular weight is computed to be 61.9, giving a molar flow rate of 71 1bmol/min. The corresponding SCFM (standard cubic feet per minute at standard conditions of 60°F and 1 atm) is (71)(379) = 26,000. Assume $k = 1.2$, giving $a = (1.2 - 1)/1.2 = 0.167$. With a decompression ratio of $12/26 = 0.462$ and $T_1 = 797$°R, Eq. (6.4) gives 1,910 THp, which is much more than 120 Hp. Therefore, according to the above heuristic, an expander should be used. The theoretical temperature of the gas exiting the expander, using Eq. (6.2) is $797(0.462)^{0.167} = 701$°R = 241°F = 116°C.

Pumping a Liquid or Compressing a Gas

When it is necessary to increase the pressure between process operations, it is almost always far less expensive to pump a liquid rather than compress a vapor. This is because the power required to increase the pressure of a flowing stream is

$$W = \int_{P_1}^{P_2} V\,dP \tag{6.6}$$

where V is the volumetric flow rate, which is normally far less for liquid streams—typically two orders of magnitude less. Hence, it is common to install pumps having approximately 10 Hp, whereas comparable compressors require approximately 1,000 Hp and are far more expensive to purchase and install. For these reasons, if the low-pressure stream is a vapor and the phase state is also vapor at the higher pressure, it is almost always preferable to condense the vapor, pump it and revaporize it rather than compress it, as illustrated in Figure 6.17. If the low-pressure stream is a liquid and the high-pressure stream is a vapor, it is preferable to increase the pressure first with a pump and then vaporize the liquid rather than vaporize the liquid and then compress it. This is the subject of Exercise 6.12 and the following example.

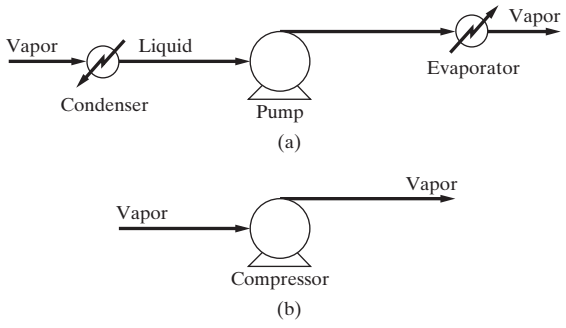

Figure 6.17 Alternatives for raising the pressure of a vapor stream: (a) pump a liquid and (b) compress the vapor.

Heuristic 43: ***To increase the pressure of a stream, pump a liquid rather than compress a gas unless refrigeration is needed.***

EXAMPLE 6.11 ***Feed Preparation of Ethylbenzene***

Ethylbenzene is to be taken from storage as a liquid at 25°C and 1 atm and fed to a styrene reactor as a vapor at 400°C and 5 atm at 100,000 1b/hr. In this example, two alternatives are considered for positioning the temperature- and pressure-increase operations.

SOLUTION

1. Pump first. Using the PUMP and HEATER subroutines in ASPEN PLUS discussed on the multimedia modules, which can be downloaded from www.seas.upenn.edu/~dlewin/multimedia.html, 12.5 brake *Hp* are required to pump the liquid followed by 4.67×10^7 Btu/hr to vaporize the liquid and heat the vapor to 400°C.
2. Vaporize the liquid first. Using the HEATER and COMPR subroutines discussed on the multimedia CD-ROM, 4.21×10^7 Btu/hr, are required to vaporize the liquid and heat it to 349.6°C, followed by 1,897 brake *Hp* to compress the vapor to 5 atm at 400°C.

Clearly, the power requirement is substantially less when pumping a liquid. Note that these results can be reproduced using the EXAM6-11.bkp file in the Program and Simulation Files folder, which can be downloaded from the Wiley Web site associated with this book.

Vacuum

When process pressures less than the ambient pressure are required, special devices and considerations are necessary. Vacuum operation is most common in crystallization, distillation, drying, evaporation, and pervaporation operations. A vacuum inside the equipment causes inleakage of ambient-pressure air. A vacuum system is used to remove this air together with any associated vapor in the process stream that passes through the equipment. For continuous processes, vacuums are predominantly in the range of 1–760 torr (0.13–101.3 kPa). In this range, it is common to use a vacuum pump, which compresses the gas from vacuum (suction pressure) to ambient pressure, or a jet-ejector system, which uses a flow of pressurized water or steam to mix with and remove the gas to create the vacuum. To design the vacuum system, it is necessary to estimate the inleakage of air, determine the total amount of gas (inleakage

plus associated vapor) to be removed, and select an appropriate system for the vacuum level required. The following heuristics are useful. Details of vacuum equipment are presented in Section 16.6.

Heuristic 44: ***Estimate inleakage of air by:***

$$w = kV^{0.667} \tag{6.7}$$

where w = lb/hr of air inleakage, $V = ft^3$ of volume of the equipment under vacuum, and $k = 0.2$ for pressures greater than 90 torr, 0.15 for pressures between 21 and 89 torr, 0.10 for pressures between 3.1 and 20 torr, and 0.051 for pressures between 1 and 3 torr.

Heuristic 45: ***To reduce the amount of gas sent to the vacuum system if its temperature is greater than 100°F, add a condenser using cooling water before the vacuum system. The gas leaving the condenser will be at a dew-point temperature of 100°F at the vacuum pressure.***

Heuristic 46: ***For pressures down to 10 torr and gas flow rates up to 10,000 ft^3/min at the inlet to the vacuum system, use a liquid-ring vacuum pump. For pressures down to 2 torr and gas flow rates up to 1,000,000 ft^3/min at the inlet to the vacuum system, use a steam-jet ejector system (one-stage for 100–760 torr, two-stage for 15–100 torr, and three-stage for 2–15 torr). Include a direct-contact condenser between stages.***

Heuristic 47: ***For a three-stage steam-jet ejector system used to achieve a vacuum of 2 torr, 100 pounds of 100 psig steam per pound of gas are required.***

Conveying Granular Solids

The movement of streams of granular solids horizontally and/or vertically is achieved with conveyors and elevators. When selecting the type of equipment, important considerations are stickiness, abrasiveness, particle size, and density of the solid particles.

Heuristic 48: ***If the solid particles are small in size, low in particle density, and not sticky or abrasive, use pneumatic conveying with air at 1–7 ft^3/ft^3 of solids and 35–120 ft/s air velocity for distances up to 400 ft. Otherwise, for sticky and/or abrasive solids of any size and density, use a screw conveyer and/or bucket elevator for distances up to 150 ft. For solid particles of any size and shape, and not sticky, use a belt conveyor with inclination up to 30° if necessary for long distances up to a mile or more.***

Changing the Pressure of Granular Solids

Continuous processes frequently involve granular solids either alone, slurried in a liquid, or fluidized in a gas. In many cases, the streams containing the solids are at ambient pressure and are moved with ease by conveyors and elevators. However, in some cases, elevated pressure or vacuum may be required. If solid particles alone are being processed, they are placed in a closed hopper where the pressure is then adjusted to the required value. The solids are then conveyed under pressure or vacuum. For a slurry, the solids are placed in a hopper from which they are discharged into a liquid at ambient pressure. The resulting slurry is then pumped to the desired pressure. A gas–solid particles mixture is formed by discharging solid particles from a hopper, through a rotary valve (also referred to as a rotary air-lock valve), into a gas stream at elevated pressure. For discharge pressures up to 15 psig, a standard rotary valve is used. For discharge pressures in the range of 15 psig to almost 100 psig, high-performance rotary valves are available. Rotary valves must be carefully designed to minimize or avoid gas leakage, prevent bridging of solids in the valve, and avoid wear of the vanes in the valve.

6.8 CHANGING THE PARTICLE SIZE OF SOLIDS AND SIZE SEPARATION OF PARTICLES

It is frequently necessary to change the particle size of solids to meet product specifications or change reaction or drying rate. Methods to accomplish changes in particle size, discussed in detail in *Chemical Process Equipment—Selection and Design* by S.M. Walas (1988) and in *Perry's Chemical Engineers' Handbook*, 7th edition (Green and Perry, 2008), include crushing, grinding, and disintegration to reduce particle size; compression, extrusion, and agglomeration to increase particle size; and size separation devices to obtain a narrow range of particle size. Crushers and grinders are used with screens in closed circuits wherein oversize material is recycled. Grindability is determined mainly by hardness as measured by the following Mohs scale, which ranges from 1 for the softest material to 10 for the hardest:

Material	Mohs Scale
Talc, $Mg_3SiO_{10}(OH)_2$	1
Gypsum, $CaSO_4 \cdot 2H_2O$	2
Calcite, $CaCO_3$	3
Fluorite, CaF_2	4
Apatite, $Ca_5(PO_4)_3(OH, F, Cl)$	5
Feldspar, Na, Ca, K, Al silicates	6
Quartz, SiO_2	7
Topaz, $Al_2SiO_4(F, OH)_3$	8
Corundum, Al_2O_3	9
Diamond, C	10

Materials with a Mohs scale from 1 to 3 are considered soft and include graphite, many plastics, asphalt, sulfur, many inorganic salts, marble, and anthracite coal. Intermediate hardness extends from a Mohs scale of 4 to 6 and includes limestone, asbestos, and glass. Hard materials are characterized by a Mohs scale of 7 to 10 and include sand, granite, and emery. The following

heuristics apply to particle-size reduction. Size of small particles is commonly stated in terms of screen mesh size according to the following U.S. standard (ASTM EII), where not all mesh sizes are given:

Mesh (openings/inch)	Sieve Opening, mm
4	4.75
6	3.35
8	2.36
12	1.70
16	1.18
20	0.841
30	0.600
40	0.420
50	0.300
70	0.212
100	0.149
140	0.106
200	0.074
270	0.053
400	0.037

Heuristic 49: ***Crushing of coarse solids. Use a jaw crusher to reduce lumps of hard, abrasive, and/or sticky materials of 4 inches to 3 feet in diameter to slabby particles of 1–4 inches in size. Use a gyratory crusher to reduce slabby materials of 8 inches to 6 feet in size to rounded particles of 1–10 inches in diameter. Use a cone crusher to reduce less hard and less sticky materials of 2 inches to 1 foot in diameter to particles of 0.2 inch (4 mesh) to 2 inches in diameter.***

Heuristic 50: ***Grinding to fine solids. Use a rod mill to take particles of intermediate hardness as large as 20 mm and reduce them to particles in the range of 10–35 mesh. Use a ball mill to reduce particles of low to intermediate hardness of 1–10 mm in size to very small particles of less than 140 mesh.***

Heuristic 51: ***Particle-size enlargement. Use compression with rotary compression machines to convert powders and granules into tablets of up to 1.5 inches in diameter. Use extruders with cutters to make pellets and wafers from pastes and melts. Use roll compactors to produce sheets from finely divided materials; the sheets are then cut into any desired shape. Use rotating drum granulators and rotary disk granulators with binders to produce particles in the size range of 2–25 mm.***

Heuristic 52: ***Size separation of particles. Use a grizzly of spaced, inclined, vibrated parallel bars to remove large particles greater than 2 inches in diameter. Use a revolving cylindrical perforated screen to remove intermediate-size particles in the size range of 0.25 inch to 1.5 inches in diameter. Use flat, inclined woven screens (U.S. standard) that are vibrated, shaken, or impacted with bouncing balls to separate small particles in the size range of 3–80 mesh. Use an air classifier to separate fine particles smaller than 80 mesh.***

6.9 REMOVAL OF PARTICLES FROM GASES AND LIQUIDS

Fine particles are most efficiently removed from dilute suspensions in gases and liquids by using centrifugal force in cyclones and hydroclones, respectively.

Heuristic 53: ***Use a cyclone separator to remove, from a gas, droplets or solid particles of diameter down to 10 microns (0.01 mm). Use a hydroclone separator to remove, from a liquid, insoluble liquid droplets or solid particles of diameter down to 5 microns (0.005 mm). However, small amounts of entrained liquid droplets are commonly removed from gases by vertical knock-out drums equipped with mesh pads to help coalesce the smallest droplets.***

6.10 CONSIDERATIONS THAT APPLY TO THE ENTIRE FLOWSHEET

The preceding discussion was directed primarily to the initial development of the process flowsheet, by considering particular sections of it and specific types of equipment within it. However, the flowsheet(s) resulting from the application of the 53 heuristics presented above need(s) additional development by applying some general considerations that may be able to improve the process, particularly with respect to efficiency, simplicity, and economics. The following general considerations, suggested by A. Brostow of Air Products and Chemicals, Inc., are typical of those used in process design by industrial chemical engineers:

(a) To increase second-law efficiency and reduce energy consumption, avoid, if possible, the mixing of streams of different temperatures, pressures, or compositions. This is considered in detail in Chapter 10 on second-law analysis.

(b) For a new process, determine how it differs from a similar conventional process and pinpoint the advantages and disadvantages of the new process, making changes where disadvantages are uncovered.

(c) For a new process, determine the maximum production rate and yield, and look for opportunities to increase the production rate and yield. Then, calculate theoretical efficiencies by applying lost-work analysis as presented in Chapter 10. Look for ways to increase the efficiency.

(d) Carefully examine the process flowsheet, looking for ways to eliminate equipment by combining, rearranging, or replacing process steps.

(e) Perform preliminary economic evaluations at different production rates and corresponding plant sizes using simple scaling methods, noting that what is not economical at a small size may be economical at a large size and vice versa.

6.11 SUMMARY

Having studied this chapter, the reader should:

1. Understand how to apply heuristics to obtain a base-case process flowsheet(s) rapidly.
2. Be able to implement the steps in Section 2.1 for process synthesis more effectively, using the many heuristics presented herein and summarized in Table 6.2. The examples and exercises should enable him or her to gain experience in their application.
3. Recognize the limitations of the heuristics in Table 6.2 and the role of the process simulator in permitting the systematic variation of parameters and the examination of alternative designs. The reader should also recognize that the heuristics listed are a subset of the many rules of thumb that have been applied by design teams in carrying out process synthesis.

Table 6.2 Heuristics in Chapter 6

	Heuristic
Reaction operations	
1	Select raw materials and chemical reactions to avoid, or reduce, the handling and storage of hazardous and toxic chemicals.
Distribution of chemicals	
2	Use an excess of one chemical reactant in a reaction operation to consume completely a valuable, toxic, or hazardous chemical reactant. The MSDSs will indicate which chemicals are toxic and hazardous.
3	When nearly pure products are required, eliminate inert species before the reaction operations when the separations are easily accomplished and when the catalyst is adversely affected by the inert but not when a large exothermic heat of reaction must be removed.
4	Introduce purge streams to provide exits for species that enter the process as impurities in the feed or are formed in irreversible side reactions when these species are in trace quantities and/or are difficult to separate from the other chemicals. Lighter species leave in vapor purge streams, and heavier species exit in liquid purge streams.
5	Do not purge valuable species or species that are toxic and hazardous, even in small concentrations (see the MSDSs). Add separators to recover valuable species. Add reactors to eliminate, if possible, toxic and hazardous species.
6	Byproducts that are produced in small quantities in *reversible* reactions are usually not recovered in separators or purged. Instead, they are usually recycled to extinction.
7	For competing reactions, both in series and parallel, adjust the temperature, pressure, and catalyst to obtain high yields of the desired products. In the initial distribution of chemicals, assume that these conditions can be satisfied. Before developing a base-case design, obtain kinetics data and check this assumption.
8	For reversible reactions especially, consider conducting them in a separation device capable of removing the products and hence driving the reactions to the right. Such reaction-separation operations lead to very different distributions of chemicals.
Separation operations—liquid and vapor mixtures	
9	Separate liquid mixtures using distillation, stripping, enhanced (extractive, azeotropic, reactive) distillation, liquid–liquid extraction, crystallization, and/or adsorption. The selection among these alternatives is considered in Chapter 9.
10	Attempt to condense or partially condense vapor mixtures with cooling water or a refrigerant. Then, use Heuristic 9.
11	Separate vapor mixtures using partial condensation, cryogenic distillation, absorption, adsorption, membrane separation, and/or desublimation. The selection among these alternatives is considered in Chapter 9.
Separation operations—involving solid particles	
12	Crystallize inorganic chemicals from a concentrated aqueous solution by chilling when solubility decreases significantly with decreasing temperature. Keep the solution at most 1 to 2°F below the saturation temperature at the prevailing concentration. Use crystallization by evaporation, rather than chilling, when solubility does not change significantly with temperature.

(*Continued*)

Table 6.2 (*continued*)

	Heuristic
13	Crystal growth rates are approximately the same in all directions, but crystals are never spheres. Crystal growth rates and sizes are controlled by limiting the extent of supersaturation, $S = C/C_{\text{saturation}}$, where C is concentration, usually in the range $1.02 < S < 1.05$. Growth rates are influenced greatly by the presence of impurities and of certain specific additives that vary from case to case.
14	Separate organic chemicals by melt crystallization with cooling, using suspension crystallization, followed by removal of crystals by settling, filtration, or centrifugation. Alternatively, use layer crystallization on a cooled surface with scraping or melting to remove the crystals. If the melt forms a solid solution instead of a eutectic, use repeated melting and freezing steps, called fractional melt crystallization, or zone melting to obtain nearly pure crystalline products.
15	Using multiple evaporators (called effects) in series, the latent heat of evaporation of water is recovered and reused. With a single evaporator, the ratio of the amount of water evaporated to the amount of external steam supplied to cause the evaporation is typically 0.8. For two effects, the ratio becomes 1.6; for three effects 2.4, and so forth. The magnitude of the boiling-point elevation caused by the dissolved inorganic compounds is a controlling factor in selecting the optimal number of effects. The elevation is often in the range of 3–10°F between solution and pure water boiling points. When the boiling-point rise is small, minimum evaporation cost is obtained with 8 to 10 effects. When the boiling-point rise is appreciable, the optimal number of effects is small, 6 or less. If necessary, boost interstage steam pressures with steam-jet or mechanical compressors.
16	When employing multiple effects, the liquid and vapor flows may be in the same or different directions. Use forward feed, where both liquid and vapor flow in the same direction, for a small number of effects, particularly when the liquid feed is hot. Use backward feed, where liquid flows in a direction opposite to vapor flows, for cold feeds, and/or a large number of effects. With forward feed, intermediate liquid pumps are not necessary, whereas they are necessary for backward feed.
17	When crystals are fragile, effective washing is required, and clear mother liquor is desired, use: gravity, top-feed horizontal pan filtration for slurries that filter at a rapid rate; vacuum rotary-drum filtration for slurries that filter at a moderate rate; and pressure filtration for slurries that filter at a slow rate.
18	When cakes of low moisture content are required, use: solid-bowl centrifugation if solids are permitted in the mother liquor; centrifugal filtration if effective washing is required.
19	For granular material, free flowing or not, of particle sizes from 3 to 15 mm, use continuous tray and belt dryers with direct heat. For free-flowing granular solids that are not heat sensitive, use an inclined rotary cylindrical dryer where the heat may be supplied directly from a hot gas or indirectly from tubes, carrying steam that run the length of the dryer and are located in one or two rings concentric to and located just inside the dryer rotating shell. For small, free-flowing particles of 1–3 mm in diameter, when rapid drying is possible, use a pneumatic conveying dryer with direct heat. For very small free-flowing particles of less than 1 mm in diameter, use a fluidized-bed dryer with direct heat.
20	For pastes and slurries of fine solids, use a drum dryer with indirect heat. For a liquid or pumpable slurry, use a spray dryer with direct heat.
Heat removal and addition	
21	To remove a highly exothermic heat of reaction, consider the use of excess reactant, an inert diluent, or cold shots. These affect the distribution of chemicals and should be inserted early in process synthesis.
22	For less exothermic heats of reaction, circulate reactor fluid to an external cooler or use a jacketed vessel or cooling coils. Also, consider the use of intercoolers between adiabatic reaction stages.
23	To control temperature for a highly endothermic heat of reaction, consider the use of excess reactant, an inert diluent, or hot shots. These affect the distribution of chemicals and should be inserted early in process synthesis.
24	For less endothermic heats of reaction, circulate reactor fluid to an external heater or use a jacketed vessel or heating coils. Also, consider the use of interheaters between adiabatic reaction stages.
Heat exchangers and furnaces	
25	Unless required as part of the design of the separator or reactor, provide necessary heat exchange for heating or cooling process fluid streams, with or without utilities, in an external shell-and-tube heat exchanger using countercurrent flow. However, if a process stream requires heating above 750°F, use a furnace unless the process fluid is subject to chemical decomposition.

Table 6.2 (*continued*)

	Heuristic
26	Near-optimal minimum temperature approaches in heat exchangers depend on the temperature level as follows: 10°F or less for temperatures below ambient. 20°F for temperatures at or above ambient up to 300°F. 50°F for high temperatures. 250 to 350°F in a furnace for flue gas temperature above inlet process fluid temperature.
27	When using cooling water to cool or condense a process stream, assume a water inlet temperature of 90°F (from a cooling tower) and a maximum water outlet temperature of 120°F.
28	Boil a pure liquid or close-boiling liquid mixture in a separate heat exchanger, using a maximum overall temperature driving force of 45°F to ensure nucleate boiling and avoid undesirable film boiling as discussed in Section 12.1.
29	When cooling and condensing a stream in a heat exchanger, a zone analysis, described in Section 12.1, should be made to make sure that the temperature difference between the hot stream and the cold stream is equal to or greater than the minimum approach temperature at all locations in the heat exchanger. The zone analysis is performed by dividing the heat exchanger into a number of segments and applying an energy balance to each segment to determine corresponding stream inlet and outlet temperatures for the segment, taking into account any phase change. A process simulation program conveniently accomplishes the zone analysis.
30	Typically, a hydrocarbon gives an adiabatic flame temperature of approximately 3,500°F when using the stoichiometric amount of air. However, use excess air to achieve complete combustion and give a maximum flue gas temperature of 2,000°F. Set the stack gas temperature in the range of 650–950°F to prevent condensation of the corrosive components of the flue gas.
31	Estimate heat-exchanger pressure drops as follows: 1.5 psi for boiling and condensing. 3 psi for a gas. 5 psi for a low-viscosity liquid. 7–9 psi for a high-viscosity liquid. 20 psi for a process fluid passing through a furnace.
32	Quench a very hot process stream to at least 1,150°F before sending it to a heat exchanger for additional cooling and/or condensation. The quench fluid is best obtained from a downstream separator as in Figure 7.31 for the toluene hydrodealkylation process. Alternatively, if the process stream contains water vapor, liquid water may be an effective quench fluid.
33	If possible, heat or cool a stream of solid particles by direct contact with a hot gas or cold gas, respectively, using a rotary kiln, a fluidized bed, a multiple hearth, or a flash/pneumatic conveyor. Otherwise, use a jacketed spiral conveyor.
Pressure increase operations	
34	Use a fan to raise the gas pressure from atmospheric pressure to as high as 40 inches water gauge (10.1 kPa gauge or 1.47 psig). Use a blower or compressor to raise the gas pressure to as high as 206 kPa gauge or 30 psig. Use a compressor or a staged compressor system to attain pressures greater than 206 kPa gauge or 30 psig.
35	Estimate the theoretical adiabatic horsepower (*THp*) for compressing a gas: $$THp = SCFM\left(\frac{T_1}{8{,}130a}\right)\left[\left(\frac{P_2}{P_1}\right)^a - 1\right] \quad (6.1)$$ where $SCFM$ = standard cubic feet of gas per minute at 60°F and 1 atm (379 SCF/1bmol); T_1 = gas inlet temperature in °R; inlet and outlet pressures, P_1 and P_2, are absolute pressures: and $a = (k-1)/k$, with k = the gas specific heat ratio, C_p/C_v. Estimate the theoretical exit temperature, T_2, for a gas compressor: $$T_2 = T_1(P_2/P_1)^a \quad (6.2)$$

(*Continued*)

Table 6.2 (*continued*)

	Heuristic
36	Estimate the number of gas compression stages, N, from the following table, which assumes a specific heat ratio of 1.4 and a maximum compression ratio of 4 for each stage.

Final Pressure/Inlet Pressure	Number of Stages
< 4	1
4–16	2
16–64	3
64–256	4

Optimal interstage pressures correspond to equal Hp for each compressor. Therefore, based on the equation for theoretical compressor Hp, estimate interstage pressures by using approximately the same compression ratio for each stage with an intercooler pressure drop of 2 psi or 15 kPa.

37 For heads up to 3,200 ft and flow rates in the range of 10–5,000 gpm, use a centrifugal pump. For high heads up to 20,000 ft and flow rates up to 500 gpm, use a reciprocating pump. Less common are axial pumps for heads up to 40 ft for flow rates in the range of 20–100,000 gpm and rotary pumps for heads up to 3,000 ft for flow rates in the range of 1–1,500 gpm.

38 For liquid flow, assume a pipeline pressure drop of 2 psi/100 ft of pipe and a control valve pressure drop of at least 10 psi. For each 10-ft rise in elevation, assume a pressure drop of 4 psi.

39 Estimate the theoretical horsepower (THp) for pumping a liquid:

$$THp = (\text{gpm})(\text{Pressure increase, psi})/1{,}714 \tag{6.3}$$

Pressure decrease operations

40 Consider the use of an expander for reducing the pressure of a gas or a pressure-recovery turbine for reducing the pressure of a liquid when more than 20 Hp and 150 Hp, respectively, can be recovered.

41 Estimate the theoretical adiabatic horsepower (THp) for expanding a gas:

$$THp = SCFM\left(\frac{T_1}{8{,}130a}\right)\left[1-\left(\frac{P_2}{P_1}\right)^a\right] \tag{6.4}$$

42 Estimate the theoretical horsepower (THp) for reducing the pressure of a liquid:

$$THp = (\text{gpm})(\text{Pressure decrease, psi})/1{,}714 \tag{6.5}$$

Pumping liquid or compressing gas

43 To increase the pressure of a stream, pump a liquid rather than compress a gas unless refrigeration is needed.

Vacuum

44 Estimate inleakage of air by:

$$w = kV^{0.667} \tag{6.7}$$

where w = lb/hr of air inleakage, V = ft^3 of volume of the equipment under vacuum, and $k = 0.2$ for pressures greater than 90 torr, 0.15 for pressures between 21 and 89 torr, 0.10 for pressures between 3.1 and 20 torr, and 0.051 for pressures between 1 and 3 torr.

45 To reduce the amount of gas sent to the vacuum system if its temperature is greater than 100°F, add a condenser using cooling water before the vacuum system. The gas leaving the condenser will be at a dew-point temperature of 100°F at the vacuum pressure.

Table 6.2 (*continued*)

	Heuristic
46	For pressures down to 10 torr and gas flow rates up to 10,000 ft^3/min at the inlet to the vacuum system, use a liquid-ring vacuum pump. For pressures down to 2 torr and gas flow rates up to 1,000,000 ft^3/min at the inlet to the vacuum system, use a steam-jet ejector system (one-stage for 100–760 torr, two-stage for 15–100 torr, and three-stage for 2–15 torr). Include a direct-contact condenser between stages.
47	For a three-stage steam-jet ejector system used to achieve a vacuum of 2 torr, 100 pounds of 100 psig steam per pound of gas are required.
Conveying granular solids	
48	If the solid particles are small in size, low in particle density, and not sticky or abrasive, use pneumatic conveying with air at 1 to 7 ft^3/ft^3 of solids and 35 to 120 ft/s air velocity for distances up to 400 ft. Otherwise, for sticky and/or abrasive solids of any size and density, use a screw conveyer and/or bucket elevator for distances up to 150 ft. For solid particles of any size and shape, and not sticky, use a belt conveyor, with inclination up to 30° if necessary, for long distances up to a mile or more.
Solid particle size change and separation	
49	Crushing of coarse solids. Use a jaw crusher to reduce lumps of hard, abrasive, and/or sticky materials of 4 inches to 3 feet in diameter to slabby particles of 1–4 inches in size. Use a gyratory crusher to reduce slabby materials of 8 inches to 6 feet in size to rounded particles of 1–10 inches in diameter. Use a cone crusher to reduce less hard and less sticky materials of 2 inches to 1 foot in diameter to particles of 0.2 inch (4 mesh) to 2 inches in diameter.
50	Grinding to fine solids. Use a rod mill to take particles of intermediate hardness as large as 20 mm and reduce them to particles in the range of 10–35 mesh. Use a ball mill to reduce particles of low to intermediate hardness of 1–10 mm in size to very small particles of less than 140 mesh.
51	Particle-size enlargement. Use compression with rotary compression machines to convert powders and granules into tablets of up to 1.5 inches in diameter. Use extruders with cutters to make pellets and wafers from pastes and melts. Use roll compactors to produce sheets from finely divided materials; the sheets are then cut into any desired shape. Use rotating drum granulators and rotary disk granulators with binders to produce particles in the size range of 2–25 mm.
52	Size separation of particles. Use a grizzly of spaced, inclined, vibrated parallel bars to remove large particles greater than 2 inches in diameter. Use a revolving cylindrical perforated screen to remove intermediate-size particles in the size range of 0.25 inch to 1.5 inches in diameter. Use flat, inclined woven screens (U.S. standard) that are vibrated, shaken, or impacted with bouncing balls to separate small particles in the size range of 3–80 mesh. Use an air classifier to separate fine particles smaller than 80 mesh.
53	Use a cyclone separator to remove, from a gas, droplets or solid particles of diameter down to 10 microns (0.01 mm). Use a hydroclone separator to remove, from a liquid, insoluble liquid droplets or solid particles of diameter down to 5 microns (0.005 mm). However, small amounts of entrained liquid droplets are commonly removed from gases by vertical knock-out drums equipped with mesh pads to help coalesce the smallest droplets.

REFERENCES

1. Baddocr, R. F., P.L.T. Brain, B. A. Logeais, and J. P. Eymery, "Steady-State Simulation of an Ammonia Synthesis Converter," *Chem. Eng. Sci.*, **20**, 281 (1965).

2. Douglas, J. M., *Conceptual Design of Chemical Processes*, McGraw-Hill, New York (1988).

3. Fogler, H. S., *Elements of Chemical Reaction Engineering*, Prentice-Hall, Englewood Cliffs, New Jersey (2011).

4. B. F. Goodrich Co., "Preparation of Vinyl Chloride," British Patent 938,824 (October 9, 1963).

5. Green, D. W., and R. H. Perry (ed.), *Perry's Chemical Engineers' Handbook*, 7th ed., McGraw-Hill, New York (2008).

6. Henley, E. J., and E. M. Rosen, *Material and Energy Balance Computations*, Wiley, New York (1969).

7. Hua, I., R. H. Hochemer, and M. R. Hoffmann, "Sonochemical Degradation of *p*-Nitrophenol in a Parallel-Plate Near-Field Acoustical Processor," *Environ. Sci. Technol.*, **29**(11), 2790 (1995a).

8. Hua, I., R. H. Hochemer, and M. R. Hoffmann, "Sonolytic Hydrolysis of *p*-Nitrophenyl Acetate: The Role of Supercritical Water," *J. Phys. Chem.*, **99**, 2335 (1995b).

9. Myers, A. L., and W. D. Seider, *Introduction to Chemical Engineering and Computer Calculations*, Prentice-Hall, Englewood Cliffs, New Jersey (1976).

10. Schmidt, L. D., *The Engineering of Chemical Reactions*, 2nd ed., Oxford University Press, Oxford, United Kingdom. (2004).

11. Walas, S. M., *Chemical Process Equipment—Selection and Design*, Butterworth, Stoneham, Massachusetts (1988).

EXERCISES

6.1 For the production of ethylene glycol, how much is the economic potential per pound of ethylene glycol reduced when chlorine and caustic are used to avoid the production of ethylene oxide?

6.2 Consider ethyl-tertiary-butyl-ether (ETBE) as an alternative gasoline oxygenate to MTBE. Although the latter appears to have the best combination of properties such as oxygen content, octane number, energy content, and cost, the former can be manufactured using ethanol according to:

$$C_2H_5OH + \textit{iso}\text{-butene} \rightleftharpoons \text{ETBE}$$

Because ethanol can be manufactured from biomass, it is potentially more acceptable to the environment.

(a) Rework Example 6.1 for this process.

(b) Is reactive distillation promising for combining the reaction and separation operations? If so, suggest a distribution of chemicals using a reactive distillation operation.

6.3 For the ammonia process in Example 6.4, consider operation of the reactor at 932°F and 400 atm. Use a simulator to show how the product, recycle, and purge flow rates, as well as the mole fractions of argon and methane vary with the purge-to-recycle ratio. How do the power requirements for compression vary, assuming 3 atm pressure drop in the reactor and 1 atm pressure drop in the heat exchanger?

6.4 *Revamp of a toluene hydrodealkylation process.* This problem considers some waste-minimization concepts involving ***recycle to extinction*** - a heuristic for process synthesis. However, in this exercise, when this heuristic is applied, analysis using process simulation is carried out. For this reason, we advise the reader to solve this exercise after studying Chapter 7 and possibly after solving Exercises 7.2 to 7.4, which simulates sections of the toluene hydrodealkylation process. Our operating toluene hydrodealkylation unit, shown in Figure 6.18, involves the hydrogenation of toluene to benzene and methane. An equilibrium side reaction produces a small quantity of biphenyl. To be more competitive and to eliminate waste, the process needs to be studied for a possible revamp. The customer for our small production of biphenyl has informed us that it will not renew its contract with us, and we have no other prospective buyer for biphenyl. Also, a membrane separator company believes that if we install their equipment, we can reduce our makeup hydrogen requirement. Make preliminary process design calculations with a simulator to compare the following two alternatives, and advise me of the technical feasibility of the second alternative and whether we should consider such a revamp further. For your studies, you will have to perform mainly material balance calculations. You will not make detailed distillation calculations, and liquid pumps need not be modeled. For the second alternative, calculate the required area in square feet of the membrane unit and determine if it is reasonable.

Alternative 1. Do no revamp and use the biphenyl for its fuel value.

Alternative 2. Eliminate operation of the toluene column and recycle the biphenyl (with the toluene) to extinction. This should increase the yield of benzene. Also, install a membrane separation unit to reduce hydrogen consumption.

Current plant operation: The current plant operation can be adequately simulated with CHEMCAD, using the equipment models indicated in the flow diagram. Alternatively, any other simulator can be used with appropriate models. Note that the flow diagram of the process includes only the reactor, separators, and recycle-gas compressor. The plant operating factor is 96% (8,410 hr/yr). The feedstock is pure toluene at a flow rate of 274.2 lbmol/hr, which is fixed for both alternatives, because any additional benzene that we can make can be sold. The makeup hydrogen is 95 mol% hydrogen and 5 mol% methane. Our reactor outlet conditions are 1,000°F and 520 psia. The hydrogen-to-toluene molar ratio in the feed to the reactor must be 4 to prevent coke formation. The toluene conversion is 70%. The biphenyl in the reactor effluent is the chemical equilibrium amount. The flash drum conditions are 100°F at 500 psia. The flash vapor is not separated into hydrogen and methane but is purged to limit methane buildup in the recycle gas. The purge gas, which has fuel value, is 25% of the vapor leaving the flash vessel. Perfect separations can be assumed for the three columns. Based on this information, you can obtain the current plant material balance.

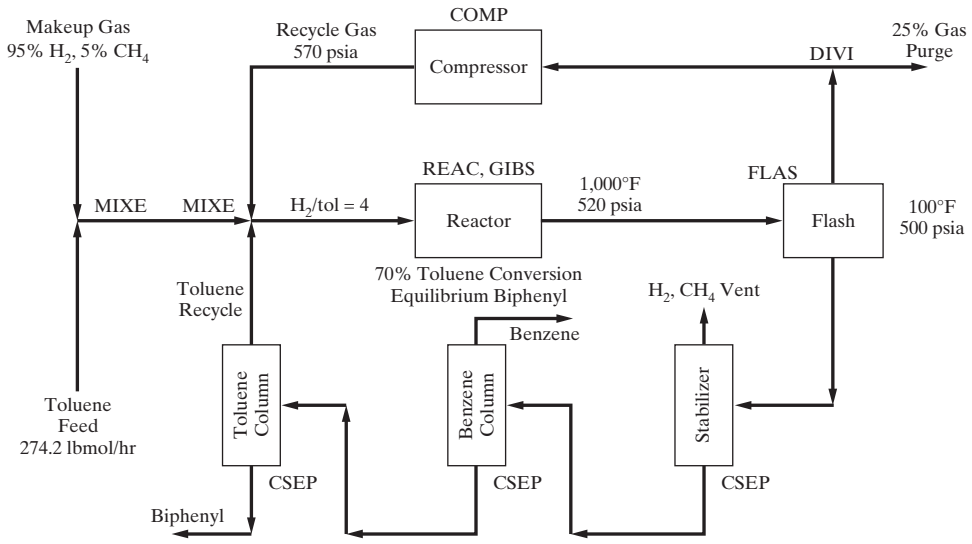

Figure 6.18 Flowsheet for the toluene hydrodealkylation process.

Alternative 1. Simulate the current plant operation. Note that the process has two recycle loops that must be converged. The SRK equation of state is adequate for *K*-values and enthalpies. From your converged material balance, summarize the overall component material balance in pounds per year (i.e., process feeds and products).

Alternative 2. Eliminate the toluene column and rerun the simulation. Because the biphenyl will be recycled to extinction, the benzene production should increase. Replace the stream divider, which divides the flash vapor into a purge and a gas recycle, with a membrane separation unit that can be modeled with a CSEP (black-box separator) unit.

For Alternative 2, the vendor of the membrane unit has supplied the following information:

Hydrogen will pass through the membrane faster than methane. Vapor benzene, toluene, and biphenyl will not pass through the membrane.

The hydrogen-rich permeate will be the new recycle gas. The retentate gas will be used for fuel.

Tests indicate that the purity of the hydrogen-rich permeate gas will be 95 mol% with a hydrogen recovery of 90%. However, the pressure of the permeate gas will be 50 psia, compared to 500 psia for the recycle gas in the current plant operation. A pressure of 570 psia is required at the discharge of the recycle-gas compression system. Thus, a new compressor will be needed.

Run the revamped process with the simulator. From your converged material balance, summarize the overall component material balance in pounds per year (i.e., process feeds and products).

The membrane unit is to be sized by hand calculations on the basis of the hydrogen flux through the membrane. Tests by the vendor using a nonporous cellulose acetate membrane in a spiral-wound module indicate that this flux is 20 scfh (60°F and 1 atm) per square foot of membrane surface area per 100 psi hydrogen partial-pressure driving force. To determine the driving force, take the hydrogen partial pressure on the feed side of the membrane as the arithmetic average between the inlet and the outlet (retentate) partial pressures. Take the hydrogen partial pressure on the permeate side as that of the final permeate.

Summarize and discuss your results in a report and make recommendations concerning cost studies.

6.5 For the reaction system:

$$\begin{array}{l} \mathrm{A + B} \xrightarrow{k_1} \mathrm{C + A} \xrightarrow{k_3} \mathrm{E} \\ \quad \searrow^{k_2} \mathrm{D + A} \nearrow_{k_4} \end{array}$$

select an operating temperature that favors the production of C. The pre-exponential factor and activation energy for the reactions are tabulated as follows:

Rxtn	k_0(m^6/kmol^2 · s)	E (kJ / kmol)
1	3.7×10^6	65,800
2	3.6×10^6	74,100
3	5.7×10^6	74,500
4	1.1×10^7	74,400

6.6 Propylene glycol mono-methyl-ether acetate (PMA) is produced by the esterification of propylene glycol mono-methyl ether (PM) in acetic acid (HOAc):

$$\underset{\text{PM}}{\mathrm{CH_3CH(OH)CH_2OCH_3}} + \underset{\text{HOAc}}{\mathrm{CH_3COOH}} \rightleftharpoons \underset{\text{PMA}}{\mathrm{CH_3CH(OC(CH_3)O)CH_2OCH_3}} + \mathrm{H_2O}$$

Conventionally, the reaction takes place in a fixed-bed reactor followed by the recovery of PMA from water, and unreacted PM and HOAc. Prepare a potential distribution of chemicals for a reactive distillation process with the feed at 203°F and 1 atm.

6.7 For the following reactions, determine the maximum or minimum temperatures of the reactor effluents assuming:

(a) Complete conversion

(b) Equilibrium conversion

The reactants are available in stoichiometric proportions at the temperature and pressure indicated.

	T_0 (°F)	P (atm)
a. $C_7H_8 + H_2 \rightarrow C_6H_6 + CH_4$	1,200	38.7
b. $SO_2 + \frac{1}{2}O_2 \rightarrow SO_3$	77	1.0
c. $CO + \frac{1}{2}O_2 \rightarrow CO_2$	77	1.0
d. $C_2H_4Cl_2 \rightarrow C_2H_3Cl + HCl$	932	26.0

Also, find the heats of reaction at the conditions of the reactants.

6.8 For Example 6.9, use a simulator to graph the effluent temperature of the methanol reactor as a function of the H_2/CO ratio.

6.9 For Example 6.10, use a simulator to graph the effluent temperature of the methanol reactor as a function of the dodecane flow rate.

6.10 Divide the methanol reaction operation in Example 6.6 into five consecutive stages in series. Feed the CO reactant entirely into the first operation at 25°C and 1 atm. Divide the H_2 reactant into five cold shots and vary the temperature of H_2 before dividing it into cold shots. Assuming that the reaction operations are adiabatic, determine the maximum temperature in the flowsheet as a function of the temperature of the cold shots. How does this compare with the adiabatic reaction temperature?

6.11 Repeat Exercise 6.10 using intercoolers instead of cold shots and an unknown number of reaction stages. The feed to the first reactor is at 25°C and 1 atm. Throughout the reactors, the temperature must be held below 300°C. What is the conversion of CO in the first reactor? How many reaction stages and intercoolers are necessary to operate between 25 and 300°C?

6.12 *Alternatives for preparing a feed.* A process under design requires that 100 1bmol/hr of toluene at 70°F and 20 psia be brought to 450°F and 75 psia. Develop at least three flowsheets to accomplish this using combinations of heat exchangers, liquid pumps, and/or gas compressors. Discuss the advantages and disadvantages of each flowsheet, and make a recommendation as to which flowsheet is best.

Chapter 7

Simulation to Assist in Process Creation

7.0 OBJECTIVES

The objective at this stage of process design is to perform model-based, steady-state *process simulations* of any process flowsheet alternative using a *process simulator*. The calculations performed here involve steady-state mass and/or energy balances with different degrees of details of the available process flowsheet. To perform a process simulation, the required flowsheet details must be available. Therefore, for a new process under creation, when not too much detailed information can be expected to be available, the designer needs to make a series of *design decisions* related to *process creation*. These design decisions, however, need to be further refined and verified before the actual process can be built and operated. On the other hand, for a process that already exists, a flowsheet with detailed information already exists. Therefore, the designer usually has sufficient information to perform process simulations, and the goal then is usually to carry out *process analysis*. That is, process simulations are performed on multiple processing options to identify those that are better than the existing process. In either case, process simulation is a fast and easy way to perform the first steps of *design verification*, that is, to check whether the design objectives have been achieved. For example, have the target product specifications been achieved? If yes, what are the associated energy and/or utility demands?

A *process simulator* is a tool for performing mass and/or energy balances of a process defined by a process flowsheet consisting of a sequence of continuous or batch operations (which, for the latter, are not at steady state). A process simulator could be considered an engineering tool that performs automated calculations covering material and/or energy balances of the chemical process under study together with physical property estimations, design/rating calculations, and/or process optimization. Note, however, it is *not* a process engineer. That is, it does not make the design decisions. It helps to verify design decisions and to generate data (information) that may be used to make design decisions.

The following questions, regarded as important for a good understanding of the issues related to process simulation, are addressed in this chapter:

- How is a process simulation problem formulated?
- What are the important steps in process simulation?
- How are the models, the needed data, and the method of solution selected?
- How is process simulation performed in a systematic and efficient manner?

Process design requires the designer to make a series of design decisions related to process creation. To verify the design decisions, process simulations are performed. The nature of the design decisions that need to be verified, however, greatly influence the selection of models that best represent operations used in the process being created or improved, and the numerical approach that may be applied to solve the model equations. In this way, a process simulator helps the designer by performing the calculations needed to verify the process design.

After studying this chapter, the reader should:

1. Be cognizant of the characteristics of various types of simulation tasks.
2. Have the ability to select the appropriate models for process simulation.
3. Be familiar with computer-aided methods and tools that are applicable for selection, design, and analysis of processes to produce many chemical products.
4. Have the ability to model (simulate), design, and analyze process flowsheets.

7.1 INTRODUCTION

The steps involved in the use of a process simulator in process design are illustrated through Figure 7.1 where the steps for steady-state process simulation of a typical chemical process represented by a flowsheet consisting of a mixer, reactor, separator, and divider (stream splitter) as unit operations, are highlighted. As illustrated in Figure 7.1, the designer defines the problem; selects-collects the appropriate models representing the unit operations in the flowsheet (note that for a steady-state simulation, the models are composed of algebraic equations); collects the data needed to satisfy the problem degrees of freedom; solves the total set of model equations using available

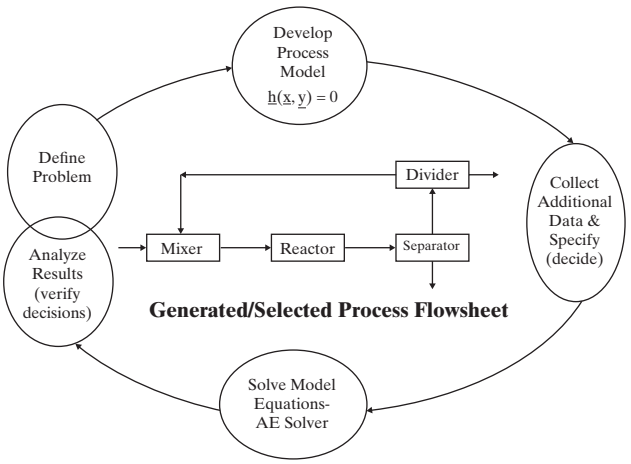

Figure 7.1 The steps involved in process simulation.

solvers; and then in the final step, checks whether the simulation results are acceptable and correct. If yes, the designer moves to the next step of the design process; if not, the designer adjusts the problem definition and repeats the steps until the desired results are obtained. Note that there are several reasons for repeating this cycle—for example, the selected models may not be appropriate, the numerical solution may not be correct, or the data specification may not be consistent. The former are associated with the function and ability of the process simulator, whereas the latter is associated with design decisions made by the designer. One way to simultaneously make design decisions and perform process simulation is to solve a process optimization problem where the optimizer (the numerical method) makes the design decisions in an outer loop (i.e., generates new values for the design variables) while process simulations are performed in an inner loop using the new design decisions until convergence in the outer loop is achieved. Therefore, process simulation helps not only to verify design decisions but also to optimize process designs and/or evaluate process operations for purposes of monitoring and control.

The starting point for a simulation problem is a process for which a flowsheet has been synthesized (Chapters 2 and 6); the raw materials are known (composition, state, flow rate); the reactions involved are known (stoichiometry, conversion, temperature, and pressure); the product specifications are known (flow rate, purity, state, etc.). Detailed information on the process unit modules involved, however, may not be available. What are not known are the flow rates, compositions, temperatures, and pressures of all streams; the enthalpies, states, and so on, of all streams [these are calculated after the feed and product streams are specified; a base-case (reference) design of the unit operations in the flowsheet (design decisions related to the flash vessels, separation columns, heat exchangers, pumps, etc.). A step-by-step hierarchical approach in which the work is divided into four sequential tasks is proposed, each task providing additional information for the next simulation task, as the process is created.

This chapter is divided into two main themes, steady-state simulation of continuous processes (Sections 7.2–7.4) and dynamic simulation of batch operations (Section 7.5).

7.2 PRINCIPLES OF PROCESS SIMULATION

Given a process flowsheet with varying degrees of details, the objective is to perform mass and energy balance calculations and establish temperatures, pressures, and compositions of all streams as the minimum information needed to totally define the process. As more details are added, the phase identities; the utilities (for heating or cooling); the pressure changes; the designs of reactors, separators, and heat exchangers; and many more process units are established. That is, process simulation is the act of representing some aspects of the real chemical process by numbers or symbols that may be manipulated to facilitate its study. To perform a process simulation, one needs to have a good understanding of the issues influencing it. Also, for efficient use of process simulators to perform process simulations, knowledge of various terms (and their meanings) is very important; for example, what are *tear streams* and how do they influence the method of solution? Finally, process simulations can be performed at various levels with different starting points and corresponding degrees of complexity of the simulation models.

Definition of Terms

A simple process flowsheet is shown in Figure 7.2, which is used to clarify and explain terms that will be used throughout this chapter and the remainder of this book.

Flowsheeting

Flowsheeting refers to performing steady-state simulations of a given process flowsheet, which is a representation of a process in terms of *unit modules* (representing unit operations) and *streams* (representing material and energy flows). Flowsheeting can be performed in many ways, depending on the *process simulator* (commercial or in-house) being used.

Unit Modules

Each unit module (Unit1, Unit2, Unit3, Unit4, and Unit5) in Figure 7.2 represents an unit operation of the actual chemical process with its corresponding model composed of a set of equations.

Streams

Material and energy flows are usually indicated in the flowsheet through directional lines, called streams (Si, $i = 0, 1, 2, 3, 4\text{-}1, 4\text{-}2, 5$, in Figure 7.2). The minimum variables representing a stream are temperature, pressure, and compositions of chemicals present in the process. Stream properties, such as phase identity, enthalpy, density, and so on, are calculated using an appropriate property model (constitutive equations). Streams can be of different types:

- ***Input Stream*:** Here the stream enters the process from the surroundings to any unit module (S0 in Figure 7.2).

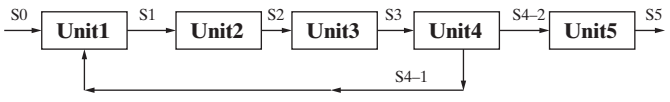

Figure 7.2 Example of a simple process flowsheet.

- ***Outlet Stream*:** Here the stream leaves the process from any unit module (S5 in Figure 7.2).
- ***Intermediate Stream*:** Here the stream connects two unit modules (S1, S2, S3, S4-1, S4-2 in Figure 7.2).
- ***Tear Stream*:** Its stream variables are used as guesses for recycle convergence (see more details below on recycle loops and convergence). For the flowsheet in Figure 7.2, the tear stream can be any one of S1, S2, S3, or S4-1.

Recycle Loops

Starting from any unit module and following the directions of the streams leaving the unit modules, when their paths lead back to the starting unit module, the set of streams and unit modules form a recycle loop. From the flowsheet of Figure 7.2, there is one recycle loop consisting of the streams S1, S2, S3, and S4-1. The corresponding unit modules are Unit1, Unit2, Unit3, and Unit4. In a chemical process, there can be multiple recycle loops.

Simulation Approach

The solution of the model equations representing the unit modules and streams depends on the simulation approach employed. There are two basic types of simulation approaches (variations of these are possible, but not covered herein):

- ***Sequential Modular*:** Here the model equations corresponding to only one unit module and its connecting streams are solved in a single step, which is repeated for all of the unit modules in the flowsheet. For this approach, a *calculation sequence* (see below) needs to be established first.
- ***Equation Oriented*:** Here the model equations for all the unit modules and connecting streams are collected together and solved simultaneously. For this approach, an *equation-ordering scheme* may be applied.

Calculation Sequence

For the sequential-modular simulation approach, a calculation sequence for the process simulation needs to be established first. For a flowsheet without a recycle stream, this is straightforward; one starts at the first unit module [with a feed stream(s) and no intermediate source streams] and proceeds one module at a time until the last module is reached. Note that, as discussed in Section 2.3, intermediate *source* streams are effluents from process units; these satisfy the *sinks* needed by process units downstream. However, if a recycle loop is present in the flowsheet, a *tear stream* first needs to be identified; calculations are started with the unit module following the tear stream, and the calculations are repeated until the starting value (before entering the first module) and the end value (after the last unit module in the recycle loop) have approximately similar values (see the subsection Recycle Convergence for more details). The tear streams in a flowsheet are identified through *flowsheet decomposition* techniques. For the flowsheet in Figure 7.2, considering stream S4-1 as the tear stream, the calculation sequence for the unit modules is to guess the variables of stream S4-1 and repeat the sequence: solve Unit1, solve Unit2, solve Unit3, and solve Unit4 until convergence (guessed and calculated values of the variables in stream S4-1 are similar); then, solve Unit5.

The sequence for solving the unit-module equations also indicates a *partitioning* (or *decomposition*) of the flowsheet into two parts: unit modules Unit1, Unit2, Unit3, and Unit4 belong to Partition-1, whereas Unit5 belongs to Partition-2. It is not necessary to solve the model equations of Unit5 until convergence of the recycle loop in Partition-1 has been achieved.

Equation-Ordering Scheme

Similar to determining the calculation sequence for the sequential-modular approach, the model equations representing all of the unit modules in the flowsheet can be ordered to find the most appropriate way to solve them. That is, the equations may be ordered to obtain a lower block-tridiagonal matrix as indicated in Figure 7.3 for the flowsheet in Figure 7.2. As in the sequential modular approach, where the unit modules are partitioned into Partition-1 and Partition-2, the equations are partitioned into Set-1 and Set-2. Then, the Set-1 equations are solved simultaneously for $\textcircled{x}$ and the remaining variables in Set-1, after which the Set-2 equations are solved simultaneously.

Important Process Simulation Issues

The following issues, considered as very important in process simulation, are briefly described in the sections below:

- Features of process simulators
- Modeling
- Degrees of freedom analysis
- Flowsheet decomposition
- Recycle convergence

Features of Process Simulators

The process simulators usually contain a library of built-in and ready-to-use mathematical models of varying degrees of complexity representing a wide collection of operations typically performed in chemical processes. It also includes associated

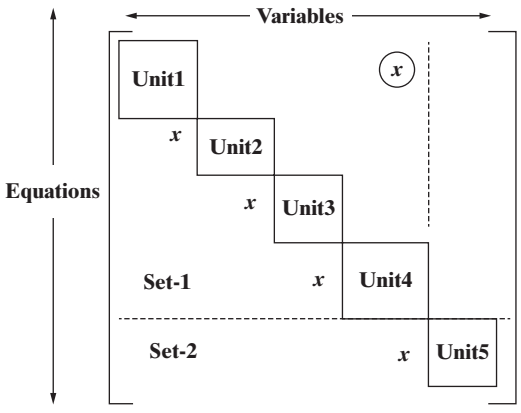

Figure 7.3 Equation-ordering for simultaneous-modular approach.

constitutive models, for example, models for thermophysical and transport property prediction, reaction kinetics, and so on that help the user define and analyze the equations representing the chemical process. The essential elements of a process simulator are as follows:

- ***User Interface*:** Through this interface, the simulator communicates with the user and its collections of models, solvers, and databases. The user interface provides templates for various types of problems and guides the user through the various problem-solving steps.
- ***Model Library*:** To save time for the user, the process simulators provide a large collection of unit modules that facilitate the solution of a broad array of process design, synthesis and analysis problems.
- ***Solver Library*:** For any model-based solution approach, a solver is always needed. Because various types of simulation problems involve different classes of models (represented by different classes of equations), the process simulators need collections of appropriate solvers.
- ***Database*:** For the design, analysis, and verification of processes, in addition to a collection of models, a set of databases is needed from which useful data are extracted, for example, data for pure-component properties of a large collection of chemicals, and, the parameters of thermophysical property models.

Well-known commercial process simulators, such as ASPEN PLUS, Aspen HYSYS, Honeywell's UniSim®Design[1], PRO/II, and CHEMCAD, employ different forms of the sequential-modular approach whereas the equation-oriented approach is employed by gPROMS (Process Systems Enterprise, Ltd.) and as options in ASPEN PLUS, Aspen HYSYS (Aspen Technology, Inc.) and UniSim®Design (Honeywell International, Inc.). Clearly, simulators employing the equation-oriented approach avoid unit-by-unit iterations for converging the recycle loops and design specifications. Given good initial guesses (for the equation solvers), this is a major advantage. One way to obtain good initial estimates is to perform an initial pass with the sequential-modular option. Furthermore, some simulators permit the creation of a hybrid simulation in which the equations associated with some process units are solved unit by unit whereas the equations associated with the remaining process units are solved simultaneously.

Modeling

As highlighted in Figure 7.1, before a process simulation can be performed, the process flowsheet must be represented by an appropriate set of process unit modules; that is, each containing the model equations for a process unit. These modules may be derived for every new process unit or retrieved from a simulator's library of process unit models. The latter option is most often favored in process design. Figures 7.4a–e show

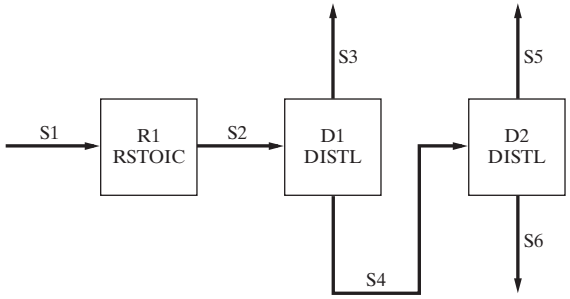

(a)

Figure 7.4 Acyclic flowsheet: (a) ASPEN PLUS simulation flowsheet using blocks; (b) ASPEN PLUS simulation flowsheet using icons; (c) UniSim®Design simulation flowsheet; (d) CHEMCAD simulation flowsheet; (e) PRO/II simulation flowsheet.

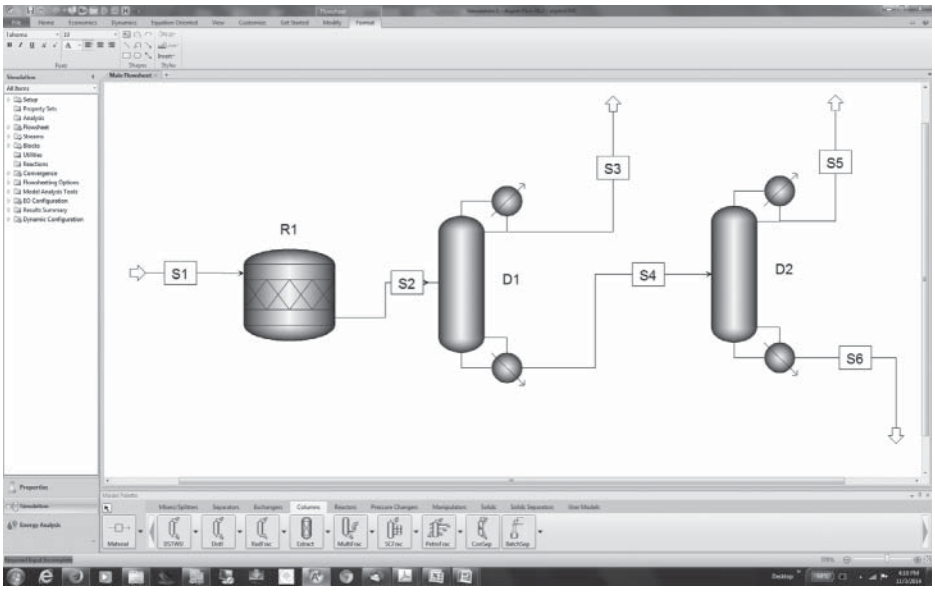

(b)

Figure 7.4 (*Continued*) (*Source:* © ASPEN PLUS).

[1]UniSim® is a registered trademark of Honeywell International Inc.

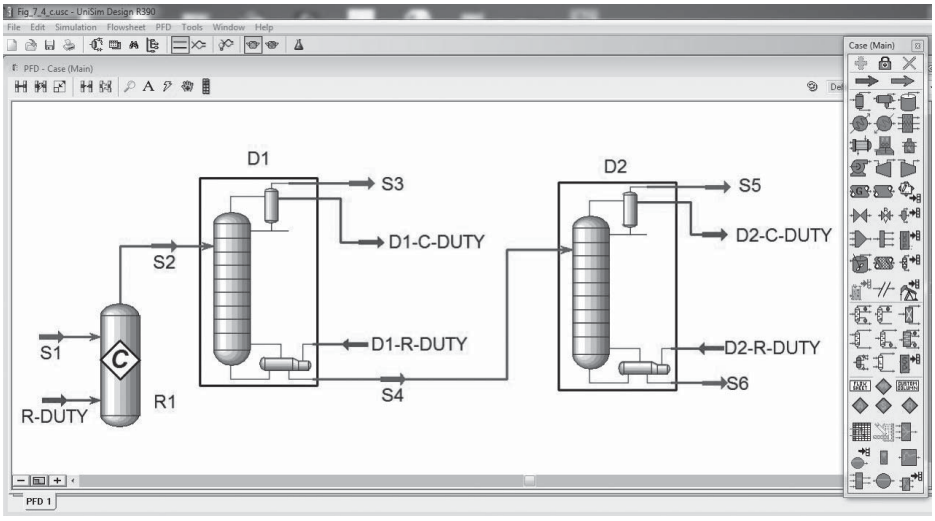

(c)

(*Source:* UniSim®Design).

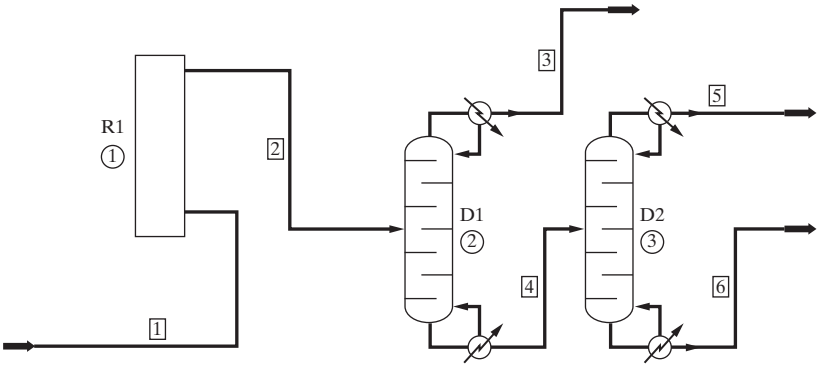

(d)

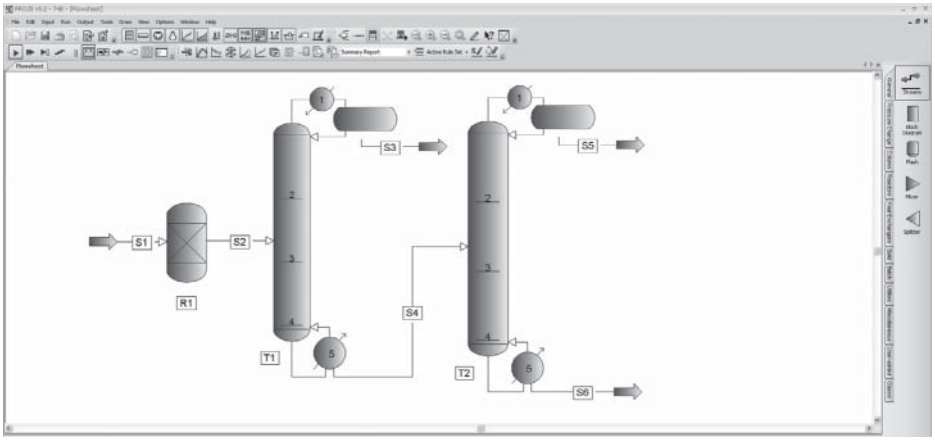

(e)

Figure 7.4 (*Continued*) (*Source:* PRO/II with permission by Schneider Electric).

simulation flowsheets using existing models in process simulator libraries. In each case, the user selects the appropriate process-unit module, which contains a preprogrammed set of model equations. Figures 7.4a,b show ASPEN PLUS simulation flowsheets, and Figures 7.4c–e show simulation flowsheets for the UniSim®Design, CHEMCAD, and PRO/II simulators.

The forms of the selected module depend very much on the mode of simulation. For a steady-state simulation, the simplest form is a set of algebraic equations for mass and energy balances. For a more detailed simulation, a steady-state model accounting for spatial variables involving sets of partial-differential equations together with algebraic equations may be considered.

For dynamic simulations, ordinary differential equations together with algebraic equations often represent the process model.

Tables 7.1 and 7.2 list the main unit operation modules available in ASPEN PLUS, PRO/II, and UniSim® Design accompanied by lists of variables in parentheses that need to be specified. These specifications can be considered as design decisions that the designer makes to determine a feasible process alternative, that is, a process design that satisfies the desired process specifications. In Table 7.1, only the simple mass-balance modules are listed, whereas in Table 7.2, the detailed rigorous modules are listed.

Simple Mass-Balance Modules

For mass-balance calculations, almost all chemical process flowsheets can be represented by a combination of mass-balance modules of mixers (representing all kinds of mixing operations), stoichiometric (conversion) reactors (representing all types of reactors), component splitters (representing all types of separation operations), and dividers (representing all types of stream-splitting operations). They are normally in-house library modules available in the process simulators (see the list of unit modules in Table 7.1). To highlight the concepts and principles, the derivation of these modules is highlighted through a case study.

Model Assumptions. For all four mass-balance models, it is assumed that the mixture is perfectly mixed and homogeneous with the temperatures and pressures perfectly controlled (therefore, unchanged). Under these conditions, the separations can be modeled using separation factors [see Eq. (9.8)] whereas for the reactions, either conversions of the limiting reactants or reaction-rate models must be supplied. These assumptions decouple the mass balances from the energy balance in each of the four unit operations.

Model Derivation. The control volumes and the stream connections are shown in Figures 7.5a–c, after which the mass-balance equations are summarized.

***Mixer Model*:** N_C is the number of compounds; i is the component counter; N_M is the number of input streams to the mixer; j is the input-stream counter; and f_{ij} is the flow rate of component i in stream j; see Figure 7.5a.

$$f_{i,N_M+1} = \sum_j f_{ij} \qquad \text{for } i = 1, \ldots, N_C;\ j = 1, \ldots, N_M \tag{7.1}$$

***Reactor Model (Single Reaction)*:** k is the limiting reactant; X_k is the fractional conversion of component k [see Eqs. (7.2) and (8.4)]; ν_i is the stoichiometric coefficient of component i in the reaction; and stream j enters the reactor; see Figure 7.5b.

$$f_{i,j+1} = f_{ij} - \frac{\nu_i}{\nu_k} X_k f_{kj} \qquad \text{for } i = 1, \ldots, N_C \tag{7.2}$$

***Component-Splitter Model*:** For one feed stream j and two product streams, $j+1$ and $j+2$; ξ_{iS} is the separation fraction of species i exiting in stream $j+1$; see Figure 7.5c.

$$f_{i,j+1} = \xi_{iS} f_{ij} \qquad \text{for } i = 1, \ldots, N_C \tag{7.3}$$

$$f_{i,j+2} = (1 - \xi_{iS}) f_{ij} \tag{7.4}$$

***Stream-Divider (Splitter) Model*:** For one feed stream j and two product streams, $j+1$ and $j+2$; β is the split fraction of stream j exiting in stream $j+1$; see Figure 7.5c.

$$f_{i,j+1} = \beta_D f_{ij} \qquad \text{for } i = 1, \ldots, N_C \tag{7.5}$$

$$f_{i,j+2} = (1 - \beta_D) f_{ij} \qquad \text{for } i = 1, \ldots, N_C \tag{7.6}$$

Note that the difference between a component splitter and a stream divider (splitter) is that in the stream divider, all the streams have the same compositions whereas in the component splitter, they are different. In this way, the stream divider is a special case of the component splitter. Note that for the reactor model a reaction-rate expression can be used instead of the conversion specification.

Rigorous Process Models

For rigorous simulations of the process flowsheet, it is preferable to perform mass and energy balance calculations, incorporating thermo-physical property models, using the rigorous unit modules in Table 7.2. These are similar to the libraries of rigorous modules available in other well-known process simulators.

Degrees of Freedom Analysis

The degrees of freedom define the data needed to fully specify the problem for the simulation model and the corresponding form of the model employed. The data to be specified could be classified in terms of variables fixed by the chemical system (usually these

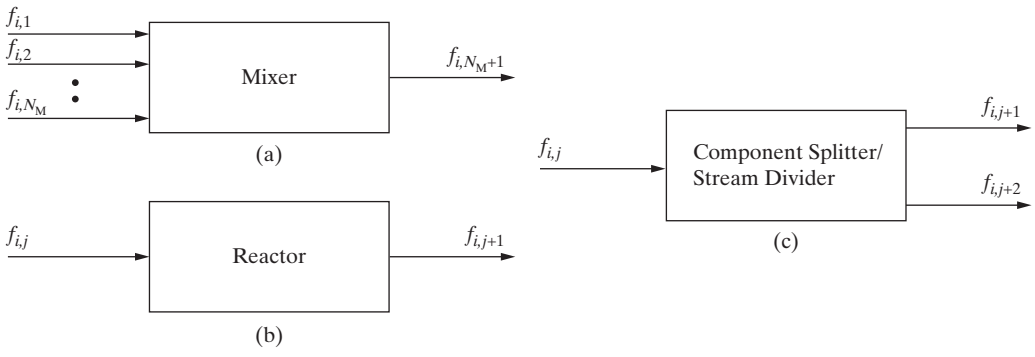

Figure 7.5 Schematics of mixer (a); reactor (b); and component splitter/divider (c).

Table 7.1 Simple Modules of Unit Operations (Mass Balances Only)

Unit Module	ASPEN PLUS	PRO/II	UniSim®Design
DIVIDER	 FSplit (feed stream, split fraction)	 Splitter (feed stream, split fraction)	 TEE (feed stream, split fraction)
MIXER	 MIXER (feed streams)	 MIXER (feed streams)	 MIXER (feed streams)
REACTOR (Stoichiometric reactor)	 RStoic (feed stream, reaction, conversion)	 Conversion reactor (feed stream, reaction, conversion)	 Conversion reactor (feed stream, reaction, conversion)
SEPARATOR	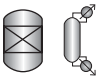 Sep (feed stream, separation fractions)	 Stream calculator (feed stream, separation fractions)	 Component splitter (feed stream, separation fractions)

Source: Images are obtained from © ASPEN PLUS, UniSim®Design, and PRO/II. Used with permission.

Table 7.2 Rigorous Models of Unit Operations

Unit Module	ASPEN PLUS	PRO/II	UniSim®Design
Simple (one stream) heater or cooler (temperature changer)	 Heater (thermal and phase state changer; models heater, cooler, condenser, and so forth; specify feed stream, temperature, pressure)	 Simple heat exchanger (thermal and phase state changer; models heater, cooler, condenser, and so forth; specify feed stream, temperature, pressure)	 Cooler  Heater  LNG exchanger (feed stream, duty, outlet temperature
Shell-and-tube heat exchanger	 HeatX (two stream heat exchanger; models cocurrent and countercurrent shell-and-tube heat exchanger; process fluid, specify service fluid, exchanger specification)	 Rigorous heat exchanger (two stream heat exchanger; models cocurrent and countercurrent shell-and-tube heat exchanger; specify process fluid, service fluid, exchanger specification)	 Heat exchanger (tube side inlet and outlet, shell side inlet and outlet)
Pump (pressure changer)	 Pump (feed stream, discharge pressure, duty)	 Pump (feed stream, discharge pressure, duty)	 Pump (feed stream, discharge pressure, duty)

Table 7.2 (*continued*)

Unit Module	ASPEN PLUS	PRO/II	UniSim®Design
Compressor and expander (pressure changer)	 Compressor or turbine (specify feed stream, discharge pressure, type, and model)	 Compressor or expander (specify feed stream, discharge pressure, type, and model)	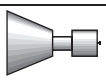 Compressor or expander (specify feed stream, discharge pressure, type, and model)
Valve	 (specify discharge pressure)	 (specify discharge pressure)	 (specify discharge pressure)
Distillation column	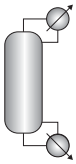 RadFrac (specify feed stream, feed and products position, calculation type, number of stages, column configuration, operating specification) 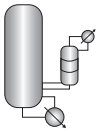 MultiFrac (rigorous fractionation for complex columns such as absorber/stripper combinations, and so on) 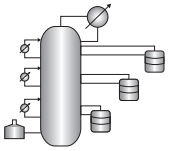 PetroFrac (rigorous fractionation for petroleum refining applications such as preflash towers, and so on: feed stream, column spec., operating specs., pressure) 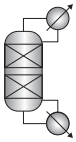 RateFrac (rigorous fractionation using rate-based non-equilibrium model; specify feed stream, column configuration, operating, reaction) 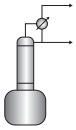 BatchFrac (rigorous 2- or 3-phase batch distillation; specify feed stream, configuration, charge-product, pressure, holdups, operation step)	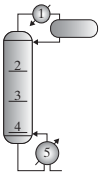 Column where reboiler and condenser are selected (specify feed stream, feed and products position, calculation type, number of stages, column configuration, operating specification, multicomponent liquid–liquid extraction, rigorous fractionation using rate-based non-equilibrium model, nonideal aqueous electrolytic model involving ionic species)	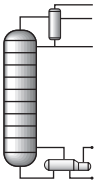 Distillation column (specify feed stream, feed and products position, calculation type, number of stages, column configuration, operating specification) 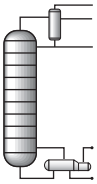 3-phase distillation

(Continued)

Table 7.2 (*continued*)

Unit Module	ASPEN PLUS	PRO/II	UniSim®Design
Absorber	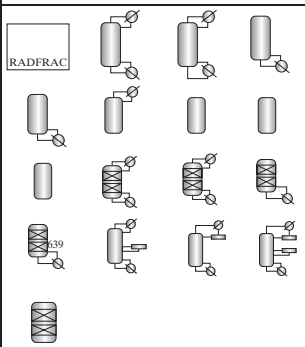 RadFrac (can use different module) (specify feed stream, feed and products position, calculation type, reaction, number of stages, column configuration, operating specification)	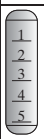 Column where reboiler and condenser are selected depending on the configuration; for example, for a reboiled absorber, a reboiler is selected	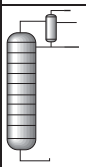 Refluxed absorber 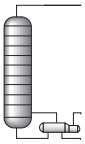 Reboiled absorber 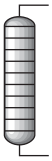 Absorber  Liquid–liquid extractor (feed stream inlet, stream outlet, number of stages)
PT-Flash	 Flash2, Flash3 (specify feed stream, pressure, temperature)	 Flash (specify feed stream, pressure, temperature, duty)	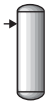 Separator (specify feed stream, pressure, temperature, duty)
Reactor	 RYield (Nonstoichiometric reactor based on known yield distribution; specify feed stream, temperature, pressure, valid phase, component yield)		 Yield shift reactor (specify feed stream, model configuration, composition shift, property shift)
	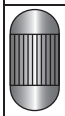 REquil (rigorous equilibrium reactor based on stoichiometric approach; specify feed stream, temperature, pressure, valid phase, reaction)	 R-EQ (rigorous equilibrium reactor based on stoichiometric approach; specify feed stream, temperature, pressure, valid phase, reaction)	 Equilibrium reactor (specify feed stream, reaction set)
	 RGibbs (rigorous reaction and/or multiphase equilibrium based on Gibbs free energy minimization; specify feed stream, temperature, pressure; calculates phase and chemical equilibrium)	 R-GIBBS Gibbs reactor (rigorous reaction and/or multiphase equilibrium based on Gibbs free energy minimization; specify feed stream, temperature, pressure; calculates phase and chemical equilibrium)	 Gibbs reactor (specify feed stream, operating conditions)

Table 7.2 (*continued*)

Unit Module	ASPEN PLUS	PRO/II	UniSim®Design
	 RCSTR (perfectly mixed continuous-stirred tank reactor with rate-controlled reactions based on specified kinetics; specify feed stream, temperature, pressure, type, valid phase, reaction)	 R-CSTR CSTR Reactor (perfectly mixed continuous-stirred tank reactor with rate-controlled reactions based on specified kinetics; specify feed stream, temperature, pressure, type, valid phase, reaction)	 CSTR Continuous-stirred tank reactor (specified feed stream, design specificaitons, reaction information)
	 RPlug (plug-flow reactor with perfect radial mixing and rate-controlled reactions based on specified kinetics; specify feed stream, reactor type, configuration of reactor, valid phase, reaction)	 RPLUG Plug-Flow Reactor (perfect radial mixing with rate-controlled reactions based on specified kinetics; specify feed stream, reactor type, configuration of reactor, valid phase, reaction)	 Plug Flow Reactor (perfect radial mixing; feed stream, design specification, reaction information)
	 RBATCH (perfectly mixed batch or semibatch reactor with rate-controlled reactions based on specified kinetics; specified feed stream, reactor operating conditions, valid phase, stop criteria, operation time)	 BR1 Batch Reactor (perfectly mixed batch or semibatch reactor with rate-controlled reactions based on specified kinetics; specified feed stream, reactor operating conditions, valid phase, stop criteria, operation time)	

Source: Images are obtained from © ASPEN PLUS, UniSim®Design, and PRO/II. Used with permission.

are data related to the chemicals and their properties); variables fixed by the process (usually these are related to process specifications; that is, related to design decisions); and variables fixed by the unit operation models (usually, these are equipment parameters, that is, related to design decisions). Therefore, different sets of data satisfying the degrees of freedom correspond to different sets of design decisions.

EXAMPLE 7.1 ***Cooler***

Consider the cooler in Figure 7.6, in which stream S1, containing benzene and toluene at a vapor fraction of $\phi_1 = 0.5$, is condensed by removing heat, Q. Carry out a degrees of freedom analysis.

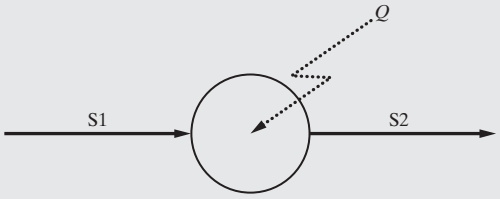

Figure 7.6 Schematic of a cooler.

SOLUTION

At steady state, the material and energy balances are

$$F_1 x_{B1} = F_2 x_{B2} \tag{7.7}$$

$$F_1 x_{T1} = F_2 x_{T2} \tag{7.8}$$

$$F_1 h_1 + Q = F_2 h_2 \tag{7.9}$$

where F_i is the molar flow rate of stream i, x_{ji} is the mole fraction of species j in stream i, and h_i is the enthalpy of stream i, which can be expressed as

$$h_i = h_i\{P_i, \phi_i, x_i\} \qquad i = 1,\ 2 \tag{7.10}$$

and $x_{Ti} = 1 - x_{Bi}$, $i = 1, 2$. Note that, in this case, the pressure, P, and vapor fraction, ϕ, accompany the mole fractions as the $C + 2$ intensive variables that provide the enthalpy and other intensive variables of each stream. For this model, $N_{\text{Equations}} = 7$ and $N_{\text{Variables}} = 13$ (F_i, h_i, P_i, ϕ_i, x_{Bi}, and x_{Ti}, $i = 1, 2$, and Q). Hence, $N_D = 13 - 7 = 6$, and one set of specifications is composed of the variables of the feed stream (F_1, P_1, ϕ_1, x_{B1}) and P_2 and Q. In the process simulators, so-called heater and cooler unit modules are provided to solve the equations for specifications like these.

EXAMPLE 7.2 ***Mixer***

Consider the mixer in Figure 7.7 in which streams S1 and S2, containing benzene and toluene, are mixed isobarically to form stream S3. Carry out a degrees of freedom analysis for this mixer module.

SOLUTION

At steady state, its material and energy balances are

$$F_1 x_{B1} + F_2 x_{B2} = F_3 x_{B3} \tag{7.11}$$

$$F_1 x_{T1} + F_2 x_{T2} = F_3 x_{T3} \tag{7.12}$$

$$F_1 h_1 + F_2 h_2 = F_3 h_3 \tag{7.13}$$

Figure 7.7 Benzene–toluene mixer.

Using temperature and pressure as the intensive variables, Eq. (7.10) becomes

$$h_i = h_i\{T_i, P, x_i\} \qquad i = 1,\ 2,\ 3 \tag{7.14}$$

and $x_{Ti} = 1 - x_{Bi}$, $i = 1, 2, 3$. For this model, $N_{\text{Equations}} = 9$, and $N_{\text{Variables}} = 16$ (F_i, h_i, T_i, x_{Bi}, and x_{Ti}, $i = 1, 2, 3$, and P). Hence, $N_D = 16 - 9 = 7$, and a common set of specifications is composed of the variables of the feed streams (F_1, x_{B1}, T_1, and F_2, x_{B2}, T_2) and P.

Flowsheet Decomposition

Flowsheets are rarely acyclic as in Figure 7.4. In process synthesis, most distributions of chemicals involve recycle streams as in Figure 7.2. For the simpler distributions, where the fractional conversions or the extents of reaction are known, the split fractions are specified, and no purge streams exist, as in the vinyl-chloride process (Figure 2.6) the flow rates of the species in the recycle streams can be calculated directly (without iteration). In most cases, however, with complex equilibrium reactions, complex separators, and purge streams, iterative recycle calculations are necessary, especially when inert chemicals enter the process as impurities with the reactants.

As shown in Figure 7.2 and discussed in the subsection Calculation Sequence, iterative recycle calculations are necessary. In this subsection, the general problem of flowsheet decomposition is introduced, given a more complex flowsheet with multiple recycle loops. For this purpose, when using the sequential-modular approach, all of the process simulators determine the number and identity of the recycle loops; and select the tear streams and the calculation order for the process units within the recycle loops.

Before considering this more general problem, for the simple process in Figure 7.2, a tear stream is easily selected, for example, S4-1. Then, with the feed stream, S0, specified and guesses for S4-1 entered (often zero), calculations begin with Unit1 and proceed around the loop until the calculations for Unit4 are completed. Then, the newly computed values for S4-1 are compared with the guess values. When not sufficiently close,

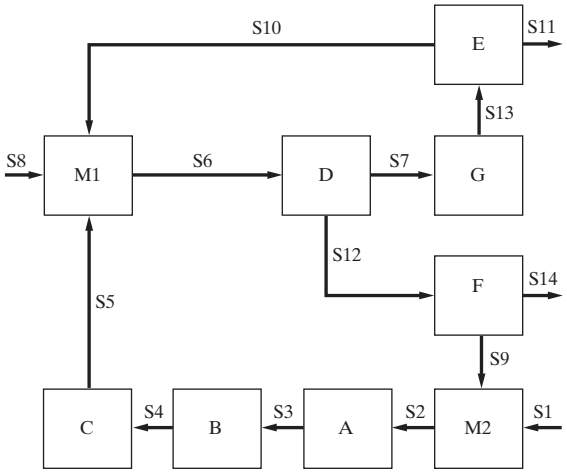

Figure 7.8 Nested recycle loops.

a numerical convergence method (e.g., successive substitutions, Wegstein's method—to be discussed in the subsection Recycle Convergence), is used to produce new guess values and the sequence around the loop is repeated.

A more complex flowsheet involves two or more recycle loops, often coupled together, often in interlocking recycle loops. Consider, for example, the flowsheet in Figure 7.8, which involves two interlocking recycle loops with feed streams S1 and S8 specified. Herein, a decomposition can be created that involves just one tear stream, S6, because it resides in both recycle loops. For this, guesses are made for S6 and the calculations begin with unit D. Then either the sequence G, E or F, M2, A, B, C is calculated. When both sequences are completed, M1 is calculated to give new values for stream S6. When not sufficiently close to the guesses, new guesses are estimated (using a numerical method) and the calculation sequence is repeated.

Alternatively, streams S10 and S5 are selected as the tear streams and a nested calculation sequence using an internal recycle loop nested with an external recycle loop. When beginning with guesses for tear stream S10, after guesses are made for tear stream S5, the internal loop involving M1, D, G, E is converged. Then, the external loop F, M2, A, B, C is computed to give new values for S10. When not sufficiently close to the guesses, new guesses for S10 are computed using a numerical method.

Another more complex flowsheet having three nested recycle loops is shown in Figure 7.9 with feed stream S1 specified. Here, three tear streams can be selected, but just two tear streams, S5 and S8, simplify the calculation sequence. S5 resides in two recycle loops, as does S8. Let S8 be in the external iteration loop. With guesses for S8, calculate units F and G. Then, begin the internal iteration loop. With guesses for S5, calculate D, A, B, C, to give new values for S5 and iterate through this internal loop until convergence is achieved. Having converged the internal loop, calculate E to give new values for S8 and, until convergence is achieved, make another iteration through the external loop.

Clearly, with process simulators using the sequential-modular approach as flowsheets become more complex, decomposition techniques gain importance. First, the number of partitions, the number of recycle loops, the tear streams, and the calculation

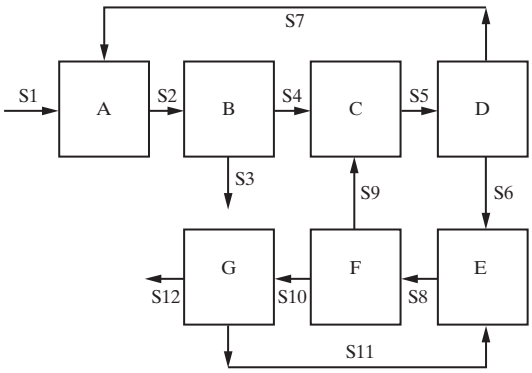

Figure 7.9 Three nested recycle loops.

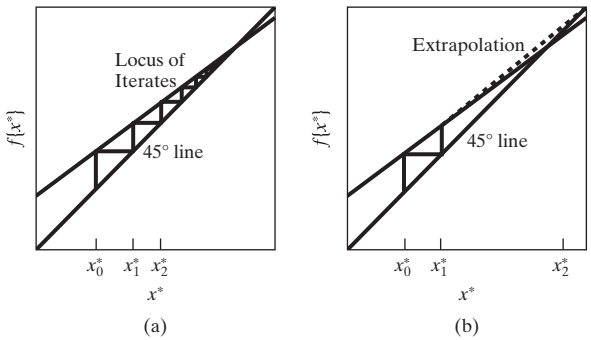

Figure 7.10 Convergence of a recycle loop: (a) successive substitution method; (b) Wegstein's method.

order for the unit operations are determined. Once the user provides the flowsheet in the form of unit modules and their connections, the simulator automatically determines the flowsheet decomposition details. It is recommended, however, that the designer/user determine whether the selected tear streams and the corresponding calculation order are optimal or could be improved. When appropriate, the process simulators permit the user to select alternate tear streams, thereby altering the calculation order. After the calculation order and the tear streams have been established, the next step is to select the recycle convergence option.

Recycle Convergence

When implementing the sequential-modular method and carrying out a flowsheet decomposition to achieve recycle convergence, all of the process simulators offer the successive substitution (direct iteration) and bounded-Wegstein methods of convergence, as well as more sophisticated methods for highly nonlinear systems where the successive substitution or Wegstein's methods may fail or may be very inefficient. These other methods include the Newton–Raphson method, Broyden's quasi-Newton method, and the dominant-eigenvalue method (Wegstein, 1958; Henley and Rosen, 1969; Myers and Seider, 1976; Westerberg et al., 1979). Each of these five methods determines whether the relative difference between the guessed and calculated variables for the tear stream (e.g., stream S4-1 in Figure 7.2) are all less than a prespecified tolerance. If not, the convergence subroutine computes new guesses for its output stream variables and iterates until the loop is converged.

To converge the recycle loop in Figure 7.2 with tear stream S4-1, let x^* be the guess value of a particular variable (element) of its stream vector, and let $f\{x^*\}$ be the corresponding value for the corresponding calculated variable in S4-1, as determined by taking x^* and calculating Unit1, Unit2, Unit3, and Unit4 in that order. When the method of successive substitutions is specified, the new guess for x is simply made equal to $f\{x^*\}$. A sequence of calculations may exhibit the behavior shown in Figure 7.10a. After a number of iterations, the locus of iterates intersects the 45° line, giving the converged value of x in stream S4-1. When the slope of the locus of iterates ($f\{x\}$, x) is close to unity (for processes with high recycle ratios), a large number of iterations may be required before convergence occurs.

Wegstein's method can be employed to accelerate convergence when the method of successive substitutions requires a large number of iterations. As shown in Figure 7.10b, the previous two iterates $f\{x^*\}$ and x^* are extrapolated linearly to obtain the next value of x as the point of intersection with the 45° line. The equation of the straight-line extrapolation is derived easily as

$$x = \left(\frac{s}{s-1}\right)x^* - \left(\frac{1}{s-1}\right)f\{x^*\} \tag{7.15}$$

where s is the slope of the extrapolated line. A more convenient form of Eq. (7.15) uses a weighting function defined by $q = s/(s-1)$, giving

$$x = qx^* + (1-q)f\{x^*\} \tag{7.16}$$

Thus, weights q and $1-q$ are applied, respectively, to x^* and $f\{x^*\}$. Equation (7.16), with q defined by the slope, is usually employed when the slope is less than 1, such that $q < 0$. Typically, q is bounded between -20 and 0 to ensure stability and a reasonable rate of convergence. Wegstein's method reduces to the method of successive substitutions, $x = f\{x^*\}$, when $q = 0$.

In the following text, the principal features of five recycle convergence methods (successive substitution, Wegstein's method, Newton–Raphson method, Broyden's quasi-Newton method, and the dominant-eigenvalue method) are compared. Consider the recycle convergence unit shown in Figure 7.11 and let

$$\underline{y} = \underline{f}\{\underline{x}^*\} - \underline{x}^* \tag{7.17}$$

where $\underline{x}^*$ is the vector of guesses for n recycle (tear) variables and $\underline{f}\{\underline{x}^*\}$ is the vector of the recycle variables computed from the guesses after one pass through the simulation units in the recycle loop. Clearly, the objective of the convergence unit is to adjust $\underline{x}^*$ so as to drive $\underline{y}$ toward zero. Note that this dashed recycle convergence unit is not shown on simulation flowsheets. However, one hidden convergence unit is implemented for each tear stream.

Figure 7.11 Recycle convergence unit.

Newton–Raphson Method. The Newton–Raphson second-order method can be written as

$$\underline{\underline{J}}\{\underline{x}^*\}\underline{\Delta x} = -\underline{y}\{\underline{x}^*\} \tag{7.18}$$

where $\underline{\Delta x} = \underline{x} - \underline{x}^*$. Substituting and rearranging, the new values of the recycle variables, $\underline{x}$, are

$$\underline{x} = \underline{x}^* - \underline{\underline{J}}^{-1}\{\underline{x}^*\}\underline{y}\{\underline{x}^*\} \tag{7.19}$$

In these equations, the Jacobian matrix:

$$\underline{\underline{J}}\{\underline{x}^*\} = \begin{bmatrix} \frac{\partial y_1}{\partial x_1} & \frac{\partial y_1}{\partial x_2} & \cdots & \frac{\partial y_1}{\partial x_n} \\ \frac{\partial y_2}{\partial x_1} & \frac{\partial y_2}{\partial x_2} & \cdots & \frac{\partial y_2}{\partial x_n} \\ \vdots & \vdots & & \vdots \\ \frac{\partial y_n}{\partial x_1} & \frac{\partial y_n}{\partial x_2} & \cdots & \frac{\partial y_n}{\partial x_n} \end{bmatrix} \underline{x}^* \tag{7.20}$$

is evaluated at $\underline{x}^*$.

In each iteration of the Newton–Raphson method when the guesses are close to the true values, the length of the error vector, $\|\underline{y}\|$, is the square of its length after the previous iteration; that is, when the length of the initial error vector is 0.1, the subsequent error vectors are reduced to 0.01, 10^{-4}, 10^{-8}, …. However, this rapid rate of convergence requires that n^2 partial derivatives be evaluated at $\underline{x}^*$. Because most recycle loops involve many process units, each involving many equations, the chain rule for partial differentiation cannot be implemented easily. Consequently, the partial derivatives are evaluated by numerical perturbation; that is, each guess, x_i, $i = 1, \ldots, n$, is perturbed, one at a time. For each perturbation, δx_i, $i = 1, \ldots, n$, a pass through the recycle loop is required to give y_j^p, $j = 1, \ldots, n$. Then the partial derivatives in the ith row are computed by difference:

$$\frac{\partial y_j}{\partial x_i} \cong \frac{y_j^p - y_j}{\delta x_i} \quad j = 1, \ldots, n \tag{7.21}$$

This requires $n + 1$ passes through the recycle loop to complete the Jacobian matrix for just one iteration of the Newton–Raphson method; that is, for $n = 10$, 11 passes are necessary, usually involving far too many computations to be competitive.

Alternatively, so-called secant methods can be used to approximate the Jacobian matrix with far less effort (Westerberg et al., 1979). These provide a superlinear rate of convergence; that is, they reduce the errors less rapidly than the Newton–Raphson method, but more rapidly than the method of successive substitutions, which has a linear rate of convergence (i.e., the length of the error vector is reduced from 0.1 to 0.01, 10^{-3}, 10^{-4}, 10^{-5}, …). These methods are also referred to as quasi-Newton methods with Broyden's method being the most popular.

Method of Successive Substitutions. To compare the method of successive substitutions with the Newton–Raphson method or the quasi-Newton methods, the former can be written:

$$\underline{x} = \underline{f}\{\underline{x}^*\} \tag{7.22}$$

Subtracting $\underline{x}^*$ from both sides:

$$\underline{x} - \underline{x}^* = \underline{f}\{\underline{x}^*\} - \underline{x}^* \tag{7.23}$$

or

$$-\underline{\underline{I}}\,\underline{\Delta x} = -\underline{y}\{\underline{x}^*\} \tag{7.24}$$

Note that the Jacobian matrix is replaced by the identity matrix, and hence, each element of the $\underline{\Delta x}$ vector is influenced only by its corresponding element in the $\underline{y}$ vector. No interactions from the other elements of the $\underline{y}$ vector influence $\underline{\Delta x_i}$.

Wegstein's Method. Rewriting Eq. (7.15) for n-dimensional vectors,

$$\underline{x} = \begin{bmatrix} \frac{s_1}{s_1 - 1} & & \\ & \ddots & \\ & & \frac{s_n}{s_n - 1} \end{bmatrix} \underline{x}^* - \begin{bmatrix} \frac{1}{s_1 - 1} & & \\ & \ddots & \\ & & \frac{1}{s_n - 1} \end{bmatrix} \underline{f}\{\underline{x}^*\} \tag{7.25}$$

and subtracting $\underline{x}^*$ from both sides,

$$\underline{x} - \underline{x}^* = \begin{bmatrix} \frac{1}{1 - s_1} & & \\ & \ddots & \\ & & \frac{1}{1 - s_n} \end{bmatrix} \underline{y}\{\underline{x}^*\} \tag{7.26}$$

or

$$-\underline{\underline{A}}\,\underline{\Delta x} = -\underline{y}\{\underline{x}^*\} \tag{7.27}$$

where $\underline{\underline{A}}$ is a diagonal matrix with the elements $1 - s_i$, $i = 1, \ldots, n$. Although Wegstein's method provides a superlinear rate of convergence, note that like the method of successive substitutions, no interactions occur.

Dominant-Eigenvalue Method. In the dominant-eigenvalue method, the largest eigenvalue of the Jacobian matrix is estimated every third or fourth iteration and used in place of s_i in Eq. (7.26) to accelerate the method of successive substitutions, which is applied at the other iterations (Orbach and Crowe, 1971; Crowe and Nishio, 1975).

Control Blocks—Design Specifications

Occasionally, the need arises to provide specifications for variables or parameters that are not permitted by a unit module in a simulator module library. To accomplish this, all of the simulators provide a facility for iterative adjustments of so-called *manipulated variables and parameters* so as to achieve the desired specifications. Guesses are made for the *manipulated variables and parameters*. Then, the simulation calculations are performed and a *control* algorithm compares the calculated values with the desired specifications, which may be called *set points*. When significant differences, or errors, are detected,

the control algorithm prepares new guesses, using numerical methods, and transfers control to repeat the simulation calculations. Because the procedure is analogous to that performed by feedback controllers in a chemical plant (which are designed to reject disturbances during dynamic operation), it is common to refer to these convergence algorithms as *feedback control* algorithms (Henley and Rosen, 1969).

EXAMPLE 7.3 ***Example 7.2 Revisited***

For an equimolar feed stream, S1, at 1,000 lbmol/hr and 100°F, the flow rate of a toluene stream, S2, at 50°F is adjusted to achieve a desired temperature of the mixer effluent (e.g., 85°F), as shown in Figure 7.12. Convergence units for feedback control (design specifications) are shown on simulation flowsheets as dotted circles connected to streams and simulation modules by dotted lines. The dotted lines represent the information flow of stream variables to the control unit and information flow of adjusted equipment parameters to simulation modules. Note that the control units of most simulators can adjust the flow rates of the streams. After the calculations by the MIXER module are completed, the control unit samples the effluent temperature. It adjusts the flow rate of stream S2 when the specified temperature is not achieved and transfers to the MIXER module to repeat the mixing calculations. This cycle is repeated until the convergence criteria are satisfied or the maximum number of iterations is exceeded. In ASPEN PLUS, the control unit is called "$OLVER" (as shown in Figure 7.12), in UniSim®Design, it is called "Adjust"; in PRO/II, it is called "Control." What is important to note is that the MIXER module is in the inner loop and the control unit is in the outer loop.

Specifications are provided in the module ASPEN → Principles of Flowsheet Simulation → Control Blocks → Design Specifications, which is part of the multimedia encyclopedia that can be downloaded from www.seas.upenn.edu/~dlewin/multimedia.html.

Based on the input specifications in this module, ASPEN PLUS generates the program in the module and the simulator reports that

SEQUENCE USED WAS: $OLVER01 M1
(RETURN $OLVER01)

The iterative procedure used by $OLVER01 is initiated in the manner shown in Figure 7.13a. As indicated above, an initial guess for the manipulated variable (800 lbmol/hr), and the minimum and maximum values of the manipulated variable (0 and 2,000 lbmol/hr) are provided. Then, $OLVER01 adjusts the manipulated variable, using one of several convergence algorithms, until the convergence tolerances are satisfied with $F_2 = 402.3$ lbmol/hr. When the upper or lower bound is reached, a message is provided that convergence has not been achieved. For this example, the secant method was used to achieve convergence, with the iteration history displayed in Figure 7.13b.

Note that replacing the MIXER module with any process flowsheet would result in a similar calculation sequence.

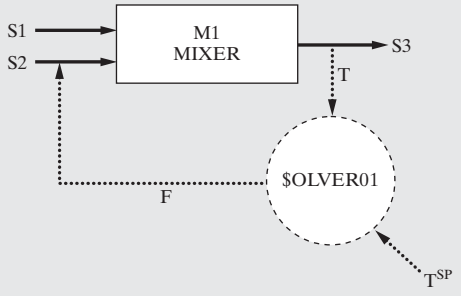

Figure 7.12 Feedback control—Design specification for the benzene–toluene mixer using ASPEN PLUS.

Flash with Recycle Problem

To master the concepts of recycle analysis, it is recommended that the reader solve several of the exercises at the end of the chapter. Of these, the so-called flash with recycle problem (Exercise 7.1a) should be solved first. Although it involves just one recycle loop, it demonstrates a very important principle. See if you can identify it!

Consider the simple process in Figure 7.14. For the three cases, compare and discuss the flow rates and compositions of the product streams.

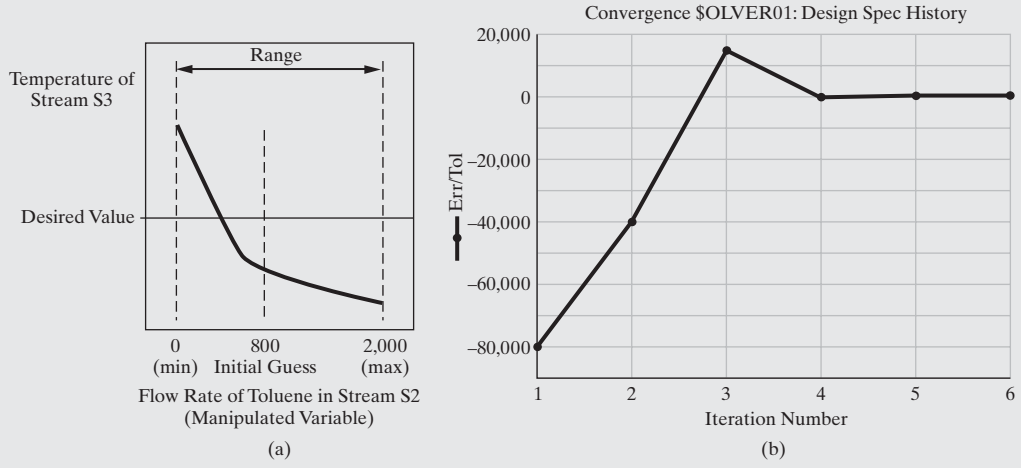

Figure 7.13 Graphical solution of the mixer control problem: (a) specifications for the manipulated variable; (b) ASPEN PLUS iteration history using the secant method.

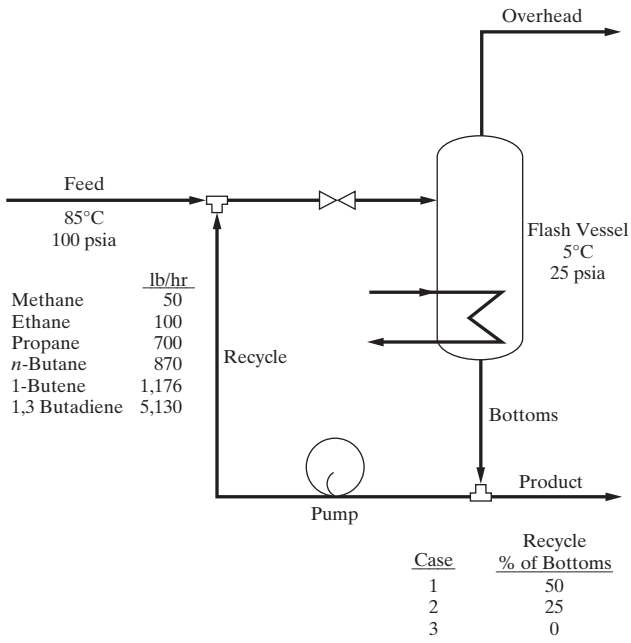

Figure 7.14 Flash with recycle process.

Note that the flash with recycle process is a good representation of a quench vessel in which hot gases, typically from an exothermic reactor, are quenched by a cold liquid recycle. Quenches are often needed to provide rapid cooling of a reactor effluent by direct-contact heat transfer. Cold liquid is showered over hot, rising gases. As some of the liquid vaporizes, the latent heat of vaporization is absorbed, and cooling occurs. Quenches are particularly effective for the rapid cooling of organic vapors so as to avoid, or at least reduce, the deposition of solid carbon by chemical reaction. Any solid that is deposited can be bled with the condensate from the vessel bottoms rather easily. The alternative, shell-and-tube heat exchangers, often become fouled with solids and must be shut down periodically for cleaning.

Flash Vessel Control

Next, it is recommended that the reader solve a variation on the flash with recycle problem. In this variation (Exercise 7.1b), case 3 is modified so as to determine the flash temperature to obtain 850 lb/hr of overhead vapor.

7.3 PROCESS CREATION THROUGH PROCESS SIMULATION

The objective of process design is process creation during which process simulation plays the important role of verification and generation of data based on the possible design decisions. The information (data) available at various stages of a process design project is (are) different. At the start, very little information is available, but near the end, almost all of the necessary information is available. This means that the simulation problems (tasks) solved at different stages of a process design project are also varied, requiring diverse forms of process models. Figure 7.15 shows how the different simulation tasks are used, depending on the available or generated information with corresponding entry points, to solve each process simulation problem.

The entry point depends on the available information and the specific process design objectives. Brief overviews for each of the entry points follow.

Entry-1

At this level, only the connectivities of the unit modules are available, but the design details of the unit modules are not yet

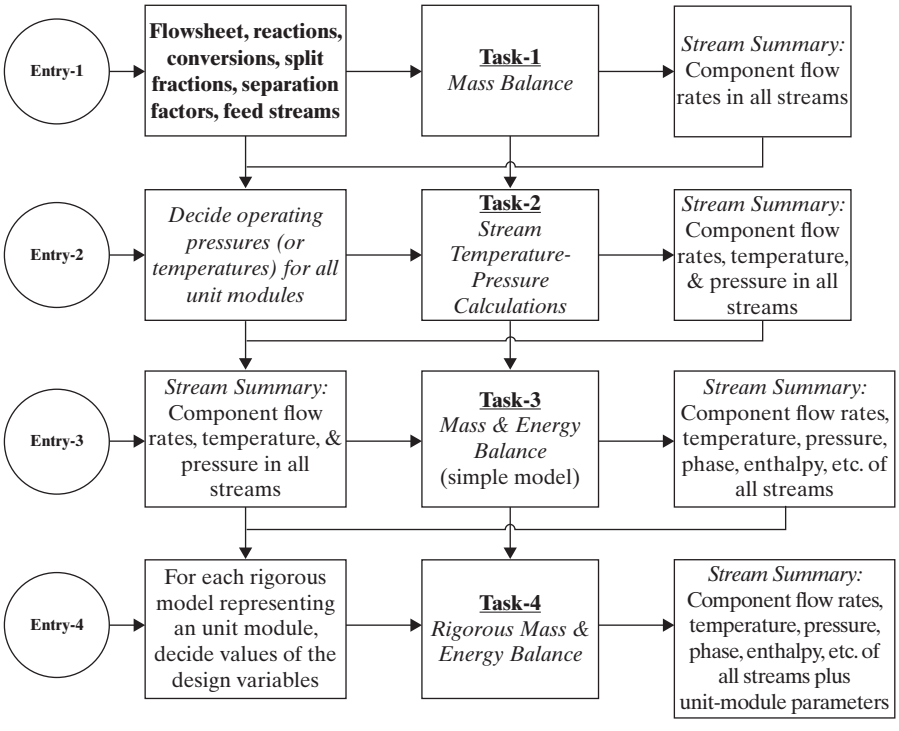

Figure 7.15 Decomposition of process simulation problem into subtasks whose data flows are highlighted.

available. Also, the temperatures, pressures, and compositions of the process streams are unknown. Most likely, the reaction stoichiometric coefficients and estimates (or desired values) of the conversions are available. For the downstream separation modules, product-recovery targets could be available (or the designer could set these values as initial estimates of the design objectives). Here, the design decisions (specifications) involve the reaction conversions, separation recoveries, and purge fractions to obtain a specified product (flow rates and purities) from given feed materials (flow rates and purities). With these specifications, only mass balances can be performed (see simulation Task-1). The results of simulation Task-1 are the component flow rates of all streams in the process flowsheet.

Entry-2

With the component flow rates of all streams available, the next level in the hierarchy of process-design calculations involves deciding on the stream (or unit module) temperatures and pressures. A good starting point is always the reactor whose temperature and pressure are usually fixed by the reaction specifications (e.g., catalyst and/or chemical equilibrium). Here, the design decisions involve the choice of two of the following variables for every process stream: temperature, pressure, and phase. Note that when modeling a distillation column with liquid distillate and bottoms products, the corresponding streams from the component-splitter module must be saturated liquids. For a component-splitter module that represents a vapor–liquid flash operation, the overhead and bottom streams of the component-splitter have the same temperature and pressure at vapor–liquid equilibrium. That is, the overhead product is at its dew point whereas the bottoms product is at its bubble point. For a reactor, when the temperature and pressure are specified, the phase identity is calculated at phase equilibrium (involving vapor, liquid, and solid phases). In summary, given the results of Task-1, design decisions for stream pressures, temperatures, and/or phase identities are made. Having completed simulation Task-2, the component flow rates, pressures, temperatures, and phase identities of all streams in the flowsheet are known.

Entry-3

With the results from simulation Task-2, the process flowsheet can be refined to include additional unit modules to model heat exchangers, pumps, compressors, valves, and so on. Then, mass and energy balance calculations are performed for all unit modules in the process flowsheet. Note that the unit modules continue to solve the equations for simple models, as in Task-1, as well as for the simple models of heat exchangers, pumps, and so on, in Table 7.2. The design decisions (specifications) are equipment parameters for the additional unit modules (for example, exit pressures for pumps, compressors, and exit temperatures for heat exchangers) based on the stream properties from simulation Task-2. The result from simulation Task-3 is a complete mass and energy balance for the entire process flowsheet using *simple* models. Additional results include the net energy addition/removal for every unit module of the process, computed from the known stream enthalpies of all streams.

Entry-4

Entry at this level requires all of the information generated (obtained) at the lower levels, and process simulation is performed with *rigorous* models involving additional design decisions (specifications), for example, the number of trays, the reflux ratio, and the position of the feed tray. These design parameters are selected such that the effluent stream conditions (temperature, pressure, and component flow rates) for the rigorous and simple models are approximately the same. Consequently, the mass and energy balance results do not change appreciably from those obtained in simulation Task-3.

During process synthesis, given a basic process flowsheet with only limited data (e.g., one branch in a synthesis tree, such as Figure 2.6, when creating a vinyl-chloride process), a designer could begin at Entry-1 and gradually move from Task-1 to the next higher-level tasks, ending at Task-4, where almost all of the process data would be available. That is, from any entry point, executing its simulation task, the designer gradually moves upward to higher-level simulation tasks. For example, when working with an existing process, for which the process flowsheet and all of the detailed design variables are known, the designer can begin at Entry-4 and perform the necessary simulations with rigorous unit modules. On the other hand, at the start of a design project, only a rough sketch of a process flowsheet is known together with reaction data and a feed-stream allocation(s); beginning at Entry-4 would require uninformed guesses for many of the decision variables. Because the degrees of freedom are normally numerous, it is more efficient to proceed step by step, increasing the amount of generated data (information) until all necessary data are available for the rigorous process simulation. The result is a feasible process flowsheet to be fine-tuned and improved through optimization, process integration, and process intensification.

Whichever simulation task is performed, the steps are those highlighted in Figure 7.1; that is, the simulation problem is defined, an appropriate process model is derived/selected, the model degrees of freedom are analyzed, the model equations are solved, and the simulation results are analyzed.

Process Simulation Task-1

This task is to perform only mass balances because sufficient information to perform mass and energy balances is unavailable. Because only mass balances are performed, the corresponding models for the unit modules are simple. For mass-balance calculations, almost all chemical process flowsheets are represented by a combination of mass-balance models of mixers (representing all kinds of mixing operations), stoichiometric (conversion) reactors (representing all types of reactors), component splitters (representing all types of separation operations), and stream dividers (representing all types of stream-splitting operations). These can also be represented by library modules available in many process simulators (see the list of unit modules in Table 7.1). Note that Examples 7.4 and 7.5 show how to carry out simulation Task-1 for the synthesis of processes to convert benzene to cyclohexane and ethylene to ethanol. These show how to assemble the simple mass balance modules; that is, to assemble mass balance Eqs. (7.1)–(7.6) to model the process flowsheets.

Process Simulation Task-2

This task is to establish temperatures, pressures, and phase identities of each stream in the process flowsheet based on the component flow rates established in Task-1 or specified by the designer. Constitutive (property) models are needed to perform its computations. At this point, knowledge of phase equilibria is necessary because phase identities need to be calculated. The problems are defined as follows (for processes with vapor and liquid phases): identify saturated vapor streams, those that are saturated liquids, those that are superheated vapor, those that are subcooled liquid, and those that contain a mix of phases. Table 7.3 gives a list of selected properties together with some details on their computation using constitutive models. A helpful reference for information on property models and their use in process-product design is given by Kontogeorgis and Gani (2009).

With the component flow rates in each stream known, the designer specifies the pressure (or temperature) of each stream and calculates the temperature (or pressure) using dew- and bubble-point calculations. To perform dew- or bubble-point calculations, a phase-equilibrium model is needed, as discussed in Section 2.3.

Process Simulation Task-3

The objective in this task is to perform mass and energy balances for the entire process flowsheet given stream temperatures, pressures, component flow rates, and phase identities. Properties of the streams are also computed. Unit modules are added that do not affect the mass balances, such as those for heat exchangers, compressors, and pumps. Given the mass-balance model, energy-balance equations (one per unit module) are added to compute the energy added/removed from each unit operation. For example, in the case of a component splitter, when the inlet stream F is liquid and outlet streams V and L are saturated vapor and liquid, respectively, the energy balance equation is,

$$H^{\mathrm{F}}(T^{\mathrm{F}},\ \underline{z})F_j = H^{\mathrm{L}}(T^{\mathrm{L}},\ \underline{x})F_{j+2} + H^{\mathrm{V}}(T^{\mathrm{V}},\ \underline{y})\,F_{j+1} + Q \quad (7.28)$$

where H^{J} is the enthalpy of stream j; $\underline{x}$, $\underline{y}$, and $\underline{z}$ are the mole fractions of the liquid, vapor, and feed streams, respectively; T^{J} is the temperature of stream j; F_j are the flow rates of stream j (i.e., j, $j+1$ and $j+2$) and Q is the heat added to or removed from the surroundings.

The data needed to perform Task-3 are highlighted under Entry-3 in Figure 7.15. That is, using the temperatures, pressures, compositions, and flow rates of each stream, mass and energy balances are calculated by either adding models for enthalpy calculations to the mass-balance model or simply asking the simulator to perform mass and energy balances for process flowsheets consisting of mixers, reactors, component splitters, and stream dividers. Note that when using Eq. (7.28), specifying stream temperatures to calculate the heat duty (Q) is easier than specifying Q and calculating an unknown stream temperature because, for the latter, Eq. (7.28) becomes nonlinear, and an iterative solution technique is necessary.

Process Simulation Task-4

The objective of this task is to perform mass- and energy-balance calculations with rigorous models, where feasible, for the unit

Table 7.3 Partial List of Thermophysical Properties

Property	Property Type	Model/Algorithm	Parameters
Activity coefficient	Liquid-phase component in a mixture	GE-models[a] (Wilson, NRTL, UNIQUAC, UNIFAC)	Size and volume parameters (molecules or groups); interaction parameters
Fugacity coefficient	Liquid- or vapor-phase component property in a mixture	Equations of state (cubic); PC-SAFT	Cubic EOS (critical properties, acentric factor, binary interaction parameters); PC-SAFT parameters
Vapor–liquid saturation point	Mixture phase equilibrium property	ΔG minimization (γ-ϕ approach or ϕ-ϕ approach)	EOS and GE-model parameters, composition of one coexisting phase plus temperature or pressure
VLE phase diagram	Multiple calculations of VL saturation points	ΔG minimization (γ-ϕ approach or ϕ-ϕ approach)	
LLE phase diagram	Multiple calculations of LL saturation points	ΔG minimization (γ-γ approach); not Wilson GE-model	GE-model parameters
VLLE phase diagrams	Two liquid phases in equilibrium with a vapor phase—ternary or more compounds	ΔG minimization (γ-ϕ approach or ϕ-ϕ approach); not Wilson GE-model	
SLE saturation	Composition of solid in equilibrium with a liquid mixture as a function of temperature	ΔG minimization (γ-approach); solid phase assumed pure	GE-model parameters plus heat of fusion and melting temperature of the solid
Density	Pure compound or mixture; function of temperature and pressure	Equation of state; corresponding states; correlations	Critical props., acentric factor, correl. coefs., mixing rules
Vapor pressures	Pure component, temperature-dependent property	Equation of state; Antoine correlation	Critical properties, acentric factor, Antoine coefs.

[a] Excess Gibbs free energy models.

modules in the process flowsheet using the information generated from the previous tasks or supplied by the designer. The simple models are replaced by their rigorous formulations with additional design decisions (specifications) needed. Table 7.2 lists the minimum variables that must be specified. This subtask yields a rigorous simulation of the base-case design.

Conceptual Example—Carry Out Tasks 1–4

Consider the flowsheet for a process to convert benzene to cyclohexane in Figure 7.16, a variation of the process presented in Figure 10.24. Here, benzene stream, S2, is mixed with hydrogen (from a steam-methane reformer containing 2.5 mol% methane) and recycle hydrogen. The combined stream, S4, is heated to 422.2 K at 33.3 atm and sent to reactor, R-1, where the exothermic reaction, $C_6H_6 + 3H_2 \rightarrow C_6H_{12}$, converts 97% of the benzene. After cooling, cyclohexane product is recovered by distillation, with hydrogen recycled and compressed to 34 atm. Note that stream S10 is purged to keep inert methane from building up in the process. Also, the H_2/C_6H_6 ratio is adjusted to 12 in reactor feed S4.

The main objective of process simulation (during the synthesis of processes for continuous steady-state operation) is to obtain the minimum information of all streams, that is, temperatures, T_j, pressures, P_j, and compositions (component flow rates, f_{ij}) in Table 7.4, where j is the stream counter and i is the component counter. Note that H_2, CH_4, C_6H_6, and C_6H_{12} are components $1, \ldots, 4$. Knowing these data, the stream properties, θ_j (e.g., phase, enthalpy, density), for each stream can also be calculated. Should a rigorous simulation be performed or should simulation subtasks be carried out as recommended above? In the former, to obtain estimates for the many additional design variables, many trial-and-error iterations may be required to achieve a feasible process design. In the latter, beginning with the simplest Task-1 for which all necessary data are known and proceeding from task to task, specifications are gradually accumulated yielding the desired simulation result.

Table 7.4 Stream Summary for a Typical Process Simulation[a]

Variables	Streams						
	S1	S2	S3	S4	S5	… …	S10
$f_{1,j}$	*	*	??	??	??	??	??
$f_{2,j}$	*	*	??	??	??	??	??
$f_{3,j}$	*	*	??	??	??	??	??
$f_{4,j}$	*	*	??	??	??	??	??
P_j	*	*	-	-	-	-	-
T_j	*	*	-	-	-	-	-
θ_j	-	-	-	-	-	-	-

[a] Illustrated for process simulation Task-1.

In Table 7.4, note that for process simulation Task-1, only the entries in the feed streams, S1 and S2, are known (denoted by *)—and the flow rates of the component entries (denoted by ??) in the remaining streams are computed using the material balances. All other entries are denoted by "-" because they do not appear in the mass balances.

In simulation Task-2, for each stream j, either P_j or T_j is specified; the other is calculated. In simulation Task-3, stream properties such as enthalpies are calculated, allowing the addition of energy-balance calculations. In simulation Task-4, the final values of all variables in Table 7.4 are calculated by replacing simple with rigorous models and using the values from simulation Task-3 as initial estimates. In addition to the variables listed in Table 7.4, the equipment parameters in Table 7.2 are determined.

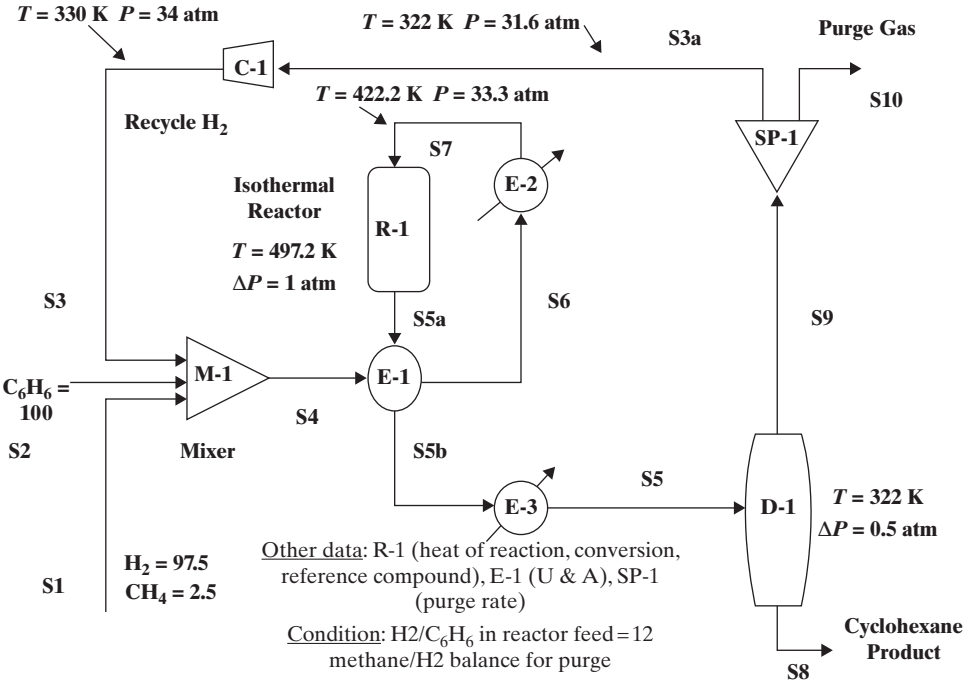

Figure 7.16 Process flowsheet for cyclohexane production.

EXAMPLE 7.4 *Benzene to Cyclohexane Process*

Develop the mass balances for the process flowsheet in Figure 7.16, perform model analysis, and propose a solution procedure. The information in Table 7.5 is known. Here, 2.5% of the recycle hydrogen stream is to be purged.

Table 7.5 Known Data for Cyclohexane Process[a]

Unit/Stream	Specifications	Specified Value
Reactor	Reaction, stoichiometric coefficients ($\underline{\nu}$), conversion (X_k), key component (k)	$C_6H_6 + 3H_2 \rightarrow C_6H_{12}$ $\underline{\nu}(-3,\ 0,\ -1,\ 1)$; $X_k(0.97, k = 3)$
Separation	Component split fractions in overhead product ($\underline{\xi}_S$)	$\underline{\xi}_S(1.0,\ 1.0,\ 0.0,\ 0.0)$
Purge	Stream-divider split fraction (β_D)	$\beta_D(0.025)$
Feed stream 1	Component flow rates ($\underline{f}_1$, kmol/hr)	$\underline{f}_1(0,\ 0,\ 45.36,\ 0)$
Feed stream 2	Component flow rates ($\underline{f}_2$, kmol/hr)	$\underline{f}_2(146.25,\ 3.75,\ 0,\ 0)$

[a] See variable definitions in Eqs. (7.1)–(7.6).

SOLUTION

Start at Entry-1 in Figure 7.15: Convert the original flowsheet to one with only mixers, reactors, component splitters, and stream dividers, as shown in Figure 7.17. Note that the unit modules for heat exchangers, pumps, and compressors are removed from the original flowsheet because they do not affect the mass-balance calculations.

Using the model Eqs. (7.1)–(7.6), a mass-balance model for the process flowsheet in Figure 7.17 is obtained. Table 7.6 lists the model equations and variables as well as the degrees of freedom and variables to be specified. Tables 7.7 and 7.8 give the ordered incidence matrix in terms of the equations as well as the unit modules. Note the off-diagonal element at the top right-hand corner due to the recycle loop.

Table 7.6 Mass-Balance Model Analysis for Cyclohexane Process

Equations		Number
Eq. (7.1): $f_{i,N_M+1} = \Sigma_j f_{ij}$	for $i = 1, N_C$; $j = 1, N_M$; $N_M = 3$	N_C
Eq. (7.2): $f_{i5} = f_{i4} + \nu_i X_k f_{k4}$	for $i = 1, N_C$; k = key compound	N_C
Eq. (7.3): $f_{i8} = \xi_{iS} f_{i5}$	for $i = 1, N_C$	N_C
Eq. (7.4): $f_{i9} = (1 - \xi_{iS}) f_{i5}$	for $i = 1, N_C$	N_C
Eq. (7.5): $f_{i10} = \beta_D f_{i9}$	for $i = 1, N_C$	N_C
Eq. (7.6): $f_{i3} = (1 - \beta_D) f_{i9}$	for $i = 1, N_C$;	N_C
Total: N_E (number of equations)		$6 \times N_C$
Variables		
Component flow rates $\underline{f}_1, \underline{f}_2, \underline{f}_3, \underline{f}_4, \underline{f}_5, \underline{f}_8, \underline{f}_9, \underline{f}_{10}$		$8 \times N_C$
Reactor parameters: $\underline{\nu}$ (stoichiometric coefficients), X_k (conversion)—these are repeated for each reaction		$N_C + 1$
Component split-fractions: $\underline{\xi}_S$		N_C
Stream-divider split-fractions: β_D		1
Total: N_V (number of variables)		$10 \times N_C + 2$
Degrees of freedom		
$N_V - N_E$		$4 \times N_C + 2$
Variables to specify (decisions)		
$\underline{f}_1, \underline{f}_2$ ($2N_C$ process variables); $\underline{\nu}, X_k, \underline{\xi}_S, \beta_D$ ($2N_C + 2$ equipment parameters)		
Unknown variables		
$\underline{f}_3, \underline{f}_4, \underline{f}_5, \underline{f}_8, \underline{f}_9, \underline{f}_{10}$ ($6N_C$ process variables)		

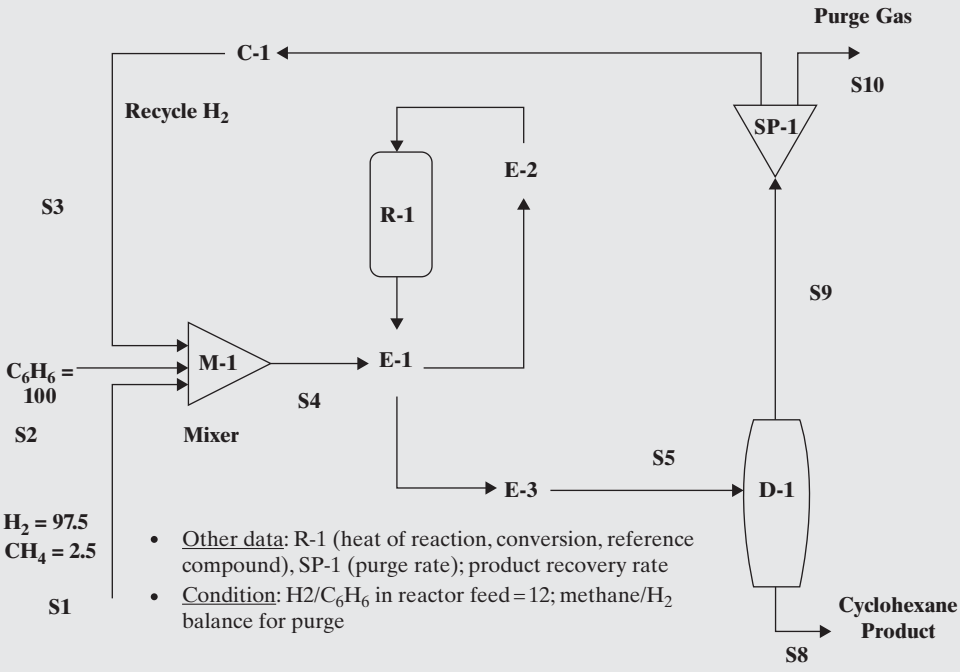

Figure 7.17 Simplified cyclohexane process flowsheet for mass balances only.

Table 7.7 Ordered Model Equations in Incidence Matrix for Cyclohexane Process

	Specified variables						Calculated variables					
	$\underline{f}_1$	$\underline{f}_2$	γ	η_k	ξ_S	β_D	$\underline{f}_5$	$\underline{f}_8$	$\underline{f}_9$	$\underline{f}_{10}$	$\underline{f}_3$	$\underline{f}_4$
Eq. (7.2)			*	*			(*)					*
Eq. (7.3)					*		*	(*)				
Eq. (7.4)					*		*		(*)			
Eq. (7.5)						*			*	(*)		
Eq. (7.6)						*			*		(*)	
Eq. (7.1)	*	*									*	(*)

Table 7.8 Ordered Model Equations in Unit Modules for Cyclohexane Process

	Specified Variables						Calculated Variables					
	$\underline{f}_1$	$\underline{f}_2$	$\underline{\gamma}$	η_k	$\underline{\xi}_S$	β_D	$\underline{f}_5$	$\underline{f}_8$	$\underline{f}_9$	$\underline{f}_{10}$	$\underline{f}_3$	$\underline{f}_4$
Reactor			*	*			(*)					*
CS					*		*	(*)				
CS					*		*		(*)			
SD						*			*	(*)		
SD						*			*		(*)	
Mixer	*	*									*	(*)

Table 7.9 Mass-Balance Simulation Results for Cyclohexane Process

	Streams							
Variables	S1	S2	S4	S5	S8	S9	S10	S3
f_{H2}(kmol/hr)	0	146.25	701.61	569.64	0	569.64	14.24	555.47
f_M (kmol/hr)	0	3.75	149.85	149.85	0	149.85	3.75	146.10
f_B (kmol/hr)	45.35	0	45.35	1.36	1.36	0	0	0
f_{CH} (kmol/hr)	0	0	0	43.99	43.99	0	0	0
Total (kmol/hr)	45.35	150.00	896.81	764.84	45.35	719.49	17.99	701.57
T (K)	Not calculated in Task-1							
P (atm)	Not calculated in Task-1							

Using the information in Tables 7.6–7.8, create your own process (mass-balance) simulator or use any commercial simulator (see the unit modules listed in Table 7.1).

Then, solve the mass-balance simulation problem. Results are given in a stream summary in Table 7.9.

Simulation Tasks 2–4 Using the compositions in each stream, fixing a pressure (or a temperature), the saturated liquid (or vapor) temperature (or pressure) can be calculated (Task-2). Also, since the reactor temperature and pressure are known ($T = 497.2$ K, $P = 34$ atm), the phase(s) of the reactor outlet stream (S5) can be calculated. Because the dew-point temperature of stream S4 is 397 K at $P = 34$ atm, the stream is a superheated vapor. Also, because of the temperature and pressure differences between the unit modules, heat exchangers, pumps, and compressors are positioned. In Task-3, these unit modules are introduced, the Task-1 mass balances are augmented with energy balances, and solutions of the mass and energy balances are obtained. In Task-4, the component-splitter module is replaced with a distillation column module. The objective is to find a distillation column design (number of stages, feed-stage location, reflux ratio) that matches the product recoveries from the component-splitter module. This is achieved with a five-stage column fed at the top stage, a vapor top product, liquid bottoms product, and reflux ratio (reflux/vapor product) at 0.0428. Other considerations include determining whether, in place of a distillation column, a TP-flash operation can be used, as well as investigating why the temperature of the top product is close to 256 K. What can be done to increase this temperature? Also, if a TP-flash operation can be used, determine whether $T = 300$ K and $P = 33.5$ atm would be appropriate. Finally, it would be helpful to check whether a 99.99 mol% cyclohexane product can be obtained if the benzene conversion is 97%, as specified.

EXAMPLE 7.5 ***Ethylene to Ethanol Process***

The process flowsheet in Figure 7.18 has been synthesized to convert ethylene to dry ethanol (> 99% pure). Note that the ethylene feed stream contains small amounts of propylene and methane. To complete the process synthesis, it is desired to perform simulation Tasks-1, Task-2, and Task-4. Three reactions, with specifications at 578 K and 68 atm (based upon prior experimentation and specified by Biegler et al., 1997), are:

Ethylene + water = Ethanol (conversion of ethylene is 7%) (R1)

Propylene + water = Isopropanol (conversion of propylene is 0.7%) (R2)

Ethanol = Diethyl ether + water (at equilibrium with $K_3 = 0.2$) (R3)

Prior to Task-1, the specified variables and their values are given in Table 7.10. In addition, the conversions for R1 and R2 are 0.07

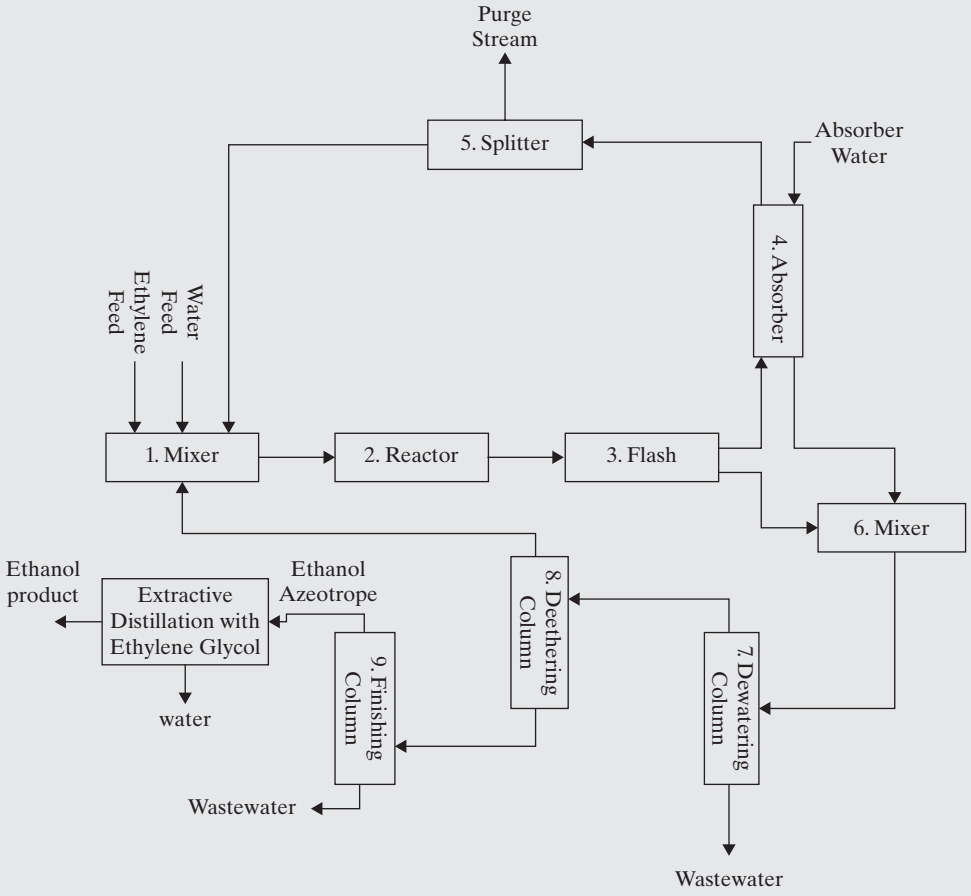

Figure 7.18 Process flowsheet for conversion of ethylene to ethanol.

Table 7.10 Specified Variables Prior to Task-1—Ethylene to Ethanol Process

	ξ_{Flash}	ξ_{Abs}	$\xi_{\text{Split}} = \beta_{\text{D}}$	$\xi_{\text{Dist-1}}$	$\xi_{\text{Dist-2}}$	$\xi_{\text{Dist-3}}$	$\xi_{\text{Dist-4}}$	$\xi_{\text{Dist-5}}$
Ethylene	0.95	1	0.995	1	1	1	-	-
Propylene	0.9	1	0.995	1	1	1	-	-
Methane	1.0	1	0.995	1	1	1	-	-
Ethanol	0.15	0.01	0.995	1	0	1	0.99	1
Isopropanol (IPA)	0.0	0.0	0.995	1	0	0	-	-
Water	0.0	0.0	0.995	0.1	0	0.33	0	1
Diethyl ether (DEE)	0.5	0.01	0.995	1	1	1	-	-
Ethylene Glycol (EG)	0.0	0	0.995	0	0	0	0	0

Note: Same values of $\xi_{\text{Split}} = \beta_{\text{D}}$ for all components indicate a stream divider (splitter).

(for ethylene) and 0.007 (for propylene), respectively. For R3, the amount of diethyl ether (DEE) formed can be calculated from ethanol (EA) and water (W):

$$f_{DEE} = K_3(f_{EA})^2/f_W \tag{7.29}$$

where f_i is the flow rate (mol/s) of compound i and K_3 is the equilibrium constant as given in Biegler et al. (1997).

SOLUTION

Simulation Task-1 with Derived Model Initially, the mass-balance model derived from Eqs. (7.1)–(7.6) was solved. The calculated stream variables for the outlet streams in Figure 7.17 are given in Table 7.11a–c. Interested readers can derive this model and check their solutions by comparing their calculated values with those in Table 7.11a–c.

Simulation Task-1 Using the PRO/II Process Simulator Here, the process flowsheet is modeled using the modules in the PRO/II module library (see Table 7.1). These include the mixer, stoichiometric reactor, stream calculator (for all the separators: PT-flash, absorber, and three distillation columns), and stream splitter. Note that the icons in Figure 7.19 are shown in Table 7.1 (a stream calculator is also known as a component splitter). The simulator organizes the model equations according to its built-in sequential-modular solution strategy. The data in Table 7.10 are used in PRO/II (and, in principle, in any other process simulator, using the same models). R1 is a stoichiometric reactor module with specified conversion (for reactions R1 and R2), whereas R2 is a stoichiometric reactor module with specified equilibrium constant for reaction R3. The PT-flash is modeled using a stream calculator module, SC1-F. Mixer M2 and stream calculator module, SC2-ABS, model the absorber. Stream calculator modules SC3-T1, SC4-T2, and SC5-T3 model three distillation columns. The top product from SC5-T3 is at the ethanol–water azeotrope from which ethanol is recovered using ethylene glycol as the solvent. This occurs in an extractive distillation column, modeled using SC6-T4, which produces a product of > 99% pure ethanol. SC7-T5 models the solvent recovery column. Water in stream S18 is the solvent for the absorber. The ethylene glycol solvent is in stream S21. The reader is encouraged to find the number of partitions, the number of recycle streams, and the corresponding number of tear streams in each partition before performing the mass-balance simulations.

Simulation to Determine the Conditions of Unit Modules and Streams (Task-2) Streams S11, S12, S13, S14, S23, and S24 are saturated liquid products at 1 atm. Their calculated bubble-point temperatures are 351.4 K, 369.2 K, 351.4 K, 460.6 K, 373.2 K, and 469.3 K, respectively. Stream S15 is a vapor product effluent from the reactor at $T = 575$ K and $P = 68$ atm. The TP-flash module needs to operate at $T = 320$ K and $P = 20$ atm. The UNIQUAC model is used as the GE-model for activity-coefficient calculations, and the vapor phase is assumed to be ideal. In simulation Task-2, all of the temperatures and pressures associated with the unit modules in Figure 7.19 are assigned. Then, in simulation Task-3, mass and energy balances are calculated using simple models to estimate the heat duties added to, or removed from, each unit module. While not carried out herein, readers are encouraged to implement Task-3.

Simulation with Rigorous Models (Task-4) In PRO/II, the separator module (modeled in Task-1 using a component-splitter module) is used to model a distillation column. For Task-4, the distillation module is selected, which includes the appropriate equations. Note, however, in this case, the user is unable to view the equations, but the user must provide values of the known variables (recoveries of the key components, number of stages, feed location, estimates of product flow rates, and reflux ratio—all other variables are calculated). The detailed simulation results are not given here. However, the corresponding PRO/II files, ethanol-process-task1.prz, and ethanol-process-task4.prz can be downloaded from

Table 7.11 Simulation Results for the (a) Inlet, (b) Outlet, and (c) Recycle Streams (flow rates in kg-mol/hr)

(a)

	Flow Rates of Components for Inlet Streams			
Components	S2	S18	S21	S30
Ethylene	342.3648	0	0	0
H_2O	0	40	0	483.49
Methane	7.1326	0	0	0
Propene	7.1326	0	0	0
DEE	0	0	0	0
IPA	0	0	0	0
Ethanol	0	0	0	0
EG	0	0	0.0041	0

(b)

	Flow Rates of Components for Outlet Streams				
Components	S8	S12	S13	S23	S28
Ethylene	69.00	0	0	0	0
H_2O	0	166.24	0	81.88	0
Methane	7.13	0	0	0	0
Propene	5.12	0	0	0	0
DEE	0.0006	0	0	0	0
IPA	0	2.00	0	0	0
Ethanol	0.0082	0	273.35	0	0
EG	0	0	0	0	0.0041

(c)

	Flow Rates of Components for Recycle Streams			
Components	S1	S7	S9	S29
Ethylene	0	3381.20	181.59	0
H_2O	2233.10	0	0	0
Methane	0	349.50	0	0
Propene	0	251.14	28.47	0
DEE	0	0.030	6.11	0
IPA	0	0	0	0
Ethanol	0	0.402	0	0.274
EG	0	0	0	409.37

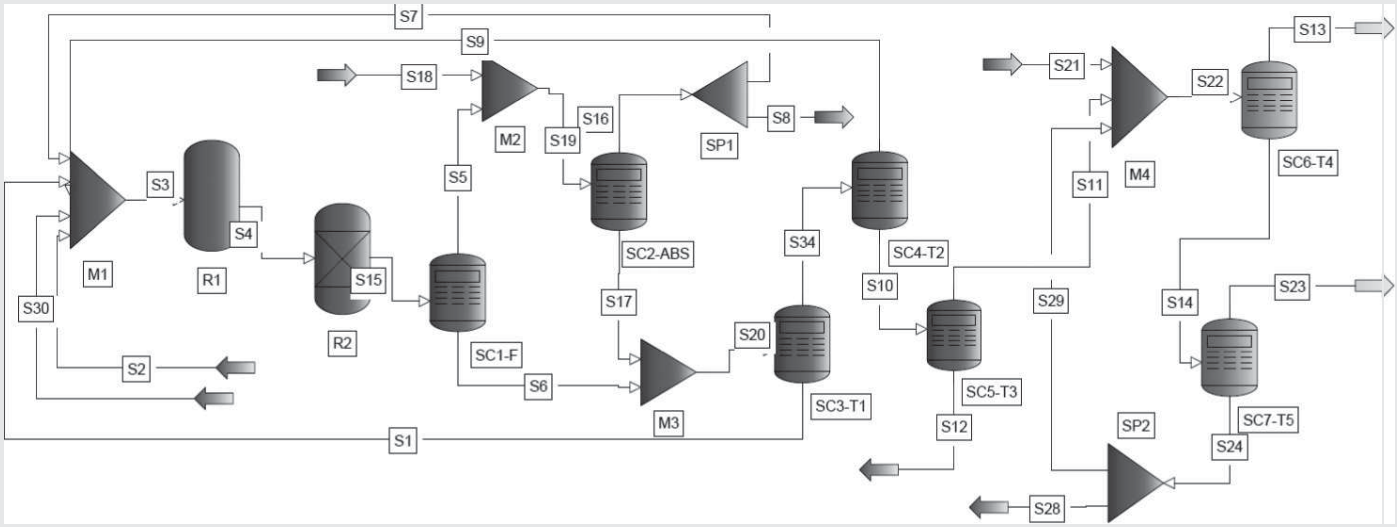

Figure 7.19 PRO/II process flowsheet for mass-balance model of the process to convert ethylene to ethanol.

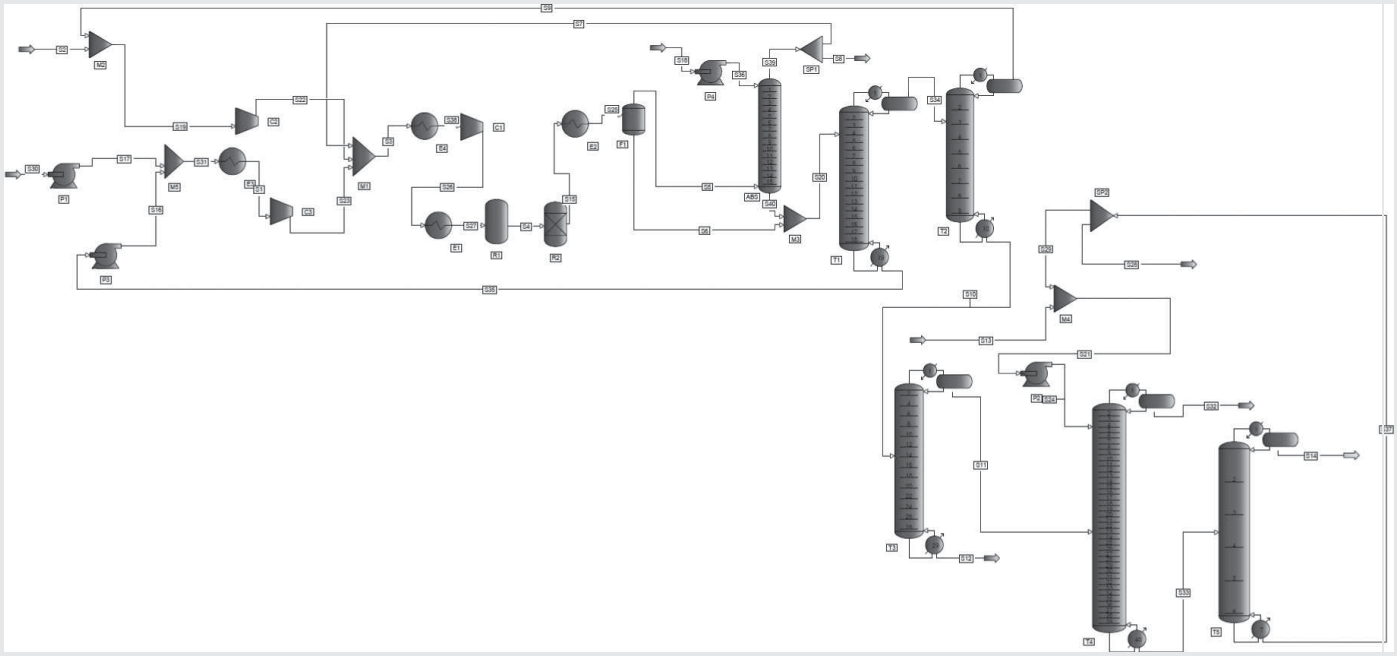

Figure 7.20 PRO/II process flowsheet for rigorous models of the process to convert ethylene to ethanol.

the Program and Simulation Files folder on the Wiley Web site associated with this textbook. Note that as equations are added for the more rigorous models, additional variables must be specified. For lists of these variables, consult the PRO/II manual. Note also that the constitutive (property) model equations are also retrieved by simply selecting the corresponding model from the constitutive (property) model library. Figure 7.20 shows the detailed flowsheet for the process to produce dry ethanol from ethylene, in which all of the stream calculators have been replaced by their respective rigorous models, and pumps, compressors, and heat exchangers have been added. Note that this is not an optimized process flowsheet, just a feasible one, with respect to conversion of the specified raw materials to the specified product.

7.4 CASE STUDIES

These case studies are intended to provide the reader with examples of process simulation tasks having different entry points into the process simulation framework in Figure 7.15. Three case studies are highlighted in this section with varying degrees of available and generated information.

Monochlorobenzene (MCB) Separation Process

Another process, which is considered throughout this book, involves the separation of a mixture consisting of HCl, benzene, and monochlorobenzene (MCB), the effluent from a reactor to

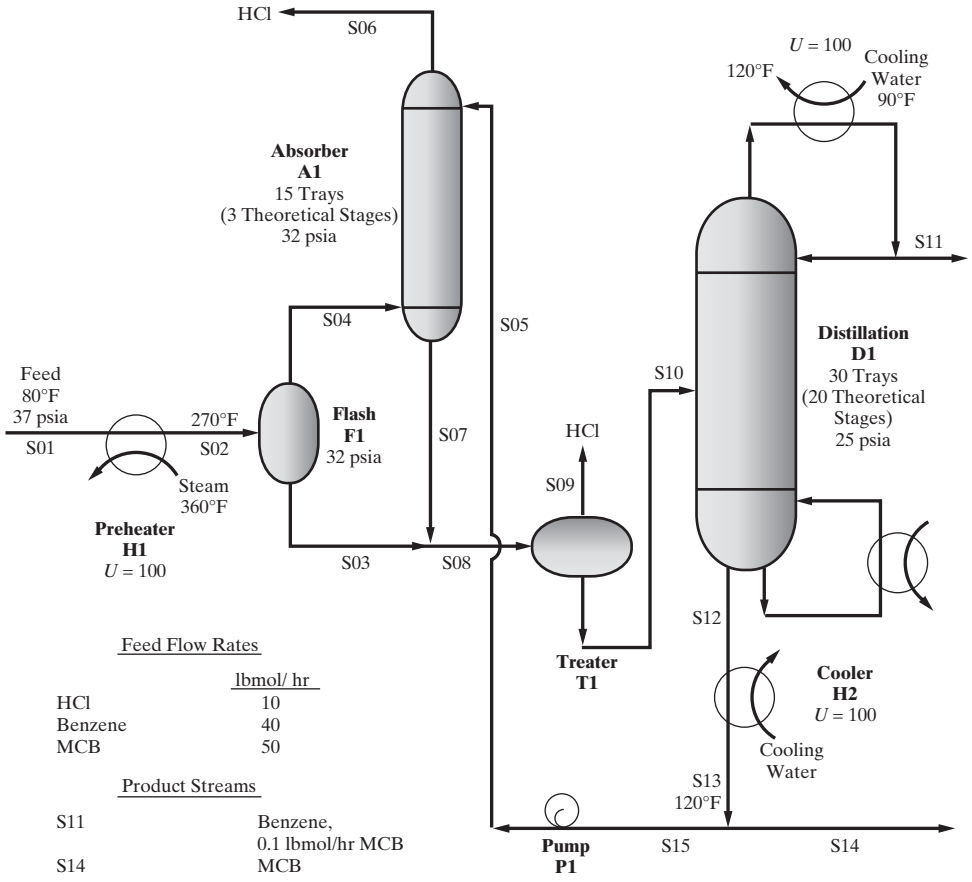

Figure 7.21 Process flowsheet for the MCB separation process.

produce MCB by the chlorination of benzene. As discussed in Chapter 9, when separating a light gaseous species, such as HCl, from two heavier species, it is common to vaporize the feed partially followed by separation of the vapor and liquid phases in a flash separator. To obtain nearly pure HCl, the benzene and MCB can be absorbed in an absorber. Then, since benzene and MCB have significantly different boiling points, they can be separated by distillation. The process that results from this synthesis strategy is shown in Figure 7.21. Included on the diagram is the design basis (or specifications). Note that a portion of the MCB product is used as the absorbent.

As shown in the flowsheet, the feed is partially vaporized in the preheater, H1, and separated into two phases in the flash vessel, F1. The vapor from F1 is sent to the absorber, A1, where most of the HCl vapor passes through, but the benzene is largely absorbed using recycled MCB as the absorbent. The liquid effluents from F1 and A1 are combined, treated to remove the remaining HCl with insignificant losses of benzene and MCB, and distilled in D1 to separate benzene from MCB. The distillate rate is set equal to the benzene flow rate in the feed to D1, and the reflux ratio is adjusted to obtain the indicated MCB impurity in the distillate. The bottoms are cooled to 120°F in the heat exchanger, H2, after which one-third of the bottoms is removed as MCB product with the remaining two-thirds recycled to the absorber. Note that this fraction recycled is specified during the distribution of chemicals in process synthesis, along with the temperature of the recycle, in an attempt to absorb benzene without sizable amounts of HCl. Furthermore, the temperature of stream S02 is specified to generate an adequate amount of vapor, three equilibrium stages are judged to be sufficient for the absorber (using the approximate Kremser–Brown equations), and the number of stages and the reflux ratio are estimated for the distillation column. Using the process simulators, these specifications are adjusted routinely to see how they affect the performance and economics of the process. Also, note that due to space limitations, a more complete, unit-by-unit description of the process and its specifications is reserved for the multimedia module, *ASPEN → Principles of Flowsheet Simulation → Interpretation of Input and Output → Sample Problem.*

Use of Process Simulators To determine the unknown temperatures and flow rates of the species, that is, to satisfy the material and energy balances, the MCB separation process is simulated in the steady state using ASPEN PLUS. This is accomplished by first creating an ASPEN PLUS simulation flowsheet as illustrated

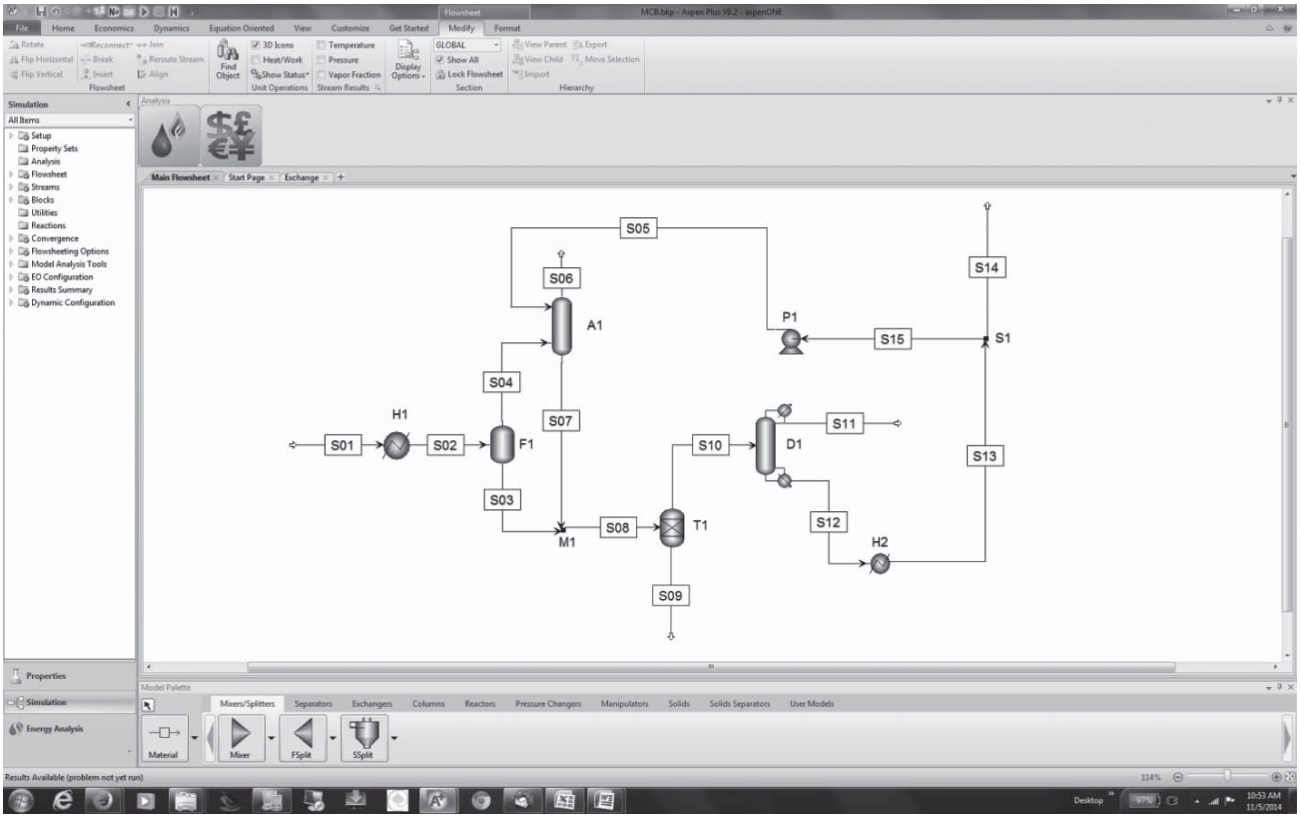

Figure 7.22 ASPEN PLUS simulation flowsheet for the MCB separation process. (*Source:* © AspenTech).

in Figure 7.22. Then, the ASPEN PLUS forms are completed and the Run button is depressed, which produces the results shown in the modules under *ASPEN → Principles of Flowsheet Simulation → Interpretation of Input and Output*, which provides a unit-by-unit description of the input and the computer output. Then, parametric studies can be carried out as recommended in Exercise 7.6.

The Aspen Process Economic Analyzer is also used to calculate equipment sizes and estimate capital costs for the MCB separation process in Section 16.8. Then, a profitability analysis is performed using the EXCEL spreadsheet described in Section 17.8. In Section 20S.5 (Case Study 20S.3), process controllers are added and their responses to various disturbances are computed using UNISIM in dynamic mode. Hence, for the MCB separation process, the process simulators have been used throughout the design process, although most design teams use a variety of computational tools to carry out these calculations.

Hydrodealkylation of Toluene to Benzene

In Chapter 6, Heuristics for Process Synthesis, a process to hydrodealkylate toluene to benzene was synthesized in Examples 6.1, 6.5, and 6.7. In this case study, process simulation Tasks-1, Task-2, and Task-4, are used to gradually accumulate specifications of the rigorous design presented at the completion of Task-4. Initially, in Task-1, a simple mass-balance model is created. Eventually, the stream calculators are replaced with distillation columns, and heat exchangers, pumps, and compressors are added. Much data for this process can be found in many published articles and books. The specifications used here for the mass-balance model are from Douglas (1985)—see Table 7.12.

Table 7.12 Specifications for Hydrodealkylation Process Mass-Balance Model

	ν (stoich. coef.)		ξ (split fractions)				
	Reaction		PT-Flash	Purge	Distillation		
Compound	1	2	S-101	TEE-101[a]	S-102	S-103	S-104
Hydrogen	−1	1	0.9998	0.12	1	1	1
Methane	1	0	0.9700	0.12	1	1	1
Benzene	1	−2	0.0500	0.12	0	1	1
Toluene	−1	0	0.0100	0.12	0	0.0008	1
Biphenyl	0	1	0	0.12	0	0	0

[a] All component split fractions = 0.12 (i.e., the stream-split fraction = 0.12).

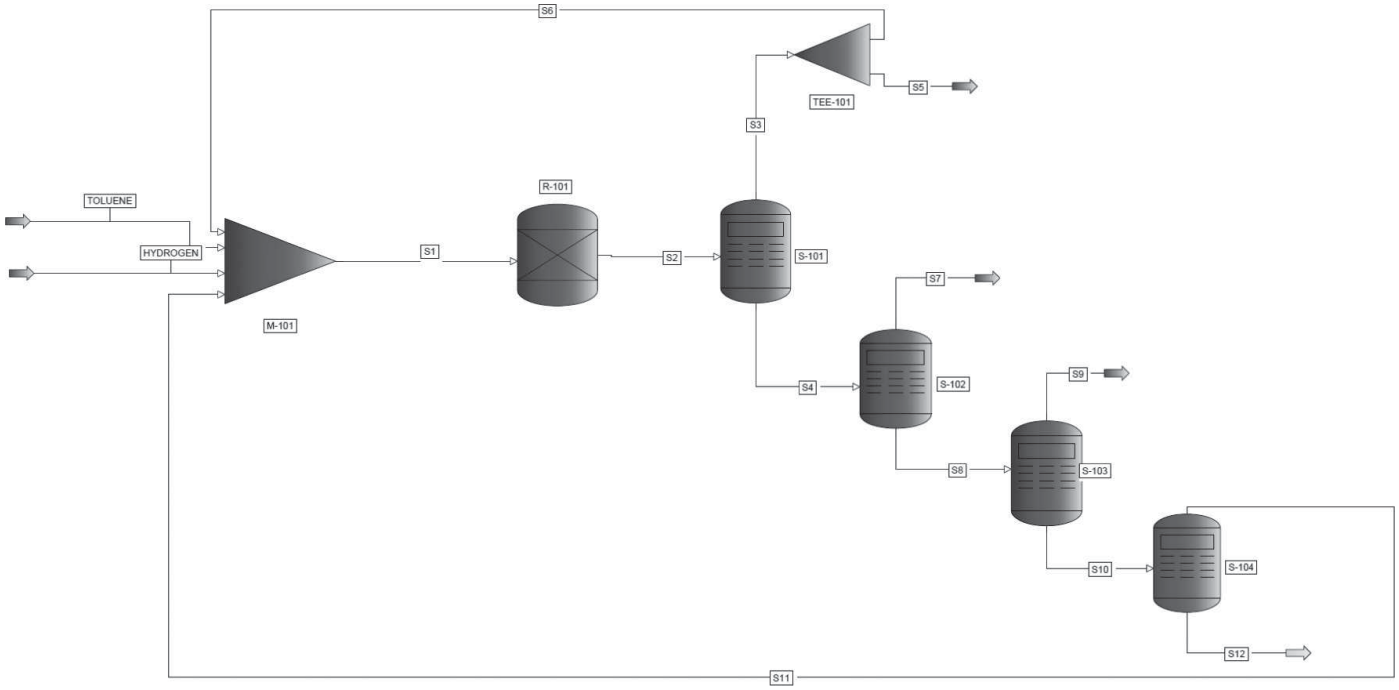

Figure 7.23 Modeling of HDA process with PRO/II—Mass-balance model.

Using the mass-balance modules in Eqs. (7.1)–(7.6), the PRO/II simulation flowsheet in Figure 7.23 is modeled for mass-balance calculations. Note that the purge module, TEE-101, with a stream split-fraction of 0.12 is used. The mass-balance results from PRO/II are shown in Table 7.13.

To convert the simple flowsheet to the detailed flowsheet, the stream calculator modules, S-102–S-104, are replaced by distillation columns. Also, heat exchangers, pumps, compressors, valves, and so on are added. To perform the rigorous simulations, additional variables must be specified for each module in PRO/II as given in Table 7.14 and the complete flowsheet is shown in Figure 7.24. For the distillation columns, the specifications in Table 7.14 indicate the minimum variables to be specified. Pressure drops in the columns are assumed to be negligible (in a more accurate design, pressure drops per stage are considered). Note that the flowsheet in Figure 7.24 is not an optimized design. Also, heat integration has not been performed. It is simply a feasible design that has been simulated with rigorous models. Analysis of these results helps to set targets for heat integration and process optimization. When estimating pressure drops in the process units, a compressor in the hydrogen recycle stream, S6, is needed.

The simulated results are shown for the inlet and outlet streams in Table 7.15. The corresponding PRO/II files hda-task1.prz (corresponding to Figure 7.23) and hda-task4 .prz (corresponding to Figure 7.24) can be downloaded from the Program and Simulation Files folder on the Wiley Web site associated with this textbook.

Bioethanol Process Simulation

This case study involves a bioethanol production process (Wooley et al., 1999), which is based upon the process developed at the U.S. National Renewable Energy Laboratory (NREL). The main operations of the process are highlighted in Figure 7.25.

Table 7.13 Simulation Results from PRO/II—Mass-Balance Only—HDA Process

Stream Name	S1	S2	S3	S4	S5	S6	S7	S8	S9	S10	S11	S12	Toluene	Hydrogen
Flow Rate (kmol/hr)	1987.63	1987.53	1814.63	172.89	217.75	1596.87	10.37	162.52	120.43	42.09	40.80	1.29	123.83	226.12
Composition														
Hydrogen	0.4679	0.4063	0.4449	0.0009	0.4449	0.4449	0.0156	0.0000	0.0000	0.0000	0.0000	0.0000	0.0000	0.9709
Methane	0.4463	0.5086	0.5514	0.0590	0.5514	0.5514	0.9844	0.0000	0.0000	0.0000	0.0000	0.0000	0.0000	0.0291
Benzene	0.0028	0.0638	0.0035	0.6964	0.0035	0.0035	0.0000	0.7408	0.9997	0.0000	0.0000	0.0000	0.0000	0.0000
Toluene	0.0830	0.0208	0.0002	0.2362	0.0002	0.0002	0.0000	0.2513	0.0003	0.9693	1.0000	0.0000	1.0000	0.0000
Biphenyl	0.0000	0.0007	0.0000	0.0075	0.0000	0.0000	0.0000	0.0080	0.0000	0.0307	0.0000	1.0000	0.0000	0.0000

Table 7.14 Specifications for the Rigorous Simulation Using PRO/II—HDA Process

Unit Operation/Stream	Variables to Specify	Specified Value
Stream toluene	*T, P, F,* $\underline{x}$	See Table 7.15
Stream hydrogen	*T, P, F,* $\underline{x}$	See Table 7.15
Compressor—C1	Outlet pressure	38 atm
Heat exchanger—E-101	Outlet temperature (process stream)	450 K
Heat exchanger—E-102	Outlet temperature (process stream)	894 K
Heat exchanger—E-103	Outlet temperature (process stream)	300 K
Reactor—R-101	Reaction, conversion, stoichiometric coefficients	See Table 7.12
PT Flash—F-101	*T, P*	300 K, 38 atm
Purge – TEE-101	Purge fraction	0.12
Valve—V-101	Exit pressure	1 atm
Distillation column—T-101	Number of stages (N_P), feed stage (N_F), product rate (distillate or bottom), recovery of compound *i* at top (ξ_{Di}), recovery of compound *i* at bottom (ξ_{Bi})	$N_P = 8$; $N_F = 4$; methane stream (top product) = 9.95 kmol/hr; recovery of methane in top product = 99.9%; recovery of benzene in bottom product = 99.5%
Distillation column—T-102	Number of stages (N_P), feed stage (N_F), product rate (distillate or bottom), recovery of compound *i* at top (ξ_{Di}), recovery of compound *i* at bottom (ξ_{Bi})	$N_P = 35$; $N_F = 10$; benzene stream (top product) = 119.55 kmol/hr; recovery of benzene in top product = 99.5%; reflux ratio = 2.48
Distillation column—T-103	Number of stages (N_P), feed stage (N_F), product rate (distillate or bottom), recovery of compound *i* at top (ξ_{Di}), recovery of compound *i* at bottom (ξ_{Bi})	$N_P = 12$; $N_F = 2$; biphenyl stream (bottom product) = 1.34 kmol/hr; recovery of toluene in top product = 99.9%; recovery of biphenyl in bottom product = 99.9%
Constitutive Models		
VLE	Model for fugacity coefficients	SRK equation of state
Pure component (temperature-dependent) properties	Vapor pressure, density, heat capacity, heat of vaporization, viscosity, etc.	DIPPR correlations
Flowsheet Decomposition	Tear stream = S1; Start calculations at module R-101	
Calculation order	R-101 → E-103 → F-101 → TEE-101 → M-101; T-101 → V-101 → T-102 → T-103 → M-102 → E-101 → C1 → M-103 → E-102[a]	

[a] Repeat from R-101 with new estimates for Stream S1.

Table 7.15 Simulated Results from PRO/II—Mass and Energy Balances with Rigorous Models—HDA Process

	Streams					
Stream Variable	Toluene	Hydrogen	Purge	Methane	Benzene	Biphenyl
Phase	Liquid	Vapor	Vapor	Vapor	Liquid	Liquid
Temperature (K)	303.15	303.15	300.00	371.90	352.25	508.60
Pressure (atm)	1	39.12	38	38	1	1
Flow rate (kmol/hr)	123.83	226.12	219.21	9.94	119.55	1.34
Component flow rate (kmol/hr)						
Hydrogen	0	219.54	96.70	0.70	0.0001	0
Methane	0	6.59	121.50	8.61	0.009	0
Benzene	0	0	0.92	0.60	119.43	0
Toluene	123.83	0	0.10	0.02	0.12	0
Biphenyl	0	0	0	0	0	1.30

Feedstock Handling. The feedstock, hardwood chips (Wooley et al., 1999), is delivered to the feed-handling area for storage and size reduction. In this case study, however, the feed stock used is cassava rhizome (Mangnimit, 2013), which is milled into small pieces before it is sent to the pretreatment section.

Pretreatment. The heart of the pretreatment process area is the "pretreatment reactor," which converts most of the hemicellulose of the feedstock to soluble sugars—primarily xylose, mannose, arabinose, and galactose—by hydrolysis using dilute sulfuric acid and elevated temperature. The hydrolysis under these conditions also solubilizes some of the lignin in the feedstock. In addition, acetic acid is released from the hemicellulose hydrolysis. Degradation products of pentose sugars (primarily furfural) and hexose sugars (primarily hydroxymethylfurfural) are also formed. Following the pretreatment reactor, the hydrolysate—consisting of a mixture of liquid and solid particles—is flash cooled. This operation vaporizes a large amount of water, a portion of acetic acid, and much of the furfural and hydroxymethylfurfural.

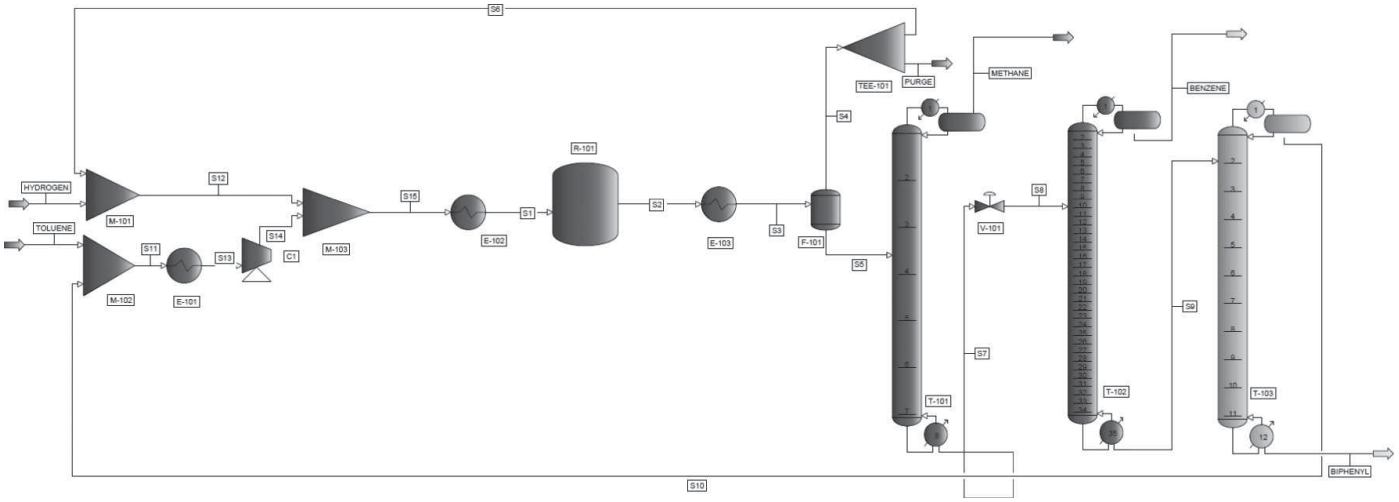

Figure 7.24 Rigorous HDA process flowsheet.

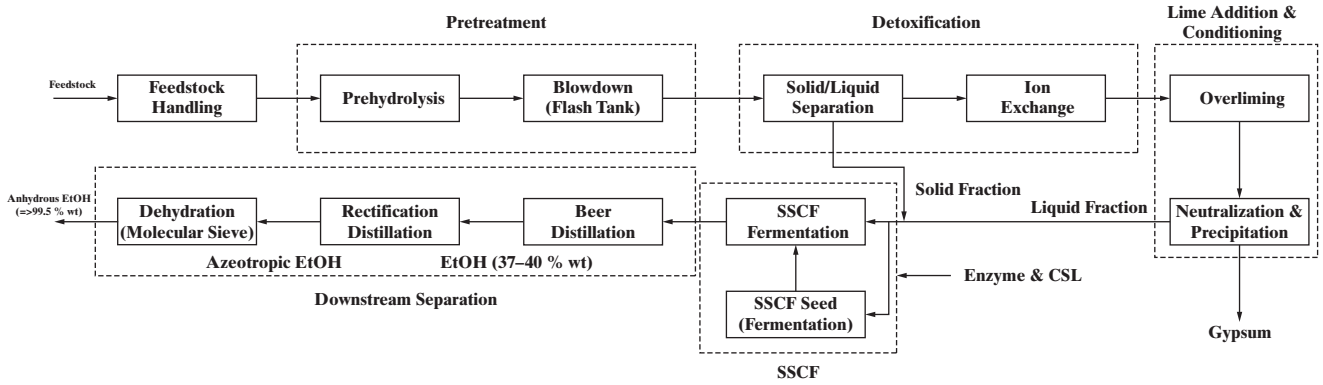

Figure 7.25 Block diagram of the bioethanol process.

Detoxification, Lime Addition, and Conditioning. The unreacted solid phase is separated from the liquid hydrolysate. The latter contains sulfuric acid and other inhibitors in addition to the hemicellulose sugars. Before fermentation, detoxification of the liquid hydrolysate is required to remove the inhibitors formed during the pretreatment of biomass. Ion exchange is used to remove acetic acid and sulfuric acid that will be toxic to the microorganisms in the fermentation (Note: for the cassava rhizome–based process simulated here, the ion-exchange operation is not used). After ion exchange, the pH is raised to 10 (by adding lime) and held at this value for a period of time. Neutralization and precipitation of gypsum follow the overliming step. The gypsum is removed using filtration, and the hydrolysate is finally mixed again with the solid fraction (from the solid–liquid detoxification separation unit) before being sent to SSCF (simultaneous saccharification and cofermentation).

SSCF. Following the lime addition, a small portion of the detoxified slurry is diverted to the SSCF seed process area for microorganism production (*Zymomonas mobilis*); the bulk of the material is sent to the (SSCF) process area. Two different operations are performed in this process area—saccharification (hydrolysis) of the remaining cellulose to glucose using cellulase enzymes and fermentation of the resulting glucose and other sugars to ethanol. For the fermentation, the recombinant *Zymomonas mobilis* bacterium is used to ferment both glucose and xylose to ethanol. The resulting ethanol broth is collected and sent to the downstream separation area.

Downstream Separation. After the SSCF, distillation and molecular sieve adsorption are used to recover the ethanol from the fermentor beer and produce nearly 100% pure ethanol. Distillation is accomplished in two columns. The first column (beer column) removes the dissolved CO_2 and most of the water, and the second distillation column concentrates the ethanol to near azeotropic composition. Subsequently, the residual water from the nearly azeotropic mixture is removed by vapor phase molecular sieve adsorption.

Following Alvarado-Morales et al. (2009), the block diagram in Figure 7.25 is translated into the process flowsheet to the bioethanol simulation flowsheet using PRO/II modules shown in Figure 7.26. Here, some of the steps involved in carrying out sequential simulations, starting with Task-1 and ending with Task-4, are described. To get started, biomass data are collected including the components in the biomass, the reactions in the pretreatment and fermentation stages, and the separation factors for the separations.

The specifications used by Mangnimit (2013), adopted from Alvarado-Morales et al. (2009), are given in Table 7.16.

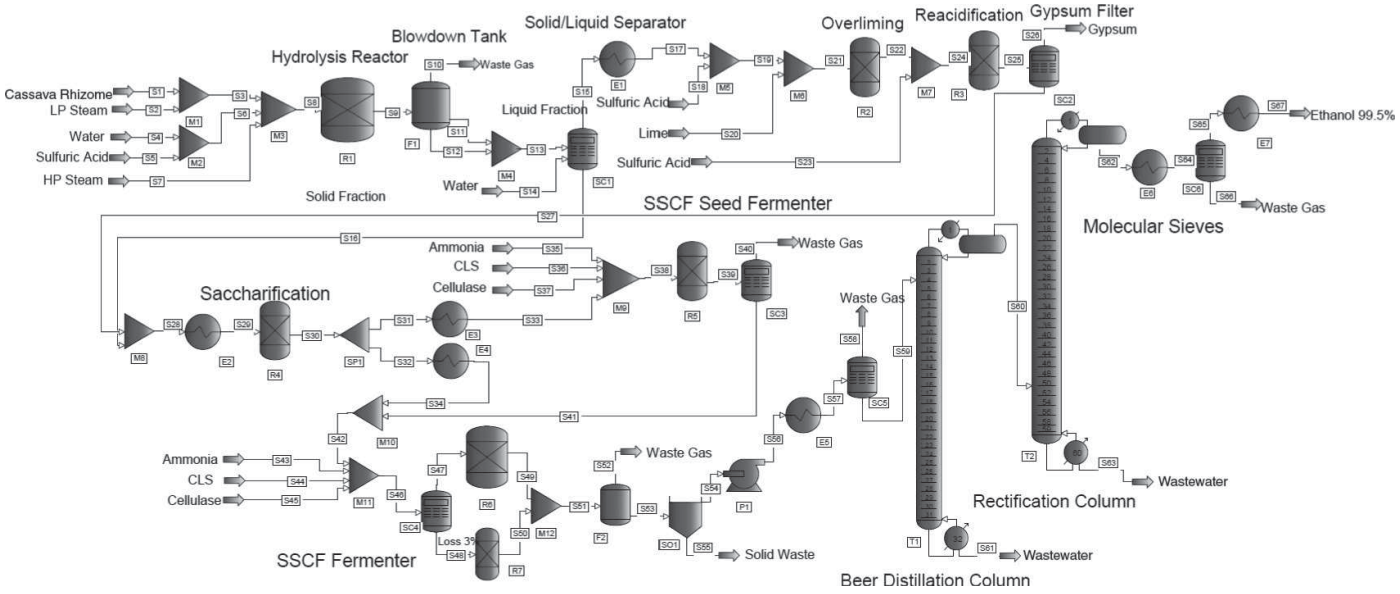

Figure 7.26 Bioethanol production simulation flowsheet using PRO/II modules. (*Source:* Mangnimit, 2013. Used with permission).

Table 7.16 Specifications for Bioethanol Production

Unit Operation	Variables Specified	Remarks
Hydrolysis reactor	Reaction set, Extent of reaction, Temperature	R1- conversion reactor
Flash	Pressure	F1- flash
Solid/Liquid separator	Recovery	SC1- stream calculator
Cooler	Hot side *T*, *U* value, Cold side utility type, Utility temperature	E1- simple heat exchanger
Overliming reactor	Reaction set, Extent of reaction, Temperature	R2- conversion reactor
Reacidification reactor	Reaction set, Extent of reaction, Temperature	R3- conversion reactor
Gypsum filter	Recovery	SC2- stream calculator
Heater	Cold side *T*, *U* value, Hot side utility type, Utility temperature	E2- simple heat exchanger
Saccharification reactor	Reaction set, Extent of reaction, Temperature	R4- conversion
Cooler	Hot side *T*, *U* value, Cold side utility type, Utility temperature	E3- simple heat exchanger
Cooler	Hot side *T*, *U* value, Cold side utility type, Utility temperature	E4- simple heat exchanger
SSCF Seed Fermenter	Reaction set, Extent of reaction, Temperature	R5- conversion reactor
Separator	Recovery	SC3- stream calculator
Splitter	Recovery	SC4- stream calculator
SSCF fermenter	Reaction set, Extent of reaction, Temperature	R6- conversion reactor
SSCF fermenter	Reaction set, Extent of reaction, Temperature	R7- conversion reactor
Flash	Pressure	F2- flash
Separator	Recovery	SO1- solid separator
Pump	Outlet Pressure	P1- pump
Heater	Cold side *T*, *U* value, Hot side utility type, Utility temperature	E5- simple heat exchanger
Separator	Recovery	SC5- stream calculator
Distillation column	Top tray pressure, Pressure drop, Feed tray, Overhead flow rate estimate, Condenser type, Column recovery, Reflux ratio	T1- distillation column
Distillation column	Top tray pressure, Pressure drop, Feed tray, Overhead flow rate estimate, Condenser type, Column recovery, Reflux ratio	T2- distillation column
Heater	Cold side *T*, *U* value, Hot side utility type, Utility temperature	E6- simple heat exchanger
Separator	Recovery	SC6- stream calculator
Cooler	Hot side *T*, *U* value, Cold side utility type, Utility temperature	E7- simple heat exchanger

Sources: Alvarado-Morales et al., 2009; Mangnimit, 2013. Used with Permission.

Tables 7.17–7.22 give the chemical reactions known to occur in the reactors. For each of the six reactors, R1–R6, known reactions together with conversions based on data from Wooley et al. (1999) are listed.

Stream calculators are used to represent the solid–liquid separator (SC1), the gypsum filter operation (SC2), splitting of the feed to the SSCF fermenters (SC4), removal of waste gases after the SSCF fermentation operation (SC3 and SC5), and molecular sieve operation (SC6) to obtain 99.5% pure ethanol.

After the simple mass-balance simulation, distillation column modules, T1 and T2, model the beer distillation operation (for recovery of ethanol from the SSCF fermentation process) and the rectification operation (to obtain the ethanol–water azeotrope), respectively. The remaining water is removed using a molecular sieve operation modeled using a stream-calculator module, SC3.

Table 7.17 Reactions for Pretreatment

Reaction	Conversion	Modeled
$C_6H_{10}O_5 + H_2O \rightarrow C_6H_{12}O_6$	Cellulose	0.065
$C_6H_{10}O_5 + 1/2H_2O \rightarrow 1/2C_{12}H_{22}O_{11}$	Cellulose	0.007
$C_5H_8O_4 + H_2O \rightarrow C_5H_{10}O_5$	Hemicellulose	0.750
$C_5H_8O_4 \rightarrow C_4H_3OCHO + 2H_2O$	Hemicellulose	0.100
$C_6H_{10}O_5 + H_2O \rightarrow C_6H_{12}O_6$	Mannan	0.750
$C_6H_{10}O_5 \rightarrow C_6H_6O_3 + 2H_2O$	Mannan	0.150
$C_6H_{10}O_5 + H_2O \rightarrow C_6H_{12}O_6$	Galactan	0.750
$C_6H_{10}O_5 \rightarrow C_6H_6O_3 + 2H_2O$	Galactan	0.150
$C_5H_8O_4 + H_2O \rightarrow C_5H_{10}O_5$	Arabinan	0.750
$C_5H_8O_4 \rightarrow C_4H_3OCHO + 2H_2O$	Arabinan	0.100
$C_2H_4O_2 \rightarrow CH_3COOH$	Acetate	1.0

Source: Wooley et al., 1999.

Table 7.18 Reaction Data for Ion Exchange

Reaction	Conversion	Modeled
$H_2SO_4 + 2NH_3 \rightarrow (NH_4)_2SO_4$	Sulfuric acid	1.0
$CH_3COOH + NH_3 \rightarrow CH_3COONH_4$	Acetic acid	1.0

Source: Wooley et al., 1999.

Table 7.19 Reaction Data for Overliming Process

Reaction	Conversion	Modeled
$H_2SO_4 + Ca(OH)_2 \rightarrow CaSO_4 2H_2O$	Lime	1.0

Source: Wooley et al., 1999.

Table 7.20 Reaction Data for SSCF Saccharification

Reaction	Conversion	Modeled
$C_6H_{10}O_5 + 1/2H_2O \rightarrow 1/2C_{12}H_{22}O_{11}$	Cellulose	0.012
$C_6H_{10}O_5 + H_2O \rightarrow C_6H_{12}O_6$	Cellulose	0.800
$C_{12}H_{22}O_{11} + H_2O \rightarrow 2C_6H_{12}O_6$	Cellobiose	1.000

Source: Wooley et al., 1999.

Table 7.21 Reaction Data for SSCF Fermentation

Reaction	Conversion	Modeled
$C_6H_{12}O_6 \rightarrow 2CH_3CH_2OH + 2CO_2$	Glucose	0.920
$C_6H_{12}O_6 + 1.2NH_3 \rightarrow 6CH_{1.8}O_{0.5}N_{0.2} + 2.4H_2O + 0.3O_2$	Glucose	0.027
$C_6H_{12}O_6 + 2H_2O \rightarrow C_3H_8O_3 + O_2$	Glucose	0.002
$C_6H_{12}O_6 + 2CO_2 \rightarrow 2HOOCCH_2CH_2COOH + O_2$	Glucose	0.008
$C_6H_{12}O_6 \rightarrow 3CH_3COOH$	Glucose	0.022
$C_6H_{12}O_6 \rightarrow 2CH_3CHOHCOOH$	Glucose	0.013
$3C_5H_{10}O_5 \rightarrow 5CH_3CH_2OH + 5CO_2$	Xylose	0.850
$C_5H_{10}O_5 + NH_3 \rightarrow 5CH_{1.8}O_{0.5}N_{0.2} + 2H_2O + 0.25O_2$	Xylose	0.029
$3C_5H_{10}O_5 + 5H_2O \rightarrow 5C_3H_8O_3 + 2.5O_2$	Xylose	0.002
$C_5H_{10}O_5 + H_2O \rightarrow C_5H_{12}O_5 + 0.5O_2$	Xylose	0.006
$3C_5H_{10}O_5 + 5CO_2 \rightarrow 5HOOCCH_2CH_2COOH + 2.5O_2$	Xylose	0.009
$2C_5H_{10}O_5 \rightarrow 5CH_3COOH$	Xylose	0.024
$3C_5H_{10}O_5 \rightarrow 5CH_3CHOHCOOH$	Xylose	0.014

Source: Wooley et al., 1999.

Table 7.22 Reaction Data for SSCF Contamination Loss

Reaction	Conversion	Modeled
$C_6H_{12}O_6 \rightarrow 2CH_3CHOHCOOH$	Glucose	1.0
$3C_5H_{10}O_5 \rightarrow 5CH_3CHOHCOOH$	Xylose	1.0
$3C_5H_{10}O_5 \rightarrow 5CH_3CHOHCOOH$	Arabinose	1.0
$C_6H_{12}O_6 \rightarrow 2CH_3CHOHCOOH$	Galactose	1.0
$C_6H_{12}O_6 \rightarrow 2CH_3CHOHCOOH$	Mannose	1.0

Source: Wooley et al., 1999.

The vapor–liquid phase equilibrium is modeled using the UNIFAC group-contribution method for the liquid-phase activity coefficient, assuming ideal vapor phases and assuming the pure-component vapor pressures using regressed Antoine constants for each compound in the system. The enthalpies for the liquid and vapor phases are calculated using regressed liquid heat capacity models and regressed heats of vaporization models. Also, lipids databases are available in ASPEN PLUS and PRO/II. Alternatively, the data for the compounds present can be downloaded from bioethanol-cassava-rhizhom.zip file in the Program and Simulation Files folder on the Wiley Web site associated with this textbook. This zip file contains the PRO/II file plus the database libraries as well as a more detailed version of Table 7.16 with all the unit specification values.

With the data in Tables 7.16–7.22 and the inlet streams in Table 7.23, a rigorous process simulation should obtain the results in Table 7.23. Note that, as this process flowsheet does not have any recycle stream, it is recommended that the flowsheet be built and simulated in stages, starting with the pretreatment section and the mixers prior to reactor R1.

Table 7.23 Selected Stream Results from Simulation with PRO/II for Production of Bioethanol from Cassava Rhizome

Stream Name		**S1**	**S2**	**S4**	**S5**	**S7**	**S10**	**S18**	**S20**	**S21**	**S23**	**S26**	**S35**	**S36**
Phase		Mixed	Vapor	Liquid	Liquid	Vapor	Vapor	Liquid	Solid	Mixed	Liquid	Mixed	Vapor	Liquid
Temperature	C	30.0	160.0	25.0	25.0	268.0	103.9	25.0	25.0	49.9	25.0	49.8	25.0	25.0
Pressure	ATM	1.0	6.0	1.0	1.0	13.0	1.0	1.0	1.0	1.0	1.0	1.0	1.0	1.0
Enthalpy	M*KJ/HR	−26.4	2.0	0.5	0.0	8.9	6.4	0.0	−0.5	4.3	0.0	0.0	0.0	0.0
Molecular Weight		103.9	18.0	18.0	98.1	18.0	18.7	98.1	74.1	23.4	98.1	137.8	17.0	18.0
Vapor Weight Fraction		1.0	1.0	0.0	0.0	1.0	1.0	0.0	1.0	0.0	0.0	1.0	1.0	0.0
Liquid Weight Fraction		0.0	0.0	1.0	1.0	0.0	0.0	1.0	0.0	1.0	1.0	0.0	0.0	1.0
Total Mass Rate	KG/DAY	377,198.4	17,633.9	118,657.3	2,376.1	76,613.9	59,531.7	2,680.9	4,296.2	481,750.8	1,129.0	8,684.2	5.0	1,430.3
Total Weight Comp. Rates														
Cellulose		112,339.2	0.0	0.0	0.0	0.0	0.0	0.0	0.0	518.4	0.0	518.4	0.0	0.0
Hemicellulose		160,185.2	0.0	0.0	0.0	0.0	0.0	0.0	0.0	40.0	0.0	40.0	0.0	0.0
Lignin		87,686.6	0.0	0.0	0.0	0.0	0.0	0.0	0.0	438.4	0.0	0.0	0.0	0.0
Glucose		0.0	0.0	0.0	0.0	0.0	0.0	0.0	0.0	6,902.6	0.0	13.8	0.0	0.0
Xylose		0.0	0.0	0.0	0.0	0.0	0.0	0.0	0.0	106,486.1	0.0	213.0	0.0	0.0
Cellobiose		0.0	0.0	0.0	0.0	0.0	0.0	0.0	0.0	655.7	0.0	0.0	0.0	0.0
Ethanol		0.0	0.0	0.0	0.0	0.0	0.0	0.0	0.0	0.0	0.0	0.0	0.0	0.0
Water		3,108.7	17,633.9	118,657.3	0.0	76,613.9	56,751.4	0.0	0.0	355,449.8	0.0	0.0	0.0	0.0
Sulfuric Acid		0.0	0.0	0.0	2,376.1	0.0	0.0	2,680.9	0.0	4,558.1	1,129.0	0.0	0.0	0.0
Furfural		0.0	0.0	0.0	0.0	0.0	2,780.3	0.0	0.0	2,405.2	0.0	4.8	0.0	0.0
Ammonia		0.0	0.0	0.0	0.0	0.0	0.0	0.0	0.0	0.0	0.0	0.0	5.0	0.0
Oxygen		0.0	0.0	0.0	0.0	0.0	0.0	0.0	0.0	0.0	0.0	0.0	0.0	0.0
Carbon Dioxide		0.0	0.0	0.0	0.0	0.0	0.0	0.0	0.0	0.0	0.0	0.0	0.0	0.0
Glycerol		0.0	0.0	0.0	0.0	0.0	0.0	0.0	0.0	0.0	0.0	0.0	0.0	0.0
Succinic Acid		0.0	0.0	0.0	0.0	0.0	0.0	0.0	0.0	0.0	0.0	0.0	0.0	0.0
Lactic Acid		0.0	0.0	0.0	0.0	0.0	0.0	0.0	0.0	0.0	0.0	0.0	0.0	0.0
HMF		0.0	0.0	0.0	0.0	0.0	0.0	0.0	0.0	0.0	0.0	0.0	0.0	0.0
Xylitol		0.0	0.0	0.0	0.0	0.0	0.0	0.0	0.0	0.0	0.0	0.0	0.0	0.0
Acetic Acid		0.0	0.0	0.0	0.0	0.0	0.0	0.0	0.0	0.0	0.0	0.0	0.0	0.0
CornSteep Liquor		0.0	0.0	0.0	0.0	0.0	0.0	0.0	0.0	0.0	0.0	0.0	0.0	1,430.3
ZM		0.0	0.0	0.0	0.0	0.0	0.0	0.0	0.0	0.0	0.0	0.0	0.0	0.0
Cellulase		0.0	0.0	0.0	0.0	0.0	0.0	0.0	0.0	0.0	0.0	0.0	0.0	0.0
Lime		0.0	0.0	0.0	0.0	0.0	0.0	0.0	4,296.2	4,296.2	0.0	0.0	0.0	0.0
$CaSO_4$		0.0	0.0	0.0	0.0	0.0	0.0	0.0	0.0	0.0	0.0	7,894.1	0.0	0.0
Ash		13,878.7	0.0	0.0	0.0	0.0	0.0	0.0	0.0	0.0	0.0	0.0	0.0	0.0

Table 7.23 (*continued*)

Stream Name		S37	S40	S43	S44	S45	S52	S55	S58	S61	S63	S66	S67
Phase		Mixed	Vapor	Vapor	Liquid	Solid	Vapor	Solid	Vapor	Liquid	Liquid	Vapor	Liquid
Temperature	C	25.0	42.6	25.0	25.0	25.0	41.0	41.0	100.0	116.7	110.0	100.0	40.0
Pressure	ATM	1.0	1.0	1.0	1.0	1.0	1.0	1.0	4.8	1.8	1.8	1.0	1.0
Enthalpy	M*KJ/HR	0.0	0.1	0.0	0.0	0.0	1.1	−6.2	0.2	9.3	0.2	0.8	0.5
Molecular Weight		18.1	44.0	17.0	18.0	22.8	42.3	67.4	42.5	19.4	18.7	18.0	46.0
Vapor Weight Fraction		0.0	1.0	1.0	0.0	1.0	1.0	1.0	1.0	0.0	0.0	1.0	0.0
Liquid Weight Fraction		1.0	0.0	0.0	1.0	0.0	0.0	0.0	0.0	1.0	1.0	0.0	1.0
Total Mass Rate	KG/DAY	924.6	11,717.2	14.9	2103.4	181.5	10,7312.6	111,206.3	15,070.6	464,600.5	9,520.6	7,573.7	119,151.8
Total Weight Comp. Rates													
Cellulose		0.0	0.0	0.0	0.0	0.0	0.0	897.0	0.0	0.0	0.0	0.0	0.0
Hemicellulose		0.0	0.0	0.0	0.0	0.0	0.0	7,969.2	0.0	0.0	0.0	0.0	0.0
Lignin		0.0	0.0	0.0	0.0	0.0	0.0	87,686.6	0.0	0.0	0.0	0.0	0.0
Glucose		0.0	0.0	0.0	0.0	0.0	0.0	0.0	0.0	5,242.6	0.0	0.0	0.0
Xylose		0.0	0.0	0.0	0.0	0.0	0.0	0.0	0.0	19,880.3	0.0	0.0	0.0
Cellobiose		0.0	0.0	0.0	0.0	0.0	0.0	0.0	0.0	0.0	0.0	0.0	0.0
Ethanol		0.0	891.3	0.0	0.0	0.0	6,212.3	0.0	364.5	1,458.2	598.4	0.0	119,092.3
Water		906.5	22.5	0.0	0.0	0.0	3,158.6	0.0	394.5	421,417.1	8,912.3	7,573.7	59.5
Sulfuric Acid		0.0	0.0	0.0	0.0	0.0	0.0	0.0	0.0	499.0	0.0	0.0	0.0
Furfural		0.0	0.0	0.0	0.0	0.0	52.6	0.0	17.8	2960.9	8.5	0.0	0.0
Ammonia		0.0	0.0	14.9	0.0	0.0	0.0	0.0	0.0	0.0	0.0	0.0	0.0
Oxygen		0.0	33.1	0.0	0.0	0.0	183.6	0.0	2.7	0.0	0.0	0.0	0.0
Carbon Dioxide		0.0	10,770.2	0.0	0.0	0.0	97,688.3	0.0	14,287.9	0.0	0.0	0.0	0.0
Glycerol		0.0	0.0	0.0	0.0	0.0	0.0	0.0	0.0	101.8	0.0	0.0	0.0
Succinic Acid		0.0	0.0	0.0	0.0	0.0	0.0	0.0	0.0	326.5	0.0	0.0	0.0
Lactic Acid		0.0	0.0	0.0	0.0	0.0	0.0	0.0	0.0	7,639.5	0.0	0.0	0.0
HMF		0.0	0.0	0.0	0.0	0.0	0.0	0.0	0.0	0.0	0.0	0.0	0.0
Xylitol		0.0	0.0	0.0	0.0	0.0	0.0	0.0	0.0	1,142.2	0.0	0.0	0.0
Acetic Acid		0.0	0.0	0.0	0.0	0.0	3.6	0.0	0.2	416.3	0.3	0.0	0.0
CornSteep Liquor		0.0	0.0	0.0	2,103.4	0.0	13.6	0.0	3.0	3,516.1	1.0	0.0	0.0
ZM		0.0	0.0	0.0	0.0	0.0	0.0	575.0	0.0	0.0	0.0	0.0	0.0
Cellulase		18.2	0.0	0.0	0.0	181.5	0.0	199.7	0.0	0.0	0.0	0.0	0.0
Lime		0.0	0.0	0.0	0.0	0.0	0.0	0.0	0.0	0.0	0.0	0.0	0.0
$CaSO_4$		0.0	0.0	0.0	0.0	0.0	0.0	0.0	0.0	0.0	0.0	0.0	0.0
Ash		0.0	0.0	0.0	0.0	0.0	0.0	13,878.7	0.0	0.0	0.0	0.0	0.0

Source: Mangnimit, 2013.

7.5 PRINCIPLES OF BATCH FLOWSHEET SIMULATION

During the task-integration step of process synthesis as equipment items are selected, key decisions are made regarding whether they operate in continuous, batch, or semicontinuous modes as discussed in Section 2.3. These decisions are based upon throughput and flexibility considerations. When the throughput is small, for example, on the laboratory scale, continuous operation is often difficult and impractical to maintain because it is usually simpler and more profitable to complete a batch in hours, days, or weeks. Even for larger throughputs where multiple products are produced with variably sized orders received regularly, batch processes offer the ease of switching from the production of one product to another, that is, flexibility, which is more difficult to achieve in continuous operation. These and other issues are discussed in more detail in Chapter 22.

As shown for the manufacture of tissue plasminogen activator (tPA) in Section 2.3, when batch operation is selected for an equipment item, either the batch time or batch size must be selected, with the other determined as a function of the throughput specification (e.g., 80 kg/yr of tPA). Furthermore, for a single product plant involving a serial sequence of processing steps when the product throughput is specified, the throughput for each process unit is determined as shown in the synthesis of the tPA process in Section 2.3. In many cases, available vessel sizes are used to determine the size of a batch.

Given the process flowsheet and the specifics of operation for each equipment item, it is the role of batch process simulators such as the ASPEN BATCH PROCESS DEVELOPER by Aspen Technology, Inc. and SUPERPRO DESIGNER by Intelligen, Inc. to carry out material and energy balances and to prepare an operating schedule in the form of a Gantt chart for the process. Then, after the equipment and operating costs are estimated and profitability measures are computed, the batch operating parameters and procedures can be varied to increase the profitability of the design.

Process and Simulation Flowsheets

As in the steady-state simulation of continuous processes, it is convenient to convert from a process flowsheet to a simulation flowsheet. To accomplish this, it is helpful to be familiar with the library of models (or procedures) and operations provided by the simulator. For example, when using SUPERPRO DESIGNER to simulate three fermentation reactors in series, the process flowsheet in Figure 7.27a is replaced by the simulation flowsheet in Figure 7.27b. In the ASPEN BATCH PROCESS DEVELOPER, however, this conversion is accomplished without drawing the simulation flowsheet, since the latter is generated automatically on the basis of the recipe specifications for each equipment item.

In the simulation flowsheets, the arcs represent the streams that convey the batches from equipment item to equipment item. Each arc bears the stream name and represents the transfer of information associated with each stream, that is, the mass of each species per batch, temperature, pressure, density, and other physical properties.

The icons represent the models for each of the equipment items. Unlike for the simulation of continuous processes, these models involve a sequence of process operations, which are specified by the designer. Typically, these operations are defined as a recipe or campaign for each equipment item and usually involve charging the chemicals into the vessel, processing the chemicals, removing the chemicals from the vessel, and cleaning the vessel. Note that in the SUPERPRO DESIGNER simulation flowsheet in Figure 7.27b, the microfiltration model represents both the microfilter and its holding tank in the process flowsheet, (Figure 7.27a).

Equipment Models

Table 7.24 lists the equipment models (or procedures) and operations in each of the two simulators. Some of the models carry out simple material balances given specifications for the feed stream(s) and the batch (or vessel) size or batch time. Others, like the batch distillation models, integrate the dynamic MESH (material balance, equilibrium, summation of mole fractions, heat balance) equations given specifications like the number of trays, the reflux ratio, and the batch time. Detailed documentation of the equipment models is provided in user manuals and help screens.

More specifically, a list of the ASPEN BATCH PROCESS DEVELOPER equipment models is provided in Table 7.24a. These are organized under the class of model, with a list of type of equipment and an indication of whether a model can be used in batch, continuous, or either mode. Similarly, for SUPERPRO DESIGNER, a list of procedures (equipment models) is provided in Table 7.24c. These are organized here as groups of equipment types.

For each equipment item, the engineer must specify the details of its operations. These include specifications for charging, processing, emptying, and cleaning. When using the ASPEN BATCH PROCESS DEVELOPER, these are specified in the steps in a recipe, with the equipment items defined as the steps are specified. A full list of the operations available is provided in Table 7.24b. In SUPERPRO DESIGNER, since the engineer provides a simulation flowsheet, the operations are specified unit by unit. Its list of operations is provided in Table 7.24d. Following this discussion, the results for a SUPERPRO DESIGNER simulation of the reactor section of the tPA process are provided in Example 7.6. In SUPERPRO DESIGNER, because the engineer provides a simulation flowsheet, the operations are specified unit by unit. Its list of operations is provided in Table 7.24d.

Combined Batch and Continuous Processes

Since it is possible to have adjacent equipment items operating in batch and continuous modes, it is important to understand the conventions used when preparing a mixed simulation with batch and continuous operations. In most cases, it is desirable to install a holding tank to moderate the surges that would otherwise occur.

In SUPERPRO DESIGNER, each flowsheet is defined by the engineer as either batch or continuous. In batch mode, stream results are reported on a per-batch basis, even for

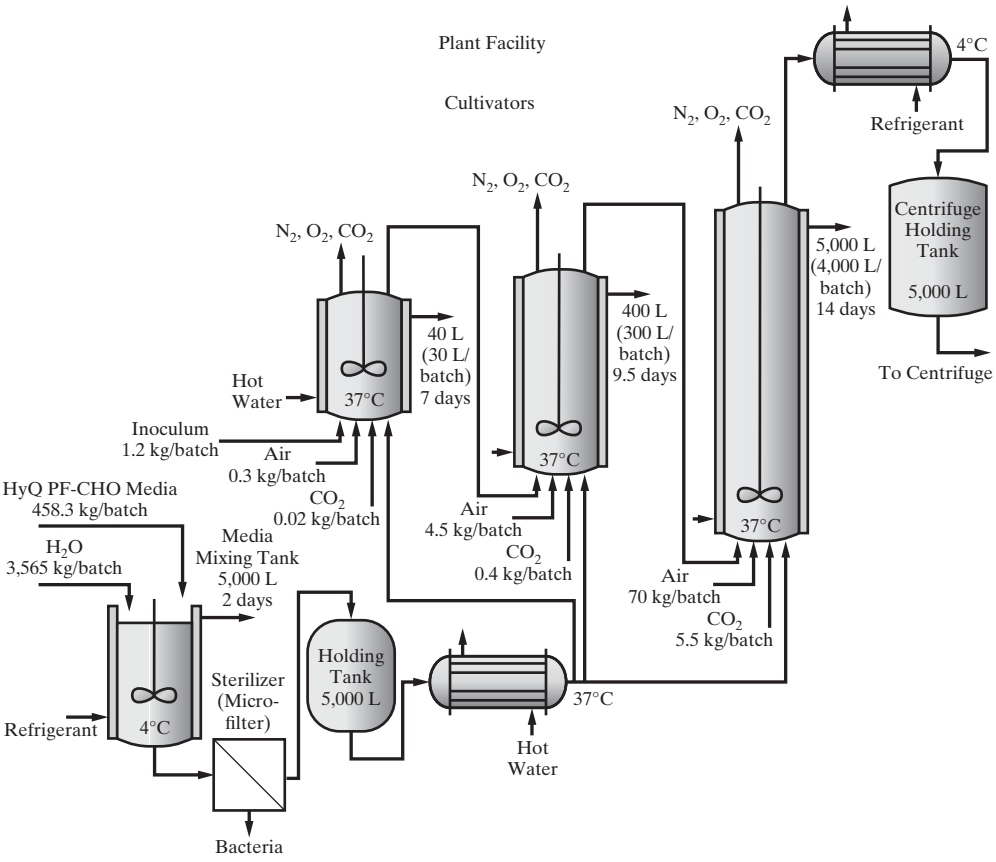

(a) Process flowsheet

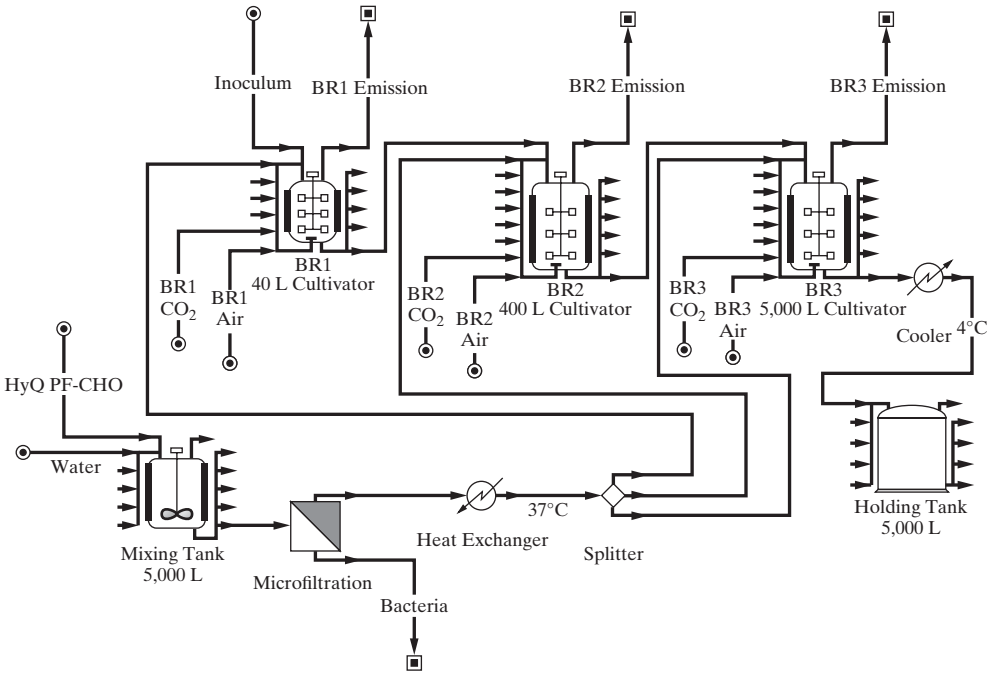

(b) SUPERPRO DESIGNER simulation flowsheet

Figure 7.27 Flowsheets.

Table 7.24 Equipment Models

(a) ASPEN BATCH PROCESS DEVELOPER Equipment Models

Class	Mode	Type
Adsorption	Batch	Adsorption system
Agitator	Continuous	Agitator—3-blade retreat impeller, helical ribbon, paddle, propeller, turbine
Biotech	Batch	Autoclave, cell factory, diafilter, filter-depth, incubator, incubator-shaker, laminar flow hood, lyophilizer, microfilter, triblender, ultrafilter
	Continuous	Bead mill, homogenizer, sterilizer, transfer panel, valve
Centrifuge	Batch	Centrifuge, centrifuge—decanter, disk-stack, filter, horizontal basket, multichamber-bowl, tubular-bowl, vertical basket
Column	Batch	Column, column—chromatography
	Continuous	Column—continuous packed, continuous tray
Compressor	Continuous	Compressor, blower, fan
Conveyor	Continuous	Conveyor—pneumatic
Crystallizer	Batch	Crystallizer
	Continuous	Crystallizer—continuous
Dryer	Batch	Dryer, dryer—agitated pan, blender, conical, freeze, fluid bed, horizontal paddle, rotary, spray, tray
	Continuous	Dryer—continuous, fluid bed—continuous
Emission control	Either	Vapor emission vent
Evaporator	Continuous	Evaporator—long tube, thin film, wiped film
Extractor	Batch	Extractor
	Continuous	Extractor—continuous
Fermenter	Batch	Fermentor
	Continuous	Fermentor—continuous
Filling	Continuous	Filling system
Filter	Batch	Filler—agitated Nutsche, air, bag, belt, cross flow, dryer, in-line, pot, press, sparkler, tank sheet
	Continuous	Filter—continuous
Formulation and packaging	Batch	Blender, coater, high gear granulator, kneader, mill-hammer, screen, sifter
	Continuous	Classifier, extruder, filling system, granulator-fluid bed, mill—continuous, jet; tableting unit
Changing component for formulation	Continuous	Air distributor plate, agitator—impeller, blade; chopper, distributor plate, filter socks, nozzle, screen—mill
Generic	Batch	Generic batch
Heat exchanger	Batch	Condenser
	Continuous	Cooling tower, electric heater, fired heater, heat exchanger, heat exchanger plate, heat exchanger shell and tube, refrigeration unit
Heat transfer	Batch	Internal helical-coil, jacket—agitated conventional, baffled conventional, conventional, dimple, halt-pipe coils
Hopper	Batch	Hopper, plate feeder
Instrument		Flow meter, moisture analyzer, scale, tester—hardness, friability, thickness; disintegration bath
Mixer	Batch	Mixer
	Continuous	Mixer—in-line
Piping	Batch	Piping
Pump	Continuous	Pump, pump—liquid ring vacuum, vacuum
Reactor	Batch	Reactor
	Continuous	Reactor—continuous
Scrubber	Batch	
Solid transport	Continuous	Screw conveyor, vacuum-pressure lock
Storage location	Batch	Inventory location, inventory location-vapor
Tank	Batch	Tank
Miscellaneous	Continuous	After burner, cyclone, demister, dust collector, ejector, hydrocyclone, steam jet

Table 7.24 (*continued*)

(b) ASPEN BATCH PROCESS DEVELOPER Operations

Batch operations	Age, centrifuge, charge, clean, cool, concentrate, crystallize, decant, distill, dry, evacuate, extract, filter, filter-in-place, heat, heat-to-reflux-and-age, line-blow, line-flush, open/close-vent, pH-adjust, pressurize, purge, QC-test, quench, quench-in-place, react, react-distill, start-sweep, stop-sweep, transfer, transfer-through-heat-exchanger, utilize, vent, wash-cake, yield-react
Chromatography operations	Elute-column. equilibrate-column, load-column, regenerate-column, wash-column
Continuous operations	Crystallize-continuously, Distill-continuously, Dry-continuously, Extract-continuously, filter-continuously, react-continuously
Biotech operations	Cell-disrupt, centrifuge-by-setting, depth-filter, diafilter, ferment, ferment-continuously, microfilter, sterilize, transfer-through-sterilizer, ultrafilter

(c) SUPERPRO DESIGNER Procedures (Equipment Models)

Group	Mode	Type
Vessel	Batch	Reactor, fermentor, seed fermentor, airlift fermentor
Continuous reaction	Continuous	Stoichiometric (CSTR, PFR, fermentor, seed fermentor, airlift fermentor)
	Continuous	Kinetics (CSTR, PFR, fermentor, seed fermentor)
	Continuous	Equilibrium (CSTR)
	Continuous	Environmental (Well-mixed aerobic, biooxidation, …)
Filtration	Batch	Microfiltration, ultrafiltration, reverse osmosis, diafiltration, dead end filtration, Nutsche filtration, plate and frame filtration, baghouse filtration, electrostatic precipitation
	Feed and Bleed (continuous)	Microfiltration, ultrafiltration, reverse osmosis
	Either	Rotary, vacuum filtration, air filtration, belt filtration, granular media filtration, baghouse filtration, electrostatic precipitation
Centrifugation	Batch	Basket centrifuge
	Either	Decanter centrifuge, disk-stack centrifuge, bowl centrifuge, Centritech centrifuge, cyclone, hydroclone
Homogenization	Either	High pressure, bead milling
Chromatography/adsorption	Batch	Gel filtration, packed bed adsorption (PBA) chromatography, granular activated carbon (GAC)—liquid and gaseous stream
Drying	Batch	Tray drying, freeze drying
	Either	Spray drying, fluid-bed drying, drum drying, rotary drying, sludge drying
Sedimentation	Either	Decanting (2-liquid phases), clarification. inclined plane (IP) clarification, thickener basin, dissolved air flotation tank, oil separator
Distillation	Batch	Shortcut batch distillation
	Either	Flash drum, shortcut distillation
Extraction	Either	Mixer-settler, differential column extractor, centrifugal extractor
Phase change	Either	Condensation for gas streams, multiple-effect evaporation, crystallization
Adsorption/stripping	Either	Absorber, stripper, degasifier
Storage	Batch	Hopper, equalization tank, junction box mixing
	Either	Blending tank, flat bottom tank, receiver, horizontal tank, vertical on legs tank, silo
Heat exchange	Either	Heating, electrical heating, cooling, heat exchanging (2-streams), heat sterilization
Mixing	Batch	Bulk flow (tumble mixer)
	Either	Bulk flow (2-9 streams), discrete flow (2-9 streams)
Splitting	Either	Bulk flow (2-9 streams), discrete flow (2-9 streams), component flow (2-9 streams)
Size reduction	Either	Grinding (bulk or discrete flow), shredding (bulk or discrete flow)
Formulation and packaging	Either	Extrusion, blow molding, injection molding, trimming, filling, assembly, printing, labeling, boxing, tableting
Transport (near)	Either	Liquid (pump)
		Gas (compressor, fan)
		Solids (belt conveyor—bulk or discrete flow, pneumatic conveyor—bulk or discrete flow, screw conveyor—bulk or discrete flow, bucket elevator—bulk or discrete flow)
Transport (far)	Either	By land (truck—bulk or discrete flow, train—bulk or discrete flow)
		By sea (ship—bulk or discrete flow)
		By air (airplane—bulk or discrete flow)

(*Continued*)

Table 7.24 (*continued*)

(d) SUPERPRO DESIGNER Operations			
Absorb	Adsorb	Agitate	Assemble
Bio-oxidize	Bioreact	Centrifuge	Charge
Clarify	Clean-in-place (CIP)	Compress	Concentrate (batch)
Concentrate (feed & bleed)	Condense	Convert to bulk	Convert to discrete
Convey	Cool	Crystallize	Cyclone
Cycloning	Decant	Degasify	Diafilter
Distill	Dry	Dry cake	Elevate
Elute	Equalize	Equilibrate	Evacuate
Exchange heat	Extract/phase split	Extrude	Ferment (kinetic)
Ferment (stoichiometric)	Fill	Filter	Flash
Flotate	Gas sweep	Grind	Handle solids flow
Heat	Hold	Homogenize	Incinerate
Label	Load	Mix	Mix solids
Mold	Neutralize	Oxidize	Pack
Pass through	Precipitate	Pressurize	Print
Pump	Pump gas	Purge/inlet	Radiate
React (equilibrium)	React (kinetic)	React (stoichiometric)	Regenerate
Separate oil	Shred	Split	Steam-in-place (SIP)
Sterilize	Store	Store solids	Strip
Tablet	Thicken	Transfer in	Transfer out
Transport	Trim	Vaporize/concentrate	Vent
Wash	Wash cake		

streams associated with continuous processes in a batch flowsheet. Each equipment item is designated as operating in batch/semicontinuous or continuous mode. Scheduling information must be included for all items designated as operating as batch/semicontinuous. Semicontinuous units operate continuously while utilized but are shut down between uses. Equipment items designated as continuous are assumed to operate at all times, and are excluded from operation schedules (and Gantt charts).

When a SUPERPRO DESIGNER flowsheet is defined to be in continuous mode, streams are reported on a per-hour basis. Scheduling information is not required, and no overall batch time is calculated. Individual batch processes can be inserted into the flowsheet with their batch and turnaround times specified.

In the ASPEN BATCH PROCESS DEVELOPER, every simulation is for an overall batch process with stream values always reported on a per-batch basis. Continuous operations, however, can be inserted. For these units, a feed is loaded, the vessel is filled to its surge volume, and an effluent stream immediately begins to transfer the product downstream. This differs from normal batch operation, which involves loading all of the feed and completing the processing steps before unloading. Specific units in the ASPEN BATCH PROCESS DEVELOPER, such as the *Fermenter*, can also operate *as fed-batch*. In such operations, a feed is added continuously to the batch while an operation is taking place.

With SUPERPRO DESIGNER and the ASPEN BATCH PROCESS DEVELOPER, caution must be exercised when introducing continuous operations into batch processes, as no warnings are provided when a continuous process unit is running dry. When a feed to a continuous unit runs dry, the simulator assumes that this unit is shut down and restarted when the feed returns. Clearly, such operation is infeasible for many units, such as distillation columns and chemical reactors. Consequently, when continuous processes are included, it is important to check the results computed by the batch simulators to be sure that unreasonable assumptions have not been made.

An advantage of adding continuous operations arises when the process bottleneck is transferred to the continuous unit. When a schedule is devised such that the continuous unit is always in operation, batch cycling is avoided.

EXAMPLE 7.6 *tPA Cultivators*

As discussed in Section 2.3, tPA-CHO cells are used to produce tPA. These cells are duplicated to a density of 3.0×10^6 cell/mL, after which the culture becomes too dense and the tPA-CHO cells die at a high rate. For this reason, engineers cultivate tPA-CHO cells in a sequence of bioreactors, each building up mass to a density of 3.0×10^6 cell/mL, with the accumulated cell mass used to inoculate the next largest reactor, until the desired cell mass is reached.

In this example, the objective is to determine the effective time between batches; that is, the *cycle time*, which is less than the total occupied time of a sequence of batch operations. The cycle time is smaller because while one batch is moving through the sequence, other batches are being processed simultaneously in other pieces of equipment both upstream and downstream. Therefore, the effective time

between batches, or the cycle time, is determined by the equipment unit that requires the most processing time. This equipment unit is known as the *bottleneck*, and consequently, to reduce the cycle time, engineers seek to reduce the processing time of the bottleneck as much as possible. Usually, the bottleneck is associated with the largest process unit, often the main bioreactor, because these reactors involve the largest cultivation times. See Chapter 22 for a more complete discussion of the cycle time and bottleneck.

For this example, the SUPERPRO DESIGNER simulator is used to determine the cycle time for a portion of the tPA process that involves just two cultivators as shown in Figure 7.28. This is intended as a practice example (with solution presented) for readers who solve Exercise 7.25, in which all three culltivators are included. Initially, a mixing tank is charged with 3,565 kg of water and 459.5 kg of HyQ PF-CHO media, with a charge time of one hour. The material in the tank is cooled to 4°C for one day and aged for two days to allow for quality-assurance testing. Then, this material is transferred to a 0.2-μm microfilter for sterilization to remove bacteria over a two-hour period, and is sent to a holding tank. Next, the first cultivator is charged with 1.2 kg of tPA-CHO cells in one hour.

Then, 21.2 kg of material from the holding tank are heated in a heat exchanger to 37°C and added to the first cultivator in 0.5 day, after which cultivation takes place over the next five days. The yield from the cultivation is 15.3 wt% tPA-CHO cells, 0.01 wt% endotoxin, 84.7 wt% water, and 0.01 wt% tPA. The products of Cultivator 1 are fed to Cultivator 2 in 0.5 day. Then, 293.5 kg of media from the holding tank are heated to 37°C and fed to Cultivator 2 in 0.5 day, after which the cultivation takes place over seven days. Immediately after Cultivator 1 is emptied, it is cleaned in place using 60 kg of water over 20 hours. Note that to override the SUPERPRO DESIGNER estimate, a charge time of one min should be entered. Then, it is sterilized at 130°C for two hours and cooled to 25°C (with one hour heat up and cool down times). The yield of the cultivation in Cultivator 2 is 11.7 wt% tPA-CHO cells, 7.67×10^{-4} wt% endotoxin, 88.3 wt% water, and 0.039 wt% tPA. After this cultivation, the contents of Cultivator 2 are cooled in a heat exchanger to 4°C and transferred to the centrifuge holding tank over 0.5 day. After Cultivator 2 is emptied, it is cleaned in place using 600 kg of water over 20 hours and sterilized using the procedure for Cultivator 1.

To determine the cycle time and the bottleneck unit, create a multiple-batch Gantt chart using SUPERPRO DESIGNER. Generate equipment content and capacity reports to determine the sizes of the equipment items. Examine the stream table report to monitor the production of tPA-CHO cells and tPA in the process.

SOLUTION

When using SUPERPRO DESIGNER, the materials are specified: tPA-CHO cells, tPA, media, water, nitrogen, oxygen, and carbon dioxide. Then, each equipment item is entered with its recipe of operations. Note that there is no cultivator model in SUPERPRO DESIGNER, and consequently, the Fermenter model is used in its place. Given this information, SUPERPRO DESIGNER generates a recipe of operations for the process shown in Figure 7.29. Also, it generates the Gantt chart, as shown in Figure 7.30. For each vessel, solid blocks show the time period during which it is in operation. Solid blocks are for the first and second batches, respectively. The bottleneck is associated with the equipment unit that is utilized at all times, that is, for which the blue and orange blocks touch each other. Clearly, this unit determines the cycle time, which is approximately nine days. Note that these results can be reproduced using the folder SUPERPRO-EXAM 7-6 in the Program and Simulation Files folder, which can be downloaded from the Wiley Web site associated with this text book. Also, to obtain detailed instructions and results, see the file Example 7.6, Detailed Instructions for Solving and Results.pdf in the PDF Folder on the Wiley Web site.

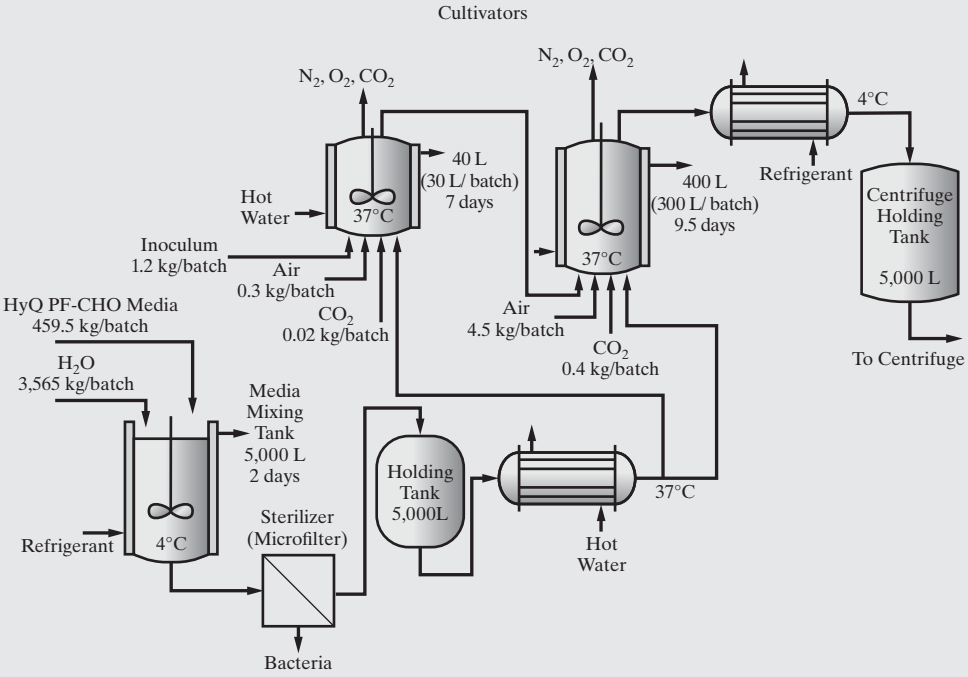

Figure 7.28 tPA reactor section with two cultivators.

1. Reactor Growth Chain

1.1. Charge Mixing Tank with 459.5 kg of Media. The charge time is 1 h. Charge Mixing Tank with 3,565 kg of WATER. The charge time is 1 h.

1.2. Cool unit Mixing Tank to 4°C. The cooling time is 1 day.

1.3. Age the contents of unit Mixing Tank for 2 days.

1.4. Microfilter the contents of Mixing Tank in Microfilter. The mode of operation is Batch Concentration. Unspecified components go to the Permeate. The operation time is 2 h. The permeate stream is sent to Holding Tank.

1.5. Charge Fermenter 1 with 1.2 kg of tPA-CHO Cells. The charge time is 1 h.

1.6. Transfer contents of unit Holding Tank to Fermenter 1 through Heat Exchanger. The final stream temperature is 37°C. Transfer 21.2 kg of vessel contents. The transfer time is 0.5 day.

1.7. Ferment in unit Fermenter 1. The yield of tPA-CHO Cells in the Solid phase is 0.153, of Endotoxin in the Liquid phase is 0.0001, of tPA in the Liquid phase is 0.0001, of WATER in the Liquid phase is 0.847, of Media in the Liquid phase is 0, of Media in the Solid phase is 0, and of tPA-CHO Cells in the Liquid phase is 0. The fermentation time is 5 days. Continuously add 0.02 kg of CARBON DIOXIDE. Continuously add 0.3 kg of AIR.

2. Final Fermentation

Start Parallel

Series

2.1. Transfer contents of unit Fermenter 1 to Fermenter 2. Transfer 100% of vessel contents. The transfer time is 0.5 day.

2.2. Transfer contents of unit Holding Tank to Fermenter 2 through Heat Exchanger. The final stream temperature is 37°C. Transfer 293.5 kg of vessel contents. The transfer time is 0.5 day.

2.3. Ferment in unit Fermenter 2. The yield of tPA-CHO Cells in the Solid phase is 0.117, of Endotoxin in the Liquid phase is 7.67e-6, of tPA in the Liquid phase is 0.00039, of WATER in the Liquid phase is 0.883, of Media in the Solid phase is 0, of Media in the Liquid phase is 0, and of tPA-CHO Cells in the Liquid phase is 0. The fermentation time is 7 days. Continuously add 0.4 kg of CARBON DIOXIDE. Continuously add 4.5 kg of AIR.

Series

2.4. Clean unit Fermenter 1. Clean with 60 kg of WATER. The feed time is 1 min. Cleaning time is 20 h.

2.5. Sterilize the contents of Fermenter 1. The sterilization temperature is 130°C. The heat-up time is 1 h. Maintain the temperature for 2 h. The cool-down time is 1 h.

End Parallel

2.6. Transfer contents of unit Fermenter 2 to Centrifuge Holding Tank through heat exchanger Cooler. The final stream temperature is 4°C. Transfer 100% of vessel contents. The transfer time is 1 day.

2.7. Clean unit Fermenter 2. Clean with 600 kg of WATER. The feed time is 1 min. Cleaning time is 68 h.

2.8. Sterilize the contents of Fermenter 2. The sterilization temperature is 130°C. The heat-up time is 1 h. Maintain the temperature for 2 h. The cool-down time is 1 h.

Figure 7.29 Recipe of process operations for 2-cultivator process.

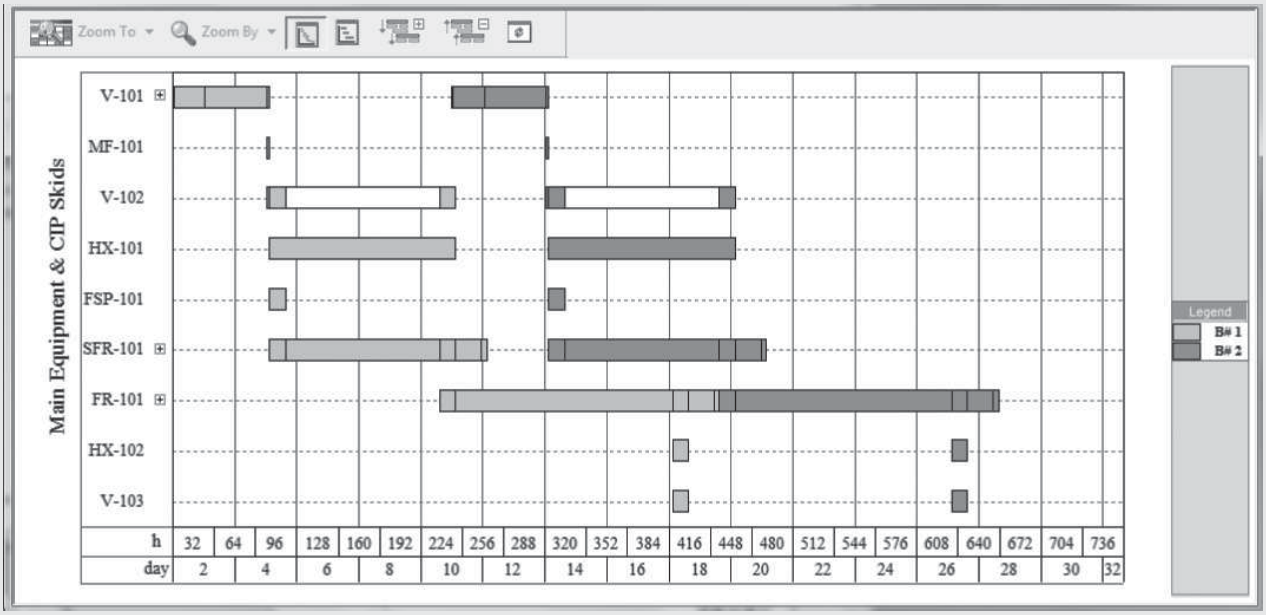

Figure 7.30 Gantt chart. See the Color Figures folder on the Wiley web site.

7.6 SUMMARY

Having studied this chapter, the reader should:

1. Understand the basic principles of process simulation, including key terminology and important process simulation issues.
2. Be able to create a simple mass-balance simulation involving just mixers, stoichiometric reaction conversions, component splitters (separators), and stream dividers.
3. Understand the importance of degrees of freedom in determining simulation specifications.
4. Understand how to decompose a flowsheet when multiple recycle loops are present.
5. Be able to use design specifications, which are implemented as control blocks.
6. Understand how to begin with simple mass-balance simulations and gradually build up information associated with the design of a chemical process.
7. Have been exposed to case studies involving multiple simulations that illustrate the role of process simulators in process synthesis.
8. Have been introduced to batch process simulators, recipes for batch process units, and their ability to schedule batch processes, that is, to create Gantt charts, determine cycle times, and identify bottlenecks in batch processing.

Process simulation plays a central role in process creation. The following work flow for design could be tried (Note that it is always possible to return to an upstream step from any of the downstream steps—that is why the design process is iterative, but few iterations are required when good decisions are made.):

- Data collection and design problem definition
- Flowsheet generation (see Chapter 6)
- Mass balances (simulation Task-1)
- Mass and energy balances (simulation Tasks 2–3)
- Rigorous simulation (simulation Task-4)
- Equipment sizing calculations (see Chapter 16)
- Equipment costing calculations (see Chapter 16)
- Economic analysis (see Chapter 17)
- Process integration (see Chapter 11)
- Process optimization (see Chapter 21)

REFERENCES

1. Alvarado-Morales, M., J. Terra, K. V. Gernaey, J. M. Woodley, and R. Gani, "Biorefining: Computer aided tools for sustainable design and analysis of bioethanol production" *Chem. Eng. Res. Des.*, **87**(9), 1171 (2009).

2. Biegler, L. T., I. E. Grossmann, and A. W. Westerberg, *Systematic Methods of Chemical Process Design, Prentice Hall International Series* (1999).

3. Crowe, C. M., and M. Nishio, "Convergence Promotion in the Simulation of Chemical Processes—The General Dominant Eigenvalue Method," *AIChE J.*, **21**, 3 (1975).

4. Douglas, J. M., *Conceptual Design of Chemical Processes*, McGraw-Hill (1988).

5. Henley, E. J., and E. M. Rosen, *Material and Energy Balance Computations*, Wiley, New York (1969).

6. Kontogeorgis, G. M., and R. Gani, *Computer-Aided Property Estimation for Process and Product Design*, CACE 19, Elsevier Science B.V., The Netherlands (2004), pp. 1–425

7. Mangnimit, S., Sustainable Process Design of Biofuels: Bioethanol Production from Cassava Rhizome, MSc-Thesis, The Petroleum and Petrochemical College, Chulalongkorn University, Bangkok, Thailand (2013).

8. Myers, A. L., and W. D. Seider, *Introduction to Chemical Engineering and Computer Calculations*, Prentice-Hall, Englewood Cliffs, New Jersey (1976).

9. Orbach, O., and C. M. Crowe, "Convergence Promotion in the Simulation of Chemical Processes with Recycle—The Dominant Eigenvalue Method," *Can. J. Chem. Eng.*, **49**, 509 (1971).

10. Wegstein, J. H., "Accelerating Convergence of Iterative Processes," *Commun. Assoc. Comp. Machinery*, **1**(6), 9 (1958).

11. Westerberg, A. W., H. P. Hutchison, R. L. Motard, and P. Winter, *Process Flowsheeting*, Cambridge University Press, Cambridge (1979).

12. Wooley, R., M. Ruth, J. Sheehan, K. Ibsen, H. Majdeski, and A. Galvez, "*Lignocellulosic Biomass to Ethanol Process Design and Economics Utilizing Co-current Dilute Acid Prehydrolysis and Enzymatic Hydrolysis–Current and Futuristic Scenarios,*" National Renewable Energy Laboratory, Golden Colorado, USA (1999).

EXERCISES

7.1 *Flash with recycle*

(a) Consider the flash separation process shown in Figure 7.1. If using ASPEN PLUS, solve all three cases using the MIXER, FLASH2, FSPLIT, and PUMP modules and the RK-SOAVE option set for themophysical properties. Compare and discuss the flow rates and compositions for the overhead stream produced by each of the three cases.

(b) Modify case 3 of Exercise 7.1a to determine the flash temperature necessary to obtain 850 lb/hr if overhead vapor. If using ASPEN PLUS, a design specification can be used to adjust the temperature of the flash drum to obtain the desired overhead flow rate.

7.2 *Toluene hydrodealkylation process—reactor section*. As discussed in Example 6.7, toluene (C_7H_8) is to be converted thermally to benzene (C_6H_6) in a hydrodealkylation reactor. The main reaction is $C_7H_8 + H_2 \rightarrow C_6H_6 + CH_4$. An unavoidable side reaction occurs that produces biphenyl: $2C_6H_6 \rightarrow C_{12}H_{10} + H_2$.

The reactor section of the process is shown in Figure 7.31 as are the conditions for the feed and two recycle streams. The flow rate of the quench stream should be such that the reactor effluent is quenched to 1,150°F. Conversion of toluene in the reactor is 75 mol%. Two mole percent of the benzene present after the first reaction occurs is converted to biphenyl. Use a process simulator to perform material and energy balances with the Soave–Redlich–Kwong equation of state (RK-SOAVE option in ASPEN PLUS).

7.3 *Toluene hydrodealkylation process—separation section*. As discussed in Example 6.7, the following stream at 100°F and 484 psia is to be separated by two distillation columns into the Products 1–3 in the following table.

Species Flow Rates (lbmol/hr)	Feed	Recycle	Gas Recycle
H_2	0	0	2,045.9
CH_4	0	0	3,020.8
C_6H_6 (benzene)	0	3.4	42.8
C_7H_8 (toluene)	274.2	82.5	5.3
$C_{12}H_{10}$ (biphenyl)	0	1.0	0

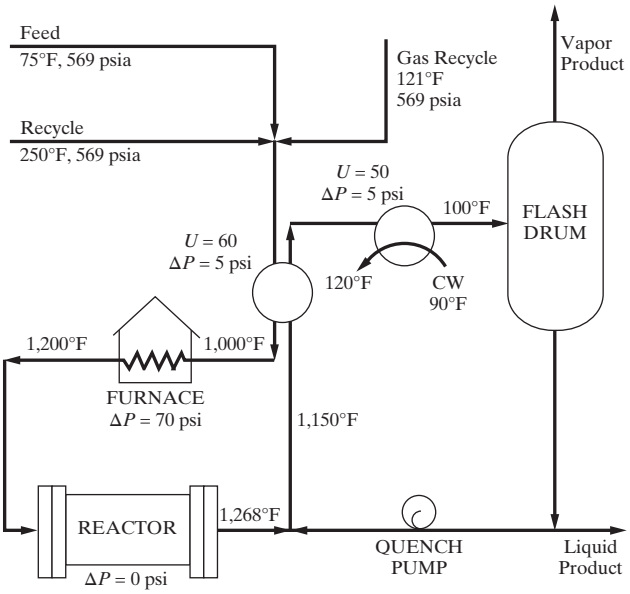

Figure 7.31 Reactor section of the toluene hydrodealkylation process.

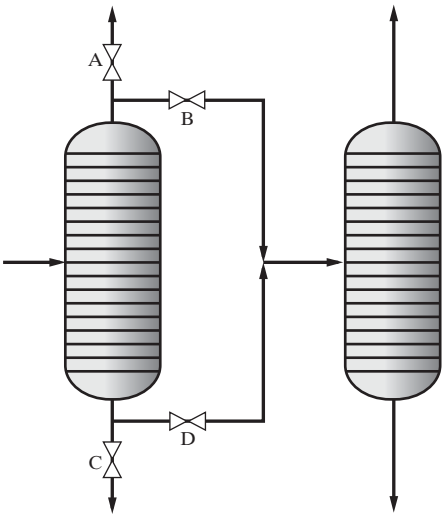

Figure 7.32 Toluene hydrodealkylation process—Distillation section.

	lbmol/hr			
Species	Feed	Product 1	Product 2	Product 3
H_2	1.5	1.5		
CH_4	19.3	19.2	0.1	
C_6H_6 (benzene)	262.8	1.3	258.1	3.1
C_7H_8 (toluene)	84.7		0.1	84.6
$C_{12}H_{10}$ (biphenyl)	5.1			5.1

Two different distillation sequences are to be examined as shown in Figure 7.32. In the first sequence, H_2 and CH_4 are removed in the first column.

If using ASPEN PLUS, the DSTWU module is used to estimate the reflux ratio and theoretical tray requirements for both sequences. In addition, the RK-SOAVE option is used. Specify a reflux ratio equal to 1.3 times the minimum. Use design specifications to adjust the isobaric column pressures so as to obtain distillate temperatures of 130°F; however, no column pressure should be less than 20 psia. Also, specify total condensers but note that a partial condenser is used when H_2 and CH_4 are taken overhead.

7.4 Complete a simulation of the entire process for the hydrodealkylation of toluene in Figure 6.14. Initially, let the purge/recycle ratio be 0.25; then, vary this ratio and determine its effect on the performance of the process. Use a design specification to determine the unknown amount of hydrogen to be added to the feed stream (equal to that lost in the purge). If using ASPEN PLUS, the distillation columns can be simulated using the RADFRAC module with the number of stages and reflux ratio previously computed by the DSTWU module. (To carry out an economic analysis of the process, see Exercise 17.21.)

7.5 (a) Complete a steady-state simulation of the vinyl-chloride process in Figure 2.6. First, create a simulation flowsheet. Assume that:

Cooling water is heated from 30 to 50°C.
Saturated steam is available at 260°C (48.4 atm).

If using ASPEN PLUS, use the UNIQUAC option set for thermophysical properties.

(b) Carry out process integration and repeat the steady-state simulation.

7.6 For the monochlorobenzene separation process in Figure 7.14, the results of an ASPEN PLUS simulation are provided in the multimedia modules under *ASPEN → Principles of Flowsheet Simulation → Interpretation of Input and Output*. Repeat the simulation with:

(a) 25% MCB recycled at 130°F; stream S02 at 250°F; 15 theoretical stages in the distillation column.

(b) Other specifications of your choice.

7.7 *Cavett Problem*. A process having multiple recycle loops formulated by R.H. Cavett [Proc. Am. Petrol. Inst., **43**, 57 (1963)] has been used extensively to test tearing, sequencing, and convergence procedures. Although the process flowsheet requires compressors, valves, and heat exchangers, a simplified ASPEN PLUS flowsheet is shown in Figure 7.33 (excluding the recycle convergence units). In this form, the process is the equivalent of a four-theoretical-stage, near-isothermal distillation (rather than the conventional near-isobaric type) for which a patent by A.Gunther [U.S. Patent 3,575,007 (April 13, 1971)] exists. For the specifications shown on the flowsheet, use a process simulator to determine the component flow rates for all streams in the process.

7.8 Use a process simulator to model a two-stage compression system with an intercooler. The feed stream consists of 95 mol% hydrogen and 5 mol% methane at 100°F and 30 psia; 440 lbmol/hr is compressed to 569 psia. The outlet temperature of the intercooler is 100°F and its pressure drop is 2 pisa. The centrifugal compressors have an isentropic efficiency of 0.9 and a mechanical efficiency of 0.98.

Determine the power requirements and heat removed for three intermediate pressures (outlet from the first three stages): 100, 130, 160 psia. If using ASPEN PLUS, use the MCOMPR module and the RK-SOAVE option.

7.9 Consider the ammonia process in which N_2 and H_2 (with impurities Ar and CH_4) are converted to NH_3 at high pressure (Figure 7.34). If using ASPEN PLUS, use the following subroutines:

Compressor	COMPR
Reactor	RSTOIC
Heat exchanger	HEATER
High-pressure separator	FLASH2
Low-pressure separator	FLASH2
Recirculating compressor	COMPR

You are given the feed stream and fraction purged in the splitter. Prepare a simulation flowsheet and, when applicable, show the calculation sequence prepared by the process simulator (if using ASPEN PLUS, complete SEQUENCE USED WAS:).

7.10 The feed (equimolar A and B) to a reactor is heated from 100°F to 500°F in a 1-2 parallel-counterflow heat exchanger with a mean overall heat-transfer coefficient of 75 Btu/hr-ft^2°F. It is converted to C by the exothermic reaction A + B → C in an adiabatic plug-flow tubular reactor (Figure 7.35). For a process simulator, prepare a simulation flowsheet and show the calculation sequence to determine:

(a) Flow rates and unknown temperatures for each stream.

(b) Heat duty and area of the countercurrent shell-and-tube heat exchanger.

Component	lbmol/hr
N_2	358.2
CO_2	4,965.6
H_2S	339.4
C_1	2,995.5
C_2	2,395.5
C_3	2,291.0
iC_4	604.1
nC_4	1,539.9
iC_s	790.4
nC_5	1,129.9
nC_6	1,764.7
nC_7	2,606.7
nC_8	1,844.5
nC_9	1,669.0
nC_{10}	831.7
nC_{12}	1,214.5

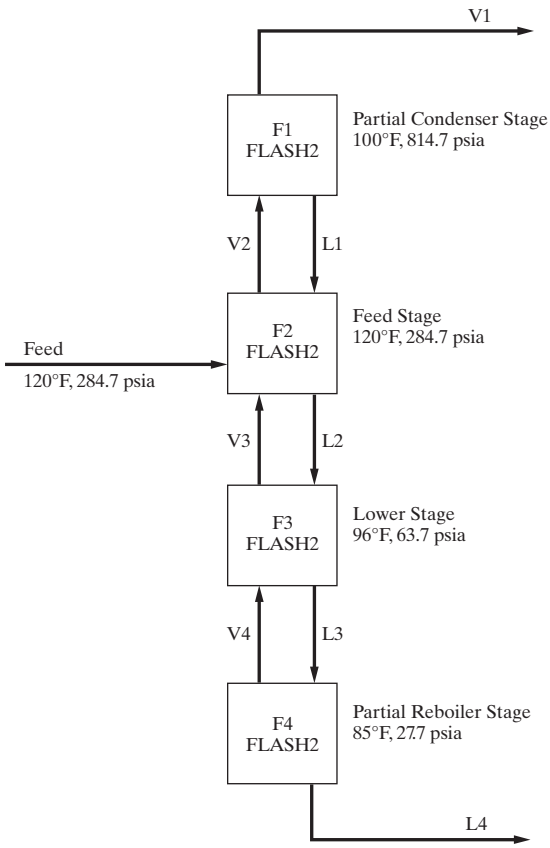

Figure 7.33 Near-isothermal distillation process.

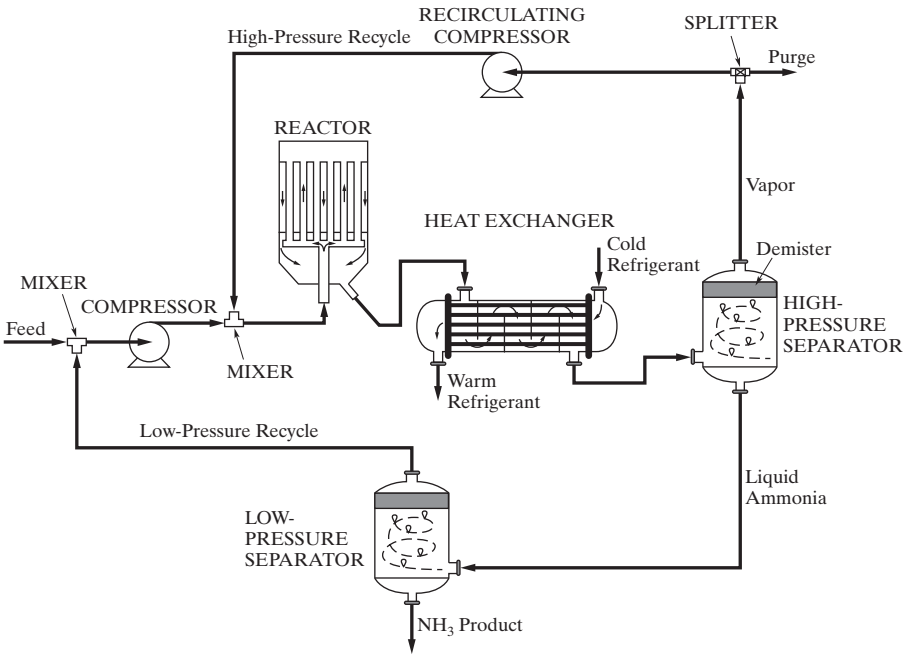

Figure 7.34 Ammonia reactor loop.

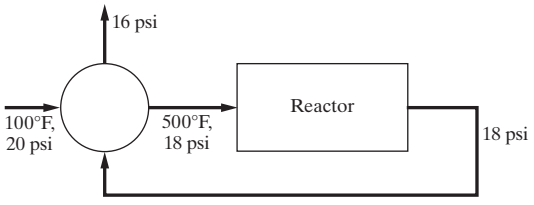

Figure 7.35 Reactor with feed/product heat exchanger.

7.11 Consider the simulation flowsheets in Figure 7.36, which were prepared for ASPEN PLUS. The feed stream, S1, is specified, as are the parameters for each process unit.

Complete the simulation flowsheets using sequences acceptable to ASPEN PLUS. If any of the streams are torn, your flowsheets should include the recycle convergence units. In addition, you should indicate the calculation sequences.

This problem is easily modified if you are working with UniSim® Design, CHEMCAD, or PRO/II.

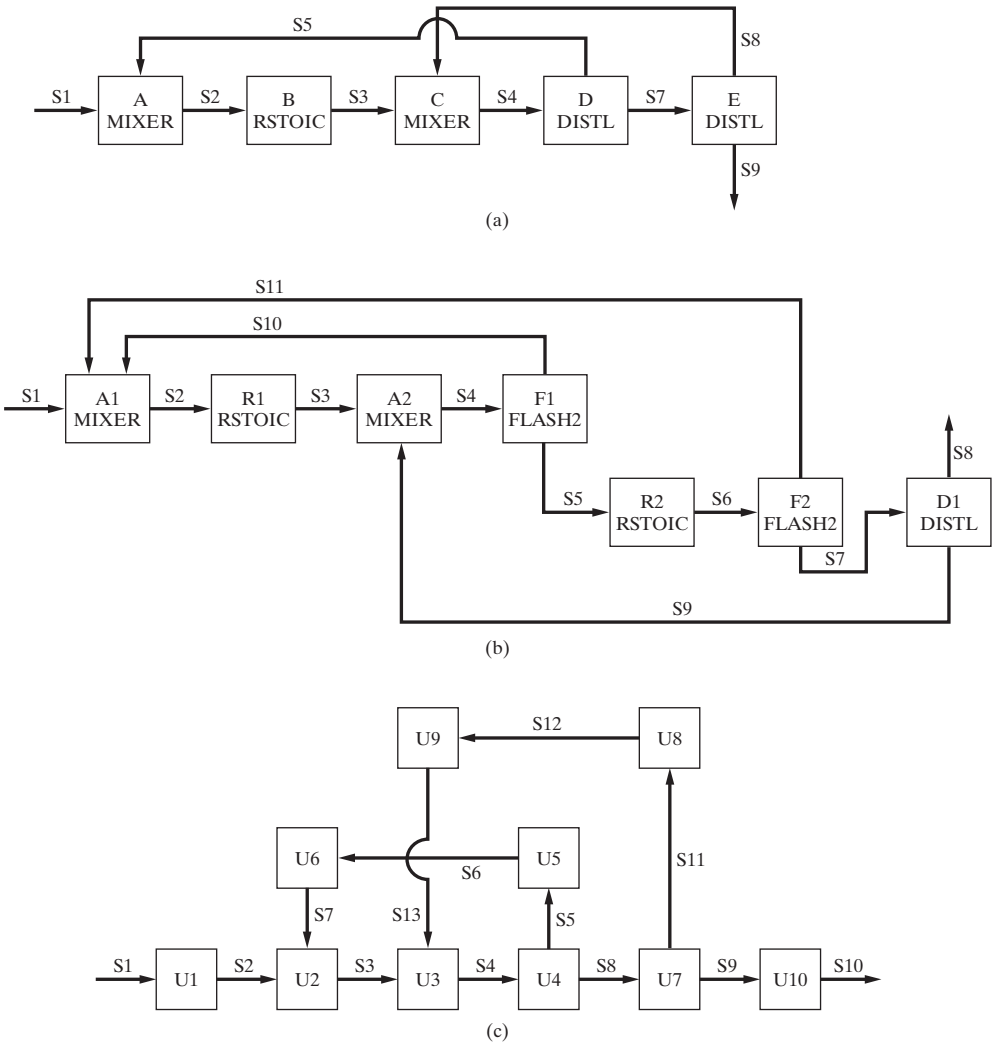

Figure 7.36 Interlinked recycle loops.

7.12 Use a process simulator to determine the flow rate of saturated vapor benzene at 176.2°F and 1 atm to be mixed with 100 lbmol/hr of liquid benzene to raise its temperature from 25 to 50°F. Prepare a good initial estimate. (*Note*: $\lambda_{NBP} = 13{,}200$ Btu/lbmol, $c_p = 0.42$ Btu/lb°F.)

7.13 A distillation tower is needed to separate an equimolar mixture at 77°F and 1 atm of benzene from styrene. The distillate should contain 99 mol% benzene and 95 mol% of the benzene fed to the tower.

Use a process simulator to determine the minimum number of trays at total reflux (N_{min}), the minimum reflux ratio (R_{min}), and the theoretical number of trays at equilibrium when $R = 1.3R_{min}$.

7.14 Use a process simulator to determine the heat required to vaporize 45 mol% of a liquid stream entering an evaporator at 150°F and 202 psia and containing

	lbmol/hr
Propane	250
n-Butane	400
n-Pentane	350

Assume that the evaporator product is at 200 psia. Use the Soave–Redlich–Kwong equation of state.

7.15 For an equimolar mixture of *n*-pentane and *n*-hexane at 10 atm, use a process simulator to compute:

(a) The bubble-point temperature.

(b) The temperature when the vapor fraction is 0.5.

7.16 Hot gases from the toluene hydrodealkylation reactor are cooled and separated as shown in the flowsheet of Figure 7.37. In a steady-state simulation, can the composition of the recycle stream be determined without iterative recycle calculations? Explain your answer.

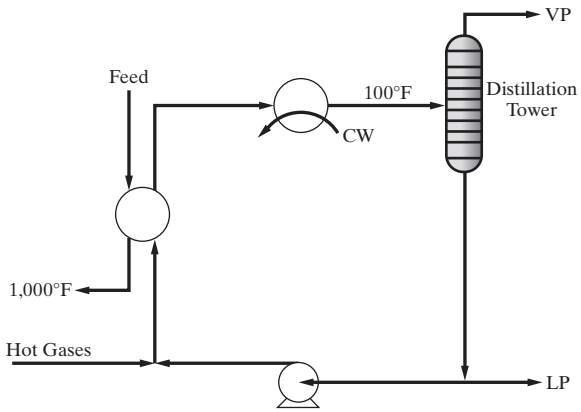

Figure 7.37 Combined quench/distillation process.

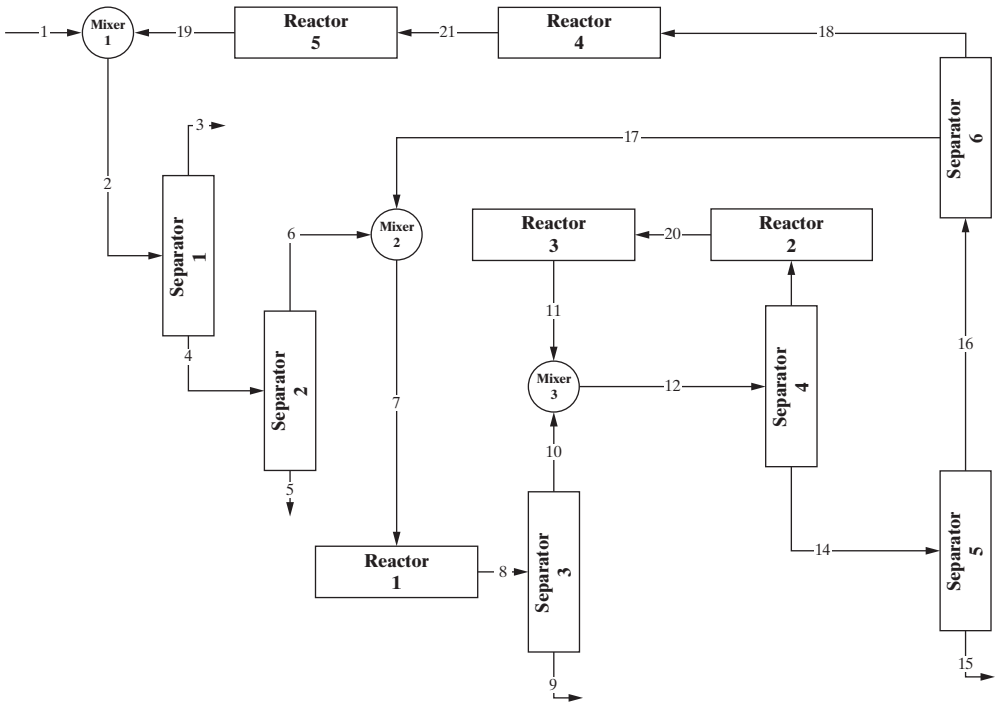

Figure 7.38 Process flowsheet.

7.17 *Flowsheet decomposition and calculation sequence*. Find the number of recycle loops, the optimal number of tear streams, and the corresponding calculation sequence for the process flowsheet in Figure 7.38.

7.18 Given the feed streams and the parameters of the process units as shown in Figure 7.38, complete the simulation flowsheet for ASPEN PLUS and show the calculation sequence (i.e., complete the statement SEQUENCE USED WAS:). If any of the streams are torn, your flowsheet should include the stream convergence units.

The simulation flowsheet can be modified for UniSim®Design, CHEMCAD, or PRO/II and the exercise repeated.

7.19 Given the feed streams and the parameters of the process units as shown in Figure 7.39, complete the simulation flowsheet for ASPEN PLUS and show the calculation sequence (i.e., complete the statement SEQUENCE USED WAS:). If any of the streams are torn, your flowsheet should include the stream convergence units.

The simulation flowsheet can be modified for UniSim®Design, CHEMCAD, or PRO/II and the exercise repeated.

7.20 *Flowsheet for mass balance*. Convert the process flowsheet in Figure 7.22 into a flowsheet for mass-balance simulation Task-1. List the model equations, the variables to be specified, and the variables to be calculated.

7.21 *Simulation Task-2*. For the streams listed in Table 7.9 (cyclohexane process) and Table 7.13 (HDA process), specify (or select) a pressure (or temperature), and calculate temperature (or pressure). Indicate the reasons for selection of the specified variable and explain the calculation procedure (including the selection of the constitutive models) to be employed. Identify also the phases of each of the streams.

7.22 *Design decisions for simulation problems*. For the following simulation problems, consult Table 7.2 and list the design decision variables.

(a) An equimolar mixture of benzene and toluene in a process stream is in the liquid state at 300 K and 1 atm. If a heat exchanger is employed to totally vaporize this stream, indicate which unit module should be used, which design variables need to be specified, and which variables will be calculated.

(b) Consider an equimolar mixture of ethanol and water at 300 K and 1 atm. In a distillation column, indicate the design variables to be specified to obtain 95 mol% of the ethanol–water azeotrope as the distillate and 99 mol% water as the bottom product. Can the distillate product be 99% ethanol?

(c) The reactor effluent from a superheated vapor needs to be separated into a vapor stream for vapor recovery and a liquid stream for a liquid recovery. Indicate which unit modules need to be employed for only mass-balance calculations and how either the temperature and/or pressure will be specified for the vapor–liquid separation operation and for rigorous simulation.

(d) From the following mixture (ethylene = 3,681.9 kmol/hr; propylene = 363.8 kmol/hr; methane = 368.2 kmol/hr; diethyl ether = 6.6 kmol/hr; water = 2,417 kmol/hr, and ethanol = 282.8 kmol/hr; at 550 K and 60 atm), 50% of diethyl ether is to be removed as a liquid product in a PT-flash operation. What should be the temperature and pressure of the PT-flash operation? What will be the distribution of products as overhead vapor and bottom liquid products? If from the overhead vapor product ethanol and diethyl ether are to be recovered through an absorption column with water as the solvent, list the variables that need to be specified and the variables that will be calculated through simulation of an absorption column.

7.23 *Rigorous process simulation: Design specifications*. The process flowsheet and list of variables to specify for the HDA process are given in Figure 7.24 and Table 7.14. Perform simulations with any process simulator to match the results given in Tables 7.13 and 7.15. Table 7.14 lists

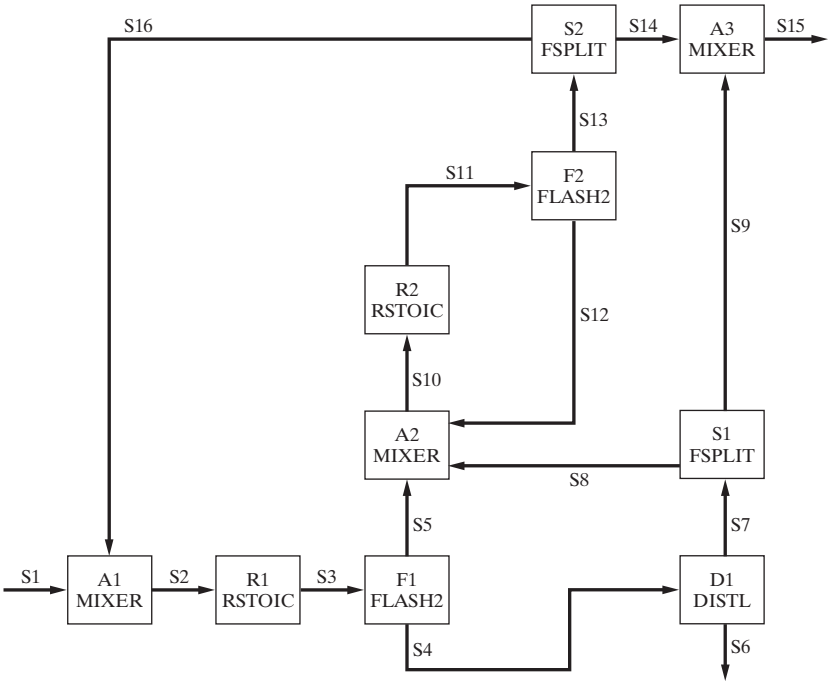

Figure 7.39 Incomplete simulation flowsheet.

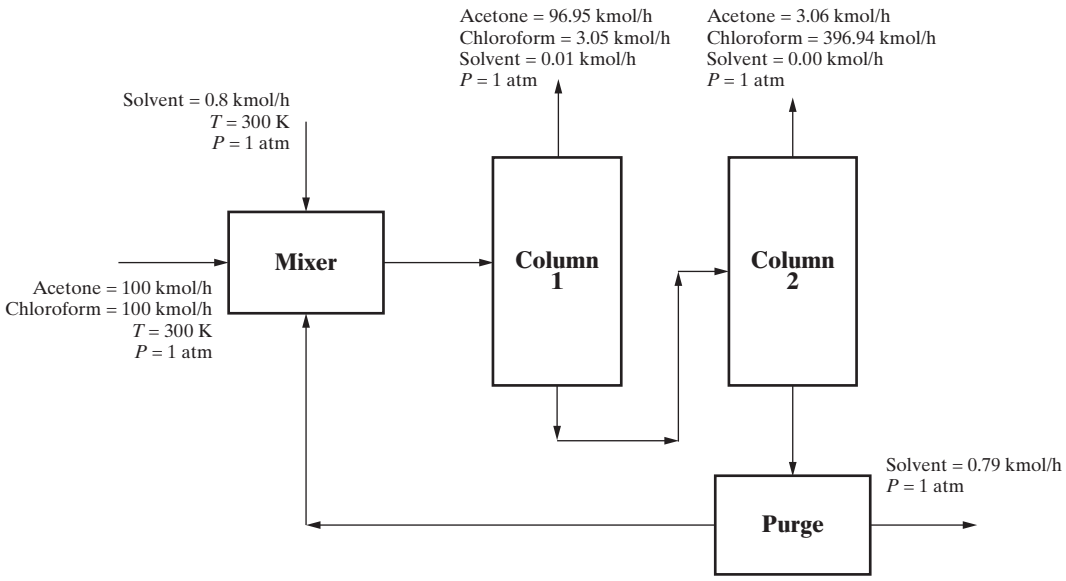

Figure 7.40 Simulation results using a simple mass-balance model.

the design variables for the distillation columns. Are there other ways to specify these distillation columns that will give the same results?

7.24 *Simulation of a solvent-based extraction process.* Consider a binary equimolar mixture of acetone and chloroform at 300 K and 1 atm. Because this mixture forms a binary azeotrope, methyl-*n*-pentyl ether solvent is used to extract the chloroform from acetone. The flowsheet in Figure 7.40 for the process shows the results of solving a simple mass-balance model. Perform a rigorous simulation of the process by converting the two component-splitter modules into distillation-column modules. This involves finding appropriate specifications for the two distillation columns to yield approximately the mass balance given in the flowsheet. Assume a pressure of 1 atm in all streams and estimate the temperatures of the other streams according to their phases (saturated liquid or vapor).

The separation in the mass-balance flowsheet gives an acetone product of approximately 96% purity from column 1 and a chloroform product of approximately 96% purity from column 2. A makeup of 0.8 kmol/hr of solvent is added to replace this amount lost from the purge stream. How can the product purity be improved and the solvent loss decreased?

Hints: First generate a Txy phase diagram for this system and identify the type of binary azeotrope formed by acetone and chloroform. Column 1 is the extraction column and needs solvent at approximately twice the amount of the mixture being separated. For column 1, try a specification of 96% acetone recovery in the distillate and 96% chloroform in the

bottoms product. For column 2, try a specification of 99.9% chloroform recovery in the distillate and 99.9% solvent in the bottoms product. For the purge, start with a purge fraction of 0.2%. Note that sufficient solvent needs to be recycled to perform the extraction in column 1.

7.25 *Debottlenecking reactor train*. When the third tPA cultivator in Example 2.3 is added to the cultivators in Example 7.6, as shown in Figure 7.27a, a significant time strain is placed on the process because the combined feed, cultivation, harvest, and cleaning time in this largest vessel is long and rigid. Consequently, the remainder of the process is designed to keep this cultivator in constant use, so as to maximize the yearly output of product. Note that, in many cases, when an equipment item causes a bottleneck, a duplicate is installed so as to reduce the cycle time.

For this exercise, the third cultivator is added to the simulation in Example 7.6 with the specifications for the mixer, filter, holding tank, heat exchanger 1, and first two cultivators identical to those in Example 7.6. After the cultivation is completed in Cultivator 2, its cell mass is transferred as inoculum to Cultivator 3 over 0.5 day. Then, the remaining media from the mixing tank is heated to 37°C and added over 1.5 days after which cultivation takes place over eight days. Immediately after the transfer from Cultivator 2 to Cultivator 3, Cultivator 2 is cleaned in place using 600 kg of water over 20 hr. The yield of the cultivation in Cultivator 3 is 11.4 wt% tPA-CHO cells, 7.7×10^{-5} wt% endotoxin, 88.9 wt% water, and 0.0559 wt% tPA. When the cultivation is completed in Cultivator 3, its contents are cooled in a heat exchanger to 4°C and transferred to the centrifuge holding tank over one day, and Cultivator 3 is cleaned using 600 kg of water over 67 hr and sterilized using the procedure for Cultivators 1 and 2.

To eliminate an undesirable bottleneck(s), and reduce the cycle time to 14 days (total operation time of Cultivator 3), it may be necessary to add an equipment units(s).

Print and submit the text recipes and three-batch schedules for both the original process and the modified process, if debottlenecking is necessary, as prepared by SUPERPRO DESIGNER.

Chapter 8

Synthesis of Networks Containing Reactors

8.0 OBJECTIVES

The design of the reaction section of the process flowsheet involves the conversion of certain chemicals in the feed to the section to the desired chemical products. More specifically, it is desired to ensure sufficient yield and selectivity of the required product species by appropriate selection of a single reactor or network of reactors. The presence of at least one chemical reactor and one or more separation sections for the separation of the effluent mixture leaving the reactor(s) characterizes many chemical processes. In many cases, one or more of the streams leaving the separation sections(s) are recycles to the reactor. The reactor section therefore needs to be designed to account also for the impact of the separation section(s) and recycle(s) on the overall performance of the process.

After studying this chapter, the reader should:

1. Be familiar with the types of reactor models available in commercial process simulators and their use in process design. Further assistance is provided in the multimedia modules, which can be downloaded from the www.seas.upenn.edu/~dlewin/multimedia.html (*ASPEN* → *Chemical Reactors* and *HYSYS* → *Chemical Reactors*).
2. Be able to determine whether a reactor network should be considered and, if so, design it using the concept of the *attainable region*.
3. Be aware of the alternative design configurations commonly used to handle heat transfer to or from the reactor so as to sustain an exothermic or endothermic reactor at its desired temperature level.
4. Be able to determine the best location for the separation section either before or after the reactor or both.
5. Be able to select an appropriate value for any necessary purge rate from a recycle loop, accounting for the trade-offs between purge-to-recycle ratio, recycle ratio, and raw-material loss, especially when dealing with inert or byproduct chemicals that are difficult to separate from the reactants.
6. Be able to determine the optimal reactor conversion, accounting for the trade-off between the cost of the reactor section and the cost of the separation section in the presence of recycle.
7. Understand the conditions under which recycle of byproducts to extinction can be employed to reduce waste and increase yield.

8.1 INTRODUCTION

As mentioned above, this chapter treats reactors as single entities and in combination with other reactors and/or separation systems, including the effect of recycle from a separation system to a reactor. Section 8.2 describes the types of single reactor models available in the process simulators. In Section 8.3, attainable-region analysis is introduced as a tool for the optimal design of reactor networks. Section 8.4 discusses the applicability of the different reactor types to model complex configurations, particularly for reactors that require heat exchange so as to sustain a stable operation at the desired temperature level. Here, examples are presented from the processing industry.

Beginning in Section 8.5, reactors are considered in combination with separation systems. The feed to a reactor section of a chemical process is often a combined feed consisting of fresh feed mixed with one or more recycle streams, as shown later in Figure 9.1. Although Figure 9.1 shows only one reactor section, multiple reactor sections are sometimes required, with separation sections located between each pair of reactor sections. Of major importance is the fact that fresh reactor feeds rarely contain only the reactants for the desired reactions. Besides the reactants, they may contain inert chemicals, potential reactants for undesired side-reactions, catalyst poisons, and products of the desired reactions. Recycle streams are intended to contain only unconverted reactants of the desired reactions. However, more commonly, recycle streams also contain products of the desired reactions, products of undesired side reactions, and inert chemicals. Reactor effluents are almost never products that meet purity specifications. Besides the products, effluents may contain reactants, inerts products of undesired side reactions, and feed impurities. Thus, almost every chemical involved in a chemical reaction also involves one or more separation sections in addition to one or more recycle streams.

A major challenge of process design is devising an optimal scheme for uniting the reaction and separation functions of a process. Section 8.5 discusses the problem of where best to locate the separation section with respect to the reaction section. Although it might seem that the reaction section should logically precede the separation section, such a sequence is not always optimal.

Section 8.6 extends the treatment in Section 8.5 by addressing the trade-offs in processes involving recycle back to the reaction section. Because of recycle from a separation section, an optimal conversion per passthrough the reactor exists, which is examined in Section 8.7. In some cases, an optimal yield and minimization or elimination of waste products can be achieved by recycling the products of undesirable reactions to extinction, as discussed in Section 8.8. Finally, control problems associated with reactor-separator-recycle systems are introduced in Section 8.9.

8.2 REACTOR MODELS IN THE PROCESS SIMULATORS

Chemical reactors, particularly for continuous processes, are often custom designed to involve multiple phases (e.g., vapor, liquid, reacting solid, and solid catalyst), different geometries (e.g., stirred tanks, tubular flows, converging and diverging nozzles, spiral flows, and membrane transport) and various regimes of momentum, heat, and mass transfer (e.g., viscous flow, turbulent flow, conduction, radiation, diffusion, and dispersion). There are so many designs involving different combinations of these attributes that attempts to develop generalized reactor models have met with limited success. Instead, most of the process simulators provide four kinds of idealized reactor models, including (1) a stoichiometric, material-balance model that permits the specification of reactant conversions and extents of reaction for one or more specified reactions; (2) a thermodynamic-equilibrium model for multiple phases (vapor, liquid, and solid) in chemical equilibrium where the approach to equilibrium for individual reactions can be specified; (3) a kinetic model for a continuous-stirred-tank reactor (CSTR) that assumes perfect mixing of homogeneous phases (liquid or vapor); and (4) a kinetic model for a plug-flow tubular reactor (PFTR or PFR), for homogeneous phases (liquid or vapor) and assuming no backmixing (dispersion). Only the latter two models compute a reactor volume. These models are used in the early stages of process synthesis when the details of the reactor designs are less important, but reactor effluents and heat duties are needed.

The ideal reactor models are replaced by custom-made models as the reaction details gain significance. For this purpose, all of the flowsheet simulators provide facilities for the insertion of user-generated models. These are refined often as the design proceeds and as reactor data from the laboratory or pilot plant are regressed. In fact, some of the simulators provide facilities for estimating the parameters of kinetic models by nonlinear regression.

When working with the ideal reactor models, the reader should refer to available textbooks on reactor analysis and design, for example, *Chemical Reactor Analysis and Design* by G. F. Froment, K. B. Bishoff, and J. De Wilde (2010); *Essentials of Chemical Reaction Engineering* by H. S. Fogler (2011); *The Engineering of Chemical Reactions* by L. D. Schmidt (1998); *Chemical Reaction Engineering* by O. Levenspiel (1999), and to the user manuals and tutorial segments of the flowsheet simulators. The following discussion of the ideal reactor models used in simulators is preceded by a brief review of reaction stoichiometry and reaction extent, which together provide the basis for calculation of the basic conversion reaction model in the simulators. Advanced models for tubular reactors that account for nonplug flow are introduced in Chapter 15.

Reaction Stoichiometry

For most of the reactor models in the flowsheet simulators, it is necessary to provide R chemical reactions involving C chemical species:

$$\sum_{j=1}^{C} \nu_{ij} A_j = 0, \quad i = 1, \ldots, R \tag{8.1}$$

where A_j is the chemical formula for species j and ν_{ij} is the stoichiometric coefficient for species j in reaction i (negative for reactants, positive for products). As an example for just one reaction for the manufacture of methanol, let the chemicals be ordered according to decreasing volatility, that is: (1) H_2, (2) CO, and (3) CH_3OH. The reaction can be written as $-2H_2-CO + CH_3OH = 0$, and the stoichiometric coefficient matrix is

$$\nu_{ij} = \begin{matrix} \\ \mathrm{H_2} \\ \mathrm{CO} \\ \mathrm{CH_3OH} \end{matrix} \begin{bmatrix} \\ -2 \\ -1 \\ 1 \end{bmatrix}$$

Extent of Reaction

Consider a single reaction. In the stoichiometric reactor models, the fractional conversion, X_k, of key reactant k,

$$X_k = \frac{n_{k,in} - n_{k,out}}{n_{k,in}}, \tag{8.2}$$

where $n_{k,in}$ and $n_{k,out}$ are the moles of species k entering and leaving the reactor with $0 \le X_k \le 1$. The extent (number of moles extent) of reaction i, given by

$$\xi_i = \frac{\Delta n_{ij}}{\nu_{ij}}, \quad j = 1, \ldots, C. \tag{8.3}$$

The molar flow rates of the components in the reactor product, $n_{j,out}$, are computed from the component molar flow rates in the reactor feed, $n_{j,in}$, by a component material-balance equation that is consistent with the reaction stoichiometry. If a specification of the fractional conversion of the key component, k, is made with Eq. (8.2):

$$n_{j,out} = n_{j,in} - n_{k,in} X_k \left(\frac{\nu_j}{\nu_k} \right), \; j = 1, \ldots, C \tag{8.4}$$

If the extent of the reaction is specified:

$$n_{j,out} = n_{j,in} + \xi \nu_j, \quad j = 1, \ldots, C \tag{8.5}$$

For example, for the conversion of CO and H_2 to CH_3OH, assuming an initial feed of 100 kmol/hr CO and 600 kmol/hr H_2 and 70% conversion of CO (the key component), using Eq. (8.4), the molar flow rates of the three components in the reactor effluent are:

$$n_{H_2,out} = 600 - 100(0.7)(-2 \,/\, -1) = 460 \text{ kmol/hr}$$
$$n_{CO,out} = 100 - 100(0.7)(-1 \,/\, -1) = 30 \text{ kmol/hr}$$
$$n_{CH_3OH,out} = 0 - 100(0.7)(1 \,/\, -1) = 70 \text{ kmol/hr}$$

The mole fraction of methanol in the reactor effluent is $y_{CH_3OH} = 100 \times [70/(460 + 30 + 70)] = 12.5$ mol%. If, instead, the extent of reaction is specified as 70 kmol/hr, then Eq. (8.5) gives the same results.

For multiple reactions, the reactions must be specified as series or parallel. The former is equivalent to having reactors in series with the feed to each reactor, except the first, being the product from the previous reactor. Each reaction can have a different key reactant. For parallel reactions, it is preferable to specify the extent of reaction for each reaction, which results in:

$$n_{j,out} = n_{j,in} + \sum_{i=1}^{R} \xi_i \nu_{i,j}, \quad j = 1, \ldots, C \tag{8.6}$$

Chemical Equilibrium

A chemical reaction can be written as a general stoichiometric equation in terms of reactants A, B, etc. and products R, S, and so on,

$$aA + bB + \cdots = rR + sS + \cdots \tag{8.7}$$

In writing this equation, it is very important that, unless otherwise stated, each reactant and product is understood to be the pure component in a separate and designated phase state: gas, liquid, or solid. A reaction is characterized by two important thermodynamic quantities, namely the heat of reaction and the Gibbs (free) energy of reaction. Furthermore, these two quantities are functions of temperature and pressure. Thermodynamic data are widely available in simulators and elsewhere for more than a thousand chemicals, for the calculation of these two quantities under standard state conditions, e.g. at a reference temperature of 25°C and 1 bar with all components in a designated phase state (e.g., as an ideal gas). The effect of temperature on the heat of reaction depends on the heat capacities of the reactants and products and the effect of temperature on those heat capacities. For many reactions, the effect of temperature on the heat of reaction is relatively small. For example, the reaction of gaseous CO and H_2 to form gaseous methanol,

$$CO + 2H_2 \rightleftharpoons CH_3OH, \tag{8.8}$$

has a standard heat of reaction, ΔH^{o}_{rxn}, at 25°C of –90,400 kJ/kmol of methanol whereas at 800°C, the heat of reaction, ΔH^{o}_{rxn}, is –103,800 kJ/kmol, a relatively small change for such a large change in temperature. At both temperatures, the heat of reaction is exothermic. By contrast, the effect of temperature on the Gibbs energy of reaction can be very large. For example, for the same methanol formation reaction, the standard Gibbs energy of reaction, ΔG^{o}_{rxn}, is –25,200 kJ/kmol at 25°C. Already, at 500°C, the Gibbs energy of reaction, ΔG^{o}_{rxn}, has undergone a drastic change to +88,000 kJ/kmol.

Such a drastic change in the Gibbs energy of reaction with temperature also results in a drastic change to the degree of conversion of a reactant to a product at chemical equilibrium. For example, by chemical thermodynamic equilibrium calculations reviewed next in this chapter, if the feed is stoichiometric (2 moles of H_2 per mole of CO) and the pressure is 1 bar, the equilibrium conversion of CO to methanol at 25°C is close to 100% ($X = 1$). However, at 500°C, the conversion is close to zero ($X = 0$). This is in agreement with Le Chatelier's principle, which when applied to the effect of temperature on the chemical equilibrium for an exothermic reaction gives the result that conversion decreases with increasing temperature. Le Chatelier's principle, when applied to the methanol reaction, also shows that the conversion at a given temperature can be increased by using an excess of one of the reactants for either a gas- or liquid-phase reaction and/or, in the case of gas-phase reaction by an increase in total pressure.

Many reactions of industrial importance are limited by chemical equilibrium where conversion of the limiting reactant is less than 100% when the rate of the backward reaction becomes equal to the rate of the forward reaction. For a specified feed composition and final temperature and pressure, the product composition at chemical equilibrium can be computed by either of two methods: (1) chemical equilibrium constants computed from the Gibbs energy of reaction combined with material balance equations for a set of independent reactions or (2) the minimization of the Gibbs energy of the reacting system. The first method is applicable when the stoichiometry can be specified for all reactions being considered. The second method requires only a list of the possible products.

For the first method, a chemical equilibrium constant, K, is computed for each independent stoichiometric reaction in the set, using the equation,

$$K = \frac{a_R^r a_S^s \cdots}{a_A^a a_B^b \cdots} = \exp\left(-\frac{\Delta G^{o}_{rxn}}{RT}\right), \tag{8.9}$$

where a_i^j is the activity of component i raised to the power j.

For a gas mixture, the activity is given by:

$$a_i = \overline{\phi}_i y_i P = \overline{\phi}_i P_i, \tag{8.10}$$

where $\overline{\phi}_i$ is the fugacity coefficient of component i in the gas mixture, equal to 1.0 for an ideal gas mixture, and P_i is the partial pressure. In general, $\overline{\phi}_i$ is a function of temperature, pressure, and composition. At low to moderate pressures, $\overline{\phi}_i = 1.0$, so that the activity is equal to the partial pressure in bar. It is common to replace the activity in Eq.(8.9) by its definition in Eq. (8.10) to give:

$$K = \frac{y_R^r y_S^s \cdots}{y_A^a y_B^b \cdots}\left(\frac{\overline{\phi}_R^r \overline{\phi}_S^s \cdots}{\overline{\phi}_A^a \overline{\phi}_B^b \cdots}\right) P^{r+s+\cdots-a-b-\cdots} = \frac{y_R^r y_S^s \cdots}{y_A^a y_B^b \cdots} K_{\overline{\phi}} P^{r+s+\cdots-a-b-\cdots} = \frac{P_R^r P_S^s \cdots}{P_A^a P_B^b \cdots} K_{\overline{\phi}} \tag{8.11}$$

where $K_{\overline{\phi}} = 1.0$ for low to moderate pressures.

For a liquid mixture, the activity is given by:

$$a_i = x_i \gamma_i \exp\left[\frac{\overline{V}_i}{RT}(P - P^{vap})\right] \tag{8.12}$$

where γ_i is the activity coefficient of component i in the liquid mixture, and is equal to 1.0 for an ideal liquid mixture, $\overline{V}_i$ is the partial molar volume of component i, and P^{vap} is the vapor pressure of component i. The pressures are in bar. In general, γ_i is mainly a function of temperature and composition. For ideal liquid mixtures at low to moderate pressures, $\gamma_i = 1.0$, so that the

activity is equal to the mole fraction. It is common to replace the activity in Eq. (8.9) for K with Eq. (8.12), after replacing y with x, to give:

$$K = \frac{y_R^r y_S^s \cdots}{y_A^a y_B^b \cdots} \left(\frac{\gamma_R^r \gamma_S^s \cdots}{\gamma_A^a \gamma_B^b \cdots} \right) = \frac{y_R^r y_S^s \cdots}{y_A^a y_B^b \cdots} K_\gamma \tag{8.13}$$

where $K_\gamma = 1.0$ for ideal liquid solutions at low to moderate pressures. Most textbooks on chemical thermodynamics present charts of $\log_{10} K$ as a function of temperature for many chemical reactions. The van't Hoff equation relates K to temperature by:

$$\left(\frac{d \ln K}{dT} \right)_P = \frac{\Delta H^\circ_{\text{rxn}}}{RT^2} \tag{8.14}$$

If the heat of reaction is assumed independent of temperature over a particular range of temperature, integration and conversion to $\log_{10}$ form gives the approximate correlating equation:

$$\log_{10} K = A + B/T \tag{8.15}$$

where T is the absolute temperature. Many chemical equilibrium curves are represented with reasonable accuracy by this equation. For example, for the gas-phase reaction of CO and H_2 to form methanol, over a temperature range of 273 to 773 K,

$$\log_{10} K = -12.275 + 4938/T \tag{8.16}$$

Typically, the methanol synthesis reaction is catalyzed by copper-zinc oxide at a pressure of 100 bar and a temperature of 300°C. A large excess of hydrogen is used to help absorb the relatively high heat of reaction. At these conditions, $K = 0.0002202$ and $K_{\overline{\phi}} = 0.61$. Therefore,

$$\frac{(y_{CH_3OH})}{(y_{CO})(y_{H_2})^2} = \frac{K}{K_\phi} P^2 = \frac{0.0002202}{0.61} (100)^2 = 3.61 \tag{8.17}$$

If X is the equilibrium fractional conversion of the limiting reactant, CO, then using the same initial feed composition as before and the stoichiometry for the reaction, the equilibrium mole fractions are:

$$y_{CH_3OH} = \frac{100X}{700 - 200X}$$
$$y_{CO} = \frac{100 - 100X}{700 - 200X}$$
$$y_{H_2} = \frac{600 - 200X}{700 - 200X}$$

Combining the above four equations to give a nonlinear equation in X and solving gives $X = 0.0709$.

The second method for computing chemical equilibrium is to apply the criterion that the total Gibbs energy, G, is a minimum at constant temperature and pressure. Alternatively, one could use the entropy, S, as a maximum or the Helmholtz energy, A, as a minimum, but the Gibbs energy is most widely applied. Two advantages of this second method are (1) the avoidance of having to formulate stoichiometric equations (only the possible products need to be specified) and (2) the ease of formulation for multiple phases and simultaneous phase equilibrium. For a single phase, the total Gibbs energy at a specified T and P is given by:

$$G = \sum_{i=1}^{C} N_i \overline{G}_i \tag{8.18}$$

where N_i is the mole number of component i and $\overline{G}_i$ is the partial molar Gibbs energy of component i in the equilibrium mixture. The components are those in the feed plus those that may be produced by chemical reactions. The Gibbs energy is minimized with respect to the values of the N_i's, which are constrained by atom balances. The method is readily extended to multiple phases. This free energy method is not suitable for hand calculations, but a numerical method of calculation that is easy to use is widely implemented in process simulators.

It would seem that for simplicity or usefulness, the second method would be preferred because when using this model, an independent set of chemical reactions need not be specified. Hence, the designer is not required to identify the reactions that take place. However, since most reactors are designed to emphasize desired reactions and curtail or exclude undesired reactions, the chemical reactions that take place in the reactor are usually known by the time the reactor is to be designed. Thus, the first model may be preferred, with the second model being useful for preliminary exploration of the thermodynamic possibilities. To make the second model more useful, restrictions should be placed on certain improbable reactions. If this is not done, the second method can produce results that are incorrect because they implicitly include reactions that may not be kinetically feasible.

For instructions on the use of equilibrium and Gibbs reactor models in the process simulators, see the multimedia modules that accompany this book.

Kinetics

Fractional conversion and equilibrium reactor models are useful in the early stages of process design when conducting material and energy balance studies. However, eventually reactor systems must be configured and sized. This requires knowledge of reaction kinetics, which is obtained from published data in the literature or by conducting laboratory experiments. For homogeneous noncatalytic reactions, power-law expressions are commonly used to fit laboratory kinetic data. These expressions are not always based on the stoichiometric equation because several elementary reaction steps may be involved, the sum of which is the stoichiometric equation, but one of which may control the overall reaction rate. Elementary steps rarely involve more than two molecules. The general power-law kinetic equation is:

$$-r_j = -\frac{dC_j}{dt} = k \prod_{i=1}^{C} C_i^{\alpha_i} \tag{8.19}$$

where $-r_j$ is the rate of disappearance of component j (in mol/time-volume), C_i is the concentration of component i (in mol/volume), t is time, k is the reaction rate coefficient, α_i is the order of reaction with respect to component i, and C is the number of components.

For gas-phase reactions, the partial pressure, P_i, is sometimes used in place of the concentration, C_i, in the kinetic equation. However, it should be noted that, in order for the kinetic equation to satisfy conditions at equilibrium, the proper composition variable should be activity, as in Eq. (8.9), rather than concentration

or partial pressure. The reaction rate coefficient is a function of temperature, usually given by the empirical Arrhenius equation:

$$k = k_o \exp(-E/RT) \tag{8.20}$$

where k_o is the pre-exponential factor and E is the activation energy.

For reactions that are catalyzed by solid porous catalyst particles, the sequence of elementary steps may include adsorption on the catalyst surface of one or more reactants and/or desorption of one or more products. In that case, a Langmuir-Hinshelwood (LH) kinetic equation is often found to fit the experimental kinetic data more accurately than the power-law expression of Eq. (8.19). The LH formulation is characterized by a denominator term that includes concentrations of certain reactants and/or products that are strongly adsorbed. The LH equation may also include a prefix, η, called an overall effectiveness factor that accounts for mass and heat transfer resistances both external and internal to the catalyst particles, such that compositions in the bulk phase may not be the same as the compositions at the catalyst surface where the reactions actually occur. As an example, laboratory kinetic data for the air-oxidation of SO_2 to SO_3 are fitted well by the following LH equation:

$$-r_{SO_2} = \frac{\eta k \left(P_{SO_2} P_{O_2} - \frac{P_{SO_3}^2}{K^2 P_{SO_2}} \right)}{[1 + K_1 P_{SO_2}^{1/2} + K_2 P_{SO_3}^{1/2}]} \tag{8.21}$$

where K is the chemical equilibrium constant, K_1 and K_2 are adsorption equilibrium constants, k is a rate constant, and partial pressures are those in the bulk phase.

Ideal Kinetic Reaction Models—CSTRs and PFRs

CSTR

The simplest kinetic reactor model is the CSTR (continuous stirred-tank reactor) in which the contents are assumed to be perfectly mixed. Thus, the composition and the temperature are uniform throughout the reactor volume and equal to the composition and temperature of the reactor effluent. However, the fluid elements do not all have the same residence time in the reactor. Rather, there is a residence-time distribution. In the early design stages, it is common to assume perfect mixing, which can be approached in well-agitated commercial reactors. But, for more accurate concentration and conversion results, computational fluid dynamics (CFD) software is increasingly being used by design engineers. See, for example, the usage of COMSOL in Section 15.6. Accordingly, a possible complication that must be considered is the existence of multiple solutions. In that case, it is necessary to determine the optimal of those solutions that are operationally stable. This is illustrated in the following example.

EXAMPLE 8.1 ***Kinetics for Hydrolysis of Propylene Oxide***

Propylene glycol (PG) is produced from propylene oxide (PO) by liquid-phase hydrolysis with excess water under adiabatic and near-ambient conditions in the presence of a small amount of soluble sulfuric acid as a homogeneous catalyst:

$$C_3H_6O + H_2O \rightarrow C_3H_8O_2 \tag{8.22}$$

Because the exothermic heat of reaction is appreciable, excess water is used to control the temperature. Because PO is not completely soluble in water, methanol is added to the feed to maintain a single liquid phase, which enters the reactor at 23.9°C with the following flows:

Propylene oxide:	18.712 kmol/hr
Water, to be determined, within the range	160 to 500 kmol/hr
Methanol:	32.73 kmol/hr

It is proposed to consider the use of an existing agitated reactor vessel, which can be operated adiabatically at 3 bar (to suppress vaporization) with a liquid volume of 1.1356 m^3. The reaction occurs in a sequence of elementary steps, with the controlling step involving two molecules of PO. The power-law kinetic equation is:

$$-r_{PO} = 9.15 \times 10^{22} \exp(-1.556 \times 10^5/RT) C_{PO}^2 \tag{8.23}$$

where C_{PO} is in kmol/m^3, $R = 8.314$ kJ/kmol-K, and T is in K. Carry out a sensitivity analysis to investigate the effect of the water feed rate on operating temperature and the PO conversion.

SOLUTION

As shown on the multimedia modules that accompany this book (following the links: HYSYS → Chemical Reactors → Setting Up Reactors → CSTR or ASPEN → Chemical Reactors → Kinetic Reactors → CSTRs → RCSTR), analysis of this process shows that there is the possibility of multiple steady states; for example, at a water flow rate of 400 kmol/hr, the following results are obtained: (1) conversion of 83% with an effluent temperature of 62°C, (2) conversion of 45% with an effluent temperature of 44°C, and (3) conversion of 3% with an effluent temperature of 25°C. The intermediate 45% conversion case is found to be unstable, whereas the other two cases are stable with the higher-conversion case being preferred.

PFR

More complex is the plug-flow tubular reactor (PFR or PFTR), in which the composition of the flowing fluid is assumed to change down the length of the reactor as a plug with no composition or temperature gradients in the radial direction. Furthermore, possible diffusion and heat transfer rates are neglected in the axial direction (referred to as axial dispersion). Thus, the PFR is completely unmixed. Unlike the CSTR model, all fluid elements in the PFR model have the same residence time in the reactor. If the reactor operates under adiabatic or nonisothermal conditions, the temperature of the flowing fluid changes down the length of the reactor. In most cases, for a given conversion, the residence time from the PFR model will be less than for the CSTR model.

Both ASPEN PLUS, UniSim®Design and Aspen HYSYS provide rigorous one-dimensional, plug-flow models that neglect axial dispersion. Thus, there are no radial gradients of temperature, composition, or pressure, and mass transfer by diffusion is assumed not to occur in the axial direction. Operation of the reactor can be adiabatic, isothermal, or nonadiabatic, nonisothermal. For the latter, heat transfer to or from the reacting mixture

occurs along the length of the reactor. Consider the case of an adiabatic operation with one chemical reaction. A mole balance for the limiting reactant, A, can be written as:

$$F_{A0}\frac{dX}{dV} = -r_A\{X, T\} \tag{8.24}$$

where F_{A0} is the molar flow rate of A entering the reactor, X is the fractional conversion of A, V is the reactor volume, and r_A is the rate of reaction of A written as a function of fractional conversion and temperature. Because the process simulators compute enthalpies referred to the elements (rather than to the components) with values for the standard enthalpy of formation built into the component properties data bank, the heat of reaction is handled automatically, and the energy balance for adiabatic operation becomes simply:

$$H\{X, T\} = H\{X = 0, T = T_0\} \tag{8.25}$$

where H is the enthalpy flow rate of the reacting mixture in energy/unit time, and T_0 is the entering temperature. Eqs. (8.24) and (8.25) are solved by numerical integration. The following example illustrates the use the simulator models for a PFR for sizing a plug-flow adiabatic reactor for the noncatalytic hydrodealkylation of toluene.

EXAMPLE 8.2 ***Toluene Hydrodealkylation Reactor***

A hydrodealkylation reactor feed at 1,200°F and 494 psia consists of:

Component	lbmol/hr
Hydrogen	2,049.1
Methane	3,020.8
Benzene	39.8
Toluene	362.0
Biphenyl	4.2
Total	5,475.9

These molar flow rates account for the small extent of reaction for the secondary reaction of benzene to biphenyl (2%) and ignore the negligible rate of the reverse reaction, leaving the main reaction to be considered:

$$H_2 + C_7H_8 \rightarrow CH_4 + C_6H_6, \tag{8.26}$$

Laboratory studies have shown that in the absence of a catalyst, this is a free-radical chain reaction that proceeds in three elementary steps:

$$\begin{aligned} H_2 &\rightleftharpoons 2H\cdot \\ H\cdot + C_6H_5CH_3 &\rightarrow C_6H_6 + CH_3\cdot \\ CH_3\cdot + H_2 &\rightarrow CH_4 + H\cdot \end{aligned} \tag{8.27}$$

Equilibrium is established rapidly in the first step to provide hydrogen-free-radicals. The sum of the next two steps is the stoichiometric equation. Step 2 is the slow or controlling step. Thus, the overall reaction rate is not proportional to the product of the hydrogen and toluene concentrations as given by the law of mass action when applied to the stoichiometric reaction. Instead, the overall reaction rate is proportional to the product of the hydrogen-free-radical and toluene concentrations as given in the second elementary step. For the above hydrodealkylation chain reaction, the power-law kinetic equation is derived as follows. Because the first elementary step is at equilibrium:

$$K_1 = \frac{C_{H\cdot}^2}{C_{H_2}} \tag{8.28}$$

Rearrangement gives

$$C_{H\cdot} = K_1^{1/2} C_{H_2}^{1/2} \tag{8.29}$$

The power-law kinetic equation for the second elementary step, which controls the overall reaction rate, is:

$$-\frac{dC_{\text{toluene}}}{dt} = k_2 C_{H\cdot} C_{\text{toluene}} \tag{8.30}$$

Combining the last two equations,

$$-\frac{dC_{\text{toluene}}}{dt} = k_2 K_1^{1/2} C_{H_2}^{1/2} C_{\text{toluene}} \tag{8.31}$$

This rate expression correlates well the laboratory kinetic data for temperatures in the range of 500–900°C and pressures in the range of 1–250 atm with $k_2K_1^{1/2} = 6.3 \times 10^{10} \exp(-52{,}000/RT)$ with concentrations in kmol/m^3, time in sec, T in K, and $R = 1.987$ cal/mol-K. Use the PFR model in a process simulator to determine the length of a cylindrical plug-flow reactor with a length-to-diameter ratio of six that yields a toluene conversion of 75%. Use the Peng-Robinson equation of state to estimate the thermophysical properties for this vapor-phase reaction.

SOLUTION

To see how an adiabatic PFR is designed to provide a 75% conversion of toluene, see the multimedia modules that accompany this book. Follow the link HYSYS → Chemical Reactors → Setting Up Reactors → PFR for a solution obtained with UniSim® Design/ASPEN HYSYS and ASPEN → Chemical Reactors → Kinetic Reactors → PFTRs → RPLUG for a solution with ASPEN PLUS. Note that the results provided by these simulators are almost identical; the UniSim®Design/ASPEN HYSYS result calls for a reactor volume of 3,690 ft^3($D = 9.2$ ft, $L = 55.3$ ft) whereas ASPEN PLUS gives a volume of 3,774 ft^3($D = 9.3$ ft, $L = 55.8$ ft). The main reason for the slight discrepancy is due to the neglected pressure drop in the UniSim®Design/ASPEN HYSYS simulation and the assumption of a pressure drop of 5 psia in the ASPEN PLUS calculation.

At high gas flow rates (high Reynolds numbers) in a long, straight, tubular reactor, the PFR model is generally valid because turbulent flow is usually achieved. without appreciable axial mass and heat transfer. For liquid-phase reactions, optimal Reynolds numbers may be below 2,100 such that laminar flow persists and the PFR model is invalid. An ideal laminar flow reactor (LFR) model assumes isothermal flow with a parabolic velocity profile. Because of the resulting residence-time distribution for the fluid elements in the laminar streamlines, the volume of an LFR must be greater than that of a PFR for a given conversion of the limiting reactant.

Figure 8.1 shows the ratio of the length of an LFR to a PFR (same as the volume ratio or average residence-time ratio) as a function of the ratio of exit concentration to entering concentration of the limiting reactant (same as 1 minus the fractional conversion of the limiting reactant) for zero-, first-, and second-order irreversible reactions. All three curves assume negligible radial

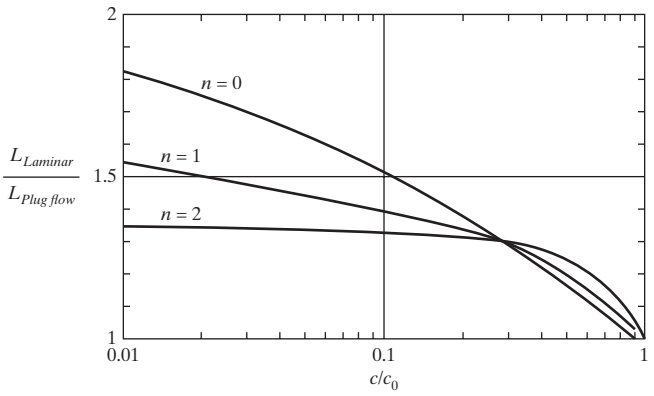

Figure 8.1 Effect of reaction order on the ratio of tubular reactor length for isothermal laminar flow with no radial diffusion to plug flow. (*Source:* Adapted from Levenspiel (1999). Used with permission).

and axial diffusion. As the conversion increases (decreasing concentration ratio), the length ratio increases. At a conversion of 90% an LFR must be 38% longer than a PFR for a first-order reaction. Although not shown on the plot, the length ratio for a zero-order reaction becomes 2 at 100% conversion. In a different approach, Schmidt (1998) shows that for a given reactor volume, the loss in conversion in an LFR compared to a PFR is only 12% at the most for first- and second-order reactions. But for a zero-order reaction, the limiting loss is 25%. If radial diffusion is taken into account, the loss is even less. Simulation programs have both CSTR and PFR models, but not laminar flow models. As discussed in Chapter 15, CFD (computational fluid dynamics) programs, such as COMSOL, can be used to design nonideal LFRs and even examine tubular reactors that are curved rather than straight. For example, Slominski et al. (2011) used CFD to design helical and lemniscate tubular reactors, operating in the laminar flow region, that more closely approximated plug flow.

For liquid-phase reactions, a single PFR or CSTR reactor is often used. For a single reaction at isothermal conditions, the volume of a PFR is smaller than that of a CSTR for the same conversion and temperature. However, for (1) autocatalytic reactions, where the reaction rate depends on the concentration of a product, or (2) autothermal reactions in an adiabatic reactor, where the feed is cold but the reaction is highly exothermic, the volume of a CSTR can be smaller than a PFR, such that axial dispersion in a tubular reactor may actually be beneficial. In general, a CSTR model is not used for a gas-phase reaction because of the difficulty in obtaining perfect mixing in the gas.

For noncatalytic homogeneous reactions, a tubular reactor is widely used because it can handle liquid or vapor feeds, with or without phase change in the reactor. The PFR model is usually adequate for an adiabatic tubular reactor if the flow is turbulent and if it can be assumed that when a phase change occurs in the reactor, the reaction takes place predominantly in one of the two phases. The nonadiabatic, nonisothermal case can be computed by one of the following three models: (1) a specified axial temperature profile with negligible radial dispersion, (2) consideration of heat transfer to or from some specified heat source or sink, with a corresponding overall heat transfer coefficient and negligible radial dispersion, or (3) a detailed heat-transfer model that takes into account radial dispersion. Either a fractional conversion of a limiting reactant or a reactor volume is specified. For either of the first two models, the calculations require the solution of ordinary differential equations (ODEs). For the third model, partial differential equations (PDEs) must be solved.

For fixed-bed catalytic reactors, a PFR model with a pseudohomogeneous kinetic equation is usually adequate for adiabatic operation and is referred to as a 1D (one-dimensional) model. It involves the solution of ODEs. However, if the reactor is nonadiabatic with heat transfer to or from the wall, the PFR model is not usually adequate and a 2D (two-dimensional) model is required, involving the solution of PDES that account for variations in temperature and composition in both the axial and radial directions. Simulators do not include 2D models, but they can be generated by the user and inserted into the simulator. Models for fluidized-bed catalytic reactors are the most complex and cannot be adequately modeled with either the CSTR or PFR models. Because some of the gas passing through the fluidized bed can bypass the suspended catalyst, the conversion in a fluidized bed can be less than that predicted by the CSTR model. Several models for fluidized-bed reactors are presented in Chapter 20 of *Chemical Reaction Engineering* by O. Levenspiel (1999).

The multimedia modules that accompany this book provide complete details of the modeling of reactions and reactors using the process simulators. For ASPEN PLUS, follow the link ASPEN → Chemical Reactors → Overview. For HYSYS, see HYSYS → Chemical Reactors → Overview.

8.3 REACTOR NETWORK DESIGN USING THE ATTAINABLE REGION

An optimal reactor section of a process may be a network of chemical reactors rather than a single reactor, particularly when the use of CSTRs are being considered. This section describes the use of the *attainable region* (AR), which defines the achievable compositions that may be obtained from a network of chemical reactors. This is analogous to the topic of feasible product compositions in distillation that is presented in Chapter 9. The idea of representing the attainable region in composition space originates from Horn (1964), with more recent developments and extensions by Glasser and co-workers (Glasser et al., 1987; Hildebrandt et al., 1990).

Figure 8.2 is a plot of effluent concentration of A and B for the attainable region for van de Vusse kinetics (van de Vusse, 1964) based on the reactions:

$$\mathrm{A} \underset{k_2}{\overset{k_1}{\rightleftharpoons}} \mathrm{B} \xrightarrow{k_3} \mathrm{C}$$

$$2\mathrm{A} \xrightarrow{k_4} \mathrm{D} \tag{8.32}$$

Reactions 1, 2, and 3 in Eq. (8.32) are first order in A and B, respectively, whereas reaction 4 is second order in A. The rate constants at a particular temperature are: $k_1 = 0.01\ \mathrm{s}^{-1}$, $k_2 = 5\ \mathrm{s}^{-1}$, $k_3 = 10\ \mathrm{s}^{-1}$, and $k_4 = 100\ \mathrm{m}^3/\mathrm{kmol} \cdot \mathrm{s}^{-1}$. The boundary of the attainable region, shown in Figure 8.2, is composed of arcs, each of which results from the application of a distinct reactor type as described next.

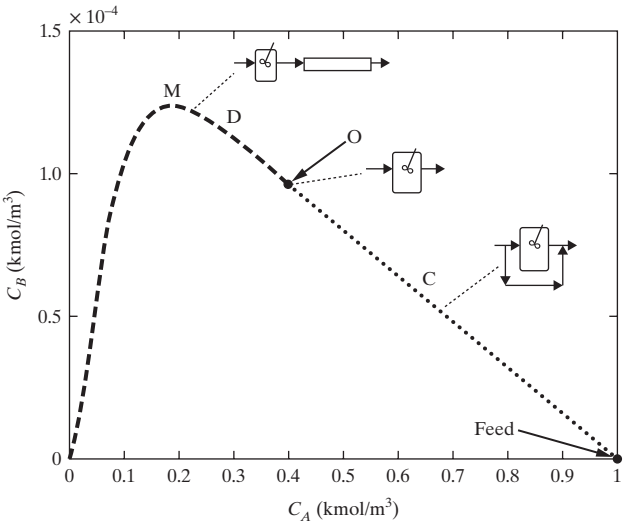

Figure 8.2 Attainable region for the van de Vusse reaction.

For the case of van de Vusse kinetics with a feed of 1 kmol/m^3 of A, Figure 8.2 indicates that the boundary on the AR is composed of an arc representing a CSTR with bypass (curve C), a CSTR (point O), and a CSTR followed by a PFR (dashed-curve D). Within the region bounded by the three arcs and the horizontal base line ($C_B = 0$), product compositions can be achieved with some combination of these reactor configurations. The appropriate reactor configuration along the boundary of the attainable region depends on the desired effluent concentration of A. Note that all effluent concentrations of B are very small. When $1 > C_A > 0.38$ kmol/m^3, a CSTR with bypass (curve C) provides the maximum concentration of B whereas when $C_A < 0.38$ kmol/m^3, this is achieved using a CSTR (point O), followed by a PFR (curve D). Note that the maximum achievable concentration, $C_B = 1.25 \times 10^{-4}$ kmol/m^3, occurs at point M and is obtained using the latter design (at point M along curve D). Evidently, the attainable region provides helpful assistance in the design of optimal reactor networks. A procedure for the construction of attainable regions is discussed next.

Construction of the Attainable Region

A systematic method for the construction of the attainable region using CSTRs and PFRs, with or without mixing and bypass, for a system of chemical reactions, as presented by Hildebrandt and Biegler (1995), is demonstrated for van de Vusse kinetics:

Step 1: *Begin by constructing a trajectory for a PFR from the feed point continuing to the complete conversion of A or chemical equilibrium.* In this case, the PFR trajectory is computed by solving simultaneously the kinetic equations for A and B:

$$\frac{dC_A}{d\tau} = -k_1 C_A + k_2 C_B - k_4 C_A^2 \qquad (8.33)$$

$$\frac{dC_B}{d\tau} = k_1 C_A - k_2 C_B - k_3 C_B \qquad (8.34)$$

where τ is the PFR residence time. Note that kinetic equations for C and D are not required for the construction of the attainable region in 2D space because their compositions do not appear in Eqs. (8.33) and (8.34). The trajectory in C_A–C_B space is plotted in Figure 8.3a as curve ABC. In this example, component A is completely converted.

Step 2: *When the PFR trajectory bounds a convex region, this constitutes a candidate attainable region. A convex region is one in which all straight lines drawn from one point on the boundary to any other point on the boundary lie wholly within the region or on the boundary. If not, the region is nonconvex. When none of the rate vectors* $[dC_A/d\tau,\ dC_B/d\tau]^T$ *at concentrations on the edge of the candidate AR point out of it, the current limits are the boundary of the AR and the procedure terminates.* In this example, as seen in Figure 8.3a, the PFR trajectory is not convex from A to B, so proceed to the next step to determine whether the attainable region can be extended beyond the curve ABC.

Step 3: *The PFR trajectory is expanded by linear arcs representing mixing between the PFR effluent and the feed stream, extending the candidate attainable region. Note that a linear arc connecting two points on a composition trajectory is expressed by the equation:*

$$\underline{c}^* = \alpha \underline{c}_1 + (1 - \alpha)\underline{c}_2 \qquad (8.35)$$

where $\underline{c}_1$ *and* $\underline{c}_2$ *are the compositions of two streams in the composition space,* $\underline{c}^*$ *is the composition of the mixed stream, and* α *is the fraction of the stream with composition* $\underline{c}_1$ *in the mixed stream. The linear arcs are then tested to ensure that no rate vectors positioned on them point out of the AR. If there are such vectors, proceed to the next step, or return to step 2.* As shown in Figure 8.3a, a linear arc, ADB, is added, extending the attainable region to ADBC. Since for this example, some rate vectors computed along this arc are found to point out of the extended AR, proceed to the next step.

Step 4: *Since there are vectors pointing out of the convex hull formed by the union between the PFR trajectory and linear mixing arcs, it is possible that a CSTR trajectory enlarges the attainable region. After placing the CSTR trajectory that extends the AR the most, additional linear arcs that represent the mixing of streams are placed to ensure that the AR remains convex.* The CSTR trajectory is computed by solving the CSTR form of the kinetic equations for A and B given by Eqs. (8.33) and (8.34) as a function of the residence time, τ:

$$C_{A0} - C_A = \tau(k_1 C_A - k_2 C_B + k_4 C_A^2) \qquad (8.36)$$

$$C_B = \tau(k_1 C_A - k_2 C_B - k_s C_B) \qquad (8.37)$$

For this example, the CSTR trajectory that extends the AR most is that computed from the feed point at C_{AO}, the largest concentration of A. This is indicated as curve AEF in Figure 8.3b, which passes through point B. Since the union of the previous AR and the CSTR trajectory is not convex, a linear arc, AGO, is augmented as shown in Figure 8.3c. This arc represents a CSTR with a bypass stream.

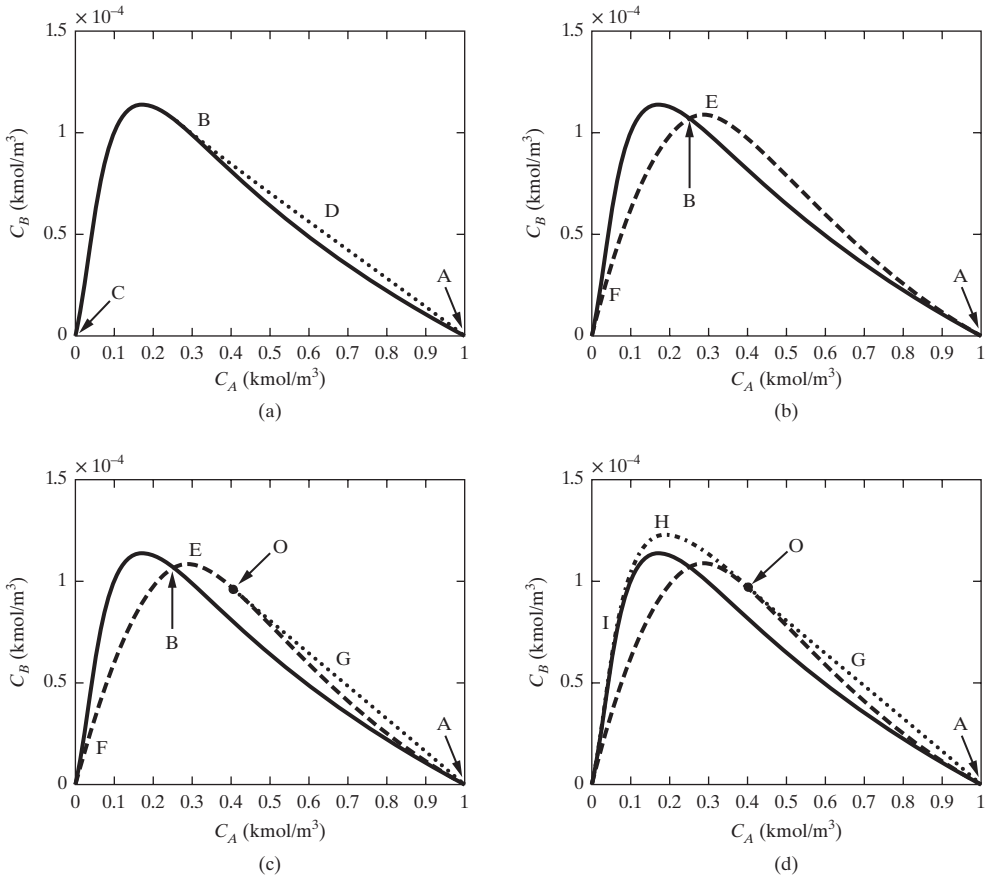

Figure 8.3 Construction of the attainable region for the van de Vusse reaction: (a) PFR trajectory from $\underline{C}(0) = [1,\ 0]^{\mathrm{T}}$ (solid line) with mixing line (dotted line); (b) CSTR trajectory from $\underline{C}(0) = [1,\ 0]^{\mathrm{T}}$ (dashed line); (c) addition of bypass to CSTR (dotted line); (d) addition of PFR in series with CSTR (dot-dashed line).

Step 5: *A PFR trajectory is drawn from the position where the mixing line meets the CSTR trajectory. If this PFR trajectory is convex, it augments the previous AR to form an expanded candidate AR. Then return to Step 2. Otherwise, repeat the procedure from Step 3.* As shown in Figure 8.3d, the PFR trajectory, OHI, leads to a convex attainable region. The boundaries of the region are (a) the linear arc, AGO, which represents a CSTR with bypass stream; (b) the point O, which represents a CSTR; and the arc OHI, which represents a CSTR followed by a PFR in series. It is noted that the maximum composition of B is obtained at point H, using a CSTR followed by a PFR.

Clearly, the optimal reactor design would be that which minimizes the annual costs computed to account for the capital and operating costs, not simply the design that maximizes the yield or selectivity. Nonetheless, the maximum attainable region identifies the entire space of feasible concentrations. The following example shows how the attainable region is used to select the most appropriate reactor network to maximize the yield of a desired product for the case where a number of competing reactions occur.

EXAMPLE 8.3 *Reaction Network Synthesis for the Manufacture of Maleic Anhydride*

Maleic anhydride is manufactured by the oxidation of benzene with excess air over vanadium pentoxide catalyst (Westerlink and Westerterp, 1988). The following reactions occur:

$$\text{Reaction 1:}\quad C_6H_6 + \tfrac{9}{2}O_2 \rightarrow C_4H_2O_3 + 2CO_2 + 2H_2O \tag{8.38}$$

$$\text{Reaction 2:}\quad C_4H_2O_3 + 3O_2 \rightarrow 4CO_2 + H_2O \tag{8.39}$$

$$\text{Reaction 3:}\quad C_6H_6 + \tfrac{15}{2}O_2 \rightarrow 6CO_2 + 3H_2O \tag{8.40}$$

Since air is supplied in excess, the reaction kinetics are approximated as first-order rate laws:

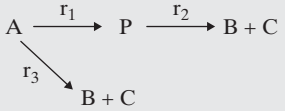

$$r_1 = k_1 C_A, r_2 = k_2 C_P \text{ and } r_3 = k_3 C_A \tag{8.41}$$

where A is benzene, P is maleic anhydride (the desired product), and B and C are the undesired byproducts (H_2O and CO_2). The kinetic rate

coefficients for Eq. (8.41) are (in m^3/kg cat.·s):

$$\left.\begin{aligned} k_1 &= 4280 \exp\left[-12{,}660/T\,(\mathrm{K})\right] \\ k_2 &= 70{,}100 \exp[-15{,}000/T(\mathrm{K})] \\ k_3 &= 26 \exp[-10{,}800/T(\mathrm{K})] \end{aligned}\right\} \quad (8.42)$$

Given that the available feed stream contains benzene at a concentration of 10 mol/m^3 with a volumetric flow rate, υ_0, of 0.0025 m^3/s (the feed is largely air), a network of isothermal reactors is proposed to maximize the yield of maleic anhydride.

The first decision that needs to be made is the selection of the appropriate reaction temperature. Following the discussion in Chapter 6, Figure 8.4 shows the effect of temperature on the three kinetic rate coefficients and indicates that in the range $366 < T < 850$ K, the kinetic rate coefficient of the desired reaction to MA is larger than those of the competing reactions, with the biggest difference in favor of the desired reaction being in the center of this temperature range.

Since all of the reaction rate expressions involve only benzene and maleic anhydride, this allows the system to be expressed in a two-dimensional composition space. For this system, the attainable region is straightforward to construct. This begins by tracing the composition space trajectory for a packed bed reactor (PBR), modeled as a PFR, which depends on the solution of the molar balances:

$$\upsilon_0 \frac{dC_A}{dW} = -k_1 C_A - k_3 C_A, C_A(0) = C_{A0} = 10 \text{ mol/m}^3 \quad (8.43)$$

$$\upsilon_0 \frac{dC_P}{dW} = k_1 C_A - k_2 C_P, C_P(0) = 0 \text{ mol/m}^3 \quad (8.44)$$

where W is the kg of catalyst. In Eqs. (8.43) and (8.44), the temperature-dependent kinetic rate constants are computed using Eq. (8.42). Figure 8.5 presents solutions of these equations as trajectories in C_A–C_P space for several operating temperatures. Since these trajectories are convex and it is found that rate vectors computed along their boundaries are tangent to them, it is concluded that each trajectory constitutes the attainable region for the corresponding temperature.

Evidently, a single plug-flow reactor (or packed-bed reactor in this case) provides for maximum production of maleic anhydride with the required space velocity being that which brings the value of C_P to its maximum in Figure 8.5. At 800 K, it is determined that the maximum concentration of maleic anhydride is 3.8 mol/m^3, requiring 4.5 kg of catalyst. At 600 K it is 5.3 mol/m^3 but at this low temperature, 1,400 kg of catalyst is needed. A good compromise is to operate the PBR at

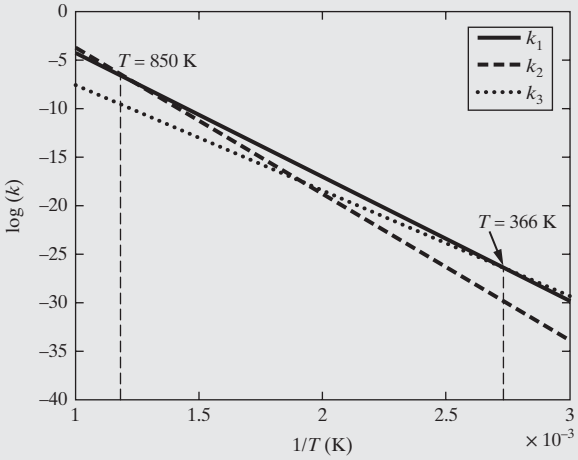

Figure 8.4 Influence on temperature of kinetic rate constants for MA manufacture.

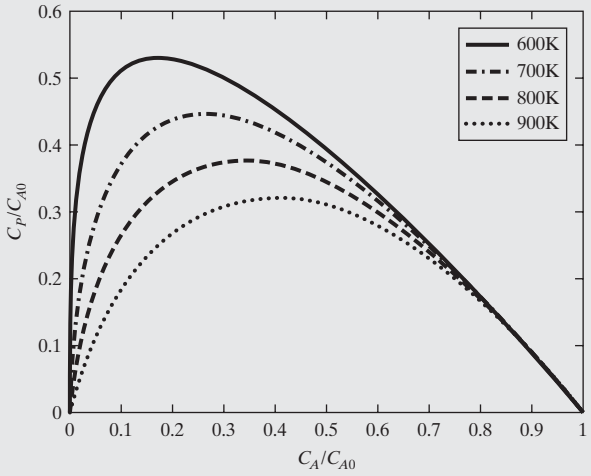

Figure 8.5 Attainable regions for MA manufacture at various temperatures.

an intermediate temperature, for example, 770 K, with a maximum concentration of maleic anhydride of 4.0 mol/m^3, requiring 8 kg of catalyst.

Figure 8.6a shows composition profiles for all species as a function of bed length (proportional to the weight of catalyst), indicating

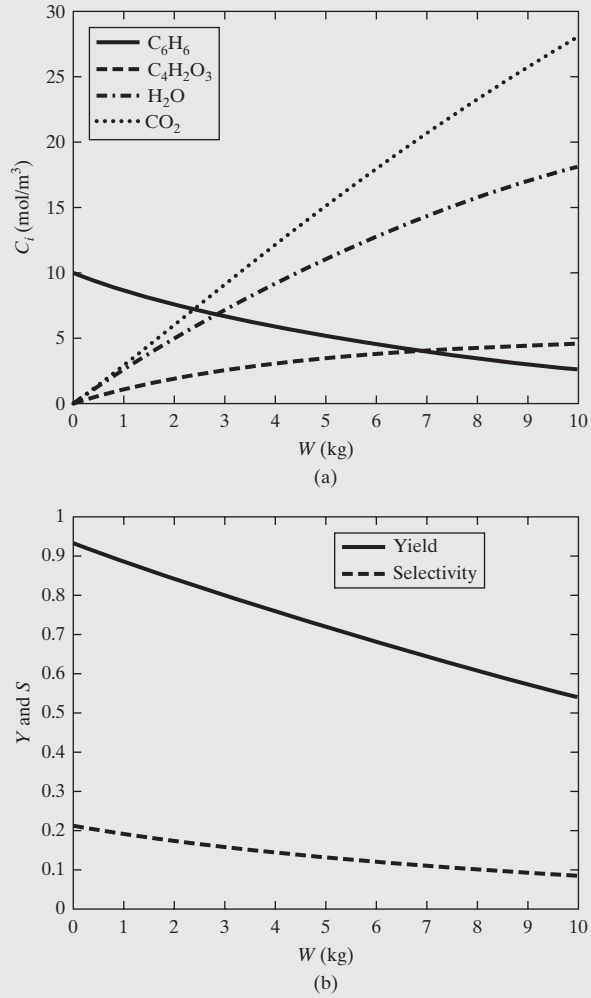

Figure 8.6 Composition profiles for MA manufacture in an isothermal PBR at 770 K: (a) composition profiles; (b) selectivity and yield.

that the optimal catalyst loading, where the concentration of maleic anhydride is a maximum, is about 8 kg for isothermal operation at 770 K. Figure 8.6b indicates that the yield in these conditions is 61%, while the selectivity is only about 10%. The selectivity for this reaction system is poor due to the large amounts of CO_2 and H_2O produced with the highest selectivity that could be achieved by repressing both of the undesired reactions being 22%.

Thus far, the attainable region has been shown for the analysis of systems with two key compositions that need to be tracked. In the following, the principle of reaction invariants is used to reduce the composition space in systems of larger dimension.

The Principle of Reaction Invariants

Since the attainable region depends on geometric constructions, it is effectively limited to the analysis of systems involving two independent species. However, as shown by Omtveit et al. (1994), systems involving higher dimensions can be analyzed by the 2D AR approach by applying the principle of reaction invariants of Fjeld et al. (1974). The basic idea consists of imposing atomic balances on the reacting species. Since these balances always hold, these additional linear constraints impose a relationship between the reacting species, and thus permit the complete system to be projected into a reduced space of independent species. The use of the AR analysis is appropriate when this reduced space is in two-dimensions.

Let the reacting system consist of n_i moles of each species i, each containing a_{ij} atoms of element j. The molar changes in the species due to reaction are combined in the vector $\Delta\underline{n}$, and the coefficients a_{ij} form the matrix $\underline{\underline{A}}$, noting that since the number of atoms for each element remain constant, $\underline{\underline{A}}\,\Delta\underline{n} = 0$. Partitioning $\Delta\underline{n}$ and $\underline{\underline{A}}$ into dependent, d, and independent, i, components:

$$\underline{\underline{A}} = \left[\underline{\underline{A}}_d \;\vdots\; \underline{\underline{A}}_i\right] \tag{8.45}$$

$$\Delta\underline{n}^T = \left[\Delta\underline{n}_d^T \;\vdots\; \Delta\underline{n}_i^T\right] \tag{8.46}$$

Assuming that $\underline{\underline{A}}_d$ is square and nonsingular, an expression for the changes in the number of moles of each dependent species is obtained by algebraic manipulation:

$$\Delta\underline{n}_d = -\underline{\underline{A}}_d^{-1}\underline{\underline{A}}_i\Delta\underline{n}_i \tag{8.47}$$

The dimension of i is equal to the number of species minus the number of chemical elements contained in the species. When this dimension is two or less, the principle of reaction invariants permits the application of the attainable region to complex reaction systems. This is illustrated in the following example introduced by Omtveit et al. (1994).

EXAMPLE 8.4 ***Attainable Region for Steam Reforming of Methane***

Construct the attainable region for the steam reforming of methane at 1050 K, and use it to identify the networks that provide for the maximum composition and selectivity of CO.

SOLUTION

The following reactions involving five species and three elements dominate in the steam reforming of methane:

$$CH_4 + 2H_2O \rightleftharpoons CO_2 + 4H_2 \tag{8.48}$$

$$CH_4 + H_2O \rightleftharpoons CO + 3H_2 \tag{8.49}$$

$$CO + H_2O \rightleftharpoons CO_2 + H_2 \tag{8.50}$$

By evoking the principle of reaction invariants, the number of species that need to be tracked for this system is reduced to two so that the attainable region can be shown in two dimensions. Accordingly, the vector of mole changes is:

$$\Delta\underline{n}^T = [\Delta\underline{n}_d^T \vdots \Delta\underline{n}_i^T] = [\Delta n_{H_2}, \Delta n_{H_2O}, \Delta n_{CO_2} \vdots \Delta n_{CH_4}, \Delta n_{CO}]^T \tag{8.51}$$

where methane and carbon monoxide have been selected as the independent components. The atom balances for the three elements, C, H and O are:

$$\text{C balance} : \Delta n_{CO_2} + \Delta n_{CH_4} + \Delta n_{CO} = 0$$

$$\text{H balance} : 2\Delta n_{H_2} + 2\Delta n_{H_2O} + 4\Delta n_{CH_4} = 0$$

$$\text{O balance} : \Delta n_{H_2O} + 2\Delta n_{CO_2} + \Delta n_{CO} = 0$$

Substituting into the matrix $\underline{\underline{A}}$ gives the following where the rows, starting at the top, correspond to C, H, and O, respectively.

$$\underline{\underline{A}} = [\underline{\underline{A}}_d \vdots \underline{\underline{A}}_i] = \left[\begin{array}{ccc:cc} 0 & 0 & 1 & 1 & 1 \\ 2 & 2 & 0 & 4 & 0 \\ 0 & 1 & 2 & 0 & 1 \end{array}\right] \tag{8.52}$$

The dependent molar changes, $\Delta\underline{n}_d$, are expressed in terms of the molar changes in methane and carbon monoxide, using Eq. (8.47):

$$\Delta\underline{n}_d = \begin{bmatrix} \Delta n_{H_2} \\ \Delta n_{H_2O} \\ \Delta n_{CO_2} \end{bmatrix} = -\underline{\underline{A}}_d^{-1}\underline{\underline{A}}_i\Delta\underline{n}_i = \begin{bmatrix} -4 & -1 \\ 2 & 1 \\ -1 & -1 \end{bmatrix}\begin{bmatrix} \Delta n_{CH_4} \\ \Delta n_{CO} \end{bmatrix} \tag{8.53}$$

For example, if $\Delta n_{CH_4} = -5$ moles and $\Delta n_{CO} = +3$ moles, Eq. (8.53) gives $\Delta n_{H_2} = +17$ moles, $\Delta n_{H_2O} = -7$ moles, and $\Delta n_{CO_2} = +2$ moles, which satisfies the atom balances. The feed would have to contain more than 5 moles of methane and more than 7 moles of water.

Xu and Froment (1989) provide the kinetic expressions for the reversible reactions in Eqs. (8.48), (8.49) and (8.50) in terms of the partial pressures of the participating species. Noting that the number of moles decreases by two in each of the reactions in which methane participates, the total number of moles in the system is given by:

$$n_T = [n_{H_2} + n_{H_2O} + n_{CO_2} + n_{CH_4} + n_{CO}]_0 - 2\Delta n_{CH_4} \tag{8.54}$$

The partial pressure of each of the five species is expressed as Pn_i/n_T, for i, where the number of moles of the dependent species, H_2, H_2O, and CO_2 are expressed in terms of CH_4 and CO using Eq. (8.53). This allows the construction of the attainable region for the steam reforming reactions at 1050 K, which was computed by Omtveit et al. (1994) as follows:

Step 1: *Begin by constructing a trajectory for a PFR from the feed point, continuing to the complete conversion of methane or chemical equilibrium.* Here, the PFR trajectory is computed by solving the kinetic equations for the reactions of Eqs. (8.48), (8.49) and (8.50) for CH_4 and CO. This leads to trajectory (1)

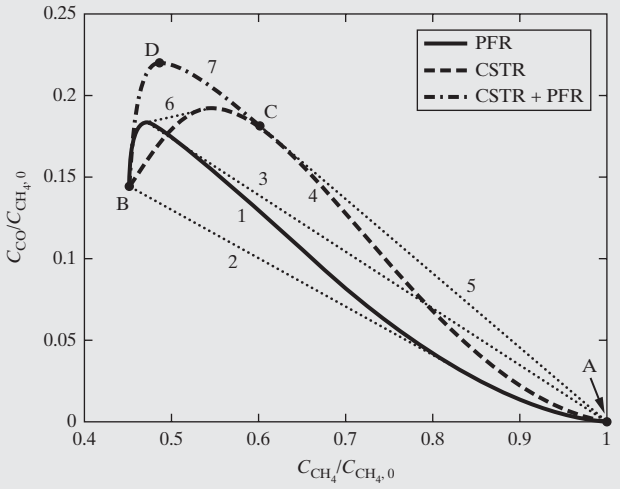

Figure 8.7 Development of the attainable region for steam reforming reactions at T = 1,050 K.

in Figure 8.7, which tracks the compositions from the feed point, A, to chemical equilibrium at point B.

Step 2: *When the PFR trajectory bounds a convex region, this constitutes a candidate attainable region. When the rate vectors at concentrations outside of the candidate AR do not point back into it, the current limits are the boundary of the AR and the procedure terminates.* In Figure 8.7, the PFR trajectory is not convex, so proceed to the next step.

Step 3: *The PFR trajectory is expanded by linear arcs, representing mixing between the PFR effluent and the feed stream, extending the candidate attainable region.* Here, two linear arcs are introduced to form a convex hull, tangent to the PFR trajectory from below, connecting to the chemical equilibrium point B (line 2) and from the feed point to a point tangent to the PFR trajectory from above (line 3). In this example, line 2 constitutes the lower boundary of the attainable region. It is found that rate trajectories point out of the convex hull, so proceed to the next step.

Step 4: *Since there are vectors pointing out of the convex hull, formed by the union between the PFR trajectory and linear mixing arcs, a CSTR trajectory may enlarge the attainable region. After placing the CSTR trajectory that extends the AR the most, additional linear arcs that represent the mixing of streams are placed to ensure that the AR remains convex.* Here, the CSTR trajectory is computed by solving the molar balances for CH_4 and CO for varying space-time, τ. This leads to the trajectory (4), which is augmented by two linear arcs connecting the feed point to a point tangent to the CSTR trajectory (line 5) at point C, and an additional line (6) connecting the CSTR to the PFR trajectories at two tangent points. This forms the new candidate attainable region, on which trajectories are identified that point outward.

Step 5: *A PFR trajectory is drawn from the position where the mixing line meets the CSTR trajectory. When this PFR trajectory is convex, it augments the previous AR to form an expanded candidate AR. Return to Step 2. Otherwise, repeat the procedure from Step 3.* As shown in Figure 8.7, the PFR trajectory (line 7) leads to a convex attainable region. The boundaries of the region are (a) the linear arc (line 5) from A to C, which represents a CSTR with bypass stream; (b) the point C, which represents a CSTR; and line 7 from C to B, which represents a CSTR followed by a PFR in series. Note that the maximum composition of CO is obtained at point D, using a CSTR and PFR in series. The maximum selectivity, defined by the ratio of CO/CH_4, is also achieved at point D, where the ratio is 0.47, as compared to point C, where the ratio is only 0.30.

8.4 REACTOR DESIGN FOR COMPLEX CONFIGURATIONS

As discussed in Section 6.5, temperature control is an important consideration in reactor design. Adiabatic operation is always considered first because it results in the simplest and least expensive reactor. However, when reactions are highly exothermic or endothermic, it may be desirable to exercise some degree of control over the temperature. Some methods for doing this, as shown in Figure 8.8, include (a) heat transfer to or from the reacting fluid across a wall to or from an external cooling or heating agent; (b) an inert or reactive heat carrier or diluent in the reacting fluid; (c) a series of reactor beds with a heat exchanger for cooling or heating between each pair of beds; and (d) cold-shot cooling (also called direct-contact quench) or hot-shot heating where the combined feed is split into two or more parts, one of which enters at the start of the reactor while the remaining parts enter the reactor at other locations. The following are industrial examples of the application of these four methods. In considering these examples, a useful measure of the degree of exothermicity or endothermicity of a reaction is the adiabatic temperature rise (ATR) for complete reaction with reactants in stoichiometric ratio.

Heat Exchange Reactor

An example of the industrial use of a heat exchange reactor in Figure 8.8a is in the manufacture of phthalic anhydride produced by the oxidation of orthoxylene with air in the presence of vanadium pentoxide catalyst particles, as discussed by Rase (1977). The reaction, which is carried out at about 375°C and 1.2 atm, is highly exothermic with an ATR of about 1,170°C, even with nitrogen in the air providing some dilution. Adiabatic operation is not feasible. The reactor resembles a vertical shell-and-tube heat exchanger. Inside the shell are hundreds of long tubes of small diameter, which are packed with catalyst particles and through which the reacting gas passes downward. Small-diameter tubes are used to minimize inside-tube heat-transfer resistance A heat-transfer medium consisting of a sodium nitrite-potassium nitrate fused salt circulates outside the tubes through the shell to remove the heat of reaction. Water is ruled out as a heat-transfer medium in this case because the required water pressure would be very high. The heat-transfer rate distribution is not adequate to maintain isothermal conditions for the reacting fluid, but its temperature changes by less than 40°C. In some applications, the arrangement is catalyst-packed beds interspersed with tubes conveying a coolant (e.g., the TVA design in Figure 6.16).

Temperature Control Using Dilutent

Styrene is produced by the catalytic dehydrogenation of ethylbenzene at 1.2 atm and a temperature of about 575°C, as described

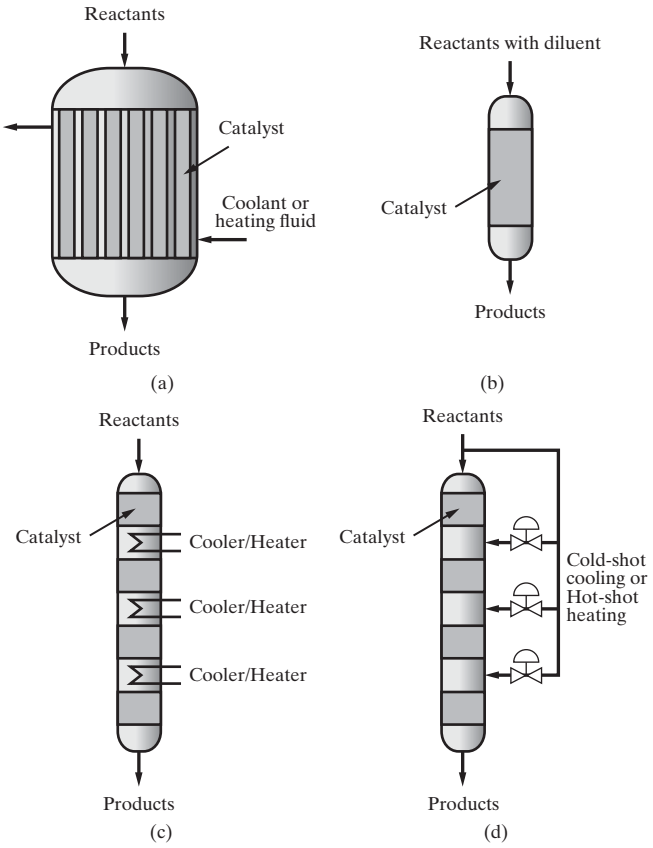

Figure 8.8 Reactors for handling large values of adiabatic temperature change: (a) heat exchanger reactor; (b) use of diluent; (c) external heat exchange; (d) hot-/cold-shot.

by Smith (1981). The reaction is sufficiently endothermic with an ATR of about −460°C, such that if the reactor were operated adiabatically with a feed of pure ethylbenzene, the temperature of the reacting fluid would decrease to such an extent that the reaction rate would be unduly compromised, resulting in a very large reactor volume. To maintain a reasonable temperature, a large amount of steam is added to the feed (typically with a molar ratio of steam to ethylbenzene of 20:1), which is preheated to 625°C before entering the reactor (Figure 8.8b). The steam is inert and is easily recovered from the reactor effluent by condensation. The presence of the steam reduces the reaction rate because the styrene concentration is reduced. However, the reactor can now be operated adiabatically in a simple manner.

Temperature Control Using External Heat Exchange or Cold-shots

Sulfur trioxide, which is used to make sulfuric acid, is produced by catalytic oxidation by air of sulfur dioxide with vanadium pentoxide catalyst particles in a packed bed operating at 1.2 atm and a temperature of about 450°C, as discussed by Rase (1977). Adiabatic operation is not feasible since the reaction is highly exothermic with an ATR of about 710°C, even with nitrogen in the air providing some dilution. Hence, the reactor system consists of four adiabatic reactor beds in series, each of the same diameter but different height, with a heat exchanger between each pair of beds, as shown in Figure 8.8c. The temperature rises adiabatically in each reactor bed, and the hot reactor effluent is cooled in the heat exchanger positioned before the next bed. When the ATR is higher, such as in the manufacture of ammonia from synthesis gas as described by Rase (1977), the cold-shot design in Figure 8.8d is recommended.

An important design consideration for fixed-bed catalytic reactors that can be designed with a 1D model is the desire to reduce the vessel volume to a minimum. As presented first by Aris (1960), this is achieved by design. If z is the direction down the length of the reactor, the trajectory of the mass- and energy-balance equations for a single reaction in $X(z)$ and $T(z)$ space is adjusted by design to match the trajectory corresponding to maximum reaction rate, $(\underline{X}^*, \underline{T}^*)$, as closely as possible. Thus, tube-cooled (or heated) reactors, cold-shot (or hot shot) converters, and multiple adiabatic beds with intercoolers (or interheaters) need to be carefully designed in such a way that $(X(z), T(z)) \approx (\underline{X}^*, \underline{T}^*)$.

As an example, consider an exothermic reversible reaction in a PFR. For this case, the rate of the backward reaction increases more rapidly with increasing temperature than does the rate of the forward reaction. Also, the backward reaction is slow and the forward reaction is fast at low temperatures. Thus, for a maximum rate of reaction, we want the temperature to be high at low conversions and low at high conversions. This is shown in Figure 8.9 adapted from Smith (1981), where reaction rate for a sequence of fractional conversions, X, starting with $X_1 = 0$, is plotted against temperature, T. For each value of X, the reaction rate curve in Figure 8.9 shows a maximum value. A locus of maximum rates is shown, corresponding to the solid and dashed lines passing through the points B and C, with the maximum reaction rate decreasing with increasing fractional conversion. At each conversion level, the desired temperature corresponds to the maximum reaction rate. In Figure 8.9, the feed enters at temperature T_A with a reaction rate at point A. Although the maximum reaction rate for X_1 is not shown, it is clear that T_A is not the temperature corresponding to the maximum rate. If the entering temperature cannot be increased, the best procedure is to operate isothermally at T_A until the conversion at point B is reached,

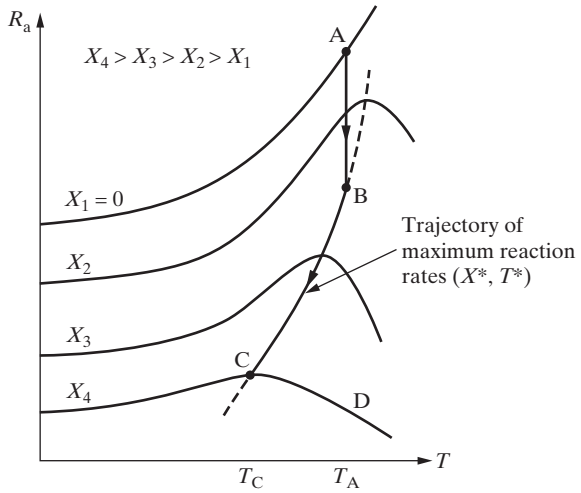

Figure 8.9 Temperature trajectories for an exothermic reversible reaction in a PFR. (*Source:* Adapted from Smith, 1981).

and then follow the optimal profile BC to the desired conversion. Suppose the reactor exit conversion is X_4. Then, the desired reactor temperature trajectory is the solid line ABC, with reactor exit temperature, T_c. Corresponding to this trajectory, but not shown in Figure 8.9 is a heat duty profile, which must be matched by heat exchange to achieve the optimal reaction rate trajectory. Alternatively, isothermal operation of the reactor at T_A corresponds to the trajectory ABD in Figure 8.9. In this case, the reaction rates are not at their maximum values except at point B, requiring a larger reactor volume. If instead of a PFR, a CSTR were used, the optimal temperature of operation for achieving conversion X_4 would be T_C, which corresponds to the maximum reaction rate for that conversion. By specifying a temperature profile for a PFR or an exit temperature for a CSTR, the optimal reactor volume can be determined together with the required corresponding heat-duty profile.

As discussed by Van Heerden (1953), the reactor feed temperature has an important effect on the stability of an autothermal reactor, that is, a reactor whose feed is preheated by its effluent. For reversible exothermic reactions such as that encountered in ammonia synthesis, the heat generation rate varies nonlinearly with the reaction temperature as shown by curve (a) in Figure 8.10. At low temperatures, the rate of heat generation is limited by the low rate of the forward reaction to ammonia. At very high temperatures, the rate of reaction is limited by equilibrium, so that again low heat generation rates are to be expected. However, at some intermediate temperature, the reaction rate exhibits a maximum value. In contrast, the rate of convective heat removal is almost linear with the reaction temperature, with a slope depending on the heat capacity of the reacting stream. Thus, the intercept of the heat removal line (b) and the heat generation line (a) sometimes leads to three possible operating conditions: (O) the nonreacting state, (I) the ignition point, and (S) the desired operating point. Both the nonreactive and the desired operating points are stable, since a small positive perturbation in reactor temperature would lead to the situation where the heat removal rate exceeds the heat generation rate and, hence, would decrease the reactor temperature. Similarly, a small negative perturbation in the reactor temperature would have the opposite effect, leading to a temperature rise. Using the same arguments, the ignition point is clearly unstable so that a small positive perturbation in temperature would lead to an inevitable jump to the desired, stable operating point, whereas a negative perturbation would lead to a so-called "blow-out," to the stable, nonreactive state.

Van Heerden (1953) for tube-cooled converters and Stephens and Richards (1973) for cold-shot converters refer to the temperature difference between operating points I and S as the "stability margin." Clearly, operation with larger stability margins would be more robust to disturbances. Thus, a design with increased extent of heat transfer, indicated by the line (b') in Figure 8.10, would clearly have a lower stability margin. In such cases, the proximity of the stable operating point to the unstable ignition point leads to an increased likelihood of loss of control to process upsets. For example, ammonia synthesis catalyst undergoes deactivation, mainly by poisoning due to feed impurities, or by high temperature sintering, which reduces the catalyst surface area. Lewin and Lavie (1984) studied the effect of catalyst deactivation on the optimal operation of a tube-cooled ammonia converter, which can lead to loss of stability since decreased catalyst activity leads to lower heat generation rates, as shown by line (a′) in Figure 8.10.

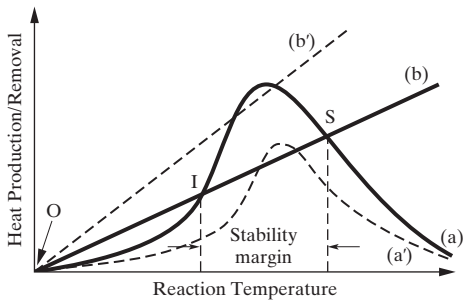

Figure 8.10 Multiple steady states in an autothermal reactor, with reaction rate limited by equilibrium: heat production rates for fully-active (a) and deactivated catalyst (a′); heat removal rates for normal (b), and increased heat transfer (b′).

The following example illustrates how a cold-shot reactor is designed to maximize conversion while satisfying stability margins.

EXAMPLE 8.5 ***Optimal Bypass Distribution in a Three-bed Cold-shot Ammonia Synthesis Converter***

A reactor for the synthesis of ammonia consists of three adiabatic beds, shown in Figure 8.11. As summarized in Table 8.1, the reactor feed consists of two sources, the first of which is a makeup feed stream of 20,000 kmol/hr at 25°C and 150 atmospheres containing mainly hydrogen and nitrogen in the stoichiometric molar ratio of 3:1. Since ammonia synthesis gas is produced from naphtha and air, it contains small concentrations of methane from naphtha and argon from air. Both of these species reduce the partial pressures of the reagents, and thus affect the reaction rate. The second feed, which contains larger concentrations of the inert components, is a recycle stream of 40,000 kmol/hr at 25°C and 150 atmospheres consisting of unreacted synthesis gas, recovered after removing the ammonia product.

The converter consists of three cylindrical, 2-m diameter adiabatic beds packed with catalyst for bed lengths of 1.5 m, 2m, and 2.5m, respectively. The reactor feed is split into three branches, with the first branch being the main feed entering the first bed after being preheated by the hot reactor effluent from the third bed. The second and third branches, with flow fractions φ_1 and φ_2, respectively, are controlled by adjusting valves V-1 and V-2. These branches provide "cold-shot" cooling at the first and second bed effluents, respectively. It is desired to optimize the allocation of the bypass fractions to maximize the conversion in the converter.

SOLUTION

Ammonia synthesis is controlled by the reversible reaction whose rate is expressed by the Tempkin equation (Tempkin and Pyzev, 1940) in terms of the partial pressures in atmospheres of the reaction species:

$$R_a = 10^4 e^{-91{,}000/RT}[P_{N_2}]^{0.5}[P_{H_2}]^{1.5} - 1.3\times 10^{10} e^{-140{,}000/RT}[P_{NH_3}], \tag{8.55}$$

where R_a is the rate of nitrogen disappearance in kmol/m^3–s, T is the temperature in K, P_i are the partial pressures of the reaction species

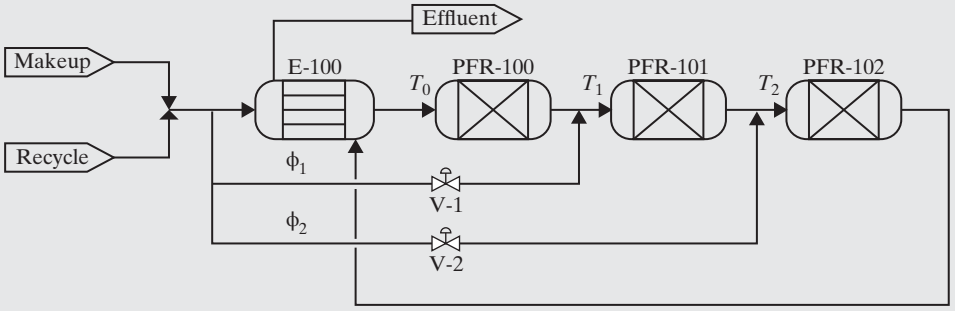

Figure 8.11 Cold-shot ammonia synthesis converter.

Table 8.1 Ammonia Converter—Makeup Feed and Recycle Streams

		Makeup Stream	Recycle Stream
Flow rate [kmol/h]		20,000	40,000
Temperature [°C]		25	
Pressure [atm]		150	
Compositions [mol%]:	H_2	72	61
	N_2	24	20
	NH_3	0	1.5
	CH_4	3	13
	Ar	1	4.5

in atm, and the activation energies for the forward and reverse reactions are in kJ/kmol. The species partial pressures can be expressed in terms of the ammonia mole fraction, x_{NH_3}, and the original feed composition:

$$P_{H_2} = \frac{F_o x_{f,H_2} - 1.5\xi}{F_o - \xi} P,\ P_{N_2} = \frac{F_o x_{f,N_2} - 0.5\xi}{F_o - \xi} P \quad \text{and}$$
$$P_{NH_3} = \frac{F_o x_{f,NH_3} + \xi}{F_o - \xi} P = x_{NH_3} P, \tag{8.56}$$

where F_o is the total molar flow rate of the combined reactor feed, the molar conversion, $\xi = F_o x_{NH_3}/(1 + x_{NH_3})$; P is the operating pressure; and $x_{f,i}$ is the feed mole fractions of species i. Consequently, the rate of reaction can be computed as a function of the temperature and x_{NH_3}, as shown in Figure 8.12a for an operating pressure of 150 atm. The ridge of maximum reaction rate in composition-temperature space defines an optimal decreasing temperature progression that is to be approximated by appropriate design and operation of the converter.

The composition-temperature trajectory in the converter is plotted over contours of reaction rate in Figure 8.12b for suboptimal bypass fractions, $\underline{\varphi} = [0.1,\ 0.1]^T$. Note that in the figure, the trajectories in the converter beds are plotted as solid lines, whereas those at the cold-shot mixing junctions appear as dotted lines. The temperature in Bed 1(PFR-100) rises to 415°C to a point close to the equilibrium limit. The first cold-shot cools the gas to 370°C. In Bed 2 (PFR-101), the temperature rises to 405°C, again to a point close to the equilibrium limit. Before entering Bed 3, the final cold-shot cools the gas to 360°C. The ammonia effluent concentration from the last bed is 12.7 mol%. Figure 8.12b also includes a dashed line for the optimal temperature progression, the locus of maximum reaction rates in composition-temperature space.

To maximize the conversion in the reactor, the following nonlinear program (NLP) of the type discussed in Chapter 21 is formulated:

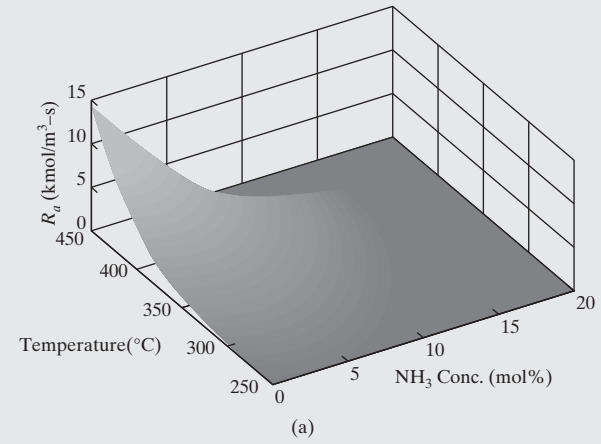

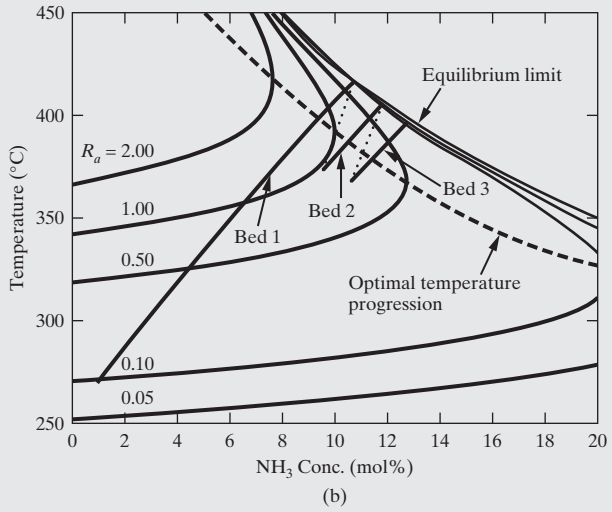

Figure 8.12 Composition-temperature space diagrams for ammonia synthesis converter design: (a) reaction rate as a function of ammonia mole fraction and temperature; (b) suboptimal cold-shot composition-temperature trajectory, plotted over reaction rate contours, with bypasses set to $\underline{\varphi} = [0.1,\ 0.1]^T$.

$$\max_{\phi_1,\phi_2} \xi \tag{8.57}$$

subject to

$$\underline{f}(\underline{x}) = 0 \tag{8.58}$$
$$T_1 > 300°\text{C} \tag{8.59}$$
$$T_2 > 300°\text{C} \tag{8.60}$$
$$\phi_1 + \phi_2 \le 0.6 \tag{8.61}$$

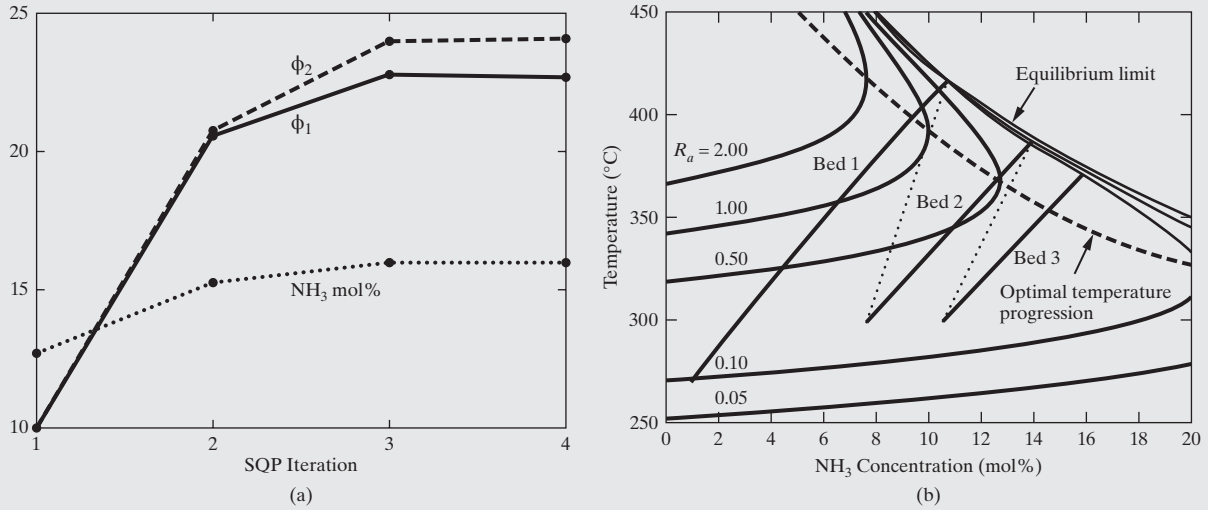

Figure 8.13 Optimal selection of bypass fractions for cold-shot ammonia converter: (a) convergence to the optimal solution; (b) optimal cold-shot profile in composition-temperature space with bypasses set to $\underline{\varphi} = [0.227,\ 0.240]^T$.

In the above, Eq. (8.58) refers to the kinetics and material and energy balances for the converter in Figure 8.11, and Eqs. (8.59) and (8.60) define lower limits for the feed temperatures of the second and third beds. These minimum values are taken arbitrarily as 300°C but are representative of minimum ignition temperatures. Note that in the first bed where the rate of reaction and with it the heat generation rate is higher, the feed temperature is maintained constant at the lower value of 270°C by appropriate design of the heat-exchanger, E-100. Finally, Eq. (8.63) ensures that a total maximum bypass of 60% is not exceeded, noting that this upper limit is arbitrary.

The NLP in Eqs. (8.57) – (8.61) is solved efficiently using successive quadratic programming (SQP) described in Chapter 21. Figure 8.13a shows the stepwise convergence to the optimal solution obtained in four iterations. The final ammonia composition in the converter effluent is 15.9 mol%, obtained with optimal bypass fractions of $\varphi_1 = 0.227$ and $\varphi_2 = 0.240$. The composition-temperature trajectories for the optimal bypass distribution shown in Figure 8.13b confirm that the overall performance of the three beds is significantly improved through increased utilization of the second and third beds. These results can be reproduced with UniSim®Design using the file NH3_CONVERTOR_OPT.usc. For full details, the reader is referred to the multimedia modules that accompany this book, where this example is presented in multimedia under HYSYS → Tutorials → Reactor Design → Ammonia Converter Design. Using simulators, complex reactor configurations are readily designed.

8.5 LOCATING THE SEPARATION SECTION WITH RESPECT TO THE REACTOR SECTION

In some chemical processes, a separation section is placed before the reactor section to remove undesirable chemicals from the feed stocks. In almost all chemical processes, a separation section is located after the reaction section, where products are purified and unconverted reactants are purged or recovered for recycle back to the reactor section. In this manner, a process involving reactions with unfavorable chemical equilibrium constants at reactor conditions can achieve high overall process conversions to desired products. Important industrial examples of such reactions are the hydrogenation of nitrogen to ammonia,

$$N_2 + 3H_2 \rightleftharpoons 2NH_3$$

and the hydrogenation of carbon monoxide to methanol,

$$CO + 2H_2 \rightleftharpoons CH_3OH$$

both of which are exothermic reactions, whose chemical equilibrium constants, K_c, therefore decrease with increasing temperature according to the van't Hoff equation:

$$\left(\frac{\partial \ln K_c}{\partial T}\right)_P = \frac{\Delta H^o_{rx}}{RT^2} \tag{8.62}$$

In these two examples, the chemical equilibrium constants are both less than unity and reactor conversions are less than 50% at temperatures high enough to achieve reasonable reaction rates. Because both reactions involve shrinkage in the number of moles (4 to 2 for the ammonia reaction and 3 to 1 for the methanol reaction), the reactor conversion can also be increased by increasing the pressure, but practical considerations limit the operating pressure. However, with the recovery and recycle of unconverted reactants, overall process conversions of 100% are approached.

Although product purification may require extreme measures to achieve product specifications, recycle streams rarely require a significant degree of purification with respect to recycled reactants. When two or more reactants are involved, they do not have to be recovered separately for recycle unless their *separation indexes* (e.g., relative volatility) are separated by the product(s), as shown in the next two examples.

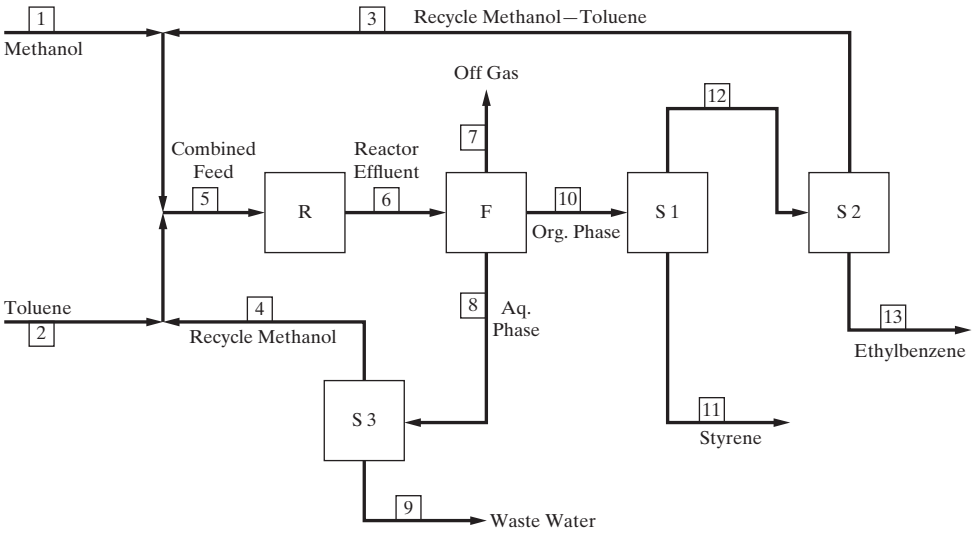

Material Balance for Styrene Process										
	Streams with flow rates in kmol/hr:									
Component	1	2	3	4	6	7	8	10	11	13
Hydrogen					352.2	352.2				
Methanol	493.4		66.0	37.0	107.3	4.3	37.0	66.0		
Water					489.1	7.9	481.2			
Toluene		491.9	104.5		107.3	1.5		105.8		1.3
Ethylbenzene			3.8		140.7	0.7		140.0		136.2
Styrene					352.2	1.6		350.6	346.7	3.9
Total	493.4	491.9	174.3	37.0	1,548.8	368.2	518.2	662.4	346.7	141.4

Figure 8.14 Styrene process.

EXAMPLE 8.6 *Styrene Manufacture*

In the styrene manufacture process of Figure 8.14, the main reaction is:

$$\text{Methanol} + \text{Toluene} \rightarrow \text{Styrene} + \text{Hydrogen} + \text{Water}$$

The following side reaction also occurs:

$$\text{Methanol} + \text{Toluene} \rightarrow \text{Ethylbenzene} + \text{Water}$$

The reactor effluent contains appreciable percentages of unreacted methanol and toluene. In this process, both styrene and ethylbenzene are products and must be purified to meet strict specifications. Water from the main reaction must be treated to the extent required for disposal to a sewer or for another use. Methanol and toluene are recovered and recycled. They are adjacent in relative volatility and, therefore, when distillation is used, they need not be separated, and because they are recycled, they need not be purified to a high degree. Typically, the recycle stream might contain 5% ethylbenzene plus styrene.

EXAMPLE 8.7 *Cumene Manufacture*

A more complex example is the manufacture of cumene (isopropyl benzene) by the alkylation of benzene with propylene taken from the 1997 National Student Design Competition of the AIChE. Cumene is widely used to make acetone and phenol. The feed streams to the process are nearly pure benzene, and a refinery cut of a propylene-propane mixture is used rather than a more expensive feed of nearly pure propylene:

Component	Propylene Feed, lbmol/hr	Benzene Feed, lbmol/hr
Water	0.1800	
Ethane	4.6440	
Propylene	1,029.2075	
Propane	465.6127	
1-Butene	0.0300	
Isobutane	0.3135	
Methylcyclopentane, MCP		1.1570
Benzene		997.5130
Methylcyclohexane, MCH		0.2030
Toluene		0.1270

The main reaction, conducted with a catalyst, is:

$$\text{Propylene} + \text{Benzene} \rightarrow \text{Isopropylbenzene (Cumene)}$$

A number of undesirable side reactions involving the main reactants also occur including:

Propylene + Benzene → n-Propylbenzene

Cumene + Propylene → m-Diisopropylbenzene (m-DIPBs)

Cumene + Propylene → p-Diisopropylbenzene (p-DIPBs)

Other alkylation reactions that produce larger molecules

All of the impurities in the propylene and benzene fresh feed streams, including the large amount of propane in the propylene feed, are essentially inert with the exception of 1-Butene, which enters into the following undesirable side reactions:

1-Butene + Benzene → t-Butylbenzene (t-BB)

1-Butene + Benzene → 1-isopropyl, 4-methyl Benzene (p-Cymene)

Potential products and byproducts include cumene, propane, DIPBs, t-BB, p-cymene, inert light hydrocarbons, inert, aromatic compounds, and water. A main objective of the process is to maximize the production of cumene and minimize the amounts of byproduct and waste streams. The cumene product must meet the following specifications:

Cumene purity, wt%	99.97	minimum
Butylbenzenes, ppm (by wt)	40	maximum
Toluene, ppm (by wt)	15	maximum
Cymene, ppm (by wt)	10	maximum
Benzene and paraffins, ppm (by wt)	10	maximum
Others, ppm (by wt)	225	maximum

The propane byproduct is used as either fuel gas or LPG. Thus, it can contain water and light hydrocarbons. However, the aromatic content cannot exceed 0.01 wt%.

Experimental alkylation data show that the two reactions that produce DIPBs can result in a serious loss (> 10%) of potential cumene product. To reduce this loss, two remedies are applied, the first of which is related to Heuristic 2 in Table 6.2: (1) the use of a large excess of benzene in the combined feed to the alkylation reactor, for example, a 4.0 molar ratio of benzene to propylene to reduce the DIPB formation reactions and (2) the addition of a trans-alkylation reactor where the DIPBs are reacted with benzene to produce cumene according to the reaction:

DIPB + Benzene → 2 Cumene

Other alkylation reactions produce larger molecules.

SOLUTION

A preliminary block flow diagram, suggested for the cumene process, is shown in Figure 8.15. The process consists of one separation section of three columns situated between two reactor sections, one for alkylation and one for trans-alkylation. The separations are all distillations, where approximate measures of separation indices for distillation, assuming ideal liquid solutions, are the differences between the normal boiling points of the components in the alkylation reactor effluent:

Component	Formula	Molecular Weight	Normal Boiling Point, °C
Water	H_2O	18.02	100
Ethane	C_2H_6	30.07	−88.6
Propylene	C_3H_6	42.08	−47.4
Propane	C_3H_8	44.11	−42.1
Isobutane	C_4H_{10}	58.13	−11.7
1-Butene	C_4H_8	56.12	−6.3
Methylcyclopentane	C_6H_{12}	84.16	71.8
Benzene	C_6H_6	78.12	80.1
Methylcyclohexane	C_7H_{14}	98.19	100.9
Toluene	C_7H_8	92.16	110.6
Cumene	C_9H_{12}	120.2	152.4
n-Propylbenzene	C_9H_{12}	120.2	159.2
t-Butylbenzene	$C_{10}H_{14}$	134.2	169.0
p-Cymene	$C_{10}H_{14}$	134.2	177.1
m-DIPB	$C_{12}H_{18}$	162.3	203.2
p-DIPB	$C_{12}H_{18}$	162.3	210.3
Trans-alkylation heavies		201.7	261.3
Alkylation heavies		206.4	278.8

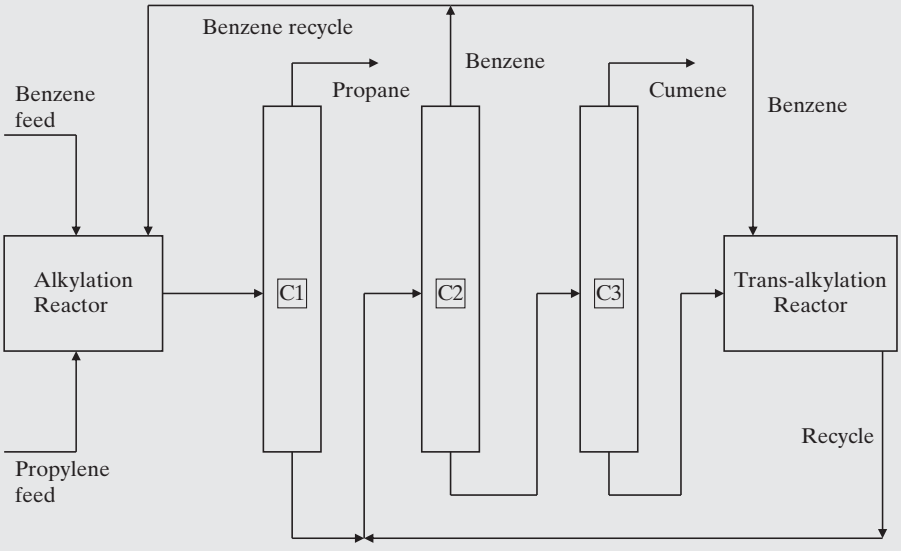

Figure 8.15 Cumene process.

Note that the fresh propylene feed contains approximately 31 mol% propane. Because propane is inert, Heuristic 3 of Table 6.2 should be considered. Propane can be removed in a separation section before or after the alkylation reactor. However, if removed before the reactor, a difficult separation between propane and propylene is required, as discussed in Section 9.2, because the boiling-point difference is only 5.3°C (relative volatility is about 1.1). In the alkylation reactor, essentially all of the propylene, as well as all of the 1-butene, are reacted. Therefore, after the reactor, propylene is not present to be separated from propane. Instead, the propane, together with water and small amounts of inert light hydrocarbons in the propylene feed, are easily removed from the excess benzene in the reactor effluent in the depropanizer, C1. Here, the difference in boiling points between the key components is 112.2°C (relative volatility > 10). Following the depropanizer is a benzene-recovery distillation column, C2, where benzene is removed, with a portion recycled to the alkylation reactor and the remainder sent to the trans-alkylation reactor. The main separation is between benzene and cumene with a boiling-point difference of 72.3°C (relative volatility > 5). Finally, cumene product is recovered as the distillate in distillation column, C3, where the bottoms product, composed of DIPBs, is sent to the trans-alkylation reactor to be converted to cumene. In the trans-alkylation reactor, a 4.0 molar ratio of benzene to total DIPBs is used. By recycling the effluent from the trans-alkylation reactor, no net production of DIPBs is incurred. Based on laboratory experiments and other considerations, the benzene recycle to the alkylation reactor can contain up to 10 mol% impurities. However, the combined feed to the alkylation reactor must not contain more than 1.3 mol% cumene.

A cardinal rule, implied in Heuristic 4 of Table 6.2, that must be adhered to when developing a process flowsheet is to provide exits from the process for all inert species that enter the process as impurities in the fresh feed(s) or are formed in irreversible side reactions. In the cumene process, these species include water and ethane, which are more volatile than propane; isobutane, MCP, MCH, and toluene, which are more volatile than cumene; and n-propylbenzene, tBB, and p-cymene, which are more volatile than the DIPBs. Based on the product specifications for the propane and cumene products, calculations show that the total amounts of these species produced do not leave with one or both products. Consequently, two alternatives, suggested in Heuristic 4 of Table 6.2, must be evaluated. The first is to add separators to the process flowsheet. When too expensive, the second includes one or more purge or drag streams, resulting in the loss of reactant(s), product(s), or both. Two drag streams, one from the distillate of the benzene recovery column and one from the bottoms of the cumene recovery column, are used, leading to a benzene loss of about 2% and a cumene loss of less than 1%. Inclusion of drag streams and the resulting material balance calculations are the subjects of Exercise 8.6 at the end of this chapter.

Some chemical processes, especially those utilizing a catalyst in the chemical reactor, may require a feed separation section, as shown in Figure 9.1, to purify the fresh feed before it enters the reactor. In this separation section, catalyst poisons are removed as well as components other than reactants for the main reaction(s) that may enter into undesirable side reactions in the reactor section. In general, inert chemicals can be removed in separation sections either before or after the reactor, wherever the separation index is more favorable as has been discussed in Example 8.7 for the cumene process. However, when removed after the reactor, a larger reactor is required because of the higher flow rate and lower reactant concentrations. As an example, consider the manufacture of sulfuric acid. The feed stocks are air and either sulfur or sulfide ores, where the first reaction is the oxidation of sulfur or sulfide to sulfur dioxide, the second reaction is the catalytic oxidation of SO_2 to SO_3, and the third reaction is the absorption of SO_3 in water to form sulfuric acid. Before the first reactor, moisture must be removed from the entering air to avoid corrosion and allow the use of carbon steel. Before entering the second reactor, dust, fluorides, and arsenic and vanadium compounds must be removed from the feed gas to prevent catalyst poisoning.

What should be done when the fresh feed contains an appreciable percentage of product chemicals? This occurs most frequently in isomerization reactions involving light paraffin hydrocarbons, as illustrated in Example 6.2. Suppose the reaction is A $\rightleftharpoons$ B. In this case, it is important to remove the product B from the fresh feed before it enters the reactor so as to increase the rate of reaction and achieve the highest equilibrium conversion possible. However, because reactor conversion is usually incomplete for isomerization reactions, A is commonly separated from B with A recovered and recycled. Unless other chemicals formed in the reactor interfere with the A-B separation, the two A-B separators are combined with the resulting separator placed before the reactor. Exercise 8.7 considers separator placement for a pentane-isomerization process.

8.6 TRADE-OFFS IN PROCESSES INVOLVING RECYCLE

Reactions with very large chemical equilibrium constants (e.g., > 10,000) at reactor conditions of temperature and pressure provide an opportunity for approaching 100% conversion during a single pass through the reactor. In addition, when the feed contains stoichiometric proportions of the reactants with no impurities and the reaction leads to only one product, then in principle no separation section is needed. One such situation exists. It is the manufacture of anhydrous hydrogen chloride gas from pure, evaporated chlorine and a stoichiometric amount of pure, electrolytic hydrogen by the reaction:

$$H_2 + Cl_2 \rightarrow 2\,HCl$$

The only pieces of equipment required are a reactor, compressors, and heat exchangers. Such a process is rare. Even when 100% reactor conversion is theoretically possible, the optimal reactor conversion is less than 100% and a separation section is necessary. The main reason for this is the rapid decline in reaction rate as the reacting mixture is depleted of reactants. Thus, in most processes where a chemical reactor is required, consideration must be given to the trade-offs between the cost of the reactor section and the cost of the separation section that follows it.

A number of factors affect the trade-off between the reactor and separation sections, many of which are introduced in Chapters 6 and 9. These include:

1. The fractional conversion in the reactor of the limiting reactant. This directly affects the need for and cost of the separation section.

2. The entering temperature to and mode of operation (adiabatic, isothermal, programmed temperature profile, etc.) for the reactor. This affects heating and/or cooling costs and reactor-effluent composition when side reactions are possible.
3. Reactor pressure, particularly for gas-phase reactions where the number of reactant molecules is greater than the number of product molecules. In this case, reaction kinetics may favor a higher pressure but at the higher cost of gas compression.
4. Use of an excess of one reactant to minimize side reactions and/or increase the rate of reaction. This increases the cost of the separation system.
5. Use of an inert diluent in an adiabatic reactor to reduce the change in temperature. This increases the cost of the separation system.
6. Use of a gas or liquid purge stream to avoid difficult separations. This reduces the cost of the separation system but results in the loss of reactants and may increase the cost of the reactor section, depending on the purge-to-recycle ratio (ratio of purge flow rate to recycle flow rate).

The use of process simulation in conjunction with optimization, as discussed in Chapter 21, allows one to determine optimal values of reactor conversion by entering temperature, mode of operation, pressure, molar ratio of reactants in a combined reactor feed, diluent ratio, and purge-to-recycle ratio.

8.7 OPTIMAL REACTOR CONVERSION

Return to the toluene hydrodealkylation process in Section 7.4 with the reaction kinetics in Example 8.2, based on a chain reaction. To illustrate the effect of achieving a high conversion on reactor size, simplify the combined reactor feed by eliminating methane and neglect biphenyl formation. Also, to avoid carbon formation, assume a molar ratio of hydrogen to toluene of 5 for the combined feed to the reactor. At typical reactor conditions, the reverse reaction is considered to be negligible, and Eq. (8.29) gives the forward reaction rate, r_f, where the Arrhenius equation for the rate constant, k_f, as a function of temperature is taken from the paragraph following Eq. (8.29). Thus,

$$r_f = -\frac{dC_{\text{toluene}}}{dt} = k_f C_{H_2}^{1/2} C_{\text{toluene}}$$
$$= 6.3 \times 10^{10} \exp\left(\frac{-52{,}000}{RT}\right) C_{H_2}^{1/2} C_{\text{toluene}} \qquad (8.63)$$

where $R = 1.987$ cal/mol − K; concentrations, C_i, are in kmol/m^3; time, t, is in sec; and temperature, T, is in K. Next, the volume of both isothermal and adiabatic PFRs is computed for a series of conversions from 1% to 99% for the following feed conditions:

Temperature, °F	1,200
Pressure, psia (0 pressure drop)	500
Component flow rates, lbmol/hr:	
Hydrogen	2,500
Toluene	500

The calculations can be performed with any process simulator. Using the CHEMCAD program, the results for the isothermal case plotted as reactor volume against fractional conversion of toluene are shown in Figure 8.16 with the adiabatic case in Figure 8.17. For the isothermal case, the reactor volume increases almost linearly as conversion increases to 0.4. The volume then increases more rapidly until at conversions near 0.8, the volume turns up sharply. The reactor volume is 4,080 ft^3 at a conversion of 0.9 but twice that at a conversion of 0.99.

As seen in Figure 8.17, the effect of conversion on reactor volume for the adiabatic case is very different from the isothermal case in Figure 8.16. At all conversions, the reactor volume is less for the adiabatic case. Furthermore, the difference in reactor volumes widens as the conversion is increased. For example, at a 50% conversion, the isothermal reactor volume is 2.25 times that of the adiabatic reactor. At a 99% conversion, the ratio becomes 8. The adiabatic case benefits by the increase in temperature with increasing conversion. The exothermic heat of reaction is considerable: between 21,000 and 22,000 Btu/lbmol of toluene reacted. However, the large excess of hydrogen acts as a heat carrier, curtailing the adiabatic rise in temperature. Nevertheless, the temperature increases by approximately 2.2°F per 1% increase in conversion. Thus, at 99% conversion, the reactor outlet temperature is approximately 1,418°F. As the conversion increases, the concentration of toluene in Eq. (8.63) decreases, causing the rate of reaction to decrease. The decrease of the hydrogen concentration is not nearly as pronounced because of its large excess in the reactor feed. In the adiabatic case, the decrease in toluene concentration with conversion is offset by the increase in the rate constant with temperature because the activation energy is moderately high at 93,600 Btu/lbmol. This results in an approximate doubling of the rate constant with every 50°F increase in temperature.

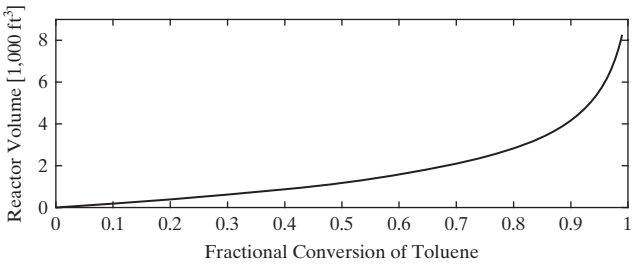

Figure 8.16 Required reactor volume for toluene hydrodealkylation in an isothermal PFR.

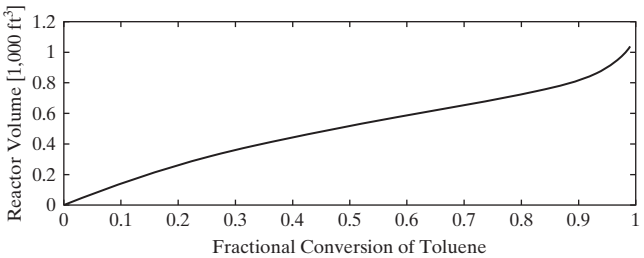

Figure 8.17 Required reactor volume for toluene hydrodealkylation in an adiabatic PFR.

Thus, in Figure 8.17 for the adiabatic case unlike the isothermal case, the increase in reactor volume is less than linear up to an inflection point at a conversion of approximately 50%. Only beyond a conversion of 90% does the reactor volume turn up sharply.

When striving for high reactor conversions, it may be necessary to consider the reverse reaction even when the reaction is considered to be irreversible. This is the case for the hydrodealkylation of toluene. A rate equation for the reverse reaction can be derived from the rate equation for the forward reaction, given by Eq. (8.63), by assuming that the two rate equations are consistent with the chemical-reaction equilibrium constant. Assume that the gas reacting mixture is ideal at the high temperature of the reaction. Then, the chemical equilibrium constant can be expressed in terms of concentrations and equated to the ratio of the rate constants by:

$$K_c = \frac{C_{CH_4} C_{benzene}}{C_{H_2} C_{toluene}} = \frac{k_f}{k_b} \tag{8.64}$$

But at chemical equilibrium, the rate of the forward reaction is equal to the rate of the backward reaction. Therefore, from Eq. (8.63), with an as yet undetermined dependence of component concentrations on the backward rate,

$$k_f C_{H_2}^{1/2} C_{toluene} = k_b C_{H_2}^{\alpha} C_{toluene}^{\beta} C_{CH_4}^{\gamma} C_{benzene}^{\delta} \tag{8.65}$$

To determine the exponents, α, β, γ, and δ, combine Eqs. (8.64) and (8.65),

$$\frac{k_f}{k_b} = \frac{C_{H_2}^{\alpha} C_{toluene}^{\beta} C_{CH_4}^{\gamma} C_{benzene}^{\delta}}{C_{H_2}^{1/2} C_{toluene}} = \frac{C_{CH_4} C_{benzene}}{C_{H_2} C_{toluene}} \tag{8.66}$$

By equating exponents in Eq. (8.66), $\alpha = -1/2$, $\beta = 0$, $\gamma = 1$, and $\delta = 1$. Therefore, the form of the rate equation for the backward reaction is:

$$r_b = k_b C_{H_2}^{-1/2} C_{CH_4} C_{benzene} \tag{8.67}$$

To determine the Arrhenius expression for k_b from Eq. (8.64), an expression for K_c as a function of temperature is needed. Based on the correlations of Yaws (1977), the standard Gibbs free energy of reaction, ΔG_{rx}^{o}, in cal/mol, as a function of the absolute temperature, T, in K, for the hydrodealkylation of toluene,

$$H_2 + C_7H_8 \rightarrow CH_4 + C_6H_6$$

is given by:

$$\Delta G_{rx}^{o} = -11{,}200 - 2.1\,T \tag{8.68}$$

From thermodynamics, ΔG_{rx}^{o} is related to the chemical-reaction equilibrium constant by the equation:

$$K_c = \exp\left(\frac{-\Delta G_{rx}^{o}}{RT}\right) \tag{8.69}$$

Combining Eqs. (8.68) and (8.69) and substituting 1.987 for R, gives:

$$K_c = \exp\left(\frac{5{,}636}{T} + 1.057\right) = 2.878 \exp\left(\frac{5{,}636}{T}\right) \tag{8.70}$$

From Eq. (8.64), using the temperature-dependent expressions for k_f in Eq. (8.63) and K_c in Eq. (8.70),

$$k_b = \frac{k_f}{K_c} = \frac{6.3 \times 10^{10} \exp\left(\frac{-52{,}000}{RT}\right)}{2.878 \exp\left(\frac{5{,}636}{T}\right)}$$
$$= 2.19 \times 10^{10} \exp\left(\frac{-63{,}200}{RT}\right) \tag{8.71}$$

Combining Eqs. (8.67) and (8.71), the rate law for the backward reaction becomes

$$r_b = 2.19 \times 10^{10} \exp\left(\frac{-63{,}200}{RT}\right) C_{H_2}^{-1/2} C_{CH_4} C_{benzene} \tag{8.72}$$

When the reactor calculations are repeated for up to 99% conversion of toluene, taking into account the reverse reaction, reactor volumes for both isothermal and adiabatic cases increase only slightly (<1%). This is largely due to the large concentration of hydrogen, which according to Eq. (8.72) decreases the rate of the reverse reaction. Reaction equilibrium calculations for this example give a 99.98% conversion for the isothermal case and a 99.96% conversion for the adiabatic case. However, when only the stoichiometric quantity of hydrogen is used in the feed, the equilibrium isothermal conversion decreases to 97.3%.

8.8 RECYCLE TO EXTINCTION

In many chemical processes, the main reaction is accompanied by one or more side reactions that produce byproducts. When the main reaction is irreversible or has a large chemical-reaction equilibrium constant, but one or more of the side reactions are so-called reversible reactions with chemical-reaction equilibrium constants on the order of 1 or less, the possibility of increasing the overall yield of the desired product(s) from the main reaction by eliminating the net production of byproduct(s) exists. This is accomplished by applying a concept sometimes referred to as *recycle to extinction*. The concept must be applied with care and must be supported by reaction rates that are sufficiently high. This is particularly true when the main reaction is catalyzed because the catalyst may not support the side reaction(s). Experimental verification is essential.

The recycle to extinction concept is introduced briefly in Example 6.4 illustrated for the toluene-hydrodealkylation process. Two alternatives are considered: (1) production of the byproduct and (2) recovery and recycle to extinction of the byproduct. In this process, the main reaction is the hydrogenation of toluene to the main products, benzene and methane:

$$H_2 + C_7H_8 \rightarrow CH_4 + C_6H_6$$

As shown in Section 8.6, this reaction, while not completely irreversible at typical reactor operating conditions, has a chemical-reaction equilibrium constant high enough to give conversions greater than 99%. When the main reaction is carried out thermally in the absence of a catalyst, it is accompanied by the following side reaction that produces the byproduct, biphenyl:

$$2C_6H_6 \rightleftharpoons H_2 + C_{12}H_{10}$$

The chemical-reaction equilibrium constant for this reaction is written as:

$$K_c = \frac{C_{H_2} C_{\text{biphenyl}}}{C^2_{\text{benzene}}} \tag{8.73}$$

Although not always considered, a further reaction to triphenyl also occurs,

$$C_6H_6 + C_{12}H_{10} \rightleftharpoons H_2 + C_{18}H_{14}$$

with a chemical-reaction equilibrium constant written as:

$$K_c = \frac{C_{H_2} C_{\text{triphenyl}}}{C_{\text{benzene}} C_{\text{biphenyl}}} \tag{8.74}$$

From Hougen and Watson (1947), the chemical-reaction equilibrium constant for Eq. (8.73) ranges from 0.045 to 0.32 over a temperature range of 700 to 1,400°F, whereas for Eq. (8.74), the constant increases from 0.23 to 0.46 over the same temperature range. When the biphenyl and triphenyl byproducts are recovered and recycled to the reactor, they build to their equilibrium concentrations at the reactor outlet, as determined from Eqs. (8.73) and (8.74), such that no net production of either biphenyl or triphenyl occurs. In effect, the byproducts are recycled to extinction. In this manner, the production of undesirable byproducts is eliminated and the overall yield of the main product(s) is increased. A disadvantage of recycle of the byproducts to extinction is that the byproducts and unconverted reactants increase the cost of recycling. However, the cost of the separation system downstream of the reactor may be reduced when the byproducts are recovered together with one or more of the reactants in a single recycle stream. This occurs in the toluene hydrodealkylation process where the biphenyl and triphenyl are recovered with toluene.

A second example where recycle to extinction should be considered is the hydrolysis of ethylene to ethyl alcohol:

$$C_2H_4 + H_2O \rightarrow C_2H_5OH$$

which is accompanied by a reversible side reaction that produces diethylether and water,

$$2C_2H_5OH \rightleftharpoons (C_2H_5)_2O + H_2O$$

for which the chemical-reaction equilibrium constant at typical reactor conditions is 0.2. By recovering and recycling diethylether and water, the overall yield of alcohol is increased.

A third example is the steam reforming of methane (or natural gas) in the presence of a nickel-supported catalyst to produce synthesis gas ($CO + H_2$), an intermediate that can be used to produce acetic acid, ammonia, gasoline, or methanol. The main reaction is:

$$CH_4 + H_2O \rightleftharpoons CO + 3H_2$$

Typically, the reactor operation at adiabatic conditions gives an outlet temperature of approximately 800°C, which limits the extent of the reaction to that of chemical equilibrium, with an equilibrium constant of 126.8, with compositions in partial pressures in atm. Reactor pressure is generally set by the available pressure of the methane and may be as high as 30 atm.

In the presence of the catalyst, a number of side reactions occur as discussed by Rase (1977). However, the only one of significance is the water-gas shift reaction:

$$CO + H_2O \rightleftharpoons CO_2 + H_2$$

At 800°C, the chemical-reaction equilibrium constant for this reaction is 0.929 with compositions in partial pressures in atm. When CO_2 is recovered and recycled to extinction, is the overall yield of synthesis gas increased? This is the subject of Example 8.8.

EXAMPLE 8.8 ***Steam Reforming of Naphtha***

The fresh feed to a steam reformer is 13.5 kmol/hr of methane and 86.5 kmol/hr of steam. If the outlet conditions of the reactor are 800°C and 12.2 atm and chemical equilibrium is achieved for both the steam reforming and water-gas shift reactions, determine the kmol/hr of synthesis gas produced when:

(a) The CO_2 produced is not recovered and recycled.

(b) The CO_2 is recovered from the reactor effluent and recycled to extinction.

SOLUTION

(a) At 800°C, the two chemical equilibrium equations are:

$$\frac{n_{CO} n^3_{H_2}}{n_{CH_4} n_{H_2O}} \left(\frac{P}{n_{\text{total}}}\right)^2 = 126.8$$

$$\frac{n_{CO_2} n_{H_2}}{n_{CO} n_{H_2O}} = 0.929$$

where $P = 12.2$ atm and n_i are in kmol/hr. Since these two equations contain five unknowns, three atom-balance equations are needed. They are:

$$\begin{aligned}
&\text{Carbon balance :} && 13.5 = n_{CH_4} + n_{CO} + n_{CO_2} \\
&\text{Hydrogen balance:} && 2(86.5) + 4(13.5) = 227.0 \\
& && \quad = 2n_{H_2} + 4n_{CH_4} + 2n_{H_2O} \\
&\text{Oxygen balance:} && 86.5 = n_{H_2O} + n_{CO} + 2n_{CO_2}
\end{aligned}$$

where the left-hand sides are in kg · atom/hr of the elements, C, H, and O in the fresh feed. Solving these five equations gives:

Component	Fresh Feed, kmol/hr	Reactor Effluent, kmol/hr
Methane	13.5	0.605
Water	86.5	66.229
Hydrogen	0	46.061
Carbon monoxide	0	5.521
Carbon dioxide	0	7.375
Total	100.0	125.791

From these results, 95.5% of the methane is reacted. The production of synthesis gas is 5.521 + 46.061 = 51.582 kmol/hr.

(b) For recycle of CO_2 to extinction, the CO_2 in the reactor effluent is recycled and added to the fresh feed to give a combined feed. At chemical equilibrium, the flow rate of CO_2 in the reactor effluent is the same as that in the combined feed. The two chemical equilibrium equations remain the same, but the three atom balance equations become:

$$\text{Carbon balance:} \quad 13.5 + n_{CO_2} = n_{CH_4} + n_{CO} + n_{CO_2}$$
$$\text{Hydrogen balance:} \quad 2(86.5) + 4(13.5) = 227.0 = 2n_{H_2} + 4n_{CH_4} + 2n_{H_2O}$$
$$\text{Oxygen balance:} \quad 86.5 + 2n_{CO_2} = n_{H_2O} + n_{CO} + 2n_{CO_2}$$

Solving the revised equations gives:

Component	Combined Feed, kmol/hr	Reactor Effluent, kmol/hr
Methane	13.5	0.549
Water	86.5	73.544
Hydrogen	0	38.859
Carbon monoxide	0	12.946
Carbon dioxide	22.763	22.763
Total	122.763	148.661

Observe that there is no net production of CO_2. The percent conversion of methane is slightly greater at 95.9% with the production of synthesis gas slightly increased to 12.946 + 38.859 = 51.805 kmol/hr. Note that in case (a), the production of CO_2 from CO by the water-gas shift reaction gives an additional mole of H_2 for every mole of CO_2 produced. Thus, by eliminating the net production of CO_2, less H_2 is produced. The usual benefit of the increased yield of the main product (s) by recycle to extinction is not achieved in this case. However, in case (b), CO_2 is not emitted to the atmosphere where it contributes to global warming. This is considered in more detail by Mulholland and Dyer (1999).

8.9 SNOWBALL EFFECTS IN THE CONTROL OF PROCESSES INVOLVING RECYCLE

In recent years, chemical engineers engaged in process design in industry have become increasingly aware of the need to understand the interaction of process design and process control when developing a control system for an entire chemical plant. When the process does not involve recycle, the development of the control system is relatively straightforward because the process can be treated in a sequential manner. However, the majority of chemical processes involve recycle, for which the development of a feasible and efficient control system, particularly for a reactor-separator-recycle network, is not at all straightforward. This is due to the possibility of the so-called *snowball effect*, which refers to a situation where a small disturbance, for example, in the fresh feed rate to a reactor, causes a very large change in the flow rate of the recycle stream. When this occurs, either the reactor or the separation system, or both, may not be able to handle the increased load. Whether or not the snowball effect occurs depends on the design of the control system.

8.10 SUMMARY

This chapter has introduced the design of chemical reactors and reactor networks. Different methods of reaction temperature control have been presented with emphasis on the use of multiple adiabatic reactors or beds, using cold-shots or heat exchangers between reactors or beds. The attainable region has been presented to define the reactor network that maximizes either the yield or the selectivity of a desired product given the feed to the reactor. However, since reactor yield is often sacrificed in favor of selectivity, conversion is rarely complete with unreacted species recycled. Thus, the optimal reactor feed conditions depend on the overall plant economics, and the reactor network should be synthesized as part of an overall plant design.

After completing this chapter and reviewing the multimedia modules that accompany this book, the reader should:

1. Be able to effectively use ASPEN PLUS and/or UniSim® Design/ASPEN HYSYS to model chemical reactors, implementing some of these complexities such as tube-cooling and cold-shots.
2. Be able to define the combination of CSTRs and/or PFRs that maximize the yield or selectivity of the desired reactor product for a particular feed composition, given the reaction kinetics, using attainable region analysis.
3. Have an appreciation for the complex configurations that are often used in commercial reactor designs, especially when it is required to handle highly exothermic or endothermic reactions, and be able to implement simplified examples using a process simulator.
4. Understand the considerations in determining the best locations of the separation sections with respect to the reactor section.
5. Be aware of the many trade-offs between the reactor section and the separation sections(s) when recycle is used, particularly when fast side reactions can occur.
6. Know that the optimal fractional conversion of the limiting reactant in the reaction section is usually less than 100% of the equilibrium conversion.
7. Be able to apply the concept of recycle to extinction to reduce waste and increase the yield of the main product.
8. Be aware that the snowball effect can occur in a reactor-separator-recycle network.

REFERENCES

1. Aris, R. "The Optimum Design of Adiabatic Reactors with Several Beds," *Chem. Eng. Sci.*, **12**, 243 (1960).

2. Fjeld, M., O. A. Asbjornsen, and H. J. Astrom, "Reaction Invariants and Their Importance in the Analysis of Eigenvectors, Stability and Controllability of CSTRs," *Chem. Eng. Sci.*, **30**, 1917 (1974).

3. Fogler, H. S., *Essentials of Chemical Reaction Engineering*, 4th ed., Prentice Hall, Upper Saddle River, New Jersey (2011).

4. Froment, G. F, K. B. Bishoff, and J. De Wilde, *Chemical Reactor Analysis and Design*, 3rd ed., John Wiley, New York (2010).

5. Glasser, D., C. Crowe, and D. A. Hildebrandt, "A Geometric Approach to Steady Flow Reactors: The Attainable Region and Optimization in Concentration Space," *Ind. Eng. Chem. Res*., **26**(9), 1803 (1987).

6. Hildebrandt, D., and L. T. Biegler, "Synthesis of Chemical Reactor Networks," *AIChE Symposium Series*, **91**(304), 52 (1995).

7. Hildebrandt, D. A., D. Glasser, and C. Crowe, "The Geometry of the Attainable Region Generated by Reaction and Mixing with and without Constraints," *Ind. Eng. Chem. Res*., **29**(1), 49 (1990).

8. Horn, F. J. M., "Attainable Regions in Chemical Reaction Technique," *Third European Symposium of Chemical Reaction Engineering*, Pergamon Press, London (1964).

9. Hougen, O. A., and K. M. Watson, *Chemical Process Principles, Part Three, Kinetics and Catalysts*, John Wiley, New York (1947).

10. Levenspiel, O., *Chemical Reaction Engineering*, 3rd ed., John Wiley, New York (1999).

11. Lewin, D. R., and R. Lavie, "Optimal Operation of a Tube Cooled Ammonia Converter in the Face of Catalyst Bed Deactivation," *I. Chem. Eng. Symp. Ser*., **87**, 393 (1984).

12. Mulholland, K. L., and J. A. Dyer, *Pollution Prevention: Methodology, Technologies and Practices*, AIChE, New York (1999).

13. Omtveit, T., J. Tanskanen, and K. M. Lien, "Graphical Targetting Procedures for Reactor Systems," *Comput. Chem. Eng*., **18**(S), S113 (1994).

14. Rase, H. F., *Chemical Reactor Design for Process Plants, Vol. 2*, *Case Studies and Design Data*, Wiley-Interscience, New York (1977).

15. Schmidt, L. D., *The Engineering of Chemical Reactions*, 2nd ed., Oxford University Press, New York (1998).

16. Slominski, C. G., W. D. Seider, S. W. Churchill, and J. D. Seader, "Helical and Lemniscate Tubular Reactors," *Ind. Eng. Chem. Res.*, **50**, 8842–8850 (2011).

17. Smith, J. M., *Chemical Engineering Kinetics,* 3rd ed., McGraw-Hill., New York (1981).

18. Stephens, A. D., and R. J. Richards, "Steady State and Dynamic Analysis of an Ammonia Synthesis Plant," *Automatica*, **9**, 65 (1973).

19. Temkin, M., and V. Pyzhev, "Kinetics of Ammonia Synthesis on Promoted Iron Catalyst," *Acta Physicochim. U.R.S.S*., **12**(3), 327 (1940).

20. Trambouze, P. J., and E. L. Piret, "Continuous Stirred Tank Reactors: Designs for Maximum Conversions of Raw Materials to Desired Product," *AIChE J.*, **5**, 384 (1959).

21. van de Vusse, J. G., "Plug Flow vs. Tank Reactor," *Chem. Eng. Sci.*, **19**, 994 (1964).

22. van Heerden, C., "Autothermic Processes—Properties and Reactor Design," *Ind. Eng. Chem.*, **45**(6), 1242 (1953).

23. Westerlink, E. J., and K. R. Westerterp, "Safe Design of Cooled Tubular Reactors for Exothermic Multiple Reactions: Multiple Reaction Networks," *Chem. Eng. Sci*., **43**(5), 1051 (1988).

24. Xu, J., and G. Froment, "Methane Steam Reforming: Diffusional Limitations and Reactor Simulation," *AIChE J.*, **35**(1), 88 (1989).

25. Yaws, C. L., *Physical Properties*, McGraw-Hill, New York (1977).

EXERCISES

8.1 A system of three parallel reactions (Trambouze and Piret, 1959) involves the following reaction scheme:

$$A \xrightarrow{k_1} B \quad A \xrightarrow{k_2} C \quad A \xrightarrow{k_3} D$$

where the reactions above are zero-order, first-order, and second-order, respectively, with $k_1 = 0.025$ mol/L-min, $k_2 = 0.2$ min^{-1}, and $k_3 = 0.4$ L/mol-min, and the initial concentration of $C_A = 1$ mol/L. Use the attainable region algorithm to find the reactor network that maximizes the selectivity of C from A.

8.2 Repeat Exercise 8.1, taking the first two reactions as first order, and the last as second order with $k_1 = 0.02$ min^{-1}, $k_2 = 0.2$ min^{-1}, and $k_3 = 2.0$ L/mol-min, and the initial concentration of $C_A = 1$ mol/L. Use the attainable region algorithm to find the reactor network that maximizes the selectivity of C from A.

8.3 For the reaction system:

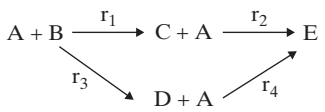

where $r_1 = k_1 C_A$, $r_2 = k_2 C_C$, $r_3 = k_3 C_A$; and $r_4 = k_4 C_A$. The rate constants are $k_1 =$ a min^{-1}, $k_2 =$ b min^{-1}, $k_3 =$ c min^{-1}, $k_4 =$ d min^{-1}, and the feed concentration of A is 1 kgmol/m^3. Use the attainable region algorithm to find the reactor network that maximizes the selectivity of C from A.

8.4 In Example 8.4, choose methane and hydrogen as independent components. Derive relationships for the remaining components in terms of methane and hydrogen.

8.5 Carry out a modified design for an ammonia converter in Example 8.5 consisting of three diabatic reactor bed sections, each of 2 m diameter and 2 m length (note that the total bed length is the same as before). Assuming the same reactor inlet temperature of 270°C, compute the optimum heat duties and effluent temperatures for each bed such that the effluent ammonia mole fraction for the reactor is maximized. Plot the temperature composition trajectory for the modified converter design and compare with the three-bed cold-shot design of Example 8.5.

8.6 *Cumene process with drag (purge) streams.* In Example 8.7, a process for producing cumene by the alkylation of benzene with propylene is described. The flowsheet for the process is given in Figure 8.14.

However, that flowsheet does not provide for the removal of water, ethane, isobutane, MCP, MCH toluene, n-propylbenzene, tBB, and p-cymene. For their removal, it is proposed to add two drag (purge) streams to the flowsheet: one from the distillate of the benzene recovery column, C2, and the other from the bottoms of the cumene recovery column, C3. Also, the flowsheet in Figure 8.14 does not provide for an exit for the heavies produced in the alkylation and trans-alkylation reactors in the event that their amounts are too large to be included in the allowable impurity in the cumene product. Thus, it may be necessary to add a fourth distillation column, C4, following C3 with the distillate from C4 fed to the trans-alkylation reactor and the bottoms from C4 being a heavies product. If so, the heavies must not contain more than 5% of the DIPBs and lighter entering C4.

Most of the data for the cumene process is given in Example 8.7. However, missing are the product distributions for the two reactors. These are as follows from laboratory studies:

	Alkylation Reactor	Trans-alkylation Reactor
Component	Change in pounds per 100 pounds of propylene in the combined feed	Change in pounds per 100 pounds of propylene in the combined feed to the Alkylation Reactor
Propylene	−100.0000	0.0000
1-Butene	−0.0039	
Benzene	−168.1835	−16.3570
Toluene	−0.0214	
Cumene	232.7018	50.7652
n-Propylbenzene	0.0346	0.0087
p-Cymene	0.0306	−0.0025
t-BB	0.0080	−0.0007
m-DIPB	20.3314	−20.2323
p-DIPB	14.7797	−14.4953
Alkylation heavies	0.3227	
Trans-alkylation heavies	0.0000	0.3121
Total change	0	0

Using the above data and those in Example 8.7, revise the flowsheet in Figure 8.14 and produce a complete material balance with the component flow rates in lbmol/hr for each stream in your flowsheet. Try to maximize the production of cumene. Be sure to add two drag streams for removal of byproducts and a fourth distillation column if necessary. Compute the overall percent conversion of benzene to cumene and the annual production of cumene in lb/yr if the operating factor is 0.95. If a heavies product is produced, what could it be used for?

8.7 The feed to a pentane isomerization process consists of 650 kmol/hr of n-pentane and 300 kmol/hr of isopentane. The effluent from the catalytic isomerization reactor will contain 6.5 moles of isopentane for every mole of n-pentane. The catalyst prevents the formation of neopentane. If the isopentane product, produced by separating isopentane from n-pentane by distillation, is to contain only 2 wt% n-pentane and the separation system is to be placed before the reactor, calculate the total flow rate and composition of the reactor effluent, the combined feed to the reactor, and the bottoms product from the distillation column. Design the distillation column. Repeat the material balance calculations and the design of the distillation column if the separation system is placed after the reactor. Based on your results and without determining any capital or operating costs, which separation system placement is preferred?

Chapter 9

Synthesis of Separation Trains

9.0 OBJECTIVES

Most chemical processes are dominated by the need to separate multicomponent chemical mixtures. In general, a number of separation steps must be employed where each step separates between two components of the feed to that step. During process design, separation methods must be selected and sequenced for these steps. This chapter discusses some of the techniques for the synthesis of separation trains. More detailed treatments are given by Douglas (1995), Barnicki and Siirola (1997), and Doherty and Malone (2001).

After studying this chapter, the reader should:

1. Be familiar with the more widely used industrial separation methods and their basis for separation.
2. Understand the concept of the separation factor and be able to select appropriate separation methods for vapor–, liquid–, and solid–fluid mixtures.
3. Understand how distillation columns are sequenced and how to apply heuristics to narrow the search for a near-optimal sequence.
4. Be able to apply algorithmic methods to determine an optimal sequence of distillation-type separations.
5. Be familiar with the difficulties in and techniques for determining feasible sequences when azeotropes can form.
6. Be able to determine feasible separation systems for gas mixtures and solid–fluid systems.

9.1 INTRODUCTION

Almost all chemical processes require the separation of mixtures of chemical species (components). In Section 6.4, three flowsheets (Figures 6.9, 6.10, and 6.11) are shown for processes involving a reactor followed by a separation system. A more general flowsheet for a process involving one reactor system is shown in Figure 9.1, where separation systems are shown before as well as after the reactor section. A *feed separation system* may be required to purify the reactor feed(s) by removing catalyst poisons and inert species, especially if they are present as a significant percentage of the feed. An *effluent separation system*, which follows the reactor system and is almost always required, recovers unconverted reactants (in gas, liquid, and/or solid phases) for recycle to the reactor system and separates and purifies products and byproducts. Where separations are too difficult, purge streams are used to prevent buildup of certain species in recycle streams. Processes that do not involve a reactor system also utilize separation operations if the feed is a mixture that requires separation. Frequently, the major investment and operating costs of a process will be those costs associated with the separation equipment, rather than with the chemical reactor(s).

Feed Separation System

As shown in Figure 9.1, the combined feed to a reactor section may consist of one or more feed streams and one or more recycle streams when conversion of reactants is incomplete. When a feed separation system is needed and more than one feed enters the process, it is usually preferable to provide separate separation operations for the individual feed streams before mixing them with each other and with any recycle streams. Some industrial examples of chemical processes that require a feed separation system are:

1. Production of polypropylene from a feed of propylene and propane. Propane, which is not involved in the propylene polymerization reaction, is removed from the propylene by distillation.
2. Production of acetaldehyde by the dehydrogenation of ethanol using a chromium-copper catalyst. If the feed is a dilute solution of ethanol in water, distillation is used to concentrate the ethanol to the near-azeotrope composition (89.4 mol% ethanol at 1 atm) before it enters the reactor.
3. Production of formaldehyde by air-oxidation of methanol using a silver catalyst. The entering air is scrubbed with aqueous sodium hydroxide to remove any SO_2 and CO_2, which are catalyst poisons.
4. Production of vinyl chloride by the gas-phase reaction of HCl and acetylene with a mercuric chloride catalyst. Small amounts of water are removed from both feed gases by adsorption to prevent corrosion of the reactor vessel and acetaldehyde formation.
5. Production of phosgene by the gas-phase reaction of CO and chlorine using an activated carbon catalyst. Both feed gases are treated to remove oxygen, which poisons the

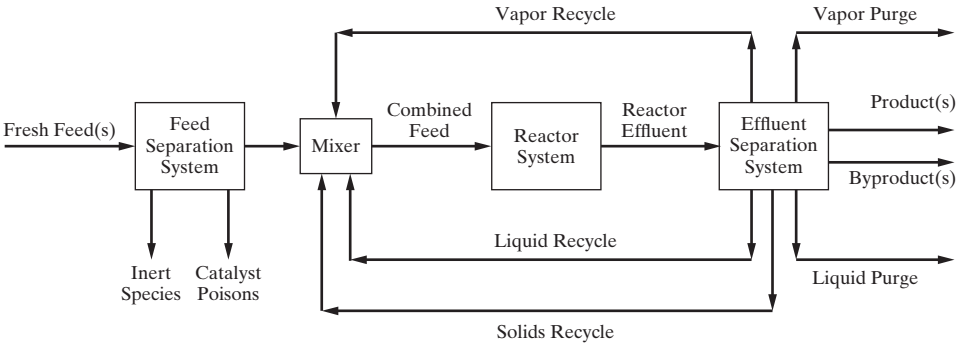

Figure 9.1 General flowsheet for a process with one reactor system.

catalyst; sulfur compounds, which form sulfur chlorides; hydrogen, which reacts with both chlorine and phosgene to form HCl; and water and hydrocarbons, which also form HCl.

Phase Separation of Reactor Effluent

In Figure 9.1, the reactor effluent may be a heterogeneous (two or more phases) mixture, but most often is a homogeneous (single-phase) mixture. When the latter, it is often advantageous to change the temperature and/or (but less frequently) the pressure to obtain a partial separation of the components by forming a heterogeneous mixture of two or more phases. Following the change in temperature and/or pressure, phase equilibrium is rapidly attained, resulting in the following possible phase conditions of the reactor effluent, where two liquid phases may form (phase splitting) when both water and hydrocarbons are present in the reactor effluent:

Possible Phase Conditions of Reactor Effluent

Vapor	Liquid
Vapor and liquid	Liquid 1 and liquid 2
Vapor, liquid 1 and liquid 2	Liquid and solids
Vapor and solids	Liquid 1, liquid 2, and solids
Vapor, liquid and solids	Solids
Vapor, liquid 1, liquid 2, and solids	

With the reasonable assumption that the phases in a heterogeneous mixture are in phase (physical) equilibrium for a given reactor effluent composition at the temperature and pressure to which the effluent is brought, process simulators can readily estimate the amounts and compositions of the phases in equilibrium by an isothermal (two-phase)-flash calculation provided that solids are not present. When the possibility of two liquid phases exists, it is necessary to employ a three-phase flash model rather than the usual two-phase flash model. The three-phase model considers the possibility that a vapor phase may also be present together with two liquid phases.

In the absence of solids, the resulting phases are separated, often by gravity, in a flash vessel for the V-L case, or in a decanter for the V-L1-L2 or L1-L2 cases. For the latter two cases, centrifugal force may be employed if gravity settling is too slow because of small liquid-density differences or high liquid viscosities. If solids are present with one or two liquid phases, it is not possible to separate completely the solids from the liquid phase(s). Instead, a centrifuge or filter is used to deliver a wet cake of solids that requires further processing to recover the liquid and dry the solids.

Several examples of phase-separation equipment are shown in Figure 9.2. Each exiting phase is either recycled to the reactor, purged from the system, or, most often, sent to separate vapor, liquid, or slurry separation systems as shown in Figure 9.3. The effluents from these separation systems are products, which are sent to storage; byproducts, which also leave the process; reactor-system recycle streams, which are sent back to the reactor; or separation-system recycle streams, which are sent to one of the other separation systems. Purges and byproducts are either additional valuable products, which are sent to storage; fuel byproducts, which are sent to a fuel supply or storage system; and/or waste streams, which are sent to waste treatment, incineration, or landfill.

Consider the following examples of phase-equilibria calculations for industrial reactor effluents:

1. ***Vapor–liquid Case.*** The reactor effluent for a toluene hydrodealkylation process, of the type discussed in Example 6.7, is a gas at 1,150°F and 520 psia. When brought to 100°F at say 500 psia by a series of heat exchangers, the result is a vapor phase in equilibrium with a single liquid phase. A two-phase flash calculation using the SRK equation of state gives the following results:

Reactor Effluent Phase Equilibrium for a Toluene Hydrodealkylation Process

Component	Effluent (lbmol/hr)	Vapor (lbmol/hr)	Liquid (lbmol/hr)
H_2	1,292	1,290	2
CH_4	1,167	1,149	18
Benzene	280	16	264
Toluene	117	2	115
Biphenyl	3	0	3
Total	2,859	2,457	402

As seen, a reasonably good separation is made between the light gases, H_2 and CH_4, and the three less-volatile

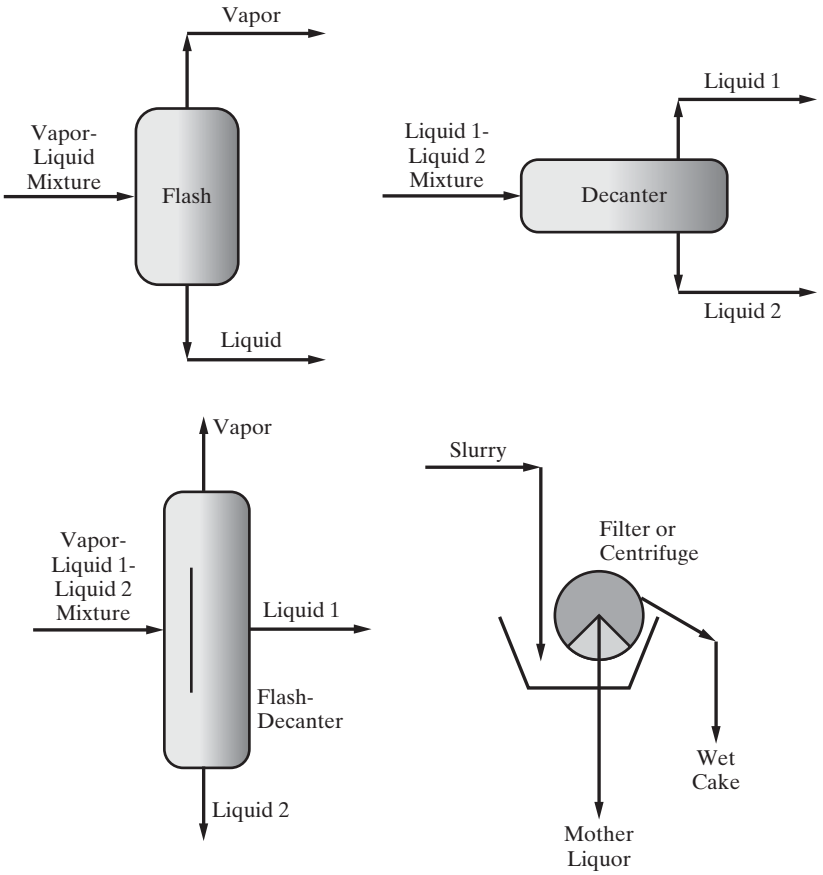

Figure 9.2 Examples of phase-separation devices.

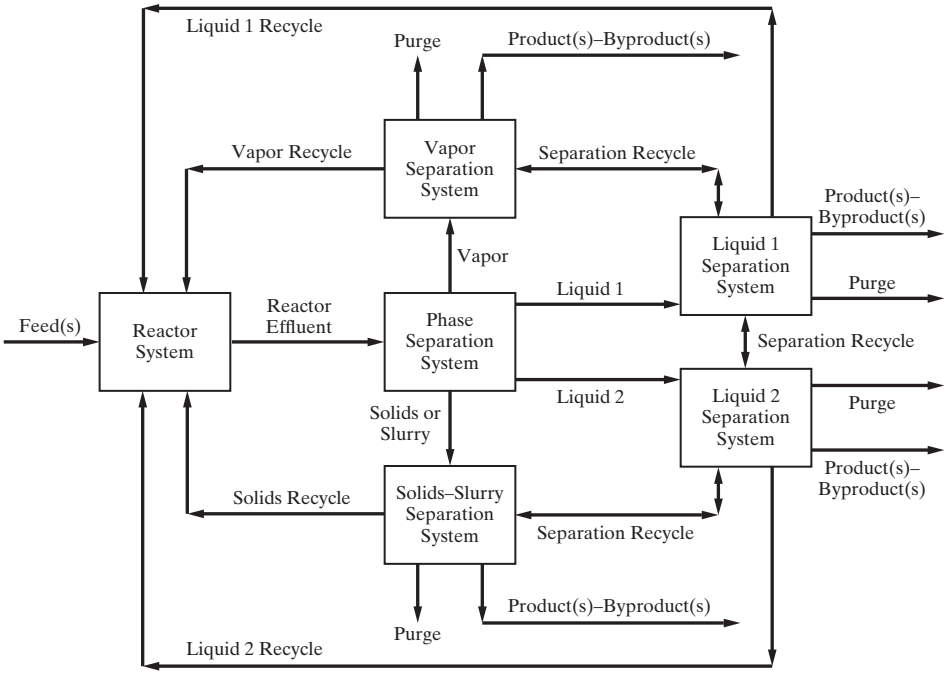

Figure 9.3 Process flowsheet showing separate separation systems with reactor-system and separation-system recycles.

aromatic hydrocarbons. The vapor is sent to a vapor separation system to recover CH_4 as a byproduct and H_2 for recycle. The liquid is sent to a liquid separation system to recover benzene as the main product, toluene for recycle to the reactor, and biphenyl as a fuel byproduct. Alternatively, the vapor can be divided without component separation into a reactor recycle stream and a vapor purge stream to prevent buildup of CH_4 whereas the biphenyl can be separated with the toluene and recycled to extinction. These two alternatives are shown in Figure 9.4.

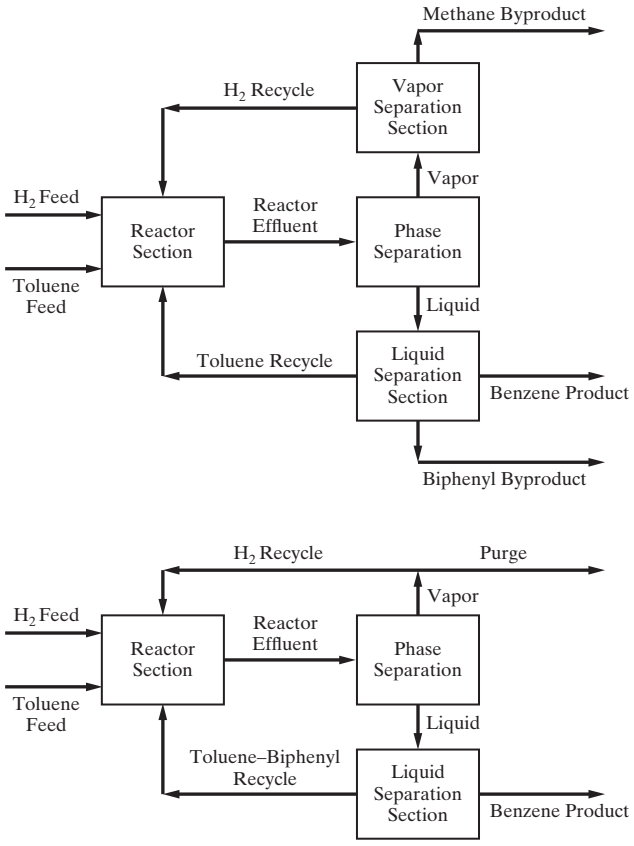

Figure 9.4 Alternative flowsheets for hydrodealkylation of toluene to benzene.

2. ***Vapor–liquid 1-liquid 2 Case.*** The reactor effluent in a styrene production process, involving the reaction:

$$\text{methanol} + \text{toluene} = \text{styrene} + \text{hydrogen} + \text{water}$$

with a side reaction of the same reactants that produces ethylbenzene and water, is a gas at 425°C and 330 kPa. When brought to 38°C at say 278 kPa by a series of heat exchangers, the result is a vapor phase in equilibrium with an organic-rich liquid phase and a water-rich liquid phase. A three-phase flash calculation using the NRTL method for estimating liquid-phase activity coefficients gives the following results:

Reactor Effluent Phase Equilibrium for a Styrene Process

Component	Effluent (lbmol/hr)	Vapor (lbmol/hr)	Liquid 1 (lbmol/hr)	Liquid 2 (lbmol/hr)
H_2	352.2	352.2	0.0	0.0
Methanol	107.3	9.9	31.0	66.4
Water	489.1	8.0	0.5	480.6
Toluene	107.3	1.7	105.5	0.1
Ethylbenzene	140.7	0.5	140.0	0.2
Styrene	352.2	2.0	350.1	0.1
Total	1,548.8	374.3	627.1	547.4

In this case, the vapor is 94 mol% H_2 for which a vapor separation section may not be needed. The organic-rich liquid phase (L1) is sent to a liquid separation section to recover a combined methanol and toluene stream for recycle to the reactor, ethylbenzene as a byproduct, and styrene as the main product. The water-rich liquid phase (L2) is sent to another liquid separation section to recover methanol for recycle to the reactor and water, which is sent to wastewater treatment to remove small quantities of soluble organic components. It is important to note that a two-phase flash calculation would produce erroneous results. If in doubt, perform a three-phase flash calculation rather than a two-phase flash calculation.

3. ***Vapor–solids Case.*** Phthalic anhydride is manufactured mainly by the vapor-phase partial oxidation of orthoxylene with excess air in a shell-and-tube fixed-bed reactor using vanadium pentoxide catalyst packed inside the tubes. Typically the reactor feed is very dilute in the orthoxylene with only 1.27 moles of orthoxylene per 100 moles of air. The main reaction consumes 80% of the orthoxylene to produce phthalic anhydride and water. The remaining 20% of the orthoxylene is completely and unavoidably oxidized to CO_2 and water vapor. Typical reactor effluent conditions are 660 K and 25 psia. The reactions are exothermic, with heat removal in the reactor by molten salt of the eutectic mixture of sodium and potassium nitrites and nitrates, which recirculates between the shell side of the reactor and a heat exchanger that produces steam. The reactor effluent is cooled, in a heat exchanger to produce steam from boiler feed water, to 180°C, which is safely above the primary dew point of 140°C, corresponding to condensation of liquid phthalic anhydride. The effluent then passes to one of two parallel desublimation condensers using cooling water, where the effluent is cooled to 70°C at 20 psia. Under these conditions, the phthalic anhydride desublimes on the outside of the extended-surface tubes of the heat exchanger as a solid because the temperature is well below its normal melting point of 131°C. The desublimation temperature of 70°C is safely above the secondary dew point of 36°C for the condensation of water. Two dew points can occur because water and phthalic anhydride are almost insoluble in each other. The water vapor will not begin to condense until its partial pressure in the vapor reaches its vapor pressure. At phase-equilibrium conditions of 70°C and 20 psia (1,034 torr), a two-phase flash calculation on the reactor effluent is performed on the reactor effluent. The calculation uses the Clausius–Clapeyron vapor-pressure equation of Crooks and Feetham (1946) for solid phthalic anhydride:

$$\text{Log}_{10}P^s = 12.249 - 4{,}632/T$$

where vapor pressure, P^s, is in torr and temperature, T, is in K. This equation is valid for temperatures in the range of 30°C to the normal melting point of 131°C and predicts a vapor pressure of 0.000517 torr at 25°C, which is in good

agreement with the often-quoted value of 0.000514 torr. Assuming that the solid phase is pure phthalic anhydride, its partial pressure in the equilibrium vapor phase is equal to its vapor pressure. The results of the two-phase flash calculation are:

Reactor Effluent Phase Equilibrium for a Phthalic Anhydride Process—Basis : 100 Moles of Reactor Effluent

Component	Effluent (moles)	Vapor (moles)	Solids (moles)
N_2	77.70	77.70	0.00
O_2	15.05	15.05	0.00
Orthoxylene	0.00	0.00	0.00
CO_2	2.00	2.00	0.00
H_2O	4.25	4.25	0.00
Phthalic anhydride	1.00	0.005	0.995
Total	100.00	99.005	0.995

At these equilibrium conditions of 70°C and 1,034 torr, the partial pressure of phthalic anhydride in the vapor is (0.005/99.005)1,034 = 0.05 torr, which is equal to its vapor pressure. The partial pressure of water in the vapor is (4.25/99.005)1,034 = 44.4 torr, which is well below its vapor pressure of 234 torr at 70°C. Thus, water does not condense at these conditions. The amount of solids in the table above corresponds to a 99.5% desublimation of phthalic anhydride. At 85°C the percent desublimation is only 98%, while at 96.4°C it is only 95%. Thus, the recovery of phthalic anhydride from the reactor effluent is sensitive to the desublimation condenser temperature.

While one desublimation condenser is removing 99.5% of the phthalic anhydride from the effluent, phthalic anhydride in the other condenser is melted with hot water at 160°C flowing inside the tubes and sent to a liquid separation section for the removal of small amounts of any impurities. Thus, the reactor effluent gas is switched back and forth between the two parallel cooling-water condensers. The vapor leaving the desublimation condenser is sent to a vapor separation section.

4. ***Vapor–liquid–solids Case.*** Magnesium sulfate as Epsom salts ($MgSO_4 \cdot 7H_2O$) is produced by the reaction of solid $Mg(OH)_2$ with an aqueous solution of sulfuric acid. A typical reactor effluent is a 10 wt% aqueous solution of $MgSO_4$ at 70°F and 14.7 psia. The effluent is concentrated to 37.75 wt% $MgSO_4$ in a double-effect evaporation system with forward feed, after which filtrate from a subsequent filtering operation is added. Crystallization is then carried out in a continuous adiabatic vacuum flash crystallizer operating at 85.6°F and 0.577 psia to produce a vapor and a magma (slurry of liquid and solid). By making an adiabatic enthalpy balance that accounts for the heat of crystallization, heat of vaporization, and the activity coefficient of water in a sulfate solution for a vapor phase of H_2O, an aqueous phase of dissolved sulfate using Figure 9.5 to obtain $MgSO_4$ solubility as a function of temperature, and a solid phase of hydrated magnesium sulfate crystals, the following phase-equilibrium conditions are calculated:

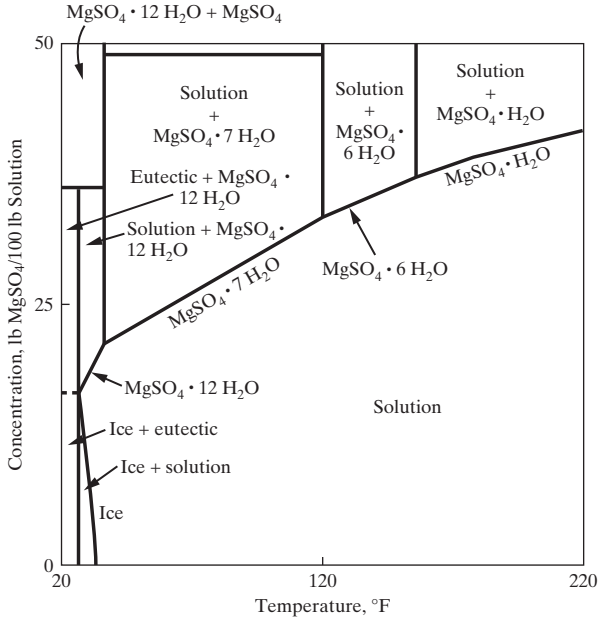

Figure 9.5 Phase diagram for the $MgSO_4 \cdot H_2O$ system.

Crystallizer Phase Equilibrium for a Magnesium Sulfate Process

Component	Effluent (lb/hr)	Vapor (lb/hr)	Liquid (lb/hr)	Solids (lb/hr)
H_2O	9,844	581	7,803	0
$MgSO_4$	4,480	0	3,086	0
$MgSO_4 \cdot 7H_2O$	0	0	0	2,854
Total	14,324	581	10,889	2,854

The vapor is condensed without further treatment. The magma of combined liquid and solids is sent to a slurry separation system to obtain a product of dry crystals of $MgSO_4 \cdot 7H_2O$.

Industrial Separation Operations

Following phase separation, the individual vapor, liquid, solids, and/or slurry streams are sent to individual separation systems, the most common of which is the liquid separation system. When the feed to a vapor or liquid separation system is a binary mixture, it may be possible to select a separation method that can accomplish the separation task in just one piece of equipment. In that case, the separation system is relatively simple. More commonly, however, the feed mixture involves more than two components.

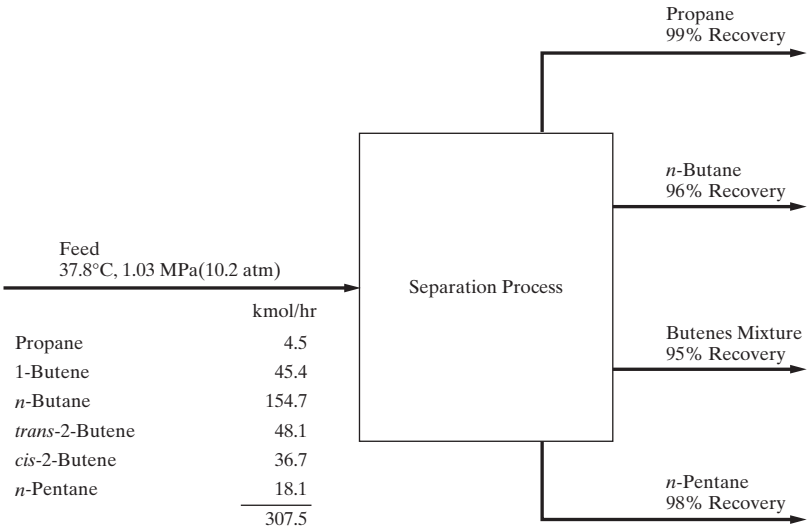

Figure 9.6 Specification for butenes recovery system.

Although some progress is being made in devising multicomponent separation systems involving a single piece of equipment, most systems involve a number of units in which the separations are sequenced, with each unit separating its feed stream into two effluent streams of different composition. The separation in each piece of equipment (unit) is made between two components designated as the key components for that particular separation unit. Each effluent is either a final product or a feed to another separation device. The synthesis of a multicomponent separation system can be very complex because it involves not only the selection of the separation method(s), but also the manner in which the pieces of separation equipment are sequenced. This chapter deals with both aspects of the synthesis problem.

As an example of the complexity of a multicomponent separation system, consider the synthesis of a separation system for the recovery of butenes from a C_4 concentrate from the catalytic dehydrogenation of *n*-butane. The specifications for the separation process are taken from Hendry and Hughes (1972) and are shown in Figure 9.6. The process feed, which contains propane, 1-butene, *n*-butane, *trans*-2-butene, *cis*-2-butene, and *n*-pentane, is to be separated into four fractions: (1) a propane-rich stream containing 99% of the propane in the feed, (2) an *n*-butane-rich stream containing 96% of the nC_4 in the feed, (3) a stream containing a mixture of the three butenes at 95% recovery, and (4) an *n*-pentane-rich stream containing 98% of the nC_5 in the feed. The C_3 and nC_5 streams are final products, the nC_4 stream is recycled to the catalytic dehydrogenation reactor, and the butenes stream is sent to another dehydrogenation reactor to produce butadienes.

Many different types of separation devices and sequences thereof can accomplish the separations specified in Figure 9.6. In general, the process design engineer seeks the most economical system. One such system, based on mature technology and the availability of inexpensive energy, is shown in Figure 9.7. The system involves two separation methods, distillation and extractive distillation. The process feed from the butane dehydrogenation unit is sent to a series of two distillation columns (1-butene columns, C-1A and C-1B), where the more volatile propane and 1-butene are removed as distillate and then separated in a second distillation column (depropanizer, C-2) into propane and 1-butene. Distillation unit C-1 consists of two columns because 150 trays are required, which are too many for a single column (since the tray spacing is typically 2 ft, giving a 300-ft high tower while most towers do not exceed 200 ft for structural reasons). The bottoms from unit C-1A, which consists mainly of *n*-butane, the 2-butene isomers, and nC_5, is sent to another distillation column (deoiler, C-3) where nC_5 product is removed as bottoms. The distillate stream from unit C-3 cannot be separated into nC_4-rich and 2-butenes-rich streams economically by ordinary distillation because the relative volatility is only about 1.03. Instead, the process in Figure 9.7 uses extractive distillation with a solvent of 96% furfural in water, which enhances the relative volatility to about 1.17. The separation occurs in columns C-4A and C-4B with nC_4 taken off as distillate. The bottoms is sent to a furfural stripper (C-5), where the solvent is recovered and recycled to unit C-4 and the 2-butenes are recovered as distillate. The 1-butene and 2-butenes streams are mixed and sent to a butenes dehydrogenation reactor. Although the process in Figure 9.7 is practical and economical, it does involve the separation of 1-butene from the 2-butenes. Perhaps another sequence could avoid this unnecessary separation.

The separation process of Figure 9.7 utilizes only distillation-type separation methods. These are usually the methods of choice for liquid or partially vaporized feeds unless the relative volatility between the two key components is less than 1.10 or extreme conditions of temperature and pressure are required. In those cases or for vapor, solid, or wet solid feeds, a number of other separation methods should be considered. These are listed in Table 9.1 in order of technical maturity as determined by Keller (1987), except for a few added separation methods not considered by Keller.

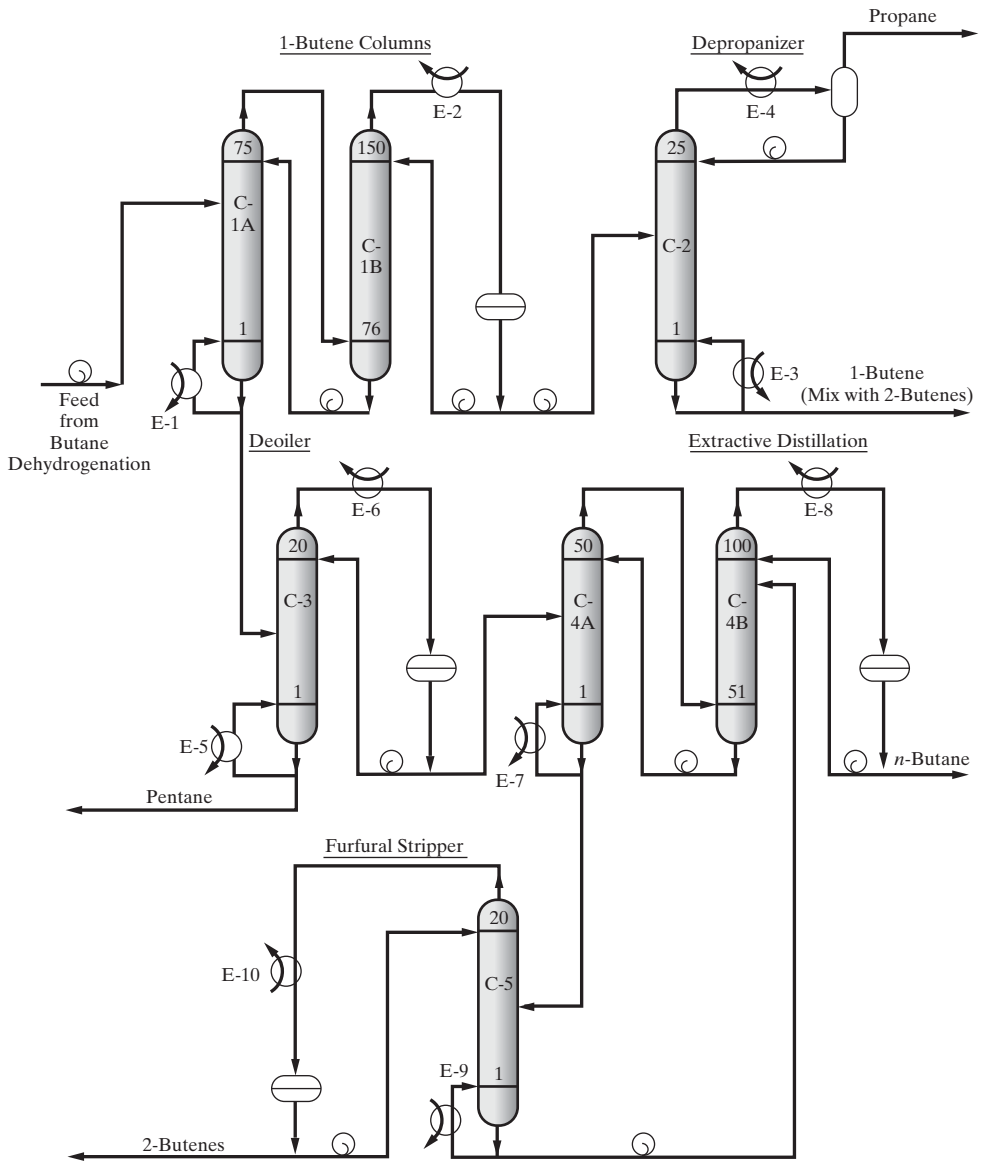

Figure 9.7 Process for butenes recovery; C = distillation column; E = heat exchanger.

As noted in Table 9.1, the feed to a separation unit usually consists of a single vapor, liquid, or solid phase. If the feed is composed of two or more coexisting phases, consideration should be given to separating the feed stream into two phases by some mechanical means of the type shown in Figure 9.2, and then sending the separated phases to different separation units, each appropriate for the phase condition of the stream.

The separation of a feed mixture into streams of differing chemical compositions is achieved by forcing individual species into different spatial locations. This is accomplished by any one or a combination of four common industrial techniques: (1) the creation by heat transfer, shaft work, or pressure reduction of a second phase; (2) the introduction into the system of a second fluid phase; (3) the addition of a solid phase on which selective adsorption can occur; and (4) the placement of a selective membrane barrier. Unlike the mixing of chemical species, which is a spontaneous process, the separation of a mixture of chemicals requires an expenditure of some form of energy. In the first technique, no other chemicals are added to the feed mixture and the separation is achieved by an energy-separating agent (ESA), usually heat transfer, which causes the formation of a second phase. The components are separated by differences in volatility, thus causing each species to favor one phase over another. In the second technique, a second phase is added to the separation unit in the form of a solvent as a mass-separating agent (MSA) that selectively dissolves or alters the volatility of certain species of the mixture. An additional separation step is usually required to recover the solvent for recycle. The third technique involves the addition of solid particles that selectively adsorb certain species of the mixture. Subsequently, the particles must be treated by another separation method to recover the adsorbed species and regenerate the adsorbent for further use. Thus, the particles act as

Table 9.1 Common Industrial Separation Methods

Separation Method	Phase Condition of Feed	Separating Agent(s)	Developed or Added Phase	Separation Property
Flash	L and/or V	Pressure reduction or heat transfer ESA	V or L	Volatility
Distillation (ordinary)	L and/or V	Heat transfer or shaft work ESA	V or L	Volatility
Gas absorption	V	Liquid absorbent MSA	L	Volatility
Stripping	L	Vapor stripping agent MSA	V	Volatility
Extractive distillation	L and/or V	Liquid solvent and heat transfer MSA	L and V	Volatility
Azeotropic distillation	L and/or V	Liquid entrainer and heat transfer MSA	L and V	Volatility
Liquid–liquid extraction	L	Liquid solvent MSA	Second L	Solubility
Crystallization	L	Heat transfer ESA	S	Solubility or melting point
Gas adsorption	V	Solid adsorbent MSA	S	Adsorbability
Liquid adsorption	L	Solid adsorbent MSA	S	Adsorbability
Membrane	L or V	Membrane ESA	Membrane	Permeability and/or solubility
Supercritical extraction	L or V	Supercritical solvent MSA	Supercritical fluid	Solubility
Leaching	S	Liquid solvent MSA	L	Solubility
Drying	S and L	Heat transfer ESA	V	Volatility
Desublimation	V	Heat transfer ESA	S	Volatility

an MSA. The fourth technique imposes a barrier that allows the permeation of some species over others. A mechanical energy loss accompanies the permeation. Thus, this technique involves an ESA. For all four techniques, mass transfer controls the rate of migration of species from one phase to another. Except for the fourth technique, the extent of mass transfer is limited by thermodynamic equilibrium between the phases. In the case of membrane separations, the exiting phases do not approach equilibrium; rather, the separation occurs strictly because of differences in the rates of permeation through the membrane.

9.2 CRITERIA FOR SELECTION OF SEPARATION METHODS

The development of a separation process requires the selection of (1) separation methods, (2) ESAs and/or MSAs, (3) separation equipment, (4) the optimal arrangement or sequencing of the equipment, and (5) the optimal operating conditions of temperature and pressure for the equipment.

When the process feed is a binary mixture and the task is to separate that mixture into two products, a single separation device may suffice if an ESA is used. If an MSA is necessary, an additional separation device will be required to recover the MSA for recycle. For a multicomponent feed that is to be separated into nearly pure components and/or one or more multicomponent products, more than one separation device is usually required. Not only must these devices be selected but also an optimal arrangement of the devices must be sought. In devising such a separation sequence, it is preferable not to separate components that must be blended later to form desired multicomponent products. However, many exceptions exist to this rule. For example, in Figure 9.6, a six-component mixture is separated into four products, one of which contains 1-butene and *cis*- and *trans*-2-butene. However, the process in Figure 9.7 shows the separation of 1-butene from the 2-butenes and subsequent blending to obtain the desired olefin mixture. The unnecessary separation is carried out because the volatility of *n*-butane is intermediate between that of 1-butene and the two 2-butene isomers. The process shown in Figure 9.7 is the most economical one known, as shown later in Example 9.3. In a multicomponent separation process, each separation operation generally separates between two components in which case the minimum number of operations is one less than the number of products. However, there are a growing number of exceptions to this rule, and cases are described later for which a single separation operation may produce only a partial separation.

Phase Condition of the Feed as a Criterion

When selecting a separation method from Table 9.1, the phase condition of the feed is considered first.

Vapor Feeds

If the feed is a vapor or is readily converted to a vapor, the following operations from Table 9.1 should be considered: (1) partial condensation (the opposite of a flash or partial vaporization), (2) distillation under cryogenic conditions, (3) gas absorption, (4) gas adsorption, (5) gas permeation with a membrane, and (6) desublimation.

Liquid Feeds

If the feed is a liquid or is readily converted to a liquid, a number of the operations in Table 9.1 may be applicable: (1) flash or partial vaporization, (2) (ordinary) distillation, (3) stripping, (4) extractive distillation, (5) azeotropic distillation, (6) liquid–liquid extraction, (7) crystallization, (8) liquid adsorption, (9) dialysis, reverse osmosis, ultrafiltration, and pervaporation with a

membrane, and (10) supercritical extraction. A flash and the different types of distillation are also applicable for feeds consisting of combined liquid and vapor phases.

Slurries, Wet Cakes, and Dry Solids

Slurry feeds are generally separated first by filtration or centrifugation to obtain a wet cake, which is then separated into a vapor and a dry solid by drying. Feeds consisting of dry solids can be leached with a selective solvent to separate the components.

Separation Factor as a Criterion

The second consideration for the selection of a separation method is the separation factor, SF, which can be achieved by the particular separation method for the separation between two key components of the feed. This factor for the separation of key component 1 from key component 2 between phases I and II for a single stage of contacting is defined as

$$\text{SF} = \frac{C_1^{\text{I}}/C_2^{\text{I}}}{C_1^{\text{II}}/C_2^{\text{II}}} \tag{9.1}$$

where C_j^i is a composition (expressed as a mole fraction, mass fraction, or concentration) of component j in phase i. If phase I is to be rich in component 1 and phase II is to be rich in component 2, then SF must be large. The value of SF is limited by thermodynamic equilibrium except for membrane separations that are controlled by relative rates of mass transfer through the membrane. For example, in the case of distillation, using mole fractions as the composition variable and letting phase I be the vapor and phase II be the liquid, the limiting value of SF is given in terms of vapor and liquid equilibrium ratios (K-values) by

$$\text{SF} = \frac{y_1/y_2}{x_1/x_2} = \frac{y_1/x_1}{y_2/x_2} = \frac{K_1}{K_2} = \alpha_{1,2} \tag{9.2}$$

where α is the relative volatility. In general, components 1 and 2 are designated in such a manner that SF > 1.0. Consequently, the larger the value of SF, the more feasible is the particular separation operation. However, when seeking a desirable SF value, it is best to avoid extreme conditions of temperature that may require refrigeration or damage heat-sensitive materials; pressures that may require gas compression or vacuum; and MSA concentrations that may require expensive means to recover the MSA. In general, operations employing an ESA are economically feasible at a lower value of SF than are those employing an MSA. In particular, provided that vapor and liquid phases are readily formed, distillation should always be considered first as a possible separation operation if the feed is a liquid or partially vaporized.

When a multicomponent mixture forms nearly ideal liquid and vapor solutions, and the ideal gas law holds, the K-values and relative volatility can be readily estimated from vapor pressure data. Such K-values are referred to as ideal or Raoult's law K-values. Then, the SF for vapor–liquid separation operations employing an ESA (partial evaporation, partial condensation, or distillation) is given by

$$\text{SF} = \alpha_{1,2} = \frac{P_1^s}{P_2^s} \tag{9.3}$$

where P_i^s is the vapor pressure of component i. When the components form moderately nonideal liquid solutions (hydrocarbon mixtures or homologous series of other organic compounds) and/or pressures are elevated, an equation-of-state, such as Soave–Redlich–Kwong (SRK) or Peng–Robinson (PR), may be necessary for the estimation of the separation factor, using

$$\text{SF} = \alpha_{1,2} = \frac{\overline{\phi}_1^L/\overline{\phi}_1^V}{\overline{\phi}_2^L/\overline{\phi}_2^V} \tag{9.4}$$

where $\overline{\phi}_i$ is the mixture fugacity coefficient of component i.

For vapor–liquid separation operations (e.g., azeotropic and extractive distillation) that use an MSA that causes the formation of a nonideal liquid solution but operate at near ambient pressure, expressions for the K-values of the key components are based on a modified Raoult's law that incorporates liquid-phase activity coefficients. Thus, the separation factor is given by

$$\text{SF} = \alpha_{1,2} = \frac{\gamma_1^L P_1^s}{\gamma_2^L P_2^s} \tag{9.5}$$

where γ_i is the activity coefficient of component i, which is estimated from the Wilson, NRTL, UNIQUAC, or UNIFAC equations and is a strong function of mixture composition.

If an MSA is used to create two liquid phases, such as in liquid–liquid extraction, the SF is referred to as the relative selectivity, β:

$$\text{SF} = \beta_{1,2} = \frac{\gamma_1^{\text{II}}/\gamma_2^{\text{II}}}{\gamma_1^{\text{I}}/\gamma_2^{\text{I}}} \tag{9.6}$$

where phase II is usually the MSA-rich phase and component 1 is more selective for the MSA-rich phase than is component 2.

In general, MSAs for extractive distillation and liquid–liquid extraction are selected according to their ease of recovery for recycle and to achieve relatively large values of SF. Such MSAs are often polar organic compounds (e.g., furfural) used in the example earlier to separate n-butane from 2-butenes. In some cases, the MSA is selected in such a way that it forms one or more homogeneous or heterogeneous azeotropes with the components in the feed. For example, the addition of n-butyl acetate to a mixture of acetic acid and water results in a heterogeneous minimum-boiling azeotrope of the acetate with water. The azeotrope is taken overhead, the acetate and water layers are separated, and the acetate is recirculated.

Although the degree of separation that can be achieved for a given value of SF is almost always far below that required to attain necessary product purities, the application of efficient countercurrent-flow cascades of many contacting stages as in distillation operations can frequently achieve sharp separations. For example, consider a mixture of 60 mol% propylene and 40 mol% propane. It is desired to separate this mixture into two products at 290 psia, one containing 99 mol% propylene and the other 95 mol% propane. By material balance, the former product would constitute 58.5 mol% of the feed and the latter 41.5 mol%. From equilibrium thermodynamics, the relative volatility for this mixture is approximately 1.12. A single equilibrium vaporization at 290 psia to produce 58.5 mol% vapor results in products that are far short of the desired compositions: a vapor containing just 61.12 mol% propylene and a liquid containing just 51.36 mol%

propane at 51.4°C. However, with a countercurrent cascade of such stages in a simple (single-feed, two-product) distillation column with reflux and boilup, the desired products can be achieved with 200 stages and a reflux ratio of 15.9.

Single-stage operations (e.g., partial vaporization or partial condensation with the use of an ESA) are utilized only if SF between the two key components is very large or if a rough or partial separation is needed. For example, if SF = 10,000, a mixture containing equimolar parts of components 1 and 2 could be partially vaporized to give a vapor containing 99 mol% of component 1 and a liquid containing 99 mol% of component 2. At low values of SF, lower than 1.10 but greater than 1.05, ordinary distillation may still be the most economical choice. However, an MSA may be able to enhance the value of SF for an alternative separation method to the degree that the method becomes more economical than ordinary distillation. As illustrated in Figure 9.8 from Souders (1964), extractive distillation or liquid–liquid extraction may be preferred if the SF can be suitably enhanced. If SF = 2 for ordinary distillation, it must be above 3.3 for extractive distillation to be an acceptable alternative and above 18 for liquid–liquid extraction.

Unless values of SF are about 10 or above, absorption and stripping operations cannot achieve sharp separation between two components. Nevertheless, these operations are used widely for preliminary or partial separations where the separation of one key component is sharp, but only a partial separation of the other key component is adequate. The degree of sharpness of separation is given by the recovery factor RF,

$$\mathrm{RF} = \frac{n_i^I}{n_i^F} \tag{9.7}$$

where n is moles or mass, I is the product rich in i, and F is the feed.

The separation of a solid mixture may be necessary when one or more (but not all) of the components are (is) not readily melted, sublimed, or vaporized. Such operations may even be preferred when boiling points are close but melting points are far apart, as is the case with many isomeric pairs. The classic example is the separation of metaxylene from paraxylene whose normal boiling points differ only by 0.8°C but whose melting points differ by 64°C. With an SF of only 1.02, as determined from Eq. (9.2), ordinary distillation to produce relatively pure products from an equimolar mixture of the two isomers would require about 1,000 stages and a reflux ratio of more than 100. For the separation by crystallization, the SF is nearly infinity because essentially pure paraxylene is crystallized. However, the mother liquor contains at least 13 mol% paraxylene in metaxylene, corresponding to the limiting eutectic composition. When carefully carried out, crystallization can achieve products of very high purity.

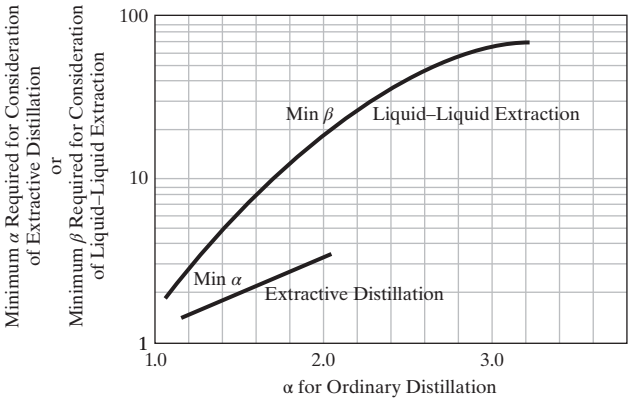

Figure 9.8 Relative selectivities for equal-cost separators. Adapted from Souders, 1964. Reproduced with permission of the American Institute of Chemical Engineers. Copyright © 1964 AIChE. All rights reserved.

The separation factor for adsorption depends on either differences in the rate of adsorption or adsorption equilibrium, with the latter being more common in industrial applications. For equilibrium adsorption, Eq. (9.1) applies where the concentrations are those at equilibrium on the adsorbed layer within the pores of the adsorbent and in the bulk fluid external to the adsorbent particles. High selectivity for adsorbents is achieved either by sieving, as with molecular-sieve zeolites or carbon, or by large differences in adsorbability. For example, in the case of molecular-sieve zeolites, aperture sizes of 3, 4, 5, 8, and 10 Å are available. Thus, nitrogen molecules, with a kinetic diameter of about 3.6 Å, can be separated from ammonia with a kinetic diameter of about 2.6 Å, using a zeolite with an aperture of 3 Å. Only the ammonia is adsorbed. Adsorbents of silica gel and activated alumina having wide distributions of pore diameters in the range of 20 to 100 Å are highly selective for water, whereas activated carbon with pore diameters in the same range is highly selective for organic compounds. When adsorption is conducted in fixed beds, essentially complete removal from the feed of those components with high selectivity can be achieved until breakthrough occurs. Before breakthrough, regeneration or removal of the adsorbent is required.

If only a small amount of one component is present in a mixture, changing the phase of the components in high concentrations should be avoided. In such a case, absorption, stripping, or selective adsorption best removes the minor component. Adsorption is particularly effective because of the high selectivity of adsorbents and is widely used for purification, where small amounts of a solute are removed from a liquid or vapor feed.

For membrane separation operations, SF may still be defined by Eq. (9.1). However, SF is governed by relative rates of mass transfer in terms of permeabilities rather than by equilibrium considerations. For the ideal case where the downstream concentration is negligible compared to the upstream concentration, the separation factor reduces to:

$$\mathrm{SF} = \frac{P_{M_1}}{P_{M_2}} \tag{9.8}$$

where P_{M_i} is the permeability of species i. In most cases, the value of SF must be established experimentally. In general, membrane separation operations should be considered whenever adsorption methods are considered. Membranes are either porous or nonporous. If porous, the permeability is proportional to the diffusivity through the pore. If nonporous, the permeability is the product of the solubility of the molecule in the membrane and its diffusivity for travel through the membrane. An example of

the use of membranes is gas permeation with nonporous hollow fibers to separate hydrogen, helium, carbon dioxide, and/or water vapor from gases containing oxygen, nitrogen, carbon monoxide, and/or light hydrocarbons. For a typical membrane, the SF between hydrogen and methane is 6. Because it is difficult to achieve large numbers of stages with membranes, an SF of this magnitude is not sufficient to achieve a sharp separation, but is widely used to make a partial separation. Sharp separations can be achieved by sieving when the kinetic molecular diameters of the components to be separated differ widely and when membrane pore diameter lies between those kinetic diameters.

Supercritical extraction utilizes the solvent power of a gas at near-critical conditions. It is the preferred method for the removal of undesirable ingredients from foodstuffs with carbon dioxide. The separation factor, which is given by Eq. (9.1), is difficult to estimate from equations of state using Eq. (9.4) and is best determined by experiment. Equation (9.1) also applies for leaching (solid–liquid extraction), often using a highly selective solvent. As with supercritical extraction, the value of SF is best determined by experiment. Because mass transfer in a solid is very slow, it is important to preprocess the solid to drastically decrease the distance for diffusion. Typical methods involve making thin slices of the solid or pulverizing it. Desublimation is best applied when a sublimable component is to be removed from noncondensable components of a gas stream, corresponding to a very large separation factor.

Reason for the Separation as a Criterion

A final consideration in the selection of a separation method is the reason for the separation. Possible reasons are (1) purification of a species or group of species, (2) removal of undesirable constituents, and (3) recovery of constituents for subsequent processing or removal. In the case of purification, the use of an MSA method may avoid exposure with an ESA method to high temperatures that may cause decomposition. In some cases, removal of undesirable species together with a modest amount of desirable species may be economically acceptable. Likewise, in the recovery of constituents for recycle, a high degree of separation from the product(s) may not be necessary.

9.3 SELECTION OF EQUIPMENT

Only a very brief discussion of equipment for separation operations is presented here. Much more extensive presentations, including drawings and comparisons, are given in Perry's *Chemical Engineers' Handbook* (Green and Perry, 2008) and by Kister (1992), Walas (1988), and Seader et al. (2016). In general, equipment selection is based on stage or mass-transfer efficiency, pilot-plant tests, scale-up feasibility, investment and operating cost, and ease of maintenance.

Absorption, Stripping, and Distillation

For absorption, stripping, and all types of distillation (i.e., vapor–liquid separation operations), either trayed or packed columns are used. Trayed columns are usually preferred for initial installations, particularly for columns 3 ft or more in diameter. However, packed columns should be given serious consideration for operation under vacuum or where a low pressure drop is desired. Other applications favoring packed columns are corrosive systems, foaming systems, and cases where low liquid holdup is desired. Packing is also generally specified for revamps. Applications favoring trayed columns are feeds containing solids, high liquid-to-gas ratios, large-diameter columns, and where operation over a wide range of conditions is necessary. The three most commonly used tray types are sieve, valve, and bubble cap. However, because of high cost, the latter is specified only when a large liquid holdup is required on the tray, for example, when conducting a chemical reaction simultaneously with distillation. Sieve trays are the least expensive and have the lowest pressure drop per tray, but they have the narrowest operating range (turndown ratio). Therefore, when flexibility is required, valve trays are a better choice. Many different types of packings are available. They are classified as random or structured. The latter are considerably more expensive than the former, but have the lowest pressure drop, the highest efficiency, and the highest capacity compared to both random packings and trays. For that reason, structured packings are often considered for column revamps.

Liquid–Liquid Extraction

For liquid–liquid extraction, an even greater variety of equipment is available, including multiple mixer-settler units or single countercurrent-flow columns with or without mechanical agitation. Very compact, but expensive, centrifugal extractors are also available. When the equivalent of only a few theoretical stages is required, mixer-settler units may be the best choice because efficiencies approaching 100% are achievable in each unit. For a large number of stages, columns with mechanical agitation may be favored. Packed and perforated tray columns can be very inefficient and are not recommended for critical separations.

Membrane Separation

Most commercial membrane separations use natural or synthetic glassy or rubbery polymers. To achieve high permeability and selectivity, nonporous materials are preferred, with thicknesses ranging from 0.1 to 1.0 micron, either as a surface layer or film onto or as part of much thicker asymmetric or composite membrane materials, which are fabricated primarily into spiral-wound and hollow-fiber-type modules to achieve a high ratio of membrane surface area to module volume.

Adsorption

For commercial applications, an adsorbent must be chosen carefully to give the required selectivity, capacity, stability, strength, and regenerability. The most commonly used adsorbents are activated carbon, molecular-sieve carbon, molecular-sieve zeolites, silica gel, and activated alumina. Of particular importance in the selection process is the adsorption isotherm for competing solutes when using a particular adsorbent. Most adsorption operations are conducted in a semicontinuous cyclic mode that

includes a regeneration step. Batch slurry systems are favored for small-scale separations whereas fixed-bed operations are preferred for large-scale separations. Quite elaborate cycles have been developed for the latter.

Leaching

Equipment for leaching operations is designed for either batchwise or continuous processing. For rapid leaching, it is best to reduce the size of the solids by grinding or slicing. The solids are contacted by the solvent using either percolation or immersion. A number of different patented devices are available.

Crystallization

Crystallization operations include the crystallization of an inorganic compound from an aqueous solution (solution crystallization) and the crystallization of an organic compound from a mixture of organic chemicals (melt crystallization). On a large scale, solution crystallization is frequently conducted continuously in a vacuum evaporating draft-tube baffled crystallizer to produce crystalline particles whereas the falling-film crystallizer is used for melt crystallization to produce a dense layer of crystals.

Drying

A number of factors influence the selection of a dryer from the many different types available. These factors are dominated by the nature of the feed, whether it be granular solids, a paste, a slab, a film, a slurry, or a liquid. Other factors include the need for agitation, the type of heat source (convection, radiation, conduction, or microwave heating), and the degree to which the material must be dried. The most commonly employed continuous dryers include tunnel, belt, band, turbo-tray, rotary, steam-tube rotary, screw-conveyor, fluidized-bed, spouted-bed, pneumatic-conveyor, spray, and drum dryers.

9.4 SEQUENCING OF ORDINARY DISTILLATION COLUMNS FOR THE SEPARATION OF NEARLY IDEAL LIQUID MIXTURES

Multicomponent mixtures are often separated into more than two products. Although one piece of equipment of complex design might be devised to produce all the desired products, a sequence of two-product separators is more common.

For nearly ideal feeds such as hydrocarbon mixtures and mixtures of a homologous series, for example, alcohols, the most economical sequence will often include only ordinary distillation columns provided that the following conditions hold:

1. The relative volatility between the two selected key components for the separation in each column is greater than 1.05.
2. The reboiler duty is not excessive. An example of an excessive duty occurs in the distillation of a mixture with a low relative volatility between the two key components where the light key component is water, which has a very high heat of vaporization.
3. The tower pressure does not cause the mixture to approach its critical temperature.
4. The overhead vapor can be at least partially condensed at the column pressure to provide reflux without excessive refrigeration requirements.
5. The bottoms temperature at the tower pressure is not so high that chemical decomposition occurs.
6. Azeotropes do not prevent the desired separation.
7. Column pressure drop is tolerable, particularly if operation is under vacuum.

Column Pressure and Type of Condenser

During the development of distillation sequences, it is necessary to make at least preliminary estimates of column-operating pressures and condenser types (total or partial). The estimates are facilitated by the use of the algorithm in Figure 9.9, which is conservative. Assume that cooling water is available at 90°F, sufficient to cool and condense a vapor to 120°F. The bubble-point pressure is calculated at 120°F for an estimated distillate composition. If the computed pressure is less than 215 psia, use a total condenser unless a vapor distillate is required, in which case use a partial condenser. If the pressure is less than 30 psia, set the condenser pressure to 30 psia and avoid near-vacuum operation. If the distillate bubble-point pressure is greater than 215 psia, but less than 365 psia, use a partial condenser. If it is greater than 365 psia, determine the dew-point pressure for the distillate as a vapor. If the pressure is greater than 365 psia, operate the condenser at 415 psia with a suitable refrigerant in place of cooling water. For the selected condenser pressure, add 10 psia to estimate the bottoms pressure (for nonvacuum duty, acceptable column pressure drops are in the range 0.05–0.15 psi/tray), and compute the bubble-point temperature for an estimated bottoms composition. If that temperature exceeds the decomposition or critical temperature of the bottoms, reduce the condenser pressure appropriately.

Number of Sequences of Ordinary Distillation Columns

Initial consideration is usually given to a sequence of ordinary distillation columns, where a single feed is sent to each column and the products from each column number just two, the distillate and the bottoms. For example, consider a mixture of benzene, toluene, and biphenyl. Because the normal boiling points of the three components (80.1, 110.8, and 254.9°C, respectively) are widely separated, the mixture can be conveniently separated into three nearly pure components by ordinary distillation. A common process for separating this mixture is the sequence of two ordinary distillation columns shown in Figure 9.10a. In the first column, the most volatile component, benzene, is taken overhead as a distillate final product. The bottoms is a mixture of toluene and biphenyl, which is sent to the second column for separation into the two other final products: a distillate of toluene and a bottoms of biphenyl, the least volatile component.

Even if a sequence of ordinary distillation columns is used, not all columns need give nearly pure products. For example,

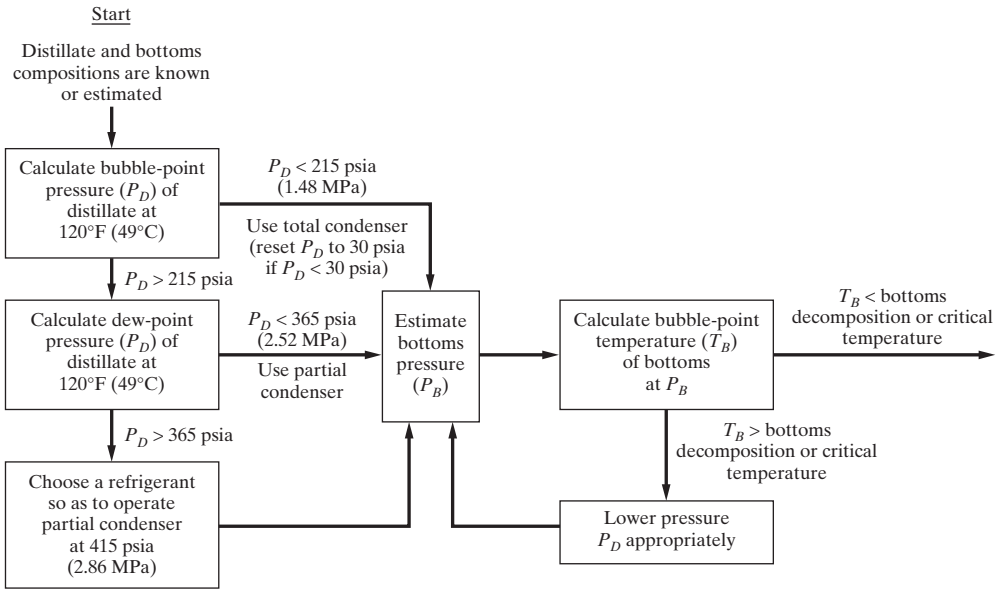

Figure 9.9 Algorithm for establishing distillation column pressure and condenser type.

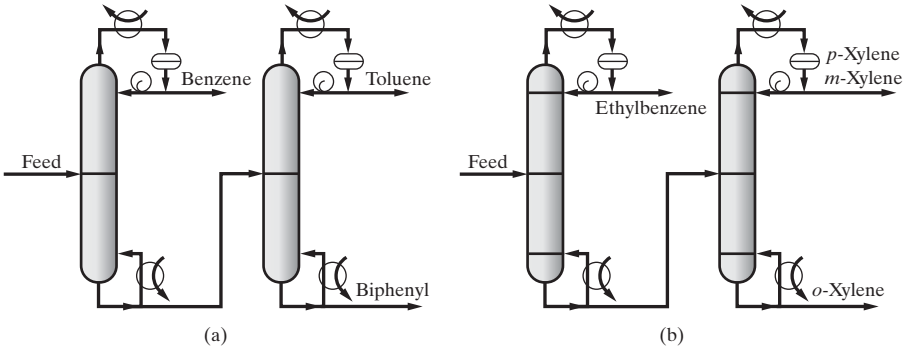

Figure 9.10 Distillation configurations for separation of ternary mixtures: (a) separation of a benzene-toluene-biphenyl mixture; (b) separation of xylene isomers.

Figure 9.10b shows a distillation sequence for the separation of a mixture of ethylbenzene, *p*-xylene, *m*-xylene, and *o*-xylene into only three products: nearly pure ethylbenzene, a mixture of *p*- and *m*-xylene, and nearly pure *o*-xylene. The para and meta isomers are not separated because the normal boiling points of these two compounds differ by only 0.8°C, making separation by distillation impractical.

Note in Figure 9.10 that it takes a sequence of two ordinary distillation columns to separate a mixture into three products. Furthermore, other sequences can produce the same final products. For example, the separation of benzene, toluene, and biphenyl shown in Figure 9.10a can also be achieved by removing biphenyl as bottoms in the first column, followed by the separation of benzene and toluene in the second column. However, the separation of toluene from benzene and biphenyl by ordinary distillation in the first column is impossible because toluene is intermediate in volatility. Thus, the number of possible sequences is limited to two for this case of the separation of a ternary mixture into three nearly pure products.

Now consider the more general case of the synthesis of all possible ordinary distillation sequences for a multicomponent feed that is to be separated into P final products that are nearly pure components and/or multicomponent mixtures. The components in the feed are ordered by volatility with the first component being the most volatile. This order is almost always consistent with that for normal boiling point if the mixture forms nearly ideal liquid solutions, such that Eq. (9.3) applies. Assume that the order of volatility of the components does not change as the sequence proceeds. Furthermore, assume that any multicomponent products contain only components that are adjacent in volatility. For example, suppose that the previously cited mixture of benzene, toluene, and biphenyl is to be separated into toluene and a multicomponent product of benzene and biphenyl. With ordinary distillation, it would be necessary first to produce products of benzene, toluene, and biphenyl and then blend the benzene and biphenyl.

An equation for the number of different sequences of ordinary distillation columns, N_s, to produce a number of products, P, can be developed in the following manner. For the first separator in the sequence, $P - 1$ separation points are possible. For example, if the desired products are A, B, C, D, and E in order of decreasing volatility, then the possible separation points are $5 - 1 = 4$,

Table 9.2 Number of Possible Sequences for Separation by Ordinary Distillation

Number of Products, P	Number of Separators in the Sequence	Number of Different Sequences, N_s
2	1	1
3	2	2
4	3	5
5	4	14
6	5	42
7	6	132
8	7	429
9	8	1,430
10	9	4,862

as follows: A–B, B–C, C–D, and D–E. Now let j be the number of final products that must be developed from the distillate of the first column. For example, if the separation point in the first column is C–D, then $j = 3$ (A, B, C). Then $P - j$ equals the number of final products that must be developed from the bottoms of the first column. If N_i is the number of different sequences for i final products, then for a given separation point in the first column, the number of sequences is $N_j N_{P-j}$. But in the first separator, $P - 1$ different separation points are possible. Thus, the number of different sequences for P products is the following sum:

$$N_s = \sum_{j=1}^{P-1} N_j N_{P-j} = \frac{[2(P-1)]!}{P!(P-1)!} \tag{9.9}$$

Application of Eq. (9.9) gives results shown in Table 9.2 for sequences producing up to 10 products. As shown, the number of sequences grows rapidly as the number of final products increases.

Equation (9.9) gives five possible sequences of three columns for a four-component feed. These sequences are shown in Figure 9.11. The first, where all final products but one are distillates, is often referred to as the *direct sequence*. It is widely used in industry because distillate final products are more free of impurities such as objectionable high-boiling compounds and solids. If the purity of the final bottoms product (D) is critical, it may be produced as a distillate in an additional column called a rerun (or finishing) column. If all products except one are bottoms products, the sequence is referred to as the *indirect sequence*. This sequence is generally considered to be the least desirable sequence because of difficulties in achieving purity specifications for bottoms products. The other three sequences in Figure 9.11 produce two products as distillates and two products as bottoms. In all sequences except one, at least one final product is produced in each column.

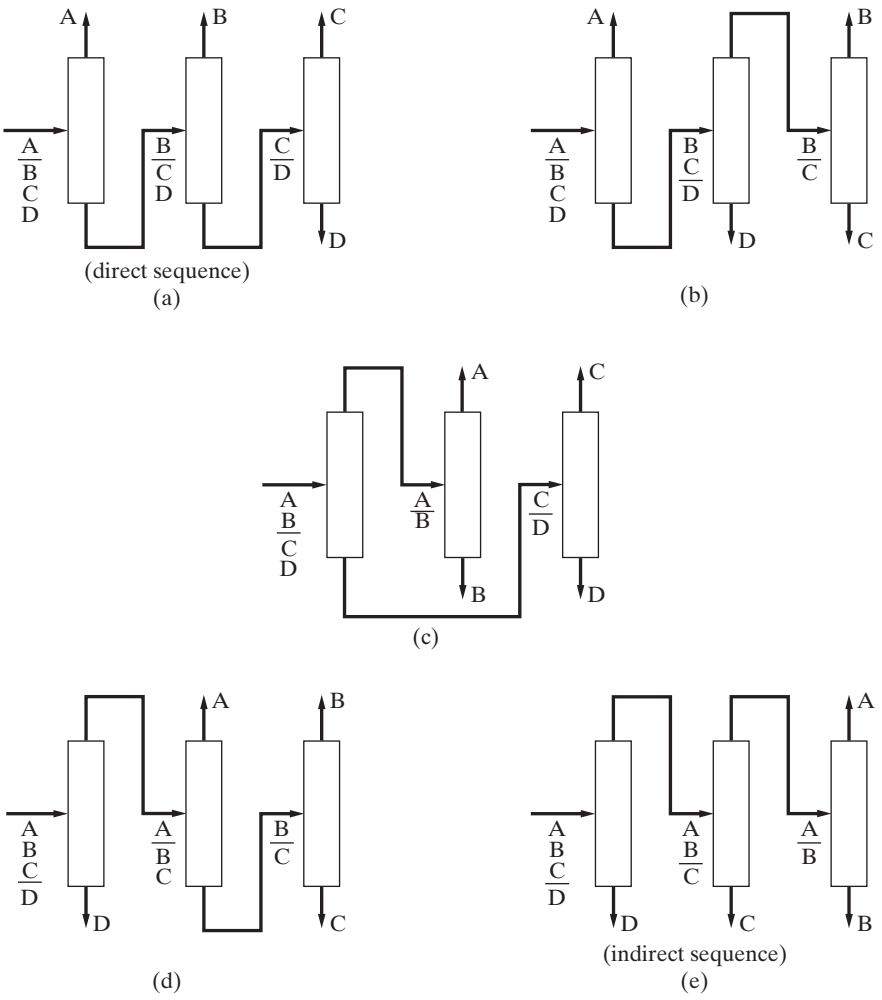

Figure 9.11 The five sequences for a four-component feed.

EXAMPLE 9.1

Ordinary distillation is to be used to separate the ordered mixture C_2, $C_3^=$, C_3, 1-$C_4^=$, nC_4 into the three products C_2; ($C_3^=$, 1-$C_4^=$); (C_3, nC_4). Determine the number of possible sequences.

SOLUTION

Neither multicomponent product contains adjacent components in the ordered list. Therefore, the mixture must be completely separated with subsequent blending to produce the ($C_3^=$, 1-$C_4^=$) and (C_3, nC_4) products. Thus, from Table 9.2 with P taken as 5, $N_s = 14$.

Heuristics for Determining Favorable Sequences

When the number of products is three or four, designing and costing all possible sequences can best determine the most economical sequence. Often, however, unless the feed mixture has a wide distribution of component concentrations or a wide variation of relative volatilities for the possible separation points, the costs will not vary much and the sequence selection may be based on operation factors. In that case, the direct sequence is often the choice. Otherwise, a number of heuristics that have appeared in the literature, starting in 1947, have proved useful for reducing the number of sequences for detailed examination. The most useful of these heuristics are:

1. Remove thermally unstable, corrosive, or chemically reactive components early in the sequence.
2. Remove final products one-by-one as distillates (the direct sequence).
3. Sequence separation points to remove, early in the sequence, those components of greatest molar percentage in the feed.
4. Sequence separation points in the order of decreasing relative volatility so that the most difficult splits are made in the absence of the other components.
5. Sequence separation points to leave last those separations that give the highest purity products.
6. Sequence separation points that favor near equimolar amounts of distillate and bottoms in each column.

None of these heuristics require column design and costing. Unfortunately, however, these heuristics often conflict with each other. Thus, more than one sequence will be developed, and cost and other factors will need to be considered to develop an optimal final design. When energy costs are relatively high, the sixth heuristic often leads to the most economical sequence. Heuristics 2–6 are consistent with observations about the effect of the nonkey components on the separation of two key components. These nonkey components can increase the reflux and boilup requirements, which, in turn, increase column diameter and reboiler operating cost. These and the number of trays are the major factors affecting the investment and operating costs of a distillation operation.

EXAMPLE 9.2

Consider the separation problem shown in Figure 9.12a except that separate isopentane and n-pentane products are also to be obtained with 98% recoveries. Use heuristics to determine a good sequence of ordinary distillation units.

SOLUTION

Approximate relative volatilities for all adjacent pairs are:

Component Pair	Approximate α at 1 atm
C_3/iC_4	3.6
iC_4/nC_4	1.5
nC_4/iC_5	2.8
iC_5/nC_5	1.35

For this example, there are wide variations in both relative volatility and molar percentages in the process feed. The choice is Heuristic 4, which dominates over Heuristic 3 and leads to the sequence shown in Figure 9.12b, where the first split is between the pair with the highest relative volatility. This sequence also corresponds to the optimal arrangement.

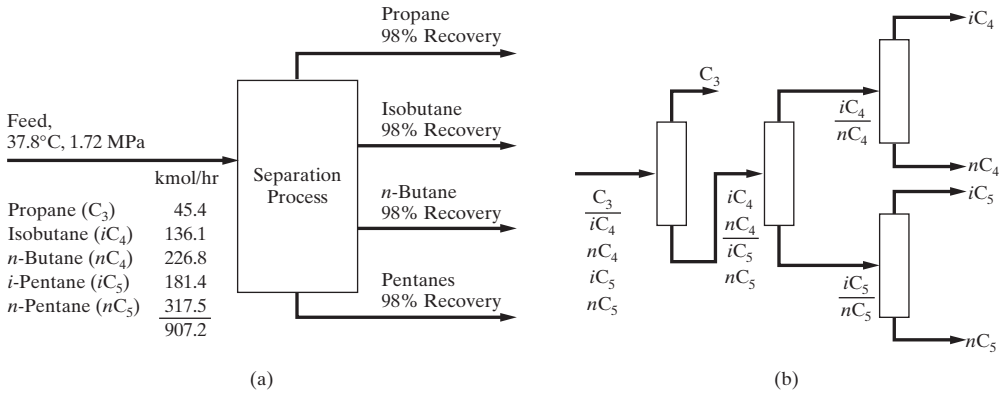

Figure 9.12 Synthesis problem and separation train for Example 9.2: (a) paraffin separation problem; (b) sequence developed from heuristics.

Sequencing of General Vapor–Liquid Separation Processes

When ordinary distillation is not practical for each separator in a sequence for separating a multicomponent mixture, other types of separators must be employed and the order of volatility or other separation index may be different for each type. Of great importance when other types of separators are used is that the number of possible sequences is greatly increased over the value calculated from Eq. (9.9). Usually the number of different types of separators to be considered is limited by applicability. If they are all two-product separators and if T equals the number of different types, then the number of possible sequences is given by

$$N_s^T = T^{P-1} N_s \tag{9.10}$$

When a separator type utilizes a recycled MSA, as, for example, with extractive distillation, homogeneous azeotropic distillation, liquid–liquid extraction, absorption, stripping, and so on, Eq. (9.10) may be applied if the MSA is recovered for recycle in the separator following the separator into which it is introduced and if these two separators are counted together as one unit. For example, if $P = 3$ and ordinary distillation, extractive distillation with solvent I, extractive distillation with solvent II, and liquid–liquid extraction with solvent III are to be considered, then $T = 4$, and the application of Eqs. (9.9) and (9.10) gives 32 possible sequences. This is an enormous increase over the two sequences resulting in considering only ordinary distillation.

Equations (9.9) and (9.10) can be applied to even more complex problems, such as those of Figure 9.1, where the feed contains six components but only four products are specified. If two separation methods (i.e., ordinary distillation and extractive distillation with aqueous furfural) are considered and only the four desired products are produced without blending, then $T = 2$, $P = 4$, and Eqs. (9.9) and (9.10) give $N_s^T = 40$. If five products, including the 2-butene isomers, are produced, with the two butene streams being blended at the end of the sequence, $N_s^T = 224$. If six products are produced with the three butene streams being blended at the end of the sequence, then $N_s^T = 1{,}344$. Therefore, the total number of sequences possible, if all three product numbers are considered, is $40 + 224 + 1{,}344 = 1{,}608$.

Because of the enormous increase in the number of possible sequences when separation methods other than ordinary distillation are considered, it may be worthwhile to forbid certain separations by certain separator types. In this manner, the number of possible sequences can be greatly reduced. For example, for the separation process shown in Figure 9.6, *cis*- and *trans*-2-butene are adjacent to each other in volatility order for ordinary distillation and for extractive distillation with aqueous furfural. Therefore, sequences that include their separation are not necessary. This reduces the total number of possible sequences to 264. Further reduction can be made by excluding other separations. For example, the relative volatility between *cis*-2-butene and *n*-pentane for ordinary distillation is approximately 2.5; accordingly, by using Figure 9.8, extractive distillation for this separation probably need not be considered.

EXAMPLE 9.3

Consider the separation problem studied by Hendry and Hughes (1972) as shown in Figure 9.6. Determine the feasibility of two-product ordinary distillation (method I), select an alternative separation technique (method II) if necessary, and forbid impractical splits. Determine the feasible separations and the number of possible separation sequences that incorporate only these separations.

SOLUTION

Data for the six species are as follows:

Species		Normal Boiling Point (°C)	Critical Temperature (°C)	Critical Pressure (MPa)
Propane	A	−42.1	96.7	4.17
1-Butene	B	−6.3	146.4	3.94
n-Butane	C	−0.5	152.0	3.73
trans-2-Butene	D	0.9	155.4	4.12
cis-2-Butene	E	3.7	161.4	4.02
n-Pentane	F	36.1	196.3	3.31

Because both *trans*- and *cis*-2-butenes are contained in the butenes product and are adjacent when species are ordered by relative volatility, they need not be separated. All ordinary distillation columns can be operated above atmospheric pressure and with cooling-water condensers. Approximate relative volatilities assuming ideal solutions at 150°F (65.6°C) are as follows for all adjacent binary pairs except trans-2-butene and cis-2-butene, which are not split.

Adjacent Binary Pair	Approximate Relative Volatility at 150°F (65.5°C)
Propane /1-Butene (A/B)	2.45
1-Butene /*n*-Butane (B/C)	1.18
n-Butane /*trans*-2-Butene (C/D)	1.03
cis-2-Butene /*n*-Pentane (E/F)	2.50

Because of their high relative volatilities, splits A/B and E/F, even in the presence of the other hydrocarbons, should be by ordinary distillation only. Split C/D is considered infeasible by ordinary distillation; split B/C is feasible, but an alternative method might be more attractive.

From Hendry and Hughes (1972), the use of approximately 96 wt% aqueous furfural as a solvent for extractive distillation increases the volatility of paraffins relative to olefins, causing a reversal in volatility between 1-Butene and *n*-Butane and giving the separation order (ACBDEF). Thus, the three olefins, which are specified as one product, are grouped together. They give an approximate relative volatility of 1.17 for split $(C/B)CH_4$. In the presence of A, this would add the additional split (A/C), which by ordinary distillation has a very desirable relative volatility of 2.89. Also, split $(\ldots C/D \ldots)_{II}$, with a relative volatility of 1.70, is more attractive than split $(\ldots C/D \ldots)_{I}$, according to Figure 9.8.

In summary, the splits to be considered with all others forbidden are $(A/B\ldots)_I$, $(\ldots B/C\ldots)_I$, $(\ldots E/F)_I$, $(A/C)_I$, $(\ldots C/B\ldots)_{II}$, and $(\ldots C/D\ldots)_{II}$. All feasible subgroups, separations, and sequences can be generated by developing an and/or-directed graph as shown for this example in Figure 9.13 where rectangular nodes designate subgroups and numbered, circular nodes represent separations. A separation includes the separator for recovering the MSA when separation method II is used. A separation sequence is developed by starting at the process feed node and making path decisions until all products are produced. From each rectangular (*or*) node, one path is taken; if present, both paths from a circular (*and*) node must be taken. Figure 9.13 is divided into four main branches, one of each of the four possible separations that come first in the various sequences. Figure 9.13 contains the 31 separations and 12 sequences listed in Table 9.3 by separation number and annual costs.

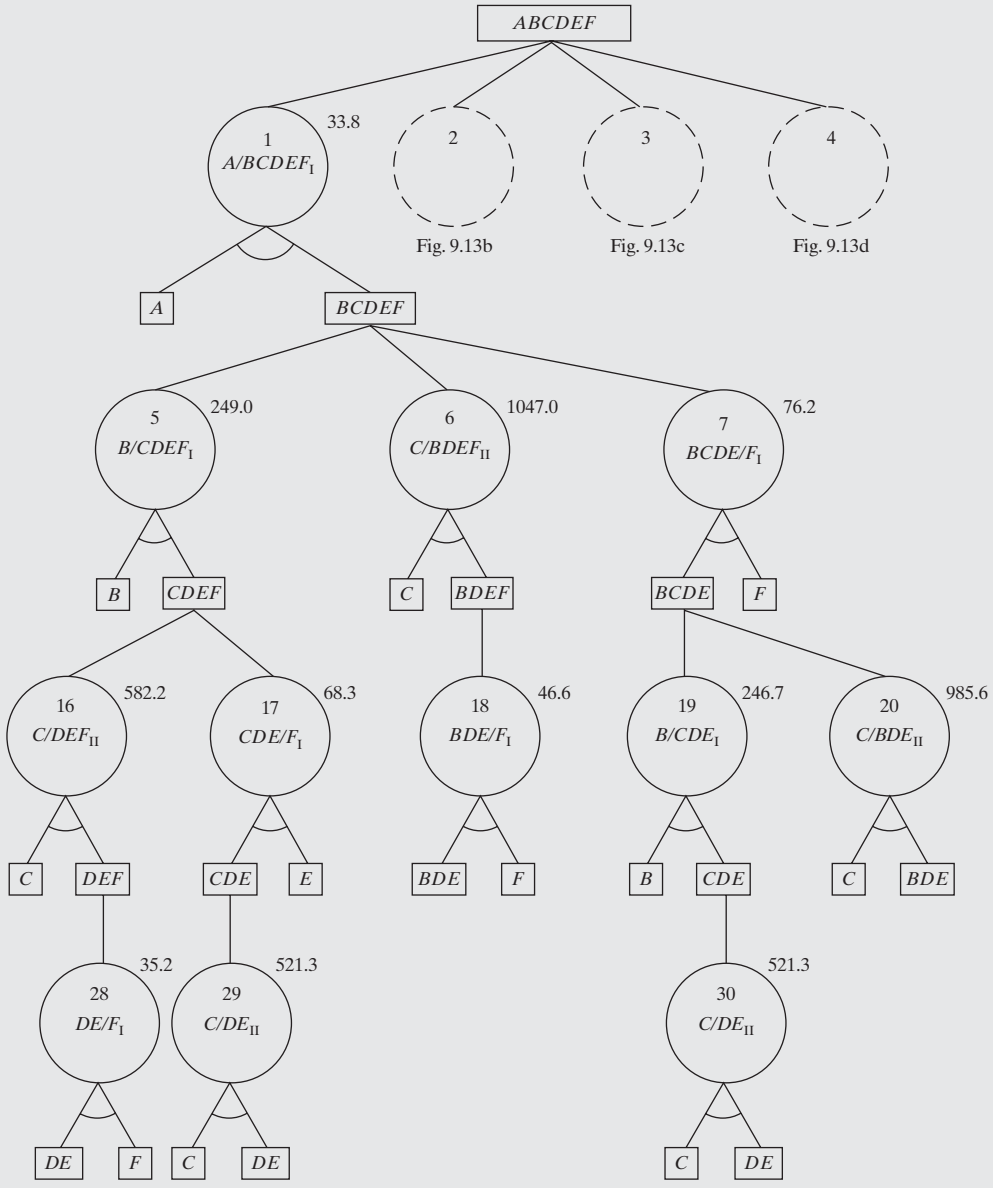

(a)

Figure 9.13 Synthesis tree for Example 9.3: (a) first branch of sequences; (b) second branch of sequences; (c) third branch of sequences; (d) fourth branch of sequences. The lowest-cost sequence in Table 9.3 with an annual cost of $860,400 is highlighted in Figure 9.13(b).

The decimal numbers in Figure 9.13 are annualized costs for the separations in thousands of dollars per year. Annualized costs, C_A, for ordinary distillation operations assuming splits of the two key components (e.g., 99 mol% recovery of the light key component in the distillate and 99 mol% recovery of the heavy key component in the bottoms product) are estimated using the following steps for columns with trays:

1. Set column condenser and reboiler pressures, P_D and P_B, using the algorithm in Figure 9.9.
2. Estimate the minimum number of stages, N_{min}, at total reflux using the Fenske or Winn methods. Estimate the minimum reflux ratio (infinite stages), R_{min}, using the Underwood equation. Estimate the theoretical number of stages, N, using $R/R_{min} = 1.3$ and the Gilliland correlation (see Chapter 13 and the multimedia modules on separation associated with this book). This is the FUG method for which all process simulators have a model (DSTWU in ASPEN PLUS, Shortcut Column in UniSim®Design/ASPEN HYSYS).
3. Select a tray spacing (typically 2 ft) and compute the height of the tower, H.
4. Estimate the flooding velocity, U_f, using the Fair correlation. Set the vapor velocity, $U = 0.85U_f$, and compute the tower diameter, D_T, using Eq. (13.11).
5. Estimate the installed cost of the distillation tower and its trays, C_{BM}, using Figure 16.13 or Eqs. (16.52), (16.57), (16.58), and (16.66).
6. Estimate the cost of the condenser utility (e.g., cooling water) and reboiler utility (e.g., steam).

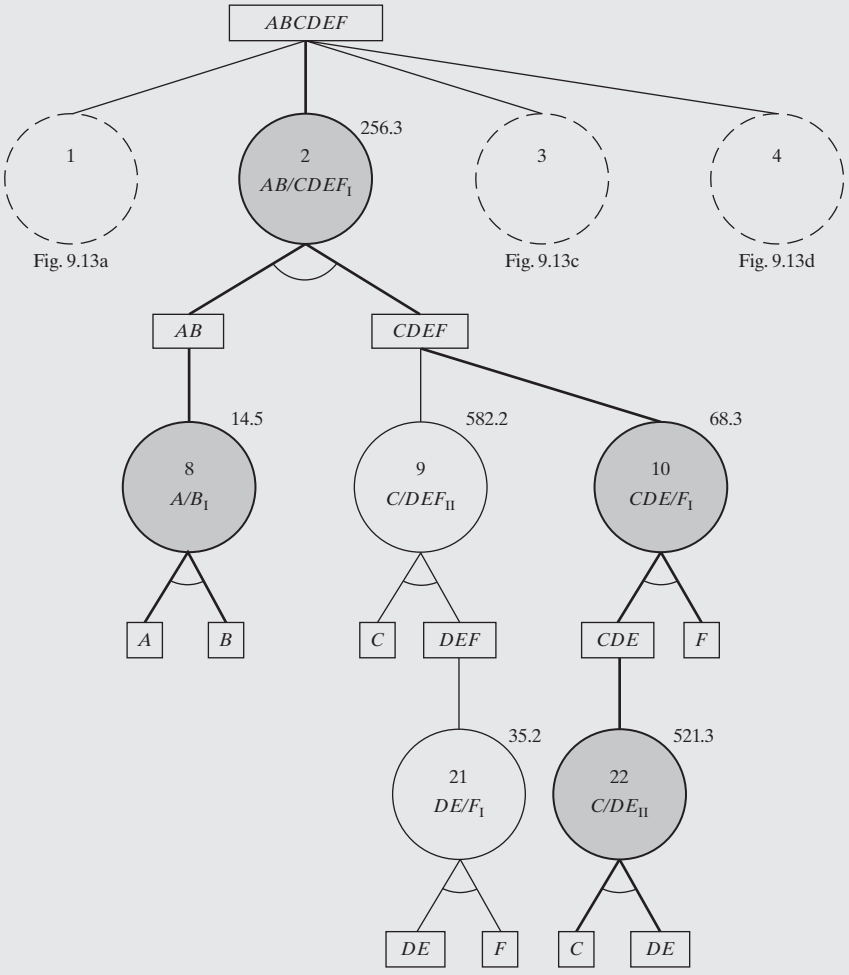

(b)

Figure 9.13 (*Continued*)

7. Estimate the areas for heat transfer in the condenser and reboiler, using Chapter 12, and estimate the installed costs for the condenser and reboiler using Figure 16.10 or Eqs. (16.39)–(16.43).
8. Size a reflux accumulator using a horizontal process vessel, a liquid residence time of 5 min for half full, and an aspect ratio of 4. Estimate its installed cost using Eqs. (16.52), (16.53), and (16.55).
9. Sum the installed costs. When comparing separation sequences, the other investment costs can be neglected when computing the total capital investment, C_{TCI}. Refer to Section 16.3. Note that the reflux and bottoms product pumps are not sized and costed because their costs are usually very small compared with the other equipment.

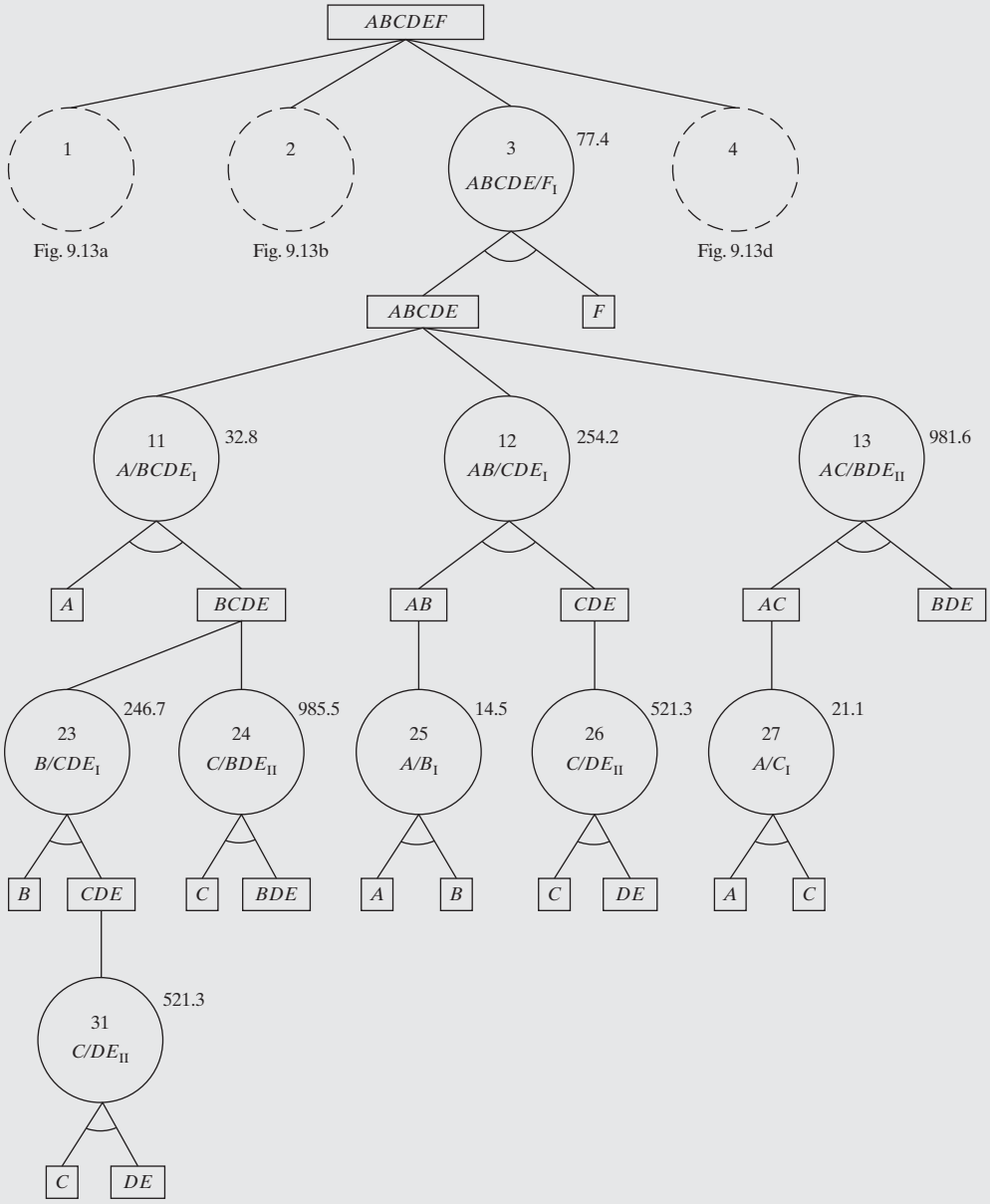

(c)

Figure 9.13 (*Continued*)

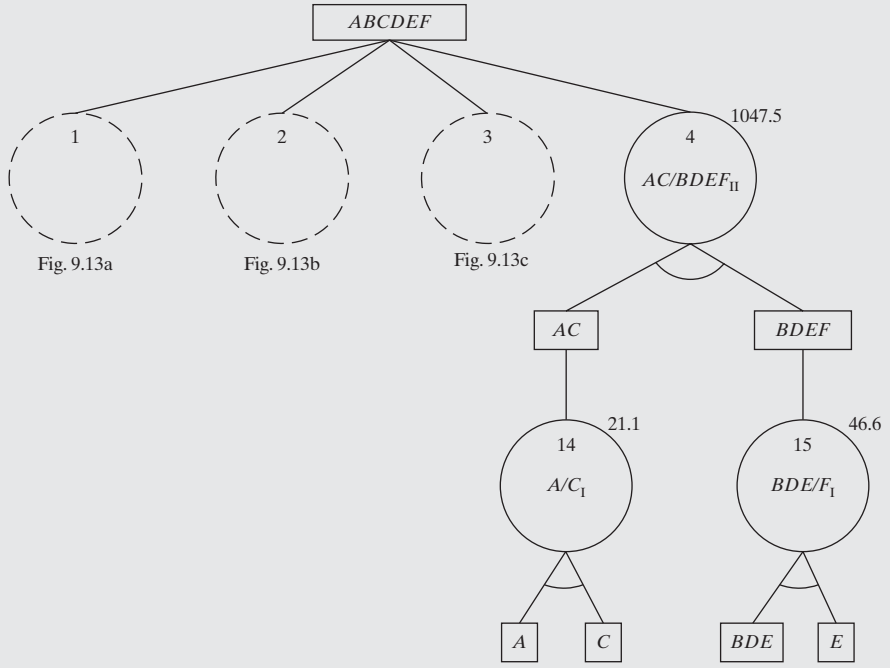

(d)

Figure 9.13 (*Continued*)

Table 9.3 Sequences for Example 9.3

	Sequence	Annual Cost, C_A (\$/yr)
	1 – 5 – 16 – 28	900,200
	1 – 5 – 17 – 29	872,400
	1 – 6 – 18	1,127,400
	1 – 7 – 19 – 30	878,000
	1 – 7 – 20	1,095,600
	8 / 2 \ 9 – 21	888,200
Lowest-cost sequence	8 / 2 \ 10 – 22	860,400
	3 – 11 – 23 – 31	878,200
	3 – 11 –24	1,095,700
	25 / 3 – 12 \ 26	867,400
	3 – 13 – 27	1,080,100
	4 – 14 – 15	1,115,200

10. Estimate the cost of sales, *COS*. For comparison of separation sequences, include only the annual cost of utilities. See Section 17.2.

11. Compute the annualized cost, C_A using Eq. (17.10) with the return on investment, $r = 0.2$.

Similar steps are used to estimate the annualized cost for the extractive distillation operation.

The lowest-cost sequence is identified in Table 9.3 and Figure 9.13(b) with its PFD presented in Figure 9.14 (which is equivalent to Figure 9.7). The highest-cost sequence is 31% higher in cost than the lowest. If only the $(A/C\ldots)_{II}$ and $(\ldots E/F)_{II}$ splits are prohibited as by Hendry and Hughes (1972), the consequence is 64 unique separations and 227 sequences. However, every one of the additional 215 sequences is more than 350% higher in cost than the lowest-cost sequence.

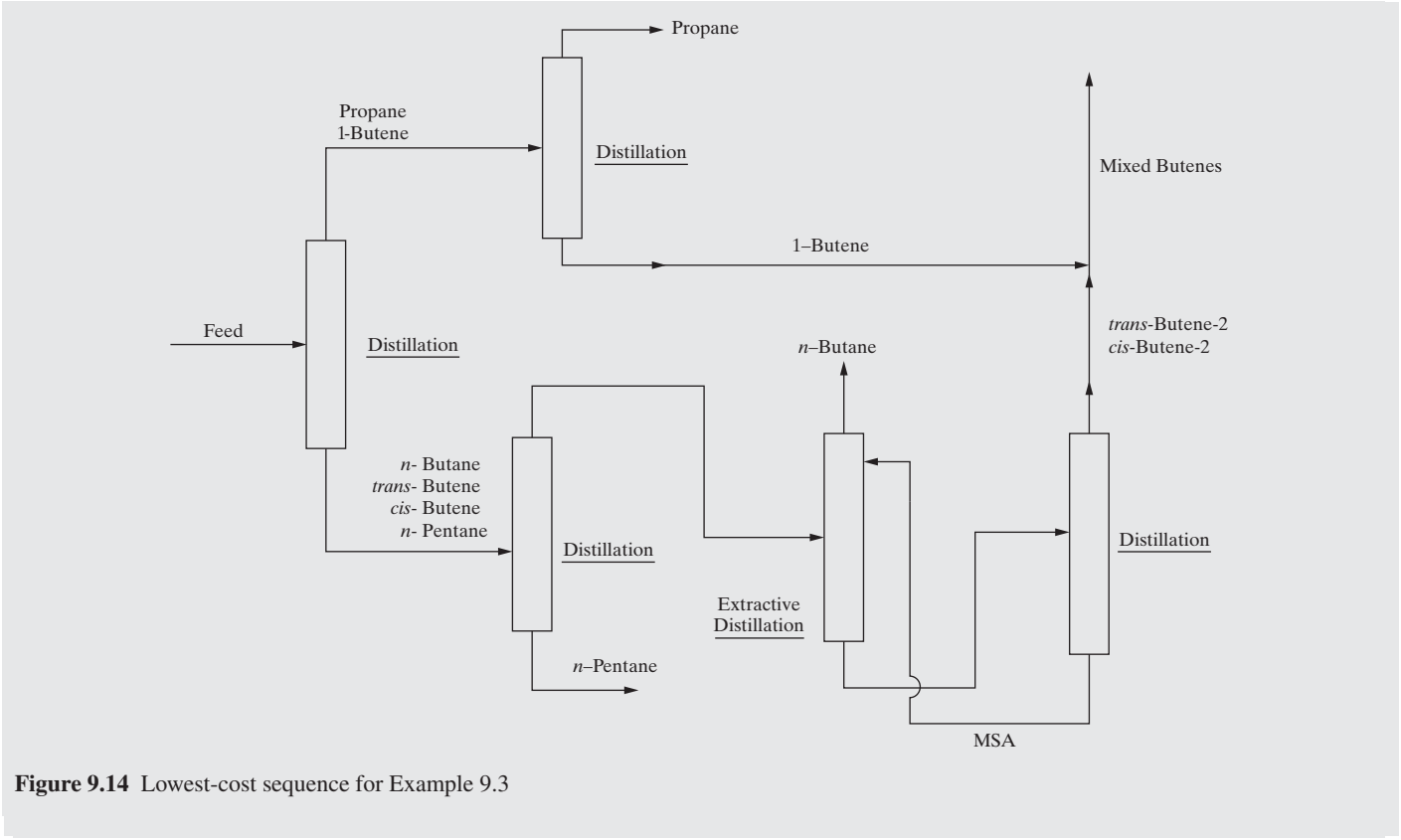

Figure 9.14 Lowest-cost sequence for Example 9.3

Marginal Vapor Rate Method

The last two sections have presented alternative strategies for sequencing ordinary distillation columns. The first of these focused on the usage of heuristics to select cost-effective separation sequences. However, reliance solely on heuristics may lead to conflicting results, and as shown in the last section, it is preferable to employ sequencing methods that rely on column design and, in some cases, cost estimation. As shown, exhaustive search to calculate the annualized cost of every sequence can determine the optimal sequence provided that column-operating conditions are optimized, and may be justified for sequences involving just three or possibly four products. However, less rigorous methods are available that can produce good sequences, although not always optimal. These methods, which attempt to reduce the search space, include those of Hendry and Hughes (1972), Rodrigo and Seader (1975), Gomez and Seader (1976), Seader and Westerberg (1977), and the marginal vapor rate (MV) method of Modi and Westerberg (1992). The latter method outperforms the other methods and can be applied without the necessity of complete column designs and calculations of costs.

For a given split between two key components, Modi and Westerberg (1992) consider the difference in costs between the separation in the absence of nonkey components and the separation in the presence of nonkey components, defining this difference as the marginal annualized cost (MAC). They show that a good approximation of MAC is the MV, which is the corresponding difference in molar vapor rate passing up the column. The sequence with the minimum sum of column MVs is selected. The good approximation is due to the fact that vapor rate is a reliable measure of cost because it is a major factor in determining column diameter as well as reboiler and condenser areas (thus, column and heat-exchanger capital costs) and reboiler and condenser duties (thus, heat-exchanger annual operating costs).

A convenient method for determining the molar vapor rate in an ordinary distillation column separating a nearly ideal system uses the Underwood equations to calculate the minimum reflux ratio, R_{min}. This is readily accomplished, as in the next example with a process simulation program. The design reflux ratio is taken as $R = 1.2R_{min}$. By material balance, the molar vapor rate, V, entering the condenser is given by $V = D(R + 1)$, where D is the molar distillate rate. With the assumption that the feed to the column is a bubble-point liquid, the molar vapor rate through the column will be nearly constant at this value of V. In making the calculations of MV, the selection of product purities is not critical because the minimum reflux ratio is not sensitive to those purities. Thus, to simplify the material balance calculations, it is convenient to assume nearly perfect separations with the light and lighter-than-light key components leaving in the distillate and the heavy and heavier-than-heavy key components leaving in the bottoms. Column top and bottom pressures are estimated with Figure 9.9. The column feed pressure is taken as the average of the top and bottom pressures.

EXAMPLE 9.4

Use the marginal vapor rate method to determine a sequence for the separation of light hydrocarbons specified in Figure 9.12(a) except (1) remove the propane from the feed, (2) ignore the given temperature and pressure of the feed, and (3) strive for recoveries of 99.9% of the key components in each column. Use a process simulation program, with the Soave-Redlich-Kwong equation of state for *K*-values and enthalpies, to set.

SOLUTION

To produce four nearly pure products from the four-component feed, five sequences of three ordinary distillation columns each are shown in Figure 9.11. Let A = isobutane, B = *n*-butane, C = isopentane, and D = *n*-pentane. A total of 10 unique separations is embedded in Figure 9.11. These are listed in Table 9.4 with the results of the calculations for the top column pressure, P_{top}, in kPa; the molar distillate rate, *D*, in kmol/hr; and the reflux ratio, *R*, using the shortcut (Fenske–Underwood–Gilliland or FUG) distillation model of the CHEMCAD process simulation program. This model applies the Underwood equations to estimate the minimum reflux ratio, as described by Seader et al. (2016). Column feeds were computed as bubble-point liquids at P_{top} + 35kPa. Also included in Table 9.4 are values of the column molar vapor rate, *V*, and marginal vapor rate, MV, both in kmol/hr. From Table 9.4, the sum of the marginal vapor rates is calculated for each of the five sequences in Figure 9.11. The results are given in Table 9.5.

Table 9.5 shows that the preferred sequence is the one that performs the two most difficult separations, A/B and C/D, in the absence of nonkey components. These two separations are far more difficult than the separation B/C. The direct sequence is the next best.

Table 9.5 Marginal Vapor Rates for the Five Possible Sequences

Sequence in Figure 9.11	Marginal Vapor Rate, MV (kmol/hr)
(a) Direct	567
(b)	725
(c)	435
(d)	776
(e) Indirect	844

Table 9.4 Calculations of Marginal Vapor Rate, MV

Separation	Column Top Pressure (kPa)	Distillate Rate, *D* (kmol/hr)	Reflux Ratio, ($R = 1.2R_{min}$)	Vapor Rate, $V = D(R+1)$ (kmol/hr)	Marginal Vapor Rate (kmol/hr)
A/B	680	136.2	10.7	1,594	0
A/BC	680	136.2	11.9	1,757	163
A/BCD	680	136.2	13.2	1,934	340
B/C	490	226.8	2.06	694	0
AB/C	560	362.9	1.55	925	231
B/CD	490	226.8	3.06	921	227
AB/CD	560	362.9	2.11	1,129	435
C/D	210	181.5	13.5	2,632	0
BC/D	350	408.3	6.39	3,017	385
ABC/D	430	544.4	4.96	3,245	613

Complex and Thermally Coupled Distillation Columns

Following the development of an optimal or near-optimal sequence of simple, two-product distillation columns, revised sequences involving complex, rather than simple, distillation columns should be considered. Some guidance is available from a study by Tedder and Rudd (1978a, b) of the separation of ternary mixtures (A, B, and C in order of decreasing volatility) in which eight alternative sequences of one to three columns were considered, seven of which are shown in Figure 9.15. The configurations include the direct and indirect sequences (I and II), two interlinked cases (III and IV), five cases that include the use of sidestreams (III, IV, V, VI, and VII), and one case (V) involving a column with two feeds. All columns in Cases I, II, V, VI, and VII have condensers and reboilers. In Cases III and IV, the first column has a condenser and reboiler. In Case III, the rectifier column has a condenser only whereas the stripper in Case IV has a reboiler only. The interlinking streams that return from the second column to the first column thermally couple the columns in Cases III and IV.

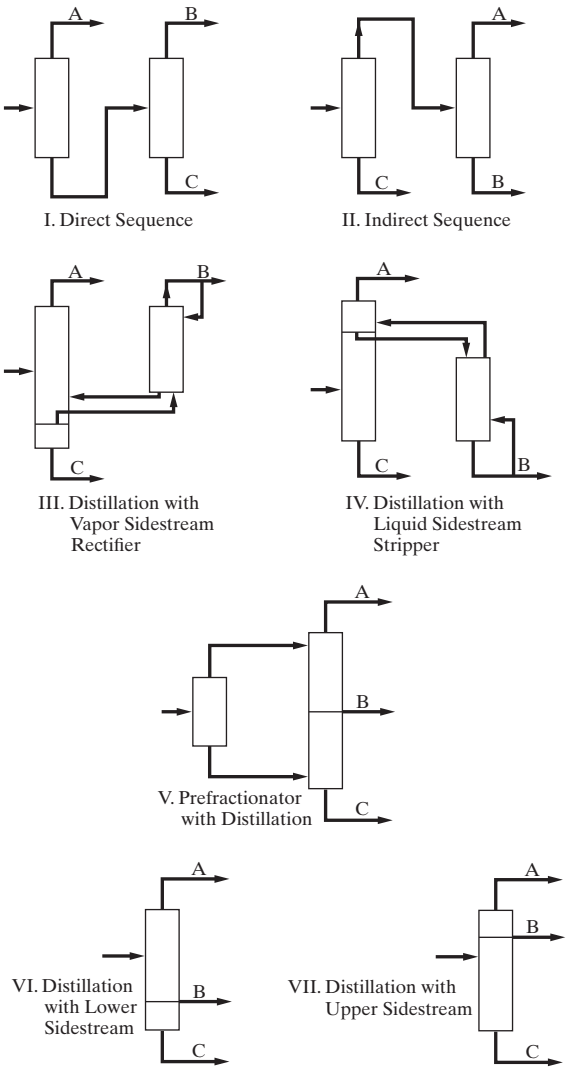

Figure 9.15 Configurations for ternary distillation.

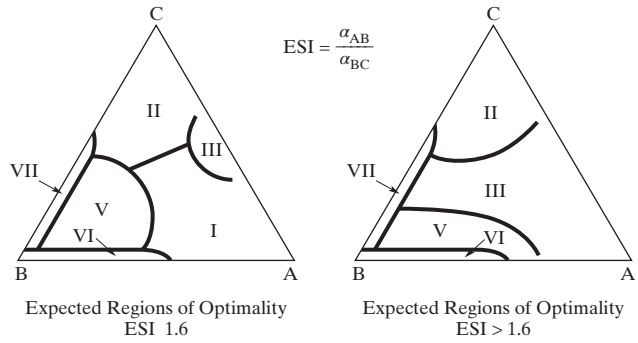

Figure 9.16 Regions of optimality for ternary distillation configurations (Adapted from Tedder and Rudd, 1978a, b). Reproduced with permission of the American Institute of Chemical Engineers. Copyright © 1978 AIChE. All rights reserved.

As shown in Figure 9.16, optimal regions for the various configurations depend on the process feed composition and on an ease-of-separation index (ESI), which is defined as the relative volatility ratio, $\alpha_{A,B}/\alpha_{B,C}$. It is interesting to note that a ternary mixture is separated into three products with just one column in Cases VI and VII in Figure 9.15, but the reflux requirement is excessive unless the feed contains a large amount of B, the component of intermediate volatility, and little of the component that is removed from the same section of the column as B. Otherwise, if the feed is dominated by B but also contains appreciable amounts of A and C, the prefractionator case (V) is optimal. Perhaps the biggest surprise of the study is the superiority of distillation with a vapor sidestream rectifier, which is favored for a large region of the feed composition when ESI > 1.6. The results of Figure 9.16 can be extended to multicomponent separation problems involving more than three components if difficult ternary separations are performed last.

Case V in Figure 9.15 consists of a prefractionator followed by a product column from which all three final products are drawn. Each column is provided with its own condenser and reboiler. As shown in Figure 9.17, eliminating the condenser and reboiler in the prefractionator and providing, instead, reflux and boilup to that column from the product column can thermally couple this arrangement, which is referred to as a Petlyuk system after its chief developer, and is described by Petlyuk et al. (1965). The prefractionator separates the ternary-mixture feed, ABC, into a top product containing A and B and a bottom product of B and C. Thus, component B is split between the top and bottom streams exiting from the prefractionator. The top product is sent to the upper section of the product column, and the bottom product is sent to the lower section. The upper section of the product column provides the reflux for the prefractionator, and the lower section provides its boilup. The product column separates its two feeds into a distillate of A, a sidestream of B, and a bottoms of C. Fidkowski and Krolikowski (1987) determined the minimum molar boilup vapor requirements for the Petlyuk system and the other two thermally coupled systems (III and IV)

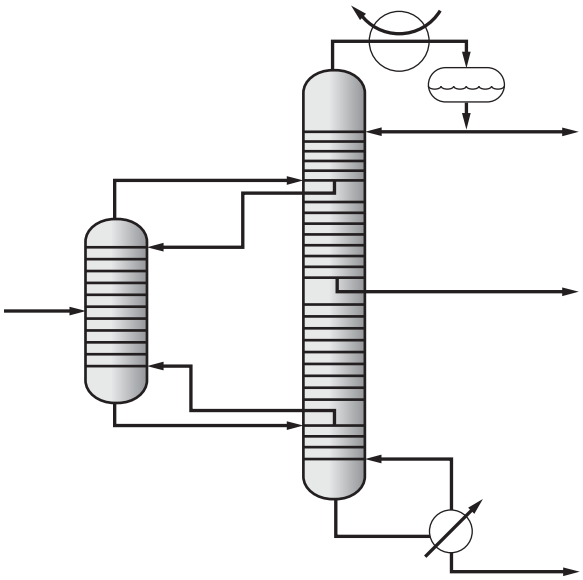

Figure 9.17 Thermally coupled Petlyuk system.

in Figure 9.15, assuming constant relative volatilities, constant molar overflow, and bubble-point liquid feed and products. Fidkowski and Krolikowski compared the requirements to those of the conventional direct and indirect sequences shown as Cases I and II in Figure 9.15 and proved that for all combinations of feed flow rates of the components A, B, and C, as well as all values of relative volatilities, that: (1) the Petlyuk system has the lowest minimum molar boilup vapor requirements and (2) Cases III and IV in Figure 9.15 are equivalent and have lower minimum molar boilup vapor requirements than either the direct or indirect sequence.

Despite its lower vapor boilup requirements, no industrial installations of a two-column Petlyuk system have been reported. Two possible reasons for this, as noted by Agrawal and Fidkowski (1998), are (1) an unfavorable thermodynamic efficiency when the three feed components are not close boiling because all of the reboiler heat must be supplied at the highest temperature and all of the condenser heat must be removed at the lowest temperature and (2) the difficulty in controlling the fractions of vapor and liquid streams in the product column that are returned to the prefractionator as boilup and reflux, respectively. The Petlyuk system can be embodied into a single column, with a significantly reduced capital cost, by using a dividing-wall column (also called divided wall and column in column), a concept described in a patent by Wright (1949) and shown by his patent drawing in Figure 9.18. Because the dividing-wall column makes possible savings in both energy and capital and because control difficulties appear to have been solved, it is attracting much attention. The first dividing-wall column was installed by BASF in 1985. A number of such columns using packing have been installed in the past 15 years, and the first dividing-wall column

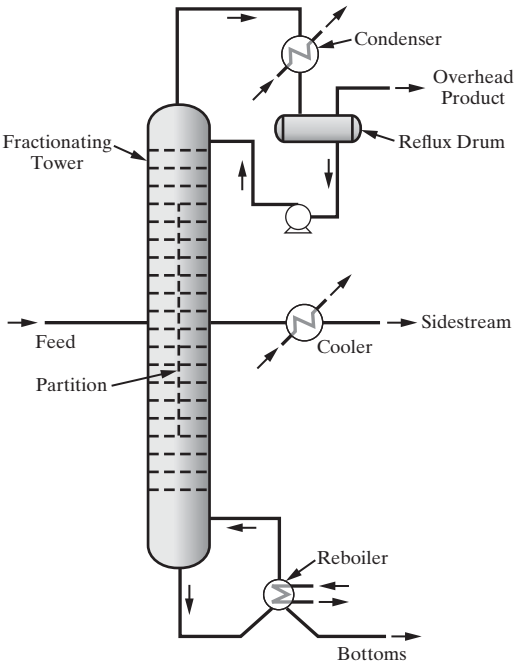

Figure 9.18 Dividing-wall (partition) column of Wright.

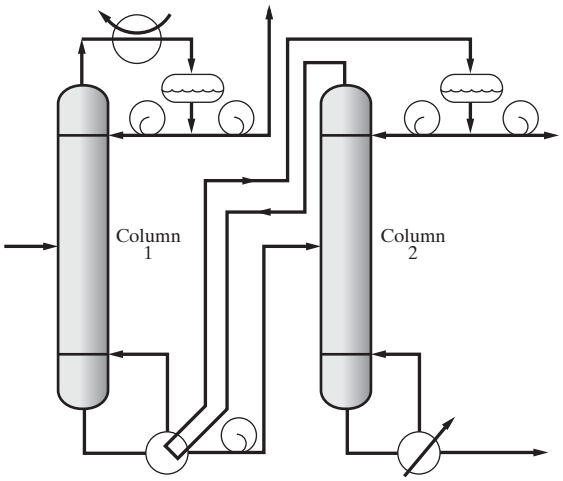

Figure 9.19 Heat-integrated direct sequence of two distillation columns.

using trays was recently announced. Agrawal and Fidkowski (1998) present other thermally fully coupled (FC) systems of distillation columns that retain the benefit of a minimum vapor requirement and afford easier control. Energy savings can also be achieved by heat-integrating the two columns in a direct sequence. In Figure 9.19, Column 2 is operated at a higher pressure than Column 1, such that the condenser duty of Column 2 can provide the reboiler duty of Column 1. Rev et al. (2001) show that heat-integrated systems are often superior in annualized cost to the Petlyuk system. For further discussion of design aspects of heat-integrated distillation columns, see Section 11.8, and Examples 11.14 and 11.25; control aspects are presented in Example 20.2 and Example 20S.8.

9.5 SEQUENCING OF OPERATIONS FOR THE SEPARATION OF NONIDEAL LIQUID MIXTURES

When a multicomponent fluid mixture is nonideal, its separation by a sequence of ordinary distillation columns will not be technically and/or economically feasible if relative volatilities between key components drop below 1.05 and, particularly, if azeotropes are formed. For such mixtures, separation is most commonly achieved by sequences composed of ordinary distillation columns, enhanced distillation columns, and/or liquid–liquid extraction equipment. Membrane and adsorption separations can also be incorporated into separation sequences, but their use is much less common. Enhanced distillation operations include extractive distillation, homogeneous azeotropic distillation, heterogeneous azeotropic distillation, pressure-swing distillation, and reactive distillation. These operations are considered in detail in Perry's *Chemical Engineers' Handbook* (Green and Perry, 2006) and by Seader et al. (2016), Stichlmair and Fair (1998), and Doherty and Malone (2001). A design-oriented introduction to enhanced distillation is presented here.

In many processes involving oxygenated organic compounds such as alcohols, ketones, ethers, and acids, often in the presence

of water, distillation separations are complicated by the presence of azeotropes. Close-boiling mixtures of hydrocarbons (e.g., benzene and cyclohexane whose normal boiling points only differ by 1.1°F) can also form azeotropes. For these and other mixtures, special attention must be given to the distillation boundaries in the composition space that confine the compositions for any one column to lie within a bounded region of the composition space. To introduce these boundaries leading to approaches for the synthesis of separation trains, several concepts concerning azeotropes, residue curves, and distillation lines are reviewed in the subsections that follow.

Azeotropy

The word *azeotrope* is derived from the Greek words ζέειν (boil) and τρόπος (turning) combined with the prefix α- (no) to give the overall meaning, "to boil unchanged," implying that the vapor emitted has the same composition as the liquid (Swietoslawski, 1963). When classifying the many azeotropic mixtures, it is helpful to examine their deviations from Raoult's law (Lecat, 1918).

When two or more fluid phases are in physical equilibrium, the chemical potential, fugacity, and activity of each species is the same in each phase. Thus, in terms of species mixture fugacities for a vapor phase in physical equilibrium with a single liquid phase,

$$\bar{f}_j^V = \bar{f}_j^L \quad j = 1, \ldots, C \tag{9.11}$$

Substituting expressions for the mixture fugacities in terms of mole fractions, activity coefficients, and fugacity coefficients,

$$y_j \bar{\phi}_j^V P = x_j \gamma_j^L f_j^L \quad j = 1, \ldots, C \tag{9.12}$$

where $\bar{\phi}$ is a mixture fugacity coefficient, γ is a mixture activity coefficient, and f is a pure-species fugacity.

For a binary mixture with an ideal liquid solution ($\gamma_j^L = 1$) and a vapor phase that forms an ideal gas solution and obeys the ideal gas law ($\bar{\phi}_j^V = 1$ and $f_j^L = P_j^s$), Eq. (9.12) reduces to the following two equations for the two components 1 and 2:

$$y_1 P = x_1 P_1^s \tag{9.13a}$$

$$y_2 P = x_2 P_2^s \tag{9.13b}$$

where P_j^s is the vapor pressure of species j. Adding Eqs. (9.13a) and (9.13b), noting that mole fractions must sum to 1,

$$\begin{aligned}(y_1 + y_2)P = P &= x_1 P_1^s + x_2 P_2^s \\ &= x_1 P_1^s + (1 - x_1) P_2^s \\ &= P_2^s + (P_1^s - P_2^s) x_1 \end{aligned} \tag{9.14}$$

This linear relationship between the total pressure, P, and the mole fraction, x_1, of the most volatile species is a characteristic of Raoult's law, as shown in Figure 9.20a for the benzene-toluene mixture at 90°C. Note that the bubble-point curve ($P - x$) is linear between the vapor pressures of the pure species (at $x_1 = 0,\ 1$), and the dew-point curve ($P - y$) lies below it. When the ($x_1,\ y_1$) points are graphed at different pressures, the familiar vapor-liquid equilibrium curve is obtained, as shown in Figure 9.20b. Using McCabe-Thiele analysis, it is shown readily that for any feed

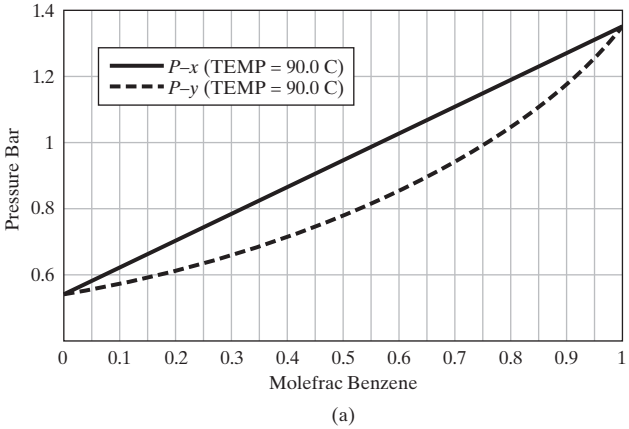

(a)

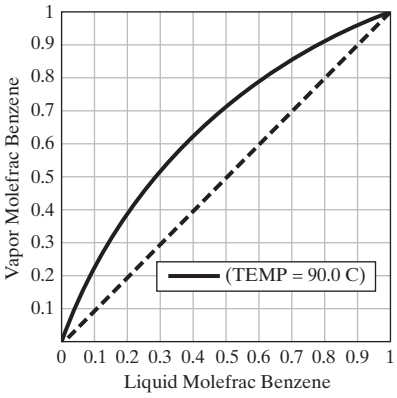

(b)

Figure 9.20 Phase diagrams for the benzene–toluene mixture at 90°C, calculated using ASPEN PLUS: (a) $P - x - y$ diagram: (b) $x - y$ diagram.

composition, there are no limitations to the values of the mole fractions of the distillate and bottoms products from a distillation tower.

However, when the mixture forms a nonideal liquid phase and exhibits a positive deviation from Raoult's law ($\gamma_j^L > 1, j = 1,2$), Eq. (9.14) becomes

$$P = x_1 \gamma_1^L P_1^s + (1 - x_1)\gamma_2^L P_2^s \tag{9.15}$$

Furthermore, if the boiling points of the two components are close enough, the bubble- and dew-point curves may reach a maximum at the same composition, which by definition is the azeotropic point. Such a situation is illustrated in Figure 9.21a for the binary mixture of isopropyl ether (1) and isopropyl alcohol (2) at 70°C. Figure 9.21b shows the corresponding $x - y$ diagram, and Figure 9.21c shows the bubble- and dew-point curves on a $T - x - y$ diagram at 101 kPa. Note the *minimum-boiling azeotrope* at 66°C, where $x_1 = y_1 = 0.76$. Feed streams having lower isopropyl ether mole fractions cannot be purified beyond 0.76 in a distillation column, and streams having higher isopropyl ether mole fractions have distillate mole fractions that have a lower bound of 0.76. Consequently, the azeotropic composition is commonly referred to as a *distillation boundary*.

Similarly, when the mixture exhibits the less-common negative deviation from Raoult's law ($\gamma_j^L < 1, j = 1,2$), both the

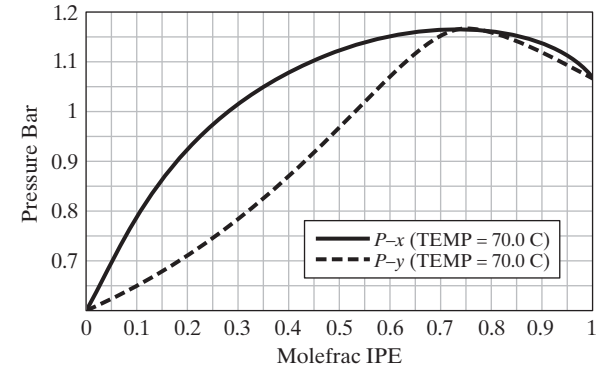

(a)

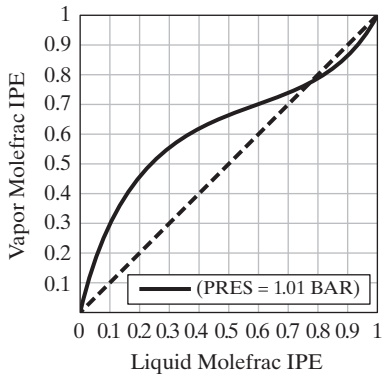

(b)

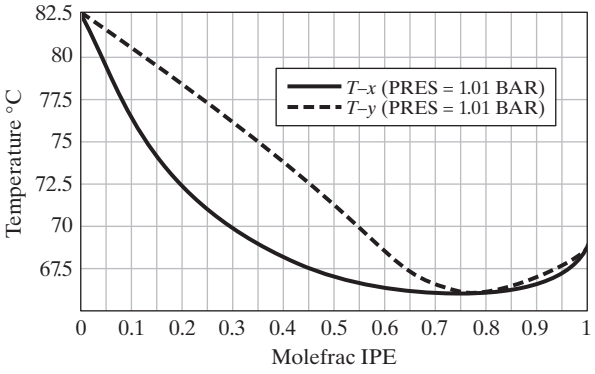

(c)

Figure 9.21 Phase diagrams for the isopropyl ether-isopropyl alcohol binary computed using ASPEN PLUS: (a) *P–x–y* diagram at 70°C; (b) *x–y* diagram at 101 kPa; (c) *T–x–y* diagram at 101 kPa.

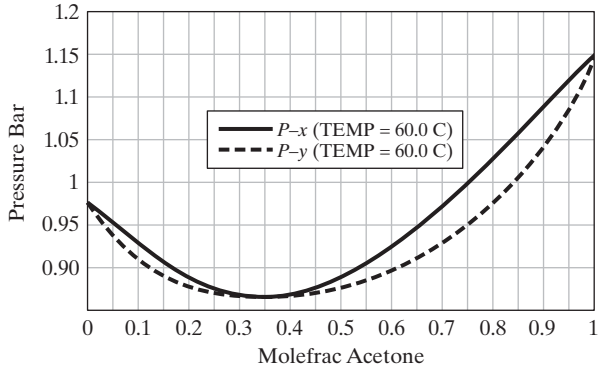

(a)

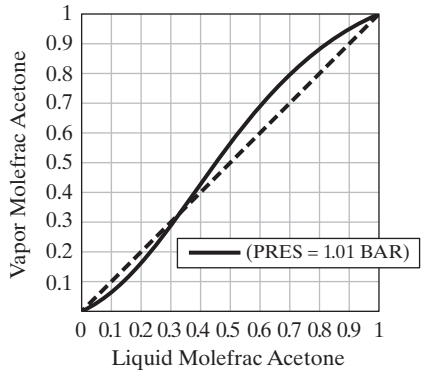

(b)

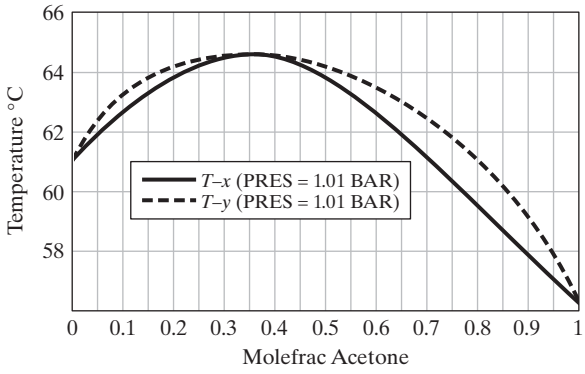

(c)

Figure 9.22 Phase diagrams for the acetone–chloroform binary computed using ASPEN PLUS: (a) *P–x–y* diagram at 60°C; (b) *x–y* diagram at 101 kPa; (c) *T–x–y* diagram at 101 kPa.

bubble- and dew-point curves drop below the straight line that represents the bubble points for an ideal mixture, as anticipated by examination of Eq. (9.15). Furthermore, when the bubble- and dew-point curves have the same minimum, an azeotropic composition is defined, as shown in Figure 9.22a for the binary mixture of acetone (1) and chloroform (2) at 64.5°C, where $x_1 = y_1 = 0.35$. For this system, Figures 9.22b and 9.22c show the corresponding *x–y* diagram and $T–x-y$ diagram at 101 kPa. On the latter diagram, the azeotropic point is at a maximum temperature, and consequently, the system is said to have a *maximum-boiling azeotrope*. In this case, feed streams having lower acetone mole fractions cannot be purified beyond 0.35 in the bottoms product of a distillation column, and streams having higher acetone mole fractions have a lower bound of 0.35 in the acetone mole fraction of the bottoms product.

In summary, at a homogeneous azeotrope, $x_j = y_j$, $j = 1, \ldots, C$, the expression for the equilibrium constant, K_j, for species j becomes unity. Based on the general phase equilibria Eq. (9.12), the criterion for azeotrope formation is given by:

$$K_j = \frac{y_j}{x_j} = \frac{\gamma_j^L f_j^L}{\overline{\phi}_j^V P} = 1 \quad j = 1, \ldots, C \tag{9.16}$$

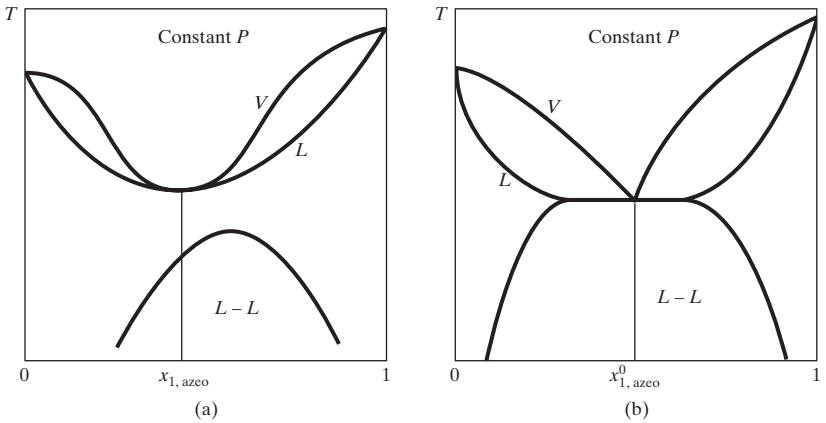

Figure 9.23 Binary phase diagram at a fixed pressure for (a) homogeneous azeotrope; (b) heterogeneous azeotrope.

where the degree of nonideality is expressed by the deviation from unity of the activity coefficients and fugacities for the liquid phase and of the fugacity coefficients for the vapor phase. At low pressure, $\overline{\phi}_j^V = 1$ and $f_j^L = P_j^s$ so that Eq. (9.16) reduces to

$$K_j = \frac{y_j}{x_j} = \gamma_j^L \frac{P_j^s}{P} = 1 \quad j = 1, \ldots, C \tag{9.17}$$

Because the K-values for all of the species are unity at an azeotrope point, a simple distillation approaches this point at which no further separation can occur. For this reason, an azeotrope is often called a *stationary* or *fixed* or *pinch point*.

For a minimum-boiling azeotrope, when the deviations from Raoult's law are sufficiently large ($\gamma_j^L \gg 1$, usually > 7), splitting the liquid phase into two liquid phases (phase splitting) may occur, and a minimum-boiling, heterogeneous azeotrope may form that has a vapor phase in equilibrium with the two liquid phases. A heterogeneous azeotrope occurs when the vapor–liquid envelope overlaps with the liquid–liquid envelope, as illustrated in Figure 9.23b. For a homogeneous azeotrope, when $x_1 = x_{1,azeo} = y_1$, the mixture boils at this composition, as shown in Figure 9.23a; for a heterogeneous azeotrope, however, when the overall liquid composition of the two liquid phases, $x_1 = x^0_{1,azeo} = y_1$, the mixture boils at this overall composition, as illustrated in Figure 9.23b, but the three coexisting phases have distinct compositions.

Residue Curves

To understand better the properties of azeotropic mixtures that contain three chemical species, it helps to examine the properties of residue curves on a ternary diagram. A collection of residue curves, which is called a *residue curve map*, can be computed and drawn by any of the major simulation programs. Each residue curve is constructed by tracing the composition of the equilibrium liquid residue of a simple (Rayleigh batch) distillation in time, starting from a selected initial composition of the charge to the still using the following numerical procedure.

Consider L moles of liquid with mole fractions $x_j (j = 1, \ldots, C)$ in a simple distillation still at its bubble point as illustrated in Figure 9.24. Note that the still contains no trays and that no reflux is provided. As heating begins, a small portion of this liquid, ΔL moles, is vaporized. The instantaneous vapor phase has mole

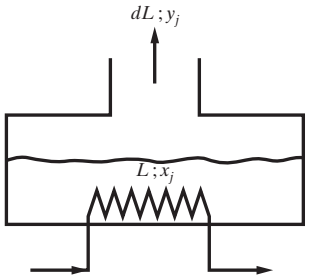

Figure 9.24 Simple distillation still.

fractions $y_j (j = 1, \ldots, C)$, assumed to be in equilibrium with the remaining liquid. Since the residual liquid, $L - \Delta L$ moles, has mole fractions $x_j + \Delta x_j$, the mass balance for species j is given by

$$Lx_j = (\Delta L)y_j + (L - \Delta L)(x_j + \Delta x_j) \qquad j = 1, \ldots, C-1 \tag{9.18}$$

In the limit, as $\Delta L \to 0$,

$$\frac{dx_j}{dL/L} = x_j - y_j = x_j(1 - K_j\{T, P, \underline{x}, \underline{y}\}) \qquad j = 1, \ldots, C-1 \tag{9.19}$$

and setting $d\hat{t} = dL/L$,

$$\frac{dx_j}{d\hat{t}} = x_j - y_j = x_j(1 - K_j\{T, P, \underline{x}, \underline{y}\}), \quad j = 1, \ldots, C-1 \tag{9.20}$$

where K_j is given by Eq. (9.16). In Eq. (9.20), $\hat{t}$ can be interpreted as the dimensionless time with the solution defining a family of residue curves, as illustrated in Figure 9.25. Note that each residue curve is the locus of the compositions of the residual liquid in time, as vapor is boiled off from a simple distillation still. Often, an arrow is assigned in the direction of increasing time (and increasing temperature). Note that the residue curve map does not show the equilibrium vapor composition corresponding to each point on a residue curve.

Another important property is that the fixed points of the residue curves are points where the driving force for a change in the liquid composition is zero; that is, $d\underline{x}/d\hat{t} = 0$. This condition is satisfied at the azeotropic points and the pure-species vertices. For a ternary mixture with a single binary azeotrope, as in Figure 9.25, there are four fixed points on the triangular

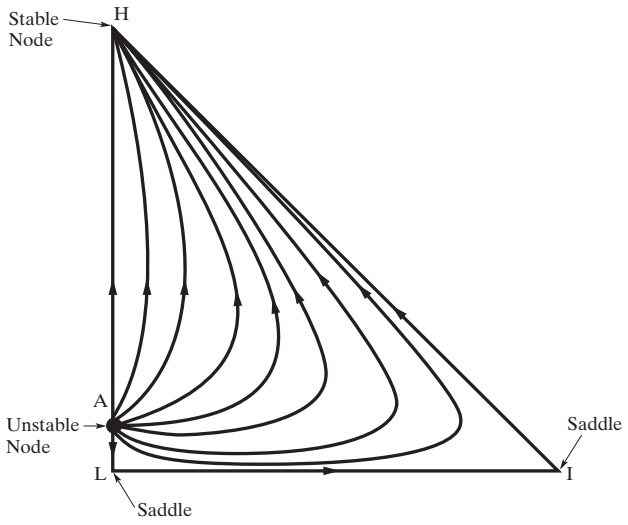

Figure 9.25 Residue curves of a ternary system with a minimum-boiling binary azeotrope.

diagram: the binary azeotrope and the three vertices. Furthermore, the behavior of the residue curves in the vicinity of the fixed points depends on their stability. When all of the residue curves are directed by the arrows to the fixed point, it is referred to as a stable node, as illustrated in Figure 9.26a; when all are directed away, the fixed point is an unstable node (as in Figure 9.26b); and finally, when some of the residue curves are directed to and others are directed away from the fixed point, it is referred to as a saddle point (as in Figure 9.26c). Note that for a ternary system, the stability can be determined by calculating the eigenvalues of the Jacobian matrix of the nonlinear ordinary differential equations that comprise Eq. (9.20).

As an example, consider the residue curve map for a ternary system with a minimum-boiling binary azeotrope of heavy (H) and light (L) species as shown in Figure 9.25. There are four fixed points: one unstable node at the binary azeotrope (A), one stable node at the vertex for the heavy species (H), and two saddles at the vertices of the light (L) and intermediate (I) species.

It is of special note that the boiling points and the compositions of all azeotropes can be used to characterize residue curve maps. In fact, even without a simulation program to compute and draw the detailed diagrams, this information alone is sufficient to sketch the key characteristics of these diagrams using the following procedure. First, the boiling points of the pure species are entered at the vertices. Then the boiling points of the binary azeotropes are positioned at the azeotropic compositions along the edges, with the boiling points of any ternary

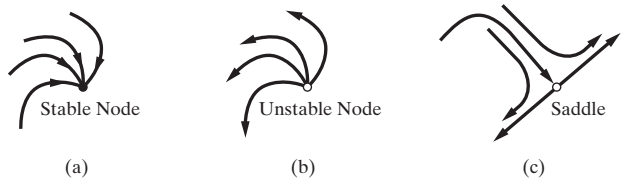

Figure 9.26 Stability of residue curves for a ternary system in the vicinity of a binary azeotrope.

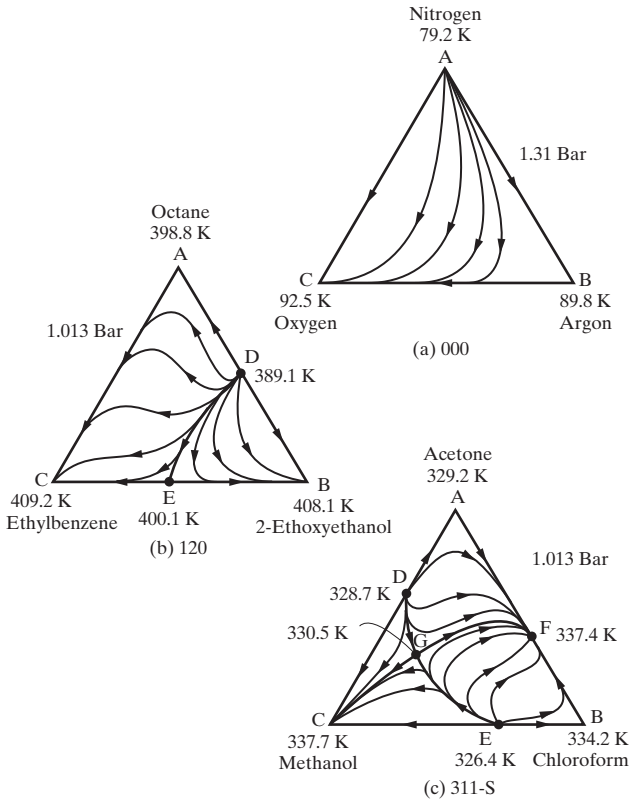

Figure 9.27 Maps of residue curves or distillation lines: (a) system without azeotropes; (b) system with two binary azeotropes; (c) system with binary and ternary azeotropes (Stichlmair et al., 1989). Reproduced with permission of the American Institute of Chemical Engineers. Copyright © 1989 AIChE. All rights reserved.

azeotropes positioned at their compositions within the triangle. Arrows are assigned in the direction of increasing temperature in a simple distillation still. As examples, typical diagrams for mixtures involving binary and ternary azeotropes are illustrated in Figure 9.27. Figure 9.27a is for a simple system, without azeotropes, involving nitrogen, oxygen, and argon. In this mixture, nitrogen is the lowest-boiling species (L), argon is the intermediate boiler (I), and oxygen is the highest-boiling species (H). Thus, along the oxygen–argon edge, the arrow is pointing to the oxygen vertex, and on the remaining edges, the arrows point away from the nitrogen vertex. Since these arrows point away at the nitrogen vertex, it is an unstable node, and all of the residue curves emanate from it. At the argon vertex, the arrows point to and away from it. Since the residue curves turn in the vicinity of this vertex, it is not a terminal point. Rather, it is referred to as a saddle point. All of the curves end at the oxygen vertex, which is a terminal point or stable node. For this ternary mixture, the map shows that pure argon, the intermediate boiler, cannot be obtained in a simple distillation.

Simple Distillation Boundaries

The graphical approach described here is effective in locating the starting and terminal points and the qualitative locations of the residue curves. As illustrated in Figures 9.27b and 9.27c,

it works well for binary and ternary azeotropes that exhibit multiple starting and terminal points. In these cases, one or more simple distillation boundaries called separatrices (e.g., curved line DE in Figure 9.27b) divide these diagrams into regions with distinct pairs of starting and terminal points. For the separation of homogeneous mixtures by simple distillation, these separatrices cannot be crossed unless they are highly curved. A feed located in region ADECA in Figure 9.27b has a starting point approaching the composition of the binary azeotrope of octane and 2-ethoxyethanol and a terminal point approaching pure ethylbenzene, whereas a feed located in region DBED has a starting point approaching the same binary azeotrope but a terminal point approaching pure 2-ethoxyethanol. In this case, a pure octane product is not possible. Figure 9.27c is even more complex. It shows four distillation boundaries (curved lines GC, DG, GF, and EG), which divide the diagram into four distillation regions.

Distillation Towers

When tray towers are modeled assuming vapor–liquid equilibrium at each tray, the residue curves approximate the liquid composition profiles at total reflux. To show this, a species balance is performed for the top n trays, counting down the tower, as shown in Figure 9.28:

$$L_{n-1}\underline{x}_{n-1} + D\underline{x}_D = V_n\underline{y}_n \tag{9.21}$$

where D and $\underline{x}_D$ are the molar flow rate and vector of mole fractions of the distillate. Similarly, L_{n-1} and $\underline{x}_{n-1}$ are for the liquid leaving tray $n-1$, and V_n and $\underline{y}_n$ are for the vapor leaving tray n. Defining h as the dimensionless distance from the top of the tower, a backward-difference approximation at tray n is given by

$$\left.\frac{d\underline{x}}{dh}\right|_n \approx \underline{x}_n - \underline{x}_{n-1} \tag{9.22}$$

Rearranging Eq. (9.21) and substituting in Eq. (9.22),

$$\left.\frac{d\underline{x}}{dh}\right|_n \approx \underline{x}_n - \frac{V_n}{L_{n-1}}\underline{y}_n + \frac{D}{L_{n-1}}\underline{x}_D \tag{9.23}$$

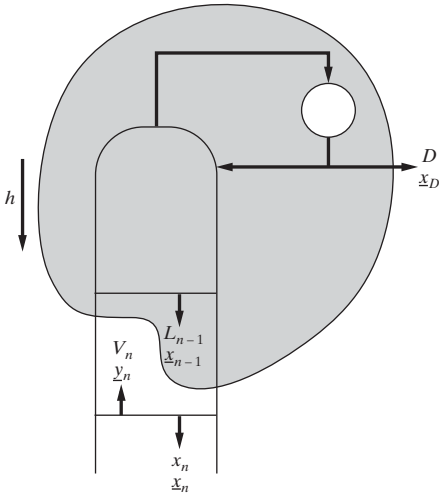

Figure 9.28 Schematic of rectifying section.

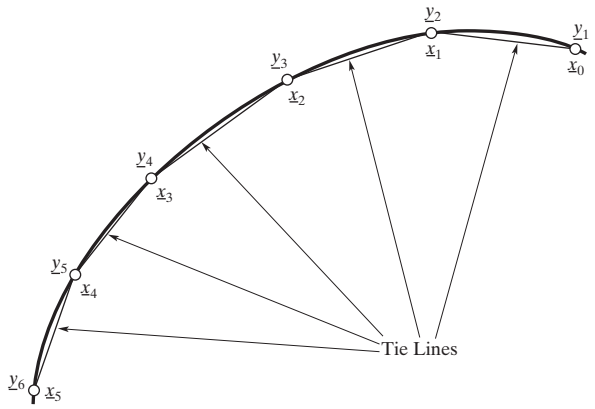

Figure 9.29 Distillation line and its tie lines.

At total reflux, with $D = 0$ and $V_n = L_{n-1}$, Eq. (9.23) becomes

$$\left.\frac{d\underline{x}}{dh}\right|_n \approx \underline{x}_n - \underline{y}_n \tag{9.24}$$

Hence, Eq. (9.24) approximates the operating lines at total reflux and, because $\hat{t}$ and h are dimensionless variables and Eq. (9.20) is identical in form, the residue curves approximate the operating lines of a distillation tower operating at total reflux.

Distillation Lines

An exact representation of the operating line for a distillation tower at total reflux, also known as a distillation line [as defined by Zharov (1968) and Zharov and Serafimov (1975)], is shown in Figure 9.29. Note that, at total reflux,

$$\underline{x}_n = \underline{y}_{n+1} \qquad n = 0,1,\ldots \tag{9.25}$$

Furthermore, assuming operation in vapor–liquid equilibrium, the mole fractions on trays n, $\underline{x}_n$, and $\underline{y}_{n+1}$ lie at the ends of the equilibrium tie lines.

To appreciate better the differences between distillation lines and residue curves, consider the following observations. First, Eq. (9.20) requires the tie line vectors connecting liquid composition x and vapor composition y, at equilibrium, to be tangent to the residue curves, as illustrated in Figure 9.30.

Since these tie line vectors must also be chords of the distillation lines, the residue curves and the distillation lines must intersect at the liquid composition x. Note that when the residue curve is linear (as for binary mixtures), the tie lines and the residue curve are collinear, and consequently, the distillation lines coincide with the residue curves.

Figure 9.31a shows two distillation lines (δ_1 and δ_2) that intersect a residue curve at points A and B. As a consequence of Eq. (9.20), their corresponding vapor compositions at equilibrium, a and b, lie at the intersection of the tangents to the residue curves at A and B with the distillation lines δ_1 and δ_2. Clearly, the distillation lines do not coincide with the residue curves, an assumption that is commonly made but that may produce significant errors. In Figure 9.31b, a single distillation line connects the compositions on four adjacent trays (at C, D, E, F) and crosses four residue curves (ρ_C, ρ_D, ρ_E, ρ_F) at these points.

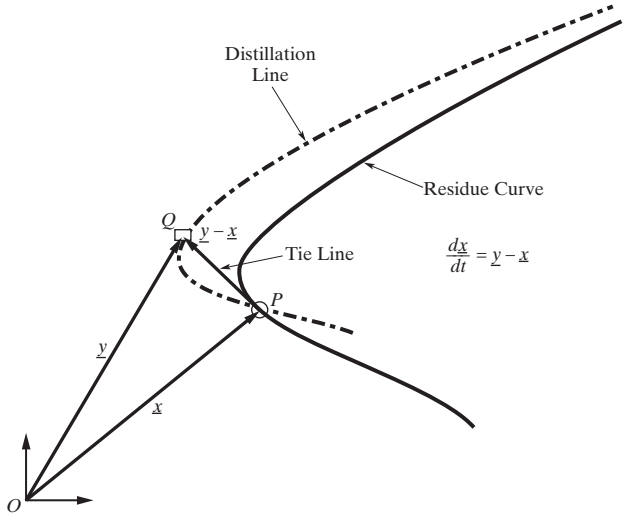

Figure 9.30 Residue curve and distillation line through *P*.

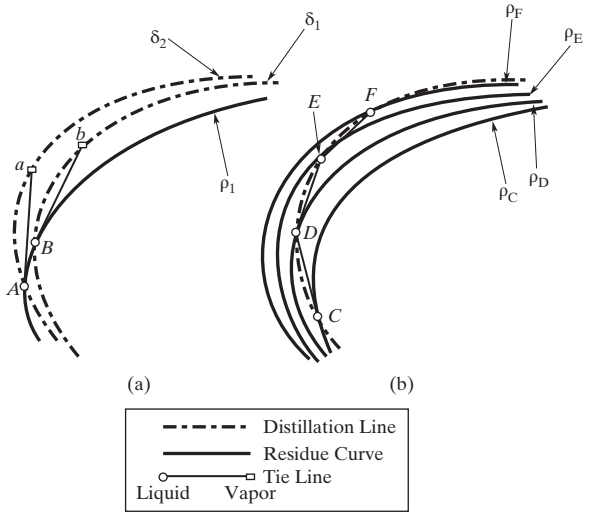

Figure 9.31 Geometric relationship between distillation lines and residue curves.

Computing Azeotropes for Multicomponent Mixtures

Gmehling (1994) provides data on more than 15,000 binary azeotropes and 900 ternary azeotropes. Undoubtedly, many more ternary azeotropes exist as well as untold numbers of azeotropes involving more than three components. When a process simulation program is used to compute a residue curve map for a ternary system at a specified pressure, compositions and temperatures of all azeotropes are automatically estimated. The results depend, of course, on the selected vapor pressure and liquid-phase activity coefficient correlations. For quaternary and higher systems, the arclength homotopy-continuation method of Fidkowski, Malone, and Doherty (1993) can be used for homogeneous systems to estimate all azeotropes. They find all roots to the following equations, which define a homogeneous azeotrope:

$$y_j - x_j = 0 \qquad j = 1,2,\ldots,C-1 \tag{9.26}$$

$$y_j = \left(\frac{\gamma_j^L P_j^s}{\overline{\phi}_j^V P}\right) x_j \qquad j = 1,2,\ldots,C-1 \tag{9.27}$$

$$\sum_{j=1}^{C} x_j = 1 \tag{9.28}$$

$$\sum_{j=1}^{C} y_j = 1 \tag{9.29}$$

$$x_j \geq 0, \qquad j = 1,2,\ldots,C \tag{9.30}$$

To find the roots, they construct the following homotopy to replace Eqs. (9.26) and (9.27) based on gradually moving from an ideal *K*-value based on Raoult's law to the more rigorous expression of Eq. (9.27):

$$\begin{aligned} y_j - x_j &= \left\{\left((1-t) + t\frac{\gamma_j^L}{\overline{\phi}_j^V}\right)\frac{P_j^s}{P} - 1\right\} x_j \\ &= H(t, x_j) = 0 \qquad j = 1,2,\ldots,C-1 \end{aligned} \tag{9.31}$$

Initially, the homotopy parameter, t, is set to 0 and all values of x_j are set to 0 except for one, which is set to 1.0. Then t is gradually and systematically increased until a value of 1.0 is obtained. With each increase, the temperature and mole fractions are computed. If the resulting composition at $t = 1.0$ is not a pure component, it is an azeotrope. By starting from each pure component, all azeotropes are computed. The method of Fidkowski, Malone, and Doherty (1993) is included in many of the process simulation programs. Eckert and Kubicek (1997) extended the method of Fidkowski, Malone, and Doherty to the estimation of heterogeneous multicomponent azeotropes.

Distillation-Line Boundaries and Feasible Product Compositions

Of great practical interest is the effect of distillation boundaries on the operation of distillation towers. To summarize a growing body of literature, it is well established that the compositions of a distillation tower operating at total reflux cannot cross the distillation-line boundaries except under unusual circumstances where these boundaries exhibit a high degree of curvature. This provides the total-reflux bound on the possible (feasible) compositions for the distillate and bottoms products.

As shown in Figure 9.32a, at total reflux, $\underline{x}_B$ and $\underline{y}_D$ reside on a distillation line. Furthermore, these compositions lie collinear with the feed composition, $\underline{x}_F$, on the overall material balance line. As the number of stages increases, the operating curve becomes more convex and in the limit approaches the two sides of the triangle that meet at the intermediate boiler. As an example, an operating line at total reflux (minimum stages) is the curve AFC in Figure 9.33a. At the other extreme, as the number of stages increases, the operating curve becomes more convex approaching ABC, where the number of stages approaches infinity (corresponding to minimum reflux). Hence, the operating line for a distillation tower that operates within these limiting regimes lies within the region ABCFA in Figure 9.33a. Note that

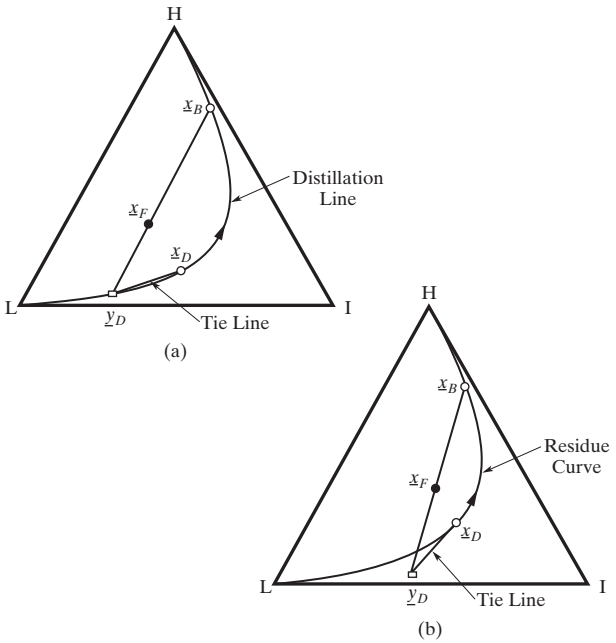

Figure 9.32 Overall mass balance line with a partial/total condenser.

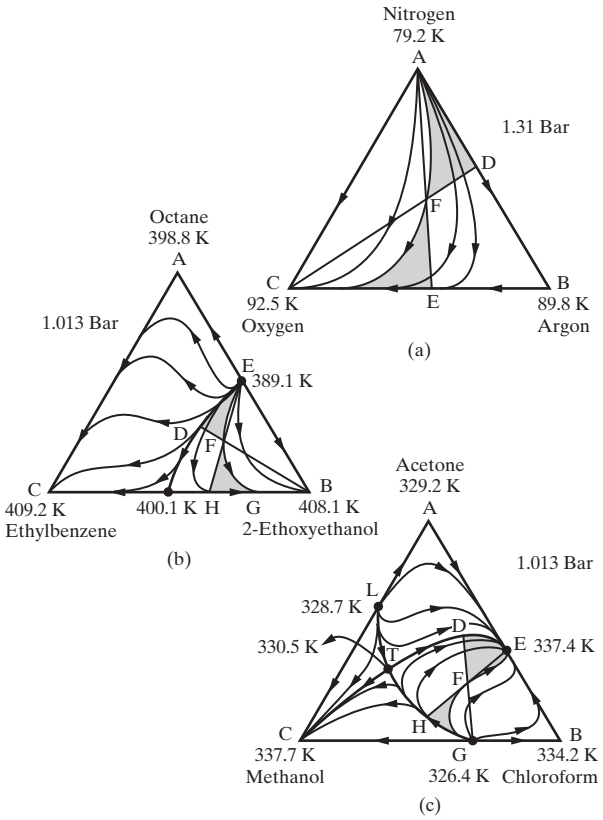

Figure 9.33 Regions of feasible distillate and bottoms product compositions (shaded) for a ternary mixture: (a) system without azeotropes; (b) system with two binary azeotropes; (c) system with binary and ternary azeotropes (Stichlmair et al., 1989). Reproduced with permission of the American Institute of Chemical Engineers. Copyright © 1989 AIChE. All rights reserved.

when a distillation tower operates with a partial condenser as the feed and product streams are decreased toward total reflux, the last bubble of vapor distillate has the mole fractions $\underline{y}_D$, as shown in Figures 9.32a and 9.32b. Consequently, as total reflux is approached, the material balance line connecting the bottoms, feed, and distillate mole fractions is shown. Figure 9.32a shows the distillation line that passes through the $\underline{x}_B$ and $\underline{y}_D$ mole fractions, and Figure 9.32b shows the residue curve that passes through the $\underline{x}_D$ mole fractions, and approximately through the $\underline{x}_B$ mole fractions.

Two additional bounds in Figure 9.33a are obtained as follows. First, in the limit of a pure nitrogen distillate, the line AFE represents a limiting overall material balance for a feed composition at point F, with point E at the minimum concentration of oxygen in the bottoms product. Similarly, in the limit of a pure oxygen bottoms, the line CFD represents a limiting overall material balance, with point D at the minimum concentration of nitrogen in the distillate along the nitrogen–argon axis. Hence, the distillate composition is confined to the shaded region ADFA, and the bottoms product composition lies in the shaded region CEFC. Operating lines that lie within the region ABCFA connect the distillate and bottoms product compositions in these shaded regions. At best, only one pure species can be obtained. In addition, only those species located at the end points of the distillation lines can be recovered in high purity. Hence, the end points of the distillation lines determine the potential distillate and bottoms products for a given feed. This also applies to the complex mixtures in Figures 9.33b and 9.33c where the location of the feed point determines the distillation region in which the potential distillate and bottoms product compositions lie. For example, in Figure 9.33b, for feed F, only pure 2-ethoxyethanol can be obtained. When the feed is moved to the left across the distillation-line boundary, pure ethylbenzene can be obtained. In Figure 9.33c, only methanol can be recovered in high purity for feeds in the region LTGCL. For a feed in the region EDTHGBE, no pure product is possible. Before attempting rigorous distillation calculations with a simulation program, it is essential to establish, with the aid of computer-generated residual curve maps, regions of product composition feasibility such as shown in Figure 9.33. Otherwise, it is possible to waste much time and effort in trying to converge distillation calculations when specified product compositions are impossible.

Heterogeneous Distillation

In heterogeneous azeotropic distillation, an entrainer is utilized that concentrates in the overhead vapor and, when condensed, causes the formation of a second liquid phase that can be decanted and recirculated to the tower as reflux. The other liquid phase, as well as the bottoms, are the products from the distillation. This is possible when the entrainer forms a heterogeneous azeotrope with one or more of the species in the feed. For example, ethanol and water form a minimum-boiling azeotrope at 89 mol% ethanol and 1 atm, but by using a suitable entrainer, it is possible to devise a process to produce pure ethanol as a product. Such a process is described next.

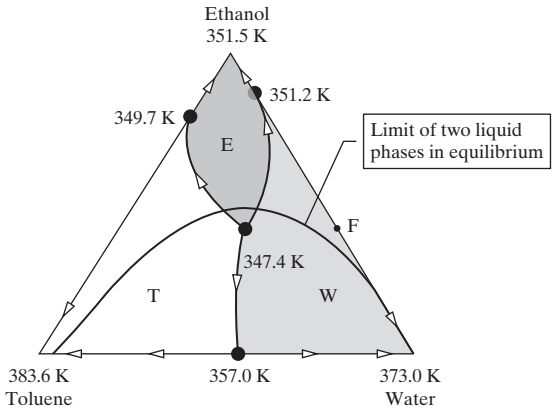

Figure 9.34 Ternary composition diagram for a mixture of ethanol, water, and toluene.

Although toluene is the highest-boiling species, it is an appropriate entrainer because it forms minimum-boiling azeotropes with both water and ethanol. As shown in the ternary composition diagram for the mixture of ethanol, water, and toluene in Figure 9.34, three binary azeotropes and a single tertiary azeotrope are formed, dividing the phase plane into three distillation regions: E within which pure ethanol can be produced, W within which pure water can be produced, and T within which pure toluene can be produced. Since the feed composition lies within distillation region W, purified ethanol cannot be produced directly from the feed stream, but purified water can be produced. It is noted that the tertiary azeotrope is a heterogeneous one because it resides inside the region in which two liquid phases are in equilibrium.

These observations guide the construction of the PFD, shown in Figure 9.35a, following the material balance lines positioned on the ternary phase diagram presented in Figure 9.35b. Noting that distillation region E can produce pure ethanol, we begin by placing the azeotropic tower, C-2, to recover ethanol as high-purity bottoms product, B2, with the overhead vapor of C-2 approaching the ternary, minimum-boiling, heterogeneous azeotrope, D2. This condenses into two liquid phases, one rich in toluene (point S2) and the other rich in water (point S1), which are separated in the decanter, represented in Figure 9.35b by the tie line S2-D2-S1. As the aqueous stream, S1, is inside distillation region W, it is mixed with F to produce M1, the feed to the preconcentrator tower, C-1, which produces high-purity water as bottoms, B1, and a distillate, D1, just to right of the simple distillation boundary separating regions E and W. The organic stream drawn from the decanter, S2, is mixed with D1 to produce M2, the feed stream to the azeotropic tower, C-2, thus completing the process.

The distillation sequence shown in Figure 9.35a is only one of several sequences involving from two to four columns that have been proposed and/or applied in industry for separating a mixture by employing heterogeneous azeotropic distillation.

Most common is the three-column sequence from the study of Ryan and Doherty (1989) as shown in Figure 9.36a. When used to separate a mixture of ethanol and water using benzene as the entrainer, the three columns perform the separation in the

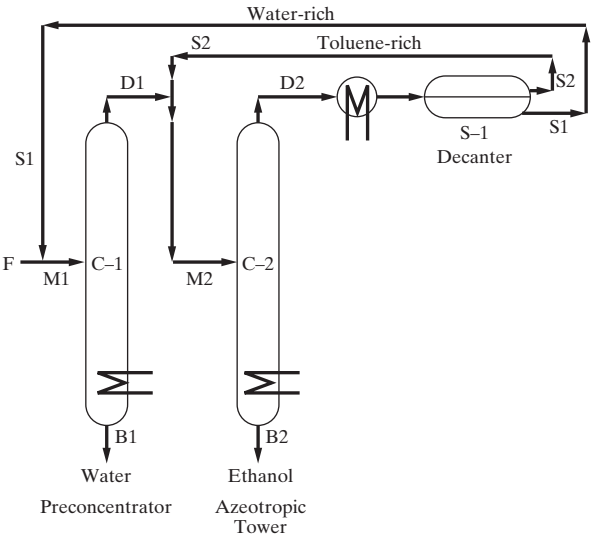

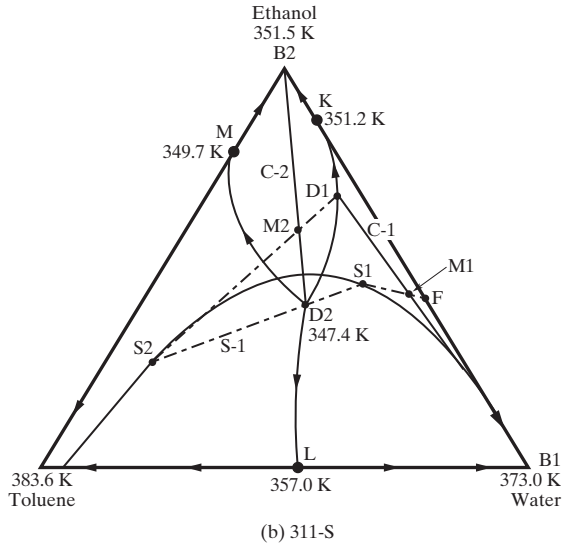

Figure 9.35 Dehydration of ethanol using toluene as an entrainer: (a) process flow diagram; (b) ternary composition diagram.

following manner, where the material-balance lines for Columns 2 and 3 are shown in Figure 9.36b. The aqueous feed, F1, dilute in ethanol, is preconcentrated in Column 1 to obtain a pure water bottoms, B1, and a distillate, D1, whose composition approaches that of the homogeneous minimum-boiling binary azeotrope. The distillate becomes the feed to Column 2, the azeotropic column, where nearly pure ethanol, B2, is removed as bottoms. The overhead vapor from Column 2, V2, is close to the composition of the heterogeneous ternary azeotrope of ethanol, water, and benzene. When condensed, it separates into two liquid phases in the decanter. Most of the organic-rich phase, L2, is returned to Column 2 as reflux. Most of the water-rich phase, D2, is sent to Column 3, the entrainer recovery column. Here, the distillate, D3, consisting mainly of ethanol but with appreciable amounts of benzene and water, is recycled to the top of Column 2. The bottoms, B3 from Column 3, is nearly pure water. All columns operate at close to 1 atm pressure.

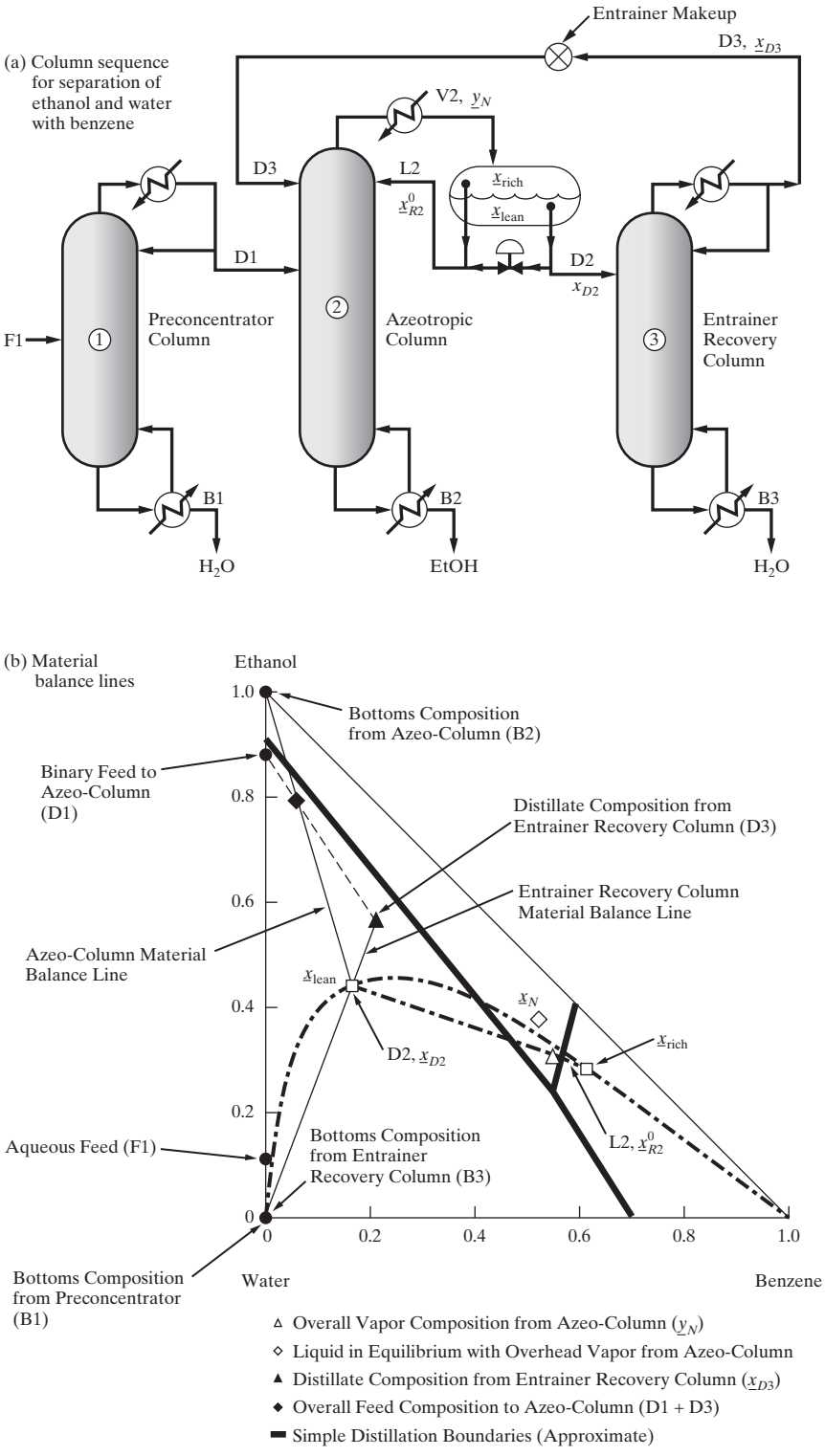

Figure 9.36 Kubierschky three-column system.

Multiple Steady States

The occurrence of multiple steady states in chemical reactors has been well recognized for at least 50 years. The most common example is an adiabatic CSTR for which, in some cases, for the same feed and reactor size, three possible products may be obtained, two of which are stable and one unstable. The product obtained in actual operation depends upon the startup procedure for the reactor. Only in the past 35 years has the existence of multiple steady states in distillation towers been shown by calculations and verified by experimental data from tower operation. In particular, azeotropic distillation is especially susceptible to multiple steady states. Disturbances during operation of an azeotropic tower can cause it to switch from one steady state to another, as shown by Prokopakis and Seider (1983).

Methods for computing multiple steady states for homogeneous and heterogeneous azeotropic distillation are presented in a number of publications. Kovach and Seider (1987) computed, by an arclength homotopy-continuation method, five steady states for the ethanol–benzene–water distillation. Bekiaris et al. (1993, 1996, 2000) studied multiple steady states for ternary homogeneous- and ternary heterogeneous-azeotropic distillation, respectively. Using the distillate flow rate as the bifurcation parameter, they found conditions of feed compositions and distillation-region boundaries for which multiple steady states can occur in columns operating at total reflux (infinite reflux ratio) with an infinite number of equilibrium stages (referred to as the 1–1 case). They showed that their results have relevant implications for columns operating at finite reflux ratios with a finite number of stages. Vadapalli and Seader (2001) used ASPEN PLUS with an arclength continuation and bifurcation method to compute all stable and unstable steady states for azeotropic distillation under conditions of finite reflux ratio and finite number of equilibrium stages. Specifications for their heterogeneous azeotropic distillation example, involving the separation of an ethanol–water mixture using benzene, are shown in Figure 9.37a. The total feed rate to the column is 101.962 kmol/hr. The desired bottoms product is pure ethanol. Using the bottoms flow rate as the bifurcation parameter, computed results for the mole fraction of ethanol in the bottoms are shown in Figure 9.37b as a function of the bifurcation parameter. In the range of bottoms flow rate from approximately 78 to 96 kmol/hr, three steady states exist, two stable and one unstable. For a bottoms rate equal to the flow rate of ethanol in the feed (89 kmol/hr), the best stable solution is an ethanol mole fraction of 0.98; the inferior stable solution is only 0.89. Figure 9.37b shows the computed points. In the continuation method, the results of one point are used as the initial guess for obtaining an adjacent point.

Although heterogeneous azeotropic distillation towers are probably used more widely than their homogeneous counterparts, care must be taken in their design and operation. In addition to the possibility of multiple steady states, most azeotropic distillation towers involve sharp fronts as the temperatures and compositions shift abruptly from the vicinity of one fixed point to the vicinity of another. Furthermore, in heterogeneous distillations, sharp fronts often accompany the interface between trays having one and two liquid phases as well. Consequently, designers must select carefully the number of trays and the reflux rates to prevent these fronts from exiting the tower with an associated deterioration in the product quality. Although these and other special properties of azeotropic towers (e.g., maximum reflux rates above which the separation deteriorates, and an insensitivity of the product compositions to the number of trays) are complicating factors, they fortunately are usually less important when synthesizing separation trains, and consequently, they are not discussed further here. For a review of the literature on this subject, see the article by Widagdo and Seider (1996).

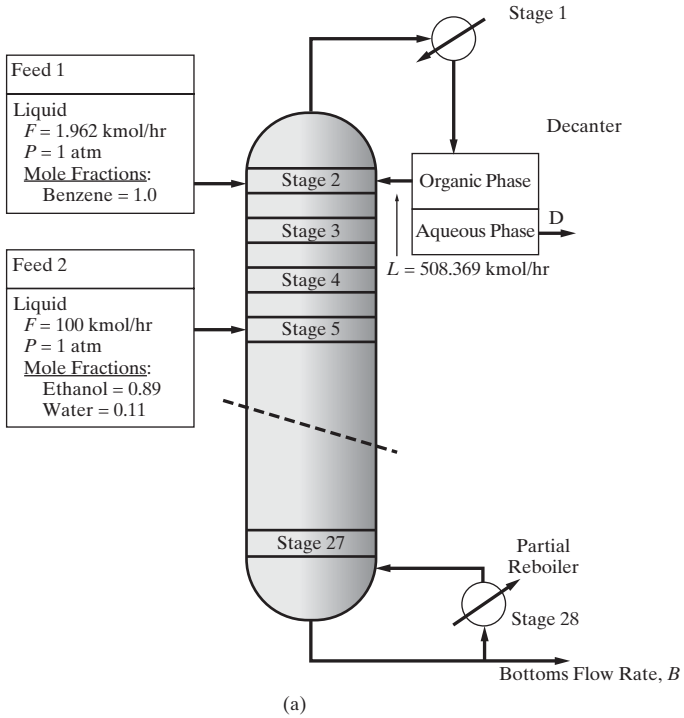

(a)

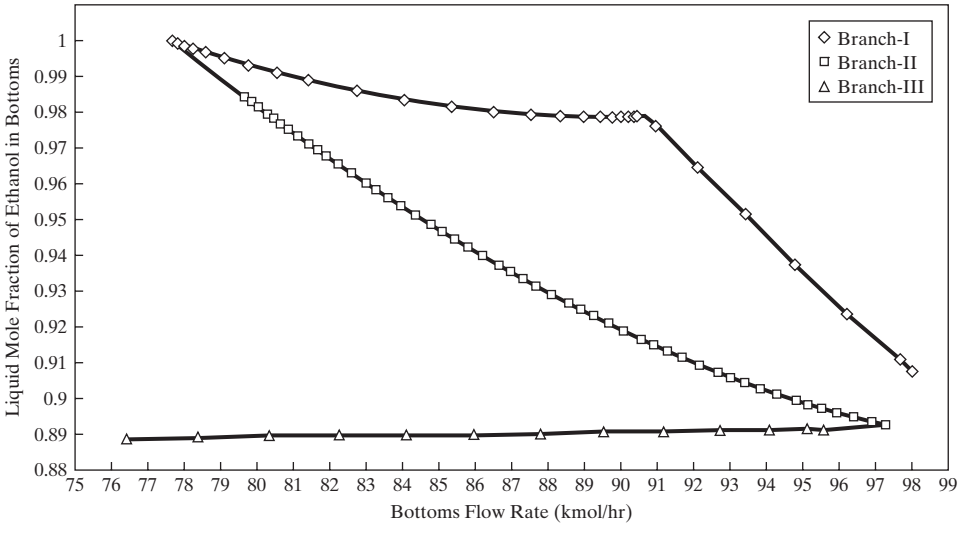

(b)

Figure 9.37 Heterogeneous azeotropic distillation: (a) specifications (b) bifurcation diagram; branches I and III—stable, branch II—unstable.

Pressure-Swing Distillation

In some situations, azeotropic points are sensitive to moderate changes in pressure. When this is the case, pressure-swing distillation can be used in place of azeotropic distillation to permit the recovery of two nearly pure species that are separated by a distillation boundary. This section introduces pressure-swing distillation.

The effect of pressure on the temperature and composition of the ethanol–water and ethanol–benzene azeotropes, two minimum-boiling binary azeotropes, is shown in Figure 9.38. For the first, as the pressure is decreased from 760 to 100 torr, the mole fraction of ethanol increases from 0.894 to 0.980. Although not shown, at a lower pressure, below 70 torr, the azeotrope disappears entirely. The temperature changes are comparable for the ethanol–benzene azeotrope, but the composition is far more sensitive. Many other binary azeotropes are pressure sensitive, as discussed by Knapp and Doherty (1992), who list 36 systems taken from the compilation of azeotropic data by Horsley (1973).

An example of pressure-swing distillation described by Van Winkle (1967) is provided for the mixture A – B having a minimum-boiling azeotrope with the $T - x - y$ curves at two pressures shown in Figure 9.39a. To take advantage of the decrease in the composition of A as the pressure decreases from P_2 to P_1, a sequence of two distillation towers is shown in Figure 9.39b. The total feed to Column 1, F_1, operating at the lower pressure, P_1, is the sum of the fresh feed, F, whose composition is richer in A than the azeotrope and the distillate, D_2, whose composition is close to that of the azeotrope at P_2 and which is recycled from Column 2 to Column 1. The compositions of D_2, and consequently F_1, are richer in A than the azeotropic composition at P_1. Hence, the bottoms product, B_1, that leaves Column 1 is nearly pure A. Since the distillate, D_1, which is slightly richer in A than the azeotropic composition, is less rich in A than the azeotropic composition at P_2, when it is fed to Column 2, the bottoms product, B_2, is nearly pure B. Another example is provided by Robinson and Gilliland (1950) for the dehydration of ethanol, where the fresh-feed composition is less rich in ethanol than the azeotrope. In this case, ethanol and water are removed as bottoms products also, but nearly pure B (water) is recovered from the first column, and A (ethanol) is

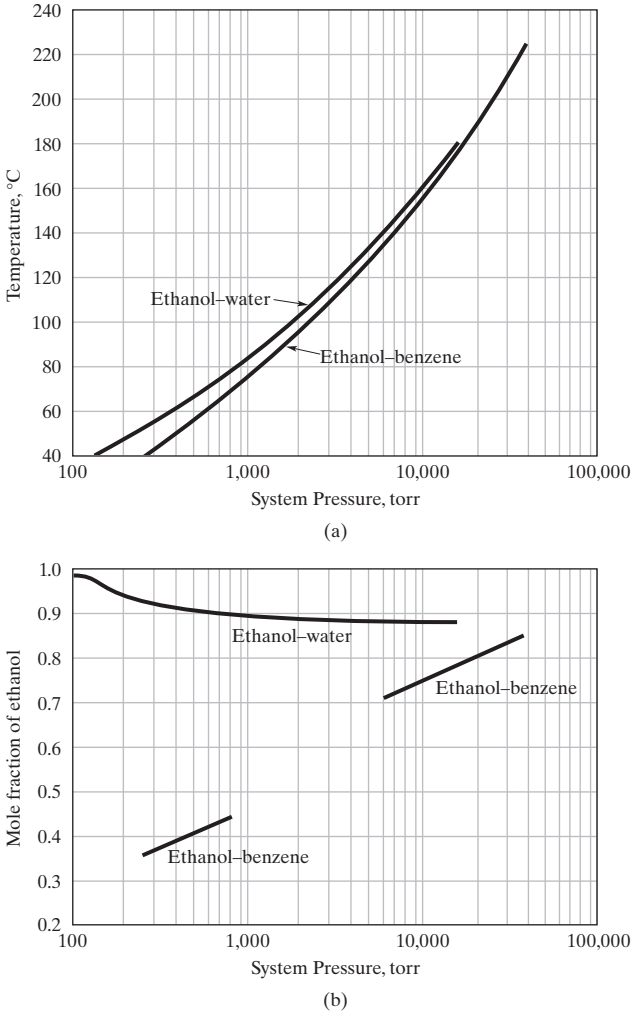

Figure 9.38 Effect of pressure on azeotrope conditions: (a) temperature of azeotrope; (b) composition of azeotrope.

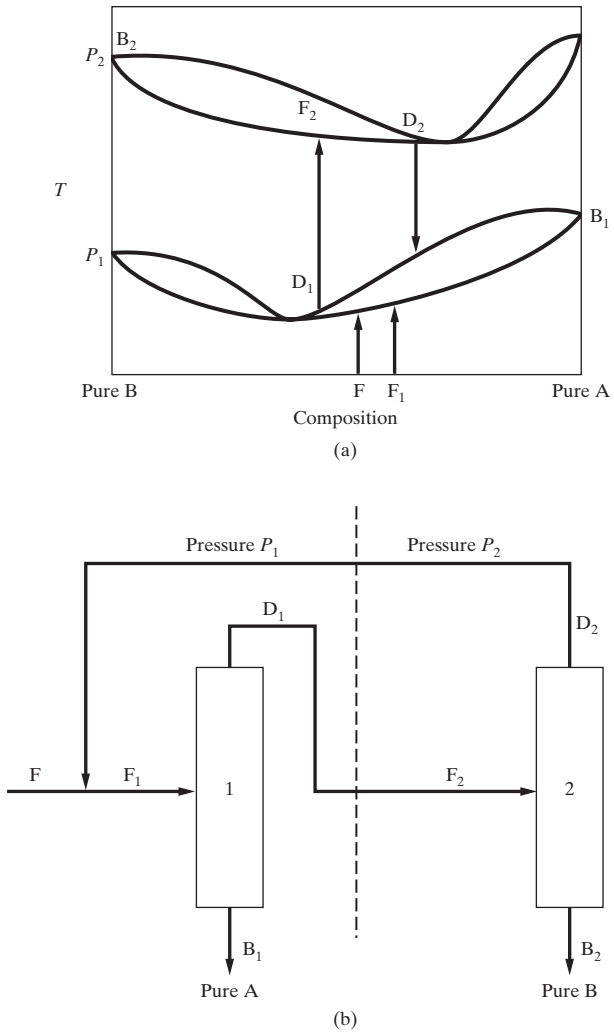

Figure 9.39 Pressure-swing distillation for the separation of a minimum-boiling azeotrope: (a) $T - x - y$ curves at pressures P_1 and P_2 for minimum-boiling azeotrope; (b) distillation sequence for minimum-boiling azeotrope.

recovered from the second. Similar pressure-swing distillations are designed to separate maximum-boiling binary azeotropes, which are less common.

When designing pressure-swing distillation sequences, the recycle ratio must be adjusted carefully. Note that it is closely related to the differences in the compositions of the azeotrope at P_1 and P_2. Horwitz (1997) illustrates this for the dehydration of ethylenediamine.

EXAMPLE 9.5

Consider the separation of 100 kmol/hr of an equimolar stream of tetrahydrofuran (THF) and water using pressure-swing distillation, as shown in Figure 9.40. The tower T1 operates at 1 bar with the pressure of tower T2 increased to 10 bar. As shown in the $T - x - y$ diagrams in Figure 9.41, the binary azeotrope shifts from 19 mol% water at 1 bar to 33 mol% water at 10 bar. Assuming that the bottoms product from T1 contains pure water and that from T2 contains pure THF, and that the distillates from T1 and T2 are at their azeotropic compositions, determine the unknown flow rates of the product and internal streams. Note that data for the calculation of vapor–liquid equilibria are provided in Table 9.6.

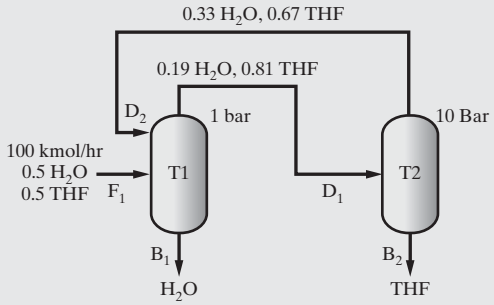

Figure 9.40 Pressure-swing distillation for dehydration of THF with stream compositions in mole fraction.

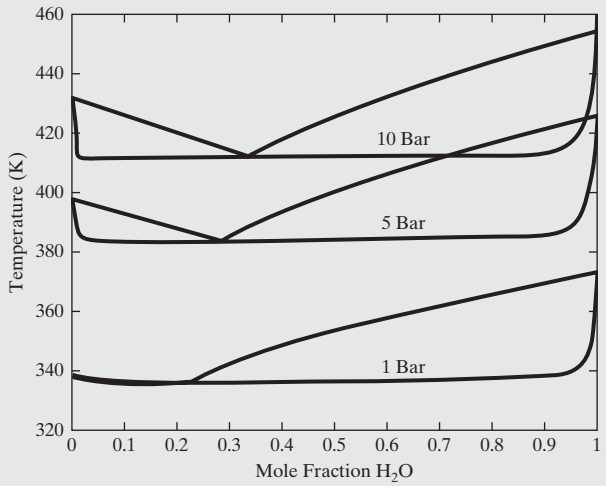

Figure 9.41 $T - x - y$ diagrams for THF and water.

SOLUTION

Since the bottoms products are pure, $B_1 = 50$ kmol/hrH_2O and $B_2 = 50$ kmol/hr THF. To determine the distillate flow rates, the following species balances apply.

$$H_2O \text{ balance on column T2}: \quad 0.19D_1 = 0.33D_2$$

$$\text{THF balance on column T1}: \quad 0.81D_1 = 0.67D_2 + 50$$

Solving these two equations simultaneously, $D_1 = 117.9$ kmol/hr and $D_2 = 67.9$ kmol/hr. Exercise 9.16 examines the effect of pressure on the internal flow rates.

Table 9.6 Data for Vapor–Liquid Equilibria for THF – H_2O

Extended Antoine Coefficients

	H_2O	THF
C^1	7.36	5.490
C^2	–7,258	–5,305
C^3	0.0	0.0
C^4	0.0	0.0
C^5	–7.304	–4.763
C^6	4.1653×10^{-6}	1.4291×10^{-17}
C^7	2.0	6.0

$\ln P_i^s = C_i^1 + C_i^2/(T + C_i^3) + C_i^4 T + C_i^5 \ln T + C_i^6 T^{C_i^7}$; P_i^s, Pascal, T, K

Wilson Interaction Coefficients

A_{ij}	H_2O	THF	B_{ij}	H_2O	THF
H_2O	0.0	−23.709	H_2O	0.0	7,500
THF	–2.999	0.0	THF	–45.07	0.0

Membranes, Adsorbers, and Auxiliary Separators

When operating homogeneous azeotropic distillation towers, a convenient vehicle for permitting the compositions to cross a distillation boundary is to introduce a membrane separator, adsorber, or other auxiliary separator. These are inserted either before or after the condenser of the distillation column and serve a similar role to the decanter in a heterogeneous azeotropic distillation tower, with the products having their compositions in adjacent distillation regions.

Reactive Distillation

Another important vehicle for crossing distillation boundaries is through the introduction of chemical reaction(s) on the trays of a distillation column. As discussed in Section 6.3, it is often advantageous to combine reaction and distillation operations so as to drive a reversible reaction(s) toward completion through the recovery of its products in the vapor and liquid streams that leave the trays. Somewhat less obvious, perhaps, is the effect the reaction(s) can have on repositioning or eliminating the distillation boundaries that otherwise complicate the recovery of nearly pure species. For this reason, the discussion that follows concentrates on the effect of a reaction on the residue curve maps. Several constructs must be introduced, however, to prepare for the main concepts.

For reactive systems, it is helpful to begin with a more rigorous definition of an azeotrope, that is, a mixture whose phases exhibit no changes in composition during vaporization or condensation. On this basis, for vapor and liquid phases with $dx_j/dt = dy_j/dt = 0, j = 1, \ldots, C$ in the presence of a homogeneous chemical reaction $\Sigma_j \nu_j A_j = 0$ at equilibrium, the conditions for a reactive azeotrope can be derived (Barbosa and Doherty, 1988a) such that

$$\frac{y_j - x_j}{\nu_j - x_j \nu_T} = \frac{d\xi}{dv} = \kappa \qquad j = 1, \ldots, C \tag{9.32}$$

where ν_j is the stoichiometric coefficient of species j, $\nu_T = \Sigma_j \nu_j$, ξ is the extent of the reaction, v is the moles of vapor, and κ is a constant. Furthermore, it can be shown that the mass balances for simple distillation in the presence of a chemical reaction can be written in terms of transformed variables (Barbosa and Doherty, 1988b):

$$\frac{dX_j}{d\tau} = X_j - Y_j \qquad j = 1, \ldots, C-1; j \neq j' \tag{9.33a}$$

where

$$X_j = \frac{x_j/\nu_j - x_{j'}/\nu_{j'}}{\nu_{j'} - \nu_T x_j} \tag{9.33b}$$

$$Y_j = \frac{y_j/\nu_j - y_{j'}/\nu_{j'}}{\nu_{j'} - \nu_T y_j} \tag{9.33c}$$

$$\tau = \frac{H}{v}\left(\frac{\nu_{j'} - \nu_T y_j}{\nu_{j'} - \nu_T x_j}\right) t \tag{9.33d}$$

Here, H is the molar liquid holdup in the still, and j' denotes a reference species. Clearly, Eq. (9.33a) corresponds to the mass balances without chemical reaction [Eq. (9.20)]. By integration of the latter equation for a nonreactive mixture of isobutene, methanol, and methyl tertiary-butyl ether (MTBE), the residue curve map in Figure 9.42a is obtained. There are two minimum-boiling binary azeotropes and a distillation boundary that separates two distillation regions.

When the chemical reaction is turned on and permitted to equilibrate, Eq. (9.33a) is integrated and at long times,

$$X_j = Y_j \qquad j = 1, \ldots, C \tag{9.34}$$

define the fixed point and are the conditions derived for a reactive azeotrope [Eq. (9.32)]. At shorter times, reactive residue curves are obtained, as shown in Figure 9.42d, where the effect of the chemical reaction can be seen. It is clear that the residue curves have been distorted significantly and pass through the reactive azeotrope or so-called equilibrium tangent pinch. Furthermore, the distillation boundary has been eliminated completely. The reactive azeotrope of this mixture is shown clearly in an $X - Y$ diagram (Figure 9.43), which is similar to the $x - y$ diagram when reaction does not occur. Finally, through the use of a kinetic model involving a well-stirred reactor, it is possible to show the residue curves as a function of the residence time (that is, the Damkohler number, Da). Figures 9.42b and 9.42c show how the residue curves change as the residence time increases (Venimadhavan et al., 1994).

Separation Train Synthesis

Beginning with the need to separate a C-component mixture into several products, alternative sequences of two-product distillation towers are considered in this section. Although the synthesis strategies are not as well defined for highly nonideal and azeotropic mixtures, several steps are well recognized and are described next. It should be mentioned that these strategies continue to be developed, and variations are not uncommon.

Step 1: ***Identify the Azeotropes***. Initially, it is very helpful to obtain estimates of the temperature, pressure, and composition of the binary, ternary, … , azeotropes associated with the C-component mixture. For all of the ternary submixtures, these can be determined, as described above, by preparing residue curve or distillation-line maps. When it is necessary to estimate the quaternary and higher-component azeotropes as well as the binary and ternary azeotropes, the methods of Fidkowski et al. (1993) and Eckert and Kubicek (1997) are recommended. When the C-component mixture is the effluent from a chemical reactor, it may be helpful to include the reacting chemicals, that is, to locate any azeotropes involving these chemicals as well as the existence of reactive azeotropes. This information may show the potential for using reactive distillation operations as a vehicle for crossing distillation boundaries that complicate the recovery of nearly pure species.

Step 2: ***Identify Alternative Separators***. Given estimates for the azeotropes, the alternatives for the separators involving all C species are identified. These separate two species

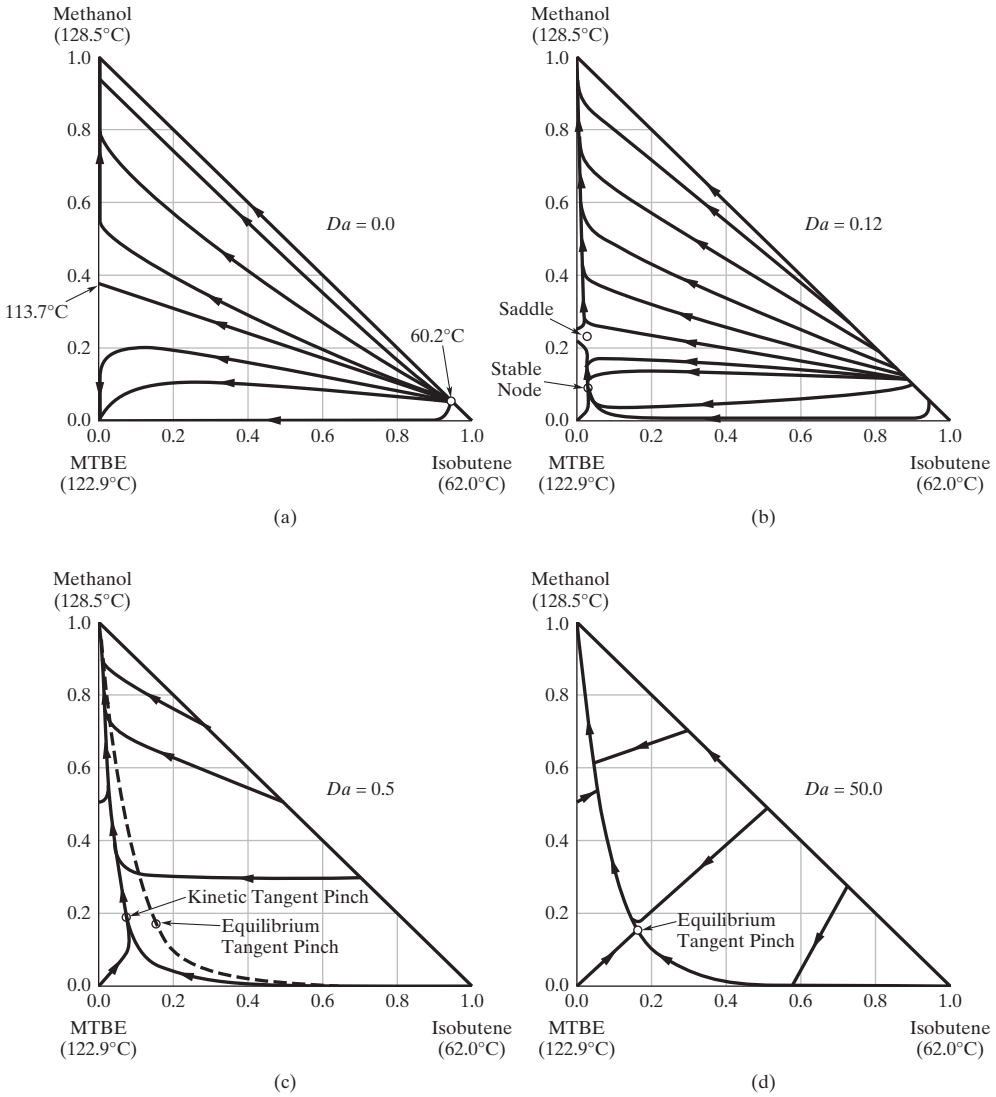

Figure 9.42 Residue curve maps for isobutene, methanol, and MTBE as a function of *Da* at 8 atm. (Reprinted from Venimadhavan et al., 1994). Reproduced with permission of the American Institute of Chemical Engineers. Copyright © 1994 AIChE. All rights reserved.

that may or may not involve a binary azeotrope. When no binary azeotrope is involved, a normal distillation tower may be adequate unless the key components are close boiling. For close-boiling binary pairs or binary pairs with an azeotrope separating the desired products, the design of an extractive distillation tower or an azeotropic distillation tower should be considered. The former is preferred when a suitable solvent is available.

Step 3: ***Select the Entrainer***. Probably the most difficult decision in designing an azeotropic distillation tower involves the selection of the entrainer. This is complicated by the effect of the entrainer on the residue curves and distillation lines that result. In this regard, the selection of the entrainer for the separation of binary mixtures alone is a large combinatorial problem complicated by the existence of 113 types of residue curve maps involving different combinations of low- and high-boiling binary and ternary azeotropes with associated distillation boundaries. This classification, which involves several indices that characterize the various kinds of azeotropes and vertices, was prepared by Matsuyama and Nishimura (1977) to aid in screening potential entrainers.

Thus, many factors need to be considered in selecting an entrainer, factors that can have a significant impact on the resulting separation train. Two of the more important guidelines are the following:

(a) When designing homogeneous azeotropic distillation towers, select an entrainer that does not introduce a distillation boundary between the two species to be separated.

(b) To cross a distillation boundary between two species to be separated, select an entrainer that induces liquid-phase splitting as in heterogeneous azeotropic distillation.

The effects of these and other guidelines must be considered as each separator is designed and as the

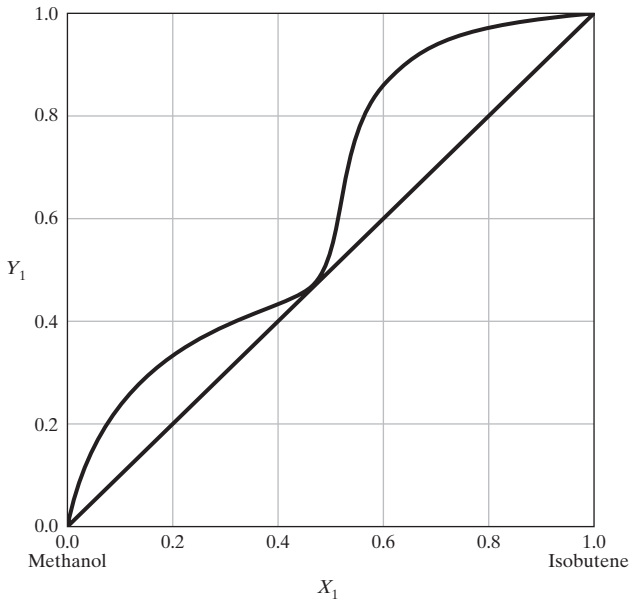

Figure 9.43 Transformed compositions for isobutene, methanol, and MTBE in chemical and phase equilibrium (Reprinted from Doherty and Buzad, 1992). Reproduced with permission of the American Institute of Chemical Engineers. Copyright © 1992 AIChE. All rights reserved.

separation sequence evolves. More recently, Peterson and Partin (1997) showed that temperature sequences involving the boiling points of the pure species and the azeotrope temperatures can be used to effectively categorize many kinds of residue curve maps. This classification simplifies the search for an entrainer that has a desirable residue curve map, for example, one that does not involve a distillation boundary.

Step 4: ***Identify Feasible Distillate and Bottoms-product Compositions***. When positioning a two-product separator, it is usually an objective to recover at least one nearly pure species or at least to produce two products that are easier to separate into the desired products than the feed mixture. To accomplish this, it helps to know the range of feasible distillate and bottoms-product compositions. For a three-component feed stream, the feed composition can be positioned on a distillation-line map and the feasible compositions for the distillate and bottoms product identified using the methods described in the subsection on distillation-line boundaries and feasible product compositions. For feed mixtures containing four or more species ($C > 3$), a common approach is to identify the three most important species that are associated with the separator being considered. Note, however, that the methods for identifying the feasible compositions assume that they are bounded by the distillation line at total reflux through the feed composition. For azeotropic distillations, however, it has been shown that the best separations may not be achieved at total reflux. Consequently, a procedure has been developed to locate the bounds at finite reflux. This involves complex graphics to construct the so-called pinch-point trajectories, which are beyond the scope of this presentation but are described in detail by Widagdo and Seider (1996). Because the composition bounds at finite reflux usually include the feasible region at total reflux, the latter usually leads to conservative designs.

Having determined the bounds on the feasible compositions, the first separator is positioned usually to recover one nearly pure species. At this point in the synthesis procedure, the separator can be completely designed (to determine number of trays, reflux ratio, installed and operating costs, etc.). Alternatively, the design calculations can be delayed until a sequence of separators is selected, with its product compositions positioned. In this case, Steps 2–4 are repeated for the mixture in the other product stream. Initially, the simplest separators are considered, that is, ordinary distillation, extractive distillation, and homogeneous azeotropic distillation. However, when distillation boundaries are encountered and cannot be eliminated through the choice of a suitable entrainer, more complex separators are considered, such as heterogeneous azeotropic distillation, pressure-swing distillation, the addition of membranes, adsorption, auxiliary separators, and reactive distillation. Normally, a sequence is synthesized involving many two-product separators without chemical reaction. Subsequently, after the separators are designed completely, steps are taken to carry out task integration as described in Section 2.3. This involves the combination of two or more separators and seeking opportunities to combine the reaction and separation steps in reactive distillation towers. As an example, Siirola (1995) describes the development of a process for the manufacture of methyl acetate and the dehydration of acetic acid. Initially, a sequence was synthesized involving a reactor, an extractor, a decanter, and eight distillation columns incorporating two mass separating agents. The flowsheet was reduced subsequently to four columns by using evolutionary strategies and task integration before being reduced finally to just two columns, one involving reactive distillation.

The next example illustrates the usage of the above procedure, as applied to the separation of a binary mixture exhibiting a minimum-boiling azeotrope and focuses of the selection of a suitable entrainer and column operating pressures.

EXAMPLE 9.6 ***Entrainer Selection and Operating Pressure***

The most economical process is sought for the separation of a feed stream containing 30 mol% of A and 70 mol% of B into highly pure product streams (at least 99 mol%). The process should utilize one or more 2-product distillation columns, with each column operating either at 2 or 10 bar. The process may include the usage of one of two entrainers, C and D. Data for the ternary systems A-B-C and A-B-D are provided in Table 9.7. As seen, both feature two homogeneous azeotropes. Your solution should provide justification for your choice of entrainer, as well as the material balance lines for the columns that comprise the separation system you devise, and a PFD for the process.

Table 9.7 Molar Compositions and Boiling Temperatures for the Systems A-B-C and A-B-D at 2 and 10 bar.

Component	Pure A	Pure B	Pure C	Azeotrope I	Azeotrope II
Data for the system A-B-C at 2 bar					
A	100%	0%	0%	50%	50%
B	0%	100%	0%	50%	0%
C	0%	0%	100%	0%	50%
Temperature	80°C	125°C	110°C	70°C	65°C
Data for the system A-B-C at 10 bar					
A	100%	0%	0%	50%	50%
B	0%	100%	0%	50%	0%
C	0%	0%	100%	0%	50%
Temperature	110°C	150°C	130°C	90°C	120°C

Component	Pure A	Pure B	Pure D	Azeotrope I	Azeotrope II
Data for the system A-B-D at 2 bar					
A	100%	0%	0%	50%	20%
B	0%	100%	0%	50%	0%
D	0%	0%	100%	0%	80%
Temperature	80°C	125°C	135°C	70°C	75°C
Data for the system A-B-D at 10 bar					
A	100%	0%	0%	50%	0%
B	0%	100%	0%	50%	80%
D	0%	0%	100%	0%	20%
Temperature	110°C	150°C	180°C	90°C	130°C

SOLUTION

First, notice in Table 9.7 that azeotrope I, which constitutes the distillation boundary between A and B, is invariant with pressure. Consequently, pressure-swing distillation alone cannot yield pure products, requiring that an entrainer be considered. Evidently, residue-curve maps must be generated for each of the two systems at both operating pressures, to assist in selecting the best entrainer. Sketches are presented in Figure 9.44.

Careful study of Figures 9.44c and 9.44d enables one to eliminate entrainer D as inappropriate for the purification of A and B: (1) At 2 bar, B cannot be produced from a two-product column as it is the intermediate boiler in its distillation region; (2) the distillation boundary separating the two distillation regions does not allow both A and B to be purified by pressure-swing distillation. This leaves entrainer C to be considered. Figures 9.44a and 9.44b show that entrainer C is promising: (1) B can be purified at 2 bar; (2) it would appear that the distillation boundaries at the two operating pressures lend themselves better for pressure swing distillation; a column operating at 10 bar can separate any binary mixture of A and C into pure products whereas a column at 2 bar can produce pure B.

These observations suggest the process sketched in Figure 9.45. The first column is operated at 2 bar with a bottoms stream, B_1, rich in B; and an overhead stream, D_1, at the binary azeotrope of A and C. D_1 is compressed to 10 bar and then fed to the high-pressure column, operating at 10 bar, which produces an overhead stream, D_2 rich in A, and a bottoms stream B_2, rich in C. B_2 is recycled and mixed with the feed stream F, to give the feed stream to the first column, M_1.

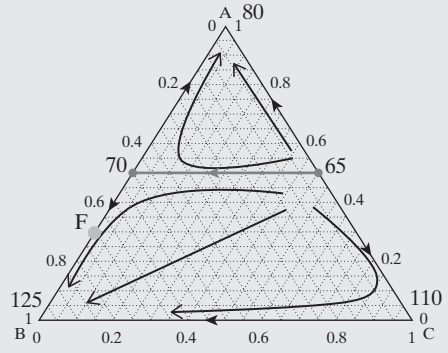

(a) A-B-C at 2 Bar

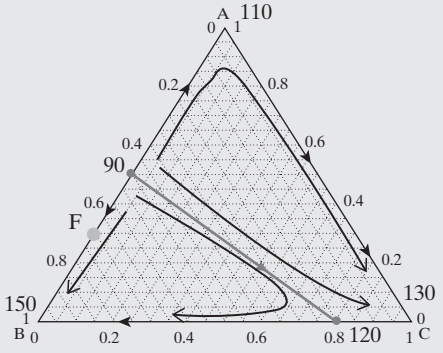

(b) A-B-C at 10 Bar

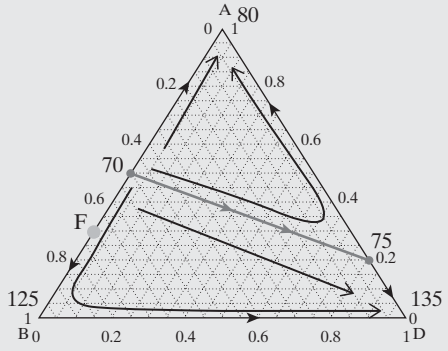

(c) A-B-D at 2 Bar

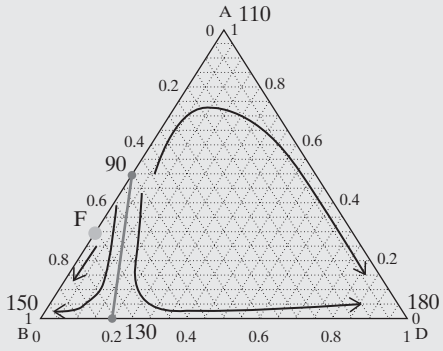

(d) A-B-D at 10 Bar

Figure 9.44 Ternary phase diagrams for the two alternative systems: A-B-C and A-B-D at two operating pressures, 2 and 10 bar.

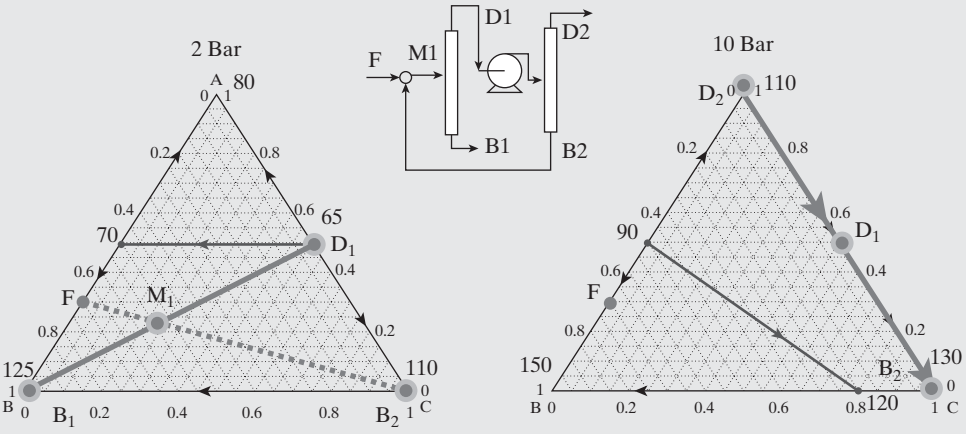

Figure 9.45 Ternary phase diagrams for system: A-B-C at two operating pressures, 2 and 10 bar, and the PFD for the separation process.

As illustrated throughout this section, process simulators have extensive facilities for preparing phase equilibrium diagrams ($T-x-y$, $P-x-y$, $x-y$, …), residue curve maps, and bimodal curves for ternary systems. In addition, related but independent packages have been developed for the synthesis and evaluation of distillation trains involving azeotropic mixtures. These include SPLIT™, developed by Aspen Technology, Inc., in the early 2000s, and DISTIL™ developed by M. F. Doherty and M. F. Malone at the University of Massachusetts (as incorporated into HYSYS and UniSim®Design). The following is an example of the capabilities afforded by such packages.

EXAMPLE 9.7 *Manufacture of Di-Tertiary-Butyl Peroxide*

This example involves the manufacture of 100 million pounds per year of di-tertiary-butyl peroxide (DTBP) by the catalytic reaction of tertiary-butyl hydroperoxide (TBHP) with excess tertiary-butyl alcohol (TBA) at 170°F and 15 psia according to the reaction

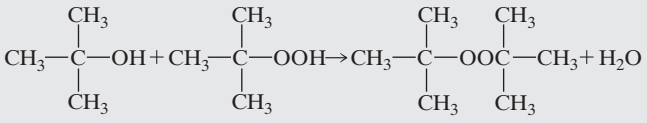

Tertiary-butyl Alcohol (TBA) | Tertiary-butyl Hydroperoxide (TBHP) | DTBP

Assume that the reactor effluent stream contains

	Ibmol/hr	Mole Fraction
TBA	72.1	0.272
H_2O	105.6	0.398
DTBP	87.7	0.330
		1.000

and small quantities of isobutene, methanol, and acetone, which can be disregarded. A separation sequence is to be synthesized to produce 99.6 mol% pure DTBP containing negligible water. It may be difficult to separate TBA and water. Therefore, rather than recovering and recycling the unreacted TBA, the conversion of TBA to isobutene and water in the separation sequence should be considered. In the catalytic reactor, the TBA dehydrates to isobutene, which is the actual molecule that reacts with TBHP to form DTBP. Thus, isobutene, instead of TBA, can be recycled to the catalytic reactor.

SOLUTION

A residue curve map at 15 psia, prepared using ASPEN PLUS (with the NRTL option set and proprietary interaction coefficients), is displayed in Figure 9.46a. There are three minimum-boiling binary azeotropes:

	T, °F	
DTBP–TBA	177	$x_{TBA} = 0.82$
TBA–H_2O	176	$x_{H_2O} = 0.38$
H_2O–DTBP	188	$x_{DTBP} = 0.47$

and the boiling points of the pure species are 181, 212, and 232°F, for TBA, H_2O, and DTBP, respectively. In addition, there is a minimum-boiling ternary azeotrope at $x_{TBA} = 0.44$, $x_{H2O} = 0.33$, and $x_{DTBP} = 0.23$, and 174°F. Consequently, there are three distinct distillation regions with the feed composition in a region that does not include the product vertex for DTBP.

To cross the distillation boundaries, it is possible to take advantage of the partial miscibility of the DTBP–H_2O system as well as the disappearance of the ternary azeotrope at 250 psia as illustrated in Figure 9.46b. One possible design is shown in Figure 9.47, where the reactor effluent is in stream S-107. Column D-102 forms a distillate in stream S-108 whose composition is very close to the ternary azeotrope and a bottoms product in stream S-109, as shown on the ternary diagram in Figure 9.48a. The latter stream, containing less than 5 mol% TBA, is split into two liquid phases in the decanter. The aqueous phase in stream S-111 enters the distillation tower, D-103, which forms nearly pure water in the bottoms product, stream S-113. The distillate

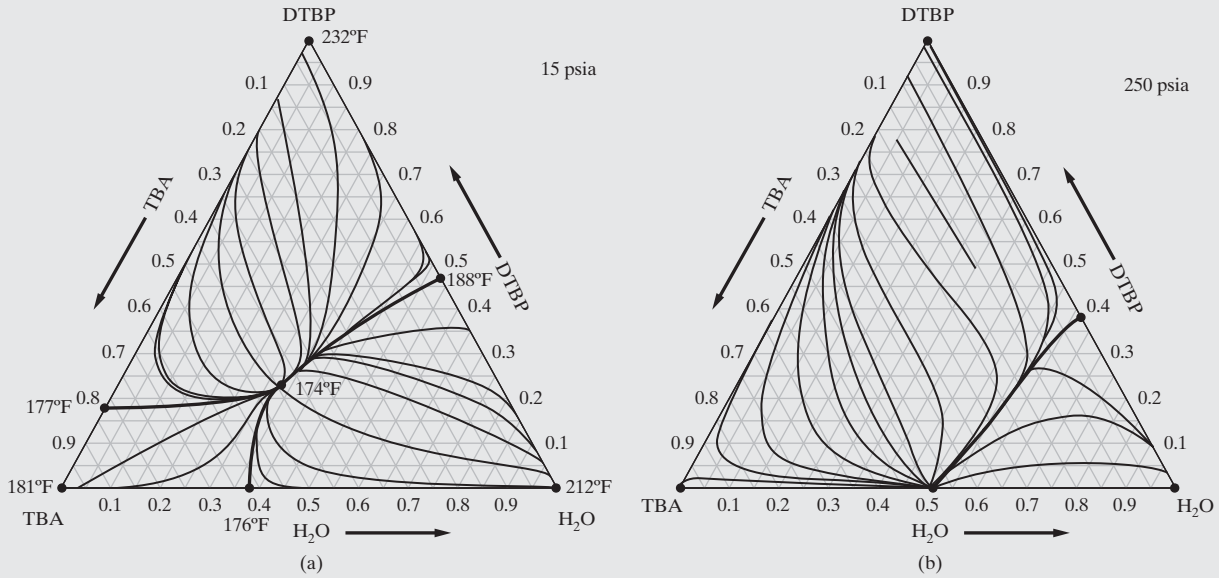

Figure 9.46 Residue curve map for the TBA–H_2O–DTBP system: (a) 15 psia; (b) 250 psia.

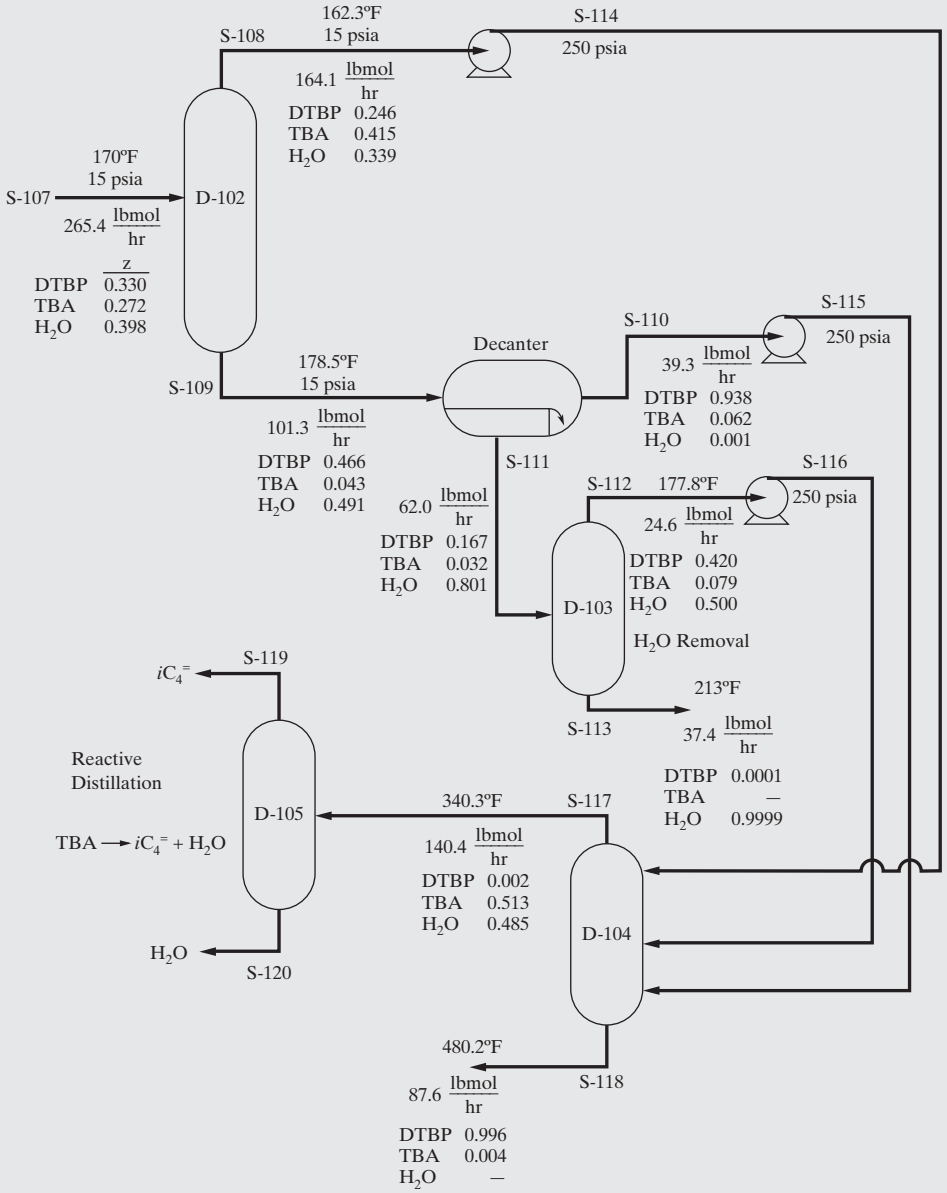

Figure 9.47 Process flowsheet for the DTBP process.

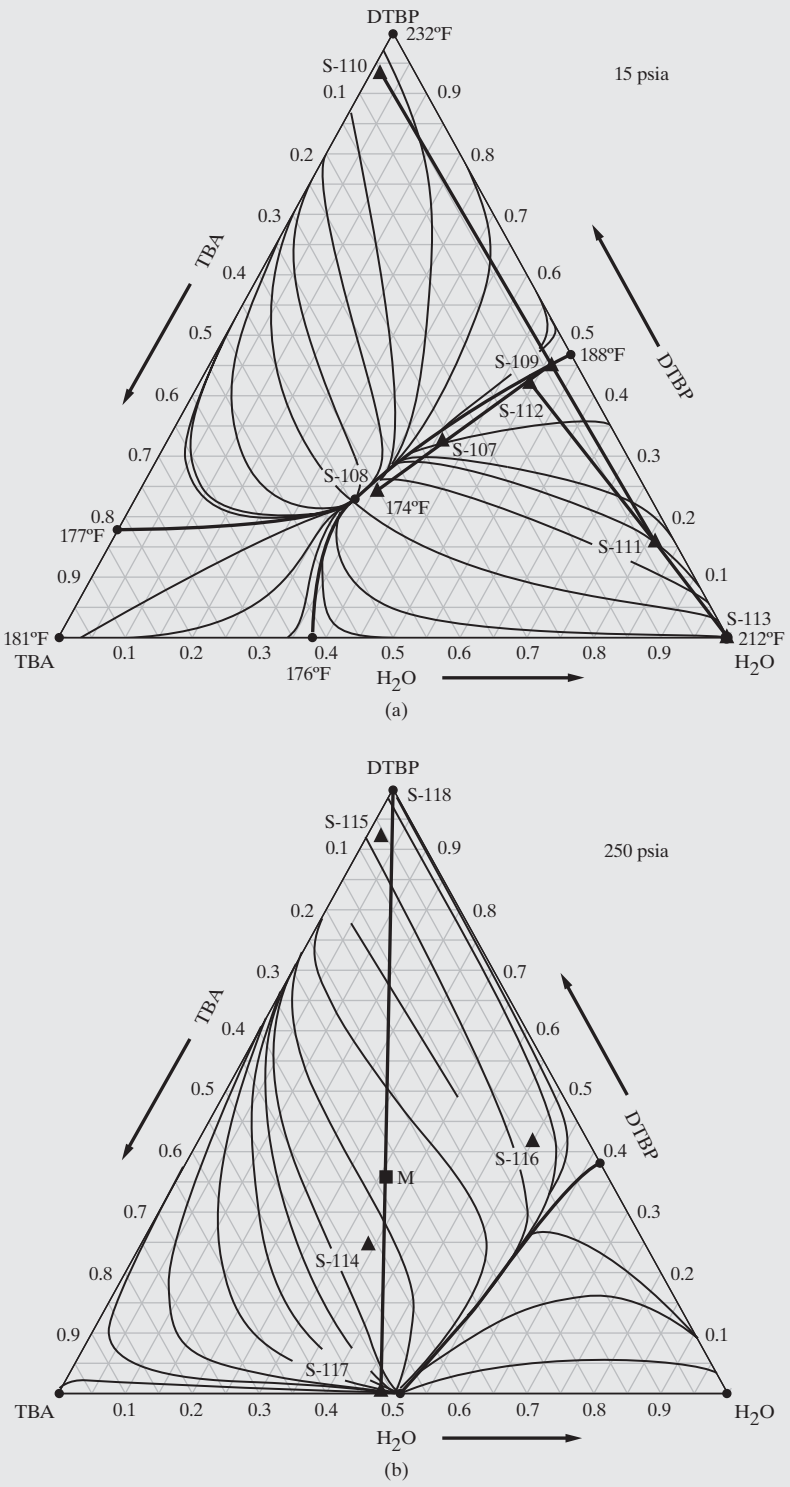

Figure 9.48 Distillation boundaries and material balance lines for the TBA–H_2O–DTBP system: (a) 15 psia; (b) 250 psia.

from tower D-102, S-108; the organic phase from the decanter, S-110; and the distillate from tower D-103, S-112 are pumped to 250 psia and sent to the distillation tower, D-104, where they enter on stages that have comparable compositions. The compositions of the streams at elevated pressure, S-114, S-115, and S-116 and the mix point, M, are shown in Figure 9.48b. Note that at 250 psia, M lies in the distillation region that contains the DTBP vertex. Consequently, tower D-104 produces nearly pure DTBP in the bottoms products, S-118, and its distillate, S-117, is sent to the reactive distillation tower, D-105, where the TBA is dehydrated according to the reaction

$$\text{TBA} \rightarrow i\text{-butene} + H_2O$$

with *i*-butene recovered in the distillate, S-119, which is recycled to the catalytic reactor, and water in the bottoms product, S-120. As seen in Figures 9.48a and 9.48b, the material balance lines associated with the distillation towers lie entirely within separate distillation regions. The process works effectively because of the phase split and because the distillation boundaries are repositioned at the elevated

pressure. Note, however, that the material balance line for the tower, D-102, would preferably be positioned farther away from the distillation boundary to allow for inaccuracies in its calculation.

Since this design was completed, the potential for DTBP to decompose explosively at temperatures above 255°F was brought to our attention. At 250 psia, DTBP is present in the bottoms product of tower D-104 at 480.2°F. Given this crucial safety concern, a design team would seek clear experimental evidence. If positive, lower pressures, with corresponding lower temperatures, would be explored, recognizing that the distillation boundaries are displaced less at lower pressures.

For additional details of this process design, see the design report by Lee et al. (1995). Also, see Problem A-IIS.1.10 in the Supplement_to_Appendix_II.pdf (in the PDF Files folder, which can be downloaded from www.seas.upenn.edu/~dlewin/design projects.html) for the design problem statement that led to this design.

9.6 SEPARATION SYSTEMS FOR GAS MIXTURES

Sections 9.4 and 9.5 deal primarily with the synthesis of separation trains for liquid–mixture feeds. The primary separation techniques are ordinary and enhanced distillation. If the feed consists of a vapor mixture in equilibrium with a liquid mixture, the same techniques and synthesis procedures can often be employed. However, as discussed in Section 9.1, if the feed is a gas mixture and a wide gap in volatility exists between two groups of chemicals in the mixture, it is often preferable to partially condense the mixture, separate the phases, and send the liquid and gas phases to separate separation systems as discussed by Douglas (1988) and shown in Figure 9.49. Note that if a liquid phase is produced in the gas separation system, it is routed to the liquid separation system and vice versa.

In some cases, it has been found economical to use distillation to separate a gas mixture, with the large-scale separation of air by cryogenic distillation into nitrogen and oxygen being the most common example. However, the separation by distillation of many other gas mixtures, such as hydrogen from methane or hydrogen from nitrogen, is not practical because of the high cost of partially condensing the overhead vapor to obtain reflux. Instead, other separation methods, such as absorption, adsorption, or membrane permeation, are employed. In just the past 35 years, continuous adsorption and membrane processes have been developed for the separation of air that economically rival the cryogenic distillation process at low to moderate production levels.

Barnicki and Fair (1992) consider in detail the selection and sequencing of equipment for the separation of gas mixtures. Whereas ordinary distillation is the dominant method for the separation of liquid mixtures, no method is dominant for gas mixtures. The separation of gas mixtures is further complicated by the fact that whereas most liquid mixtures are separated into nearly pure components, the separation of gas mixtures falls into the following three categories: (1) sharp splits to produce nearly pure products, (2) enrichment to increase the concentration(s) of one or more species, for example, oxygen and nitrogen enrichment, and (3) purification to remove one or more low-concentration impurities. The first category is often referred to as *bulk separation*, the purpose of which is to produce high-purity products at high recovery. Separations in this category can be difficult to achieve for gas mixtures. The best choices are cryogenic distillation, absorption, and adsorption. By contrast, the second category achieves neither high purity nor high recovery and is ideally suited for any of the common separation methods for gas mixtures including membrane separation by gas permeation. To produce high-purity products by purification, adsorption and absorption with chemical reaction are preferred.

The synthesis of a separation train for a gas mixture can be carried out by first determining the feasible separation methods, which depend on the separation categories and the separation factors, and then designing and costing systems involving these methods to determine the optimal train. The design of equipment for absorption, adsorption, distillation, and membrane separations is covered by Seader et al. (2016). Besides the separation category and separation factor, the production scale of the process is a major factor in determining the optimal train because economies of scale are most pronounced for cryogenic distillation and absorption, and least pronounced for adsorption and membrane separations. For example, for the separation of air into nitrogen- and oxygen-enriched products, membrane separations are most economical at low production rates, adsorption at moderate rates, and cryogenic distillation at high rates.

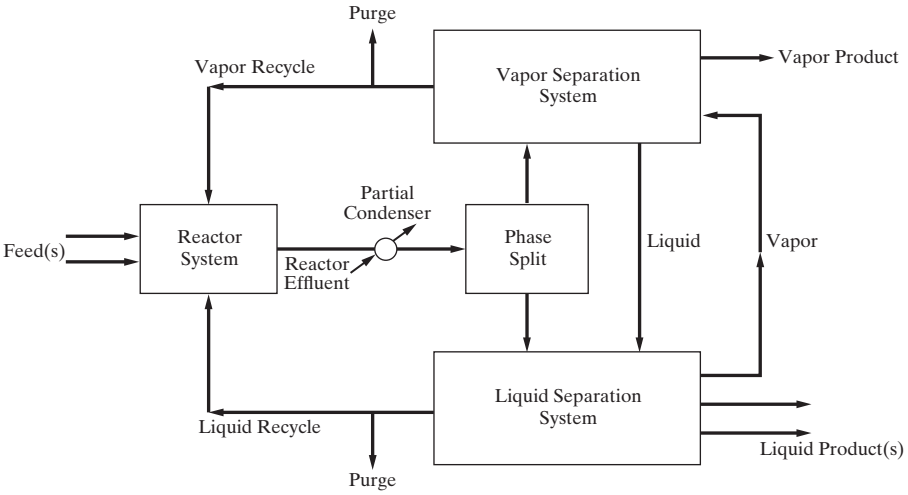

Figure 9.49 Process with vapor and liquid separation systems. (*Source:* Modified and reprinted with permission from Douglas, 1988).

Membrane Separation by Gas Permeation

In gas permeation, the gas mixture is compressed to a high pressure and brought into contact with a very thin membrane to produce two products: (1) a permeate that passes through the membrane and is discharged at a low pressure and (2) a retentate that does not pass through the membrane and is maintained at close to the high pressure of the feed. The separation factor defined by Eqs. (9.2) and (9.8) can be applied to gas permeation when the retentate-side pressure is much greater than the permeate-side pressure, if y is the mole fraction in the permeate and x is the mole fraction in the retentate. The relative volatility is replaced by the ratio of the membrane permeabilities for the two key components of the feed–gas mixture, sometimes called the permselectivity. Most commercial membranes for gas permeation are nonporous (dense) amorphous or semicrystalline polymers. To pass through such polymers, the gas molecules first dissolve in the polymer and then pass through it by diffusion. Thus, the permeability depends on both solubility and diffusivity in the particular polymer at the conditions of temperature and pressure. The permeability is the product of the solubility and diffusivity. Permeabilities are best determined by laboratory measurements. However, a predictive method given by Barnicki (1991) for a number of glassy and rubbery polymers, which depends on species van der Waals volume and critical temperature, can be applied in the absence of data. In general, gas permeation is commercially feasible when the ratio of permeabilities (permselectivity) for the two components is greater than 15. However, some processes that require only rough enrichments use membranes having permselectivities of only 5. Commercial applications include the recovery of carbon dioxide from hydrocarbons, the adjustment of the hydrogen-to-carbon monoxide ratio in synthesis gas, the recovery of hydrocarbons from hydrogen, and the separation of air into nitrogen- and oxygen-enriched streams.

Adsorption

Adsorption differs from the other techniques in that it is a cyclic operation with adsorption and desorption steps. However, adsorption is a very versatile separation technique. To be economical, the adsorbent must be regenerable. This requirement precludes the processing of gas mixtures that contain (1) high-boiling organic compounds because they are preferentially adsorbed and are difficult to remove during the regeneration part of the cycle, (2) lower-boiling organic compounds that may polymerize on the adsorbent surface, and (3) highly acidic or basic compounds that may react with the adsorbent surface. In some cases, such compounds can be removed from the gas mixture by guard beds or other methods prior to entry into the adsorption system.

Selectivity in adsorption is controlled by (1) molecular sieving or (2) adsorption equilibrium. When components differ significantly in molecular size and/or shape, as characterized by the kinetic diameter, zeolites and carbon molecular-sieve adsorbents can be used to advantage because of the strong selectivity achieved by molecular sieving. These adsorbents have very narrow pore-size distributions that prevent entry into the pore structure of molecules with a kinetic diameter greater than the nearly uniform pore aperture. Zeolites are readily available with nominal apertures in angstroms of 3, 4, 5, 8, and 10. Thus, for example, consider a gas mixture containing the following components with corresponding kinetic diameters in angstroms in parentheses: nitrogen (<3), carbon dioxide (>3 and <4), and benzene (>7 and <8). The zeolite with a 3-Å aperture could selectively adsorb the nitrogen, leaving a mixture of carbon dioxide and benzene that could be separated with a zeolite of 4-Å aperture. Barnicki (1991) gives methods for estimating kinetic diameters. In effect, the separation factor for a properly selected sieving-type adsorbent is infinity.

Adsorbents made of activated alumina, activated carbon, and silica gel separate by differences in adsorption equilibria, which must be determined by experiment. Equilibrium-limited adsorption can be applied to all three categories of separation, but is usually not a favored method when the components to be selectively adsorbed constitute an appreciable fraction of the feed gas. Conversely, equilibrium-limited adsorption is ideal for the removal of small quantities of selectively adsorbed impurities. At a given temperature, the equilibrium loading of a given component, in mass of adsorbate per unit mass of adsorbent, depends on the component's partial pressure and to a lesser extent on the partial pressures of the other components. For equilibrium-limited adsorption to be feasible, Barnicki and Fair (1992) suggest that the ratio of equilibrium loadings of the two key components be used as a separation factor. This ratio should be based on the partial pressures in the feed gas. A ratio of at least 2, and preferably much higher, makes equilibrium adsorption quite favorable. However, two other conditions must also be met: (1) the more highly adsorbed component should have a concentration in the feed of less than 10 mol% and (2) for an adsorption time of 2 hr, the required bed height should not exceed 20 ft. Equilibrium-limited adsorption is usually the best alternative for the removal of water and organic chemicals from mixtures with light gases and should also be considered for enrichment applications.

Absorption

Absorption of components of a gas mixture into a solvent may take place by physical or chemical means. When no chemical reaction between the solute and absorbent occurs (physical absorption), the separation factor is given by Eq. (9.2). Thus, if component 1 is to be selectively absorbed, a small value of SF is desired. Alternatively, Barnicki and Fair (1992) suggest that consideration of physical absorption should be based on a selectivity, $S_{1,2}$, defined as the ratio of liquid-phase mole fractions of the two key components in the gas mixture. This selectivity can be estimated from the partial pressures of the two components in the gas feed and their K-values for the given solvent. For components whose critical temperatures are greater than the system temperature,

$$S_{1,2} = \frac{x_1}{x_2} = \frac{\gamma_2^{\infty} p_1 P_2^s}{\gamma_1^{\infty} p_2 P_1^s} \tag{9.35}$$

where γ^{∞} is the liquid-phase activity coefficient at infinite dilution, p is partial pressure, and P^s is vapor pressure. For components whose critical temperatures are less than the system

temperature, the selectivity can be estimated from Henry's law constants:

$$S_{1,2} = \frac{x_1}{x_2} = \frac{H_2 p_1}{H_1 p_2} \tag{9.36}$$

where $H = yP/x$. For enrichment, the selectivity should be 3 or greater; for a sharp separation, 4 or greater. The number of theoretical stages should be at least 5. For the removal of readily soluble organic compounds from light gases, Douglas (1988) recommends the use of 10 theoretical stages and a solvent molar flow rate, L, based on an absorption factor, A, for solute of 1.4, where

$$A = \frac{L}{KV} \tag{9.37}$$

with V = gas molar flow rate. When the partial pressure in the gas feed of the component to be absorbed is very small and a high percentage of it is to be removed, physical absorption may not be favorable. Instead, particularly if the solute is an acid or base, chemical absorption may be attractive.

Partial Condensation and Cryogenic Distillation

The previously discussed separation techniques for gas mixtures all involve a mass separating agent. Alternatively, thermal means are employed with partial condensation and cryogenic distillation. Barnicki and Fair (1992) recommend that partial condensation be considered for enrichment when the relative volatility between the key components is at least 7. For large-scale ($>10-20$ tons/day of product gas) enrichment and sharp separations, cryogenic distillation is feasible when the relative volatility between the key components is greater than 2. However, if the feed gas contains components, such as carbon dioxide and water that can freeze at the distillation temperatures, those components must be removed first.

9.7 SEPARATION SYSTEMS FOR SOLID-FLUID MIXTURES

The final product from many industrial chemical processes is a solid material. This is especially true for inorganic compounds, but is also common for a number of moderate- to high-molecular-weight organic compounds. Such processes involve the separation operations of leaching, evaporation, solution crystallization (solutes with high melting points that are crystallized from a solvent), melt crystallization (crystallization from a mixture of components with low to moderate melting points), precipitation (rapid crystallization from a solvent of nearly insoluble compounds that are usually formed by a chemical reaction), desublimation, and/or drying, as well as the phase-separation operations of filtration, centrifugation, and cyclone separation. In addition, because specifications for solid products may also include a particle size distribution, size-increase and size-reduction operations may also be necessary. If particle shape is also a product specification, certain types of crystallizers and/or dryers may be dictated. Even when the final product is not a solid, solid–liquid or solid–gas separation operations may be involved. For example, liquid mixtures of *meta*- and *para*-xylene cannot be separated by distillation because their normal boiling points differ by only 0.8°C. Instead, because their melting points differ by 64°C, they are separated industrially by melt crystallization. Nevertheless, the final products are liquids. Another example is phthalic anhydride, which, although a solid at room temperature, is usually shipped in the molten state. It is produced by the air oxidation of napthalene or *ortho*-xylene. The separation of the anhydride from the reactor effluent gas mixture is accomplished by desublimation followed by distillation to remove impurities and produce a melt.

A common flowsheet for the separation section of a process for the manufacture of inorganic salt crystals from their aqueous solution is shown in Figure 9.50. If the feed is aqueous $MgSO_4$, a typical process proceeds as follows. A 10 wt% sulfate feed is concentrated, without crystallization, to 30 wt% in a double-effect evaporation system. The concentrate is mixed with recycled mother liquors from the hydroclone and centrifuge before being fed to an evaporative vacuum crystallizer, which produces, by solution crystallization, a magma of 35 wt% crystals of $MgSO_4 \cdot 7H_2O$, the stable hydrate at the temperature in the crystallizer. The magma is thickened to 50 wt% crystals in a hydroclone and then sent to a centrifuge, which discharges a cake containing 35 wt% moisture. The cake is dried to 2 wt% moisture in a direct-heat rotary dryer. Approximately 99 wt% of the dried crystals are retained on a 100-mesh screen and 30 wt% are retained on a 20-mesh screen. The crystals are bagged for shipment. Rossiter (1986) presents

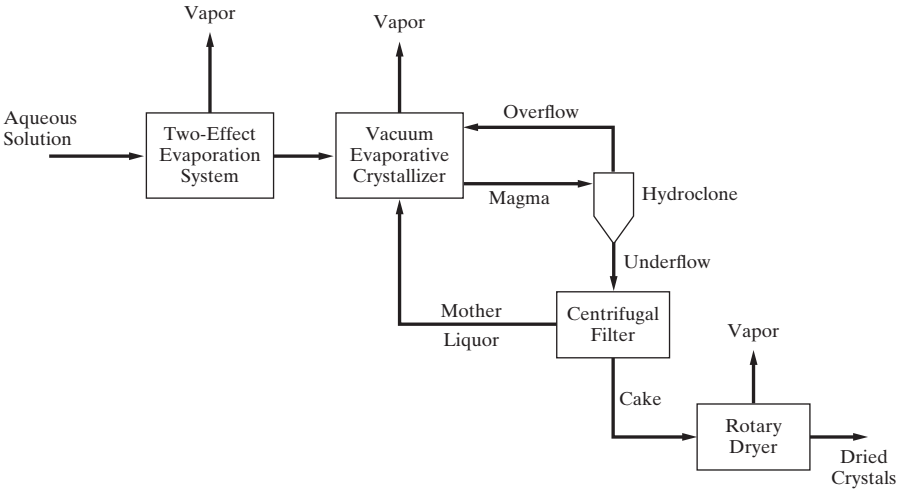

Figure 9.50 Process for producing inorganic salt crystals.

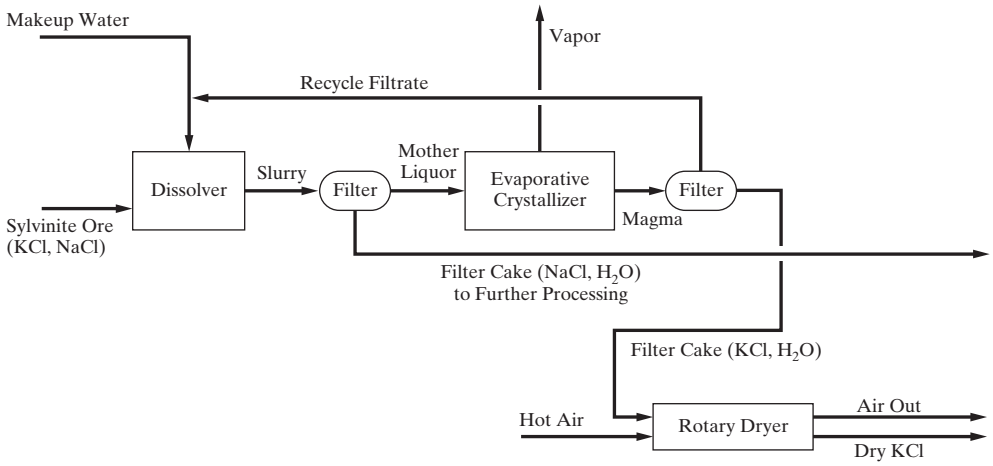

Figure 9.51 Process for separating a solid mixture.

a similar flowsheet for the separation of aqueous NaCl where a fluidized-bed dryer replaces the rotary dryer in Figure 9.50.

When a solid mixture of two components is to be separated, the process is more complicated. Such a process using solution crystallization and shown in Figure 9.51, is considered by Rajagopal et al. (1988) for the production of crystalline potash (KCl) from sylvinite ore (mixture of 40 wt% KCl and 60 wt% NaCl). The separation scheme is feasible because KCl is less soluble than NaCl in water, and the solubility of KCl in water decreases with decreasing temperature, whereas the reverse is true for NaCl. In the first step of the process, KCl is completely dissolved (leached) by a mixture of makeup water and filtrate from the second filter. The NaCl in the ore is not dissolved because conditions are selected so that the water in the dissolver is saturated with NaCl. Thus, a slurry of solid (undissolved) NaCl and aqueous KCl–NaCl leaves the dissolver. The slurry is filtered in a rotary vacuum filter, which sends the wet cake of NaCl to further processing and the mother liquor to an evaporative crystallizer. There, evaporation lowers the temperature below that in the dissolver, causing crystallization only of the KCl. The magma from the crystallizer is sent to a rotary vacuum filter, from which the mother liquor is recycled to the dissolver, and the filter cake is sent to a direct-heat rotary dryer to produce crystalline potash. Other sequences for multicomponent mixtures are considered by Rajagopal et al. (1991), Cisternas and Rudd (1993), and Dye and Ng (1995b).

In both of the processes just described, a crystallizer produces a solid and, following a solid–liquid phase separation, a dryer removes the moisture. In some cases, all three of these operations can be carried out in a single piece of equipment, a spray dryer or a drum dryer, but at the expense of increased utility cost because all of the solvent is evaporated. Such dryers are used extensively to produce dried milk and detergents. For these products, spray dryers are particularly desirable because the drying process produces porous particles that are readily dissolved in water. Spray dryers can also handle slurries and pastes.

As discussed by Barnicki and Fair (1990), melt crystallization is an alternative to other separation techniques for liquid mixtures, including ordinary distillation, enhanced distillation, liquid–liquid extraction, adsorption, and membrane permeation.

Melt crystallization should be considered only when ordinary distillation is not feasible, but may be an attractive alternative when the melting-point difference between the two key components exceeds 20°C and a eutectic is not formed. If a eutectic is formed, high recovery may not be possible, as discussed by King (1980). Methods for circumventing the eutectic limitation are discussed by Dye and Ng (1995a).

9.8 SUMMARY

Having studied this chapter, the reader should:

1. Know how each of the important industrial separation methods can be applied to the separation of multicomponent mixtures.
2. Know the importance of the separation factor.
3. Know how to determine near-optimal and optimal distillation sequences for nearly ideal systems.
4. Know how to develop separation sequences for nonideal systems that involve the formation of azeotropes.
5. Know how to develop a sequence for separating a gas mixture.
6. Know how to separate solid–fluid and multicomponent solid mixtures.

REFERENCES

1. Agrawal, R., and Z. T. Fidkowski, "More Operable Arrangements of Fully Thermally Coupled Distillation Systems," *AIChE J.*, **44**, 2565–2568 (1998).

2. Barbosa, D., and M. F. Doherty, "The Influence of Equilibrium Chemical Reactions on Vapor-Liquid Phase Diagrams," *Chem. Eng. Sci.*, **43**, 529 (1988a).

3. Barbosa, D., and M. F. Doherty, "The Simple Distillation of Homogeneous Reactive Mixtures," *Chem. Eng. Sci.*, **43**, 541 (1988b).

4. Barnicki, S. D., *Separation System Synthesis: A Knowledge-Based Approach*, Ph.D. dissertation, Department of Chemical Engineering, University of Texas at Austin (1991).

5. Barnicki, S. D., and J. R. Fair, "Separation System Synthesis: A Knowledge-Based Approach. 1. Liquid Mixture Separations," *Ind. Eng. Chem. Res.*, **29**, 421–432 (1990).

6. Barnicki, S. D., and J. R. Fair, "Separation System Synthesis: A Knowledge-Based Approach. 2. Gas/Vapor Mixtures," *Ind. Eng. Chem. Res.*, **31**, 1679–1694 (1992).

7. Barnicki, S. D., and J. J. Siirola, "Separations Process Synthesis," in J. I. Kroschwitz and M. Howe-Grant (eds.), *Kirk-Othmer Encyclopedia of Chemical Technology*, 4th ed., Vol. **21**, pp. 923–962, Wiley, New York (1997).

8. Bekiaris, N., T. E. Guttinger, and M. Morari, "Multiple Steady States in Distillation: Effect of VL(L)E Inaccuracies," *AIChE J.*, **46**(5), 955–979 (2000).

9. Bekiaris, N., G. A. Meski, C. M. Radu, and M. Morari, "Multiple Steady States in Homogeneous Azeotropic Distillation," *Ind. Eng. Chem. Res.*, **32**, 2023–2038 (1993).

10. Bekiaris, N., G. A. Meski, C. M. Radu, and M. Morari, "Multiple Steady States in Heterogeneous Azeotropic Distillation," *Ind. Eng. Chem. Res.*, **35**, 207–227 (1996).

11. Cisternas, L. A., and D. F. Rudd, "Process Designs for Fractional Crystallization from Solution," *Ind. Eng. Chem. Res.*, **32**, 1993–2005 (1993).

12. Crooks, D. A., and F. M. Feetham, *J.Chem. Soc.*, 899–901 (1946).

13. Doherty, M. F., and G. Buzad, "Reactive Distillation by Design," *Trans. I Chem E*, **70**, 448–458 (1992).

14. Doherty, M. F., and M. F. Malone, *Conceptual Design of Distillation Systems*, McGraw-Hill, Boston (2001).

15. Douglas, J. M., *Conceptual Design of Chemical Processes*, McGraw-Hill, New York (1988).

16. Douglas, J. M., "Synthesis of Separation System Flowsheets," *AIChE J.*, **41**, 2522–2536 (1995).

17. Dye, S., and K. M. Ng, "Bypassing Eutectics with Extractive Crystallization: Design Alternatives and Tradeoffs," *AIChE J.*, **41**, 1456–1470 (1995a).

18. Dye, S., and K. M. Ng, "Fractional Crystallization: Design Alternatives and Tradeoffs," *AIChE J.*, **41**, 2427–2438 (1995b).

19. Eckert, E., and M. Kubicek, "Computing Heterogeneous Azeotropes in Multicomponent Mixtures," *Comput. Chem. Eng.*, **21**, 347–350 (1997).

20. Fidkowski, Z., and L. Krolikowski, "Minimum Energy Requirements of Thermally Coupled Distillation Systems," *AIChE J.*, **33**, 643–653 (1987).

21. Fidkowski, Z. T., M. F. Malone, and M. F. Doherty, "Computing Azeotropes in Multicomponent Mixtures," *Comput. Chem. Eng.*, **17**, 1141 (1993).

22. Gmehling, J., *Azeotropic Data*, VCH Publishers, Deerfield Beach, Florida (1994).

23. Gomez, A., and J. D. Seader, "Separation Sequence Synthesis by a Predictor Based Ordered Search," *AIChE J.*, **22**, 970–979 (1976).

24. Green, D. W., and R. H. Perry Ed., *Perry's Chemical Engineers' Handbook*, 8th ed., McGraw-Hill, New York (2008).

25. Heaven, D. L., Optimum Sequencing of Distillation Columns in Multicomponent Fractionation, Master of Science Thesis in Chemical Engineering, University of California, Berkeley, 1969.

26. Hendry, J. E., and R. R. Hughes, "Generating Separation Process Flowsheets," *Chem. Eng. Prog.*, **68**(6), 69 (1972).

27. Horsley, L. H., *Azeotropic Data–III*, Advances in Chemistry Series No. 116, American Chemical Society, Washington, DC (1973).

28. Horwitz, B. A., "Optimize Pressure-Sensitive Distillation," *Chem.Eng. Prog.*, **93**(4), 47 (1997).

29. Keller, G. M., "Separations: New Directions for an Old Field," *AIChE Monogr. Ser. No.* **17**, 83 (1987).

30. King, C. J., *Separation Processes*, 2nd ed., McGraw-Hill, New York (1980).

31. Kister, H. Z., *Distillation Design*, McGraw-Hill, New York (1992).

32. Knapp, J. P., and M. F. Doherty, "A New Pressure-Swing Distillation Process for Separating Homogeneous Azeotropic Mixtures," *Ind. Eng. Chem. Res.*, **31**, 346 (1992).

33. Kovach III, J. W., and W. D. Seider, "Heterogeneous Azeotropic Distillation: Homotopy-Continuation Methods," *Comput.Chem. Eng.*, **11**, 593 (1987).

34. Lecat, M., *L'azcotropism: la tension de vapeur des melanges de liquides. 1. ptie., Donnes experimentales. Bibliographie*, A. Hoste, Gand, Belgium (1918).

35. Lee, K.-S., C. Levy, and N. Steckman, Ditertiary-Butyl Peroxide Manufacture, Towne Library, University of Pennsylvania, Philadelphia (1995).

36. Matsuyama, H., and H. Nishimura, "Topological and Thermodynamic Classification of Ternary Vapor–Liquid Equilibria," *J. Chem. Eng. Jpn.*, **10**(3), 181 (1977).

37. Modi, A. K., and A. W. Westerberg, "Distillation Column Sequencing Using Marginal Price," *Ind. Eng. Chem. Res.*, **31**, 839–848 (1992).

38. Peterson, E. J., and L. R. Partin, "Temperature Sequences for Categorizing All Ternary Distillation Boundary Maps," *Ind. Eng. Chem. Res.*, **36**, 1799–1811 (1997).

39. Petlyuk, F. B., V. M. Platonov, and D. M. Slavinskii, "Thermodynamically Optimal Method for Separating Multicomponent Mixtures," *Int. Chem. Eng.*, **5**, 555 (1965).

40. Prokopakis, G. J., and W. D. Seider, "Dynamic Simulation of Azeotropic Distillation Towers," *AIChEJ.*, **29**, 1017–1029 (1983).

41. Rajagopal, S., K. M. Ng, and J. M. Douglas, "Design of Solids Processes: Production of Potash," *Ind. Eng. Chem. Res.*, **27**, 2071–2078 (1988).

42. Rajagopal, S., K. M. Ng, and J. M. Douglas, "Design and Economic Trade-offs of Extractive Crystallization Processes," *AIChE J.*, **37**, 437–447 (1991).

43. Rev, E., M. Emtir, Z. Szitkai, P. Mizsey, and Z. Fonyo, "Energy Savings of Integrated and Coupled Distillation Systems," *Comput. Chem. Eng.*, **25**, 119–140 (2001).

44. Robinson, C. S., and E. R. Gilliland, *Elements of Fractional Distillation*, McGraw-Hill, New York (1950).

45. Rodrigo, B. F. R., and J. D. Seader, "Synthesis of Separation Sequences by Ordered Branch Search," *AIChEJ.*, **21**(5), 885 (1975).

46. Rossiter, A. P., "Design and Optimisation of Solids Processes. Part3—Optimisation of a Crystalline Salt Plant Using a Novel Procedure," *Chem. Eng. Res. Des.*, **64**, 191–196 (1986).

47. Ryan, P. J., and M. F. Doherty, "Design/Optimization of Ternary Heterogeneous Azeotropic Distillation Sequences," *AIChE J.*, **35**, 1592–1601 (1989).

48. Seader, J. D., E. J. Henley, and D. K. Roper, *Separation Process Principles*, 4th ed., John Wiley, New Jersey (2016).

49. Seader, J. D., and A. W. Westerberg, "A Combined Heuristic and Evolutionary Strategy for Synthesis of Simple Separation Sequences," *AIChE J.*, **23**, 951 (1977).

50. Siirola, J. J., "An Industrial Perspective of Process Synthesis," in L. T. Biegler and M. F. Doherty, (eds.) *Foundations of Computer-Aided Process Design*, *AIChE Symp. Ser. No. 304*, **91**, 222–233 (1995).

51. Souders, M., "The Countercurrent Separation Process," *Chem. Eng. Prog.*, **60**(2), 75–82 (1964).

52. Stichlmair, J. G., and J. R. Fair, *Distillation–Principles and Practice*, Wiley-VCH, New York (1998).

53. Stichlmair, J. G., J. R. Fair, and J. L. Bravo, "Separation of Azeotropic Mixtures via Enhanced Distillation," *Chem. Eng. Prog.*, **85**(63), 1 (1989).

54. Swietoslawski, W., *Azeotropy and Polyazeotropy*, Pergamon Press, New York (1963).

55. Tedder, D. W., and D. F. Rudd, "Parametric Studies in Industrial Distillation: I. Design Comparisons," *AIChEJ.*, **24**, 303 (1978a).

56. Tedder, D. W., and D. F. Rudd, "Parametric Studies in Industrial Distillation: II. Heuristic Optimization," *AIChEJ.*, **24**, 316 (1978b).

57. Vadapalli, A., and J. D. Seader, "A Generalized Framework for Computing Bifurcation Diagrams Using Process Simulation Programs," *Comput. Chem. Eng.*, **25**, 445–464 (2001).

58. Van Winkle, M., *Distillation*, McGraw-Hill, New York (1967).

59. Venimadhavan, G., G. Buzad, M. F. Doherty, and M. F. Malone, "Effect of Kinetics on Residue Curve Maps for Reactive Distillation," *AIChEJ.*, **40**(11), 1814 (1994).

60. Walas, S. M., *Chemical Process Equipment–Selection and Design*, Butterworth, Boston (1988).

61. Widagdo, S., and W. D. Seider, "Azeotropic Distillation," *AIChE J.*, **42**(1), 96 (1996).

62. Wright, R. O., "Fractionation Apparatus," U.S. Patent 2,471,134 (May 24, 1949).

63. Zharov, V. T., "Phase Representations and Rectification of Multicomponent Solutions," *J. Appl. Chem. USSR*, **41**, 2530 (1968).

64. Zharov, V. T., and L. A. Serafimov, *Physicochemical Fundamentals of Distillations and Rectifications* (in Russian), Khimiya, Leningrad, USSR (1975).

EXERCISES

9.1 Stabilized effluent from a hydrogenation unit as given below is to be separated by ordinary distillation into five relatively pure products. Four distillation columns will be required. According to Eq. (9.9) and Table 9.2, these four columns can be arranged into 14 possible sequences. Draw sketches, as in Figure 9.11, for each of these sequences.

Component	Feed Flow Rate (lbmol/hr)	Approximate Relative Volatility Relative to C5
Propane (C3)	10	8.1
Butene-1 (B1)	100	3.7
n-Butane (NB)	341	3.1
Butene-2 isomers (B2)	187	2.7
n-Pentane (C5)	40	1.0

9.2 Consider the problem of separation, by ordinary distillation, of propane, A; isobutane, B; *n*-butane, C; isopentane, D; and *n*-pentane, E. Using the heuristics of Section 9.4, develop flowsheets for:

(a) Equimolar feed with required product streams A, (B, C), and (D, E) required

(b) Feed consisting of A = 10, B = 10, C = 60, D = 10, and E = 20 (relative moles) with products A, B, C, D, and E.

Component	Average Relative Volatility
A >	2.2
B >	1.44
C >	2.73
D >	1.25
E	

9.3 Thermal cracking of naphtha yields a gas that is to be separated by a distillation train into the products indicated in Figure 9.52. If reasonably sharp separations are to be achieved, determine by the heuristics of Section 9.4 two good sequences.

9.4 The effluent from a reactor contains a mixture of various chlorinated derivatives of the hydrocarbon RH_3, together with the hydrocarbon itself and HCl. Based on the following information and the heuristics of Section 9.4, devise the best two feasible separation sequences. Explain your reasoning. Note that HCl may be corrosive.

Species	lbmol/hr	α Relative to RCl_3	Purity Desired
HCl	52	4.7	80%
RH_3	58	15.0	85%
RCl_3	16	1.0	98%
RH_2Cl	30	1.9	95%
$RHCl_2$	14	1.2	98%

9.5 Investigators at the University of California at Berkeley have studied all 14 possible sequences for separating the following mixture at a flow rate of 200 lbmol/hr into its five components at about 98% purity each (D.L. Heaven, M.S. thesis in Chemical Engineering, University of California, Berkeley, 1969).

Species	Symbol	Feed Mole Fraction	Approximate Volatility Relative to *n*-Pentane
Propane	A	0.05	8.1
Isobutane	B	0.15	4.3
n-Butane	C	0.25	3.1
Isopentane	D	0.20	1.25
n-Pentane	E	0.35	1.0
		1.00	

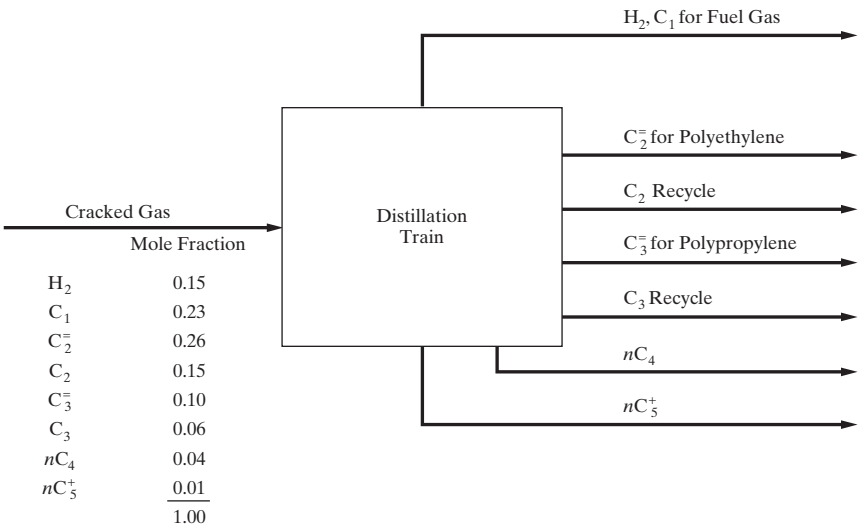

Figure 9.52 Thermal cracking of naphtha.

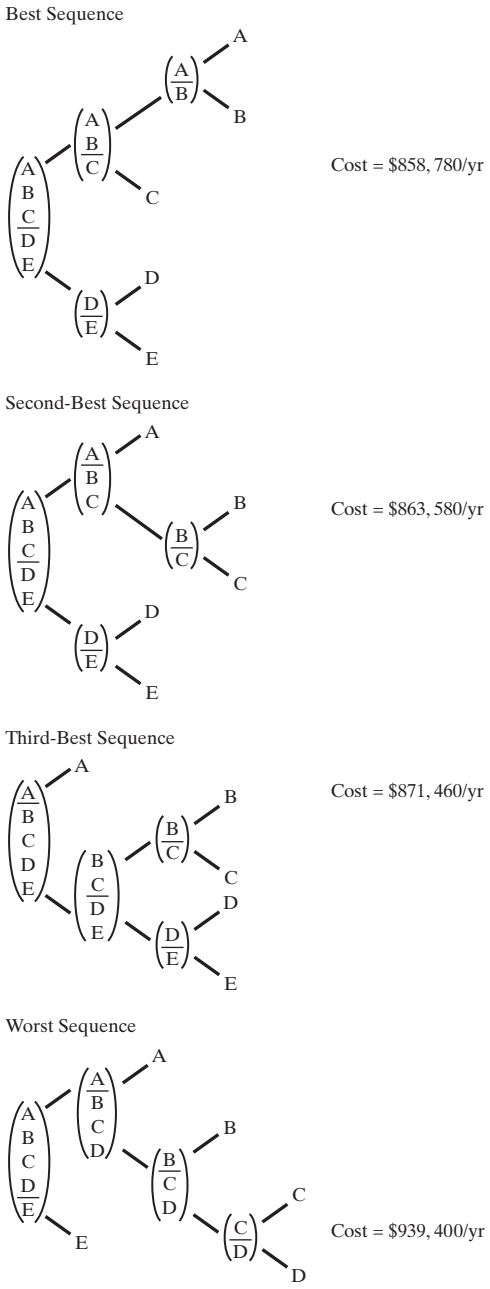

Figure 9.53 Cost data for Exercise 9.5.

For each sequence, they determined the annual operating cost including depreciation of the capital investment. Cost data for the best three sequences and the worst sequence are in Figure 9.53. Explain in detail, as best you can, why the best sequences are best and the worst sequence is worst using the heuristics. Which heuristics appear to be the most important?

9.6 The following cost data, which include operating cost and depreciation of capital investment, pertain to Exercise 9.1. Determine by finding the total cost for each of the 14 possible sequences:

(a) The best sequence

(b) The second-best sequence

(c) The worst sequence

Are the heuristics of Section 9.4 in agreement with the results based on costs?

Split	Cost ($/yr)
C3/B1	15,000
Bl/NB	190,000
NB/B2	420,000
B2/C5	32,000
C3, Bl/NB	197,000
C3/B1, NB	59,000
Bl, NB/B2	500,000
Bl/NB, B2	247,000
NB, B2/C5	64,000
NB/B2, C5	460,000
C3, Bl, NB/B2	510,000
C3, Bl/NB, B2	254,000
C3/B1, NB, B2	85,000
Bl, NB, B2/C5	94,000
Bl, NB/B2, C5	530,000
Bl/NB, B2, C5	254,000
C3, Bl, NB, B2/C5	95,000
C3, Bl, NB/B2, C5	540,000
C3, Bl/NB, B2, C5	261,000
C3/B1, NB, B2, C5	90,000

9.7 The feed to a separation process consists of the following species:

Species Number	Species
1	Ethane
2	Propane
3	Butene-1
4	*n*-Butane

It is desired to separate this mixture into essentially pure species. The use of two types of separators is to be explored:

(a) Ordinary distillation

(b) Extractive distillation with furfural (species 5)

The separation orderings according to relative volatility are:

	Separator Type	
	1	**2**
Species number	1	1
	2	2
	3	4
	4	3
		5

Notice that the addition of furfural causes n-Butane (4) to become more volatile than Butene-1 (3). Determine the number of possible separation sequences.

9.8 The following stream at 100°F and 250 psia is to be separated into the four indicated products. Also, given is the cost of each of the unique separators. Determine:

(a) The best sequence

(b) The second-best sequence

Percent Recovery						
Species	Symbol	Feed (lbmol/hr)	Product 1	Product 2	Product 3	Product 4
Propane	A	100	98			
i-Butane	B	300		98		
n-Butane	C	500			98	
i-Pentane	D	400				98

Unique Separator	Cost ($/yr)
A/B	26,100
B/C	94,900
C/D	59,300
A/BC	39,500
AB/C	119,800
B/CD	112,600
BC/D	76,800
A/BCD	47,100
AB/CD	140,500
ABC/D	94,500

9.9 The following stream at 100°F and 300 psia is to be separated into four essentially pure products. Also given is the cost of each unique separator. Determine the best sequence.

Species	Symbol	Feed rate (lbmol/hr)
i-Butane	A	300
n-Butane	B	500
i-Pentane	C	400
n-Pentane	D	700

Unique Separator	Cost ($/yr)
A/B	94,900
B/C	59,300
C/D	169,200
A/BC	112,600
AB/C	76,800
B/CD	78,200
BC/D	185,300
A/BCD	133,400
AB/CD	94,400
ABC/D	241,800

9.10 The following stream at 100°F and 20 psia is to be separated into the four indicated products. Determine the best distillation sequence by the heuristics of Section 9.4. Compare your result with that obtained by applying the Marginal Vapor Rate method.

Species	Feed (lbmol/hr)	Product 1	Product 2	Product 3	Product 4
Benzene	100	98			
Toluene	100		98		
Ethylbenzene	200			98	
p-Xylene	200			98	
m-Xylene	200			98	
o-Xylene	200				98

9.11 A hypothetical mixture of four species, A, B, C, and D, is to be separated into four separate components. Two different separator types are being considered, neither of which requires a mass separating agent. The order of separation for each of the two types is:

Separator Type I	Separator Type II
A	B
B	A
C	C
D	D

Annual cost data for all the possible splits follow. Determine by considering each possible sequence:

(a) The best sequence

(b) The second-best sequence

(c) The worst sequence

For each answer, draw a diagram of the separation train, being careful to label each separator as to whether it is type I or II.

Subgroup	Split	Type Separator	Annual Cost × $ 10,000
(A, B)	A/B	I	8
		II	15
(B, C)	B/C	I	23
		II	19
(C, D)	C/D	I	10
		II	18
(A, C)	A/C	I	20
		II	6
(A, B, C)	A/B, C	I	10
	B/A, C	II	25
	A, B/C	I	25
		II	20
(B, C, D)	B/C, D	I	27
		II	22
	B, C/D	I	12
		II	20
(A, C, D)	A/C, D	I	23
		II	10
	A, C/D	I	11
		II	20
(A, B, C, D)	A/B, C, D	I	14
	B/A, C, D	II	20
	A, B/C, D	I	27
		II	25
	A, B, C/D	I	13
		II	21

9.12 A multicomponent mixture is boiled in a flask at 1 atm. The vapors are condensed and recovered as a liquid product. It is desired to examine the mole fractions of the residual liquid in the flask as vaporization proceeds. Although sketches of the residue-curve maps are called for in (b)–(d), a process simulator can be used to prepare the drawings accurately.

(a) For a mixture of 60 mol% n-butane (1) and 40 mol% n-pentane (2), determine the residual mole fraction of n-butane after 10% of the liquid has vaporized.

(b) Consider mixtures of n-butane (1), n-pentane (2), and n-hexane (3). For three typical feed compositions:

	Mole Fractions		
Component	I	II	III
I	0.7	0.15	0.15
2	0.15	0.7	0.15
3	0.15	0.15	0.7

Sketch the residue curves (solutions of the ODEs; do not solve them analytically or numerically) on triangular graph paper. Use arrows to show the direction along the trajectories in time.

(c) Repeat (b) for mixtures of acetone (1), choroform (2), and benzene (3). Note that the acetone-chloroform binary exhibits a maximum-boiling azeotrope (64°C) at 35 mol% acetone with no other azeotropes existing. Sketch any boundaries across which the residue curves cannot traverse.

(d) Repeat (c) for mixtures of methyl acetate (1), methanol (2), and n-hexane (3). Note the existence of four azeotropes, where compositions are in mol%.

	T°*C*
Methyl acetate (65%)-methanol (35%)	53.5
Methanol (51%)-*n*-hexane (49%)	50.0
Methyl acetate (60%)-*n*-hexane (40%)	51.8
Methyl acetate (31%)-*n*-hexane (40%)-methanol (29%)	49.0

9.13 Prepare residue-curve maps using a process simulation program for the following mixtures at 1 atm. Identify any distillation boundaries.

(a) Acetone, n-heptane, toluene

(b) Methanol, ethanol, water

(c) Acetone, chloroform, ethanol

9.14 For a mixture of 70 mol% chloroform, 15 mol% acetone, and 15 mol% ethanol at 1 atm, show on a residue curve map the feasible compositions of the distillate and bottoms product.

9.15 For the manufacture of di-tertiary-butyl peroxide in Example 9.7, synthesize an alternative process and show the flow rate and composition of each stream.

9.16 For the pressure-swing dehydration of THF, determine the internal flow rates when the high-pressure column is at 5 bar.

9.17 Design a process for the separation of 1,000 kgmol/hr of a mixture composed of 50 mol% acetone (A) and 50 mol% heptane (C) to highly pure product streams (at least 99 mol% each), noting that acetone and heptane form a minimum-boiling azeotrope. Consider using benzene (B) as an entrainer. Your design should consist of as few distillation columns as possible, with each column having only two product streams (distillate and bottoms), operating at 1 bar. Boiling temperature data for the system is given as follows.

Data for P = 1 bar

Component				Azeo-I
A	100%	0%	0%	95%
B	0%	100%	0%	0%
C	0%	0%	100%	5%
Temperature	56°C	80°C	98°C	55°C

9.18 Design a process for the separation of 1,000 kgmol/hr of a mixture comprising 50 mol% A and 50 mol% B to highly pure product streams (at least 99 mol% each). Your design should consist of at most two columns, with each column having only two product streams (distillate and bottoms), operating at either 2 or 5 bar. You may consider the usage of entrainer C. Boiling temperature data for the system A-B-C is provided in Table 9.8 for the two possible operating pressures.

(a) Design a separation process for the production of highly pure A and B (each at least 99 mol%). Sketch the operating lines for your process on a ternary phase diagram and provide a PFD indicating key compositions and temperatures.

(b) If your solution includes the usage of entrainer C, estimate the required feed rate of C in kgmol/hr.

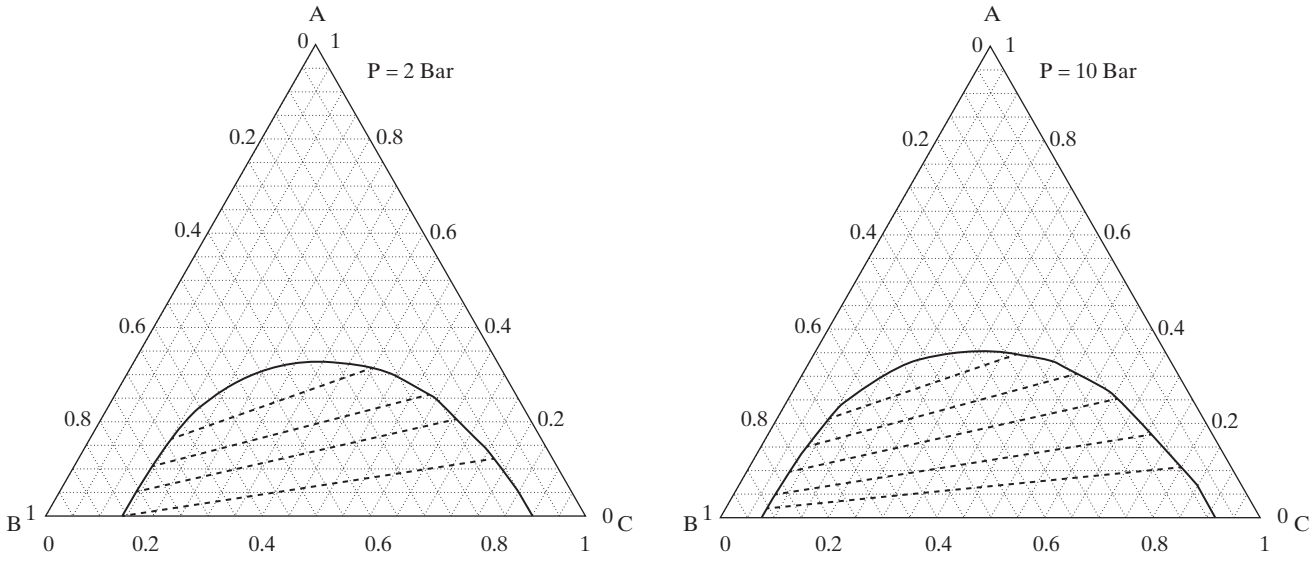

Figure 9.54 Ternary phase diagrams for Exercise 9.19 at two operating pressures.

Table 9.8 Boiling Temperature Data for the System A-B-C in Exercise 9.18

Data for P = 2 bar							
Component				Azeo-I	Azeo-II	Azeo-III	Azeo-IV
A	100%	0%	0%	50%	0%	40%	40%
B	0%	100%	0%	50%	30%	0%	25%
C	0%	0%	100%	0%	70%	60%	35%
Temperature	120°C	90°C	80°C	80°C	70°C	75°C	65°C

Data for P = 5 bar							
Component				Azeo-I	Azeo-II	Azeo-III	Azeo-IV
A	100%	0%	0%	50%	0%	25%	15%
B	0%	100%	0%	50%	70%	0%	70%
C	0%	0%	100%	0%	30%	75%	15%
Temperature	150°C	120°C	110°C	105°C	95°C	90°C	80°C

9.19 Design a process for the separation of 1,000 kgmol/hr of a mixture composed of 50 mol% A and 50 mol% B (water) to product streams: a highly pure stream of A (at least 99 mol%) and a purified water stream (at least 90 mol%). Your design should consist of as few distillation columns as possible, with each column having only two product streams (distillate and bottoms), with each column operating either at 2 or 10 bar. You may consider the usage of entrainer C. Boiling temperature data for the system A-B-C are provided in Table 9.9 for the two possible operating pressures. Ternary diagrams at the two pressures are provided in Figure 9.54 noting that the system exhibits regions of liquid–liquid equilibrium at both of the operating pressures.

Table 9.9 Boiling Temperature Data for the System A-B-C in Exercise 9.19

(a) P = 2 bar							
	Pure A	Pure B	Pure C	Azeo-I	Azeo-II	Azeo-III	Azeo-IV
A	1.00	0.00	0.00	0.70	0.40	0.00	0.15
B	0.00	1.00	0.00	0.30	0.00	0.30	0.30
C	0.00	0.00	1.00	0.00	0.60	0.70	0.55
Temperature (°C)	100	120	130	95	90	110	85

(b) P = 10 bar							
	Pure A	Pure B	Pure C	Azeo-I	Azeo-II	Azeo-III	Azeo-IV
A	1.00	0.00	0.00	0.70	0.25	0.00	0.10
B	0.00	1.00	0.00	0.30	0.00	0.20	0.15
C	0.00	0.00	1.00	0.00	0.75	0.80	0.75
Temperature (°C)	150	170	180	135	145	160	130

(a) Design a separation process for the production of A and B as specified above. Draw the operating lines for your process on the ternary phase diagram(s) provided in Figure 9.54, and provide a PFD indicating key compositions and temperatures.

(b) If your solution includes the usage of entrainer C estimate the required feed rate of C at steady state in kgmol/hr.

Table 9.10 Effect of Reactor Operating Temperature on Effluent Composition

Operating Point	Operating Temperature (°C)	CSTR Effluent Composition (mol%) A	B	C
1	180	60	10	30
2	160	45	25	30
3	120	30	40	30
4	100	15	55	30

Table 9.11 Boiling Temperature Data for the System A-B-C in Exercise 9.20

(a) Data for $P = 5$ bar					
Component				Azeo-I	Azeo-II
A	100%	0%	0%	40%	15%
B	0%	100%	0%	60%	0%
C	0%	0%	100%	0%	85%
Temperature	50°C	80°C	120°C	40°C	45°C

(b) Data for $P = 15$ bar					
Component				Azeo-I	Azeo-II
A	100%	0%	0%	65%	45%
B	0%	100%	0%	35%	0%
C	0%	0%	100%	0%	55%
Temperature	60°C	100°C	150°C	50°C	55°C

9.20 In a process for the manufacture of C from A and B, streams of A and B are fed to a CSTR, where they undergo reversible reaction to the product: A + B ⇌ C. Because the reaction is highly exothermic, the reactor needs to be cooled. And because the reaction is reversible, all three species are present in the reactor effluent in compositions according to the operating temperature of the CSTR as presented in Table 9.10. The CSTR effluent is fed to a distillation column, designed to separate the product C from the reagents A and B, which are recycled to the reactor.

In addition to selecting the most appropriate operating temperature for the CSTR, you must also design a separation system to produce highly pure C (at least 99 mol%) consisting of as few distillation towers as possible, each having only two product streams (distillate and bottoms), with each column operating either at 5 or 15 bar. Boiling temperature data for the system A-B-C are provided in Table 9.11 for the two operating pressures. You are asked to keep plant operating costs to a minimum!

Chapter 10

Second-Law Analysis

10.0 OBJECTIVES

The first law of thermodynamics is widely used in design to make energy balances around equipment. Much less used are the entropy balances based on the second law of thermodynamics. Although the first law can determine energy transfer requirements in the form of heat and shaft work for specified changes to streams or batches of materials, it cannot indicate whether energy is being used efficiently. As shown in this chapter, calculations with the second law or a combined first and second law can determine thermodynamic efficiency, an indicator of energy efficiency. The calculations are difficult to do by hand but are readily carried out with a process simulation program. When the thermodynamic efficiency of a process is found to be low, it needs to be improved, or a better process should be sought. The average thermodynamic efficiency for chemical plants is in the range of only 20–25%. Therefore, chemical engineers need to spend more effort in improving energy efficiency. In particular, more attention needs to be directed to designing energy-efficient separation sequences and heat exchanger networks. In general, mechanical equipment such as pumps and compressors operate at high energy efficiency.

After studying this chapter, the reader should:

1. Understand the limitations of the first law of thermodynamics.
2. Understand the usefulness of the second law and a combined statement of the first and second laws.
3. Be able to specify a system and surroundings for conducting a second-law analysis.
4. Be able to derive and apply a combined statement of the first and second laws for the determination of lost work or exergy.
5. Be able to use a process simulation program to perform a second-law analysis of a process.
6. Be able to pinpoint the major areas of inefficiency (lost work).
7. Understand the causes of lost work and how to remedy them.

10.1 INTRODUCTION

A chemical process uses physical and/or chemical operations to transform feed materials into products of different composition. Table 10.1 lists the types of operations that are most widely used. Depending on the production rate and the operations used, the process is conducted batchwise, continuously, semicontinuously, or cyclically. A continuous, heat-integrated process that illustrates several of the operations in Table 10.1 is shown in Figure 10.1 where benzene and a mixture of xylene isomers are produced by the disproportionation of toluene. The heart of the process is a fixed-bed catalytic reactor, R-1, where the main chemical change is the reaction:

$$2C_7H_8 \rightarrow C_6H_6 + C_8H_{10} \text{ isomers}$$

This reaction is conducted in the presence of hydrogen to minimize the undesirable formation of coke by condensation reactions. However, other undesirable side reactions such as

$$C_7H_8 + H_2 \rightarrow C_6H_6 + CH_4$$

occur that produce light paraffins. Chemicals in the reactor effluent are separated from each other as follows. Hydrogen is recovered for recycle by partial condensation in exchanger E-2 with phase separation in flash drum D-1; light paraffin gases are removed in fractionator C-1; benzene is recovered and purified in fractionator C-2; and mixed xylenes are recovered and purified, and unreacted toluene is recovered for recycle in fractionator C-3. Compressors K-1 and K-2 bring fresh hydrogen and recycled hydrogen, respectively, to reactor pressure. Pump P-1 brings

Table 10.1 Common Operations in Chemical Processing

Operation	Examples of Equipment Used
Change in chemical species	Reactor
Separation of chemicals	Distillation, absorption, liquid–liquid extraction
Separation of phases	Settler
Pressure change	Pump, compressor, valve, turbine, expander
Temperature or phase change	Heat exchanger, condenser
Mixing	Agitated vessel, in-line mixer
Dividing	Pipe tee
Size enlargement of solids	Pellet mill
Size reduction of solids	Jaw crusher
Separation of solids by size	Screen

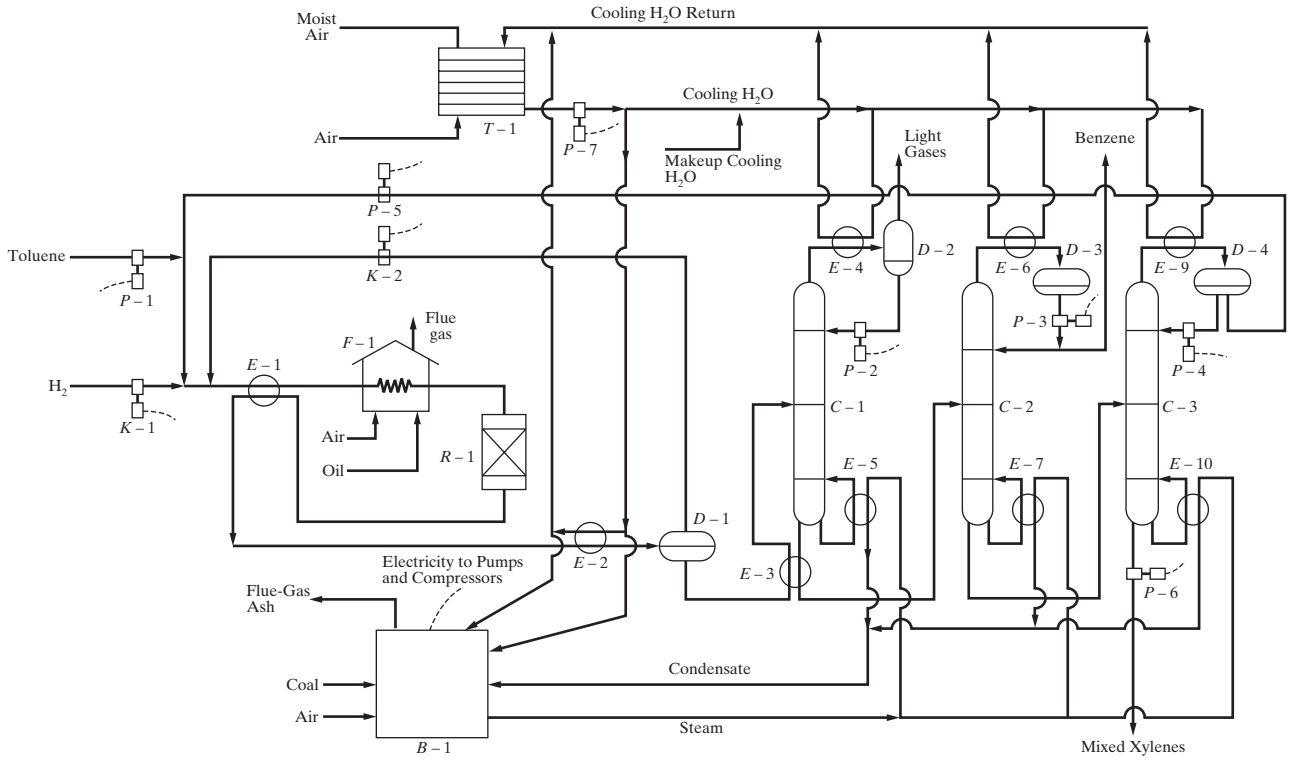

Figure 10.1 Process for disproportionation of toluene to benzene and xylene.

fresh toluene to reactor pressure. Pumps P-2, P-3, and P-4 deliver reflux to fractionators C-1, C-2, and C-3, respectively. Pumps P-3 and P-6 deliver benzene and xylene products, respectively, to storage, and pump P-5 recycles toluene. Furnace F-1 uses the combustion of fuel oil with air to bring reactants to reactor temperature after preheater E-1 has recovered a portion of the thermal energy in the reactor effluent. Cooling water is used in overhead condensers E-4, E-6, and E-9, and steam is used in reboilers E-5, E-7, and E-10 of fractionators C-1, C-2, and C-3, respectively. Benzene and xylene products are cooled by water in coolers E-8 and E-11 (not shown in Figure 10.1) before being sent to storage. Exchanger E-3 preheats feed to fractionator C-1 with bottoms from the same fractionator. Cooling water is supplied mainly by recycle from cooling tower T-1 by pump P-7. Electricity for all pumps and compressors as well as steam for reboilers is produced from coal-fired power plant B-1. The overall input to and output from the process is represented schematically in Figure 10.2.

Ideally, each operation in a process would be conducted in a reversible manner to achieve the minimum energy input or the maximum energy output, corresponding to a second-law thermodynamic efficiency of 100%. Even if this were technically feasible, such a process would be uneconomical because of excessive capital investment in equipment, which would have to be essentially infinite in size to minimize transport (heat, mass, and momentum transfer) gradients. Nevertheless, it is economical to modify existing processes to reduce energy consumption and to design new processes to operate at higher thermodynamic efficiencies. A second-law thermodynamic analysis identifies inefficient processes and the operations within these processes that are the most wasteful of energy, so that the process engineer can direct his or her efforts to conserving energy.

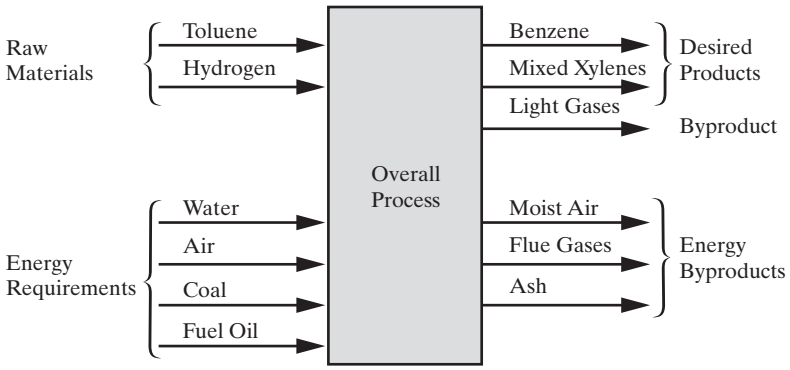

Figure 10.2 Overall process streams for toluene disproportionation.

10.2 THE SYSTEM AND THE SURROUNDINGS

To conduct a second-law analysis, a process is divided into a system and surroundings. The *system* is the matter and its internal energy contained in the operating unit (s) on which the engineer wishes to focus. Everything not in the system is in the *surroundings*. The boundaries of the system may be real or imaginary, rigid or movable, and open or closed to the transfer of matter and energy (enthalpy) between the system and the surroundings. Some references call a *closed system* simply a *system*, and an *open system*, into and/or out of which matter can flow, a *control volume*. They refer to the boundary of the control volume as the *control surface* across which matter can flow.

Batch, cyclic, and continuous processes are shown schematically in Figure 10.3. Batch and cyclic processes are usually divided into a closed system (or simply a system) and surroundings; continuous processes are divided into an open system (or control volume) and surroundings.

The division of a process into system and surroundings is the choice of the one performing the thermodynamic analysis. Many choices are possible for a chemical process. For example, in Figure 10.1, the system can be the complete process, with the surroundings being the ambient air, water, and so forth, surrounding the equipment (commonly referred to as the *infinite surroundings*, *dead state*, or *infinite heat reservoir*), and the storage tanks for the raw materials and products.

More commonly, utility plants (e.g., the steam power plant and cooling-water system) are considered separately from the rest of the process. This is shown schematically in Figure 10.4 where the process is divided into three systems. The benzene-mixed xylenes plant is sufficiently complex that it is advisable to divide it into a reaction section and a separation section as shown in Figure 10.5. Any individual operation in the process—for example, fractionator C-2 — can be the system and everything else the surroundings. Finally, a portion of a single operation can be the system—for example, one tray in fractionator C-2.

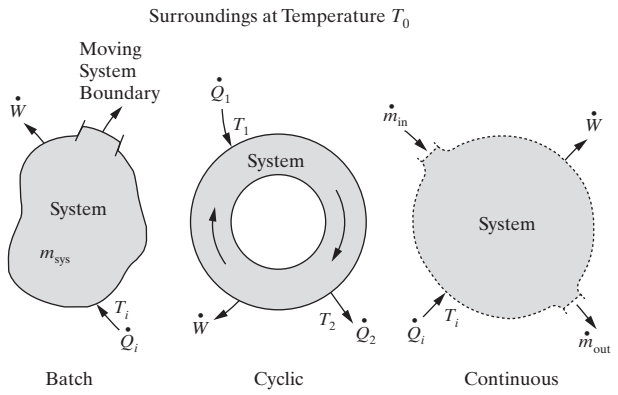

Figure 10.3 Common methods of processing.

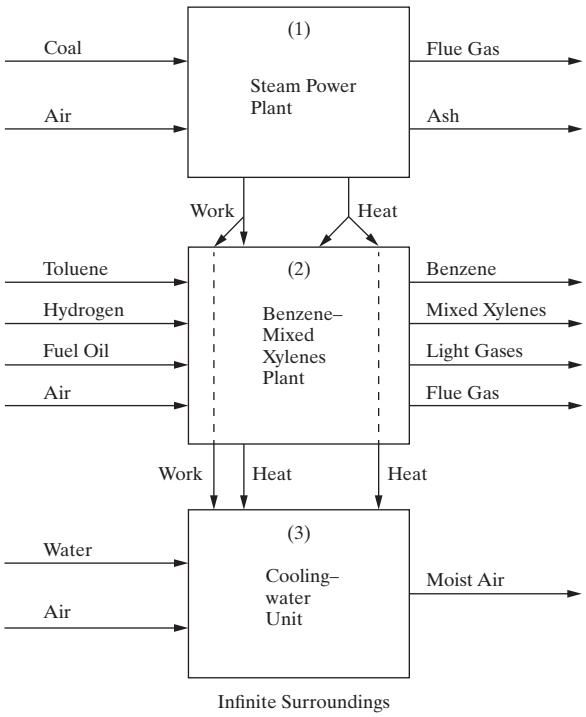

Figure 10.4 Partitioning of the toluene disproportionation plant.

10.3 ENERGY TRANSFER

Heat, work, or both can be transferred across the boundaries of closed or open systems. If no heat is transferred across its boundaries, the system is said to be adiabatic or thermally isolated; and if neither work nor heat is transferred, the system is said to be totally isolated.

The most efficient form of energy transfer is *work*, for example, a rotating or reciprocating shaft at the boundary of a system causing *shaft work*. Less efficient, but more common,

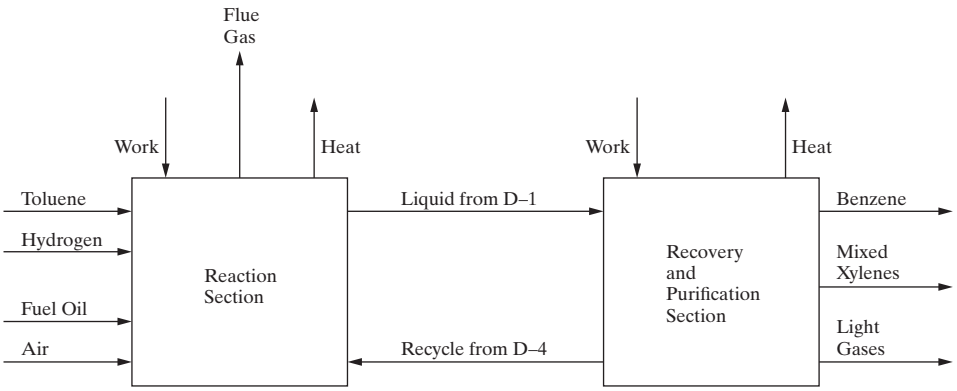

Figure 10.5 Partitioning of the toluene disproportionation process.

is *heat transfer*, which occurs when the temperatures of the system and the surroundings differ. If the system is at the higher temperature, it loses energy and the surroundings gain energy; and if the system is at the lower temperature, it gains energy and the surroundings lose energy.

A number of devices are used in processes to transfer work between a system and its surroundings. Pumps, compressors, blowers, and fans convert shaft work into fluid momentum for the main purpose of increasing fluid pressure. Turbines and expanders take energy from a fluid, causing a pressure decrease and converting the energy to shaft work. A motor converts electrical work to shaft work. A generator converts shaft work to electrical work. In general these devices are the most efficient operations in a process.

As an example of energy transfer by work, consider Figure 10.6a, where an incompressible liquid at 25°C having a specific volume, V, of 0.001 m^3/kg is pumped continuously at a rate $\dot{m}$ of 10 kg/s from a pressure P_1 of 0.1 MPa to a pressure P_2 of 2.0 MPa, with no change in kinetic or potential energy, by a rotating shaft driven by an electrical motor. In the absence of electrical resistance, shaft friction, and fluid friction,

Electrical work input to the electric motor

= shaft work delivered to the pump by the motor

= shaft work delivered to the liquid by the pump

= isothermal, isokinetic, isopotential energy increase of liquid

$= \dot{W} = \dot{m}V(P_2 - P_1) = 10(0.001)(2{,}000{,}000 - 100{,}000)$

= 19 kN-m/s (kJ/s or kW)

In actual equipment [as shown in Figure 10.6(b)], electrical resistance may permit only a 95% transfer of electrical work to the motor shaft, shaft friction may permit only a 90% transfer of shaft work to the fluid, and fluid friction may cause a rise in fluid temperature equivalent to a 5% loss of the shaft work (1 kW increase in U). For the same increase in fluid pressure, the electrical work input to the electric motor is then

$$\dot{W}_{\text{input}} = \frac{19}{(0.95)(0.90)(0.95)} = 23.39 \text{ kW}$$

The difference, 23.39 − 19.00 = 4.39 kW, between the rate of electrical work input to the motor and the rate of energy required to increase the fluid pressure is the power not used in accomplishing the desired goal. This excess power causes temperatures in the system and/or the surroundings to rise.

If the temperature of a system or a part of the surroundings remains reasonably constant when heat transfer between these two regions occurs, then the system or the part of the surroundings is called a *heat reservoir*. Heat reservoirs include heating media, such as steam, hot water, Dowtherm (the diphenyl (26.5 wt%)-diphenyloxide (73.5%) eutectic), oil, molten salts, mercury, and flue gases produced by combustion; and cooling media such as air, water, chilled water, ammonia, propane, and other refrigerants. For each of these reservoirs, it is convenient to assign a temperature. It is also convenient to distinguish between finite-sized heat reservoirs, which are designed to operate at certain desired temperatures, T_i, and the essentially infinite heat reservoirs that exist in the natural environment, such as atmospheric air, oceans, and large lakes or rivers at temperatures designated as T_0.

10.4 THERMODYNAMIC PROPERTIES

When work and/or heat is transferred to or from a system, energy changes occur. The most common forms of energy in chemical processing are those associated with (1) macroscopic motion

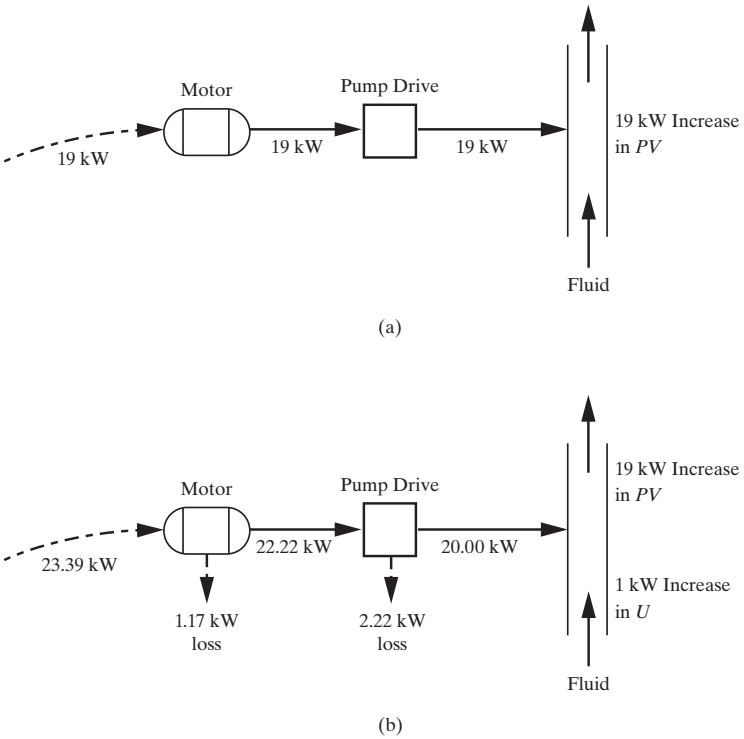

Figure 10.6 Comparison of reversible and irreversible pumping operations.

(*kinetic energy*), (2) location in a gravitational field (*potential energy*), and (3) *internal energy* due to translational, rotational, and vibrational motions of molecules, atoms, and electrons together with the potential energy due to forces acting between molecules, atoms, electrons, and nuclei. The first two forms of energy are taken relative to some arbitrary reference, such as a point on the surface of the earth. In most chemical processes, changes to these two forms of energy are relatively small and are often ignored. An exception is the combustion chamber and nozzle of a rocket engine where the heat of reaction (internal energy) is converted to kinetic energy. Internal energy is most important in chemical processing and is taken relative to some arbitrary reference condition.

The internal energy of a substance is a *state property* because its value depends on the state or condition of the substance, which is determined by temperature, pressure, composition, phase (if more than one phase is possible), and the reference condition. Changes in internal energy are independent of the path employed in moving from one state to another.

Another state property, closely related to internal energy, is *enthalpy*, defined by the relation

$$H = U + PV \tag{10.1}$$

This property is particularly convenient for continuous processes because the two terms on the right-hand side frequently appear together in energy balance equations.

The most desirable reference conditions for internal energy and enthalpy in processes where chemical reactions take place are 0 K or 25°C, zero pressure or 1 atm, and standard chemical elements, such as C (graphite), H_2 (gas), O_2 (gas), N_2 (gas), Cl_2 (gas), and S (rhombic sulfur) rather than the chemical species themselves that are in the mixture. With this reference condition, internal energy and enthalpy changes automatically take into account heat of reaction. Felder and Rousseau (2000) discuss this reference condition. As an example, the enthalpy of 1 kg of superheated steam at 300°C and 1 MPa relative to the elements H_2 (gas) and O_2 (gas) at 0 K and 0 Pa is determined to be −12,209.3 kJ. Alternatively, from the steam tables in Borgnakke and Sonntag (2013) for a reference condition of saturated liquid water at 0°C, the enthalpy is 3,051.2 kJ/kg.

It is well known from thermodynamic principles that energy transferred as work is more useful than energy transferred as heat. Work can be completely converted to heat, but only a fraction of heat can be converted to work. Furthermore, as the temperature of a system is decreased, heat transferred from the system becomes less useful, and less of the heat can be converted to work. A state property that accounts for the differences between heat and work is entropy, *S*. When heat is transferred into a closed system at temperature, *T*, the entropy of the system increases because entropy transfer accompanies heat transfer. By contrast, work transfer (shaft work) is not accompanied by entropy transfer. When heat is transferred at a rate $\dot{Q}$ from a surrounding heat reservoir at a constant temperature, $T_{\text{reservoir}}$, into a system, the heat reservoir experiences a decrease in entropy given by

$$\Delta \dot{S}_{\text{reservoir}} = \frac{-\dot{Q}}{T_{\text{reservoir}}} \tag{10.2}$$

where $\Delta \dot{S}$ is the entropy change in Btu/hr-°R. The lower the value of *T*, the greater is the decrease in entropy.

For a pure, ideal gas, only temperature affects *U* and *H*. However, the entropy, *S*, of an ideal gas is affected by both temperature and pressure. Accordingly, the reference pressure for *U* and *H* is usually taken as zero. For *S*, the reference pressure is usually taken as 1 atm to avoid a value of *S* equal to minus infinity. At a reference temperature of 0 K, the entropy of a crystalline substance is zero by the third law of thermodynamics.

Typical Entropy Changes

In general, when heat is transferred to a nonisothermal system, its entropy change, $\Delta \dot{S}$, is:

$$\Delta \dot{S} = \int_1^2 \frac{d\dot{Q}}{T} \tag{10.3}$$

Using Eq. (10.3), entropy changes can be computed for several common systems, as illustrated next.

Isobaric Heat Transfer

Consider the stream at constant *P* in Figure 10.7. According to the first law of thermodynamics, the rate of heat transfer to the differential section, $d\dot{Q}$, is:

$$d\dot{Q} = \dot{m} dH = \dot{m} c_p dT \tag{10.4}$$

where $\dot{m}$ is the mass flow rate and c_p is the heat capacity. Substituting in Eq. (10.3):

$$\Delta S_{1\to 2} = \int_{T_1}^{T_2} \frac{c_p dT}{T} \tag{10.5}$$

Here, *S* is the specific entropy, that is, $\dot{S}/\dot{m}$. For constant c_p:

$$\Delta S_{1\to 2} = c_p \ln \frac{T_2}{T_1} \tag{10.6}$$

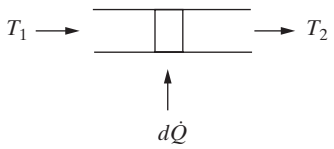

Figure 10.7 Isobaric flow through a pipe.

Ideal Gas at Constant Temperature

Figure 10.8 shows the isothermal flow of an ideal gas with a decrease of pressure from P_1 to P_2. For this system, the differential change in the specific enthalpy is:

$$dH = TdS + VdP = c_p dT = 0 \tag{10.7}$$

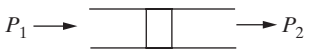

Figure 10.8 Isothermal flow through a pipe

where V is the specific volume. Rearranging:

$$dS = -\frac{V}{T}dP \tag{10.8}$$

Substituting for an ideal gas, $V = RT/P$:

$$dS = -R\,\frac{dP}{P} \tag{10.9}$$

and integrating:

$$\Delta S_{1\to 2} = R\ \ln\ \frac{P_1}{P_2} \tag{10.10}$$

Ideal Gas Mixing

When C species are mixed at constant pressure and temperature as illustrated in Figure 10.9, the change in the entropy flow rate is given by Eq. (10.10), applied separately for each species j:

$$\dot{m}_j \Delta S_{1\to 2_j} = \dot{m}_j R\ \ln\ \frac{P}{P_j} \tag{10.11}$$

where $P_j = x_j P$ is the partial pressure of species j, x_j is its mole fraction, and $\dot{m}_j$ is the molar flow rate. Summing over all of the species, the change in the enthalpy flow rate for the mixing process is:

$$\dot{m}\Delta S_{1\to 2} = \sum_{j=1}^{C} \dot{m}_j R\ \ln\ \frac{P}{P_j} \tag{10.12}$$

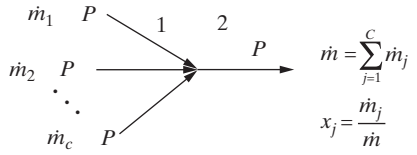

Figure 10.9 Isothermal mixing of C ideal gas species.

or

$$\Delta S_{1\to 2} = -\sum_{j=1}^{C} x_j R\ \ln\ x_j \tag{10.13}$$

where $x_j = P_j/P = \dot{m}_j/\dot{m}$.

Thermodynamic Availability

When matter is taken from state 1, at a given velocity, elevation, composition, temperature T, and pressure P, to state 2, at a different velocity, elevation, composition, T, and P, it is of interest to determine the maximum amount of useful work that can be extracted or the minimum amount of work that is needed. Ignoring kinetic energy and potential energy differences and referring enthalpies to the elements, the first law of thermodynamics can be used to determine the *net* amount of energy transferred by heat and/or work in moving from state 1 to state 2, which is simply the change in enthalpy. The first law cannot be used to determine the maximum or minimum amount of useful work, which depends on the details of the process used to effect the change in state. The maximum or minimum is achieved only if the process is reversible.

To determine the maximum rate at which work is performed, $\dot{W}_{\max}$, in bringing a stream to equilibrium with its surroundings, a reversible path can be selected, as illustrated in Figure 10.10. A stream at molar flow rate, $\dot{m}$, in state 1, at T_1 and elevated pressure, P_1, is fed to turbine I, which operates adiabatically and reversibly. It is expanded to P_2 and the environmental temperature, T_0, while producing shaft work at the rate, $\dot{W}_{s_I}$. The effluent stream from turbine I is expanded isothermally (non-adiabatically) and reversibly in turbine II to the environmental pressure, P_0. The path is shown in the P-V and T-S diagrams, the second of which shows the isentropic behavior of turbine I.

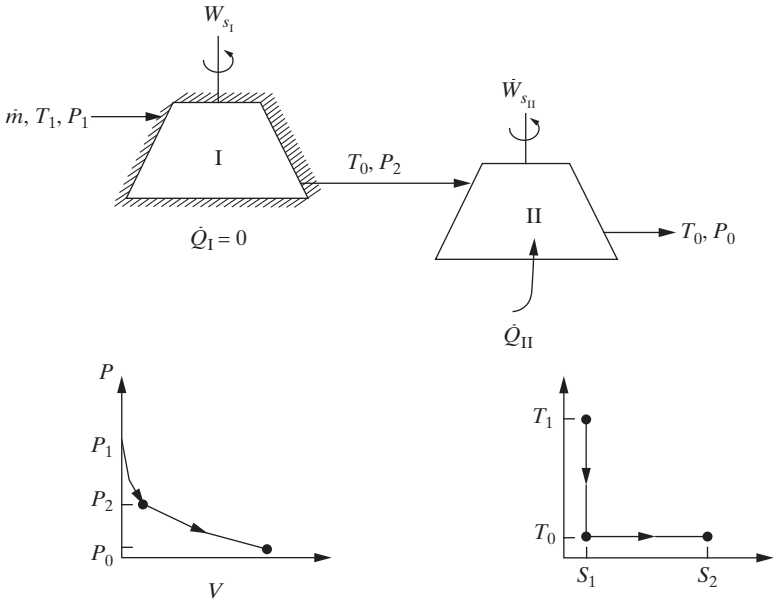

Figure 10.10 Reversible path.

Ignoring kinetic and potential energy changes, the first law of thermodynamics applied to the overall process is:

$$\dot{m}\Delta H_{1\to 0} = \dot{Q} - \dot{W}_s \tag{10.14}$$

where $\dot{Q}$ is the rate of heat transfer to turbine II, and $\dot{W}_s$ is the sum of the shaft work rates delivered by the two turbines.

For turbine II, applying the differential form of Eq. (10.3):

$$\dot{m}dS = \frac{d\dot{Q}}{T_0} \tag{10.15}$$

and integrating:

$$\dot{Q} = \dot{m}\int T_0 dS = T_0\dot{m}\Delta S_{1\to 0} \tag{10.16}$$

Substituting in the first law, Eq. (10.14):

$$\dot{m}\Delta H_{1\to 0} = T_0\dot{m}\Delta S_{1\to 0} - \dot{W}_s \tag{10.17}$$

and rearranging:

$$\dot{W}_s = \dot{W}_{s_{\text{I}}} + \dot{W}_{s_{\text{II}}} = -\dot{m}(\Delta H_{1\to 0} - T_0\Delta S_{1\to 0}) \tag{10.18}$$

This reversible work is the maximum work "available" in bringing the feed stream to the environmental conditions; that is, $\dot{W}_s$ is the maximum rate of obtaining work, which can be written $\dot{m}A_{1\to 0}$. The intensive property, $A_{1\to 0}$, was initially referred to as the *thermodynamic availability* and is commonly referred to as the *exergy*. The term *exergy* (from the Greek *ex* = out and *erg* = work), coined by Rant (1956), is also used for $A_{1\to 0}$. The concept of availability was first developed in detail by Keenan (1951).

It follows that the change in availability of a stream when it is converted from state 1 to state 2 in a chemical process as shown in Figure 10.11 is:

$$\Delta A_{1\to 2} = A_2 - A_1 = \Delta H_{1\to 2} - T_0\Delta S_{1\to 2} \tag{10.19}$$

That is, the change in the maximum work available from the stream is a function solely of its changes in enthalpy and entropy and the environmental temperature. Like H and S, A is a state function, independent of path but dependent on the temperature, T_0, and pressure, P_0, of the dead state. If chemical reactions occur, the availability also depends on the composition of the dead state.

Typical Availability Changes

In this subsection, availability changes are computed for several simple processes to show the significant impact of the change in entropy. These are taken from the monograph by Sussman (1980), who presents many other excellent examples, including three that take into account chemical reaction, one of which deals with a complete methane reforming process. In all cases, the environmental (dead-state) temperature in the following examples is taken as 298 K = 537°R.

Figure 10.11 Availability change upon processing.

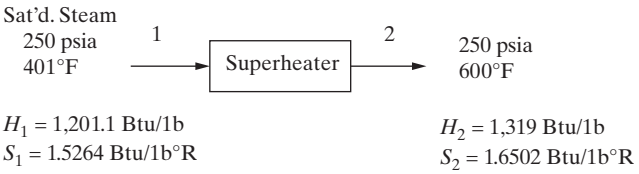

Figure 10.12 Steam superheater.

Superheating Steam

As shown in Figure 10.12, saturated steam at 250 psia and 401°F is superheated isobarically to 600°F with the enthalpy and entropy values taken from the steam tables. Substituting in Eq. (10.19):

$$\begin{aligned}\Delta A_{1\to 2} &= \Delta H_{1\to 2} - T_0\Delta S_{1\to 2}\\ &= (1{,}319 - 1{,}201.1) - 537(1.6502 - 1.5264)\\ &= 117.9 - 66.5\\ &= 51.4\ \frac{\text{Btu}}{\text{lb}}\end{aligned}$$

Although the enthalpy of the stream is increased by 117.9 Btu/lb, which equals the heat transferred to the stream, the maximum work that can be obtained from stream 2, if it is taken to the environmental conditions, is increased by only 51.4 Btu/lb, which is less than 50 % of the heat transferred because the entropy term increases so significantly.

Liquefying Air

As shown in Figure 10.13, air at 25°C and 1 atm is condensed isobarically to a saturated liquid at −194.5°C. Substituting in Eq. (10.19):

$$\begin{aligned}\Delta A_{1\to 2} &= \Delta H_{1\to 2} - T_0\Delta S_{1\to 2}\\ &= (25.74 - 127.11) - 298(0 - 0.9260)\\ &= -101.37 + 275.95\\ &= 174.6\ \frac{\text{kcal}}{\text{kg}}\end{aligned}$$

Note that the enthalpy and entropy data are obtained from the air tables where the reference state is saturated liquid air at 25°C. The change in enthalpy, −101.37 kcal/kg, is the heat removed from the condenser by using a refrigerator that requires considerable compression work. In this case, the entropy change is sufficiently negative to cause the entropy to be about three times more positive than the negative enthalpy change. This causes a large increase in the availability of the liquid air. Stated differently, 174.6 kcal/kg is the maximum work obtained from the liquid air in returning it to the environmental state and is the minimum work of refrigeration in liquefying air.

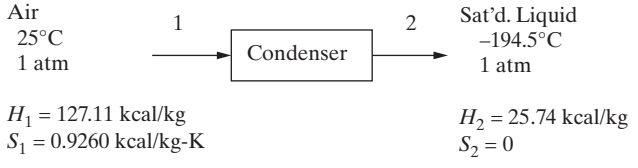

Figure 10.13 Condensation of air.

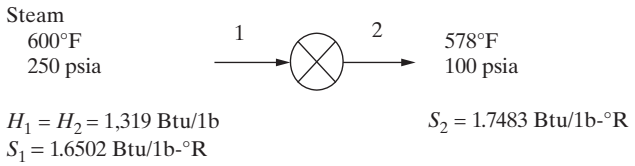

Figure 10.14 Throttling steam.

Throttling

As shown in Figure 10.14, superheated steam is throttled adiabatically across a valve from 600°F and 250 psia to 100 psia. Using the steam tables for this isenthalpic process, its temperature is reduced to 578°F, and its entropy is increased from 1.6502 Btu/lb-°R to 1.7483 Btu/lb-°R. Substituting in Eq. (10.19):

$$\begin{aligned}\Delta A_{1\to 2} &= \Delta H_{1\to 2} - T_0 \Delta S_{1\to 2} \\ &= 0 - 537(1.7483 - 1.6502) \\ &= 0 - 52.68 \\ &= -52.68 \ \frac{\text{Btu}}{\text{lb}}\end{aligned}$$

When throttling, the entire change in availability is due to the negative change in entropy. Stated differently, the entropy term is the maximum loss of the ability of the stream to do work in transferring to its environmental (dead) state. Using Eq. (10.19), A_1 is computed to be 432.8 Btu/lb [$H_0 = S_0 = 0$ at $T_0 = 460°\text{R}$ and $P_0 = 0$ atm, $A_1 = (1{,}319 - 0) - 537(1.6502 - 0) = 432.8$ Btu/lb], and consequently, 12% of its "available" work is lost in throttling. As considered subsequently in this chapter, the possibility of replacing the valve with a turbine to recover power should be considered when the pressure of a stream must be reduced.

Isothermal Mixing

In Figure 10.15, nitrogen and oxygen gases are mixed isobarically and adiabatically to give concentrations proportional to those in air. To obtain the change in availability, Eq. (10.19) applies with Eq. (10.13) substituted to give

$$\begin{aligned}\Delta A_{1\to 2} &= \Delta H_{1\to 2} - T_0 \Delta S_{1\to 2} \\ &= 0 + T_0 \sum_{j=1}^{2} x_j R \ \ln x_j \\ &= 0 + 298(0.79 \ \ln 0.79 + 0.21 \ \ln 0.21)\ 1.987 \\ &= -304.3 \ \frac{\text{cal}}{\text{mol air}}\end{aligned}$$

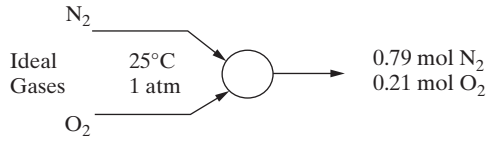

Figure 10.15 Isothermal mixing to air.

The positive entropy change upon mixing results in the negative change in availability. Stated differently, 304.3 cal of work is the minimum required to separate air into nitrogen and oxygen gases.

Thermal Mixing

In Figure 10.16, 0.5 kg/s of water at 100°C and 1 atm is mixed adiabatically and isobarically with 0.5 kg/s of water at 0°C and 1 atm. The resulting temperature is 50°C. Using Eq. (10.19) with Eq. (10.6) substituted, the availability of the mixed stream is computed:

$$\begin{aligned}A_2 &= -\left(\Delta H_{2\to 0} - T_0 \Delta S_{2\to 0}\right) \\ &= -\left[c_p\left(T_0 - T_2\right) - T_0 c_p \ln\left(\frac{T_0}{T_2}\right)\right] \\ &= -\left[(1)\,(298 - 323) - 298(1)\ \ln\frac{298}{323}\right] \\ &= -\left[-25 + 24.01\right] \\ &= 0.99 \ \frac{\text{kcal}}{\text{kg}}\end{aligned}$$

Similarly, the availabilities of the hot and cold feed streams are computed: $A_{1,\text{hot}} = 8.1$ kcal/kg and $A_{2,\text{cold}} = 1.11$ kcal/kg. Consequently, the availability change upon thermal mixing is:

$$\Delta(\dot{m}A)_{1\to 2} = (1)(0.99) - (0.5)(8.1) - (0.5)(1.11) = -3.62 \ \frac{\text{kcal}}{\text{s}}$$

The availability change upon thermal mixing is illustrated conveniently in an *availability flow diagram* as shown in Figure 10.17 where the widths of the arrows are proportional to the availability flow rates. Combining the availability flow rates for the hot and cold streams, the availability flow rate entering the mixer is $4.05 + 0.555 = 4.61$ kcal/s. In the mixer, this is divided into 0.99 kcal/s, which leaves in the mixed effluent stream, and 3.62 kcal/s, which is lost to the environment; that is, approximately 78% of the *availability* to do work is lost upon thermal mixing. Clearly, this loss decreases as the temperatures of the hot and cold streams approach each other. Sussman (1980) makes extensive use of availability flow diagrams like that in Figure 10.17.

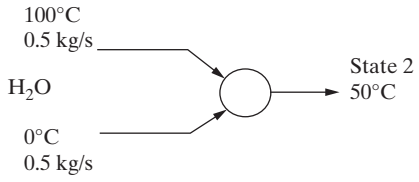

Figure 10.16 Thermal mixing of water.

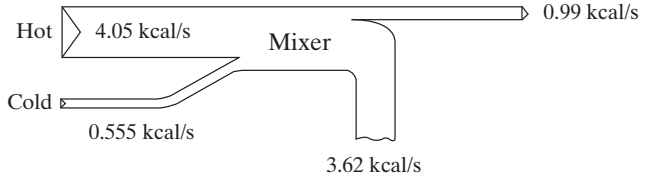

Figure 10.17 Availability flow diagram for thermal mixing of water.

10.5 EQUATIONS FOR SECOND-LAW ANALYSIS

In this section, the first and second laws of thermodynamics are used to derive useful equations for computing the lost work of any process. A general energy balance (first law of thermodynamics) can be written for a system bounded by the control volume shown in Figure 10.18. Streams at certain fixed states flow at fixed rates into or out of the control volume; heat and work are transferred at fixed rates across the boundaries of the control volume; matter within the control volume undergoes changes in amount and state; and the boundaries of the control volume expand or contract. The energy balance for such a control volume over a period of time, Δt, is

$$\frac{\Delta(mU)_{\text{sys}}}{\Delta \text{t}} + \Delta(\dot{m}H)_{\text{flowing streams}} = \dot{Q}_0 + \sum_i \dot{Q}_i - \sum_i \dot{W}_i \tag{10.20}$$

where $\Delta(mU)_{\text{sys}}$ is the change in internal energy of the system, $\Delta(\dot{m}H)_{\text{flowing streams}}$ is the sum of enthalpy flows leaving the system minus the sum of those entering the system, $\dot{Q}_0$ is positive for heat transfer from the infinite surroundings at T_0 to the control volume, and $\dot{Q}_i$ is positive for heat transfer to the control volume from a heat reservoir at temperature T_i different from T_0. Eq. (10.20) ignores changes in kinetic energy and potential energy for both the system and the flowing streams. The term $\sum_i W_i$ is positive for work done by the system on the surroundings and includes mechanical shaft work, electrical work, and work resulting from the expansion (or contraction) of the control volume itself against the surroundings ($P_{\text{surr}}\Delta V_{\text{sys}}$).

An entropy balance for the system in Figure 10.18 can be written in a manner analogous to that used for the energy balance, Eq. (10.20), except that here we prefer to write an entropy balance for both the control volume and the surroundings. The result is

$$\frac{\Delta(mS)_{\text{sys}}}{\Delta t} + \Delta(\dot{m}S)_{\text{flowing streams}} - \frac{\dot{Q}_0}{T_0} - \sum_i \frac{\dot{Q}_i}{T_i} = \Delta\dot{S}_{irr} \tag{10.21}$$

where $\Delta(mS)_{\text{sys}}$ is the change of entropy of the system, $\Delta(\dot{m}S)_{\text{flowing streams}}$ is the sum of entropy flows leaving the system minus the sum of those entering the system, $-\dot{Q}_0/T_0$ is the rate of decrease in entropy of the infinite surroundings when heat is transferred from the infinite surroundings at T_0 to the system in the control volume, and $-\sum_i \dot{Q}_i/T_i$ is the sum of the rates of entropy decrease of the various heat reservoirs at various temperatures, T_i, that are used to transfer heat into the system. Unlike energy, entropy is not conserved. The term $\Delta\dot{S}_{irr}$ is the increase in entropy of the universe due to the process. It is zero only for a reversible process. Otherwise, it is positive and is a measure of the irreversibility of the process. It cannot be negative.

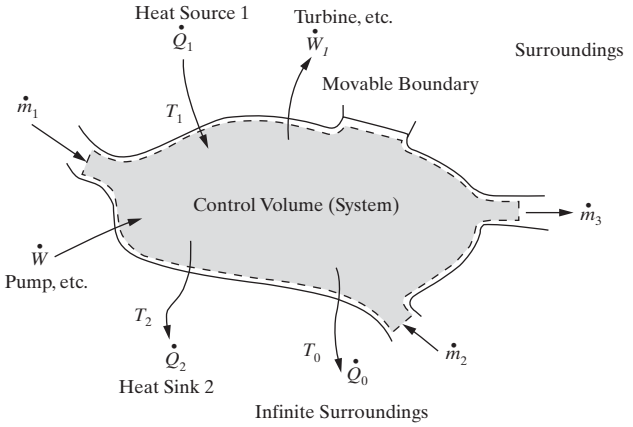

Figure 10.18 Control volume for open system

Although $\Delta\dot{S}_{irr}$ is a fundamental quantity, it is of limited practical use because of the difficulty in interpreting the significance of its magnitude. As with another fundamental thermodynamic quantity, chemical potential, chemical engineers prefer to use a surrogate property. For chemical potential, that quantity is fugacity; for $\Delta\dot{S}_{irr}$, it is availability (exergy), which was defined earlier and arises naturally, as will be shown next, when the first and second laws of thermodynamics are combined.

To derive availability, combine Eqs. (10.20) and (10.21) by eliminating $\dot{Q}_0$. The result is

$$\frac{\Delta[m(U - T_0S)]_{\text{sys}}}{\Delta t} + \Delta[\dot{m}(H - T_0S)]_{\text{flowing streams}} - \sum_i \dot{Q}_i\left(1 - \frac{T_0}{T_t}\right) + \sum_i \dot{W}_i + T_0\Delta\dot{S}_{irr} = 0 \tag{10.22}$$

In this equation, we see in the second term on the left-hand side that the enthalpy and entropy appear together to form a combined factor that is similar to the Gibbs free energy. However, the entropy is multiplied by the dead-state temperature, T_0, instead of the stream temperature, T. In addition, the first term on the left side can be rewritten to give the same combination, $H - T_0S$, by substituting Eq. (10.1), the definition of enthalpy, for the internal energy. The result is

$$\frac{\Delta[m(H - T_0S - PV)]_{\text{sys}}}{\Delta t} + \Delta[\dot{m}(H - T_0S)]_{\text{flowing streams}} - \sum_i \dot{Q}_i\left(1 - \frac{T_0}{T_t}\right) + \sum_i \dot{W}_i + T_0\Delta\dot{S}_{irr} = 0 \tag{10.23}$$

We now define an *availability function*, B, for the combination of enthalpy and entropy in Eq. (10.23):

$$B = H - T_0S \tag{10.24}$$

The availability function in Eq. (10.24) and availability in Eq. (10.19) differ from each other in that the availability is referenced to a dead state at T_0, P_0, and a composition for every element in the periodic table) and is, therefore, an absolute quantity. The availability function, by contrast, can be referenced to any state and is not an absolute quantity. In Eq. (10.23), however, only the change in availability function appears. By their definitions, the change in availability function is exactly equal to the change in availability. When evaluating a process, only the change in availability or availability function, ΔA or ΔB, respectively, is important. If one is interested in the maximum useful work that can be extracted from a material that is brought to equilibrium with the dead state, then the availability, A, is

of importance. In the second-law analysis of a process, we will use ΔB.

In addition, we also note in Eq. (10.22) that $\Delta\dot{S}_{irr}$ is multiplied by T_0 and that their product has the units of energy flow. Accordingly, it is given the name lost work, $L\dot{W}$, or loss of availability or exergy:

$$L\dot{W} = T_0\Delta\dot{S}_{irr} \tag{10.25}$$

Substitution of Eqs. (10.24) and (10.25) into Eq. (10.23) gives

$$\frac{\Delta[m(B-PV)]_{\text{sys}}}{\Delta t} + \Delta[\dot{m}(B)]_{\text{flowing streams}} - \sum_i \left(1 - \frac{T_0}{T_i}\right)\dot{Q}_i + \sum_i \dot{W}_i + L\dot{W} = 0 \tag{10.26}$$

Alternatively, Eq. (10.26) may be rearranged to the following form:

$$\sum_i \dot{W}_i + L\dot{W} = -\frac{\Delta[m(B-PV)]_{\text{sys}}}{\Delta t} - \Delta[\dot{m}(B)]_{\text{flowing streams}} + \sum_i \left(1 - \frac{T_0}{T_i}\right)\dot{Q}_i \tag{10.27}$$

For a reversible process, $\Delta\dot{S}_{irr}$ and, therefore, $T_0\,\Delta\dot{S}_{irr}$ and $L\dot{W}$, are zero. For an irreversible process, $\Delta\dot{S}_{irr}$ and $L\dot{W}$ are positive. The lost work represents the energy flow (power) lost because of irreversibilities in the process. The lost work is much easier to relate to than $\Delta\dot{S}_{irr}$.

The significance of Eq. (10.27) is best illustrated by a simple case. For a continuous, steady-state, adiabatic process, Eq. (10.27) simplifies to

$$\sum_i \dot{W}_i + L\dot{W} = -\Delta[\dot{m}(B)]_{\text{flowing streams}} \tag{10.28}$$

If the process decreases the availability function for the flowing streams, then the right-hand side of Eq. (10.28) will be a positive quantity. That decrease will be converted to useful work done on the surroundings and/or lost work. However, if the lost work is greater than the decrease in availability, work will have to be transferred from the surroundings to the processing system. If the process is also reversible, then $\sum_i W_i$ is the maximum work that can be extracted from the decrease in availability. Thus, for such a reversible process,

$$\sum \dot{W}_{\max} = -\Delta[\dot{m}(B)]_{\text{flowing streams}} \qquad \text{for } \Delta B = (-) \tag{10.29}$$

If the process increases the availability function for the flowing streams, then the right-hand side of Eq. (10.28) will be a negative quantity. That increase will require work to be done by the surroundings on the process (i.e., a negative value for $\sum_i W_i$). If lost work (a positive quantity) occurs in the process because of irreversibilities, then, according to Eq. (10.28), an equivalent amount of additional work must be done on the process by the surroundings to satisfy the change in the availability function. If the process is reversible, then $\sum_i W_i$ is the minimum work required for the increase in availability. Thus, for such a reversible process,

$$\left(\sum_i \dot{W}_i\right)_{\min} = -\Delta[\dot{m}(B)]_{\text{flowing streams}} \text{ for } \Delta B = (+) \tag{10.30}$$

Eqs. (10.26) and (10.27) are availability balances. The heat and the work terms are transfers of availability to or from the process. For a continuous, steady-state process, let us compare an energy balance to an availability balance. The comparison is facilitated by rewriting Eq. (10.20) for the energy balance and Eq. (10.26) for the availability balance, respectively, in the following forms where work and heat terms are all positive because they are labeled into or out of the system:

Energy balance:

$$0 = \sum(\dot{m}H)_{\text{in}} - \sum(\dot{m}H)_{\text{out}} + \sum\dot{W}_{\text{in}} - \sum\dot{W}_{\text{out}} + \sum\dot{Q}_{\text{in}} - \sum\dot{Q}_{\text{out}} \tag{10.31}$$

Availability balance:

$$L\dot{W} = \sum(\dot{m}B)_{\text{in}} - \sum(\dot{m}B)_{\text{out}} + \sum\dot{W}_{\text{in}} - \sum\dot{W}_{\text{out}} + \sum\left[\dot{Q}\left(1 - \frac{T_0}{T}\right)\right]_{\text{in}} - \sum\left[\dot{Q}\left(1 - \frac{T_0}{T}\right)\right]_{\text{out}} \tag{10.32}$$

By comparing these two equations, we note the following:

1. The left-hand side of Eq. (10.31) is zero. That is, energy is conserved. The left-hand side of Eq. (10.32) is zero only for a reversible process. Otherwise, the left-hand side is positive and availability is not conserved. In an irreversible process, some availability is lost.
2. In the energy balance, work and heat are counted the same. In the availability balance, work and heat are not counted the same. All work input increases the availability of material flowing through the process. Only a portion of heat transferred into a system is available to increase the availability of flowing streams. The heat is degraded by a coefficient equal to $1 - (T_0/T)$. This coefficient is precisely the Carnot cycle efficiency for a heat engine that takes heat from a source at temperature, T, and converts a portion of it to useful work, discharging the balance to a sink at a lower temperature, T_0. Note that in the availability balance, T is not the temperature of the process stream within the system, but is the temperature of the heat source or sink outside the system.
3. The energy balance, which is valid whether the process is reversible or not, has no terms that take into account irreversibility. Thus, the energy balance cannot be used to compute the minimum or maximum energy requirements

when taking material from inlet to outlet states. The availability balance does have a term $L\dot{W}$ that is a measure of irreversibility. When the lost work is zero, the process is reversible and Eq. (10.32) can be used to determine the maximum or minimum energy requirements to cause a change in availability.

Regardless of whether a net availability of heat or work is transferred to or from a process, the energy balance must be satisfied. Thus, the energy and availability balances are used together to determine energy requirements and irreversibilities that lead to lost work. The more efficient a process, the smaller the lost work.

10.6 EXAMPLES OF LOST-WORK CALCULATIONS

Before proceeding with a discussion of the second-law thermodynamic efficiency in the next section, two examples are provided to illustrate the calculation of lost work for chemical processes.

EXAMPLE 10.1 ***Two-stage Compression***

For the first example, consider the continuous two-stage compression of nitrogen gas shown in Figure 10.19, which is based on actual plant operating conditions. The system or control volume is selected to exclude the electric power generation plant and cooling-water heat sink. Assume that the temperature, T, of the cooling water is essentially equal to the dead-state temperature, T_0. Calculate the lost work.

SOLUTION

For this process, Eq. (10.32) reduces to

$$L\dot{W} = (\dot{m}B)_1 - (\dot{m}B)_2 + \dot{W}_{\text{electrical in}} \tag{10.33}$$

where $B = H - T_0S$.

The enthalpies and entropies of the entering and exiting nitrogen gas, computed from a modified Benedict-Webb-Rubin (BWR) equation of state, are:

$$H_1 = 132.46 \text{ Btu/lb} \qquad H_2 = 182.49 \text{ Btu/lb}$$
$$S_1 = 1.6335 \text{ Btu/lb-°R} \qquad S_2 = 1.5758 \text{ Btu/lb-°R}$$

The electrical work input is given as 107.3 kW and T_0 is given as 536.7°R. The entering and exiting availability functions are:

$$B_1 = 132.46 - (536.7)(1.6335) = -744.24 \text{ Btu/lb}$$
$$B_2 = 182.49 - (536.7)(1.5758) = -663.24 \text{ Btu/lb}$$

The flow rate of nitrogen through the process is 3,600 lb/hr. Therefore, the change in availability of nitrogen is:

$$3{,}600[-663.24 - (-744.24)] = 291{,}600 \text{ Btu/hr}$$

Because the availability increases, energy must be transferred into the system. The electrical power input of 107.3 kW is equivalent to 366,400 Btu/hr. This is greater than the availability increase, which represents the minimum energy input corresponding to a reversible process. Thus, the compression process has irreversibility. To determine the extent of the irreversibility, substitute the change in availability of the nitrogen and the work input into the availability balance, Eq. (10.33), for the lost work:

$$L\dot{W} = (\dot{m}B)_1 - (\dot{m}B)_2 + \dot{W}_{\text{electrical in}} = -291{,}600 + 366{,}400$$
$$= 74{,}800 \text{ Btu/lb}$$

which is equivalent to 21.9 kW or 29.4 hp.

Where does the irreversibility occur? To answer this, separate second-law analyses are needed for each of the two compressors and the intercooler. Unfortunately, data on the nitrogen leaving the first compressor and leaving the intercooler are not provided. Therefore, these separate analyses cannot be made.

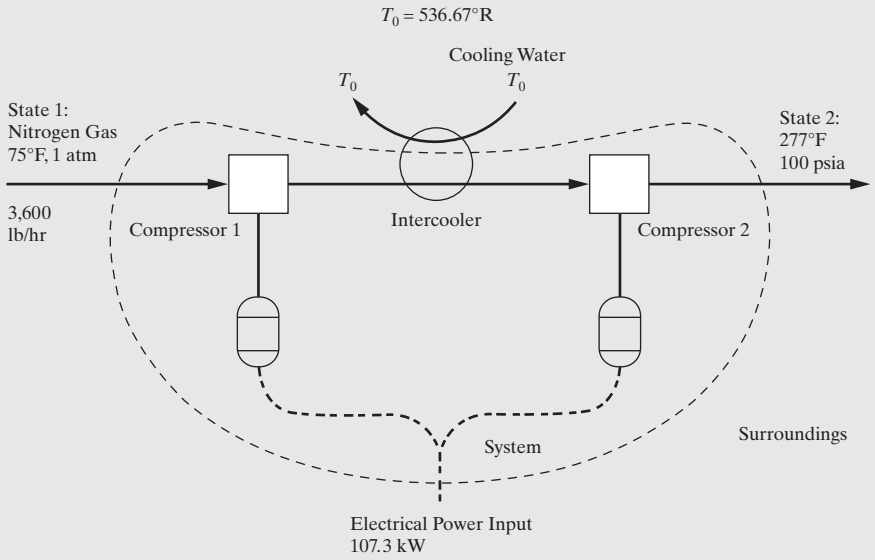

Figure 10.19 Continuous process for compression of nitrogen.

How can we apply the first law of thermodynamics to the nitrogen compression problem? We can apply an energy balance to calculate how much heat must be transferred from the nitrogen to cooling water in the intercooler:

$$\dot{W}_{\text{electrical in}} = \dot{Q}_{\text{out}} + \dot{m}(H_2 - H_1) \tag{10.34}$$

Therefore,

$$\dot{Q}_{\text{out}} = 366{,}400 - (3{,}600)(182.49 - 132.46) - 366{,}400 - 180{,}100$$
$$= 186{,}300 \text{ Btu/hr}$$

Note that the enthalpy increase of 180,100 Btu/hr is far less than the minimum amount of energy of 291,600 Btu/hr that must be added. Even if the compressors and the intercooler were reversible, 291,600 − 180,100 = 111,500 Btu/hr of energy would have to be transferred out of the system. Although this is considerably less than the 186,300 Btu/hr for the actual process, it is still a large amount.

EXAMPLE 10.2 *Propane Refrigeration Cycle*

As a second example, consider the plant operating data shown in Figure 10.20 for a propane refrigeration cycle. Saturated propane vapor (state 1) at 0°F and 38.37 psia for a flow rate of 5,400 lb/hr is compressed to superheated vapor (state 2) at 187 psia and 113°F. The propane is then condensed with cooling water at 77°F in the refrigerant condenser to state 3 at 98.7°F and 185 psia. Reducing the pressure across the valve to 40 psia causes the propane to become partially vaporized (state 4) at the corresponding saturation temperature of 2°F. The cycle is completed by passing the propane through the refrigerant evaporator where the propane absorbs heat from the matter being refrigerated and from which it emerges as a saturated vapor (state 1), thus completing the cycle. Calculate the lost work.

SOLUTION

Let the system be circulating propane and the electric motor drive of the compressor, but not the cooling water used in the condenser or the matter being refrigerated in the evaporator.

For each pass through the cycle, there is no net enthalpy change for the propane. The energy balance, if applied incorrectly, would therefore indicate that no energy is required to run the cycle. But, of course, energy input is required at the compressor, and heat is transferred to the system from the matter being refrigerated at the evaporator. By an energy balance, the sum of these two energy inputs is transferred out of the system to cooling water at the condenser.

Again, it is emphasized that the first law of thermodynamics cannot be used to determine minimum or maximum energy transfer to or from a system. Instead, we must use the second law or the availability balance (combined first and second laws). For the propane refrigeration cycle, the availability balance of Eq. (10.32) simplifies to

$$L\dot{W} = \dot{W}_{\text{in}} + \left(1 - \frac{T_0}{T_{\text{Evaporator}}}\right)\dot{Q}_{\text{in}} - \left(1 - \frac{T_0}{T_{\text{Condenser}}}\right)\dot{Q}_{\text{out}} \tag{10.35}$$

Note that the control volume contains the refrigerant fluid (propane), the matter being refrigerated is treated as a heat reservoir at 10°F, and the condenser releases heat to a heat reservoir at T_0.

For a reversible cycle, the lost work would be zero, and this form of the availability balance is the classical result for the refrigeration (reverse Carnot) cycle. To prove this, the first law gives

$$\dot{W}_{\text{in}} + \dot{Q}_{\text{in}} = \dot{Q}_{\text{out}} \tag{10.36}$$

Substitution of this equation into the lost-work equation, Eq. (10.35), with $L\dot{W} = 0$, so as to eliminate $\dot{Q}_{\text{out}}$, gives the following widely used equation for the coefficient of performance (COP) of a refrigeration cycle:

$$\text{COP} = \frac{\dot{Q}_{\text{in}}}{\dot{W}_{\text{in}}} = \frac{T_{\text{Evaporator}}}{T_{\text{Condenser}} - T_{\text{Evaporator}}} \tag{10.37}$$

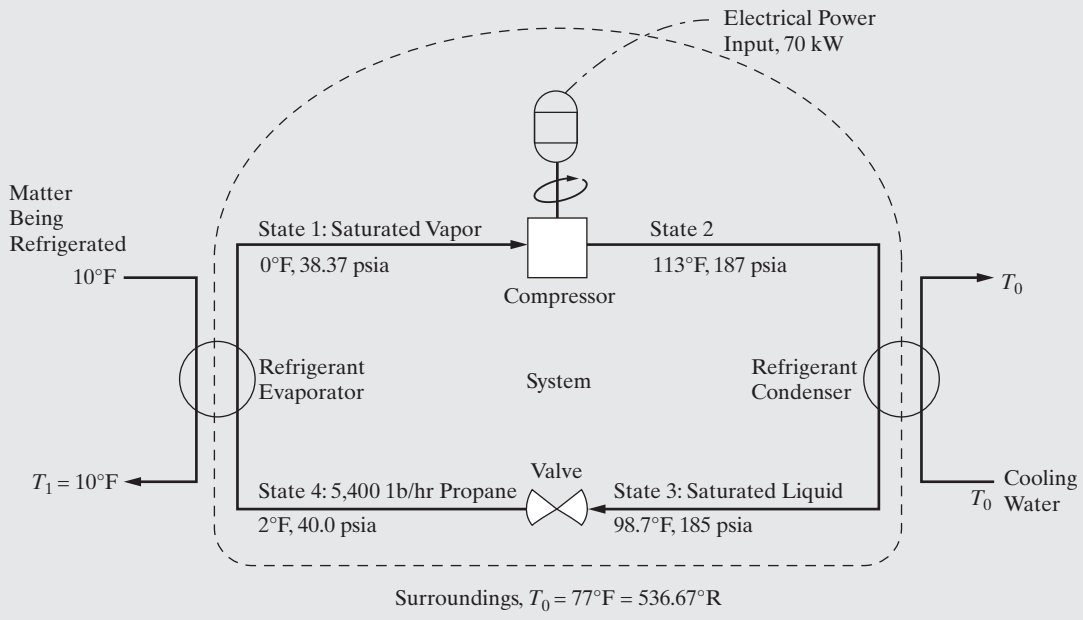

Figure 10.20 Operating conditions for propane refrigeration cycle.

The lost work for the cycle is computed in the following manner. First, we take the dead-state temperature, T_0, to be the cooling-water temperature, $T_{\text{Condenser}}$. The lost work then reduces to

$$L\dot{W} = \dot{W}_{\text{in}} + \left(1 - \frac{T_0}{T_{\text{Evaporator}}}\right)\dot{Q}_{\text{in}} \tag{10.38}$$

The electrical work input is given in Figure 10.20 as 70 kW. The heat transferred in the evaporator is obtained most readily from an energy balance on the propane as it flows from state 3 (saturated liquid at 185 psia) to state 1 (saturated vapor at 38.37 psia), noting that no enthalpy change occurs across the valve:

$$\dot{Q}_{\text{in}} = \dot{m}_{\text{propane}}\,(H_1 - H_4) = \dot{m}_{\text{propane}}\,(H_1 - H_3) \tag{10.39}$$

From the Example 10.2 problem statement, the propane circulation rate is 5,400 lb/hr. Again, we estimate enthalpies and entropies from a modified Benedict-Webb-Rubin (BWR) equation of state, which gives

$$H_1 = -686.6 \text{ Btu/lb} \quad \text{and} \quad H_3 = H_4 = -797.2 \text{ Btu/lb}$$

Thus,

$$\dot{Q}_{\text{in}} = 5{,}400[(-686.6) - (-797.2)] = 597{,}200 \text{ Btu/hr} = 174.9 \text{ kW}$$

The temperatures are

$$T_0 = 77 + 459.7 = 536.7\ ^\circ\text{R} \text{ and } T_{\text{Evaporator}} = 10 + 459.7 = 469.7\ ^\circ\text{R}$$

The second term on the right-hand side of the lost-work equation, Eq. (10.38), for the propane refrigeration cycle is the reversible work input that corresponds to the heat input. It is

$$\left(1 - \frac{536.7}{469.7}\right)174.9 = -24.95 \text{ kW}$$

The lost work is

$$L\dot{W} = 70 + (-24.95) = 45.05 \text{ kW}$$

In a reversible cycle, with $L\dot{W} = 0$, only $70 - 45.05$ or 24.95 kW of electrical work input would be required.

10.7 THERMODYNAMIC EFFICIENCY

The thermodynamic efficiency of an operation or an entire process depends on its main goal and the work lost in accomplishing that goal. Goals differ from application to application. For example, the main goal of an adiabatic turbine operating continuously might be to produce work. The main goal of a refrigeration cycle might be the transfer of heat from the stream being refrigerated to the refrigerant. In continuous chemical processes that involve reactors, separators, heat exchangers, and shaft-work devices, the main goal is the increase or decrease of the availability function of the streams flowing across the boundaries of the system. For a complex batch chemical process, the main goal is the increase or decrease of the batch availability function $m(B - PV)$ of the system.

Table 10.2 Possible Main Goals of an Operation or Process

Main Goal	Explanation
$-\dot{W}$	Work transfer
$-\Delta(\dot{m}B)$	Change in availability function of flowing streams
$\left(1 - \frac{T_0}{T_1}\right)\dot{Q}_i$	Work equivalent of heat transfer
$-\frac{\Delta[m(B - PV)]_{sys}}{\Delta t}$	Change in batch availability function of system

To derive general expressions for thermodynamic efficiency, we write Eq. (10.26), the combined energy and entropy balance, in the form

$$L\dot{W} = -\sum_i \dot{W}_i - \Delta(\dot{m}B)_{\text{flowing streams}} + \sum_i \left(1 - \frac{T_0}{T_i}\right)\dot{Q}_i - \frac{\Delta[m(B - PV)]_{\text{sys}}}{\Delta t} \tag{10.40}$$

Each of the terms on the right-hand side of Eq. (10.40) represents a possible main goal. The availabilities of some main goals are listed in Table 10.2. The thermodynamic efficiency is computed from one of two equations, depending on the sign of the term that represents the main goal on the right-hand side of Eq. (10.40). If the sign is positive, the thermodynamic efficiency is given by

$$\eta_{(+)\text{goal}} = \frac{\text{main goal} - L\dot{W}}{\text{main goal}} \tag{10.41}$$

If the numerical value of the main goal selected is negative, the thermodynamic efficiency is given by

$$\eta_{(-)\text{goal}} = \frac{\text{main goal}}{\text{main goal} - L\dot{W}} \tag{10.42}$$

The application of Eq. (10.42) always results in a positive efficiency that is equal to or less than unity (i.e., 100%) because the main goal has a negative sign and the lost work is greater than or equal to zero. On the other hand, Eq. (10.41) can give values ranging from less than zero up to unity. A negative efficiency results when the lost work is greater than the absolute value of the main goal. For example, consider a continuous process whose main goal is to decrease the availability function of the flowing streams. If the process is reversible and exchanges heat only with the infinite surroundings, then $L\dot{W} = 0$ and work could be done on the surroundings. If, however, the process is so irreversible that, instead, work must be done on the system by the surroundings, then $L\dot{W}$ will be greater than the main goal, $-\Delta(\dot{m}B)_{\text{flowing streams}}$, and Eq. (10.41) will yield a negative efficiency. Thermodynamic efficiencies greater than unity are impossible.

The application of Eqs. (10.41) and (10.42) for the calculation of thermodynamic efficiency may be illustrated by considering the two examples in the preceding section. For the continuous, steady-state, steady-flow, two-stage compression process shown

in Figure 10.19, the main goal is to change the availability function of the nitrogen gas. The calculations previously presented give

$$\text{Main goal} = \dot{m}(B_2 - B_1) = -291{,}600 \text{ Btu/hr}$$
$$L\dot{W} = 74{,}800 \text{ Btu/hr}$$

Because the main goal has a negative value, we apply Eq. (10.42) to obtain

$$\eta = \frac{-291{,}600}{-291{,}600 - 74{,}800} = 0.796, \text{ or } 79.6\%$$

This is consistent with the previous calculation of 20.4% for the loss of input electrical energy.

In the refrigeration cycle of Figure 10.20, the main goal—the transfer of heat from the matter being refrigerated at 10°F to the propane refrigerant—requires the work of a reversible Carnot cycle, which was calculated to be −25 kW. This work was accompanied by 45 kW of lost work. Thus, Eq. (10.42) gives

$$\eta = \frac{-25}{-25 - 45} = 0.357, \text{ or } 35.7\%$$

10.8 CAUSES OF LOST WORK

Lost work is caused by irreversibilities. Major causes are:

1. ***Mixing of Two or More Streams or Batches of Material That Differ in Temperature, Pressure, and/or Composition.*** Such mixing leads to significant increases in entropy, but may be unavoidable when preparing a composite feed for chemical reaction. Often, however, such mixing can be avoided when recycling material. Quenching a hot stream with a cold stream increases entropy.
2. ***Finite Driving Forces for Transport Processes.*** For reasonable-size processing equipment, finite driving forces are needed for heat transfer and mass transfer. However, the smaller the driving forces, the smaller is the lost work. In distillation, small driving forces are best achieved with countercurrent flow of vapor and liquid at reflux ratios close to minimum. For heat exchangers, small temperature-driving forces are achieved with countercurrent flow and small temperature approaches at either end of the exchanger.
3. ***Fluid Friction and Drag.*** Significant decreases in skin friction for flow of fluids in pipes can be achieved by increasing pipe diameter, thereby reducing fluid velocity. Reducing the velocity or streamlining the shape of the object can reduce form drag for flow of fluid past submerged objects.
4. ***Chemical Reactions Occurring Far from Equilibrium.*** To minimize lost work, reactions should be carried out with little or no dilution, with minimal side reactions, and at maximum yields to avoid separations and byproduct formation. This is best achieved by using selective catalysts. If the reaction is exothermic, it is best carried out at high temperature to maximize the usefulness of the energy produced. If the reaction is endothermic, it is best carried out at below ambient temperature to utilize heat from the dead state.
5. ***Transferring Heat to Cooling Water, Especially When That Heat is Available at an Elevated Temperature.*** Good uses should be found for waste heat.
6. ***Mechanical Friction in Machinery Such as Pumps, Compressors, and Turbines.***

Second-law thermodynamic efficiency of the majority of chemical processes is in the range of 25 to 30%. Economic analyses have shown that it is worthwhile to seek ways to improve this efficiency to at least 60%. Machinery is available with efficiencies of 80% and higher.

10.9 THREE EXAMPLES OF SECOND-LAW ANALYSIS

In this section, three detailed examples of second-law analysis are presented for chemical processes. Each example includes the calculation of lost work, the determination of where the lost work occurs, and consideration of how the lost work can be reduced. The examples involve (1) the propane refrigeration cycle introduced in Section 10.6, (2) the separation of a mixture of propylene and propane by distillation, and (3) a process for the hydrogenation of benzene to cyclohexane. The third example is computed with ASPEN PLUS.

EXAMPLE 10.3 ***Propane Refrigeration Cycle—Example 10.2 Revisited***

In Sections 10.6 and 10.7, the total rate of lost work and overall thermodynamic efficiency of a propane refrigeration cycle, shown in Figure 10.20, is calculated. Now, consider this cycle in detail to determine where the lost work occurs with respect to each of the four steps in the cycle. Then, attempt to improve the efficiency of the cycle by concentrating on those steps where most of the lost work occurs. Although the overall process is a cycle, each separate step in the cycle can be treated as a continuous process so that Eq. (10.27) applies.

SOLUTION

Compressor: State 1 to State 2
For this step,

$$L\dot{W}_{1-2} = \dot{m}[(H_1 - T_0S_1) - (H_2 - T_0S_2)] - \dot{W}_{\text{elec}}$$

The thermodynamic properties of propane are obtained from a modified BWR equation as in Example 10.2. Note that states 1 and 2 are both vapor. The rate of lost work in kilowatts is calculated as follows:

$$\begin{aligned} L\dot{W}_{1-2} &= (2.929 \times 10^{-4})(5{,}400)\{[-686.60 - (536.67)(1.3507) \\ &\quad - [-655.41 - (536.67)(1.3501)]\} - (-70) \\ &= -49.83 + 70 = 20.17 \text{ kW} \end{aligned}$$

This represents 20.17/45.05 = 0.448, or 44.8% of the total lost work for the cycle. This lost work results because of motor and compressor irreversibilities.

Refrigerant Condenser: State 2 to State 3
For heat rejection from the propane refrigerant to cooling water at the temperature of the infinite surroundings, T_0,

$$\mathrm{L}\dot{W}_{2-3} = \dot{m}[(H_2 - T_0S_2) - (H_3 - T_0S_3)]$$

State 3 is a saturated liquid, so

$$\begin{aligned}\mathrm{L}\dot{W}_{2-3} &= (2.929 \times 10^{-4})(5{,}400)\{[-655.41 - (536.67)(1.3501)] \\ &\quad - [-797.2 - (536.67)(1.0963)]\} \\ &= 8.83 \text{ kW}\end{aligned}$$

This represents $8.83/45.05 = 0.196$, or 19.6% of the total lost work for the cycle. This lost work results because of a frictional pressure drop of 2 psi through the heat exchanger and the rather large temperature driving force for heat transfer.

Valve: State 3 to State 4
Assume that this step is adiabatic with $H_3 = H_4$. Then

$$\mathrm{L}\dot{W}_{3-4} = \dot{m}[(-T_0S_3) - (-T_0S_4)]$$

Because state 4 is a partially vaporized condition, the fractions of vapor and liquid must be determined to obtain S_4. That is, if ψ is the weight fraction vaporized, then

$$S_4 = \psi(S_4)_\mathrm{V} + (1 - \psi)(S_4)_\mathrm{L}$$

where V and L represent vapor and liquid, respectively. The weight fraction vaporized can be determined by noting that

$$H_3 = H_4 = \psi(H_4)_\mathrm{V} + (1 - \psi)(H_4)_\mathrm{L}$$

and by solving for ψ to obtain

$$\psi = \frac{H_3 - (H_4)_\mathrm{L}}{(H_4)_\mathrm{V} - (H_4)_\mathrm{L}} = \frac{-797.2 - (-855.7)}{-686.1 - (-855.7)} = 0.345$$

Therefore,

$$S_4 = (0.345)(1.3501) + (1 - 0.345)(0.9831) = 1.1097 \text{ Btu/lb-°R}$$

and thus

$$\begin{aligned}\mathrm{L}\dot{W}_{3-4} &= (2.929 \times 10^{-4})(5{,}400)\{[-(536.67)(1.0963)] \\ &\quad - [-(536.67)(1.1097)]\} \\ &= 11.37 \text{ kW}\end{aligned}$$

This represents $11.37/45.05 = 0.252$, or 25.2% of the total lost work for the cycle. This lost work occurs because of the frictional pressure drop across the valve.

Refrigerant Evaporator: State 4 to State 1
For this step,

$$L\dot{W}_{4-1} = \dot{m}[(H_4 - T_0S_4) - (H_1 - T_0S_1)] + \left(1 - \frac{T_0}{T_i}\right)\dot{Q}_i$$

where T_i, the temperature of the matter being refrigerated, is 10°F (469.7°R). From the energy balance, the heat transfer rate in the refrigerant evaporator is

$$\dot{Q}_i = \dot{m}(H_1 - H_4)$$

Therefore,

$$L\dot{W}_{4-1} = \dot{m}[(H_4 - T_0S_4) - (H_1 - T_0S_1)] + \left(1 - \frac{T_0}{T_i}\right)\dot{m}(H_1 - H_4)$$

Simplifying,

$$\begin{aligned}L\dot{W}_{4-1} &= \dot{m}T_0\left[\left(S_1 - S_4\right) - \frac{H_1 - H_4}{T_i}\right] \\ &= (2.929 \times 10^{-4})(5{,}400)(536.67) \\ &\quad \left[(1.3507 - 1.1097) - \frac{(-686.60) - (-797.20)}{469.67}\right] \\ &= 4.68 \text{ kW}\end{aligned}$$

This represents $4.68/45.05 = 0.104$, or 10.4% of the total lost work for the cycle. This lost work occurs because of frictional pressure drop through the heat exchanger and the small but finite temperature driving force for heat transfer. Table 10.3 summarizes the preceding analysis.

Table 10.3 Lost Work for Propane Refrigeration Cycle

Step in Cycle	State to State	$L\dot{W}$(kW)	Percentage of Total $L\dot{W}$
Compressor	1–2	20.17	44.8
Refrigerant condenser	2–3	8.83	19.6
Valve	3–4	11.37	25.2
Refrigerant evaporator	4–1	4.68	10.4
		45.05	100.0

How can the thermodynamic efficiency of this refrigeration cycle be improved? Table 10.3 shows that the major loss is due to the compressor, with moderate losses in the refrigerant condenser and the valve, but only a small loss in the refrigerant evaporator. Some improvements can be made by maintaining the same basic cycle, but adjusting the operating conditions and changing the equipment to accomplish the following:

1. Increase the efficiency of the compressor.
2. Reduce the frictional pressure drop in the refrigerant condenser. Use a higher-temperature coolant for the refrigerant condenser or reduce the compressor discharge pressure to lower the temperature of the refrigerant at states 2 and 3.
3. Replace the valve with a power-recovery turbine.
4. Reduce the frictional pressure drop in the refrigerant evaporator. Increase the pressure at state 4 to reduce the temperature-driving force in the refrigerant evaporator.

A revised cycle that incorporates these improvements is shown in Figure 10.21. Comparison of the cycle with the original one in Figure 10.20 shows the following:

1. The valve is replaced by a power-recovery turbine that supplies a portion of the power required by the compressor.
2. The frictional pressure drop in the refrigerant evaporator is reduced from 1.63 psi (40.0 − 38.37) to 0.5 psi (44.85 − 44.35).
3. The frictional pressure drop in the refrigerant condenser is reduced from 2 psi (187 − 185) to 0.5 psi (154.9 − 154.4).

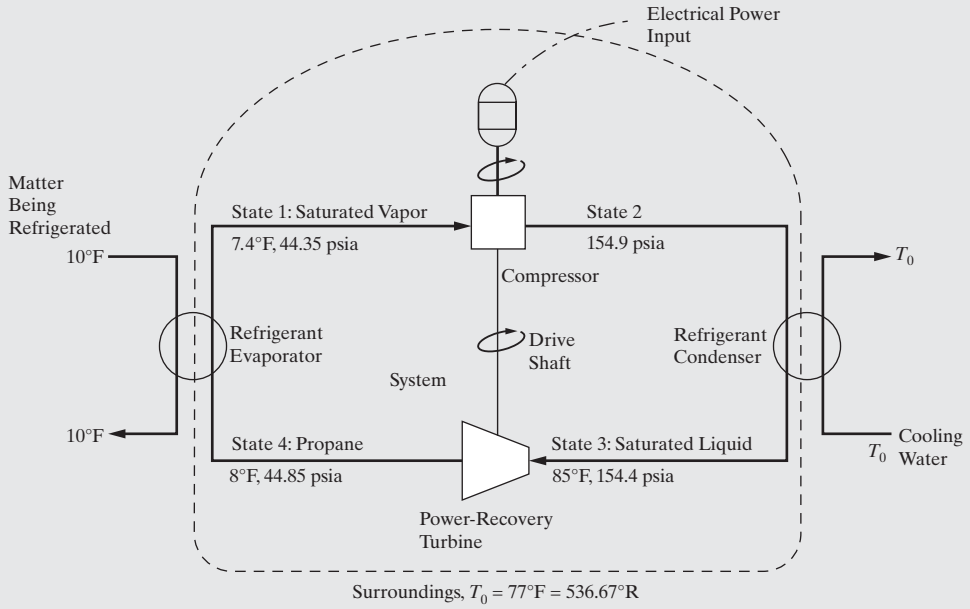

Figure 10.21 Revised propane refrigeration cycle.

4. The compressor inlet and discharge pressures are changed from 38.37 psia to 44.35 psia and from 187 psia to 154.9 psia, respectively, thus reducing the compression ratio from 4.874 to 3.493. The corresponding changes in refrigerant temperature cause reductions in the minimum temperature-driving forces in the condenser and evaporator from 21.7°F (98.7 − 77) to 8°F(85 − 77) and from 8°F (10 − 2) to 2°F (10 − 8), respectively.

Next, the lost work is calculated assuming that the power-recovery turbine and the compressor operate isentropically. Also, the rate of heat transfer in the refrigerant evaporator is assumed to be the same as for the original cycle (597,200 Btu/hr, as calculated above). Required thermodynamic properties of propane for the revised cycle are given in the following table.

Temperature (°F)	Pressure (psia)	Phase	Enthalpy (Btu/lb)	Entropy (Btu/lb-°R)
85.0	154.40	Sat'd. liquid	−806.1	1.0805
8.0	44.85	Sat'd. vapor	−684.4	1.3485
8.0	44.85	Sat'd liquid	−852.3	0.9899
7.4	44.35	Sat'd vapor	−684.6	1.3486
100.0	154.90	Vapor	−658.1	1.3518
90.0	154.90	Vapor	−663.0	1.3431

It is worthwhile to begin calculations with the refrigerant condenser where the known heat duty permits us to determine the propane flow rate.

From State 4 to State 1

$$\dot{Q}_i = \dot{m}(H_1 - H_4)$$

Therefore,

$$\dot{m} = \frac{\dot{Q}_i}{H_1 - H_4} = \frac{597{,}200}{-684.6 - H_4}$$

To obtain H_4, note that since the power-recovery turbine is assumed to operate isentropically, $S_4 = S_3 = 1.0805$ Btu/lb-°R. Also note that $(S_4)_V > 1.0805 > (S_4)_L$. Therefore, state 4 is partially vaporized propane. If Ψ is the weight fraction vaporized,

$$S_4 = S_3 = \psi(S_4)_V + (1 - \psi)(S_4)_L$$

and therefore,

$$\psi = \frac{S_3 - (S_4)_L}{(S_4)_V - (S_4)_L} = \frac{1.0805 - 0.9899}{1.3485 - 0.9899} = 0.2526$$

$$H_4 = \psi(H_4)_V + (1 - \psi)(H_4)_L$$

$$= 0.2526(-684.4) + (1 - 0.2526)(-852.3) = -809.9 \text{ Btu/lb}$$

Thus,

$$\dot{m} = \frac{597{,}200}{-684.6 - (-809.9)} = 4{,}766 \text{ lb/hr}$$

From State 3 to State 4

Letting $\dot{W}_T$ = rate of work transferred from the propane by the turbine,

$$-\dot{W}_T = \dot{m}(H_4 - H_3)$$

$$= 4{,}766[-809.9 - (-806.1)] = -18{,}110 \text{ Btu/hr}$$

or

$$\dot{W}_T = 18{,}110 \text{ Btu/hr}$$

From State 1 to State 2

Letting $-\dot{W}_C$ = rate of work transferred by the compressor to the propane,

$$-\dot{W}_C = \dot{m}(H_2 - H_1)$$

The enthalpy, H_2, depends on the temperature of the propane leaving the compressor. It can be obtained by noting that

$$S_2 = S_1 = 1.3486 \text{ Btu/lb-°R}$$

because of the isentropic compression assumption. From the thermodynamic data given,

$$(S_{100°F})_V > (S_2)_V > (S_{90°F})_V$$

By interpolation, $T_2 = 96.32°F$ and $H_2 = -659.9$ Btu/lb. Therefore,

$$\dot{W}_C = -4{,}766[-659.9 - (-684.6)] = -117{,}720 \text{ Btu/hr}$$

Of this amount, 18,110 Btu/hr is supplied from the power-recovery turbine. Therefore, the theoretical electrical power input, $\dot{W}_E$, is

$$\dot{W}_E = -117{,}720 + 18{,}110 = -99{,}610 \text{ Btu/hr}$$

For the cycle,

$$L\dot{W} = -\dot{W}_E + \dot{Q}_i\left(1 - \frac{T_0}{T_i}\right)$$

$$= 99{,}610 + 597{,}200\left(1 - \frac{536.67}{469.67}\right) = 14{,}420 \text{ Btu/hr}$$

or

$$\frac{(14{,}420)(1.0544)}{3{,}600} = 4.22 \text{ kW}$$

This rate of lost work represents a large reduction from the value of 45.05 kW computed for the original cycle. The reduction is so large because isentropic compression and expansion has been assumed unrealistically for the revised cycle. To account for irreversibilities in compression and expansion, refer to Exercise 10.22.

EXAMPLE 10.4 *Separation of a Propylene-Propane Mixture by Distillation*

The initial design of a distillation operation for the continuous, steady-state, steady-flow separation of a propylene-propane mixture is shown in Figure 10.22. Conventional distillation is used with a bottoms pressure of 300 psia so that cooling water can be used in the partial condenser to provide reflux. The relative volatility of propylene to propane is quite low, varying from 1.08 to 1.14 for conditions at the top of the fractionator to conditions at the bottom of the fractionator, respectively; thus, a large external reflux ratio of 15.9 is required at operation near the minimum reflux. Because of high product purities as well as the low average relative volatility, 200 stages are required at 100% tray efficiency. With 24-in. tray spacing, two columns in series are needed because a single column would be too tall. Therefore, an intercolumn pump is shown in addition to the reflux pump. Total pressure drop for the two columns is 20 psi.

As shown in Figure 10.22, the system is chosen so that it does not include the 77°F cooling water used as the coolant in the partial condenser or the 220°F saturated steam used as the heating medium in the partial reboiler. Enthalpies of the feed stream and the two product streams are given in Table 10.4 with reference to the elements H_2 (gas) and C (graphite) at 0°R and 0 psia using the Soave-Redlich-Kwong (SRK) equation of state with standard heats of formation. Entropies given are referred to 0°R and 1 atm.

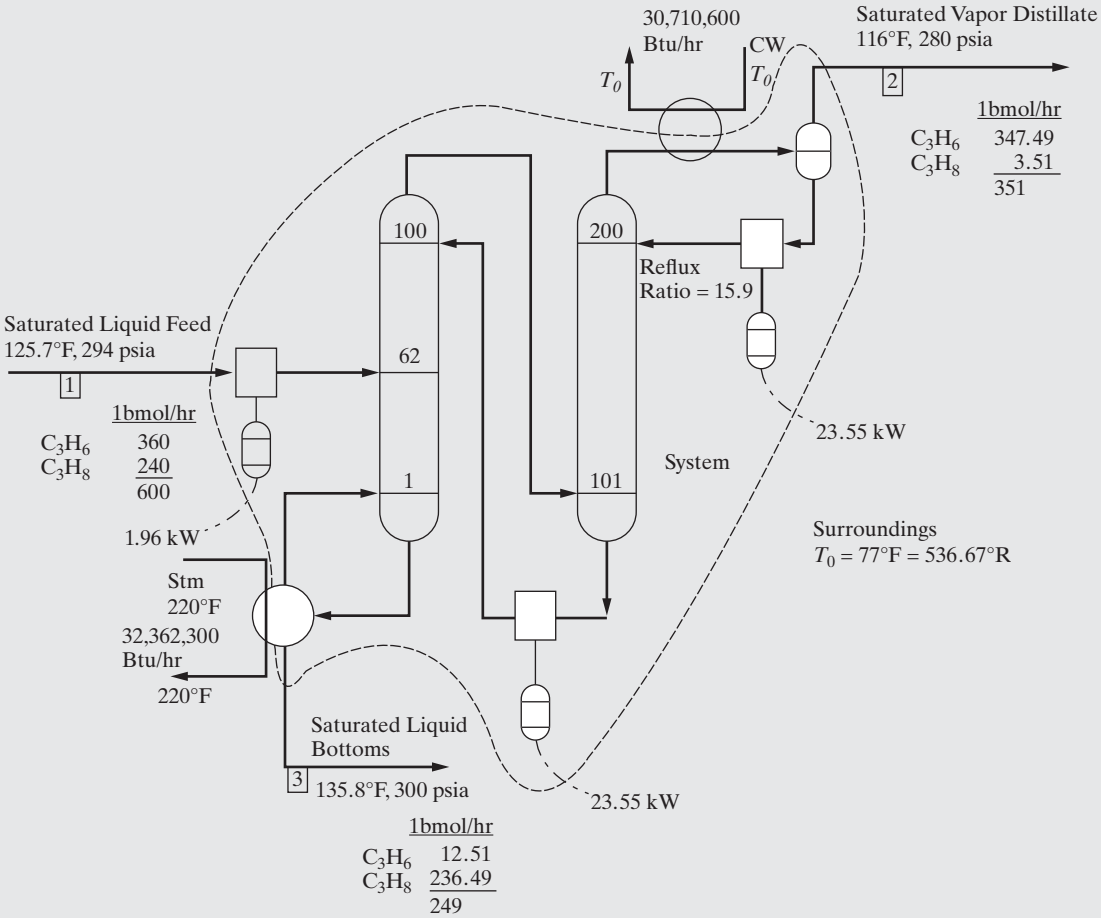

Figure 10.22 Distillation system for propylene-propane separation.

Table 10.4 Properties for Propylene-Propane Separation

State	Stream	Phase Condition	T(°F)	P(psia)	$\dot{m}$(lbmol/hr)	H(Btu/lbmol)	S(Btu/lbmol-°R)
1	Feed	Saturated liquid	125.7	294	600	−4, 133.4	50.92
2	Distillate	Saturated vapor	116.0	380	351	20,239.7	57.81
3	Bottoms	Saturated liquid	135.8	300	249	−31, 218.8	51.16

The rate of lost work is

$$L\dot{W} = -\sum_i \dot{W}_{elec_i} + [\dot{m}_1(H_1 - T_0S_1) - \dot{m}_2(H_2 - T_0S_2) - \dot{m}_3(H_3 - T_0S_3)] + \left(1 - \frac{T_0}{T_{\text{stm}}}\right)\dot{Q}_{\text{reboiler}}$$

where the work equivalent of the heat transferred to the condenser is zero because the temperature of the cooling water is assumed to be T_0. Thus, $L\dot{W}$ (in kilowatts) is given by

$$\begin{aligned} L\dot{W} &= -(-1.96 - 23.55 - 23.55) \\ &\quad + (2.929 \times 10^{-4})\left\{\begin{matrix} 600\,[-4{,}133.4 - (536.67)\,(50.92)] \\ -351[20{,}239.7 - (536.67)(57.81)] \\ -249[-31{,}218.8 - (536.67)(51.16)] \end{matrix}\right\} \\ &\quad + (2.929 \times 10^{-4})\left(1 - \frac{536.67}{679.67}\right)(32{,}362{,}300) \\ &= 49.06 - 140.81 + 1{,}994.33 = 1{,}902.58 \text{ kW} \end{aligned}$$

The thermodynamic efficiency is computed from Eq. (10.41) because the main goal is to change the availability function of the streams, which is

$$-\Delta(\dot{m}B)_{\text{flowing streams}} = -140.81 \text{ kW}$$

Thus, as in most continuous separation operations, the availability function of the flowing streams has been increased. In this example, the increase is brought about mainly by the transfer of heat in the reboiler, giving

$$\eta = \frac{-\Delta(\dot{m}B)}{-\Delta(\dot{m}B) - L\dot{W}} = \frac{-140.81}{-140.81 - 1{,}902.58} = 0.0689, \text{ or } 6.89\%$$

This is a very low efficiency but is typical of conventional distillation of mixtures with a low relative volatility because of the large energy expenditures required in the reboiler. Therefore, other separation methods, such as adsorption, have been explored for this separation. Also, elaborate schemes for reducing the reboiler heat duty in distillation have been devised, including multieffect distillation and operation at lower pressures using heat pumps as discussed in Section 11.8. One such alternative scheme, using reboiler-liquid flashing, for the separation of propylene from propane is shown in Figure 10.23. The feed is reduced in pressure to 108 psia by a power-recovery turbine and

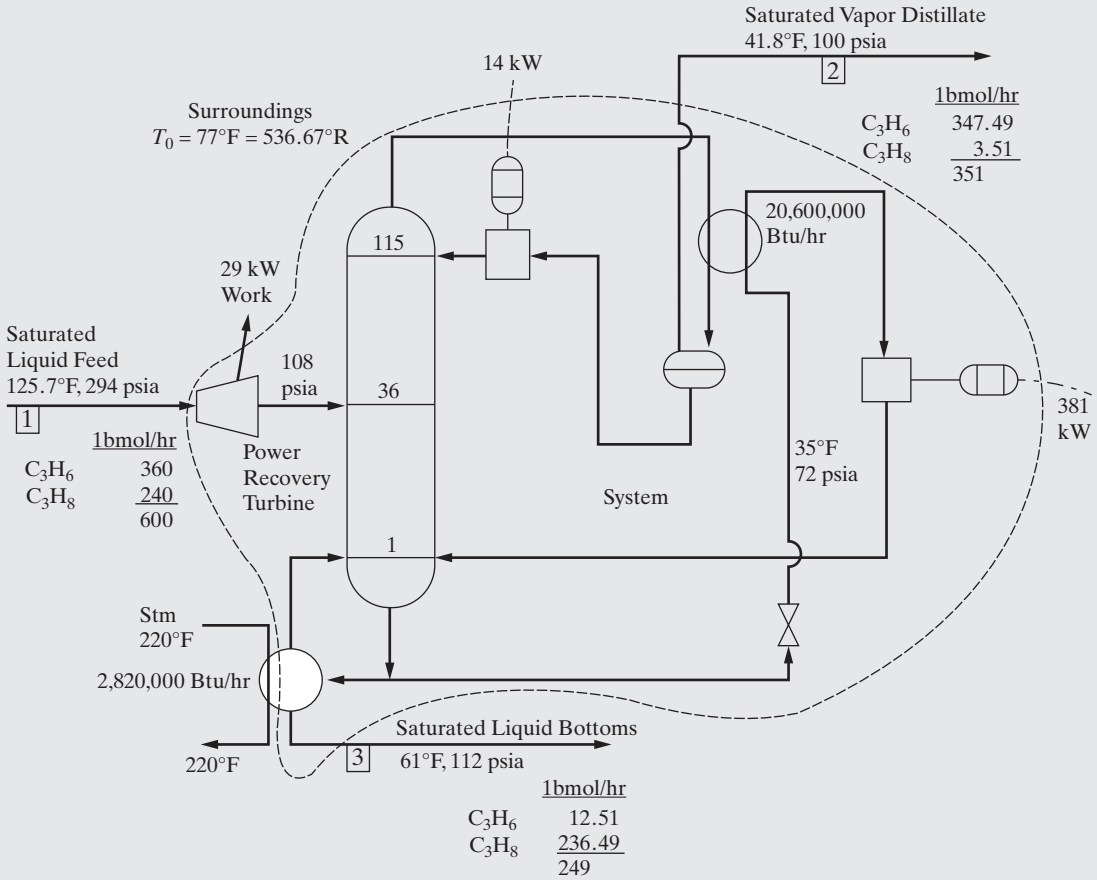

Figure 10.23 Low-temperature distillation with reboiler-liquid flashing for propylene-propane separation.

then distilled in a single column operating at a bottoms pressure of 112 psia. Liquid leaving the bottom tray is flashed across an expansion valve to a pressure corresponding to a saturation temperature lower than the saturation temperature of the overhead vapor so that the partial condenser can be used as a reboiler. A compressor is needed to return the reboiled vapor to the bottom of the column. Because the required reboiler duty is somewhat larger than the required condenser duty, an auxiliary steam-heated reboiler is needed. The large reduction in reboiler steam is somewhat offset by the power requirement of the compressor.

The following enthalpy and entropy data apply to Figure 10.23.

Stream	Phase	Enthalpy (Btu/lbmol)	Entropy (Btu/lbmol-°R)
Feed	Saturated liquid	−4,133.4	50.92
Distillate	Saturated vapor	19,672.6	58.40
Bottoms	Saturated liquid	−33, 682.1	46.87

The rate of lost work for the system is given by

$$\begin{aligned} L\dot{W} &= -\sum_i \dot{W}_{elec_i} + [\dot{m}_1(H_1 - T_0S_1) - \dot{m}_2(H_2 - T_0S_2) \\ &\quad - \dot{m}_3(H_3 - T_0S_3)] + \left(1 - \frac{T_0}{T_{\text{stm}}}\right)\dot{Q}_{\text{reboiler}} \\ &= -(29 - 14 - 381) \\ &\quad + (2.929 \times 10^{-4})\left\{\begin{array}{l} 600\,[-4{,}133.4 - (536.67)\,(50.92)] \\ -351[19{,}672.6 - (536.67)(58.40)] \\ -249[-33{,}682.1 - (536.67)(46.87)] \end{array}\right\} \\ &\quad + (2.929 \times 10^{-4})\left(1 - \frac{536.67}{679.67}\right)(2{,}820{,}000) \\ &= 366.0 - 38.2 + 173.8 = 501.6 \text{ kW} \end{aligned}$$

Since $-\Delta(\dot{m}B)_{\text{flowing streams}} = -38.2$ kW,

$$\eta = \frac{-\Delta(\dot{m}B)}{-\Delta(\dot{m}B) - L\dot{W}} = \frac{-38.2}{-38.2 - 501.6} = 0.07, \text{ or } 7.0\%$$

Although the lost work is much lower than the value of 1,902.58 kW computed for the system in Figure 10.22, the thermodynamic efficiency is still low. The two cases are not really comparable because the product conditions are not the same.

EXAMPLE 10.5 *A Process for Converting Benzene to Cyclohexane*

Here, a process is considered that involves a chemical reactor as well as separators, heat exchangers, and pumps. A continuous, steady-state, steady-flow process for manufacturing approximately 10 million gallons per year of high-purity cyclohexane by the catalytic hydrogenation of high-purity benzene, at elevated temperature and pressure, is shown in Figure 10.24. The heart of the process is a reactor in which liquid benzene from storage, together with makeup hydrogen and recycle hydrogen in stoichiometric excess, take part in the reaction:

$$C_6H_6 + 3H_2 \rightarrow C_6H_{12}$$

Figure 10.24 includes all major equipment and streams together with a set of operating conditions for making a preliminary design and second law analysis. As shown, 92.14 lbmol/hr of pure liquid benzene feed (S1) at 100°F and 15 psia is pumped by P1 to 335 psia and mixed in-line and adiabatically at M1 with impure hydrogen makeup gas (S3) containing 0.296 mol% nitrogen at 120°F and 335 psia, gas recycle (S4), and a cyclohexane recycle (S5) to produce the combined reactor feed (S6). In the cooled reactor, R1, 99.86% of the benzene in stream S6 is hydrogenated to produce the saturated-vapor reactor effluent (S7) at 392°F and 315 psia. This effluent is reduced in temperature to 120°F at 300 psia by the cooler, H1, and then separated at these conditions in the high-pressure flash drum, F1, into a hydrogen-rich vapor and a cyclohexane-rich liquid. A total of 8.166% of the vapor from this flash drum is purged to stream S11 at line tee D1 with the remaining vapor (S12) recycled to the reactor, R1, to provide an excess of hydrogen. At the line tee, D2, 62% of the liquid (S10) from flash drum F1 is sent in stream S14 to a low-pressure adiabatic flash drum, F2, at 15 psia. Gas from F2 is vented to stream S15 while liquid is taken as cyclohexane product S16. The remaining liquid S13 from F1 is recycled by pump P2 to reactor R1 to control the pressure of the saturated-vapor reactor effluent.

It is convenient to use computer simulation to perform mass and energy balance calculations automatically for continuous-flow, steady-state processes like the one in Figure 10.24. For this example, ASPEN PLUS is used. This requires that the process flow diagram be converted to a simulation flowsheet as discussed in Section 7.3. That flowsheet is shown in Figure 10.25, in which each stream has a unique name the same as or similar to that shown in Figure 10.24. Each operation is a simulation unit within which two names appear. The top name (e.g., R1 for the reactor) is a unique user-specified unit name or so-called block i.d. The bottom name (e.g., RSTOIC for the reactor) refers to the selected ASPEN PLUS model, or module, for the operation. As discussed earlier, in many cases, a particular operation can be simulated with two or more models. The information given in Figures 10.24 and 10.25 is sufficient to prepare the input for a simulation. As discussed earlier, specifications can be entered interactively in the ASPEN PLUS program. Specifications entered on input forms are converted by ASPEN PLUS to a compact listing that can be displayed if desired. The listing is given in Figure 10.26 where the flowsheet topology is followed by the list of components with user-selected names followed by databank names. Thermodynamic properties are computed by option CHAO-SEA, which is the Chao-Seader method with the Grayson-Streed constants for estimating K values and the Redlich-Kwong equation of state for obtaining the departure functions for the effect of pressure on enthalpy and entropy. All mixture enthalpies and entropies are referenced to the elements at 25°C. Therefore, energy and entropy balances automatically account for enthalpy and entropy changes due to chemical reaction. This greatly simplifies the calculations when chemical reactions occur as is this cyclohexane process. The availablity function, B, is readily computed from its definition, Eq. (10.24), for a selected value of T_0. Specifications for the two inlet streams, S1 and S3, follow. The ASPEN PLUS program concludes with the operating conditions for each simulation unit.

In Figure 10.25, two recycle loops are clearly seen. However, no recycle convergence method is specified in the ASPEN PLUS program, and the flowsheet does not show the convergence units. Accordingly, ASPEN PLUS selects, by default, the tear streams, initial component flow rates of zero for the tear streams, and a convergence method. The converged results of the simulation for the ASPEN PLUS program in Figure 10.26 are given in Figure 10.27 where component

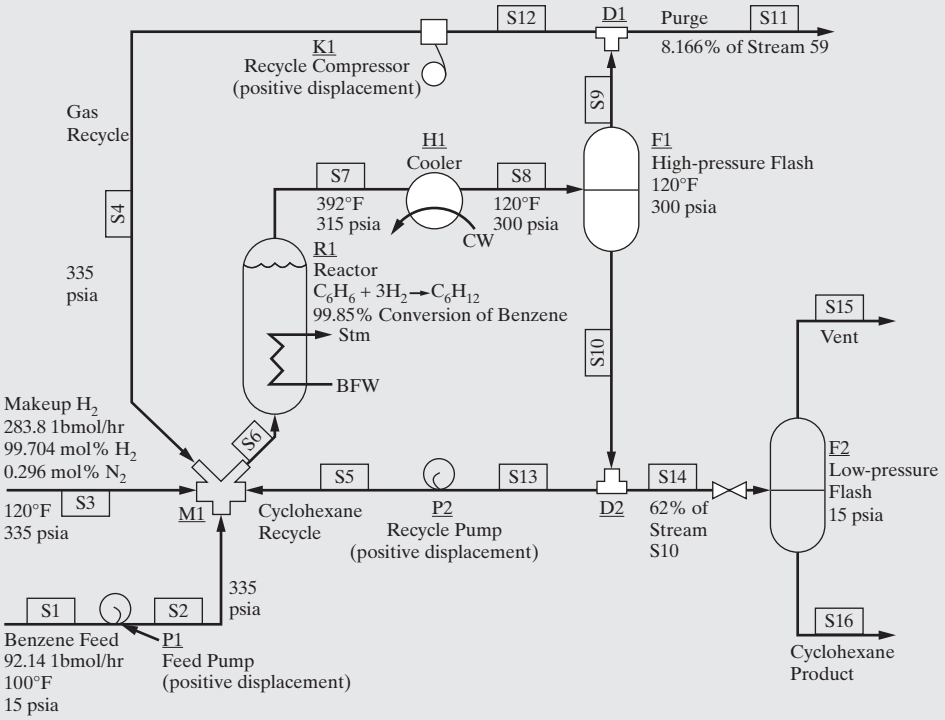

Figure 10.24 Process flow diagram and design for hydrogenation of benzene to cyclohexane.

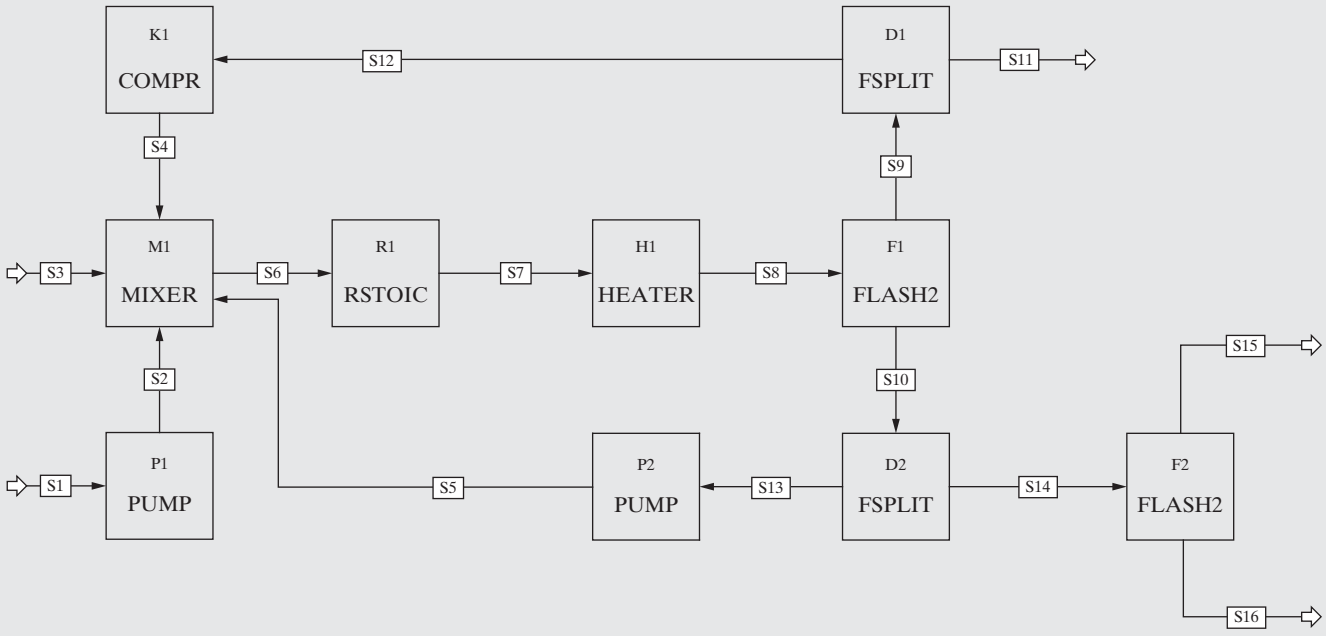

Figure 10.25 ASPEN PLUS flowsheet for the cyclohexane process.

and total molar flow rates, temperature, pressure, molar enthalpy, molar vapor and liquid fractions, molar entropy, density, and average molecular weight are listed. By comparing streams S1 and S16, it is seen that the overall yield of cyclohexane from the process is 91.24955/92.1400, or 99.03%. By comparing streams S3 and S16, it is seen that an overall excess of [(282.9599/3)/91.24955] – 1.0, or only 3.36% H_2, is used. Examination of stream S4 or S12 shows that relatively little N_2 is recycled, although the amount is large relative to the N_2 in the makeup hydrogen. The amount of cyclohexane recycle in stream S5 or S13 is considerable compared to the benzene feed S1. The energy balance results are summarized in Table 10.5 where the net energy transfer rates are listed for each operation, and are considerable for the reactor, R1, and the partial condenser, H1.

```
IN-UNITS ENG
DEF-STREAMS CONVEN ALL
MODEL-OPTION
DATABANKS 'APV82 PURE28' / 'APV82 AQUEOUS' / 'APV82 SOLIDS' /  &
        'APV82 INORGANIC' / NOASPENPCD
PROP-SOURCES 'APV82 PURE28' / 'APV82 AQUEOUS' / 'APV82 SOLIDS' &
         / 'APV82 INORGANIC'
COMPONENTS
    HYDRO-01 H2 /
    NITRO-01 N2 /
    BENZE-01 C6H6 /
    CYCLO-01 C6H12-1
SOLVE
    RUN-MODE MODE=SIM
FLOWSHEET
    BLOCK M1 IN=S3 S5 S4 S2 OUT=S6
    BLOCK R1 IN=S6 OUT=S7
    BLOCK H1 IN=S7 OUT=S8
    BLOCK F1 IN=S8 OUT=S9 S10
    BLOCK D1 IN=S9 OUT=S12 S11
    BLOCK D2 IN=S10 OUT=S14 S13
    BLOCK P2 IN=S13 OUT=S5
    BLOCK P1 IN=S1 OUT=S2
    BLOCK K1 IN=S12 OUT=S4
    BLOCK F2 IN=S14 OUT=S15 S16
PROPERTIES CHAO-SEA
STREAM S1
    SUBSTREAM MIXED TEMP=100. PRES=15.
    MOLE-FLOW BENZE-01 92.14
STREAM S3
    SUBSTREAM MIXED TEMP=120. PRES=335.
    MOLE-FLOW HYDRO-01 282.9599 / NITRO-01 0.84
BLOCK M1 MIXER
    PARAM
BLOCK D1 FSPLIT
    FRAC S12 0.91834
BLOCK D2 FSPLIT
    FRAC S14 0.62
BLOCK H1 HEATER
    PARAM TEMP=120. PRES=300.
BLOCK F1 FLASH2
    PARAM TEMP=120. PRES=300.
BLOCK F2 FLASH2
    PARAM PRES=15. DUTY=0.
BLOCK R1 RSTOIC
    PARAM TEMP=392. PRES=315.
    STOIC 1 MIXED BENZE-01 -1. / HYDRO-01 -3. / CYCLO-01 1.
    CONV 1 MIXED BENZE-01 0.9986
BLOCK P1 PUMP
    PARAM PRES=335.
BLOCK P2 PUMP
    PARAM PRES=335.
BLOCK K1 COMPR
    PARAM TYPE=ASME-ISENTROP PRES=335. SB-MAXIT=30  & SB-TOL=0.0001
EO-CONV-OPTI
STREAM-REPOR MOLEFLOW
```

Figure 10.26 ASPEN PLUS input in paragraph form for the cyclohexane process.

Heat and Material Balance Table																	
Stream ID		S1	S2	S3	S4	S5	S6	S7	S8	S9	S10	S11	S12	S13	S14	S15	S16
From			P1		K1	P2	M1	R1	H1	F1	F1	D1	D1	D2	D2	F2	F2
To		P1	M1	M1	MI	MI	R1	H1	F1	D1	D2		K1	P2	F2		
Phase		LIQUID	LIQUID	VAPOR	VAPOR	LIQUID	MIXED	VAPOR	MIXED	VAPOR	LIQUID	VAPOR	VAPOR	LIQUID	LIQUID	VAPOR	LIQUID
Substream: MIXED																	
Mole Flow	lbmol/hr																
HYDRO-01		0.0	0.0	282.9599	65.20195	.5983471	348.7571	72.57440	72.57440	70.99980	1.574598	5.797844	65.20195	.5983471	.9762505	.94663	.0296110
NITRO-01		0.0	0.0	.8400000	7.507531	.1053847	8.452439	8.452439	8.452439	8.175111	.2773283	.6675795	7.507531	.1053847	.1719435	.16403	7.91323E-3
BENZE-01		92.14000	92.14000	00	1.56136E-3	.0483989	92.18996	.1290659	.1290659	1.70020E-3	.1273657	1.38838E-4	1.56136E-3	.0483989	.0789667	6.58663	.0783081
CYCLO-OI		0.0	0.0	00	1.602711	56.33650	57.93828	149.9992	149.9992	1.745226	148.2538	.1425151	1.602711	56.33650	91.91745	.66785	91.24955
Total Flow	lbmol/hr	92.14000	92.14000	283.7999	74.31376	57.08863	507.3378	231.1551	231.1551	80.92183	150.2332	6.608077	74.31376	57.08863	93.14461	1.7792	91.36538
Total Flow	lb/hr	7197.391	7197.391	593.9445	476.7595	4749.291	13017.29	13017.29	13017.29	519.1536	12498.13	42.39408	476.7595	4749.291	7748.843	62.766	7686.077
Total Flow	Cuft/hr	134.1836	134.8476	5339.719	1454.162	102.2477	6896.312	5903.728	1964.081	1695.167	268.9142	138.4273	1556.740	102.1874	166.7268	735.17	164.4343
Temperature	F	100.0000	107.4571	120.0000	144.3024	120.8454	108.5906	392.0000	120.0000	120.0000	120.0000	120.0000	120.0000	120.0000	120.0000	121.07	121.0760
Pressure	psia	15.00000	335.0000	335.0000	335.0000	335.0000	335.0000	315.0000	300.0000	300.0000	300.0000	300.0000	300.0000	300.0000	300.0000	15.000	15.00000
Vapor Frac		0.0	0.0	1.000000	1.000000	0.0	.7127575	1.000000	.3500760	1.000000	00	1.000000	1.000000	00	00	1.0000	0.0
Liquid Frac		1.000000	1.000000	00	0.0	1.000000	.2872425	0.0	.6499240	0.0	1.000000	0.0	00	1.000000	1.000000	00	1.000000
Sol Frac		0.0	0.0	00	0.0	0.0	0.0	0.0	0.0	0.0	00	0.0	00	00	00	00	0.0
Enthalpy	Btu/lbmol	21987.30	22278.98	300.8400	−649.0018	−64339.81	−3120.447	−27208.10	−42131.82	−829.3708	−64379.03	−829.3708	−829.3708	−64379.03	−64379.03	−19266.68	−65257.53
Enthalpy	Btu/lb	281.4784	285.2124	143.7480	− 101.1616	−773.3937	−121.6168	−483.1491	−748.1577	−129.2762	−773.8651	−129.2762	−129.2762	−773.8651	−773.8651	−546.1531	−775.7246
Enthalpy	Btu/hr	2.02591E + 6	2.05279E + 6	85378.37	−48229.76	−3.6731E + 6	−1.5831E + 6	−6.2893E + 6	−9.7390E + 6	−67114.21	−9.6719E + 6	−5480.546	−61633.66	−3.6753E + 6	−5.9966E + 6	−34279.74	−5.9623E + 6
Entropy	Btu/lbmol-R	−60.59916	−60.37874	−5.645173	−7.188212	−141.9280	−30.73357	−74.63910	−94.80521	−7.272376	− 141.9540	−7. −7.272376	−7.272376	−141.9540	−141.9540	−43.77821	−143.2864
Entropy	Btu/lb-R	−.7757820	−.7729603	−2.697389	−1.120445	−1.706039	−1.197815	−1325407	−1.683508	−1.133564	−1.706352	−141.9540	−1.133564	−1.706352	−1.706352	−1.240983	−1.703264
Density	lbmol/cuft	.6866711	*.6832901*	.0531488	.0511041	.5583368	.0735665	.0391540	.1176912	.0477367	.5586660	.0477367	.0477367	.5586660	.5586660	242013	.5556345
Density	lb/cuft	53.63838	53.37428	.1112314	.3278556	46.44889	1.887572	2.204927	6.627673	.3062551	46.47629	.3062551	.3062551	46.47629	46.47629	.08597	46.74254
Average MW		78.11364	78.11364	2.092829	6.415495	83.19154	25.65803	56.31409	56.31409	6.415495	83.19154	6.415495	6.415495	83.19154	83.19154	35.277	84.12461
Liq Vol 60F	Cuft/hr	130.6342	130.6342	243.4758	65.14532	97.85171	537.1024	328.4426	328.4426	70.93813	257.5045	5.792807	65.14532	97.85171	159.6528	2.1059	157.5469

Figure 10.27 Converged results for process streams of the cyclohexane process.

Table 10.5 Net Energy Transfer Rate for the Simulation Units in the Cyclohexane Process

Operation	Net Energy Transfer Rate
R1	4,706,200 Btu/hr out
H1	3,449,700 Btu/hr out
K1	5.268 Bhp
P1	10.56 Bhp
P2	0.880 Bhp

The results in Figure 10.27 and Table 10.5 are used to perform a second-law analysis. The dead-state temperature is taken as 77°F. The calculation of lost work for the entire process and the corresponding second-law efficiency is carried out in Figure 10.28. Note that the availability function for each stream can be computed and printed by ASPEN PLUS. The overall efficiency is only 34.8%. Similar analyses are carried out readily for the separate operations in the process. The fraction of the total lost work for each operation is as follows:

Operation	Percentage of Total Lost Work
Feed pump P1	0.34
Recycle pump P2	0.02
Recycle compressor K1	0.10
Mixer M1—Reactor R1	68.0
Cooler H1—Flash F1	30.7
Flash F2 with valve	0.87
Total	100.00

This table shows clearly that the reactor and cooler are, by far, the largest contributors to the inefficiency of the process. Some reduction in lost work can be achieved by replacing the partial condenser with two or three heat exchangers operating with coolants at different temperature levels. But what can be done with the reactor? Would it be better to operate it at a lower or higher temperature? Should a larger excess of hydrogen be used? Clearly, there is room for considerable improvement in the reactor operation. See Exercise 10.23.

Stream Availabilities

	H 1000s of Btu/hr	S 1000s of Btu/hr	$B = H - T_0S$ 1000s of Btu/hr
S1	2,025.9	−5.583	5,024.3
S3	85.38	−1.602	945.7
S11	−5.48	−0.0481	20.33
S15	−34.30	−0.0779	7.55
S16	−5,962	−13.092	1,068.0

Overall change in stream availability

$1{,}000 \times (-20.33 - 7.55 - 1{,}068 + 5{,}024.2 + 945.7) = -4{,}874.11$ Btu/hr

Shaft Work

	W_S, BHp	W_S, Btu/hr
P1	−10.56	−26,641
P2	−0.88	− 2,220
K1	−5.268	−13,290

Overall addition of shaft work: −26,641 − 2,220 − 13,290 = −42,152 Btu/hr

Heat Transfer

	Q, Btu/hr	$Q \times (1 - T_0/T)$, Btu/hr
R1	4,706,200	1,739,968
H1	3,449,700	0

Overall transfer of heat as equivalent work: 1,739,968 + 0 = 1,739,968 Btu/hr

Lost Work: $-(-4{,}874{,}110) + (42{,}152) - (1{,}739{,}968) = 3{,}176{,}564$ Btu/hr = 1,259 Hp

Thermodynamic Efficiency: $100 \times (4{,}874{,}110 - 3{,}176{,}564)/4{,}874{,}110 = 34.8\%$

Figure 10.28 Second-law analysis of the cyclohexane process. System is overall process with utilities in surroundings. $T_0 = 537$°R(77°F).

10.10 SUMMARY

Having studied this chapter, the reader should:

1. Know the differences between and the limitations of the first and second laws of thermodynamics.
2. Understand the concepts of the irreversible change in entropy and lost work or exergy.
3. Be able to use a process simulator to compute lost work and second-law efficiency.
4. Be able to pinpoint major causes of lost work in a process and determine ways to improve the efficient use of energy.

REFERENCES

1. Borgnakke, C., and R. E. Sonntag, *Fundamentals of Thermodynamics*, 8th ed., Wiley, New York (2013).

2. Felder, R. M., and R. W. Rousseau, *Elementary Principles of Chemical Processes*, 3rd edition, Wiley, New York (2000).

3. Keenan, J. H., "Availability and Irreversibility in Thermodynamics," *British Journal of Applied Physics*, **2**, 183–192 (1951).

4. Rant, Z., Exergie, Ein Neues Wort Fur Technische Arbeitfahrigkeit, *Forschung Ing-Wes*, **22**, 1, 36–37 (1956).

5. Sommerfeld, J. T., "Analysis and Simulation of a Solar-powered Refrigeration Cycle," *Chem. Eng. Educ.*, Winter (2001).

6. Sussman, M. V., *Availability (Exergy) Analysis—A Self Instruction Manual*, Tufts University, Medford, Massachusetts (1980).

EXERCISES

10.1 A stream of hot gases at 1,000°C, having a specific heat of 6.9 cal/mol-°C, is used to preheat air fed to a furnace. Because of insufficient insulation, the hot gas cools to 700°C before it enters the air preheater. How much availability per mole does it lose?

10.2 An ideal gas, with $C_p = 7$ cal/mol-°C, is compressed from 1 to 50 atm while its temperature rises from 25 to 150°C. How much does its availability per mole change?

10.3 Superheated steam at 250 psia and 500°F is compressed to 350 psia. The isentropic efficiency of the compressor is 70%. For the compressor, compute its:

(a) Lost work

(b) Thermodynamic efficiency

10.4 Steam at 400°F, 70 psia, and 100 lb/hr is compressed to 200 psia. The electrical work is 4.1 kW. Determine the:

(a) Lost work

(b) Thermodynamic efficiency

(c) Isentropic efficiency

10.5 The rate of heat transfer between Reservoir A at 200°F and Reservoir B at 180°F is 1,000 Btu/hr.

(a) Compute the lost work.

(b) Adjust the temperature of Reservoir A to 10°F. For the same heat duty and lost work, compute the temperature of Reservoir B. How does the approach temperature, ΔT_{AB}, compare with the original value of 20°F?

10.6 Nitrogen gas at 25°C and 1 atm, with $C_p = 7$ cal/mol-K, is cooled to −100°C at 1 atm. Assuming an ideal gas, calculate the minimum work per mole required for cooling. What is the maximum work per mole that can be obtained when the gas is returned to 25°C and 1 atm?

10.7 An equimolar stream of benzene and toluene at 1,000 lbmol/hr and 100°F is mixed with a toluene stream at 402.3 lbmol/hr and 50°F. Assuming ideal vapor and liquid mixtures, use a process simulator to compute the:

(a) Change of availability upon mixing

(b) Lost work

(c) Thermodynamic efficiency

10.8 Consider the cooler, H2, in the monochlorobenzene separation process in Figures 7.21and 7.22. Assume that the heat is transferred to an infinite reservoir of cooling water at 77°F.

(a) Using the enthalpy and entropy values in the results for the sample problem in the ASPEN PLUS section of the multimedia modules that can be downloaded from www.seas.upenn.edu/∼dlewin/multimedia.html, determine the lost work associated with the cooler.

(b) Let the reservoir be at 100°F and repeat (a).

10.9 Two streams, each containing 0.5 lb/hr steam at 550 psia, are mixed as shown in Figure 10.29:

(a) Compute the heat loss to an environmental reservoir at 77°F.

(b) Compute the lost work and thermodynamic efficiency.

10.10 1,000 lb/hr of saturated water at 600 psia is superheated to 650°F and expanded across a turbine to 200 psia as illustrated in Figure 10.30. Calculate the:

(a) Isentropic efficiency of the turbine

(b) Lost work for the process

(c) Thermodynamic efficiency of the process

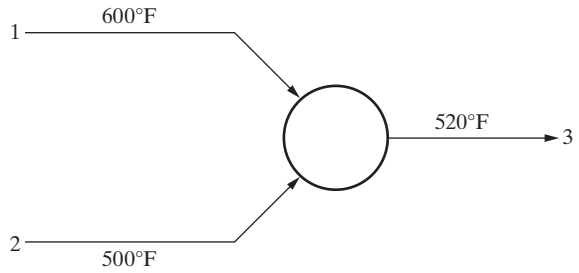

Figure 10.29 Two-stream mixer.

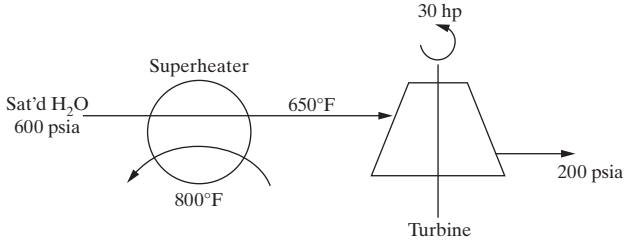

Figure 10.30 Superheater and turbine.

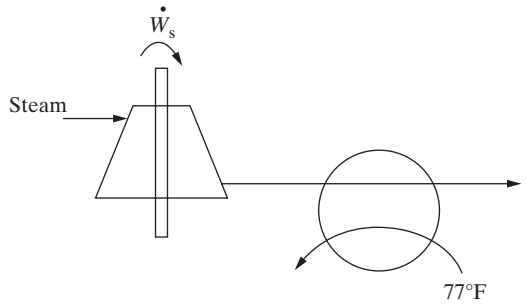

Figure 10.31 Turbine and cooler.

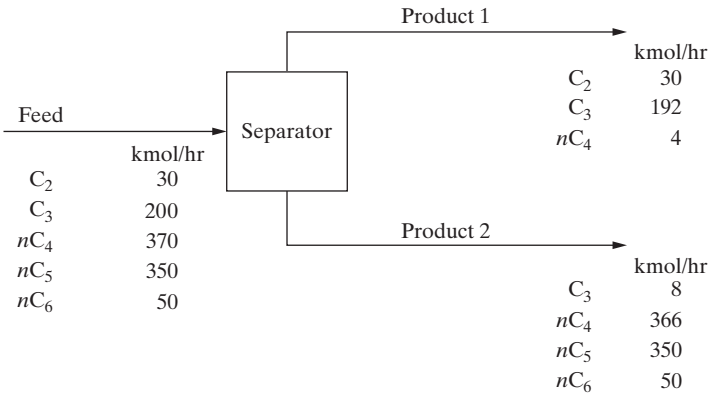

Figure 10.32 Separator.

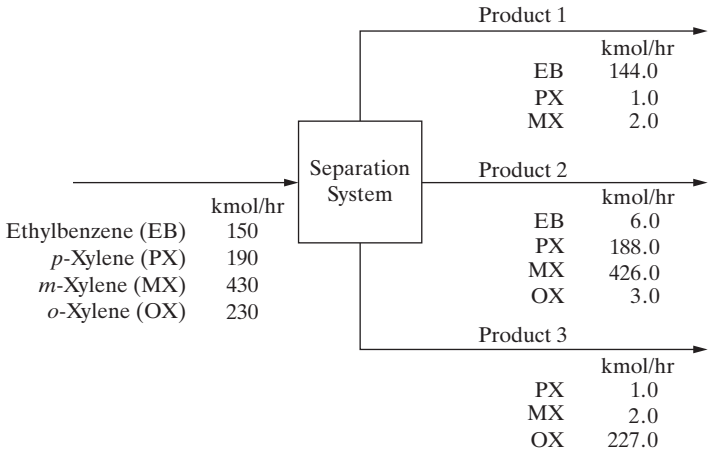

Figure 10.33 Separation system.

10.11 Superheated steam at 580°F and 500 psia is expanded across a turbine, as shown in Figure 10.31, to 540°F and 400 psia. 0.9 kW of shaft work is produced. The turbine exhaust is cooled by a 77°F reservoir to its dew point at 400 psia.

Determine the:

(a) Flowrate of steam in lb/hr

(b) Isentropic efficiency of the turbine

(c) Lost work

(d) Thermodynamic efficiency

10.12 Calculate the minimum rate of work in watts for the gaseous separation at ambient conditions indicated in Figure 10.32.

10.13 Calculate the minimum rate of work in watts for the gaseous separation at ambient conditions of the feed into the three products shown in Figure 10.33.

10.14 For the adiabatic flash operation shown in Figure 10.34, calculate the following:

(a) Change in availability function ($T_0 = 100$°F)

(b) (b) Lost work

(c) Thermodynamic efficiency

10.15 Consider the results of an ASPEN PLUS simulation of the flash vessel in Figure 10.35:

Heat is obtained from a large reservoir at 150°F. Calculate the following:

(a) Rate of heat addition

(b) Lost work

(c) Thermodynamic efficiency

10.16 A partial condenser operates as shown in Figure 10.36. Assuming that $T_0 = 70$°F, calculate the following:

(a) Condenser duty

(b) Change in availability function

(c) Lost work

(d) Thermodynamic efficiency

10.17 A light-hydrocarbon mixture is to be separated by distillation as shown in Figure 10.37 into ethane-rich and propane-rich fractions. Based on the specifications given and use of the Soave-Redlich-Kwong equation for thermodynamic properties, use ASPEN PLUS with the RADFRAC distillation model to simulate the column operation. Using the results of the simulation with $T_0 = 80$°F, a condenser refrigerant temperature of 0°F, and a reboiler steam temperature of 250°F, calculate the following:

(a) Irreversible production of entropy, Btu/hr-°R

(b) Change in availability function in Btu/hr

(c) Lost work in Btu/hr, kW, and Hp

(d) Thermodynamic efficiency

10.18 A mixture of three hydrocarbons is to be separated into three nearly pure products by thermally coupled distillation at 1 atm as shown in Figure 10.38.

Based on the specifications given and other specifications of your choice to achieve reasonably good separations, together with use of the Peng-Robinson equation for thermodynamic properties, use ASPEN PLUS with the MULTIFRAC distillation model to simulate the column. Using the results of the simulation with $T_0 = 100$°F, calculate the following:

(a) Irreversible production of entropy, Btu/hr-°R

(b) Change in availability function in Btu/hr

(c) Lost work in Btu/hr, kW, and Hp

(d) Thermodynamic efficiency

10.19 Consider the hypothetical perfect separation of a mixture of ethylene and ethane into pure products by distillation as shown in Figure 10.39.

Two schemes are to be considered: conventional distillation and distillation using a heat pump with reboiler liquid flashing. In both cases, the column will operate at a pressure of 200 psia, at which the average relative volatility is 1.55. A reflux ratio of 1.10 times minimum, as computed from the Underwood equation, is to be used. Other conditions

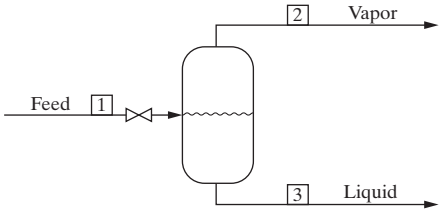

	Flow Rate, lbmol/hr		
	Stream 1	**Stream 2**	**Stream 3**
H_2	0.98	0.95	0.03
N_2	0.22	0.21	0.01
Benzene	0.08	0.00	0.08
Cyclohexane	91.92	0.69	91.23
	Stream 1	**Stream 2**	**Stream 3**
Temperature, °F	120	119.9	119.9
Pressure, psia	300	15	15
Enthalpy, 1,000 Btu/hr	–3,642.05	–14.27	–3,627.78
Entropy, 1,000 Btu/hr-°R	4.920	0.094	4.860

Figure 10.34 Adiabatic flash separator.

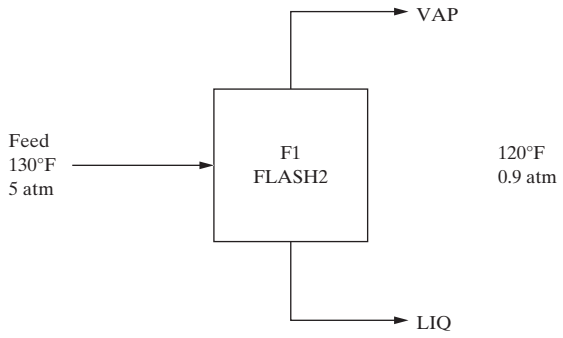

STREAM ID	FEED	LIQ	VAP
FROM :	-------	F1	F1
TO :	F1	-------	-------
SUBSTREAM: MIXED			
PHASE:	LIQUID	LIQUID	LIQUID
COMPONENTS: LBMOL/HR			
C5H12–1	0.5000	0.2168	0.2832
C6H14–1	0.5000	0.3471	0.1528
TOTAL FLOW:			
LBMOL/HR	1.0000	0.5639	0.4360
LB/HR	79.1645	45.5578	33.6067
CUFT/HR	2.0847	1.1807	205.0349
STATE VARIABLES:			
TEMP F	130.0000	120.0000	120.0000
PRES PSI	73.5000	13.2300	13.2300
VFRAC	0.0	0.0	1.0000
LFRAC	1.0000	1.0000	0.0
SFRAC	0.0	0.0	0.0
ENTHALPY:			
BTU/LBMOL	–7.7433+04	–7.9182+04	–6.4768+04
BTU/LB	–978.1301	–980.1487	–840.4011
BTU/HR	–7.7433+04	–4.4653+04	–2.8243+04
ENTROPY:			
BTU/LBMOL–R	–137.7615	–141.4483	–114.8608
BTU/LB–R	–1.7401	–1.7509	–1.4903
DENSITY:			
LBMOL/CUFT	0.4796	0.4776	2.1268–03
LB/CUFT	37.9725	38.5848	0.1639
AVG MW	79.1645	80.7854	77.0682

Figure 10.35 Flash separator.

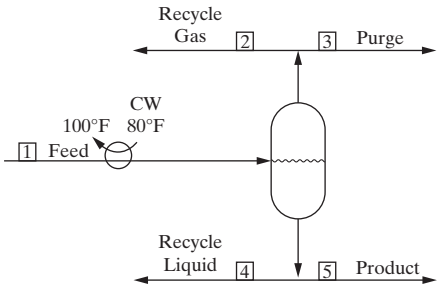

	Flow Rate, lbmol/hr				
	Stream 1	**Stream 2**	**Stream 3**	**Stream 4**	**Stream 5**
H_2	72.53	65.15	5.80	0.60	0.98
N_2	7.98	7.01	0.62	0.13	0.22
Benzene	0.13	0.00	0.00	0.05	0.08
Cyclohexane	150.00	1.61	0.14	56.33	91.92
	Stream 1	**Stream 2**	**Stream 3**	**Stream 4**	**Stream 5**
Temperature, °F	392	120	120	120	120
Pressure, psia	315	300	300	300	300
Enthalpy, 1,000 Btu/hr	–2,303.29	241.76	21.61	–2,231.84	–3,642.05
Entropy, 1,000 Btu/hr-°R	14.68	2.13	0.19	3.02	4.92

Figure 10.36 Partial Condenser.

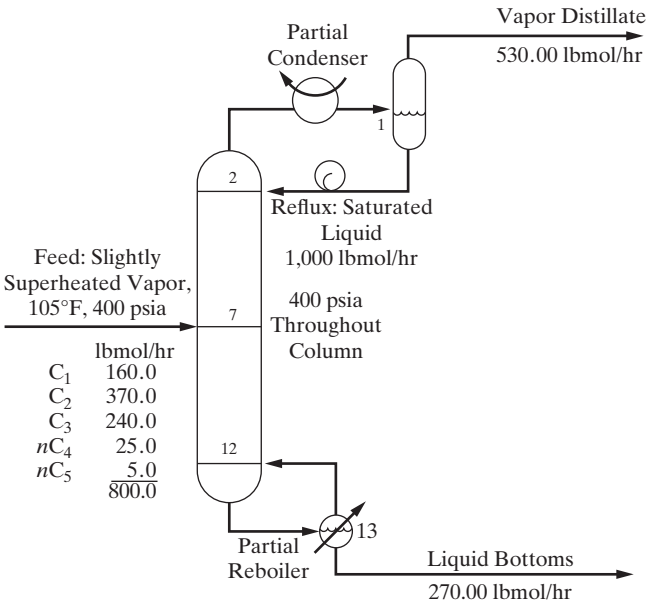

Figure 10.37 Distillation process for Exercise 10.17.

for the scheme using reboiler liquid flashing follow. Calculate the following for each scheme:

(a) Change in availability function ($T_0 = 100°F$)

(b) Lost work

(c) Thermodynamic efficiency

Other thermodynamic data are:

	Latent Heat of Vaporization (Btu/lbmol)
Ethylene at 200 psia	4,348
Ethane at 200 psia	4,751
Ethane at 90 psia	5.473

10.20 Consider a steam engine that operates in a Rankine cycle as shown in Figure 10.40:

The turbine exhaust is a saturated vapor.

(a) Find the saturation temperature of the turbine exhaust.

(b) For an isentropic efficiency of 90%, determine the shaft work delivered by the turbine. What is the temperature of the feed to the turbine?

(c) Compute the lost work for the turbine.

(d) Compute the thermodynamic efficiency for the turbine.

10.21 A reactor is to be designed for the oxidation of sulfur dioxide, with excess oxygen from air, to sulfur trioxide. The entering feed, at 550 K and 1.1 bar, consists of 0.219 kmol/s of nitrogen, 0.058 kmol/s of oxygen, and 0.028 kmol/s of sulfur dioxide. The fractional conversion of sulfur dioxide is 50%. The reaction is very exothermic. Three cases are to be considered:

(a) Adiabatic reaction

(b) Isothermal reaction with the heat of reaction transferred to boiler feed water at 100°C

(c) Isothermal reaction with the heat of reaction transferred to boiler feed water at 200°C

For each case, compute the lost work in kW.

10.22 For the revised propane refrigeration cycle in Figure 10.21 (Example 10.3), let the isentropic efficiencies of the turbine and compressor be 0.9 and 0.7, respectively. Compute the following:

(a) Lost work for the four process units and the entire cycle.

(b) Thermodynamic efficiency of the cycle.

10.23 Alter the design of the cyclohexane process in Example 10.5 to reduce the lost work and increase the thermodynamic efficiency. Use a simulation program to complete the material and energy balances, and compute the entropies and availability functions for all of the streams as well as the lost work for each piece of equipment.

10.24 The chilled-water plant at the University of Pennsylvania sends chilled water to the buildings at 42°F and receives warmed water at 55°F. A refrigerant is vaporized in the refrigerant condenser at 38°F as it removes heat from warmed water. The refrigerant is condensed to

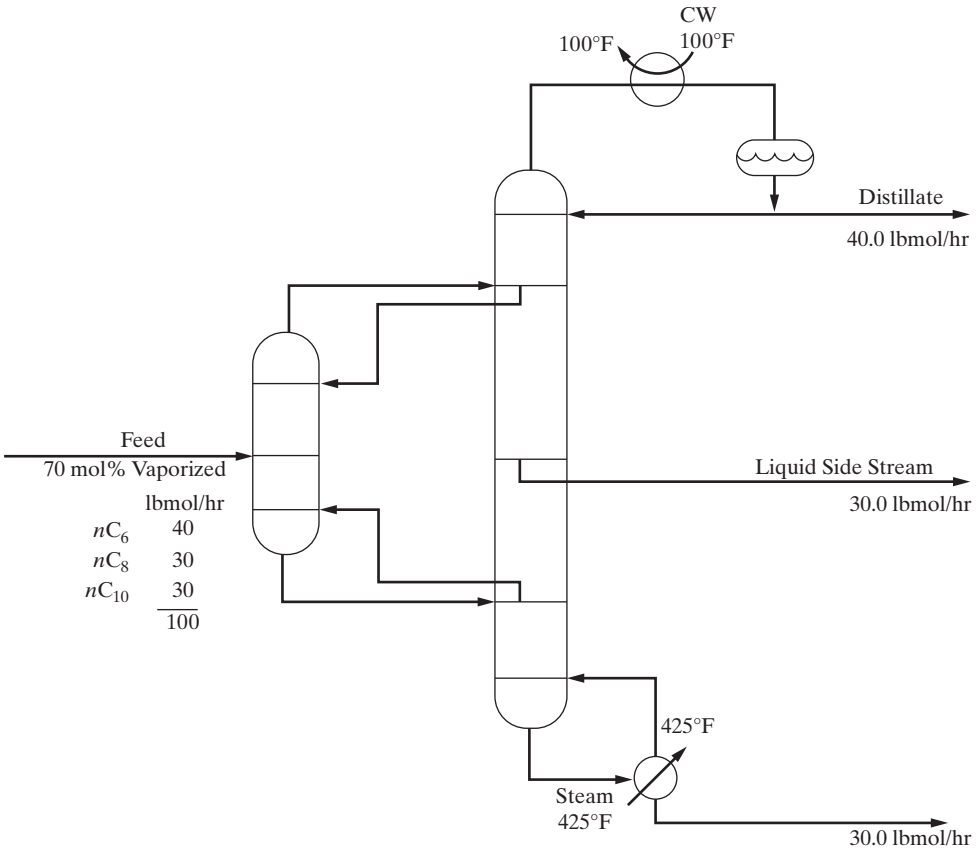

Figure 10.38 Thermally coupled distillation process for Exercise 10.18.

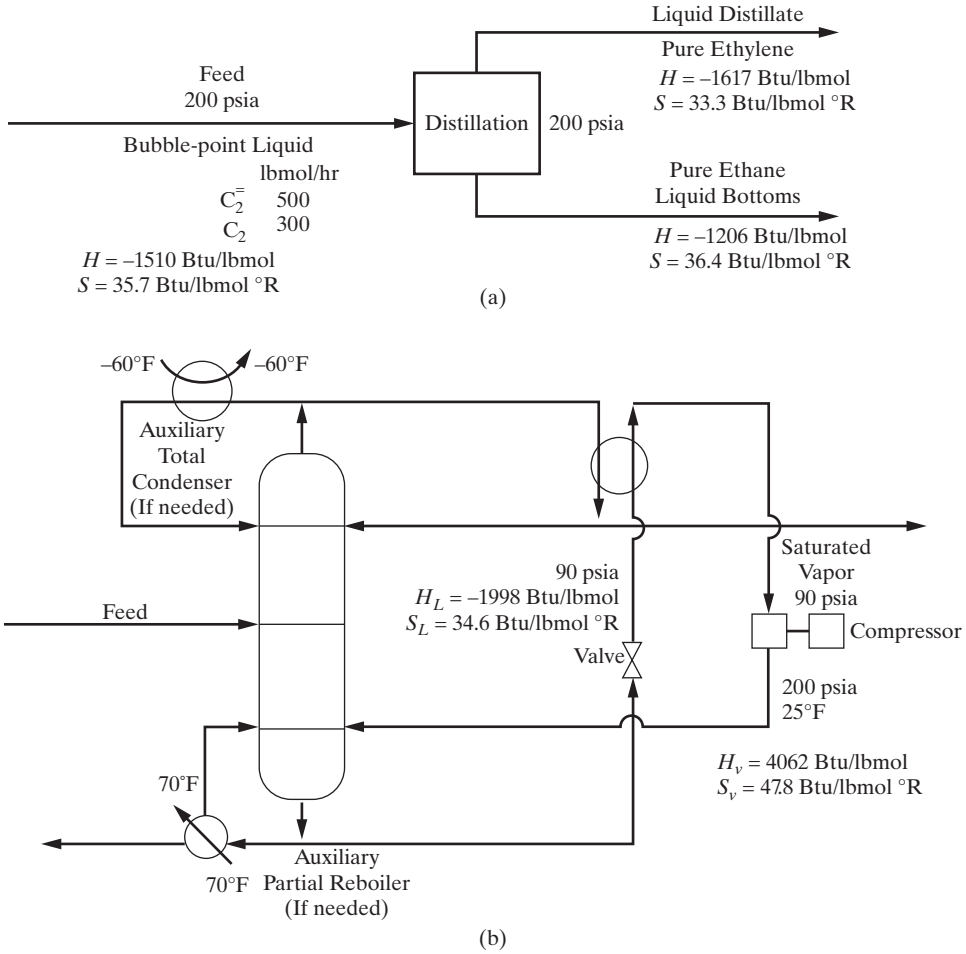

Figure 10.39 Distillation process and data for Exercise 10.19: (a) distillation; (b) reboiler.

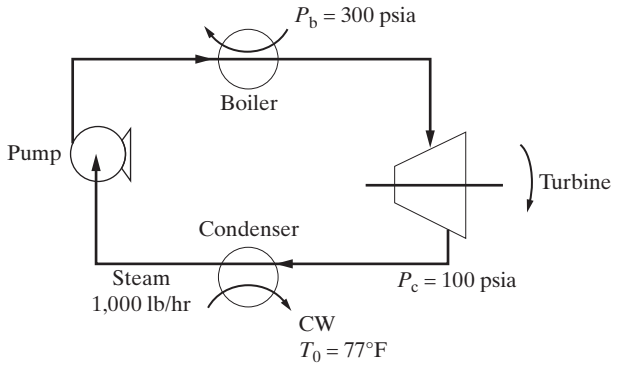

Figure 10.40 Rankine Cycle.

a saturated liquid at 98°F. The condensing medium is water at 85°F, which is heated to 95°F as it absorbs heat rejected from the refrigerant. The warmed condenser water is cooled in a cooling tower in which it is sprayed over a stream containing ambient air. Assume that the ambient air is at 100°F and 95% humidity on a hot summer day and is rejected at 100% humidity. For Phase I of the plant, the cooling capacity is 20,000 tons.

(a) Calculate the flow rates of the chilled water and condenser water in gal/min.

(b) Select a refrigerant and its operating pressures. Assuming an isentropic efficiency of 70% for the compressor, determine the refrigerant flow rate and the brake horsepower for the compressor.

(c) Calculate the lost work and thermodynamic efficiency.

10.25 Consider the solar or waste-heat refrigeration cycle in Figure 10.41, which was proposed by Sommerfeld (2001). In addition to the conventional refrigeration loop, a portion of the condensate is pumped to an elevated pressure, where it is vaporized using solar energy or low-temperature waste energy in a chemical complex. Its saturated vapor effluent is expanded to recover power in a turbine and mixed with the gases from the compressor.

Use a process simulator to solve the material and energy balances for the following specifications:

R-134a refrigerant

4-ton refrigeration load at 20°F

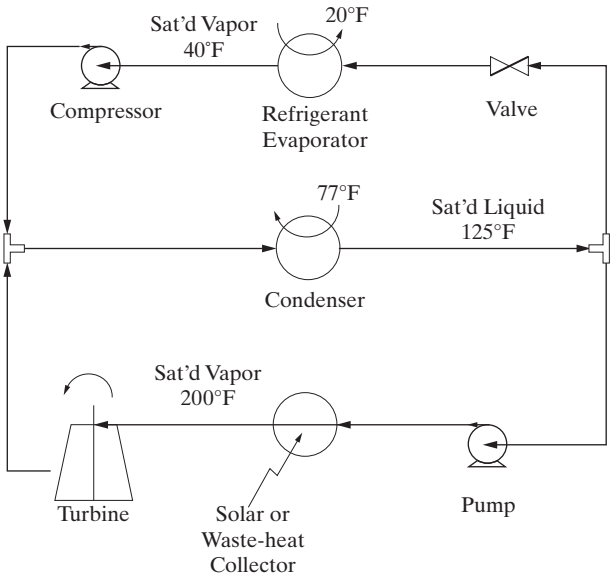

Figure 10.41 Solar or waste-heat refrigeration cycle.

Refrigerant evaporator effluent-saturated vapor at 40°F

Condenser heat rejected to environment at 77°F

Condenser effluent-saturated liquid at 125°F

Solar or waste-heat available at 220°F

Solar or waste-heat collector effluent-saturated vapor at 200°F

Isentropic efficiency of the compressor = 70%

Isentropic efficiency of the turbine = 90%

Isentropic efficiency of the pump = 100%

(a) Determine the flow rates of refrigerant in both loops; the three operating pressures; the condenser and collector heat duties; the power consumed or generated by the compressor, pump, and turbine; and the coefficient of performance, lost work, and thermodynamic efficiency for the refrigerator.

(b) Vary the condenser effluent temperature to determine its effect on the solution in (a).

Chapter 11

Heat and Power Integration

11.0 OBJECTIVES

This chapter introduces several *algorithmic* approaches that have been developed for process integration to satisfy the cooling, heating, and power demands of a process. After studying this material, the reader should:

1. Be able to determine minimum energy requirement (MER) targets, that is, to compute the minimum usage of heating and cooling utilities when exchanging heat between the hot and cold streams in a process.
2. Be able to design a network to meet the MER targets, that is, to position heat exchangers in a network, assuming overall heat transfer coefficients. This is accomplished using a unit-by-unit method beginning at the closest-approach temperature difference (the *pinch*).
3. Be able to reduce the number of heat exchangers in MER networks by relaxing the MER target and *breaking the heat loops* (i.e., allowing heat to flow across the pinch) or by employing *stream splitting*.
4. Be able to design a network when the minimum approach temperature is below a threshold value at which either heating or cooling utility is used but not both.
5. Understand the importance of the specified minimum approach temperature difference on the design of a heat exchanger network (HEN).
6. Be able to use the grand composite curve to assist in the selection and positioning of appropriate types of hot and cold utilities in the network.
7. Be able to use the grand composite curve to optimally position reactors and distillation columns to minimize usage of hot and cold utilities in the network.
8. Be able to apply several approaches to designing energy-efficient distillation trains, including the adjustment of tower pressure, multiple-effect distillation, heat pumping, vapor recompression, and reboiler flashing.
9. Know how to correctly position *heat engines* and *heat pumps*, to reduce the demand for heating and cooling using utilities.

11.1 INTRODUCTION

At the start of the task-integration step in process synthesis, the source and target temperatures, T^s and T^t, and power demands for pumping and compression of all streams are known. Heat and power integration seeks to utilize the energy in the high-temperature streams that need to be cooled and/or condensed to heat and/or vaporize the cold streams and provide power to compressors from turbines and heat engines where possible. In most designs, it is common initially to disregard power demands in favor of designing an effective network of heat exchangers by heat integration without using the energy of the high-temperature streams to produce power. To accomplish this, N_H hot process streams with specified source and target temperatures $T^s_{h,i}$ and $T^t_{h,i}$, $i = 1, \ldots, N_H$ are cooled by N_C cold process streams with specified source and target temperatures, $T^s_{c,i}$ and $T^t_{c,i}$, $i = 1, \ldots, N_C$, as shown schematically in Figure 11.1a. When (1) the sum of the heating requirements does not equal the sum of the cooling requirements, (2) some source temperatures may be insufficiently high or low to achieve some target temperatures through heat exchange, or (3) other restrictions exist, as discussed in Section 11.2, it is always necessary to provide one or more auxiliary heat exchangers for heating or cooling through the use of utilities such as steam and cooling water. Furthermore, it is common to refer to the heat exchangers between the hot and cold process streams as comprising the *interior network*, and those between the hot or cold streams and the utilities as comprising the *auxiliary network* as shown schematically in Figure 11.1b.

Since it is assumed that the stream heat capacities are con stant, each stream can be represented on a temperature-enthalpy diagram as a directed linear graph as illustrated in Figure 11.2. Noting that the heat-capacity flow rate, C, is defined for each stream as the product of its flow rate and specific heat capacity, $C = \dot{m}C_p$, then for each stream, $C = \Delta H/\Delta T$, and clearly the gradient of a stream trajectory on the temperature-enthalpy diagram is inversely proportional to C. By convention, hot streams will be represented as graphs from left to right, whereas cold streams will be indicated by directed graphs from right to left.

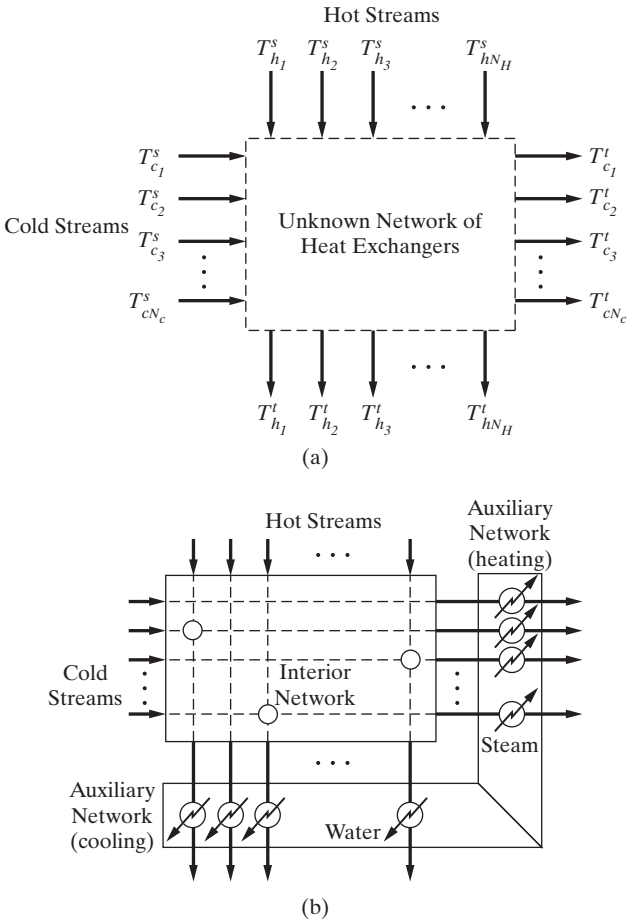

Figure 11.1 Heat-integration schematics: (a) source and target temperatures for heat integration; (b) interior and auxiliary networks of heat exchangers.

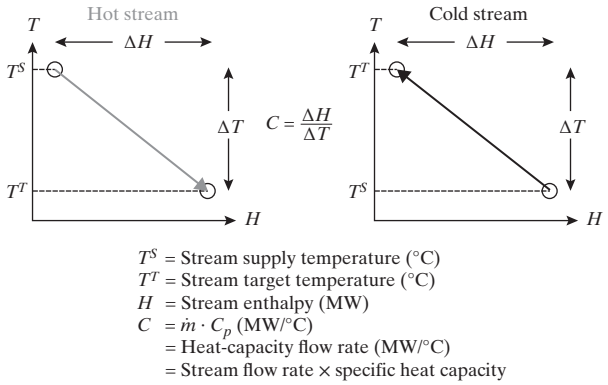

Figure 11.2 Hot and cold streams on temperature-enthalpy diagrams.

The temperature trajectories of the hot- and cold-side streams in a countercurrent heat exchanger can also be represented on temperature-enthalpy diagrams as shown in Figure 11.3. The figure presents two countercurrent heat exchangers in both of which a hot stream, whose temperature is reduced from 100 to 60°C, exchanges heat with a cold stream that is to be heated from

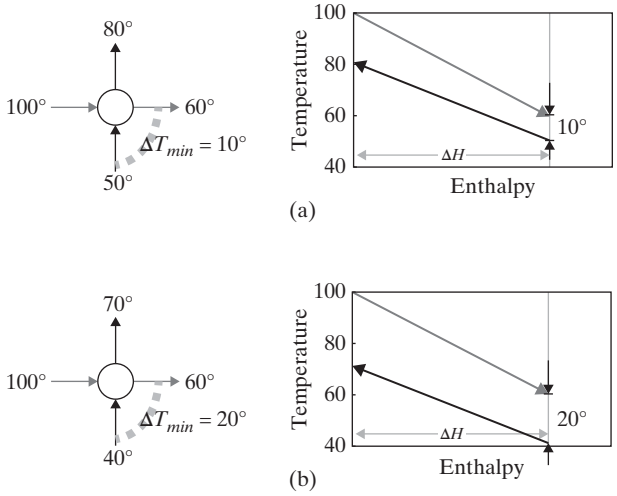

Figure 11.3 Heat exchangers on temperature-enthalpy diagrams for two heat exchangers with different values of ΔT_{min}.

50 to 80°C in case (a) and a cold stream is heated from 40 to 70°C, in case (b). Since all of the heat transferred occurs in the heat exchangers, the hot-side trajectory is positioned vertically above the cold-side trajectory in each of the corresponding enthalpy-temperature diagrams. Furthermore, since the temperature trajectories are linear, the minimum approach temperature, ΔT_{min}, occurs either on the left-hand side (the hot end) if $C_c < C_h$ or on the right-hand side (the cold end) if $C_c > C_h$ as is the case in this example.

The selection of the minimum approach temperature, ΔT_{min}, for the heat exchangers is a key design variable in the synthesis of HENs because of its impact on lost work associated with heat transfer. Consider the heat transfer between the high- and low-temperature reservoirs in Figure 11.4. Equation (10.27), which is the result of combining the first and second laws of thermodynamics for the general process in Figure 10.18, can be simplified to eliminate the term involving the flowing streams, the work term, and the term for unsteady operation to give

$$LW = \left(1 - \frac{T_0}{T_1}\right) Q + \left(1 - \frac{T_0}{T_2}\right)(-Q) \tag{11.1a}$$

$$= QT_0 \frac{\Delta T}{T_1 T_2} \tag{11.1b}$$

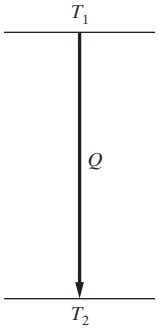

Figure 11.4 Heat exchanger between two reservoirs.

where LW is the rate of lost work, and T_0 is the absolute temperature of the environment. Note that a simpler notation suffices in Chapter 10 in which all analysis is in the steady state; hence, $LW \equiv L\dot{W}$, $Q \equiv \dot{Q}$, and $m \equiv \dot{m}$. It can be seen that, for a given rate of heat transfer and a given ΔT approach, the rate of lost work increases almost inversely with the decrease in the square of the absolute temperature level. Thus, as the temperature levels move lower into the cryogenic region, the approach temperature difference, ΔT_{min}, must decrease approximately as the square of the temperature level to maintain the same rate of lost work. This explains the need to use very small approach temperature differences on the order of 1°C in the cold boxes of cryogenic processes. If the approach temperature differences were not reduced, the large increases in the rate of lost work would sharply increase the energy requirements to operate these processes, especially the operating and installation costs for compressors.

When designing a heat-integrated system, the imposition of a desired value of ΔT_{min} generally affects the quantities of utility heating and cooling required. Figure 11.5a shows the process flow and temperature-enthalpy diagrams for the first heat exchanger introduced in Figure 11.3 in which the minimum approach temperature is $\Delta T_{min} = 10$°C. In this case, the heat required by the cold stream, ΔH, is provided in full by heat transfer from the hot stream with no utility heating or cooling needed. However, if the design is required to satisfy $\Delta T_{min} \geq 20$°C, the cold end of the heat exchanger in design (a) now violates this requirement, and the only way to comply would be to increase the effluent temperature of the hot stream from 60 to 70°C, thus reducing the duty in the heat exchanger by 25%. The reduced amount of heat thus transferred from the hot to the cold stream is offset by utilities: The hot stream is cooled from 70 to 60°C by a cooler, and the cold stream is heated from 67.5 to 80°C by a heater. These changes are indicated in the temperature-enthalpy diagram

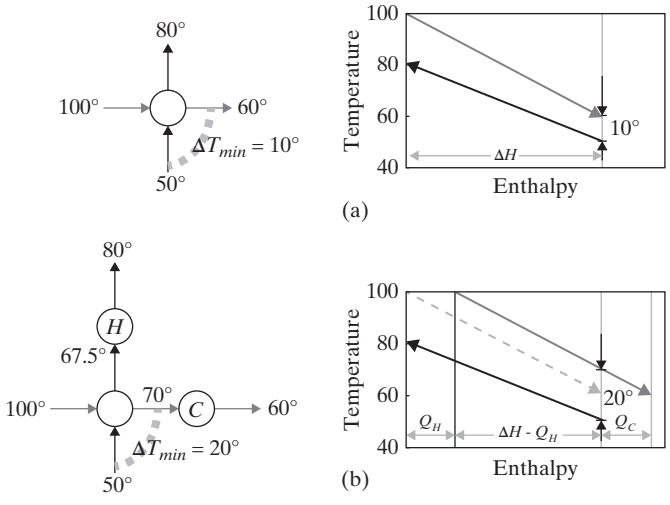

Figure 11.5 Designing a simple network to meet $\Delta T_{min} \geq 20$°C: (a) Design involving a single heat-exchanger for $\Delta T_{min} = 10$°C; (b) Modified network for $\Delta T_{min} = 20$°C, involving one heat-exchanger, one heater and one cooler.

by shifting the two trajectories relative to one other. Arbitrarily, the figure shows a shift in the hot stream to the right until the two trajectories are separated by 20°C, the minimally acceptable value of ΔT_{min}, at the right-hand side of the cold-side trajectory. The shift in enthalpy imposed on the hot trajectory, Q_h, is the required duty of the new heater, and for this example where the heating and cooling demands are equal, Q_h also equals Q_c, the required duty of the new cooler. In this example, these external duties are equal to 25% of the duty demanded by two process streams, with the heat transferred between the two process streams reduced to the remaining 75% ($\Delta H - Q_h = \Delta H - Q_c = 0.75\Delta H$), corresponding to the portion of the hot stream temperature trajectory that remains aligned vertically above the cold stream trajectory.

When carrying out the design given the states of the source and target streams (flow rates of the species, temperature, pressure, and phase), it is desired to synthesize the most economical network of heat exchangers. Several measures of economic goodness are possible as discussed in Section 17.4. Usually, when generating and comparing alternative flowsheets, an approximate profitability measure is sufficient such as the annualized cost:

$$C_A = i_m(C_{TCI}) + C \tag{11.2}$$

where C_{TCI} is the total capital investment as defined in Table 16.9, i_m is a reasonable return on investment annually (e.g., when $i_m = 0.33$, a chemical company charges itself annually for one-third of the cost of the capital invested), and C is the annual cost of sales as defined in the *cost sheet* of Table 17.1. In Tables 16.9 and 17.1, many factors are involved, most of which are necessary for a detailed profitability analysis. However, to estimate an approximate profitability measure for the comparison of alternative flowsheets, it is adequate to approximate C_{TCI} as the sum of the purchase costs for each of the heat exchangers (without including installation costs and other capital investment costs). The purchase costs can be estimated based on the area for heat transfer, A, estimated from the heat transfer rate equation discussed in Section 12.2 [Eq. (12.7)]:

$$A = Q/(U\, F_T \Delta T_{LM}) \tag{11.3}$$

where Q is the heat duty, U is the overall heat transfer coefficient, F_T is the correction factor for a multiple-pass exchanger, and ΔT_{LM} is the log-mean temperature-driving force for countercurrent flow based on the approach-temperature differences at the two ends. Equation (11.3) must be used with care because of its restrictions as discussed in Chapter 12. If both a phase change and a significant temperature change occur for one or both streams, U is not constant and a ΔT_{LM} is not appropriate. Furthermore, multiple-pass exchangers may be required for which F_T is in the range 0.75–0.9. Nevertheless, to develop a reasonably optimal heat exchanger network, it is common to apply Eq.(11.3) with $F_T = 1.0$. It is adequate to approximate C as the annual cost of the utilities for heating and cooling, typically using steam and

cooling water. In summary, with these approximations, Eq. (11.2) is rewritten as

$$C_A = i_m \left[\sum_i C_{P,I,i} + \sum_i C_{P,A,i} \right] + sF_s + (cw)F_{cw} \qquad (11.4)$$

where $C_{P,I,i}$ and $C_{P,A,i}$ are the purchase costs of the heat exchangers in the interior and auxiliary networks, respectively, F_s is the annual flow rate of steam (e.g., in kilograms per year), s is the unit cost of steam (e.g., in dollars per kilogram), F_{cw} is the annual flow rate of cooling water, and cw is the unit cost of cooling water. Clearly, when other utilities, such as fuel, cool air, boiler feed water, and refrigerants, are used, additional terms are needed.

Many approaches have been developed to optimize Eq. (11.4) and similar profitability measures, several of which are presented in this chapter. Probably the most widely used, an approach developed immediately after the Arab oil embargo in 1973, which triggered a global energy crisis, utilizes a two-step procedure:

Step 1: A network of heat exchangers is designed having the *minimum usage of utilities* (that is, an MER network), usually requiring a large number of heat exchangers. However, when the cost of fuel is extremely high, as it was in the late 1970s and early 2010s, a nearly optimal design is obtained.

Step 2: The number of heat exchangers is reduced toward the minimum, possibly at the expense of increasing the consumption of utilities.

Clearly, as step 2 is implemented one heat exchanger at a time, capital costs are reduced due to the economy of scale in equations of the form:

$$C_P = K \cdot A^n \qquad (11.5)$$

where K is a constant and n is less than unity, typically 0.6. As each heat exchanger is removed with the total area for heat transfer approximately constant, the area of each of the remaining heat exchangers is increased, and because $n < 1$, the purchase cost per unit of area is decreased. In addition, as step 2 is implemented, the consumption of utilities is normally increased. At some point, the increased cost of utilities overrides the decreased cost of capital and C_A increases beyond the minimum. When the cost of fuel is high, the minimum C_A is not far from that for a network of heat exchangers using the minimum utilities.

11.2 MINIMUM UTILITY TARGETS

A principal objective in the synthesis of HENs is the efficient utilization of energy in the hot process streams to heat cold process streams. Thus, it is desirable to compute the MER before synthesizing the HEN, that is, to determine the minimum hot and cold utilities in the network given the heating and cooling requirements of the process streams. This important first step is referred to as *MER targeting* and is useful in that it determines the utility requirements for the most thermodynamically efficient network. To introduce this targeting step, an example involving only sensible heat is introduced. Later, examples are presented that also involve the latent heat of phase change and the heat of reaction under either isothermal or nonisothermal conditions.

EXAMPLE 11.1 ***A Typical Heat-integration Problem***

Figure 11.6 shows a typical heat integration problem specified in terms of a process flowsheet, that is, a table of stream data, composed of source and target temperatures, the required enthalpy changes in each stream, and the heat-capacity flow rates of each stream. As can be seen in the figure, there are two hot streams: H1, the hot effluent of reactor R-1 that needs to be cooled from 180°C to 80°C, removing 100 kW (C = 1 kW/°C); and H2, the bottoms stream of column C-1 that needs to be cooled from 130°C to 40°C, removing 180 kW (C = 2 kW/°C); and two cold streams: C1, the distillate stream of column C-1, that needs to be heated from 60°C to 100°C, receiving 160 kW (C = 4 kW/°C), and C2, the feed stream of reactor R-1, that needs to be heated from 30°C to 120°C, receiving 162 kW (C = 1.8 kW/°C). The figure also indicates that a heat-integrated solution is desired for this process with a minimum

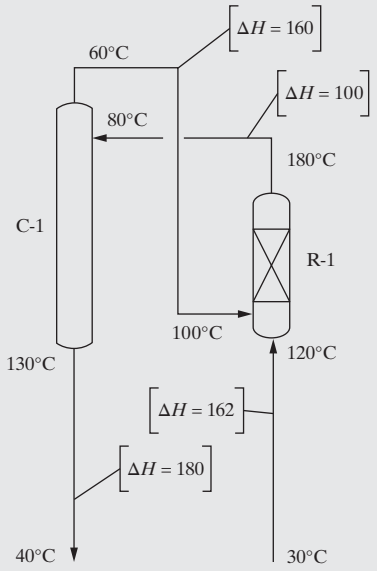

$\Delta T_{min} = 10°C$

Stream	T^S (°C)	T^T (°C)	ΔH (kW)	C (kW/°C)
H1	180	80	100	1.0
H2	130	40	180	2.0
C1	60	100	160	4.0
C2	30	120	162	1.8

Utilities. Stream@150°C, cw@25°C

Design a network of steam heaters, water coolers, and exchangers for the process streams. Where possible, use exchangers in preference to utilities.

Figure 11.6 Typical heat integration problem.

temperature difference of $\Delta T_{min} = 10°C$ and that the two utilities that are available are cooling water at 25°C and steam at 150°C. The solution to this problem consists of a heat exchanger network, that is, the optimum arrangement of heat exchangers in the interior and auxiliary networks and their heat transfer duties.

SOLUTION

For this system, a total of 280 kW must be removed from the two hot streams compared with a total of 322 kW that is demanded by the two cold streams. Hence, from the first law of thermodynamics, a minimum of 42 kW must be supplied by steam. As will be shown, this is the lower limit on the minimum utility usage, which, from the second law of thermodynamics, depends on ΔT_{min}. Figure 11.7 shows a possible solution to the problem, composed of an interior network of two heat exchangers and an auxiliary network involving one cooler and one heater. The two interior-network heat exchangers are a unit transferring 100 kW from stream H1 to stream C1 and a second unit transferring 162 kW from stream H2 to stream C2. The two auxiliary units are a 60 kW heater using utility steam to provide the remaining duty to stream C1 not acquired from stream H1 and an 18 kW cooler using cooling water utility to provide the additional cooling duty required by stream H2 not provided by stream C2. Note that the *difference* between the hot and cold utility duties equals that given by the first law of thermodynamics.

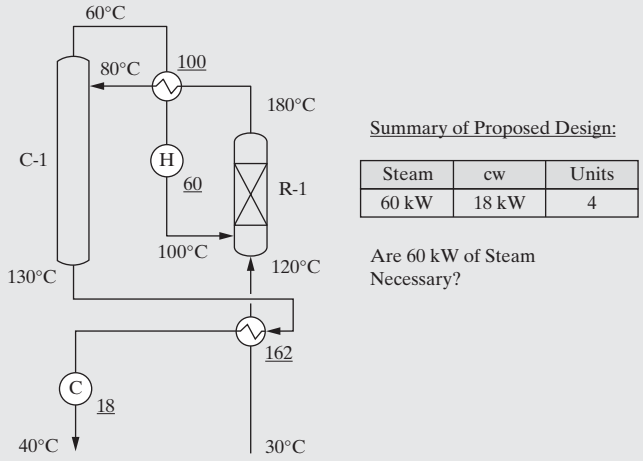

Figure 11.7 Summary of proposed solution to the heat integration problem.

Since the design of this HEN has neither considered the MER targets nor utilized procedures for optimal HEN synthesis, its assessment focuses on two questions: (1) How do the heating and cooling utility duties of 60 and 18 kW compare with the MER targets? and (2) is it possible to synthesize a HEN with fewer than the four heat exchangers used here, and if so, what are its utility requirements? In this section, the first of these two questions is addressed with the second, which usually involves higher utility costs and decreased capital costs, postponed until later. Two methods are introduced to estimate MER targets: (1) a graphical method using *composite heating and cooling* curves to be defined and (2) the temperature-interval method. It is also possible to compute MER targets from the solution of a suitably formulated linear program, as described in the supplementary materials that accompany this chapter.

Composite Curve Method

The usage of temperature-enthalpy diagrams to represent trajectories in a single heat exchanger has been demonstrated in the previous section. The Composite Curve method, introduced by Umeda et al. (1978), is an extension of the same representation but used to compute MER targets for a network of several process streams. The method involves the following steps:

Step 1: Generate the *hot composite curve*, which is a temperature-enthalpy trajectory representing the enthalpy availability from all of the hot streams in the process, as a function of temperature.

Step 2: Generate the *cold composite curve*, the temperature-enthalpy trajectory representing the enthalpy demand by all of the cold streams in the process, as a function of temperature.

Step 3: Given that the absolute value of enthalpy on the ordinate is arbitrary, displace the two composite curves relative to each other by an amount of enthalpy necessary to ensure the required minimum temperature approach, ΔT_{min}. This step is equivalent to the manipulation demonstrated for a single heat exchanger in Figure 11.5.

Step 4: Once the hot and cold composite curves are aligned to satisfy the required value of ΔT_{min}, one can identify the MER target attributes directly from the enthalpy-temperature diagram, namely, the minimum amounts of utility heating and cooling duties, Q_{Hmin} and Q_{Cmin}, respectively, and the hot and cold pinch temperatures, T_H^{pinch} and T_C^{pinch}.

EXAMPLE 11.2 ***A Typical Heat-integration Problem (Example 11.1 Revisited)***

In this example, the minimum utility requirements for a HEN involving the four streams in Example 11.1 are determined for $\Delta T_{min} = 10°C$ using the Composite Curve method.

SOLUTION

To generate hot and cold composite curves, one must first identify the temperature intervals, that is, a rank-ordered list of all of the source and target temperatures starting with the highest temperature with hot and cold streams treated separately. For example, Table 11.1a shows the analysis of the hot streams. The first interval, Hot-1, begins at 180°C and ends at 130°C, and in this interval, only stream H1 is present, and so the total flowing heat capacity in this interval is that of H1, $C = 1$ kW/°C with the enthalpy available being $\Delta T \times \sum C = 50$ kW. Note that it is helpful to indicate which streams are present in each interval as shown in the incidence columns in the table. Similarly, the second interval, Hot-2, begins at 130°C and ends at 80°C with both H1 and H2 present, and so the total flowing heat capacity in this interval is $\sum C = 3$ kW/°C with the enthalpy available being

Table 11.1a Temperature Intervals and Enthalpy Flows for Cold Streams

Interval	T_{start} (°C)	T_{end} (°C)	ΔT(°C)	H1	H2	ΣC(kW/°C)	ΔH(kW)
Hot-1	180	130	50			1.0	50
Hot-2	130	80	50			3.0	150
Hot-3	80	40	40			2.0	80

Table 11.1b Temperature Intervals and Enthalpy Flows for Cold Streams

Interval	T_{start} (°C)	T_{end} (°C)	ΔT(°C)	C1	C2	ΣC(kW/°C)	ΔH(kW)
Cold-1	120	100	20			1.8	36
Cold-2	100	60	40			5.8	232
Cold-3	60	30	30			1.8	54

$\Delta T \times \sum C = 150$ kW. The last interval includes only H2 between 80°C and 40°C with 80 kW available. The hot composite curve is then drawn as follows, assuming for now, no offset in enthalpy. The first segment of the trajectory begins at the coordinate (0 kW, 180°C), and terminates at (50 kW, 130°C). The next segment begins at the coordinate (50 kW, 130°C), and using the computed results in Table 11.1a, ends at the coordinate (200 kW, 80°C). The last segment is the line from (200 kW, 80°C) to (280 kW, 40°C). In a similar fashion, using data in Table 11.1b, the cold composite curve joins the coordinates: (0 kW, 120°C), (36 kW, 100°C), (268 kW, 60°C), and (322 kW, 30°C).

The hot and cold composite curves as computed in Table 11.1 are shown in Figure 11.8a and indicate an infeasible solution since there is a crossover in the trajectories; indeed, to be feasible, the hot composite curve must lie above the cold composite curve. This is remedied by adjusting the horizontal position of one of the curves relative to the other. Shifting the hot composite curve to the right by 30 kW as shown in Figure 11.8b eliminates the crossover at the limit; here, the curves are coincident at the so-called "pinch point," which occurs for this example at cold stream temperature of 60°C. Increasing the magnitude of the enthalpy shift on the hot composite curve, say

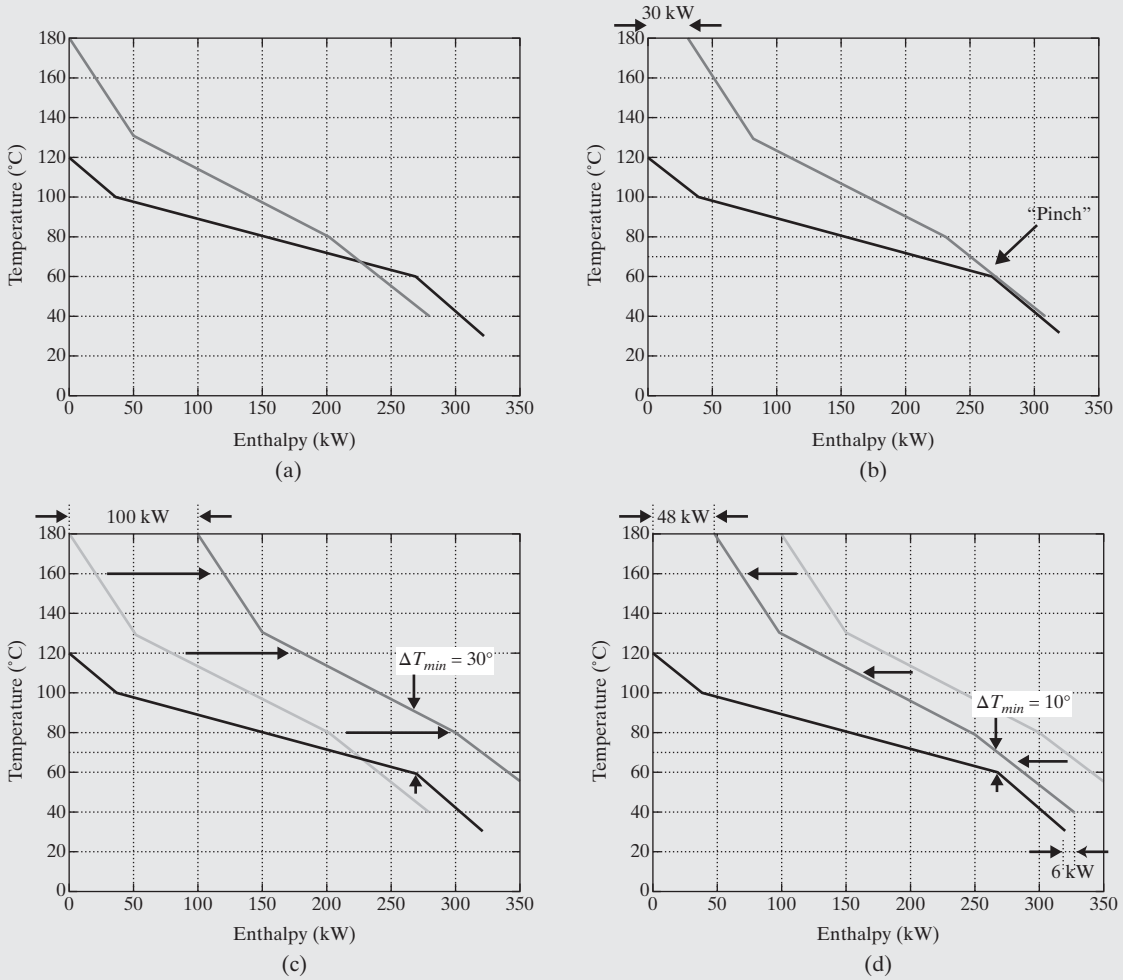

Figure 11.8 Hot and cold composite curves: (a) with no enthalpy offset; (b) with hot composite curve offset by 30 kW, identifying the "pinch"; (c) with hot composite curve offset by 100 kW, giving $\Delta T_{min} = 30$°C; (d) with hot composite curve offset by 48 kW, giving $\Delta T_{min} = 10$°C.

to 100 kW as shown in Figure 11.8c, gives a minimum temperature approach of $\Delta T_{min} = 30°C$. Finally, in Figure 11.8d, the desired value of $\Delta T_{min} = 10°C$ is achieved by adjusting the horizontal enthalpy shift to 48 kW, which is also the amount of hot utility required ($Q_{Hmin} =$ 48 kW) since it is the amount of enthalpy by which the cold composite curve extends to the left beyond the start of the hot composite curve. The amount of cold utility required can be read off by measuring the amount of enthalpy that the hot composite curve extends beyond the limit of the cold composite curve, in this case, $Q_{Cmin} =$ 6 kW. The cold pinch temperature is 60°C with the hot pinch temperature being, of course, ΔT_{min} higher at 70°C. These are referred to as the *MER targets*; evidently, the HEN in Figure 11.7 exceeds these targets by 12 kW.

Many additional observations are noteworthy in connection with the hot and cold composite curves. One is that the slopes of the composite curves *always* decrease at the inlet temperature of a stream and increase at the outlet temperature of a stream. It follows that points at which the slope decreases are candidate pinch points, and furthermore, when a pinch temperature exists, one of the inlet temperatures is *always* a pinch temperature. Hence, to locate a potential pinch temperature, one needs only to examine the inlet temperatures of the streams.

Another observation is that for some ΔT_{min} there are no pinch temperatures. In such cases, either hot or cold utilities (not both) are required in an amount equal to the difference between the total energy to be removed from the hot streams and that to be added to the cold streams. The ΔT_{min} at which the pinch disappears is referred to as the *threshold* ΔT_{min}, as discussed in Section 11.5.

Temperature-Interval (TI) Method

The *temperature-interval method* was developed by Linnhoff and Flower (1978a, 1978b) following the pioneering work of Hohmann (1971). It is a systematic procedure for determining the minimum utility requirements over all possible HENs given just the heating and cooling requirements for the process streams and the minimum approach temperature in the heat exchangers, ΔT_{min}, and consists of the following steps:

Step 1: Adjusting the hot and cold stream temperatures to bring them to the same reference.

Step 2: Determining the temperature intervals and carrying out enthalpy balances in each interval.

Step 3: Computing the enthalpy cascade, the residual enthalpy flows, determining the location of the "pinch," and computing MER targets.

EXAMPLE 11.3 *A Typical Heat-integration Problem (Example 11.1 Revisited)*

Returning to Example 11.1, the temperature-interval method is used for the calculation of MER targets for $\Delta T_{min} = 10°C$.

SOLUTION

The first step in the TI method is to adjust the source and target temperatures using ΔT_{min}. Somewhat arbitrarily, this is accomplished by reducing the temperatures of the hot streams by ΔT_{min} while leaving the temperatures of the cold streams untouched as follows:

			Adjusted Temperatures		
	T^s(°C)	T^t(°C)	T^s(°C)	T^t(°C)	
H1	180		170		T_0
		80		70	T_3
H2	130		120		T_1
		40		30	T_5
C1	60		60		T_4
		100		100	T_2
C2	30		30		T_5
		120		120	T_1

The adjustment of the hot stream temperatures by $-\Delta T_{min}$ brings both the hot and cold streams to a common frame of reference so that when performing an energy balance involving hot and cold streams at the same temperature level, the calculation accounts for heat transfer with at least a driving force of ΔT_{min}. Note that the adjusted temperatures are rank ordered, beginning with T_0, the highest temperature. These are used to create a cascade of *temperature intervals* within which energy balances are carried out. As shown in Table 11.2 and Figure 11.9, each interval, i, displays the enthalpy difference, ΔH_i, between the energy to be removed from the hot streams and the energy to be taken up by the cold streams in that interval. Just as in the table used to generate data for the preparation of the composite curves, it is helpful to indicate which streams are present in each interval by color coding incidence columns in the table. Thus, in interval 1, 170°C to 120°C ($\Delta T = 50°C$), only stream H1 is involved. Hence, the enthalpy difference is:

$$\Delta H_1 = \left(\sum C_h - \sum C_c\right)_1 (T_0 - T_1) = (1) \times (170 - 120) = 50 \text{ kW}$$

It is noted that initially, no energy is assumed to enter this interval from a hot utility at a higher temperature, that is, $Q_h = 0$. Hence, 50 kW are available and flow down as a residual, R_1, into the next lowest interval 2; that is, $R_1 = 50$ kW. Interval 2 involves streams H1, H2 and C2 between, 120°C and 100°C ($\Delta T_2 = 20°C$), and hence, the enthalpy difference is:

$$\Delta H_2 = \left(\sum C_h - \sum C_c\right)_2 (T_1 - T_2) = (1 + 2 - 1.8) \times (120 - 100) = 24 \text{ kW}$$

When this is added to the residual from interval 1, R_1, this makes the residual from interval 2, $R_2 = 74$ kW. Interval 3, 100°C to 70°C ($\Delta T_3 = 30°C$), involves all four streams, with an enthalpy difference of −84 kW as detailed in Table 11.2, making the residual from interval 3 equal to −10 kW. Similarly, the enthalpy differences in intervals 4 and 5 are −38 and 6 kW, respectively, with the residuals leaving these intervals being −48 and −42 kW. Note that for $Q_h = 0$, the largest negative residual is from interval 3,

Table 11.2 Enthalpy Differences for Temperature Intervals

Interval	$T_{i-1} - T_i$ (°C)	H1	H2	C1	C2	$\Sigma C_h - \Sigma C_c$(kW/°C)	ΔH_i(kW)
1	170 – 120 = 50					1	50
2	120 – 100 = 20					1 + 2 –1.8 = 1.2	24
3	100 – 70 = 30					1 + 2 –1.8 –4 = –2.8	–84
4	70 – 60 = 10					2 –1.8 –4 = –3.8	–38
5	60 – 30 = 30					2 –1.8 = 0.2	6

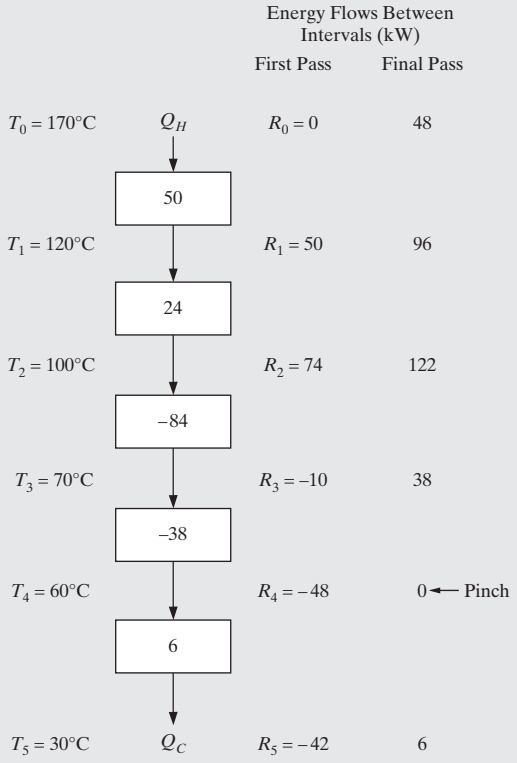

Figure 11.9 Cascade of temperature intervals, energy balances, and residuals.

$R_3 = -48$ kW. Clearly, to satisfy the second law of thermodynamics, all negative residuals must be removed because heat cannot flow from a low- to a high-temperature interval. The only way to avoid negative residuals is to add energy at higher temperatures. This is achieved using a hot utility stream above 170°C. In Figure 11.9 note that when $Q_h = 48$ kW, R_1 becomes 96 kW, $R_2 = 122$ kW, $R_3 = 38$ kW, $R_4 = 0$ kW, and $R_5 = Q_c = 6$ kW. Thus, $Q_h = 48$ kW is the smallest amount of energy that must be added above 170°C, and hence, it becomes a lower bound on the hot utility duty, just as $Q_c = 6$ kW becomes the lower bound on the cold utility duty. As with the composite curve method, these are referred to as the *MER targets*.

Note $Q_h - Q_c = 42$ kW, which is consistent with the first law. Furthermore, at minimum utilities, no energy flows between intervals 4 and 5. This is referred to as the *pinch* with associated temperatures of 60°C for the cold streams and $60 + \Delta T_{min} = 70$°C for the hot streams. To maintain minimum utilities, it is recognized that *no energy is permitted to flow across the pinch*. If, as in the HEN in Figure 11.7, Q_h would be increased to 60 kW; R_3, the transfer of heat across the pinch, would be 12 kW; and Q_c would increase to 18 kW.

HEN synthesis is facilitated using the stream representation in Figure 11.10 in which arrows moving from left to right denote the hot streams, whereas arrows moving from right to left denote the cold streams. The arrows for the hot and cold streams either pass through or begin at the pinch temperatures. To maintain minimum utilities, two separate HENs *must* be designed, one on the hot side and one on the cold side of the pinch. Energy is not permitted to flow across the pinch. Energy is added from hot utilities on the hot side of the pinch ($Q_{Hmin} = 48$ kW), and energy is removed using cold utilities on the cold side of the pinch ($Q_{Cmin} = 6$ kW). If energy were exchanged between a hot stream on the hot side of the pinch and a cold stream on the cold side of the pinch, this energy would not be available to heat the cold streams on the hot side of the pinch, and additional energy from the hot utilities would be required. Similarly, the cold stream on the cold side of the pinch would not have the ability to remove this energy from the hot streams on the cold side of the pinch, and the same amount of additional energy would have to be removed from the cold streams on the cold side of the pinch using cold utilities.

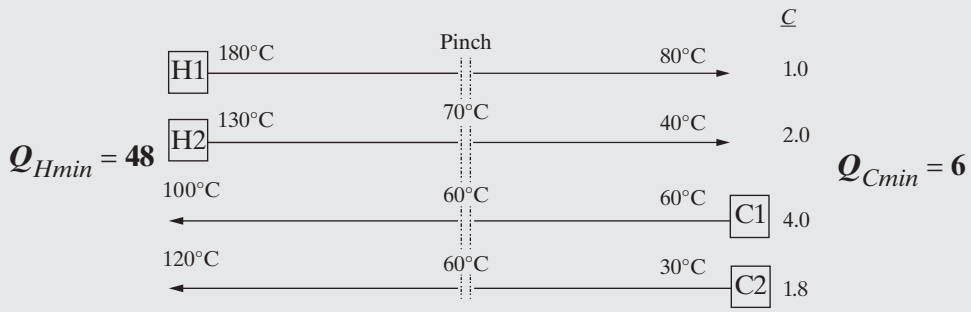

Figure 11.10 Pinch decomposition of the hot and cold streams for Example 11.3.

Although the two methods for MER targeting described above are equivalent, the TI method is more convenient because it does not rely on the graphical skills of the designer and it can be easily coded or automated on a spreadsheet.

Thus far, only sensible heat changes have been considered. Furthermore, the specific heat or heat capacity has been assumed constant over the range between the source and target temperatures so that the stream heat-capacity flow rates are constant. In many processes, latent heat of phase change, heat of reaction, and heat of mixing may also be involved under isothermal or nonisothermal conditions. In addition, the specific heat may not be constant, or sensible heat may be combined with latent heat, heat of reaction, or heat of mixing, such as for multicomponent mixtures passing through condensers, vaporizers, reboilers, and nonadiabatic reactors and mixers. In such cases, a fictitious heat-capacity flow rate can be used based on the change in enthalpy flow due to all applicable effects over a temperature range. In general, a plot of stream enthalpy flow as a function of temperature will be curved but can be discretized into straight-line segments. Particular attention should be paid to the accuracy of the discretization in the vicinity of the pinch temperatures. Note that a conservative approach is recommended in which the linear approximations provide a bound for the cold stream temperature-enthalpy curves from above and for the hot stream curves from below. This conservative approach ensures that the true temperature approach is greater than that computed in terms of the linear approximations. The following example shows how linear piecewise approximations are used to generate stream data for a design problem involving both vaporization and condensation of process streams.

EXAMPLE 11.4 *MER Targeting for a Process Exhibiting Phase Changes and Variable Heat Capacities*

Figure 11.11 shows a process for the manufacture of toluene by dehydrogenation of n-heptane. Note that a furnace heats the feed stream of pure n-heptane, S1, at 65°F to the reactor feed, S2, at 800°F. Furthermore, the reactor effluent, S3, containing a multicomponent mixture of n-heptane, hydrogen, and toluene at 800°F is cooled to 65°F and fed to a separator as stream S4. It is planned to install a heat exchanger to heat the feed stream, S1, using the hot reactor effluent, S3, and thus reduce the required duty of the preheater, E-100. (a) Generate stream data using piecewise linear approximations for the heating and cooling curves for the reactor feed and effluent streams. (b) Using the stream data, compute the MER targets for $\Delta T_{min} = 10°F$.

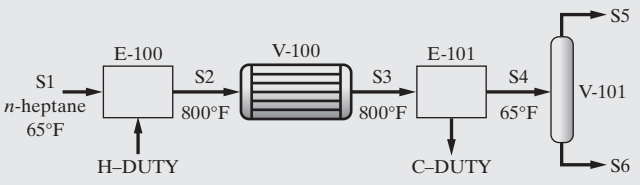

Figure 11.11 Process flow diagram for dehydrogenation of n-heptane.

SOLUTION

(a) Generation of Stream Data UniSim®Design is used to simulate the process in Figure 11.11, as shown in the multimedia modules, which can be downloaded from www.seas.upenn.edu/~dlewin/multimedia.htlm (see HYSYS → Tutorials → Heat Transfer → Toluene Manufacture). The Peng-Robinson equation of state is used to estimate thermodynamic properties. Sensitivity analyses are performed in which enthalpies for S2 and S4 are computed as a function of temperature, giving the temperature-enthalpy diagrams in Figures 11.12 and 11.13. In Figure 11.12, which is for pure n-heptane feed, only liquid sensible heat is involved from 65°F to 209°F where isothermal vaporization occurs as represented by the horizontal line. From there until 800°F, only vapor sensible heat is involved. In Figure 11.13 , which is for the ternary reactor effluent, only vapor sensible heat is involved from 800°F down to 183°F, which is the dew point. Then, condensation occurs, involving both latent heat and sensible heat down to the target temperature of 65°F. Shown in the diagrams are the piecewise linear approximations defined by critical coordinates on the original heating and cooling curves. The piecewise linear approximations are defined in terms of temperature-enthalpy coordinates, (h_k, T_k) and (h_{k+1}, T_{k+1}) through which linear arcs are drawn to approximate the true heating or cooling curves. Each arc represents a new stream with the source and target temperatures being the abscissa coordinates, T_k and T_{k+1}, and the heat-capacity flow rate is given by:

$$C_k = \frac{h_{k+1} - h_k}{T_{k+1} - T_k}, \tag{11.6}$$

where h is the enthalpy flow rate and MM stands for million. This is the inverse of the gradient of each linear segment in Figures 11.12 and 11.13.

A reasonably accurate linear approximation is obtained using four segments for stream S2 and six for stream S4 whose coordinates are positioned to ensure accuracy in the vicinity of the temperature pinches. The temperature coordinates are determined to the nearest degree. Thus, in Figure 11.12, the horizontal line for the vaporization of n-heptane at 209°F is taken to occur over a 1°F interval from 209 to 210°F, giving a fictitious heat-capacity flow rate, C, of 1.4282 MMBtu/hr/1°F = 1.4282 MMBtu/hr-°F.

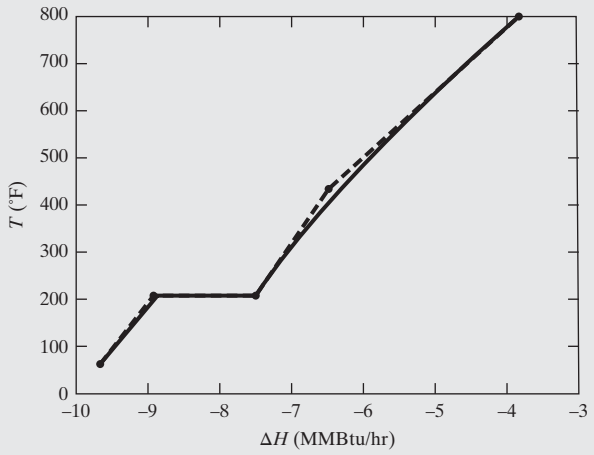

Figure 11.12 Temperature-enthalpy diagram for the cold stream, S2, showing simulation results (solid line) and piecewise linear approximation (dashed line).

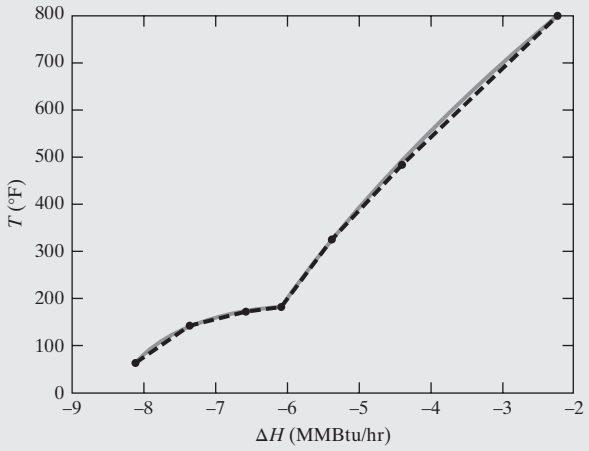

Figure 11.13 Temperature-enthalpy diagram for the hot stream, S4, showing simulation results (solid line) and piecewise linear approximation (dashed line).

Having determined the coordinate positions, the stream data for the four cold and six hot streams are computed directly where the heat-capacity flow rate for the *k*th stream is given by Eq. (11.6), as shown in Table 11.3. Note the increased values of heat-capacity flow rate in the region where streams exhibit phase change and, in particular, the large value for the case of the cold stream (pure n-heptane) where vaporization is assumed to occur over 1°F.

(b) Computing MER Targets The TI method is applied using the data in Table 11.3 with the hot temperatures reduced by ΔT_{min}. The results, summarized in Table 11.4, indicate that the cold pinch temperature is 173°F, giving the hot and cold utility targets of Q_{Hmin} = 1.421 MMBtu/hr and Q_{Hmin} = 1.471 MMBtu/hr. The location of the cold pinch temperature in the UniSim®Design simulation of the heat-integrated process designed for ΔT_{min} = 10°F is 172°F with the heat duties of the preheater and cooler being 1.396 MMBtu/hr and 1.446 MMBtu/hr, respectively. These differences are the result of the linear approximations used for the heating and cooling curves.

Table 11.3 Stream Data for Example 11.4

(a) Cold Streams				
Stream	T^s(°F)	T^t(°F)	Duty (MMBtu/hr)	C (MMBtu/hr °F)
S2A	65	209	0.7446	0.5171×10^{-2}
S2B	209	210	1.4282	1.4282
S2C	210	435	1.0492	0.4663×10^{-2}
S2D	435	800	2.6446	0.7245×10^{-2}
(b) Hot Streams				
Stream	T^s(°F)	T^t(°F)	Duty (MMBtu/hr)	C (MMBtu/hr °F)
S4A	800	485	2.1745	0.6903×10^{-2}
S4B	485	326	0.9823	0.6178×10^{-2}
S4C	326	183	0.7304	0.5108×10^{-2}
S4D	183	172	0.4863	4.421×10^{-2}
S4E	172	143	0.7780	2.683×10^{-2}
S4F	143	65	0.7652	0.9810×10^{-2}

Table 11.4 Computation of MER Targets Using the TI Method

		MMBtu/hr		
Interval	$T_{i-1} - T_i$(°F)	ΔH_i	$R_i(Q_{Hmin} = 0)$	$R_i(Q_{Hmin} = 1.4208)$
			0	1.4208
1	800 − 790 = 10	−0.0725	−0.0725	1.3483
2	790 − 475 = 315	−0.1077	−0.1802	1.2406
3	475 − 435 = 40	−0.0427	−0.2229	1.1979
4	435 − 316 = 119	0.1803	−0.0426	1.3782
5	316 − 210 = 106	0.0472	0.0046	1.4254
6	210 − 209 = 1	−1.4231	−1.4185	0.0023
7	209 − 173 = 36	−0.0023	−1.4208	0.0000←Pinch
8	173 − 162 = 11	0.4294	−0.9913	0.4294
9	162 − 133 = 29	0.6281	−0.3633	1.0575
10	133 − 65 = 68	0.3155	−0.0478	1.3729
11	65 − 55 = 10	0.0981	0.0502	1.4710

11.3 NETWORKS FOR MAXIMUM ENERGY RECOVERY

Having determined the minimum utilities for heating and cooling, it is common to design two networks of heat exchangers, one on the hot side and one on the cold side of the pinch. This section presents a method introduced by Linnhoff and Hindmarsh (1983), which places emphasis on positioning the heat exchangers by working out from the pinch. An alternative algorithmic strategy that utilizes a mixed-integer linear program (MILP), introduced by Papoulias and Grossmann (1983), is presented in the supplementary materials that accompany this chapter.

Stream Matching at the Pinch

To explain the approach of Linnhoff and Hindmarsh (1983), it helps to refer to a diagram showing the *pinch decomposition* of the hot and cold streams as shown in Figure 11.10 for the four streams in Example 11.1. Attention is focused at the pinch where the temperatures of the hot and cold streams are separated by ΔT_{min}. This, of course, is the location of the closest temperature approach.

Consider the schematic of a countercurrent heat exchanger in Figure 11.14. The hot stream, having a heat-capacity flow rate of C_h, enters at $T_{h,i}$ and exits at $T_{h,o}$. It transfers heat, Q, to the cold stream that has a heat-capacity flow rate of C_c, entering at $T_{c,i}$ and exiting at $T_{c,o}$. On the cold end of the heat exchanger where the temperatures of the hot and cold streams are the lowest, the

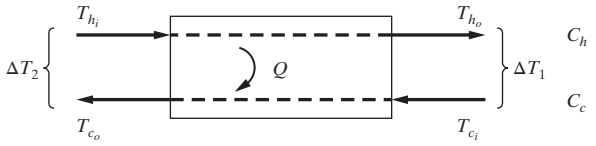

Figure 11.14 Schematic of a countercurrent heat exchanger.

approach temperature difference is ΔT_1. On the hot end where the temperatures are the highest, the approach temperature difference is ΔT_2. Carrying out energy balances for the hot and cold streams:

$$Q = C_h(T_{h,i} - T_{h,o}) \text{ or } T_{h,i} - T_{h,o} = \frac{Q}{C_h} \tag{11.7}$$

$$Q = C_c(T_{c,o} - T_{c,i}) \text{ or } T_{c,o} - T_{c,i} = \frac{Q}{C_c} \tag{11.8}$$

and subtracting Eq. (11.8) from Eq. (11.7):

$$(T_{h,i} - T_{c,o}) - (T_{h,o} - T_{c,i}) = Q\left(\frac{1}{C_h} - \frac{1}{C_c}\right) \tag{11.9}$$

or:

$$\Delta T_2 - \Delta T_1 = \frac{Q(C_c - C_h)}{C_h C_c} \tag{11.10}$$

Following the approach introduced by Linnhoff and Hindmarsh (1983), the potential locations for the heat exchangers at the pinch are considered next. When a heat exchanger is positioned on the hot side of the pinch, which is considered first arbitrarily, $\Delta T_1 = \Delta T_{min}$, and Eq. (11.10) becomes:

$$\Delta T_2 = \Delta T_{\min} + \frac{Q(C_c - C_h)}{C_h C_c} \tag{11.11}$$

Then, to assure that $\Delta T_2 \geq \Delta T_{\min}$ since $Q > 0$ and the heat-capacity flow rates are positive, it follows that $C_c \geq C_h$ is a necessary and sufficient condition. That is, for a match to be *feasible* at the pinch on the hot side, $C_c \geq C_h$ must be satisfied. If two streams are matched at the pinch with $C_c < C_h$, the heat exchanger is *infeasible* because $\Delta T_2 < \Delta T_{\min}$.

When a heat exchanger is positioned on the cold side of the pinch, $\Delta T_2 = \Delta T_{\min}$, and Eq. (11.10) becomes:

$$\Delta T_1 = \Delta T_{\min} - \frac{Q(C_c - C_h)}{C_h C_c} \tag{11.12}$$

In this case, to assure that there are no approach temperature violations (i.e., $\Delta T_1 \geq \Delta T_{\min}$), it is necessary and sufficient that $C_h \geq C_c$. Note that this condition is just the reverse of that on the hot side of the pinch. These stream-matching rules are now applied to design a HEN for Example 11.1.

EXAMPLE 11.5 ***A Typical Heat-integration Problem (Example 11.1 Revisited)***

Design a HEN to meet the MER targets for Example 11.1: $Q_{\text{Hmin}} = 48$ kW and $Q_{\text{Cmin}} = 6$ kW where Q_{Hmin} and Q_{Cmin} are the minimum hot and cold utility loads. The cold and hot pinch temperatures are 60 and 70°C, respectively.

SOLUTION

As stated previously, when designing a HEN to meet MER targets, no heat is transferred across the pinch, and hence, two HENs are designed, one on the hot side and one on the cold side of the pinch as shown in Figure 11.15. Since only two streams exist below the pinch, namely, H2 and C2, the HEN on the cold side of the pinch is designed first. At the pinch, the only possible match is between C2 and H2, which is a feasible match as $C_{C2} < C_{H2}$, and thus, interior heat exchanger 1 is installed, with a heat duty equal to 54 kW, the entire heating requirement of stream C2 on the cold side of the pinch. The cooling requirement of stream H2 is then satisfied by installing a cooler (labeled C) with a heat duty of 6 kW, which matches the MER cooling target.

On the hot side of the pinch, the cooling demands of both of the hot streams need to be satisfied using cold streams because no cooling utility is allowed above the pinch. The first match to be selected is that for the hot stream with the largest value of C_H, namely, H2. This is matched with C1 because $C_{C1} > C_{H2}$ (C2 is an unsuitable match as $C_{C2} > C_{H2}$), and interior heat exchanger 2 is installed with a heat duty equal to 120 kW, the entire cooling requirement of stream H2 on the hot side of the pinch. Similarly, because $C_{C2} \geq C_{H1}$, streams H1 and C2 are matched on the hot side of the pinch, using interior heat exchanger 3 with a heat duty equal to 100 kW, the entire cooling requirement of H1 on the hot side of the pinch. Since these two heat exchangers bring streams C1 and C2 to 90 and 115.5°C respectively, utility heaters (labeled H) are added to complete the design on the hot side of the pinch with a total duty of 48 kW, which matches the MER heating target. Note that each unit exchanges heat between two process streams in countercurrent flow, with the inlet and outlet temperatures for each stream shown on either side of circles, identified by the heat exchanger number, connected by a vertical line to represent the match and the heat duty annotated below the circle associated with the cold stream.

The final design, shown in Figure 11.15, meets the MER targets with a total number of six heat exchangers. These are displayed in the flowsheet in Figure 11.16, which should be compared with the HEN in Figure 11.7. Note that the former meets the MER energy targets, whereas in the latter, both the cold and hot utility targets are exceeded

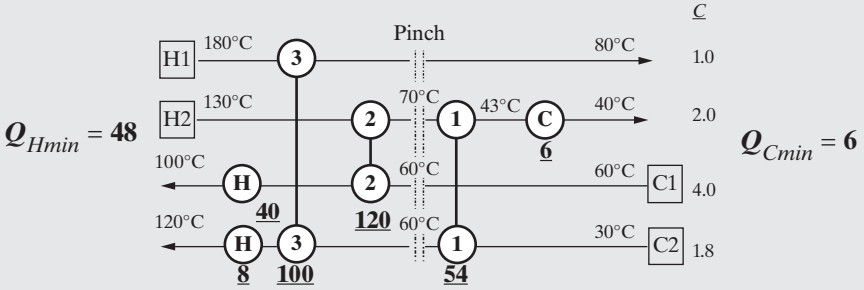

Figure 11.15 Interior heat exchangers (1–3) and auxiliary heat exchangers (C, H). Heat duties in kW and heat-capacity flow rates in kW/°C.

by 12 kW. In contrast, the latter involves only four units compared to six utilized in the MER design. Cost estimates are needed to select between these and other alternatives. As will be seen in later examples, the trade-off between capital and operating costs is at the heart of HEN synthesis.

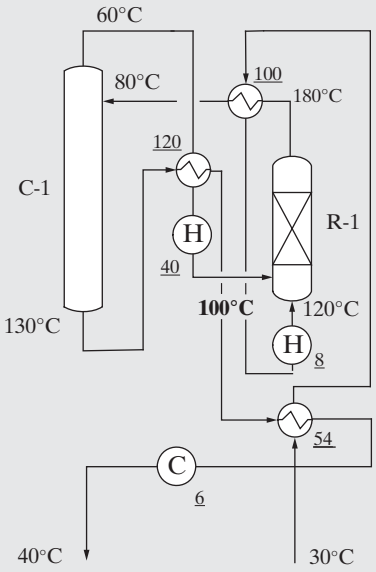

Figure 11.16 Flowsheet for HEN in Figure 11.15.

In summary, the HEN design procedure to meet MER targets consists of the following steps:

Step 1: MER Targeting: The pinch temperatures are determined together with minimum hot and cold utility targets, Q_{Hmin} and Q_{Cmin}, respectively.

Step 2: The synthesis problem is decomposed at the pinch, yielding two independent HENs to be designed, using the representation shown in Figure 11.10. It is helpful to list the heat-capacity flow rates for each stream in a column to the right for reference.

Step 3: The HEN is designed on the hot side of the pinch, *starting at the pinch*, and working outward. *At the pinch*, streams are paired such that $C_c \geq C_h$. In general, the heat duty of each interior heat exchanger is selected to be as large as possible, to reduce the total number of exchangers. In some cases (e.g., Example 11.6), duties are selected to retain sufficient temperature driving forces for additional matches. Finally, hot utilities are added to meet cold temperature targets (up to a total of Q_{Hmin}). *Cold utilities are not used on the hot side of the pinch.*

Step 4: The HEN is designed on the cold side of the pinch *starting at the pinch* and working outward. *At the pinch*, streams are paired such that $C_h \geq C_c$. In general, the duty of each interior heat exchanger is selected to be as large as possible to reduce the total number of exchangers. As mentioned above, it may be necessary to select duties to retain sufficient temperature driving forces for additional matches. Finally, cold utilities are added to meet cold temperature targets (up to a total of Q_{Cmin}). *Hot utilities are not used on the cold side of the pinch.*

In this synthesis procedure, the designer positions the first heat exchangers *at the pinch* where the approach temperature difference at one end of each heat exchanger is constrained at $\Delta T_{\min}$. Then, working outward, the utility exchangers are positioned last. In cases that do not require stream splitting (to be considered in Section 11.4), this simple procedure is sufficient to guarantee compliance with the MER targets. However, it tends to create designs with a large number of heat exchangers as illustrated in the following example.

EXAMPLE 11.6 ***HEN Optimal Annualized Cost***

Consider the design of a HEN for the four streams below in a problem presented by Linnhoff and Flower (1978a, 1978b):

Stream	T^s (°C)	T^t (°C)	C (kW/°C)	Q (kW)
C1	60	180	3	360
C2	30	130	2.6	260
H1	180	40	2	280
H2	150	40	4	440

Let $\Delta T_{min} = 10°C$, with the following specifications:

Cooling water (cw): $T^s = 30°C,\ T^t \leq 80°C$,
cost of $cw = 0.00015$ \$/kg

Steam (sat'd.,s): $T = 258°C,\ \Delta H^v = 1{,}676$ kJ/kg, cost of $s = 0.006$ \$/kg

Overall heat-transfer coefficients:

$$U_{heater} = 1 \text{ kW/m}^2\text{°C},\ U_{cooler} = U_{exch} = 0.75 \text{ kW/m}^2\text{°C}$$

Purchased cost of heat exchangers:

$$C_P = 3{,}000A^{0.5}\ (\$,\ \text{m}^2)$$

Equipment operability = 8,500 hr/yr, return on investment = i_m = 0.1 (for Eq. (11.4)).

SOLUTION

First, the MER targets are computed using the TI method as summarized in the cascade diagram of Figure 11.17 where the pinch temperatures are 140 and 150°C, and the minimum hot and cold utility duties are 60 kW and 160 kW, respectively.

Next, the MER synthesis procedure is used to design the HEN. Since only streams H1 and C1 appear on the hot side of the pinch and $C_{\text{H1}} < C_{\text{C1}}$, a heat exchanger is installed between streams H1 and C1 as shown in Figure 11.18a with a heat duty equal to 60 kW, the cooling demand of H1 on the hot side of the pinch. Finally, a 60 kW heater is installed to complete heating stream C1.

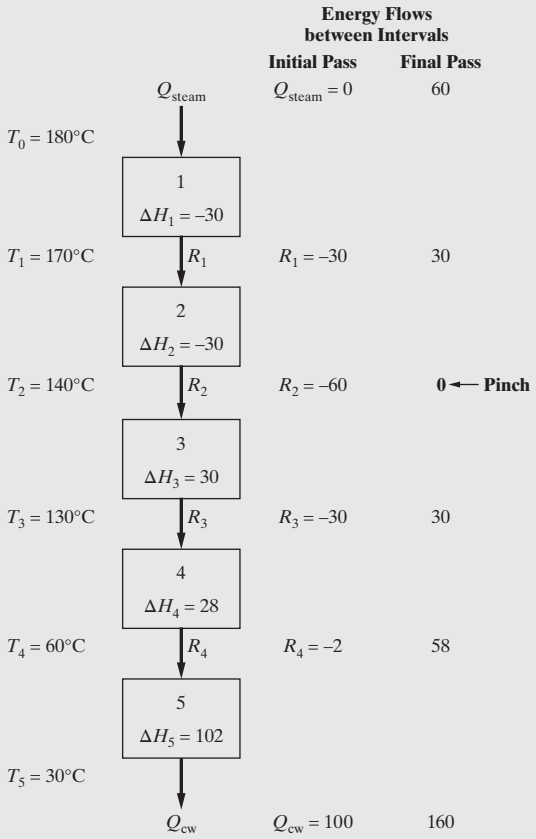

Figure 11.17 Cascade diagram for Example 11.6 showing temperature intervals, heat balances, and residuals; ΔH_i and R_i in kW.

On the cold side, all four streams are present, but only streams H1, H2, and C1 exist at the pinch, since the target temperature of stream C2 is 130°C below 140°C, the pinch temperature of the cold streams. Only the H2-C1 match is feasible since $C_{H2} > C_{C1}$ whereas $C_{H1} < C_{C1}$. Following the guidelines, one would be tempted to install an internal heat exchanger with a duty of 240 kW as shown in Figure 11.18b, which would satisfy the entire energy requirement of stream C1 on the cold side of the pinch. Furthermore, the H1-C2 match is possible even though $C_{H1} < C_{C2}$ because stream C2 does not reach the pinch. Thus, a heat exchanger can be installed between these streams, but since $\Delta T_1 < \Delta T_2$ and $\Delta T_1 \geq \Delta T_{min} = 10°C$, only 86.58 kW can be transferred as shown in Figure 11.18b. Unfortunately, this requires that a portion of stream C1 be heated with hot utility (173.42 kW). The addition of heat from a hot utility on the cold side of the pinch requires that an equivalent amount of heat be removed from the hot streams using cooling water, thereby exceeding the minimum cold utility (160 kW).

Alternatively, a more careful design is performed in which heat exchangers are added with duties assigned such that sufficient temperature differences are retained for additional matches as shown in Figure 11.18c. The first match, H2-C1, is assigned a heat duty of only 40 kW so that the H2 effluent temperature is reduced to only 140°C. This allows H2 to be used to heat stream C2 with a heat duty of 120 kW, which reduces the effluent temperature of H2 to 110°C, allowing H2 subsequent use to heat stream C1 and so on. As seen in Figure 11.18c, this rather complicated design, involving six heat exchangers, meets the MER cooling target of 160 kW.

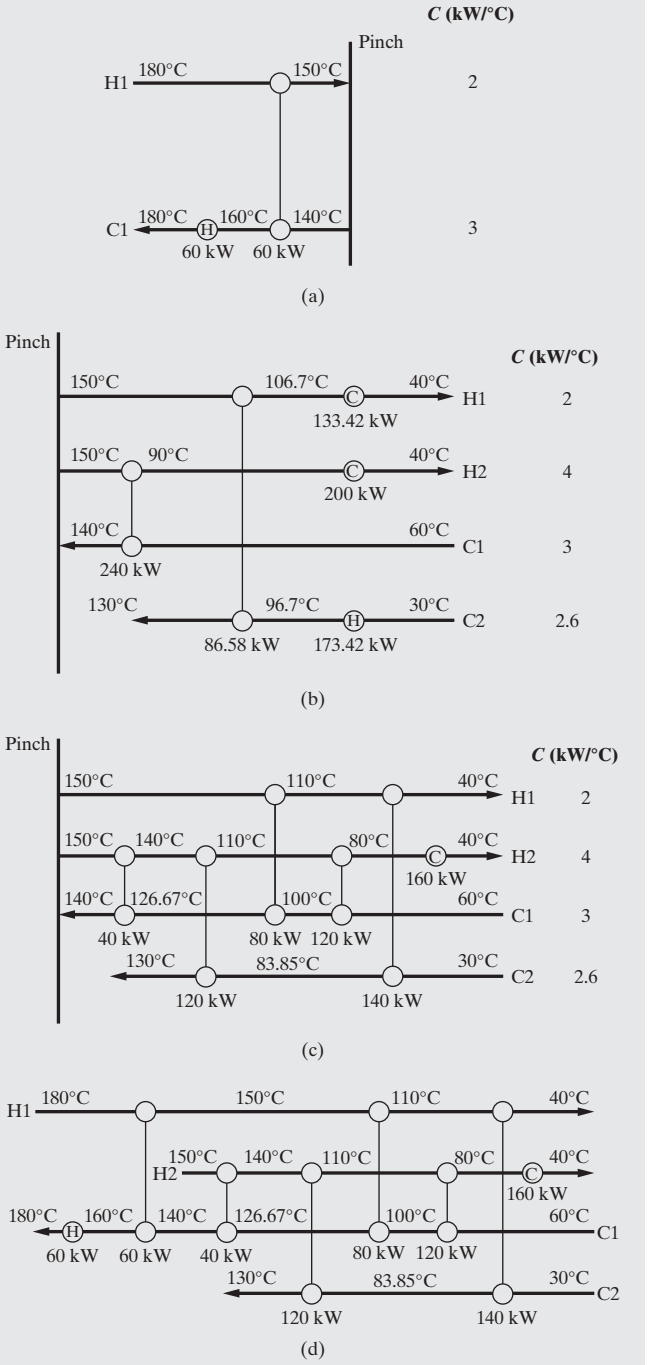

Figure 11.18 MER design for Example 11.6: (a) network on the hot side of the pinch; (b) network on the cold side of the pinch—additional utilities required; (c) network on the cold side of the pinch—minimum utilities; (d) combined network involving eight heat exchangers.

When combined with the network in Figure 11.18a, the resulting HEN involves six interior heat exchangers, an auxiliary heater, and an auxiliary cooler as shown in Figure 11.18d. Note that this network utilizes the minimum hot and cold utilities but involves eight heat exchangers, three above the minimum, as discussed in Section 11.4. The next step is to consider the possibilities for reducing the number of heat exchangers by removing the *heat loops*, or to introduce stream splitting, as demonstrated in Section 11.4.

11.4 MINIMUM NUMBER OF HEAT EXCHANGERS

Having designed a HEN that meets the MER targets, it is common to reduce the number of heat exchangers toward the minimum while permitting the consumption of utilities to rise, particularly when small heat exchangers can be eliminated. In this way, lower annualized costs may be obtained, especially when the cost of fuel is low relative to the purchase cost of the heat exchangers. Alternatively, an attempt can be made to design the HEN to minimize the number of exchangers *and satisfy the MER target* by invoking stream splitting.

Reducing the Number of Heat Exchangers—Breaking Heat Loops

Before proceeding, it is important to recognize that, as pointed out by Hohmann (1971), the minimum number of heat exchangers in a HEN is

$$N_{HX,min} = N_S + N_U - 1 \tag{11.13}$$

where N_S is the number of streams and N_U is the total number of distinct hot and cold utility sources. Thus, for hot utilities, fuel, steam at high pressure (hps), intermediate pressure (ips), and low pressure (lps) and for cold utilities, boiler feed water (bfw), cooling water (cw), and refrigeration, each counts as distinct utility sources. Hence, for the networks in Example 11.6, which involve four streams and two utilities (steam and cooling water), $N_{HX,min} = 5$. Eq. (11.12) indicates that the minimum number of heat exchangers, and with it the minimum capital cost of the HEN, increase with each distinct utility source utilized in a design. However, as shown in Section 11.7, the operating costs of a HEN are reduced by replacing a portion of the utility duty requirement provided by a costly utility (e.g., refrigeration) by one at a lower cost (e.g., cooling water).

In a more general result, Douglas (1988) shows that the minimum number of heat exchangers is also dependent on the number of *independent networks*, N_{NW}, that is, the number of subnetworks consisting of linked paths between the connected streams:

$$N_{HX,min} = N_S + N_U - N_{NW} \tag{11.14}$$

When all streams in a process are connected directly or indirectly by heat exchangers as in Figure 11.19a, $N_{NW} = 1$, and Eq. (11.13) reverts to Eq. (11.12) with $N_{HX,min} = 4$, noting that the HEN in Figure 11.19a has seven heat exchangers, three in excess of the minimum possible. In contrast, Figure 11.19b illustrates a network of five streams and two utilities composed of two independent subsystems: one connecting streams H1, C1 and the cold utility, and the second connecting streams H2, C2, C3 and the hot utility. In this case, $N_{HX,min} = N_S + N_U - N_{NW} = 5 + 2 - 2 = 5$, which is the number of heat exchangers in the HEN shown.

In one of the first studies of the methods for heat integration, Hohmann (1971) showed that in a HEN with N_{HX} heat exchangers, $N_{HX} - N_{HX,min}$ independent *heat loops* exist, that is, subnetworks that exhibit cyclic heat flows between two or more streams. The simplest case of a heat loop is shown in Figure 11.20a, noting that streams H1 and C1 are matched twice with heat exchangers 1 and 3. A similar heat loop is shown in Figure 11.20b, where heat flows between streams H1 and C2

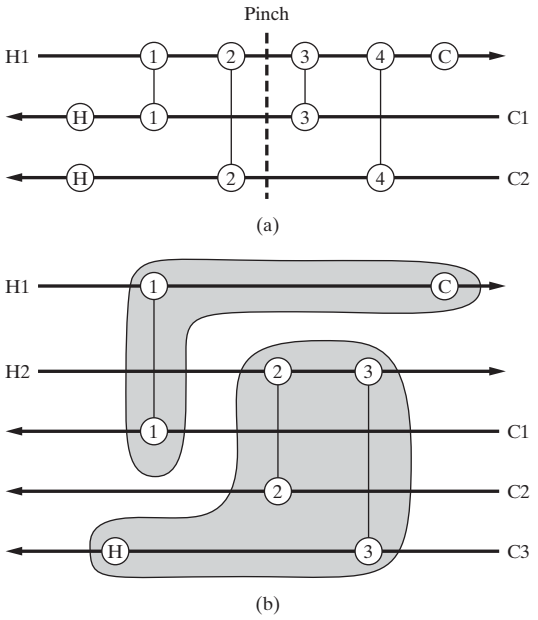

Figure 11.19 HENs involving: (a) one network; (b) two independent networks.

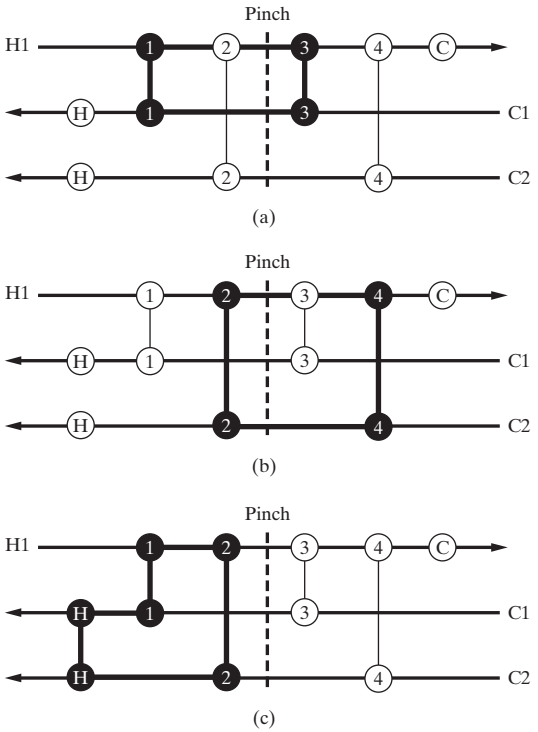

Figure 11.20 The three heat loops in the HEN in Figure 11.19.

in two matches, in heat exchangers 2 and 4. A more complex heat loop is shown in Figure 11.20c in which heat flows between streams H1 and C1 in heat exchanger 1, between H1 and C2 in heat exchanger 2, and between C1 and C2 and the hot utility, forming a closed heat cycle. Note that if C1 and C2 were to be serviced by two distinct sources of hot utility, there would be no heat loop in Figure 11.20c. Note also that the three heat loops identified in Figure 11.20 explain why the HEN has three heat exchangers more that $N_{HX,min}$.

Since a pinch exists in Figure 11.20, a HEN that meets the MER targets consists of two *independent* networks, one on each side of the pinch, so that: $N^{+}_{HX,\min} = N^{-}_{HX,\min} = N_S + N_U - 1 = 3 + 1 - 1 = 3$, noting that the + and − superscripts indicate the hot and cold side of the pinch, respectively. Thus, the HEN in Figure 11.20 can be designed to meet the MER targets with just six heat exchangers ($N^{MER}_{HX,\min} = N^{+}_{HX,\min} + N^{-}_{HX,\min} = 6$). The simplest change is to eliminate heat exchanger 1, transferring its duty to heat exchanger 2, decreasing the duty of the heater on stream C2 by this amount and increasing the duty of the heater on stream C1 by this amount. This is referred to as *loop breaking*. Often, the smallest heat exchanger in the heat loop is eliminated because the cost of the area saved by eliminating a small exchanger is usually more than the cost incurred in increasing the area of a large exchanger by the same amount.

As will be shown in Example 11.7, each heat loop is broken by removing a heat exchanger and adjusting the heat loads accordingly, which often leads to heat flow across the pinch, moving the HEN away from the MER targets.

EXAMPLE 11.7 ***HEN Optimal Annualized Cost (Example 11.6 revisited)***

Return to the HEN in Figure 11.18d, which was designed to meet the MER targets and involves eight heat exchangers, three more than $N_{HX,min}$ given by Eq. (11.12). In this example, the heat loops are identified and removed, one by one, taking note of the impact on the capital cost, the cost of the utilities, and the annualized cost, C_A, in Eq. (11.4).

SOLUTION

Beginning with the HEN in Figure 11.18d, using the specifications at the start of Example 11.6, the heat transfer area for each heat exchanger is computed [Eq. (11.3)], the purchase costs are estimated using $C_P = 3{,}000A^{0.5}$, and the total purchase cost is computed to be \$66,899. The annual cost of steam and cooling water is \$10,976/yr, which combines with the purchase cost multiplied by a return on investment ($i_m = 0.1$) to give C_A = \$17,666/yr.

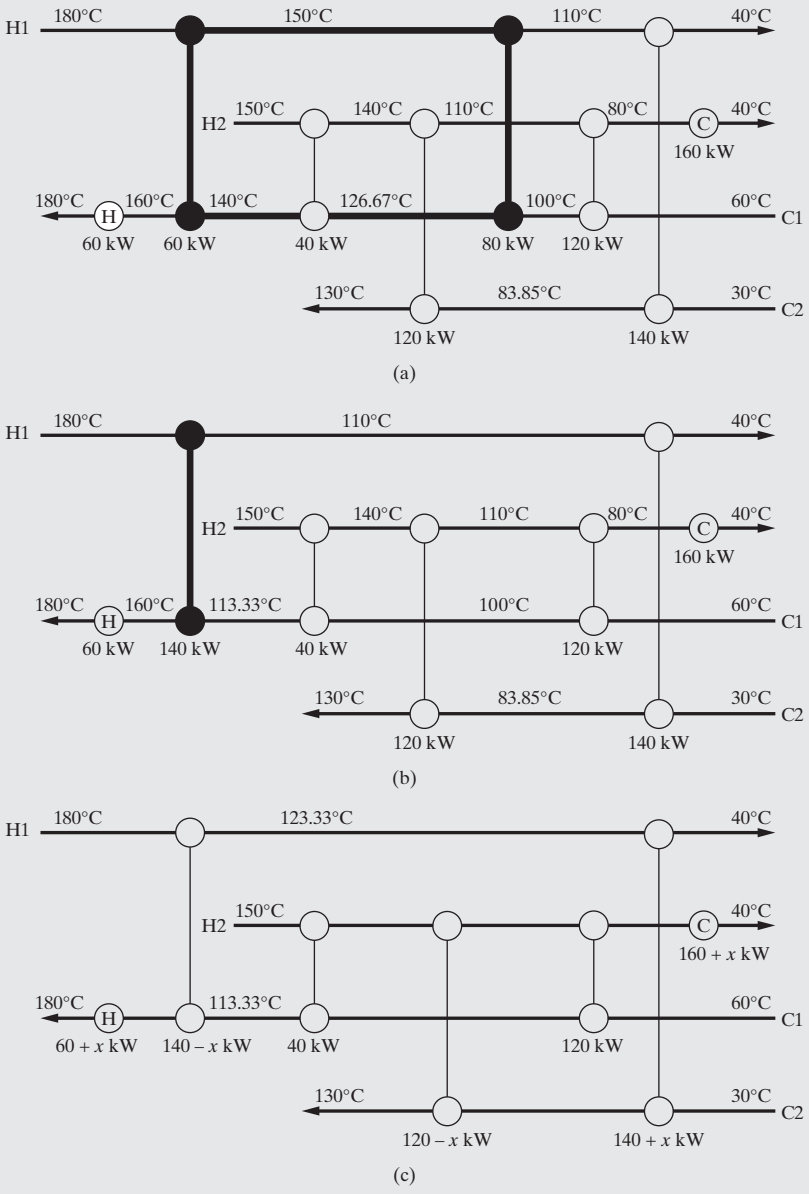

Figure 11.21 Breaking heat loops—Example 11.7: (a) eight heat exchangers, first heat loop; (b) seven heat exchangers, ΔT_{min} violation; (c) seven heat exchangers, shifting heat loads.

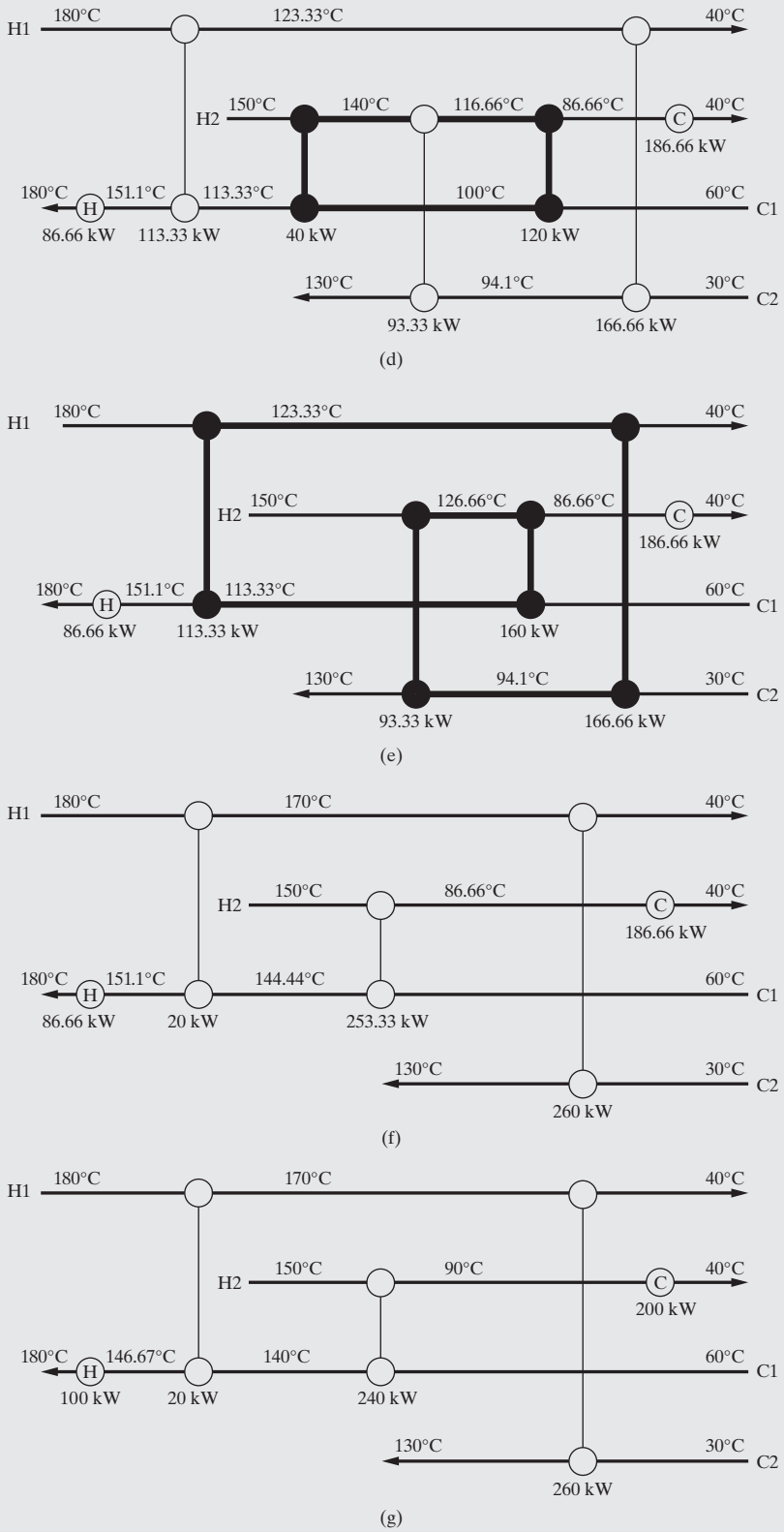

Figure 11.21 (*Continued*) (d) seven heat exchangers, second heat loop; (e) six heat exchangers, third heat loop; (f) five heat exchangers, ΔT_{min} violation.

To eliminate the first heat loop, in which heat is exchanged in two heat exchangers between streams H1 and C1, as shown in Figure 11.21a, the 80 kW exchanger is combined with the 60 kW exchanger as shown in Figure 11.21b. This causes an approach-temperature violation (110°C − 113.33°C = −13.33°C), which must be eliminated by transferring less heat, x, in this heat exchanger. This amount of heat is computed so as to give $\Delta T_{min} = 10°C$ on the cold side; that is, the temperature of stream H1 is reduced to 123.33°C. Then, by heat balance,

$$140 - x = 2(180 - 123.33)$$

and the reduction in the heat load is $x = 26.66$ kW. The results of the above calculations can be checked on the spreadsheet SS1.xlsx that can be downloaded from the Program and Simulation Files folder on the Wiley Website.

Furthermore, to account for this reduction, the steam consumption must be increased by x to heat stream C1 to 180°C, and the loads of five other exchangers must be adjusted by the same amount as shown in Figure 11.21c. This includes the same increase in the consumption of cooling water because x units of heat are transferred across the pinch. After the heat loads are adjusted, the resulting network is shown in Figure 11.21d. A glance at Table 11.5 shows the total purchase cost of the seven heat exchangers is reduced to \$57,469, but the cost of utilities is increased to \$13,897/yr, and hence, C_A is increased to \$19,644/yr.

To eliminate the second heat loop in which heat is exchanged in two heat exchangers between streams H2 and C1 as shown in Figure 11.21d, the 40 kW exchanger is combined with the 120 kW exchanger as shown in Figure 11.21e. Normally, the exchanger with the smaller load is eliminated and its load transferred to the large one unless the loads are comparable (as in the case of the first heat loop). In this case, since there are no temperature-approach violations, no adjustments in the loads of the heat exchangers are needed. Hence, as shown in Table 11.5, the cost of utilities is unchanged and the total purchase cost is reduced to \$53,767, which reduces C_A to \$19,273/yr.

The final heat loop has four heat exchangers involving four streams as shown in Figure 11.21e. One of these can be eliminated by shifting the load of the smallest exchanger around the heat loop. The network in Figure 11.21f results, but it has a temperature approach violation ($150 - 144.44 = 5.56 \leq 10°C$). To eliminate this, the 253.33 kW heat load is reduced by y where:

$$253.33 - y = 3(140 - 60)$$

to enable stream C1 to leave the heat exchanger at 140°C. This amount of heat ($y = 13.33$ kW) must be supplied and removed by additional steam and cooling water, respectively, as shown in Figure 11.21g where the final HEN is displayed, with only five heat exchangers.

In Table 11.5 for this network, the total purchase cost is reduced to \$45,931, but the cost of utilities is increased to \$15,359/yr, resulting in the largest C_A at \$19,951. Hence, for this system, the HEN with eight heat exchangers has the lowest C_A when $\Delta T_{min} = 10°C$. Of course, the trade-off between the total purchase cost and the cost of utilities shifts as the cost of fuel decreases and the capital cost or the return on investment increases. Under different conditions, another configuration can have the lowest annualized cost. These results can be checked on the spreadsheet SS1.xlsx.

Table 11.5 Cost Comparison for Example 11.7

Network	Utilities Cost (\$/yr)	C_P, Purchase Cost (\$)	C_A, Annualized Cost (\$/yr)
Design for MER:			
8 HXs	10,976	66,899	17,666
7 HXs	13,897	57,469	19,644
6 HXs	13,897	53,767	19,273
Design for $N_{HX,min}$:			
5 HXs	15,358	45,931	19,951
Design for MER: stream-split design, 6 HX[a]	10,976	54,889	16,465

[a] See Example 11.9 for details of the stream-split design to meet $N^{MER}_{HX,\min}$.

Table 11.5, an alternative design involving stream splitting gives the lowest value of the annualized cost. Indeed, as will be shown in the next section, the use of stream splitting can often enable the design of HENs that satisfy the MER targets with the minimum number of heat exchangers.

Reducing the Number of Heat Exchangers—Stream Splitting

When designing a HEN to meet MER targets, stream splitting *must* be employed if the number of hot streams *at the pinch*, on the cold side, is less than the number of cold streams. Below the pinch, hot utilities cannot be employed, so each cold stream must be paired with a hot stream, to ensure all matches satisfy the desired ΔT_{min}. Thus, when the number of hot streams at the pinch is less than the number of cold streams, hot streams have to be split to create opportunities for feasible stream-matches. Similarly, stream splitting **must** also be employed if the number of cold streams *at the pinch*, on the hot side, is less than the number of hot streams. Moreover, stream splitting helps to reduce the number of heat exchangers in a HEN without increasing the utility duties, which often occurs when heat loops are broken. The following example illustrates the use of stream splitting to achieve simultaneously the MER targets and the minimum units for a HEN involving two hot streams and one cold stream.

EXAMPLE 11.8 *Stream Splitting*

It is required to design a HEN with a minimum number of heat exchangers that satisfy $\Delta T_{min} = 10°C$ and a hot utility MER target of 300 kW for three streams on the hot side of the pinch:

Stream	T^s (°C)	T^t (°C)	C (kW/°C)	Q (kW)
H1	200	100	5	500
H2	150	100	4	200
C1	90	190	10	1,000

SOLUTION

Since no cold utility is allowed, Eq. (11.13) gives $N_{HX,min} = 3$. Furthermore, because the two hot streams need to be cooled entirely by the single cold stream to avoid an approach-temperature violation (i.e., $\Delta T_1 < \Delta T_{min}$), the cold stream must be split as shown in Figure 11.22a. Note that the duties of all three heat exchangers have been set to satisfy the MER targets, but the portion of the heat-capacity flow rate assigned to the first stream, x, must be determined by solving the energy balances for the split streams:

$$x(T_1 - 90) = 500 \tag{11.15}$$

$$(10 - x)(T_2 - 90) = 200 \tag{11.16}$$

subject to the constraints:

$$200 - T_1 \geq \Delta T_{min} = 10°\text{C} \tag{11.17}$$

$$150 - T_2 \geq \Delta T_{min} = 10°\text{C} \tag{11.18}$$

To minimize lost work, as explained in Section 10.4, it is desirable to mix the split streams isothermally, that is, to select $T_1 = T_2 = 160°\text{C}$ with $x = 7.143$ kW/°C. Unfortunately, isothermal mixing is infeasible since inequality (11.18) limits T_2 to be less than or equal to 140°C. Arbitrarily, the equality is set *active*, that is, $T_2 = 140°\text{C}$, giving $x = 6$ kW/°C and $T_1 = 173.33°\text{C}$. Note that by making a minor structural change in which the heater is moved upstream of the mixing junction as in Figure 11.22b, the design is improved to provide isothermal mixing as desired.

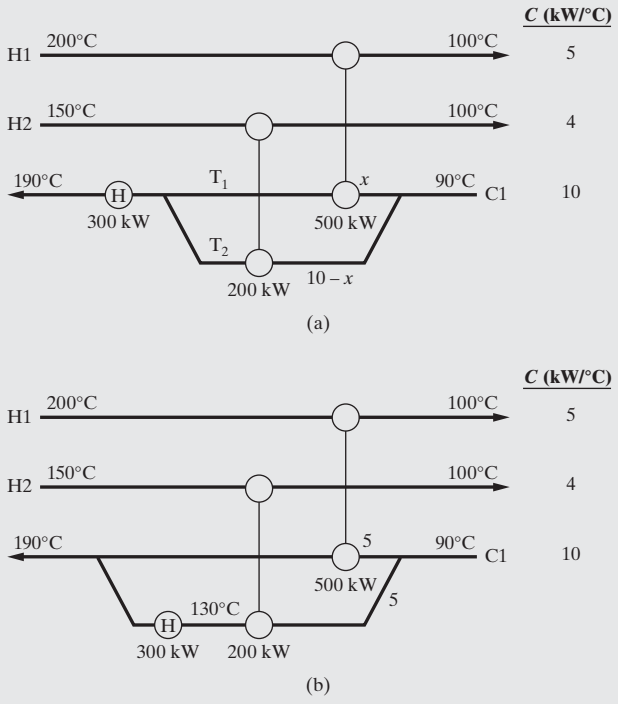

Figure 11.22 MER design for Example 9.9: (a) split determination; (b) improved design.

As illustrated in Example 11.9 and in accordance with Linnhoff and Hindmarsh (1983), generalized rules for stream splitting on both sides of the pinch to satisfy MER requirements are:

Hot Side of Pinch

H-1 Let N_H and N_C be the number of hot and cold streams at the pinch. Noting that cold utilities cannot be used on the hot side of the pinch, if $N_H > N_C$, *a cold stream must be split* since for feasibility, $N_H \leq N_C$.

H-2 On the hot side of the pinch, all feasible matches must ensure that $C_h \leq C_c$. If this is not possible for every match, split one or more hot streams as necessary. If hot streams are split, return to step H-1.

Cold Side of Pinch

C-1 Let N_H and N_C be the number of hot and cold streams at the pinch. Note that hot utilities cannot be used on the cold side of the pinch; if $N_C > N_H$, *a hot stream must be split* since for feasibility, $N_C \leq N_H$.

C-2 On the cold side of the pinch, all feasible matches must ensure $C_c \leq C_h$. If this is not possible for every match, split one or more cold streams as necessary. If cold streams are split, return to step C-1.

As mentioned previously, stream splitting is also used to reduce the number of heat exchangers for HENs that satisfy the MER targets as shown in the following example.

EXAMPLE 11.9 *HEN Optimal Annualized Cost (Examples 11.6 and 11.7 revisited)*

Return to Example 11.7 and recall that as heat loops are broken to reduce the number of heat exchangers, heating and cooling utilities are normally increased. Here, stream splitting is used to reduce the number of heat exchangers while satisfying MER targets.

SOLUTION

Since an MER design implies separate HENs on both sides of the pinch, it is helpful to compute the minimum number of heat exchangers in each HEN. On the hot side of the pinch, only streams H1 and C1 exist, and so $N^{+}_{HX,\text{min}} = 2$, whereas on the cold side of the pinch, all streams participate, and $N^{-}_{HX,\text{min}} = 4$. Thus, $N^{MER}_{HX,\text{min}} = N^{+}_{HX,\text{min}} + N^{-}_{HX,\text{min}} = 6$. The HEN in Figure 11.18a has the minimum number of heat exchangers whereas that in Figure 11.18c exceeds the minimum by two heat exchangers.

Figure 11.23 shows a possible design in which stream H2 is split *at the pinch*, ensuring that $C_c \leq C_h$, with the largest portion of its heat-capacity flow rate, $4 - x$, paired with stream C1 using heat exchanger 1. The remaining branch is paired with a portion of stream C2, y, using heat exchanger 2. The remaining portion of stream C2, with a heat-capacity flow rate of $2.6 - y$, is paired with stream H1. To determine x and y, the energy balances associated with the stream splits are solved to ensure isothermal mixing, giving $x = 40/70 = 0.57$ kW/°C and $y = 40/100 = 0.4$ kW/°C. Note

that $C_c \le C_h$ is satisfied only in match 1, the only heat exchanger having both streams at the pinch. The overall HEN, a combination of Figures 11.18a and 11.23, satisfies the MER targets and has the minimum number of heat exchangers (six). Consequently, the cost of utilities is at the minimum, $10,976, with the total purchase cost, $54,889, providing an annualized cost of $16,465 the lowest of all of the alternatives analyzed in the spreadsheet SS1.xlsx in which can be downloaded from the Wiley Website.

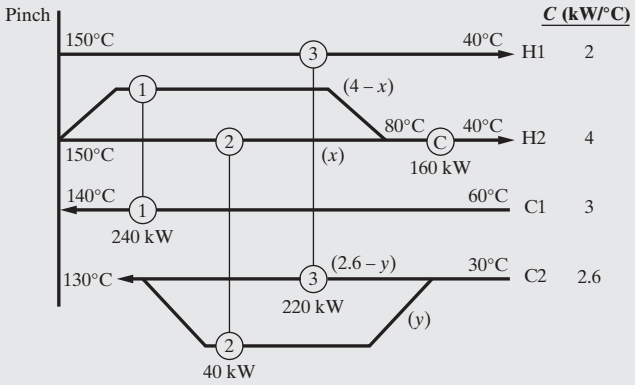

Figure 11.23 Stream splitting on the cold side of the pinch to achieve $N^{-}_{HX,\min}$ for Example 11.9.

Although stream splitting provides these advantages, its use should be considered with caution because it reduces flexibility and complicates process operability. When possible, it is usually preferable to break heat loops without stream splitting as shown later in Example 11.13.

11.5 THRESHOLD APPROACH TEMPERATURE

In many cases, the selected ΔT_{min} is such that no pinch exists, and MER design calls for either hot or cold utility to be used, but not both. The critical ΔT_{min} below which no pinch exists is referred to as the *threshold approach temperature difference*, ΔT_{thres}. Figure 11.24 shows the effect of changing the required ΔT_{min} on the composite curve diagrams for a typical process in which the total enthalpy demand of the cold streams is ΔH_C whereas the hot streams require a total of ΔH_H of cooling. In this example, it is noted that $\Delta H_H > \Delta H_C$. The selected value of ΔT_{min} affects the minimum amounts of hot and cold utilities that are required. The Q-T diagram labeled ❶ in Figure 11.24 shows the situation where the ΔT_{min} value leads to minimum values of Q_{Hmin} external heating and Q_{Cmin} external cooling where these duties are just the enthalpy overhangs at each end of the diagram. Reduction of the value of ΔT_{min} implies a relative shift of the hot composite curve to the left. And at a critical value shown in the Q-T diagram labeled ❷, the shift is such that no hot utility is required with the required cold utility, now reduced to

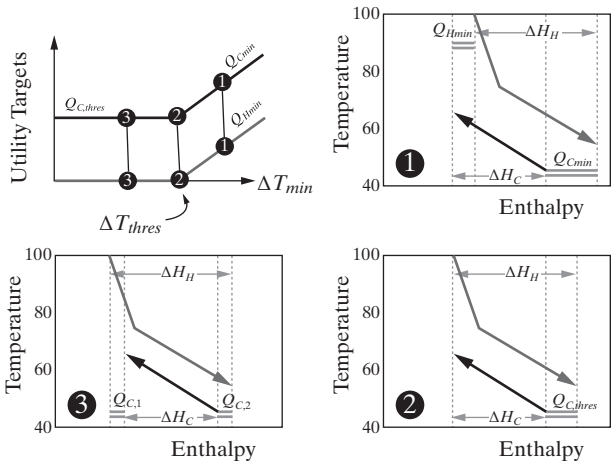

Figure 11.24 The definition of *threshold approach temperature difference*, ΔT_{thres}, for the case where only external cooling utility is required for $\Delta T_{min} < \Delta T_{thres}$.

$Q_{C,thres} = \Delta H_H - \Delta H_C$, the required cooling duty as defined by the first law. It is noted that that the value of ΔT_{min} that makes this come about is the *threshold approach temperature difference*, ΔT_{thres}.

As shown in the Q-T diagram labeled ❸, any further shift of the hot composite curve to the left will, of course, not reduce the required amount of cold utility below $Q_{C,thres}$, but rather, it will split the required cooling duty into a portion at the hot end, $Q_{C,1}$, and a portion at the cold end, $Q_{C,2}$ (such that $Q_{C,1} + Q_{C,2} = Q_{C,thres}$). In summary, as shown on the plot of utility targets as a function of ΔT_{min} on the top left of Figure 11.24 for the case where $\Delta H_H > \Delta H_C$, only $Q_{C,thres}$ cooling utility is required for values of $\Delta T_{min} < \Delta T_{thres}$. For values of ΔT_{min} in excess of ΔT_{thres}, the process pinch exists, and external cooling duties of $Q_{C,min} = \Delta H_H - \Delta H_C + x$, and external heating duties $Q_{H,\min} = x$, where the value of x increases with increasing ΔT_{min}.

The next example shows how MER targets are computed as a function of ΔT_{min}. This is followed by Example 11.11, which demonstrates how the guidelines presented previously are adapted for HEN design in threshold problems.

EXAMPLE 11.10

Compute MER targets for the following streams as a function of the minimum approach temperature:

Stream	T^s (°C)	T^t (°C)	C (kW/°C)	Q (kW)
H1	300	200	1.5	150
H2	300	250	2	100
C1	30	200	1.2	204

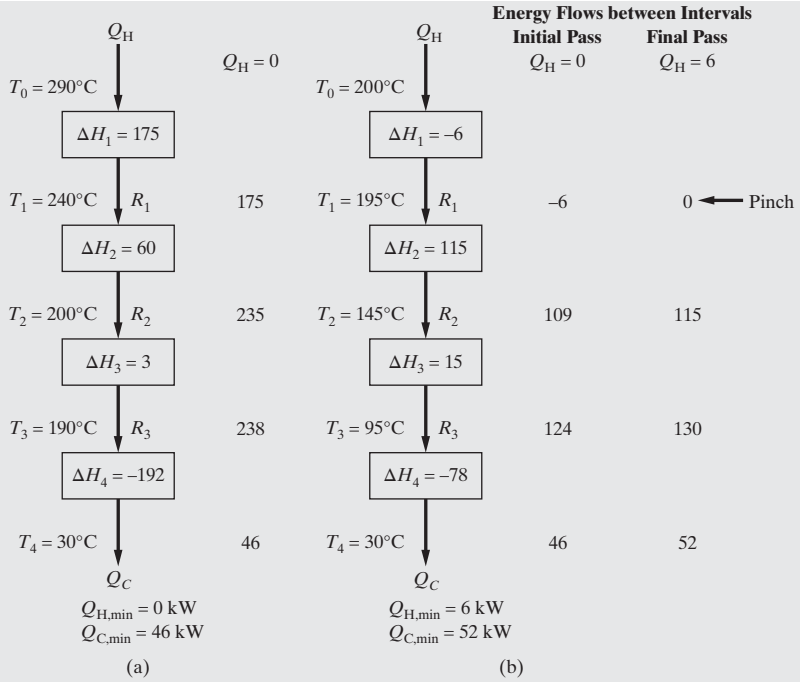

Figure 11.25 Temperature intervals, energy balances, and residuals for Example 11.10 at: (a) $\Delta T_{min} = 10°C$; (b) $\Delta T_{min} = 105°C$.

SOLUTION

For $\Delta T_{min} = 10°C$, no pinch exists as shown in Figure 11.25a using the TI method. Note that 46 kW of cold utility is required. When the analysis is repeated as ΔT_{min} is varied for $\Delta T_{min} > 100°C$, a pinch exists as illustrated in Figure 11.25b for $\Delta T_{min} = 105°C$. Figure 11.26 shows the threshold, $\Delta T_{min} = \Delta T_{thres}$, at which the pinch appears. Since no heating utility is required for $\Delta T_{min} < \Delta T_{thres}$ where the cooling requirement is constant at 46 kW, no energy is saved while capital costs are increased as ΔT_{min} is decreased. The impact of ΔT_{min} on the economics of HENs is considered in Section 11.6.

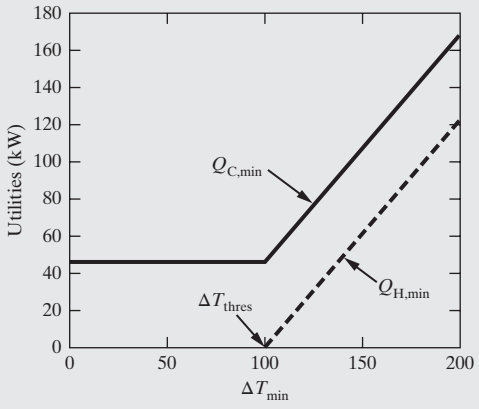

Figure 11.26 Minimum utility requirements as a function of ΔT_{min} for Example 11.10.

EXAMPLE 11.11

For the following streams:

Stream	T^s (°C)	T^t (°C)	C (kW/°C)	Q (kW)
H1	590	400	2.376	451.4
H2	471	200	1.577	427.4
H3	533	150	1.320	505.6
C1	200	400	1.600	320.0
C2	100	430	1.600	528.0
C3	300	400	4.128	412.8
C4	150	280	2.624	341.1

design a HEN at the threshold approach temperature difference, $\Delta T_{min} = \Delta T_{thres} = 50°C$ to meet the MER targets: $Q_{Hmin} = 217.5$ kW and $Q_{Cmin} = 0$ kW as well as the $N_{HX,min}$ target of seven exchangers.

SOLUTION

Although no pinch exists, the MER design procedure is used, starting at the cold end, where matches are placed with $\Delta T_1 = \Delta T_{min} = 50°C$, and reserving the allocation of the utility heaters until last. Furthermore, matches at the limiting ΔT_{min} must have $C_h \leq C_c$, as dictated by the MER design procedure for the hot side of the pinch.

As seen in Figure 11.27, the first match is made bearing in mind that no cooling utility is allowed and stream H3 must be cooled to 150°C. Since C2 is the only cold stream that can be used, internal heat exchanger 1 is installed with a heat duty of 505.6 kW, which completes the cooling requirement of stream H3. Similarly, the second match is between streams H2 and C4 with a heat duty of 341.1 kW,

which completes the heating requirement of stream C4. The remaining matches are far less constrained and are positioned with relative ease. Note that the last units positioned are the auxiliary heaters with a total duty equal to the MER target. Also, seven heat exchangers are utilized (five internal heat exchangers and two auxiliary heaters). Note that this network has no heat loops and stream splitting is not employed.

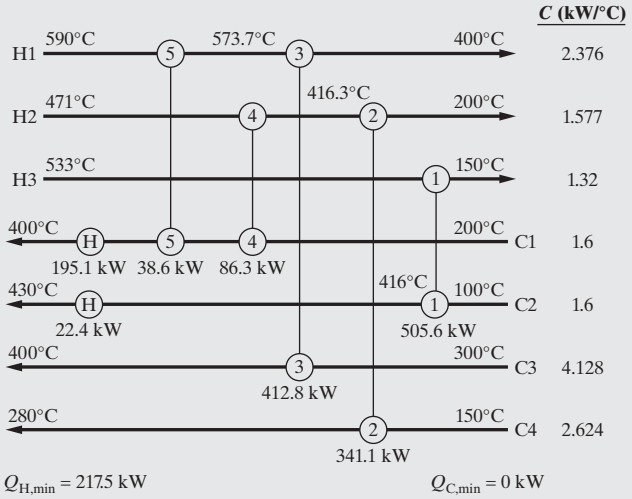

Figure 11.27 HEN with minimum number of exchangers to meet MER target at $\Delta T_{min} = \Delta T_{thres} = 50°C$ in Example 11.11.

11.6 OPTIMUM APPROACH TEMPERATURE

The importance of the minimum approach temperature, ΔT_{min}, has been emphasized in the previous sections. Clearly, as $\Delta T_{min} \to 0$, the true pinch is approached at which the area for heat transfer approaches infinity while the minimum utility requirements are reduced to the absolute minimum. At the other extreme, as $\Delta T_{min} \to \infty$, the heat transfer area approaches zero and the utility requirements are increased to the maximum with no heat exchange between the hot and cold streams. The variations in heat transfer area and utility requirements with ΔT_{min} translate into the variations in capital and operating costs shown schematically in Figure 11.28. As discussed in the previous section, as ΔT_{min} decreases, the cost of utilities decreases linearly until a threshold temperature, ΔT_{thres}, is reached; below it the cost of utilities is not reduced. Furthermore, when $\Delta T_{min} \le \Delta T_{thres}$, there is no pinch, and consequently, the trade-offs between the capital and utility costs as ΔT_{min} decreases become less straightforward. The first impression would suggest that since the cost of utilities is fixed, decreasing ΔT_{min} increases capital costs, implying that the optimal ΔT_{min} must lie on or above ΔT_{thres}. In fact, capital costs depend on ΔT_{lm} rather than on ΔT_{min}, and in practice, only a few of the heat exchangers in a network are actually designed at the ΔT_{min} design constraint, so the effect on capital costs of the number of units in a design may be more significant than that of the value of ΔT_{min} as illustrated in the next example.

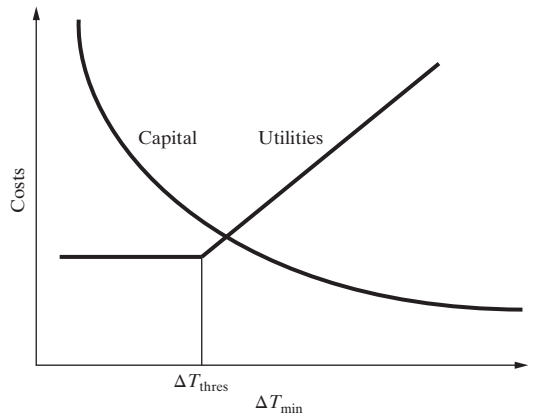

Figure 11.28 Trade-off between capital and utilities costs as a function of ΔT_{min}.

EXAMPLE 11.12

Consider the design of a HEN for four streams in a problem generated initially by Nishida et al. (1977):

Stream	T^s(K)	T^t (K)	C (kW/K)	Q (kW)
C1	269.3	488.7	36.93	8,102.44
H1	533.2	316.5	10.55	2,286.19
H2	494.3	383.2	26.38	2,930.82
H3	477.5	316.5	15.83	2,548.63

The following specifications apply:

Cooling water (cw): $T^s = 310.9$ K, $T^t \le 355.4$ K,
cost of $cw = 0.11023$ \$/1,000kg
Steam (sat'd.,s): $T = 508.7$ K, $\Delta H^v = 1{,}785.2$ kJ/kg,
cost of $s = 2.2046$ \$/1,000kg

Overall heat-transfer coefficients:

$U_{heater} = 0.3505$ kW/m^2 K, $U_{cooler} = U_{exch} = 0.2629$ kW/m^2 K

Purchase cost of heat exchangers:

$$C_P = 1{,}456.3A^{0.6} \quad (\$, \text{ m}^2)$$

Equipment operability = 8,500 hr/yr

Return on investment = $i_m = 0.1$ (for Eq. 11.2)

SOLUTION

For this example, when $\Delta T_{min} \ge \Delta T_{thres,} = 25.833$ K, two pinches exist. This is because the heat-capacity flow rates of streams H1 and H2 sum to the heat-capacity flow rate of stream C1. Consequently, when $\Delta T_{min} = 30$ K, at the first pinch the hot and cold stream temperatures are 494.3 K and 464.3 K, and at the second pinch the temperatures are 477.5 K and 447.5 K. The temperature interval between these temperatures involves just streams H1, H2, and C1 and hence $\Delta T = 30$ K throughout this interval. Above the pinches, steam provides 490.7 kW and below the pinches, cooling water removes 153.89 kW. These minimum utility requirements at $\Delta T_{min} = 30$ K are shown in Figure 11.29a.

When $\Delta T_{min} = \Delta T_{thres} = 25.833$ K, the temperatures of the hot streams at the pinches are unchanged, but the temperatures of the cold streams are 468.5 K and 451.7 K. In this case, on the low-temperature

side of the pinches, no cooling water is required because the composite cold curve begins where the composite hot curve ends as shown in Figure 11.29b.

Figure 11.30 shows the designs for three HENs having minimum utilities at three ΔT_{min}: 30, 25.833, and 16.9 K. For the first two in Figure 11.30a and 11.30b, using the method of Linnhoff and Hindmarsh (1983), stream splitting is required below the first pinch. Stream C1 is split into two streams between the pinches because just streams H1 and H2 are present. Below the second pinch, stream C1 is split into three streams to maximize the temperature driving forces in the three heat exchangers installed between the split stream and the three hot streams. As shown in Table 11.6 , both the purchase and utility costs are lower at ΔT_{thres}. The former is reduced because the cooling water exchanger is no longer needed. At $\Delta T_{min} = 16.9$ K, the HEN is much simpler because no pinches exist as shown in Figure 11.30c. Hence, the purchase cost is lower and the cost of utilities is equal to that at ΔT_{thres}. When compared with the other two networks having minimum utilities, the latter has a lower annualized cost. This result is a counterexample to what one might expect: Even though the design is for a ΔT_{min} value lower than ΔT_{thres}, the capital costs are lower than those for the design at the threshold. The results presented in this example can be checked by running the spreadsheet SS2.xlsx, which can be downloaded from the Program and Simulation File folder on the Wiley Website.

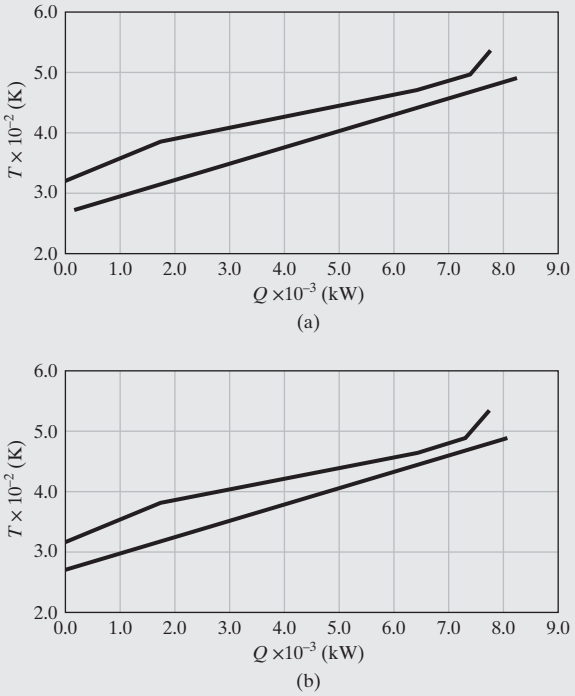

Figure 11.29 Composite heating and cooling curves for Example 11.12: (a) $\Delta T_{min} = 30$ K; (b) $\Delta T_{min} = \Delta T_{thres} = 25.833$ K.

Table 11.6 Cost Comparisons for Example 11.11.

Network	Utilities Cost ($/yr)	C_P, Purchase Cost ($)	C_A, Annualized Cost ($/yr)
$\Delta T_{min} = 30$ K	27,354	213,309	48,685
$\Delta T_{min} = 25.833$ K	12,728	158,183	28,546
$\Delta T_{min} = 16.9$ K	12,728	138,232	26,556

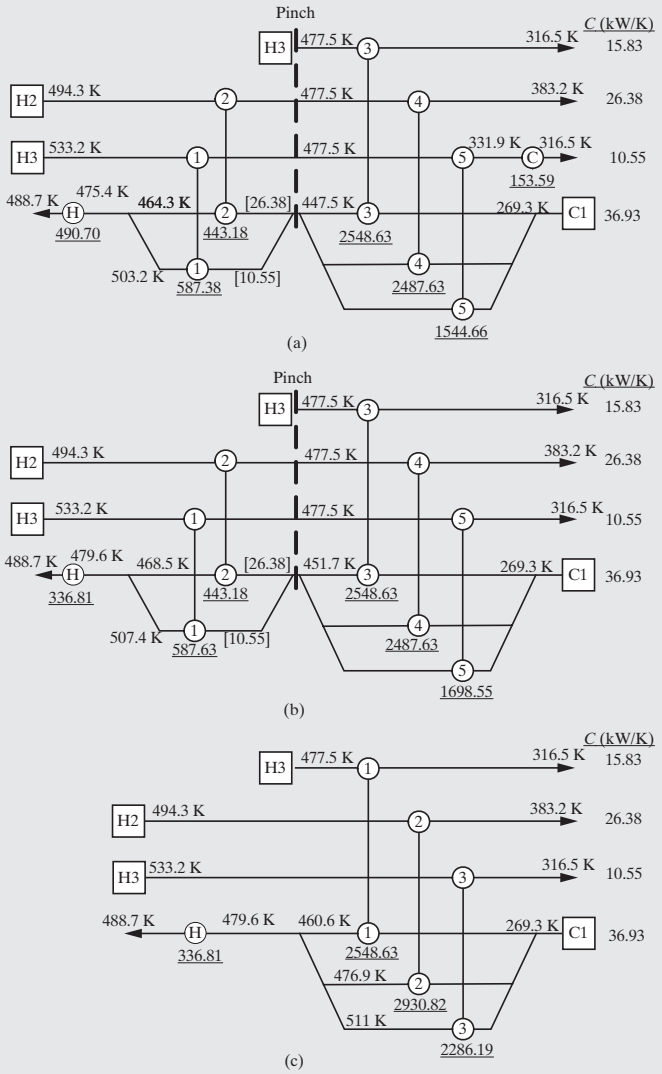

Figure 11.30 HENs for Example 11.12: (a) $\Delta T_{min} = 30$ K; (b) $\Delta T_{min} = 25.833$ K; (c) $\Delta T_{min} = 16.9$ K.

11.7 MULTIPLE UTILITIES

Thus far, multiple sources of hot and cold utilities have not been considered. For example, steam is normally available at several pressures with its cost a function of the pressure (and temperature) level as discussed in Section 17.2 (Table 17.1). To lower the cost of utilities, as well as the lost work, Section 11.7 shows how to use the *grand composite curve* (GCC) to reduce the temperature driving force in the auxiliary heat exchangers.

Designing HENs Assisted by the Grand Composite Curve

Using the TI Method as described above, temperature intervals are identified and residuals computed to estimate the minimum heating and cooling utilities and to locate the pinch temperatures. For example, in the cascade diagram of Figure 11.31 computed for $\Delta T_{min} = 10°C$, the cold pinch temperature is 190°C with the minimum hot and cold utility levels being 1,000 kW each. The residual enthalpies leaving each temperature interval indicate the excess heating or cooling capacity of the cascade above and

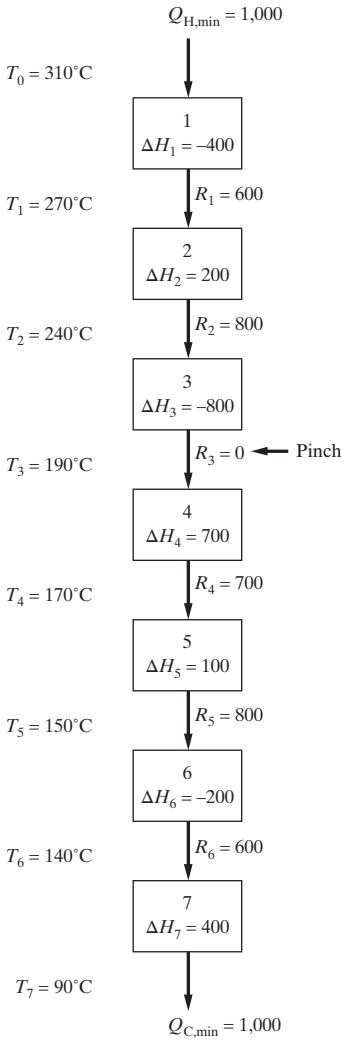

Figure 11.31 Temperature intervals, energy balances, and residuals; ΔH_i, R_i, $Q_{H\,\min}$, and $Q_{C\,\min}$ in kW.

including the temperature interval. This suggests the representation shown in Figure 11.32 referred to as the *grand composite curve* (GCC) in which the enthalpy residuals are displayed as a function of the interval temperatures. The enthalpy residuals corresponding to the highest and lowest interval temperatures are the minimum heating and cooling utility duties, respectively. Furthermore, as seen previously, the process is divided into a portion above the pinch (indicated by a solid circle at the temperature at which the residual enthalpy equals zero) in which there is excess heating demand and a portion below the pinch in which there is excess cooling demand.

In addition to this information, Figure 11.32 provides the following insights:

1. The local rise in the enthalpy residual along the arc BC, which indicates an increase in the residual heat available, can be used to supply the increased demand denoted by the decrease in the enthalpy residual along the arc CD. This is accomplished using internal heat exchange. Similarly, the heat demand along the arc FG can be supplied by internal heat exchange with the arc EF.

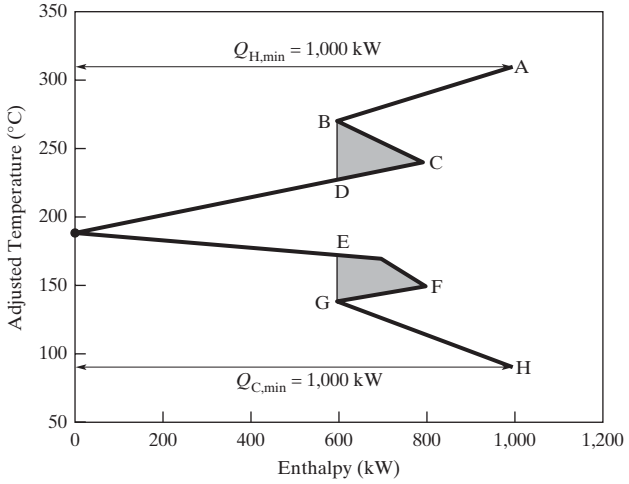

Figure 11.32 Grand composite curve for the temperature intervals in Figure 11.31.

2. When 1,000 kW is provided at 330°C, a fired-heater is required that burns fuel. Alternatively, the GCC replotted in Figure 11.33 shows that up to 600 kW can be provided at 230°C using less expensive high-pressure steam at 400 psi, noting that the alternative utility temperature level and duty are limited by the intercept D. This leaves only 400 kW to be supplied in the fired heater. Similarly, instead of removing 1,000 kW at 90°C using cooling water, up to 600 kW can be removed at 170°C by heating boiler feed water, leading to further savings in operating costs. As before, the temperature level that can be exploited is limited by intercept E. Evidently, significant savings in operating costs are revealed by the GCC.

The GCC is a helpful tool to assist in the targeting of appropriate distributions of types of utilities as illustrated in the next two examples. The first one involves a design for a type of four-stream problem seen previously, but the emphasis is on reducing costs through appropriate selection of utilities.

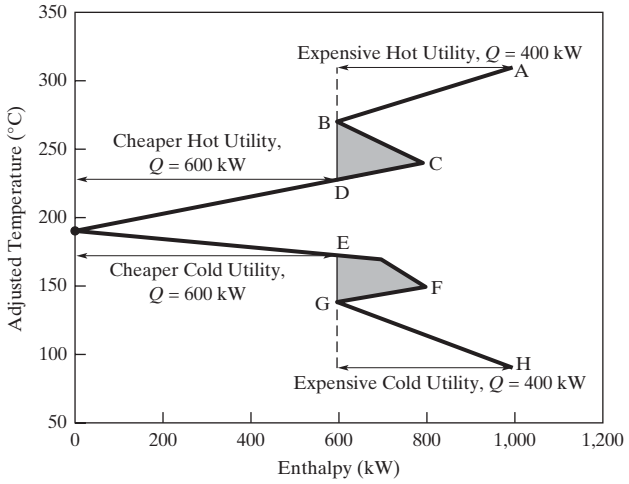

Figure 11.33 Grand composite curve for the temperature intervals in Figure 11.31 showing possible savings by utilizing hps and bfw.

EXAMPLE 11.13

Consider the design of a HEN for the four streams below with $\Delta T_{min} = 10°C$:

Stream	T^s (°C)	T^t (°C)	C (kW/°C)
H1	180	40	20
H2	160	40	40
C1	60	220	30
C2	30	180	22

To reduce operating costs, the design should consider alternative utility sources: high-pressure (hps) and intermediate-pressure (ips) steam, boiler feed water (bfw), and cooling water (cw).

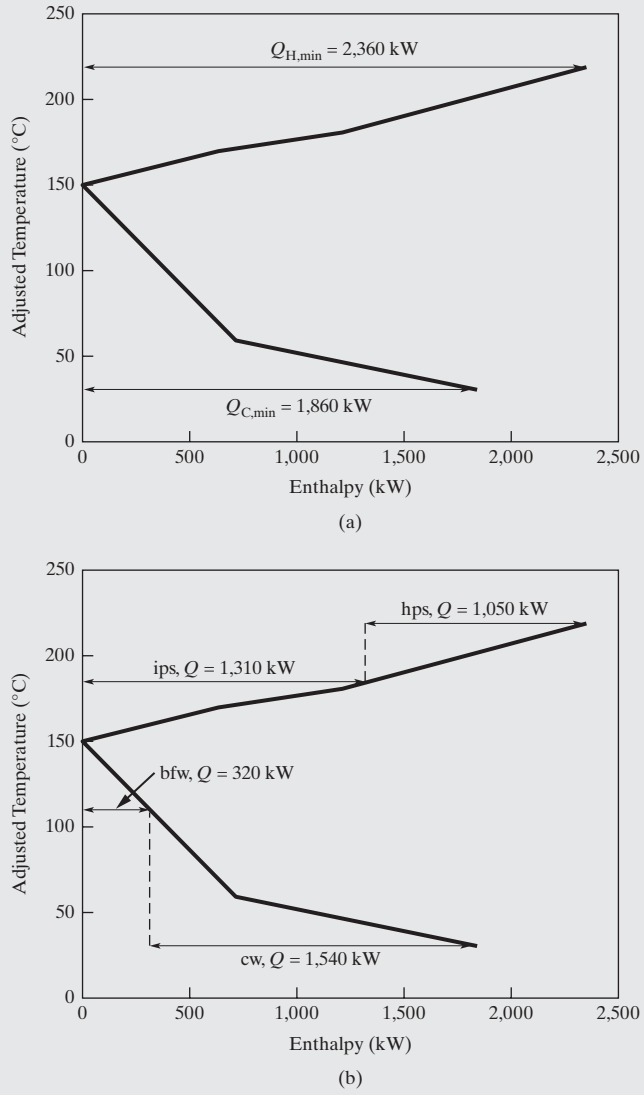

Figure 11.34 Grand composite curve for Example 11.13: (a) MER targets; (b) possible positioning of multiple utilities.

SOLUTION

The TI method is used to construct the grand composite curve shown in Figure 11.34a, which indicates that MER targets are $Q_{Hmin} = 2{,}360$ kW and $Q_{Hmin} = 1{,}860$ kW with pinch temperatures of 150 and 160°C. Since stream H2 does not appear on the hot side of the pinch, the minimum number of exchangers that meets MER targets, $N^{MER}_{HX,\min} = N^{+}_{HX,\min} + N^{-}_{HX,\min} = 3 + 4 = 7$. A HEN designed for $N^{MER}_{HX,\min} = 7$ is shown in Figure 11.35a in which cooling water and HP steam are used. A simpler design obtained by eliminating heat exchanger 3 and thus, breaking one of the heat loops in Figure 11.35a is shown in Figure 11.35b, noting that this involves 240 kW of additional heating and cooling utilities.

An alternative design is suggested in Figure 11.34b in which a portion of the hot utility, 1,310 kW, is supplied as ips steam at 195°C (at an adjusted temperature of 185°C). Furthermore, a portion of the cold utility duty, 320 kW, is used to generate boiler feed water (bfw) at 110°C. These substitutions lead to the more complex design in Figure 11.36 involving three pinches: a process pinch at 150–160°C, utility pinches at 110–120°C, and 185–195°C. The two utility pinches arise because of the infinite heat-capacity flow rates associated with the utility streams. Note that the $N^{MER}_{HX,\min}$ target of 12 heat exchangers is met by stream splitting and careful matching to permit a feasible design. Furthermore, the number of heat exchangers can be reduced by (1) combining heat exchangers 6 and 10; (2) eliminating exchanger 1, reducing the capital costs at the expense of shifting 650 kW of hot utility duty from ips to hps stream; (3) eliminating heat loops, probably at the expense of additional utilities (see Exercise 11.19).

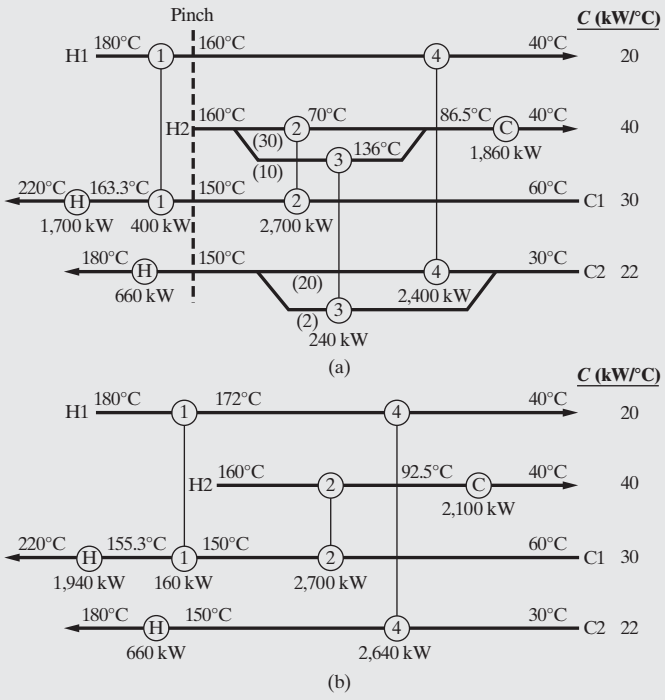

Figure 11.35 HENs for Example 11.13: (a) design to meet the $N^{MER}_{HX,\min}$ target; (b) simplified design after breaking a heat loop.

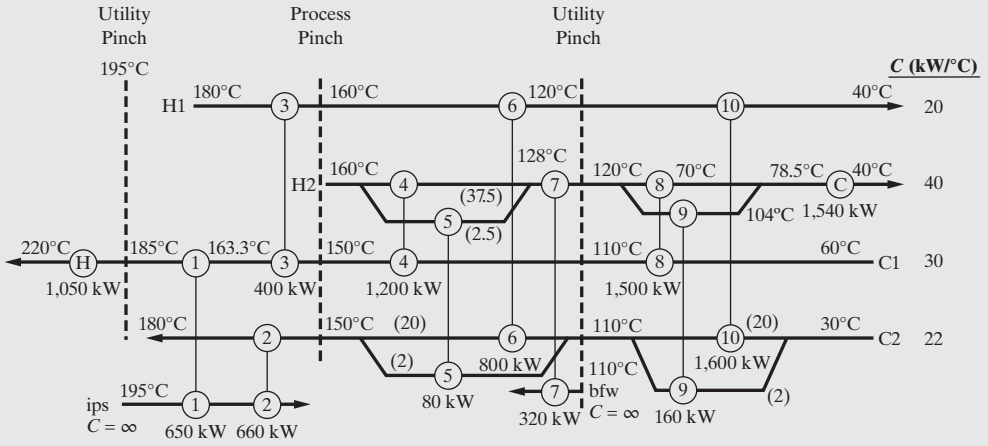

Figure 11.36 HEN for Example 11.13 utilizing cheaper utilities while meeting the $N_{HX,\min}^{MER}$ target.

The next example of the application of the GCC in design introduces the heat integration of a distillation column, which is dealt with in greater detail in Section 11.8.

EXAMPLE 11.14 *Designing a HEN for an Air Separation Column*

Figure 11.37 is the process flow diagram (PFD) for an air separation column fed with hot compressed air. Design a HEN for this process that meets MER targets with $\Delta T_{min} = 5°C$ to minimize operating costs. Utilities are to be selected from among those available on-site from the list in Table 11.7.

Table 11.7 List of available utilities for Example 11.14.

Utility	Type	T^s (°C)
bfw@hp	Cooling	215
bfw@ip	Cooling	185
cw	Cooling	20
NH_3_Refrig	Cooling	−30
CH_4_Refrig	Cooling	−160
N_2_Refrig	Cooling	−190
lps	Heating	150

SOLUTION

Four process streams are extracted from the PFD in Figure 11.37 as shown in the following table:

Stream	T^s (°C)	T^t (°C)	ΔH (kW)	C (kW/°C)
H1	255	−145	2400	6
H2	−150	−151	1500	1500
C1	−150	0	900	6
C2	−130	−129	1400	1400

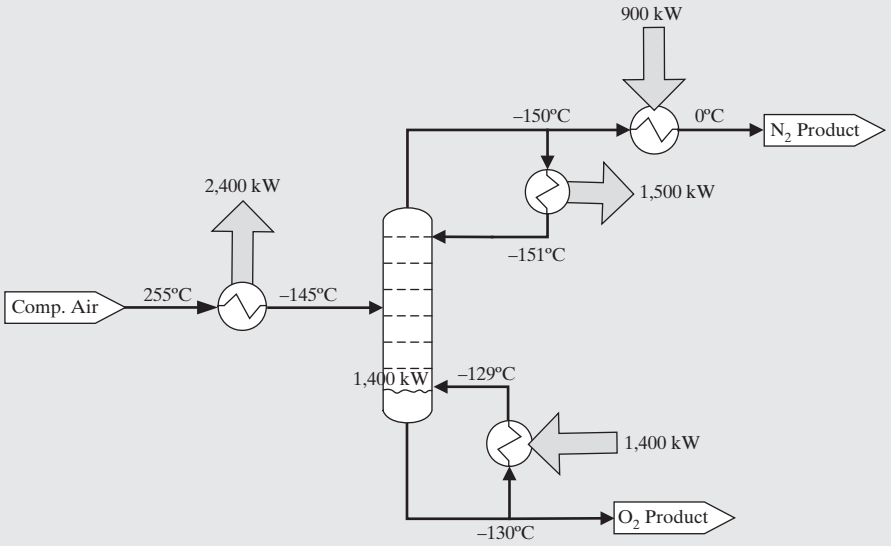

Figure 11.37 Process flow diagram for the separation of compressed air.

MER Targeting for $\Delta T_{min} = 5°C$:

Interval	$T_{i-1} - T_i$ (°C)	H1	H2	C1	C2	$\sum C_h - \sum C_c$	ΔH(kW)
1	250 – 0 = 250					+6	1,500
2	0 – (–129) = 129					0	0
3	–129 – (–130) = 1					–1,400	–1,400
4	–130 – (–150) = 20					0	0
5	–150 – (–155) = 5					0	0
6	–155 – (–156) = 1					+1,500	+1,500

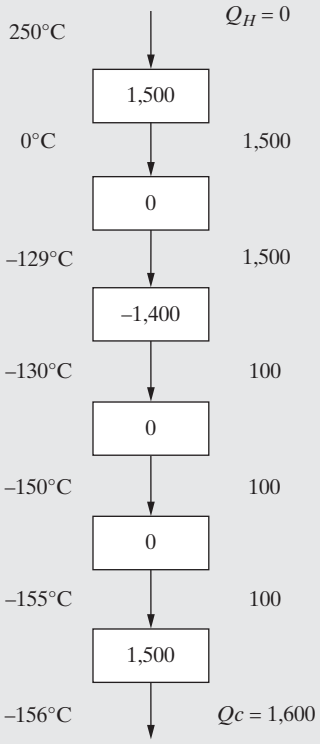

Figure 11.38 Enthalpy cascade for Example 11.14.

The enthalpy cascade is shown in Figure 11.38. Clearly, this is a threshold problem with $Q_{Hmin} = 0$ kW and $Q_{Cmin} = 1{,}600$ kW. Note the jumps in residual enthalpy from 1,500 to 100 kW at −130°C, and then back to 1,600 kW at −156°C, which are the adjusted temperatures corresponding to the reboiler and condenser of the air separation column, resulting in a "notch" in the GCC.

The GCC shown in Figure 11.39 enables the partitioning of the total cold utility requirements of 1,600 kW into two parts: (1) 100 kW at about 240°C, which can be satisfied using hp bfw, and (2) 1,500 kW at −156°C, which can be satisfied using methane refrigerant. These selections ensure minimization of operating costs as the usage of high-pressure bfw as a coolant provides revenue, and the choice of methane as refrigerant is the cheapest on the list that provides a driving force for heat transfer in the condenser. A HEN that meets the MER targets, as partitioned into these two types of cold utility, is shown in Figure 11.40.

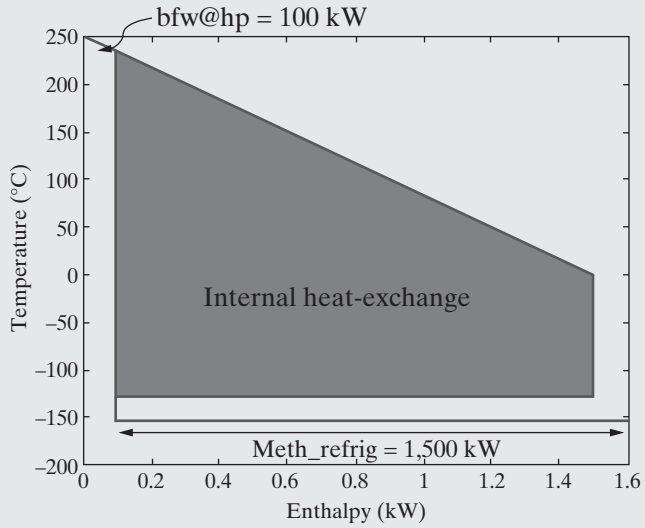

Figure 11.39 Grand composite curve for Example 11.14.

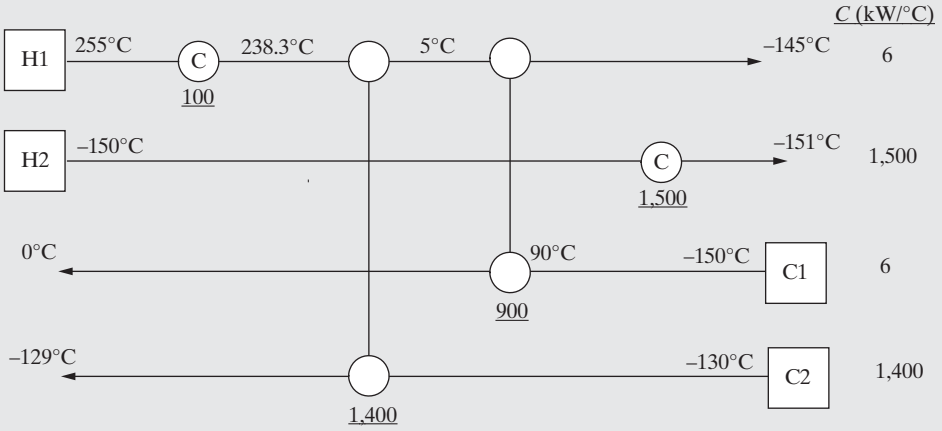

Figure 11.40 HEN for Example 11.14.

11.8 HEAT-INTEGRATED REACTORS AND DISTILLATION TRAINS

Although distillation is highly energy intensive, having a low thermodynamic efficiency (less than 10% for a difficult separation as shown in Example 10.4), it continues to be widely used for the separation of organic chemicals in large-scale chemical processes. As discussed in Chapter 9, the designer normally seeks to utilize more effective separation processes, but in many cases has no choice but to resort to distillation because it is more economical, especially in the manufacture of commodity chemicals.

In the previous sections of this chapter, methods have been discussed for exchanging heat between high-temperature sources and low-temperature sinks. When distillation operations are present in a process flowsheet, it is particularly important to consider the heating requirements in the reboilers and the cooling requirements in the condensers as HENs are designed. Furthermore, over the past two decades, several approaches have been suggested for the energy-efficient incorporation of distillation columns into a process flowsheet. This section is intended to present some of these approaches. Before pursuing a detailed discussion of the heat integration of distillation columns, this section begins with a summary of rules concerning the appropriate placement of reactors and distillation columns (Smith, 2005).

Appropriate Placement of Reactors and Distillation Columns

The basic rule that applies in the guidance of appropriate placement of both reactors (Glavic et al., 1988) and distillation columns (Smith and Linnhoff, 1988) is to ensure that external heating occurs only above the pinch and that external cooling only occurs below the pinch. Figure 11.41 summarizes the possible options regarding the placement of reactors within an existing background process, expressed in the form of its enthalpy cascade, computed without accounting for the reactor.

Figure 11.41a shows the placement of an exothermic reactor above the pinch whereas Figure 11.41b shows its insertion below the pinch. Because the exothermic reactor is an external heat source from the point of view of the background process, placing the exothermic reactor above the pinch reduces the demand on external heating utilities by an amount equal to the enthalpy released by the reactor, Q_{react}. In contrast, placing the exothermic reactor below the pinch is equivalent to introducing utility heating and must be compensated by additional utility cooling equal to the enthalpy released by the reactor. Evidently, the appropriate placement of exothermic reactors is above the pinch. As shown in Figures 11.41c and 11.41d, the appropriate placement of endothermic reactions is below the pinch because they are heat sinks with respect to the background process.

Turning to the appropriate placement of distillation columns, consider Figure 11.42, which shows alternative positioning of a distillation column in the enthalpy cascade of an existing background process, computed without consideration of the column's condenser and reboiler duties. Figure 11.42a shows the consequence of placing the column across the pinch (i.e., positioning the reboiler above the pinch and the condenser below the pinch).

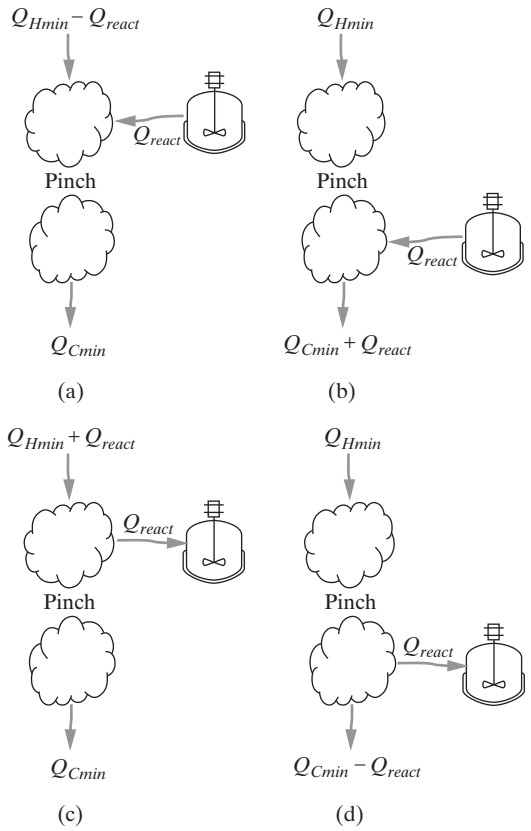

Figure 11.41 Alternative placements of exothermic and endothermic reactors in the enthalpy cascade of a background process: (a) exothermic reactor placed above the pinch; (b) exothermic reactor incorrectly placed below the pinch; (c) endothermic reactor incorrectly placed above the pinch; (d) endothermic reactor placed below the pinch.

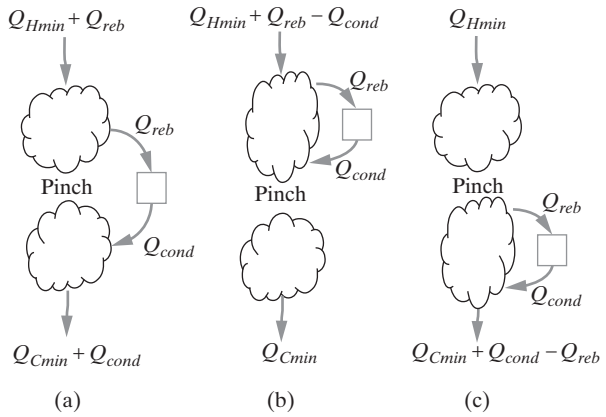

Figure 11.42 Alternative placements of a distillation column in the enthalpy cascade of a background process.

In this case, the hot utility load on the process is increased above its original Q_{Hmin} by an amount equal to the reboiler duty, Q_{reb}, and its cold utility load is increased from Q_{Hmin} by an amount equal to the condenser duty, Q_{cond}. In other words, the column has not been heat integrated at all, and placement across the pinch merely transfers heat across the pinch. In fact, the correct

placement of a distillation column is either completely above the pinch as shown in Figure 11.42b or completely below the pinch as shown in Figure 11.42c. In the former case, the hot utility duty is changed from Q_{Hmin} to $Q_{Hmin} + Q_{reb} - Q_{cond}$, and the cold utility duty demand remains unchanged. In the latter case, the hot utility duty remains unchanged and the cold utility duty changes from Q_{Cmin} to $Q_{Cmin} + Q_{cond} - Q_{reb}$. As will be shown, because the reboiler and condenser duties for many columns are comparable, this implies that ***the correct placement of a distillation column is either above or below but not across the pinch***.

In summary, three heuristics result:

1. **When positioning exothermic reactors to reduce the total utilities, place them entirely *above* the pinch.**
2. **When positioning exothermic reactors to reduce the total utilities, place them entirely *below* the pinch.**
3. **When positioning distillation columns to reduce the total utilities, place them either *above* or *below* the pinch but *never across* the pinch.**

Impact of Operating Pressure of Distillation Columns

As discussed in Section 9.4, the column pressure of a distillation column is a key design variable because it determines the temperature levels in the reboiler and condenser and, consequently, the possible heating and cooling media. Earlier, when synthesizing the vinyl-chloride process in Figure 2.6, it was noted that: "… heat is needed to drive the reboiler in the first distillation column at 93°C, but the heat of reaction (available from the direct chlorination of ethylene at 90°C) cannot be used for this purpose unless the temperature levels are adjusted." Furthermore, the question was raised: "How can this be accomplished?"

The principal vehicle for enabling these kinds of energy exchanges in most processes is through the adjustment of the pressure of the distillation towers, although in many cases it is possible to operate the reactor at a higher temperature. For the direct chlorination of ethylene in the liquid phase, it should be possible to increase the reactor temperature without increasing the rate of undesirable side reactions; and consequently, this alternative should be considered. The other alternative is to reduce the pressure of the distillation tower, thereby reducing the reboiler temperature and permitting the condensation of the dichloroethane product in the reboiler of the first tower. This reduces the usage of cooling water and steam or eliminates them entirely, depending upon the cooling and heating demands. Also, as the distillation pressure is reduced, the separation is made easier and the number of stages is decreased. On the down side, however, the temperature of the condenser is reduced. If it is reduced below the temperature at which cooling water can be used, the cost of refrigeration becomes a significant cost factor (largely through an increased compression load). Furthermore, the integrated process is more difficult to control. In many cases, however, the combined savings in the utilities and the capital cost of the heat exchangers and the column exceeds the added refrigeration costs, and a reliable control system can be designed for the heat-integrated process as discussed in Chapter 20.

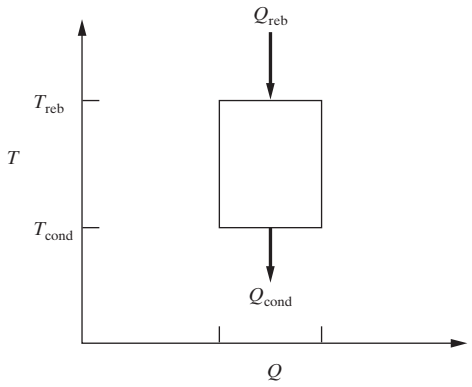

Figure 11.43 T–Q diagram for a distillation column.

As introduced by Dhole and Linnhoff (1993), when working with the grand composite curve for the background process into which a distillation column is to be heat integrated, it helps to examine the column's heating and cooling requirements using a T–Q diagram, as shown in Figure 11.43. This diagram shows the heat provided to the reboiler, Q_{reb}, at temperature, T_{reb}. Similarly, the diagram shows the heat removed from the condenser, Q_{cond}, at temperature, T_{cond}. The principal assumption in Figure 11.43 is that $Q_{reb} \approx Q_{cond}$. At first, this assumption may appear unjustified, but is reasonable for most distillation towers, especially when the feed and product streams are saturated liquids. To justify this for the distillation tower in Figure 11.44, the energy balance in the steady state is:

$$FH_F - DH_D - BH_B + Q_{reb} - Q_{cond} = 0 \tag{11.19}$$

Then, for saturated liquids where $T_{cond} < T_F < T_{reb}$, a reasonable approximation is:

$$FH_F - DH_D - BH_B \approx 0 \tag{11.20}$$

and consequently,

$$Q_{reb} \approx Q_{cond} \tag{11.21}$$

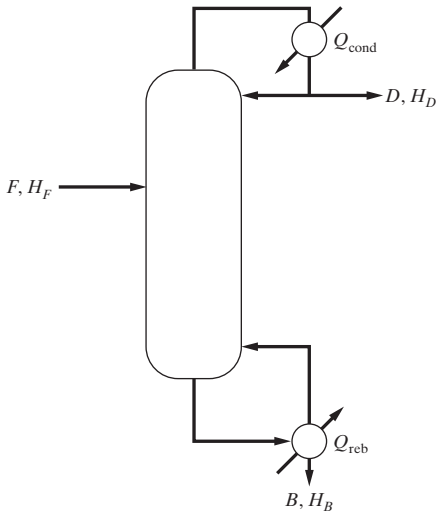

Figure 11.44 Schematic of a distillation tower.

It is important to note that the heat duty, $Q \approx Q_{reb} \approx Q_{cond}$, is related directly to the reflux ratio. When Q is reduced because the cost of fuel is high, the number of trays (or the height of the packing) increases. Clearly, the trade-offs between operating and capital costs significantly influence the optimal design.

To see how T–Q rectangles are used in conjunction with the grand composite curve to assist in heat-integrating columns with process streams, consider the integration of two distillation columns, both requiring 6 MW in condenser and reboiler duties, into an existing background process as represented by the GCC in Figure 11.45. The operating pressures of these two columns have been adjusted so the T–Q rectangle positioned between reboiler and condenser operating temperatures provides a match with the GCC trajectory, more specifically:

1. The T–Q rectangle for column A has been adjusted to lie under the pinch, and it receives all its 6 MW reboiler duty and half of its condenser duty requirements by heat exchange with the background process; the remaining half of its condenser duty is used to raise steam using boiler feed water (bfw). A balance of 3.5 MW of cooling required by the background process is satisfied by cooling water.
2. The T–Q rectangle for column B has been adjusted to lie above the pinch, and it receives all of its 6 MW reboiler utility duty from furnace heat and then transfers its condenser duty to meet lower temperature heating requirements of the background process, which requires only a balance of 3.5 MW of additional heating that is met by high pressure steam (hps). It is noted that this positioning of column B introduces a second process pinch at that column's condenser temperature.

Unfortunately, it can be difficult to position a tower like Column A in Figure 11.45 unless the chemical species being separated are close boiling. Alternatively, the pressure of the tower can be adjusted and the tower positioned so that the reboiler receives its energy from a hot utility and the condenser rejects its energy to the cold process streams above the pinch as with Column B in Figure 11.45.

After matching the column energy requirements with the energy availability in the background process by adjusting the positions of the column T–Q rectangles on the GCC constructed for the background process alone, one can then treat the column condenser and reboiler duties as additional hot and cold process streams, respectively, recompute the updated enthalpy cascade, and redraw the GCC for the resulting integrated process (i.e., including the columns) as shown in Figure 11.46. Note the "notches" introduced into the GCC by the two columns, and the additional pinch at 280°C, the condenser temperature of column B. Note that in the HEN design for an air-separation column in Example 11.14, a threshold problem requiring only cold utility, the column appears as a "notch" in the GCC (see Figure 11.39) with the column's reboiler duty supplied by heat exchange with the background process and its condenser duty supplied using methane refrigerant utility.

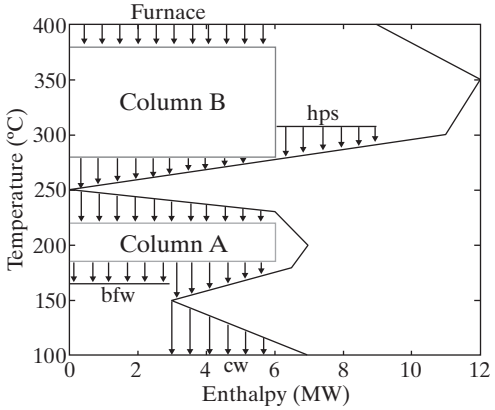

Figure 11.45 Use of the GCC to integrate two columns (indicated by the T–Q rectangles) into a background process (GCC).

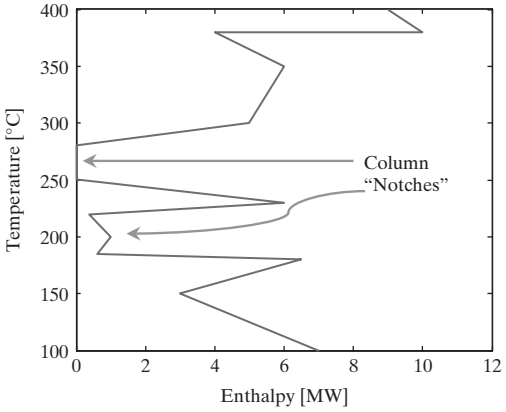

Figure 11.46 The GCC for the process in Figure 11.45 after including the columns' condenser and reboiler streams.

Multiple-Effect Distillation

For separations where the T–Q rectangle for a distillation tower cannot be positioned appropriately in the GCC as in Figure 11.45, several possibilities exist for creating a more energy-efficient distillation operation. One widely used configuration for distilling water is *multiple-effect distillation* in which the feed stream is split into approximately equal portions and sent to the same number of separate distillation towers, each operating at a different pressure as illustrated in Figure 11.47a for a cascade of two effects. The pressures in the towers decrease from the bottom to the top of the cascade so that the temperatures of the adjacent condensing vapors and boiling liquids differ by ΔT_{min}. In this way, heat from the condensing vapor in the tower below at a pressure of P_2 is transferred to boil the bottoms liquid from the tower above at the lower pressure of P_1. Note that the flow rates of the feed streams are adjusted to equate the duties of the adjacent condensing and boiling streams. In this way, the heat duties associated with condensation and boiling, Q_{effect}, are approximately equal to the heat duty for a single effect, Q, divided by the number of effects, N_{effect}; that is, $Q_{effect} \approx Q/N_{effect}$. When the price of fuel is high, this represents a substantial reduction in the operating costs. On the down side, however, the pressure level is increased in $N_{effect} - 1$ of the distillation towers, and multiple towers are needed. While pumping costs to increase

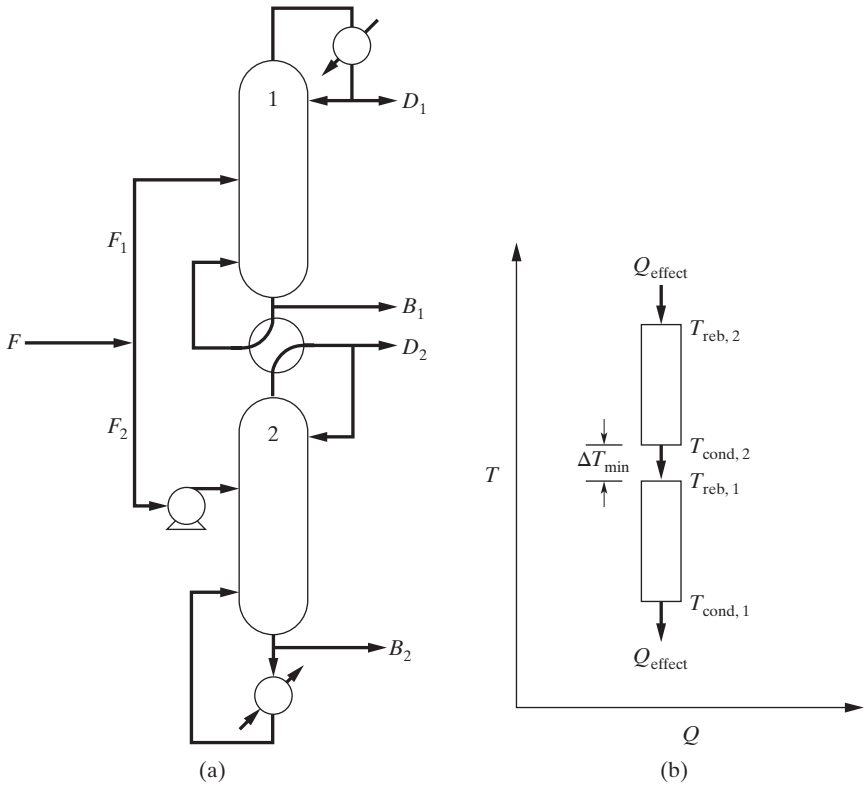

Figure 11.47 Two-effect distillation: (a) tower and heat exchanger configuration; (b) T–Q diagram

the pressure of liquid feed streams are low, the tower walls are thicker, increasing the purchase costs, and the relative volatility is decreased at higher pressures, increasing the number of trays (or height of the packing) required to maintain the same reflux, that is, the same Q_{effect}. In many cases, these increases in the operating and purchase costs are small when compared with the large savings in the utilities for condensing and especially boiling. The net effect of dividing the feed stream into N_{effect} nearly equal portions is to elongate the T–Q diagram as shown in Figure 11.47b.

Two variations on multiple-effect distillation do not involve *feed splitting* (FS) as described above and shown in Figure 11.48a. For these configurations as shown in Figures 10.48b and 10.48c, the entire feed stream is sent to the first tower. In the *light split/forward heat integration* (LSF) configuration (Figure 11.48b), the feed is pumped and sent to the high-pressure column. About half of the light key component is removed in the distillate at high purity. The bottoms product, which contains the remainder of the light key component, is fed to the low-pressure column. In this case, the heat integration is in the direction of the mass flow. For the other variation in Figure 11.48c, referred to as the *light split/reverse heat integration* (LSR) configuration, the feed is sent to the low-pressure column. Here, also about half of the light key component is removed in the distillate with the

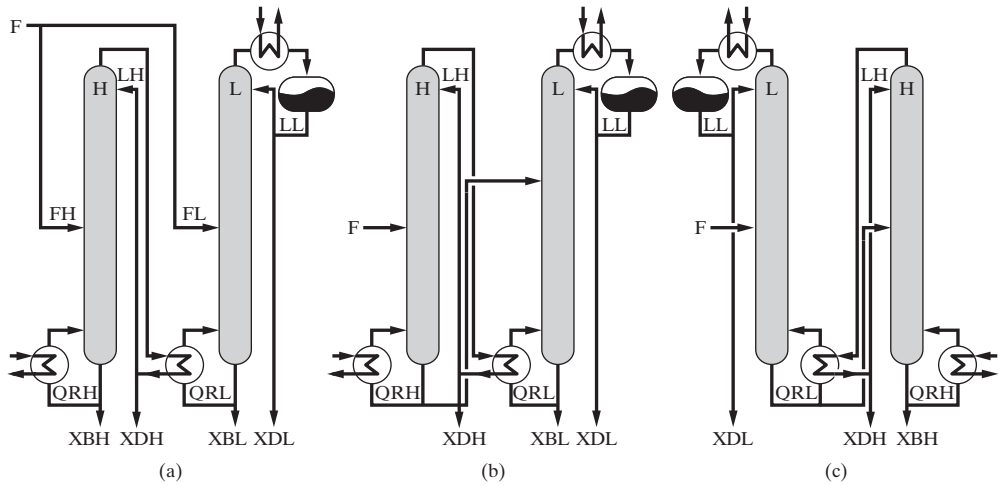

Figure 11.48 Variations on two-effect distillation: (a) FS; (b) LSF; (c) LSR.

bottoms product pumped and sent to the high-pressure column. In this case, the heat integration is in the reverse direction of the mass flow. Note that these configurations are compared among themselves and with a single column in Example 20S.8, where the dehydration of methanol is examined. First, the configurations are compared when operation is in the steady state. Then, the controllability and resiliency (C&R) of each configuration is assessed in response to typical disturbances and verified by dynamic simulations of the FS and LSR configurations, confirming the findings of the C&R analysis.

The following example illustrates how an exothermic reactor and a separation system, involving two distillation columns operating at suitably selected pressures, can be integrated with a background process to minimize operating costs.

EXAMPLE 11.15 *Heat Integration in a Methanol Synthesis Loop*

Figure 11.49 shows the PFD of methanol plant's synthesis loop. The synthesis feed gas is compressed from 13 to 48 bar in compressor K-100, mixed with the recycle stream and then raised to 50 bar in K-101. The compressed synthesis gas is heated to 200°C in E-100 and then fed to the converter, R-100, which partially converts the feed gas to methanol and water, exiting the reactor at 300°C. The reactor effluent is cooled to 30°C in E-101 and then fed to a flash vessel, V-100, which produces a vapor overhead product and a liquid bottoms product. The overhead product is partly purged before returning to K-101 as recycle. The liquid product from V-100 undergoes pressure reduction to 10 bar before flashing in V-101 into a small vent stream and a liquid stream that is fed to column T-100. T-100 produces some of the methanol product as distillate and a mixture of methanol and water as bottoms, whose pressure is reduced to 2 bar before being fed to a second column, T-101, which produces the remainder of the methanol product as distillate and water as bottoms.

1. Compute the MER targets for $\Delta T_{min} = 10°C$.
2. Sketch the GCC using your targeting results from (1). Because utilities are available as shown in Table 11.8 and noting the costs per MW of each type of utility (given relative to the cost of cooling water), use the GCC to define the amounts of each utility that should be used to minimize operating costs.
3. Design a HEN with the minimum number of units to meet MER targets for $\Delta T_{min} = 10°C$ and to minimize the utility costs.

Table 11.8 Temperatures and Costs of Utilities

Utility Type	C/H	T^S (°C)	T^T (°C)	Annual Cost/MW (relative to cw)
Cooling water, cw	C	20°C	40°C	1
Boiler feed water, bfw	C	185°C	185°C	−12[a]
Low press. steam, lps	H	145°C	145°C	20
Inter. press. steam, ips	H	185°C	185°C	25
High press. steam, hps	H	250°C	250°C	30

[a] As usage of bfw generates revenue, its relative cost is negative.

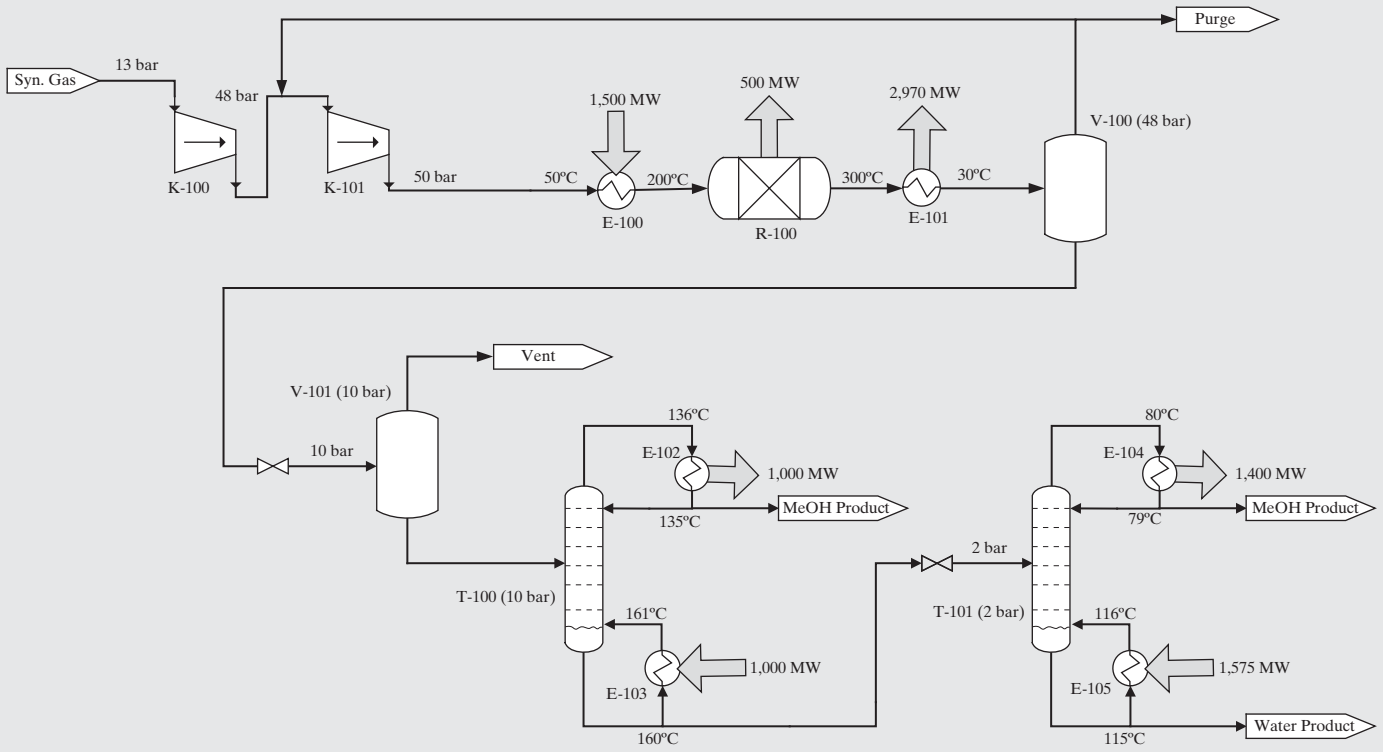

Figure 11.49 PFD for a process for the manufacture of methanol from synthesis gas.

SOLUTION

Data extraction and MER targeting: The following stream table can be extracted from the information on the PFD:

Stream	T^S (°C)	T^T (°C)	ΔH (MW)	C (MW/°C)
C1	50	200	1500	10
C2	160	161	1000	1000
C3	115	116	1575	1575
H1	200	300	500	5
H2	300	30	2970	11
H3	136	135	1000	1000
H4	80	79	1400	1400

The above data can be used to complete the interval table (hot stream temperatures reduced by $\Delta T_{min} = 10$°C):

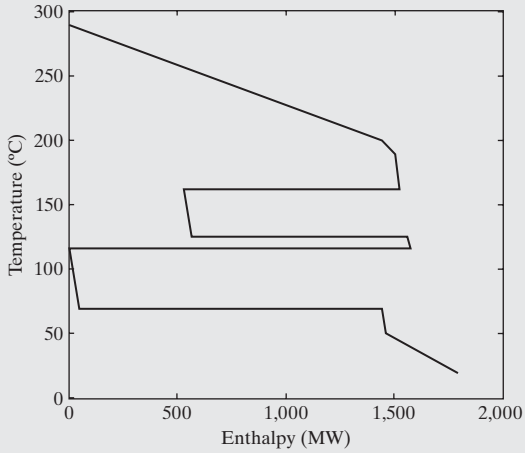

Figure 11.50 GCC for Example 11.15.

Interval	$T_i - T_{i-1}$(°C)	H1	H2	H3	H4	C1	C2	C3	$\sum C_H - \sum C_C$	ΔH(MW)
1	290 – 200 = 90								+16	+1,440
2	200 – 190 = 10								+6	+60
3	190 – 161 = 29								+1	+29
4	161 – 160 = 1								–999	–999
5	160 – 126 = 34								+1	+34
6	126 – 125 = 1								+1,001	+1,001
7	125 – 116 = 9								+1	+9
8	116 – 115 = 1								–1,574	–1,574
9	115 – 70 = 45								+1	+45
10	70 – 69 = 1								+1,401	+1,401
11	69 – 50 = 19								+1	+19
12	50 – 20 = 30								+11	+330

Using the table above, one can construct an enthalpy cascade from which MER targeting is determined: the cold pinch temperature is 115°C, and the hot and cold utility targets are $Q_{H,Min} = 0$ MW and $Q_{C,Min} = 1795$ MW, respectively (i.e., this is a threshold problem). The GCC prepared using these results shown in Figure 11.50 indicates that the total external cooling duty required can be satisfied using cooling water. Note that this GCC is also characterized by two "notches" corresponding to the locations of the two columns and that the process pinch at 115°C is introduced by the reboiler of column T-101. Guidance for the correct placement of the two columns, that is, for the selection of their operating pressures, is facilitated by plotting the GCC first for the background process excluding the two columns, and then adjusting the positions of the column T–Q rectangles to obtain good fits as seen previously in this section.

HEN synthesis to meet MER targets: Figure 11.51 shows a possible HEN that satisfies the MER targets. In this design:

1. Above the pinch we are not allowed to use cold utilities and the MER target for the hot utility is 0 MW. Thus, because neither hot nor cold utilities can be employed above the pinch, all of the heat required by the three cold streams needs to be provided by the hot streams. The first thing to notice is that the two hottest streams, H1 and H3, need to be matched against C2 and C3, respectively, consuming all of their heat. Note that these two matches are critical to satisfy the MER targets, and because the cold streams matched are both associated with reboilers, the order that hot streams match to them is unimportant (because the temperatures of those two streams are almost constant). These matches satisfy the requirements of both hot streams, leaving C2 short by 500 MW and C3 short by 575 MW.
2. This leaves only one hot stream, H2, at the pinch, which must supply heat to two cold streams at the pinch, C1 and C3, meaning that H2 must be split. H2 is split and heat exchangers are introduced, connecting to C1 with duty 850 MW (satisfying the requirements of C1) and with C3 having duty 575 MW (satisfying the requirements of C3). Split C's are selected to ensure isothermal mixing at the splits.
3. Finally, a heat exchanger is installed between H2 and C2 with duty 500 MW, completing the hot side.

The design below the pinch is trivial.

There are five units above and three below the pinch, which are the minimum number of units that allow the MER to be matched (above the pinch, $N^+_{HX,\min} = 6_{\text{streams}} + 0_{\text{utilities}} - 1 = 5$, and below the pinch, $N^-_{HX,\min} = 3 + 1 - 1 = 3$).

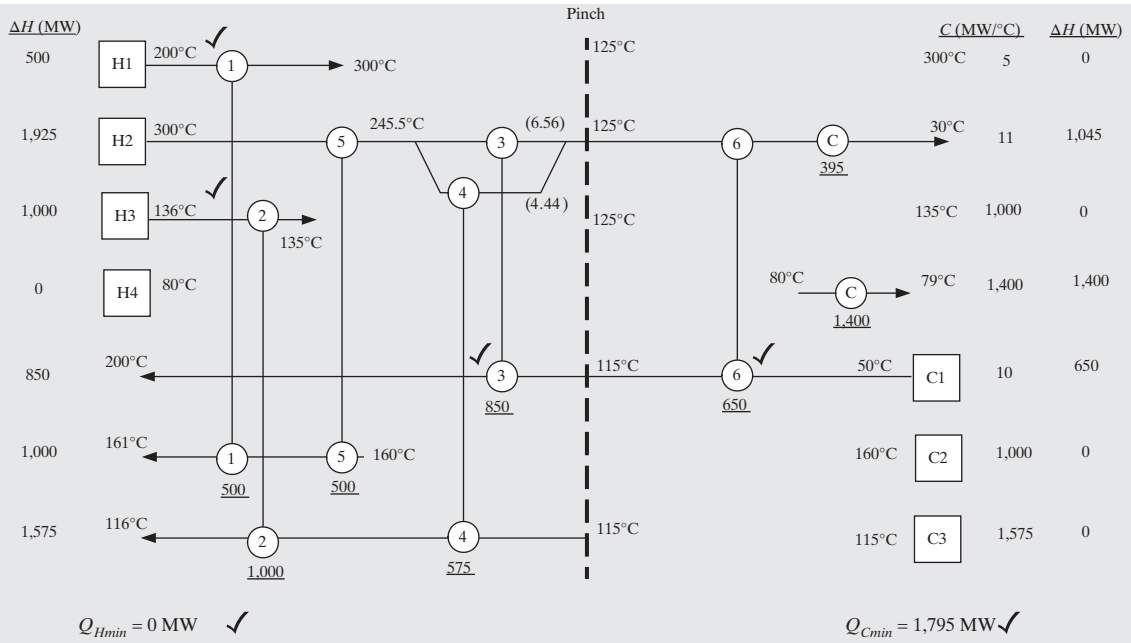

Figure 11.51 HEN for Example 11.15.

Heat Pumping, Vapor Recompression, and Reboiler Flashing

Other more sophisticated configurations designed to increase the thermodynamic efficiency permit the vapor overhead to be condensed with the bottoms liquid from the *same* distillation column. Each of three configurations, *heat pumping*, *vapor recompression*, and *reboiler flashing*, involves expensive compression of a vapor stream as shown in Figure 11.52. The heat pump operates like a refrigeration cycle and requires an external fluid as the working medium. It pumps available heat from the low-temperature level of the condenser up to a higher temperature level at the reboiler, thus reducing the need for external utilities. The other two configurations do not have external working fluids. Instead, they use the internal process fluids. To be effective, the savings in the cost of utilities and purchase costs for the heat exchangers must be greater than the increased utility and capital costs associated with the compressor.

For a detailed analysis of the reboiler-flashing configuration, which is usually the most financially attractive of the three configurations, the reader is referred to Example 10.4, in which the lost work and thermodynamic efficiency are computed for the separation of propylene and propane. Note that these configurations are most attractive for the separation of close-boiling mixtures because relatively small pressure changes are required, and consequently, the cost of compression is not too high.

11.9 HEAT ENGINES AND HEAT PUMPS

When processes have significant power demands, usually in compressor loads, it is normally sound practice to operate at or near the minimum utilities for heating and cooling. This is because the annualized cost is dominated often by the operating and capital costs associated with satisfying these power demands. Given the desirability of operating these processes at minimum utilities, Townsend and Linnhoff (1983a and 1983b) make

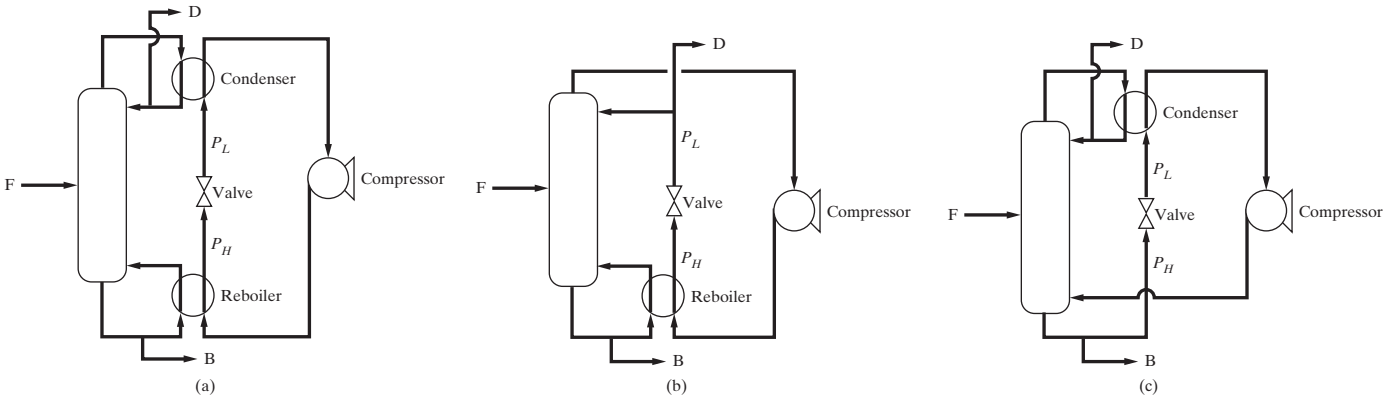

Figure 11.52 Distillation configurations involving compression: (a) heat pumping; (b) vapor recompression; (c) reboiler flashing.

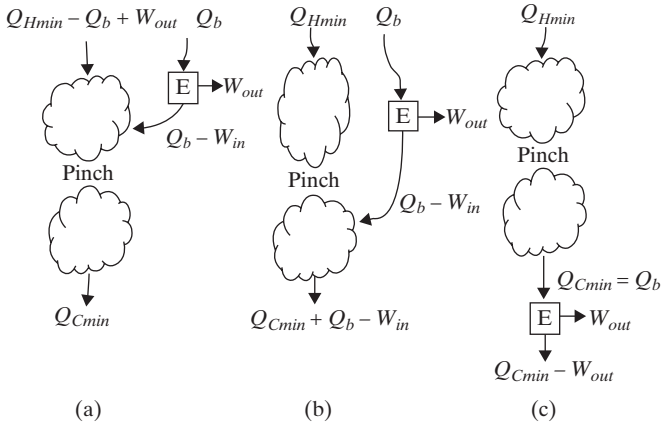

Figure 11.53 Alternatives for the placement of heat engines: (a) above the pinch; (b) across the pinch; (c) below the pinch.

recommendations concerning the positioning of heat engines and heat pumps relative to the pinch as discussed next.

Figure 11.53 shows a schematic of the enthalpy cascade for the streams to be heated and cooled in a background chemical process separated into two sections above and below the pinch. Consider the three alternatives for positioning a typical heat engine as shown in Figure 11.54. The latter is a closed cycle in which condensate, at T_1 and P_c, is pumped to T_2 and P_b and sent to a boiler where it leaves as a superheated vapor at T_3 and P_b. The boiler effluent is expanded across a turbine to T_4 and P_c, before it is condensed. The net heat energy, Q_b–Q_c, is converted to the net power, W_{out}–W_{in}, typically at a thermodynamic efficiency (see Section 10.7 and Exercise 10.20) of about 35%. Returning to Figure 11.53a, where the heat engine is positioned above the pinch to satisfy the demand for hot utilities, Q_{Hmin}, Q_b is required by the boiler and the net power produced is W_{out}, neglecting the small power requirement of the pump. Hence, W_{out} is produced by adding the equivalent heat to Q_{Hmin}. In Figure 11.53c where the heat engine is positioned below the pinch, the heat that would be rejected to cold utilities, Q_{Cmin}, is sent to the boiler. W_{out} is recovered from the turbine and the remainder is rejected to the cold utilities. The alternative to these two placements in Figure 11.53b has the heat engine accepting heat above the pinch and rejecting heat below the pinch. As shown, the total utilities above the pinch are incremented by Q_b, and below the pinch, the cold utilities are incremented by Q_b–W_{out}. Clearly, when the heat engine is positioned across the pinch, both the hot and cold utility loads

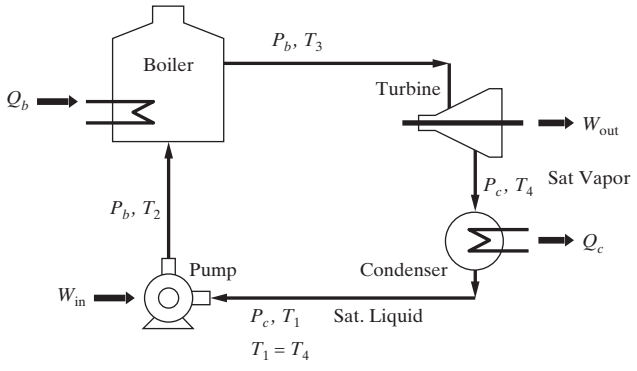

Figure 11.54 Heat engine.

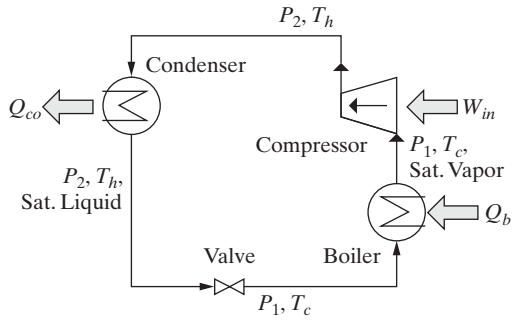

Figure 11.55 Heat Pump.

are incremented, and this configuration is less profitable than the configurations with the heat engine entirely above or below the pinch.

A heat pump, illustrated in Figure 11.55, is a closed loop of auxiliary fluid designed to accept heat at a low temperature, T_c, and transfer it at a higher temperature, T_h. The auxiliary fluid enters an evaporator operating at T_c as a saturated liquid at pressure P_1, and in so doing, accepts latent heat at a rate Q_b. The saturated vapor is then compressed to pressure P_2, and its temperature increases to T_h, though the application of W_{in} shaft work. The hot pressurized auxiliary fluid is then fed to a condenser where the hot vapor condenses back to saturated liquid while transferring latent heat at a rate Q_{co}, noting that by the first law, $Q_{co} = Q_b + W_{in}$. Next, the hot compressed liquid is fed to an expansion valve where the pressure is reduced back to P_1 and the temperature back to T_c, closing the circuit.

Figure 11.56 presents the three alternatives for positioning heat pumps relative to the pinch. In Figure 11.56c, where the heat pump is positioned across the pinch, heat is removed from a temperature interval below the pinch and rejected to a temperature interval above the pinch, causing a reduction in both the hot and cold utility loads but at the expense of shaft work. Alternatively, when the heat pump is positioned above the pinch as in Figure 11.56a, its compression load, W_{in}, reduces the hot utility load by this amount, but does not reduce the cold utility load below the pinch. In this case, expensive power is converted directly to less valuable heat to reduce the hot utility load. Finally, when the heat pump is positioned below the pinch, as in Figure 11.56b, its compression load, W_{in}, increases the cold

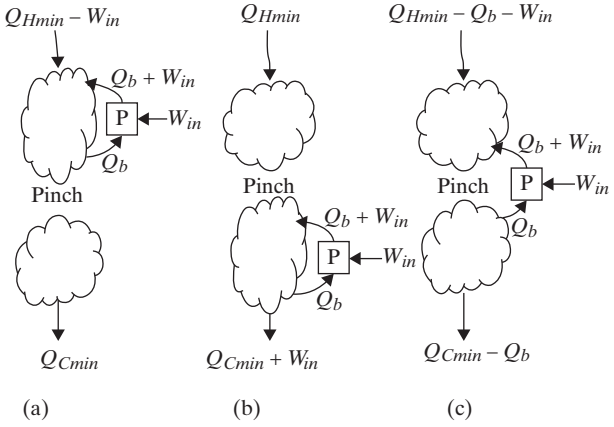

Figure 11.56 Alternatives for the placement of heat pumps: (a) above the pinch; (b) below the pinch; (c) across the pinch.

utility load by the same amount without affecting the hot utility load. Clearly, this is less desirable than when the heat pump is positioned across the pinch where both the hot and cold utilities are decreased.

When designing heat pumps, one needs to keep in mind that the shaft work, W_{in}, required to pump Q_{co} units of enthalpy to a hot sink at T_h from a cold source at T_c is given by:

$$W_{in} = \frac{Q_{co}}{\eta_m}\left(\frac{T_h - T_c}{T_h}\right) \tag{11.22}$$

where η_m is the mechanical efficiency of the compressor equaling unity for a reversible process and temperatures are in absolute units. The coefficient of performance, COP, for a heat pump is COP $= Q_{co}/W_{in}$. As shown in Example 11.16, these design equations have implications on the selection of the desirable *temperature lift*, T_h–T_c.

In summary, two heuristics result:

1. **When positioning heat engines to reduce the total utilities, place them entirely *above* or *below* the pinch.**
2. **When positioning heat pumps to reduce the total utilities, place them *across* the pinch.**

The following example illustrates the practical application of the second of these heuristics.

EXAMPLE 11.16 ***Placement of a Heat Pump***

Figure 11.57a shows the enthalpy cascade for a background process designed for $\Delta T_{min} = 10°C$, which has MER targets of $Q_{Hmin} = 9$ MW, $Q_{Cmin} = 8$ MW, and a cold pinch temperature of 250°C. Which is the best possible placement of a heat pump, assumed to have 60% mechanical efficiency, to reduce the external hot and cold utility requirements of the background process?

SOLUTION

Following the guidelines discussed above, one should place a heat pump across the pinch, and in this case, there are two reasonable alternatives shown in Figure 11.56b and Figure 11.56c. In option A (Figure 11.56b), heat is transferred from the background process below the pinch at 200°C (i.e., $T_c = 210°C$, recalling that heat is transferred from hot streams that are ΔT_{min} hotter than the cold stream scale used in GCCs) and transferred to the process at 300°C (i.e., $T_h = 300°C$). Option B (Figure 11.56c) differs from option A in that heat is transferred from 100°C (i.e., $T_c = 110°C$). For both options, the quantity of heat that can be transferred to the process at 300°C while ensuring all residuals are positive is $Q_{co} = 9$ MW (i.e., $Q_b + W_{in} = 9$ MW)-so that $Q_H = 0$ and therefore, the two options differ by the shaft work required, which computed using Eq.(11.22) with $\eta_m = 0.6$. Its consequences are summarized in the following table:

Option	T_c (°C)	W_{in} (MW)	Q_b (MW)	Q_c (MW)	COP
A	210	2.36	6.64	1.36	3.82
B	110	4.97	4.03	3.97	1.81

The results overwhelmingly favor option A although both options completely eliminate the need for external hot utility (i.e., $Q_H = 0$, reduced from 9 MW in the original background process). Option A achieves this result while requiring only 2.36 MW

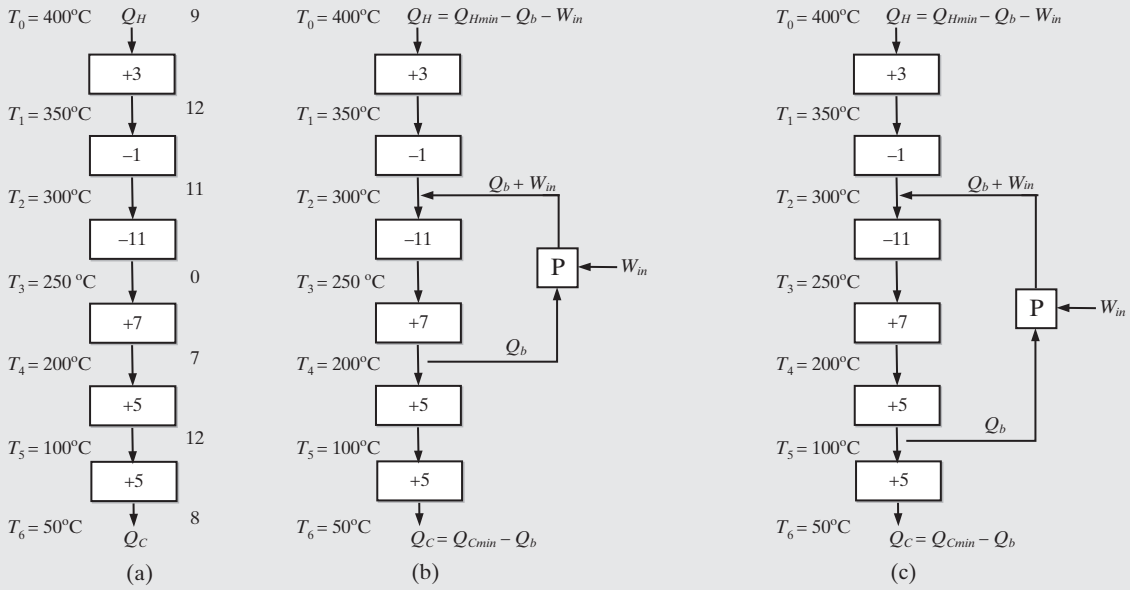

Figure 11.57 Heat pump installation in enthalpy cascade for Example 11.16: (a) background process; (b) placement of heat pump, option A; (c) placement of heat pump, option B.

of shaft work (less than half of the requirement of option B), and recovers 83% of the 8 MW of low-temperature waste heat in the original process (compared with only about 50% recovery in option B). The COP values are consistent with these results: The value for option A is about twice that of option B. The significantly improved performance of option A confirms that in principle, heat loops should be designed to reduce the *temperature lift* as much as possible.

11.10 SUMMARY

Having studied this chapter and having solved many of the exercises, the reader should have learned how to achieve effective heat integration using several approaches that do not require formal optimization methods. More specifically, the reader should:

1. Be able to determine the minimum cooling and heating utilities (MER targets) for a network of heat exchangers using the temperature-interval (TI) method or the composite-curve method.
2. Be able to design a network to meet the MER targets, that is, to position heat exchangers in a network assuming overall heat transfer coefficients. This is accomplished using a unit-by-unit method beginning at the closest approach temperature difference (the *pinch*).
3. Be able to reduce the number of heat exchangers in MER networks by relaxing the MER target and *breaking the heat loops* (i.e., allowing heat to flow across the pinch), or alternatively, by employing *stream splitting*.
4. Be able to design a network when the minimum approach temperature is below a threshold value at which either heating or cooling utility is used, but not both.
5. Understand the importance of the specified minimum approach temperature difference on the design of a heat exchanger network (HEN).
6. Be able to use the grand composite curve to assist in the selection and positioning of appropriate types of hot and cold utilities in the network.
7. Be able to use the grand composite curve to optimally position reactors and distillation columns to minimize usage of hot and cold utilities in the network.
8. Be able to apply several approaches to designing energy-efficient distillation trains, including the adjustment of tower pressure, multiple-effect distillation, and heat pumping, vapor recompression, and reboiler flashing.
9. Know how to correctly position *heat engines* and *heat pumps*, to reduce the demand for heating and cooling using utilities.

Alternatively, and as described in more detail in the supplementary materials that accompany this chapter, optimization problems are formulated and solved using GAMS, including linear programs (LPs) to perform MER targeting and mixed-integer linear programs (MILPs) and nonlinear programs (NLPs) for the design and optimization of HENs. See the outline for the supplement below.

Heat Integration Software

Most of the methods introduced in this chapter, especially those for the design of HENs, are implemented in commercial software. Of special note are ADVENT^{TM} by Aspen Tech (in the Aspen Engineering Suite), HEXTRAN^{TM} by Simulation Sciences Inc., and TARGET^{TM} by the Linnhoff–March Corp. As mentioned in the chapter, many of the methods involve the solution of linear and nonlinear programs (LPs and NLPs)—whose fundamentals are introduced in Chapter 21—and their mixed-integer counterparts (MILPs and MINLPs).

SUPPLEMENTS TO CHAPTER 11

MILP and MINLP Applications in HEN Synthesis

A supplement to Chapter 11, "MILP and MINP Applications in HEN Synthesis," is provided in the PDF Files folder, which can be downloaded from the Wiley Web site (See the file Supplement_to_Chapter 11–1.pdf). The contents of this supplement are:

11S-1.0 Objectives
11S-1.1 MER Targeting Using Linear Programming (LP)
11S-1.2 MER Design Using Mixed-Integer Linear Programming (MILP)
11S-1.3 Superstructures for Minimization of Annual Costs
11S-1.4 Case Studies
- Case Study 11S-1.1 Optimal Heat-Integration for the ABCDE Process
- Case Study 11S-1.2 Optimal Heat-Integration for an Ethylene Plant

11S-1.5 Summary
11S-1.6 References

Mass Integration

Another supplement to Chapter 11, "Mass Integration" is provided in the PDF Files folder; Supplement_to_Chapter 11–2.pdf. In this supplement, the parallels between heat and mass integration are presented with examples similar to those in Chapter 11. The contents of this supplement are:

11S-2.0 Objectives
11S-2.1 Introduction
11S-2.2 Minimum Mass-Separating Agent
11S-2.3 Mass Exchange Networks for Minimum External Area
11S-2.4 Minimum Number of Mass Exchangers
11S-2.5 Advanced Topics
11S-2.6 Summary
11S-2.7 References

REFERENCES

1. Dhole, V. R., and B. Linnhoff, "Distillation Column Targets," *Comput. Chem. Eng.*, **17**(5–6) (1993).

2. Douglas, J. M. *Conceptual Design of Chemical Processes*, McGraw-Hill, New York (1988).

3. Glavic, P., Z. Kravanja, and M. Homsak, "Heat Integration of Reactors; I. Criteria for the Placement of Reactors into Process Flowsheets, " *Chem. Eng. Sci.*, **43**, 593 (1988).

4. Hohmann, E. C., *Optimum Networks for Heat Exchange*, Ph.D. dissertation, University of Southern California (1971).

5. Linnhoff, B., and J.R. Flower, "Synthesis of Heat Exchanger Networks: I. Systematic Generation of Energy Optimal Networks," *AIChE J.*, **24**, 633 (1978a).

6. Linnhoff, B., and J. R. Flower, "Synthesis of Heat Exchanger Networks: II. Evolutionary Generation of Networks with Various Criteria of Optimality," *AIChE J.*, **24**, 642 (1978b).

7. Linnhoff, B., and E. Hindmarsh, "The Pinch Design Method for Heat Exchanger Networks," *Chem. Eng. Sci.*, **38**, 745 (1983).

8. Linnhoff, B., D. W. Townsend, D. Boland, G. E. Hewitt, B. E. A. Thomas, A. R. Guy, R. H. Marsland, *A User Guide on Process Integration for the Efficient Use of Energy*, Revised 1st Ed., The Institution of Chemical Engineers (IChemE), Rugby, England (1994).

9. Nishida, N., Y. A. Liu, and L. Lapidus, "Studies in Chemical Process Design and Synthesis: III. A Simple and Practical Approach to the Optimal Synthesis of Heat Exchanger Networks," *AIChE J.*, **23**, 77 (1977).

10. Papoulias, S., and I. E. Grossmann, "A Structural Optimization Approach in Process Synthesis—II: Heat Recovery Networks," *Comput. Chem. Eng.*, **7**, 707 (1983).

11. Smith, R., and B. Linnhoff, "The Appropriate Placement of Distillation Columns," *Trans. IChemE ChERD*, **66**, 195 (1988).

12. Smith, R., *Chemical Process Design and Integration*, John Wiley, The Atrium, Southern Gate, Chichester, England (2005)

13. Townsend, D. W., and B. Linnhoff, "Heat and Power Networks in Process Design. 1. Criteria for Placement of Heat Engines and Heat Pumps in Process Networks," *AIChE J.*, **29**, 742 (1983a).

14. Townsend, D. W., and B. Linnhoff, "Heat and Power Networks in Process Design. II. Design Procedure for Equipment Selection and Process Matching," *AIChE J.*, **29**, 748 (1983b).

15. Umeda, T., J. Itoh, and K. Shiroko, "Heat Exchange System Synthesis," *Chem. Eng. Prog.*, **74**, 70, July (1978).

16. Yee, T. F., and I. E. Grossmann, "Simultaneous Optimization Models for Heat Integration—II: Heat Exchanger Network Synthesis," *Comput. Chem. Eng.*, **10**, 1165 (1990).

EXERCISES

11.1 Four streams are to be cooled or heated:

Stream	T^s (°C)	T^t (°C)	C (kW/°C)
H1	180	60	3
H2	150	30	1
C1	30	135	2
C2	80	140	5

(a) For $\Delta T_{min} = 10°C$, find the minimum heating and cooling utilities. What are the pinch temperatures?

(b) Design a heat exchanger network for MER on both the hot and cold sides of the pinch.

11.2 (a) For $\Delta T_{min} = 10°C$, find the minimum utility requirements for a network of heat exchangers involving the following streams:

Stream	T^s (°C)	T^t (°C)	C (kW/°C)
C1	60	180	3
C2	30	105	2.6
H1	180	40	2
H2	150	40	4

(b) Repeat (a) for the following streams:

Stream	T^s (°C)	T^t (°C)	C (kW/°C)
C1	100	430	1.6
C2	180	350	3.27
C3	200	400	2.6
H1	440	150	2.8
H2	520	300	2.38
H3	390	150	3.36

(c) For (a) and (b), design HENs that require the minimum utilities.

11.3 Consider the design of a network of heat exchangers that requires the minimum utilities for heating and cooling. Is it true that a pinch temperature can occur *only* at the inlet temperature of a hot or cold stream? (*Hint*: Sketch typical composite hot and cold curves for two hot and two cold streams.)

11.4 The PFD in Figure 11.58 shows a process for the manufacture of X and Y. The process feed is heated in furnace F-100 to 800°C and is then fed to an adiabatic and isothermal PFR, R-100, where the reaction to X and Y occurs. The reactor effluents at 800°C are cooled to 70°C in heat exchanger E-100 and then fed to distillation column T-100 where X is obtained as distillate and Y as bottoms. Figure 11.58 shows the stream temperatures as well as the heat duties of all proposed heat exchangers. Explain (in words) why this process must have a pinch.

11.5 Consider the following heating and cooling demands:

Stream	T^s (°C)	T^t (°C)	C (kW/°C)
H1	525	300	2
H2	500	375	4
H3	475	300	3
C1	275	500	6

A HEN is to be designed with $\Delta T_{min} = 30°C$:

(a) Find the MER targets.

(b) Design a subnetwork of heat exchangers below the pinch that meets the MER targets.

11.6 Consider the process flowsheet in Figure 11.59 where the duties required for each heat exchanger are in MW, and the source and target stream temperatures are:

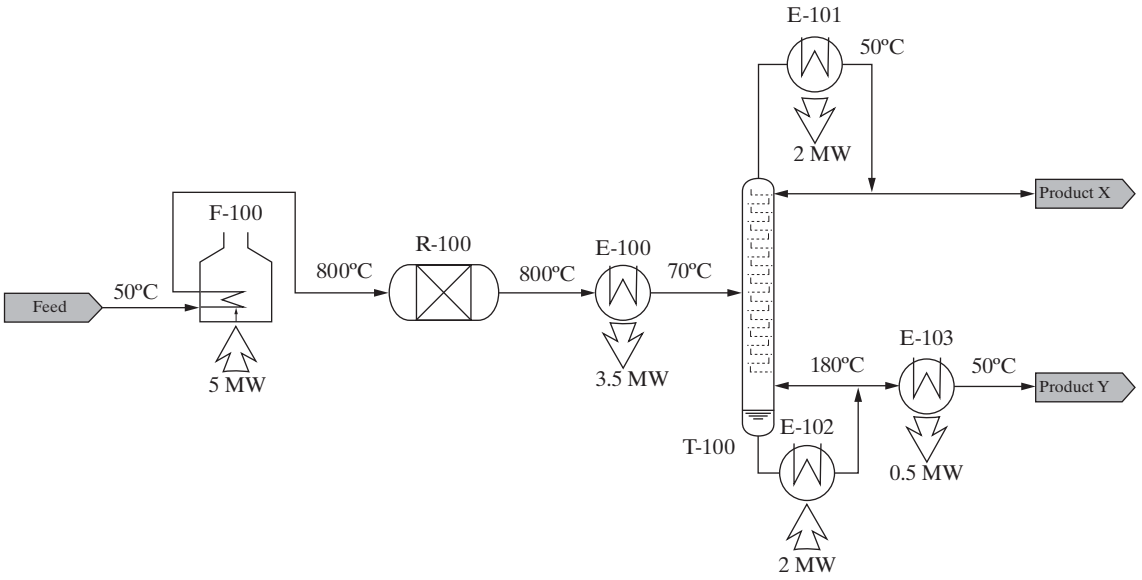

Figure 11.58 PFD for a process for the manufacture of X and Y.

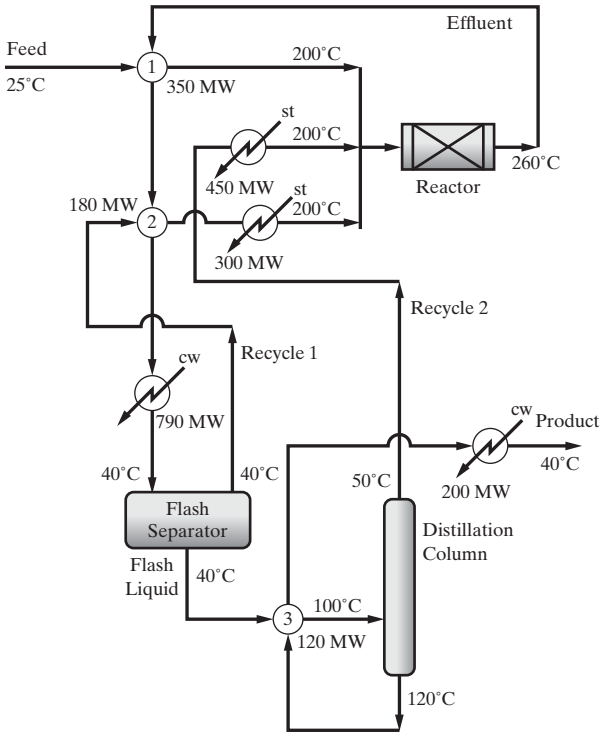

Figure 11.59 Flowsheet for Exercise 11.6.

Process Stream	T^s (°C)	T^t (°C)
Feed	25	200
Effluent	260	40
Recycle 1	40	200
Flash Liquid	40	100
Recycle 2	50	200
Product	120	40

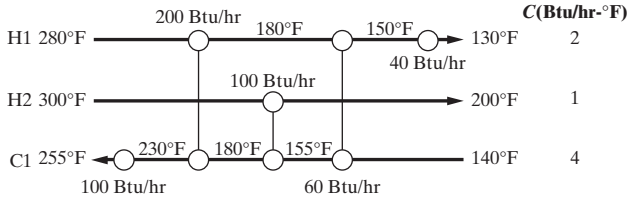

Figure 11.60 HEN for Exercise 11.7.

(a) The flowsheet calls for 990 MW to be removed by cooling water and 750 MW to be provided by steam. It is suspected that this design does not meet MER targets for $\Delta T_{min} = 10°C$. Verify or refute this suspicion.

(b) If verified, design a HEN to meet MER targets for $\Delta T_{min} = 10°C$.

11.7 Consider the network of heat exchangers in Figure 11.60:

(a) Determine $N_{HX,min}$.

(b) Identify the heat loop.

(c) Show one way to break the heat loop using $\Delta T_{min} = 10°F$. For the resulting network, prepare a revised diagram, showing all temperatures and heat duties.

11.8 To exchange heat between four streams with $\Delta T_{min} = 20°C$, the HEN in Figure 11.61 is proposed. Determine whether the network has the minimum utility requirements. If not, design a network with the minimum utility requirements. As an alternative, design a network with the minimum number of heat exchangers. Using the specifications in Example 11.6, which alternative is preferred?

11.9 A process has streams to be heated and cooled above its pinch temperatures as illustrated in Figure 11.62. Complete a design that satisfies MER targets with the minimum number of heat exchangers.

11.10 Consider a process with the following streams:

Stream	T^s (°F)	T^t (°F)	C ($\times 10^{-4}$ Btu/hr°F)
H1	480	250	2.0
H2	430	180	3.0
C1	100	400	2.5
C2	150	360	2.5
C3	200	400	2.5

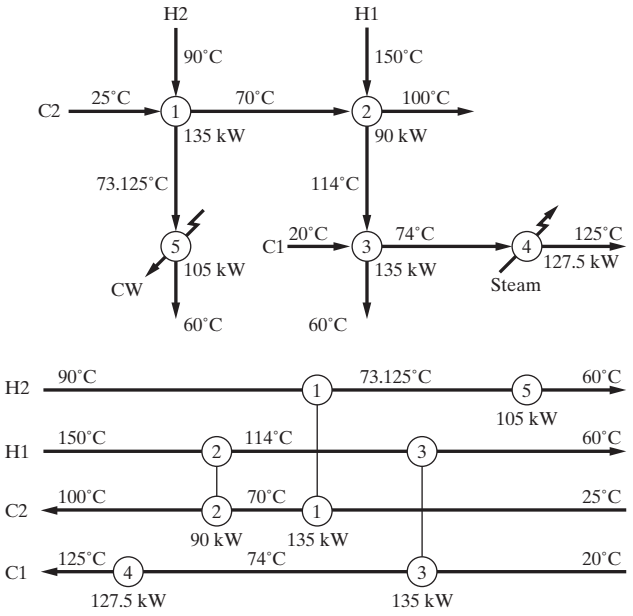

Figure 11.61 HEN for Exercise 11.8.

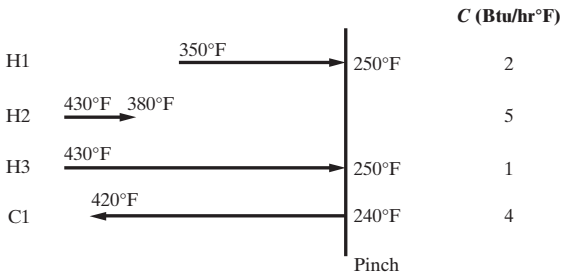

Figure 11.62 HEN for Exercise 11.9.

(a) Compute ΔT_{thres} as well as the minimum external heating and cooling requirements as a function of ΔT_{min}.

(b) Design a HEN to meet the MER targets with $N^{MER}_{HX,\min}$ heat exchangers for $\Delta T_{min} = 20°F$. Show the heat duties and temperatures for each heat exchanger.

11.11 Design a HEN to meet the MER targets for $\Delta T_{min} = 10°C$ and $N_{HX,min}$ for a process involving five hot streams and one cold stream as introduced by Yee and Grossmann (1990):

Stream	T^s (K)	T^t (K)	C (kW/K)
H1	500	320	6
H2	480	380	4
H3	460	360	6
H4	380	360	20
H5	380	320	12
C1	290	670	18

11.12 The PFD in Figure 11.63 shows a process in which two liquid products, A and B, are produced from a feed stream of raw material R. In the process, the reactor feed is preheated to 300°C and fed to an isothermal PFR, R-100, where the two products are produced. The reactor effluent at 300°C is cooled to 180°C and fed to column T-100, where Product A is withdrawn as distillate. The bottoms stream of T-100 is cooled to 120°C and fed to column T-101 in which Product B is withdrawn as distillate and the unreacted raw materials withdrawn as bottoms, cooled to 100°C and recycled. Figure 11.63 shows the stream temperatures and C values as well as the heat duties of all proposed heat exchangers.

(a) Compute MER targets and pinch temperatures for $\Delta T_{min} = 10°C$.

(b) Design a HEN with the minimum number of heat exchangers that meets the MER targets.

11.13 Consider a process with the following streams:

Stream	T^s (°C)	T^t (°C)	C (kW/°C)
H1	350	160	3.2
H2	400	100	3
H3	110	60	8
C1	50	250	4.5
C2	70	320	2
C3	100	300	3

When $\Delta T_{min} = 10°C$, the minimum utilities for heating and cooling are 237 kW and 145 kW, respectively, with pinch temperatures at 110°C and 100°C. Design a HEN that satisfies the MER targets and has the minimum number of heat exchangers, $N^{MER}_{HX,\min}$. Show the heat duties and temperatures for each heat exchanger.

11.14 Consider a process with the following streams:

Stream	T^s (°C)	T^t (°C)	C (kW/°C)
H1	500	50	5
H2	400	100	4
H3	400	100	3
H4	200	50	2
C1	250	450	10
C2	30	430	6

(a) Determine MER targets for $\Delta T_{min} = 10°C$.

(b) Design a HEN for MER using no more than 10 heat exchangers (including auxiliary heaters and coolers).

(c) Add an additional stream to your HEN without increasing the total number of exchangers. The data for the additional stream are:

Stream	T^s (°C)	T^t (°C)	C (kW/°C)
C3	40	200	4

11.15 Figure 11.64 presents the PFD of a process for the production of organic fibers (Smith, 2005). In the process, the organic solvent is removed from the fibers in dryer D-100 using circulated warmed air, which is then cooled before entering adsorbing column A-100 where the

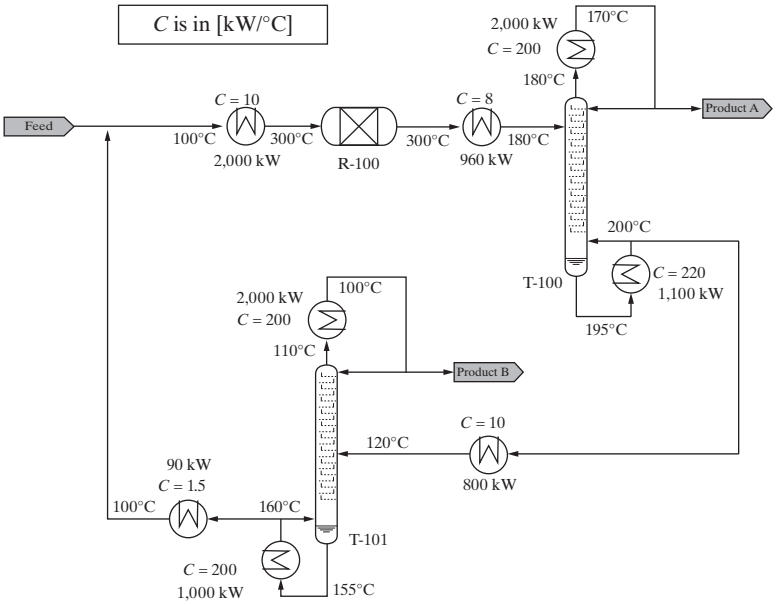

Figure 11.63 PFD for a process for the manufacture of products A and B from R.

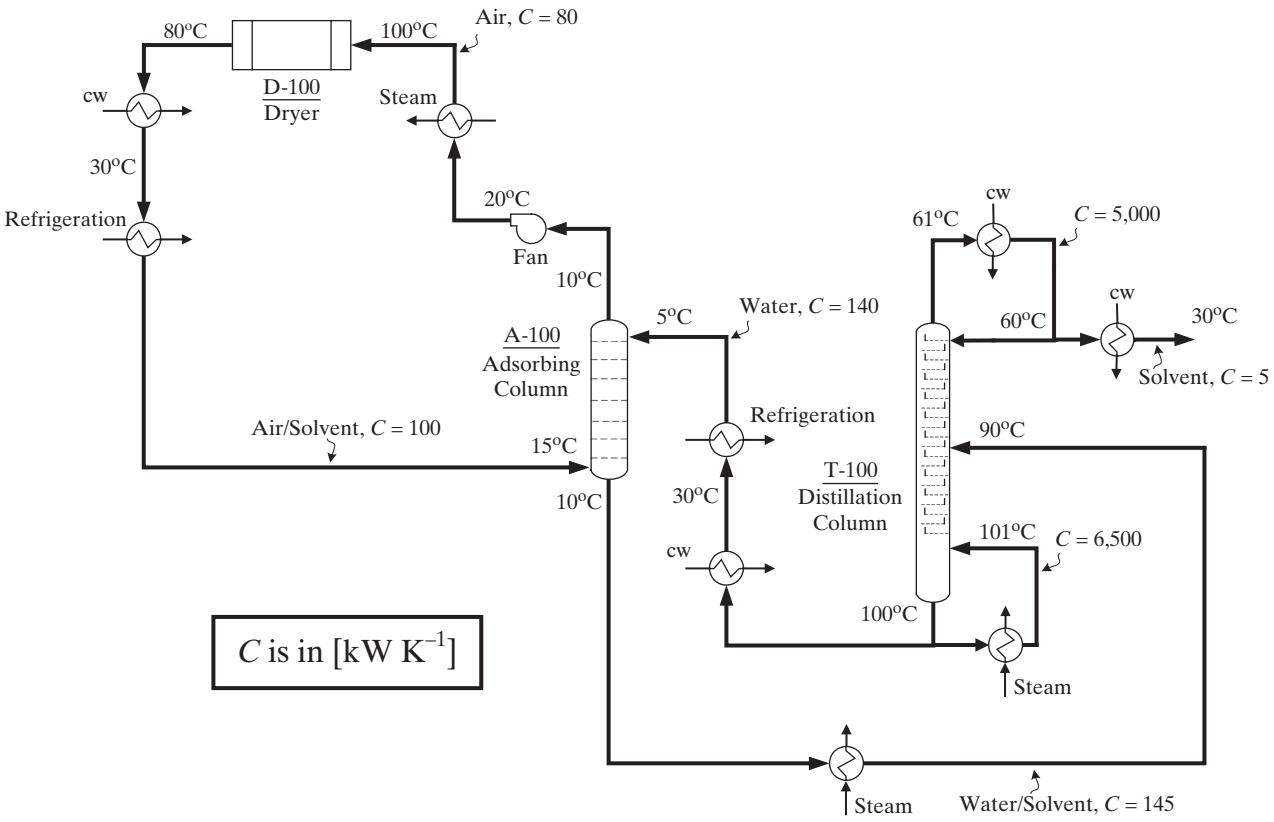

Figure 11.64 Process flow diagram of a process for the production of organic fibers.

solvent is removed by a stream of water. The mixture of water and solvent is then separated in distillation column T-100, and the water is recycled. The process is serviced by three types of utilities: steam at 150°C, cooling water at 20°C, and refrigerant at −5°C; possible changes in sensible heat of both the cooling water and refrigerant can be neglected.

(a) Compute MER targets for this process at $\Delta T_{min} = 10°C$.

(b) Design a HEN to meet the MER targets at $\Delta T_{min} = 10°C$. The design should utilize no more than 12 heat exchangers (including utility coolers and heaters).

11.16 Design a heat exchanger network for MER with at most 15 heat exchangers (including utility heaters) and $\Delta T_{min} = 10°C$ for the following streams:

Stream	T^s (°C)	T^t (°C)	C (kW/°C)
H1	140	50	10
H2	320	20	9
H3	370	20	8
C1	50	130	10
C2	130	430	8
C3	100	300	6
C4	30	230	5
C5	30	130	4
C6	30	430	1

When MER targets are satisfied, the hot pinch temperature is 140°C with Q_{Hmin} = 760 kW and Q_{Cmin} = 960 kW.

11.17 Figure 11.65 presents the PFD of a process for the recovery of methane from a feed stream consisting of 75% methane and 25% nitrogen. The process feed is first cooled from 90 to −160°F, and because of partial condensation in the feed stream under these conditions, the stream is split into two portions as shown in the PFD: from 90 to −120°F where C = 20 kBtu/hr°F and from −120 to −150°F where C = 50 kBtu/hr°F. After cooling, the feed is separated in the cryogenic column operating at 600 psia. The column bottoms, rich in methane, are expanded to a pressure of 100 psia, heated from −250 to −100°F, and then fed to a compressor that raises its pressure to 1,000 psia. The column distillate heated from −180 to 80°F also undergoes phase changes and, like the feed stream, is divided into two portions. Note that the design of the HEN for this process is limited to the usage of one type of cold utility and one type of hot utility.

(a) Compute MER targets for this process, at ΔT_{min} = 10°F.

(b) Design a HEN to meet the MER targets with the minimum number of units at ΔT_{min} = 10°F given that the design can utilize only one type of cold utility and one type of hot utility.

11.18 Design a heat exchanger network for MER with at most 18 heat exchangers (including utility heaters) and ΔT_{min} = 10°C for the following streams:

Stream	T^s (°C)	T^t (°C)	C (kW/°C)
H1	400	20	10
H2	200	50	15
H3	350	230	5
H4	400	100	8
C1	80	450	7
C2	20	320	10
C3	50	450	5
C4	50	350	4
C5	100	500	1

When MER targets are satisfied, the hot pinch temperature is 200°C, with Q_{Hmin} = 1,170 kW and Q_{Cmin} = 1,170 kW.

11.19 In Example 11.13, HENs are designed for a process involving two hot and two cold streams. Note that three designs are proposed: (1) involving only HP steam and cooling water that meets the $N^{MER}_{HX,\min}$ target (shown in Figure 11.35a); (2) involving HP steam and cooling water with no stream splitting and one less heat exchanger (shown in Figure 11.35b); and (3) utilizing HP and IP steam, cooling water, and boiler feed water (shown in Figure 11.36). Which of these designs has the lowest annualized cost given the following specifications?

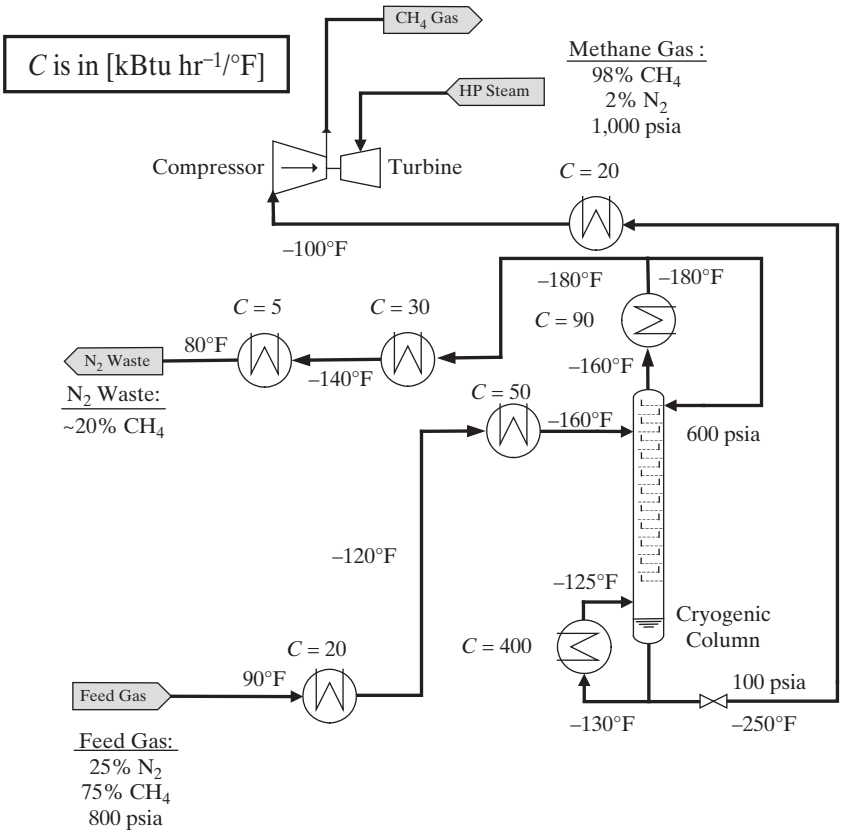

Figure 11.65 Process flow diagram of a process for methane recovery.

Cooling water (*cw*): $T^s = 30°C,\ T^t \leq 80°C$, cost of *cw* = 0.00015 \$/Kg

Boiler feed water (bfw): $T = 110°C,\ \Delta H^v = 2{,}230$ kJ/kg, revenue on bfw = 0.001 \$/kg

IP Steam (sat'd, *ips*): $T = 195°C,\ \Delta H^v = 1{,}958$ kJ/kg, cost of *ips* = 0.003 \$/kg

HP Steam (sat'd, *hps*): $T = 258°C,\ \Delta H^v = 1{,}676$ kJ/kg, cost of *hps* = 0.006 \$/kg

Overall heat-transfer coefficients: $U_{heater} = U_{cooler} = U_{exch} =$ 1 kW/m^2 °C

Purchase cost of heat exchangers: $C_P = 3{,}000A^{0.5}$ (\$, m^2)

Return on investment, $i_m = 0.1$.

Bonus: Adapt the design in Figure 11.36 to produce a cheaper HEN.

11.20 The following table presents stream data for a background process.

Stream	Feed Temp. (°C)	Target Temp. (°C)	*C* (MW/°C)
H1	500	100	4
C1	50	450	1
C2	60	400	1
C3	40	420	0.75

(a) Compute MER targets for this process at $\Delta T_{min} = 20°C$.

(b) Design a HEN to meet the MER targets at $\Delta T_{min} = 20°C$ with the minimum number of units.

(c) Investigate the feasibility of substituting boiler feed water (BFW) at 180°C to raise steam for part of the cooling water requirement implemented in (b). What is the maximum amount of steam (in MW) that can be raised from this process?

(d) Redesign the HEN, again with the minimum number of units, to meet the MER targets at $\Delta T_{min} = 20°C$ and at the same time, produce as much 180°C steam as possible.

11.21 A HEN is to be designed to meet MER targets for the following stream data:

Stream	T^s (°C)	T^t (°C)	*C* (kW/°C)
H1	850	400	4
H2	600	30	3
H3	400	300	10
C1	80	300	15
C2	150	650	3
C3	100	200	2
C4	60	180	1

(a) Compute MER targets for this process at $\Delta T_{min} = 10°C$.

(b) Design a HEN to meet the MER targets at $\Delta T_{min} = 20°C$ with no more than 10 heat exchangers (including utility heaters and coolers).

(c) Draw the GCC for this process and use it to suggest changes to the HEN to reduce operating costs. In so doing, note that there are no restrictions in the number of units.

11.22 The following table presents residual heat flows in the enthalpy cascade of a process computed at $\Delta T_{min} = 10°C$ (Smith, 2005):

Interval Temperature (°C)	Residual Heat Flow (MW)
295	18.3
285	19.8
185	4.8
145	0
85	10.8
45	12.0
35	14.3

(a) It is desired to efficiently heat integrate a distillation column for the separation of a binary mixture of toluene and biphenyl with this process. The column produces essentially pure product streams and is originally designed to operate at 1.013 bar. At that pressure, toluene boils at 107°C, and biphenyl at 197°C. The condenser and reboiler duties are both 4 MW. What will be the consequences of attempting to heat integrate the column operating at 1.013 bar?

(b) What is your recommendation for an appropriate operating pressure for the column, assuming that the condenser and reboiler duties as stated above are independent of operating pressure and that vapor pressure of toluene and biphenyl are estimated using the Antoine equation:

$$\ln P_i = A_i - \frac{B_i}{T + C_i}$$

where P_i is the vapor pressure (bar), T_i is the temperature (K), and the remaining parameters are listed in the following table. The selection of operating pressure should be made to maintain the reboiler temperature as low as possible while avoiding operation in vacuum conditions.

Parameter values for Antoine equation:

Component	A_i	B_i	C_i
Toluene	9.4	3,100	−50
Biphenyl	10.0	4,000	−70

Chapter 12

Heat Exchanger Design

12.0 OBJECTIVES

Storage tanks, reactors, and separation units in a chemical process are operated at specified temperatures, pressures, and phase conditions. In continuous processes, pressure conditions are established by valves and pumps for liquids and valves, compressors, and turbines or expanders for gases. Valves are also used to partially or completely convert liquids to gases. Temperature and phase conditions are established mainly by heat exchangers, which are the subject of this chapter.

After studying this chapter, and the multimedia materials on heat exchangers, which can be downloaded from www.seas.upenn.edu/~dlewin/multimedia.html, the reader should:

1. Understand how the temperature and phase conditions of a stream can be changed by using a heat exchanger.
2. Be able to specify a heat exchanger when modeling just the process side.
3. Be able to select heat-transfer media for the other side of the exchanger.
4. Understand the importance of heating and cooling curves and how to generate them and use them to avoid crossover violations of the second law of thermodynamics.
5. Be familiar with the major types of heat exchange equipment and how they differ in flow directions of the two fluids exchanging heat and the corresponding effect on the temperature-driving force for heat transfer.
6. Be able to specify a heat exchanger when modeling both sides.
7. Know how to estimate overall heat-transfer coefficients, including the effect of fouling.
8. Understand the limitations of boiling heat transfer.
9. Be able to design a shell-and-tube heat exchanger with the help of a simulator.

12.1 INTRODUCTION

This chapter begins with consideration of the effects of changing temperature, pressure, and phase condition for a single stream on stream enthalpy and heat duty. Then heating and cooling media are discussed, and the temperature-driving force for effecting a desired change in stream conditions is considered. Selection of heat exchange equipment is followed by a discussion of methods of determining exchanger sizes from estimates of overall heat-transfer coefficients. The chapter concludes with a comprehensive design problem for a shell-and-tube heat exchanger. In addition, the multimedia modules, which can be downloaded from the www.seas.upenn.edu/~dlewin/multimedia.html, show how to model heat exchangers using ASPEN PLUS and HYSYS; see *ASPEN → Heat Exchangers and HYSYS → Heat Exchangers*.

Heat Duty

In the early stages of process design, heating and cooling of liquids and vapors, partial and complete vaporization of liquids, partial and complete condensation of vapors, and sensible and latent heat changes for streams containing solids are treated without regard to (1) the source or sink of thermal energy transferred to or from the stream, (2) the rate at which the energy is transferred, or (3) the type and size of heat exchanger needed. Only of interest are the overall enthalpy change (*heat duty*) of a process stream for the specified heat exchanger inlet and outlet conditions, and the variation of enthalpy with intermediate conditions. The variation is represented most conveniently by *heating and cooling curves*. The heat duty and these curves are most easily obtained, especially for streams that are multicomponent mixtures undergoing phase change, with a steady-state process simulator. The calculations are not simple because effects of temperature, pressure, and composition on enthalpy are taken into account, and the phase condition is established by a phase equilibrium calculation.

Consider the heat exchanger in Figure 12.1. The continuous, steady-state heat duty is given by

$$Q = m(H_{out} - H_{in}) \tag{12.1}$$

where Q is the heat duty (rate of heat transfer), m is the flow rate of the stream (mass or molar), H_{in} is the enthalpy of the stream entering (per unit mass or mole), and H_{out} is the enthalpy of the stream leaving (per unit mass or mole). Simulation programs refer to this type of model as a *one-sided heat exchanger* because only one of the two streams exchanging heat is considered. The calculations are illustrated in the following example.

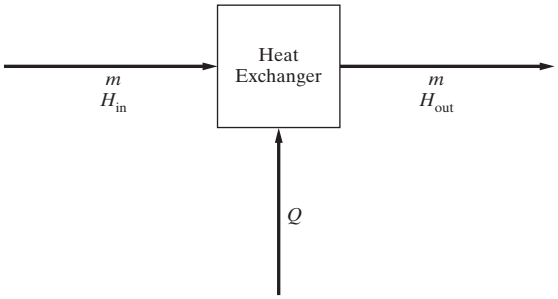

Figure 12.1 One-sided heat exchanger.

EXAMPLE 12.1

In Figure 2.5, the reactor effluent vapor from the pyrolysis reactor consists of 58,300 lb/hr of HC1, 100,000 lb/hr of vinyl chloride, and 105,500 lb/hr of 1,2-dichloroethane at 500°C and 26 atm. Before entering the separation section, this stream is cooled and condensed to 6°C at 12 atm. Assume that this is to be done in three steps: (1) cooling in heat exchanger 1 at 26 atm to the dew-point temperature, (2) adiabatic expansion across a valve to 12 atm, and (3) cooling and condensation in heat exchanger 2 at 12 atm to 6°C. Determine the heat duties and cooling curves for each heat exchanger. Note that the pressure drop in each of the two exchangers is neglected.

SOLUTION

This example was solved using ASPEN PLUS. The flowsheet is shown in Figure 12.2 where the HEATER model (for a one-sided heat exchanger) is used for heat exchanger 1 (E-1) and heat exchanger 2 (E-2). The pressure is dropped using the VALVE model for valve (V-1). The Soave-Redlich-Kwong (SRK) equation of state was used to compute thermodynamic properties. The results of the simulation are included in Figure 12.2 where the heat duties computed from Eq. (12.1) are shown to be 46,780,000 Btu/hr for E-1 and 53,000,000 Btu/hr for E-2. Stream conditions leaving E-1 are at the dew-point temperature of 157.6°C at 26 atm. The stream leaves valve V-1 as a vapor at 140.2°C and 12 atm. Thus, the adiabatic expansion lowers the temperature by 17.4°C. Stream conditions leaving E-2 are liquid at 6°C and 12 atm.

The cooling curve for E-1 is given in Figure 12.3a. Vapor conditions persist throughout E-1; thus, the enthalpy change is all sensible heat. Because the vapor heat capacity changes only slowly with temperature, the graph of the temperature as a function of the

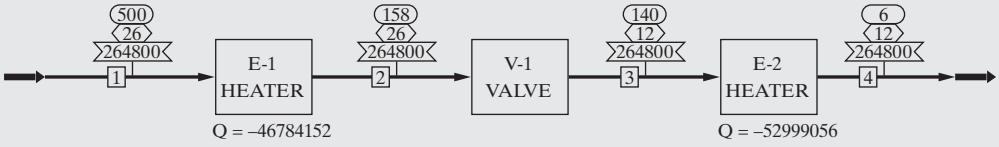

Temperature (C)
Pressure (ATM)
Flow Rate (LB/HR)
Heat duty (BTU/HR)
Power (HP)
Q Heat duty (BTU/HR)
W Power (HP)

Heat and Material Balance Table					
Stream ID		1	2	3	4
Temperature	C	500.0	157.6	140.2	6.00
Pressure	ATM	26.00	26.00	12.00	12.00
Vapor Frac		1.000	1.000	1.000	0.000
Mole Flow	LBMOL/HR	4275.224	4275.224	4275.224	4275.224
Mass Flow	LB/HR	264800.000	264800.000	264800.000	264800.000
Volume Flow	CUFT/HR	165314.984	77820.844	177819.281	3933.389
Enthalpy	MMBTU/HR	–47.128	–93.912	–93.912	–146.911
Mass Flow	LB/HR				
HCL		58300.000	58300.000	58300.000	58300.000
VC		100000.000	100000.000	100000.000	100000.000
DCE		105000.00	105000.00	105000.00	105000.00

Figure 12.2 ASPEN PLUS flowsheet for Example 12.1.

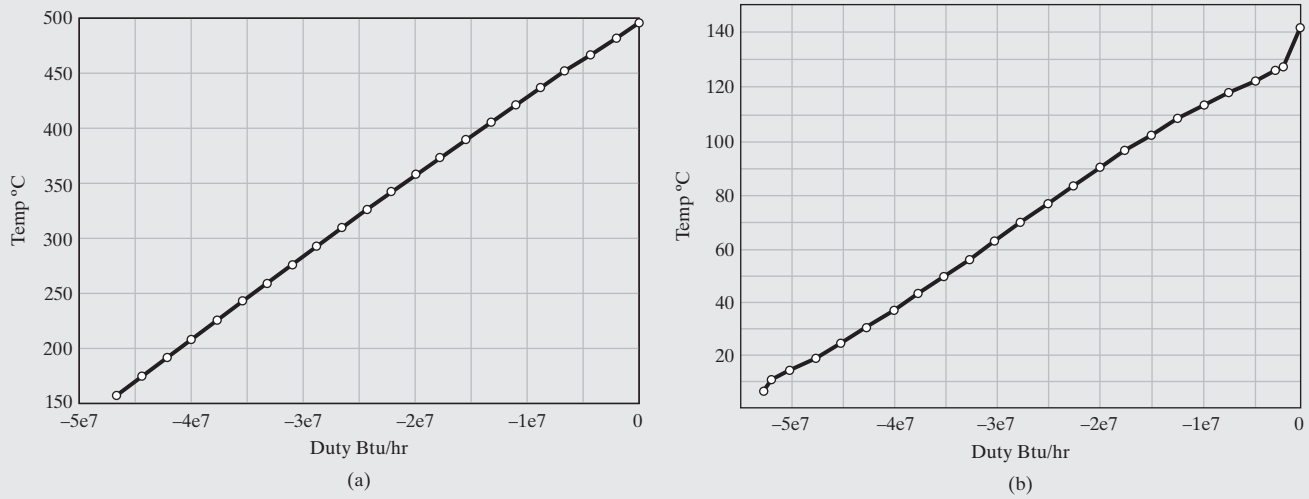

Figure 12.3 Cooling curves for Example 12.1: (a) exchanger E-1; (b) exchanger E-2.

enthalpy change is almost linear. The cooling curve for E-2 is given in Figure 12.3b. Entering E-2, the stream is slightly superheated at 140.2°C, with the dew point occurring at 126°C, as seen by the significant change in the slope of the curve in Figure 12.3b as condensation occurs. Another significant change in slope occurs at 10°C, which is the bubble point. Between the dew point and the bubble point, both sensible and latent heat changes occur with the curve deviating somewhat from a straight line.

Heat-Transfer Media

Heat is transferred to or from process streams using other process streams or *heat-transfer media*. In a final process design, every effort is made to exchange heat between process streams so as to minimize the use of heat-transfer media (usually referred to as *utilities*). Inevitably, however, some use of media, mostly cooling water, steam, and the products of combustion, is necessary. When media must be used, the heat exchangers are called *utility exchangers*.

Heat-transfer media are classified as *coolants* (heat sinks) when heat is transferred to them from process streams and as *heat sources* when heat is transferred from them to process streams. Process design includes the selection of appropriate heat-transfer media, data for which are listed in Table 12.1 where the media are ordered by temperature range of application.

The most common coolant, by far, is cooling water, which is circulated through a cooling tower. As indicated in Heuristic 27 of Chapter 6, the water typically enters the utility exchanger at 90°F and exits at no higher than 120°F. The cooling tower restores the cooling water temperature to 90°F by contacting the water with air, causing evaporation of a small amount of the water. The enthalpy of evaporation is supplied mainly from the water, causing it to cool. The evaporated water is replaced by treated water. With cooling water, process streams can be cooled and/or condensed to temperatures as low as about 100°F (depending on seasonal variations). When the plant is located near an ocean or river, that water is sometimes used for cooling without using a cooling tower. When water is scarce at the plant location, air is used for cooling, but air can only cool process streams economically to about 120°F.

When exchanger inlet temperatures of process streams to be cooled are higher than 250°F, consideration is given to transferring at least some of the heat to treated boiler feed water to produce steam. The steam is produced at as high a pressure and corresponding saturation temperature as possible, subject to a reasonable temperature-driving force for heat transfer in the utility exchanger. For process design purposes, the boiler feed water enters the utility exchanger as a saturated liquid at the selected pressure and exits without temperature change as a saturated vapor. The steam is available for use elsewhere in the process. For process stream temperatures above the critical temperature of water, supercritical water is sometimes used as the coolant.

When process streams must be cooled below 100°F in utility exchangers, refrigerants are used, which are designated with an R number by the American Society of Heating, Refrigerating and Air-Conditioning Engineers (ASHRAE). When the process involves light hydrocarbons, the refrigerant can be one of the hydrocarbons, for example, propane (R-290). Otherwise, a commercial refrigerant, for example, R-717 (ammonia) or R-134a (tetrafluoroethane), is selected. A widely used refrigerant, R-12 (dichloro-difluoromethane) is phased out because of the accepted hypothesis that chlorine and bromine atoms from halocarbons (but not fluorine) deplete desirable ozone in the atmosphere when released to the air. Feasible refrigerants are included in Table 12.1 for a range of coolant temperatures. When the refrigerant is a pure compound, as it often is, the process design calculation assumes that the refrigerant enters the utility exchanger at a specified pressure as a saturated liquid and exits without temperature change as a saturated vapor. The refrigerant is circulated through a refrigeration cycle, often consisting of a compressor (to increase the pressure), a condenser (to condense the compressed vapor), a throttle valve (to reduce the pressure), and the utility exchanger (also called the refrigerant boiler) as discussed in Example 10.2. The refrigerant boiling temperature is chosen to avoid freezing the process stream at the wall of the exchanger unless it is a crystallizer. When process streams are to be cooled to temperatures between 45 and 90°F, chilled water is often used as the coolant rather than a boiling refrigerant. Chilled aqueous brines can be used to temperatures as low as 0°F. Extensive information on refrigerants is given in the *ASHRAE Handbook* (2015).

The most common heat source for heating and/or vaporizing process streams in a utility exchanger is steam, which is available in most chemical plants, from a boiler at two, three, or more pressure levels. For example, the available levels might be 50, 150, and 450 psig, corresponding to saturation temperatures of 298, 366, and 459°F, respectively, for a barometric pressure of 14.7 psia. For process design purposes, the steam enters the utility exchanger as a saturated vapor and exits without pressure change as a saturated liquid (condensate), which is returned to the boiler. A steam trap is positioned on the exit line to purge all

Table 12.1 Heat-Transfer Media

Medium	Typical Temperature Range (°F)	Mode
Coolants		
Ethylene	–150 to –100	Vaporizing
Propylene	–50 to 10	Vaporizing
Propane	–40 to 20	Vaporizing
Ammonia	–30 to 30	Vaporizing
Tetrafluoroethane	–15 to 60	Vaporizing
Chilled brine	0 to 60	Sensible
Chilled water	45 to 90	Sensible
Cooling water	90 to 120	Sensible
Air	90 to 140	Sensible
Boiler feed water	220 to 450	Vaporizing
Heat Sources		
Hot water	100 to 200	Sensible
Steam	220 to 450	Condensing
Heating oils	30 to 600	Sensible
Dowtherm A	450 to 750	Condensing
Molten salts	300 to 1,100	Sensible
Molten metals	100 to 1,400	Sensible
Combustion gases	30 to 2,000	Sensible

of the condensate, thus ensuring only saturated steam participates in heat transfer.

Although condensing steam can be used as a heat source to temperatures as high as about 700°F (critical temperature of water = 705.4°F), steam pressures become very high at high temperatures (3,206 psia at the critical temperature). It is more common to use other media for temperatures above about 450°F. As listed in Table 12.1, these include the diphenyl (26.5 wt%)—diphenyloxide (73.5 wt%), and eutectic (Dowtherm A) for temperatures from 450 to 750°F, and various heating oils, molten salts, and molten metals for higher temperatures. Alternatively, as indicated in Heuristic 25 of Chapter 6, a furnace (fired heater), burning gas, fuel oil, or coal is often used in place of a utility heat exchanger when the chemicals being heated are not subject to decomposition and heating is required above 750°F.

Temperature-driving Force for Heat Transfer

When streams on both sides of a heat exchanger are considered in process design with a simulation program, a *two-sided heat exchanger* model is used. The model applies Eq. (12.1) to each side under conditions of equal heat-transfer rates, assuming that the exchanger is well insulated such that heat losses are negligible. Thus, all of the heat released by one side is taken up by the other side. In addition, a transport equation is applied to compute the heat-transfer area of the exchanger:

$$Q = UA\Delta T_m \tag{12.2}$$

where U is the overall heat-transfer coefficient, A is the area for heat transfer, and ΔT_m is the mean temperature-driving force for heat transfer.

The driving force is a critical component of Eq. (12.2). For a given heat exchange task, the rate of heat transfer, Q, is computed from Eq. (12.1). Depending on the geometry and extent of fouling of the heat exchanger and the conditions of the streams passing through the exchanger, the overall coefficient, U, can be computed from correlations described later in this chapter. The mean driving force, ΔT_m, then determines the heat exchanger area, A. The driving force depends on the entering and exiting stream temperatures, the variation of enthalpy with temperature and pressure of each of the two streams as they pass through the exchanger (as given by the heating and cooling curves), and the stream flow patterns in the exchanger. The latter requires careful consideration.

Examples of a few standard flow patterns are shown in Figure 12.4. The standard and most efficient pattern is countercurrent flow of the two streams. For this case, reference temperature-driving forces are those at the two ends of the exchanger. At one end, ΔT is the difference between the temperatures of the entering hot stream and exiting cold stream. At the other end, ΔT is the difference between the temperatures of the exiting hot stream and the entering cold stream. The smaller of the two differences is called the *closest* or *minimum temperature approach*. It is common to specify the design of a two-sided heat exchanger in terms of inlet conditions for each stream, the pressure drop across the exchanger for each stream, and a minimum approach temperature that reflects economics as shown in Section 11.6. The simulation program determines to which end of the exchanger the minimum applies and then calculates the exiting stream temperatures and the heat duty.

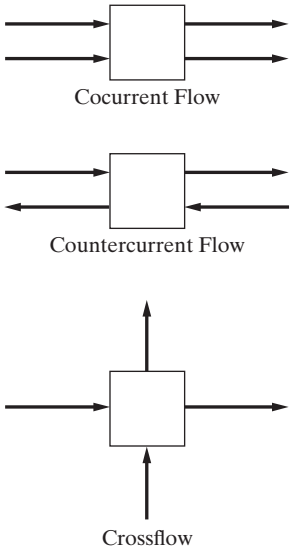

Figure 12.4 Standard flow patterns in heat exchangers.

The optimal minimum approach temperature is a function mainly of the temperature levels of the two streams as indicated in Heuristic 26 of Chapter 6 and the lost work analysis in Section 10.4. At temperatures below ambient, the optimal minimum approach temperature is less than 10°F and may be only 1–2°F at highly cryogenic conditions. At ambient temperature, it is about 10°F. At temperatures above ambient, up to 300°F, it is about 20°F. At higher temperatures, it may be 50°F. In a furnace, the flue gas temperature may be 250 to 350°F above the inlet process stream temperature. When one stream is boiled, a special consideration is necessary. Evaporation can take place in any of four different modes as shown in Figure 12.5. At temperature-driving forces on the boiling side of less than about 10°F, natural convection is dominant, and heat-transfer rates are low. At driving forces between 20 and 45°F, *nucleate boiling* occurs with rapid heat-transfer rates because of the turbulence generated by the bubbles. For driving forces above 100°F, *film boiling* takes place, and heat-transfer rates are again low because the mechanism is conduction through the gas film. The region between 50 and 100°F is in transition and is usually avoided. Heat exchangers for vaporization and reboiling avoid film boiling and are designed for the nucleate boiling region to maximize heat-transfer rates. A conservative rule of thumb is to employ Heuristic 28 of Chapter 6, which suggests using a mean overall temperature-driving force of 45°F. This driving force can be achieved by adjusting the pressure at which boiling takes place or the temperature of the heating medium.

EXAMPLE 12.2

Toluene is converted to benzene by hydrodealkylation. Typically, a 75% conversion is used in the reactor, which necessitates the recovery and recycle of unreacted toluene. In addition, a side reaction occurs that produces a small amount of a biphenyl byproduct, which is separated from the toluene. A hydrodealkylation process is being

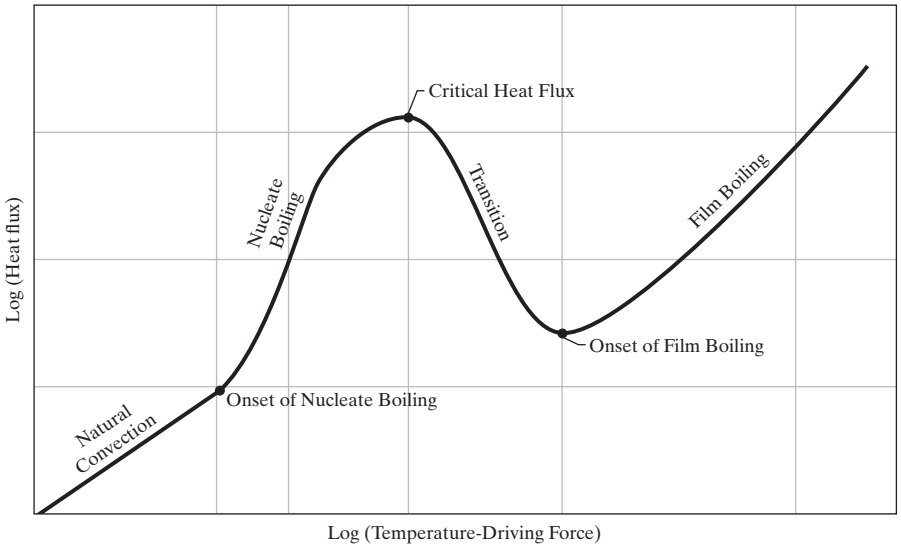

Figure 12.5 Modes in boiling heat transfer.

designed that includes a distillation column for separating toluene from biphenyl. The feed to the column is 3.4 lbmol/hr of benzene, 84.6 lbmol/hr of toluene, 5.1 lbmol/hr of biphenyl at 264°F and 37.1 psia. The distillate is to contain 99.5% of the toluene and 2% of the biphenyl. If the column operates at a bottoms pressure of 38.2 psia, determine the bottoms temperature and select a suitable heat source for the reboiler. Steam is available at pressures of 60, 160, and 445 psig. The barometer reads 14 psia.

SOLUTION

Assume that no benzene is present in the bottoms because it has a much higher vapor pressure than toluene, and a sharp separation between toluene and biphenyl is specified. By material balance, the bottoms contains 0.423 lbmol/hr of toluene and 4.998 lbmol/hr of biphenyl. A bubble-point calculation for this composition at 38.2 psia, using ASPEN PLUS with the SRK equation of state for K values, gives a temperature of 510.5°F. The highest-pressure steam available is at 459 psia with a saturation temperature of 458°F. Thus, steam cannot be used as the heat source for the reboiler. Instead, Dowtherm A is selected, assumed to enter the exchanger as a saturated vapor and exit as a saturated liquid. To ensure nucleate boiling, the overall temperature-driving force for reboiling the biphenyl bottoms is taken as 45°F. Thus, the condensing temperature for the Dowtherm A is 555.5°F. From data supplied by Dow Chemical Co., the saturation pressure at this temperature is only 28.5 psia, and the heat of vaporization is 116 Btu/lb. If saturated steam at 555.5°F were available, the pressure would be 1,089 psia with a heat of vaporization of 633 Btu/lb. Thus, the use of Dowtherm A at high temperatures results in much lower pressures, but its low heat of vaporization requires a higher circulation rate.

EXAMPLE 12.3

A mixture of 62.5 mol% ethylene and 37.5 mol% ethane is separated by distillation to obtain a vapor distillate of 99 mol% ethylene with 98% recovery of ethylene. When the pressure in the reflux drum is 200 psia, determine the distillate temperature and select a coolant for the condenser. What pressure is required to permit the use of cooling water in the condenser?

SOLUTION

Using the CHEMCAD simulator, the dew-point temperature for 99 mol% ethylene and 1 mol% ethane at 200 psia is −42°F. Assuming a minimum approach temperature of 5°F and a boiling refrigerant, the refrigerant temperature is −47°F. From Table 12.1, a suitable refrigerant is propylene, but ethylene, which is available at 99 mol% purity in the plant, is also a possibility with a boiling pressure of 185 psia.

The critical temperatures of ethylene and ethane are 49 and 90°F, respectively, at critical pressures of 730 and 708 psia, respectively. The critical point for 99 mol% ethylene is approximately at 50°F and 729 psia. Therefore, it is not possible to use cooling water in the condenser because it can only achieve a condensing temperature of 100°F.

When a process stream is both heated and vaporized or both cooled and condensed, the minimum approach temperature can occur within the exchanger away from either end. This can be determined from heating and cooling curves as illustrated in the following example.

EXAMPLE 12.4

A mixture of 100 lbmol/hr of ethyl chloride and 10 lbmol/hr of ethanol at 200°F and 35 psia is cooled with 90 lbmol/hr of ethanol at 90°F and 100 psia in a countercurrent-flow heat exchanger. Determine the stream outlet conditions and the heat duty for a minimum approach temperature of 10°F. Assume a pressure drop of 5 psi on the hot side and 10 psi on the cold side.

SOLUTION

The calculations are made with the CHEMCAD program using the HTXR (two-sided heat exchanger) model with the UNIFAC method for computing *K* values. The hot stream is found to enter the exchanger as superheated vapor and exit partially condensed. The cold stream is found to be a liquid throughout the exchanger. The *plot* menu is used to generate heating and cooling curves, which are shown in Figure 12.6a.

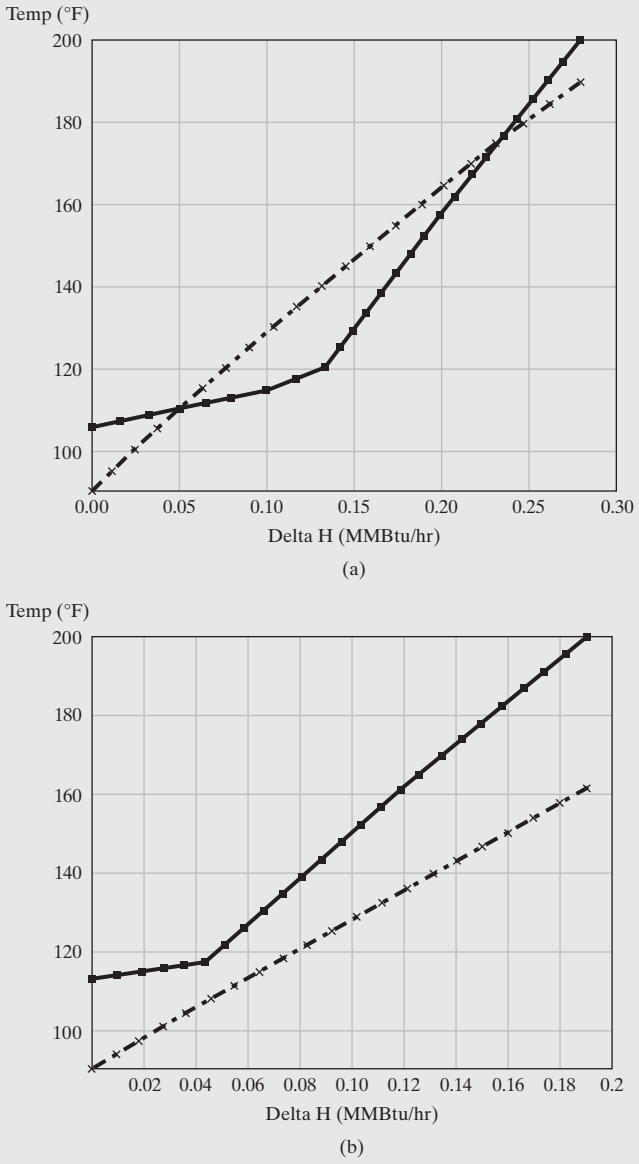

Figure 12.6 Heating and cooling curves for Example 12.4: (a) temperature crossover; (b) no temperature crossover.

It is seen that the minimum approach temperature of 10°F is placed by the HTXR model at the 200°F hot stream feed end to give a cold stream outlet temperature of 190°F. At the other end of the exchanger, the hot stream exits at 105.5°F, so the driving force at that end is 105.5–90 = 15.5°F. The heat duty is 277,000 Btu/hr. However, Figure 12.6a shows that the temperature of the hot stream crosses over the temperature of the cold stream within the exchanger. This is a *temperature crossover*, which violates the second law of thermodynamics. This crossover is caused by the condensation of the hot stream, which begins at a dew-point temperature of approximately 120°F. This results in a sharp change in slope of the temperature-enthalpy curve for the hot stream. From 120°F to the exit temperature, the hot stream undergoes partial condensation to an exit condition of 93 mol% vapor. The HTXR model has an option that can be used to detect a crossover during execution. This option, which is suggested in Heuristic 29 of Chapter 6, is a zone analysis called *Number of Zones*. If, for example, 20 zones across the exchanger are specified, stream temperatures are computed at 19 intermediate points in the exchanger. From these temperatures, the intermediate temperature-driving forces for the heat exchanger are checked to determine whether any are negative. If so, the HTXR model terminates with a warning to the user.

When a crossover occurs, a trial-and-error procedure can be applied to place the minimum approach temperature within the exchanger. This involves increasing the specified minimum approach temperature, which, as mentioned above, is placed at one end or the other. For this example, the result is shown in Figure 12.6b where it is seen that the minimum approach temperature occurs at the dew-point temperature of the hot stream. This is achieved by specifying a minimum approach temperature of 23°F, which is placed by the HTXR model at the hot stream exit end of the exchanger. Now the hot stream is cooled only to 113°F and the cold stream is heated only to 161°F. The heat duty is reduced to 190,000 Btu/hr. The hot stream exits with 97.8 mol% vapor.

Pressure Drop

The final design of a heat exchanger includes pressure-drop calculations on each side. These pressure drops cannot be computed by the simulator until a detailed design is completed for the heat exchanger. For process design when using a simulation program, preliminary conservative estimates of pressure drops due to friction are provided by the user. Some suggested values from Heuristic 31 of Chapter 6 are as follows. An additional pressure change occurs if the exchanger is placed vertically due to energy conversions between pressure head and potential energy.

	Pressure Drop	
Liquid streams with no phase change	5 to 9 psi	35 to 62 kPa
Vapor streams with no phase change	3 psi	21 kPa
Condensing streams	1.5 psi	10 kPa
Boiling streams	1.5 psi	10 kPa
Process streams passing through a furnace	20 psi	140 kPa

Methods for determining pressure drop when heat exchanger geometry is known are discussed in Section 12.3.

12.2 EQUIPMENT FOR HEAT EXCHANGE

As listed in Table 12.2, a wide variety of standard-size equipment is available for conducting heat exchange. Commercial units range in size from very small, *double-pipe heat exchangers*, with less than 1 ft^2 of heat-transfer surface to the very common shell-and-tube heat exchangers in a variety of configurations in sizes from 50 to 8,000 ft^2. Also available are large, air-cooled units called *fin-fan heat exchangers* because they consist of tubes with external peripheral fins and fans to force air past the tubes. Finned area in a single unit is as large as 20,000 ft^2. For specialized applications, *compact* (plate and other nontubular) *heat exchangers* are available. These are considered only briefly here but are discussed in more detail in *Perry's Chemical Engineers' Handbook* (2008).

Table 12.2 Heat Exchange Equipment

Double pipe
Shell and tube
Countercurrent flow
Parallel (cocurrent) flow
Crossflow
1–2, 1–4, 1–6, 1–8
2–4, 2–8
3–6
4–8
6–12
Air cooled (fin-fan)
Compact
Plate and frame
Spiral plate
Spiral tube
Plate fin

Double-Pipe Heat Exchangers

A typical double-pipe unit is shown in Figure 12.7a. In its simplest form, it consists of an inner straight pipe of circular cross section concentric to and supported within an outer straight pipe by means of packing glands. One stream flows through the inner pipe, and the other stream flows countercurrently through the annular passage between the outer wall of the inner pipe and the inner wall of the outer pipe. When the inner pipe is a 12-ft-long, 1 1/4-in., schedule 40 pipe, the heat-transfer area from Table 12.3 is 5.22 ft^2 based on the outside wall of the inner pipe. When the inner pipe is a 20-ft-long, 3-in., schedule 40 pipe, the heat-transfer area is 18.34 ft^2. When more heat-transfer area is needed, return bends and heads are used with additional pipes to build a hairpin unit as shown in Figure 12.7b. Hairpin units are available in sizes up to about 200 ft^2 of heat-transfer area and are competitive with shell-and-tube exchangers in the range of 100 to 200 ft^2. To prevent sagging of the inner pipe with a resulting distortion of the annular cross section, pipe length is limited to 20 ft. Therefore, a 200-ft^2 unit of 3-in.-diameter inner pipes requires 10 hairpin connections. When one stream is at high temperature and/or high pressure and/or is corrosive, it is passed through the inner pipe. If the other stream is a gas, longitudinal fins can be added to the outside surface of the inner pipe to help balance the inner and outer heat-transfer resistances. If crystallization occurs from a liquid stream flowing through the inner pipe, scrapers can be added inside that pipe to prevent buildup of crystals on the inner wall. Double-pipe exchangers are not recommended for use in boiling or vaporization services.

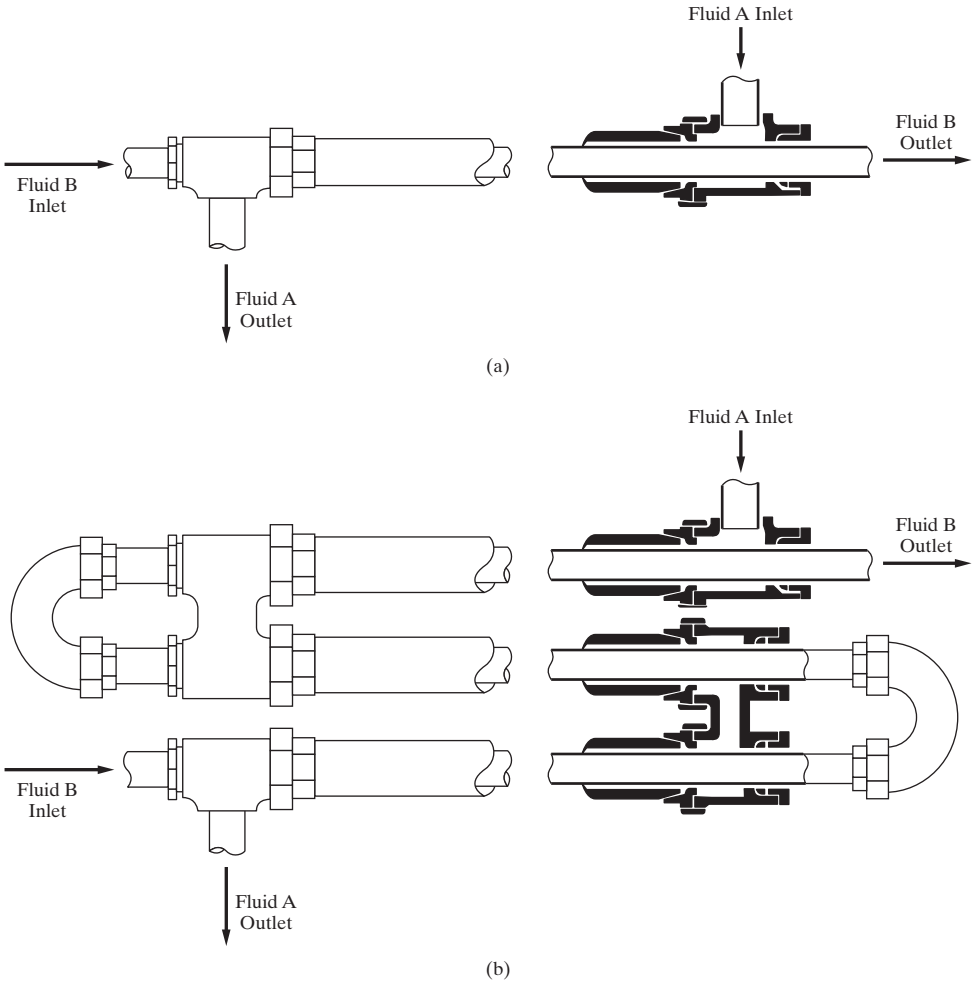

Figure 12.7 Double-pipe heat exchangers: (a) single unit; (b) hairpin unit.

Table 12.3 Steel Pipe Data

Nominal Pipe Size (in.)	O.D. (in.)	Schedule No.	I.D. (in.)	Flow Area per Pipe (in.^{2})	Surface per Linear Foot (ft^2)		Weight per Linear Foot (lb steel)
					Outside	Inside	
1/8	0.405	40†	0.269	0.058	0.106	0.070	0.25
		80‡	0.215	0.036	0.106	0.056	0.32
1/4	0.540	40	0.364	0.104	0.141	0.095	0.43
		80	0.302	0.072	0.141	0.079	0.54
3/8	0.675	40	0.493	0.192	0.177	0.129	0.57
		80	0.423	0.141	0.177	0.111	0.74
1/2	0.840	40	0.622	0.304	0.220	0.163	0.85
		80	0.546	0.235	0.220	0.143	1.09
3/4	1.05	40	0.824	0.534	0.275	0.216	1.13
		80	0.742	0.432	0 275	0.194	1.48
1	1.32	40	1.049	0.864	0.344	0.274	1.68
		80	0.957	0.718	0.344	0.250	2.17
1 1/4	1.66	40	1.380	1.50	0.435	0.362	2.28
		80	1.278	1.28	0.435	0.335	3.00
1 1/2	1.90	40	1.610	2.04	0.498	0.422	2.72
		80	1.500	1.76	0498	0.393	3.64
2	1.38	40	2.067	3.35	0.622	0.542	3.66
		80	1.939	2.95	0.622	0.508	5.03
2 1/2	2.88	40	2.469	4.79	0.753	0.647	5.80
		80	2.323	4.23	0.753	0.609	7.67
3	3.50	40	3.068	7.38	0.917	0.804	7.58
		80	2.900	6.61	0.917	0.760	10.3
4	4.50	40	4.026	12.7	1.178	1.055	10.8
		80	3.826	11.5	1.178	1.002	15.0
6	6.625	40	6.065	28.9	1.734	1.590	19.0
		80	5.761	26.1	1.734	1.510	28.6
8	8.625	40	7.981	50.0	2.258	2.090	28.6
		80	7.625	45.7	2 258	2.000	43.4
10	10.75	40	10.02	78.8	2.814	2.62	40.5
		60	9.75	74.6	2.814	2.55	54.8
12	12.75	30	12.09	115	3.338	3.17	43.8
16	16.0	30	15.25	183	4.189	4.00	62.6
20	20.0	20	19.25	291	5.236	5 05	78.6
24	24.0	20	23.25	425	6.283	6.09	94.7

†Schedule 40 designates former "standard" pipe.

‡Schedule 80 designates former "extra-strong" pipe.

Shell-and-tube Heat Exchangers

Heat-transfer area per unit volume is greatly increased by placing a large number of small-diameter tubes inside a shell, that is, a pressure vessel. Shell-and-tube heat exchangers whose design is standardized by the Tubular Exchanger Manufacturers Association (TEMA) and has changed little in almost 70 years is shown in one configuration in Figure 12.8a. Data for heat exchanger tubes are given in Table 12.4. The following heuristic is useful in making preliminary calculations:

Heuristic 54: ***For shell-and-tube heat exchangers, tubes are typically 3/4-in. O.D, 16 ft long, and on 1-in. triangular spacing. A shell of 1-ft diameter accommodates 100 ft^2; 2-ft, 400 ft^2, and 3 ft, 1100 ft^2.***

As a further example of this type of exchanger, a standard 37-in. I.D. shell can accommodate 1,074 3/4 -in. O.D., 16 BWG (Birmingham wire gauge, which determines the tube wall thickness) tubes on a 1-in. triangular pitch (tube center-to-center distance). When the tubes are 20-ft long, the heat-transfer area based on the outside tube surface is 4,224 ft^2. The inside volume of the shell is 149 ft^3, resulting in almost 30 ft^2 of heat-transfer surface area per cubic foot of exchanger volume. A double-pipe heat exchanger consisting of a 1- 1/4 -in., schedule 40 pipe inside a 2-in., schedule 40 pipe has only 1.17 ft^2 of heat-transfer surface area per cubic foot of exchanger volume.

Many configurations of shell-and-tube exchangers are available, with Figure 12.8a being the simplest. It is a one-tube-pass,

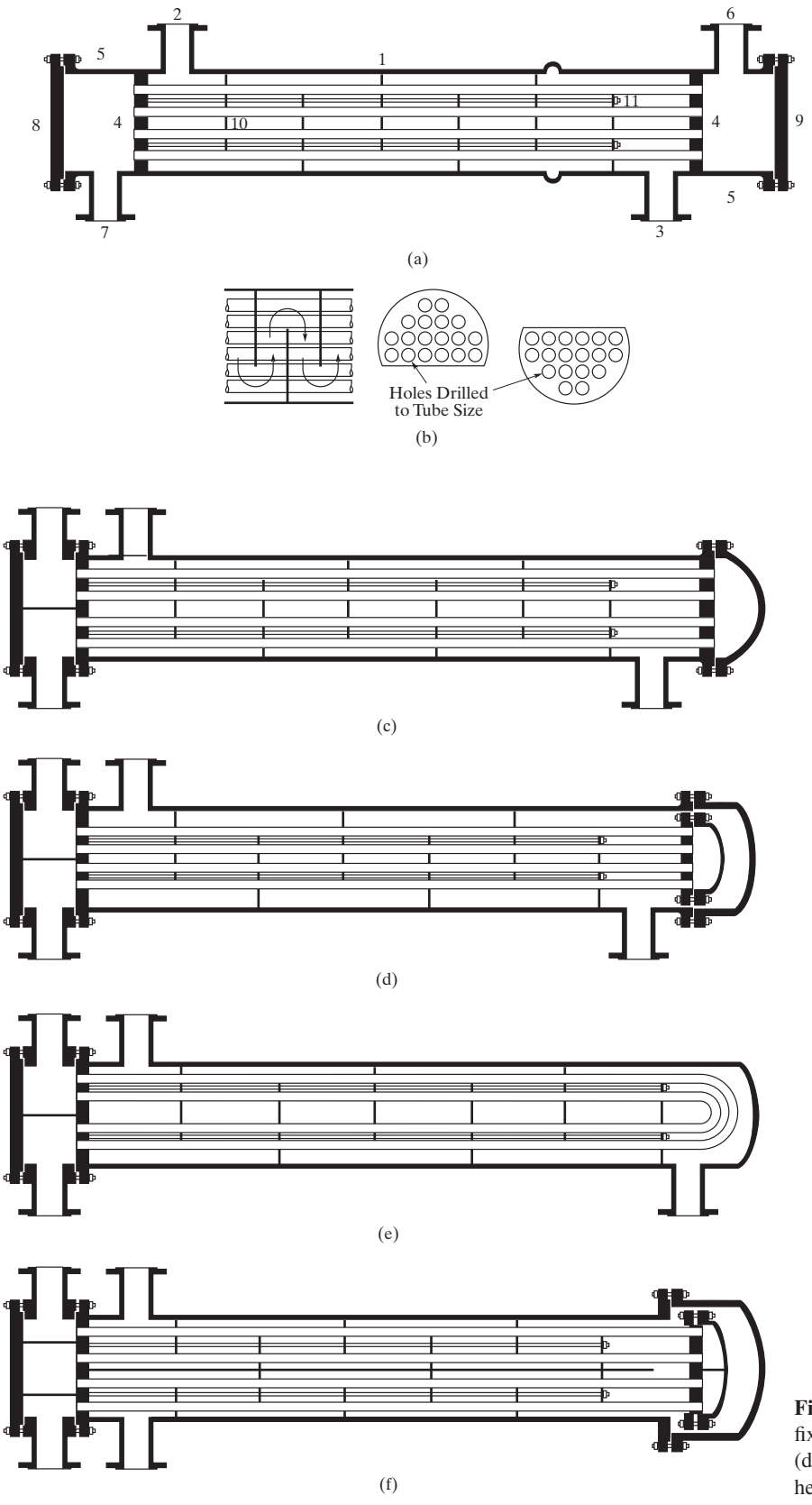

Figure 12.8 Shell-and-tube heat exchangers: (a) 1-1 fixed head; (b) segmental baffles; (c) 1-2 fixed head; (d) 1-2 floating head; (e) 1-2 U-tube; (f) 2-4 floating head.

Table 12.4 Heat Exchanger Tube Data

Tube OD. (in.)	BWG	Wall Thickness (in.)	I.D. (in.)	Flow Area per Tube ($in.^2$)	Surface per Linear Foot (ft^2)		Weight per Linear Foot (lb steel)
					Outside	Inside	
½	12	0.109	0.282	0.0625	0.1309	0.0748	0.493
	14	0.083	0.334	0.0876	0.1309	0.0874	0.403
	16	0.065	0.370	0.1076	0.1309	0.0969	0.329
	18	0.049	0.402	0.127	0.1309	0.1052	0.258
	20	0.035	0.430	0.145	0.1309	0.1125	0.190
¾	10	0.134	0.482	0.182	0.1963	0.1263	0.965
	11	0.120	0.510	0.204	0.1963	0.1335	0.884
	12	0.109	0.532	0.223	0.1963	0.1393	0.817
	13	0.095	0.560	0.247	0.1963	0.1466	0.727
	14	0.083	0.584	0.268	0.1963	0.1529	0.647
	15	0.072	0.606	0.289	0.1963	0.1587	0.571
	16	0.065	0.620	0.302	0.1963	0.1623	0.520
	17	0.058	0.634	0.314	0.1963	0.1660	0.469
	18	0.049	0.652	0.334	0.1963	0.1707	0.401
1	8	0.165	0.670	0.335	0.2618	0.1754	1.61
	9	0.148	0.704	0.389	0.2618	0.1843	1.47
	10	0.134	0.732	0.421	0.2618	0.1916	1.36
	11	0.120	0.760	0.455	0.2618	0.1990	1.23
	12	0.109	0.782	0.479	0.2618	0.2048	1.14
	13	0.095	0.810	0.515	0.2618	0.2121	1.00
	14	0.083	0.834	0.546	0.2618	0.2183	0.890
	15	0.072	0.856	0.576	0.2618	0.2241	0.781
	16	0.065	0.870	0.594	0.2618	0.2277	0.710
	17	0.058	0.884	0.613	0.2618	0.2314	0.639
	18	0.049	0.902	0.639	0.2618	0.2361	0.545
1 ¼	8	0.165	0.920	0.665	0.3271	0.2409	2.09
	9	0.148	0.954	0.714	0.3271	0.2498	1.91
	10	0.134	0.982	0.757	0.3271	0.2572	1.75
	11	0.120	1.01	0.800	0.3271	0.2644	1.58
	12	0.109	1.03	0.836	0.3271	0.2701	1.45
	13	0.095	1.06	0.884	0.3271	0.2775	1.28
	14	0.083	1.08	0.923	0.3271	0.2839	1.13
	15	0.072	1.11	0.960	0.3271	0.2896	0.991
	16	0.065	1.12	0.985	0.3271	0.2932	0.900
	17	0.058	1.13	1.01	0.3271	0.2969	0.808
	18	0.049	1.15	1.04	0.3271	0.3015	0.688
1 ½	8	0.165	1.17	1.075	0.3925	0.3063	2.57
	9	0.148	1.20	1.14	0.3925	0.3152	2.34
	10	0.134	1.23	1.19	03925	0.3225	2.14
	11	0.120	1.26	1.25	0.3925	0.3299	1.98
	12	0.109	1.28	1.29	0.3925	0.3356	1.77
	13	0.095	1.31	1.35	0.3925	0.3430	1.56
	14	0.083	1.33	1.40	0.3925	0.3492	1.37
	15	0.072	1.36	1.44	0.3925	0.3555	1.20
	16	0.065	1.37	1.47	0.3925	0.3587	1.09
	17	0.058	1.38	1.50	0.3925	0.3623	0.978
	18	0.049	1.40	1.54	0.3925	0.3670	0.831

one-shell-pass, fixed (stationary)-head exchanger. One stream (tube-side fluid) flows through the tubes; the other (shell-side fluid) flows (usually countercurrently) through the shell across the outside of the tubes. The exchanger consists of a shell (1) to which are attached an inlet nozzle (2) and an outlet nozzle (3) for the shell-side fluid. At either end of the shell are tube sheets (4) into which tubes are expanded to prevent leakage of streams between the tube side and the shell side. Attached to the tube sheets are channels (5) with inlet and outlet nozzles (6, 7) for the tube-side fluid. Attached to channels are covers (8, 9). To induce turbulence and increase the velocity of the shell-side fluid, transverse baffles (10) through which the tubes pass are employed on the shell side. The baffles shown in Figure 12.8b cause the shell-side fluid to flow mainly at right angles to the axes of the tubes. Baffle spacing (*baffle pitch*) is fixed by baffle spacers (11), which consist of through-bolts screwed into the tube sheets and covered with pipes of length equal to the baffle spacing. Minimum spacing is 20% of the shell inside diameter; maximum is 100%. Various types of baffles are available, but the segmental is the most common with a segment height equal to 75% of the shell inside diameter. This is often referred to as a *baffle cut* of 25%. Maximum baffle cut is 45%. It is not practical to fit the baffles snugly to the inside surface of the shell. Instead, there is a shell-to-baffle clearance, which depends on shell inside diameter. The diametric shell-to-baffle clearance (twice the clearance) varies from approximately $\frac{1}{8}$ in to $\frac{3}{8}$ in. for shell inside diameters of 12 to 84 in.

Several different tube layout patterns are used, four of which are shown in Figure 12.9. Tube spacing is characterized by the *tube pitch*, which is the closest center-to-center distance between the adjacent tubes or by *tube clearance*, which is the shortest distance between two adjacent tube holes. The most common tube layouts are shown in Figure 12.9 and in the table that follows it.

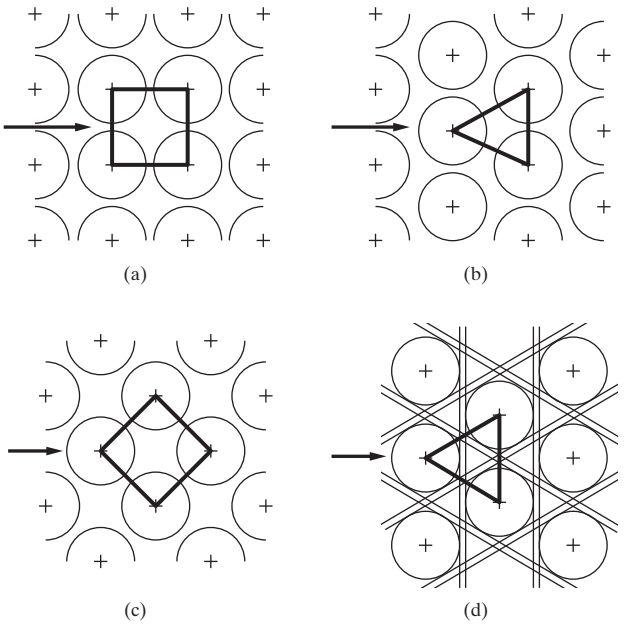

Figure 12.9 Tube layout patterns: (a) square pitch; (b) triangular pitch; (c) square pitch rotated; (d) triangular pitch with cleaning lanes.

Layout	Tube O.D. (in.)	Tube Pitch (in.)
Square	$\frac{3}{4}$	1
Square	1	$1\frac{1}{4}$
Triangular	$\frac{3}{4}$	$1\frac{5}{16}$
Triangular	$\frac{3}{4}$	1
Triangular	1	$1\frac{1}{4}$

It is not practical to fit tubes tightly to the baffles. Accordingly, some shell-side fluid leaks through the clearance between the tubes and the baffle holes. This leakage is in addition to the leakage through the clearance between the shell and the baffles. Although tubes can completely fill the shell, there must be a clearance between the outermost tubes and the shell. Typical clearance between the outer-tube limit (OTL) and the shell inside diameter is $\frac{1}{2}$ in. Common tube lengths are 8, 12, 16, and 20 ft.

The 1-1 fixed-head shell-and-tube heat exchanger of Figure 12.8a has several limitations:

1. The inside surfaces of the tubes can be cleaned when necessary by removing the end covers of the shell and reaming out the tubes, but the outside surfaces of the tubes cannot be cleaned because the tube bundle is fixed inside the shell.
2. If large temperature differences exist between the shell-side and tube-side fluids, differential expansion between the shell and tubes may exceed limits for bellows or expansion joints.
3. The velocity of the tube-side fluid may be too low to obtain a reasonable heat-transfer coefficient.

These limitations are avoided by other configurations in Figure 12.8. The floating-head unit of Figure 12.8d eliminates the differential expansion problem. Also, the pull-through design permits removal of the tube bundle from the shell so that the outside surfaces of the tubes can be cleaned. The square-pitch tube layout is preferred for cleaning.

To increase the tube-side fluid velocity so as to increase the inside heat-transfer coefficient, a one-shell-pass, two-tube-pass (1-2) exchanger shown in Figures 12.8c, 12.8d, and 12.8e is used, which are, respectively, fixed-head, floating-head, and U-tube units. A disadvantage of the U-tube unit is the inability to clean the insides of the tubes completely.

With the one-tube pass exchangers of Figures 12.8a and 12.8b, efficient countercurrent flow between the tube-side and shell-side fluids is closely approximated. This is not the case with the 1-2 exchangers of Figures 12.8c, 12.8d, and 12.8e because of the reversal of the tube-side fluid flow direction. The flow is countercurrent in one tube pass and cocurrent (parallel) in the other. As shown later in this section, this limits heat recovery because of the reduction in the mean temperature-driving force for heat transfer. Note that a video of an industrial 1-2 exchanger is provided on the multimedia modules that accompanies this text. See *ASPEN → Heat Exchangers → Introduction with Video* or *HYSYS → Heat Exchangers → Theory*.

The shell-side fluid velocity is increased and the exchanger heat recovery is improved with the two-shell-pass, four-tube-pass (2-4) configuration shown in Figure 12.8f where a longitudinal

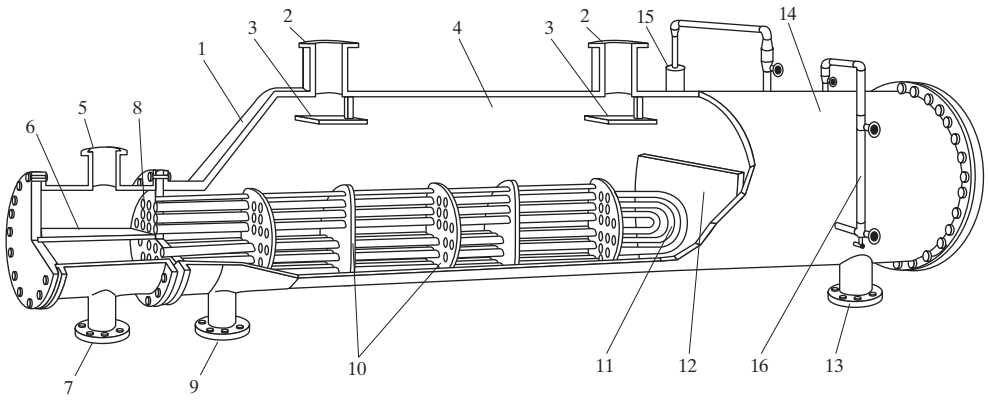

Figure 12.10 Kettle reboiler: (1) shell; (2) shell outlet nozzles (vapor); (3) entrainment baffles; (4) vapor-disengaging space; (5) channel inlet nozzle; (6) channel partition; (7) channel outlet nozzle; (8) tube sheet; (9) shell inlet nozzle; (10) tube support plates; (11) U-tube returns; (12) weir; (13) shell outlet nozzle (liquid); (14) liquid holdup (surge) section; (15) top of level-instrument housing (external displacer); (16) liquid level gauge.

baffle creates the two-shell passes in a single shell. Alternatively, two exchangers in series, each with a single shell pass and two tube passes, can be employed. Further improvements are achieved with 3-6 and 4-8 exchangers but at the cost of more complexity in the exchanger design. Customarily, not more than two shell passes are provided in a single shell. Thus, a 3-6 pass exchanger would consist of three shells (exchangers) in series, each with two tube passes. When even higher tube-side velocities are desired, 1-4, 1-6, or 2-8 exchangers can be specified. Heat recovery for these various combinations of shell-and-tube passes is considered in detail later in this section.

The exchangers in Figure 12.8 are suitable for heating, cooling, condensation, and vaporization. However, a special design, the *kettle reboiler* shown in Figure 12.10, is also in common use for vaporization or boiling, particularly with distillation columns. Compared to a 1-2 exchanger, the kettle reboiler has a weir to control the liquid level in the shell and a disengagement region in the space above the liquid level. In a typical service, steam is condensed inside the tubes and liquid is vaporized from the pool of liquid outside the tubes. The circulation of the boilup stream in distillation column reboilers can be driven by either natural or forced convection. In a reboiler circuit driven by natural convection as shown in Figure 12.11a for a so-called *once-through thermosyphon reboiler*, the driving force for the circulation is the difference in hydrostatic heads of the downcomer and riser lines. A *kettle reboiler* circuit is often driven by natural convection. For a reboiler circuit driven by forced convection illustrated in Figure 12.11b, the driving force is provided by a pump installed in the downcomer line.

When employing a shell-and-tube heat exchanger, a decision must be made as to which fluid passes through the tubes (tube side) and which passes through the shell outside the tubes (shell side). The following heuristic is useful in making this decision:

Heuristic 55: ***The tube side is for corrosive, fouling, scaling, hazardous, high-temperature, high-pressure, and more expensive fluids. The shell side is for more viscous, cleaner, lower-flow rate, evaporating, and condensing fluids.***

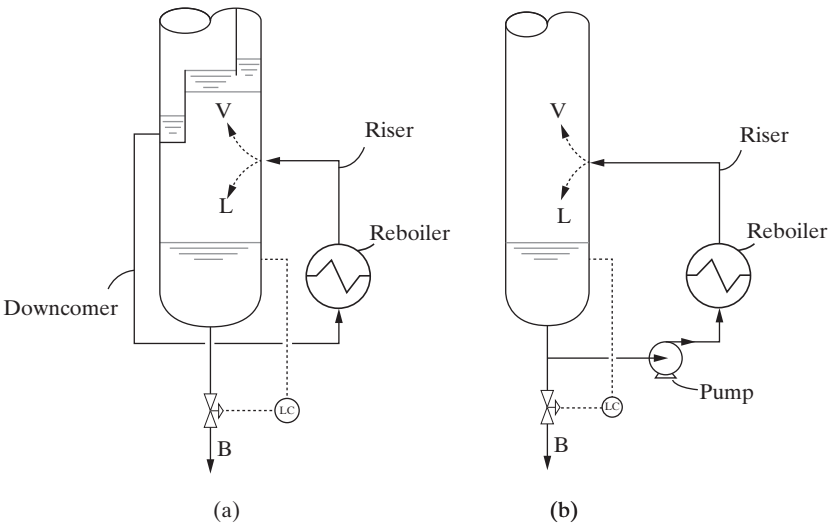

Figure 12.11 Examples of reboiler circuits: (a) a once-through thermosyphon reboiler; (b) reboiler circuit driven by forced convection.

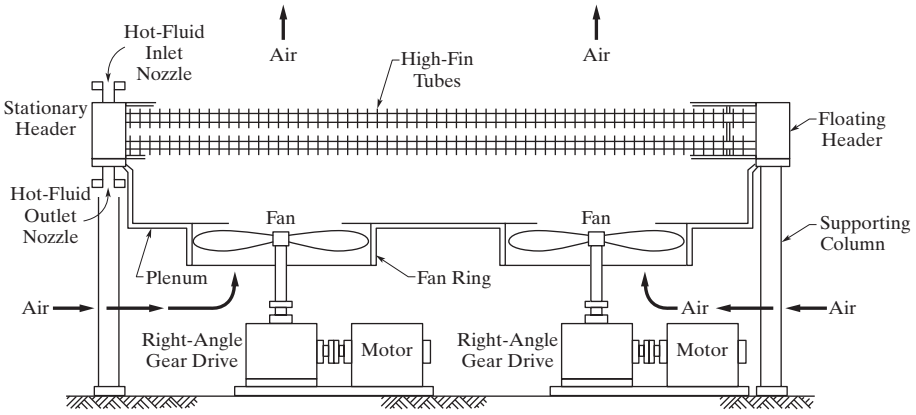

Figure 12.12 Fin-fan heat exchanger.

Air-Cooled Heat Exchangers

When cooling water is scarce, air is used for cooling and condensing liquid streams in fin-fan heat exchangers. A common configuration is shown in Figure 12.12. See also a video of an industrial fin-fan cooler in the multimedia modules that accompanies this text. The liquid to be cooled and/or condensed passes through the inside of the tubes. Peripheral fins on the outside of the tubes across which the air flows increase the outside heat-transfer area and thereby lower the outside thermal resistance so that it approaches the tube inside resistance. The tubes are arranged in banks with the air forced across the tubes in crossflow by one or more fans. No shell is needed, fouling on the outside of the tubes does not occur, and inside tube cleaning is readily accomplished. For initial design, the following heuristic is useful:

Heuristic 56: ***For an air-cooled exchanger, the tubes are typically 0.75–1.00-in. in outside diameter. The ratio of fin surface area to tube outside bare area is large at 15–20. Fan power requirement is in the range of 2–5 hp per million Btu/hr transferred, or about 20–hp per 1,000 ft^2 of tube outside bare surface (fin-free) area. Minimum approach temperature is about 50°F, which is much higher than with water-cooled exchangers. Without the fins, overall heat-transfer coefficients would be about 10 Btu/hr-ft^2-°F With the fins, U = 80–100 Btu/hr-ft^2-°F based on the tube outside bare surface area.***

Design is usually based on an entering air temperature of 90°F (hot summer day) for which the process stream can be assumed to exit the air-cooled heat exchanger at 140°F. For air at 70°F, a stream can be cooled typically to 120°F. Special design considerations may be required for the use of air coolers in the Middle East where air temperatures may vary from 130°F during the day to 35°F at night. Overhead condensers sometimes combine an air cooler with a cooling-water condenser to reduce the cooling-water load.

Compact Heat Exchangers

Compact heat exchangers have been available for more than a century but have been slow to replace shell-and-tube exchangers. This has been due to the standards established by TEMA for shell-and-tube exchangers and their applicability to high pressures and temperatures and to streams containing particulate matter. Nevertheless, for non-demanding services, compact exchangers deserve consideration because they can offer significant economies.

When the two fluids exchanging heat must be kept clean, *plate-and-frame heat exchangers* made of stainless steel are commonly used. A typical configuration as shown in Figure 12.13a consists of a series of pressed corrugated plates on close spacing. Hot and cold fluids flow on opposite sides of a plate. Heat-transfer coefficients are high because of the enhancement of turbulence by the corrugations. Fouling of the surfaces is low, and the heat-transfer surfaces are readily cleaned. Because gasket seals are necessary in the grooves around the periphery of the plates to contain and direct the fluids, operating pressures and temperatures are limited to 300 psig and 400°F. Plate-and-frame units with as much as 16,000 ft^2 of heat-transfer surface area are available. They are suitable only for heating and cooling with no phase change. They can be designed for very small minimum approach temperatures and are ideal for viscous, corrosive fluids. They are also well suited for high sanitation services where in stainless-steel construction they may be 25–50% of the cost of a shell-and-tube unit.

Heat-transfer coefficients can also be enhanced by using spiral-flow passageways as in the *spiral-plate heat exchanger* shown in Figure 12.13b. This unit provides true countercurrent flow. Typically, the hot fluid enters at the center of the spiral and flows outward while the cold fluid enters at the periphery and flows inward. This unit is competitive with the shell-and-tube exchanger for heating and cooling of highly viscous, corrosive, fouling, and scaling fluids at ambient to moderate pressures. Units with up to 2,000 ft^2 of heat-transfer surface area are available.

For operation at high pressures, a spiral of adjacent tubes can be used. One fluid flows through the tube coil while the other fluid flows counter-currently in the spiral gap between turns of the coil. The shell side is readily cleaned, but the tube side is not. Sizes of the *spiral-tube heat exchanger* are limited to 500 ft^2 of heat-transfer surface area.

When sensible heat is to be exchanged between two gases, extended heat-transfer surface in the form of fins is desirable on both sides. This is accomplished by *plate-fin heat exchangers*, an example of which is shown in Figure 12.13c. These compact units achieve heat-transfer surface areas of 350 ft^2/ft^3 of unit,

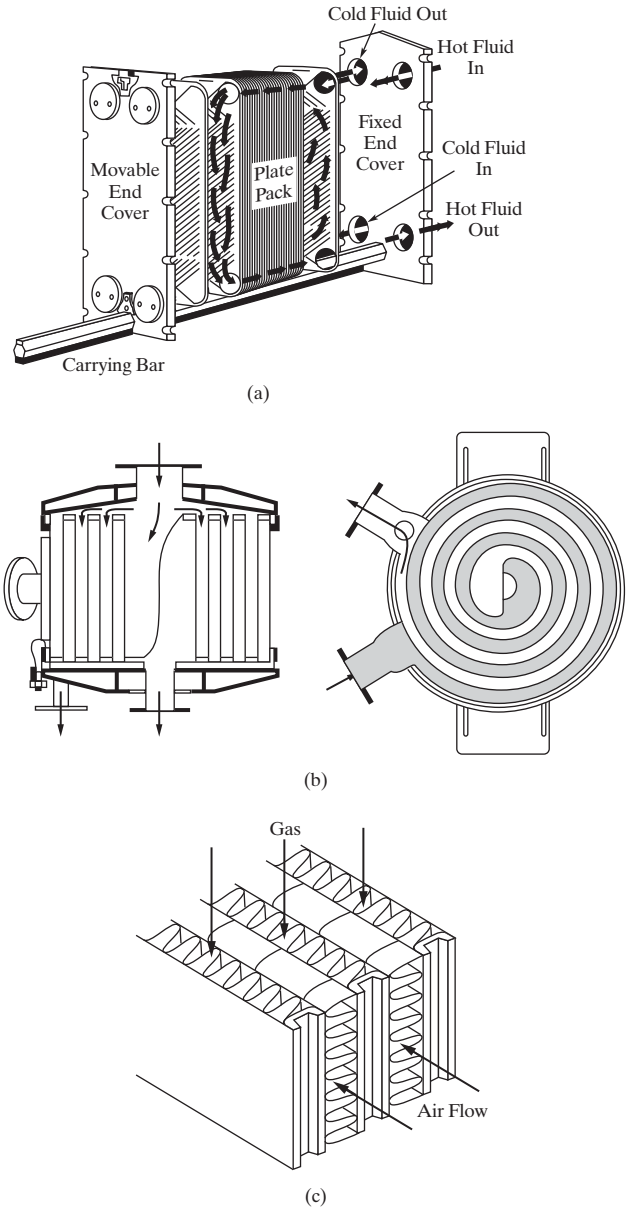

Figure 12.13 Compact heat exchangers: (a) plate and frame; (b) spiral plate; (c) plate fin.

which is much higher (up to 4 times) than for shell-and-tube heat exchangers. The fins consist of corrugated surfaces of 0.2- to 0.6-mm thickness and 3.8- to 11.8-mm height. Fin density is 230–700 fins/m. Plate-fin units can be designed for high pressures and for countercurrent or crossflow. Two, three, or more streams can exchange heat in a single unit.

Furnaces

Furnaces (also called fired heaters) are often used to heat, vaporize, and/or react process streams at high temperatures and high flow rates. Heat duties of commercial units are in the range of 3 to 100 MW (10,000,000 to 340,000,000 Btu/hr). A number of different designs exist using either rectangular or cylindrical steel chambers and lined with fire brick. The process fluid flows through tubes that are arranged in a so-called *radiant section* around the inside wall of the furnace enclosure. In this section, heat transfer to the outer surface of the tubes is predominantly by radiation from combustion gases resulting from burning the furnace fuel with air. To recover as much energy as possible from the combustion gases, a so-called *convection section* where the gases flow over a bank of extended-surface tubes surmounts the radiant section. In this section, heat transfer from the gases to the tubes is predominantly by forced convection. In some cases, plain tubes are placed in the bottom part of the convection section to shield the extended-surface tubes from excessive radiation. Furnaces are purchased as package units with preliminary estimates of purchase cost based on the heat duty. Typical designs are based on the following heuristic:

Heuristic 57: ***Typical heat fluxes in fired heaters are 12,000 Btu/hr-ft^2 in the radiant section and 4,000 Btu/hr-ft^2 in the convection section with approximately equal heat duties in the two sections. Typical process liquid velocity in the tubes is 6 ft/s. Thermal efficiency for modern fired heaters is 80–90 % while older fired heaters may have thermal efficiencies of only 70–75 %.***

As stated in Heuristic 30 of Chapter 6, stack gas (exit) temperatures are in the range 650 to 950°F. However, the flue gas must not be cooled below its dew point, called the *acid dew point*. Otherwise, corrosion of the stack may occur.

Temperature-driving Forces in Shell-and-tube Heat Exchangers

The rate of heat transfer between two streams flowing through a heat exchanger is governed by Eq. (12.2). Except for a few simple, idealized cases, the mean temperature-driving force, ΔT_m, is a complicated function of the exchanger flow configuration and the thermodynamic and transport properties of the fluids. When a phase change occurs, an additional complication enters into its determination.

The simplest expression for ΔT_m is determined when the following assumptions hold:

1. Stream flows are at steady state.
2. Stream flows are countercurrent or cocurrent to each other.
3. The overall heat-transfer coefficient is constant throughout the exchanger.
4. Each stream undergoes only sensible enthalpy changes (heating or cooling) with constant specific heat.
5. Heat losses are negligible.

For these assumptions, changes in the stream temperatures with distance through the exchanger or with stream enthalpy are linear as shown in the heating and cooling curves of Figure 12.14a for countercurrent flow and Figure 12.14b for cocurrent flow. The ΔT_m is then a function only of the driving forces at the two ends of the exchanger, ΔT_1 and ΔT_2, in the form of a log mean:

$$\Delta T_{LM} = \frac{\Delta T_1 - \Delta T_2}{\ln(\Delta T_1/\Delta T_2)} \tag{12.3}$$

If at most one or of the streams undergoes isothermal condensation or boiling, the specific heat is constant for a stream not undergoing phase change and the above assumptions 1, 3, and 5 apply, the log-mean temperature difference applies to all heat

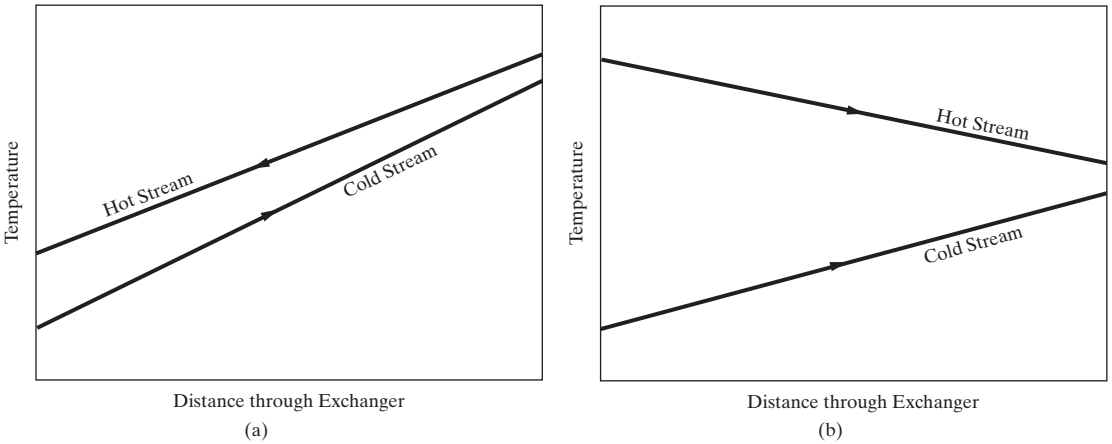

Figure 12.14 Ideal heating and cooling curves: (a) countercurrent flow; (b) cocurrent flow.

exchanger configurations, including multiple tube- or shell-pass arrangements. When both streams undergo isothermal condensation or boiling, $\Delta T_1 = \Delta T_2$ can be used for ΔT_{LM}.

When shell-and-tube exchangers with multiple-tube passes or multiple shell-and-tube passes are used, the flow directions of the two fluids are combinations of countercurrent and cocurrent flow. The resulting ΔT_m for given values of ΔT_1 and ΔT_2 based on countercurrent flow is less than ΔT_{LM} given by Eq. (12.3). For assumptions 1, 3, 4, and 5 above, the true mean temperature-driving force for a 1-2 exchanger was derived by Nagle (1933) and Underwood (1934). The resulting equation is commonly expressed in terms of the ratio, F_T = correction factor = $\Delta T_m/\Delta T_{LM}$:

$$F_T = \frac{\sqrt{R^2+1}\,\ln[(1-S)/(1-RS)]}{(R-1)\ln\left[\dfrac{2-S\left(R+1-\sqrt{R^2+1}\right)}{2-S\left(R+1+\sqrt{R^2+1}\right)}\right]} \tag{12.4}$$

where

$$R = \frac{T_{\text{hot in}} - T_{\text{hot out}}}{T_{\text{cold out}} - T_{\text{cold in}}} \tag{12.5}$$

$$S = \frac{T_{\text{cold out}} - T_{\text{cold in}}}{T_{\text{hot in}} - T_{\text{cold in}}} \tag{12.6}$$

Since $T_{\text{hot in}} > T_{\text{cold out}}$, S must take a value between 0 and 1. In contrast, the ratio R is a positive value that can be greater than or less than unity, depending on the ratio of the flowing heat capacities of the hot and cold streams. The rate of heat transfer in multipass exchangers then becomes

$$Q = UAF_T\Delta T_{\text{LM for countercurrent flow}} \tag{12.7}$$

A graph of Eq. (12.4) appears in Figure 12.15 with F_T as a function of S and R as a parameter. Values of F_T are always less than 1. In heat exchanger applications, it is desirable to have a value of F_T of 0.85 or higher. Values of less than 0.75 are generally unacceptable because below this value, curves in Figure 12.15 turn sharply downward. Thus, small errors in R and S or small deviations from the above assumptions can result in values of F_T much lower than anticipated. Values of F_T are not significantly decreased further by using exchangers with additional tube passes, such as 1-4, 1-6, or 1-8. At most, F_T for a 1-8 exchanger differs by less than 2% from that for a 1-2 exchanger.

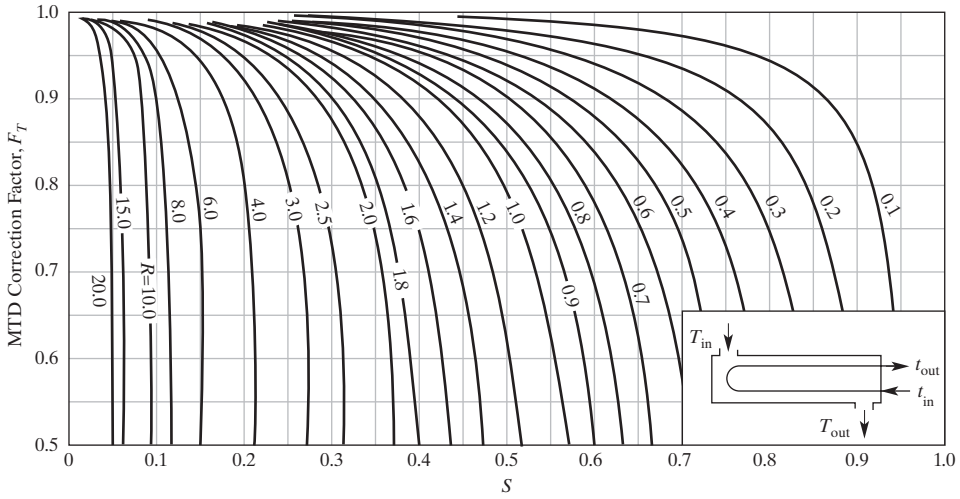

Figure 12.15 Temperature-driving-force correction factor for 1-2 shell-and-tube heat exchanger. (*Source:* Adapted from Bowman (1940)).

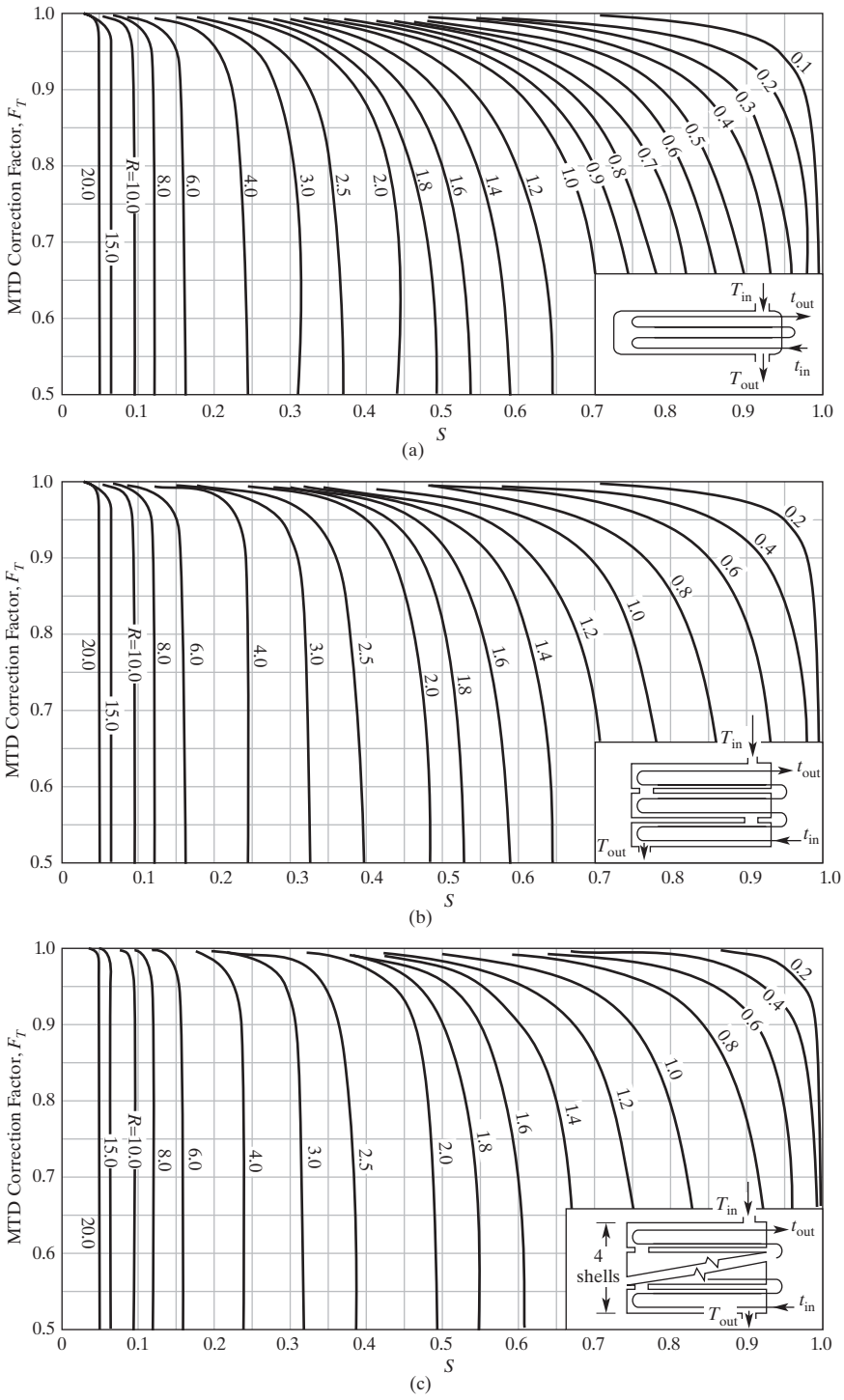

Figure 12.16 Temperature-driving-force correction factor for multiple-shell-pass heat exchangers: (a) 2-4 exchanger; (b) 3-6 exchanger; (c) 4-8 exchanger. (*Source:* Adapted from Bowman et al., (1940)).

When F_T is unsatisfactory, a multiple-shell-pass heat exchanger is used. The more shell passes, the higher is the value of F_T. Charts for correction factors of multiple-shell-pass exchangers are given in Figure 12.16 from the work of Bowman et al. (1940). Crossflow exchangers are also less efficient than countercurrent exchangers. Charts of correction factors for cross-current flow are given in Figure 12.17. In Figures 12.15 to 12.17, the symbols T and t differentiate between shell- or tube-side fluids. Use of Figures 12.15 to 12.17 with Eqs. (12.5) to (12.7) is independent of whether the hot fluid flows on the shell or tube side. The use of the correction-factor charts is illustrated by the following example.

EXAMPLE 12.5

A hot stream is being cooled from 200°F to 140°F by a cold stream that enters the exchanger at 100°F and exits at 190°F. Select an appropriate multiple-tube-pass shell-and-tube exchanger configuration and determine the true mean temperature-driving force.

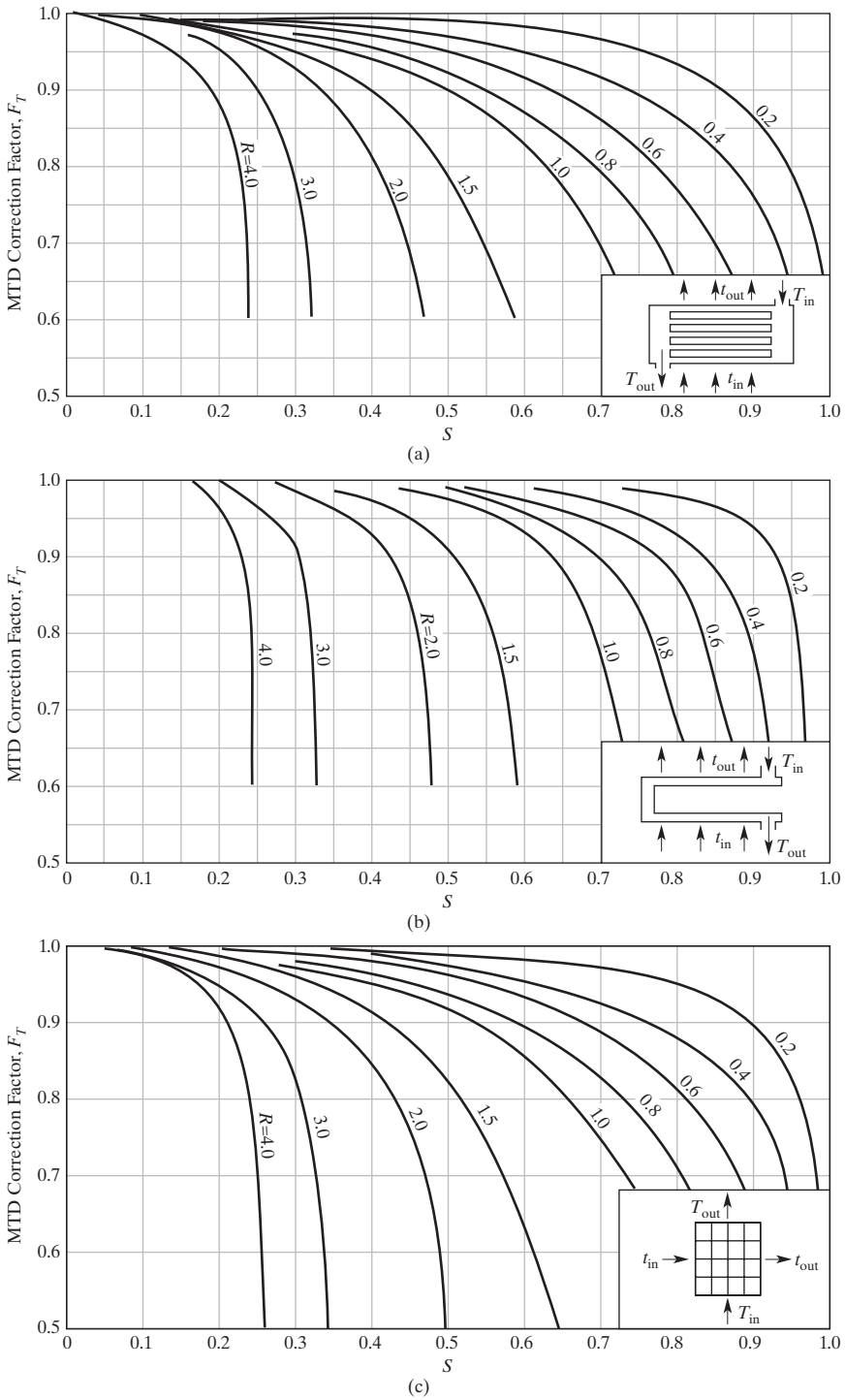

Figure 12.17 Temperature-driving-force correction factor for crossflow heat exchangers: (a) one shell pass, one or more parallel rows of tubes; (b) two shell passes, two rows of tubes (for more than two passes, use $F_T = 1$); (c) one shell pass, one tube pass, both fluids unmixed. (*Source:* Adapted from Bowman et al., (1940)).

SOLUTION

For countercurrent flow, the temperature-driving forces at the two ends of the exchanger are $200 - 190 = 10°F$ and $140 - 100 = 40°F$. The log-mean driving force, using Eq. (12.3), is

$$\Delta T_{LM} = \frac{40 - 10}{\ln(40/10)} = \frac{30}{1.386} = 21.6^{o}F$$

For multiple-pass exchangers, using Eqs. (12.5) and (12.6),

$$R = \frac{200 - 140}{190 - 100} = 0.667 \text{ and } S = \frac{190 - 100}{200 - 100} = 0.9$$

For a 1-2 exchanger, using Figure 12.15, the value of F_T cannot be read because it is less than 0.5. When it is computed from Eq. (12.4), the argument of the natural log term in the denominator of Eq. (12.4) is negative. Thus, a real value of F_T cannot be computed. This indicates that a temperature crossover occurs in a 1-2 exchanger.

For a 2-4 exchanger, using Figure 12.16a, F_T is again less than 0.5. For a 3-6 exchanger, using Figure 12.16b, $F_T = 0.7$, which is risky. For a 4-8 exchanger, using Figure 12.16c, $F_T = 0.85$, which is satisfactory, and so this is the configuration that should be adopted for this application. The mean temperature-driving force is $F_T \Delta T_{LM} = 0.85(21.6) = 18.4°F$.

12.3 HEAT-TRANSFER COEFFICIENTS AND PRESSURE DROP

To determine the heat-transfer area of a heat exchanger from Eq. (12.7), an overall heat-transfer coefficient is required. It can be estimated from experience or from the sum of the calculated individual thermal resistances. For double-pipe and shell-and-tube heat exchangers, the area changes across the wall of the cylindrical pipes or tubes. Accordingly, the overall heat-transfer coefficient is based on the inner wall, i, the outer wall, o, or, much less frequently, a mean, m. The three coefficients are related by

$$\frac{1}{UA} = \frac{1}{U_o A_o} = \frac{1}{U_i A_i} = \frac{1}{U_m A_m} \tag{12.8}$$

When the outer wall is used, the area is A_o and

$$U_0 = \frac{1}{R_{f,o} + \left(\frac{1}{h_o}\right) + \left(\frac{t_w A_o}{k_w A_m}\right) + \left(\frac{A_o}{h_i A_i}\right) + R_{f,i}\left(\frac{A_o}{A_i}\right)} \tag{12.9}$$

where $R_{f,o}$ is the outside fouling factor, $R_{f,i}$ is the inside fouling factor, h is the individual heat-transfer coefficient, k_w is the thermal conductivity of the cylindrical wall, t_w is the thickness of the cylindrical wall,

$$A_o = \pi D_o L \quad A_i = \pi D_i L \quad A_m = \frac{\pi L(D_o - D_i)}{\ln(D_o/D_i)}$$

D is the tube or pipe diameter, and L is the tube or pipe length. When the inner wall is used, the area is A_i and

$$U_i = \frac{1}{R_{f,o}\left(\frac{A_i}{A_o}\right) + \left(\frac{A_i}{h_o A_o}\right) + \left(\frac{t_w A_i}{k_w A_m}\right) + \left(\frac{1}{h_i}\right) + R_{f,i}} \tag{12.10}$$

Estimation of Overall Heat-transfer Coefficients

For preliminary design, the heat-transfer area is computed from Eq. (12.7) using an estimate of the overall heat-transfer coefficient, U, based on the service. Because the values are approximate, the basis for the area is of no concern. Typical estimates of U for shell-and-tube heat exchangers are given in Table 12.5. The values include a fouling-factor contribution referred to as *total dirt*, equal to $R_{f,o} + R_{f,i}$. For example, for gasoline on the shell side and water in the tubes, U is given as 60 – 100 Btu/°F-ft^2-hr with total dirt of 0.003 (hr-ft^2-°F)/Btu. The U in Table 12.5 can be referred to as U_{dirty}. Thus, $1/U_{dirty} = 0.010 - 0.017$(hr-ft^2-°F)/Btu. For a clean exchanger, $1/U_{clean} = 1/U_{dirty} - (R_{f,o} + R_{f,i}) = 0.007 - 0.014$ (hr-ft^2-°F)/Btu or $U_{clean} = 70$–140 Btu/°F-ft^2-hr.

EXAMPLE 12.6

A mixture of 60 mol% propylene and 40 mol% propane at a flow rate of 600 lbmol/hr is distilled at 300 psia to produce a distillate of 99 mol% propylene and a bottoms of 95 mol% propane. The bottoms temperature is 138°F and the heat duty of the reboiler, Q, is 33,700,000 Btu/hr. When waste heat, consisting of saturated steam at 220°F, is used as the heating medium in the reboiler, estimate the area of a shell-and-tube reboiler.

SOLUTION

Assume that the bottoms is on the shell side and steam is inside the tubes. Because the bottoms is almost pure, assume that it vaporizes at 138°F, whereas the steam condenses at 220°F. Therefore, $\Delta T_{LM} = \Delta T_m = 220 - 138 = 82$°F. From Table 12.5, under vaporizers with propane on the shell side and steam condensing on the tube side, $U = 200$–300 Btu/°F-ft^2-hr. Note that this includes a fouling resistance of 0.0015 (hr-ft^2-°F)/Btu. The correction factor, F_T, is 1, regardless of the number of passes or flow directions because at least one fluid is at a constant temperature in the exchanger. From Eq. (12.7), using 200 Btu/°F-ft^2-hr for U,

$$A = \frac{Q}{UF_T \Delta T_{\text{LM}}} = \frac{33{,}700{,}000}{(200)(1.0)(82)} = 2{,}050 \text{ ft}^2$$

The heat flux in the reboiler is

$$\frac{Q}{A} = \frac{33{,}700{,}000}{2{,}050} = 16{,}400 \text{ Btu/ft}^2\text{-hr}.$$

Note that ΔT_m greatly exceeds the maximum value of 45°F suggested earlier for reboilers. However, that value pertains to just the portion of the ΔT on the boiling side of the exchanger. In this example, when the total driving force of 82°F is divided among the five resistances, it is possible that the maximum value might not be exceeded. Alternative limits on reboilers for the vaporization of organic chemicals are maximum heat fluxes of 12,000 Btu/ft^2-hr for natural circulation and 20,000 Btu/ft^2-hr for forced circulation. Therefore, with a heat flux of 16,400 Btu/ft^2-hr, neither a once-through thermosyphon reboiler nor a kettle reboiler should be specified. Instead, a pump-through reboiler should be used to pump the bottoms through the shell side of the reboiler (as illustrated in Figure 12.11b). Alternatively, the heating steam temperature could be reduced. However, this would result in vacuum steam, which is very undesirable because air that leaks into the steam can interfere with condensation.

Estimation of Individual Heat-transfer Coefficients and Frictional Pressure Drop

An enormous amount of experimental work on convective heat-transfer and skin-friction pressure drop were reported during the twentieth century. This has been accompanied by theoretical developments. For laminar flow, heat-transfer coefficients and friction factors for well-defined, simple geometries can be accurately predicted from theory. For turbulent flow, both theoretical equations and empirical correlations of data are available. No attempt is made in the brief space permitted here to present recommended methods for predicting convective heat-transfer coefficients and friction factors for the wide variety of commercial heat exchanger geometries. Instead, the reader is referred to the *Handbook of Heat Exchanger Design*, edited by G.F. Hewitt (1992), which provides a comprehensive coverage by experts in the field. A brief discussion is given here of turbulent-flow convective heat-transfer and skin friction without phase change. In general, turbulent flow is preferred in heat exchangers because of the higher heat-transfer coefficients that can be achieved.

Table 12.5 Typical Overall Heat-Transfer Coefficients for Shell-and-Tube Heat Exchangers [U = Btu/(°F - ft^2 - hr)]

Shell Side	Tube Side	Design U	Includes Total Dirt
Liquid–Liquid Media			
Aroclor 1248	Jet fuels	100–150	0.0015
Cutback asphalt	Water	10–20	0.01
Demineralized water	Water	300–500	0.001
Ethanol amine (MEA or DEA) 10–25% solutions	Water or DEA, or MEA solutions	140–200	0.003
Fuel oil	Water	15–25	0.007
Fuel oil	Oil	10–15	0.008
Gasoline	Water	60–100	0.003
Heavy oils	Heavy oils	10–40	0.004
Heavy oils	Water	15–50	0.005
Hydrogen-rich reformer stream	Hydrogen-rich reformer stream	90–120	0.002
Kerosene or gas oil	Water	25–50	0.005
Kerosene or gas oil	Oil	20–35	0.005
Kerosene or jet fuels	Trichloroethylene	40–50	0.0015
Jacket water	Water	230–300	0.002
Lube oil (low viscosity)	Water	25–50	0.002
Lube oil (high viscosity)	Water	40–80	0.003
Lube oil	Oil	11–20	0.006
Naphtha	Water	50–70	0.005
Naphtha	Oil	25–35	0.005
Organic solvents	Water	50–150	0.003
Organic solvents	Brine	35–90	0.003
Organic solvents	Organic solvents	20–60	0.002
Tall oil derivatives, vegetable oil, etc.	Water	20–50	0.004
Water	Caustic soda solutions (10–30%)	100–250	0.003
Water	Water	200–250	0.003
Wax distillate	Water	15–25	0.005
Wax distillate	Oil	13–23	0.005
Condensing Vapor–liquid Media			
Alcohol vapor	Water	100–200	0.002
Asphalt 450°F	Dowtherm vapor	40–60	0.006
Dowtherm vapor	Tall oil and derivatives	60–80	0.004
Dowtherm vapor	Dowtherm liquid	80–120	0.0015
Gas-plant tar	Steam	40–50	0.0055
High-boiling hydrocarbons V	Water	20–50	0.003
Low-boiling hydrocarbons A	Water	80–200	0.003
Hydrocarbon vapors (partial condenser)	Oil	25–45	0.004
Organic solvents A	Water	100–200	0.003
Organic solvents high NC, A	Water or brine	20–60	0.003
Organic solvents low NC, V	Water or brine	50–120	0.003
Kerosene	Water	30–65	0.004
Kerosene	Oil	20–30	0.005
Naphtha	Water	50–75	0.005
Naphtha	Oil	20–30	0.005
Stabilizer column vapor	Water	80–120	0.003
Steam	Feed water	400–1,000	0.0005
Steam	No. 6 fuel oil	15–25	0.0055
Steam	No. 2 fuel oil	60–90	0.0025
Sulfur dioxide	Water	150–200	0.003
Tall oil derivatives, vegetable oils (vapor)	Water	20–50	0.004
Water	Aromatic vapor–stream azeotrope	40–80	0.005

Table 12.5 (Continued)

Shell Side	Tube Side	Design U	Includes Total Dirt
Gas–liquid Media			
Air, N_2, etc. (compressed)	Water or brine	40–80	0.005
Air,N_2, etc. A	Water or brine	10–50	0.005
Water or brine	Air, N_2, etc. (compressed)	20–40	0.005
Water or brine	Air, N_2, etc. A	5–20	0.005
Water	Hydrogen containing natural-gas mixtures	80–125	0.003
Vaporizers			
Anhydrous ammonia	Steam condensing	150–300	0.0015
Chlorine	Steam condensing	150–300	0.0015
Chlorine	Light heat-transfer oil	40–60	0.0015
Propane, butane, etc.	Steam condensing	200–300	0.0015
Water	Steam condensing	250–400	0.0015

NC = Noncondensable gas present

V = Vacuum

A = Atmospheric pressure

Dirt (or fouling factor) units are (hr-ft^2-°F/Btu).

To convert British thermal units per hour-square foot-degrees Fahrenheit to joules per square meter-second-Kelvin, multiply by 5.6783; to convert from hr-ft^2-°F/Btu to sec-m^2-K/joule, multiply by 0.1761.

Turbulent Flow in Straight, Smooth Ducts, Pipes, and Tubes of Circular Cross Section

In double-pipe and shell-and-tube heat exchangers, fluids flow through straight, smooth pipes and tubes of circular cross section. Many correlations have been published for the prediction of the inside-wall, convective heat-transfer coefficient, h_i, when no phase change occurs. For turbulent flow, with Reynolds numbers, $N_{\mathrm{Re}} = D_i G/\mu$, greater than 10,000, three empirical correlations have been widely quoted and applied. The first is the Dittus–Boelter equation (Dittus and Boelter, 1930) for liquids and gases in fully developed flow ($D_i/L < 60$) and with Prandtl numbers, $N_{\mathrm{Pr}} = C_p\mu/k$, between 0.7 and 100:

$$N_{\mathrm{Nu}} = \frac{h_i D_i}{k_b} = 0.023\left(\frac{D_i G}{\mu_b}\right)^{0.8}\left(\frac{C_{\mathrm{p}_b}\mu_b}{k_b}\right)^{n} \tag{12.11}$$

where D_i is the inside duct, pipe, or tube diameter; G is the fluid mass velocity (flow rate/cross-sectional area for flow); k is the fluid thermal conductivity; C_p is the fluid specific heat; μ is the fluid viscosity; subscript b refers to average bulk fluid conditions; and exponent $n = 0.4$ for heating the fluid and 0.3 for cooling.

The Colburn equation (Colburn, 1931) also applies to liquids and gases and is almost identical to the Dittus–Boelter equation but is usually displayed in a j-factor form in terms of a Stanton number, $N_{\mathrm{St}} = h_{\mathrm{i}}/GC_p$. It is considered valid to a Prandtl number of 160:

$$\frac{h_i}{GC_{\mathrm{p}_b}}\left(\frac{C_{\mathrm{p}_f}\mu_f}{k_f}\right)^{2/3} = 0.023\left(\frac{D_i G}{\mu_f}\right)^{-0.2} \tag{12.12}$$

where the subscript f refers to a film temperature midway between the wall and bulk condition.

The Sieder–Tate equation (Sieder and Tate, 1936) is specifically for liquids, especially for viscous liquids where the viscosities at the wall and in the bulk may be considerably different. It is claimed to be valid for very high Prandtl numbers. In Nusselt number form, it is

$$N_{\mathrm{Nu}} = \frac{h_i D_i}{k_b} = 0.027\left(\frac{D_i G}{\mu_b}\right)^{0.8}\left(\frac{C_{\mathrm{p}_b}\mu_b}{k_b}\right)^{1/3}\left(\frac{\mu_b}{\mu_w}\right)^{0.14} \tag{12.13}$$

where the subscript w refers to the temperature at the wall.

In Section 2.5.1 of Hewitt (1992), prepared by Gnielinski, a more accurate and more widely applicable correlation is given, which accounts for tube diameter-to-tube length ratio for $0 < D_i/L < 1$, and is applicable to wide ranges of Reynolds and Prandtl numbers of 2,300 to 1,000,000 and 0.6 to 2,000, respectively. The correlation has a semitheoretical basis in the Prandtl analogy to skin friction in terms of the Darcy friction factor, f_D:

$$N_{\mathrm{Nu}} = \frac{h_i D_i}{k_b} = \frac{(f_D/8)(N_{\mathrm{Re}} - 1{,}000)N_{\mathrm{Pr}}}{1 + 12.7\sqrt{f_D/8}(N_{\mathrm{Pr}}^{2/3} - 1)}\left[1 + \left(\frac{D_i}{L}\right)^{2/3}\right] \tag{12.14}$$

where

$$f_D = (1.82\log_{10}N_{\mathrm{Re}} - 1.64)^{-2} \tag{12.15}$$

The Darcy friction factor is related to the Fanning friction factor by $f_D = 4f$. The application of Eq. (12.14) is made easy because all properties are evaluated at the bulk fluid conditions. However, for viscous liquids, the right-hand side is multiplied by a correction factor K where

$$K = \left(\frac{N_{\mathrm{Pr}_b}}{N_{\mathrm{Pr}_w}}\right)^{0.11} \tag{12.16}$$

For gases being heated, a different correction factor is employed:

$$K = \left(\frac{T_b}{T_w}\right)^{0.45} \tag{12.17}$$

where T is absolute temperature. The Gnielinski equations are preferred for computer calculations in heat exchanger design programs.

The pressure drop for the flow of a liquid or gas under isothermal conditions without phase change through a straight circular tube or pipe of constant cross-sectional area is given by either the Darcy or Fanning equation:

$$-\Delta P = \frac{f_D G^2 L}{2 g_c \rho D_i} = \frac{2 f G^2 L}{g_c \rho D_i} \tag{12.18}$$

where:

$-\Delta P = P_{\text{in}} - P_{\text{out}} =$ pressure drop
$L =$ length of tube or pipe
$g_c =$ conversion factor $= 32.17$ ft-lbm/lbf-s^2
$= 1$ in SI units

For turbulent flow at $N_{\text{Re}} > 10{,}000$ with a smooth wall, f_D is given by Eq. (12.15), or a Fanning friction factor chart can be used to obtain f .

Equation (12.18) accounts for only skin friction at the inside wall of the tube or pipe. Pressure drop also occurs as the fluid enters (by contraction) or leaves (by expansion) the tube or pipe from or to, respectively, the header, and as the fluid reverses flow direction in exchangers with multiple-tube passes. In addition, pressure drop occurs as the fluid enters the exchanger from a nozzle and passes out through a nozzle. For nonisothermal flow in a multitube-pass exchanger, Eq. (12.18) is modified to:

$$-\Delta P = K_{\text{p}} \frac{N_p f_D G^2 L}{2 g_c \rho D_i \phi} = K_p \frac{2 N_p f G^2 L}{g_c \rho D_i \phi} \tag{12.19}$$

where:

$K_{\text{p}} =$ correction factor for contraction, expansion, and reversal losses
$N_p =$ number of tube passes
$\phi =$ correction factor for nonisothermal turbulent flow $= 1.02(\mu_{\text{b}}/\mu_{\text{w}})^{0.14}$, where subscript w refers to the average inside wall temperature

A reasonable value for K_{p} is 1.2. If the exchanger is vertical and flow is upward, the outlet pressure is further reduced by the height of the heat exchanger times the fluid density. If the flow is downward, the outlet pressure is increased by the same amount.

Turbulent Flow in the Annular Region Between Straight, Smooth, Concentric Pipes of Circular Cross Section

In double-pipe heat exchangers, one fluid flows through the annular region between the inner and outer pipes. To predict the heat-transfer coefficient at the outside of the inner pipe, Eqs. (12.14) and (12.15) with the K corrections can be used by (1) replacing D_i by D_2–D_1 where D_2 is the inside diameter of the outer pipe and D_1 is the outer diameter of the inner pipe. Then the following correction is made:

$$\frac{N_{\text{Nu,annulus}}}{N_{\text{Nu,tube}}} = 0.86 \left(\frac{D_1}{D_2} \right)^{-0.16} \tag{12.20}$$

When the flow is through the annulus of a double-pipe heat exchanger, Eqs. (12.15) and (12.19) can be used to estimate the frictional pressure drop, provided that the inside diameter, D_i, of the tube or pipe is replaced by the hydraulic diameter, D_H, which is defined as four times the channel cross-sectional area divided by the wetted perimeter. For an annulus, $D_H = D_2 - D_1$.

Turbulent Flow on the Shell Side of Shell-and-tube Heat Exchangers

Accurate predictions of the shell-side heat-transfer coefficient and pressure drop are difficult because of the complex geometry and resulting flow patterns. A number of correlations are available, none of which is as accurate as those above for the tube side. All are based on crossflow past an ideal tube bank, either staggered (triangular pitch pattern) or inline (square pitch pattern). Corrections are made for flow distortion due to baffles, leakage, and bypassing. From 1950 to 1963, values of h_o, the shell-side, convective heat-transfer coefficient, were most usually predicted by the correlations of Donohue (1949) and Kern (1950), which are suitable for hand calculations. Both of these correlations are of the general Nusselt number form

$$N_{\text{Nu}} = \frac{h_o D}{k_b} = C \left(\frac{DG}{\mu_b} \right)^n \left(\frac{C_{\text{p}_b} \mu_b}{k_b} \right)^{1/3} \left(\frac{\mu_b}{\mu_w} \right)^{0.14} \tag{12.21}$$

The two correlations differ in how D and G are defined and how C and n are determined. For D, Donohue uses the tube outside diameter whereas Kern uses the hydraulic diameter. For the mass velocity, G, Donohue uses a geometric mean of (1) the mass velocity in the free area of the baffle window, parallel with the tubes, and (2) the mass velocity normal to the tubes for the row closest to the centerline of the exchanger; Kern uses just the latter mass velocity. Donohue uses $n = 0.6$ and $C = 0.2$; Kern uses 0.55 and 0.36, respectively. Kern's correlation is valid for N_{Re} from 2,000 to 1,000,000. Donohue's correlation is considered to be conservative.

For flow of a gas or liquid across the tubes on the shell side of a shell-and-tube heat exchanger, a preliminary estimate of the shell-side pressure drop can be made by the method of Grimison (1937). The pressure drop is given by a modified Fanning equation:

$$-\Delta P_t = K_S \frac{2 N_R f' \cdot G_S^2}{g_c \rho \phi} \tag{12.22}$$

where K_S is a correction factor for friction due to inlet and outlet nozzles and the presence of shell-side baffles that cause reversal of the flow direction, recrossing of tubes, and variation in cross-sectional area for flow. K_S may be taken as approximately 1.10 times (1 + number of baffles). N_R is the number of tube rows across which the shell fluid flows, which equals the total number of tubes at the center plane minus the number of tube rows

Table 12.6 Tube Sheet Layouts

	One Pass		Two Pass		Four Pass	
Shell I.D.,in.	Square Pitch	Triangular Pitch	Square Pitch	Triangular Pitch	Square Pitch	Triangular Pitch
			¾-in. O.D. Tubes on 1-in. Pitch			
8	32	37	26	30	20	24
12	81	92	76	82	68	76
15 ¼	137	151	124	138	116	122
21 ¼	277	316	270	302	246	278
25	413	470	394	452	370	422
31	657	745	640	728	600	678
37	934	1,074	914	1,044	886	1,012
			1-in.O.D.Tubes on1 ¼-in.Pitch			
8	21	21	16	16	14	16
12	48	55	45	52	40	48
15 ¼	81	91	76	86	68	80
21 ¼	177	199	166	188	158	170
25	260	294	252	282	238	256
31	406	472	398	454	380	430
37	596	674	574	664	562	632

that pass through the cut portions of the baffles. For 25% cut baffles, N_R may be taken as 50% of the number of tubes at the center plane. For example, if the inside shell diameter is 25 in., the tube outside diameter is 0.75 in., and the tube clearance is 0.25 in. (pitch = 1 in.), and the number of tubes in the row at the center plane is 25. With 25% cut baffles, $N_R = 0.5 \times 25 \cong 13$. G_S is the fluid mass velocity based on the flow area at the center plane, which equals the distance between baffles times the tube clearance times the number of tubes at the center plane. f' is the modified friction factor such that:

$$f' = b\left(\frac{D_o G_S}{\mu_b}\right)^{-0.15} \tag{12.23}$$

where b for triangular pitch (staggered tubes) is:

$$b = 0.23 + \frac{0.11}{(x_T - 1)^{1.08}} \tag{12.24}$$

and for tubes in line (e.g., square pitch), b is:

$$b = 0.044 + \frac{0.08x_L}{(x_T - 1)^{0.43+1.13/x_L}} \tag{12.25}$$

Here, x_T is the ratio of the pitch transverse to flow-to-tube outside diameter, and x_L is the ratio of pitch parallel to flow-to-tube outside diameter. For square pitch, $x_T = x_L$.

In 1963, Bell and co-workers at the University of Delaware published a comprehensive method for predicting the shell-side pressure drop and convective heat-transfer coefficient. This method is often referred to as the Bell–Delaware method and is described in detail in Section 11 of the 8th edition of *Perry's Chemical Engineers' Handbook* (2008). Experts in Hewitt (1992) consider it to be the best method available. To use the method, geometric and construction details of the exchanger must be known. The calculations are best carried out with a computer. The method considers the effects of tube layout, bypassing, tube-to-baffle leakage, shell-to-baffle leakage, baffle cut, baffle spacing, and adverse temperature gradients. These effects are applied as corrections to an equation of the form of Eq. (12.21). However, the exponent n on the Reynolds number depends on the Reynolds number.

When making estimates of the heat-transfer coefficients and pressure drop for shell-and-tube heat exchangers, using the methods discussed previously or the more accurate methods in *Perry's Chemical Engineers' Handbook* (2008), tubesheet layouts must be known as a function of shell-and-tube diameters. These data are given in Table 12.6 for shell diameters ranging from 8 to 37 in., and for ¾ - and 1-in. O.D. tubes.

Heat-transfer Coefficients for Laminar-flow, Condensation, Boiling, and Compact Heat Exchangers

Correlations are available for predicting pressure drops and convective heat-transfer coefficients for laminar flow inside and outside of ducts, tubes, and pipes; for pipes with longitudinal and peripheral fins; for condensation and boiling; and for several different geometries used in compact heat exchangers. No attempt is made to discuss or summarize these correlations here. They are presented by Hewitt (1992).

12.4 DESIGN OF SHELL-AND-TUBE HEAT EXCHANGERS

The design of a shell-and-tube heat exchanger is an iterative process because heat-transfer coefficients and pressure drop depend on many geometric factors, including shell and tube diameters, tube length, tube layout, baffle type and spacing, and the numbers of tube and shell passes, all of which are initially unknown and are determined as part of the design process.

A procedure for an iterative design calculation is as follows, where it is assumed that the inlet conditions (temperature, pressure, composition, flow rate, and phase condition) are known for the two streams entering the heat exchanger and that an exit temperature or some equivalent specification is given for one of the two streams. If a heating or cooling utility is to be used for one of the two streams, it is selected from Table 12.1, together with its entering and leaving temperatures. A decision is made as to which stream will flow on the tube side and which will flow on the shell side. Shell-and-tube side pressure drops are estimated using the values suggested at the end of Section 12.1. With this information, an overall energy balance is used, as discussed in Section 12.1, to calculate the heat duty and the remaining exiting conditions for the two streams. If a heating or cooling utility is to be used, its flow rate is calculated from an energy balance.

A one-tube-pass, one-shell-pass, countercurrent-flow exchanger is assumed. A check is made to make sure that the second law of thermodynamics is not violated and that a reasonable temperature-driving force exists at the two ends of the exchanger as discussed in Section 12.1. If a phase change occurs on either side of the exchanger, a heating and/or cooling curve is calculated as discussed in Section 12.1, and a check is made to make sure that a temperature crossover is not computed within the exchanger.

A preliminary estimate of the heat exchanger area is made by using Table 12.5 to estimate first the overall heat-transfer coefficient and then using the heating and/or cooling curves or Eq. (12.3) to compute the mean driving force for heat transfer, followed by Eq. (12.7) to estimate the heat exchanger area with $F_T = 1$. If the area is greater than 8,000 ft^2, multiple exchangers of the same area are used in parallel. For example, if an area of 15,000 ft^2 is estimated, then two exchangers of 7,500 ft^2 each are used.

From the estimated heat-transfer area, preliminary estimates are made of the exchanger geometry. A tube-side velocity in the range of 1 to 10 ft/s is selected with a typical value being 4 ft/s. The total inside-tube cross-sectional area is then computed from the continuity equation. A tube size is selected (e.g., 3/4-in. O.D., 14 BWG), which, from Table 12.4, has an inside diameter of 0.584 in. and an inside flow area, based on the inside cross-sectional area, of 0.268 in^2. From this, the number of tubes per pass per exchanger is calculated. A tube length is selected (e.g., 16 ft), and the number of tube passes per exchanger is calculated. The tube-side velocity and tube length are adjusted if necessary to obtain an integer number for the number of tube passes.

If more than one tube pass is necessary, the log-mean temperature-driving force is corrected, using Figures 12.15 through 12.17. This may require using more than one shell pass as discussed in Section 12.2 and illustrated in Example 12.5. A tube-sheet layout is then selected from Table 12.6, and a baffle design and spacing are selected for the shell side. This completes a preliminary design of the heat exchanger.

A revised design is made next by using the geometry of the preliminary design to estimate an overall heat-transfer coefficient from calculated individual heat-transfer coefficients and estimated fouling factors as well as pressure drops, using the methods discussed in Section 12.3. Then, the entire procedure for sizing the heat exchanger is iterated until a reasonable design is achieved. The iterations seek to minimize the exchanger area without unduly increasing the pressure drop.

The previous procedure is tedious if done by hand calculations. Therefore, it is more convenient to conduct the design with available computer programs. For example, the HEATX subroutine of the ASPEN PLUS simulator computes heat-transfer coefficients, pressure drops, and outlet conditions for a shell-and-tube heat exchanger of known geometry, as illustrated in Example 12.7. It can be used by trial-and-error with the iterative procedure to design an exchanger.

EXAMPLE 12.7

An existing 2-8 shell-and-tube heat exchanger in a single shell (equivalent to two shells in series with 4 tube passes in each shell) is to be used to transfer heat to a toluene feed stream from a styrene product stream. The toluene enters the exchanger on the tube side at a flow rate of 125,000 lb/hr at 100°F and 90 psia. The styrene enters on the shell side at a flow rate of 150,000 lb/hr at 300°F and 50 psia. The exchanger shell and tubes are carbon steel. The shell has an inside diameter of 39 in. and contains 1,024 3/4-in., 14 BWG, 16-ft-long tubes on a 1-in. square pitch. Twenty-two segmental baffles are used with a baffle cut of 25%. Shell inlet and outlet nozzles are 6.0-in., schedule 40 pipe, and tube-side inlet and outlet nozzles are 4-in., schedule 40 pipe. Fouling factors are estimated to be 0.002 (hr-ft^2-°F)/Btu on each side. Determine the exit temperatures of the two streams, the heat duty, and the pressure drops.

SOLUTION

The HEATX subroutine (block) of the ASPEN PLUS simulator is used to make the calculations. It has built-in correlations of the type described above for estimating shell-side and tube-side heat-transfer coefficients and pressure drops. The following results are obtained (both streams are liquid):

Toluene exit temperature = 259.67°F

Styrene exit temperature = 175.85°F

Tube-side tube pressure drop = 1.54 psi

Tube-side nozzle pressure drop = 0.33 psi

Toluene exit pressure = 88.46 psia

Shell-side baffle pressure drop = 1.46 psia

Shell-side nozzle pressure drop = 0.15 psia

Styrene exit pressure = 48.54 psia

Heat-transfer area (tube outside) = 3,283.5 ft^2 each of two shells
= 6,567.1 ft^2 total surface

Heat duty = 9,395,996 Btu/hr

Estimated U_o, *clean* = 59.99 Btu/(hr-ft^2-°R)

Estimated U_o, *dirty* = 47.68 Btu/(hr-ft^2-°R)

Log-mean temperature difference based on countercurrent flow = 56.2°F.

Correction factor for 2-8 exchanger, $F_T = 0.525$

Note: A correction factor of less than 0.7 is the lowest practically allowed value. The value computed here indicates that the configuration given is not recommended for this application. More than two shells would be required for a new design.

Velocity in the tubes = 1.21 ft/ sec

Maximum Reynolds number in the tubes = 22,077

Crossflow velocity in the shell = 2.45 ft/ sec

Maximum crossflow Reynolds number in the shell = 34,850

Flow regime on tube and shell sides = turbulent

The file EXAM12-7.bkp can be used to reproduce these results. It will run on any ASPEN PLUS VERSION of 8.6 and above. It can be found in the Program and Simulation Files folder in the Wiley Web site that supports this book. Any user will have to read the special instructions for requirements to run an ASPEN PLUS file containing a HEATX block.

Of even greater utility are the Exchanger Design and Rating programs of Aspen Technology, which are a suite of five programs: (1) Shell and Tube for the detailed thermal design, rating, and simulation of shell-and-tube heat exchangers, including sensible heating and cooling, condensation, and vaporization; (2) AirCooled, (3) Fired Heater, (4) Plate, and (5) Plate and Fin. Of particular importance is Shell and Tube, which can determine the optimal geometry for a shell-and-tube heat exchanger. This program evaluates all possible baffle and shell- and tube-pass arrangements and seeks the exchanger with the smallest shell diameter, longest tube length, minimum reasonable baffle spacing, and maximum reasonable number of tube passes, subject to allowable shell- and tube-side pressure drops. The result is a complete TEMA (Tubular Exchanger Manufacturers Association) specification sheet.

EXAMPLE 12.8

Design a new shell-and-tube heat exchanger for the conditions of Example 12.7 but with maximum shell-side and tube-side pressure drops of 10 psi each.

SOLUTION

In this case, it is convenient to use a heat-exchanger design program such as Shell and Tube within Exchanger Design software. For this example, the inlet conditions for the toluene and styrene streams are taken from Example 12.7. That example used physical properties of ASPEN PLUS. In this example, the physical property correlations provided with the Exchanger Design programs were used. The results showed less than a 2.6% difference. To provide the best comparison with Example 12.7, the same two exit temperatures computed in Example 12.7 (175.85°F for styrene and 259.67°F for toluene) were specified. To maintain the same heat requirement, both flow rates were increased by 2.65%. The Shell and Tube software considered 42 designs, all having two to five shell passes in series and total tube passes ranging from two to four. Maximum tube length was limited to 20 ft. Most designs resulted in pressure drops that ranged from 1.5 to 15 psi on both shell and tube sides. The recommended design was a 3-6 exchanger with three exchangers in series, each with one shell pass and 2 tube passes. Tubes of 0.75-in. O.D., 0.065-in. thickness, 20-ft long, and on 0.9375-in. triangular spacing were selected. Each of the three shells contains 738.4 ft^2 for a total of 2,215 ft^2.

Other results are as follows in the same order as in Example 12.7:

Toluene exit temperature = 259.7°F

Styrene exit temperature = 175.85°F

Tube-side tube pressure drop = 4.45 psi

Tube-side nozzle pressure drop = 0.06 psi

Toluene exit pressure = 85.55 psia

Shell-side pressure drop = 7.52 psi

Shell-side baffle pressure drop = 3.9 psi

Shell-side nozzle pressure drop = 0.18 psi

Styrene exit pressure = 42.48 psia

Heat-transfer area (tube outside) = 2.215 ft^2 or 738.4 ft^2 in each of the three shells

Heat duty = 9,396,321 Btu/hr

Estimated heat-transfer coefficient on the tube side = 249 Btu/hr-ft^2-°F

Estimated heat-transfer coefficient on the shell side = 317 Btu/hr-ft^2-°F

Estimated overall heat-transfer coefficient, clean = 136.7 Btu/hr-ft^2-°F

Estimated overall heat-transfer coefficient, fouled = 86.1 Btu/hr-ft^2-°F

Log-mean temperature difference based on countercurrent flow = 56.23°F

Correction factor for 3-6 exchanger, $F_T = 0.877$

Velocity in the tubes = 3.4 ft/s

Nominal Reynolds number in the tubes = 58,180,000

Velocity in the shell = 3.22 ft/s

Nominal Reynolds number in the shell = 68,000

Flow regime on tube and shell sides = turbulent

Additional results were 22 baffles in each shell on an 9.5-inch spacing and with a 35% baffle cut, 190 tubes in each shell for a total of 570 tubes, and a shell inside diameter of 17.25 inches. The setting plan and tube layout for each of the three shells in series is shown in Figure 8.18, and the heat exchanger specification sheet is shown in Figure 8.19.

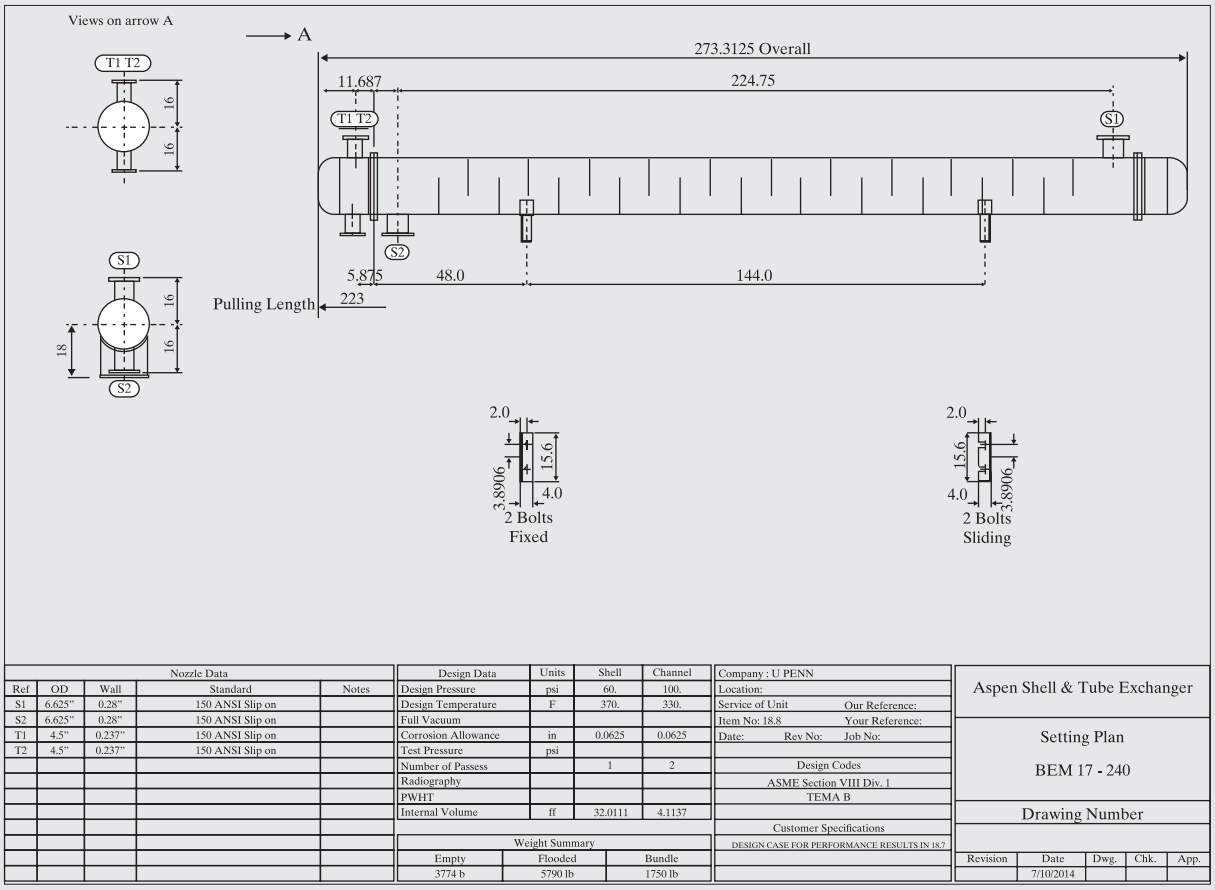

Nozzle Data				
Ref	OD	Wall	Standard	Notes
S1	6.625"	0.28"	150 ANSI Slip on	
S2	6.625"	0.28"	150 ANSI Slip on	
T1	4.5"	0.237"	150 ANSI Slip on	
T2	4.5"	0.237"	150 ANSI Slip on	

Design Data	Units	Shell	Channel
Design Pressure	psi	60.	100.
Design Temperature	F	370.	330.
Full Vacuum			
Corrosion Allowance	in	0.0625	0.0625
Test Pressure	psi		
Number of Passess		1	2
Radiography			
PWHT			
Internal Volume	ff	32.0111	4.1137

Weight Summary		
Empty	Flooded	Bundle
3774 b	5790 lb	1750 lb

Company : U PENN
Location:
Service of Unit — Our Reference:
Item No: 18.8 — Your Reference:
Date: — Rev No: — Job No:

Design Codes
ASME Section VIII Div. 1
TEMA B

Customer Specifications
DESIGN CASE FOR PERFORMANCE RESULTS IN 18.7

Aspen Shell & Tube Exchanger

Setting Plan

BEM 17 - 240

Drawing Number

Revision	Date	Dwg.	Chk.	App.
	7/10/2014			

(a)

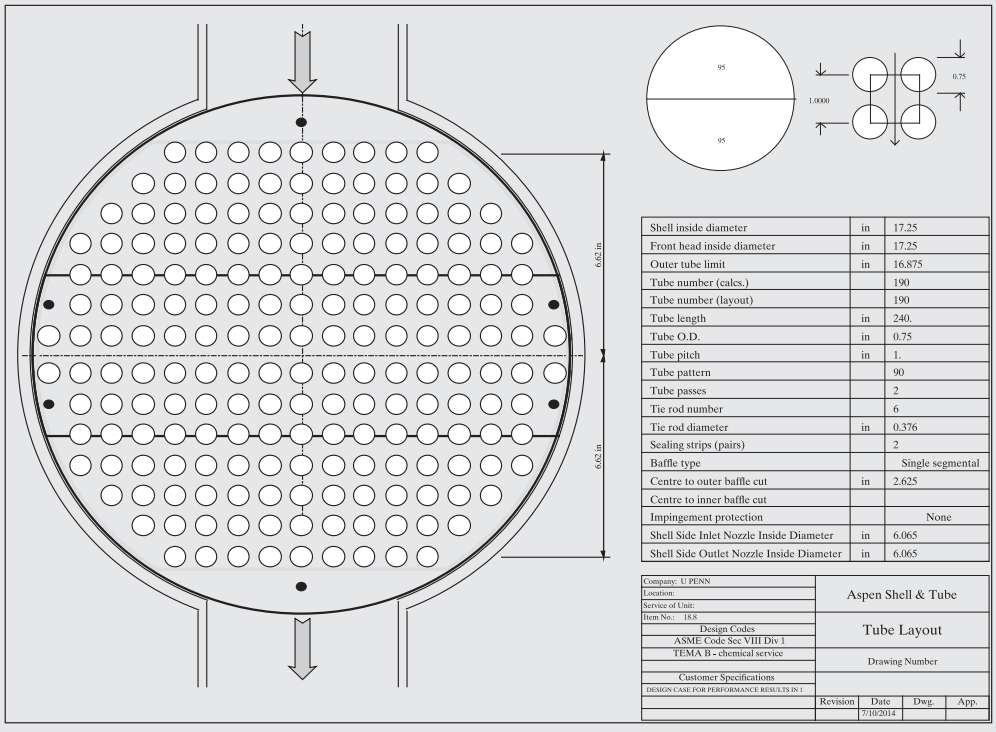

Shell inside diameter	in	17.25
Front head inside diameter	in	17.25
Outer tube limit	in	16.875
Tube number (calcs.)		190
Tube number (layout)		190
Tube length	in	240.
Tube O.D.	in	0.75
Tube pitch	in	1.
Tube pattern		90
Tube passes		2
Tie rod number		6
Tie rod diameter	in	0.376
Sealing strips (pairs)		2
Baffle type		Single segmental
Centre to outer baffle cut	in	2.625
Centre to inner baffle cut		
Impingement protection		None
Shell Side Inlet Nozzle Inside Diameter	in	6.065
Shell Side Outlet Nozzle Inside Diameter	in	6.065

Company: U PENN
Location:
Service of Unit:
Item No.: 18.8
Design Codes
ASME Code Sec VIII Div 1
TEMA B - chemical service
Customer Specifications
DESIGN CASE FOR PERFORMANCE RESULTS IN 1

Aspen Shell & Tube

Tube Layout

Drawing Number

Revision	Date	Dwg.	App.
	7/10/2014		

(b)

Figure 12.18 Heat exchanger for Example 12.8: (a) setting plan; (b) tube layout.

Heat Exchanger Specification Sheet

1	Company: U PENN							
2	Location:							
3	Service of Unit		Our Reference:					
4	Item No.: 18.8		Your Reference:					
5	Date:	Rev No.:	Job No.:					
6	Size 17–240 in	Type BEM	Hor	Connected in	1 parallel	3 series		
7	Surf/unit(eff.) 2215.1 ft^2	Shells/unit 3		Surf/shell (eff.)	738.4 ft^2			
8	PERFORMANCE OF ONE UNIT							
9	Fluid allocation	Shell Side		Tube Side				
10	Fluid name	STYRENE		TOLUENE				
11	Fluid quantity, Total Ib/h	154000		128300				
12	Vapor (In/Out) Ib/h	0	0	0	0			
13	Liquid Ib/h	154000	154000	128300	128300			
14	Noncondensable Ib/h	0	0	0	0			
15								
16	Temperature (In/Out) ºF	300	175.85	100	259.68			
17	Dew / Bubble point ºF			367.85	367.85			
18	Density Vapor/Liquid Ib/ft^3	/ 48.622	/ 52.663	/ 53.289	/ 47601			
19	Viscosity cp	/ 0.214	/ 0.3589	/ 0.4781	/ 0.2249			
20	Molecular wt, Vap							
21	Molecular wt, NC							
22	Specific heat BTU/(Ib F)	/ 0.5492	/ 0.453	/ 0.4235	/ 0.4816			
23	Thermal conductivity BTU/(ft h F)	/ 0.066	/ 0.073	/ 0.077	/ 0.062			
24	Latent heat BTU/Ib							
25	Pressure (abs) psi	50	42.48	90	85.55			
26	Velocity ft/s	3.22		3.4				
27	Pressure drop, allow./calc. psi	10	7.52	10	4.45			
28	Fouling resistance (min) ft^2 h F/BTU	0.002		0.002	0.0023 Ao based			
29	Heat exchanged 9396321 BTU/h			MTD corrected 49.3 ºF				
30	Transfer rate, Service 86.04	Dirty 86.1		Clean 136.72				BTU/(h ft^2 F)
31	CONSTRUCTION OF ONE SHELL					Sketch		
32		Shell Side		Tube Side				
33	Design/vac/test pressure:g psi	60/ /		100/ /				
34	Design temperature ºF	370		330				
35	Number passes per shell	1		2				
36	Corrosion allowance in	0.0625		0.0625				
37	Connections In in	1	6/ 150 ANSI	1	6/ 150 ANSI			
38	Size/rating Out	1	6/ 150 ANSI	1	4/ 150 ANSI			
39	Norminal Intermediate	1	6/ 150 ANSI	1	4/ 150 ANSI			
40	Tube No. 190 OD 0.75	Tks-Avg 0.049 in	Length 240 in	Pitch 1 in				
41	Tube type Plain	#/in Material Carbon Steel		Tube pattern 90				
42	Shell Carbon Steel ID 17.25	OD 18 in	Shell cover -					
43	Channel or bonnet Carbon Steel		Channel cover -					
44	Tubesheet-stationary Carbon Steel -		Tubesheet-floating -					
45	Floating head cover -		Impingement protection None					
46	Baffle-cross Carbon Steel	Type Single segmental	Cut(%d) 34.78	H Spacing: c/c 9.5 in				
47	Baffle-long -	Seal type	Inlet 19 in					
48	Supports-tube	U-bend 0	Type					
49	Bypass seal	Tube-tubesheet joint	Exp. 2 grv					
50	Expansion joint -	Type None						
51	RhoV2-Inlet nozzle 935	Bundle entrance 170	Bundle exit 157	$Ib/(ft\ s^2)$				
52	Gaskets - Shell side -	Tube Side	Flat Metal Jacket Fibe					
53	Floating head -							
54	Code requirements ASME Code Sec VIII Div 1		TEMA class B - chemical service					
55	Weight/Shell 3773.7	Filled with water 5789.9	Bundle 1750.3 Ib					
56	Remarks DESIGN CASE FOR PERFORMANCE RESULTS IN 18.7							
57								
58								

Figure 12.19 Heat exchanger specification sheet for Example 12.8.

12.5 SUMMARY

After studying this chapter, the reader should:

1. Know how the temperature and phase conditions of a stream can be changed by using a heat exchanger.
2. Be able to specify and use a simulation program to calculate a heat exchanger when modeling just one side.
3. Be able to select heat-transfer media for the other side of the exchanger.
4. Know the importance of heating and cooling curves and how to generate them with a simulation program and use them to avoid crossover violations of the second law of thermodynamics.
5. Know the major types of heat exchange equipment and how they differ in flow directions of the two fluids exchanging heat and how to determine the corrected temperature driving force for heat transfer.
6. Know how to specify a heat exchanger when modeling both sides with a simulation program.
7. Know how to estimate overall heat-transfer coefficients, including the effect of fouling.
8. Know the limitations of boiling heat transfer.
9. Be able to design a shell-and-tube heat exchanger with the help of a simulator.

REFERENCES

1. Bowman, R. A., A. C. Mueller, and W. M. Nagle, "Mean Temperature Difference in Design," *Trans. ASME*, **62**, 283–293 (1940).

2. Colburn, A. P., "A Method of Correlating Forced Convection Heat Transfer Data and a Comparison with Fluid Friction," *Trans. AIChE*, **29**, 166 (1931).

3. Dittus, F. W., and L. M. K. Boelter, "Heat Transfer in Automobile Radiators of the Tubular Type," Univ. Calif. (Berkeley) Pub. Eng., **2**, 443 (1930).

4. Donohue, D. A., *Ind. Eng. Chem.*, **41**, 2499 (1949).

5. Grimison, E. D., *Trans. ASME*, **59**, 583 (1937).

6. Hewitt, G. F., (ed.), *Handbook of Heat Exchanger Design*, Begell House, New York (1992).

7. Kern, D. Q., *Process Heat Transfer*, McGraw-Hill, New York (1950).

8. Nagle, W. M., "Mean Temperature Differences in Multipass Heat Exchangers," *Ind. Eng. Chem.*, **25**, 604–609 (1933).

9. Green, D. W., and R. H. Perry, *Perry's Chemical Engineers' Handbook*, 8th ed., McGraw-Hill, New York (2008).

10. Sieder, E. N., and G. E. Tate, "Heat Transfer and Pressure Drops of Liquids in Tubes," *Ind. Eng. Chem.*, **28**, 1429–1436 (1936).

11. Underwood, A. J. V., "The Calculation of the Mean Temperature Difference in Multipass Heat Exchangers," *J. Inst. Petroleum Technol*, **20**, 145–158 (1934).

EXERCISES

12.1 In Example 12.7, an existing exchanger is used to transfer sensible heat between toluene and styrene streams. A minimum approach temperature of 31.3°F is achieved. Design a new shell-and-tube heat exchanger for a 10°F minimum approach temperature.

12.2 A heat exchange system is needed to cool 60,000 lb/hr of acetone at 250°F and 150 psia to 100°F. The cooling can be achieved by exchanging heat with 185,000 lb/hr of acetic acid, which is available at 90°F and 75 psia, and needs to be heated. Four 1-2 shell-and-tube heat exchangers are available. Each has an inside shell diameter of 21.25 in. and contains 270-3/4-in.-O.D., 14 BWG, 16-ft-long carbon steel tubes in a square layout on a 1-in. pitch. Segmental baffles with a 25% baffle cut are spaced 5 in. apart. Determine whether one or more of these exchangers can accomplish the task. Note that if two, three, or four of the exchangers are connected in series, they will be equivalent to one 2-4, 3-6, or 4-8 exchanger, respectively. If the exchangers are not adequate, design a new exchanger or exchanger system that is adequate. Assume a combined fouling factor of 0.004 (hr-ft^2-°F)/Btu.

12.3 A trim heater is to be designed to heat 116,000 lb/hr of 57 wt% ethane, 25 wt% propane, and 18 wt% n-butane from 80 to 96°F. The stream will enter the exchanger at 520 psia and must not reach the bubble point in the exchanger. The stream will be heated with gasoline, which will enter at 240°F and 95 psia, with a flow rate of 34,000 lb/hr. Standard practice of the company is to use 1-2 shell-and-tube heat exchangers with $\frac{3}{4}$-in., 16 BWG carbon steel tubes, 20 ft long, 1-in. square pitch. Tube count depends on shell diameter, with the following diameters available:

Shell I.D. (in.)	Tube Count
10	52
12	78
13.25	96
15.25	136
17.25	176
19.25	224

The gasoline will flow on the shell side. Assume a combined fouling factor of 0.002 (hr-ft^2-°F)/Btu. Design a suitable heat exchange system, assuming a 25% overdesign factor.

12.4 Design a 1-4 shell-and-tube heat exchanger to cool 60,000 lb/hr of 42° API kerosene from 400 to 220°F by heating a 35° API distillate from 100 to 200°F under the following specifications. Allow a 10-psi pressure drop for each stream and a combined fouling factor of 0.004 (hr-ft^2-°F)/Btu. Neglect the tube-wall resistance. Use $\frac{3}{4}$-in., 16 BWG tubing, O.D. = 0.75 in., I.D. = 0.620 in., flow area/tube = 0.302 in^2, surface/linear foot = 0.1963 ft^2 outside and 0.1623 ft^2 inside. Use 1-in. square pitch. Place kerosene on the shell side. If necessary, change the configuration to keep the tube lengths below 20 ft and the pressure drops below 10 psi.

DATA

	42° API		25° API	
	400°F	**225°F**	**200°F**	**100°F**
$C_{p,}$ Btu/1b °F	0.67	0.56	0.53	0.47
μ, cP	0.20	0.60	1.3	3.4
k, Btu/hr-ft-°F	0.074	0.078	0.076	0.078
Sp. gr.	0.685	0.75	0.798	0.836

12.5 Hot water at 100,000 lb/hr and 160°F is cooled with 200,000 lb/hr of cold water at 90°F, which is heated to 120°F in a countercurrent shell-and-tube heat exchanger. The exchanger has 20-ft steel tubes with 0.75-in. O.D. and 0.62-in. I.D. The tubes are on a 1-in. square pitch. The thermal conductivity of copper is 25.9 Btu/(ft-hr-°F). The mean heat-transfer coefficients are estimated as $h_i = 200$ Btu/hr-ft^2-°F and $h_o = 200$ Btu/hr-ft^2-°F. Estimate:

(a) The area for heat transfer

(b) The diameter of the shell

12.6 A horizontal 1-4 heat exchanger is used to heat gas oil with saturated steam. Assume that $h_o = 1{,}000$ Btu/hr-ft^2-°F for condensing steam and the fouling factor = 0.004 (hr-ft^2-°F)/Btu [1 bbl = 42 gal].

(a) For a tube-side velocity of 6 ft/ sec, determine the number and length of tubes and the shell diameter.

(b) Determine the tube-side pressure drop.

	Shell Side		Tube Side	
	Inlet	**Outlet**	**Inlet**	**Outlet**
Fluid	Steam condensate		Gas oil	
Flow rate (bbl/hr)			1,200	
Temperature (°F)			60	150
Pressure (psig)	50	50	60	
Viscosity (cP)			5.0	1.8
Sp. gr.			0.840	0.810
Thermal conductivity [Btu/(ft-hr-°F)			0.078	0.083
Heat capacity (Btu/1b-°F)			0.480	0.461

The tubes are 1-in. O.D. by 16 BWG on a 1.25-in. square pitch.

12.7 An alternative heating medium for Exercise 12.6 is a distillate:

	Shell Side	
	Inlet	**Outlet**
Fluid	–35° API distillate –	
Flow rate		
Temperature (°F)	250	150
Pressure (psig)	80	
Viscosity (cP)	1.3	3.4
Sp. gr.	0.798	0.836
Thermal conductivity Btu/(ft-hr-°F)	0.076	0.078
Heat capacity (Btu/1b-°F)	0.53	0.47

Determine the tube-side velocity, number and length of tubes, and shell diameter for a 1-6 shell-and-tube heat exchanger using the 1-in.-O.D. by 16 BWG tubes on a 1.25-in. square pitch. Design to avoid pressure drops greater than 10 psia. If necessary, change the configuration to keep the tube length below 20 ft.

12.8 Ethylene glycol at 100,000 lb/hr enters the shell of a 1-6 shell-and-tube heat exchanger at 250°F and is cooled to 130°F with cooling water heated from 90 to 120°F. Assume that the mean overall heat-transfer coefficient (based on the inside area of the tubes) is 100 Btu/(ft^2-hr-°F) and the tube-side velocity is 5 ft/ sec. Use $^3/_4$-in., 16 BWG tubing (O.D. = 0.75 in., I.D. = 0.62 in.) arranged on a 1-in. square pitch.

(a) Calculate the number of tubes, length of the tubes, and tube-side heat-transfer coefficient.

(b) Calculate the shell-side heat-transfer coefficient to give an overall heat-transfer coefficient of 100 Btu/(ft^2-hr-°F).

DATA

	Ethylene Glycol	**Water**
	190°F	105°F
$C_{p,}$ Btu/1b°F	0.65	1.0
μ, cP	3.6	0.67
k, Btu/hr-ft-°F	0.154	0.363
Sp. gr.	1.110	1.0

Chapter 13

Separation Tower Design

13.0 OBJECTIVES

The most commonly used separation method in industrial chemical processes is distillation, including enhanced distillation (extractive, azeotropic, and reactive), which is carried out in towers of cylindrical shape containing either plates or packing for contacting the vapor flowing up the tower with the liquid flowing down. The process design of such towers consists of a number of calculations, which are described and illustrated in this chapter. Most of these calculations are readily made with a simulator. The same calculations apply to any multistage separation involving mass transfer between vapor and liquid phases, including absorption and stripping.

After studying this chapter and the materials on distillation on the multimedia modules that accompany this book, (these can be downloaded from www.seas.upenn.edu/∼dlewin/multimedia.html) the reader should be able to:

1. determine the tower operating conditions of pressure and temperature and the type of condenser to use.
2. determine the number of equilibrium stages and reflux required.
3. select an appropriate contacting method (plates or packing).
4. determine the number of actual plates or packing height required together with feed and product locations.
5. determine the tower diameter.
6. determine other factors that may influence tower operation.

13.1 OPERATING CONDITIONS

Multistage towers for separations involving mass transfer between vapor and liquid phases can operate anywhere within the two-phase region, but proximity to the critical point should be avoided. Typical operating pressures for distillation range from 1 to 415 psia. For temperature-sensitive materials, vacuum distillation is very common with pressures as low as 5 mm Hg. Except for low-boiling components and when a vapor distillate is desired, a total condenser is used. Before determining a feasible and, hopefully, a near-optimal operating pressure, a preliminary material balance must be made to estimate the distillate and bottoms product compositions. As a starting point for establishing a reasonable operating pressure and a type of condenser, the graphical algorithm in Figure 9.9 can be applied in the following manner, noting that it is based on the use of cooling water that enters the condenser at 90°F and exits at 120°F. The pressure at the exit of the condenser (or in the reflux drum), P_D, is determined so as to permit condensation with cooling water if possible. This pressure is computed as the bubble-point pressure at 120°F. If this pressure is less than 215 psia, a total condenser is used. However, if the pressure is less than 30 psia, set the condenser outlet pressure at 20 to 30 psia to avoid vacuum operation. If the pressure at 120°F is greater than 215 psia, calculate the dew-point pressure of the distillate at 120°F. If that pressure is less than 365 psia, use a partial condenser; if it is greater than 365 psia, select a refrigerant that gives a minimum approach temperature of 5 to 10°F, in place of cooling water, for the partial condenser such that the distillate dew-point pressure does not exceed 415 psia. Up to this point, the tower operating pressure has been determined by the composition of the distillate. Conditions based on the composition of the bottoms product must now be checked. Using the determined condenser outlet pressure, assume a condenser pressure drop in the range of 0–2 psia. Assume a tower pressure drop of 5 to 10 psia. This will give a pressure at the bottom of the column, P_B, in the range of 5–12 psia higher than the condenser-outlet pressure. Almost all reboilers are partial reboilers that produce a bottoms product at or close to the bubble point. Therefore, determine the bottoms temperature, T_B, by a bubble-point calculation based on the estimated bottoms composition and the bottoms pressure. If this exceeds the decomposition, polymerization, or critical temperature of the bottoms, then compute a bottoms pressure based on a bottoms temperature safely below the limiting temperature. Then using the assumed pressure drops, calculate a new condenser outlet pressure and corresponding temperature. This may require a change in the coolant used in the condenser and the type of condenser. Also, the new condenser outlet pressure may be less than about 15 psia in which case a vacuum system for the tower will be necessary as discussed later in Section 16.5.

In some distillations, the overhead vapor may contain components covering a wide range of volatility. For example, the overhead vapor from a vacuum tower will contain air from leakage into the tower mixed with other components that could be condensed with cooling water or a modest refrigerant. In other

cases, the overhead vapor may contain hydrogen and other light gases mixed with easily condensable components. In those cases, neither a total nor partial condenser is used. Instead, the condenser is designed to produce both a vapor distillate and a liquid distillate. The latter has the same composition as the reflux. For vacuum operation, the vapor distillate is sent to a vacuum pump. To determine the pressure, P_D, compositions of the vapor distillate and the liquid distillate are calculated for a series of pressures at a temperature of 120°F for cooling water or at a lower temperature if a refrigerant is necessary to recover a higher percentage of the less-volatile components in the liquid distillate. When using a refrigerated condenser, one should always consider placing a water-cooled partial condenser ahead of it. From the results of the calculations, a reasonable pressure is selected.

For extractive and azeotropic distillation, the condenser outlet pressure is usually near ambient pressure in the range of 20–30 psia, and a total condenser is used. An exception is azeotropic distillation when a low molecular-weight entrainer is used that necessitates a higher pressure. For reactive distillation, the pressure must be sufficiently high to give corresponding temperatures in the range of reasonable reaction rates.

Absorbers and strippers usually involve components that cover a very wide range of volatility. For example, an absorber might have a feed gas that contains methane whereas the absorbent might be an oil of 150 molecular weight. For these two separation operations, which frequently do not utilize either a condenser or reboiler, the tower operating pressure cannot be determined from bubble- and/or dew-point calculations because they can be extremely sensitive to assumed product vapor and/or liquid compositions. Instead, the following rules may apply:

Absorption favors high pressures and low temperatures. Therefore, cool the feed gas and absorbent with cooling water or a refrigerant. If the internal temperature rise in an absorption column is large, interstage coolers can be added. However, because of the high cost of gas compression, it may not be economical to increase the pressure of the feed gas. But do not decrease the pressure of the feed gas.

Stripping favors low pressures and high temperatures. Therefore, heat the liquid feed and stripping agent and lower the pressure to near ambient but not to a vacuum.

13.2 FENSKE-UNDERWOOD-GILLILAND (FUG) SHORTCUT METHOD FOR ORDINARY DISTILLATION

For ordinary distillation of a single feed to give only distillate and bottoms products, the FUG method, which is included in the library of equipment models of all simulators, is useful for making an initial estimate of the reflux ratio, the number of equilibrium stages, and the location of the feed stage. The method is quite accurate for ideal mixtures of a narrow-boiling range. However, for nonideal mixtures, particularly those that form azeotropes, and for wide-boiling feeds, the FUG method can be quite inaccurate. Therefore, before applying the method, the vapor–liquid equilibrium of the feed should be carefully examined for the magnitude of liquid-phase activity coefficients and the possibility of azeotropes over the range of possible compositions. Note that for nonideal mixtures, especially, design engineers often skip this approximate method in preference to running a few iterations using a rigorous model as discussed in Section 13.4. Often, reasonable guesses can be provided for the number of stages and reflux ratio to achieve a satisfactory simulation that can be fine-tuned to satisfy product specifications.

The FUG method, which applies to binary and multicomponent feeds, is described in detail by Seader et al. (2016) and in *Perry's Chemical Engineers' Handbook* (Green and Perry, 2008). Only the procedure is discussed here. The method involves five steps based on the desired separation of two key components in the feed. It includes an estimation of the separation of the nonkey components.

Step 1: *Estimation by the Fenske equation of the minimum number of equilibrium stages, $N_{\min}$ (corresponding to total reflux or infinite reflux ratio), needed to separate the two key components*. The Fenske equation is simple and readily applied, even by hand. It involves only one assumption, that of an average relative volatility, $\alpha_{LK,HK}$, between the two key components throughout the tower. This may be the geometric average of the distillate and bottoms or the geometric average of the feed, distillate, and bottoms. The Fenske equation may be written as follows:

$$N_{\min} = \frac{\log\left[\left(\frac{d_{LK}}{b_{LK}}\right)\left(\frac{b_{HK}}{d_{HK}}\right)\right]}{\log \alpha_{LK,HK}} \tag{13.1}$$

where d is a component flow rate in the distillate and b is a component flow rate in the bottoms product.

Step 2: *Estimation by the Fenske equation of the distribution, d/b, of each nonkey component between distillate and bottoms at total reflux using the value of $N_{\min}$ computed in Step 1, the b/d ratio for the heavy key, and the relative volatility between the nonkey and the heavy key, $\alpha_{NK,HK}$*. Although this estimate is for total reflux conditions, it is a surprisingly good estimate for the distribution of the nonkey components at finite reflux conditions for nearly ideal mixtures.

Step 3: *Estimation by the Underwood equations of the minimum reflux ratio, $R_{\min}$ (corresponding to an infinite number of equilibrium stages), needed to separate the two key components*. This calculation is complicated because it involves the solution of nonlinear equations and requires a calculation of the distribution of the nonkey components at minimum reflux even though that distribution is not used for any other purpose. The application of the Underwood equations involves two serious assumptions: (1) The molar liquid flow rate is constant throughout the rectifying section and (2) the relative volatility is constant in the pinch region. When these assumptions are not valid, the

estimated minimum reflux ratio can be less than the true value, making the method nonconservative. More details of the use of the Underwood equations are given by Seader et al. (2016).

Step 4: *Estimation by the Gilliland correlation of the actual number of equilibrium stages, N, for a specified ratio of actual reflux ratio, R, to minimum reflux ratio,* $R_{\min}$. The Gilliland correlation, which is shown in Figure 13.1, has no theoretical foundation but is an empirical fit of many rigorous binary and multicomponent calculations when plotted as $(N - N_{\min})/(N + 1)$ as a function of $(R - R_{\min})/(R + 1)$. The accuracy of the Gilliland method is limited because it ignores the effect of the feed condition (from subcooled to superheated) and can be badly in error when stripping is much more important in the separation than rectification. For optimal design, the recommended value of $R/R_{\min}$ to use with the Gilliland method is typically in the range of 1.1 to 1.5 with the lower value for difficult separations requiring more than 100 equilibrium stages and the higher value for easy separations of less than 10 equilibrium stages. At $R/R_{\min} = 1.3$, $N/N_{\min}$ is often equal to approximately 2.

Step 5: *Estimation of the feed-stage location by the Fenske equation*. The calculation is made with Eq. (13.1) by applying it to the section of stages between the feed composition and the distillate composition to obtain the minimum number of rectification stages, $N_{R,\min}$, and then to the section of stages between the feed and bottoms product to obtain the minimum number of stripping stages, $N_{S,\min}$. The ratio of $N_{R,\min}$ to $N_{S,\min}$ is assumed to be the same as the ratio of N_R to N_S at finite reflux conditions. Alternatively, the empirical, but often more accurate, Kirkbride equation can be applied, as discussed by Seader et al. (2016).

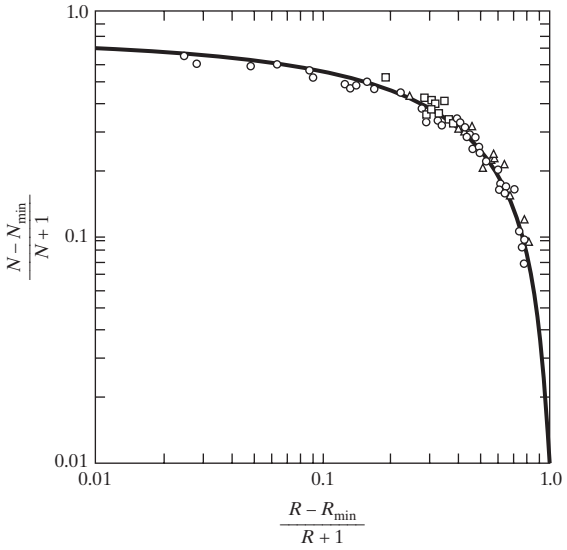

Figure 13.1 Comparison of rigorous calculations with Gilliland correlation.

13.3 KREMSER SHORTCUT METHOD FOR ABSORPTION AND STRIPPING

For adiabatic absorbers and strippers with one feed, one absorbent or stripping agent, and two products, a simple and useful shortcut method for estimating the minimum absorbent or stripping agent flow rate is the Kremser method. It applies in the limit of an infinite number of equilibrium stages for the specified absorption or stripping of one component, the key component, from the feed. It also applies for a finite number of equilibrium stages, N. Although the method is not included in the library of equipment models of most simulators, it is quite straightforward to apply the Kremser method using hand calculations or a spreadsheet. The derivation of the equations is presented in detail by Seader et al. (2016), and in *Perry's Chemical Engineers' Handbook* (Green and Perry, 2008).

The separation factor in the Kremser method is an effective absorption factor, A_e, for absorption and a stripping factor, S_e, for stripping, rather than a relative volatility as in the FUG method for distillation. These two factors, which are different for each component, are defined by:

$$A_e = L/KV \tag{13.2}$$

$$S_e = KV/L \tag{13.3}$$

The total molar liquid rate down the tower, L, the total molar vapor rate up the tower, V, and the K-value all vary from the top stage to the bottom stage of the tower. However, sufficiently good estimates by the Kremser method can be achieved by using average values based on the flow rates and temperatures of the two streams entering the tower.

For an absorber, the design basis is the tower pressure; the flow rate, composition, temperature, and pressure of the entering vapor feed; the composition, temperature, and pressure of the absorbent; and the fraction to be absorbed of one key component. The minimum molar absorbent flow rate is estimated from:

$$L_{\min} = K_K V_{in}(1 - \phi_{A_K}) \tag{13.4}$$

where K_K is the K-value of the key component computed at the average temperature and pressure of the two entering streams and $(1 - \phi_{A_K})$ is the fraction of the key component in the feed gas that is to be absorbed. Typically, the operating absorbent rate is 1.5 times the minimum value. Then, the following equation, due to Kremser and shown in Figure 13.2, is used to compute the number of equilibrium stages required. This equation assumes that the absorbent does not contain the key component.

$$\phi_{A_K} = \frac{A_{e_K} - 1}{A_{e_K}^{N+1} - 1} \tag{13.5}$$

With the value of N computed for the key component, Eq. (13.5) is then used to compute the values of ϕ_A for the other components in the feed gas using their absorption factors. From this, a material balance around the tower can be completed.

For a stripper, the design basis is the tower pressure; the flow rate, composition, temperature, and pressure of the entering liquid feed; the composition, temperature, and pressure of the stripping

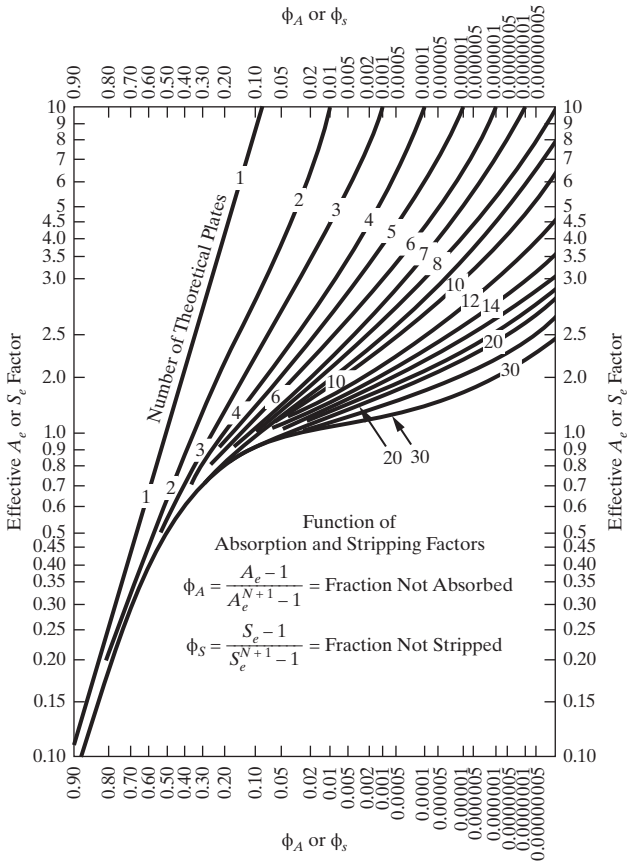

Figure 13.2 Plot of the Kremser equation for absorbers and strippers.

agent; and the fraction of a key component to be stripped. The minimum molar stripping agent flow rate is estimated from:

$$V_{\min} = \frac{L_{in}}{K_K}(1 - \phi_{S_K}) \tag{13.6}$$

where K_K is the K-value of the key component computed at the average temperature and pressure of the two entering streams and $(1 - \phi_{S_K})$ is the fraction of the key component in the feed gas that is to be stripped. Typically, the stripping agent rate is 1.5 times the minimum value. Then, the following equation is used to compute the number of equilibrium stages required. This equation assumes that the stripping agent does not contain the key component.

$$\phi_{S_K} = \frac{S_{e_K} - 1}{S_{e_K}^{N+1} - 1} \tag{13.7}$$

With the value of N computed for the key component, Eq. (13.7) is then used to compute the values of ϕ_S for the other components in the feed liquid using their stripping factors. From this, a material balance around the tower can be completed.

EXAMPLE 13.1

The feed gas to an absorber at 105°F and 400 psia contains 150 kmol/hr of methane, 350 kmol/hr of ethane, 250 kmol/hr of propane, and 50 kmol/hr of *n*-butane. The absorber is to absorb 90% of the *n*-butane with an oil at 90°F and 50 psia. With the Kremser equation, estimate the number of stages required and the amounts absorbed of the other three components in the feed gas.

SOLUTION

Set the absorber pressure at the feed gas pressure of 400 psia and neglect the pressure drop in the absorber. Use a pump to increase the pressure of the absorbent to 400 psia. The entering vapor rate is $V = 150 + 350 + 250 + 50 = 800$ kmol/hr. The average temperature of the two entering streams is $(105 + 90)/2 = 97.5$°F. The K-value for the key component, *n*-butane, at 400 psia and 97.5°F, is 0.22 by the SRK equation of state. Using Eq. (13.4) with $(1 - \phi_{A_K}) = 0.90$, the minimum absorbent rate is

$$L_{\min} = 0.22(800)(0.90) = 158 \text{ kmol/hr}$$

Select an operating absorbent flow rate of $L = 1.5\ L_{\min} = 1.5(158) = 237$ kmol/hr. The absorption factor for *n*-butane, from Eq. (13.2), is

$$A_e = 137/[0.22(800)] = 1.35$$

This is close to 1.40, which is often quoted as the optimal value of the absorption factor. Equation (13.5), which is nonlinear in N, is now applied with $(1 - \phi_{A_K}) = 0.90$, which gives $\phi_{A_K} = 0.10$.

$$0.1 = \frac{1.35 - 1}{1.35^{N+1} - 1}$$

Solving gives $N = 4$ equilibrium stages. The result for this exercise is very useful as a first approximation for a rigorous equilibrium-stage method using a simulator as described in the next section.

13.4 RIGOROUS MULTICOMPONENT, MULTIEQUILIBRIUM-STAGE METHODS WITH A SIMULATOR

Almost all multistage, multicomponent, vapor–liquid separation towers, whether plate or packed, are routinely designed with simulators. The calculations are usually based on the assumption of equilibrium stages, but more realistic mass-transfer models are also available (e.g., see Chapter 12 of Seader et al. 2016). The equilibrium-stage calculations apply component mole balances, enthalpy balances, and vapor–liquid phase equilibrium at each stage and utilize any of a number of reasonably rigorous thermodynamic correlations based on equations of state or liquid-phase activity coefficients to estimate K-values and enthalpies. The resulting large set of equations is nonlinear and is solved iteratively for stagewise profiles of vapor flows and compositions, liquid flows and compositions, and temperatures from a set of starting guesses by either an *inside-out method* or a *Newton method*, both of which are described in some detail by Seader et al. (2016) and in *Perry's Chemical Engineers' Handbook* (Green and Perry, 2008). The inside-out method is fast and is the most widely used, but Newton's method is sometimes preferred for highly nonideal systems. However, convergence of the solution of the nonlinear equations is not guaranteed for either method. When a method fails to converge within the default number of iterations (usually 20): (1) more iterations can be specified, (2) a damping factor can be applied to limit the changes made by the method to the guesses of the unknowns

between iterations to prevent wild swings, and/or (3) the initial guesses of the unknowns can be changed. In this way, most problems, unless infeasibly specified, can be converged. Infeasible specifications include those where an inadvertent attempt is made to violate the order of volatility of the components.

Equilibrium-stage methods are usually adequate for nearly ideal distillation systems when coupled with calculations of plate efficiency to estimate actual trays or, in the case of packed towers, when HETS (height equivalent of a theoretical stage) or HETP (height equivalent to a theoretical plate) values are known from experience or from experiment to enable the estimation of packed height. For absorbers, strippers, and nonideal distillation systems, mass-transfer models are preferred, but their use requires a value for the tower diameter and a tray layout or type and size of packing. Even when mass-transfer models are preferred, initial calculations are usually made with equilibrium-stage models. Also, note that data for reliable mass-transfer coefficients are often difficult to obtain.

Both of the equilibrium-stage methods can handle almost any tower configuration, including multiple feeds, vapor and liquid sidestreams, and interheaters and intercoolers. Some of these methods can also handle pumparounds (liquid side draws returned to the column at a higher tray after heat exchange with other streams), bypasses, two liquid phases, chemical reaction, interlinked towers, and specified plate efficiencies. Thus, these models can be applied to ordinary and complex distillation, extractive distillation, homogeneous azeotropic distillation, heterogeneous azeotropic distillation, reactive distillation, absorption, stripping, reboiled stripping, and reboiled absorption.

When using an equilibrium-stage model, the following must be specified: (1) all stage pressures; (2) type of condenser (total, partial, or mixed) and type of reboiler; (3) all tower feed streams and feed stage locations, including total feed flow rate, composition, temperature, and pressure; (4) and number of equilibrium stages. In addition, stage locations for side streams, intercoolers, and interheaters are necessary. From a degrees-of-freedom analysis, as discussed by Seader et al. (2016), in *Perry's Chemical Engineers' Handbook* (Green and Perry, 2008) and in Section 7.2, this leaves one additional specification for each stream leaving the tower and each intermediate heat exchanger. In addition, some models require the user to provide initial guesses of vapor and liquid flow rates at the top of the tower and stage temperatures at the top and bottom of the tower.

For ordinary distillation of nearly ideal systems, the FUG method, described in Section 13.2, provides an excellent starting point because it estimates the number of equilibrium stages, the feed stage location, and the reflux ratio. The latter can be used for the degree-of-freedom for the distillate product. For the degree-of-freedom of the bottoms product, a preferred initial specification is the bottoms flow rate because it almost always results in a converged solution. However, these two specifications may not give the desired split of the two key components. If not, the calculation is repeated by specifying the desired heavy-key flow rate or mole fraction in the distillate and the desired light-key flow rate or mole fraction in the bottoms product, using the results of the previous calculation as an initial approximation of the solution. The reflux ratio and bottoms flow rate now become initial guesses that are varied to achieve the desired split of the two key components.

If convergence for the desired split is not achieved, then estimates of the reflux ratio and/or the bottoms product flow rate may have to be revised to achieve convergence when specifying the desired split of the two key components. It is usually not difficult to judge the direction in which these estimates should be revised. Rarely does the number of equilibrium stages have to be increased or decreased. However, the degree of separation as high purities are approached is more sensitive to the number of stages than to the reflux ratio. Finally, it is useful to vary the feed stage location to determine its optimal value, which corresponds to the lowest necessary reflux ratio.

For converged calculations, simulators can provide tables and graphs of temperature, vapor and liquid flow rates, and vapor and liquid compositions as a function of stage number. These profiles should be examined closely to detect the existence of any pinch points where little or no change occurs over a section of stages. If a pinch point is found, say over a region of four stages, then the number of stages in that section of the column can probably be reduced by four without changing the degree of separation. This should be confirmed by calculations.

For simple absorbers and strippers, the Kremser method described in Section 13.3 can be used to obtain an initial approximation to the number of equilibrium stages and the flow rate of the absorbent or stripping agent. Then, with the rigorous method, the latter can be varied to achieve the desired separation of the key component for a fixed number of stages.

When the FUG method is not valid for obtaining initial estimates for use with the rigorous methods, the following procedure may be useful. It focuses on an attempt to at least estimate the number of equilibrium stages required for each section of stages bounded by feeds and/or products. These estimates are provided by the Fenske equation, applied to key-component concentrations at either end of the section where the computed N_{min} is multiplied by 2 to approximate the necessary N. This is illustrated in the following example.

EXAMPLE 13.2

A distillation column for the separation between propane and *n*-butane is to have the following two feeds:

	Upper Feed	Lower Feed
Temperature, °F	170	230
Pressure, psia	245	245
Component feed rates, lbmol/hr:		
Ethane	2.5	0.5
Propane	14.0	6.0
n-butane	10.0	18.0
n-pentane	5.0	30.0
n-hexane	0.5	4.5

Use the Fenske equation to estimate the number of stages that should be placed between the two feeds.

SOLUTION

First compute the relative volatility between propane and *n*-butane at 245 psia and the average temperature of the two feeds of

$(170 + 230)/2 = 200°F$. The respective average K-values by the SRK equation of state are 1.76 and 0.84, giving $\alpha_{LK,HK} = 1.76/0.84 = 2.10$. Applying the Fenske equation [Eq. (13.1)] between the two feeds, using the key component feed flow rates, gives:

$$N_{min} = \frac{\log\left[\left(\frac{14}{6}\right)\left(\frac{18}{10}\right)\right]}{\log(2.10)} = \frac{0.623}{0.322} = 1.93$$

Therefore, $N = 2(1.93) = 3.86$. If this is rounded up to a value of 4, then four equilibrium stages should be placed between the two feed stages.

Rigorous calculations for extractive distillation are usually readily converged once the user determines which components the solvent forces to the bottom of the tower. The Fenske equation can be applied in a manner similar to that in Example 13.2 to determine at which stage down from the top to bring in the solvent so as to minimize its loss to the distillate. Rigorous calculations for azeotropic distillation are another matter. Before even attempting a rigorous calculation, a triangular residue-curve map, which can be drawn by the simulators, should be used to determine feasible entrainer flow rates and product compositions as described in Section 9.5. In addition, for heterogeneous azeotropic distillation, a triangular liquid–liquid phase equilibrium diagram should be used to determine preliminary values for the flows and compositions of the phase split that occurs in the overhead decanter. Failure to make these preliminary studies can result in much time and effort spent in trying to converge an infeasible tower specification. Most difficult of all are reactive distillation calculations. Again, preliminary calculations are necessary, including (1) independent reactor calculations with a CSTR model to determine an operating temperature range that gives reasonable reaction rates and (2) flash calculations to determine component volatilities of reaction mixtures.

13.5 PLATE EFFICIENCY AND HETP

If a mass-transfer (rate-based) model of the type described by Seader et al. (2016) is used, the stages will be actual trays or packed height in the case of packings. If an equilibrium-stage model is used, plate efficiencies for tray towers or HETP values for packed towers must be estimated to convert equilibrium stages to actual trays or to packed height. One of the major factors that influences mass transfer is the viscosity of the liquid phase. In distillation, liquid viscosities are generally low, often in the range of 0.1 to 0.2 cP, and overall plate efficiencies, E_o, are relatively high, in the range of 50 to 100%. Because of a liquid crossflow effect in large-diameter distillation towers, efficiencies even higher than 100% have been measured. Liquid viscosity in absorbers and some strippers is often in the range of 0.2 to 2.0 cP, and overall plate efficiencies are in the range of 10 to 50%. Very approximate estimates that are sometimes used are 70% for distillation, 50% for strippers, and 30% for absorbers. The number of actual plates required is

$$N_{actual} = N_{equilibrium}/E_o \tag{13.8}$$

A better estimate of overall plate efficiency can be made with the Lockett and Leggett version of the empirical O'Connell correlation as shown in Figure 13.3. In this plot, the overall plate efficiency depends on the product of the average liquid-phase viscosity in cP and a dimensionless volatility factor. For distillation, the volatility factor is the average relative volatility between the light and heavy key components, $\alpha_{LK,HK}$. For absorbers and strippers, the volatility factor is 10 times the average K-value of the key component. If an even better estimate of the plate efficiency is desired, particularly one that depends on plate location and component, semitheoretical methods based on the definition of the Murphree vapor phase efficiency can be applied as discussed by Seader et al. (2016).

For packed columns, HETP values are usually used to convert equilibrium stages to packed height even though the alternative concept of HTU (height of a transfer unit) together with NTU (number of transfer units) is on a firmer theoretical foundation. Values of HETP (in ft) are generally derived from experimental data for a particular type and size of packing and are often available from packing vendors. Typically cited in the absence of data is an HETP of 2 ft for modern random packings and 1 ft for structured packings. However, Kister (1992) suggests the following, where D_p is the nominal diameter of random packings

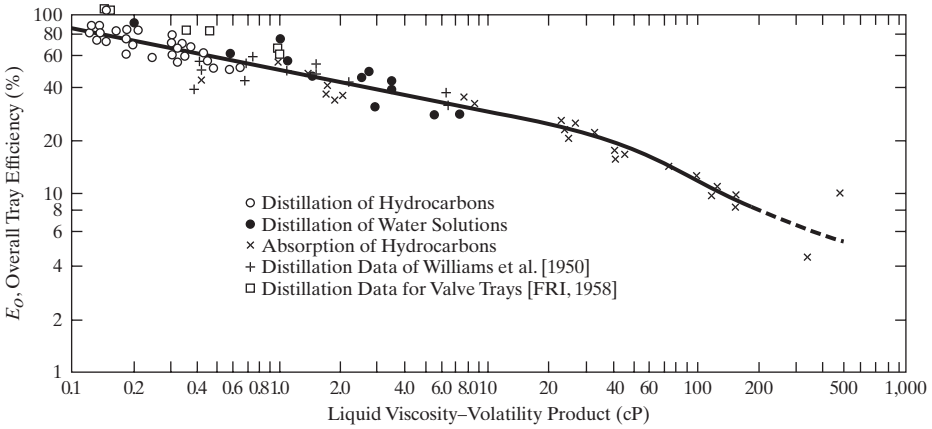

Figure 13.3 Lockhart and Leggett version of O'Connell correlation for plate efficiency.

(in in.), a is the specific surface area of structured packings (in ft^2/ft^3 packing), and HETP is in ft.

1. For modern random packings with low-viscosity liquids:

$$\text{HTEP} = 1.5D_p$$

2. For structured packings at low-to-moderate pressures and low-viscosity liquids:

$$\text{HTEP} = 100/a + 0.333$$

3. For absorption with a viscous liquid:

$$\text{HTEP} = 5 \text{ to } 6$$

4. For vacuum service:

$$\text{HTEP} = 1.5D_p + 0.50$$

5. For high-pressure service with structured packing:

$$\text{HTEP} > 100/a + 0.333$$

6. For small-diameter towers less than 2 ft in diameter:

$$\text{HTEP} = \text{tower diameter in feet, but not less than 1}$$

The packed height is given by:

$$\text{Packed height} = N_{equilibrium}\,(\text{HETP}) \tag{13.9}$$

If a more accurate estimate of packed height is desired, correlations of experimental mass-transfer coefficients or heights of transfer units should be used for the particular packing selected. Some of these correlations are provided in simulators, and the method of calculation is given in detail by Seader et al. (2016).

13.6 TOWER DIAMETER

The tower diameter depends on the vapor and liquid flow rates and their properties up and down the tower. The tower diameter is computed to avoid flooding where the liquid begins to fill the tower and leaves with the vapor because it cannot flow downward at the required rate.

Tray Towers

For a given vapor flow rate in a tray tower, downcomer flooding occurs when the liquid rate is increased to the point where the liquid froth in the downcomer backs up to the tray above. This type of flooding is not common because most tray towers have downcomers with an adequate cross-sectional area for liquid flow. A common rule is to compute the height of clear liquid in the downcomer. At low to moderate pressures if the height is less than 50% of the tray spacing, it is unlikely that downcomer flooding will occur. However, at high pressures, this value may drop to 20–30%. Another rule is to provide a downcomer cross-sectional area of at least 10–20% of the total tower cross-sectional area with the larger percentage pertaining to high pressure.

More commonly, the diameter of a tray tower is determined to avoid entrainment flooding. For a given liquid rate as the vapor rate is increased, more and more liquid droplets are carried by the vapor to the tray above. Flooding occurs when the liquid entrainment by the vapor is so excessive that column operation becomes unstable.

The tower inside cross-sectional area, A_T, is computed at a fraction, f (typically 0.75 to 0.85), of the vapor flooding velocity, U_f, from the continuity equation for one-dimensional steady flow, applied to the vapor flowing up to the next tray through area $(A_T - A_d)$:

$$\dot{m}_V = G = (fU_f)(A_T - A_d)\rho_G \tag{13.10}$$

where G = mass flow rate of vapor, A_d = downcomer area, and ρ_G = vapor density. Substituting $A_T = \pi(D_T)^2/4$ for a circular cross section into Eq. (13.10) and solving for the tower inside diameter, D_T, gives

$$D_T = \left[\frac{4G}{(fU_f)\,\pi\left(1 - \frac{A_d}{A_T}\right)\rho_G}\right]^{1/2} \tag{13.11}$$

The flooding velocity is computed from an empirical capacity parameter, C, based on a force balance on a suspended liquid droplet:

$$U_f = C\left(\frac{\rho_L - \rho_G}{\rho_G}\right)^{1/2} \tag{13.12}$$

The capacity parameter is given empirically by:

$$C = C_{SB}F_{ST}F_FF_{HA} \tag{13.13}$$

The parameter, C_{SB}, for towers with perforated (sieve) plates is given by the correlation of Fair (1961) based on data from commercial-size towers, covering tray spacings from 6 to 36 in. A revision by Fair of the original correlation, shown in Figure 13.4, applies to all common crossflow plates (sieve, valve, and bubble-cap), with plate spacing from 6 to 36 in, and C_{SB} in ft/s. The abscissa in Figure 13.4 is a flow ratio parameter, $F_{LG} = (L/G)(\rho_G/\rho_L)^{1/2}$, where both the liquid rate, L, and vapor rate, G, are mass flow rates. The surface tension factor, F_{ST}, is equal to $(\sigma/20)^{0.20}$, where the surface tension, σ, is in

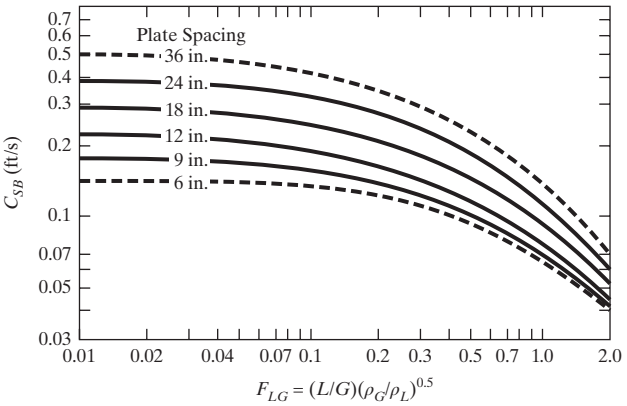

Figure 13.4 Flooding correlation for sieve, valve, and bubble-cap trays.

dyne/cm. The foaming factor, F_F, is 1 for nonfoaming systems, typical of distillation, and 0.5 to 0.75 for foaming systems, typical of absorption with heavy oils. The hole-area factor, F_{HA}, is 1 for valve and bubble-cap trays. For sieve trays, it is 1 for $(A_h/A_a) > 0.10$, and $[5(A_h/A_a) + 0.5]$ for $0.06 < (A_h/A_a) < 1.0$ where A_h is the total hole area on a tray and A_a is the active area of the tray, $A_a = (A_T - 2A_d)$, where bubbling occurs.

In Eq. (13.11), the ratio (A_d/A_T) may be estimated by

$$\frac{A_d}{A_T} = \begin{Bmatrix} 0.1, & F_{LG} \le 0.1 \\ 0.1 + \dfrac{(F_{LG} - 0.1)}{9}, & 0.1 \le F_{LG} \le 1.0 \\ 0.2, & F_{LG} \ge 1.0 \end{Bmatrix}$$

Example 13.3 illustrates the calculation of the tower diameter for a sieve tray.

Packed Towers

If a packed tower is irrigated from a good distributor by a downflow of liquid, the liquid flows over the packing surface, and a volumetric holdup of liquid in the tower is observed. As vapor is passed up the tower at low flow rates, countercurrent to the liquid, little or no drag is exerted by the vapor on the liquid and the liquid holdup is unchanged. The liquid has no difficulty leaving the tower as fast as it enters. However, if the gas flow rate is increased, a point is eventually reached where, because of drag, the liquid holdup begins to increase significantly with increasing vapor rate. This is called the loading point. Further increases in the vapor rate eventually reach the point where liquid begins to fill the tower, causing a rapid increase in pressure drop. The flooding point can be defined as the point where the pressure drop rapidly increases with a simultaneous decrease in mass-transfer efficiency. Typically, the flooding point is accompanied by a pressure head of approximately 2 in. of water/ft of packing. For a given liquid flow rate, the loading gas flow rate, which is typically 70% of the flooding gas flow rate, is often used to compute the tower inside diameter.

The diameter of a packed tower is calculated from an estimated flooding velocity with a continuity equation similar to Eq. (13.11) for tray towers:

$$D_T = \left[\frac{4G}{(fU_f)\,\pi\rho_G} \right]^{1/2} \tag{13.14}$$

For towers with random packing, the generalized correlation of Leva (1992) gives reasonable estimates of the flooding velocity in terms of a packing factor, F_P, which depends on the type and size of packing, and the same flow ratio parameter, F_{LG}, used for tray towers. The Leva flooding correlation fits the following equation

$$Y = \exp[-3.7121 - 1.0371(\ln F_{LG}) - 0.1501(\ln F_{LG})^2 - 0.007544(\ln F_{LG})^3] \tag{13.15}$$

where

$$Y = \frac{U_f^2 F_P}{g} \left(\frac{\rho_G}{\rho_{H_2O_{(L)}}} \right) f\{\rho_L\} f\{\mu_L\} \tag{13.16}$$

Table 13.1 Packing Factors for Calculating Flooding Velocity

Type Packing	Material	Nominal Diameter, D_P (in.)	Packing Factor, F_P(ft^2/ft^3)
Raschig rings	Ceramic	1.0	157
		2.0	58
		3.0	33
Raschig rings	Metal	1.0	165
		2.0	71
		3.0	40
Intalox saddles	Ceramic	1.0	92
		2.0	30
		3.0	15
Intalox saddles	Plastic	1.0	36
		2.0	25
Pall rings	Metal	1.0	56
		1.5	29
		2.0	27
		3.5	16
Pall rings	Plastic	1.0	53
		2.0	25
		3.5	15

The flooding velocity factor Y is dimensionless with U_f in ft/s, F_P in ft^2/ft^3, and $g = 32.2$ ft/s^2. Values of F_P for several representative packings are listed in Table 13.1. Equation (13.15) is valid for Y in the range 0.01 – 10.

The density function in Eq. (13.16), valid for density ratios in the range 0.65–1.4, is given by:

$$f\{\rho_L\} = -0.8787 + 2.6776 \left(\frac{\rho_{H_2O_{(L)}}}{\rho_L} \right) - 0.6313 \left(\frac{\rho_{H_2O_{(L)}}}{\rho_L} \right)^2 \tag{13.17}$$

For random packings of 1 in. or greater nominal diameter, the viscosity function in Eq.(13.16), valid for liquid viscosities in the range 0.3–20 cP, is given by:

$$f\{\mu_L\} = 0.96\mu_L^{0.19} \tag{13.18}$$

For a value of F_{LG}, Y is computed from Eq. (13.15), U_f is then computed from Eq. (13.16) for a given packing type and size with F_P from Table 13.1 and using Eqs. (13.17) and (13.18). Then for $f = 0.7$, the tower diameter is computed from Eq. (13.14). The tower inside diameter should be at least 10 times the nominal packing diameter (see Table 13.1) and preferably closer to 30 times. Table 13.1 is extended to other random packings by Seader, et al. (2016).

The determination of the flooding velocity in structured packings is best carried out by using interpolation of the flooding and pressure drop charts for individual structured packings in Chapter 10 of Kister (1992).

13.7 PRESSURE DROP AND WEEPING

In general, pressure drop per unit height is least for towers with structured packings and greatest for tray towers with randomly packed towers in between. For sieve trays, the components of the pressure drop are (1) pressure drop through the holes in

the tray, which depends on the hole diameter, hole area, and vapor volumetric flow rate; (2) pressure drop due to surface tension; and (3) the head of equivalent clear liquid on the tray, which depends on the weir height, weir length, and froth density. Detailed methods of calculation of tray pressure drop are presented by Kister (1992), Seader et al. (2016), and in *Perry's Chemical Engineers' Handbook* (Green and Perry, 2008). Most simulators perform this calculation. However, the user should minimize the hydraulic gradient of the liquid flowing across the tray before requesting the calculation by considering the number of liquid passes to use. Columns of diameter larger than 4 ft and operating with liquid rates greater than 500 gal/min frequently employ multipass trays to increase weir length and shorten the liquid flow path across the tray. Figure 13.5 shows three multipass arrangements and a correlation for selecting the number of passes to use. For preliminary design, a pressure drop of 0.10 psi/tray can be assumed for columns operating at ambient pressure or higher. For vacuum operation, trays should be designed so as not to exceed 0.05 psi/tray or packing should be considered as a substitute for trays to give an even lower pressure drop. Methods for estimating pressure drop in packed towers are found in Kister, and in *Perry's Chemical Engineers' Handbook* and are performed by simulators.

For sieve trays, the possibility of weeping of liquid through the holes in the trays should be checked, particularly when the vapor flow rate is considerably below the flooding point. Methods for checking this are used by the simulators. Note that, in general, weeping rates as high as 10% do not affect the tray efficiency, primarily because the weeping liquid is in contact with the vapor as it falls to the tray below.

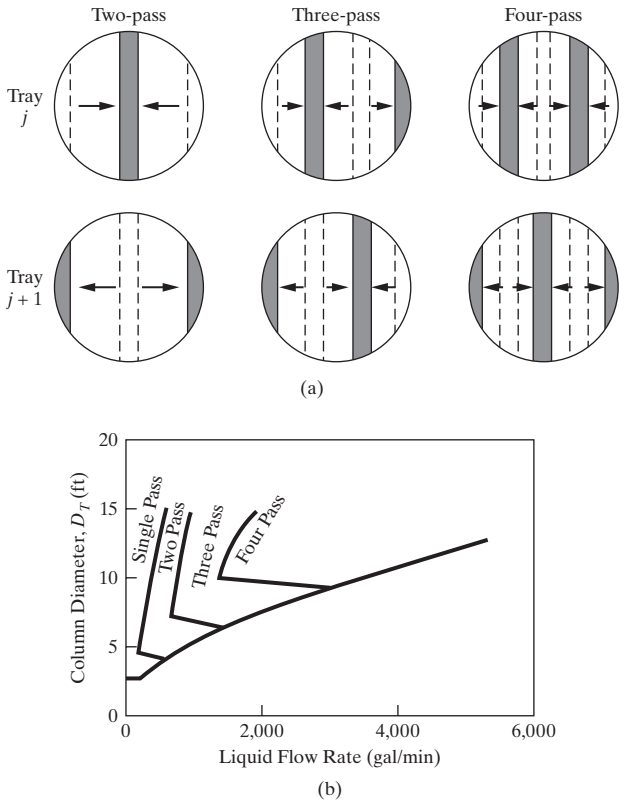

Figure 13.5 Selection of multipass trays. (a) multipass trays: (1) two-pass; (2) three-pass; (3) four-pass. (b) flow pass correlation. (*Source:* Based upon *Koch Flexitray Design Manual, Bulletin 960*, Koch Engineering Co., Inc., Wichita, Kansas, 1960).

EXAMPLE 13.3

Several alternative distillation sequences are being examined for the separation of a mixture of light hydrocarbons. The sequences are to be compared on the basis of annualized cost, discussed in Chapter 17 and given by Eq. (17.10). This requires estimates of the total capital cost and the annual operating cost of the columns, trays, condensers, reboilers, and reflux accumulators. To estimate these costs, equipment sizes must be determined. In this example, calculations of the height and diameter are illustrated for one column in one of the sequences.

The column to be sized is a deisobutanizer with a saturated liquid feed of 500 lbmol/hr of isobutane and 500 lbmol/hr of *n*-butane. The distillate is to be 99 mol% isobutane and the bottoms 99 mol% *n*-butane. The column shell is carbon steel with carbon-steel sieve trays on 24-in. spacing. The trays have 0.25-in. diameter holes with a hole area to active area ratio of 0.1. The weir height is 2 in.

SOLUTION

Following the procedure outlined above, the following results are obtained:

1. Using a simulator with the Soave–Redlich–Kwong (SRK) equation of state for thermodynamic properties, a bubble-point pressure of 98 psia is computed at 120°F for the distillate composition. Therefore, from Figure 9.9, a total condenser should be used with cooling water. Assuming a pressure drop of 2 psia across the condenser, the pressure at the top of the column is 100 psia. Assuming a 10-psi drop across the tower, the tower bottoms pressure is 110 psia. This gives a bubble-point bottoms temperature of 152°F, which is far below the decomposition temperature of *n*-butane. The assumed tower pressure drop is checked by a simulator after the column diameter is determined.
2. Using the Fenske–Underwood–Gilliland shortcut model with a process simulator, for a reflux-to-minimum reflux ratio of 1.10 (because this is a difficult separation with a relative volatility predicted by the SRK equation of state of approximately 1.30) gives 36.4 minimum stages, a minimum reflux ratio of 6.6, 85.6 equilibrium stages at a reflux ratio of 7.25, and a feed-stage location of 43 stages from the top (approximately at the middle stage). Using these results as a first approximation, a rigorous equilibrium-stage calculation for 84 equilibrium stages in the column, an equilibrium-stage reboiler, and a total condenser (86 stages in all) with a feed stage at the middle gives a reflux ratio of 7.38 (only 2% greater than the FUG value) to achieve the specified distillate and bottoms purities. Thus, for this nearly ideal system, the FUG method is in close agreement with a rigorous method. The computed condenser duty is 31,600,000 Btu/hr and the reboiler duty is 31,700,000 Btu/hr.
3. Use Figure 13.3 to estimate the plate efficiency for average conditions in the tower. Using a simulator, the estimated average liquid viscosity = 0.12 cP, whereas the average relative volatility = 1.30. Using the product of these two factors = 0.12(1.3) = 0.156, Figure 13.3 predicts $E_O = 0.80$. Therefore, the number of actual trays = 84/0.80 = 105 with the partial reboiler counted as an additional stage.

4. For a 24-in. tray spacing, allowing a 10-ft-high liquid bottoms storage (sump) below the bottom tray and a 4-ft disengagement height above the top tray, the tower height is 222 ft (tangent-to-tangent, i.e., not including the top and bottom tower heads).
5. Assume that the tower diameter will be determined from the entrainment flooding velocity rather than by downcomer flooding. The clear liquid height in the downcomer is one of a number of items computed by a simulator when a tray design is specified. That height should be checked to determine whether it is less than 50% of the tray spacing. If not, to prevent downcomer flooding, the downcomer cross-sectional area should be increased. For conditions at the top stage of the column, a process simulation program gives the following results.

Liquid Phase

Surface tension = 7.1 dyne/cm

Flow rate = 215,000 lb/hr

Density = 32.4 lb/ft^3 or 4.33 lb/gal

Molecular weight = 58.12

Vapor Phase

Flow rate = 244,000 lb/hr

Density = 1.095 lb/ft^3

Molecular weight = 58.12

The flow ratio parameter =

$$F_{LG} = (215,000/244,000) \times (1.095/32.4)^{0.5} = 0.162$$

From Figure 13.4 for 24-in. tray spacing, $C_{SB} = 0.09$ m/s

The surface-tension factor = $F_{ST} = (7.1/20)^{0.2} = 0.81$. Assume $F_F = 1$. Also, $F_{HA} = 1$. Therefore, from Eq. (13.13), $C = 0.09(0.81)(1)(1) = 0.073$ m/s. From Eq. (13.12), $U_f = 0.073\ [(32.4-1.095)/1.095]^{0.5} = 0.390$ m/s = 4,610 ft/hr. Assume operation on the top tray of 80% f flooding ($f = 0.80$). To determine the ratio A_d/A_T, $0.1 + (F_{LG}–0.1)/9 = 0.1 + 0.062/9 = 0.107 = A_d/A_T$.

From Eq. (13.11),

$$D_T = \left[\frac{4\,(244,000)}{0.8(4,610)(3.14)(1-0.107)(1.095)}\right]^{1/2} = 9.3 \text{ ft}$$

For this large a tower diameter, the need for a multipass tray needs to be considered using Figure 13.5. The volumetric liquid flow rate = $(215,000/60)/4.33 = 828$ gpm. For this diameter and liquid flow rate, a three-pass tray is indicated. For a one-pass tray, a simulator gives a tower diameter of 9.5 ft, when the diameter is restricted to increments of 0.5 ft. For a three-pass tray, the tower diameter remains at 9.5 ft.

Other calculations from a simulator for both single-pass and three-pass trays are as follows:

	Single-Pass Sieve Tray	Three-Pass Sieve Tray
Weir length, ft	7.3	23.3
Flow path length, ft	6.1	2.2
Active area, ft^2	70.9	70.9
Weeping tendency	Barely	No
Pressure drop, psi	0.067	0.056
Downcomer backup, ft	0.70	0.54
Downcomer area/Tower area	0.122	0.122

Both the single-pass and three-pass trays have the same ratio of downcomer area to tower area, which is only 14% greater than the assumed value of 0.107. The much shorter flow path length of the three-pass tray reduces the hydraulic gradient so that a more uniform vapor distribution over the tray active area is achieved. The weeping tendency is not a problem with either tray. The total pressure drop for the 105 trays is 7.0 psi for the single-pass tray and 5.9 psi for the three-pass tray compared to the assumed 10-psi drop. The downcomer backups, which are based on clear liquid, are safely below a possible problem of downcomer flooding provided that the volume fraction of vapor in the downcomer froth is not much greater than the commonly assumed value of 0.50.

13.8 SUMMARY

After studying this chapter and completing a few exercises, the reader should be able to:

1. select an appropriate operating pressure for a multistage tower and a condenser type for distillation.
2. determine the number of equilibrium stages required for a separation and a reasonable reflux ratio for distillation.
3. determine whether trays, packing, or both should be considered.
4. determine the number of actual trays or packing height required.
5. estimate the tower diameter.
6. consider other factors for successful tower operation.

REFERENCES

1. Fair, J. R., "How to Predict Sieve Tray Entrainment and Flooding," *Petro./Chem. Eng.*, **33**, 211–218 (1961).

2. FRI (Fractionation Research Institute) report of Sept. 3, 1958, *Glitsch Ballast Tray*, published as Bulletin No. 159 of Fritz W. Glitsch and Sons, Inc., Dallas, Texas (1958).

3. Green, D. W., and Perry, R. H., (eds.), *Perry's Chemical Engineers' Handbook*, 8th ed., McGraw-Hill, New York (2008).

4. Kister, H. Z., *Distillation Design*, McGraw-Hill, New York (1992).

5. *Koch Flexitray Design Manual, Bulletin 960*, Koch Engineering Co. Inc., Wichita, Kansas (1960).

6. Leva, M., "Reconsider Packed-Tower Pressure-Drop Correlations," *Chem. Eng. Prog.*, **88** (1), 65–72 (1992).

7. Seader, J. D., E. J. Henley, and D. K. Roper, *Separation Process Principles*, 4th ed., John Wiley, New Jersey (2016).

8. Williams, G. C., E. K. Stigger, and J. H. Nichols, "A Correlation of Plate Efficiencies in Fractionating Columns," *Chem. Eng. Prog.*, **46**, 1, 7–16 (1950).

EXERCISES

13.1 In Example 13.1, an absorber with an absorbent rate of 237 kmol/hr and 4 equilibrium stages absorbs 90% of the entering *n*-butane. Repeat the calculations for:

(a) 474 kmol/hr of absorbent (twice the flow) and four equilibrium stages.

(b) Eight equilibrium stages (twice the stages) and 237 kmol/hr of absorbent.

Which case results in the most absorption of *n*-butane? Is this result confirmed by the trends of the curves in the Kremser plot of Figure 13.2.

13.2 The feed to a distillation tower consists of 14.3 kmol/hr of methanol, 105.3 kmol/hr of toluene, 136.2 kmol/hr of ethylbenzene, and 350.6 kmol/hr of styrene. The bottoms product is to contain 0.1 kmol/hr of ethylbenzene and 346.2 kmol/hr of styrene. Determine a suitable operating pressure at the top of the tower noting that the bottoms temperature is limited to 145°C to prevent the polymerization of styrene.

13.3 A mixture of benzene and monochlorobenzene is to be separated into almost pure products by distillation. Determine an appropriate operating pressure at the top of the tower.

13.4 In a reboiled absorber, operating as a deethanizer at 400 psia to separate a light hydrocarbon feed, conditions at the bottom tray are:

Liquid Phase

Molar flow = 1,366 lbmol/hr

MW = 91.7

Density = 36.2 lb/ft^3

Surface tension = 10.6 dyne/cm

Vapor Phase

Molar flow = 735.2 lbmol/hr

MW = 41.2

Density = 2.83 lb/ft^3

If sieve trays are used with a hole area of 10% and a 24-in. tray spacing, determine the tower diameter. Assume 80% of flooding and a foaming factor of 0.75.

13.5 A distillation tower with sieve trays is to separate benzene from mono-chlorobenzene. Conditions at a plate near the bottom of the column are:

Vapor Phase

Mass flow rate = 24,850 lb/hr

Density = 0.356 lb/ft^3

Liquid Phase

Mass flow rate = 41,850 lb/hr

Density = 59.9 lb/ft^3

Surface tension = 24 dyne/cm

Determine a reasonable tower diameter.

13.6 Water is to be used to absorb acetone from a dilute mixture with air in a tower packed with 3.5-in. metal Pall rings. Average conditions in the tower are:

Temperature = 25°C; pressure = 110 kPa

Liquid Phase

Water = 1,930 kmol/hr; acetone = 5 kmol/hr

Density = 62.4 lb/ft3

Surface tension = 75 dyne/cm

Vapor Phase

Air = 680 kmol/hr

Water = 13 kmol/hr

Acetone = 5 kmol/hr

Determine the column diameter for operation at 70% of flooding.

Chapter 14

Pumps, Compressors, and Expanders

14.0 OBJECTIVES

This chapter presents brief descriptions and some theoretical background of the most widely used pumps for liquids as well as compressors and expanders for gases, all of which are modeled in simulators. Heuristics for the application of these devices during the synthesis of a chemical process are presented in Chapter 6. Further information on their selection and capital cost estimation is covered in Chapter 16. More comprehensive coverage of the many types of pumps, compressors, and expanders available is presented in Sandler and Luckiewicz (1987) and in *Perry's Chemical Engineers' Handbook* (Green and Perry, 2008). After studying this chapter and the materials on pumps, compressors, and turbines on the multimedia modules that accompany this book that can be downloaded from www.seas.upenn.edu/~dlewin/multimedia.html, the reader should be able to explain how the more common types of pumps, compressors, and expanders work and how a simulator computes their power input or output.

14.1 PUMPS

The main purpose of a pump is to provide the energy needed to move a liquid from one location to another. The net result of the pumping action may be to increase the elevation, velocity, and/or pressure of the liquid. However, in most process applications, pumps are designed to increase the pressure of the liquid. In that case, the power required is

$$\dot{W} = Fv(\Delta P) \tag{14.1}$$

where F is the molar flow rate, v is the molar volume, and P is pressure. Because the liquid molar volume is usually much smaller than that of a gas, pumps require relatively little power compared to gas compressors for the same molar flow rate and increase in pressure. Therefore, when a vapor stream is produced from a liquid stream with increased pressure and temperature, it is generally more economical to increase the pressure while the stream is a liquid. Except for very large changes in pressure, the temperature of the liquid being pumped increases only slightly.

The main methods used to move a liquid are centrifugal force, displacement, gravity, electromagnetic force, and transfer of momentum from another fluid, with the first two methods being the most common for chemical processes. Pumps that use centrifugal force are sometimes referred to as kinetic pumps but more commonly as *centrifugal* pumps. Displacement of one part of a fluid with another part takes place in so-called *positive-displacement* pumps, whose action is either reciprocating or rotary. The use of electromagnetic force is limited to fluids that can conduct electricity. Jet pumps, either eductors or injectors, are simple devices that transfer momentum from one fluid to another. Their application is also limited because the motive and pumped fluids contact each other and may mix together, and the efficiency of transfer is very low.

The two most important characteristics of a pumping operation are the *capacity* and the *head*. The capacity refers to the flow rate of the fluid being pumped. It may be stated as a mass flow rate, a molar flow rate, or a volumetric flow rate. Most common is the volumetric flow rate, Q, in units of either m^3/hr or gal/min (gpm). The head, or pump head, H, refers to the increase in total head across the pump from the suction, s, to the discharge, d, where the head is the sum of the velocity head, static head, and pressure head. Thus,

$$H, \text{ pump head} = \left(\frac{V_d^2}{2g} + z_d + \frac{P_d}{\rho_d g}\right) - \left(\frac{V_s^2}{2g} + z_s + \frac{P_s}{\rho_s g}\right) \tag{14.2}$$

where V is the average velocity of the liquid, z is the elevation, P is the pressure of the liquid, g is the gravitational acceleration ($32.2\ ft/s^2$, $9.81\ m/s^2$), and ρ is the liquid density. The head is expressed in units of ft or m of liquid. The required pump head or pressure increase is determined by an energy balance as discussed with a heuristic and example in Section 6.7.

Centrifugal Pumps

As shown in Figure 14.1, a centrifugal pump consists of an impeller mounted on a shaft and containing a number of blades rotating within a stationary casing that is provided with an inlet

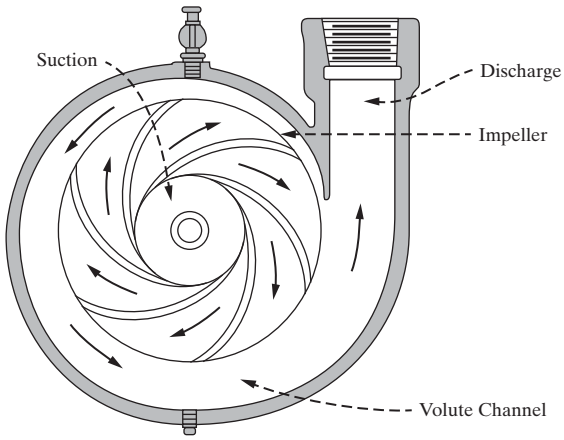

Figure 14.1 Schematic of centrifugal pump.

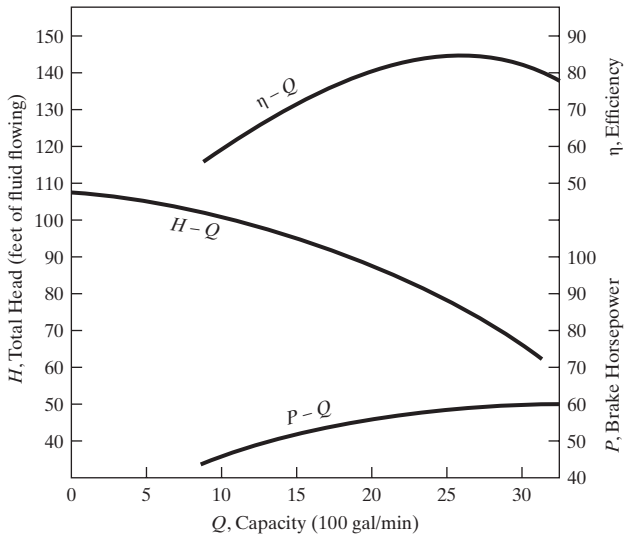

Figure 14.2 Characteristic curves for a centrifugal pump.

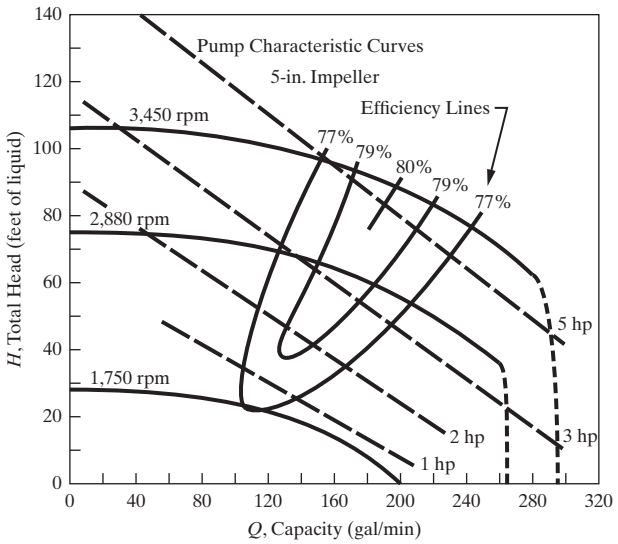

Figure 14.3 Effect of rate of rotation on characteristic curves.

and outlet for the liquid being pumped. Power, usually from an electric motor, rotates the shaft, which rotates the impeller. The rotating blades reduce the pressure at the inlet or eye of the impeller, causing liquid to enter the impeller from the suction of the pump. This liquid is forced outward along the blades to the blade tips at an increasing tangential velocity. At this point the liquid has acquired an increased velocity head from the power input to the pump. The velocity head is then reduced and converted to a pressure head as the liquid passes into the annular (volute) chamber within the casing and beyond the blades, and then to the pump outlet or discharge.

When a centrifugal pump is installed in a pumping system and operated at a particular rotational rate, N, (usually 1,750 to 3,450 rpm), the flow rate can be varied by changing the opening on a valve located in the pump discharge line. The variation of H with Q defines a unique characteristic curve for the particular pump operating at N with a fluid of a particular viscosity. Each make and model of a centrifugal pump is supplied by the manufacturer with a characteristic curve determined by the manufacturer when pumping water. Corrections are necessary when other fluids are pumped. Corresponding to the variation of H with Q, curves representing the effect of Q on the brake horsepower, P, and the pump efficiency, η, are shown in Figure 14.2. Typically, the pump head decreases with increasing flow rate while the brake horsepower increases with increasing flow rate. The pump efficiency passes through a maximum. The pump will only operate at points on the characteristic curve. Therefore, for a particular pumping task, the required head-volumetric flow rate point must lie somewhat below the characteristic curve. The difference between the two heads (pump head, required head) can be throttled across a control valve in the discharge line. Ideally, a centrifugal pump should be selected so that the operating point is located on the characteristic curve at the point of maximum efficiency.

For a given centrifugal pump, the characteristic curve moves upward with increasing rate of rotation, N, as shown in Figure 14.3. Similarly, for a pump of a particular design, the characteristic curve moves upward with increasing impeller diameter, D, as shown in Figure 14.4. When a characteristic curve

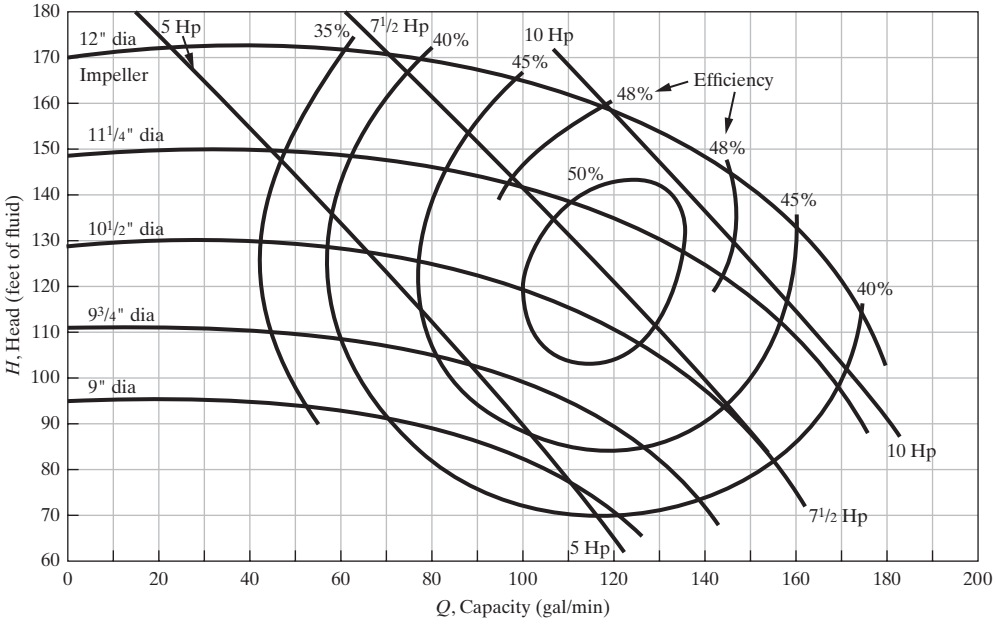

Figure 14.4 Effect of impeller diameter on characteristic curves.

for just one rotation rate and/or impeller diameter is available and an approximate characteristic curve is desired for another rotation rate and/or impeller diameter, the affinity laws for a centrifugal pump can be applied:

$$Q_2 = Q_1\left(\frac{N_2}{N_1}\right) \tag{14.3}$$

$$H_2 = H_1\left(\frac{N_2}{N_1}\right)^2 \tag{14.4}$$

$$Q_2 = Q_1\left(\frac{D_2}{D_1}\right) \tag{14.5}$$

$$H_2 = H_1\left(\frac{D_2}{D_1}\right)^2 \tag{14.6}$$

More difficult is the correction for viscosity. In general, increasing viscosity for a fixed capacity, Q, decreases the pump head and the pump efficiency and increases the brake horsepower (Hp). Typical effects of viscosity are shown in Figure 14.5. As seen, the effect of viscosity can be substantial.

Because centrifugal pumps operate at high rates of rotation, the imparted high liquid velocities can lower the local pressure. If that pressure falls below the vapor pressure of the liquid, vaporization will produce bubbles that may collapse violently against surfaces where a higher pressure exists. This phenomenon is called cavitation and must be avoided. Otherwise, besides a lowering of efficiency and flow rate, the pump may be damaged. The tendency for cavitation is measured by a quantity peculiar to each pump and available from the manufacturer called required NPSH (net positive-suction head) expressed as a head. It is typically in the range of 2–10 ft of head. The available NPSH is defined as the difference between the liquid pressure at the pump inlet and the vapor pressure of the liquid expressed as a head. To avoid cavitation, the available NPSH must be greater than the manufacturer's value for the required NPSH. An example of the application of the NPSH is given later in Example 16.6.

Centrifugal pumps are limited by the rate of rotation of the impeller to the pump head they can achieve in a single stage. A typical maximum head for a single stage is 500 ft. By going to multiple stages, heads as high as at least 3,200 ft can be achieved.

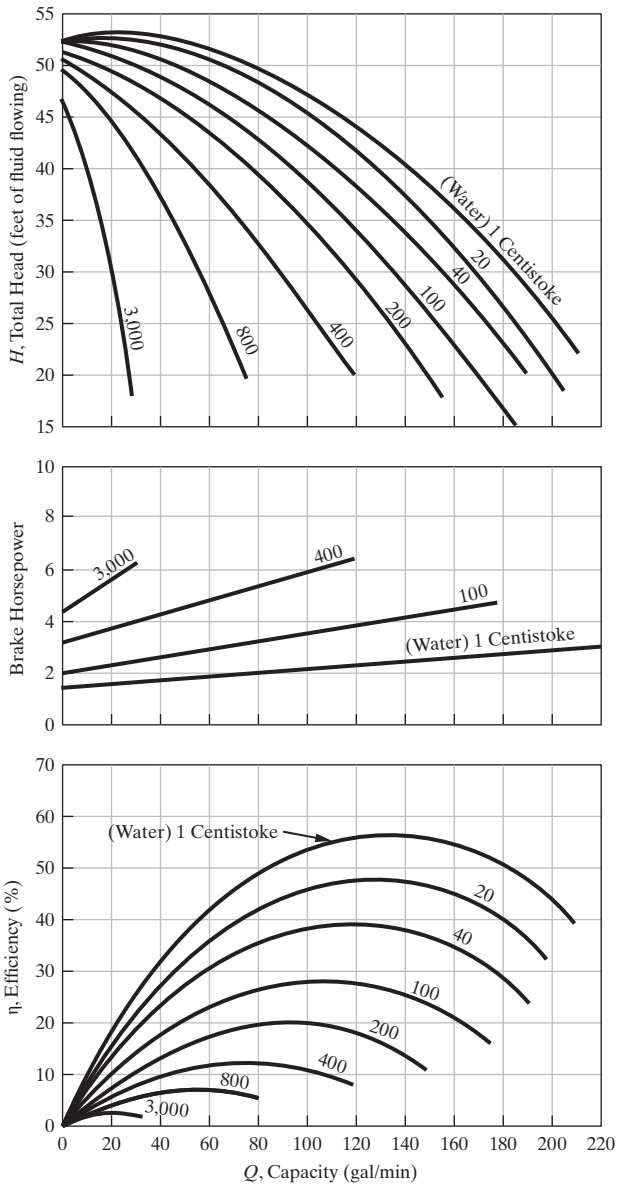

Figure 14.5 Effect of viscosity on characteristic curves.

Positive-displacement Pumps

Positive-displacement pumps, either reciprocating or gear, are essentially metering pumps designed to deliver a volumetric flow rate, Q, that is independent of the required pump head, H. Thus, the characteristic curve of a positive displacement pump, if it can be called that, is a vertical line on a plot of Q as a function of H. The pump head is limited only by the Hp of the driver, the strength of the pump, and/or possible leakage through clearances between moving pistons, plungers, gears, or screws and stationary cylinders or casings. Unlike centrifugal pumps, where the flow rate can be changed (while staying on the characteristic curve) by adjusting a valve on the discharge line, the flow rate of a positive-displacement pump must be changed by a bypass or with a speed changer on the motor. The efficiency of positive-displacement pumps is greater than for centrifugal pumps because less friction occurs in the former, and cavitation is not usually a concern with positive-displacement pumps.

The three main classes of reciprocating pumps are piston, plunger, and diaphragm, which are shown schematically in Figure 14.6. They all contain valves on the inlet and outlet. During suction, a chamber is filled with liquid with the inlet valve open and the outlet valve closed. During discharge of the liquid from the chamber, the inlet valve is closed and outlet valve opened. This type of action causes pressure pulsations, which cause a fluctuating flow rate and discharge pressure. These fluctuations can be reduced by employing a gas-charged surge chamber in the discharge line and/or by using multiple cylinders in parallel. In addition, if pistons are used, the pump can be double-acting with chambers on either side of the piston. With a plunger, only a single-action is used. Reciprocating pumps with a flexible diaphragm of metal, rubber, or plastic eliminate packing and seals, making them useful for hazardous or toxic liquids.

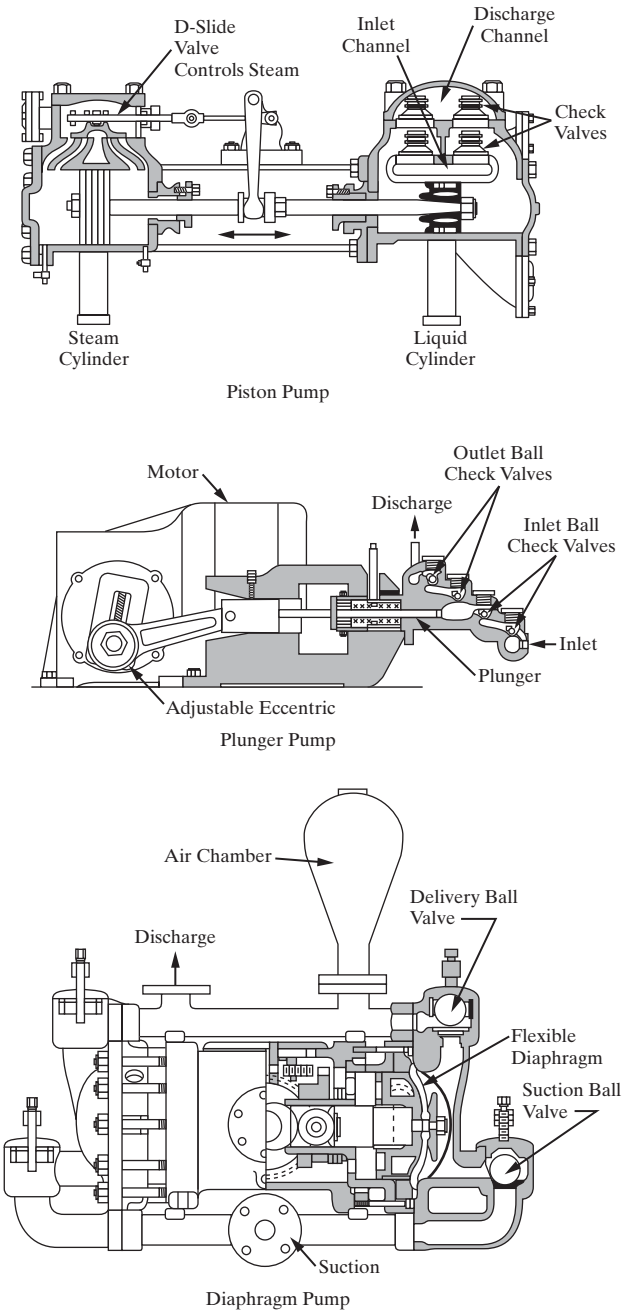

Figure 14.6 Reciprocating pumps.

Rotary pumps include gear pumps and screw pumps, which are shown schematically in Figure 14.7. These must be designed to tight tolerances to avoid binding and excessive wear. They are best suited for liquids of high viscosity. Flow rates are more steady than for reciprocating pumps but less steady than for centrifugal pumps.

Pump Models in Simulators

The pump models in process simulators do not differentiate between centrifugal pumps and positive-displacement pumps when calculating theoretical power requirement from the product

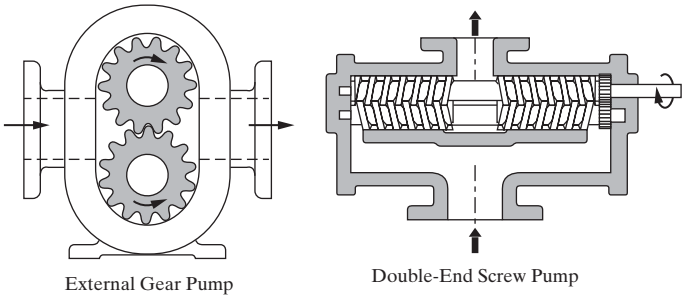

Figure 14.7 Rotary pumps.

of the capacity and required head [Eq. (14.1)]. In some cases, the models do utilize built-in efficiency equations, which differentiate between the two types of pumps when computing the brake horsepower. Most models calculate a discharge temperature, which is based on the small variation of density with temperature and an assumption that all of the pump inefficiency produces friction that causes an increase in the liquid temperature. In most cases, the temperature and enthalpy changes of the liquid across the pump are small. Simulators do not provide built-in characteristic curves to help select a suitable centrifugal pump, nor do they consider multiple stages or cylinders. Pump subroutines are discussed further on the multimedia modules accompanied by a video of an industrial-scale centrifugal pump (ASPEN → Pumps, Compressors & Expanders → Pumps and HYSYS → Pumps, Compressors & Expanders → Pumps).

EXAMPLE 14.1

In a toluene hydrodealkylation process, 25,000 lb/hr of toluene feed is pumped from 75°F and 30 psia to 570 psia. Use a process simulator to compute the capacity in gpm, the pump head in ft of toluene, the exit temperature, and brake horsepower (BHp) for:

1. A pump efficiency of 100%.
2. A pump efficiency of 75%.

SOLUTION

Using the SRK equation of state for thermodynamic properties, the following results are obtained:

	Pump Efficiency = 100%	Pump Efficiency = 75%
Capacity, gpm	57.3	57.3
Pump head, ft of toluene	1,440	1,440
Outlet temperature, °F	75.78	77.37
Brake horsepower, BHp	18.2	24.3

The temperature rise is very small even for the 75% efficiency case. The pump head is well above the limit of 500 ft for a single-stage centrifugal pump. Therefore, a multistage centrifugal pump would be required.

14.2 COMPRESSORS AND EXPANDERS

Gas compressors (including fans and blowers), unlike pumps, are designed to increase the velocity and/or pressure of gases rather than liquids. In fact, small amounts of liquid can cause significant amounts of degradation to the compressor blades, and, consequently, most compressor systems are designed to prevent liquid from entering the compressor and to avoid condensation in the compressor. The main methods used to move a gas are centrifugal force, displacement, and transfer of momentum. There are no sharp boundaries among fans, blowers, or compressors, but one convenient classification is based on discharge pressure or compression ratio. By this classification, a fan mainly increases the kinetic energy of the gas with a discharge pressure of no more than 110% of the suction pressure. A blower increases the pressure head more than the velocity head with a compression ratio of not more than 2. A compressor increases the velocity head very little with a compression ratio of greater than 2.

Centrifugal Compressors

Centrifugal fans, blowers, and compressors are widely used in chemical processes because they produce a continuous flow, are relatively small, and are free of vibration. Because gases are compressible, the temperature difference between the compressed gas and the feed gas is significant at even moderate compression ratios and may limit the compression ratio possible in a single stage. However, the need for multiple stages in centrifugal compressors is usually dictated instead by impellor rotation-rate limitations, which limit the compression ratio that can be achieved.

Like pumps, the feed (stream 1) to a centrifugal compressor at its suction pressure enters the eye of the impeller unit, as shown in Figure 14.8. The compressed gas leaves as stream 2.

A large amount of power input compared to pumps is required to increase the pressure of a gas, primarily because of the large molar volume of a gas. Although compressors are much larger than pumps, they can be well insulated so that heat losses are negligible compared to their power requirements. Accordingly, adiabatic operation is usually assumed. The characteristic curves for centrifugal compressors are similar to those for a centrifugal pump, as shown in Figures 14.2–14.4, except that the coordinates may be static pressure (in place of head) and actual ft^3/min (ACFM) at inlet conditions (in place of gpm). Also, for some impeller designs, as ACFM is increased from zero, the static pressure first decreases, goes through a minimum, rises to a maximum, and then drops sharply. As with a centrifugal pump, a centrifugal fan, blower, or compressor should be selected for operation at the point of maximum efficiency on the characteristic curve.

Positive-displacement Compressors

Positive-displacement fans, blowers, and compressors are similar in action to positive-displacement pumps and include reciprocating compressors, two- or three-lobe blowers, and screw compressors. However, with gases, the almost vertical characteristic curves bend to the left more than for liquids because of the greater tendency for slip.

Reciprocating compressors use pistons with either single- or double-action. As discussed in Section 16.5, compression ratios

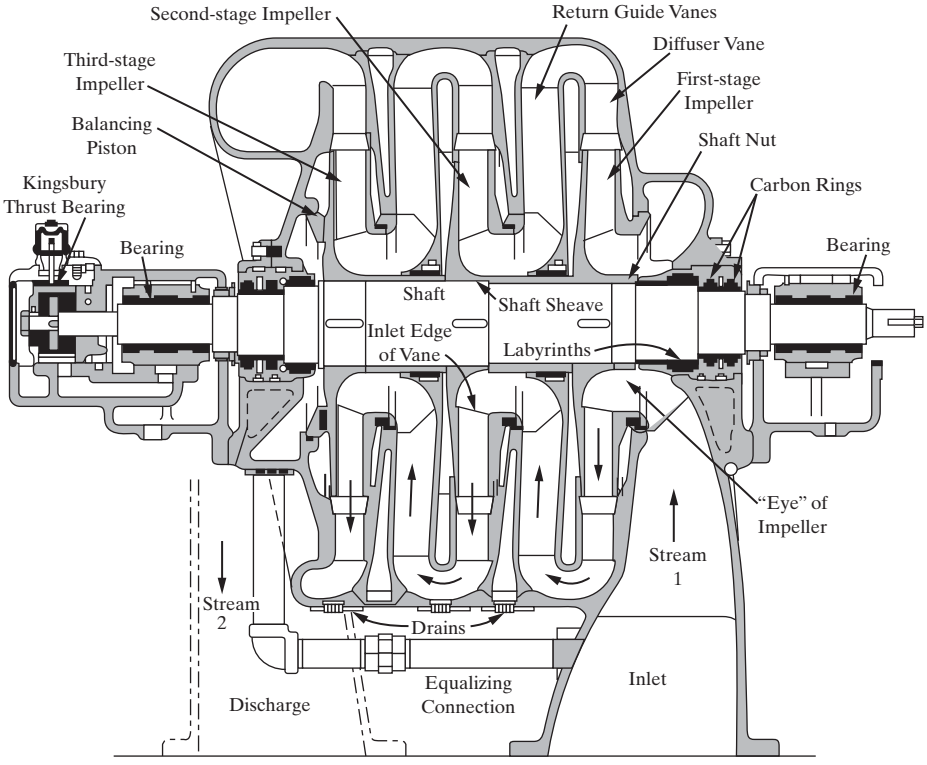

Figure 14.8 Cross section of a three-stage centrifugal compressor.

in a single stage are limited to a discharge temperature of 400°F. This corresponds to compression ratios about 2.5–6 as the specific heat ratio of the gas decreases from 1.67 (monatomic gas) to 1.30 (methane). Compression ratios of even 8 are possible with high molecular-weight gases. If higher compression ratios are needed, a multistage reciprocating compressor is used with intercooling, usually by water. See, for example, the video of a two-stage reciprocating compressor with an intercooler on the multimedia modules that accompany this book (ASPEN → Pumps, Compressors & Expanders → Compressors & Expanders and HYSYS → Pumps, Compressors & Expanders → Compressors & Expanders). Reciprocating compressors must be protected by knock-out drums to prevent the entry of liquid.

A lobed blower shown in Figure 14.9 is similar to a gear pump. Both two- and three-lobe units are common. They are limited to low capacity and low heads because shaft deflection must be kept small to maintain clearance between the rotating lobes and the casing. If higher compression ratios are required, multiple stages can be used. A screw compressor as shown in Figure 14.10 with two screws, male and female, that rotate at speeds typical of centrifugal pumps can operate at higher capacities to give higher compression ratios that may be limited by temperature. If so, higher compression ratios can be achieved with multiple stages separated by intercoolers. Screw compressors can run dry or can be flooded with oil.

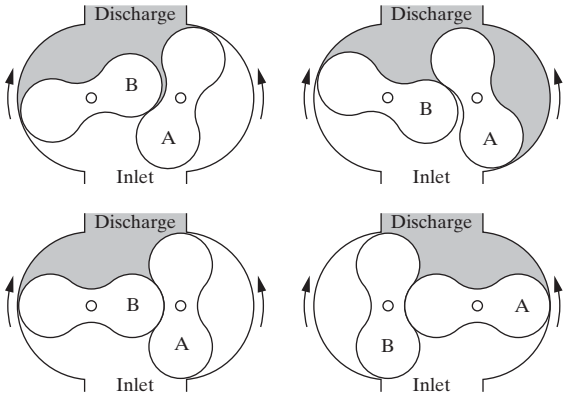

Figure 14.9 Lobed blower.

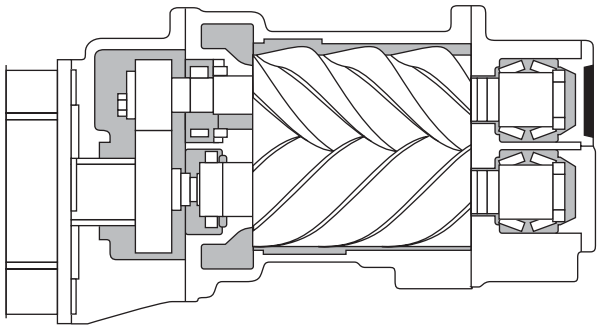

Figure 14.10 Screw compressor.

Expanders

Expanders (also called turboexpanders and expansion turbines) are often used in place of valves to recover power from a gas when its pressure must be decreased. At the same time, the temperature of the gas is reduced, and often the chilling of the gas is more important than the power recovery. Most common is the radial-flow turbine as shown in Figure 14.11, which resembles a centrifugal pump and can handle inlet pressures to 3,000 psi and temperatures to 1,000°F. With an impeller tip speed of 1,000 ft/s,

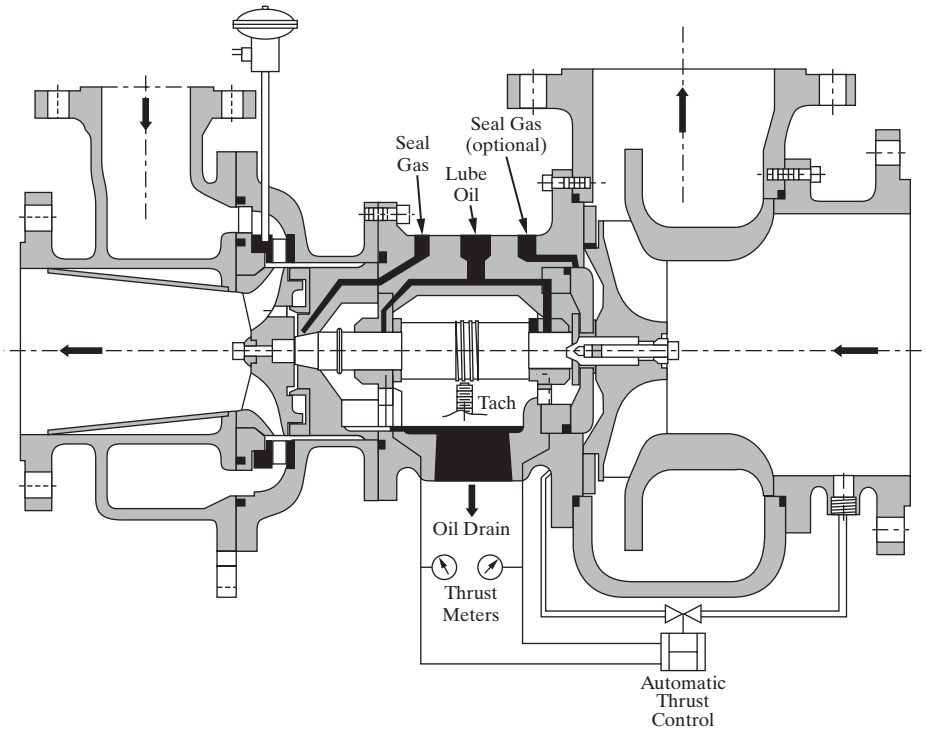

Figure 14.11 Radial-flow turbine.

a single stage of expansion can reduce the enthalpy of the gas by as much as 50 Btu/lb (116 kJ/kg). When calculations show that condensation may occur during the expansion, the expander must be designed to avoid erosion of the impeller. Expanders are widely used at cryogenic conditions. Although power can also be recovered by decreasing the pressure of a liquid with a turbine, it is usually not economical to do so.

Compressor and Expander Models in Simulators

Either of two methods can be used to take into account efficiency when calculating power requirements for compressors whether they are centrifugal, reciprocating, or screw. One method is the polytropic method based on the expression, PV^n = constant during compression, where V is the gas volume and n is the polytropic coefficient, which lies between 1 and the specific heat ratio.

Since the advent of simulation programs that routinely calculate entropy, the second method, called the isentropic method, has become preferred because it has a sound theoretical basis. The theoretical horsepower delivered to the gas is computed for a reversible, adiabatic (isentropic) compression from inlet 1 to outlet 2. The entropy balance in terms of the molar entropy, s, is

$$s\{T_1, P_1\} = s\{T_{2,\text{isentropic}}, P_2\} \tag{14.7}$$

Since T_1, P_1, and P_2 are known, Eq. (14.7) is solved iteratively for $T_{2,\text{isentropic}}$. With T_2 known, the exit enthalpy can be computed. Then the first law of thermodynamics for an adiabatic compression of molar gas flow, F, assuming no change in potential or kinetic energy of the gas and written in terms of molar enthalpy, h, can be applied to calculate the theoretical or isentropic power:

$$\dot{W}_{\text{isentropic}} = F(h_{2,\text{isentropic}} - h_1) \tag{14.8}$$

The excess power required, because of inefficiency of the compressor, is the difference between the brake power, $\dot{W}_{\text{brake}}$, and the isentropic power, $\dot{W}_{\text{isentropic}}$. These two powers define an isentropic efficiency, with the assumption that the excess power increases the enthalpy to an actual value, h_2:

$$\eta_s = \frac{\dot{W}_{\text{isentropic}}}{\dot{W}_{\text{brake}}} = \frac{h_{2,\text{isentropic}} - h_1}{h_2 - h_1} \tag{14.9}$$

The actual temperature of the discharged compressed gas, T_2, is then computed iteratively from the actual enthalpy, h_2. The actual temperature T_2 can be significantly higher than the isentropic temperature, $T_{2,\text{isentropic}}$.

The isentropic method is also applied to an expander. Eq. (14.7) is used for calculating the isentropic exit temperature but taking into account possible condensation of the gas. Like the exit pressure, the exit temperature will be less than the inlet value. Then, the exit isentropic enthalpy is computed, from which Eq. (14.8) is used to calculate the power recovered, which will be a negative value. The effect of the expander efficiency is just the opposite of the compressor efficiency, as indicated by a revision of Eq. (14.9) for applicability to expanders:

$$\eta_s = \frac{\dot{W}_{\text{brake}}}{\dot{W}_{\text{isentropic}}} = \frac{h_1 - h_2}{h_1 - h_{2,\text{isentropic}}} \tag{14.10}$$

Because of inefficiency, the brake horsepower recovered is less than the isentropic horsepower and the exit temperature is higher than the isentropic exit temperature. Thus, inefficiency will reduce the tendency for condensation to occur.

EXAMPLE 14.2

A natural gas stream of 5,000 kmol/hr at 25°C and 1,500 kPa contains 90% methane, 7% ethane, and 3% propane. Currently, this gas is expanded adiabatically across a valve to 300 kPa. Use a process simulator to determine the exit temperature and recovered power if the valve is replaced with:

1. An isentropic expansion turbine
2. An expansion turbine with an isentropic efficiency of 75%

SOLUTION

Using the SRK equation of state for thermodynamic properties, the following results are obtained.

	Valve	Isentropic Expander	Expander
Isentropic efficiency, η_s	—	1.00	0.75
Exit temperature, °C	18.5	−69.7	−47.1
Power recovered, kW	0	4,480	3,360
Power recovered, BHp	0	6,010	4,510

The results show that not only does the expander recover a significant amount of power, but it is also very effective in reducing the temperature compared to the valve. However, the actual exit temperature is almost 20°C higher than the isentropic value. In all cases, no condensation is found to occur since the dew point of the exit gas at 300 kPa is computed to be −83.2°C.

14.3 SUMMARY

After studying this chapter and the materials on pumps, compressors, and turbines on the multimedia modules that accompany this book, the reader should:

1. Be able to explain how the more common types of pumps, compressors, and expanders work.
2. Understand the types of calculations made by a simulator for pumps, compressors, and expanders.

REFERENCES

1. Green, D. W., and R. H. Perry (eds.), *Perry's Chemical Engineers' Handbook*, 8th ed., McGraw-Hill, New York (2008).

2. Sandler, H. J., and E. T. Luckiewicz, *Practical Process Engineering*, McGraw-Hill, New York (1987).

EXERCISES

14.1 Liquid oxygen is stored in a tank at −298°F and 35 psia. It is to be pumped at 100 lb/s to a pressure of 300 psia. The liquid oxygen level in the tank is 10 ft above the pump, and friction and acceleration losses from the tank to the pump suction are negligible. If the pump efficiency is 80%, calculate the BHp, the oxygen discharge temperature, and the available NPSH using a simulator to make the calculations.

14.2 Use a simulator to design a compression system with intercoolers to compress 600 lb/hr of a mixture of 95 mol% hydrogen and 5 mol% methane at 75°F and 20 psia to a pressure of 600 psia if the maximum exit temperature from a compressor stage is 400°F and compressor efficiency is 80%. Assume gas outlet temperatures from the intercoolers at 120°F. For each compressor stage, compute the BHp. For each intercooler, compute the heat duty in Btu/hr.

14.3 Superheated steam available at 800 psia and 600°F is to be expanded to a pressure of 150 psia at the rate of 100,000 lb/hr. Calculate with a simulator the exit temperature, phase condition, and Hp recovered for an:

(a) Adiabatic valve

(b) Isentropic expansion turbine

(c) Expansion turbine with an isentropic efficiency of 75%

14.4 Propane gas at 300 psia and 150°F is sent to an expansion turbine with an efficiency of 80%. What is the lowest outlet pressure that can be achieved without condensing any of the propane?

Chapter 15

Chemical Reactor Design

15.0 OBJECTIVES

In Chapter 8, Synthesis of Networks Containing Reactors, emphasis is placed on the synthesis of chemical reactor networks involving continuous stirred-tank and tubular reactors. During process synthesis and simulation, in the early stages of process design, it is common to focus on reaction rates and heat transfer, while assuming perfect mixing in stirred-tank reactors, and plug flow and perfect radial mixing in tubular reactors, as taught in apparently all chemical reactor design textbooks (e.g., Fogler, 2011; Levenspiel, 1999; Rawlings and Ekerdt, 2002; Hill, 1977). To review this approach, in Section 8.2, these assumptions were applied to create CSTR (continuous stirred-tank reactor) and PFR (plug-flow tubular reactor) models in Examples 8.1 and 8.2. Two additional approaches are often introduced to account for intermediate backmixing. These involve partial recycle about tubular reactor models that assume plug flow and perfect radial mixing and the decomposition of a tubular reactor into several perfectly mixed, stirred tanks in series. However, these approaches do not accurately account for momentum, heat, and mass transfer.

In this chapter, after examining the limitations of the plug flow and perfect radial mixing assumptions in tubular reactors, the effects of fully developed laminar flow and radial mass transfer are considered. Together, these lead to partial differential equations that require finite-element approximations to solve in computational fluid dynamic (CFD) codes, such as COMSOL (COMSOL, 2014) and FLUENT (ANSYS, 2014). After these are introduced, complex mixing patterns in tubular reactors are modeled and solved using CFD codes. Finally, several kinds of stirred-tank reactor models are considered.

After studying this chapter, the reader should:

1. Be able to use COMSOL to create and solve numerically isothermal tubular reactor models involving momentum and mass balances—and, in so doing, show how reaction conversion increases as the reactants are better mixed—reaching a maximum when plug flow and perfect radial mixing are assumed.
2. Understand how secondary circulating flows lead to better mixing and higher conversions in coiled tubular reactors.
3. Be able to use COMSOL to create and solve numerically nonisothermal tubular reactor models involving momentum, heat, and mass balances—when heats of reaction are significant.
4. Understand how the COMSOL Mixing Module models the degrees of mixing in stirred-tank reactors approaching the assumption of total backmixing as the fluid residence times distribute uniformly.

A key objective is to show readers that often there is a need to put aside the classical PFR and CSTR assumptions when designing chemical reactors. As shown, the assumption of perfect mixing often leads to large errors in reaction conversions. For this reason, interfaces are being created to permit the use of CFD packages within process simulators, for example, for use of FLUENT within ASPEN PLUS (Zitney, 2002).

COMSOL displays profiles of velocity, temperature, and species compositions in a spectrum of colors ranging from dark purple (black) through yellow, green, and blue, to dark red. All figures in this textbook are printed in just one color—black-and-white, grey-scale. Please obtain the original color figures from the Color Figures folder on the Wiley website for this book. Also, a file, Chapter 15.pdf, that includes the color figures can be downloaded from the PDF Files folder on the website.

15.1 INTRODUCTION

To show the need for computational fluid dynamics (CFD) packages, this chapter begins the discussion with Section 15.2 on PFR Models for Tubular Reactors. Two limiting cases in which CFD is not needed are illustrated, one assuming plug flow and the other assuming fully developed laminar flow without molecular diffusion. Then, Section 15.3 introduces the COMSOL CFD package, and Section 15.4 shows how to use COMSOL to create and solve more rigorous tubular reactor models, which are needed to model mixing effects. Sections 15.2–15.4 involve isothermal tubular reactors, and Section 15.5 considers the effects of heats of reaction in nonisothermal tubular reactors. Finally, in Section 15.6, methods for modeling mixing in agitated stirred-tank reactors are introduced.

15.2 LIMITING APPROXIMATE MODELS FOR TUBULAR REACTORS

In this section, the first of two limiting models, in Example 15.1, is a PFR model assuming plug flow and perfect radial mixing of species. This significantly overestimates reaction conversion and,

thus, significantly underestimates the reactor length required to achieve a specified conversion. The second, in Example 15.2, assumes fully developed laminar flow without molecular diffusion, underestimating reaction conversion and overestimating reactor length to achieve a specified conversion.

EXAMPLE 15.1 ***PFR Model***

For the liquid-phase saponification of ethyl acetate by sodium hydroxide in an aqueous solution to produce ethyl alcohol and sodium acetate:

$$\text{EtAc} + \text{NaOH} \rightarrow \text{EtOH} + \text{NaAc}$$

determines the reaction conversion in a straight tube assuming plug flow and perfect radial mixing of species and isothermal operation.

A schematic of the tubular reactor is shown in Figure 15.1. The conditions are as follows:

Feed at 0.05 mol/L of sodium hydroxide and 0.05 mol/L of ethyl acetate.

Tube radius at 2 cm (0.7874 in).

Temperature is 30°C.

Density of the reacting fluid (assumed to be pure water) is 996 kg/m^3 and viscosity of the reacting fluid is 0.000798 Pa-s at 30°C.

Inlet volumetric flow rate of solution at 2 L/min (assumed to remain constant).

Second-order irreversible reaction (first-order in each reactant) with rate constant, k = 8.9 L/mol-min at 30°C.

Note that these specifications are comparable to those of Seader and Southwick (1982). For a reactor volume of 1,977 cm^3 (length of 157.3 cm), compute the conversion.

SOLUTION

The saponification reaction has the form:

$$\text{A} + \text{B} \rightarrow \text{C} + \text{D}$$

The reaction is second order and irreversible at 30°C. Using the plug-flow assumption, the radial velocity and diffusivity are zero, and the axial velocity is constant in the radial and axial directions. The intrinsic rate of consumption of reactant A (ethyl acetate) is:

$$r_A = u_{mean}\left(-\frac{dc_A}{dZ}\right) = kc_Ac_B \tag{15.1}$$

and for reactant B (sodium hydroxide) is:

$$r_B = u_{mean}\left(-\frac{dc_B}{dZ}\right) = kc_Ac_B \tag{15.2}$$

where Z is the axial coordinate, k is the reaction-rate constant, and c_A and c_B are the concentrations of A and B. The inlet concentrations and intrinsic rates of consumption of both reactants are equal. Consequently, throughout the reactor:

$$c_A = c_B,\ r = r_A = r_B \tag{15.3}$$

and

$$r = u_{mean}\left(-\frac{dc_A}{dZ}\right) = u_{mean}\left(-\frac{dc_B}{dZ}\right) = kc_A^2 \tag{15.4}$$

Only reactant A will be considered in the calculations that follow. The fractional conversion of reactants A and B, X, is:

$$X = 1 - \frac{c_A}{c_{A0}} \tag{15.5}$$

where c_{A0} is the inlet concentration of reactant A. Substituting Eq. (15.5) into (15.4):

$$r = u_{mean}\left(\frac{dX}{dZ}\right) = kc_{A0}(1-X)^2 \tag{15.6}$$

Integrating from $Z = 0$ to L:

$$X_{PFR} = \frac{1}{\left(1 + \frac{u_{mean}}{kc_{A0}L}\right)} \tag{15.7}$$

where $L = 157.3$ cm is the tube length. For a similar derivation, see Churchill (2005). Substituting the specifications,

$$U_{mean} = \frac{V}{A_c} = \frac{2\frac{\text{L}}{\text{min}}}{\pi \times 2\ \text{cm}^2} \times \frac{1{,}000\ \text{cm}^3}{1\ \text{L}} = 159.15\frac{\text{cm}}{\text{min}}$$

$$X_{PFR} = \frac{1}{1 + \frac{159.15\frac{\text{cm}}{\text{min}}}{8.9\frac{\text{L}}{\text{mol} \times \text{min}} \times 0.05\frac{\text{mol}}{\text{L}} \times 157.3\ \text{cm}}} \times 100 = 30.55\%$$

Next, consider Hagen-Pousiulle flow, that is, fully developed laminar flow.

EXAMPLE 15.2 ***Laminar Flow (Example 15.1 Revisited)***

In this example, the feed liquid is assumed to be in fully developed laminar flow. First, compute the Reynolds number to check this assumption. Next, determine the radial velocity profile. Then, determine the conversion in the reactor.

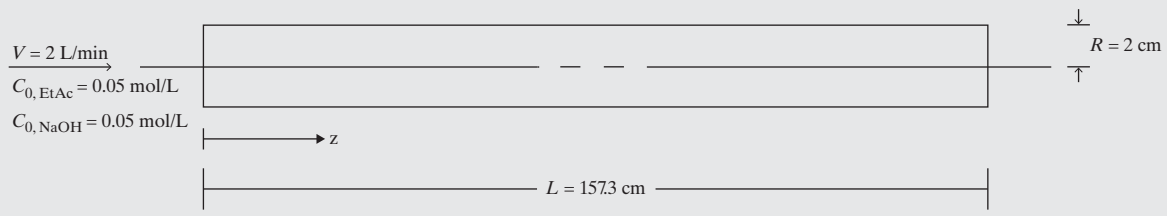

Figure 15.1 Schematic of straight-tube reactor.

SOLUTION

The Reynolds number is:

$$Re = \frac{\rho\, u_{\text{mean}}\, D}{\mu} = \frac{996\frac{\text{kg}}{\text{m}^3} \times 0.0265\frac{\text{m}}{\text{s}} \times 0.04\ \text{m}}{0.000798\frac{\text{kg}}{\text{m} \times \text{s}}} = 1{,}323 < 2{,}300$$

Analytical solutions can also be found for laminar flow in a straight tube *with no radial mixing* (i.e., negligible diffusion). This idealized reactor is referred to as laminar with zero diffusion ($D = 0\ \text{m}^2/\text{s}$) (i.e., LD0). The variation of the axial velocity, u, is given by the well-known parabolic profile; zero velocity at the tube wall, R_t; and $2u_{\text{mean}}$ at the centerline, $R = 0$:

$$\frac{u\{R\}}{u_{\text{mean}}} = 2\left(1 - \left(\frac{R}{R_{\text{t}}}\right)^2\right) \tag{15.8}$$

where R is the radial coordinate. As in the PFR model, $c_{\text{A}} = c_{\text{B}}$, but Eq. (15.6) becomes:

$$r\{R\} = 2u_{\text{mean}}\left(1 - \left(\frac{R}{R_{\text{t}}}\right)^2\right)\left(\frac{\partial X\{R\}}{\partial Z}\right) = kc_{\text{A0}}(1 - X\{R\})^2 \tag{15.9}$$

which is a partial-differential equation in coordinates Z and R. Integrating with respect to Z:

$$X_{\text{LD0}}\{R\} = \frac{1}{\left(1 + \dfrac{2u_{\text{mean}}\left(1 - \left(\dfrac{R}{R_{\text{t}}}\right)^2\right)}{kc_{\text{A0}}L}\right)} \tag{15.10}$$

The mixed-mean conversion is:

$$\overline{X}_{\text{LD0}} = 2\pi\int_0^{R_{\text{t}}} X_{\text{LD0}}\{R\}\, u\{R\}\, RdR \tag{15.11}$$

Substituting Eqs. (15.8) and (15.10) gives:

$$\overline{X}_{\text{LD0}} = 2\varphi\left(1 - \varphi\ln\left(1 + \frac{1}{\varphi}\right)\right) \tag{15.12}$$

where

$$\varphi = \frac{kc_{\text{A0}}L}{2u_{\text{mean}}}$$

See also Churchill (2005). Substituting the specifications:

$$\varphi = \frac{kc_{\text{A0}}L}{2u_{\text{mean}}} = \frac{8.9\frac{\text{L}}{\text{mol} - \text{min}} \times 0.05\frac{\text{mol}}{\text{L}} \times 157.3\ \text{cm}}{2 \times 159.15\frac{\text{cm}}{\text{min}}} = 0.2199$$

$$\overline{X}_{\text{LD0}} = 2(0.2199)\left(1 - 0.2199\ln\left(1 + \frac{1}{0.2199}\right)\right)100 = 27.41\%$$

As expected, this conversion is less than that assuming plug flow −9% less.

15.3 THE COMSOL CFD PACKAGE

CFD packages, like COMSOL (COMSOL 2014), are needed to show the impact of momentum, heat, and mass transfer on the degree of mixing of chemical reactants as it affects the reaction conversion.

As an introduction to COMSOL, this section takes the inexperienced user through a procedure to solve the Navier-Stokes equations in a tubular reactor to determine the velocity profile for laminar flow [i.e., Eq. (15.8)]. This velocity profile is used later in Example 15.3. Note: This description and all COMSOL solutions in this text use Version 4.4. Also, due to space limitations, all screenshots cannot be shown. To follow the detailed steps, it is recommended that readers use COMSOL to implement the step-by-step instructions.

Start by opening the COMSOL Multiphysics package. This opens the *Model Wizard*. Select the option for 2D axisymmetric geometry and click *Add Geometry* in the top right corner of the *Model Wizard* to initialize the model. The 2D axisymmetric setting allows the user to create geometries and system conditions in two dimensions to be symmetrically rotated about an axis. This option is appropriate for tubes, pipes, and other geometries that are axisymmetric. Later in this chapter, the 3D model is explored as well. Once selected, many new functions become available in the *Model Builder* on the left side of the screen. These tabs are used to set up the model with boundary conditions and initial parameters.

First, the parameters used throughout the model are defined in the *Global Definitions* tab. This is done by right-clicking on the *Global Definitions* heading and selecting the *Parameters* option. In the newly created *Parameters* tab, the global constants are entered as shown in Figure 15.2. This defines variables to be used throughout the simulation. For example, typing *dens* into any COMSOL prompt returns the value of the parameter *dens*, $996\ \text{kg}/\text{m}^3$.

Once these specifications are input into COMSOL, the geometry must be created. This process is carried out similarly to the parameter definition. Right-click on the *Geometry* tab and select the *Rectangle* geometry. This creates and selects the *Rectangle1* tab in the *Model Builder*. Enter the parameters for the tubular reactor into the dialogue boxes as shown in Figure 15.3. Recall that the model is axisymmetric, so the width should be the tube radius, Rt, and the height (length) should be 1.573 m. Center the rectangle at the origin and click the *Build All* option at the top of the *Rectangle1* tab. This creates the specified geometries in the model. The user should experiment with creating different geometries in 2D and 3D modes to gain familiarity with the user interface.

After the parameters and specified geometries are entered, different *physics* options can be added to define the momentum, heat, and species transport balances. The *physics* packages are the main functional components in COMSOL. These packages create the various balances and equations to be solved. Next, in this section, the laminar flow physics is introduced to create the momentum balances, and later in the chapter, the chemical

Name	Expression	Value	Description
Rt	2[cm]	0.020000 m	Tube Radius
dens	996[kg/m^3]	996.00 kg/m^3	Density
visc	0.000798[Pa*s]	7.9800E-4 Pa·s	Dynamic Viscosity
flow	2[L/min]	3.3333E-5 m…	Flow Rate
Umean	flow/(pi*Rt^2)	0.026526 m/s	Avg. Velocity
c0	0.05[mol/L]	50.000 mol/…	Initial Reactant Conc.
D	1.2*10^-5[cm^…	1.2000E-9 m…	Diffusivity
k	8.9[L/mol/min]	1.4833E-4 m…	Reaction Rate Constant

Figure 15.2 Parameters for the tubular reactor.

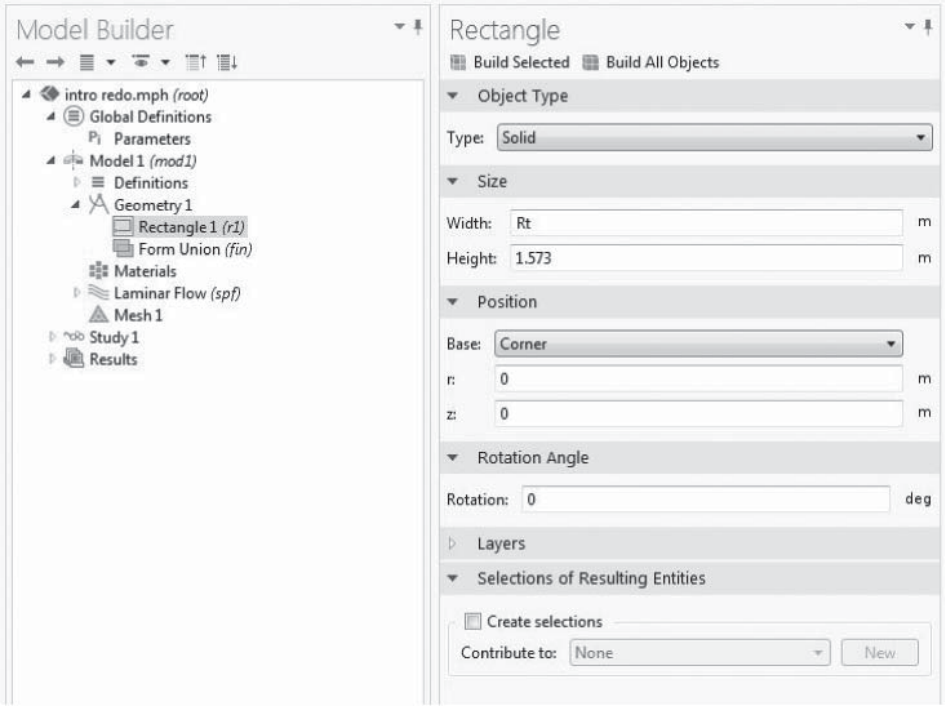

Figure 15.3 Model builder interface. (*Source:* Image made using the COMSOL Multiphysics software and is provided courtesy of COMSOL).

transport and heat-transfer physics are used to create the heat and species transport balances. Note that similar steps are followed to set up and specify all of the physics packages.

Physics options are added by right-clicking on the *Model1* tab and selecting the option *Add Physics*. This opens a menu with all the physics packages available in COMSOL. To add the momentum balances for laminar flow to the model, expand the *Fluid Flow* tab followed by the *Single-Phase Flow* tab. Then select the *Laminar Flow* option and click *Add to Selection* in the top right corner of the *Model Wizard* as shown in Figure 15.4. The newly created *Laminar Flow* tab can then be filled in with the proper initial and boundary conditions for the system. Notice that the rectangle created previously is automatically selected as the domain in which laminar physics applies. The domains in the model to which the physics are applied can be changed by using the plus and minus buttons to select or deselect domains, respectively. In this case, the appropriate domain is already selected.

The variables and assumptions for the laminar flow physics and the boundary conditions must now be specified. Under the *Laminar Flow* (*spf*) tab, select the *incompressible* option in the *Compressibility* menu. Under the *Equations* tab, COMSOL shows the momentum balance, Eq. (15.13), and continuity balance, Eq. (15.14), to be solved to compute the laminar velocity profile:

$$\rho(\boldsymbol{u}\cdot\nabla)\boldsymbol{u} = \nabla\cdot[-p\boldsymbol{I} + \mu(\nabla\boldsymbol{u} + (\nabla\boldsymbol{u})^T] + \boldsymbol{F} \tag{15.13}$$

$$\rho\nabla\cdot\boldsymbol{u} = 0 \tag{15.14}$$

where $\boldsymbol{u}$ represents the velocity vector, p is the pressure, $\boldsymbol{F}$ is an applied force vector (zero in this example), $\boldsymbol{I}$ is the identity matrix, T is the transpose of the gradient vector, and "inverted delta" is the gradient vector.

Then, select the *Fluid Properties* tab and select the *user defined* option for density and viscosity and enter the parameters *dens* and *visc*, respectively. The centerline at $r = 0$ (COMSOL uses r as the radial coordinate and z as the axial coordinate) is automatically selected as the sole axial symmetry boundary, and the rest of the edges of the created rectangle are automatically selected as walls (to be modified for the inlet and outlet below). Select the *Wall*

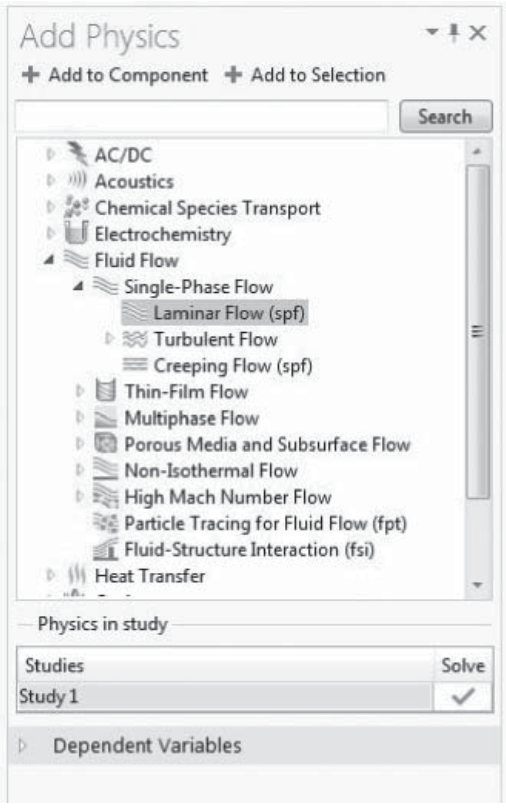

Figure 15.4 Selecting the *physics* options. (*Source:* Image made using the COMSOL Multiphysics software and is provided courtesy of COMSOL).

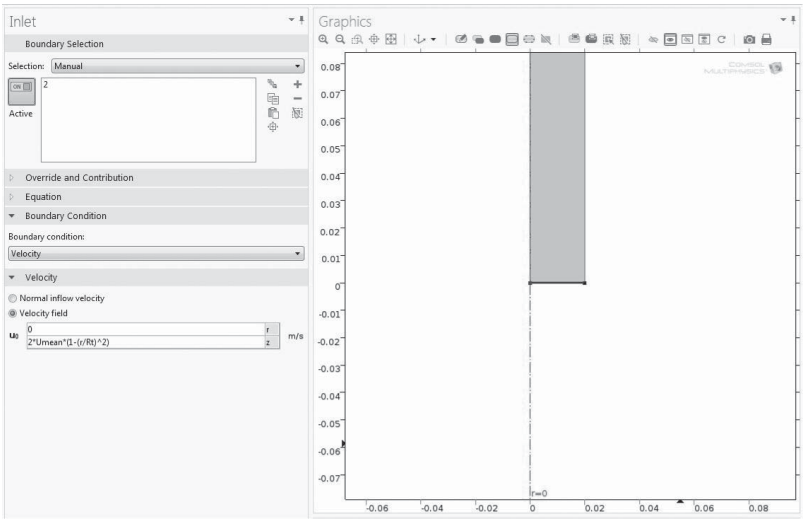

Figure 15.5 Selecting boundary conditions. (*Source:* Image made using the COMSOL Multiphysics software and is provided courtesy of COMSOL).

tab to view the different options for the wall boundary condition. The appropriate boundary condition for the tube wall is the *no slip* (zero velocity) option.

Now, boundary conditions for the inflow and the outflow of the tube must be created. This is done by right-clicking on the *Laminar Flow* (*spf*) tab and selecting the inlet and outlet options, respectively. Once these tabs are created, the parameters and conditions for the entrance and exit are entered. The parameters and entrance dialogues are shown in Figure 15.5.

After selecting the *Inlet* tab, set the boundary condition to *velocity* and select the *velocity field* option. This allows the user to specify the radial and axial velocities at the inlet. For this example, the radial velocity, denoted by *r*, is left at 0, and the axial velocity, denoted by *z*, is set to a laminar profile, 2*Umean*(1 − (r/Rt)^2). Finally, this boundary condition is applied to the bottom edge (2) of the created rectangle by selecting that edge and clicking the plus button in the *Boundary Selection* area. This sets the velocity vector entering the tube to a parabolic laminar profile. Next, the outlet conditions are specified. For this example, the appropriate condition is *pressure*, *no viscous stress*, and the pressure is set to 1 [atm]. The top of the rectangle (edge 3) is then selected for the outlet boundary condition. This sets the boundary at the exit of the reactor to have no viscous stress at the indicated pressure. Notice that once these conditions are selected under the *Wall* boundary tab, (*overridden*) appears next to the boundaries numbered 2 and 3 at the bottom and top of the rectangle. The equations used for the boundary conditions can be viewed in the same way that the equation for the momentum balance was viewed. That is, under each boundary condition tab there is an *Equations* tab that shows the equations COMSOL will use for the boundaries. The boundary equations are shown in Table 15.1. Here, $\mathbf{u_0}$ represents the specified velocity vector at the inlet.

The initial values are then specified under the *Initial Values* tab. There is a place to enter the initial velocity field and the initial pressure in this tab. In this example, the initial velocity field is left at zero and the initial pressure is set at 1 [atm]. This gives COMSOL an initial guess of the zero velocity throughout the reactor, allowing it to solve for the laminar velocity profile throughout the reactor. Now the model is fully specified and ready to be solved.

Table 15.1 Boundary Conditions

Boundary Condition	Boundary Selection	Equation
Wall	4	$\boldsymbol{u} = \mathbf{0}$
Inlet	2	$\boldsymbol{u} = \boldsymbol{u_0}$
Outlet	3	$p = p_{0,}\ [\mu(\nabla \boldsymbol{u} + (\nabla \boldsymbol{u})^T]n = \mathbf{0}$

Before solving, a mesh must be specified. To specify a mesh, select the *Mesh* tab. COMSOL has the option of using a physics-controlled mesh. This option is generally the best choice if it is possible to use since it tailors the mesh to the selected *physics*. Select the *normal* option for the mesh and select the *Build All* option to build the mesh. It may take COMSOL a minute to prepare the mesh. The mesh should look similar to the one in Figure 15.6. Notice that this mesh is tailored to laminar flow physics with a higher concentration of mesh points near

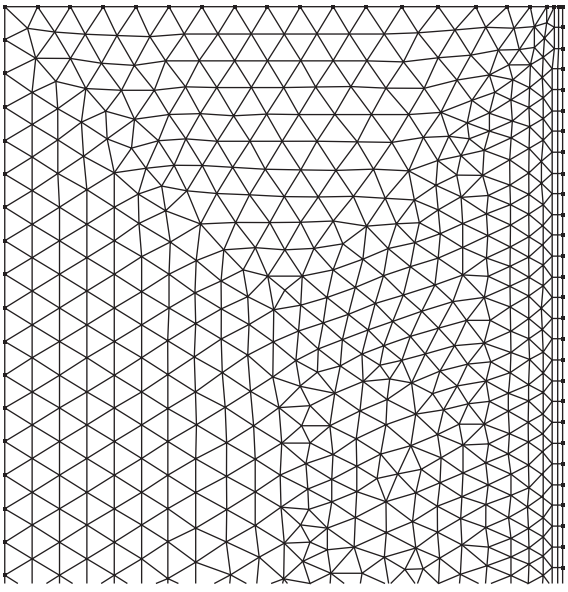

Figure 15.6 Typical *normal* mesh.

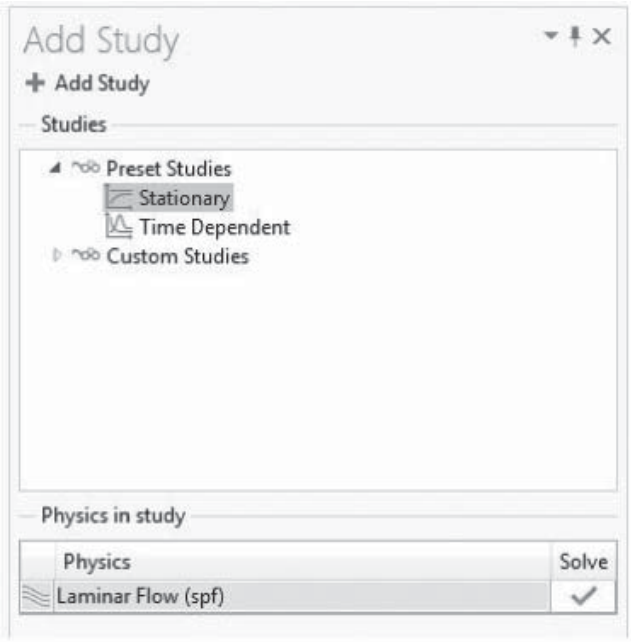

Figure 15.7 Selecting study type. (*Source:* Image made using the COMSOL Multiphysics software and is provided courtesy of COMSOL).

the wall and in the entrance and exit regions. Once the mesh is specified, COMSOL is ready to solve the partial differential equations using a finite-element method.

To solve the simulation (PDEs), a study must be created. To create a study, right-click on the top tab in the *Model Builder* with the file name on it. Select the *Add Study* option. Once this option is selected, a menu automatically opens. Select the *Stationary* option since this example is solved at steady state, and click *Add Study* to create the study as shown in Figure 15.7. Once created, a new tab entitled *Study1* is created. Select the newly created tab and select the *compute* option. This will execute the simulation (i.e., solve the PDEs). COMSOL automatically displays the velocity and pressure results. The former is the laminar flow profile in Figure 15.8. Notice that the aspect ratio is changed in the figure to display the results more clearly. Also, the ordinate and abscissa are Axial Distance [m] and Radial Distance [m].

Different views and plots can be created by right-clicking the *Results* tab and adding other plot groups. Once a plot group is created, a different plot can be added by right-clicking the plot group and selecting different plot types. Try plotting different results such as streamlines or contour maps to become more familiar with plotting results. One-dimensional plot groups such as the velocity at different axial distances can also be created.

There are many different *physics* options and boundary conditions to choose from in COMSOL. The user should experiment with other conditions to become more familiar with the package and setting up simulations. When a simulation gives the error message *maximum number of Newton iterations reached*, the number of Newton iterations allowed should be increased using the study folder as shown in Figure 15.9. Initially, a maximum of 25 Newton iterations is specified; however, as more complex physics are added to the model, this specification should be increased to allow COMSOL more iterations to solve the system.

15.4 CFD FOR TUBULAR REACTOR MODELS

This section shows how to create various tubular reactor models and how to solve them using finite-element methods with the COMSOL CFD code.

Initially, we return to Example 15.2, in which fully developed laminar flow occurs, but molecular diffusion in the radial direction is ignored. To account for molecular diffusion, the mass balance for species A becomes a partial differential equation:

$$2u_{\text{mean}}\left(1-\left(\frac{R}{R_t}\right)^2\right)\left(\frac{\partial c_A}{\partial Z}\right) = D\left(\frac{\partial^2 c_A}{\partial R^2}+\frac{1}{R}\left(\frac{\partial c_A}{\partial R}\right)+\left(\frac{\partial^2 c_A}{\partial Z^2}\right)\right)-kc_A{}^2 \qquad (15.15)$$

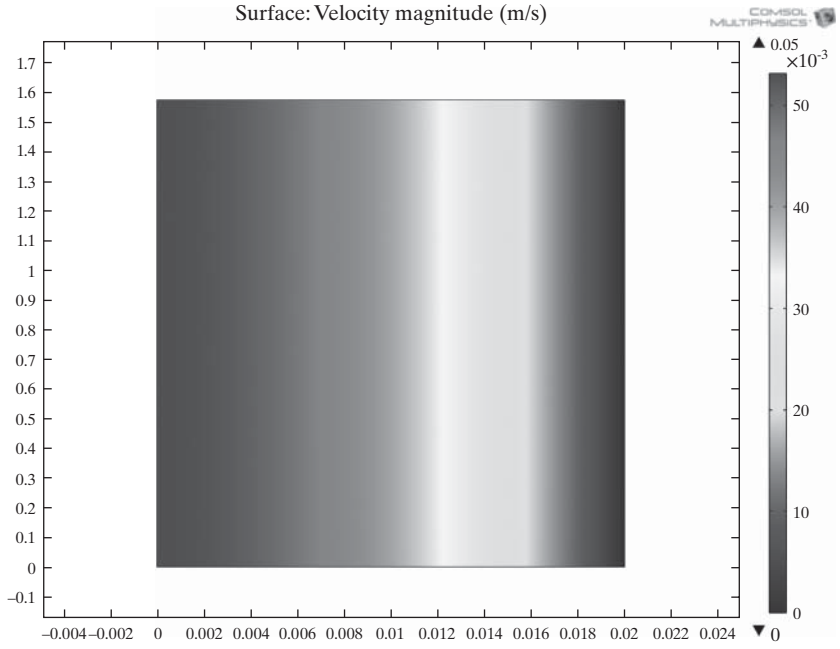

Figure 15.8 Computed axial-velocity profiles from centerline to tube wall (see the **Color Figure** folder on the Wiley Web site associated with this book).

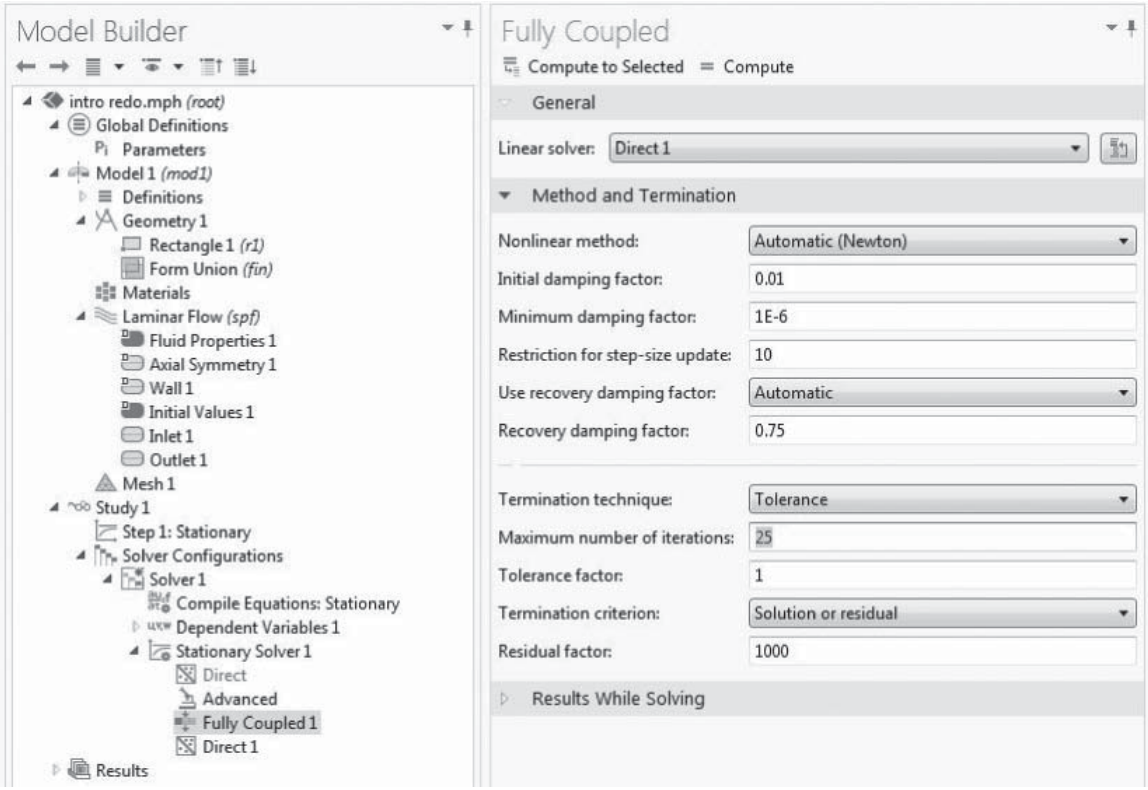

Figure 15.9 Specifying iteration parameters and error tolerances. (*Source:* Image made using the COMSOL Multiphysics software and is provided courtesy of COMSOL).

Here, the second-order term on the right-hand side accounts for molecular diffusion.

Next, Example 15.3 shows how to create and solve this model using COMSOL.

EXAMPLE 15.3 ***Laminar Flow with Diffusion (Examples 15.1 and 15.2 Revisited)***

In the straight-tube reactor with fully developed parabolic flow, the diffusivities of ethyl acetate and NaOH are $1.2 \times 10^{-5}\text{cm}^2/\text{s}$; that is $D = D_A = D_B$, and consequently, $c_A = c_B$. Because Eq. (15.15) does not have an analytical solution, use COMSOL to compute the fractional conversion.

SOLUTION

To solve this system with radial diffusion, a new COMSOL simulation must be created. The beginning stages of creating this simulation are similar to those described in Section 15.3. A 2D axisymmetric model is created, the parameters in Figure 15.2 are added to the global definitions, and a rectangle with the dimensions in Figure 15.3 is created as described in Section 15.3. For this simulation, the *Transport of Diluted Species* (*chds*) physics is added instead of the *Laminar Flow* (*spf*) physics, as shown in Figure 15.10.

A laminar flow profile is specified as a *user-defined velocity field* in this physics package, rather than independently solving for the velocity profile. This saves COMSOL computation time and complexity. Once the new physics tab is created, the boundary and initial conditions are entered.

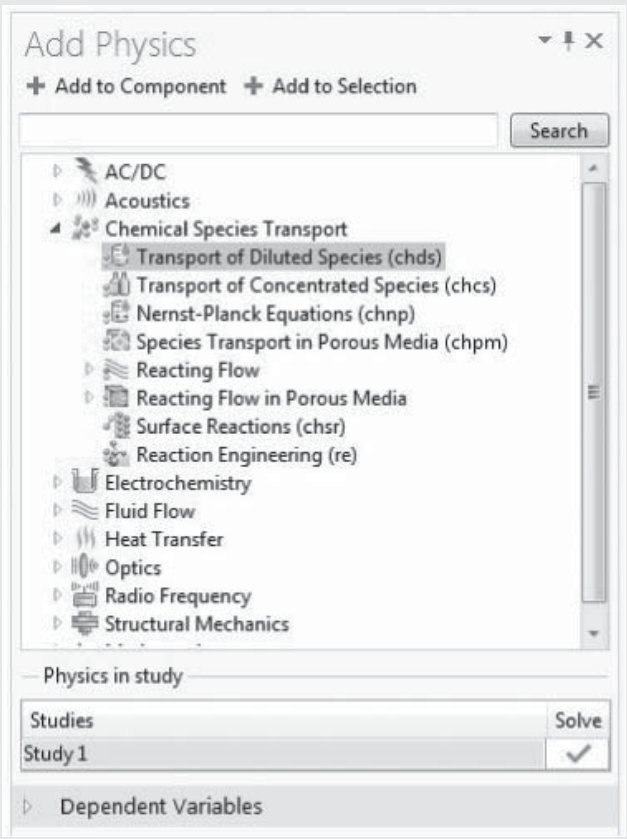

Figure 15.10 Transport of diluted species. (*Source:* Image made using the COMSOL Multiphysics software and is provided courtesy of COMSOL).

First, under the *Convection and Diffusion* tab, the velocity profile and the diffusivity are defined as shown in Figure 15.11. Laminar axial velocities are defined as a function of radius, 2*Umean*[1 − (r/Rt)^2], to be applied at all axial positions, and radial velocities are specified at zero. Also, the Temperature specification is inactive because the heat-balance physics has not been specified.

Next, the concentrations of A are set to the variable *c0* throughout the rectangle. Then, the *Inflow*, *Outflow*, and *Reactions* tabs are added in the same way that the *Inlet* and *Outlet* tabs were added to the laminar flow example in Figure 15.5 by right-clicking on the *Transport of Diluted Species* (*chds*) tab and selecting the appropriate options. In this case, the Inflow condition is set to the variable *c0* as well. The bottom edge of the rectangle is set as the inflow boundary, and the top of the rectangle is set as the outflow boundary. Finally, the reaction conditions are specified under the newly created *Reactions* tab. The reaction rate is set to −k*c^2, and the rectangle is selected as the domain in which the reaction is active, as shown in Figure 15.12.

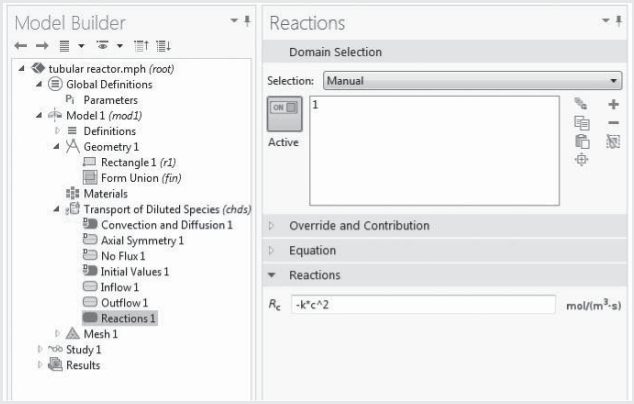

Figure 15.12 Reaction specifications. (*Source:* Image made using the COMSOL Multiphysics software and is provided courtesy of COMSOL).

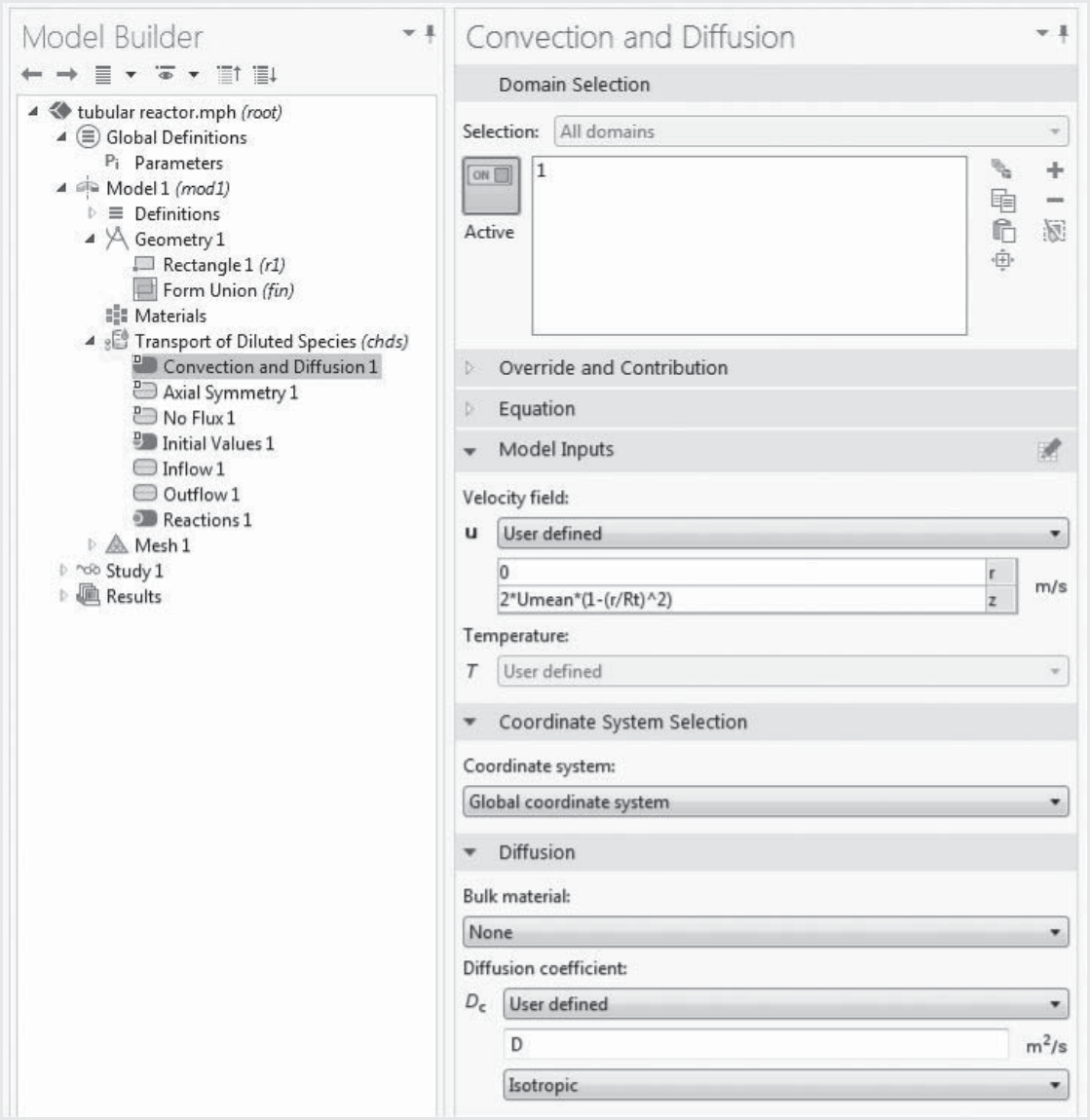

Figure 15.11 Convection and diffusion specifications. (*Source:* Image made using the COMSOL Multiphysics software and is provided courtesy of COMSOL).

Table 15.2 Species Transport Boundary Conditions

Boundary Condition	Bondary Selection	Equation
No flux	4	$-\boldsymbol{n}^*\boldsymbol{N}_i = 0$
Inflow	2	$c_i = c_{0,i}$
Outflow	3	$-\boldsymbol{n}^* D_i^* \nabla c_i = 0$

The equations for the concentration boundary conditions and the species mass balances can be viewed as described for the momentum balances in Section 15.3 (Table 15.1). That is, the equations can be viewed by simply expanding the *Equations* tab under the different headings for the boundaries. The boundary conditions are described by the set of equations given in Table 15.2. Note that at the tube outlet, the diffusive flux is set to zero (i.e., assuming that all species transport at the outlet is due to convection).

Next, a mesh must be specified. For this system, the physics-controlled meshes are not sufficiently accurate (because the momentum balances are not being solved). To solve the species balance accurately, a user-defined mesh is created as shown in Figure 15.13. This is accomplished by selecting the *user-defined* option under the *mesh* tab. Then, the *Size* tab is selected and the parameters shown in Figure 15.13 are entered. This creates a mesh with 78,684 elements. Once the mesh is created, a stationary study (at steady state) is created and the finite-element equations are solved.

The c_A solution is automatically plotted in the results tab, as shown in Figure 15.14. The ordinate and abscissa are Axial Distance [m] and Radial Distance [m]. Note that c_A is depleted near the wall, where the axial velocities are low, providing large residence times. Also, notice that the aspect ratio is changed in the figure to display the results more clearly.

The concentration plot at the exit of the reactor can be displayed by creating a new 1D plot group. This is accomplished by right clicking on *Results* and selecting the *1D Plot Group* option. Once the *1D Plot Group* is created, right-click on it and select the *Line Graph* option. The outlet boundary is then selected and the plot option is selected in the top left corner. This creates a 1D plot of $\boldsymbol{c}_A$ at the exit, as shown in Figure 15.15. Note that the concentration gradient at the wall approaches zero because the wall is impervious to species transfer.

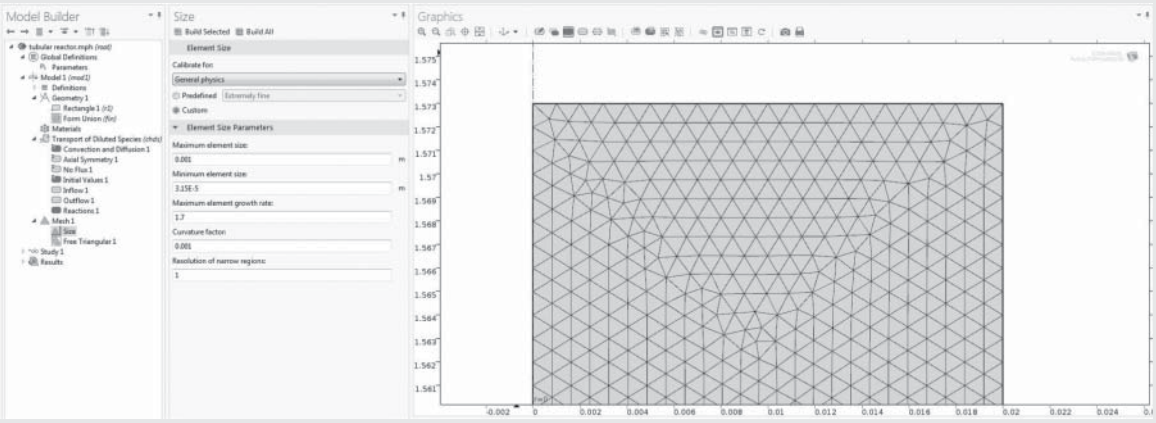

Figure 15.13 User-created mesh. (*Source:* Image made using the COMSOL Multiphysics software and is provided courtesy of COMSOL).

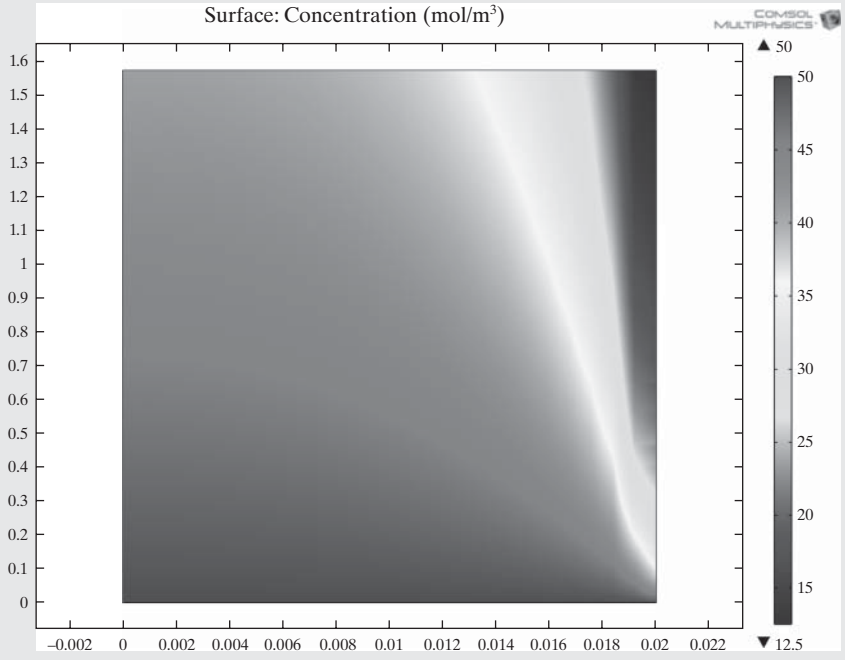

Figure 15.14 Reactant concentration results (see the **Color Figure** folder on the Wiley Web site associated with this book).

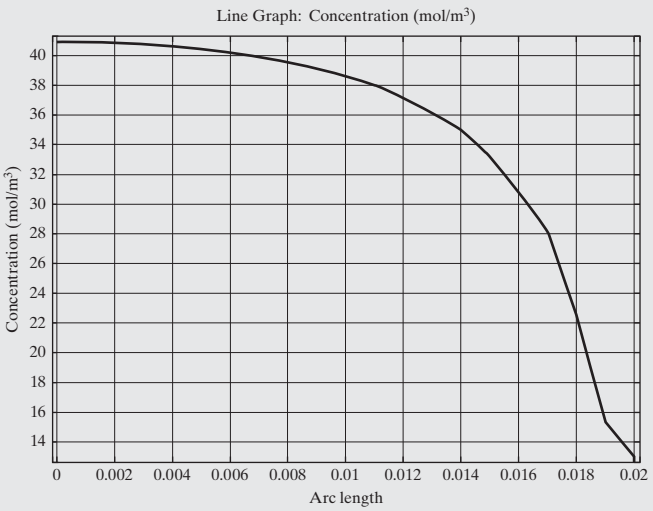

Figure 15.15 Radial c_A profile at the exit.

To compute the conversion of A, the total flow rate of reactant entering and leaving the reactor must be calculated. This is done by computing a surface integral of the variable *chds.ntflux_ c* along the entrance and the exit of the reactor. This calculation is achieved using the *Derived Values* tab under the *Results* heading in COMSOL. To create the line integral calculations, right-click on the *Derived Values* tab and select the *Line Integral* option, which creates a new tab for a line integral calculation. Two of these calculations should be completed to find the total flow rates at the entrance and exit. The appropriate boundary must be selected for each calculation. Then, the variable name *chds.ntflux_c* is entered in the *Expression* area to specify that the total flux is the expression to be integrated. This automatically sets the *Units* to [mol/s]. The *Compute Surface Integral* option is selected under the *Integration Settings* tab to indicate that the variable specified is to be calculated over the specified surface of the revolved geometry rather than over just the indicated line as shown in Figure 15.16.

Calculating the total flow rates in this manner gives that the flux entering the tubular reactor as −0.001666677 mol/s (note that the

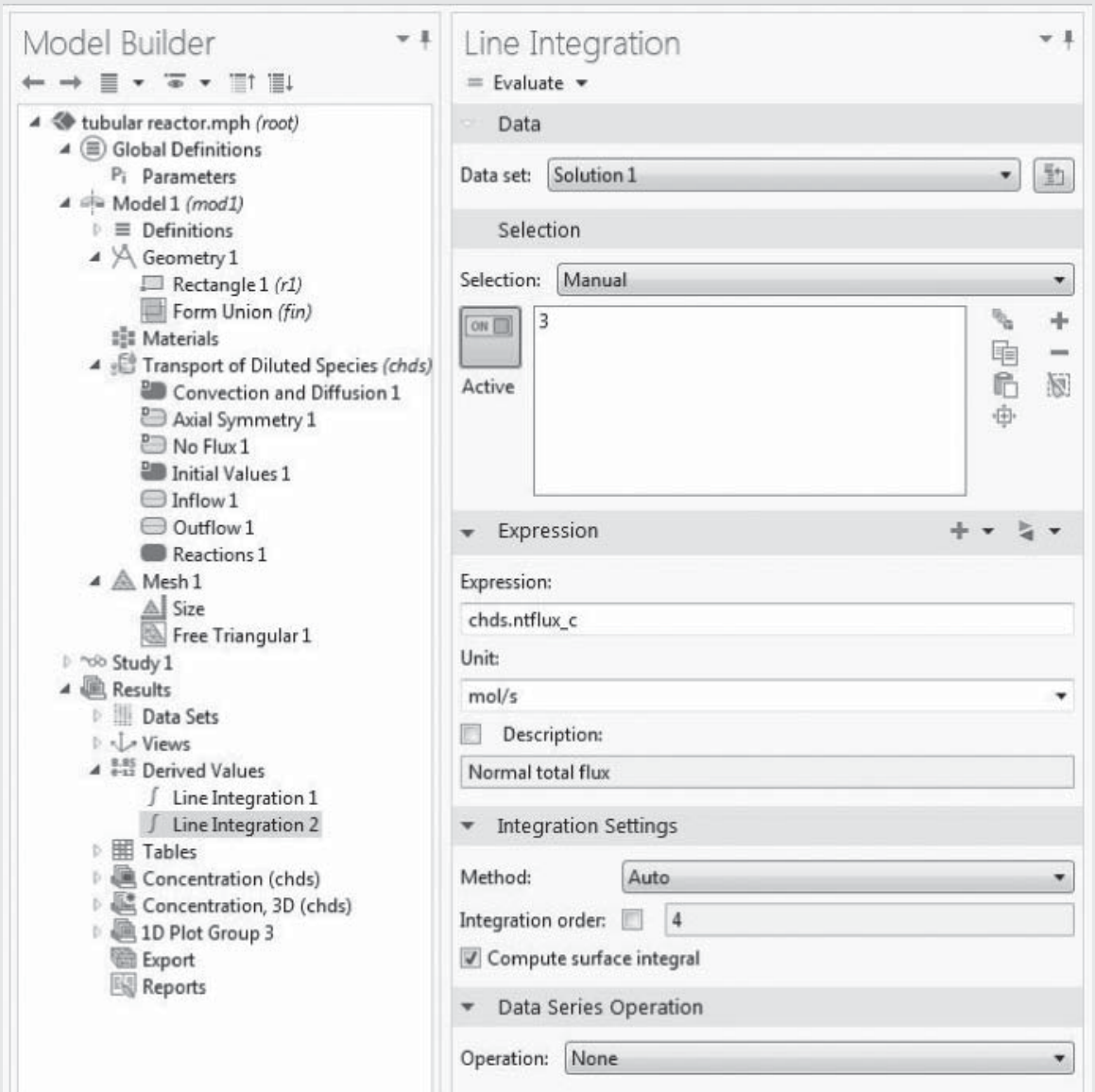

Figure 15.16 Integration specifications. (*Source:* Image made using the COMSOL Multiphysics software and is provided courtesy of COMSOL).

flux is negative since it is going into the reactor; a positive value is used in the equations as convention) and the total flux exiting as 0.001208069 mol/s. Substituting in Eq. (15.16), the conversion in the reactor is:

$$\overline{X}_{\text{LD1}} = \left(1 - \frac{chds.ntflux\_c_{out}}{chds.ntflux\_c_{in}}\right) 100\%$$
$$= \left(1 - \frac{0.001208 \frac{\text{mol}}{\text{s}}}{0.001667 \frac{\text{mol}}{\text{s}}}\right) 100\% = 27.52\% \qquad (15.16)$$

Clearly, diffusion increases the radial mixing as compared to the conversion without diffusion (zero radial mixing) in Example 15.2 (27.41%). As the diffusivity increases, conversion increases with increased mixing.

EXAMPLE 15.4 *Helical Flow*

As a further example of how mixing impacts the conversion in a tubular reactor, helical flow is examined (Slominski et al., 2011) for the following conditions:

Feed at 0.05 mol/L of sodium hydroxide and 0.05 mol/L of ethyl acetate.

Minor radius at 2 cm (0.7874 in)

Major radius at 25 cm (9.8425 in)

Pitch at 5 cm (1.9685 in)

Temperature is 30°C.

Density of the reacting fluid (assumed to be pure water) is 996 kg/m^3 and viscosity of the reacting fluid is 0.000798 Pa − s at 30°C.

Inlet volumetric flow rate of solution at 2 L/min (assumed to remain constant).

Second-order irreversible reaction (first-order in each reactant) with rate constant, $k = 8.9$ L/mol-min at 30°C.

These conditions were used to set the tubular reactor length used in Examples 15.1–15.3 based on the characteristic length, L_c, of the helix as described by Eq. (15.17):

$$L_c = 2\pi\sqrt{(R_t + R_m)^2 + \left(\frac{P_t}{4}\right)^2}$$
$$= 2\pi\sqrt{(2+23)^2 + \left(\frac{5}{4}\right)^2} = 157.3 \text{ cm} \qquad (15.17)$$

where R_t is the tube (minor) radius, R_m is the mandrel radius (i.e., the helix is wrapped about a solid mandrel), and P_t is the axial pitch of the helix. The tubular reactors in Examples 15.1–15.3 are assigned the characteristic length of the helix to compare the mixing effects in the four examples.

For this COMSOL simulation, the 3D option is selected from the *Model Wizard* rather than the 2D axisymmetric option used for the straight-tube reactors. This option generates various 3D geometries. Once created, the parameters from Figure 15.2 are added to the *Global Definitions* tab. Once the parameters are entered, the geometry is specified by right-clicking on the *Geometry* tab and selecting the *Helix* option. The *Helix* option is found under the *More Primitives* menu. Once created, the dimensions are entered under the *Helix1* tab as shown in Figure 15.17.

This creates a single turn of a helix with a major radius (distance from the mandrel axis to the center of the tube) of 25 cm, a minor radius (tube radius) of 2 cm, and an axial pitch (vertical rise of a single turn) of 5 cm. Normally, the centerline of the mandrel is at the origin. Instead, in Figure 15.17, the axis of the helix tube is positioned at the origin. Hence, the centerline of the mandrel is located at ($x = -0.25$, $y = 0$, $z = 0$), which centers the axis of the tube at the origin. This lateral shift in the x-direction simplifies positioning a 3D laminar profile at the tube inlet.

Once the geometry is created, *physics* must be added to the model. For this example, both the *Laminar Flow (spf)* and the *Transport of Diluted Species (chds)* physics must be added. Once added, the initial and boundary conditions are specified for both physics.

The *Laminar Flow (spf)* physics are specified in the same way as for Example 15.1. But for the helix, the boundary selections and inlet velocity field must reflect the 3D geometry. First, the *Inlet* and *Outlet* boundary conditions are added as in the last examples, that is, by right-clicking on the *Laminar Flow (spf)* tab and selecting the

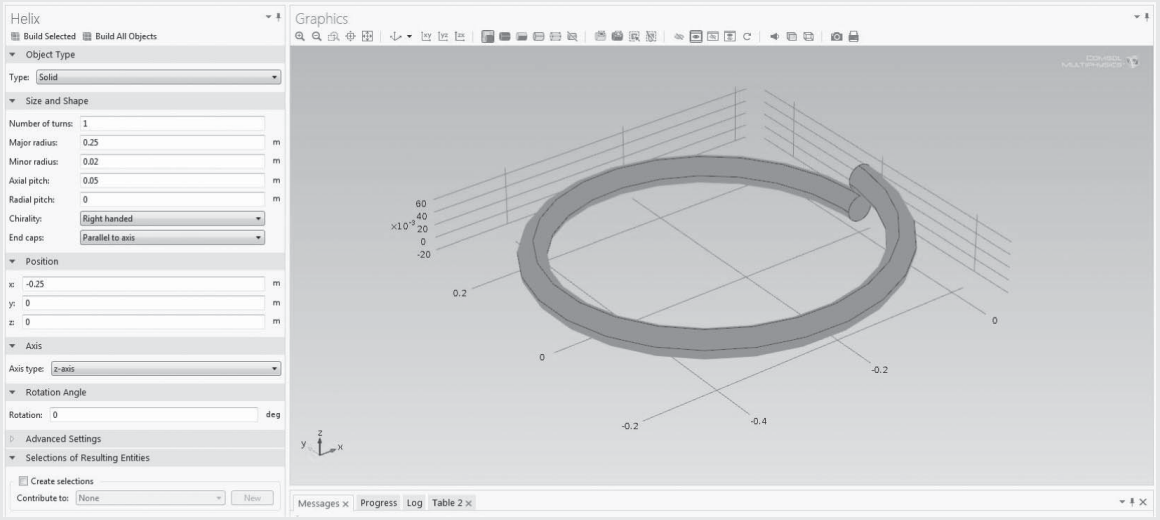

Figure 15.17 Helix dimension entry. (*Source:* Image made using the COMSOL Multiphysics software and is provided courtesy of COMSOL).

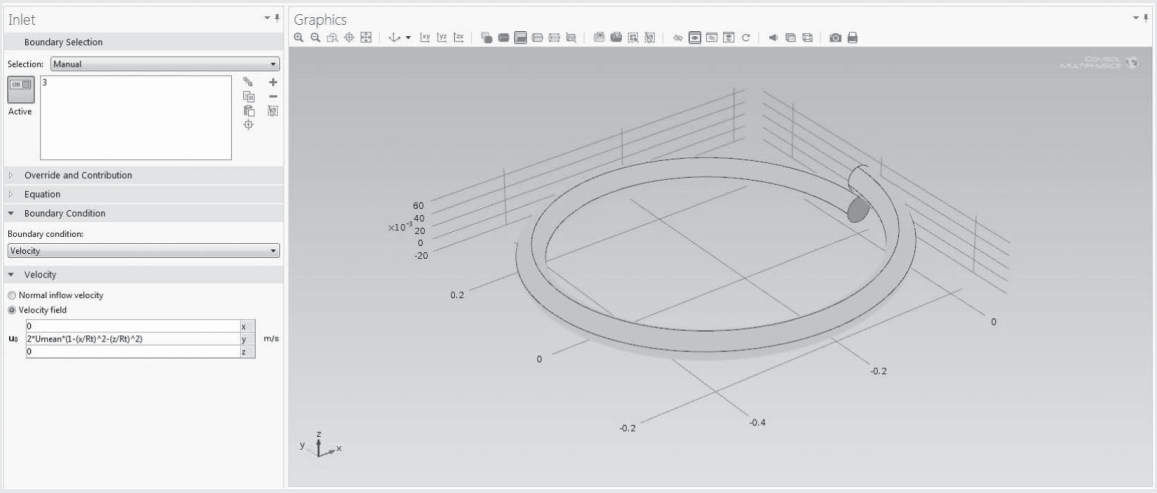

Figure 15.18 Inlet conditions. (*Source:* Image made using the COMSOL Multiphysics software and is provided courtesy of COMSOL).

appropriate conditions. Once created, the boundary and initial conditions are entered.

The conditions under the *Laminar Flow (spf)* tab must be changed to *Incompressible flow* with the helical domain, 1, selected. Under the *Fluid Properties* tab, the density and viscosity are set in helical domain, 1. Once these conditions are set, the *Initial Conditions* are set. For this example, the initial velocity field is left at zero. Although it can be preferable to give COMSOL better initial guesses, due to the complexity of the helical geometry, initial velocities cannot be readily defined—and are left at zero. The initial pressure is set to 1 [atm].

Once the initial conditions are set, the boundary conditions are set. The *Inlet* boundary condition is set as shown in Figure 15.18.

The inlet boundary is selected to be the circle centered at the origin, which is automatically numbered as boundary 3 by COMSOL. The boundary is added to the condition by selecting it and clicking the plus button. The *Velocity* option is selected as the boundary condition and the *Velocity field* option is specified. The velocity field is set as zero in the *x* and *z* directions and at 2*Umean*(1 − (x/Rt)^2 − (z/Rt)^2), a 3D laminar velocity profile, in the *y* direction. The *Outlet* boundary is set to be *Pressure*, *no viscous stress*, as in Example 15.3. The pressure is set at 1 [atm] and the other end of the helix, boundary 4, is selected as the outlet boundary. This fully specifies the laminar physics.

Now the *Transport of Diluted Species (chds)* conditions must be specified. Under the *Transport of Diluted Species (chds)* tab, all of the appropriate conditions are already specified. That is, the helical domain, 1, is selected and the convection option is selected. Under the *Convection and Diffusion* tab the option for ***u*** is set to *Velocity field (spf/fp1)* rather than the *user-defined* option. This connects the *Transport of Diluted Species (chds)* and *Laminar Flow (spf)* physics by the velocity field. This setting uses the velocities calculated in the *Laminar Flow* physics as the input for the concentration calculations. The diffusion is set to the diffusion parameter, *D*, under the *Convection and Diffusion* tab as well. The *Initial Values* tab is then selected and the initial concentration is set to *c*0.

The extra boundary conditions for inlet, outlet, and reaction must be added to the model as in Example 15.3; That, is by right-clicking on the *Transport of Diluted Species (chds)* tab and selecting the *Inflow*, *Outflow*, and *Reactions* options. Under the *Inflow* tab, the entering concentration is set at *c0* for the entrance to the helix, boundary 3 in COMSOL. Under the *Outflow* tab, the exit of the helix, boundary 4 in COMSOL, must be selected. Finally, under the *Reactions* tab, the reaction rate is set to −k*c^2 and the helical domain, 1, is selected as

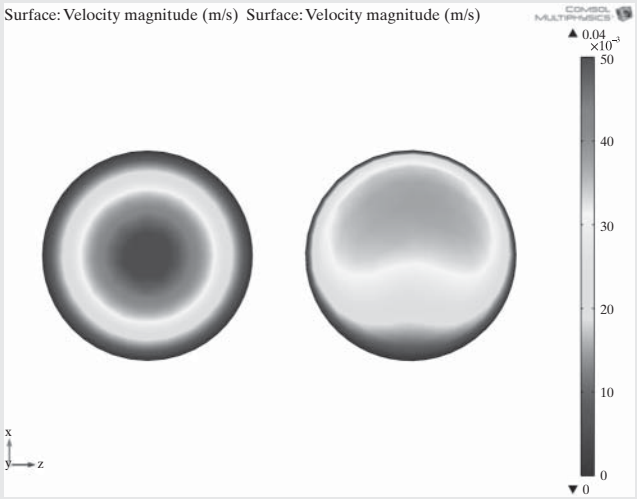

Figure 15.19 Velocity profile in a helix (see the **Color Figure** folder on the Wiley Web site associated with this book).

the active domain for the reaction. Now the model is fully specified for the momentum and species balances.

Next, an appropriate mesh is created. In this case, the physics-controlled meshes are sufficient to achieve an acceptable solution to the model. To begin, select the *finer* option for the physics-controlled mesh and select *Build All* at the top of the mesh toolbox. This creates a mesh with 296,850 elements. Next, a study is created by right-clicking on the heading with the file name and selecting the *Add Study* option. Then, select the stationary option and click *Add Study* to create the study. Finally, select the *Compute* option to solve the finite-element equations. The calculation takes approximately seven minutes to solve on an Intel® core™ i7 processor.

The study automatically creates plots for the velocity profile and the pressure contour maps. The velocity profiles at the entrance (at left) and exit (at right) of the helix are shown in Figure 15.19. Notice that the image for the exit is oriented such that the outside of the helix is at the top of the image. Additional results are plotted in Figure 15.20 to view the reactant concentration along the axis of the helix and compute the conversion in the helical reactor to compare the effects of mixing. To view the concentration of reactant at various points in the helical

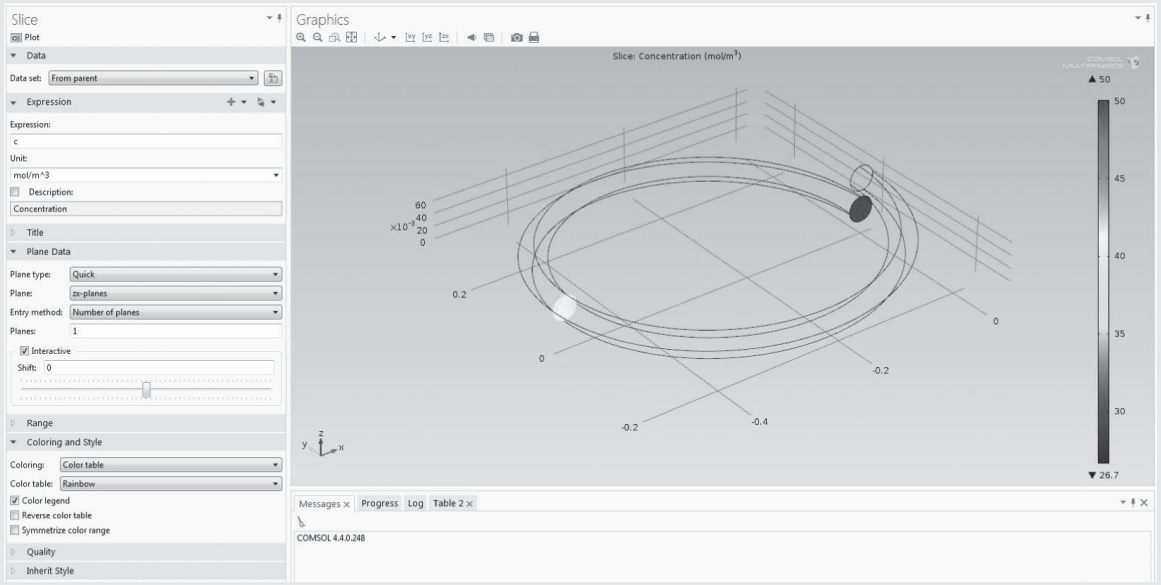

Figure 15.20 Concentration slice plot (see the Color Figure folder on the Wiley Web site associated with this book). (*Source:* Image made using the COMSOL Multiphysics software and is provided courtesy of COMSOL).

reactor, a 3D result is added by right-clicking the *Results* tab and selecting the *3D Plot Group* option to create a new 3D plot group. Once created, right-click the *3D Plot Group* tab and select the *Slice* option. This creates a 2D slice that can be moved throughout the helix to view 2D concentrations at different axial distances. The *expression* under the *Slice* tab is then changed to *c*, indicating that concentrations are to be graphed as shown in Figure 15.20. The *shift* shown in the image indicates how far from the origin the slice is placed.

The concentrations entering and exiting the helix are shown in Figure 15.21. Notice that the exiting concentrations are nearly uniform except for a small area of lower concentration near the inner wall of the helix. This indicates that the helical reactor for this system creates a very well-mixed region. This is consistent with the velocity plot in Figure 15.19, which shows a horseshoe shape at the outer wall, indicating that the fluid recirculates from the outer wall due to centrifugal forces in three dimensions. The mixing in this region is further confirmed by the secondary velocity plot at the helix exit shown in Figure 15.22. In this plot, the arrows represent the velocity in the *xz*-plane at the helix exit, showing the velocity field orthogonal to the main direction of travel through the helix. This plot shows strong recirculation patterns in the helix, creating a nearly uniform concentration profile, similar to that assuming plug flow with perfect radial mixing in a straight tube.

To have COMSOL compute reaction conversions, the strategy described in the solution to Example 15.3 is followed. This involves calculating the surface integral of the total normal flux of the concentration at the entrance and exit to compute the species flow rates and using Eq. (15.16). The resulting conversion is 30.79%—a result that exceeds 30.54% for the assumption of plug flow and perfect radial mixing in a straight-tube reactor.

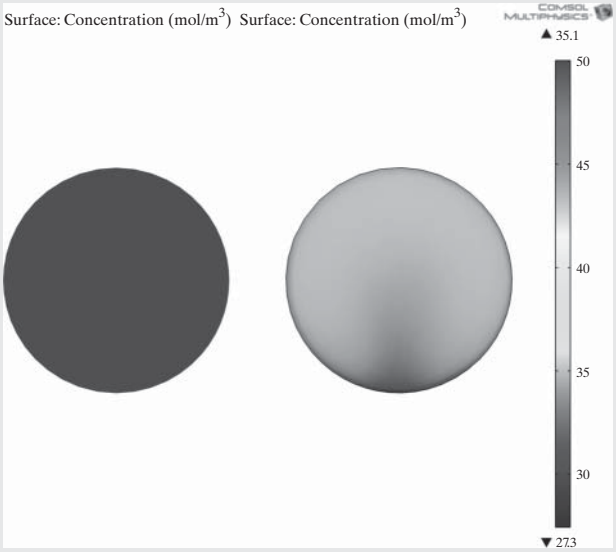

Figure 15.21 Concentration profile in a helical reactor (see the **Color Figure** folder on the Wiley Web site associated with this book).

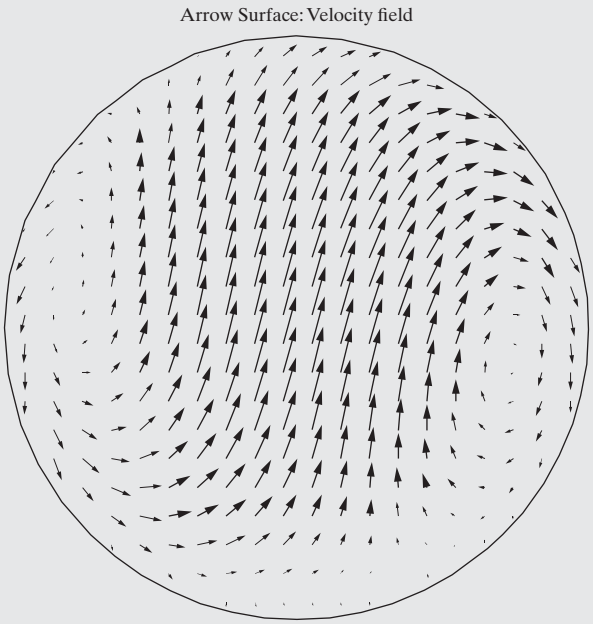

Figure 15.22 Recirculation at helix exit.

Table 15.3 Results for Varying Mesh Sizes

Mesh	Extremely Coarse	Extra Coarse	Coarser	Coarse	Normal	Fine
No. of domain elements	6,729	12,345	14,904	23,628	45,619	106,265
Total flux in (mol/s)	−0.001435137	−0.001601617	−0.001552344	−0.001592523	−0.001605556	−0.001628923
Total flux out (mol/s)	0.000921029	0.00107946	0.00104071	0.001091324	0.001100405	0.001123202
Conversion	35.82292964	32.60185926	32.95885335	31.47197961	31.46270631	31.04636242
ln(conversion)	3.578588181	3.484369319	3.495259915	3.449097614	3.448802918	3.435481649
1/(domain elements)	0.00014861	8.10045E-05	6.70961E-05	4.23227E-05	2.19207E-05	9.41044E-06

Clearly, the helical reactor results are not converged. To obtain convergence, results are computed using smaller mesh sizes as summarized in Table 15.3. Using linear regression, Figure 15.23 shows a linear relationship between $y = \ln(X)$ and $x = (\text{no. of domain elements})^{-1}$. Extrapolating to an infinite number of domain elements, the y-intercept = 3.419. Hence, X at zero mesh size is extrapolated as exp(3.419) = 30.40%, slightly less than 30.55%. Here, $R^2 = 0.9497$ shows a strong linear correlation of the data, giving good confidence in the extrapolation result.

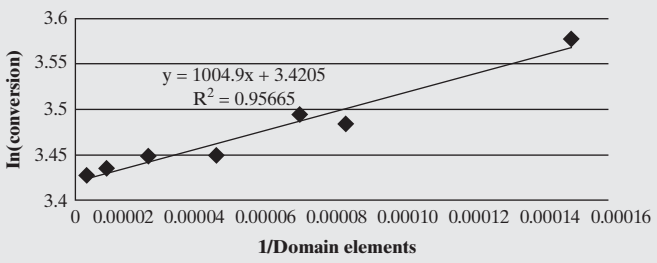

Figure 15.23 Regression of ln(conversion) vs. (no. of elements)$^{-1}$.

15.5 NONISOTHERMAL TUBULAR REACTOR MODELS

As the heat of reaction increases, either exothermically or endothermically, temperature increases or decreases in the tubular reactor gain importance. When designing a chemical reactor, the maximum or minimum temperatures achieved, which occur under adiabatic conditions, should be estimated. For exothermic reactions, as temperatures rise, vessel yield stresses must not decrease below safe operating conditions. For endothermic reactions, as temperatures decrease, the reaction rates must not fall too low. Initially, it helps to calculate the adiabatic flame temperature as discussed in Section 6.5, that is, the maximum temperature achievable assuming a perfectly insulated vessel. Consequently, in this section, Example 15.5 begins by examining the ethyl acetate—NaOH reactor under adiabatic conditions.

Then, heat transfer is considered to lower or increase the reactor temperatures. It is said that the reactor operates *diabetically*. Example 15.6 considers operation with heat transfer through the tube wall, assuming a constant wall temperature at 30°C, the cooling water temperature.

EXAMPLE 15.5 ***Nonisothermal–Adiabatic (Example 15.3 Revisited)***

Returning to Example 15.3, let's compute the heat of reaction, ΔH_{rxn}, for the reaction:

$$\text{EtAc} + \text{NaOH} \rightarrow \text{EtOH} + \text{NaAc}$$

using

$$\Delta H_{\text{rxn}} = \sum_{j=1}^{N_{\text{P}}} \Delta H_{\text{f,prod } j} - \sum_{i=1}^{N_{\text{R}}} \Delta H_{\text{f,react } i} \tag{15.18}$$

where ΔH_{f} is the enthalpy of formation of product species j or reactant species i at temperature, T, and N_{P} and N_{R} are the numbers of products and reactants. Here, ΔH_{f} is calculated using the standard enthalpy of formation, $\Delta H_{\text{f}}^{\circ}$ at 25°C, and the specific heat, c_p, of the products and reactants:

$$\Delta H_{\text{f}} = \Delta H_{\text{f}}^{\text{o}} + c_{\text{p}}(T - 298) \tag{15.19}$$

The heats of formation and heat capacities of the products and reactants are listed in Table 15.4.

Using Eqs. (15.18) and (15.19), the enthalpy of reaction is −36.08 kJ/mol at 303.15 K; that is, just mildly exothermic, too low to create significant temperature increases. Rather than select a more exothermic reaction, to demonstrate the use of COMSOL, Example 15.3 is extended using all prior specifications but artificially increasing the heat of reaction by a factor of 150 to −5, 412 kJ/mol.

SOLUTION

Because the temperature varies, the Arrhenius equation gives the reaction-rate constant:

$$k = Ae^{-\frac{E_{\text{a}}}{RT}} \tag{15.20}$$

where the pre-exponential factor, A, is 3.202×10^7 L/mol-s; the activation energy, E_a, is 48.367 kJ/mol; and R is the universal gas constant. Note that at 303.15 K, $k = 8.9$ L/mol-min.

Table 15.4 Heats of Reaction and Heat Capacities

Species	ΔH_{f}^{o}(kJ/mol)	C_{p}(kJ/mol-K)
Ethyl acetate	−480.3125	0.169
Sodium hydroxide	−469.15	0.08785
Ethanol	−276	0.112
Sodium acetate	−709.32	0.10083

Name	Expression	Value	Description
Rt	2[cm]	0.020000 m	Tube Radius
dens	996[kg/m^3]	996.00 kg/m^3	Density
visc	0.000798[Pa*s]	7.9800E-4 Pa·s	Dynamic Viscosity
flow	2[L/min]	3.3333E-5 m^3/s	Flow Rate
Umean	flow/(pi*Rt^2)	0.026526 m/s	Avg. Velocity
c0	0.05[mol/L]	50.000 mol/m^3	Initial Reactant Conc.
D	1.2*10^-5[cm^2/s]	1.2000E-9 m^2/s	Diffusivity
k	8.9[L/mol/min]	1.4833E-4 m^3/(s·mol)	Reaction Rate Constant
dH	36.0776*150[kJ/mol]	5.4116E6 J/mol	Enthalpy of Reaction
Ea	48.367[kJ/mol]	48367 J/mol	Activation Energy
R	8.314[J/mol/K]	8.3140 J/(mol·K)	Gas Constant
A	3.202*10^7[L/mol/s]	32020 m^3/(s·mol)	Pre-exponential Factor

Figure 15.24 Parameters.

Next, the energy balance is included by adding heat transfer *physics* to the COMSOL file in Example 15.3. First, the heat of reaction, which does not vary significantly with temperature, and the Arrhenius rate constants are added to the *Parameters* tab as shown in Figure 15.24. Note that the liquid properties are nearly constant over the temperature range in question.

The *Geometry* is unchanged and the *Reaction* tab under the *Transport of Diluted Species* (*chds*) tab is changed to $-[A^*\exp(-Ea/R/T)]^*$ c^2, that is, the Arrhenius equation.

To add heat-transfer physics, right-click on the *Model* tab and select *Add Physics*. Then, select the *Heat Transfer in Fluids* (*ht*) option under the *Heat Transfer* tab as shown in Figure 15.25, and click the checkered flag in the top right corner.

Next, the specifications for heat transfer are added to the model. Under the *Heat Transfer in Fluids* (*ht*) tab, Domain 1 is automatically selected in which the heat transfer is active. Under the *Heat Transfer in Fluids 1* tab, the constants for heat transfer are specified as shown in Figure 15.26.

As in Example 15.3, the laminar velocity profile is defined under the *Heat Transfer in Fluids* (*ht*) tab. The pressure, not shown in

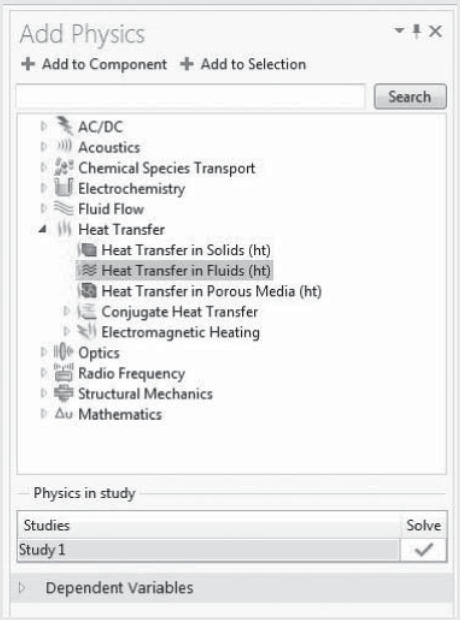

Figure 15.25 Adding heat transfer. (*Source:* Image made using the COMSOL Multiphysics software and is provided courtesy of COMSOL).

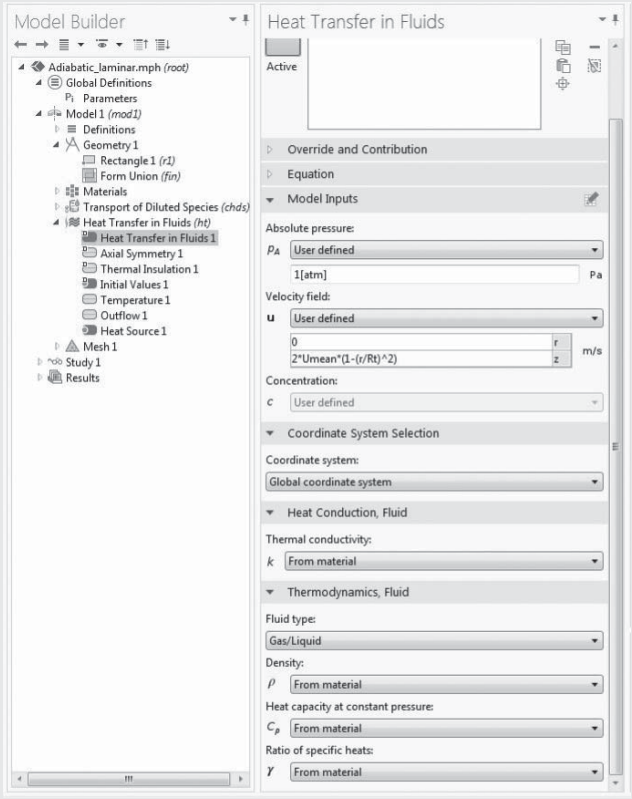

Figure 15.26 Heat-transfer specifications. (*Source:* Image made using the COMSOL Multiphysics software and is provided courtesy of COMSOL).

Figure 15.26, is specified at 1 [atm]. The remaining constants are taken from the *Materials* tab, which specifies the material constants in a given domain. To specify a material for Domain 1, right-click on the *Materials* tab and select the *Material* option. This creates the *Material 1* tab, which automatically shows the constants to be specified for heat transfer as shown in Figure 15.27. Note that γ is the ratio of the specific heat at constant volume to that at constant pressure, c_v/c_p. For an incompressible fluid, $c_v = c_p$ and $\gamma = 1$. These constants are entered in the Value column as shown in Figure 15.28. Note that the fluid is approximated as pure water at 303.15 K because the products and reactants are extremely dilute.

After the constants are specified, the initial conditions are entered under the *Initial Values* tab. In this case, the initial temperature is set to 303.15 K.

Next, the boundary conditions for the energy balance are added. To add these conditions, right-click on the *Heat Transfer in Fluids* (*ht*) tab and select the *Temperature*, *Outflow* option. This will add tabs of the same names to the model. Under the *Temperature* tab, the inlet temperature is set to 303.15 K and the inlet boundary, in this case boundary 2, is selected as the constant temperature boundary. The *Outflow* boundary is set at boundary 3 with the diffusive flux at the outlet set at zero, that is, permitting just convective heat transfer through the tube outlet. Boundary 4, the tube wall, is the only active boundary remaining in the *Thermal Insulation 1* tab; that is, the zero-flux boundary condition is set at the tube wall.

Also, a heat source is added. This is accomplished by right-clicking the *Heat Transfer in Fluids* (*ht*) tab and selecting the *Heat Source 1* option. Then, enter the rate of heat generated as the reaction rate multiplied by the enthalpy of reaction, *dH*, and set it to be active in Domain 1. This is shown in Figure 15.29.

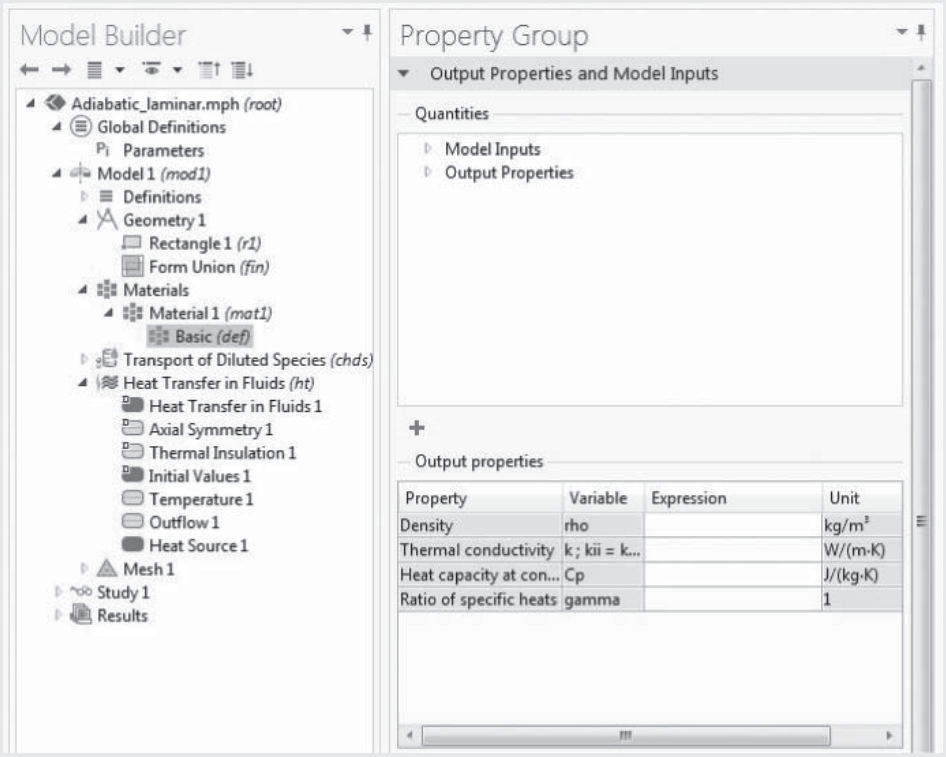

Figure 15.27 Materials tab. (*Source:* Image made using the COMSOL Multiphysics software and is provided courtesy of COMSOL).

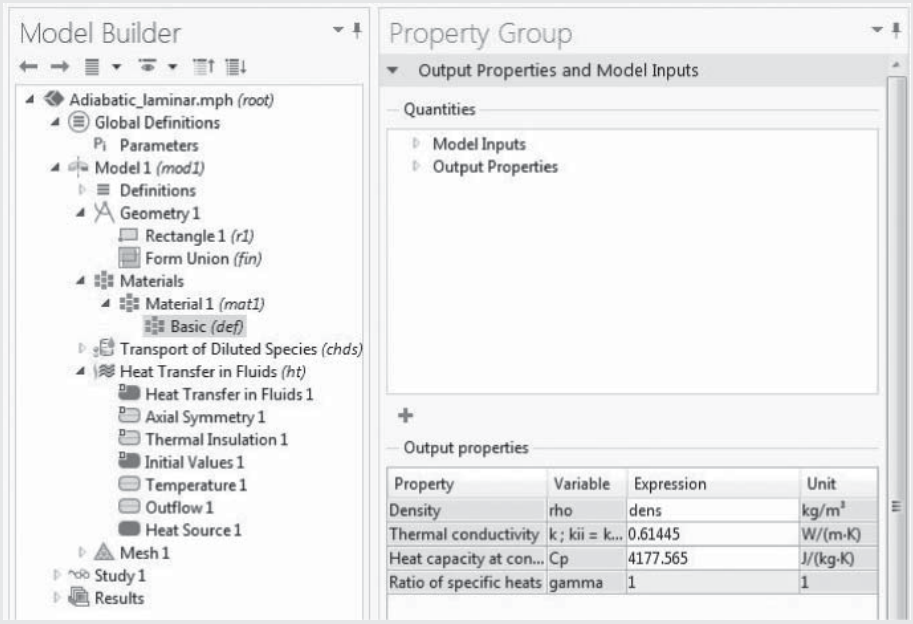

Figure 15.28 Material constants. (*Source:* Image made using the COMSOL Multiphysics software and is provided courtesy of COMSOL).

The differential equations that COMSOL solves for the heat-transfer physics (i.e., the energy balance) and the boundary conditions are viewed by using the *Equation* tabs as presented in the previous examples. A summary of the partial differential equation and boundary conditions is presented in Table 15.5. In these equations, Q_{vh} represents viscous heating (heat created by friction in the fluid) and W_p represents the pressure work. For this example, both are zero. In the energy balance (heat-transfer equation), $\rho^* Cp^* u \cdot \nabla T$ is the convective rate of heat transfer, and $\nabla \cdot (k \nabla T)$ is the rate of conductive heat transfer.

The heat-transfer model is automatically added to the *Study 1* tab. The mesh used in Example 15.3 remains applicable. To solve the model, click the *compute* option under the *Study 1* tab. Eleven seconds are required using an Intel® core™ i7 processor. The results are similar to those in Example 15.3 with the concentration profiles shown in Figure 15.30 [ordinate and abscissa are Axial Distance (m) and Radial Distance (m)]. But the rates of reaction and conversion are significantly higher (at higher temperatures) as shown.

To plot the temperature profiles, right-click on the *Results* tab and select the *2D Plot Group* option. Then, right-click the newly created *2D Plot Group* tab and select the *Surface* option to create a new surface plot. Under the surface tab, enter *T* as the expression to be plotted and select the *plot* option in the top left corner. The temperature profiles in Figure 15.31 are similar to the concentration profiles. Close to the

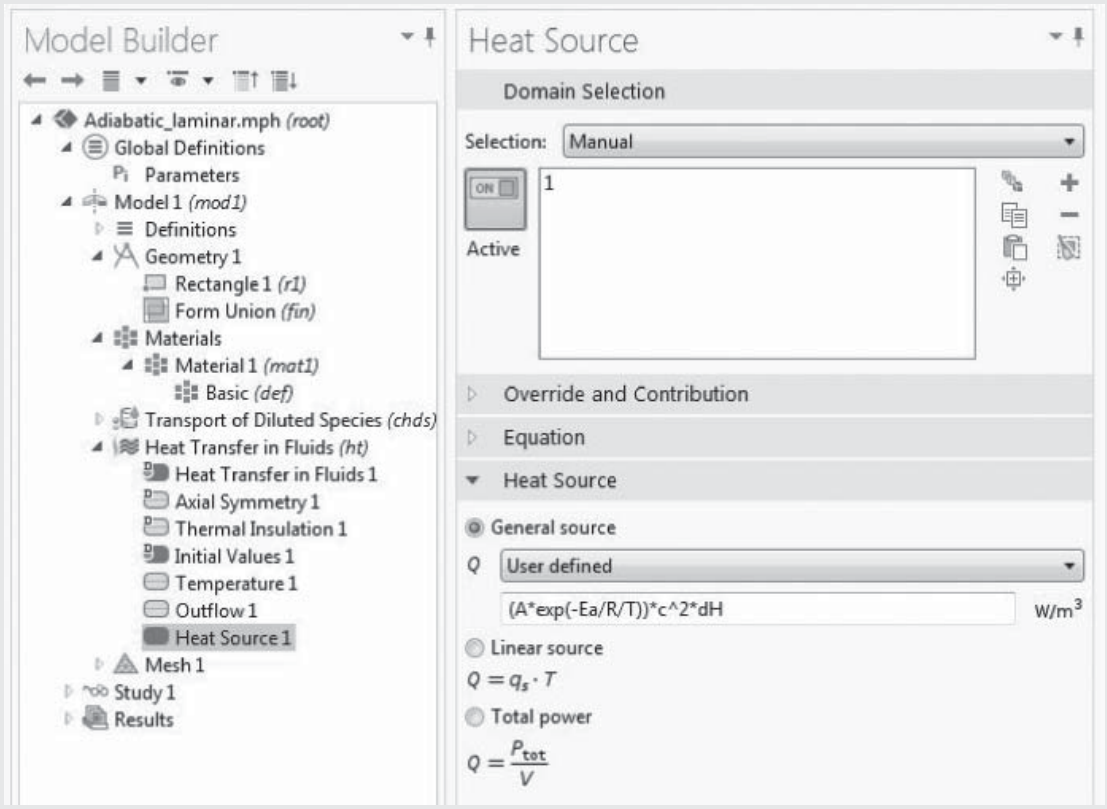

Figure 15.29 Heat source. (*Source:* Image made using the COMSOL Multiphysics software and is provided courtesy of COMSOL).

Table 15.5 Equations for Heat Transfer and the Boundary Conditions

Condition	Equation	Applicable Area
Heat transfer	$\rho^* Cp^* u \cdot \nabla T = \nabla \cdot (k\nabla T) + \mathrm{Q} + \mathrm{Qvh} + W\mathrm{p}$	Domain 1
Temperature	$T = T0$	Boundary 2
Outflow	$-n \cdot (-k\nabla T) = 0$	Boundary 3
Insulation	$-n \cdot (-k\nabla T) = 0$	Boundary 4
Heat source	$\mathrm{Q} = [A^* \exp(-E\mathrm{a}/R/T)]^*\mathrm{c}\hat{}2^*\mathrm{dH}$	Domain 1

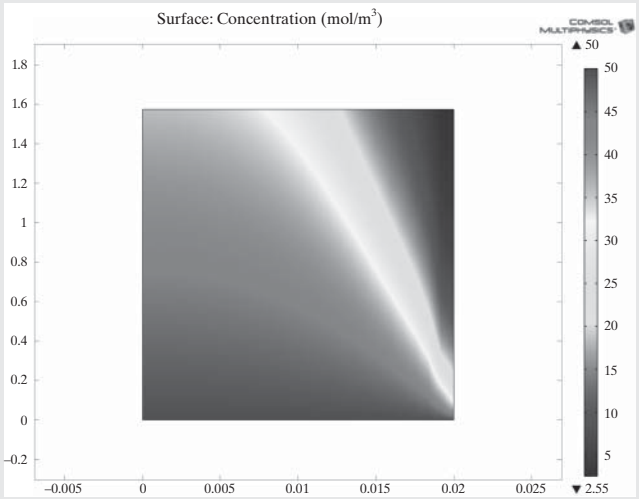

Figure 15.30 Concentration profile (see the **Color Figure** folder on the Wiley Web site associated with this book).

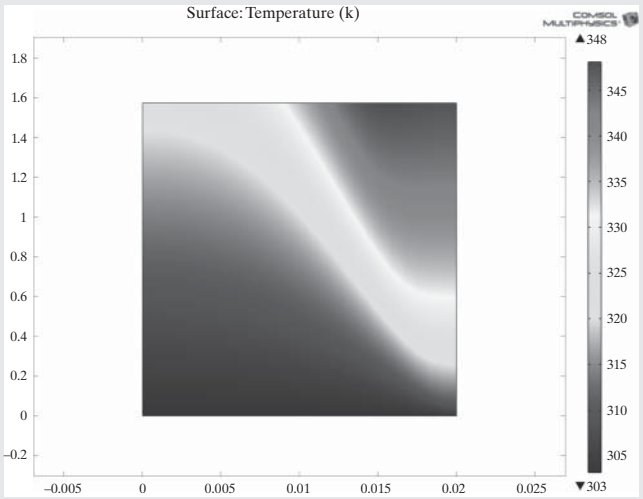

Figure 15.31 Temperature profile (see the **Color Figure** folder on the Wiley Web site associated with this book).

wall at lower velocities, conversions are higher, more heat is liberated, and temperatures are higher as expected.

Finally, to calculate the reactor conversion, use the *Line Integration* tabs under the *Derived Values* tab in the *Results* section as in Example 15.3. The reactant flow in the reactor effluent is 0.000801 mol/s. Given the inlet flow, −0.001667 mol/s, using Eq. (15.16), the conversion is 52.0%, much higher than 27.5% at 30°C (isothermal).

EXAMPLE 15.6 *Nonisothermal–Diabatic (Example 15.5 Revisited)*

To assess a diabetic tubular reactor (with heat transfer at the walls), consider the assumption of a uniform wall temperature at 303.15 K (cooling water temperature). Compare the conversions, assuming:

1. Fully developed laminar flow with radial diffusion
2. Plug flow

SOLUTION

1. **Fully Developed Laminar Flow with Radial Diffusion** Beginning with the COMSOL model in Example 15.5, the only change involves the boundary condition at the tube wall. To set this boundary condition, a new *Temperature* tab is added by right-clicking on the *Heat Transfer in Fluids* (*ht*) tab and selecting the *Temperature* option. A *Temperature 2* tab is created, permitting the wall (boundary 4) temperature to be set at 303.15 K. Given this specification, click the *Compute* option under the *Study 1* tab to execute the solver.

   The computed concentration and temperature fields are shown in Figures 15.32 and 15.33 [ordinate and abscissa are Axial Distance (m) and Radial Distance (m)], respectively. When compared with results computed under adiabatic operation with heat transfer at the wall, the fluid temperatures near the wall are drastically reduced. This reduction leads to significantly less reaction near the wall.

   To compute the conversion, the *Line Integral* tabs set up for the previous examples are reevaluated. As before, the reactant flow rate into the reactor is 0.0016667 mol/s. In this case, the reactant in the effluent stream is increased to 0.0008989 mol/s, which decreases the conversion to 46.07% compared with 51.95% for adiabatic operation. This is expected since the temperatures throughout the reactor are reduced due to heat transfer. For adiabatic operation, the temperature peaks at 348.1 K (at the tube entrance, about 0.7 cm from the tube wall), whereas for the diabatic case, it only peaks at 334.0 K (along the tube centerline at the entrance to the tube).

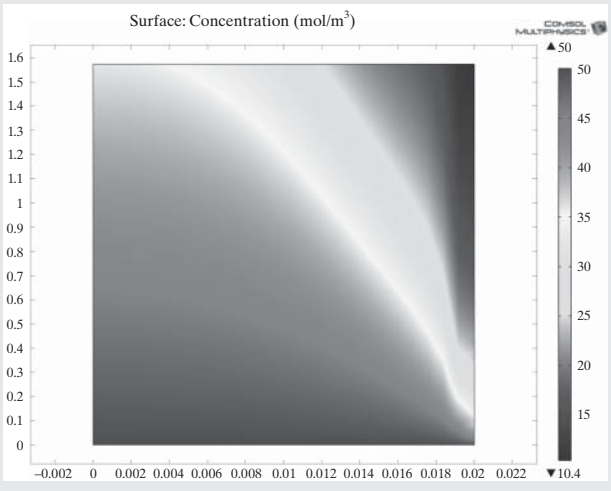

Figure 15.32 Concentration profile—fully developed laminar flow (see the **Color Figure** folder on the Wiley Web site associated with this book).

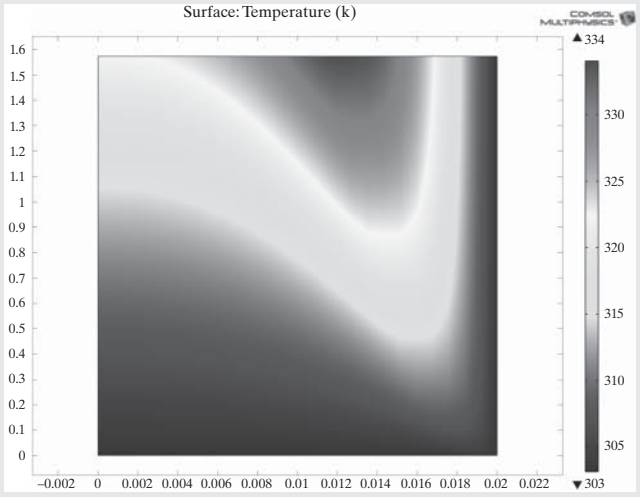

Figure 15.33 Temperature profile—fully developed laminar flow (see the **Color Figure** folder on the Wiley Web site associated with this book).

2. **Plug flow** The COMSOL model is exactly the same as for part (1) except that a uniform radial velocity, Umean, is specified. For part (2) the velocity profiles in the *Transport of Diluted Species (chds)* and the *Heat Transfer in Fluids* (*ht*) tabs must be changed from 2*Umean*(1 − (r/Rt)^2)) to Umean.

   The computed concentration and temperature fields are shown in Figures 15.34 and 15.35 [ordinate and abscissa are Axial Distance (m) and Radial Distance (m)], respectively. For plug flow, the temperatures and concentrations remain relatively constant across the tube radius; however, near the wall, the temperature approaches the constant wall temperature, lowering the reactant conversion near the wall.

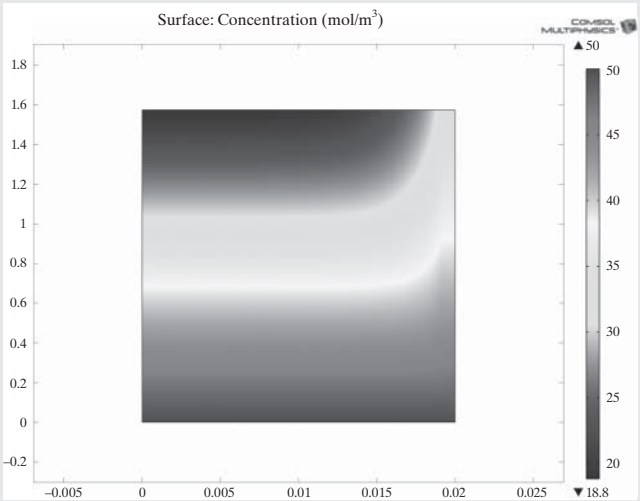

Figure 15.34 Concentration profile—plug flow (see the **Color Figure** folder on the Wiley Web site associated with this book).

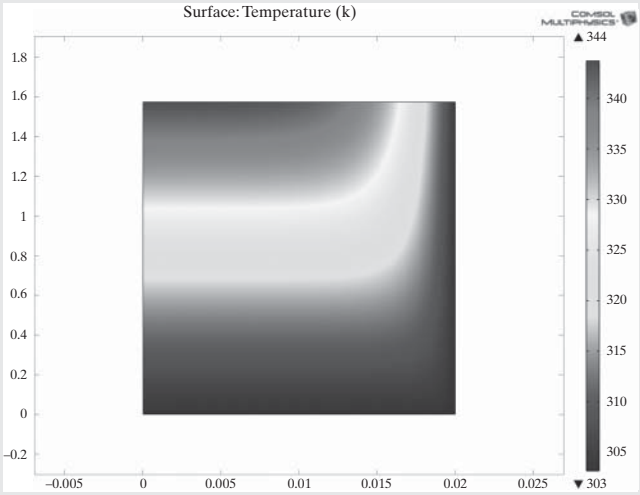

Figure 15.35 Temperature profile—plug flow (see the **Color Figure** folder on the Wiley Web site associated with this book).

Finally, for the plug-flow case, the reactant flow into the tube is 0.0016667 mol/s and 0.0007601 mol/s in the effluent from the reactor, yielding a 54.40% conversion. As expected, this exceeds 46.07% for fully developed laminar flow.

15.6 MIXING IN STIRRED-TANK REACTORS

Continuous-stirred-tank reactors (CSTRs) involve agitators and mixing patterns more complex than in most tubular reactors. For these reactors, the assumption of total back mixing often leads to large over estimates in reaction conversions. To properly model the mixing patterns, usually involving large turbulent eddies, COMSOL includes a *Mixer Module* (COMSOL, 2014), often not purchased by universities and colleges. This section provides a brief introduction to the module and presents some of the results attainable from it.

The *Mixer Module* allows for the modeling of a few types of mixers commonly found in industry. Models are available for either flat- or dish-bottomed mixers. Also, baffles can be added to the reactor walls. Finally, the mixer can be modeled with a pitched-blade impeller or a Rushton turbine. Once the geometry has been specified, the user can add many *physics* balances as in the normal CFD module, that is, balances for heat transfer, species transport, and chemical reactions and models of laminar or turbulent flow.

Once the model is specified, the *Mixer Module* offers two solution options for the stirred-tank reactor. The first is a full, time-dependent solution, which is carried out by creating two domains. One domain is defined by the area encapsulated around the rotors and deals with the geometric motion of its parts. The other domain is in the surrounding tank, including additive features such as baffles. These domains are connected by COMSOL's new "sliding-mesh technology." This solution technique offers the greatest accuracy, but is much more computationally expensive.

The other solution technique is called a frozen-rotor solution. This feature treats the rotor and its surroundings as stationary and solves the system based on a rotating reference frame. This technique is less computationally expensive, but much more limited, giving acceptable answers for simple systems (e.g., without baffles). Note that often the frozen-rotor solution is used to initialize guess values for complex systems involving full, time-dependent solutions.

The *Mixer Module* also offers free-surface modeling in a stirred-tank reactor. This feature allows the user to specify the surface-tension coefficient and contact angles for two-phase fluid pairs in the reactor. COMSOL then models the interface between the fluids. It also provides many parameters for different liquid/liquid and liquid/gas pairs for use with its free-surface modeling feature.

Some of the results from the *Mixer Module* are shown in Figure 15.36.

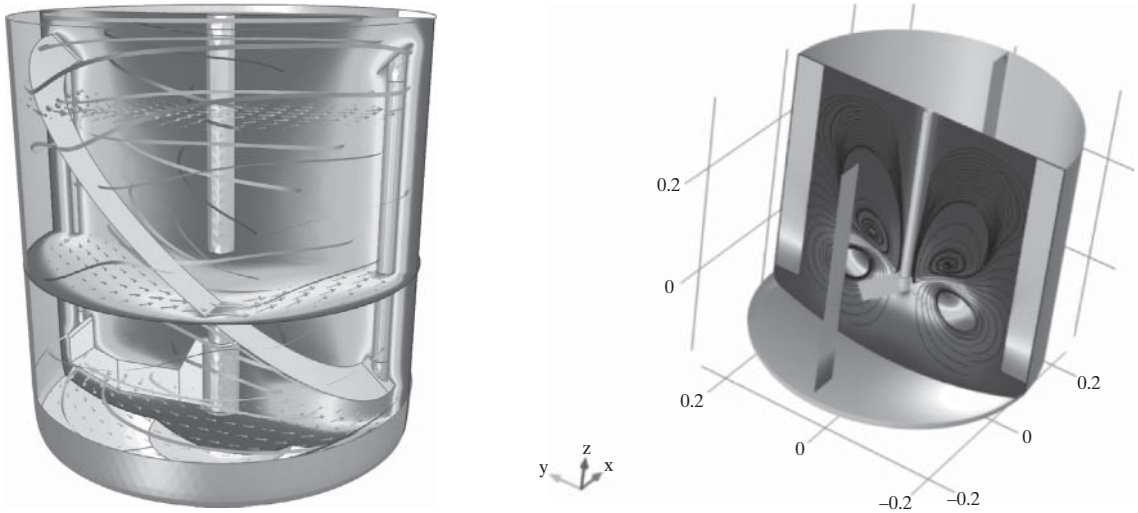

(a) (b)

Figure 15.36 *Mixer Module* results: (a) mixer showing particle trajectories and horizontal-arrow surfaces with velocities and slice plots showing the temperature; (b) a dish-bottomed mixer with baffles and a pitched-blade impeller showing streamlines and velocity map (see the **Color Figure** folder on the Wiley Web site associated with this book).

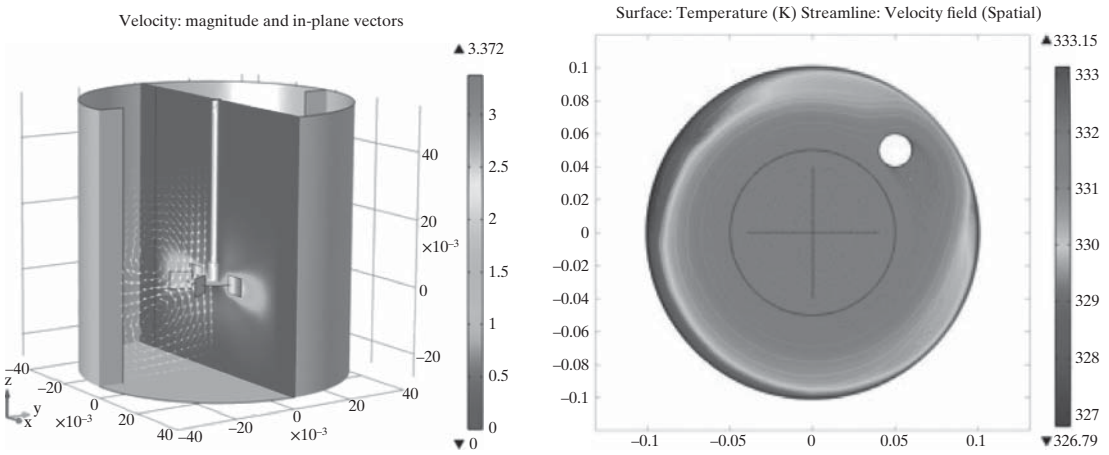

(c) (d)

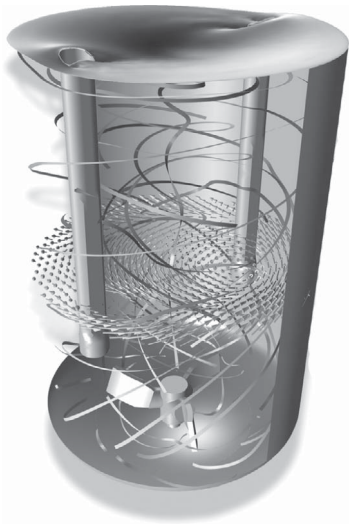

(e)

Figure 15.36 (*Continued*) (c) a flat-bottomed reactor with baffles and a Rushton turbine showing a velocity map and secondary mixing via an arrow surface; (d) 2D nonisothermal mixer showing streamlines and temperature; (e) flat-bottomed reactor and three-blade impeller and two vertical cylinders to break up flow. This model shows a particle tracing and the free surface modeling features as well, as seen at the top of the reactor (See the **Color Figure** folder on the Wiley Web site associated with this book). (*Source:* Image made using the COMSOL Multiphysics software and is provided courtesy of COMSOL).

15.7 SUMMARY

After studying this chapter, the reader should:

1. Understand the limitations of the assumptions of plug flow and perfect radial mixing in tubular reactor models.
2. Be able to use COMSOL to account for laminar flow and radial diffusion in straight-tubular reactors.
3. Be able to use COMSOL to model 3-dimensional laminar flow in helical flow reactors and understand their increased mixing and reaction due to secondary flows.
4. For exothermic or endothermic tubular reactors, be able to model adiabatic and diabatic operation using COMSOL.
5. Understand the kinds of stirred-tank reactor models available using COMSOL.

REFERENCES

1. ANSYS, "FLUENT 6.3 User's Guide," *FLUENT 6.3 User's Guide*, ANSYS, (20 September 2006). Web. Accessed August 21, 2014, from aero jet.engr.ucdavis.edu.

2. Churchill, S. W., "Interaction of Chemical Reactions and Transport. 1. An Overview," *Ind. Eng. Chem. Res.*, **44**(14), 5199–5212 (2005).

3. COMSOL, "COMSOL Multiphysics User's Guide," COMSOL, Burlington, Massachusetts, (2005). COMSOL, May 2012, Web. Accessed August 21, 2014, from nf.nci.org.au.

4. COMSOL, "Mixer Module" *Fluid Mixing Software*., Web. Accessed August 21, 2014, from www.comsol.com/mixer-module.

5. Fogler, H. S., *Essentials of Chemical Reaction Engineering*, Prentice-Hall (2011).

6. Hill, C. G., *An Introduction to Chemical Engineering Kinetics and Reactor Design*, Wiley (1977).

7. Levenspiel, O., *Chemical Reaction Engineering*, 3rd ed., John Wiley, New York (1999).

8. Rawlings, J. B., and J. G. Ekerdt, *Chemical Reactor Analysis and Design Fundamentals*, Nob Hill (2002).

9. Seader, J. D., and L. M. Southwick, "Saponification of Ethyl Acetate in Curved-Tube Reactors," *Chem. Eng. Commun.*, **9**, 175–183 (1981).

10. Slominski, C. G., W. D. Seider, S. W. Churchill, and J. D. Seader, "Helical and Lemniscate Tubular Reactors," *Ind. Eng. Chem. Res.*, **50**, 8, 842–8, 850 (2011).

11. Zitney, S. E., and S. Madhava, "Integrated Process Simulation and CFD for Improved Process Engineering," *Computer-Aided Chem. Eng.*, **10**, 397–402 (2002).

EXERCISES

15.1 Consider the tubular reactor to saponify ethyl acetate with sodium hydroxide in Example 15.1.

(a) Assuming plug flow and perfect radial mixing, determine the length of the reactor to convert 50% of the reactants.

(b) For the reactor in part (a), assuming fully developed laminar flow and no radial diffusion, what is the conversion of the reactants?

15.2 For the saponification of ethyl acetate with sodium hydroxide in a tubular reactor with fully developed laminar flow at 75°C, use COMSOL to account for radial diffusion. Estimate the conversion of the reactants.

15.3 Revisit the helical flow reactor in Example 15.4.

(a) Increase the mandrel radius to 50 cm and increase the volumetric flow rate to achieve the same residence time. Determine the conversion of the reactants in one cycle of the helix. What is the effect of increasing the mandrel radius.

(b) Increase the pitch to 10 cm and adjust the flow to achieve the same residence time. What is the effect of increasing the pitch?

15.4 Consider the mixing of ethyl acetate and sodium hydroxide in a confined jet tubular reactor as shown in the following figure. In this system, ethyl acetate is fed through the confined jet tube while sodium hydroxide is fed through the annular region. The confined jet creates a wake into which fluid from the jet and annular region enter, causing mixing to occur.

(a) Set up a confined jet geometry in COMSOL as shown in the following figure and define fully developed laminar flow profiles at the entrances to the tube and annulus. Use COMSOL to solve for the flow profiles (including axial velocity and streamlines) throughout the jet-mixing device (including the jet tube and the annular region) and to plot streamlines. Assume a 1-mm jet-tube wall thickness.

(b) Include the mass balances for species transport. Use COMSOL to find the concentration profiles and conversion.

(c) For parts (a) and (b), what is the effect of reducing the radius of the jet tube? Consider $r = 0.3$ cm.

15.5 Rework Example 15.6, assuming convective heat transfer to cooling water that surrounds the tube. Let the heat-transfer coefficient be $h_o = 100$ Btu/ft^2-hr-°F.

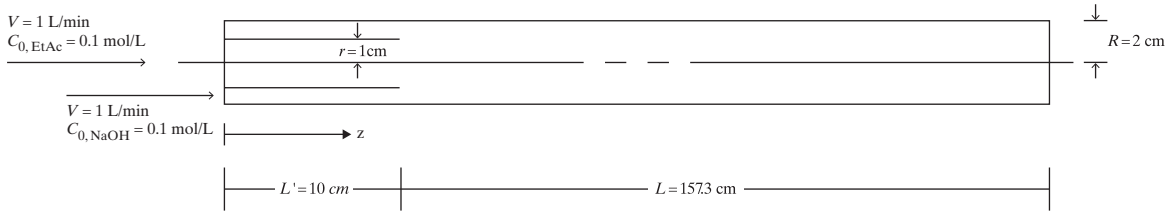

Chapter 16

Cost Accounting and Capital Cost Estimation

16.0 OBJECTIVES

Throughout the design process, as discussed in the previous chapters, estimates of the cost of equipment and other costs related to the capital investment play a crucial role in selecting from among the design alternatives. This chapter presents the various methods in common use for making preliminary estimates of capital costs of ventures for new products and processing plants or revamps of existing plants and should be studied in connection with the other chapters as needed. Some readers may prefer to study Sections 16.2 to 16.6 before working with the previous chapters, especially when exploring the techniques for process synthesis that require estimates of capital costs. In Chapter 17, capital cost estimates prepared according to the information presented in this chapter are combined with process operating costs and other expenses to determine the profitability of a proposed venture. However, even though a venture is predicted to be profitable, the financial condition of the company exploring the venture may not be sufficient to justify a decision to proceed with the venture, or competing ventures may be more attractive. In the former case, it is important to understand measures used to determine the financial condition of a company. These measures are intimately tied to the field of cost accounting, which is the subject of Section 16.1.

After studying this chapter, the reader should be able to:

1. Assess the financial condition of a company from its annual report.
2. Use the equations provided to estimate the purchase cost of representative types of process equipment and, when applicable, components of functional chemical products (devices) as well as the Equipment Costing.xlsx spreadsheet, available from the Wiley Web site associated with this textbook.
3. Estimate the cost of installation of the equipment units, including the cost of materials, labor, and indirect costs.
4. Estimate the total capital investment for the process, including the costs of spare equipment, storage tanks, surge vessels, site preparation and service facilities, allocated costs for utilities and related facilities, contingencies, land, royalties, startup, and working capital.
5. Understand the need to reestimate the working capital after preparing the cost sheet as discussed in Chapter 17.
6. Use the Aspen Process Economic Analyzer (APEA) to rigorously estimate the purchase and installation costs of chemical processing equipment.

16.1 ACCOUNTING

Accounting is the systematic recording, reporting, and analysis of the financial transactions of a business. Accounting is necessary and valuable to a company because it:

1. Provides a record of property owned, debts owed, and money invested.
2. Provides a basis for the preparation of a report that gives the financial status of the company.
3. Gives assistance and direction to those managing the affairs of the company.
4. Provides a basis for stockholders and others to evaluate management of the company.

Debits and Credits

By tradition, since the fifteenth century, the recording of financial transactions by accountants is carried out by the *double-entry method* of *debits* and *credits*. Surprisingly, debits are increases (not decreases) in assets, where an *asset* is anything of economic value that is owned by the company. Credits are just the opposite; that is, they are decreases in assets. One possible explanation for the definitions of debits and credits is that the giver receives a credit while the receiver acquires a debit. By custom, all transactions are initially recorded chronologically in terms of debits and credits in *a journal*, where for every debit, there is a credit of equal amount. The debits and credits apply to different accounts (cash, land, equipment,

bank account, etc.), which are maintained in separate *ledgers* for each account. Entries in the journal are posted to the ledgers, usually with the debit entry going to one ledger and the corresponding credit entry going to a different ledger. Although the journal might seem superfluous, it serves two useful purposes besides being a chronological record: (1) It reduces the possibility of error because for each transaction, the debit and corresponding credit are recorded together and (2) if desired, a detailed explanation for a transaction is easily entered into the journal. In both the journal and the separate account ledgers, debits are entered to the left of the credits. At any point in time, the sum of debit entries for all ledgers must equal the sum of credit entries for all ledgers. Although it is not necessary for engineers to be accountants, it is important for engineers to understand what accountants do and why they do it.

Tables 16.1 and 16.2 show an example of double-entry bookkeeping with a journal and ledgers for the following transactions. The company purchases a heat exchanger for $80,450, paid for by a check. The next day the company sells $125,000 of ammonia product with payment by check. Two more days later, the company purchases land for $265,000 paid for by check. In all cases, the checks are handled with the same bank account. Note that four separate accounts are involved. Suppose they have been assigned the following account numbers: Bank Account, 11; Plant Equipment, 15; Sales of Products, 12; and Land, 20. The journal page (say page 43) is shown in Table 16.1 where the ledger account numbers are added in the column to the left of the debits column when the journal entries are posted to the ledgers. Postings to the ledger page (page 5 of this ledger) for the Bank Account are shown in Table 16.2. Included to the left of the debits and credits columns are the corresponding pages in the journal, in this case just page 43. This ledger page is for the month of June for which the initial balance in the bank account, page 42, was the amount of $500,000. At the end of June 6, the bank account balance was $500{,}000 + 125{,}000 - 80{,}450 - 265{,}000 = \$279{,}550$. Balances may be entered into the ledger at the end of each month.

The Annual Report (Form 10-K)

Every publicly held company in the United States is required by the Securities and Exchange Commission (SEC) to submit an annual report of financial condition, referred to as Form 10-K. In addition to the 10-K, most companies also issue a more user-friendly, attractive annual report of financial condition written primarily for stockholders that typically provides the following useful information:

1. Nature of the company's business.
2. Summary of important events and new developments of the year.
3. New acquisitions and formation of partnerships.
4. Plans for the near future.
5. Summary of concerns that might influence the company's business.
6. Collection of financial statements from Form 10-K, including:
   - **(a)** Balance Sheet
   - **(b)** Income Statement
   - **(c)** Cash Flow Statement

The current financial condition of a company can be assessed by an analysis of the financial statements in its annual report. Annual

Table 16.1 Typical Journal Page

JOURNAL Page 43

2008				Debit ($)	Credit ($)
June	3	Heat Exchanger	15	80,450	
		Cash	11		80,450
		Purchase of a heat exchanger for ammonia plant			
	4	Cash	11	125,000	
		Ammonia Product	12		125,000
		Sales of product from ammonia plant to ABC			
	6	Land	20	265,000	
		Cash	11		265,000
		Purchase of land in Iowa from XYZ			

Table 16.2 Typical Ledger Page

BANK ACCOUNT, LEDGER 11 Page 5

2008				Debit ($)	2008				Credit ($)
June	2	Balance forward	42	500,000	June				
	4	Sales	43	125,000		3	Purchase	43	80,450
						6	Purchase	43	265,000

reports of more than 11,000 U.S. companies can be viewed at the Web site www.irin.com.

The Balance Sheet

The *balance sheet*, also called the *consolidated balance sheet* or *statement of consolidated financial condition*, is a quantitative summary of a company's financial condition at a specific point in time (at the end of the calendar or fiscal year), including *assets, liabilities*, and *net worth* (share owners' equity, stockholders' equity, or proprietorship). *Equity* means ownership, generally in the form of common stock or as a holding company. The balance sheet is prepared from balances in the ledger accounts. The overall entries in the balance sheet must conform to the fundamental accounting equation:

$$\text{Assets} = \text{Liabilities} + \text{Net Worth} \tag{16.1}$$

For publicly held companies, the net worth is the stockholders' equity. Bankers and other grantors of credit to companies are concerned with the margin of security for their loans. The balance sheet provides them with two important measures: (1) the assets owned by the company and (2) the liabilities owed by the company. A representative consolidated balance sheet for a large fictitious corporation, U. S. Shale Gas, Inc., is given in Table 16.3 for the calendar year ending December 31, 2013. In the United States, a corporation is the most common form of business organization, one that is chartered by a state and given many legal rights as an entity separate from its owners. It is characterized by the limited liability of its owners, the issuance of shares of easily transferable stock, and existence as a going concern. The balance sheet is divided, according to Eq. (16.1), into three sections: Assets, Liabilities, and, in this case, Shareholders' Equity (in place of Net Worth). Each section is divided into accounts in which entries are the balances in the ledger accounts as of the date of the balance statement. All numbers in the table represent millions of U.S. dollars.

As shown in Table 16.3, assets for this corporation are divided into Current Assets, Investments, Property, and Other Assets. *Current assets* are items of economic value that could be converted to cash in less than one year, including cash and cash equivalents, marketable securities, accounts receivable, inventories, prepaid expenses, and deferred income taxes. The current assets total $4,630,000,000. *Investments* pertain to investments in companies in which ownership interest by U.S. Shale Gas is 50% or less, but over which U. S. Shale Gas exercises significant influence over operating and financial policies. *Property* constitutes fixed assets, including land, buildings, machinery, equipment, and software, and is listed at its *book value*, which is the original cost (the so-called *basis*), corrected for accumulated depreciation. *Depreciation* is the allocation of the cost of an asset over a period of time for accounting and tax purposes. It accounts for a decline in the value of a property due to general wear and tear or obsolescence. Property still in use remains on the books and the balance sheet even after it is completely depreciated. *Goodwill* is an intangible asset that provides a company a competitive advantage, such as a well-known and accepted brand name, reputation, or high employee morale. In addition to goodwill, other intangible assets may be listed, such as patents and trademarks. The total assets are shown as $14,211,000,000.

The second part of the balance sheet in Table 16.3 lists the liabilities and stockholders' equity. *Current liabilities* include all payments that must be made by the company within one year. The total for U. S. Shale Gas is $4,153,000,000. *Long-term debts*, often in the form of bonds, are due after more than one year from the date of the balance sheet. They total $3,943,000,000. *Other noncurrent liabilities* total $1,754,000,000 and include pension and other postretirement benefits as well as reserves for any company operations that are discontinued. Total liabilities are $9,850,000,000. We note that liabilities are less than assets by $4,361,000,000. Thus, by Eq. (16.1), this difference must be the stockholders' equity. This equity includes the par value of issued common stock, which totals $1,000,000,000. The par value of a share of stock is an arbitrary amount that has no relationship to the market value of the stock, but is used to determine the amount credited to the stock account. If the stock is issued for more than its par value, the excess is credited to the account shown as *Capital in Excess of Par Value*. In Table 16.3, the par value is $1.00 per share, but the stock was issued at $4.23 per share. Companies frequently repurchase shares of their common stock, resulting in a reduction of stockholders' equity. Because the shares are placed in a treasury, the transaction appears as *Treasury Stock at Cost*. In Table 16.3, that amount is $3,428,000,000. The other account under stockholders' equity is *Retained Earnings*, which is the accumulated retained earnings that are increased each year by net income. The amount of this entry must be such that Eq. (16.1) is satisfied. This is seen to be the case in Table 16.3, where the net stockholders' equity is $4,361,000,000, giving total liabilities

Table 16.3 Consolidated Balance Sheet for U. S. Shale Gas in Millions of Dollars as of 31 December 2013

ASSETS			
Current Assets			
Cash and Cash Equivalents	107		
Marketable Securities	45		
Accounts Receivable	2,692		
Inventories:			
Finished Products and Work in Progress	1,420		
Materials and Supplies	312		
Deferred Income Tax Assets	54		
Total current assets		4,630	
Investments			
In Nonconsolidated Affiliates	544		
Other	1,476		
Total investments		2,020	
Property			
Land	200		
Buildings	2,190		
Plant Machinery and Equipment	7,684		
Office equipment	645		
Computer Software	242		
Less accumulated depreciation	(6,006)		
Net property		4,955	
Other Assets			
Goodwill	952		
Other Intangible Assets	1,654		
Total other assets		2,606	
TOTAL ASSETS			14,211
LIABILITIES			
Current Liabilities			
Short-term Debt (payable within one year)	150		
Accounts Payable	2,773		
Income Taxes Payable	130		

(*Continued*)

Table 16.3 (*continued*)

Deferred Income Tax Liabilities	21		
Dividends Payable	104		
Accrued Current Liabilities	975		
Total Current Liabilities		4,153	
Long-term Debt		3,943	
Other Noncurrent Liabilities			
Pension and Other Postretirement Benefits	892		
Reserve for Discontinued Operations	78		
Other Noncurrent Obligations	784		
Total Other Noncurrent Liabilities		1,754	
TOTAL LIABILITIES			9,850
STOCKHOLDERS' EQUITY			
Common Stock (authorized 2,000,000,000 shares at $1.00 par value; 1,000,000,000 issued)	1,000		
Capital in Excess of Par Value of Common Stock	4,230		
Retained Earnings	2,559		
Less Treasury Stock at Cost, 300,000,000 shares	(3,428)		
NET STOCKHOLDERS EQUITY			4,361
TOTAL LIABILITIES + STOCKHOLDERS' EQUITY			14,211

plus stockholders' equity as $14,211,000,000, which is equal to total assets by Eq. (16.1).

The Income Statement

An annual report also contains *the income statement*, also called the *statement of consolidated income* (loss) or *statement of consolidated operations*, which is an accounting of sales, expenses, and net profit (same as net earnings and net income) for a given period. In the annual report, the period is for one calendar or fiscal year. However, many companies also issue quarterly statements. Bankers, other grantors of credit, and investors and speculators pay close attention to the income statement because it provides the net profit of the company, which is an indication of the ability of the company to pay its debts and grow. *Net profit* is defined as *revenues* (sales) minus cost of sales, operating expenses, and taxes over a given period of time with *gross profit* (gross earnings or gross income) being revenues minus just cost of sales and operating expenses (i.e., profit before taxes).

A representative consolidated income statement for the large fictitious corporation U. S. Shale Gas is given in Table 16.4 for the calendar year 2013. *Net sales* is gross sales minus returns, discounts, and allowances. The *cost of goods sold* (cost of sales) is the cost of purchasing the necessary *raw materials* to produce the goods plus the *cost of manufacturing* the finished products. Operating expenses are expenses other than those of manufacture and include research and development expenses; selling, general, and administrative expenses; insurance and finance company operations; and amortization and adjustments of goodwill. *Amortization* is the gradual elimination of a liability, such as a mortgage, in regular payments over a specified period of time and whose payments are sufficient to cover both principal and interest. Income from operations equals gross profit minus operating expenses. From this, interest expenses are subtracted to give gross income (sometimes called net profit before income taxes). Interest expenses pertain to interest payments to bond holders and interest on loans. Subtraction of income taxes gives net income. Table 16.4 shows that from an annual net sales of $11,504,000,000, the net profit is $803,000,000 or 6.98%.

The Cash Flow Statement

The *cash flow statement*, also called the *consolidated statement of cash flow* or *statement of consolidated cash flow*, is a summary

Table 16.4 Consolidated Income Statement for U. S. Shale Gas in Millions of Dollars for the Calendar Year 2013

Net sales	11,504	
Cost of goods sold	9,131	
GROSS PROFIT		2,373
OPERATING EXPENSES		
Research and development expenses	446	
Selling, general, and administrative expenses	439	
Insurance and finance company operations	34	
Amortization and adjustments of goodwill	64	
TOTAL OPERATING EXPENSES		983
INCOME FROM OPERATIONS		1,390
Interest expense	185	
GROSS INCOME		1,205
Provision for income taxes	402	
NET INCOME		803

Table 16.5 Consolidated Cash Flow Statement for Toledo Chemicals in Millions of Dollars for Calendar Year 2013

OPERATING ACTIVITIES		
Net income available for common stockholders	3,151	
Adjustments to reconcile net income to net cash:		
Depreciation	675	
Depletion	383	
Amortization	486	
Provision for deferred income tax	125	
Net gain (loss) on sales of property	(103)	
Changes in assets and liabilities involving cash:		
Accounts and notes receivable	(441)	
Inventories	(389)	
Accounts payable	315	
CASH PROVIDED BY OPERATING ACTIVITIES		4,202
INVESTING ACTIVITIES		
Capital expenditures	(1,227)	
Sales of property	231	
Sales (purchases) of investments	2,221	
CASH PROVIDED IN INVESTING ACTIVITIES		1,225
FINANCING ACTIVITIES		
Payments on long-term debt	(524)	
Purchases of treasury stock	(15)	
Proceeds from sales of preferred stock	620	
Dividends paid to stockholders	(485)	
CASH PROVIDED (USED) IN FINANCING ACTIVITIES		(404)
INCREASE (DECREASE) IN CASH AND CASH EQUIVALENT		5,023

of the cash flow of a company over a given period of time. The *cash flow* equals cash receipts minus cash payments over a given period of time or, equivalently, net profit plus amounts charged off for depreciation, depletion, and amortization. These latter three items are added back because they do not represent any cash transactions. *Depletion*, which is similar to depreciation, accounts for the exhaustion of natural resources owned by the company, such as oil, timber, and minerals. The cash flow statement is a measure of a company's financial health and, in recent years, has become a very important feature of the annual report.

A representative consolidated cash flow statement for a fictitious company, Toledo Chemicals, is given in Table 16.5 for the calendar year 2013. The statement is divided into three parts: operating activities, investing activities, and financing activities. Cash flows are either into or out of the company. In this statement, cash flows out of the company are stated in parentheses. Under operating activities, to the net income available for holders of common stock are added depreciation, depletion, amortization, and provision for deferred income tax; subtracted is a net loss on sales of property. Since the cash is not yet in hand, receivables and inventory are subtracted, but accounts payable (not yet paid)

is added. The resulting cash flow into the company for operating activities for the year 2013 is $4,202,000,000. Under investing activities, capital expenditures by the company are subtracted from the sum of sales of property and sales of investments to give a cash flow of $1,225,000,000 into the company. Under financing activities, cash flows out of the company due to payments of long-term debt, purchases of treasury stock, and dividends paid to stockholders are partially offset by proceeds to the company from sales of preferred stock to give a cash flow out of the company of $404,000,000. For the combined three activities, the cash flow into the company is $5,023,000,000.

Financial Ratio Analysis

The analysis of the performance and financial condition of a company is carried out by computing several ratios from information given in its annual report. Such analysis must be done carefully because seemingly good performance might be due more to such factors as inflation and reduction of inventory than to improvements in company operations.

Current Ratio

The *current ratio* is defined as current assets divided by current liabilities. It is an indication of the ability of a company to meet short-term debt obligations. The higher the current ratio, the more liquid the company is. However, too high a ratio may indicate that the company is not putting its cash or equivalent cash to good use. A reasonable ratio is 2, but it is better to compare current ratios of companies in a similar business. From Table 16.3, the current ratio of U.S. Shale Gas is $4{,}630/4{,}153 = 1.11$, which is a low value. On Aug. 31, 2013, Monsanto Co. had a much better current ratio of 2.32.

Acid-Test Ratio

The *acid-test ratio*, also called the *quick ratio*, is a modification of the current ratio with the aim of obtaining a better measure of the liquidity of a company. In place of current assets, only assets readily convertible to cash, called *quick assets*, are used. Thus, it is defined as the ratio of current assets minus inventory to current liabilities. Marketable securities, accounts receivable, and deferred income tax assets are considered to be part of quick assets. From Table 16.3, the quick assets for U. S. Shale Gas, in millions of dollars, are $4{,}630 - 1{,}420 - 312 = 2{,}898$. This gives an acid-test ratio of $2{,}898/4{,}153 = 0.70$, which is not a desirable ratio since it is less than unity. As of August 31, 2013, Monsanto Company had a much better acid-test ratio of 1.64.

Equity Ratio

The *equity ratio* is defined as the ratio of stockholder's equity to total assets. It measures the long-term financial strength of a company. From Table 16.3, the equity ratio for U. S. Shale Gas is $4{,}361/14{,}211 = 0.31$, which, again, is too low a value. The ratio should be about 0.50. If the equity ratio is too high, the company may be curtailing its growth. As of August 31, 2013, Monsanto Company had a satisfactory equity ratio of 0.61.

These three financial ratios use only data from the balance sheet. We next consider two ratios that use both the balance sheet and the income statement and then two ratios that use data from the income statement only. These ratios are particularly susceptible to economic conditions, which can, sometimes, change quickly from year to year.

Return on Total Assets (ROA)

One measure of how a company uses its assets is the *return on total assets*, which is defined as the ratio of income before interest and taxes to total assets. Using data from Tables 16.3 and 16.4, this ratio for U. S. Shale Gas is $1{,}390/14{,}211 = 0.098$ or 9.8%, which is less than the 12.01% achieved by Monsanto Company in the fiscal year of 2013.

Return on Equity (ROE)

A more widely quoted return measure is the *return on stockholders' equity*, which measures the ability of a company to reinvest its earnings to generate additional earnings. It is identical to ROA except that the divisor in the ratio is common stockholders' equity instead of total assets. For U.S. Shale Gas, the ROA from data in Tables 16.3 and 16.4 is $1{,}390/4{,}361 = 0.319$ or 31.9%, which is higher than the 19.76% achieved by Monsanto Company in the year 2013. Historically, the norm for ROE in the United States is approximately 11%. However, in 2011, the 30 companies that make up the Dow Jones Industrial Average (DJIA) had an average ROE of 25%. For the five-year period of 2009–2013, the three DJ (Dow Jones) companies with the highest ROE were Boeing (104%), IBM (71%), and Microsoft (40%).

Operating Margin

The operating margin is defined as the ratio of income from operations (called revenues) to net sales. For some industrial groups, it is highly susceptible to general economic conditions. For U. S. Shale Gas, Table 16.4 gives an operating margin of $1{,}390/11{,}504 = 12.1\%$, which is somewhat lower than the 16.7% achieved by Monsanto Company in the year 2013.

Profit Margin

The *profit margin*, also called the *net profit ratio*, is defined as the ratio of net income after taxes to net sales. It is more widely quoted than the operating margin and is also more susceptible to general economic conditions. When used over a period of years, it is a very useful measure of the growth of a company. Using the data of Table 16.4, the profit margin for U. S. Shale Gas was $803/11{,}504 = 0.070$ or 7.0%. In the third quarter of the recession year 2001, the average operating margin for 900 companies in the United States was only 3.0%, with the 25 largest publicly held chemical companies averaging a dismal 0.9%. A year earlier, when general economic conditions were much more favorable, these two values were higher at 6.8% and 6.6%, respectively. For some companies, operating margins can be quite high. From 2002 to 2006, Microsoft had an average profit margin of 25.3%, compared to an industry average of 18.3% and an S&P 500 company

average of 11.7%. In 2006, Pfizer achieved 25.2% whereas 3M, Questar Gas, DuPont, EXXON/Mobil, IBM, and Starbucks had lower profit margins of 17.0%, 14.2%, 10.8%, 10.5%, 10.3%, and 7.5%, respectively. The average profit margin for companies in the S&P 500 bottomed in 2009 to approximately 1%. By 2013, it had climbed back to approximately 9%.

Cost Accounting

Cost accounting is a branch of accounting that deals specifically with the identification, recording, tracking, and control of costs. Accountants allocate these costs among (1) *direct costs*, both labor and materials, (2) *indirect costs or overhead*, and (3) other miscellaneous expenses. Direct costs are those costs directly attributable to a project such as the construction of a new plant or the operation of an existing plant. Indirect costs or overhead are costs that are generally shared among several projects and are allocated to the individual projects by a formula or some other means. Miscellaneous expenses include administration, distribution and selling, research, engineering, and development. Direct costs can be more accurately identified, measured, and controlled, and are generally the largest fraction of the total cost.

Cost accounting is of great interest in plant construction and plant operation. It is also of importance when making an economic evaluation of a process design to determine whether a plant should be built. By studying company cost accounting records for existing manufacturing plants, chemical engineers preparing economic evaluations of proposed new processing plants or revamps of existing processes are less likely to omit or neglect costs that may have a significant influence on estimated process profitability measures. Large companies that engage in a number of plant construction and plant operation projects use cost accounting records to make comparisons of costs. These records are invaluable to company process design engineers when preparing estimates of investment and operating costs for new projects.

Cost accounting for direct costs is accomplished in terms of unit cost and quantity. The product of these two is the cost. For example, an existing process may have used 11.2 million kg/yr of a raw material with an average unit cost of \$0.52/kg. The cost is then \$5,824,000/yr. At the beginning of the year, a standard cost and a standard quantity are established for the year, for example, 10,500,000 kg and \$0.51/kg. The budgeted cost for the year is $10{,}500{,}000 \times 0.51 = \$5{,}355{,}000$. The differences between the actual and standard unit costs and quantities are called variances. Accountants can set variance flags to warn process managers of possible cost overruns. In this example, the quantity variance is $11.2 - 10.5$ or 0.7 million kg/yr. This is a percentage variance of $0.7/10.5 \times 100\% = 6.7\%$. The cost variance is \$0.01/kg or a percentage variance of $0.01/0.51 \times 100\% = 2.0\%$.

A *variance in quantity* may reveal the extent of waste. For example, suppose a plant is scheduled to produce 22,700,000 kg for the coming year. Design calculations indicate that 1.2 kg of raw material is required to produce each kilogram of product. The actual production rate for the year is 21,800,000 kg. The design rate for the raw material at the actual production rate is $1.2 \times 21{,}800{,}000 = 26{,}160{,}000$ kg/yr. However, the accounting records show for the raw material a beginning inventory of 1,070,000 kg, an ending inventory of 1,120,000 kg, and a purchase of 26,980,000 kg. Thus, the amount of raw material used is $26{,}980{,}000 + 1{,}070{,}000 - 1{,}120{,}000 = 26{,}930{,}000$ kg. If the design calculations are accepted as the basis, the waste is $26.93 - 26.16 = 0.77$ million kg. At \$0.52/kg, this represents a loss for the year of $\$0.52 \times 770{,}000 = \$400{,}400$, a significant amount of money and an incentive to find the reasons for the waste and eliminate it. Similar calculations can be made for utility usage by expressing both the design and the actual values for the quantities of utilities on a per-kilogram production of product basis.

The analysis of *variance in cost* is complicated when the price of the material, whether it be the raw material or the finished product, varies during the year. This is because of the need for the company to maintain inventories of raw materials and finished products. Two methods of costing in common use are: (1) *first-in, first-out*, and (2) *last-in, first-out*. In the first method, abbreviated *as FIFO*, the cost of the oldest material in the inventory is used first. In the second method, abbreviated as *LIFO*, the cost of the most recent material in the inventory is used first; that is, the older material is kept in the inventory. Companies may also use any of several average costing methods. To illustrate the possible significance to the company of choosing between the FIFO and LIFO methods, consider the following example. At the beginning of the year 2012, ABC Oil Producing Company had an inventory of 100,000 barrels (bbl) of crude oil with a unit cost of \$50/barrel. During the first quarter of 2012, purchases of crude oil were made at three different prices as follows:

Month	Barrels Purchased	Cost (\$/bbl)
January	80,000	50
February	100,000	60
March	150,000	30

At the end of March, the inventory is 75,000 barrels. Determine the cost of the barrels sold during the quarter. The total number of barrels sold during the quarter is $100{,}000 - 75{,}000 + 80{,}000 + 100{,}000 + 150{,}000 = 355{,}000$.

FIFO method:

Cost of barrels sold by first-in, first-out is

$$\begin{aligned} 100{,}000 \times 50 &= \$5{,}000{,}000 \\ 80{,}000 \times 50 &= 4{,}000{,}000 \\ 100{,}000 \times 60 &= 6{,}000{,}000 \\ 75{,}000 \times 30 &= 2{,}250{,}000 \\ \text{Total barrels sold} &= 355{,}000 \\ \text{Total cost of barrels sold} &= \$17{,}250{,}000 \end{aligned}$$

LIFO method:

Cost of barrels sold by first-in, first-out is

$$\begin{aligned} 150{,}000 \times 30 &= \$4{,}500{,}000 \\ 100{,}000 \times 60 &= 6{,}000{,}000 \\ 80{,}000 \times 50 &= 4{,}000{,}000 \\ 25{,}000 \times 50 &= 1{,}250{,}000 \\ \text{Total barrels sold} &= 355{,}000 \\ \text{Total cost of barrels sold} &= \$15{,}750{,}000 \end{aligned}$$

The total cost of barrels sold by the LIFO method is \$1,500,000 less than that of the FIFO method. The unit costs are

$48.59/bbl for the FIFO method and $44.37/bbl for the LIFO method.

16.2 COST INDEXES AND CAPITAL INVESTMENT

In all stages of the design process, estimates of both the total capital investment (TCI) and annual cost of manufacture (COM) are crucial for the evaluation of product and processing alternatives. As discussed in Chapters 6 and 8, many heuristics have been developed to create process flowsheets that reduce costs and increase the profitability of the processes being designed. In Chapters 9 and 11, approximate measures are used such as the annualized cost (involving both the capital investment and the annual manufacturing cost) for the comparison of alternative process flowsheets. In some cases, when the manufacturing costs, especially the costs of fuel, are high, it is possible to compare the alternatives on the basis of the lost work or thermodynamic efficiency. This is the subject of Chapter 10 in which several considerations are presented for adjusting the minimum approach temperature in heat exchangers, replacing valves with turbines, and reducing pressure drops in pipelines.

In this chapter and the next, commonly used methods are developed for assessing the profitability of product and process designs. This chapter focuses on the so-called *direct permanent* (capital) *investment,* C_{DPI}, that is, the estimation of the purchase cost of required equipment and the cost of its installation in a potential chemical process. To this is added a contingency, the cost of land, any applicable royalties, and the cost of starting up the plant to give the *total permanent investment*, C_{TPI}. The *contingency* accounts for uncertainty in the estimate and the possibility of not accounting for all of the costs involved. *Royalties* are payments made for the use of property, especially a patent, copyrighted work, franchise, or natural resource through its use. In Chapter 17, the *annual manufacturing costs*—together with the general annual expenses such as administration and marketing, which are listed in a *cost sheet*—are considered. These costs are the basis for an estimate of the *working capital* needed to compute the *total capital investment* for a chemical process. Then, together with depreciation and tax schedules, cash flows are computed that lead to profitability measures such as the *investor's rate of return* (IRR), also known as the *discounted cash flow rate of return* (DCFRR).

Cost Indexes

Sections 16.5–16.8 describe various approaches for estimating the purchase costs of processing equipment items. In the simplest approach (Sections 16.5–16.7), graphs and equations are provided that give cost estimates as a function of equipment sizes. But, these prices generally increase with time, and the graphs and equations are based upon prices in mid-2014. Hence, at later dates, these estimates are adjusted using cost indexes as shown below. Section 16.8 describes the Aspen Process Economic Analyzer (APEA), which estimates purchase costs using an extensive database of material and construction labor costs and detailed, though preliminary, design methods. The APEA database is updated regularly, and consequently, cost estimates do not need to be adjusted using cost indexes. Finally, quotes from vendors should be the most accurate and up-to-date.

When using purchase cost estimates from an earlier date, an estimate of the cost at the later date is made by multiplying the cost from an earlier date by the ratio of a *cost index, I*, at that later date to a base cost index, I_{base}, that corresponds to the date that applies to the purchase cost:

$$Cost = Base\ cost \left(\frac{I}{I_{\text{base}}} \right) \tag{16.2}$$

The indexes most commonly considered by chemical engineers are:

1. ***The Chemical Engineering (CE) Plant Cost Index.*** It is published in each monthly issue of the magazine *Chemical Engineering* with $I = 100$ for 1957–1959. A complete description of the index appears in *Chemical Engineering*, **109**(1), 62–70(2002) in an extensive revision by W.M. Vatavuk.
2. ***The Marshall & Swift (MS) Equipment Cost Index.*** It was published in each monthly issue of the magazine *Chemical Engineering* through 2011, with $I = 100$ for 1926. A complete description of the index appears in *Chemical Engineering*, **54**(11), 124 (1947); **85**(11), 189 (1978); and **92**(9), 75 (1985).
3. ***The Nelson-Farrar (NF) Refinery Construction Cost Index.*** It is published in the first issue each month of the magazine *Oil & Gas Journal* with $I = 100$ for 1946. A complete description of the index appears in the magazine *Oil & Gas Journal*, **63**(14), 185 (1965); **74**(48), 68(1976); and **83**(52), 145 (1985).
4. ***The Engineering News-Record (ENR) Construction Cost Index.*** It is published each week in the magazine *Engineering News-Record* and in each monthly issue of *Chemical Engineering* with $I = 100$ for 1967. A complete description of the index appears in *Engineering News-Record*, **178**(11), 87 (1967).

The CE and NF indexes pertain to the entire processing plant, taking into account labor and materials to fabricate the equipment, deliver it, and install it. However, the NF index is restricted to the petroleum industry whereas the CE index pertains to an average of all chemical processing industries. The ENR index, which is a more general index that pertains to the average of all industrial construction, is a composite of the costs of structural steel, lumber, concrete, and labor. The MS index pertains to an all-industry average equipment purchase cost. However, the MS index is accompanied by a more useful process industries average equipment cost index, averaged mainly for the chemicals, petroleum products, paper, and rubber industries. The CE and NF indexes also provide cost indexes for only the purchase cost of several categories of processing equipment, including heat exchangers, pumps and compressors, and machinery.

Figure 16.1 compares, on a semilogarithmic plot, the value of the CE Plant Cost Index, MS Process Industries Average Cost Index, NF Refinery Cost Index, and ENR Construction Cost

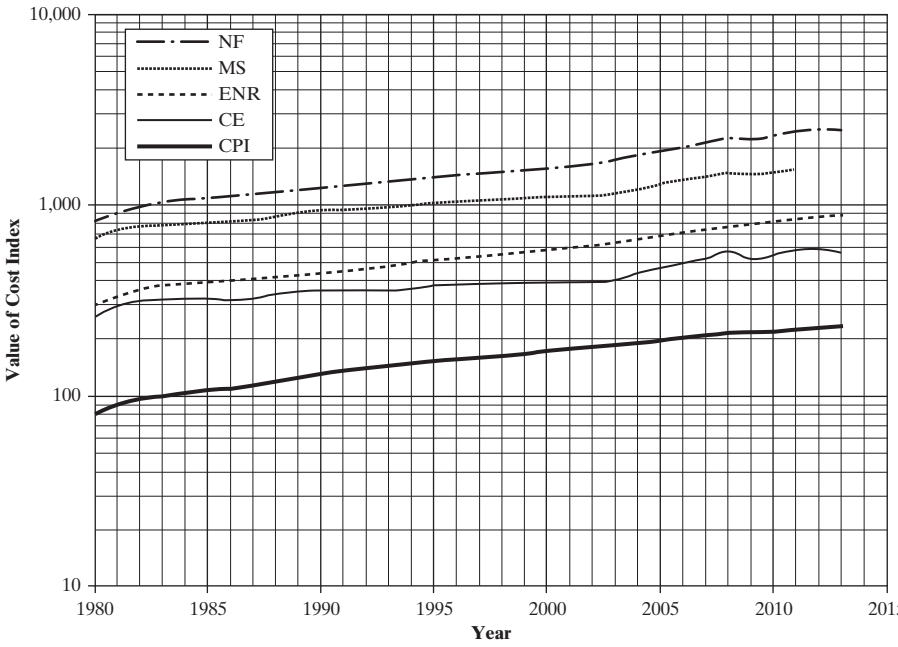

Figure 16.1 Comparison of annual average cost indexes.

Index for the period of 1980 to 2013. The same values are tabulated in Table 16.6. It can be seen that costs increased steadily through 2006 but oscillated significantly while increasing from 2008 through 2013—probably due to the serious recession. In the 33-year period of Table 16.6, the cost indexes increased by factors of 2.172 for CE, 2.277 for MS, 3.026 for NF, and 2.934 for ENR. These factors correspond to the following respective increases per year: 3.55%, 4.12%, 6.14%, 5.86%, respectively. Included in Figure 16.1 and Table 16.6 are values for the U. S. Consumer Price Index (CPI) published by the federal government and used to measure the rate of inflation with a basis of 10.0 for the year 1914. In the 33-year period from 1980 to 2013, the CPI increased by a factor of 2.828, giving an average consumer inflation rate of 5.54% per year, very close to the ENR index rate.

Commodity Chemicals

Manufactured chemicals, also referred to as basic chemical products, can be classified as either (1) primary chemicals, usually referred to as *commodity chemicals* or *bulk chemicals*, or (2) secondary chemicals, which include *fine chemicals* and *specialty chemicals*. Commodity chemicals have a known chemical structure, are most often produced by continuous processing, and are characterized by high production rates (typically more than 10 million lb/yr), high sales volumes, low selling prices, and global competition. Secondary chemicals are most often produced by batch processing and are characterized by low production rates (typically less than 1 million lb/yr), low sales volume, and high selling prices.

Many of the high-volume commodity chemicals are listed in Table 16.7, including U. S. production rates in the year 2005 from the July 10, 2006, issue of *Chemical & Engineering News*, and the typical sales price in the year 2014 from *ICIS Chemical Business*. Note that 14 commodity chemicals are produced at total rates of more than 10 billion lb/yr, equivalent to about 125,000 lb/hr. A large petroleum refinery producing many products feeds 100,000 barrels of crude oil per day, equivalent to about 1,300,000 lb/hr. Also, note that more recent production rates have not been published by *C&E News* since 2006—probably because commodity chemicals production in the United States has remained level, as companies built new plants closer to the sources of fossil fuels outside the United States. Recently, however, with the vast expansion of U.S. shale-gas production, large new plants are being announced for construction near gas drilling rigs.

Prices for the commodity chemicals in Table 16.7 range from as low as \$0.04/lb for hydrochloric acid to \$0.95/lb for acrylonitrile. These prices may be compared to regular grade gasoline at the pump before state and federal taxes are added at \$3.50/gal, equivalent to \$0.59/lb. Most fine and specialty chemicals cost much more than commodity chemicals. For example, cetyl (palmityl) alcohol in crystalline flake form, which is used as a textile conditioner, an emulsifier, and a component of cosmetics, costs above \$4/lb. Many pharmaceuticals cost significantly more. For example, tPA, a drug to degrade blood clots, costs as much as \$200 for a 100-mg dose!

Economy-of-scale and the Six-tenths Factor

When demand is high for commodity chemicals, advantage can be taken of the *economy of scale*. This principle holds as long as each major piece of equipment in the plant can be made larger as the production rate is increased. This makes possible a single-train plant with no or few pieces of equipment duplicated. However, when the equipment size exceeds the maximum size that can be fabricated and shipped, then equipment must be duplicated and the economy of scale is lost because two or

Table 16.6 Comparison of Annual Average Cost Indexes

	CE	MS	NF	ENR	CPI
Years	Chemical Engineering Plant Cost Index Year 1957–1959 = 100	Marshall-Swift Process Industry Index Year 1926 = 100	Nelson-Farrar Refinery Construction Index Year 1946 = 100	Engineering News-Record Construction Index Year 1967 = 100	U.S. Federal Government Consumer Price Index Year 1914 = 10
1980	261	675	823	303	82.4
1981	297	745	904	330	90.9
1982	314	774	977	357	96.5
1983	317	786	1,026	380	99.6
1984	323	806	1,061	387	103.9
1985	325	813	1,074	392	107.6
1986	318	817	1,090	401	109.6
1987	324	830	1,122	412	113.6
1988	343	870	1,165	422	118.3
1989	355	914	1,196	429	124.0
1990	358	935	1,226	441	130.7
1991	361	952	1,253	450	136.2
1992	358	960	1,277	464	140.3
1993	359	975	1,311	485	144.5
1994	368	1,000	1,350	503	148.2
1995	381	1,037	1,392	509	152.4
1996	382	1,051	1,419	524	156.9
1997	387	1,068	1,449	542	160.5
1998	390	1,075	1,478	551	163.0
1999	391	1,083	1,497	564	166.6
2000	394	1,110	1,543	579	172.2
2001	394	1,109	1,580	590	177.1
2002	396	1,121	1,642	609	179.9
2003	402	1,143	1,710	623	184.0
2004	444	1,202	1,834	662	188.9
2005	468	1,295	1,919	693	195.3
2006	500	1,365	2,008	722	201.6
2007	525	1,399	2,107	742	207.3
2008	575	1,478	2,251	774	215.3
2009	522	1,446	2,218	798	214.5
2010	551	1,477	2,338	819	218.1
2011	586	1,537[a]	2,436	844	224.9
2012	585		2,465	867	229.6
2013	567		2,490	889	233.0

[a] Data from *Chemical Engineering* until April 2012.

more trains of equipment are required. The economy of scale is embedded in the following relationship, which correlates the variation of cost with capacity:

$$\frac{Cost_2}{Cost_1} = \left(\frac{Capacity_2}{Capacity_1}\right)^m \tag{16.3}$$

This relationship has been found to give reasonable results for individual pieces of equipment and for entire plants. Although, as shown by Williams (1947a,b), the exponent, m, may vary from 0.48 to 0.87 for equipment and from 0.38 to 0.90 for plants, the average value is close to 0.60. Accordingly, Eq. (16.3) is referred to as the "six-tenths rule." Thus, if the capacity is doubled, the 0.6 exponent gives only a 52% increase in cost. Equation (16.3) is used in conjunction with Eq. (16.2) to take cost data from an earlier year at a certain capacity and estimate the current cost at a different capacity. As an example, suppose the total depreciable capital investment for a plant to produce 1,250 tonne/day (1 tonne = 1,000 kg) of ammonia was $140 million in 1990. In the year 2013, the estimated investment

Table 16.7 Major U. S. Commodity Chemicals

Chemical	U.S. Production in 2005 (millions of pounds)	Typical Price in 2014 ($/lb)	Typical Raw Materials Required
Sulfuric acid	80,512	0.05	Sulfur dioxide, oxygen, water
Ethylene	52,853	0.68	Petroleum
Propylene	33,803	0.70	Petroleum
Phosphoric acid	25,571	0.37	Phosphorum, oxygen, water
Ethylene dichloride	24,930	0.18	Ethylene, chlorine
Chlorine	22,432	0.12	Sodium chloride, water
Ammonia	21,550	0.29	Nitrogen, hydrogen
Sodium hydroxide	18,483	0.29	Sodium chloride, water
Benzene	14,635	0.54	Coal tar, petroleum
Ammonium nitrate	14,006	0.086	Ammonia, nitric acid
Nitric acid	13,951	0.11	Ammonia, oxygen
Urea	12,789	0.26	Carbon dioxide, ammonia
Ethylbenzene	11,576	0.57	Benzene, ethylene
Styrene	11,116	0.73	Ethylbenzene
Hydrochloric acid	9,713	0.04	Byproduct of chemical processes
Cumene	7,736	0.062	Benzene, propylene
Ethylene oxide	6,980	0.76	Ethylene, oxygen
Ammonium sulfate	5,683	0.066	Ammonia, sulfuric acid
Vinyl acetate	2,926	0.067	Ethylene, acetic acid, oxygen
Acrylonitrile	2,917	0.95	Propylene, ammonia, oxygen
Sodium chlorate	2,577	0.24	Chlorine, sodium hydroxide

for a 2,500 tonne/day plant is as follows, where the CE index in Table 16.6 is used:

Estimated investment, millions of U.S. dollars,

$$= 140\left(\frac{2{,}500}{1{,}250}\right)^{0.6}\left(\frac{567}{358}\right) = 140(1.52)(1.584) = 337$$

Note that Sections 16.5 to 16.7 provide equations more accurate than Eq. 16.3 for each equipment type. Then, Section 16.8 shows how to use the APEA, which provides even more accurate estimates for determining the effect of scale on capital cost. The APEA can be used to estimate costs for the equipment items simulated in many of the major process simulators (e.g., ASPEN PLUS, Aspen HYSYS, UniSim®Design, ChemCAD, and PRO/II).

Typical Plant Capacities and Capital Investments for Commodity Chemicals

Because of the economy of scale, one might ask: How large are the capacities of the plants used to produce commodity chemicals and what are the corresponding capital investments? Haselbarth (1967) presented investment and plant capacity data for 60 types of chemical plants. This was followed by a more extensive compilation by Guthrie (1970, 1974) for 54 chemical processes. Unfortunately, because competition for the manufacture of commodity chemicals has become so keen in recent years, companies are now reluctant to divulge investment figures for new plants. However, Table 16.8 presents data for many of the commodity chemicals in Table 16.7. Plant production rates are large, 0.360 to 4.0 billion lb/yr. Corresponding total depreciable capital investments are also large, ranging from 20 million to 400 million U.S. dollars in 1995.

Note that in several cases, the plants produce combined products. Both ethylene and propylene are produced from a naphtha cut obtained from the fractionation of crude oil. A combined ammonia-urea fertilizer plant is common. The electrolysis of a brine solution produces both chlorine and sodium hydroxide. Recent literature data are usually given for plant capacities in tons per year (1 tonne = 1,000 kg) or tons per day (1 ton = 2,000 lb) of product, but the capacity data in Table 16.8 are given in pounds of product per year. Also included in the table is the value of C_b for use in the following modification of Eq. (16.3):

$$C_{TDC} = C_b\left(\frac{\text{Pounds/Year}}{\text{Production rate in Table 16.8}}\right)^{0.6}\left(\frac{I}{I_b}\right) \quad (16.4)$$

where C_{TDC} is the total depreciable capital (TDC) investment for the desired production rate and year. The data in Table 16.8 are indexed to the year 2005, when, according to Table 16.6, the Chemical Engineering Plant Cost Index was 381. Thus, for the year 2013, the right-hand side of Eq. (16.4) would include a cost index ratio of 567/381 = 1.49.

Table 16.8 Representative Plant Capacity and Capital Investment for Some Commodity Chemicals

Commodity Chemical(s)	Production Rate(s) (millions of pounds/year)	Capital Investment Factor [C_b in Eq. (16.4) for 1995]
Ethylene and propylene	1,200 and 600	$300,000,000
Sulfuric acid	4,000	$30,000,000
Ethylene dichloride	1,000	$80,000,000
Ammonia and urea	400 and 1,500	$400,000,000
Chlorine and sodium hydroxide	360 and 400	$80,000,000
Ethylbenzene	2,800	$80,000,000
Phosphoric acid	3,200	$50,000,000
Styrene	2,500	$200,000,000
Nitric acid	1,400	$50,000,000
Ethylene oxide	600	$80,000,000
Cumene	600	$30,000,000
Ammonium nitrate	800	$20,000,000

EXAMPLE 16.1

Estimate the total depreciable capital investment in the year 2013 for a plant to produce 90 ton/day of chlorine and 100 ton/day of sodium hydroxide. Assume that the plant will operate continuously for 330 days of the 365-day year.

SOLUTION

The production rate can be based either on the chlorine or the sodium hydroxide since both are produced in the same plant. The annual production rate of, say, chlorine in lb/year = 90(2,000)(330) = 59,400,000 lb/year. In Table 16.8, C_b = $80,000,000 for a chlorine production rate of 360,000,000 lb/yr. Using Eq. (16.4),

$$C_{TDC} = \$80 \text{ million} \left(\frac{59.4}{360}\right)^{0.6} \left(\frac{567}{381}\right) = \$40.4 \text{ million}$$

16.3 CAPITAL INVESTMENT COSTS

The total capital investment (TCI) of a chemical plant or a chemical product manufacturing facility is a one-time expense for the design, construction, and startup of a new plant or a revamp of an existing plant. It is analogous to the purchase price of a new house whose price includes purchase of the land, building-permit fees, excavation of the land, improvements to the land to provide utilities and access, preparation of architectural and construction drawings, construction of the house, landscaping, and contractor's fee. For convenience in cost accounting and cost estimation, Busche (1995) divides the TCI into the components listed in Table 16.9.

Before Table 16.9 is discussed, it is important to make a few distinctions. A new chemical processing plant may be an addition to an existing *integrated complex*, such as the addition of a polyethylene plant to a petroleum refinery that produces ethylene as one of its products; or it may be a *grass-roots plant* with no other chemical plants nearby. In both cases, a new plant requires *auxiliary facilities*, including utilities such as steam, cooling water, and electricity and other services, such as waste treatment and railroad facilities. A grass-roots plant may also require other new facilities, such as a cafeteria and a maintenance shop. In the integrated complex, the auxiliary facilities may be shared among the various plants in the complex. For either an integrated complex or a grass-roots plant, it is customary to separate the processing equipment directly associated with the manufacturing process from the auxiliary facilities by an imaginary fence that defines so-called *battery limits*, with the chemical processing plant inside the limits in an *on-site* area. The utilities and other services are outside the battery limits and are referred to as *offsite facilities*. Figure 16.2 shows typical offsite auxiliary facilities that might be associated with a grass-roots plant. Depending on the extent of the offsite facilities, they can be a significant fraction of the total capital investment.

Table 16.9 begins with the sums of so-called bare-module costs for fabricated process equipment and process machinery. These refer to the on-site part of the plant, which can be divided into modules, each of which contains a processing unit that may be a piece of *fabricated process equipment*, such as a heat exchanger, vessel, or distillation column; or an item of *process machinery*, such as a pump, compressor, centrifuge, conveyor, or robot arm. Fabricated equipment is custom designed, usually according to the pressure vessel code and other design standards, for any size and shape that can be shipped. Process machinery is selected from a vendor-supplied list of standard sizes and often includes a driver, such as an electric motor. A module contains not only the piece of equipment or machinery, but also all other materials for installing it (setting it up and connecting it to equipment in other modules), including the piping to and from other modules; the concrete (or other) foundation; ladders and other steel supporting structures; the instruments, controllers, lighting, and electrical wiring; insulation; and painting. Also, depending on plant location and size, some equipment may be housed in process buildings or shelters.

Given the purchase cost of a process unit, the installed cost is obtained by adding the cost of installation. It is common to estimate the cost of installation using *factored-cost methods* based

Table 16.9 Components of Total Capital Investment (TCI)

Total bare-module costs for fabricated equipment	C_{FE}				
Total bare-module costs for process machinery	C_{PM}				
Total bare-module costs for spares	C_{spare}				
Total bare-module costs for storage and surge tanks	$C_{storage}$				
Total cost for initial catalyst charges	$C_{catalyst}$				
Total bare-module costs for computers and software, including distributed control systems, instruments, and alarms	C_{comp}				
Total bare-module investment, TBM		C_{TBM}			
Cost of site preparation		C_{site}			
Cost of service facilities		C_{serv}			
Allocated costs for utility plants and related facilities		C_{alloc}			
Total of direct permanent investment, DPI			C_{DPI}		
Cost of contingencies and contractor's fee			C_{cont}		
Total depreciable capital, TDC				C_{TDC}	
Cost of land				C_{land}	
Cost of royalties				C_{royal}	
Cost of plant startup				$C_{startup}$	
Total permanent investment, TPI					C_{TPI}
Working capital					C_{wc}
Total capital investment, TCI					C_{TCI}

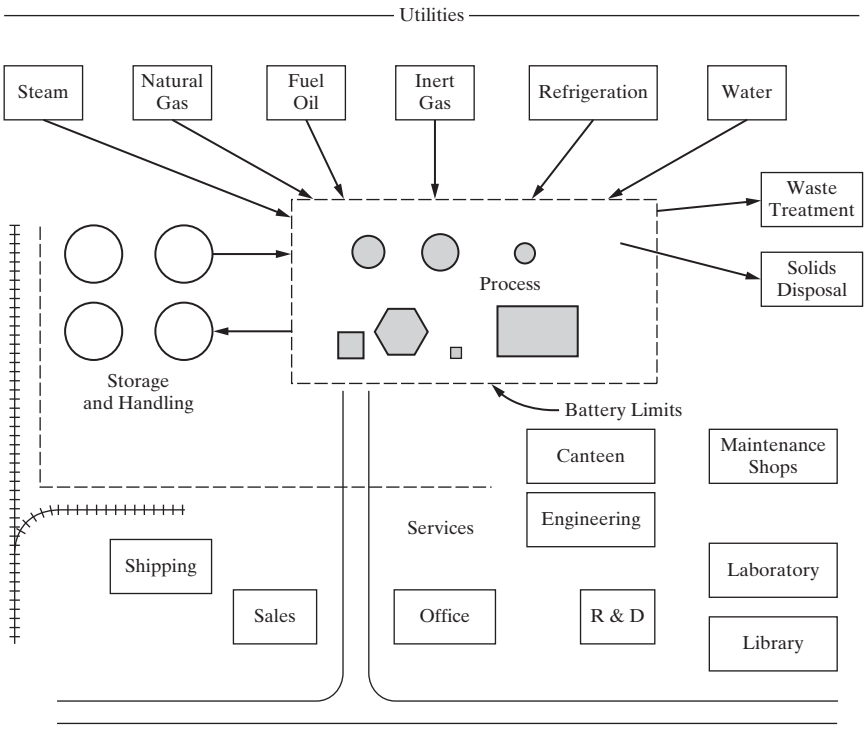

Figure 16.2 Plant services outside of process battery limits. (*Source:* Courtesy of C. A. Miller).

on the free on board (f.o.b.) purchase cost of the process equipment. For each piece of equipment, Guthrie (1969, 1974) provides factors to estimate the direct costs of materials and labor as well as indirect costs involved in the installation procedure. When these costs are added to the purchase cost, Guthrie calls the result the *bare-module* cost instead of the installed cost. As an illustration, see Table 16.10 in which the installation costs for a heat exchanger are given as a fraction of the f.o.b. purchase cost, C_P (i.e., the purchase cost does not include the delivery cost to the plant site). Although the f.o.b. purchase cost is \$10,000, the bare-module cost is \$32,910. The components of the installed cost are as follows.

Table 16.10 Example of Installation Costs for a Heat Exchanger to Give the Bare-Module Costs

	Cost ($)	Total Costs ($)	Fraction of f.o.b. Purchase Cost C_P
Direct module expenses			
Equipment purchase price, f.o.b., C_P		10,000	1.00 C_P
Field materials used for installation			
Piping	4,560		
Concrete	510		
Steel	310		
Instruments and controllers	1,020		
Electrical	200		
Insulation	490		
Paint	50		
Total of direct field materials, C_M		7,140	$C_M = 0.714\ C_P$
Direct field labor for installation			
Material erection	5,540		
Equipment setting	760		
Total of direct field labor, C_L		6,300	$C_L = 0.63\ C_P$
Indirect module expenses			
Freight, insurance, taxes, C_{FIT}	800		$C_{\text{FIT}} = 0.08\ C_P$
Construction overhead, C_O	5,710		$C_O = 0.571\ C_P$
Contractor engineering expenses, C_E	2,960		$C_E = 0.296\ C_P$
Total indirect expenses, C_{IE}		9,470	$C_{\text{IE}} = 0.947\ C_P$
Bare-module cost, C_{BM}		32,910	$C_{\text{BM}} = 3.291\ C_P$
			$F_{\text{BM}} = 3.291$

Direct Materials and Labor (M&L)

The costs of materials, C_M, for installation include the costs of concrete for the foundations, steel for structural support, piping from and to the other modules, instruments and controllers, lighting and electrical materials, insulation, and paint. Piping costs can be very substantial. Guthrie (1969, 1974) indicates that the cost of piping for a heat exchanger is typically 45.6% of the f.o.b. purchase cost whereas the total cost of materials for installation is estimated at 71.4% of the f.o.b. purchase cost as shown in Table 16.10. Hence, for a $10,000 heat exchanger, the cost of materials for installation is $7,140.

Similarly, Guthrie provides a field labor factor of 0.63 for installation; that is, the cost of labor for installation of the heat exchanger in Table 16.10, C_L, is 63% of the f.o.b. purchase cost or $6,300. The field labor cost accounts for the setting in place of the exchanger, installation of the associated piping, and all other labor costs utilizing the field materials. Combined with the cost of materials, the total cost of direct materials and labor for installation of the heat exchanger is $13,440, corresponding to a combined *materials and labor factor* of 1.344.

When using a factored-cost method like that of Guthrie, it is important to check the materials and labor factors for a specific job. Piping costs are usually underestimated and, in some cases, rival the purchase cost of the equipment. In this respect, separation towers often have the highest piping costs. Instruments and controllers can also be very expensive (with factors from 0.1 to 0.75) when they include analyzers, distributed control systems, and so on. The larger factor applies to a high degree of instrumentation and control of small equipment.

Other considerations involve materials of construction and the design pressure. As discussed later in this chapter, equations provide estimates of purchase costs based on the use of carbon steel at low-to-moderate pressures with multiplication factors to estimate the purchase costs for more expensive materials and higher pressures. Often the materials and labor factors are applied incorrectly to the resulting purchase costs. More specifically, the concrete foundation for a titanium vessel is no more expensive than that for a carbon steel vessel and is, therefore, a much smaller percentage of the vessel cost. Instrument and electrical costs are also a smaller percentage of the vessel cost. An example of the correct application of materials and labor factors is given later in Example 16.4.

The above discussion supposes that the vendor assembles all fabricated process equipment before shipping it to the plant for installation. In some cases, equipment cannot be shipped to the plant site in one piece and pre-installation field assembly will be required. Examples are furnaces and very large distillation columns and other vessels that cannot be trucked, barged, or sent by rail in one piece to the plant site. Large columns may be fabricated in sections in the shops of the vendor and transported to the plant site, where the sections are welded in a horizontal orientation before the column is erected to a vertical position. In this chapter, the purchase cost of field-assembled equipment includes the cost of pre-installation assembly at the plant site. Field-assembly costs are usually included in the purchase-cost quote from a vendor.

Indirect Costs

Other costs, such as the costs of freight to deliver the equipment to the plant site, with associated insurance and taxes, are considered to be *indirect expenses*, C_{FIT}. As shown in Table 16.10, these are estimated to be approximately 8% of C_P, that is, \$800 for the heat exchanger. These are accompanied by construction overhead, C_o, which includes fringe benefits for the workers (health insurance, vacation pay, sick leave, etc.), so-called *burden* (Social Security taxes, unemployment insurance, etc.), and salaries, fringe benefits, and burden for the supervisory personnel. The construction overhead also includes the costs of temporary buildings, roads, parking areas, cranes and machinery (purchased or rented), job site cleanup, security costs, and so on. These costs are estimated at approximately 57.1% of the f.o.b. purchase cost of the equipment, or \$5,710 for a \$10,000 heat exchanger. Contractor engineering expenses, C_E, are also included in the indirect expense category. This covers the costs of engineering, including salaries for project and process engineers, designers, procurement expenses, home office expenses, and so on. They are estimated to be 29.6% of C_P, that is, \$2,960 for a \$10,000 heat exchanger.

Summing the indirect module expenses (\$9,470) and combining the result with the cost of materials and labor, the *bare-module cost* for the \$10,000 heat exchanger, C_{BM}, is \$32,910, and, hence, the *bare-module factor,* F_{BM}, is 3.291.

Guthrie also computes and lists factors for starting with the f.o.b. purchase cost and arriving at the bare-module cost. For the heat exchanger example of Table 16.10, the factors are derived as follows:

Start with the equipment purchase price, f.o.b. of \$10,000.

The direct field materials, including the equipment, total (10,000 + 7,140) = \$17,140.

Guthrie defines the direct materials factor as (17,140)/10,000 = 1.714.

The direct field labor totals \$6,300.

Guthrie defines the direct labor factor as (6,300)/10,000 = 0.630.

The combined direct field materials and labor total \$23,440.

Guthrie defines the combined direct field materials and labor factor as (23,440/10,000) = 2.344.

The indirect module expenses total \$9,470.

Guthrie defines the indirect factor as (23,440 + 9,470)/23,440 = 1.404.

The total bare-module factor is 2.344 times 1.404 = 3.291, the same as above.

Bare-module factors vary among the various types of fabricated equipment and process machinery, decreasing somewhat with increasing size. The extent of this variation for ordinary materials of construction and low-to-moderate pressures can be seen in Table 16.11, which is taken from Guthrie (1974), based on single units of smaller size, where the factors are as much as 10% lower for multiple units of the same type. For the solids-handling equipment, the indirect factor is taken from Guthrie (1969) as 1.29. The bare-module factors vary from a value of 1.39 for crushers to separate solid particles by size to 4.16 for vertical pressure vessels, which are widely used for distillation, absorption, stripping, and flash drums. All of the equipment for handling solids and fluid-solids mixtures have factors less than 2.45. In Table 16.9, the sum of the bare-module costs for all items of fabricated equipment is C_{FE} whereas the sum of the bare-module costs for all items of process machinery is C_{PM}.

Table 16.11 Bare-Module Factors of Guthrie (1974) for Ordinary Materials of Construction and Low-to-Moderate Pressures

	Bare-Module Factor (F_{BM})
Furnaces and direct-fired heaters, shop-fabricated	2.19
Furnaces and direct fired heaters, field-fabricated	1.86
Shell-and-tube heat exchangers	3.17
Double-pipe heat exchangers	1.80
Fin-tube air coolers	2.17
Vertical pressure vessels	4.16
Horizontal pressure vessels	3.05
Pumps and drivers	3.30
Gas compressors and drivers	2.15
Centrifuges	2.03
Horizontal conveyors	1.61
Bucket conveyors	1.74
Crushers	1.39
Mills	2.30
Crystallizers	2.06
Dryers	2.06
Evaporators	2.45
Filters	2.32
Flakers	2.05
Screens	1.73

Other Investment Costs

In addition to the bare-module costs associated with the process equipment in a flowsheet, capital costs are incurred for spare items of equipment, C_{spare}; for storage and surge tanks, C_{storage}; for initial charges of catalyst, C_{catalyst}; and for computers and software, including instruments, distributed control systems, and alarms, C_{comp}. As shown in Table 16.9, these costs are added to the bare-module costs for the on-site equipment to give the *total bare-module investment*, C_{TBM}. Other investment costs include site preparation or development, C_{site}; service facilities (e.g., utility lines and industrial buildings), C_{serv}; and allocated costs to purchase or upgrade the utility plants and other offsite facilities (e.g., for steam and electricity generation and waste disposal), C_{alloc}, shown in Figure 16.2. These are added to C_{TBM} to give the *direct permanent investment*, C_{DPI}. After adding funds (typically 18% of C_{DPI}) to cover contingencies and a contractor fee, the *total depreciable capital*, C_{TDC}, is obtained. Depreciation is very important to companies that use equipment to manufacture goods because it permits companies to reduce their taxes. As will be discussed in detail in the next chapter, depreciation is the allocation of the cost of an asset, such as a processing plant,

Table 16.12 Allocated Capital Investment Costs for Utility Plants (CE cost index = 567)

Utility	Size Factor, S	Range of S	Allocated Cost, \$
Steam	Flow rate, lb/hr	20,000 – 1,000,000 1b/hr	$C_{alloc} = 930\ S^{0.81}$
Electricity	Power, MW	0.5 – 1,000 MW	$C_{alloc} = 2{,}900{,}000\ S^{0.83}$
Cooling water	Flow rate, gpm	1,000 – 200,000 gpm	$C_{alloc} = 1{,}100\ S^{0.68}$
Process water	Flow rate, gpm	5 – 10,000 gpm	$C_{alloc} = 1{,}700\ S^{0.96}$
Refrigeration (evaporator temperature = −20°F)	Tons	3 – 1,000 tons	$C_{alloc} = 12{,}500\ S^{0.77}$

over a period of time for accounting and tax purposes. Depreciation accounts for the decline in the value of equipment due to general wear and tear. To the C_{TDC} is added the investment in nondepreciable items— including the cost of land, the cost of royalties for the use of processes patented by others, and costs for plant startup—to give the *total permanent investment*, C_{TPI}, also referred to as *total fixed capital*. After the working capital is added, the *total capital investment*, C_{TCI}, is obtained.

The working capital is described in detail in the next chapter. It includes the initial investment in temporary and consumable materials, as well as cash for initial payments of salaries and other operating expenses prior to the receipt of payments for plant products. Other costs, which represent a significant fraction of the total capital investment, are considered next.

Spares, Storage Tanks, Surge Vessels, Catalyst Costs, and Computer Costs

In addition to the bare-module costs for each process unit in the flowsheet as discussed above, it is often recommended to provide funds for *spares*, C_{spare}, especially for liquid pumps, to permit uninterrupted operation when a process unit becomes inoperable. Pumps are relatively inexpensive but require frequent maintenance to prevent leaks. Funds are also provided for storage units and surge tanks, $C_{storage}$, to provide improved control and intermediate storage between sections of the plant, so that one section can continue operation when an adjoining section is down or operating under capacity. The amount of storage depends on the anticipated periods of downtime and the importance of maintaining steady, uninterrupted operation. In addition, it is common to include the cost of the initial charge of catalyst, $C_{cataiyst}$, which is a sizable investment cost in some plants. Finally, the cost of computers and software with associated instruments, distributed control systems, and alarms, C_{comp}, is gaining importance in many plants, especially those that manufacture industrial and configured consumer products. These costs are included in C_{TBM}, as indicated in Table 16.9.

Site Preparation

Site preparation typically involves making land surveys, dewatering and drainage, surface clearing, rock blasting, excavation, grading, and piling and the addition of fencing, roads, sidewalks, railroad sidings, sewer lines, fire protection facilities, and landscaping. Costs for site preparation and development, C_{site}, can be quite substantial for grass-roots plants, in the range of 10–20% of the total bare-module cost of the equipment. For an addition to an existing integrated complex, the cost may only be in the range of 4–6% of the total bare-module cost of the equipment.

Service Facilities

Costs for service facilities, C_{serv}, include utility lines, control rooms, laboratories for feed and product testing, maintenance shops, and other buildings. Service facility costs can be substantial for a grass-roots plant when administrative offices, medical facilities, cafeterias, garages, and warehouses are needed.

Allocated Costs for Utilities and Related Facilities

Allocated costs, C_{alloc}, are included to provide or upgrade offsite utility plants (steam, electricity, cooling water, process water, boiler feed water, refrigeration, inert gas, fuels, etc.) and related facilities for liquid waste disposal, solids waste disposal, off-gas treatment, and wastewater treatment. Some typical capital investment costs for utility plants are shown in Table 16.12. Cogeneration plants can provide both steam and electricity by burning a fuel. When utilities such as electricity are purchased from vendors at so many cents per kilowatt-hour, that cost includes the vendor investment cost. Thus, a capital cost for the plant is then not included in the capital cost estimate.

Contingencies and Contractor's Fee

Contingencies are unanticipated costs incurred during the construction of a plant. To account for the cost of contingencies, it is common to set aside 15% of the direct permanent investment, C_{DPI}, which is composed of the components in Table 16.9. In addition, Guthrie (1969) adds a contractor fee of 3% of the direct permanent investment. When this total of 18%, designated C_{cont}, is added, the total depreciable capital, C_{TDC}, is obtained.

The cost of contingencies varies considerably with 15% being a useful estimate when the design team is unable to make a better estimate. With processes for which the company has considerable experience, the cost of contingency is much lower than when a plant is being designed to produce a new chemical product just discovered by a research group. When deciding on a contingency cost, the design team should address the following three groups of questions:

1. How well is the product or process known? Has the process been demonstrated commercially in a pilot plant or in a laboratory? How long has the process run? Are the corrosion

rates associated with the equipment well established? Has a demonstration of the process included all of the recycle streams?

2. How complete is the design? Has a simulation model been prepared? Is the detailed design complete? How much is known about the plant site?
3. How accurate are the estimates? Is the equipment conventional, or are there new and complex equipment items with which the company has little experience and cost history? In most cases, a 15% contingency is low except when the experience factor is very great. Typical designs, which are representative of most designs by student groups at universities, are likely to require 35% for contingency costs. When the chemistry is new and not well understood, 100% might be more realistic.

Land

The cost of land, C_{land}, is nondepreciable because land rarely decreases in value, and in the absence of data can be taken as 2% of the total depreciable capital, C_{TDC}.

Royalties

When a company desires to use a product or process that is covered by patents owned by another company, a license may sometimes be negotiated. The license fee may be a one-time fee in which case that fee is included in the capital investment as a one-time royalty or paid-up license, C_{royal}. A more common arrangement is to pay an initial license fee, included in the capital investment, and an annual royalty based on the amount or dollar value of product sold as discussed in Section 17.2 under Licensing Fees. The amount of the annual royalty depends on the uniqueness of the process and the chemical being produced, with a range of 1–5% of product sales. In the absence of data, an initial royalty fee of 2% of C_{TDC} may be assumed together with an annual royalty of 3% of product sales.

Startup

The cost of plant startup, C_{startup}, is typically estimated as 10% of C_{TDC}, However, according to Feldman (1969), if the process and equipment are well known to skilled operators and the new process is not dependent on the operation of another plant, the startup cost may be as low as 2% of C_{TDC}, At the other extreme, if the process and the equipment are radically new, and the new process is dependent on another plant, the startup cost may be as high as 30% of C_{TDC}. In this latter case, it may be necessary to modify the process and add more equipment. With respect to startup, it is important that the process design include additional equipment, such as heat exchangers, to achieve the startup. This is particularly important for processes involving significant recycle streams and/or a high degree of energy integration. Startup time depends on the same factors as startup costs and is generally taken as a percentage of construction time, varying from 10 to 40%.

Some company accountants may prefer to divide plant startup costs into two categories: (1) those costs incurred by the contractor in checking equipment performance, calibrating controllers and other plant equipment, and commissioning the plant and (2) those costs incurred by plant operating personnel when starting up and shutting down the plant. The former costs are included in the capital cost whereas the latter are considered operating costs.

Table 16.13 Typical Investment Site Factors, F_{ISF}

U.S. Gulf Coast	1.00
U.S. Southwest	0.95
U.S. Northeast	1.10
U.S. Midwest	1.15
U.S. West Coast	1.25
Western Europe	1.20
Mexico	0.95
Japan	1.15
Pacific Rim	1.00
India	0.85

Investment Site Factors

In many companies, *investment site factors*, $F_{\text{I\$F}}$, are used to multiply the total permanent investment, C_{TPI}, to account for different costs in different localities based on the availability of labor, the efficiency of the workforce, local rules and customs, union status, and other items. Typical factors in recent use by one of the major chemical companies are provided in Table 16.13, in which a plant in the U.S. Gulf Coast area is given a base factor of 1.0. The factors range from 0.85 in India to 1.25 in the U.S. West Coast area. The corrected total permanent investment is computed as:

$$C_{\text{TPI}_{\text{corrected}}} = F_{\text{ISF}} C_{\text{TPI}}$$

Working Capital

Working capital funds, C_{WC}, are needed to cover operating costs required for the early operation of the plant, including the cost of the inventory and funds to cover accounts receivable. Because they involve the costs of the raw materials and the values of the intermediates, products, and byproducts, the working capital is normally estimated in connection with the calculation of the operating "Cost Sheet," which is presented in Table 17.1 and discussed in Section 17.2. Note that funds are usually allocated for a spare charge of catalyst, often kept in a warehouse, as a backup in case an operating problem causes the catalyst to become ineffective.

Example of an Estimate of Capital Investment

An example of an estimate of the total capital investment for a processing plant is given in Tables 16.14 and 16.15 for an ammonia plant producing 1 billion lb/yr. The costs are for the year 2000 at a U.S. Midwest location. The plant is part of an integrated complex. The process involves a variety of equipment, including gas compressors, pumps, heat exchangers, a catalytic reactor, a distillation column, an absorber, a flash drum, a gas adsorber, and gas permeation membrane separators. The material of construction is almost exclusively carbon steel.

Table 16.14 Capital Cost of Bare-Module Equipment Cost for an Ammonia Plant—Costs in Millions of U.S. Dollars (Year 2006)

	C_P	F_{BM}	C_{BM}
Fabricated equipment			
Heat exchangers	6.67	3.3	22.01
Flash drum	0.01	4.3	0.04
Distillation column	0.09	4.3	0.38
Adsorbers	0.23	4.3	0.98
Absorber	0.25	4.3	1.09
Membrane separators	4.52	3.2	14.46
Reactor	0.43	4.3	1.86
Process machinery			
Gas compressors	27.72	3.5	97.00
Pumps	0.09	3.4	0.30
Total bare-module cost for on-site equipment			138.12

For the ammonia process, which operates at high pressure (200 atm) mostly in the gas phase, the total f.o.b. purchase cost of the on-site process equipment is $40,010,000. Installation costs boost this amount by a factor of 3.452 to a total bare-module cost of $138,120,000. As seen in Table 16.14, this cost is dominated by the gas compressors with significant contributions from the heat exchangers and the membrane separators. Surprisingly, the reactor cost is a small fraction of the total cost. This is often the case for chemical plants. The reactor may not cost much, but it is the heart of the process, and it had better produce the desired results.

Table 16.15 continues the cost estimate to obtain the total capital investment. After all other investment costs are added to the total bare-module cost of the on-site equipment, the total capital investment becomes $228,080,000. The total permanent investment is $215,280,000, which is a factor of 5.38 times the total f.o.b. purchase cost of the on-site process equipment. The startup cost here is taken as 8% of C_{TDC}.

16.4 ESTIMATION OF THE TOTAL CAPITAL INVESTMENT

As the project for manufacturing a new or existing chemical by a new process progresses from laboratory research through pilot-plant development to a decision for plant construction, a number of process design studies of increasing complexity may be made, accompanied at each step by capital cost estimates of increasing levels of accuracy as follows:

1. *Order-of-magnitude estimate* based on bench-scale laboratory data sufficient to determine the type of equipment and its arrangement to convert the feedstock(s) to product(s).
2. *Study estimate* based on a preliminary process design.
3. *Preliminary estimate* based on detailed process design studies leading to an optimized process design.
4. *Definitive estimate* based on a detailed plant design, including detailed drawings and cost estimates, sufficient to apply cost accounting.

If the process is well known and has been verified by one or more commercial operating plants, only estimate levels 3 and 4 are necessary. Methods for making capital investments at the first three levels are discussed next. This chapter is concluded with an example of a definitive estimate using APEA, which is part of AspenOne that includes ASPEN PLUS. APEA, which is discussed in Section 16.8, has more than 40 years of field-testing on commercial plants and is in use by worldwide owner companies and engineering design and construction firms. In our experience, application of APEA is rather quickly understood and applied by chemical engineering students and practitioners after having studied the simpler, but less accurate, costing methods presented here in Sections 16.2 to 16.7.

Table 16.15 Total Capital Investment for an Ammonia Plant—Costs in Millions of U.S. Dollars (Year 2006)

Total bare-module cost for on-site equipment	138.12				
Cost for spares	0.66				
Cost for storage and surge tanks	0.57				
Cost for initial catalyst charge	0.63				
Cost of computers, software, and associated items					
Total bare-module investment		139.98			
Cost of site preparation		4.20			
Cost of service facilities		2.09			
Allocated costs for utility plants and related facilities		19.61			
Direct permanent investment			165.88		
Cost of contingencies and contractor's fee			29.86		
Total depreciable capital				195.74	
Cost of land				3.91	
Cost of plant startup				15.63	
Total permanent investment					215.28
Working capital					12.80
Total capital investment					228.08

Note: In Table 16.15, the cost of computers, software, and associated items is included in the total bare-module cost for on-site equipment.

Method 1. Order-of-Magnitude Estimate (based on the method of Hill, 1956)

This estimation method can be applied rapidly and is useful in determining whether a new process is worth pursuing, especially when there are competing routes. The method is particularly useful for low-pressure petrochemical plants, where it has an accuracy of approximately ±50%. For moderate-to-high pressure processes, the actual cost may be as much as twice the estimate. To produce the estimate, only two things are needed: a production rate in pounds per year and a flowsheet showing the gas compressors, reactors, and separation equipment required. Heat exchangers and liquid pumps are not considered in making the estimate. Also, it is not necessary to compute a mass and energy balance or to design or size the equipment, but it is important that the process has been sufficiently studied that the flowsheet is complete with all the major pieces of gas movement, reactors, and separation equipment and their required materials of construction. Another important factor in making the estimate is the design pressure of each major piece of equipment if it is greater than 100 psi. The method proceeds as follows based on a year 2006 Marshall and Swift Process Industries Average Cost Index of 1,365, a base production rate of 10,000,000 lb/yr for the main product, carbon steel construction, and a design pressure of less than 100 psi.

Step 1 : Establish the production rate of the main product in pounds per year. Compute a production rate factor, F_{PR}, using the six-tenths rule:

$$F_{PR} = \left(\frac{\text{Main product flow rate, lb/yr}}{10{,}000{,}000} \right)^{0.6} \tag{16.5}$$

Step 2: Using a process flowsheet, calculate from the following equation a module cost, C_M, for purchasing, delivering, and setting in place each major piece of equipment, including gas compressors and blowers (but not low-compression ratio recycle compressors and blowers); and reactors; separators such as distillation columns, absorbers, strippers, adsorbers, membrane units, extractors, electrostatic precipitators, crystallizers, and evaporators (but not heat exchangers, flash and reflux drums, or liquid pumps):

$$C_M = F_{PR} F_M \left(\frac{\text{design pressure, psia, if } > 100 \text{ psi}}{100} \right)^{0.25} \times (\$160{,}000) \tag{16.6}$$

where F_M is a material factor, as follows:

Material	F_M
Carbon steel	1.0
Copper	1.2
Stainless steel	2.0
Nickel alloy	2.5
Titanium clad	3.0

Step3: Sum the values of C_M; multiply the sum by the factor F_{PI} to account for piping, instrumentation and automatic controls, and indirect costs; and update with the current MS cost index, giving the total bare-module investment, C_{TBM}:

$$C_{TBM} = F_{PI} \left(\frac{\text{MS index}}{1{,}365} \right) \Sigma C_M \tag{16.7}$$

where the factor F_{PI} depends on whether the plant processes solids, fluids, or a mixture of the two, as follows:

Type of Process	F_{PI}
Solids handling	1.85
Solids-fluids handling	2.00
Fluids handling	2.15

Step 4: To obtain the direct permanent investment, C_{DPI}, multiply C_{TBM} by the following factors to account for site preparation, service facilities, utility plants, and related facilities:

$$C_{DPI} = (1 + F_1 + F_2)\, C_{TBM} \tag{16.8}$$

where the factors F_1 and F_2 are

	F_1
Outdoor construction	0.15
Mixed indoor and outdoor construction	0.40
Indoor construction	0.80
	F_2
Minor additions to existing facilities	0.10
Major additions to existing facilities	0.30
Grass-roots plant	0.80

Outdoor construction is common except where winters are very severe and/or solids handling is critical.

Step 5: Obtain the total permanent investment and the total capital investment by the following equations where a large contingency of 40% is used because of the approximate nature of the capital cost estimate, and the costs of land, royalties, and plant startup are assumed to add an additional 10%. Working capital is taken as 15% of the total permanent investment.

$$C_{TPI} = 1.50 C_{DPI}$$
$$C_{TCI} = 1.15 C_{TPI}$$

EXAMPLE 16.2

Make an order-of-magnitude estimate of the total capital investment as of early 2007 with MS = 1,400 to produce benzene according to the toluene hydrodealkylation process shown in Figure 6.14. Assume an overall conversion of toluene to benzene of 95% and 330 days of operation per year. Also assume the makeup gas enters at the desired pressure and a clay adsorption treater must be added to the flowsheet after the stabilizer. The treater removes contaminants that would prevent the benzene product from meeting specifications. In addition, in order for the reactor to handle the high temperature, it must have a brick lining on the inside, so take a material factor of $F_M = 1.5$. Otherwise, all major equipment is constructed of carbon steel. The plant will be constructed outdoors with major additions to existing facilities.

SOLUTION

Step 1: The plant will operate 330(24) = 7,920 hr/yr. For a toluene feed rate of 274.2 lbmol/hr, the annual benzene production rate is 0.95(274.2)(78.11)(7,920) = 161,000,000 lb/yr. Thus,

$$F_{PR} = \left(\frac{161{,}000{,}000}{10{,}000{,}000}\right)^{0.6} = 5.3$$

Step 2: The flowsheet includes one reactor (with $F_M = 1.5$) operating at 570 psia, three distillation columns operating at pressures less than 100 psia, one compressor operating at 570 psia, and one adsorption tower, assumed to operate at less than 100 psia. Therefore, the sum of the C_M values is

$$\Sigma C_M = 5.3\left[1.5\left(\frac{570}{100}\right)^{0.25} + 3 + 1\left(\frac{570}{100}\right)^{0.25} + 1\right] \times (\$160{,}000) = \$6{,}670{,}000$$

Step 3: From Eq. (16.7), the total bare-module investment for a fluids handling process is

$$C_{TBM} = 2.15\left(\frac{1{,}400}{1{,}365}\right)(\$6{,}650{,}000) = \$14{,}700{,}000$$

Steps 4 and 5:

$$C_{DPI} = (1 + 0.15 + 0.30)(\$14{,}700{,}000) = \$21{,}300{,}000$$
$$C_{TPI} = 1.50(\$21{,}400{,}000) = \$32{,}100{,}000$$
$$C_{TCI} = 1.15(\$32{,}100{,}000) = \$36{,}900{,}000$$

Method 2. Study Estimate (based on the overall factor method of Lang, 1947a, b, and 1948)

In a series of three articles from 1947 to 1948, Lang developed a method for estimating the capital cost of a chemical plant using overall factors that multiply estimates of the delivered cost of the major items of process equipment. This method requires a process design complete with a mass and energy balance as well as equipment sizing. In addition, materials of construction for the major items of equipment, including the heat exchangers and pumps, must be known. Considerably more time is required for making a study estimate than for the preceding order-of-magnitude estimate. But the accuracy is improved to ±35%. To apply the method, the f.o.b. purchase cost of each piece of major equipment must be estimated. F.o.b purchase costs of a wide range of chemical processing equipment are given in the next section of this chapter. The Lang method proceeds by steps as follows:

Step 1: From the process design, prepare an equipment list giving the equipment title, label, size, material of construction, design temperature, and design pressure.

Step 2: Using the data in Step 1 with f.o.b. equipment cost data, add to the equipment list the cost and the corresponding cost index of the cost data. Update the cost data to the current cost index, sum the updated purchase costs to obtain the total f.o.b. purchase cost, C_P, and multiply by 1.05 to account for delivery of the equipment to the plant site. Then, multiply the result by an appropriate Lang factor, f_L, to obtain the total permanent investment (fixed capital investment), C_{TPI} (i.e., without the working capital) or the total capital investment, C_{TCI} (i.e., including an estimate of the working capital at 15% of the total capital investment or 17.6% of the total permanent investment).

$$C_{TPI} = 1.05\, f_{L_{TPI}} \sum_i \left(\frac{I_i}{I_{b_i}}\right) C_{P_i} \tag{16.9}$$

$$C_{TCI} = 1.05\, f_{L_{TCI}} \sum_i \left(\frac{I_i}{I_{b_i}}\right) C_{P_i} \tag{16.10}$$

The original Lang factor, based on capital costs for 14 different chemical plants, was found to depend on the extent to which the plant processes solids or fluids. Lang's factors, which at that time did not account for working capital, are given in the second column of Table 16.16.

A more detailed development of the Lang factors, based on an analysis of 156 capital cost estimates, was published by the editors of *Chemical Engineering* magazine in the September 30, 1963, issue on pages 120 and 122 as "Cost File 81." A further refinement by Peters, Timmerhaus, and West (2003) gives the most widely accepted values of the Lang factors, which are included in Table 16.16 and are the factors recommended here for use in Eqs. (16.9) and (16.10). The detailed breakdown of costs by Peters et al. is given in Table 16.17, which assumes that major plant

Table 16.16 Original and Recommended Lang Factors

	Original Lang Factors, *Not* Including Working Capital	$f_{L_{TPI}}$ Recommended Lang Factors of Peters et al. *Not* Including Working Capital	$f_{L_{TCI}}$ Recommended Lang Factors of Peters et al. Including Working Capital
Solids processing plant	3.10	3.97	4.67
Solids-fluids processing plant	3.63	4.28	5.03
Fluids processing plant	4.74	5.04	5.93

Table 16.17 Breakdown of Lang Factors by Peters et al. (2003)

	Percent of Delivered Equipment Cost for		
	Solids Processing Plant	Solids-Fluids Processing Plant	Fluids Processing Plant
Delivered cost of process equipment	100	100	100
Installation	45	39	47
Instrumentation and control	18	26	36
Piping	16	31	68
Electrical	10	10	11
Buildings (including services)	25	29	18
Yard improvements	15	12	10
Service facilities	40	55	70
Total direct plant cost	269	302	360
Engineering and supervision	33	32	33
Construction expenses	39	34	41
Total and indirect plant costs	341	368	434
Contractor's fee and legal expenses	21	23	26
Contingency	35	37	44
Fixed capital investment	397	428	504
Lang factor, $f_{L_{TPI}}$, for use in Eq. (16.9)	3.97	4.28	5.04
Working capital	70	75	89
Total capital investment	467	503	593
Lang factor, $f_{L_{TCI}}$, for use in Eq. (16.10)	4.67	5.03	5.93

additions are made to an existing site. The numbers in the table are based on a value of 100 for the total delivered cost of the process equipment. Here, the delivered cost is estimated as 1.05 times the f.o.b. purchase cost. The Lang factors apply to total permanent investments of up to approximately $100 million U.S. dollars. Note that the combined contractor's fee and legal expenses, as well as the contingency, are quite generous. If Eq. (16.9) is used, a detailed estimate of the working capital should be made according to the method presented in Section 17.3. No provision is made in the Lang-factor estimates for spares, storage and surge tanks, initial catalyst charge, royalties, or plant startup. However, these additional items can be added when desired. The fixed capital investment in Table 16.17 is the same as the total permanent investment in Table 16.9.

EXAMPLE 16.3

Use the Lang-factor method to estimate the total capital investment as of the year 2006 (MS = 1,365) to produce cyclohexane according to the benzene hydrogenation process shown in Figure 10.24. However, the makeup H_2 feed is not available at 335 psia but at 75 psia. Therefore, a feed-gas compressor, K2, has been added. Also two heat exchangers have been added. Reactor effluent stream S7 now enters new exchanger H2, which cools the effluent to 260°F by producing 10 psig steam from boiler feed water. The effluent leaves H_2 as stream S7A and enters new exchanger H3, where it is heat exchanged with the feed benzene, heating the benzene to 235°F while being cooled to 201°F and leaving as stream S7B, which now enters existing exchanger H1. The process design has been completed, with the equipment sizes in the "Equipment List" of Table 16.18. Also included in Table 16.18 are estimates of the f.o.b. purchase costs in the year 1977 (MS index of 514). All equipment is fabricated from carbon steel.

SOLUTION

Referring to Table 16.18, the total f.o.b. purchase cost corresponding to an MS index of 514 is $176,900. However, if we provide spares for the two pumps, the total becomes $178,600. From Eq. (16.10), using a Lang factor for fluids processing of 5.93 from Table 16.16 and an updated MS index of 1,365, the estimated capital investment is

$$C_{TCI} = 1.05(5.93)\left(\frac{1,365}{514}\right)\$178,600 = \$2,950,000$$

For this example, the order-of-magnitude estimate of Method 1 gives $4,700,000.

Table 16.18 Equipment List, Including Purchase Costs, for the Cyclohexane Process

Equipment Name	Equipment Label	Size	Design Temperature (°F)	Design Pressure (psia)	C_P, f.o.b. Purchase Cost (MS Index = 514)
Recycle compressor	Kl	3 Hp	120	350	2,000
Feed-gas compressor	K2	296 Hp	450	350	80,000
Benzene feed pump	PI	4Hp	120	350	1,200
Recycle pump	P2	1 Hp	120	350	500
Cooler	HI	210 ft^2	210	300	4,000
Effluent-BFW HX	H2	120 ft^2	400	320	2,500
Effluent-benzene HX	H3	160 ft^2	270	310	3,200
High-pressure flash	Fl	2 ft diam. × 8 ft height	120	300	5,000
Low-pressure flash	F2	2 ft diam. × 8 ft height	120	20	3,500
Reactor	Rl	8 ft diam. × 30 ft height	400	330	75,000

Method 3. Preliminary Estimate (Based on the Individual Factors Method of Guthrie, 1969, 1974)

This method is best carried out after an optimal process design has been developed, complete with a mass and energy balance, equipment sizing, selection of materials of construction, and development of a process control configuration as incorporated into a P&ID. More time is required for making a preliminary estimate than for the preceding study estimate, but the accuracy is improved to perhaps ±20%. To apply the method, the f.o.b. purchase cost of each piece of major equipment must be estimated, as was the case with the Lang method. However, instead of using an overall Lang factor to account for installation of the equipment and other capital costs, individual factors for each type of equipment given in Table 16.11 are used as developed first by Hand (1958) and later in much more detail by Guthrie (1969, 1974), who introduced the bare-module concept.

Furthermore, the Guthrie method recognizes that the foundation, supporting structures, and ladders, as well as electrical, insulation, and paint will cost the same irrespective of the materials of construction used for equipment, or whether the equipment is designed to withstand high pressure.

The only difference is in the cost of the attached piping because it is stainless steel, for example, instead of carbon steel and may have to be thicker for high pressure. This is illustrated by Example 16.4. F.o.b. purchase costs of a wide range of chemical processing equipment are given in the next section. The Guthrie method involves the summation of estimates of module costs for the four different modules that comprise the total capital investment (C_{TPI}) shown in Eq. (16.11). To this summation is added a contingency and contractor fee in terms of a factor to obtain the total permanent investment. An appropriate estimate of the working capital is added to obtain the total capital investment. Thus, the components of the total permanent investment are accounted for in a manner somewhat different from Table 16.9, but the overall result is the same. The equation for the total capital investment by the Guthrie method is

$$\begin{aligned} C_{TCI} &= C_{TPI} + C_{WC} \\ &= 1.18(C_{TBM} + C_{site} + C_{buildings} \\ &\quad + C_{offsite\ facilities}) + C_{WC} \end{aligned} \tag{16.11}$$

Equation (16.11) does not account for royalties or plant startup. These additional costs should be added if they are known or can be estimated.

The total bare-module cost, C_{TBM}, refers to the summation of bare-module costs for all items of process equipment, including fabricated equipment, process machinery, spares, storage tanks, surge tanks, and computers and software. The initial charge of catalyst is included with the corresponding catalytic reactor cost. As shown in the heat exchanger example of Table 16.10, the bare-module cost is based on the f.o.b. equipment purchase cost, to which is factored in direct field materials and labor, and indirect expenses such as freight, insurance, taxes, overhead, and engineering.

Site development costs, C_{site}, are discussed previously in the section on capital investment costs. In lieu of a detailed estimate, which is not normally prepared at this stage of cost estimation, a value of 10–20% of C_{TBM} may be assigned for a grass-roots plant and 4–6% for an addition to an integrated complex.

Building costs, $C_{buildings}$, are also discussed previously in the section on capital investment costs. In the Guthrie method, buildings include process buildings and nonprocess buildings. Again,

a detailed estimate is not generally made at this stage of cost estimation. Instead, an approximate estimate is sufficient, but must consider whether some or all the process equipment must be housed in buildings because of weather or other conditions, and whether a grass-roots location or an addition to an integrated complex is being considered. If the equipment is housed, the cost of process buildings may be estimated at 10% of C_{TBM}. If a grass-roots plant is being considered, the nonprocess buildings may be estimated at 20% of C_{TBM}. If the process is to be an addition to an integrated complex, the nonprocess buildings may be estimated at 5% of C_{TBM}.

Offsite facilities include utility plants when the company provides its own utilities, pollution control, ponds, waste treatment, offsite tankage, and receiving and shipping facilities. The utility plants may be estimated with the help of Table 16.12. To this may be added 5% of C_{TBM} to cover other facilities.

The factor 1.18 in Eq. (16.11) covers a contingency of 15% and a contractor fee of 3%. As with the Lang-factor method, the working capital can be estimated at 15% of the total capital investment, which is equivalent to 17.6% of the total permanent investment, or it can be estimated in detail by the method discussed in Section 17.3.

The Guthrie method proceeds by steps as follows:

Step 1: From the process design, prepare an equipment list, giving the equipment title, label, size, material of construction, design temperature, and design pressure.

Step 2: Using the data in Step 1 with f.o.b. equipment purchase cost data, add to the equipment list the cost, C_{P_b}, and the corresponding cost index, I_b, of the cost data. In the Guthrie method, the f.o.b. purchase cost is a base cost corresponding to a near-ambient design pressure, carbon steel as the material of construction, and a base design.

Step 3: Update the cost data to the current cost index. For each piece of equipment, determine the bare-module cost—using bare-module factors, F_{BM}, from Table 16.11, being careful to determine it properly when the material of construction is not carbon steel and/or the pressure is not near ambient—as given by Eq. (16.12) and illustrated by the following example before moving to Step 4. As discussed earlier, the bare-module cost accounts for delivery, insurance, taxes, and direct materials and labor for installation.

$$C_{\text{BM}} = C_{P_b}\left(\frac{I}{I_b}\right)[F_{\text{BM}} + (F_d F_p F_m - 1)] \qquad (16.12)$$

where:

F_{MB} = bare-module factor
F_d = equipment design factor
F_p = pressure factor
F_m = material factor

Step 4: Obtain the total bare-module cost, C_{TBM}, by summing the bare-module costs of the process equipment.

Step 5: Using Eq. (16.11), estimate the total permanent investment. Add to this an estimate of the working capital to obtain the total capital investment.

EXAMPLE 16.4

The base f.o.b. purchase cost for a fabricated vertical pressure vessel, 6 ft in inside diameter and 100 ft in height (tangent-to-tangent) made of carbon steel for a design pressure of not greater than 50 psig, is given as \$102,000 as of 1995 (CE index = 381). Calculate the bare-module cost for the year 2006 (CE index = 500) if the vessel is made of 316 clad stainless steel for a design pressure of 200 psig. For these conditions, Guthrie (1974) gives $F_{\text{BM}} = 4.16$, $F_d = 1$, $F_p = 1.55$, and $F_m = 2.60$.

SOLUTION

Using Eq. (16.12),

$$C_{\text{BM}} = \$102{,}000\left(\frac{500}{381}\right)[4.16 + (1 \times 1.55 \times 2.60 - 1)]$$
$$= \$962{,}000$$

EXAMPLE 16.5

The total bare-module cost for a process to produce 40,000,000 lb/yr of butyl alcohols by the catalytic hydration of butylenes is \$12,900,000 indexed to the year 2006. Estimate the total capital investment. The process will be an addition to an existing integrated complex and no process buildings will be required. Offsite utility plants have been estimated at \$1,500,000, and the working capital has been estimated at \$1,700,000.

SOLUTION

$$C_{\text{TBM}} = \$12{,}900{,}000$$

Estimates of the other terms in Eq. (16.11) are as follows:

$$C_{\text{site}} = 0.05C_{\text{TBM}} = 0.05(12{,}900{,}000) = \$645{,}000$$
$$C_{\text{buildings}} = 0.05C_{\text{TBM}} = 0.05(12{,}900{,}000) = \$645{,}000$$
$$C_{\text{offsite facilities}} = 1{,}500{,}000 + 0.05C_{\text{TBM}} = 1{,}500{,}000 + 0.05(12{,}900{,}000) = \$2{,}145{,}000$$
$$C_{\text{TPI}} = 12{,}900{,}000 + 645{,}000 + 645{,}000 + 2{,}145{,}000 = \$16{,}335{,}000$$
$$C_{\text{WC}} = \$1{,}700{,}000$$
$$C_{\text{TCI}} = 16{,}335{,}000 + 1{,}700{,}000 = \$18{,}035{,}000$$

For a grass-roots plant, an additional 25% of C_{TBM} is added for site development and buildings. This amounts to \$3,225,000, giving a total capital investment of \$21,260,000.

16.5 PURCHASE COSTS OF THE MOST WIDELY USED PROCESS EQUIPMENT

The Lang and Guthrie methods for estimating the total capital investment require f.o.b. purchase costs for all major items of process equipment. Since 1949, a number of literature articles and book chapters have presented such data. Some of the more widely used sources of equipment cost data are given in Table 16.19. Included is the cost index of the cost data. Typically, equipment

Table 16.19 Sources of Purchase Costs of Process Equipment

Author	Reference	Cost Index
Chilton, E.H.	*Chemical Engineering*, **56** (6), 97–106 (1949)	
Walas, S.M., and Spangler, CD.	*Chemical Engineering*, **67** (6) 173–176 (1960)	MS = 234.3
Bauman, H.C.	*Fundamentals of Cost Engineering in the Chemical Industry*, Reinhold (1964)	MS = 237.3
Mills, H.E.	*Chemical Engineering*, **71** (6), 133 (1964)	MS = 238.8
Guthrie, K.M.	*Chemical Engineering*, **76** (6), 114–142 (1969)	MS = 273.1
Guthrie, K.M.	*Process Plant Estimating Evaluation and Control*, Craftsman Book (1974)	MS = 303.3
Woods, D.R.	*Financial Decision Making in the Process Industry*, Prentice-Hall (1975)	MS = 300
Pikulik, A., and Diaz, H.E.	*Chemical Engineering*, **84** (21), 107–122 (1977)	MS = 460
Hall, R.S., Matley, J., and McNaughton, K.J.	*Chemical Engineering*, **89** (7), 80–116 (1982)	CE = 305
Walas, S.M.	*Chemical Process Equipment*, Butterworth (1988)	CE = 325
Turton, R., Bailie, R.C., Whiting, W.B., and Shaeiwitz, J.A.	*Analysis, Synthesis, and Design of Chemical Processes*, 2nd ed., Prentice Hall (2003)	CE = 397
Peters, M.S., Timmerhaus, K.D., and West, R.E.	*Plant Design and Economics for Chemical Engineers*, 5th ed., McGraw-Hill (2003)	CE = 390.4
Ulrich, G.D., and Vasudevan, P.T.	*Chemical Engineering Process Design and Economics—A Practical Guide*, 2nd ed., Process Publishing (2004)	CE = 400

cost data are presented in the form of graphs and/or equations of f.o.b. purchase cost as a function of one or more equipment size factors. Graphs show clearly the effect of the size factors on the cost and may be quickly read; however, equations are more consistent, especially compared to graphs using logarithmic coordinates. Furthermore, equations are easily incorporated into computer programs. In this section, equations and graphs are presented for f.o.b. purchase costs of the most widely used chemical processing equipment: pumps, electric motors, fans, blowers, compressors, shell-and-tube and double-pipe heat exchangers, general-purpose fired heaters (furnaces), pressure vessels and towers, trays, and packings. Then, in Section 16.6, equations alone are presented for a wide variety of other chemical processing equipment. The equipment cost equations should be used, even when one of the following graphs might apply.[1]

Recently, an equipment-costing EXCEL spreadsheet that implements the equations presented in Sections 16.5 and 16.6 was prepared by Russell Dunn at Vanderbilt University. This spreadsheet can be downloaded from the Program and Simulation file section of the Wiley Web site associated with this textbook. Its usage is discussed in Section 16.7.

The form of the equations is a modification of the equation $C_P = A\ (size\ factor, S)^b$ (where A and b are constants) obtained by taking the natural logarithm of both sides, adding additional higher-order terms as with a polynomial, and solving for C_P to obtain

$$C_P = \exp\{A_0 + A_1[\ln(S)] + A_2[\ln(S)]^2 + \cdots\}$$

The equations are usually based on the more common materials of construction, such as carbon steel. For other materials, multiplying factors are provided. Assistance in choosing the materials of construction is given in Appendix III.

As discussed by Woods (1975) and Walas (1988), when cost data are assembled from vendor quotes, they exhibit scatter due to differing qualities of equipment fabrication, design differences, market conditions, vendor profit, and other considerations. Accordingly, the accuracy of published equipment cost data, such as referenced in Table 16.19, may be no better than ±25%. More accurate estimates can be obtained from APEA, discussed in Section 16.8. Final equipment cost estimates can only be obtained by bids from the equipment manufacturers. These require special requests that are sometimes costly to prepare and, for that reason, are often not obtained until a decision has been made to construct the plant and a final detailed capital cost estimate is needed for making an appropriation request. For some proprietary equipment systems, even a preliminary cost estimate might have to be requested from a vendor.

Some chemical products, for example, home hemodialysis devices, involve small storage vessels, membrane mass exchangers, adsorption cartridges, and circulating pumps. Most often, the equations for cost estimation do not apply for these laboratory-scale equipment items. In these cases, cost estimates can often be obtained from the distributors of laboratory equipment and vendors. Note that as the production level increases, volume discounts should be negotiated.

Pumps and Electric Motors

Pumps are used widely in chemical processing plants to move liquids through piping systems from one piece of equipment to another. The three most commonly used pumps are radial

[1] In developing the cost equations for the purchase cost of processing equipment presented in this chapter, available literature sources as far back as 1960 were consulted. After determining a suitable equipment size factor, all or much of the cost data were plotted. When a wide spread in the data was evident, which was not uncommon, an attempt was made to assess the validity of the data by comparison with costs of similar equipment. When the validity could not be determined, the data were averaged. In some cases, especially where available data were sparse, cost data were obtained from vendors of the equipment. It must be understood that the only accurate cost data are bids from a vendor and that bids from different vendors can sometimes differ significantly.

centrifugal, piston or plunger reciprocating, and external rotary gear, as discussed in some detail in Section 14.1. Of these three, the radial centrifugal pump (referred to here as just the centrifugal pump) is selected for industrial service approximately 90% of the time because it is:

1. Relatively inexpensive to purchase and install.
2. Operated at high speed so that it can be driven directly with an electric motor.
3. Relatively simple in construction with no closely fitting parts that might wear, resulting in a low maintenance cost.
4. Available from a large number of vendors, many of whom comply with industry standards, such as those of the American Petroleum Institute (API), American Society of Mechanical Engineers (ASME), and the International Organization for Standardization (ISO).
5. Available in a wide range of materials of construction.
6. Applicable over a wide range of volumetric flow rate and temperature.
7. Applicable by staging for the achievement of heads up to 3,200 ft.
8. Capable of pumping a liquid at a constant flow rate with a constant discharge pressure.
9. Capable of handling slurries.
10. Easy to operate with control of the flow rate by a valve on the discharge line.
11. Free from damage if the valve on the discharge line is inadvertently or purposely closed.

However, the centrifugal pump has the following limitations:

1. It cannot efficiently pump liquids with a kinematic viscosity greater than 100 centistokes.
2. The maximum efficiency of a particular pump is limited to a narrow range of its characteristic curve (flow rate versus head).
3. For most models, it cannot produce heads greater than 3,200 ft.
4. For most models, the volumetric flow rate must be greater than 10 gpm.
5. Most models are subject to air binding and must be primed.
6. Because of potential cavitation and the net positive suction head (NPSH) limitation, most models cannot pump liquids that are close to their bubble point.
7. Spares are normally specified because seals to prevent leakage may require attention more often than scheduled maintenance.

Pump Selection

A centrifugal pump of the common radial type should be given first consideration when the pumping requirements fall in the following ranges:

1. Volumetric flow rate from 10 gpm (0.000631 m^3/s) to 5,000 gpm (0.3155 m^3/s).
2. Head from 50 ft (15.24 m) to 3,200 ft (975.4 m).
3. Kinematic viscosity less than 100 centistokes (0.0001 m^2/s).
4. Available NPSH greater than 5 ft (1.52 m).

When one or more of these requirements is outside the above ranges, a suitable centrifugal pump may still be available. This is particularly the case for the volumetric flow rate where centrifugal pumps may be found for capacities up to 15,000 gpm or more. Alternatively, two or more centrifugal pumps may be placed in parallel. However, when one or more of the other three requirements cannot be met, one of the following two types of pumps should be considered for the service.

External rotary gear pumps are particularly suitable for moderate-to-very-high-kinematic viscosity liquids in the range of 100 to 500,000 centistokes for flow capacities to at least 1,500 gpm (0.252 m^3/s) and heads to at least 3,000 ft (914.4 m). They are moderately priced, but usually more expensive than radial centrifugal pumps. They cannot be used with liquids containing particles and do not give as smooth a flow rate as do radial centrifugal pumps.

Reciprocating pumps of the plunger type can achieve the highest heads of up to at least 20,000 ft and flow rates to at least 500 gpm, at a maximum Hp of 200, using 3 to 5 cylinders to reduce flow pulsations. The piston type can achieve heads to at least 5,000 ft and flow rates to at least 100 gpm, at a maximum Hp of 90, using 2 to 3 cylinders. For a given horsepower, the highest heads are only achieved with the lowest flow rates and vice versa. Reciprocating pumps can handle liquids of moderate kinematic viscosity up to 100,000 centistokes. Reciprocating pumps are more expensive than gear pumps and deliver a pulsating, rather than a smooth, steady flow, which is reduced but not eliminated when multiple cylinders are used.

Many other specialized pumps are available for services that cannot be handled by radial centrifugal, external rotary gear, and plunger and piston reciprocating pumps. Specialized pumps are not considered here. Purchase-cost data are given next for only the three most commonly used types of pumps.

Pump and Motor Purchase Costs

Centrifugal Pumps

Much purchase-cost data for centrifugal pumps of the most common radial type have been published. The cost most often includes the pump, a base plate, and a direct-drive coupling. In some cases, an electric motor drive is included. There is no general agreement on the equipment size factor to be used for correlating purchase costs. Most common are (1) brake horsepower and (2) the product of the capacity and the head (or pressure increase). Here, the cost correlation method used is that of the Monsanto Company in their FLOWTRAN simulation program, which was subsequently adopted by Corripio et al. (1982a). Their size factor, S, which recognizes the fact that a given centrifugal pump can operate over a range of flow rate and head combinations, is

$$S = Q(H)^{0.5} \tag{16.13}$$

where Q is the flow rate through the pump in gallons per minute and H is the pump head in feet of fluid flowing (pressure rise/liquid

Table 16.20 Typical Types of Radial Centrifugal Pumps and F_T Factors

No. of Stages	Shaft rpm	Case-Split Orientation	Flow Rate Range (gpm)	Pump Head Range(ft)	Maximum Motor Hp	Type Factor [F_T in Eq. (16.15)]
1	3,600	VSC	50–900	50–400	75	1.00
1	1,800	VSC	50–3,500	50–200	200	1.50
1	3,600	HSC	100–1,500	100–450	150	1.70
1	1,800	HSC	250–5,000	50–500	250	2.00
2	3,600	HSC	50–1,100	300–1,100	250	2.70
2+	3,600	HSC	100–1,500	650–3,200	1,450	8.90

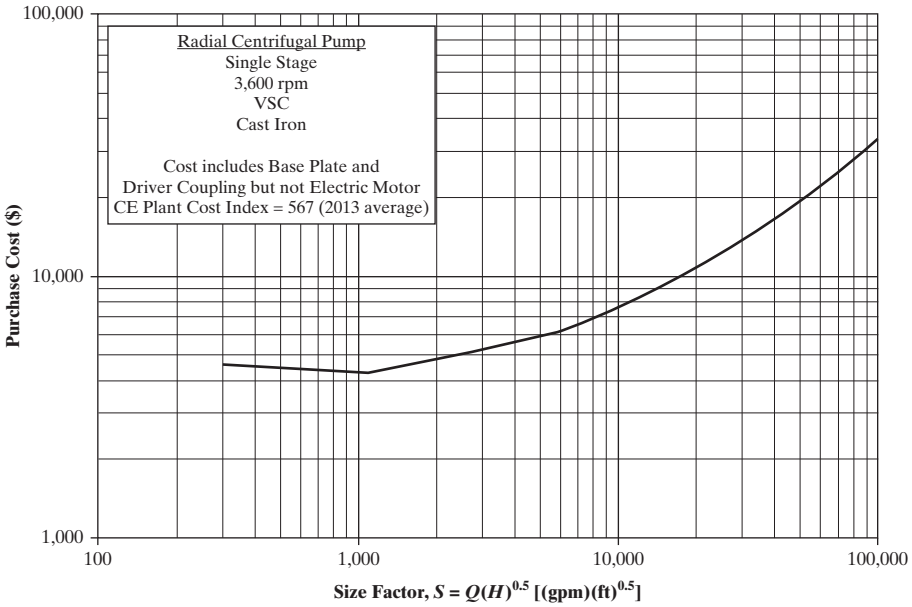

Figure 16.3 Base f.o.b. purchase cost for radial centrifugal pumps.

density). The pump purchase cost is correlated with the maximum value of S that the pump can handle.

In addition to the size factor, the purchase cost of a centrifugal pump depends on its rate of rotation (usually in the range of 1,800 to 3,600 rpm); the number of impellers (usually in the range of 1 to 4) in series (called stages) to reach the desired head; the orientation of the splitting of the bolted-together pump case (HSC, horizontal split case, or VSC, vertical split case); and the material of construction. Typical ranges of flow rate and head and maximum horsepower of the electric motor used to drive the pump, taken from Corripio et al. (1982a), are given in Table 16.20. From their cost data, indexed to 2013 (CE = 567), the f.o.b. purchase cost of a single-stage centrifugal pump with VSC construction of cast iron and operating at 3,600 rpm (referred to here as the base cost, C_B), is plotted in Figure 16.3. The cost includes the base plate and driver coupling but not the electric motor. The cost curve in Figure 16.3 is given by the following equation, which is valid from $S = 400$ to $S = 100{,}000$:

$$C_B = \exp\{12.1656 - 1.1448[\ln(S)] + 0.0862\ln(S)]^2\} \quad (16.14)$$

For other types of centrifugal pumps and other materials of construction, the f.o.b. purchase cost is given by:

$$C_P = F_T F_M C_B \quad (16.15)$$

Table 16.21 Materials of Construction Factors, F_M, for Centrifugal Pumps

Material of Construction	Material Factor [F_M, in Eq. (16.15)]
Cast iron	1.00
Ductile iron	1.15
Cast steel	1.35
Bronze	1.90
Stainless steel	2.00
Hastelloy C	2.95
Monel	3.30
Nickel	3.50
Titanium	9.70

where F_M is a material factor given in Table 16.21, and F_T is a pump-type factor included in Table 16.20.

Electric Motors

A centrifugal pump is usually driven by an electric motor whose cost is added to the pump cost from Eq. (16.15). The size parameter for the motor is its power consumption, P_C, which is determined from the theoretical horsepower of the pump, P_T; its fractional efficiency, η_P; and the fractional efficiency of the

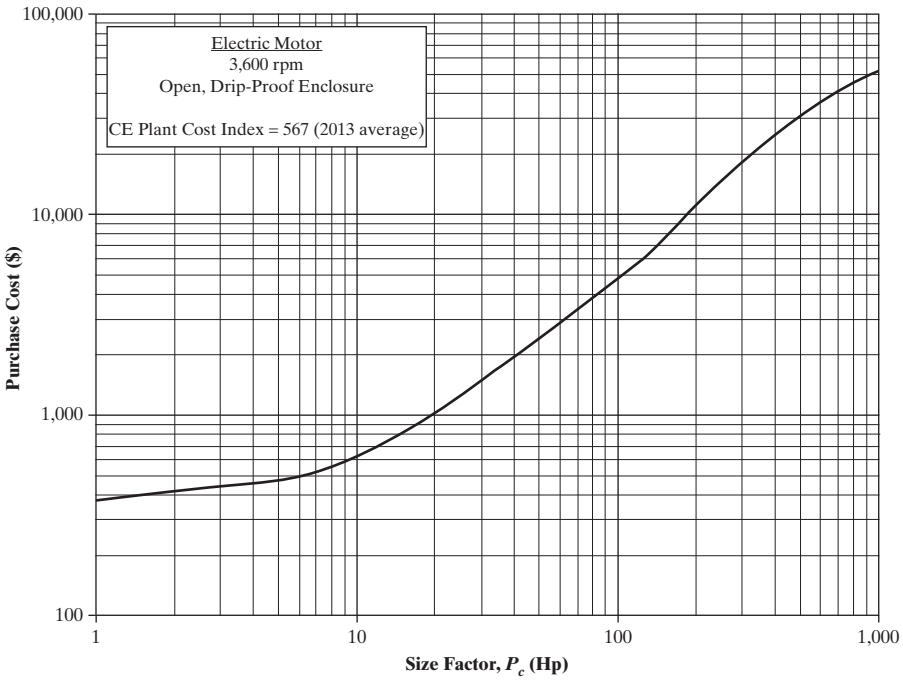

Figure 16.4 Base f.o.b. purchase cost for electric motors.

electric motor, η_M, by the equation:

$$P_C = \frac{P_{\mathrm{T}}}{\eta_P \eta_M} = \frac{P_B}{\eta_M} = \frac{QH\rho}{33{,}000\eta_P\eta_M} \tag{16.16}$$

where, as previously, Q is the flow rate through the pump in gallons per minute, H is the pump head in feet of fluid flowing, and P_B is the pump brake horsepower with ρ equal to the liquid density in pounds per gallon. Corripio et al. (1982a) give the following equations for estimating η_P as a function of the volumetric flow rate, and η_M as a function of pump brake horsepower:

$$\eta_P = -0.316 + 0.24015(\ln Q) - 0.01199\ (\ln Q)^2 \tag{16.17}$$

for Q in the range of 50 to 5,000 gpm;

$$\eta_M = 0.80 + 0.0319(\ln P_B) - 0.00182\ (\ln P_B)^2 \tag{16.18}$$

for P_B in the range of 1 to 1,500 Hp.

The f.o.b. purchase cost of an electric motor depends on its power consumption, P_C, the rotation rate of its shaft, and the type of motor enclosure. Cost data are given here for two common motor speeds (3,600 rpm and 1,800 rpm) and three common types of motor enclosures:

1. *Open, drip-proof enclosure*, which is designed to prevent the entrance of liquid and dirt particles but not airborne moisture, dust, and corrosive fumes into the internal working parts of the motor.
2. *Totally enclosed, fan-cooled* (TEFC) *enclosure*, which prevents any air from getting inside, thus protecting against moisture, dust, dirt, and corrosive vapors.
3. *Explosion-proof enclosure*, which protects the motor against explosion hazards from combustible gases, liquids, and dust by pressurizing the enclosure with a safe gas.

From the electric motor cost correlations of Corripio et al. (1982a), indexed to 2013 (CE = 567), the f.o.b. purchase cost of an electric motor operating at 3,600 rpm with an open, drip-proof enclosure (referred to here as the base cost, C_B) is plotted in Figure 16.4 as a function of the horsepower consumption, P_C. The cost curve is given by the equation:

$$\begin{aligned} C_{\mathrm{B}} = \exp\{&5.9332 + 0.16829[\ln(P_C)] \\ &- 0.110056\ [\ln(P_C)]^2\ + 0.071413\ [\ln(P_C)]^3 \\ &- 0.0063788\ [\ln(P_C)]^4\} \end{aligned} \tag{16.19}$$

which applies over the range of 1 to 700 Hp. For other motor speeds and type enclosures, the f.o.b. purchase cost is given by:

$$C_P = F_{\mathrm{T}} C_B \tag{16.20}$$

where F_T is a motor-type factor given in Table 16.22, applicable within a range of electric motor power consumption, P_C, from 1 to 1,500 Hp.

External Gear Pumps

Purchase-cost data for external gear pumps are not as widely available as they are for radial centrifugal pumps. The cost most often includes the gear pump, a base plate, and a driver coupling. In some cases, an electric motor drive is included. There is no

Table 16.22 F_{T} Factors in Eq. (16.20) and Ranges for Electric Motors

Type Motor Enclosure	3,600 rpm	1,800 rpm
Open, drip-proof enclosure, 1 to 700 Hp	1.0	0.90
Totally enclosed, fan-cooled, 1 to 250 Hp	1.4	1.3
Explosion-proof enclosure, 1 to 250 Hp	1.8	1.7

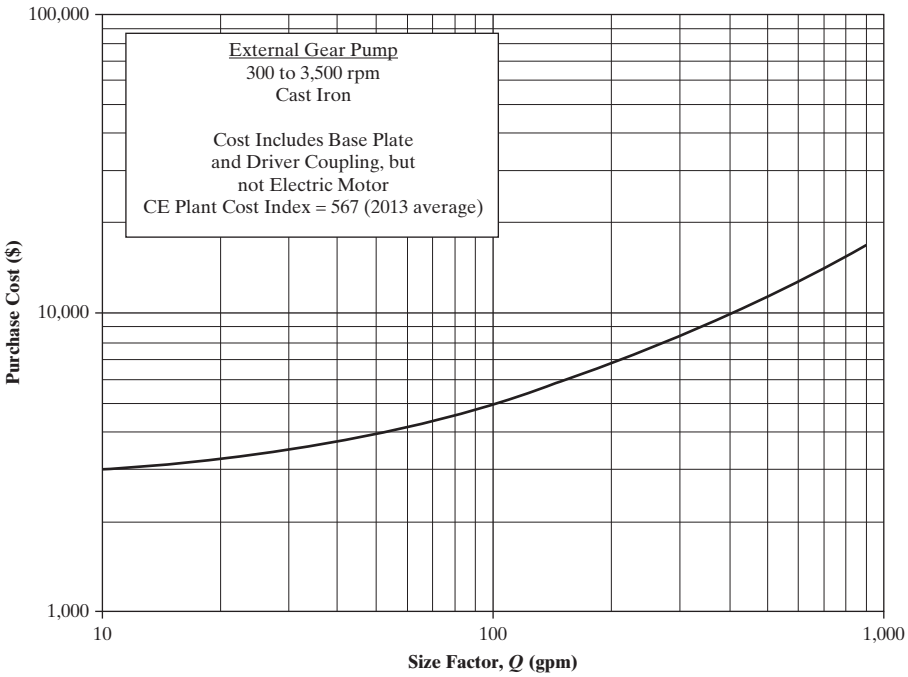

Figure 16.5 Base f.o.b. purchase cost for external gear pumps.

general agreement on what equipment size factor to use for correlating purchase costs. Most common are (1) brake horsepower and (2) flow capacity. Here, the cost correlation method used is in terms of flow capacity, Q, in gallons per minute, as used by Walas (1988).

In addition to the size factor, the purchase cost of a gear pump depends on the material of construction. Although gear pumps can be designed to operate over a wide range of flow rates and discharge pressure, typical ranges are 10 to 1,500 gpm and up to 200 psia for high-viscosity fluids. Typical pump efficiencies are 80% for low-kinematic viscosity liquids (20 centistokes) and 50% for high-kinematic viscosity liquids (500 centistokes). The f.o.b. purchase cost of an external gear pump of cast iron construction and for a cost index for 2013 (CE = 567) (referred to here as the base cost, C_B) is plotted in Figure 16.5. The cost includes the base plate and driver coupling, but not the electric motor. The cost curve in Figure 16.5 is given in terms of Q by the equation:

$$C_{\mathrm{B}} = \exp\{8.2816 - 0.2918[\ln(Q)] + 0.0743\,[\ln(Q)]^2\} \quad (16.21)$$

which is applicable over a range of 10 to 900 gpm. For other materials of construction, the f.o.b. purchase cost is given by:

$$C_{\mathrm{P}} = F_{\mathrm{M}} C_{\mathrm{B}} \quad (16.22)$$

where F_{M} is a material factor given in Table 16.21. The power requirement for the electric motor to drive the pump depends on the head, H, and the flow rate, Q, as given by Eq. (16.16).

Reciprocating Plunger Pumps

Although piston pumps are common, the plunger type is the best choice for the most demanding applications and is available for a wider range of flow rates. Purchase-cost data for reciprocating plunger pumps are not as widely available as they are for radial centrifugal pumps. The cost most often includes the pump and a driver coupling for a motor or a V-belt drive. In most cases, an electric motor drive is not included. There is no general agreement on what equipment size factor to use for correlating purchase costs. Most common are (1) brake horsepower and (2) flow capacity. The cost of most models is based on the brake horsepower. By changing the plunger and cylinder diameter, a reciprocating pump of a specified horsepower can operate over a 10-fold range of flow rate and head. Here, the cost correlation method used is in terms of brake horsepower, P_B, as given by Eq. (16.16) where the pump efficiency, η_P, is typically 0.90 (90%).

In addition to the size factor, the purchase cost of a reciprocating plunger pump depends on the material of construction. The f.o.b. purchase cost of a reciprocating plunger pump of ductile iron construction and a cost index for 2013 (CE = 567) (referred to here as the base cost, C_B), is plotted in Figure 16.6. The cost includes a V-belt drive but not the electric motor. The cost curve in Figure 16.6 is given by the equation:

$$C_{\mathrm{B}} = \exp\{7.9361 + 0.26986[\ln(P_{\mathrm{B}})] + 0.06718\,[\ln(P_{\mathrm{B}})]^2\} \quad (16.23)$$

which is applicable over the range of 1 to 200 BHp. For other materials of construction, the f.o.b. purchase cost is given by Eq. (16.15), where F_M is a material factor, as follows:

Ductile iron $F_m = 1.00$
Ni–Al–Bronze $F_m = 1.15$
Carbon steel $F_m = 1.50$
Stainless steel $F_m = 2.20$

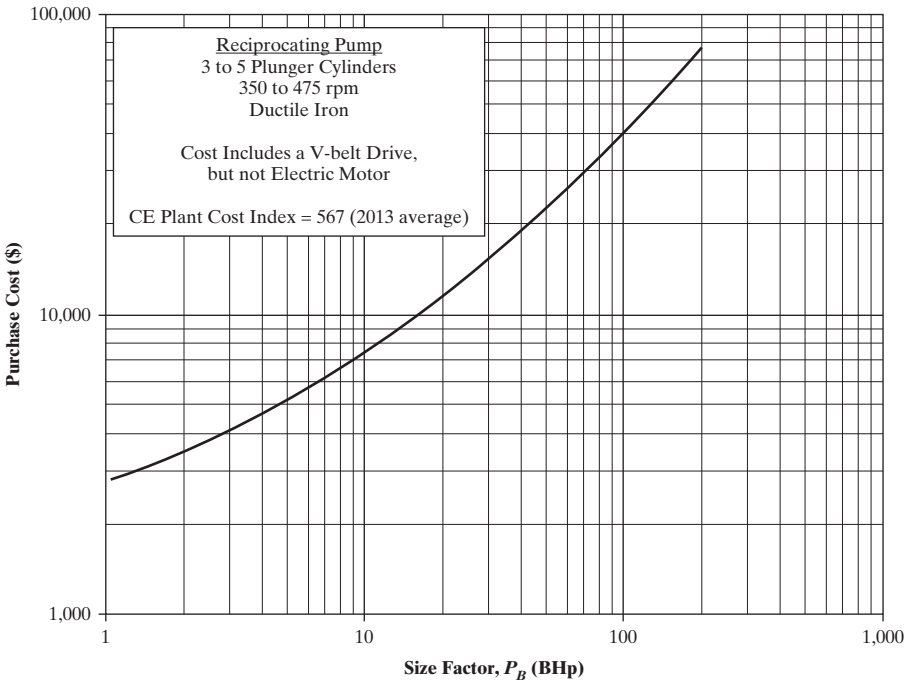

Figure 16.6 Base f.o.b. purchase cost for reciprocating plunger pumps.

EXAMPLE 16.6

In Chapter 2, a vinyl-chloride process is synthesized with a detailed process flow diagram shown in Figure 2.17. In that process, Reactor Pump P-100 takes stream 4 (a mixture of streams 3 and 16) of 263,800 lb/hr of 1, 2-dichloroethane at 90°C and 1.5 atm and delivers it to an evaporator operating at a much higher pressure of 26 atm. Select a suitable pump and electric motor and estimate the f.o.b. purchase cost at a CE index of 600.

SOLUTION

A process simulation program is used to obtain the density, viscosity, and vapor pressure of the feed at 90°C and 1.5 atm. The density is 9.54 lb/gal (71.4 lb/ft^{3}or 1.14 g/cm^3), the viscosity is 0.37 cP, and the vapor pressure is 1.212 atm.

The feed volumetric flow rate is $263{,}800/[(60)(9.54)] = Q =$ 461 gpm.

The pressure increase across the pump is 26 − 1.5 − 24.5 atm.

The pump head is (24.5) (14.696) (144)/71.4 = H = 726 ft.

The kinematic viscosity is 0.37/1.14 = 0.32 centistokes, which is quite low.

Choose a radial centrifugal pump.

However, it is necessary to first check the available NPSH as discussed in Section 14.1.

$$\text{NPSH}_A = \frac{\text{Suction pressure} - \text{Vapor pressure}}{\text{Liquid density}}$$

$$= \frac{(1.5 - 1.212)(14.696)(144)}{71.4} = 8.54 \text{ ft}$$

Assume we can purchase a radial centrifugal pump with a required NPSH > 5.

From Eq. (16.13), the centrifugal pump size parameter is

$$S = Q(H)^{0.5} = 461\ (726)^{0.5} = 12{,}420(\text{gpm})(\text{ft})^{0.5}$$

$$\text{and In (S)} = 9.427$$

From Eq. (16.14), the base pump purchase cost at a CE cost index of 567 is

$$C_B = \exp\{12.1656 - 1.1448[\ln(12{,}420)] + 0.0862\ [\ln(12{,}420)]^2\} = \$8{,}380$$

From Table 16.20, for the given flow rate and relatively high head, choose a 2-stage, 3600-rpm, HSC centrifugal pump, with $F_T = 2.70$.

From Table 16.21, choose cast steel with $F_M = 1.35$ because of the relatively high discharge pressure.

From Eq. (16.15) and correcting for a CE cost index of 600,

$$C_P = (2.70)(1.35)(600/567)(\$8{,}380) = \$32{,}300$$

From Eq. (16.17), the pump efficiency for $Q = 461$ gpm and $\ln(Q) = 6.13$ is

$$\eta_P = -0.316 + 0.24015(6.13) - 0.01199\ (6.13)^2 = 0.706$$

From Eq. (16.16), the pump brake horsepower, P_B, is

$$P_B = \frac{QH\rho}{33{,}000\eta_P} = \frac{(461)(726)(9.54)}{33{,}000(0.706)} = 137 \text{ BHp}$$

From Eq. (16.18), the motor efficiency for $\ln(P_B) = 4.92$ is

$$\eta_M = 0.80 + 0.0319(4.92) - 0.00182(4.92)^2 = 0.913$$

From Eq. (16.16), the power consumption of the motor is

$$P_C = \frac{P_B}{\eta_M} = \frac{137}{0.913} = 150 \text{ Hp}$$

From Eq. (16.19), the base cost of the motor for ln (Pc) = 5.01 and a CE index of 567 is

$$C_B = \exp\{5.9332 + 0.16829(5.01) - 0.110056\,(5.01)^2 + 0.071413\,(5.01)^3 - 0.0063788\,(5.01)^4\} = \$7{,}910$$

Because of the possible flammability hazard of 1,2-dichloroethane, specify an explosion-proof electric motor to drive the pump. From Table 16.22, for 3,600 rpm, $F_T = 1.8$ and using Eq. (16.20) but with added updating of the CE cost index to 600,

$$C_P = F_T C_B = (1.80)\left(\frac{600}{567}\right)(\$7{,}910) = \$15{,}070$$

Total cost of centrifugal pump and motor = \$32,300 + \$15,070 = \$47,400. Consideration should be given to purchasing a spare pump and motor.

Fans, Blowers, and Compressors

When energy input is required to move a gas through various pipelines or ducts in a chemical processing plant, a fan, blower, or compressor is used. As discussed in Section 14.1, the power input to the gas mover increases the total head of the gas, which, ignoring a change in potential energy of the gas due to change in elevation above sea level, includes the velocity (dynamic) head and the pressure (static) head. According to Papanastasiou (1994), the gas mover is defined as (1) a *fan*, if almost all of the energy input increases the velocity head; (2) a *blower*, if the energy input increases both the velocity head and the pressure head; and (3) a *compressor*, if almost all of the energy input increases the pressure head. However, that definition is not widely accepted. In practice, one vendor may refer to a particular gas mover as a fan, and another vendor may refer to it as a blower. The same situation applies to blowers and low-compression-ratio compressors. Here, we classify a fan as a gas mover that is generally limited to near-ambient suction pressures and pressure increases of less than 10%. Blowers can operate at any suction pressure, with compression ratios of up to 2. Thus, the main purpose of a fan is to move large quantities of gas with an increase in pressure head of up to 40 in. of H_2O head where a blower can take a gas at 1 atm and deliver it at up to 2 atm. For larger compression ratios, a compressor is generally specified.

Fans are widely used for high-flow, low-pressure-increase applications such as heating and ventilating systems; air supply to cooling towers, low-pressure-drop dryers, and finned-tube air coolers; and removal of fumes, flue gas, and gas from a baghouse. Blowers are used for supplying combustion air to boilers and fired heaters, air to strippers, purge gas for regeneration of fixed-bed adsorbers, and air to dryers with more pressure drop than a fan can handle and for pneumatic conveying of particles. Compressors are widely used with a variety of gases and gas mixtures to increase their pressure to required levels for chemical reaction and separation.

Because a gas is compressible with a density much lower than that of a liquid, the temperature of a gas rises when compressed, and this temperature rise is a limiting factor in determining the permissible compression ratio for a single-stage gas compressor. As discussed in Section 14.2, fractional dissipation in the gas mover causes a further rise in the gas temperature. Although some specialized compressors permit a gas discharge temperature of up to 600°F, the more widely used compressors are limited to discharge temperatures in the range of 375 to 400°F. For a diatomic gas or gas mixture (e.g., air) with a specific heat ratio of 1.4, a 400°F limit corresponds to a maximum single-stage compression ratio of 3.75 after taking into account an assumed compressor isentropic efficiency of 85%. This limiting compression ratio decreases to 2.50 for a monatomic gas with a higher specific heat ratio of 1.67, but increases to 6.0 for a gas with a lower specific heat ratio of 1.30 (e.g., methane). For gases with a specific heat ratio less than 1.30, even higher compression ratios may be possible, but most compressors are limited to a compression ratio of 8.0. If a higher compression ratio is required, the compression is accomplished in stages that are separated by heat exchangers that cool the gas to about 100°F before entering the next stage. Because the cooling may cause some condensation, a vapor-liquid separator, which is usually a vertical vessel containing a demister pad to coalesce small liquid droplets and is called a *knock-out drum*, must be provided after each intercooler to remove liquid from the gas prior to its entry into the next stage of compression. Because most compressors cannot tolerate any liquid in the gas, compressor inlet and outlet phase conditions should always be checked. As discussed in the subsection Compressors, the maximum compression ratio for a centrifugal compressor may be limited by the maximum velocity at the blade tips rather than by the exit temperature.

Fans

Most fans are of the centrifugal or axial-flow type. *Centrifugal fans* achieve the highest discharge pressures whereas *axial-flow fans* provide the highest flow rates. Although forward-curved and airfoil blade designs are available for centrifugal fans, the two most popular are the *backward-curved blade* and the *straight-radial blade*. The former is the cheapest for a given flow capacity and the most efficient, but the discharge pressure decreases rapidly from its maximum value as the flow rate is increased. It is suitable only for air and clean gases. The straight-radial centrifugal fan is less efficient, but is suitable for dust-laden gases and maintains the discharge pressure, up to a compression ratio of 1.2, over a wider range of flow rates. However, at this level of pressure increase, a fan may be called a blower. Axial-flow fans come in two main types: *vane axial* (compression ratio to 1.04) and *tube axial* (compression ratio to 1.025). Less efficient are propeller fans. Typical operating ranges of centrifugal and axial-flow fans are given in Table 16.23.

Table 16.23 Typical Operating Ranges of Fans

Fan Type	Flow Rate (ACFM)[a]	Total Head (in. H_2O)
Centrifugal backward curved	1,000–100,000	1–40
Centrifugal straight radial	1,000–20,000	1–30
Vane axial	1,000–800,000	0.02–16
Propeller	1,000–15,000	0.00–1

[a] ACFM = actual cubic feet per minute.

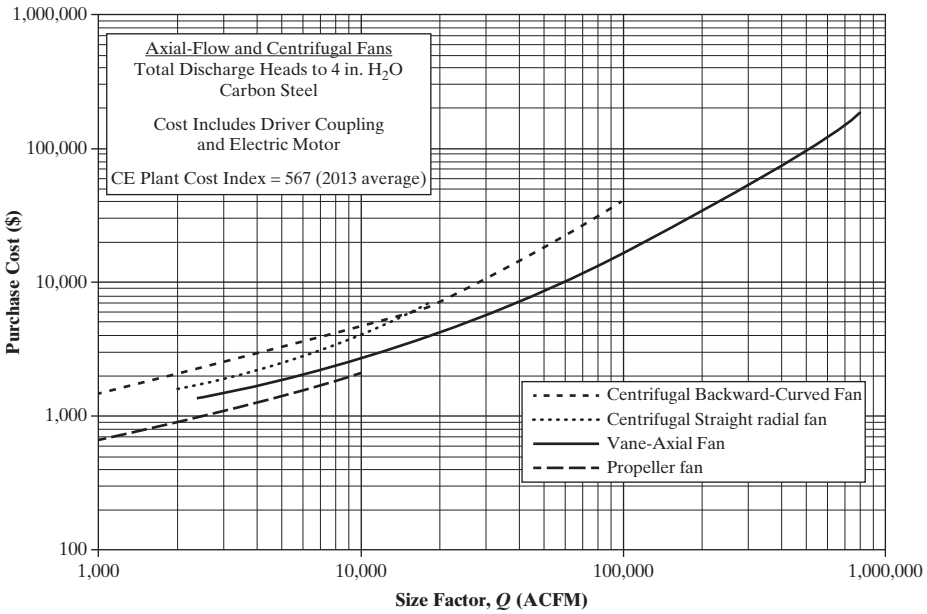

Figure 16.7 Base f.o.b. purchase costs for axial-flow and centrifugal fans.

The equipment size factor for a fan is the actual cubic feet per minute, ACFM, entering the fan. Fans are usually driven by an electric motor with either a direct drive or a belt. Base f.o.b. purchase costs, C_B, for the four most common types of fans, averaged from several published sources listed in Table 16.19 and vendor quotes, are plotted in Figure 16.7 as a function of Q in ACFM at a cost index for 2013 (CE = 567). The base cost, which includes an electric motor drive, is for carbon-steel construction and total discharge heads to 4 in. H_2O. For other materials of construction and higher discharge heads, the f.o.b. purchase cost is given by

$$C_P = F_H F_M C_B \tag{16.24}$$

where the following values of F_M apply to other materials of construction:

Fiberglass $F_M = 1.8$
Stainless steel $F_M = 2.5$
Nickel alloy $F_M = 5.0$

The head factor, F_H, for total heads greater than 4 in. H_2O is given in Table 16.24.

Table 16.24 Head Factor, F_H, for Fans in Eq. (16.24)

Head (in. H_2O)	Centrifugal Backward Curved	Centrifugal Straight Radial	Vane Axial	Propeller
5–8	1.15	1.15	1.15	—
9–15	1.30	1.30	1.30	
16–30	1.45	1.45		
31–40	1.55			

The base cost curves in Figure 16.7 for a CE cost index of 567 are given by the following equations, with Q in actual cubic feet per minute (ACFM) of gas entering the fan.

Centrifugal backward-curved fan (valid from $Q = 1{,}000$ to 100,000 ACFM):

$$C_B = \exp\{11.4152 - 1.3805[\ln(Q)] + 0.1139\,[\ln(Q)]^2\} \tag{16.25}$$

Centrifugal straight-radial fan (valid from $Q = 1{,}000$ to 20,000 ACFM):

$$C_B = \exp\{12.1667 - 1.6407[\ln(Q)] + 0.1328\,[\ln(Q)]^2\} \tag{16.26}$$

Vane-axial fan (valid from $Q = 1{,}000$ to 800,000 ACFM):

$$C_B = \exp\{9.6487 - 0.97566[\ln(Q)] + 0.08532\,[\ln(Q)]^2 \tag{16.27}$$

Propeller fan (valid from $Q = 1{,}000$ to 15,000 ACFM):

$$C_B = \exp\{6.16328 - 0.28635[\ln(Q)] + 0.04866\,[\ln(Q)]^2\} \tag{16.28}$$

The brake horsepower for a fan may be computed in any of three ways, depending on whether the total change in head is mostly dynamic, static, or a mixture of the two. The corresponding nominal fan efficiency, η_F, is 40% for mostly a dynamic change, 60% for mostly a static change, and 70% for a mixture of the two. The power consumption is given by the following equation, which is similar to Eq. (16.16) and where the electric motor efficiency, η_M, can be taken as 90%:

$$P_C = \frac{P_B}{\eta_M} = \frac{QH_t}{6{,}350\eta_F\eta_M} \tag{16.29}$$

where Q = gas inlet flow rate in cubic feet per minute, and H_t = change in total head in inches of water.

EXAMPLE 16.7

A flue gas at 200°F and 740 torr with an average molecular weight of 31.3 is to be discharged at a rate of 12,000 standard cubic feet per minute (SCFM) at 60°F and 1 atm to a pressure of 768 torr in a duct where the velocity, V, will be 150ft/s. Calculate the actual inlet flow rate in cubic feet per minute and the power consumption. Select a suitable fan and estimate the purchase cost for CE = 600.

SOLUTION

The actual fan inlet flow rate is $12{,}000\left(\frac{660}{520}\right)\left(\frac{740}{760}\right) = 14{,}830\ \text{ft}^3/\text{min}$.

Assume the inlet velocity is zero.

The increase in dynamic head is $\frac{V^2}{2g_c} = \frac{150^2}{2\,(32.2)} = 349$ ft-lbf/lbm of gas.

From the ideal gas law, the average density of the gas in passing through the fan, assuming no change in temperature, is 0.0644 lb/ft^3.

The increase in pressure head $= \frac{\Delta P}{\rho} = \frac{\frac{(768-740)}{760}(14.7)(144)}{0.0644} =$ 1,211 ft-lbf/lbm of gas. The total change in head is 349 + 1,211 = 1,560 ft-lbf/lbm of gas = 19.3 in. of H_20. Because static head is predominant, let $\eta_F = 0.60$. From Eq. (16.29),

$$P_C = \frac{14{,}830(19.3)}{6{,}350(0.60)(0.90)} = 83.5\ \text{Hp}$$

Because the head is greater than 16 in. of H_2O and the flue gas is not likely to be clean, using Table 16.23, select a centrifugal fan with a straight-radial impeller. From Table 16.24, the head factor, F_H, is 1.45. From Eqs. (16.24) and (16.26), correcting for the cost index, the purchase cost, including the motor, is

$$C_B = 1.45\left(\frac{600}{567}\right)\exp\{12.1667 - 1.6407[\ln(14{,}830)] + 0.1328\,[\ln(14{,}830)]^2\} = \$8{,}840$$

Blowers

Most blowers with compression ratios up to 2 are of the multistage centrifugal (often called turboblower) type or the rotary positive-displacement type. Axial-flow units can also be used, but must be multistaged. The centrifugal units are similar to centrifugal fans with the same type of blades, but operate at higher speeds and are built to withstand higher discharge pressures. The most common rotary blower is the straight-two-lobe (Roots) blower developed by the Roots brothers in 1854 or a modification with three straight lobes. Typical operating ranges are 100 to 50,000 ICFM for centrifugal blowers and 20 to 50,000 ICFM for rotary straight-lobe blowers with two lobes where ICFM is the cubic feet per minute at inlet conditions. Typical mechanical efficiencies, η_B, are 70–80% for centrifugal blowers and 50–70% for straight-lobe blowers. However, with straight-lobe blowers, the higher efficiency is achieved only for compression ratios from 1.2 to 1.3; from 1.3 to 2.0, the efficiency falls off rapidly. The centrifugal blower delivers a smooth flow rate, but as discussed in Section 14.2, the straight-lobe units deliver a somewhat pulsing flow. As with pumps, rotary blowers deliver a fixed volumetric flow rate with varying inlet and outlet pressures whereas the volumetric throughput of centrifugal blowers varies with changes in inlet or discharge pressures. Both types of blowers have found a wide range of applications, but centrifugal blowers are more common in chemical processing plants and are widely used to supply air to strippers, dryers, and combustion devices. Rotary blowers are useful for pneumatic conveying and are well suited to other applications when a fixed volumetric flow rate is essential.

The equipment size factor for a blower is the brake horsepower, P_B, which is computed from the inlet volumetric flow rate, Q_I in cubic feet per minute and pressures in lbf/in^2 at the inlet, P_I and outlet, P_O, by the following equation, which assumes the ideal gas law and a constant specific heat ratio, k:

$$P_B = 0.00436\left(\frac{k}{k-1}\right)\frac{Q_I P_I}{\eta_B}\left[\left(\frac{P_O}{P_I}\right)^{\frac{k-1}{k}} - 1\right] \qquad (16.30)$$

Blowers are usually driven by an electric motor with a direct drive for the centrifugal type and a belt or chain drive for the rotary type. Except for very large units, centrifugal blowers must be staged to achieve pressures greater than 40 in. of H_2O gauge. Base f.o.b. purchase costs, C_B, for the two major types of blowers based on data from Garrett (1989) and recent data from vendors are plotted in Figure 16.8 as a function of P_C in horsepower for a cost index in 2013 (CE = 567). The base cost, which includes an electric motor drive, is for a cast-iron construction housing with compression ratios up to 2. The centrifugal blower uses sheet metal blades. For other materials of construction, the f.o.b. purchase cost is given by:

$$C_P = F_M C_B \qquad (16.31)$$

where the metal material factors given above for fans can be used. In addition, centrifugal blowers are available with cast aluminum blades with $F_M = 0.60$.

The base blower purchase cost curves in Figure 16.8 for a CE cost index of 567 are given by the following equations with P_C in horsepower:

Centrifugal (turbo) blower (valid from $P_C = 5$ to 1,000 Hp):

$$C_B = \exp\{7.0187 + 0.7900[\ln(P_C)]\} \qquad (16.32)$$

Rotary straight-lobe blower (valid from $P_C = 1$ to 1,000 Hp):

$$C_B = \exp\{7.71751 + 0.79320[\ln(P_C)] - 0.012900\,[\ln(P_C)]^2\} \qquad (16.33)$$

EXAMPLE 16.8

Air available at 70°F and 14.5 psia is to be supplied by a blower at 6,400 ACFM to a column with 15 plates to strip VOCs (volatile organic compounds) from 1,000 gpm of wastewater. The column is 6 ft in diameter. The pressure drop through the inlet line, the column, and the outlet line has been estimated to be at 3 psi. The gas exiting from the column is to be sent to the next unit at a pressure of 18 psia. Select and size a blower, calculate the required power consumption, and estimate the f.o.b. purchase cost for a CE cost index of 600.

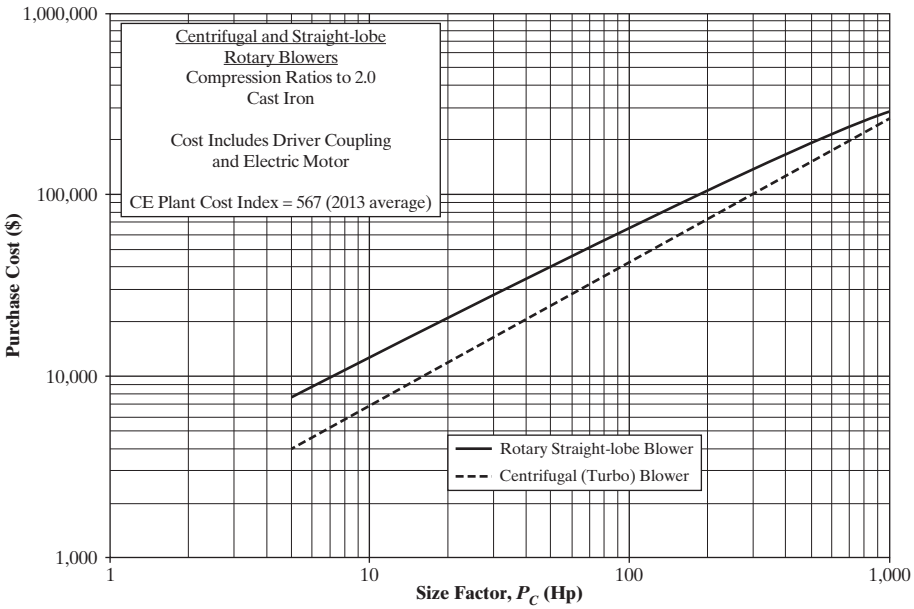

Figure 16.8 Base f.o.b. purchase costs for centrifugal and straight-lobe blowers.

SOLUTION

The total pressure increase required across the blower is $18.0 - 14.5 + 3.0 = 6.5$ psi. At the blower inlet, the pressure is 14.5 psia, giving an air density of 0.074 lbm/ft^3. This gives an inlet pressure head of $(14.5)(144)/0.074 = 28{,}200$ ft-lbf/lbm. At the blower exit, the pressure is $18.0 + 3.0 = 21.0$ psia, giving an air density of approximately 0.095 lbm/ft^3 and an outlet pressure head of $(21)(144)/0.095 = 31{,}800$ ft-lbf/lbm. This gives a change in pressure head of $31{,}800 - 28{,}200 = 3{,}600$ ft-lbf/lbm. For the increase in kinetic-energy head, assume the blower inlet velocity is zero and the blower discharge air velocity in the exit line is 75 ft/s. The increase in kinetic energy is $(75)^2/[2(32.2)] = 87.3$ ft-lbf/lbm. In this example, the change in kinetic-energy head is only about 2.5% of the total increase in head. Neglecting the increase in kinetic-energy head, the blower brake horsepower from Eq. (16.30), using $k = 1.4$ and $\eta_B = 0.75$ for a centrifugal blower, is:

$$P_B = 0.00436\left(\frac{1.4}{1.4-1}\right)\frac{6{,}400(14.5)}{0.75}\left[\left(\frac{21}{14.5}\right)^{\frac{1.4-1}{1.4}} - 1\right]$$

$$= 211 \text{ BHp}$$

Using Eq. (16.18), the motor efficiency = $\eta_M = 0.92$. From Eq. (16.16), the consumed power for a centrifugal blower is $211/0.92 = 229$ Hp. A straight-lobe blower with $\eta_B = 0.65$ requires a consumed power of 265 Hp. For this application, either the centrifugal blower or straight-lobe blower is suitable, but with a compression ratio of $21/14.5 = 1.45$, the centrifugal blower is more efficient and is more widely used for this application. Using Eq. (16.2), with a CE cost index of 567, the estimated f.o.b. purchase cost of the centrifugal blower of iron and steel construction, which would be a multistage unit, including an electric motor with a direct drive, is

$$C_B = \frac{600}{567}\exp\{7.0187 + 0.7900[\ln(229)]\} = \$86{,}500$$

A centrifugal blower with aluminum blades, $F_M = 0.60$, is also suitable and reduces the f.o.b. purchase cost to 0.6 ($86,500) = $51,900.

Compressors

Compressors are used widely to move gases for compression ratios greater than 2. As discussed in Section 16.3, the major types are the trunk-piston and crosshead reciprocating compressors, diaphragm compressors, centrifugal compressors, axial compressors, and the screw, sliding-vane, and liquid-ring (piston) rotary compressors. Of these, the most commonly used in chemical processing plants are the (1) double-acting crosshead reciprocating compressor, (2) multistage centrifugal compressor, and (3) rotary twin-screw compressor. These are referred to here as simply reciprocating, centrifugal, and screw compressors.

Reciprocating compressors can handle the widest range of pressure, from vacuum to 100,000 psig, but the narrowest range of flow rates, from 5 to 7,000 ACFM, with horsepowers up to 20,000 per machine. By using many stages, centrifugal compressors can deliver pressures up to 5,000 psig for the largest flow rates from 1,000 to 150,000 ACFM with horsepowers to 2,000 per machine. Screw compressors have the smallest pressure range, up to 400 psig, for flow rates from 800 to 20,000 ACFM with horsepowers to 6,000 per machine.

Because reciprocating and screw compressors are of the positive-displacement type, they are designed for a particular flow rate, with their discharge pressure set by the downstream system, provided that the power input to the compressor is sufficient. The maximum compression ratio per stage is set by a limiting temperature rise of the gas being compressed as discussed at the beginning of this subsection. Compared to the screw compressor, the reciprocating compressor is more efficient (80–90% compared to 75–85%), more expensive, larger in size, somewhat more flexible in operation, accompanied in operation by large shaking forces that require a large foundation and more maintenance, is less noisy, and does not deliver as smooth a flow rate. Reciprocating compressors cannot tolerate the presence of liquid or solid particles in the feed gas, and consequently, must be protected by a knock-out drum.

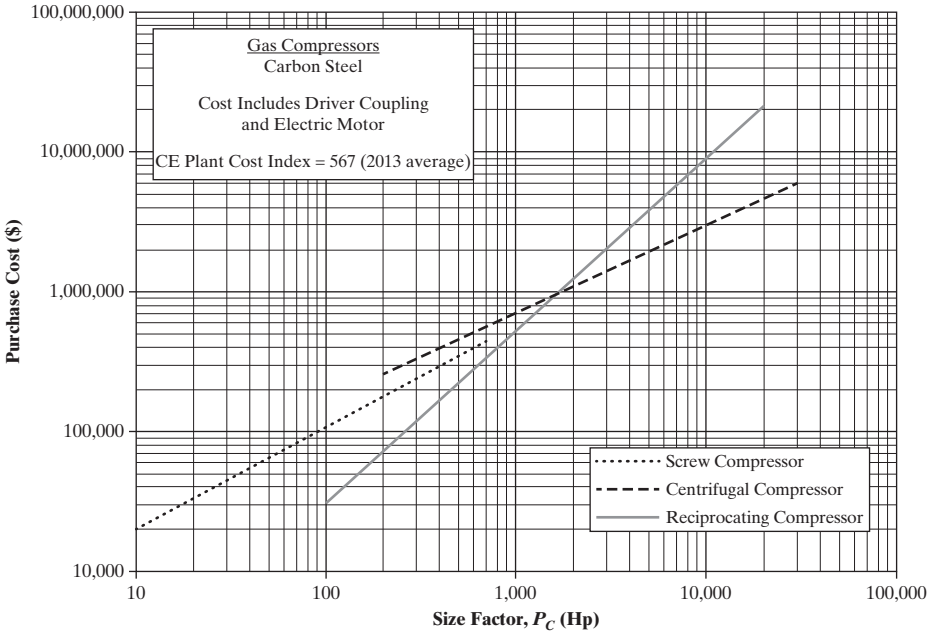

Figure 16.9 Base f.o.b. purchase costs for centrifugal, reciprocating, and screw compressors.

The centrifugal compressor has become exceedingly popular in the last few decades because it is easily controlled, delivers a smooth flow rate (which, however, is dependent on the required discharge pressure), has small foundations and low maintenance, and can handle large flow rates and fairly high pressures. However, it is less efficient (70–75%) and more expensive than a screw compressor for the same application. The velocity of the blade tips sets the maximum compression ratio per machine stage. This limitation almost always translates into multiple stages in a single machine for compression ratios greater than 2 even though a limiting temperature is not achieved. Single machines may have as many as 10 stages. Further compression after reaching the temperature limit requires an intercooler followed by another machine.

Process simulation programs are preferred to compute the theoretical and brake horsepower requirements, as well as the exit temperature of a compressor because the ideal gas law is not usually applicable for pressures above two atmospheres. However, Eq. (16.30) can be used to obtain a preliminary estimate of the brake horsepower. An estimate of the exit temperature, including the effect of compressor efficiency, η_c, can be made with the following modification of the equation for the isentropic exit temperature:

$$T_O = T_I + \frac{T_I\left[\left(\frac{P_O}{P_1}\right)^{\frac{k-1}{k}} - 1\right]}{\eta_C} \tag{16.34}$$

Compressors may be driven by electric motors, steam turbines, or gas turbines, but the former are the most common driver and the gas turbine is the least common. All drivers are available up to at least 20,000 Hp. For applications below about 200 Hp, electric motors are used almost exclusively. Most efficient is the electric motor; least efficient is the gas turbine. Efficiencies of all three drivers increase with horsepower. At 1,000 Hp, typical efficiencies are 95%, 65%, and 35% for the electric motor, steam turbine, and gas turbine, respectively. Therefore, unless excess steam or low-cost combustion gas is available, the electric motor is the driver of choice over the entire horsepower range. An exception is sometimes made for centrifugal compressors, where the steam turbine is an ideal driver because the speeds of the two devices can be matched. See Section 16.6 and Table 16.32 there for cost equations for steam and gas turbines.

Base f.o.b. purchase costs, C_B, for the three major types of compressors based on data from Garrett (1989) and Walas (1988) in Table 16.19, are plotted in Figure 16.9 as a function of consumed power, P_C, in horsepower for a cost index in 2013 (CE = 567). The base cost, which includes an electric motor drive, is for cast iron or carbon-steel construction. For other drives and materials of construction, the f.o.b. purchase cost is given by:

$$C_P = F_D F_M C_B \tag{16.35}$$

where, in place of an electric motor drive, $F_D = 1.15$ for a steam turbine drive and 1.25 for a gas turbine drive, and $F_M = 2.5$ for stainless steel and 5.0 for nickel alloy.

The base compressor purchase cost curves in Figure 16.9 for a CE cost index of 567 are given by the following equations with P_C in horsepower:

Centrifugal compressor (valid from $P_C = 200$ to 30,000 Hp):

$$C_B = \exp\{9.1553 + 0.63[\ln(P_C)]\} \tag{16.36}$$

Reciprocating compressor (valid from $P_C = 100$ to 20,000 Hp):

$$C_B = \exp\{4.6762 + 1.23[\ln(P_C)]\} \tag{16.37}$$

Screw compressor (valid from $P_C = 10$ to 750 Hp):

$$C_B = \exp\{8.2496 + 0.7243[\ln(P_C)]\} \tag{16.38}$$

EXAMPLE 16.9

In an ammonia process in which hydrogen and nitrogen are combined at high temperature and high pressure in a catalytic reactor, a multistage gas compression system with intercoolers is needed to compress the feed gas to the reactor pressure. For one of the compression stages, the feed gas, at 320 K, 30 bar, and 6,815 kmol/hr, has a composition in mol% of 72.21 H_2, 27.13 N_2, 0.61 CH_4, and 0.05 Ar. It is to be compressed to 70 bar in an uncooled, adiabatic compressor. Size and select the compressor and the drive and estimate the f.o.b. purchase cost for a CE index of 600.

SOLUTION

At the high-pressure conditions, the ideal gas law does not apply and, therefore, it is preferred to size the compressor with a process simulation program. Using the SRK equation of state, the results give an inlet volumetric flow rate of 6,120 m^3/hr or 3,602 cfm. This is in the range of all three compressor types. However, the discharge pressure of 70 bar or 1,016 psi is beyond the range of the screw compressor. Select a centrifugal compressor of steel construction with an assumed isentropic efficiency of 75%. This gives a discharge temperature of 439 K or 331°F, which is below the suggested 400°F discharge limit for a compressor. The corresponding theoretical kilowatts is 4,940 or 6,630 THp (theoretical horsepower). With a 75% compressor efficiency, the brake horsepower is 8,840. Assume a 95% efficiency for the motor. This gives P_C = 9,300 Hp. From Eq. (16.36), the f.o.b. purchase cost for CE = 600 is

$$C_B = \left(\frac{600}{567}\right) \exp\{9.1553 + 0.63[\ln(9{,}300)] = \$3{,}170{,}000$$

An alternative that might be considered is the use of two identical centrifugal compressors, each delivering 50% of the required flow, in place of the single compressor.

Heat Exchangers

As discussed in Chapter 12, a wide variety of heat exchangers is available for heating, cooling, condensing, and vaporizing process streams, particularly liquids and gases. The most important types are shell-and-tube, double-pipe, air-cooled fin-fan, and compact heat exchangers, including plate-and-frame, spiral-plate, spiral-tube, and plate-fin types. For most applications in chemical processing plants, shell-and-tube heat exchangers, which are governed by TEMA (Tubular Exchanger Manufacturers Association) standards and ASME (American Society of Mechanical Engineers) pressure-vessel code as well as other standards, are selected. However, for heat exchanger areas less than 200 ft^2, double-pipe heat exchangers are often selected, and when streams are cooled by air, fin-fan units are common. Compact heat exchangers are usually reserved for nondemanding applications. In this section, graphs and equations are presented only for shell-and-tube and double-pipe heat exchangers. Equations for air-cooled fin-fan and compact heat exchangers that are described in Section 12.2 are presented in Section 16.6 and Table 16.32.

Shell-and-Tube Heat Exchangers

These exchangers cover a wide range of geometrical variables including tube diameter, wall thickness, length, spacing, and arrangement; baffle type and spacing; numbers of tube and shell passes; and fixed-head, floating-head, U-tube, and kettle designs. However, most published purchase-cost data are correlated in terms of heat exchange surface area (usually based on the outside surface area of the tubes) for a base-case design with correction factors only for pressure and materials for the shell and tubes. In some cases, corrections for tube length are given. Here, the following cost correlations are based on several of the references in Table 16.19 and in Corripio et al. (1982b). The base cost curves in Figure 16.10 for a CE cost index of 567 are given by

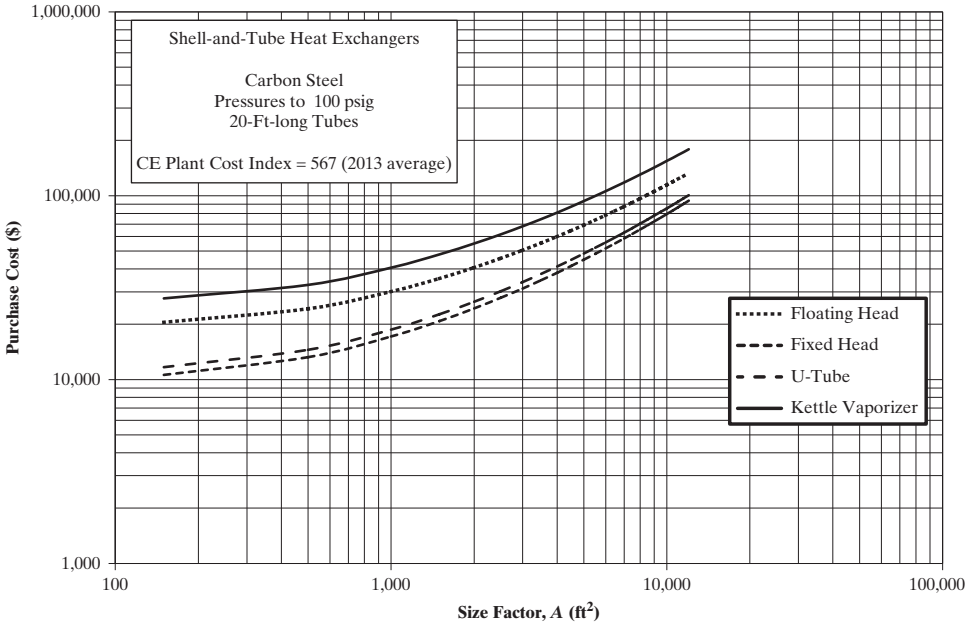

Figure 16.10 Base f.o.b. purchase costs for shell-and-tube heat exchangers.

the following equations with tube outside surface area, A, in square feet, ranging from 150 to 12,000 ft^2. These base-case exchangers include 3/4-in. or 1-in. O.D., 16 BWG (Birmingham Wire Gage) carbon-steel tubes, 20 ft long, on square or triangular pitch in a carbon-steel shell for use with shell-side pressures up to 100 psig.

Floating head:

$$C_B = \exp\{12.0310 - 0.8709[\ln(A)] + 0.09005\,[\ln(A)]^2\} \quad (16.39)$$

Fixed head:

$$C_B = \exp\{11.4185 - 0.9228[\ln(A)] + 0.09861\,[\ln(A)]^2\} \quad (16.40)$$

U-tube:

$$C_B = \exp\{11.5510 - 0.9186[\ln(A)] + 0.09790\,[\ln(A)]^2\} \quad (16.41)$$

Kettle vaporizer:

$$C_B = \exp\{12.3310 - 0.8709[\ln(A)] + 0.09005\,[\ln(A)]^2\} \quad (16.42)$$

The f.o.b. purchase cost for each of these four types of heat exchangers is determined from

$$C_P = F_P F_M F_L C_B \quad (16.43)$$

where F_M is a material factor for various combinations of tube and shell material, as given in Table 16.25 as a function of the surface area, A, in square feet according to the equation:

$$F_M = a + \left(\frac{A}{100}\right)^b \quad (16.44)$$

The factor F_L is a tube-length correction as follows:

Tube Length (ft)	F_L
8	1.25
12	1.12
16	1.05
20	1.00

Table 16.25 Materials of Construction Factors, F_M, for Shell-and-Tube Heat Exchangers

Materials of Construction Shell/Tube	a in Eq. (16.44)	b in Eq. (16.44)
Carbon steel/carbon steel	0.00	0.00
Carbon steel/brass	1.08	0.05
Carbon steel/stainless steel	1.75	0.13
Carbon steel/Monel	2.1	0.13
Carbon steel/titanium	5.2	0.16
Carbon steel/Cr-Mo steel	1.55	0.05
Cr-Mo steel/Cr-Mo steel	1.70	0.07
Stainless steel/stainless steel	2.70	0.07
Monel/Monel	3.3	0.08
Titanium/titanium	9.6	0.06

The pressure factor, F_P, is based on the shell-side pressure, P, in psig and is given by Eq. (16.45), which is applicable from 100 to 2,000 psig:

$$F_P = 0.9803 + 0.018\left(\frac{P}{100}\right) + 0.0017\left(\frac{P}{100}\right)^2 \quad (16.45)$$

Double-Pipe Heat Exchangers

For heat exchange surface areas of less than 200 ft^2 and as low as 2 ft^2, double-pipe heat exchangers are often selected over shell-and-tube heat exchangers. The area, A, is usually based on the outside surface area of the inner pipe. The cost correlation here is based on the average of several of the references in Table 16.19. The base cost curve in Figure 16.11 for a CE cost index of 567 is for carbon-steel construction for pressures to 600 psig with the area in square feet. The correlating equation is:

$$C_B = \exp\{7.2718 + 0.16[\ln(A)]\} \quad (16.46)$$

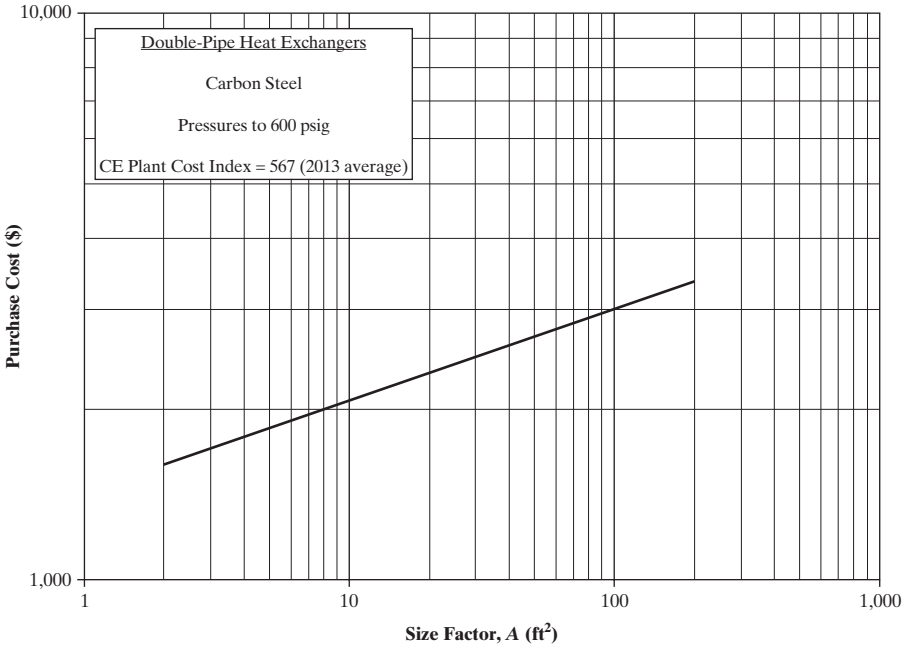

Figure 16.11 Base f.o.b. purchase costs for double-pipe heat exchangers.

The f.o.b. purchase cost is determined from

$$C_P = F_P F_M C_B \tag{16.47}$$

where the material factor, F_M, is 2.0 for an outer pipe of carbon steel and an inner pipe of stainless steel. If both pipes are stainless steel, the factor is 3.0. The pressure factor, F_P, for the range of pressure, P, from 600 to 3,000 psig is given by:

$$F_P = 0.8510 + 0.1292\left(\frac{P}{600}\right) + 0.0198\left(\frac{P}{600}\right)^2 \tag{16.48}$$

EXAMPLE 16.10

In Examples 6.1, 6.5, and 6.7, a toluene hydrodealkylation process is synthesized. Material- and energy-balance calculations on that process give a combined feed to the hydrodealkylation reactor of 5,802 lbmol/hr, containing mainly 35 vol% hydrogen, 58 vol% methane, and 7 vol% toluene at 127.6°F and 569 psia. This stream is heated to 1,000°F in a heat exchanger by 6,010 lbmol/hr of quenched reactor effluent (which also contains a significant percentage of hydrogen), entering the exchanger at 1,150°F and 494 psia and exiting at 364.2°F and 489 psia. The calculated heat duty, Q, is 69,360,000 Btu/hr. Estimate the area of the heat exchanger and the f.o.b. purchase cost at a CE index of 600.

SOLUTION

The combined feed enters the heat exchanger with a molar vapor fraction of 93.1% and leaves as a superheated vapor. The quenched effluent enters and exits as a superheated vapor. Thus, some vaporization occurs on the combined feed side. A zone analysis for a countercurrent heat exchanger gives a mean temperature driving force, ΔT_M, of 190.4°F compared to end driving forces of 150°F and 236.6°F. Assuming an overall heat-transfer coefficient, U, of 50 Btu/hr-ft^2-°F, the heat exchanger area is

$$A = \frac{Q}{U(\Delta T_M)} = \frac{69{,}360{,}000}{50(190.4)} = 7{,}290 \text{ ft}^2$$

For these size- and temperature-difference conditions, select a floating-head shell-and-tube heat exchanger with 20-ft-long tubes. Pressures on both the shell and tube sides are in the range of 500 to 600 psig. Select a design pressure of 700 psig. Because temperatures are as high as 1,000 to 1,150°F, carbon steel cannot be used as the material of construction for either the shell or tubes. Because the hydrogen content of both streams is significant, Cr–Mo alloy steel, which is often used in the temperature range of this exchanger, is not suitable either, and stainless steel must be selected. From Eq. (16.39), the base purchase cost at a CE index of 567 is

$$C_B = \exp\{10.292 - 0.5905[\ln(7{,}290)] + 0.08414\,[\ln(7{,}290)]^2\}$$
$$= \$120{,}100$$

From Eq. (16.44) and Table 16.25, for stainless steel construction, $F_M = 2.70 + (7{,}290/100)^{0.07} = 4.05$. For a pressure of 700 psig, using Eq. (16.45):

$$F_P = 0.9803 + 0.018\left(\frac{700}{100}\right) + 0.0017\left(\frac{700}{100}\right)^2 = 1.19$$

From Eq. (16.43), the f.o.b. purchase cost for a CE index of 600 is:

$$C_P = 1.19(4.05)(600/567)(120{,}100) = \$613{,}000$$

Fired Heaters

Indirect-fired heaters of the box type, also called fired heaters, process heaters, and furnaces, are commonly used to heat and/or vaporize nonreacting process streams at elevated temperatures beyond where steam is normally employed. The fuel for combustion is either gas or fuel oil. As discussed in Section 12.2, heat duties of fired heaters are in the range of 10 to 340 million Btu/hr (3,000 to 100,000 kJ/s or 3 to 100 MW). Typically, fired heaters are complete package units with standard horizontal tubes of carbon steel, adequate for temperatures to 1,100°F and pressures to 500 psig. For higher temperatures and/or pressures, other materials of construction may be needed and tubes must have an increased wall thickness. Thermal efficiencies range from 70 to 90% with the higher value corresponding to units designed for energy conservation. The base cost depends on the heat duty, Q, absorbed by the process stream in Btu/hr. The cost correlation, shown in Figure 16.12, is for gas-fired heaters and is based on the average of several of the references in Table 16.19. For CE = 567, the base cost for Q from 10 to 500 million Btu/hr is:

$$C_B = \exp\{-0.15241 + 0.785[\ln(Q)]\} \tag{16.49}$$

The f.o.b. purchase cost is determined from:

$$C_P = F_P F_M C_B \tag{16.50}$$

where the material factor, F_M, is 1.4 for tubes of Cr–Mo alloy steel and 1.7 for stainless steel. The pressure factor, F_P, for the range of pressure, P, from 500 to 3,000 psig is given by:

$$F_P = 0.986 - 0.0035\left(\frac{P}{500}\right) + 0.0175\left(\frac{P}{500}\right)^2 \tag{16.51}$$

Fired heaters for specific purposes are discussed in Section 16.6.

EXAMPLE 16.11

After being heated to 1,000°F and before entering the reactor, the combined feed in Example 16.10 is heated further to 1,200°F in a fired heater. Determine the f.o.b. purchase cost of a gas-fired heater at a CE index of 600.

SOLUTION

The calculated absorbed heat duty, Q, is 18,390,000 Btu/hr. Assume a design pressure for the tubes of 700 psig. Because of the significant hydrogen concentration in the combined feed, stainless steel tubes are required. From Eq. (16.49), the base cost is

$$C_B = \exp\{-0.15241 + 0.785[\ln(18{,}390{,}000)]\} = \$433{,}000$$

From stainless steel tubes, $F_M = 1.7$. For a pressure of 700 psig, using Eq. (16.51):

$$F_P = 0.986 - 0.0035\left(\frac{700}{500}\right) + 0.0175\left(\frac{700}{500}\right)^2 = 1.015$$

From Eq. (16.50), the f.o.b. purchase cost for CE index = 600 is

$$C_P = 1.015(1.7)(600/567)(433{,}000) = \$791{,}000$$

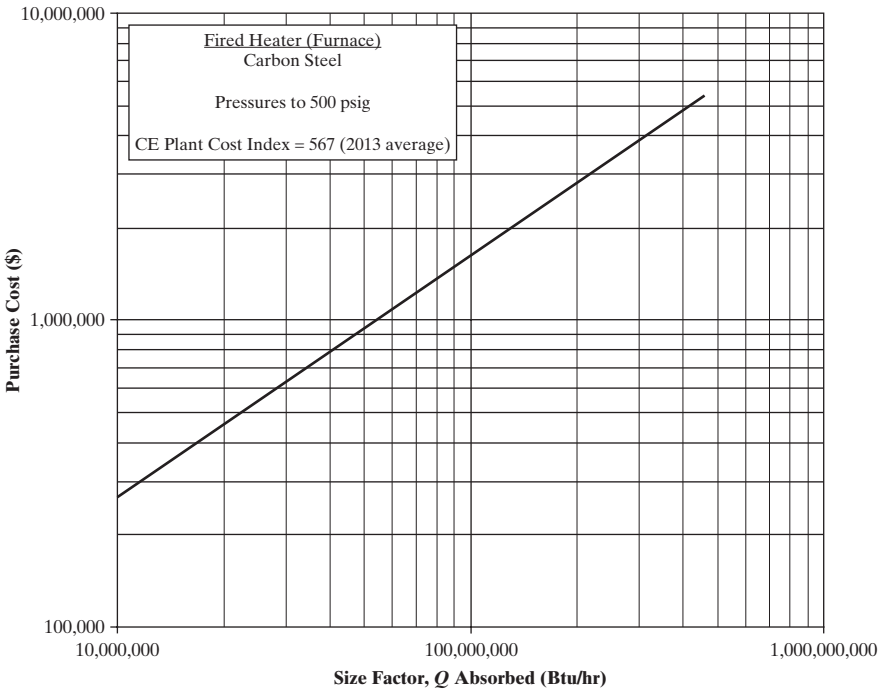

Figure 16.12 Base f.o.b. purchase costs for indirect gas-fired heaters of the box type.

Pressure Vessels and Towers for Distillation, Absorption, and Stripping

Pressure vessels containing little or no internals (largely empty) are widely used in chemical processing plants. Applications include reflux drums, flash drums, knock-out drums, settlers, chemical reactors, mixing vessels, vessels for fixed-bed adsorption, and storage drums. These vessels are usually cylindrical in shape with an inside diameter, D_i, and consist of a cylindrical shell of length L (often referred to as the *tangent-to-tangent length*), to which are welded two ellipsoidal or torispherical (dished) heads at opposite ends. In addition, the vessel includes nozzles for entering and exiting streams, manholes for internal access, connections for relief valves and instruments, skirts or saddles for support depending on whether the vessel is oriented horizontally or vertically, and platforms and ladders. Shell and head thicknesses are usually determined from the ASME Boiler and Pressure Vessel Code and may include allowance for corrosion, vacuum operation, wind loading, and earthquake.

Because many factors can affect the purchase cost of a pressure vessel, it is not surprising that a wide selection of size factors has been used to estimate the purchase cost; however, all methods differentiate between vertical and horizontal orientation of the vessel. The simplest methods base the cost on the inside diameter and tangent-to-tangent length of the shell with a correction for design pressure. The most elaborate method is based on a complete design of the pressure vessel to obtain the vessel weight and a sizing and count of the nozzles and manholes. Here, the method of Mulet, Corripio, and Evans (1981a, b) is employed, which is a method of intermediate complexity based on the weight of the shell and two 2:1 elliptical heads. The f.o.b. purchase cost, which is for carbon-steel construction and includes an allowance for platforms, ladders, and a nominal number of nozzles and manholes, is given by

$$C_P = F_M C_V + C_{PL} \tag{16.52}$$

The f.o.b. purchase cost—at a CE index = 567 of the empty vessel, C_V, but including nozzles, manholes, and supports, based on the weight in pounds of the shell and the two heads, W—depends on orientation as shown in Figure 16.13. The correlating equations are:

Horizontal vessels for $1{,}000 < W < 920{,}000$ lb:

$$C_V = \exp\{5.6336 + 0.4599[\ln(W)] + 0.00582\,[\ln(W)]^2\} \tag{16.53}$$

Vertical vessels for $4{,}200 < W < 1{,}000{,}000$ lb:

$$C_V = \exp\{7.1390 + 0.18255[\ln(W)] + 0.02297\,[\ln(W)]^2\} \tag{16.54}$$

The added cost, C_{PL}, for platforms and ladders depends on the vessel inside diameter, D_i, in feet and, for a vertical vessel, on the tangent-to-tangent length of the shell, L, in feet, and is given by:

Horizontal vessels for $3 < D_i < 12$ ft:

$$C_{PL} = 2275\,(D_i)^{0.2094} \tag{16.55}$$

Vertical vessels for $3 < D_i < 21$ ft and $12 < L < 40$ ft:

$$C_{PL} = 410\,(D_i)^{0.73960}(L)^{0.70684} \tag{16.56}$$

Towers are vertical pressure vessels for various separation operations, including distillation, absorption, and stripping. They contain plates and/or packing plus additional nozzles and manholes as well as internals for multiple feed entries and management of bottoms liquid and its withdrawal. Figure 16.13 includes a curve for the f.o.b. purchase cost in U.S. dollars, as of a CE index = 567 of vertical towers, C_T, including nozzles,

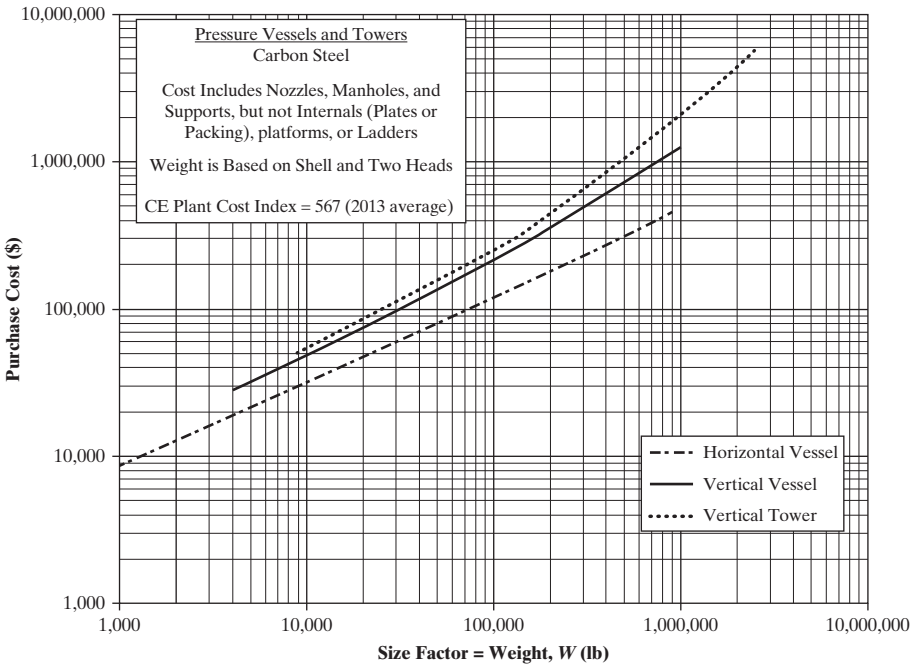

Figure 16.13 Base f.o.b. purchase costs for pressure vessels and towers.

manholes, a skirt, and internals (but not plates and/or packing), based on the weight in pounds of the shell and the two heads, W. The correlating equation is

Towers for $9{,}000 < W < 2{,}500{,}000$ lb:

$$C_V = \exp\{10.5449 - 0.4672[\ln(W)] + 0.05482\,[\ln(W)]^2\} \tag{16.57}$$

The added cost, C_{PL}, for platforms and ladders for towers depends on the tower inside diameter, D_i, in feet and on the tangent-to-tangent length of the shell, L, in feet, and is given by:

Towers for $3 < \mathrm{D}_i, < 24$ ft and $27 < L < 170$ ft:

$$C_{PL} = 341\ (D_i)^{0.63316}(L)^{0.80161} \tag{16.58}$$

The weight, W, in the cost corrrelations for a pressure vessel or tower depends on the wall thicknesses of the shell and the two heads. Although the thickness of the heads may be required to be somewhat thicker than the shell, particularly at high pressures, it is sufficient for cost-estimation purposes to assume head thicknesses equal to the shell thickness, t_s. Then, with 2:1 elliptical heads, the weight of the shell and the two heads is approximately:

$$W = \pi(D_i + t_s)(L + 0.8D_i)t_s\rho \tag{16.59}$$

where the term L accounts for the cylinder, the term in $0.8D_i$ accounts for the two heads, and ρ is the density of the carbon steel, which can be taken as 490 lb/ft^3 or 0.284 lb/in^3. Note that in Eq. (16.59), D_i, L, and t_S are in inches.

In the absence of corrosion, wind, and earthquake considerations and for internal pressures greater than the external pressure (i.e., excluding vacuum operation), the cylindrical shell wall thickness is computed from the ASME pressure-vessel code formula:

$$t_p = \frac{P_d D_i}{2SE - 1.2P_d} \tag{16.60}$$

where t_p = wall thickness in inches to withstand the internal pressure, P_d = internal design gauge pressure in psig, $\mathrm{D_i}$ = inside shell diameter in inches, S = maximum allowable stress of the shell material at the design temperature in pounds per square inch, and E = fractional weld efficiency. Sandler and Luckiewicz (1987) recommend that the design pressure, P_d in psig, be greater than the operating pressure, P_o. The following recommendations are similar to theirs. For operating pressures between 0 and 5 psig, use a design pressure of 10 psig. In the range of operating pressure from 10 psig to 1,000 psig, use the following equation:

$$P_d = \exp\{0.60608 + 0.91615[\ln(P_o)] + 0.0015655[\ln(P_o)]^2\} \tag{16.61}$$

For operating pressures greater than 1,000 psig, use a design pressure equal to 1.1 times the operating pressure. However, safety considerations may dictate an even larger difference between design pressure and operating pressure, especially when runaway reactions are possible.

The maximum allowable stress, S, in Eq. (16.60) depends on the design temperature and the material of construction. The design temperature may be taken as the operating temperature plus 50°F. However, again, safety considerations may dictate an even larger difference. At a given temperature, different steel compositions have different values for the maximum allowable stress. In the design temperature range of –20°F to 650°F in a noncorrosive environment that is free of hydrogen, a commonly used carbon steel is SA-285, grade C, with a maximum

allowable stress of 13,750 psi. In the temperature range from 650°F to 900°F, in a noncorrosive environment including the presence of hydrogen, a commonly used low-alloy (1% Cr and 0.5% Mo) steel is SA-387B. Its maximum allowable stress in its recommended temperature range is as follows:

Temperature (°F)	Maximum Allowable Stress (psi)
–20 to 650	15,000
700	15,000
750	15,000
800	14,750
850	14,200
900	13,100

The weld efficiency, E, in Eq. (16.60) accounts mainly for the integrity of the weld for the longitudinal seam. For carbon steel up to 1.25 in. in thickness, only a 10% spot X-ray check of the weld is necessary and a value of 0.85 for E should be used. For larger wall thicknesses, a 100% X-ray check is required, giving a value of 1.0 for E.

At low pressures, wall thicknesses calculated from Eq. (16.60) may be too small to give sufficient rigidity to vessels. Accordingly, the following minimum wall thicknesses should be used:

Vessel Inside Diameter (ft)	Minimum Wall Thickness (in.)
Up to 4	1/4
4–6	5/16
6–8	3/8
8–10	7/16
10–12	1/2

Equation (16.60) is suitable for calculating the thickness of a horizontal pressure vessel, but does not account for the effect of wind or an earthquake on a vertical vessel or column, and is not applicable to vessels or columns under vacuum. Mulet et al. (1981a) present a method for determining average wall thickness, t_V, of a vertical vessel or tower to withstand the internal pressure at the top of the column, and to withstand the wind load or an equivalent earthquake, in addition to the internal pressure, at the bottom of the column. The method assumes a substantial wind load based on a wind velocity of 140 miles/hr, acting uniformly over the height of the column. Their simplified equation is as follows, where t_W = the necessary thickness in inches to withstand the wind load or earthquake at the bottom of the column, D_o = the outside diameter of the vertical vessel in inches, L = the tangent-to-tangent vessel height in inches, and S = the maximum allowable stress in pounds per square inch.

$$t_W = \frac{0.22(D_o + 18)L^2}{SD_o^2} \tag{16.62}$$

where the term 18 (in inches) accounts for column cage ladders. The average vessel wall thickness, t_V, is then computed from the average of the thickness at the top, t_P, and the thickness at the bottom, $t_P + t_W$.

Equation (16.60) does not apply to vacuum vessels for which the internal pressure is less than the external pressure. Such vessels must be sufficiently thick to withstand a collapsing pressure, or they must be provided with stiffening rings around their outer periphery. For the former alternative, Mulet et al. (1981a) present a method for computing the necessary wall thickness, t_E, based mainly on the vessel length-to-outside diameter ratio and the modulus of elasticity, E_M, of the metal wall. A simple approximation of their method, which is applicable to $t_E/D_o < 0.05$, is given by Eq. (16.63) where D_o = outside diameter:

$$t_E = 1.3D_o\left(\frac{P_d L}{E_M D_o}\right)^{0.4} \tag{16.63}$$

However, to the value of t_E the following correction, t_{EC}, must be added:

$$t_{\mathrm{EC}} = L(0.18D_i - 2.2) \times 10^{-5} - 0.19 \tag{16.64}$$

where all variables are in in. The total thickness for a vacuum vessel is

$$t_V = t_E + t_{\mathrm{EC}} \tag{16.65}$$

The modulus of elasticity, E_M, depends on temperature with the following values for carbon steel and low-alloy steel:

E_M, Modulus of Elasticity, psi (multiply values by 10^6)

Temperature (°F)	Carbon Steel	Low-Alloy Steel
−20	30.2	30.2
200	29.5	29.5
400	28.3	28.6
650	26.0	27.0
700	—	26.6
800	—	25.7
900	—	24.5

Even for noncorrosive conditions, a corrosion allowance, t_C, of $\frac{1}{8}$ in. should be added to t_V to give the value of t_S to be used in Eq. (16.59) for vessel weight. In addition, it is important to note that vessels are generally fabricated from metal plate whose thicknesses can be assumed to come in the following increments:

1/16-in. increments for 3/16 to 1/2 in. inclusive

1/8-in. increments for 5/8 to 2 in. inclusive

1/4-in. increments for 2 1/4 to 3 in. inclusive

The final vessel thickness is obtained by rounding up to the next increment.

The material-of-construction factor for pressure vessels and towers, F_M, is given in Table 16.26.

Before presenting cost data for plates and packings in distillation, absorption, and stripping towers, the following example is presented to estimate the purchase cost of an adiabatic, homogeneous gas-phase reactor.

Table 16.26 Materials-of-Construction Factors, F_M, for Pressure Vessels

Material of Construction	Material Factor [F_M in Eq. (16.52)]
Carbon steel	1.0
Low-alloy steel	1.2
Stainless steel 304	1.7
Stainless steel 316	2.1
Carpenter 20CB-3	3.2
Nickel-200	5.4
Monel-400	3.6
Inconel-600	3.9
Incoloy-825	3.7
Titanium	7.7

The purchase cost of the vessel given by Eq. (16.53) is

$$C_V = \exp\{5.6336 + 0.4599[\ln(72{,}500)] + 0.00582\,[\ln(72{,}500)]^2\}$$
$$= \$99{,}700$$

From Table 16.26, the material factor is 1.20. Thus, $F_M C_V$ = \$119,600.

To this is added the cost of the platforms and ladders from Eq. (16.55):

$$C_{PL} = 2275\,(78)^{0.2094} = \$5660$$

Using Eq. (16.52), the purchase cost at a CE index of 600 is

$$C_P = \left(\frac{600}{567}\right)(119{,}600 + 5{,}660) = \$132{,}500$$

EXAMPLE 16.12

An adiabatic reactor consists of a cylindrical vessel with elliptical heads, with an inside diameter of 6.5 ft (78 in.) and a tangent-to-tangent length of 40 ft (480 in.). Gas enters the reactor at a pressure of 484 psia and 800°F. Exit conditions are 482 psia and 850°F. The vessel will be oriented in a horizontal position. Estimate the vessel thickness in inches, weight in pounds, and purchase cost in dollars for a CE cost index of 600. The vessel contains no internals and the gas is noncorrosive. The barometric pressure at the plant site is 14 psia.

SOLUTION

The operating pressure, based on the higher pressure, is (484 − 14) = 470 psig. Using Eq. (16.61), the design pressure is

$$P_d = \exp\{0.60608 + 0.91615[\text{In}(470)] + 0.0015655\,[\text{In}(470)]^2\}$$
$$= 546 \text{ psig.}$$

The higher operating temperature is 850°F. Take a design temperature of 50°F higher or 900°F. A suitable material of construction is low-alloy steel. From a table above, its maximum allowable stress, S, is 13,100 psi. Assume that the wall thickness will be greater than 1.25 in., giving a weld efficiency, E, of 1.0. From the pressure-vessel code formula of Eq. (16.60),

$$t_P = \frac{(546)(78)}{2(13{,}100)(1.0) - 1.2(546)} = 1.667 \text{ in.}$$

which is greater than the assumed 1.25 in. and also greater than the minimum value of $\frac{3}{8}$ in. required for rigidity. Because the orientation of the vessel is horizontal, the vessel is not subject to wind load or earthquake considerations. Adding a corrosion allowance of $\frac{1}{8}$ in. gives a total thickness of 1.792 in. Since this is in the range of $\frac{5}{8}$ to 2 in., the steel plate comes in increments of $\frac{1}{8}$ in. Since 1.792 in. is greater than $1\frac{6}{8}$ in., specify a plate thickness, t_S, of $1\frac{7}{8}$ in. or 1.875 in. for use in Eq. (16.59) to give a vessel weight of:

$$W = (3.14)(78 + 1.875)[480 + 0.8(78)](1.875)(0.284)$$
$$= 72{,}500 \text{ lb}$$

Plates

Vertical towers for absorption, distillation, and stripping utilize trays (plates) and/or packing. Mulet et al. (1981b) present a method for estimating the purchase cost of trays installed in a vertical tower. This cost is added to Eq. (16.52) to obtain the total purchase cost. The cost for the installed trays, C_T, all with downcomers, is given by

$$C_T = N_T F_{NT} F_{TT} F_{TM} C_{BT} \tag{16.66}$$

Here, the base cost, C_{BT}, is for sieve trays at a CE cost index of 567, where the inside diameter of the tower is in feet and the equation is valid for 2 to 16 ft.

$$C_{BT} = 468 \exp(0.1482\, D_i) \tag{16.67}$$

In Eq. (16.66), N_T = the number of trays. If that number is greater than 20, the factor $F_{NT} = 1$. If $N_T < 20$, the factor is greater than 1, as given by

$$F_{NT} = \frac{2.25}{1.0414^{NT}} \tag{16.68}$$

The factor F_{TT} accounts for the type of tray:

Tray Type	F_{TT}
Sieve	1.0
Valve	1.18
Bubble cap	1.87

The factor F_{TM}, which depends on column diameter in feet, corrects for the material of construction:

Material of Construction	F_{TM}
Carbon steel	1.0
303 Stainless steel	$1.189 + 0.0577\, D_i$
316 Stainless steel	$1.401 + 0.0724\, D_i$
Carpenter 20CB-3	$1.525 + 0.0788\, D_i$
Monel	$2.306 + 0.1120\, D_i$

EXAMPLE 16.13

A distillation column is to be used to separate isobutane from *n*-butane. The column, which is equipped with 100 sieve trays, has an inside diameter of 10 ft (120 in.) and a tangent-to-tangent length of 212 ft (2,544 in.). Operating conditions are 110 psia and 150°F at the bottom of the tower and 100 psia and 120°F at the top. The material of construction is carbon steel. The barometric pressure at the plant location is 14.5 psia. Estimate the purchase cost of the distillation column at a CE index of 600.

SOLUTION

The operating pressure, based on the higher pressure, is (110 − 14.5) = 95.5 psig. Using Eq. (16.61), the design pressure is

$$P_d = \exp\{0.60608 + 0.91615[\ln(95.5)] + 0.0015655\,[\ln(95.5)]^2\} = 123 \text{ psig}$$

The higher operating temperature is 150°F. Take a design temperature of 50°F higher, or 200°F. For carbon steel at this temperature, the maximum allowable stress, S, is 15,000 psi. Assume that the wall thickness will be less than 1.25 in., giving a weld efficiency, E, of 0.85. From the pressure-vessel code formula, Eq. (16.60),

$$t_P = \frac{(123)(120)}{2(15{,}000)(0.85) - 1.2(123)} = 0.582 \text{ in.}$$

which is greater than the minimum value of $^7/_{16}$ (or 0.4375) in. required for rigidity. Because orientation of the vessel is vertical and because it is quite tall, the tower may be subject to wind load or earthquake. From Eq. (16.62), assuming a wall thickness of 1.25 in., which gives an outside diameter, D_o, of 122.5 in., the additional tower wall thickness at the bottom of the tower is

$$t_W = \frac{0.22(122.5 + 18)[(212)(12)]^2}{15{,}000\,(122.5)^2} = 0.889 \text{ in.}$$

Therefore, at the bottom of the column, the required thickness to withstand internal pressure and wind load (or earthquake) is 0.582 + 0.889 = 1.471 in., compared to 0.582 in. at the top of the column. The average thickness = t_V = (0.582 + 1.471)/2 = 1.027 in. To this, add a corrosion allowance of $^1/_8$ in., giving a thickness of 1.027 + 0.125 = 1.152 in. Therefore, specify a steel plate thickness, t_S, of 1.250 in. From Eq. (16.59), the vessel weight, W, is

$$W = (3.14)(120 + 1.250)[2{,}544 + 0.8(120)](1.250)(0.284) = 356{,}800 \text{ lb}$$

The purchase cost of the vertical tower given by Eq. (16.57) is

$$C_V = \exp\{10.5449 - 0.4672[\ln(356{,}800)] + 0.05482\,[\ln(356{,}800)]^2\} = \$753{,}400$$

From Table 16.26, the material factor is 1.00. Thus, $F_M C_V$ = $753,400. To this is added the cost of the platforms and ladders from Eq. (16.58), which, however, is applied outside of its range of 27 to 170 ft for the tangent-to-tangent length of the shell.

$$C_{PL} = 341(10)^{0.63316}(212)^{0.80161} = \$107{,}300$$

The purchase cost at the CE index of 600 for just the tower, platforms, and ladders is

$$C_P = \left(\frac{600}{567}\right)(753{,}400 + 107{,}300) = \$910{,}800$$

To this must be added the cost of 100 sieve trays. From Eq. (16.67),

$$C_{BT} = 468 \exp[0.1482(10)] = \$2060 \text{ per tray}$$

Using Eq. (16.66), and upgrading the cost index to 600,

$$C_T = N_T F_{NT} F_{TT} C_{BT} = 100(1.0)(1.0)(2060)\left(\frac{600}{567}\right) = \$218{,}000$$

The total purchase cost of the distillation column is

$$\$910{,}800 + \$218{,}000 = \$1{,}130{,}000$$

Packings

Packings for towers are classified as dumped (random) or structured. When packings are used, the total purchase cost of the packed tower becomes

$$C_P = F_M C_V + C_{\text{PL}} + V_{\text{P}} C_{\text{PK}} + C_{\text{DR}} \tag{16.69}$$

where F_M for the vessel is given in Table 16.26, C_V for a vertical tower is given by Eq. (16.57), C_{PL} for the platforms and ladders is given by Eq. (16.58), V_{P} is the volume of the packing in cubic feet, C_{PK} is the installed cost of the packing in dollars per cubic foot, and C_{DR} is the installed cost of high-performance liquid distributors and redistributors required for obtaining satisfactory performance with packings.

Installed costs for dumped packings are given by several of the references in Table 16.19. Table 16.27, which was developed by taking averages of those costs, indexed to CE = 567, and adding some additional values from vendors, includes costs for six different dumped packings and five different materials.

Compared to dumped packings and trays, structured packings offer reduced pressure drop, higher stage efficiency in terms of reduced HETS (height equivalent to a theoretical stage), and capacity in terms of reduced diameter. However, they are more expensive in dollars per cubic foot of packing and are not normally available in carbon steel. They are most often installed when revamping existing towers to reduce pressure drop, increase capacity, and/or increase purity of products. Accordingly, installed costs of structured packings are not widely available. In the absence of a vendor quote and for a very approximate estimate, the installed cost of structured packing of the corrugated-sheet type in stainless steel can be taken as \$285/ft^3.

Installed-cost data for high-performance liquid distributors and redistributors are also not widely available. Distributors should be placed at every feed point and, conservatively, redistributors should be used every 20 ft. In the absence of a vendor quote and for a very approximate estimate, the installed cost of a liquid distributor can be taken as \$140/ft^2 of column cross-sectional area.

Table 16.27 Installed Costs of Some Dumped Packings

	Installed Cost ($/ft^3)				
Size	1 in.	1.5 in.	2 in.	3 in.	4 in.
Berl saddles					
Ceramic	50	40	32		
Raschig rings					
Carbon steel	50	50	30	30	
Stainless steel	150	116	80	80	
Ceramic	20	20	20	20	
Intalox saddles					
Ceramic	40	40	30	22	
Polypropylene	42		26	14	
Pall rings					
Carbon steel	56	42	36		
Stainless steel	160	130	100		
Polypropylene	50	30	20	18	
Cascade minirings					
Stainless steel	130	100	80	60	50
Ceramic	90		80	50	
Polypropylene	90		80	50	
Tellerettes					
Polyethylene	100				

EXAMPLE 16.14

A distillation column has two sections. The one above the feed is 14 ft in inside diameter with a 20-ft height, 15 ft of which is packed with structured packing of the corrugated-sheet type. The bottom section is 16 ft in diameter with a 70-ft height, 60 ft of which is packed with 4-in. Cascade minirings. The column is made of carbon steel, but both packings are of stainless steel. The column will operate under vacuum with conditions of 55 kPa and 60°C at the top and 60 kPa and 125°C at the bottom. A total of four liquid distributors or redistributors will be used. Estimate the f.o.b. purchase cost of the column, including installed packings, distributors, and redistributors, for a CE cost index of 600. The barometric pressure is 100 kPa.

SOLUTION

Take a design temperature of 50°F higher than the highest temperature of 125°C (257°F), or 307°F. For a vacuum vessel, use Eq. (16.63) to estimate the wall thickness. The maximum pressure difference between the inside and outside of the vessel is 100 − 55 = 45 kPa or 6.5 psig. Use this as the design pressure, P_d. From a table above, the modulus of elasticity for carbon steel at 307°F is 28.9×10^6 psi. For the top section, D_i = 14 ft or 168 in. Assume for this large a diameter that $D_i = D_0$. But for L, use the total length of (20 + 70) = 90 ft. Then the wall thickness for the top section is

$$t_E = 1.3(168)\left(\frac{6.5\,(90)}{28.9 \times 10^6(14)}\right)^{0.4} = 1.01 \text{ in.}$$

This is well within the limit of applicability of $t_E/D_O < 0.05$. To this must be added the correction of Eq. (16.64):

$$t_{EC} = (90)(12)[0.18(168) - 2.2] \times 10^{-5} - 0.19 = 0.11 \text{ in.}$$

The total thickness for the top section, from Eq. (16.65), is t_V = 1.01 + 0.11 = 1.12 in. Adding a $^1/_8$ in. corrosion allowance gives 1.245 in. and, therefore, use a plate thickness including the next $^1/_8$-in. increment or 1.25 in. Similar calculations for the bottom section give a wall thickness of 1.375 in.

The weights of the two sections are estimated from Eq. (16.59) but with only one head per section. However, as recommended by Mulet et al. (1981a) for a two-diameter tower, the weight of each section is based on the total length. The base cost for the two sections is then calculated from:

$$C_V = \frac{L_1 C_{V1} + L_2 C_{V2}}{L_1 + L_2} \tag{16.70}$$

For the top section,

$$W_1 = 3.14(168 + 1.25)[1{,}080 + 0.8(168)](1.25)(0.284)$$
$$= 229{,}100 \text{ lb}$$

A similar calculation for the bottom section gives W_2 = 319,300 lb. Base purchase costs for a tower section are given by Eq. (16.57). For the top section,

$$C_{V1} = \exp\{10.5449 - 0.4672[\ln(229{,}100)] + 0.05482\,[\ln(229{,}100)]^2\} = \$503{,}400$$

A similar calculation for the bottom section gives C_{V2} = $679,600. Using Eq. (16.70), the purchase cost of the entire empty tower is

$$C_V = \frac{20(503{,}400) + 70(679{,}600)}{20 + 70} = \$640{,}400$$

To this is added the costs of the platforms and ladders for the tower. The concept of Eq. (16.70) is again applied after substituting C_{PL} for C_V for each section. From Eq. (16.58) for the top section, again using the total length of the tower:

$$C_{PL1} = 341(14)^{0.63316}(90)^{0.80161} = \$66{,}800$$

A similar calculation for the bottom section gives C_{PL2} = $72,700. Using the form of Eq. (16.70), the total cost of the platforms and ladders is

$$C_{PL} = \frac{20(66{,}800) + 70(72{,}700)}{20 + 70} = \$71{,}400$$

The structured packing occupies a volume, V_{P1}, of $3.14(14)^2(15)4 = 2{,}310$ ft^3. The estimated installed cost, $C_{PK,1}$, is $\$285/ft^3$. The random packing occupies a volume, V_{P2}, of $3.14(16)^2(60)/4 = 12{,}060$ ft^3. From Table 16.27, the installed cost of 4-in. cascade minirings in stainless steel = $C_{PK,2} = \$50/ft^2$. For the four distributors, assume one has a diameter of 14 ft and the other three have a diameter of 16 ft. This corresponds to areas of 154 ft^2 and 201 ft^2, respectively. At a cost of $\$140/ft^2$, the total installed cost of the four distributors or redistributors is

$$C_{DR} = 154(140) + 3(201)(140) = \$105{,}900$$

From Equation (16.67), after including the CE cost index ratio, the f.o.b. purchase cost of the vacuum tower, complete with packings, distributors and redistributors, platforms, and ladders, is

$$C_P = (600/567)[(1.0)(640{,}400) + 71{,}400 + [2{,}310(285) + 12{,}060(50)] + 105{,}900]$$
$$= (600/567)[640{,}400 + 71{,}400 + 1{,}261{,}400 + 105{,}900]$$
$$= \$2{,}200{,}000$$

Note that the packings are a large fraction of the total cost of the tower.

16.6 PURCHASE COSTS OF OTHER CHEMICAL PROCESSING EQUIPMENT

In this section, equations are presented for the estimation of the f.o.b. purchase cost of chemical processing equipment not covered in Section 16.5. In each equipment category, so many different designs are available that it is not possible to consider them all. Instead, an attempt has been made to include only the most widely used designs for which, in some cases, heuristics are included for estimating equipment sizes. This should be sufficient for preliminary estimates of capital cost. For final plant design, vendors of the different types of equipment should be consulted for assistance in selecting and sizing the most suitable design and to obtain more accurate estimates of purchase cost so as to achieve the most operable and economical process. The purchase-cost equations for the equipment in this section, which are based on a size factor, S, valid for a stated range and an average cost index for the year 2013 (CE = 567), are listed in Table 16.32, which appears at the end of this section. For the most part, the purchase-cost equations were developed from the sources of cost data given in Table 16.19 and the data at the Internet site www.matche.com/EquipCost. When the pressure and material of construction are not mentioned in Table 16.32, low-to-moderate pressures and conventional materials of construction such as carbon steel may be assumed. In lieu of data for other materials of construction, the purchase cost for another material may be estimated by multiplying the cost obtained from the equation in Table 16.32 by one of the following factors:

Material	Factor
Carbon steel	1.0
Copper	1.2
Stainless steel	2.0
Nickel	2.5
Monel	2.7
Titanium clad	3.0
Titanium	6.0

Table 16.32 is accompanied by the following brief equipment descriptions, which include, in some cases, heuristics for estimating the size factor when design data are not readily available. More equipment descriptions and detailed methods for determining size for most of the types of equipment described below may be found in *Perry's Chemical Engineers' Handbook* (Green and Perry, 2008).

Adsorption Equipment

Adsorption from liquids is carried out in stirred vessels *(slurry adsorption)* or in fixed beds, while *fixed-bed adsorption* is used for gases. For slurry adsorption, which is usually conducted batchwise, the purchase cost includes the vessel, a motor-driven agitator, and the adsorbent particles. The size of the vessel and the amount of adsorbent required depend on the amount of solute to be adsorbed from the feed, the adsorption equilibrium, the solids content of the slurry in the vessel, and the desired time of treatment. A reasonable slurry composition is 5 vol% solids. An agitator sized at 10 Hp/1,000 gal being stirred is generally sufficient to keep the solid particles in suspension. Costs of adsorbents and motor-driven agitators are included in Table 16.32.

For fixed-bed adsorption of gases, a reasonable superficial gas velocity through the bed is 100 ft/min, whereas for liquids, it is 1 ft/min. Typical bed heights are 1 to 3 times the bed diameter. A conservative equilibrium adsorbent loading is 10 lb of adsorbate per 100 lb of adsorbent. Breakthrough times should account for mass-transfer resistance effects by adding 2 ft to the bed height calculated on the basis of equilibrium loading.

Agitators (propellers and turbines)

Motor-driven propellers and turbines are the most widely used devices for agitation in vessels. Propellers are small in diameter and use high rates of rotation by direct coupling with motors running typically at 1,150 or 1,750 rpm. They are often used to agitate large liquid storage tanks by mounting several propellers sideways at locations around the periphery of the tank. Turbines are larger in diameter, typically one-third of the vessel diameter and, by using speed reducers with electric motors, rotate at 37 to 320 rpm. Turbines, which are available in several designs, are more versatile than propellers and are usually the preferred type of agitator for applications involving mixing of miscible and immiscible liquids in reactors, mixing of immiscible liquids in liquid-liquid extraction vessels, suspension of fine adsorbent particles in slurry adsorption, enhancement of heat transfer to or from a liquid in a jacketed tank, and dispersion of a gas into a liquid in a tank. Typical horsepower requirements for turbines, based on the fluid volume in the vessel or tank, are

Application	Hp/1,000 Gallons
Blending miscible liquids	0.5
Homogeneous liquid reaction	1.5
Reaction with heat transfer	3
Liquid–liquid reaction or extraction	5
Gas dispersion in a liquid	10
Suspension of solid particles	10

Autoclaves

An autoclave is predominantly a vertical, cylindrical stirred-tank reactor. It can be operated continuously or batchwise over a wide range of production rates, temperatures, and pressures. The stirring is achieved by internal agitators (turbines or propellers) or by forced circulation through the vessel with an external pump. However, the contents of small autoclaves are stirred by rocking, shaking, or tumbling the vessel. Most autoclaves are provided with a means of transferring heat to or from the contents of the vessel. That means may be a jacket, internal coils or tubes, an external pump-heat exchanger combination, an external reflux condenser when vapors are evolved, an electrically heated mantel, or direct firing by partial submergence of the autoclave in a furnace. In Table 16.32, equations for estimating f.o.b. purchase

costs are listed for autoclaves made of steel, stainless steel, and glass-lined steel. These autoclaves are provided with turbine agitators and heat-transfer jackets.

Crystallizers

Most industrial crystallization operations are *solution crystallization* involving the crystallization of inorganic compounds from aqueous solutions. Only the inorganic compound crystallizes. However, a growing number of applications are being made for *melt crystallization*, which involves a mixture of two or more organic components whose freezing points are not far removed from each other. In that case, impure crystals (solid solutions) may be obtained that require repeated melting and freezing steps to obtain pure crystals of the component with the highest freezing temperature. Only solution crystallization is considered here.

Solution crystallization occurs from a supersaturated aqueous solution, which is achieved from the feed by cooling, evaporation, or a combination of cooling and evaporation. The application of cooling crystallization is limited because for many dissolved inorganic compounds, the decrease in solubility with decreasing temperature is not sufficient to make the method practical. Therefore, evaporative crystallizers are more common. Table 16.32 contains f.o.b. purchase costs for four types of crystallizers. The continuous jacketed scraped-wall crystallizer is based on length, which can be estimated by a heat-transfer rate using a scraped-surface cooling area of 3 ft^2 per foot of length and an overall heat-transfer coefficient of 20 $Btu/hr\text{-}ft^2\text{-}°F$. The heat-transfer rate is obtained by an energy balance that accounts for both sensible heat and the heat of crystallization. The purchase costs of continuous forced-circulation evaporative crystallizers or the popular continuous draft-tube baffled (DTB) crystallizers are based on the rate of production of crystals in tons (2,000 lbs) per day. The purchase cost of batch evaporative crystallizers, which usually operate under vacuum, depends on the vessel size.

Drives Other than Electric Motors

When the required shaft horsepower for power input to an item of process equipment is less than 100 Hp, an electric motor is usually the selected drive. For higher horsepower input, consideration is given to combustion gas turbines, steam turbines, and internal combustion gas engines. However, except for remote, mobile, or special situations, steam turbines are the most common alternative to electric motors. Furthermore, steam turbines are considerably more efficient, 50–80%, than gas turbines or engines, which have efficiencies of only 30–40%. Equations for f.o.b. purchase costs of steam and gas turbine drives are included in Table 16.32 as a function of shaft horsepower.

Dryers

No single drying device can handle efficiently the wide variety of feed materials, which includes granular solids, pastes, slabs, films, slurries, and liquid. Accordingly, many different types of commercial dryers have been developed for both continuous and batchwise operation. Batch dryers include tray and agitated types. Continuous dryers include tunnel, belt, tray, direct and indirect rotary, screw conveyor, fluidized-bed, spouted-bed, pneumatic-conveyor, spray, drum, infrared, dielectric, microwave, and freeze types. The selection and sizing of dryers often involve testing on a pilot-plant level. The f.o.b. purchase costs for several of the more widely used dryers are included in Table 16.32. Different size factors are used depending on the type of dryer. In the *batch compartment dryer*, the feed is placed in stacked trays over which hot air passes. Trays typically measure $30 \times 30 \times 3$ in. Typical drying time is a few hours. The cost depends on the tray surface area.

Two types of *rotary dryers* are available for continuous drying. In the direct-heat type, longitudinal flights, which extend inward radially from the inner periphery of the slightly inclined rotating dryer cylinder, lift and shower the granular solids through hot air flowing through the cylinder. The inclination of the cylinder causes the solids to flow from the feed end to the discharge end of the cylinder. Moisture evaporation rates are generally in the range of 0.3–3 $lb/hr\text{-}ft^3$ of dryer volume depending on the amount of free moisture and the desired moisture content of the product. Direct-heat rotary dryers vary in size from 1-ft diameter by 4-ft long to 20-ft diameter by 150-ft long. The cost depends on the peripheral area of the shell. Typical length-to-diameter ratios vary from 4 for small dryers to 8 for large dryers. In the indirect-heat type, the material is dried by contact with the outer surface area of tubes arranged in one or two circular rows around the inner periphery of the rotating shell. The purchase cost depends on the outside surface area of the tubes that carry condensing steam. Typical heat fluxes range from 600 to 2,000 $Btu/hr\text{-}ft^2$. Indirect-heat rotary dryers vary in size from 3 ft in diameter by 15 ft long to 15 ft in diameter by 80 ft long.

Drum dryers take a solution or thin slurry and spread it as a thin film over a rotating drum heated internally by condensing steam to produce a flaked product. Typical moisture evaporation rates are 3–6 $lb/hr\text{-}ft^2$. One or two drums (side by side) may be used. Drum dimensions range from 1 ft in diameter by 1.5 ft long to 5 ft in diameter by 12 ft long. The cost of drum dryers depends on the surface area of the drum.

Spray dryers produce small porous particles, such as powdered milk and laundry detergent, from a liquid solution by evaporation of the volatile component of the feed, with the purchase cost correlated with the evaporation rate. Size and cost data for other dryers as well as considerations in dryer selection are found in Section 12 of *Perry's Chemical Engineers' Handbook* (Green and Perry, 2008).

Dust Collectors

The removal of dust particles, typically 1 to 1,000 microns in diameter, from gas streams (also called gas cleaning) is accomplished on an industrial scale by four main types of equipment: (1) *bag filters*, (2) *cyclones* using centrifugal force, (3) *electrostatic precipitators*, and (4) *venturi scrubbers* using washing with a liquid. Reasons for dust collection include air pollution control, elimination of safety and health hazards, recovery of a valuable product, improvement in the quality of other products, and reduction of equipment maintenance. Typical ranges of particle size

that can be efficiently removed by each of the four methods are as follows:

Equipment	Dust Particle Range (microns)
Bag filters	0.1 to 50
Cyclones	10 to 1,000
Electrostatic precipitators	0.01 to 10
Venturi scrubbers	0.1 to 100

Bag filters, also referred to as fabric filters and baghouses, use natural or synthetic woven fabrics or felts. Typically, the openings in the filter fabric are larger than the particles to be removed. Therefore, an initiation period must take place during which particles build up on the fabric surface by impingement. After this occurs, the collected particles themselves act as a precoat to become the actual filter medium for subsequent dust removal. Bag filters are automatically cleaned periodically by shaking, using reverse flow of clean gas, or pulsing with clean gas. Dust collection efficiencies approach 100%.

The theory of particle removal by cyclones is well developed and equipment dimension ratios are well established, making it possible to design cyclones to remove particles of a known size range with reasonable estimates of particle collection efficiency as a function of particle size. However, the efficiency of cyclones is greater for larger particles. Smaller particles can be removed only with cyclones of small diameter. Pressure drops in cyclones can be substantial and often limit the smallest particle size that can be removed. Multiple cyclones are sometimes used in series or parallel.

Electrostatic precipitators operate in a fashion that is just the opposite of a cyclone, removing the smallest particles at the highest collection efficiencies. They can remove the smallest dust particles as well as even smaller particles in the fume and smoke ranges down to 0.01 μm. In the precipitator, the particles are charged by passing the gas between two electrodes charged to a potential difference of tens of thousands of volts. This requires that the gas contain ionizable components such as carbon dioxide, carbon monoxide, sulfur dioxide, and water vapor. If not, water vapor can be added. The ions attach to the particles, carrying them to a collecting electrode. The particles are continuously or periodically removed from the electrode by rapping the collecting electrode.

The venturi scrubber usually consists of a venturi contactor followed by a cyclone separator. The particle-laden gas flows downward to the approach section of the venturi, where water is injected tangentially to flood the wall. After achieving intimate contact of the particles with the liquid in the throat of the venturi, the stream then turns and enters the cyclone where clean gas leaves at the top and a slurry leaves at the bottom. Venturi scrubbers are particularly effective at high concentrations of particles.

Equations for estimating the f.o.b. purchase costs of dust collectors are given in Table 16.32 where the size factor is the actual gas flow rate. All collectors are of mild steel construction. For relatively large dust particles, cyclones are adequate and are the least expensive alternative. For gases containing a wide range of particle sizes, a cyclone followed by an electrostatic precipitator is a common combination.

Evaporators

Aqueous solutions of inorganic salts and bases are concentrated without crystallization in evaporators. Because the volatility of water is much higher than that of the dissolved inorganic salts and bases, only water is evaporated. Evaporators are also used with aqueous solutions of organic compounds that have little volatility. Most popular is the *long-tube vertical (rising-film) evaporator* with tubes from 12 to 35 ft long with boiling inside the tubes. For viscous solutions, a pump is added to give a. *forced-circulation evaporator*. Less efficient, but less expensive, is the *horizontal-tube evaporator* where boiling occurs outside the tubes. For temperature-sensitive applications, a (long-tube vertical) *falling-film evaporator* is used, typically with a small overall temperature driving force of less than 15°F. Many evaporators operate under vacuum and are frequently multistaged to reduce the cost of the heating steam. The f.o.b. purchase costs for evaporators are included in Table 16.32 in terms of the heat-transfer area, for carbon-steel construction and pressures to 10 atmospheres. Typical ranges of overall heat-transfer coefficients, U, which increase with the boiling temperature, are as follows for a boiling-point range of 120 to 220°F:

Evaporator Type	U (Btu/hr-ft^2 -°F)
Horizontal tube	80–400
Long-tube vertical	150–650
Forced circulation	450–650
Falling film	350–750

Fired Heaters for Specific Purposes

Fired heaters are available for providing heat-transfer media of the types described in Section 12.2, including hot water, steam, mineral oils, silicon oils, chlorinated diphenyls (Dowtherm A), and molten (fused) salts. Fired heaters are also used as reactors, such as reformers in petroleum refineries and for pyrolysis of organic chemicals. Purchase costs for these specific types of fired heaters, based on heat duty, are presented in Table 16.32.

Liquid–Liquid Extractors

A wide variety of commercial equipment is available for carrying out separations by liquid-liquid extraction. The most efficient are those that provide mechanical agitation of the liquid phases. When the number of equilibrium stages is small, for example, five or less, and floor space is available but headroom is at a premium, a battery of *mixer-settler vessels* may be the best choice. For preliminary cost estimates, and in lieu of mass-transfer data, the mixing vessels can be pressure vessels that have a height-to-diameter ratio of 1 and provide 5 min or less residence time, depending on the liquid viscosity and the interfacial tension. The mixers are equipped with vertical side baffles and a flat-blade turbine agitator that delivers 4 Hp/1,000 gal. The settlers can be horizontal vessels with inlet baffles and a length-to-diameter ratio of 4. The capacity of the settler can be determined based on 5 gal/min of feed/ft^2 of phase disengaging area (diameter × length) provided that the specific-gravity difference between the two liquid phases

is greater than 0.10. Each mixing vessel in the battery will approximate an equilibrium stage. Purchase costs of mixers and settlers can be estimated from the costs for pressure vessels and agitators discussed above.

When headroom is available, a number of column designs with mechanical agitation from impellers on a vertical shaft can be used. Typical of these is the *rotating-disk contactor (RDC)*, which has a maximum diameter of 25 ft and maximum total liquid throughput of 120 ft^3 of liquid/hr-ft^2 of column cross-sectional area. Typical HETP (height equivalent to a theoretical stage) values range from 2 to 4 ft, depending on column diameter and interfacial tension. The f.o.b. purchase cost for an RDC unit is included in Table 16.32, where the size factor is the product of the column diameter raised to a 1.5 exponent and the column height.

EXAMPLE 16.15

An aqueous feed of 30,260 lb/hr of 22 wt% acetic acid is contacted with 71,100 lb/hr of a solvent of 96.5 wt% ethyl acetate at 100°F and 25 psia to extract 99.8% of the acetic acid. A process simulation program computes six equilibrium stages for the separation. The densities of the two entering liquid phases are 62.4 lb/ft^3 for the feed and 55.0 lb/ft^3 for the solvent. Estimate the size and f.o.b. purchase cost of an RDC liquid-liquid extraction column for a CE cost index of 600.

SOLUTION

The volumetric flow rate of the feed = 30,260/62.4 = 485 ft^3/hr.

The volumetric flow rate of the solvent = 71,100/55.0 = 1,293 ft^3/hr.

The total volumetric flow rate through the column = 485 + 1,293 = 1,778 ft^3/hr.

For a maximum throughput of 120 ft^3/hr-ft^2, cited above, the minimum cross-sectional area for flow = 1,778/120 = 14.8 ft^2.

Assume a throughput of 60% of the maximum value.

Actual cross-sectional area for flow = 14.8/0.6 = 24.7 ft^2.

Column diameter = $[24.7(4)/3.14]^{0.5}$ = 5.6 ft. Specify a diameter, D, of 5.5 ft.

Assume an HETP of 4 ft. This gives a total stage height of 4(6) = 24 ft. Add an additional 3 ft at the top and 3 ft at the bottom to give a total tangent-to-tangent height, H, of 24 + 3 + 3 = 30 ft.

From Table 16.32, the size factor $= S = H(D)^{1.5} = 30\,(5.5)^{1.5} =$ 387 $ft^{2.5}$.
For carbon steel at a CE index of 567, the f.o.b. purchase cost is

$$C_P = 363(387)^{0.84} = \$54{,}100$$

Because the feed contains water and acetic acid, assume stainless steel construction with a material factor of 2.0 and correct for the cost index. This gives an estimated f.o.b. purchase cost of

$$C_P = 54{,}100(2.0)(600/567) = \$114{,}500$$

Membrane Separations

Commercial membrane-separation processes include *reverse osmosis, gas permeation, dialysis, electrodialysis, pervaporation, ultrafiltration, and microfiltration*. Membranes are mainly synthetic or natural polymers in the form of sheets that are spiral wound or hollow fibers that are bundled together. Reverse osmosis, operating at a feed pressure of 1,000 psia, produces water of 99.95% purity from seawater (3.5 wt% dissolved salts) at a 45% recovery, or with a feed pressure of 250 psia from brackish water (less than 0.5 wt% dissolved salts). Bare-module costs of reverse osmosis plants based on purified water rate in gallons per day are included in Table 16.32. Other membrane-separation costs in Table 16.32 are f.o.b. purchase costs.

Gas permeation is used to separate gas mixtures, for example, hydrogen from methane. High pressures on the order of 500 psia are used to force the molecules through a dense polymer membrane, which is packaged in pressure-vessel modules, each containing up to 4,000 ft^2 of membrane surface area. Membrane modules cost approximately \$45/ft^2 of membrane surface area. Multiple modules are arranged in parallel to achieve the desired total membrane area.

Pervaporation is used to separate water–organic and organic–organic mixtures that form azeotropes and may be difficult to separate by enhanced distillation. Typical membrane modules cost \$38/ft^2 of membrane surface area.

Ultrafiltration uses a microporous polymer membrane, which allows water and molecules of less than some cut-off molecular weight to pass through, depending on the pore diameter, while retaining larger molecules. A typical membrane module may contain 30 ft^2 of membrane surface area at a cost of \$10 to \$25/ft^2 of surface area.

Mixers for Powders, Pastes, and Doughs

A wide variety of designs is available for mixing powders or pastes, polymers, and doughs of high viscosity. Among the more widely used designs are *ribbon and tumbler mixers* for dry powders, and *kneaders and mullers* for pastes and doughs. Equations for f.o.b. purchase costs of these devices are included in Table 16.32 in terms of the volumetric size. All designs operate batchwise; some can operate continuously. Typical residence times for mixing are less than 5 min. A comprehensive treatment of this type of mixing is given in *Perry's Chemical Engineers' Handbook* (Green and Perry, 2008).

Power Recovery

Valves are often used to reduce the pressure of a gas or liquid process stream. By replacing the valve with a turbine, called an *expander, turboexpander*, or *expansion turbine* in the case of a gas and a *liquid expander* or *radial-inflow, power-recovery turbine* in the case of a liquid, power can be recovered for use elsewhere. Power recovery from gases is far more common than from liquids because for a given change in pressure and mass flow rate, far more power can be recovered from a gas than from a liquid because of the lower density of the gas. Equations for f.o.b. purchase costs of

power-recovery devices are included in Table 16.32 in terms of horsepower that can be extracted. Typical efficiencies are 75–85% for gases and 50–60% for liquids. Condensation of gases in expanders up to 20% can be tolerated, but vapor evolution from liquid expansion requires a special design. Whenever more than 100 Hp for a gas and more than 150 Hp for a liquid can be extracted, a power-recovery device should be considered.

Screens

Solid particles are separated according to particle size by screening. Ideally, particles of size smaller than the opening of the screen surface, called *undersize* or *fines*, pass through whereas larger particles, called *oversize* or *tails*, do not. However, a perfect separation is not possible. If the undersize is the desired product, the screen efficiency is the mass ratio of undersize obtained from the screen to the undersize in the feed. A typical efficiency might be 75%. For particles with sizes greater than 2 in., a vibrating, inclined *grizzly*, which consists of parallel bars of fixed spacing, is commonly used. The opening between adjacent parallel bars may be from 2 to 12 in. Inclined *vibrating screens* are used to separate particles smaller than 2 in. Standard screen sizes of the U.S. Sieve Series are used. The screens consist of woven wire with square apertures (openings). Screen sizes are quoted in millimeters above 8 mm and in *mesh* for 8 mm and lower. Mesh refers to the number of openings per inch. However, because wire diameter is not constant, the actual opening size cannot be easily calculated from the mesh. Instead, a table, such as is found in *Perry's Chemical Engineers' Handbook* (Green and Perry, 2008), must be used to obtain the opening size. For example, a 20-mesh (No. 20) screen has square openings of 0.841 mm. Purchase costs of grizzlies and vibrating screens, included in Table 16.32, depend on the screen surface area. Screen capacities are directly proportional to screen surface area and approximately proportional to the opening between bars or the screen aperture. However, capacity for vibrating screens drops off dramatically for particle sizes below that for 140 mesh (0.105 mm). Typical capacities for grizzly screens range from 1 to 4 tons of feed/ft^2 of screen surface-hr-inch of opening between bars with the lower value for coal and the higher value for gravel. For vibrating screens, typical capacities range from 0.2 to 0.8 ton/ft^2-hr-mm of aperture. Vibrating screens are available in single-, double-, and triple-deck machines where the screen surface area refers to the total area in square feet of all screens in the deck. For the separation of very small particles of less than 0.1 mm in diameter, air classifiers are used, which can be costed as a cyclone separator.

Size Enlargement

Solid products are frequently produced in preferred shapes, such as tablets, rods, sheets, and so on. Such shapes are produced by a variety of size enlargement or agglomeration equipment by pressure compaction as by a *pellet mill, pug mill extruder, roll-type press, screw extruder*, or *tableting press* or by tumbling compaction in *disk or pan agglomerators*. Equations for f.o.b. purchase costs of these devices are included in Table 16.32 in terms of the feed rate. A comprehensive treatment of size enlargement is given in *Perry's Chemical Engineers' Handbook* (Green and Perry, 2008).

Size Reduction Equipment

The size of solid particles can be reduced by one or more of the following actions: (1) impact by a single rigid force, (2) compression between two rigid forces, (3) shear, and (4) attrition between particles or a particle and a wall. The energy required to reduce the size of particles is far more than that theoretically required to increase the surface area of the particles with the excess energy causing an increase in the temperature of the particles and the surroundings. A wide variety of equipment is available for particle size reduction, but except for special cases, most crushing and grinding tasks can be accomplished with the types of equipment listed in Table 16.28, which is taken from Walas (1988) and is organized by feed particle size. Included in the table are representative solids' feed rates and power consumption. In general, primary and secondary crushers, including *jaw crushers, gyratory crushers*, and *cone crushers*, are used with feed particle sizes greater than about 2 in. They accomplish a size (diameter) reduction ratio of approximately 8. For feeds of smaller particle sizes, grinding is used with *hammer mills* and *ball mills* but at lower capacities, especially with hammer mills. With these two mills, the size reduction ratio is much larger, 100 to 400, to achieve particle sizes in the 0.01 to 0.1 mm range. For the production of even smaller particles in the range of 3 to 50 μm, a. *jet mill* (pulverizer), which uses gas jets, can be used. The f.o.b. purchase costs of the crushers and grinders in Table 16.28, including electric motor drives, are listed in Table 16.32.

Solid–liquid Separation Equipment (thickeners, clarifiers, filters, centrifuges, and expression)

Slurries of solid particles and liquid are separated into more concentrated slurries or wet cakes and relatively clear liquid (overflow) by means of gravity, pressure, vacuum, or centrifugal force. The solid particles and/or the clear liquid may be the product of value. Continuous *clarifiers* remove small concentrations of solid particles by settling (sedimentation) to produce a clear liquid. Continuous *thickeners* are similar in design to clarifiers, but the emphasis is on producing a more concentrated slurry that can be fed to a filter or centrifuge to produce a wet cake. With thickeners, the solid particles are usually more valuable. Clarifiers and thickeners operate continuously, most often with gravity causing the solid particles to settle to the bottom of the equipment where a rake is used to remove concentrated slurry. Typically, the feed to a thickener is 1–30 wt% solids whereas the underflow product is 10–70 wt% solids. For a clarifier, the wt% solids in the feed is usually less than 1%. The f.o.b. purchase costs for thickeners and clarifiers listed in Table 16.32 are based on a size factor of the settling area. Most thickeners and clarifiers are circular with a

Table 16.28 Operating Ranges of Widely Used Crushing and Grinding Equipment[a]

Equipment	Feed Size (mm)	Product Size (mm)	Size Reduction Ratio	Capacity [ton/hr (1 ton = 2,000 lb)]	Power (Hp)
Gyratory crushers	200–2,000	25–250	8	100–500	135–940
Jaw crushers	100–1,000	25–100	8	10–1,000	7–270
Cone crushers	50–300	5–50	8	10–1,000	27–335
Hammer mills	5–30	0.01–0.1	400	0.1–5	1.3–135
Ball mills	1–10	0.01–0.1	100	10–300	65–6,700
Jet mills	1–10	0.003–0.05	300	0.1–2	2.7–135

[a] *Source:* Reprinted with permission from Walas, (1988).

diameter from 10 to 400 ft. Below 100 ft, construction is usually of carbon steel whereas concrete is used for diameters greater than 100 ft. The required settling area is best determined by scaling up laboratory sedimentation experiments. In the absence of such data, very preliminary cost estimates can be made by estimating a settling area based on the equation: Settling area, $ft^2 = C_1$ (tons solids/day), where C_1 typically is in the range of 2–50, with the lower value applying to large particles of high density and the higher value applying to fine particles of low density. The settling area for a clarifier can be estimated by the equation: Settling area, $ft^2 = C_2$ (gpm of overflow liquid), where C_2 is typically 0.5 to 1.5. Power requirements for thickeners and clarifiers are relatively low because of the low rotation rate of the rake. For example, a 200-ft-diameter unit requires only 16 Hp.

Continuous wet classifiers, of the *rake* and *spiral* type, and *hydroclones* (hydrocyclones) can also produce concentrated slurries, but the overflow liquid is not clear because it contains the smaller particles. A separation of particles by size and density occurs. Hydroclones are inexpensive, typically 6 in. in diameter or less, and a single unit can handle only low flow rates. For high flow rates, parallel units are employed in a *multiclone*. Table 16.32 contains f.o.b. purchase costs for wet classifiers and hydroclones. The size factor is the solids flow rate for classifiers and the liquid flow rate for hydroclones.

Wet cakes can be produced by sending concentrated slurries to filters operating under pressure or vacuum. Liquid passes through a porous barrier (filter media), which retains most of the solid particles to form a wet cake. Filters are designed to operate either continuously (e.g., the *continuous rotary-drum vacuum filter* or the *rotary pan filter)* or batch-wise (e.g., the *plate-and-frame filter* or the *pressure leaf filter)*. Table 16.32 contains f.o.b. purchase costs for most of the widely used filters. All costs are based on filtering area, which must be determined by laboratory experiments with a handheld vacuum or pressure leaf filter. For preliminary cost estimates, in the absence of such tests, select a continuous rotary-drum vacuum filter operating at a rotation rate of 20 rev/hr, with a filtering area estimated for fine particles (e.g., those produced by a precipitation reaction to produce relatively insoluble inorganic particles) at a filtrate rate of 1,500 lb/day-ft^2 (vacuum of 18–25 in. of Hg) and, for coarse solids (e.g., those produced by crystallization) at a filtrate rate of 6,000 lb/day-ft^2 (vacuum of 2–6 in. of Hg).

An alternative to a filter is a centrifuge that accomplishes the removal of some of the liquid in the feed under a high centrifugal force, up to 50,000 times the gravitational force on the earth, by sedimentation with a solid bowl or by filtration with a perforated bowl, either continuously or batchwise. Table 16.32 contains f.o.b. purchase costs for many of the more widely used centrifuges in 304 stainless steel. Included are two manual *batch centrifugal filters*, two *automatic-batch centrifugal filters*, and two *continuous centrifuges*. The size factor for the latter two centrifuges is the ton/hr of solid particles whereas the size factor for the other four centrifuges is the bowl diameter. With auto-batch operation, from 1 to 24 ton/hr of solids can be processed. For manual batch operation, a cycle time of 2 min for coarse particles and 30 min for fine particles is representative. From 0.15 to 5 ton/hr of solids can be processed in a 40-in.-diameter manual batch centrifuge.

Some wet solids consist of fibrous pulps or other compressible materials from which liquid cannot be removed by settling, filtering, or centrifuging. Instead *expression* is used with *screw presses* or *roll presses*. Table 16.32 provides f.o.b. purchase costs for these two presses in stainless steel.

EXAMPLE 16.16

Consider a process similar to that of Figure 9.45 for the continuous production of crystals of $MgSO_4 \cdot 7H_2O$ from an aqueous solution of 10 wt% $MgSO_4$. However, replace the hydroclone-centrifugal filter combination with a rotary-drum vacuum filter. Thus, in Figure 9.45, the magma goes directly to the filter, which produces filtrate (mother liquor) that is recycled to the crystallizer and a wet cake that is sent to the dryer. The crystallizer operates adiabatically. Therefore, the filtrate is heated with an external heat exchanger before being recycled to the crystallizer. For the production of 3,504 lb/hr of $MgSO_4 \cdot 7H_2O$, containing 1.5 wt% moisture from a feed of a 10 wt% aqueous solution of $MgSO_4$ at 14.7 psia and 70°F, estimate the f.o.b. purchase costs of all major items of equipment at a CE cost index of 567, using the following results from material and energy balances obtained with a process simulation program and preliminary equipment sizing:

Feed to the process:

$$H_2O = 15{,}174 \text{ lb/hr}$$

$$MgSO_4 = 1{,}686 \text{ lb/hr}$$

Evaporator effect 1 (long-tube vertical):

Operating pressure = 7.51 psia
Evaporation rate = 6,197 lb/hr
U = 450 Btu/hr-ft^2-°F
ΔT = 30°F
Heat duty = 7,895,000 Btu/hr
Area, A = 585 ft^2

Evaporator effect 2 (long-tube vertical):

Operating pressure = 2.20 psia
Evaporation rate = 6,197 lb/hr
U = 250 Btu/hr-ft^2-°F
ΔT = 40°F
Heat duty = 5,855,000 Btu/hr
Area, A = 585 ft^2

Feed to crystallizer from evaporator effect 2:

H_2O = 2,780 lb/hr
$MgSO_4$ = 1,686 lb/hr

Recycle filtrate (mother liquor) to crystallizer from external heater:

H_2O = 7,046 lb/hr
$MgSO_4$ = 2,792 lb/hr
Temperature after being heated = 180°F

Crystallizer (continuous adiabatic draft-tube baffled):

Operating pressure = 0.577 psia
Temperature = 85.6°F
Solubility of $MgSO_4$ at these conditions = 28.3 wt% $MgSO_4$
H_2O evaporation rate = 583 lb/hr

Magma flow rate to filter:

H_2O = 7,783 lb/hr
Dissolved $MgSO_4$ = 3,084 lb/hr
$MgSO_4 \cdot 7H_2O$ crystals produced = 2,854 lb/hr or 34.2 ton/day

Filter (continuous rotary vacuum):

Cake, assumed to contain 73.5 wt% solids = 3,883 lb/hr
Total filtrate = 9,838 lb/hr = 236,100 lb/day
Assumed filtrate flux = 5,000 lb/day-ft^2 because crystals are fairly coarse
Filter area = 236,100/5,000 = 47 ft^2

Drier (continuous direct-heat rotary):

Production rate of crystals with 1.5 wt% moisture = 3,504 lb/hr
Moisture evaporation rate by contact with hot air = 379 lb/hr
Moisture in crystals = 52 lb/hr
Outlet temperature of crystals = 113°F
Assumed volumetric moisture evaporation rate = 2 lb/hr/ft^3 of dryer volume because crystal moisture will be mainly free and final moisture content is not particularly low.
Dryer volume = 379/2 = 190 ft^3
Dryer dimensions: 3.5 ft diameter by 20 ft long
Peripheral area = 220 ft^2

SOLUTION

The process system consists of two long-tube vertical evaporators, a draft-tube baffled crystallizer, a rotary-drum vacuum filter, and a direct-heat rotary dryer. Also, pumps are needed to move the solution from evaporator 1 to evaporator 2, to recycle the filtrate from the filter to the crystallizer, and to move the magma from the crystallizer to the filter; and a heat exchanger is needed to heat the recycle filtrate. However, the purchase costs for the three pumps and the heat exchanger are not considered here because examples for these types of equipment are presented in Section 16.5. For the equipment considered here, assume fabrication from stainless steel with a material factor of 2 for the ratio of stainless steel cost to carbon steel cost. For the process, using the following size factors and the equations in Table 16.32, the estimated f.o.b. equipment purchase costs at a CE index of 567 are included in the following table.

Equipment	Type	Size Factor	f.o.b. Purchase Cost, in Carbon Steel	f.o.b. Purchase Cost, in Stainless Steel
Evaporator 1	Long-tube vertical	A = 585 ft^2	$215,000	$430,000
Evaporator 2	Long-tube vertical	A = 585 ft^2	$215,000	$430,000
Crystallizer	Draft-tube baffled	W = 34.2 ton/day	$296,000	$592,000
Filter	Rotary vacuum	A = 47 ft^2	$145,000	$290,000
Dryer	Direct-heat rotary	A = 220 ft^2	—	$223,000

Solids-Handling Systems

The handling of bulk solids in a chemical process is considerably more complex than the handling of liquids and gases, and requires much more attention by operators. A typical handling system may include a storage bin, hopper, or silo; a feeder; and a conveyor and/or elevator to send the bulk solids to a piece of processing equipment. The selection of equipment for handling bulk solids depends strongly on the nature of the solids. The classification scheme of the FMC Corporation as presented in Section 21 of *Perry's Chemical Engineers' Handbook* (Green and Perry, 2008) is particularly useful. In that scheme, bulk solids are classified by size, flowability, abrasiveness, and other special characteristics. For example, fine sodium chloride is classified as being particles between 100 mesh and $^1/_8$ in. diameter, free flowing with an angle of repose of 30 to 45°, mildly abrasive, mildly corrosive, and hygroscopic. Titanium dioxide particles, widely used as a pigment for whiteness, are particularly difficult to handle because of their small particle size (minus 325 mesh), irregular shape, and stickiness. In general, increased moisture content, increased temperature, decreased particle size, and increased time of storage at rest cause increased cohesiveness of the particles and decreased flowability.

A typical storage vessel for bulk solids, called a *bin*, consists of an upper section with vertical walls and a lower section with at least one sloping side, referred to as a hopper. The upper part of the bin is square or circular in cross section whereas the hopper is frequently conical in shape. Below the hopper is a chute, gate, or a rotary star valve. The design of a bin is best accomplished by a method devised by Andrew W. Jenike in the 1960s and described in *Perry's Chemical Engineers' Handbook* (Green and Perry, 2008). This method differentiates between the more desirable uniform mass flow with all particles moving downward and the less desirable funnel flow where all particles are not in motion and solids flow downward only in a channel in the center of the vessel. The elimination of bridging and assistance in obtaining uniform flow across the cross section of the bin can often be achieved by using a vibrating hopper. Typically, bin storage is provided for 8 hrs of operation. Most bins are constructed of carbon steel with or without rubber lining, fiberglass, or stainless steel. An equation for estimating the f.o.b. purchase cost of carbon steel bins is included in Table 16.32.

Bins may discharge bulk solids directly into a piece of processing equipment. Alternatively, the solids may be dropped onto a conveyor or into a feeder. Feeders are classified as volumetric or gravimetric. Volumetric feeders, which are the most common, discharge a volume of material per unit time whereas more expensive gravimetric feeders weigh the solids being discharged. If the bulk density of the solids is reasonably constant, volumetric feeders can confine mass flow rates to within a range of 5%. Volumetric feeders include *belts* (aprons), *rotary valves, screws, tables*, and *vibratory feeders*. Screw feeders are best for sticky materials, but belt and vibratory feeders also work in some cases. Gravimetric feeders work only with free-flowing solids and include weigh belts, loss-in-weight systems, and gain-in-weight systems. Purchase-cost equations for belt, screw, and vibratory feeders are included in Table 16.32.

Bulk solids are moved to other locations by conveyors (usually horizontal) or elevators (usually vertical). A wide range of conveyors is available, but the most common are the belt, screw, and vibratory conveyors. *Belt conveyors* can move coarse, corrosive, and abrasive particles of 100 mesh to several inches in size for distances up to 1,000 ft with a modest degree of inclination but at temperatures normally limited to 150°F. Typical belt widths range from 14 in. to 60 in. with belt speeds ranging from 100 to 600 ft/min. Typical heights of bulk solids on the belt range from 1 in. for the narrowest belt to 6 in. for the widest belt. Typical volumetric flow capacities range from 660 ft^3/hr for a 14-in.-wide belt moving at 100 ft/min to 86,000 ft^3/hr for a 60-in.-wide belt moving at 600 ft/min.

Screw conveyors consisting of a screw mounted in a trough are widely used. They can move particles of any size up to a few inches, in any straight direction, for distances up to 300 ft horizontally and up to 30 ft vertically, and at temperatures up to 900°F. Screw conveyors can be fitted with special screws for sticky materials, can be sealed to keep in dust and keep out moisture, and can be jacketed for cooling and heating. The screw, which ranges from 6 to 20 in. diameter, typically rotates at 25 to 100 rpm. Volumetric flow capacities when the trough is 30% full and the screw is rotating at 50 rpm range from 75 ft^3/hr for a 6-in.-diameter screw to 3,000 ft^3/hr for a 20-in.-diameter screw.

Vibratory conveyors are limited to straight distances, usually horizontal, up to 100 ft, but are not suited for fine particles less than 100 mesh in size. Solids must be free flowing, but temperatures up to 250°F can be handled. Widths range from 1 to 36 in. with pan heights to at least 5 in. Experiments are usually necessary to properly size a vibratory conveyor. For an 18-in.-wide conveyor with a 5-in. pan height and a 20-ft length, a typical mass flow capacity is 70,000 lb/hr or 700 ft^3/hr for solid particles having a bulk density of 100 lb/ft^3.

A *bucket elevator*, consisting of an endless chain of buckets, is best for moving solids vertically. The elevator loads at one level and discharges at another. Vertical distances of more than 3,000 ft have been spanned, but commonly available elevators are limited to 150 ft. Most often, discharge is by centrifugal force from buckets moving at speeds up to 1,200 ft/min. However, for materials that are sticky or that tend to pack, discharge is by gravity by completely inverting the buckets, which travel at lower speeds, up to 400 ft/min. Typical buckets range in width from 6 to 20 in. with bucket volumes from 0.06 to 0.6 ft^3 at bucket spacings from 1 to 1.5 ft. For a bucket speed of 150 ft/min, typical volumetric capacities range from 300 to 7,500 ft^3/hr.

Equations for estimating the purchase costs for the above four conveyor and elevator systems are included in Table 16.32. Belt and vibratory conveyors are priced by the width and the length of the conveyor. Screw conveyors are priced by the diameter of the screw and the length of the conveyor. Bucket elevators are priced by the width of the bucket and the elevated height. The costs do not include the electric motor or drive system. The required horsepower input of the electric motor drive, which depends on

Table 16.29 Power Requirements of Mechanical Conveyors[a]

Conveyor Type	Power Equation[b]
Belt	$P = 0.00058\ (m)^{0.82}L$
Screw	$P = 0.0146\ (m)^{0.85}L$
Bucket	$P = 0.020\ m(L)^{0.63}$

[a] *Source:* Reproduced with permission from Ulrich (1984).

[b] Units: P = Hp, m = lb/s, L = ft. For an elevation change, h, in ft, add or subtract $P = 0.00182\ mh$.

the mass flow rate, m, and the length of the conveyor, L, may be estimated from the equations given in Table 16.29 taken from Ulrich (1984). Additional power must be added to the equations for elevating the material by a height, h. The screw conveyor requires the largest amount of power, whereas the belt conveyor requires the least.

EXAMPLE 16.17

Flakes of phthalic anhydride with a bulk density of 30 lb/ft^3 are to be conveyed a horizontal distance of 40 ft from a bin to a packaging facility at the rate of 1,200 ft^3/hr. Size and cost a bin and conveying system as of a CE index of 567.

SOLUTION

Assume a bin storage time of 8 hr. Therefore, the bulk solids volume is 8(1,200) = 9,600 ft^3. Assume an outage (gas space above the bulk solids) of 20%. Thus, the bin volume above the hopper = 9,600/(1 − 0.20) = 12,000 ft^3. Neglecting the volume of the hopper below the bin and assuming a cylindrical bin with a height equal to 150% of the diameter, the hopper dimensions are 22 ft in diameter by 33 ft high. From Table 16.32, the purchase cost of the bin in carbon steel is $646\ (12{,}000)^{0.46}$ = $48,600. Because flakes may tend to mat and interlock, consideration should be given to the addition of a vibrator to the hopper.

A screw conveyor is a reasonable choice to transport the flakes, and it can also act as a feeder to remove the flakes from the hopper. From the above discussion, for a trough running 30% full at 50 rpm, a 6-in. screw can transport 75 ft^3/hr whereas a 20-in. screw can transport 3,000 ft^3/hr. Assume that the flow rate is proportional to the screw diameter raised to the exponent x. Then, the exponent is computed as 3. Therefore, the required screw diameter is computed as 15 in. From the equation in Table 16.32 for a length of 40 ft, the purchase cost of the screw conveyor is $80(15)(40)^{0.59}$ = $10,600. The cost of the motor and a belt drive must be added. From Table 16.29, for a mass flow rate, m, equal to (1,200/3,600)30 = 10 lb/s and with no elevation change, the electric motor Hp is $0.0146(10)^{0.85}40 = 4.13$. Assume a 5-Hp motor. From Table 16.22, select a totally enclosed, fan-cooled motor rotating at 1,800 rpm. Thus, F_T in Eq. (16.20) is 1.3. From Eq. (16.19), for P_C = 5 Hp, the base cost is C_B = approximately $480, giving a purchase cost of 1.3(480) = $624. This gives a total of $11,200 for the conveyor with motor or a total of $59,800 for the bin and conveyor. Add 10% to vibrate the hopper, cover the conveyor, and add a belt drive to the motor. This gives a total purchase cost for the system of $65,800.

Bulk solids may also be conveyed pneumatically as a dilute suspension in a gas, often air, through a piping system over distances of up to several hundred feet. Materials ranging in size from fine powders to 1/4-in.-diameter pellets and in bulk densities up to 200 lb/ft^3 have been routinely conveyed in this manner. A pneumatic conveying system usually includes a blower to move the gas, a rotary air lock valve to control the rate of addition of the bulk solids to the gas, a piping system, and a cyclone to separate the solids from the gas at the discharge point. The pressure in the piping system may be below or above ambient pressure. Air velocities required to convey the solids typically range from 50 ft/s for low-bulk-density solids to 200 ft/s for high-bulk-density solids. The purchase cost of a *pneumatic conveying* system depends mainly on the bulk solids flow rate and the equivalent length (pipe plus fittings) of the piping system, but the particle size and bulk density of the solids are also factors. Table 16.32 includes an equation for estimating the purchase cost of a system to convey solids having a bulk density of 30 lb/ft^3. The power requirement, P, in horsepower depends mainly on the solids flow rate, m, in pounds per second as estimated by:

$$P = 10\ m^{0.95} \tag{16.71}$$

Storage Tanks and Vessels

Storage tanks and vessels are used to store process liquid and gas feeds and products as well as to provide intermediate storage between sections of a plant operating continuously or between operations for a batch or semicontinuous process. For liquid storage at pressures less than approximately 3 psig, so-called atmospheric tanks are used. These tanks may be open (no roof), cone roof, or floating-roof types. *Open tanks*, which may be made of fiberglass, are commonly used only for water and some aqueous solutions because they are subject to moisture, weather, and atmospheric pollution. *Cone-roof* (or *other fixed-roof*) *tanks* require a vent system to prevent pressure changes due to changes in temperature and during changes in liquid level during filling or emptying. When the vapor pressure of the liquid over the expected range of storage temperature causes a significant rate of evaporation, *a. floating-roof* (or *other variable volume*) *tank* should be used. Such tanks do not vent. Current EPA regulations dictate the use of a floating-roof tank when, at the maximum atmospheric temperature at the plant site, the vapor pressure of the liquid is greater than 3.9 psia for storage of less than 40,000 gal or greater than 0.75 psia for storage of more than 40,000 gal.

Storage of liquid feeds and products is usually provided off-site with residence times varying from one week to one month, depending on the frequency of delivery and distribution. The capacity of atmospheric liquid storage tanks should be at least 1.5 times the size of the transportation equipment, typically 4,000 to 7,500 gal for tank trucks and up to 34,500 gal for tank cars. A shipment by barge may be as large as 420,000 gal. The maximum size for a single cone-roof or floating-roof tank is approximately 20,000,000 gal, which corresponds to a diameter of about 300 ft and a height of about 50 ft. Storage of liquid feeds, products, and intermediates may also be provided on-site in so-called surge tanks or day tanks, which provide residence times of 10 min to one day. Equations for estimating the f.o.b. purchase costs of open, cone-roof, and floating-roof tanks are included in Table 16.32.

For liquid stored at pressures greater than 3 psig or under vacuum, spherical or horizontal (or vertical) cylindrical (bullet) pressure vessels are used. Vertical vessels are not normally used for volumes greater than 1,000 gal. Horizontal pressure vessels for storage are at least as large as 350,000 gal. Spherical pressure vessels are also common with more than 5,000 having been constructed worldwide. For liquid storage, spheres as large as 94 ft in diameter (3,000,000 gal) have been installed. The design and costing of cylindrical pressure vessels is considered in detail in Section 16.5. Purchase costs are plotted in Figure 16.13. For spherical pressure vessels, Eq. (16.60) for cylindrical pressure vessels is revised to:

$$t_p = \frac{P_d D_i}{4SE - 0.4P_d} \tag{16.72}$$

Equations for estimating the f.o.b. purchase costs of spherical pressure vessels, based on just the vessel volume, are included in Table 16.32 for two different pressure ranges.

Pressure vessels are also used for the storage of gases at pressures greater than 3 psig. For pressures between 0 and 3 psig, a *gas holder*, similar to a floating-roof tank for liquids, is used. An equation for estimating the f.o.b. purchase cost of a gas holder is included in Table 16.32.

Vacuum Systems

In some chemical processes, operations are conducted at pressures less than ambient. To achieve such pressures, vacuum systems are required. Pressures below ambient are commonly divided into four vacuum regions:

Vacuum Region	Pressure Range (torr)
Rough	760 to 1
Medium	1 to 0.001
High	0.001 to 10^{-7}
Ultrahigh	10^{-7} and below

Of greatest interest to chemical processing is the rough region, which covers most polymer reactors, vacuum distillation columns, vacuum stripping columns, pervaporation membrane separations, vacuum-swing adsorbers, and vacuum crystallizers, evaporators, filters, and dryers.

In the rough region, the available vacuum systems include (1) one-, two-, and three-stage *ejectors* driven with steam and with or without interstage surface or barometric (direct-contact) condensers, (2) one- or two-stage *liquid-ring pumps* using oil or water as the sealant, and (3) *dry vacuum pumps* including rotary lobe, claw, and screw compressors. Although the first two systems have been the most widely used, dry vacuum pumps are gaining attention because they are more efficient and do not require a working fluid such as steam, water, or oil, which can contribute to air pollution. Typical flow capacities and lower limits of suction pressure for process applications of these three types of vacuum systems are given in Table 16.30 taken from Ryans and Bays (2001). This table is useful in making a preliminary selection of candidate vacuum systems based on the flow rate and pressure at suction conditions.

Table 16.30 Lower Limits of Suction Pressure and Capacities of Vacuum Systems[a]

System Type	Lower Limit of Suction Pressure (torr)	Volumetric Flow Range at Suction Conditions (ft^3/min)
Steam-jet ejectors		10–1,000,000
One stage	100	
Two stage	15	
Three stage	2	
Liquid-ring pumps		3–18,000
One-stage water sealed	50	
Two-stage water sealed	25	
Oil sealed	10	
Dry vacuum pumps		
Three-stage rotary lobe	1.5	60–240
Three-stage claw	0.3	60–270
Screw compressor	0.1	50–1,400

[a] *Source:* Reprinted with permission from Ryans, and Bays, (2001).

For batch processes where a vessel is being evacuated, the flow rate to be handled by the vacuum system depends on the selected time period for evacuation and on the contents of the vessel. When the flow contains condensables, a precondenser upstream of the vacuum system should be considered so as to reduce the flow rate to the vacuum pump. For continuous processes, the flow rate to be handled by the vacuum system is usually based on an estimate of air leakage into the equipment operating under vacuum. Air leakage occurs at gasketed joints, porous welds, and cracks and fissures in vessel walls. A simple but often adequate estimate can be made based on the equipment volume and operating pressure with the following equation, derived from recommendations of the Heat Exchange Institute:

$$W = 5 + \{0.0298 + 0.03088[\ln(P)] - 0.0005733 \times [\ln(P)]^2\} V^{0.66} \tag{16.73}$$

where W is the air leakage rate in lb/hr, P is the absolute operating pressure in torr assuming a barometric pressure of 760 torr, and V is the vessel volume in ft^3. For many pieces of equipment operating under a vacuum, the air leakage leaving the equipment will be accompanied by volatile process components. To partially recover these components and reduce the load on the vacuum pump, the exiting gas should first pass through a precondenser before proceeding to the vacuum system. The flow rates of process components still in the gas leaving the precondenser with the air can be determined by a flash calculation as illustrated in Example 16.18.

Note in Table 16.30 that steam-jet ejector systems can handle a very wide range of conditions. They have no moving parts and are inexpensive to maintain, but are very inefficient because of the high usage of motive steam. The maximum compression ratio per stage is approximately 7.5. The required motive steam rate for each stage depends on the ratio of suction pressure-to-discharge pressure, steam pressure, temperature, gas properties, and ejector nozzle-to-throat ratio. A reasonably conservative range for the total motive steam requirement for all stages, when using

Table 16.31 Multiplying Factors for Steam-jet Ejector Vacuum Systems

Items	Cost Multiplying Factors
1 Stage	1.0
2 Stages	1.8
3 Stages	2.1
1 Surface condenser	1.6
2 Surface condensers	2.3
1 Barometric condenser	1.7
2 Barometric condensers	1.9
Carbon steel	1.0
Stainless steel	2.0
Hastelloy	3.0

100-psig steam to evacuate mostly air, is 5–10 lb of steam per pound of gas being pumped. A detailed procedure for designing an ejector vacuum system is given by Sandler and Luckiewicz (1987).

Liquid-ring pumps are limited to a suction pressure of 10 torr with a moderate capacity and efficiency (25–50%). Dry vacuum pumps can achieve very low pressures at higher efficiencies, but only for low capacities. Since vacuum pumps are actually gas compressors, a tendency exists for the gas temperature to increase in an amount corresponding to the compression ratio. However, this temperature rise is greatly minimized or eliminated in ejector systems and with the liquid-ring pump because of the addition of another fluid. The temperature rise must not be overlooked with dry vacuum pumps.

The f.o.b. purchase costs for vacuum systems are included in Table 16.32. The equation for the one-stage ejector system in carbon steel is based on indexed data from Pikulik and Diaz (1977). Use the multiplying factors in Table 16.31 to add stages and interstage condensers to and change materials of construction. For the other vacuum systems, f.o.b. purchase costs in Table 16.32 were taken from Ryans and Bays (2001).

EXAMPLE 16.18

A vacuum distillation column produces an overhead vapor of 1,365 kmol/hr of ethylbenzene and 63 kmol/hr of styrene at 30 kPa. The volume of the column, vapor line, condenser, and reflux drum is 50,000 ft^3. The overhead vapor is sent to a condenser where most of the vapor is condensed. The remaining vapor at 50°C and 25 kPa is sent to a vacuum system. Determine the air leakage rate in the distillation operation and the flow rate to the vacuum system. Select an appropriate vacuum system and determine its f.o.b. purchase cost at a CE cost index of 600.

SOLUTION

The amount of air leakage, W, is estimated from Eq. (16.73). Using a pressure of 25 kPa = 188 torr:

$$W = 5 + \{0.0298 + 0.03088[\ln(188)] - 0.0005733[\ln(188)^2]\}50{,}000^{0.66} = 227 \text{ lb/hr}$$

This is equivalent to 103 kg/hr or 3.6 kmol/hr. Adding this to the overhead vapor and performing a flash calculation at 50°C and 25 kPa (188 torr) gives a vapor leaving the reflux drum and entering the vacuum system of 3.6 kmol/hr of air and 0.7 kmol/hr of ethylbenzene. The volumetric flow rate to the vacuum system is 272 ft^3/min. The flow rate in pounds per hour is 394. From Table 16.30, applicable vacuum systems are a single-stage steam-jet ejector, a single-stage liquid-ring pump, and a screw compressor. The three-stage claw unit is just out of the range of the volumetric flow rate.

From Table 16.32, the size factor for the ejector = S = 394/188 = 2.1. From the cost equation in Table 16.32, the f.o.b. purchase cost of the ejector in carbon steel and for a cost index of 600 is

$$C_P = (600/567)(1915)(2.1)^{0.41} = \$2{,}750$$

The estimated 100-psig steam consumption is 10(394) = 3,940 lb/hr. Assuming a steam cost of \$7.00/1,000 lb and operation for 8,000 hr/yr, the annual steam cost is 3.94(7.00)(8,000) = \$220,600/yr, which is far more than the cost of the ejector.

Next, consider the liquid-ring pump. From Table 16.32, with a size factor of 272 ft^3/min, in stainless steel and at CE = 600, the f.o.b. purchase cost is

$$C_P = (600/567)(8{,}250)(272)^{0.37} = \$65{,}700$$

At an overall efficiency of 40% for compression to 100 kPa, the calculated horsepower input is 16.8 or 12.6 kW. Assuming an electricity cost of \$0.07 kW/hr for 8,000 hr/yr, the annual electricity cost is 12.6(0.07)(8,000) = \$7,060/yr, which is much less than the ejector system.

These two vacuum systems can be compared on an annualized cost basis as discussed in Section 17.4, but it seems clear that the higher cost of the liquid-ring pump is more than offset by the much higher utility cost to operate the ejector system. The screw compressor is also a candidate, but its purchase cost, \$96,900, is significantly higher and the annual electricity cost, at an overall efficiency of 70%, is only about \$2,940/yr less than for the liquid-ring pump.

Wastewater Treatment

Wastewater can contain inorganic and organic compounds in soluble, colloidal, insoluble liquid, and solid particulate forms. Before wastewater can be sent to a sewer or converted to drinking water, process water, boiler-feed water, or cooling water, it must be treated to remove certain impurities. Such treatment may consist of as many as three major treatment steps: primary, secondary, and tertiary. Primary treatment involves physical separation operations such as screening to remove large solids and sedimentation to remove smaller particulate matter, which settles to the bottom, and insoluble organic liquid, which floats to the top and is skimmed. Secondary treatment removes dissolved organic compounds by biological degradation with aerobic or anaerobic microorganisms in a recirculating activated sludge. This may produce settleable solids, which are removed by filtration. Removal of nitrogen and phosphorus nutrients, residual organic compounds, and dissolved inorganic compounds is accomplished in a tertiary treatment, which involves such operations as carbon adsorption, demineralization, and reverse osmosis. The water

Table 16.32 Purchase Costs (f.o.b.) of Other Chemical Processing Equipment (CE Index = 567. Equations for pumps, compressors, motors, heat exchangers, and pressure vessels are in Section 16.5)

Equipment Type	Size Factor (S)	Range of S	f.o.b. Purchase Cost Equation ($)	Notes
Adsorbents				
Activated alumina	Bulk volume, ft^3		$C_P = 72\ S$	
Activated carbon	Bulk volume, ft^3		$C_P = 41\ S$	
Silica gel	Bulk volume, ft^3		$C_P = 210\ S$	
Molecular sieves	Bulk volume, ft^3		$C_P = 85\ S$	
Agitators				Includes motor and shaft
Propeller, open tank	Motor Hp	1–8 Hp	$C_P = 2{,}610\ S^{0.34}$	Direct coupling to motor
Propeller, closed vessel	Motor Hp	1–8 Hp	$C_P = 3{,}740\ S^{0.17}$	Direct coupling to motor, pressures to 150 psig
Turbine, open tank	Motor Hp	2–60 Hp	$C_P = 3{,}730\ S^{0.54}$	Includes speed reducer
Turbine, closed vessel	Motor Hp	2–60 Hp	$C_P = 4{,}105\ S^{0.57}$	Includes speed reducer, pressures to 150 psig
				Includes turbine agitator and heat-transfer jacket
Autoclaves				
Steel	Vessel volume, gal	30–8,000 gal	$C_P = 1{,}185\ S^{0.52}$	Pressures to 300 psig
Stainless steel	Vessel volume, gal	30–2,000 gal	$C_P = 2{,}245\ S^{0.58}$	Pressures to 300 psig
Glass lined	Vessel volume, gal	30–4,000 gal	$C_P = 2{,}085\ S^{0.54}$	Pressures to 300 psig
Crystallizers				
Continuous cooling				
Jacketed scraped wall	Length, L, ft	15–200 ft	$C_P = 16{,}440\ L^{0.67}$	Stainless steel
Continuous evaporative				
Forced circulation	Tons crystals/day, W	10–1,000 ton/day	$C_P = 39{,}575\ W^{0.56}$	Carbon steel
Draft-tube baffled	Tons crystals/day, W	10–250 ton/day	$C_P = 31{,}980\ W^{0.63}$	Carbon steel
Batch evaporative	Volume, V, ft^3	50–1,000 ft^3	$C_P = 46{,}380\ V^{0.41}$	Stainless steel
Drives other than electric motors				
Steam turbines (noncondensing)	Shaft power, P, Hp	250–10,000 Hp	$C_P = 10{,}660\ P^{0.41}$	Carbon steel
Steam turbines (condensing)	Shaft power, P, Hp	250–10,000 Hp	$C_P = 28{,}350\ P^{0.405}$	Carbon steel
Gas turbines	Shaft power, P, Hp	100–10,000 Hp	$C_P = 2{,}835\ P^{0.76}$	Carbon steel
Internal combustion engines	Shaft power, P, Hp	100–4,000 Hp	$C_P = 1{,}588\ P^{0.75}$	Carbon steel
Dryers				
Batch tray	Tray area, A, ft^2	20–200 ft^2	$C_P = 4{,}400\ A^{0.35}$	Stainless steel
Direct-heat rotary	Drum peripheral area, A, ft^2	200–3,000 ft^2	$C_P = \exp\{10.522 + 0.1003[\ln(A)] + 0.04303\ [\ln(A)]^2\}$	Stainless steel
Indirect-heat steam-tube rotary	Heat-transfer area, A, ft^2	100–1,400 ft^2	$C_P = 1{,}520\ A^{0.80}$	Stainless steel

(Continued)

Table 16.32 (*continued*)

Equipment Type	Size Factor (S)	Range of S	f.o.b. Purchase Cost Equation ($)	Notes
Dryers (continued)				
Drum	Heat-transfer area, A, ft^2	60–480 ft^2	$C_P = 32{,}000\ A^{0.49}$	Stainless steel
Spray	Evaporation rate, W, lb/hr	30–3,000 lb/hr	$C_P = \exp\{8.5133 + 0.9847[\ln(W)] - 0.0561[\ln(W)]^2\}$	Stainless steel
Dust collectors				
Bag filters	Gas flow rate, actual ft^3 /min	5,000–2,000,000	$C_P = \exp\{10.3838 - 0.4381[\ln(S)] + 0.055563[\ln(S)]^2\}$	Carbon steel
Cyclones	Gas flow rate, actual ft^3 /min	200–100,000	$C_P = \exp\{9.3485 - 0.7892[\ln(S)] + 0.08487[\ln(S)]^2\}$	Carbon steel
Electrostatic precipitators	Gas flow rate, actual ft^3/min	10,000–2,000,000	$C_P = \exp\{11.8058 - 0.5300[\ln(S)] + 0.05454[\ln(S)]^2\}$	Carbon steel
Venturi scrubbers	Gas flow rate, actual ft^3 /min	2,000–20,000	$C_P = \exp\{9.7413 - 0.3281[\ln(S)] + 0.0500[\ln(S)]^2\}$	Carbon steel
Evaporators				
Horizontal tube	Heat-transfer area, A, ft^2	100–8,000 ft^2	$C_P = 4{,}604\ A^{0.53}$	Carbon steel
Long-tube vertical (rising film)	Heat-transfer area, A, ft^2	100–8,000 ft^2	$C_P = 6{,}464\ A^{0.55}$	Carbon steel
Forced circulation	Heat-transfer area, A, ft^2	150–8,000 ft^2	$C_P = \exp\{8.0369 + 0.6994[\ln(A)] - 0.00004[\ln(A)]^2\}$	Carbon steel
Falling film	Heat-transfer area, A, ft^2	150–4,000 ft^2	$C_P = 13{,}700\ A^{0.68}$	Stainless steel tubes, carbon steel shell
Fired heaters for specific purposes				
Reformer	Heat absorbed, Q, Btu/hr	10–50 million Btu/hr	$C_P = 0.974\ Q^{0.81}$	Carbon steel, pressure to 10 atm
Pyrolysis	Heat absorbed, Q, Btu/hr	10–500 million Btu/hr	$C_P = 0.737\ Q^{0.81}$	Carbon steel, pressure to 10 atm
Hot water	Heat absorbed, Q, Btu/hr	0.5–70 million Btu/hr	$C_P = \exp\{9.7188 - 0.3769[\ln(Q)] + 0.03434[\ln(Q)]^2\}$	
Molten salt, mineral and silicon oils	Heat absorbed, Q, Btu/hr	0.5–70 million Btu/hr	$C_P = 13.97\ Q^{0.64}$	
Dowtherm A	Heat absorbed, Q, Btu/hr	0.5–70 million Btu/hr	$C_P = 14.45\ Q^{0.65}$	
Steam boiler	Heat absorbed, Q, Btu/hr	0.5–70 million Btu/hr	$C_P = 0.416\ Q^{0.77}$	Carbon steel, pressure to 20 atm
Heat exchangers, other				
Air-cooled fin-fan	Bare-tube heat-transfer area, A, ft^2	40–150,000 ft^2	$C_P = 2{,}835\ A^{0.40}$	Carbon steel
Compact units				
Plate and frame	Heat-transfer area, A, ft^2	150–15,000 ft^2	$C_P = 10{,}070\ A^{0.42}$	Stainless steel
Spiral plate	Heat-transfer area, A, ft^2	20–2,000 ft^2	$C_P = 7{,}030A^{0.42}$	Stainless steel
Spiral tube	Heat-transfer area, A, ft^2	1–500 ft^2	$C_P = \exp\{8.2015 + 0.4343[\ln(A)] + 0.03812[\ln(A)]^2\}$	Stainless steel
Liquid–liquid extractors	S = (Height, H, ft) (Diameter, D, ft)$^{1.5}$	3–2,000 ft$^{2.5}$	$C_P = 363\ S^{0.84}$	Carbon steel
Rotating-disk contactors (RDC)				

Membrane separations				
Reverse osmosis, seawater	Purified water, Q, gal/day	2–50 million gal/day	$C_{BM} = \exp\{.1258+1.802[\ln(Q)] + 0.01775[\ln(Q)]^2\}$	Bare-module cost
Reverse osmosis, brackish water	Purified water, Q, gal/day	0.2–14 million gal/day	$C_{BM} = 3.1\ Q$	Bare-module cost
Gas permeation	Membrane surface area, A, ft^2	—	$C_p = 51\ A$	Membrane module
Pervaporation	Membrane surface area, A, ft^2	—	$C_p = 43\ A$	Membrane module
Ultrafiltration	Membrane surface area, A, ft^2	—	$C_p = 10A$ to $25A$	Membrane cartridge
Mixers for powders, pastes, polymers, and doughs				
Kneaders, tilting double arm	Volume, V, ft^3	10–56 ft^3	$C_p = 2{,}041\ V^{0.58}$	Carbon steel
Kneaders, sigma double arm	Volume, V, ft^3	20–380 ft^3	$C_p = 18{,}705\ V^{0.60}$	Carbon steel
Muller	Volume, V, ft^3	10–380 ft^3	$C_p = 15{,}875\ V^{0.56}$	Carbon steel
Ribbon	Volume, V, ft^3	25–320 ft^3	$C_p = 2{,}438\ V^{0.60}$	Carbon steel
Tumblers, double cone	Volume, V, ft^3	50–270 ft^3	$C_p = 3{,}856\ V^{0.42}$	Carbon steel
Tumblers, twin shell	Volume, V, ft^3	35–330 ft^3	$C_p = 1{,}700\ V^{0.60}$	Carbon steel
Power-recovery turbines				
Gas expanders (pressure discharge)	Power extracted, P, Hp	20–5,000 Hp	$C_p = 600\ P^{0.81}$	Carbon steel
Gas expanders (vacuum discharge)	Power extracted, P, Hp	200–8,000 Hp	$C_p = 1{,}350\ P^{0.81}$	Carbon steel
Liquid expanders	Power extracted, P, Hp	150–2,000 Hp	$C_p = 1{,}590\ P^{0.70}$	Carbon steel
Screens				
Vibrating grizzlies	Surface area, A, ft^2	6–40 ft^2	$C_p = 6{,}575\ A^{0.34}$	Carbon steel
Vibrating screens, 1 deck	Surface area, A, ft^2	32–60 ft^2	$C_p = 1{,}588\ A^{0.71}$	Carbon steel
Vibrating screens, 2 decks	Surface area, A, ft^2	32–192 ft^2	$C_p = 1{,}395\ A^{0.78}$	Carbon steel
Vibrating screens, 3 decks	Surface area, A, ft^2	48–192 ft^2	$C_p = 1{,}010\ A^{0.91}$	Carbon steel
Size enlargement				
Disk agglomerators	Feed rate, F, lb/hr	800–80,000 lb/hr	$C_p = \exp\{10.8587 - 0.4915[\ln(F)] + 0.03648[\ln(F)]^2\}$	Carbon steel
Drum agglomerators	Feed rate, F, lb/hr	800–240,000 lb/hr	$C_p = \exp\{11.5525 - 0.5981\ [\ln(F)] + 0.04451\ [\ln(F)]^2\}$	Carbon steel
Pellet mills	Feed rate, F, lb/hr	800–80,000 lb/hr	$C_p = 7938\ F^{0.11}$	Carbon steel
Pug mill extruders	Feed rate, F, lb/hr	80–40,000 lb/hr	$C_p = \exp\{9.6126 - 0.01453[\ln(F)] + 0.01019[\ln(F)]^2\}$	Carbon steel
Screw extruders	Feed rate, F, lb/hr	8–800 lb/hr	$C_p = \exp\{10.9186 + 0.02099[\ln(F)]^2\}$	Carbon steel
Roll-type presses	Feed rate, F, lb/hr	8,000–140,000 lb/hr	$C_p = 130\ F^{0.59}$	Carbon steel
Tableting presses	Feed rate, F, lb/hr	800–8,000 lb/hr	$C_p = \exp\{9.2828 + 0.1050[\ln(F)] + 0.01885[\ln(F)]^2\}$	Carbon steel
Size reduction equipment				
Gyratory crushers	Feed rate, W, ton/hr	25–1,200 ton/hr	$C_p = 11{,}910\ W^{0.60}$	Includes motor and drive
Jaw crushers	Feed rate, W, ton/hr	10–200 ton/hr	$C_p = 2{,}610\ W^{0.89}$	Includes motor and drive
Cone crushers	Feed rate, W, ton/hr	20–300 ton/hr	$C_p = 2{,}041 W^{1.05}$	Includes motor and drive

Table 16.32 (*continued*)

Equipment Type	Size Factor (S)	Range of S	f.o.b. Purchase Cost Equation ($)	Notes
Side reduction equipment (continued)				
Hammer mills	Feed rate, W, ton/hr	2–200 ton/hr	$C_P = 4{,}310\ W^{0.78}$	Includes motor and drive
Ball mills	Feed rate, W, ton/hr	1–30 ton/hr	$C_P = 64{,}640\ W^{0.69}$	Includes motor and drive
Jet mills	Feed rate, W, ton/hr	1–5 ton/hr	$C_P = 38{,}560\ W^{0.39}$	Includes motor and drive
Solid-liquid separators				
Thickener, steel	Settling area, A, ft^2	80–8,000 ft^2	$C_P = 3{,}810\ A^{0.58}$	Carbon steel
Thickener, concrete	Settling area, A, ft^2	8,000–125,000 ft^2	$C_P = 2{,}720\ A^{0.58}$	Concrete
Clarifier, steel	Settling area, A, ft^2	80–8,000 ft^2	$C_P = 3{,}460\ A^{0.58}$	Carbon steel
Clarifier, concrete	Settling area, A, ft^2	8,000–125,000 ft^2	$C_P = 2{,}450\ A^{0.58}$	Concrete
Filters				
Plate and frame	Filtering area, A, ft^2	130–800 ft^2	$C_P = 5{,}445\ A^{0.52}$	Carbon steel
Pressure leaf	Filtering area, A, ft^2	30–2,500 ft^2	$C_P = 1{,}385\ A^{0.71}$	Carbon steel
Rotary-drum vacuum	Filtering area, A, ft^2	10–800 ft^2	$C_P = \exp\{11.796 - 0.1905[\ln(A)] + 0.0554[\ln(A)]^2\}$	Carbon steel
Rotary pan	Filtering area, A, ft^2	100–1,100 ft^2	$C_P = 28{,}010\ A^{0.48}$	Carbon steel
Wet classifiers (rake and spiral)	Solids feed rate, F, lb/hr	8,000–800,000 lb/hr	$C_P = 0.018\ F^{1.33}$	Carbon steel
Hydroclones	Liquid feed rate, Q, gal/min	8–1,200 gal/min	$C_P = 275\ Q^{0.5}$	Carbon steel
Centrifuges				
Batch top-drive vertical basket	Bowl diameter, D, in.	20–43 in.	$C_P = 2{,}270\ D^{0.95}$	Stainless steel
Batch bottom-drive vertical basket	Bowl diameter, D, in.	20–43 in.	$C_P = 975\ D^{1.00}$	Stainless steel
Vertical auto-batch	Bowl diameter, D, in.	20–70 in.	$C_P = 6{,}180\ D^{0.94}$	Stainless steel
Horizontal auto-batch	Bowl diameter, D, in.	20–43 in.	$C_P = 2{,}440\ D^{1.11}$	Stainless steel
Continuous reciprocating pusher	Tons solids/hr, S	1–20 tons solids/hr	$C_P = 170{,}100\ S^{0.30}$	Stainless steel
Continuous scroll solid bowl	Tons solids/hr, S	2–40 tons solids/hr	$C_P = 68{,}040\ S^{0.50}$	Stainless steel
Expression				
Screw presses	Wet solids flow rate, F, lb/hr	150–12,000 lb/hr	$C_P = \exp\{11.0991 - 0.3580[\ln(F)] + 0.05853\ [\ln(F)]^2\}$	Stainless steel
Roll presses	Wet solids flow rate, F, lb/hr	150–12,000 lb/hr	$C_P = \exp\{10.9807 - 0.4467[\ln(F)] + 0.06136[\ln(F)]^2\}$	Stainless steel
Solids-handling systems				
Bins	Volume, ft^3	10–100,000 ft^3	$C_P = 646\ S^{0.46}$	Carbon steel at atmospheric pressure
Feeders				
Belt	Volumetric flow rate, ft^3 /hr	120–500 ft^3/hr	$C_P = 813\ S^{0.38}$	Includes motor and belt drive
Screw	Volumetric flow rate, ft^3 /hr	400–10,000 ft^3/hr	$C_P = 1{,}094\ S^{0.22}$	
Vibratory	Volumetric flow rate, ft^3 /hr	40–900 ft^3/hr	$C_P = 46.6\ S^{0.90}$	Includes motor and belt drive

Conveyors				
Belt	Width, *W,* in. Length, *L,* ft	14–60 in., up to 300 ft	$C_P = 24.4\ WL$	Does not include motor or drive
Screw	Diameter, *D,* in. Length, *L,* ft	6–20 in., up to 300 ft	$C_P = 80\ DL^{0.59}$	Does not include motor, drive, lid, or jacket
Vibratory	Width, *W,* in. Length, *L,* ft	12–36 in., up to 100 ft	$C_P = 92.5\ W^{0.57}\ L^{0.87}$	Does not include motor or drive
Bucket elevators	Bucket width, *W,* in. height, *L,* ft	6–20 in., 15–150 ft	$C_P = 692\ W^{0.5}\ L^{0.57}$	Does not include motor or drive
Pneumatic conveyors	solids flow rate, *m,* lb/s equivalent length, *L,* feet	3–30 lb/s, 30–600 ft	$C_P = 17{,}240\ M^{0.63} L^{0.2}$	Includes blower, motor, piping, rotary valve, and cyclone
Storage tanks				
Open	Volume, *V,* gal	1,000–30,000 gal	$C_P = 18\ V^{0.73}$	Fiberglass
Cone roof	Volume, *V,* gal	10,000–1,000,000 gal	$C_P = 265\ V^{0.513}$	Carbon steel, pressure to 3 psig
Floating roof	Volume, *V,* gal	30,000–1,000,000 gal	$C_P = 475\ V^{0.507}$	Carbon steel, pressure to 3 psig
Spherical, 0–30 psig	Volume, *V,* gal	10,000–1,000,000 gal	$C_P = 68\ V^{0.72}$	Carbon steel
Spherical, 30–200 psig	Volume, *V,* gal	10,000–750,000 gal	$C_P = 53\ V^{0.78}$	Carbon steel
Gas holders	Volume, *V,* ft^3	4,000–400,000 ft^3	$C_P = 3{,}595\ V^{0.43}$	Carbon steel, pressure to 3 psig
Vacuum systems				
One-stage jet ejector	(lb/hr)/(suction pressure, torr)	0.1–100 lb/hr-torr	$C_P = 1{,}915\ S^{0.41}$	See Table 16.31 for multistage units and condensers
Liquid-ring pumps	Flow at suction, ft^3/min	50–350 ft^3/min	$C_P = 8{,}250\ S^{0.37}$	Stainless steel with sealant recirculation
Three-stage lobe	Flow at suction, ft^3 /min	60–240 ft^3/min	$C_P = 8{,}075\ S^{0.41}$	Includes intercoolers
Three-stage claw	Flow at suction, ft^3/min	60–270 ft^3/min	$C_P = 9{,}785\ S^{0.36}$	Includes intercoolers
Screw compressors	Flow at suction, ft^3/min	50–350 ft^3/min	$C_P = 10{,}875\ S^{0.38}$	With protective controls
Wastewater treatment				
Primary	Wastewater rate, *Q,* gal/min	75–75,000 gal/min	$C_P = 16{,}785\ Q^{0.64}$	Bare-module cost
Primary + Secondary	Wastewater rate, *Q,* gal/min	75–75,000 gal/min	$C_P = 48{,}760\ Q^{0.64}$	Bare-module cost
Primary + Secondary + Tertiary	Wastewater rate, *Q,* gal/min	75–75,000 gal/min	$C_P = 99{,}790\ Q^{0.64}$	Bare-module cost

may also be disinfected with chlorine, ozone, or ultraviolet light. Equations for typical investment costs for wastewater treatment are included in Table 16.32. These are bare-module costs rather than f.o.b. purchase costs.

16.7 EQUIPMENT COSTING SPREADSHEET

For the most widely used process equipment in Section 16.5, Professor Russell Dunn at Vanderbilt University created the EXCEL Equipment Costing Spreadsheet, which implements the equations that estimate purchase costs. This spreadsheet, Equipment Costing.xlsx, can be downloaded from the Program and Simulation Files folder on the Wiley Web site associated with this textbook.

After opening the spreadsheet, seek a brief set of instructions for its usage on the Title Page tab. Note that a separate tab is provided for each equipment type. Also, to see data and results for a typical example, download Equipment Costing Example.xlsx on the Wiley Web site associated with this textbook.

16.8 EQUIPMENT SIZING AND CAPITAL COST ESTIMATION USING ASPEN PROCESS ECONOMIC ANALYZER (APEA)

Aspen Process Economic Analyzer (APEA) is a software system provided by Aspen Technology, Inc., for evaluation of capital expenditures, operating costs, and the profitability of a process design. It can be accessed independently of or from within ASPEN PLUS. APEA has an automatic, electronic *expert system* that links to process simulation programs. It is used to (1) extend the results of process simulations, (2) generate size and cost estimates for processing equipment, (3) perform preliminary mechanical designs, and (4) estimate purchase and installation costs, indirect costs, the total capital investment, the engineering-procurement-construction planning schedule, and (5) perform profitability analyses. Section 16.8 places emphasis on items (1)–(4) but not item (5). Instead, in Chapter 17, Annual Costs, Earnings, and Profitability Analysis, Section 17.8 describes an EXCEL profitability analysis spreadsheet using total capital investment estimates generated with the methods in Sections 16.2–16.7 and with APEA. This spreadsheet, Profitability Analysis 4.0.xlsx, permits entry of capital-cost estimates in the format of Table 16.9 and the cost-sheet entries in Table 17.1. Note that APEA is often used to generate profitability analyses, but its entries are not closely aligned with the entries and default values in Tables 16.9 and 17.1.

When using a process simulator, the user can request that APEA accomplish items (1)–(5) after completing a simulation—adjusting simulation parameters and repeating the economic analysis. Alternatively, APEA can be used independently after completing a simulation run. In this section, only use with a process simulator is covered. Five key steps are necessary:

Step 1: ASPEN PLUS simulation results are *loaded* automatically into APEA.

Step 2: Process simulation units (that is, blocks, modules, or subroutines) are *mapped* into more descriptive models of process equipment (e.g., mapping a HEATX simulation unit into a floating-head, shell-and-tube heat exchanger, and mapping a RADFRAC simulation unit into a tray tower complete with reboiler, condenser, reflux accumulator) and associated *plant bulks*, which include installation items, such as piping, instrumentation, insulation, paint, and so on.

Step 3: Equipment items are *sized* and *re-sized* when modified.

Step 4: Capital costs, operating costs, and the total investment are *evaluated* for a project.

Step 5: Results are presented to be *reviewed*, with modifications as necessary and re-evaluation.

APEA accepts simulation results from ASPEN PLUS, ASPEN HYSYS, UniSim®Design, CHEMCAD, PRO/II, and other simulators. To estimate equipment sizes and costs with satisfactory accuracy, it is often necessary to augment the simulation file in two ways. First, to estimate equipment sizes, APEA requires estimates of mixture properties not needed for the material and energy balances or phase equilibria calculations. For this reason, the simulation report files are augmented (using built-in files) with estimates by the simulators of mixture properties, such as viscosity, thermal conductivity, and surface tension, for each of the streams in the simulation flowsheet. Second, when the simulator models (blocks) are not sufficiently detailed to permit APEA to obtain accurate equipment sizes and cost estimates, the designer replaces them with more rigorous models (blocks); for example, the approximate HEATER and RSTOIC models (blocks) in ASPEN PLUS are often replaced with more rigorous HEATX and RPLUG models (blocks). After the simulation file is augmented, the revised simulation is run and the results are sent to APEA.

This section presents estimates of equipment sizes and purchase and installation costs using APEA for two examples involving (1) a depropanizer distillation tower and (2) the monochlorobenzene (MCB) separation process introduced in Section 7.4. The details of using APEA for these two examples are presented in the file Aspen Process Economic Analyzer (APEA) Course Notes.pdf. on the Web site associated with this book.

Equipment Sizing and Costing in ASPEN PLUS Using Built-in APEA Features

When executing an ASPEN PLUS simulation, the user can request estimates of equipment sizes and costs using built-in default specifications. This is accomplished using the *Economics* tab on the ASPEN PLUS ribbon as shown in Figure 16.14.

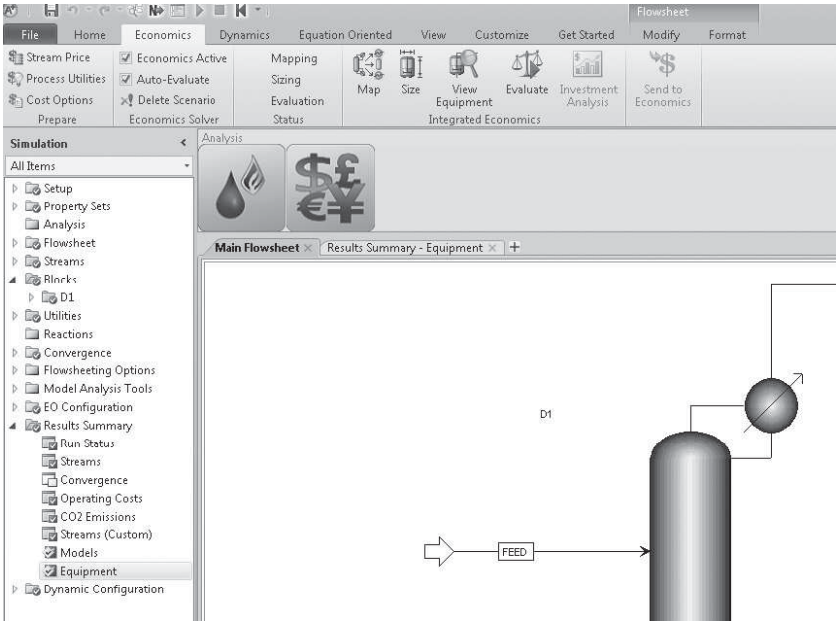

Figure 16.14 Economics tab in the ASPEN PLUS ribbon. (*Source:* Reprinted with permission by Aspen Tech).

Several options are possible. Here, the *Economics Active* checkbox is checked, indicating that after the simulation is completed, costing (and sizing) is to be achieved without leaving ASPEN PLUS. This permits the economics to be recalculated when simulation parameters are updated. Note that when not checked, the *Send to Economics* icon is active and control is transferred out of ASPEN PLUS to APEA.

After the *Economics Active* checkbox is checked, the *Map* icon is clicked. Then, the process simulation units (i.e., blocks, modules, or subroutines) are mapped into more descriptive models of the process equipment (e.g., mapping a RADFRAC simulation unit into a tray tower, condenser, reflux accumulator, and so on) and associated *plant bulks*, which include installation items such as piping, instrumentation, insulation, paint, and so on. Note that during mapping, the default equipment types can be altered. For the details about mapping, see the Aspen Process Economic Analyzer (APEA) Course Notes.pdf file on the Web site associated with this book.

After the mapping is completed, click the *Size* icon to obtain equipment sizes using the default equipment parameters (e.g., default tray spacing). Then, click the *View Equipment* icon to display the *Results Summary-Equipment* form, which contains the equipment parameters that can be adjusted. Once you have adjusted the parameters, you can view the updated sizes/costs by clicking the *Evaluate* button. Note that clicking the size or evaluate buttons in the *Results Summary-Equipment* form does not update the costs and sizes (for Version 8.2 and earlier versions). You can export the *Result Summary-Equipment* form to EXCEL by clicking the *Send to Excel* button in the form. The *Aspen Summary Grid* dialog box appears. Click the *Export tables to Excel* button and choose a name for the EXCEL file. The tab containing sizing information for the tray tower is shown in Figure 16.15.

Although you can add equipment during the mapping process, you may not be able to edit its connectivity. For the depropanizer example, for instance, you are not able to modify the RADFRAC block to include a reboiler pump between the tower and the reboiler. Therefore, all information for the added pump must be entered manually.

If you would like ASPEN PLUS to update cost and size estimates every time you run the simulation, check the *Auto-Evaluate* check box.

For more detailed equipment costing, after the costs are evaluated, click on the *Investment Analysis* icon. This generates an EXCEL workbook similar to the one obtained in APEA (when you click the *Evaluate Project* icon in APEA ribbon and choose to view the results as a spreadsheet (under *Tools-Options-View Spreadsheets in Excel*). The workbook has 10 worksheets: *Equipment, Utility Summary, Project Summary, Executive Summary, Utility Resource Summary, Product Summary, Cash Flow, Raw Material*, and *Run Summary*. Of particular interest is the *Equipment* worksheet in the EXCEL workbook. This worksheet contains details about the direct and installed costs and weights. A screen capture of the *Equipment* worksheet is shown in Figure 16.16.

Note that the stream splitters and mixers are not sized and/or costed by ASPEN PLUS as they are treated as *Quoted equipment*. The costs and weights above are based on ASPEN PLUS defaults.

When using the *Economics Tab* in ASPEN PLUS, it is not possible to choose a *Standard Basis* for the equipment size/cost evaluation. Note that the default project type is *Grass roots/Clear field*. To change the *Standard Basis* and other defaults, use the *Send to Economics* icon in the ASPEN PLUS ribbon to export the simulation results to APEA.

In the next two examples, equipment sizing and costing were performed using APEA. For more details about the procedure, please consult Aspen Process Economic Analyzer (APEA) Course Notes.pdf file available on the Web site associated with this book.

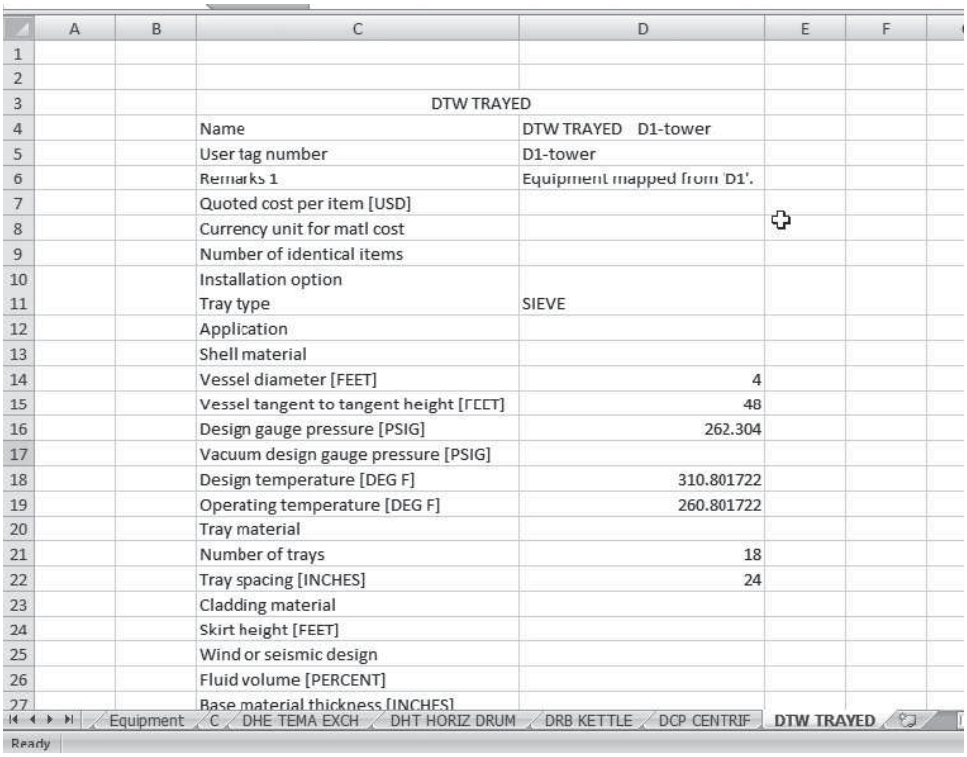

	DTW TRAYED	
Name	DTW TRAYED D1-tower	
User tag number	D1-tower	
Remarks 1	Equipment mapped from 'D1'.	
Quoted cost per item [USD]		
Currency unit for matl cost		
Number of identical items		
Installation option		
Tray type	SIEVE	
Application		
Shell material		
Vessel diameter [FEET]	4	
Vessel tangent to tangent height [FEET]	48	
Design gauge pressure [PSIG]	262.304	
Vacuum design gauge pressure [PSIG]		
Design temperature [DEG F]	310.801722	
Operating temperature [DEG F]	260.801722	
Tray material		
Number of trays	18	
Tray spacing [INCHES]	24	
Cladding material		
Skirt height [FEET]		
Wind or seismic design		
Fluid volume [PERCENT]		
Base material thickness [INCHES]		

Figure 16.15 Default tray tower parameters.

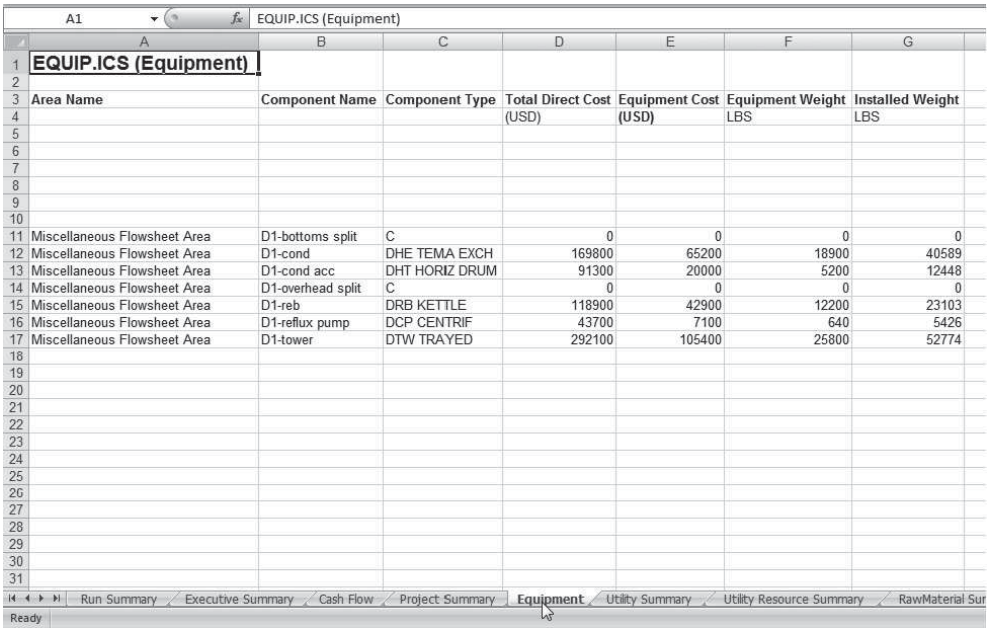

EQUIP.ICS (Equipment)

Area Name	Component Name	Component Type	Total Direct Cost (USD)	Equipment Cost (USD)	Equipment Weight LBS	Installed Weight LBS
Miscellaneous Flowsheet Area	D1-bottoms split	C	0	0	0	0
Miscellaneous Flowsheet Area	D1-cond	DHE TEMA EXCH	169800	65200	18900	40589
Miscellaneous Flowsheet Area	D1-cond acc	DHT HORIZ DRUM	91300	20000	5200	12448
Miscellaneous Flowsheet Area	D1-overhead split	C	0	0	0	0
Miscellaneous Flowsheet Area	D1-reb	DRB KETTLE	118900	42900	12200	23103
Miscellaneous Flowsheet Area	D1-reflux pump	DCP CENTRIF	43700	7100	640	5426
Miscellaneous Flowsheet Area	D1-tower	DTW TRAYED	292100	105400	25800	52774

Figure 16.16 Equipment worksheet in EXCEL workbook.

EXAMPLE 16.19 ***Depropanizer***

The depropanizer distillation tower in Figure 16.17 is designed and simulated using ASPEN PLUS as follows. First, for the pressures shown, using the DSTWU subroutine for the specification, $R = 1.75R_{min}$, the reflux ratio, number of equilibrium stages, and the feed stage are estimated to be $R = 6.06$, $N = 14$, and $N_{Feed} = 7$, respectively. When the tower is simulated with these specifications and $D/F = 0.226$, to achieve the desired distillate purity, the RADFRAC model (block, subroutine) adjusts the reflux ratio to 8.88. In this example, it is desired to estimate the total permanent investment, C_{TPI}, using APEA. The material of construction is A515 Carbon Steel for the tower and A285C Steel for the condenser, reboiler, reflux accumulator, and pumps. Note that these are default materials. For the details about specifying the materials of construction, see the Aspen Process Economic Analyzer (APEA) Course Notes.pdf file on the Wiley Web site associated with this textbook.

SOLUTION

For the depropanizer system, APEA performs mechanical designs and estimates sizes, purchase costs, and associated installation materials and labor costs for the distillation tower, condenser, reflux accumulator, reflux pump, and reboiler. The designer can add a reboiler pump (to pump liquid from the sump to the reboiler) as was done in obtaining this solution. APEA uses many parameters to estimate equipment sizes and to specify the characteristics of utilities with built-in defaults that can be replaced by user-specified values. Particular attention should be paid to APEA *Design Basis* parameters, such as the design pressure and temperature, the overdesign allowances, the residence times in the process vessels, and the tower specifications. Changes can be made to the default parameters, including the tray efficiency, bottom sump height, vapor disengagement height, and others. The default parameters are listed in Appendix II of the file, Aspen Process Economic Analyzer (APEA) Course Notes.pdf.

For the condenser, APEA uses the cooling water utility. However, its default inlet and outlet temperatures were changed from 75 and 95°F to 90 and 120°F. Also, APEA has three built-in utilities for steam at 100, 165, and 400 psia. Because 100 psia steam condenses at 377.8°F and the bubble-point temperature of the bottoms product at 252 psia is 260.8°F, when 100 psia steam is used in the reboiler, $\Delta T = 117$°F, which often results in undesirable film boiling as discussed in Section 12.1. To reduce the approach temperature difference, and ensure nucleate boiling, a low-pressure steam utility at 50 psia is defined.

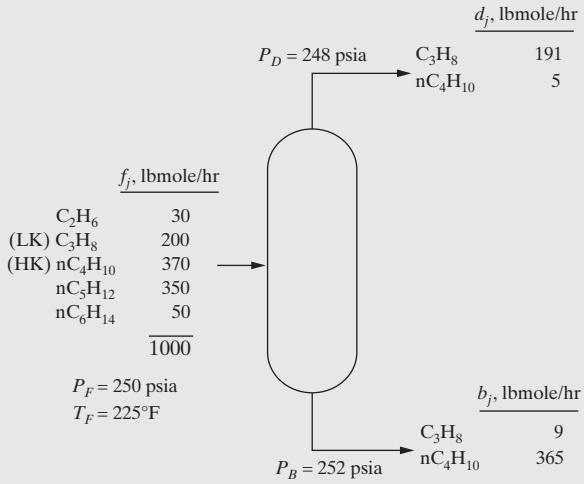

Figure 16.17 Specifications for design of the depropanizer distillation tower.

After the parameters for estimating equipment sizes and the utility parameters are adjusted and a new steam utility is defined, the simulation units (blocks, modules, or subroutines) are *mapped* into APEA. In this case, there is only one distillation unit, D1, to be mapped. The default mapping results in (1) a tray tower, (2) TEMA shell-and-tube heat exchanger, (3) a horizontal drum for the reflux accumulator, (4) a centrifugal reflux pump, and (5) a kettle reboiler with U tubes. To use a kettle reboiler with a floating head one of the other built-in reboilers, the default mapping (U-tube reboiler) is changed to the preferred mapping. The default mapping for the condenser in this example is the TEMA shell-and-tube heat exchanger. When the mapping for the simulation unit, D1, is completed, sizes have been estimated by APEA for all of the equipment items. Note that for this distillation system, a reboiler pump is added by the designer and mapped separately by APEA. Note also that the equipment sizes can be adjusted by the designer before APEA estimates equipment costs. Custom sizes can be entered or sizing parameters are entered and APEA does the sizing based on the parameters. This was done for the distillation tower in the course notes.

In the next step, APEA estimates the purchase and installation costs. Before proceeding, the designer can (1) apply one of six engineering contractor profiles, which determine the engineering execution procedure and (2) adjust the *standard basis*, which defines the nature of the site and workforce. Here, the default values may correspond to inappropriate costs for the following reasons. When designing small plants, the *Plant Engineer* or *Local Contractor* profiles are preferable. For this distillation system, which is added to a large plant complex, it is important to replace the default *project type* (*grass roots/clear field*) with *plant addition—suppressed infrastructure*. The latter instructs APEA to omit items involving electrical switchgear and transformers, which are not needed when adding this distillation system to an existing process facility. After the standard basis has been adjusted, APEA *evaluates* all of the equipment items in the project. During the evaluation, purchase and installation costs are estimated. For this purpose, APEA utilizes design, work-item, and cost models that have been developed and updated annually in accordance with industry design codes and costs for numerous process plants since the mid-1970s. Given the broad spectrum of APEA users worldwide, APEA purchase cost estimates are based upon an extensive database of material and construction labor costs and detailed, although preliminary, design methods.

For installation costs, APEA does *not* use bare–module factors as discussed in Section 16.3. Rather, rigorous methods are used to estimate the costs of materials, labor, and construction equipment. These methods are based upon detailed design calculations for foundations, platforms, piping, instrumentation, electrical connections, insulation, and painting, among other items involved in the installation. For example, for concrete foundations, the dimensions of the foundation and the amount of concrete are estimated based upon the height and weight of the tower, soil conditions, wind velocity, and seismic zone. For piping and instrumentation types, quantities, and sizes, APEA uses self-contained, user-adjustable, P&ID templates that are unique to each type of equipment. APEA uses its library of piping and instrumentation models, mechanical design methods, and equipment and stream information, to develop lists of materials for piping and

Table 16.33 APEA Estimates of Equipment Sizes, Purchase Costs, and Direct Materials and Labor Costs for Installation of the Depropanizer Distillation Complex

	Equipment Sizes	Purchase Cost, C_P, $	Direct Materials and Labor Cost, C_{DML}, $
Tray tower			
	No. of trays = 15	$ 91,400	$271,700
	Tangent-to-tangent height = 42 ft		
	Diameter = 4 ft		
	Vessel weight = 22,100 lb		
Condenser			
	Heat-transfer area =11,100 ft^2 (5,550 ft^2/shell)	242,700	407,400
Reflux accumulator			
	Volume = 1,175 gal	20,000	91,300
	Diameter = 4 ft		
	Length =12.5 ft		
	Vessel weight = 5,200 lb		
Reflux pump			
	Fluid head = 225 ft	7,100	43,700
	Driver power = 20 Hp		
Reboiler			
	Heat-transfer area = 3,580 ft^2	94,900	176,100
Reboiler pump			
	Fluid head = 20 ft	6,700	49,500
	Driver power = 3 Hp		
	TOTAL	$462,800	$1,039,700

```
                    LICENSED FOR USE BY **                                                          14
                                          PROJECT:
                     0201    Miscellaneous Flowsheet  -  Miscellaneous Flowsheet
                                    C O M P O N E N T    L I S T

=============================================================================================================================
:          :          :                          :                                                          : PURCHASED:
: ORIGIN   :ITEM TYPE :          I T E M           :---------------------- D E S I G N   D A T A ----------------------: EQUIPMENT:
:          :          :  D E S C R I P T I O N   :                                                          : COST USD :
=============================================================================================================================
 Equipment mapped from 'D1'.
 TW -    28 TRAYED      D1-tower                   Shell material                        A 516                          91400
                        CODE OF ACCOUNT:     111  Number of trays                         15
                        TAG NO.: D1-tower         Vessel diameter                       4.000 FEET
                                                  Vessel tangent to tangent height      42.00 FEET
                                                  Design temperature                   310.80 DEG F
                                                  Design gauge pressure                262.30 PSIG
                                                  Application                          DISTIL
                                                  Tray type                            SIEVE
                                                  Tray spacing                          24.00 INCHES
                                                  Tray material                         A285C
                                                  Tray thickness                        0.188 INCHES
                                                  Base material thickness               0.563 INCHES
                                                  Total weight                          22100 LBS

                    I T E M          :--- M A T E R I A L ---:********* M A N P O W E R *********:--- L/M ---:
                                     :                FRACTION :                FRACTION          :   RATIO   :
                                     :     USD         OF PE   :       USD       OF PE  MANHOURS  : USD/USD  :
                    EQUIPMENT&SETTING:    91400.      1.0000  :       1919.     0.0210        63  :    0.021  :
                    PIPING           :    36837.      0.4030  :      20304.     0.2221       682  :    0.551  :
                    CIVIL            :     2239.      0.0245  :       3276.     0.0358       135  :    1.463  :
                    STRUCTURAL STEEL :    11392.      0.1246  :       2031.     0.0222        73  :    0.178  :
                    INSTRUMENTATION  :    52922.      0.5790  :      23188.     0.2537       760  :    0.438  :
                    ELECTRICAL       :     1902.      0.0208  :       1103.     0.0121        38  :    0.580  :
                    INSULATION       :    10658.      0.1166  :       8942.     0.0978       396  :    0.839  :
                    PAINT            :     1062.      0.0116  :       2508.     0.0274       112  :    2.361  :
                                     ----------------------------------------------------------------------------
                    SUBTOTAL         :   208412.      2.2802  :      63271.     0.6922      2259  :    0.304  :
                    TOTAL MATERIAL AND MANPOWER COST    =USD    271700.   INST'L COST/PE RATIO =  2.973

=============================================================================================================================
```

Figure 16.18 Estimates of equipment sizes and purchase and installation costs for the depropanizer tray tower.

instruments with associated material costs and installation hours. Consequently, the installation cost estimates by APEA are more accurate than those obtained using bare-module or factored-cost methods.

For the six equipment items in the depropanizer distillation system, including the added reboiler pump, the key equipment sizes and cost estimates are shown in Table 16.33. Note that APEA designed the condenser to be a TEMA shell-and-tube heat exchanger with two parallel units, each having one tube pass and a correction factor, $F_T = 0.64$. It should be possible to improve this design by resizing the unit to obtain a correction factor close to unity, eliminating one of the parallel units. Figure 16.18 shows more details for the tray tower from the *Capital Estimate Report*. With specifications of tray efficiency at 0.8, tray spacing at 2 ft, bottom-sump height at 10 ft, and a vapor disengagement region at 4 ft, APEA sized the tower to have a diameter of 4 ft, a tangent-to-tangent height of 42 ft, 15 trays, and installed weight of 22,100 lb. Details about other equipment items are contained in the Aspen Process Economic Analyzer (APEA) Course Notes.pdf. APEA chose the default tray type to be sieve, default shell material to be A516, and default tray material to be A285C.

For details of the other equipment items, see Appendix III of the file, Aspen Process Economic Analyzer (APEA) Course Notes.pdf. Also, the DEC3RP folder (in the Program and Simulation Files folder on the Wiley Web site associated with this book) can be accessed to recompute these results at a later date. Note that the DEC3 folder does not include the reboiler pump. The calculations were carried out using APEA, Version 8.2, with the design and cost basis date being the First Quarter of 2012.

Total Permanent Investment

APEA also computes the total permanent investment, C_{TPI}, as defined in Table 16.9. However, here, the total permanent investment is computed by the spreadsheet, Profitability Analysis-4.0.xls, which is discussed in Section 17.8. When using APEA option in the spreadsheet, the user enters the following values, which are obtained from APEA:

Total direct materials and labor costs	$1,161,800
Material and labor G&A overhead and contractor fees	90,700
Contractor engineering costs	553,400
Indirect costs	361,400

Note that the total direct materials and labor costs, $1,161,800, includes items not chargeable to the individual equipment items in Table 16.33. For the details of obtaining these values from APEA, see the file, Aspen Process Economic Analyzer (APEA) Course Notes.pdf.

EXAMPLE 16.20 *Monochlorobenzene (MCB) Separation Process*

The monochlorobenzene (MCB) separation process in Figure 16.19 is designed and simulated using the procedures described in Section 7.4. In this example, it is desired to estimate the total permanent investment, C_{TPI}, using APEA.

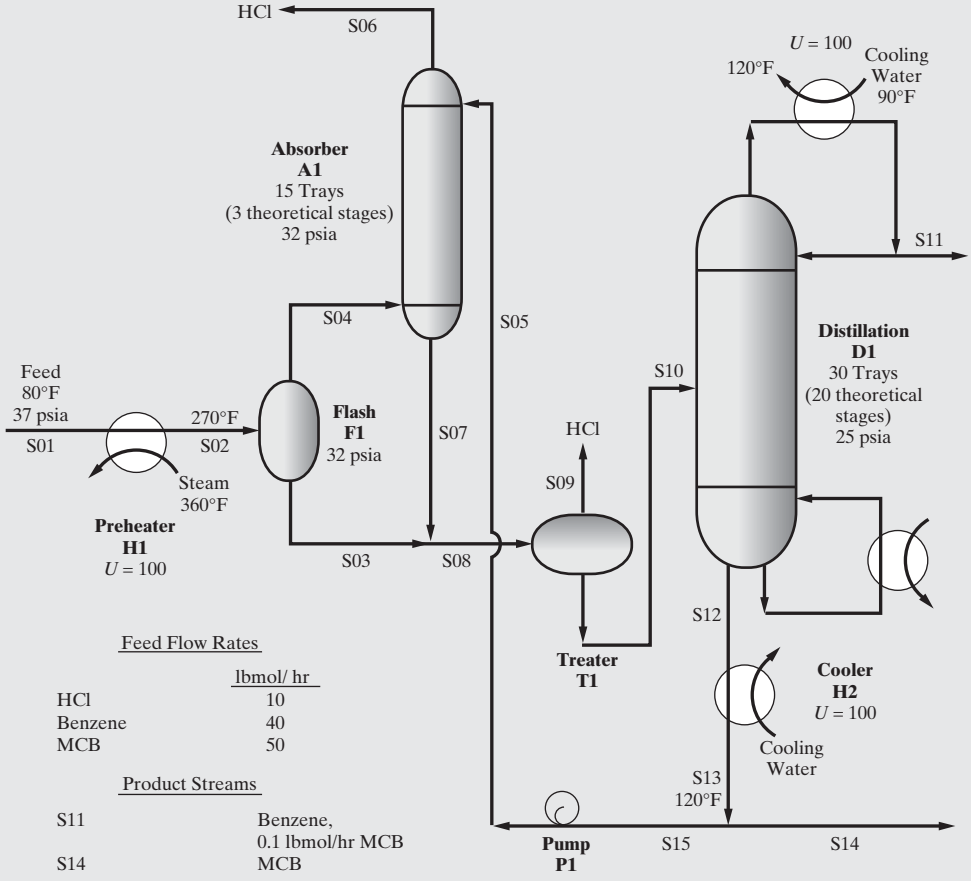

Figure 16.19 Process flowsheet for the MCB separation process.

SOLUTION

The simulation results were computed initially using the DISTL model (block) in ASPEN PLUS. When this is replaced by the RADFRAC model (block), the reflux ratio is adjusted from 4.29 to 3.35 and the stream flow rates differ slightly (< 1%).

Because the absorber has a tray efficiency of 20% and the tray efficiency of the distillation column is 60%, the two towers must be resized after mapping. Finally, the units M1 (for the stream mixer), S1 (for the stream splitter), and T1 are mapped as *Quoted equipment* having zero cost. Note these unit names appear on the simulation flowsheet in Section 7.4 (Figure 7.22).

After the mapping and sizing are completed (i.e., the equipment sizes are computed), as for the depropanizer in Example 16.19, the MCB separation process can be viewed as representing an addition to an existing plant. Consequently, the standard basis is selected as *plant addition—suppressed infrastructure*. This is because a full *grass roots/clear field* installation would provide an unnecessary supporting power distribution substation and control system equipment for this small separation plant, which typically would be supported as a neighboring facility but not built as a separate entity. After the standard basis has been adjusted, APEA *evaluates* all of the equipment items in the mapping. During the evaluation, purchase and installation costs are estimated. For 10 equipment items, the key equipment sizes and cost estimates are shown in Table 16.34 with details of the equipment items provided in Appendix IV of the file, Aspen Process Economic Analyzer (APEA) Course Notes.pdf. Also, the MCB folder (in the ASPEN folder on the Wiley Web site associated with this book) can be accessed to recompute these results at a later date. The calculations were carried out using APEA, Version 8.2, with the design and cost basis date being the First Quarter 2012.

Table 16.34 Equipment Sizes and Purchase Costs for the MCB Separation Process

	Equipment Sizes	Purchase Cost, C_P, $	Direct Materials and Labor Cost, C_{DML}, $
Tray tower, D1			
	No. of trays = 30	$ 111,200	$ 296,100
	Tangent-to-tangent height = 72 ft		
	Diameter = 3 ft		
	Vessel weight = 23,700 lb		
Condenser, D1			
	Heat-transfer area =129 ft^2	11,000	61,200
Reflux accumulator, D1			
	Liquid volume = 212 gal	10,500	75,000
	Diameter = 3 ft		
	Length = 4 ft		
	Vessel weight = 1,400 lb		
Reflux pump, D1			
	Fluid head = 225 ft	5,100	33,100
	Driver power = 3.0 Hp		
Reboiler, D1			
	Heat-transfer area = 923 ft^2	33,900	101,900
Absorber, A1			
	No. of trays = 15	39,700	177,800
	Tangent-to-tangent height = 42 ft		
	Diameter = 1.5 ft		
	Vessel weight = 6,000 lb		
Flash vessel, F1			
	Liquid volume = 635 gal	15,100	105,900
	Diameter = 3 ft		
	Length = 12 ft		
	Vessel weight = 2,600 lb		
Heat exchanger, H1			
	Heat-transfer area = 58 ft^2	8,800	59,300
Heat exchanger, H2			
	Heat-transfer area = 134 ft^2	11,100	62,000
Pump, P1			
	Fluid head = 62.4 ft	3,900	31,800
	Driver power = 1.5 Hp		
	TOTAL	$250,300	$1,004,100

Total Permanent Investment

APEA also computes the total permanent investment. However, in this textbook, the total permanent investment is computed by the spreadsheet, Profitability Analysis-4.0.xls, which is discussed in Section 17.8. When using APEA option in the spreadsheet, the user enters the following values, which are obtained from APEA:

Total direct materials and labor costs	$1,183,100
Material and labor G&A overhead and contractor fees	102,500
Contractor engineering costs	839,200
Indirect costs	525,400

Note that the total direct materials and labor costs, $1,183,100, includes items not chargeable to the individual equipment items in Table 16.34. For the details of obtaining these values from APEA, see the file, Aspen Process Economic Analyzer (APEA) Course Notes.pdf.

16.9 SUMMARY

Having completed this chapter and some of the associated exercises, the reader should:

1. Be able to assess the financial condition of a company by applying financial ratio analysis to data given in its annual report.
2. Be able to estimate the purchase costs of equipment items using the provided equations and cost indexes to update those costs.
3. Be able to estimate each of the other costs included in the capital cost of a plant and apply the concept of the bare-module cost.
4. Be able to estimate the total capital investment of a plant by using three methods of increasing complexity that range from order-of-magnitude to preliminary estimates.
5. Be able to use the Aspen Process Economic Analyzer (APEA) provided by Aspen Technology, Inc., to prepare a more definitive estimate of capital costs—one that uses regularly updated purchase costs and provides detailed estimates of installation costs for all process units. Also, be able to use APEA to carry out economic analysis when carrying out a process simulation (e.g., using ASPEN PLUS and Aspen HYSYS).

REFERENCES

1. Bauman, H. C., *Fundamentals of Cost Engineering in the Chemical Industry*, Reinhold (1964).

2. Busche, R. M., *Venture Analysis: A Framework for Venture Planning—Course Notes*, Bio-en-gene-er Associates, Wilmington, Delaware (1995).

3. Chilton, E. H., *Chemical Engineering*, **56**(6), 97–106 (1949).

4. Corripio, A. B., K. S. Chrien, and L. B. Evans, "Estimate Costs of Centrifugal Pumps and Electric Motors," *Chem. Eng.*, **89**, 115–118 (1982a).

5. Corripio, A. B., K. S. Chrien, and L. B. Evans, "Estimate Costs of Heat Exchangers and Storage Tanks via Correlations," *Chem. Eng.*, **89**,125–127 (1982b).

6. Feldman, R. P., "Economics of Plant Startups," *Chem. Eng.*, **76**, 87–90 (1969).

7. Garrett, D. E., *Chemical Engineering Economics*, Van Nostrand-Rineholt, New York (1989).

8. Green, D. W., and R. H. Perry (eds.), *Perry's Chemical Engineers' Handbook*, 8th ed., McGraw-Hill, New York (2008).

9. Guthrie, K. M., "Data and Techniques for Preliminary Capital Cost Estimating," *Chem. Eng.*, **76**, 114–142 (1969).

10. Guthrie, K. M., "Capital and Operating Costs for 54 Chemical Processes," *Chem. Eng.*, **77**(13), 140 (1970).

11. Guthrie, K. M., *Process Plant Estimating, Evaluation, and Control*, Craftsman, Solano Beach, California (1974).

12. Hall, R. S., J. Matley, and K. J. McNaughton, *Chemical Engineering*, **89**(7), 80–116 (1982).

13. Hand, W. E., "From Flow Sheet to Cost Estimate," *Petroleum Refiner*, **37**(9), 331–334 (1958).

14. Haselbarth, J. E., "Updated Investment Cost for 60 Types of Chemical Plants," *Chem. Eng.*, **74**(25), 214–215 (1967).

15. Hill, R. D., "What Petrochemical Plants Cost," *Petroleum Refiner*, **35**(8), 106–110 (1956).

16. Lang, H. J., "Engineering Approach to Preliminary Cost Estimates," *Chem. Eng.*, **54**(9), 130–133 (1947a).

17. Lang, H. J., "Cost Relationship in Preliminary Cost Estimation," *Chem. Eng.*, **54**(10), 117–121 (1947b).

18. Lang, H. J., "Simplified Approach to Preliminary Cost Estimates," *Chem. Eng.*, **55**(6), 112–113 (1948).

19. Mills, H. E., *Chemical Engineering*, **71**(6), 133 (1964).

20. Mulet, A., A. B. Corripio, and L. B. Evans, "Estimate Costs of Pressure Vessels via Correlations," *Chem. Eng.*, **88**(20), 145–150 (1981a).

21. Mulet, A., A. B. Corripio, and L.B. Evans, "Estimate Costs of Distillation and Absorption Towers via Correlations," *Chem. Eng.*, **88**(26), 77–82 (1981b).

22. Papanastasiou, T. C., *Applied Fluid Mechanics*, Prentice-Hall, Englewood Cliffs, New Jersey (1994).

23. Peters, M. S., K. D. Timmerhaus, and R. E. West, *Plant Design and Economics for Chemical Engineers*, 5th ed., McGraw-Hill, New York (2003).

24. Pikulik, A., and H. E. Diaz, *Chemical Engineering*, **84**(21), 107–116 (1977).

25. Ryans, J., and J. Bays, "Run Clean with Dry Vacuum Pumps," *Chem. Eng. Prog.*, **97**(10), 32–41 (2001).

26. Sandler, H. J., and E. T. Luckiewicz, *Practical Process Engineering*, McGraw-Hill, New York (1987).

27. Turton, R., R. C. Bailie, W. B. Whiting, and J. A. Shaeiwitz, *Analysis, Synthesis, and Design of Chemical Processes*, 2nd ed., Prentice Hall, Upper Saddle River, New Jersey (2003).

28. Ulrich, G. D., *A Guide to Chemical Engineering Process Design and Economics*, John Wiley, New York (1984).

29. Ulrich, G. D., and P. T. Vasudevan, *Chemical Engineering Process Design and Economics—A Practical Guide*, 2nd ed., Process Publishing, Lee, New Hampshire (2004).

30. Walas, S. M., *Chemical Process Equipment*, Butterworth, London (1988).

31. Walas, S. M., and C. D. Spangler, *Chemical Engineering*, **67**(6), 173–176, (1960).

32. Williams, R., "Standardizing Cost Data on Process Equipment," *Chem. Eng.*, **54**(6), 102, (1947a).

33. Williams, R., "Six-Tenths Factor Aids in Approximating Costs," *Chem. Eng.*, **54**(12), 124–125 (1947b).

34. Woods, D. R., *Financial Decision Making in the Process Industry*, Prentice-Hall, Englewood Cliffs, New Jersey (1975).

EXERCISES

16.1 On the Internet, find a recent annual report for the company Merck & Co., Inc. Based on information in that report, determine the following:

(a) The nature of the business of Merck.

(b) The new developments by Merck.

(c) The new acquisitions or partnerships if any.

(d) Stated concerns of the company.

(e) A financial ratio analysis, including:

- **(1)** Current ratio.
- **(2)** Acid-test ratio.
- **(3)** Equity ratio.
- **(4)** Return on total assets.
- **(5)** Return on equity.
- **(6)** Operating margin.
- **(7)** Profit margin.

(f) Your stock purchase recommendation, including reasons for buying or selling the stock.

16.2 At the beginning of the year 2013, Company XYZ had an inventory of 8,000 widgets with a unit cost of $6.00. During that year, the following purchases of widgets were made:

Month of Purchase	Number of Units	Unit Cost ($)
February	10,000	$7.00
May	5,000	$8.00
June	15,000	$9.00
August	25,000	$10.00
November	20,000	$10.50

At the end of 2013, the number of units in the inventory was 2,900. Use both the FIFO and LIFO methods to determine the cost of goods sold for 2013.

16.3 Based upon the following data for the reactors, compressors/expanders, and distillation columns of a plant to produce 1,500 metric ton/day of methanol with an operating factor of 0.95, estimate by using Method 1 (order-of-magnitude estimate) the total capital investment. The two methanol reactors are of the shell-and-tube type. The plant will be constructed outdoors and is a major addition to existing facilities. Use a CE cost index of 600.

Equipment	Size	Material	Pressure (kPa)	Temperature (°C)
Steam reformer	620 million Btu/hr	316 ss	2,000	350
2 Methanol reactors	Each with 4,000 1.5-in. o.d. tubes by 30-ft long on 2.25-in. triangular pitch	cs shell 316 ss tubes	6,000	320
Reformed gas centrifugal compressor	16,000 kW	cs	6,000	200
Recycle gas centrifugal compressor	5,000 kW	cs	6,000	200
Tail-gas expander	4,500 kW	cs	6,000	200
Light ends tower	3-ft diameter 60 sieve trays	ss	500	200
Finishing tower	18-ft diameter 80 sieve trays	ss	200	200

Note: ss = stainless steel, cs = carbon steel

16.4 The feed to a sieve-tray distillation column operating at 1 atm is 700 lbmol/hr of 45 mol% benzene and 55 mol% toluene at 1 atm with a bubble-point temperature of 201°F. The distillate contains 91.6 mol% benzene and boils at 179.4°F. The bottoms product contains 94.6 mol% toluene and boils at 226.6°F. The column has 23 trays spaced 18 in. apart, and its reflux ratio is 1.25. Column pressure drop is neglected. Estimate the total bare-module cost of the column, condenser, reflux accumulator, combined reflux and distillate pump, reboiler, and reboiler pump. Also, estimate the total permanent investment using either the Lang or Guthrie methods. Compute the results using (1) the equations in Sections 16.5 and 16.6 (possibly using the Equipment Costing.xlsx spreadsheet in Section 16.7), and/or APEA. Compare the results.

Data

Overall U of total condenser = 100 Btu/hr-ft^2-°F

Cooling water from 90°F to 120°F

Reboiler heat flux to avoid film boiling = 12,000 Btu/hr-ft^2

Reflux accumulator residence time = 5 min at half full.

$L/D = 2$.

Centrifugal pump pressure rise = 100 psi (for each pump).

Suction pressure = 1 atm.

Use sieve trays with $A_h/A_a = 0.1$.

Calculate the flooding velocity of the column using the procedure in Example 13.3. Use 35% of the flooding velocity to determine the column diameter.

Saturated steam is available at 60 psia.

Notes

The file BENTOLDIST.bkp is included in the Program and Simulation Files folder, which can be downloaded from the Wiley Web site associated with this book. It contains the simulation results using the RADFRAC subroutine in ASPEN PLUS. This file should be used to determine the physical properties, flow rates, and heat exchanger duties needed for the above calculations. Also, the file should be used to prepare the report file for APEA. Note that the simulation was carried out using 18 trays at 100% efficiency. When using APEA, set the tray efficiency to 80% and APEA will adjust the number of trays to 23.

Since APEA does not size and cost a bottoms pump, a centrifugal pump should be added.

APEA estimates the physical properties and heat-transfer coefficients. Do not adjust these.

In APEA, reset the temperatures of cooling water (90°F to 120°F) and add a utility for 60 psia steam. Use the steam tables to estimate the physical properties.

Use a kettle reboiler with a floating head.

APEA sizes the tower using a 24-in. tray spacing as a default. After sizing (mapping) is complete, adjust the tray spacing to 18 in. Note that the height of the tower must be adjusted accordingly.

Note that APEA estimates the *Direct Material and Manpower* for each equipment item. These are also referred to as the cost of direct materials and labor, $C_{DML} = C_P + C_M + C_L$.

16.5 Figure 16.20 shows a system designed to recover argon from the purge stream in an ammonia synthesis plant. Estimate the total bare-module cost associated with the addition of this argon recovery system to an existing plant. Assuming no allocated costs for utilities and related facilities, estimate the direct permanent investment, the total depreciable capital, and the total permanent investment for the process. Include only the equipment shown in the flowsheet and specified below. Use CE = 600.

Equipment Specifications

Molecular sieve adsorbers (ignore packing):

	Al	A2
Diameter (ft)	10	10
Height (ft)	7	7
Pressure (psia)	2,000	1,000
Material	ss	ss

Absorber and distillation columns:

	ABl	Dl	D2
Material	ss	ss	ss
Diameter (ft)	2	3.5	1.7
Height (ft)	45	50	15
Pressure (psia)	1,000	70	14.7
No. of trays	40	45	12
Tray spacing (ft)	1	1	1
Tray type	Sieve	Sieve	Sieve

Heat exchangers, reboilers, and condensers

	El	E2	E3	E4	E5	E6	E7
Area (ft^2)	993	401	891	2,423	336	2,828	55
Pressure (psia)	1,000	1,000	1,000	70	70	14.7	14.7

El, E2, E3, E4, and E6 are shell-and-tube, floating-head, stainless steel heat exchangers.

E5 and E7 are stainless steel kettle reboilers.

Compressors:

	CI	C2
Type	Centrifugal	Centrifugal
Material	ss	ss
Efficiency (%)	80	80
Hydraulic horsepower (theoretical work)	122.4	130.4

Turbine (Tl)

Type	**Axial Gas Turbine**
Material	ss
Theoretical power	228.6 Hp
Efficiency (%)	90

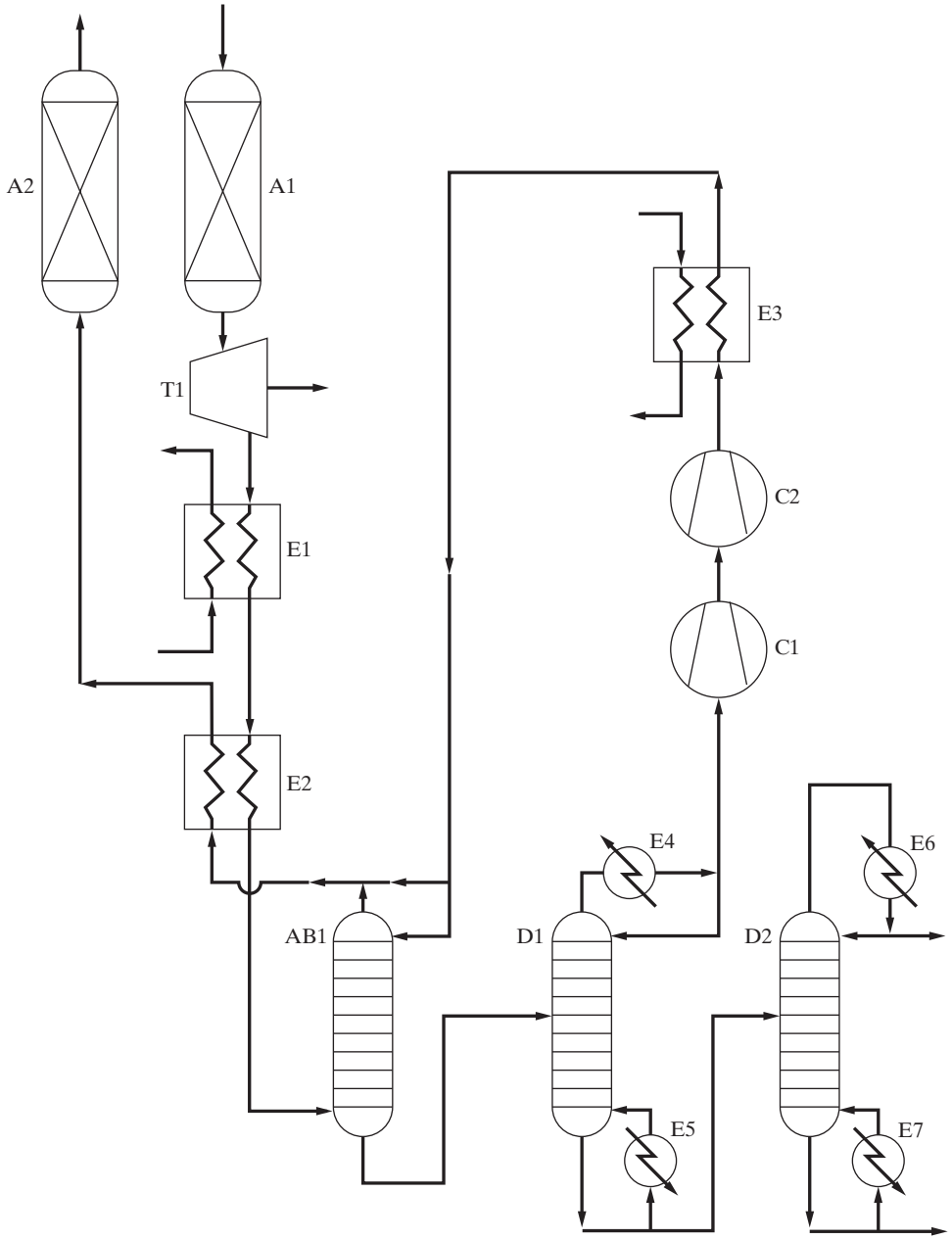

Figure 16.20 Argon recovery process.

16.6 The following are the major units in a chemical plant. Evaluate the bare-module cost for each unit and for the entire process. Assuming no allocated costs for the utilities and related facilities, estimate the direct permanent investment, the total depreciable capital, and the total permanent investment for the process. Use CE = 600.

(a) Two cast-steel centrifugal pumps (one a standby), each to handle 200 gal/min and producing a 200-psia head. The suction pressure is 25 psia and the temperature is ambient.

(b) A process heater with heat duty of 20,000,000 Btu/hr. The tube material is carbon steel. The pressure is 225 psia.

(c) A distillation column with 5-ft diameter, 25 sieve plates, and 2-ft tray spacing. The pressure is 200 psia and the material of construction is 316 stainless steel.

(d) A distillation column with 2-ft diameter, 15 sieve plates, and 2-ft tray spacing. The pressure is 200 psia and the material of construction is 316 stainless steel.

(e) A shell-and-tube heat exchanger with 3,200 ft^2 transfer surface, floating heads, a carbon-steel shell, and stainless steel tubes at 200 psia.

(f) A shell-and-tube heat exchanger with 7,800 ft^2 transfer surface, floating heads, and stainless steel shell and tubes at 200 psia.

16.7 Determine the total bare-module cost for the flowsheet in Figure 16.21 at ambient temperature and pressure. Use CE = 600.

Design Specifications

Pumps: reciprocating, motor driven, 25 psia head

Heat exchangers: floating-head, $\Delta T_{LM} = 30°F$, $U = 15$ Btu/hr-ft^2-°F

Reslurry vessel and crystallizer: vertical, with $H/D = 2$

All equipment: carbon steel

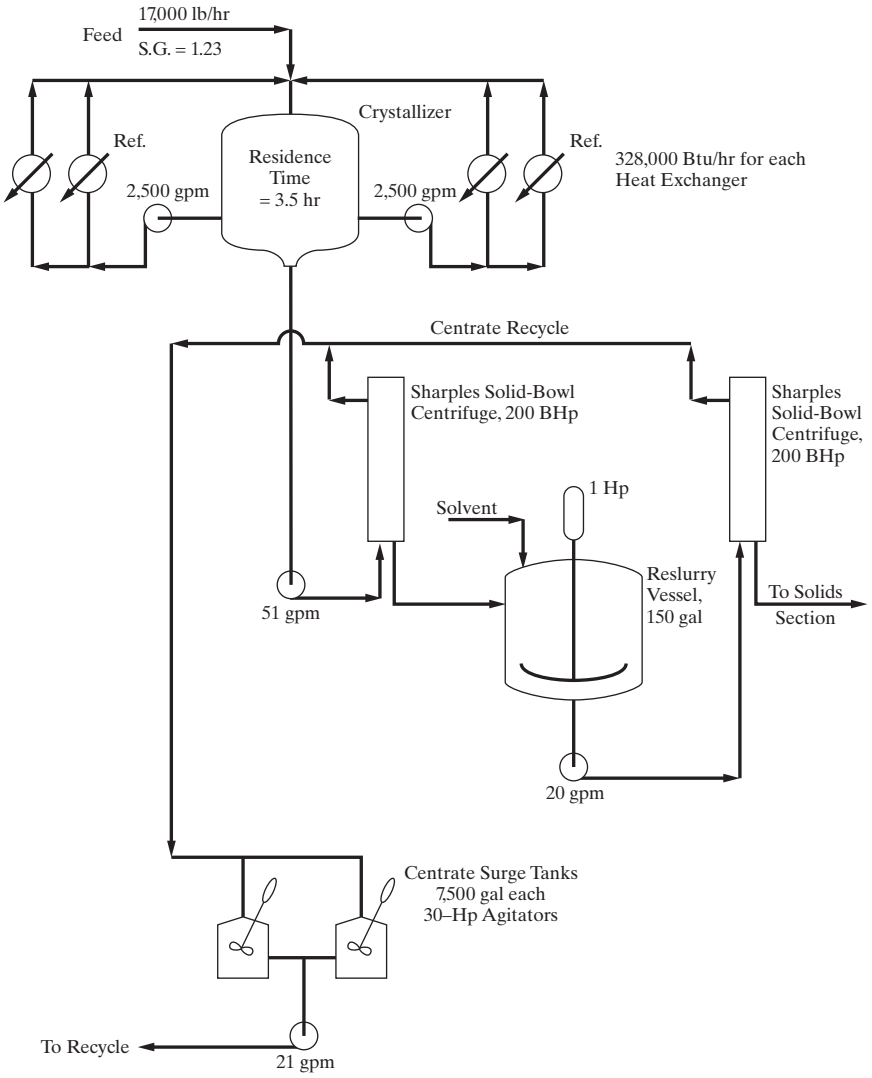

Figure 16.21 Flowsheet for Exercise 16.7.

16.8 A chemical plant contains the following equipment:
(a) Two gas-fired heaters, each with a heat duty of 20,000,000 Btu/hr. The tubes are carbon steel and the heaters operate at 225 psia. (b) Three distillation columns with 8-ft diameter, 25 sieve trays, and 2-ft tray spacing constructed using solid 316 stainless steel and operating at 200 psia.

Evaluate the total bare-module cost for the equipment and for the entire plant. Assuming no allocated costs for utilities and related facilities, estimate the direct permanent investment, the total depreciable capital, and the total permanent investment for the process. Use a CE cost index of 600.

16.9 Estimate the total bare-module cost for installation of nine 600-Hp centrifugal compressors of carbon steel with explosion-proof electric motors, a stainless steel direct-heat rotary dryer of 6-ft diameter by 30 ft long, and a continuous stainless steel scroll solid-bowl centrifuge processing 20 ton/hr of solids. Use CE = 600.

16.10 A plant contains

2 centrifugal compressors of carbon steel and 500-kW rating with explosion-proof electric motors

1 jaw crusher at 10 kg/s capacity

3 floating-head shell-and-tube heat exchangers of stainless steel, rated at 400 m^2 and 100 barg on the tube side

Calculate the total bare-module cost using CE = 600.

16.11 Consider a 1-2, shell-and-tube heat exchanger:

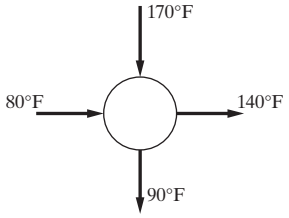

The cold stream has a heat-capacity flow rate $C = 40{,}000$ Btu/hr-°F. Its heat-transfer coefficients are $h_i = h_0 = 50$ Btu/(ft -hr-°F). For a stainless steel heat exchanger with a floating head built to withstand pressures up to 100 barg, estimate the bare-module cost. Use a CE cost index = 600.

16.12 A chemical plant contains

3 drum dryers of nickel alloy, each containing 540 ft^2.

40 kettle reboilers with a carbon-steel shell and copper tubes at 1,450 psia, each containing 325 ft^2.

Calculate the total bare-module cost for CE = 600.

Chapter 17

Annual Costs, Earnings, and Profitability Analysis

17.0 OBJECTIVES

Like the capital cost estimates of Chapter 16, methods presented in this chapter for the estimation of annual costs, annual earnings, and profitability measures play a crucial role throughout the design process in helping the design team to select the best design alternatives. The methods presented are those in common use and should be studied in connection with other chapters in this book as needed. In many cases, readers may prefer to study Sections 17.1 to 17.7 even before reading other chapters, especially when creating a business case for a new chemical product or studying the techniques for process synthesis that require estimates of capital costs, annual costs, and annual earnings, followed by the calculation of profitability measures.

After studying this chapter, the reader should be able to:

1. Estimate annual costs using a standard cost sheet and to estimate the annual cash flows and the working capital. The latter completes the estimation of the total capital investment, C_{TCI}, in Table 16.9.
2. Compute approximate profitability measures, such as return on investment (ROI), payback period (PBP), venture profit (VP), and annualized cost (C_A). These measures provide a snapshot view of the economic goodness, usually in the third year of operation, of a process or a product manufacturing plant. They do not include the time value of money, that is, compound interest.
3. Compute the present worth and future worth of single payments and annuities and the capitalized cost perpetuity. These measures are often used to compare proposals for the purchase of two competitive equipment items.
4. Compute cash flows and depreciation and to use them to project the net present value and investor's rate of return (IRR) (also known as the discounted cash flow rate of return, DCFRR), two measures that account for projections of revenues and costs over the life of the proposed process, and the time value of money.
5. Use Aspen Process Economic Analyzer (APEA) and an economic spreadsheet to carry out a profitability analysis for a potential process.

17.1 INTRODUCTION

Having completed an estimate for the total permanent investment, C_{TPI}, in Table 16.9, of a proposed plant or of a proposed chemical product manufacturing facility, it remains to estimate the total annual sales revenue, S, the total annual production cost, C, and the annual pre-tax and after-tax earnings. This includes the development of the so-called *cost sheet.* Then the working capital can be estimated and added to the total permanent investment to give the total capital investment for the plant or product manufacturing facility, as shown in Table 16.9. These provide the ingredients for a measure of economic goodness, called the *return on investment,* defined by

$$\text{Return on investment} = \frac{\text{Annual earnings}}{\text{Capital investment}} \qquad (17.1)$$

which is generally stated as a percentage per year. This definition includes a number of alternatives, depending on whether the annual earnings are before or after taxes and whether the capital investment includes land and working capital. The most common alternative for return on investment is based on the annual earnings after taxes and the total capital investment. This alternative is referred to here as ROI. A new commercial venture must compete with the *commercial interest rate (*or *cost of capital), i*, which is the annual rate at which money is returned to investors for the use of their capital, say, in the purchase of high-grade bonds. The commercial interest rate is considered to be essentially without risk. Investments in chemical processing plants and product manufacturing facilities always entail *risk.* Therefore, to be attractive, an investment in a venture involving a new or revamped chemical processing plant or product manufacturing facility must have an ROI greater than *i.* The greater the risk of the venture, the greater must be the difference between a financially attractive ROI and *i.* Establishment of the degree of risk involves answers to the following questions:

1. Is a new chemical product to be produced? If so, are uses for it established and is there a sure market for it at its projected price?
2. Is an already commercially available chemical product to be produced? If so, is the new plant going to utilize new technology that is predicted to reduce investment and/or operating costs? If so, how certain is the new technology? Does the technology involve potential environmental,

safety, and/or control issues? Does the technology involve uncertainties with respect to materials of construction? If the new plant is going to use established, mature technology, is future demand for the chemical predicted to be greater than the current supply?

3. For the new plant, is the availability of the feedstocks (raw materials) ensured at a known price, or are the feedstocks controlled and/or produced by the company installing the new process or product manufacturing facility?

As an example, suppose the current commercial interest rate is 10%. The proposed venture involves the manufacture of a new chemical product at conditions of high temperature and pressure using new technology. The uses of the new chemical product have been established and buyers have signed contracts to purchase the new chemical product at an agreed-upon price. The feedstocks are produced by and available from the company that will produce the new chemical product. This degree of risk might be considered moderate, requiring an (ROI – *i*) of 15% or an ROI of at least 25%. A high-risk venture might require an (ROI – *i)* of 50%.

This chapter begins with the methods for estimating the remaining elements of the approximate ROI measure, as well as other comparable measures such as the *venture profit* (VP), *payback period* (PBP), and *annualized cost* (C_A), which are utilized often to compare alternatives during the early stages of product/process design, particularly during process synthesis. Rigorous profitability measures, which involve consideration of the *time value of money* and estimates of the *cash flows* throughout the life of the proposed product/process, are applied before making a final decision on a project when a company must assess carefully how it expends its limited capital. These measures, which include the *net present value* (NPV) and the *investor's rate of return* (IRR) (also referred to as the *discounted cash flow rate of return,* DCFRR), incorporate one of a number of equipment depreciation schedules, based on U.S. tax laws, and account for the time value of money over the life of the product/process. These rigorous measures permit the design team to account for anticipated changes as well—for example, the need to replace the catalyst charge every four years, or the recognition that in seven years the company patent will expire and the selling price will be reduced, and so on. To initiate the discussion of these rigorous measures, several subjects that involve the time value of money are discussed, including compound interest, annuities, and perpetuities such as capitalized costs. The effects of depreciation, inflation, depletion, and salvage value at the end of the life of a product and/or processing plant are also discussed.

The chapter concludes with a discussion of an economics spreadsheet to calculate profitability measures.

17.2 ANNUAL SALES REVENUES, PRODUCTION COSTS, AND THE COST SHEET

Many continuing costs are associated with the operation of a chemical plant or product manufacturing facility. These are included in the cost sheet shown in Table 17.1, which is patterned after one prepared by Busche (1995) and includes representative unit costs (typical factors) that can be used for early estimates when more exact costs are not available.

Sales Revenue

Before estimating the annual costs listed on the cost sheet, the total annual sales revenue, *S*, should be estimated. If *S* is not greater than the costs of the feedstock(s), there is no need to consider the process design further. Typically, this calculation of the *economic potential* is made early, during the preliminary process synthesis stage, as discussed in Section 2.3 and shown in Table 2.3 for the development of a vinyl-chloride process. As the process design proceeds, the calculation needs to be repeated after conversions and yields are better established. The total sales revenue is based on the unit selling price(s) and on the quantity of product(s) produced for sale. If the process produces more than one main product, such as in Table 16.8, where plants produce ethylene–propylene, ammonia–urea, and chlorine–sodium hydroxide, the total sales revenue can include both products as coproducts. Otherwise, additional products can be considered byproducts for which an annual credit can be taken toward the cost of manufacture. Other possible credits include (1) gas, liquid, or solid effluents that can be used for fuel, (2) steam produced from boiler-feed water, and (3) electrical energy produced from a gas expander (turbine). If the streams with fuel value, steam, and/or electricity are used within the process, then the credit will be automatically accounted for. Otherwise, if to be used elsewhere, a transfer cost can be assigned to determine the credit against the cost of manufacture. The quantity of product(s) is obtained from the process design material balance and the estimated plant-operating factor or annual hours of plant operation.

Feedstocks

A major consideration in determining the cost of manufacture are the costs of the feedstocks, which may be natural resources such as petroleum, commodity chemicals such as chlorine, or fine chemicals. In the production of commodity chemicals, feedstock costs can be a significant contribution to the cost of manufacture, often in the range of 40 to 60% and even higher. The required quantity of feedstock is obtained from the process design material balance and the estimated plant operating factor. For example, in the earlier discussion in Chapter 2 of the production of vinyl chloride at the rate of 100,000 lb/hr, the process design material balance gives a chlorine feedstock flow rate of 113,400 lb/hr. If the plant-operating factor is based on 330 days/yr (operating factor = 330/365 = 0.904), the annual chlorine flow rate is 113,400(24)(365)(0.904) = 898.02 million lb/yr. If the delivered purchase cost of the chlorine is \$0.18/lb, the annual chlorine feedstock cost is \$161,644,000/yr. Similarly, the annual flow rate of ethylene, the other feedstock, is 44,900 lb/hr or 355.56 million lb/yr. At \$0.30/lb, the annual ethylene feedstock cost is \$106,668,000/yr. The total annual feedstock cost is \$268,312,000. The process produces 100,000 lb/hr of vinyl chloride or 791.90 million lb/yr. At a selling price of \$0.35/lb, the annual sales revenue is \$277,165,000, which is greater than the total annual feedstock costs. The process also produces a byproduct of gaseous HCl, which, if it could be sold, could enhance the potential earnings of the process.

Table 17.1 Cost Sheet Outline[a]

Cost Factor	Typical Factor in American Engineering Units	Typical Factor in SI Units
Feedstocks (raw materials)		
Utilities		
Steam, 450 psig[b]	$8.00/1,000 lb	$17.60/1,000 kg
Steam, 150 psig[b]	$7.00/1,000 lb	$15.30/1,000 kg
Steam, 50 psig[b]	$6.00/1,000 lb	$13.20/1,000 kg
Electricity[b]	$0.070/kW-hr	$0.070/kW-hr
Cooling water (cw)[b]	$0.10/1,000 gal	$0.027/$m^3$
Process water[b]	$0.80/1,000 gal	$0.27/$m^3$
Boiler-feed water (bfw)[b]	$2.00/1,000 gal	$0.56/$m^3$
Refrigeration, – 150°F[b]	$10.00/ton-day	$33.20/GJ
Refrigeration, – 90°F[b]	$7.00/ton-day	$23.30/GJ
Refrigeration, –30°F[b]	$4.00/ton-day	$13.17/GJ
Refrigeration, 10°F[b]	$2.00/ton-day	$6.47/GJ
Chilled water, 40°F[b]	$1.50/ton-day	$5.00/GJ
Natural gas	$5.00/1,000 SCF	$0.213/SCM
Fuel oil	$3.50/gal	$933/$m^3$
Coal—Appalacia, 12,500–13,000 Btu/lb	$60/ton	$66/1,000 kg
Coal—Powder River Basin, 8,800 Btu/lb	$13/ton	$14.34/1,000 kg
Wastewater treatment[c]	$0.15/lb organic removed	$0.33/kg organic removed
Landfill	$0.08/dry lb	$0.17/drykg
Operations (labor-related) (O) (See Table 17.3)		
Direct wages and benefits (DW&B)	$40/operator-hr	$40/operator-hr
Direct salaries and benefits	15% of DW&B	15% of DW&B
Operating supplies and services	6% of DW&B	6% of DW&B
Technical assistance to manufacturing	$60,000/(operator/shift)-yr	$60,000/(operator/shift)-yr
Control laboratory	$65,000/(operator/shift)-yr	$65,000/(operator/shift)-yr
Maintenance (M)		
Wages and benefits (MW&B)		
Fluid handling process	3.5% of C_{TDC}	3.5% of C_{TDC}
Solids–fluids handling process	4.5% of C_{TDC}	4.5% of C_{TDC}
Solids-handling process	5.0% of C_{TDC}	5.0% of C_{TDC}
Salaries and benefits	25% of MW&B	25% of MW&B
Materials and services	100% of MW&B	100% of MW&B
Maintenance overhead	5% of MW&B	5% of MW&B
Operating overhead		
General plant overhead	7.1% of M&O-SW&B	7.1% of M&O-SW&B
Mechanical department services	2.4% of M&O-SW&B	2.4% of M&O-SW&B
Employee relations department	5.9% of M&O-SW&B	5.9% of M&O-SW&B
Business services	7.4% of M&O-SW&B	7.4% of M&O-SW&B
Property taxes and insurance	2% of C_{TDC}	2% of C_{TDC}
Depreciation (see also Section 17.6)		
Direct plant	8% of (C_{TDC} – 1.18 C_{alloc})	8% of (C_{TDC} – 1.18C_{alloc})
Allocated plant	6% of 1.18C_{alloc}	6% of 1.18C_{alloc}
Rental fees (office and lab space)	(no guideline)	(no guideline)
Licensing fees	(no guideline)	(no guideline)
COST OF MANUFACTURE (COM)	Sum of above	Sum of above
General Expenses		
Selling (or transfer) expense	3% (1%) of sales	3% (1%) of sales
Direct research	4.8% of sales	4.8% of sales
Allocated research	0.5% of sales	0.5% of sales
Administrative expense	2.0% of sales	2.0% of sales
Management incentive compensation	1.25% of sales	1.25% of sales
TOTAL GENERAL EXPENSES (GE)		
TOTAL PRODUCTION COST (C)	COM + GE	COM + GE

[a] DW&B = direct wages and benefits; MW&B = maintenance wages and benefits; M&O-SW&B = maintenance and operations salary, wages, and benefits. See Table 16.9 for C_{TDC} and C_{alloc}. 1 ton of refrigeration = 12,000 Btu/hr.
[b] assumes natural gas is the energy source.
[c] normal wastewater and organics – amenable to aerobic and anaerobic digestion.
Source: Busche, 1995 with modifications.

The feedstocks may be purchased from suppliers, or the company itself may produce one or more of the feedstocks or have control over a required natural resource. If a feedstock is to be purchased, availability from more than one supplier can keep the cost down. However, a long-range contract can ensure the availability of the feedstock. In the absence of price quotations from prospective suppliers of feedstocks, especially for early cost evaluations when the raw materials are commodity chemicals, the weekly newspaper *ICIS Chemical Business Americas,* formerly *Chemical Market Reporter,* can be consulted, where most of the costs are for tank-car quantities. The prices quoted are representative of prices in the United States, but they are not location specific and may require an added delivery cost. Furthermore, the prices do not reflect the discounts that usually accompany long-term contracts. Also, larger production rates can increase the supply to such an extent that the price is reduced for a given demand. For specialty chemicals such as pharmaceuticals, prices can be obtained from their manufacturers. If the company manufactures a feedstock or controls it, a *transfer price* must be assigned. The transfer price is an agreed-upon price between the company division that supplies the feedstock and the division that manufactures the products from the feedstock. The transfer price may be (1) the market price or (2) a price negotiated between the two divisions, recognizing that the price influences the selling division's revenue and the buying division's cost.

Utilities

Except for certain processes involving inexpensive feedstocks, such as the manufacture of oxygen, nitrogen, and argon from air or the production of hydrogen and oxygen from water, the annual cost of utilities, while much smaller than the feedstock costs, is not an insignificant contribution to the selling price of the product(s), often in the range of 5 to 10%. As listed in the cost sheet of Table 17.1, utilities include steam for heating at two or more pressure levels, electricity, cooling water, process water, demineralized boiler-feed water, refrigeration at different temperature levels, fuels such as natural gas, wastewater treatment, waste disposal, and landfill. Often, the largest utility cost is that of steam.

The company may purchase utilities from a public or private utility company or build its own utility plants. Credit can be taken for any utilities, for example, fuel, steam, and electricity, produced by the process. Purchased utility costs are based on consumption. For company-owned utilities, both capital costs and operating costs apply. A cogeneration unit using a fuel can supply electricity accompanied by low-, medium-, and high-pressure steam. For early estimates, the purchase of utilities can be assumed by using the unit costs in Table 17.1.

Steam

Steam has many potential uses in a process, both as a process fluid and as a utility. In the former category, it may be used as a feedstock, as an inert diluent in a reactor to absorb heat of reaction, as a direct heating agent, and as a stripping agent in absorbers and adsorbers. As a utility, it can be used in place of electricity to drive pumps and compressors, and in ejectors to produce a vacuum. Steam is used in heat exchangers to heat liquids and gases and vaporize liquids. Typical pressure levels for steam are 50, 150, and 450 psig, with high-pressure steam more costly than steam at the lower pressures. In computing steam utility requirements, credit is taken only for the latent heat of vaporization. No credit is taken for sensible heat of the steam even though the steam may arrive at the heat exchanger superheated and leave as subcooled condensate. This is illustrated in the following example.

EXAMPLE 17.1

A kettle reboiler is used to evaporate toluene at 375°F with a heat duty of 3,000,000 Btu/hr. Steam is available at 50,150, and 450 psig. Determine the steam pressure level to use, the steam flow rate in lb/hr and lb/yr, and the estimated annual steam cost if the plant-operating factor is 0.90.

SOLUTION

Assuming a barometric pressure of 14 psia, the saturation temperature of 150-psig steam is 365°F. Since this is lower than 375°F, 450-psig steam must be used. However, to avoid film boiling as discussed in Chapter 12, use an overall temperature-driving force of 45°F, which sets the steam condensing temperature at 375 + 45 = 420°F, corresponding to a saturated steam pressure of 309 psia. With a valve assumed to operate adiabatically, the pressure of the high-pressure steam is reduced from 464 psia to 309 psia, producing a superheated vapor. However, the steam is assumed to enter the heat exchanger as a saturated vapor at 420°F and 309 psia and leave as a saturated liquid at 420°F. At these conditions, the latent heat of vaporization of steam is 806 Btu/lb. By an energy balance, the hourly steam requirement is 3,000,000/806 = 3,722 lb/hr or 3,722(24)(365)(0.9) = 29,350,000 lb/yr. From Table 17.1, the cost of 450-psig steam is $8.00/1,000 lb. Therefore, the annual steam cost = 29,350,000(8.00)/1,000 = $234,800/yr.

Electricity

The operation of many items of processing equipment requires energy input in the form of a drive or motor. This equipment includes pumps, compressors, blowers, fans, agitators and mixers, feeders, conveyors, elevators, crushers, grinders, mills, scraped-wall crystallizers, agitated-film evaporators, agitated and centrifugal liquid–liquid extractors, centrifuges and rotary vacuum filters, rotary dryers and kilns, and spray and drum dryers. Although many types of drives are available, including air expanders, combustion gas turbines, internal combustion engines, and steam turbines, the most common drives are electric motors because they are very efficient (> 90%); very reliable; readily available in a wide range of wattages (Hp), shaft speeds, and designs; and long lasting; and offer convenience, small footprint, favorable cost, and ease of maintenance. Electric motors are almost always used for power up to 200 Hp and are even available for applications requiring in excess of 10,000 Hp.

Alternating, rather than direct, current is used almost exclusively in electric motors. In the United States, the alternating current cycles from positive to negative and back to positive 60 times a second, referred to as 60 hertz (Hz). This rate works well with electric clocks, since there are 60 seconds in a minute. In Europe,

for some reason, 50 Hz is used. Alternating current originates at offsite private, public, governmental, or company facilities, generally at 18, 22, or 24 kilovolts (kV). For transmission to the plant on-site location, transformers step up the voltage to as high as 700 kV and then step it down to user voltages that are mainly in the range of 120 to 600 volts, but may be as high as 13,800 volts for motors of very high horsepower. Of the many electric motor designs, the most common is the three-phase, alternating-current, constant-speed, squirrel-cage induction motor. Induction motors of 60 Hz are capable of being operated satisfactorily on 50 Hz circuits if their voltage and horsepower ratings are reduced by a factor of 50/60. Motor enclosures may be explosion-proof (for locations near combustible fluids and dust), open-drip proof (to prevent entrance of liquid drips and dirt particles, but not vapor, dust, or fumes), or totally enclosed. For a given amount of energy transfer, the cost of electricity usually is greater than the cost of steam, as illustrated in the following example.

EXAMPLE 17.2

An electric motor is to be used to drive a compressor of 1,119 brake horsepower (BHp). The efficiency of the motor is 95%. Therefore, the electrical input to the motor must be 1,119(0.7457)/0.95 = 878 kW. This is equivalent to 3,000,000 Btu/hr, which is the basis for Example 17.1. Calculate the kW-hr required per year for the motor if the plant-operating factor is 0.9, and calculate the cost of electricity per year.

SOLUTION

The plant will operate (365)(24)(0.9) = 7,884 hr/yr. Therefore, the motor requires 878(7,884) = 6,922,000 kW-hr/yr. From Table 17.1, the cost of the electricity is 6,922,000(0.07) = $484,500/yr.

Cooling Water

Cooling water is used to cool liquids and gases and condense vapors. Typically, cooling water circulates between a cooling tower and process heat exchangers by means of a pump. For preliminary design purposes, it can be assumed that the cooling water enters a heat exchanger at 90°F and exits at 120°F. In the cooling tower, direct contact of downward-flowing water with air, forced upward by a fan, causes the water temperature to approach within about 5°F of the wet-bulb temperature of the air. Approximately 80% of the reduction of the temperature of the cooling water is accomplished by evaporation of a small amount of the cooling water; the balance is caused by the transfer of heat from the cooling water to the surrounding air. In addition to the evaporation in the cooling tower, cooling water is also lost by drift (entrained water droplets in the cooling tower air discharge) and blowdown (deliberate purging of untreated cooling water to prevent buildup and subsequent precipitation) of dissolved salts in the cooling water. Typically, makeup cooling water is 1.5 to 3% of the circulating cooling water rate. Alternatives to cooling towers include spray ponds and cooling ponds. Warm water spread out over a large area of impervious ground in an open pond can cool by evaporation, convection, and radiation. The rate of cooling can be increased by recirculating the water through spray nozzles, much like a fountain.

When a plant is located near a river or large body of water, cooling water can be drawn off at one location, pumped to the heat exchangers, and discharged downstream in a river or to another location in a lake, bay, or ocean. It is customary to filter this water, but not treat it to remove salts and similar impurities.

In general, the cost of cooling water is much less than the cost of steam for a given heat exchanger duty, as illustrated in the following example.

EXAMPLE 17.3

Cooling water is used in the overhead condenser of a distillation column with a heat duty of 3,000,000 Btu/hr. Determine the gallons per minute (gpm) of cooling water required and the annual cost of the cooling water if the plant has an operating factor of 0.90.

SOLUTION

Assume the cooling water enters the condenser at 90°F and exits at 120°F. Water has a specific heat of 1 Btu/lb-°F and a density of 8.33 lb/gal. Therefore, by an energy balance, the condenser requires 3,000,000/[(1)(120 − 90)] = 100,000 lb/ hr or 100,000/ [(60)(8.33)] = 200 gpm. The total gallons per year = 200(60)(24)(365)(0.9) = 94,600,000. From Table 17.1, the cost of cooling water = $0.10/ 1,000 gal. Therefore, the annual cost = 0.10(94,600,000)/(1,000) = $9,460/yr.

Process Water and Boiler-Feed Water

Water is needed for many purposes in a chemical processing plant, including cooling water (discussed above), boiler-feed water, and process water, which is water that enters directly into the process, rather than being used indirectly as a heat-transfer agent. Process water must be purified to the extent necessary to avoid introduction of any undesirable chemicals into the process that could poison catalysts, foul equipment, and/or introduce impurities into products. Boiler-feed water (bfw) is used to produce steam in offsite boiler or cogeneration facilities. bfw can also be used, in place of cooling water, as a cooling agent in a process when the temperature of a process stream to be cooled exceeds approximately 300°F. In the heat exchanger, the bfw is vaporized to steam, which may find use elsewhere in the process. Whether bfw is used on-site or offsite, it must be demineralized before use to avoid fouling heat exchanger tubes. Sources of water include municipal water, well water, river water, lake water, ocean water, brackish water, treated wastewater, and condensate. The cost of process water, given in Table 17.1 as $0.80/1,000 gal, corresponds to only a moderate degree of pretreatment. The annual cost of process water, when needed, is usually very small compared to other feedstocks. When bfw is used to produce steam in a process heat exchanger, the cost of the bfw is partially offset by the value of the steam produced from it. This value is taken as a credit. In Table 17.1, the cost of bfw is given as $2.00/1,000 gal, which accounts for the credit. Extensive treatment of water containing large amounts of impurities can raise the cost to as much as $6.00/1.000 gal.

Sterilized water for the manufacture of pharmaceuticals can cost as much as \$550/1,000 gal. The use of bfw in a process heat exchanger is illustrated in the following example.

EXAMPLE 17.4

A process for hydrogenating benzene to cyclohexane, described in Example 10.5, includes a well-mixed reactor, where an exothermic reaction occurs at 392°F and 315 psia. A total of 4,706,200 Btu/hr of heat must be transferred out of the reactor. Although this heat could be transferred into cooling water, the temperature in the reactor is sufficiently high to consider transferring the heat, by means of a heat exchanger, to boiler-feed water to produce steam. Determine the pressure level of the steam that could be produced, the pounds per hour of bfw required, and the annual cost of the bfw. The plant-operating factor is 0.9.

SOLUTION

To ensure nucleate boiling of the bfw, assume an overall driving force of 45°F, as described in Chapter 12. Thus, the bfw will be converted to steam at (392 − 45) = 347°F. This corresponds to a saturation pressure of 130 psia. Assume the bfw enters the heat exchanger as liquid at 90°F and exits as saturated vapor at 347°F. The change in enthalpy = 1,134 Btu/lb. Therefore, by an energy balance, the steam produced from the bfw = 4,706,200/1,134 = 4,150 lb/hr. The annual cost of the bfw at \$2.00/1,000 gal with water at a density of 8.33 lb/gal is 4,150(24)(365)(0.9)(2.00)/[(8.33)(1,000)] = \$7,860/yr.

Refrigeration

The two most common coolants are cooling water and air. In general, cooling water from a cooling tower or pond can be used to cool a process stream to 100°F whereas air, which is used in desert locations or where water is in short supply, can cool to only 120°F. To cool and/or condense process streams to temperatures below 100°F, chilled water, chilled brine, or a refrigerant is necessary, with the latter category being the most common. Several refrigerants are listed in Table 12.1. Prior to 1995, when the U.S. Clean Air Act Amendments of 1990 went into effect, two of the most popular refrigerants were CFC Freon R-12 (dichlorodifluoromethane) and HCFC Freon R-22 (chlorodifluoromethane). The chlorine atoms in these refrigerants were found to be released in the stratosphere, causing a depletion of the ozone layer. Since 1995, production of these two refrigerants and other chlorofluorocarbons has ceased or has been curtailed as discussed in Section 4.3. The case study there shows how to carry out molecular structure design to synthesize 1,1,1,2-tetrafluoroethane (R-134a, which is the same as HFC-134a), a common replacement refrigerant. According to the EPA, R-134a does not propagate a flame under normal conditions in open air, shows no evidence of toxicity below 400 ppm, and does not deplete the ozone layer. This refrigerant, as well as ammonia and several light hydrocarbons, cools by transferring heat from the process stream in a heat exchanger where the refrigerant is evaporated. A typical propane refrigeration system is shown in Figure 10.20, where the propane is circulated by a compressor through a condenser, a valve or turbine, and an evaporator where the cooling takes place. The temperature-driving force in the refrigerant evaporator is typically in the range of 2 to 10°F. Thus, with R-134a, which from Table 12.1 has an operating range of −15 to 60°F, a process stream can be cooled down to within 2°F of –15°F or −13°F. For lower temperatures, ammonia or the light hydrocarbons can be used. For example, an ethylene refrigerant can cool a stream down to as low as −148°F. The lower-limit temperature of operation of the refrigerant corresponds approximately to its normal boiling point. Lower temperatures would require an undesirable vacuum on the refrigerant side of the evaporator.

Typically, a chemical plant must provide its own refrigeration, either offsite, or more typically on-site. Petroleum refineries use light-hydrocarbon refrigerants whereas other plants may consider ammonia and R-134a, unless very low temperatures (< −30°F) are required in which case cascade refrigeration systems are often used. These systems are often included with the equipment in the process flowsheet.

The temperature level is the key factor in determining the cost of refrigeration. For moderate temperatures, estimates of annual operating cost are based on a ton-day of refrigeration, where a ton is defined as the heat removal to freeze 1 ton (2,000 lb) per day of water at 32°F, which corresponds to 12,000 Btu/hr. Calculation of the annual refrigeration cost is illustrated in the following example. For a given energy-transfer rate, the cost of a moderate level of refrigeration compares to the cost of steam for heating.

EXAMPLE 17.5

A process stream in a petroleum refinery is to be partially condensed and cooled to 10°F with a cooling duty of 3,000,000 Btu/hr. Select a suitable refrigerant, and calculate the tons of refrigeration required and the annual operating cost if the plant-operating factor is 0.9.

SOLUTION

From Table 12.1, a suitable refrigerant for a petroleum refinery is propane since it has an evaporation range of −40 to 20°F. The propane evaporation temperature would be approximately 5°F. The tons of refrigeration = 3,000,000/12,000 = 250 tons. The annual refrigeration is 250(365)(0.9) = 82,130 ton-day. From Table 17.1 for this temperature level, the annual operating cost = 82,130(4.00) = \$328,500/yr. Most of this cost is the cost of electricity to drive the propane compressor.

Fuels

Various fuels may be combusted in a chemical process to provide heat or work. In addition to the fuels needed for the offsite facilities such as boilers, electrical power generation, and cogeneration, fuels such as coal, natural gas, manufactured gas, and/or fuel oil may be needed for high-temperature heating in furnaces and fired heaters. Also, fuels may be used to drive pumps and compressors. Typically, the fuel, whether it be solid, liquid, or gas, is burned completely with an excess amount of air. To determine the amount of fuel required, the heating value (heat of combustion) of the fuel must be known. Two heating values are in common use, the *higher heating value* (also called the gross heating value),

Table 17.2 Typical Heating Values of Fuels

Fuel	HHV	LHV
Pennsylvania anthracite coal	13,500 Btu/lb	
Illinois bituminous coal	12,500 Btu/lb	
Wyoming subbituminous coal	9,500 Btu/lb	
North Dakota lignite coal	7,200 Btu/lb	
No. 2 fuel oil (33° API)	139,000 Btu/gal	131,000 Btu/gal
No. 4 fuel oil (23.2° API)	145,000 Btu/gal	137,000 Btu/gal
Low-sulfur No. 6 fuel oil (12.6° API)	153,000 Btu/gal	145,000 Btu/gal
Methyl alcohol	9,550 Btu/lb	
Ethyl alcohol	12,780 Btu/lb	
Benzene	17,986 Btu/lb	17,259 Btu/lb
Hydrogen	322 Btu/SCF	272 Btu/SCF
Carbon monoxide	321 Btu/SCF	321 Btu/SCF
Methane	1,012 Btu/SCF	907 Btu/SCF
Ethane	1,786 Btu/SCF	1,601 Btu/SCF
Propane	2,522 Btu/SCF	2,312 Btu/SCF
Natural gas (85–95 vol% methane)	1.020–1,090 Btu/SCF	920–990 Btu/SCF

HHV, and the *lower heating value* (also called the net heating value), LHV. The heating value is the total heat evolved by complete combustion of a fuel with dry air when the fuel and air are at 60°F before combustion and all of the flue gas (product from combustion) is brought to 60°F after combustion. If the water vapor in the cooled flue gas is not condensed, the total heat is the LHV. If the water vapor is condensed, additional heat is evolved, giving the HHV. Some typical heating values for common fuels are given in Table 17.2. A manufactured gas is not listed; typically, it contains mainly H_2, CO, CH_4, and N_2 over wide ranges of composition. Note that heating values for solid and liquid fuels are usually quoted on a mass basis whereas gaseous fuels are on a volume basis, usually standard cubic feet (SCF) at 1 atm and 60°F. For a given heat-transfer rate to a process stream being heated and/or vaporized in a fired heater, the amount of fuel required is greater than that based on its HHV because of heat losses, a flue gas temperature much greater than 60°F, and the presence of water as vapor in the flue gas. The ratio of the amount of fuel based on the HHV to the actual amount is the fired heater thermal efficiency, which may range from 50 to 80%. Typical fuel costs are included in Table 17.1. The calculation of the fuel requirement for a fired heater is illustrated in the following example.

EXAMPLE 17.6

A fired heater is to be used to heat and vaporize the feed to a reactor from 1,000 to 1,200°F. The heat duty is 3,000,000 Btu/hr. The fuel is natural gas with an HHV of 1,050 Btu/SCF. The thermal efficiency is 70%. If the plant-operating factor is 0.9, compute the SCF/hr and SCF/yr of natural gas required and the annual fuel cost.

SOLUTION

For an efficiency of 70%, the heat evolved from combustion of the fuel is 3,000,000/0.7 = 4,286,000 Btu/hr. The natural gas must be supplied at a rate of 4,286,000/1,050 = 4,082 SCF/hr or a rate of 4,082(24)(365)(0.9) = 32,180,000 SCF/yr. From Table 17.1, the cost of natural gas is $5.00/1,000 SCF. Therefore, the annual cost is 32,180,000(5.00)/1,000 = $160,900/yr.

Waste Treatment

Most chemical processes produce waste streams: gaseous (with or without particles), liquid (with or without particles, dissolved gases, and dissolved solids), solids (wet or dry), and slurries. In some cases, valuable byproducts can be removed from waste streams by additional processing. However, when this is not economical, federal regulations require that waste streams be treated to remove pollutants before being sent to the surrounding air, a sewer, a pond, a nearby river, a lake, an ocean, or a landfill.

Air Pollution Abatement

Waste gases may contain particulates and/or gaseous pollutants, inorganic or organic. Additional equipment must be added to the process to remove these pollutants. If that equipment requires utilities, their costs must be added to the other utility costs. The removal of particles is usually accomplished with cyclone collectors, wet scrubbers, electrostatic precipitators, and fabric-filter systems. Inorganic gaseous pollutants such as ammonia; chlorine and fluorine; oxides of sulfur, carbon, and nitrogen; hydrogen sulfide, chloride, fluoride, and cyanide; and organic gaseous pollutants such as hydrocarbons and oxygenated organic compounds can be removed by absorption, adsorption, condensation, and/or combustion.

Wastewater Treatment

When water is fed into a process and/or the process produces water, wastewater is usually one of the process effluents. This wastewater must be treated for the removal of pollutants before being discharged to a sewer, pond, or body of water. In the United

States, the treatment is regulated by the U.S. Clean Water Act of 1977. The treatments necessary depend on the nature of the foreign material, that is, whether it is suspended or dissolved in the water. When private or municipal sewage treatment plants are nearby, the wastewater can be sent directly to those plants. However, pretreatment may be required to neutralize the water, remove large solids, and remove grease and oil. If the treatment facilities are located on-site or offsite, equipment for several treatments should be considered. *Primary treatment,* using gravity sedimentation or clarification, is used to remove suspended solids. *Secondary treatment* adds aerobic biological organisms (those requiring molecular oxygen for metabolism) in the form of a sludge to cause oxidation of the dissolved biodegradable organic compounds to carbon dioxide, water, sulfates, and so on. Excess flocculated suspension (activated sludge) is removed from the water by clarification or air flotation. A measure of the biodegradability is the biochemical oxygen demand (BOD), which is the amount of oxygen required in parts per million of water by mass and in milligrams per liter of water. *Tertiary treatment* adds one or more additional chemical treatments to remove acids, alkalies, colloidal matter, color, odor, metals, and other pollutants not removed in earlier steps. Of most concern in chemical processing plants is the removal of dissolved organic compounds, particularly those that are carcinogenic, such as benzene. The following example illustrates the calculation of the cost of removal of dissolved organic compounds by biodegradation.

EXAMPLE 17.7

A wastewater stream of 500 gpm at 70°F contains 150 mg/L of benzene that is to be removed by biodegradation. If 99.9% of the benzene is removed, determine the amount of benzene removed per year and the operating cost of removal using a cost from Table 17.1 of \$0.15/lb benzene and a plant-operating factor of 0.9.

SOLUTION

First, determine whether all of the benzene is dissolved in the wastewater. The solubility of benzene in water at 70°F is a mole fraction of 0.00040. The mole fraction of benzene (MW = 78) in the wastewater (55.5 mol/L) is (0.150/78)/55.5 = 0.000035. Therefore, all of the benzene is dissolved. The flow rate of 500 gpm is equivalent to 500(3.785)(60) = 113,600 L/hr. The pounds of benzene removed per year = (0.150/454)(113,600)(24)(365)(0.9) = 296,000 lb/yr. The cost of benzene removal = 0.15(296,000) = \$44,400/yr.

Solid Wastes

According to U.S. federal regulations, solid wastes must be classified as hazardous or nonhazardous. Due to their ignitability, corrosivity, reactivity, and/or toxicity, hazardous wastes pose a substantial threat to human, plant, or animal life and must be treated on-site or near-site by physical, chemical, thermal, or biological means before being put in containers and removed. Nonhazardous solid wastes may be placed in containers and removed to a landfill or, in some cases, incinerated. The annual cost of solid waste treatment and disposal varies widely. Typical costs are \$0.03/lb of waste for nonhazardous dry or wet solids and \$0.10/lb for hazardous dry or wet solids.

Labor-related Operations, O

One of the most difficult annual costs to estimate is direct wages and benefits (DW&B) for operating a chemical plant. It and the other annual costs that are proportional to it are often an important fraction of the cost of manufacture. Table 17.1 lists the labor-related charges associated with operations. These include *direct wages and benefits* (DW&B), calculated from an hourly rate for the operators of a proposed plant. To estimate all labor-related operations, it is necessary to estimate the number of operators for the plant per shift and to account for three shifts daily, except for small businesses that operate over one shift daily, five days per week. Typically, each shift operator works 40 hr per week, and, hence, for each operator required during a 7(24) = 168-hr week, 4.2 shifts must be covered. In practice, due to illness, vacations, holidays, training, special assignments, overtime during startups, and so on, it is common to provide for 5 shifts for each operator required.

Estimates of the number of plant operators needed per shift are based on the type and arrangement of the equipment, the multiplicity of units, the amount of instrumentation and control for the process, whether solids are handled, whether the process is continuous or batchwise or includes semicontinuous operations, and company policy in establishing labor requirements, particularly as it relates to operator unions. For preliminary estimates of the number of operators required per shift, the process may be divided into sections as discussed in Chapter 9 and shown in Figures 9.1 and 9.3. These sections may include: (1) feed preparation system using separation steps, (2) reactor system, (3) vapor recovery system, (4) liquid-seperation system, (5) solids separation and purification system, and (6) pollution abatement system. When a process includes two or more reactor systems and/or two or more liquid-separation systems, each is counted separately. As given in Table 17.3 for a continuously operating, automatically controlled fluids-processing plant with a low-to-medium capacity of 10 to 100 ton/day of product, one operator/shift is assigned to each section. For solids–fluids processing and solids processing, the number of operators per shift is increased as noted in Table 17.3. For large capacities, for example, 1,000 ton/day of product, the number of operators/shift in Table 17.3 are doubled

Table 17.3 Direct Operating Labor Requirements for Chemical Processing Plants. Basis: Plant with Automatic Controls and 10–100 Ton/Day of Product

Type of Process	Number of Operators per Process Section[a]
Continuous operation	
Fluids processing	1
Solids–fluids processing	2
Solids processing	3
Batch or semibatch operation	
Fluids processing	2
Solids–fluids processing	3
Solids processing	4

[a] For large continuous-flow processes (e.g., 1,000 ton/day of product), multiply the number of operators by 2.

for each section. Batch and semicontinuous processing also require more operators than a continuous process as indicated in Table 17.3. A process should always have at least two operators present per shift. Each shift operator is paid for 40 hr/week and 52 weeks/yr or a total of 2,080 hr/yr. The annual cost of direct wages and benefits (DW&B) is obtained from:

$$\text{DW\&B, \$/yr} = (\text{operators/shift})(5 \text{ shifts}) \times (2{,}080 \text{ hr/yr-operator})(\$/\text{hr}) \quad (17.2)$$

where the \$/hr covers wages and benefits, and depends on locality and whether operators are unionized. In Table 17.1, a figure of \$40/hr is typical in the United States.

To obtain the total annual labor-related operations cost, O, direct salaries and benefits for supervisory and engineering personnel at 15% of DW&B and operating supplies and services at 6% of DW&B are added to DW&B. In addition, \$60,000/(operator/shift)-yr for technical assistance to manufacturing and \$65, 000)/(operator/shift)-yr for control laboratory are added. An estimate of the total annual cost of labor-related operations is illustrated in the following example.

EXAMPLE 17.8

The vinyl-chloride process discussed in Example 2.2 and Section 2.5 and shown in Figures 2.6, 2.16, and 2.17 produces 100,000 lb/hr of vinyl chloride or 1,200 ton/day. Estimate the annual cost of labor-related operations, O.

SOLUTION

This is a continuous fluids process of large capacity. Assume it is automatically controlled. From the block flow diagram, the process is comprised of two reactor sections and one liquid-separation section. Therefore, from Table 17.3, three operators per shift are required for a moderate-capacity plant. However, this is a large-capacity plant, requiring twice that number or 6 operators per shift and five shifts or a total of 30 shift operators. Also, a large-capacity plant requires one labor-yr each for technical assistance and control laboratory. Using Eq. (17.2), the annual costs are

$$\text{Annual DW\&B} = (30 \text{ operators})(2{,}080 \text{ hr/yr})(\$40.00/\text{hr}) = \$2{,}496{,}000$$

Using Table 17.1, the other annual labor-related operation costs are

$$\text{Direct salaries and benefits} = 0.15(\$2{,}496{,}000) = \$374{,}400$$

$$\text{Operating supplies and services} = 0.06(\$2{,}496{,}000) = \$149{,}800$$

$$\text{Technical assistance to manufacturing} = \$60{,}000(5) = \$300{,}000$$

$$\text{Control Laboratory} = \$65{,}000(5) = \$325{,}000$$

The total labor-related operations annual cost, O, is:

$$\text{O} = \$2{,}496{,}000 + \$374{,}400 + \$149{,}800 + \$300{,}000 + \$325{,}000 = \$3{,}645{,}200/\text{yr}$$

Maintenance, M

A second category of labor-related costs is associated with the maintenance of a proposed plant. Processing equipment must be kept in acceptable working order with repairs and replacement of parts made as needed. Annual maintenance costs, M, are sometimes greater than the cost of labor-related operations, O. Included in Table 17.1 under annual maintenance costs, M, is the main item, maintenance wages and benefits (MW&B), which is estimated as a fraction of the total depreciable capital, $C_{\text{TDC,}}$. depending on whether the process handles fluids, solids, or a combination of fluids and solids. The range is from a low of 3.5% for fluids to 5.0% for solids, with 4.5% for solids–fluids processing. Salaries and benefits for the engineers and supervisory personnel are estimated at 25% of MW&B. Materials and services for maintenance are estimated at 100% of MW&B, and maintenance overhead is estimated at 5% of MW&B. Thus, the total annual cost of maintenance varies from 8.05 to 11.5% of C_{TDC}. Maintenance costs can be controlled by selecting the proper materials of construction for the processing equipment, sparing pumps, avoiding high rotation speeds of shafts, restricting the highest fouling streams to the tube side of heat exchangers, selecting long-life catalysts for reactors, scheduling routine maintenance, and practicing preventive maintenance based on experience, supplier information, and record-keeping. Routine maintenance includes cleaning of heat exchanger tubing and lubrication and replacement of packing and mechanical seals in pumps, compressors, blowers, and agitators. A main goal should be to provide most of the maintenance during scheduled plant shutdowns, which might be during a two- or three-week period each year.

EXAMPLE 17.9

The total depreciable capital investment, C_{TDC}, for a plant to produce 300,000 tons per year of cumene is estimated to be \$31,000,000. The process involves only fluids processing. Estimate the annual plant maintenance cost, M.

SOLUTION

Using Table 17.1, the annual maintenance costs are

$$\text{Wages and benefits (MW\&B) at 3.5\% of } C_{\text{TDC}} = \$1{,}085{,}000$$

$$\text{Salaries and benefits at 25\% of MW\&B} = 271{,}000$$

$$\text{Materials and services at100\% of MW\&B} = 1{,}085{,}000$$

$$\text{Maintenance overhead at 5\% of MW\&B} = 54{,}000$$

The total annual maintenance cost, M, is \$2,495.000/yr.

Operating Overhead

To this point in Table 17.1, all costs have been directly related to plant operation. However, a company always incurs many other expenses, which while not directly related to plant operation can be estimated as a fraction of the combined salary, wages, and benefits for maintenance and labor-related operations, referred to here as M&O-SW&B. Overhead expenses include the costs of providing the following services: cafeteria; employment and

personnel; fire protection, inspection, and safety; first aid and medical; industrial relations; janitorial; purchasing, receiving, and warehousing; automotive and other transportation; and recreation. In Table 17.1, overhead costs are divided into four categories: general plant overhead, provision for the services of the mechanical department and for the employee relations department as well as business services with the total annual operating overhead cost equal to the sum of these four categories or (7.1 + 2.4 + 5.9 + 7.4) = 22.8% of M&O-SW&B.

EXAMPLE 17.10

Estimate the annual cost of operating overhead for the cumene plant of Example 17.9, assuming that the cost of labor-related operations is the same as in Example 17.8.

SOLUTION

The previous two examples provide the following wages, salaries, and benefits per year for labor-related operations and maintenance:

Direct wages and benefits (DW&B) = $2,496,000
Direct salaries and benefits = 374,400
Maintenance wages and benefits (MW&B) = 1,085,000
Maintenance salaries and benefits = 271,000

The total annual M&O-SW&B is the sum, which equals $4,226,000/yr.

The total annual operating overhead cost is 22.8% of the M&O-SW&B or $963,500.

Property Taxes and Insurance

Annual property taxes are assessed by the local municipality as a percentage of the total depreciable capital, C_{TDC}, with a range from 1% for plants located in sparsely populated areas to 3% when located in heavily populated areas. Property taxes are not related to federal income taxes levied by the Internal Revenue Service and considered later. Liability insurance costs depend on the pressure and temperature levels of plant operation and on whether flammable, explosive, or toxic chemicals are involved. The annual cost of insurance is also estimated as a percentage of the total depreciable capital, C_{TDC}, with a range of 0.5 to 1.5%. In the absence of data, annual property taxes and insurance may be estimated at 2% of C_{TDC}, as given in Table 17.1. This corresponds to a process of low risk located away from a heavily populated area.

Depreciation, D

The subject of depreciation is complex and often confusing because depreciation has several definitions and applications. Most commonly, it is simply a measure of the decrease in value of an asset over time. Some companies use depreciation as a means to set aside a fund to replace a plant when it is no longer operable. In its most complex application, depreciation is an annual allowance whose calculation is controlled by the U.S. federal government when determining federal income tax. The larger the depreciation in a given year, the smaller the federal income tax and the greater the net profit. This is considered in detail in the discussion of cash flow in Section 17.6.

For use with approximate profitability measures, as applied here to the preliminary calculation of the annual manufacturing cost, depreciation, D, is estimated as a constant percentage of the total depreciable capital, C_{TDC}. This type of depreciation is referred to as *straight-line* (*SL*) *depreciation.* Although it has been customary to take that percentage as 10% for each of 10 yr, in Table 17.1, the direct plant (on-site) depreciation is taken as 8% of ($C_{TDC} - 1.18C_{alloc}$) (equivalent to a plant life of about 12 yr). Also, the allocated plant (offsite) depreciation is taken as 6% of the contribution of the allocated costs for utilities and related facilities to the total depreciable capital, C_{TDC}, and $1.18C_{alloc}$ (equivalent to a life of about 16 yr) where the 1.18 factor accounts for the share of the contingency and contractor's fee, C_{cont}.

Rental Fees

In product design, especially in the early years of startup companies, it is frequently necessary to rent office and laboratory space. These facilities are often available in research-oriented complexes and science centers that are often located in the vicinity of universities, at beltways surrounding large cities, and so on. Often the laboratory facilities are available at different cleanliness ratings with high levels usually required for the manufacture of pharmaceuticals, electronic materials, and the like.

Licensing Fees

When chemical products and processes under patent protection are utilized, an annual licensing fee may be negotiated, often based on the amount or dollar value of product sold. The amount of the annual licensing fee depends on the uniqueness of the process and the chemical being produced, with a range of 1–5% of product sales. In many cases, an initial royalty fee, as a portion of the capital investment, is included. In the absence of data, an initial royalty fee of 2% of C_{TDC} may be assumed, with an annual licensing fee of 3% of product sales, as discussed in Section 16.3.

Cost of Manufacture, COM

The total annual cost of manufacture, COM, as shown in Table 17.1, is the sum of (1) *direct manufacturing costs:* feedstocks, utilities, labor-related operations, and maintenance; (2) *operating overhead;* and (3) *fixed costs:* property taxes, insurance, and depreciation.

Total Production Cost, C

The total annual production cost equals the sum of the cost of manufacture and general expenses,

$$C = COM + \text{general expenses} \tag{17.3}$$

General expenses refer to activities that are conducted by the central operations of a company, perhaps at the corporate

headquarters, and are financed from profits made by the company from their operating plants. In Table 17.1, general expenses comprise five categories: selling (or transfer) expense, research (direct and allocated), administrative expense, and management incentive compensation. The *selling expense* covers all the costs involved in selling the products, including expenses of the sales office, advertising, traveling sales representatives, containers and shipping, commissions, and technical sales service. The research expense covers both research and development costs for new products and new manufacturing methods for existing products. Administrative expense covers those top-management and general administrative activities that are not direct manufacturing costs. In Table 17.1, all general expenses are estimated as a percentage of the total sales revenue. The total general expenses range from 9.55 to 11.55% of S. Note that the direct research allocation by pharmaceutical companies often exceeds 4.8% of sales (Pisano, 1997).

EXAMPLE 17.11

For the MCB separation process in Section 7.4, estimate the annual production cost, C, where products will be used in-house, with a total annual sales, S. Base your estimate on:

Continuous plant operation	330 day/yr or 7,920 hr/yr
Feedstock	9,117 lb/hr @ $0.50/lb
MCB product	5,572 lb/hr @ $0.68/lb
Benzene byproduct	3,133 lb/hr @ $0.54/lb
HCl gas byproduct	355 lb/hr @ $0.04/lb

Note: Benzene and HCl are treated as byproducts, and credit is taken for them.

Total bare-module costs, C_{TBM}	$1,230,000
Cost of site preparation and service facilities, $C_{site} + C_{serv}$	$123,000
Cost of land @2% of C_{TDC}	
Cost of contingencies @18% of C_{DPI}	
150-psig steam	1,365.5 lb/hr@$7.00/1,000 lb
Electricity	9.60 kW@$0.07/kW-hr
Cooling water	258 gpm@$0.10/1,000 gal
Operators	one/shift

SOLUTION

The total depreciable capital, using Table 16.9, is computed as:

$$C_{DPI} = \$1{,}230{,}000 + \$123{,}000 = \$1{,}353{,}000$$
$$C_{cont} = 0.18\, C_{DPI} = 0.18(1{,}353{,}000) = \$243{,}500$$
$$C_{TDC} = C_{DPI} + C_{cont} = \$1{,}353{,}000 + \$243{,}500 = \$1{,}596{,}500$$

For this moderate-size plant with one section, use one operator/shift (five shifts).

Using Table 17.1 with the data, the following annual costs are computed:

Cost Factor	Annual Cost
Feedstocks (raw materials)	$36,103,300
Utilities	
Steam, 150 psig	75,700
Electricity	5,300
Cooling water (cw)	12,300
Total Utilities	$93,300
Operations (O)	
Direct wages and benefits (DW&B)	416,000
Direct salaries and benefits	62,400
Operating supplies and services	25,000
Technical assistance to manufacturing	300,000
Control laboratory	325,000
Total labor-related operations	$1,128,400
Maintenance (M)	
Wages and benefits (MW&B)	55,900
Salaries and benefits	14,000
Materials and Services	55,900
Materials overhead	2,800
Total maintenance	$128,600
Total of M&O-SW&B	$548,300
Operating overhead	
General plant overhead	38,900
Mechanical department services	13,200
Employee relations department	32,300
Business services	40,600
Total operating overhead	$125,000
Property taxes and insurance	$31,900
Depreciation (D)	
Direct plant	127,700
Allocated plant	-
Total depreciation	$127,700
Credit on Byproducts	(13,511,700)
COST OF MANUFACTURE (COM)	$24,101,500
General Expenses (GE)	
Transfer expenses	435,200
Direct research	2,089,000
Allocated research	217,600
Administrative expense	870,400
Management incentive compensation	544,000
TOTAL GENERAL EXPENSES (GE)	$4,156,200
TOTAL PRODUCTION COST (C)	$28,257,700
Sales	
Monochlorobenzene product	30,008,600
TOTAL SALES, S	$30,008,600

Table 17.4 Federal Income Tax Rate Schedule for Corporations

Gross Earnings Over	But Not Over	Income Tax
$ 0	$ 50,000	15%
50,000	75,000	$7,500 + 25% over $50,000
75,000	100,000	$13,750 + 34% over $75,000
100,000	335,000	$22,250 + 39% over $ 100,000
335,000	10,000,000	$113,900 + 34% over $335,000
10,000,000	15,000,000	$3,400,000 + 35% over $10,000,000
15,000,000	81,333,333	$5,150,000+38% over $15,000,000
18,333,333	—	$6,416,667 + 35% over $18,333,333 (equivalent to 35% on total gross earnings)

Note that these results are for operation of the MCB plant at full (100%) capacity. They are equivalent to the results in Example 17.32 using the Profitability Analysis-4.0.xls spreadsheet. Also, there are no allocated plant costs for utilities, and general expenses are estimated using transfer expenses rather than selling expenses.

Pre-Tax (Gross) Earnings and After-Tax (Net) Earnings (Profit)

The annual *pre-tax earnings or profit,* also called the *gross earnings or profit,* is the difference between the annual sales revenue and the annual product cost:

$$\text{Gross earnings or profit} = S - C \tag{17.4}$$

The annual *after-tax earnings or profit,* also called the *net earnings or profit,* is the gross earnings minus U.S. federal and state income taxes on the gross earnings. Since at least the year 1913, U.S. corporations have been subject to federal income tax on gross earnings. During the period from 1913 to 2007, the federal corporation income tax was as low as 1% and as high as 52%. During World War II and the Korean War, an additional excise tax brought the total tax to as high as 80%. The current schedule for U.S. corporate income tax rates, shown in Table 17.4, was established in September 2000. The smallest corporations have a rate of only 15%. Above gross earnings of $50,000, the rate increases in steps until it reaches 35% for corporations with gross earnings that equal or exceed $18,333,333. Corporations are also subject to state income tax, which for large corporations varies widely from as low as 3% in Illinois to as high as 9.5% in Vermont, with 5% being a reasonable assumption for preliminary economic analyses. Here, we will use a combined federal and state income tax rate, t, of 35 + 5 = 40%. Thus,

$$\begin{aligned}\text{Net earnings or profit} &= (1 - t)\ \text{gross earnings} \\ &= 0.60\,(S - C)\end{aligned} \tag{17.5}$$

EXAMPLE 17.12

For the data and results of Example 17.11, calculate the annual gross earnings and annual net earnings.

SOLUTION

From Eq. (17.4),

$$\begin{aligned}\text{Annual gross earnings or profit} &= S - C \\ &= \$30{,}008{,}600 - \$28{,}257{,}700 \\ &= \$1{,}750{,}900/\text{yr}\end{aligned}$$

From Eq. (17.5),

$$\begin{aligned}\text{Annual net earnings or profit} &= 0.6(1{,}750{,}900) \\ &= \$1{,}050{,}500/\text{yr}\end{aligned}$$

Of the costs in the cost sheet of Table 17.1, only the costs for labor-related operations, maintenance, operations overhead, property taxes and insurance, and depreciation are considered to be *fixed costs,* which do not vary with the production rate of the plant. Fixed costs are contrasted with the costs of feedstocks, utilities, and general expenses, which are referred to as *variable costs* because they vary directly with the production rate. For a large plant with a large total capital investment and significant economies of scale, the profitability can be sharply increased by substantial savings in utilities such as steam. A smaller plant, in contrast, has a larger fraction of its costs in the investment and the fixed costs of operation; hence, the same percentage decrease in the utilization of steam results in a smaller increase in its profitability. This is one of the reasons that small plants usually have difficulty competing with larger plants in the chemical industry. The reader should keep this in mind while studying the profitability measures in Sections 17.4 and 17.7. Before leaving Table 17.1, the reader is reminded that the prices listed there refer to the year 2014 and should be adjusted in subsequent years, possibly escalated by the rate of inflation.

17.3 WORKING CAPITAL AND TOTAL CAPITAL INVESTMENT

To complete the estimation of the total capital investment, a more accurate estimate of working capital is needed to replace the 15% of total capital investment used in conjunction with Eq. (16.10). In general, working capital refers to funds, in addition to fixed capital and startup funds, needed by a company to meet its obligations until payments are received from others for goods the company has sold them. Accountants define working capital as current assets minus current liabilities; current assets consist of cash reserves, inventories, and accounts receivable, and current liabilities include accounts payable. It is fairly standard to provide working capital for a one-month period of plant operation, because those buying the product are usually given 30 days to make their payments, and the company has 30 days to pay for raw materials. Inventories of products may be much less than a 30-days supply. Here, seven days are assumed. Working capital is fully recoverable and, therefore, is not depreciated. If we apply the definition of working capital to the operation of a chemical plant, working capital is

$$\begin{aligned}C_{WC} = {} & \text{Cash reserves} + \text{Inventory} \\ & + \text{Accounts receivable} - \text{Accounts payable}\end{aligned} \tag{17.6}$$

with the following basis for calculation that follows general accounting practices:

1. Thirty days of cash reserves for raw materials, utilities, operations, maintenance, operating overhead, property taxes, insurance, and depreciation. This amounts to 8.33% of the annual cost of manufacture, COM (assuming 30 days is 1/12 of a year).
2. Seven days of inventories of liquid and solid (but not gas) products at their sales price, which assumes that these products are shipped once each week, whereas gas products are not stored, but are pipelined. This amounts to 1.92% of the annual sales of liquid and solid products.
3. Thirty days of accounts receivable for product at the sales price. This amounts to 8.33% of the annual sales of all products.
4. Thirty days of accounts payable by the company for feedstocks at the purchase price. This amounts to 8.33% of the annual feedstock costs.

EXAMPLE 17.13

For the MCB plant considered in Example 17.11, estimate the working capital and compute the total capital investment if land and royalty costs are zero, but the startup cost is taken as 2% of C_{TDC}. Note that the MCB plant is a small addition to a large benzene-manufacturing process. Include 30 days of accounts receivable, but just 4 days of MCB inventory and 2 days of feedstock as the basis for your estimation. An allocation for cash reserves is not necessary.

SOLUTION

$$\text{MCB inventory} = 0.011(30{,}008{,}600) = \$330{,}100$$
$$\text{Accounts receivable} = 0.0833(30{,}008{,}600) = \$2{,}499{,}700$$
$$\text{Raw materials} = 0.0055(36{,}103{,}300) = \$198{,}600$$

From Eq. (17.6):

$$\text{Working capital} = C_{WC} = \$0.00 + \$330{,}100 + \$2{,}499{,}700 + \$198{,}600 = \$3{,}028{,}400$$

which is much greater than the total depreciable capital.

$$\text{Startup cost} = C_{start} = 0.10(1{,}596{,}500) = \$159{,}700$$
$$\text{Total capital investment} = C_{TCI} = C_{TDC} + C_{start} + C_{land} + C_{WC}$$
$$= \$1{,}596{,}500 + \$159{,}700 + \$31{,}900 + \$3{,}028{,}400 = \$4{,}816{,}500$$

Note that for this case, the working capital is 63% of the total capital investment and much more than the commonly used approximate estimate of 15% of total capital investment. In this example, it appears that working capital is more a function of annual sales (perhaps 10%) than of total depreciable capital.

17.4 APPROXIMATE PROFITABILITY MEASURES

To be a worthwhile investment, a venture for the installation of a new chemical product manufacturing facility, a new chemical plant, or a revamp of an existing plant must be profitable. However, it is not sufficient that a venture make a large net profit. That profit over the life of the venture must be more than the original capital investment for the venture. The greater the excess of profits over investment, the more attractive is the venture. To compare alternative ventures that vie for capital investment, a number of profitability measures have been developed. They are all based on the estimates of capital investment and annual earnings that have been presented in Chapter 16 and the previous sections of this chapter. The simpler, approximate measures discussed in this section and summarized in Table 17.5 ignore the effect of inflation or so-called time value of money and use simple straight-line depreciation. Therefore, they are useful only in the early stages of project evaluation. The rigorous measures that account for the time value of money and faster depreciation are considered in the three subsequent sections and must be considered before a final decision is made on whether to proceed with a new venture.

Return on Investment (ROI)

This profitability measure, introduced earlier as Eq. (17.1), is also called rate of return on investment (ROROI), simple rate of return (ROR), return on original investment, engineer's method, and operator's method. ROI is the annual interest rate made by the profits on the original investment. ROI provides a snapshot view of the profitability of the plant, normally using estimates of the elements of the investment in Table 16.9 and the pre-tax or after-tax earnings in, say, the third year of operation and assuming that they remain unchanged during the life of the process. For ROI and all of the approximate profitability measures of this section, the production cost is computed using straight-line depreciation, and, after some startup period, the plant is assumed to operate each year at full capacity (or at some percentage of full capacity) for the same number of days per year. As was stated earlier, many definitions of ROI have been suggested and used. Here, the most common definition is applied.

$$\text{ROI} = \frac{\text{Net earnings}}{\text{Total capital investment}} = \frac{(1-t)(\text{S}-\text{C})}{C_{TCI}} \qquad (17.7)$$

The calculation of ROI is readily made and the concept is easy to understand. However, as stated above, the definition of ROI involves many assumptions. Furthermore, ROI does not consider the size of the venture. Would a large company favor many small projects over a few large projects when the small projects have just slightly more favorable values of ROI?

Payback Period (PBP)

The *payback period* is the time required for the annual earnings to equal the original investment. Payback period is also called payout time, payout period, payoff period, and cash recovery period. Because it is simple and even more understandable than ROI, PBP is widely used in early evaluations to compare alternatives. Like ROI, the payback period in years has several definitions, but the following is used here. This definition is not consistent with the definition of ROI in Eq. (17.7) because only the depreciable capital is used and the annual depreciation, D, is added back

Table 17.5 Approximate Profitability Measures
Time Value of Money is Ignored and Straight-Line Depreciation is Used.
(details presented in Section 17.4)

Approximate Profitability Measure	Formula[a]
Return on investment (ROI)	$\text{ROI} = \dfrac{\text{Net earnings}}{\text{Total capital investment}} = \dfrac{(1-t)(\text{S}-\text{C})}{C_{\text{TCI}}}$
Payback period (PBP)	$\text{PBP} = \dfrac{C_{\text{TDC}}}{(1-t)(\text{S}-\text{C})+\text{D}}$
Venture profit (VP)	$\text{VP} = (1-t)(\text{S}-\text{C}) - i_{\min}\,(C_{\text{TCI}})$
Annualized cost (AC)	$\text{AC} = C_{\text{A}} = \text{C} + i_{\min}\,(C_{\text{TCI}})$

[a] $i_{\min}$ = reasonable return on investment; t = sum of U.S. federal and state income tax rates; C = annual production cost; D = annual depreciation; S = annual sales revenues; C_{TCI} = total capital investment; C_{TDC} = total depreciable capital.

to the net earnings because that depreciation is retained by the company.

$$\begin{aligned}\text{PBP} &= \frac{C_{\text{TDC}}}{(1-t)(\text{S}-\text{C})+\text{D}} \\ &= \frac{C_{\text{TDC}}}{\text{Net earnings} + \text{Annual depreciation}} \\ &= \frac{C_{\text{TDC}}}{\text{Cash flow}} \end{aligned} \tag{17.8}$$

High-risk ventures should have payback periods of less than 2 yr. In these times of rapid progress in technology, most companies will not consider a project with a PBP of more than 4 yr. PBP is especially useful for simple equipment replacement problems. For example, should an old, inefficient pump be replaced with a new, energy-efficient model? This decision is clear if the PBP is less than 1 yr. PBP should never be used for final decisions on large projects because it gives no consideration to the period of plant operation after the payback period.

EXAMPLE 17.14

A process, projected to have a total depreciable capital, C_{TDC}, of \$90 million, with no allocated costs for outside utilities, is to be installed over a 3-yr period (2014–2016). Just prior to startup, \$40 million of working capital is required. At 90% of production capacity (projected for the third and subsequent operating years), sales revenues, S, are projected to be \$150 million/yr and the total annual production cost, excluding depreciation, is projected to be \$100 million/yr. Also, the plant is projected to operate at 0.5 of 90% and 0.75 of 90% of capacity during the first and second operating years. Thus, during those years, S = \$75 million/yr and \$113 million/yr, respectively. Take straight-line depreciation at 8%/yr. Using the third operating year as a basis, compute

(a) Return on investment (ROI)

(b) Payback period (PBP)

SOLUTION

$$\begin{aligned}\text{Depreciation} &= 0.08(\$90{,}000{,}000) = \$7{,}200{,}000/\text{yr} \\ \text{Total production cost} &= \$100{,}000{,}000 + \$7{,}200{,}000 \\ &= \$107{,}200{,}000/\text{yr} \\ \text{Pre-tax earnings} &= \$150{,}000{,}000 - \$107{,}200{,}000 \\ &= \$42{,}800{,}000/\text{yr} \\ \text{Income taxes} &= 0.40(\$42{,}800{,}000) = \$17{,}100{,}000/\text{yr} \\ \text{After-tax earnings} &= \$42{,}800{,}000 - \$17{,}100{,}000 \\ &= \$25{,}700{,}000/\text{yr} \\ C_{\text{TCI}} &= \$90{,}000{,}000 + \$40{,}000{,}000 \\ &= \$130{,}000{,}000 \end{aligned}$$

(a) From Eq. (17.7),

$$\text{ROI} = \frac{\$25{,}700{,}000}{\$130{,}000{,}000} = 0.198 \text{ or } 19.8\%$$

(b) From Eq. (17.8)

$$\text{PBP} = \frac{\$90{,}000{,}000}{\$25{,}700{,}000 + \$7{,}200{,}000} = 2.74 \text{ yr}$$

In this example, values of both ROI and PBP are sufficient to merit some interest in the project, but they are not sufficient to attract a high degree of interest unless the process is of very low risk and only less-profitable ventures are under consideration.

Venture Profit (VP)

An approximate measure of the profitability of a potential process or product that does take into account the size of the project is venture profit. It is used often for preliminary estimates when comparing alternative flowsheets during the process synthesis stage of process design and/or the *concept* stage of product design. VP is the annual net earnings in excess of a minimum acceptable return on investment, $i_{\min}$. Thus,

$$\begin{aligned}\text{VP} &= (1-t)(\text{S}-\text{C}) - i_{\min}C_{\text{TCI}} \\ &= \text{Net earnings} - i_{\min}C_{\text{TCI}} \end{aligned} \tag{17.9}$$

Sometimes, for crude comparisons of flowsheets with different arrangements of process units, the total capital investment in Eq. (17.9) is estimated as the sum of the bare-module costs, or even the sum of the purchase costs; and annual production cost, C, includes only the cost of the raw materials, the utilities, and the labor-related operations. The return on investment, i_{min}, is that desired by the company. Here, we take $i_{min} = 0.20$ (20%).

EXAMPLE 17.15

For the MCB process considered in Examples 17.11 and 17.13, calculate

(a) Return on investment (ROI)

(b) Payback period (PBP)

(c) Venture profit (VP)

SOLUTION

From the previous examples,

$$C_{TCI} = \$4{,}816{,}500$$
$$C_{TDC} = \$1{,}596{,}500$$
$$\text{Net earnings} = \$1{,}050{,}500$$
$$\text{Depreciation} = \$127{,}700$$

(a) From Eq. (17.7),

$$\text{ROI} = \frac{1{,}050{,}500}{4{,}816{,}500} = 0.2196 \textit{ or } 21.96\%$$

(b) From Eq. (17.8),

$$\text{PBP} = \frac{1{,}596{,}500}{1{,}050{,}500 + 127{,}700}$$
$$= 1.36 \text{ yr or about 17 months}$$

(c) From Eq. (17.9),

$$\text{VP} = \$1{,}050{,}500 - 0.20(\$4{,}816{,}500) = \$87{,}200/\text{yr}$$

These results are promising. The ROI is sufficiently high and the PBP is good. The VP is fairly good for a high interest rate.

Annualized Cost (C_A)

A measure of economic goodness, which does not involve sales revenues for products and is also used for preliminary estimates when comparing alternative flowsheets during process synthesis or alternative product concepts during the *concept* stage of product design, is the *annualized cost*. It is the sum of the production cost and a reasonable return on the original capital investment where, again, the reasonable return on investment, i_{min}, is taken here as 0.2. Thus,

$$C_A = C + i_{min}(C_{TCI}) \tag{17.10}$$

This criterion is also useful for comparing alternative items of equipment in a process or alternative replacements for existing equipment.

EXAMPLE 17.16

Several alternative distillation sequences are being examined for the separation of a mixture of light hydrocarbons. The sequences are to be compared on the basis of annualized cost given by Eq. (17.10). However, for the total capital investment, only the bare-module costs of the columns, trays, condensers, reboilers, and reflux accumulators will be summed. For the total annual production cost, C, only the annual utility costs for the condenser cooling water and reboiler steam will be summed. For one of the columns, design calculations have been completed and the costs have been computed with the following results. The column is a deisobutanizer with a saturated liquid feed of 500 lbmol/hr of isobutane and 500 lbmol/hr of *n*-butane. The distillate is 99 mol% isobutane and the bottoms is 99 mol% *n*-butane. The column shell is carbon steel with carbon-steel sieve trays on 24-in. spacing. The trays have 0.25-in.-diameter holes with a hole area of 10%. The weir height is 2 in. The column pressure is set at 100 psia at the top so that cooling water can be used in the total condenser; the bottoms pressure is 110 psia. Calculations give 100 trays at a reflux ratio of 7.4. This corresponds to a condenser duty of 33,600.000 Btu/hr and a reboiler duty of 33,800,000 Btu/hr. For 24-in. tray spacing, allowing a 10-ft-high bottoms sump below the bottom tray and a 4-ft disengagement height above the top tray, the column height is 212 ft (tangent to tangent). Based on entrainment flooding, the column diameter is determined to be constant at 10 ft.

The bare-module cost of the tower vessel is estimated to be \$3,350,000 and the accompanying tray cost is \$300,000, giving a total bare-module cost for the column of \$3,650,000. The bare-module costs for the column auxiliaries are computed to be

2 Condensers in parallel	\$680,000
Reboiler	170,000
Reflux drum	200,000
Reflux pump + a spare	120,000

The total bare-module cost for the column and its auxiliaries = \$4,820,000

The annual heating steam cost for the reboiler = \$2,180,000/yr

The annual cooling water cost for the two condensers = \$90,000/yr

The annual electricity cost for the reflux pump = \$48,000/yr

The total utility cost = \$2,318,000/yr

Compute the annualized cost.

SOLUTION

For purposes of comparison of alternatives, the bare-module cost of the distillation column and its auxiliary equipment replaces C_{TCI}. The annual utility cost replaces the total annual production cost.

From Eq. (17.10), $C_A = \$2{,}318{,}000 + 0.20(\$4{,}820{,}000) = \$3{,}282{,}000/\text{yr}$.

Product Selling Price for Profitability

In some cases, especially when a new chemical product is to be produced, the selling price may not be known or easily established. For basic chemical products, especially, rather than guess a selling price, a desired return on investment (say, 20%) can be assumed and Eq. (17.7) can then be used to back-calculate the selling price necessary to achieve this objective. Another useful procedure is to set the venture profit to zero and use Eq. (17.9) to back-calculate a minimum selling price. More elaborate methods for determining a selling price are implemented using the rigorous profitability measures in Section 17.7 that account for the time value of money.

For new configured consumer chemical products, such as home hemodialysis products and labs-on-a-chip for high-throughout screening, pricing strategies depend on the consumer market. As discussed in Section 19.4, there are no simple recipes for setting prices.

EXAMPLE 17.17

In Example 17.15, approximated profitability measures when applied to the MCB plant are favorable, assuming MCB is sold for \$0.68/lb. Alternatively:

(a) Use the ROI measure of Eq. (17.7) to estimate a selling price for a 20% return on investment.

(b) Use the VP measure of Eq. (17.9) to estimate a minimum selling price.

SOLUTION

(a) From Example 17.11, C = \$28,257,700/yr and from Example 17.13, C_{TCI} = \$4,783,500. Substitution in Eq. (17.7) gives

$$\text{ROI} = 0.20 = \frac{(1 - 0.4)(44{,}131{,}000x - 28{,}257{,}700)}{4{,}816{,}500}$$

Solving, x = selling price of MCB = \$0.6764/lb, which is slightly lower than \$0.68/lb. To achieve a higher ROI, the selling price increases.

(b) Substitution into Eq. (17.9), with VP = 0, gives

$$\text{VP} = 0 = (1 - 0.4)[44{,}131{,}000x - 28{,}257{,}700] - 0.20(4{,}816{,}500)$$

Solving, x = selling price of MCB = \$0.6767/lb, which is the same result as in part (a). This not surprising because Eqs. (17.7) and (17.9) are identical when VP is set to zero and ROI = $i_{\min}$.

17.5 TIME VALUE OF MONEY

All of the profitability measures discussed so far give only a snapshot view at a given point in time. The total annual sales revenues, S, and the total annual production cost, C, are estimated at critical points, normally for the third operating year. Furthermore, a simple depreciation schedule, typically straight-line depreciation, is used. As mentioned earlier, company resources are often sufficiently limited so as not to justify a more careful examination of the revenues and costs over the life of a proposed product and/or plant at the early stages of consideration. However, because of the compounding effect of interest and inflation, it eventually becomes important to account for the time value of money and to charge for depreciation in accordance with the schedule required by the U.S. Internal Revenue Service since 1986 (modified in 1988). In the next section, the methods of calculating cash flows for each year in the life of a proposed product and/or plant project are presented. With these methods, rigorous profitability measures can be computed as shown in Section 17.7. Before doing this, however, it is necessary to examine in this section how interest is compounded and to discuss annuities and perpetuities. A number of useful formulas are derived and/or presented for single-payment interest in this section. They are summarized in Table 17.6

Compound Interest

The time value of money recognizes the fact that an amount of money at the current time, referred to as *present amount, present sum, present value,* or *present worth* and given the symbol *P,* may not be the same at a future date. Instead, if that money is invested at an *interest rate, i,* and the interest is added to *P,* the amount of money at the future date will be a *future amount, future value,* or *future worth,* here given the symbol *F.* The *interest,* which is the compensation for the use of the money or capital over a period of time, is the difference between *F* and *P.* The concept of interest is complicated because (1) the *interest period* is not necessarily 1 yr, (2) interest may be simple or compound, and (3) compounding may be discrete or continuous.

Let us call the starting present worth or present sum the capital or principal, *P.* Simple interest over several interest time periods is calculated only on *P.* No interest is calculated on interest accrued in previous interest periods, Thus, the total amount of simple interest for n interest periods when i is the simple interest rate per period, is

$$\text{Simple interest} = I_S = F - P = niP \tag{17.11}$$

Simple interest is rarely used. It has been largely replaced by compound interest, which is calculated at each period on the principal plus the accumulated interest. The interest rate, *i,* is now referred to as the compound interest rate per period. The effect of compounding is shown in Table 17.7 in which the future worth, *F,* of the principal, *P,* is calculated for n periods. Beginning at the start of the first period with principal (present worth) *P,* the interest accumulated during the first period is *Pi,* which when added to *P* gives the future worth at the end of the first period as $F = P + Pi = P(1 + i)^1$. After each period, the power to which $(1 + i)$ is raised increases, and consequently, after n compound-interest periods, the principal has grown to

$$F = P(1 + i)^n \tag{17.12}$$

With compound interest, the total amount of interest after n periods is

$$\text{Compound interest} = I_C = F - P = P[(1 + i)^n - 1] \tag{17.13}$$

The factor $(1 + i)^n$ in Eqs. (17.12) and (17.13) is commonly referred to as the *discrete single-payment compound-amount factor.* As shown in Eq. (17.12), when this factor is multiplied by *P*, we obtain the future worth, *F,* after n periods with interest rate per period, i. If Eq. (17.12) is solved for *P*, we obtain

$$P = F\left[\frac{1}{(1 + i)^n}\right] \tag{17.14}$$

where the factor $[1/(1 + i)^n]$ is the discrete single-payment present-worth factor. When applied in this manner, this factor is a *discount factor* because the present worth is less than (is discounted from) the future worth.

Table 17.6 Time Value of Money: Interest, Formulas, Single Payments

Interest Type	Formula[a]
Amount of simple interest	$I_S = F - P = niP$
Single-payment simple-amount factor	$\frac{F}{P} = 1 + ni$
Single-payment simple present-worth factor	$\frac{P}{F} = \frac{1}{1 + ni}$
Compound interest	
Amount of compound interest	$I_C = F - P = P[(1 + i)^n - 1]$
Single-payment compound-amount factor	$\frac{F}{P} = (1 + i)^n$
Single-payment present-worth factor	$\frac{P}{F} = \frac{1}{(1 + i)^n}$
Nominal interest rate per year	$r = im$
Effective discrete compound interest	
Effective discrete annual compound interest rate	$i_{\text{eff}} = (1 + i)^m - 1 = \left(1 + \frac{r}{m}\right)^m - 1$
Amount of discrete compound interest	$I_C = F - P = P\,[(1 + i_{\text{eff}})^{n_y} - 1]$
Discrete single-payment compound-amount factor	$\frac{F}{P} = (1 + i_{\text{eff}})^{n_y}$
Discrete single-payment present-worth factor	$\frac{P}{F} = \frac{1}{(1 + i_{\text{eff}})^{n_y}}$
Effective continuous compound interest	
Effective continuous annual compound interest rate	$i_{\text{eff}} = e^r - 1 = e^{im} - 1$
Amount of continuous compound interest	$I_C = F - P = P\,[(1 + i_{eff})^{n_y} - 1]$
Continuous single-payment compound-amount factor	$\frac{F}{P} = (1 + i_{\text{eff}})^{n_y} = e^{rn_y}$
Continuous single-payment present-worth factor	$\frac{P}{F} = \frac{1}{(1 + i_{\text{eff}})^{n_y}} = e^{-rn_y}$

[a] $i =$ interest rate per period; $m =$ number of periods per year: $r =$ nominal interest rate per year; $n_y =$ number of years; $i_{\text{eff}} =$ effective annual compound interest rate; $n =$ number of interest periods.

Table 17.7 Compound Interest

No. of Periods	Capital at Start of Period	Interest Paid during Period	F = Future Worth at End of Period
1	P	Pi	$P + Pi = P(1 + i)$
2	$P(1 + i)$	$P(1 + i)i$	$P(1 + i)^2$
3	$P(1 + i)^2$	$P(1 + i)^2 i$	$P(1 + i)^3$
.	.	.	.
.	.	.	.
.	.	.	.
n	$P(1 + i)^{n-1}$	$P(1 + i)^{n-1} i$	$P(1 + i)^n$

EXAMPLE 17.18

Determine the interest rate per year required to double $10,000 in 10 yr if the interest rate is

(a) simple

(b) compound

SOLUTION

$$P = \$10{,}000,\ F = 2(10{,}000) = \$20{,}000,\ n = 10 \text{ yr},$$
$$F - P = \$20{,}000 - \$10{,}000 = \$10{,}000$$

(a) From Eq. (17.11), $\$10{,}000 = niP = 10i(\$10{,}000)$

$$\text{Solving, } i = 0.10 \text{ or } 10\%$$

(b) From Eq. (17.13), $\$10{,}000 = P[(1 + i)^n - 1] = \$10{,}000 \times [(1 + i)^{10} - 1]$

$$\text{Solving, } i = 0.0718 \text{ or } 7.18\%$$

Thus, money can double in 10 yr with an interest of just over 7% compounded annually.

As seen in Example 17.18, there is a significant difference between simple interest and compound interest. Looking at this example from another perspective, if the compound interest rate for 10 yr were 10%, from Eq. (17.13), the future worth would be

$25,937 compared to $20,000 for simple interest. When investing money, one should always seek compound interest so that interest is obtained on the interest.

Nominal and Effective Interest Rates

The interest period can be a day, week, month, year, and so on. However, it is commonly defined in fractions of a year, for example, 1 yr, 1/2yr, … , 1/*m* yr, where *m* is the number of periods per year. When the interest period is not 1 yr, it is common to use the concepts of *nominal interest rate* and *effective interest rate* for compound interest, both based on 1 yr. The use of these two concepts permits the calculations to be carried out on an annual basis.

Given the value of *m,* the number of times per year to calculate interest at *i,* and the interest rate per period of 1/*m* yr (*m* times per year), the *nominal interest rate* per year, *r*, is

$$r = im \tag{17.15}$$

If the interest rate is 3%/quarter, then with four quarters per year, the nominal interest rate, *r,* is 0.03(4) = 0.12 or 12%/yr. In the case of simple interest (no compounding), $1,000 at the beginning of a year would yield 1,000(1.12) = $1,200. But more commonly, nominal interest rates are stated on an annual basis with a compounding period, for example, 12% compounded quarterly.

To handle compound interest when the interest period is some fraction of a year, (1/*m*), an effective interest rate per year, i_{eff}, is defined by

$$F_{\text{end of 1 yr}} = P(1 + i_{\text{eff}}) \tag{17.16}$$

Based on *i,* the actual interest rate per 1/*m* yr, we can also write

$$F_{\text{end of 1 yr}} = P(1 + i)^m = P\left(1 + \frac{r}{m}\right)^m \tag{17.17}$$

Equating Eqs. (17.16) and (17.17) and solving for i_{eff} gives

$$i_{\text{eff}} = (1 + i)^m - 1 = \left(1 + \frac{r}{m}\right)^m - 1 \tag{17.18}$$

EXAMPLE 17.19

An interest rate is reported as 3% compounded quarterly. Determine the nominal and effective interest rates per year.

SOLUTION

$$i = 3\%/\text{quarter of a year}, \quad m = 4 \text{ times per year}$$

The nominal interest rate per year, from Eq. (17.15), is

$$r = 0.03(4) = 0.12 \text{ or } 12\%/\text{yr compounded quarterly}$$

From Eq. (17.18), the effective interest rate per year is

$$i_{\text{eff}} = \left(1 + \frac{0.12}{4}\right)^4 - 1 = 0.1255 \text{ or } 12.55\%$$

which is larger than the nominal rate.

Continuous Compounding of Interest

In the limit, as the number of periods per year approaches infinity, that is, as $m \to \infty$, *continuous compounding* occurs, and i_{eff} tends to a maximum value for a given value of *i.* Equation (17.18) becomes

$$i_{\text{eff,cont}} = \lim_{m\to\infty}\left(1 + \frac{r}{m}\right)^m - 1 = \lim_{m\to\infty}\left(1 + \frac{1}{(m/r)}\right)^{(m/r)} - 1$$

Since

$$\lim_{x\to\infty}\left(1 + \frac{1}{x}\right)^x = e = 2.71828\ldots$$

$$\text{and } \lim_{x\to\infty}\left(1 + \frac{1}{x}\right)^{xr} = e^r$$

therefore,

$$i_{\text{eff}} = e^r - 1 \tag{17.19}$$

where *r* is now the nominal annual interest rate compounded continuously, and i_{eff} is the effective annual interest rate compounded continuously. If *r* = 10% per year, from Eq. (17.18), $i_{\text{eff}} = \exp^{0.1} - 1 = 0.10517$ or 10.517%.

With continuous compounding, Eq. (17.12) for the future worth in terms of i_{eff} and the number of years, n_y, becomes

$$F = P(1 + i_{\text{eff}})^{n_y} = Pe^{rn_y} \tag{17.20}$$

With continuous compound interest, the total amount of interest after n_y years is

$$\begin{aligned}\text{Continuous compound interest} &= F - P \\ &= P[(1 + i_{\text{eff}})^{n_y} - 1]\end{aligned} \tag{17.21}$$

The factor $(1 + i_{eff})^{n_y}$ in Eqs. (17.12) and (17.13), which from Eq. (17.19) equals e^{rn_y}, is commonly referred to as the *continuous single-payment compound-amount factor*.

EXAMPLE 17.20

If it is assumed that $200,000 will be needed for a 4-yr college education starting 10 yr from now, how much must be invested today at a 6% nominal annual interest rate compounded (a) continuously and (b) twice annually?

SOLUTION

F = $200,000, r = 0.06,

(a) For continuous compounding, from Eq. (17.19), $i_{\text{eff}} = e^{0.06} - 1 = 0.06184$
From Eq. (17.20), with n_y = 10yr,

$$P = \frac{F}{(1 + i_{\text{eff}})^{n_y}} = \frac{\$200{,}000}{(1 + 0.06184)^{10}} = \$109{,}760$$

(b) Eq. (17.17) gives the future worth for *m* periods per year of compounding at the end of the first year. For n_y years, that equation becomes

$$F = P\left(1 + \frac{r}{m}\right)^{mn_y} \tag{17.22}$$

For compounding twice annually ($m = 2$),

$$P = \frac{F}{\left(1 + \frac{r}{m}\right)^{mn_y}} = \frac{\$200{,}000}{\left(1 + \frac{0.06}{2}\right)^{2(10)}} = \$110{,}740$$

Note that the minimum capital is obtained when the interest is compounded continuously, with a difference of $980 between it and the result for semiannual compounding.

Annuities

Early in this section, only two sums of money were considered, one at the beginning, called present worth, P, and one at the end, called future worth, F. One of these was referred to as the single payment. The two were related by equations involving the interest rate/period and the number of periods that interest was applied. The use of compound interest to determine sums earlier in time (e.g., present worth) that are equivalent to a later, larger sum (e.g., future worth) was referred to as *discounting*. Factors such as $1/(1 + i)^n$ are called *discount factors*. The concepts in the previous section can be extended to a very common situation, called the *annuity*, where instead of a single payment, a series of equal payments is made at equal time intervals. Annuities also involve discounting and discount factors.

Everyday applications of annuities include house, automobile, and other loan payments (installments), when the total amount paid back over the loan period includes not only the principal (original amount of the loan), but also interest, sometimes in substantial amounts. Those saving for retirement put payments into an annuity over a period of years, with interest added to their payments. Upon retirement, retirees receive periodic payments over a specified period of years, with the unpaid amount at any period still accumulating interest. Periodic payments are also made to life insurance policies. Other kinds of annuities are created for corporations to accumulate capital, perhaps for building a new chemical processing plant.

In this section, so-called *ordinary annuities* are defined, in which the payments are made at the end of each of n interest periods and interest, i, is compounded per period. The annuity begins at the start of the first period and finishes at the end of the last period, with the duration referred to as the *annuity term.* At the close of the last period, the future worth, F, of all of the payments made is known as the *amount of the annuity*. A number of formulas are derived or presented in this and the subsequent subsection of Section 17.5. For convenience, they are summarized in Table 17.8. Less common than ordinary annuities and not discussed here are *annuity due*, in which payments are made at the beginning of the period, and the *deferred annuity*, in which the first payment is delayed to a specified date. A *perpetuity* is another form of annuity that continues payments forever.

Discrete Compounding

To determine F when discrete uniform payments of A each are made at the end of each of the n discrete interest periods, the future worth of all the accumulated amounts, payments, and interest is summed to give the amount of the annuity. Thus, starting with the first payment at the end of the first period and finishing with the last payment at the end of the last period,

$$F = A(1 + i)^{n-1} + A(1 + i)^{n-2} + \ \ldots \ + A(1 + i) + A \qquad (17.23)$$

Note that because the first payment is made at the end of the first period, it is compounded over the remaining $(n - 1)$ periods. Also, the last payment is made at the end of the last period, and consequently it is not compounded. Because as n becomes large, Eq. (17.23) becomes cumbersome to evaluate, it is useful to simplify the equation. This is accomplished by multiplying both sides of Eq. (17.23) by $(1 + i)$ to give

$$F(1 + i) = A(1 + i)^n + A(1 + i)^{n-1} + \ \ldots \\ + A(1 + i)^2 + A(1 + i) \qquad (17.24)$$

Then, if Eq. (17.23) is subtracted from Eq. (17.24), we obtain

$$Fi = A(1 + i)^n - A \qquad (17.25)$$

which, when rearranged, gives

$$F = A\left[\frac{(1 + i)^n - 1}{i}\right] \qquad (17.26)$$

Table 17.8 Time Value of Money: Annuity Factors and Uniform-Series Payments[a]

Discrete or Continuous Factor	Periodic Interest A, End of Year, Discrete Factor	Continuous Interest A, End of Year, Continuous Factor	Continuous Interest A, Continuous Factor
Uniform-series sinking-fund deposit factor	$\frac{A}{F} = \frac{i}{(1 + i)^n - 1}$	$\frac{\overline{A}}{F} = \frac{e^r - 1}{e^{rn_y} - 1}$	$\frac{\overline{A}}{F} = \frac{r}{e^{rn_y} - 1}$
Uniform-series compound-amount factor	$\frac{F}{A} = \frac{(1 + i)^n - 1}{i}$	$\frac{F}{\overline{A}} = \frac{e^{rn_y} - 1}{e^r - 1}$	$\frac{F}{\overline{A}} = \frac{e^{rn_y} - 1}{r}$
Uniform-series capital-recovery factor	$\frac{A}{P} = \frac{i(1 + i)^n}{(1 + i)^n - 1}$	$\frac{\overline{A}}{P} = \frac{e^r - 1}{1 - e^{-rn_y}}$	$\frac{\overline{A}}{P} = \frac{r}{1 - e^{-rn_y}}$
Uniform-series present-worth factor	$\frac{P}{A} = \frac{(1 + i)^n - 1}{i(1 + i)^n}$	$\frac{P}{\overline{A}} = \frac{1 - e^{-rn_y}}{e^r - 1}$	$\frac{P}{\overline{A}} = \frac{1 - e^{-rn_y}}{r}$

[a] i = periodic interest rate; A = payment per interest period; n = number of interest periods; $\overline{A}$ = total annual payments per year; r = nominal annual interest rate.

where the factor $[(1+i)^n - 1]/i$ is referred to as the *discrete uniform-series compound-amount factor.* If Eq. (17.26) is solved for A, we obtain

$$A = F\left[\frac{i}{(1+i)^n - 1}\right] \tag{17.27}$$

where the factor $i/[(1+i)^n - 1]$ is referred to as the *discrete uniform-series sinking-fund deposit factor.* A sinking fund consists of periodic deposits that accumulate with interest up to a maturity date. In the past, some companies have used a sinking fund as a depreciation allowance to recover an original capital investment.

Sometimes, periodic payments, A, are made two or more times per year and interest is compounded the same number of times per year, that is, m times each year. In that case, it is convenient to express the annual total of all annuity payments by the variable $\overline{A}$. Then, the payment per period, A, is simply $\overline{A}/m$. Since $i = r/m$ and $n = mn_y$, Eq. (17.26) can be rewritten as

$$F = \frac{\overline{A}}{m}\left[\frac{\left(1+\frac{r}{m}\right)^{mn_y} - 1}{r/m}\right] = \overline{A}\left[\frac{\left(1+\frac{r}{m}\right)^{mn_y} - 1}{r}\right] \tag{17.28}$$

If, in the more general case, equal payments are made p times per year while interest is compounded m times per year, then, according to Bauman (1964), the future worth becomes

$$F = \widehat{A}\left[\frac{\left(1+\frac{r}{m}\right)^{mn_y} - 1}{\left(1+\frac{r}{m}\right)^{m/p} - 1}\right] \tag{17.29}$$

where $\widehat{A}$ is the amount of each payment and $\overline{A} = p\widehat{A}$. Equation (17.29) is not included in Table 17.8, but is considered in Example 17.21.

Continuous Compounding

For continuous compounding of interest with continuous payments, as $m \to \infty$, Eq. (17.26) can be expressed as follows with the limit obtained, as before, from the derivation of Eq. (17.19):

$$\begin{aligned} F &= \lim_{m\to\infty} \overline{A}\left[\frac{(1+r/m)^{(m/r)(rn_y)} - 1}{r}\right] \\ &= \overline{A}\left(\frac{e^{rn_y} - 1}{r}\right) \end{aligned} \tag{17.30}$$

The factor $\left(\frac{e^{rn_y}-1}{r}\right)$ is referred to as the *continuous uniform-series compound-amount factor.* Equation (17.30) seems hypothetical because, although interest can be credited continuously, payments cannot be made continuously.

More practical is continuous compounding of interest, but with equal discrete payments at p times per year and totaling $\overline{A}$ each year, giving the limit of Eq. (17.29) as $m \to \infty$ as

$$\begin{aligned} F &= \lim_{m\to\infty} \widehat{A}\left[\frac{(1+r/m)^{(m/r)(rn_y)} - 1}{\left(1+\frac{r}{m}\right)^{(m/r)(r/p)} - 1}\right] \\ &= \widehat{A}\left(\frac{e^{rn_y} - 1}{e^{(r/p)} - 1}\right) \end{aligned} \tag{17.31}$$

Equation (17.31) is not included in Table 17.8, but the case for just one payment per year, $p = 1$, with continuous compounding, is included.

EXAMPLE 17.21

For the college education savings plan considered in Example 17.20, which is estimated to require \$200,000 10 yr from now, calculate the total of the payments made each year to an annuity at a 6% nominal interest rate for the following conditions:

(a) Interest compounded continuously and payments continuous
(b) Interest compounded continuously but payments quarterly
(c) Interest compounded continuously but payments annually
(d) Interest compounded quarterly and payments quarterly
(e) Interest compounded semiannually and payments semiannually
(f) Interest compounded quarterly and payments monthly

For the lowest and highest payments, on an annual basis, compute the total amount of payments.

SOLUTION

For this example, $r = 0.06$, $F = \$200{,}000$, $n_y = 10$ yr.

Use the $\widehat{A}/F$ or $\overline{A}/F$ uniform-series sinking-fund deposit factors.

(a) Equation (17.30) applies:

$$\overline{A} = F\frac{r}{e^{rn_y} - 1} = \$200{,}000\frac{0.06}{e^{0.06(10)} - 1} = \$14{,}596/\text{yr}$$

(b) Equation (17.31) applies with $p = 4$ payments/yr and $\widehat{A} = \$/\text{payment}$, $\overline{A} = p\widehat{A} = 4\widehat{A}$:

$$\begin{aligned} \widehat{A} &= F\left(\frac{e^{(r/p)} - 1}{e^{rn_y} - 1}\right) = \$200{,}000\left(\frac{e^{0.06/4} - 1}{e^{0.06(10)} - 1}\right) \\ &= \$3{,}677/\text{payment} \end{aligned}$$

Therefore, $\overline{A} = 4(\$3{,}677) = \$14{,}706/\text{yr}$

(c) Equation (17.31) applies with $p = 1$ payments/yr. Therefore, $\overline{A} = \widehat{A}$.

$$\begin{aligned} \overline{A} = \widehat{A} &= F\left(\frac{e^{(r/p)} - 1}{e^{rn_y} - 1}\right) = \$200{,}000\left(\frac{e^{0.06/1} - 1}{e^{0.06(10)} - 1}\right) \\ &= \$15{,}043/\text{yr} \end{aligned}$$

(d) Equation (17.28) applies with $m = p = 4$ payment/yr.

$$\begin{aligned} \overline{A} &= F\left[\frac{r}{\left(1+\frac{r}{m}\right)^{mn_y} - 1}\right] = \$200{,}000\left[\frac{0.06}{\left(1+\frac{0.06}{4}\right)^{4(10)} - 1}\right] \\ &= \$14{,}742/\text{yr} \end{aligned}$$

(e) Equation (17.28) applies with $m = p = 2$ payment/yr.

$$\begin{aligned} \overline{A} &= F\left[\frac{r}{\left(1+\frac{r}{m}\right)^{mn_y} - 1}\right] = \$200{,}000\left[\frac{0.06}{\left(1+\frac{0.06}{2}\right)^{2(10)} - 1}\right] \\ &= \$14{,}886/\text{yr} \end{aligned}$$

(f) Equation (17.29) applies with $m = 4$ payment/yr and $p = 12$ payment/yr. $\overline{A} = p\widehat{A}$.

$$\widehat{A} = F\left[\frac{\left(1+\frac{r}{m}\right)^{m/p}-1}{\left(1+\frac{r}{m}\right)^{mn_y}-1}\right] = \$200{,}000\left[\frac{\left(1+\frac{0.06}{4}\right)^{4/12}-1}{\left(1+\frac{0.06}{4}\right)^{4(10)}-1}\right]$$

$$= \$1{,}222/\text{payment}$$

$$\overline{A} = p\widehat{A} = 12\,(\$1{,}222) = \$14{,}669/\text{yr}$$

Because the nominal interest rate is relatively low, the differences between the answers are not large, ranging from a low of $14,596/yr for continuous compounding of interest and continuous payments to a high of $15,043/yr for annual payments with interest compounded continuously. Thus, the total amount of payments over the 10 yr of payments ranges from $145,960 to $150,430. The annual payment is even higher for discrete annual payments with interest compounded annually: $15,174/yr or a total of $151,740 for 10 yr.

EXAMPLE 17.22

An engineer begins employment at the age of 25 and plans to invest enough money to have $1,000,000 at the retirement age of 65. Assume that payments to the retirement fund will be made each month and that the money will receive interest at 3% compounded quarterly. Calculate the amount of each payment and the total amount of the payments made during the 40-yr savings period.

SOLUTION

Equation (17.29) applies with $F = \$1{,}000{,}000$, $r = 0.03$, $m = 4$ times/yr, and $p = 12$ time/yr.

$$\widehat{A} = F\left[\frac{\left(1+\frac{r}{m}\right)^{m/p}-1}{\left(1+\frac{r}{m}\right)^{mn_y}-1}\right]$$

$$= \$1{,}000{,}000\left[\frac{\left(1+\frac{0.03}{4}\right)^{4/12}-1}{\left(1+\frac{0.03}{4}\right)4(40)-1}\right] = \$1{,}081.77/\textit{month}$$

For the $12(40) = 480$ payments, the total amount of payments is only $480($1,082) = $519,360. The growth of the future worth is exponential as shown in the following table, where 10 years of additional payments are added, giving a future worth of $1,495,731

End of Year	Future Worth ($)	Total Payments ($)
10	150,733	129,812
20	353,974	259,625
30	628,014	389,437
40	997,515	519,250
50	1,495,731	649,062

This example shows the power of compounding.

Present Worth of an Annuity

The *present worth of an annuity, P,* is the amount of money at the present time that, if invested at a compound interest rate, will yield the amount of the annuity, *F,* at a future time. This is useful for determining the periodic payments from an annuity that can be made over a specified number of years in the future.

Annuity equations relating F and the periodic payments, A, are converted to equations relating P to A by combining them with Eq. (17.12) for discrete interest or Eq. (17.20) for continuous interest. This is often referred to as discounting the amount of the annuity to determine its present worth. In Table 17.8 under periodic interest, the discrete uniform-series sinking-fund deposit factor becomes the discrete uniform-series capital-recovery factor in the following manner:

$$P = \frac{F}{(1+i)^n} = A\left[\frac{(1+i)^n-1}{i(1+i)^n}\right] \tag{17.32}$$

Similarly, the continuous, uniform-series capital-recovery with payments, A, at the end of each year is obtained:

$$P = \frac{F}{e^{rn_y}} = \frac{A}{e^{rn_y}}\left[\frac{e^{rn_y}-1}{e^r-1}\right] = A\left[\frac{1-e^{-rn_y}}{e^r-1}\right] \tag{17.33}$$

When comparing two annuities involving many payments into the future, it can be very helpful to discount all of the payments to their present worth. This gives the principal required at the current time, invested at the current interest rate, to enable the payments to be made at the end of each annuity period. While the annuity is making payments, interest continues to be paid on the remaining balance. At the end of the term of the annuity, the balance is zero.

EXAMPLE 17.23

Upon retirement at the age of 65, an employee has a retirement fund of $1,000,000. If this fund is invested at 3% compounded quarterly, how much can be paid to the retiree at the end of each month if the fund is to diminish to zero at the end of 20 yr when the retiree would be 85?

$$r = 0.03,\ m = 4,\ p = 12,\ \text{and } P = \$1{,}000{,}000$$

SOLUTION

Since the period of compounding and the payment period are different, none of the equations in Table 17.8 apply. Instead, use the following extension of Eq. (17.14),

$$P = \frac{F}{(1+i)^n} = \frac{F}{\left(1+\frac{r}{m}\right)^{mn_y}} \tag{17.34}$$

with Eq. (17.29), to give:

$$\widehat{A} = P\left[\frac{\left(1+\frac{r}{m}\right)^{m/p}-1}{1-\left(1+\frac{r}{m}\right)^{-mn_y}}\right]$$

$$\widehat{A} = \$1{,}000{,}000\left[\frac{\left(1+\frac{0.03}{4}\right)^{\frac{4}{12}}-1}{1-\left(1+\frac{0.03}{4}\right)^{-4(20)}}\right]$$

$$= \$5{,}542.24/\text{month or } \$66{,}506.90/\text{yr}$$

Comparing Alternative Equipment Purchases

It is often desirable to compare the purchases of two or more alternative items of equipment, each having a different installed cost and estimated performance life, maintenance cost, and salvage value. The two main methods for comparison, *present worth* and *capitalized cost,* are covered in this subsection. At the outset, it is important to recognize that these measures are examined, often on an ad hoc basis, primarily for the purchase of an equipment item after the plant has been designed. During the comparison of alternative plant designs or major retrofits, when it is important to account for sales revenues, the calculation of *cash flows* is recommended for use in computing the *net present value* (NPV) or the *investor's rate of return* (IRR or DCFRR) as described in the next section. Note, however, that the present worth and NPV are identical when there are no revenues, for example, when comparing alternative methods for treating a waste stream. In general, when making comparisons of alternatives, it is not necessary to consider so-called *sunk costs,* which are costs that occurred in the past but have no effect on current or future decisions.

Present Worth

In the present-worth technique, all of the costs and revenues are discounted to calculate the *present worth* of each alternative. Note that it is crucial to compare the alternatives over the same time period. This approach is illustrated in Example 17.24, in which diagrams show the projected costs and the recovery of the salvage values in time.

EXAMPLE 17.24

Two alternative pumps, A (carbon steel) and B (aluminum), have different installed and maintenance costs, salvage values, and anticipated service lives, as indicated. It is desired to select one of the pumps on the basis of present worth when the effective interest rate is 10%.

	A	B
Installed cost	\$18,000	\$25,000
Uniform end of-year maintenance	\$4,000	\$3,000
Salvage value	\$500	\$1,500
Service life	2 yr	3 yr

SOLUTION

Six years is the shortest time period for which the two pumps can be compared on a common basis because six is the smallest number divisible by both two and three. Thus, pump A is replaced twice and salvaged three times over 6 yr, during which time pump B is replaced once and salvaged twice. For pump A, the costs and salvage values are shown on the following diagram in which the installed and maintenance costs are represented by downward vectors (i.e., negative, compared to zero along the horizontal axis) and the salvage values are represented by upward vectors (i.e., positive). Notice that at the end of the second, fourth, and sixth years, the maintenance costs appear even though the pump is being salvaged and replaced. These are charges that have accumulated over the prior year.

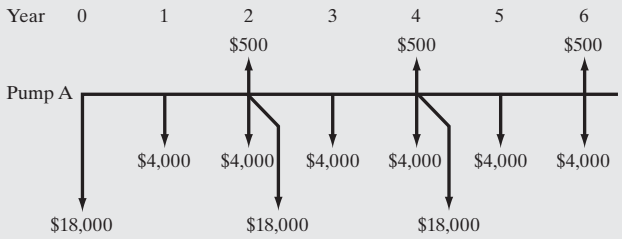

When discounting the costs and salvage values, the maintenance costs can be treated as an annuity, computed using Eq. (17.32) with $i = 0.10$ and $n = 6$, because the cost is periodic and constant at \$4,000/yr. Also, the salvage value can be credited against the purchase cost, giving \$18,000 − \$500 = \$17,500 because they both occur at the end of the second and fourth years. Thus,

$$P_A = -\$18{,}000 - \$4{,}000\left[\frac{(1+0.1)^6-1}{0.1(1+0.1)^6}\right] - \frac{\$17{,}500}{(1+0.1)^2} - \frac{\$17{,}500}{(1+0.1)^4} + \frac{\$500}{(1+0.1)^6}$$
$$= -\$61{,}554$$

The corresponding diagram for pump B is

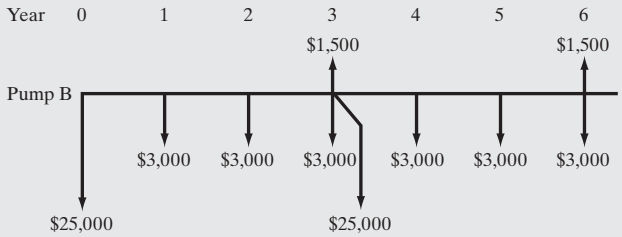

and the discounted costs and salvage values are

$$P_B = -\$25{,}000 - \$3{,}000\left[\frac{(1+0.1)^6-1}{0.1(1+0.1)^6}\right] - \frac{\$23{,}500}{(1+0.1)^3} + \frac{\$1{,}500}{(1+0.1)^6} = -\$54{,}875$$

Although pump B has the higher installation cost, it is selected because its present worth is lower than that of pump A.

Capitalized Costs and Perpetuities

Another method for comparing alternatives, which leads to conclusions identical to those of present worth, is to compute *capitalized costs.* This involves the creation of a *perpetuity* in which periodic replacements continue indefinitely for each alternative. The capitalized cost, K, is defined as the original cost, C_I, plus the present value of the perpetuity for an infinite number of replacements made every n_R years. When a replacement is made, it is common to assign a salvage value, S_{equip}. Thus, if inflation of costs is ignored, the replacement cost is constant at $C_R = C_I - S_{\text{equip}}$. Note that better estimates for the replacement costs, taking into account inflation, likely market conditions, and similar factors, are not normally justified for comparisons involving perpetuities. To account for such factors, the cash flow analysis in the next section is preferred. Assuming a nominal interest rate r compounded m times per year and using the general form of

the discount factor in Eq. (17.34), the investment must provide a future worth, F, every n_y years, sufficient to pay for the replacement of the equipment item and replace the principal, P, so that it can be reinvested for another n_y years. Thus,

$$F_{n_y} = C_R + P = P\left(1 + \frac{r}{m}\right)^{mn_y} \tag{17.35}$$

Rearranging Eq. (17.35), the present value of the perpetuity is

$$P = \frac{C_R}{\left(1 + \frac{r}{m}\right)^{mn_y} - 1} \tag{17.36}$$

From the definition of the capitalized cost,

$$K = C_I + P = C_I + \frac{C_R}{\left(1 + \frac{r}{m}\right)^{mn_y} - 1} \tag{17.37}$$

EXAMPLE 17.25

Select one of the two pumps in Example 17.24 on the basis of capitalized costs.

SOLUTION

To use capitalized costs when annual operating costs are also required (in this case for maintenance), it is appropriate to discount the operating cost payments to present worth, using the annuity equation [Eq. (17.32)], and to add this to the equipment installed cost. For pump A, the initial adjusted installed cost is

$$C_{I_A} = \$18{,}000 + \$4{,}000\left[\frac{(1+0.1)^2 - 1}{0.1(1+0.1)^2}\right] = \$18{,}000 + \$6{,}940$$
$$= \$24{,}940$$

and the equipment cost, using Eq. (17.37) with $r = 0.1$, $m = 1$, and $n_y = 2$, is

$$K_A = \$24{,}940 + \frac{\$24{,}940 - \$500}{(1+0.1)^2 - 1} = \$24{,}940 + \$116{,}380$$
$$= \$141{,}320$$

Turning to pump B,

$$C_{I_B} = \$25{,}000 + \$3{,}000\left[\frac{(1+0.1)^3 - 1}{0.1(1+0.1)^3}\right] = \$25{,}000 + \$7{,}460$$
$$= \$32{,}460$$

and

$$K_B = \$32{,}460 + \frac{\$32{,}460 - \$1{,}500}{(1+0.1)^3 - 1} = \$32{,}460 + \$93{,}540$$
$$= \$126{,}000$$

Indeed, pump B has the lower capitalized cost, a result consistent with the comparison in Example 17.24 of the two present worths. In fact, P_A/P_B in Example 17.24 equals K_A/K_B in Example 17.25.

17.6 CASH FLOW AND DEPRECIATION

The approximate profitability measures in Section 17.4—although often used to select the most promising new products during the *concept* stage of product design or the most promising chemical processes for the manufacture of existing chemical products—are often inadequate to enable management to make a final decision regarding the financial feasibility of a potential new design. Dr. Robert M. Busche, former President of Bio-en-gene-er Associates and a long-time engineer and venture analyst at DuPont, often reminds students that chemical companies like DuPont were awash in cash assets during the period following World War II and throughout the 1950s and 1960s. At that time, the principal challenges were to develop new products and commercialize them quickly. Approximate measures of financial goodness, like the return on investment (ROI), were used routinely to decide whether a chemical product or process was sufficiently promising to fund. In the 1970s and 1980s, however, cash assets became less plentiful, and the competition among potential chemical products and processes for the limited resources of a company became much stiffer. To arrive at decisions, management required more accurate assessments of the financial aspects of potential processes, and consequently, companies began to require cash flow estimates for each year of operation of the most promising chemical products and processes. This change in perspective was signaled in a pioneering paper by Souders (1966). Note, however, that the ROI, as well as the PBP, continue to be computed, primarily because they are easy to calculate. They permit a quick comparison of investments with relatively few calculations and are especially useful when the costs and revenues are not anticipated to change significantly over the life of the project.

As was discussed in Chapter 16, *cash flow* for a company has become an important financial factor. Cash flow is defined as the net passage of money into or out of a company due to an investment. It may be positive (into) or negative (out of). For investment evaluation, investments are considered a negative cash flow, whereas after-tax profits plus depreciation are positive cash flows. During the years of plant construction or creation of a chemical product manufacturing facility, the cash flow, CF, for a particular year, is

$$\text{CF} = -fC_{\text{TDC}} - C_{\text{WC}} - C_{\text{land}} \tag{17.38}$$

where f is the fraction of the total depreciable capital, C_{TDC}, expended that year, and C_{WC} and C_{land} are the working capital and the cost of land that are expended, respectively if any, during that year of construction.

To estimate the cash flow for a particular year of plant operation, the pre-tax earnings are computed from Eq. (17.4) and the after-tax earnings from Eq. (17.5). However, in the calculation of the production cost, a more elaborate depreciation schedule, discussed in the next section, replaces the straight-line depreciation used in Section 17.2. The cash flow from plant and product manufacturing operations is the after-tax earnings plus the depreciation:

$$CF = (1 - t)(\text{S} - \text{C}) + \text{D} = 0.60(\text{S} - \text{C}) + \text{D} \tag{17.39}$$

During the first year of operation, startup costs may occur. During all years of operation, there may be royalty and additional investment costs. At the conclusion of plant operations, there may be a salvage value for used equipment, S_{equip}. The annual cash

flow, *CF,* for any year of the project, including the construction phase and possible salvage at the end of operation, is

$$CF = (1 - t)\,(\mathrm{S} - \mathrm{C}) + \mathrm{D} - fC_{\mathrm{TDC}} - C_{\mathrm{WC}} - C_{\mathrm{land}} - C_{\mathrm{startup}} - C_{\mathrm{royal}} + S_{\mathrm{equip}} \qquad (17.40)$$

In Eq. (17.40), the depreciable capital is normally expended before operation of the plant or product manufacturing facility begins, and the working capital is usually expended in the year preceding the beginning of operation. The working capital is recovered during the last year of operation as a negative entry (to give a positive cash flow) in Eq. (17.40). A common convention is that all cash transactions take place at the end of the year. It is also common to project cash flows for new commodity chemical products over 10-plus years, typically 15 yr, whereas cash flows are projected for established commodity chemical products for 20 yr or more. Another convention recommended by Busche (1995) is to design commodity chemical plants on a capacity basis to operate during 330 days (7,920 hr) per year with 35 days for shutdowns due to maintenance needs and malfunctions. This corresponds to an operating factor of 0.9041. Some companies prefer to round this figure to 8,000 hr/yr. In addition, Busche recommends that the total production cost, C (computed using the cost sheet of Table 17.1), and sales, S, be computed for production at less than 100% of capacity during the first and, perhaps, second year of operation, while the plant is being started up and any design flaws are being remedied.

For specialty chemicals, including many pharmaceuticals and many new consumer products, the rapid development of new technologies shortens the projected life of the new chemical products. Chapter 19, Business Decision Making in Product Development, covers typical cash flow considerations for new chemical products.

Depreciation

Depreciation is the reduction in value of an asset. Recall from the cost sheet of Table 17.1 that a company is allowed to treat depreciation as a cost of production, thereby reducing its income tax liability even though depreciation is not an actual cash flow out of the company. When calculating approximate profitability measures such as the return on investment (ROI), it is common to calculate the cost of sales using straight-line (SL) depreciation as in Table 17.1. Since the approximate profitability measures give just a snapshot view of the economic goodness of a proposed project, usually projected for the third year of operation, no other method of accounting for the depreciation of the total depreciable capital is justified.

Two profitability measures discussed here that provide more rigor—net present value (NPV) and investor's rate of return (IRR)—involve the discounting of cash flows to present worth, as discussed in the next section. These measures increase in magnitude when a larger fraction of the total depreciation is taken in the early years of operation, when the plant or product manufacturing facility is probably operating below capacity and the discount factors are low. For these reasons, it is advantageous for a company to rapidly depreciate its capital investment early in the life of a process instead of using straight-line depreciation. Depreciation methods that favor the earlier years include the *declining-balance* (DB) *method*, the *double declining-balance* (DDB) *method*, and the *sum-of-the-years digits* (SYD) *method*. More recently, in 1981, the U.S. federal income tax regulations provided an *Accelerated Cost Recovery System* (ACRS) for early depreciation. A *Modified Accelerated Cost Recovery System* (MACRS) went into effect in 1987. The ACRS and MACRS methods combine aspects of the DB or DDB methods with the SL method. These five methods are discussed next and compared to straight-line depreciation. Another depreciation method that is sometimes referred to is the sinking-fund method. However, it decelerates rather than accelerates depreciation and, therefore, is not of interest to most industries and is not considered here. It is important to note that a company may use two or more different depreciation methods, most commonly (1) one method for *book depreciation* for internal financial accounting and (2) one method for *tax depreciation* that follows government regulations.

All of the depreciation methods to be discussed are based on the asset *book value,* which at any year is defined as the original cost of the asset (e.g., the depreciable capital investment) minus the sum of the depreciation charges made to the asset up to that year. This is in contrast to the *market value,* which is the price that could be obtained for the asset if it were placed for sale in the open market, and to the *replacement value,* which is the cost of replacing the asset. The book value is the value shown on the accounting records. The book value decreases each year until it reaches a salvage value, at which time it is completely depreciated. The number of years, *n,* over which an asset can be depreciated is usually related to an estimate of the useful life of the asset, which is discussed here.

Declining-Balance (DB) *and Double Declining-Balance* (DDB) *Methods*

The declining-balance method is also referred to as the fixed percentage or uniform percentage method because the amount of depreciation each year is a fixed fraction, *d,* of the book value of the depreciable asset. Let B = the original cost of the asset, which is usually called the *basis*; t = years of service of the asset; and BV_t = book value at the end of year t. Then, the amount of annual depreciation, D_t, for the year t is given by

$$D_t = BV_{t-1} - BV_t = dBV_{t-1} \qquad (17.41)$$

Consequently, after $t - 1$ yr, the book value is

$$BV_{t-1} = B(1 - d)^{t-1} \qquad (17.42)$$

Combining Eqs. (17.41) and (17.42) gives

$$D_t = dB(1 - d)^{t-1} \qquad (17.43)$$

Limits are placed on the value of d, allowing it to range only from $1/n$ to $2/n$ with $1.5/n$ (150% declining balance) and $2/n$ (200% or double declining balance) being common values. With the declining-balance methods, a salvage value is not used. However, the book value, which never reaches zero because it is only decreased each year by a fixed fraction, is not permitted to drop below the estimated salvage value. To force the book value

to the salvage value at the end of year *n,* it is considered desirable to use the *combination method,* which involves switching from the declining-balance method to the straight-line method partway through the service life. Another scheme is to back-calculate the value of d that will give a book value equal to the salvage value at year $t = n$. This value of d is obtained from Eq. (17.42) by setting $(t - 1) = n$. Thus,

$$S_{\text{equip}} = B(1 - d)^n \tag{17.44}$$

Solving Eq. (17.44) for d gives

$$d = 1 - \left(\frac{S_{\text{equip}}}{B}\right)^{1/n} \tag{17.45}$$

However, if the computed $d > 0.2$, it is out of the accepted range and cannot be used. In that case, the only alternative declining-balance method is the combination method as illustrated in the following example.

EXAMPLE 17.26

A new instrument is purchased for the control laboratory of a plant at a cost of $200,000. It is estimated to have a 10-yr useful life with a salvage value of $30,000. Estimate the amount of depreciation each year by the following methods:

(a) Straight-line depreciation over 10 yr based on $200,000 − $30,000 = $170,000

(b) Declining-balance depreciation with $d = 1/n$

(c) 150% declining-balance depreciation

(d) Double declining-balance depreciation

(e) Combination method of double declining-balance depreciation switching to straight-line depreciation after 5 yr.

SOLUTION

(a) The amount of depreciation each year is constant at $170,000/10 = $17,000.

From Eq. (17.45), for declining-balance methods,

$$d = 1 - \left(\frac{S_{\text{equip}}}{B}\right)^{1/n} = 1 - \left(\frac{\$30{,}000}{\$200{,}000}\right)^{1/10} = 0.173$$

Therefore, the 100% and 150% declining-balance methods will not be attractive since this $d > 0.10$ and 0.15. The 200% declining-balance method and the combination method will lead to good results.

(b) The depreciation each year is computed from Eq. (17.41) with $B = \$200{,}000$ and $d = 1/10 = 0.10$. See the following table.

(c) Use Eq. (17.41) with $B = \$200{,}000$ and $d = 1.5/10 = 0.15$. See the following table.

(d) Use Eq. (17.41) with $B = \$200{,}000$ and $d = 2/10 = 0.20$. See the following table.

(e) Use Eq. (17.41) with $B = \$200{,}000$ and $d = 1.5/10 = 0.15$. for the first five years and then subtract the salvage value from the book value and continue with straight-line depreciation. See the following table.

The results of the calculations, which are readily carried out on a spreadsheet, are as follows: For parts (a), (b), and (c):

	Straight-Line Depreciation		Declining Balance ($d = 0.1$)		Declining Balance ($d = 0.15$)	
End of Year	D ($/yr)	*BV* ($)	D ($/yr)	*BV* ($)	D ($/yr)	*BV* ($)
0		200,000		200,000		200,000
1	17,000	183,000	20,000	180,000	30,000	170,000
2	17,000	166,000	18,000	162,000	25,500	144,500
3	17,000	149,000	16,200	145,800	21,675	122,825
4	17,000	132,000	14,580	131,220	18,424	104,401
5	17,000	115,000	13,122	118,098	15,660	88,741
6	17,000	98,000	11,810	106,288	13,311	75,430
7	17,000	81,000	10,629	95,659	11,314	64,115
8	17,000	64,000	9,566	86,093	9,617	54,498
9	17,000	47,000	8,609	77,484	8,175	46,323
10	17,000	30,000	7,748	69,736	6,949	39,375

Note in the table for parts (b) and (c) that the salvage value of $30,000 is not reached by year 10. Thus, these are not good methods to apply.

For parts (d) and (e):

	Declining Balance ($d = 0.20$)		Combination Method	
End of Year	D ($/yr)	*BV* ($)	D ($/yr)	*BV* ($)
0		200,000		200,000
1	40,000	160,000	40,000	160,000
2	32,000	128,000	32,000	128,000
3	25,600	102,400	25,600	102,400
4	20,480	81,920	20,480	81,920
5	16,384	65,536	16,384	65,536
6	13,107	52,429	7,107	58,429
7	10,486	41,943	7,107	51,322
8	8,389	33,554	7,107	44,214
9	3,554	30,000	7,107	37,107
10	0	30,000	7,107	30,000

For part (d), the double declining-balance method with $d = 0.2 > 0.173$ the salvage value is reached by the book value before 10 yr. As shown in the table, it is reached in year 9, so that no depreciation is taken in year 10. In part (e), the combination method switches from the double declining-balance method to the straight-line method in year 6, such that the book value becomes the salvage value in year 10. For these two methods, the depreciation is greatly accelerated over the straight-line method in the first 4 yr.

Sum-of-the-Years Digits (SYD) *Method*

This is a classic depreciation acceleration method that has the advantage of being able to handle a salvage value including zero. Its disadvantage is that the depreciation acceleration is less than the double declining-balance method. Its name is derived from

the use of the sum of the digits from 1 to n, the number of years of useful life of the asset. This sum in compact form is given by

$$\text{SUM} = \sum_{j=1}^{n} j = \frac{n(n+1)}{2} \tag{17.46}$$

Thus, for $n = 10$ yr, SUM $= 10(10 + 1)/2 = 55$. The annual depreciation is

$$D_t = \frac{\text{Depreciable years remaining}}{\text{SUM}}(B - S_{\text{equip}}) \tag{17.47}$$

Thus, if $n = 10$ yr, the fraction depreciated the first year is $10/55 = 0.1818$, which is almost twice that of the straight- line method. For the next year, the fraction is $9/55 = 0.1636$. In year 6, the fraction is $5/55 = 0.0909$, which is now less than the straight-line depreciation of 0.10. If Example 17.26 is applied to the SYD method, the following results are obtained, which are compared to the DDB method:

	Sum-of-the-Years Digits		Declining Balance ($d = 0.20$)	
End of Year	D ($/yr)	*BV* ($)	D ($/yr)	*BV* ($)
0		200,000		200,000
1	30,909	169,091	40,000	160,000
2	27,818	141,273	32,000	128,000
3	24,727	116,545	25,600	102,400
4	21,636	94,909	20,480	81,920
5	18,545	76,364	16,384	65,536
6	15,455	60,909	13,107	52,429
7	12,364	48,545	10,486	41,943
8	9,273	39,273	8,389	33,554
9	6,182	33,091	3,554	30,000
10	3,091	30,000	0	30,000

In the first three years, the DDB method accelerates the depreciation much more than the SYD method, although the depreciation in the first year of the SYD method, $30,909, is considerably higher than the $17,000 of the straight-line method.

ACRS *and* MACRS *Methods for Tax Depreciation*

From 1982 to 1986, the U.S. federal income tax regulations required companies to use the Accelerated Cost Recovery System (ACRS) to depreciate property when computing federal income tax. In 1987, the Modified Accelerated Cost Recovery System (MACRS) replaced that system.

Both systems are based on the declining-balance method with a switch to the straight-line method when it offers a faster depreciation write-off. However, both methods assume that assets are placed in service at the midpoint of the tax year. Therefore, for both methods, only 50% of the DB depreciation is allowed in the first year. Another departure occurs for the MACRS method, because the depreciation is continued for 1 yr beyond the life, but only 50% of the straight-line depreciation is taken in that final year. For both methods, the service life (called *class life*) is fixed by regulations for from 3 to 15 yr, and to 20 yr and even longer (in the case of some structures) for the MACRS method.

Table 17.9 MACRS Tax-Basis Depreciation

	Percent of Total Depreciable Capital (C_{TDC}) for Class Life of			
Year	5 Years	7 Years	10 Years	15 Years
1	20.00	14.29	10.00	5.00
2	32.00	24.49	18.00	9.50
3	19.20	17.49	14.40	8.55
4	11.52	12.49	11.52	7.70
5	11.52	8.93	9.22	6.93
6	5.76	8.92	7.37	6.23
7	100.00	8.93	6.55	5.90
8		4.46	6.55	5.90
9		100.00	6.56	5.91
10			6.55	5.90
11			3.28	5.91
12			100.00	5.90
13				5.91
14				5.90
15				5.91
16				2.95
				100.00

The depreciation calculations are best carried out using the U.S. tables. The MACRS depreciation table is shown in Table 17.9 for the class lives of 5, 7, 10, and 15 yr. The selection of class life is also regulated by the U.S. federal government, which offers two options: (1) the General Depreciation System (GDS) and (2) the Alternative Depreciation System (ADS). The GDS allows a more desirable, shorter class life and is the preferred choice. However, the ADS is sometimes used by new businesses that do not need the tax benefit of accelerated depreciation.

Table 17.10 gives the GDS class life for a number of different kinds of assets. For most new chemical plant projects, a class

Table 17.10 GDS Class Life for Use with the MACRS Depreciation Method

Type of Asset	GDS Class Life (years)
Special manufacturing and handling devices (e.g., tractors)	3
Autos, trucks, buses; cargo containers, computers and peripherals; copy and duplicating equipment; some manufacturing equipment	5
Railroad cars, engines, tracks; agricultural machinery; office furniture; petroleum and natural gas equipment and some other manufacturing equipment; all other business assets not listed in another class	7
Equipment for water transportation, petroleum refining, agriculture product processing, durable-goods manufacturing, and shipbuilding	10
Land improvements, docks, roads, drainage, bridges, pipelines, landscaping, nuclear-power production, and telephone distribution	15
Farm buildings, telephone switching buildings, power production equipment, municipal sewers, and water utilities	20
Residential rental property, including mobile homes	27.5
Nonresidential real property attached to the land	39

life of 5, 7, or 10 yr is used. For these three class lives, Table 17.9 shows that depreciation begins with the double declining-balance method. For example, for a class life of 10 yr, depreciation in the first year is 50% of $2/n = 2/10 = 0.20$, which gives the 10% shown in the table. When 10% of the basis, B, is subtracted from B, the book value is 90% of the basis. In year 2, the DDB depreciation is 20% of the 90% or 18%, which is the value shown in the table. Also, for a same class life of 10 yr, the table shows a switch to straight-line depreciation of 6.55% in year 7 because the calculated DDB depreciation would be lower at 5.90%

EXAMPLE 17.27

In Example 17.14, the total depreciable capital of a new plant is projected to be $90 million. Compute the annual depreciation by the MACRS method for class lives of 5, 7, and 10 yr and the income taxes saved because of depreciation during an 11-year period for a combined federal and state income tax rate of 37% rather than the recommended 40%. Assume no salvage value.

SOLUTION

The basis for depreciation is $90,000,000. The amount of depreciation for each year is the product of the basis and the fractional percentage depreciation from Table 17.9. The savings in income tax each year is 37% of the amount of depreciation. The calculations are readily made with a spreadsheet, which gives the following results.

These results show for the three cases the same total depreciation of $90,000,000. which equals the basis, and the same total income tax savings of $33,300,000 because of depreciation. However, when the present values of the tax savings for each year are computed from Eq. (17.14) and summed for each of the three cases, the results are different, with the shorter class life favored, as shown below for a nominal interest rate of 10% compounded annually.

The class life of 5 yr is superior to 7 yr, and even more so to 10 yr.

Class Life (years)	Present Value of Income Tax Savings
5	$25,750,000
7	$24,024,000
10	$21,783,000

Before leaving this complex topic, it is important to emphasize that depreciation does not involve a transfer of cash; it is just an accounting artifact. In the calculation of cash flows, it is needed to calculate the taxable earnings from which income tax is computed [Income tax $= 0.40(S - C)$]. Then, as shown in Eq. (17.39), depreciation is added back to the after-tax earnings to obtain cash flows. From an income tax standpoint, depreciation should be taken as rapidly as the law permits.

Depletion

Whereas depreciation applies to assets that can be replaced, *depletion* applies to natural resources, which when removed for processing disappear forever or are renewed only by nature over a period of many years. Depletion is applicable to fisheries, forests, mineral deposits, natural gas wells, oil deposits, orchards, quarries, vineyards, and so on. The U.S. federal government permits those using natural resources a depletion allowance, which acts like depreciation as an expense against sales revenue. Two methods are used to calculate the annual depletion allowance: *cost* (or factor) *depletion* and *percentage depletion*.

Cost Depletion

This method is based on the usage of the resource each year, starting with an estimate of the amount of resource that can be removed (recovered) and its cost. Since it may be difficult to make an initial estimate of the amount of recoverable resource, the estimate can be revised at a later date. To use this method, a cost depletion factor, p_t, for the year t is defined as

$$p_t = \frac{\text{First cost of the resource}}{\text{Estimated units of recoverable resource}} \tag{17.48}$$

where the units are barrels for oil, tons for ore, standard cubic feet for gas, board feet for lumber, and so on. The depletion charge for year t is the product of the cost depletion factor and the recovered number of units in year t. The total depletion charge cannot exceed the first cost of the resource.

	Class Life = 5 years		Class Life = 7 years		Class Life = 10 years	
Year	D ($/yr)	Taxes Saved ($/yr)	D ($/yr)	Taxes Saved ($/yr)	D ($/yr)	Taxes Saved ($/yr)
1	18,000,000	6,660,000	12,861,000	4,758,570	9,000,000	3,330,000
2	28,800,000	10,656,000	22,041,000	8,155,170	16,200,000	5,994,000
3	17,280,000	6,393,600	15,741,000	5,824,170	12,960,000	4,795,200
4	10,368,000	3,836,160	11,241,000	4,159,170	10,368,000	3,836,160
5	10,368,000	3,836,160	8,037,000	2,973,690	8,298,000	3,070,260
6	5,184,000	1,918,080	8,028,000	2,970,360	6,633,000	2,454,210
7	0	0	8,037,000	2,973,690	5,895,000	2,181,150
8	0	0	4,014,000	1,485,180	5,895,000	2,181,150
9	0	0	0	0	5,904,000	2,184,480
10	0	0	0	0	5,895,000	2,181,150
11	0	0	0	0	2,952,000	1,092,240
Total $	90,000,000	33,300,000	90,000,000	33,300,000	90,000,000	33,300,000

Table 17.11 Allowable Percentages of Gross Income for Depletion of Natural Resources When Using Percentage Depletion

Natural Resource	Percentage of Gross Income
Gravel, peat, sand, and some stones	5
Coal, lignite, and sodium chloride	10
Most other minerals and metal ores	14
Copper, gold, iron ore. and silver	15
Oil and gas wells (only for small producers)	15
Lead, nickel, sulfur, uranium, and zinc	22

Percentage Depletion

For the natural resources listed in Table 17.11, a special consideration is given. A constant percentage of the sales revenue (referred to as the gross income) from the resource may be depleted, provided that it does not exceed 50% of the taxable income (before the depletion allowance) of the company. Total depletion charges are allowed to exceed the first cost of the resource. The allowable percentage depends on the type of resource as given in Table 17.11. However, for oil and gas, only small producers are allowed to use percentage depletion.

When percentage depletion is applicable, cost depletion is also computed and the method giving the largest annual depletion charge is used.

EXAMPLE 17.28

A mining property containing an estimated 900,000 tons of lead and zinc ore is purchased for $4,500,000. In the first year of operation, 100,000 tons of the ore is mined and sold for $20/ton. The expenses that year are $1,200,000. Calculate the net profit and cash flow by (a) cost depletion and (b) percentage depletion. Assume a tax rate of 40%.

SOLUTION

The sales revenue (gross income) = 20(100,000) = $2,000,000.

(a) From Eq. (17.48), p_t = $4,500,000/900,000 = $5/ton

Depletion charge = 5(100,000) = $500,000

Profit before taxes = $2,000,000 − $1,200,000 − $500,000 = $300,000

Income tax = 0.40(300,000) = $120,000

Net profit (after tax) = $300,000 − $120,000 = $180,000

Cash flow = net profit + depletion charge = $180,000 + $500,000 = $680,000

(b) From Table 17.11, the allowable % of gross income for depletion = 22%

Depletion allowance = 0.22($2,000,000) = $440,000

Taxable income before depletion = $2,000,000 − $1,200,000 = $800,000

The percentage depletion allowance of $440,000 exceeds 50% of the taxable income before the depletion allowance. Therefore, the depletion allowance can only be 0.50 ($800,000) = $400,000.

Profit before taxes = $800,000 − $400,000 = $400,000

Income tax = 0.40($400,000) = $160,000

Net profit (after tax) = $400,000 − $160,000 = $240,000

Cash flow = $240,000 + $400,000 = $640,000

In this example, cost depletion is better than percentage depletion.

17.7 RIGOROUS PROFITABILITY MEASURES

The two principal profitability measures that involve the time value of money in terms of discounted cash flows are the net present value or worth (NPV) and the investor's rate of return (IRR), which is also referred to as the discounted cash flow rate of return (DCFRR). These measures are anomalous in that, when used to compare alternative chemical products and processes, they often give different results. This has led to substantial disagreement within the finance community (Brealey and Myers, 1984).

When using NPV and IRR, the discounting is normally made with Eq. (17.34) using a nominal interest rate, r, that is compounded annually ($m = 1$), with n_y starting from the beginning of the first year of chemical product or plant design. It is possible to account for *investment creep* in the projection of the cash flows. This usually arises through small annual increases in the investment, on the order of 1–1.5%, due to small projects to install additional equipment as the capacity of the process or product manufacturing facility is increased or process modifications are needed. The additional investment is depreciated on the same schedule as the original investment. The calculations are more complex, but are readily made when calculating cash flows.

When carrying out a rigorous profitability analysis, some design teams adopt the convention of reducing the process yield by a small amount, such as 2%, to account for the loss of raw materials and products during startups, shutdowns, and periods when there are malfunctions. Often, raw materials are vented or flared during startup. In other cases, one part of the plant shuts down while the remainder continues to operate, with small amounts of intermediate products vented when they are nontoxic and not easily stored, until the idle portion of the plant is restarted.

Finally, when calculating the cash flow for the last year of operation, it is common to take credit for the working capital investment. Some companies also take credit for a projection of the salvage value of the plant or the product manufacturing facility, assuming that it is dismantled and sold at the end of its useful life. Because salvage values are difficult to estimate and in some cases distort the NPV and IRR, many companies prefer to be conservative and assume a zero salvage value.

The NPV method is simpler to implement than the IRR method and is well defined, whereas the IRR is not defined in all situations. Because the latter involves an iterative computation of the net present value, the simpler to calculate NPV is discussed first.

Net Present Value (NPV)

To evaluate the *net present value* (NPV) of a proposed plant or product manufacturing facility, its cash flows are computed for each year of the projected life of the plant or product manufacturing facility, including construction and startup phases. Then, given the interest rate specified by company management (typically 15%), each cash flow is discounted to its present worth. The sum of all the discounted cash flows is the net present value. The NPV provides a quantitative measure for comparing the capital required for competing products and processes in current terms. However, the result is usually quite sensitive to the assumed interest rate, with proposed products and processes changing favor as the interest rate varies. An illustration of the calculation of NPV is given in Example 17.29, following a discussion of the IRR method.

Investor's Rate of Return (IRR or DCFRR)

The *investor's rate of return* (IRR), also called the *discounted cash flow rate of return* (DCFRR), is the interest rate that gives a net present value of zero. Since the net present value is a complex nonlinear function of the interest rate, an iterative procedure (easily accomplished using a spreadsheet) is required to solve

$$\text{NPV}\{r\} = 0 \quad \text{for } r \tag{17.49}$$

When comparing proposed products and processes, the largest IRR is the most desirable. Note, however, that sometimes the product and process with the largest IRR have the smallest NPV. In many cases, especially when the alternatives have widely disparate investments, both the NPV and the IRR are effective measures. This is especially true when the alternatives are comparable in one measure but are very different in the other. The following example computes both the NPV and the IRR.

EXAMPLE 17.29 ***(Example 17.14 Revisited)***

For the process considered in Example 17.14, but with MACRS depreciation for a 5-yr class life as determined in Example 17.27, calculate over an estimated life of 15 yr, including years 2014–2016 when the plant is being constructed (a) the NPV for a nominal interest rate of 15% compounded annually and (b) the nominal interest rate for the IRR method (i.e., for NPV = 0). For the first 2 yr of plant operation, when at 45 and 67.5% of capacity, the cost of production, exclusive of depreciation, is \$55 million and \$78 million, respectively.

SOLUTION

(a) The cash flows are listed in the following table in millions of dollars per year. Note that the total depreciable capital of \$90 million is divided into three equal parts for the first 3 yr. The working capital of \$40 million appears in the third year. Plant startup costs in the years 2018 and 2019 are not included and no salvage is taken at the end of the project. In the year 2016, the investment in millions is $-\$30 - \$40 = -\$70$ and the discount factor is $1/(1 + 0.15)^2 = 0.7561$. Therefore, the PV is $0.7561(-70) = -52.93$ or $-\$52.93$ million. Instead of showing negative signs in the table, negative values are enclosed in parentheses. When added to the $-\$56.09$ million for the cumulative PV for 2015 a cumulative PV of $-\$109.02$ million is obtained for 2016. In the first year of plant operation, 2017, sales revenue is \$75 million, MACRS depreciation is \$18 million, and production cost exclusive of depreciation is \$55 million. Therefore, pre-tax earnings are $75 - 55 - 18 = \$2$ million. The combined federal and state income tax is $0.40(2) = \$0.80$ million. This gives an after-tax or net earnings of $2 - 0.80 = \$1.20$ million. The cash flow for year 2017 is 1.20 + the \$18 million depreciation allowance = \$19.20 million. The discount factor for that year is $1/1.15^3 = 0.6575$. Therefore, the PV for 2017 is 0.6575(19.20) or \$12.62 million. When added to the cumulative PV

Calculation of Cash Flows (Millions of Dollars) for Example 17.29 (nominal interest rate = 15 %)

Year	Investment		D	$C_{\text{Excl. Dep.}}$	S	Net Earnings	Cash Flow	Discounted Cash Flow	Cum. PV
	fC_{TDC}	C_{WC}							
2014	(30.00)						(30.00)	(30.00)	(30.00)
2015	(30.00)						(30.00)	(26.09)	(56.09)
2016	(30.00)	(40.00)					(70.00)	(52.93)	(109.02)
2017			18.00	55.00	75.00	1.20	19.20	12.62	(96.39)
2018			28.80	78.00	113.00	3.72	32.52	18.59	(77.80)
2019			17.28	100.00	150.00	19.63	36.91	18.35	(59.45)
2020			10.37	100.00	150.00	23.78	34.15	14.76	(44.68)
2021			10.37	100.00	150.00	23.78	34.15	12.84	(31.85)
2022			5.18	100.00	150.00	26.89	32.07	10.48	(21.36)
2023				100.00	150.00	30.00	30.00	8.53	(12.83)
2024				100.00	150.00	30.00	30.00	7.42	(5.42)
2025				100.00	150.00	30.00	30.00	6.45	1.03
2026				100.00	150.00	30.00	30.00	5.61	6.64
2027				100.00	150.00	30.00	30.00	4.88	11.51
2028		40.00		100.00	150.00	30.00	70.00	9.89	21.41

Net earnings = $(\text{S} - \text{C}_{\text{Excl. Dep.}} - \text{D}) \times (1.0 - \text{income tax rate})$

Annual cash flow = C = (net earnings + D) $- fC_{\text{TDC}} - C_{\text{WC}}$

of −$109.02 million, a cumulative PV of −$96.39 is obtained. The calculations for the remaining years of the project are carried out in a similar manner, most conveniently with a spreadsheet. The final NPV at the end of year 2028 is $21.41 million. Notice that the cumulative PV remains negative until the year 2025. This is equivalent to a payback time of more than 8 yr from the start of plant operation. This is very different from the 2.74-yr payback period computed in Example 17.14, where both the time value of money and the first 2 yr of operation at reduced capacity were ignored.

(b) The IRR (or DCFRR) is obtained iteratively by conducting the same calculations as in part (a), but with a sequence of values for the nominal interest rate until an NPV of zero is obtained. Since an interest rate of 15% in part (a) produced a positive NPV, we know that the interest rate for a zero NPV must be greater than 15%. In fact, an IRR of 18.5% is obtained.

It is of interest to examine the annual cash flows on non-discounted and discounted bases as shown in the following bar graphs. Graph (a) is for the former. For discounted cash flows, graphs (b) and (c) are for an interest rate of 15%, and graph (d) is for the IRR of 18.5%. Note that discounted cash flows during the time of plant operation are much smaller than those for the nondiscounted cash flows in the first graph.

Finally, when calculating annual discounted cash flows, it is not difficult to account for inflation in estimating revenues and costs when the inflation factors are known. Inflation, considered in the following subsection, was not included in this example so as to enable the reader to trace the calculations of the cash flows more easily.

Inflation

Inflation is the change in the value of a currency over time. Most often, the change is a loss in value. The effect of inflation on a profitability analysis is difficult to include because the future inflation rate is not known and there is no general agreement on how the effect of inflation should be incorporated into present-worth calculations. Some argue that revenues and costs increase in the same proportion to the inflation rate factor, making it unnecessary to consider inflation when using a rigorous profitability measure. However, this ignores the fact that depreciation allowances are not adjusted for inflation and, therefore, if revenues and costs increase by the same percentage, the gross earnings increase, making it necessary to pay more income tax as shown in the following example.

EXAMPLE 17.30

Consider the years 2019 and 2020 of the results in the table of Example 17.29. In 2019 and 2020 income tax in millions of dollars is, respectively,

$$0.40(150.00 - 100.00 - 17.28) = 13.09$$

$0.40(150.00 - 100.00 - 10.37) = 15.85$, with a cash flow of 34.15

Assume that the results of 2019 are unchanged, but that the sales revenue and production cost, excluding depreciation, both increase by 8% due to inflation. Recompute the entries in the table in Example 17.29.

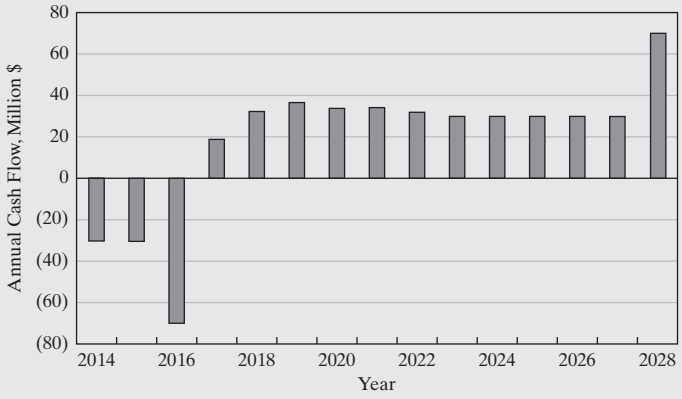

(a) Annual cash flows

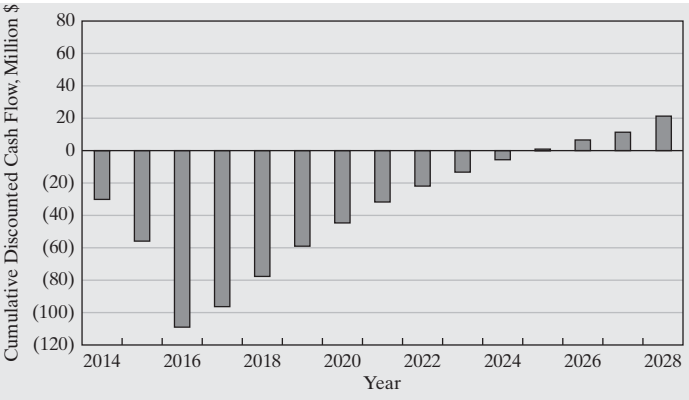

(c) Cum. discounted cash flows (cum. present values)
nominal interest rate = 15%

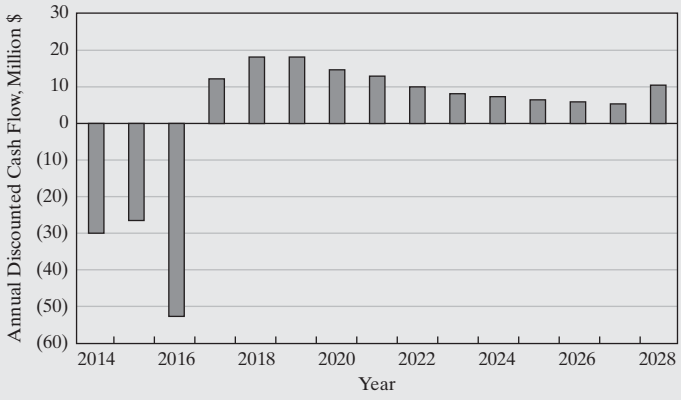

(b) Annual discounted cash flows (annual present values)
nominal interest rate = 15%

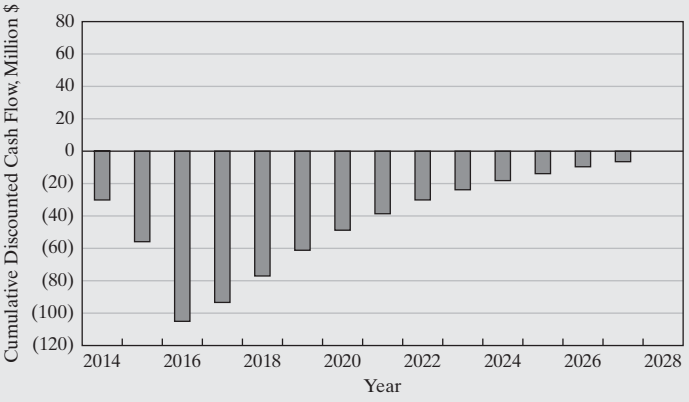

(d) Cum. discounted cash flows (cum. present values)
nominal interest rate = 18.5% (IRR or DCFRR)

SOLUTION

Now the income tax in millions of dollars for 2019 is

$$0.40[150(1.08) - 100(1.08) - 10.37)]$$
$$= 17.45, \text{ a } 10.1\% \text{ increase in income tax}$$

The cash flow for 2020 is now 36.55, an increase of about 7% over the 34.15 million dollars of the first case of no inflation in 2020. Based on the effect of inflation on the value of currency, the company has fallen behind somewhat. Thus, it would appear that it is important to make some correction for inflation if the rate is high.

The historic effect of inflation on costs was seen in Chapter 16 in Table 16.6, where four cost indexes and the Consumer Price Index (CPI) were compared. From that table, the following average annual inflation rates shown in Table 17.12 are obtained for the 10-yr periods of 1980–1990 and 1990–2000, and for the 5-yr period 2000–2005. Also included in the table are the average hourly percentage rate increases in labor wages of private production workers in the United States for the same periods taken from the Bureau of Labor Statistics. In the period 1980–1990, the average hourly labor wage increased from \$6.85 to \$10.20, whereas for 1990–2000, the increase was from \$10.20 to \$14.01. For 2000–2005, the increase was from \$14.01 to \$16.12. Thus, assuming a 40-hr workweek for 52 weeks/yr, the private production worker had an average annual wage of \$33,530 in 2005.

The data in Tables 16.6 and 17.12 show that attempts in the United States to curb inflation during the 25-yr period of 1980–2005 met with some success when compared to the great inflation of the 1970s. The average annual increase in the cost of building a chemical plant has been only 2.63%. Average annual inflation as measured by the Consumer Price Index has been only 3.64%, whereas hourly wages have increased at an average rate of 3.48%, only 5% lower than the increase in the CPI. During the 1970s, the average annual increase in the CPI was almost 8%, while the average increase in wages was 7%.

It is also of interest to consider the effect of inflation on the prices of commodity chemicals, such as those in Table 16.7. In the past 50 yr, the prices of the inorganic chemicals in that list have changed at the most by a factor of 2. This represents an average annual inflation rate of only 1.4%. However, in the case of petrochemicals, their prices, like the price of gasoline, are tied to the price of oil, which has fluctuated greatly since the 1950s. For example, the price of ethylene was \$0.05/lb in 1963, \$0.24/lb in 1990, and as much as \$0.43/lb in 2006, making it impossible to predict the effect of inflation unless the future price of oil can be predicted. In addition, for a new chemical plant, raw-material prices and product prices are often negotiated with contracts for at least a few years.

Table 17.12 Average Annual Inflation Rates of Cost Indexes and Hourly Labor Wages as Average Percent Increase per Year

Period	CE	MS	ENR	CPI	Hourly Labor Wages
1980–1990	3.21	3.31	3.82	4.72	4.06
1990–2000	0.97	1.67	2.76	2.80	3.22
2000–2005	3.50	3.13	3.66	2.55	2.85

For the purpose of comparing alternative processes with rigorous profitability measures and in the absence of future inflation rates, the following average inflation rates can be used.

Cost of raw materials and price of products	2.5%/yr
Cost of utilities	2.5%/yr
Cost of processing equipment	2.5%/yr
Cost of hourly labor	3.0%/yr

In effect, these rates correspond to approximately 2.5% for material and 3.0% for labor.

Another aspect of inflation is its effect on purchasing power for both consumers and companies. Equation (17.12) gives the future worth of a present amount of money if it earns compound interest.

$$F = P(1 + i)^n$$

However, if inflation occurs, the purchasing power of that future sum will not be the same as that of the present sum. To account for a constant rate of inflation, Eq. (17.12) is modified to give the future worth in terms of the purchasing power of present dollars. Let the nominal interest rate compounded annually $= r = i$, the number of years $= n$, the annual inflation rate $= f$, and the future worth in present purchasing power $= F_{PP,0}$. Then,

$$F_{PP,0} = \frac{F}{(1+f)^n} = P\left[\frac{(1+i)^n}{(1+f)^n}\right] \tag{17.50}$$

EXAMPLE 17.31

A present sum of money of \$10,000 is invested for 10 yr at an interest rate of 7% compounded annually. During that 10-yr period, the inflation rate is constant at 3%. Compute the future worth, F, and the future worth in terms of purchasing power at the beginning of the investment, $F_{PP,0}$.

SOLUTION

$$P = \$10{,}000,\ i = 0.07,\ f = 0.03$$

From Eq. (17.12),

$$F = \$10{,}000\ (1 + 0.07)^{10} = \$19.672$$

Thus, when inflation is not taken into account, the future worth after 10 yr is almost twice as much as the present amount.

From Eq. (17.50),

$$F_{PP,0} = \frac{\$19{,}672}{(1 + 0.03)^{10}} = \frac{\$19{,}672}{1.3439} = \$14{,}638$$

When inflation is taken into account, the future purchasing power is only about 50% (rather than 100%) more than that of the present amount.

17.8 PROFITABILITY ANALYSIS SPREADSHEET

This section describes how to use the Profitability Analysis-4.0.xls spreadsheet by Brian K. Downey (2008), which estimates the approximate and rigorous profitability measures for a potential chemical process. This EXCEL spreadsheet has been designed to permit specifications using the entries in Table 16.9 to compute the total capital investment (TCI); Table 17.1 to compute the total production cost; and the cash flow table to compute the net present value in the solution to Example 17.29. It is in the Program and Simulation Files folder, which can be downloaded from the Wiley Web site associated with this book. An example analysis is shown for the monochlorobenzene (MCB) separation process, which was introduced in Section 7.4. The example uses two sources of installed equipment cost estimates. First, it uses the purchase and installation costs estimated by the purchase-cost equations in Sections 16.5 and 16.6. Then, it uses the more accurate installed equipment costs estimated by the Aspen Process Economic Analyzer (APEA).

General Instructions for Use of Profitability Analysis—4.0.xls

Upon opening the file Profitability Analysis-4.0.xls, the user will notice 10 EXCEL tabs at the bottom of the screen, 4 of which are shaded in green. These 4 tabs are "protected," intended only for printing outputs after the specifications have been entered. No changes can be made to the entries in these tabs. All are calculated based upon the entries in the other tabs. These tabs are:

1. ***Input Summary.*** Includes all specifications including the project chronology.
2. ***Cost Summary.*** Includes Variable Cost, Fixed Cost, and Investment Summaries.
3. ***Cash Flows.*** Summarizes the project annual cash flows.
4. ***Profitability Measures.*** Includes the net present value (NPV), investor's rate of return (IRR), and return on investment (ROI) for the project.

The other six tabs are used for the input specifications. They include the:

1. ***General Input***
2. ***Selling Price***
3. ***Variable Costs and Working Capital*** (abbreviated Var Costs & WC)
4. ***Total Permanent Investment***
5. ***Equipment Costs***
6. ***Fixed Costs***

Next, the input specifications in each tab are discussed.

General Input Tab

It is suggested that users begin with the *General Input* tab. First, the Process Title, Product name, and Plant location are entered. Note that these entries appear in the *Input Summary* for printing. Next, the following should be entered:

Timeline entries specify the project starting year and the number of years of design, construction, and production. Normally, production begins after design and construction are completed; that is, the years of design and construction occur before production begins. However, it is possible to allocate a portion of the total permanent investment to be expended during the early production years as will be discussed in the *Total Permanent Investment* tab. The Total Number of Years for Project is automatically calculated, and then entries are provided for both the Start Year and Site Factor (see Table 16.13).

Continuous Operation occurs 24 hr/day, 7 day/wk, but with shutdowns for maintenance and related reasons. To account for the latter, days/yr, hr/yr, or the Operating Factor (fraction of hours in operation per year) is entered. Only one of the three entries is required in this section; however, if the user supplies more than one value, the Operating Factor is used by default. This mode applies for the production of commodity chemicals as well as specialty chemicals, for example, the manufacture of pharmaceuticals in batch processes that operate "continuously."

Discrete Operation occurs over x hr/day and y day/yr, where entries are often $x = 8$ *hr/day* and $y = 260$ *day/yr*. This is typical of a startup company that operates in just one shift, 5 day/wk, and 52 wk/yr. Since a process cannot be both discrete and continuous, only one of these two sections should be completed. If entries are made in both, the spreadsheet uses the Discrete values by default.

Next, the Production Capacity (i.e., the percent of design capacity) is specified. Production will begin at the specified "Start production at" percent of design capacity, and then will ramp linearly (over the number of "Years to achieve full capacity") until it reaches its "Production Capacity." A drop-down menu allows for the selection of the applicable MACRS depreciation schedule (shown to the right of the selection) along with an entry to specify the number or worker shifts.

In addition to those entries, it is necessary to specify financial information for calculation of the return on investment (ROI), the net present value (NPV), and the investor's rate of return (IRR), also known as the discounted cash flow rate of return (DCFRR). Entries are provided for the income tax rate, the cost of capital (for the NPV calculation), and the inflation rate. Note that a general inflation rate applicable to all operating costs can be specified, or separate inflation rates can be specified for the product price, fixed costs, and variable costs.

Product Information is supplied by entering both the units (lb, gram, gallon, etc.) and price per unit along with the total number of units produced per year, day, or hour (specify one). *Raw Materials*, *Byproducts*, and *Utilities* entries are similar. The names for the raw materials, byproducts, and utilities are entered in the left column, the units in the second column, and the amounts required [specified as the "Required Ratio"; that is, the ratio of the raw material/byproduct/utility per unit of product (e.g., lb high pressure steam/lb MCB)] in the third column. The price is specified in the fourth column (e.g., $/kWhr), and up to 10 entries can be made in each section.

Selling Price Tab

Entries are made in the *Selling Price* tab when it is desired to adjust the product selling prices in one or more of the project years. As a default, user input prices, adjusted by the inflation rate, are displayed annually in the "Calculated Unit Price" column. In any year, a user-specified price is entered in the "Manual Input Price" column to override the price in the "Calculated Unit Price" column. The "Price to Be Used" column shows the prices year-by-year.

Variable Costs & Working Capital Tab

The *Var Costs & WC* tab permits the specification of percentages of product sales charged for selling/transfer expenses, direct research, allocated research, administrative expenses, and management incentives compensation. The defaults are those in the cost sheet of Table 17.1, as discussed in Section 17.2.

In addition, the numbers of days entered for the accounts receivable, cash reserves, accounts payable, and inventories, as discussed in Section 17.3, can be altered from default values. For the inventories, working capital can be allocated for the product and the raw materials. Note that when the production is increased in a subsequent year, the spreadsheet makes increments to working capital accordingly. Also, credit is taken for the total working capital at the finish of the last production year.

Total Permanent Investment Tab

The first entries in the *Total Permanent Investment* tab designate the percentage of the total permanent investment assigned to one or more years, beginning with the first year of construction. Note that for new products, percentages of the total permanent investment can be assigned to three of the production years.

Next, for each of the pertinent entries in Table 16.9, the default entry can be altered.

Equipment Costs Tab

In the *Equipment Costs* tab, the total equipment costs for the life of the project are entered. Then, using the *Total Permanent Investment* tab, as discussed above, percentages of the total permanent investment can be assigned to the individual project years.

To enter equipment costs, start with the equipment name in the left-most column. Next is the equipment type—in which equipment items are identified to be in one of seven categories in the drop-down menu: Fabricated Equipment, C_{FE}; Process Machinery, C_{PM}; Spares, C_{spare}; Storage, $C_{storage}$; Other Equipment, C_{OE}; Catalysts, $C_{catalyst}$; or Computers, Software, and so on, C_{comp}; as grouped in Table 16.9 and discussed in Section 16.3. It is suggested that equipment items of the same type be grouped on sequential lines.

The user may enter (1) the purchase cost only, (2) the purchase cost and bare-module factor, or (3) the bare-module cost. For each equipment item, a default bare-module factor, 3.21, is used to calculate the Bare-Module Cost—which can be overridden as desired. Alternatively, the "Bare-Module Factor Calculator," to the right of this tab, uses the factors in Table 16.10 as fractions of the purchase cost to compute the cost of installation materials, C_M; labor, C_L; freight, insurance, and taxes, C_{FIT}; construction overhead, C_o; and contractor engineering, C_E. These factors are summed to give the total bare-module factor, which can be used to replace the default values. Each purchase cost is multiplied by its bare-module factor to give the bare-module costs. Alternatively, for any equipment item, the bare-module cost can be entered, with entries for the purchase cost and bare-module factors disregarded.

APEA Specifications. When APEA is used to estimate purchase and installation costs for the entire plant, use the "APEA Inputs" section at the bottom of the *Equipment Costs* tab. Note that APEA specifications override any equipment costs entered above. Note also that APEA must be used to estimate the purchase and installation costs for all of the equipment items. It is not possible to use APEA for selected equipment items. The Total Direct Materials and Labor Costs, Material and Labor G&A Overhead and Contractor Fees, Contractor Engineering Costs, and Indirect Costs are obtained from the APEA *Capital Estimate Report* as discussed in Section 16.8. Other costs can be entered (e.g., for pipe racks, sewers, sumps) under Miscellaneous Installation Costs if desired.

Fixed Costs Tab

In the *Fixed Costs* tab, the entries appear in six subsections: Operations, Maintenance, Operating Overhead, Property Taxes and Insurance, Straight-line Depreciation, and Depletion Allowance. The default entries, found in Table 17.1, can be replaced as desired. However, under Operations, entries must be made for (1) the number of operators per shift, (2) the technical assistance to manufacturing, and (3) the control laboratory. Typical entries are in Tables 17.1 and 17.3. If a depletion allowance applies, see the subsection Depletion in Section 17.6 for estimating it.

Running the Analysis

Results are automatically tabulated and updated as the specifications are entered. The results are found in the four aforementioned green tabs, *Input Summary, Cost Summary, Cash Flows,* and *Profitability Measures.* The *Cost Summary* tab includes all of the entries associated with the total permanent investment, the working capital, and the total capital investment (i.e., the entries in Table 16.9). Also included are sections on Variable Costs at design capacity (not production during a specific year) of operations and for Fixed Costs. These correspond to the entries in Table 17.1. Then, the *Cash Flows* tab contains the cash flows for each year during the life of the project. Finally, the *Profitability Measures* tab contains NPV, IRR, and ROI.

Also, the results of an IRR sensitivity analysis are displayed in two dimensions. To define the two dimensions, click on the

variable name on the *x* and *y* axes and select the desired choice using the drop-down menus. Choices include product price, variable cost, fixed cost, total investment, and rate of inflation. Analysis ranges can be adjusted using the "Vary Initial Value by +/−" option. The number in boldface on each axis is the base-case value; by default, these are varied from 50 to 150% of the base-case value. After all sensitivity inputs are specified, press the "F9" key to run the analysis.

Saving or Loading an Analysis

At any point, when entering specifications or after completing an analysis, the contents of the worksheet can be saved as a normal EXCEL file. No special loading or saving techniques are required; simply open a new, blank version of the Profitability Analysis-4.0.xls spreadsheet to start a new analysis or continue with an existing analysis by opening the spreadsheet like any other EXCEL file.

Having described the details of data entry into the Profitability Analysis-4.0.xls spreadsheet, Example 17.32 is provided to illustrate its use for the MCB separation process.

EXAMPLE 17.32

It is desired to carry out a profitability analysis for the monochlorobenzene (MCB) separation process in Section 7.4 using (a) purchase costs and bare-module factors and (b) purchase and installation costs estimated by APEA. In Example 16.20, the latter estimates were computed, beginning with ASPEN PLUS simulation in the file, MCB.bkp. The plant location is the Gulf Coast. The design time is estimated to be 1 yr with the construction time at 1 yr and the total operating life of the project at 15 yr. During the first 3 years, the production rate increases linearly to 90% of design capacity from 50% to 100% of 90%; that is, in years 1, 2, and 3, the production rate is 45%, 67.5%, and 90%, respectively, of design capacity. It is assumed that all of the equipment items are installed during the construction year. The cost of capital is taken to be 15% annually.

SOLUTION

From the simulation results:

$$\text{MCB production rate} = 5{,}572.1\frac{\text{lb}}{\text{hr}} \times 24\frac{\text{hr}}{\text{day}} \times 330\frac{\text{day}}{\text{yr}}$$
$$= 44{,}131{,}000\ \frac{\text{lb}}{\text{yr}}$$

The MCB product (stream S14) is valued at \$0.68/lb. Furthermore, from the simulation results

$$\frac{9{,}117.1\text{ lb S01/hr}}{5{,}572.1\text{ lb S14/hr}} = 1.636\frac{\text{lb S01}}{\text{lb S14}}$$

and the price of the feed stream (S01) is \$0.50/lb.

The utility costs are estimated as follows with the quantities per pound of product determined based upon the simulation results.

$$\text{Medium pressure steam} = 7.00\frac{\$}{1{,}000\text{ lb}} = 0.007\frac{\$}{\text{lb}}$$

$$\frac{1.365.5\text{ lb steam/hr}}{5{,}572.1\text{ lb S14/hr}} = 0.2451\frac{\text{lb steam}}{\text{lb S14}}$$

$$\text{Cooling water} = \frac{\$0.10}{1{,}000\text{ gal}} = 10^{-4}\frac{\$}{\text{gal}} = 1.2\times10^{-5}\frac{\$}{\text{lb}}$$

$$\frac{1.2927\times10^{5}\text{ lb H}_2\text{O/hr}}{5{,}572.1\text{ lb S14/hr}} = 23.2\frac{\text{lb H}_2\text{O}}{\text{lb S14}}$$

$$\text{Electricity} = 0.07\frac{\$}{\text{KWhr}}$$

$$\frac{9.60\text{ kW}}{5{,}572.1\text{ lb S14/hr}} = 0.00172\frac{\text{kWh}}{\text{lb S14}}$$

The byproduct benzene (stream S11) is valued at \$0.54/lb, and the quantity per pound of product is determined from the simulation results:

$$\frac{3{,}132.7\text{ lb S11/hr}}{5{,}572.1\text{ lb S14/hr}} = 0.5622\frac{\text{lb S11}}{\text{lb S14}}$$

The byproduct HCl (stream S06) is valued at \$0.04/lb, and the quantity per pound of product is determined from the simulation results:

$$\frac{355.45\text{ lb S06/hr}}{5{,}572.1\text{ lb S14/hr}} = 0.06379\ \frac{\text{lb S06}}{\text{lb S14}}$$

Results from the Profitability Analysis Spreadsheet—Part (a) Purchase Costs and Bare-Module Factors

Included are the following:

1. ***Input Summary.*** Note that all specifications are shown, with the default values used in most cases.
2. ***Investment Summary.***
3. ***Variable Cost Summary.*** These costs are estimated for the third operating year.
4. ***Fixed Cost Summary.***
5. ***Cash Flow Summary.***
6. ***Profitability Measures.*** As seen, the IRR is 32.2%, the ROI is 34.8%, and the NPV is \$3,924,000. Note in Examples 17.11, 17.13, and 17.15 that the production rate is at full (100%) plant capacity rather than the linearly increasing rate in this example. Consequently, the ROI computed in Example 17.15 is somewhat higher at 38.2%. Also, due to the linearly increasing production rate in this example, working capital is invested before the first, second, and third production years.
7. ***Sensitivity Analyses.*** Here, the IRR is studied as the product price, and variable costs are adjusted.

1. ***Input Summary—Part (a) Purchase Costs and Bare-Module Factors***

General Information

Process Title:	**Monochlorobenzene Separation Process**
Product:	**MCB**
Plant Site Location:	**Gulf Coast**
Site Factor:	**1.00**
Operating Hours per Year:	**7920**
Operating Hours per Year:	**330**
Operating Factor:	**0.9041**

Product Information

This Process will Yield

	5,572	lb of MCB per hour
	133,732	lb of MCB per day
	44,131,000	lb of MCB per year
Price	**$0.68**	**/lb**

Chronology

Year	Action	Distribution of Permanent Investment	Production Capacity	Depreciation 5 year MACRS	Product Price
2014	Design		0.0%		
2015	Construction	100%	0.0%		
2016	Production	0%	45.0%	20.00%	$0.68
2017	Production	0%	67.5%	32.00%	$0.68
2018	Production	0%	90.0%	19.20%	$0.68
2019	Production		90.0%	11.52%	$0.68
2020	Production		90.0%	11.52%	$0.68
2021	Production		90.0%	5.76%	$0.68
2022	Production		90.0%		$0.68
2023	Production		90.0%		$0.68
2024	Production		90.0%		$0.68
2025	Production		90.0%		$0.68
2026	Production		90.0%		$0.68
2027	Production		90.0%		$0.68
2028	Production		90.0%		$0.68
2029	Production		90.0%		$0.68
2030	Production		90.0%		$0.68

Equipment Costs

Equipment Description		Bare-Module Cost
Distillation Column	Fabricated Equipment	$462,600
Absorber	Fabricated Equipment	$165,200
Heat Exchangers	Fabricated Equipment	$237,800
Flash Vessels, Accumulator and Storage Tanks	Fabricated Equipment	$319,500
Pumps	Process Machinery	$44,800
Total		***$1,230,000***

Raw Materials

	Raw Material:	Unit:	Required Ratio:	Cost of Raw Material
1	FEED	lb	1.636 lb per lb of MCB	$0.500 per lb
	Total weighted Average:			$0.818 per lb of MCB

Byproducts

	Byproduct:	Unit:	Ratio to Product	Byproduct Selling Price
1	Benzene	lb	0.5622 lb per lb of MCB	$0.540 per lb
2	HCI	lb	0.0638 lb per lb of MCB	$0.040 per lb
	Total weighted Average:			$0.306 per lb of MCB

Utilities

	Utility:	Unit:	Required Ratio	Utility Cost
1	Medium Pressure Steam	lb	0.2451 lb per lb of MCB	$7.000E-03 per lb
2	Low Pressure Steam	lb	0 lb per lb of MCB	$0.000E+00 per lb
3	Process Water	gal	0 gal per lb of MCB	$0.000E+00 per gal
4	Cooling Water	lb	23.2 lb per lb of MCB	$1,200E-05 per lb
5	Electricity	kWh	0.00172 kWh per lb of MCB	$0.070 per kWh
	Total Weighted Average:			$2.115E-03 per lb of MCB

Variable Costs

General Expenses:

Selling / Transfer Expenses:	**1.00% of Sales**
Direct Research:	**4.80% of Sales**
Allocated Research:	**0.50% of Sales**
Administrative Expense:	**2.00% of Sales**
Management Incentive Compensation:	**1.25% of Sales**

Working Capital

Accounts Receivable	⇒	**30**	**Days**
Cash Reserves (excluding Raw Materials)	⇒	**0**	**Days**
Accounts Payable	⇒	**0**	**Days**
MCB Inventory	⇒	**4**	**Days**
Raw Materials	⇒	**2**	**Days**

Total Permanent Investment

Cost of Site Preparations:	**5.00%**	**of Total Bare-Module Costs**
Cost of Service Facilities:	**5.00%**	**of Total Bare-Module Costs**
Allocated Costs for utility plants and related facilities:	**$0**	
Cost of Contingencies and Contractor Fees:	**18.00%**	**of Direct Permanent Investment**
Cost of Land:	**2.00%**	**of Total Depreciable Capital**
Cost of Royalties:	**$0**	
Cost of Plant Start-Up:	**10.00%**	**of Total Depreciable Capital**

Fixed Costs

Operations

Operators per Shift:	**1**	**(assuming 5 shifts)**
Direct Wages and Benefits:	**$40**	**/operator hour**
Direct Salaries and Benefits:	**15%**	**of Direct Wages and Benefits**
Operating Supplies and Services:	**6%**	**of Direct Wages and Benefits**
Technical Assistance to Manufacturing:	**$60,000.00**	**per year, for each Operator per shift**
Control Laboratory:	**$65,000.00**	**per year, for each Operator per shift**

Maintenance

Wages and Benefits:	**3.50%**	**of Total Depreciable Capital**
Salaries and Benefits:	**25%**	**of Maintenance Wages and Benefits**
Materials and Services:	**100%**	**of Maintenance Wages and Benefits**
Maintenance Overhead:	**5%**	**of Maintenance Wages and Benefits**

Operating Overhead

General Plant Overhead:	**7.10%**	**of Maintenance and Operations Wages and Benefits**
Mechanical Department Services:	**2.40%**	**of Maintenance and Operations Wages and Benefits**
Employee Relations Department:	**5.90%**	**of Maintenance and Operations Wages and Benefits**
Business Services:	**7.40%**	**of Maintenance and Operations Wages and Benefits**

Property Taxes and Insurance

Property Taxes and Insurance:	**2%**	**of Total Depreciable Capital**

Straight line Depreciation

Direct Plant:	8.00%	**of Total Depreciable Capital, less 1.18 times the Allocated Costs for Utility Plants and Related Facilities**
Allocated Plant:	6.00%	**of 1.18 times the Allocated Costs for Utility Plants and Related Facilities**

Other Annual Expenses

Rental Fees (Office and Laboratory Space):	**$0**
Licensing Fees:	**$0**
Miscellaneous:	**$0**

Depletion Allowance

Annual Depletion Allowance:	**$0**

2. ***Investment Summary—Part (a) Purchase Costs and Bare-Module Factors***

Investment Summary

Bare-Module Costs		
Fabricated Equipment	$1,185,100	
Process Machinery	$ 44,800	
Spares	$ -	
Storage	$ -	
Other Equipment	$ -	
Catalysts	$ -	
Computers, Software, Etc.	$ -	
Total Bare Module Costs:		**$1,230,000**
Direct Permanent Investment		
Cost of Site Preparations:	$ 61,500	
Cost of Service Facilities:	$ 61,500	
Allocated Costs for utility plants and related facilities:	$ -	
Direct Permanent Investment		**$1,353,000**
Total Depreciable Capital		
Cost of Contingencies & Contractor Fees	$ 243,500	
Total Depreciable Capital		**$1,596,500**
Total Permanent Investment		
Cost of Land:	$ 31,900	
Cost of Royalties:	$ -	
Cost of Plant Start-Up:	$ 159,700	
Total Permanent Investment - Unadjusted		$1,788,100
Site Factor		1.00
Total Permanent Investment		**$1,788,100**

Working Capital

	2015	**2016**	**2017**
Accounts Receivable	$1,109,925	$ 554,962	$554,962
Cash Reserves	$ -	$ -	$ -
Accounts Payable	$ -	$ -	$ -
MCB Inventory	$ 147,990	$ 73,995	$ 73,995
Raw Materials	$ 89,012	$ 44,506	$ 44,506
Total	**$1,346,926**	**$ 673,463**	**$673,463**
Present Value at 15%	*$1,171,240*	*$ 509,235*	*$442,813*
Total Capital Investment		**$3,911,388**	

3. ***Variable Cost Summary—Part (a) Purchase Costs and Bare-Module Factors***

Variable Cost Summary		
Variable Costs at 100% Capacity:		
General Expenses		
Selling / Transfer Expenses:		$ 300,091
Direct Research:		$ 1,440,436
Allocated Research:		$ 150,045
Administrative Expense:		$ 600,182
Management Incentive Compensation;		$ 375,114
Total General Expenses		$ 2,865,867
Raw Materials	$0.818000 per lb of MCB	$36,099,158
Byproducts	$0.306140 per lb of MCB	($13,510,264)
Utilities	$0.002115 per lb of MCB	$93,300
Total Variable Costs		**$ 25,548,100**

4. ***Fixed Cost Summary—Part (a) Purchase Costs and Bare-Module Factors***

Fixed Cost Summary		
Operations		
Direct Wages and Benefits	$ 416,000	
Direct Salaries and Benefits	$ 62,400	
Operating Supplies and Services	$ 25,000	
Technical Assistance to Manufacturing	$ 300,000	
Control Laboratory	$ 325,000	
Total Operations		$ **1,128,400**
Maintenance		
Wages and Benefits	$ 55,900	
Salaries and Benefits	$ 14,000	
Materials and Services	$ 55,900	
Maintenance Overhead	$ 2,800	
Total Maintenance		$ **128,600**
Operating Overhead		
General Plant Overhead:	$ 38,929	
Mechanical Department Services:	$ 13,159	
Employee Relations Department:	$ 32,350	
Business Services:	$ 40,574	
Total Operating Overhead		$ **125,000**
Property Taxes and Insurance		
Property Taxes and Insurance:	$ 31,900	
Other Annual Expenses		
Rental Fees (Office and Laboratory Space):	$ -	
Licensing Fees:	$ -	
Miscellaneous:	$ -	
Total Other Annual Expenses		$ -
Total Fixed Costs		$ **1,413,900**

5. *Cash Flow Summary—Part (a) Purchase Costs and Bare-Module Factors*

Cash Flow Summary

Year	Percentage of Design Capacity	Product Unit Price	Sales	Capital Costs	Working Capital	Var Costs	Fixed Costs	Depreciation	Depletion Allowance	Taxale Income	Taxes	Net Earnings	Cash Flow	Cumulative Net Present Value at 15%
2014	0%		-	-	-	-	-	-	-	-	-	-	-	-
2015	0%		-	(1,788,100)	(1,346,900)	-		-	-	-	-	-	(3,135,000)	(2,726,100)
2016	45%	$0.68	13,504,100	-	(673,500)	(11,496,600)	(1,413,900)	(319,300)	-	274,200	(101,500)	172,800	(181,400)	(2,863,300)
2017	68%	$0.68	20,256,100	-	(673,500)	(17,245,000)	(1,413,900)	(510,900)	-	1,086,400	(402,000)	684,400	521,00	(2,520,200)
2018	90%	$0.68	27,008,200	-	-	(22,993,300)	(1,413,900)	(306,500)	-	2,294,500	(848,900)	1,445,500	1,752,000	(1,518,400)
2019	90%	$0.68	27,008,200	-	-	(22,993,300)	(1,413,900)	(183,900)	-	2,417,100	(894,300)	1,522,800	1,706,700	(669,900)
2020	90%	$0.68	27,008,200	-	-	(22,993,300)	(1,413,900)	(183,900)	-	2,417,100	(894,300)	1,522,800	1,706,700	67,900
2021	90%	$0.68	27,008,200	-	-	(22,993,300)	(1,413,900)	(92,000)	-	2,509,000	(928,300)	1,580,700	1,672,600	696,700
2022	90%	$0.68	27,008,200	-	-	(22,993,300)	(1,413,900)	-	-	2,601,000	(962,400)	1,638,600	1,638,600	1,232,400
2023	90%	$0.68	27,008,200	-	-	(22,993,300)	(1,413,900)	-	-	2,601,000	(962,400)	1,638,600	1,638,600	1,698,200
2024	90%	$0.68	27,008,200	-	-	(22,993,300)	(1,413,900)	-	-	2,601,000	(962,400)	1,638,600	1,638,600	2,103,200
2025	90%	$0.68	27,008,200	-	-	(22,993,300)	(1,413,900)	-	-	2,601,000	(962,400)	1,638,600	1,638,600	2,455,400
2026	90%	$0.68	27,008,200	-	-	(22,993,300)	(1,413,900)	-	-	2,601,000	(962,400)	1,638,600	1,638,600	2,761,700
2027	90%	$0.68	27,008,200	-	-	(22,993,300)	(1,413,900)	-	-	2,601,000	(962,400)	1,638,600	1,638,600	3,028,000
2028	90%	$0.68	27,008,200	-	-	(22,993,300)	(1,413,900)	-	-	2,601,000	(962,400)	1,638,600	1,638,600	3,259,600
2029	90%	$0.68	27,008,200	-	-	(22,993,300)	(1,413,900)	-	-	2,601,000	(962,400)	1,638,600	1,638,600	3,461,000
2030	90%	$0.68	27,008,200	-	2,693,900	(22,993,300)	(1,413,900)	-	-	2,601,000	(962,400)	1,638,600	4,332,500	3,924,000

6. ***Profitability Measures—Part (a) Purchase Costs and Bare-Module Factors***

Profitability Measures	
The Internal Rate of Return (IRR) for this project is	32.17%
The Net Present Value (NPV) of this project in 2014 is	$ 3,924,000

ROI Analysis (Third Production Year)

Annual Sales	**27,008,172**
Annual Costs	**(24,407,190)**
Depreciation	**(127,720)**
Income Tax	**(915,107)**
Net Earnings	**1,558,155**
Total Capital Investment	**4,481,980**
ROI	**34.76%**

7. ***Sensitivity Analyses—Part (a) Purchase Costs and Bare-Module Factors***

Sensitivity Analyses

	Vary Initial Value by +/−
x-axis	50%
y-axis	50%

		Variable Costs										
		$12,774,050	$15,328,860	$17,883,670	$20,438,480	$22,993,290	***$25,548,100***	$28,102,910	$30,657,720	$33,212,530	$35,767,340	$38,322,150
Product Price	$0.34	8.14%	Negative IRR	Negative IRR	Negative IRR	Negative IRR	Negative IRR	Negative IRR	Negative IRR	Negative IRR	Negative IRR	Negative IRR
	$0.41	48.03%	14.62%	Negative IRR	Negative IRR	Negative IRR	Negative IRR	Negative IRR	Negative IRR	Negative IRR	Negative IRR	Negative IRR
	$0.48	79.53%	51.00%	19.95%	Negative IRR	Negative IRR	Negative IRR	Negative IRR	Negative IRR	Negative IRR	Negative IRR	Negative IRR
	$0.54	107.39%	80.95%	53.70%	24.53%	−15.10%	Negative IRR	Negative IRR	Negative IRR	Negative IRR	Negative IRR	Negative IRR
	$0.61	132.65%	107.65%	82.25%	56.16%	28.56%	−5.63%	Negative IRR	Negative IRR	Negative IRR	Negative IRR	Negative IRR
	$0.68	155.80%	131.96%	107.88%	83.45%	58.42%	32.17%	1.52%	Negative IRR	Negative IRR	Negative IRR	Negative IRR
	$0.75	177.19%	154.33%	131.32%	108.10%	84.56%	60.50%	35.44%	7.27%	Negative IRR	Negative IRR	Negative IRR
	$0.82	197.05%	175.06%	152.96%	130.73%	108.30%	85.59%	62.43%	38.43%	12.14%	Negative IRR	Negative IRR
	$0.88	215.56%	194.35%	173.06%	151.68%	130.17%	108.49%	86.55%	64.21%	41.17%	16.38%	−15.54%
	$0.95	232.86%	212.36%	191.81%	171.19%	150.48%	129.65%	108.66%	87.45%	65.88%	43.70%	20.15%
	$1.02	249.09%	229.25%	209.36%	189.43%	169.43%	149.35%	129.16%	108.83%	88.29%	67.43%	46.05%

Results from the Profitability Analysis Spreadsheet—Part (b) Purchase and Installation Costs Estimated by APEA

Included are the following:

1. ***Input Summary.*** Note that all specifications are shown, with the default values used in most cases.
2. ***Investment Summary.***
3. ***Variable Cost Summary.*** These costs are estimated for the third operating year.
4. ***Fixed Cost Summary.***
5. ***Cash Flow Summary.***
6. ***Profitability Measures.*** As seen, the IRR is 21.1%, the ROI is 20.11%, and the NPV is $1,886,200. These values are significantly lower than those estimated using the purchase cost equations in Sections 16.5 and 16.6 coupled with bare-module factors. APEA installation costs are calculated more rigorously, including costs not accounted for in the bare-module factors.
7. ***Sensitivity Analyses.*** Here, the IRR is studied as the product price and variable costs are adjusted.

1. ***Input Summary—Part (b) Purchase and Installation Costs Estimated by APEA***

General Information

Process Title: **Monochlorobenzene Separation Process**

Product: **MCB**

Plant Site Location: **Gulf Coast**

Site Factor: **1.00**

Operating Hours per Year: **7920**

Operating Days Per Year: **330**

Operating Factor: **0.9041**

Product Information

This Process will Yield

5,572 lb of MCB per hour
133,732 lb of MCB per day
44,131,000 lb of MCB per year

Price **$0.68** **/lb**

Chronology

Year	Action	Distribution of Permanent Investment	Production Capacity	Depreciation 5 year MACRS	Product Price
2014	Design		0.0%		
2015	Construction	100%	0.0%		
2016	Production	0%	45.0%	20.00%	$0.68
2017	Production	0%	67.5%	32.00%	$0.68
2018	Production	0%	90.0%	19.20%	$0.68
2019	Production		90.0%	11,52%	$0.68
2020	Production		90.0%	11,52%	$0.68
2021	Production		90.0%	5.76%	$0.68
2022	Production		90.0%		$0.68
2023	Production		90.0%		$0.68
2024	Production		90.0%		$0.68
2025	Production		90.0%		$0.68
2026	Production		90.0%		$0.68
2027	Production		90.0%		$0.68
2028	Production		90.0%		$0.68
2029	Production		90.0%		$0.68
2030	Production		90.0%		$0.68

Raw Materials

	Raw Material:	Unit:	Required Ratio:	Cost of Raw Material:
1	FEED	lb	1.636 lb per lb of MCB	$0.500 per lb
	Total weighted Average:			$0.818 per lb of MCB

Byproducts

	Byproduct:	Unit:	Ratio to Product	Byproduct Selling Price
1	Benzene	lb	0.5622 lb per lb of MCB	$0.540 per lb
2	HCI	lb	0.066379 lb per lb of MCB	$0.040 per lb
	Total weighted Average:			$0.306 per lb of MCB

Utilities

	Utility:	Unit:	Required Ratio	Utility Cost
1	Medium Pressure Steam	lb	0.2451 lb per lb of MCB	$7.000E-03 per lb
2	Low Pressure Steam	lb	0 lb per lb of MCB	$0.000E+00 per lb
3	Process Water	gal	0 gal per lb of MCB	$0.000E+00 per gal
4	Cooling Water	lb	23.2 lb per lb of MCB	$1,200E-05 per lb
5	Electricity	kWh	0.00172 kWh per lb of MCB	$0.070 per kWh
	Total Weighted Average:			$2.115E-03 per lb of MCB

Total Permanent Investment		
Cost of Site Preparations:	**5.00%**	**of Total Bare-Module Costs**
Cost of Service Facilities:	**5.00%**	**of Total Bare-Module Costs**
Allocated Costs for utility plants and related facilities:	**$0**	
Cost of Contingencies and Contractor Fees:	**18.00%**	**of Direct Permanent Investment**
Cost of Land:	**2.00%**	**of Total Depreciable Capital**
Cost of Royalties:	**$0**	
Cost of Plant Start-Up:	**10.00%**	**of Total Depreciable Capital**
Fixed Costs		
Operations		
Operators per Shift:	**1**	**(assuming 5 shifts)**
Direct Wages and Benefits:	**$40**	**/operator hour**
Direct Salaries and Benefits:	**15%**	**of Direct Wages and Benefits**
Operating Supplies and Services:	**6%**	**of Direct Wages and Benefits**
Technical Assistance to Manufacturing:	**$60,000.00**	**per year, for each Operator per shift**
Control Laboratory:	**$65,000.00**	**per year, for each Operator per shift**
Maintenance		
Wages and Benefits:	**3.50%**	**of Total Depreciable Capital**
Salaries and Benefits:	**25%**	**of Maintenance Wages and Benefits**
Materials and Services:	**100%**	**of Maintenance Wages and Benefits**
Maintenance Overhead:	**5%**	**of Maintenance Wages and Benefits**
Operating Overhead		
General Plant Overhead:	**7.10%**	**of Maintenance and Operations Wages and Benefits**
Mechanical Department Services:	**2.40%**	**of Maintenance and Operations Wages and Benefits**
Employee Relations Department:	**5.90%**	**of Maintenance and Operations Wages and Benefits**
Business Services:	**7.40%**	**of Maintenance and Operations Wages and Benefits**
Property Taxes and Insurance		
Property Taxes and Insurance:	**2%**	**of Total Depreciable Capital**
Straight-line Depreciation		
Direct Plant:	**8.00%**	**of Total Depreciable Capital, less 1.18 times the Allocated Costs for Utility Plants and Related Facilities**
Allocated Plant:	**6.00%**	**of 1.18 times the Allocated Costs for Utility Plants and Related Facilities**
Other Annual Expenses		
Rental Fees (Office and Laboratory Space):	**$0**	
Licensing Fees:	**$0**	
Miscellaneous:	**$0**	
Depletion Allowance		
Annual Depletion Allowance:	**$0**	

2. ***Investment Summary—Part (b) Purchase and Installation Costs Estimated by APEA***

Investment Summary

Installed Equipment Costs		
Total Direct Materials And Labor Costs	$ 1,183,100	
Miscellaneous Installation Costs	$ -	
Material and Labor G&A Overhead and Contractor Fees	$ 102,500	
Contractor Engineering Costs	$ 839,200	
Indirect Costs	$ 525,400	
Total:		**$2,650,000**
Direct Permanent Investment		
Cost of Site Preparations:	$ 132,500	
Coat of Service- Facilities:	$ 132,500	
Allocated Costs for utility plants and related facilities:	$ -	
Direct Permanent Investment		**$2,915,000**
Total Depreciable Capital		
Cost of Contingencies & Contractor Fees	$ 524,700	
Total Depreciable Capital		**$3,439,700**
Total Permanent Investment		
Cost of Land:	$ 68,794	
Cost of Royalties:	$ -	
Cost of Plant Start-Up:	$ 343,970	
Total Permanent Investment – Unadjusted		$3,852,500
Site Factor		1.00
Total Permanent Investment		**$3,852,500**

Working Capital

	2015	2016	2017
Accounts Receivable	$1,109,925	$ 554,962	$554,962
Cash Reserves	$ -	$ -	$ -
Accounts Payable	$ -	$ -	$ -
MCB Inventory	$ 147,990	$ 73,995	$ 73,995
Raw Materials	$ 89,012	$ 44,506	$ 44,506
Total	**$1,346,926**	**$ 673,463**	**$673,463**
Present Value at 15%	*$1,171,240*	$ *509,235*	*$442,813*
Total Capital Investment		**$5,975,800**	

3. ***Variable Cost Summary—Part (b) Purchase and Installation Costs Estimated by APEA***

Variable Cost Summary		
Variable Costs at 100% Capacity:		
General Expenses		
Selling / Transfer Expenses:		$ 300,091
Direct Research:		$ 1,440,436
Allocated Research:		$ 150,045
Administrative Expense:		$ 600,182
Management Incentive Compensation:		$ 375,114
Total General Expenses		$ 2,865,867
Raw Materials	$0.818000 per lb of MCB	$36,099,158
Byproducts	$0.306140 per lb of MCB	($13,510,247)
Utilities	$0.002115 per lb of MCB	$93,315
Total Variable Costs		**$25,548,093**

4. ***Fixed Cost Summary—Part (b) Purchase and Installation Costs Estimated by APEA***

Fixed Cost Summary		
Operations		
Direct Wages and Benefits		$ 416,000
Direct Salaries and Benefits		$ 62,400
Operating Supplies and Services		$ 24,960
Technical Assistance to Manufacturing		$ 300,000
Control Laboratory		$ 325,000
Total Operations		$**1,128,360**
Maintenance		
Wages and Benefits		$ 120,390
Salaries and Benefits		$ 30,097
Materials and Services		$ 120,390
Maintenance Overhead		$ 6,019
Total Maintenance		$ **276,896**
Operating Overhead		
General Plant Overhead:		$ 44,651
Mechanical Department Services:		$ 15,093
Employee Relations Department:		$ 37,104
Business Services:		$ 46,538
Total Operating Overhead		$ **143,386**
Property Taxes and Insurance		
Property Taxes and Insurance:		$ 68,794
Other Annual Expenses		
Rental Fees (Office and Laboratory Space):		$ -
Licensing Fees:		$ -
Miscellaneous:		$ -
Total Other Annual Expenses		$ -
Total Fixed Costs		$**1,617,436**

5. ***Cash Flow Summary—Part (b) Purchase and Installation Costs Estimated by APEA***

Cash Flow Summary														
Year	Percentage of Design Capacity	Product Unit Price	Sales	Capital Costs	Working Capital	Var Costs	Fixed Costs	Depreciation	Depletion Allowance	Taxable Income	Taxes	Net Earnings	Cash Flow	Cumulative Net Present Value at 15%
2014	0%		-	-	-	-	-	-	-	-	-	-	-	-
2015	0%		-	(3,852,500)	(1,346,900)	-	-	-	-	-	-	-	(5,199,400)	(4,521,200)
2016	45%	$0.68	13,504,100	-	(673,500)	(11,496,600)	(1,617,400)	(687,900)	-	(297,900)	110,200	(187,700)	(173,200)	(4,652,200)
2017	68%	$0.68	20,256,100	-	(673,500)	(17,245,000)	(1,617,400)	(1,100,700)	-	293,000	(108,400)	184,600	611,800	(4,249,900)
2018	90%	$0.68	27,008,200	-	-	(22,993,300)	(1,617,400)	(660,400)	-	1,737,000	(642,700)	1,094,300	1,754,800	(3,246,600)
2019	90%	$0.68	27,008,200	-	-	(22,993,300)	(1,617,400)	(396,300)	-	2,001,200	(740,400)	1,260,800	1,657,000	(2,422,800)
2020	90%	$0.68	27,008,200	-	-	(22,993,300)	(1,617,400)	(396,300)	-	2,001,200	(740,400)	1,260,800	1,657,000	(1,706,400)
2021	90%	$0.68	27,008,200	-	-	(22,993,300)	(1,617,400)	(198,100)	-	2,199,300	(813,800)	1,385,600	1,583,700	(1,111,100)
2022	90%	$0.68	27,008,200	-	-	(22,993,300)	(1,617,400)	-	-	2,397,500	(887,100)	1,510,400	1,510,400	(617,300)
2023	90%	$0.68	27,008,200	-	-	(22,993,300)	(1,617,400)	-	-	2,397,500	(887,100)	1,510,400	1,510,400	(188,000)
2024	90%	$0.68	27,008,200	-	-	(22,993,300)	(1,617,400)	-	-	2,397,500	(887,100)	1,510,400	1,510,400	185,400
2025	90%	$0.68	27,008,200	-	-	(22,993,300)	(1,617,400)	-	-	2,397,500	(887,100)	1,510,400	1,510,400	510,000
2026	90%	$0.68	27,008,200	-	-	(22,993,300)	(1,617,400)	-	-	2,397,500	(887,100)	1,510,400	1,510,400	792,300
2027	90%	$0.68	27,008,200	-	-	(22,993,300)	(1,617,400)	-	-	2,397,500	(887,1001	1,510,400	1,510,400	1,037,800
2028	90%	$0.68	27,008,200	-	-	(22,993,300)	(1,617,400)	-	-	2,397,500	(887,100)	1,510,400	1,510,400	1,251,300
2029	90%	$0.68	27,008,200	-	-	(22,993,300)	(1,617,400)	-	-	2,397,500	(887,100)	1,510,400	1,510,400	1,436,900
2030	90%	$0.68	27,008,200	-	2,693,900	(22,993,300)	(1,617,400)	-	-	2,397,500	(887,100)	1,510,400	4,204,200	1,886,200

6. ***Profitability Measures—Part (b) Purchase and Installation Costs Estimated by APEA***

Profitability Measures	
The Internal Rate of Return (IRR) for this project is	21.06%
The Net Present Value (NPV) of this project in 2014 is	$1,886,200

ROI Analysis (Third Production Year)

Annual Sales	27,008,172
Annual Costs	(24,610,720)
Depreciation	(308,200)
Income Tax	(773,023)
Net Earnings	1,316,229
Total Capital Investment	6,546,353
ROI	20.11%

7. ***Sensitivity Analyses—Part (b) Purchase and Installation Costs Estimated by APEA***

Sensitivity Analyses

	Vary Initial Value by +/−
x-axis	50%
y-axis	50%

		Variable Costs										
		$12,774,047	$15,328,856	$17,883,665	$20,438,475	$22,993,284	***$25,548,093***	$28,102,903	$30,657,712	$33,212,521	$35,767,331	$38,322,140
Product Price	$0.34	0.30%	Negative IRR	Negative IRR	Negative IRR	Negative IRR	Negative IRR	Negative IRR	Negative IRR	Negative IRR	Negative IRR	Negative IRR
	$0.41	30.55%	6.11%	Negative IRR	Negative IRR	Negative IRR	Negative IRR	Negative IRR	Negative IRR	Negative IRR	Negative IRR	Negative IRR
	$0 48	52.10%	33.14%	10.72%	Negative IRR	Negative IRR	Negative IRR	Negative IRR	Negative IRR	Negative IRR	Negative IRR	Negative IRR
	$0 54	70.95%	53.78%	35.52%	14.61%	Negative IRR	Negative IRR	Negative IRR	Negative IRR	Negative IRR	Negative IRR	Negative IRR
	$0.61	88.15%	72.03%	55.35%	37.74%	18.01%	−10.68%	Negative IRR	Negative IRR	Negative IRR	Negative IRR	Negative IRR
	$0.68	104.13%	88.76%	73.05%	56.84%	39.81%	21.06%	−3.76%	Negative IRR	Negative IRR	Negative IRR	Negative IRR
	$0.75	119.13%	104.35%	89.34%	74.02%	58.25%	41.75%	23.83%	1.55%	Negative IRR	Negative IRR	Negative IRR
	$0.82	133.29%	119.01%	104,56%	89.90%	74.95%	59.59%	43.58%	26.37%	5.90%	Negative IRR	Negative IRR
	$0 88	146.73%	132.68%	118.90%	104.77%	90.44%	75.83%	60.86%	45.31%	28.73%	9.62%	Negative IRR
	$0.95	159.53%	146.05%	132.48%	118.80%	104.97%	90.94%	76.68%	62.06%	46.94%	30.93%	12.90%
	$1.02	171.74%	158.61%	145.40%	132.10%	118.70%	105.15%	91.43%	77.48%	63.22%	48.49%	32.98%

17.9 SUMMARY

After studying this chapter and completing several of the exercises, the reader should be able to:

1. estimate annual costs using a standard cost sheet similar to the one in Table 17.1
2. estimate annual cash flows, working capital, and the total capital investment in Table 16.9.
3. compute approximate profitability measures, ROI, PBP, VP, and annualized cost.
4. compute present and future worth of single payments and annuities.
5. compute profitability measures that account for the time value of money, including the net present value, NPR, and the investor's rate of return, IRR.
6. use Aspen Process Economic Analyzer (APEA) and an economics spreadsheet to perform a profitability analysis.

REFERENCES

1. Bauman, H. C., *Fundamentals of Cost Engineering in the Chemical Industry,* Reinhold, New York (1964).

2. Brealey, R., and S. Myers, *Principles of Corporate Finance*, McGraw-Hill, New York (1984).

3. Busche, R. M., *Venture Analysis: A Framework for Venture Planning,* Course Notes, Bio-en-gene-er Associates, Wilmington, Delaware (1995).

4. Downey, B. K., *Profitability Analysis Spreadsheet*, University of Pennsylvania, Philadelphia (2008).

5. Pisano, G. P., *The Development Factory: Unlocking the Potential of Process Innovation*, Harvard Business School Press, Cambridge (1997).

6. Souders, M., Engineering Economy, *Chem. Eng. Prog.,* **62**(3), 79–81 (1966).

EXERCISES

17.1 In the design of a chemical plant, the following costs and revenues (in the third year of production) are projected:

Total depreciable capital, excluding allocated power	$10,000,000
Allocated power utility	$ 2,000,000
Working capital	$ 500,000
Annual sales	$ 8,000,000/yr
Annual cost of sales excluding depreciation	$ 1,500,000/yr

Assume the costs of land, royalties, and startup are zero. Determine

(a) The return on investment (ROI)

(b) The payback period (PBP)

17.2 For Exercise 17.1, the return on investment desired by the chemical company is 20%. Determine the venture profit.

17.3 It is desired to have $9,000 available 12 yr from now. If $5,000 is available for investment at the present time, what discrete annual rate of compound interest on the investment would be necessary to yield the desired amount?

17.4 What will be the total amount available 10 yr from now if $2,000 is deposited at the present time with nominal interest at the rate of 6% compounded semi-annually?

17.5 An original loan of $2,000 was made at 6% simple interest per year for 4 yr. At the end of this time, no interest had been paid and the loan was extended for 6 yr more at a new effective compound interest rate of 8%/yr. What is the total amount owed at the end of the 10^{th} yr if no intermediate payments are made?

17.6 A concern borrows $50,000 at an annual effective compound interest rate of 10%. The concern wishes to pay off the debt in 5 yr by making equal payments at the end of each year. How much will each payment have to be?

17.7 How many years are required for money to double when invested at a nominal interest rate of 14% compounded semiannually? Determine the shortest time in years, allowing any number of compounding periods.

17.8 A person at age 30 is planning for retirement at age 60. He projects that he will need $100,000 a year until age 80. Determine the uniform annual contribution (by him and his company) needed to provide these funds. Assume that the effective interest rate is 8%/yr and the rate of inflation is zero.

17.9 A heat exchanger has been designed for use in a chemical process. A standard type of heat exchanger with a negligible scrap value costs $4,000 and will have a useful life of 6 yr. Another proposed heat exchanger of equivalent design capacity costs $6,800 but will have a useful life of 10 yr and a scrap value of $800. Assuming an effective compound interest rate of 8%/yr, determine which heat exchanger is cheaper by comparing the capitalized costs.

17.10 Two machines, each with a service life of 5 yr, have the following cost comparison. If the effective interest rate is 10%/yr, which machine is more economical?

	A	B
First cost	$25,000	$15,000
Uniform end of-year maintenance	2,000	4,000
Overhaul, end of third year		3,500
Salvage value	3,000	
Benefit from quality as a uniform end-of-year amount	500	

17.11 Two pumps are being considered for purchase:

	A	B
Initial cost	$8,450	$10,000
Salvage value	1,500	4,000

Determine the service life, n_y, at which the two pumps are competitive. The annual effective interest rate is 10%.

17.12 Two heat exchangers are being considered for installation in a chemical plant. It is projected that:

	A	B
Installed cost	$70,000	$80,000
Uniform end of-year maintenance	?	$4,000
Salvage value	$7,000	$8,000
Service life	8 yr	7 yr

For an effective interest rate of 10%, determine the uniform end-of-year maintenance for heat exchanger A at which the two are competitive.

17.13 Consider the following two alternatives for the installation of a pump:

	A	B
Installed cost	$30,000	$16,000
Uniform end-of-year maintenance	$1,600	$2,400
Salvage value	?	$1,000
Life	5 yr	3 yr

The effective annual interest rate is 10%. Determine the salvage value for pump A when the two pumps are competitive.

17. 14 You are offered two options to finance a compressor with a nominal interest rate at 7.25% compounded monthly.

(a) You pay $590 per month for 134 months.

(b) You pay $545 per month for 151 months.

Compare these with the alternative of $590 per month for 151 months (at a nominal interest rate of 8.75% compounded monthly.)

Compared to the alternative, it is claimed that (a) saves $10,030 and (b) saves $6,795. Do you agree? Justify your response.

(*Hint*: Use present value analysis.)

17.15 Two pumps are under consideration:

	A	B
Installed cost	$10,000	$18,000
Service life	1 yr	2 yr

Determine the interest rate at which the two pumps are competitive.

17. 16 A chemical plant constructed in 2007 began operating in 2008. In 2010, the plant is projected to operate at 90% of capacity, with

Sales	$10 MM
Cost of sales (excl. dep.)	$ 5 MM

(a) Calculate the return on investment (ROI) in 2010 given that the total depreciable capital is $18 MM and the working capital is $2 MM. Assume straight-line depreciation at 8% per year.

(b) Calculate the cash flow in 2010 and discount it to present value assuming an effective interest rate of 15%. Use the MACRS depreciation schedule for a class life of 5 yr.

17.17 A proposed chemical plant has the following projected costs and revenues in millions of dollars:

	Investment	Working Capital	Cost of Sales (excl. dep.)	Sales
2003	(40.0)	(4.0)		
2004			4.0	10.0
2005			5.6	14.0
2006			7.0	17.5
2007			8.0	20.0
2008			9.0	22.5
2009			9.6	24.0
2010		4.0	10.0	25.0

Using an MACRS depreciation schedule having a class life of 5 yr,

(a) Compute the cash flows.

(b) At an effective interest rate of 20%, determine the net present value.

(c) Is the investor's rate of return less than or greater than 20%? Explain

(d) Compute the investor's rate of return.

17.18 An engineer in charge of the design of a plant must choose either a batch or a continuous system. The batch system offers a lower initial outlay but, owing to high labor requirements, exhibits a higher operating cost. The cash flows relevant to this problem have been estimated as follows:

	Year		Investor's Rate of Return	Net Present Worth at 10%
	0	1–10		
Batch system	−$20,000	$5,600	25%	$14,400
Continuous system	−$30,000	$7,650	22	$17,000

Check the values given for the investor's rate of return and net present worth. If the company requires a minimum rate of return of 10%, which system should be chosen?

17. 19 An oil company is offered a lease of a group of oil wells on which the primary reserves are close to exhaustion. The major condition of the purchase is that the oil company must agree to undertake a water-flood project at the end of 5 yr to make possible secondary recovery. No immediate payment by the oil company is required. The relevant cash flows have been estimated as follows:

Year				Investor's	Net Present
0	1–4	5	6–20	Rate of Return	Worth at 10%
0	$50,000	−$650,000	$100,000	?	$227,000

Should the lease-and-flood arrangement be accepted? How should this proposal be presented to the company board of directors, who understand and make it a policy to evaluate by the investor's rate of return?

17.20 *Sequencing of two distillation columns*. The demand for styrene monomer continues to increase. Other companies produce styrene by alkylating benzene with ethylene to ethylbenzene, followed by dehydrogenation to styrene. Our chemists have developed a new reaction path to styrene that involves other chemicals that appear to be available from our own supplies at a relatively low cost. These chemicals are toluene and methanol. We have been asked to prepare a preliminary design and economic evaluation for this new route to determine whether it merits further consideration. If so, we will consider entering the styrene manufacturing business.

The new process can be broken down into four sections: (1) the reactor section where toluene is partially reacted with methanol to produce styrene, water, and hydrogen, with an unfortunate side reaction that produces ethylbenzene and water; (2) an aqueous stream separation system; (3) an organic stream separation system; and (4) a vapor separation system. Fortunately, we have a potential buyer for the ethylbenzene byproduct. We are assigning you the design and economic calculations of just the organic stream separation system. Others are preparing the designs for the other three sections.

The chemical engineer working on the reactor section has already calculated the following reactor effluent:

Component	kmol/hr
Hydrogen	352
Methanol	107
Water	484
Toluene	107
Ethylbenzene	137
Styrene	352

This effluent is cooled to 38°C and enters a flash-decanter vessel at 278 kPa. Three phases leave that vessel. The vapor phase (hydrogen rich) is sent to the vapor separation system. The aqueous phase (mostly water with some methanol) is sent to the aqueous stream separation system. The organic-rich phase is sent to the organic stream separation system, which you will design. To obtain the composition of the feed to your section, use a simulator with the UNIFAC method to perform a three-phase flash for the above conditions. If the resulting organic liquid stream contains small amounts of hydrogen and water, assume they can be completely removed at no cost before your stream enters your separation section.

Your separation system must produce the following streams with two distillation operations in series:

A methanol–toluene-rich distillate stream for recycle back to the reactor. This stream should not contain more than 5 wt% of combined ethylbenzene and styrene.

An ethylbenzene byproduct stream containing 0.8 wt% max. toluene and 3.9 wt% max. styrene.

A styrene product stream containing 300 ppm (by wt) max. ethylbenzene.

We have a serious problem with styrene. If any stream contains more than 50 wt% styrene, the temperature of the stream must not exceed 145°C. Otherwise, the styrene will polymerize. This must be carefully considered when establishing the operation conditions for the two distillation operations. You may have to operate one or both columns under vacuum. This will require you to estimate the amount of air that leaks into the vacuum columns and select and cost vacuum systems. In designing the distillation system, you are to consider the direct sequence and the indirect sequence.

Please submit a report on the two designs and cost estimates (fixed capital and utility operating costs only). For the capital cost of each of the two alternative sequences, sum the purchase costs of the distillation columns, heat exchangers, and any vacuum equipment. Multiply that cost by the appropriate Lang factor. To annualize the capital cost, multiply by 0.333. Add to this annualized cost the annual utility cost for steam and cooling water. Call this the total annualized cost for the alternative.

Use a simulator to do as many of the calculations as possible, including the very important column pressure-drop calculations (because of the need for vacuum in one or more columns). Assume a condenser pressure drop of 5 kPa and no pressure drop across the reboiler. You may select column internals from the following list:

Sieve trays on 18-in. spacing with overall tray efficiency of 75%.

Pall rings random packing with HETP = 24 in.

Mellapak structured packing with HETP = 12 in.

Submit your results as a short report complete with an introduction to the problem, a process description, process flow diagram, discussion of equipment operating conditions and how you arrived at them, a material-balance table, cost tables, conclusions, and your recommendations. Make it clear which alternative you favor and whether it might offer some technical challenges if it is selected for final design.

17.21 *Toluene hydrodealkylation process-economic analysis using ASPEN PLUS, APEA, and the profitability analysis spreadsheet.*

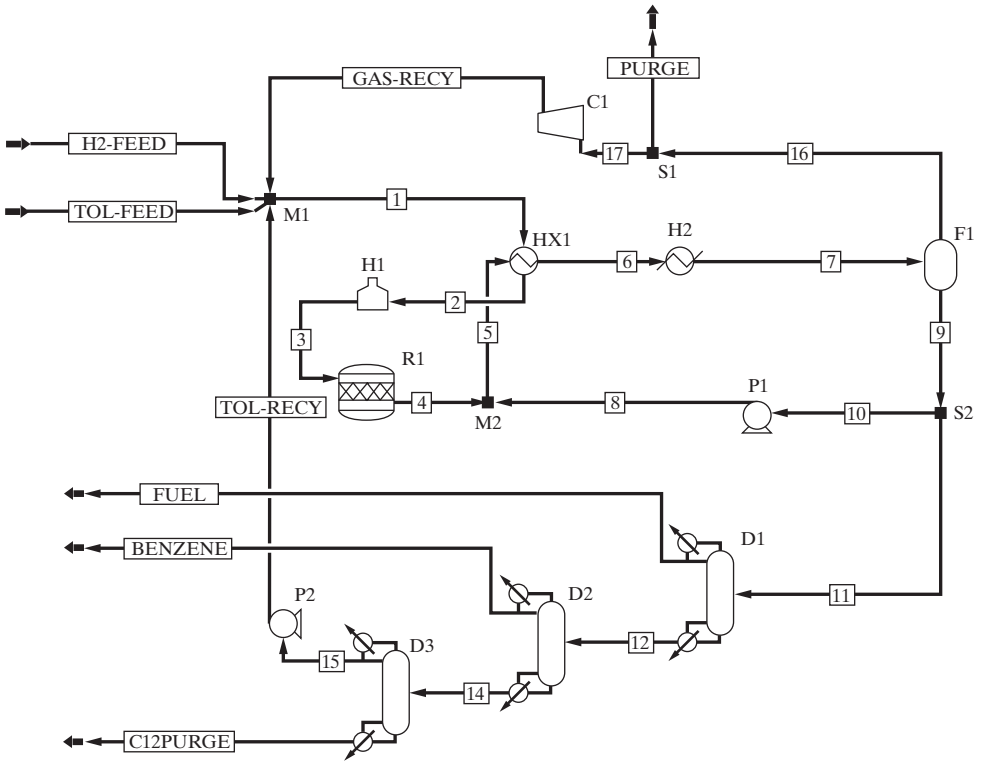

Figure 17.1 ASPEN PLUS simulation flowsheet for the toluene hydrodealkylation process.

This assignment begins with a completed simulation of the toluene hydrodealkylation process in Figure 17.1 and involves the completion of an economic evaluation. Note that the simulation results for this process were developed in solution of Exercise 7.4 and can be reproduced using the HDA.bkp file in the Program and Simulation Files folder on the Wiley Web site associated with this textbook. APEA will be used for equipment and capital cost estimation. The spreadsheet, Profitability Analysis – 4.0.xls, also in the Program and Simulation Files folder, will be used for economic analysis. This spreadsheet will enable you to enter the specifications recommended for capital investment costs (Section 16.3, Tables 16.9 and 16.12) and for the cost sheet (Section 17.2, Table 17.1), and using the approximate profitability measures in Section 17.4 and those involving cash flows in Section 17.6. In most cases, only the nondefault APEA entries are provided in this problem statement. This, together with the description in Section 16.8, should enable you to understand the items on APEA input forms.

Cost Options

The project startup date is January 2016 and the project duration is 16 yr (15 production yrs). For simplicity, the effect of inflation is disregarded in this assignment.

Equipment

Unless otherwise stated, the default equipment types and materials of construction are acceptable.

Tanks

Toluene storage tank
Create a tank to store a two-day supply of toluene.

Benzene storage tank
Create a tank to store a two-day supply of the benzene product.

Stream 11 storage tank
Create a tank to store a two-day supply of the intermediate stream 11.

Flash vessel F1

Size a vertical flash vessel to have a 10-minute liquid retention time.

Reactor R1

The elevated temperature (1,268°F) and pressure (494 psia) present special complications when designing and sizing the hydrodealkylation reactor. This is a large-diameter vessel that is lined with refractory brick to insulate the steel alloy that composes the retaining wall. Initially, use APEA to design a vessel that has a 10-ft diameter and a 60-ft tangent-to-tangent length. To estimate the thickness of the refractory brick and the temperature at the brick-steel interface, a heat balance is necessary. In practice, the brick thickness is adjusted to give an interface temperature of 900°F. When using APEA, select refractory-lined carbon steel. Using the pull-down menu, select a 9-inch layer of 90% alumina fire brick, symbol 9FB90. Also, consider the possibility of using two or three smaller-diameter vessels in parallel. Finally, compare the costs of horizontal and vertical vessels.

Before mapping the reactor model in the ASPEN PLUS simulation, replace the RSTOIC model (block) with the RPLUG model (block) in ASPEN PLUS. Note, however, that the kinetics of the side reaction cannot be modeled using the RPLUG model (block). Since the conversion of this reaction is small, its kinetics can be neglected in the reactor design. Rather, it is sufficient to account for the reaction using a dummy reactor unit, R1D, modeled with the RSTOIC block, which follows the reactor unit R1, modeled with the RPLUG block. Do not permit APEA to size and cost unit R1D.

Heat Exchangers

H2
Use cooling water.

D1, D2, and D3 condensers
Use cooling water.

D1, D2, and D3 reboilers
Use steam.

Distillation Towers

In the ASPEN PLUS simulation, for each distillation column, use the RADFRAC model (block) in place of the DISTL model (block). As a result, the reflux ratios change somewhat to achieve the same product specifications using the same number of trays.

In APEA, set the tray efficiency of the three columns to 90%.

The reflux accumulators should be horizontal vessels with a liquid holdup time of 10 min.

Pumps

Toluene pump
Create a pump to bring the toluene feed from atmospheric pressure to 569 psia.

Benzene pump
Increase the pressure of the benzene product stream by 25 psia.

D1 condenser pump
Increase the pressure of the D1 reflux by 25 psia.

D1 reboiler pump
Increase the pressure of the D1 reboiler pump by 25 psia.

D2 condenser pump
Increase the pressure of the D2 reflux by 25 psia.

D2 reboiler pump
Increase the pressure of the D2 reboiler pump by 25 psia.

D3 condenser pump
Increase the pressure of the D3 reflux by 25 psia.

D3 reboiler pump
Increase the pressure of the D3 reboiler pump by 25 psia.

Other Equipment

Compressor C1
Use a centrifugal compressor.
Use a motor drive and an electrical utility.

Fired heater H1

In the ASPEN PLUS simulation, the HEATER model (block) was used. By default, units modeled with the HEATER block are mapped as heat exchangers by APEA. Instead, this unit must be mapped as a furnace. Furthermore, before estimating the cost of the furnace, the default material, carbon steel, must be replaced by a material that can withstand temperatures up to 1,200°F in the furnace. Note that Inconel is selected from among the materials available in APEA that can withstand this temperature. To replace carbon steel, in row nine of the window that displays the equipment sizes for the furnace, double-click on the equipment item, scroll to locate *tube material*

selection, which opens the pull-down menu on the right. Then, select *Inconel.* These changes must be saved before leaving this window.

Labor Costs

Use a wage rate of $40/hr.

Materials

For the feed, product, and byproduct streams H2-FEED. TOL-FEED, BENZENE, PURGE, FUEL, and C12PURGE, the following prices are typical:

Hydrogen feed	$1.00/lb
Toluene feed	$1.50/gal
Benzene product	$2.50/gal
FUEL, PURGE	$3.00/MM Btu heating value
C12PURGE	0

The prices are for toluene and benzene at 1 atm and 75°F. You can use ASPEN PLUS to estimate the densities needed to obtain the prices on a mass basis. (You can also use ASPEN PLUS to estimate the heating value of a stream rather than calculate it independently.) To compute and display the heating values of all streams, access the Property Sets folder, press *New*, and enter an ID (e.g., PS-5) to obtain the *Property Sets* tab. From the pull-down menu, select HHV-0 or HHV-15. Then, follow the sequence: *Setup→Report Options→Stream→Property Sets.* This produces the *Property Sets* dialog box. From the *Available Property Sets*, move your ID to the *Selected Property Sets* and press *Close.* Then, run ASPEN PLUS and obtain the stream report. Heating values will be displayed for each stream.

Utilities

For this process, cooling water, steam, electricity, and fuel are purchased.

Cooling water: $0.10/1,000 gal. Use inlet and outlet temperatures of 90°F and 120°F.

Steam: Use prices in Table 17.1.

Electricity: $0.07/kW-hr.

Fuel (to heater H1): Assume the heater is gas fired at a cost of $2.60/MM Btu.

Operating Costs

The plant is anticipated to operate 330 days a year.

Average hourly wage rate is $40/hr with two operators per shift.

Profitablity Analysis

Project a 15-yr life for the plant.

Assume a 15% interest rate to calculate the net present value.

For cash flow analysis, use the 5-yr MACRS depreciation schedule. Estimate the effective tax rate to be 40% with no investment tax credit.

Assume a production schedule such that the plant operates at 50% of full scale (90% of capacity) in the first year, 75% of full scale in the second year, and 100% of full scale thereafter.

Provide for the cost of startup at 20% of the total materials and labor cost of the process units.

Provide for working capital to cover 2 days of raw material inventory, 2 days of in-process chemicals, 2 days of finished-product inventory, and 30 days of accounts receivable.

Part Three

Design Analysis—Product and Process

With the advent of digital computers, it is now possible and desirable to economically analyze designs so as to greatly improve controllability and profitability and to achieve optimal operation of continuous and batch processes. Part III considers these topics in five chapters.

Avoiding manufacturing defects in products and abnormal operation in processing is key to a successful and profitable venture. Chapter 18 introduces the six-sigma structured methodology for product quality analysis that is applicable to the design of new products and processes. Variables that are critical to ensuring quality are measured and checked to determine whether they are within control limits. The methodology is then directed to reducing the variance of the critical variables by integrating design and control strategies. The strategy is illustrated by two examples, one dealing with the design of a process for manufacturing penicillin; the other for the design of an Espresso machine.

The business aspects of product development are treated in Chapter 19. The material in this chapter covers the entire development cycle. It goes beyond the cost reductions sought in conventional product and process design to include the use of cash flow diagrams, product-development budgeting, make-buy decisions, microeconomics, and consideration of other company and societal factors. Four examples illustrate the application of these aspects to business decision making.

It is of great importance to consider controllability, resiliency, and operability issues early in process design. Chapter 20 deals with procedures and guidelines to do this including (1) identification of potential control problems in flowsheets as they are generated, (2) selection of controlled and manipulated variables for a plantwide control system, and (3) synthesis of a plantwide control system. With control systems incorporated in the designs, computer-aided dynamic simulations can be conducted to verify the controllability, resiliency, and operability of competing flowsheets. The material presented in this chapter is illustrated in 12 practical examples.

The use of process simulators provides opportunities to optimize a process design with respect to flowsheet structure and/or selected operating conditions. Chapter 21 begins with a general discussion of the fundamentals of optimization using linear programming and nonlinear programming, including the formulation of an objective function that is minimized or maximized and the selection of design variables and equality or inequality constraints. The chapter concludes with two case studies using process simulators, one for a recycle with purge process involving just one decision variable and one inequality constraint; the other case study is for a complex distillation operation involving four decision variables and five inequality constraints.

Batch processes are widely used to produce seasonal specialty chemicals, pharmaceuticals, and electronic materials. In addition to the need for optimizing the operating conditions, it is also necessary to schedule the reactor and distillation operations in the process. These topics are covered in Chapter 22. Three batch modes—batch, fed-batch, and batch-product removal—are discussed with five examples to reactors, distillation, and combined reactor-separator batch processes. The chapter concludes with a treatment of batch cycle times using Gantt charts.

Chapter 18

Six-Sigma Design Strategies

18.0 OBJECTIVES

This chapter introduces six-sigma methodology and shows how it is used to improve product designs and process operations. After studying this chapter, the reader should:

1. Be able to compute the sigma level of a specific process in a product manufacturing facility.
2. Have an appreciation of how integrated design and control can assist in improving the sigma level of a specific process or the entire product manufacturing facility through the reduction of variance in the most critical manufacturing steps.

18.1 INTRODUCTION

Espresso coffee is prepared in a machine that injects water under high-pressure steam through a cake of ground coffee. In a conventional espresso machine, the user manually loads ground coffee into a metal filter cup, locks the cup under the water head, and then activates the water heater. A manufacturer of espresso machines would like to guarantee that each cup of coffee processed by the machine has a consistent quality. It is noted that the quality of each cup of espresso depends on a large number of variables, among them the grade and freshness of the coffee beans, the extent to which the beans have been ground, the machine's operating temperature and pressure, the degree to which the ground coffee is packed into the metal filter holder, and the total amount of water used. Since many of the sources of product variability cannot be controlled by the manufacturer, the development of an improved espresso machine would be driven by the desire to either reduce the influence of these variables or eliminate as many as necessary to ensure a satisfactory product.

This chapter describes the role of integrated design and control together with six-sigma methodology (Rath and Strong, 2000, 2002) in the manufacture of products such as espresso machines, integrated circuits, and drugs and specialty chemicals, which are either defect-free in the case of manufactured items or delivered on specification in the case of pharmaceuticals. It will be shown that these aims can be achieved by utilizing six-sigma methodology and additional statistical tools to quantify quality and, more importantly, the loss of quality and its cost. These tools assist in identifying the main sources of product variance, which are then attenuated or eliminated by improving the integrated design of the manufacturing process and its control system.

This chapter begins by describing the mathematical basis for six-sigma methodology and its role in quantifying the cost of manufacturing defects or abnormal operation in processing steps and in guiding manufacturing to reduce product variance. Next, its role in product design is described, showing how six-sigma methodology is enhanced by incorporating integrated design and control into the product design process. The chapter concludes with examples of how the combined approach assists in improving product manufacturing and processing.

18.2 SIX-SIGMA METHODOLOGY IN PRODUCT DESIGN AND MANUFACTURING

Definitions

Six-sigma (6σ) is a structured methodology for eliminating defects and, hence, improving product quality in manufacturing and services. The methodology aims to identify and reduce the variance in product quality and involves a combination of statistical quality control, data analysis methods, and personnel training.

The critical-to-quality (CTQ) variables are monitored and used to track production to ensure that a sufficient number of measurements are within the control limits, commonly using the Shewart Chart shown in Figure 18.1. The measurements shown in the chart could be the composition of the chemical produced from a reactor when producing a basic chemical product or a characteristic attribute associated with finished items from the production line for a configured consumer product. The degrees to which both of these products are satisfactory are quantified by the proportion of measurements that lie within the specification bounds demarcated from above by the upper control limit (UCL) and from below by the lower control limit (LCL). In both cases, improved production involves reducing the number of off-specification measurements, which in six-sigma methodology is expressed as the *number of defects per million opportunities* (DPMO) with the term six-sigma defining a desired level of quality: 3.4 defects per million opportunities. For example, the data in Figure 18.1 show 1 defect in 24 opportunities; that is, 1 off-specification measurement in 24.

As discussed by Lewin et al. (2007), on many production lines, open-loop, recipe-driven, feedforward control strategies are implemented. Often, the desired operating point

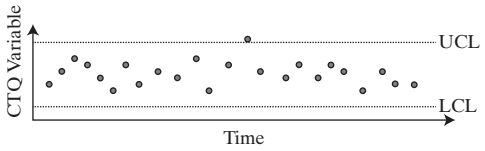

Figure 18.1 Monitoring product quality in a Shewart Chart.

is determined following a statistical design-of-experiment (DOE) study that locates a "stable" processing window. Subsequently, the degrees-of-freedom of the process (the manipulated variables) are fixed according to the DOE results. Feedback control, if implemented at all, is usually limited to single proportional-integral-derivative (PID) control loops, usually only the lower-level loops (e.g., for temperature control). The main disadvantages of feedforward control are well recognized: (1) Unmeasured and/or unknown disturbances are neglected and (2) because the feedforward correction is based on an imperfect process model, generally the product is not produced consistently on target even in the absence of unknown disturbances. Process models are usually not implemented, and, when used, are usually limited to empirical, polynomial-like formulations. Typically, when loss-of-control (LOC) incidents occur, the process is shut down with associated production losses, and a new DOE study is initiated to diagnose the problem and suggest corrections.

Figure 18.2 shows typical performances using three alternative control strategies. The solid line (a) shows the expected distribution of a CTQ variable when using only feedforward control, which ignores the effects of unmeasured disturbances, leading in this case to a large fraction of CTQ measurements below the LCL. The dashed line (b) indicates the anticipated improvement when implementing a feedback-control strategy designed to maintain the average CTQ measurement on target. To significantly improve the product yield, however, in addition to feedback control, the CTQ variance must be reduced, corresponding to the dashed-dotted line (c).

The symbol σ (sigma) is the standard deviation of the value of a quality variable, a measure of its variance, which is assumed to have a normal distribution. Figure 18.3a shows such a distribution of measurements with $\sigma = 2$. Note that the distribution is

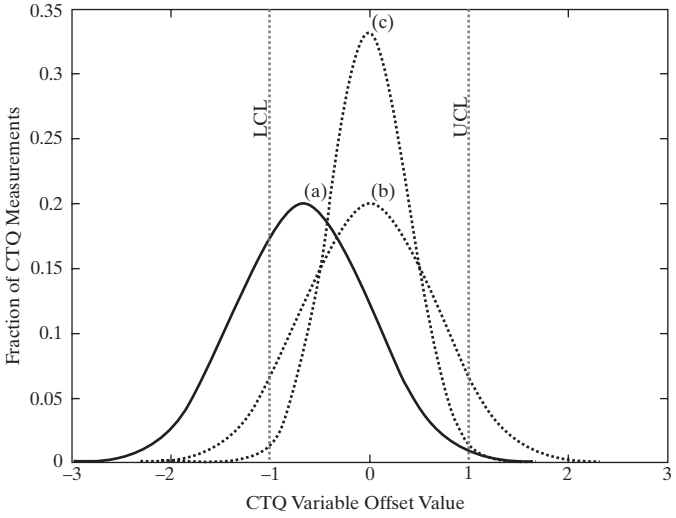

Figure 18.2 Probability distributions for CTQ variable: (a) solid line—without regulatory control; (b) dashed line—with regulatory control but with a large variance; (c) dashed-dotted line—with regulatory control and a lower variance.

normalized such that the total area under the curve is unity with a probability density function given by:

$$f(x) = \frac{1}{\sigma\sqrt{2\pi}} \exp\left[-\frac{1}{2}\left(\frac{x-\mu}{\sigma}\right)^2\right] \tag{18.1}$$

where $f(x)$ is the probability of the quality at a value of x and μ is the average value of x. Assuming that operating conditions are considered normal if the quality is maintained within 3σ of μ, then the UCL is at $\mu + 3\sigma$ and the LCL is at $\mu - 3\sigma$. As shown in Figure 18.3a, the number of DPMO above the UCL is:

$$\begin{aligned} \text{DPMO} &= 10^6 \int_{\mu+3\sigma}^{\infty} f(x)dx \\ &= \frac{1}{2}10^6 \left(1 - \int_{\mu-3\sigma}^{\mu+3\sigma} f(x)\,dx\right) = 1{,}350 \end{aligned} \tag{18.2}$$

This means that 1,350 DPMO are expected in a normal sample above the UCL and the same number are expected below the

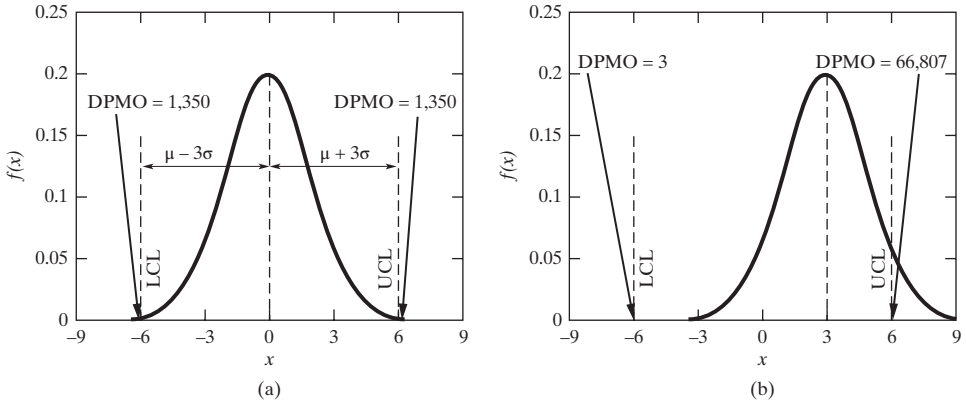

Figure 18.3 Distribution of product quality at 3σ with $\sigma = 2$: (a) normal operation at $\mu = 0$; (b) abnormal operation shifted to $\mu + 1.5\sigma$.

LCL. It is important, however, that the manufacturing process be insensitive to process drifts. In accepted six-sigma methodology, a worst-case shift of 1.5σ in the distribution of quality is assumed, giving a new average value of $\mu + 1.5\sigma$ as shown in Figure 18.3b. For operation at 3σ, that is, at a sigma level of 3—or in other words, *when the distance from the normal average value to one of the control limits is equal to three times the standard deviation*—the expected DPMO above the UCL is 66,807 and below the LCL is 3. This gives a total expected DPMO of 66,810, a significant deterioration in quality. Clearly, to improve the reliability of manufacturing, one needs to reduce the variance in the product and, thus, increase its sigma level.

Suppose that by improvements in either the process design or its control system, the variance can be reduced to $\sigma = 1$. An operation at 6σ—that is, at a sigma level of 6 on either side of the average value of the distribution $\mu = 0$—defines the UCL at $\mu + 6\sigma$ and the LCL at $\mu - 6\sigma$ as shown in Figure 18.4a. Here, there is 1 defect per billion opportunities on either side of the acceptance limits, which are insignificant defect levels. The improvement in performance is apparent when considering a shift of 1.5σ as before; for 6σ operation, or in other words, *when the distance from the normal average value to one of the control limits is equal to six times the standard deviation*, the DPMO (above the UCL) increases to only 3.4 as shown in Figure 18.4b.

Cost of Defects

Table 18.1 and Figure 18.5 present the effect of the sigma level on the DPMO, assuming a 1.5σ shift in mean as in Figures 18.3b and 18.4b. Note that Figure 18.5 accounts for the total DPMO above the UCL and below the LCL. For example, for the data in Figure 18.1 with 1 defect recorded in 24 measurements, the DPMO is $(1/24) \times 10^6 = 41{,}667$, which from Figure 18.5 is equivalent to a sigma level of approximately 3.3. Although originally developed for the analysis of product manufacturing, it is relatively easy to compute the sigma level for a continuous process (Trivedi, 2002). As an example, suppose that on average, the distillate from a distillation column fails to meet its specifications during 5 hr/mo of production. The sigma level for this process is computed by first estimating the DPMO:

$$\text{DPMO} = 10^6 \times \frac{5}{30 \times 24} = 6{,}944$$

Table 18.1 Effect of Sigma Level on Expected DPMO with 1.5σ Shift in Mean, μ

Sigma Level	Expected DPMO
1.0	697,672
2.0	308,770
3.0	66,810
3.5	22,750
4.0	6,210
4.5	1,350
5.0	233
5.5	32
6.0	3.4

Figure 18.5 gives the sigma level for this DPMO at 3.8.

If improved operations were to reduce the specification violations to 0.5 hr/month, the DPMO would be reduced by a factor of 10, giving an increase in the sigma level to 4.7. The increased sigma level is a consequence of the reduction in the variance in the CTQ variable. This improved operation is normally achieved by enhancements in the process and/or its control system. Evidently, lower sigma levels are achieved for processes in which abnormal operation is prevalent compared to processes in which abnormal operation seldom occurs. Thus, for example, a crude-oil distillation unit with frequent feedstock changes is expected to have a lower sigma level than one relying on a single feedstock. This is because feedstock changes cause process upsets that propagate throughout the entire unit, leading to off-specification product until corrections are made by the feedback-control system.

The expected number of defects presented in Figure 18.5 applies to a single manufacturing step. Usually, the manufacture of devices involves a number of steps. For n steps, assuming that all defective components of the device are removed from the production sequence at the step where they occur, the overall defect-free throughput yield (TY) is:

$$\text{TY} = \prod_{u=1}^{n} \left(1 - \frac{\text{DPMO}_i}{10^6}\right) \tag{18.3}$$

where DPMO_i is the expected number of defects per million opportunities in step i. If the DPMO is identical in each step,

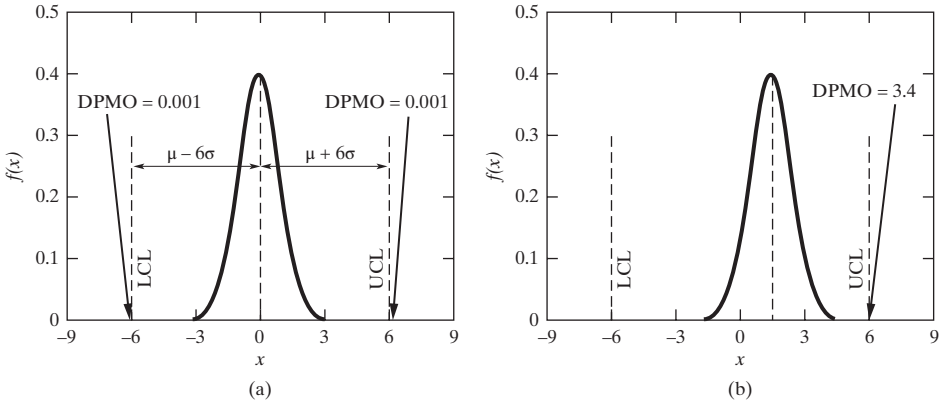

Figure 18.4 Distribution of product quality at 6σ, with $\sigma = 1$: (a) normal operation at $\mu = 0$; (b) abnormal operation shifted to $\mu + 1.5\sigma$.

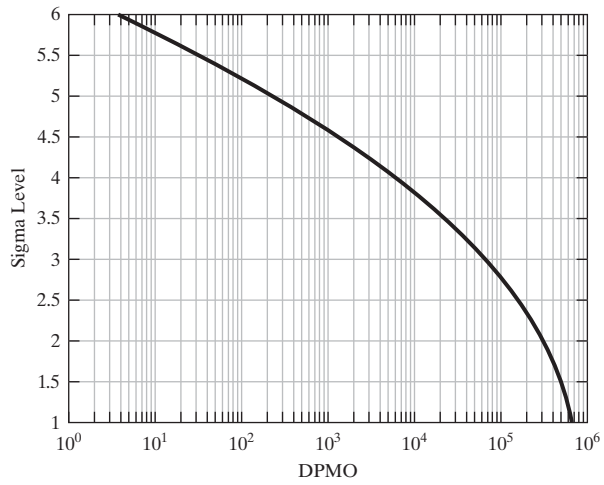

Figure 18.5 The relationship between DPMO and the sigma level.

Eq. (18.3) reduces to:

$$\mathrm{TY} = \left(1 - \frac{\mathrm{DPMO}}{10^6}\right)^n \tag{18.4}$$

The fraction of the production capacity lost due to defects is $1 - \mathrm{TY}$. For example, consider the manufacture of a device involving 40 steps, each of which operates at 4σ. From Figure 18.5, the expected DPMO is 6,210 per step, so $\mathrm{TY} = (1 - 0.00621)^{40} = 0.779$. Thus, 22% of production capacity is lost due to defects, rendering the overall manufacturing operation a 2.3σ process (noting that Figure 18.5 shows that 22% defects, or 220,000 DPMO, corresponds to a sigma level of 2.3). In contrast, if each of the 40 steps operates at 6σ, $\mathrm{TY} = (1 - 3.4/10^6)^{40} = 0.99986$, corresponding to about 1 faulty device for every 10,000 produced; in this case, the overall operation is a 5.2σ process.

In the preceding discussion, it has been assumed that defective devices are eliminated in production, leaving only the impact on reduced throughput yield. In the likely event that a fraction of the defects is undiscovered and leads to shipped devices that are faulty, the impact on sales resulting from customer dissatisfaction could be much greater. Noting that many manufacturing operations involve hundreds of steps (e.g., integrated-circuit chip manufacturing), it is clear that high levels of reliability as expressed by low DPMO values are generally required to ensure profitable manufacture. This is the driving force behind the extensive proliferation of six-sigma methodology (Wheeler, 2002).

Methods to Monitor and Reduce Variance

As described in detail by Rath and Strong (2000), an iterative five-step procedure is followed to progressively improve product quality. The five steps are: (1) **d**efine, (2) **m**easure, (3) **a**nalyze, (4) **i**mprove, and (5) **c**ontrol, referred to by the acronym DMAIC:

Step 1: ***Define.*** First, a clear statement is made defining the intended improvement. Next, the project team is selected, and the responsibilities of each team member assigned. To assist in project management, a map is prepared showing the suppliers, inputs, process, outputs, and customers (referred to by the acronym SIPOC). A simplified block diagram usually accompanies a SIPOC, showing the principal steps in the process (usually four to seven steps). At this stage, the main focus is on customer concerns, which are used to define CTQ output variables. As an example, suppose the company ACME Tubes, Inc., manufactures PVC tubing by extrusion of PVC melt. A SIPOC describing its operations is presented in Figure 18.6. The quality of the PVC tubing measured in terms of its impact strength is considered to be the principal CTQ, and customer specifications define the LCL and UCL.

Step 2: ***Measure.*** The CTQ variables are monitored to check their compliance with the LCLs and UCLs. Most commonly, univariate statistical process control (SPC) techniques, such as the Shewart Chart, are utilized (see Chapter 28 in Ogunnaike and Ray, 1994). The data for the CTQ variables are analyzed and used to compute the DPMO. This enables the sigma level of the process to be assessed using Figure 18.5. As noted above, the DPMO is relatively easy to compute for device manufacture and is readily applied to improve continuous processes (Trivedi, 2002; Wheeler, 2002). Continuing the PVC extrusion example, suppose this analysis indicates operation at 3σ with a target to attain 5σ performance.

Step 3: ***Analyze.*** When the sigma level is below its target, steps are taken to increase it, starting by defining the most significant causes for the excessive variability. This is assisted by a systematic analysis of the sequence of steps in the manufacturing process and the interactions between them. Using this analysis, the common root cause of the variance is identified.

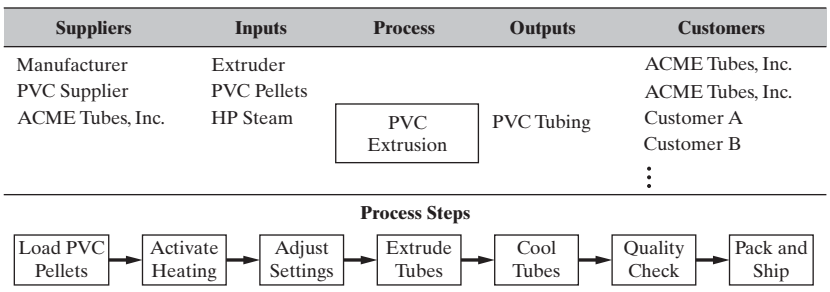

Figure 18.6 SIPOC for PVC tubing extrusion by ACME Tubes, Inc.

Continuing the PVC extrusion example, note that several factors contribute to an excessively high variance in product quality, among them the variance in the purity of the PVC pellets, the variance in the fraction of volatiles in the pellets, and the variance in the operating temperature of the steam heater. Clearly, all of these factors interact; but suppose that after analysis, it is determined that the variance in the operating temperature has the greatest impact on quality.

Step 4: ***Improve.*** Having identified the common root cause of variance, it is eliminated or attenuated by redesign of the manufacturing process or by employing process control. Continuing the PVC tubing example, one possible solution would be to redesign the steam heater. As will be demonstrated, systematic process redesign can improve the controllability and resiliency of a process and, hence, reduce the variance in the controlled output variables. Alternatively, a feedback controller could be installed to manipulate the steam valve to enable tighter control of the operating temperature (through control of the steam pressure). In this way, the variance in the temperature is transferred to that of the mass flow rate of steam.

Step 5: ***Control.*** After implementing steps to reduce the variance in the CTQ variable, the effect of the change is quantified, analyzed, and used to drive the DMAIC procedure further. Thus, steps (2) to (5) are repeated to improve process quality in a stepwise fashion. Note that achieving 6σ performance is rarely the goal and is seldom achieved. In fact, six-sigma methodology aims at incrementally improving the sigma level of a manufacturing process with the most likely outcome being that eventually, as 6σ performance is being approached, the manufacturing process is often superseded by an improved one.

Six-Sigma for Product Design

As detailed in Rath and Strong (2000), the DMAIC procedure is combined with ideas specific to product design to create a methodology that assists in applying the six-sigma approach to product design. Again, a five-step procedure is recommended:

Step 1: ***Define Project.*** In this step, the market opportunities are identified, a design team is assigned, and resources are allocated. Typically, the project time line is summarized in a Gantt chart (see Section 22.4).

Step 2: ***Identify Requirements.*** As in DMAIC, the requirements of the product are defined in terms of the needs of customers. For the design of a process such as a heat exchanger network, appropriate specifications would quantify the desired dynamic performance of the process—with the objective to reduce the occurrence of violations of the UCLs and LCLs defined for each target temperature.

Step 3: ***Select Concept.*** Innovative concepts for the new design are generated, first by brainstorming. These are evaluated with the best selected for further development. Often for product design, a rather qualitative approach is applied to make progressive improvements. As will be seen in the first example of Section 18.3, this can be strengthened by adopting a quantitative, model-based methodology.

Step 4: ***Develop Design.*** Often, several teams work in parallel to develop and test competing designs, making modifications as necessary. The goal of this step is to prepare a detailed design together with a plan for its management, manufacture, and quality assurance.

Step 5: ***Implement Design.*** The detailed designs in Step 4 are critically tested. The most promising design is pilot tested and if successful, proceeds to full-scale implementation.

18.3 EXAMPLE APPLICATIONS

This section presents two examples that show how product quality is improved by reducing the variance in the CTQ variables as guided by six-sigma principles. In the first example, a six-sigma approach guides improvements to a process for the manufacture of penicillin with the main goal being to satisfy the highest possible sigma level while improving the penicillin yield. The second example, which is more qualitative, shows how similar ideas are applied in the design of a new product, that is, an improved espresso machine.

EXAMPLE 18.1 ***Improving the Design and Control of Penicillin Manufacture***

The production of an active pharmaceutical ingredient (API) usually involves two principal phases: reaction/fermentation in which the API is produced from its biosystem and separation/purification in which product quantity and quality specifications are satisfied. Whereas upstream processing (i.e., in bioreactors) is important, downstream processing (i.e., in product purification operations) is often more important because a product that fails to meet purity specifications cannot be marketed. For these reasons, a plantwide approach to the design and operation of an API process is greatly assisted by six-sigma methodology, which is the driving force for continuous improvement. Six-sigma methodology identifies the root cause or causes of low yields due to excessive variance in the desired performance of one or more processing units (Dassau et al., 2006).

A typical pharmaceutical process, as illustrated in Figure 18.7 for the production of penicillin, involves batch and semibatch operations rather than continuous processing. Although these operations are inherently transient, typically with nonlinear dynamics, they nonetheless enable the flexible production of high-value-added products in the pharmaceutical industry. These unit operations, often referred to as "unit procedures," are well known, including size reduction and classification, sterilization, mixing, filtration, evaporation and distillation, crystallization, solid–liquid extraction, drying, and bioreactors. In this example, six-sigma methodology is used for a simplified penicillin process that considers only the fermentation and the first downstream

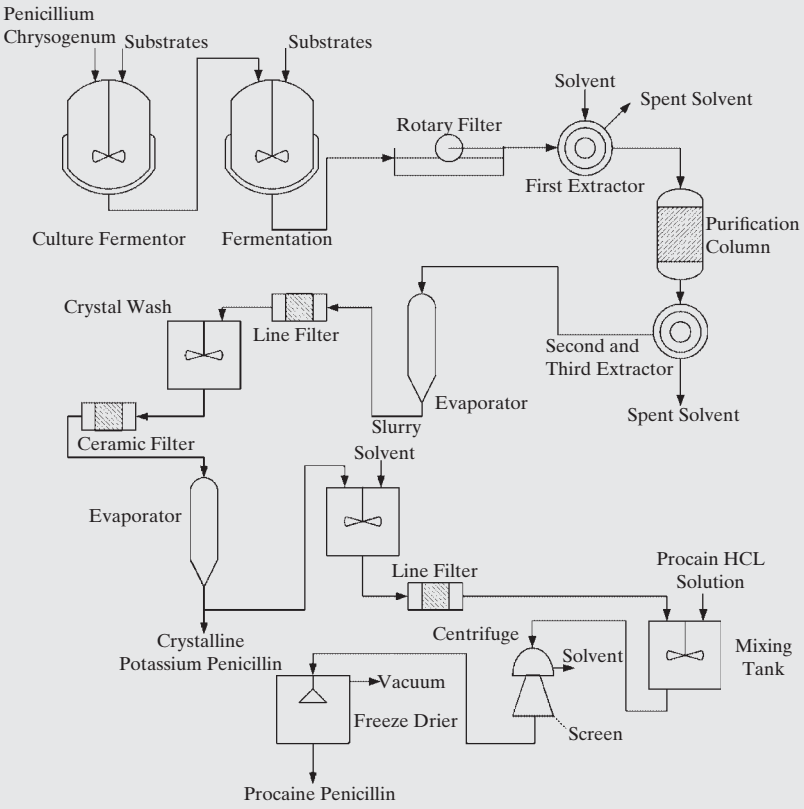

Figure 18.7 Penicillin process.

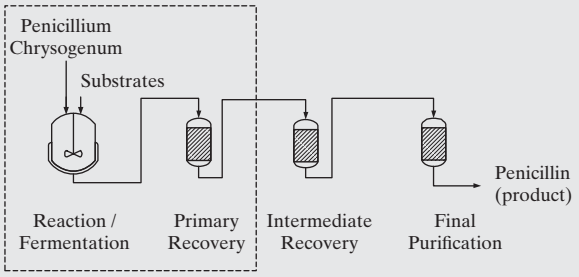

Figure 18.8 Schematic of simplified penicillin process.

processing steps in Figure 18.8. The following solution begins with a discussion of the process models.

SOLUTION

Modeling

The models of the fermenter and extractors for primary recovery and their control systems are presented in the file Supplement_to_Chapter_18.pdf. These were implemented in Matlab® and Simulink® and calibrated using nonlinear regression to compute key model parameters by minimizing the sum-of-the-square errors between the model predictions and data reported in the literature.

Fermenter

The penicillin fermentation stage is simulated using the model described in Section 18S.1. Its control system shown in Figure 18.9

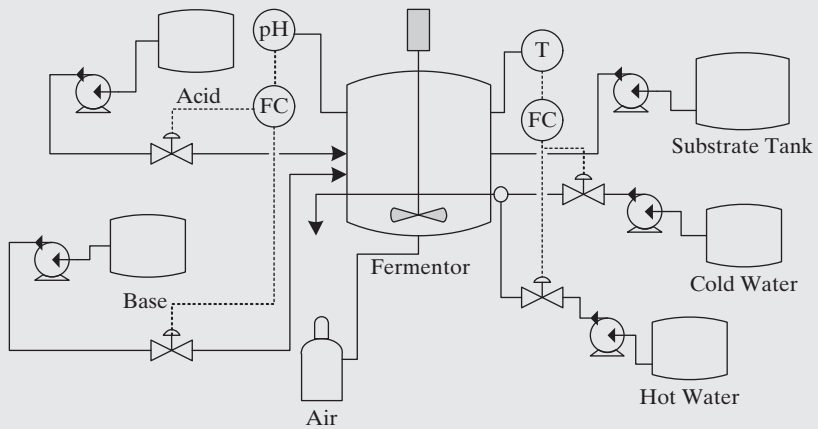

Figure 18.9 Fermenter and its control system.

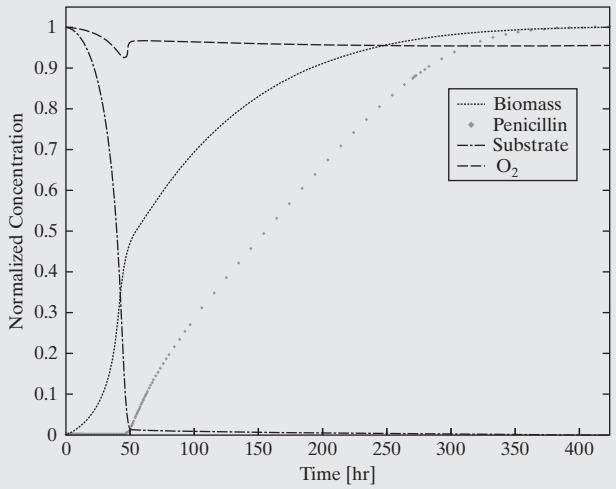

Figure 18.10 Fermentation trajectories (base case).

manipulates the coolant flow rate using a PI controller to regulate the fermenter temperature and manipulates the flow rates of the acid and base streams to the fermenter using a PI controller with a nonlinear gain to regulate the pH. The latter is intended to approximately "invert" the titration curve, as discussed in Section 18S.3. The product recipe calls for a makeup stream of substrate to be introduced when the substrate concentration is reduced to a threshold value with the oxygen flow rate held constant. The simulation results presented in Figure 18.10 are in good agreement with the published results of Bajpai and Reuss (1980) and Birol et al. (2002) where the temperature and pH setpoints were 25°C and 5, and the substrate threshold concentration was 0.3 g/l. About 422 simulation hrs are needed to reach the maximum penicillin concentration, 1.5 g/l. Makeup substrate is introduced after 48 hrs.

Primary Recovery

To recover penicillin from the fermentation broth, reactive extraction is often used with typical organic solvents being *n*-butyr-acetate and amines such as Amberlite LA-2. Although Reschke and Schuegerl (1984, 1985, 1986) present a model describing the reactive extraction of penicillin, it lacks the degrees-of-freedom (DOFs) to enable the control of both the pH and the solvent and extract flow rates. To add DOFs permitting improved control, Dassau et al. (2006) developed a two-film model as described in Section 18S.2.

Using the DMAIC Procedure for Process Refinement

For the penicillin production process described above, the DMAIC procedure is applied to define the base-case conditions in Table 18.2. As shown for the control limits on the CTQ variables, large DPMO values are computed, accompanied by large production times and low TYs. Subsequently, as summarized in Table 18.3, cycles of the DMAIC procedure are implemented to improve the process iteratively with improvements at each cycle implemented to reduce the variance of the unit exhibiting the highest DPMO value.

Cycle I

For the base-case operation, the reactive extractor has the highest DPMO, 462,456. As shown in Figure 18.11, only 73% of the penicillin is extracted after 5 hrs, and the pH value settles slowly toward its setpoint of 5. Moreover, the value of C_x, the concentration of degradation products, rises throughout the batch. The TY of the process is 63% and the production time is 432 hrs. Evidently, this poor performance is due to the absence of pH control in the reactive re-extractor. Consequently, the process is improved by installing a control system to maintain the pH at 5, which, as shown in Figure 18.11, not only regulates the pH as required but also reduces the impurities by 74%, increasing the TY of the unit to 89%, and the overall TY to 77%.

Cycle II

Note that the pH control implemented in Cycle I improves the quality of the feed to the reactive re-extractor, thereby reducing its DPMO from 31,264 to 13,378. Moreover, the fermenter is selected for the Cycle II improvement because it dominates the overall production time and its DPMO exceeds that of the reactive re-extractor. The DMAIC cycle is repeated with a significant decrease in the fermentation time achieved by increasing the glucose concentration at the feed outlet (i.e., the threshold value) from 0.3g/l to above 15 g/l. This reduces the time needed to achieve a maximum penicillin concentration of 1.5 g/l, from 422 to 258 hrs as shown in Figure 18.12. But the pH and temperature distributions have significantly higher variances than in the base case with DPMO levels of 49,628 and 15,625, both exceeding the base-case values of 45,445 and 465. These increases must be weighed against the 40% reduction in batch time with no decrease in the total TY.

Table 18.2 Summary of Control Limits, DPMO, and Throughput Yield for the Base-Case Conditions

	LCL	UCL	DPMO	Production Time (hr)
Fermenter				422
pH	4.9	5.1	45,445	
Temperature	22	28	465	
Reactive extractor—TY=73%				5
pH	4.8	5.2	462,456	
C_x(mole/liter)	6.75×10^{-5}			
Reactive re-extractor—TY=86%				5
pH	7	9	31,264	
C_x(mole/liter)	$4{,}2 \times 10^{-5}$			
Total production time (hr)				432
Total TY (%)				63

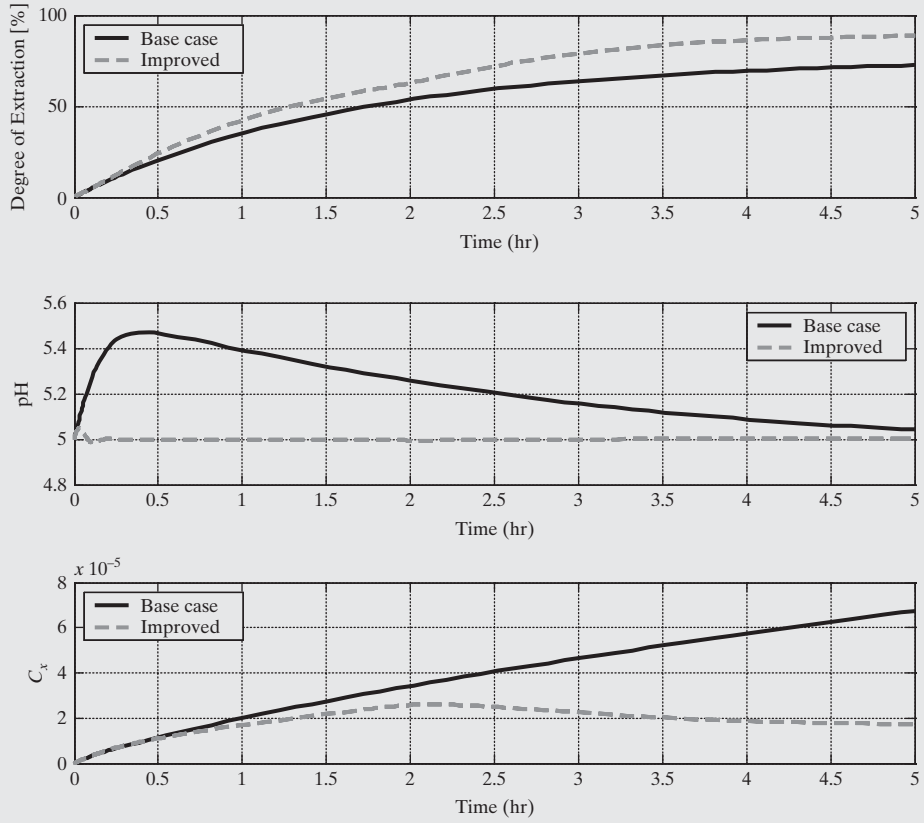

Figure 18.11 Comparison between trajectories in the reactive extractor before and after Cycle I improvements.

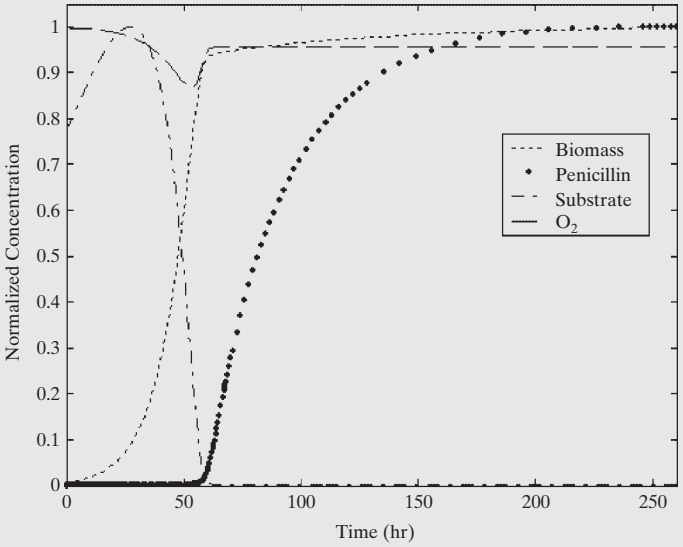

Figure 18.12 Fermentation trajectories after Cycle II improvements.

Cycle III

Once again, the DMAIC procedure is repeated, this time with improvements in the reactive re-extractor unit. For the base case without pH control, the degree of extraction reaches 86%, as shown in Figure 18.13. Note, however, that penicillin degradation is rather high. Here also, a pH controller is introduced, decreasing the concentration of impurities in this unit by 33%. But there is a slight decrease in the degree of extraction from 86% to 83%, reducing the total TY to 74%. Consequently, the 33% decrease in impurity level must be weighed against a 3% decrease in penicillin yield.

Summary

As demonstrated, the DMAIC approach involving a combination of improved process control, modified substrate feeding profiles in the fermenter, and improvements in the downstream processing section can achieve a 40% reduction in batch time, a 17% increase in throughput yield, and a 33% reduction of impurities as summarized

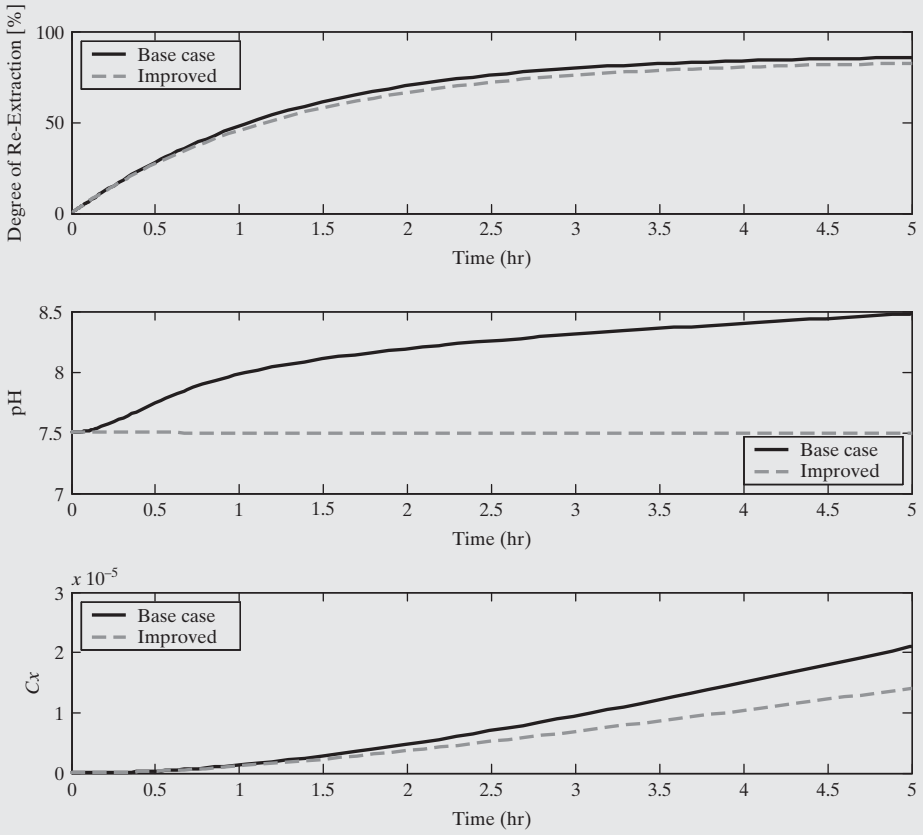

Figure 18.13 Re-extractor trajectories before and after Cycle III.

Table 18.3 Summary of Improvements Using the DMAIC Procedure

	Base Case	Cycle I	Cycle II	Cycle III
Fermenter				
DPMO—pH	45,445	45,445	49,628	49,628
DPMO—Temperature	465	465	15,625	15,625
Reactive extractor				
DPMO—pH	462,456	<1	<1	<1
C_x(mole/liter)	6.75×10^{-5}	1.74×10^{-5}	1.74×10^{-5}	1.74×10^{-5}
Reactive re-extractor				
DPMO—pH	31,264	13,378	13,378	<1
C_x(mole/liter)	4.2×10^{-5}	2.1×10^{-5}	2.1×10^{-5}	1.4×10^{-5}
Total production time (hr)	432	432	268	268
Total TY %	63	77	77	74

in Table 18.3. These improvements arise from adopting a plantwide approach, noting that each improvement has its price tag, budget, and time constraints, which usually limit the total number of improvements performed. Evidently, this systematic approach can have a substantial impact on the pharmaceutical industry through improved overall process yield, quality, and return on investment.

EXAMPLE 18.2 *Designing the Ultimate Espresso Machine*

Today, the coffee industry is globally situated, employing more than 20 million people. As a commodity, coffee ranks second only to petroleum in dollars traded worldwide. Furthermore, coffee is the most popular beverage in the world with over 400 billion cups consumed annually. Espresso, a relatively recent innovation in the preparation of coffee, originated in 1822 with the innovation of the first crude espresso machine in France that was later perfected and first manufactured in Italy. Espresso has become an integral part of Italian life and culture with over 200,000 espresso bars currently in Italy.

Espresso coffee is prepared in a machine that pumps cold water at high pressure (commonly 10–20 bar) into a hot water boiler, which displaces near-boiling hot water. This water is then forced through a cake of ground coffee as illustrated in Figure 18.14. In a conventional machine, the user manually loads ground coffee into a metal filter housing, referred to as a *portafilter*, ensuring that the ground coffee is adequately packed, locks the portafilter under the hot water exit head, and activates the heater. A coffee cup placed under the portafilter is then filled with the freshly extracted espresso coffee, which is produced by the leaching action of the high-pressure hot water as it passes through the bed of ground coffee.

Suppose that a new product is envisaged as an alternative to a conventional espresso machine with the objective being to improve the quality of the espresso obtained by a home user. The solution that follows describes a typical scenario using the DMAIC procedure.

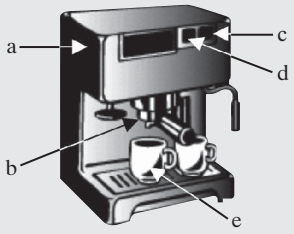

Figure 18.14 A typical espresso machine: (a) pressure vessel; (b) portafilter holding ground coffee; (c) on/off switch, with built-in pressure indicator; (d) solenoid valve for espresso coffee; (e) cup holding leached espresso coffee.

SOLUTION

Applying the DMAIC procedure could lead to the following sequence of events:

Step 1: ***Define.*** A typical SIPOC shown in Figure 18.15 identifies the principal steps that a home user would follow when using the machine. At this stage, the main focus would be on ensuring customer satisfaction with the quality of the espresso produced by the new machine. The quality of the coffee is considered to be the principal CTQ variable, and customer specifications define its LCL and UCL. Note that the control chart in Figure 18.16 identifies conditions under which acceptable coffee is prepared, which are constrained in a tight operating window delineated between 18–22% extraction of solubles and 1.15–1.35% solubles concentration (Sivetz and Desrosier, 1979). Note, however, that for such a food product, the issue of quality is complex because flavor and odor attributes are difficult to quantify. As described by Andueza et al. (2002, 2003, 2007), a panel of judges typically conducts a sensory descriptive analysis. In their assessment, the appearance of foam is defined by color (clear, hazelnut, or dark), consistency (consistent or inconsistent), and persistence (with a hole in the center, evanescent, or persistent), noting the percentage of judges who observe each attribute. Attributes such as odor intensity, body, acidity, bitterness, astringency, flavor intensity, and aftertaste intensity are typically assessed on a scale of "none'" (0) to "very high" (10). More specifically, the judges gauge odor/flavor attributes, making a distinction between positive flavor attributes such as fruity/winey, malty/cereal, fresh, strawlike, caramel-like, chocolatelike, spicy, nutty, tobaccolike, and buttery and negative attributes such as woody/papery, burnt/roasty, acrid, fermented, earthy/musty, rancid, burnt rubbery, sulphurous, flat, grassy/green/herbal, animal-like, motoroily, and ashy. The flavor profile of each sample is then defined by the percentage of judges that perceive each positive and negative flavor attribute. A typical result is shown in Figure 18.17.

Step 2: ***Measure.*** The CTQ variables are monitored to check their compliance with the LCLs and UCLs. Suppose this analysis indicates that using the existing machine, one cup in three on average has attributes outside the ideal operating window in Figure 18.16, indicating operation at lower than 2σ with an immediate target to reduce this to 1 in 250, that is, to attain 4σ performance.

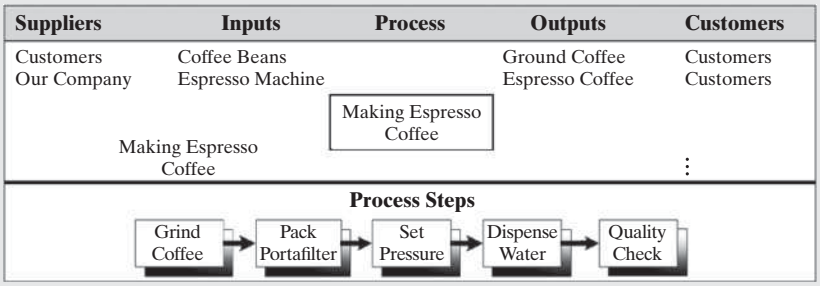

Figure 18.15 SIPOC for the preparation of espresso coffee.

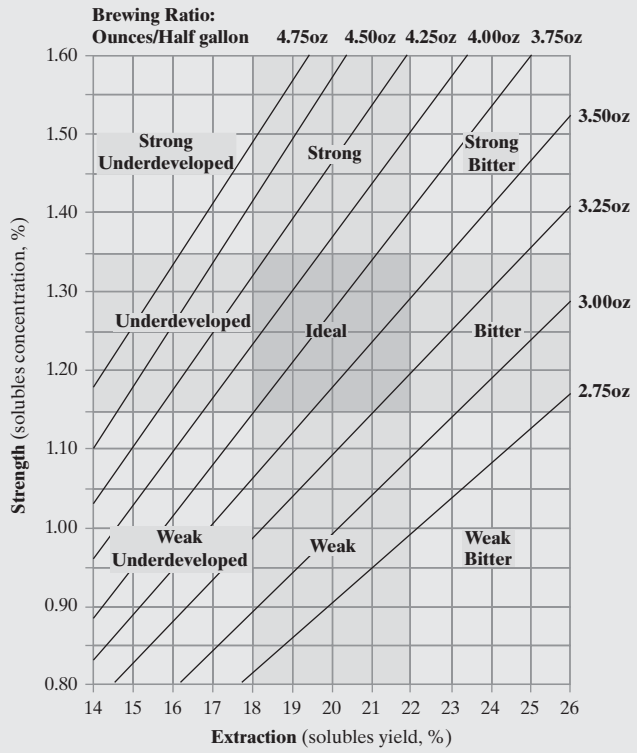

Figure 18.16 Coffee brewing control chart. (*Source:* Based upon chart developed by Ernest E. Lockhart, Pan American Coffee Bureau, and the National Coffee Association of U.S.A., 1957).

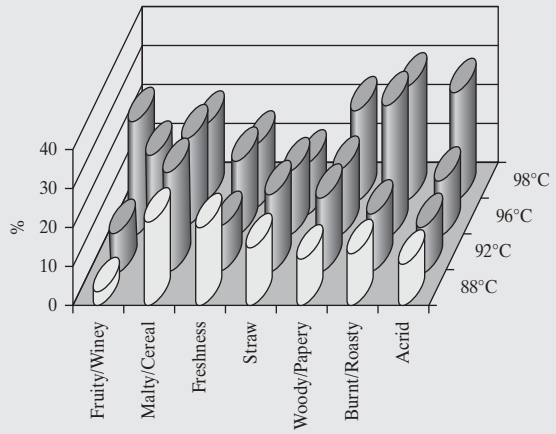

Figure 18.17 Influence of water temperature on flavor characteristics of Arabica espresso coffee samples (Andueza et al., 2003), noting the unacceptably high percentage of responders indicating undesirable flavor attributes at temperatures higher than 92°C. Copyright Society of Chemical Industry. Reproduced with permission. Permission is granted by John Wiley & Sons Ltd on behalf of SCI.

Step 3: ***Analyze*.** Several factors contribute to an excessively high variance in product quality (Sivetz and Desrosier, 1979; llly, 2002; Andueza et al., 2002, 2003, 2007):

(a) Freshness of the Ground Coffee. When the coffee is stale, the taste of the coffee is affected.

(b) Grade of the Ground Coffee. When too coarse, leaching is insufficient, affecting the taste of the coffee. In contrast, when the coffee beans are ground too fine, the pressure drop across the packed grinds is too high, detrimentally affecting the leaching and producing harsh, bitter flavors. Serious espresso drinkers prepare their own roasted coffee beans and personally grind them fresh. However, such extreme behavior is atypical.

(c) Ground Coffee Packed Evenly in the Portafilter to the Correct Degree. Since the brew water is under high pressure, it finds the path of least resistance through the coffee. Uneven packing leads to channeling with the coffee in and in the proximity of the channels overextracted and underextracted elsewhere. The resulting beverage is bitter and astringent with many potentially good flavors remaining in the portafilter basket. In contrast, when the ground coffee is evenly and tightly packed, the water flows uniformly through all of the coffee.

(d) Correct Amount of Coffee Loaded. An insufficient amount of coffee leads to overextraction and to a flat and watery drink (see Andueza et al., 2007).

(e) Sufficiently High Water Pressure. This controls the temperature at which the leaching takes place (see Andueza et al., 2002).

(f) Proper Amount of Water Passed through the Ground Coffee. As indicated in Figure 18.16, the degree of extraction is critical to ensuring an acceptable product (see also Illy, 2002, and Andueza et al., 2007).

(g) Quality of the Water. Since espresso coffee is 99% water, poor water quality (e.g., involving chlorine impurities, organic content, hardness, and alkalinity) to extract coffee has a detrimental effect on the quality of the product (Sivetz and Desrosier, 1979).

Step 4: ***Improve*.** Having identified the root cause of variance, it is eliminated or attenuated by redesign of the manufacturing process or by employing process control. For the espresso machine, there are several ways to reduce the sources of variance identified above. These include equipping the espresso machine with a water filter to reduce the variance due to item (g). In some machines, a solenoid valve is installed to dispense a precise amount of water, thus attenuating the variance due to item (f). Furthermore, by increasing the degrees-of-freedom in the design through installation of a pressure-control loop, the pressure can be maintained between its UCL and LCL, reducing the variations due to item (e). Note, however, that items (a) to (d) constitute sources of variance not under the control of the manufacturer of the espresso machine as described in the introduction. To eliminate these four sources of variance, the manufacturer of a novel espresso machine can provide its users with vacuum-sealed capsules of ground coffee having a built-in filter. On insertion into the machine, the capsule is perforated and used to prepare a single cup of coffee. Since the capsules are vacuum sealed, this ensures that the ground coffee is fresh, reducing the variance due to item (a). These capsules of coffee must be manufactured by a process with a sufficiently high sigma level to ensure that variations due to items (b) and (d) do not occur. Furthermore, rather than relying on suitable packing of the ground coffee into the portafilter, a fixed flow resistance can be arranged in

the coffee capsules themselves to ensure the correct degree of coffee extraction, reducing variations due to item (c). Moreover, when the manufacturer of the espresso machines also controls the coffee supply, the revenue from sales of coffee capsules are likely to far exceed that of the new espresso machines.

Step 5: ***Control.*** After implementing steps to reduce the variance in the CTQ variables, the results are evaluated, and possible improvements are considered. Thus, Steps (2) to (5) in the DMAIC procedure are repeated to improve the process quality in a stepwise fashion. For the espresso example, it is evident that a manufacturer of espresso machines would not necessarily implement all of the alternatives identified previously for the reduction of the variances in the CTQ variables. Rather, the manufacturer would first introduce the most practical alternative, the cheapest, or those alternatives with the greatest impact.

18.4 SUMMARY

This chapter has introduced the potential advantages of using six-sigma methodology to quantify and ensure product and process quality when integrating design and control strategies.

After studying this chapter, the reader should:

1. Be able to compute the sigma level of a specific process in a product manufacturing facility.
2. Have an appreciation of how integrated design and control can assist in improving the sigma level of a specific process of the entire product manufacturing facility through the reduction of variance in the most critical manufacturing steps.

As shown in the examples, this design methodology benefits from reducing the variance in the critical-to-quality variables by exploiting, and when necessary, increasing, the process degrees-of-freedom by using integrated design and control procedures. Although product manufacturing has traditionally relied solely on statistical process control, the trend to improve profitability through increasing yields is driving many industries to embrace six-sigma methodology and advanced control strategies. For example, in integrated circuit manufacturing, the increased reliance on advanced process control (APC) and in particular on multivariable control reflects the need to utilize the potential degrees-of-freedom in processes to assist in the reduction of CTQ variable variance.

REFERENCES

1. Andueza, S., L. Maeztru, B. Dean, M. Paz de Peña, J. Bello, and C. Cid, "Influence of Water Pressure on the Final Quality of Arabica Espresso Coffee. Application of Multivariate Analysis," *J. Agricul. & Food Chem.*, **50**(25), 7426–7431 (2002).

2. Andueza, S., L. Maeztru, L. Pascual, C. Ibañez, M. Paz de Peña, and C. Cid, "Influence of Extraction Temperature on the Final Quality of Espresso Coffee," *J. Sci. Food & Agricul.*, **83**(3), 240–248 (2003).

3. Andueza, S., M. A. Vila, M. Paz de Peña, and C. Cid, "Influence of Coffee/water Ratio on the Final Quality of Espresso Coffee," *J. Sci. Food & Agricul.*, **87**(4), 586–592 (2007).

4. Bajpai, R. K., and M. Reuss, "A Mechanistic Model for Penicillin Production," *J. Chem. Tech. & Biotech.*, **30**(6), 332–344 (1980).

5. Birol, G., C. Undey, and A. Cinar, "A Modular Simulation Package for Fed-Batch Fermentation: Penicillin Production," *Comput. Chem. Eng.*, **26**(11), 1553–1565 (2002).

6. Dassau, E., I. Zadok, and D. R. Lewin, "Combining Six-Sigma with Integrated Design and Control for Yield Enhancement in Bioprocessing," *Ind. Eng. Chem. Res.*, **45**(25), 8299–8309 (2006).

7. Illy, E. "The Complexity of Coffee," *Scien. Amer.*, 72–77 (2002 June).

8. Lachman-Shalem, S., B. Grosman, and D. R. Lewin, "Nonlinear Modeling and Multivariable Control of Photolithography," *IEEE Trans. of Semiconductor Manufact.*, **15**(3), 310–322 (2002).

9. Lewin, D. R., S., Lachman-Shalem, and B. Grosman, "The Role of Process System Engineering (PSE) in Integrated Circuit (IC) Manufacturing," *Cont. Eng. Prac.*, **15**(7), 293–309 (2007).

10. Ogunnaike, B. A., and W. H. Ray, *Process Dynamics, Modeling and Control*, Oxford University Press, New York (1994).

11. Rath and Strong, *Six Sigma Pocket Guide*, Rath and Strong Management Consultants/AON Management Consulting, Lexington, Massachusetts (2000).

12. Rath and Strong, *Design for Six Sigma Pocket Guide*, Rath and Strong Management Consultants/AON Management Consulting, Lexington, Massachusetts (2002).

13. Reschke, M., and K. Schuegerl, "Reactive Extraction of Penicillin I, II and III," *Chem. Eng. Jour.*, **28**(1), B1–B29 (1984).

14. Reschke, M., and K. Schuegerl, "Continuous Reactive Extraction of Penicillin G in a Karr Column," *Chem. Eng. Jour.*, **31**(3), B19–B26 (1985).

15. Reschke, M., and K. Schuegerl, "Simulation of the Continuous Reactive Extraction of Penicillin G in a Karr Column," *Chem. Eng. Jour*, **32**(1), B1–B5 (1986).

16. Sivetz, M., and N. W. Desrosier, *Coffee Technology*, AVI Publishing Co., Westport, Connecticut (1979).

17. Trivedi, Y. B., "Applying 6 Sigma," *Chem. Eng. Prog.*, **98**(7), 76–81 (2002).

18. Wheeler, J. M., "Getting Started: Six-Sigma Control of Operations," *Chem. Eng. Prog.*, **98**(6), 76–81 (2002).

EXERCISES

18.1 For the manufacture of the hemodialysis device in Chapter 24,

(a) Prepare a SIPOC.

(b) Identify all of the sources of variance in the urea concentration in treated blood after a 4-hr treatment. Suggest improvements in the design to increase the sigma level of the product.

18.2 Photolithography is an important process in integrated circuit manufacture in which a circuit pattern is transferred from a mask onto a photosensitive polymer (the PR), ultimately replicating that pattern on the surface of a silicon wafer (Lachman-Shalem et al., 2002). A typical photolithography process consists of seven steps: spin coat of the PR, prebake, chill, expose, post-exposure bake (PEB), chill, and development. The overall objective is to produce printed lines with accurate and consistent width (referred to as the critical dimension, CD). The following table shows the steps required with the sigma level of each step.

Steps in Photolithography and Their Sigma Levels

Step	Subprocess	Function	Sigma Level
1	PR coating	Coats wafer with a thick layer of PR	3.5
2	Prebake	Hardens the PR before exposure in the stepper	4.5
3	Chill 1	Cools the wafer after prebake	5.0
4	Stepper	Exposes the PR through a negative of the pattern to be reproduced	4.0
5	PEB	Fully hardens the PR after exposure	4.5
6	Chill 2	Cools the wafer after PEB	5.0
7	Development	Develops the image imprinted on the PR	3.0

(a) Compute the sigma level of the complete process.

(b) You are required to reduce the variance in this process by "process improvements." Given the limited engineering time available, you can allocate only three instances of process improvements, each of which will increase the sigma level of the selected step by 0.5. Allocate process improvements optimally to maximize the increase in sigma level for the overall process.

Chapter 19

Business Decision Making in Product Development

19.0 OBJECTIVES

The aim of a product-development project is to market a product that meets a consumer's needs and to serve the society at large while making a profit for the company. The design of molecular products and mixture-blended products is covered in Chapter 4. The identification of the desirable consumer product and its attributes and the determination of the product specifications through conceptual product design are covered in Chapters 1 and 5, respectively. This chapter discusses the financial, economic, organizational, and societal aspects of product development and, more importantly, decision making on the relevant issues.

After studying this chapter, the reader should:

1. Be familiar with the concepts of project cash flow and the pertinent financial terms.
2. Be able to decide whether a product project should be undertaken by considering the financial return and other nonfinancial issues.
3. Understand how make-or-buy decisions in product manufacture are generated.
4. Appreciate the microeconomics of launching a product in the marketplace.
5. Be able to quantify the various trade-offs in product development using sensitivity analysis.

19.1 INTRODUCTION

In response to the rapid development of innovative technologies and the fast-changing global marketplace, companies have to redouble their effort to commercialize new products to stay competitive. No company, irrespective of its size, can prosper or merely survive if it does not innovate to meet consumers' wants and needs. As an example of the relevant statistics, DuPont commercialized 1,753 new products in 2013, and 28% of its sales in 2013 was derived from new products launched within the past four years. This trend of rapid product introduction is expected to continue and even accelerate for B2C products.

To manage these product-development projects efficiently, the multidisciplinary framework addresses three questions systematically. The first is *what to make* by performing market study and product design. The second is *how to make* by performing prototyping, process design, feasibility study, and engineering design. The third, the topic of this chapter, is concerned with business decision making to arrive at a successful product. Since success is often measured by profitability, this may seem to be the economic analysis task in Figure 1.3, which involves the calculation of various financial metrics such as the net present value (NPV) and investor's rate of return (IRR). However, these calculated financial metrics are only as good as the assumed parameters such as the target sales volume (i.e., the supply), marketing budget, and so on used in the calculations. There is often a trade-off associated with each decision on an assumed parameter. For example, if the supply is set too high, there would be a depressing effect on the selling price. If the marketing budget is excessive, the incremental increase in sales might not justify the marketing cost. Note that the business decisions and the associated economic analysis are done repeatedly throughout the entire product-development project. This is because the accuracy of the parameters for financial predictions tends to improve with time as information on all aspects of the project ranging from engineering data to market intelligence becomes available or firms up. The course of action for the product-development project is constantly adjusted to obtain the optimal outcome.

There is an important difference between the economic evaluation of a B2C product and that of a B2B product. An implicit assumption in the process design of many B2B chemical products is that the company will build a manufacturing plant. This is not the case in product design. B2C products, such as the air purifier in Example 5.1, are composed of many discrete components. The production of these components can be done in-house or outsourced. In some cases, all of the components can simply be purchased on the market. These so-called make-or-buy decisions can have significant impact on project economics.

Some important business decisions in product development are not financial or technical in nature. With finite resources in terms of people and money, it is essential to leverage the existing know-how, in-house resources, and external business and technology connections to launch new products with minimum effort. These organizational factors, as well as societal factors that would impact a product-development project, are discussed in this chapter as well.

19.2 ECONOMIC ANALYSIS

The analysis is based on the *stand-alone principle*, meaning that the product-development project in question is considered in isolation from other development projects (Ross et al., 2012). From the point of view of economic analysis, a product-development

project is viewed as a single firm producing the product of interest. Of course, this may not be true, particularly for a large corporation with many related products. Consider the air purifier in Example 5.1. Even if the catalyst division of the home appliances company can supply a powerful photocatalyst at a discounted price, the air purifier project should be treated as a stand-alone project so that it is judged entirely on its own merit. Whether to buy internally or externally depends on the catalyst price and required performance.

Cash Flow Diagram

The economic analysis of a product project is predicated on the income and cash flow statements discussed in Chapter 17. Figure 19.1 shows the relationship among the financial terms that are essential in economic analysis in the form of the *cash flow diagram* (Vrana, 1995).

Thus, *income from operations* (IFO) for a given year is obtained by subtracting the costs from *net sales* (S). There are two types of costs. *Fixed costs* are those that do not change with sales volume whereas *variable costs* do. Examples of fixed costs include rent and wages. Variable costs include raw materials and commissions. These costs (C_{ED}) exclude depreciation as signified by the subscripts. *Earnings before income tax* (EBIT) is obtained by subtracting *depreciation* (D) from income from operations. After deducting federal and state corporate taxes from EBIT, we have the *after-tax operating income* (ATOI). The dollar amount of depreciation is determined solely for the purpose of calculating income tax. Governments use depreciation as a way to encourage capital investment by reducing the corporate income tax. Actually, the depreciation money has never left the company. Thus, the *operating cash flow* (OCF) is obtained by summing the ATOI and depreciation. This bookkeeping nature of depreciation is represented by the bypass channel in the cash flow diagram. The following equations capture the discussion above:

$$\text{IFO} = \text{S} - C_{ED} \tag{19.1}$$

$$\text{EBIT} = \text{IFO} - \text{D} = \text{S} - C_{ED} - \text{D} \tag{19.2}$$

$$\text{ATOI} = (1 - t)\,\text{EBIT} = (1 - t)(\text{S} - C_{ED} - \text{D}) \tag{19.3}$$

$$\begin{aligned}\text{OCF} &= \text{ATOI} + \text{D} = (1 - t)(\text{S} - C_{ED} - \text{D}) + \text{D} \\ &= (1 - t)(\text{S} - C_{ED}) + t\,\text{D}\end{aligned} \tag{19.4}$$

Here, t is the tax rate. Note that Eq. (19.4) is a form of Eq. (17.40) where $\text{C} = C_{ED} + \text{D}$ and other costs are explicitly considered. The operating cash flow becomes part of the *project cash flow* (PCF), which can be used for debt repayment, dividends to shareholders, and construction of new plants. PCF can also come from borrowing or accepting new investment. For a new product project, it is normally necessary to inject cash for equipment acquisition and capital for the routine operations of the single firm according to the stand-alone principle. *Working capital* is the money tied up in providing goods and services and includes short-term assets such as inventory and accounts receivable. *Net working capital* (NWC) is working capital minus short-term liabilities such as accounts payable. The net working capital is represented by a spinning circle in Figure 19.1, signifying the fact that the money within the NWC pool is continuously consumed and replenished. In addition, when there is no new investment/borrowing, debt repayment or dividend distribution,

$$\begin{aligned}\text{PCF} = \text{OCF} &- \text{Increase in net working capital } (\Delta\text{NWC}) \\ &- \text{Project capital spending}\end{aligned} \tag{19.5}$$

Eq. (19.5) shows that when money is removed from OCF to increase the amount of NWC or to fund a construction project, the project cash flow would decrease by this amount. Note that when the NWC is decreased, ΔNWC is negative, and the PCF increases as money is returned to the project cash flow pool.

Total capital spending, such as the construction of manufacturing plants and purchase of equipment over the years, is the *net permanent investment*. The data are captured under the property heading in the balance sheet (Table 16.3). Similarly, the *accumulated depreciation* is the total amount of depreciation over the years. The two dotted lines emanating from the depreciation bypass in Figure 19.1 represent how the data on depreciation accumulated over time are recorded in the balance

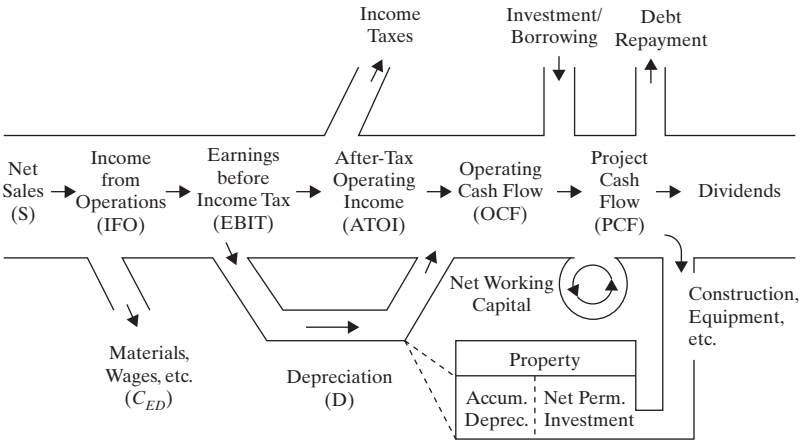

Figure 19.1 Cash flow diagram for a product-development project based on the stand-alone principle.

sheet as well. The book value of the fixed assets of this firm is the difference between net permanent investment and accumulated depreciation. Note that the book value is not the market value the company receives when the assets are sold (at that moment in time). The gain, if any, between the actual cash (referred to as the *salvage value*) the company receives in the event of a sale and the book value is taxable.

Economic Analysis for Product Development

There are two distinct periods for a product-development project: a relatively short period of product development from idea to production and a long product life cycle consisting of introduction, growth, maturity, and decline phases (Figure 1.2). In the early stage of the product-development period, information is often inaccurate and incomplete. Approximate profitability measures such as return on investment and payback period (Table 17.5) can be used to obtain a rough idea of whether the project is worthwhile. As more accurate information becomes available, project profitability should be evaluated using the net present value (NPV) or investor's rate of return (IRR). The NPV is given by

$$\text{NPV} = \sum_{j=-n}^{m} \frac{(\text{Project cash flow})_j}{(1+\text{r})^j} \tag{19.6}$$

Here, r is the discount rate, and n and m are the number of periods of the product-development and product life cycle, respectively. The length of a period can be in terms of weeks, months, or years. The product-development period is represented by $j < 0$, where the project cash flow tends to be negative. Investment is needed to develop the new product but there is no income. The product life cycle is represented by $j \geq 0$ in which the project cash flow is supposedly positive. In the initial phase of the product life cycle, sales volume tends to be low as the consumer gains familiarity with the product, resulting in negative cash flows.

In the NPV approach, the project cash flow is discounted to the time when the product life cycle starts [i.e., $j = 0$ in Eq. (19.6)]. The discount rate is a figure set by management. It represents the sum of the expected inflation rate and a reasonable rate of return for the company's investment. The terms for $j < 0$ in Eq. (19.6) represent the principal and interest earned by the money invested. Note that each term $(\text{Project cash flow})_j(1+\text{r})^j$ has the same form as Eq. (17.12) for calculating the principal plus the compound interest. Similarly, the terms for $j \geq 0$ in Eq. (19.6) represent the present value of the funds earned throughout the product life cycle. Each term $(\text{Project cash flow})_j(1+\text{r})^{-j}$ has the same form as Eq. (17.14). Thus, we compare the money invested to the money earned at the same time point of $j = 0$. A positive NPV implies that the product under consideration meets, and indeed exceeds, management's expectation on financial return.

In the IRR approach, the discount rate is treated as an unknown in Eq. (19.6) and is calculated by setting NPV to zero. The discount rate thus calculated is referred to as the investor's rate of return, which should be as large as possible. It represents the interest rate for the investment made by the company. The terms for $j < 0$ in Eq. (19.6) represent the total investment, principal plus compound interest, at the time point $j = 0$. The terms for $j \geq 0$ in Eq. (19.6) represent the present value of the total return at $j = 0$. As discussed in Chapter 17, the investor's rate of return can be compared with the bank interest rate. When the IRR is higher than the prevailing bank interest rate, the investment money can be borrowed from the bank and invested in the project, paying the prevailing interest to the bank with the remaining funds earned by the company. When the IRR is below the bank interest rate, the project is a poor investment. Even when the company has money to invest, it may be preferable to deposit funds in the bank to earn basically risk-free interest. The following example illustrates these evaluations. Conceptually, the first example, while similar to Example 17.29, which is for process design, extends beyond that example.

EXAMPLE 19.1 ***Preliminary Economic Evaluation for an Air Purifier Project***

The marketing team of the home appliances company in Example 5.1 submits a three-year sales projection to management. It is expected that 50,000 units of the air purifier can be sold per year at \$300/unit. An annual advertising budget of \$2.5MM is proposed. The engineering team estimates that the manufacturing equipment costs \$3MM. The development time is estimated to be one year at a cost of \$2MM. The net working capital is \$2MM. The fixed cost is \$1.5MM per year, and the variable cost is \$80 per unit. Should the project be undertaken based on the NPV with a 20% discount rate? Also, consider the investor's rate of return given that the prevailing bank interest rate is 5%. Use the five-year class life in the Modified Accelerated Cost Recovery System for depreciation. Assume a negligible market value of the equipment after three years. Use an overall tax rate of 40% which is a combination of the 35% federal rate and the average rate levied by the states. Management needs to know the amount of cash required to carry out this project.

SOLUTION

The depreciation and the equipment book value are calculated using the depreciation percentages given in Table 17.9.

Year	MACRS Tax Basis Depreciation, %	Depreciation × \$1,000	Book Value × \$1,000
1	20.00	$3{,}000 \times 0.2 = 600$	2,400
2	32.00	$3{,}000 \times 0.32 = 960$	1,440
3	19.20	$3{,}000 \times 0.192 = 576$	864

To calculate the NPV and IRR, the project cash flow for each year of the four-year project is needed. The following table shows the project cash flow for the entire project. The IFO, EBIT, ATOI, and OCF are calculated using Eqs. (19.1), (19.2), (19.3), and (19.4), respectively. The project cash flow calculated using Eq. (19.5) changes from year to year. A total of \$7MM must be injected into the project before product manufacturing begins. In the following table, the numbers within parentheses are negative.

	$ in Thousands				
Year	−1	0	1	2	3
Sales	0	0	15,000	15,000	15,000
Fixed + Advertising costs			(4,000)	(4,000)	(4,000)
Variable costs			(4,000)	(4,000)	(4,000)
IFO			7,000	7,000	7,000
Depreciation			(600)	(960)	(576)
EBIT			6,400	6,040	6,424
Taxes (40%)			(2,560)	(2,416)	(2,570)
ATOI			3,840	3,624	3,854
OCF			4,440	4,584	4,430
NWC		(2,000)			2,000
Capital spending		(3,000)			
Development cost	(2,000)				
PCF	−2,000	−5,000	4,440	4,584	6,430

A discount rate of 20% is suggested by management, and the NPV is calculated using Eq. (19.6):

$$\text{NPV} = -2{,}000(1+\text{r}) - 5{,}000 + \frac{4{,}440}{(1+\text{r})} + \frac{4{,}584}{(1+\text{r})^2} + \frac{6{,}430}{(1+\text{r})^3}$$
$$= \$3{,}204.4$$

Because the NPV is positive, the project remains attractive. Note that the NPV is calculated at five time points to keep it simple. In reality, the money is spent at different times of the year. For example, capital spending does not occur exactly at year 0. More time periods can be used when higher accuracy is desirable. To determine the IRR, the NPV in Eq. (19.6) is set to zero.

$$2{,}000(1+\text{r}) = -5{,}000 + \frac{4{,}440}{(1+\text{r})} + \frac{4{,}584}{(1+\text{r})^2} + \frac{6{,}430}{(1+\text{r})^3}$$

Using the solver function in EXCEL, r = 0.4043. Since the IRR is much higher than the prevailing bank interest rate, again, the project remains attractive. The accuracy of these profitability measures improves as more realistic projections become available.

The cumulative project cash flow is plotted against time in Figure 19.2. The company spends $2MM in the product-development period. Another $5MM is used for working capital and equipment to start up the production, resulting in a negative cumulative project cash flow of $7MM. The cash flow becomes positive after year 0 whereas the cumulative project cash flow becomes positive after year 1.

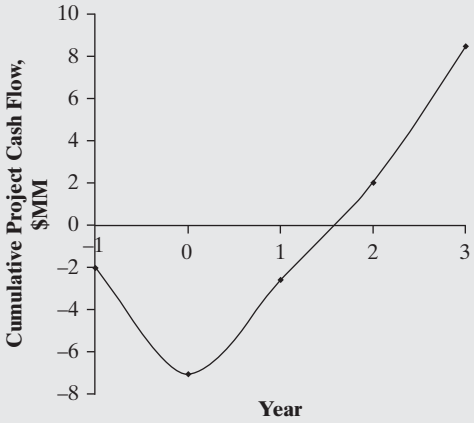

Figure 19.2 Cumulative project cash flow as a function of time.

EXAMPLE 19.2 *Economic Evaluations with More Realistic Sales Projection*

Sales are expected to pick up slowly after product launch as consumers start to take note of the air purifier. However, sales and the unit price tend to decrease at some point in time (Figure 1.2). After a careful review, the marketing team suggests a more realistic estimate of the sales volume and a pricing strategy in the following table.

Year	Unit Sales	Selling Price, $	Revenues × $1,000
1	30,000	300	9,000
2	70,000	275	19,250
3	50,000	250	12,500

To accommodate the increased production in the second year, the engineering team recommends that the equipment cost be increased to $5MM. Use the five-year class life in the Modified Accelerated Cost Recovery System for depreciation. The market value of the equipment after three years is now estimated to be $2.5MM.

SOLUTION

The depreciation and the equipment book value are calculated using the depreciation percentages given in Table 17.9.

Year	MACRS Tax Basis Depreciation, %	Depreciation × $1,000	Book Value × $1,000
1	20.0	5,000 × 0.2 = 1,000	4,000
2	32.0	5,000 × 0.32 = 1,600	2,400
3	19.2	5,000 × 0.192 = 960	1,440

The following table shows the project cash flow (PCF) for the new sales estimates. After three years, the after-tax proceeds recovered from selling the equipment (in thousands of dollars) = ($2,500 − $1,440) (1 − 0.40) = 636. See the last column, third row from the bottom.

	$ in Thousands				
Year	−1	0	1	2	3
Sales	0	0	9,000	19,250	12,500
Fixed + Advertising costs			(4,000)	(4,000)	(4,000)
Variable costs			(2,400)	(5,600)	(4,000)
Income from operations			2,600	9,650	4,500
Depreciation			(1,000)	(1,600)	(960)
EBIT			1,600	8,050	3,540
Taxes (40%)			(640)	(3,220)	(1,416)

(Continued)

(*Continued*)

	$ in Thousands				
Year	−1	0	1	2	3
ATOI			960	4,830	2,124
OCF			1,960	6,430	3,084
NWC		(2,000)			2,000
Capital spending		(5,000)			
Equipment sales					636
Development cost	(2,000)				
PCF	−2,000	−7,000	1,960	6,430	5,720

By setting the *NPV* to zero in Eq. (19.6),

$$2{,}000\,(1+\mathrm{r}) = -7{,}000 + \frac{1{,}960}{(1+\mathrm{r})} + \frac{6{,}430}{(1+\mathrm{r})^2} + \frac{5{,}720}{(1+\mathrm{r})^3}$$

Using the solver function in EXCEL, r = 0.2005, which is smaller than 0.4043 obtained in Example 19.1. However, because the IRR is still much higher than the prevailing bank interest rate, the project remains attractive.

Note that for large companies with many concurrent new product-development projects, these profitability measures are compared across the companywide product portfolio. A positive NPV or high IRR of a new product-development project does not guarantee management approval to proceed and is subject to further product portfolio management scrutiny. There are cases in which top management elects to proceed with a new product-development project with less favorable profitability measures for clear strategic reasons, such as entering a new market or to establish a presence in a new geographic location.

19.3 MAKE-OR-BUY DECISIONS

The manufacture of almost all products tends to begin with chemical precursors or ingredients that are bought from another company. For example, a chemical company would purchase para-xylene from an oil company to make terephthalic acid and react the terephthalic acid with ethylene glycol perhaps also purchased from another supplier to make polyethylene terephthalate. For the air purifier in Example 5.1, the company probably buys the HEPA filter, PCO catalysts, the air purifier housing, and so on from different suppliers. Then, the catalysts are impregnated on the filter and all the parts are assembled together at a plant site. Clearly, few companies make a B2C or B2B final product all the way from the natural resources. The aim of make-or-buy decision making is to address these issues systematically and effectively.

Table 19.1 is a list of factors that influence make-or-buy considerations and the reasons for favoring either the make or the buy option. For instance, a company may consider outsourcing part

Table 19.1 Factors Influencing Make-or-Buy Decisions and the Heuristics for Decision Making

Factors	Situations Favoring "Make"	Situations Favoring "Buy/Subcontracting"
Manufacturing technology	• The technology is newly developed in-house • The company is in a leadership position	• The company has limited production experience • The supplier has better knowledge in the manufacturing technology
Resources	• Existing idle facilities to perform the production in-house • The production can leverage or share the existing facilities for in-house production • No competent supplier is available • Available suppliers are not reliable • The quality of available ingredients does not meet the specifications • Need to ensure undisrupted supply	• The company has limited facilities or insufficient capacity • The company has limited space for new production lines • It is necessary to reduce time to market
IP ownership	• Design secrecy is required to protect proprietary technology	• The supplier owns the patent of the technology for manufacturing the particular ingredients or parts
Economic benefits	• Projected sales are large, and building new production capacity can reap economic benefit	• There is limited budget for initial investment • The supplier offers a cheaper price
Quality assurance	• Need to exert direct control of product quality	• The supplier provides a customer-preferred brand in terms of quality and reliability
Regulatory restrictions	• The company has already gotten the license to produce the product of interest	• The company does not have the required certification or license to handle or manufacture certain materials
Strategic plan	• The manufacturing technology is considered strategic by the company • There is a need to gain experience to manage a family of products	• The company cannot take the additional risk or does not have enough time to manage a new production line

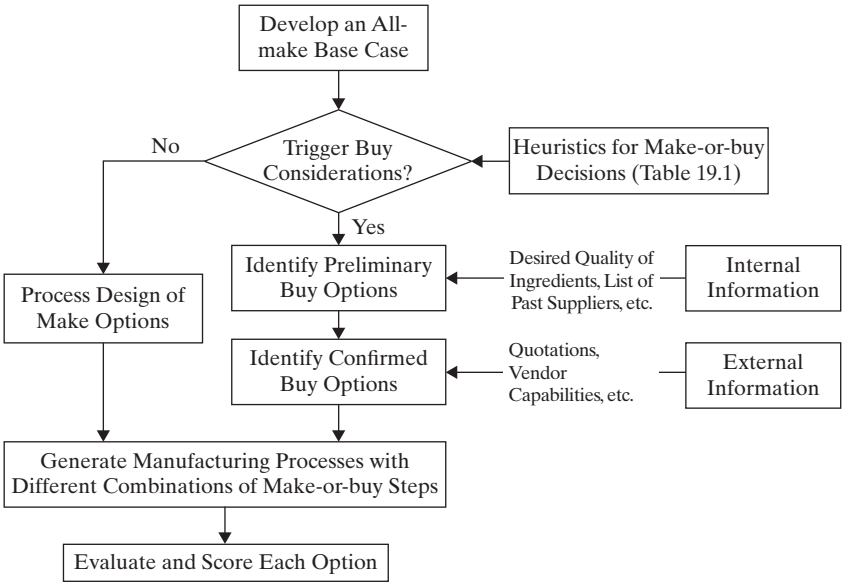

Figure 19.3 Activities involved in the make-or-buy analysis of product development.

of the manufacturing process to vendors to save capital investment and time rather than build its own manufacturing facilities. Another reason may be the superiority of vendors' technology. However, when the product involves a proprietary formulation or a company-owned manufacturing process or design that offers a unique competitive advantage in the marketplace, it is preferable to keep the process in-house. The remainder of Table 19.1, which lists other factors, is provided for the reader to explore. Even when a company decides to purchase ingredients or outsource manufacturing, it tends not to rely on a single supplier. This is related to the failure risk and the economic bargaining power of a single supplier, which can disrupt production, cause severe customer dissatisfaction, and increase product cost.

Figure 19.3 shows the activities in a make-or-buy analysis. To begin such an analysis, an all-make base case in which all manufacturing steps are performed internally, is prepared. This base case is critiqued considering the factors in Table 19.1. For B2C products, it is expected that many ingredients and components are purchased. Internal information including the desired quality of the ingredients or components, expected time of delivery, target price range, in-house manufacturing experiences and technical know-how, list of past suppliers, and so on is collected from various departments of the company. Many preliminary buy options can be generated. At this point, external information such as quotations from potential vendors, location and capabilities of the vendor, and so forth is obtained. The preliminary buy options become confirmed buy options if the availability and acceptability of such options can be established. Concurrently, the make options are identified, the processes designed, and the costs estimated. Combining the buy options and make options generates manufacturing processes with different make-or-buy steps. These make-or-buy options are then evaluated to identify two to three top options for a final decision by top management.

EXAMPLE 19.3 ***Economic Evaluation with Outsourced Manufacturing***

After reviewing the recommendation by the product-development team to spend an additional $2MM for equipment acquisition, management prefers to outsource a portion of manufacturing to a contract manufacturer in the second year of production. There are two main reasons:

1. ***Uncertainty about Sales Projections.*** If the demand for air purifiers were to exceed the projected 70,000 units in the second year, the company might remain low on capacity even after spending $5MM on equipment whereas the external supplier provides reserve capacity at little cost to the company.
2. ***Know-how.*** Because the company manufactures most of the air purifiers, there is sufficient know-how to guide the supplier on quality assurance.

Given that the outsourcing of 20,000 units is expected to increase the variable cost by $30 to $110 per unit and the salvage value of the $3MM equipment is $1.5MM, what is the impact on the product economics?

SOLUTION

The calculations are similar to those in Example 19.2. Because of the contract manufacturing of 20,000 units in year 2, the variable cost for year 2 is $(80 \times 50 + 110 \times 20) = \$6{,}200$ (in thousands of dollars). The after-tax revenue from selling the equipment = ($1,500 − $864)(1 − 0.4) = 382. Note that the book value is calculated as (3,000 − 600 − 960 − 576 = $864). The following table shows the calculations for the project cash flow (PCF).

	$ in Thousands				
Year	−1	0	1	2	3
Sales	0	0	9,000	19,250	12,500
Fixed + Advertising costs			(4,000)	(4,000)	(4,000)
Variable costs			(2,400)	(6,200)	(4,000)
Income from operations			2,600	9,050	4,500
Depreciation			(600)	(960)	(576)
EBIT			2,000	8,090	3,924
Taxes (40%)			(800)	(3,236)	(1,570)
ATOI			1,200	4,854	2,354
OCF			1,800	5,814	2,930
NWC		(2,000)			2,000
Capital spending		(3,000)			
Equipment sales					382
Development cost	(2,000)				
PCF	−2,000	−5,000	1,800	5,814	5,312

By setting the NPV to zero in Eq. (19.6),

$$2{,}000(1+\mathrm{r}) = -5{,}000 + \frac{1{,}800}{(1+\mathrm{r})} + \frac{5{,}814}{(1+\mathrm{r})^2} + \frac{5{,}312}{(1+\mathrm{r})^3}$$

Using the solver function in EXCEL, r = 0.2751, which is larger than 0.2005 obtained in Example 19.2. This indicates that contracting out part of the manufacturing to an original equipment manufacturer (OEM) is an excellent business decision. This gives the company extra capacity when needed, saves upfront investment, and results in a higher return.

19.4 MICROECONOMICS OF PRODUCT DEVELOPMENT

Profits arise from sales revenue, which is the number of units sold, multiplied by the unit selling price. Clearly, fixing the sales volume or, equivalently, demand, d_n, and selling price, p_n, of the new product are two key decisions in product development. These two parameters are closely coupled and depend on the consumer preference for the company's product, H_n, and that of the competition, H_c, the competition's selling price, p_c, and demand, d_c. Following Bagajewicz (2007) and Whitnack et al. (2009), an expression that relates all of these parameters is:

$$p_n {d_n}^{1-\rho} = \alpha^{\rho} \left(\frac{H_n}{H_c}\right)^{\rho} p_c \left(\frac{Y - p_n d_n}{p_c}\right)^{1-\rho} \tag{19.7}$$

In Eq. (19.7), the projected market size, Y (i.e., anticipated maximum sales revenues), satisfies:

$$Y \geq p_n d_n + p_c d_c \tag{19.8}$$

Although Eq. (19.7) may not be quantitatively valid for the product under consideration and the parameters, α and ρ, are hard to determine *a priori*, it provides insights for business decision making. The left-hand side of Eq. (19.7) shows the well-known fact that the demand is expected to be inversely proportional to the price of the new product. Here, ρ is an adjustable parameter less than or equal to unity, and α is a parameter between 0 and 1, which measures the consumers' familiarity with the new product. Even when the quality of the company's product exceeds that of the competition's product, consumers may not recognize the value proposition and be willing to pay for it. When α equals zero, the demand for the new product is zero as well, irrespective of the product price. The value of α can be raised by increasing the marketing budget. Advertisements tend to give sales a boost, particularly during the advertising period. When the consumer preference for the new product measured in some arbitrary units is higher than the competition's preference, both the price of and demand for the new product can be increased. The right-hand side of Eq. (19.7) shows that a decrease in the price of the competing product has the opposite effect of suppressing the price of and demand for the new product. Equation (19.8) indicates that the projected market size exceeds or equals the revenues for the new product and the competitor's products.

Sometimes, it is tempting to attempt to capture a significant fraction of the market. A larger sales volume implies a larger manufacturing plant. Because of the economies of scale, this means that the unit production cost can be reduced. According to Eq. (19.7), the price can be lowered to achieve the desired market share because of the built-in ceteris paribus assumption (i.e., all other things being equal), which presumes that the company's action does not affect the competitor's actions. In reality, a lower price may not result in higher sales. There is a substantial risk that the competitor might retaliate by lowering its own product price in response to the new product's price, thereby creating a price war and a lower profit margin for all producers. Alternatively, the company can increase the marketing budget to increase market share. However, the cost of advertisements would reduce the profit per unit of product sold, and an increase in sales may not lead to a larger total profit. Note that this simplified model does not account for changes in the total market size or multiple competitors with similar products among others.

Sensitivity Analysis

It should be clear that there is much uncertainty in launching a new product. The projected sales volume may be overly optimistic or the impact of advertisements on sales exaggerated. For these reasons, it is often helpful to carry out a large number of what-if analyses to discover the possible impact of these uncertain parameters or scenarios on financial returns. The aim of such an exercise is to form a mental picture of all possible outcomes of a product-development project so as to minimize the number of surprises and to decide on the best course of actions. Often, an upper bound (the best-case scenario) and a lower bound (the worst-case scenario) of the projected sales volume can be considered in an economic evaluation. Similarly, when there is uncertainty about the fixed cost, it can be changed to quantify its effect on financial returns. In fact, completely different scenarios can be used in an economic evaluation to give the product-development team a good sense of the potential impact.

The main objective of a sensitivity analysis is to determine the most important factors or assumptions that affect the profitability measures significantly so that the prediction of these parameters can be improved during the course of the product development. This is illustrated in the example below.

EXAMPLE 19.4 ***Price and Sales Uncertainty (Example 19.1 Revisited)***

Because of the uncertainty in projected product prices and sales figures, management would like to quantify how the following changes impact the net present value:

1. If the best- and worst-case scenario product prices in Example 19.1 are \$400 and \$200 per unit, respectively, how would the net present (NPV) value change? Again, assume a discount rate of 20%.
2. The sales volume is related to the advertising budget as follows:

Advertising Budget, \$MM	Number of Units Sold
1.0	35,000
2.5	50,000
4.0	55,000

Determine whether it is beneficial to change the advertising budget to realize a higher NPV. Assume that the same equipment budget of \$3MM is sufficient to produce the number of units sold.

SOLUTION

(a) Referring to Example 19.1, for a price of \$400 per unit, the PCF values (in thousands of dollars) are: −2,000, −5,000, 7,440, 7,584, and 9,430, for years −1, 0, 1, 2, and 3, respectively. If a discount rate of 20% is assumed, the NPV can be calculated using Eq. (19.6) as follows. For the best-case scenario,

$$\text{NPV} = -2{,}000(1+\text{r}) - 5{,}000 + \frac{7{,}440}{(1+\text{r})} + \frac{7{,}584}{(1+\text{r})^2} + \frac{9{,}430}{(1+\text{r})^3} = \$9{,}524$$

For a price of \$200 per unit, the PCF values (in thousands of dollars) are −2,000, 5,000, 1,440, 1,584, and 3,430 for years −1, 0, 1, 2, and 3, respectively. For the worst-case scenario,

$$\text{NPV} = -2{,}000(1+\text{r}) - 5{,}000 + \frac{1{,}440}{(1+\text{r})} + \frac{1{,}584}{(1+\text{r})^2} + \frac{3{,}430}{(1+\text{r})^3} = -\$3{,}115$$

The NPV greatly improves from the base-case value of \$3,204.4 (Example 19.1) in the best-case scenario but is negative in the worst-case scenario.

(b) For an advertising budget of \$4MM, the PCF values (in thousands of dollars) are −2,000, 5,000, 4,200, 4,344, and 6,190 for years −1, 0, 1, 2, and 3, respectively. If a discount rate of 20% is assumed, the *NPV* can be calculated using Eq. (19.6) as follows:

$$\text{NPV} = -2{,}000(1+\text{r}) - 5{,}000 + \frac{4{,}200}{(1+\text{r})} + \frac{4{,}344}{(1+\text{r})^2} + \frac{6{,}190}{(1+\text{r})^3} = \$2{,}699$$

For an advertisement budget of \$1MM,

$$\text{NPV} = -2{,}000(1+\text{r}) - 5{,}000 + \frac{3{,}360}{(1+\text{r})} + \frac{3{,}504}{(1+\text{r})^2} + \frac{5{,}350}{(1+\text{r})^3} = \$930$$

The NPV at a high advertisement budget is lower than the base-case value of \$3,204.4. This clearly shows that a higher sales volume does not necessarily yield a higher return. Surprisingly, the NPV at a lower advertisement budget is also inferior to the base-case value, underscoring the importance of sensitivity analysis when there are multiple uncertain factors influencing the economics of the product-development project.

19.5 COMPANY AND SOCIETAL FACTORS AFFECTING PRODUCT DEVELOPMENT

As discussed previously, a wide range of decisions are made in a product-development project taking into account the views of the consumers, competitors, and suppliers. Business decision making is based on economic analysis, make-or-buy analysis, sensitivity analysis, and so on. In addition to market issues, the product-development project is also significantly influenced by considerations related to the parent company and the society at large, as described in the following subsections.

Company-level Factors

Leveraging Existing Expertise and Resources

It is common practice for a company to focus on a *product line* with products designed to satisfy a single need. For example, a company can have a product line of water filters including those mounted on a faucet and those used on top of a water pitcher. This product line can be extended to other water treatment devices such as home-use RO modules, domestic ozone water purifiers, and so on. All of these products can be designed by the same team of engineers and scientists because related physicochemical phenomena—adsorption, ion-exchange, membrane filtration, and ozone generation—are involved. In fact, the same laboratory with equipment such as chemical oxygen demand (COD) meters; biochemical oxygen demand (BOD) apparatuses; setups for bacterial cultivation, isolation, and identification; inductively coupled plasma atomic emission spectroscopy for the detection of trace metals; and so on can be used for water characterization irrespective of the water treatment device. Similarly, the idle time of some production facilities can also be reduced by using them for these related products. This strategy of developing and marketing related products can be extended to a *product mix* with complementary product lines. If the key ingredients for a water filter—ion exchange resin and activated carbon—are purchased from a supplier who sells the same ingredients to all competitors, the only way to have a product that stands out in the market is to have a sleek structure, form, shape, and configuration of the water filter. However, if the company also has a product line of water treatment chemicals, it is possible to explore new and unique adsorbents or ion exchange resins, thereby offering a competitive advantage to the product line of water treatment devices.

Company Strategy

The senior management team of a company is responsible for creating shareholder value through allocation of resources. Thus, company strategy has a significant impact on all product-development projects. For example, management might view the domestic air purifier project as a stepping stone to enter the market of central air purifiers for hospitals and commercial buildings. In addition to PCO catalysis, technologies such as plasma and UV irradiation for killing bacteria and viruses are also important. In this case, it is desirable to invest more than the $2MM set aside and more time than the one year planned for product development (Example 19.1). An innovation map that delineates the technology platform for air purification and sterilization would be very helpful at this time.

Societal Factors

Societal Needs

All products are created to meet the needs of consumers and to serve society at large. It is helpful to identify the emerging needs and develop the product ahead of the competitors. In many cases, the product-development team is in a better position than the senior management team to spot the technologies that meet those needs. For example, the shortage of potable water and the remediation of industrial wastewater have been identified as two of the global grand challenges. A technical team designing domestic water filters and reverse osmosis modules can consider the development of similar equipment units for large-scale water treatment. Another megatrend is to minimize the risk of spreading infectious diseases in a densely populated world. To meet this challenge, an air purifier product line can be extended to rid air of airborne pathogens in public places.

The sustainability issues and indicators discussed in Section 3.5 should be considered in a product-development project. In fact, sustainability reporting is gradually becoming a requirement, similar to financial reporting, for organizations around the world.

Global Supply Chain

All companies, large or small, operate in an increasingly connected global environment. Manufacturing is distributed around the world for different reasons. One is proximity to market. It may be advantageous to locate the manufacturing plant near the market to reduce the transportation cost. Another reason is labor cost. There is often a huge difference in wage levels among workers in developed and emerging economies. Since labor cost often constitutes a significant fraction of the B2C product cost, savings can more than cover shipping costs. The third reason is product quality. The more sophisticated products are dominated by countries with advanced technologies. The fourth is local content legislation. Some governments might demand that some parts of a foreign company's product on sale in their country be produced locally instead of being imported. The make-or-buy decisions have to consider all of these factors.

Government Regulations and Policies

Government policy has enormous impact on product development. Consider the Restriction of Hazardous Substances Directive (RoHS) issued by the European Union. The use of lead, mercury, cadmium, hexavalent chromium, polybrominated biphenyls, and polybrominated biphenyl ether in household appliances, consumer equipment, medical devices, electronic products, and so on is severely restricted. Clearly, this has an impact on the choice of materials in conceptual product design.

Government initiatives can encourage the development of certain new products. For example, many governments have decided to heavily subsidize the development of solar renewable energy. This precipitates the production of a wide range of chemical products ranging from crystalline silicon to ethylene vinyl acetate film for the fabrication of solar panels. A similar initiative applies for energy storage. Subsidies and research funds are given to companies and research organizations to develop new battery materials such as lithium nickel manganese cobalt oxide, and novel batteries such as flow batteries.

19.6 SUMMARY

This chapter discussed the essence of product development: cash flow diagrams, product-development budgeting, make-or-buy decisions, and microeconomics as well as company and societal factors affecting product development. This coverage goes beyond cost reduction emphasized in conventional process design (Table 1.1). By having an understanding of the entire product-development cycle (Figure 1.3), the chemical engineer has become part of the management team consisting of technical and businesspeople with different backgrounds to drive a product-development project. This coverage also reflects the worldwide trend of emphasizing entrepreneurship in education in which an individual is encouraged to start a new business and accept both the risks and rewards associated with the business venture.

The cash flow diagram is predicated on the income and cash flow statements. Various metrics for financial return can be determined with an estimation of project cash flow (PCF). Most common are the net present value and investor's rate of return, but return on investment, payback period, and metrics that are firm specific can also be used.

The variables in the cash flow diagram depend on decisions made throughout the project duration. For example, the net sales depend on the sales volume and the product price. The sales volume, in turn, depends not only on product quality but also on the advertisement budget. The pricing strategy has to be set relative to the competitor's product quality and price.

The stand-alone principle is normally assumed for calculating the potential financial return so that the product-development project is evaluated on its own merits. In practice, many other factors that blur this view interfere. For example, it is not unusual to spend more research and development effort than needed for the intended product during the product-development period. This paves the way for the development of follow-up or related products. Also, production and research equipment for the new

product may be available within the company, and the true equipment cost may not be adequately accounted for in the economic evaluation of a new product project. Finally, governments and societies at large have their own goals and needs. Many start-up firms and large corporations take advantage of the financial incentives offered by the government. Such public money can significantly affect the financial return of a product-development project.

REFERENCES

1. Bagajewicz, M. J., "On the Role of Microeconomics, Planning, and Finances in Product Design," *AIChE J.*, **53**, 3155 (2007).

2. Ross, A., R. W. Westerfield, and B. D. Jordan, *Fundamentals of Corporate Finance*, McGraw-Hill, Boston (2012).

3. Vrana, B. M., DuPont in-house course notes (1995).

4. Whitnack, C., A. Heller, M. T. Frow, S. Kerr, and M. J. Bagajewicz, "Financial Risk Management in the Design of Products under Uncertainty," *Computers and Chemical Engineering*, **33**, 1056 (2009).

EXERCISES

19.1 A company is considering a new three-year expansion project that requires an initial fixed investment of \$1.8MM. The fixed asset is depreciated based on the five-year class life in the Modified Accelerated Cost Recovery System. After three years of use, the salvage value is assumed to be zero. The project is estimated to generate \$1,850,000 in annual sales with costs of \$650,000/yr. If the tax rate is 40%, what is the operating cash flow for this project?

19.2 Calculate the net present value and investor's rate of return in Example 19.1 if the product life cycle is extended from three to five years. All other input data remain unchanged.

19.3 Similarly, calculate the investor's rate of return in Example 19.2 with the following changes:

(a) The product life cycle is extended from three to seven years.

(b) In year 3, spend \$1MM to develop an improved product, which will be on sale in year 4.

(c) In years 4, 5, and 6, increase the advertising budget from \$2.5MM to \$3.5MM.

Because of (b) and (c), the estimated sales volume and selling price are given as follows:

Year	Unit Sales	Selling Price, \$
4	60,000	300
5	70,000	275
6	55,000	250
7	40,000	250

(d) Instead of having a fixed amount of working capital, it is suggested that the working capital be adjusted from year to year at \$40/unit.

Plot the cumulative project cash flow from the beginning of product development to the end of product life cycle.

19.4 Regarding market share and government support, consider the following:

(a) The product project team decides to seek a larger market share by lowering the price. Repeat Example 19.2 with the following sales projection:

Year	Unit Sales	Selling Price, \$	Revenues, \$1000
1	50,000	300	12,500
2	90,000	275	20,250
3	70,000	250	14,000

To accommodate the increased production, the engineering team recommends that the equipment cost be increased to \$7MM. Use the five-year property class in the Modified Accelerated Cost Recovery System for depreciation. The market value of the equipment after three years is \$3.5MM.

(b) If the government supports the product-development project with a \$5MM grant payable at the start of the product-development period, what is the impact on the investor's rate of return?

19.5 Regarding the innovation map for an air purifier, do the following:

(a) The company decides to develop a long-term strategy for the development of air purifiers. HEPA filters are used to remove solid particulates; plasma (http://www.plasma-air.com/how-it-works), UV (http://en.wikipedia.org/wiki/Ultraviolet_germicidal_irradiation), and ozone (http://www.understandingozone.com/about.asp) are used to kill bacteria and viruses; PCO is used to decompose VOCs. Develop an innovation map for using these materials for a product line of air purifiers.

(b) Make a survey of existing air purifiers on the market, and compare with the products identified in part (a).

19.6 Perform economic analysis for the water pitcher product-development project in Exercise 5.12. Specifically, determine the investor's rate of return for this product. There is no correct answer to this question because it depends on assumptions such as the cost of product development, revenues, product cost, the length of product life, and so on. Instead, the solution will be judged by its clarity, thoughtfulness, completeness, and logic.

Chapter 20

Plantwide Controllability Assessment

20.0 OBJECTIVES

In this chapter, the importance of considering controllability and operability issues early in the design process is demonstrated by showing how controllability considerations can help to differentiate between processes that are easy and processes that are difficult to control. The chapter provides a recommended methodology to initiate the design of attractive plantwide control systems.

After studying this chapter, the reader should be able to:

1. Identify potential control problems in a process flowsheet.
2. Classify and select controlled and manipulated variables for a plantwide control system.
3. Perform a conceptual synthesis of plantwide control structures (pairings) based on degrees-of-freedom analysis and qualitative guidelines.

20.1 INTRODUCTION

The design of a continuous chemical process is usually carried out at steady state for a given operating range, assuming that a control system can be designed to maintain the process at the desired operating level and within the design constraints. However, unfavorable process static and dynamic characteristics could limit the effectiveness of the control system, leading to a process that is unable to meet its design specifications. A related issue is that alternative designs usually are judged based on economics alone without taking controllability into account. This may lead to the elimination of easily controlled but slightly less economical alternatives in favor of slightly more economical designs that may be extremely difficult to control. It is becoming increasingly evident that design based on steady-state economics alone is risky because the resulting plants are often difficult to control (i.e., inflexible, with poor disturbance-rejection properties), resulting in off-specification product, excessive use of energy, and associated profitability losses.

Consequently, there is a growing recognition of the need to consider the controllability and resiliency (C&R) of a chemical process during its design. Controllability can be defined as the ease with which a continuous plant can be held at a specific steady state. An associated concept is switchability, which measures the ease with which the process can be moved from one desired stationary point to another. Resiliency measures the degree to which a processing system can meet its design objectives despite external disturbances and uncertainties in its design parameters. Clearly, it would be greatly advantageous to be able to predict as early as possible in the design process how well a given flowsheet meets these dynamic performance requirements.

Table 20.1 summarizes the four main stages in the design of a chemical process. In the conceptual and preliminary stages, a large number of alternative process flowsheets in the steady state (SS) are generated. Subsequent stages involve more detailed analysis in the SS, followed by the testing of the dynamic (Dyn) performance of the controlled flowsheets. Here, considerably more engineering effort is expended than in the preliminary stages. Therefore, far fewer designs are considered with many of the initial flowsheets having been eliminated from further consideration by screening in the preliminary stages.

The need to account for the controllability of competing flowsheets in the early design stages is an indication that simple screening measures using the limited information available should be employed to select from among the flowsheets. Here, if high-fidelity, closed-loop, dynamic modeling were used, the engineering effort and time required for development and analysis would slow the design process significantly. The right-hand columns in Table 20.1 show that the shortcut C&R tools provide a bridge between SS simulation for process design and the rigorous dynamic simulation required to verify switchability and other attributes of the closed-loop dynamics of the final design. ASPEN PLUS, PRO/II, ASPEN HYSYS, UniSim® Design, and CHEMCAD are commonly used simulation packages, all of which enable both SS and dynamic simulation.

In the following examples, the impact of design decisions on controllability and resiliency is introduced for four processes. The supplement to this chapter (Section 20S in the file Supplement_to_Chapter_20.pdf in the PDF Files folder, which can be downloaded from the Wiley Web site associated with this book) expands upon this introduction and shows how to eliminate the less desirable alternatives and validate the performance of the most promising designs.

Table 20.1 Process Design Stages, Issues, and Tools

Design Stage	Issues	What Gets Fixed	Tools		
			SS	C&R	Dyn
1. Process creation	Selecting between alternative material pathways and flowsheets	Material pathways			
2. Development of base-case design	Feasibility studies based on fixed material pathways Unit operations selection Heat integration superstructure	Flowsheet structure			
3. Detailed design	Optimization of key process variables Analysis of process sensitivity to disturbances and uncertainties	Optimal flowsheet parameters			
4. Plantwide controllability assessment	Flowsheet controllability Dynamic response of the process to disturbances Selection of the control system structure and its parameters	Control structure and its parameters			

EXAMPLE 20.1 ***Heat Exchanger Networks***

The network shown in Figure 20.1a, which was introduced by McAvoy (1983), cools hot stream 1 from 500 to 300°F using cold streams 2 and 3 having feed temperatures of 300 and 200°F and corresponding target temperatures of 371.4 and 400°F, respectively, with the heat-capacity flow rates in MMBtu/hr-°F. Furthermore, the feed rate and temperature of the hot stream are considered as disturbances.

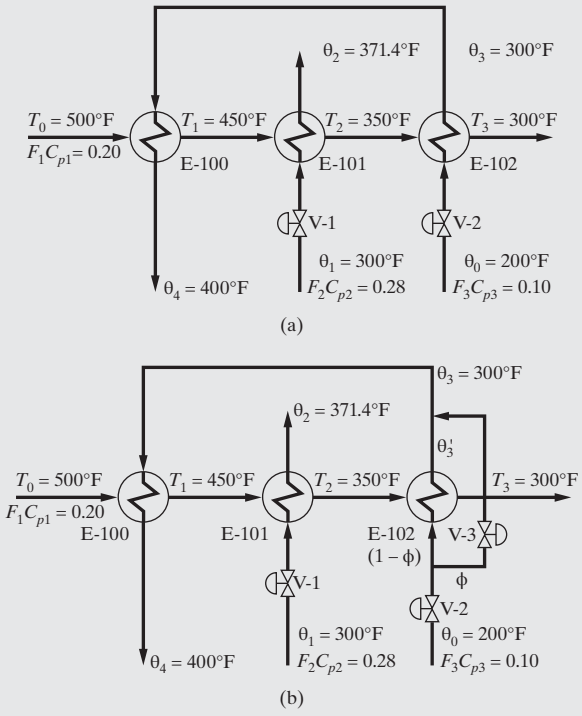

Figure 20.1 Heat exchanger network: (a) original configuration; (b) modification with bypass.

As shown in Figure 20.1a, two of the target temperatures can be controlled by manipulating the flow rates of the two cold streams. This means that one of the target temperatures is left uncontrolled in the face of disturbances in the hot stream. An alternative design, involving a bypass around exchanger E-102, is illustrated in Figure 20.1b. As shown, this simple modification allows all three target temperatures to be regulated. Because the selection of the appropriate bypass flow fraction, ϕ, and of the most effective control configuration is not trivial, controllability analysis should be carried out on the alternative networks and their candidate control structures. This will assist in selecting one of the two designs as shown in the supplement to this chapter.

EXAMPLE 20.2 ***Heat-integrated Distillation Columns***

The production of methanol is carried out in a moderate-pressure synthesis loop by the direct hydrogenation of carbon dioxide,

$$CO_2 + 3H_2 \rightleftharpoons CH_3OH + H_2O, \tag{20.1}$$

which generates a liquid product that contains a binary mixture of methanol and water in approximately equal proportions. To provide commercial methanol that is nearly free of water, dehydration is achieved commonly by distillation. To reduce the sizable energy costs, three double-effect, heat-integrated configurations shown in Figure 20.2 are commonly considered as alternatives to a single distillation column (SC):

Feed Split (FS)

The feed is split nearly equally ($F_H \approx F_L$) between two columns to achieve optimal operation. The overhead vapor product of the high-pressure column supplies the heat required in the low-pressure column.

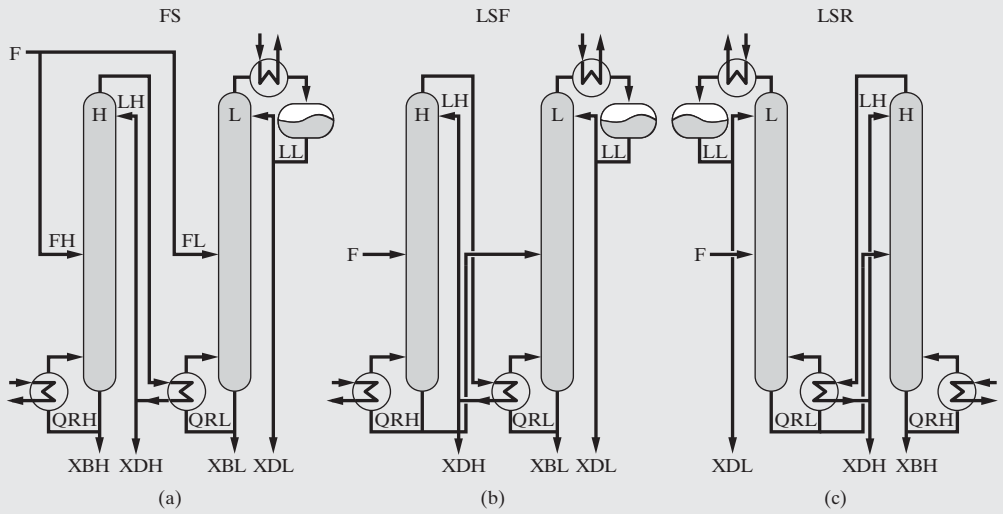

Figure 20.2 Three heat-integrated alternatives to a single distillation column.

Light-split/Forward Heat Integration (LSF)

The entire feed is fed to the high-pressure column. About half of the methanol product is removed in the distillate from the high-pressure column, and the bottoms product is fed into the low-pressure column. In this configuration, heat integration is in the same direction as the mass flow.

Light-split/Reverse Heat Integration (LSR)

The entire feed is fed to the low-pressure column with the bottoms product from the low-pressure column fed into the high-pressure column. Here, heat integration is in the opposite direction to that of the mass flow.

As discussed in Section 11.8, Multiple-Effect Distillation, these configurations reduce the energy costs by using the heat of condensation of the overhead stream from the high-pressure column (H) to supply the heat of vaporization of the boilup in the low-pressure column (L). Although they are more economical, assuming steady-state operation, they are more difficult to control because the configurations (1) are more interactive and (2) have one less manipulated variable for process control because the reboiler duty in the low-pressure column can no longer be manipulated independently.

To show the energy savings, the four flowsheets were simulated on the basis of an equimolar feed of 2,700 kmol/hr, producing 96 mol% methanol in the distillate and 4 mol% methanol in the bottoms product, assuming 75% tray efficiency and no heat loss to the surroundings as well as using UNIFAC to estimate the liquid-phase activity coefficients. The total energy requirements for the four alternatives were computed as follows:

SC: 2.12×10^7 kcal/hr LSR: 1.23×10^7 kcal/hr

LSF: 1.33×10^7 kcal/hr FS: 1.23×10^7 kcal/hr

Clearly, the LSR and FS configurations save the most energy, although the energy consumption in the LSF configuration is only 8% higher. Based on steady-state economics alone, one of these three configurations would be selected. However, disturbance resiliency analysis (Chiang and Luyben, 1988; Weitz and Lewin, 1996) shows that either the LSR or LSF configurations are preferred for disturbance rejection because they provide performance only slightly worse than that of a single column, SC. The FS configuration, on the other hand, does considerably worse. The supplement to this chapter shows how to obtain this information when selecting from among these alternatives.

EXAMPLE 20.3 *Heat Recovery from an Exothermic Reactor*

Often, the heat from an exothermic reactor is used to preheat the reactor feed, thus saving energy, as discussed in Section 6.5. Figure 20.3b shows a configuration using a feed/product heat exchanger that is commonly preferred to the configuration with independent preheat in Figure 20.3a. However, the heat-integrated configuration shares the same disadvantages as the heat-integrated distillation systems discussed in the Example 20.3 (i.e., one less manipulated variable and possibly unfavorable dynamic interactions). Furthermore, the feed-effluent heat exchanger introduces positive feedback and the possibility of thermal runaway.

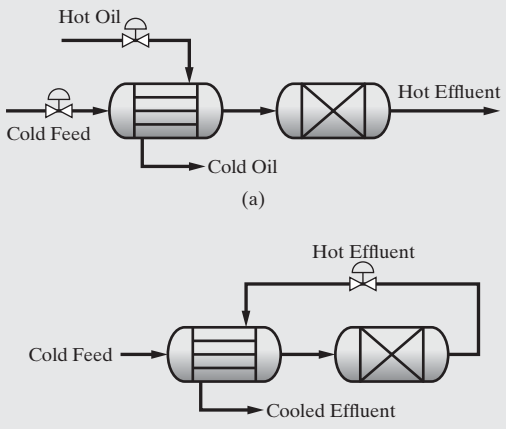

Figure 20.3 Two configurations for an exothermic reactor requiring feed preheating: (a) reactor with independent preheat; (b) heat-integrated (autothermal) reactor.

EXAMPLE 20.4 ***Reactor-flash-recycle System***

Reactor design for complete conversion may be impossible thermodynamically or undesirable because of reduced yields when byproducts are formed. In such cases, an economic alternative is to design a combined reactor-separator-recycle system as illustrated in the simple example in Figure 20.4. Here, the reaction A → B is carried out in a CSTR whose liquid feed is a stream containing pure A. In the event that B is sufficiently more volatile than A, the separation can be performed using a flash vessel with unreacted A recycled to the reactor. As will be seen in the plantwide control examples at the end of this chapter and in the quantitative analysis in the supplement to this chapter, the presence of the recycle complicates control of the process and requires special attention.

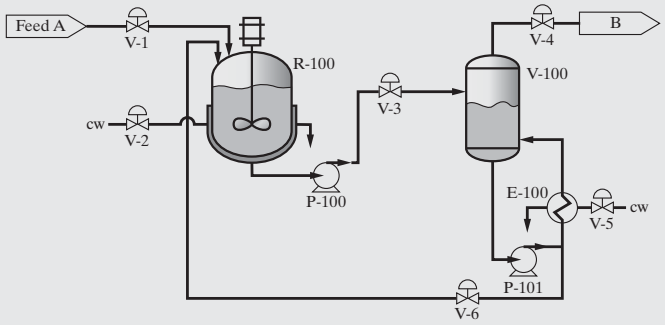

Figure 20.4 Reactor-flash-recycle system for the production of B.

To enable the evaluation of the controllability and resiliency of alternative process configurations, it is important to consider two aspects of the design of plantwide control systems:

1. The classification and selection of controlled and manipulated variables
2. The qualitative synthesis of plantwide control structures based on degrees-of-freedom analysis and qualitative guidelines.

These are examined in the next two sections.

20.2 CONTROL SYSTEM CONFIGURATION

The design of a control system for a chemical plant is guided by the objective to maximize profits by transforming raw materials into useful products while satisfying product specifications, safety constraints, operational limitations, and environmental regulations. All four constraints require special consideration.

1. ***Product Specifications.*** To satisfy customer expectations, it is important that product quality and production rate meet specifications. This has been the driving force for the implementation of online, optimal process control in the chemical industry. More recently, statistics-based approaches such as six-sigma methodologies have been harnessed for this purpose, as discussed in Chapter 18.
2. ***Safety Constraints.*** The plant must be operated safely to protect the well-being of plant personnel, the plant itself, and nearby communities. As an example, a typical safety-driven constraint requires that the temperature and pressure of a steel vessel not exceed upper limits dictated by metallurgy. For other examples, see Section 3.6.
3. ***Operational Limitations.*** Examples of these are upper and lower bounds on the vapor velocity in distillation columns to avoid flooding and weeping, respectively, and upper bounds on the reactor temperatures to prevent degradation of the catalyst or the onset of undesirable side reactions.
4. ***Environmental Regulations.*** These require that processing plants comply with constraints on air and water quality as well as waste disposal. Many examples are discussed in Section 3.4.

Classification of Process Variables

When designing a plantwide control system, it is common to view the process in terms of its input and output variables. These variables include flow rates of streams entering and leaving process equipment and temperatures, pressures, and compositions in entering and leaving streams and/or within equipment.

Process *output variables* are those that give information about the state of the process. They are usually associated with streams leaving the process or with measurements inside a process vessel. When designing a control system, output variables are usually referred to as *controlled variables*, which are measured (online or off-line).

Process *input variables* are independent variables that affect the output variables of a process. They can be subdivided into two categories: (1) *manipulated variables* (also called *control variables*), which can be adjusted freely by an operator or a control mechanism, and (2) *disturbance variables* (also called externally defined variables), which are subject to the external environment and thus cannot be controlled. These variables are associated typically with the inlet and outlet streams. In a control system, manipulated variables cause changes to controlled variables.

There are three main reasons why it may be impossible to control all of the output variables of a process.

1. It may not be possible to measure online all of the output variables, especially compositions. Even when it is possible, it may be too expensive to do so.
2. By a degrees-of-freedom analysis, described later, there may not be enough manipulated variables available to control all of the output variables.
3. Potential control loops may be impractical because of slow dynamics, low sensitivity to the manipulated variables, or interactions with other control loops.

Qualitative criteria have been suggested by Newell and Lee (1988) to guide the selection of controlled and manipulated variables that are suitable for an initial configuration of a plantwide

control system. These guidelines, which are presented next, are driven by the plant and control objectives and should not be applied without due consideration. When two guidelines conflict, the most important of the two should be adopted. In critical cases, the more reliable quantitative screening approaches discussed in the supplement to this chapter should be considered. Following presentation of the guidelines, examples of the selection of variables are given.

Selection of Controlled (Output) Variables

Guideline 1: ***Select Output Variables That Are Either Non–self-regulating or Unstable.*** A *self-regulating process* is one that is described by a state equation of the form $\dot{x} = f\{x, u\}$ where x is an output variable and u is an input variable. A change in u will result in the process moving to a new steady state. A *non-self-regulating process* is described by $\dot{x} = f\{u\}$. As a result, changes in the input variable, u, affect the process output as a pure integrator. An example of a non-self-regulating output variable is the liquid level of a surge tank whose effluent feeds a pump followed by a control valve. Clearly, if the control valve is left uncontrolled, a positive feed disturbance to the surge drum may cause the vessel to overflow. When the process is *unstable* in the open loop (that is, in the absence of feedback control), a change in the input variable causes the system to become unstable. Clearly, non-self-regulating and unstable process output variables must be selected as controlled variables.

Guideline 2: ***Choose Output Variables That Would Exceed the Equipment and Operating Constraints without Control.*** Clearly, when safety or operational constraints are imposed, it is important to measure and control these output variables to comply with the constraints.

Guideline 3: ***Select Output Variables That Are Direct Measures of the Product Quality or That Strongly Affect It.*** Examples of variables that are a direct measure of the product quality are the composition and refractive index whereas those that strongly affect it are temperature and pressure.

Guideline 4: ***Choose Output Variables That Exhibit Significant Interactions with Other Output Variables.*** Plantwide control must handle the potential interactions in the process. Improved closed-loop performance is achieved by stabilizing output variables that interact significantly with each other.

Guideline 5: ***Choose Output Variables That Have Favorable Static and Dynamic Responses to the Available Manipulated Variables.*** This guideline assists in the selection between alternative output variables that match up on the other guidelines.

Selection of Manipulated Variables

Guideline 6: ***Select Manipulated Variables That Significantly Affect the Controlled Variables.*** For each control loop, select an input variable with as large a SS gain as possible and sufficient range to adjust the controlled variable. For example, when a distillation column operates with a large reflux ratio, that is, values greater than 4 (Luyben et al., 1999), it is much easier to control the level in the reflux drum using the reflux flow rate rather than the distillate flow rate.

Guideline 7: ***Select Manipulated Variables That Rapidly Affect the Controlled Variables.*** This precludes the selection of inputs that affect the outputs with large delays or time constants.

Guideline 8: ***Select Manipulated Variables That Affect the Controlled Variables Directly rather than Indirectly.*** For example, when appropriate for the design of an exothermic reactor, it is preferable to inject a coolant directly rather than use a cooling jacket.

Guideline 9: ***Avoid Recycling Disturbances.*** It is usually better to eliminate the effect of disturbances by allowing them to leave the process in an effluent stream rather than having them propagate through the process by the manipulation of a feed or recycle stream.

Selection of Measured Variables

Both input and output variables may be measured variables with online measurement preferred to off-line measurement. Seborg et al. (1989) discuss the importance of measurements in control and provide three guidelines for the selection of variables to be measured and the location of the measurements.

Guideline 10: ***Reliable, Accurate Measurements Are Essential for Good Control.*** An example of a poorly designed measurement would be an orifice positioned to measure flow rate with an insufficient entry length of piping.

Guideline 11: ***Select Measurement Points That Are Sufficiently Sensitive.*** Consider, for example, the indirect control of the product compositions from a distillation column by the regulation of a temperature near the end of the column. In high-purity distillation columns with almost flat terminal temperature profiles, it is preferable to move the temperature measurement point closer to the feed tray.

Guideline 12: ***Select Measurement Points That Minimize Time Delays and Time Constants.*** Large time delays and dynamic lags in the process limit the achievable closed-loop performance. These should be reduced whenever possible in the process design and the selection of measurements.

Degrees-of-Freedom Analysis

Before selecting the controlled and manipulated variables for a control system, one must determine the number of manipulated variables permissible. As discussed in Section 7.2, the number of manipulated variables cannot exceed the number of degrees of freedom, which are determined using a process model according to

$$N_D = N_V - N_E \tag{20.2}$$

where N_D is the number of degrees of freedom, N_V is the number of process variables, and N_E is the number of independent equations that describe the process. However, the number of manipulated variables, N_M, is generally less than the number of degrees of freedom because one or more variables may be externally defined (i.e., N_{ED}, the disturbances); that is, $N_D = N_M + N_{ED}$. Consequently, the number of manipulated variables can be expressed in terms of the number of externally defined variables:

$$N_M = N_V - N_{ED} - N_E \tag{20.3}$$

The number of manipulated variables equals the number of controlled variables that can be regulated. When a manipulated variable is paired with a regulated-output variable, its degree of freedom is transferred to the output's setpoint, which becomes the new independent variable.

Next, degrees-of-freedom analyses are carried out and their implications for control system design are considered for heat exchanger networks, jacketed stirred-tank reactors, a utility system, a flash vessel, and a distillation column.

EXAMPLE 20.5 ***Control Configurations for Heat Exchanger Networks (Example 20.1 revisited)***

Referring to Figure 20.1a, the process can be described in terms of 15 variables: F_1, F_2, F_3, T_0, T_1, T_2, T_3, θ_0, θ_1, θ_2, θ_3, θ_4, Q_1, Q_2, and Q_3. Of these, assume that four variables can be considered to be externally defined: F_1, T_0, θ_0; and θ_1. A steady-state model for the process consists of three equations for each heat exchanger. For example, for the first heat exchanger, the following equations apply:

$$Q_1 = F_1 C_{P1}(T_0 - T_1) \tag{20.4}$$

$$Q_1 = F_3 C_{P3}(\theta_4 - \theta_3) \tag{20.5}$$

$$Q_1 = U_1 A_1 \frac{(T_0 - \theta_4) - (T_1 - \theta_3)}{\ln\left\{\dfrac{T_0 - \theta_4}{T_1 - \theta_3}\right\}} \tag{20.6}$$

In these equations, Q_i, U_i, and A_i are the heat duty, heat-transfer coefficient, and heat-transfer area, respectively, for heat exchanger i. Values for the latter two are assumed known, so they are not process variables. Similar equations are written for the other two heat exchangers, making a total of nine equations. Consequently, the number of manipulated variables is computed: $N_M = N_V - N_{ED} - N_E = 15 - 4 - 9 = 2$

Thus, two variables can be manipulated. Two candidates are the flow rates of the two cold streams: F_2 and F_3. Ideally, for the selection of the controlled variables, it would be desirable to regulate all three target temperatures: T_3, θ_2, and θ_4. However, with only two manipulated variables, only two controlled variables can be selected. The guidelines presented above are insufficient to select which two of the three should be picked because all three provide a direct measure of the product quality (Guideline 3), and there are clearly significant interactions among all three of the variables (Guideline 4). Without quantitative analysis, one cannot gauge which of the three have the most favorable static and dynamic responses to the manipulated variables. If only T_3, θ_2, and θ_4 are considered as potential controlled variables, three possible control systems should be investigated. As an illustration, Figure 20.5 shows one possible configuration of two control loops. One loop adjusts the flow rate, F_2, to control θ_2, and the other loop adjusts F_3 to control θ_4. An alternative configuration with reversed pairings (i.e., $\theta_4 - F_2$, $\theta_2 - F_3$) is unstable as shown in Case Study 20S.2.

The design in Figure 20.1b involving a bypass on exchanger E-102 permits the regulation of all three target temperatures. In this case, the number of variables is increased by 2 (the bypass flow fraction, ϕ, and the temperature, θ_3'), giving a total of 17 variables with the same four disturbance variables. For constant heat capacities and no phase change, the process is modeled by one additional energy balance for the mixer,

$$\theta_3 = (1 - \phi)\theta_0 + \phi\theta_3' \tag{20.7}$$

where ϕ is the E-102 bypass flow fraction and θ_3' is the temperature leaving heat exchanger E-102. Because $N_M = N_V - N_{ED} - N_E = 17 - 4 - 10 = 3$, three variables can be manipulated, namely, F_2, F_3, and ϕ. The flow rate of the second cold stream, F_3, affects two of the three heat exchangers whereas F_2 affects only the second one directly, and ϕ affects T_3 directly (Guidelines 6, 7, and 8). The control structure shown in Figure 20.6 is the most resilient and controllable regulatory structure as is demonstrated in Case Study 20S.2.

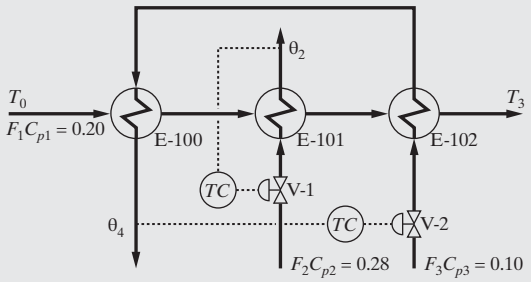

Figure 20.5 Control system for original heat exchanger network.

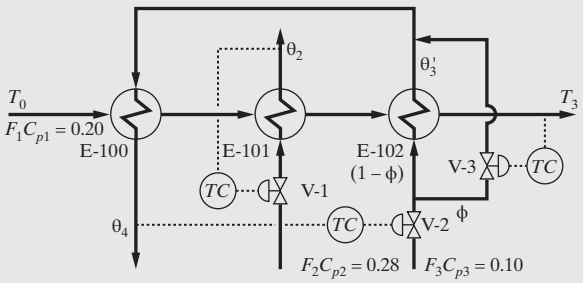

Figure 20.6 Control system for the modified heat exchanger network.

EXAMPLE 20.6 *Control Configuration for a Jacketed CSTR*

Consider the control of a jacketed continuous-stirred-tank reactor (CSTR) in which the exothermic reaction A → B is carried out. This system can be described by 10 variables as shown in Figure 20.7: $h, T, C_A, C_{Ai}, T_i, F_i, F_o, F_c, T_c$, and T_{co}, three of which are considered to be externally defined: C_{Ai}, T_i, and T_{co}. Its model involves four equations, assuming constant fluid density.

1. Overall mass balance:

$$A\frac{dh}{dt} = F_i - F_o \tag{20.8}$$

2. Mass balance on component A:

$$A\frac{d}{dt}(hC_A) = F_iC_{Ai} - F_oC_A - Ah \cdot r\{C_A, T\} \tag{20.9}$$

3. Energy balance on the reacting mixture:

$$A\rho c_p\frac{d}{dt}(h \cdot T) = F_i\rho c_pT_i - F_o\rho c_pT - Ah \cdot r\{C_A, T\}(-\Delta H) - UA_s(T - T_c) \tag{20.10}$$

4. Energy balance on the jacket coolant:

$$V_c\rho_c c_{Pc}\frac{dT_c}{dt} = F_c\rho_c c_{pc}T_{co} - F_c\rho_c c_{pc}T_c + UA_s(T - T_c) \tag{20.11}$$

where A is the cross-sectional area of the vessel, h is the liquid level in the reactor, A_s is the area for heat transfer, U is the overall heat transfer coefficient, C_{Ai} and C_A are the inlet and reactor concentrations of A, T_i and T are the inlet and reactor temperatures, F_i and F_o are the inlet and outlet volumetric flow rates, ρ is the fluid density, F_c is the coolant volumentric flow rate, ρ_c is the coolant density, T_{co} and T_c are the inlet coolant and jacket temperatures, V_c is the volume of fluid in the cooling jacket, r is the intrinsic rate of reaction, ΔH is the heat of reaction, and c_p and c_{pc} are the specific heats of the reacting mixture and coolant, respectively.

Here, the number of variables that can be manipulated independently is $N_M = N_V - N_{ED} - N_E = 10 - 3 - 4 = 3$.

Selection of Controlled Variables. C_A should be selected because it affects the product quality directly (Guideline 3). T should be selected because it must be regulated properly to avoid safety problems (Guideline 2) and because it interacts with C_A (Guideline 4). Finally, h must be selected as a controlled output because it is non-self-regulating (Guideline 1).

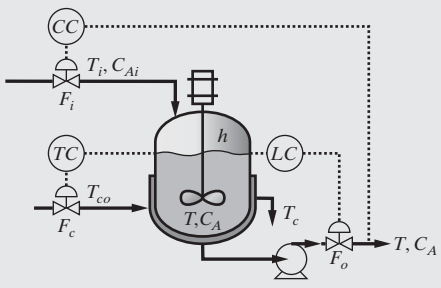

Figure 20.7 Control system for a jacketed CSTR.

Selection of Manipulated Variables. The volumetric feed flow rate, F_i, should be selected because it directly and rapidly affects the conversion (Guidelines 6, 7, and 8). Using the same reasoning, F_c is selected to control the reactor temperature, T; and the flow rate of the reactor effluent, F_o, is selected to control h. This configuration, which is shown in Figure 20.7, should be compared with other pairings using the quantitative analysis presented in the supplement to this chapter, it being noted that there are several opportunities for improvement.

EXAMPLE 20.7 *Control Configuration for a Utilities Subsystem*

Often, the contents of a chemical batch reactor are heated initially to achieve ignition and then cooled to remove the heat generated in reaction. In such cases, it is common to install a jacket supplied with both cooling and heating utility streams as shown in Figure 20.8. The utilities subsystem involves eight variables: $P_{cf}, T_{cf}, F_{c1}, T_{c1}, F_{c2}, T_{c2}, F_c$, and T_{co}. Of these, two are externally defined and constitute disturbance variables: P_{cf} and T_{cf}. Four material and energy balances relate the subsystem variables: (1) an energy balance for the cooling branch, (2) an energy balance for the heating branch, (3) an energy balance for the mixing junction, and (4) a mass balance for the mixing junction. Hence, the number of variables to be manipulated independently is $N_M = N_V - N_{ED} - N_E = 8 - 2 - 4 = 2$. This is also the number of subsystem variables that can be controlled independently.

Selection of Controlled Variables. The guidelines presented earlier are not helpful because no output variable has a direct effect on the product quality, all are self-regulating, and none is directly associated with equipment or operating constraints. Nonetheless, F_c and T_{co} are obvious choices for the controlled variables because the objective of this subsystem is to control the temperature and flow rate of the utility stream fed to the reactor jacket.

Selection of Manipulated Variables. The two obvious candidates are F_{c1} and F_{c2} because both affect the two outputs directly and rapidly (Guidelines 7 and 8). However, linear and nonlinear combinations of these flow rates are also possible. As shown in Example 20S.4, a quantitative analysis is needed to make the best selection.

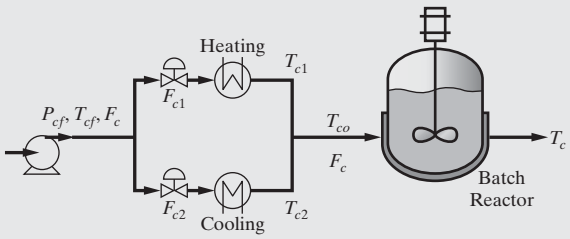

Figure 20.8 Utilities subsystem for a batch chemical reactor.

EXAMPLE 20.8 *Control Configuration for a Flash Drum*

The flash drum in Figure 20.9 illustrates a situation in which a stream containing a binary mixture of two components, A and B, is flashed through a valve and separated in a flash drum into an overhead vapor stream and a residual liquid product stream. External heat exchange with liquid recycle is provided with a fixed recycle ratio. This process is modeled with 11 variables: F_i, T, C_A, F_W, P_f, h, T_f, F_V, y_A, F_L, and x_A. Two variables are considered to be externally defined, T and C_A. The model involves five equations: a total mass balance, a mass balance for component A, an overall energy balance, and a vapor–liquid equilibrium equation for each component. Thus, the number of variables to be manipulated independently is $N_M = N_V - N_{ED} - N_E = 11 - 2 - 5 = 4$.

Selection of Controlled Variables. P_f is selected because of the potential safety problems (Guideline 2) and because it affects the product concentrations (Guideline 3). T_f should be selected because it directly affects the product quality (Guideline 3). The liquid level in the drum, h, must be selected because it is not self-regulating (Guideline 1), and F_i is selected because it controls the product flow rate directly, one of the overall control objectives (Guideline 3). Note that all of these outputs exhibit significant interaction.

Selection of Manipulated Variables. F_i is designated as the *production handle*, that is, the manipulated variable selected to maintain the desired production rate. It is adjusted to achieve its setpoint (Guideline 8). F_V has a rapid, direct effect on the vessel pressure, P_f, but almost no effect on any other output (Guidelines 7 and 8). For similar reasons, F_L is selected to control the liquid level, h. F_W is selected because it directly controls the flash temperature, T_f (Guideline 8).

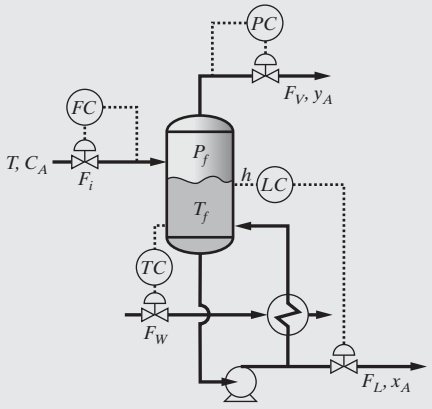

Figure 20.9 Control configuration for a flash drum.

EXAMPLE 20.9 *Control Configurations for a Binary Distillation Column*

This analysis of the distillation operation in Figure 20.10 is based on the following assumptions and specifications: (1) constant relative volatility, (2) saturated liquid distillate, (3) negligible vapor holdup

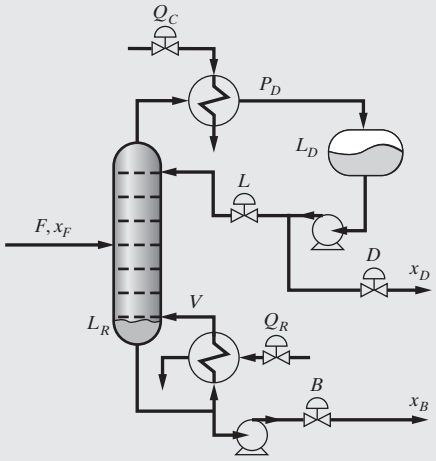

Figure 20.10 A distillation column with two liquid products.

in the column, (4) constant tray pressure drops (Luyben, 1990), and (5) negligible heat losses except for the condenser and reboiler. A column consisting of N_T trays is modeled in terms of the following $4N_T + 13$ variables:

Vapor and liquid compositions on each tray	$2N_T$
Tray liquid flow rates and holdups	$2N_T$
Reflux drum holdup and composition	2
Reflux and distillate flow rates	2
Column sump vapor and liquid compositions	2
Column sump liquid holdup	1
Bottoms product and reboiler steam flow rates	2
Feed flow rate and composition	2
Condenser pressure	1
Condenser duty	1

The system is described by $4N_T + 6$ equations:

Species mass balances (trays, sump, reflux drum)	$N_T + 2$
Total mass balances (trays, sump, reflux drum)	$N_T + 2$
Vapor–liquid equilibrium (trays, sump)	$N_T + 1$
Tray hydraulics for tray holdup	N_T
Total vapor dynamics	1

Assuming that the feed flow rate and composition are externally defined, the number of variables to be manipulated independently is $N_M = N_V - N_{ED} - N_E = 4N_T + 13 - 2 - (4N_T + 6) = 5$.

Selection of Controlled Variables The condenser pressure, P_D, should be regulated because it strongly affects the product compositions (Guidelines 3 and 4). The reflux drum and sump liquid inventory levels, L_D and L_R, need to be regulated because they are not self-regulating (Guideline 1). This leaves two additional variables that can be regulated. When distillate and bottoms streams are product streams, their compositions, x_D and x_B, respectively, are often selected as controlled variables (Guideline 3). Because significant delay times

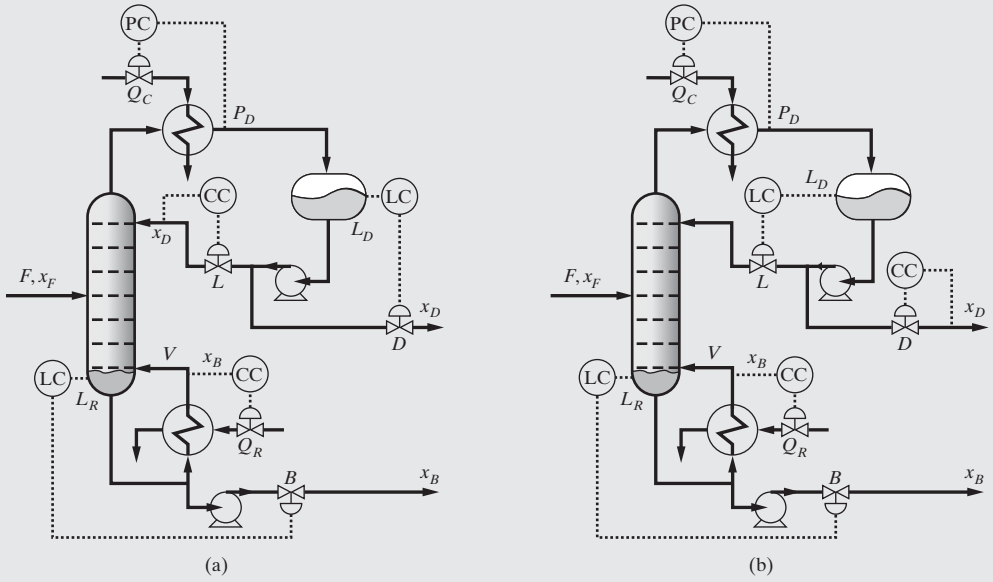

Figure 20.11 Two control configurations for a binary distillation column: (a) LV; (b) DV.

compositions (Guideline 12). In this regard, temperatures must be measured on trays that are sensitive to column upsets (Guideline 11).

Selection of Manipulated Variables. As shown in Figure 20.10 by labels on the valves, the five manipulated variables are the flow rates of the reflux, distillate, and bottoms streams L, D, and B, respectively, and the cooling and heating duties, Q_C and Q_R, respectively. It is most common to control P_D in columns with a liquid overhead product by manipulating Q_C. This leaves two compositions and two liquid inventories to control. A commonly employed configuration is to use the reflux, L, to control the top composition, x_D, and the reboiler duty, Q_R (which is closely related to V), to control the bottoms composition, x_B, in the so-called LV-configuration shown in Figure 20.11a. This leaves the distillate and bottoms streams, D and B, to control the reflux and sump liquid inventory levels, L_D and L_R, respectively. In columns operating with large reflux ratios (above 4), the flow of distillate will be insufficient to adequately regulate the reflux level, and in such cases, it is advisable to use L to control L_D (Guideline 6). Then, D regulates x_D, in the so-called DV-configuration, shown in Figure 20.11b, noting that the dynamic performance of this scheme is inferior to the LV-configuration. Alternative configurations involve ratios of manipulated variables intended to decouple the control loops by reducing the interaction between them (Shinskey, 1984; Luyben et al., 1999). The dynamic performance of a column control system should be verified using the quantitative methods described in the supplement to this chapter.

20.3 QUALITATIVE PLANTWIDE CONTROL SYSTEM SYNTHESIS

As pointed out by Luyben et al. (1999), the design of a plantwide control system should be driven by the objectives of the overall process rather than by considerations of the individual processing units as in the preceding section. Their strategy for control system design utilizes the available degrees of freedom to achieve these objectives in order of importance by adopting a "top-down" approach in common with successful programming practice. Alternatively, in a simpler "bottom-up" approach (Stephanopoulos, 1984), the process is divided into subsystems with each subsystem often composed of several process units that share a common processing goal. Then, a control system is formulated for each subsystem by relying on the qualitative guidelines in Section 20.2 or the quantitative analysis to be described in the supplement to this chapter. Finally, an integrated system is synthesized by eliminating possible conflicts among the subsystems. The main disadvantage of this bottom-up approach is that good solutions at the subsystem level may not satisfy the process objectives. This can occur when manipulated variables are assigned to meet the control objectives of a subsystem, leaving less attractive inputs to satisfy those of the overall process. As will be demonstrated, interactions among subsystems, such as those resulting from heat integration and material recycle, are not addressed in this decomposition approach, which often leads to unworkable solutions.

The qualitative design procedure for plantwide control by Luyben et al. (1999) consists of the following steps:

Step 1: ***Establish the Control Objectives.*** As mentioned, the control objectives are related closely to the process objectives. For example, one may wish to impose a given production rate while ensuring that the products satisfy the quality specified by the market and guaranteeing that the process meets environmental and safety constraints.

Step 2: ***Determine the Control Degrees of Freedom.*** In practice, the degrees-of-freedom analysis in Section 20.2 may be too cumbersome for the synthesis of plantwide control systems. In a more direct approach, the number of control valves in the flowsheet equals the degrees of freedom (Luyben et al., 1999). As the valves are positioned on the flowsheet, care must

be taken to avoid the control of a flow rate by more than one valve. When the degrees of freedom are insufficient to meet all of the control objectives, it may be necessary to add control valves, for example, by adding bypass lines around heat exchangers as shown in Example 20.5 or by adding trim heaters or coolers serviced by utility streams.

Step 3: ***Establish the Energy-management System.*** In this step, control loops are positioned to regulate exothermic and endothermic reactors at desired temperatures. In addition, temperature controllers are positioned to ensure that disturbances are removed from the process through utility streams rather than recycled by heat-integrated process units.

Step 4: ***Set the Production Rate.*** This is accomplished by placing a flow control loop on the principal feed stream (referred to as *fixed feed* or *fresh feed*) or on the principal product stream (referred to as *on-demand product*), noting that these two options lead to different plantwide control configurations. Alternatively, the production rate is controlled by regulating the reactor operating conditions, for example, by controlling reactor hold-up.

Step 5: ***Control the Product Quality and Handle Safety, Environmental, and Operational Constraints.*** Having regulated the production rate and the effect of temperature disturbances, secondary objectives to regulate product quality and satisfy safety, environmental, operational, and process constraints are addressed in this step.

Step 6: ***Fix a Flow Rate in Every Recycle Loop and Control Vapor and Liquid Inventories (vessel pressures and levels).*** Process unit inventories, such as liquid holdups and vessel pressures (measures of vapor holdups), are relatively easy to control. Although vessel holdups are usually non-self-regulating (Guideline 1), the dynamic performance of their controllers is usually less important. In fact, level controllers are usually detuned to allow the vessel accumulations to dampen disturbances in the same way that shock absorbers cushion an automobile as demonstrated in the supplement to this chapter. Less obvious is the need to handle plantwide holdups in recycle loops. As will be shown qualitatively in several examples that follow and quantitatively in the supplement to this chapter, failure to impose flow control on each recycle stream can result in the loss of control of the process.

Step 7: ***Check Component Balances.*** In this step, control loops are installed to prevent the accumulation of individual chemical species in the process. Without control, chemical species often build up, especially in material recycle loops.

Step 8: ***Control the Individual Process Units.*** At this point, the remaining degrees of freedom are assigned to ensure that adequate local control is provided in each process unit. Because this step comes after the main plantwide issues have been handled, it often requires no additions to the control system.

Step 9: ***Optimize Economics and Improve Dynamic Controllability.*** When control valves remain to be assigned, they are utilized to improve the dynamic and economic performance of the process.

The above procedure is demonstrated next on three processes of increasing complexity: (1) an acyclic process, (2) the reactor-flash-recycle process in Example 20.4, and (3) the vinyl-chloride process discussed in Sections 2.3 and 2.5. The second and third examples feature recycle loops.

EXAMPLE 20.10 ***Plantwide Control System Configurations for an Acyclic Process***

The chemical process shown in Figure 20.12 is based on an example by Stephanopoulos (1984). It consists of a CSTR in which species A reacts to form B in an exothermic reaction. The reactor effluent is fed to a flash vessel where the heavier product B is concentrated in the liquid stream, and unreacted A is discarded in the vapor stream. A preheater recovers heat from the hot reactor effluent with a so-called trim heater installed to ensure that the liquid reactor feed is at the desired temperature. To ensure that the reactor temperature remains on target, the CSTR is equipped with a jacket fed with cooling water to attenuate the heat released.

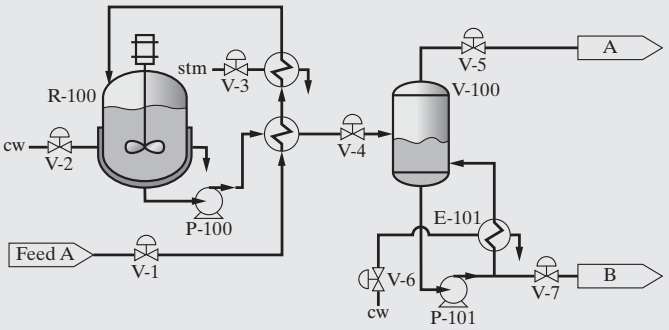

Figure 20.12 Process flowsheet for the acyclic process.

Applying the nine-step design procedure for plantwide control by Luyben and co-workers (1999), and using when possible the guidelines of Section 20.2:

Step 1: ***Set Objectives.*** The control objectives for this process are as follows:

1. Maintain the production rate of component B at a specified level.
2. Keep the conversion of the plant at its highest permissible value.
3. Achieve constant composition in the liquid effluent from the flash drum.

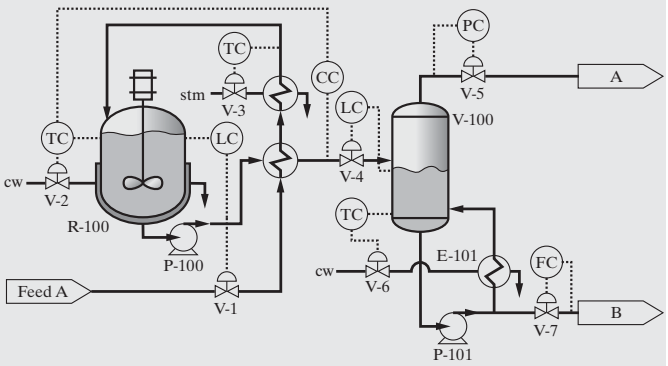

Figure 20.13 Control structure for *on-demand product* in the acyclic process.

The structure of the plantwide control system depends on the primary control objective, that is, to maintain a desired production rate. The two possible interpretations of this goal are to ensure (1) a desired flow rate of the product stream by flow control using valve V-7, which leads to the *on-demand product* configuration shown in Figure 20.13 or (2) a desired production level by *fixed feed* using valve V-1, which leads to the control configuration shown in Figure 20.14. The *on-demand product* configuration is considered first.

Step 2: ***Define Control Degrees of Freedom.*** As shown in Figure 20.12, the process has seven degrees of freedom for manipulated variables. Having decided to design a configuration for *on-demand product*, the valve controlling the B product flow rate (V-7) is reserved for independent flow control (i.e., it directly controls the flow rate).

Step 3: ***Establish the Energy-management System.*** The critical energy management for the CSTR is handled next because loss of control of the reactor would have serious plantwide consequences. Using the guidelines for controlled and manipulated variable selection, the reactor feed and effluent temperatures are identified as critical for safety (Guideline 2) and quality assurance (Guideline 3). The obvious choices for valves to control these two temperatures are V-3, the steam valve for the trim heater, and V-2, the jacket coolant valve, both of which have a direct effect (Guidelines 6 and 7). These are assigned to temperature control loops.

Step 4: ***Set the Production Rate.*** As mentioned, the B product valve, V-7, is assigned to a flow controller whose setpoint directly regulates the production rate.

Step 5: ***Control Product Quality, and Meet Safety, Environmental, and Operational Constraints.*** The product quality is controlled by maintaining the operating temperature and pressure in the flash vessel at setpoints (Guideline 3). The former is regulated by adjusting the coolant water flow rate through V-6, and the latter is controlled by adjusting the vapor flow rate through overhead valve V-5. These valves are selected because of their rapid and direct effect on the outputs (Guidelines 6, 7, and 8). In addition, these two control loops satisfy the third control objective, that is, to provide tight product-quality control.

Step 6: ***Fix Recycle Flow Rates and Vapor and Liquid Inventories.*** The liquid inventories in the flash vessel and reactor are non-self-regulating and, therefore, need to be controlled (Guideline 1). Because the liquid product valve from the flash vessel has been assigned to control the product flow rate, the inventory control must be in the reverse direction to the process flow. Thus, the reactor effluent valve, V-4, controls the flash vessel liquid level, and the feed valve, V-1, controls the reactor liquid level. Both of these valves have rapid, direct effects on the liquid holdups (Guidelines 6, 7, and 8). The vapor product valve, V-5, which has been assigned to control the pressure in V-100, thereby controls the vapor inventory.

Step 7: ***Check Component Balances.*** With the controllers assigned above, A and B cannot build up in the process, and consequently, this step is not needed.

Step 8: ***Control the Individual Process Units.*** Because all of the control valves have been assigned, no additional control loops can be designed for the process units, nor are they needed because both are already adequately controlled.

Step 9: ***Optimize Economics and Improve Dynamic Controllability.*** While a temperature control system for the CSTR is in place, its setpoint needs to be established. To meet the second control objective, which seeks to maximize conversion, a cascade controller is installed in which the setpoint of the reactor temperature controller (TC on V-2) is adjusted to control the concentration of B (CC) in the reactor effluent. If the reaction is irreversible, conversion is maximized by operating the reactor at the highest possible temperature, making this controller unnecessary. This completes the control system design for the on-demand product configuration in Figure 20.13. The performance of the control system needs to be verified by using controllability and resiliency assessment and by applying dynamic simulation as described in the supplement to this chapter.

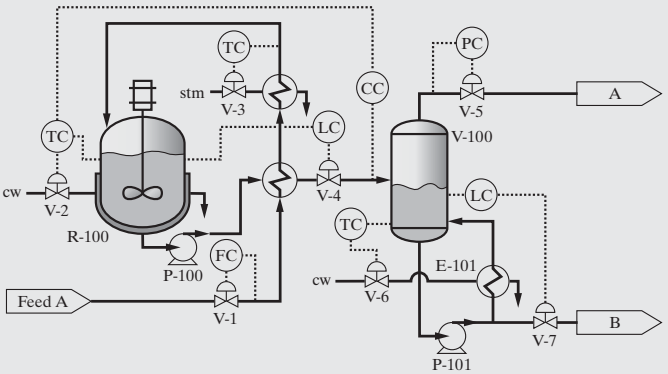

Figure 20.14 Control structure for *fixed feed* in the acyclic process.

As an alternative to the *on-demand product* configuration, the production level can be maintained by fixing the feed flow rate, which leads to the control system shown in Figure 20.14. This control configuration is derived using the same procedure as with Figure 20.13 with the only difference being in Step 6 where the liquid levels are controlled in the direction of the process flow because here, valve V-1 is in use as the production handle, and valve V-7 is free for use in inventory control. For the fixed feed configuration, reaction kinetics may dictate that the reactor holdup be manipulated in concert with throughput changes. In this case, it may be necessary to coordinate the reactor level setpoint with the feed flow rate.

EXAMPLE 20.11 ***Plantwide Control System Configuration for Reactor-flash-recycle Process (Example 20.4 revisited)***

For the reactor-flash-recycle process introduced in Example 20.4, Figure 20.15 shows a control system with the control objectives to:

1. Maintain the production rate of component B at a specified level.

2. Keep the conversion of the plant at its highest permissible value.

The control configuration consists of six control loops: (1) production rate controlled using valve V-1 on the fresh feed stream, (2) temperature control using valve V-2 to ensure isothermal operation of R-100, (3) level control in R-100 holdup using valve V-3, (4) level control in V-100 using valve V-6, (5) pressure control in V-100 using the vapor-product valve, V-4, and (6) temperature control in V-100 (controlling product quality) using the coolant valve, V-5. This control system results from using a unit-by-unit design approach with each vessel inventory controlled by manipulation of its liquid effluent flow. Although the control pairings are acceptable for each process unit in isolation, the overall control system does not establish flow control of the recycle stream. Consequently, a change in the desired feed rate that keeps the reactor inventory constant with level control causes an excessive increase in the reactor effluent flow, which is transferred rapidly to the recycle flow by the flash level controller. This undesirable positive feedback is referred to as the "snowball effect" by Luyben and co-workers (1999) and is the consequence of not ensuring flow control of the recycle stream.

Since Luyben identified the snowball effect (Luyben, 1994), the sensitivity of reactor-separator-recycle systems to external disturbances has been the subject of several studies (e.g., Wu and Yu, 1996; Skogestad, 2002). Recent work by Bildea and co-workers (2000; Kiss et al., 2002) has shown that a critical reaction rate can be defined for each reactor-separator-recycle system using the Damköhler number, *Da* (dimensionless rate of reaction, proportional to the reaction rate constant and the reactor holdup). When the Damköhler number is below a critical value, Bildea et al. show that the conventional unit-by-unit approach in Figure 20.15 leads to the loss of control. Furthermore, they show that controllability problems associated with exothermic CSTRs and PFRs are often resolved by controlling the total flow rate of the reactor feed stream.

The extent of the snowball effect is shown next by analysis of the controlled process in Figure 20.15. The combined feed of pure A and recycle is partially converted to B in reactor R-100 by the isothermal, liquid-phase, irreversible reaction A → B, which has first-order kinetics. The reactor effluent is flashed across valve V-3 to give a vapor-product stream assumed to be pure B and a liquid-product stream assumed to be pure A. The liquid stream is recycled to the reactor where it is mixed with fresh feed A to give the combined feed. What happens when the fresh feed flow rate changes? The equations that apply are:

Combined molar feed to the CSTR	$F_0 + B$
Molar material balance around the flash vessel	$F_0 + B = D + B$
Overall molar material balance	$F_0 = D$

where F_0, D, and B are the molar flow rates of the feed, flash vapor, and flash liquid streams. Finally, the rate of consumption of A in the reactor is:

$$r_A = kc_A \tag{20.12}$$

where r_A is the intrinsic rate of reaction, k is the first-order rate constant, and c_A is the molar concentration of A in the reactor effluent. Defining c_{total} as the total molar concentration and x_A as the mole fraction of A in the reactor effluent, Eq. (20.12) becomes:

$$r_A = kx_A c_{\text{total}} \tag{20.13}$$

The molar flow rate of B in the reactor effluent is:

$$(1 - x_A)(F_0 + B) = kx_A c_{\text{total}} V_R \tag{20.14}$$

where V_R is the volume of the reactor holdup. Then, substituting $c_{\text{total}} V_R = n_T$:

$$(1 - x_A)(F_0 + B) = kx_A n_T \tag{20.15}$$

where n_T is the total molar holdup in the reactor. Rearranging Eq. (20.15) for the flash liquid stream flow rate (recycled to the reactor), B:

$$B = \frac{x_A(F_0 + kn_T) - F_0}{1 - x_A} \tag{20.16}$$

With the reactor temperature and holdup fixed, a change to the fresh feed flow rate by a disturbance causes the mole fraction of A in the reactor effluent to change. Therefore, to obtain the effect of a change in F_0 on B, x_A must be eliminated from Eq. (20.16). For a perfect separation, an overall balance on the disappearance of A gives:

$$F_0 = kx_A n_T \tag{20.17}$$

Rearranging Eq. (20.17) for x_A and substituting in Eq. (20.16) gives:

$$B = \frac{F_0^2}{kn_T - F_0} \tag{20.18}$$

Equation (20.18) indicates that B increases by more than quadratically with increases in F_0. As an example, consider F_0 in the range of 50 to 150, with $kn_T = 200$. Then, Eq. (20.18) gives the recycle rate, B, as a function of F_0:

F_0	B
50	16.7
75	45.0
100	100
125	208
150	450

Thus, when the feed rate is tripled from 50 to 150, the recycle rate increases by a factor of 450/16.7 = 27. This result assumes a fixed

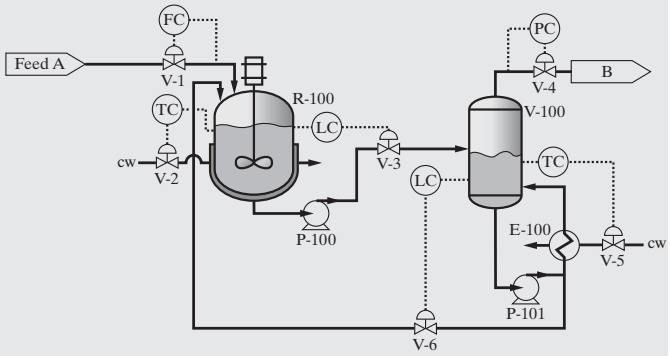

Figure 20.15 Control structure for reactor-flash-recycle process based on unit-by-unit design approach.

kn_T. A more general result relies on reformulating Eq. (20.18) in terms of the Damköhler number, $Da = kn_T/F_0$, giving:

$$B = \frac{F_0}{Da - 1} \tag{20.19}$$

Equation (20.19) shows that for values of *Da* much larger than unity, no snowball effect is expected. The snowball effect occurs as *Da* approaches a critical value of 1 and is eliminated by controlling the recycle flow rate as shown next.

To generate a workable plantwide control system as shown in Figure 20.16, the design procedure for plantwide control by Luyben and co-workers (1999) is applied:

Step 1: ***Set Objectives.*** To achieve the primary control objective, the production level is maintained by flow control of the feed stream using valve V-1.

Step 2: ***Define Control Degrees of Freedom.*** The process has six degrees of freedom.

Step 3: ***Establish the Energy-management System.*** The reactor temperature, which affects the process yield and stability (Guidelines 2 and 3), is controlled by adjusting the coolant flow rate, using valve V-2.

Step 4: ***Set the Production Rate.*** As stated previously, the feed valve, V-1, is assigned to a flow controller, whose setpoint regulates the production rate.

Step 5: ***Control Product Quality, and Meet Safety, Environmental, and Operational Constraints.*** A conventional pressure and temperature control system is set up for the flash vessel as in the previous example.

Step 6: ***Fix Recycle Flow Rates and Vapor and Liquid Inventories.*** To eliminate the snowball effect, the recycle flow rate must be controlled by installing a flow controller either on the reactor effluent or on the flash liquid effluent. As shown in Figure 20.16, the second option forces the reactor effluent valve, V-3, to control the flash vessel liquid inventory in the absence of other alternatives. Then, to regulate the reactor inventory, a cascade control system is designed in which the reactor level controller (LC) adjusts the setpoint of the feed flow controller (FC on V-1). This does not conflict with the objective to set the production rate by fixing the feed flow rate because in stable operation, the reactor level and feed flow rate vary proportionally through higher conversion in the CSTR. The vapor product valve, V-4, which has been assigned to control the pressure, thereby controls the vapor inventory.

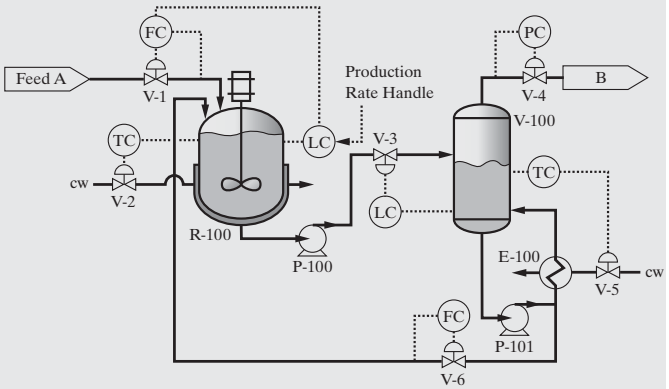

Figure 20.16 Workable plantwide control structure for reactor-flash-recycle process.

Steps 7 and 8: ***Check Component Balances and Control Individual Process Units.*** As in Example 20.10, the controllers assigned thus far prevent the buildup of A and B in the process. Both of the individual units are adequately controlled already, and in any case, no valves are left unassigned.

Step 9: ***Optimize Economics and Improve Dynamic Controllability.*** To maximize conversion, a cascade controller is installed as in the previous example in which the setpoint of the reactor temperature controller (TC on V-2) is adjusted to control the concentration of B in the reactor effluent. Again, for an irreversible reaction, it is enough to operate the reactor at the highest possible temperature.

EXAMPLE 20.12 *Plantwide Control System Configuration for the Vinyl-chloride Process*

For the vinyl-chloride process synthesized in Section 2.3 and shown in Figure 20.17, a preliminary design of its plantwide control system helps to assess the ease of maintaining the desired production level. This is achieved following the design procedure of Luyben and co-workers (1999):

Step 1: ***Set Objectives.*** Note that nearly 100% conversion is achieved in the dichloroethane reactor (R-100). Assuming that the conversion in the pyrolysis furnace (F-100) cannot be altered, the production level can be maintained by flow control of the ethylene feed flow rate using valve V-1.

Step 2: ***Determine the Control Degrees of Freedom.*** Twenty control valves have been positioned in the PFD, as shown in Figure 20.17.

Step 3: ***Establish the Energy-management System.*** The coolant valve, V-3, in the overhead condenser of the exothermic dichloroethane reactor, R-100, is used for temperature control. The yield in the pyrolysis furnace, F-100, is controlled by maintaining the outlet temperature at 500°C using the fuel gas valve, V-6. To attenuate the effect of temperature disturbances, the flow rates of the utility streams are adjusted to regulate effluent temperatures in the evaporator, E-101 (using V-5); the quench tank, V-100 (using the cooler E-102 and manipulating V-7); the partial condenser, E-103 (using V-8); and the recycle cooler, E-108 (using V-20). All of these valves act rapidly and directly on the controlled outputs (Guidelines 6, 7, and 8). Note that the temperature control loops using utility exchangers ensure that temperature disturbances are not recycled (Guideline 9).

Step 4: ***Set the Production Rate.*** As stated previously, the feed valve, V-1, is assigned to a flow controller, whose setpoint regulates the production rate.

Step 5: ***Control Product Quality and Meet Safety, Environmental, and Operational Constraints.*** The overhead product compositions in both distillation columns are regulated by adjusting the reflux flow rates using valves V-11 and V-16, both of which provide fast, direct control action (Guidelines 6, 7, and 8). The bottoms product compositions are controlled using the reboiler steam valves, V-13 and V-18. Thus, the control systems for both columns are in the LV-configuration. Valve V-9 is used to regulate the pressure in the feed to T-100. Because V-14 is needed for sump level control in T-100, it is not available for regulation of the feed pressure of T-101, and the addition of a pressure regulator should be considered for this purpose.

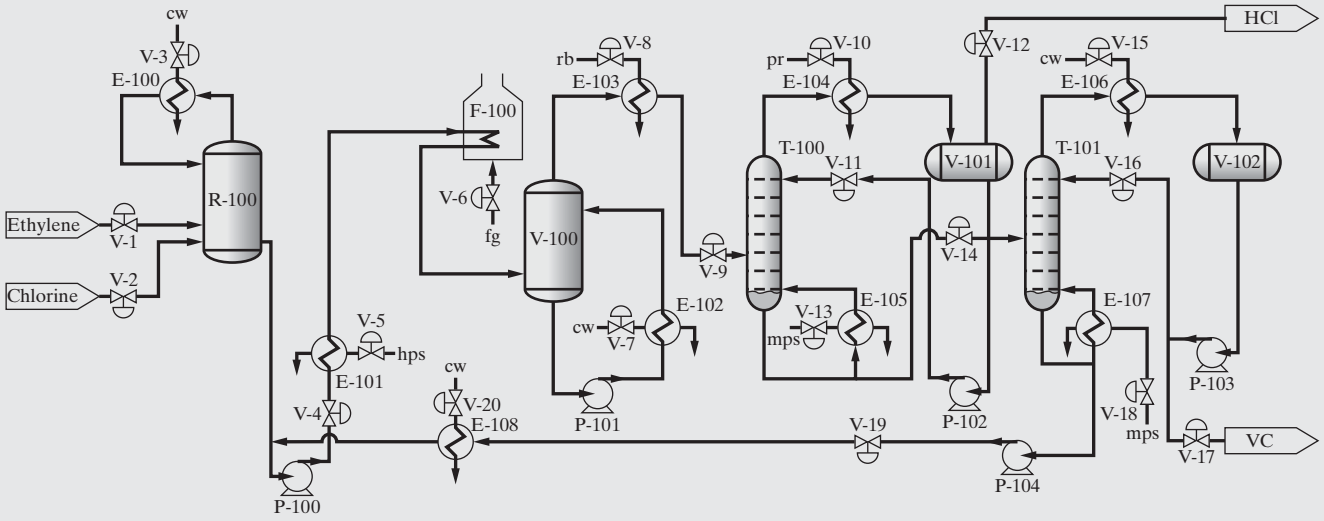

Figure 20.17 Control valve placement for the vinyl-chloride process.

Step 6: ***Fix Recycle Flow Rates and Vapor and Liquid Inventories.*** Inventory control of T-101 is assigned first. The bottoms flow rate in T-101, adjusted by valve V-19, is used for sump level control. The liquid level in reflux drum V-102 is controlled by manipulating the distillate valve, V-17. Inventory control for T-101 is completed by controlling the overhead pressure using the coolant valve, V-15. Turning to the HCl column, T-100, the bottoms product valve, V-14, is assigned to control the sump level. Because the overhead product is vapor, the condenser pressure is regulated using the distillate valve, V-12. Inventory control of T-100 is completed by assigning the condenser coolant valve, V-10, to regulate the reflux drum liquid level. The recycle flow rate must be held constant by flow control, and since V-19 is not available, a flow controller is installed to fix the combined recycle and feed flow rates using V-4. The level controller for R-100 is cascaded with the ethylene flow controller, making the level setpoint the production handle as in Example 20.11 (see Figure 20.16).

Steps 7 *and* 8: ***Check Component Balances and Control Individual Unit Operations.*** At this point, all but one of the valves (V-2) has been assigned. To ensure a stoichiometric ratio of reagents entering reactor R-100, the chlorine feed is adjusted to ensure complete conversion of the ethylene using a composition controller on the reactor effluent.

Step 9: ***Optimize Economics and Improve Dynamic Controllability.*** As in the previous example, to improve the range of production levels that can be tolerated, the setpoint of the recycle flow controller is set in proportion to the feed flow rate, suitably lagged for synchronization with the propagation rate through the process.

The complete control system is shown in Figure 20.18. Many of the qualitative decisions need to be checked by quantitative analysis or by simulation. For example, the interaction between the control systems of the two columns may require careful controller tuning. These refinements are discussed in the supplement to this chapter.

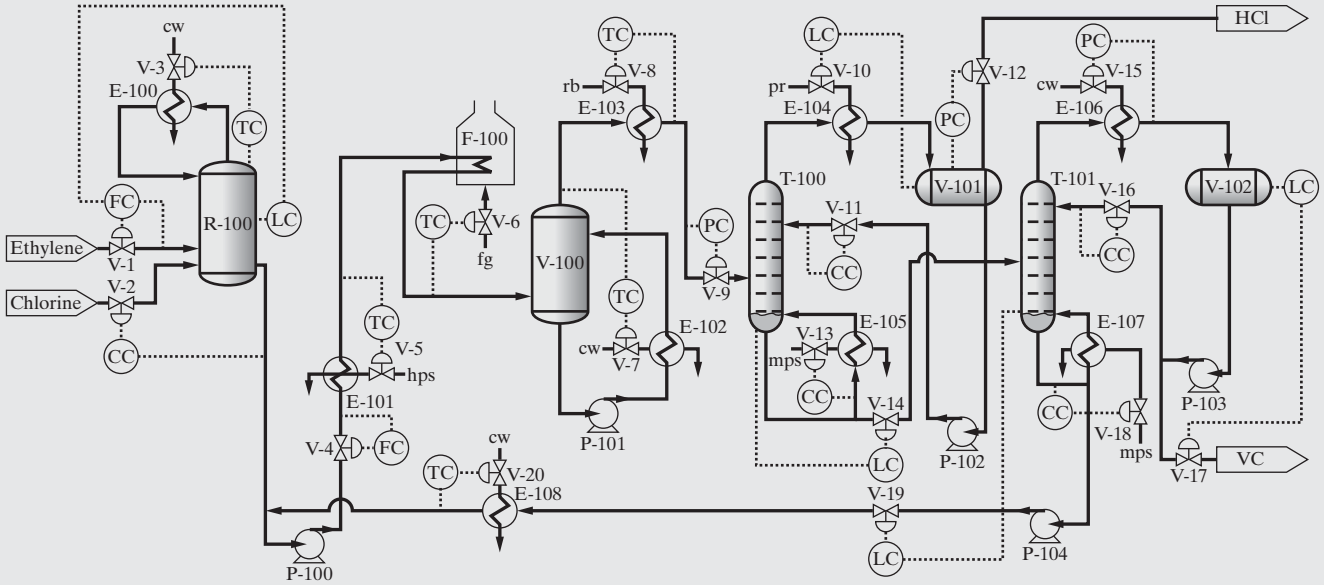

Figure 20.18 Control system for the vinyl-chloride process.

20.4 SUMMARY

This chapter has introduced the importance of considering plantwide control early in the design process. A qualitative control synthesis method combining the approaches suggested by Newell and Lee (1988) and Luyben and co-workers (1999) was presented to show how to generate alternative control configurations. The limitations of this qualitative approach have been highlighted, and the need for the quantitative approach presented in the supplement to this chapter, which involves analysis and dynamic simulation, has been established.

After studying this chapter, the reader should be able to:

1. Identify potential control problems in a process flowsheet.
2. Classify and select controlled and manipulated variables for a plantwide control system.
3. Perform a conceptual synthesis of plantwide control structures (pairings) based on degrees-of-freedom analysis and qualitative guidelines.

SUPPLEMENT TO CHAPTER 20—FLOWSHEET CONTROLLABILITY ANALYSIS

A supplement to Chapter 20, Flowsheet Controllability Analysis, is provided in the PDF Files folder, which can be downloaded from the Wiley Web site associated with this textbook. (See the file Supplement_to_Chapter 20.pdf.) The contents of this supplement are:

REFERENCES

1. Al-Arfaj, M. A., and W. L. Luyben, "Control of Ethylene Glycol Reactive Distillation Column," *AIChE J.*, **48**, 905–908 (2002).

2. Bildea, C. S., A. C. Dimian, and P. D. Iedema, "Nonlinear Behavior of Reactor-separator-recycle Systems," *Comput. Chem. Eng.*, **24**(2), 209–215 (2000).

3. Chiang, T., and W. L. Luyben, "Comparison of the Dynamic Performances of Three Heat-Integrated Distillation Configurations," *Ind. Eng. Chem. Res.*, **27**, 99–104 (1988).

4. Kiss, A. A., C. S. Bildea, A. C. Dimian, and P. D. Iedema, "State Multiplicity in CSTR-Separator-Recycle Systems," *Chem. Eng. Sci.*, **57**(4), 535–546 (2002).

5. Luyben, W. L., *Process Modeling, Simulation, and Control for Chemical Engineers*, 2nd ed., McGraw-Hill, New York (1990).

6. Luyben, W. L., "Snowball Effects in Reactor/Separator Processes with Recycle," *Ind. Eng. Chem. Res.*, **33**, 299–305 (1994).

7. Luyben, W. L., B. D. Tyreus, and M. L. Luyben, *Plantwide Process Control*, McGraw-Hill, New York (1999).

8. Mcavoy, T. J., *Interaction Analysis*, Instrument Society of America, Research Triangle Park, North Carolina (1983).

9. Newell, R. B., and P. L. Lee, *Applied Process Control*, Prentice-Hall of Australia, Brookvale, NSW (1988).

10. Seborg, D. E., T. F. Edgar, and D. A. Mellichamp, *Process Dynamics and Control, Chapter 28*, Wiley, New York (1989).

11. Shinskey, F. G., *Distillation Control*, 2nd ed., McGraw-Hill, New York (1984).

12. Skogestad, S., "Plantwide Control: Towards a Systematic Procedure," in J. Grievink and J. van der Schijndel (eds.), *Computer Aided Chemical Engineering-10*, European Symposium on *Computer Aided Process Engineering-12*, Elsevier (2002).

13. Stephanopoulos, G., *Chemical Process Control, Chapter 23*, Prentice-Hall, Englewood Cliffs (1984).

14. Weitz, O., and D. R. Lewin, "Dynamic Controllability and Resiliency Diagnosis Using Steady State Process Flowsheet Data," *Comput. Chem. Eng.*, **20**(4), 325–336 (1996).

15. Wu, K. L., and C. C. Yu, "Reactor/Separator Process with Recycle-1. Candidate Control Structures for Operability," *Comput. Chem. Eng.*, **20**(11), 1,291–1,316 (1996).

EXERCISES

20.1 Perform a degrees-of-freedom analysis for the noninteracting exothermic reactor shown in Figure 20.3a. Suggest an appropriate control structure. Carry out the same exercise for the heat-integrated reactor shown in Figure 20.3b. Compare the results.

20.2 Consider the mixing vessel shown in Figure 20.19. The feed stream flow rate, F_1, and composition, C_1, are considered to be disturbance variables. The feed is mixed with a control stream of flow rate F_2 and constant known composition, C_2. To ensure a product of constant composition, it is also possible to manipulate the flow rate, F_3, of the product stream. Perform a degrees-of-freedom analysis and suggest alternative control system configurations. Note that unsteady-state balances are required.

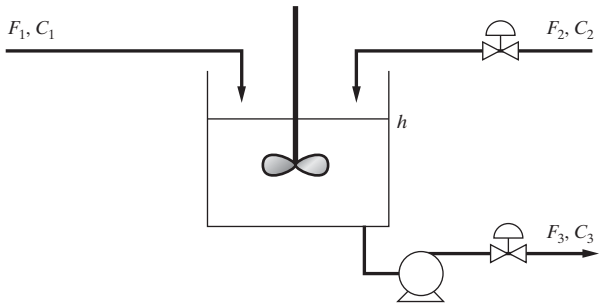

Figure 20.19 Mixing vessel.

20.3 Consider the FS two-column configuration for the separation of methanol and water in Figure 20.2 and (a) determine the number of degrees of freedom for the overall system, (b) determine the number of controlled and manipulated variables, and (c) select a workable control configuration using qualitative arguments.

20.4 Repeat Exercise 20.3 for the LSF configuration in Figure 20.2.

20.5 A control system is suggested for the exothermic reactor in Figure 20.7. Suggest alternative configurations and compare them with the original configuration.

20.6 Figure 12.20 shows a process for the isothermal production of C from A and B (A + B → C). The two reagents are fed to a CSTR, R-100, where complete conversion of B is assumed. The reactor effluent stream consisting of C and unreacted A is separated in a distillation column, T-100, where the more volatile A is withdrawn in the distillate and recycled, and product C is withdrawn in the bottoms stream. Your task is to devise a conceptual plantwide control system for the process.

Hint: It may be helpful to reposition the feed stream of A.

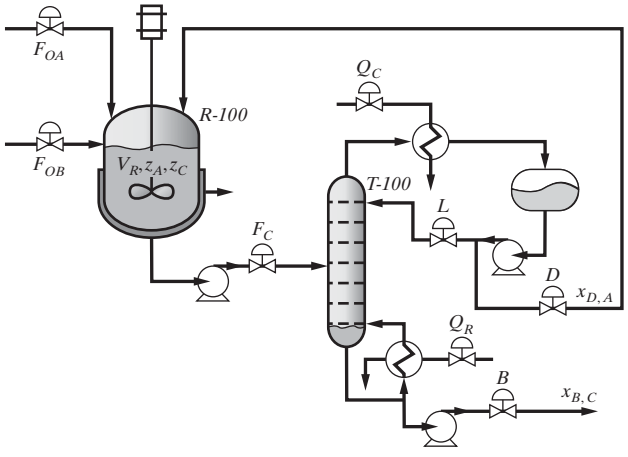

Figure 20.20 Process flowsheet for Exercise 20.6.

20.7 Figure 20.21 shows the flowsheet for a reactive distillation column for the production of ethylene glycol (EG) from ethylene oxide (EO) and water (Al-Arfaj and Luyben, 2002):

$$EO + H_2O \rightarrow EG$$

Note that the reaction proceeds to 100% conversion in the column with part of the EG undergoing a secondary (undesired) reaction to diethylene glycol (DEG):

$$EO + EG \rightarrow DEG$$

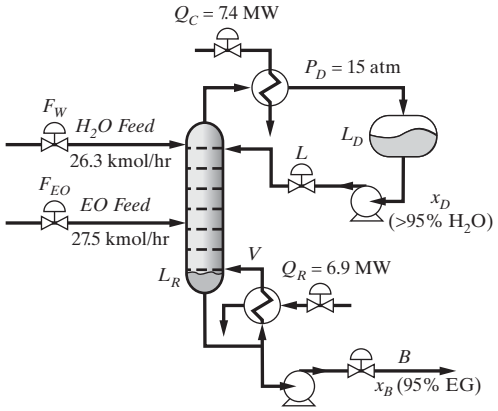

Figure 20.21 Ethylene glycol reactive distillation column.

For this reason, the EO is fed to the column in slight excess. The EG product is withdrawn as the bottoms stream, and almost pure water concentrates at the top of the column. Your task is to use the procedure of Luyben and co-workers, showing all steps, to devise a conceptual plantwide control system for the process with the following objectives:

(a) Control production rate.

(b) Ensure the EG product is at the required concentration.

20.8 Figure 20.22 shows the monochlorobenzene separation process introduced in Section 7.4. The process involves a flash vessel, V-100; an absorption column, T-100; a distillation column, T-101; a reflux drum, V-101; and three utility heat exchangers. As shown in Figure 20.22, most of the HCl is removed at high purity in the vapor effluent of T-100. However, in contrast with the design shown in Chapter 7, the design in Figure 20.22 does not include a "treater" to remove the residual HCl; instead, it is purged in a small vapor overhead product stream in T-101. The benzene and monochlorobenzene are obtained at high purity as distillate and bottoms liquid products in T-101. Note that the 12 available control valves are identified. Your task is to design a conceptual control system to ensure that the process provides stable production at a desired level while meeting quality specifications.

20.9 Figure 20.23 shows a heat-integrated process for the manufacture of vinyl chloride. This design sharply reduces the utilization of utilities in Figure 20.17 without requiring additional heat exchangers. Design a conceptual control system for the same control objectives in Example 20.12.

Hint: To provide sufficient degrees of freedom, it may be necessary to add heat exchanger bypasses and/or trim utility exchangers.

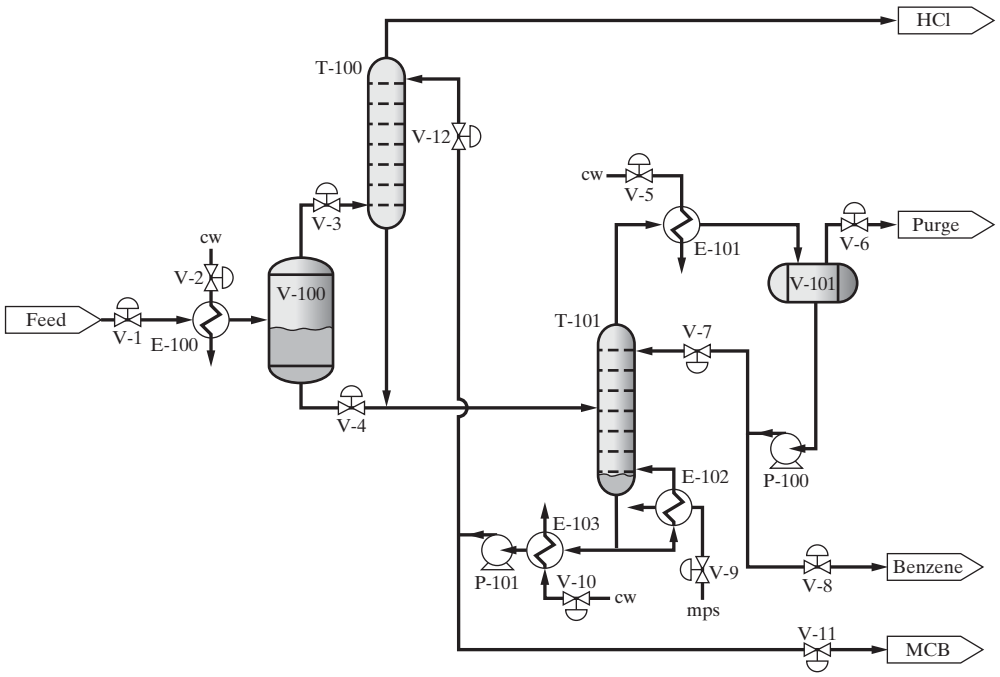

Figure 20.22 Process flowsheet for the MCB separation process.

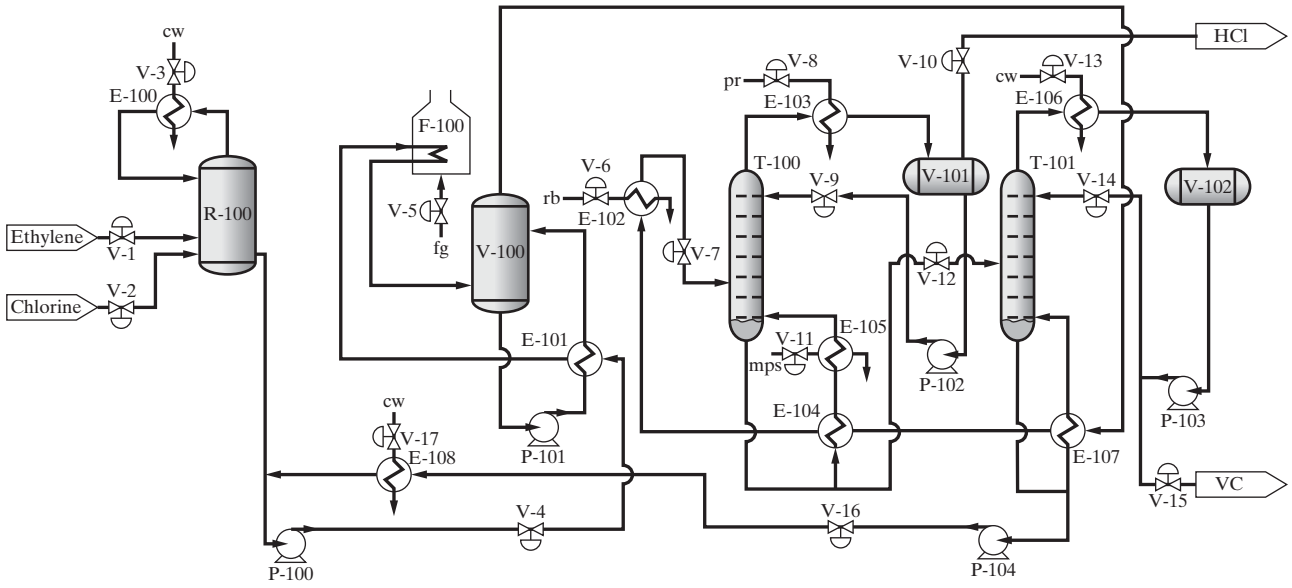

Figure 20.23 Process flowsheet for the heat-integrated vinyl-chloride process.

20.10 How would the control configuration for the vinyl-chloride process in Figure 20.18 change if the primary control objective is to provide on-demand vinyl-chloride product?

20.11 Figure 20.24 shows the flowsheet for a process for the production of methanol from synthesis gas (a mixture of hydrogen, carbon monoxide, and carbon dioxide and a small quantity of residual methane, which is inert in this process). In the process, the feed stream undergoes compression from 13 to 48 bar in compressor K-100, is then mixed with the recycle, and then is further compressed to 50 bar in compressor K-101. Both of the compressors are driven by turbines fed with high-pressure steam (hps). The high-pressure combined feed is heated to ignition temperature in heat exchanger E-100 and is then fed to the adiabatic reactor R-100, where it undergoes partial conversion to methanol and water as limited by the equilibrium conditions. The hot reactor effluent is used to preheat the feed in E-100, and is then further cooled in E-101 before being flashed in V-100. The vapor stream product from V-100 is recycled after a fraction is purged (to remove the inert methane fed in the process feed). The pressure of the liquid product stream from V-100 is reduced to 10 bar in pressure regulator V-7 and is then fed to distillation column T-100, where it is separated into a water/methanol mixture in the distillate and high-purity water in the bottoms. The distillate from T-100 undergoes further pressure reduction to 2 bar in pressure regulator V-13 and is then fed to a second

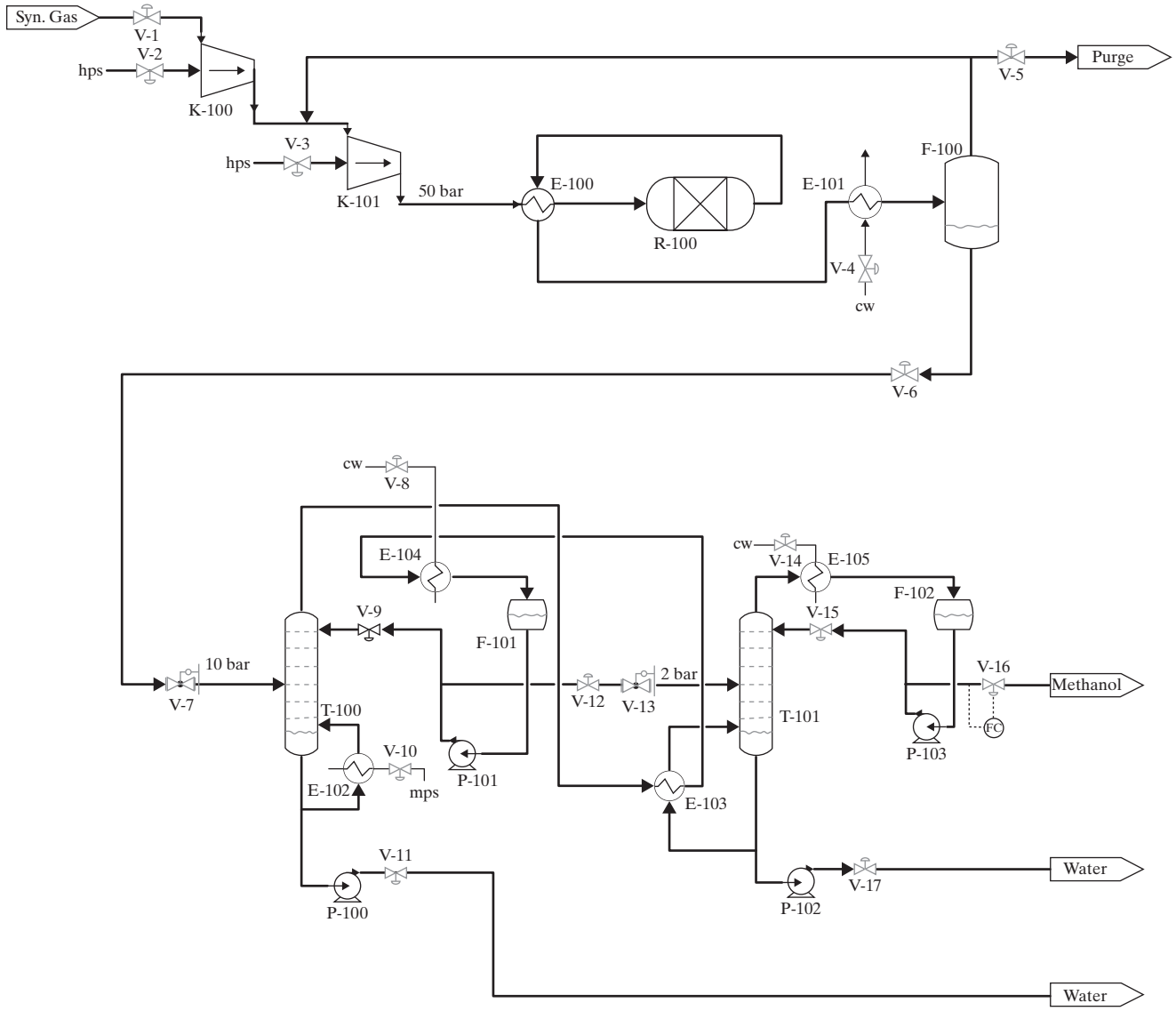

Figure 20.24 Process flowsheet for the production of methanol from synthesis gas.

column, T-101, which produces high-purity methanol as the distillate and high-purity water as bottoms. This arrangement enables the partial condensation of the overhead stream in T-100 to provide all of the heat of evaporation needed in the reboiler of T-101 in heat exchanger E-103, with the remaining condensation duty provided by the cooler E-104.

You are requested to suggest a plantwide control system to enable stable operation of the process in Figure 20.24, while satisfying the following requirements:

(a) Methanol production on demand; thus, valve V-16 is already assigned to accomplish flow control of the product stream as shown in Figure 20.24.

(b) Methanol product composition on specification.

(c) Maximum methanol recovery from the process.

(d) Maximum conversion to methanol in R-100.

Note: As indicated in Figure 20.24, the dispositions of three valves have already been resolved: V-16 is assigned to flow control for on-demand product, and both V-7 and V-13 are assigned for pressure regulation of column feed streams. Your solution should follow the procedure of Luyben et al. and include the positioning of all control loops in the PFD of Figure 20.24. You are allowed to add control valves to those already in place in the PFD, but only if these are absolutely necessary to meet the requirements.

20.12 Figure 20.25 shows the flowsheet for a process for the production of synthesis gas (a mixture of hydrogen, carbon monoxide, and carbon dioxide and a small quantity of unreacted residual methane) from methane, steam, and oxygen. The feed stream of methane is mixed with steam that is generated using waste heat generated in the process, heated in E-100 and then fed to the reformer R-100, where partial conversion of the methane to hydrogen and CO takes place. The heat demanded by this endothermic reaction is provided by the combustion of fuel gas (fg) in R-100. The hot reformer effluent stream first feeds E-100 to preheat the reformer feed as stated and is then further cooled in E-101, mixed with the oxygen feed stream, and then fed to the adiabatic oxidation reactor, R-101, where the remaining methane reacts to produce more hydrogen and CO_2. The effluent from R-101 is cooled in E-102 and then fed to the adiabatic shift reactor, R-102, where it is possible to control the ratio of $CO : CO_2$ (depending on the feed temperature to R-102). The effluent stream from R-102 is cooled in E-103 and then fed to the flash vessel

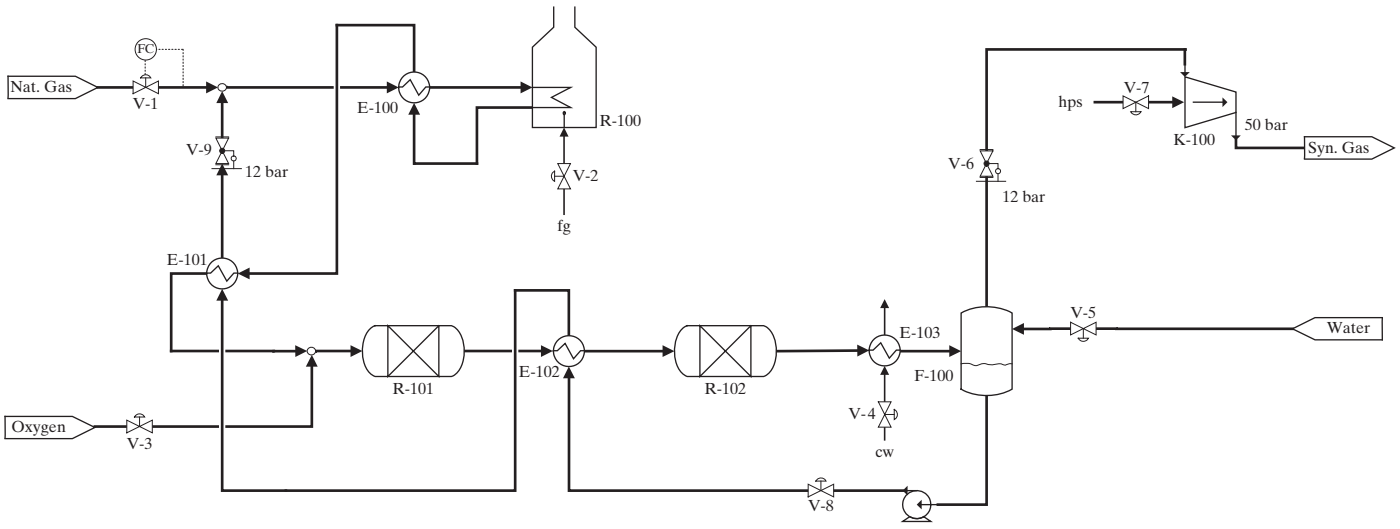

Figure 20.25 Process flowsheet for the production of synthesis gas from natural gas.

F-100, where the water in the synthesis gas condenses and is drawn off as the liquid effluent stream, which is recycled back to the process feed after being converted to saturated steam by heat exchange with hot process streams in E-102 and E-101. The vapor effluent from F-100 is compressed in K-100 to 50 bar and is the desired synthesis gas.

You are requested to suggest a plantwide control system to enable stable operation of the process in Figure 20.25 while satisfying the following requirements:

(a) *Fixed feed* methane consumption; thus, valve V-1 is already assigned to accomplish flow control of the methane feed stream as shown in Figure 20.25.

(b) Controlled hydrogen production rate in the reformer by regulation of the methane/steam ratio in the feed to R-100.

(c) Control of the $H_2 : CO_2$ ratio in the oxidation reactor (R-101) effluent.

(d) Control of the $CO : CO_2$ ratio in the shift reactor (R-102) effluent.

(e) Minimization of the energy consumption in the reformer.

Note: As indicated in Figure 20.25, the dispositions of three valves have already been resolved: V-1 is assigned to flow control for fixed-feed configuration, V-6 is assigned for pressure regulation of F-100 vapor flow, and V-9 is used to maintain the desired pressure of the saturated steam generated using the water recycle stream. Your solution should follow the procedure of Luyben et al. and should include the positioning of all control loops in the PFD of Figure 20.24. You are allowed to add control valves to those already in place in the PFD, but only if these are absolutely necessary to meet the requirements.

20.13 Figure 20.26 shows the flowsheet for a process for the production of G from A. The feed stream of A (entering through valve V-1) is mixed with a makeup stream of B (entering through valve V-2) and a recycle stream composed mostly of B, and the resulting stream is heated in E-100 and then fed to adiabatic PFR, R-100 in which occurs the exothermic reaction: $A + B \rightarrow C + D$. The R-100 effluent is separated in column T-100 into a bottoms stream rich in D, and a distillate rich in C. The distillate is mixed with a makeup stream of F (entering through valve V-8) and an F-rich recycle stream, and the resulting stream is heated in E-103 and then fed to adiabatic PFR, R-101 in which occurs the exothermic reaction: $C + F \rightarrow E + B$. The R-101 effluent is separated in column T-101 into a bottoms stream rich in E and a distillate rich in B, which is recycled. The bottoms from T-101 (rich in E) is mixed with the bottoms from T-100 (rich in D) and a makeup stream of E (entering through valve V-14), and the resulting stream is heated in E-106 and then fed to adiabatic PFR, R-102 in which occurs the exothermic reaction: $D + E \rightarrow F + G$. The R-102 effluent is separated in column T-102 into a bottoms stream rich in G and a distillate rich in F, which is recycled. The relative volatilities of the participating components are in the order: $\alpha_A > \alpha_B > \alpha_C > \alpha_D > \alpha_E > \alpha_F > \alpha_G$.

You are requested to suggest a plantwide control system to enable stable operation of the process providing G on demand. Your solution should follow the procedure of Luyben et al. and should include the positioning of all control loops in the PFD of Figure 20.26. You are allowed to add control valves to those already in place in the PFD, but only if these are absolutely necessary to meet the requirements.

20.14 Figure 20.27 shows the flowsheet for a process for the production of gasoline (mainly octane) from an olefins feed (propane, propene, and butene). The feed to the process is heated in E-100, and then E-101, and then fed to a cascade of three PFRs operating at 500 psia where it is partially converted to gasoline (mainly octane), with temperature control affected using cold shots of propane. The hot reactor effluent stream is used to preheat the reactor feed in E-100 and is then fed to the first column, T-100, after pressure reduction to 200 psia by the pressure regulator, PRV-1, where the propane is removed as the distillate with the remaining components leaving as bottoms. Part of the propane is recycled at 500 psia for use as cold shot in the reactor cascade. The bottoms from T-100 are reduced to 90 psia by the pressure regulator, PRV-2, and then fed to the second column, T-101, which separates it into butane as distillate and gasoline as bottoms. All of the product streams are cooled using cooling water.

You are requested to suggest a plantwide control system to enable stable operation of the process providing gasoline on demand. Your solution should follow the procedure of Luyben et al. and should include the positioning of all control loops in the PFD of Figure 20.27. You are allowed to add control valves to those already in place in the PFD, but only if these are absolutely necessary to meet the requirements.

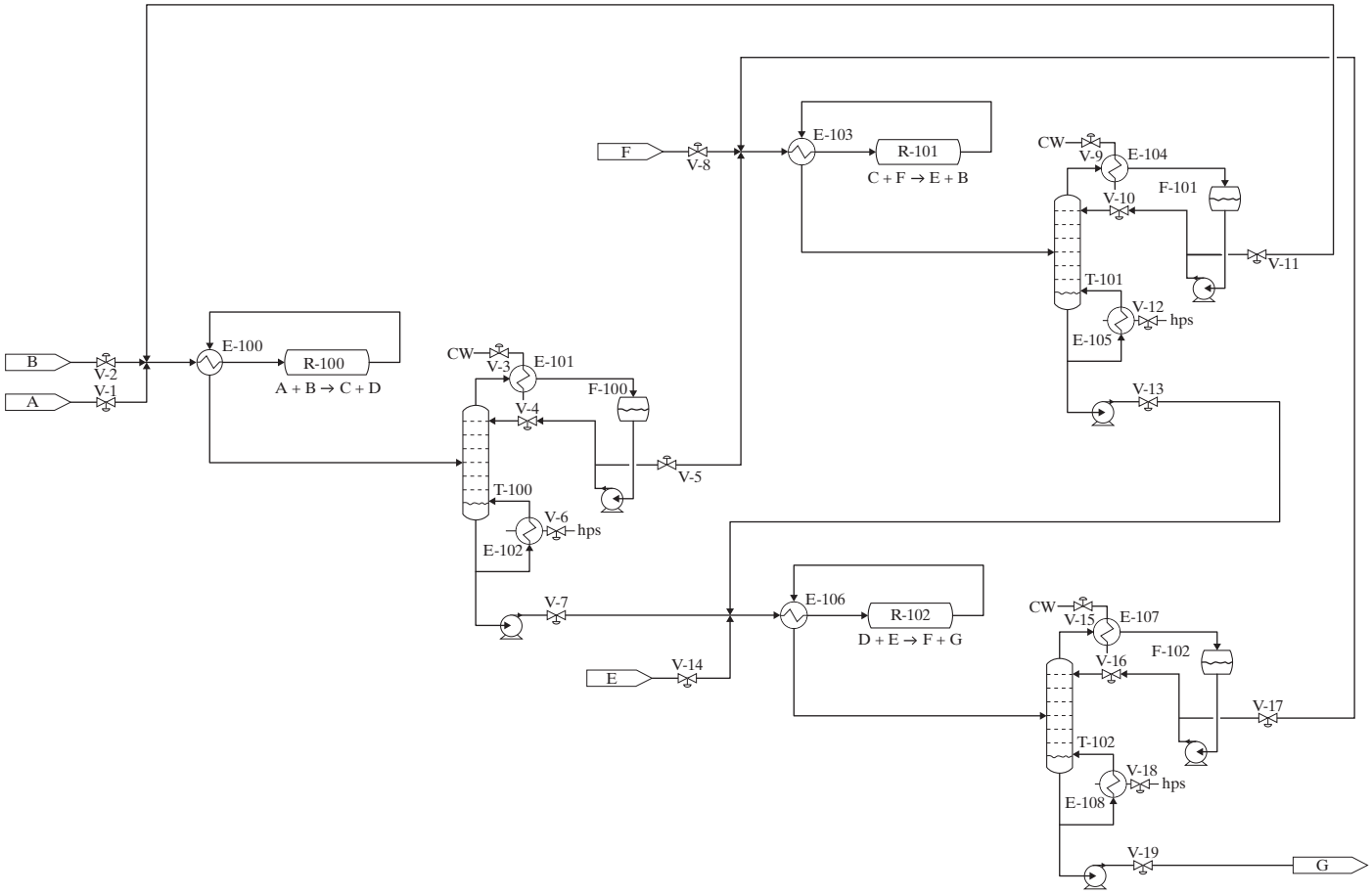

Figure 20.26 Process flowsheet for the production of G from A.

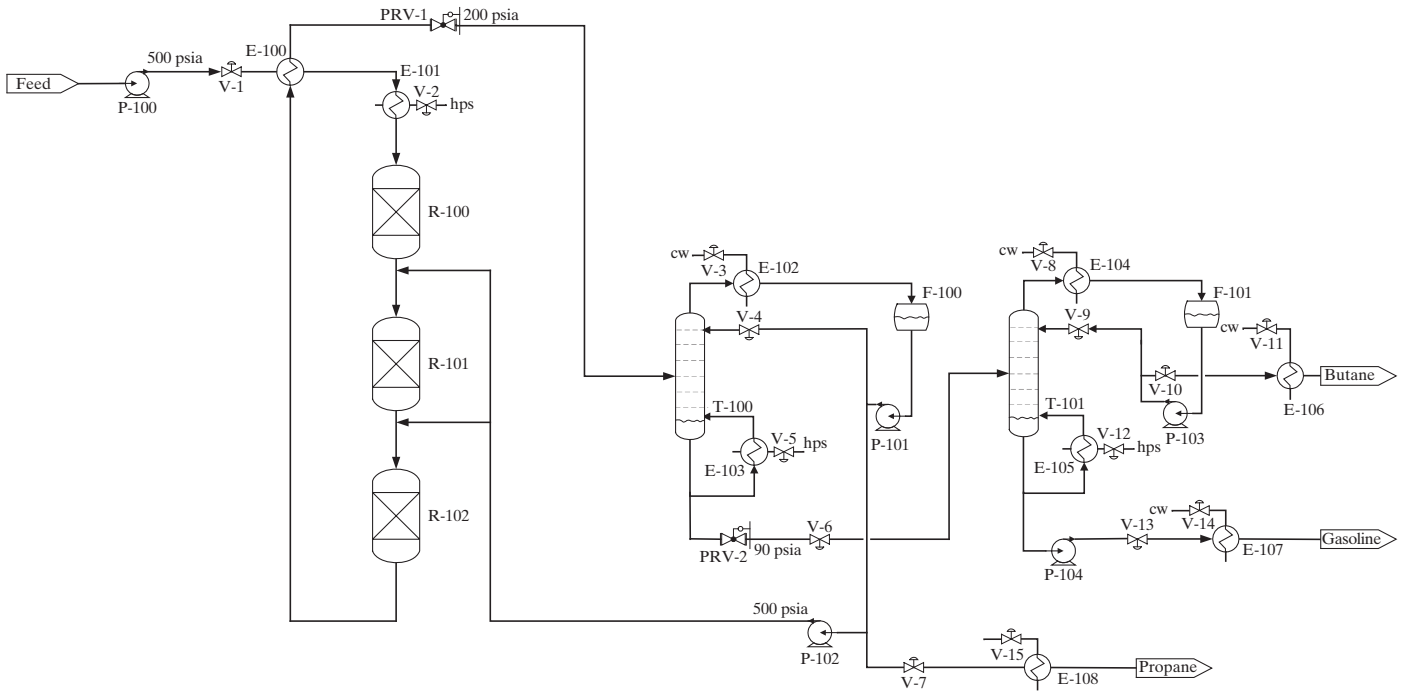

Figure 20.27 Process flowsheet for the production of gasoline from olefines.

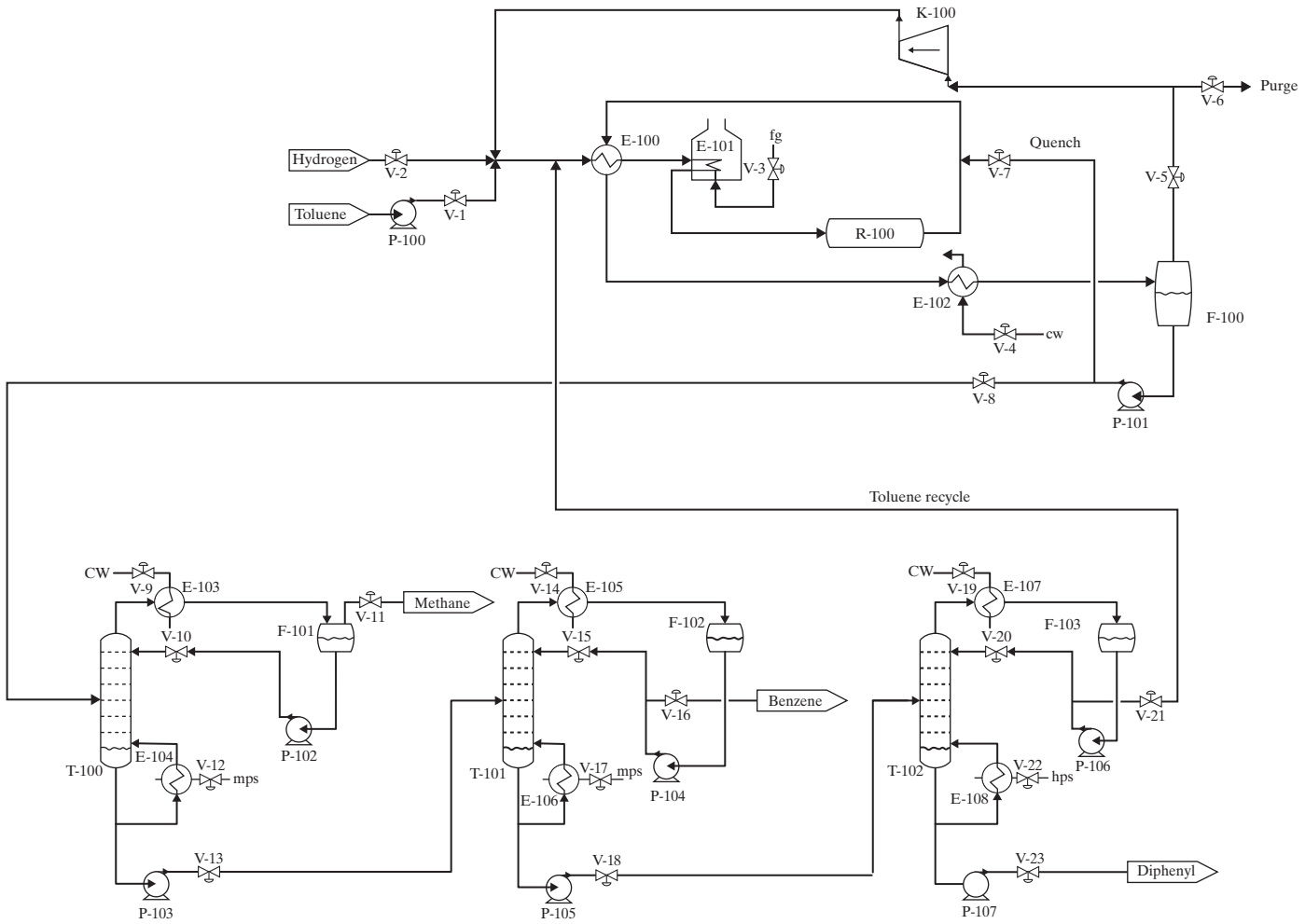

Figure 20.28 Process flowsheet for the HDA process.

20.15 Figure 20.28 shows the flowsheet for the HDA process for the production of benzene from toluene and hydrogen. Feed streams of toluene (entering through valve V-1) and hydrogen (entering through valve V-2) are mixed with a liquid recycle stream rich in toluene and a vapor recycle stream rich in hydrogen, and the combined stream is preheated first in E-100, and then vaporized and superheated in furnace E-101. The vaporized mixture of toluene and hydrogen is fed to the adiabatic PFR, R-100, where they mostly undergo partial conversion to the desired main products, benzene and methane, as well a small portion to the undesired byproduct, diphenyl. The hot reactor effluent is cooled by heat exchange with the reactor feed in E-100 and then by cooling water in E-102 before being flashed in F-100. A portion of the hydrogen-rich vapor product stream from F-100 is purged through valve V-6 to attenuate the methane content and then compressed in K-100 and recycled. The compressor is operated at maximum capacity to enable production rate to be maximized. A portion of the liquid product stream from F-100 is recycled and mixed with the reactor effluent stream to cool it before it enters E-100, but most of it is fed to a separation system consisting of three columns in series.

In the first column, T-100, the reactor products are separated into a methane-rich distillate with the other components exiting as a feed stream to the second column, T-101, which produces a benzene-rich distillate and a mixture of toluene and diphenyl as bottoms. This is fed to the last column, T-102, which separates it into a toluene-rich distillate, which is recycled, and a bottoms stream consisting largely of diphenyl.

You are requested to suggest a plantwide control system to enable stable operation of the process, while regulating the production rate. Your solution should follow the procedure of Luyben et al. and should include the positioning of all control loops in the PFD of Figure 20.28. You are asked not to add control valves to those already in place in the PFD or any additional utility heaters and coolers.

Chapter 21

Design Optimization

21.0 OBJECTIVES

This chapter begins with a brief discussion of the fundamental principles of optimization, which are presented in much more detail by Beveridge and Schechter (1970), Edgar et al. (2001), and Ravindran et al. (2006). These principles are then applied to the use of flowsheet simulators to optimize the most promising flowsheets during process design. Two process examples are presented. The first involves maximizing the venture profit (VP) of a process for the production of ethyl chloride. In the second example, the separation afforded by a distillation column with sidestreams is maximized, typical of an optimization carried out during the development of a base case design.

After studying this chapter and the multimedia modules, which can be downloaded from www.seas.upenn.edu/~dlewin/multimedia.htlm, the reader should:

1. Be able to explain the fundamentals of optimization to a layperson.
2. Be conversant with the theory of analytical or numerical methods for treating optimization problems.
3. Be able to solve linear programming (LP) problems that can be expressed in one or two decision variables by hand and problems of higher dimension using MATLAB.
4. Be able to use the golden-section search to solve a constrained nonlinear programming (NLP) problem in one decision variable.
5. Be able to formulate a nonlinear optimization problem (NLP) to maximize or minimize an objective function by adjusting continuous decision variables in the model of the process.
6. Be able to use process simulators to solve an NLP.

21.1 INTRODUCTION

From a mathematical point of view, chemical engineers deal with three types of problems when solving equations. The first type, which is the subject of most undergraduate textbooks in chemical engineering and has been the main subject of this book to this point, is the *completely specified* case in which the number of equations, N_E, to be solved is equal to the number of variables, N_V, to be determined. The equations to be solved are usually at least partially nonlinear, and the challenge is to find a method that will solve them. This case is complicated by the fact that more than one practical solution may exist, a challenge that has been largely ignored in process simulators. The second type is common in experimental work and process operations, where $N_V < N_E$. This is the *overspecified* case, which is commonly referred to as the reconciliation (or data reconciliation and rectification) problem. An example of this case is a piece of equipment operating under steady-state conditions with all or some of the variables (e.g., component flow rates, measured). Because the measurements are subject to error, they do not satisfy material-balance equations. The task with this case is to determine the most likely values for the variables. This case is not covered in this book, but is discussed by Mah (1990). The third case is the subject of this chapter, *optimization*, in which the problem is *underspecified* such that $N_V > N_E$. The problem is to select from the set of variables, $\underline{x}$, a subset of size

$$N_V - N_E = N_D \tag{21.1}$$

called the *decision variables*, $\underline{d}$, and to iteratively adjust the decision variables to achieve the optimal solution to a specified objective.

Optimization is normally applied to improve all designs, both product and process, at various stages in the design process. In the *concept* stage, optimization usually involves approximate models and objective functions sufficient to select from among numerous alternatives. Gradually, through the feasibility and development stages after eliminating less promising alternatives, the models and objectives become more rigorous. The optimization of process designs is very important, especially for the manufacture of commodity chemicals, which are produced in large quantities at relatively low prices. After having studied the steps in process creation and solved problems involving the synthesis of alternative process flowsheets in previous chapters (Chapters 2 and 6–11), it is appropriate to question whether a given flowsheet can and should be optimized by adjusting its key equipment parameters to increase some measure of its economic attractiveness. This optimization step is applied to the most promising process flowsheets after a base case has been evaluated in which the equipment has been sized, the capital and operating

costs have been estimated, and a profitability analysis has been completed. In many cases, however, optimizations are performed much earlier in process design using more approximate cost and profitability measures as shown in Examples 21.4 and 21.5.

As introduced in Supplement 11-1 to Chapter 11, formal methods of optimization can be utilized to optimize a superstructure of process units with streams that can be turned on and off using binary (integer) variables. The *mixed-integer formulation* (both continuous and integer variables) of the optimization problem in principle permits the optimizer to select simultaneously the best flowsheet and then optimize it with respect to its continuous variables, such as pressure levels, reflux ratios, residence times, and split fractions. In practice, however, most design problems are not solved using superstructures and mixed-integer optimization algorithms. Rather, as described throughout the earlier chapters, heuristics—many of which are presented in Chapter 6 with simulation and algorithmic methods presented in Chapter 7—are utilized to build and analyze *synthesis trees*. Although substructures, such as networks of heat exchangers, can be optimized conveniently using mixed-integer methods, it is impractical except for simple processes to attempt the optimization of entire process flowsheets in this manner. Accordingly, this chapter is restricted to the case of optimization problems involving continuous variables of either linear programming (LP) type or the nonlinear programming (NLP) type. Thus, mixed-integer linear programming (MILP) and mixed integer non-linear programming (MINLP) are mentioned only briefly.

This chapter focuses on the usage of process simulators to carry out the optimization simultaneously with converging the recycle loops and/or decision variables. To do the optimization efficiently, simulators use one of three methods: (1) *successive linear programming* (SLP), (2) *successive quadratic programming* (SQP), and (3) *generalized reduced gradient* (GRG). Emphasis in this chapter is placed on SQP used by ASPEN PLUS and UniSim® Design/ASPEN HYSYS. GRG, which is used by CHEMCAD, is not discussed here but is covered by Edgar et al. (2001).

21.2 GENERAL FORMULATION OF THE OPTIMIZATION PROBLEM

The formulation of an optimization problem involves:

1. A set of N_V variables, $\underline{x}$.
2. The selection of a set of appropriate *decision variables*, $\underline{d}$, from the set $\underline{x}$.
3. A measure of goodness called an *objective function*, $f\{\underline{x}\}$. (21.2)
4. A set of N_E equality constraints, $\underline{c}\{\underline{x}\} = 0$. (21.3)
5. A set of N_I inequality constraints, $\underline{g}\{\underline{x}\} \leq 0$. (21.4)
6. Lower and upper bounds on some or all of the variables, $\underline{x}^L \leq \underline{x} \leq \underline{x}^U$. (21.5)

A general optimization problem is stated as follows:

$$\begin{aligned} &\text{Minimize (or Maximize)} && f\{\underline{x}\} \\ &\quad \text{with respect to} && \qquad\qquad \textbf{(NLP1)} \\ &\quad \text{(w. r. t.) } \underline{d} \\ &&& \text{subject to (s. t.):} \\ &&& \underline{c}\{\underline{x}\} = 0 \\ &&& \underline{g}\{\underline{x}\} \leq 0 \\ &&& \underline{x}^L \leq \underline{x} \leq \underline{x}^U \end{aligned}$$

Objective Function and Decision variables

Candidates for the objective function, $f\{\underline{x}\}$, are often the profitability measures of Chapter 17 beginning with the approximate measures, such as the return on investment (ROI), the venture profit (VP), the payback period (PBP), and the annualized cost (C_A). For more thorough analyses, the rigorous measures that involve the time value of money and cash flows are used. These include the net present value (NPV) and the investor's rate of return (IRR). Other objective functions may involve measures that are related to costs or may involve safety, control, or pollution aspects. A multiobjective function consisting of two or more measures, each with a weighting coefficient, may also be employed, but such approaches are problematic with regards to how each term in the objective function is weighted. In any case, the objective function is a function of all of the decision variables, $\underline{d}$, and may also be a function of some or all of the other variables of the set, $\underline{x}$. Depending upon its nature, the objective function is minimized or maximized analytically or numerically by adjusting the values of the decision variables until the optimal solution is reached. When possible, it is best to select decision variables for which significant trade-offs are anticipated in the objective function. It is common to begin an optimization study with an approximate measure of goodness and switch to more rigorous measures when the design continues to be promising as the model of the flowsheet is refined.

Equality Constraints

In process design, the largest fractions of equality constraints, $\underline{c}\{\underline{x}\}$, are the modeling equations (usually algebraic) associated with processing equipment. For example, a distillation column with equilibrium stages may be modeled with hundreds of material balance, energy balance, and phase-equilibria equations in terms of the set of variables, $\underline{x}$. The NLP problem often involves hundreds and even thousands of equations. However, in the implementation of most simulators, these equations are solved for each process unit given equipment parameters and stream variables (usually for the feed streams) by using subroutines in a program library. Hence, when using simulators, the equations for the process units are not shown explicitly in the statement of the nonlinear programming problem. Given assumed values for the decision variables, the simulators call upon these subroutines to solve the appropriate equations and obtain the unknowns that

are needed to perform the optimization. However, certain specifications, especially those that involve more than one process unit, may require the user to formulate an equality constraint. As discussed in Chapter 7, process simulators are increasingly offering the option of using libraries of equality constraints in place of subroutines. This option is available in ASPEN PLUS and UniSim® Design.

Inequality Constraints

Inequality constraints, $\underline{g}\{\underline{x}\}$, are expressions that involve any or all of the set of variables, $\underline{x}$, and are used to bound the feasible region of operation. For example, when operating a centrifugal pump, the head developed decreases with increasing flow rate according to a pump characteristic curve. Hence, if the flow rate is varied when optimizing the process, care must be taken to make sure that the required pressure increase (head) does not exceed that available from the pump. The expression might be of the form,

$$\text{Pump head} \leq \text{a} - \text{b(Flowrate)} - \text{c (Flowrate)}^2$$

One can also introduce constraints to ensure compliance with operability, for example, the reflux ratio in distillation, which must exceed the minimum value for the required separation. If the distillation tower pressure is adjusted, the minimum reflux ratio will change and the actual ratio must be maintained above the minimum value. Important additional classes of inequality constraints are those that reflect on pollution prevention, safety, and controllability. For example, the operating temperature of an exothermic reactor should be maintained below a safe upper limit. Even when optimization is not performed, the decision variable values must be selected to avoid violating these inequality constraints. In some cases, the violations can be detected when examining the simulation results. In other cases, the unit subroutines are unable to solve the equations, for example, when the reflux ratio is adjusted to a value below the minimum value for a specified split of the key components.

Lower and Upper Bounds

Some inequality constraints simply place lower and upper bounds, $x^L \leq x \leq x^U$, on any or all of the variables, $\underline{x}$. Others permit the specification of just a lower bound or just an upper bound; for example, a lower bound on the fractional recovery of a species in a product stream. Sometimes the upper and lower bounds are included with the inequality constraints, but here, they are considered separately.

21.3 CLASSIFICATION OF OPTIMIZATION PROBLEMS

The combination of the equality constraints, inequality constraints, and lower and upper bounds defines a *feasible region*. A *feasible solution* is one that satisfies the equality constraints, the inequality constraints, and the upper and lower bounds for a feasible set of decision variables. If the solution also minimizes (or maximizes) the objective function, it is a *local optimal solution*. Sometimes, other local optimal solutions exist in the feasible region with one or more being a *global optimal solution*.

Many numerical methods have been devised for solving optimization problems. The choice of method depends upon the nature of the formulation of the problem. Therefore, it is useful to classify optimization problems with respect to certain categories.

When the objective function, equality constraints, and inequality constraints are linear with respect to the variables, $\underline{x}$, the problem is referred to as a *linear programming* (LP) problem. If the objective function, any of the equality constraints, and/or any of the inequality constraints are nonlinear with respect to the variables, the problem is referred to as a *nonlinear programming* (NLP) problem. The simplest optimization problems are those without equality constraints, inequality constraints, and lower and upper bounds. They are referred to as *unconstrained optimization*. Otherwise, if one or more constraints apply, the problem is one in *constrained optimization*.

For just a single decision variable (*unidimensional*), the feasible region and optimal solution(s) are conveniently displayed on a plot of $f\{x\}$ against x. The types of optimal solutions obtained depend both on the nature of the objective function and of the constraints. Figure 21.1 shows two different linear cases in which the only variable is designated x for the abscissa. An unconstrained *linear* objective function is shown in Figure 21.1a. In the absence of inequality constraints, no solution exists, unless one at $\pm\infty$ is meaningful. In Figure 21.1b, a linear objective function is again shown, but an upper bound is placed on x. Therefore, the feasible region is to the left of this upper bound as indicated by the arrows pointing to the left. When the maximum objective function is desired, the optimal solution is the bound. For linear objective functions, it can be shown that optimal solutions always occur at intersections between the objective function and the inequality constraints and/or lower and upper bounds.

Two cases of a nonlinear objective function that passes through a maximum are shown in Figure 21.2 with both constraints being a simple bound. The objective function is to be maximized. In Figure 21.2a, the constraint is a lower limit on x. Because the constraint is at a value of x less than the value at the maximum value of the objective function, the optimal value of x is that corresponding to the maximum value of the objective function and the

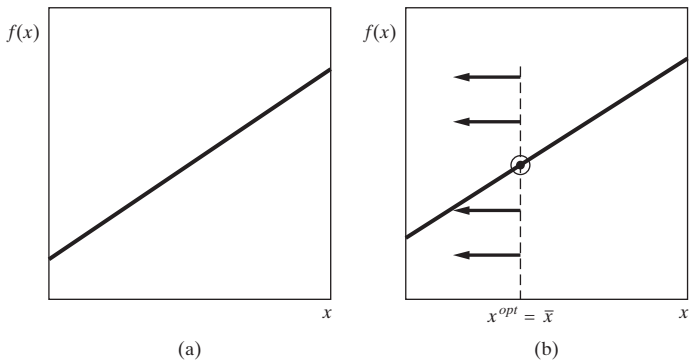

Figure 21.1 Linear objective function: (a) unconstrained; (b) subject to linear inequality constraint, $x \leq \bar{x}$.

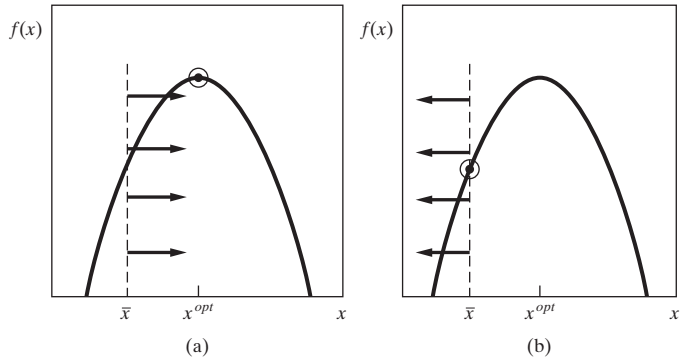

Figure 21.2 Nonlinear objective function: (a) subject to a slack constraint at $x \geq \bar{x}$; (b) subject to a binding constraint at $x \leq \bar{x}$.

constraint is referred to as a slack constraint. In Figure 21.2b, an upper bound is placed on x, and that bound is below the value at the maximum value of the objective function. Therefore, the optimal value of x is its upper bound, and the constraint is referred to as a binding constraint.

For two decision variables, a common display for the feasible region and optimal solution(s) is a plot of one decision variable against the other with contours of the objective function as shown in Figure 21.3. The optimization problem is to minimize the objective function:

$$f\{\underline{x}\} = y = 4x_1^2 + 5x_2^2$$

Two solutions are shown in Figure 21.3. The first is the unconstrained case in which the entire region is feasible. The solution, shown in Figure 21.3a, is at $x_2 = 0$ and $x_1 = 0$ where $y = 0$. The second is a constrained case with the inequality constraint:

$$g\{\underline{x}\} = 1 - x_1 \leq 0$$

This is a linear constraint that is easily converted to the constraint, $x_1 \geq 1$. Now, the feasible (valid) region is situated to the right of the constraint, as shown in Figure 21.3b. The optimal point for the unconstrained case is not located in the feasible region. Now, the minimum value of the objective function occurs at $x_2 = 0$ and $x_1 = 1$ where $y = 4$. For more than two decision variables (*multivariable*), a graphical representation is not usually attempted.

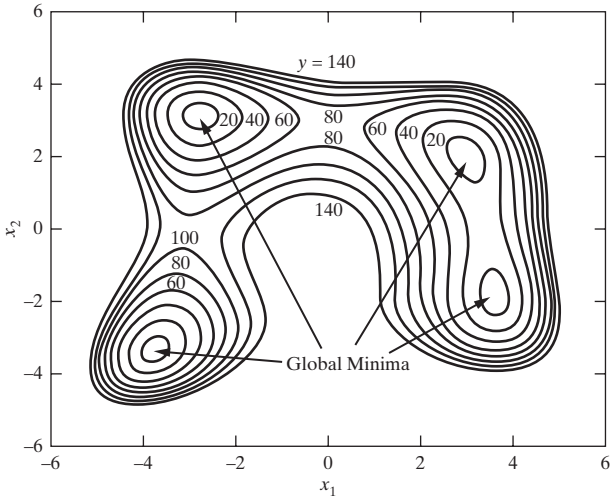

Figure 21.4 Example of a multimodal problem, Himmelblau's function.

When one optimal solution exists in the feasible region, the objective function is *unimodal*. If two optimal solutions exist, it is bimodal; if more than two, it is *multimodal*. LP problems are unimodal unless the constraints are inconsistent such that no feasible region exists. The solutions in Figures 21.1 to 21.3 are unimodal. A two-dimensional, multimodal case is shown in Figure 21.4, taken from Ravindran et al. (2006) and called the Himmelblau problem. This is an unconstrained problem with the objective function:

$$f\{x_1, x_2\} = y = (x_1^2 + x_2 - 11)^2 + (x_1 + x_2^2 - 7)^2 \qquad (21.6)$$

The contours of the objective function shown in Figure 21.4 range from 5 to 140. It can be shown that a point $y = 0$ exists at the center of each of the four closed contours identified as the global minima.

In some cases by using calculus by forming derivatives, nonlinear optimization problems can be solved analytically. For a one-dimensional problem, it is only necessary to differentiate the objective function with respect to the decision variable, set that derivative to zero, solve for the decision variable, and examine it. If more than one solution exists, each solution is obtained and examined. For n decision variables, take n partial derivatives of

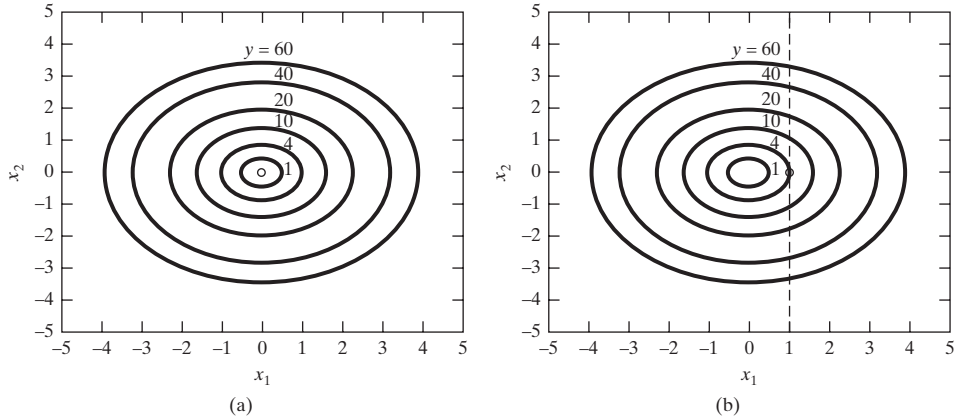

Figure 21.3 Two-variable optimization: (a) unconstrained; (b) constrained.

the objective function, one each with respect to each decision variable; set each derivative to zero; and solve the resulting set of n equations for all solutions of the decision variables. Examine each solution. The following example illustrates the use of calculus on the Himmelblau function of Figure 21.4.

EXAMPLE 21.1 ***Determining Extrema for the Himmelblau Function***

Use calculus to determine all minimum and maximum values of the unconstrained Himmelblau function given by Eq. (21.6).

SOLUTION

The two partial derivatives are:

$$\frac{\partial y}{\partial x_1} = F_1 = 4x_1(2x_1^2 + x_2 - 11) + 2(x_1 + x_2^2 - 7) = 0 \qquad (21.7)$$

$$\frac{\partial y}{\partial x_2} = F_2 = 2(x_1^2 + x_2 - 11) + 4x_2(x_1 + x_2^2 - 7) = 0 \qquad (21.8)$$

The first equation is a third-degree polynomial, and the second is also third degree. By the Theorem of Bezout, as discussed by Morgan (1987), the maximum number of solutions to a set of polynomial equations is the product of the highest degrees of the equations, which is called the total degree of the set of functions, and is equal to nine for the set, Eqs. (21.7) and (21.8). Using a solver for a set of polynomial equations, nine solutions are found as listed in Table 21.1.

Table 21.1 Solutions to Himmelblau's Function

x_1	x_2	$f\{x_1, x_2\}$	Type Solution
−0.2709	−0.9230	181.62	Local maximum
−0.1279	−1.9538	178.34	Saddle point
3.5844	−1.8481	0	Global minimum
3.3852	0.0739	13.31	Saddle point
3.0000	2.0000	0	Global minimum
0.0867	2.8843	67.72	Saddle point
−2.8051	3.1313	0	Global minimum
−3.0730	−0.0814	104.02	Saddle point
−3.7793	−3.2832	0	Global minimum

The nine solutions, referred as *stationary points*, correspond well with the contours of constant values of the objective function plotted on Figure 21.4. The type of solution is also listed in Table 21.1. There is one maximum at an objective function with a value of 181.62. Larger values of the objective function occur as values of the two decision variables are increased to infinity. Four minima occur at an objective function of zero, which is the global minimum. There are four saddle points. Edgar et al. (2001) give necessary and sufficient conditions for determining whether a stationary point is a local maximum, local minimum, or saddle point. The former two types of points are referred to as *extrema*. For a maximum, any combination of small changes in $\underline{x}$ can only decrease the value of the objective function. For a minimum, the opposite is true. For a saddle point from which small changes in $\underline{x}$ are made, some directions will increase and some decrease the value of the objective function.

Much more common in applications to problems in chemical processing is the use of numerical methods for either nonlinear or linear problems. These methods, which are covered in the following sections of this chapter, are mostly *search* methods that start from an assumed solution for $\underline{d}$ and then move $\underline{d}$ in a series of iterations, by some strategy, to reduce (increase) the value of the objective function to achieve a minimum (maximum).

Additional complications can be present in optimization problems. For example, the objective function and/or one or more equality constraints may be *discontinuous*. This might occur, for example, when steam is available to a process at two or three pressure levels with a different cost for each level. If steam is to be used where pressure is a variable, the steam cost could change abruptly at a certain value of the pressure, causing a discontinuity in the objective function.

Another complication arises when one or more of the decision variables is an integer rather than continuous. The most common case is when that integer is binary with just two values, 1 or 0. This gives rise to MILP or MINLP formulations. Although not covered in this chapter, examples of mixed-integer applications are presented in Supplement 11-1 to Chapter 11. MILP and MINLP arise in process optimization from the need to deal with binary as well as continuous decision variables, the former being a convenient way of representing alternative locations of a given equipment item in a flowsheet. MILP formulations are appropriate when both the objective function and the constraints are linear, such as in Example 11S-1.2, which shows how an MILP is formulated and solved for a design of a heat exchanger network (HEN) having the minimum energy requirement (MER). More commonly, both the objective function and the constraints are nonlinear, leading to a MINLP formulation. Example 11S-1.4 shows how a MINLP is set up and solved to minimize the annual cost of a HEN. The *superstructure* for the MINLP, which incorporates all possible heat exchanger locations and flow configurations in the HEN using binary decision variables, is described in Example 11S-1.3. For comprehensive coverage of MILP and MINLP formulation in process design, the reader is referred to Floudas (1995) and Biegler et al. (1997).

21.4 LINEAR PROGRAMMING (LP)

Although LP problems are not common when optimizing a process design, they are common in many other applications of chemical engineering. Furthermore, a numerical solution of an NLP problem is sometimes achieved by approximating the nonlinear functions with their linear approximations at each step of the iterative procedure by using a method called *successive linear programming* (SLP). Therefore, it is useful to have a basic understanding of LP methods.

Some of the common applications of LP methods are for (1) assignment, (2) blending, (3) distribution, (4) determining network flows, (5) scheduling, (6) transportation, and (7) scheduling traveling salesmen. Example 11S-1.1 demonstrates how an LP is used to determine the minimum hot and cold utilities for a HEN. For small-scale problems that can be reduced to two decision variables, a graphical solution is instructive. The graphical solution method involves (1) a definition of the decision variables, (2) formulation of the objective function, (3) formulation

of a model, (4) reduction of the number of decision variables using equality constraints, applying Eq. (21.1), and (5) solution of the LP graphically when the number of decision variables remaining is less than three. The following example with three decision variables, although solved graphically, illustrates some of the characteristics of all LP problems.

EXAMPLE 21.2 ***Production Plan for the ABC Distillery***

You have been requested to prepare a production plan for the ABC Distillery that produces a malt beer, A, and two kinds of malt whiskey, B and C. The available equipment is as follows: (1) Fermenter 1, (2) Fermenter 2, and (3) Still 3. The production of 100 gallons of A requires 5 hours in Fermenter 1 and 10 hours in Fermenter 2. For Whiskey B, 100 gallons of product require 10 hours in Fermenter 1 and 10 hours in Still 3. For Whiskey C, 100 gallons of product require 10 hours in Fermenter 1 and 20 hours in Still 3. Each week, there are 150 production hours available for each of the three equipment items. The profit expected on each product is \$5/gal for A, \$10/gal for B, and \$15/gal for C. Formulate an LP, whose solution is the production in gallons of each product per week, for maximum profit and solve it graphically. How will the solution change if, in addition to the above, one is also required to produce B and C in equal quantities?

SOLUTION

Let A, B, and C be the number of gallons produced of each product per week. In this case, the LP for this problem is:

$$\max_{A,B,C} J = 5A + 10B + 15C \tag{21.9}$$

Such that:

$$5\left(\frac{A}{100}\right) + 10\left(\frac{B}{100}\right) + 10\left(\frac{C}{100}\right) \le 150 \quad \text{(Fermenter 1 weekly capacity)} \tag{21.10}$$

$$10\frac{A}{100} \le 150 \quad \text{(Fermenter 2 weekly capacity)} \tag{21.11}$$

$$10\left(\frac{B}{100}\right) + 20\left(\frac{C}{100}\right) \le 150 \text{ (Still 3 weekly capacity)} \tag{21.12}$$

$$0 \le A, B, C$$

Noting that the profit, J, increases monotonically with the amount of product produced, and that all three products require the usage of Fermenter 1, it seems obvious that we will want to utilize Unit 1 at its maximum capacity of 150 hours:

$$5\left(\frac{A}{100}\right) + 10\left(\frac{B}{100}\right) + 10\left(\frac{C}{100}\right) = 150 \Rightarrow A = 3{,}000 - 2B - 2C \tag{21.13}$$

Thus, the LP can be expressed in terms of B and C:

$$\max_{A,B,C} J = 15{,}000 + 5C \tag{21.14}$$

Such that:

$$B + C \ge 750 \text{ (Fermenter 2 } - \text{ max capacity)} \tag{21.15}$$

$$B + 2C \le 750 \text{ (A} \le 0) \tag{21.16}$$

$$B + 2C \le 1{,}500 \text{ (Still 3 } - \text{ max capacity)} \tag{21.17}$$

$$0 \le B, C$$

See Figure 21.5 for the graphical solution.

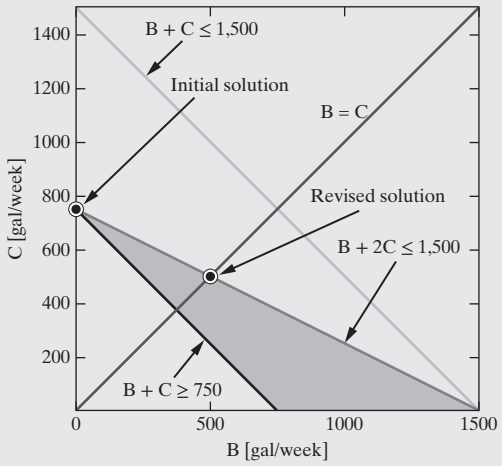

Figure 21.5 Graphical solution of Example 24.2.

The feasible region is indicated in Figure 21.5. Because the objective function is monotonically increasing with C, clearly, the optimal solution is $C = 750$, $B = 0$, and $A = 1{,}500$, giving a weekly profit of \$18,750. For the case requiring equal quantities of B and C, the LP is augmented by an additional equality constraint, $B = C$, shown graphically in Figure 21.5 by the grey line. Now the feasible region is this line (the solution must lie on the gray line) constrained by the previous feasibility region. The optimum is now $C = 500$, $B = 500$, and $A = 1{,}000$ so that the weekly profit is only \$17,500.

For large LP problems, which may involve more than 10,000 decision variables, one of two methods is applied. The first method, developed by Dantzig (1949) in the 1940s, is referred to as the *simplex meth*od. It is an iterative method that begins with initial values for the design variables (iterates) that satisfy the constraints at one of the vertices and for which the objective function is computed. The optimal solution must be at this or another vertex. Therefore, subsequent iterations generate, in a systematic procedure, a sequence of iterates that move from one vertex of the feasible region to an adjacent vertex, each time finding an improved value for the objective function, until the vertex corresponding to the optimal solution is found. As described by Edgar et al. (2001), LP problems can be solved by the simplex method with the linear model of the Solver routine of the Microsoft Excel spreadsheet. An LP solver is also available in MATLAB and GAMS. For assistance in the usage of MATLAB's *linprog* for the solution of LPs, see the link: MATLAB → Numerical Methods → Linear Programing in the multimedia modules.

When the number of iterations required by the simplex method is found to increase exponentially with the number of decision variables, the second method, which is also iterative and was developed in the 1980s, may be more efficient because it may require far fewer iterations, although each iteration requires more calculations. This method, announced by Karmarkar in 1984 and described in detail by Vanderbei (1999), is called the *interior-point method*. It differs from the simplex method in that all iterates are not required to satisfy the constraints and,

therefore, need not be located on vertices. This allows the iterates to be points interior to the feasible region, which on successive iterations can cut clear across the feasible region to locate the optimal point more quickly. Software for both LP methods is widely available from the Internet and is included in the libraries of mathematical software.

21.5 NONLINEAR PROGRAMMING (NLP) WITH A SINGLE VARIABLE

Nonlinear optimization problems in just a single decision variable frequently arise in chemical engineering applications. If the objective function is unconstrained, the optimal solution(s) can often be obtained analytically using derivatives from calculus. When they are subject to constraints, the use of numerical methods is frequently necessary. Some applications that have appeared often in chemical engineering textbooks include the following, many of which involve a balance between capital costs and operating costs. Solutions to optimization problems such as these have led to many of the heuristics that are presented in Chapter 6.

1. Optimal thickness of insulation for a pipe carrying steam for which the insulation cost is balanced against the heat loss causing steam condensation.
2. Optimal reflux ratio for a distillation column for which the capital cost of the column and heat exchangers is balanced against the utility costs for the condenser cooling utility (e.g., cooling water) and for the reboiler heating utility (e.g., steam).
3. Optimal absorbent (stripping agent or extraction solvent) flow rate in an absorber (stripper or liquid–liquid extractor) for which the number of stages is balanced against the column diameter and absorbent (stripping agent or extraction solvent) cost.
4. Optimal pipe diameter for a flowing liquid for which the capital cost of the pipe and the pump is balanced against the operating cost of the pump.
5. Optimal length (or height) and diameter of a cylindrical pressure vessel of a given volume to minimize the capital cost (try Exercise 21.6).
6. Optimal number of stages in a multieffect evaporation system for which the capital cost is balanced against the cost of heating utility (e.g., steam).
7. Optimal interstage pressures of a multistage gas compression system with intercoolers for which the total power requirement is to be a minimum (try Exercise 14.2).
8. Optimal cooling water outlet temperature from a heat exchanger for which the capital cost of the heat exchanger is balanced against the cost of the cooling water.
9. Optimal filter cake thickness in a batch filter for which the rate of filtration is balanced against the cost of removing the cake.
10. Optimal number of CSTRs in series for which the capital cost is to be minimized.

When the NLP problem consists of only one decision variable (or can be reduced to one) with lower and upper bounds, the optimal solution can be found readily using a spreadsheet or one of several structured and efficient search methods, including *region-elimination*, *derivative-based*, and *point-estimation* as described in detail by Ravindran et al. (2006). Of the search methods, the golden-section method (involving region elimination) is reasonably efficient, reliable, easily implemented, and widely used. Therefore, it is described and illustrated by example here.

Golden-section Search

The golden-section search method determines the optimal solution to a bounded objective function that is one-dimensional and unimodal. However, the function need not be continuous in either the function or its derivative. Thus, the method can solve functions like those shown in Figure 21.6.

The golden-section algorithm is now demonstrated on the minimization of a function $f(x)$. Referring to Figure 21.7a, let a and b equal the lower and upper bounds of x, noting that it is not necessary to compute $f(x)$ at these two bounds. In the first iteration of the algorithm, the distance between the two points, $b - a = L^{(1)}$. The strategy employed in the golden-section search begins by locating two points in x that are symmetrically placed within the interval from a to b by means of a factor, τ. Thus, if the point farthest from a, x_1, is located at $(a + \tau L^{(1)})$, then the other point, x_2, is located at $(b + \tau L^{(1)})$, which is equal to $[a + (1 - \tau)L^{(1)}]$. The objective function is then computed for each of these two points, and suppose after doing so that $f(x_1) > f(x_2)$ as illustrated in Figure 21.7a. Because $f(x)$ is assumed to be unimodal, the minimum value of $f(x)$ cannot lie to the right of x_1, and hence, on the basis of the results computed, the range from x_1 to b can be eliminated from the search range, thus reducing the search space by a fraction $1 - \tau = 0.38197$ (about 38.2%). This leaves a new search region of distance $x_1 - a = L^{(2)} = \tau L^{(1)}$ as shown in Figure 21.7b, marking the beginning of the second iteration. Next, a new point, x_3, is inserted, positioned symmetrical to the remaining point within the new interval. This enables the value of τ to be determined. Note that the interior point retained from the previous iteration at x_2, which was located at $[a + (1 - \tau)L^{(1)}]$ is now located on the new interval at $(a + \tau L^{(2)})$, which is the same as $(a + \tau^2 L^{(1)})$. Hence, $(1 - \tau) = \tau^2$, whose positive solution is $\tau = 0.61803$.

Using this value of τ, subsequent steps in the golden-section method add new points symmetrical to the remaining point, calculate the objective function for the new point, and eliminate a point and the region between it and the closest bound of the remaining region. How many steps are required? Because each step reduces

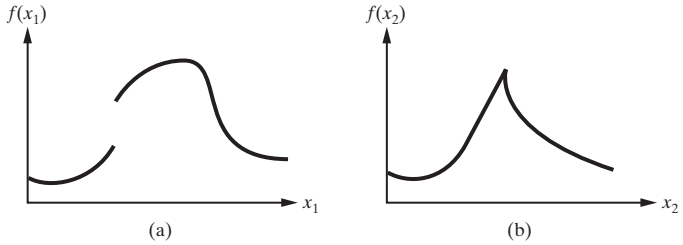

Figure 21.6 Objective function with discontinuities in (a) the function and (b) the derivative of the function.

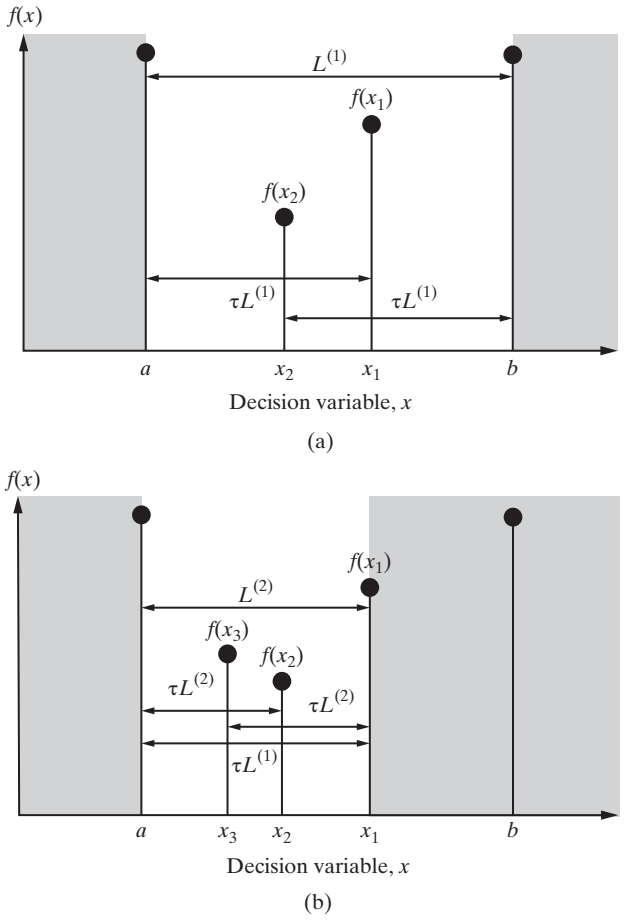

Figure 21.7 Development of the golden-section method: (a) first iteration, showing initial search region (unshaded); (b) second iteration, showing remaining search region (unshaded).

the search space by a factor $\tau = 0.61803$, the fraction of the search interval remaining after M steps is τ^M, requiring the computation of $M + 1$ objective functions. Thus, in 10 steps, the optimal solution is located in an interval that is less than 1% of the distance between the original lower and upper bounds. In 20 steps, that interval is reduced to less than 0.01% of that distance.

Rudd and Watson (1968) point out that $1 + \tau = \varphi = (1 + \sqrt{5})/2 = 1.61803$ was known in ancient times as the Golden Ratio. Greek temples were designed with this ratio because it was most pleasing to the eye. The ancient Badge of the Pythagoreans, the Pentagram, a five-pointed star, consists of five isosceles triangles whose bases are the sides of a pentagon, where the ratio of each hypotenuse (the "legs" of the isosceles triangles) to the base is φ. Numerous instances of the Golden Ratio abound in nature.

EXAMPLE 21.3 *Design of Heat Exchanger to Minimize Annual Costs*

In a petroleum refinery, 80,000 lb/hr of a light gas oil at 440°F from a sidecut stripper of a crude distillation tower is currently being cooled with cooling water before being sent to storage. The heat being lost could be used to help preheat 500,000 lb/hr of the crude oil, which is available at 240°F and is being heated by other means at a cost of \$3.00/million Btu. The plant operates 8,200 hr/yr. Based on the following data, determine what should be done, if anything, if a reasonable return on investment is $i_m = 0.20$. The savings in cooling water cost can be assumed negligible.

Data

Average specific heat of light gas oil = 0.50 Btu/lb-°F

Average specific heat of crude oil = 0.45 Btu/lb-°F

Use a floating-head, shell-and-tube heat exchanger for areas greater than 200 ft^2.

For areas greater than 12,000 ft^2, use parallel units.

Delivered cost of a heat exchanger = 1.05 times Equation (16.38)
$= 1.05\, C_P\{A\}$

Bare module factor for a heat exchanger = 3.17 from Table 16.11
$= F_{BM}$

Add 5% for site preparation and 18% for contingency and contractor's fee.

SOLUTION

For an objective function, use annualized cost given by Eq. (17.10). Thus, if q is the duty, in Btu/yr, of the light gas oil-to-crude oil heat exchanger of area, A, in ft^2, the annualized cost, to be minimized, is given by:

$$C_A = C + i_m(C_{TCI}) = -\frac{8{,}200(3.00)q}{1{,}000{,}000} + 0.20(1.05)^2(1.18)(3.17)C_P\{A\},$$
$$= -0.0246\, q + 0.8248\, C_P\{A\}, \quad (21.18)$$

Noting that the purchase cost of a floating-head heat exchanger, $C_P\{A\}$, is taken as that computed using Eq. (16.39). Thus, to be attractive, the annualized cost must be negative so that the absolute value of the savings in the current annual cost of heating the crude oil (a negative quantity) is greater than the annualized cost of the heat exchanger installation. The more negative C_A is, the better.

From Table 12.5, for gas oil-to-oil, the overall heat-transfer coefficient, U, is given as 20 to 35 Btu/hr-°F-ft^2. Because the gas oil is a light gas oil, use $U = 35$ Btu/hr-°F-ft^2. Because pure countercurrent flow should not be assumed, use a value of 0.7 for a correction factor (see Chapter 12 for a discussion of this issue), giving a mean temperature driving force of 0.7 times the log mean = $0.7\,\Delta T_{LM}$.

The equality constraints are:

1. Energy balances:

$$q = 80{,}000(0.50)(440 - T_{LGO,out}) \quad (21.19a)$$

$$q = 500{,}000(0.45)(T_{CO,out} - 240) \quad (21.19b)$$

2. Heat-transfer rate:

$$q = 0.7\, UA\Delta T_{LM} = 0.7\,(35)A\Delta T_{LM} \quad (21.20)$$

3. Definition of log-mean temperature driving force:

$$\Delta T_{LM} = \frac{(440 - T_{CO,out}) - (T_{LGO,out} - 240)}{\ln\left(\frac{440 - T_{CO,out}}{T_{LGO,out} - 240}\right)} \quad (21.21)$$

Thus, we have four equations relating five independent variables: $T_{LGO,out}$, $T_{CO,out}$, ΔT_{LM}, q, and A. This gives one decision variable, which must be selected from the five variables. The best choice is the exit temperature of the light gas oil, $T_{LGO,out}$ because it is easily bounded and permits the remaining four variables to be calculated sequentially from the four equality constraints. An upper bound on its value is for no heat exchange where $T_{LGO,out} = 440^{o}$F and $C_A = \$0$. A lower limit assumes infinite heat-exchange area where $T_{LGO,out} = 240^{o}$F, the inlet temperature of the crude oil, because the light gas oil has a much lower flow rate than the crude oil and C_A is infinite.

The optimization problem is one-dimensional with a nonlinear objective function, which may be discontinuous, depending on the heat-exchanger area. The single decision variable is bounded. Therefore, the golden-section search is a suitable method for determining the optimal solution. The calculations can be carried out conveniently in the following manner for each selection of $T_{LGO,out}$:

1. Calculate q using Eq. (21.19a).
2. Calculate $T_{CO,out}$ using Eq. (21.19b).
3. Calculate ΔT_{LM} using Eq. (21.21).
4. Calculate A using Eq. (21.20).
5. Calculate C_A using Eq. (21.18).

To begin the steps in the golden-section search, note that the interval on the decision variable is $440 - 240 = 200^{o}$F. With $\tau = 0.61803$, the first two points are located at $T_{LGO,out} = [240 + 0.61803(200)] = 363.606^{o}$F and $[240 + (1 - 0.61803)(200)] = 316.394^{o}$F.

Table 21.2 gives the results of the golden-section search, indicating that it is attractive to install the heat exchanger. The optimal exit temperature of light gas oil from the heat exchanger is approximately 250^{o}F, giving an annualized cost of approximately $\$ -144{,}200$ or a savings of \$ 144,200 per year. The final interval for search is less than 1^{o}F. More steps could reduce this interval further, but the area of the heat exchanger would change less than 2%. The crude oil outlet temperature from the heat exchanger is approximately 274^{o}F, so it is heated up only 34^{o}F, compared to a decrease of 190°F in temperature of the light gas oil. The optimal minimum approach temperature is approximately $(250 - 240) = 10^{o}$F. The heat exchangers in the table are all within the range of 200 to 12,000 ft^2 in area so that a single shell-and-tube heat exchanger is sufficient, giving a smooth curve for the objective function. That function is plotted in Figure 21.8 where it is observed that the optimum is not particularly sharp such that other factors, such as operability and reliability, might enter into a final decision on the size of heat exchanger to purchase.

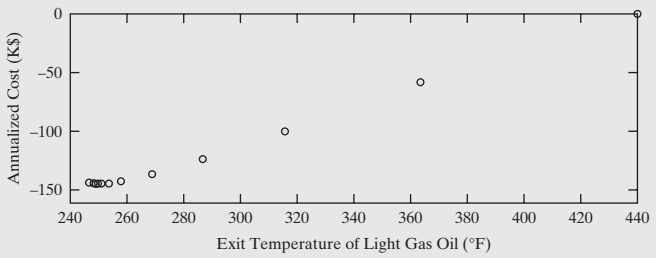

Figure 21.8 Golden-section search results for Example 21.3.

21.6 CONDITIONS FOR NONLINEAR PROGRAMMING (NLP) BY GRADIENT METHODS WITH TWO OR MORE DECISION VARIABLES

Optimization problems encountered in product and process design are often NLP problems with two or more decision variables. Accordingly, much effort has been expended by researchers in the development of efficient search methods for finding an optimal solution. The remainder of this chapter deals with some of these methods, particularly those that are implemented in process simulators.

The formulation of the NLP for application to large process design problems begins with the steady-state simulation of the process flowsheet for a *nominal* set of specifications or decision variables. As described in Section 7.2, during the creation of the simulation model (involving the material and energy balances, kinetic equations, etc., for the process units), an analysis of degrees of freedom is performed. For the simulation model, the number of variables, N_V, normally exceeds the number of

Table 21.2 Golden-section Search Results for Example 21.3

Point	$T_{LGO,out}$, °F	$T_{CO,out}$, °F	ΔT_{LM}, °F	q, $\times 10^6$ Btu/hr	A, ft^2	C_A, $\times 10^3$\$
1	316.39	261.97	120.12	4.94	1,680	−100.2
2	363.61	253.58	152.87	3.06	815.8	−59.1
3	287.21	267.16	96.80	6.11	2,577	−123.7
4	269.18	270.37	79.80	6.83	3,495	−136.4
5	258.03	272.35	67.10	7.28	4,428	−142.4
6	251.15	273.57	57.44	7.55	5,368	−144.2
7	246.89	274.33	49.93	7.72	6,314	−143.4
8	253.77	273.10	61.38	7.45	4,954	−143.8
9	249.52	273.86	54.77	7.62	5,678	−144.2
10	252.15	273.39	58.99	7.51	5,199	−144.1
11	250.52	273.68	56.53	7.58	5,482	−144.2
12	250.14	273.75	55.81	7.59	5,554	−144.2
13	250.76	273.64	56.82	7.57	5,437	−144.2

equations, N_E, with the difference between them referred to as the number of degrees of freedom or decision variables, N_D. The best procedure is to carry out a base-case simulation where the specifications for the decision variables are set using heuristics, such as those of Chapter 6. Then, gradually, as experience is gained by carrying out several simulations, the values of the decision variables are adjusted to better achieve the design objectives. In addition, the process units are simulated with more accurate models, the thermodynamic and transport properties are tuned, often using experimental and pilot-plant data, and profitability measures are computed. Having completed these steps and having gained a good appreciation of the operation of the process and some indication of the key optimization trade-offs, the engineer is well prepared to formulate a detailed NLP problem for solution by a process simulator.

General Formulation

The general formulation of the NLP problem is given at the beginning of Section 21.2. The NLP is usually solved using gradient-based methods. By using numerical partial derivatives of the objective function with respect to the decision variables, gradient-based methods are faster than nongradient methods with the advantage increasing with an increasing number of decision variables. The use of these methods requires conditions for optimality, referred to as *stationary* or *stationarity conditions*. These conditions involve slack variables and Lagrangian functions and are described next used with *successive quadratic programming* (SQP), which is a widely used gradient method in process simulators. Readers who prefer to skip these details should follow the text from Section 21.7.

Stationarity Conditions

To obtain the stationarity conditions, the Lagrangian is formed and differentiated with the details of this procedure described by McMillan (1970) and by Beveridge and Schecter (1970). The development begins by converting the inequality constraints to equality constraints through the addition of *slack variables*, z_i^2, $i = 1, \ldots, N_{Inequal}$, such that constraints (21.4) become:

$$\underline{g}_i\{\underline{x}\} + z_i^2 = 0 \quad i = 1, \ldots, N_I \tag{21.22}$$

where z_i^2 takes up the slackness when $\underline{g}_i\{\underline{x}\} < 0$. Then, the *unconstrained objective function*, or Lagrangian, is formed:

$$L\{\underline{x}, \underline{\pi}, \underline{\lambda}, \underline{z}\} = f\{\underline{x}\} + \underline{\pi}^T \underline{c}\{\underline{x}\} + \underline{\lambda}^T[\underline{g}\{\underline{x}\} + \underline{z}^2] = 0 \tag{21.23}$$

where $\underline{\pi}$ and $\underline{\lambda}$ are vectors of the Lagrange and Kuhn-Tucker multipliers. At the minimum,

$$\nabla L = 0 \tag{21.24}$$

which can be expanded to give the *stationarity conditions* or the Karush-Kuhn-Tucker (KKT) conditions:

$$\nabla_x L = \nabla_x f\{\underline{x}\} + \underline{\pi}^T \nabla_x \underline{c}\{\underline{x}\} + \underline{\lambda}^T \nabla_x \underline{g}\{\underline{x}\} = 0 \tag{21.25}$$

$$\nabla_\pi L = \underline{c}\{\underline{x}\} = 0 \tag{21.26}$$

$$\nabla_{z_i} L = g_i \lambda_i = 0, \; i = 1, \ldots, m \tag{21.27}$$

$$\underline{\lambda} \geq 0 \tag{21.28}$$

Note that $\nabla_\lambda L = 0$ gives Eqs. (21.22), which are the definitions of the slack variables and need not be expressed in the KKT conditions. Note also that $\nabla_{z_i} L = 2\lambda_i z_i = 0$, and, using Eqs. (21.22), Eqs. (21.27) results. These are the so-called *complementary slackness* equations. For constraint i, either the residual of the constraint is zero, $g_i = 0$, the Kuhn-Tucker multiplier is zero, $\lambda_i = 0$, or both are zero; that is, when the constraint is *inactive* ($g_i > 0$), the Kuhn-Tucker multiplier is zero, and when the Kuhn-Tucker multiplier is greater than zero, the constraint must be *active* ($g_i = 0$). Stated differently, there is slackness in either the constraint or the Kuhn-Tucker multiplier. Finally, it is noted that $\nabla_x \underline{c}\{\underline{x}\}$ is the Jacobian matrix of the equality constraints, $\underline{\underline{J}}\{\underline{x}\}$, and $\nabla_x \underline{g}\{\underline{x}\}$ is the Jacobian matrix of the inequality constraints, $\underline{\underline{K}}\{\underline{x}\}$.

Solution of the Stationarity Equations

The KKT conditions are a set of $N_V + N_E + N_I$ nonlinear equations (NLEs) in $N_V + N_E + N_I$ unknowns that can be solved, in principle, using an algorithm for the solution of NLEs such as the Newton-Raphson method, which for the equations:

$$\underline{F}\{\underline{X}\} = 0 \tag{21.29}$$

takes the form:

$$\underline{\Delta X}^{(k)} = -\underline{\underline{J}}\{\underline{X}^{(k)}\}\underline{F}\{\underline{X}^{(k)}\} \tag{21.30}$$

$$\underline{X}^{(k+1)} = \underline{X}^{(k)} + \underline{\Delta X}^{(k)} \tag{21.31}$$

Here, $\underline{X}^{(k)}$ is the vector of guessed values at the kth iteration (the initial guesses when $k = 0$), $\underline{F}\{\underline{X}^{(k)}\}$ is the vector of residuals at $\underline{X}^{(k)}$, $\underline{\underline{J}}\{\underline{X}^{(k)}\}$ is the Jacobian at $\underline{X}^{(k)}$, $\underline{\Delta X}^{(k)}$ is the vector of corrections computed using the Newton-Raphson linearization, and $\underline{X}^{(k+1)}$ is the vector of unknowns after the kth iteration.

When the Newton-Raphson method is applied to solve the KKT Eqs. (21.25) – (21.27), $\underline{X}^{\mathrm{T}} = [\underline{x}^{\mathrm{T}}\ \underline{\pi}^{\mathrm{T}},\ \underline{\lambda}^{\mathrm{T}}]$, and Eqs. (21.30) and (21.31) can be rewritten in terms of these variables. This was accomplished by Jirapongphan (1980) who showed that beginning with the vector of guesses, $\underline{X}^{(k)}$, one iteration of the Newton-Raphson method is equivalent to solving the following quadratic program (QP):

Minimize $\nabla_x f\{\underline{x}^{(k)}\}^{\mathrm{T}} \underline{\Delta x}^{(k+1)} + (1/2)\underline{\Delta x}^{(k+1)^{\mathrm{T}}} \nabla^2_{xx} L\{\underline{x}^{(k)},$

w. r. t. $\underline{\pi}^{(k)}, \underline{\lambda}^{(k)}\}\underline{\Delta x}^{(k+1)}$ **(QP)**

$\underline{\Delta x}^{(k+1)},\ \underline{\Delta \pi}^{(k+1)},\ \underline{\Delta \lambda}^{(k+1)}$

s. t.

$$\underline{\underline{J}}\{\underline{x}^{(k)}\}\underline{\Delta x}^{(k+1)} + \underline{c}\{\underline{x}^{(k)}\} = 0 \tag{21.32}$$

$$\underline{\underline{K}}\{\underline{x}^{(k)}\}\underline{\Delta x}^{(k+1)} + \underline{g}\{\underline{x}^{(k)}\} = 0 \tag{21.33}$$

Algorithms for the solution of quadratic programs, such as the Wolfe (1959) algorithm, are reliable and readily available. Hence, these have been used in preference to the implementation of the Newton-Raphson method. For each iteration, the quadratic objective function is minimized subject to linearized equality and inequality constraints. Clearly, the most computationally expensive step in carrying out an iteration is in the evaluation of the Laplacian of the Lagrangian, $\nabla^2_{xx}L\{\underline{x}^{(k)}, \underline{\pi}^{(k)}, \underline{\lambda}^{(k)}\}$, which is also the Hessian matrix of the Lagrangian, that is, the matrix of second derivatives with respect to $\underline{x}^{(k)}$, $\underline{\pi}^{(k)}$, and $\underline{\lambda}^{(k)}$.

To circumvent this calculation, Powell (1977) used the Broyden, Fletcher, Goldfarb, Shanno (BFGS) quasi-Newton method to approximate $\nabla^2_{xx}L\{\underline{x}^{(k)}, \underline{\pi}^{(k)}, \underline{\lambda}^{(k)}\}$. This saves considerable computation time and is the basis of Powell's SQP method. A key problem that arises in the implementation of Powell's algorithm is due to the linearization that produces a quadratic objective function and linear constraints, which often lead to infeasible solution vectors, $\underline{X}^{\mathrm{T}} = [\underline{x}^{(k)}, \underline{\pi}^{(k)}, \underline{\lambda}^{(k)}]$. This problem manifests itself in solutions, $\underline{x}^{(k+1)}$, that violate the inequality constraints as well as multipliers that are often driven to zero prematurely. Assuming that the initial guesses do not violate the inequality constraints, Han (1977) designed a unidirectional search in the direction of $\underline{\Delta X}^{(k)}$ that is designed to reduce the step taken to keep the solution vector within the feasible space.

For more complete presentations of the SQP algorithm, the reader is referred to the textbooks by Biegler et al. (1997), Edgar et al. (2001), and Ravindran et al. (2006).

21.7 OPTIMIZATION ALGORITHM

The most straightforward way to improve the objective function is by *repeated simulation*. In this procedure, the designer selects values of the decision variables and completes a simulation. Then, usually using a systematic strategy, the decision variables are adjusted and the simulation is repeated, for example, using *sensitivity analysis* in the process simulators in which simulation results are recomputed as a decision variable is adjusted using uniform increments between bounds specified by the user. However, sensitivity analyses can be very time consuming and can generate large files of information, much of which is associated with suboptimal processes. More efficiently, the designer can select a formal optimization algorithm built into the simulator to adjust the decision variables. However, when many recycle loops are present, the simulation calculations can be very time consuming with on the order of 20 or more iterations required to achieve an optimum and, for each of these iterations, as many as 20 iterations to converge each of the recycle and control loops (involving design specifications). To overcome these inefficiencies, especially for integrated flowsheets, the latest strategies adjust the decision variables and the tear variables to converge the recycle loops simultaneously (Lang and Biegler, 1987; Seader et al., 1987). In these strategies, the optimization algorithm does not converge the recycle loops for each set of decision variables. Instead, it performs just one pass through the recycle loops before adjusting the decision variables, and consequently, the strategies are referred to as *infeasible path algorithms* because the solution for that path is not converged. In most cases, the infeasible path strategy is successful in ultimately converging the recycle loops to a feasible design while optimizing the process.

To clarify the infeasible path strategy, consider the simulation flowsheets in Figure 21.9. In Figure 21.9a, the ASPEN PLUS simulation flowsheet—in which a continuous stirred-tank reactor (CSTR) followed by a recycle loop involving another CSTR, a distillation column, a purge splitter, and a heater—is optimized. In this case, the recycle convergence unit, \$OLVER01, is positioned arbitrarily so as to tear stream S9 with $\underline{x}^*$ being the vector of guessed values for the tear variables and $\underline{w}\{\underline{d}, \underline{x}^*\}$ being the vector of tear variables after one pass through the recycle loop. In Figure 21.9b, the UniSim®Design/ASPEN HYSYS PDF, which consists of a recycle loop involving a conversion reactor, a component splitter, and a tee, is optimized. Note that in HYSYS, a recycle convergence unit is explicitly positioned to tear stream R with $\underline{x}^*$ being the vector of guessed values for the tear variables

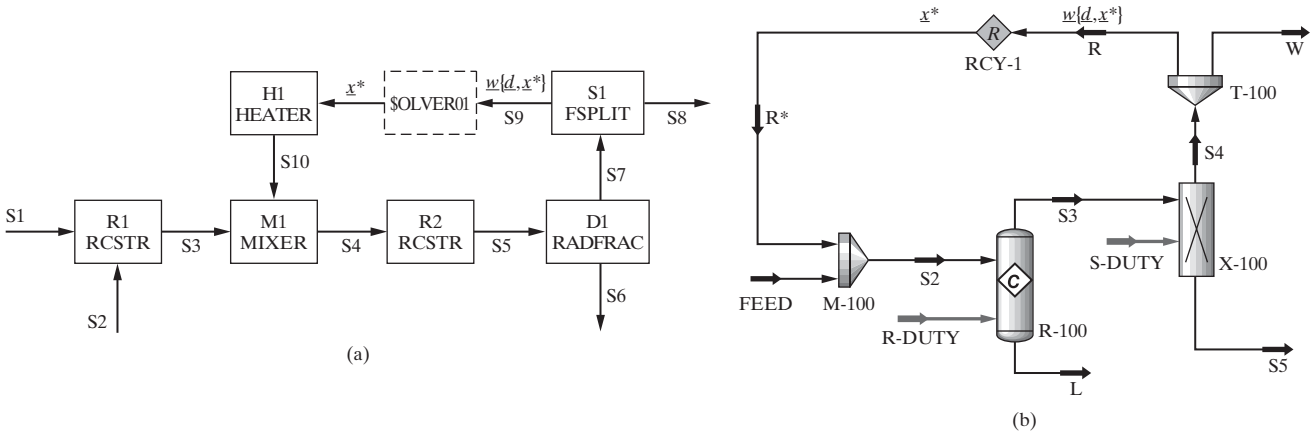

Figure 21.9 Process flowsheet with material recycle and tear stream: (a) ASPEN PLUS; (b) UniSim® Design.

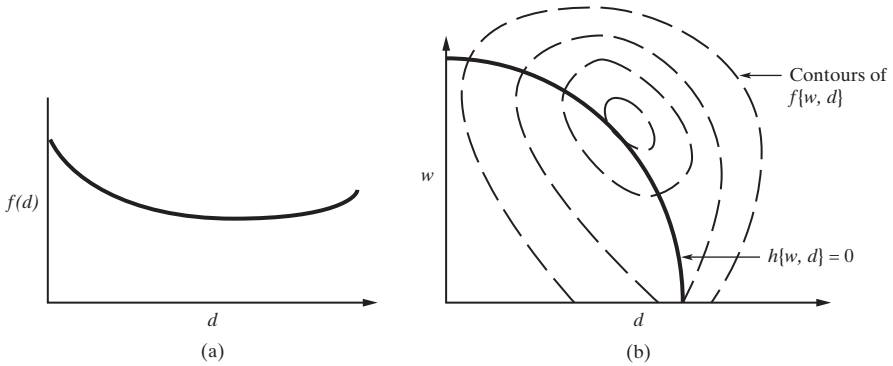

Figure 21.10 Optimization of a process with recycle: (a) objective function; (b) level contours and tear equation.

and $\underline{w}\{\underline{d}, \underline{x}^*\}$ being the vector of tear variables after one pass through the recycle loop. The revised NLP is:

Minimize $f\{x\}$ **(NLP2)**

w. r. t.

$\underline{d}$

s. t.

$\underline{h}\{\underline{x}^*\} = \underline{x}^* - \underline{w}\{\underline{x}^*\} = 0$ (tear equations)

$\underline{c}\{\underline{x}\} = 0$

$\underline{g}\{\underline{x}\} \leq 0$

$\underline{x}^L \leq \underline{x} \leq \underline{x}^U$

Here, the equality constraints are augmented by the tear equations, $\underline{h}\{\underline{x}^*\} = 0$, which must be satisfied as well at the minimum of $f\{\underline{x}\}$. For this and similar flowsheets, the decision variables include the residence times in the reactors, the reflux ratio of the distillation tower, and the purge/recycle ratio. In one-dimensional space (i.e., with one decision variable), as $\underline{d}$ varies, the objective function can be displayed as shown in Figure 21.10a. Clearly, the optimizer seeks to locate the minimum efficiently, a task that is complicated when multiple minima exist and it is desired to locate the *global* minimum.

As the decision variables are adjusted by the optimizer, the values of the tear variables and the objective function change, and it is helpful to show these functionalities in a more explicit form of the NLP:

Minimize $f\{\underline{x}, \underline{d}\}$ **(NLP3)**

w. r. t.

$\underline{d}$

s. t.

$\underline{h}\{\underline{x}^*, \underline{d}\} = \underline{x}^* - \underline{w}\{\underline{x}^*, \underline{d}\} = 0$

$\underline{c}\{\underline{x}, \underline{d}\} = 0$

$\underline{g}\{\underline{x}, \underline{d}\} \leq 0$

$\underline{x}^L \leq \underline{x} \leq \underline{x}^U$

Here, $\underline{x}$ is the vector of process variables excluding the decision variables, and $\underline{x}^*$ are guessed values for the tear variables (which equal $\underline{w}$ at the minimum). As will be seen later, it helps to show the variations of the objective function, f, and the tear functions, h, in the schematic diagram of Figure 21.10b. In this diagram, level contours are displayed as a function of just one decision variable and one tear variable, and the locus of points is displayed at which the tear equation is satisfied as d varies along the abscissa. Clearly, the minimum of f must lie on the latter curve with the minimum of $f\{w, d\}$ being infeasible.

Repeated Simulation

The repeated simulation approach is illustrated in Figure 21.11a. Beginning with an initial guess for the decision and tear variables, a simulation is completed in which the recycle loop is converged; that is, the tear equation is satisfied. Then, d is adjusted, somewhat arbitrarily, by Δ_d, and the simulation is repeated using the previous solution for w as the initial guess. This strategy is repeated until convergence to the minimum is achieved.

Infeasible Path Approach

In the infeasible path approach, as illustrated in Figure 21.11b, both d and w are adjusted simultaneously by the optimizer (with $w \rightarrow x^*$ for the next iteration), usually using the SQP algorithm. This algorithm involves just one pass through the flowsheet per iteration, so the tear equations are normally not satisfied until the optimum is located. As will be seen in the examples that follow, convergence is usually achieved in a few iterations. Figure 21.11b shows a schematic of $\underline{\Delta}$, the vector of the changes in d, Δ_d, and w, Δ_w, as computed by the SQP algorithm.

Compromise Approach

In a compromise approach, which is often necessary to achieve convergence, after the SQP step is taken (i.e., $\underline{\Delta}$), the tear equations, $\underline{h}\{\underline{x}^*\} = 0$, are converged as shown in Figure 21.11c. Often, the tear equations are converged loosely using a convergence method, typically Wegstein's method, with a maximum number of iterations assigned, typically three or four. This compromise approach is often utilized when convergence cannot be achieved after several attempts using the infeasible path approach.

Practical Aspects of Flowsheet Optimization

In most flowsheet simulations, design specifications (or control loops) are included. The iterative calculations to achieve convergence of these specifications are embedded, often within the recycle loops and are converged during each pass through the recycle loops. In other cases, these specifications are implemented as outer loops with the recycle loops converged entirely during each iteration of the outer loop. Another alternative is

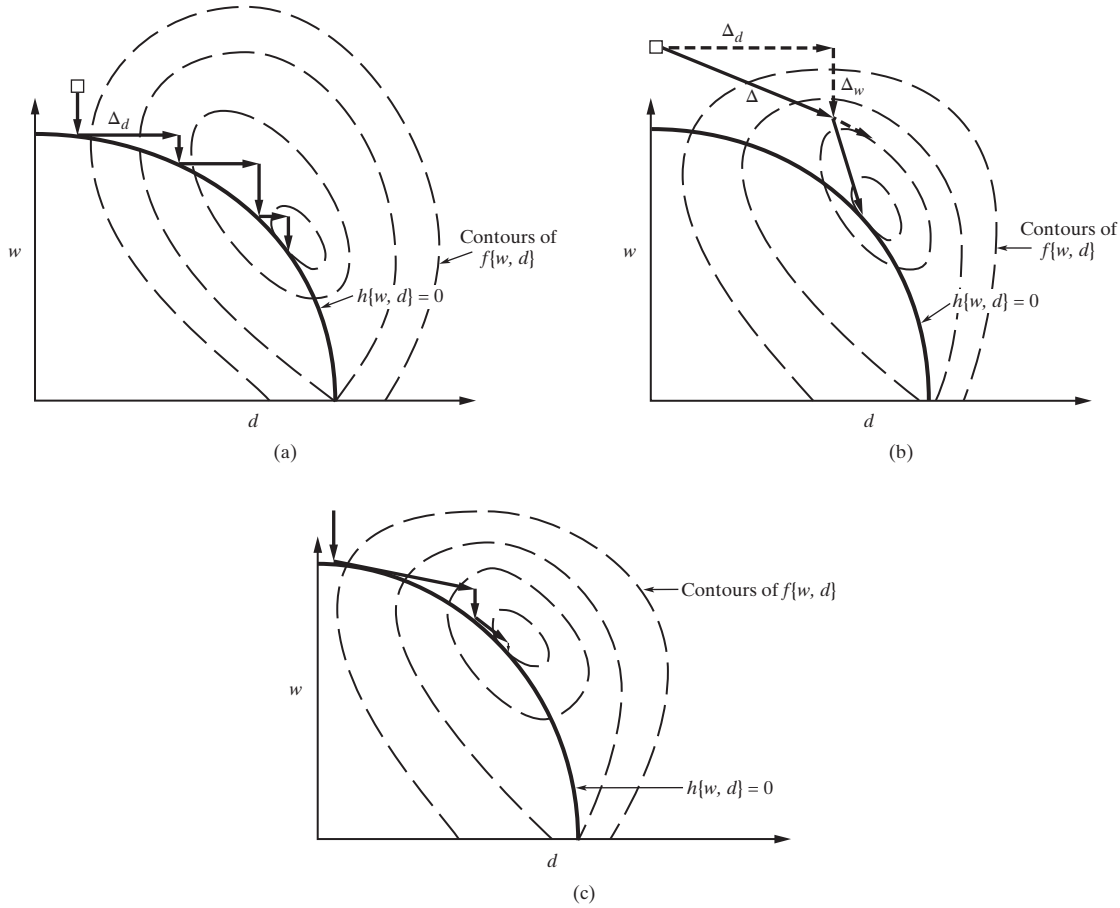

Figure 21.11 Optimization of a process with recycle: (a) repeated simulation (feasible path approach); (b) infeasible path approach; (c) compromise approach.

to converge these loops simultaneously, usually using just one pass through the unit subroutines in the recycle and design specification loops.

When solving an NLP to optimize a flowsheet, another alternative exists. In many cases, it is preferable to incorporate the design specifications as equality constraints, $\underline{c}\{\underline{x}, \underline{d}\} = 0$, as shown in NLP3. Then, it is necessary to remove these design specifications when adding the optimization convergence unit. The latter usually replaces the recycle convergence units in the simulation flowsheet.

Before implementing an infeasible path optimization, it is very helpful to carry out preliminary searches by varying the key decision variables, somewhat randomly, to gain insights into the key trade-offs. For these searches, it is probably best not to use optimization algorithms that require derivatives, or approximations to them, such as SQP. A common approach is to use the sensitivity analysis facilities of the process simulators referred to earlier.

As a final caution, be sure not to use a gradient-based approach, such as SQP, when selecting a discrete decision variable such as the number of trays in a distillation tower. In these cases, it is meaningless to estimate partial derivatives in expressions for the gradient of the objective function or its Hessian matrix because the decision variables are restricted to integer quantities. Similar problems arise when there are discrete changes in the installation costs of equipment, which can arise when a single unit is replaced with two or more units. This often occurs when size variables exceed upper bounds embedded in the subroutines for the calculation of equipment sizes and costs. These kinds of discrete changes are more difficult to detect when sizes and costs are computed for many process units in a complex profitability analysis. For this reason, carrying out the optimization initially using a simpler objective function that does not involve such discontinuities is often recommended. Then, after the optimum is computed, more rigorous measures can be computed and further optimized by using simpler methods (that do not involve derivatives) in the vicinity of the optimum.

21.8 FLOWSHEET OPTIMIZATIONS—CASE STUDIES

In this section, two case studies are presented. The first is a relatively simple example involving one decision variable and one constraint in which the venture profit for a process for the manufacture of ethyl chloride is maximized. In the second example, it is desired to optimize the operation of a multidraw distillation column in which a mixture of normal paraffins is separated into four product streams, two of which are sidestreams. This involves four decision variables and a number of constraints. Although neither of the examples involves the optimization of accurate measures of plant profitability, detailed costing could be included.

EXAMPLE 21.4 *Maximizing the Venture Profit in Ethyl Chloride Manufacture*

In this example, the venture profit of the ethyl chloride process in Figure 21.12 introduced in the multimedia modules that can be downloaded from www.seas.upenn.edu/~dlewin/multimedia.html (see HYSYS → Tutorials → Material and Energy Balances → Ethyl chloride Manufacture; and ASPEN → Tutorials → Material and Energy Balances → Ethyl chloride Manufacture) is maximized by adjusting the purge (W) flow rate. To estimate the venture profit, the following information is supplied:

$$\text{Installed cost of equipment } 500\left(\frac{330\times 24}{1000}\left(F_R\right)\right)^{0.6} \text{ monetary units}$$

Cost of ethylene	1.5×10^{-3} monetary units/kg
Cost of HCl	1.0×10^{-3} monetary units/kg
Revenue for ethyl chloride	2.5×10^{-3}monetary units/kg

where F_R is the reactor feed rate in kg/hr. The venture profit [Eq. (17.9)] is formulated (in monetary units), assuming a 10% return on investment (ROI) and 330 operating days/yr:

$$VP = 330\times 24\times 10^{-3}[2.5P-(1.5x_{Et}+x_{HCl})F] - 0.1\left[500\left(\frac{330\times 24}{1000}\left(F_R\right)\right)^{0.6}\right] \tag{21.34}$$

where x_{Et} and x_{HCl} are the mass fractions of ethylene and HCl in the feed stream, respectively, and F and P are the feed and product flow rates in kg/hr, respectively. The NLP is:

$$\text{Maximize} \quad VP \tag{21.35}$$

w. r. t.

W

s. t.

$$\underline{c}\{\underline{x}\} = 0 \quad \text{(material balances)} \tag{21.36}$$

$$R < 300 \text{ kg/hr} \tag{21.37}$$

SOLUTION

As shown in the multimedia modules (see HYSYS → Principles of flowsheet simulation → Getting started in HYSYS → Advanced features → Optimization and ASPEN → Principles of flowsheet simulation → Optimization), the VP is optimized with relative ease. As usual, the optimization is initialized from a feasible solution for $W = 5$ kmol/hr. The SQP method is used, requiring four iterations of the SQP method with 13 evaluations of the material and energy balances. The UniSim®Design spreadsheet is used to compute the VP based on flowsheet information, and the optimizer is then invoked to formulate the NLP objective function and constraints, the decision variables and numerical method parameters. The unconstrained solution [i.e., neglecting Eq. (21.37) in the NLP] gives the global maximum VP of 4,730 units obtained with a value of $W = 7.27$ kmol/hr. Augmenting the NLP with the inequality constraint in Eq. (21.37) gives $VP = 4{,}450$ units obtained with a value of $W = 8.96$ kmol/hr for which R is at its upper bound of 300 kg/hr. Use the file ETHYLCHLORIDE_OPT.usc in the Program and Simulation Files folder, which can be downloaded from the Wiley Web site that accompanies this textbook, to reproduce the results presented above.

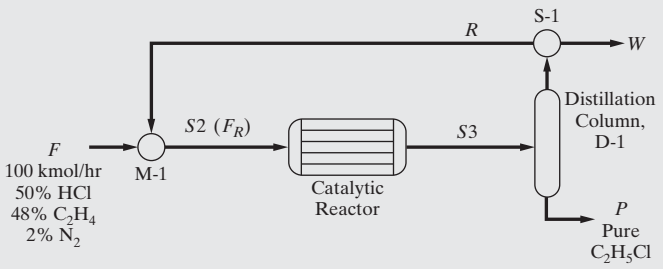

Figure 21.12 Process for the production of ethyl chloride.

EXAMPLE 21.5 *Optimization of a Distillation Tower with Sidedraws*

In this example, the distillation tower in Figure 21.13 is optimized. A feed containing the normal paraffins from nC$_5$to nC$_9$ is fed to the 25-stage tower (including the condenser and reboiler) on stage 15, counting upward from the reboiler stage. The objective is to adjust the operating conditions so as to achieve a distillate (D) concentrated in nC$_5$, a sidedraw at stage 20 ($S1$) concentrated in nC$_6$, a second sidedraw at stage 10 ($S2$) concentrated in nC$_7$ and nC$_8$, and a bottoms product (B) concentrated in nC$_9$. No costing is involved. The operating conditions to be adjusted are the reflux ratio and flow rates of the distillate and two sidedraws.

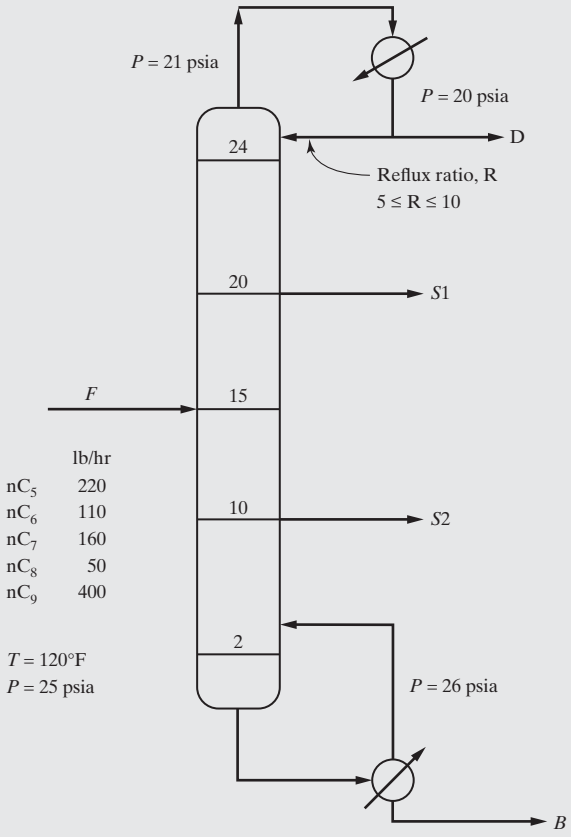

Figure 21.13 Distillation tower with sidedraws.

This is accomplished by formulating an NLP in which the feed stage and the stages of the sidedraws are held fixed during the optimization:

$$\text{Maximize} \quad D_{C5} + S1_{C6} + S2_{C7} + S2_{C8} + B_{C9} \tag{21.38}$$

w. r. t.

$R, D, S1, S2$

s. t.

$$5 \le R \le 10 \tag{21.39}$$

$$0.1 \le D/F \le 0.7 \tag{21.40}$$

$$0.1 \le S1/F \le 0.7 \tag{21.41}$$

$$0.1 \le S2/F \le 0.7 \tag{21.42}$$

$$(D + S1 + S2)/F \le 0.95 \tag{21.43}$$

where R is the reflux ratio; F, D, $S1$, $R2$, and B are the molar flow rates of the feed, distillate, two sidedraws, and bottoms product streams, respectively; and the subscript denotes the molar flow rate of a specific chemical species in that stream. Note that the product streams are withdrawn as saturated liquids at the low pressures shown. The liquid and vapor phases are assumed to be ideal and at equilibrium on the stages of the tower. All of the decision variables have inequality constraints as indicated by Eqs. (21.39)–(21.43). This example does not involve recycle convergence or any user-supplied equality constraints.

SOLUTION

As shown in the multimedia modules, (see HYSYS → Tutorials → Process Design → Multi-draw Tower Design → Multi-draw Tower Optimization and ASPEN → Tutorials → Process Design → Multi-draw Design → Multi-draw Tower Optimization), the solution of this NLP requires care because the gradient-based SQP method is sensitive to the numerical estimates of the derivatives in the Jacobian matrices $\underline{J}\{\underline{x}\}$ and $\underline{\underline{K}}\{\underline{x}\}$. The optimization is initialized at a feasible solution: $R = 5, D = S1 = S2 = 2$ lbmol/hr for which the composition profiles in the column are given in Figure 21.14a and the product recoveries summarized in Table 21.3.

Table 21.3 Product Recoveries in the Multidraw Column

	Percentage Molar Recovery					Objective
	D-C_5	S1-C_6	S2-C_7	S2-C_8	B-C_9	Function
Initial design	65	72	74	18	87	6.87
Optimized design	96	65	96	68	91	8.44

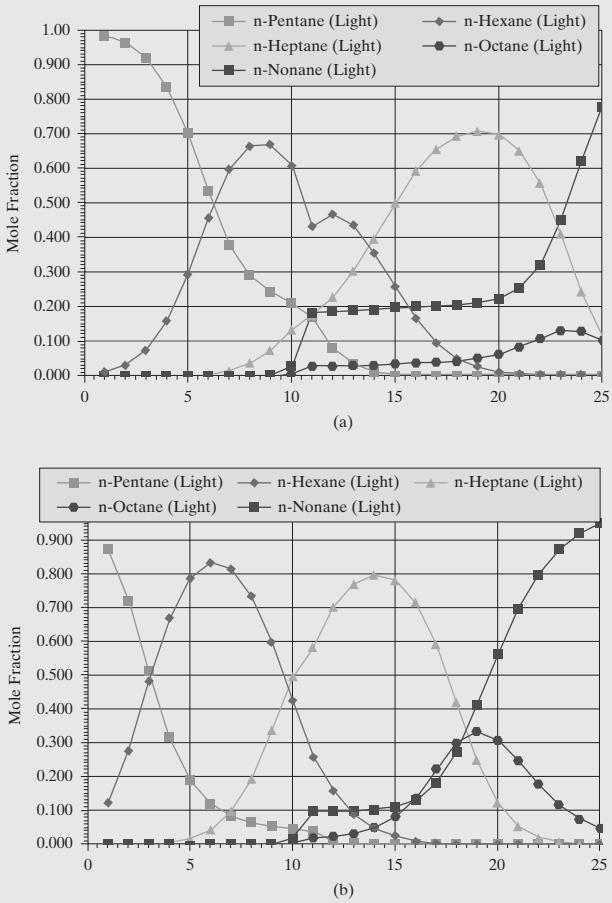

Figure 21.14 Composition profiles in multidraw column as a function of the tray number, counting from the top: (a) initial design; (b) optimized design.

Note that the peaks in the composition profiles are not at the draw stream locations, which explains the rather poor product recoveries, especially for C_8. After optimization, the decision variables are: $R = 10, D = 3.35$ lbmol/hr, $S1 = 1$ lbmol/hr, and $S2 = 2.16$ lbmol/hr, giving the composition profiles in Figure 21.14b, which show a marked improvement in positioning the composition peaks. This explains the significant improvement in product recoveries shown in Table 21.3. Use the files MULTIDRAW_OPT.usc and MULTIDRAW_OPT.bkp in the Program and Simulation Files folder, which can be downloaded from the Wiley Web site that accompanies this textbook.

21.9 SUMMARY

After studying this chapter and the relevant multimedia modules that accompany this textbook, the reader should:

1. Be able to explain the fundamentals of optimization to a layperson.
2. Be conversant with the theory of analytical or numerical methods for treating optimization problems.
3. Be able to solve linear programming (LP) problems that can be expressed in one or two decision variables by hand and problems of higher dimension using MATLAB.
4. Be able to create a nonlinear program (NLP) to optimize a process using equality and inequality constraints.
5. Be able to use the golden-section search to solve a constrained NLP problem in one decision variable.
6. Recognize the advantages of calculating the objective function and constraints for at least a base case of the decision variables before using an optimization algorithm.

7. Understand the advantages of performing optimization and converging recycle calculations and design specifications simultaneously as implemented using an *infeasible path* optimization algorithm.

8. Be able to optimize a process using ASPEN PLUS and UniSim® Design beginning with the results of a steady-state simulation.

REFERENCES

1. Beveridge, G. S. G., and R. S. Schecter, *Optimization: Theory and Practice*, McGraw-Hill, New York (1970).

2. Biegler, L. T., I. E. Grossmann, and A. W. Westerberg, *Systematic Methods of Chemical Process Design*, Prentice-Hall, Englewood Cliffs, New Jersey (1997).

3. Dantzig, G. B., "Programming of Independent Activities, II, Mathematical Model," *Econometrica*, **17**, 200–211 (1949).

4. Edgar, T. F., D. M. Himmelblau, and L. S. Lasdon, *Optimization of Chemical Processes*, 2nd ed., McGraw-Hill, New York (2001).

5. Floudas, C. A., *Nonlinear and Mixed-integer Optimization: Fundamentals and Applications*, Oxford University Press (1995).

6. Han, S.-P., "A Globally Convergent Method for Nonlinear Programming," *J. Optimization and Applications*, **22**, 297 (1977).

7. Jirapongphan, S., *Simultaneous Modular Convergence Concept in Process Flowsheet Optimization*, Sc.D. Thesis, Massachusetts Institute of Technology., Cambridge, Massachusetts (1980).

8. Lang, Y.-D., and L.T. Biegler, "A Unified Algorithm for Flowsheet Optimization," *Comput. Chem. Eng.*, **11**, 143 (1987).

9. Mah, R. S. H., *Chemical Process Structures and Information Flows*, Butterworth, Boston (1990).

10. McMillan, Jr., C., *Mathematical Programming: An Introduction to Design and Application of Optimal Decision Machines*, Wiley, New York (1970).

11. Morgan, A., *Solving Polynomial Systems Using Continuatiion for Engineering and Scientific Problems*, Prentice-Hall, Englewood Cliffs, New Jersey (1987).

12. Powell, M. J. D., "*A Fast Algorithm for Nonlinearly Constrained Optimization Calculations*," AERE Harwell, England (1977).

13. Ravindran, A., K. M. Ragsdell and G. V. Reklaitis, *Engineering Optimization—Methods and Applications*, 2nd ed., Wiley-Interscience, New York (2006).

14. Rudd, D. F., and C. C. Watson, *Strategy of Process Engineering*, John Wiley, New York (1968).

15. Seader, J. D., W. D. Seider, and A. C. Pauls, *FLOWTRAN Simulation—An Introduction*, 3rd ed., CACHE, Austin, Texas (1987).

16. Vanderbei, R. J., *Linear Programming Foundations and Extensions*, Kluwer, Norwell, Massachusetts (1999).

17. Wolfe, P., "The Simplex Method of Quadratic Programming," *Econometrica*, **27**, 382–398 (1959).

EXERCISES

21.1 During the 2002 Winter Olympics in Salt Lake City, Utah, a local microbrewery received a rush order for 100 gallons of beer containing at least 4.0 volume % alcohol. Although no 4% beer was in stock, large quantities of Beer A with 4.5% alcohol at a price of \$6.40/gallon and Beer B with 3.7% alcohol priced at \$5.00/gallon were available as was water suitable for adding to the blend at no cost. The brewery manager wanted to use at least 10 gallons of Beer A. Neglecting any volume change due to mixing, set up a suitable LP and solve it to determine the volumes (in gallons) of Beer A, Beer B, and water that should be blended to produce the desired order at the minimum cost.

21.2 A batch distillation facility has a bank of columns of Type 1 and another bank of Type 2. Type 1 columns are available for processing 6,000 hr/week, and Type 2 columns are available for 10,000 hr/week. It is desired to use these columns to manufacture two different products, A and B. Distillation time to produce 100 gal of product A is 2 hr on Type 1 columns and 1 hr on Type 2 columns. Distillation time to produce 100 gal of product B is 1 hr on Type 1 columns and 4 hr on Type 2 columns. The net profit is \$5.00/gal for product A and \$3.50/gal for product B. Use an LP with a graph to determine the production schedule that maximizes the net profit in \$/week.

21.3 Willy Wonka has engaged your consultation services to assist in the recipe formulation of a new brand of chocolate bar, weighing 100 g, which he plans to name "Super-choc." Each chocolate bar contains two types of chocolate, African and Belgian, with the balance consisting of sugar. Mr. Wonka has requested you to define the optimal composition of the new chocolate bar for minimum cost such that the following conditions are satisfied:

(a) Each bar should contain at most 60 g of chocolate.

(b) The amount of African chocolate in each bar should not be more than 10 g in excess of the amount of Belgian chocolate.

(c) The sweetness of each bar, S, should not exceed 30 units. Each gram of African chocolate reduces S by 0.3 units (relative to sugar), and each gram of Belgian chocolate raises S by one unit.

(d) The "mouth feel" of each bar, M, should be at least 40 units. Each gram of African chocolate increases M by 2.2 units, and each gram of Belgian chocolate increases M by only one unit.

(e) The "lustre" of each bar, L, should be at least 70 units. Each gram of African chocolate increases L by one unit, and each gram of Belgian chocolate increases L by 3.9 units. An example follows:

A bar of Super-choc containing 35 g of African chocolate and 25 g of Belgian chocolate has these properties:

$$S = -0.3 \times 35 + 25 = 14.5$$
$$M = 2.2 \times 35 + 25 = 102$$
$$L = 35 + 3.9 \times 25 = 132$$

Given that the cost of Belgian chocolate is three times that of African chocolate, and the cost of sugar can be neglected, set up a suitable LP and solve it to compute the optimal mass of each of the ingredients of a bar of Super-choc.

21.4 King Henry V of England has decided to wage war on France and has engaged your services to assist him to assemble an appropriate army, which can consist of four types of troops: cavalry, men at arms, archers,

Table 21.4 Data for Each Type of Unit

Unit Type	Cost/Week (gold coins)	Offensive Strength (OS)	Defensive Strength (DS)
Cavalry	10	30	10
Men at arms	5	15	20
Archers	2	20	5
Bombards	20	40	0

and bombards (crude, and sometimes effective, artillery). Table 21.4 lists the weekly salary, offensive strength (OS), and defensive strength (DS) of each type of soldier.

For example, if the army is composed of 50 cavalry, 100 men at arms, 100 archers, and one bombard, then we have:

$$\text{Weekly cost} = 50 \times 10 + 100 \times 5 + 100 \times 2 + 1 \times 20 = 1{,}220 \text{ GCs}$$

$$\text{OS} = 50 \times 30 + 100 \times 15 + 100 \times 20 + 1 \times 40 = 5{,}040$$

$$\text{DS} = 50 \times 10 + 100 \times 20 + 100 \times 5 + 1 \times 0 = 3{,}000$$

The King requests your advice on the composition of an army with the maximum possible OS but with DS of at least 7,000. The King is limiting his budget to 2,000 gold coins per week for this endeavor. Set up an LP and solve it.

21.5 Using calculus, determine all maxima, m inima, and saddle points for the following unconstrained two-dimensional objective functions:

(a) $f\{x_1, x_2\} = 2x_1^3 + 4x_1x_2^2 - 10x_1x_2 + x_2^2$

(b) $f\{x_1, x_2\} = 1000x_1 + 4 \times 10^9 x_1^{-1}x_2^{-1} + 2.5 \times 10^5 x_2$

(c) $f\{x_1, x_2\} = (1 - x_1)^2 + 100(x_2 - x_1^2)^2$

21.6 Use 10 steps of the golden-section search method to find the optimal dimensions for the cylindrical reactor vessel in Example 16.12. In that example, the dimensions of the vessel are given as the inside diameter, $D = 6.5$ ft and tangent-to-tangent length, L = 40 ft. These dimensions are not critical as long as the volume is maintained. Determine the optimal diameter and length if the permissible range of the aspect ratio, *L*/*D*, is 1 to 50.

21.7 As shown in the ASPEN PLUS simulation flowsheet in Fig. 21.15, liquid toluene is to be heated from 100 to 350°F while liquid styrene is to be cooled from 300 to 100°F. Auxiliary heat exchangers E2 and E3, which use steam and cooling water, respectively, are provided to meet the target temperatures when they cannot be achieved by the heat exchanger E1. The process is to be optimized with respect to the minimum temperature of approach in E1, which is to be between 1°F and 50°F. The temperature of stream S3 is constrained to be less than or equal to 200°F, and the temperature of stream S4 is constrained to be less than or equal to 300°F. The annualized cost is to be minimized with the return on investment, i_{min}, equal to 0.5. All of the necessary data are included in Figure 21.15.

21.8 A process to separate propylene and propane to produce 99 mol% propylene and 95 mol% propane is shown in Figure 21.16. Because of the high product purities and the low relative volatility, 200 stages may be required. Assuming 100% tray efficiency and a tray spacing of 24 in., two towers are installed because a single tower would be too tall. The distillate is vapor at 280 psia, and a pressure increase of 0.1 psi is assumed on each tray with a 0.2-psi increase in the condenser. Note that the stage numbers and reflux ratio are for a nominal design. In this exercise, a suitable objective function is to be selected and the number of stages and reflux ratio are to be adjusted to find the optimum. Pay close attention to the determination of the proper feed stage to avoid pinch or near-pinch conditions.

21.9 A process design for the disproportionation of toluene to benzene and the xylene isomers is being completed. Your assistance is needed on the design of the liquid separation section. It has been established that the feed to this section is at 100°F and 50 psia with the following flows in lbmol/hr:

Benzene	16.3
Toluene	70.9
p-Xylene	4.0
m-Xylene	7.5
o-Xylene	3.5

From this feed, it is desired to produce 99.5 mol% benzene, 98 mol% toluene for recycle, and 99 mol% mixed xylenes by distillation in two

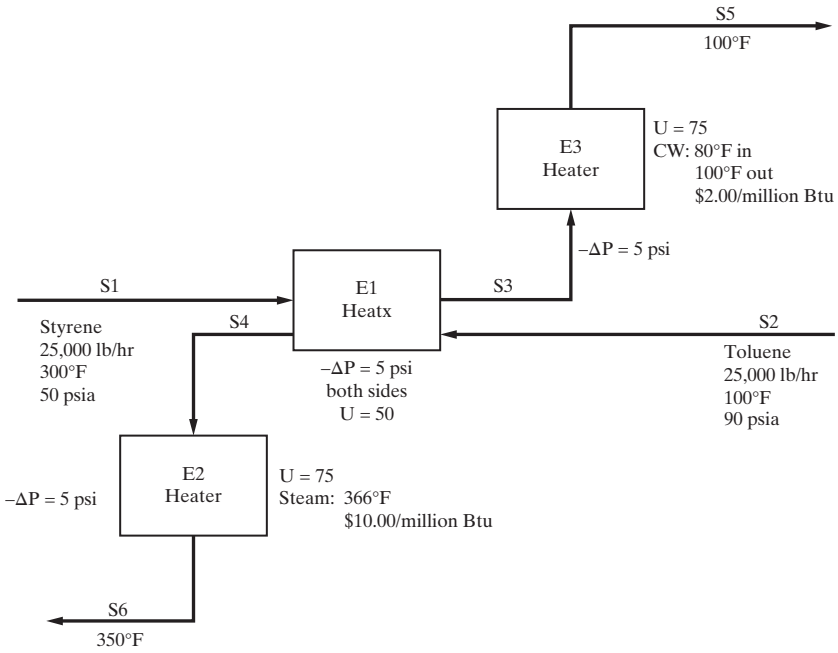

Figure 21.15 Heat exchange network.

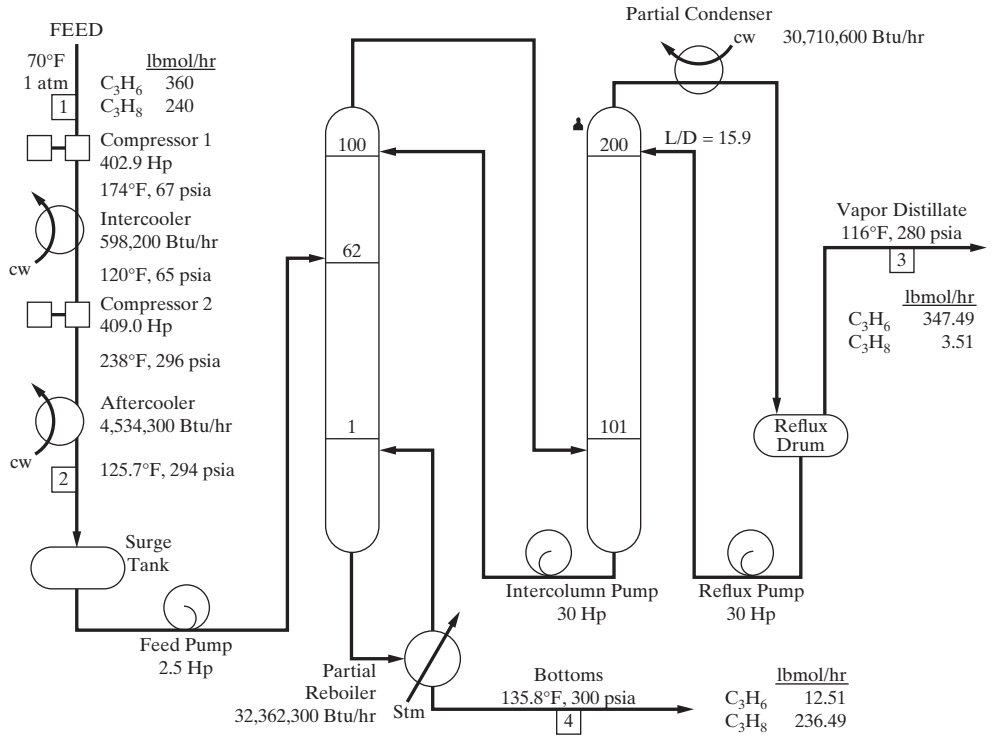

Figure 21.16 Propylene-propane distillation tower.

columns. The assigned plant operators have informed us that they prefer the direct sequence of two columns. However, because of the high percentage of toluene in the feed, a thermally coupled system shown in Figure 21.17, known as Petlyuk towers after the Russian inventor, may be a less expensive alternative.

Please prepare process designs for these two alternatives, together with estimates of capital and operating costs, and indicate whether the Petlyuk towers are attractive. The plant-operating factor is assumed to be 95%. The following data and instructions are provided for the design of the towers:

(a) Determine optimal feed preheat using the bottoms product where applicable.

(b) Determine optimal reflux ratios.

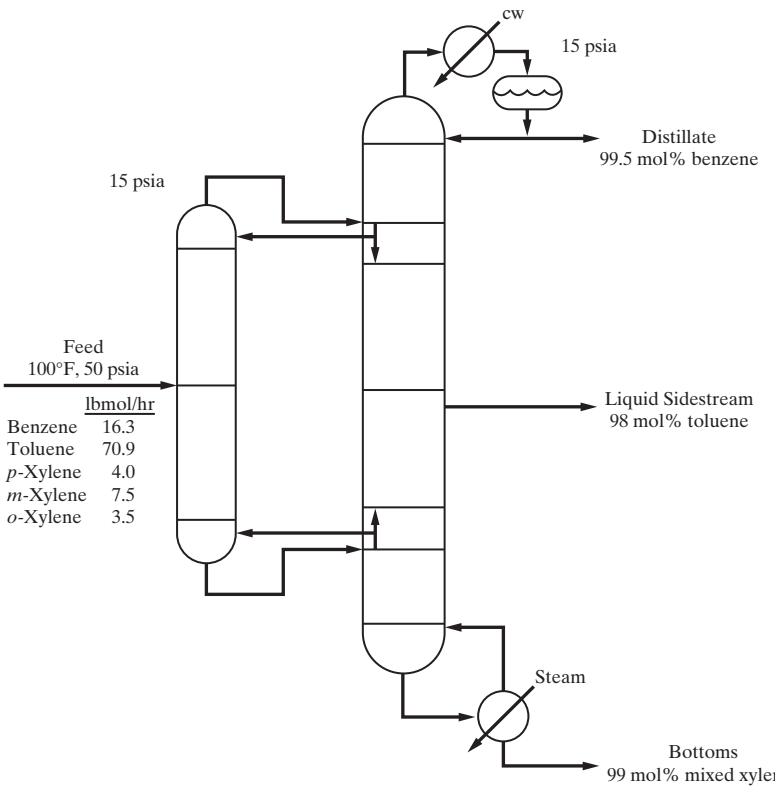

Figure 21.17 Petlyuk towers.

(c) Set a pressure of 15 psia at the top of each column, assuming no pressure drop through the condenser. Determine column bottom pressure drop from tray pressure drops.

(d) Use standard sieve trays. Overall tray efficiency is estimated to be 90% for operation at 85% of flooding.

(e) Determine column diameters to the next increment of 0.5 ft for each section and swedge the columns, when section diameters differ by more than 0.5 ft.

(f) Use reflux subcooled to 120°F from each condenser.

(g) Standard materials of construction, for example, carbon steel, can be used.

(h) Minimum shell thickness for columns and vessels is as follows:

1/4 in. for diameters less than 4 ft
5/16 in. for diameters from 4 to 5.5 ft
3/8 in. for diameters from 6 to 7.5 ft
7/16 in. for diameters from 8 to 11.5 ft
1/2 in. for diameters from 10 to 12 ft

(i) Provide horizontal reflux drums that can hold liquid reflux and distillate for 5 min at half full.

(j) Include all necessary liquid pumps with spares.

Chapter 22

Optimal Design and Scheduling of Batch Processes

22.0 OBJECTIVES

This chapter introduces strategies for designing and scheduling batch processes. It begins with single equipment items focusing on methods for achieving the optimal batch time and batch size. Then, reactor-separator processes are examined where trade-offs exist between the reaction conversion as it varies with reaction time: the cost of separation, which decreases with conversion; and the batch cycle time. Subsequently, methods of scheduling batch processes with recipes having numerous tasks and equipment items are considered. Initially, schedules are considered for plants involving a single product made in production trains that are repeated from batch to batch. The chapter concludes with strategies for designing multiproduct batch plants.

After studying this chapter, the reader should:

1. Be knowledgeable about process units operated in batch mode and approaches for optimizing their designs and operations.
2. Know how to determine the optimal reaction time for a batch reactor-separator process.
3. Be able to schedule recipes for the production of a single chemical product.
4. Understand how to schedule batch plants for the production of multiple products.

22.1 INTRODUCTION

Continuous processes are dominant in the chemical process industries for the manufacture of commodity chemicals, plastics, petroleum products, paper, and so on. When production rates are low, however—say, in the manufacture of specialty chemicals, pharmaceuticals, and electronic materials—it is difficult to justify the construction of a continuous plant composed of small vessels and pipes. In these cases, it is common to design *batch processes* or *semicontinuous processes* that are hybrids of batch and continuous processes. The alternatives are illustrated schematically in Figure 22.1 with a continuous process shown in Figure 22.1a. In the batch process of Figure 22.lb, the chemicals are fed *before* (Step 1) and the products are removed *after* (Step 3) the processing (Step 2) occurs. *Fed-batch processes* combine the first two steps with some or all chemicals being fed continuously during the processing. Then, when the processing is finished, the products are removed batchwise as shown in Figure 22.lc. In *batch-product removal*, the chemicals are fed to the process before processing begins and Steps 2 and 3 are combined; that is, the product is removed continuously as the processing occurs, as shown in Figure 22.1d. In effect, fed-batch and batch-product removal processes are semicontinuous processes.

The challenge in designing a batch, fed-batch, or batch-product removal process is in deciding on the size of the vessel and the processing time. This is complicated for the latter two processes whose flow rate and concentration of the feed stream or the flow rate of the product stream as a function of time strongly influences the performance of the process. Note that the determination of optimal operating profiles is referred to as the solution to the *optimal control problem.* This subject is introduced in the next section.

Batch and semicontinuous processes are utilized often when production rates are small, residence times are large, and product demand is intermittent, especially when the demand for a chemical is interspersed with the demand for one or more other products and the quantities needed and the timing of the orders are uncertain. Even when the demand is continuous and the production rates are sufficiently large to justify continuous processing, batch and semicontinuous processes are often designed to provide a reliable, although inefficient, route to the production of chemicals. For example, in the emulsion polymerization of resins, large batch reactors are installed, often to avoid carrying out these highly exothermic reactions in continuous stirred-tank reactors. Note, however, that whereas operation at a low-conversion steady state is often less profitable than batch or semicontinuous processing, operation at an open-loop, unstable steady state is often more profitable. Rather than install a control system to stabilize the operation, many companies prefer to operate in batch or semicontinuous mode. Similarly, design teams often opt for batch and semicontinuous processes when the chemicals are hazardous or toxic or when safety aspects are of great concern.

Because the designs for continuous and batch processes are usually very different, the choice of processing mode is made

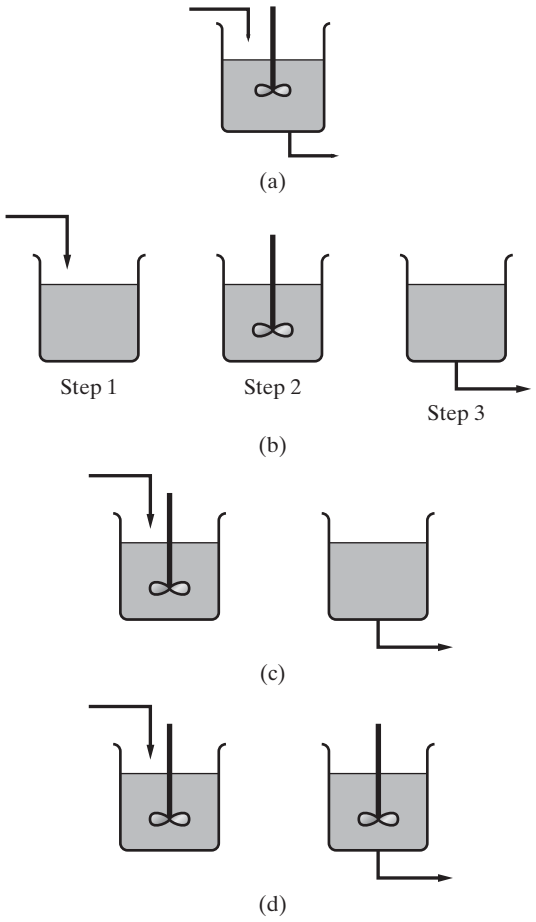

Figure 22.1 Continuous and batch processes: (a) continuous process; (b) batch process; (c) fed-batch process; (d) batch-product removal process.

commonly during process synthesis during the task-integration step as discussed in Section 2.3. At this stage, the decision to reject continuous processing is based upon rules of thumb rather than a detailed comparison of the alternatives. Through process simulation as discussed in Chapter 7 and the optimization methods presented in this chapter, more algorithmic methods are available for selecting from among the various batch and continuous processes.

Usually, for the production of small quantities of high-priced chemicals, such as in the manufacture of pharmaceuticals, foods, electronic materials, and specialty chemicals, batch, fed-batch, and batch-product removal processes are preferred. This is often the case in bioprocessing, for example, when drugs are synthesized in a series of chemical reactions, each having small yields, and requiring difficult separations to recover small amounts of product. This is also the case for banquet facilities in hotels, which prepare foods in batches, and for many unit operations in the manufacture of semiconductors. As discussed in Example 2.3 and Section 7.5, these processes usually involve a *recipe*, that is, a sequence of *tasks,* to be carried out in various items of equipment. In the latter sections of this chapter, variations on batch process schedules are discussed as are methods for optimizing the schedules.

Before proceeding, the reader should note the excellent coverage of both modeling and design of batch chemical processes in the book by Diwekar (2014).

22.2 DESIGN OF BATCH PROCESS UNITS

When designing a process unit to operate in batch mode, it is usually desired to determine the *batch time*, τ, and the *size factor, S*—which is usually expressed as the volume per unit mass of product—that maximize an objective like the amount of product. To accomplish this, a dynamic model of the process unit is formulated and the degrees of freedom adjusted as illustrated in the examples that follow. As will be seen, there are many ways to formulate this *optimal control problem.* To simplify the discussion, models for various input profiles are presented and studied to see how they affect the objectives. Emphasis is not placed on the formal methods of optimization.

Batch Processing

For conventional batch processing with no material transfer to or from the batch, performance is often improved by adjusting the operating variables such as temperature and agitation speed. Through these adjustments, reactor conversion is improved, thereby reducing the batch time to achieve the desired conversion. An example presented next shows how to achieve this objective by optimizing the temperature during batch processing.

EXAMPLE 22.1 ***Exothermic Batch Reactor***

Consider a batch reactor to carry out the exothermic reversible reaction:

$$n_1\mathrm{A} \rightleftharpoons n_2\mathrm{B}$$

where the rate of consumption of A is

$$r\{c_\mathrm{A}, c_\mathrm{B}, T\} = c_\mathrm{A}^{n_1} k_1^0 e^{\frac{-E_1}{RT}} - c_\mathrm{B}^{n_1} k_2^0 e^{\frac{-E_2}{RT}} \tag{22.1}$$

and where $E_1 < E_2$ for the exothermic reaction. The reaction is charged initially with A and B at concentrations c_{A_0} and c_{B_0}. To achieve a specified fractional conversion of A, $X = (c_{\mathrm{A}_0} - c_\mathrm{A})/c_{\mathrm{A}_0}$, determine the profile of operating temperature in time that gives the minimum batch time. This example is based upon the development by Denn (1969).

SOLUTION

The minimum batch time, $\tau_{\min}$, is achieved by integrating the mass balances:

$$\frac{\mathrm{d}c_\mathrm{A}}{\mathrm{d}t} = -r\{c_\mathrm{A}, c_\mathrm{B}, T\} \tag{22.2}$$

$$c_\mathrm{B}\{t\} = c_{\mathrm{B}_0} + \frac{n_1}{n_2}[c_{\mathrm{A}_0} - c_\mathrm{A}\{t\}] \tag{22.3}$$

while adjusting T at each point in time to give the maximum reaction rate.

The temperature at the maximum rate is obtained by differentiation of Eq. (22.1) with respect to T:

$$\frac{\mathrm{d}r}{\mathrm{d}T} = 0 \tag{22.4}$$

Rearranging:

$$T_{\text{opt}} = \frac{E_2 - E_1}{R \ln \dfrac{c_B^{n_2} k_2^0 E_2}{c_A^{n_1} k_1^0 E_1}} \tag{22.5}$$

When an upper bound in the temperature, T^U, is assigned, the typical solution profile is as shown in Figure 22.2. Initially, when $T_{\text{opt}} > T^U$, the reactor temperature is adjusted to the upper bound, T^U. Then, as conversion increases, the reactor temperature decreases, leveling off to the equilibrium conversion. In practice, this optimal temperature trajectory is approached using feedback control, with the coolant flow rate adjusted to give temperature measurements that track the optimal temperature trajectory.

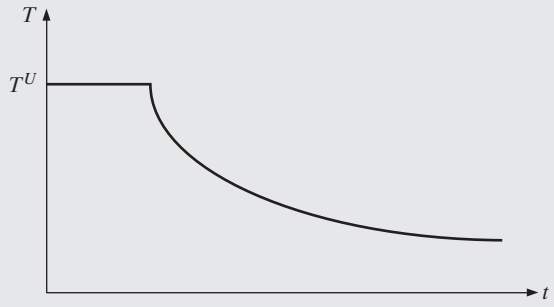

Figure 22.2 Temperature profile to minimize batch reactor time.

Fed-batch Processing

Fermentation processes for the production of drugs are usually carried out in fed-batch reactors. In these reactors, it is desirable to find the best profile for feeding substrate into the fermenting broth, as illustrated in the next example.

EXAMPLE 22.2 *Biosynthesis of Penicillin*

Consider the fed-batch reactor in Figure 22.3. Initially, the reactor is charged with an aqueous volume, $V\{0\}$, containing *E. coli* cells (referred to as biomass) in concentration $X\{0\}$. Then, an aqueous solution of sucrose (referred to as the substrate; i.e., the substance being acted on) at a concentration S_f(g/L) is fed to the reactor at a variable flow rate, $F\{t\}$(g/hr). The reactor holdup, $V\{t\}$, contains *E. coli* cells in concentration $X\{t\}$(g/L), penicillin product in concentration $P\{t\}$(g/L), and sucrose in concentration $S\{t\}$(g/L). Using Monod kinetics, the specific growth rate of the cell mass (g cell growth/g cell) is

$$\mu = \mu_{\max}\left(\frac{S}{K_x X + S}\right)$$

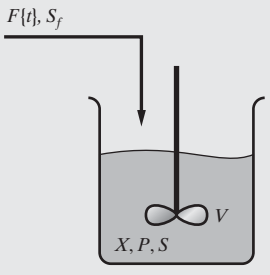

Figure 22.3 Batch penicillin reactor.

Lim and co-workers (1986) developed the following expressions for the specific rate of penicillin production (g penicillin/g cell):

$$\rho = \rho_{\max}\left(\frac{S}{K_p + S\left(1 + S/K_{\text{in}}\right)}\right)$$

and for the specific consumption rate of substrate (g substrate/g cell):

$$s = m_s\left(\frac{S}{K_m + S}\right)$$

Using mass balances for the cell mass, penicillin, and substrate, as well as the overall mass balance, the following rate equations can be derived (see Exercise 22.2):

$$\dot{X}\{t\} = \mu\{X,S\}X - \frac{X}{S_f V}F$$

$$\dot{P}\{t\} = \rho\{S\}X - K_{\text{deg}}P - \frac{P}{S_f V}F$$

$$\dot{S}\{t\} = \mu\{X,S\}\frac{X}{Y_{X/S}} - \rho\{S\}\frac{X}{Y_{P/S}} - s\{S\}X + \left(1 - \frac{S}{S_f}\right)\frac{F}{V}$$

$$\dot{V}\{t\} = \frac{F}{S_f}$$

where $Y_{X/S}$ and $Y_{P/S}$ are the yield coefficients that relate the rate of substrate consumption to the rates of cell growth and penicillin production, respectively.

Using the feed concentration $S_f = 500\ g$ S/L, with the kinetic parameters by Lim and co-workers (1986)—$\mu_{\max} = 0.11\ \text{hr}^{-1}$, $K_x = 0.006$ g S/g X, $K_P = 0.0001$ g S/L, $\rho_{\max} = 0.0055$ g P/(g X · hr), $K_{\text{in}} = 0.1$ g S/L, $K_{\text{deg}} = 0.01\ \text{hr}^{-1}$, $m_s = 0.029$ g S/(g X · hr), $K_m = 0.0001$ g S/L, $Y_{X/S} = 0.47$ g X/g S}, and $Y_{P/S} = 1.2$ g P/g S—for the initial conditions $V\{0\} = 7$ L, $X\{0\} = 1.5$ g/L, and $P\{0\} = S\{0\} = 0$ and for the constraints

$$0 \le X\{t\} \le 40$$

$$0 \le S\{t\} \le 100$$

$$0 \le V\{t\} \le 10$$

$$0 \le F\{t\} \le 50$$

$$72 \le X\{\tau\} \le 200$$

Cuthrell and Biegler (1989) maximize the production of penicillin, $P\{T\}V\{T\}$, where τ is the batch time by using variational calculus (Pontryagin maximum principle) to obtain the solution in Figure 22.4. As seen, at the optimum, the batch time is 124.9 hr, with the production of 87.05 g of penicillin. It is notable that the optimal feed flow rate is 50 g/hr for the first 11.21 hr, after which the feed stream is turned off until 28.79 hr, when it is held constant at 10 g/hr. This "on–off" control strategy is commonly referred to as *bang-bang control.* To confirm the cell mass, penicillin, and substrate concentration profiles, the differential equations can be integrated using a mathematical software package such as MATLAB. Furthermore, Cuthrell and Biegler show how to solve numerically for the optimal solution, which is often referred to as the "optimal control profile," by using orthogonal collocation on finite elements to discretize the differential equations and successive quadratic programming (SQP).

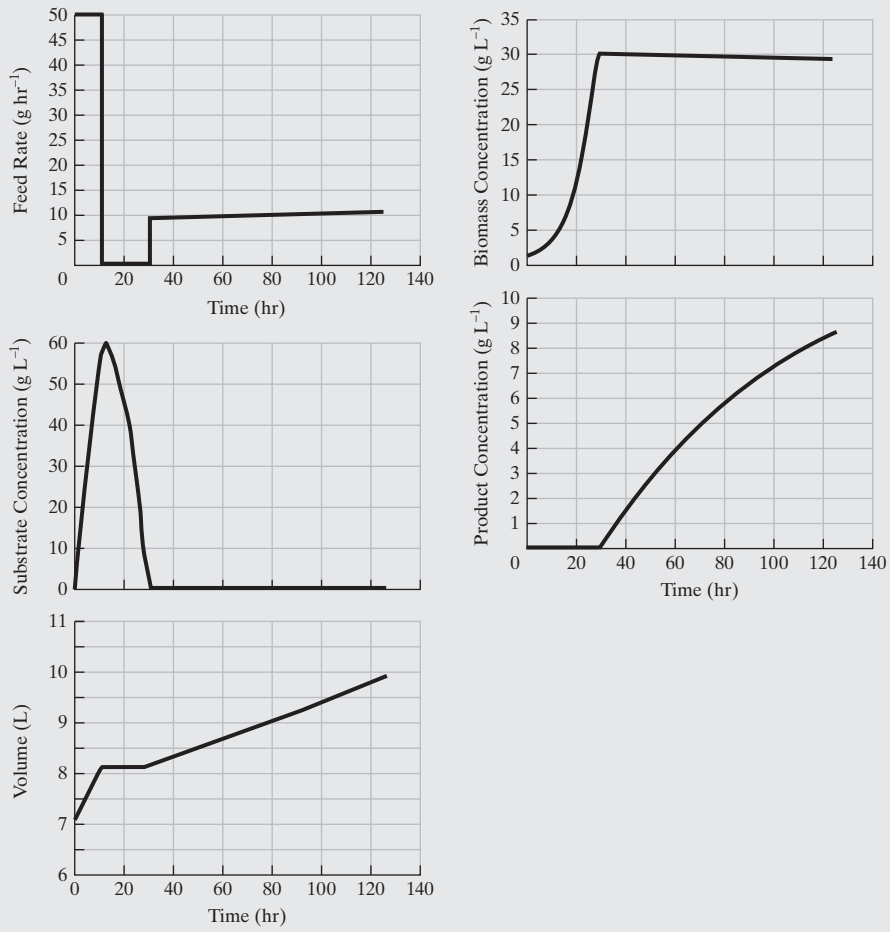

Figure 22.4 Optimal profiles for the penicillin reactor.

Batch-product Removal

When distillations are carried out in batch mode, the still is charged with the feed mixture, and the heat is turned on in the reboiler. The lightest species concentrate in the distillate, which is condensed and recovered in *batch-product removal* mode. As the light species is recovered, it is accompanied by increasing fractions of the heavier species unless a strategy is applied to maintain a high concentration of light species.

For multicomponent separations, to simplify operation, it is often satisfactory to adjust the reflux rate once or twice while recovering each species. When the purity of a species that is being collected in the product accumulator drops below its specification, the contents of the product accumulator are dumped into its product receiver, and the reflux rate is adjusted. Stated differently, the reflux rate is increased as the difficulty of the separation between the light and heavy key components increases. This is illustrated in the next example.

EXAMPLE 22.3 *Batch Distillation*

A 100-lbmol mixture of methanol, water, and propylene glycol with mole fractions 0.33, 0.33, and 0.34, is separated using a 15-tray batch distillation operation as shown in Figure 22.5. Assume operation at 16 psia in the condenser with a pressure increment of 0.1 psia on each tray. The tray liquid holdups are 0.1 ft^3/tray with 1 ft tray diameters. The still is a cylindrical vessel having 1 ft diameter and 10 ft elevation.

To seek a satisfactory operating strategy that recovers nearly pure methanol and propylene glycol products, the following recipe (also called a campaign) is proposed:

Methanol Recovery

1. Aspen Batch Modeler default—start at total reflux
2. Change reflux ratio to 3 in zero elapsed time.
3. Remove distillate at the rate of 5 lbmol/hr until the mole fraction of water in stage 2 (top tray) is 0.001 (trigger approached from below).
4. Bring column to total reflux by setting distillate rate to zero over an arbitrary elapsed time of 0.1 hr.
5. Set the reflux ratio to 5 in zero elapsed time.
6. Remove distillate at the rate of 2.5 lbmol/hr until the mole fraction of water in Receiver 1 is 0.001 (trigger approached from below).

Slop Cut Recovery

7. Bring column to total reflux by setting distillate rate to zero over an arbitrary elapsed time of 0.1 hr.
8. Set the reflux ratio to 3 in zero elapsed time.
9. Remove distillate at the rate of 20 lbmol/hr, to be sent to Receiver 2, until the mole fraction of water in the still pot is 0.001 (trigger approached from above).

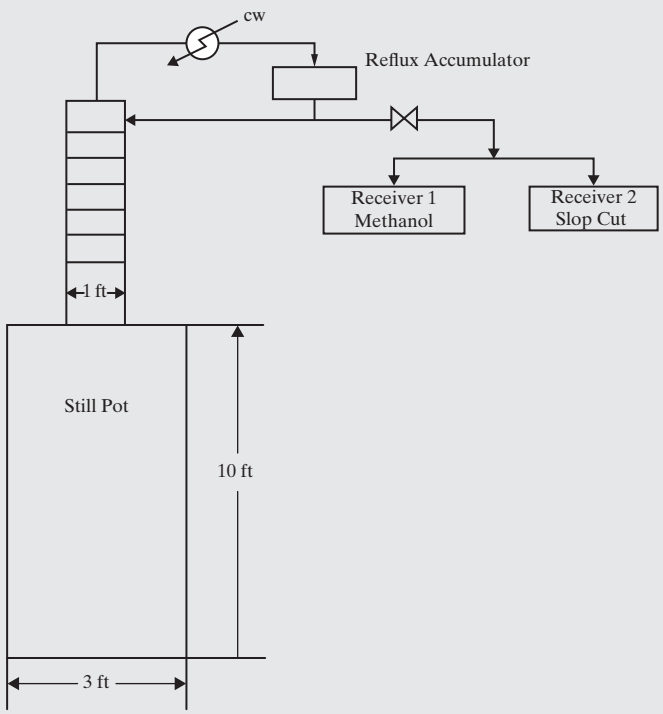

Figure 22.5 Batch distillation operation.

Propylene Glycol Recovery

10. After the slop cut is recovered, the propylene glycol product remains in the still pot.

To examine the performance of this recipe, it is helpful to use a batch distillation program similar to that introduced by Boston et al. (1981) and subsequently provided as the Aspen Batch Modeler by Aspen Technology, Inc. Then, a processing objective can be specified (such as minimum batch time, energy consumption, or reject chemicals, or some combination of these), and variations on the recipe can be explored in an effort to achieve more optimal operation as in Exercise 22.3.

SOLUTION

Using the Aspen Batch Modeler, 11.7 hr are required to complete Steps 1–9, and the results are as follows:

	Mole Fraction						
	Methanol	Water	Propylene Glycol	Methanol (lbmol)	Water (lbmol)	Propylene Glycol (lbmol)	Total (lbmol)
Receiver 1	0.999	0.001	—	30.96	0.031	—	30.99
Receiver 2	0.0581	0.9382	0.0036	2.041	32.96	0.127	35.13
Still Pot	—	0.0001	0.9999	—	0.0084	32.98	32.99
Total				**33.00**	**33.00**	**33.11**	**99.11**

Note that 30.96 lbmol methanol is recovered in the nearly pure methanol product. The remainder appears in the slop cut, which could possibly be recovered from water in a subsequent batch processing separation. Most of the water, 32.96 lbmol, appears in the slop cut, with a small amount, 0.0084 lbmol, in the propylene glycol product. Most of the propylene glycol, 32.98 lbmol, is recovered in the still pot with just 0.0084 lbmol of water. Note that the remaining 0.893 lbmol (i.e., 34.00 – 32.98 – 0.127 1bmol) of propylene glycol resides in the tray holdups after Step 9 is completed. These results can be reproduced using the Aspen Batch Modeler file, EXAM22-3.bspf in the Program and Simulation Files folder, which can be downloaded from the Wiley Web site associated with this textbook.

22.3 DESIGN OF REACTOR–SEPARATOR PROCESSES

In this section, an approach to solving the optimal control problem is introduced for reactor–separator processes. The approach involves the simultaneous determination of the batch times and size factors for both of the process units. Furthermore, the interplay between the two units involves trade-offs between them that are adjusted in the optimization. It should be noted that simpler models than employed in normal practice and in Example 22.3 are used here to demonstrate the concept to provide an analytical solution that is obtained with relative ease.

EXAMPLE 22.4

Consider the batch reactor–separator combination in Figure 22.6, initially presented by Rudd and Watson (1968). In the reactor, the isothermal irreversible reaction A → B is carried out. The separator recovers product B from unreacted A. The rate constant for the reaction is $k = 0.534\ \text{day}^{-1}$. It is assumed that the cost of A is negligible compared to the value of product B, $C_B = \$2.00/\text{lb}$; that the operating costs of the reactor are proportional to the batch time (that is, $C_o = \alpha t$, where $\alpha = \$100/\text{day}$); and that the cost of separation per batch, C_S, is inversely proportional to the conversion of A in the reactor, X (that is, $C_S = KV/X$), where K is the proportionality constant and V is the holdup volume in the reactor. Find the batch time for the reactor when the economic potential, EP (defined in Example 2.2) in \$/day is maximized. Let $c_{Ao} = 10\ \text{lb/ft}^3$, $V = 100\ \text{ft}^3$, and $K = 1.0\ \$/(\text{ft}^3 \cdot \text{batch})$. Note that as the conversion of A to product B increases, the cost of separation decreases, as shown in Figure 22.7b.

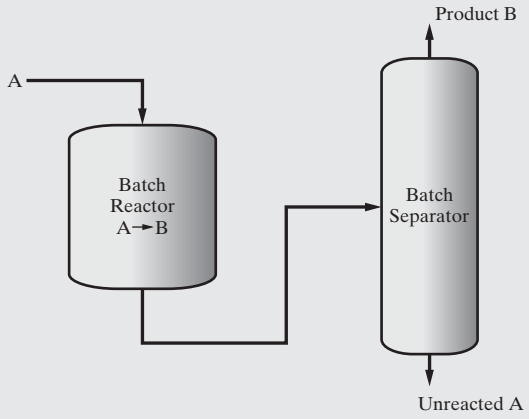

Figure 22.6 Reactor–separator process.

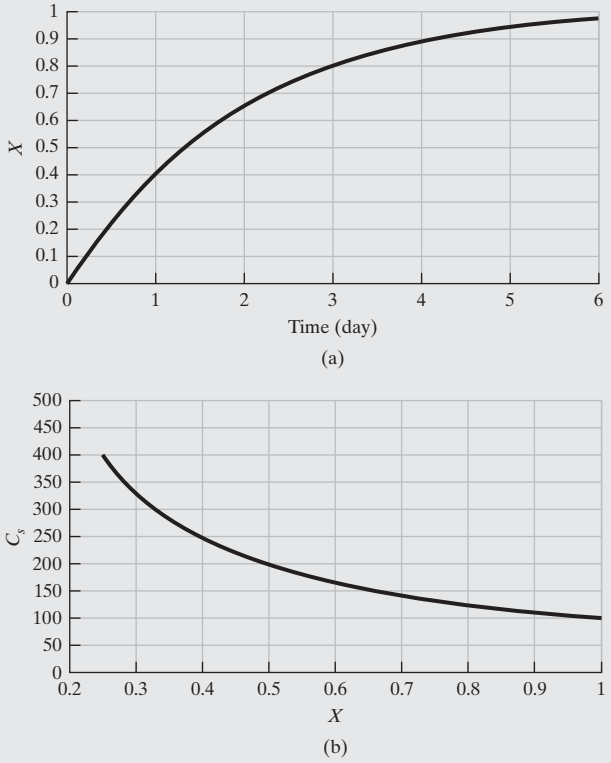

Figure 22.7 Conversion and cost of separation: (a) first-order response of conversion; and (b) cost of separation as a function of conversion.

SOLUTION

For the first-order reaction, it can be shown (Exercise 22.4) that

$$X = 1 - e^{kt} \tag{22.6}$$

as illustrated in Figure 22.7a, and

$$c_{\mathrm{B}} = c_{\mathrm{A}_0} X \tag{22.7}$$

It is desired to maximize the economic potential, *EP* (defined in Example 2.2), in \$/day; that is:

$$\max_t EP = \frac{1}{t}[C_{\mathrm{B}} V c_{\mathrm{B}}\{t\} - C_0\{t\} - C_S\{X\{t\}\}] \tag{22.8}$$

To locate the maximum, substitute the equations above and differentiate:

$$\frac{\mathrm{d}EP}{\mathrm{d}t} = 0$$

It can be shown (Exercise 22.4) that at the maximum, the reactor batch time is $\tau_{\mathrm{opt}} = 1.35$ day, with a fractional conversion, x_{opt}, of 0.514. At longer times, while the revenues increase due to increased conversion and the separation cost decrease, the economic potential decreases due to the increase in the batch time in the denominator of Eq. (22.8). At shorter times, the revenues decrease due to smaller conversion, and the separation costs increase due to a more difficult separation, more than countering the decrease in the denominator and leading to smaller economic potential. At the maximum, EC_{opt} is \$516.8/day. Note that $EP < 0$ when $t < 0.507$ day.

EXAMPLE 22.5

Figure 22.8 shows an isothermal batch reactor in which the irreversible reactions A → B → C take place with B the desired product and C an undesired byproduct. The reactions are irreversible and first order in the reactants. The reaction rate constants are $k_1 = 0.628$ hr^{-1} and $k_2 = 0.314$ hr^{-1}. The reactor products are fed from an intermediate storage tank (not shown) to a batch distillation column, from which the most volatile species, A, is removed first in the distillate, followed by product B, which is the intermediate boiler. For specified reactor volume V_r and column volume V_c, it is desired to determine the batch times for the reactor and column that minimize the cost of producing the desired amount of product B, B_{tot} moles, in a single campaign. Following Barrera and Evans (1989), the analysis is simplified by assuming that the distillation column produces pure A until it is depleted from the still, followed by pure B. Furthermore, specifications include the total molar concentration in the reactor, C; the distillate flow rate, F_d; the time horizon within which the campaign must be completed, τ_{hor}; and the cleaning times between batches for the reactor and distillation column, t_{cr} and t_{cc}. In addition, several cost coefficients are specified, including the cost of fresh feed, P_{A}(\$/mol); recycling credit for A, P_{rA}; cost or credit for the byproduct C, P_{C}; the rental rates of the reactor, r_r(\$/hr), intermediate storage, r_s, and distillation column, r_c; the costs of cleaning the reactor, C_{clr} (\$/batch), and distillation column, C_{clc}; and the utility cost per mole of distillate, P_u. These specifications are given in Table 22.1.

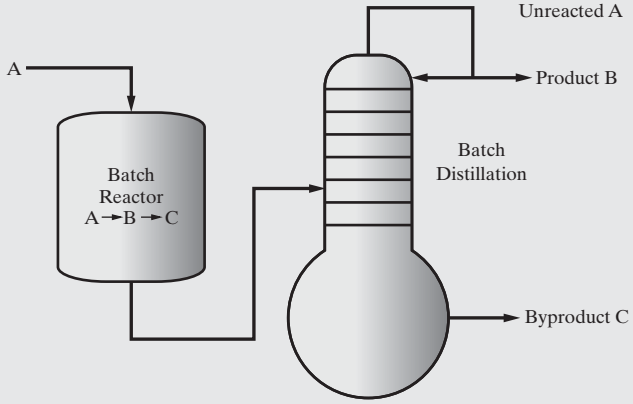

Figure 22.8 Reactive-distillation process.

Table 22.1 Specifications for Example 22.5

$V_r = 3,503$ L, $V_c = 784$ L
$B_{\mathrm{tot}} = 800$ mol
$C = 0.5$ mol/L
$F_d = 206.2$ mol/hr
$T_{\mathrm{hor}} \leq 24$ hr
$t_{cr} = 0.8$ hr, $t_{cc} = 0.5$ hr
$P_A = 1$ \$/mol, $P_{rA} = 0.2$ \$/mol, $P_C = 0.4$ \$/mol
$r_r = 100$ \$/hr, $r_s = 20$ \$/hr, $r_c = 100$ \$/hr
$C_{clr} = 100$ \$/batch, $C_{clc} = 100$ \$/batch
$P_u = 0.45$ \$/mol

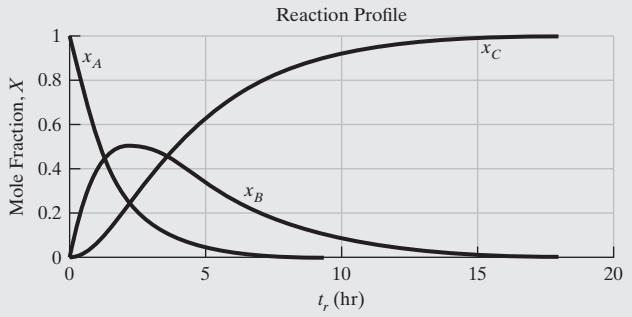

Figure 22.9 Mole fraction profiles for batch reactions: $k_1 = 0.628\ \text{hr}^{-1}$ and $k_2 = 0.314\ \text{hr}^{-1}$.

SOLUTION

By integration of the kinetic rate equations, it can be shown (Exercise 22.5) that the mole fraction profiles in time are given by:

$$x_A = e^{-k_1 t_r} \tag{22.9}$$

$$x_B = \frac{k_1(e^{-k_1 t_r} - e^{-k_2 t_r})}{k_2 - k_1} \tag{22.10}$$

$$x_C = 1 - x_A - x_B \tag{22.11}$$

These profiles are graphed in Figure 22.9.

The minimization of the campaign costs is expressed as:

$$\min_{t_r,\tau} \phi = \phi_{rm} + \phi_{eq} + \phi_{cl} + \phi_u$$

where t_r is the reaction time (reactor operating time), τ_c is the batch time for the distillation column, and the campaign costs for the raw materials, equipment rental, cleaning, and utilities, are

$$\phi_{rm} = CV_r\left[P_A + P_{rA}x_A + P_C x_C\right]\tau_{\text{tot}}/\tau_r$$
$$\phi_{eq} = \left[r_r + r_s + r_c\right]\tau_{\text{tot}}$$
$$\phi_{cl} = \left[C_{clr}/\tau_r + C_{clc}/\tau_c\right]\tau_{\text{tot}}$$
$$\phi_u = P_u F_d t_c \tau_{\text{tot}}/\tau_c$$

Note that the quantity $P_u F_d$ is the \$/hr charge for utilities, t_c/τ_c is the fraction of column batch time during which the column is operational (and using utilities), and τ_{tot} is the total batch time. These quantities are multiplied to give ϕ_u, the cost of utilities per batch. This assumes that the utilities are applied during a t_c/τ_c fraction of the reactor operation. The minimization is carried out subject to a mass balance for the reactor:

$$B_{\text{tot}} = CV_r x_B \tau_{\text{tot}}/\tau_r,$$

an equation that ensures periodicity in the storage tank (i.e., equal volumes processed per unit time):

$$\frac{V_r}{\tau_r} = \frac{V_c}{\tau_c},$$

a mass balance for the distillation column:

$$t_c = V_r C(1 - x_C)/F_d$$

and the total campaign time:

$$\tau_{\text{tot}} = \tau_r + \tau_c$$

where τ_r is the batch time for the reactor and t_c is the column operating time. In addition, as the optimization proceeds, it is necessary to satisfy the following inequality constraints:

$$\tau_{\text{tot}} \le \tau_{\text{hor}}$$
$$\tau_r - (t_r + t_{cr}) \ge 0$$
$$\tau_c - (t_c + t_{cc}) \ge 0$$

For the specifications in Table 22.1, the following solution was obtained using successive quadratic programming (SQP) in GAMS (see Section 21.6). The reactor operates for $t_r = 4.44$ hr to produce a product containing 0.062, 0.373, and 0.565 mole fractions of A, B, and C. For periodic cycling, its batch time is $\tau_r = 18.74$ hr, which exceeds the total of the reactions and cleaning times. The distillation column operates for $t_c = 3.69$ hr, which together with its cleaning time, $t_{cc} = 0.5$ hr, gives a batch time for the column, $\tau_c = 4.19$ hr. The total time, or cycle time, is $\tau_{\text{tot}} = 22.93$ hr, which falls within the horizon time specified, $\tau_{\text{hor}} = 24$ hr. These times correspond to the minimum cost, $\phi = \$10{,}240$. By varying t_r, it can be shown that this is the minimum cost.

22.4 DESIGN OF SINGLE-PRODUCT PROCESSING SEQUENCES

Having examined small optimal control problems for batch process units in Section 22.2 and for reactor-separator sequences in Section 22.3, it should be clear that the determination of optimal batch times, given batch sizes expressed as batch volumes per unit mass of product, can be demanding computationally. Because most processes in practice have recipes with numerous tasks and a comparable number of processing units (e.g., the tPA process in Chapters 2 and 7), it is normally not practical to optimize the batch times for the individual processing units when preparing a schedule of tasks and equipment items for the manufacture of a product. Consequently, when preparing a schedule of tasks and equipment items, it is common to specify batch times for tasks to be performed in specific units, usually with batch sizes, and to optimize cycle times for a specific recipe. In some cases, using the rates of production and yields, the vessels are designed as well; that is, vessel sizes are determined to minimize the cost of the plant while determining the cycle times for a specific recipe. In this section, schedules are determined for the batch processes that involve only single products. In the next section, the methodology is extended for multiproduct batch processes.

Batch process design begins with the specification of a *recipe* of *tasks* to produce a product. In continuous processing, each task is carried out in a specific equipment item, with one-to-one correspondence between them, and shown on a flowsheet that remains fixed in time. Similarly, in batch processes, the tasks are assigned to equipment items, but over specific intervals of time, which vary with batch size, which is often determined by the available equipment sizes. For example, in the tPA process in Sections 2.3 and 7.5, given the rate of tPA production [50 pg tPA/(cell-day), here pg are picograms $= 10^{-12}$ g] and the cell concentration (between 0.225×10^6 and 3×10^6 cell/mL), the availability of a 5,000-L cultivator determines the 14-day batch time and the batch size (2.24 kg of tPA, produced in 4,000 L of medium, yielding 1.6 kg of final product) for the cultivator. As discussed

in Section 2.3, process synthesis involves the creation of a sequence or flowsheet of operations, which can be referred to as a *recipe* of operations or tasks. During the *task-integration* step, tasks are often combined to be carried out in a single equipment item, for example, heating and reaction in a pyrolysis furnace. Also during this step, the decision to use continuous or batch processing is made. At this point, the available equipment sizes often determine the batch sizes and times.

Batch Cycle Times

When scheduling and designing batch processes, several formalisms are widely used, as reviewed by Reklaitis (1995). In this section, and those that follow, portions of the presentation are derived from his article.

In batch processes, it is common for a task to consist of a sequence of *steps* to be carried out in the same equipment unit. For example, Figure 22.10 shows a typical recipe with its tasks and steps. Note that each step involves a *batch time,* which is determined by the processing rates and the *batch size*, that is, the amount of the *final* product manufactured in one batch. Furthermore, a *production line* is a set of equipment items assigned to the tasks in a recipe to produce a product. When a production line is used to produce a sequence of identical batches, the *cycle time* is the time between the completions of batches. To better visualize the schedule of production, an equipment occupation diagram known as a *Gantt chart* is prepared, showing the periods of time during which each equipment item is utilized, as shown in Figure 22.11a. Note that the unit having the longest batch time (6 hr), U2, is the *bottleneck* unit because it is always in operation. Note also that the second batch is begun in time to produce the feed to unit U2 when the latter becomes available after processing the first batch. In this diagram, the batches are transferred from unit-to-unit immediately (so-called *zero-wait* strategy with no intermediate storage utilized). Clearly, the cycle time, 6 hr, is the batch time of U2.

In the schedule in Figure 22.11a, the serial process has a distinct task assigned to each equipment item. Often, to utilize the equipment more efficiently, it is possible to use an equipment item to carry out two or more tasks. Note that this may not be possible when manufacturing specialty chemicals that are very sensitive to contamination as in the manufacture of pharmaceuticals. Returning to the schedule in Figure 22.11a, when the fourth task can be carried out in Ul, this unit is better utilized, and U4 can be released for production elsewhere in the batch plant, as shown in Figure 22.11b. Note that to achieve this schedule without adding intermediate storage, it is necessary to retain the batch within U3 until U1 becomes available. Furthermore, to increase the efficiency of the schedule, that is, to reduce the cycle time, it is common to add one or more units in parallel. When in phase, it is clear that the batch time for the unit is reduced to τ_j/n_j, where n_j is the number of units in parallel for task *j.* For example, when two U2 units, each half size, are installed in parallel, the effective batch time for unit U2 is reduced to 3 hr, and the cycle time is reduced to 4 hr, with U3 the bottleneck unit. Alternatively, the parallel units can be sequenced out of phase, without altering their batch time, as shown in Figure 22.11c. In both cases, the U2 bottleneck is eliminated, and the cycle time is reduced to 4 hr.

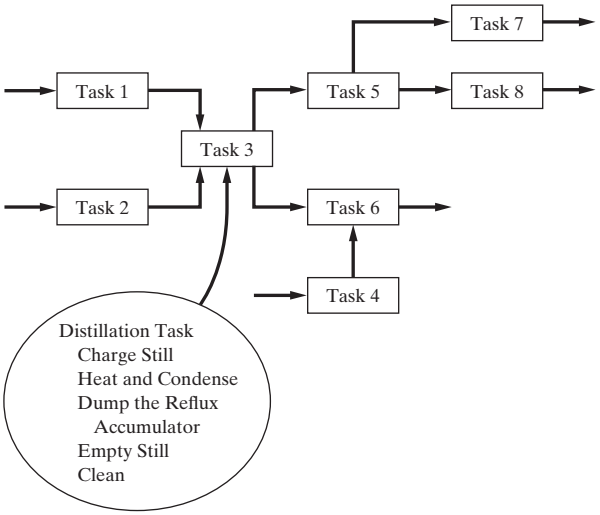

Figure 22.10 Recipes, tasks, and subtasks.

$$CT = \max_{j=1,\ldots,M} \tau_j \tag{22.12}$$

where M is the number of unique equipment units. With n_j units in parallel and in phase, the cycle time is given by:

$$CT = \max_{j=1,\ldots,M} \frac{\tau_j}{n_j} \tag{22.13}$$

Returning to the example, when two units U2 are installed in parallel to perform Task 2:

$$CT = \max_{j=1,\ldots,M} \frac{\tau_j}{n_j} = \max\left\{2, \tfrac{6}{2}, 4, 3\right\} = 4 \text{ days} \tag{22.14}$$

Intermediate Storage

Thus far, two storage options have been illustrated. No storage is used in the schedules of Figures 22.11a and 22.11c; the contents of each unit are transferred immediately to the next unit, experiencing no delay after its task has been completed. As mentioned, this is the so-called *zero-wait* (ZW) strategy. In the schedule of Figure 22.11b, U3 provides intermediate storage until Ul becomes available. Hence, a zero-wait strategy is implemented with some intermediate storage when necessary. This is referred to as an *intermediate storage* (IS) strategy. The third strategy involves unlimited intermediate storage (UIS), sufficient to hold the contents of the products from a unit having a lengthy batch time to be used repeatedly in a unit having half the batch time or less, as illustrated in Figure 22.12. Here, U1 is utilized at all times, and the cycle time is reduced from 9 to 3 hr. To produce a specified amount of product, the batch size is reduced by a factor of one-third because the cycle time is divided by 3.

Batch Size

It is convenient to define the size factor S_j for task j as the capacity required per unit of product. Commonly, it is defined as the volume required to produce a unit mass of product. For example,

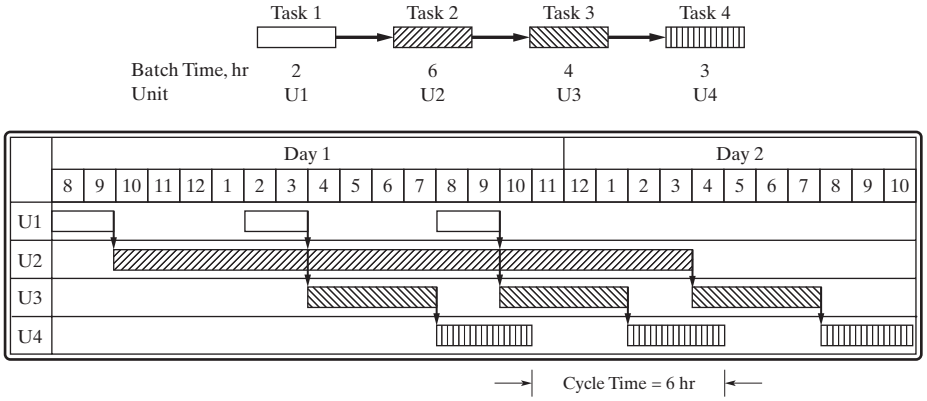

(a)

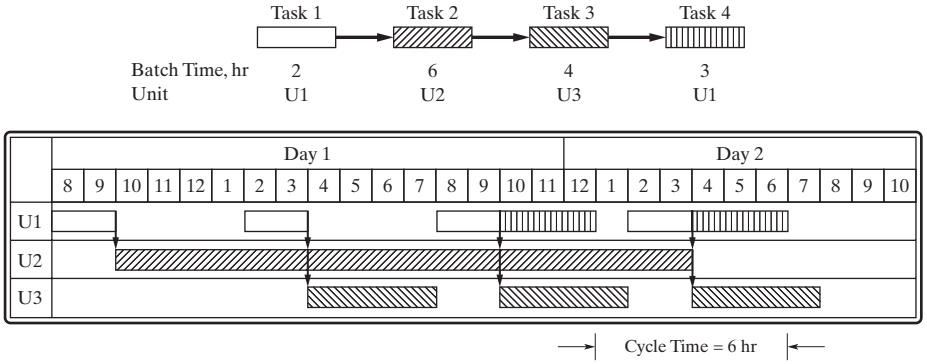

(b)

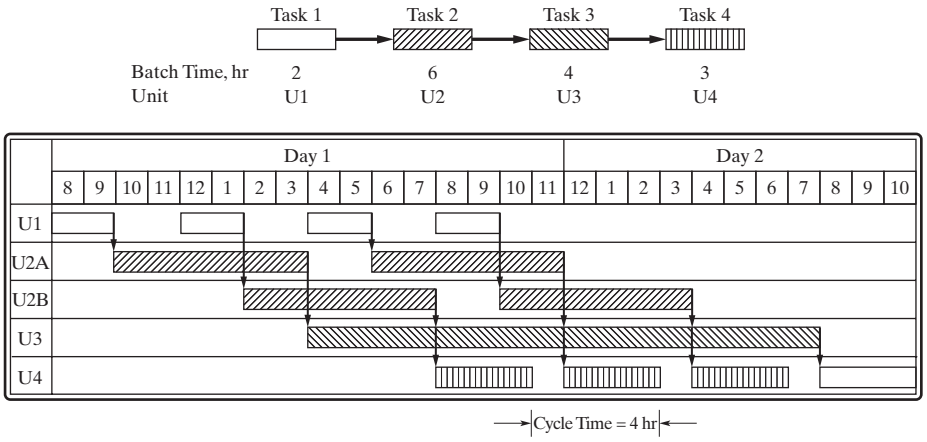

(c)

Figure 22.11 Serial recipe and Gantt charts: (a) Distinct task assigned to each unit; (b) multiple tasks assigned to same unit; (c) parallel units.

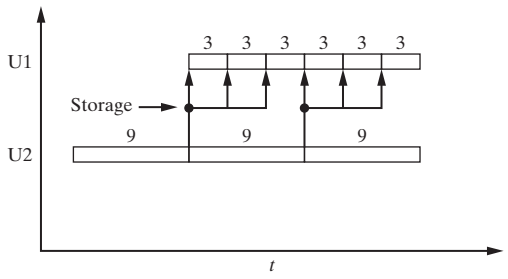

Figure 22.12 Gantt chart with unlimited intermediate storage (UIS).

for the third cultivator in the tPA process of Sections 2.3 and 7.5, 4,000 L of medium yields 2.24 kg of tPA, which eventually yields 1.6 kg of final tPA product. Consequently, its size factor is 4,000 L/1.6 kg = 2,500 L/kg tPA product. Size factors can be computed for each task in a recipe. Normally, equipment vessel sizes are selected that exceed batch volume by 10 to 20%. Clearly, the batch factor in volume/mass produced is determined by the rate of processing the batch (e.g., kg/hr) multiplied by the batch time (hr) and divided by the density of the batch (kg/L) and the mass of product produced (kg).

22.5 DESIGN ON MULTIPRODUCT PROCESSING SEQUENCES

A *multiproduct batch plant* produces a set of products whose recipe structures are the same or nearly identical. One example is a foundry that manufactures integrated circuit (IC) chips in which several different devices are produced simultaneously, each involving hundreds of tasks and utilizing several equipment items. In these plants, each product is produced in the same production line, with multiple processing tasks carried out using the same equipment items. The recipes are expressed in serial campaigns for each product. Figure 22.13 shows schedules in which a campaign of two batches to produce product A is followed by a campaign of two batches to produce product B. It should be noted, however, that because the tasks for products A and B differ in equipment utilized, the plant is not a multiproduct batch plant; instead, it is referred to as a *multipurpose batch plant.* Although the cycle times for both products are identical (4 hr), it is common for the product cycle times to be unequal. The use of alternating product cycles is a limitation that does not apply to *general multipurpose plants*, in which there are no well-defined production lines and no cyclic patterns of batch completion, as shown in Figure 22.14. Such plants are more flexible and effective for a large number of products that are produced in small volumes, where their vessels are cleaned easily and the presence of trace contaminants in the products is not a concern. Their equipment items are utilized more completely, without the idle-time gaps in plants with cyclic campaigns for each product. Consequently, multiproduct batch plants are used for larger-volume products having similar recipes, as is often the case for plants that produce a family of grades of a specific product.

Scheduling and Designing Multiproduct Plants

For an existing plant, the scheduling problem involves a specification of the (1) product orders and recipes, (2) number and capacity of the equipment items, (3) listing of the equipment

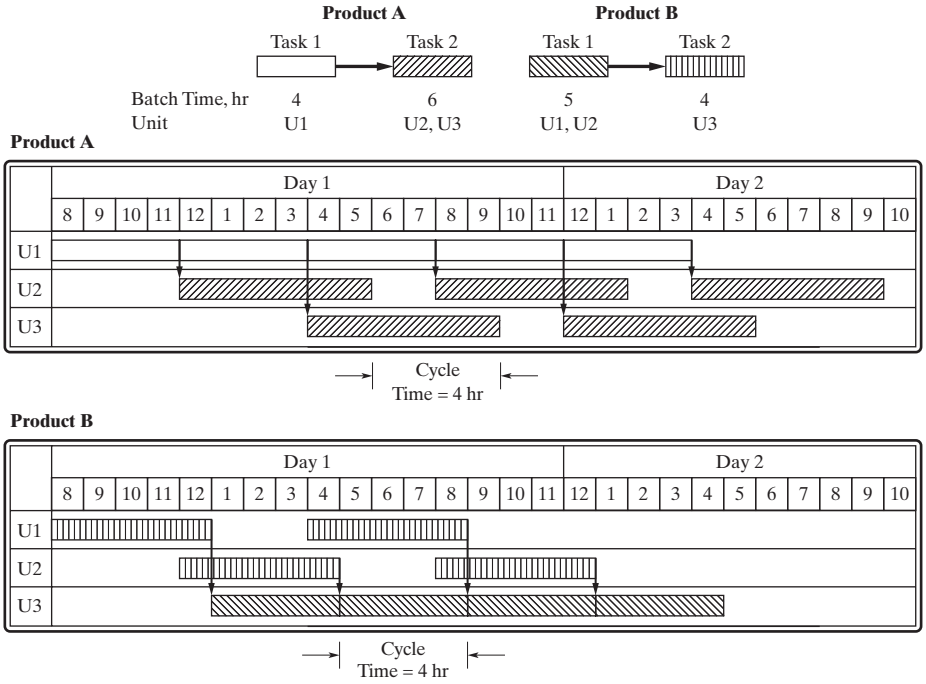

Figure 22.13 Gantt charts for a multipurpose plant.

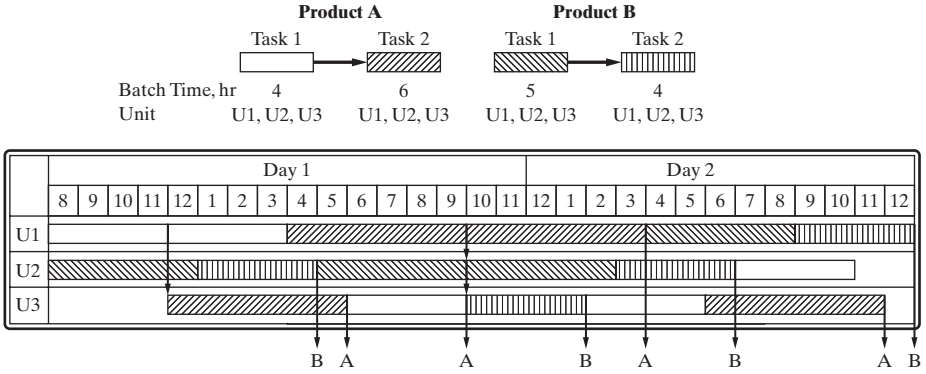

Figure 22.14 Gantt chart for a general multipurpose plant.

items available for each task, (4) limitations on the shared resources (e.g., involving the usage of utilities and manpower), and (5) restrictions on the use of equipment because of operating or safety considerations. In solving the problem, that is, determining an optimal schedule, the order in which tasks use the equipment and resources is determined, with specific timings of the tasks provided that optimize the plant performance (which can be specified in many ways, e.g., to maximize the gross profit).

When the plant does not exist, that is, when a new plant is to be designed, the product orders are usually not well defined. Otherwise, the specifications are identical. In fact, the design problem encompasses the scheduling problem in that its solution involves determining the number and capacity of the equipment items in addition to the optimal schedule. For the design problem, these are determined to optimize an objective that includes the investment costs of the equipment, such as the annualized cost. Because the product orders are not as well known during the design stage, it is common to solve the scheduling problem less rigorously.

As mentioned earlier, it is common to specify size factors and input/output ratios as known constants when defining recipes. Also, batch times for each task are often specified as constant or known functions of the batch size. These can be determined by optimizing the operation of each equipment item, as discussed in Section 22.2.

It is common to formulate the design problem for a multiproduct batch plant involving the processing of batch campaigns in series (i.e., one-at-a-time—commonly referred to as a *flowshop plant*) as a mixed-integer nonlinear program (MINLP). Then, the formulation is simplified for solution using strategies that are beyond the scope of this book (Biegler et al., 1998). Herein, as an introduction, a typical formulation is presented without simplification. It begins with the objective, that is, to minimize the total investment cost, C:

$$\min C = \sum_{j=1}^{M} m_j a_j V_j^{\alpha j}$$

where m_j is the number of out-of-phase units assigned to task j (integer variables), M is the number of tasks, and V_j is the size of the unit assigned to task j (usually in L; a_j and α_j are cost coefficients). This objective is minimized commonly subject to inequalities that involve the vessel size:

$$V_j \geq B_i S_{ij}$$

where B_i is the batch size of product i (i.e., the final product size, typically in kg), and S_{ij} is the size factor for task j in producing product i (typically in L/kg). This inequality ensures that the unit size exceeds the smallest size required to produce all of the products. In addition, lower and upper bounds are specified on the equipment sizes in accordance with manufacturing limitations:

$$V_j^L \leq V_j \leq V_j^U$$

Inequalities are associated also with the cycle time and time horizon:

$$CT_i \geq \tau_{ij}/m_j$$

$$\sum_{i=1}^{N} \frac{Q_i}{B_i} CT_i \leq H$$

where CT_i is the cycle time for producing product i [which can be determined using Eqs. (22.12) and (22.13)], τ_{ij} is the batch time for task j in producing product i, Q_i is the annual demand for product i (typically, in kg/yr), and H is the production hours available annually.

22.6 SUMMARY

After studying this chapter, the reader should be able to:

1. design batch processing units with emphasis on reducing the batch time and batch size.
2. design batch reactor-separator processes with emphasis on the trade-offs in adjusting their batch times.
3. determine operating schedules for single- and multi-product batch plants.

REFERENCES

1. Barrera, M. D., and L. B. Evans, "Optimal Design and Operation of Batch Processes," *Chem. Eng. Comm.,* **82**, 45–66 (1989).

2. Biegler, L. T., I. E. Grossmann, and A. W. Westerberg, *Systematic Methods of Chemical Process Design*, Prentice-Hall, Englewood Cliffs, New Jersey (1998).

3. Boston, J. F., H. I. Britt, S. Jirapongphan, and V. B. Shah, "An Advanced System for Simulation of Batch Distillation Operations," in R. S. H. Mah and W. D. Seider, (eds.), *Foundations of Computer-aided Process Design*, Vol. 2, AIChE, New York (1981).

4. Cuthrell, J. E., and L. T. Biegler, "Simultaneous Optimization and Solution Methods for Batch Reactor Control Profiles," *Comput. Chem. Eng.,* **13**, 49–62 (1989).

5. Denn, M. M., *Optimization by Variational Methods*, McGraw-Hill, (1969).

6. Diwekar, U., *Batch Processing: Modeling and Design*, CRC Press, Taylor & Fancis Group (2014).

7. Lim, H. C., Y. J. Tayeb, J. M. Modak, and P. Bonte, "Computational Algorithms for Optimal Feed Rates for a Class of Fed-batch Fermentations: Numerical Results for Penicillin and Cell Mass Production." *Biotechnol. Bioeng.*, **28**, 1408–1420 (1986).

8. Reklaitis, G. V., "Computer-aided Design and Operation of Batch Processes," *Chem. Eng. ed.*, Spring, 76–85 (1995).

9. Rudd, D. F., and C. C. Watson, *Strategy of Process Engineering.* Wiley, New York (1968).

EXERCISES

22.1 In Example 22.2, derive the mass balances for the cell mass, penicillin, and substrate, and the overall mass balance.

22.2 For the penicillin reactor in Example 22.2, using repeated simulations, search for the optimal feed profile to maximize:

$$0.025P\{\tau\}V\{\tau\} - 1.68\tau - 0.00085\int_0^\tau F\{t\}dt$$

where τ is the batch time. This objective function maximizes the penicillin produced while penalizing long batch times and the cost of the substrate feed stream. Indicate how the penalty terms affect the feed rate profile.

22.3 For the batch distillation column in Example 22.3, devise a recipe that will decrease the batch time without reducing the amount of product recovered. Estimate the increase in the utility usage.

22.4 In Example 22.4, derive Eqs. (22.6) and (22.7). Then, graph the economic potential as a function of the reactor batch time for various values of the rate constant, k, over the range 0.4–0.6 day^{-1}.

22.5 In Example 22.5, derive Eqs. (22.9)–(22.11).

22.6 For the reactor-distillation process in Example 22.5, recompute the solution when the reactor and column volumes are decreased by 20%.

22.7 Construct a Gantt chart for the general multipurpose plant in Figure 22.14, but with the unit assignments specified in Figure 22.13.

22.8 A batch process requires the following operations to be completed in sequence: 3 hr of mixing, 5 hr of heating, 4 hr of reaction, 7 hr of purification, and 2 hr of transfer.

(a) When the five operations are carried out in vessels U1, U2, U3, U4, and U5, respectively, determine the cycle times, and construct Gantt charts corresponding to the zero-wait, intermediate storage, and unlimited intermediate storage inventory strategies.

(b) When a new purification vessel U4A is purchased so that two 7-hr purifications can take place in parallel, determine the system bottleneck using the intermediate storage inventory strategy.

Part Four

Design Reports—Product and Process

In this part of the book, Chapter 23 presents the contents of a written design report, with recommendations concerning its completion. Particular attention is given to the many differences between the content of a product design report and a process design report. Emphasis is placed on the need for those involved to document the design throughout the design process, including the project charter, the innovation map, and the data used. For a product, the documentation should include marketing and customer considerations, a prototype design, and a business plan. For a process design, the documentation should include the flowsheets considered, summaries of material and energy balances and equipment sizing from process simulators, together with cost estimates and the profitability analysis. To accomplish this, the design team needs to maintain a repository of material entered day-to-day in project notebooks. When documented properly, such materials will be invaluable during the preparation of oral reports at project meetings and in the preparation of the final design report.

In addition, the presentation of an oral report on a design is discussed and suggestions are made for the organization of the oral presentation, the media available for presenting it, and the use of printed handouts. Also discussed is the use of DVDs and YouTube segments to record oral presentations to help improve future presentations.

Chapter 23

Written Reports and Oral Presentations

23.0 OBJECTIVES

At the completion of their design work, design teams are required to prepare reports documenting the details of the designs and how they were produced, projecting their profitabilities, and making recommendations as to whether management should invest in the products and/or processes. Also, design reports identify the key assumptions in the designs and their potential impact on the performance and profitability of the products and/or processes. This is particularly important for designs completed by undergraduate students at universities where facilities, funds, and time for pilot-plant testing cannot be arranged—and where laboratory work and testing of product prototypes are usually difficult to arrange.

It is these uncertainties, especially when data are lacking, that engineers encounter throughout their careers. Even when laboratories and pilot plants are available, engineering judgments are needed to determine when the investment of money and time is justified to organize an experimental program. In this respect, engineers are asked regularly to estimate the profitability of products and processes about which they have too little information. For these reasons, design teams usually expend considerable effort in trying to eliminate as much of the uncertainty as possible (by locating data in the literature, conducting process simulations, etc.). Invariably, however, uncertainties remain, and it is important that the design report identify the uncertainties and, when it recommends that a product be launched and/or a process be constructed, make recommendations as to how the uncertainties should be resolved.

A design report documents all of the steps leading up to the design of the product and/or process. This includes a discussion of the need for the new product and/or process, a summary of the possible ways the design team considered to satisfy the need, the rationale behind the selection of the best ideas, the one ultimately selected, and the design of the new product and/or process. In industry, the report might also include the development of a pilot plant as well as the performance of a product prototype and manufacturing tests. However, in universities, undergraduate students may not have the time and/or funds to produce a prototype of the product and determine its performance. On the other hand, a product design developed by a student design team in a previous year could be given to a new design team for further development and assessment of a prototype.

The design team should view its design report as an opportunity to showcase for management its most creative engineering efforts. Wherever possible, a design report should highlight the engineering work that the team believes will lead to greater economies than are achievable using alternative or conventional technologies—emphasizing the soundness of its ideas, but the need for data to prove their validity. A product design should emphasize the superiority of the new product over available products with similar functions.

For most student design teams, the design report is the first extensive report they prepare in their professional careers. It is the culmination of a major engineering effort and, when done well, is deserving of considerable attention from other students, faculty, industrial consultants, and prospective employers. In this respect, the professional reputation of the design team depends, in part, on how well the design problem has been analyzed, how ingeniously the product has been developed and/or the process laid out, and how thoroughly the engineering calculations and design work have been done. The efforts of a design team are judged almost entirely by the quality of the engineering report provided to its supervisor that describes the work that has been accomplished. Of particular importance to management are the strength of and justification for the recommendations made in the report. Almost always, the report will be accompanied by an oral presentation by the design team, where questions can be asked by management.

There is perhaps a tendency to view the preparation of the design report and the oral presentation to management as activities reserved for the completion of a design project. Indeed, the level of activity in writing builds steadily toward the end, especially as the design becomes more promising, but an objective of this chapter is to present the many reasons for documenting the results gradually, as the design proceeds.

After studying this chapter, the reader should:

1. Understand the template that prescribes the items in most design reports, and have a good appreciation of the materials to be included in each item.
2. Be prepared to coordinate the preparation of the design report with the other members of the design team, beginning early in the design process, and to recognize the important milestones, that is, those portions of the report that are best prepared before work begins on the next step in the design process.
3. Understand the role and format of a typical oral presentation, including the alternative media for the presentation and related topics such as the need for rehearsals and the desirability of a written handout.

23.1 CONTENTS OF THE WRITTEN REPORT

This chapter begins with a list of items to be included in most design reports and is followed by a discussion of several techniques found to be helpful in their preparation in addition to recommendations for the page formats to permit PDF files to be distributed electronically and printed copies of the design report to be bound for distribution.

Items of the Report

Before examining a list of items normally included in a design report, the reader should decide whether he or she is describing a new *product design*, a new *process design*, or possibly both new *product and process designs*. For assistance, consider Table 23.1, which identifies typical features of product and process designs.

Having made this decision, it is recommended that the reader consider the following list of 28 items, which are typically presented in the sequence shown. Note the product design items (PROD) are included *only* for product designs, and the process design items (PROC) are included *only* for process designs. When both a new product has been designed and a new process is proposed to manufacture a product, it is normally preferable for a design report to include the product design items before the process design items as follows:

Table 23.1 Features of Product and Process Designs

Product Design	Process Design
A new chemical product is proposed in one of three types (Figure 1.4, Section 5.1), either: Molecules or mixtures of molecules Functional (devices, …) Formulated	A new chemical process has been proposed to manufacture either: An existing chemical product A new chemical product
New product uses new technologies as identified in an innovation map (Figure 1.11)	Raw materials have been selected and process synthesis carried out (Section 2.3)
Product is intended for a specific market, possibly to compete with other products	A database has been assembled including: Thermophysical properties Kinetic rate constants Toxicity information Chemical prices
Product satisfies customer requirements	A process flowsheet has been created and material balances completed
A prototype design has been completed	Energy balances and utility requirements have been completed
A business case has been prepared	Equipment items have been designed (i.e., key sizes determined and costs estimated)
An IP analysis has been prepared, see Example 1.5	Operating costs have been estimated and profitability analyses completed

1. ***Letter of Transmittal.*** This letter on professional letterhead is normally directed to the supervisor who requested that the design work be done. It should be signed by all members of the design team.
2. ***Title Page.*** In addition to the title, the authors and their affiliations are listed in uppercase, as the publication date. The title should be short, but very descriptive.
3. ***Table of Contents.*** All items in the report should be listed, including the page numbers on which they begin. Hence, all pages in the report *without exception* must be numbered. This applies to text pages for which the word processor will probably have provided the page numbers, as well as the tables, figures, and appendixes, whose pages may have to be numbered manually. Note that the unnumbered pages are not readily found by the reader, who may resent the time wasted thumbing through the report to find pages that are missing or not numbered.
4. ***Abstract.*** This is a brief description of the design report, focusing on its key conclusions, special features, and assumptions in one or two paragraphs. These include projections of any applicable economic measures of goodness (e.g., the return on investment and the net present value) and recommendations to management. Care should be taken to report only *significant* figures.
5. ***Introduction and Objective-time Chart.*** This presents the origin of the design project and focuses on the objective-time chart of the tasks needed to be accomplished over the project duration (see Figure 1.6). Included are the specific goals, a project scope, and the deliverables and time line followed.
6. ***Innovation Map (PROD).*** This item of the report could be titled Technology Readiness Assessment. An innovation map should be presented showing the new technologies (materials, process/manufacturing, and product technologies) upon which the new product is based. A brief history of the technologies is helpful when discussing the innovation map, which should show how the voice of the customer for the new product is linked to the new technologies. Questions to be answered include whether all technologies are ready or can be used with minor variations.
7. ***Market and Competitive Analyses.*** These describe the market(s) for the new product and identify the principal competitors. When available, the production levels and annual sales of existing products are provided. Also, sales projections for the new product are included.
8. ***Customer Requirements (PROD).*** The voice of the customer is presented in the form of customer requirements. Although student design groups have limited access to customers, expressions of need should be stated based upon information from trade journals, advertisements, Web searches, and industrial consultants to design courses

at universities. The customer requirements should be classified as fitness-to-standard (FTS) or new-unique-difficult (NUD).

9. ***Critical-to-quality (CTQ) Variables—Product Requirements (PROD).*** This item should begin by identifying the CTQ variables, which are normally the NUD variables. Then, the translation of the customer requirements (CTQ variables) into technical requirements should be discussed. Their relationships should be discussed in the rectangular section of the House of Quality (HOQ). The triangular interaction matrix, showing the synergistic technical requirements, should be added to the HOQ.
10. ***Product Concepts (PROD).*** The alternative product concepts should be presented. The advantages and disadvantages of each product concept should be discussed relative to a reference concept (normally the best existing product).
11. ***Superior Product Concepts (PROD).*** The superior concept should be presented with justification for its selection.
12. ***Competitive (patent) Analysis (PROD).*** Having identified the superior concept for the new product, normally the competitive analysis is revisited. In this discussion, the results of more specific market analysis are presented. Also, the results of a more specific patent search are discussed in a so-called IP assessment.
13. ***Preliminary Process Synthesis (PROC).*** The alternative process flowsheets should be presented and possibly the synthesis tree (see Figure 2.7) with a discussion of the most promising flowsheets.
14. ***Assembly of Database (PROC).*** The principal thermophysical and transport property data should be presented with chemical kinetics data and toxicity data and prices for the principal chemicals.
15. ***Process Flow Diagram and Material Balances (PROC).***
    (a) **Process Flow Diagram and Material Balances.** This is the detailed process flow diagram discussed in Section 2.5 and shown for a vinyl-chloride process in Figure 2.17. All of the streams are numbered clearly and all of the process units are labeled. At some point on the arc for each stream, the temperature and pressure should appear or the information should be tabulated (e.g., see Table 2.7). Note that, as mentioned in Section 2.5, many software packages are available to simplify the preparation of flow diagrams, most notably those associated with the process simulators.

    In addition, the drawing should contain a *material-balance block* similar to the one shown for the vinyl-chloride process in Table 2.7, that is, a table showing for each numbered stream:

    (1) Total flow rate

    (2) Flow rate of each chemical species

    (3) Temperature

    (4) Pressure

    and other properties of importance (density, enthalpy, etc.). It is desirable that the flow diagram and the material-balance block appear on a single sheet for continuous reference, preferably 8½ by 11 inches, so that it can be bound easily with the remainder of the report. Alternatively, two pages can be used, one for the flowsheet and the other for the material-balance block. Following the instructions in part (d) of the discussion on *Page Format* of Section 23.2, both should appear sideways (broadside), with the flowsheet on an even page and the material-balance block on the next odd page. Most commonly, both the flowsheet and the material-balance block are prepared by computer using the latest software, such as Microsoft VISIO. The symbols on the flowsheet should follow a standard list such as those provided in Figure 2.18 and by Peters et al. (2003), Sandler and Luckiewicz (1993), and Ulrich and Vasudevan (2004). Note that simulator flowsheets are normally inadequate because many simulator blocks represent several equipment items (e.g., a distillation block does not show the condenser, reflux accumulator, reboiler, and pumps).
16. ***Process Description (PROC).*** This report item provides an explanation of the flow diagram. It best begins, however, with reference to a block flow diagram similar to that in Figure 2.16, which shows just the process steps that involve chemical reactions and the separation of chemical mixtures. Then, a more detailed description is presented that refers to all steps in the process that are shown in the process flow diagram (e.g., Figure 2.17). The detailed description describes the function of each equipment item and discusses the reasons for each particular choice. Note that the details of each major equipment item are presented in Item 18 on unit descriptions. To aid the reader, however, the discussion of each equipment item should be accompanied by a reference to the page number in Item 18. As in the introduction, when the flow diagram has been selected from among alternatives, it is appropriate to present the alternative flow diagrams and process descriptions, and to describe the reasons for the final choice.
17. ***Energy Balance and Utility Requirements (PROC).*** In describing most chemical processes, it is desirable to have a section that discusses the energy requirements of the process, and the measures adopted to improve the plant economics by energy and mass conservation, usually through the application of the methods described in Chapter 10, Second Law Analysis, and in Chapter 11, Heat and Power Integration. In this report item, all of the heating, cooling, power, and other utility demands should be identified (with numerical values provided), and the methods of satisfying these demands shown. A list should provide each demand (e.g., 500,000 Btu/hr to heat stream 5 from 80 to 200°F) and the vehicle for its satisfaction (e.g., 500,000 Btu/hr from stream 15 as it is cooled from 250 to 100°F). When power generated by a turbine is used to drive a compressor and pumps, these integrations should be listed as well.

18. ***Equipment List and Unit Descriptions (PROC).*** In this report item, every process unit in the flow diagram is described in terms of its specifications and the design methodologies (e.g., the methods for estimating the heat-transfer coefficients, the rigorous design of a distillation tower by means of a simulation program, the recommendations of industrial consultants), and the data employed (e.g., to characterize the reaction kinetics and vapor–liquid equilibria). The important approximations should be discussed as well as any difficulties encountered in performing the design calculations (e.g., in converging equilibrium-stage calculations with a simulator). In addition, the materials of construction should be indicated with the reasons for their selection.

    Each process unit description should refer to the page number in the appendix on which the design calculations appear or are described. Note that, as described under Item 28, the latter calculations are either hand printed neatly or done by computer. In addition, the description of each process unit should refer to a corresponding specification sheet, discussed subsequently, that is assembled with the other specification sheets in Item 19. Finally, the descriptions should refer to the estimated installed and operating costs for the process unit in cost summaries discussed later.

    The identification of each process unit (e.g., Unit No. E-154, the condenser on an ethanol still) should be very clear, so that the concerned reader is able, without confusion, not only to relate each unit description to the corresponding specification sheet, its estimated costs in the cost summaries, and its design calculations in the appendix, but also to locate that additional information readily and to check it when necessary.

    The process unit descriptions should include (1) storage facilities for the feed, product, byproduct, and intermediate chemicals; (2) spare equipment items (pumps, adsorption towers, etc.) required to avoid shutdowns in the event of operating difficulties; and (3) equipment for startup, which is often not needed during normal operation.

    The descriptions are accompanied by an equipment list, which includes the unit number, unit type, brief function, material of construction, size, and operating conditions of temperature and pressure.

19. ***Specification Sheets (PROC).*** Specification sheets are required to guide purchasing agents in locating vendors of desired equipment and to enable vendors to prepare bids. These sheets provide the design specifications for each of the process units in the process flow diagram referred to in the unit descriptions. A typical example is shown in Figure 23.1.

    It is recommended that before preparing specification sheets, students at universities have more experienced individuals (e.g., faculty and industrial consultants) review the specifications to identify, hopefully, impractical specifications and significant inconsistencies.

20. ***Equipment Cost Summary (PROC).*** In this report item, a table is prepared that contains the estimated purchase price of every equipment unit in the process flow diagram, identified according to the unit number and unit type on the process flow diagram and in the equipment list. The sources of the prices should be identified (graphical or tabulated cost data, a quotation from a specific manufacturer, etc.).

21. ***Fixed-capital Investment Summary (PROC).*** In this report item, the fixed capital investment is related to the estimated purchase cost of the equipment items. If desired, the equipment list and the list of equipment purchase costs can be combined. The methods for estimating the fixed capital investment, beginning with the purchase costs, should be clearly stated. If a factored cost estimate is used, the overall factor or individual equipment factors should be noted.

22. ***Operating Cost—Cost of Manufacture (PROC).*** This report item begins with a presentation of the estimated annual costs of operating the proposed plant; that is, the cost sheet, as discussed in Section 17.2 and shown in Table 17.1. In addition to the total production cost on the cost sheet, it should provide an estimate of the cost per unit weight of the product (e.g., $ per lb, kg, ton, or tonne). Note that when cash flows are computed for different production rates from year to year, a separate cost sheet is required for each unique production rate. Note also that in addition to appearing on the cost sheet, the utilities for each equipment unit and their costs should be summarized in a separate table.

23. ***Other Important Considerations.*** In most design reports, the following considerations deserve separate subparts. Often, they are sufficiently important to warrant coverage apart from any discussion in the other parts of the report. These include those aspects of the design that address:

    (a) Environmental problems and methods used to eliminate them.

    (b) Process controllability and instrumentation, including plantwide control (see Chapter 20) and a piping and instrumentation diagram (P&ID). Note that P&IDs are included only when instruments are needed to resolve special problems, for example, safety and product quality related problems (see Section 3.6).

    (c) Safety and health concerns, including a HAZOP (hazard and operability) study, as discussed in Section 3.6.

    (d) Plant startup, including additional equipment and costs.

    (e) Plant layout when critical. Here, students probably need assistance from experienced plant designers.

    To the extent that these matters influence the choice of particular or additional items of equipment as well as operating strategies, at least some discussion should be included. This report item is intended to allow for a more thorough discussion of these subjects than might be appropriate elsewhere and to enable the design team to draw attention to their importance in developing their design.

DISTILLATION COLUMN

Identification: **Item** *Distillation Column*
Item No. T-*700*
No. required 1

Date: *9 April 1997*
By: *SFG*

Function: Separate Benzoic Acid and Benzaldehyde from VCH, Styrene, and other organics.

Operation: Continuous

Materials handled:	*Feed*	*Feed 2*	*Liquid Dist.*	*Bottoms*	*Vapor Dist.*
Quantity (lb/hr):	161,527		153,022	6947	1558
Composition:					
Butadiene	4 PPB		2 PPB	trace	236 PPB
VCH	0.059		0.061	2 PPM	0.109
Styrene	0.861		0.899	0.087	0.630
Butene	10 PPB		5 PPB	trace	604 PPB
Cis-Butene	29 PPB		16 PPB	trace	2 PPM
Trans-Butene	9 PPB		5 PPB	trace	545 PPB
n-butane	3 PPB		1 PPB	trace	171 PPB
Isobutylene	7 PPB		3 PPB	trace	454 PPB
Isobutane	trace		trace	trace	9 PPB
Ethyl Benzene	0.039		0.041	96 PPM	0.041
Benzoic Acid	0.011		trace	0.244	trace
Benzaldehyde	0.028		31 PPM	0.647	10 PPM
H_2O	0.004		0.002	trace	0.205
N_2	139 PPM		2 PPM	trace	0.014
CO_2	6 PPB		1 PPB	trace	559 PPB
O_2	150 PPB		5 PPB	trace	15 PPM
Tar	902 PPM		trace	0.021	trace
Stabilizer					
Temperature (°F):	70.0		126.3	255.9	126.3

Design Data: Number of trays: 23
Pressure: 3.2 psig
Functional height: 70.5 ft
Material of construction: Carbon steel
Recommended inside diameter: 21.0 ft
Tray efficiency: 0.70
Feed stage: 13
Feed 2 stage:
Sidestream stage: 1
Molar reflux ratio: 10
Tray spacing: 3.0 ft
Skirt height: 14.5 ft

Utilities: Cooling water at 1.09 MM lb/hr and 370.52 M lb/hr 100 # stream
Controls:
Tolerances:
Comments and drawings: See Process Flow Sheet, 7 and Appendix F, 222-4.

Figure 23.1 Typical specification sheet for a process unit.

24. ***Profitability Analysis—Business Case.*** For a profitability analysis, begin by adding the working capital to the total permanent investment to give the total capital investment. Then, present estimates of one or more of the approximate profitability measures, such as the return on investment (ROI) and the venture profit (VP), and one or more of the rigorous methods that involve cash flows, such as the net present value (NPV) and the investor's rate of return (IRR). The latter is also referred to as the discounted cash flow rate of return (DCFRR). In all cases, it is important to indicate clearly the depreciation schedule and, for the rigorous methods, to provide a table that shows the calculation of the annual cash flows as shown in Example 17.29. Finally, the design team should present its judgment of the profitability of the proposed investment. Where possible, the results of sensitivity analyses and optimization should be presented.

    For new product designs, it is common to include the profitability analysis within a business case study (see Section 19.2).

25. ***Conclusions and Recommendations.*** The principal conclusions of the design study should include a clear statement of the recommendations accompanied by justifications for management. At this point, it is important to emphasize that an engineering supervisor may find it necessary to check the calculations of the engineers in the design team. For this purpose, when documenting the designs, Items 16–19 in the design report and the associated items of the appendix are very important. References to the specific pages in each of these items for every equipment unit are equally important. Neither the supervisor responsible for the work of the design team nor the faculty member who grades the design report will favorably regard references to various report items, including the appendix, that are absent or difficult to locate. The same is true of an industrial supervisor who causes such a report to be created.

26. ***Acknowledgments.*** Most design teams obtain considerable assistance and advice from industrial consultants, equipment vendors, librarians, other students, faculty,

and the like. This report item provides an opportunity to acknowledge their contributions with an expression of appreciation and thanks.

27. ***Bibliography.*** All works referred to in the design report, including the appendix, should be listed in this report item. It is recommended that the references appear in the form shown in the Reference sections near the end of each chapter in this textbook.
28. ***Appendix.*** The following items are typically included in the report's appendix, whose pages should be numbered sequentially with the body of the report.
    - **(a)** For each *process design*, the design procedures and detailed calculations for all of the equipment items in report Item 18 must be included here. These are normally not typed but must be sufficiently neat to be easily read and understood. Photocopies of legible calculation sheets with erasures or lined-out corrections are adequate.
    - **(b)** Computer programs developed for the design should be listed with sufficient documentation to enable the principal sections to be identified. This can normally be accomplished through the use of comment statements, including definitions of the key variables, at the beginning of each section.
    - **(c)** Relevant portions of the computer output (the variables at each stage of a distillation column, a graph showing the variables as a function of the stage number, etc.) should be included here. It is important that the output be sufficiently well annotated to permit the reader to read it intelligently. In some cases, handwritten annotations are helpful and adequate.
    - **(d)** Pertinent printed material (e.g., materials provided by equipment vendors that describe their products) should be included here. At the risk of stating the obvious, it cannot be emphasized too strongly that the appendix is not a repository in which large quantities of computer printouts, pertinent or not, are included to increase the weight and thickness of the report. Unless the information in the appendix can readily be located by appropriate references throughout the report, a responsible supervisor may doubt the results that appear in the foregoing items. This can only adversely affect the evaluation of the report and the quality of the proposed design.

23.2 PREPARATION OF THE WRITTEN REPORT

Coordination of the Design Team

As mentioned in the introduction to this chapter, it is important for a design team to document its work throughout the design process. In this regard, each member is normally assigned responsibilities for a portion of the design work and for its documentation. In industry, the assignments are usually coordinated by the head of the design team, who is normally appointed by the project supervisor. At a university, it is also recommended that a member of a student design team be appointed the team leader. The team leader schedules meetings to review progress of the team, plan its next steps, make assignments, and set due dates. The faculty advisor is often very helpful in advising the team as it reviews its progress and plans its next steps.

Project Notebook

When carrying out a design, the design team normally maintains a project notebook, most likely a loose-leaf binder, in which important sources of information are placed. These include articles from the literature, data from the laboratory or the literature, design calculations, and computer programs and printed outputs. This repository of information is updated regularly and is particularly helpful during the meetings of the design team, especially when visitors, such as the team's faculty advisor and industrial consultants, are present.

Milestones

Because no two design projects follow exactly the same sequence of steps, it is not possible to suggest a timetable with specific milestones to be met by all design teams. Rather, in this timetable, it should suffice to identify the milestones, with emphasis on the steps to be accomplished and the portions of the design report that can be written. It is up to the team leader to prepare the timetable so that the final completion date can be met. The following pertain to process designs. Similar steps not given here can be formulated for product designs.

Step 1: ***Complete the Block Flow Diagram and Detailed Process Flow Diagram Showing the Material Balances.*** Most design teams spend considerable time in the process creation steps, identifying alternative process flow diagrams and creating the synthesis tree as discussed in Section 2.3. These steps are very important in leading to the most profitable processes, but it is crucial not to spend too much time generating alternatives. Fairly early in the design process, the team should begin to focus its attention on the base-case design discussed in Section 2.5. This involves the preparation of a detailed process flow diagram (see Figure 2.17) and the completion of the material balances. While this is completed, the design team should prepare a draft of report Items 15 and 16. Should the base-case design be modified, the report Items 15 and 16 are revised accordingly to show how the modifications improve upon the original design.

Step 2: ***Complete the Heat Integration.*** In many cases, an attempt to achieve a high degree of heat and power integration is not undertaken until after mass integration is complete and the reactor(s) and separation equipment have been designed. After heat and power integration is complete and the heat exchangers, pumps, and compressors are installed in the base-case design, it is recommended that report Item 17 on the energy balance be completed.

Step 3: ***Complete the Detailed Equipment Design.*** After this step is completed, report Items 18 and 19 on the unit descriptions and specification sheets should be written for each process design in the report. Note that it helps to complete hand calculations neatly so that they can be inserted into the appendix without any additional work. Furthermore, it is recommended that the important sections of the computer outputs be removed and annotated when necessary for insertion into the appendix.

Step 4: ***Complete the Fixed-capital Investment and the Profitability Analysis.*** After these steps are completed, report Items 20, 21, 22, and 24, should be written for each process design.

For the novice design team, it is hoped that the preceding pointers will help to simplify both the preparation of the design report and the design process. Although many pointers merely follow common sense, they are included to help the design team set milestones to achieve throughout the design process.

Word Processing

The advent of the word processor has had a major impact on the preparation of the design report. Because sections of text can be cut and pasted with ease, it is possible to write drafts of many sections as discussed previously. As the base-case design is modified, new sections can be composed and added easily to the previously prepared sections, which can usually be included with minor modifications. For technical writing, Word and LaTeX are the most commonly used word processors. Except for highly mathematical manuscripts, the former is preferred.

Many design reports have on the order of 100 pages that include the sections discussed earlier. Because there are many cross-references between the report items, it can be very helpful to add headers to the pages that identify the report item numbers and titles. Furthermore, in addition to the table of contents, an index can be very helpful when the reader is searching for coverage of a specific topic.

Editing

No matter how careful an author is, it is difficult to compose concise text without redundant terms and the use of words that add little, if any, meaning. Most novice designers and writers examine their manuscripts carefully for spelling errors with the help of the spelling checkers in their word processors. They also seek to confirm that their statements are technically correct. However, many are inexperienced in the art of editing.

To obtain a more tightly structured document, it is recommended that the design team read its text carefully with the objectives of improving the grammatical constructions (eliminating split infinitives, avoiding the use of long strings of adjectives, etc), avoiding the usage of redundant terms, and eliminating terms that add no meaning to the sentence. This step is important even for the most experienced writers, who can take advantage of recent versions of word processors that include grammar checkers. Checks are made and suggestions sometimes given for:

1. Incomplete sentences
2. Use of passive voice when active voice would give more punch
3. Improper use of *who*, *whom*, *which*, and *that*
4. Capitalization
5. Hyphenation
6. Punctuation
7. Subject and verb agreement
8. Possessives and plurals
9. Sentence structure
10. Wordiness

It must be noted, however, that grammar checkers are not always correct and suggested corrections should, therefore, not always be accepted.

Page Format

At many companies and universities, design reports are bound for storage in technical libraries and repositories and/or distributed in PDF files. The following guidelines are recommended for the preparation of a manuscript for binding to save space on the bookshelves and simplify the usage of the reports. They are also helpful when preparing PDF files, which may eventually be printed.

(a) The pages of the report, including the appendix, should be numbered at the bottom center of each page.

(b) The pages of the report should be printed back-to-back (two-sided) with the odd page numbers appearing on the right-hand page as shown.

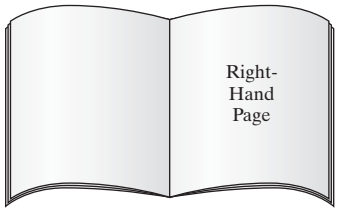

(c) All pages, including the appendix, should have left and right margins that are at least 1-inch wide as shown.

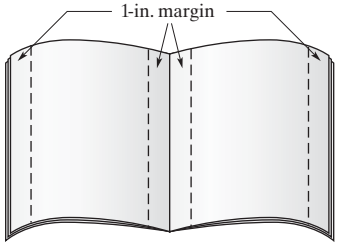

(d) Sheets that appear sideways (broadside) should be mounted so that their tops are on the left margin, as shown. Remember that for sideways sheets, the top and bottom (which

become the left and right side of the page when rotated, must have 1-inch margins.)

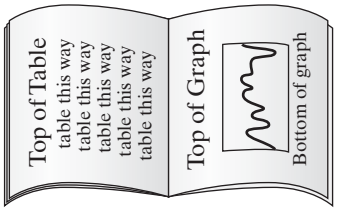

(e) Black ink should be used for the printed calculations to ensure that the pages will photocopy adequately.

Sample Design Reports

Samples of design reports are available from libraries and repositories of technical reports maintained by companies and universities. In recent years, many have become available in PDF files, for example, the design reports prepared by students at the University of Pennsylvania. Note that the titles of the problem statements that led to these reports are reproduced in Appendix II of this textbook with full problem statements included in the file Supplement_to_Appendix_II.pdf in the PDF file folder, which can be downloaded from www.seas.upenn.edu/~dlewin/UPenn Design Problem Statements.html.

23.3 ORAL DESIGN PRESENTATIONS

It is probably most common for the oral design report in industry to be presented to the immediate supervisor of a design team and managers who are responsible for deciding upon the prudence of investing funds in the proposed design. Similar presentations to a somewhat different audience (including industrial consultants, faculty, and fellow students) are prepared at universities, usually to provide the students an experience similar to what they are likely to encounter in industry. It should be noted, however, that only occasionally do young engineers have the opportunity to attend a meeting where their work and ideas are presented to the decision makers among their employers, especially to make the presentation in person.

Typical Presentation

A typical oral design presentation by a team of three to four students at a university is scheduled for 30 minutes with an additional 10 minutes for questions and discussion. This provides sufficient time to:

1. Introduce the design problem and the objective-time chart.
2. Provide an overview of the technologies involved and, for a product design, introduce the customer needs and the innovation map.
3. For a product design, present the superior concept(s), emphasizing their strengths. For a process design, discuss the sections of the proposed process (emphasizing the strengths of the design).
4. Present the results of the economic analysis.
5. Discuss other considerations.
6. Summarize the design and make recommendations.

Normally the presentation time is split evenly among the students, and it is not uncommon to split the presentation into as many as six or seven segments, with each member of the design team covering those portions of the design with which he or she is most familiar.

Media for the Presentation

Computer Projection Software

In recent years, most technical presentations are made using computer projection software displayed by LCD projectors or large-screen LCDs. PowerPoint is a software program widely used to prepare and display the images. This software is capable of displaying animated sequences, halftones, and videos.

Overhead Projector

Overhead transparency projectors continue to be available to display graphs, figures, and tables, especially in rooms equipped with just one projection device. These permit presenters to display images that accompany slides being displayed in a PowerPoint presentation, especially figures (e.g., flowsheets) and tables.

Preparation of Exhibits

To avoid duplicate work effort, it is recommended that design teams prepare all of the figures and tables for their written reports in such a way that they are displayed properly in PowerPoint slide presentations. This requires that the figures and tables be prepared with sufficiently large fonts and the information placed less compactly than would be the case when an oral presentation is not required.

Rehearsing the Presentation

One of the most difficult tasks a design team encounters is the organization of a 30-minute presentation to summarize the most salient features of an extensive written report. It is especially challenging because the members of the team have usually been so involved in the details of the design calculations that they find it difficult to summarize the really important results without overemphasizing the details. For this reason and to help the team see the forest through the trees, it is important for them to rehearse the presentation in the presence of a colleague or teacher. In the best situation, this person will have attended many design presentations in the past and will be well positioned to recommend that certain topics be expanded upon while others be deemphasized or eliminated entirely.

In one format for the rehearsal, the team makes a complete presentation without any interruptions to the critic sitting toward the back of the room to check that the exhibits can be seen and that the speakers can be heard easily. In addition, the critic takes notes and records the time that each speaker begins his or her presentation. Then, when the presentation is completed, the critic reviews the timing and offers some general comments. Often, the design team makes a brief pass through its exhibits to enable the critic to offer more specific criticisms. The critic often has a major

impact on the organization of the report and, more specifically, in helping the design team to achieve a well-balanced presentation.

Written Handout

In some situations, design teams find it easier to make their points through the preparation of a small written handout. Often, this includes an innovation map for the new technologies associated with the product, a 3D sketch of the product, or a detailed process flow diagram similar to that shown in Figure 2.17.

Evaluation of the Oral Presentation

When preparing an oral design presentation, it helps the speakers to have an appreciation of the criteria by which their presentation will be judged. Similarly, when serving on a team to evaluate oral presentations, it is important for the evaluators to understand the criteria and to apply them fairly, especially when they play an important role in the preparation of a course grade and the selection of an award winner.

One possible list of items is shown in Figure 23.2. For the product designs, items that should be included are the objective-time

Name of Presenter(s):
Title of Presentation:
Date of Presentation:
Name of Examiner/Appraiser:

Content	**Noteworthy**	**Acceptable**	**Needs Improving**
Product design			
Objective-time chart			
Innovation map			
Customer requirements			
Superior concept			
Economics			
Totals			
Process design			
Process description			
Unit descriptions			
Economics			
Novelty of design			
Totals			

Figure 23.2 Oral design presentation evaluation form. (*Continued*)

Presentation—Organization	Noteworthy	Acceptable	Needs Improving
Core message			
Clear objectives			
Overall structure			
Visible logic			
Totals			

Presentation—Execution	Noteworthy	Acceptable	Needs Improving
Confident, enthusiastic, forceful, convincing			
Controlled pace/natural finish			
Voice quality (clear, calm, understandable)			
Frequent eye contact			
Totals			

Visual Aids	Noteworthy	Acceptable	Needs Improving
Interesting, relevant			
Easy to read			
Totals			

Figure 23.2 (*Continued*)

chart and the innovation map, the description of the customer and technical requirements, the quality of the superior concept, and the discussion of the economic analysis; for the process designs, the quality of the process description, the descriptions of the process units, and the discussion of the economic analysis are included. These are at the heart of the design presentation and deserve the most attention. The next item, novelty, is more difficult to judge because some design problems provide more opportunity to be creative than others. This is recognized by most judges, who attempt to rate the creativity of the design work in the context of the design problem and the opportunities it provides to develop novel solutions. The next items address the organization of the presentation and its execution. Then, the quality of the exhibits and visual aids is evaluated. Finally, the

overall presentation is rated, which includes a recommendation for a grade when the design report is the work of a student design team.

DVDs and YouTube

Increasingly, oral design presentations are recorded on DVDs or YouTube segments to provide a record of the presentations and to enable each design team to critique its own presentation with a view toward improving the next one. In most cases, a portable video device (e.g., tablet, cell phone) mounted on a tripod or tabletop is adequate to capture the bulk of the presentation.

23.4 AWARD COMPETITION

At many universities, awards are presented to the design teams that prepare the design(s) judged to be the most outstanding. Normally, the criteria are a combination of those discussed for both the written and oral design reports. However, because the written reports are often submitted for regional competitions in which judges select from among designs completed at other universities, it is common to place more emphasis on the written reports.

Usually, a small awards committee of academic and industrial members is appointed to make the judgment. It begins by reading the reports of those design teams whose oral presentations were judged to be among the best.

At many universities, the design award is presented to the design team at the commencement exercises, either for the chemical engineering department, the engineering school, or the entire university. It often involves a small stipend and a certificate or plaque.

Finally, it is important to mention the annual National Student Design Competition prepared by AIChE members from industry and academia for the AIChE student chapters. The design contest is timed to be completed by the end of the spring semester after which the awardees are selected to receive their awards at the Annual Meeting of the AIChE, usually in November, and to make oral presentations at the associated student chapter meeting.

23.5 SUMMARY

After studying this chapter, the reader should:

1. Be able to complete the report items in a written product and/or process design report.
2. Be prepared to create an oral design presentation describing the innovative aspects and the advantages and disadvantages of a product and/or process design.

REFERENCES

1. Peters, M. S., K. D. Timmerhaus, and R. West, *Plant Design and Economics for Chemical Engineers*, 5th ed., McGraw-Hill, New York (2003).

2. Sandler, H. J., and E. T. Luckiewicz, *Practical Process Engineering,* XIMIX. Philadelphia, Pennsylvania (1993).

3. Ulrich, G. D., and P. T. Vasudevan, *Chemical Engineering Process Design and Economics: A Practical Guide*, 2nd ed., Process (Ulrich) Publishing, www.ulrichvasudesign.com (2004).

Part Five

Case Studies—Product and Process Designs

Chapter 1 introduced a Stage-Gate development procedure for conceiving a product or a process and proceeding through five stages to bring a product to market and a processing plant online. The five stages were concept, feasibility, development, manufacturing, and product introduction. The previous four parts of this book explored the stages dealing with the design of the product or the process. Those stages depend upon the major facets of chemical engineering: thermodynamics of mixtures; heat, mass, and momentum transfer; chemical kinetics; and materials science.

The final part of this book applies the principles of product and process design in four case studies, the first three of which deal with product design and the last one with process design. Chapter 24 presents the design of a hemodialysis device using cartridges containing hollow-fiber membranes to replace the function of diseased kidneys by removing waste products and excess fluids from the bloodstream and maintaining a proper chemical balance in the blood. Such devices are used in dialysis treatment centers or in machines in the home. Mass-transfer and material balance calculations are given to illustrate the method for sizing the device.

In Chapter 25, a high throughput screening device for kinase inhibitors is developed. Kinases are proteins that modify other proteins by adding phosphate groups to them, which cause functional changes in their activity. These inhibitors help regulate the growth and division of specific kinases so as to prevent them from forming growths that lead to and spread cancer. The use of kinase inhibitors represents a major change in cancer treatment from general to molecular methods. In this case study, the conceived screening device is a lab-on-a-chip designed to operate rapidly with very small quantities of very expensive biochemicals.

Chapter 26 deals with the design of an improved adhesive for attaching semiconductor LED chips to ceramic substrates to produce longer-lasting and higher-power efficiency LED light bulbs. The improvement is accomplished by increasing the thermal conductivity of the polymeric adhesive by blending silver in various shapes with the polymer. As a result, the bulb operates at a more efficient, lower temperature.

An improved process for manufacturing ammonia from natural gas is presented in Chapter 27 with added attention to the concept and feasibility stages to address particular problems associated with plant location. The process design includes steps to (1) minimize CO byproduct production by optimizing methane reforming and shift reactions, (2) improve energy efficiency by heat integration, (3) reduce gas compression costs by minimizing the operating pressure of the ammonia synthesis loop, and (4) minimize hydrogen loss in the synthesis loop purge by adding a membrane separation step.

Chapter 24

Case Study 1—Home Hemodialysis Devices

24.0 OBJECTIVES

New product-development programs are often plagued by the need for technological inventions that prolong the product development process. It is often thought that both product and technology developments should be carried out concurrently to reduce the product-development time. Yet it is recommended that these two activities be decoupled as much as possible. Most of the technology development should be completed prior to initiating a product development program. During product development, minor changes to product formulations and constructions are often necessary to meet required product performance.

In two case studies, in this chapter and in Chapter 25, the innovation map is used to show how perceived customer needs are coupled to the development of new technologies. The utility of these innovation maps is shown for converting material, process/manufacturing, and product technologies into inventions from which products that are necessary and sufficient to meet perceived customer requirements are developed. The case studies include two products: home hemodialysis devices in this chapter and high throughput screening devices for kinase inhibitors in Chapter 25.

After studying this chapter, the reader should:

1. Be able to construct an innovation map.
2. Be able to identify critical inventions for materials, process/manufacturing, and product technologies.
3. Appreciate the need for technology-protection strategies.
4. Be able to translate customer requirements into technical requirements and set product technical specifications.
5. Be able to set the initial cost target.
6. Be able to estimate the market opportunity.

24.1 HEMODIALYSIS TECHNOLOGY

Hemodialysis is one of two types of artificial dialysis treatments (the other being peritoneal dialysis) that replaces the function of diseased kidneys. The kidneys regulate the composition of the bloodstream by removing waste products and excess fluids from the bloodstream while maintaining the proper chemical balance of the blood, which consists of red cells, white cells, platelets, and the accompanying plasma. The plasma, which accounts for about 55 vol% of the blood, consists of about 92% water with the balance being inorganic salts, organic chemicals, and dissolved gases. A typical male adult has a blood volume of 5 L with a resting cardiac output of 5L/min and a systemic blood pressure of 120/80 mmHg. The most common application of hemodialysis is for patients with temporary or permanent kidney failure. It is the only treatment available for patients with end-stage renal disease (ESRD) whose kidneys are no longer capable of their function. This treatment, which is required three times per week, for an average of three to four hours per dialysis, was performed on 398,861 people in 2009. Of these, 95% were on hemodialysis and 5% on peritoneal dialysis.

A hemodialysis device consists of two major components: the dialyzer and the control and monitoring subsystem (Misra, 2005), as shown in Figure 24.1.

Most hemodialysis treatments are still performed at major hospitals or hemodialysis clinics. Only about 1–2% of renal disease patients choose to have dialysis treatment at their homes. Despite many advantages of a home dialysis treatment, the adoption rate is low due to several factors, such as the initial purchase cost of the device, the added cost to retrofit the home to accommodate the device, and the ease of use and safety. One of the key success factors in designing a home hemodialysis device is to address the ease of use and safety in the absence of a healthcare professional during the dialysis operation. The design of the control and monitoring subsystem is essential to meet this need. In this case study, we focus on the design of the dialyzer and place less emphasis on the design of the control and monitoring subsystem.

Hemodialysis Device Inventions

Before creating an *innovation map* for a hemodialysis device, one of the first steps in product design, it is important to be knowledgeable about the available technologies, including several that are of historical interest.

Enzyme Reactor

One of the first technologies, a column packed with microcapsules containing the enzyme urease and/or aspartase in a

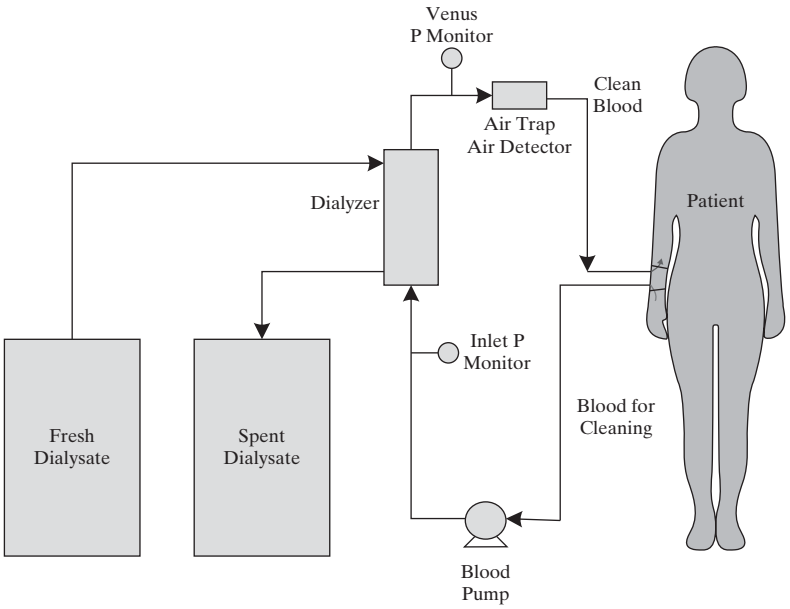

Figure 24.1 A hemodialysis device.
http://en.wikipedia.org/wiki/Dialysis

membrane gel lattice of a semipermeable polymer, was introduced by Chibata et al. (U.S. Patent 3,865,726) in 1975. In the microcapsules, urea is decomposed by the urease into NH_3 and CO_2. The NH_3 reacts with fumarate in the dialysis solution to form aspartic acid by the action of the aspartase. The aspartic acid is nontoxic to human beings and can be readily eliminated using an ion-exchange resin.

Hollow-fiber Module

A very common commercial device for hemodialysis is the C-DAK 4000 Artificial Kidney of Cordis Dow Corporation. This device is covered largely by U.S. Patent 4,276,173 (Kell and Mahoney), issued on June 3, 1981. This disposable, sterilized membrane module, shown in Figure 24.2, resembles a shell-and-tube heat exchanger. The tubes, which number 10,000, are hollow fibers, 200 microns i.d. by 10 microns wall thickness by 22 cm long, made of hydrophilic microporous cellulose acetate of 15 to 100 Å pore diameter. Alternatively, fibers of polycarbonate, polysulfone, and other polymers are used. The shell, made of acrylonitrile-butadiene-styrene (ABS) plastic with inlet and outlet side ports of polycarbonate, is 24 cm long by 4 cm in outside diameter with centered ports in the heads (caps) at either end of the shell for delivering blood into and out of the hemodialyzer. The fibers are potted at each end into polyurethane, sliced at each end to open the fibers, and sealed into the shell heads (caps) to prevent leakage between the tube side and the shell side. The total membrane area based on the inside area of the hollow fibers is 1.38 m^2. The packing density is 4,670 m^2 of membrane area/m^3 of membrane module volume. In 1992, 60 million of these units, which weigh less than 100 g each, were sold at U.S.$5 to $6 each. Based on total membrane area used and dollar value, artificial kidneys are the single largest application of membranes.

A hemodialysis treatment with a C-DAK 4000 Artificial Kidney involves the insertion of two needles into the patient's vein attached to plastic tubes to carry the patient's blood to and from the artificial kidney. The blood flows through the hollow fibers at

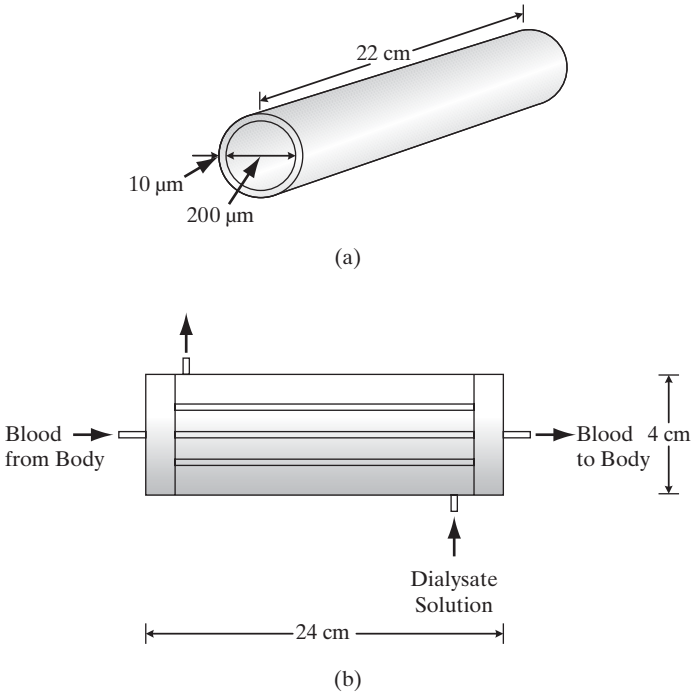

Figure 24.2 Hemodialysis device: (a) single tube; and (b) complete module.

a flow rate monitored by and controlled at 200 mL/min by a dialysis machine. A sweep dialysate solution of water, glucose, and salt passes countercurrently to the blood through the shell side of the artificial kidney at a rate of 500 mL/min. The pressure difference across the membrane from the tube side to the shell side is approximately equal to the diastolic pressure of the patient (e.g., 120 to 150 mmHg), because the dialysate is pulled through the module with suction. The pressure drop on the tube side is 30 mmHg, whereas that on the shell side is 12 mmHg. The pressure difference across the membrane causes excess fluids in the bloodstream to pass to the dialysate. Concentration differences

between the blood and the dialysate cause urea (CH_4ON_2), uric acid ($C_5H_4O_3N_4$), creatinine ($C_4H_7ON_3$), phosphates, and other low-molecular-weight metabolites to transfer by diffusion from the blood to the dialysate; and glucose and salts to transfer by diffusion from the dialysate to the blood. When the kidneys of an adult function normally, the urea content of the blood is maintained in the range of 10–20 mg of urea nitrogen per 100 mL (1 deciliter, dL).

For the design of the C-DAK 4000 Artificial Kidney, and the many similar hemodialysis devices (Daugirdas and Ing, 1988), rates of permeation of the species through the candidate membranes are necessary. Estimates for the permeability of pure species in a microporous membrane can be made from the molecular diffusivity, and pore diameter, porosity, and tortuosity of the membrane (Seader et al., 2011), as shown in Example 24.1. For this reason, considerable laboratory experimentation is required when selecting membranes in the molecular structure design step.

Home Hemodialysis Devices

The inconvenience of patient travel to a center for hemodialysis three times weekly, for four-hour treatments, has prompted medical experts to evaluate a different form of delivering hemodialysis, specifically at night, at home, while the patient is sleeping (Talamini, 2005). Of 281,600 patients in the United States in 2002, only 843 (0.3%) were home dialysis patients with no commercial home hemodialysis products available. In conventional dialysis centers, many devices accompany the hemodialysis device, including blood and dialysis pumps, pressure and temperature transducers, and an air detection system. Also included are numerous alarms associated with instruments that measure pressure and temperature as well as the occurrence of blood leaks, air embolism, and vascular access disconnects. For home dialysis, additional devices are envisioned, including a sorbent dialysis device (to recover urea from the dialysate solution), safeguards to prevent blood access disconnections, alarms to detect fluid (blood or dialysate) leaks, software allowing connection to the Internet for remote monitoring, central monitoring of treatment and patient parameters (e.g., blood pressure, pulse, venous, and arterial pressures), and the like. With the large number of home dialysis clinics being established throughout the United States, it is expected that home dialysis will increase rapidly in the coming years.

Innovation Map

For the product development of a hemodialysis device, consider the *innovation map* in Figure 24.3, which is a typical one that might have been prepared in the mid-2010s.

To construct the *innovation map*, the historical information presented here coupled with an observation of customer needs

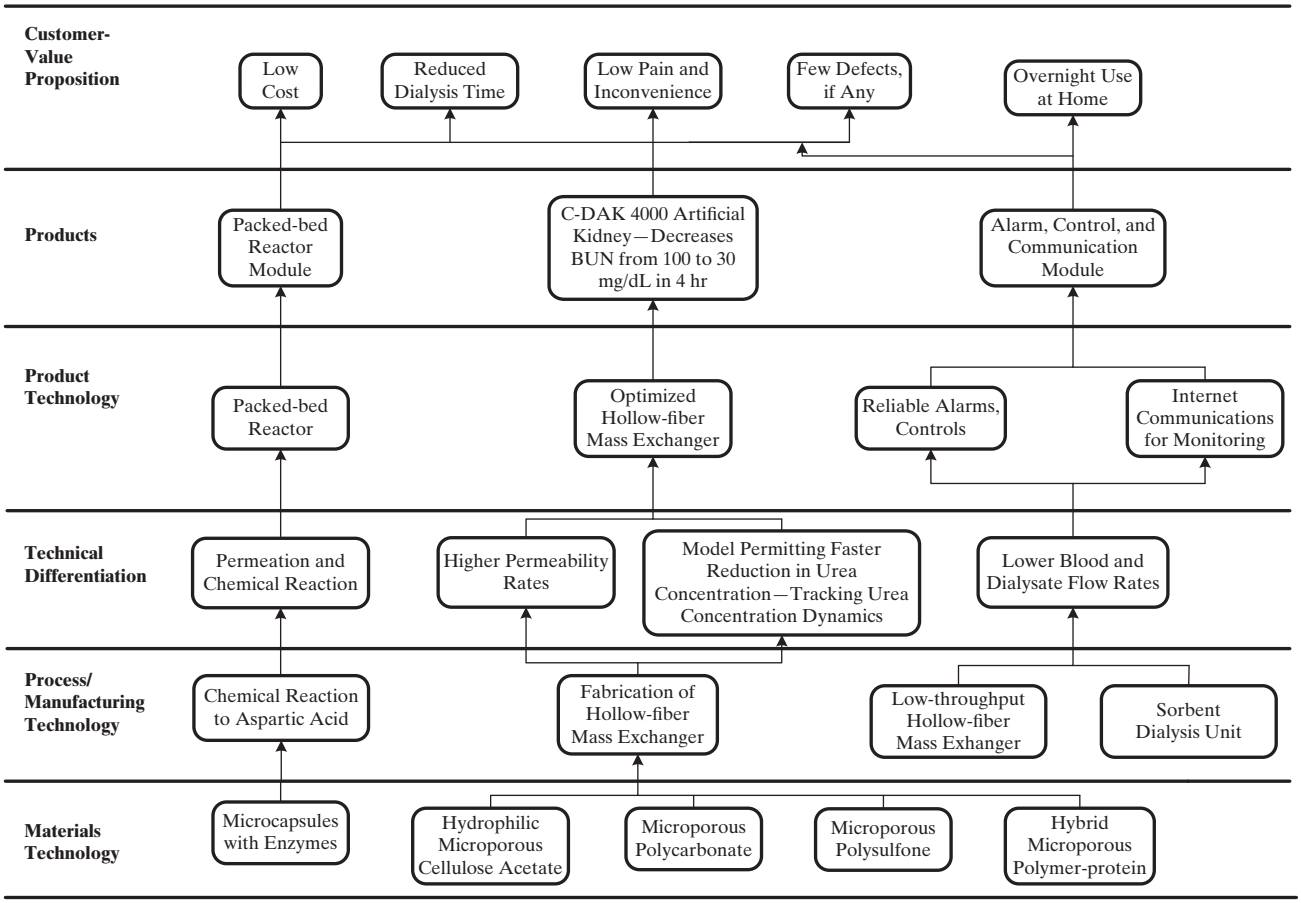

Figure 24.3 Innovation map for hemodialysis device.

provides the elements to be positioned in its six levels, moving from the bottom to the top of the map:

1. ***Materials Technology:*** Microcapsules with enzymes; hydrophobic microporous cellulose acetate, polycarbonate, and polysulfone; and hybrid microporous polymer-protein.
2. ***Process/Manufacturing Technology:*** Chemical reaction to aspartic acid, fabrication of hollow-fiber mass exchanger, low-throughput hollow-fiber mass exchanger, and sorbent dialysate unit.
3. ***Technical Differentiation (technical-value proposition):*** Permeation and chemical reaction, higher permeability rates, model permitting faster reduction in urea concentration—tracking urea concentration dynamics, and lower blood and dialysate flow rates.
4. ***Product Technology:*** Packed-bed reactor, optimized hollow-fiber mass exchanger, reliable alarms and controls, and Internet communications and monitoring.
5. ***Products:*** Packed-bed reactor module; C-DAK 4000 Artificial Kidney; alarm, control, and communication module(s).
6. ***Customer-value Proposition:*** Low-cost, reduced dialysis time, low pain and inconvenience, few defects, overnight use at home.

Given these elements, the connectivity is added to show the interplay between the technological elements, the *technical-value proposition*, and the *customer-value proposition*. As unmet customer needs are encountered, they can be added for the next generation of products.

The initial inventions involved *microcapsules with enzymes* (materials technology) with *chemical reaction to aspartic acid* (process/manufacturing technology) to provide the technical differentiation, *permeation*, and *chemical reaction*. This led to the *packed-bed reactor* (product technology) and the *packed-bed reactor module* product, which was created to satisfy the customer needs: *low cost*, *reduced dialysis time*, *low pain and inconvenience*, and *few defects* (customer-value proposition).

Then, in the 1970s, it became possible to extrude hollow fibers reliably. Several materials technologies, including *microporous cellulose acetate*, *polycarbonate*, and *polysulfone*, led to the *fabrication of hollow-fiber mass exchangers* (process/manufacturing technology). Note that a potential new material technology, involving the development of a *hybrid microporous polymer-protein*, is also shown on the innovation map. This process/manufacturing technology led to technical differentiations: *higher permeability rates* and a *model permitting faster reduction in urea concentration and tracking urea concentration dynamics*. In turn, these led to an *optimized hollow-fiber mass exchanger* (product technology) and the *C-DAK 4000 Artificial Kidney* product, which better satisfied the customer-value proposition.

Finally, in the 2000s, the customer need for *overnight home use* is likely to take advantage of new product/manufacturing technologies: *low-throughput hollow fiber mass exchanger,* and *sorbent dialysis unit*. In turn, their technical differentiation *lower blood and dialysate flow rates*—might lead to *new* product technologies: *reliable alarms and controls* and *Internet communications for monitoring*, which may provide a new product(s), that is, alarm, control, and communication module(s).

In the remainder of this section, aspects of these promising technological inventions are discussed in subsections on (1) Process/Manufacturing Technology and (2) Technology Protection.

Process/Manufacturing Technology

Hemodialysis Device. Having selected the candidate polymer membranes as discussed, which must be available in hollow-fiber membranes, a key challenge in the development of the C-DAK 4000 Artificial Kidney was to fabricate a new hollow-fiber mass exchanger (new process/manufacturing technology). This, together with a model for tracking its urea concentration dynamics, provided the technical differentiation that permitted an optimized configuration (product technology). In practice (for normal dialysis rather than potential home dialysis), blood flow rates range from 100 to 400 mL/min, and dialysate flow rates range from 200 to 800 mL/min. Decisions regarding the inside diameter, wall thickness, and length of the fiber and the number of fibers influence the pressure for the fluids on each side, the surface area for mass transfer, and the rates of mass transfer. To illustrate the development of this model and demonstrate its use for creating optimized designs, Example 24.1 is provided next.

EXAMPLE 24.1 ***Design Procedure for Hollow-fiber Hemodialysis Device***

Develop a design procedure for a hollow-fiber hemodialysis device of the type shown in Figure 24.1. Base the design on a blood flow rate of 200 mL/min and a dialysate flow rate of 500 mL/min. Assume that the design will be controlled by mass transfer of one of the blood plasma components to be removed, for example, urea. The blood will flow through the hollow fibers, and the dialysate will flow past the outside surface of the fibers in a direction countercurrent to the flow of the blood plasma. A typical patient will require hemodialysis when the blood reaches a urea nitrogen level (BUN) of 100 mg/dL. A target for the hemodialysis device is to reduce the BUN to 30 mg/dL within 4 hr, which corresponds to normal operation at a hemodialysis center.

SOLUTION

Several key steps in the design procedure are presented next, beginning with the estimation of the mass-transfer coefficient for transport of urea across the membrane. Next, pressure drops are estimated both in and outside of the hollow fibers. Then, a mass-transfer model is solved for the concentration of urea in the bloodstream as a function of time, which assists in sizing the dialysis device.

Step 1: ***Overall Mass-transfer Coefficient for Urea.*** The rate of mass transfer of urea from the blood plasma through the membrane and to the dialysate is given by

$$n = K_i A_i \Delta C_{LM} \tag{24.1}$$

where:

n = rate of mass transfer of urea nitrogen, mg/min
K_i = overall mass-transfer coefficient based on the inside area, cm/min
A_i = mass-transfer area based on the inside area of the hollow fibers, cm^2
ΔC_{LM} = log-mean urea-nitrogen concentration difference for mass transfer

The overall mass-transfer coefficient, which must consider the resistances of the blood plasma, the membrane, and the dialysate, is given by

$$\frac{1}{K_i} = \frac{1}{k_b} + \frac{l_M}{P_M}\frac{A_i}{A_m} + \frac{1}{k_d}\frac{A_i}{A_o} = \frac{1}{k_b} + \frac{l_M}{P_M}\frac{D_i}{D_m} + \frac{1}{k_d}\frac{D_i}{D_o} \tag{24.2}$$

where:

k_b = mass-transfer coefficient on the inside where the blood flows, cm/min
k_d = mass-transfer coefficient on the outside where the dialysate flows, cm/min
A_o = mass-transfer area based on the outside area of the hollow fibers, cm^2
A_m = arithmetic mean of A_i and A_o, cm^2
l_M = membrane wall thickness, cm
P_M = membrane permeability, cm^2/min

The mass-transfer coefficients, k_b and k_d, can be estimated by analogy from available dimensionless empirical correlations for heat transfer, which are taken from Knudsen and Katz (1958). These analogous correlations depend on the flow regime and relate the Sherwood number to the Reynolds and Schmidt numbers.

For the flow of blood plasma inside the hollow fibers, the flow regime will be laminar because of the very small fiber diameter and the need to avoid high flow velocities that would stress the blood cells to destruction. For example, for the C-DAK Artificial Kidney described earlier, 200 mL/min (200 cm^3/min), Q_b, of blood flows through 10,000 fibers, each of 200 microns (0.02 cm) inside diameter. D_i, with 20 microns wall thickness, t_w, rather than the 10 micron thickness shown in Figure 24.1, and 22 cm in length, L. The cross-sectional area for flow in each fiber is $3.14(0.02)^2/4 = 0.000314$ cm^2. The total flow area, S_i, for 10,000 fibers is $10{,}000(0.000314) = 3.14$ cm^2. The average blood velocity, V_b, is $(200)/3.14 = 63.7$ cm/min = 1.062 cm/s. Blood has a density, ρ_b, of 1.06 g/cm^3 and a viscosity, μ_b, of approximately 0.014 g/cm-s. This gives a Reynolds number for blood flow through the fibers, $N_{Re_b} = D_i V_b \rho_b/\mu_b = 0.02(1.062)(1.06)/0.014 = 1.608$, which is in the laminar flow regime. Because the fully developed parabolic velocity profile for laminar flow is obtained by a fiber length, $L = 0.05 D_i N_{Re_b}$, the velocity profile will be developed in less than one fiber diameter. Thus, for mass transfer of urea through the blood plasma, the important criterion is the Peclet number for mass transfer, N_{Pe_M}, which is the product of the Reynolds number and the Schmidt number, $N_{Sc_b} = \mu_b/\rho_b D_{urea}$ or

$$N_{Pe_M} = \frac{D_i V_b}{D_{urea}} \tag{24.3}$$

where D_{urea} = molecular diffusivity of urea in blood plasma, cm^2/s. The diffusivity for urea in blood plasma at a body temperature of 37°C is $0.8 \times 10^{-5} cm^2/s$. Thus, the Peclet number = $0.02(1.062)/(0.8 \times 10^{-5}) = 2{,}650$. The Sherwood number depends on the ratio of N_{Pe_M} to (L/D_i), which equals $2{,}650/(22/0.02) = 2.41$. For this condition, the Sherwood number, $N_{Sh} = D_i k_b/D_{urea}$, is approximately constant at a value of 4.364. Thus, $k_b = 4.364(0.8 \times 10^{-5})/0.02 = 0.00175$ cm/s.

Estimation of the mass-transfer coefficient in the dialysate outside the fibers is considerably more difficult because of the complex geometry. In a shell-and-tube heat exchanger, baffles are used to help direct the shell-side fluid to flow back and forth in directions largely normal to the tube length. It would be extremely difficult to include such baffles in a hollow-fiber hemodialysis unit. Instead, as shown in Figure 24.2, the dialysate leaves the inlet port at one end to enter the shell normal to the fibers, turns 90° and flows parallel to the fibers, and then turns 90° to enter the exit port at the other end. Presumably, the dialysate flow is largely parallel to the fibers along their length. For the example being considered here, assume the inside diameter of the shell to be 3.8 cm, giving a cross-sectional area of $3.14(3.8)^2/4 = 11.34$ cm^2. The 10,000 fibers, with an outside diameter of $200 + 40 = 240$ microns or 0.024 cm, occupy a cross-sectional area of $10{,}000(3.14)(0.024)^2/4 = 4.52$ cm^2. Thus, the area for flow of the dialysate is $11.34 - 4.52 = 6.82$ cm^2. As an approximation, estimate the shell-side mass-transfer coefficient, k_d, from a circular tube inside-flow correlation, as for k_b, by replacing tube inside diameter by an equivalent diameter equal to $4r_H$, where r_H is the hydraulic radius, which is equal to the cross-sectional area for flow divided by the wetted perimeter. For 10,000 fibers of 0.024 cm diameter on a square pitch, the wetted perimeter is $3.14(0.024)(10{,}000/4) = 188.4$ cm. This gives a hydraulic radius of $6.82/188.4 = 0.0362$ cm. The equivalent diameter = $4(0.0362) = 0.145$ cm. Assume dialysate properties at 37°C of $\rho_d = 1.05$ g/cm^3 and $\mu_d = 0.007$ g/cm-s. Take a dialysate flow rate of 500 cm^3/min. The average velocity of the dialysate, V_d, is $(500/60)/6.82 = 1.22$ cm/s. The dialysate Reynolds number, $N_{Re_d} = 4r_H V_d \rho_d/\mu_d$, is $0.145(1.22)(1.05)/0.007 = 26.5$, which is much higher than for the tube side, but is still in the laminar-flow region. The estimated entry length using the shell-side version of the tube-side equation is $0.05(0.145)(26.5) = 0.192$ cm, making it possible to again assume a fully developed flow. The molecular diffusivity of urea through the dialysate solution is $1.8 \times 10^{-5} cm^2/s$. The Peclet number, using a shell-side version of equation, is $N_{Pe_M} = (0.145)(1.22)/(1.8 \times 10^{-5}) = 9{,}830$. The ratio of N_{Pe_M} to $(L/4r_H)$, which equals $9{,}830/(22/0.145) = 64.8$. For this condition, the Sherwood number, $N_{Sh} = 4r_H k_d/D_{urea}$, is approximately 7. Thus, $k_d = 7(1.8 \times 10^{-5})/0.145 = 0.00087$ cm/s.

For a microporous membrane, the membrane permeability is the effective diffusivity for urea. For the microporous membrane of 20 microns (0.002 cm) wall thickness, assume a porosity, ε, of 0.25 and a tortuosity, τ, of 1.5. The effective diffusivity or permeability in the membrane is given by $(D_{urea})_{eff} = P_M = \varepsilon(D_{urea})_d/\tau = 0.25(1.8 \times 10^{-5})/1.5 = 3 \times 10^{-6}$ cm^2/s. The permeance, $P_M/l_M = 3 \times 10^{-6}/0.002 = 0.0015$ cm/s.

The overall mass-transfer coefficient based on the inside area of the hollow fibers is obtained from Eq. (24.2):

$$\frac{1}{K_i} = \frac{1}{0.00175} + \frac{1}{0.0015}\left(\frac{0.020}{0.022}\right) + \frac{1}{0.00087}\left(\frac{0.020}{0.024}\right)$$

$$= 571 + 606 + 958 = 2{,}135 \text{ s/cm}$$

This result shows that 27% of the mass-transfer resistance is on the blood side, 28% is in the membrane, and 45% is on the dialysate side. These percentages change as the fiber geometry is changed. Taking the reciprocal, the overall mass-transfer coefficient is $K_i = 0.000468$ cm/s.

Step 2: ***Pressure Drop for Blood Flow Through the Hollow Fibers.*** Because the blood flow through the hollow fibers of the hemodialyzer is laminar, the pressure drop is computed from the Hagen–Poiseuille equation:

$$-\Delta P_b = \frac{32\mu_b L V_b}{D_i^2} = \frac{32(0.014)(22)(1.062)}{0.02^2}$$

$$= 26{,}170 \text{ g/cm-s}^2 \text{ or } 2.617 \text{ kPa or } 19.6 \text{ mmHg}$$

This pressure drop compares well with the pressure drop of 30 mmHg cited above for the commercial C-DAK 4000 Artificial Kidney.

Step 3: ***Pressure Drop for Dialysate Flow Past the Hollow Fibers.*** The flow on the shell side is also laminar. Using the hydraulic-radius concept, an estimate can be made of the pressure drop by replacing D_i in the Hagen–Poiseuille equation with $4r_H$. Thus, the pressure drop is

$$-\Delta P_d = \frac{32\mu_d L V_d}{(4r_H)^2} = \frac{32(0.007)(22)(1.22)}{(0.145)^2}$$

$$= 286 \text{ g/cm-s}^2 \text{ or } 0.0286 \text{ kPa or } 0.2 \text{ mmHg}$$

This is far less than the 12 mmHg quoted above for the C-DAK 4000. This difference could be due to the entering and exiting flow of dialysate normal to the fibers, which would increase the pressure drop considerably. A better estimate could be made with a computational fluid dynamics (CFD) program. Here, r_H is the hydraulic radius for flow on the dialysate side of the hollow fibers. It is defined as the area for flow divided by the wetted perimeter outside the fibers.

This pressure-drop calculation also sheds some doubt on the above calculation of the mass-transfer coefficient on the shell side, which could also be greater than that calculated by assuming flow parallel to the length of the fibers.

Step 4: ***Urea Mass Transfer and Time Required to Reduce Its Concentration in the Blood.*** A compartment model, shown in Figure 24.4 has been successful in following changes in solute concentrations with time for a patient undergoing hemodialysis. The model consists of three perfectly mixed compartments and one membrane separator. Streams that are assumed to have negligible volume connect the compartments and separator. The upper compartment, of volume, V_p, represents a patient's body fluid other than blood. A solute, such as urea, is transferred to the body fluid at the constant mass rate, G. The second compartment of volume, V_B, represents the patient's blood, which circulates between these two compartments at a volumetric rate, Q_P. Below the second compartment is the hemodialysis unit, which transfers solutes, such as urea, across hollow-fiber membranes to a dialysate. Blood circulates at a volumetric rate, Q_B, between the hemodialyzer and the second compartment. Dialysate circulates at a volumetric rate, Q_D, between the bottom compartment (dialysate holding tank) and the hemodialyzer, through which it flows countercurrently to the blood flow. From the dialysate holding tank, a constant volumetric flow rate of waste dialysate, Q_W, is withdrawn. An equal volumetric flow rate of fresh dialysate of zero waste solute concentrations, for example, urea, is added to the circulating dialysate before it enters the hemodialyzer. Also indicated in Figure 24.4 are symbols, C_j, for solute (e.g., urea) concentrations in the various streams in units of mass/unit volume. Because of the assumption of perfectly mixed compartments, concentrations of solutes in the three compartments are equal to the solute concentrations in the streams leaving the corresponding compartments.

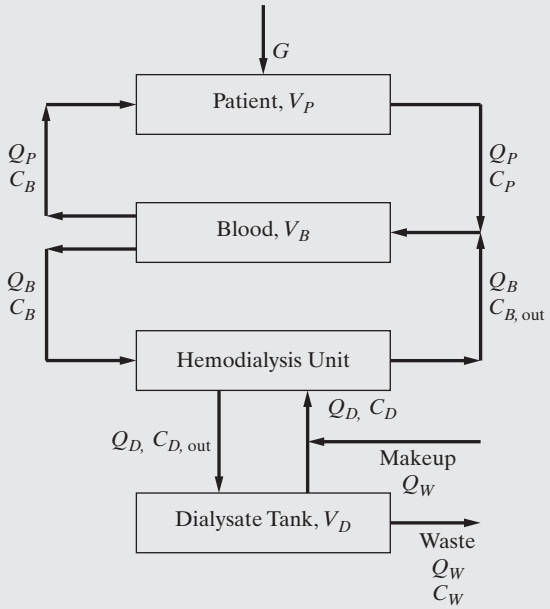

Figure 24.4 Hemodialysis model.

Model equations for a system similar to that of Figure 24.4 were developed and solved by Spaeth (1970), whose equations are applied here. Because solute concentrations change with time, the following solute mass balance equations apply to the three compartments:

$$V_P \frac{dC_P}{dt} = G - Q_P(C_P - C_B) \tag{24.4}$$

$$V_B \frac{dC_B}{dt} = Q_P(C_P - C_B) - Q_B(C_B - C_{B,\text{out}}) \tag{24.5}$$

$$V_D \frac{dC_W}{dt} = Q_D(C_{D,\text{out}} - C_W) \tag{24.6}$$

Equations for the rate of mass transfer of a solute across the walls of the hollow fibers in the membrane unit and a solute mass balance are as follows, where countercurrent flow is

assumed in the hemodialyzer, with a corresponding log-mean concentration driving force:

$$Q_B(C_B - C_{B,\text{out}}) = K_i A_i \Delta C_{LM} = K_i A_i \left[\frac{(C_B - C_{D,\text{out}}) - (C_{B,\text{out}} - C_D)}{\ln \dfrac{(C_B - C_{D,\text{out}})}{(C_{B,\text{out}} - C_D)}} \right] \tag{24.7}$$

$$Q_B(C_B - C_{B,\text{out}}) = Q_D(C_{D,\text{out}} - C_D) \tag{24.8}$$

Finally, a solute mass balance around the mixing point, assuming that the makeup dialysate contains no solute, gives

$$Q_D C_D = (Q_D - Q_W) C_W \tag{24.9}$$

Equations (24.4)–(24.9) constitute six equations in the six variables, C_P, C_B, C_D, C_W, $C_{B,\text{out}}$, and $C_{D,\text{out}}$, all of which vary with time. The six equations can be reduced to the following three ordinary differential equations in the three variables, C_P, C_B, and C_D:

$$\frac{dC_P}{dt} = \frac{G}{V_P} - \left(\frac{Q_P}{V_P}\right)(C_P - C_B) \tag{24.10}$$

$$\frac{dC_B}{dt} = \left(\frac{Q_P}{V_B}\right)(C_P - C_B) - \left(\frac{Q_B}{V_B}\right) E(C_B - C_D) \tag{24.11}$$

$$\frac{dC_D}{dt} = \left[E\left(\frac{Q_B}{V_D}\right)\left(1 - \frac{Q_W}{Q_D}\right)\right] C_B - \left[\left(\frac{Q_W}{V_D}\right) + E\left(\frac{Q_B}{V_D}\right)\left(1 - \frac{Q_W}{Q_D}\right)\right] C_D \tag{24.12}$$

where the parameter, E, is defined by

$$E \equiv \frac{C_B - C_{B,\text{out}}}{C_B - C_D} \tag{24.13}$$

and is computed from

$$E = \frac{1 - \exp\left[\dfrac{K_i A_i}{Q_B}\left(1 - \dfrac{Q_B}{Q_D}\right)\right]}{\dfrac{Q_B}{Q_D} - \exp\left[\dfrac{K_i A_i}{Q_B}\left(1 - \dfrac{Q_B}{Q_D}\right)\right]} \tag{24.14}$$

which is derived from Eqs. (24.7) and (24.8).

Equations similar to Eqs. (24.10)–(24.12), but for a two-compartment model, are solved analytically by Bird et al. (2002). However, a numerical solution, suitable for a spreadsheet is used here, beginning with conditions at time, $t = 0$, for the three solute concentrations. Once, C_P, C_B, and C_D are obtained as functions of time, the other three concentrations, C_W, $C_{B,\text{out}}$, and $C_{D,\text{out}}$ are computed as functions of time from Eqs. (24.9), (24.13), and (24.8), respectively.

As an example of the application of the above equations to urea, the following values are used:

$V_P = 40{,}000\ \text{cm}^3$, $V_B = 5{,}000\ \text{cm}^3$, and $V_D = 1{,}000\ \text{cm}^3$

$Q_P = 5{,}000\ \text{cm}^3/\text{min}$, $Q_B = 200\ \text{cm}^3/\text{min}$,

$Q_D = 500\ \text{cm}^3/\text{min}$, $Q_W = 250\ \text{cm}^3/\text{min}$

$G = 5\ \text{mg/min}$, $K_i = 0.000468\ \text{cm/s}$ (from above) = $0.0281\ \text{cm/min}$, and $A_i = 13{,}800\ \text{cm}^2$

Initial conditions for the three concentrations are

$$C_P = 1\ \text{mg/cm}^3,\ C_B = 1\ \text{mg/cm}^3,\ \text{and}\ C_D = 0\ \text{mg/cm}^3$$

The numerical solution gives the following results over a 6-hr period; all three concentrations are given in mg urea/cm^3.

Time (hr)	C_P	C_B	C_D
0	1.00	1.00	0.00
1	0.86	0.84	0.20
2	0.74	0.73	0.18
3	0.64	0.63	0.15
4	0.55	0.54	0.13
5	0.48	0.47	0.11
6	0.42	0.41	0.10

Thus, in 4 hr, which is a typical treatment time, the urea concentrate has been reduced by 45%. It is left to Exercise 24.3 at the end of the chapter for a study of the effect on the rate of urea removal of changing the hemodialyzer geometry, the blood and dialysate flow rates to the dialyzer, the rate of waste withdrawal, the volume of the dialysate tank, and the sensitivity of the rate of urea mass transfer to the mass-transfer coefficient. In particular, the estimate of the coefficient on the shell side may be low because the entry to and exit from the hemodialyzer of the dialysate is normal to rather than parallel to the fibers. This should enhance the shell-side coefficient.

Finally, the model in Example 24.1 can be used to redesign the hemodialysis device for overnight home usage. In this case, dialysis could be accomplished seven nights per week for, say, six hours per night. This would permit much smaller blood and dialysate flow rates. See Exercise 24.4 at the end of the chapter.

Sorbent Dialysis. At most hemodialysis centers, the rich dialysate from hemodialysis devices is not regenerated and recycled, but is disposed of through drains and replaced by freshly diluted solution. This process, known as single-pass dialysis, requires large volumes of ultrapure water, typically prepared using reverse osmosis, activated carbon, deionization, and the like. The necessary equipment and holding tanks are expensive and require much space and, consequently, are not well suited for home hemodialysis products.

In the Allient® Sorbent Hemodialysis System (see *Sorbent Dialysis Primer* and *History of Sorbent Dialysis in the References*), the spent dialysate is chemically regenerated by passing through a disposable cartridge containing layers of activated carbon, the urease enzyme, and ion-exchange membranes. A small amount of makeup solution, called the infusate, replenishes any essential ions lost in the filter. Thanks to this regeneration process, only 6 L are required for each treatment session compared with greater than 120 L for single-pass dialysis. In addition to removing urea from the dialysate, the cartridge removes bacteria, heavy metals, and other contaminants from ordinary tap water, eliminating the need for water treatment equipment. New devices are completely portable, requiring only a source of electricity (see *Sorbent Dialysis Primer* Web site).

The first sorbent dialysis system was developed in the early 1970s and was sold under the REDY® brand name (for REcirculating DYalysis). Its use continued throughout the 1980s and, in 1993, a portable device was created. FDA approval for this device was not completed, however, and production was suspended until 1999 when SORB™ Technology, Inc., obtained the REDY® brand and renewed interest in sorbent dialysis. After merging with Renal Solutions, Inc., in 2001, they began to develop a system for home use. Renal Solutions, Inc. recently obtained FDA approval to market their product, the Allient® Sorbent Dialysis System, for both in-center and home treatment [see Shapiro (2004) for further discussion of sorbent dialysis].

As shown in Figure 24.5, the used dialysate from the hemodialysis unit enters a purification layer consisting of activated carbon to remove particulate matter, heavy metals, and so on. Next, the dialysate passes through a layer of the urease enzyme, which converts urea to ammonium and carbonate ions, that is, ammonium carbonate. It next passes through a zirconium phosphate layer (cation exchanger) where the dangerous ammonium ions are exchanged for hydrogen and sodium. A layer of zirconium oxide (anion exchanger) binds fluorides and phosphates that have been removed from the blood. Because the urease enzyme can break down unlimited amounts of urea, the main limitation of the cartridge is its capacity to bind ammonia. Current cartridges (known as SORB™ and HISORB™) can process 20–30 g of urea nitrogen before losing their ability to bind ammonia. A breakthrough of ammonia when its concentration exceeds 2 wt% indicates that the capacity has been exceeded and the cartridge must be changed (*Sorbent Dialysis Primer*, page 6).

Technology Protection

To protect its technology prior to designing a new home hemodialysis product, product development teams need to be aware of existing patents. In July 2007, an advanced Google patent search for the term "home hemodialysis" returned 37 patents. The breakdown by decade is as follows:

Decade	Patents
1960s	1
1970s	1
1980s	0
1990s	33
2000s	2

As seen, far more patents were issued in the 1990s than the other decades. Many of the inventors cited the low percentage of patients undergoing dialysis at home and offered solutions they believed would increase the popularity of this treatment. The following categories were well represented in the search results:

Category	Patents
Dialysis machines and components	12
Dialysate solution	6

On the basis of this search, it seems clear that the principal technologies associated with the hemodialysis device and the sorbent dialysis cartridge have been developed. Before initiating the design of the home hemodialysis product in Section 24.3, a more specific search should be carried out for patents associated with devices that improve safety and for machine disinfection. When significant technologies are located, these can be added to the innovation map.

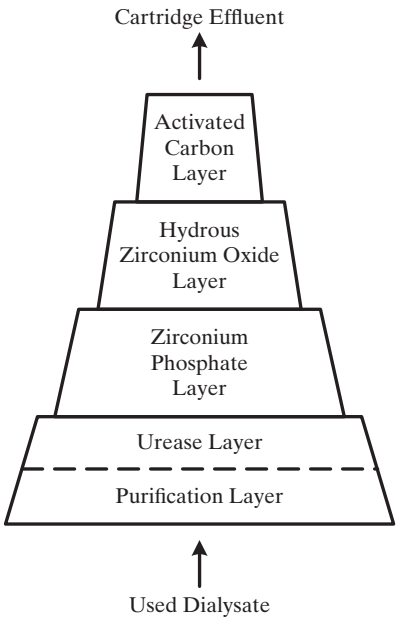

Figure 24.5 Schematic of the Allient® sorbent cartridge.

24.2 DESIGN SPECIFICATIONS OF HOME HEMODIALYSIS DEVICE

This case study is based upon a document prepared for a panel of medical experts assembled to evaluate the potential for delivering hemodialysis at home, specifically at night, while the patient is sleeping (Talamini, 2005). The underlying new technologies presented in Section 24.1, and developed during the 1970s and 1980s, were positioned in the *innovation map* of Figure 24.3, which shows the linkages between these new technologies and the products that satisfy the needs of hemodialysis patients, that is, the *customer-value proposition*. In this case study, emphasis is placed on developing the key objectives of the product development of a new home hemodialysis device (Project Charter—Objective-Time Chart) and setting the desired product performance by translating the customer requirements into a set of technical and economic requirements.

Project Charter—Objective Time Chart

Initially, the design team prepares a project charter–objective time chart as shown in Table 24.1. Clearly, the challenge is to develop a product that will permit safe, convenient use of a hemodialysis device at home at night while patients sleep. Under

Table 24.1 Project Charter—Objective Time Chart of the Home Hemodialysis Device

Project name	Home hemodialysis device
Project champions	Business Director of the Hemodialysis Business
Project leader	John Doe
Specific goals	Hemodialysis devices that operate at home while patients sleep. The product involves an array of devices to be installed at home, including alarms, with sensors, to detect and provide notifications of malfunctions with alerts to medical personnel at hemodialysis centers.
Project scope	In scope • Determination of home hemodialysis schedules • Reconfiguration of the hemodialysis device to adhere to the adjusted schedules Out of scope: • Installation of the equipment, instrumentation, and alarms • Retrofitting of bedrooms to achieve high standards of cleanliness
Deliverables	• Business opportunity assessment • Technical feasibility assessment
Timeline	Product prototypes for market testing within 12 months

the Project Scope, the design team recognizes the need to set home hemodialysis schedules and to reconfigure the hemodialysis device to adhere to these schedules. A product involving the hemodialysis device and associated operating equipment (pumps, holding tanks, sorbent dialysis, etc.), sensors, and alarms, is envisioned, but the installation of the operating system is not included in the product package. Installation instructions, but not an installation service, would be provided. Also retrofitting a bedroom to provide high standards of cleanliness is not covered by the cost of the new product. The design team envisions the demonstration of a working prototype system within 12 months.

Opportunity Assessment

A product development team needs to answer two fundamental economic questions before a company will make an investment in developing a new product. These involve the total market size and the opportunity size for the home dialysis device.

In 2011, chronic renal failure or end-stage renal disease (ESRD) impacted more than two million patients worldwide, including 571,414 in the United States—a number growing by 3.8% annually. Annual care costs in the United States approached $82,000 per patient for a total cost of care exceeding $42.5 billion. Yet the dialysis treatment itself represents less than one-third of this cost, or approximately $14.4 billion. This represents the total U.S. market opportunity, which is about 29% of the total global market. This is an attractive market with a respectable growth rate of around 4% annually.

The size of the market for the home hemodialysis device can be estimated from the adoption rate of this relatively new device as an alternative to in-center hemodialysis treatment. Prior to FDA clearance of the NxStage System One™, home hemodialysis in the United States had experienced significant decline. According to the 2011 U.S. Renal Data System's Annual Data Report, the number of patients adopting home hemodialysis treatments in the United States had dropped from approximately 3,000 patients in 1990 to 1,761 patients in 2002. The NxStage System One™ helped ignite a new wave of home hemodialysis therapy adoption, more than doubling the number of patients performing hemodialysis in their homes in its first five years on the market (NxStage Medical, Inc., www.nxstage.com/homehemodialysis/growth).

In 2011, 5,500 patients had adopted the home hemodialysis system representing merely about 1% of the total patients having chronic renal failure disease in the United States. From 2006 to 2010, the adoption of NxStage home hemodialysis grew from 1,000 to 5,000 patients, that is, about 38% annual growth or an average of 1,000 units of new sales annually. NxStage System One™ prices range from $25,000–$40,000 per unit. Thus, the annual revenue of home hemodialysis units was between $25 and $40 million.

By the end of 2010, NxStage Medical, Inc. was the market leader of the home hemodialysis device with a market share of 91%. The adoption rate of home hemodialysis was very low (1%), providing ample room for a new home hemodialysis product. Given this incentive, the next task was to determine the design specifications that offered significant advantages over the current market leader at the same or lower price.

Technical Requirements: Design Objectives

Considering the inconvenience of traveling to hemodialysis centers to receive time-consuming treatments during daytime hours that limited other activities, customer interviews indicate that low-cost home treatment while patients sleep would be far preferable. According to Talamini (2005), these potential customers need hemodialysis systems that operate reliably at home in the absence of medical personnel with comfortable, less-disruptive treatments. Potentially, these systems should involve lower blood and dialysate flow rates with no noticeable effects (i.e., smooth continuous operation without surging) while the person is sleeping. Because the treatments would be administered over longer periods—as many as seven days weekly—concentrations of urea in the blood should be lower on average, requiring smaller amounts of dialysate solution per treatment. If possible at low cost, it would be desirable to recover urea from the dialysate before recirculation to the hemodialysis device, rather than discarding the spent solution without recycling.

The most desirable customer needs are summarized in Table 24.2 with their weighting factors that were obtained either through primary customer research (e.g., using customer surveys) or by a discussion within the product development team.

Table 24.2 Customer Requirements for Home Hemodialysis Device

Customer Requirement	Weighting Factor
Reliable operation at home	50
More comfortable, less-disruptive treatments	50
No noticeable disturbances while sleeping	

Next, these customer requirements were translated into the set of technical requirements in Table 24.3. Note that they are normally adjusted by the design team as the product-development process proceeds.

Reliable home operation requires careful monitoring of many variables, such as the pressure, temperature, and flow rates, throughout the treatment session. The critical-to-quality (CTQ) variables selected must be monitored and controlled within the ranges shown in Table 24.3. The dialysate temperature is an important measure, which should be kept near body temperature. Temperatures above 42°C may lead to protein denaturation whereas temperatures above 45°C can cause hemolysis (rupturing of red blood cells). Pressures are typically measured at two points: upstream of the blood pump (arterial pressure) and downstream of the dialyzer (venous pressure). Safety alarms should be triggered when the pressure moves ±10% from the setpoint value, P^{SP} (which depends on the flow rate). Pressures are monitored similarly in the dialysate circuit. Finally, monitors must detect air embolisms and blood leakage.

For the extended dialysis schedule, 7 days/wk, 6 hr/day, the urea concentration in a patient's blood, $C_{P,i}$, builds to just 0.6 mg/cm^3 as seen by solving the following equation:

$$\frac{1.0\ \text{mg/cm}^3 - 0.30\ \text{mg/cm}^3}{56\ \text{hr}} = \frac{C_{P,i} - 0.30\ \text{mg/cm}^3}{24\ \text{hr}}$$

Most sources of home hemodialysis products suggest lower flow rates than at dialysis centers, that is, blood and dialysate flow rates at 200 and 300 cm^3/min, respectively. Note, however, that the model in Example 24.1, with the same specifications except for the initial urea concentration in the blood reduced to 0.6 mg/cm^3, indicates that the urea concentration in the blood can be reduced to 0.3 mg/cm^3 in 6 hr, using flow rates of 125 and 150 cm^3/min, respectively. In this regard, blood and dialysate pumps are available for the lower flow rates.

To keep patients comfortable during dialysis, surges in the blood flow rate must be controlled. In the *concept* stage, bounds at ±10% of the setpoint flow rate seem reasonable. This range must be carefully assessed in the *feasibility* stage when prototype products are constructed and tested.

Given the more frequent dialysis schedule, the average urea concentration is reduced to 0.45 mg/cm^3, midway between 0.6 and 0.3 mg/cm^3. This is the basis for setting the design objective for the urea concentration shown in Table 24.3.

Finally, when the dialysate is recycled, an upper bound on the urea concentration of 1 ppm seems reasonable. This upper bound must also be assessed during the construction and testing of a prototype system. Also, when sorbent dialysis is implemented, urea decomposes to ammonia, which must not exceed 2 wt% in the recycled dialysate. Note that the cartridges hold up to 20–30 g of urea, more than accumulated in a single dialysis treatment. When full, the ammonia concentration in the dialysate effluent builds as ammonia begins to break through. Another consideration is a bound on the dialysate concentration of bacteria, which must not exceed 200 colony-forming units of bacteria per milliliter (200 cfu/cm^3).

Another important aspect of reliable home operation is the user interface, which will typically be a computer or touch screen. During normal operation, this displays details such as pressure, temperature, and flow rates. When an alarm is triggered, the user interface must clearly communicate the problem to the patient and provide instructions for correcting it.

Table 24.3 Technical Requirements for the Home Hemodialysis Product

Customer Requirement	Technical Requirement Critical to Quality (CTQ)	Typical Values
Reliable operation at home	Lower average urea concentration	≤ 0.45 mg/cm^3
	Remove urea and recirculate dialysate	Residual urea concentration $\leq$ 1ppm
	Monitoring systems—P, T, air detection, blood leak detection Alarms—P, T, blood leak, air embolism, vascular access	$36 \leq T \leq 40$°C $0.9P^{SP} \leq P \leq 1.1P^{SP}$ $0.25 \leq BLS \leq 0.35$ mL/L blood Alarms $\geq$ 70 decibel
More comfortable, less-disruptive treatments No noticeable disturbances while sleeping	Lower blood and dialysate flow rates	$Q_B = 200$ cm^3/min $Q_D = 300$ cm^3/min
	Surge-free pumps	$\Delta Q_B \leq \pm 0.1 Q_B^{SP}$ $\Delta Q_D \leq \pm 0.1 Q_D^{SP}$
	Dialysis schedule	7 night/wk, 6 hr/night

Note: Blood leak sensitivity—mL/L blood; Q_B is the blood flow rate; Q_D is the dialysate flow rate; T is the temperature; P is the pressure.

Having defined the CTQ variables, it remains to generate the product concepts and evaluate these concepts against the best existing solution (hemodialysis center). This leads to the selection of the superior concept. In this case, the most promising product would include sorbent dialysis to eliminate the need for water treatment equipment and dialysate storage.

Manufacturing Cost Target

Having defined the product technical requirements, it is desired to set a cost target for the new product. The target cost often comes from the marketing and/or business development functions based on current selling prices of similar products, preferably the market leaders, and an acceptable profit margin. This target cost is the *ready-to-sell* price including packaging, delivery, distribution, marketing, and sales expenditures. As a rule of thumb, the manufacturing cost is at a maximum of one-half of the manufacturer's selling price. But, for the healthcare industry, the standard manufacturing cost is 30% of the manufacturer's selling price to cover the high R&D cost and the long FDA approval process (up to 10 years).

NxStage Medical, Inc. sells their Home Hemodialysis Device (System One™) at a price between US $25,000 and $40,000. At a manufacturer's selling price of $30,000 and using the standard gross-profit margin for the healthcare industry, the manufacturing cost is 33% of $30,000, that is, $10,000. Note that this is the target cost of the entire system including the dialyzer and the control system. Often it is desirable to break this target cost down to set the target costs for each subsystem, which are used as targets cost by the design teams associated with each subsystem.

The product development team at this point has a daunting task to develop a preliminary design within the cost target. This manufacturing cost target is revised many times during the course of a product development and keeps increasing while the product performance to be delivered keeps decreasing. Synergistic interactions between the business-development and product-development teams are key to the success of launching a successful new product.

24.3 SUMMARY

After studying this chapter, the reader should:

1. Understand the steps in the design of a new home hemodialysis product. These begin with a survey of the hemodialysis technology (Section 24.1), are summarized using an innovation map (Figure 24.3), and are followed by IP analysis. For the latter, appreciate the need to protect advances in hemodialysis technology and product applications long before the product is conceived.
2. Recognize the role of the objective-time chart, that is, the project charter, in setting goals, deliverables, and a time line in developing the new product. Also, recognize the importance of the opportunity assessment when setting the product specifications and the manufacturing cost target.

REFERENCES

1. Bird, R. B., W. E. Stewart, and E. N. Lightfoot, *Transport Phenomena*, 2nd ed., Wiley, New York (2002).

2. Chibata, I., T. Tosa, T. Sato, and T. Mori, *Blood Urea Removal Device*, U.S. Patent 3,865,726 (1975).

3. Daugirdas, J. T., and T. S. Ing (eds.), *Handbook of Dialysis*, Little, Brown Boston, Massachusetts (1988).

4. *History of Sorbent Dialysis*, Renal Solutions, Inc. Web site: www.renalsolutionsinc.com.

5. Knudsen, J. G., and D. L. Katz, *Fluid Dynamics and Heat Transfer*, McGraw-Hill, New York (1958).

6. Misra, M., "The Basics of Hemodialysis Equipment," *Hemodialysis Int'l.*, **9**, 30–36 (2005).

7. NxStage Medical, Inc. Web site: www.nxstage.com/homehemodialysis/growth.

8. Seader, J. D., E. J. Henley, and D. K. Roper, *Separation Process Principles*, 3rd ed., Wiley, New York (2011).

9. Shapiro, W. B., "Sorbent Dialysis" (Chapter 38), in *Clinical Dialysis*, 4th ed., (eds.), A. R. Nissenson and R. N. Fine, McGraw-Hill, New York (2004).

10. *Sorbent Dialysis Primer*, SORB Technologies. Web site: www.sorb.net.

11. Spaeth, E. E., *Washington University Case Study 9, Analysis and Optimization of an Artificial Kidney System*, Department of Chemical Engineering, Washington University, St. Louis, Missouri (1970).

12. Talamini, M., "Guidance for Nocturnal Home Hemodialysis Devices," *Nocturnal Home Hemodialysis Devices Panel Meeting*, 2005.

13. U.S. Renal Data System, *USRDS 2011 Annual Data Report: Atlas of End-Stage Renal Disease in the United States*, National Institutes of Health, National Institute of Diabetes and Digestive and Kidney Diseases, Bethesda, Maryland (2011).

BIBLIOGRAPHY

PATENTS—HEMODIALYSIS DEVICES—GENERAL

Kell, M. J., and R. D. Mahoney, *Cellulose Acetate Hollow Fiber and Method for Making Same*, U.S. Patent 4,276,173 (1981).

Humphreys, L. R., D. Barone, F. C. Baker, III, T. S. Bowers, and J. E. Jamieson, *Processor for a Portable Recirculatory Hemodialysis Unit*, U.S. Patent D 282,578 (1986).

Chibata, I., T. Tosa, T. Sato, and T. Mori, *Blood Urea Removal Device*, U.S. Patent 3,865,726 (1975).

PATENTS—HEMODIALYSIS DEVICES—HOLLOW-FIBER MEMBRANES

Uenishi, T., I. Yamamoto, K. Okamoto, H. Sido, Y. Shiota, H. Shikurai, S. Watanuki, and M. Suzuki, *Cellulose Acetate Hemodialysis Membrane*, U.S. Patent 5,783,124 (1998).

PATENTS—HEMODIALYSIS DEVICES—DIALYSATE REGENERATION

Marantz, L. B., *Treatment of Dialysate Solution for Removal of Urea*, U.S. Patent 3,669,878 (1972).

Michaels, A. S., A. J. Appleby, and J. C. Wright, *Flowthrough Electrochemical Hemodialysis Regeneration*, U.S. Patent 4,473,449 (1984).

Thompson, R. P., *Filter Cartridge Assemblies and Methods for Filtering Fluids*, U.S. Patent 6,878,283 (2005).

PATENTS—HEMODIALYSIS DEVICES—ALARMS/USER INTERFACE

Yin, C., *Blood Pressure Alarms for Dialysis Machines*, U.S. Patent 4,148,314 (1979).

Balschat, K., H. Ender, A. Gagel, and R. Spickermann, *Method and Device for Detecting a Leakage in a Fluid System of a Blood Treatment Apparatus*, U.S. Patent 6,804,991 (2004).

EXERCISES

24.1 Consider the hemodialysis device using the hollow-fiber module in Figure 24.1, operating 12 hr/wk (3 days, 4 hr/day) at a dialysis center. As shown in Example 24.1, with a blood flow rate of 200 mL/min and a dialysate flow rate of 500 mL/min, its overall mass-transfer coefficient is estimated to be $K_i = 0.000468$ cm/s.

(a) To design a *home* hemodialysis device, assume operation 42 hr/wk (7 days, 6 hr/day) while the patient sleeps. Reduce the blood flow rate by one-third (to 133 mL/min) and the dialysate flow rate to (300 mL/min)—a big advantage when sleeping. As a first step in redesigning the module, assume no changes in its geometry and estimate the mass-transfer coefficient inside the fiber, k_b (where the blood flows). Use the correlation:

$$N_{\text{Sh}} = 3.254 \left[\frac{L/D_i}{N_{\text{Pe}_\text{M}}} \right]^{-1/3}$$

where L is the hollow-fiber length, D_i is its inside radius, N_{Sh} is the Sherwood Number, and N_{Pe_M} is the Peclet Number for mass transfer. Then, assuming no change in the mass-transfer coefficient on the outside of the fibers, k_d (where the dialysate flows), estimate the reduction in K_i.

(b) Increase the membrane permeability by a factor of 10. Estimate the increase in K_i.

Note: These calculations are just the first steps in an iterative process to redesign the hollow-fiber module for home hemodialysis as carried out in Exercise 24.5.

24.2 For the home hemodialysis device operating with a blood flow rate of 133 mL/min and a dialysate flow rate of 300 mL/min, the fiber-side (blood-side) mass-transfer coefficient is 0.00152 cm/s, the permeability is 3×10^{-5} cm^2/s, and the overall mass-transfer coefficient is 0.000597 cm/s.

(a) Estimate the dialysate-side mass-transfer coefficient.

(b) When the *overall* mass-transfer coefficient is *doubled*, how must the dialysate-side mass-transfer coefficient be adjusted. That is, compute a new value for the dialysate-side mass-transfer coefficient.

24.3 Consider the hemodialysis device in Example 24.1. Examine the effect on the rate of urea removal of changing the hemodialyzer geometry, the blood and dialysate flow rates to the dialyzer, the rate of waste withdrawal, the volume of the dialysate tank, and the sensitivity of the rate of urea mass transfer to the mass-transfer coefficient. In particular, the estimate of the coefficient on the shell side in the solution to Example 24.1 may be low because the entry to and exit from the hemodialyzer of the dialysate is normal to rather than parallel to the fibers. This should enhance the shell-side coefficient.

24.4 Repeat Exercise 24.3 for a hemodialysis device designed for overnight home use. Assume that the device will be used 7 nights/wk for 6 hr/night.

24.5 Consider the home hemodialysis product.

(a) Complete Exercise 24.4; that is, design a hemodialysis device that lowers the urea concentration in the blood to 0.3 mg/cm^3, operating 7 nights/wk for 6 hr/night.

(b) Complete a product design, including all units; that is, the hemodialysis device, sorbent recovery unit, pumps, holding tanks, sensors, alarms, computer, and display. Estimate their purchase costs.

(c) Set a product price and complete a business plan, including estimates of the return on investment, net present value (at 15% annual interest rate), and investor's rate of return.

Chapter 25

Case Study 2—High Throughput Screening Devices for Kinase Inhibitors

25.0 OBJECTIVES

One of the key success factors of a product development effort is the ability of the technical team (engineers and scientists) to develop a superior product concept and/or construction. In addition to those steps and tools presented in Chapter 24, this chapter presents a case study of the development of high throughput screening devices for kinase inhibitors. The emphasis is placed on the development of a superior product concept. Similar steps and tools including the background for the new technologies, the innovation map, and technology protection are discussed.

After studying this chapter, the reader should:

1. Be able to construct an innovation map.
2. Be able to identify critical inventions for materials, process/manufacturing, and product technologies.
3. Appreciate the need for technology-protection strategies.
4. Be able to develop a superior product concept.
5. Be able to perform profitability analysis using the techniques described in Chapters 17 and 19.

25.1 BACKGROUND TECHNOLOGY FOR HIGH THROUGHPUT SCREENING OF KINASE INHIBITORS

Much research and development in the pharmaceuticals industry involves the discovery of new therapeutics. These are often biochemicals that are synthesized in small quantities, often tested in vitro with small quantities of proteins, peptides, and the like, which are synthesized biochemically or extracted from the body. Because screening devices need to be small, often involving nanoliter samples, and operate quickly, handling many samples in parallel over periods on the order of minutes, there is growing interest in the design of *lab-on-a-chip* products.

This section addresses the creation of lab-on-a-chip products for the screening of kinase inhibitors (KIs), which, among other things, are promising cancer therapeutics. These are small molecules that reduce the phosphorylation activity of one or more of the ~500 kinase enzymes in the human body (examples include gleevec, temserolimus, gefitinib, staurosporine, and so on). To be useful, a KI must be specific, targeting one or a small number of kinase enzymes without significantly affecting the activity of the others. In 2004, it was estimated that pharmaceutical companies were spending ~$100 million U.S./year screening potential therapeutic KI compounds created by their drug discovery efforts.

One potential lab-on-a-chip product would perform standardized kinase inhibition assays on compounds developed by pharmaceutical companies at high speed. All reagents would be purchased commercially or easily synthesized in house using benchtop-scale equipment. Because of the high cost of the purified kinase enzymes (typically $5 million/g), the use of at most 10–100 nl total reaction volume per assay is required, with the reagents and samples handled and mixed using microfluidic methods. Ideally, kinase enzyme (KE) function and reactant concentration would be followed in real time using nondestructive, noncontact methods such as fluorescence polarization (FP), fluorescent resonance energy transfer (FRET), or luminescence, which can be readily parallelized so that a single charge-coupled device (CCD) detector/scanner can monitor several hundred or thousand assays in parallel.

In this section, an *innovation map* is created to examine the key technological inventions that have accompanied chemical products closely related to the lab-on-a-chip being designed. These inventions, either in materials, or processing/manufacturing, or product technologies, are critical to attracting customers and satisfying their perceived needs. To illustrate the creation of an *innovation map* for a lab-on-a-chip to screen kinase inhibitors, the technologies related to its design are reviewed next. Then, in Section 25.2, the designs for potential lab-on-a-chip products are presented. This review begins with a brief discussion of the normal functioning of kinase enzymes and the role of kinase inhibitors.

Kinase Reactions and Lab-on-a-chip Inventions

Kinase Enzyme Reactions

In general, each kinase enzyme is a protein that phosphorylates a target protein or a set of proteins, affecting their function much

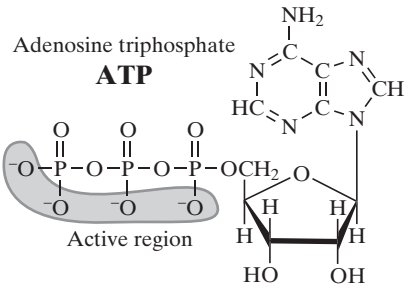

Figure 25.1 Adenosine triphosphate.

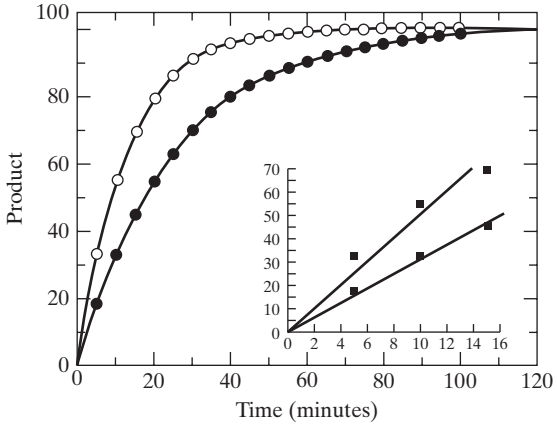

Figure 25.2 Product concentration of the phosphorylation reaction with and without kinase inhibitor. (*Source:* Copeland, 2003. Used with permission).

like an on/off switch. Along with phosphatases that remove phosphate groups, these enzymes are largely responsible for the biochemical regulation within living cells. In general, the reaction resembles:

$$\text{KE} + \text{Target protein} + \text{ATP} \rightarrow \text{KE} + (\text{Target protein})\text{PO}_4 + \text{ADP} \quad \text{(R1)}$$

That is, the kinase enzyme binds adenosine triphosphate (ATP), which is illustrated in Figure 25.1, and an active site on a target protein moves one phosphate group onto the target protein and unbinds, releasing the target protein and ADP. As an enzyme, the kinase enzyme is not modified and repeats the reaction as long as target protein and ATP are available. About 100 KEs have been cloned and purified to date and are commercially available.

The function of the KI is to compete with the target protein by binding to the KE's active site. When binding is strong, it effectively blocks access to the target protein and significantly slows the above reaction. Figure 25.2 shows the product concentration of the phosphorylation reaction as a function of time with and without the kinase inhibitor present.

The lab-on-a-chip product would create inhibitor concentration 50% ($IC_{50} = [KI]_{50}$) data; that is, it would determine the KI concentration at which a given KE's activity (rate of reaction, r_P) drops by 50%. This is traditionally determined by performing multiple assays varying the KI concentration over many orders of magnitude, and finding the crossover (if any) in the resulting

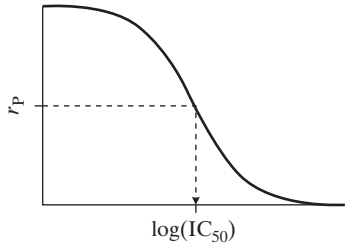

Figure 25.3 IC_{50} curve.

"S"-shaped inhibition curve (rate of reaction, r_P, as a function of inhibitor concentration), shown schematically in Figure 25.3.

One approach is to use luminescence to report the concentration of ATP at some point in time, say 1 hour or less. Firefly luciferase and similar compounds produce light using an ATP-dependent chemical reaction; the brightness of the light is essentially proportional to the concentration of ATP [ATP]. Thus, a high-resolution camera, such as a low-light CCD camera, can integrate the light signal for a short period with the brightness of a few pixels proportional to [ATP]. The time rate of change of [ATP] is then proportional to the consumption of ATP by the KE (assuming that the amount consumed by the luciferase is negligible by comparison).

Lab-on-a-chip Inventions

During the first decade of the 21st century, two promising lab-on-a-chip technologies were invented, one by the Fluidigm® Corporation and the other by the RainDance® Technologies Company, two successful startup companies.

Fluidigm Corporation Two-layer Soft Lithography. In the early 2000s, Fluidigm Corporation designed two-layer chips using poly(dimethylsiloxane), PDMS, a soft polymer known for its low cost, flexibility, and optical transparency and whose chemical structure is shown in Figure 25.4. As shown, PDMS is a repeating polymer, consisting of multiple $–OSi(CH_3)_2–$ units in series. Its flexibility allows for deflections that permit the implementation of valves and peristaltic pumps as described subsequently. To prevent protein denaturation resulting from the hydrophobicity of the $–CH_3$ groups, the PDMS is treated with air plasma, which converts its surface from hydrophobic to hydrophilic.

Fluidigm used soft lithography to create a PDMS mold. First, the chip designer, using a computer-aided design (CAD) program, devised a master mold that contained all of the microstructures to be placed on the chip. Then, the master mold was created using UV-photolithography as shown in Figure 25.5. To prevent irreversible bonding between the PDMS and the master mold, the

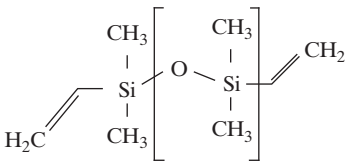

Figure 25.4 Chemical structure of PDMS composed of repeating $–OSi(CH_3)_2–$ units. Usual polymer lengths are approximately $n = 60$.

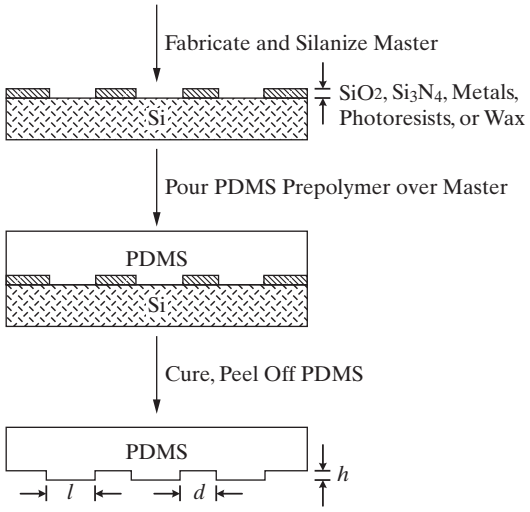

Figure 25.5 Schematic representation of the creation of PDMS molds. Each master mold fabricates 50 PDMS molds. Height, depth, and length range from 0.2–20, 0.5–200, and 0.5–200 μm, respectively. (*Source:* Copyright Wiley-VCH Verlag GmbH & Co. KGaA. Reproduced with permission).

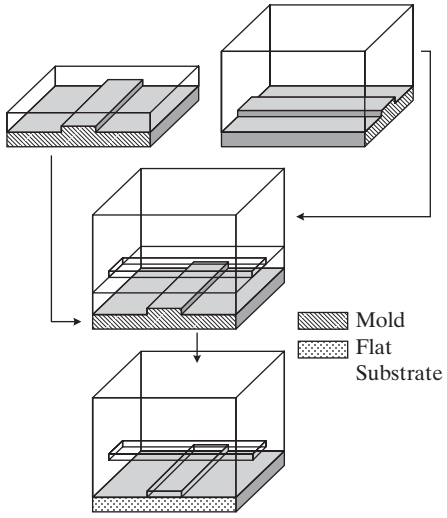

Figure 25.6 Schematic of multilayer soft lithography. The bonding between the bottom and top layers requires 1.5 hr at 80°C. (*Source:* Unger et. al., 2000. Reproduced with permission).

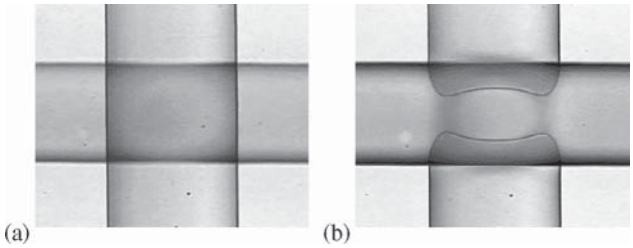

Figure 25.7 (a) Magnified close-up of Nanoflex™ valve in open position. Notice the overlap between the control and the flow channel. (b) Valve in closed position when the control channel flexes, clamping down on the flow channel and creating a tight seal. (*Source:* Reproduced with permission from the Fluidigm Corporation).

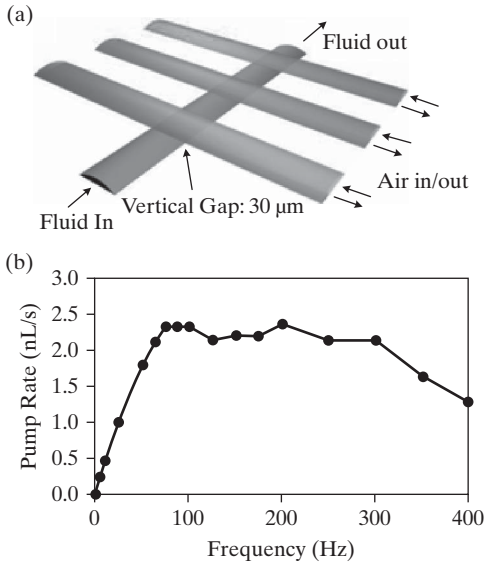

Figure 25.8 (a) When three control channels are actuated by the pattern 101, 100, 110, 010, 011, and 001 where 0 = open valve and 1 = closed valve, peristaltic pumping occurs. (b) Pump rate as a function of the frequency of pumping. In the approximate frequency range of 75 Hz–100 Hz, pump rate is constant, ~2.4 nL/s. (*Source:* Unger et al., 2000. Reproduced with permission).

latter was coated with fluorinated silanes. And, to complete the process, a liquid PDMS prepolymer was poured onto the master to create the mold. These PDMS molds are highly reproducible and precisely made in less than a day.

To add devices for control (that is, valves and peristaltic pumps) to the chip, an addition-cure process called multilayer soft lithography was developed by Quake et al. (2000). This process bonds two PDMS molds into effectively a monolithic mold. The bottom layer is a PDMS mold containing vinyl groups and a platinum catalyst, and the top layer is a PDMS mold containing a cross-linker with silicon hydride (Si-H) groups. When the two layers are joined, the latter covalently bonds to form a hermetic seal. Because the entire mold is monolithic, interlayer adhesion failures and thermal stress problems are avoided.

The pressure-driven top channels, which run orthogonal to the lower channels, control the fluid flow in the lower channels as shown in Figure 25.6. The latter contain the reagents for all of the assays to be carried out.

Due to the flexibility of PDMS, as the pressure increases, the channels deflect. Thus, as pressure is exerted on a top channel, it bends downward by as much as 30 μm until it touches and even deflects the bottom layer. With an applied pressure of approximately 100 kPa, a typical response time is on the order of 1 ms. Given sufficient pressure, a top channel seals off the bottom channels under it as shown in Figure 25.7.

To control the fluid movement in the bottom channels, peristalsis is used. Three microfabricated valves are placed in series, generating wavelike contractions, and essentially forming a peristaltic pump, as shown in Figure 25.8a. The pump uses the pattern 101, 100, 110, 010, 011, and 001, where 0 and 1 represent open and closed valves, respectively.

As shown is Figure 25.8b, the pumping rate for the bottom channels is a function of the pattern repeat frequency of the top channels. To control the flow rate, the *sensible* region of the graph is used; that is, the left-most portion, where the flow rate varies linearly for frequencies between 0 and ~75 Hz. In the design here,

a typical frequency is 100 Hz, which corresponds to a flow rate of 2.4 nL/s, or 24 pL pump cycle. Note that Section 25.2 presents a Fluidigm chip design for the HTS of kinase inhibitors.

RainDance Micron-sized Droplets. By the mid-2000s, RainDance Technologies, another startup company, had introduced a microfluidic chip that utilizes an electronically gated emulsion gun to form nanoliter droplets at very high frequencies, as high as 20,000 droplets per second. As syringe pumps force low-viscosity oil through a microfabricated chip, referred to as a Personal Laboratory System™ (PLS), emulsion guns form aqueous droplets (containing various reactants). These droplets have volumes on the order of nanoliters that can be diluted and merged to contain reactants at varying concentrations. Then, by adjusting the environment, typically the temperature, chemical reactions are carried out in the so-called "reactor droplets," and the concentrations are measured using optical monitors and cameras.

To form the small aqueous droplets, the RainDance electronic gun is pointed orthogonally to a microchannel of flowing oil. The water is forced around the point of the gun impinging into the oil, forming a meniscus, and creating charged droplets after each voltage alternation at high frequency (20,000 Hz), yielding as many as 20,000 droplets per second. Often, two guns create two streams of droplets, each containing different reactants and having opposite charges. Then, on the PLS, as shown in Figure 25.9, the droplets, flowing side-by-side, are attracted to each other. Eventually, the droplets coalesce to contain two or more reagents, for example, a kinase enzyme (KE) and a potential kinase inhibitor (KI).

To permit the combination of various reagents at differing concentrations, the PLS is configured by RainDance personnel for specific applications involving two or more emulsion guns, mixers, and splitters. The latter allow droplets to be split, with portions (say one-third volume) recycled to be met by water droplets for dilution purposes.

Because the droplets are formed at high frequencies and contain different reagents at differing concentrations, it is normally important to label the contents of each droplet using so-called *bar codes.* This led Molecular Probes®, another startup company, to develop TransFluoSphere™ fluorescent microspheres. Using three dyes (say, red, green, and blue) at three significantly different concentrations, each droplet can be assigned a unique code that is detected by recording the emission wave lengths after laser excitation.

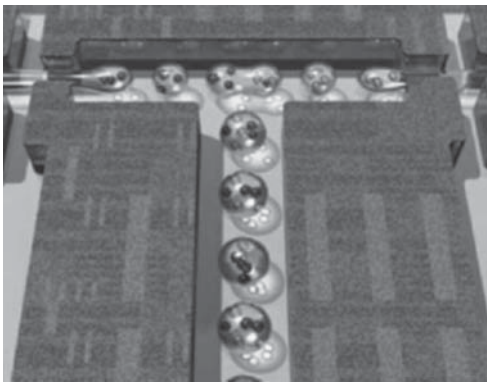

Figure 25.9 Aqueous droplets flowing in low-viscosity oil on the RDT PLS™ chip. (*Source:* Reproduced with permission. © RainDance Technologies, Inc).

Another advance was necessary to measure the concentration of the reaction products in each reactor droplet to be related to the rate of reaction. Consider the phosphorylation reaction, R1, with KIs bound to KEs to slow the rate of conversion of ATP to ADP. To measure the ADP concentration, BellBrook Laboratories, another startup company, introduced a Transcreener® Assay, a fluorescence polarization technique. This assay uses a fluorescent tracer, bound to a large antibody, which is selected carefully to be specific to ADP. When this complex is exposed to polarized light, the ADP concentration, [ADP], is proportional to the intensity of the depolarized light emitted. To measure the depolarized light emitted, Agilent Technologies developed the Agilent® SureScan™ microarray reader, which uses AlexaFluor 633™, a very bright, stable dye that is excited by the 633 nm line of the He-Ne laser. The latter is included in the Transcreener kit, which provides a mixture of ADP and AexaFluor 66™ to be blended with the kinase enzyme. Note that Section 25.2 presents a product design using a combination of these new technologies.

Innovation Map

For the product development of a lab-on-a-chip for the high throughput screening of kinase inhibitors, consider the *innovation map* in Figure 25.10, which is typical of one prepared in the mid-2000s.

To construct the *innovation map*, the historical information presented here, coupled with an observation of customer needs, provides the elements to be positioned in its six levels, moving from the bottom to the top of the map:

1. *Materials Technology.* PDMS soft polymer, 10–100 μm aqueous droplet in carrier oil, Molecular Probes TransFluoSphere fluorescent microspheres, and Transcreener Assay fluorescence polarization technique to measure [ADP].
2. *Process/Manufacturing Technology.* Fluidigm two layer soft lithography to create PDMS mold, photon generation using luciferase, RainDance® electronically gated emulsion gun–oil wets aqueous droplets, microarray reader.
3. *Technical Differentiation (technical-value proposition).* Peristaltic pumping for mixing/dilution, form aqueous droplets with embedded particle bar-codes–controlled fusion/dilution droplets containing various concentrations.
4. *Product Technology.* Mixing and nanoreactor layer + control layer, automated image analysis and storage in database, serially create large libraries of microreactors–positioned on the microfluidic chip.
5. *Products.* Fluidigm two-layer lab-on-a-chip, RDT PLS microfluidic chip.
6. *Customer-value Proposition.* Low-cost assays ($100/assay), high throughput (333 assay/day), service laboratory, lower-cost assays ($0.05/assay), higher throughput (10^6 assay/day), chip for in-house laboratory.

Given these elements, the connectivity is added to show the interplay between the technological elements, the *technical-value*

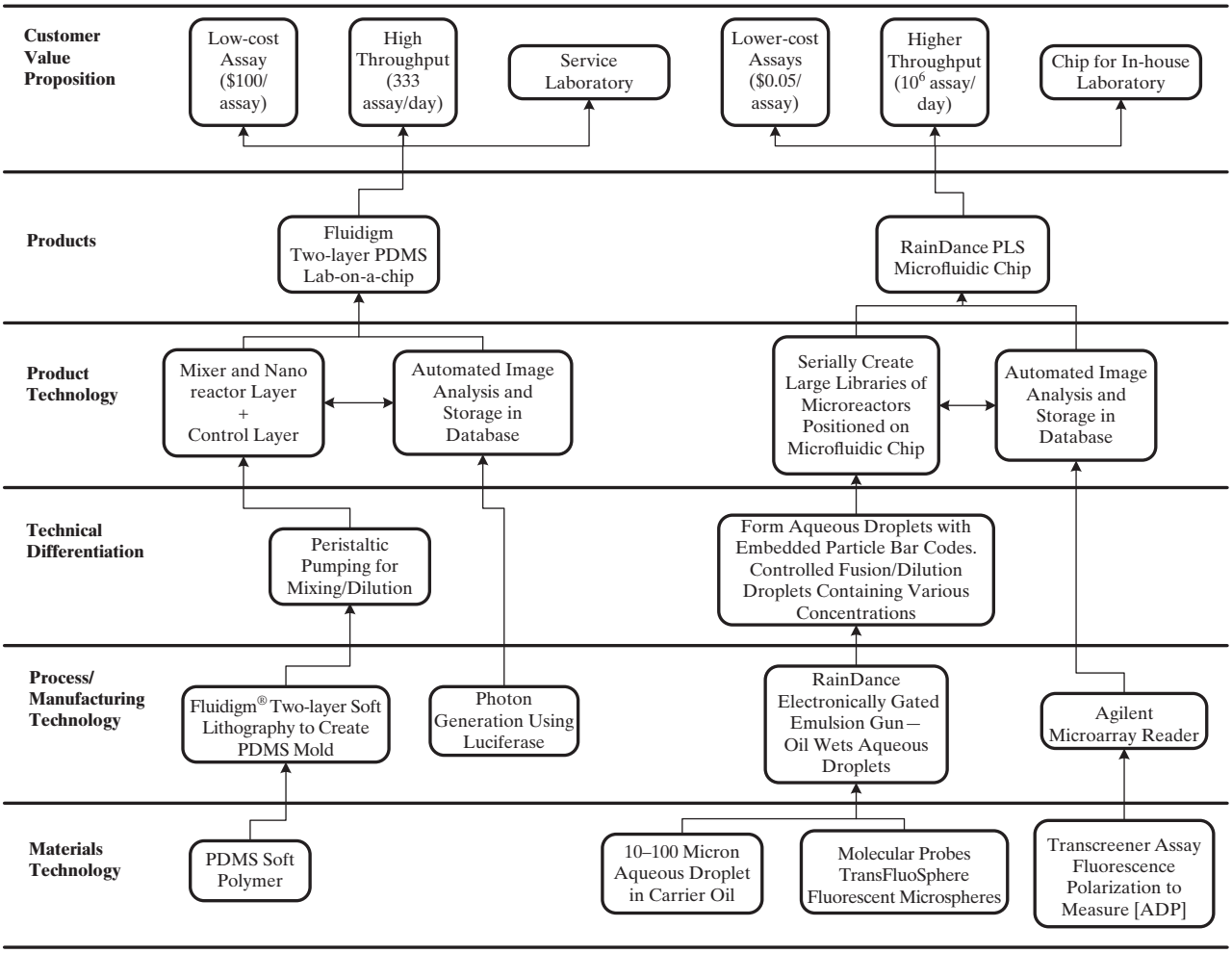

Figure 25.10 Innovation map for the lab-on-a-chip.

proposition and the *customer-value proposition*. As unmet customer needs are encountered, they can be added for the next generation of products.

In 2000, the initial inventions involved the use of PDMS *soft polymer* (materials technology) with *Fluidigm two-layer soft lithography to create a PDMS mold* (process/manufacturing technology) to provide the technical differentiation, *peristaltic pumping for mixing and dilution*. This led to the *mixer and nanoreactor layer plus a control layer* (product technology) and the *Fluidigm two-layer PDMS lab-on-a-chip* product, which was created to satisfy the customer needs: *low-cost assay* ($\$100/assay$), *high throughput* (333 $assay/day$), and *service laboratory* (customer-value proposition). In parallel, photon generation using luciferase (process/manufacturing technology) permitted the *automated image analysis and storage in database* (product technology), which led to the lab-on-a-chip product.

By 2004, the new materials and process/manufacturing technologies in the innovation map had led to a key technical differentiation. The new materials technologies permitted the generation of micron-sized aqueous droplets in a carrier oil, TransFluoSphere labels for the droplets, and Transcreener fluorescence polarization to measure [ADP]. RainDance Technologies introduced the new processing technology that permitted nanoliter aqueous droplets to be formed at high frequency with varying compositions of reagents. This, in turn, led to a new product technology involving the creation of large libraries of microreactors on microfluidic chips. Together with new image analysis techniques, the new product, the RainDance PMS chip, was introduced; it satisfied the customer needs for lower cost assays, higher throughputs and a chip configured for in-house laboratories.

In the remainder of this section, aspects of these promising technological inventions are discussed in the subsections Process/Manufacturing Technology and Technology Protection.

Process/Manufacturing Technology

This section introduces enzyme kinetics with emphasis on dual-substrate enzyme kinetics and inhibition associated with the kinase enzymes and their inhibitors. This is needed to understand the usage of the new Fluidigm process/manufacturing technology for the lab-on-a-chip product, which will be described in Section 25.2. More specifically, the kinetics model is needed to determine the concentration of ATP, [ATP], to be catalyzed by luciferase to produce sufficient photons for the CCD camera, while maintaining sufficiently high levels of [ATP], that is,

[ATP] ~1 μM. Also, the method for estimating the droplet reactor volume to produce sufficient photons is discussed, taking into account the incident photon fraction, quantum fraction, quantum efficiency, and similar factors.

Dual-substrate Enzyme Kinetics. To design the screening device presented in Section 25.2, rate data are needed for the phosphorylation reaction, R1, and for the reaction involving the kinase inhibitor, to be discussed shortly. Before considering these data, which are provided by suppliers of the kinases such as Caliper Life Sciences, Inc., and applied for the dual-substrate reaction, a brief review of Michaelis-Menton enzyme kinetics is included for reactions involving just a single substrate:

$$\mathrm{E} + \mathrm{S} \rightleftharpoons \mathrm{E\text{-}S} \rightarrow \mathrm{E} + \mathrm{P} \tag{R2}$$

where E is the enzyme, S is the substrate, E-S is the intermediate enzyme-substrate complex, and P is the product. To derive the rate of formation of the product, rate constants are defined for the reversible and irreversible reactions:

$$\mathrm{E} + \mathrm{S} \xrightarrow{k_1} \mathrm{E\text{-}S} \tag{R3}$$

$$\mathrm{E\text{-}S} \xrightarrow{k_{-1}} \mathrm{E} + \mathrm{S} \tag{R4}$$

$$\mathrm{E\text{-}S} \xrightarrow{k_2} \mathrm{E} + \mathrm{P} \tag{R5}$$

Because the enzyme is a catalyst, its total concentration, $[\mathrm{E_T}]$, remains constant such that:

$$[\mathrm{E_T}] = [\mathrm{E}] + [\mathrm{E\text{-}S}] \tag{25.1}$$

where [E] is the enzyme concentration, and [E-S] is the concentration of the enzyme bonded to the substrate.

The mass balance for the enzyme-substrate complex gives its rate of formation, $r_{\mathrm{E\text{-}S}}$, as a function of its rates of generation and consumption in reactions R3–R5:

$$r_{\mathrm{E\text{-}S}} = k_1[\mathrm{E}][\mathrm{S}] - k_{-1}[\mathrm{E\text{-}S}] - k_2[\mathrm{E\text{-}S}] = k_1[\mathrm{E}][\mathrm{S}] - (k_{-1} + k_2)[\mathrm{E\text{-}S}] \tag{25.2}$$

Because [E-S] is an intermediate in the reactions, $r_{\mathrm{E\text{-}S}}$ is commonly approximated using the pseudo-steady-state assumption, $r_{\mathrm{E\text{-}S}} = 0$, which gives:

$$[\mathrm{E}][\mathrm{S}] = (k_{-1} + k_2)/k_1[\mathrm{E\text{-}S}] = K_m[\mathrm{E\text{-}S}] \tag{25.3}$$

where K_m is referred to as the Michaelis-Menten constant. Using Eq. (25.1) to substitute for E:

$$([\mathrm{E_T}] - [\mathrm{E\text{-}S}])[\mathrm{S}] = K_m[\mathrm{E\text{-}S}] \tag{25.4}$$

Rearranging for [E-S] and multiplying by k_2, gives the rate of production of the product, P:

$$r_{\mathrm{P}} = k_2[\mathrm{E\text{-}S}] = \frac{k_2[\mathrm{S}][\mathrm{E_T}]}{K_m + [\mathrm{S}]} \tag{25.5}$$

Furthermore, because the maximum rate of production is $r_{\mathrm{P,max}} = k_2[\mathrm{E_T}]$, Eq. (25.5) can be written as:

$$r_{\mathrm{P}} = \frac{r_{\mathrm{P,max}}[\mathrm{S}]}{K_m + [\mathrm{S}]} \tag{25.6}$$

which is the familiar form of the Michaelis-Menten equation. Note that at low substrate concentrations, where $K_m \gg [\mathrm{S}]$, the rate of production is first-order in [S]. At high concentrations, where $K_m \ll [\mathrm{S}]$, substrate inhibition occurs and the rate becomes zero-order in [S].

Returning to the phosphorylation reaction, R1, which involves the two substrates, ATP and target protein (which is replaced by a polypeptide in the lab), the kinetics mechanism can be represented as:

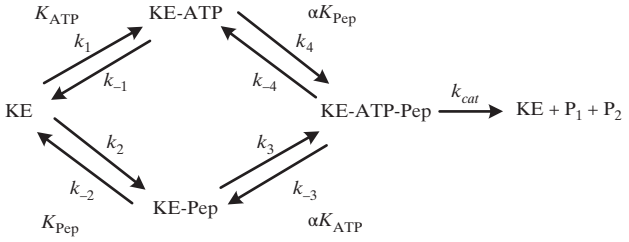

(R6)

where KE is the kinase enzyme, KE-ATP and KE-Pep are single-substrate complexes, KE-ATP-Pep is the dual-substrate complex, and P_1 and P_2 are two reaction products. Assuming *rapid equilibrium binding* (that is, equal forward and back reaction rates), and defining the dissociation equilibrium constants:

$$K_{\mathrm{ATP}} = \frac{k_{-1}}{k_1},\ \alpha K_{\mathrm{ATP}} = \frac{k_{-3}}{k_3},\ K_{\mathrm{Pep}} = \frac{k_{-2}}{k_2},\ \alpha K_{\mathrm{Pep}} = \frac{k_{-4}}{k_4} \tag{25.7}$$

and using the pseudo-steady-state assumption for the rates of production of the intermediate complexes, the rate of production of the products is:

$$r_{\mathrm{P}} = \frac{k_{cat}[\mathrm{KE_T}][\mathrm{ATP}][\mathrm{Pep}]}{\alpha K_{\mathrm{ATP}}K_{\mathrm{Pep}} + \alpha K_{\mathrm{Pep}}[\mathrm{ATP}] + \alpha K_{\mathrm{ATP}}[\mathrm{Pep}] + [\mathrm{ATP}][\mathrm{Pep}]} \tag{25.8}$$

where $[\mathrm{KE_T}]$ is the total concentration of the kinase enzyme, [ATP] is the concentration of adinosine triphosphate, and [Pep] is the concentration of the polypeptide. Note that α multiplies the equilibrium constant for single-substrate binding to give the equilibrium constant for binding after the other substrate has been bound, it being assumed that α is independent of the binding sequence. Note also that the pseudo-steady-state assumption is redundant when all of the reversible reactions are assumed to be in local equilibrium. Finally, because the maximum rate of production of products, $r_{\mathrm{P,max}}$, is $k_{cat}[\mathrm{KE_T}]$, Eq. (25.8) can be written:

$$r_{\mathrm{P}} = \frac{r_{\mathrm{P,max}}[\mathrm{ATP}][\mathrm{Pep}]}{\alpha K_{\mathrm{ATP}}K_{\mathrm{Pep}} + \alpha K_{\mathrm{Pep}}[\mathrm{ATP}] + \alpha K_{\mathrm{ATP}}[\mathrm{Pep}] + [\mathrm{ATP}][\mathrm{Pep}]} \tag{25.9}$$

Note that, typically, $K_{\mathrm{ATP}} \cong 1 - 10\ \mu\mathrm{M}$ and $K_{\mathrm{Pep}} \cong 1 - 10\ \mu\mathrm{M}$.

Kinase Inhibition Reactions. An enzyme inhibitor binds to the enzyme, preventing the enzyme from catalyzing the enzyme reaction. It competes with the substrate(s) for the enzyme's *active sites*, thereby reducing the rate of the enzyme reaction and the rate of substrate consumption. Cheng and Prusoff (1973) describe three kinetic mechanisms for the binding of an inhibitor to an enzyme that catalyzes a single-substrate reaction. These are described next for an enzyme reaction involving a single substrate before returning to the dual-substrate phosphorylation reaction.

Single-substrate Competitive Inhibitor. The first occurs when a *competitive* inhibitor is present, that is, one that competes with the substrate for the binding site on the enzyme:

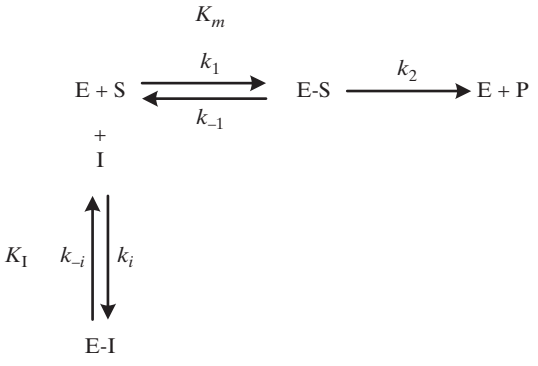

(R7)

Assuming *rapid equilibrium binding* and defining the dissociation equilibrium constant:

$$K_I = \frac{k_{-i}}{k_i} \tag{25.10}$$

and using the pseudo-steady-state assumption for the rate of production of E-S, the rate of production of the products is:

$$r_{P,I} = \frac{r_{P,max}[S]}{K_m\left(1 + \frac{[I]}{K_I}\right) + [S]} \tag{25.11}$$

where $r_{P,I}$ is the rate of production with the inhibitor present, and $r_{P,max} = k_2[E_T]$. Then, to determine $[I_{50}]$, set $r_P = 2r_{P,I}$, and solve:

$$[I_{50}] = K_I\left(1 + \frac{[S]}{K_m}\right) \tag{25.12}$$

Single-substrate Noncompetitive Inhibitor. When a *noncompetitive* inhibitor is present, it can bind to both the substrate, E, and enzyme-substrate complex, E-S:

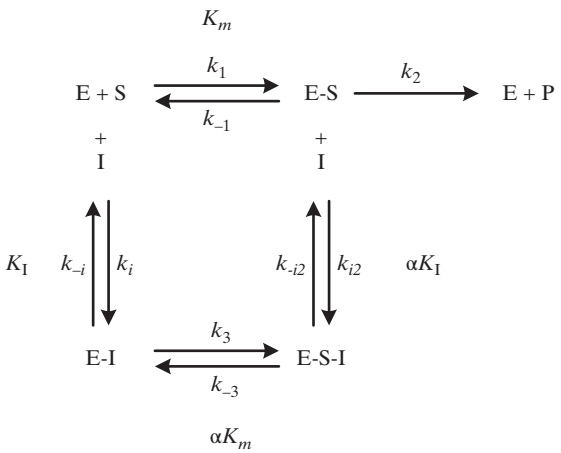

(R8)

Again, assuming *rapid equilibrium binding* and defining the dissociation equilibrium constants:

$$K_I = \frac{k_{-i}}{k_i},\ \alpha K_I = \frac{k_{-i2}}{k_{i2}},\ \alpha K_m = \frac{k_{-3}}{k_3} \tag{25.13}$$

and using the pseudo-steady-state assumption for the rate of production of E-S, the rate of production of the products is:

$$r_{P,I} = \frac{r_{P,max}[S]}{K_m\left(1 + \frac{[I]}{K_I}\right) + [S]\left(1 + \frac{[I]}{\alpha K_I}\right)} \tag{25.14}$$

Then, to determine $[I_{50}]$, set $r_P = 2r_{P,I}$, and solve:

$$[I_{50}] = \frac{K_m + [S]}{\frac{K_m}{K_I} + \frac{[S]}{\alpha K_I}} \tag{25.15}$$

Single-substrate Uncompetitive Inhibitor. For an *uncompetitive* inhibitor, binding is with the enzyme-substrate complex, E-S, only:

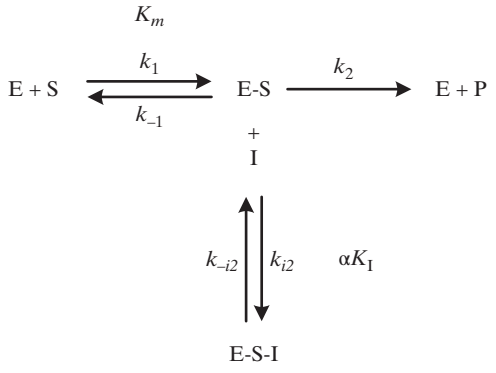

(R9)

Also, assuming *rapid equilibrium binding* and using the pseudo-steady-state assumption for the rate of production of E-S, the rate of production of the products is:

$$r_{P,I} = \frac{r_{P,max}[S]}{K_m + [S]\left(1 + \frac{[I]}{\alpha K_I}\right)} \tag{25.16}$$

and,

$$[I_{50}] = \alpha K_I\left(1 + \frac{K_m}{[S]}\right) \tag{25.17}$$

Dual-substrate Competitive Inhibitor. The competitive kinase inhibitor, KI, binds only with the kinase enzyme, KE:

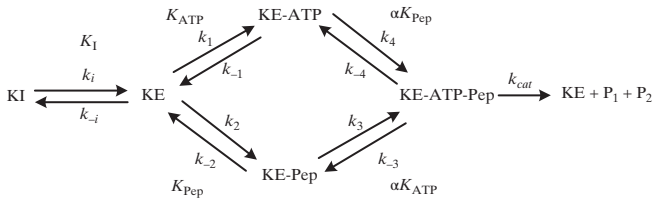

(R10)

Assuming *rapid equilibrium binding* and using the pseudo-steady-state assumption for the rates of production of the

intermediate complexes, the rate of production of the products is:

$$r_{P,I} = \frac{r_{P,max}[ATP][Pep]}{\alpha K_{ATP} K_{Pep}\left(1 + \frac{[KI]}{K_I}\right) + \alpha K_{Pep}[ATP] + \alpha K_{ATP}[Pep] + [ATP][Pep]} \quad (25.18)$$

Note that, when designing KIs, it is common to target the ATP binding site on the KE, primarily because the steric structure of the ATP binding sites are well understood. In contrast, the steric structures of the protein binding sites are not known.

Inhibition Detection Methods. For the phosphorylation reaction (R1), the rate loss due to the binding of kinase inhibitors is normally determined at high [ATP], [ATP_h], where the reaction is zero-order in [ATP]. In this case, the rate of production of products, r_{P,I,ATP_h}, in Eq. (25.18) is simplified to:

$$r_{P,I,ATP_h} = \frac{R_{ATP_h}[Pep]}{K_{m.ATP_h} + [Pep]} \quad (25.19a)$$

where

$$R_{ATP_h} = \frac{r_{P,max}[ATP_h]}{\alpha K_{ATP} + [ATP_h]}, \quad (25.19b)$$

$$K_{m,ATP_h} = \frac{\alpha K_{Pep}\left(K_{ATP}\left(1 + \frac{[KI]}{K_I}\right) + [ATP_h]\right)}{\alpha K_{ATP} + [ATP_h]} \quad (25.19c)$$

Then, the rate of reaction can be measured by monitoring [Pep]. Alternatively, the rates can be measured at high [Pep], [Pep_h], where the reaction is zero-order in [Pep], by monitoring [ATP]. In this case, the rate of production of products, r_{P,I,Pep_h}, in Eq. (25.18) is simplified to:

$$r_{P,I,Pep_h} = \frac{R_{Pep_h}[ATP]}{K_{m.Pep_h} + [ATP]} \quad (25.20a)$$

where

$$R_{Pep_h} = \frac{r_{P,max}[Pep_h]}{\alpha K_{Pep} + [Pep_h]}, \quad (25.20b)$$

$$K_{m,Pep_h} = \frac{\alpha K_{ATP}\left(K_{Pep}\left(1 + \frac{[KI]}{K_I}\right) + [Pep_h]\right)}{\alpha K_{Pep} + [Pep_h]} \quad (25.20c)$$

At [ATP_h], in the homogeneous, time-resolved, fluorescence (HTRF) assay, antibodies specific to the phosphorylated peptide product are used to generate a fluorescence, resonance, energy-transfer (FRET) signal proportional to [Pep]. This technique has the disadvantage of requiring an antibody specific to each kinase enzyme. Also, the fluorescent group can alter the kinetics of the phosphorylation reaction.

Alternatively, at [Pep_h], a simpler approach involves the use of firefly luciferase, which catalyzes the reaction of luciferin with ATP to yield light whose intensity is proportional to [ATP]. The reaction occurs in two steps:

$$\text{Luciferin} + \text{Luciferase} + \text{ATP} \equiv \text{Luciferin-Luciferase-AMP} + PP_i\text{-Luciferin-AMP}$$

$$\text{Luciferin-Luciferase-AMP} + PP_i\text{-Luciferin-AMP} + O_2 \rightarrow \text{Luciferase} + \text{Oxyluciferin} + \text{AMP} + CO_2 + \text{Light} \quad (R11)$$

Yellow-green light, having a maximum wave length of 575 nm with a quantum yield of 0.9, permits the luciferase to detect low ATP concentrations. At [ATP] > 8 μM, there is a flash of light followed by a fast decline in light production. Hence, to avoid rapid signal loss and decreased sensitivity, thermostable versions of firefly luciferase are being marketed (e.g., by Promega), which claim a stable signal for up to 4 hr. Fairly uniform streams of light are produced with [ATP] on the order of 1 μM.

To obtain an accurate measure of [ATP], the rate of consumption of ATP when generating light through reactions R11 must be small compared with the rate of consumption in the kinase-inhibited phosphorylation reaction, R1. This is accomplished by adjusting the luciferase concentration such that the rate of R11 is one-tenth the rate of R1.

The smallest useable reaction volume is ultimately set by the number of photons emitted; surely [ATP] cannot be accurately followed if only a few photons are emitted by the luciferase reaction. Electronically, this issue is manifested by what is called "shot noise," an irreducible source of noise related to the statistical number of fluctuations in the electrons in a signal. Briefly, the photons that strike an electronic detector are converted to electrons by the photoelectric effect, the electrons are accumulated during an exposure time interval amplified by a low noise amplifier and digitized. In the same way that 200 flips of a coin result in $100 \pm \sqrt{100}$, rather than exactly 100 heads, any electronic measurement that should yield N_{e^-} electrons will actually yield $N_{e^-} \pm \sqrt{N_{e^-}}$, corresponding to a fractional standard error:

$$\text{Shot noise} = \frac{\sqrt{N_{e^-}}}{N_{e^-}} = \frac{1}{\sqrt{N_{e^-}}}. \quad (25.21)$$

For example, if a 1% error is desired, 10,000 electrons are required, or 10^6 electrons to give a 0.1% expected error. In practice, well-made CCD cameras achieve a noise performance comparable to this irreducible limit. The fact that the light is spread over several pixels is irrelevant provided that the signals from the pixels are pooled together to give the total light emitted. Thus, if 10 measurements with 0.1% error are desired to follow [ATP] accurately, the reaction must yield $10 \times 10^6 = 10^7$ photoelectrons.

To calculate the photoelectrons collected per unit reaction volume, E:

$$E = [ATP] \times N_A \times (\text{ATP conv.}) \times (\text{incid. photon frac.}) \times (\text{quantum frac.}) \times (\text{quantum effic.}) \quad (25.22)$$

where N_A = Avogadro's number = 6.023×10^{23}photons/mole; ATP conv. is the fraction of ATP consumed by luciferase = 0.1; incid. photon frac. is the fraction of photons incident upon the Research STL-1001E charge-coupled device (CCD) camera lens = 0.5; quantum fraction is the luciferase quantum yield = 0.9; and the quantum efficiency of light capture = 0.7 (fraction of photons converted to electrons). Substituting, at [ATP] = 1 μM:

$$E = 10^{-6} \times (6.023 \times 10^{23}) \times 0.1 \times 0.5 \times 0.9 \times 0.7 = 1.9 \times 10^{16} e^-/\text{L}$$

Using the calculated value of E, the total volume per bolus can be sized to give 10^7 electrons:

$$V_{bolus} = \frac{10^7}{1.9 \times 10^{16}} = 0.53 \times 10^{-9}\text{L} = 0.53 \text{ nL}$$

Conservatively, the lab-on-a-chip will be designed to accommodate bolus' having a 1 nL volume, as shown in Section 25.2.

25.2 PRODUCT CONCEPT

A design team has been formed with the goal to create a lab-on-a-chip for the high throughput screening of kinase inhibitors. The chip would be available in a commercial laboratory, which carries out assays of kinase inhibitors sent by pharmaceutical companies, or the chip would be licensed to pharmaceutical companies to be installed in their in-house laboratories. This case study begins with the *innovation map* presented earlier in Figure 25.10, which shows consumer needs and two principal new technologies for the lab-on-a-chip product. Note that other technologies are available, but these two are the technologies to be considered in this limited case study.

Due to space limitations, only the principal steps in this design are presented. In brief, the objective time chart requires that a design be completed in six months. The time frame for the design project is the middle of the 2000–2010 decade. The design team has received endorsement for its *innovation map* and is proceeding into the Stage-Gate Product-Development Process (SGPDP; see Section 1.3).

Generating Product Concepts

In the mid-2000s, it is estimated that pharmaceutical companies are spending approximately $200 million/yr for screening potential therapeutic kinase inhibitors. The market and competitive analyses suggest that the design team should strive to achieve the highest speed throughput practical, performing on the order of 1 million IC_{50} assay/day, which on an 8-hr day, 5 day/wk schedule, corresponds to 250 million assay/yr. On the order of 10,000 kinase inhibitors would be tested daily against 100 kinase enzymes, giving 1 million IC_{50} assays/day.

The customers (pharmaceutical companies) seek low-cost and high throughput screening products available in a commercial service laboratory or, preferably, in their in-house laboratories. The innovation map in Figure 25.10 shows rough price expectations associated with the Fluidigm® and RainDance® technologies. Reliable assays are required, involving considerable redundancy to achieve six-sigma performance, that is, 3.4 defective assays per million. These customer requirements are translated into product requirements as follows. First, for both Fluidigm and RainDance chips, configurations are needed to create nanoliter boluses (i.e., reactor droplets) involving 100 kinase enzymes and 10,000 kinase inhibitors at different concentrations. Then, to determine the rates of the phosphorylation reaction (R1), an optical means of measuring the concentrations [ATP] or [ADP] is needed. As shown on the innovation map, two different technologies are selected for use with the Fluidigm and RainDance chips.

Several critical-to-quality (CTQ) variables are identified next. For both chips, these include:

1. The number of reactor droplets at different [KI] to achieve accurate IC_{50} concentrations [KI_{50}]. Six is the minimum commonly selected.
2. The number of redundant droplets having the same [KI] to achieve accurate IC_{50} concentrations, [KI_{50}]. Five is selected.
3. The ranges of [ATP] and [Pep] concentrations are in the reactor droplets, which influence the kinetics of the phosphorylation reaction and the rate of photon generation. In Section 25.1, these concentrations are set at [ATP] = 1 μM and [Pep] = 60 μM.
4. The volume of the reactor droplets. In Section 25.1, 1 nL is selected.
5. The reaction, or incubation, time at 37°C. In Section 25.1, 1 hr is selected.

Using these CTQ variables, two product concepts involving two chip designs are considered, and are described next.

Fluidigm Chip

Figure 25.11 shows a typical configuration of the bolus (reactor droplet) preparation system on the Fluidigm chip. For a discussion of the components of Fluidigm chips, see Section 25.1. Two reservoirs (A and B) on the lower PDMS mold, that is, the *process layer*, contain the kinase enzyme, ATP (1 μM), luciferase, luciferin, substrate peptide, flourophore (AlexaFluor 350), and

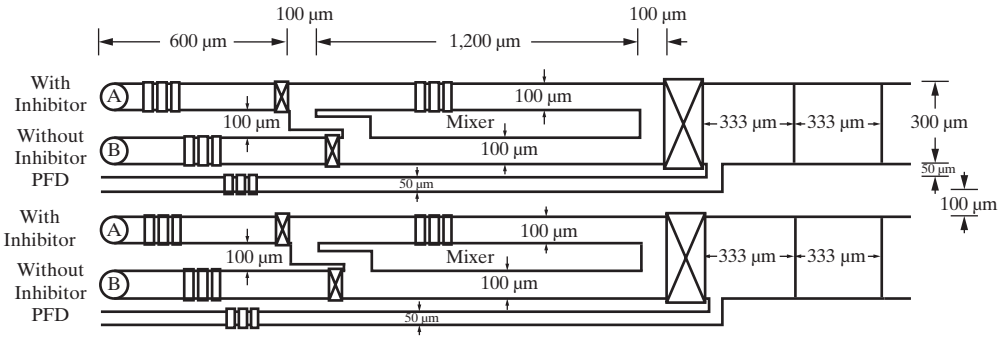

Figure 25.11 Schematic of Bolus preparation system.

buffer (to maintain pH = 7.5). In addition, reservoir A contains the kinase inhibitor. Each reservoir is 10 μm high and has a diameter of 100 μm. Reservoir B is referred to as *without inhibitor* and reservoir A as *with inhibitor*. The two reservoirs are connecting to channels, 10 μm high and 100 μm wide, each of which is crossed by three orthogonal channels in the upper PDMS mold, that is, the *control layer*. Each set of three channels, 50 μm wide per channel, serves as a peristaltic pump. Note that the two channels are separated by 100 μm. In addition, a third line, 50 μm wide, lies 50 μm below the kinase inhibitor line. For this line, a peristaltic pump is sufficient to insert perfluorodecalin (PFD), a spacer to separate the mixed boluses. Note also that these three lines are repeated 48 times in the process layer, permitting assays to be obtained in parallel for 48 kinase inhibitors.

The effluent lines from reservoirs A and B pass through valves into a 3 nL Fluidigm® mixer. Note the dimensions in Figure 25.11: All lines are 10 μm high and 100 μm wide, giving a volume of $(2 \times 1{,}200 \times 100 + 2 \times 300 \times 100) \times 10\ \mu m^3 = 3 \times 10^6 \mu m^3 = 3{,}000$ pL = 3 nL. For the initial bolus, both inlet valves are open, and the effluent valve is closed as the solutions are pumped into the mixer. Then, the inlet valves are closed and the mixer pump is operated for approximately 3 sec of mixing time, after which the three valves are opened and additional fluid from reservoirs A and/or B are pumped to displace the fluid into the effluent line. Just prior to the next mixing operation, with the effluent valve closed, 1 nL of PFD spacer is pumped to displace the first bolus in the effluent line. This process is repeated to form 15 reacting boluses in each effluent line, each having a different inhibitor concentration. Note that because the effluent line is 300 μm wide, the length of each bolus and spacer is 333 μm, to give 1 nL volume.

The dilution process is accomplished by varying the number of cycles for either or both of the pumps associated with reservoirs A and B, thereby changing the concentrations in each bolus. In each pumping cycle, 1 nL of fresh reactants displace 1 nL of fluid from the mixer. See Table 25.1 for a typical dilution schedule, that is, for each pumping cycle, the volumes of inhibitor (from reservoir A) in the mixer after pumping, the pumping times for the two pumps, and the inhibitor/total volume ratio in the mixer. As shown, in the initial cycle (1), 2,700 pL of fluid from reservoir A is pumped in 1,125 ms, and 300 pL from reservoir B is pumped in 125 ms. During cycle (2), 1,000 pL of fluid are displaced from the mixer (containing 900 pL of fluid A and 100 pL of fluid B) and replaced by 1,000 pL of fluid B. The resulting contents of the mixer are 1,800 pL of fluid A and 1,200 pL of fluid B, that is, 60% of fluid A. To pump 1,000 pL of fluid B, 416.7 ms are required. During each of the remaining 13 pumping cycles, an additional 1,000 pL of fluid B is added.

After 15 pumping cycles, which take approximately 1 min, a heating plate is activated, heating the 15 boluses to 37°C, the temperature at which the phosphorylation reaction takes place. For the next hour, photons generated by the luciferase reaction (R11 in Section 25.1) are collected by a charge-coupled device (CCD) detector/scanner to measure [ATP] and the related rate of the phosphorylation reaction (R1).

Figure 25.12 shows a top view of the chip design discussed thus far. There are two sets of 48 three-channel devices side-by-side, requiring 2.54 cm = 1 in. These two sets are separated by a trough. For a given kinase enzyme, each three-channel device involves 48 different kinase inhibitors. For each inhibitor, on each side of the trough, 15 boluses at different inhibitor concentrations are generated, giving a total of 30 boluses for each inhibitor. The length of the lines on each side of the trough is determined by adding the length of the entrance region (600 μm), the length of the mixer (1,400 μm), and the length of the bolus region ($2 \times 333 \times 15 = 10{,}000$ μm), to give a total length of 12,000 μm = 1.2 cm. Hence, 2.54 cm = 1 in. is sufficient to contain the lines on both sides of the trough, including the trough, where spent reagents are accumulated and removed.

In summary, using two channels for each inhibitor, six decades of dilution are generated. On a single chip, there are 96 three-channel devices, providing a total of 48 IC_{50}s that are generated every 90 minutes (30 min for preparation and 1 hr for reaction). With one CCD camera, over an 8 1/2-hr day, seven chips were processed, giving some time to spare. Consequently, 10,080 boluses per day, providing 336 IC_{50} curves per day

Table 25.1 Typical Dilution Schedule

Cycle	Inhibitor Volume (pL)	Inhibitor/Mixer Volume Ratio	Pump A (ms)	Pump B (ms)
1	2,700	0.9	1,125	125
2	1,800	0.6	0	417
3	1,200	0.4	0	417
4	800	0.267	0	417
5	533	0.178	0	417
6	355	0.119	0	417
7	237	0.0790	0	417
8	158	0.0527	0	417
9	105	0.0351	0	417
10	70.2	0.0234	0	417
11	46.8	0.0156	0	417
12	31.2	0.0104	0	417
13	20.8	0.00694	0	417
14	13.9	0.00462	0	417
15	9.25	0.00308	0	417

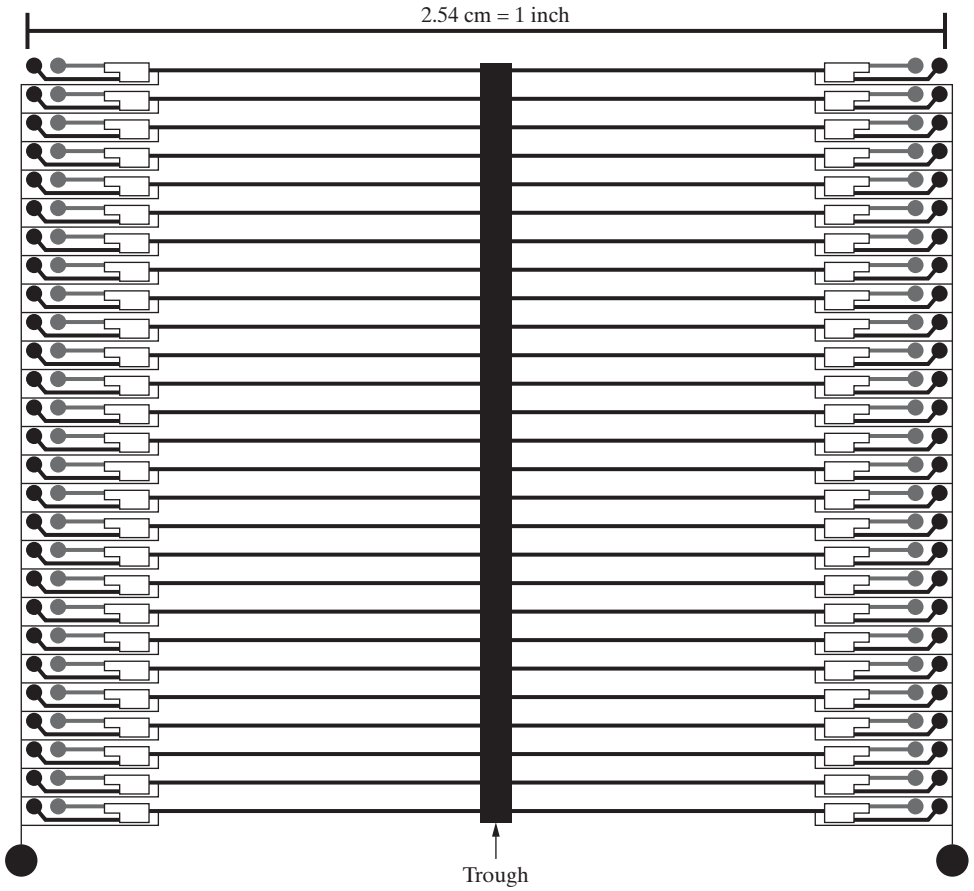

Figure 25.12 Top view of chip layout. Two arrays of 48 three-channel devices, each containing 15 boluses on each side of the trough. The PFD spacer is stored in one large reservoir on each side of the trough.

(that is, 30 boluses per IC_{50} curve) are carried out. Each chip is discarded after one utilization, providing 48 IC_{50} curves. Hence, 336 IC_{50} curves are produced using seven chips. This product design is presented by Chen et al. (2005).

Clearly, this product concept can be improved significantly, and this would be the case if it were selected as the superior product concept. If the number of boluses per IC_{50} is reduced to six, each 1-in. × 1-in. chip would produce $5 \times 48 = 240$ IC_{50}/chip and $7 \times 240 = 1{,}680$ IC_{50}/day.

Note, however, that the RainDance emulsion guns, introduced three years after the Fluidigm chips, produce reactor droplets on the order of 1,000 times faster than the Fluidigm mixer. This led to the customer request for 1 million IC_{50}/day. For this reason, the Fluidigm chip is rejected in favor of the RainDance chip.

RainDance Chip

As presented earlier in Section 25.1, RainDance chips utilize emulsion guns, which produce as many as 20,000 microdroplets/sec. These chips are configured with mixers and splitters to meet user specifications. Rather than show the detailed geometry of the custom-made chip, which is proprietary, Figure 25.13 shows a schematic of the operations to be carried out on and off the chip with timings specified.

The well plates at the top of the diagram are received from external suppliers often in mailers. When operating as a commercial service laboratory, one well plate containing 10,000 KIs is received daily from a pharmaceutical company. In the design shown, the first kinase enzyme, KE_1, is transferred by a JANUS® robot arm from its well plate to a Labcyte® ECHO 555™ liquid handler, where it is mixed with peptide and buffer solution from their well plates. Note that typical transfer times for the JANUS robot are 1.5 sec, but the robot is washed and evacuated after each kinase enzyme is transferred, requiring an additional 1.65 sec. In parallel, the JANUS robot transfers a mixture of TransFluoSpheres™ (fluorescent beads), which serves as a *bar code* for KE_1. The resulting mixture, KE_1/Pep, is transferred by the JANUS robot to an emulsion gun on the first RainDance PLS chip, which produces nanoliter droplets at 20,000 drop/sec, as discussed in Section 25.1, that are conveyed to a microcentrifuge tube.

Note that the enzymes are mixed one at a time, each enzyme being labeled with a unique combination of three of four colors at three concentration levels, that is, 12C3 = 220. Because 112 combinations involve different concentrations of the same color that cannot be distinguished, these are discarded, leaving 108 unique labels (for 100 kinase enzymes). The resulting mixtures, KE_1/Pep, … , KE_{100}/Pep, are transferred one-by-one by the JANUS robot to the emulsion gun on the first RainDance PLS chip.

As discussed subsequently, sufficient droplets are generated to mix with droplets of the 10,000 kinase inhibitors.

For each KI, five copies (for redundancy to counter measurement errors) of six droplets at different KI concentration levels are needed. Hence, for each kinase enzyme, 5 drop/conc. × 6 conc./KI × 10,000 KI = 300,000 droplets are generated at 20,000 drop/sec, requiring 15 sec. In addition, 3.15 sec/KE are required for robot transfer, washing, and evacuation. Consequently, the total time to create 30,000,000 droplets of KE_1/Pep, … , KE_{100}/Pep is (15 + 3.15) sec/KE × 100 KE = 1,815 sec ≈ 30 min, which can be prepared one day in advance. The bar-coded droplets in the microcentrifuge tube can be randomized by agitation overnight. Note that 1.65 sec are also required to wash and evacuate the emulsion gun before the next KE is loaded, but this can be accomplished during the 3.15 sec/KE required for robot transfer, washing, and evacuation.

Subsequently, these randomized droplets are transferred by the JANUS robot to an emulsion gun on the second RainDance PLS chip where they are released, carefully synchronized at 1,000 drop/sec, to be mixed with droplets of the ADP/Transcreener assay solution. The latter is transferred by robot to an emulsion gun, which also operates at 1,000 drop/sec. The two trains of droplets are combined as shown in Figure 25.9 to give complete (randomized and bar-coded) kinase enzyme droplets.

The product concept in Figure 25.13 shows an approach for generating kinase inhibitor droplets serially without labels. In this approach, the 10,000 kinase inhibitors are transferred one-by-one from their well plates to the emulsion gun by the JANUS robot. For each KI, six droplets are generated at 167 drop/sec. In a splitter, one-third of each droplet is recovered and combined with droplets from a diluent emulsion gun generated at 833 drop/sec. These are also sent to the splitter. Hence, for each KI droplet, five additional droplets at decreasing [KI] are generated in series. Note, however, that the KI emulsion gun releases its droplets

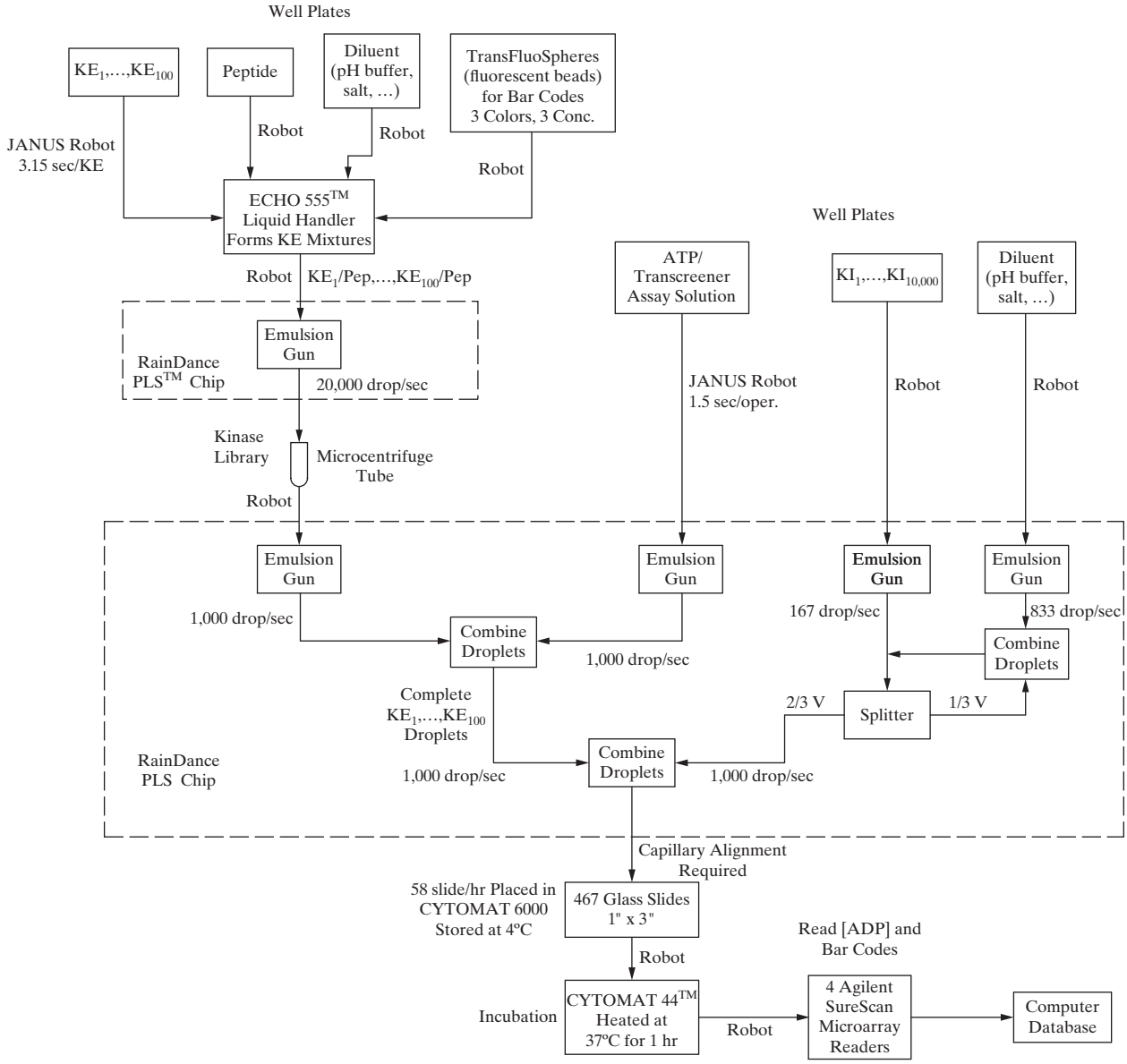

Figure 25.13 Schematic of operations on and off RainDance PLS chip.

slightly delayed to avoid intersecting with the last diluted droplet, and the splitter has a gate that turns off after the lowest concentration droplet is created. This is repeated for each of the droplets from the KI emulsion gun. To provide redundancy to overcome experimental errors, five sets of six droplets are created, that is 30 drop/KI. Because 30 drop/KI are needed for each KE, a string of 30 drop/KI × 100 KE/KI = 3,000 drop/KI at 1,000 drop/sec, requiring 3 sec/KI. The emulsion gun is loaded (1.5 sec/KI), washed (1.5 sec/KI), and evacuated (0.15 sec/KI), totaling 3.15 sec/KI. Consequently, to generate the string of droplets for 10,000 KIs, 31,500 sec/day = 8.75 hr/day are required. These KI droplets are combined with the randomized, complete KE droplets at 1,000 drop/sec.

The resulting droplets are transmitted to 1-in. × 3-in. glass slides, which have been etched with 100 μm channels (10 μm high), permitting 127 channels in parallel. Each channel receives 485 droplets, giving 61,600 drop/slide. Hence, with 467 slides, 30MM drop/day are stored. Note that a precise robot is required to align rapidly the outlet capillary from the PLS chip with the capillaries on the glass slides, moving from capillary to capillary in sequence.

At a rate of 58 slide/hr, the JANUS robot places the loaded slides into a Heraeus CYTOMAT® 6000 for storage at 4°C. These, in turn, are transferred by the robot to a CYTOMAT® 44 where they are heated at 37°C for 1 hr, the incubation time. Then, the slides are transferred one-by-one to Agilent SureScan microarray readers, which require 1 min to scan each slide; that is, 467 slide/day × 4 scan/slide × 1 min/scan = 1,868 min/day = 31.1 hr/day. Note that one scan records [ADP] for each droplet and a second scan detects its bar code. Two additional scans are performed per slide to counter errors by the microarray readers. Consequently, four microarray readers are required to complete the scanning during an 8-hr day. The resulting data are transmitted to a computer database for determination of the IC_{50} for each of the 10,000 KIs. For more specifics of this product concept, the reader is referred to the design report by Levin et al. (2007).

With all operations having batch times on the order of 8 hr or less, it is possible to design a serial train of operations with a cycle time of 9–10 hr, which can be accomplished in one working day. In one design, two KI emulsion guns are installed in parallel, permitting one gun to undergo loading, washing, and evacuation (3.15 sec/KI) while the other generates droplets (3 sec/KI). The two emulsion guns handle alternate KIs.

One possible schedule of operations for this product concept is shown in Figure 25.14. Operations begin with the preparation of the kinase enzyme library as shown in Figure 25.14a. The first kinase enzyme, KE_1, is loaded by a JANUS robot arm onto the first PLS chip in 1.5 sec after which the emulsion gun forms 300,000 droplets in 15 sec. Then, the robot arm loads the washout fluid onto the chip in 1.5 sec, and the chip is evacuated for 0.15 sec. This sequence is repeated for the remaining 99 enzymes. For the entire KE library, 1,815 sec = ∼30 min = 0.5 hr are required, which can be prepared during the preceding afternoon.

The schedule for the preparation of KI droplets at six different concentrations is shown in Figure 25.14b. Here, the first robot arm loads KI_1 onto the second chip in 1.5 sec, after which the first emulsion gun forms 500 KI_1 droplets at 167 drop/sec in 3 sec. Each of these droplets is split, and merged with droplets from the diluent emulsion gun at 833 drop/sec giving a total of 3,000 droplets of KI_1. Then, the robot arm loads the washout fluid onto the chip in 1.5 sec, after which the KI emulsion gun is evacuated. The second kinase inhibitor, KI_2, is loaded by the second robot arm after which the second emulsion gun forms KI_2 droplets. While the latter being formed, the first robot arm loads KI_3 onto the chip after which the first emulsion gun forms KI_3 droplets. Note that the two robots and emulsion guns alternate between the kinase inhibitors. While one inhibitor is being loaded and emulsified, the other robot arm and emulsion gun are being loaded with washout fluid and evacuated. Meanwhile, the diluent emulsion gun forms droplets of diluent nearly continuously, except for brief periods in which neither KI emulsion gun is in operation. Note that 6.15 sec are required to form droplets for two KIs, and, consequently, the time for the preparation of droplets for 10,000 KIs is:

$$\frac{6.15 \text{ sec}}{2 \text{ KI}} \times 10{,}000 \frac{\text{KI}}{\text{day}} = 30{,}750 \frac{\text{sec}}{\text{day}} = 8.5 \frac{\text{hr}}{\text{day}}$$

Finally, the Gantt chart in Figure 25.14c shows that the slide-loading robot arm operates with negligible delay following the formation of reaction droplets and loading onto the glass slides. Note that the Cytomat® 6000 is delayed by the 1 hr incubation time and the Agilent® Microarray readers begin shortly after the first batch of glass slides leave the incubator. Consequently, 1 million IC_{50} assays are completed in ∼9.5 hr.

Selection of Superior Product Concept

Clearly, the RainDance chip concept, having been developed three years after the Fluidigm chip concept, is preferable. In short, the generation of droplets by emulsion guns is approximately three orders of magnitude faster than by mixers driven by peristaltic pumps. If the performances were less differentiated, the design team would generate approximate cost estimates and profitability analyses to influence its decision.

25.3 PROTOTYPING

In practice, the *prototyping* stage would begin with a technical feasibility analysis to show that the Raindance PLS chip can deliver the desired performance requirements. This would involve creating and testing a prototype. In addition, alternate configurations for the PLS would be suggested and tested. For example, as proposed in Exercise 25.2, strategies would be considered involving (1) no bar codes, that is, sequential generation of both kinase enzymes and inhibitors and (2) bar codes for both the kinase enzymes and inhibitors.

Note that the product concept in Figure 25.14 presumes that the combined reaction droplets can be loaded onto the glass slides without excess pressure drops. This can be checked using estimates of the Darcy friction factor as requested in Exercise 25.3.

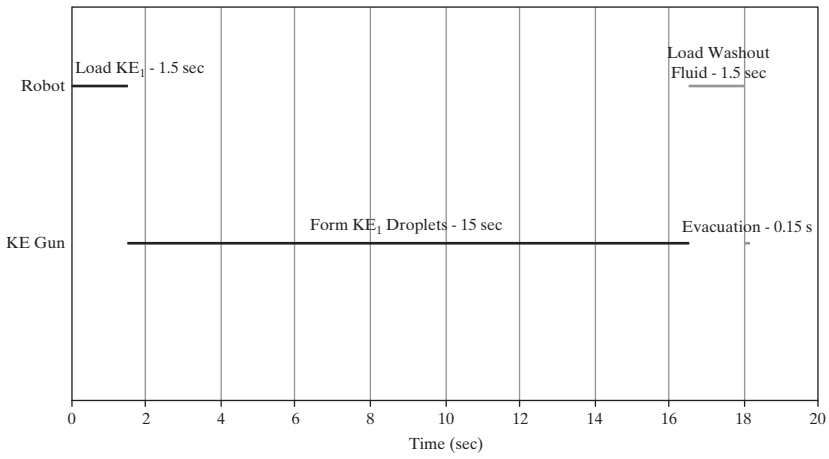

(a)

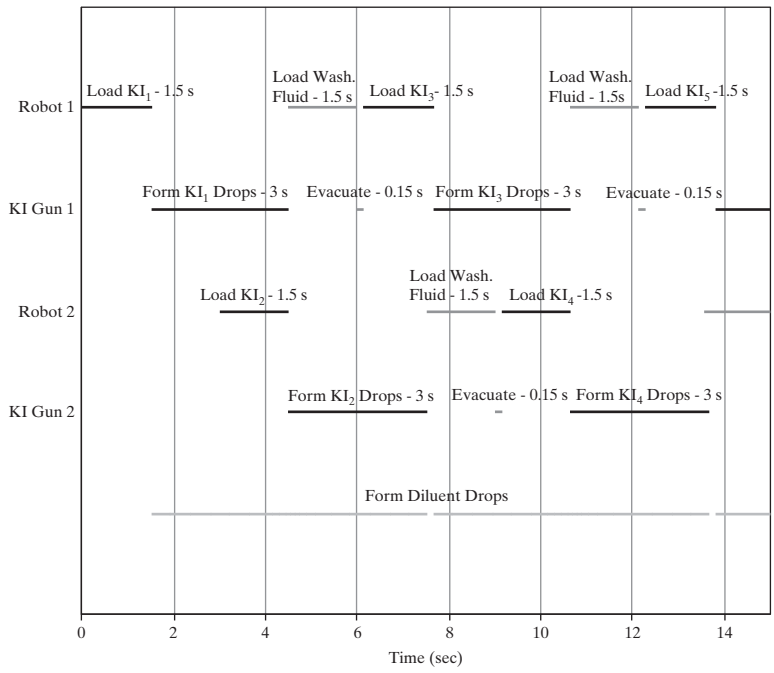

(b)

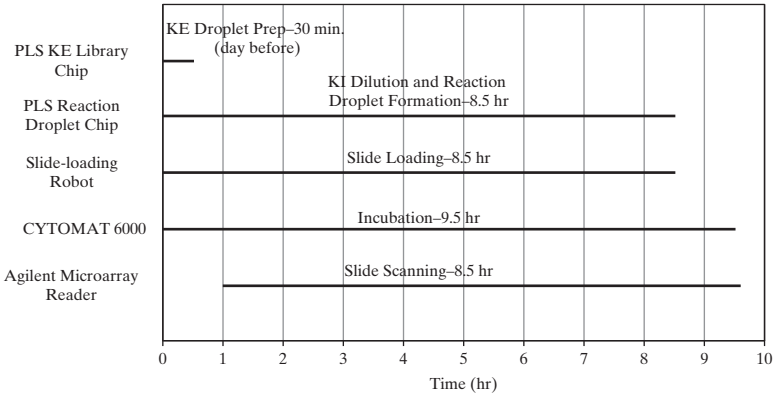

(c)

Figure 25.14 Gantt charts for high throughput screening process: (a) KE library preparation; (b) KI droplet preparation and dilution; (c) overall process.

Table 25.2 Equipment and Software Costs

	Installed Cost ($)
RainDance PLS chips	200,000
Computer system	5,000
4 Agilent microarray readers	504,000
Labcyte ECHO liquid handler	330,750
Perkin-Elmer JANUS Robotic Arm	150,000
Heraeus CYTOMAT 6000 Incubator	20,000
Refrigerator	18,000
Heraeus CYTOMAT 44	35,000
Lab management software	100,000
Security system	2,000
Total	1,364,750

Business Case

For the product concept shown in Figure 25.13, it is proposed to operate a commercial service laboratory approximately 10 hr/day, 5 days/wk in the United States. At full production, customers will send 1 well plate/day containing 10,000 kinase inhibitors to be tested against 100 kinase enzymes. Each IC_{50} assay will be priced at $0.05. A scenario is envisioned in which the development and installation of the processing equipment takes place over one year, beginning in January 2007 with operations over a four-year period beginning in January 2008. During the first year of operation, only 20% of the design production capacity is assumed, increasing to 60% in the second year, and 100% in the third and fourth years. To judge the potential profitability of the product concept, estimates of the return on investment, the net present value, and the investor's rate of return are computed.

See Table 25.2 for a list of estimates of the installed equipment costs, most of which have been obtained from equipment and software vendors. All items will be purchased and installed just prior to the first production year except for two Agilent microarray readers, which will be added at the beginning of the second production year.

Variable operating costs include the costs of reagents and raw materials (see Table 25.3). There, a unit of kinase enzyme is the amount of enzyme needed to transfer x mol of phosphate to enzyme per unit time where x is specific to each enzyme. Given 100 kinase enzymes, a representative unit price was selected. For full production (1 million IC_{50} assays/day), the total cost of reagents and raw materials is $\$0.0056/IC_{50}$, or $1.358 million/yr. Other variable costs include the cost of sales and research and development estimated at 6% and 5%, respectively, of the total sales, that is, $750,000/yr and $625,000/yr at full production. These sum to $2,732,600/yr of variable costs.

The fixed operating costs include operations, maintenance, lab and office space rental, licensing and security, and property insurance and taxes. Three operators are assumed at $85,000/oper/yr (40 hr/wk × 50 wk/yr × $42.50/hr) and five professionals at $125,000/prof/yr. Due to the maintenance of expensive automated equipment, approximately $175,000/yr is allocated for maintenance. Lab space is estimated at $\$35/ft^2$, and consequently, for 2,500 ft^2, the cost is $87,500/yr during the four operating years. For office space, the figures are $\$25/ft^2$, 2,000 ft^2, and $50,000/yr. The costs of licensing and security are estimated at $100,000/yr and $50,000/yr, respectively. At 2% of the total depreciable capital, insurance and tax costs are $34,000/yr. These fixed costs sum to approximately $1.4 million/yr.

Added to the $1,365,000 total cost of equipment and software, is the cost of lab preparation, that is, 5% of the total cost of equipment and software, or $68,200. This gives a total permanent investment of $1,433,000. Adding 18% for the cost of contingencies and fees, gives a total depreciable capital of $1,690,900. Another $250,000 is added for startup costs to give $1,940,900. Finally, the cost of working capital is estimated as the accounts receivable for 21 days of sales, that is, $1,050,000. This gives a total capital investment of $2,990,900.

Three profitability measures are computed, all showing very favorable results. An approximate measure, the return on investment, estimated in the third production year is 181.4%. Two more rigorous measures based upon the time value of money, are the investor's rate of return (IRR) at 90% and the net present value (NPV) at $5.795 million based upon a 19% annual interest rate. On this basis, it seems clear that the business case for further developing this lab-on-a-chip product is very strong. It is helpful to examine the price sensitivity of these profitability measures. This is the purpose of Exercise 25.4.

Table 25.3 Reagent and Raw Materials Costs

	Unit Cost	Unit/IC_{50}	Cost/IC_{50} ($)
Kinase enzymes	$0.044/unit	0.101 unit	4.45×10^{-3}
Peptide	$494/mg	3.72×10^{-7} mg	1.84×10^{-4}
Transcreener kits	$19,500/L	1.50×10^{-8} L	2.92×10^{-4}
TransFluoSpheres	5.667×10^{-6}/unit	30 unit	1.70×10^{-4}
DMSO (dimethyl sulfoxide)	$439/L	9.43×10^{-10} L	4.14×10^{-7}
HEPES (pH buffer)	$439/L	4.71×10^{-10} L	2.07×10^{-7}
EGTA (ethylene glycol tetraacetic acid)	$2,089/kg	1.89×10^{-11} kg	3.91×10^{-8}
Brij-35 (nonionic detergent)	$60/kg	9.43×10^{-8} kg	5.68×10^{-6}
Glass slides	$1/slide	4.87×10^{-4} slide	4.87×10^{-4}

Table 25.4 Results of Google Patent Search for "Microfluidic" and "Lab-on-a-Chip"

Category	Patents
Fluid movement and mixing	44
Microfluidic devices and applications	47
Fabrication	21
Scanning, detection, and measurement	16
Sorting and separation	10

Intellectual Property Assessment

Having prepared a strong business case for the lab-on-a-chip product, the patent landscape was examined in July 2007. At that time, an advanced Google patent search using the key words "microfluidic" and "lab-on-chip" returned 194 patents, only 12 of which were filed prior to 2000. These patents are classified roughly in the categories shown in Table 25.4, with some patents having entries in more than one category.

Patents under fluid movement and mixing introduce pumps, valves, and other methods of moving fluids on chips. Those under microfluidic devices and applications concentrate on the chip architecture (substrate, channels, pumps, etc.) and potential applications. Under fabrication, the emphasis is on the methods of manufacture such as microcontact printing and photochemistry. Those under scanning, detection, and measurement emphasize optical probes and electrical instruments to measure activities on chips. Finally, those under sorting and separation introduce devices for separation of particles based upon size and other properties.

Although several companies had filed for several patents [Syrrx, Inc. (9), Caliper Life Science (8), Caliper Technologies Corp. (7), Nanostream, Inc. (5), and Fluidigm (4)], no patents appeared to threaten the foundations of the business venture proposed. Clearly, there had been much patent activity since 2000, and, consequently, it was advisable to project only four operating years, assuming that new technologies would lead to more competitive products.

It is noteworthy that no patents filed by RainDance Technologies were identified in the Google search. In view of this, before signing a contract with RainDance to produce the PLS chips to the specifications of Figure 25.13, it is important to check that RainDance had not violated patents filed by others given the danger that the proposed commercial laboratory could be shut down due to IP violation claims.

In addition, it was important to confirm that all of the technology inventions in the *innovation map* (Figure 25.10) were protected by patents as well. See Exercise 17.8. Patent protection strengthens the business position of the commercial laboratory by preventing competition from firms that provide comparable products at lower fees.

25.4 PRODUCT DEVELOPMENT

In the development stage, the key design variables that can be adjusted to optimize the design are adjusted. These include the emulsion-gun frequencies because they influence the throughput. By optimizing the operating variables, it should be possible to significantly increase the throughput and profitability.

Also, in the development stage, more advanced prototypes are developed with more extensive testing at a pilot-scale level. More quantitative performance measures are examined to determine the extent of redundancy necessary to reduce the errors in high throughput screening.

25.5 SUMMARY

After studying this case study, the reader should:

1. Appreciate how the new materials, product/manufacturing, and product technologies are expressed in the innovation map to create the lab-on-a-chip products that satisfy customer needs.
2. Understand typical superior lab-on-a-chip product concepts that can be generated using new technologies. Two example products are described using the Fluidigm and RainDance technologies.
3. Appreciate the need to construct prototypes that demonstrate the effectiveness of the proposed lab-on-a-chip products, to create a business case, and to carry out an IP analysis before proceeding further into product development.

REFERENCES

1. Chen, Q. M., L. B. Heend, and J. Waring, *NANOLUX Screening Technologies*, Towne Library, University of Pennsylvania (2005).

2. Cheng, Y. C., and W. H. Prusoff, "Relationship Between the Inhibition Constant (K_I) and the Concentration of Inhibitor Which Causes 50% Inhibition (I_{50}) of an Enzyme Reaction," *Biochem. Pharma.*, **22**, 3099–3108 (1973).

3. Copeland, R. A., "Review: Mechanistic Considerations in High-Throughput Screening," *Anal. Biochem.*, **320**, 1–12 (2003).

4. Levin, J. J., J. Chung, and J. Irving, *Novel High-Throughput Screening of Kinase Inhibitors Using RainDance Technologies' Personal Laboratory System*, University of Pennsylvania Library (2007).

5. Unger, M. A., H. P. Chou, T. Thorsen, A. Scherer, and S. R. Quake, "Monolithic Microfabricated Valves and Pumps by Multilayer Soft Lithography," *Science*, **288**, 113–116 (2000).

6. Xia, Y., and G. M. Whitesides, "Soft Lithography," *Angew. Chem. Int. Ed.*, **37**, 550–575 (1998).

PATENTS

U.S. Patent 6,951,632. Unger, M. A., H. -P. Chou, I. D. Manger, D. Fernandes, and Y. Yi, *Microfluidic Devices for Introducing and Dispensing Fluids from Microfluidic Systems* (2005).

EXERCISES

25.1 Data for the phosphorylation reaction, R1, are provided by Caliper Life Sciences, Inc., in Figure 25.15 at high [Pep] = 1.5 μM and in Figure 25.16 at high [ATP] = 250 μM, both with [KE] = 2.5 μM. Using these two curves, find the reaction rate at [Pep] = 60 μM and [ATP] = 1 μM, which are well suited to test typical kinase inhibitors and provide a uniform stream of photons for the CCD camera.

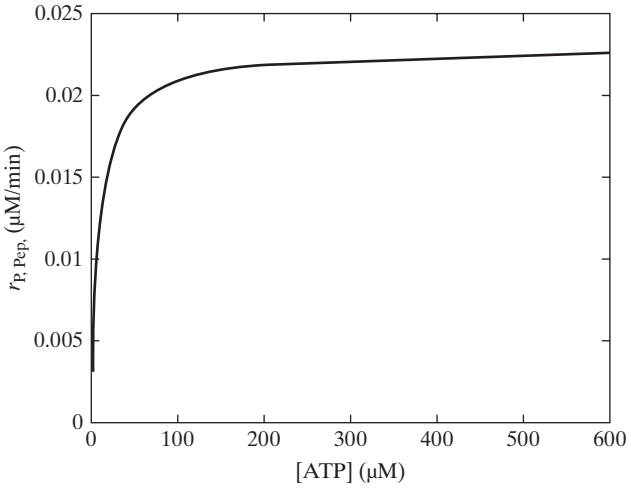

Figure 25.15 Caliper Life Sciences Data. [KE] = 2.5 μM, [Pep] = 1.5 μM, $R_{\text{Pep}_h} = 0.0229$ μM/min, and $K_{m.\text{Pep}_h} = 9.9$ μM.

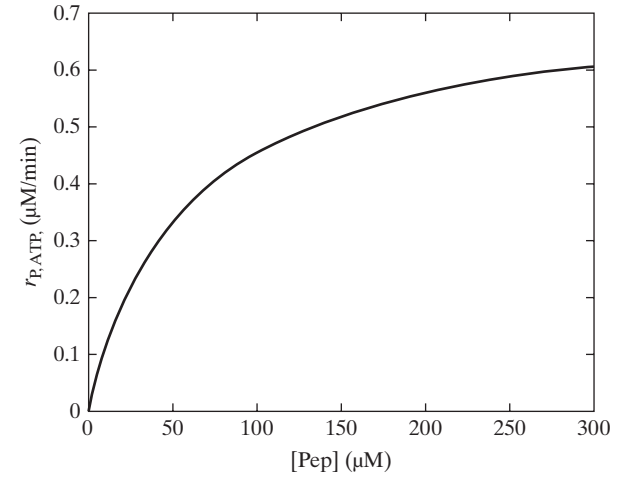

Figure 25.16 Caliper Life Sciences. [KE] = 2.5 μM, [ATP] = 250 μM, $R_{\text{ATP}_h} = 0.73$ μM/min, and $K_{m.\text{ATP}_h} = 61.6$ μM.

25.2 Consider the product concept in Figure 25.13 for the high throughput screening of kinase inhibitors. Two competitive concepts are proposed:

(a) Use no bar codes; that is, use sequential generation of both the kinase enzymes and inhibitors.

(b) Use bar codes for both the kinase enzymes and inhibitors. Determine the number of colors and concentrations necessary to provide bar codes for 10,000 kinase inhibitors.

Estimate the operation times and compare the purchase costs and net present values of the three concepts over three years.

25.3 Given the 1-in. × 3-in. glass slides upon which 1,000 aqueous drop/sec. are loaded into 100 × 10 μm parallel channels, estimate the pressure drop. Is it sufficiently low to permit usage of the glass slides? *Hint:* Use the Darcy friction factor.

25.4 Re-estimate the profitability measures in Section 25.3 as the price of IC_{50} assays varies. Use a spreadsheet to increase and decrease the price from $\$0.05/IC_{50}$ assay.

25.5 The lab-on-a-chip product in Figure 25.13 incorporates the inventions in the innovation map of Figure 25.10. Carry out a patent search to determine whether all of the technological inventions in Figure 25.10 have been protected by patents.

Chapter 26

Case Study 3—Die Attach Adhesive: A Case Study of Product Development

26.0 OBJECTIVES

Product development is a complex task that involves a multidisciplinary team and covers activities ranging from product conceptualization to commercialization. To gain a deeper appreciation of the steps required for such an effort, this chapter presents a case study on the development of a die attach adhesive (DAA). It discusses selected tasks that are likely to involve chemical engineers. The multidisciplinary product development framework in Figure 1.3 shows the general nature of these tasks. Emphasis is placed on the flow of the events and the activities in this product development project.

After studying this chapter, the reader should:

1. Have an appreciation of the application of chemical engineering science and process design in product design.
2. Be able to contribute to the development of a business model as a technical member of a multidisciplinary team.
3. Be able to analyze how a chemical product competes against similar products in terms of cost and performance.
4. Understand the concurrency nature of product design and process design.
5. Be aware of the importance of performance tests in product development.
6. Be able to estimate product cost taking make-or-buy analysis into consideration.

26.1 BACKGROUND OF TECHNOLOGY

All chemical products perform one or more functions for the user. Both the design of such a product and the way in which it delivers its function(s) depend on certain physicochemical properties and principles. A thorough understanding of the science and technology related to the product under consideration is essential to product design. This is illustrated using the design of a die attach adhesive that is used in light-emitting diode (LED) packaging.

For approximately 100 years, incandescent light bulbs (Figure 26.1a) dominated the household electric light bulb market. However, starting in the early 1980s, more efficient bulbs entered the market, including the compact fluorescent lamp (CFL), Figure 26.1b and, more recently, the LED lamp (Figure 26.1c). Because LED lamps have a significantly longer life span (at least 25,000 hours) and emit significantly more visible light per unit of power input (at least 75 lumens/watt) than incandescent light bulbs and CFLs, they are expected to dominate the household light bulb market by 2020.

The key component of an LED lamp is the LED chip made of semiconductor materials such as gallium nitride (GaN). The chip undergoes electroluminescence by emitting light when an electric current passes through it. To fabricate an LED lamp, the chip is first attached to a substrate such as alumina (Al_2O_3) (Figure 26.2) and then is connected to a power supply with bond pads and wires. To obtain white light, the light with a certain color from the chip is mixed with light of a different color from another source. For example, the blue light from a blue LED can be mixed with the yellow light from a phosphor, cerium-doped yttrium aluminum garnet, to obtain white light (Figure 26.3). Despite its relatively high efficiency in converting energy to light, most of the power to an LED is still dissipated as heat. This can result in a high junction temperature between the die and the substrate that can significantly shorten the lifetime of the LED chip. The illustration in Figure 26.4 shows the light output (as a percentage of the initial light output) of an LED lamp as a function of time at three different junction temperatures. At 135°C, 70% of light output remains after about 8,500 hours whereas at 115°C, it takes approximately 65,000 hours to drop to the same light output level. Hence, it is crucial that the heat generated by the chip be removed as fast as possible. This requires a DAA with high thermal conductivity.

26.2 MARKET STUDY

A new DAA must offer a lower cost, or better performance than similar products on the market to succeed in the marketplace. Thus, it is important to study competing products. Information on the competition, including product specifications, price, and manufacturing process is available in the public domain.

Competitive Analysis

A detailed survey of similar heat-curable DAA products on the market was conducted. Readers are encouraged to conduct their

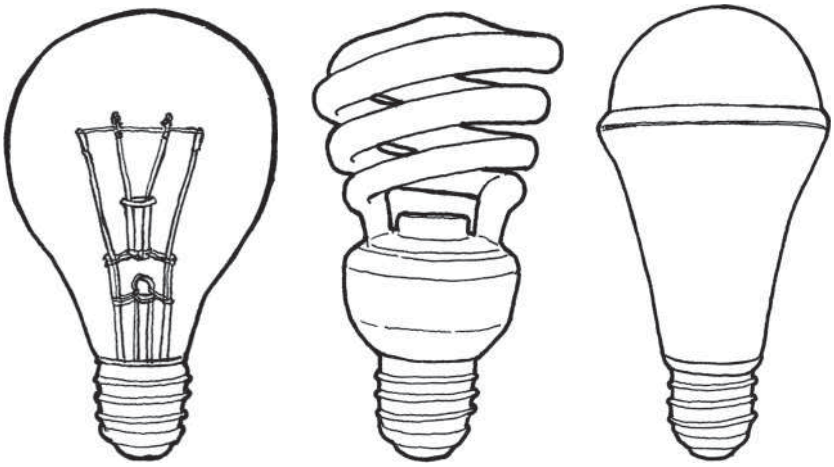

Figure 26.1 Household light bulbs: (a) incandescent light bulb; (b) CFL; (c) LED bulb.

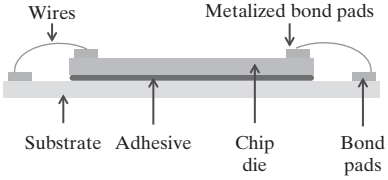

Figure 26.2 LED chip die attached to a dielectric substrate using a die attach adhesive with high thermal conductivity.

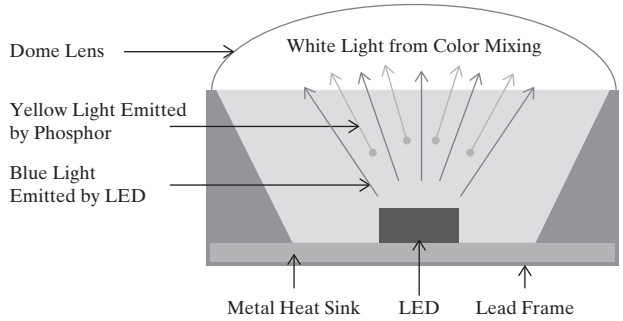

Figure 26.3 A blue LED chip inside a cavity with a yellow phosphor. White light is obtained by mixing blue light and yellow light.

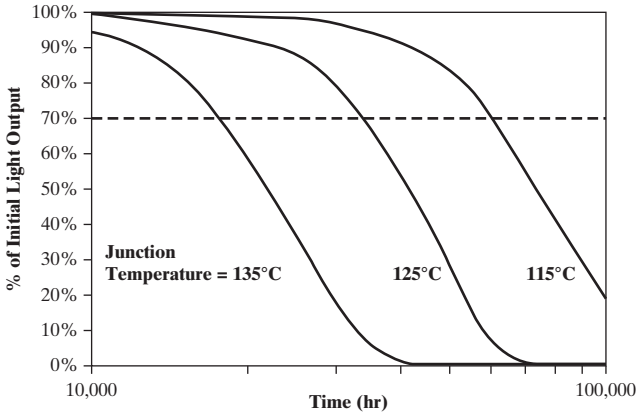

Figure 26.4 Effect of junction temperature on light output (as a percentage of initial light output) of an LED lamp during its lifetime. (*Source:* Data from Philips LumiLEDs Co).

own review. The key conclusions are presented in Table 26.1 in which the most important specifications are listed. Based on these data, the product development team decided to design a DAA with three improved product attributes. First, the thermal conductivity of the DAA would be increased in order to lower the junction temperature and, thereby, increase the lifetime of the bulb as indicated in Figure 26.4. The target was set at 25–40 W/m.K. This value is much higher than that of a typical DAA and is competitive against even the high-end products on the market. Second, existing products would have to be stored at −40°C before use to prevent curing from taking place. The storage temperature would be raised to −10°C to lower the transportation and storage costs. Third, the temperature for curing the adhesive would be lowered from a range of 150–180°C for existing products to around 100°C for the new product in order to expedite the manufacturing process. In addition to improving the product performance, it was decided to lower the price of the new DAA product. Often, the combination of improved specifications and a lower price is the key to a successful new venture.

Market Size

In terms of customer segments or, more appropriately, market segments in this case, a major market for DAA is high-brightness LED (HB-LED), which is predicted to reach sales of about $13.9 billion (Mukish, 2013). It was necessary to have the component costs of an LED package to estimate the market size of DAA for this market segment. Figure 26.5 shows the cost breakdown of a 1 W LED with a 1x1mm chip on a ceramic substrate (such as alumina) and a dome lens on top of it (Snob, 2010). Because 0.8% of the LED package was attributable to DAA, the market size of DAA for HB-LED was estimated to be around $111 million. As a new entrant to this market, a 10–15% market share within the first two years of product launch was targeted. Die attach adhesives would also be used in other market segments such as power electronics, which would be addressed at a later stage.

At this point, the product development team formulated an objective-time chart for the overall product development project, RAT^{2}IO for the tasks, and a preliminary business model canvas.

Table 26.1 Performance Targets for the New DAA Product

Product Specifications	New DAA Product	DAA Products on the Market	
		Typical	High End
Thermal conductivity (W/m.K)	25–40	2–8	20–25; Selected few >40
Storage temperature	−10°C	−40°C	−40°C
Curing temperature and time	80°C for 2h, or 100°C for 1h	150°C or above for 1–2h	180–220°C for 1h
Price	~$5/g	~$6/g	~$10/g

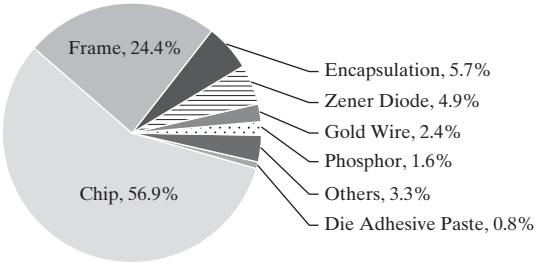

Figure 26.5 Costs of the various components of an LED package. (*Source:* Snob, 2010. Used with permission).

As in any other product development project, it took the manager much effort to secure the necessary resources–(money, technical people, space, equipment)–for the project and to persuade colleagues in other departments to join in.

EXAMPLE 26.1 ***Objective-time Chart for the DAA Development Project***

Figure 26.6 illustrates an example of an objective-time chart for the 12-month DAA project. It follows the multidisciplinary product development framework. Although Tasks 1–5 belong to the job function of business and marketing, the technical team was expected to be involved in all these activities. The aim of this group of tasks was to propose a new DAA product concept that could compete in the market. Product launch was planned in the last month of the project (Task 5). Tasks 6–12 were handled by a team of chemists and chemical engineers with the primary aim of delivering the envisioned DAA product efficiently. Note that the tasks handled by the technical team are indicated in Figure 26.6 with a dark color, and the tasks handled jointly by the business and technical teams appear in a light color and have a diagonal in the square.

The product specifications of the new DAA are set soon after studying the competing products (Task 8). There is considerable overlap between chemical synthesis handled by chemists (Task 11) and conceptual process design handled by chemical engineers (Task 12). This

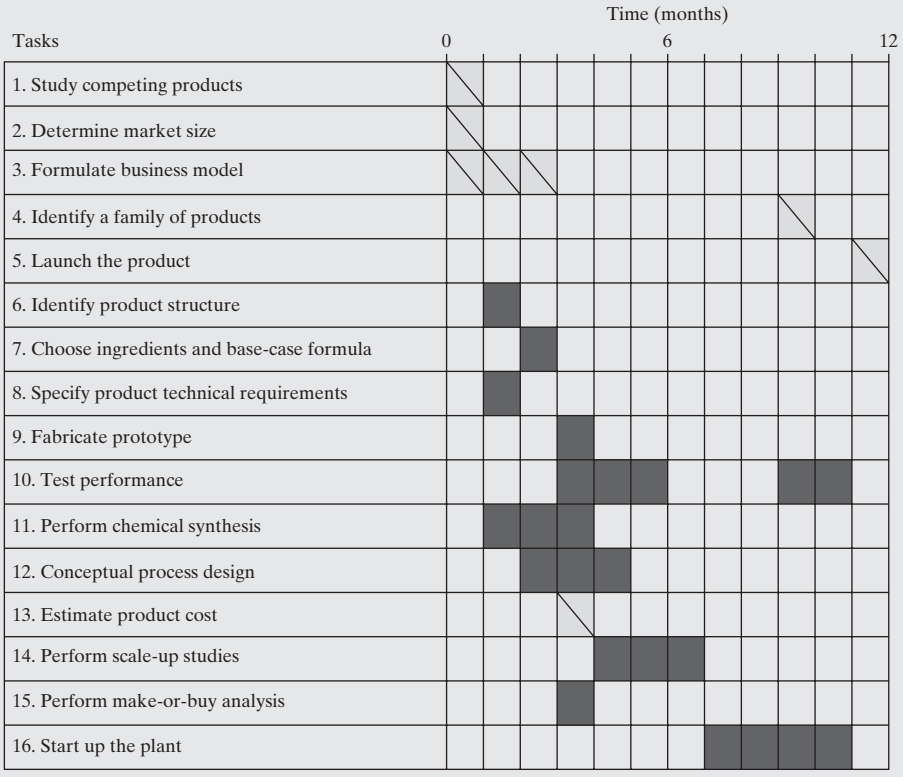

Figure 26.6 Simplified objective-time chart for the development of a DAA product.

is because the chemical engineer can propose additional experiments to the chemist. For example, a chemist tends to focus on high reaction yield. However, it is sometimes more economical to use a cheaper reactant, pay for a separation system to isolate the unconverted reactant from the reactor effluent, and recycle the recovered reactant to extinction in the reactor. In other words, even if the per pass yield is low, the overall yield can be nearly 100%. Product cost is often estimated jointly by business and technical people. The business team provides the administrative and advertising costs, and the technical personnel calculate the material and processing costs (Task 13). Tasks 14–16 are the responsibility of the chemical engineers. Plant startup (Task 16) normally takes a long time to achieve a smooth and efficient plant operation. It is important to carry out performance tests to ensure that the DAA produced in the production equipment has the same quality as that produced in the laboratory (Task 10). Before launching sales of the product, it is the opportune time to look into other market segments that might require a DAA of different product specifications (Task 4). Note that this objective-time chart shown here is simplified to retain only the essentials for the reader.

EXAMPLE 26.2 ***RAT²IOs for Selected Tasks***

RAT²IO (resources, activities, time and tools, input/output information and objective) is needed for each entry of the objective-time chart in Figure 26.6. Provide the RAT²IO for Tasks 9–11 (chemical synthesis, fabricate prototype, and performance tests).

SOLUTION

See Table 26.2 for some components of RAT²IO for DAA. Some input information such as product microstructure is the output information from earlier tasks in the product development project. The output information is used for other tasks later in the development project. Often, not all the tools have to be available in-house because some of the tasks can be outsourced. The estimated time is closely tied to the expertise and experience of the technical team. People are the key factor in deciding whether a project succeeds or fails.

26.3 PRODUCT DESIGN

Conceptualization of Product Microstructure

The DAA must offer sufficient adhesion power to keep the chip die attached to the substrate while providing a high thermal conductivity for heat removal. Thus, a conventional DAA consists of micron-sized silver particles that have a high thermal conductivity embedded in a polymer matrix that has a low thermal conductivity. An obvious way to raise the thermal conductivity is to increase the amount of silver, but this would decrease the adhesion power and even compromise the mechanical integrity of the DAA because of a corresponding decrease in the amount of polymer. The product development team speculated that using a mixture of silver in the form of both microparticles and nanorods as fillers could achieve a higher thermal conductivity while keeping the total amount of silver constant. This concept is depicted in Figure 26.7 (Lu et al., 2011). Silver nanorods with a high aspect ratio serve as bridges connecting the silver microparticles, thereby creating direct silver conductive paths for heat transfer (Figure 26.7a). It was further speculated that the addition of silver nanoparticles to the void space between the microparticles could also enhance heat transfer (Figure 26.7b).

Selection of Ingredients

The DAA consisted of five components: thermally conductive fillers, a polymer, a curing agent, a solvent, and a dispersing agent.

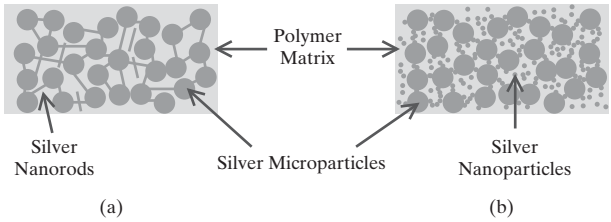

Figure 26.7 Microstructure of a conceptual die attach adhesive product.

Table 26.2 Simplified RAT²IO for the Tasks: Chemical Synthesis, Fabricate Prototype, and Performance Tests

Objectives	Input Information	Output Information	Time
Develop a prototype that meets the product specifications	• Product microstructure • Product specifications • Physicochemical property database for the ingredients	• DAA composition and ingredients • Characteristics of synthesized ingredients • Measured product specifications	• 5 months (months 2–6)

Tools	Activities	Resources
• Laboratory equipment such as reactor, mixer, centrifuge, oven • DAA test equipment such as thermal conductivity measuring device, viscometer, automatic die bonder, die shear test equipment. • Analytical instruments such as scanning electron microscope, particle sizer	• Develop the chemistry recipes for the nanomaterial ingredients • Fabricate the prototypes and test their performance • Develop the manufacture process • Obtain necessary process data	• Four synthetic chemists, two chemical engineers, and one mechanical engineer specializing in electronic packaging • Laboratory space and facilities • Budget for manpower, space, and tools

Metals such as silver, copper, and nickel with thermal conductivity of 429, 386, and 91 W/(m.K), respectively, were identified as possible candidates. Silver is roughly 100 times more expensive than copper, but its thermal conductivity is only 10% higher than that of copper. The technical team ruled out copper nanoparticles and copper nanowires although they could be either synthesized or purchased. The nagging problem was the fact that nanocopper is easily oxidized in air to form copper oxide with low thermal conductivity. Although the thermal conductivity of nickel is much lower than both silver and copper, it was thought that, similar to silver nanorods, nickel nanochains made up of connected nickel nanoparticles could link up the silver microparticles to enhance the thermal conductivity.

Because of its availability and performance, an epoxy resin with a thermal conductivity of around 0.15 W/(m.K) was used for the new product. Note that a wide variety of epoxy compounds was available (Forray et al., 2007). The curing agent could be ammonium antimony hexafluoride, imidazole-containing compounds, or a combination of them. The solvent could be toluene, xylene, propylene carbonate, acetone, methyl isobutyl ketone, ethanol, and so forth. Possible dispersing agents included glycerine fatty acids and their polymers, organic silane coupling agents having hydrophilic or hydrophobic groups, and so on.

26.4 PROCESS DESIGN

The first task was to choose between a continuous and a batch process. Based on a selling price of \$5/g and 10% of the \$111 million of the HB-LED DAA market, the annual production was expected to be 2,200 kg and revenue of \$11 million. This quantity was so small that a batch process was chosen. Another task was to develop a DAA with the desired properties. After deciding on a base-case formula of 5–10wt% metal for the DAA product, the technical team started to order the ingredients for making the DAA with the intended microstructure and product specifications. One potential problem was that the nanoparticles, nanorods, or nanochains could simply agglomerate among themselves instead of linking together the microparticles. There was no theory to predict whether a certain microstructure could be realized given the physicochemical properties, the amount of ingredients, and the way in which they were mixed together. Indeed, the technical team did not have even the most basic black-box model (Table 5.1) on hand. Thus, they proceeded by iteration, guided by their extensive experience in product formulation. Silver microparticles in the form of silver flakes were on the market. Silver nanorods, silver nanoparticles, and nickel nanochains of the desirable quality, quantity, and price were not readily available. It was decided to develop a synthesis procedure for all the nanomaterials. As an example, the procedure for synthesizing silver nanoparticles is briefly described next.

Synthesis of Ingredients: Silver Nanoparticles

An amount of silver (I) acetate monohydrate was added to a 28wt% aqueous ammonia solution to form a transparent solution. Then, an ammonium acetate solution was mixed into the silver precursor solution under vigorous stirring. The solution was purged with nitrogen, and a 55wt% aqueous hydrazine solution was added to it with vigorous stirring at room temperature under a nitrogen atmosphere. Note that hydrazine is highly toxic and unstable unless handled in solution. After 2 hours, the reaction mixture became gray. The spherical silver nanoparticles were passivated to prevent corrosion by adding dodecanethiol into the mixture. The silver nanoparticles were collected by centrifugation and were washed with deionized water and ethanol sequentially.

Preparation of DAA Product

The silver fillers were treated to enhance their dispersity (Liu et al., 2012a). A dispersing agent such as thiol, silane, or siloxane either synthesized in-house or purchased from an external supplier was added to the silver fillers in ethanol. The solution was stirred for at least 2 hours at room temperature. The treated fillers were recovered by centrifugation and washed with ethanol several times to remove the extra surfactant. The washed fillers were dried in an oven at 110°C before dispersing them in a solvent at room temperature. This was followed by the addition of the epoxy resin and curing agent. The entire mixture was mixed using a planetary mixer to get a homogeneous adhesive product. The proper selection of the mixing conditions and the type and amount of ingredients, dispersing agents, and solvent were crucial to obtain a product that upon curing yielded the desired microstructure. The homogenized adhesive was filled into a syringe dispenser and stored below −10°C, and the final product was ready for shipment and use.

Collection of Process Data for DAA

The role of the chemical engineers in the product and process development team was to translate the chemistry recipe into a production process. Reaction data such as reaction time, selectivity, and yield are used for reactor design. An experienced process engineer can spot what needs to be done in process scale-up while working with the chemists in the laboratory. By developing the chemistry recipe and engineering design concurrently, it is possible to reduce the time to market considerably. For example, mass transfer effects might adversely affect reaction selectivity. If a reaction is judged to be fast, the chemical engineer can carry out a set of experiments to determine the reaction kinetics, and select the proper reactor type and reaction conditions for production. Similarly, nanomaterials might be hard to filter. The chemical engineer can perform filtration, washing, and deliquoring experiments to determine parameters such as cake permeability, filter medium resistance, and diffusivity, which are difficult to predict (Cheng et al., 2010).

26.5 PROTOTYPING

Fabrication of Prototypes and Performance Tests

DAA samples in the form of a thin, circular patch were prepared by filling the DAA into a mold and curing it at 100°C for 1 hour. These samples were used in a large number of performance tests

Table 26.3 Characteristics of the Final DAA Product Ready for Product Launch

Filler Type	**Curing Temperature**	**Storage Temperature**	**Shelf Life**	**Thermal Conductivity**
Silver	100°C for 1hr	−10°C	>12 months	25–42 W/m·K
Lap Shear Strength	**Viscosity**	**Glass Transition Temperature**	**Coefficient of Thermal Expansion**	**Pot Life**
2.8–5.2 MPa	5k–120k cP	132°C	8–12 ppm/°C	>1hr

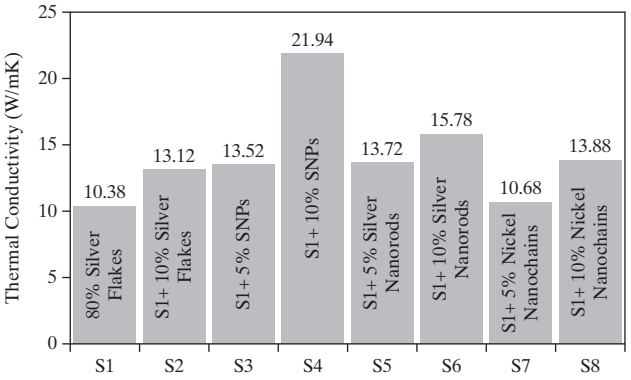

Figure 26.8 Thermal conductivity of DAA samples with different types and amounts of filler.

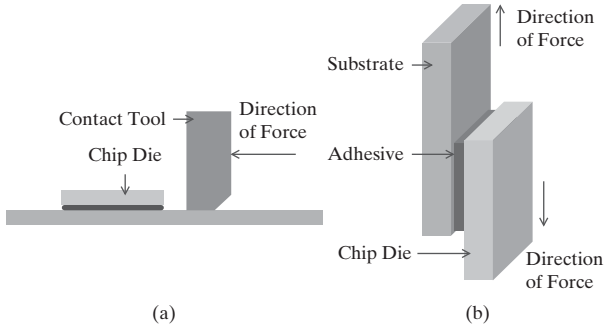

Figure 26.9 Test equipment: (a) die shear; (b) lap shear.

to ensure that the DAA product met the target product specifications. Extensive data were obtained throughout product design and prototyping. Figure 26.8 shows the thermal conductivity data of eight DAA samples (labeled S1 to S8) with different fillers and compositions (Lu et al., 2011). Sample S1 was filled with commercial microsized silver flakes in epoxy. Sample S2 was the same as Sample S1 except for an additional 10wt% of the microsized silver flakes. S3 and S4 were S1 with an additional 5% and 10% of silver nanoparticles, respectively. S5 and S6 were S1 with an additional 5% and 10% of silver nanorods, respectively. S7 and S8 were S1 with an additional 5% and 10% of nickel nanochains, respectively. Sample S4 with 10wt% of silver nanoparticles showed the highest thermal conductivity with a 111% improvement over that of S1. In comparison to the 26% improvement of S2 over S1, these data clearly showed that the nanoparticles and the resulting product microstructure had a significant effect on the thermal conductivity. Sample S6 with 10wt% of silver nanorods had the second highest thermal conductivity but was inferior to S4. Although the thermal conductivity of S8 with 10wt% of nickel nanochains showed merely 34% improvement over S1, S8 possibly offered a price advantage because the price of nickel metal was about one-thirtieth of silver. Based on these performance tests, the project team selected S4 for mass production.

The junction temperature for a reference chip die was measured using thermocouples. The viscosity of the adhesive before curing was measured using various rheometers such as a cone-and-plate viscometer. The viscosity had to be adjusted depending on the die bonder used for applying the adhesive to attach the die to the substrate. In a die shear test, the force needed to detach the chip die bonded on the substrate was measured by applying a force parallel to the substrate of the chip die (Figure 26.9a). In a lap shear test, the DAA was bonded to both the substrate and the chip die, and the force to separate them was measured (Figure 26.9b). The use of these equipment items had been anticipated in the project objective-time chart (see Example 26.2) and was secured in advance to avoid any project delay.

The recipe for the DAA product was finalized after many iterations. Patents were filed to protect the intellectual property (Liu et al., 2012b, 2014). The product characteristics are given in Table 26.3. Here, shelf life was the period of storage within which the product remains useable. Pot life was the period for which the adhesive remains usable after raising it to the working temperature.

26.6 ESTIMATION OF PRODUCT COST

Silver microparticles and nanoparticles, epoxy resin, curing agent, dispersing agent, solvent, and syringe dispensers can all be purchased on the market. Refer to Table 26.4 for the composition of the final DAA product, the approximate unit price of the raw materials on the retail market, and the cost of each component for the DAA product.

The total cost of the components (in Table 26.4) in the DAA was \$1,385.53/kg, or \$1.39/g, which can be compared to the targeted selling price of \$5.00/g in Table 26.1. The dominant cost was that of the silver fillers. Based on a cost of silver metal at \$600/kg, and the estimated processing cost for manufacturing silver microparticles and nanoparticles in-house, the technical team was confident that the silver filler cost could be further reduced by about one-third, resulting in a total component cost of \$0.92/g DAA. In addition, the quality of the silver nanoparticles on the market was not sufficiently reliable. Therefore, the product team decided to make the silver fillers in-house. The component cost in Table 26.1 includes the processing cost for the silver fillers, leaving enough room for potential profit by selling the DAA at \$5/g. An economic evaluation using investor's rate of return as well as other financial metrics as discussed in Chapter 19 convinced

Table 26.4 The Composition and Component Cost of the DAA Product for the Buy Option

Ingredient	Composition (wt%)	Unit Cost ($/kg ingredient)	Component Cost ($/kg DAA)
Silver flakes	79	1,500	1,185
Silver nanoparticles	10	2,000	200
Epoxy resin	5	5	0.25
Curing agent	5	3	0.15
Dispersing agent	1	2	0.02
Solvent	NA	1.5	0.06
Syringe dispenser (10 mL)	NA	0.05	0.05
Total	100	NA	1,385.53

senior management to allow the project to proceed further. The understanding was that the production could begin once the first customers could be secured by the marketing team. New projects have been known to fail when first customers are not secured before production.

26.7 SUMMARY

The development and commercialization of a die attach adhesive was used to illustrate many of the activities in a typical product development project. The first step was to gain an understanding of the technology background (Section 26.1) required to ensure that the development team, including management, business managers, scientists, and engineers were on common ground. This was followed by a market study and, in particular, a competitive analysis to fix the specifications of a profitable DAA product (Table 26.1). Technical team members should challenge themselves to offer a product with distinct competitive advantages in terms of specifications and cost. In product design, physical insights played a significant role in deciding the DAA microstructure (Figure 26.7). The ingredients of the product were chosen based on their physicochemical properties, cost, safety, and many other factors. There were two processing steps. One was the synthesis of the nanofillers. This was a classical team effort with the chemists working on the laboratory scale synthesis while the chemical engineers performed the process design and scale-up (Anderson, 2000). The second step was to mix the ingredients to produce the die attach adhesive. All aspects of the product in terms of technical performance, reliability, and so on had to be confirmed both in the laboratory and at the production line. Often, what was achievable on the laboratory bench could not be immediately reproduced in mass production. A proper scale-up study might be essential. The final product cost was fixed following a make-or-buy analysis that favored making silver fillers in-house.

Finally, a disclaimer is in order. This case study as presented is not supposed to lead the reader to repeat the development project. Although the overall flow of events has been captured, many twists and turns have been omitted. The actual DAA development project did not happen as smoothly and systematically as the account described here may have conveyed. This chapter illustrates the process with a concrete example, but it takes practice to be able to develop a product with speed, efficiency, and quality (Wheelwright and Clark, 1992).

REFERENCES

1. Agari, Y., and T. Uno, "Estimation on Thermal Conductivities of Filled Polymers," *J. Appl. Polym. Sci.*, **32**, 5705 (1986).

2. Anderson, N. G., *Practical Process Research & Development*, Academic Press, San Diego (2000).

3. Cheng, Y. S., K. W. Lam, K. M. Ng, and C. Wibowo., "Workflow for Managing Impurities in an Integrated Crystallization Process," *AIChE J.*, **56**, 633 (2010).

4. Forray, D. D., P. Liu, and B. delos Santos, "B-Stageable Die Attach Adhesives," U.S. Patent No. 7,176,044 B2 (2007).

5. Liu, C., D. Lu, X. Lang, A. Choi, and P. W. M. Lee, "Effect of Surface Treatments on the Performance of High Thermal Conductive Die Attach Adhesives (DAAs)," 14th International Conference on Electronic Materials and Packaging, 1 (2012a).

6. Liu, C., D. Lu, X. Lang, B. Wang, and Z. Li, "High Performance Die Attach Adhesives (DAAs) Nanomaterials for High Brightness LED," WO Patent Application No. 2012126391 A9, 2012b; U.S. Patent Application No. 2014/0001414 A1.

7. Lu, D., C. Liu, X. Lang, B. Wang, Z. Li, W. M. P. Lee, and S. W. R. Lee, "Enhancement of Thermal Conductivity of Die Attach Adhesives (DAAs) Using Nanomaterials for High Brightness Light-Emitting Diode (HBLED)," *2011 Electronic Components and Technology Conference*, 667 (2011).

8. Lumileds, "Understanding Power LED Lifetime Analysis," Technology White Paper.

9. Mukish, P., "Yole Développement 'Status of the LED Industry' Shows that Low Price LED Solutions Are Pushing Technology Adoption Toward General Lighting," *LED Professional* (September 2013), www.led-professional.com.

10. Snob, H. K., "How to Capture This Business Opportunity of LED Market 2009–2012?" (2010), http://led-fever.blogspot.hk/2010/06/how-to-capture-this-business.html.

11. Wang, M., and N. Pan, "Predictions of Effective Physical Properties of Complex Multiphase Materials," *Mat. Sci. Eng. R.*, **63**, 1 (2008).

12. Wheelwright, S. C., and K. B. Clark, *Revolutionizing Product Development*, The Free Press, New York, (1992).

13. Wibowo, C., and K. M. Ng, "Product-Oriented Process Synthesis and Development: Creams and Pastes," *AIChE J.*, **47**, 2746 (2001).

EXERCISES

26.1 Search the Internet to identify three or more companies marketing die attach adhesives. For example, check 3M and Henkel.

26.2 Conduct a competitive analysis by collecting information on the product specifications of one of the DAA products from each of the companies identified in Exercise 26.1. Specifically, the data should include (a) filler type and concentration; (b) curing temperature; (c) storage temperature; (d) shelf life; (e) thermal conductivity; (f) lap shear strength; (g) viscosity; (h) glass transition temperature; (i) coefficient of thermal expansion; and (j) pot life.

26.3 Search the Internet to identify market segments other than HB-LED that use die attach adhesives. Identify the different products in those market segments.

26.4 A business model evolves over time. Given the information in this chapter and elsewhere, fill out a business model canvas for DAA as completely as possible.

26.5 Many models of a composite's effective thermal conductivity are available in the literature (Wang and Pan, 2008). Even if a model cannot accurately predict the DAA product performance, physical insights that are beneficial to product development can be obtained from a simplified model.

(a) For a parallel model, consider a two-component composite consisting of strips of epoxy (light) and silver (dark) aligned in the same direction as the heat flow. The volume fraction of silver in the composite is ϕ.

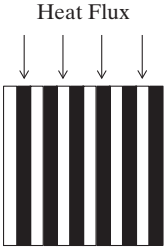

Prove that the effective thermal conductivity of the composite k_{eff} is

$$k_{eff} = (1-\phi)k_e + \phi k_s$$

where the conductivities of epoxy and silver are $k_e = 5\ \mathrm{Wm^{-1}K^{-1}}$ and $k_s = 420\ \mathrm{Wm^{1}K^{-1}}$, respectively. Calculate and plot the dependency of k_{eff} on ϕ in the range of $0.2 < \phi < 0.8$.

(b) For a series model, the microstructure is in the form of strips of epoxy and silver aligned perpendicular to the direction of heat flow.

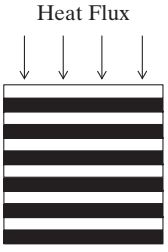

Prove that the effective thermal conductivity of the two-component composite is

$$k_{eff} = \left(\frac{1-\phi}{k_e} + \frac{\phi}{k_s}\right)^{-1}$$

Calculate and plot the dependency of k_{eff} on ϕ in the range of $0.2 < \phi < 0.8$.

(c) A mixture of parallel and series configurations is expected for the DAA product. A model was proposed for such a microstructure (Agari et al., 1986):

$$k_{eff}^{n} = (1-\phi)(C_e k)_e^{\ n} + \phi k_s^{C_s \cdot n}$$

Here, C_e is an adjustable parameter for the epoxy phase $C_s \in (0,1]$; it represents the degree of difficulty in forming a conductive silver path in the DAA. In the limit of $C_s \to 0$, the impact of k_s on k_{eff} is greatly minimized. The parameter $n \in [-1,1]$. The parallel model and the series model are recovered when n equals 1 and -1, respectively. For the DAA having a microstructure between the parallel and series models, $n \approx 0$, prove that in the limit of $n \to 0$

$$\log k_{eff} = \phi[C_s \log k_s - \log (C_e k_e)] + \log (C_e k_e)$$

(d) Figure 26.8 shows the thermal conductivities of different DAA prototypes. Sample S1 is a mixture of silver flakes (80wt%) and epoxy (20wt%).

(1) Determine C_e and C_s from S1 and S2 by data fitting.

(2) Assuming C_e is a constant, calculate C_s from S1 and S3.

(3) Using C_e and C_s from (2) calculate k_{eff} of S4. Compare the calculated value with the experimental value and explain what may cause the difference, if any.

26.6 It is desired to develop a day cream with sun-blocking, antioxidant, and moisturizing functions. The cream has to be transparent because it is used indoors. The skin has a variety of antioxidants localized in the epidermis and, to a certain extent, in the dermis to protect skin against damaging effects from reactive oxygen species. The supplementation of a sunscreen cream with antioxidants provides a rational approach to ameliorate the solar UV-induced skin damage. The cream has to be water based so that the cream does not feel oily even with a moisturizing agent. Perform the following tasks for this product development project:

(a) Prepare a comprehensive review of the technical background for this product emphasizing the role of antioxidants (see Example 5.3).

(b) Summarize the desired product attributes for this day cream.

(c) Identify antioxidant candidates.

(d) Perform a competitive analysis for this day cream.

(e) Create an objective-time chart for the overall project.

(f) Generate the RAT^{2}IOs for the main tasks in the objective-time chart in (e).

(g) Provide process flowsheet alternatives for manufacturing this cream (see Wibowo and Ng, 2001).

26.7 Figure 26.8 shows that the thermal conductivity of S3 and S4 increased by 30.25% and 111.37% by adding 5wt% and 10wt% of silver nanoparticles (NPs), respectively, to S1 with 80wt% silver flakes. There are many more NPs than silver flakes, to be represented by spherical microparticles (MPs), because the NPs are much smaller. The way in which the MPs mix with the NPs is also not known. However, to better understand the effect of the type and amount of silver filler on thermal conductivity, the four configurations in Figure 26.10 are assumed.

Thus, configuration 1, representing sample S1, does not contain any NPs. Configuration 2, representing S2, and configuration 3, representing S4, have one. Configuration 4, also representing sample S4, has four NPs. As shown in the following cross-sectional cut for configuration 3, each configuration is a unit cell, which repeats itself within the adhesive layer. There is one microparticle in each unit cell.

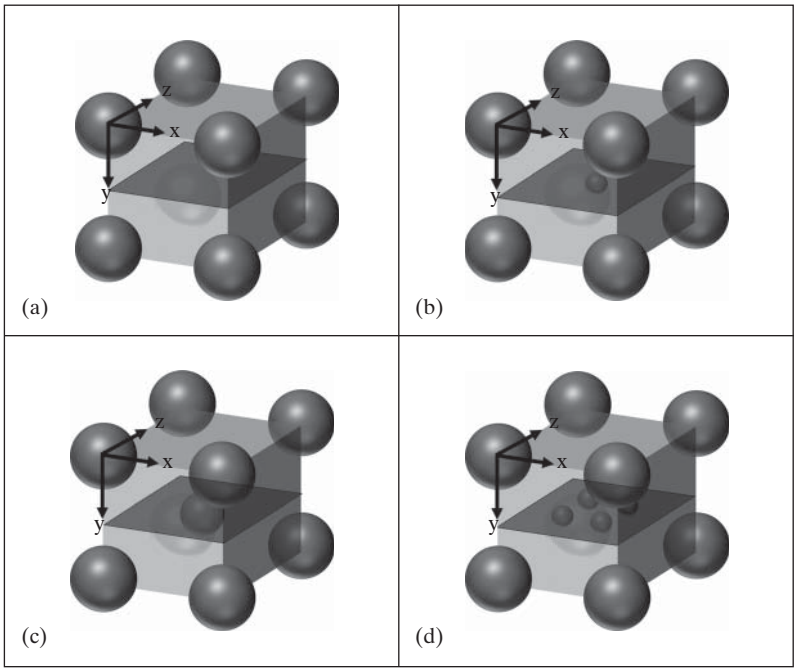

Figure 26.10 DAA microstructure: (a) Configuration 1, 80% MP, 0% NP, 20% epoxy; (b) Configuration 2, 80% MP, 5% NP, 15% epoxy; (c) Configuration 3, 80% MP, 10% NP, 10% epoxy; (d) Configuration 4, 80% MP, 10% NP, 10% epoxy.

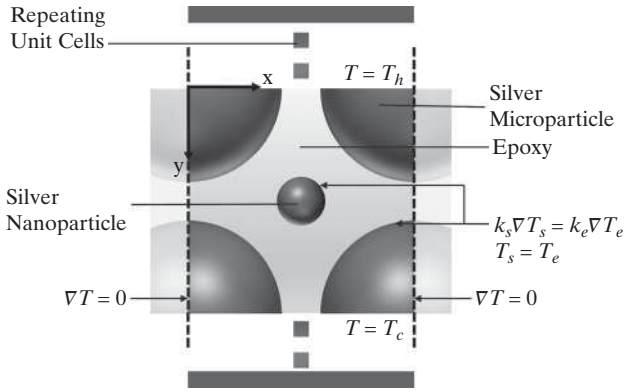

This steady-state, heat conduction problem is governed by the following equation:

$$k\nabla^2 T = 0$$

for both silver and epoxy phases and the boundary conditions:

$k_s \nabla T_s = k_e \nabla T_e$ and $T_s = T_e$	at all silver epoxy interfaces
$T = T_h$	at the top of the unit cell
$T = T_c$	at the bottom of the unit cell
$\nabla T = 0$	at the four sides of the unit cell (due to symmetry)

The thermal conductivity, specific heat, and density are given in the following table (http://www.engineeringtoolbox.com):

Properties	Silver	Epoxy
Thermal conductivity, k (W/m·K)	429	0.35
Specific heat, Cp (J/kg·K)	235	1,000
Density, ρ (kg/m^3)	10,500	1,500

In addition, it is given that the microparticles have a radius of 1.2 μm. The adhesive layer has a thickness of 51 μm. The temperature on the LED chip is 127°C, and the temperature on the substrate is 110°C.

Based on these data, determine the effective thermal conductivity of each configuration using simulation packages such as COMSOL Multiphysics. The following procedure can be used for configuration 4 (see the following cross-sectional cut) although it can be used for other configurations with minor modifications.

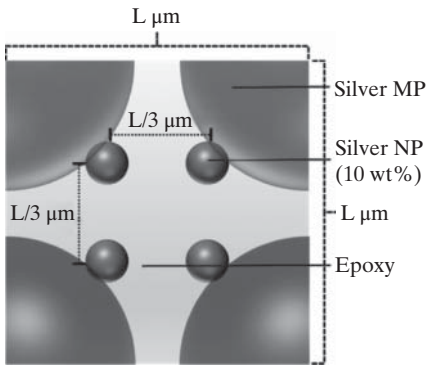

(a) Calculate the length of each side of the cubic unit cell, L for the given weight percentages of the components.

(b) Determine the diameter of the NP if any is present.

(c) Calculate the number of unit cells across the adhesive layer.

(d) Assuming a linear temperature profile across the adhesive layer, calculate the temperature at the top (T_h) and the bottom (T_c) of the unit cell.

(e) Run the software with the data and the parameters calculated.

(f) Finally, compare the trend of the calculated effective thermal conductivity with the trend of the experimental data in Figure 26.8.

Chapter 27

Case Study 4—Ammonia Process

27.0 OBJECTIVES

This chapter presents a detailed design developed for the manufacture of a commodity chemical. As such, it fulfils several functions. Firstly, it illustrates the steps in the design of *basic* chemical products using the Stage-Gate™ Product-Development Process (SGPDP) described in Chapter 1 with emphasis on the *concept* and *feasibility* stages. It also introduces Mind Maps and provides an example of their use as a means to pursue design refinement steps intended to improve the profitability of a process in development.

After studying this chapter, the reader should:

1. Be able to use the elements of the Stage-Gate™ Product-Development Process for the design of *basic* chemical products.
2. Appreciate how appropriate design methodology is implemented as needed using the Stage-Gate™ Product-Development Process.
3. Be able to prepare a Mind Map, possibly using brainstorming, and use it to drive the refinement steps intended to improve the profitability of a process design.
4. Be able to apply the skills developed through the study of Part II of this book to benefit the profitable design on a chemical process.

27.1 INTRODUCTION

Before proceeding with the ammonia case study, the reader should be conversant with the key steps in process design as introduced in Part II specifically in Chapters 6 to 11. Furthermore, because this case study is driven by economics, it is helpful to be familiar also with capital cost estimation methods introduced in Chapter 16 and with profitability analysis introduced in Chapter 17.

Project Charter—Objective Time Chart and New Technologies

As described in Chapter 1, it is recommended that a design team begin to develop a new product and process by creating a project charter. Before introducing the initial project charter prepared by the design team, a brief history of the manufacture and/or purchase of ammonia by Haifa Chemicals is reviewed.

Haifa Chemicals (ww.haifa-group.com) is an international corporation established in 1967 that produces and markets specialty fertilizers, food additives, and technical chemicals. Their production plants are located in Israel at Haifa Bay and in the Northern part of the Negev region and in Lunel, France. In the 1970s, a 250 ton/day ammonia plant was located in close proximity to the Haifa Refinery, which provided naphtha that was converted to hydrogen in a reformer. Then, because demand exceeded the plant's capacity in the late 1980s, it was shut down, and ammonia was supplied by ship from external producers. To ensure continuous operation, a refrigerated 12,000-ton storage vessel containing a month's supply of ammonia at ambient temperature was erected in Haifa Bay. The principal usage of ammonia in Israel is in the manufacture of $(NH_4)_3PO_3$ in the form of fertilizer pellets for use in farming. Haifa Chemicals operates manufacturing facilities for ammonium phosphate in Ramat Hovav in the Negev Desert in southern Israel and in Haifa Bay. It transports ammonia by truck to Ramat Hovav and phosphate rock by train to Haifa. As a result of the heightened security threat posed by the Lebanese Hezbollah in the summer of 2006, the State of Israel considered alternatives to relocate the storage tank to a remote location, such as the Negev Desert. A feasibility study for the possible manufacture of ammonia from natural gas was carried out by the final-year students of the Faculty of Chemical Engineering at the Technion with the design basis being a production rate of 350-metric tons/day (MTD) at the 2007 market price of ammonia of \$270/MT. As described in Chapter 13 of the third edition of this book, the principal conclusions of that feasibility study were:

(a) The cost-effective production of ammonia at the Israeli national demand of 350 MTD was dependent on the availability of natural gas at about half of its cost at the time. Given that methane prices were expected to rise, this effectively eliminates the feasibility of production to satisfy the Israeli market alone.

(b) A plant that produces approximately twice the Israeli national demand would be feasible if the cost of methane was subsidized by 25%. However, the surplus ammonia produced would have to be exported, probably by sea, requiring bulk storage facilities in population centers—an infeasible option.

(c) A plant to produce three times the Israeli national demand, that is, 1,000 T/day [MTD], was feasible economically.

If this solution were adopted in Haifa, the storage facilities would be doubled, with two-thirds of the production exported using the city's port facilities, which was also an infeasible option. Alternatively, a joint venture with Jordan, whose ammonia demand is approximately twice that of Israel's, could be encouraged. The combined Israeli–Jordanian demand matched the minimum level of production that was then economically viable. This suggested a production facility in the Negev Desert, close to the Israel–Jordan border.

Since 2007, two things have happened to change those conclusions. First, huge deposits of natural gas have been discovered in gas fields off the coast of Israel. These fields will provide the energy and feedstock required by Israel for many years and, of course, will also affect the feasibility of ammonia production. The second change has been the significant inflation in the market price of ammonia; the price by 2012 rising to over \$600/MT as shown in Figure 27.1. These changes motivated a new feasibility study, possibly relying on alternative technologies, that is presented in this chapter.

Consider an example project charter in Table 27.1 assembled by a typical design team. The goals of this project charter are centered on supplying an expected demand of 450 MTD ammonia while circumventing the safety hazard created by the storage of toxic ammonia in the Haifa area. To protect the population and given the prices established by external suppliers of natural gas and ammonia, it might be necessary for the government to consider providing tax breaks and low-cost loans to encourage investment in developing ammonia production facilities. This initial project charter identifies the production of synthesis gas using natural gas as the source of hydrogen and air as the source of nitrogen as *in-scope*. On the other hand, solutions involving the storage of ammonia in port cities, such as Haifa and Ashdod, are considered to be *out-of-scope*.

The first deliverable is a business opportunity assessment involving a profitability analysis. In addition, a technical feasibility assessment will be provided, including the results of process simulations. And, finally, a product life cycle assessment will be conducted that addresses (1) the danger of an ammonia release from a storage facility, (2) the release of carbon dioxide byproduct to the atmosphere, and (3) the possible conversion of ammonia to urea by reaction with carbon dioxide as a vehicle for curbing the release of the carbon dioxide byproduct. Note, however, that due to space limitations, this life-cycle assessment is relegated to Exercises 27.5–27.7. Finally, the product timeline requires the delivery of a feasible process package within six months.

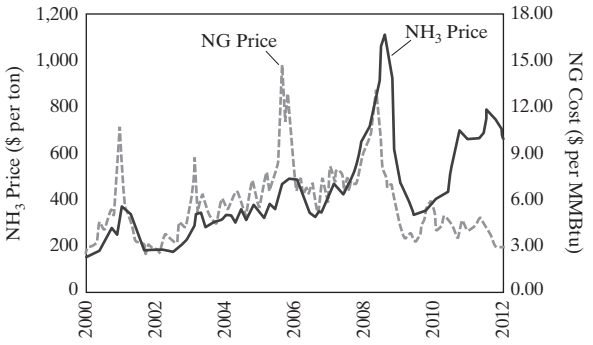

Figure 27.1 Variation of ammonia and natural gas prices by year.

Table 27.1 Initial Project Charter—Objective Time Chart

Project Name	Ammonia Production in Israel
Project Champions	Business Director of Haifa Chemicals, Inc.
Project Leaders	Speedy and Ploni Gonzales
Specific Goals	Produce and store NH_3 from synthesis gas beginning with natural gas, noting its availability from the recently discovered off-shore fields. Consider relocating the facility to a remote location to reduce the risk to population centers in the event of the release of NH_3 that might result from terrorist rocket fire.
Project Scope	In-scope: • H_2 from natural gas • N_2 from air Out-of-scope: • Production and storage in port cities with large populations (e.g., Haifa, Ashdod)
Deliverables	• Business opportunity assessment • Technical feasibility assessment • Product life cycle assessment
Timeline	Feasible processing package within 6 months.

Innovation Map

Having created a project charter, the design team next turns to an examination of the customer needs (that is, the *customer-value proposition*) and the new technologies likely to play an important role in providing the ammonia product as introduced in Chapter 1. These are shown linked together in the *innovation map* in Figure 27.2.

To construct this *innovation map*, one must first identify the elements in its four levels, moving from the bottom to the top of the map:

1. ***Process/Manufacturing Technology.*** The new technologies that should be considered to enhance the profitability of the process under development are: Improved heat integration, membrane separation to recover H_2 from the purge stream, pressure-swing adsorption to recover CO_2 from synthesis gas, and heat and mass exchange (HME) technology to enhance conversion in the NH_3 synthesis loop and provide enhanced heat recovery.
2. ***Technical Differentiation (technical-value proposition).*** Higher thermodynamic efficiency resulting from improved heat-integration methods, efficient recovery of valuable H_2 by utilizing membrane-separation technology, and reduced separation and recirculation costs in the synthesis loop by incorporating HME technology.
3. ***Products.*** NH_3 and oxygen. The CO_2 byproduct of the process is assumed to be consumed by other processes but at no revenue.

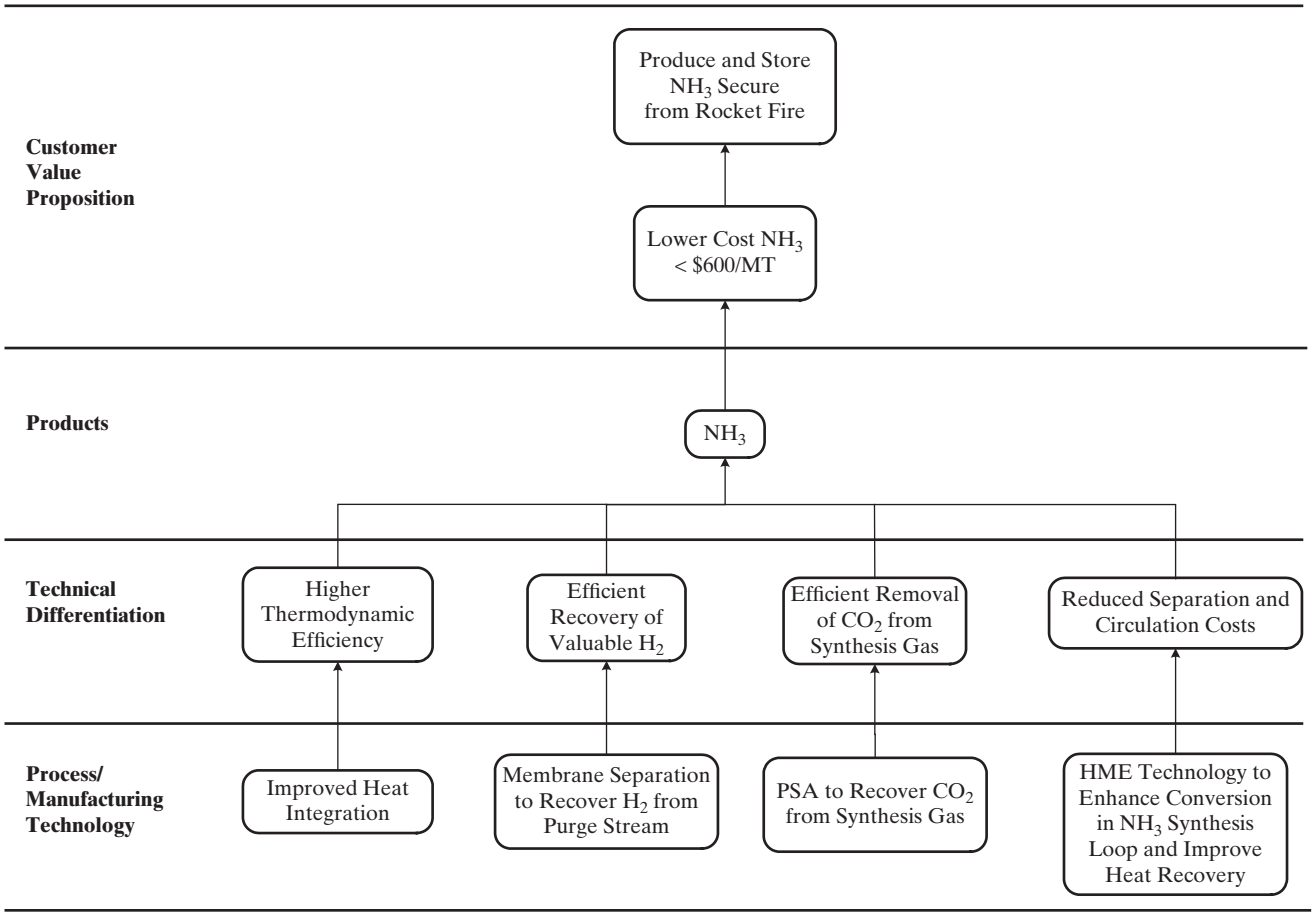

Figure 27.2 Innovation map for ammonia product.

4. ***Customer-value Proposition.*** Produce NH_3 to sell for \$0.60/kg (\$600/MT) or less while reducing the potential security impact of a rocket attack and produce O_2 to sell for \$170/MT. Note that the market price of NH_3 in 2007, when the first feasibility study was conducted, was only \$270/MT, less than half of the 2012 value. As expected, this large increase in the price of the product significantly impacts the profitability of the process and, more importantly, the minimum size of a profitable process.

After identifying the elements at all four levels of the innovation map, their connectivity in the map is added to show the interplay between the technological elements, the *technical-value proposition*, and, ultimately, the *customer-value proposition*.

In this case, for a well-known commodity chemical product, such as NH_3 the new technologies that have the potential to satisfy the customer needs are process and manufacturing technologies. The first is the Linde Concept (Figure 27.3) in which pure hydrogen and nitrogen are produced in two parallel processes and then combined as a synthesis gas that is fed to

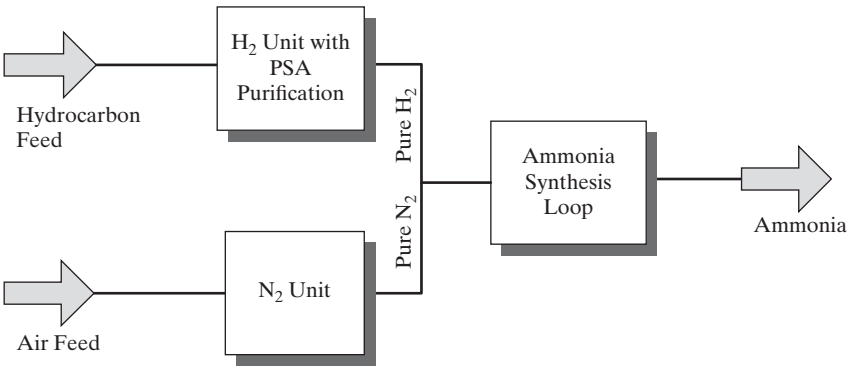

Figure 27.3 The Linde Concept for ammonia production.

an ammonia synthesis loop. The Linde Concept (http://www.linde-engineering.com/en/index.html) relies on pressure swing adsorption (PSA) to purify hydrogen while producing a CO_2-rich byproduct and air-separation distillation to generate pure nitrogen and an oxygen byproduct. Additional technologies to be considered are (1) the potential for improved heat integration using the algorithmic methods discussed in Chapter 11, (2) membranes to recover valuable H_2 from the vapor-purge stream that exits from the NH_3 synthesis loop, and (3) heat and mass exchange (HME) technology to significantly increase the conversion to NH_3 while providing enhanced heat recovery. The relevant separation technologies affecting this case study are discussed next.

Heat and Mass Exchange Technology

HME technology (Lavie, 1987) involves a heat-insulated pair of adsorbent vessels that perform their normal role of adsorption while transferring heat from the hot regenerant stream to the cold process stream from which one or more species are removed by adsorption as depicted schematically in Figure 27.4. In NH_3 production, the synthesis gas directed to the converter must be preheated while the effluent stream from the converter must be cooled to condense the ammonia. This is normally accomplished by heat exchange between the two streams. Also, the maximum concentration of ammonia in the converter effluent is limited by equilibrium and is, therefore, essentially independent of the ammonia concentration in the feed to the converter. However, by installing an HME unit to completely or partially replace the heat exchanger, the converter effluent can also be enriched at the expense of its feed. This can increase the conversion-per-pass in the converter by a few percent ages, which translates into an increase of 10–20% in ammonia production from the same loop. The hot & rich stream fed to the HME unit should be at least 150°C.

Membrane Separation of Hydrogen from Synthesis Gas

The MEDAL™ membrane technology commercialized by Air Liquide separates, hydrogen from synthesis gas as permeate, and the remaining gases are removed as residue (retentate). A schematic of a typical separator taken from the Air Liquide Web site, is shown in Figure 27.5; note that stream pressures and compositions shown do not apply directly to its application in an ammonia process. The usage of highly selective polyvinylchloride membranes enables almost perfect separation of the hydrogen with a 95% recovery of >98 mole% pure H_2. As discussed in the next section, this technology was not adopted in the initial design but is a strong candidate for the recovery of hydrogen from the purge gas stream.

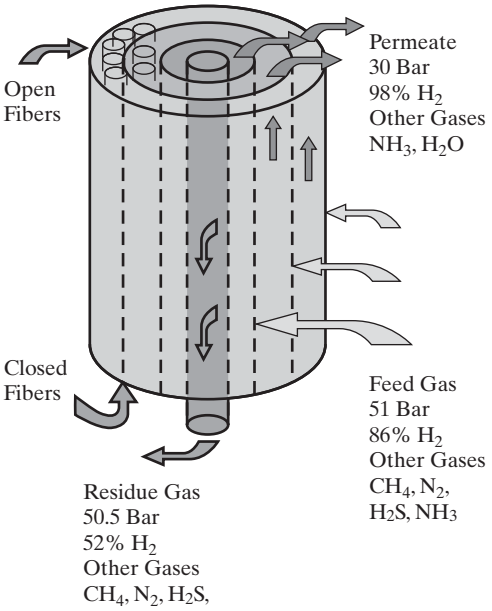

Figure 27.5 Typical membrane separator.

The innovation map links these new technologies to their related technical differentiations, which permit the generation of the NH_3 product to satisfy the customer needs identified under the *customer-value proposition*. The first, which is imperative to achieve lower costs in energy-intensive processes that produce commodity chemicals, is to yield a high thermodynamic efficiency through the extensive use of heat integration. The second, which has been enabled by hollow-fiber membranes in recent years, is to recover valuable H_2 in purge streams rather than burn it in a flare device. Finally, the application of HME technology leads directly to reduced separation and circulation costs. The combination of these technical differentiations has the potential to permit the production and storage of NH_3 in a remote environment secure from possible nearby conflagrations and to generate a product steam to be used in related chemical processes, such as for the manufacture of $(NH_4)_3PO_3$

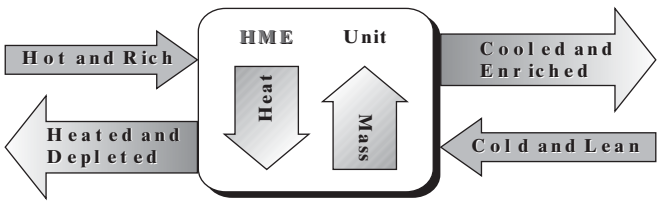

Figure 27.4 HME schematic.

27.2 INITIAL BASE CASE DESIGN

Concept Stage

Having assembled a promising *innovation map* after obtaining approval to begin the SGPDP as shown in Figure 1.6, the design team normally begins the *concept* stage with a market assessment to identify the *value creation* and *value capture* and to create the *value proposition*.

Market Assessment

For this NH_3 product, the added value to customers is unusual. In this case, the production and storage of NH_3 in a remote location

sharply reduces the danger of exposure to toxic NH_3 in the event of terrorist rocket attacks, a significant threat in Haifa, Israel.

The answers to the following questions also help to define the *value creation*. Who are the customers? These are the fertilizer manufacturers, that is, the producers of $(NH_4)_3PO_3$, and the manufacturers of industrial refrigeration units in both Israel and, possibly, Jordan. Of these customers, who are most likely to buy? Clearly, the Israelis are the most likely customers.

Turning to the *value capture*, in this case, there is no clear competition. Although the NH_3 can be purchased from external suppliers, especially from the new NH_3 plant being constructed by Egypt, unfortunately, it is not possible to import and store NH_3 in the Israeli ports, Haifa and Ashdod, which are large population centers.

Finally, the design team identifies a concise statement that summarizes the need for the new remote facility to produce the product NH_3. A likely *value proposition* statement, in this case, is: "To remove its dependence on imported NH_3, the Government of the State of Israel supports the construction of a new plant to produce NH_3 in the Negev Desert. This will permit the dismantling of the hazardous NH_3 storage facility in Haifa Bay."

Customer and Technical Requirements and Superior Product Concepts

For this commodity chemical, NH_3, the customer requirements are well established when creating the project charter. These are not further developed here in the *concept* stage. Their translation into technical requirements is rather straightforward for this case to produce 99.5 mol% NH_3. Normally, the next steps toward creating superior product concepts are to create a preliminary database and to carry out preliminary process synthesis. In this case, the most promising flowsheets of process operations are well established for the conversion of natural gas to synthesis gas and for the NH_3 synthesis loop. For this reason, as discussed next, the design team adopts initially a preliminary feasible process flowsheet for the base-case design. This flowsheet (Figures 27.6 and 27.7), is described next and further developed in the *feasibility* stage of the SGPDP.

Initial Feasible Design

Figures 27.6 and 27.7 show an initial feasible design for the production of 450 MTD of ammonia from methane using the Linde Concept on the basis of assumed raw material and product prices given in Table 27.2. The process involves two main sections: one for synthesis gas generation (Figure 27.6) and the other for the ammonia synthesis loop (Figure 27.7). Full details of the initial design, as well as a complete project tender including information about materials specifications and equipment-costing information can be accessed in the file Ammonia Project.pdf**,** which can be downloaded from the Wiley Web site that accompanies this textbook. The reader can reproduce the base-case design by running the UniSim® Design case file NH3_PROCESS_4E_STEP_0.usc. The initial design returns a venture profit [VP, computed as the profit minus a 20% return on investment; see Eq. (17.9)] of −$48.5MM/year, that is, an annual **loss** of almost $50 million. Note also that the initial economic potential is only $24MM/year.

Table 27.2 Prices of Raw Materials and Products

Commodity	Assumed Price ($/kg)
Ammonia	0.60
Carbon dioxide[a]	0.00
Methane	0.20
Oxygen	0.17
Process steam	0.05

[a] Although the CO_2 produced in the process is assumed to be adsorbed as a raw material at no charge, any CO_2 emitted in the stack of the furnace is penalized at $0.05/kg.

Synthesis Gas Generation (see Figure 27.4)

The objectives of this section are to maximize the production of synthesis gas and to ensure its purity, for which the following specifications apply: (1) a molar ratio of hydrogen to nitrogen of 3 (ideally, this ratio needs to be stoichiometric in the feed to the NH_3 converter rather than in the feed to the synthesis loop), (2) water free, (3) CO and CO_2 under 1 ppm each, and (4) minimum inerts (argon and CH_4). To achieve these objectives, the following steps are employed:

Step 1: Methane is combined with reformer steam and fed to the reformer in which most of the methane is converted to hydrogen. The reformer is a furnace in which the reaction mixture flows through tubes arranged along the furnace wall. It is modeled in UniSim® Design as a pair of coupled PFRs: One PFR, fed by fuel and air (with flow rates set to a ratio of 1:18.8 in SET-3 to ensure excess air of 15%) models the furnace, whose duty is equal to that required by the second PFR, R-100, modeling the reformer tubes. R-100 is fed by a mixture of methane and reformer steam with molar flow rates in a desired ratio set by SET-1, initially at 1.4. In the initial design, the effluent temperature of the reformer tubes is set to 1,230°C, with the effluent temperature of the furnace set to be 50°C hotter by adjusting the furnace fuel flow rate (using ADJ-1). The following reactions take place in the reformer tubes:

$$CH_4 + H_2O \rightleftharpoons 3H_2 + CO \tag{27.1}$$

$$CO + H_2O \rightleftharpoons CO_2 + H_2 \tag{27.2}$$

According to Parisi and Laborde (2001), reaction rates for these two reactions are:

$$-r_{CH_4} = k_{1,\infty} \cdot \exp[-E_1/RT] \cdot \left(P_{CH_4} P_{H_2O} - \frac{P_{CO} P_{H_2}^3}{\exp\left[\frac{-27464}{T} + 30.707\right]} \right) \quad [\text{kgmol/m}^3 - \text{s}] \tag{27.3}$$

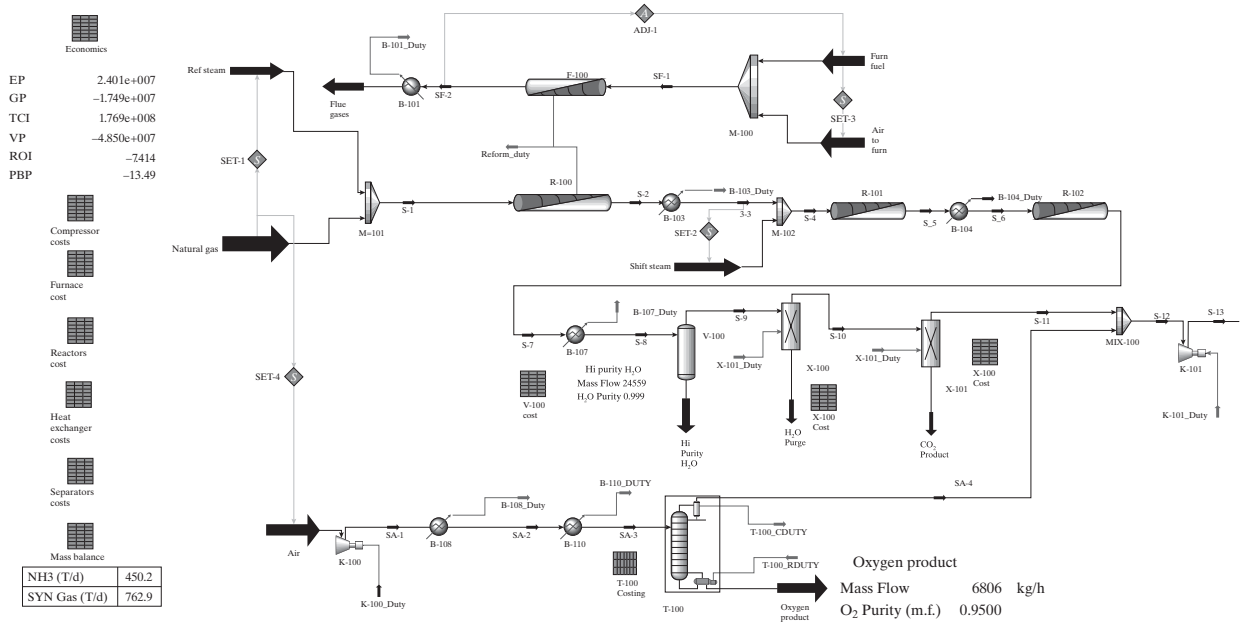

Figure 27.6 UniSim® Design PFD for the base-case design: Synthesis gas section.

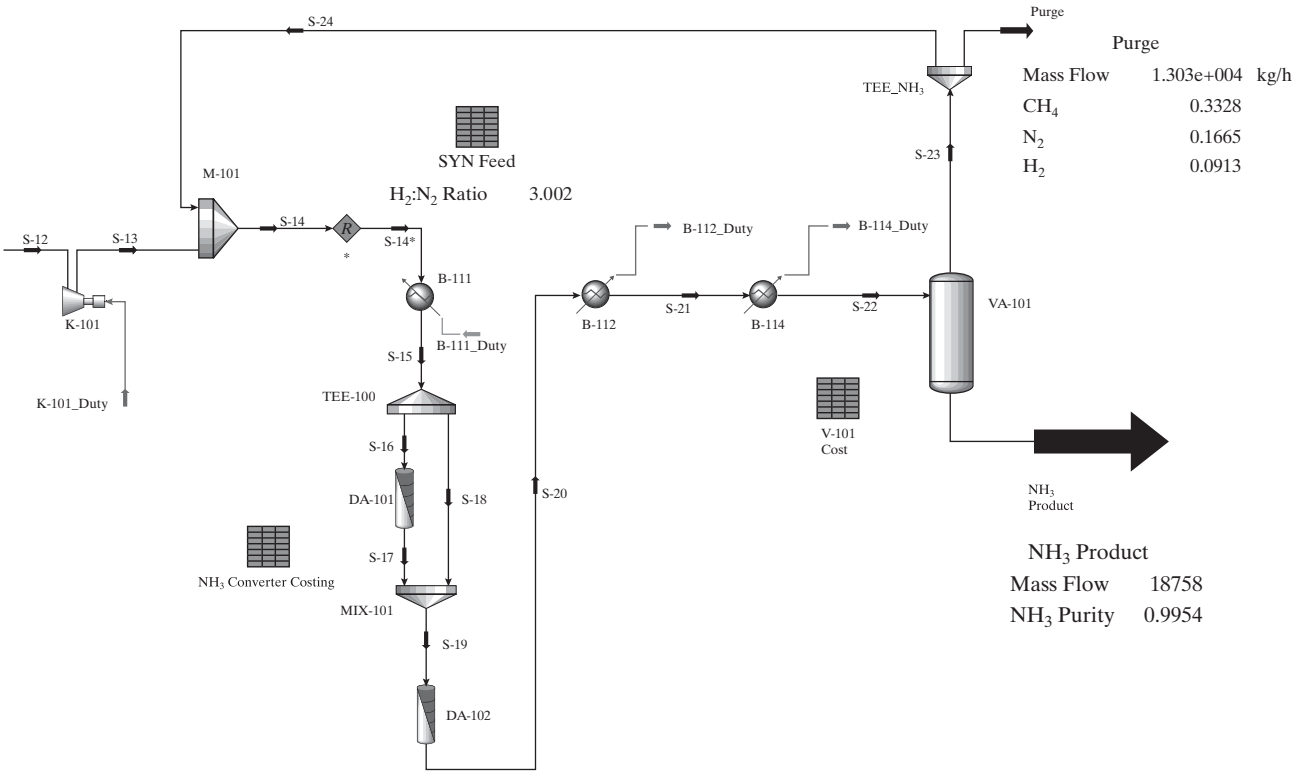

Figure 27.7 UniSim® Design PFD for the base-case design: Synthesis loop section.

$$-r_{CO} = k_{2,\infty} \cdot \exp[-E_2/RT] \cdot \left(P_{CO} P_{H_2O} - \frac{P_{CO_2} P_{H_2}}{\exp\left[\frac{4048}{T} - 3.765\right]} \right)$$

$$[\text{kgmol/m}^3 - \text{s}] \qquad (27.4)$$

Note that in the above equations, the species partial pressures are in atm, and T is the temperature in K. These authors provide the following kinetic parameters:

$$E_1 = E_2 = 16{,}000 \text{ kJ/kgmol},$$
$$k_{1,\infty} = 200 \text{ kgmol/m}^3 - \text{s},$$
$$\text{and } k_{2,\infty} = 100 \text{ kgmol/m}^3 - \text{s}.$$

The furnace is fired by combustion of the fuel, assumed to be pure methane:

$$CH_4 + 2O_2 \rightarrow CO_2 + 2H_2O \qquad (27.5)$$

According to Wolf et al. (1997), the reaction rate for the above reaction takes the mathematical form:

$$-r_{CH_4} = \frac{k_{3,\infty} \cdot \exp[-E_3/RT] \cdot P_{CH_4} P_{O_2}}{(1 + K_{CH_4} P_{CH_4} + K_{O_2} P_{O_2} + K_{CO_2} P_{CO_2} + K_{H_2O} P_{H_2O})^2}$$

$$[\text{kgmol/m}^3 - \text{s}] \qquad (27.6)$$

Note that in these equations, the species partial pressures are expressed in kPa, and T is the temperature in K. Wolf et al. (1997) provide kinetic parameters as follows:

$$K_{CH_4} = 1.1 \times 10^{-6} \cdot (-E_{CH_4}/RT),$$
$$E_{CH_4} = 34{,}200 \text{ kJ/kgmol}$$
$$K_{O_2} = 1.1 \times 10^{-2} \cdot (-E_{O_2}/RT),$$
$$E_{O_2} = 28{,}400 \text{ kJ/kgmol}$$
$$K_{CO_2} = 1.5 \times 10^{-4} \cdot (-E_{CO_2}/RT),$$
$$E_{CO_2} = 32{,}900 \text{ kJ/kgmol}$$
$$K_{H_2O} = 5.3 \cdot (-E_{H_2O}/RT),$$
$$E_{H_2O} = 27{,}300 \text{ kJ/kgmol}$$

The two remaining principal kinetic parameters were selected to be:

$$E_3 = 32{,}000 \text{ kJ/kgmol and}$$
$$k_{3,\infty} = 1{,}000 \text{ kgmol/m}^3 - \text{s}.$$

Step 2: Because the first reaction step also generates CO, which would poison the ammonia synthesis catalyst, a shift reactor is employed to convert CO to CO_2, modeled in UniSim® Design as an adiabatic PFR. In the initial design, the reformer effluent is fed to a cooler, B-103, which allows the adjustment of the feed temperature to a single shift reactor, R-101, while generating HP steam. In R-101, the

so-called water-gas shift reaction takes place in the shift reactors:

$$CO + H_2O \rightleftharpoons CO_2 + H_2 \tag{27.2}$$

The same kinetic form is used as in Eq. (27.4).

Step 3: The shift effluent is cooled using B-104 and then fed to a methanator, R-102, modeled in UniSim® Design as an adiabatic PFR where any remaining CO reacts reversibly to methane. Note that the reaction rate in Eq. (27.3) applies with the operating temperature sufficiently low to ensure that the reverse reaction dominates. In the initial design, the methanator feed temperature is selected as 50°C.

Step 4: The water produced in the previous reaction steps is removed next. In the initial design, heat exchanger B-107 cools the methanator effluent to 40°C, condensing the water, which is removed largely in the flash vessel, V-100. Residual water is removed using adsorption beds, modeled using a separator, X-100, in UniSim® Design.

Step 5: The CO_2 produced in the previous steps is removed next. The proposed design uses PSA to remove the CO_2 which is modeled in UniSim® Design as a separator, X-101. In the initial design, the overhead produced from X-101 is a stream of 85 mol% hydrogen and 15 mol% methane, requiring nitrogen to be added before being fed to the synthesis loop.

Step 6: In parallel with the preceding process, the Linde Concept also involves an additional section to produce nitrogen from air. In the initial design, air is compressed in compressor K-100 to 13 bar and then cooled, first by cooling water in B-108 and then using liquid nitrogen in B-110, and is then fed to the air separation column, T-100, which produces 99.9 mol% nitrogen as a distillate, which is mixed with the overhead product of X-101 for synthesis gas, and 95 mol% oxygen and a bottoms byproduct. The column's condenser is cooled using liquid nitrogen, and its reboiler is heated by low pressure steam.

Ammonia Synthesis Loop (see Figure 27.7)

The objectives of this section are to maximize the ammonia production and to ensure its purity (99.5 mol%). To achieve these objectives, the following steps are employed:

Step 1: The synthesis gas is compressed to the operating pressure of the synthesis loop in compressor K-101, 150 bar in the initial design.

Step 2: The synthesis gas is combined with the recycle stream from the vapor effluent of the flash vessel, VA-101.

Step 3: The combined feed from the mixer, MIX-101, is fed to heat exchanger, B-111, where it is preheated to the ignition temperature before being split into a feed stream to the first packed bed reactor, PFR-1, and its bypass stream. The two split streams are then combined and fed into a second packed bed reactor, PFR-2. The reaction in the adiabatic beds is:

$$0.5\ N_2 + 1.5\ H_2 \rightleftharpoons NH_3 \tag{27.7}$$

The rate of reaction is given by the following kinetic expression (Tempkin and Pyzhev, 1940):

$$-r_{N_2} = 10^4 \exp\left[-9.1 \times 10^4/RT\right]^{-91{,}000/RT} P_{N_2}^{0.5} P_{H_2}^{1.5} - 1.3 \times 10^{10} \exp[-1.4 \times 10^5/RT] P_{NH_3}, \tag{27.8}$$

where $-r_{N_2}$ is the rate of nitrogen disappearance in kmol/m^3–s, T is the temperature in K, P_i are the partial pressures of the reacting species in atm, and the activation energies for the forward and reverse reactions are in kJ/kmol.

Step 4: In the initial design, the hot reactor effluent is first cooled using cooling water in heat exchanger B-112 and then further cooled in heat exchanger B-114 with expensive liquid methane refrigerant. The cooled converter effluent is flashed in VA-101 to liquid ammonia product with the vapor stream is recycled.

Step 5: A purge stream is withdrawn from the vapor recycle in TEE-NH3 composed of 14% of the vapor stream from VA-101.

Profitability Measures. The economic potential and gross profit are computed as follows:

$$EP = \sum_i R_i - \sum_i C_{RM,i} \tag{27.9}$$

$$GP = EP - \sum_i C_{WA,i} - COS \tag{27.10}$$

where EP and GP are the economic potential and gross profit in \$/year, R_i is the revenue on product i in \$/year, $C_{RM,i}$ is the cost of raw material i in \$/year, $C_{WA,i}$ is the penalty associated with waste stream i in \$/year, and COS is the annual *cost of sales*, which accounts for the costs associated with utilities and labor:

$$COS = \sum_i C_{U,i} + L$$

where $C_{U,i}$ is the cost of utility i in \$/year, and L is the total annual cost of paying salaries to staff. Following Chapter 17, it is estimated that six operators, one lab technician, and one control technician will be needed per shift with five shifts required, giving a value of L = \$2,775,000/year.

Obviously, the objective is to design a process that maximizes GP while minimizing the total capital investment (TCI), computed by summing the equipment purchase costs and multiplying by a factor, F, that includes the additional costs associated with equipment installation, storage and utility facilities, and other contingencies (see Chapter 16 for more details):

$$TCI = F \cdot \sum_i C_{CP,i} + CAT \tag{27.11}$$

where $C_{P,i}$ is the purchase cost of equipment item i in \$, the term *CAT* accounts for the one-time charges such as the cost of catalysts and membranes, and the factor $F = 5.38$ is selected, following the example in Chapter 16 (see Tables 16.14 and 16.15 and accompanying explanations). The revenues and raw material costs are estimated on the basis of 24 hr/day, 330 day/year operation of the process and using the material balances obtained from UniSim® Design. Methods for the estimation for equipment purchase costs are itemized in Chapter 16.

The three profitability measures (discussed in Chapter 17) that will be used to assess the design are as follows:

1. Return on investment (ROI), computed as:

$$\text{ROI} = 100\frac{\text{GP}(1-t)}{\text{TCI}}\ [\%] \tag{27.12}$$

where t is the tax rate ($t = 0.25$ will be used). Note that Eq. (27.13) does not account for the time value of money. More accurate expressions could be used such as those described in Chapter 17. For the assessment of the design, the expression of Eq. (27.13) suffices. A value of 25% for ROI is considered promising.

2. Pay back period (PBP), approximated by the expression:

$$\text{PBP} \approx \frac{\text{TCI}}{\text{GP}(1-t)} = \frac{100}{\text{ROI}}\ [\text{years}] \tag{27.13}$$

Note that a more accurate estimate for PBP accounts for depreciation of capital investment. It is unlikely that a project with a PBP of more than four years would be considered.

3. Venture profit (VP), approximated by:

$$\text{VP} = \text{GP}(1-t) - i_m\text{TCI}\ [\$/\text{year}] \tag{27.14}$$

where i_m is the minimum acceptable rate of return payable to venture capitalists that finance the project, taken here as $i_m = 0.2$. Clearly, one is interested in a positive value for VP, and the larger the better!

Sensitivity Analysis. For a complex process, it helps to identify the decision variables having the greatest effect on the profitability with a comparable effect on the plant feasibility, such as the critical-to-quality (CTQ) variables in product design. These decision variables are:

- ***Production Rate.*** Because the desired production rate is 450 MTD of ammonia, the feed rate of methane to the synthesis gas section must be adjusted to maintain it. The objective should be to minimize the required feed rate of natural gas to keep costs of raw materials as low as possible. Furthermore, because the furnace must be maintained hotter than the reformer operating temperature (we assume 50°C is a sufficient excess), this will also fix the required furnace fuel feed rate.
- ***Steam/methane Ratio.*** This strongly affects the conversion of methane to hydrogen. Two such ratios need to be selected: the ratio feeding the reformer and a second ratio between the reformer effluent stream and the feed rate of additional shift steam before the shift reactor section.
- ***Feed Temperatures of the Shift Reactor(s).*** These control the conversion of CO to CO_2. Note that the initial design includes only one shift reactor with poor temperature control, and, consequently, the CO composition in the methanator feed is almost 8 mol%. This CO is subsequently converted to methane in the methanator, leading to high inert (CH_4) concentrations in the synthesis loop, significantly reducing its efficiency and profitability.
- ***Air/methane Ratio.*** The feed rate of air is adjusted to maintain H_2/N_2 ratio in the synthesis gas fed to the converter at 3:1.
- ***Synthesis Loop Pressure.*** The synthesis loop of the initial design operates at 150 bar. The conversion per pass increases with increasing pressure as do the equipment and operating costs.
- ***Feed Temperature to the Ammonia Converter.*** This should be adjusted to the lowest possible value that guarantees a reasonable stability margin, that is, avoids operation in the vicinity of multiple steady states (see Figure 8.10). It is noted that the initial design has a poorly designed ammonia converter.
- ***Control of "Cold-shot" Bypasses in the Ammonia Converter.*** The fractions of feed in the bypasses permit the conversion per pass to be maximized as discussed in Example 8.5.
- ***Energy Management.*** There are several opportunities for energy savings, following several examples introduced in Chapter 11, involving heat transfer between hot and cold streams as well as improved selection of utility streams as will be shown.

The initial design returns an economic potential of \$24 MM/year, and it fair to ask how this value compares with the maximum that could be achieved. This estimate is based on the following assumptions:

1. ***Reactions.*** Because the synthesis gas section must be designed to avoid the production of CO, which would poison the synthesis reaction catalyst, the overall methane reforming is assumed to follow this stoichiometry:

$$CH_4 + 2H_2O \rightleftharpoons 4H_2 + CO_2 \tag{27.15}$$

For the ammonia synthesis reaction, we have:

$$3H_2 + N_2 \rightleftharpoons 2NH_3 \tag{27.16}$$

Combining these two reactions produces the basis for the economic potential calculation:

$$\tfrac{3}{8}CH_4 + \tfrac{3}{4}H_2O + \tfrac{1}{2}N_2 \rightleftharpoons NH_3 + \tfrac{3}{8}CO_2 \tag{27.17}$$

The following table presents the molecular masses (MW) and assumed prices of all of the species that appear in the basis equation, noting that each mole of CH_4 consumed produces one mole of CO_2, assumed to be transferred at no cost or revenue to other processes as a raw material.

Commodity	MW(kg/kgmol)	Assumed Revenue($/kg)
Ammonia	17.031	0.60
Methane	16.04	−0.20
Process Steam	18.015	−0.05
Nitrogen[a]	28.015	0.00
Carbon dioxide	44.01	0.00

[a]Nitrogen is assumed to be available from air for free.

2. ***Reaction Extents.*** Both main reactions (27.9) and (27.10) are assumed to have 100% conversion, although this is not true in either case. However, as will be shown, the profitability of the overall process depends on the methane conversion and indeed, conversions of over 99% are possible. As for the ammonia conversion, by recycling and optimally operating the process, it is also possible to bring the overall hydrogen conversion to over 99%.

The following table summarizes the economic potential calculation based on 100% conversion on the basis of reaction (27.18).

Stoichiometry	$\frac{3}{8}CH_4$ +	$\frac{3}{4}H_2O$ +	$\frac{1}{2}N_2$ ⇌	NH_3 +	$\frac{3}{8}CO_2$
Molar balance (kgmol/kgmol NH_3)	$\frac{3}{8}$	$\frac{3}{4}$	$\frac{1}{2}$	1	$\frac{3}{8}$
Mass balance (kg)	6.015	13.5113	14.007	17.031	16.5038
kg/kg NH_3	0.3532	0.7933	0.8225	1	0.9690
Revenue ($/kg)	−0.20	−0.05	0	0.60	0

Thus, the revenue would be $0.60 - 0.2 \times 0.3532 - 0.05 \times 0.7933 - 0 \times 0.9690 = \$0.4897/\text{kg NH}_3$. For a production rate of 450 MTD, this is equivalent to an economic potential of $\$72.72 \times 10^6$/year, that is, about three times larger than that attained by the initial design. Evidently, further refinement of the initial design is justified. Note that the estimation of the economic potential neglects three items: (1) the possible revenue from the oxygen separated from the nitrogen in air (the actual revenue would be $0.17/kg, (2) the cost of the additional methane used to fire the furnace that drives the endothermic reforming of methane (the actual cost would be $0.2/kg), and (3) the environmental penalty incurred from CO_2 emissions from the furnace (the actual cost would be $0.05/kg). It is also noted that at 2007 prices for ammonia of $0.27/kg, the economic potential is reduced to only $\$23.71 \times 10^6$/year, explaining why an ammonia plant at 350 MTD was infeasible in 2007.

27.3 DESIGN REFINEMENT

A mind map, such as the one shown in Figure 27.8 for the analysis of the low profitability in the initial design, could be the useful result of a brainstorming exercise performed by the design team. In a mind map, the main idea being analyzed, in this case the low productivity of the process, is positioned in the center of the diagram to which associated ideas are attached. The degree to which the additional concepts are important can be emphasized by the font size used to present them and/or by the thickness of the lines connecting them to the previous concept. As shown in the diagram, the low profitability of the initial design is caused by three main weaknesses: low economic potential, high equipment costs, and high operating costs. These are analyzed in detail next.

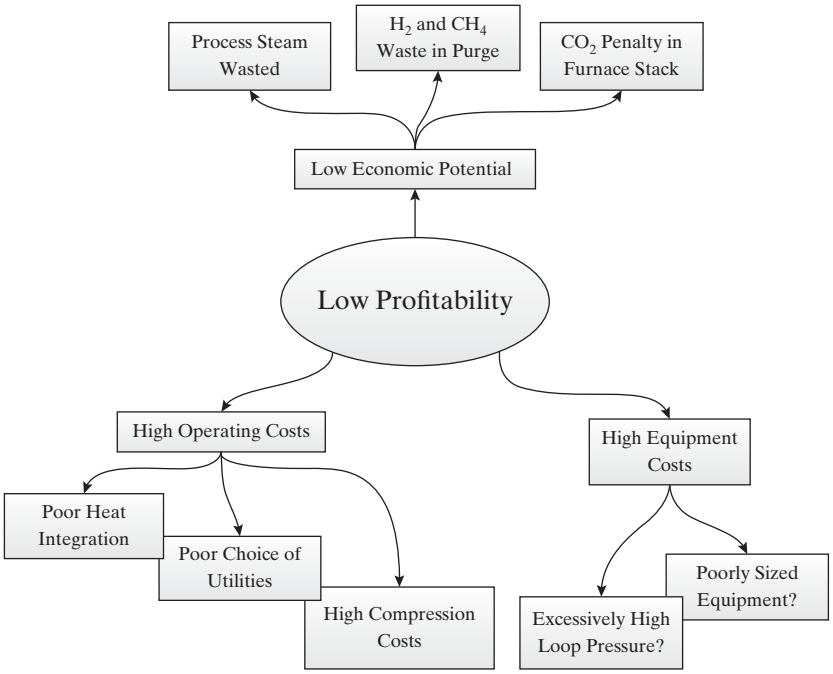

Figure 27.8 Analysis of low profitability using a mind map.

Low Economic Potential

This is due to a combination of three effects:

1. ***Water Waste.*** The reforming and shift reactions are both favored by excess steam, and, as a consequence, the combined process feed contains huge quantities of steam, leading to a large production rate of high purity water. Because this is not recycled in the initial design, the economic potential is unnecessarily reduced.
2. ***Wasted Hydrogen and Methane in the Synthesis Loop Purge.*** The large purge rate required is due to: (a) The percentage of inerts in the synthesis gas, especially CH_4, is excessive (the composition of methane is 11.8 mol%), mainly due to the relatively large concentration of CO remaining in the synthesis gas effluent from the shift converter, which is subsequently converted to methane in the methanator, and (b) the low conversion rate; the ammonia composition in the NH_3 converter effluent is about 11.5 mol% due to the excessive amount of inerts in the converter feed (over 26 mol%, despite the relatively large purge rate) and the poor performance of the converter.
3. ***High CO_2 Emission Penalties.*** This is a consequence of the large furnace used to heat the reformer, partly due to its relatively high operating temperature and partly due to the large methane feed that is required.

High Equipment Costs

The initial design has a TCI of \$177 MM, which reduces the VP by about \$35 MM/year. This relatively large value is partly due to the high operating pressure of the synthesis loop and possibly to poorly designed and sized equipment.

High Operating Costs

In the initial design, the high operating costs reduce the VP by \$17 MM/year. This excessively high cost of sales is mostly due to poor energy management characterized by the lack of heat integration, the relatively expensive utilities selected, and the high compression costs associated with the high-pressure synthesis loop.

Stepwise Process Improvements

All of weaknesses identified in the mind map analysis are addressed in a stepwise procedure aimed at systematically improving profitability. Due to space limitations, only the key improvements are highlighted next:

Step 1: ***Recycling water.*** The first and simplest modification is to recycle the high-purity water produced in the synthesis gas section. As shown in Figure 27.9, this involves the addition of pump P-100 and a heat exchanger B-105, heated by high pressure (HP) steam, to produce process steam at 15 bar used to largely offset the plant's process steam requirements. This simple change increases the economic potential by almost \$10 MM/year.

(You can test this out for yourself. Start with the initial design in the UniSim® Design case file NH3 _PROCESS_4E_STEP_0.usc and, try to reproduce the results in the file NH3 _PROCESS_4E_STEP_1.usc.) These files, as well as the rest of the case files referred to in this chapter, can be downloaded from the Wiley site associated with this book.

Step 2: ***Optimization of Methane Reforming.*** First, the operating temperature in the reformer is reduced to 1,050°C, which ensures almost complete methane conversion while reducing both the cost of the reformer and the magnitude of the CO_2 emission penalty (the amount of fuel required by the furnace after this step is reduced by almost 50%). Increasing the steam/methane ratio improves hydrogen production, but it also increases costs, and so reasonable values are selected: a molar ratio of 1.9 for the feed to the reformer and a molar ratio of 0.9 for the shift section. To improve CO conversion, the shift section is expanded to include two reactors, and the feed temperatures to each reactor are adjusted to minimize the CO composition in the effluent of each of the two units: The optimal temperature of stream S-3 is found to be 650°C whereas that of stream S-5 is found to be 390°C, lowering the CO composition in the methanator feed to under 0.8 mol%. As a consequence, the methane composition in the synthesis gas drops to 1.9 mol%. Both of the shift-reactor coolers generate HP steam, providing significant revenues. As shown in Figure 27.10 and Table 27.3, these changes lead to an increase of the economic potential to \$56.42 MM/year, equivalent to a GP of \$4.86 MM/year, and a VP of −\$29.81 MM/year. Although the profitability is improved, it remains unacceptable. (You can test this out for yourself. Starting Starting with the design in the UniSim® Design case file NH3_ PROCESS_4E_STEP_1.usc, try and reproduce the results in the file NH3_PROCESS-4E_STEP_2.usc). Additional improvements are needed in the NH_3 synthesis loop.

Step 3: ***Improvements in the Ammonia Synthesis Loop.*** First, notice that the conversion in the ammonia converter is low. In the initial design, the preheater is positioned incorrectly; it is therefore repositioned after the stream splitter, so that only the feed to the first PFR is heated, thus allowing true "cold shots" to the remaining reactor beds. In addition, as shown in Figure 27.11, the converter is expanded to include three optimally sized fixed beds. Furthermore, as shown in the multimedia modules that can be downloaded from www.seas.upenn .edu/~dlewin/multimedia.html (*HYSYS → Tutorials → Process Design Principles → Ammonia Converter* Design; and *ASPEN → Tutorials → Reactor Design* Principles → *Ammonia Converter Design*), the conversion can be significantly enhanced by adjusting

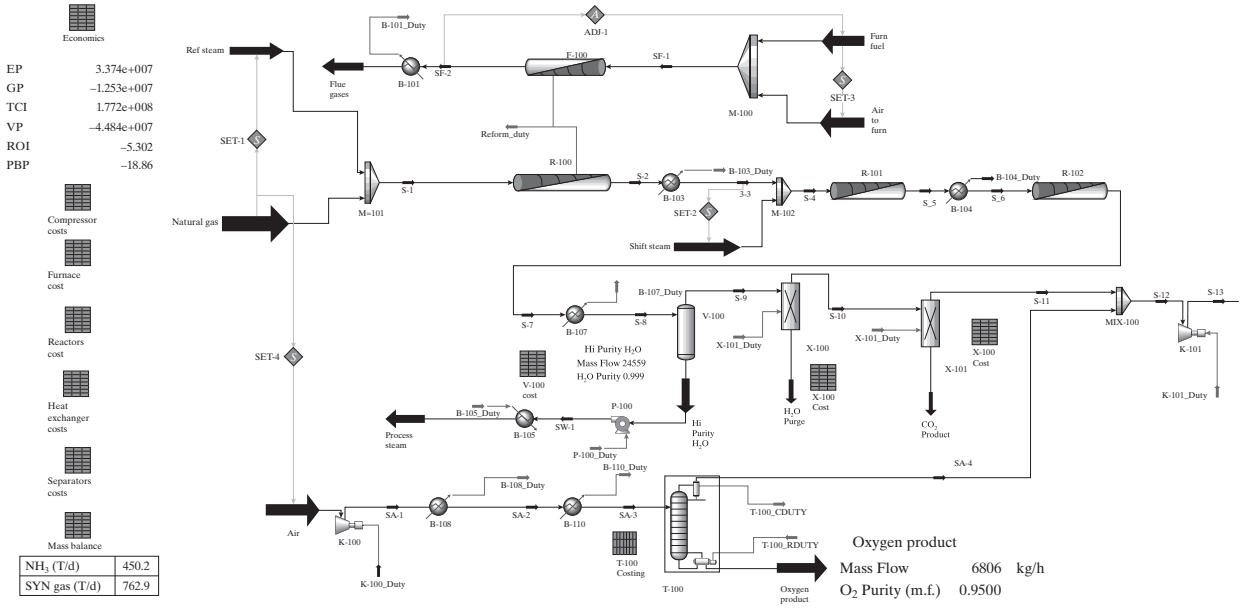

Figure 27.9 UniSim® Design PFD for Step 1: Water recycled as process steam in the synthesis gas section.

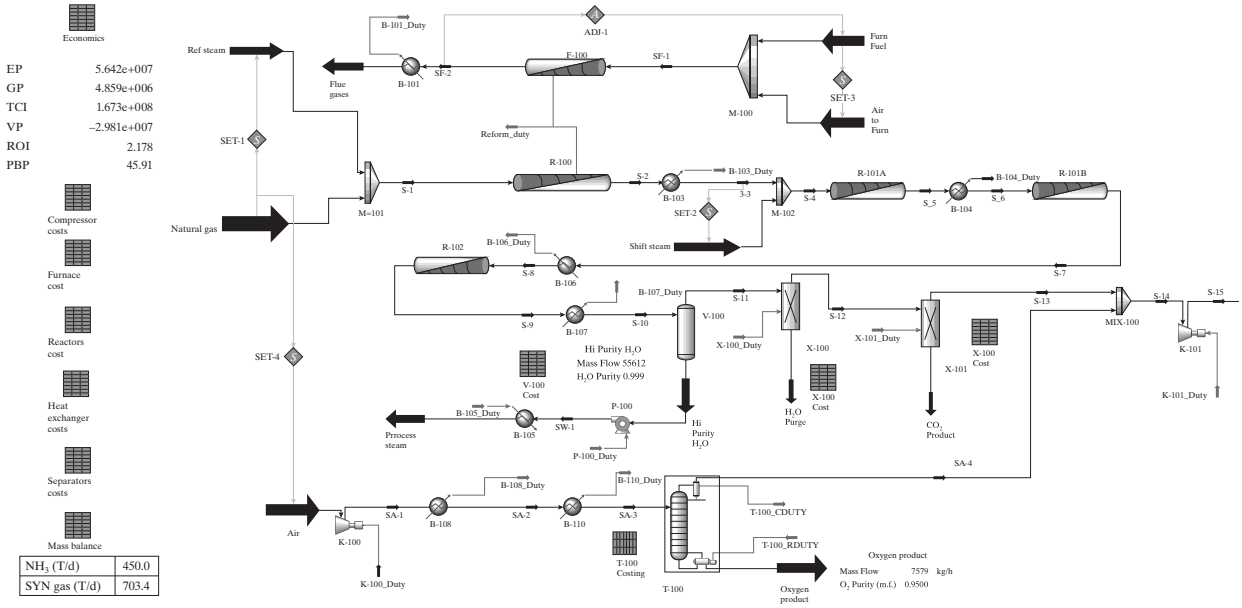

Figure 27.10 UniSim® Design PFD for Step 2: Optimization of methane reforming in the synthesis gas section.

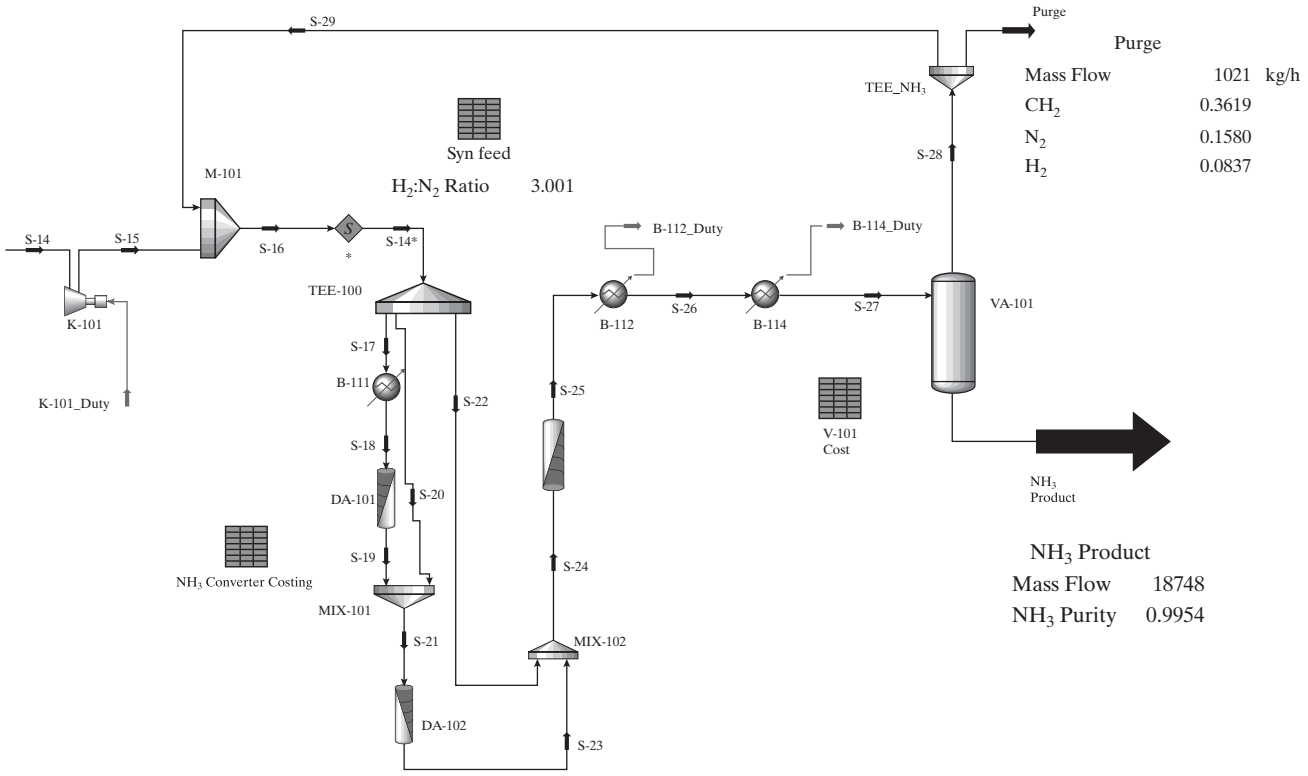

Figure 27.11 UniSim® Design PFD for Step 3: Synthesis loop section for improvements in the NH3 synthesis loop step.

Table 27.3 Profitability Analysis by Improvement Step

Step	Description	EP ($MM/year)	GP ($MM/year)	TCI ($MM)	VP ($MM/year)
0	Initial feasible design. Synthesis loop operates at 150 bar.	24.01	−17.49	176.9	−48.50
1	Water product recycled as process steam.	33.74	−2.53	177.2	−44.84
2	Optimization of methane reforming, and shift reactions to fully convert methane while minimizing CO production.	56.42	4.86	167.3	−29.81
3	Ammonia converter redesigned, synthesis loop purge reduced from 14 to 1.5%, and the methane content in purge stream is recycled as furnace fuel.	67.25	27.73	124.6	−4.13
4	Improvements in unit operations: T-100 sizing, reactor sizing, and improved selection of cooling utilities to reduce costs. Purge adjusted to meet product specifications.	62.04	32.24	141.9	−4.21
5	Design of HEN to reduce operating costs.	62.04	45.82	141.6	6.05
6	Synthesis loop operating pressure reduced to 100 bar. Purge adjusted to meet product specifications.	63.26	47.82	126.5	10.56
7	Synthesis loop operating pressure reduced to 90 bar. Purge adjusted to meet product specifications.	63.83	48.65	120.6	12.06
8	Recovery and recycle of hydrogen from purge using membrane separation in 90 bar synthesis loop design.	68.75	53.86	119.6	16.47

the cold-shot fractions. Consequently, both cold-shot fractions are increased from 0.1 to 0.2. Finally, because the methane composition in the synthesis loop feed has been reduced in the previous step, the purge rate can be lowered from 14% to just 1.5%. It is also assumed that the methane content in the purge stream can be used to partially offset the furnace fuel requirement. As shown in Table 27.3, these changes increase the economic potential to $67.25 MM/year, equivalent to a GP of $27.73 MM/year, and a VP

of −$4.13 MM/year. Note also that the TCI is sharply decreased to a value of $124.6 MM as a consequence of this step (You can test this out for yourself. Starting with the design in the UniSim® Design case file NH3_PROCESS_4E_STEP_2.usc, try and reproduce the results in the file NH3_PROCESS_4E_STEP_3.usc.).

Step 4: ***Improvements in the Individual Unit Operations.*** Several changes are introduced to improve the local performance of unit operations: (a) the air-separation column, T-100, is resized, increasing the number of theoretical trays from 35 to 50, reducing the duties of the condenser and reboiler, thus decreasing operating costs; (b) the length of the first shift reactor is reduced by one-half with no significant effect on the overall performance of the shift section; (c) the feed temperature to T-100 is increased from −161 to −150°C, thus allowing liquid methane refrigerant to replace the liquid nitrogen used before in heat exchanger B-110; (d) the feed temperature to flash drum VA-101 is increased from −130 to −80°C, thus allowing liquid ethane refrigerant to replace the liquid methane used before in heat exchanger B-114. This last change causes an increase in the methane composition in the overhead vapor line from VA-101 compensated for by increasing the purge rate. All of these changes reduce operating costs at the expense of increased equipment costs. (You can test this out for yourself. Starting with the design in the UniSim® Design case file NH3_PROCESS_4E_STEP_3.usc, try and reproduce the results in the file NH3_PROCESS_4E_STEP_4.usc.).

Step 5: ***Heat Integration.*** As shown in Figures 27.12 and 27.13, there are numerous opportunities to save operating costs through heat integration: (a) the water recycle heat exchanger, B-105, is positioned in the process line to cool the effluent of shift reactor R-101B, saving all of the HP steam used in Step 1; (b) similarly, the preheater B-111 is heated by the effluent from PFR-3, saving the HP steam used there; and (c) the air-separation column, T-100, is integrated as in Example 11.14 so that its reboiler is heated by cooling the compressed air fed to the column, thus saving the LP steam used previously. The other changes involve substituting cheaper coolants to the extent possible: (d) B-109 is installed, using liquid ammonia refrigerant to reduce the load on B-110 that uses more expensive methane refrigerant; and (e) B-113 is installed, using liquid ammonia refrigerant to reduce the load on B-114 that uses more expensive ethane refrigerant. It is noted that the three instances of heat integration eliminate the need for external heating utilities. All of these changes have no effect on the economic potential but increase both the GP to $45.82 MM/year and the VP, to $6.05 MM/year as seen in Table 27.3. It is noted that the ROI is now in excess of 24%, meaning that the process is henceforth an attractive proposition! (You can test this out for yourself. Starting with the design in the UniSim® Design case file NH3_PROCESS_4E_STEP_4.usc, try and reproduce the results in the file NH3_PROCESS_4E_STEP_5.usc).

It is quite possible that a formal pinch analysis of the type discussed in Chapter 11 may yield even better results. This is left as an exercise to the reader (try Exercise 27.4).

Step 6: ***Reducing the Synthesis Loop Operating Pressure to 100 bar*** With the synthesis loop at 150 bar, the compressor K-101 contributes about 50% of the capital investment and 100% of the operating costs for the entire process. Clearly, the next step in cost savings involves attempting to reduce the operating pressure of the loop. A reduction to 100 bar makes significant savings, increasing the GP to $47.82 MM/year, the VP to $10.56 MM/year, and the ROI to 28.4%, largely though the reduction of the TCI to $126.5 MM. (You can test this out for yourself. Starting with the design in the UniSim® Design case file NH3_PROCESS_4E_STEP_5.usc, try and reproduce the results in the file NH3_PROCESS_4E_STEP_6.usc.)

Step 7. ***Reducing the Synthesis Loop Operating Pressure to 90 bar.*** An additional decrease in the operating pressure of the synthesis loop makes more savings, increasing the VP to 12.06 MM/year and the ROI to 29.9%. (You can test this out for yourself. Starting with the design in the UniSim® Design case file NH3_PROCESS_4E_STEP_6.usc, try and reproduce the results in the file NH3_PROCESS_4E_STEP_7.usc.)

Step 8. ***Introducing Membrane Separation to Recover Hydrogen from the Purge Stream.*** Noting that at 90 bar, the purge stream carries away 600 kg/hr (about 20%) of the hydrogen fed to the loop, it makes sense to explore the feasibility of using membrane separation to recover this. As shown in Figures 27.14 and 27.15, a membrane separator is positioned to receive the purge stream as its feed, returning a hydrogen-rich stream as recycle to the loop compressor K-101, and a residual stream

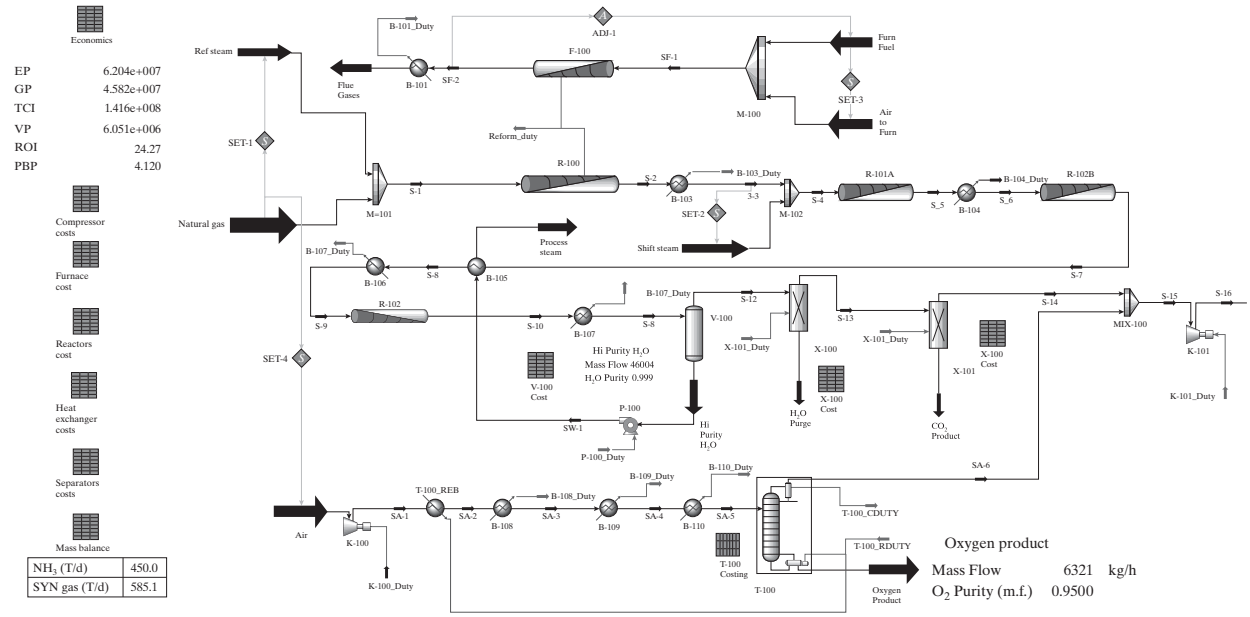

Figure 27.12 UniSim® Design PFD for Step 5: Synthesis gas section: Heat integration step.

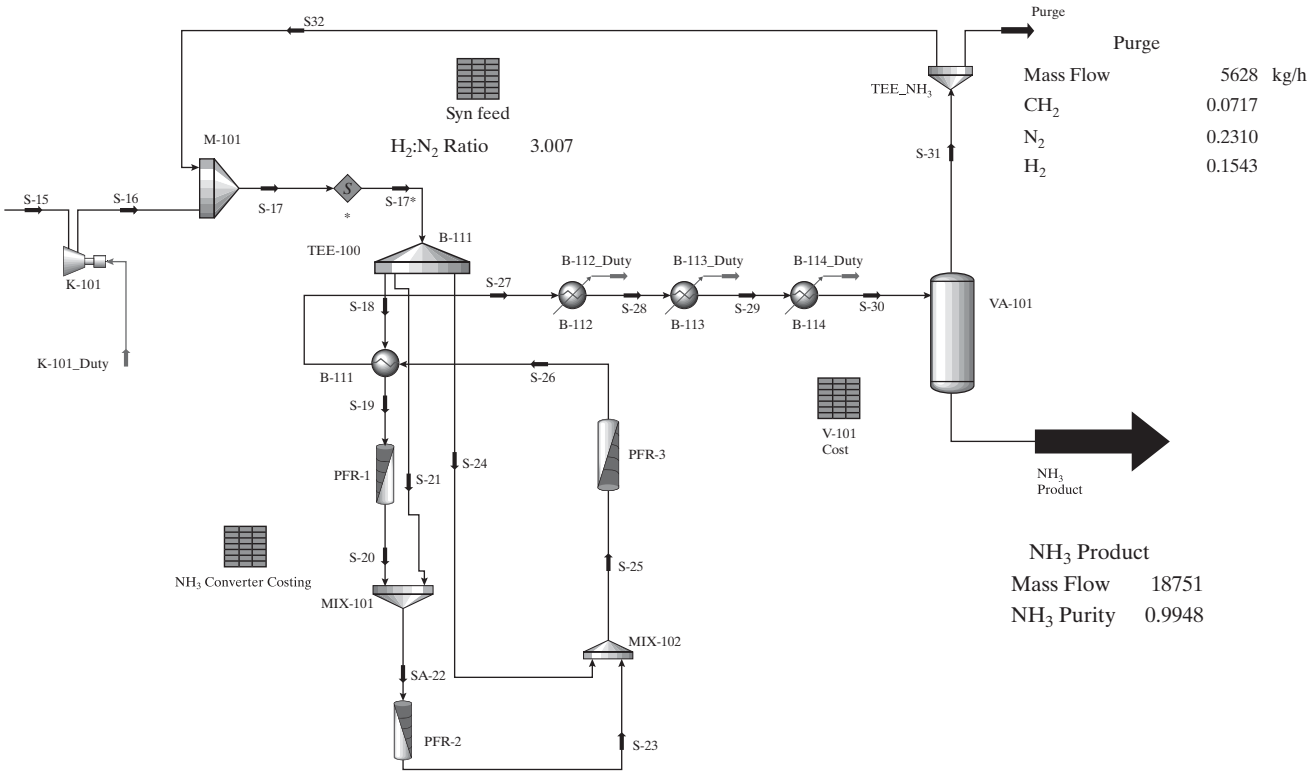

Figure 27.13 UniSim® Design PFD for Step 5: Synthesis loop section: Heat integration step.

containing mainly methane and nitrogen to partially offset the furnace fuel requirement. This component increases the profitability of the process to a VP of \$16.5 MM/year, largely due to the marked increase in economic potential to \$68.75 MM/year (because almost no raw materials are now being wasted). This final step has an ROI of almost 34% with a PBP of just under three years. (You can test this out for yourself. Starting with the design in the UniSim® Design case file NH3_PROCESS_4E_STEP_7.usc, try and reproduce the results in the file NH3_PROCESS_4E_STEP_8.usc.)

Although the economic performance achieved after Step 8 is acceptable, there may be additional opportunities to improve it even further:

- The hot reformer effluent is used to raise steam in heat exchanger B-103. Instead, one might consider using it to preheat the reformer feed, thus reducing the duty of the furnace (see Exercise 27.2).
- No formal MER targeting has been carried out. This is worth doing to check whether there are additional opportunities for energy savings (see Exercise 27.4).
- A heat-mass exchanger was not implemented; doing so also may improve the economics (see Exercise 27.3).

Development Stage

As indicated in Chapter 1, the main task in the *development* stage of the SGPDP, as applied for design of *basic chemical* products, is to carry out a detailed plant design and draw conclusions about the feasibility of the project. This stage remains to be implemented for the ammonia product. See Exercise 27.7.

Postscript

This case study documents the final year of the design project undertaken by undergraduate students of the Wolfson Department of Chemical Engineering at the Technion, Class of 2012. The students addressed a project tender, similar to the file Ammonia Project.pdf addressed in this chapter (download it from the Wiley Web site that accompanies this textbook.) The project results attracted considerable media attention in the wake of the 2006 Lebanese War and the missile bombardment of Haifa, and had a modest contribution to the subsequent decision of the Israeli government to pursue the development of ammonia production capabilities in Israel. Following the completion of the students' projects, the following letter was sent to the Israel Comptroller's Office:

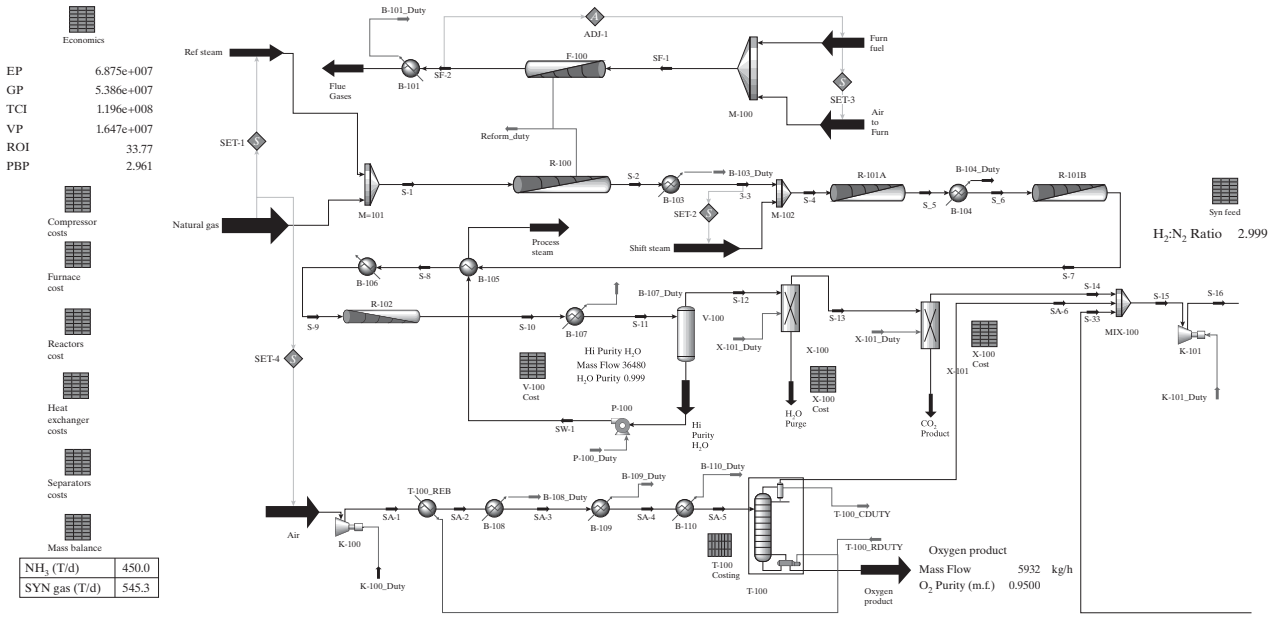

Figure 27.14 UniSim® Design PFD for Step 8: Synthesis gas section with operating pressure lowered to 90 bar, and hydrogen recovery for the purge stream.

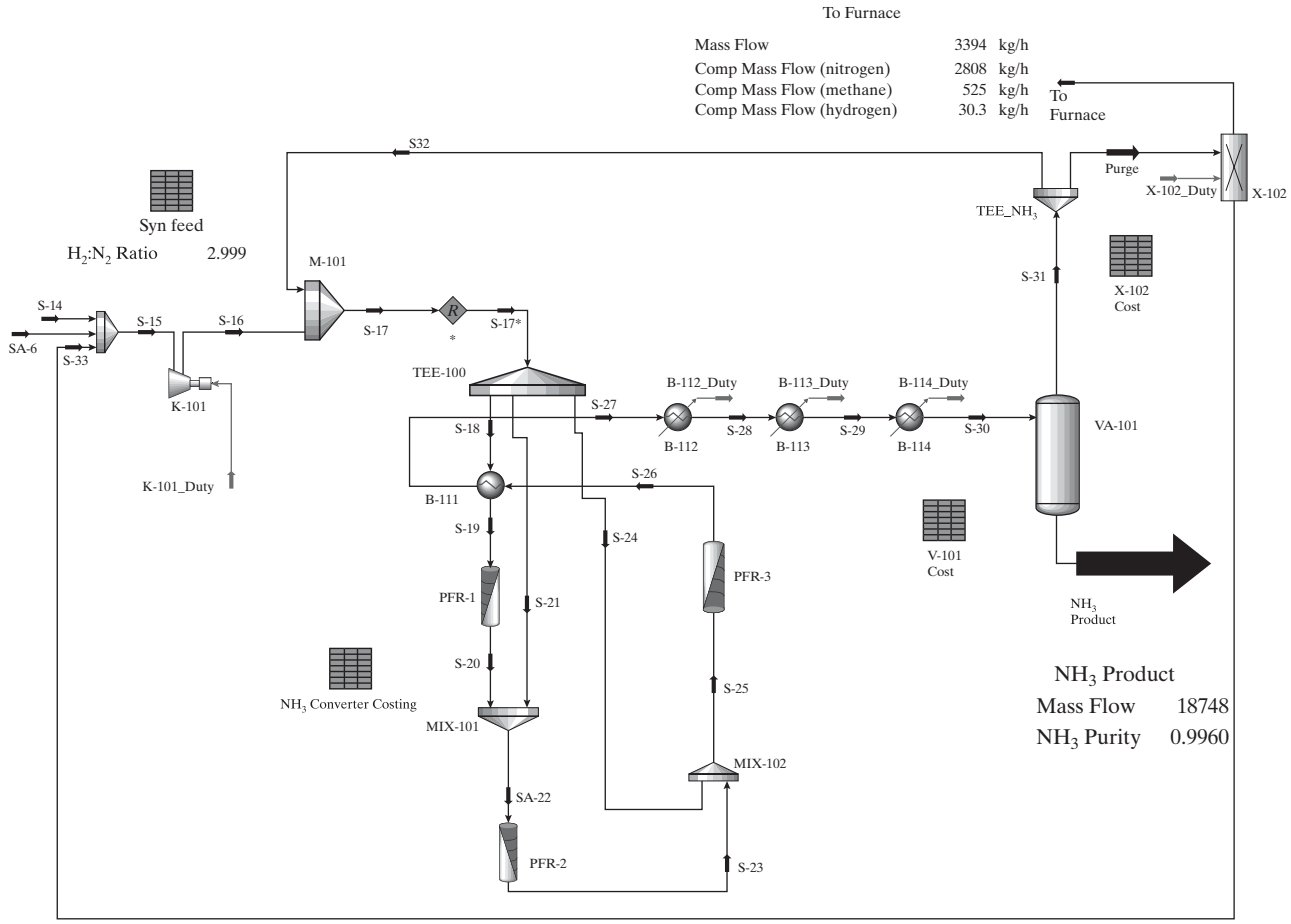

Figure 27.15 UniSim® Design PFD for Step 8: Synthesis loop section with operating pressure lowered to 90 bar, and hydrogen recovery for the purge stream.

The Wolfson Department of Chemical Engineering
Technion, Haifa 32000, Israel
Daniel R. Lewin, Professor
Churchill Family Chair
Tel. +972-4-8292006 Fax. +972-4-8295672
email: dlewin @ techunix.technion.ac.il
http://pse.technion.ac.il

Mr. Yossi Hirsh
Israel Comptroller's Office
Jerusalem

Ref: Ammonia Plant Feasibility Study

Haifa, 25th June 2012

I have been teaching Chemical Process Design at the Technion's Department of Chemical Engineering for approximately 15 years. Each year, I assign my students an extended design project involving a complete chemical plant, culminating in complete chemical process packages. Feasibility studies for processes to manufacture ammonia from natural gas (taken as methane) have been set as design projects twice – once in 2007 and again this year, 2012.

In 2007, the process design involved the use of **conventional technology** (as summarized in Chapter 13 of the Third Edition of the textbook "Product and Process Design Principles," published by Wiley in 2009 (of which I am co-author). I should also note that the sales price taken for ammonia was significantly lower than its price

today (in fact, the market price for ammonia has more than doubled since then, with no significant change to the price of natural gas). The salient conclusions of that study were that the break-even point for the manufacture of ammonia from natural gas is approximately 600 MT/Day (Metric Tons per Day).

In contrast, this year, my students were asked to carry out a feasibility study for the manufacture of 450 MT/Day of ammonia from methane, assuming the following:

- Sales price of ammonia: \$600/MT
- Cost of methane: \$200/MT
- Assumed sales price for CO_2 manufactured: \$100/MT (One mole of CO_2 is produced from each mole of methane consumed)[a]
- Assumed sales price for O_2 manufactured: \$170/MT (approximately 1/3 mole of O_2 is produced for each mole of nitrogen consumed)
- **Linde technology** (separate production train for hydrogen using PSA for the purification step and air separation column for nitrogen, and a conventional ammonia synthesis loop).

The following table summarizes the distribution of results obtained by the sixteen groups of students:

	VP	REV	RAW	OPCOST	GP	TCI
Min	15.12	110.80	20.40	0.05	52.35	106.60
Max	39.92	124.50	42.47	17.66	90.73	158.71
Best	39.92	111.80	21.48	5.95	81.60	106.60

Key:
VP = annual venture profit (after returning 20% interest to venture profit partners, and assuming 15% tax), REV = product revenue, RAW = cost of raw materials (mostly natural gas), OPCOST = annual operating cost, GP = annual gross profit, and TCI = total capital investment (TCI in \$MM, the remaining values in \$MM/year).

Note that all 16 groups of students submitted designs which showed a profit. Based on the findings of this year's design, it would appear that:

a. The construction of a plant to produce 450 MT/Day of ammonia from methane is economically feasible using Linde Technology, with the best designs providing venture profits of the range \$30 – 40 Million/Year.

b. Since most of the market for ammonia is for the manufacture of fertilizer, most of which is produced at Rotem, it would make sense to erect the plant there.

c. The details provided in this letter are preliminary results, obtained by 82 students working in 16 design groups as part of the course "054402 Design and Analysis."

d. The best three designs submitted were refined all the way to comprehensive design packages (including detailed design of all major equipment items and P&IDs of the complete processes) by 57 students enrolled in the course "054410 Plant Design." The final designs were presented on 18th June 2012, and confirmed that it is indeed possible to make 450 MT/Day of ammonia at a healthy profit.

The construction of such a plant would eliminate the need to import ammonia, to store it at the currently unsafe location in the vicinity of Haifa, and will greatly reduce the need for its transportation by road. Of particular interest to your office should be the following:

a. The UK recommendation for the appropriate frequency of inspection is: "First inspection after 6 years, then every 12 years depending on inspection results." Inspection of the ammonia storage tank is only possible after first emptying and completely evacuating the storage tank. As this will of course require the tank to go off-line, the only way to ensure continuous operation is to install a second tank. Jordan imports approximately twice as much ammonia as Israel does, and their storage facilities consist of two tanks, making it possible for them to adhere to the UK inspection recommendations without disturbing production. Regrettably, the Haifa ammonia storage facility consists of a single 12,000 Ton tank, which has never been inspected in almost 30 years of continuous operation.

[a]In the project undertaken by the students, revenue was assumed on the CO_2 produced by the process.

b. Every additional day that the storage facility operates plays with the lives of the residents of Haifa, and the responsibility lies with the operators, the Haifa Municipality and the Government of the State of Israel.

c. The decision in principle to close down the storage facility and to move to ammonia production in the Negev is a welcome one, but actions speak louder than words.

I am at your disposal should you feel a need to further consult with me.

Sincerely,

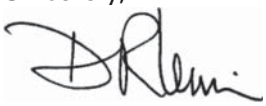

Daniel R. Lewin

REFERENCES

1. Lavie, R., "Ammonia Synthesis Enhancement through Heat-Mass-Exchange," *Plant-Operations Progress,* **6**(2), 122–126 (1987).

2. Parisi, D. R., and M. A. Laborde, "Modeling Steady-state Heterogeneous Gas-solid Reactors Using Feedforward Neural Networks," *Comput. Chem. Eng.*, **25**, 1241–1250 (2001).

3. Tempkin, M. and V. Pyzhev, "Kinetics of Ammonia Synthesis on Promoted Iron Catalyst," *Acta Physicochim. U.R.S.S.*, **12**(3), 327 (1940).

4. Wolf, D., M. Höhenberger, and M. Baerns, "External Mass and Heat Transfer Limitations for the Partial Oxidation of Methane over a Pt/MgO Catalyst—Consequences for Adiabatic Reactor Operation," *Ind. Eng. Chem. Res.*, **36**, 3345–3353 (1997).

EXERCISES

27.1 Sketch the composition-temperature trajectory for the proposed ammonia converter shown in Figure 27.7 and use it to explain why it performs poorly. On the same plot, sketch the composition-temperature trajectory for the modified design shown in Figure 27.11, and comment on the differences.

27.2 Consider the effect on the reductions of CO_2 emissions of introducing a preheater to exchange heat from the effluent of the reformer with the reformer feed. What would be the impact of this change on the profitability of the process, and what are your recommendations as a consequence?

27.3 Consider the effect on profitability of introducing a heat-mass exchanger into the ammonia synthesis loop operating at 90 bar. What is the optimal operating temperature of the flash vessel VA-101 in this case?

27.4 Carry out a formal pinch analysis of the process design presented as Step 8, using the UniSim® Design file NH3_PROCESS_4E_STEP_8_opt_V3.usc:

(a) Compute the MER targets assuming $\Delta T_{min} = 10°C$, and compare them with the total external heat duties implemented in Step 8.

(b) Plot the GCC and estimate the duties of each type of utility, again comparing the results with those implemented in Step 8.

(c) If there is a significant difference between the MER targets and the total external duties implemented in Step 8, suggest an alternative heat exchanger network to the one implemented to more closely match the MER targets, and modify the UniSim® Design case file to realize your HEN. Compute the profitability measures for your modified design and comment on the results.

27.5 As part of an NH_3-product life cycle assessment, evaluate the danger of an ammonia release from a missile attack from a 12,000 ton storage tank. Note that the existing facility is a refrigerated tank at atmospheric pressure.

27.6 As part of an NH_3-product life cycle assessment, consider the alternative of converting ammonia to urea by reaction with CO_2 as a vehicle for curbing the release of the CO_2 byproduct.

27.7 For the ammonia product, carry out the *development* stage of the SGPDP as suggested in Section 27.3.

Appendix I

Residue Curves for Heterogeneous Systems

Beginning with Eq. (9.20), which also applies for heterogeneous systems, the liquid mole fractions, x_j, are replaced by the overall liquid mole fractions, x_j^o. These are accompanied by the equations that define the vapor–liquid and liquid–liquid equilibrium constants, K_j^{VL} and K_j^{LL}, respectively, and the component mass balances, to give

$$\frac{dx_j^o}{d\hat{t}} = x_j^o - y_j, \qquad j = 1,\ldots,C \tag{A-I.1a}$$

$$y_j = x_j^I K_j^{VL}\{T, P, \underline{x}^I, \underline{y}\} \qquad j = 1,\ldots,C \tag{A-I.1b}$$

$$x_j^{II} = x_j^I K_j^{LL}\{T, P, \underline{x}^I, \underline{x}^{II}\} \qquad j = 1,\ldots,C \tag{A-I.1c}$$

$$x_j^o = \alpha x_j^I + (1-\alpha)x_j^{II} \qquad j = 1,\ldots,C \tag{A-I.1d}$$

$$\sum_{j=1}^{C} x_j^I - \sum_{j=1}^{C} x_j^{II} = 0 \tag{A-I.1e}$$

$$\sum_{j=1}^{C} y_j = 1 \tag{A-I.1f}$$

where x_j^I and x_j^{II} are the mole fractions of species j in the first and second liquid phases, respectively, and α is the mole fraction of the first liquid phase in the total liquid. To trace a residue curve from some starting composition, this system of differential-algebraic equations is solved by numerical integration. Equations (A-I.1b)–(A-I.1f) are solved to determine the compositions in vapor–liquid–liquid equilibrium as $\hat{t}$ is advanced in the integration.

Appendix II[1]

Design Problem Statements by Area

[1]The complete Appendix II appears in the file Supplement_to_Appendix_II.pdf, which can be downloaded from the Web site www.seas.upenn.edu/~dlewin/UPenn Design Problem Statements.html. Only the titles of the design problem statements are listed here.

Pharmaceuticals

Biomedicals

Polymers

Electronic Materials

Environment—Air Quality

Environment—Water Treatment

This appendix contains the problem statements for 93 design projects, each prepared for design teams of three or four students at the University of Pennsylvania by chemical engineers in the local chemical industry and by the chemical and biomolecular engineering faculty. At Penn, each team selects its design project during the first lecture course in the fall and spends the spring semester completing the design. In the spring, each group meets regularly with its faculty advisor and industrial consultants, including the individual who provided the problem statement, to report on its progress and gain advice.

The problem statements in the file Supplement_to_Appendix_II.pdf are in their original forms as they were presented to the student design teams on the date indicated. Some provide relatively little information whereas others are fairly detailed concerning the specific problems that need to be solved to complete the design. The reader should recognize that, in nearly every case, as the design team proceeded to assess the problem statement and carry out a literature search, the specific problems it formulated were somewhat different than stated here. Still, these problem statements should be useful to students and faculty in several respects. For students, the statements should help to show the broad spectrum of design problems that chemical engineers have been undertaking in recent years. For faculty members, the statements should provide a basis for similar design projects to be created for their courses.

In formulating design problem statements, the industrial consultants and faculty have sought to create product and process opportunities that lead to timely and challenging designs and that offer a reasonable likelihood that the final design will be attractive economically. Every effort is made to formulate problems that chemical engineering seniors can undertake without unduly gross assumptions and for which good sources of data for the reaction kinetics and thermophysical and transport properties exist. This was accomplished in each of the problems included here; furthermore, a student design team completed successful designs for most of these problems.

As seen in the contents, the projects have been assigned to one of the following areas, in some cases arbitrarily: chemicals, fuel products, gas manufacture, foods, pharmaceuticals, biomedicals, polymers, electronic materials, and environment.

Most of the problem statements focus on process design (PROC), although in recent years, emphasis has been shifting toward product design (PROD). See especially the recent projects under pharmaceuticals, biomedicals, and electronic materials.

Credit is given to each of the formulators for their problem statements. In addition, the names of the contributors are listed here with many thanks; their contributions in preparing these design problems have been crucial to the success of the design course.

Rakesh Agrawal	Air Products and Chemicals (now at Purdue Univ.)
E. Robert Becker	Environex, Wayne, Pennsylvania
Richard Bockrath	Consultant (formerly DuPont)
David D. Brengel	Air Products and Chemicals (now at Avalence LLC)
Adam A. Brostow	Air Products and Chemicals
Robert M. Busche	Bio-en-gene-er Associates, Wilmington, Delaware
Leonard A. Fabiano	CDI Corporation (formerly ARCO Chemical and Lyondell)
Brian E. Farrell	Air Products and Chemicals
Mike Herron	Air Products and Chemicals
F. Miles Julian	DuPont
Ralph N. Miller	DuPont
Robert Nedwick	Pennsylvania State University (formerly ARCO Chemical and Lyondell)
Frank Petrocelli	Air Products and Chemicals
Mark R. Pillarella	Air Products and Chemicals
Matthew J. Quale	Mobil Technology Company
Tiffany Rau	Eli Lilly Corporation – Puerto Rico
William B. Retallick	Consultant, West Chester, Pennsylvania
Gary Sawyer	Consultant (formerly Lyondell Chemical Company)
David G.R. Short	University of Delaware (formerly DuPont)
Peter Staffeld	Exxon/Mobil (now at Villanova University)
Albert Stella	General Electric (formerly AlliedSignal)
Edward H. Steve	Consultant (formerly CDI Engineering Group)
Matthew Targett	LP Amina (Beijing, China)
Steven M. Tieri	DuPont
Bjorn D. Tyreus	DuPont
Kamesh G. Venugopal	Air Products and Chemicals
Bruce Vrana	DuPont
Andrew Wang	Air Products and Chemicals
Steve Webb	Air Products and Chemicals
John Wismer	Arkema, Inc. (formerly Atochem North America)
Jianguo Xu	Air Products and Chemicals

Appendix III

Materials of Construction

The selection of materials of construction based on strength, corrosivity, and cost of fabrication is vital to product and process design and economic evaluation. The most common materials for process equipment, which include metals, glass, plastics, and ceramics, are listed in Table A-III.1 with typical applications. Much more extensive tables are given by M. S. Peters, K. D. Timmerhaus, and R. E. West in *Plant Design and Economics for Chemical Engineers*, fifth edition (McGraw-Hill, New York, 2003); by G. D. Ulrich and P. T. Vasudevan in *Chemical Engineering Process Design and Economics: A Practical Guide*, second edition (Process (Ulrich) Publishing, Durham, New Hampshire, 2004); and in Section 25 of the eighth edition of *Perry's Chemical Engineers' Handbook* (McGraw-Hill, New York, 2008). Table A-III.1 should be used only for preliminary process design and economic evaluation. For final process design, corrosion and strength data as functions of temperature are needed for the expected chemical compositions within the process. Equipment vendors can also assist in the final selection of materials. In general, carbon steel is used whenever possible because of its low cost and ease of fabrication.

Table A-III.1 Materials of Construction for Process Equipment

Material	Maximum Temperature, °C (°F)	Typical Applications
Carbon steel (e.g., SA-285C) Cast iron (not strong) Ductile iron (stronger)	400 (750)	Cooling-tower water, boiler-feed water, steam, air, hydrocarbons, glycols, mercury, molten salts, acetone
Low alloy (Cr-Mo) steel (e.g., SA-387B)	500 (930)	Same as carbon steel, hydrogen
Stainless steel	700 (1,300)	Aqueous salt solutions, aqueous nitric acid, aqueous basic solutions, food intermediates, alcohols, ethers, freons, hydrogen, hydrogen sulfide, molten salts, molten metals
Aluminum	150 (300)	Aqueous calcium hydroxide, hydrogen, oxygen
Copper and copper alloys, aluminum bronze, brass, bronze	150 (300)	Aqueous sulfate and sulfite solutions, hydrogen, nitrogen, alcohols and other organic chemicals, cooling-tower water, boiler-feed water
Nickel-based alloys (e.g., Hastelloy, Inconel, Monel, Incoloy, Carpenter 20)	400 (750)	Aqueous nitric and organic acids, flue gases, chlorine, bromine, halogenated hydrocarbons, ammonia, sulfur dioxide, sulfur trioxide, organic solvents, brackish water, seawater
Titanium-based alloys	400 (750)	Aqueous solutions, carbon dioxide, organic solvents
Conventional plastics (polyethylene, polypropylene, ABS)	50–120 (120–250)	Aqueous solutions at near-ambient temperatures

(Continued)

Table A-III.1 (*Continued*)

Material	Maximum Temperature, °C (°F)	Typical Applications
Fluorocarbon plastics	250 (480)	Almost everything except halogens and halogenated chemicals
Rubber lining	250 (480)	Aqueous salt solutions and aqueous basic solutions at near-ambient temperatures
Glass lining	250 (480)	Aqueous sulfuric acid solutions, almost everything except fluorine and hydrogen fluoride
Ceramics	2,000 (3,630)	Almost all aqueous solutions except hydrogen fluoride and sodium hydroxide at near-ambient temperatures; most gases except fluorine and hydrogen fluoride; most solvents; water
Graphite	2,000 (3,630)	Aqueous salt and base solutions; organic solvents Cl_2, HCl, H_2, H_2S, N_2, Hg; hydrocarbons; molten salts

Table of Acronyms

Acronym	Description
•OH	Hydroxyl Radical
2,4-D	2,4-Dichlorophenoxyacetic Acid
3M	Minnesota Mining and Manufacturing
ABET	Accreditation Board for Engineering and Technology
ABS	Acrylonitrile-butadiene-styrene
ACFM	Actual Cubic Feet per Minute
ACRS	Accelerated Cost Recovery System
ADP	Adenosine Diphosphate
AIChE	American Institute of Chemical Engineers
AM-LCD	Active Matrix Liquid Crystal Display
APC	Advanced Process Control
APEA	Aspen Process Economic Analyzer
API	American Petroleum Institute
ASCE	American Society of Civil Engineers
ASHRAE	American Society of Heating, Refrigerating, and Air-Conditioning Engineers
a-Si	Amorphous Silicon
ASME	American Society for Mechanical Engineers
ATOI	After Tax Operating Income
ATP	Adenosine Triphosphate
ATR	Adiabatic Temperature Rise
B2B	Business-to-Business
B2C	Business-to-Consumer
BFD	Block Flow Diagram
bfw	Boiler Feed Water
BOD	Biochemical Oxygen Demand
BWG	Birmingham Wire Gauge
C&R	Controllability and Resiliency
CAD	Computer-aided design (CAD)
CAGR	Compounded Annual Growth Rate
CAMbD	Computer-aided Tools for Mixture-blend Design
CAPEC	Computer Aided Product-Process Engineering Center
CAS	Chemical Abstract Service (number)
CC	Composition Controller

Acronym	Description
CCD	Charge Coupled Device
CCPS	Center for Chemical Process Safety
CD	Compact Disc
CD-ROM	Compact Disc Read Only Memory
CE	Chemical Engineering Plant Cost Index
CEO	Chief Executive Officer
CFC	Chlorofuorocarbon
CFD	Computational Fluid Dynamics
CFL	Compact Fluorescent Lamp/Light
CHO	Chinese Hamster Ovary
CI	Composition Interval; Concentration Interval
CIP	Clean In Place
COD	Chemical Oxygen Demand
COG	Coke Oven Gas
COM	Cost of Manufacture
CPI	Consumer Price Index
CSB	Chemical Safety and Hazard Investigation Board
CSTR	Continuous Stirred Tank Reactor
CTE	Coefficient of Thermal Expansion
CTQ	Critical to Quality
cw	Cooling Water
DAA	Die Attach Adhesive
DB	Declining Balance
DBEF	Dual Brightness Enhancement Film
DC	Disturbance Cost
DCFRR	Discounted Cash Flow Rate of Return
DDB	Double Declining Balance
DDT	Dichloro-diphenyl Trichloroethane
DEE	Diethyl Ether
DIERS	Design Institute for Emergency Relief Systems
DIPPR	Design Institute for Physical Properties
DJIA	Dow Jones Industrial Average
DMAIC	Define, Measure, Analyze, Improve, and Control
DOE	Design of Experiment
DOF	Degree of Freedom
DPI	Direct Permanent Investment
DPMO	Defects per Million Opportunities
DSC	Differential Scanning Calorimetry

Acronym	Description
DTB	Draft Tube Baffled
DTBP	Di-tertiary-Butyl Peroxide
DVD	Digital Video Disc
DW&B	Direct Wages and Benefits
EBIT	Earnings before Income Tax
EDGE	Enhanced Data rates for Global Evolution
EDTA	Ethylenediaminetetraacetic Acid
EG	Ethylene Glycol
ENIAC	Electronic Numerical Integrator And Computer
ENR	Engineering News Record Construction Cost Index
EOS	Equation of State
EPA	Environmental Protection Agency
EPL	Emek Project Ltd
ESA	Energy Separating Agent
ESRD	End State Renal Disease
FC	Flow Controller; Fully Coupled
FDA	Food and Drug Administration
fg	Fuel Gas
FMC	Food, Machinery, and Chemical
FP	Fluorescence Polarization
FRET	Fluorescent Resonance Energy Transfer
FTS	Fitness To Standard
FUG	Fenske Underwood Gilliland
FWR	Flash With Recycle
GAC	Granular Activated Carbon
GAMS	General Algebraic Modeling System
GC	Group Contribution
GCA	Group Contribution Assembly
GCC	Grand Composite Curve
GE	General Electric; General Expenses; Gibbs Energy (Excess)
GRG	Generalized Reduced Gradient
GUI	Graphical User Interface
GWP	Global Warming Potential
HAP	Hazardous Air Pollutant
HAZAN	Hazard Analysis
HAZOP	Hazard and Operability
HB-LED	High-Brightness Light Emitting Diode
HDA	Hydrodelakylation

Acronym	Description
HEN	Heat Exchanger Network
HEPA	High Efficiency Particulate Absorption
HETP	Height Equivalent of a Theoretical Plate
HETS	Height Equivalent of a Theoretical Stage
HF	Hydrofluoric Acid
HFC	Hydrofluorocarbon
HHV	Higher Heating Value
HLB	Hydrophilic-Lipophilic Balance
HME	Heat and Mass Exchanger
HOQ	House of Quality
hps	High-Pressure Steam
HSC	Horizontal Split Case
HTML	HyperText Markup Language
HTRF	Homogeneous Time-Resolved Fluorescence
HTU	Height of a Transfer Unit
HX	Hydrogen Halides
IC	Integrated Circuit
IEEE	Institute of Electrical and Electronics Engineers
IFO	Income from Operations
IMC	Internal Model Control
IND	Investigational New Drug
IP	Intellectual Property
IPA	iso-Propanol
IPE	Icarus Process Evaluator
ips	Intermediate Pressure Steam
IR	Infrared
IRR	Investor's Rate of Return
IS	Intermediate Storage
ISO	International Organization for Standardization
ITO	Indium Tin Oxide
KE	Kinase Enzyme
KI	Kinase Inhibitor
KJ	Kawakita, Jiro
KKT	Karush–Kuhn–Tucker
LC	Level Controller
LCD	Liquid Crystal Display
LCL	Lower Control Limit
LDPE	Low-density Polyethylene

Acronym	Description
LED	Light Emitting Diode
LFL	Lower Flammability Limit
LHV	Lower Heating Value
LLE	Liquid Liquid Equilibrium
LOC	Loss of Control
LP	Linear Program
lps	Low Pressure Steam
M&O-SW&B	Maintenance and Operations—Salary, Wages, & Benefits
MAC	Marginal Annualized Cost
MACRS	Modified Accelerated Cost Recovery System
MBBA	4-Methoxy Benzylidene-4-Butylaniline
MCB	Monochlorobenzene
MD	Molecular Dynamics
MEN	Mass Exchange Network
MER	Minimum Energy Requirement; Maximum Energy Recovery
MESH	Material balance, Equilibrium, Summation of mole fractions, Heat balance
M-G	Marerro-Gani (property model)
MI	Main Ingredient
MIC	Methyl Isocyanate
MILP	Mixed Integer Linear Program
MINLP	Mixed Integer Nonlinear Program
MIT	Massachusetts Institute of Technology
ML	Direct Materials & Labor
MO	Magneto Optical
MOC	Materials of Construction; Minimum Operating Cost; Minimum Oxygen Concentration
MOCVD	Metal Organic Chemical Vapor Deposition
mps	Medium Pressure Steam
MS	Marshall & Swift Equipment Cost Index
MSA	Mass Separating Agent
MSDS	Material Safety Data Sheet
MTBE	Methyl Tertiary-butyl Ether
MVR	Marginal Vapor Rate
MW&B	Maintenance, Wages, and Benefits
NF	Nelson Farrar Refinery Construction Cost Index
NFPA	National Fire Protection Association
NLP	Nonlinear Program
Nortel	Northern Telecom
NPSH	Net Positive Suction Head

Acronym	Description
NPV	Net Present Value
NREL	National Renewable Energy Laboratory
NRTL	Non-Random Two Liquid (GE model)
NSF	National Science Foundation
NSPE	National Society of Professional Engineers
NTU	Number of a Transfer Unit
NUD	New, Unique, and Difficult
NWC	Net Working Capital
O/W	Oil-in-Water
OCF	Operating Cash Flow
ODP	Ozone Depletion Potential
ODP	Ozone Depletion Potential
OEC	Online Ethics Center
OPEC	Organization of the Petroleum Exporting Countries
OSHA	Occupational Safety and Health Agency
OTL	Outer Tube Limit
P&G	Proctor & Gamble
P&ID	Piping and Instrumentation Diagram
PBA	Packed Bed Adsorption
PBP	Payback Period
PBS	Phosphate Buffer Solution
PC	Pressure Controller
PCF	Project Cash Flow
PCO	Photocatalytic Oxidation
PC-SAFT	Perturbed Chain Statistical Association Fluid Theory
PDA	Personal Data Assistant
PDMS	Poly-dimethylsiloxane
PDP	Plasma Display Panel
PET	Polyethylene Terephthalate
PFD	Process Flow Diagram
PFR	Plug Flow Reactor
PFTR	Plug Flow Tubular Reactor
PI	Proportional-Integral Controller
PID	Proportional-Integral-Derivative Controller
PLS	Personal Laboratory System
pr	Propane Refrigerant
PR	Peng-Robinson
ProCAMD	Software tool for CAMD

Acronym	Description
p-Si	Polymorphous Silicon
PVA	Polyvinyl Alcohol
PVAc	Polyvinyl Acetate
PVC	Polyvinylchloride
PVP	Polyvinylpyrrolidone
QFD	Quality Functional Deployment
QSAR	Quantitative Structure Activity Relationship
R&D	Research and Development
RAT2IO	Resources, Activities, Time and Tools, Input/Output Information, and Objective
rb	Refrigerated Brine
RDC	Rotating Disk Contactor
RDT	RainDance Technology
RGA	Relative Gain Array
RH	Relative Humidity
RO	Reverse Osmosis
ROA	Return On Total Assets
ROE	Return On Equity
ROI	Return On Investment
RON	Research Octane Number
ROR	Simple Rate of Return
ROROI	Rate of Return On Investment
RVP	Reid Vapor Pressure
SARS	Severe Acute Respiratory Syndrome
SCC	Stress Corrosion Crack
SCFM	Standard Cubic Feet per Minute
SCN	Steam Cracked Naphtha
SGPDP	Stage-Gate Product-Development Process
SGTDP	Stage-Gate Technology-Development Process
SIP	Steam In Place
SL	Straight Line
SLE	Solid Liquid equilibrium
SLP	Successive Linear Programming
SMART	Specific, Measurable, Agreed-upon, Realistic, and Time-based
SMILES	Simplified Molecular-Input Line-Entry System
SQP	Successive Quadratic Programming
SRI	Stanford Research Institute
SRK	Soave Redlich-Kwong
SS	Steady State
SSCF	Simultaneous Saccharification and Fermentation

Acronym	Description
SYD	Sum of the Years Digits
TBA	Tertiary-butyl Alcohol
TBM	Total Bare Module
TC	Temperature Controller; Total Capital
TCI	Total Capital Investment
TDC	Total Depreciable Capital
TDE	Thermodynamic Data Engine
TEFC	Totally Enclosed Fan Cooled
TEMA	Tubular Exchangers Manufacturers Association
TFT	Thin Film Transistor
TGA	Thermo Gravimetric Analysis
TI	Temperature Interval
TNT	Trinitro-toluene
tPA	Tissue Plasminogen Activator
TPI	Total Permanent Investment
TRC	Thermodynamics Research Center
TRI	Toxic Chemical Release Inventory
TY	Throughput Yield
UCL	Upper Control Limit
UFL	Upper Flammability Limit
UIS	Unlimited Intermediate Storage
UL	Underwriters Laboratories
UNIFAC	Universal Functional-Activity Coefficients (GE model)
UNIQUAC	UNIversal QUasi-chemical Activity Coefficients (GE model)
UV	Ultraviolet
VED	Viscous Energy Dissipation
VLE	Vapor Liquid Equilibrium
VLLE	Vapor Liquid-Liquid Equlibrium
VOC	Voice of the Customer; Volatile Organic Compound
VOCs	Volatile Organic Compounds
VOM	Voice of the Market
VP	Venture Profit
VPPD-lab	Virtual Product-Process Design Laboratory (software tool)
VSC	Vertical Split Case
W/O	Water-in-Oil
WC	Working Capital
WFI	Water For Injection
WWW	World Wide Web
ZW	Zero Wait

Author Index

Page Numbers	*Definitions*
1, 2,...	Page numbers in textbook
C11S-1.X	Section number X in Supplement_to_Chapter_11-1.pdf in PDF Files folder on Web Site
C11S-2.X	Section number X in Supplement_to_Chapter_11-2.pdf in PDF Files folder on Web Site
C18S.X	Section number X in Supplement_to_Chapter_18.pdf in PDF Files folder on Web Site
C20S.X	Section number X in Supplement_to_Chapter_20.pdf in PDF Files folder on Web Site

Subject Index

Page Numbers	*Definitions*
1, 2,…	Page numbers in textbook
C11S-1.X	Section number X in Supplement_to_Chapter_11-1.pdf in PDF Files folder on Web Site
C11S-2.X	Section number X in Supplement_to_Chapter_11-2.pdf in PDF Files folder on Web Site
C18S.X	Section number X in Supplement_to_Chapter_18.pdf in PDF Files folder on Web Site
C20S.X	Section number X in Supplement_to_Chapter_20.pdf in PDF Files folder on Web Site
AIIS-X to Y	Page X to Y in Supplement_to_Appendix_II.pdf in PDF Files folder on Web Site
PDF-APEA	In Aspen APEA Course Notes.pdf in PDF Files folder on Web Site

WILEY END USER LICENSE AGREEMENT

Go to www.wiley.com/go/eula to access Wiley’s ebook EULA.